TRANSACTIONS

OF THE

AMERICAN SOCIETY

OF

CIVIL ENGINEERS

(INSTITUTED 1852)

VOLUME 120

1955

Edited by the Executive Secretary, under the direction of the Committee on Publications.

Reprints from this publication, which is copyrighted, may be made on condition that the full title of paper, name of author, and page reference (or paper number) are given.

NEW YORK
PUBLISHED BY THE SOCIETY

1955

Transp.
TA
1
.A526
v.120

Copyright 1955, by the AMERICAN SOCIETY OF CIVIL ENGINEERS

NOTE.—The Society is not responsible for any statement made or opinion expressed in its publications.

nsportation
Library
EB 3 '56

CONTENTS

PAPERS AND DISCUSSIONS

(Alphabetical Indexes Begin on Page 1583)

No. PAGE

2722 FLOCCULATION AND FLOCCULATION BASINS
By Thomas R. Camp 1

2723 SELECTION AND DESIGN OF HIGH-VOLUME, LOW-HEAD PUMPS
By George F. Snodgrass 17

2724 DETERMINATION OF RADII OF CURVATURE OF TAXIWAYS
By John Hugh Jones and Robert Horonjeff 27

2725 PHOTOELASTIC ANALOGY FOR NONHOMOGENEOUS FOUNDATIONS
By Allen J. Curtis and F. E. Richart, Jr. 35

2726 PLANNING AND OPERATING TURNPIKES
By Charles M. Noble 54

2727 DEFLECTIONS OF A CIRCULAR BEAM OUT OF ITS INITIAL PLANE
By Enrico Volterra 65
Discussion:
By I. Oesterblom 87
Enrico Volterra 87

2728 UNUSUAL FOUNDATION CONDITIONS IN THE EVERGLADES
By Paul H. Shea 92

2729 WELDED STRUCTURES: A SYMPOSIUM 103
STEEL REQUIREMENTS
By Simon A. Greenberg 104

DESIGN AND RESEARCH
By La Motte Grover 112

Discussion:
By Jack R. Benjamin 134
George W. Lamb 135
F. J. Tamanini 140
Norman B. Jones 143
La Motte Grover 144

FABRICATION AND CONSTRUCTION
By C. L. Kreidler 147

No. Page

2730 SAND COMPACTION BY VIBROFLOTATION
By Elio D'Appolonia, Callix E. Miller, Jr., and Thomas M. Ware 154

2731 WIND VELOCITIES DURING HURRICANES
By Robert C. Gentry 169

2732 INELASTIC BEHAVIOR OF REINFORCED CONCRETE MEMBERS
By Lawrence H. N. Lee 181

Discussion:
By Boris Bresler 203
Alfred J. Ashdown 205
Lawrence H. N. Lee 205

2733 ERECTION OF MAIN RIVER SPAN, PASSAIC RIVER BRIDGE
By Jonathan Jones 208

2734 THE IMPORTANCE OF SHORAN SURVEYING
By Carl I. Aslakson 225

2735 STRUCTURAL WELDING INSPECTION
By John L. Beaton and Paul G. Jonas 235

2736 CHESAPEAKE BAY BRIDGE
By Ethan F. Ball 245

2737 OPEN CHANNELS WITH NONUNIFORM DISCHARGE
By Wen-Hsiung Li 255

Discussion:
By Turgut Sarpkaya 275
Wen-Hsiung Li 278

2738 CORRECTION OF LANDSLIDES AND SLIPOUTS
By Arthur W. Root 281

2739 DISCHARGE CHARACTERISTICS OF TAINTER GATES
By Arthur Toch 290

2740 CONSTRAINED CIRCULAR BEAMS ON ELASTIC FOUNDATIONS
By Enrico Volterra and Randall Chung 301

2741 DEAD-LOAD-STRESS MEASUREMENT IN A LONG SPAN BRIDGE
By Lawrence T. Wyly, Maurice B. Lagaard, Ralph W. Kluge, Kenneth H. Lenzen, Edward W. Larson, Jr., and Lewis B. McCammon, Jr. 311

Discussion:
By Almon H. Fuller 336
Lawrence T. Wyly, Maurice B. Lagaard, Ralph W. Kluge, Kenneth H. Lenzen, Edward W. Larson, Jr., and Lewis B. McCammon, Jr. 337

2742 ISSUES IN HIGHWAY ENGINEERING EDUCATION
By Harmer E. Davis and Ralph A. Moyer 340

2743 SEWAGE AERATION PRACTICE IN CHICAGO
By Norval E. Anderson 351

No. PAGE

2744 **TRAFFIC AT AN INTERNATIONAL AIRPORT**
By **Walther Prokosch** 364

2745 **FLOW IN ROUGH CONDUITS**
By **Henry M. Morris, Jr.** 373

Discussion:
By VICTOR L. STREETER 399
WALTER RAND 400
HARRY H. AMBROSE 402
HENRY M. MORRIS, JR. 406

2746 **INDUSTRIAL DEVELOPMENT IN THE SOUTH**
By **Carl O. Hoyer** 411

Discussion:
By ROLAND A. KAMPMEIER 422

2747 **CONSTRUCTION OF THE ELIZABETH RIVER TUNNEL**
By **Joseph Peraino** 423

2748 **BACKWATER FUNCTIONS BY NUMERICAL INTEGRATION**
By **Clint J. Keifer and Henry Hsien Chu** 429

Discussion:
By FRANCIS F. ESCOFFIER 443
HENRY J. MILES 444
RICHARD SILVESTER 445
CLINT J. KEIFER AND HENRY HSIEN CHU 448

2749 **COMMUNITY AND NEIGHBORHOOD DEVELOPMENT**
By **Russell H. Riley** 449

2750 **TOTAL SEDIMENT LOAD MEASURED IN TURBULENCE FLUME**
By **Paul C. Benedict, Maurice L. Albertson, and Donald Q. Matejka** 457

Discussion:
By W. H. CORBETT, O. C. HANSEN, AND W. M. BORLAND 485
PAUL C. BENEDICT, MAURICE L. ALBERTSON, AND DONALD Q. MATEJKA 488

2751 **STATUTORY CONTROL OF GROUND WATER IN THE WESTERN UNITED STATES**
By **S. T. Harding** 490

2752 **IMPULSIVE MOTION OF ELASTO-PLASTIC BEAMS**
By **Hans H. Bleich and Mario G. Salvadori** 499

Discussion:
By P. S. SYMONDS 516
HANS H. BLEICH AND MARIO G. SALVADORI 518

2753 **TRANSIT LINING OF HIGH-SPEED TRACK**
By **Neil R. Berndt** 521

Discussion:
By HARRY RUBEY 538

No. PAGE
2754 MODERNIZATION OF THE HALES BAR PLANT
By **Adolf A. Meyer** 539

Discussion:
By GEORGE R. RICH 557
CLARENCE E. BLEE 558
GEORGE A. JESSOP 559
ADOLF A. MEYER 562

2755 EFFECT OF WELL SCREENS ON FLOW INTO WELLS
By **Jack S. Petersen, Carl Rohwer, and Maurice L. Albertson** 563

Discussion:
By WEN-HSIUNG LI 586
ARTHUR L. COLLINS 590
MOHAMMAD NAZIR AND NAZIR AHMAD 593
MATTHEW I. RORABAUGH 595
DEAN F. PETERSON, JR. 597
G. COHEN DE LARA 598
GÉRARD TISON, JR. 601
JACK S. PETERSEN, CARL ROHWER, AND MAURICE L. ALBERTSON 604

2756 THE TRAINING OF CITY PLANNERS
By **Howard K. Menhinick** 608

Discussion:
By JORMA J. SALOVAARA 613

2757 ANALYSIS AND TESTS OF A CYLINDRICAL SHELL ROOF MODEL
By **Bruno Thürlimann and Bruce G. Johnston** 615

Discussion:
By G. C. ERNST 644
CHARLES S. WHITNEY 645
BOYD G. ANDERSON 646
BRUNO THÜRLIMANN AND BRUCE G. JOHNSTON 648

2758 APPLICATIONS OF THE RELAXATION TECHNIQUE IN FLUID MECHANICS
By **John S. McNown, En-Yun Hsu, and Chia-Shun Yih** 650

Discussion:
By FRED W. BLAISDELL 670
HENRY M. PAYNTER AND RONALD F. SCOTT 671
MLADEN BORELI 677
TURGUT SARPKAYA 681
JOHN S. MCNOWN, EN-YUN HSU, AND CHIA-SHUN YIH 684

2759 SEDIMENT SAMPLING IN TIDAL WATERWAYS
By **Edward A. Schultz** 687

2760 PRESSURE SURGES IN PUMP INSTALLATIONS
By **John Parmakian** 697

Discussion:
By CARROLL E. WITHERS 717
PETER LINTON 717
JOHN PARMAKIAN 719

No. Page

2761 AERODYNAMIC STABILITY OF SUSPENSION BRIDGES: 1952 REPORT OF THE ADVISORY BOARD ON THE INVESTIGATION OF SUSPENSION BRIDGES..... 721

2762 ASEISMIC DESIGN OF FIRMLY FOUNDED ELASTIC STRUCTURES
By Lawrence E. Goodman, Emilio Rosenblueth, and Nathan M. Newmark....... 782

2763 REDUCTION IN SOIL STRENGTH WITH INCREASE IN DENSITY
By Charles R. Foster.. 803

Discussion:
By Edward S. Barber.. 816
George R. Halton.. 817
Charles R. Foster.. 821

2764 EVALUATION OF THE PERFORMANCE OF BIOFILTRATION PLANTS
By Renville S. Rankin.. 823

Discussion:
By Peter Homack.. 836
Renville S. Rankin.. 841

2765 FINANCING OF SEWAGE WORKS IN PENNSYLVANIA
By Samuel I. Zack.. 843

2766 HIGH-VELOCITY TESTS IN A PENSTOCK
By Maxwell F. Burke.. 863

Discussion:
By Steponas Kolupaila.. 884
Frank B. Campbell.. 887
Arthur L. Collins.. 888
R. Clifford Youngquist.. 893
Maxwell F. Burke.. 894

2767 STABILIZATION OF MUNICIPAL REFUSE BY COMPOSTING
By Percy H. McGauhey and Harold B. Gotaas.. 897

Discussion:
By Arthur W. Furbank.. 916
Percy H. McGauhey and Harold B. Gotaas.. 918

2768 MOTION OF PARTICLES ON BED OF A TURBULENT STREAM
By Arthur T. Ippen and Ramjee P. Verma.. 921

2769 STRESS MEASUREMENTS, SAN LEANDRO CREEK BRIDGE
By Ray W. Clough and Charles F. Scheffey.. 939

2770 TRANQUIL FLOW THROUGH OPEN-CHANNEL CONSTRICTIONS
By Carl E. Kindsvater and Rolland W. Carter.. 955

Discussion:
By Emmett M. Laursen and Arthur Toch.. 981
Fred W. Blaisdell.. 981
Pin-Nam Lin.. 982
Carl F. Izzard.. 985
Chesley J. Posey.. 990
Carl E. Kindsvater and Rolland W. Carter.. 991

No. Page

2771 BACKWATER EFFECTS OF OPEN-CHANNEL CONSTRICTIONS
By **Hubert J. Tracy and Rolland W. Carter** 993

Discussion:
By Paul V. Hodges 1007
Carl F. Izzard 1008
Harold R. Henry 1013
Hubert J. Tracy and Rolland W. Carter 1017

2772 PLASTIC STRENGTH OF STRUCTURAL MEMBERS: A SYMPOSIUM 1019
FOREWORD
By **the Committee of the Engineering Mechanics Division on Plasticity Related to Design** 1020

PLASTIC DEFORMATION OF WIDE-FLANGE BEAM-COLUMNS
By **Robert L. Ketter, Edmund L. Kaminsky, and Lynn S. Beedle** 1028

Discussion:
By George Winter 1062
Robert L. Ketter, Edmund L. Kaminsky, and Lynn S. Beedle 1065

ECCENTRICALLY LOADED, END-RESTRAINED COLUMNS
By **Paul P. Bijlaard, Gordon P. Fisher, and George Winter** 1070

Discussion:
By Robert L. Ketter and Lynn S. Beedle 1097
John F. Baker and Michael R. Horne 1104
Paul P. Bijlaard, Gordon P. Fisher, and George Winter 1105

ECCENTRICALLY LOADED ALUMINUM COLUMNS
By **John W. Clark** 1116

INVESTIGATION AND LIMIT ANALYSIS OF NET AREA IN TENSION
By **W. Gordon Brady and Daniel C. Drucker** 1133

Discussion:
By William H. Munse 1155
Paul P. Bijlaard 1156
W. Gordon Brady and Daniel C. Drucker 1163

2773 LATERAL BUCKLING OF I-BEAMS
By **Mario G. Salvadori** 1165

Discussion:
By Robert V. Whitman 1178
Michael R. Horne 1179
Mario G. Salvadori 1182

2774 MOVEMENTS IN STRUCTURAL CONCRETE IN A POWERHOUSE
By **Stanley Moyer and Viggo Hansen** 1183

Discussion:
By E. A. Woodhead 1193
Herbert A. Kammer 1196
Stanley Moyer and Viggo Hansen 1198

2775 THE UNDISTURBED CONSOLIDATION BEHAVIOR OF CLAY
By **John H. Schmertmann** 1201

Discussion:
By Robert L. Crisp, Jr. 1228
John H. Schmertmann 1229

No. PAGE

2776 DESIGN OF STABLE CHANNELS
By **Emory W. Lane** 1234
Discussion:
By Serge Leliavsky 1261
A. Nizery and G. Braudeau 1266
N. K. Bose 1269
José S. Gandolfo 1271
Emory W. Lane 1275

2777 STRUCTURAL OBSERVATIONS OF THE KERN COUNTY EARTHQUAKE
By **Henry J. Degenkolb** 1280

2778 HIGH-STRENGTH BOLTS IN STRUCTURAL JOINTS: A SYMPOSIUM 1295
HISTORY OF THE USE OF HIGH-STRENGTH BOLTS
By **W. C. Stewart** 1296

LABORATORY TESTS OF BOLTED JOINTS
By **William H. Munse, D. T. Wright, and Nathan M. Newmark** 1299
Discussion:
By A. J. Francis 1319
William H. Munse, D. T. Wright, and Nathan M. Newmark 1320

COMPARISON OF BOLTED AND RIVETED JOINTS
By **Frank Baron and Edward W. Larson, Jr.** 1322

SLIP OF JOINTS UNDER STATIC LOADS
By **R. A. Hechtman, D. R. Young, A. G. Chin, and E. R. Savikko** 1335

FATIGUE IN RIVETED AND BOLTED SINGLE-LAP JOINTS
By **Jack W. Carter, Kenneth H. Lenzen, and Lawrence T. Wyly** 1353
Discussion:
By Glenn B. Woodruff 1381
Karl de Vries 1381
Harry C. Prince 1382
Jack W. Carter, Kenneth H. Lenzen, and Lawrence T. Wyly 1383

STRUCTURAL USES OF HIGH-STRENGTH BOLTS
By **T. R. Higgins and E. J. Ruble** 1389

2779 HYDRAULIC MODEL STUDIES OF MARTIN DAM DRAFT TUBES
By **Carl E. Kindsvater and Richard R. Randolph, Jr.** 1399
Discussion:
By Richard S. Woodruff 1416
Carl E. Kindsvater and Richard R. Randolph, Jr. 1418

2780 STRENGTH CHARACTERISTICS OF COMPACTED CLAYS
By **Gerald A. Leonards** 1420
Discussion:
By Harold J. Gibbs and Jack W. Hilf 1455
James K. Mitchell 1462
Preston T. Bennett and Paul E. Wohlt 1467
Gerald A. Leonards 1474

No. PAGE

2781 **SOME ECONOMIC ASPECTS OF WATERWAY PROJECTS**

By **Haywood R. Faison** 1480

Discussion:

By Duane Orr 1526
L. Perry Cookingham 1528
Marvin B. Marsh 1530
Owen G. Stanley 1532
Herman W. Schull, Jr. 1536
Nels C. Magnuson 1537
Braxton B. Carr 1538
Cyril E. Childe 1539
Francis J. Wilson and Newton R. Graham 1542
Charles L. Hall 1543
James Warren Davis 1545
Haywood R. Faison 1546

2782 **BACKSIGHTS AND FORESIGHTS: ADDRESS AT THE SUMMER CONVENTION, ST. LOUIS, MO., JUNE 15, 1955**

By **William Roy Glidden, President** 1550

MEMOIRS OF DECEASED MEMBERS: ABSTRACTS 1557

SUBJECT INDEX 1583

AUTHOR INDEX 1628

PAPERS PUBLISHED AUGUST, 1953-JANUARY, 1955, INCLUSIVE, AS ASCE PROCEEDINGS-SEPERATES, ACCEPTED FOR FUTURE PUBLICATION IN TRANSACTIONS, BUT NOT INCLUDED IN VOL. 120*

No.		*Proceedings-Separates*
234	APPRAISAL OF ONE-WAY STREET SYSTEM IN SACRAMENTO, CALIFORNIA By D. J. Faustmann	August, 1953
250	NUMERICAL ANALYSIS OF FRAMES WITH CURVED GIRDERS By James Michalos	August, 1953
300	DESIGNING ALUMINUM ALLOY MEMBERS FOR COMBINED END LOAD AND BENDING By H. N. Hill, E. C. Hartmann, and J. W. Clark	October, 1953
306	AN ENGINEERING APPROACH TO BLAST RESISTANT DESIGN By N. M. Newmark	October, 1953
316	THE EFFECT OF JET AIRCRAFT ON AIRPORT PAVEMENTS: INVESTIGATIONS CONDUCTED BY THE CORPS OF ENGINEERS By Gayle McFadden	October, 1953
324	PILE LOADING TESTS, MORGANZA FLOODWAY CONTROL STRUCTURE By Charles I. Mansur and John A. Focht, Jr.	November, 1953
342	THE PROBLEMS OF CIVIL AND STRUCTURAL DESIGN OF STEAM ELECTRIC PLANTS FOR THE PACIFIC GAS AND ELECTRIC COMPANY IN CENTRAL CALIFORNIA By W. L. Dickey	November, 1953
351	VERTICAL SAND DRAINS FOR STABILIZATION OF MUCK-PEAT SOILS By J C Carpenter and Edward S. Barber	November, 1953
352	CONCEPTS OF ENGINEERING BIOTECHNOLOGY IN OCCUPATIONAL HEALTH By Alvin F. Meyer	November, 1953
369	UNSTEADY FLOW IN OPEN TYPE PIPE IRRIGATION SYSTEMS By E. H. Taylor, A. F. Pillsbury, T. O. Ellis, and G. A. Bekey	December, 1953
387	AN EXPERIMENTAL STUDY OF BUBBLES MOVING IN LIQUIDS By W. L. Haberman and R. K. Morton	January, 1954
393	SURVEYS AND MAPS FOR PIPELINES By George E. MacDonald	January, 1954
406	DEVELOPMENT OF AN INTERNATIONAL AIRPORT By Earle M. Rader	February, 1954
422	TREATMENT AND DISPOSAL OF ATOMIC ENERGY INDUSTRY WASTES By Joseph A. Lieberman and Arthur E. Gorman	March, 1954
431	MORNING-GLORY SHAFT SPILLWAYS: PROTOTYPE BEHAVIOR By J. N. Bradley	April, 1954
432	MORNING-GLORY SHAFT SPILLWAYS: DETERMINATION OF PRESSURE-CONTROLLED PROFILES By W. E. Wagner	April, 1954

---

* Also to be included: "Experimental Studies of Air Entrainment in Open Channel Flow," by Lorenz G. Straub and Owen P. Lamb, *Proceedings*, Minnesota International Hydraulics Convention, August, 1953, p. 425.

No.		
433	MORNING-GLORY SHAFT SPILLWAYS: PERFORMANCE TESTS ON PROTOTYPE AND MODEL By A. J. Peterka	April, 1954
449	NON-UNIFORM TORSION OF PLATE GIRDERS By Gerald G. Kubo, Bruce G. Johnston, and William J. Eney	June, 1954
462	FACTORS INFLUENCING IRRIGATION IN HUMID AREAS By Tyler H. Quackenbush	July, 1954
468	SAFETY AND THE PROBABILITY OF STRUCTURAL FAILURE By A. M. Freudenthal	August, 1954
471	INCINERATION AND ALTERNATIVE REFUSE DISPOSAL PROCESSES By Ralph Stone and F. R. Bowerman	August, 1954
475	SAFE LOADS ON DOG-LEG PILES By James D. Parsons and Stanley D. Wilson	August, 1954
505	IMPROVING THE LOAD CARRYING CAPACITIES OF SUBGRADES By Charles M. Noble	September, 1954
524	A MODERN MILITARY GRID SYSTEM By Floyd W. Hough	October, 1954
526	VERIFICATION OF THEORY FOR OBLIQUE STANDING WAVES By Arthur T. Ippen and Donald R. F. Harleman	October, 1954
527	LATERAL BUCKLING OF CANTILEVERED I-BEAMS UNDER UNIFORM LOADS By Stanley Poley	October, 1954
528	ANALOG COMPUTERS APPLIED TO ELASTIC-PLASTIC SYSTEMS By Leo Schenker and Gunther Martin	October, 1954
529	BEAM RESTRAINTS PROVIDED BY WALLS WITH OPENINGS By I. A. Mohammed and E. P. Popov	October, 1954
534	THE BOX INLET DROP SPILLWAY AND ITS OUTLET By Fred W. Blaisdell and Charles A. Donnelly	November, 1954
540	THE VIBRATION OF STEEL STACKS By Walter L. Dickey and Glenn B. Woodruff	November, 1954
541	RESONANT VIBRATION OF STEEL STACKS By E. A. Dockstader, W. F. Swiger, and Emory Ireland	November, 1954
542	THE OCTAGONAL GIRDER FOUR COLUMN SPACE FRAME By P. C. Disario, J. S. Podolan, and N. A. Weil	November, 1954
544	EXAMPLES OF TIMBER STRUCTURE FAILURES By Michael N. Salgo	November, 1954
558	AN INFLUENCE LINE ANALYSIS FOR SUSPENSION BRIDGES By David J. Peery	December, 1954
562	MOMENTS AND DEFLECTIONS IN STEEL GRID BRIDGE FLOORS By H. J. Greenberg	December, 1954
565	THE PRESENT STATUS OF RESEARCH ON SEDIMENT TRANSPORT By Ning Chien	December, 1954

No.		*Proceedings-Separates*
566	SIMILARITY OF DISTORTED RIVER MODELS WITH MOVABLE BED By H. A. Einstein and Ning Chien	December, 1954
567	FLOW EXPANSION AND PRESSURE RECOVERY IN FLUIDS By Harold Tults	December, 1954
570	EFFECT OF SAMPLE DISTURBANCE ON THE STRENGTH OF A CLAY By Max L. Calhoon	December, 1954
583	ULTIMATE SLOPES AND DEFLECTIONS—A BRIEF FOR LIMIT DESIGN By George C. Ernst	January, 1955
587	WIND LOADS ON GIRDER BRIDGES By John M. Biggs, Saul Namyet, and Jiro Adachi	January, 1955
599	PRIVATE ENTERPRISE CAN MEET THE PARKING DEMAND By C. T. McGavin	January, 1955
602	ORGANIZATION FOR METROPOLITAN TRAFFIC AND TRANSPORTATION PLANNING By Charles A. Blessing	January, 1955
604	A NEW APPROACH TO TURBULENT BOUNDARY LAYER PROBLEMS By Donald Ross	January, 1955

ERRATA

Transactions, Vol. 119, 1954

Page 198, Fig. 3, the curve labeled Eq. 6*b* should also be labeled "B H" to indicate that the Blume-Hesselmeyer procedure and Eq. 6*b* lead to identical results.

Page 200, Table 10, the value in Col. 8 for $i = 1$ should be -0.6132.

Page 200, Fig. 5, the abscissa should read "Value of the Left Side of Eq. 77×10^{-3}."

Page 1209, Fig. 12(*c*), the right-hand load, $P/2$, should be shown acting upward.

Page 1284, Fig. 21, the two distances denoted as "27.2 ft" should be "27.2 kips."

Page 1368, line 5, "Ingo County" should be "Inyo County."

Transactions, Vol. 120, 1955

Page 297, Eq. 11 should read

$$\frac{H_L}{\dfrac{V^2}{2g}} = \left(\frac{y_2}{y_1}\right)^2 - 4\,\frac{\left(\dfrac{y_2}{y_1}\right)^2 - \left(\dfrac{y_2}{y_1}\right)}{\left(\dfrac{y_2}{y_1}\right) + 1} - 1 \ldots\ldots\ldots\ldots (11)$$

Page 331, Fig. 16, the panel point designated as L_{14} should read U_{14}.

Page 356, Table 3, the final-settling sludge index according to F. W. Mohlman for the Calumet Works should be 58 and not 8, and the final-settling sludge index according to W. Donaldson for the Calumet Works should be 1.72 and not 51.72.

Page 361, the word "less" should be substituted for the word "more" in the second line of the fourth paragraph.

AMERICAN SOCIETY OF CIVIL ENGINEERS
Founded November 5, 1852
TRANSACTIONS

Paper No. 2722

FLOCCULATION AND FLOCCULATION BASINS

By Thomas R. Camp,[1] M. ASCE

Synopsis

An important process in the treatment of water, sewage, and industrial wastes is the formation of suspended flocs which can be effectively removed from the liquid by settling or filtration. This process is known as flocculation or coagulation. Prior to 1920, the nature of the process was not well understood by sanitary engineers and was frequently confused with mixing—the purpose of which is to distribute the coagulating chemicals in the liquid being treated so as to promote solution of the chemicals and completion of the chemical reactions. It has since been learned that flocculation is a physical process requiring gentle turbulence and time. Little progress has been made, however, in the scientific development of the principles involved and their application to design.

The fundamental theory of the physical process of floc formation is presented in this paper, together with evidence of experimental verification. The paper also includes procedures in the practical application of the theory to design of flocculation apparatus and basins.

Notation

The letter symbols adopted for use in this paper are defined where they first appear and are arranged alphabetically, for convenience of reference, in the Appendix.

Theory of Flocculation

The completion of the chemical reactions in a coagulation or softening process is almost instantaneous after the chemicals are fully dissolved. The precipitates first formed by the chemical reactions are crystals of molecular size. The initial increase in size of these colloidal crystals is caused by true diffusion or Brownian motion. At this stage the particles are still too small to be seen by the naked eye. The completion of the coagulation process requires gentle turbulent mixing of the suspension. It has been shown by D. A. Root, A. M.

Note.—Published, essentially as printed here, in September, 1953, as *Proceedings-Separate No. 283*. Positions and titles given are those in effect when the paper was received for publication.

[1] Cons. Engr., Camp, Dresser & McKee, Boston, Mass.

ASCE, B. V. Bhoota, M. ASCE, and the writer[2] that the Brownian-motion phase of coagulation is completed in a few seconds and is therefore of negligible importance in fixing tank dimensions as compared to the turbulent-mixing phase.

It has been demonstrated[3,4] that the rate of flocculation caused by the motion of the fluid (at a point in a fluid) is directly proportional to the absolute velocity gradient or space rate of change of velocity at that point and is directly proportional to the concentration of flocculable particles at that point. This relationship has been independently developed by others,[5] and experimental verification has been obtained with small glass spheres having an average diameter of 137 microns, suspended in high-viscosity corn syrup. The experimental verification was obtained in streamline motion of the fluid.

It has also been demonstrated[3] that the absolute velocity gradient at a point in a fluid in motion is equal to the square root of the ratio of the power loss by shear per unit of volume of fluid to the viscosity of the fluid. The velocity gradients at any instant throughout a vessel or chamber in use for flocculation vary considerably in magnitude, being greatest at the solid boundaries of the paddles or other devices used to introduce the mixing motion and being least in the corners of the chamber farthest from the point of introduction of the motion. Also, the velocity gradients in a conduit in which coagulation is taking place by means of the flow of the fluid are greatest at the walls. Under steady conditions of work input, however, there is a mean velocity gradient that corresponds with the mean value of the rate of power dissipation throughout the tank or conduit.

The rate of power dissipation (the work of shear per unit of volume per unit of time at a point) is known as the "dissipation function."[6] The mean value of the dissipation function, herein designated as W, is equal to the total power dissipation divided by the volume of the chamber or conduit. The root-mean-square velocity gradient is defined by the following relationship:

$$G = \sqrt{\frac{W}{\mu}} \qquad \text{(1)}$$

in which G is the root-mean-square velocity gradient in the chamber and μ is the absolute viscosity of the fluid.

As the rate of floc formation is directly proportional to the velocity gradient G, it should follow that the greater the magnitude of G the less should be the time required to form the floc. Hence, for economy in the size of flocculation chambers, the velocity gradients should be made as large as practicable. The practical limit of the velocity gradient for any flocculation process is determined by the size of floc particles required because there is a maximum size of floc particle associated with each velocity gradient. This statement will be explained by examining the concept of viscosity.

---

[2] "Effects of Temperature on Rate of Floc Formation," by D. A. Root, B. V. Bhoota, and Thomas R. Camp, *Journal*, A.W.W.A., Vol. 32, 1940, p. 1913.

[3] "Velocity Gradients and Internal Work in Fluid Motion," by Thomas R. Camp, and P. C. Stein, *Journal*, Boston Soc. of Civ. Engrs., October, 1943, p. 219.

[4] 'Sedimentation and the Design of Settling Tanks," by Thomas R. Camp, *Transactions*, ASCE, Vol. 111, 1946, p. 920.

[5] 'Particle Motions in Sheared Suspensions: II, Collisions of Uniform Spheres," by R. St. J. Manley and S. G. Mason, *Journal of Colloid Science*, Vol. 7, August, 1952, pp. 354–369.

[6] "On the Theories of Internal Friction of Fluids in Motion," by G. G. Stokes, *Cambridge Philosophical Transactions*, Vol. 8, 1845.

The viscosity of a fluid is the proportionality constant between the unit shearing force, τ, and the velocity gradient at a point, G':

$$\tau = \mu G' \dots\dots\dots\dots\dots\dots (2)$$

It is evident from Eq. 2 that the higher the velocity gradients become, the greater will be the shearing forces in a fluid. As floc particles grow they become weaker and are more easily sheared apart. Thus, to form small floc particles, relatively high velocity gradients may be used; for large floc particles lower velocity gradients are required.

Experience in water-treatment plants and sewage-treatment plants shows that too-violent mixing in flocculation chambers will prevent the formation of floc particles that are large enough to settle out effectively. Microscopic studies of water flow in rapid sand filters by P. C. Stein,[7] A. M. ASCE, in which the computed value of the mean velocity gradient was approximately 200 sec^{-1}, showed that no appreciable flocculation was taking place in the pores. Experiments by C. E. Hubley, A. A. Robertson, and S. G. Mason[8] showed that suspensions of aged latex particles in water had very little tendency to flocculate at velocity gradients exceeding 10 sec^{-1}, whereas suspensions of wood pulp fibers required velocity gradients in excess of 50 sec^{-1} to break up the flocs appreciably. Experiments by Mr. Stein[7] on the formation of hydrous ferric oxide floc in laboratory jar tests indicated that 20 sec^{-1} was the optimum velocity gradient for flocculation and that 40 sec^{-1} disrupted the flocs.

As data regarding limiting velocity gradients are extremely meager in the field of water and sewage treatment, an effort has been made to provide more information on this subject by computing the mean velocity gradients available in flocculation basins of existing water-treatment plants. For this purpose, the data[9] in *ASCE Manual of Engineering Practice No. 19* were used. Table 2 of the manual contains information on forty-two flocculation basins. The velocity gradients have been computed for twenty of these basins, with the omission of those gradients on which the data were incomplete or for which the detention period was less than 10 min. The results of the computations are shown in Table 1, in which the velocity gradients are based on a water temperature of 50°F, at which the absolute viscosity is 0.273×10^{-4} lb-sec per sq ft. The values of W are expressed in foot-pounds per second per cubic foot.

The velocity gradients in Table 1 are those at the full capacity of the plants. The values for the dissipation function W are based on the capacity of the plants as shown in Col. 2 and the values for head loss or horsepower as shown in Col. 7. It is probable that even at full plant capacity the water horsepower is much less than the connected horsepower. For the baffled basins, the value of W has been based on the retention periods and head losses, as shown in

---

[7] "A Study of the Theory of Rapid Filtration of Water Through Sand," by P. C. Stein, thesis presented to the Massachusetts Inst. of Technology, Cambridge, Mass., in 1940, in partial fulfilment of the requirement for the degree of Doctor of Science.

[8] "Flocculation in Suspensions of Large Particles," by C. E. Hubley, A. A. Robertson, and S. G. Mason, *Canadian Journal of Research*, B, 28, December, 1950, pp. 770–787.

[9] "Water Treatment Plant Design," *Manual of Engineering Practice No. 19*, ASCE, 1940, p. 29, Table 2.

Cols. 6 and 7, respectively, which are those for the full plant capacity. At lesser rates the head loss will be less and the retention period will be greater. Thus, it may be concluded that the range of values for the mean velocity gradients as shown in Table 1 represent maxima, and the optimum values are probably much smaller.

TABLE 1.—FLOCCULATION BASIN

Line	Plant (1)	Capacity, in millions of gallons per day (2)	Date built (3)	Type of agitation (4)	Velocity, in feet per second (5)
a	Albany, N. Y. (Helderberg)	40	1932	Over-and-under, around-end baffles	0.9
b	Atlanta, Ga.	42	1923	Around-end baffles	2.0
c	Baltimore, Md. (new)	112	1928	Around-end baffles	1.3
d	Cleveland, Ohio (Division Ave.)	140	1918	Over-and-under baffles	0.4
e	Denver, Colo.	60	1924	Around-end baffles	0.3
f	Detroit, Mich. (Springwells)	272	1931	Around-end baffles	0.4
g	Erie, Pa. (Chestnut St.)	37	1925	Vertical baffles	0.1
h	Flint, Mich.	28	1924	Over-and-under baffles	0.6
i	Fort Worth, Tex.	20	1923	Around-end baffles	0.5
j	Grand Rapids, Mich.	40	1924	Around-end baffles	1.0
k	Kansas City, Kans.	25	1927	Around-end baffles	1.1
l	Kansas City, Mo.	100	1928	Spiral flow	...
m	Knoxville, Tenn.	15	1927	Mechanical agitators	1.5
n	Miami, Fla.	20	1926	Mechanical agitators	1.0
o	New Orleans, La.	40 72	1909 1928	Around-end baffles	0.8
p	Oakland, Calif.	12	1927	Mechanical agitators	1.7
q	Oklahoma City, Okla.	16	1923	Over-and-under baffles	0.6
r	St. Louis, Mo. (Howard Bend)	80	1929	Spiral flow	0.7
s	Tampa, Fla.	14	1926	Mechanical agitators	0.8
t	Washington, D. C.	80	1927	Around-end baffles	1.5

As the rate of flocculation varies directly with the magnitude of the mean velocity gradient G, satisfactory flocculation should be produced with particular values of the product $G\ T$, in which T is the flocculation period. If G and T are expressed in seconds, the product $G\ T$ is a dimensionless number. The values of $G\ T$ for the flocculation basins in Table 1 are shown in Col. 11. Table 1 indicates that the maximum velocity gradients used in the United States range from approximately 20 sec^{-1} to 74 sec^{-1} and that the values of the product $G\ T$ at plant capacity range from approximately 23,000 to 210,000. It may be assumed that these values represent coagulation basins that are operating fairly satisfactorily.

Since, as stated previously, higher velocity gradients may be used for small floc particles rather than for large floc particles, the best economy should result where flocculation is carried out in several stages in a series of tanks with the velocity gradients progressively decreasing as the floc particles grow in size. This procedure was first developed by W. F. Langelier, and is known as the Langelier process. The sum of the ($G\ T$)-values for the series of basins should be the same as the sum for a single basin to obtain satisfactory floc, but the detention period, and hence the cost for the series, should be less.

MEANS FOR PRODUCING VELOCITY GRADIENTS

The earliest flocculation basins were the so-called baffled mixing chambers with over-and-under baffles or around-the-end baffles. Such basins were usually designed with a channel velocity of from 0.3 ft per sec to 1.0 ft per sec.

For baffled mixing channels or conduits of any type, the value of the dissipation function W may be computed from the discharge and head loss as follows:

$$W = \frac{Q \gamma h_f}{V} = \frac{\gamma h_f}{T} \qquad (3)$$

IN WATER-TREATMENT PLANTS

Retention period, in minutes (6)	Head loss for mixing, in feet (7)	Horsepower per million gallons per day (8)	W, in foot-pounds per second per cubic foot (9)	G, in seconds^{-1} (10)	$G\,T$ (T, in seconds) (11)	Line
20	3		0.156	74	88,800	a
25	1		0.041	39	58,500	b
30	3		0.104	61	110,000	c
39	0.4		0.011	20	46,800	d
20	0.5		0.026	31	37,200	e
17	0.5 ±		0.030	33	33,600	f
19	1.3		0.068	50	57,000	g
35	1.2		0.036	36	75,600	h
40	1 ±		0.026	31	74,400	i
45	1		0.023	29	78,000	j
10	0.4		0.041	39	23,400	k
30	3.5		0.121	67	121,000	l
20	(6 hp)	0.4	0.120	66	79,200	m
20	(3 hp)	0.15	0.045	40	48,000	n
60	1 ±		0.017	25	90,000	o
20	(4 hp)	0.33	0.098	60	72,000	p
30	2		0.071	51	92,000	q
16	0.5 ±		0.032	34	32,600	r
100	(8 hp)	0.57	0.034	35	210,000	s
27	0.5 to 2		0.077	53	86,000	t

in which Q represents the discharge; γ, the unit weight of the fluid; h_f, the head loss by friction; V, the volume of liquid in the conduit or chamber; and T, the retention period (in seconds).

Baffled mixing chambers are not satisfactory for flocculation purposes because most of the head loss occurs at the 180-degree bends so that the velocity gradients are too great at the bends and not great enough in the straight channels. Another objection to this type of flocculation basin is that the magnitude of the dissipation function, hence the magnitude of the velocity gradients, is directly porportional to the rate of discharge and cannot be varied at will by the operator. In modern plants, mechanical stirring devices are used, in which case the velocity gradients are independent of the rate of discharge. Mechanical stirring devices enable the operator to change the velocity gradient if variable-speed drives are provided. Flocculation may also be accomplished by means of diffused air, in which case the magnitude of the mean velocity gradient may be controlled by the quantity of air used.

In some treatment plants, turbulent mixing for coagulation has been induced by bringing the water tangentially into a basin (circular or square) at high velocity. In such basins a spiral motion is induced. The value of the dissipation function W may be computed for such basins by means of Eq. 3 with h_f taken as the velocity head at the inlet. In such basins the turbulence is not uniformly distributed as it is introduced at only one point. Basins of this type are not satisfactory in series because the floc will be broken up in passage from one basin to the next.

When turbulence is induced by mechanical mixing or by air, the value of the dissipation function W may be estimated from the drag force of the stirring blades or air bubbles in the water and the distance moved per second. The drag force for any body immersed in still water is, by Newton's law,

$$F_D = C_D A \gamma \frac{v^2}{2g} \qquad (4)$$

in which C_D represents the drag coefficient; A, the cross-sectional area of the submerged object in a plane perpendicular to the direction of motion; and v, the relative velocity of the object with respect to the fluid.

The distance moved per second by the submerged blade or air bubble is equal to its velocity with respect to the liquid. Unfortunately, the relative velocity of the stirring blade of most types of stirring devices and of the liquid immediately surrounding the blade is difficult to determine. Rotary stirring devices set the liquid in spiral motion with an average angular velocity less than the velocity of the rotors and with the velocity beyond the central core diminishing with distance from the center. With reciprocating agitators, such as the so-called "walking beam" type, the velocity of the blade with respect to the tank varies throughout the stroke. During the stroke, motion is induced in the surrounding liquid. As the direction of stroke is changed periodically, the effect is to retard the motion of the liquid. Nevertheless, the relative motion of blade and tank is not the same as the relative motion of blade and surrounding liquid. Rising air bubbles also tend to impart motion to the surrounding liquid, which in turn will result in faster rise of the air bubbles with respect to the tank.

THE EFFECT OF SHORT-CIRCUITING

In order to facilitate the design of stirring mechanisms, most tanks with paddles mounted on vertical shafts are made circular or approximately square, and most tanks with paddles mounted on horizontal shafts are made approximately square in cross-sectional area. The mixing process short-circuits some of the water quickly from the entrance to the outlet port of each basin. This portion of the liquid will be inadequately coagulated.

Short-circuiting in a tank may be measured experimentally by introducing a slug of tracer, such as dye or salt, at the inlet port and by measuring its concentration after various intervals of time at the outlet port. If the mixing is assumed to be violent enough to accomplish a uniform dispersion of the slug of tracer throughout the contents of the tank instantaneously, the concentration of the tracer at the outlet may be computed by means of the following:

$$\frac{C}{C_o} = e^{-t/T} \qquad (5)$$

in which C denotes the concentration of tracer at the outlet after time t, C_o is the initial concentration if the tracer is instantaneously dispersed throughout the contents of the tank, T equals the retention period of the tank, and e is the base of Napierian logarithms.

Fig. 1 is a dimensionless plot of Eq. 5. Also shown in Fig. 1 is an experimental curve determined from a model of a cubical mixing tank with a moderate degree of mixing. The area under the curve represents the tracer slug. It will be noted from both the theoretical and experimental curves that a large part of the tracer is passed through the tank in less than the theoretical retention period. In the case of the theoretical curve, 40% of the slug leaves the tank in less than one half the retention period and 22%, in less than one fourth the retention period.

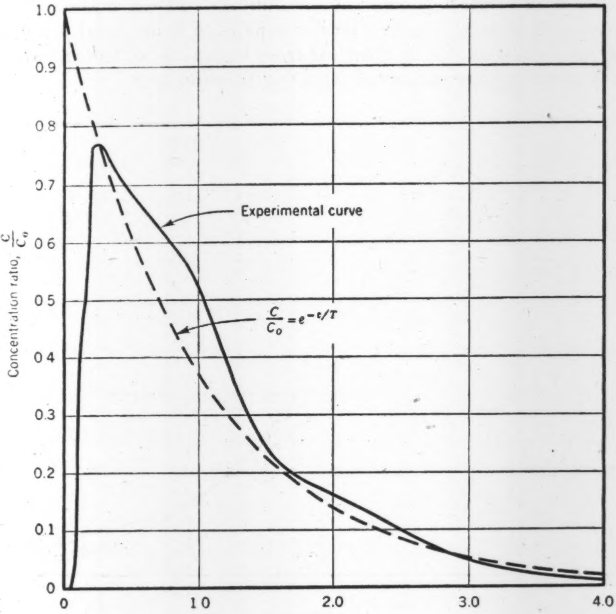

Fig. 1.—Tracer-Solution Concentration

In order to compensate for this short-circuiting, several tanks should be placed in series so that the liquid which passes through the upstream tank in a short period will have a chance to stay in the downstream tanks for a longer period.

Mr. Stein has developed the equation for the instantaneous dispersion curve for n tanks of equal size in series as follows:

$$\frac{C}{C_o} = \frac{n^n}{(n-1)\,!}\left(\frac{t}{T}\right)^{n-1} e^{-n\,t/T} \quad \ldots\ldots\ldots\ldots\ldots (6)$$

in which C_o and T are based on the total volume of n tanks in series.

In Fig. 2 are shown the theoretical curves for one, two, three, four, and ten instantaneous-dispersion tanks in series. A study of the curves shows that with three tanks in series approximately 4% of the slug will pass through in one fourth the retention period and approximately 19% of the slug, in one half the retention period.

Flocculation by Diffused-Air Aeration

The work done on water in a flocculation tank by means of rising air bubbles may be computed either from the work of expansion of the air in the bubbles or from the drag forces between the air bubbles and the liquid. The results will be approximately the same whether expansion is assumed to be adiabatic or isothermal, and the results obtained from expansion of the gas are approximately the same as those computed from the drag forces.

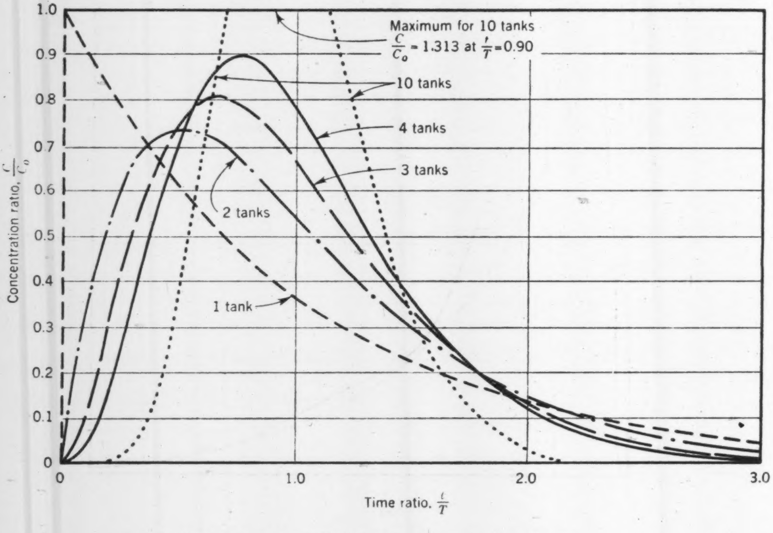

Fig. 2.—Dispersion Curves for Tanks in Series

The work done by the drag forces on air bubbles in still water is equal to the drag force times the distance traveled by the bubbles (that is, the depth of the diffusers below the water surface). The drag force is nearly equal to the weight of the water displaced by the air bubbles. Hence, the value in water of the dissipation function (in foot-pounds per second per cubic foot), computed from the drag force, is given by

$$W = \frac{62.4\, Q_a}{V} \frac{34\, H}{\frac{H}{2} + 34} \quad \ldots\ldots\ldots\ldots\ldots\ldots \quad (7a)$$

in which Q_a equals the flow of free air, in cubic feet per second; V, the volume of liquid in the tank; and H, the depth of the diffusers. Thus, $Q_a \dfrac{34}{(H/2) + 34}$ equals the flow of air, in cubic feet per second, at depth $H/2$, and 624 $Q_a \dfrac{34}{(H/2) + 34}$ equals the drag force, in pounds per second.

If the work is computed by isothermal expansion of the air as the bubbles rise through the depth H, the value of the dissipation function is given by

$$W = \frac{4{,}890\, Q_a}{V} \log \frac{H + 34}{34} \qquad \text{(7b)}$$

For a flocculation tank of volume V, the quantity of diffused air required in cubic feet per second for any mean velocity gradient G is given by Eqs. 8:

From the drag force—

$$Q_a = \frac{G^2 \mu V}{2{,}120 \dfrac{H}{(H/2) + 34}} \qquad \text{(8a)}$$

From isothermal expansion—

$$Q_a = \frac{G^2 \mu V}{4{,}890 \log \dfrac{H + 34}{34}} \qquad \text{(8b)}$$

It will be noted from the foregoing equations that the quantity of air required to produce a given mean velocity gradient is independent of the bubble size. For good flocculation, air bubbles should be distributed uniformly throughout the volume V and should be small enough so that the velocity gradients close to the bubbles are not great enough to disrupt the floc. As the regions of high velocity gradient are much more numerous and more widely dispersed if diffused air is used than if paddle flocculators are used, the precaution concerning bubble size is of great importance.

It may be shown that individual bubbles rising in still water will conform to the Stokes law for bubble diameters less than 1.4 mm. The rising velocity of each bubble with respect to the water surrounding it is given by the Stokes law:

$$v = \frac{1}{18} \frac{g}{\mu} (\rho_1 - \rho)\, D^2{}_b \qquad \text{(9)}$$

in which v is the rising velocity; g, the gravity constant; ρ_1, the mass density of air in a bubble; ρ, the mass density of water; and D_b, the diameter of the bubble.

In the Stokes-law region the maximum value of the velocity gradient $G'_{\max}$ occurs at the interface between the bubble and the water and is given by

$$G'_{\max} = \frac{1}{6} \frac{g}{\mu} (\rho_1 - \rho)\, D_b \qquad \text{(10)}$$

The sizes of air bubbles corresponding to various values of the maximum velocity gradient as computed from Eq. 10 are shown in the following tabulation (water at 50°F):

G'_{max}, in seconds^{-1}	Bubble diameter, D_b, in millimeters
100	0.08
200	0.16
500	0.40
1,000	0.80
2,000 ±	2.0

It is apparent from this table that bubbles must be small to prevent destruction of the floc in the final compartment of a flocculation basin where a mean velocity gradient of approximately 10 is required. In a typical case with diffusers at a depth of 14 ft, the quantity of air required at a water temperature of 50°F for a G-value equal to 10 is estimated from Eq. 8 to be 0.00315 cu ft per min per sq ft of tank area. This is a small flow of air by comparison with the capacity of porous-plate diffusers available commercially.

If in the foregoing example the size of the air bubbles is 2 mm (a common size for commercially available porous plates), the number of bubbles required per second per square foot of tank area is only about 300, and the bubbles must be spaced about 1½ in. apart. In this case there will be velocity gradients of 2,000 sec^{-1} at intervals of 1½ in. throughout the tank.

If in this example the bubble size is made 0.16 mm so as to limit the maximum velocity gradient to about 200 sec^{-1}, the number of bubbles per second per square foot of tank area is estimated at 5,830, and the bubbles will be spaced ¼ in. apart.

It is evident from the foregoing discussion that much research and development will be required in order to obtain satisfactory diffusers so that flocculation by aeration may be controlled within optimum limits. Experience indicates that with air flocculation most of the floc particles will be carried upward by the air bubbles to form a scum at the surface of the water. This will reduce the concentration of flocculable particles and thus increase the time required for flocculation. However, the floc can be removed by the skimming of the surface of the aeration tank rather than by sedimentation in a separate unit following coagulation. Flocculation by aeration, therefore, offers an opportunity for a saving in the initial cost of the plant. Attempts are now being made to exploit this advantage commercially.

Flocculation by Rotating Blades

Most of the commercially available apparatus for flocculation is the revolving-paddle type, with either vertical or horizontal shafts. In most installations only rotor paddles are provided, and the only resistance to rotation of the water with the paddles is the drag on the walls of the tank. It is known that the water does move with the paddles, but little is known about the relative velocity of the paddles and the water.

In some existing plants, the width of the paddles is so great that the water in front of them is carried along at approximately the velocity of the paddles. The only mixing in such installations occurs between the outside edges of the paddles and the walls of the tank.

Elwood L. Bean,[10] A. M. ASCE, recommends that the area of the paddles in a basin without stator blades should not be greater than from 15% to 20% of the cross-sectional area of a basin if rolling of the water is to be prevented. Mr. Bean further states that, if the paddle area is 25% of the cross-sectional area, major rotation of the water will result. No evidence has been presented to indicate that the speed of the water relative to the paddles can be maintained proportional to the shaft speed unless stators are used to stabilize the motion.

In order to change the magnitude of the mean velocity gradient in an existing basin provided with rotor paddles, it is necessary to change the speed of rotation of the paddles. For effective control of the velocity gradient, the power dissipation must be definitely related to the speed of rotation after equilibrium is reached following starting of the paddles. In order to simplify design, it is desirable that the rotor paddles be mounted parallel to the shaft on arms attached to the shaft. The velocity of a paddle with respect to the tank is then proportional to its distance from the shaft.

The expression for the dissipation function for a single rotor blade at distance r_b from the center of the shaft is

$$W = \frac{F_D\, v}{V} = \frac{C_D\, A\, \frac{62.4}{64.4}\, v^3}{V} = \frac{C_D\, A\, \frac{62.4}{64.4}\left[2\,\pi\, r_b\,(1-k)\,S_s\right]^3}{V}$$

$$= \frac{239\, C_D\, A\, r^3_b\,(1-k)^3 S^3_s}{V} \quad \text{.\,.\,.\,.\,.\,.\,.\,.\,.\,.\,.\,.\,.\,.\,.\,.\,(11}a\text{)}$$

in which v equals the velocity of the blade with respect to the water; r_b, the distance of the center of the blade from the shaft; S_s, the speed of the shaft, in revolutions per second; and $k\, S_s$, the speed of the water, in revolutions per second. The validity of Eq. 11*a* depends on the existance of a constant ratio between the rotating speed of the shaft and the velocity of the water surrounding the paddle. In the Cambridge, Mass., water-treatment plant, where stators have been used, measurements have shown that the assumption is valid and that the power dissipation is directly proportional to the cube of the shaft speed.

A flocculation tank must have several rotor paddles, at varying distances out from the shaft and possibly with varying paddle areas. The value of the dissipation function W for all the paddles in a tank is given by Eq. 11*b* as follows:

$$W = \frac{239\, C_D\,(1-k)^3\, S^3_s}{V}\, \Sigma\, A\, r^3_b \quad \text{.\,.\,.\,.\,.\,.\,.\,.\,.\,.\,.\,.\,.\,.\,(11}b\text{)}$$

in which $\Sigma\, A\, r^3_b$ is the sum of the values of $A\, r^3_b$ for all rotors.

Eqs. 11*a* and 11*b* show that, if the rotors start at full speed, the starting power will be much greater than the power after the water is rotated at its equilibrium velocity. At the start the value of k is 0. If, for example, the speed of the water after equilibrium is one half the speed of the shaft with a value of k equaling 0.5, the starting power will be eight times the equilibrium power. Therefore, drive motors must be greatly oversized, or provisions must be made to bring the paddles up to speed slowly during starting.

---

[10] "Study of Physical Factors Affecting Flocculation," by Elwood L. Beam, *Water Works Engineering*, January, 1953, p. 33.

In Fig. 3 are shown a half plan and sections of four new flocculation chambers constructed (in 1951–1952) for the Cambridge water works. This plant is the first practical application of the theory of flocculation described in the paper. Stators have been provided in each compartment with a value of $\Sigma A r^3_b$ approximately equal to the value of $\Sigma A r^3_b$ for the rotors. Nothing was known about the velocity of the rotors relative to the surrounding water or about the amount of power loss to be expected in the transmission, bearings, and stuffing boxes; therefore, provisions were made in the specifications for testing to evaluate the unknowns after the first chamber was equipped with the flocculating mechanisms and for changing the size of sprocket wheels.

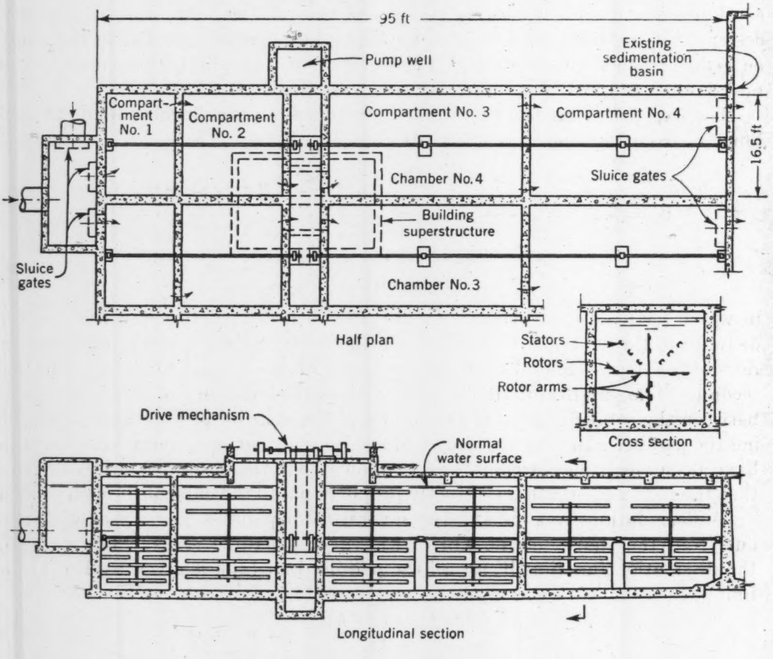
95 ft
Pump well
Existing sedimentation basin
Compartment No. 1
Compartment No. 2
Compartment No. 3
Compartment No. 4
16.5 ft
Chamber No. 4
Sluice gates
Building superstructure
Sluice gates
Chamber No. 3
Half plan
Stators
Rotors
Rotor arms
Cross section
Drive mechanism
Normal water surface
Longitudinal section

FIG. 3.—FLOCCULATION CHAMBERS, CAMBRIDGE, MASS.

There are two shafts (Fig. 3) for driving the flocculating rotors in each chamber—a high-speed shaft for the smaller compartments and a low-speed shaft for the larger compartments. With the sprockets finally selected, the speed of the high-speed shaft is 78% greater than the speed of the low-speed shaft. The mechanism for each chamber is driven by a single 10-hp, variable-speed, electric motor of the movable-brush type, having a three-to-one speed range. The minimum speed of the motor is approximately 833 rpm; after testing, the stop on the speed change was set to limit the top speed at 2,200 rpm.

The results of the tests on the flocculator mechanism at Cambridge are shown by the curves in Fig. 4. The tests showed that approximately 1 hp is lost through transmission, stuffing boxes, and bearings, regardless of the speed. The tests also showed that, after equilibrium is established, the water revolves at approximately 24% of the speed of the rotors in the high-speed compartments and at approximately 32% of the speed of the rotors in the low-speed compartments. That is, the values of *k* were found to be 0.24 and 0.32.

The speed of the low-speed shaft at Cambridge can be adjusted from approximately 1.1 rpm to approximately 2.9 rpm, and the speed of the high-speed shaft can be adjusted from approximately 2 rpm to approximately 5.2 rpm.

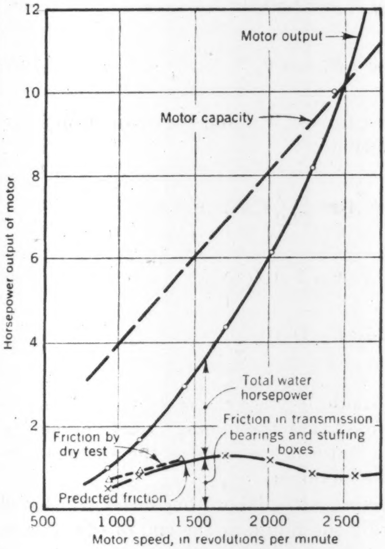

FIG. 4.—RESULTS OF FLOCCULATOR TESTS

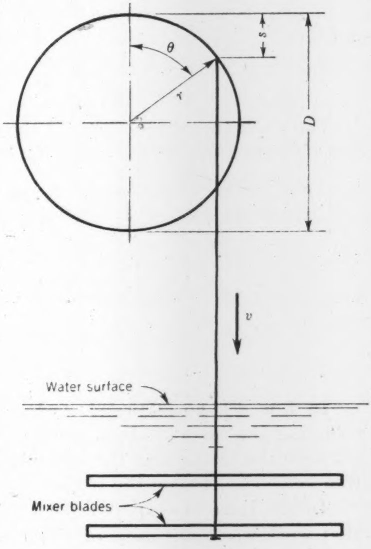

FIG. 5.—RECIPROCATING PADDLES

The mean velocity gradient in the last compartment at minimum speed ranges from approximately 5 in winter to approximately 7.6 in summer and can be increased approximately 4.3-fold by an increase in speed. For any speed and water temperature, the mean velocity gradients in the first three compartments are, respectively, 5.6, 3.8, and 1.9 times the mean velocity gradient in the fourth compartment.

FLOCCULATION BY RECIPROCATING BLADES

An analysis of the work input in a flocculation tank with reciprocating paddles may be made readily for the case of simple harmonic motion, as illustrated in Fig. 5, in which the angular velocity ω is $d\theta/dt = 2\pi S_s$. Successful measurements have been made of the work input with laboratory stirring devices of this type by Krause Ignacio[11] with electrical strain gages.

In reciprocating motion, the relative velocity of blade and liquid is changing continuously throughout a cycle. In order to obtain values for the mean velocity gradient, therefore, it is necessary to compute the mean value of the dissipation function throughout a cycle.

The basic equations for the distance traveled (s), vertical velocity (v), and vertical acceleration (a) at any point of the stroke in reciprocating motion as illustrated in Fig. 5 are:

$$s = r - r\cos\theta \qquad (12a)$$

$$v = \frac{ds}{dt} = r\sin\theta\,\frac{d\theta}{dt} = 2\,\pi\,r\,S_s\sin\theta \qquad (12b)$$

and

$$a = \frac{dv}{dt} = 4\,\pi^2\,r\,S^2{}_s\cos\theta \qquad (12c)$$

The work (per cycle) done by the drag forces (W_c) and the dissipation function (W) are given by the following equations:

$$W_c = 2\int_0^{\pi} F_D\,v\,\frac{d\theta}{2\,\pi\,S_s} = 4\,\pi^2\,\frac{62.4}{32.2}\,C_D\,\Sigma\,A\,r^3\,S^2{}_s \int_0^{\pi}\sin^3\theta\,d\theta = 12.74\,C_D\,\Sigma\,A\,D^3\,S^2{}_s \qquad (13a)$$

and

$$W = \frac{W_c\,S_s}{V} = \frac{12.74\,C_D\,D^3\,S^3{}_s}{V}\,\Sigma\,A \qquad (13b)$$

In Eqs. 13, no allowance has been made for movement of the water surrounding the blades. It has been assumed that the average relative velocity between the blades and the surrounding water is the same as the average relative velocity between the blades and the chamber.

In Mr. Ignacio's experience with a reciprocating laboratory mixer,[11] he found that work was being done on the mixer by the liquid at the end of the strokes. This was undoubtedly due to the inertia effect of liquid masses maintaining the velocity imparted by the mixer until after the mixer reversed its stroke. The resulting effect of the inertia force of the liquid was to increase the total work done per cycle, particularly at the higher speeds of the mixer.

The actual work done per cycle was measured by Mr. Ignacio, and the value of the drag coefficient was computed for each run by means of Eq. 13*a*. In still water, for isolated blades of the shape used by Mr. Ignacio, the drag coefficient should have a value of from 1.5 to 2. The experimental values of the drag coefficient ranged from approximately 3 to 5.2, the values of the Reynolds number ranging from 150 to 700. The values of the Reynolds number were based on the blade widths and the mean velocity of the blades with respect to the container throughout the stroke. Assuming that the correct value for the drag coefficient was 2, and that the apparent values found in the experiments were produced by higher relative velocities between the mixer and the water, the actual relative velocities should be from 20% greater than the assumed average velocity at the lower speed to 60% greater at the higher speed.

---

[11] "Measurement of Work Input in Liquids by Reciprocating Mixing Devices," by Krause Ignacio, thesis presented to the Massachusetts Inst. of Technology, Cambridge, Mass., in 1943, in partial fulfilment of the requirement for the degree of Master of Science.

The mixing device used by Mr. Ignacio in his experiments was a grid system which occupied 11% of the total volume of the water in the container. Undoubtedly, part of the reason for the high values for the drag coefficients was the large displacement volume of the mixer. The relative displacement volume for mixing blades in water-treatment plants and sewage-treatment plants would be negligible by comparison. For design purposes, therefore, a drag coefficient of 3 for flat blades should give approximately correct values of the dissipation function when used in Eq. 13*b*.

APPENDIX. NOTATION

The following symbols, used in this paper, conform essentially to "American Standard Letter Symbols for Hydraulics" (ASA—Z10.2–1942), prepared by a committee of The American Standards Association with ASCE representation, and approved by the Association in 1942:

A = the cross-sectional area of the submerged object in a plane perpendicular to the direction of motion with respect to the submerging fluid;
a = the vertical acceleration of reciprocating paddles;
C = the concentration of tracer solution at the tank outlet after time t from introduction at the inlet;
C_o = the initial concentration of tracer solution in the tank if the solution is instantaneously dispersed;
C_D = the drag coefficient;
D = the length of the stroke of paddles in reciprocating motion;
D_b = the diameter of air bubble in the Stokes law;
e = the base of Napierian logarithms;
F_D = the drag force;
G = the root-mean-square velocity gradient, in seconds^{-1};
G' = the velocity gradient at a point, in seconds^{-1};
$G'_{\max}$ = the maximum value of the velocity gradient in a fluid field, in seconds^{-1};
g = acceleration due to gravity;
H = the depth of diffusers in an aeration tank;
h_f = head lost by friction;
k = the ratio of the rotating velocity of fluid to the rotating velocity of blades;
n = the number of tanks of equal volume in series;
Q = the rate of discharge of fluid;
Q_a = the flow of free air, in cubic feet per second;
r = the radius of simple harmonic motion for reciprocating blades;

r_b = the distance of the center of the rotating blade from the center of the shaft;
S_s = the speed of a rotating shaft, in revolutions per second;
s = the vertical distance traveled by reciprocating blades in time t;
T = the retention period in a tank or conduit;
t = the time of appearance of tracer in concentration C at tank outlet, also the time required for reciprocating blades to travel vertical distances;
V = volume of liquid in tank, series of tanks, or conduit;
v = relative velocity of submerged object with respect to fluid;
W = dissipation function or the work of shear in a fluid, per unit volume per unit time;
W_c = the work done by shear forces in a fluid by reciprocating motion, per unit volume per cycle;
γ = unit weight of fluid;
θ = angle of rotation corresponding to vertical distance traveled, s, in simple harmonic motion;
μ = the absolute viscosity of a fluid;
ρ = the mass density of the fluid;
ρ_1 = the mass density of the air in a bubble;
τ = unit shearing force in fluid caused by velocity gradient; and
ω = the angular velocity in simple harmonic motion.

AMERICAN SOCIETY OF CIVIL ENGINEERS
Founded November 5, 1852
TRANSACTIONS

Paper No. 2723

SELECTION AND DESIGN OF HIGH-VOLUME, LOW-HEAD PUMPS

By George F. Snodgrass[1]

Synopsis

The design of pumping stations for drainage facilities involves the selection of the correct type of pump from the many that utilize centrifugal action. It must also be decided whether to mount the pump vertically or horizontally. With these decisions made, one must design the intake system and the discharge system on the basis of the method for powering the pump and transmitting the power from the prime mover to the pump shaft. Many of these decisions can be reached by the use of good judgment, but more of them depend on detailed investigation and study. When these studies have been completed, a sound plan should be evolved which (1) is capable of some operational flexibility from the design conditions, (2) is economical on a first-cost basis and annual-cost basis, and (3) lends itself to operation by ordinary skilled labor.

Introduction

The flood-control project in central and southern Florida is based on the construction of eight major and one minor pumping station (as of 1954). Each station should be able to remove $\frac{3}{4}$ in. of runoff from the acreage of its tributary area. The nominal pumping heads of all the stations can be considered low as they vary from 4 ft to 13 ft. The eight major stations have capacities ranging from 2,900 cu ft per sec to 4,800 cu ft per sec.

The head of water on the pump is of importance in the selection of the type of pump to be used. For example, six pumps at the pumping plant near Tracy, Calif., pump 2×10^6 gal per min (4,400 cu ft per sec) against a head of 197 ft. This pumping is accomplished by 84-in., single-stage, centrifugal pumps powered by 22,500-hp motors. On the flood-control project in Florida, where the pumps are of a similar capacity, the use of axial-flow pumps is indicated. These two illustrations represent part of the range within which are found centrifugal pumps suitable for drainage work. Within this range also are

---

Note.—Published, essentially as printed here, in July, 1953, as *Proceedings-Separate No.* 229. Positions and titles given are those in effect when the paper was received for publication.

[1] Civ. Engr., Corps of Engrs., U. S. Dept. of the Army, Jacksonville, Fla.

mixed-flow pumps, having the combined characteristics of both the centrifugal and the axial-flow pumps, the degree of either characteristic being determined by the shape of the impeller.

TYPES OF PUMPS

The characteristics of the pumps previously cited vary widely within the range of design from centrifugal flow to axial flow; when compared to the working head, the centrifugal pump has a low cutoff head and the axial-flow pump has a high cutoff head. However, for high-volume application it is known that within the given general head ranges the following types of pumps are used:

Head, in feet	Type of pump	Relative cost
Over 30	Centrifugal	Highest
10 to 50	Mixed flow	....
2 to 30	Axial flow	Lowest

It can be seen from this tabulation that, for the Florida flood-control project, the more costly centrifugal pump can be eliminated and the selection narrowed down to the mixed-flow pump or the axial-flow pump.

In Fig. 1(*a*) is shown a typical performance curve for a mixed-flow, open-impeller pump, and in Fig. 1(*b*) is shown the typical performance curves for an axial-flow, propeller pump. In both cases the abscissa and ordinates are expressed in percentage of values at the maximum efficiency point and in terms of total dynamic head. An examination of Fig. 1 indicates that either pump appears to have good characteristics for solving the problem of pumping drainage or floodwaters. It is also apparent that the mixed-flow pump has a less steep head-capacity curve, a lower cutoff value, and a flatter brake-horsepower curve when approaching cutoff. The axial-flow pump has a steep head-capacity curve, a higher cutoff value, and a brake-horsepower curve which at cutoff requires 250% of the power at the best efficiency point.

The pump with the characteristics illustrated in Fig. 1(*a*) has a specific speed of approximately 6,250. The pump illustrated in Fig. 1(*b*) has a specific speed of approximately 11,000. Although the efficiency-capacity curve of a centrifugal pump with a low specific speed is flatter than that of a propeller pump, it should be noted that low-head pumps are used primarily when the head varies as a result of a variation in the suction level, and maximum capacity is usually required at any head. In this case, axial-flow propeller pumps with steep head-capacity curves have a definite advantage; they will deliver more water within a given head range and at a better efficiency than mixed-flow, centrifugal pumps. This fact is illustrated by the two curves in Fig. 2 which show that, when efficiency is plotted against head, the pumps with higher specific speeds have flatter efficiency curves.

From Fig. 1 it can be seen that, for pumps driven by synchronous electric motors, the head-horsepower relationship is more satisfactory for the mixed-flow pump than it is for the axial-flow pump. This more satisfactory relationship results because—for the mixed-flow pump—the horsepower throughout the full range of capacity usually does not exceed 125% of the horsepower required at the best efficiency point. For the axial-flow pump, the horsepower at cutoff is approximately 250% of that at the best efficiency point. However, for pumps driven by internal combustion engines, satisfactory and safe operation of axial-flow pumps is possible because the variations of head, capacity, and brake horsepower with pump speed follow definite rules (termed "affinity laws") which are favorable to this combination. When applied to every point on the head-capacity curve for a pump, these laws stipulate that—when the speed is changed—the capacity varies directly with the speed, the head varies as the square of the speed, and the brake horsepower varies with the cube of the speed. The brake-horsepower output of a diesel engine, however, can be considered directly proportional to the rotative speed. Should the head on the pump increase during operation to a point requiring more power than the engine can deliver, the diesel engine will slow down, and its power output will decrease in proportion to the speed while the power required by the pump

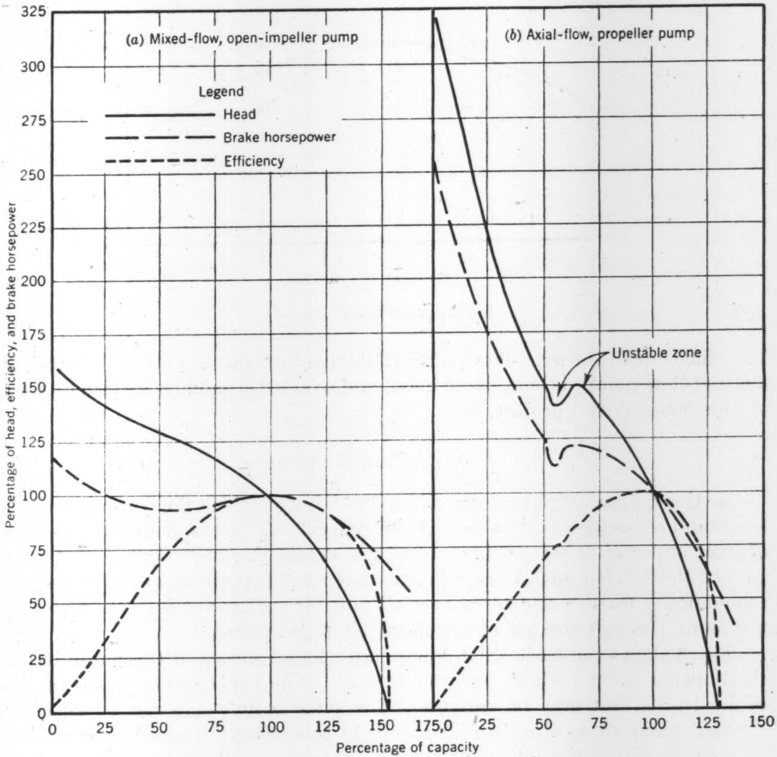

FIG. 1.—PERFORMANCE CURVES

(which slows down proportionately) drops off as the cube of the speed. Thus, it is evident that pumps driven by oil engines can be operated safely when the engine is at full power.

Axial-flow, propeller pumps are less costly than mixed-flow pumps because the pump casing is less complicated, lighter in weight, and occupies less space.

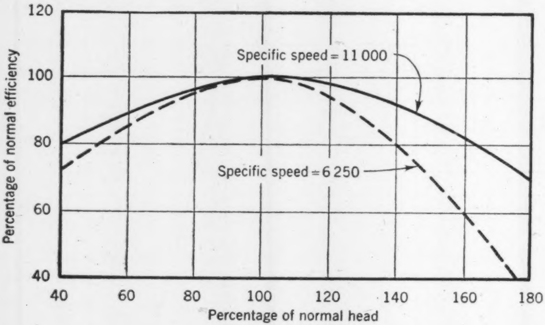

Fig. 2.—Efficiency Curves

The efficiency of the axial-flow pump (although probably slightly below that of a mixed-flow pump) is considered good, and over-all economics dictated its use on this flood-control project.

Axial-Flow Pumps

In the design of pumps for a low-head installation, the various friction losses and other losses in the system are generally of such a magnitude as to be of great importance because in terms of percentage they represent a substantial part of the total head. Care must be taken to keep all losses as low as it is economically feasible and to recover all possible energy put into the water by the pump through the use of a siphon-discharge system.

Fig. 3 shows the basic axial-flow pump which consists of the pump barrel, the impeller (or propeller), and the diffuser. The vanes or blades are usually of fixed pitch but may be variable. The same basic pump can be used as a vertical pump or as a horizontal pump; in this latter instance the drive shaft may be on either the intake or the discharge side. Basic pumps have been tested giving efficiencies as high as 93% on the basis of the total dynamic head. The hydraulic thrust is usually carried to a bearing outside the water column.

In economic studies of various methods of powering the pumps, including electric motors utilizing purchased power, it was concluded that, with the indicated load factor (equivalent to fifty days of full-capacity operation per year), diesel engines were the most economical. Oil engines also made possible the use of variable-speed operation of the pumps—an important factor.

It is considered good practice in designing pumping stations to install not less than three pumps in any primary station so that at least 66% of capacity is available when one unit is closed for repairs. Considering that the economic life of a station is fifty years, the wisdom of this is apparent.

Economic studies have shown that, on the basis of flow, larger pumps are less expensive than smaller ones. It has also been shown that, other factors being equal, the pumps should be as large as possible—within the range of suitable power-transmission systems. The pumps, power-transmission systems, and prime movers should be within a range where competition between manufacturers exists. It has been determined that pumps having a capacity of between 730 cu ft per sec and 960 cu ft per sec meet all these requirements. Pumps of this size have rotative speeds of between 105 rpm and 145 rpm, a range well below that of modern (1954) diesel engines. Therefore, it is necessary to use some form of power-transmission system for speed changes between the engine and pump.

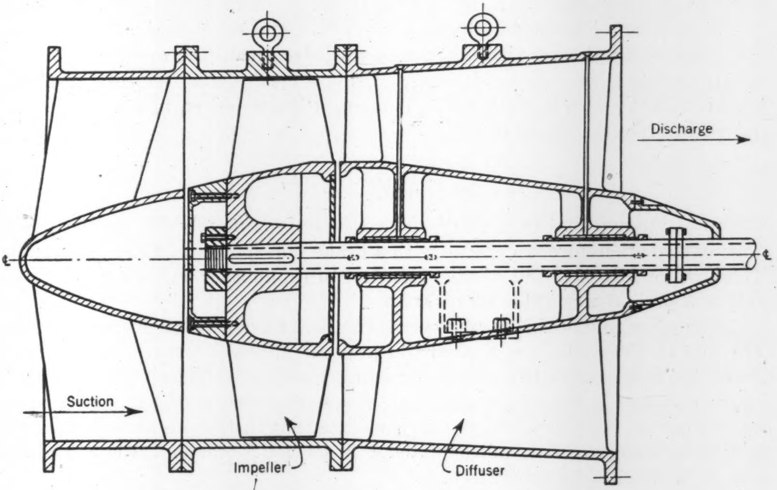

Fig. 3.—Section Through an Axial-Flow Pump

Power Required to Drive Pumps

When a tentative pump size has been selected, the power required to drive the pump must be determined. The head is ascertained by examining the discharge-bay hydrograph to arrive at the highest discharge-pool elevation at which pumping at rated quantity is to be conducted (or at that elevation which is economically justified) and also to determine the average discharge-pool elevation. It is also necessary to study the water-surface elevations of the sump and to determine the water-surface elevation in the feeder canal when pumping the rated quantity of water. The difference in these two elevations determines the pool-to-pool head at the rated point. At one station in Florida where six pumps have been installed, these characteristics were:

Item	Value
Maximum discharge-pool elevation, in feet above mean sea level	19.4
Sump elevation, in feet above mean sea level	8.3
Head, in feet, at rated point	11.1
Head, in feet, at average pool	9.2
Discharge, in cubic feet per second	4,610

Studies of several axial-flow pumps showed that efficiencies in the pump alone should be within the range of 85% to 90%. A preliminary computation of the losses of a low-head pumping system from the sump pool through to the discharge pool indicates that these losses will be within the range of 1.5 ft to 2.1 ft, including velocity-head losses. Using a mean value, the total dynamic head is 11.1 ft + 1.8 ft = 12.9 ft. The approximate power, in horsepower, required to drive the pump is

$$\frac{800 \times 62.4 \times 12.9}{550 \times 0.875} = 1{,}340.$$

The transmission loss in a speed reducer is approximately 3% of the power transmitted; therefore, an engine with a brake horsepower of 1,385 is required. To allow for loss of power as the engine matures, another 5% is allowed to result in a preliminary value of 1,450 hp.

A diesel engine of this horsepower rating will have a rotative speed of from 275 rpm to 850 rpm, as compared to the pump speed of 105 rpm to 145 rpm. To reduce from engine to pump speed requires a speed reducer. For operation equivalent to fifty-two days per year, the service factor of the transmission system can be fairly low—when one considers that the load is almost shockless and the prime mover is multicylinder. A service factor of 1.0 is considered adequate and 1.25, conservative.

For the delivery of this horsepower, several methods of power transmissions can be used, such as silent-chain drives, right-angle gear drives, and parallel-shaft gear drives. These drives have sufficient latitude to allow the use of a basic axial-flow pump for both horizontal and vertical pumps. From the standpoint of efficiency, there is little choice between the two applications.

Horizontal or Vertical Pumps

An axial-flow pump mounted horizontally can be driven from either the suction side or the discharge side; for pumps working under a high suction lift, the shaft through the discharge column of water seems more desirable. For drainage work it is also desirable to have the invert of the pump barrel above both pool levels in order to facilitate inspection of the pump. The ultimate lift of water, from the drawn-down surface of the sump to the top of the highest part of the pump, should not exceed 20 ft for even the slowest specific-speed pumps. A chart[2] for axial-flow pumps shows the safe limits of suction lift for pumps of various specific speeds. For example, at the previously cited installation, the specific speed is 10,920, and the total dynamic head is 13.0 ft. The chart for this case allows a suction lift, measured from the water surface in the sump to the center line of the pump, of 13 ft. The distance in the actual installation is 11.2 ft; therefore, the pumps can be considered safe and should operate quietly and without cavitation.

---

[2] "Standards," Hydr. Inst., New York, N. Y., 1951, Fig. No. B-24.

An axial-flow pump mounted vertically is usually of the wet-pit type, with the propeller submerged during normal operating conditions. This pump is then under a suction head, and the pump may have a considerably higher specific speed—and may be somewhat smaller—then a horizontally mounted pump of the same capacity. The suction side of a submerged vertical pump is invariably equipped with a bell, the diameter of which is such that its area is approximately twice that of the impeller eye.

PREVENTION OF BACKFLOW

Several methods can be used to prevent backflow through the pumps when they are not operating. Gates can be used in the discharge column but, because of the high cutoff heads of the axial-flow pump, the gates should open automatically. In the vertical pump application, with siphon, the lip of the siphon is usually placed above the highest tailwater elevation against which pumping is to be conducted. During nonoperating periods for both vertical and horizontal pumps, the pump can be put under air pressure which will balance the head of water above the siphon lip, or pump invert, against the depression of water inside the suction system below the water level in the sump basin. This method is limited by the submergence of the suction bell and the fact that 1 lb of air pressure will balance 2.310 ft of water at 62°F. With horizontal pumps, this can be accomplished by piping the vacuum pumps to discharge either into or from the pumps.

SUCTION-BAY WIDTH

The pump is only a part of a pumping system, and the hydraulic design of the system external to the pump is reflected in the over-all (pool-to-pool) economy of the station. It is necessary to guard against factors that adversely affect the performance of the pump. In multiple-unit stations (especially where vertical pumps are installed) the small floor space occupied by each unit is a temptation to reduce the size of the station by placing the units closer together. This results in a poor flow of water approaching the suction bell of the pumps.

The intake end of the suction system of a horizontal pump is elliptical and considerably larger than the pump barrel. The intake end of a vertical pump consists of a bell. The width of the intake bay should be not less than twice the diameter of the bell to allow proper distribution of water approaching the bell. This dimension can be decreased slightly if the sump floor is deep and increased slightly if the sump floor is shallow. These changes usually result in some decrease in efficiency.

SUBMERGENCE

The vertical distance, when pumping, between the water-surface elevation of the suction bay and the bottom of the bell or suction piece is termed "submergence." This distance should not be less than 5 ft for pumps of the cited capacity. This minimum value is stipulated to prevent vortices which originate at the impeller from reaching the water surface and allowing air to enter the pump. Submergence is a factor in determining the elevation of the sump floor because the distance between the bottom of the bell or suction piece and the top of the suction-bay floor should be not less than one half the diameter of the bell. This distance can be somewhat larger without sacrificing efficiency, but it should rarely be less unless a special device, such as an umbrella, is installed.

Other Considerations

The trash rack is the only screen provided to prevent material other than water from entering the pump. Water hyacinth, small pieces of wood, and similar objects can easily pass through the pump; hence the openings in the trash rack can be approximately 5 in. wide. This will prevent floating objects such as dead animals or automobile tires from entering the sump; a power trash-rack cleaner should be provided. The 5-in. opening in the trash rack will cause a head loss of less than 0.1 ft as the velocities through the screen are less than 3 ft per sec.

The water enters the suction system of the pump at from 4 ft per sec to 6 ft per sec and is accelerated as the diameter of the bell or suction piece decreases. The water column is "squeezed" which increases the pressure; little difficulty caused by convergence is encountered on the suction side of the pump. The water, when leaving the diffuser section of the pump, is traveling at approximately 15 ft per sec, and (unless the water column is increased in size) the velocity-head loss at exit is large. This expansion results in a decreasing piezometer pressure. Unless the expansion process is accomplished correctly, it will result in a poorly operating discharge system. The discharge column for horizontal pumps may be expanded safely with approximately 8° of divergence; for vertical pumps with siphons, the expansion may be carried out in a similar manner but somewhat more rapidly.

The discharge end of the pump should be at—or below—the minimum discharge-pool elevation to assure priming of the horizontal pump and the establishment of a siphon in the vertical pump.

Variable Speed Operations

In Fig. 1 (*b*), an unstable zone is noted at approximately 150% of the head at the best efficiency point. It is not considered good practice to operate an axial-flow pump in the unstable zone, nor economical to operate at heads above it. In Fig. 4 there are shown the characteristics of a 106-in.-diameter, axial-flow pump designed to pump 800 cu ft per sec against a head of 11.3 ft (pool-to-pool) at a rotative speed of 124 rpm. Head-capacity curves are shown in Fig. 4 for speeds higher and lower than the design conditions, together with curves of equal efficiency and equal brake horsepower on the pump shaft. This pump is designed to operate at—or to the right of—the best efficiency point. It can be seen that, for heads lower than 10 ft, the pump cannot operate at peak efficiency when pumping the rated quantity of water and when running at rated speed. Similarly, it is apparent that, when the pump is slowed, the efficiency

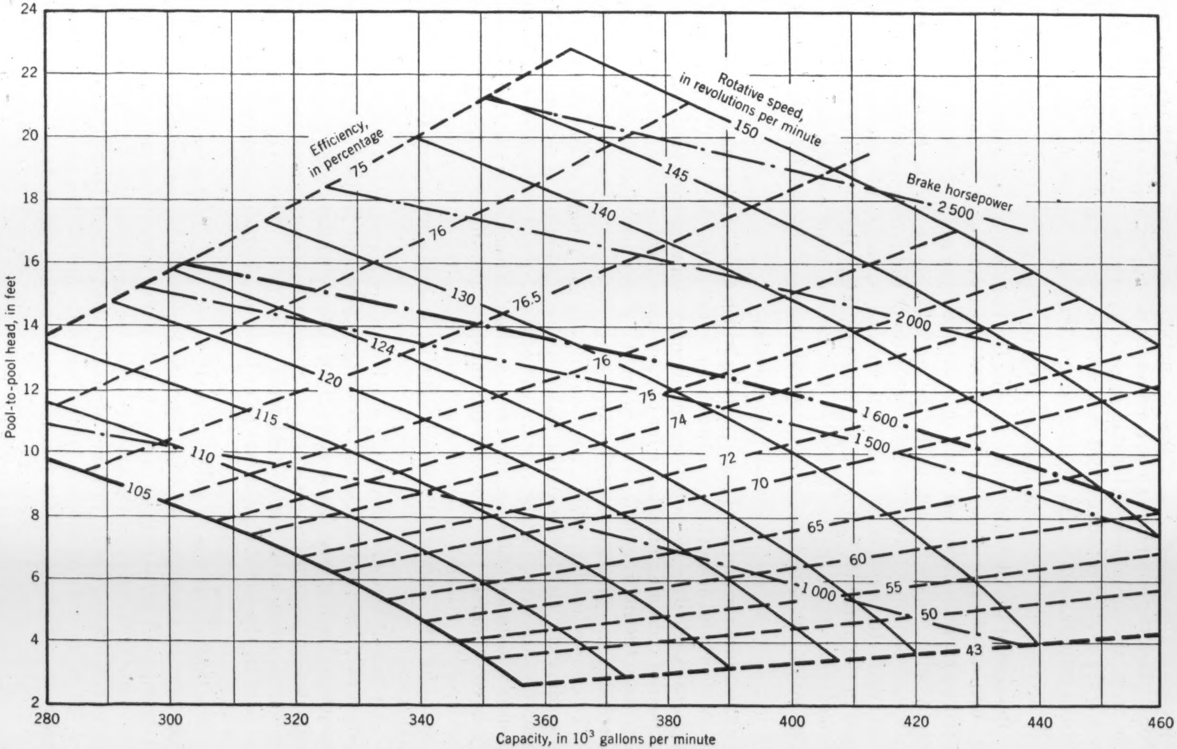

FIG. 4.—CHARACTERISTICS OF AN AXIAL-FLOW PUMP

improves. The area of Fig. 4 that is enclosed by heavy lines shows the zone within which the pumping can be conducted; the upper limit is the power available from the variable-speed diesel engine driving the pump, and the lower limit is the slowest rotative speed at which the pumps can be operated without causing critical vibration in the engine and transmission system.

Model and Field Tests

Because of the difficulty of measuring the large volume of water discharged by pumps of the size which has been cited, the results of an homologous model tested under prototype heads will probably be more accurate than a field test. For example (to be analogous to the prototype), an 18-in. model required 11,000 gal per min of water because the ratio of the prototype diameter to the model diameter was 5.90. This relatively small quantity of water can be measured in the pump laboratory much more accurately than 800 cu ft per sec can be measured in the field. Likewise, the various head conditions can be reproduced in the model much more accurately than in the field.

Conclusions

The hydraulic and mechanical criteria which must be formulated before the actual structural design is begun have been described herein. On the basis of deductions reached in the analysis, preliminary drawings are prepared for the purpose of obtaining machinery for the pumping plant. These drawings need only show the information necessary for the pump manufactureres to prepare their bids.

The model testing, design, and manufacture of pumps of this size require approximately eighteen months; engines and transmission systems require somewhat less time. A substantial part of the pump is embedded in concrete when it is installed; thus, ample time is available after the contract for machinery is consummated to complete the substructure and superstructure plans. The separate purchase of machinery is usually limited to the pumps, the prime movers for the pumps, the speed-reducing transmissions, and the pertinent auxiliaries.

A plant of the size previously cited requires innumerable small electrical motors to drive vacuum pumps, air compressers, and heat-exchanger pumps. Because of the fact that the electrical load of these motors cannot be accurately estimated until the main machinery is determined, the procurement of auxiliary generating equipment and switchboards is deferred. This equipment is then included in the structure contract as delivery can be accomplished in less than a year.

No unusual problems other than those of underseepage require special treatment in the design of the structure to house the pumps and auxiliary equipment. The vibrations caused by the pump and engines are of relatively low frequencies, and the foundation loads are approximately 4 tons per sq ft. These conditions pose no problem when the plant is built on rock foundations, but for piling they require special treatment to prevent the sand from moving under the structure. Mass concrete construction rather than cellular construction is preferred if the cost is within the same range. As with all hydraulic structures, stability under all conditions must be provided.

AMERICAN SOCIETY OF CIVIL ENGINEERS
Founded November 5, 1852
TRANSACTIONS

Paper No. 2724

DETERMINATION OF RADII OF CURVATURE OF TAXIWAYS

By John Hugh Jones,[1] J. M. ASCE, and
Robert Horonjeff,[2] A. M. ASCE

Synopsis

A series of tests to develop the relationship between turning radius and aircraft speed, type of landing gear, total angle of turn, and passenger comfort revealed that only the speed of the aircraft was significant. The relationship between speed and turning radius was obtained by photographing the paths taken by three types of aircraft as they were taxied at a condition of impending skid over a painted grid. The paths were approximated by multicentered circular arcs.

It was found that the expression used in the design of highway curves to relate radial force and friction was applicable to the design of taxiways. The computed friction factor remained sensibly constant with changes in aircraft speed. A design curve relating aircraft speed and turning radius is offered.

Introduction

Consultation with the Airport Engineering Division of the Civil Aeronautics Administration, United States Department of Commerce (CAA), in 1951 revealed the lack of quantitative information on the relationship of aircraft speed to the radius of turning while taxiing. This relationship is an important consideration in the layout of taxiways, particularly those used for clearing aircraft from runways.

In order to increase the rate at which aircraft can land at the busier terminals, taxiway patterns must be developed which will permit minimum occupancy of runways by landing aircraft. This led airport designers to the concept of "lead-off taxiways" which would permit aircraft to leave the runway at speeds as great as 50 miles per hr. Studies[3] conducted by the CAA indicate

---

Note.—Published, essentially as printed here, in August, 1953, as *Proceedings-Separate No. 233.* Positions and titles are those in effect when the paper was received for publication.

[1] Asst. Prof. of Civ. Eng., Univ. of California, Berkeley, Calif.

[2] Lecturer and Research Engr., Inst. of Transportation and Traffic Eng., Univ. of California, Berkeley, Calif.

[3] "Preliminary Report on Airport Configuration Studies," *Airport Engineering Bulletin No. 1,* Civ. Aeronautics Administration, U. S. Dept. of Commerce, Office of Airports, June 15, 1951.

suitable positions for lead-off taxiways along the runways. The present investigation, which complements the work of the CAA, provides information on suitable radii for these lead-off taxiways.

APPARATUS

Three models of aircraft were used in these tests. These aircraft, shown in Fig. 1, are currently (1954) used for commercial operations throughout the world. Maximum gross take-off weights for these aircraft are: DC-3, 25,000 lb; DC-6, 92,000 lb; and CV-340, 47,000 lb. These aircraft are equipped with two types of landing gear: The nose-wheel type on the CV-340 and DC-6 and the tail-wheel type on the DC-3. The main landing gear of the CV-340 and DC-6 is equipped with dual wheels; the DC-3 has single-tire main wheels. The principal dimensions and wheel sizes of the landing gear are shown in Fig. 2.

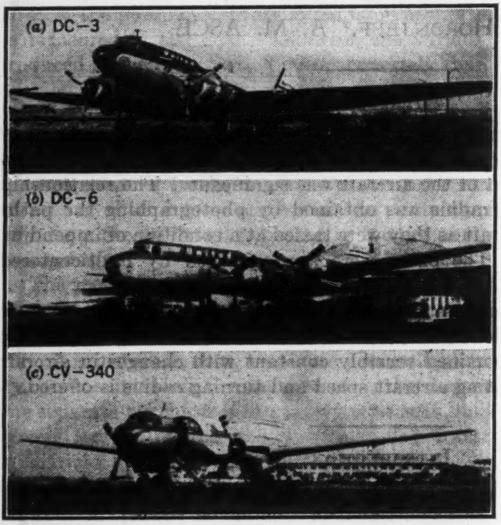

FIG. 1.—TEST AIRCRAFT

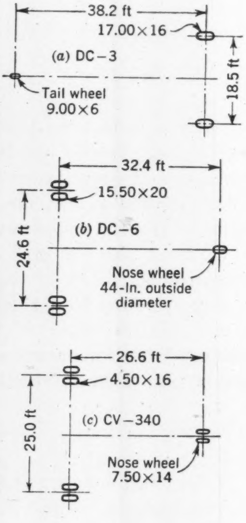

FIG. 2.—LANDING-GEAR CONFIGURATIONS

The equipment used to determine the paths and speeds of the aircraft consisted of a 16-mm motion-picture camera mounted on an outrigger extending from the cockpit window on the right side of the aircraft. A grid formed of 20-ft by 20-ft squares was painted on the northwest end of the northwest-southeast runway at the San Francisco (Calif.) International Airport, as shown in Fig. 3. The camera was adjusted to photograph vertically downward and thus record the path of the aircraft as it maneuvered over the grid. The camera was operated at a nominal speed of 32 frames per sec, but the exact speed was determined by photographing a stop watch.

TEST PROGRAM

The test program was designed to indicate how aircraft speed, type of landing gear, total angle of turn, and passenger comfort imposed limits on the turning radius. An initial series of tests was sufficient, however, to show that the speed of the aircraft is the only variable having a significant effect on the minimum permissible radius. This limiting speed was taken as that of impending skid and was determined by pilot judgment. However, the observer riding in the aircraft was often able to note such confirming symptoms of impending skid as nose-wheel chatter or tail-wheel bounce, and tire squeal; outside the aircraft the condition was implied by tire marks on the pavement.

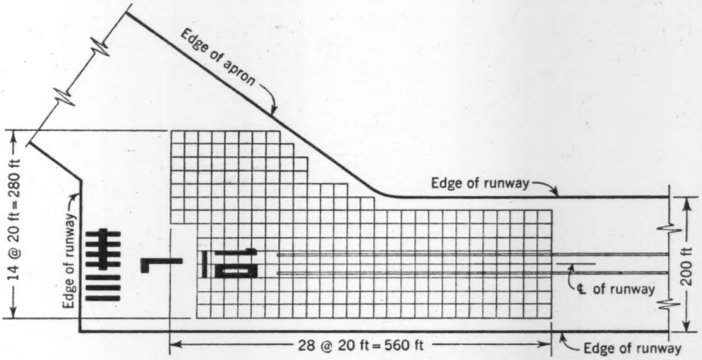

FIG. 3.—GRID LAYOUT

The methods of steering the aircraft differed for the two types of landing gear. The tail-wheel aircraft (DC-3) was steered by the use of wheel-brakes, engines, and rudder in various combinations. The CV-340 and the DC-6 were steered exclusively by use of the nose wheel.

The aircraft were taxied on the grid a total of fifty-seven times at ground speeds ranging from 16 miles per hr to 53 miles per hr. For each run at impending skid, the path of the aircraft was recorded by the motion-picture camera. During the tests the winds were usually less than 15 miles per hr. Observations of the aircraft from the ground by visual and photographic methods indicated negligible "body roll" even during the tightest turns.

ANALYSIS OF DATA

The photographs of the aircraft's travel over the grid were viewed as still pictures. Each time the center of the camera crossed a grid line, the ground position of the camera with respect to an intersection of grid lines was plotted on a drawing of the grid. The relative positions of camera and landing gear being known, the path of the landing gear could be plotted. In this manner the path of the turning aircraft was established. The radii of curvature were determined from the circular arcs which were used to fit smooth curves to the plotted points. The speed of the aircraft was readily determined from the

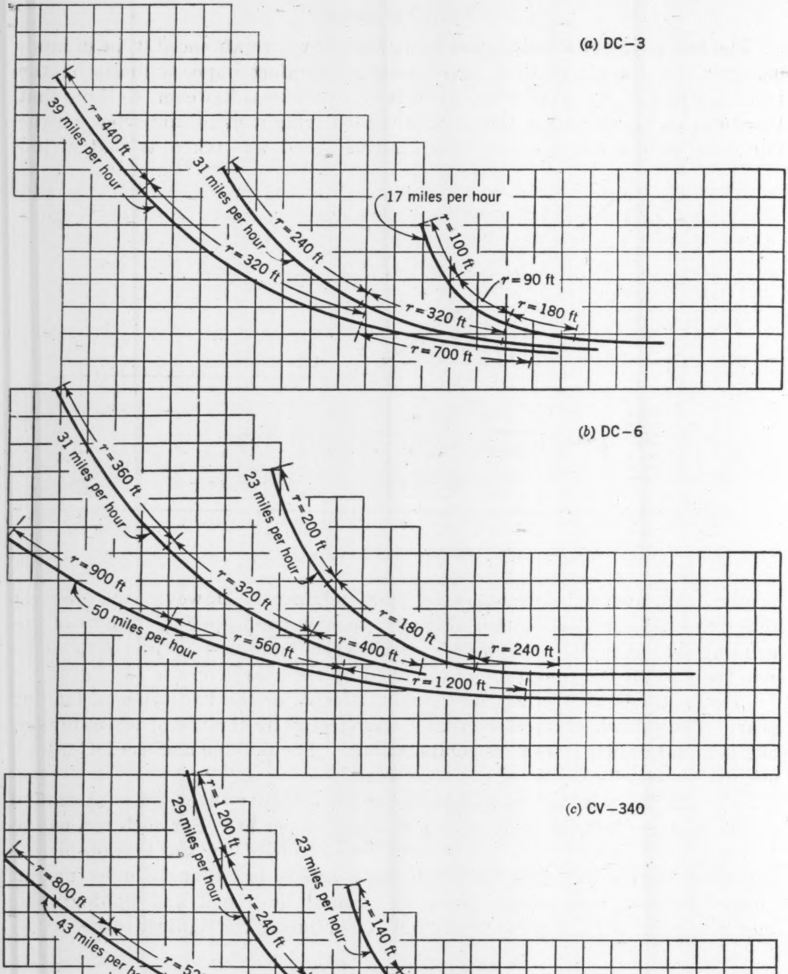
(a) DC-3
r = 440 ft
39 miles per hour
31 miles per hour
r = 240 ft
r = 320 ft
17 miles per hour
r = 100 ft
r = 90 ft
r = 180 ft
r = 320 ft
r = 700 ft
(b) DC-6
r = 360 ft
31 miles per hour
23 miles per hour
r = 200 ft
r = 900 ft
50 miles per hour
r = 320 ft
r = 180 ft
r = 240 ft
r = 560 ft
r = 400 ft
r = 1 200 ft
(c) CV-340
r = 1 200 ft
29 miles per hour
23 miles per hour
r = 800 ft
43 miles per hour
r = 240 ft
r = 140 ft
r = 520 ft
r = 200 ft
r = 120 ft
r = 600 ft
r = 320 ft
r = 600 ft

FIG. 4.—TYPICAL CENTER-LINE PATHS OF AIRCRAFT AT VARIOUS SPEEDS, IMPENDING SKID CONDITIONS

number of exposed frames of film between crossings of grid lines and the known camera timing in terms of frames per second. The paths of each aircraft at the impending skid condition for three different average speeds are shown in Fig. 4. From these and similar plots the corresponding speed of the aircraft and the radius of curvature were obtained. The observed paths of the aircraft were best approximated by three-centered or four-centered compound curves although the actual curves were probably circular arcs with spirals at each end. The data were plotted from the observed radius and the corresponding speed for each run at the impending skid condition, as shown in Fig. 5.

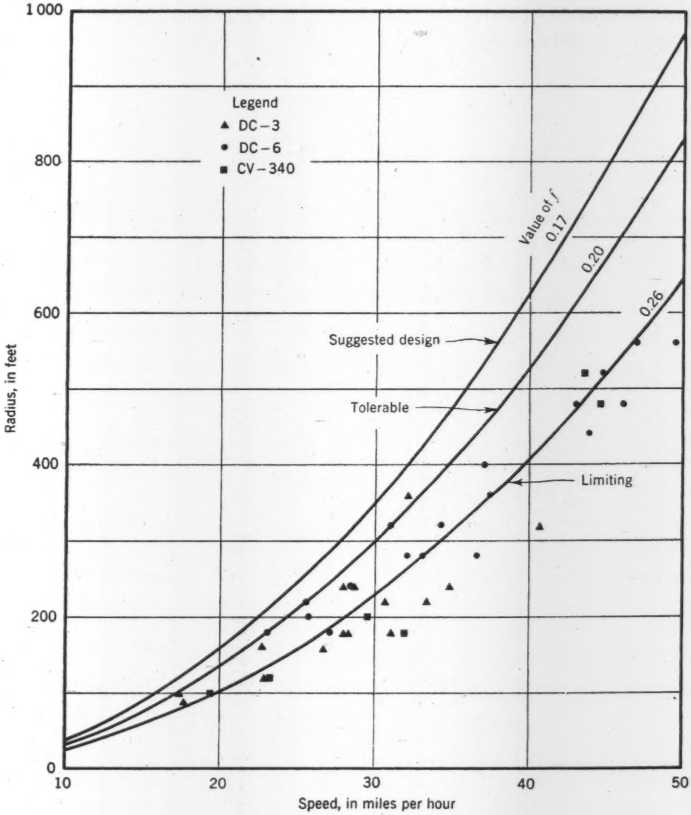

FIG. 5.—RELATIONSHIP BETWEEN TURNING RADIUS AND AIRCRAFT SPEED

Following the fitting of various curves to these data, it was found that a curve representing the fundamental equation of radial force opposed by frictional force used in the design of highway curves was entirely satisfactory.

This expression is

$$\frac{W\,v^2}{g\,r} = W f \qquad (1)$$

in which W is weight, v denotes velocity, g is the acceleration of gravity, r represents radius, and f is the friction factor. The friction factor is the horizontal acceleration resulting from the turn and is expressed as a fraction of g, the acceleration due to gravity. When Eq. 1 is solved for r in feet, with v in miles per hour, it becomes

$$r = \frac{v^2}{15 f} \qquad (2)$$

TABLE 1.—Computed Friction Factors

Aircraft	Speed, in miles per hour	Radius, in feet	Friction factor[a]
DC-3	17.6	100	0.21
	17.8	90	0.24
	22.9	120	0.29
	22.9	160	0.22
	26.8	160	0.30
	28.0	240	0.22
	28.1	180	0.29
	28.5	180	0.30
	28.8	240	0.23
	30.7	220	0.29
	31.2	180	0.36
	32.3	360	0.19
	33.5	220	0.34
	35.0	240	0.34
	40.9	320	0.35
DC-6	23.2	180	0.20
	25.7	220	0.20
	25.8	200	0.22
	27.2	180	0.27
	28.6	240	0.23
	31.1	320	0.22
	32.2	280	0.25
	33.1	280	0.26
	34.4	320	0.25
	36.7	280	0.32
	37.2	400	0.23
	37.5	360	0.26
	39.3	480	0.21
	43.1	480	0.26
	44.0	440	0.29
	44.9	520	0.26
	46.2	480	0.30
	47.1	560	0.26
	49.6	560	0.29
CV-340	19.5	100	0.25
	23.1	120	0.30
	29.6	200	0.29
	32.0	180	0.37
	36.8	480	0.19
	43.7	520	0.24
	44.7	480	0.28

[a] Computed from Eq. 2.

It is recognized that Eq. 1 is not strictly applicable to the case of an aircraft because the weight in the term $W f$ is reduced by whatever lift is developed at a particular speed, whereas the mass term, W/g, remains unaffected. However, as an aircraft turns off from a runway, the wind creates a force opposite to the outward radial force, which may partly offset the effect of lift. Other factors, such as the distribution of load on the landing gear and the tire condition, may also have their effect. Nevertheless, the curve expressed by a friction factor of 0.26 shows a good fit (Fig. 5), well within the practicable limits of accuracy of the measurements; this curve represents the observed limiting condition for operation on dry bituminous pavements when wind velocities are low.

The particular friction factor of 0.26 is the mean value of the f-values computed from Eq. 2 for each of the forty-one observations shown in Fig. 5. These f-values are shown in Table 1. An examination of these values indicates no marked change in friction factor at higher speeds, as might be expected if lift were effective and if there were no other compensating factors.

The curve designated as "Tolerable" in Fig. 5 is one which envelops all the plotted points and which was established on the basis of a constant friction factor of 0.20 in Eq. 2. For a particular speed, the radius should not be less than that indicated by this curve; otherwise, skidding might occur.

The curve designated as "Suggested Design" in Fig. 5 was determined from a friction factor of 0.17 in Eq. 2. This curve provides a margin of safety of 50% over the radii established by the "Limiting" curve. From Fig. 5 the following approximate, suggested-design values are obtained:

Speed, in miles per hour	Radius, in feet
10	50
20	150
30	350
40	650
50	1,000

This margin of safety (50%) is necessary to account for the difference between the favorable conditions under which the tests were conducted and conditions more frequently encountered in service. The effects of pavement condition, wind velocity and relative direction, tire condition, wing lift, distribution of weight on the landing gear, uncertainty of steering, and a multitude of similar factors were not evaluated separately in this investigation. Until the magnitude of these variables has been determined, a margin of safety of 50% is justified.

CONCLUSIONS

Within the limits of the tests, it was determined that the type of landing gear and the size of the aircraft do not affect the speed-radius relationship. For a given type of surface, only speed has a significant effect on the limiting values of the radius of turning.

ACKNOWLEDGMENTS

The aircraft designated as DC-3 and DC-6 were manufactured by the Douglas Aircraft Corporation of Santa Monica, Calif. The CV-340 was manufactured by the Consolidated-Vultee Aircraft Corporation of San Diego, Calif.

Appreciation is expressed to the maintenance staff of United Air Lines, Incorporated, at San Francisco, Calif., and to the management of the San Francisco International Airport for their cooperation in this investigation. W. E. Rhoades and J. D. Beaumont made the arrangements for the use of the aircraft, and H. C. Holloway and M. C. Casserly were the test pilots. F. V. Philpot, A. M. ASCE, and his maintenance staff at the airport assisted in laying out and painting the grid.

R. A. Moyer, A. M. ASCE, offered many helpful suggestions throughout the test program, and Wayne Snowden critically reviewed the manuscript.

AMERICAN SOCIETY OF CIVIL ENGINEERS
Founded November 5, 1852
TRANSACTIONS

Paper No. 2725

PHOTOELASTIC ANALOGY FOR NON-HOMOGENEOUS FOUNDATIONS

BY ALLEN J. CURTIS,[1] AND F. E. RICHART, JR.,[2]
A. M. ASCE

SYNOPSIS

The stress distributions in a semi-infinite body—in which Poisson's ratio is constant but in which the modulus of elasticity varies with depth—are considered herein. The general equations of elasticity for such a point-isotropic material are derived. These equations establish the fact that superposition of correct solutions is permissible. There is shown to be an analogy between the stresses in a constrained slice, which has a modulus of elasticity that varies with depth, and the stresses in a plate whose thickness varies in the same manner if the state of stress in the plate can be considered to be two-dimensional. Thus, the stress distributions beneath infinite line loads or infinite strip loads on such a foundation can be determined experimentally by the use of photoelasticity. The photoelastic analogy is confirmed by experiments, and its use is outlined.

NOTATION

Compressive stresses will be assumed positive. Also, the term "solutions" is used to indicate a solution for the stress distribution caused by a surface loading on a semi-infinite body.

The letter symbols adopted for use in this paper are defined where they first appear, in the illustrations or in the text, and are arranged alphabetically, for convenience of reference, in the Appendix.

INTRODUCTION

For certain problems in soil mechanics the stress-strain relationships of the soil agree with Hooke's law. In these problems the theory of elasticity will give satisfactory results for stresses and displacements if the properties of the

---

NOTE.—Published, essentially as printed here, in July, 1953, as *Proceedings-Separate No. 211*. Positions and titles given are those in effect when the paper was received for publication.

[1] Member of the Technical Staff, Research and Development Labs., Hughes Aircraft Co., Culver City, Calif.

[2] Associate Prof. of Civ. Eng., Univ. of Florida, Gainesville, Fla.

theoretical material are similar to the physical properties of the soil mass.[3] If the soil mass is homogeneous and isotropic as well as elastic, a solution involving only two elastic constants will be applicable. Such solutions as that by J. Boussinesq,[4] for a concentrated normal load, and that by V. Cerruti,[5] for a concentrated tangential load, each load acting on the free surface of a semi-infinite body, have been used satisfactorily for the study of stresses and deformations beneath foundations. By suitable integration of the equations for stresses given by these fundamental problems, it has been possible to evaluate the stress distributions beneath line loads, strip loads, and area loads.

However, the materials encountered in soil mechanics are seldom both homogeneous and isotropic. Consequently, actual results are often at variance with theoretical predictions. As a result of this discrepancy numerous studies have been made, based on the theory of elasticity, in which the idealized elastic material is assumed to have properties more nearly like those of soils. For various analyses, the elastic material has been assumed to be (*a*) homogeneous but aelotropic, such as a soil having different elastic properties in the horizontal and vertical directions, (*b*) made up of layered systems, each layer being homogeneous and isotropic, or (*c*) point-isotropic, in which the material is assumed to be isotropic at each point but is nonhomogeneous as the elastic constants vary throughout the mass.

This investigation is concerned with the analyses based on an assumption of point-isotropic materials for which Poisson's ratio is constant throughout, but for which the modulus of elasticity varies with depth. First, the general equations of elasticity are derived for this particular type of point-isotropic material. Then, by comparing the general equations of elasticity with those equations which represent the stress distribution in a plate of variable thickness, an analogy is established which permits the analysis of stress distributions in the point-isotropic material by the use of a photoelastic model which has a variable thickness.

EQUATIONS OF ELASTICITY FOR POINT–ISOTROPIC MATERIALS

The theory of elasticity is based on Hooke's law which (for the general case) establishes a possible total of thirty-six independent elastic constants at each point of the material. However, if the material is assumed to be isotropic (that is, if the elastic properties are independent of a rotation of the coordinate axes), only two independent elastic constants are obtained at any point. If, in addition, the assumption is made that the material is homogeneous, only two elastic constants are obtained throughout the body. Because the mathematical procedures are simplified greatly by using only two elastic constants, the greater part of the work in the theory of elasticity has been based on the assumptions that the material is isotropic and homogeneous.

For point-isotropic material only two independent elastic constants are obtained at each point in the body. These two quantities, however, may each have different values at various locations within the elastic body. The values of Poisson's ratio, μ, and the modulus of elasticity, E, are used in this study as the two independent elastic constants. It is assumed that Poisson's ratio has the same value throughout the body, but that the modulus of elasticity is solely a function of depth.

---

[3] "Theoretical Soil Mechanics," by K. Terzaghi, John Wiley & Sons, Inc., New York, N. Y., 1943, p. 367.

[4] "Applications des Potentiels," by J. Boussinesq, Gauthier-Villars, Paris, France, 1885.

[5] "Ricerche intorno all'equilibrio de corpi elastici isotropi," by V. Cerruti, *Memoria fisica e matematica*, Academia Lincei, Rome, Italy, 1882.

These assumptions regarding the elastic constants do not affect the usual stress-strain relationships as these relationships are concerned with the conditions at a point of the body. Also the strain-displacement equations are unaffected by the assumed variation of the elastic constants.

The equilibrium equations, in terms of stress, express the equations of statics which must be satisfied throughout a body. Thus, variations of elastic constants cannot affect the equations in this form. In terms of stresses, the equations of equilibrium (for Cartesian coordinates) can be written as

$$\frac{\partial \sigma_x}{\partial x} + \frac{\partial \tau_{xy}}{\partial y} + \frac{\partial \tau_{xz}}{\partial z} + X = 0 \cdots (x, y, z) \ldots\ldots\ldots\ldots\ldots (1)$$

in which σ is the normal component of internal force per unit area; τ denotes the tangential component of internal force per unit area; a single subscript signifies the direction of the normal component of the internal force; a double subscript denotes the plane in which the tangential component of internal force is acting; x, y, and z are the Cartesian coordinates; and X is the component of body or inertia force in the x-direction. The notation (x, y, z) to the right of Eq. 1 indicates that similar equations, for the other coordinate directions, can be written by a cyclic interchange of subscripts.

In the problem under consideration, the only body forces encountered will be the gravity loading of the soil. It will be shown, however, that the differential equations to be satisfied in this point-isotropic medium are linear, so that the law of superposition is valid. Thus, the effects of gravity loading can be added separately to any solution obtained; consequently the body forces are neglected in the analysis.

In addition to the equilibrium equations, boundary conditions, and stress-strain relationships, a complete solution of a problem by use of the theory of elasticity must also satisfy the equations of compatibility. In terms of strains, the compatibility equations for a three-dimensional system are

$$\frac{\partial^2 \epsilon_x}{\partial y^2} + \frac{\partial^2 \epsilon_y}{\partial x^2} = \frac{\partial^2 \gamma_{xy}}{\partial x\, \partial y} \cdots (x, y, z) \ldots\ldots\ldots\ldots\ldots\ldots (2)$$

and

$$\frac{2\, \partial^2 \epsilon_x}{\partial y\, \partial z} = \frac{\partial}{\partial x}\left(-\frac{\partial \gamma_{yz}}{\partial x} + \frac{\partial \gamma_{zx}}{\partial y} + \frac{\partial \gamma_{xy}}{\partial z}\right) \cdots (x, y, z) \ldots\ldots\ldots\ldots (3)$$

in which ϵ is the deformation per unit length (strain) and γ_{xy} denotes the shearing strain or detrusion between the xz-plane and the yz-plane. Eqs. 2 and 3 are independent of the elastic constants E and μ in this form. However, one convenient method of solving problems in elasticity is to transform Eqs. 2 and 3 so that they are in terms of stresses. This transformation is performed by use of the stress-strain relationships and equilibrium equations.[6] When the boundary conditions are known in terms of stresses, as is the case for the problem under consideration, this seems to be preferable.

---

[6] "Theory of Elasticity," by S. Timoshenko and J. N. Goodier, McGraw-Hill Book Co., Inc., New York, N. Y., 1951, p. 230.

In accordance with the usual practice, the z-direction has been chosen as the direction of increasing depth, so that E or the modulus of elasticity in shear, G, is a function of z only; that is,

$$\frac{\partial E}{\partial x} = \frac{\partial G}{\partial x} = \frac{\partial E}{\partial y} = \frac{\partial G}{\partial y} = 0 \ldots\ldots\ldots\ldots (4)$$

Substituting the stress-strain relationships into Eqs. 2 and 3, and using the equilibrium equations to eliminate shearing stresses, the three-dimensional equations of compatibility in terms of stresses become

$$\left(\nabla^2\theta - \nabla^2\sigma_z - \frac{\partial z^2}{\partial^2\theta}\right) - \frac{\mu}{1+\mu}\left(\nabla^2\theta - \frac{\partial^2\theta}{\partial z^2}\right) = 0 \ldots\ldots\ldots (5)$$

$$\left(\nabla^2\theta - \nabla^2\sigma_x - \frac{\partial^2\theta}{\partial x^2}\right) - \frac{\mu}{1+\mu}\left(\nabla^2\theta - \frac{\partial^2\theta}{\partial x^2}\right) - 2\left[\frac{\partial}{\partial z}\left(\sigma_y - \frac{\mu}{1+\mu}\theta\right)\right.$$
$$\left. - \frac{\partial \tau_{yz}}{\partial y}\right]\frac{\partial \log_e G}{\partial z} + \left(\sigma_y - \frac{\mu}{1+\mu}\theta\right)\left[\left(\frac{\partial \log_e G}{\partial z}\right)^2 - \frac{\partial^2 \log_e G}{\partial z^2}\right] = 0 \ldots (6)$$

$$\left(\nabla^2\theta - \nabla^2\sigma_y - \frac{\partial^2\theta}{\partial y^2}\right) - \frac{\mu}{1+\mu}\left(\nabla^2\theta - \frac{\partial^2\theta}{\partial y^2}\right) - 2\left[\frac{\partial}{\partial z}\left(\sigma_x - \frac{\mu}{1+\mu}\theta\right)\right.$$
$$\left. - \frac{\partial \tau_{xz}}{\partial x}\right]\frac{\partial \log_e G}{\partial z} + \left(\sigma_x - \frac{\mu}{1+\mu}\theta\right)\left[\left(\frac{\partial \log_e G}{\partial z}\right)^2 - \frac{\partial^2 \log_e G}{\partial z^2}\right] = 0 \ldots (7)$$

$$\nabla^2\tau_{yz} + \frac{1}{1+\mu}\frac{\partial^2\theta}{\partial y\,\partial z} + \left[\frac{\partial \tau_{xy}}{\partial x} - \frac{\partial}{\partial y}\left(\sigma_x - \frac{\mu}{1+\mu}\theta\right)\right]\frac{\partial \log_e G}{\partial z} = 0 \ldots (8)$$

$$\nabla^2\tau_{xz} + \frac{1}{1+\mu}\frac{\partial^2\theta}{\partial x\,\partial z} + \left[\frac{\partial \tau_{xy}}{\partial y} - \frac{\partial}{\partial x}\left(\sigma_y - \frac{\mu}{1+\mu}\theta\right)\right]\frac{\partial \log_e G}{\partial z} = 0 \ldots (9)$$

and

$$\nabla^2\tau_{xy} + \frac{1}{1+\mu}\frac{\partial^2\theta}{\partial x\,\partial y} + \left(\frac{\partial \tau_{xz}}{\partial y} + \frac{\partial \tau_{yz}}{\partial x} - 2\frac{\partial \tau_{xy}}{\partial z}\right)\frac{\partial \log_e G}{\partial z}$$
$$+ \tau_{xy}\left[\left(\frac{\partial \log_e G}{\partial z}\right)^2 - \frac{\partial^2 \log_e G}{\partial z^2}\right] = 0 \ldots (10)$$

In Eqs. 5 through 10,

$$\nabla^2 = \left(\frac{\partial^2}{\partial x^2} + \frac{\partial^2}{\partial y^2} + \frac{\partial^2}{\partial z^2}\right) \ldots\ldots\ldots\ldots (11)$$

and is the Laplacian operator. In these equations θ denotes the sum of the principal stresses.

Adding Eqs. 5, 6, and 7 and again using the equilibrium equations to eliminate shear stresses results in

$$\nabla^2\theta - 2\frac{\partial\theta}{\partial z}\frac{\partial \log_e G}{\partial z} + \left(\theta - \frac{1+\mu}{1-\mu}\sigma_z\right)\left[\left(\frac{\partial \log_e G}{\partial z}\right)^2 - \frac{\partial^2 \log_e G}{\partial z^2}\right] = 0 \ldots (12)$$

It is evident that, if G is constant, the compatibility equations reduce to those given by S. Timoshenko and J. N. Goodier.[7]

In the system which corresponds to plane strain in the xz-plane, the compatibility relationships are reduced from six to one because

$$\epsilon_y = \gamma_{yz} = \gamma_{yx} = \frac{\partial}{\partial y} = 0 \qquad (13)$$

By substituting the relationships from Eq. 13 into Eqs. 2 and 3, and using the stress-strain relationships and equilibrium equations, the compatibility equation, in terms of stress, is determined for plane strain to be

$$\nabla^2\theta' - 2\frac{\partial\theta'}{\partial z}\frac{\partial \log_e G}{\partial z} + \left(\sigma_x - \frac{\mu}{1-\mu}\sigma_z\right)\left[\left(\frac{\partial \log_e G}{\partial z}\right)^2 - \frac{\partial^2 \log_e G}{\partial z^2}\right] = 0 \qquad (14)$$

in which

$$\theta' = \sigma_x + \sigma_z \qquad (15)$$

A slice is considered to be in a state of plane stress if the faces of the slice are free of surface tractions and if it is thin enough—in comparison with its other dimensions—so that variations of stress normal to the plane of the slice can be considered negligible. This condition requires that, for plane stress in the xz-plane,

$$\sigma_y = \tau_{xy} = \tau_{zy} = \frac{\partial}{\partial y} = 0 \qquad (16)$$

Under these assumptions, the compatibility relationships reduce to

$$\frac{\partial^2\epsilon_x}{\partial z^2} + \frac{\partial^2\epsilon_z}{\partial x^2} = \frac{\partial^2\gamma_{xz}}{\partial x\,\partial z} \qquad (17)$$

and

$$\frac{\partial^2\epsilon_y}{\partial x^2} = \frac{\partial^2\epsilon_y}{\partial z^2} = \frac{\partial^2\epsilon_y}{\partial x\,\partial z} = 0 \qquad (18)$$

Eq. 18 is satisfied if

$$\epsilon_y = -\frac{\mu\,\theta}{E} = a\,x + b\,y + c \qquad (19)$$

in which a, b, and c are constants. It is customary to solve plane-stress problems by neglecting Eq. 18 which also involves disregarding two shear stress-strain relationships that relate Eqs. 16 and 18. E. Reissner has shown[8] that the error caused by this simplification is small if the change in the normal stresses is moderate in a distance equal to the thickness of the slice. In addition, by integrating the correction to the stresses obtained in this manner across the thickness of the plate, the result is zero. Consequently, in photoelastic work the fringe patterns will agree with this average stress distribution.

The compatibility equations for the case of plane stress in the xz-plane can be transformed into terms of stress to give

---

[7] "Theory of Elasticity," by S. Timoshenko and J. N. Goodier, McGraw-Hill Book Co., Inc., New York, N. Y., 1951, p. 231.

[8] "On the Calculation of Three-Dimensional Corrections for the Two-Dimensional Theory of Plane Stress," by E. Reissner, *Proceedings*, 15th Semi-Annual Eastern Photoelasticity Conference, Addison-Wesley Press, Inc., Cambridge, Mass., June, 1942, p. 23.

$$\nabla^2\theta' - 2\frac{\partial\theta'}{\partial z}\frac{\partial \log_e G}{\partial z} + (\sigma_x - \mu\,\sigma_z)\left[\left(\frac{\partial \log_e G}{\partial z}\right)^2 - \frac{\partial^2 \log_e G}{\partial z^2}\right] = 0 \quad \text{..(20)}$$

Inspection of Eqs. 12, 14, and 20 shows the following: (1) All the equations are linear, so that the solutions for different surface loadings or displacements can be superimposed. Thus, the solutions for a concentrated force or a line load of infinite length are fundamental solutions for the three-dimensional problem and the two-dimensional problem, respectively. (2) The rate of change of $\log_e G$ (or $\log_e E$), rather than the actual value or rate of change of G (or E), influences the stress distribution. (3) The solutions of two-dimensional problems depend on the value of Poisson's ratio, in contrast to the solutions ordinarily obtained under the assumption of a constant modulus of elasticity.

SOLUTIONS FOR POINT–ISOTROPIC MATERIALS

A solution for stresses which has been used in connection with nonhomogeneous foundations is that given by O. K. Fröhlich.[9] Mr. Fröhlich assumed that a radial stress distribution existed in the semi-infinite body beneath a point load P, and he derived the expression for σ_R, the radial stress,

$$\sigma_R = \frac{n\,P}{2\,\pi\,R}\cos^{n-2}\psi \quad \text{.....................(21)}$$

in which ψ is the angle between the radial direction and the z-axis and n is an arbitrary parameter. The value of n has been interpreted as a "stress concentration factor" in order to relate the changes in the stress field produced by varying the characteristics of the modulus of elasticity of the foundation material.

When Eq. 21 is used in connection with a material whose modulus of elasticity is described by

$$E = k\,z^w \quad \text{.........................(22)}$$

the results were found to be correct only if

$$n = w + 3 = 1 + \frac{1}{\mu} \quad \text{...................(23)}$$

in which k and w are constants for the particular material. This restriction on the use of Mr. Fröhlich's solution was established by J. Ohde.[10]

The special case for which the foundation modulus of elasticity varies as

$$E = k\,z \quad \text{.........................(24)}$$

has been studied by H. Borowicka.[11] By representing the stresses and displacements by an infinite power series with unknown constant coefficients, Mr. Borowicka obtained a solution for the case of a point load which can be evaluated for any value of Poisson's ratio. The vertical stress along the loading axis in a material which satisfies Eq. 24 is as follows:

---

[9] "Druckverteilung im Baugrund," by O. K. Fröhlich, Julius Springer, Vienna, Austria, 1934.

[10] "Zur Theorie der Druckverteilung im Baugrund," by J. Ohde, *Der Bauingenieur*, Vol. 20, 1939, p. 451.

[11] "Die Druckausbreitung im Halbraum bei linear zunehmenden Elastizitätsmodul," by H. Borowicka, *Ingenieur-Archiv*, Vol. 14, 1945, p. 75.

Poisson's ratio, μ	$\left(\frac{\sigma_z}{\frac{3P}{2\pi z^2}}\right)_{\rho=0}$
$\frac{1}{2}$	1.00
$\frac{1}{3}$	1.33
$\frac{1}{4}$	1.47
0	1.76

in which $\rho = (x^2 + y^2)^{\frac{1}{2}}$. These results indicate that the value of the vertical stress on the axis of loading depends on the value of Poisson's ratio. For a change in Poisson's ratio from $\frac{1}{2}$ to 0, a corresponding increase in stress of 76% occurs, at any depth. Consequently, the use of the solution obtained by Mr. Fröhlich can result in considerable error if the conditions of Eq. 23 are not satisfied.

Tables 1 and 2 are a summary of the correct solutions for the vertical stresses along the loading axis in semi-infinite, point-isotropic materials.

TABLE 1.—VERTICAL STRESS σ_z CAUSED BY A POINT LOAD P, ACTING VERTICALLY AT THE SURFACE OF A SEMI-INFINITE BODY

Expression for E	Value of μ	Expression[a] for σ_z	Value of $\left(\frac{z^2\sigma_z}{P}\right)_{\rho=0}$	Expression for σ_R
Constant	$0 < \mu < \frac{1}{2}$	$\frac{3P}{2\pi}\frac{z^3}{R^5}$	0.477	$\frac{P}{\pi R^2}\left[(2-\mu)\cos\psi - \frac{1-2\mu}{2}\right]$
kz	$\frac{1}{2}$	$\frac{3P}{2\pi}\frac{z^3}{R^5}$	0.477	$\frac{3P}{2\pi}\frac{\cos\psi}{R^2}$
kz	$\frac{1}{3}$	$\frac{2P}{\pi}\frac{z^4}{R^6}$	0.637	$\frac{2P}{\pi}\frac{\cos^2\psi}{R^2}$
kz	$\frac{1}{4}$	Infinite series	0.699	Infinite series
kz	0	Infinite series	0.839	Infinite series
$kz^{\frac{1}{2}}$	0.40	$\frac{7P}{4\pi R^2}\cos^{7/2}\psi$	0.557	$\frac{7P}{4\pi R^2}\cos^{3/2}\psi$
kz^w	$\frac{1}{n-1} = \frac{1}{w+2}$	$\frac{nP}{2\pi R^2}\cos^n\psi$	$\frac{n}{2\pi}$	$\frac{nP}{2\pi R^2}\cos^{n-2}\psi$

[a] In which $R = (x^2 + y^2 + z^2)^{\frac{1}{2}}$.

THE PHOTOELASTIC ANALOGY

Data from soil tests indicate that elastic soils often have a modulus of elasticity which increases with increasing depth. Such soils can be considered to be composed of an infinite number of thin horizontal layers of homogeneous, isotropic materials. With increasing depth, each layer is somewhat more rigid so that a given uniform pressure on two adjacent layers will produce a smaller contraction in the lower layer. Such a physical concept has been used by

K. Terzaghi,[12] Hon. M. ASCE, and N. M. Newmark,[13] M. ASCE, as a basis for methods of estimating the stress distribution in nonhomogeneous foundations. By these methods the vertical thicknesses of layers were adjusted in proportion to their relative stiffnesses; the Boussinesq solution[4] was then applied to this transformed material.

TABLE 2.—VERTICAL STRESS σ_z RESULTING FROM A LINE LOAD OF q PER UNIT LENGTH, ACTING VERTICALLY AT THE SURFACE OF A SEMI-INFINITE BODY

Expression for E	Value of μ	Expression[a] for σ_z	Value of $\left(\frac{z\,\sigma_z}{q}\right)_{x=0}$	Expression for σ_r
Constant	$0 < \mu < \frac{1}{2}$	$\frac{2}{\pi}\frac{q}{}\frac{\cos^3\theta}{r}$	$\frac{2}{\pi}$	$\frac{2\,q}{\pi}\frac{\cos\theta}{r}$
$k\,z$	$\frac{1}{2}$	$\frac{3\,q}{4}\frac{\cos^4\theta}{r}$	$\frac{3}{4}$	$\frac{3\,q}{4}\frac{\cos^2\theta}{r}$
$k\,z^{\frac{1}{2}}$	0.40	$f_{\frac{1}{2}}\,q\,\frac{\cos^{7/2}\theta}{r}$	$f_{\frac{1}{2}}$	$f_{\frac{1}{2}}\,q\,\frac{\cos^{3/2}\theta}{r}$
$k\,z^w$	$\frac{1}{n-1} = \frac{1}{w+2}$	$f\,q\,\frac{\cos^n\theta}{r}$	f	$f\,q\,\frac{\cos^{n-2}\theta}{r}$
$\frac{k}{z}$	$\frac{1}{2} > \mu > 0$	$\frac{4\,q}{\pi^2}\frac{z\,\text{arc tan}\,(z/x)}{r^2}$	$\frac{2}{\pi}$	$\frac{4\,q}{\pi^2}\frac{1}{z}\,\text{arc tan}\,(z/x)$

[a] In which $f = \dfrac{1}{2\int_0^{\pi/2}\cos^{n-1}\theta\,d\theta}$, $f_{\frac{1}{2}} = 0.7218$, and $r = (x^2 + z^2)^{\frac{1}{2}}$.

A similar physical interpretation of the problem can be gained by considering a thin slice from a semi-infinite body of homogeneous, isotropic material which is loaded along a region of the free surface. If the slice has a constant thickness, the stress distribution will correspond to that produced by an infinite line loading or an infinite strip loading on the semi-infinite body. If the thickness of the slice varies as a function of the depth (increased thickness with increased depth), and if the thickness changes smoothly and not too rapidly, it is reasonable to expect the stress distribution to be two-dimensional and the variations of stress across the thickness of the slice to be negligible. The slice may thus be considered to be an infinite number of thin strips, each strip being somewhat wider with an increase in depth. If a uniform pressure is applied over the top surface of such a slice, the stress and accompanying vertical contractions will decrease with depth. Thus, there appears to be a physical analogy between the soil with a varying modulus and the slice with a varying thickness. It can be shown that this relationship is mathematically valid, thus establishing a method for determining the stress distribution in a point-isotropic material by the use of photoelasticity.

The stress distribution in a semi-infinite body produced by a line load or strip load on the surface can be analyzed as a problem of plane strain. A photoelastic model, however, represents a problem of plane stress. In order to use the results from photoelastic tests to describe stress distribution for a case of plane strain, it is necessary to use the plane stress-plane strain (or free slice-constrained slice) analogy which has been cited by H. M. Westergaard[14] and by R. D. Mindlin, A. M. ASCE, and M. G. Salvadori,[15] M. ASCE.

---

[12] "Bodenpressung und Bettungsziffer," by K. Terzaghi, *Oesterreichiesche Bauzeitung*, No. 25, June 18, 1932.

[13] Discussion by N. M. Newmark of "Distribution of Stresses under a Foundation," by A. E. Cummings, *Transactions*, ASCE, Vol. 101, 1936, p. 1115.

In a plane-stress system with elastic constants, E', G', and μ', and in a plane-strain system with constants, E, G, and μ, it can be shown that the substitution of

$$E' = \frac{E}{1 - \mu^2} \qquad (25a)$$

$$G' = G \qquad (25b)$$

and

$$\mu' = \frac{\mu}{1 - \mu} \qquad (25c)$$

into the stress-strain relationships for plane stress yields the equation for plane strain. Similarly, the substitution of

$$E = E' \frac{1 + 2\mu'}{(1 + \mu')^2} \qquad (26a)$$

$$G = G' \qquad (26b)$$

and

$$\mu = \frac{\mu'}{1 + \mu'} \qquad (26c)$$

into the stress-strain relationships for plane strain yields the equations for plane stress. The equilibrium equations in terms of stress are equal, and, by inspection of Eqs. 14 and 20, it can be seen that the compatibility equations also become identical if these substitutions are made.

Thus, a free slice and a constrained slice which have the same physical dimensions and the same boundary loading will have the same stress distribution if Poisson's ratios for the two materials are related as previously shown and if the moduli of elasticity are directly proportional. From Eqs. 25 it can be seen that practical use of the free slice-constrained slice analogy is limited to a certain range of values for Poisson's ratio. If the value in the plane-strain system is $\frac{1}{3}$, the corresponding value for plane stress is $\frac{1}{2}$. Because it is impossible for a material to have a value of Poisson's ratio which is greater than $\frac{1}{2}$, the limiting value for the analogy is $\mu = \frac{1}{3}$ (plane strain), corresponding to $\mu' = \frac{1}{2}$ (plane stress).

If a semi-infinite, thin, free slice (whose thickness H is a function of the depth z) is subjected to a given boundary loading, the equations of equilibrium of an infinitesimal element of this slice can be written as

$$\frac{\partial(H\,\sigma_z)}{\partial z} + \frac{\partial(H\,\tau_{xz})}{\partial x} = 0 \qquad (27a)$$

and

$$\frac{\partial(H\,\sigma_x)}{\partial x} + \frac{\partial(H\,\tau_{xz})}{\partial z} = 0 \qquad (27b)$$

---

[14] "Graphostatics of Stress Functions," by H. M. Westergaard, *Transactions*, ASME, Vol. 56, No. 3, 1934, p. 141.

[15] "Analogies," by R. D. Mindlin and M. G. Salvadori, in "Handbook of Experimental Stress Analysis," edited by M. Hetenyi, John Wiley & Sons, Inc., New York, N. Y., 1950, Chapter VII.

if the thickness is assumed to vary gradually, so that the state of stress can be considered to be two-dimensional. The stress-strain relationships can be written as

$$\epsilon_x = \frac{1}{E'}\,(\sigma_x - \mu'\,\sigma_z) = \frac{1}{E'\,H}\,(H\,\sigma_x - \mu'\,H\,\sigma_z)\cdots(x, z)\ldots\ldots(28a)$$

and

$$\gamma_{xz} = \frac{\tau_{xz}}{G'} = \frac{2\,(1+\mu)}{E'\,H}\,(H\,\tau_{xz})\ldots\ldots\ldots\ldots\ldots\ldots(28b)$$

and the compatibility relationship is given in Eq. 17. By use of Eqs. 17, 27, and 28, the compatibility equation for the variable-thickness slice is given, in terms of stresses, as

$$\nabla^2\,(H\,\sigma_x + H\,\sigma_z) - 2\,\frac{\partial}{\partial z}\,(H\,\sigma_x + H\,\sigma_z)\,\frac{\partial \log_e H}{\partial z} + (H\,\sigma_x - \mu'\,H\,\sigma_z)\left[\left(\frac{\partial \log_e H}{\partial z}\right)^2 - \frac{\partial^2 \log_e H}{\partial z^2}\right] = 0\ldots(29)$$

By comparing Eq. 29 with Eqs. 14 and 20, and by comparing the equilibrium equations, it is seen that the two systems are mathematically identical, except for the boundary conditions, as follows:

Plane strain $E = E(z)$	Plane stress $H = H(z)$
σ_x	$H\,\sigma_x$
σ_z	$H\,\sigma_z$
τ_{xz}	$H\,\tau_{xz}$
$E(z)$	$H(z)$
μ	$\mu' = \dfrac{\mu}{1-\mu}$

Therefore, if a semi-infinite free slice with varying thickness is loaded on the top surface, the stress multiplied by the thickness at a given point is equal to the stress at a corresponding point in a semi-infinite constrained slice of varying modulus (loaded similarly) providing that the relationships of the previous tabulation are maintained. Thus, the analogy is proved mathematically. It should be noted that, in the compatibility relationship, it is merely the derivatives of the ($\log_e G$)-term and the ($\log_e H$)-term which must correspond so that the thickness of the free slice can be scaled geometrically to any desired value.

As it is obviously impossible to test a semi-infinite slice, either photoelastically or otherwise, a finite model must be used. A. J. Durelli[16] and M. M. Frocht[17] have used relatively small sheets of Bakelite as photoelastic models to check the Flamant solution[18] for the semi-infinite plate. The results agreed with the theoretical analysis as the distance from the edges of the model increased. Thus, by comparing the stress distribution in two plates of the same size under the same load—one plate having a constant thickness and the other having a variable thickness—it appears possible to determine, by use of this analogy, the effect of a variable modulus of elasticity on the stress distribution caused by infinite line loads or infinite strip loads.

---

[16] "Distribution of Stresses in Partial Compression and a New Method of Determining the Isostatics in Photoelasticity," by A. J. Durelli, *Proceedings*, 13th Semi-Annual Eastern Photoelasticity Conference, Massachusetts Inst. of Technology, Cambridge, Mass., June 12, 13, 14, 1941, p. 25.

[17] "Photoelasticity," by M. M. Frocht, John Wiley & Sons, Inc., New York, N. Y., Vol. II, 1948.

[18] "Sur la repartition des pressions dans un solide rectangulaire charge transversalement," by Flamant, *Comptes Rendues*, Vol. 114, 1892.

The photoelastic method provides a means of determining at each point in the model (*a*) the difference between the principal stresses from the fringe patterns, and (*b*) the direction of the principal stresses from the isoclinics. For a complete study of the stress distribution, it is also necessary to determine the sum of the principal stresses at each point. This can be done by any one of the usual methods.[17]

For this type of problem, it appears that a numerical method is the most expedient as the models have rectangular boundaries. The boundary conditions consist of a load applied at a point, or distributed over a small area, on the top edge of the plate and a known, or assumed, distribution of stress on the bottom edge. The vertical edges of the plate are free from external loads. A comparison is made between the stress distribution in the plate of constant thickness, as obtained by the usual methods, and that in the plate whose thickness varies with depth.

For the case of the constant-thickness plate, the photoelastic fringe pattern will determine the values of the difference of the principal stresses, $p - q$, at each point of the model by the relationship,

$$\frac{p - q}{2} = \frac{j\,m}{H} \quad \text{. . . . . (30)}$$

in which j is the fringe constant for the material and m denotes the fringe order.

In the case of the photoelastic model having a variable thickness, Eq. 30 can be rewritten as

$$\frac{H\,(p - q)}{2} = j\,m \quad \text{. . . . . (31)}$$

and the compatibility equation to be satisfied is given by Eq. 29 if $H\,(p + q)$ is substituted for $H\,(\sigma_x + \sigma_z)$. The boundary values of $H\,(p + q)$ are established by the fringe order at each point. In order to solve Eq. 29, it is necessary to express $h\,\sigma_x - \mu'\,h\,\sigma_z$ in terms of $H\,(p + q)$ and other known quantities. By introducing the angle, α, between the z-axis and the direction of the principal stress, p, Eq. 29 becomes

$$\nabla^2(H\,p + H\,q) - 2\,\frac{\partial}{\partial z}\,(H\,p + H\,q)\,\frac{\partial \log_e H}{\partial z} + \left[\left(\frac{1 - \mu'}{2}\right)(H\,p + H\,q) - \frac{1 + \mu'}{2}\,(H\,p - H\,q)\cos 2\,\alpha\right]\left[\left(\frac{\partial \log_e H}{\partial z}\right)^2 - \frac{\partial^2 \log_e H}{\partial z^2}\right] = 0 \quad \text{. . (32)}$$

The only unknown in Eq. 32 is $H\,(p + q)$ at interior points, as the values of α are unknown from the isoclinics, and $H\,(p - q)$ is known from the fringe pattern. Thus Eq. 32 can be solved numerically, and the complete stress distribution in the model can be obtained.

The finite-difference form for the square net shown in Fig. 1 is as follows:

For a Constant-Thickness Plate.—

$$4\,F(0) = F(1) + F(2) + F(3) + F(4) \qquad \text{(33a)}$$

in which

$$F(n) = (p + q)\,(n) \qquad \text{(33b)}$$

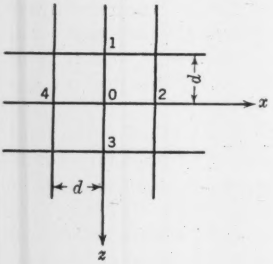

FIG. 1.—SQUARE NET

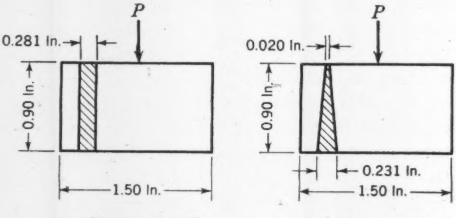

(a) Plate, constant E (b) Wedge, $E = k\,z$

FIG. 2.—BAKELITE MODELS

For a Varying-Thickness Plate.—

$$A(0)\,F(0) = B(0)\,F(1) + C(0)\,F(3) + F(2) + F(4) - D(0) \qquad \text{(34a)}$$

in which

$$F(n) = H\,(p - q)\,(n) \qquad \text{(34b)}$$

$$A(n) = 4 - d^2\,\frac{1-\mu}{2}\left[\left(\frac{\partial \log_e H}{\partial z}\right)^2 - \frac{\partial^2 \log_e H}{\partial z^2}\right]_n \qquad \text{(34c)}$$

$$B(n) = 1 + d\left(\frac{\partial \log_e H}{\partial z}\right)_n \qquad \text{(34d)}$$

$$C(n) = 1 - d\left(\frac{\partial \log_e H}{\partial z}\right)_n \qquad \text{(34e)}$$

and

$$D(n) = \left\{\frac{1+\mu}{2}\,(H\,p - H\,q)\cos 2\,\alpha\left[\left(\frac{\partial \log_e H}{\partial z}\right)^2 - \frac{\partial^2 \log_e H}{\partial z^2}\right]\right\}_n \qquad \text{(34f)}$$

If the variation in thickness is not easily expressed analytically, the required derivatives may also be obtained graphically or by the use of finite differences.

SELECTION OF PHOTOELASTIC MODEL

The analogy has been proved mathematically, but it is necessary to evaluate its suitability as a tool for experimental stress studies. The first consideration must be the choice of a photoelastic model which corresponds, by analogy, to a given variation of elastic modulus in the semi-infinite body. Of the known solutions, the only one which is valid for any given value of Poisson's ratio is the solution offered by Mr. Borowicka[11] using Eq. 24. The photoelastic model which represents this modulus has a thickness which corresponds to $H = k\,z$, or a wedge. The obvious difficulties encountered in applying a load to the sharp edge of a wedge are partly offset by the simple machining operations involved in the preparation of the model.

After a consideration of the photoelastic behavior, machinability, and availability of the various materials ordinarily used for photoelastic models, Bakelite[19] BT 61-893 was selected for the wedge. The material fringe value was found, by use of standard tension specimens, to be 44.3 lb per sq in. of shear per fringe per in. of thickness for the ½-in. plate, and 41.5 lb per sq in. of shear per fringe per in. for the ¼-in. plate. Poisson's ratio for this material was found to be 0.366 from lateral and longitudinal strain measurements on a tension strip. The longitudinal strains were measured with two 1-in. gage length (Huggenberger) strain gages. and the lateral strains were measured by use of an interferometer[20] strain gage.

As it was evident that the dimensions of a finite model would affect the stress distribution, considerable study was given to this problem. A series of tests was conducted to determine the most desirable height-to-width ratio for a plate loaded by a concentrated load and supported by a distributed reaction. From these tests a height-to-width ratio of 0.60 was chosen. The final model was 0.90 in. high and had a wedge angle of 14°, as shown in Fig. 2(*b*).

It is obvious that a top-surface thickness of zero would develop infinite stress under any load. Consequently, the edge would chip out, or flow plastically, even under small loads. Also, this chipping effect would be likely to occur during machining of the Bakelite; thus, it is doubtful if such an edge could be machined, even if it were desired. Preliminary experiments showed that a top thickness of 0.020 in. was satisfactory.

EXPERIMENTAL PROCEDURE

The wedge was loaded along its plane of symmetry by a concentrated force acting on the top edge. The lower edge of the model rested on several thicknesses of cardboard. The cardboard rested on a Plexiglas block which in turn was supported by a steel block. Steel rollers were placed between the steel block and the steel base plate so as to eliminate any horizontal force which might be introduced by the loading device. The method of loading the models is shown diagrammatically in Fig. 3, and the actual test arrangement is shown in Fig. 4. The load was applied through a lever system and was indicated by the deformation of a series of isoelastic springs.

Because the wedge was loaded along its axis of symmetry, its faces were not perpendicular to the optical axis of the polariscope. Thus, it was necessary to immerse the wedge in a liquid bath which had the same index of refraction as that of the model material. A satisfactory liquid was prepared by mixing one part of Bayol F. White oil with two parts of Halowax 1007 oil. The container for the oil was made from sheets of ⅛-in. and ½-in. Plexiglas and is shown in Fig. 4.

The thin top edge of the wedge caused large stresses to appear in this region, even when relatively light loads were imposed. In order to obtain fringe values close to the load before the pin dug into the edge, photographs were taken of the fringe pattern for a series of increasing loads. Thus, the values obtained are most accurate in the top part of the model for small loads and are more accurate at lower depths for large loads. Fig. 2 shows the shapes of the models and Fig. 5 shows the representative fringe patterns.

---

[19] "Photoelasticity," by M. M. Frocht, John Wiley & Sons, Inc., New York, N. Y., Vol. I, 1948.

[20] "An Application of the Interferometer Strain Gage in Photoelasticity," by R. W. Vose, *Transactions*, ASME, 1935, p. A-99.

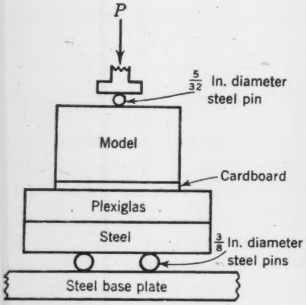
P
$\frac{5}{32}$ In. diameter steel pin
Model
Cardboard
Plexiglas
Steel
$\frac{3}{8}$ In. diameter steel pins
Steel base plate

FIG. 3.—DIAGRAM OF LOADING

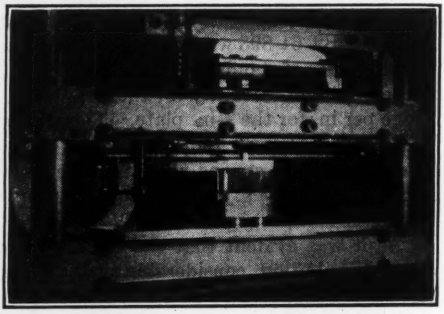

FIG. 4.—LABORATORY ARRANGEMENT

TEST RESULTS FOR THE CONSTANT–THICKNESS PLATE

The value for the difference between the principal stresses, $p - q$, at each point in the plate can be computed from Eq. 30. By dividing the right side of Eq. 30 by P/H to obtain the stresses caused by a unit line load, Eq. 30 becomes

$$\frac{p - q}{2} = \frac{j\,m}{P} \ldots\ldots\ldots\ldots\ldots\ldots\ldots\ldots (35)$$

The position of the fringes on the z-axis was obtained from the photographs (Fig. 5) and was correlated to the percentage of the model height. The values of $p - q$ from tests and theory were then plotted for corresponding values of the percentage of the model height, as shown in Fig. 6(a).

From Fig. 6(a) it can be seen that the test values of $p - q$ are within 5% of the theoretical values in the region between 8% and 30% of model height. The values are low at 8%, high at 30%, and in good agreement at 15% of model height. The values are low near the top region of the plate because of the plastic flow under the pins which caused a redistribution of the stresses. For the lower region of the plate, the stresses are high as a result of the shape of the model and the method of support

TEST RESULTS FOR THE WEDGE

By use of the analogy the values of $H\ (p - q)$ in the wedge were compared with the values of $p - q$ obtained from Mr. Borowicka's solution using the value $\mu = 0.268$ (obtained from Eq. 26, using $\mu' = 0.366$ for Bakelite). By integration of Mr. Borowicka's solution to determine the effect of an infinite line load, the value for the difference of the principal stresses was found to be

$$p - q = 1.225\,\frac{2\,q}{\pi\,z} \ldots\ldots\ldots\ldots\ldots\ldots\ldots (36)$$

Eq. 36 corresponds to an increase of 22.5% over the value obtained for a constant modulus of elasticity.

If the wedge is loaded by a total load of P lb, then the obtained values of $H\ (p - q)$ correspond to the values of $p - q$ caused by a line load of P lb per unit length in the point-isotropic material. The values for a unit line load are given by Eq. 35.

It is seen in Figs. 5(*c*) and 5(*d*) that the loading pin has dug into the top of the wedge so that the load is no longer concentrated at a point. In order to correct for this, it was assumed that the load on the top surface was distributed parabolically over the bearing width. As it was desired to compare the results for several wedges and loads, and thus different bearing widths, the correction was applied to the experimental values rather than to the theoretical values. To obtain a correction factor, the ratio of $p - q$ for a parabolic distribution of load to $p - q$ for a concentrated load on the z-axis was computed, assuming the radial-stress distribution for $E = k\,z$ and $\mu = \frac{1}{3}$ (Table 2). Fig. 7 shows the plot of this ratio as a function of the angle β, in which $2\,\beta$ is the angle subtended by the load at the point under consideration.

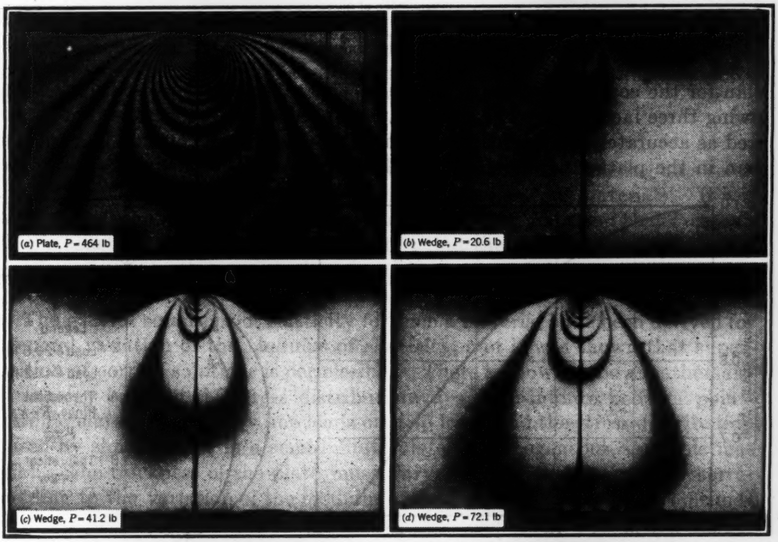

FIG. 5.—REPRESENTATIVE FRINGE PATTERNS

The experimental values of $p - q$ given by Eq. 35 were then divided by the factor obtained from Fig. 7 and were plotted against the percentage of model height in Fig. 6(*b*). The theoretical values of $p - q$ for the constant modulus and for $E = k\,z$ are also plotted in Fig. 6(*b*).

The test results for the wedge, corrected for spreading of the load, are lower than the theoretical solution in the upper 45% of the model height. In Fig.

6(*b*) no curve was drawn through the experimental values. However, a curve drawn through the average of the plotted points indicates variations from theory (curve A) of 4%, 6%, 5%, and 4% at 10%, 15%, 20%, and 30% of model height, respectively. The scatter of results for the wedge is considerably larger than for the constant-thickness models. This scattering is caused by the following three factors: (*a*) The small loads applied to the wedge were not measured as accurately by the loading frame. (*b*) The fringe count is much lower than in the plate; therefore, any residual stresses in the model become more significant. (*c*) The lower stress gradient produces broader fringes so that the location of their mid-position is more susceptible to personal errors.

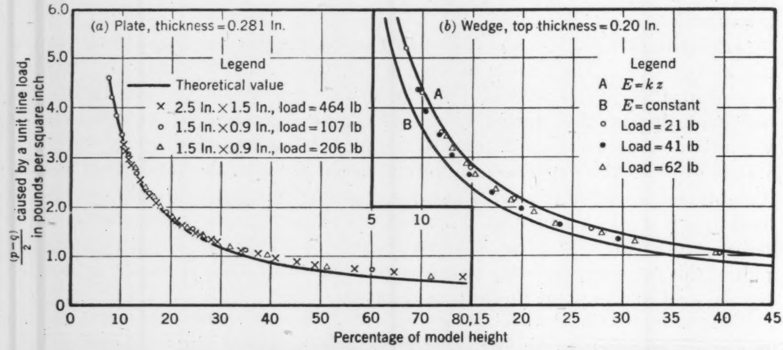

FIG. 6.—RELATIONSHIP BETWEEN DIFFERENCE OF PRINCIPAL STRESSES AND PERCENTAGE OF MODEL HEIGHT

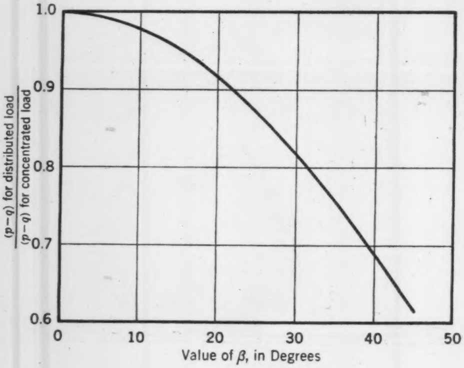

FIG. 7.—CORRECTION FACTOR FOR PARABOLIC DISTRIBUTION OF LOADS

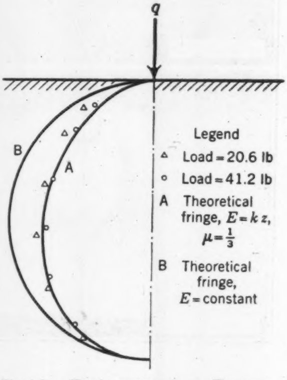
q
B
A
Legend
△ Load = 20.6 lb
○ Load = 41.2 lb
A Theoretical fringe, E = kz, μ = 1/3
B Theoretical fringe, E = constant

FIG. 8.—THEORETICAL AND EXPERIMENTAL FRINGE SHAPES FOR WEDGE MODEL

These results for $p - q$ on the axis of the wedge are not satisfactory because of the large correction factor required to account for the distribution of the load.

An additional corroboration of the analogy, however, was obtained by comparing the shape of the fringes to the shape of the theoretical fringes. This comparison was made for fringes in the region of the wedge which corresponds to the region of the constant-thickness plate for which the fringes are circular. As the stress distribution for $E = k z$ and $\mu = \frac{1}{3}$ is not much different from that for $\mu = 0.268$, the fringes in the wedge were compared with the theoretical shape for $\mu = \frac{1}{3}$. For this solution, it is shown in Table 2 that σ_r is the only principal stress not equal to zero, and as a result the expression for $p - q$ is given as

$$\sigma_r = p - q = \frac{3\,q}{4}\frac{\cos^2\theta}{r} \qquad (37)$$

Therefore, the theoretical fringes are lines denoting

$$\frac{\cos^2\theta}{r} = \text{a constant} \qquad (38)$$

Fig. 8 shows a theoretical fringe determined by Eq. 38 and a circle which corresponds to the theoretical fringe for a constant-thickness plate. The plotted points indicate the shape of the fringes in a wedge 1.50 in. by 0.90 in., 0.014 in. thick at the top, obtained for loads of 20.6 lb and 41.2 lb. The experimental and theoretical shapes are seen to be in close agreement except near the top surface, where the spreading of the load caused fringe distortion. This correspondence between the theoretical and test fringe shapes is thus considered to be an acceptable confirmation of the mathematical analogy.

CONCLUSIONS

The problem of the stress distribution caused by surface loading on a semi-infinite body has been analyzed for certain nonhomogeneous materials. It was assumed that the material is isotropic at any particular point and that Poisson's ratio is constant throughout the region, but that the modulus of elasticity is a function of the depth beneath the top surface although it is constant at any given depth. This is termed a "point-isotropic material."

The general equations of elasticity for such a material have been derived for a general variation of the modulus of elasticity, and it was shown that superposition of correct solutions is permissible. There is shown to be a mathematical analogy between the stress distribution in a semi-infinite body of point-isotropic material caused by line loads or strip loads and the stress disbribution caused by similar loads in a semi-infinite plate of homogeneous, isotropic material. The thickness of the plate must vary with depth in a manner corresponding to the variation of the modulus of elasticity in the point-isotropic material. Thus, it is possible to use the photoelastic method to determine stresses in point-isotropic materials. The mathematical analogy is confirmed experimentally by use of a wedge-shaped photoelastic model. This model was analogous to a point-isotropic material for which the modulus of elasticity increased linearly with an increase in depth from a zero value at the top surface.

It is suggested that the photoelastic analogy can be used in two ways:

1. A complete stress distribution of the model can be obtained and compared with the complete stress distribution in a plate of similar size. In using

such a comparison, considerations must be made with regard to the method of support and the stress-concentrating effects induced thereby.

2. The ratio of $p - q$ along the z-axis of the model to the value of $p - q$ along the z-axis of a similarly supported plate is determined in the region between 10% and 20% of the model height. This ratio can then be used to obtain appropriate values of the stress-concentration factor, n. This value of n can then be used in Mr. Fröhlich's equations to give an approximation for the stress distribution in the point-isotropic material. The validity of this method depends on the relationship between n and the elastic constants of the material. If the approximation is reasonable, however, this method is convenient as these equations can be integrated easily.

A limitation of the method is that solutions can be obtained only for values of Poisson's ratio between 0.23 and 0.33, as presently available (1954) photoelastic materials have Poisson's ratios varying from about 0.30 to 0.50.

ACKNOWLEDGMENTS

This study of the stress distribution in nonhomogeneous materials was undertaken at the suggestion of A. Casagrande, M. ASCE, whose helpful advice is sincerely appreciated. The method of verifying the analogy, as represented in Fig. 8, was proposed by C. E. Pearson.

The Division of Applied Science of Harvard University, at Cambridge, Mass., provided the materials and equipment for the experimental work involved in this study, except for the determination of Poisson's ratio for the Bakelite. The latter determination was performed in the Experimental Stress Laboratory of the Massachusetts Institute of Technology, at Cambridge, through the courtesy of W. M. Murray and W. L. Walsh. The Department of Civil Engineering at the University of Florida, at Gainesville, assisted in the preparation of the manuscript.

APPENDIX

The following symbols, adopted for use in the paper and for the guidance of discussers, conform essentially with "Soil Mechanics Nomenclature," *Manual of Engineering Practice No. 22* of the ASCE:

A = finite-difference function defined in Eq. 34c;
a = constant defined in Eq. 19;
B = finite-difference function defined in Eq. 34d;
b = constant defined in Eq. 19;
C = finite-difference function defined in Eq. 34e;
c = constant defined in Eq. 19;
D = finite-difference function defined in Eq. 34f;
d = distance in Fig. 1;
E = modulus of elasticity for three-dimensional system and plane-strain system;

E' = modulus of elasticity for plane-stress system;
F = finite-difference function defined in Eqs. 33*b* and 34*b*;
f = function defined in Table 2;
$f_{\frac{1}{2}}$ = function defined in Table 2;
G = modulus of elasticity in shear for a plane-strain system;
G' = modulus of elasticity in shear for a three-dimensional system and a plane-stress system;
H = thickness of the plate;
j = fringe constant for the material;
k = constant in Eq. 22 describing variation of modulus of elasticity;
m = fringe order;
n = arbitrary parameter termed the "stress-concentration factor";
P = point force;
p = principal stress;
q = principal stress;
$\bar{q}$ = line load per unit length;
R = defined in Table 1;
r = defined in Table 2;
w = constant in Eq. 22 describing variation of modulus of elasticity;
X = component of body force in x-direction;
x, y, and z = Cartesian coordinates, with z denoting depth;
α = angle between the z-axis and the principal stress, p;
β = one half of the angle subtended by the load at the point under consideration;
γ_{xy} = shearing strain or detrusion between the xz-plane and yz-plane;
∇^2 = the Laplacian operator defined in Eq. 11;
ϵ = deformation per unit length (strain);
θ = sum of the principal stresses;
θ' = defined in Eq. 15;
μ = Poisson's ratio in the plane-strain system;
μ' = Poisson's ratio in the plane-stress system;
$\rho = (x^2 + y^2)^{\frac{1}{2}}$;
σ = normal component of internal force per unit area:
    σ_R = normal stress in the R-direction;
    σ_r = normal stress in the r-direction;
τ = tangential component of internal force per unit area; and
ψ = angle between radial direction and z-axis.

AMERICAN SOCIETY OF CIVIL ENGINEERS
Founded November 5, 1852
TRANSACTIONS

Paper No. 2726

PLANNING AND OPERATING TURNPIKES

By Charles M. Noble,[1] M. ASCE

SYNOPSIS

The planning of turnpikes is a task that makes demands on all the resources of the engineer. Legal, economic, and engineering considerations are of great importance. Following the passage of suitable enabling legislation, reports must be prepared which provide the investor with a clear picture of the project and an indication as to how the money is to be spent and returned.

Because the interest on the indebtedness is highest during the construction phase when income is nonexistent, it is imperative that construction schedules be as accelerated as possible. The phases of construction should be so arranged that there is little time lost because of poor planning.

The operation of a turnpike is an involved problem of maintenance and training. The conditions on the turnpike must be of the highest quality as the driver who is paying for the use of the roadway is exacting in his demands. Conditions which exist on toll-free roads cannot be tolerated on turnpikes. The operation of a turnpike is a "big business," and the project must be conducted on this basis.

INTRODUCTION

There is little relationship between the present-day (1954) turnpike and the turnpike of the eighteenth century. The latter, more often than not, was a private venture that was engaged in at a time when highway transportation was powered by animals, and traffic volume was low. As a result of the development of canals and railways, these ventures were financial failures. The modern turnpike, however, was germinated in the automotive era when great volumes of mixed traffic were involved, and it was constituted as a government activity. Generally these roads have been financed on the revenue-bond principle, on a self-liquidating basis, and with capital (raised from private sources) repaid solely from tolls and other charges assessed against the users of the facility. The combination of government sponsorship, heavy traffic demand, and the revenue bond has assured success for projects in operation as of

---

Note.—Published, essentially as printed here, in July, 1953, as *Proceedings-Separate No. 214*. Positions and titles given are those in effect when the paper was received for publication.

[1] Chf. Engr., New Jersey Turnpike Authority, New Brunswick, N. J.

1954. However, in order to justify the expense of establishing a turnpike organization and of performing the studies necessary to determine the financial feasibility of a given project, there must be sufficient traffic and an economic and public demand.

LEGISLATION

Of fundamental importance to the eventual construction of a turnpike is the drafting of the enabling turnpike legislation; the best legal talent should be employed for this task. In present (1954) practice, the turnpike body is a state agency which has delegated to it specific and general powers of sufficient breadth to enable the agency to perform its function quickly, unhindered by outside forces. The form may be either a commission or an authority although the latter has attained stature by reason of a long history of favorable court decisions and familiarity of investors with its structure. Usually the act provides that when all loans are repaid the facility shall revert to the state to become an integral part of the state highway system. A desirable innovation would provide that, before being freed of tolls, a capital fund be accumulated in sufficient amount to maintain and operate the facility from the proceeds of the interest in perpetuity. This accumulation should require a relatively short time as the earnings are then at a maximum.

The act should establish the number of commissioners and how they are to be appointed, the length of their terms, their manner of succession, and their compensation (if any). Usually the governor of the state is the appointing officer, and often the approval of the legislative is stipulated. The first commissioners are usually appointed for unequal terms to avoid the expiration of their terms occurring within the same year—and so that succeeding terms will be staggered. Often the chairman of the state highway commission serves as an ex-officio member of the turnpike commission.

Other essential features of the act are:

1. The turnpike body should pledge that revenues will be used solely for maintenance, operation, payment of interest, and amortization of the bonds. The property is not mortgaged—in case of default the title to the facility remains with the turnpike. In the case of revenue-bond financing the faith and credit of the state is not pledged specifically. Hence, indebtedness is not charged against the debt limit of the state.

2. Advance funds should be provided in order to finance preliminary expenses and engineering and traffic reports suitable for negotiating and consummating the sale of bonds. Usually the advance is repaid out of the proceeds of the bonds. The preliminary expenses of the New Jersey Turnpike Authority exceeded $1,000,000—which included the cost of final surveys, designs, plans, and borings up to the date of the sale of the bonds.

3. Representatives of the turnpike should be authorized to enter private and public property, without constituting a trespass, for the purpose of making surveys, soundings, test pits, and borings.

4. The turnpike body should have the right of eminent domain and the authority of immediate possession of property on the filing of condemnation papers. It is usual to require the turnpike to file a bond or a cash deposit with the court to cover the appraised value of the property.

5. The turnpike authority should be able to relocate utilities or cause them to be relocated. Authority should also be provided for the bridging, closing, or relocation of streets, highways, and railways.

6. The bonds should be tax-free securities.

7. The turnpike body should have complete freedom in contracting for concessions on the turnpike.

8. The life of the bonds should be established. Some issues have been limited to thirty years, but on expensive projects the bond life may be extended to thirty-five years as some projects would not have sufficient "coverage" with a thirty-year bond.

9. The body should be authorized to establish appropriate rules and regulations affecting traffic or conduct on the turnpike.

In order to avoid delays, particularly during the construction period when substantial bond interest is accumulating, the turnpike body must be allowed complete freedom of action and decision; veto or supervisory powers in the hands of other agencies can be disastrous. If the adoption of the turnpike principle is considered necessary to the public interest, the commissioners entrusted with the project must be provided with the widest powers and the greatest latitude for discretion.

Finally, every precaution must be taken to assure the constitutionality of the act. The laws of each state differ, and the act must be drawn in harmony with the state laws and court decisions. Almost invariably it will be necessary to test the constitutionality of the act in the courts of the state before buyers will purchase bonds.

PRELIMINARY REPORTS

After passage of the enabling legislation, appointment of the commissioners, organization of the authority, and determination of a project, it is necessary to take two steps: (1) A preliminary engineering survey must be made. This survey should include a feasibility investigation and an estimate of cost and should be followed by a formal report. (2) A traffic and revenue report should be made.

Engineering Report.—It is customary to have the engineering survey and report prepared by a consulting engineer who has experience in the field and who has the confidence of fiscal experts. On large projects and when time is of the essence, the turnpike body may engage several groups of engineers and, in addition, an organization of general consultants to review the findings and consolidate the reports of the other consultants into a report to be utilized in the financing. At the outset the turnpike body and its consulting engineers should agree on the geometric design standards, including the roadway cross section, right-of-way width, and general policy on cross roads and utility relocations. The cost of the highway is closely related to these features.

Of primary importance is the determination of the engineering feasibility of the project. Map and field reconnaissance examinations are made in sufficient detail that the route of the turnpike can be selected from one of several routes studied. In this work, consideration is given to natural travel routes; centers of traffic generation as indicated by population, industry, and motor-vehicle registration; traffic counts; and the economic features of the region. Consultation with the planning agency of the state and close liaison with the planning division of the state highway department are desirable in order that the route selected will serve the people of the state and region most effectively, supplement and complement the state and interstate highway system, and result in attracting the maximum traffic in the territory.

The number and location of traffic interchanges are important considerations; careful thought must be given to the origin and destination of traffic. The condition and suitability of existing connecting routes, traffic congestion, focal points of population and industry, and traffic desire lines (not only for long-distance travel but also for local movements) are all pertinent factors.

The policy concerning concessions should be established by the turnpike body as to scope, frequency, and general design. It should also be decided whether the authority will develop the sites and construct the buildings or have the concessionaires provide them with reversion to the authority at the end of an amortization period.

The preliminary engineering report should be a comprehensive document suitable for perusal by financial experts. The report should include a complete description of the project, the service it will perform, the design standards, interchanges, concessions, maintenance facilities, toll facilities, construction schedule, estimate of cost, estimate of administrative and operating expenses, and a review of the traffic and revenue report, including copies of the estimated results of operation and the amortization schedule from that report. Suitable illustrations and exhibits should be included to make the project and the report thoroughly understandable and complete.

The estimate of cost includes all items required to place the highway in operation and is composed of administration (including legal and financial advice); repayment of preliminary expenses; interest during construction (and generally for a year thereafter); engineering, including the making of borings; construction of maintenance buildings, police buildings, toll booths, administration buildings, and concession facilities; installation of lighting, radio equipment, fencing, guard rails, traffic aids and safety devices, signs, and toll-collection equipment; landscaping and erosion control; procurement of equipment for maintenance and police operations; employment and training of police, toll collection, toll audit, and maintenance personnel; provision for utility services, maintenance of traffic, utility and railroad relocation and restoration, and acquisition of real estate; and contingencies. After financing, this cost is the construction fund.

Traffic and Revenue Report.—Again, the services of an experienced consulting engineer who specializes in traffic and revenue work and who has an established reputation with the financial experts should be sought to conduct the studies and to make the traffic and revenue report. The fate of the project will probably depend on the accuracy of the report.

The traffic engineers should peruse all information available from the highway department concerning traffic counts and origin and destination surveys; economic, population, industrial, and commercial markets; and vehicular registration trends from other state or governmental agencies. In addition, the operating records of ferries and toll bridges in the area should be studied.

With these data, a determination is made of the scope and location of additional origin and destination surveys and of a traffic-desire sampling program. It is customary for the state and local police to assist the on-the-road survey crews in handling traffic and preventing disorder.

In addition, a survey is made of current and planned highway, bridge, ferry, and tunnel construction in order that the effect of this construction on the proposed turnpike and on prospective traffic and revenues can be evaluated properly.

The completed report should contain estimates of the amount of traffic that will patronize the various parts of the turnpike, an assumed toll schedule based on the value of the service, and estimates of the revenues from traffic and concessions. The main part of the report is contained in the "Estimated Results of Operation" and the "Amortization Schedule."

Preliminary Organization.—In the preliminary phases of a turnpike project —when the financial feasibility of the project is unknown—it is unsound to engage a large staff other than that employed by the consulting engineers. Consequently, it has been customary to secure the services of a limited number of personnel from the state highway department on a loan basis. In conjunction with the consulting highway engineer and with the concurrence of the commissioners, this small group headed by a chief engineer establishes the characteristics, scope, general routing, design standards, and tentative interchange locations of the proposed turnpike. As an example, the New Jersey Turnpike Authority operated at first with a chief engineer and one stenographer, and with counsel and a recording secretary on a part-time basis to take minutes of commission meetings. Later, a director of public information and another stenographer were added; this small staff performed all necessary duties until it became apparent that the project would be self-liquidating. Only then was the staff augmented in anticipation of financing and construction. In addition to the staff, bond counsel and a financial adviser were engaged.

FINANCING

The word, turnpike, connotes financing by the sale of revenue bonds, such bonds to be repaid solely from the revenue earnings of the facility itself. It is, of course, necessary to borrow the money in advance of construction when earning power and cost of the project are estimated, and there is no history of actual earnings; thus, risk capital is involved. The tax-free character of the bonds is an attractive feature. On the other hand, the market is to some extent limited as revenue bonds are purchased by certain investors only. Until the sale of bonds for the Ohio Turnpike in 1952, the largest single issue on record was $220,000,000.

The sale of the bonds can be handled by negotiation or by public bidding. Each has its advantages. In the case of a negotiated issue, terms advantageous to the authority can be secured by shrewd bargaining. It is important that the turnpike body be assured of the exact rate of interest and the amount of discount that will be charged (if any) before it is committed to sell the issue to a particular group. It is a source of satisfaction to the turnpike body to learn that it has secured (1) the best possible terms concerning the date and the terms of call for refunding or redeeming the bonds and (2) other advantages that will limit the ultimate cost through to the end of the amortization period. For example, the New Jersey Turnpike Authority negotiated a sale with the unique provision that the bonds need be "taken down" only as and when required to pay the contractors. This saved the authority $11,000,000 in interest and financing costs over the two-year construction period.

The public-advertisement method of selling bonds protects the turnpike body from accusations of favoritism or bad bargaining. This method has the disadvantage that all the terms of the bond resolution or trust indenture, including the interest rate, must be determined in advance—with the possibility that the best terms were not anticipated and secured, although bids presumably take the stated terms into consideration. In both cases the skill, experience, and financial acumen of bond counsel and financial adviser are indispensable.

Because interest starts as soon as the bonds are sold and must be paid during the construction period, it would be advantageous if sufficient funds could be made available to defray the cost of final surveys, designs, preparation of contract drawings, property drawings, and right-of-way acquisition. In cases where the total bond issue is sold initially, this will reduce interest cost materially.

CONSTRUCTION

When the financing of a project appears assured, it is essential to assemble rapidly the engineering organization required to establish final alinement; to prepare designs, contract drawings, specifications, and property maps; and to supervise and administer the construction and materials testing. From this point on to completion there is a "race" against time and bond interest.

Prior to World War II the original Pennsylvania Turnpike Commission assembled its own staff of engineers for both design and construction supervision, primarily from the staff of the highway department. Materials testing was performed in the state highway laboratory. Following World War II, however, a shortage of engineers made this impractical. Therefore, turnpike authorities have engaged private consulting engineers of national reputation who are able to assemble quickly adequate staffs of engineers. On some projects the consultant surveys the final alinement and prepares designs, specifications, and contract drawings; supervision and administration of construction are performed by the owner. In other cases, the consultant designs and supervises construction under the administrative direction of the owner. Usually, private laboratories are engaged to test materials and to make the shop inspections.

On large projects it is desirable to divide the project into sections and assign a consulting engineer to each section in order to engage sufficient personnel so that the plans and the work can be placed under contract at the earliest possible date. In some cases a separate bridge-engineering organization and a separate highway-engineering group are assigned the same section. In some instances this is desirable although it does increase the problem of coordination.

Bond resolutions and trust indentures usually require that the authority employ a general consulting engineer who acts in the dual capacity of safeguarding the interests of the owner and the bond holder. This engineer's duties are generally delineated in those documents. In addition, it is desirable to designate an engineering organization to develop, under the direction of the owner, design standards (both geometric and structural); standards of drainage design; standard details and drawings for the guard rail, fencing, signs, and traffic-safety devices; and uniform systems of lighting, toll collection, and radio operation. The negotiation and preparation of application permits for crossing over navigable waters are also suitable assignments for this organization. It is also customary to utilize the forms of contracts and specifications used by the highway department of the state as contractors and material producers are familiar with their provisions. Considerable saving of time is accomplished by developing the state specifications, with suitable modifications, into a document termed the "Standard Contract and Specifications" for the turnpike and by using supplementary specifications to cover unit-bid schedules and the special features of each contract. Finally, it is necessary to engage an architect for designing the various buildings required for the turnpike.

Turnpikes have invariably been constructed by contractors, usually under the competitive-bidding system, although in some cases it has proved advantageous to negotiate contracts. Because of the speed at which the work must progress and the disastrous consequences of default, it is desirable that an adequate system of contractor prequalification be adopted. This will not guarantee against default, but it does minimize the danger.

A master plan for the conduct of the entire design and construction operation must be developed at the start of the project. The entire work, section by section, is subdivided into appropriate contracts. The size of contract and the class of work included depend on the number, size, and versatility of available contracting organizations that may be interested in bidding for the work.

The contracts are so arranged with respect to time in the plan that the entire project can be finished on a predetermined date. Contracts must be arranged in proper sequence so that the work of contractors will follow in logical order, one after the other. This is particularly true when grading, bridging, and paving are in separate contracts. The process is similar to an assembly line. Weekly reports covering progress of both design and construction will indicate quickly where progress lags and where intensification of activity is necessary.

Organization.—At the outset of the design period, the staff of the turnpike organization must be enlarged for coordination, progress control, avoidance of delayed decisions, handling financial affairs and legal problems, and properly servicing the organization. An appropriate organization chart for a large project is shown in Fig. 1.

Acquisition of Right of Way

One of the most important activities of the turnpike body is the acquisition of right of way. Construction cannot begin until a right of entry has been obtained. Therefore, top priority must be given to completing property maps as appraisals and negotiations cannot begin until these maps are in the field.

It is obvious that parcels on which buildings are located should be given first priority as time is required not only for evacuation of occupants but also for demolition or moving operations.

After the contractor begins work, it is necessary to coordinate the acquisition of real estate with his schedule of operations so that continuous stretches of right of way will be available to him as needed. Weekly consultation with the contractor as to his plans and needs and a listing of critical parcels will reveal the urgent requirements so that the negotiators for real estate will intensify their activities at the proper places. All too often extraordinary measures are necessary to keep the acquisition of property abreast of the construction schedule.

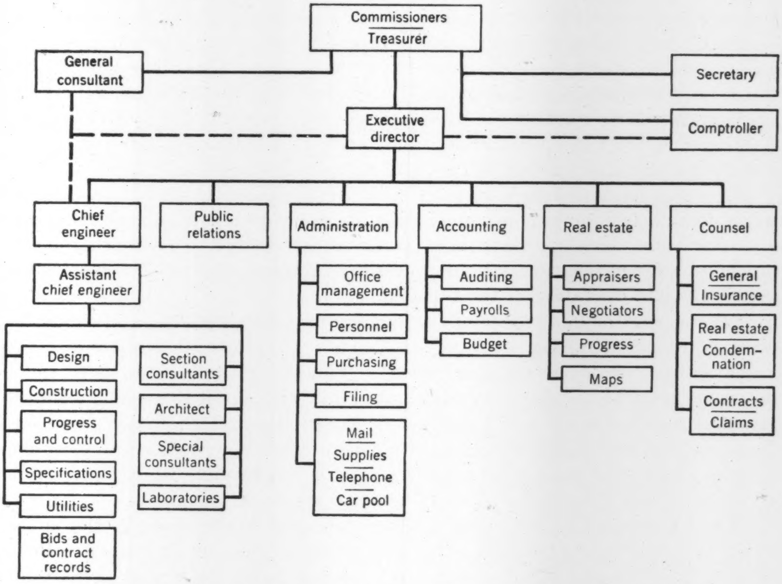
Commissioners
Treasurer
General consultant
Secretary
Executive director
Comptroller
Chief engineer
Public relations
Administration
Accounting
Real estate
Counsel
Assistant chief engineer
Office management
Personnel
Purchasing
Filing
Mail
Supplies
Telephone
Car pool
Auditing
Payrolls
Budget
Appraisers
Negotiators
Progress
Maps
General
Insurance
Real estate
Condemnation
Contracts
Claims
Design
Construction
Progress and control
Specifications
Utilities
Bids and contract records
Section consultants
Architect
Special consultants
Laboratories

FIG. 1.—SUGGESTED ORGANIZATION DURING THE DESIGN AND CONSTRUCTION PHASE

OPERATION

Planning for operation usually begins from six months to nine months before the scheduled opening of the project. At the beginning it is advantageous to establish the operation organization chart, job classifications, salary and wage ranges, number of personnel required in each category, and a personnel policy; this will give direction and simplify recruitment. Obviously, personnel should be utilized from the existing staff to as great an extent as possible. It is also desirable to appoint the superintendent of maintenance six months or more before the opening date. The date of purchase of the maintenance equipment will depend on the lead time that is necessary. Lists of equipment are compiled by the superintendent of maintenance, and orders are placed on the basis of the specifications to assure delivery in time for them to be utilized in the training of maintenance personnel. The superintendent also prepares a safety manual to be followed by maintenance personnel, with particular emphasis on the high speed and density of traffic on turnpikes. The preparation of a servicing manual with greasing schedules for each model is a necessity, together with a system for assuring that each piece of equipment is actually serviced in accordance with the schedule.

Well in advance of the opening date the vehicle-classification system and the toll rates for trips between the various interchanges for each classification should be established. This will allow ample time for the printing of toll schedules and tickets (if a ticket system is used) for the opening day. The selection of the type and amount of toll-auditing tabulating equipment is an important decision as well as whether the machines will be purchased outright or rented. A service contract for maintenance and repair is usually negotiated with the stipulation that new models will replace outmoded machines.

It is also necessary to determine whether the turnpike will have its own police force or will employ a unit of the state police as a turnpike detachment.

After these decisions have been made, it is possible to establish routine procedures for purchasing, inventory control, accounting, and cost-keeping to assure efficient operation of the turnpike.

Several months in advance of the opening day, specifications and contracts must be prepared for the letting of contracts for the operation of concessions (such as fuel, oil, accessories, and food). The terms and conditions of these contracts must be written with sufficient clarity and detail to avoid misunderstanding during operation. Usually these contracts run for a five-year period. It is essential that the best and most efficient service be rendered to turnpike patrons; otherwise there is an adverse effect on toll revenue which is far more significant than the revenue received from concessions.

From two months to three months in advance of the opening, the police chief and the superintendent of toll collection should be appointed. Both officers must become familiar with the project in every detail and prepare for the training of their organizations. In both cases, operating manuals must be prepared, and in the case of toll collection a mastery of the toll-collection system is essential.

Similarly, arrangements must be made in advance with local fire and ambulance companies for service on an at-call basis, and territories must be mapped out. Their names, addresses, and telephone numbers should be listed for the use of police, toll collectors, and maintenance personnel. Arrangements are then made for towing, wrecking, and repair services, usually with reputable private garages adjacent to the interchanges. Territories, rules, regulations, and maximum charges are determined; once again unsatisfactory service or unreasonable charges will result in patron dissatisfaction and may affect toll revenue adversely.

Approximately two months before the opening of the turnpike, employment of toll collection, police, maintenance, and toll-audit personnel should begin. Selection of uniform style and contracts for manufacture should precede employment of personnel so that measurements and fittings can be made as rapidly as persons are employed. Toll-collection personnel and police must, of necessity, be organized on a 24-hour day, seven-day week basis, and, in the case of collectors, expected traffic volumes and peak hourly rates must be anticipated in order that sufficient personnel will be trained and will be available at proper locations. The maintenance organization should include men on night duty or on call in case of emergency. Generally, it is advantageous to employ more men than those actually needed in case traffic exceeds estimates. Surplus personnel can be eliminated quickly on the basis of comparative merit after the actual work load is demonstrated by operating experience. In order that the organization does not remain over-organized, it is desirable to have a well-planned "yardstick" to determine a reasonable expected daily output per man in each job classification. Scientific job-test questionnaires completed prior to employment will minimize turnover resulting from misfits and incompatibility of temperament. Nevertheless, turnover may be expected to be high in the initial months of operation in areas having a high level of employment.

Immediately after the employment of a sufficient number of persons, the training period should be initiated. The training curricula must be well planned, and competent instructors should be assigned. In the case of police, maintenance and toll-audit personnel, experienced leaders are available, and it is usually possible to assemble a strong nucleus of experienced personnel around which to develop an organization. Toll collection, however, is a comparatively new field in so far as turnpikes are concerned. The system, of necessity, differs from a toll facility in which the origin and destination are not considered. Therefore, training is not only more important but also more difficult. For this reason alone it is desirable to reduce vehicle classifications to a minimum and arrange the classifications in a manner that will enable collectors to identify them at a glance. Thorough drilling in the collection manual is essential, and collectors must become proficient in making change rapidly and in detecting counterfeit bills. An efficient collector should collect from approximately three hundred vehicles per hour.

Maintenance personnel need training; emphasis must be placed on the difference between maintaining an ordinary highway and a turnpike. The public expects and is entitled to superior maintenance on a turnpike. Conditions that would be tolerated on a toll-free highway will be bitterly criticized by turnpike patrons. The personnel must be indoctrinated with the spirit of giving a high order of service.

A training period during which the actual equipment purchased for the turnpike is used is important, particularly from the standpoint of safety. In addition, instruction in the care, servicing, and handling of equipment is essential. The details of the cost-accounting system and the inventory and accountability program should be explained to all maintenance personnel, not only to obtain compliance but also to impress on them that slip-shod methods and practices will not be tolerated. Finally, all personnel that will use the radiotelephone must be indoctrinated and licensed for radio operation.

At this point, the personnel should be ready to operate the completed turnpike. A suggested organization chart is shown in Fig. 2. The scale of the organization will, of course, depend on the scope of the project and the volume of traffic. On small projects, one man can handle several of the functions delineated on the chart.

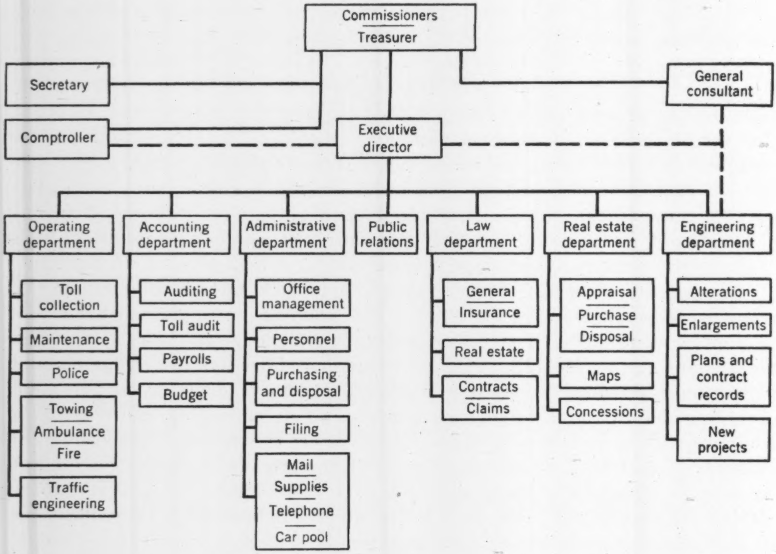
Commissioners
Treasurer
Secretary
Comptroller
Executive director
General consultant
Operating department
Toll collection
Maintenance
Police
Towing
Ambulance
Fire
Traffic engineering
Accounting department
Auditing
Toll audit
Payrolls
Budget
Administrative department
Office management
Personnel
Purchasing and disposal
Filing
Mail
Supplies
Telephone
Car pool
Public relations
Law department
General
Insurance
Real estate
Contracts
Claims
Real estate department
Appraisal
Purchase
Disposal
Maps
Concessions
Engineering department
Alterations
Enlargements
Plans and contract records
New projects

FIG. 2.—SUGGESTED ORGANIZATION DURING THE OPERATION PHASE

CONCLUSION

The organization, financing, planning, design, construction, and operation of turnpikes is "big business." Usually the smallest project costs more than $40,000,000 whereas the larger projects approach $300,000,000 in capital expenditure. Revenues are commensurate with capital cost, as evidenced by receipts on the New Jersey Turnpike, which amounted to $17,830,000 in 1952. Turnpike earnings increase yearly until amortization.

It is evident, therefore, that engineering and management must be of a high caliber and that the most modern and efficient business practices must be utilized in addition to the latest advances in design and construction engineering. The motoring public is discerning and will be satisfied with only the best, not only in engineering but also in maintenance and operation.

AMERICAN SOCIETY OF CIVIL ENGINEERS
Founded November 5, 1852
TRANSACTIONS

Paper No. 2727

DEFLECTIONS OF A CIRCULAR BEAM OUT OF ITS INITIAL PLANE

BY ENRICO VOLTERRA[1]

WITH DISCUSSION BY MESSRS. I. OESTERBLOM, AND ENRICO VOLTERRA

SYNOPSIS

The Saint-Venant equations for a circular beam bent out of its plane of initial curvature are applied to the study of the deflections of beams subjected to uniformly distributed forces and supported at symmetric points, and of the deflections of circular-arc bow girders supporting distributed or concentrated forces. The solutions are given in explicit form. Curves of the deflections, angles of twist, and bending and twisting moments are presented for certain cases.

NOTATION

The letter symbols in this paper are defined where they first appear, in the text or by diagram, and are assembled alphabetically in Appendix I.

INTRODUCTION

In previous papers (1)[2], the Saint-Venant equations (2) for circular beams bent out of their plane of initial curvature have been applied to the study of deflections of beams resting on elastic foundations and loaded by concentrated symmetric forces. The same equations can also be applied to the study of the deflections of circular beams subjected to uniformly distributed loads and supported at equidistant points (Fig. 1) and to the study of the deflections of circular-arc bow girders with uniformly distributed or concentrated loads (Fig. 2). The solution can be expressed in explicit form and the final results presented in tabular form.

NOTE.—Published essentially as printed here, in December, 1953, as *Proceedings-Separate No. 375*. Positions and titles given are those in effect when the paper or discussion was received for publication.

[1] Prof. of Mechanics, Rensselaer Polytechnic Inst., Troy, N. Y.

[2] Numbers in parentheses, thus: (1) refer to the Bibliography at the end of the paper.

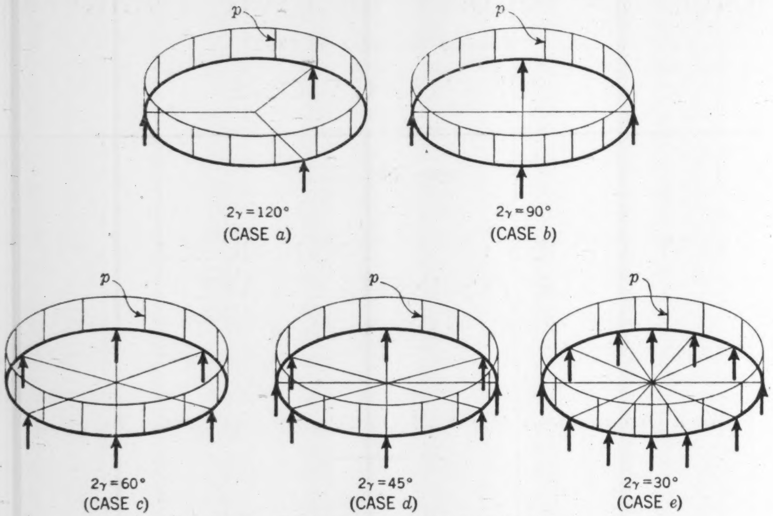

$2\gamma = 120°$ (CASE *a*)

$2\gamma = 90°$ (CASE *b*)

$2\gamma = 60°$ (CASE *c*)

$2\gamma = 45°$ (CASE *d*)

$2\gamma = 30°$ (CASE *e*)

FIG. 1.—CIRCULAR BEAMS UNIFORMLY LOADED

The problem of the bending of beams of simple or double curvature is important in strength of materials. Many writers have contributed to this field of research. Among them are Barré de Saint-Venant (1), H. Resal (3), B. G. Kannenberg (4), H. Marcus (5)(6), F. Düsterbehn (7), F. Schleicher (8), C. B. Biezeno (9), A. J. S. Pippard, M. ASCE, and F. L. Barrow (10)(11), and more recently Mervin B. Hogan (12)(13)(14)(15)(16), Robert B. B. Moorman, M. ASCE, and Manford B. Tate, A.M. ASCE (17), and Becla Velutini (18).

Many of the methods proposed are derived from considerations of strain energy; others are graphical in nature. In the particular case of a circular beam bent out of its plane of initial curvature, it is possible in the most common cases encountered in practice—especially in that of reinforced concrete struc-

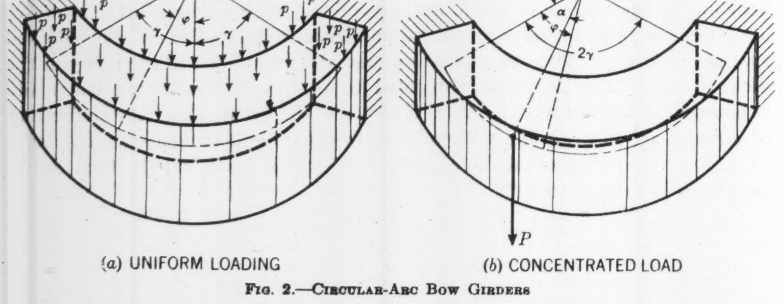

(*a*) UNIFORM LOADING

(*b*) CONCENTRATED LOAD

FIG. 2.—CIRCULAR-ARC BOW GIRDERS

tures—to express the final results in a simple explicit form. Tables can provide the engineer with the required data, thus reducing the labor involved in computations.

The object of the paper is to demonstrate this fact, and for this reason every case considered is followed by a specific numerical example to show how the corresponding tables can be used.

BENDING OF A CURVED BEAM OUT OF ITS PLANE OF INITIAL CURVATURE

A curved beam, built-in at one end, having constant inertia characteristics is to be considered (Fig. 3). The beam will be referred to a system of rectangular coordinates x, y, and z with the origin O at the centroid of the cross section, the axes x and y coinciding with the principal axes of inertia of the cross section and the axis z with the tangent to the center line at O. The plane xz coincides with the horizontal plane of the initial curvature of the beam, with the positive direction of x toward the center of curvature, y directed positive downward, z taken positive away from the built-in end, and the arc s of the center line measured from the fixed end.

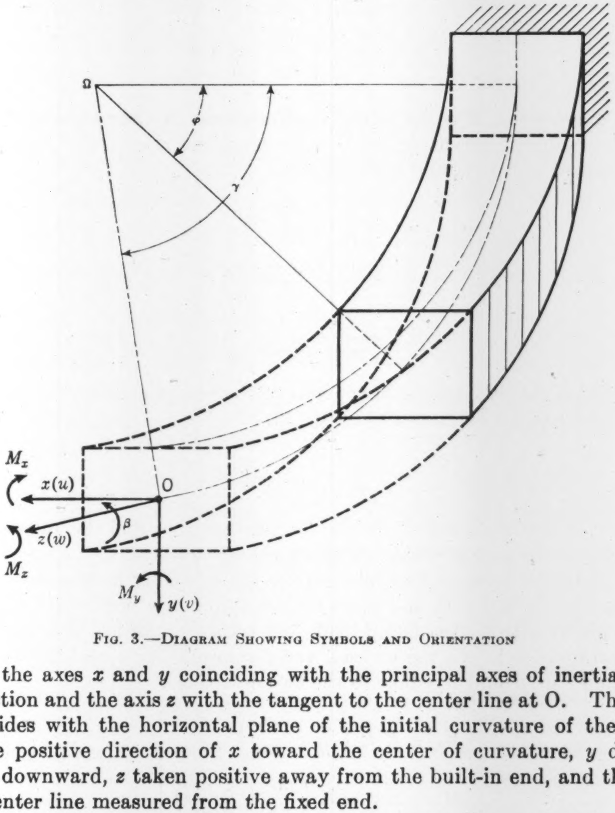

FIG. 3.—DIAGRAM SHOWING SYMBOLS AND ORIENTATION

The displacement of the centroid O during bending is resolved into three components, u, v, and w, in the directions of the x, y, and z axes, respectively. The angle of twist β of the cross section about the z-axis is considered positive when the rotation is counterclockwise with respect to the z-axis. The deformation of an element of the curved bar, bounded by two adjacent cross sections, consists of bending in the principal planes xz and yz and twist about the z-axis. If M_x, M_y, and M_z are the moments on the cross section at O about the x-axis, y-axis, and z-axis, respectively (their positive directions are shown in Fig. 3), $E\,I_x$ and $E\,I_y$ the flexural rigidity about the axes indicated by subscripts, K the torsional rigidity, and $1/R$ the initial curvature of the center line of the bar, the equations for determining the changes in curvature $\left(\frac{1}{R_1}; \frac{1}{R_2}\right)$ and the twist are (19) (20)

$$\left.\begin{aligned} M_x &= \frac{E\,I_x}{R_1} \\ M_y &= E\,I_y\left(\frac{1}{R_2} - \frac{1}{R}\right) \end{aligned}\right\} \qquad (1)$$

In these expressions, E is the modulus of elasticity, I the moment of inertia, and R the radius of curvature. The expressions for the curvatures and twist as functions of u, v, w, and β are (19) (20)

$$\left.\begin{aligned} \frac{1}{R_1} &= \frac{\beta}{R} - \frac{d^2v}{ds^2} \\ \frac{1}{R_2} &= \frac{1}{R} - \frac{u}{R^2} + \frac{d^2u}{ds^2} \\ \theta &= \frac{d\beta}{ds} + \frac{1}{R}\frac{dv}{ds} \end{aligned}\right\} \qquad (2)$$

The condition that the length of the axis of the bar remain unchanged during bending and twist is expressed by (19) (20)

$$\frac{dw}{ds} - \frac{u}{R} = 0 \qquad (3)$$

By the use of Eqs. 1, 2, and 3, the displacement u, v, w, and the angle β can be determined in the case of small deflections of curved beams.

The particular cases to be explained are (a) a circular beam subjected to a uniformly distributed load and supported at symmetric points, (b) a circular-arc bow girder with a distributed load, and (c) a circular-arc bow girder with a concentrated load. In these cases, the displacements u and w can be neglected and Eqs. 1 and 2 reduce to the two equations,

$$\left.\begin{aligned} M_x &= E\,I_x\left(\frac{\beta}{R} - \frac{d^2v}{ds^2}\right) \\ M_z &= K\theta = K\left(\frac{d\beta}{ds} + \frac{1}{R}\frac{dv}{ds}\right) \end{aligned}\right\} \qquad (4)$$

Circular Beam Subjected to a Uniformly Distributed Load and Supported Symmetrically.—If p is the uniformly distributed load, per unit length of the beam, if 2γ is the angular distance between the points of support (Fig. 1), and with the following notation,

$$\left.\begin{aligned} Y &= \frac{v}{R} \\ a &= \frac{E\,I_x}{R} \\ \mu &= \frac{K}{E\,I_x} \\ \nu &= \frac{p\,R^3}{E\,I_x} \end{aligned}\right\}\ldots\ldots\ldots\ldots\ldots\ldots (5)$$

Eqs. 4 become

$$\left.\begin{aligned} a\left(\beta - \frac{d^2Y}{d\phi^2}\right) &= M_x \\ \mu\,a\left(\frac{d\beta}{d\phi} + \frac{dY}{d\phi}\right) &= M_z \end{aligned}\right\}\ldots\ldots\ldots\ldots\ldots\ldots (6)$$

For equilibrium, however, the equations,

$$\left.\begin{aligned} \frac{dM_z}{d\phi} - M_x &= 0 \\ \frac{d^2M_x}{d\phi^2} + \frac{dM_z}{d\phi} - a\,\nu &= 0 \end{aligned}\right\}\ldots\ldots\ldots\ldots\ldots\ldots (7)$$

must be verified with the boundary conditions:

$$\left.\begin{aligned} \beta(\gamma) &= \beta(-\gamma) \\ \frac{d\beta(\gamma)}{d\phi} &= \frac{d\beta(-\gamma)}{d\phi} \end{aligned}\right\}\ldots\ldots\ldots\ldots\ldots\ldots (8a)$$

$$\left.\begin{aligned} Y(\gamma) &= Y(-\gamma) \\ \frac{dY(\gamma)}{d\phi} &= \frac{dY(-\gamma)}{d\phi} \end{aligned}\right\}\ldots\ldots\ldots\ldots\ldots\ldots (8b)$$

and

$$\left.\begin{aligned} \frac{d^2Y(\gamma)}{d\phi^2} &= \frac{d^2Y(-\gamma)}{d\phi^2} \\ \frac{dM_x(-\gamma)}{d\phi} - \frac{dM_x(\gamma)}{d\phi} &= 2\,a\,\gamma\,\nu \end{aligned}\right\}\ldots\ldots\ldots\ldots\ldots\ldots (8c)$$

The angle ϕ is measured from the center between the points of support. From Eqs. 6, 7, and 8 are obtained

$$\frac{\beta}{\nu} = \frac{\mu + 1}{2\,\mu}\left[2 - \frac{\gamma}{\sin\gamma}\,\phi\sin\phi - \frac{\gamma}{\sin\gamma}\,(1 + \gamma\cot\gamma)\cos\phi\right]\ldots\ldots (9a)$$

$$\frac{Y}{\nu} = \frac{1}{2\,\mu}\left\{\phi^2 - 2 + \frac{(\mu + 1)\,\gamma}{\sin\gamma}\,\phi\sin\phi + \frac{\gamma}{\sin\gamma}\,[\mu + 3 + (\mu + 1)\,\gamma\cot\gamma]\cos\phi + A'\right\}\ldots (9b)$$

$$\frac{M_x}{a\,\nu} = 1 - \frac{\gamma}{\sin\gamma}\cos\phi\ldots\ldots\ldots\ldots\ldots\ldots (9c)$$

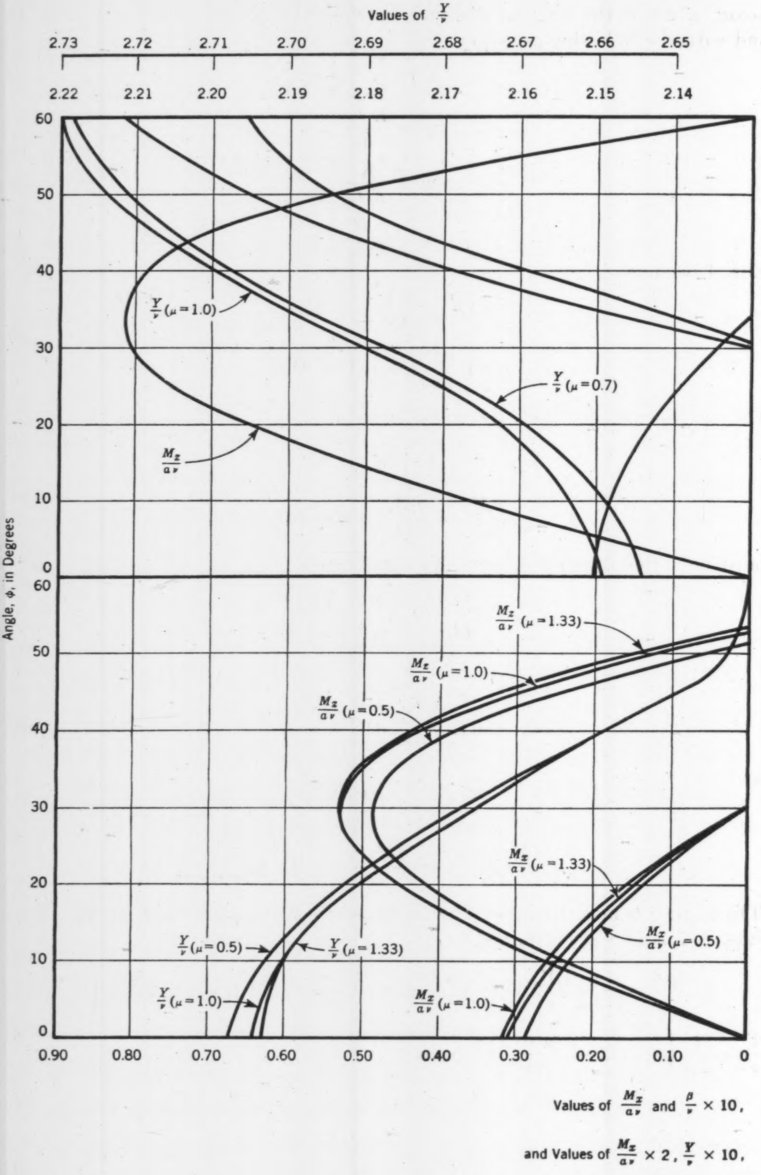

FIG. 4.—FUNCTIONS FOR

[for $\mu = 0.7$ in Fig. 4(a)]

[for $\mu = 1.0$ in Fig. 4(a)]

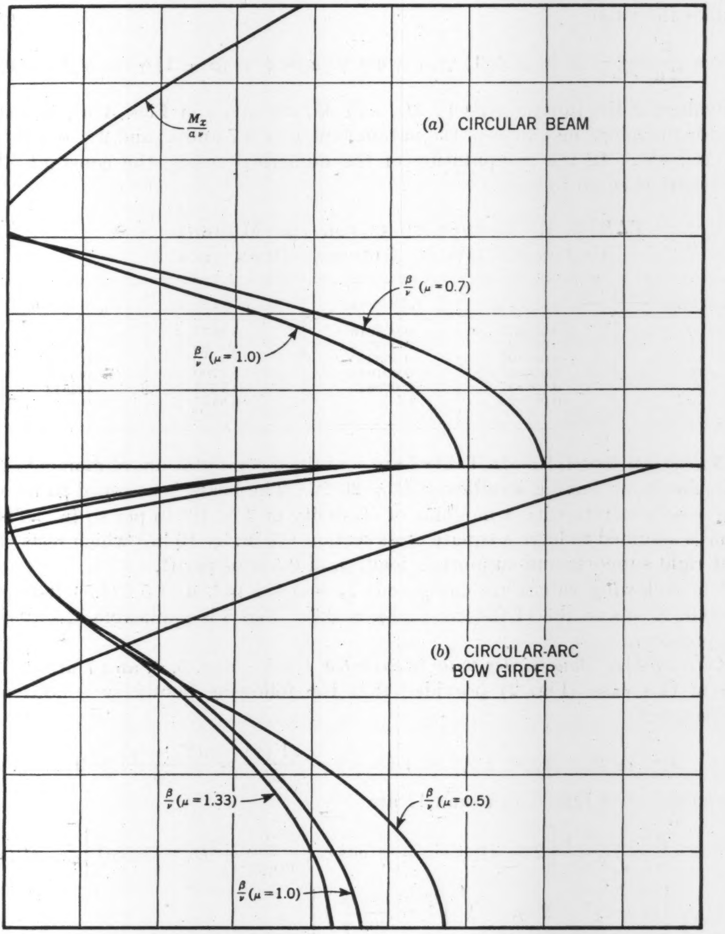

Each in Fig. 4(a); Values of $\frac{M_z}{a\nu} \times 10$;

and $\frac{\beta}{\nu} \times 5$, Each in Fig. 4($b$)

UNIFORM LOAD, $2\gamma = 120°$

and

$$\frac{M_z}{a\,\nu} = \phi - \frac{\gamma}{\sin\gamma}\sin\phi \quad \text{(9}d\text{)}$$

In the case of rigid supports $Y = 0$ for $\phi = \gamma$, and the constant of Eq. 9*b* assumes the value,

$$A' = -\frac{1}{2\,\mu}\{\gamma^2 - 2 + (\mu + 1)\,\gamma^2 + \gamma\cot\gamma\,[\mu + 3 + (\mu + 1)\,\gamma\cot\gamma]\} \quad (10)$$

The values of the functions β, Y, M_x, and M_z are given in Figs. 4(*a*), 5, and 6(*a*) for the following values of the parameters, $\mu = 0.7$ and 1; and $2\,\gamma = 120°$, 90°, and 45°. In the computation of the numerical scales, the constant A' was taken as equal to zero.

TABLE 1.—COMPUTATIONS FOR THE MOMENTS IN A UNIFORMLY LOADED CIRCULAR BEAM (FIG. 5)

ϕ, in degrees	β, in radians	v, in inches	M_x, in foot-tons	M_z, in foot-tons
0	−0.000812	0.005616	3.4875	0
5	−0.000644	0.005064	2.9683	0.2888
10	−0.000191	0.003360	1.4110	0.4872
15	0.000391	0.001680	−1.1700	0.5045
20	0.000847	0.000820	−4.7533	0.2542
22.5	0.000924	0	−6.9137	0

Numerical Example.—In Table 1 are contained computations of moments in a circular beam having a radius of $R = 20$ ft. The beam is assumed to be of reinforced concrete with a modulus of elasticity of 3×10^6 lb per sq in. The beam is assumed to have a square cross section (16 in. by 16 in.) which rests on eight rigid supports and supports a load, p, of 0.5 tons per ft.

The following values are computed: $I_x = 5{,}451$ in.^{4}, $a = 5{,}688.54$ ft-tons, $\nu = 0.0239$, $a\,\nu = 133.11$ ft-tons, and $\mu = 0.7$. Fig. 5 is applicable in solving this problem.

Circular-Arc Bow Girder with Distributed Load.—Eqs. 5, 6, and 7 are valid also in this case (Fig. 2) provided that the following boundary conditions are assumed:

$$\beta(\gamma) = \beta(-\gamma) = Y(\gamma) = Y(-\gamma) = \frac{dY(\gamma)}{d\phi} = \frac{dY(-\gamma)}{d\phi} = 0 \quad (11)$$

The solutions of Eqs. 5, 6, 7, and 11 are

$$\frac{\beta}{\nu} = \frac{\mu + 1}{2\,\mu}\left[2 + D_1\,\phi\sin\phi - \cos\phi\left(\frac{2}{\cos\gamma} + D_1\,\gamma\tan\gamma\right)\right] \quad \text{(12}a\text{)}$$

$$\frac{Y}{\nu} = \frac{1}{2\,\mu}\left[\phi^2 - \gamma^2 - 2\,(\mu + 1)\left(1 - \frac{\cos\phi}{\cos\gamma}\right)\right]$$
$$+ \frac{D_1}{2\,\mu}\{-\,(\mu + 1)\,\phi\sin\phi + [(\mu + 1)\,\gamma\tan\gamma - 2]\cos\phi + 2\cos\gamma\} \quad \text{(12}b\text{)}$$

$$\frac{M_x}{a\,\nu} = 1 + D_1\cos\phi \quad \text{(12}c\text{)}$$

$$\frac{M_z}{a\,\nu} = \phi + D_1\sin\phi \quad \text{(12}d\text{)}$$

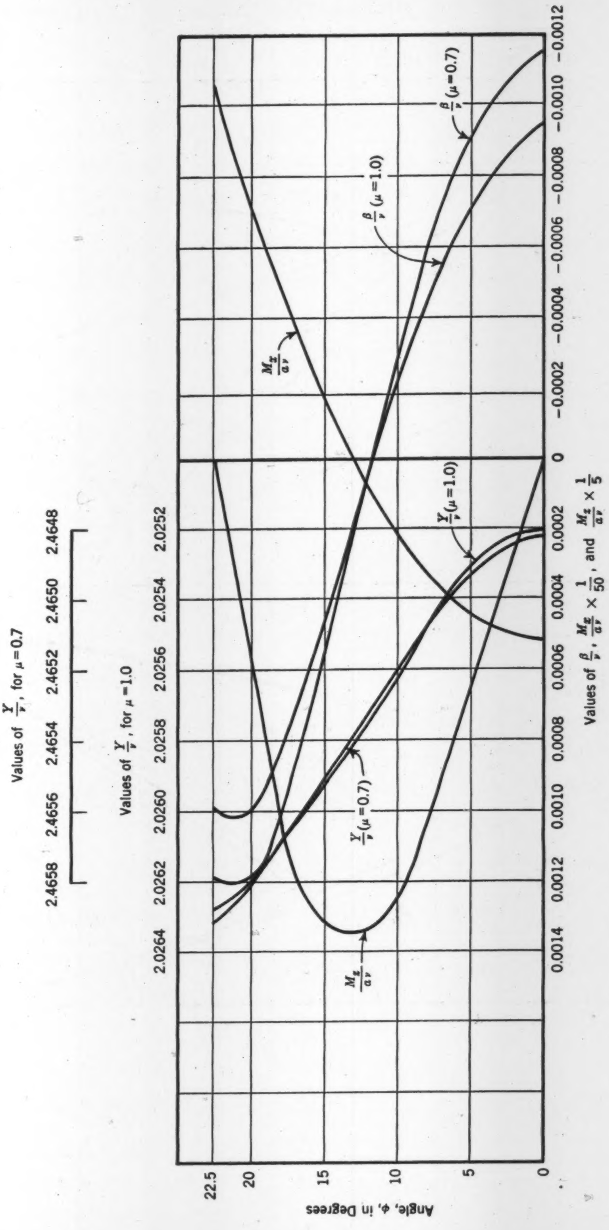

FIG. 5.—FUNCTIONS FOR A CIRCULAR BEAM WITH A DISTRIBUTION LOAD ($2\gamma = 45°$, AND $\mu = 0.7$ AND 1)

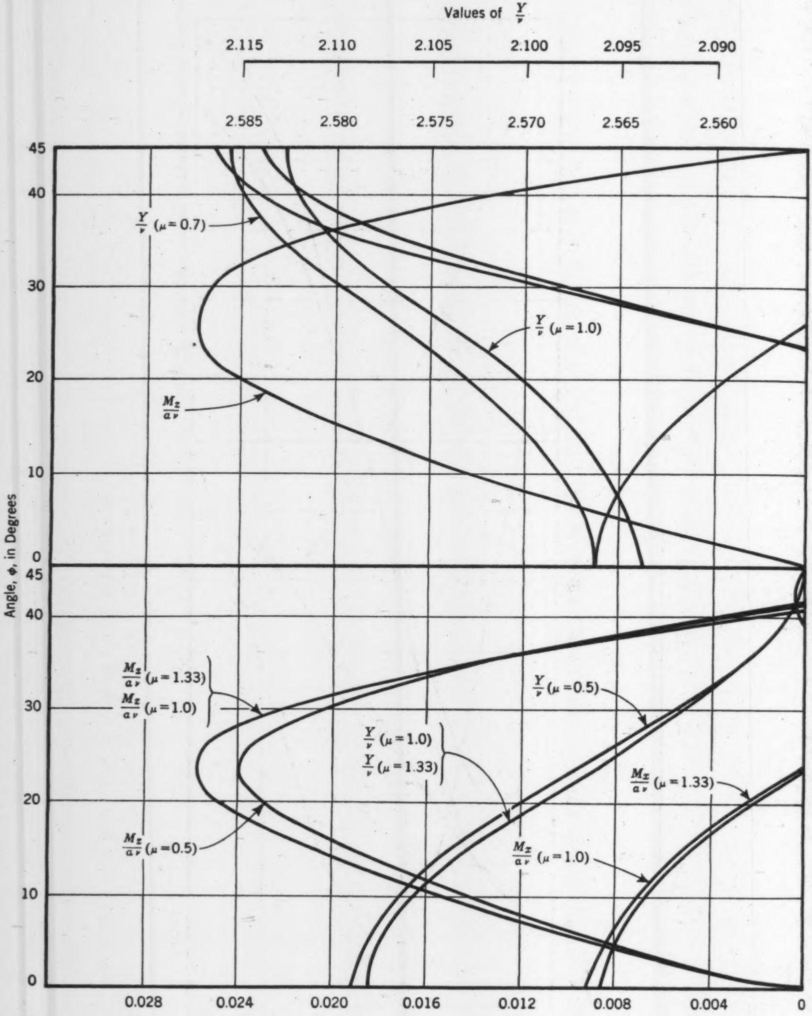

Values of $\frac{M_z}{a\nu} \times \frac{4}{5}$ and $\frac{M_z}{a\nu} \times \frac{2}{25}$,

Values of $\frac{M_z}{a\nu}$, $\frac{M_z}{a\nu} \times \frac{1}{10}$, $\frac{Y}{\nu}$,

Values of $\frac{\beta}{\nu}$ for $\mu = 0.7$ in Fig. 6(*a*);

FIG. 6.—FUNCTIONS FOR

[for $\mu = 1.0$ in Fig. 6(a)]

[for $\mu = 0.7$ in Fig. 6(a)]

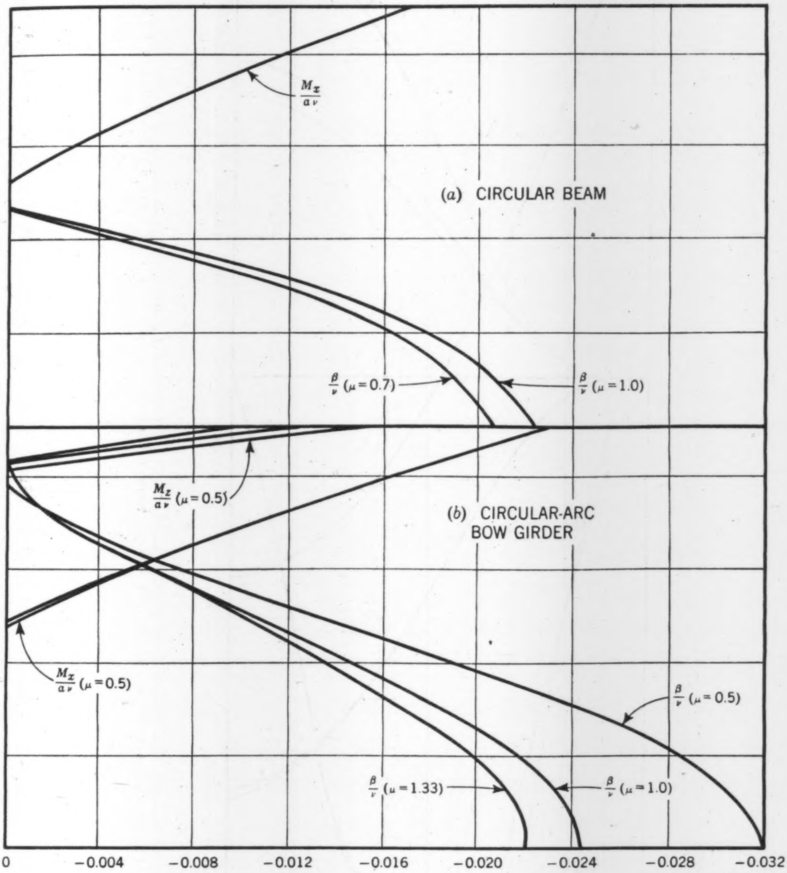

Each in Fig. 6(a);

and $\frac{\beta}{\nu} \times \frac{4}{5}$, Each in Fig. 6($b$);

and Values of $\frac{\beta}{\nu} \times \frac{4}{3}$ for $\mu = 1.0$ in Fig. 6(a)

UNIFORM LOAD, $2\gamma = 90°$

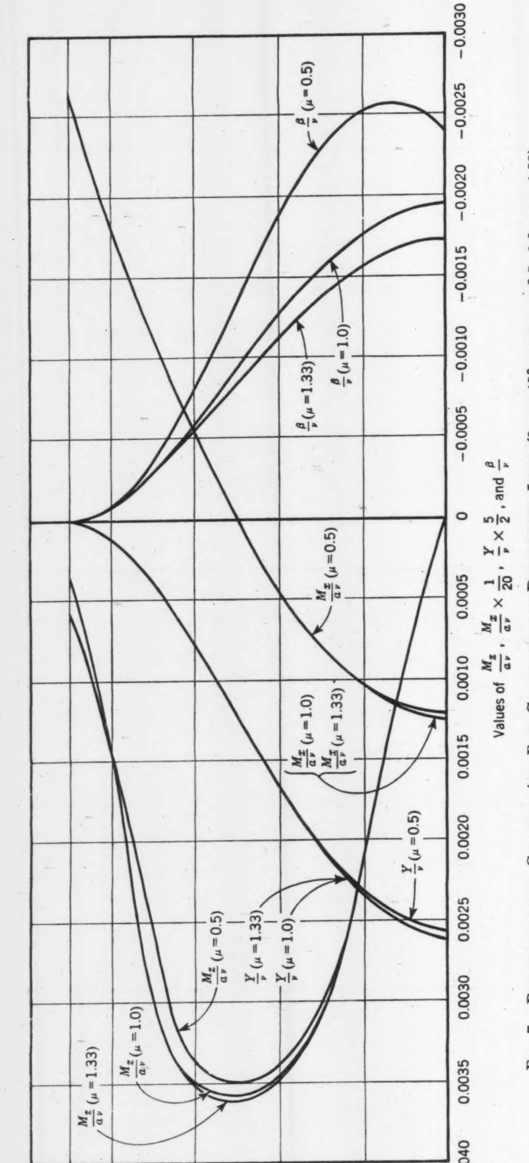

FIG. 7.—FUNCTIONS FOR A CIRCULAR-ARC BOW GIRDER WITH A DISTRIBUTED LOAD ($2\gamma = 45°$; AND $\mu = 0.5$, 1.0, AND 1.33)

in which

$$D_1 = 2 \frac{\gamma \cos \gamma - (1 + \mu) \sin \gamma}{(1 + \mu) \gamma + (\mu - 1) \sin \gamma \cos \gamma} \ldots \ldots \ldots \ldots (13)$$

In the particular case in which $\gamma = 90°$,

$$D_1 \gamma \tan \gamma + \frac{2}{\cos \gamma} = \frac{\pi^2 + 4 (\mu - 1)}{\pi (1 + \mu)} \ldots \ldots \ldots \ldots (14)$$

The values of the functions β, Y, M_x, and M_z are given in Figs. 4(*b*), 6(*b*), and 7 for the following values of the parameters: $\mu = 0.5$, 1, and 1.33; and $2\gamma = 120°$, 90°, and 45°.

Numerical Example; Bow Girder.—A circular bow girder is assumed to be subjected to a uniformly distributed load, p, of 0.25 tons per ft. The beam is of reinforced concrete ($E = 3 \times 10^6$ lb per sq in.), and its rectangular cross section is 20 in. wide and 12 in. deep. The angular distance between the built-in ends is $2\gamma = 120°$.

TABLE 2.—COMPUTATIONS FOR THE MOMENTS IN A UNIFORMLY LOADED CIRCULAR-ARC BOW GIRDER (FIG. 4(*b*))

ϕ, in degrees	β, in radians	v, in inches	M_x, in foot-tons	M_z, in foot-tons
0	0.0003468	0.02415	3.6290	0
10	0.0003222	0.02275	3.1940	0.6080
20	0.0002535	0.01881	1.9025	1.0650
30	0.0001572	0.01315	− 0.2065	1.2245
40	0.0000588	0.007030	− 3.0690	0.9490
50	0.00000702	0.002052	− 6.5977	0.1145
60	0	0	−10.6855	−1.3865

The following values are computed: $I_x = 8 \times 10^3$ in.^{4}, $a = 8{,}333.33$ ft-tons, $\nu = 3 \times 10^{-3}$, $a\,\nu = 25$ ft-tons and $\mu = 0.5$. The computations for this example are in Table 2, and are based on Fig. 4(*b*).

Circular-Arc Bow Girder with Concentrated Load.—If P is the concentrated load, 2γ the angular distance between the extremities of the beam, and α the angular distance between the end of the beam ($\phi = 0$) and the point where the concentrated force is applied (Fig. 3), it follows that $\nu = (P\,R^2)/(E\,I_x)$ and that Eqs. 6 are still valid. For equilibrium, the following equations must be verified:

$$\left.\begin{array}{l} \dfrac{dM_z}{d\phi} - M_x = 0 \\ \dfrac{d^2M_x}{d\phi^2} + \dfrac{dM_z}{d\phi} = 0 \end{array}\right\} \ldots \ldots \ldots \ldots \ldots \ldots (15)$$

The boundary conditions and the conditions of continuity are, in this case,

$$\beta(0) = \beta(2\gamma) = Y(0) = Y(2\gamma) = \frac{dY(0)}{d\phi} = \frac{dY(2\gamma)}{d\phi} = 0 \ldots. (16a)$$

$$\frac{dM_x(\alpha + 0)}{d\phi} - \frac{dM_x(\alpha - 0)}{d\phi} = -\,a\,\nu \ldots \ldots \ldots \ldots (16b)$$

and β, $\frac{d\beta}{d\phi}$, Y, $\frac{dY}{d\phi}$, and $\frac{d^2Y}{d\phi^2}$ are all continuous for $\phi = a$. Because of the discontinuity at $\phi = \alpha$, the analytical expression for the bending and twisting moments M_x and M_z for the displacement v and the angle of twist β are different in the intervals $0, \alpha$ and $\alpha, 2\gamma$. If $\beta = \bar{\beta}$, $y = \bar{y}$, $M_x = \bar{M}_x$, and $M_z = \bar{M}_z$ for $0 \leq \phi \leq \alpha$ and $\beta = \bar{\beta} + \beta^*$ and if $Y = \bar{Y} + Y^*$, $M_x = \bar{M}_x + M^*_x$, and $M_z = \bar{M}_z + M^*_z$ for $\alpha \leq \phi \leq 2\gamma$, the solution of Eqs. 6, 15, and 16 is

$$\beta^* = \frac{\mu + 1}{2\mu} \nu \left[(\phi - \alpha) \cos (\phi - \alpha) - \sin (\phi - \alpha)\right] \qquad (17a)$$

$$Y^* = -\frac{\nu}{2\mu} [2 (\phi - \alpha) + (\mu + 1) (\phi - \alpha) \cos (\phi - \alpha) - (\mu + 3) \sin (\phi - \alpha)] \qquad (17b)$$

$$M^*_x = -a\nu \sin (\phi - \alpha) \qquad (17c)$$

and

$$M^*_z = -a\nu [1 - \cos (\phi - \alpha)] \qquad (17d)$$

Finally,

$$\bar{\beta} = \nu A (\mu + 1) \phi \sin \phi + \nu B [-(\mu + 1) \phi \cos \phi + (\mu - 1) \sin \phi] + 2\nu C \sin \phi \qquad (18a)$$

$$\bar{Y} = \nu A [2 - (\mu + 1) \phi \sin \phi - 2 \cos \phi] + \nu B (\mu + 1) (\phi \cos \phi - \sin \phi) + 2\nu C (\phi - \sin \phi) \qquad (18b)$$

$$\bar{M}_x = 2\mu\nu a (A \cos \phi + \beta \sin \phi) \qquad (18c)$$

$$\bar{M}_z = 2\mu\nu a (A \sin \phi - B \cos \phi + C) \qquad (18d)$$

The constants A, B, and C are determined from the following equations:

$$A = [(\mu + 1)\gamma^2 - 2 + 2 \cos \gamma] \frac{L_1}{D_2} \sin \gamma + [-(\mu + 1)\gamma^2 \cos \gamma + (\mu - 1)\gamma \sin \gamma + 2 \sin^2 \gamma] \frac{L_2}{D_2} - (1 - \cos \gamma) \frac{L_3}{D_2} \qquad (19a)$$

$$B = -[(\mu + 1)\gamma^2 \cos \gamma + (\mu - 1)\gamma \sin \gamma + 2 (1 - \cos \gamma)^2] \frac{L_1}{D_2} + [-(\mu + 1)\gamma^2 + 2 - 2 \cos \gamma] \frac{L_2}{D_2} \sin \gamma + \sin \gamma \frac{L_3}{D_2} \qquad (19b)$$

and

$$C = -\sin \gamma \frac{L_1}{D_2} - (1 - \cos \gamma) \frac{L_2}{D_2} + [(\mu + 1)\gamma - (\mu - 1) \sin \gamma] \frac{L_3}{D_2} \qquad (19c)$$

in which

$$D_2 = [(\mu + 1)\gamma + (\mu - 1) \sin \gamma] \Delta \qquad (20)$$

$$\Delta = 4 (1 - \cos \gamma) - \gamma [(\mu + 1)\gamma - (\mu - 1) \sin \gamma] \qquad (21)$$

$$L_1 = \frac{\mu + 1}{2\mu} [(\gamma - \alpha) \cos (\gamma - \alpha) - \sin (\gamma - \alpha)] \qquad (22a)$$

$$L_2 = \frac{1}{2\mu} [(\mu + 1) (\gamma - \alpha) \sin (\gamma - \alpha) + 2 \cos (\gamma - \alpha) - 2] \qquad (22b)$$

and

$$L_3 = \frac{1}{\mu}\left[\sin\,(\gamma - \alpha) - (\gamma - \alpha)\right] \qquad \text{(22c)}$$

The values of the constants *A*, *B*, and *C* are given in Figs. 8, 9, 10, and 11 for the following values of the parameters: $\mu = 0.564$, 0.7, 0.85, 1.15, and 1.33; $2\gamma = 120°$, 90°, and 45°; and for the angle ϕ varying in the interval $(0, \gamma)$ by 10°.

Numerical Example: Bow Girder with Point Load.—A reinforced concrete ($E = 3 \times 10^6$ lb per sq in.) circular bow girder, 24 in. by 24 in. in cross section,

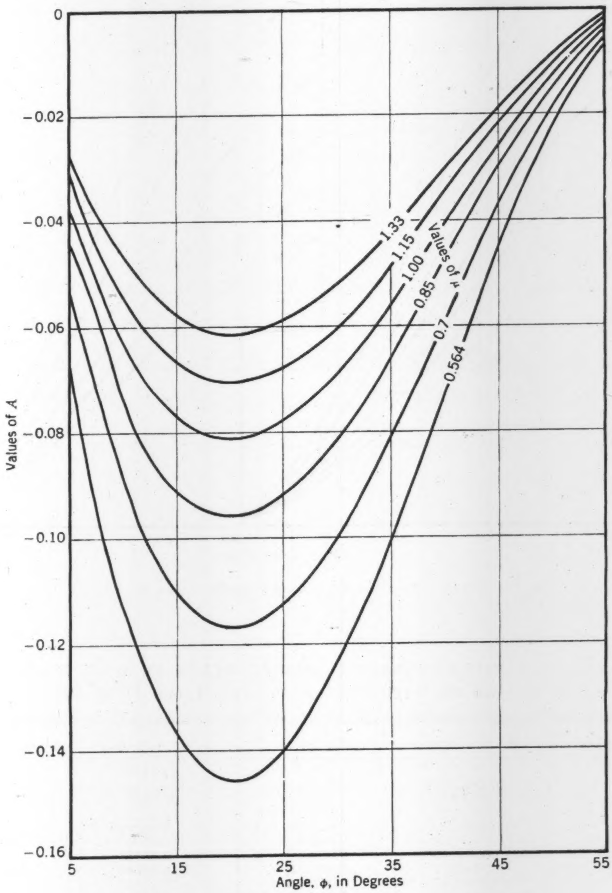

FIG. 8.—RELATIONSHIPS FOR A CIRCULAR-ARC BOW GIRDER WITH A CONCENTRATED LOAD, $2\gamma = 120°$

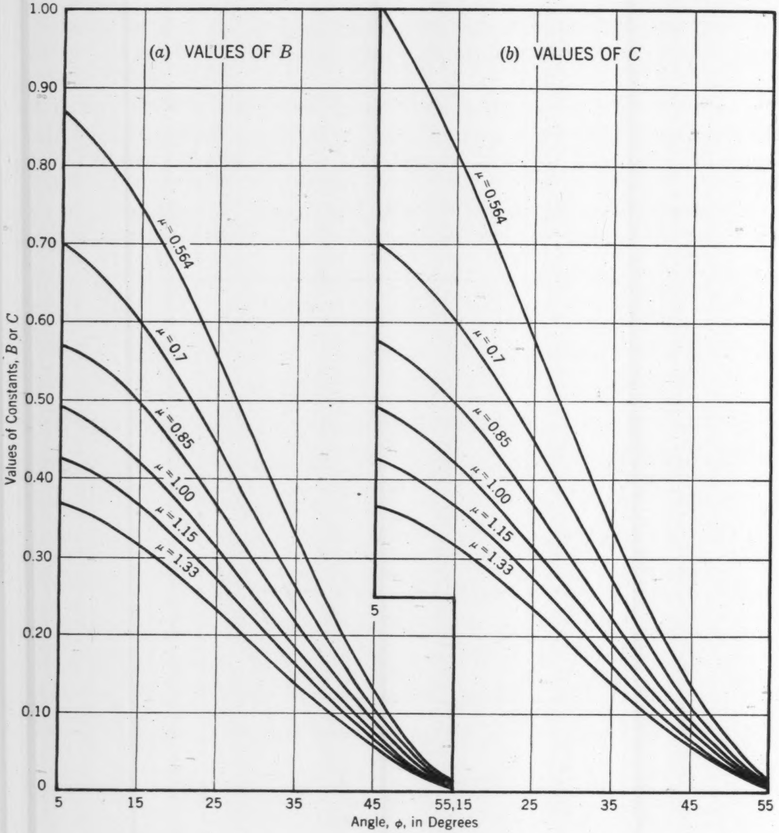

FIG. 9.—RELATIONSHIPS FOR A CONCENTRATED LOAD, 2 γ = 120°

TABLE 3.—COMPUTATIONS FOR THE MOMENTS IN A CIRCULAR-ARC BOW GIRDER WITH CONCENTRATED LOAD (FIG. 10)

ϕ, in degrees	β, in radians	v, in inches	M_x, in foot-tons	M_z, in foot-tons
0	0	0	−44.7104	3.2872
5	−0.00002012	0.002544	−36.1116	−0.2408
10	−0.00004321	0.009888	−27.2356	−3.0072
15	−0.0001223	0.020520	−18.1552	−4.9840
20	−0.0002243	0.033168	− 8.9376	−6.1712
25	−0.0003358	0.046584	0.3500	−6.5464
30	−0.0004443	0.059328	9.6348	−6.1124
35	−0.0005371	0.070032	18.8468	−4.8664
40	−0.0006015	0.077376	27.9160	−2.8252
45	−0.0006257	0.080352	36.7696	0.0000

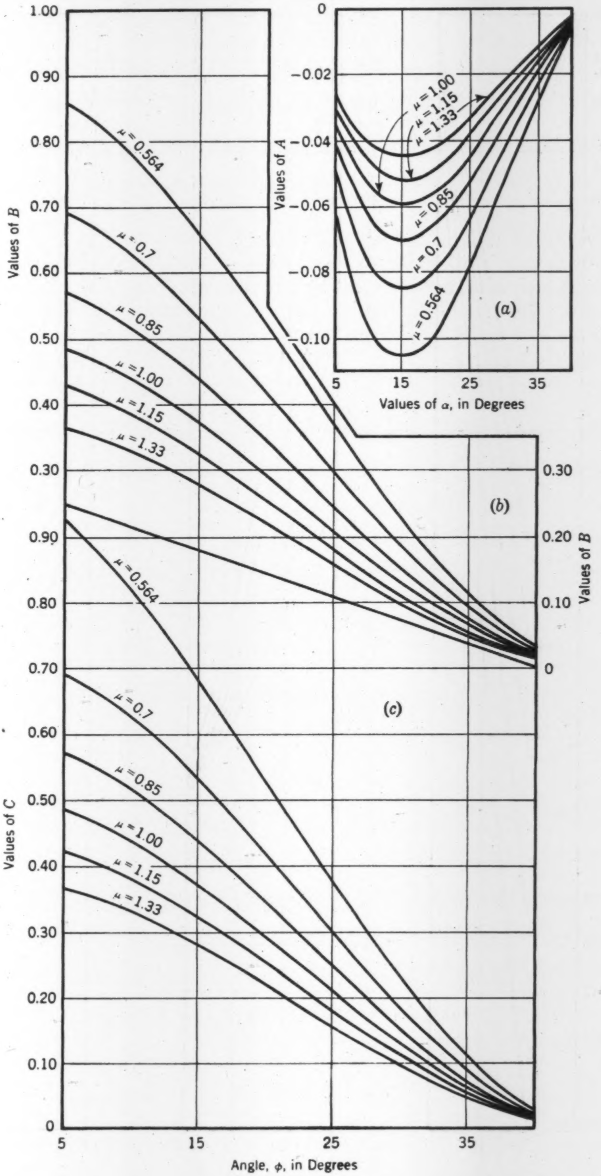

FIG. 10.—RELATIONSHIPS FOR A CONCENTRATED LOAD, $2\gamma = 90°$

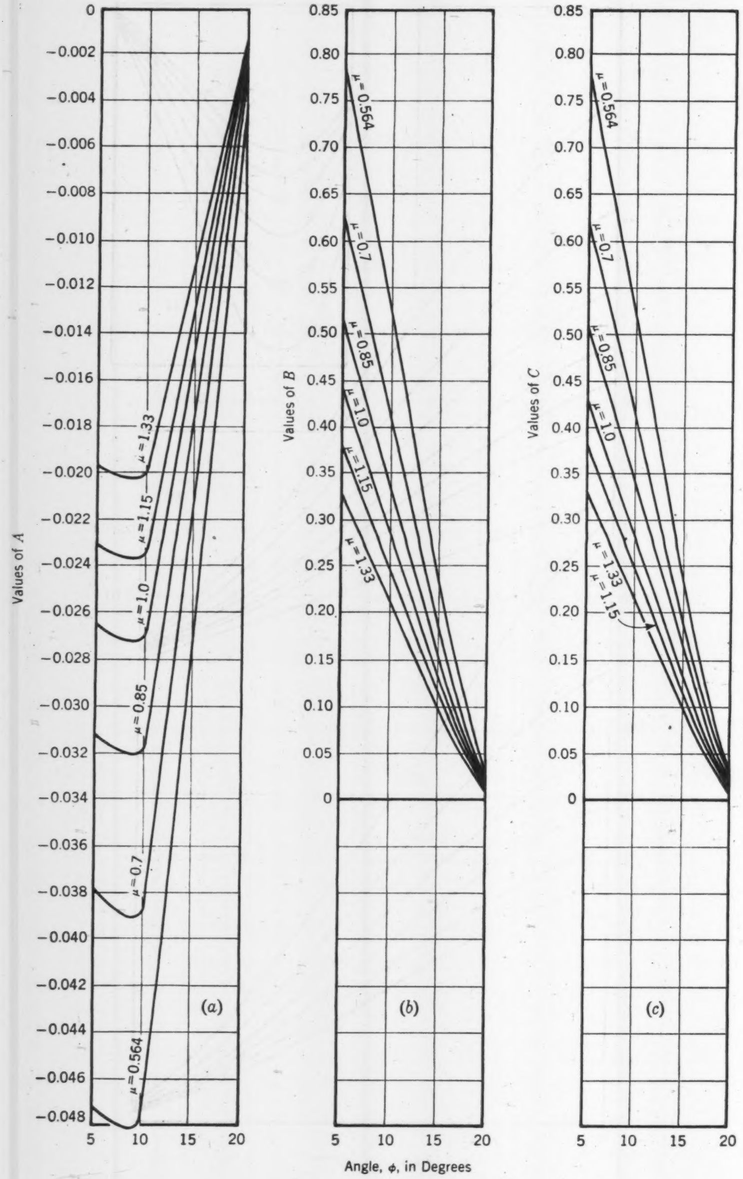

FIG. 11.—RELATIONSHIPS FOR A CONCENTRATED LOAD, $2\gamma = 45°$

is assumed to support a concentrated load, $P = 10$ tons, at the center. The angle between the built-in ends is $2\gamma = 90°$ so that P is at $\alpha = 45°$.

From this information, the following are computed: $I_z = 27{,}648$ in.^{4}, $\mu = 0.7$, $\nu = 0.013889$, $a = 14{,}400$ ft-tons, and $2\mu\nu a = 280$ ft-tons. From Fig. 10 are obtained: $A = -0.16$, $B = 0.345$, and $C = 0.357$. In Table 3 are the results obtained for this particular case by applying Eqs. 18.

ACKNOWLEDGMENT

The writer wishes to express his appreciation and thanks to members of the Instituto per le Applicazioni del Calcolo in Rome, Italy, for having checked the formulas and for the help received in the numerical computation of some of the tables presented in the paper.

APPENDIX I. NOTATION

The following symbols, adopted for use in the paper, and for the guidance of discussers, conform essentially with American Standard Letter Symbols for Structural Analysis (ASA Z10.8—1949), prepared by a committee of the American Standards Association, with ASCE representation, and approved by the Association in 1949:

A, A' = constants;

$a = \frac{E I_z}{R}$;

B = a constant;

C = a constant;

D_1, D_2 = terms defined in Eqs. 13 and 20, respectively;

E = the modulus of elasticity;

I = the rectangular moment of inertia;

K = the torsional rigidity;

L_1, L_2, L_3 = terms defined in Eqs. 22;

M_y, M_z = bending moments;

M_s = twisting moments;

P = intensity of the concentrated load;

p = intensity of the distributed load;

R = the initial curvature of the center line of the beam;

s = arc length;

u, v, w = displacements along axes x, y, and z, respectively;

x, y, z = rectangular coordinate axes;

$Y = \frac{v}{R}$;

α = an angle defined in Fig. 2(*b*);

β = the angle of twist;

γ = one half the angular distance between points of support;

Δ = a term defined in Eq. 21;

θ = the angle of twist per unit length;

$\mu = \frac{K}{E\, I_z}$;

$\nu = \frac{P R^2}{E\, I_z}$; and

ϕ = an angle defined in Fig. 2.

APPENDIX II. BIBLIOGRAPHY ON CURVED BEAMS

(1) **"Bending of a Circular Beam Resting on an Elastic Foundation,"** by Enrico Volterra, *Journal of Applied Mechanics*, March, 1952, pp. 1–4.

(2) **"Mémoire sur le calcul de la résistance et de la flexion des pièces solides à simple ou à double courbure, en prenant simultanément en consideration les divers efforts auxquels elles peuvent être soumises dans tous les sens,"** by Barré de Saint-Venant, *Comptes-Rendus*, l'Académie des Sciences de Paris, Vol. XVII, 1843, pp. 942 and 1020–1031.

(3) **"De la déformation qu'éprouve une pièce à simple ou à double courbure sous l'action de forces qui lui font subir en même temps une flexion et une torsion,"** by H. Resal, *Journal de Mathématiques pures et appliqués*, Société Mathématique Française, Vol. III, 1877, pp. 307–322.

(4) **"Zur Theorie torsionsfester Ringe,"** by B. G. Kannenberg, *Der Eisenbau*, 1913, pp. 329–334.

(5) **"Abriss einer allgemeinen Theorie des eigenspannten Tragers mit raumlich gefundener Mittelinie,"** by H. Marcus, *Zeitschrift für Bauwesen,* 1914, pp. 198–223.

(6) **"Die elastische Linie des Doppelt gekrümmten Trägers,"** by H. Marcus, *ibid.,* 1919, pp. 163–180.

(7) **"Ringsformige Träger,"** by F. Düsterbehn, *Der Eisenbau,* 1920, pp. 73–80.

(8) **"Die elastische Verschiebungen gekrümmter Stabe als Drehungen beziehungsweise Schraubungen um Achsen von Momentenflachen,"** by F. Schleicher, *Zeitschrift für Angewandte Mathematik und Mechanik,* Vol. IV, 1924, p. 475.

(9) **"Über die quasi-statische Berechnung geschlossener Kreisformiger Ringe Konstanten Querschnittes,"** by C. B. Biezeno, *ibid.,* Vol. VIII, 1928, p. 237.

(10) **"The Stress Analysis of Bow Girders,"** by A. J. S. Pippard and F. L. Barrow, *Building Research Technical Paper No. 1,* Department of Scientific and Industrial Research, His Majesty's Stationery Office, London, England, 1926, pp. 1–27.

(11) **"An Application of the Principle of Superposition to Certain Structural Problems,"** by A. J. S. Pippard, *Journal,* Inst. of C. E., London, England, 1938, pp. 447–454.

(12) **"The Solution of Closed Rings with Equally Spaced Supports,"** by Mervin B. Hogan, *Bulletin,* University of Utah, Ogden, Utah, Vol. 34, November, 1943.

(13) **"The Solution of Closed Rings with Equally Spaced Supports and Moments-Loadings,"** by Mervin B. Hogan, *ibid.,* Vol. 34, May, 1944.

(14) **"Moment Distribution Applied to Combined Flexure and Torsion,"** by Mervin B. Hogan, *ibid.,* Vol. 35, February, 1945.

(15) **"The Deflection of Circular Arcs Subjected to Combined Flexure and Torsion,"** by Mervin B. Hogan, *ibid.,* Vol. 35, April, 1947.

(16) **"The Derivation of Two–Five Moment Theorems for Continuous Plane Curved Beams,"** by Mervin B. Hogan, *ibid.,* Vol. 36, April, 1947.

(17) **"Influence Lines for Horizontally Curved Fixed-End Beams of Circular Arch Plan,"** by Robert B. B. Moorman and Manford B. Tate, *The University of Missouri Bulletin,* Vol. 48, No. 26 (Eng. Series No. 35), Columbus, Mo., pp. 1–39.

(18) **"Analysis of Continuous Circular Curved Beams,"** by Becla Velutini, *Journal,* Am. Concrete Inst., Vol. 22, November, 1950, pp. 217–228.

(19) **"The Mathematical Theory of Elasticity,"** by A. E. H. Love, Dover Publications, New York, N. Y., 4th Ed., 1944. (*a*) Chapter XXI.

(20) **"Strength of Materials—Advanced Theory and Problems,"** Pt. II by S. Timoshenko, Macmillan Co., New York, N. Y., 1936, pp. 467–473.

(21) **"Deflections of Circular Beams Resting on Elastic Foundations Obtained by Methods of Harmonic Analysis,"** by Enrico Volterra, *Journal of Applied Mechanics,* June, 1953, pp. 227–232.

(22) **"A Study of the Circular Arc Bow Girder,"** by A. H. Gibson and E. G. Ritchie, Constable, New York, N. Y., 1914.

(23) **"Analysis of Engineering Structures,"** by A. J. S. Pippard and F. L. Barrow, Edward Arnold, London, England, 2d Ed., 1945.

(24) **"Stresses in Curved Beams Under Loads Normal to the Plane of Its Axis,"** by R. B. Moorman, *Bulletin No. 145*, Iowa State College, Ames, Iowa, 1940.

(25) **"Studies in Elastic Structures,"** by A. J. S. Pippard, Arnold and Co., London, England, 1952. (*a*) pp. 224–226.

(26) **"Bending of a Constrained Circular Beam Resting on an Elastic Foundation,"** by Enrico Volterra and R. Chung, *Transactions*, ASCE, Vol. 120, 1955.

DISCUSSION

I. Oesterblom,[3] M. ASCE.—In the English language, the subject of the paper was ably treated as early as 1914 by A. H. Gibson and E. G. Ritchie (22). Two distinguished authorities, Messrs. Pippard and Barrow, made extensive studies of and published papers and books on the arc bow girder (10) (11). One could ask for no more complete treatment of the theory of bow girder deflections and of the application of this theory. A book (23) which is a résumé of many years work has been published by Messrs. Pippard and Barrow. The German references are also extensive, but none that specifically refer to the subject or have usefulness in design was published earlier than the English works. Thus, one questions whether or not the paper advances new theories in the design or construction of civil engineering work, especially as the selected solutions do not include a graph for the almost universal case, $2\gamma = 180°$. Arc bow girders are usually supported at right angles to the structural frame and, when they are close to the frame (these are usually only ornamental in purpose), the designing engineer need not—and cannot afford to—spend time on extensive calculations. The author suggests (Fig. 1) five equidistant cuts of the circle, without explanation in the text, and develops three of them into helpful graphs. However, if wall wedges of 120° and 45° were common, the arc bow girders would be placed not at the point of the wedge but somewhere on the face of the wall so that 2γ would equal 180°.

Solutions to more comprehensive, varied, and real problems than those of this paper may be found in papers and books previously published. The author has referred to some that seem superior to his own presentation from the standpoint of the progress indicated and the utility shown. A bulletin (24) by Mr. Moorman provides an objective understanding of past work in this field, an experimental verification of the theory, and (best of all) a clarification of what the engineer may expect and should demand from the mathematician.

The paper fails to elaborate on the relation of stress to deflection; yet, because of the combination of longitudinal and rotational deformations, this subject is important, particularly in reinforced concrete design. The practicing engineer would stand defeated at this point even if the author's graphs would otherwise suit his needs. The paper would have been much more important if the author had attempted such an interesting problem.

In Appendix II, one of the books (19) seems to have no reference to the subject; two of them (3) (20) refer to mechanical engineering problems; and a fourth (1) is so broad and fundamental that it is the basis for all elastic problems. The writer does not consider these works proper for inclusion in the Bibliography on Curved Beams.

Enrico Volterra,[4] M. ASCE.—The writer thanks Mr. Oesterblom for contributing to the discussion of the paper.

---

[3] Rutherfordton, N. C.

[4] Prof. of Mechanics, Rensselaer Polytechnic Inst., Troy, N. Y.

The purpose of the paper was the study of deflections of circular beams in three particular and distinct cases: (1) Circular rings rigidly supported at symmetrical points and subjected to uniformly distributed forces; (2) circular-arc bow girders built in at both ends and subjected to uniformly distributed forces; and (3) circular-arc bow girders built in at both ends and subjected to concentrated forces.

Fig. 1 refers to case 1 of the circular ring and not to case 2 of the circular-arc bow girder (Fig. 2(*a*)) as erroneously interpreted by the discusser.

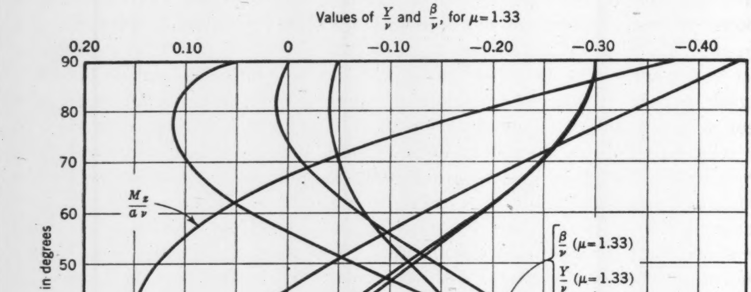

FIG. 12.—FUNCTIONS FOR A CIRCULAR-ARC BOW GIRDER WITH A DISTRIBUTED LOAD ($2\gamma = 180°$; AND $\mu = 0.5$, 1.0, AND 1.33)

Originally, the writer prepared many more graphs than those that were finally published; among the unpublished graphs were those for the case of circular-arc bow girders with a center angle $2\gamma = 180°$ to which Mr. Oesterblom refers. Graphs for this case are presented in Figs. 12 and 13.

The writer is aware of the works previously published on the subject, particularly those of English authors. He presented a bibliography which he thought was almost complete, containing all the works published on curved

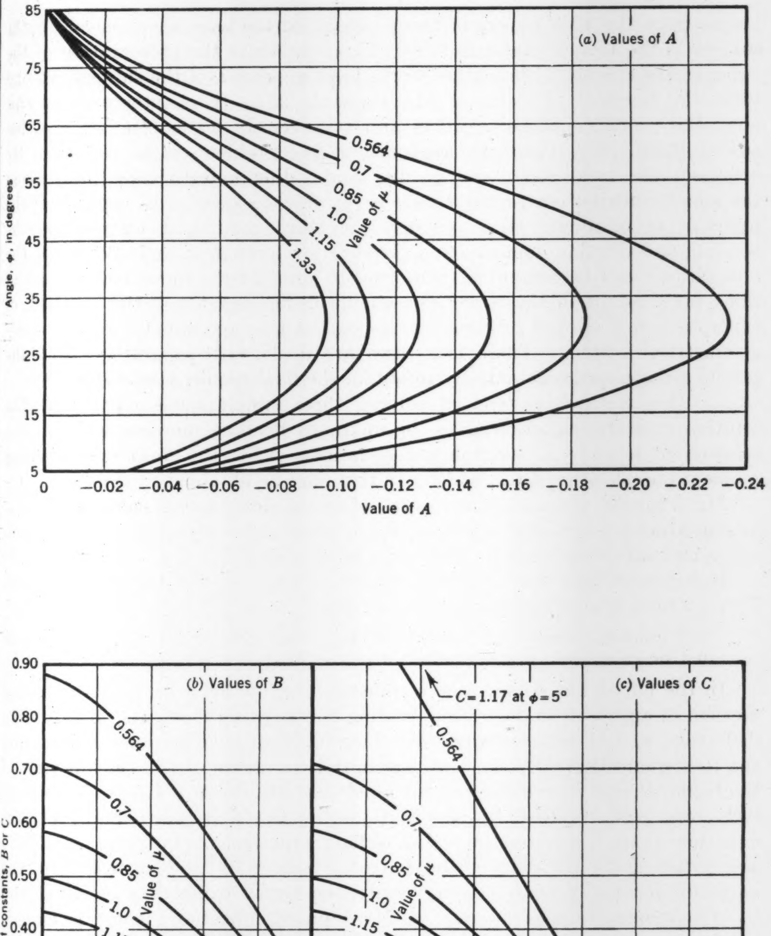

FIG. 13.—RELATIONSHIPS FOR A CIRCULAR-ARC BOW GIRDER WITH A CONCENTRATED LOAD ($2\gamma = 180°$)

beams from the 1843 papers of Saint-Venant to the papers published on the subject in the United States in 1950. However, since the presentation of the paper in the spring of 1952, other works have appeared on the subject, among them the excellent textbook of Mr. Pippard (25). In chapter nine of this book the problems of bow girders and transversely loaded frames are discussed (25*a*). Mr. Pippard's approach to the problems is as follows. He expresses the total strain energy due to bending and twisting, neglecting the small contribution to the total energy due to shear. By applying the principle of minimum strain energy, the three redundant unknowns—the bending and twisting moments and the shearing force in the midsection of the bow girder—can be computed. In order to simplify the numerical computations involved in solving the three simultaneous equations, the method of superposition is applied by dividing the loading into a symmetrical and skew-symmetrical system. These two cases are dealt with separately, and the results are summed algebraically to obtain the final required solutions.

By this method, instead of solving three simultaneous equations, the solution of a first equation gives the unknown bending moment whereas the solution of a pair of simultaneous equations yields the unknown twisting moment and shearing force, which can therefore be obtained explicitly.

Mr. Pippard discusses many cases of arc girders of engineering interest, among which are the cases of a circular-arc bow girder with a concentrated load and a circular-arc bow girder with a distributed load.

However, in the more general cases of noncircular-arc bow girders, Mr. Pippard finds that the resulting expressions

> "* * * cannot usually be integrated by exact mathematical process but must be calculated approximately by graphical or arithmetical methods."

In the paper, the writer used a different and, he believes, a more general method of approach to determine bending and twisting moments, M_x and M_z, deflection, v, and twisting angle, β. Four differential equations, connecting the four quantities, M_x, M_z, v, β, the initial curvature of the central line of the beam, R, and its inertial and torsional characteristics, $E\,I$ and K, respectively, are used. Two of these equations are the well-known Saint-Venant equations (Eqs. 1) whereas the two subsidiary equations of equilibrium (Eqs. 7) are obtained by minimizing the potential energy of the system. In the equation for the potential energy only the terms expressing bending and twisting moments appear because, as Mr. Pippard indicated, the energy caused by shear can be neglected. By solving these four differential equations under different load and boundary conditions, the results for the three special cases mentioned were obtained in closed form.

The same differential equations under appropriate load conditions and boundary conditions were used in earlier papers by the writer for solving problems of circular rings resting on elastic foundations and submitted to symmetric or antisymmetric concentrated loads (2)(21)(26).

Moreover, by using the same approach it is possible to solve in closed form particular cases of the more general problem of the deflection of a noncircular bow girder. In fact, it can also be shown that, in the case of a noncircular bow girder built-in at both ends and subjected to a uniformly distributed load, the results can be expressed in closed form if the central line of the curved beam is a cycloid, a catenary, or a parabola. The writer is preparing a paper (1954) on the subject of deflections of noncircular bow girders in which the results for these special cases will be given in closed form.

Mr. Oesterblom's criticism that the paper fails to elaborate on the relation of stress to deflection is certainly not correct. In fact—as the formulas presented in the paper give in closed form the relationships existing among bending and twisting moments, deflections and angles of twist, initial curvatures, inertial and torsional characteristics of the beam, and external loading—it is possible in each specific case to derive from these formulas the relationships between stresses and deflections.

The textbook (19) to which the discusser refers as having no reference to the subject contains an entire chapter (Chapter XXI) dealing with small deformation of naturally curved rods (19*a*).

The two references (3) and (20), which according to the discusser apply to mechanical engineering problems and should not have been quoted, are Mr. Resal's fundamental work on bending and twisting of a curved beam and the textbook of S. Timoshenko, many pages (of the second volume) of which deal with the problem of bending of a curved beam out of its plane of initial curvature and give useful references on the entire subject.

Finally, the fourth work, which Mr. Oesterblom does not consider proper for inclusion in the bibliography on curved beams, is Saint-Venant's original papers (1). In these papers the theory of small deformations of initially curved beams was first developed.

AMERICAN SOCIETY OF CIVIL ENGINEERS
Founded November 5, 1852
TRANSACTIONS

Paper No. 2728

UNUSUAL FOUNDATION CONDITIONS IN THE EVERGLADES

BY PAUL H. SHEA[1]

SYNOPSIS

Unusual foundation conditions encountered on that part of the Central and Southern Florida Project to be built in the Everglades include (1) very pervious solution-riddled limestone in the foundations of water-retention works, (2) thick layers of soft peat in levee foundations, and (3) structure foundations of interbedded sand and porous limestone.

Prevention of seepage losses by grouting or cutoff walls is not economically feasible. Water-control works on the landside of the levees must be designed to include the underseepage flow. Quantitative determinations of the probable underseepage have been based on permeabilities computed from the results of well-pumping tests. A few discharge measurements made since completion of the levees show good agreement with computed seepage losses.

Provision must be made for large embankment settlements in designing levees on deep peat. Nearly all the peats encountered on the project have low shearing strengths.

Many structures to be built for the project must be founded on formations consisting of thin layers of porous limestone underlaid or interbedded with fine sand. It is believed that a thin rock layer has value in that it acts as a foundation raft to reduce differential settlement. Great care must be exercised in excavating and unwatering these foundations.

INTRODUCTION

The Central and Southern Florida Project (still incomplete in 1954) will eventually be an integrated system of water-control works for flood control, drainage, and water conservation—covering all eastern Florida from the latitude of Orlando southward. Included in the project will be hundreds of miles of canals and levees, numerous small dams and spillways, and several large pumping stations.

Much of the Central and Southern Florida Project is to be built in the

---

NOTE.—Published, essentially as printed here, in July, 1953, as *Proceedings-Separate No. 227*. Positions and titles given are those in effect when the paper was received for publication.

[1] Civ. Engr., Jacksonville (Fla.) Dist. Corps of Engrs., U. S. Dept. of the Army.

grassy, swampy plain of the Everglades. The region is flat, having an average slope from north to south of about 1 ft in 5 miles. Throughout the Everglades the surface soil is peat varying in thickness from a few inches to more than 15 ft. Underlying the peat along many miles of the alinements of levees to be built for the project is a series of extremely pervious, solution-riddled Pleistocene limestone formations 50 ft thick. The limestones are Miami oolite, which is only a few feet thick along most of the levee alinements, and the underlying Fort Thompson formation. In areas where the thick series of limestones is absent, the materials below the peat are interbedded sands, marls, and limestones.

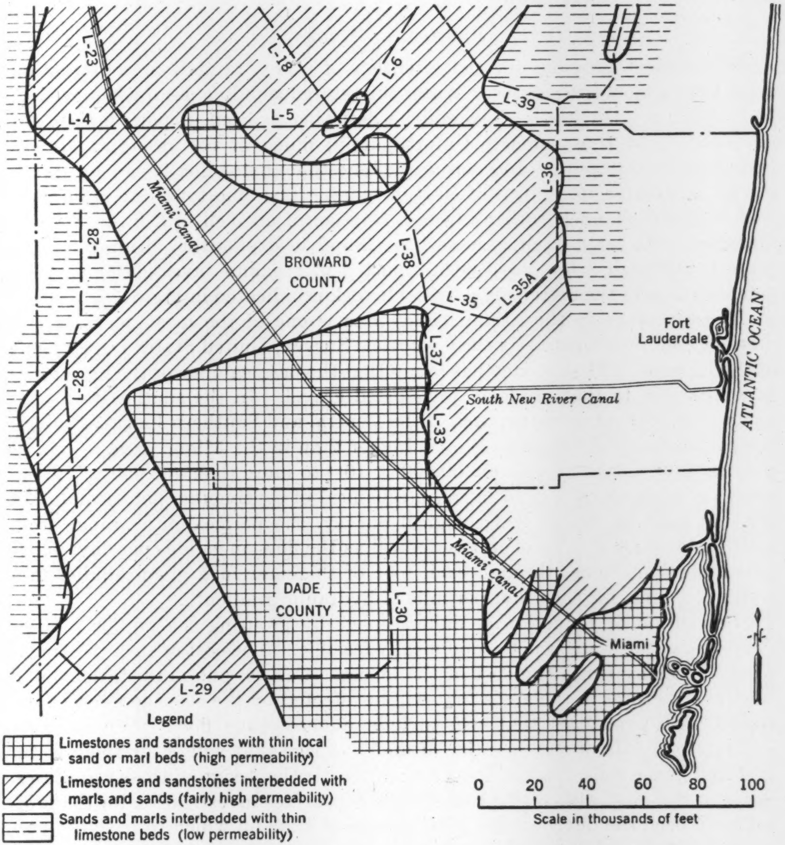
L-23
L-18
L-6
L-39
L-4
L-5
L-36
Miami Canal
L-28
BROWARD COUNTY
L-38
L-35
L-35A
Fort Lauderdale
L-37
South New River Canal
ATLANTIC OCEAN
L-33
L-28
DADE COUNTY
L-30
Miami Canal
Miami
L-29
Legend
▦ Limestones and sandstones with thin local sand or marl beds (high permeability)
▨ Limestones and sandstones interbedded with marls and sands (fairly high permeability)
☰ Sands and marls interbedded with thin limestone beds (low permeability)
0
20
40
60
80
100
Scale in thousands of feet

FIG. 1.—AREAS OF PERMEABLE ROCK

The three major foundation conditions (characteristic of the region) found on the project are: (1) The presence of extremely pervious rock in the foundations for water-retention works, (2) thick layers of weak, compressible peat in embankment foundations, and (3) structure foundations of interbedded porous limestone and sand. As one or more of these conditions exist at each levee or structure site, it may be said that all foundation conditions found on the project are somewhat extraordinary.

PERMEABLE ROCK

The project provides for the retention of excess rainfall in conservation areas to be ringed with levees. Water thus stored could be used, when needed, for irrigation. Obviously, it would be desirable to keep seepage losses at a minimum from those areas. Unfortunately, much of the reservoir area is underlaid by very porous and permeable limestones extending from—or near—the ground surface to depths of 50 ft or more. The limestones are perforated with solution channels ranging from a fraction of an inch to 6 in. or 8 in. in diameter. No large cavities have been found in exploratory drilling for the project, although a few have been reported in previous investigations. The extent in area of the extremely permeable rock is indicated in Fig. 1.

The limestone in the Miami (Fla.) area is one of the most pervious formations ever investigated by the Geological Survey, United States Department of the Interior. That agency has found that the permeability of the limestones is comparable to that of clean, well-sorted gravel. In the southeastern part of the southern conservation area of the Central and Southern Florida Project, the permeability of the rocks is even higher than in the Miami area. Typical permeability values range from $60,000 \times 10^{-4}$ to more than $400,000 \times 10^{-4}$ in units (most commonly used in soil mechanics) of centimeters per second. In the unit used by the U. S. Geological Survey, the permeabilities range from 130,000 to 900,000. That unit is defined as the flow, in gallons per day, under prevailing conditions, through each foot of thickness of a given aquifer in a width of 1 mile, for each foot per mile of hydraulic gradient.

Prevention or reduction of underseepage by grouting the porous rock or providing cutoff walls is not economically feasible. The cost of such treatment would be many times the cost of the levees. Canals, pumping stations, and control structures in the areas that will be affected by the seepage must be designed with capacities that will include underseepage flow. A reasonably accurate estimate of the quantity of underseepage that will occur when water is stored in the conservation areas is required for the design of these structures. Some of the most difficult features of the subsurface investigation for the project have been the devising and performance of tests on which to base the necessary estimates of foundation permeability and the interpretation of the results of the tests.

In December, 1950, a series of well-pumping tests to determine foundation permeabilities was begun. Tests were performed in the usual manner by pumping from a central well and observing the drawdown produced in observation wells at various distances from the pump well. An unusual feature of the tests was that drawdowns were extremely small because of the high permeability, and particularly accurate measurement was required. Electric point gages, accurate to 0.001 ft, were used for measuring drawdowns. Soon after the pumping tests were begun, it became apparent that none of the published methods for computing permeabilities from such tests was applicable to the physical conditions encountered. In the Everglades, the porous limestone is overlaid by sawgrass peat of varying thickness. Throughout most of the area, the uppermost limestone is much less pervious than the remainder because of the sealing of pores and solution channels by peat, marl, or redeposited calcite. The thickness of the relatively tight layer varies from a few inches to 2 ft or 3 ft. The water surface in the Everglades almost always lies either above the ground surface or in the peat. In the vicinity of a pumping well, the water seeps downward through the dense top layer into the aquifer and then flows toward the pump well to replace water removed during a pumping test.

Nearly all published methods for computing the permeabilities of porous materials by means of field pumping tests are based on one of the following assumptions: (1) The aquifer extends upward to the ground surface, or (2) the aquifer lies beneath a layer of completely impervious material. It is also assumed that water removed during a pumping test is supplied by depletion of the water stored in the aquifer, or by a distant source, or by both. It is evident that those assumptions do not apply to pumping tests in the Everglades where water is supplied by vertical flow from above the aquifer through a layer of lower permeability. A further complication in performing the pumping tests and interpreting the results is the presence of horizontal beds of relatively impervious fresh-water limestone dividing the more pervious marine limestone into two or three aquifers. Wherever that condition exists, sets of piezometers must be installed in all aquifers to make the required determination of hydraulic gradients.

Details of the mathematical treatment required for derivation of the necessary formulas for the computation of permeability and underseepage quantities for foundations of the type found in the Everglades are beyond the scope of this paper.

The derivation of the formulas is based on the following assumptions: (1) The blankets and the aquifers are homogeneous and of uniform thickness; (2) the aquifers have constant horizontal permeabilities; (3) the Darcy law applies; (4) flow is vertical in the blankets and virtually horizontal in the aquifers (this assumption is essentially correct when the permeability of the blanket is much less than that of the aquifer); (5) the head at the top of the top blanket is constant; and (6) flow is steady. Application of the methods developed to the results of a given pumping test is limited by the degree to which the physical conditions at the test site fulfil the requirements of the foregoing assumptions. In Fig. 2, relationships for permeability and underseepage in the simplest case—that of a single aquifer with an overlying blanket of relatively low permeability—are: For radial flow, $a\,r_e = 1.123$, $Q = 2.73\,k_2\,z_2\,\frac{\Delta h}{\Delta(\log r)}$, and $a = \sqrt{\frac{k_1}{k_2\,z_2\,z_1}}$; and for sheet flow, $x_r = \frac{1}{a}$ and $Q = \frac{k_2\,z_2\,H}{L + x_r + R}$, in which $R = B$ if $B \leq x_r$ and $R = x_r$ if $B \geq x_r$. In these expressions, Q denotes flow, r denotes radius, and k_1 and k_2 are the vertical permeability of the blanket and the horizontal permeability of the aquifer, respectively.

The formulas presented here were derived by Preston T. Bennett,[2] M. ASCE. Those for sheet flow were published or implied in the paper by Mr. Bennett.

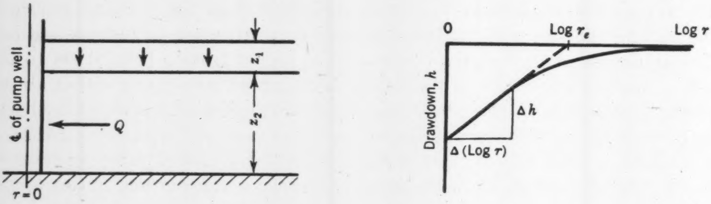
℄ of pump well
z_1
z_2
Q
$r=0$
0
Log r_e
Log r
Drawdown, h
Δh
Δ (Log r)

(a) Radial flow

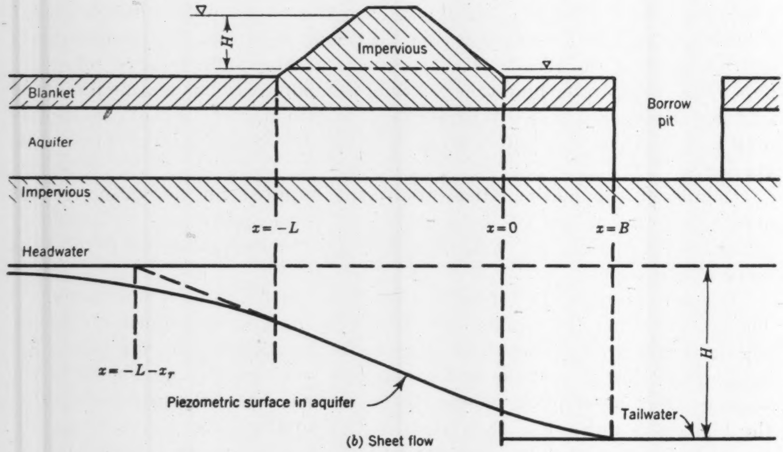
H
Impervious
Blanket
Aquifer
Impervious
Borrow pit
$x = -L$
$x=0$
$x=B$
Headwater
$x = -L - x_r$
Piezometric surface in aquifer
Tailwater
H

(b) Sheet flow

FIG. 2.—DIAGRAMS FOR COMPUTING SEEPAGE FROM WELL-PUMPING TEST (SINGLE-BLANKETED AQUIFER)

The much more complicated systems of two or three aquifers with intervening blankets require long computations for their solution, the formulas for which have been published by the Jacksonville (Fla.) District Corps of Engineers,[3] United States Department of the Army.

---

[2] "The Effect of Blankets on Seepage Through Pervious Foundations," by Preston T. Bennett, *Transactions*, ASCE, Vol. 111, 1946, p. 215.

[3] "Permeability Investigations by Well-Pumping Tests," Pt. I, Supplement 7, Partial Definite Project Report, Central and Southern Florida Project, Jacksonville (Fla.) Dist. Corps of Engrs., U. S. Dept. of the Army, February 16, 1952.

Well-pumping tests have provided the only means of arriving at a quantitative determination of foundation permeabilities. Such tests were expensive, and only a limited number could be made. To extend the information from the pumping tests, so-called "recharge" tests have been made in core borings along the levee alinements and at structure sites. The procedure followed is to test the drill holes in 5-ft sections by pumping water into the holes at a rate which will maintain a constant head. The "take" in gallons per minute per foot of head is used as a rough index of the permeability of the material tested. Attempts to compute actual permeabilities from recharge tests have been found to give misleading results.

Information from the pumping tests, recharge tests, geologic studies, and other available data were used in making the required estimate of underseepage flow. In the area of highest permeability, along levee L-30 and the south end of levee L-33 (Fig. 1), it is estimated that the underseepage will exceed 100 cu ft per sec per mile of levee for each foot of head acting. Underseepage in that area will not be directly proportional to the head because seepage flow will be turbulent at heads exceeding 1 ft, according to the data obtained from the pumping tests.

Since the completion of levees L-30, L-33, and L-37, which are founded on very pervious rock (as indicated by Fig. 1), a few discharge measurements have been made in the continuous borrow pits on the landside of the levees. These measurements have been made to determine the quantity of underseepage intercepted by the continuous landside borrow pit. Lines of piezometers have been installed to permit observation of the hydraulic gradients in the foundations. From these observations it is possible to compute the approximate percentage of underseepage flow intercepted by the borrow pits. Opportunity for such measurements has been limited because the manner in which the control structures have been operated has resulted in free flow in only one short length of borrow pit. That reach, the L-30 borrow pit between the Dade-Broward Dike and the Miami Canal, has been metered on several occasions. The agreement between the measured and predicted discharges has been highly satisfactory. With head differentials of slightly less than 2 ft, underseepage has been about 200 cu ft per sec per mile.

The solution-riddled limestone is responsible for another serious difficulty in the construction of the project—the extremely high cost of unwatering excavations. Wherever it is necessary to perform work "in the dry" below the water table, almost incredibly high rates of pumping are required. For example, in unwatering a small excavation for a culvert headwall at the intersection of levee L-33 and the Miami Canal, the contractor was forced to pump at a rate of more than 20,000 gal per min, although the hole was completely ringed with steel sheet piling. The head acting was only 8 ft. Another example of the high permeability of the rock is furnished by an experience with an experimental ring levee built near the south end of levee L-30. The area surrounded by the ring levee was filled by pumping from the borrow pit in the course of investigations that were being performed. The borrow pit was L-shaped and about 100 ft wide by a total length of 600 ft measured on the center line. Pumping from the pit at a rate of 10,400 gal per min for more than 30 hr caused no measurable drawdown on a recording gage set near the midpoint of the area, although the total volume of water pumped would have filled a hole having the same area as the borrow pit to a depth of approximately 35 ft.

The first large structure to be built in the pervious rock area will be a pumping station at the intersection of levee L-37 and the South New River Canal (Fig. 1). This structure is now (August, 1954) under contract, and attempts to unwater the excavation have been made. The contractor elected to use well points set in holes drilled in the rock in his initial unwatering plan. An area approximately 180 ft by 130 ft was ringed with well points. A total of 483 well points on two 12-in.-diameter headers were installed, and eleven pumps of 10-in. and 12-in. impeller diameters were used on the headers. In addition to the well-point pumps, two 24-in. propeller-type pumps and five 10-in. and 12-in. centrifugal pumps were used, pumping directly from the excavated area. The total pump capacity was estimated to be 60,000 gal per min. With this capacity, the water was drawn down about 9 ft of the 25 ft required for the construction of the station. The use of well points has been abandoned, and the contractor plans to divide the area into small units to be unwatered and to use steel sheet-pile cofferdams and tremie-concrete seals.

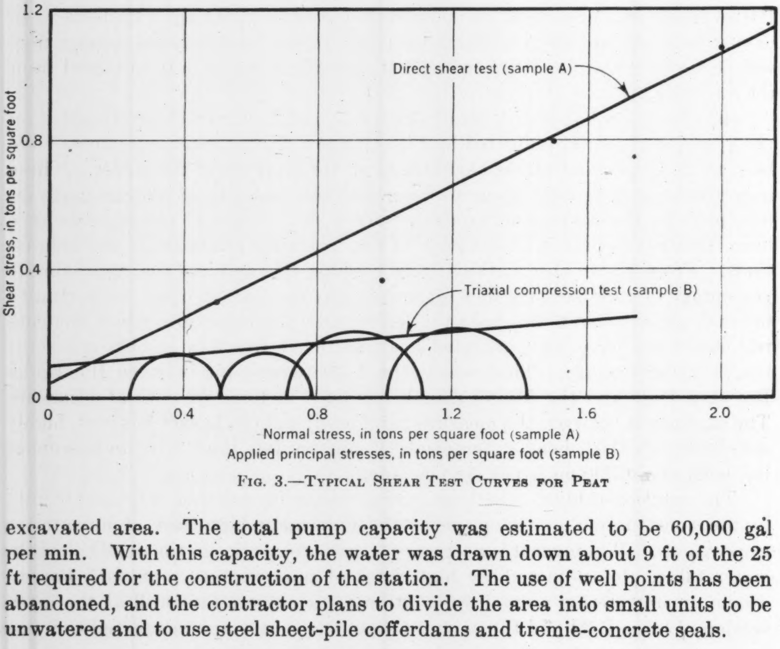

FIG. 3.—TYPICAL SHEAR TEST CURVES FOR PEAT

PEAT

Methods of embankment construction in the Everglades are dictated by the physical conditions under which the levees must be built. Because of the presence of a layer of soft peat at the surface throughout almost the entire area, conventional methods using hauled-in fill and layer-compaction are not practicable. Embankment materials are cast-in-place from continuous adjacent borrow pits by draglines supported on mats. In areas of deep peat, mats alone are not sufficient to support the equipment, and it is necessary to place a layer of sand or rock excavated from the borrow pit ahead of the machines for a working base. On several occasions, borrow-pit banks have yielded under the weight of the draglines, causing the machines to slide into the borrow pit.

In designing levees on peat foundations, the first step is to determine the shearing strength of the peat. For almost all soils, sufficiently accurate values of shearing strength can be obtained from the results of direct shear tests. Peat is not a soil, however, as the following characteristics demonstrate. Typical qualities of Everglades peat are: (1) Dry unit weight, from 5 lb per cu ft to 10 lb per cu ft; (2) natural water content, usually more than 500% and often more than 1,000%; and (3) loss on ignition, more than 90%.

A material that is over 90% plant fiber can hardly be called a soil. Direct shear tests on peat give completely erroneous results. The predetermined failure plane cuts across the fibers, and the apparent angle of internal friction is usually between 20° and 25°. If the same material is tested in a confined compression apparatus in which failure can occur on any plane, low shearing strength is observed. Angles of internal friction from triaxial tests are usually less than 5°. In Fig. 3 is shown the comparison between the results obtained by the two test methods on similar samples. Cohesion of about 0.1 ton per sq ft is the only shearing strength considered in design. The following data apply to Fig. 3:

Item	Sample A	Sample B
Dry unit weight, in pounds per cubic foot	10	8
Water content, in percentage	462	655
Loss on ignition, in percentage	90.7	91.3
Angle of internal friction, ϕ, in degrees	27	5
Cohesion, c, in tons per square foot	0.04	0.10

Comparatively steep embankment slopes (1 on 2 and 1 on 3) have been adopted for almost all levees constructed on the project to date. In the areas of deepest peat, a few small slides have occurred during construction, but after the failed areas were repaired, the completed levees gave no further trouble. The embankment materials have been excavated under water and cast into the levees. These materials were completely saturated and provided a greater load on the foundation than will ever occur after the construction period.

In the design of a levee, now (August, 1954) under construction, in which the embankment is to be founded on deep peat having little strength, a mat of rock, sand, and marl is being provided, extending approximately 30 ft outside the toes of the embankment; it will act somewhat as a "spread footing" for the levee. Stripping of the foundation was limited to the cutting and removal of trees and large brush. Experience has taught that the strength imparted by the surface root mat is of great value in supporting superimposed loads. Tractors equipped with special tracks can traverse the peat as long as the root mat is not ruptured, but they bog down as soon as that support is destroyed. Some idea of the difficulties anticipated in building this levee may be gained from the fact that construction by draglines was considered impracticable because it was thought to be impossible to operate such equipment in the area. The embankment is being placed by use of a hydraulic dredge, and final shaping will be done by light drag lines and bulldozers after sufficient fill has been placed to support their weight. The adequacy of the design has not been tested because embankment construction is not yet complete.

From the inception of the project, it was recognized that large settlements of embankments founded on peat were inevitable. Early estimates, based both on experience in the construction of levees around Lake Okeechobee in Florida, and on incomplete consolidation test data, were that settlement would be equal to 50% of the peat thickness and that half the settlement would occur during construction. Because the heights of the first levees built varied within the narrow range of 10 ft to 15 ft, no correction was made for the load variation thus produced. For the first levees built in the project, construction grades were placed above final design grade by an additional height equal to 25% of the peat thickness, in accordance with the method used for estimating the settlement. Profiles of those levees, surveyed a year after completion, show no significant change in elevation since the completion of the embankments. Apparently, nearly all the settlement occurred during construction.

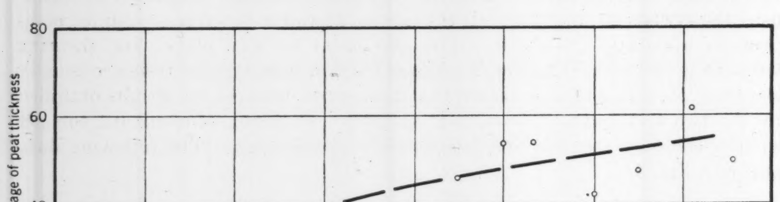

Fig. 4.—Relation Between Settlement of Peat and Embankment Height

Settlement plates were installed at many points along the levee alinements immediately before the fill was placed. At each plate, the thickness of the peat was determined by auger borings. Elevations of the plates have been checked several times since the completion of the embankments. Although individual settlements differ considerably, the average of all the readings approximates the original estimate of 50% of the peat thickness. There has been little change in the elevations of the plates since the first reading, confirming the evidence furnished by the post-construction profiles that nearly 100% of the settlement occurred during construction. Although the average settlement was 50% of the peat thickness, the settlement was not independent of the levee height. Fig. 4 is a curve showing the observed variation of the settlement with the variation of the embankment height.

Use of consolidation tests for predicting settlement has been only partly successful. Although the depth of settlement can be determined with fair accuracy, the predicted length of time required for the settlement is not even approximately correct. On samples for which the consolidation tests indicate from 15 years to 20 years for a settlement of 90%, the actual settlement occurs in a few days or weeks. The reason for this discrepancy has not been investigated (as of 1954).

INTERBEDDED ROCK AND SAND FOUNDATIONS

It will be necessary (1954) to build several fairly large structures on foundations of rock and sand. Some of those structures are now under construction. In some cases, the structures will be founded on beds of rock both overlaid and underlaid by sand, and in others on formations composed of alternating beds of consolidated and unconsolidated materials. To those not familiar with the geology of the coastal plain areas of the unglaciated parts of the United States, the occurrence of rock interbedded with—and underlaid by—unconsolidated materials may seem strange, but such conditions are found throughout a large part of the Florida peninsula. Whenever possible, structures such as pumping stations and spillways will be founded on rock. Even if the rock layer is relatively thin, it is believed that it will have somewhat the effect of a large foundation raft, which will minimize differential settlement. Cutting through the rock bed on which the structure rests will be avoided, if possible. In some cases, drains and spillway apron sills may require excavation through the rock. Thin rock beds with essentially vertical solution channels are considered analogous to concrete slabs with weep holes. Continuous toe drains cut through the rock and into the sand will be provided at the downstream end of structures on such foundations to relieve the uplift pressure in the sand beds and prevent subsurface erosion of the sand. The drains will be filled with graded filter material and will contain perforated collector pipes that will be vented to tailwater through riser pipes.

Some difficulty is experienced in unwatering foundations of interbedded rock and sand. To date (1954) both open-sump pumping and well-point systems have been used. Pumping from sumps, which is common practice in rock foundations, can be done safely only if special precautions are observed. Concentration of flow into sumps would almost certainly cause movement of sand and consequent damage to the foundation. Such movement is prevented by filling the pump sumps with properly graded filter material and setting the pump intakes in perforated pipes. Continuous trenches through the rock bed on which a structure is to be founded cannot be tolerated, and in many cases a large number of sumps would be required because of the lack of interconnection. All in all, it is believed that heterogeneous foundations of the type found on this project can best be unwatered by the use of well-point systems. Such systems, when properly installed and operated, tend to stabilize the fine sands rather than render them "quick" and result in completed excavations having firm floors and side slopes.

Great care must be taken in excavating for the foundations of structures to be placed on thin rock layers. In a massive rock foundation, overexcavation will simply increase costs, but in the case of a foundation layer only a few feet thick, overexcavation can have disastrous consequences. It is possible to destroy the foundation completely by excessive blasting. Blasting to grade one foot or two feet below the surface of a thin rock layer is impracticable and should not be attempted. Rock removal by rooter, rock plow, air spade, or some other easily controllable method is required.

The Effect on Design and Construction

The unusual conditions described present problems in design and construction, some of which have no ready solution. Large seepage losses and unusually great settlements of embankments are difficulties for which allowance can be made; however, they cannot be prevented without spending an amount of money disproportionate to the benefits gained. High unwatering costs are inevitable and must be considered in estimating the cost of proposed structures.

All structures are designed for 100% uplift on the full base area. Wherever any possibility of piping or flotation of foundation sand exists, drainage facilities are provided to relieve the uplift pressures. Structures proposed for the project (1954) are relatively small, and foundation loads rarely exceed 2 tons per sq ft or 3 tons per sq ft. The rocks and sands on which the structures are to be founded usually have more than adequate bearing capacities for the loads. Pile foundations have not been required for any of the structures designed to date (1954).

Careful inspection of foundation excavation work is required to prevent damage to foundations by improper unwatering or excavation procedures. Wherever other considerations permit, foundation grades are raised to the highest possible level to obtain the maximum thickness of rock under the structures and to reduce concrete quantities.

Summary

Highly porous rock, thick beds of soft peat, and foundations of interbedded rock and sand complicate the design and construction of levees and structures for the Central and Southern Florida Project. The design and construction of engineering works adequate for their intended purpose can be accomplished in spite of the unfavorable foundation conditions, but only by recognizing the foundation problems and by making the necessary allowances in design.

AMERICAN SOCIETY OF CIVIL ENGINEERS
Founded November 5, 1852
TRANSACTIONS

Paper No. 2729

WELDED STRUCTURES

A SYMPOSIUM

PAGE

Steel Requirements
By Simon A. Greenberg 104

Design and Research
By La Motte Grover, M. ASCE 112

Fabrication and Construction
By C. L. Kreidler 147

STEEL REQUIREMENTS

By Simon A. Greenberg[1]

Synopsis

The properties for steel that is to be welded must be more carefully specified than those for steel that is to be fabricated by other joining methods. The type of construction—bridges or buildings—also affects these requirements. Both the chemical composition and the mechanical properties that are necessary to make a steel readily and efficiently weldable are reviewed. The establishment of special conditions of manufacture and physical attributes necessarily adds to the unit cost of the steel, but it is shown that the decrease in the weight of the structure more than balances this increased cost for each ton of steel. Following the acceptance of welding as an economically sound process, it is expected that welded structures will become widely used.

Introduction

There are thirty-seven different welding processes in use at the present time (1953).[2] Manual shielded metal-arc welding is most commonly used for structural fabrication. Oxy-acetylene welding and submerged arc welding are used to a lesser extent; spot welding is used in the fabrication of light-gage structural members.

Structural joints made by welding differ from joints made by other methods in two principal respects:

1. There is a difference in stress distribution, as a result of the continuous, integral nature of the mass of weld metal across the joint (as distinguished from a row of rivets, for example).
2. The heating of the base metal incident to welding, has a metallurgical effect on the metal's properties, and this effect must be considered and controlled.

When using joining methods other than welding, designers of bridges and buildings have disregarded the metallurgical properties of steel. These designers know that A 7 steel,[3] for example, has certain specified mechanical properties from which safe allowable stresses for various loading conditions can be established. However, these same engineers, when designing a welded structure, are impatient with the necessity for a better understanding of what makes a particular type of steel behave as it does. Curiously enough, these engineers when designing a concrete structure become greatly concerned with water-cement ratios, consistencies, and setting properties.

Note.—Presented at the Centennial Convocation, Chicago, Ill., September, 1952. Published, essentially as printed here, in November, 1953, as *Proceedings-Separate No. 344*. Positions and titles given are those in effect when the paper was received for publication.

[1] Technical Secy., Am. Welding Soc., New York, N. Y.

[2] "Standard Master Chart of Welding Processes and Process Charts," Am. Welding Soc., 1949.

[3] "Steel for Bridges and Buildings," Pt. 1, Ferrous Metals, A7-52T, A.S.T.M., 1952.

METALLURGICAL CONSIDERATIONS

In addition to its mechanical properties, the facts which should be known about a steel for its proper use in welded construction include:

1. The chemistry of the steel—principally the carbon and manganese contents and the kind and amount of alloying elements present, if any. The usual limits of phosphorus and sulfur are acceptable.
2. How the steel is made—whether it is rimmed, semi-killed, or fully-killed, and whether it is made to fine-grain practice.
3. The thicknesses of the plates and shapes to be used. Where a joint includes different thicknesses of steel, the greatest thickness is significant.

Chemistry of the Steel.—The chemical analysis of a steel affects its tensile strength, yield point, ductility, and the ratio of these mechanical properties to each other. Carbon, and to a lesser extent, manganese affect the mechanical properties; carbon and manganese are also hardening elements. Alloying elements may impart strength, "hardenability," corrosion resistance, machinability, or some other specific property to the steel.

Method of Manufacture.—How a steel is made has an influence on the types of loading to which it can be subjected in a structure. A fully-killed steel, made to fine-grain practice, will (mechanical properties being the same) have the best resistance to impact and dynamic loadings. The "transition temperature" of the fully-killed steel (the temperature at which it changes from being ductile to brittle) will be lower and, hence, the steel will better resist loadings under severe changes in temperature and will behave better at low temperatures.

Steel Thickness.—The thickness of a steel section will have a bearing on the heat effect of welding. When a weld is made between two pieces of steel, some of the heat flows into the base metal away from the joint. This flow produces a heat gradient from the edge of the steel at the joint (where the temperature is greatest) to some point away from the joint (where the base metal is at the ambient temperature). The heating and subsequent cooling produced during welding alter, to some extent, the metallurgical properties of that part of the steel which has undergone this cycle. The distance from the joint that this heat effect extends into the base metal is known as the "heat-affected zone."

When a thick piece of steel is heated during welding, the heat-affected zone is narrower than for a thin section—that is, a given heat input is absorbed by the larger mass of the thick section in a shorter distance from the point of welding than the same input would be absorbed in the lesser mass of a thin section. A narrow heat-affected zone provides a less gradual transition in the metallurgical structure of the metal. Among other things, this narrow zone results in a tendency toward greater hardening and higher shrinkage deformations.

STEEL FOR USE IN STRUCTURES

Fortunately, most of the steels used for bridge and building construction are readily welded, with a minimum of metallurgical effect on their load-carrying properties. Because the practical aspects of the previously cited considerations are different for bridges and buildings, it is desirable to separate these two types of structures.

Steel for Buildings.—A single code[4] forms the basis for the welding requirements in almost every city of significant size in the United States. This code provides for the use of A 7 steel,[5] which is the type of steel normally used in building construction. The specification for this steel is based solely on mechanical properties, with special limitations on the sulfur and phosphorus contents. This code further provides[6] that

> "When welds are being made in parts where thicknesses of more than 1½ inches are involved, the base material adjacent to the welding shall in no case be at a temperature of less than 70°F."

The provision for the use of A 7 steel is based on this steel's general suitability for buildings or other structures subjected, essentially, to static loading. The additional requirement for preheat is intended to account for the effect of thickness plus the fact that the carbon and manganese contents of A 7 steel usually increase with increasing thickness.

Almost all the welded buildings erected prior to 1953 were made of A 7 steel, and no difficulty has been encountered in service. Although the thickness limitation of 1½ in. probably accounts for 90% of this construction, some of the sections have been 2 in. thick or greater.

At the present time (1953) the American Welding Society (AWS) is reviewing the base metal requirements of the code.[4] There are two schools of thought to be reconciled—one advocates the use of a steel (other than A 7) with a specified chemistry when thicknesses greater than 1 in. are involved, and the other group favors the exclusive use of A 7 steel with special, specific workmanship requirements enforced for thicknesses that exceed 1 in. Both approaches are valid and arrive at the same result. From a practical standpoint the question is resolved on the basis of whether it is more economical to pay an extra charge for a steel or to spend additional funds for special workmanship requirements. The decision rests with the fabricator and engineer and depends on the particular conditions.

Pending the adoption of revised provisions in the AWS building code, the following recommendations are advanced:

1. The A 7 steel should be used for plates and shapes in all thicknesses up to and including 1½ in. A mill report should be obtained for each heat of steel. If this ladle analysis shows the percentage of carbon plus ⅙ of the percentage of manganese (the "carbon equivalent") to be greater than 0.43% (equal to about 0.31% C and 0.75% Mn), particularly for steel thicknesses which exceed 1 in., some special requirement should be imposed—as recommended for thicker sections.

2. The A 7 steel should be used for plates and shapes that are thicker than 1½ in. but thinner than 2 in. If the mill report shows that the carbon equivalent is in excess of 0.43%, either (*a*) low-hydrogen electrodes[7] should be used, or

---

[4] "Standard Code for Arc and Gas Welding in Building Construction," Am. Welding Soc., 1946.

[5] *Ibid.*, p. 5, Article 106.

[6] *Ibid.*, p. 17, Article 403(h).

[7] "Specifications for Mild Steel Electrodes," Am. Welding Soc. and A.S.T.M., 1948.

(*b*) a preheat of between 100°F and 150°F should be used. Another alternative would be to use a steel, other than A 7, having a controlled chemistry.

3. For plates and shapes thicker than 2 in. and thinner than 3 in., A 7 steel may be used. If the mill report does not exceed the chemistry given in item 1, then low-hydrogen electrodes[7] or a preheat of from 100°F to 150°F, or a combination of both should be used. If the carbon equivalent is in excess of 0.43%, a preheat of between 250°F and 300°F, or low-hydrogen electrodes and a preheat of from 100°F to 150°F or higher, should be used according to the analysis and thickness of the steel. As an alternative, a steel other than the A 7 can be used. This steel should have a controlled chemistry and should be used with low-hydrogen electrodes or with low preheat temperatures according to the analysis and thickness.

4. For plates and shapes which are more than 3 in. thick (not usual in building construction) special provisions should be established—based on items 1 to 3.

The welding technique that is used should prevent weld cracking during the process. To avoid cracking, one can use many narrow string beads instead of fewer and wider weave beads for butt welds, or, perhaps, multiple passes for fillet welds.

The compilation and checking of mill reports are helpful to the fabricator. At some steel mills the desirable chemical limitations for A 7 steel will be exceeded with only rare exception; at other mills carbon and manganese contents in excess of these values will be usual. Knowing the type of steel to expect from a mill will make it possible to determine the best alternative, which can then be followed as a routine matter. Where only an occasional piece of steel exceeds the desirable chemical limitations, low-hydrogen electrodes or preheating can be used without any appreciable effect on the cost. Where higher carbon and manganese contents are normal and usual, preheating, low-hydrogen electrodes, or steel with a guaranteed chemistry (all at an extra cost) must be used regularly.

The recommendations for steel to be used in building construction are based on normal conditions. Stricter requirements should be imposed in designing for special conditions—such as an airplane hangar located in the middle of the plains of northern Montana, exposed to the hot sun and bitter cold weather, both possibly within a single day.

These recommendations may seem to be conservative and needlessly severe. However, they are valid as a general over-all basis from which engineers and fabricators can depart in either direction as their experience indicates.

Steel for Bridges.—In several respects the problems involved in bridge construction and design differ from the problems encountered in building fabrication and design. Bridge loadings are dynamic and produce repetitive stresses in one or more of the members. These stresses may vary from zero to some maximum value, or they may revert from full or partial tension to full or partial compression. In addition to these fatigue stresses, high impact stresses may also be imposed on a bridge structure.

More particularly from a welding standpoint, the usual bridge structure is an open framework which is exposed to all changes in weather, and its principal members are often of greater thickness than those that are usually encountered in building construction.

The AWS has studied steels and stresses for highway and railway bridges at great length. The pattern which has been evolved for allowable stresses for various numbers of repetitions of loading can be applied to all bridge joint designs, regardless of the joining method. In an AWS publication[8] are listed the base metal requirements for various conditions as well as the allowable stresses.

TABLE 1.—REQUIREMENTS FOR

Items	RECOMMENDED SPECIFICATIONS				
	(a) PLATES			(b) STRUCTURAL SHAPES	
	Thickness of Thinnest Plate			Thickness of Thickest Element[a]	
	Up to and including ½ in.	Greater than ½ in. Up to and including 1 in.	Greater than 1 in. Up to and including 4 in.	Up to and including 1 in.	Greater than 1 in.
Chemical Constituents:					
Carbon[b]	0.27	0.27	0.27	0.29	0.29
Manganese[c]	...	0.50 to 0.90	0.75 to 1.15	...	0.50 to 0.90
Silicon[c]	...	...	0.15 to 0.30	...	...
Phosphorous[b]	0.040	0.040	0.040	0.040	0.040
Sulfur[b]	0.050	0.050	0.050	0.050	0.050
Mechanical Properties:					
Tensile strength[d]	60 to 75			60 to 72	
Yield point[e]	33			½ Tensile strength or 33	
Elongation in 2 in.[b]	22			21	
Elongation in 8 in.[f]	1,500 ÷ Tensile strength			22	

[a] Web or flange thickness, whichever is greater. [b] Maximum percentage. [c] Percentage. [d] In kips per

In the United States, the history of welded bridges, like the history of buildings, indicates that A 7 steel has been used satisfactorily and without any difficulty in service. The record shows that an ever-increasing number of highway bridges (mostly girder spans) and a lesser number of new railway bridges have been built and that many existing railway bridges have been strengthened by welding to carry the increasing loads of improved locomotives and cars.

Despite this favorable record of A 7 steel, the AWS has studied possible revisions to the steel requirements with the idea of specifying a steel with a controlled chemistry for most, if not all, thicknesses. It is felt that the specifications should take into account the greater use of welding for bridge construction and should include more extreme cases of thickness and weather conditions.

In February, 1952, steel mill representatives were consulted by the AWS in an effort to arrive at practical specifications for the chemical requirements and mechanical properties of a weldable bridge steel. At this time it was agreed to extend the specifications to cover thicknesses up to and including 4 in. for structural members and not more than 8 in. for such incidental parts as shoes, saddles, and the like. The specification requirements arrived at as a result of the conference are shown in Table 1(*a*).

---

[8] "Standard Specifications for Welded Highway and Railway Bridges: Design Construction and Repair," Am. Welding Soc., 4th Ed., 1947.

The analyses shown in Table 1 are all ladle analyses, which means that the carbon may possibly be as much as 0.04% higher in the delivered steel (check analysis). The silicon content specified for steel which is greater than 1 in. thick is to assure a fully-killed steel. Although it would be preferable to use a fine-grained steel, this was not found to be practical. A fully-killed steel is desirable because of its lower transition temperature and its greater resistance to impact at lower temperatures. The proposed mechanical properties for these plates in all thicknesses are also shown in Table 1(*a*).

WELDABLE BRIDGE STEEL

California State Highway Department Specifications					Items
(*c*) PLATES			(*d*) STRUCTURAL SHAPES		
Thickness of Thinnest Plate			Thickness of Thickest Element[a]		
Up to and including ½ in.	Greater than ½ in. Up to and including 1 in.	Greater than 1 in.	Up to and including 1 in.	Greater than 1 in.	
			A 7 Steel		Chemical Constituents:
...	0.25	0.25		0.18	Carbon[b]
...	0.50 to 0.90	1.15 maximum		1.30 maximum	Manganese[c]
...	...	0.15 to 0.30		0.15 to 0.30	Silicon[c]
0.040	0.040	0.040		...	Phosphorous[b]
0.050	0.050	0.050		...	Sulfur[b]
					Mechanical Properties:
58 to 75				92 to 85	Tensile strength[d]
32				50 to 42	Yield point[e]
23[g]				20	Elongation in 2 in.[f]
21				20	Elongation in 8 in.[f]

square inch. [e] Maximum value, in kips per square inch. [f] Minimum percentage. [g] More than ½ in. only.

For structural shapes having various nominal mean thicknesses, in either the web or flange, whichever is the thicker, the chemical constituents should be as given in Table 1(*b*). In all cases the mechanical properties of the structural shapes remain the same as for A 7 steel (Table 1(*b*)).

The California State Highway Department has specified[9] the chemical requirements shown in Table 1(*c*) for plate steel used in the viaduct of the Division Street Interchange in San Francisco, Calif. These chemical-constituent values are determined from a ladle analysis. The silicon is specified in the thicker members to assure a fully-killed steel. The mechanical properties for this plate steel, in all thicknesses, are also shown in Table 1(*c*).

For structural shapes not exceeding 1 in. in thickness, A 7 steel was specified by the California State Highway Department. For shapes of greater thicknesses, steel conforming to MIL-S-16113 (ships) grade HT steel was specified. This steel, in addition to those constituents shown in Table 1(*d*), contains small amounts of copper, nickel, vanadium, titanium, chromium, and molybdenum. The mechanical properties of this steel are given in Table 1(*d*). The tensile strengths and yield points decrease, as shown, as the thicknesses of the members increase.

---

[9] "Weldability of Structural Steel," by E. L. Erickson, *The Welding Journal*, December, 1953, pp. 1155–1159.

On the basis of the requirements for welding, the specifications of the California State Highway Department are preferred to the recommended specifications. However, the improvement in chemistry is obtained by a reduction of the yield point from 33 kips per sq in. to 32 kips per sq in. and a reduction of 2 kips per sq in. in the minimum tensile strength—from 60 kips per sq in. to 58 kips per sq in. This decrease causes a corresponding increase in the elongation—from 22% to 23% (for plates, for example).

The AWS has encountered reluctance on the part of bridge designers to accept these slight reductions in mechanical properties. This reluctance should not exist because the final designs in both cases would probably produce the same section in all but a few cases.

TABLE 2.—COST INCREASE, IN DOLLARS PER TON, AS A RESULT OF USING THE RECOMMENDATIONS OF TABLE 1 RATHER THAN A 7 STEEL FOR PLATES

Thickness	Steel from Table 1(*a*)	Steel from Table 1(*c*)
Up to and including ½ in.	1.00	none
Greater than ½ in. Up to and including 1 in.	3.00	3.00
Greater than 1 in. Up to and including 1½ in.	15.00	15.00
Greater than 1½ in.	5.00	5.00

It is of interest to compare the costs of the steel from each of the two specifications with A 7 steel of the same thickness (as of 1953). In Table 2 is shown the increase in cost for plate material in dollars per ton over A 7 steel of the same thickness.

The increased costs shown in Table 2 serve as a guide in deciding whether, in any given case, it will be more practical and economical to specify a better steel or to use A 7 steel in combination with preheating, low-hydrogen electrodes, and special welding procedures and techniques.

Because the workmanship requirements of the AWS specifications have not yet been modified (as of 1953), it is recommended—with a caution that these suggestions are general and should be made more rigid where special circumstances (particularly low-temperature service) are involved—that

1. For plates and shapes up to and including those 1 in. thick, A 7 steel should be used. If the mill report indicates a carbon equivalent greater than 0.40%, mild preheating or low-hydrogen electrodes should be used.

2. For plates and shapes thicker than 1 in. and up to and including 2 in., the steel recommended in Table 1(*c*) and Table 1(*d*) should be used without further precautions. Alternatively the steel recommended in Table 1(*a*) and Table 1(*b*) could be used with low-hydrogen electrodes or a 100°F preheat. The

A 7 steel can be used with a 200°F preheat or a 100°F preheat and low-hydrogen electrodes. These suggestions relative to A 7 steel should be modified according to the chemical analysis shown in the mill report and the specific thickness involved.

3. For plates and shapes thicker than 2 in., the steel prescribed in Table 1(*c*) and Table 1(*d*) can be used with a preheat of 100°F (or more) or low-hydrogen electrodes. These supplementary procedures can be used separately or in combination, according to the thicknesses involved. Alternatively the steel recommended in Table 1(*a*) and Table 1(*b*) can be used with a 200°F (or higher) preheat. This steel can be used with a lower preheat and low-hydrogen electrodes, dependent on the thickness. In general, it is desirable not to use the A 7 steel.

Where welding is done at low temperatures all work should be preheated so that it is at least warm to the touch for at least 3 in. on either side of the joint.

ECONOMICS OF WELDING

Welding, when properly done, may be the most economical method of making structural joints. In the last analysis of any fabrication problem, the economics will determine what joining method will be used.

Effective and economical use of welding for structural purposes does not depend solely on the selection of the proper steel. The design must be based on the use of welding, and the fabrication operations must be planned to minimize the steps involved in the shop and in the field. Even with an increase in the unit cost of the steel, the total cost may be less because less steel is required, or because the total fabricating cost is reduced.

For example, Robert E. Robertson, Jr., M. ASCE, cites a case in which 20% of the weight of a truss was saved by eliminating gusset plates and other connection details and by welding the joints.[10] Mr. Robertson also gives an example of a railroad bridge with a 120-ft span in which 30 tons of steel were saved by using 10-ft-deep, through, welded girders. The total saving was estimated to be $12,000.

John F. Willis, M. ASCE, has reported on the complete change-over to welded construction by the Connecticut State Highway Department. In one case[11] Mr. Willis described a deck girder bridge having a 165-ft center span and two 80-ft cantilever end spans, in which 32% of the weight and $6,600 were saved by welding the joints.

A fourteen-story building in Richmond, Va., was welded at a saving of $60,000 in comparison to a similar riveted structure.

CONCLUSION

The number of welded structures is increasing daily. As more fabricators acquire welding equipment and learn to use it more effectively and as more engineers become better acquainted with welding and the advantages it offers—then will welded structures become more widely accepted.

---

[10] "Economical Design of Welded Buildings," by Robert E. Robertson, Jr., *The Welding Journal*, December, 1949, pp. 1152–1161.

[11] "Welded Plate Girder Bridge Separates Connecticut Highways," by John F. Willis, *ibid.* April, 1944, pp. 315–317.

DESIGN AND RESEARCH

By La Motte Grover,[1] M. ASCE

With Discussion by Messrs. Jack R. Benjamin, George W. Lamb, F. J. Tamanini, Norman B. Jones, and La Motte Grover

---

Synopsis

During World War II welded steel construction received an impetus. Advances in this type of construction resulted from the extensive use of welding in the building of ships. These very ships, however, were also a source of concern as to the proper materials, details of design, and construction procedures to be used in welding large structures. The welding experience that was gained during this shipbuilding program provides an important part of the basis for the ever-increasing use of structural welding.

As in all other types of construction, welded structures have been subjected to innumerable tests—tests which have provided further bases for improving both the techniques of welding and the method of designing these structures.

A few welded bridges in Belgium and Germany have failed when subjected to a severe drop in temperature during cold weather. Their failures, however, can be attributed to a deficiency in the steel material. In the case of the one failure in America (Canada) forces induced by nonthermal growth of the concrete floor are believed to be a major contributing factor.

Introduction

A number of questions have been asked repeatedly by designers since the introduction of welded steel construction in the early 1920's. They are questions that naturally arise in the mind of one who contemplates the use of a type of structure or a method of construction with which he is unfamiliar.

The questions that are most frequently asked are as follows: How can one be sure that the welded joints will be adequate and that the structure will be safe? Must there be special requirements in the specifications for the structural-steel material to assure its weldability? How do welded joints and members behave under repeated stress, impact, and vibration? Do residual welding stresses reduce the strength of a welded joint or member? These questions have been prompted, to some extent, by difficulties encountered in a few of the preliminary welded-bridge projects in Europe and in the large welded ships constructed during World War II.

Although experience with welding has provided satisfactory answers to many of these questions, extensive research was needed to answer the others.

Note.—Presented at the Centennial Convocation, Chicago, Ill., September, 1952. Published, essentially as printed here, in November, 1953, as *Proceedings-Separate No. 348*. Positions and titles given are those in effect when the paper was received for publication.

[1] Welding Engr., Air Reduction Co., New York, N. Y., and Chairman, Structural Research Committee of the Welding Research Council, Engineering Foundation.

In welding, as in other fields, research is never-ending. This research contributes to an understanding of the behavior and the design of welded structures.

SHIP FRACTURES

Both experience and research indicate that the problems concerning ship fractures are quite different from those normally encountered by structural engineers. However, not only welded ships have failed; riveted ships, also, have developed fractures from time to time, and some of them have split in two.

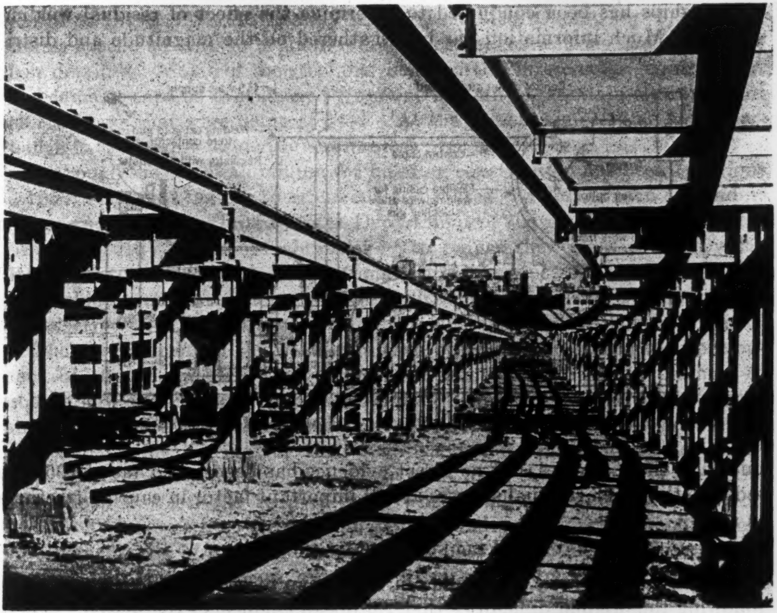

FIG. 1.—DIVISION STREET INTERCHANGE OF THE BAY SHORE FREEWAY IN SAN FRANCISCO, CALIF.

The wide expanses of relatively thick plating in the hull of a large ocean-going ship present a special problem of stress distribution. Research and study of the ship-fracture problem have been concentrated mainly on the steel material, but improvements have also been made in the design details. These improvements have eliminated serious notch effects, or geometrical stress raisers, and details that did not provide suitable access for the making of sound welds.

The satisfactory record of the ships built during the latter part of World War II, as compared with those built earlier, is most significant. In the later-built ships, hatch corners were rounded to reduce the notch effect. These corners and the hatch-side girders were arranged so as to eliminate the details that made sound welding difficult or impossible. Such details occurred in some parts of the earlier-built ships. Similar, important improvements were made in other design details to accomplish the same objectives. Some of the improvement in performance can doubtless be ascribed to better workmanship. At the beginning of the shipbuilding program many of the workmen had virtually no mechanical or construction experience or training. In some of the later ships, built during the period from 1945 to 1953, improvements in details of design and in workmanship were supplemented by the use of a higher grade of steel for the hull. No major fractures have occurred in these newer ships.

An extensive program of research on large-scale specimens and on large welded ships has been conducted to determine the effect of residual welding stresses. Much information has been gathered on the magnitude and distribution of these stresses, but no direct evidence has been found (as of 1953) to indicate that such residual stresses are an important factor in causing fractures in ships.[2]

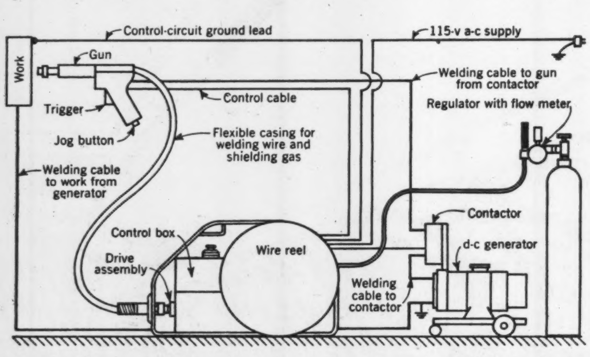
Control-circuit ground lead
115-v a-c supply
Work
Gun
Welding cable to gun from contactor
Control cable
Regulator with flow meter
Trigger
Jog button
Flexible casing for welding wire and shielding gas
Welding cable to work from generator
Contactor
Control box
d-c generator
Drive assembly
Wire reel
Welding cable to contactor

FIG. 2.—EQUIPMENT USED IN THE INERT-GAS METAL-ARC WELDING PROCESS

WELDED BRIDGES IN EUROPE

Improvements have been made in the design of welded bridges in Europe following the original difficulties that European engineers experienced. These difficulties seem to be attributable principally to the grade of steel that was in use at that time (1938)—a basic Bessemer steel (with bad segregations) which was subject to serious strain aging. This steel differs greatly from the structural-steel material that is customarily used in bridges and buildings in the United States.

Some rolled beams made from this Thomas steel (reclaimed war-surplus material), with butt-welded splices, were tested in France following World War II. The beams failed with a brittle fracture under a static load at a stress of only 21,300 lb per sq in. In contrast, to fracture some of the welded beams made from A 7 steel[3] in a research program at Columbia University in New

---

[2] "The Design and Methods of Construction of Welded Steel Merchant Vessels, July 15, 1946," U. S. Govt. Printing Office, Washington, D. C., 1947.

[3] "Steel for Bridges and Buildings," Pt. 1 Ferrous Metals, A7-52T, A.S.T.M., 1952.

York, N. Y., a combination of low temperature and very severe impact (roughly equivalent to a static-load stress of from 70,000 lb per sq in. to 90,000 lb per sq in.) was required. The impact was much more severe than that experienced under actual service conditions for a railway or highway bridge.

PROCESSES USED FOR STRUCTURAL WELDING

Manual, shielded, metal-arc welding is the most extensively used process for structural work. In structural welding, for the most part, the comparatively short welding runs are not suited to fully-automatic welding.

For structures with complicated framing, such as the Division Street Interchange of the Bay Shore Freeway in San Francisco, Calif. (Fig. 1), welding offers a special advantage in simplifying structural connections and facilitating their detailing. Some of the steel pier bents in this interchange required that the beams or caps be cantilevered from one column to maintain clearances for the roadways that were being crossed. At the present time (1953) this interchange is the largest welded-bridge project ever undertaken.

Although the use of aluminum for building construction has been (previous to 1953) restricted mainly to ornamental purposes and details such as window frames and sash, the United States Department of the Navy makes extensive use of the 61ST-6 alloy of aluminum[4,5] to reduce the weight caused by the alterations to its ships. A semi-automatic welding process is used—the inert-gas-shielded metal-arc welding process—with a continuously fed, consumable wire electrode. The apparatus used in this welding process is shown in Fig. 2.

The development of this semi-automatic welding process and the development of the newer high-strength weldable alloys of aluminum promise to provide new uses for structural aluminum. The older high-strength, aluminum-magnesium-silicon alloys, such as 61ST, depend on a solution heat treatment and artificial aging for their high yield and tensile strengths. Consequently, in the zone affected by the heat of welding, the tensile strength of the older alloys is drastically reduced, even when using the equipment shown in Fig. 2. The newer high-strength alloys of aluminum contain comparatively high percentages of magnesium as a principal constituent. These alloys develop high joint efficiencies, especially when welded by the inert-gas metal-arc welding process. This process, in both the semi-automatic and fully-automatic forms, can also be used to join other metals such as bronzes and stainless steel. The process also has been adopted for the special-application welding of mild and structural grades of steel.

EXPERIENCE AND RESEARCH AS A BACKGROUND FOR DESIGN

All welding experience is important as a basis for using structural welding in railway and highway bridges and buildings. A large part of this experience was gained in the shipbuilding program of World War II.

Outstanding programs of welded-bridge construction—such as those in Kansas, in Connecticut, and in the Province of Quebec in Canada—have been especially valuable proving grounds. In these particular programs excellent service of welded structures for periods that exceed seventeen years has been

---

[4] "The Aluminum Data Book," Reynolds Metal Co., Louisville, Ky., 1950.

[5] "Alcoa Aluminum and Its Alloys," Aluminum Co. of America, Pittsburgh, Pa., 1950.

recorded. The states of New York and California have also initiated programs of welded-bridge construction.

Gilbert D. Fish, M. ASCE, contributed greatly to the advancement of welded building construction. For the rapid advancements and improvements in the economical design of large, welded, rigid-frame office buildings (especially in the southwestern part of the United States) much credit must be given to Boyd S. Meyer.[6]

However, this rapid progress would not have been possible without the benefit of practical research and testing of large-scale welded specimens. This testing and research were part of the programs of the Structural Steel Committee of the Welding Research Council (WRC) and the Fatigue Testing Committee, WRC, at the University of Illinois (Urbana).[7,8,9]

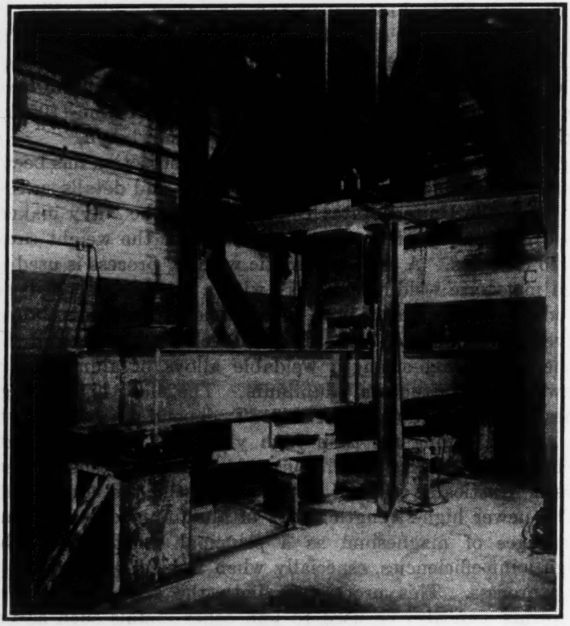

FIG. 3.—TEST ARRANGEMENT FOR THE IMPACT TESTING OF A WELDED BEAM

The specifications and codes of the American Welding Society (AWS) for bridge and building construction[10,11] have been based on the results of this research. Design practices, likewise, have made use of these results and have become standardized. These practices and specifications and some of the supporting research have been described by the writer.[12,13,14,15]

---

[6] "Problems of Welded Fabrication," Pt. I by Boyd S. Meyer and Pt. II by W. L. Perry, *Proceedings*, National Eng. Conference, A.I.S.C., 1952.

[7] "Fatigue Strength of Butt Welds in Ordinary Bridge Steel," *Research Supplement, The Welding Journal*, May, 1943, pp. 189s–211s.

[8] "Fatigue Strength of Fillet, Plug and Slot Welds in Ordinary Bridge Steels," *ibid.*, July, 1945, pp 378s–400s.

[9] "Fatigue Strength of Steel Beams, Flexural," by Wilbur M. Wilson, *ibid.*, August, 1948, pp. 409s–417s.

[10] "Standard Code for Arc and Gas Welding in Building Construction," Am. Welding Soc., 1946.

[11] "Standard Specifications for Welded Highway and Railway Bridges: Design Construction and Repair," Am. Welding Soc., 4th Ed., 1947.

IMPACT TESTS OF WELDED BEAMS

To determine the best design details and procedure for making a welded splice in a beam or girder, a project of the WRC was performed at Columbia University under the direction of W. J. Krefeld, M. ASCE, E. C. Ingalls, and George B. Anderson.[16] Experience had shown welded girder construction to be economical, but there was a question as to whether the residual stresses produced by welding might not combine with the load stresses and thus reduce the strength of a welded girder, particularly under suddenly applied loads.

Wide-flange beams (16WF71) of 12-ft span, with butt-welded splices at midspan, were first tested at room temperature under a load at midspan. Following the static control tests, impact tests were made by dropping a heavy tup on the beam, using a rig similar to a pile driver (Fig. 3). Residual stresses of considerable magnitude were measured on one of the beams by the destructive method of relaxation by trepanning plugs upon which SR-4 electric strain gages had been mounted.[17]

In the drop-hammer impact tests conducted at room temperature, the rolling-mill residual stresses, together with the residual welding stresses, and the stress concentrations at the point of load application merely served to lower the apparent proportional limit. There was no evidence of any adverse effect on the carrying capacity of the beams. The beams all failed by lateral buckling or web crippling. The program was then redirected toward a study of the behavior of welded beams under impact at low temperatures and an investigation of the temperature of transition from the ductile-buckling type of failure to failure by brittle fracture.

Beams of two grades of material were tested, both conforming to the specifications for A 7 steel: One grade was semi-killed steel as normally supplied; the other was a silicon-aluminum, fully-killed steel. This latter steel was not A 94 steel, a high-carbon steel which is not recommended for welded construction. Various types of small-specimen tests were made to compare the two steels with regard to the transition temperature from ductile fracture to brittle fracture. The tests used were the Charpy keyhole and V-notch impact tests and tear tests.[18] For the Charpy V-notch tests the specimens were taken from similar locations in the various beams. The fully-killed steel withstood temperatures that were from 40°F to 70°F lower (based on an energy level of 15 ft-lb) than those that the semi-killed steel withstood. Specimens taken from the flange or web adjacent to the fillets proved to be of poorer material than

---

[12] "Manual of Design for Arc Welded Steel Structures," by La Motte Grover, Air Reduction Co., New York, N. Y., 1946.

[13] "Welded Bridges," by La Motte Grover, *The Welding Journal*, October, 1948.

[14] "Interpretive Report on Box Girders and Small Specimens," by La Motte Grover, E. M. MacCutcheon, W. S. Pellini, W. Spraragen, and J. Vasta, *Research Supplement*, *ibid.*, July, 1951.

[15] "Welding Trims Steel from Heavy Trusses," by La Motte Grover and Gilbert D. Fish, *Engineering News-Record*, August 2, 1951.

[16] "Transition Temperatures of Structural Steel Beams with Butt-Welded Splices," by W. J. Krefeld and George B. Anderson, *Research Supplement*, *The Welding Journal*, November, 1953, pp. 538s–576s.

[17] "A Method for the Measurement of Residual Welding Stresses," by J. L. Meriam, E. Paul DeGarmo, and Finn Jonassen, *ibid.*, June, 1946, pp. 340s–343s.

[18] "Notch Sensitivity of Steel Evaluated by Tear Test," *ibid.*, March, 1949, pp. 153s–165s.

the specimens taken from the edges of the flange or the center of the web. This variation could have been caused by the difference in the amount of hot-working of the material in the steel mill and by the different temperatures and rates of cooling during the finishing passes in the steel mill. It has been reported that, in general, lower finishing-pass temperatures in rolling the steel material are beneficial in controlling its grain size and reducing the transition temperature.[19] Also, the flange-to-web junction in a steel beam has been recognized by others as a critical location.[20]

Throughout this investigation careful control was exercised by the laboratory technicians. Ingenious and quite elaborate instrumentation was devised for measuring and recording the instantaneous values of the strains and deflections. Much valuable fundamental information was gathered concerning the behavior of steel material under impact.

The testing conditions were much more severe than the conditions encountered in a railway or highway bridge. However, plastic deformation was produced readily in beam tests at room temperature when instantaneous rates of deformation in the material were as great as 2 in. per in. per sec. This rate of deformation is much greater than would be expected in any highway or railway bridge. Also, some of the testing temperatures were approximately −120°F. Such exaggerated conditions are sometimes necessary to provide complete data on trends in behavior and to establish the correlation between tests of full-size structural members and tests of small specimens of the same material. Furthermore, such extreme conditions of impact might be produced by collisions, bombings, or similar incidents.

Many tests were conducted at temperatures that would be expected to exist in cold climates, but the severity of the impact and the strain rates were exaggerated in order to produce the actual fractures. Under static loading, however, no fractures could be produced, even at −100° F.

The criterion for evaluating the results of the impact tests of these beams was the transition temperature (of testing) when the type of failure changed from buckling and crippling to failure by fracture. Beams of both types of steel were tested in several conditions; (1) As-welded, (2) welded and subsequently given a 1150° F "stress relief" (or post heating), and (3) welded with preheat of from 350° F to 400° F to reduce the rate of cooling after welding.

EFFECTS OF LOW-HYDROGEN ELECTRODES, PREHEAT, AND STRESS RELIEF

In some of the later tests conducted at Columbia University, the benefit derived from using electrodes with low-hydrogen content in their coatings,[21] such as E-6016, was investigated. The use of these electrodes cannot be considered a panacea which will permit the elimination of other precautions in the welding of very thick material or some types of steel material that are especially difficult to weld. Nevertheless, a substantial benefit from their use has been reported. One structural fabricator has reported that heavy press frames with material 5 in. thick were welded successfully and with very little preheat when low-hydrogen electrodes were used.

---

[19] "Research under the Ship Structure Committee," by E. A. Wright, Finn Jonassen, and H. G. Acker, *Transactions*, Soc. of Naval Architects and Marine Engrs., Vol. 60, 1952, pp. 223–272.

[20] "Static Load Tests of Rolled Steel Beams with Butt Welded Splices, Carried to Destruction," by A. Lazard, *Publications*, International Assn. for Bridge and Structural Eng., Vol. X, No. 19.

[21] "Tentative Specification for Mild Steel Arc-Welding Electrodes," Designation A233–48T, A.S.T.M., 1948.

Research has indicated that the weld metal produced by low-hydrogen electrodes (when they are properly conditioned and stored) has substantially greater low-temperature notch toughness than ordinary carbon-steel weld metal produced with the common types of electrodes. Impact tests on beams have shown that there is substantial improvement in low-temperature impact resistance when low-hydrogen electrodes are used.

On the basis of the tests, the transition temperatures were well defined for beams welded with ordinary types of mild-steel electrodes[21] (E-6011 and E-6020). These transition temperatures are listed in Table 1, along with data from tests of some beams welded with low-hydrogen electrodes, and from tests on other beams welded without the provision of the coped holes shown in Fig. 4.

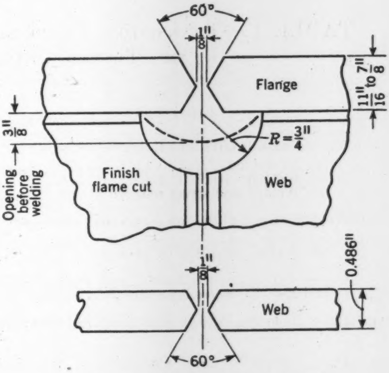

FIG. 4.—DETAILS OF A COPED HOLE

In examining Table 1 it should be realized that the low-hydrogen electrodes used for the semi-killed steel were not stored or conditioned to control the moisture as they were in the case of the fully-killed beams of the low-hydrogen series. Hence, somewhat lower transition temperatures for the semi-killed beams might have been found if they, too, had been welded with moisture-controlled, low-hydrogen electrodes.

It can be noted from Table 1 that preheating is more beneficial than a stress relief performed at some time subsequent to cooling after welding. Similar benefits from preheat have been demonstrated by other investigators. Fortunately, such preheating is a much more practical operation than the furnace "stress relieving," when the preheating is of a reasonable temperature, such as 150° F, or less. There is evidence that a post-heat, immediately following the welding—to retard the cooling rate—is at least as beneficial as preheat, but such post-heating is not practical. From Table 1, it can be noted that, for beams of the type involved in these tests, the use of low-hydrogen electrodes is equivalent to the provision of preheat. Other research and experience have indicated that, for this type of steel and for the thicknesses involved, a preheat of 100° F, or less, would have been adequate. However, a preheat of 350° F was used for these specimens. When tested, semi-killed steel beams welded with low-hydrogen electrodes were as satisfactory as the fully-killed beams welded with ordinary electrodes. No additional benefit was derived from preheating before welding for the fully-killed beams welded with low-hydrogen electrodes. For the chemistry and thicknesses of steel involved in these beams, the benefits of preheat and the use of low-hydrogen electrodes would be expected to be about equal and not additive.

Because of the unusually severe impact and high strain rates involved in these tests, it is believed that even for the semi-killed steel, welded beams of this type could be expected to behave in a satisfactory manner at low temperatures. For built-up girders with very thick flanges, welding specifications should include requirements that will assure the provision of fully-killed steel material, which would normally be furnished by most mills supplying A 7 steel for bridge and building construction.

TABLE 1.—Transition Temperatures[a] (in Degrees Fahrenheit) of Beams Tested Under Drop–Hammer Impact

Beam condition	Fully-killed steel beams	Semi-killed steel beams
1. Welded with E-6011 and E-6020 electrodes:		
(a) As-welded	−29	− 5
(b) Welded with 350° F preheat	−57	−17
(c) Welded and stress relieved	−45	− 5
2. Welded with E-6016 (low-hydrogen) electrodes:		
(a) As-welded	−65	−25[b]
(b) Welded with 350° F preheat	−55	−36[b]
3. Coped web holes eliminated, and welded with E-6011 and E-6020 electrodes	−70	
4. Plain, unwelded beams with machined coped holes and sharp pressed notch	+25[c]	+85[c]
5. Plain, unwelded beams with coped web holes made by flame-cutting	−30	−60 to −115[d]

[a] Based on the temperature at which the mode of failure changes from buckling to fracture, except as noted for beams with pressed notches. [b] This temperature or lower. [c] Approximately the lowest temperature at which failure will occur by buckling rather than by propagation of a small tear or crack. [d] Too few tests to give more than a range of values.

Effect of Coped Holes in Web of Beam

Semicircular holes were coped in the webs of most of the welded test beams (Fig. 4) to provide access for making butt welds in the flanges. The holes then were enlarged slightly to remove any defects at the ends of the butt weld in the web. It was realized that any hole or geometrical discontinuity causes stress concentrations and raises the transition temperature of the steel. However, this is a practical detail that has been used widely to facilitate the making of sound flange welds. These small holes are left open because of the difficulty of closing or filling them without leaving defects.

In most of the test beams that fractured at low temperatures, the fracture in the bottom flange and at the top of the coped hole of the web began under the same blow of the tup. It could not be determined whether stress concentrations at the coped hole were an important factor, but high local plastic deformations were found at these holes at temperatures approaching the transition range. In a few beams it could be ascertained definitely that fracture began at the coped hole, prior to the blow of the tup that caused extensive fracturing in both the web and the flange.

Further tests of unwelded beams were made to investigate independently the effect of flame-cut copes and the condition of their edges. Tests were made of three such beams of fully-killed steel and of three beams of semi-killed steel. The fully-killed beams showed a transition temperature of about −30° F, approximately the same as for the as-welded beams of Table 1. For some reason the semi-killed beams performed much better than the fully-killed beams, and their transition temperature was below −60° F. However, there were too few tests to be able to reach conclusions in comparing the effect on the two steels. It should be realized that all these tests represent exaggerated conditions of impact and high strain rate and also that, when flame-cutting is used in preparing beveled edges for welding, any effects of flame-cutting are removed by the local melting and fusion of the welding process. Furthermore, the flame cutting on these specimens was quite rough.

In unwelded beams with the holes made by drilling and then by carefully filing the edge to a smooth surface, no cracks developed at the lowest test temperature of −115° F. This led to the belief that the surface condition of the edge of the hole was the important factor. Although there is evidence that a suitable flame treatment will increase the resistance to propagation of cracks from such small surface defects, this effect was believed to be geometrical rather than metallurgical. This belief seems to have been confirmed by further impact tests of three unwelded beams of each type of steel, which were prepared with "crack starters" in the form of drilled and mechanically notched holes in the web. A fine notch, 0.10 in. deep, having a 45° angle and a root radius of 0.00075 in., was pressed at the top edge of the lower hole, after first filing the notch almost to size. This technique (which has been used by several investigators) produces a sharp notch without any appreciable cold-working that might influence the results. All six of these beams were tested under virtually identical conditions except for varying the test temperature.

A small tear or crack began from the pressed notch in all six of these beams (Table 1), but in the case of buckling failures, this short crack terminated in a zone of comparatively high tensile stress. Therefore, one might consider that the criterion for the transition temperature of these six beams is actually based on the ability of the steel material to resist propagation of cracks or to inhibit free-running cracks.

Brittle failure occurred in all these beams with pressed notches when tested at temperatures of −30° F and −60° F. A semi-killed beam tested at 30° F likewise failed by brittle fracture, but a fully-killed beam tested at 30° F failed by buckling. Only one beam, one made from fully-killed steel, was tested at a higher temperature of 60° F. This beam developed only a very short crack of fibrous texture, 1/16 in. long, and then it continued to buckle without further propagation of the crack.

The test results indicate that the tendency for crack propagation is dependent on the temperature. It appears that, in the case of a brittle fracture, at a relatively low temperature, a large part of the total absorbed energy is utilized to start the fracture, and a comparatively small part, to propagate the crack. In a ductile fracture at a comparatively high temperature, these proportions seem to be approximately reversed, with the greater part of the energy being utilized for crack propagation.

Because a sizable brittle fracture or crack developed in the fully-killed beam tested at −30° F, this unwelded beam with a pressed notch might be considered to have behaved as a beam of the same material in the as-welded condition, or as a beam with a flame-cut hole.

These tests demonstrate a fact that has been proved in fatigue testing. Any practical method of fabricating and joining steel material usually introduces at least minor geometrical notch effects that reduce the resistance of the material, particularly under dynamic loading.

To investigate the benefit of eliminating the coped holes in the webs of the beams adjacent to the top and bottom flange welds, a series of six fully-killed beams without such copes were fabricated and tested. To provide a comparison with a larger number of previous tests, the butt-welded splices of these test beams were made with E-6011 and E-6020 electrodes, rather than with low-hydrogen electrodes. Although the execution of sound flange welds is more difficult when there are no copes (special care and procedures being necessary), the precautions required are entirely practical.

As indicated in Table 1, the welded beams without coped holes showed a transition temperature of approximately −70° F, although cutting the beams for examination showed some appreciable weld defects in the flange near the flange-to-web junction. This transition temperature is approximately 40° F lower than for similar beams having web holes.

There is a further advantage of using test conditions that are more severe than those that are likely to be encountered in practice. This severity magnifies the effects of design details so that the details can be studied critically. Whenever difficulties are encountered in any type of engineering construction, they usually result from a combination of factors or from faulty details and practices. The best practical details of design necessarily involve some notch effects, but a well-advised designer can avoid very unfavorable details.

Plastic Analysis in Structural Design

There are many advantages to the use of welding to develop highly efficient and economical connections in continuous or rigid-frame construction. Consequently, as welding has come into wider use for building construction, much interest has arisen among designers and researchers in the method of plastic analysis of continuous frames and their components.[22,23,24] (This method of analysis has been referred to as "load limit design," "plastic design," and "load factor design.")

The objective in using a plastic-analysis method is to apply a suitable safety factor to the true ultimate load that a structure can carry without excessive deformations or deflections occurring, and to produce a design that is as nearly balanced as practical among the component members and connections of a continuous frame. It is thereby possible to attain maximum economy in material and construction costs.

---

[22] "Theory of Limit Design," by J. A. Van den Broek, John Wiley & Sons Inc., New York, N. Y., 1948.

[23] "Plastic Design and the Deformation of Structures: Progress Report No. 3—Welded Continuous Frames and Their Components," by L. S. Beedle, A. A. Topractsoglou, and B. G. Johnston, *Research Supplement, The Welding Journal*, Vol. 30, 1951, pp. 348s–356s.

[24] "Plastic Behavior of Mild Steel Plate Girders," by A. Lazard, *Proceedings*, Fourth Cong. International Assn. for Bridge and Structural Eng., Cambridge and London, England, August and September, 1952.

Conventional methods of analysis, based solely on elastic behavior, usually presume that failure is imminent when a yield-point stress is developed at any point in a frame. A critical examination of practical engineering structures shows that this is far from true in most rigid-frame structures, and that continuous frames possess much unrecognized reserve strength.

The concept of "plastic hinges," which causes a favorable redistribution of moments and stresses, was introduced in Hungary[25] (in 1914) and has been investigated extensively in Belgium, France, Germany, and England. In the United States the reserve strength accompanying continuity has been recognized, to some extent, by allowing increased working stresses for combined gravity loads and lateral forces. Furthermore, in practical engineering structures, sizable plastic deformations must actually occur, as the members and connections (whether welded or riveted) become adjusted while initial loads are being applied.

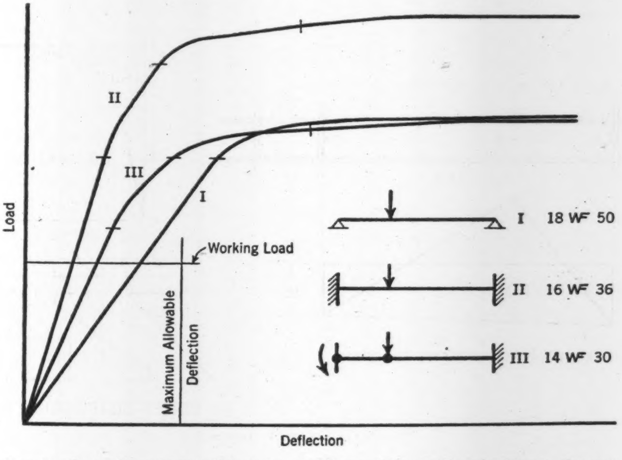

Fig. 5.—Load-Deflection Diagram for Three Beams Having Equal Spans

Interest in this method was revived[26] by J. F. Baker, A. M. ASCE. Mr. Baker showed that in some special cases the actual failure load of a continuous frame may be eight or ten times that computed by conventional analysis, and, in many cases of continuous framing, large economies can be realized by extending the design analysis to take into account the reserve strength in the plastic range. Localized, abrupt stress peaks, such as those indicated by elastic analysis at points of negative moment over supports, are not significant. Even in columns with rigid connections of beams, there is often a great reserve of strength after the yield-point stress has been reached.

---

[25] "Experiments with Clamped Girders," by Gábor Kazinczy, *Betonszemle*, Vol. 2, June 1, 1914, pp. 101–102.

[26] "A Review of Recent Investigations into the Behavior of Steel Frames in the Plastic Range," by J. F. Baker, *Journal*, Inst. of C. E., London, England, Vol. 3, 1949, pp. 185–240.

To be conservative, the method of analysis can be devised in such a way that, under the assumed working loads for a structure, the computed stresses would not exceed the yield-point stress. However, the true ultimate load capacity, as limited by excessive deformations or deflections, would be determined by recognizing the reserve strength after plastic yielding has begun. Thus, in effect, a sliding scale of generally increased working stresses would result when a given factor of safety is applied.

The opportunity to develop a comprehensive rational method of plastic analysis has been enhanced in the United States because of the feasibility of making large-scale tests to determine the basic behavior of beams, columns, welded joints, and frames in both the elastic and plastic ranges. Most of the research for this method of design has been conducted at Lehigh University at Bethlehem, Pa., by Bruce Johnston, M. ASCE, and Lynn S. Beedle, A. M. ASCE. The program is (1953) under the general direction of an advisory subcommittee of the Structural Steel Committee of the WRC.

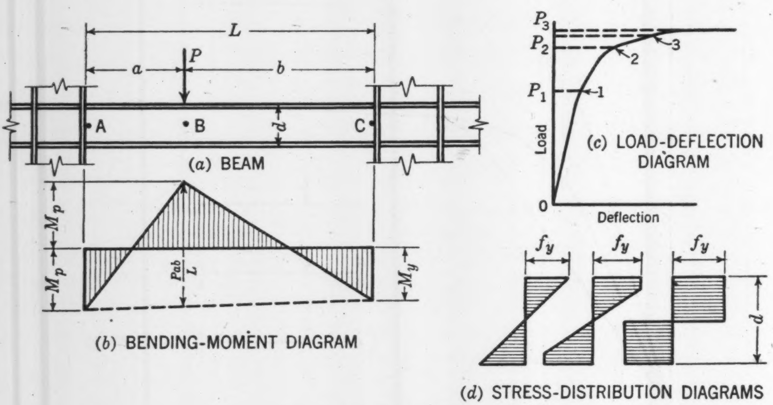

(a) BEAM

(b) BENDING-MOMENT DIAGRAM

(c) LOAD-DEFLECTION DIAGRAM

(d) STRESS-DISTRIBUTION DIAGRAMS

FIG. 6.—PLASTIC ANALYSIS

Mr. Beedle has cited[27] the examples shown in Fig. 5 as illustrating quite an ordinary case in which the plastic design of continuous framing, Case III, shows a saving of 20% as compared with Case II, designed by the elastic theory. This design provides the same actual load capacity as Case I, designed for simple supports. There is a 40% saving as compared with Case I. In a structure which contains some rigid frames and some simply supported beams, all designed by the elastic theory (Case I and Case II), the design as a whole is unbalanced. The beam of Case II is obviously overdesigned. The beam diagram for Case III depicts the state when the first plastic hinge has formed at the left support and a second hinge is beginning to form under the load. When a third plastic hinge forms at the right support, the true load capacity of the beam will have been reached.

---

[27] "Welded Continuous Frames and Their Components," by C. H. Yang, L. S. Beedle, and B. G. Johnston, *Research Supplement, The Welding Journal*, July, 1951, pp. 348s–356s.

The basis for the plastic theory of design, as applied to the beam in Fig. 6(*a*), is illustrated in an elementary manner by the simplified load-deflection curve (Fig. 6(*c*)) and stress-distribution diagrams (Fig. 6(*d*)). Slightly below point 1 in Fig. 6(*c*), the yield-point stress has barely been reached at the point of maximum moment at the left support. The distribution of stress across the beam section is still triangular, and the resisting moment of the section when yielding begins is designated as M_y. Slightly above point 1, there is some plastic deformation in the outer fibers, and the stress distribution becomes trapezoidal. A plastic hinge then develops at this point of maximum moment—at the left support in the case illustrated. A rectangular stress distribution can be assumed to exist at the plastic hinge. The resisting moment, M_p, is the yield-point stress multiplied by the static moment of the entire beam section about its neutral axis.

As the load on the beam is increased further, the beam behaves as though it were hinged at the left support, with a constant moment applied at that point, until the process of forming a plastic hinge has occurred under the load (point B, Fig. 6(*a*)). This occurs in the vicinity of point 2 on the load-deflection curve in Fig. 6(*c*). At point 3 of this curve, a final hinge begins to form at the right support. From this point on the deflection continues at an uncontrolled rate; therefore, the load at this point is the load capacity of the beam. If the rotation at any plastic hinge actually proceeds far enough, the stresses in the beam fibers will begin to increase again as strain hardening becomes appreciable, but this does not occur until the strain or local degree of curvature is approximately fifteen times the value at the elastic limit.

In the case of a symmetrical, simple, portal frame having two similar legs rigidly connected to a beam, with symmetrical loading and no sidesway, the first hinge might develop at midspan. Then, as the load is increased, the moment and stresses at the knees would increase until two more plastic hinges were developed. Collapse would not begin until virtually full plastic-hinge action had developed at all three hinges, after which the deflections would increase at an uncontrolled rate.

In the simple case shown in Fig. 6, only the stresses and rotations caused by the bending moment were considered. In an actual case, however, there are sometimes other limiting factors that must be considered. The rotation capacity of each section must be evaluated to determine whether all the assumed plastic hinges can actually be developed before local buckling, excessive deflection, or fracture occurs. There are also other limitations similar to those that must be investigated in design by the elastic theory. The effect of shear deformations may be important—for example, in rigid-frame rectangular knees formed by the intersection of rolled-beam sections (without haunching), there is no wide-flange shape that has sufficient web thickness to prevent premature web yielding caused by shear, without added stiffening. Expressions have been developed for the required thickness of the web in simple rigid-frame connections, which apply in the case of elastic analysis as well as plastic analysis.[28]

---

[28] "Connections for Welded Continuous Portal Frames," Progress Report No. 4, Pt. III, Discussion of Test Results and Conclusions, by L. S. Beedle, A. A. Topractsoglou, and B. G. Johnston, ***Research Supplement, The Welding Journal***, November, 1952, p. 546s.

An analysis of a case such as that illustrated in Fig. 6, made by C. H. Yang, Mr. Beedle and Mr. Johnston, showed the maximum deflection of a beam designed by plastic analysis to be less than that of a beam designed for a simply

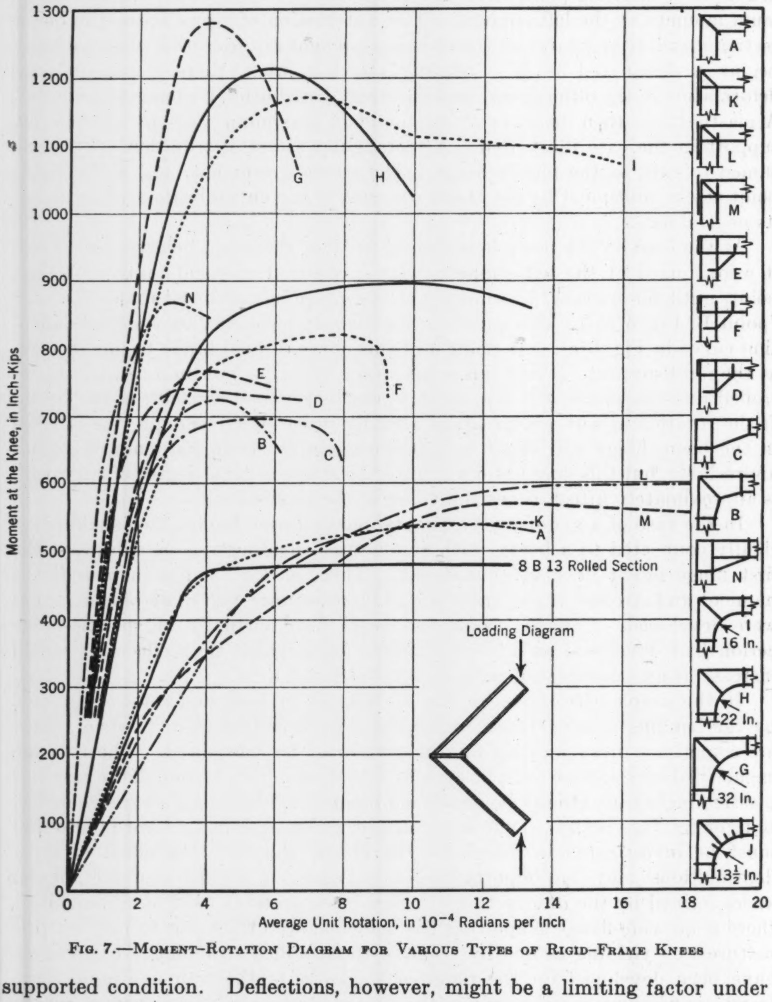

Fig. 7.—Moment-Rotation Diagram for Various Types of Rigid-Frame Knees

supported condition. Deflections, however, might be a limiting factor under some circumstances.

In investigating such factors as rotation capacity and web yielding caused by shear, there is a special advantage to large-scale tests which use structures fabricated from commercial rolled-steel sections, such as those actually used in practical construction. Tests of this kind have been performed to gain information for the reliable prediction of moment-rotation characteristics.

TESTS OF RIGID–FRAME KNEES

Typical results of tests of various types of rigid-frame knees are shown in Fig. 7. Also included therein is an (M/ϕ)-curve for the plain beam section, determined from beam tests made prior to the testing of the knees. In Fig. 7 it is shown that straight knees with parallel flanges can be proportioned easily and economically to develop capacities for moment and rotation considerably in excess of those required to meet the design predictions. Knees with curved haunches showed excellent strength when proportioned according to the procedures recommended[29] by the American Institute of Steel Construction (AISC).

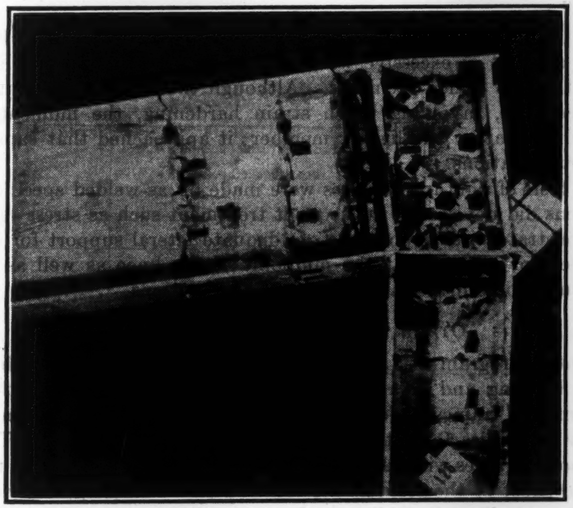

FIG. 8.—THE EXCESS DEFORMATION INHERENT IN A TYPE P CONNECTION

To compute the distribution of moments in rigid-frame members, approximate expressions have been developed[30] for determining the relationship between the average unit rotations of haunched connections and simple rectangular knees.

All the sections tested eventually failed by local and lateral instability rather than by fracture. The larger sections collapsed more suddenly. It would appear that if haunched knees were used in plastic design, they should be proportioned so as to be strong enough to cause plastic hinges to develop in the adjacent members. Additional tests of complete frames would be desirable to determine the suitability of such an arrangement.

---

[29] "Single Span Rigid Frames in Steel," by J. D. Griffiths, A.I.S.C., October, 1948.

[30] "Connections for Welded Continuous Portal Frames," Progress Report No. 4, Pt. III, Discussion of Test Results and Conclusions, by L. S. Beedle, A. A. Topractsoglu, and B. G. Johnston, *Research Supplement, The Welding Journal*, November, 1952, p. 551s.

Of course, information concerning the elastic range is useful in the design of rigid frames, even though plastic analysis is not used. Design practices have always been predicated on the use of a steel material that can deform plastically.

The type A connection (Fig. 7), which has the lowest fabrication cost, showed less rotation capacity in the plastic range than did rectangular knees such as those of type L and type M with more stiffening; those of type A collapsed more suddenly after reaching the maximum load capacity. However, the type A connection appears to behave well within the elastic range and might possibly be used for some cases in plastic design where only limited rotation capacity is needed.

The type P connection without a diagonal stiffener, shown in Fig. 8, deformed as a result of excessive web shear at half the moment value for the lighter of the two joined members. Although the rotation was large at the point of collapse, involving much strain hardening, the moment capacity never reached that of the lighter member; it approached that capacity only at very large rotations.

All the tests of rigid-frame knees were made on as-welded specimens—that is, specimens did not receive subsequent treatment such as stress relief. The tests demonstrated the importance of adequate lateral support for any rigid-frame knee—for example, at the midpoint of the knee as well as at splices between built-up haunches and adjacent beam sections.

OTHER TESTS FOR PLASTIC DESIGN

The entire program at Lehigh University included tests of columns with combined bending and axial loading[31] to simulate conditions in the vertical members of rigid frames. Tests were also made of continuous beams to determine their capacities for rotation so as to form plastic hinges. Three rigid frames—portal frames with rectangular knees—were tested virtually to destruction. The effect of the residual stresses caused by welding, as well as those resulting from cooling after rolling in the steel mill, were investigated in columns and beams.

The portal frames tested were composed of a 14-ft beam spanning between the vertical legs, with two symmetrically located concentrated loads (Fig. 9).

When the midspan deflection had reached approximately 10% of the length of the span, frame 1 (composed of 8WF40 sections) was still able to resist increasing loads. As a result of strain hardening, this frame carried loads considerably in excess of the collapse load that had been predicted by plastic analysis. Large unit rotations were developed in this section.

Frame 2 (composed of 8B13 sections) almost developed the predicted collapse strength, despite the fact that this shape is one of the least suitable shapes available to resist local buckling. In the test of a third frame, the effect of combined lateral and vertical loading was studied. The results conformed closely to those predicted by plastic analysis.

---

[31] "Column Strength Under Combined Bending and Thrust," by R. L. Ketter, L. S. Beedle, and B. G. Johnston, *Research Supplement, The Welding Journal*, December, 1952, pp. 607s–621s.

In a test of a 16-ft-long, 8WF31 column with hinged ends and an axial load and bending moment applied at the top, the maximum resistance of the column exceeded not only the predicted yield moment but also the plastic-hinge moment for this beam section as determined for pure bending. These excesses indicate that in many cases the influence of axial load can be neglected in portal-frame columns when designing by plastic analysis.

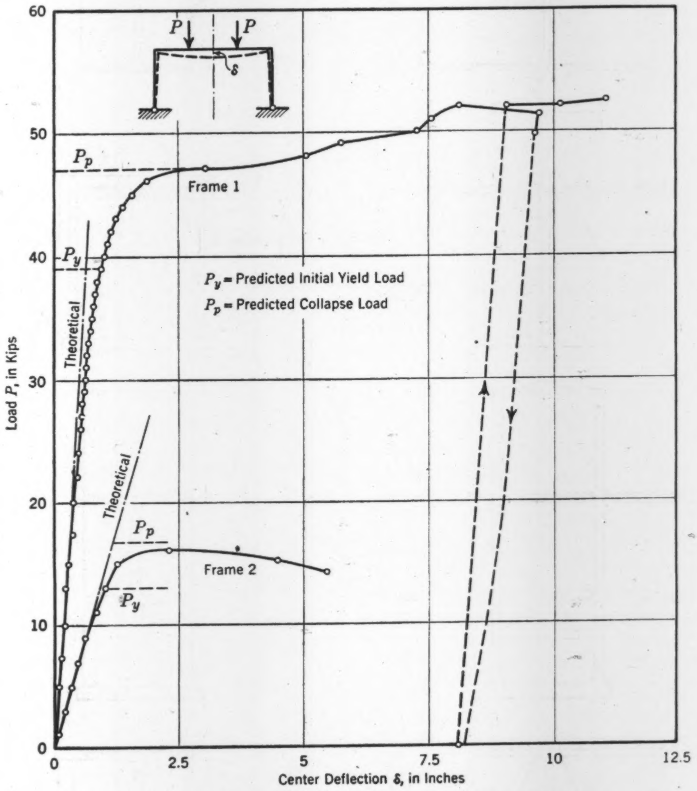

FIG. 9.—LOAD-DEFLECTION CURVES FOR TWO PORTAL FRAMES

Much fundamental information was derived from the various tests of columns performed at Lehigh University. This information can be used to develop rational methods for designing columns which include the interaction or combined effect of bending and axial loading.

Tests were also made of beams which were continuous over two supports, with loaded overhanging cantilever arms to simulate a portal frame, prior to the tests of the actual frames. This arrangement afforded flexibility in regu-

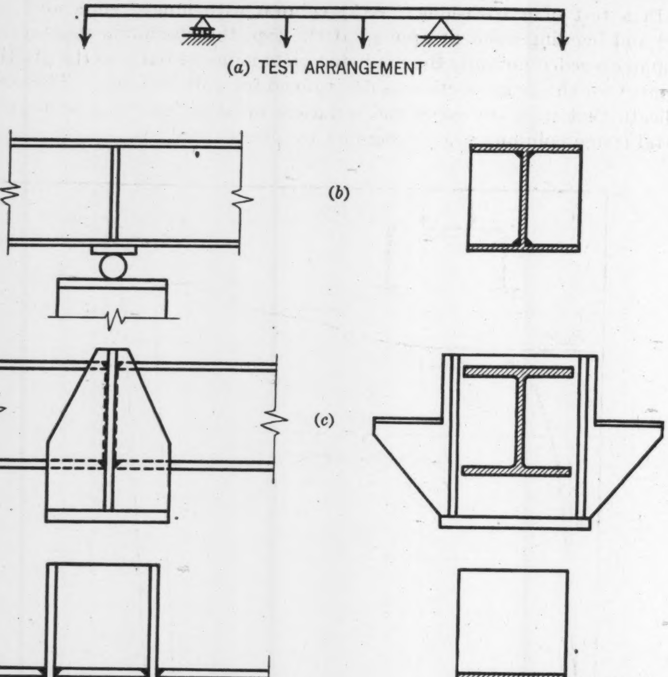
(a) TEST ARRANGEMENT
(b)
(c)
(d)
(e) LOAD CARRIER

FIG. 10.—LOAD CARRIER AND SUPPORTS USED IN TESTS OF CONTINUOUS BEAMS

lating the slope of the beam over the supports so as to simulate various conditions of behavior. Four different tests were made of such continuous beams, as delivered, with rolling-mill residual stresses and some localized residual welding stresses at the supports. In the early part of the plastic range, there was approximately a 10% reduction in the moment capacity as compared with the computed values. This reduction was attributed to the effect of the rolling-mill residual stresses. However, with continued straining, the full plastic-hinge moment can be developed. Even a 14WF30 beam, lightest of its series and therefore one which tends to buckle locally, showed quite a good combination of plastic strength and rotation capacity.

Of the three types of stiffening details used over the supports for the continuous beams, the one shown in Fig. 10(*d*) resulted in the least deflection, and the detail shown in Fig. 10(*b*) resulted in the largest deflection.

In the continuous-beam tests, the effect of residual stresses[32] and stress concentrations seemed to be only a moderate increase in deflections. Substantially the predicted ultimate strengths were developed in all tests. A test made of an 8WF67 beam after stress-relief annealing showed moment-rotation characteristics which conformed to the theoretical values.

The behavior of the beams in these various tests, together with other considerations, leads to a belief that residual stresses caused by welding are not usually as influential as those resulting from cooling after rolling. The welding stresses are highly localized whereas the rolling-mill stresses are widespread and would be expected to cause somewhat premature yielding over a wider area, and thus influence the deflections.

The portal-frame tests, and the tests of columns under combined bending and axial loads of the order to be expected in the legs of portal frames, all indicated little if any effect of axial loads on the load capacity. Therefore, residual stresses would not be an important factor. In members subjected to large axial loads, these stresses might exert more influence, especially in the case of a pin-ended column.

This method of plastic analysis is mainly applicable to building frames. Before it can be applied to bridge design, there must be an investigation of the effect of small plastic deformations on the fatigue strength. To apply the method widely and to the fullest extent of its benefits, further studies would be desirable to determine the local buckling characteristics of the various rolled sections that are available for use in design. Local buckling of the edges of beam flanges in the plastic range was the immediate cause of collapse for almost all the specimens that were loaded to their ultimate capacity. One of the objectives of the current (1953) program at Lehigh University is the development of a specification for the most suitable geometrical shape or cross section for rolled-steel sections.

As more thought is given to resistance to bombing, the matter of reserve strength becomes increasingly important. Whether it is recognized or not in design analysis, experience confirms the fact that welded rigid frames and continuous construction usually provide a large amount of reserve strength as compared with simple beam and column design.

---

[32] "Residual Stress and the Yield Strength of Steel Beams," by C. H. Yang, L. S. Beedle, and B. G. Johnston, *ibid.*, April, 1952, pp. 205s–229s.

DIFFICULTIES WITH WELDED BRIDGES IN CANADA

Prior to 1953 fifteen large welded-girder bridges were constructed in the Province of Quebec, Canada. With the exception of one bridge at Three Rivers, these bridges have given trouble-free service. The Three Rivers Bridge is composed of two groups of continuous plate-girder spans, totaling approximately 2,000 ft in length, and composed of span lengths of up to 180 ft. This bridge was put in service in November, 1947. In February, 1950, a fracture developed[33] in each of two girders when the temperature dropped quite rapidly from +40° F to −10° F. Repairs were made, and riveted cover straps were added at all welded tension joints similar to those where fractures had occurred, because an investigation had shown some of the $2\frac{1}{2}$-in.-thick flange plates at the fractures to be of an inferior rimmed steel of high average carbon and sulfur content, containing marked segregations. This steel differed greatly from that ordinarily furnished for bridge construction in the United States and Canada, although it conformed to the specifications.

On January 31, 1951, at 3 a.m., with a temperature of −30° F, four spans of this continuous-girder bridge collapsed completely. Design, fabrication, and erection operations and welding methods, procedures, and sequences were all investigated and found not to have contributed to the failure. An examination of the steel after removal from the stream revealed innumerable fractures throughout the members; but none of them occurred at welded joints or splices in the flanges or webs. The fractures did, however, traverse longitudinal fillet welds in some cases. The girders were composed of single-thickness flanges, fillet-welded to the webs. The findings of the judicial commission were inconclusive—attributing the failure to an "unknown scientific cause" or to "sabotage." A demolition expert who examined the steel after collapse testified that the local appearance at one point and conditions in general indicated that collapse had been caused by an explosion.

The shortcomings of the steel material, resulting in poor low-temperature notch toughness, can be considered the cause for the very brittle behavior as the spans collapsed. However, the primary cause for collapse has not yet (1953) been determined. It does not appear that the design or the welding methods were at fault, in view of the locations of the fractures during the collapse, especially when riveted straps had been added at critical points during the earlier repairs.

A plausible hypothesis has been advanced by disinterested groups to account for the forces causing initiation of such a failure with virtually no live load on the bridge. This hypothesis is that nonthermal expansion or growth of the concrete floor slab provided such forces. From photographs of the partial fractures that occurred in 1950, it appears that the steel had parted about $\frac{3}{8}$ in., but the adjacent concrete slab had not. This condition seems to indicate the existence of a high compression stress in the floor slab. There is particularly strong adherence to this theory by bridge engineers who have had experience with this kind of expansive concrete in the middle western parts of the United States where certain kinds of aggregates have been used. Such concrete has been found in various parts of the United States and Canada, some of it in places near the Three Rivers Bridge.

---

[33] "Canadian Welded Girder Bridge Practices," by D. B. Armstrong, *Abstract*, Highway Research Board, National Research Council, Washington, D. C., June, 1951.

The floor slab of this bridge was well anchored to the steel girders and floor beams, although composite action was not assumed in the design computations. A thorough investigation of the concrete is being conducted (1953), with particular emphasis on the nonthermal expansion or growth phenomenon. The results should help to determine the interaction of stresses that existed between the girder flanges and the concrete deck of this particular bridge. George W. Lamb, M. ASCE, has made computations which indicate that the amount of nonthermal expansion that might have occurred in the floor slab of this bridge could easily cause fracture and failure under these circumstances. Concrete of this type has "grown" as much as 2 in. per 100 ft in some bridge floors in Kansas. With no anchorage to continuous steel beams, the floor has slid along them and sheared off back walls of abutments. In a bridge composed of a series of simple spans, in which the steel was not continuous, the steel moved along with the concrete, displacing the superstructure with respect to the pier bents. The greater part of the growth of such concrete has been found to occur during the first two to five years.

Whether or not expansive concrete is established eventually as the major contributing factor in the collapse of the Three Rivers Bridge, it is well for designers to be aware of this phenomenon, especially if composite construction is used, or if concrete floor slabs are tied into steel girders for other reasons, in comparatively long structures. Under such circumstances it is especially important to make suitable tests to assure the furnishing of materials that will not produce this expansive type of concrete. Such tests have now been undertaken.

For evidence of the adequacy of other welded steel bridges in Canada to withstand the low temperatures that occur, one need but examine the service record of the bridge at Ste. Anne de la Perade (erected in 1936). Fabricated and erected by the same organization that built the Three Rivers Bridge, this structure has had a perfect record of performance for seventeen years (as of 1953).

CONCLUSION

Welded structures have failed, as have other structures. Investigation, however, reveals that the failures are attributable not to the welding process but for the most part to the occasional use of unsuitable materials of construction. Advances in the control of materials and improvements in the details of design and construction methods have been made to prevent such failures.

DISCUSSION

Jack R. Benjamin,[34] A. M. ASCE.—The structural engineer's basic problem involves the method of securing the necessary structural performance with a maximum of economy. The action of various welding details is almost unknown, with the result that engineers tend to penalize welding. A usual design approach is to compute the necessary amount of weld and then double it. This procedure does not constitute good design, but it reflects the attitude of many engineers toward welding. Research reports, such as those offered by Mr. Grover, assist greatly in overcoming this attitude.

Most of the investigations of brittle fractures are based on a temperature-metallurgical approach. Is there any basis for ignoring stresses and detailing? In particular, will joints where distortions are restricted by the use of large amounts of light welding tend to show brittle fracture?

The structural engineer has a great deal of freedom in the design of welded joints, but he must decide whether some details are better than others. The designer must feel that he can control the joint behavior by his design details. If a shear connection is desired between a beam and a column, a detail must be chosen which will act as a hinge with respect to moment resistance. Web plates plus light seats tend to provide moment resistance but, if this moment is not considered in the design, the joint can be overstressed. If detailing will not allow local yielding without damage, the entire joint integrity is endangered. If the moment is included in the design, the size of the connection is increased until it becomes a costly assembly. It is therefore necessary to determine what types of joints can yield safely under low moments. Full continuity is not always the solution.

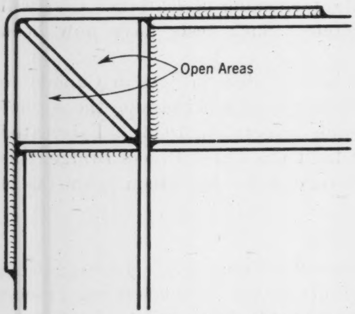

Fig. 11.—A Rigid-Frame Knee

The current (1954) research trend toward ultimate design must satisfy one basic problem of the designer before it can be accepted. Under prevailing specifications the designer is relatively confident of his designs—their performance is known. Not only must plastic design prove more economical, it must be predictable; the engineer must be able to control the behavior of his structure. Full continuity with expensive joint details unfortunately involves the problem of mode of failure. Not only are these failure modes complex, but such factors as torsional failure of the structure as a whole must be considered.

One possible solution to this problem would be to provide for less than full plastic strength by including points of predictable plastic moment. In this manner the mode of failure could be controlled. The acceptance of plastic-design procedures by the practicing engineer will be influenced to a greater extent by guaranteed performance than by the saving of a few pounds of steel.

---

[34] Associate Prof. of Structural Eng., Stanford Univ., Stanford, Calif.

The tests of rigid-frame knees (Fig. 7) illustrate this problem. The use of very heavy knees to force the development of plastic hinges in the adjacent members makes the plastic design more complex. Perhaps a knee detail should be developed with predictable characteristics and less welding. A suggested joint is shown in Fig. 11. This joint is designed to fail by buckling of the diagonal strut. A joint of this type should show good plastic characteristics, be capable of shakedown without damage, and be economical.

GEORGE W. LAMB,[35] M. ASCE.—Many of the problems encountered in the design of welded structures have been solved by research and experience as has been shown by Mr. Grover. Research has been by far the most economical process for solving many of these problems. Observations of and experience with actual structures (also considered to be research) likewise provide solutions. The main features that distinguish actual-structure observations from laboratory research are the cost, the size of the specimen, the nonaccelerated rate of the test, and the integration into the results of many conditions that cannot be accurately reproduced in the laboratory.

Research, as reflected by laboratory tests, produces a series of facts which justifies certain limited conclusions. Such facts, however, will not support full conclusions nor give all the answers. In citing (under the heading, "Difficulties with Welded Bridge in Canada") the partial failure of the Three Rivers Bridge in 1950 and the collapse of four of the eight spans in 1951, the author draws attention to the value of correlating laboratory research with field observations and experience in order to obtain logical answers to some of the questions that have been raised by designers. Inasmuch as the writer advanced the hypothesis of an expansive concrete floor having been the cause of, or a major contributing factor in, these failures, this hypothesis should be explained. It will be shown that, when different materials are combined—with or without intent—in such a way as to require close functioning in a structure, the results of coordinated research for the different materials are required to explain fully difficulties which can arise.

The Three Rivers Bridge (Fig. 12) consisted of two bridges, one over the east channel and one over the west channel of the St. Maurice River. Both bridges were all-welded, continuous, haunched, deck-girder structures. Both bridges had two main girders spaced 32 ft apart, which supported a 42-ft concrete roadway and two 5-ft sidewalks. Floor beams and brackets spaced at 10 ft on centers supported the roadway and sidewalks between, and outside, the girders. Both bridges were constructed in 1947. These structures were conservatively designed and well constructed. The details of the design were conventional and had been used many times.

The east bridge is a five-span structure, composed of two 108-ft end spans and three 140-ft intermediate spans. The girders are 10 ft deep at the piers and $6\frac{1}{2}$ ft deep at midspan. The west bridge, which collapsed in 1951, was an eight-span structure. The end spans were 148 ft, and the six intermediate spans were 180 ft. The girders were 12 ft deep at the piers and 8 ft deep at midspan.

---

[35] Dist. Engr., Am. Inst. of Steel Constr., Inc., Topeka, Kans.

The fractures that occurred in one of the girders of each of these bridges in 1950 were located, in each case, on the river side of the first pier, and approximately a distance equal to the depth of the girder from the piers. These fractures extended through the upper or (in this case) tension part of the web and flange (Fig. 13, Line A and line B). The spans did not collapse as a result of these fractures, and they were repaired by replacing the welded tension splices with 100% riveted joints.

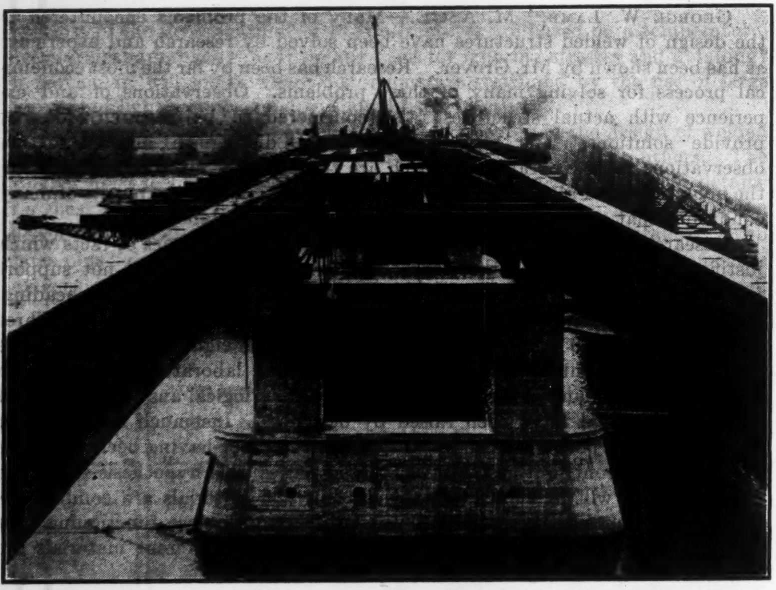

FIG. 12.—THREE RIVERS BRIDGE (QUEBEC, CANADA) DURING CONSTRUCTION

The initial point of rupture in the 1951 collapse of the west bridge could not be exactly located, but photographs of the collapsed structure show a point of large structural damage on the river side of the first pier at the opposite end of the bridge from the 1950 fracture (Fig. 13(*a*), line C).

Some data relative to the properties of the steel near the first fractures of these bridges have been published.[33] The mechanical properties of the steel indicated that it was more than adequate for the design loads. Adjacent to these fractures, the elastic limit of the steel ranged from 28,000 lb per sq in. to 58,000 lb per sq in.; in the core of some of the plates the carbon content was approximately 0.40%, and the sulfur content was approximately 0.116%. Mill tests indicated that all the steel was A 7 steel,[3] and in all but two cases in ninety tests additional check analysis confirmed this.

No data have been published relative to the expansive characteristics of the concrete in the floor of these bridges. By customary standards, the concrete was of good quality and adequate for the purpose; it had an ultimate compressive strength at an age of four years of from 3,500 lb per sq in. to 5,900 lb per sq in.

Concrete having the characteristic of expanding under conditions of wetting, drying, and freezing is not uncommon. A map is available[36] which shows where expansive concrete is common and has been definitely found and recognized. Expansive concrete is believed to be present in the Jacques Cartier Bridge in Montreal, Que., Canada, which is 90 miles from the Three Rivers Bridge.

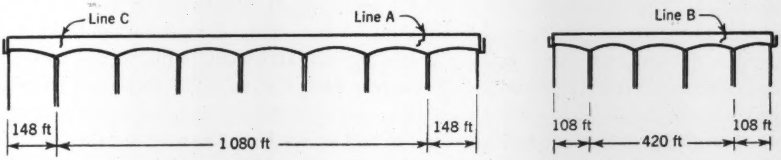

(a) West Bridge

(b) East Bridge

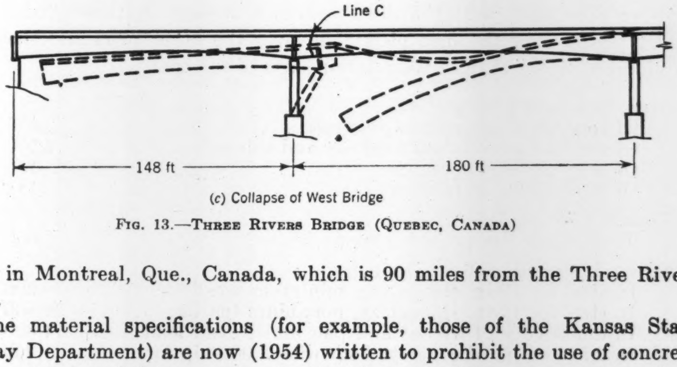

(c) Collapse of West Bridge

FIG. 13.—THREE RIVERS BRIDGE (QUEBEC, CANADA)

Some material specifications (for example, those of the Kansas State Highway Department) are now (1954) written to prohibit the use of concrete having wetting and drying expansion (as determined by a one-year test) of more than 0.7 in. per 100 ft, or 0.00058 in. per in. Even this concrete expansion will cause difficulties in some structures if combined with other strains and a contributing section geometry.

The concrete floors of the Republican River Bridge at St. Francis, Kans., and the Cimarron River Bridge near Sitka, Kans., expanded under wetting and drying (or freezing) 2 in. per 100 ft, or 0.00167 in. per in. In the Republican River Bridge the forces resisting this expansion were estimated to be 1,000,000 lb, which caused compressive stresses in the concrete floor slab of 450 lb per sq in. This resisting force did not prevent expansion of the concrete floor. As a result, differential movement between the floor and the steel girders took place when the supports for the end expansion joint failed by tearing free from the girders.

---

[36] "Modern Concepts Applied to Concrete Aggregate," by R. F. Blanks, *Transactions*, ASCE, Vol. 115, 1950, p. 417.

The writer has reason to believe that the floors of both bridges of the Three Rivers Bridge were made of concrete having a net wetting and drying expansion of more than 0.00073 in. per in., with perhaps as much expansion as that which occurred in the Republican River Bridge. There is also reason to believe that, in addition, this concrete had the characteristic of expanding under freezing and thawing cycles. Net wetting and drying expansion of 0.00073 in. would have tended to stretch the 1,376-ft girders in the west bridge of the Three Rivers Bridge approximately 12 in. This elongation would have produced a total tension in one girder of approximately 3,000 kips, with a corresponding compressive stress in the concrete floor slab of 1,200 lb per sq in. or less.

The girder of the Three Rivers Bridge had a variable cross section; therefore, if the tensile force caused by expansion were considered to be applied on the neutral axis of the girder rather than on the upper flange, the resulting tensile stress in the steel would vary from 16,600 lb per sq in. at the interior supports to 26,800 lb per sq in. near the inflection points. It should be noted from the following tabulation that the dead-load unit stresses in these girders were slightly higher over the first piers than over the other piers and they were considerably higher than in the interior parts of the span.

Area, in square inches	
Of concrete roadway and sidewalk	5,000
Of one half of concrete roadway and sidewalk	2,500
Of steel girder, maximum	180
Of steel girder, minimum	112
Tensile force, in kips	
To elongate the 1,376-ft girder	3,000
Stress, in pounds per square inch	
In steel for 12-in. elongation, minimum tensile	16,600
In steel for 12-in. elongation, maximum tensile	26,800
In upper edge of web at first pier under dead load	14,600
In 2,500 sq in. of concrete floor with 3,000-kip force	1,200
Strain in Republican River Bridge concrete, in inches per inch	
Measured expansion	0.00167
Shortening with compressive stress of 450 lb per sq in.	0.00030
Unrestrained expansion	0.00197
Shortening under compressive stress of 1,200 lb per sq in.	0.00080
Strain in the floor of the Three Rivers Bridge if it were made with Republican River Bridge concrete, in inches per inch	
Net expansion caused by wetting and drying	0.00117
Potential expansion caused by fifteen thawing-and-freezing cycles	0.00200
Elongation of 1,376-ft girder, in feet	
Caused by wetting and drying	1.61
Caused by thawing and freezing	2.76
Necessary for rupture	1.00

A tensile force is produced in the girders when adequately connected expansion joint devices at each end of the bridge—together with friction, floor-beam embedment, and anti-creep bars—restrict the elongation of the expansive concrete floor. This tensile force creates tension and shear stresses in the girder, in addition to the stresses produced by the dead load. The tensile force caused by expansion is distributed, in varying proportions, across the full cross-sectional area of the girders. This distribution results in horizontal and vertical shear in the web, which—when combined with the direct tension—produces diagonal tension in the web. The direction of this diagonal tension in the web is downward and toward the center of the entire structure. Dead-load tension in the upper part of this girder, caused by bending combined with vertical shear, produces diagonal tension in the web of the girder. The direction of this diagonal tension on the river side of all piers is downward and toward the center of the entire structure, and on the bank side of all piers is downward and toward the bank. On the bank side of all piers these tensile stresses are not in the same general direction and tend to nullify each other. The stresses on the river side of the piers, however, are in the same general direction; their components are additive, and the maximum stress therefore occurs at this point.

If the expansive-floor stresses—which were variable in intensity because of the variable girder section—were added to the variable dead-load bending stresses, the total unit stress near the section where fracture occurred would be the highest. As the force caused by restricting the elongation of the expansive floor slowly increased, this critical point in the cross section of the girder reached the elastic limit before the remainder of the girder. Then, any additional elongation would be concentrated at this point and in time would cause rupture.

The web of this girder was restricted from "necking-down" under tension by the stiffeners and the floor-beam connections located at alternate spaces of 5 ft. The web was also subjected to biaxial stress which prevented the ductility of the metal from being effective. The web under this condition could be expected to break in a brittle manner and it could also be expected to break before the unrestricted and uniaxially stressed flange.

The 1950 fractures indicated that the initial fracture began at the top of the web and propagated downward through the web and upward through the flange. The flange had a brittle fracture, most likely as a result of absorbing a shock load caused by the sudden release of the web stress at failure—probably at a time when the temperature was low. In the 1951 collapse of the four spans of the west bridge, the initial rupture would have been expected to occur at a point of maximum stress and extensive structural damage both of which were on the river side of the first pier.

The fracture probably extended from the top to the bottom of the girder, running almost vertically and missing the stiffeners and floor-beam connections which had prevented collapse in 1950 (Fig. 13(*a*), line C). As a result, the hanger effect that saved the span from falling in 1950 was not effective. The transfer of dead load to the previously highly stressed adjacent girder broke that girder. As the long end of these girders deflected from under the roadway slab, the unsupported slab, heavily reinforced parallel to the center line and capable of taking considerable tension, sagged and buckled downward into a catenary. The tension forces set up by this catenary action pulled the first pier over toward the river and pulled the end of the girders approximately 70 ft off the abutment toward the river (Fig. 13(*c*)).

The collapse of these two spans caused the collapse of the adjacent span because its end moment was removed. In turn, the fourth span fell for the same reason. The progression of this failure was probably halted at the center of the bridge—which was also the center of expansion of the floor slab—because the force causing the failure had dissipated at this point, and because the disrupting force on the remaining four spans of the bridge had been partly relieved the previous year by the first fracture.

The true cause of a structural failure of this type can never be definitely proved; it has to be arrived at by logical deduction. The basic cause of this failure can be explained as already shown. It is presented as the most obvious explanation, but it is also one that is easily overlooked. It could not have been predicted without using the coordinated results of research and observations on the materials used in the bridge.

This failure—as is usually the case—opens up new fields for research, especially those in which two materials of completely different characteristics are combined and are required to act together. The failure draws attention to one of the faults of research: Research data can support only limited conclusions; secondary conclusions, extended beyond the range of the known facts, are not justified.

The design and construction of the Three Rivers Bridge were conservative and conventional. The failure of a supposedly adequate structure of this type undoubtedly discourages the use of welding and the use of continuous steel structures until the failure has been satisfactorily explained. The failure tends to increase the cost of all steel-bridge construction to the extent that a higher quality (and higher priced) steel and additional costly requirements in fabrication procedure are demanded.

It would certainly not be practicable or economical to attempt to furnish a steel of such ductility that it could accommodate the type of progressive growth that is characteristic of expansive concrete. The use of such an improved and more costly steel would probably not have prevented this failure—nor would it offer protection against other failures of the same type which result from stresses induced by the growth of expansive concrete.

F. J. Tamanini,[37] A. M. ASCE.—An excellent report on welded structures has been made by the author. Although primarily concerned with welded steel structures, Mr. Grover cited aluminum welding developments and uses under the heading, "Processes Used for Structural Welding."

Welded-aluminum design was successfully used by the Corps of Engineers, United States Department of the Army, in the military bridges that were used to make the major river crossings in Korea (from 1950 to 1954). Since 1943, the Engineer Research and Development Laboratories (Fort Belvoir,

---

[37] Chf., Structural Design Branch, Eng. Research and Development Labs., Fort Belvoir, Va.

Va.), with the cooperation of fabricators and aluminum producers, have successfully incorporated welding in aluminum bridge structures to satisfy stringent military requirements. During the design and development of these bridges (1943 to 1945), various aluminum alloys were used in full-size, welded stringer beams which, in military terminology, are termed "balk." Although carbon-arc welding and metallic-arc welding were used in early balk fabrications, no weld failures, as primary deficiencies, were noted in testing full-size balks to ultimate failure. The original failures (1943 to 1945) were primarily caused by attachment details and compressive buckling, which were remedied by subsequent redesign.

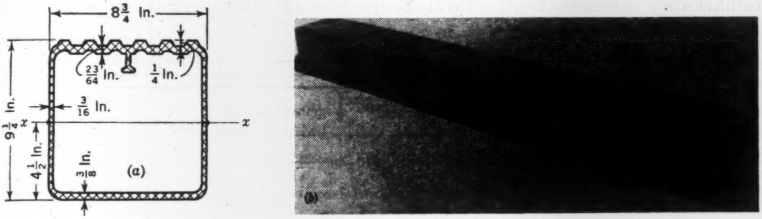

FIG. 14.—ALUMINUM NORMAL BALK

Aluminum alloy[4,5] 14S–T6 and inert-gas, shielded arc welding are now (1954) specified for fabrication of the balk. Both helium and argon as the shielding gases together with tungsten electrodes have been used successfully by various manufacturers, many of whom have designed their own automatic welding fixtures by combining commercially available welding equipment with specially fabricated fixtures.

The balk is basically a 9-in. by 9-in. watertight, square box approximately 15 ft long to which are attached connection lugs. The lugs make it adaptable for use as the articulated-continuous roadway of a floating or simple-span bridge. The balk is composed of two extruded special channels butt-welded together on the neutral axis with plates welded to the ends to complete the watertight box. Such a balk is shown in Fig. 14. The properties of the balk section shown in Fig. 14(*a*) are as follows:

Item	Value
Area, in inches^2	10.26
Moment of inertia, in inches^4	148.2
Section modulus, in inches^3	32.9
Modulus of elasticity, in pounds per square inch	10.6×10^6

During fabrication of 20,000 balk, sample balk taken at frequent intervals were tested to ultimate failure as a beam. The deflection at a 30,000-lb load and the maximum measured deflection occurring immediately prior to failure were recorded. The balk were welded by a production-line welding apparatus which utilized one of several available automatic welding devices. Basically, the apparatus was an automatic, helium gas, shielded, consumable wire, electrode-type welding arrangement. Welding speeds as high as 120 in. per min were obtained; however, in order to reduce porosity and achieve maximum tensile strength of welds, a speed of 90 in. per min was used. Except for removing grease and dirt from the welding surfaces, no cleaning was necessary.

Forty-four sample balk were tested to failure in the manner depicted in Fig. 15. As a result of optimum aluminum welding and section design, excellent welding equipment, and choice of efficient welding procedures, high and remarkably consistent structural properties for the balk were evidenced.

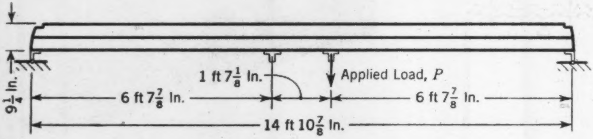

Fig. 15.—Laboratory Arrangement for Testing Balk

Under the application of the specified 30,000-lb load, the measured deflections were observed to fall within a narrow range—from 2.25 in. to 2.50 in. The numerical average for all forty-four beams was 2.33 in. It is interesting to note that, by using the balk properties shown in Fig. 14(*a*) and by taking E (the modulus of elasticity) as 10.6×10^6 lb per sq in., the computed deflection is 2.30 in. The stipulated 30,000-lb test load corresponds to the imposed field loading. It is under this condition that the allowable working stress of 40,000 lb per sq in. in bending occurs. The factor of safety for designing military bridges in steel or aluminum is 1.25—based on the yield strength.

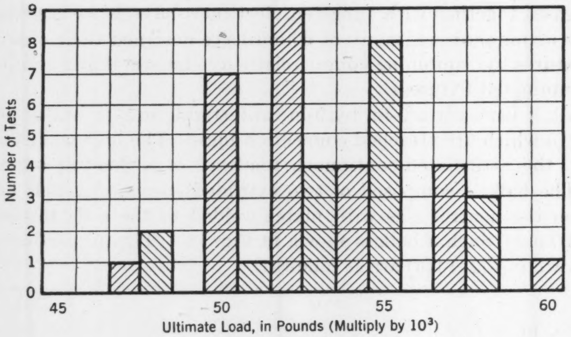

Fig. 16.—Ultimate Test Loads

With a few exceptions, the ultimate load for all forty-four balk produced identical structural ruptures—that is, weld-zone fracture was followed by a combined maximum-tension failure and vertical-shear failure of the lower balk-channel extrusion. The average ultimate load was 53,200 lb, and the average of the maximum measured deflections was 4.49 in. The ultimate-load data are shown in Fig. 16.

Because of the size of the balk and insufficient extrusion facilities for making the hollow box extrusion in one piece, welding appeared to be the only acceptable method of obtaining the desired section. Tests and field use, even under the high-stress conditions for military loads, have certainly justified its acceptance. During the development of military bridges utilizing aluminum welding from 1943 to 1954, experience and tests have shown that welding can be used successfully not only for jointing sections on the neutral axis but also for obtaining watertightness, and it can also be used in other areas where the low ductility of the zone affected by the heat of welding is not considered to be deficient or detrimental to the end product.

NORMAN B. JONES,[38] J. M. ASCE.—A valuable summary of research on welded structures has been presented by Mr. Grover. It is believed, however, that several comments are necessary regarding the type of portal frame beam-to-column connection exemplified in Fig. 8. These comments are based primarily on the source[39] of Fig. 7.

The type P connection (Fig. 8) consisted of a 14WF30 beam and an 8WF31 column. At a moment value equivalent to 20 kips per sq in. on the column, the joint stiffness compares as favorably with the 8WF31 rolled section as the type A joint (Fig. 7) compares with the 8B13 rolled section at a moment equivalent to 20 kips per sq in. Slightly below a moment equivalent to 22 kips per sq in. on the 8WF31 column the type P joint started a plastic rotation as a result of web yielding. The type A connection continued to function with an almost constant relative stiffness until a moment of 400 in.-kip was reached.

Because these observations indicate that the type P connection performed satisfactorily at a moment equivalent to 20 kips per sq in. on the 8WF31 column, it is of interest to compute the approximate web unit shear:

$$\text{Shear force} = \frac{550}{7.57} = 72.7 \text{ kips}$$

$$v = \frac{72.7}{13.86 \times 0.27} = 19.4 \text{ kips per sq in.}$$

This value indicates that web yield is probably imminent, according to the various theories of shear failure.[40]

The author states (under the heading, "Tests of Rigid-Frame Knees"):

> "The type P connection without a diagonal stiffener, * * * deformed as a result of excessive web shear at half the moment value for the lighter of the two joined members."

It should be emphasized that the "moment value" referred to is the "full plastic moment" which has a value of 1,190 in.-kip for an 8WF31 section.

---

[38] Structural Engr., Whittier, Calif.

[39] "Connections for Welded Continuous Portal Frames," Progress Report No. 4, Pt. 1, by L. S. Beedle, A. A. Topractsoglou, and B. G. Johnston, *Research Supplement, Welding Journal*, July, 1951, pp. 359s–384s.

[40] "Strength of Materials," by S. Timoshenko, D. Van Nostrand Co., Inc., New York, N. Y., 2d Ed., 1941, Pt. II, p. 477.

This moment capacity is that which must be developed when the desirable benefits of plastic design are to be utilized. When conventional designs are made by elastic analysis and design methods, it is not necessary to rely on the moment-carrying capacity of connections beyond the elastic limit.

It is believed that the type P connection is usually adequate to develop moments permitted by the ordinary working stresses and elastic analysis, but that it is definitely lacking in any measurable "factor of safety." For a greater moment capacity for the connection (and therefore a more uniform factor of safety throughout the structure) the joint web should be reinforced to maintain the unit shear stresses at values less than 13 kips per sq in.

La Motte Grover,[41] M. ASCE.—Attention has been called by Mr. Benjamin to the practice of penalizing welded construction because of the lack of sufficient knowledge concerning the behavior of welded details. This condition has improved, but much educational work remains to be done. To a large extent it is a matter of disseminating information; also—as in other fields—there is a continual need for further study and research. In many respects there is available much more research information about welded details than about other types of construction. Furthermore, it should be realized that welding has a long history of satisfactory performance in the United States.

It was principally the first research studies of flexible and semi-rigid welded beam-end connections, begun in the late 1920's, that prompted subsequent researchers to determine the actual behavior of riveted and bolted connections. Many such connections had been in use for years with little thought given to how they actually behaved and what end moments might be transferred to columns by relatively rigid wind-bracing connections of beams and quite rigid connections of relatively deep building trusses.

It is true that a large part of the study of the brittle-fracture phenomenon has been in the field of metallurgy to determine the behavior of materials under various conditions of temperature, state of stress, and strain rate. This type of investigation has been necessary for a complete understanding of the fundamental problem. However, details of design and the effect of fabricating procedures have also been studied in large-scale tests of welded structural members, hatch-corner details of ships, end connections of longitudinals in tanker ships, reinforcements around openings, and other practical details of design. A committee of the WRC is now (1954) preparing a manual to provide interpretation of much of this research for use in practical designing and detailing.

With regard to design stresses, the trend in Europe as well as in the United States is to place more emphasis on deformations than on stresses, or at least to make the designer equally conscious of deformations. The work of the Structural Steel Committee, WRC, is being continued to provide more thorough answers to some of the questions that Mr. Benjamin has posed.

Mr. Lamb has made a noteworthy contribution to the explanation of the failure of the Three Rivers Bridge. He has presented data on the expansive properties of concrete similar to that used in the floor of the bridge. It has been shown that there is a strong probability that the growth of this rather unusual concrete created sufficiently high stresses to rupture the steel material. This rupture occurred despite good control over fabrication operations and design provisions that would normally be adequate for this type of welded structure. An even stronger case could have been made if Mr. Lamb had not neglected (in the interests of being conservative in his estimate) the eccentricity of the expansive force on the girders. Also, under the conditions of a very rapid drop in atmospheric temperature, a considerable difference of temperature between the floor slab and the web of the girder could have helped increase the tensile stress in the steel.

---

[41] Welding Engr., Air Reduction Co., New York, N. Y.

With regard to the brittle appearance of the fractures, it is known that, when a structural-steel material fractures at a relatively low temperature, regardless of the cause, the fracture will have the characteristic crystalline appearance that was observed. Although very high strain rates cause brittle fractures, the rates of strain associated with impact loads from traffic on a bridge are not believed to be great enough to exercise much influence (apart from the dynamic increment of the load).

As Mr. Lamb has mentioned, advantage can often be taken of engineering failures to accumulate research data. This is possible only when adequate construction records are available and when conditions attending failure can be determined with reasonable accuracy. Apparently, this information was available for the Three Rivers Bridge. A careful examination of the wreckage, supplemented by engineering data and considerations, has made it possible to establish the behavior and sequence of events as the bridge collapsed. Accordingly, the conditions of a controlled test were realized. These conditions represented actual service behavior which would have been too costly or impossible to reproduce in a research project. In the same general manner, tests of full-scale structural members made under carefully controlled conditions have provided valuable information to supplement the fundamental information derived from tests of smaller and more simple specimens. The results of such full-scale tests have complemented each other despite the complexity of such specimens as compared with specimens used to develop fundamental information.

The facts presented by Mr. Lamb do not necessarily invalidate the opinions expressed by demolition experts who examined the failure of the Three Rivers Bridge and testified that the collapse appeared to have been caused by an explosion—thus suggesting sabotage. The steel could have been in a high state of tension as a result of the "internal loading" resulting from the growth of the concrete. Even though some slipping had occurred between the floor slab and the steel, the tension stress could have remained relatively high so that an explosion would have "triggered" the collapse.

An important distinction should be made between the nature of the internal loading caused by the growth of a concrete floor slab and the localized internal residual stresses resulting from welding. The former would act in the same manner as an external load and is in fact external with reference to the steel. Therefore, this loading would maintain a field of high elastic stress with sufficient energy to start a fracture and propogate it. On the other hand, residual stresses caused by welding are localized, self-limiting, and disappear under very small local yielding. Therefore, residual stresses cannot maintain a field of high elastic stress and energy.

Mr. Tamanini has offerred an interesting example of a successful application of the inert-gas-shielded metal-arc welding process in aluminum structural work. The unfavorable influence of the heat of welding on the strength of the solution heat treated and artificially aged structural alloys of aluminum was cited under the heading, "Processes Used for Structural Welding." Despite this handicap, it is often possible for a designer to locate welded joints in aluminum in such a manner that the reduced strength of the heat-affected zone will not influence the over-all strength of a member. Even though the longitudinal welds in the balk were located in a plane of maximum shear, the test beams developed virtually the full strength of the base metal in bending, and measured deflections conformed closely to the computed deflections. Accordingly, the beams could be used at the full allowable working stresses that had been adopted for the base metal.

For the benefit of those who have been accustomed to think only of conventional elastic analysis and allowable working stresses, Mr. Jones had emphasized that the moment value for the 8W31 section is the maximum moment or full plastic moment developed by the testing of this rolled beam section. As Mr. Jones has implied, the type P connection would fulfil conventional design requirements based on elastic analysis and customary working stresses. If it were to be evaluated solely on this basis, under conditions that do not make allowance for its shortcomings with respect to reserve strength or over-all factor of safety for the entire structure, this detail would be favored over a more expensive detail of superior behavior at stresses greater than conventional working stresses. However, there might well be a legitimate use in certain types of construction for a detail with somewhat less reserve strength, such as the type A knee of lowest fabrication cost; for example, it could be used in a structure with definitely controlled loading, which could not be expected to be subjected to such hazards as bombing, earthquakes, tornados, or other serious overloading.

FABRICATION AND CONSTRUCTION

By C. L. Kreidler[1]

Synopsis

During the latter part of the nineteenth century the development of the elevator contributed to an increased demand for taller buildings; height limitations on masonry walls do not lend themselves to tall-building construction, but structural-steel construction met this demand. The introduction of welding in the 1920's proved to be another impetus to the use of structural steel.

Steel fabrication is detailed and involved. The arrangement of departments and assignment of duties and responsibilities may vary from one fabricator to the next, but the aim of all is to fabricate structural steel at a reduced cost so as to meet competition successfully. The use of welding has done much to approach this goal.

Introduction

On October 8, 1871, a fire was started in Chicago, Ill., in a barn on DeKovan Street not far from Canal Street. In 48 hours the fire destroyed $192,000,000 worth of property (out of a total property evaluation of $575,000,000), and 100,000 persons were homeless.

Catastrophe that it was, the Chicago fire offered unprecedented opportunities to architects and engineers. Their success in taking advantage of this opportunity is attested to by scores of beautiful and useful buildings which represent the largest existing (1953) concentration of first-rate commercial architecture in the world. In the two decades following the fire, buildings worth $316,220,000 were constructed in Chicago. The impetus of this construction forced on the designers the necessity for developing a new form and technique of building.

The invention of the elevator caused a demand for buildings of increased height. The fact that the thickness of a masonry bearing wall increases in direct proportion to its height places a restriction on the height of the building. Consequently, approximately ten stories is the practical limiting height for a building with masonry bearing walls. The Monadnock Building in Chicago, however, is the tallest masonry building ever constructed. This building is sixteen stories high and rests on walls that are 72 in. thick at the base.

In 1885, the Home Insurance Building in Chicago was completed; this was the first truly skeletal building. The frame was a serial column-and-beam type of construction, formed from round cast iron columns, wrought iron box columns of built-up section, and wrought iron I-beams. The lintels and mullions were cast iron. The building was originally ten stories high; two stories

---

Note.—Presented at the Centennial Convocation, Chicago, Ill., September, 1952. Published essentially as printed here, in November, 1953, as *Proceedings-Separate No. 345*. Positions and titles given are those in effect when the paper was received for publication.

[1] Chf. Structural Engr., Lehigh Structural Steel Co., Allentown, Pa.

were added in 1890, and in 1931 the structure was demolished. The outermost floor beams carried not only their part of the floor load but also one bay of the exterior wall, up to the beam next above. This method of carrying the outer envelope is standard practice for the construction of tall steel-framed structures. Without this technique, the skyscraper would be impossible.

In addition to originating the steel-frame structure, engineers from Chicago are credited with creating hollow-tile fireproofing and developing the use of large areas of glass in walls. These features are presently (1953) common in construction.

THE ORGANIZATION OF A STEEL COMPANY

Each structural-steel company has a different organizational arrangement for estimating, bidding, preparing shop drawings, and fabricating. With the objective of fabricating at minimum costs so as to meet competition, all the companies strive to eliminate duplication of work and unnecessary departments. The smaller companies operate one plant and a general office which performs all the functions of the business. The larger companies operate several plants and various offices.

Whether the company is large or small, the functions can be classified into twelve departments: (1) The contracting department submits bids and takes contracts. (2) The engineering department prepares designs, makes estimates of weights and costs, and supervises the work of the plant engineers. (3) The drafting department requisitions the materials needed to perform the contract and prepares the working drawings. (4) The operating department performs the operations specified on the shop drawings. (5) The auditing department renders invoices to the customers and compiles data of cost and accounts. (6) The purchasing department buys all materials and supplies for the company. (7) The treasury department approves the credits of prospective customers, collects bills, pays any indebtedness, and disburses the salaries and wages of employees. (8) The erecting department maintains the erection equipment and erects the fabricated structural steel in the field. (9) The mechanical engineering department solves problems pertaining to the fuel, power, and machinery of the plant. (10) The traffic department issues instructions for the routing of all shipments, furnishes instructions for shipping clearances, investigates shipping rates, and adjusts all claims with shippers. (11) The personnel and public relations department maintains relations with the public and supervises the welfare of the employees. (12) The safety department requires no description. Its work is of paramount importance in operating an efficient plant.

THE FUNCTIONS OF A STEEL COMPANY

Obtaining a Contract.—The first step in securing a contract consists of preparing a bid. From plans and specifications prepared by architects and engineers (selected by the contracting department), an estimate of cost is prepared by the engineering department. Most contracts are taken on a unit price or lump-sum basis. Both types of estimates are composed of the same elements: The cost of the raw material, the cost of the direct shop labor, the general expenses of operating the shop, the drawing costs, and the estimated overhead expenses. To these costs are added shipping charges, insurance, taxes, and miscellaneous items so as to arrive at an estimated cost. To the estimated cost the contracting department adds a margin and submits a proposal to the customer which states the selling price and the delivery date. Frequently, the time of delivery may determine who is to be the successful bidder.

Fulfiling a Contract: Preliminary Steps.—When a contract is awarded, the designs, specifications, and pertinent information are released to the drafting department for the preparation of the shop-working and detail drawings. Good designs, specifications, and complete information without subsequent revisions are the ideal conditions for making detail drawings quickly and economically with the least chance for error. A structural-steel building is similar to a gigantic, skeletal, jig-saw puzzle. The drafting department must devise an identifying system for each piece so that the erection department will be informed how and where to place each element of the structure. At the start of the project, the types of connections, the location of shop and field joints, the connection medium, and the sequence of erection must be determined. All material that goes into the completed structure must be requisitioned from the purchasing department by the drafting department. The drafting department prepares the preliminary bills of material for the use of the purchasing department in ordering each principal piece of material from the rolling mill to its exact size.

From the design drawings, the drafting department prepares a framing plan which is very similar to the design drawing except that typical connections and identifying markings are added. This drawing is diagrammatic and is made to a small scale. With the framing plan to identify the pieces, column details and beam details are prepared. These details are usually schematic, and as such, are not drawn completely to scale. Similarly, girder details are prepared. On each of the drawings is given complete information for identifying the shipping piece, the description and size of all the material which is to be assembled to form the shipping piece, the weight of each item, and complete information required for fabrication.

The fabricator's drawings are then submitted to the customer's engineer for approval. The engineer's examination may be complete or merely a survey of the general design, the size of material used, and the strength of the connections. The structural steel company is responsible for the accuracy of the shop drawings, the approval by the customer's engineer being merely the authority to proceed with the fabrication.

Shop and shipping bills are prepared from the approved detail drawings by the operating department. The shop bills contain a list of all the members on the contract with the material used to fabricate each member, the weight of each piece of material, the weight of the completed member, a list of the mill material with item order numbers showing the lengths from which the pieces are cut, and the sections to be taken from stock material.

The shipping bills contain a list of all the shipping pieces with descriptions and shipping marks, give the over-all dimensions of each member for purposes of identification, and include the computed weights. Actual scale weights are seldom used in structural steel contracts; computed weights are preferred.

Fabricating Shop.—Shop organization, equipment, and the routine of handling work will vary for different operating departments. The usual plan is to have a large structural shop and a small auxiliary shop for fabricating light material. Other buildings are devoted to machine work, forge work, and such departments as are required for plant operation. All equipment, however, is located so that material can move progressively from the receiving yard to the shipping yard with the least handling of the material.

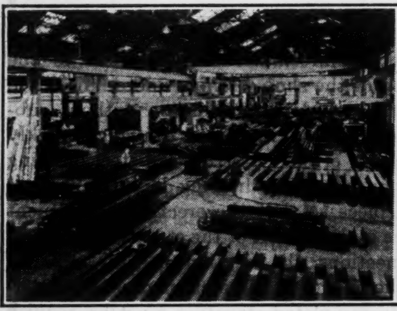

FIG. 1.—FABRICATING SHOP

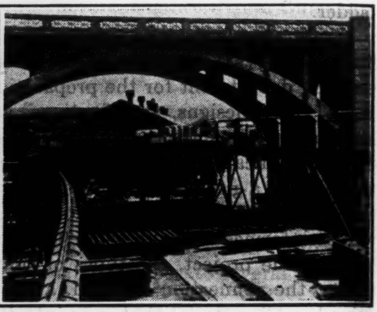

FIG. 2.—SHIPPING YARD

During the time the drawings are being prepared and the templets made, the material is received from the mills. As the material arrives, each item is checked against the mill orders. The material is sorted and piled on skids for later consignment to the fabricating shop.

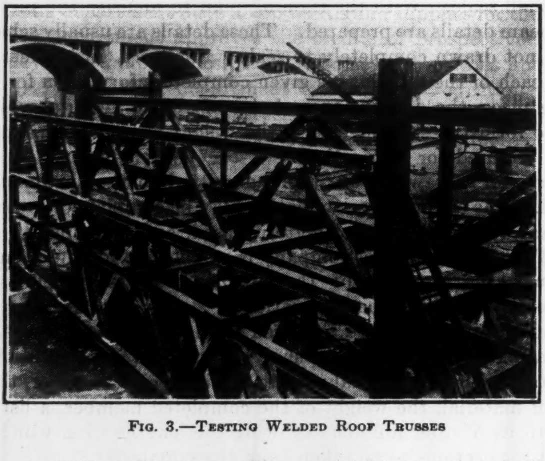

FIG. 3.—TESTING WELDED ROOF TRUSSES

Various methods and devices are used for locating holes and cuts on the steel. Generally this is accomplished by the use of templets or by marking the steel directly from the drawings, without the use of templets—a process termed "scratching." The templet is usually made of wood or cardboard or a combination of both to full size.

The first operation in the fabricating shop consists of marking the material—termed "laying out"—by the use of templets or scratching. The assembly mark, the contract number, and other information are then painted on the steel. Before leaving the lay-out skids, the cuts and copes are usually made on the steel by flame-cutting. The steel is then moved to the punches and drills.

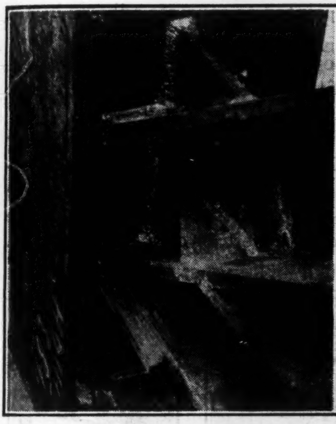
FIG. 4.—WELDED JOINT AT COLUMN AND BOTTOM CHORD

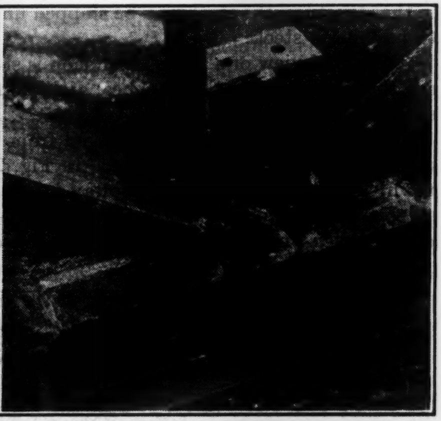
FIG. 5.—WELDED BOTTOM CHORD PANEL POINT

FIG. 6.—FABRICATED GIRDER

FIG. 7.—ERECTED GIRDER

After the detail pieces and main material of a member have been punched, the next operation is that of "fitting" or assembling the various parts of a member for welding. All the pieces are fitted by direct reference to the shop drawings. The main sections are identified by the description painted on the steel by the lay-out man. This process of fitting is probably the most difficult and responsible of any work in the structural shop. The shop connections are then welded; these are usually made by the manual shielded metal-arc welding process.

The next operation is to clean the fabricated members. Scrapers, brushes, shot-blasting, flame-cleaning, or chemical baths may be used to remove dirt, scale, rust, and other foreign matter. If the steel is to be encased in concrete in the structure, the steel may be shipped unpainted as concrete adheres better to unpainted steel.

A general view of a fabricating shop is shown in Fig. 1. In the foreground are the lay-out area, the punches, and the fitting area; at the far end of the shop are the painting skids.

The fabricated steel is transferred from the shop to the shipping yard for dispatch to the field for erection. In Fig. 2 part of a shipping yard in Allentown, Pa., is shown. The craneway in the foreground is curved so that the steel may be moved directly from the shop through the bridge arch. The crane travels on a curve to the right, a curve to the left, or on a straight track.

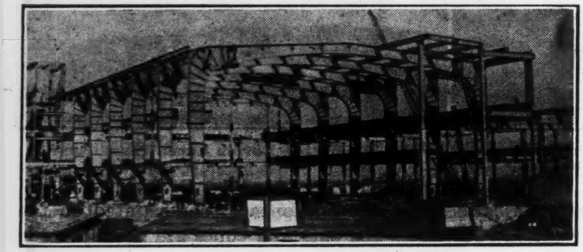

FIG. 8.—WELDED RIGID FRAMES

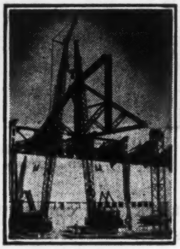

FIG. 9.—ERECTING A WELDED TRUSS

Throughout the fabrication process, the matter of inspection to maintain accuracy and quality is important. The structural steel companies have their own inspectors as a safeguard against errors as the correction of errors in the field is an expensive matter. In addition, purchasers of structural steel usually employ inspectors to assure themselves that specifications and plan are followed in the rolling and fabrication.

On special contracts the engineer may require additional inspection or testing. In Fig. 3 is shown an arrangement for testing welded roof trusses. By using hydraulic jacks placed between a pair of trusses with the top truss inverted, 150% of the design loads were applied to the trusses. The observed center deflections of the trusses agreed with the computed deflections, and the original joint designs were adopted without alteration. In Fig. 4 is shown the detail of the joint of the column and the bottom chord of the truss, and in Fig. 5 is shown one of the bottom chord panel points.

Erection.—Following the preparation and approval of the detail drawing of a welded cantilever girder, the girder is fabricated (Fig. 6); it is then erected (Fig. 7) by the erection department. The erectors have a choice of a large variety of hoisting equipment. By using the hoisting equipment and following the drawings prepared by the drafting department, the fabricated pieces are placed in their assigned locations in the structure. The members are then welded into position.

SOME WELDED STRUCTURES

In Fig. 8 are shown the welded rigid frames in the grit chamber of the Owls Head Sewage Disposal Plant in New York, N. Y. The rigid frames span 66 ft, have a 23-ft rise, and weigh 6½ tons each. The column section is 20 in. deep at the base, the knee is 4 ft 9 in. deep, and the beam section is a 30WF172. The knee and column web is a ½-in. plate, and each flange at the knee is composed of a 16-in. by 1⅛-in. plate and a 14-in. by 1⅛-in. plate.

The raising of the east half of a camel-back truss which supports the roof and monorail cranes in an aircraft factory addition is shown in Fig. 9. The complete all-welded truss spans 200 ft and has a rise of 40 ft at midspan. The bottom chord is 36 ft above floor level. The main members are 36WF sections with the webs parallel to the ground line. The tower on the right is used for erection purposes only. The half-truss in process of being erected weighs 37 tons. To the verticals of this truss are connected parallel-chord trusses with a span of 125 ft.

CONCLUSION

Since the introduction of modern (1953) construction, long strides in material quality and fabrication techniques have been made. Forecasts for the future predict continued advancements. To provide a structure which has an enduring framework that is incombustible and has the economic advantages of strength, compactness, adaptability, salvage, and speed of erection, one should build welded-steel structures.

AMERICAN SOCIETY OF CIVIL ENGINEERS
Founded November 5, 1852
TRANSACTIONS

Paper No. 2730

SAND COMPACTION BY VIBROFLOTATION

BY ELIO D'APPOLONIA[1] AND CALLIX E. MILLER, JR.,[2] ASSOCIATE MEMBERS ASCE, AND THOMAS M. WARE[3]

SYNOPSIS

Borings made at the site of a proposed phosphate plant revealed the existence of a very loose sand that was quite susceptible to significant changes in volume when subjected to vibration or sudden shock. Because the operations of the plant were such that vibrations would be prevalent, it was necessary that the soil be compacted prior to construction so that no significant settlements would occur following the completion of the plant. Studies made prior to construction revealed that the process that was most likely to give the required compaction was that of vibroflotation.

Before applying the vibroflotation process to this project, it was necessary to determine the pattern in which the vibroflot should be used. These tests and the settlement studies are outlined; the resulting settlement was 50% less than the computed value.

INTRODUCTION

Vibration and sudden shocks are known to change a sand deposit from a loose state to a dense state. This change is accompanied by surface settlements that may be as great as 1 in. per ft of depth of sand deposit. To avoid the severe damage that would result to a structure subjected to such settlements, it is necessary to compact the sand prior to construction or to by-pass the deposit of loose sand by the use of piles.

Many methods of sand compaction have been used; some of these are the driving of short, stubby piles, blasting,[4] rolling,[5] vibrating plates, and vibroflotation.[6,7,8] A method is selected for a particular project because of its

---

NOTE.—Published, essentially as printed here, in July, 1953, as *Proceedings-Separate No. 200*. Positions and titles given are those in effect when the paper was received for publication.

[1] Associate Prof. in Civ. Eng., Carnegie Inst. of Technology, Pittsburgh, Pa.

[2] Constr. Project Engr., International Minerals and Chemical Corp., Chicago, Ill.

[3] Vice-Pres., Eng. Div., International Minerals and Chemical Corp., Chicago, Ill.

[4] "Compaction of Cohesionless Foundation Soils by Explosives," by A. K. B. Lyman, *Transactions*, ASCE, Vol. 107, 1942, p. 1330.

[5] "Compaction Studies on Sand Subgrade," Soil Compaction Investigation Report No. 3, *Technical Memo No. 3-271*, Waterways Experiment Station, Vicksburg, Miss., October, 1949.

[6] "A New Soil Compaction Device," by S. Steuerman, *Engineering News-Record*, July 20, 1939.

[7] "Wet Vibration Puts Strength in Sand," by B. Fruhauf, *ibid.*, July 23, 1949.

[8] "Vibroflotation Experiments at Enders Dam, Frenchman Cambridge Unit, Missouri Basin Project," Bureau of Reclamation, U. S. Dept. of the Interior, Research and Geology Div., Denver, Colo., July 27, 1948.

effectiveness and economy. Cost comparisons made for a phosphate plant near Bartow, Fla., showed that the vibroflotation process was the most economical. A comparison of the effectiveness and certainty of each of the several methods of compacting sand similarly resulted in the selection of this process. The method is simple, and good compaction is assured with adequate field control.

Although vibroflotation has been used extensively in Europe—notably in Germany[9]—the process has hitherto (as of 1952) been little applied in the United States. The first large-scale compaction of loose sand by vibroflotation in the United States occurred at Bartow. In this project approximately 156,000 sq ft of foundation area were compacted to an average depth of 12 ft at a cost of approximately $0.10 per cu ft. Compaction proceeded at an average rate of 1,400 sq ft per day, requiring 25 to 30 penetrations of the vibroflot during each 8-hr shift.

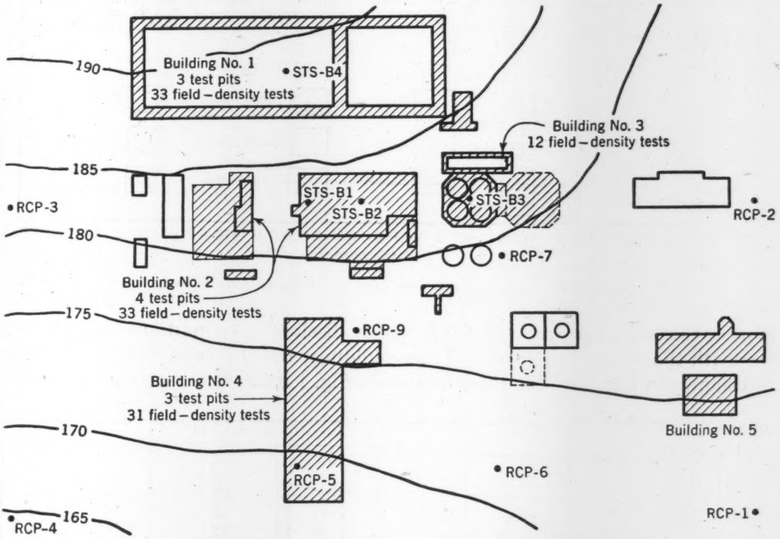
190
Building No. 1
3 test pits
33 field-density tests
STS-B4
Building No. 3
12 field-density tests
185
STS-B1
STS-B2
STS-B3
RCP-3
RCP-2
180
RCP-7
Building No. 2
4 test pits
33 field-density tests
175
RCP-9
Building No. 4
3 test pits
31 field-density tests
170
Building No. 5
RCP-6
RCP-5
165
RCP-4
RCP-1

FIG. 1.—PHOSPHATE PLANT LAYOUT AND LOCATION OF BORINGS

The soil conditions and foundation loads that led to the selection of the vibroflotation process will be reviewed subsequently. Also summarized will be the field tests and laboratory tests that were conducted to establish the effectiveness of the process.

SOILS

The site of the phosphate plant is a relatively high rise of land with a gradual fall to the west. The high point of the site is at El. 190, and the low point is at El. 160. Examination of aerial photographs disclosed a uniformity in vegetation throughout the area; there were no thick rings of vegetation to indicate the existence of old swamps. Exploratory borings were made to check this apparent uniformity of the soils and to disclose soil conditions immediately beneath the major structures. These buildings and the location of the borings are shown in Fig. 1. The shaded areas in Fig. 1 indicate those areas which are compacted by vibroflotation. A generalized boring log with results of the standard penetration tests (the number of blows required to cause 1 ft of penetration of a 2-in. split spoon under a weight of 140 lb falling through a

---

[9] "Grain Elevator Foundations upon Vibroflot-Piles," by A. Scheidig, *Die Bautechnik*, No. 25, June 14, 1940, p. 277.

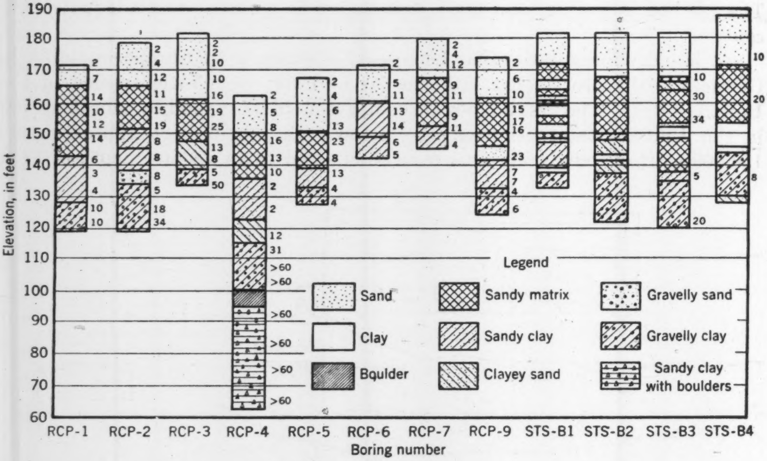

FIG. 2.—GENERALIZED BORING LOGS AND RESULTS OF STANDARD PENETRATION TESTS

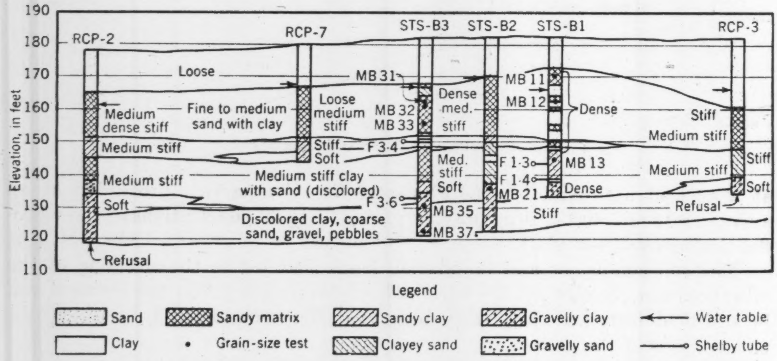
Elevation, in feet
190
180
170
160
150
140
130
120
110
RCP-2
RCP-7
STS-B3
STS-B2
STS-B1
RCP-3
Loose
Medium dense stiff
Fine to medium sand with clay
Loose medium stiff
MB 31
MB 32
MB 33
Dense med. stiff
MB 11
MB 12
Dense
Stiff
Medium stiff
Medium stiff
Stiff
Soft
F 3-4
Med. stiff
Soft
F 1-3
F 1-4
MB 21
MB 13
Dense
Medium stiff
Stiff
Soft
Medium stiff
Medium stiff clay with sand (discolored)
Soft
F 3-6
MB 35
MB 37
Stiff
Refusal
Discolored clay, coarse sand, gravel, pebbles
Refusal
Legend
Sand
Clay
Sandy matrix
• Grain-size test
Sandy clay
Clayey sand
Gravelly clay
Gravelly sand
Water table
Shelby tube

FIG. 3.—NORTH-SOUTH SOIL PROFILE FROM RCP-2 TO RCP-3

height of 30 in.) is shown in Fig. 2. The soil profiles illustrated in Figs. 3 and 4 show an area covered with clean, loose, wind-blown sand varying in thickness from 10 ft to 15 ft. Penetration tests disclosed that the density increased with the depth of the sand deposit; the number of blows per foot ranged from 2 at the surface to 10 at the bottom of the layer. Such low values indicate the presence of a very loose sand that is susceptible to significant changes in volume when subjected to vibration or sudden shock.

Below the sand is a sandy "matrix" deposit (a local term that is used to denote a stiff conglomerate of sand, clay, and phosphate granules) containing reddish-brown and yellow clay and some phosphate granules. The average thickness of this layer is 15 ft. Penetration tests revealed a material that was medium dense or fairly well compacted. The matrix has high bearing strength, and vibrations would have little effect on this deposit.

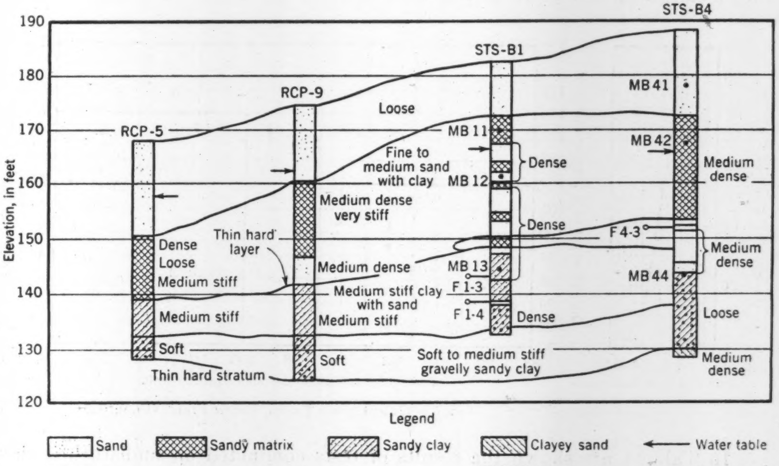

Elevation, in feet
190
180
170
160
150
140
130
120
RCP-5
RCP-9
STS-B1
STS-B4
Loose
MB 11
Fine to medium sand with clay
MB 12
Dense
Dense
MB 41
MB 42
Medium dense
Medium dense very stiff
Thin hard layer
Dense
Loose
Medium stiff
Medium dense
F 4-3
Medium dense
MB 13
F 1-3
F 1-4
MB 44
Medium stiff clay with sand
Medium stiff
Medium stiff
Dense
Loose
Soft
Soft
Soft to medium stiff gravelly sandy clay
Medium dense
Thin hard stratum
Legend
Sand
Sandy matrix
Sandy clay
Clayey sand
Water table
Clay
Grain-size test
Gravelly clay
Shelby tube

FIG. 4.—EAST-WEST SOIL PROFILE FROM RCP-5 TO STS-B4

Beneath the matrix are layers of sandy clay and gravelly clay interspersed with layers of sand and matrix. The clay deposits vary in thickness from a few inches to 3 ft. For the most part, the sandy clay deposits are firmly cemented (as indicated by the penetration tests) and would be classified as medium stiff to stiff. The reddish-brown to yellow discoloration of the originally white clay above El. 135 is probably caused by exposure to air and subsequent desiccation.

The clay deposits below El. 135 contain coarse gravel, rocks, and traces of phosphate granules. Penetration tests were erratic—indicating deposits of soft material with sporadic refusal near El. 120. Because of the rocks and boulders, the results of the penetration tests below El. 120 were interpreted with caution. Resistance to a penetration of comparable magnitude might not have been encountered during the driving of piles because the rocks would be easily pushed aside. Observations of deep cuts (made by mining operations) in similar soils have disclosed alternate layers of stiff and soft clay matrix which were erratic in extent and depth. Such deposits could be classified (erroneously) by a driller as gravelly clay. Hence, the resistance to penetration below El. 120, as recorded by' the driller, is not reliable for the design of the foundations. Below El. 130 the gravelly clay layer has a blue to black discoloration because of pre-existing vegetation at these lower elevations.

Soil Tests

Mechanical-analysis tests conducted on samples taken from different depths of the upper sand deposit indicate a very uniform sand (Fig. 5). In all cases the grain sizes are greater than 0.06 mm. These tests clearly indicate a windblown sand which is unstable in a loose state.

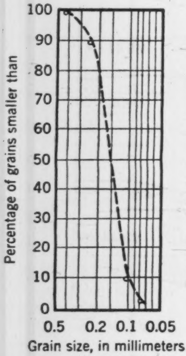

Fig. 5.—Grain-Size Curve

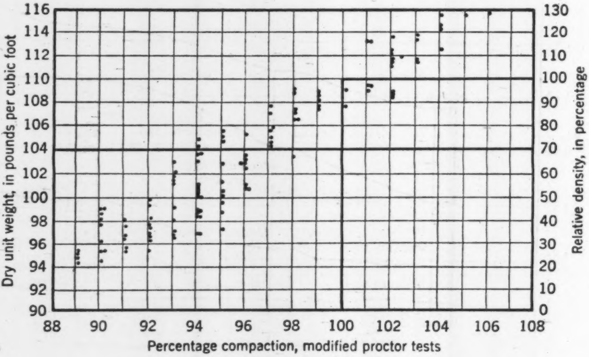

Fig. 6.—Compaction Tests, Eglin Field (Florida)

In Table 1 are shown the results of tests conducted on undisturbed clay samples. The location of each sample is shown in Figs. 3 and 4. The high-moisture contents and liquid limits obtained for the clay samples would normally indicate a fairly compressible material. However, this is not borne out by the compression indices. The low values for the compression index indicate a material of low to medium compressibility, which probably can be attributed to the precompression by desiccation that occurred during the formation of the deposits.

Field-density tests conducted at various points throughout the foundation area and at different depths below the surface (to a maximum of 12 ft) disclosed a loose sand with a relative density ranging from 30% to 47% and averaging 33%. The sand had an average dry unit weight of 90 lb per cu ft and 110 lb per cu ft in its loosest and densest states, respectively. The dry unit weight of the sand in a dense state was obtained by the vibration of a saturated sample under a surcharge of 2.2 kips per sq ft. The minimum dry unit weight was obtained by tremming the sand through a funnel.

The value of the maximum dry unit weight is dependent on the test procedure. Different methods of compaction produced variations in the dry unit weight from 106 lb per cu ft to 114 lb per cu ft. The question arose as to whether or not the average value of 110 lb per cu ft was reasonable. The results of the surcharge method of compaction were compared with modified Proctor tests[5] conducted on a similar sand found at Eglin Field, Florida. Because modified Proctor tests were not available for the Bartow sands, test results obtained at Eglin Field were used for comparison. In Fig. 6 it is seen that a modified Proctor value of 100% corresponds approximately to a 100% relative density at a dry unit weight of 110 lb per cu ft. Because of this agreement, it was felt that field control of the vibroflotation process based on maximum and minimum values of the dry unit weight of 110 lb per cu ft and 90 lb per cu ft was adequate.

TABLE 1.—SOIL DATA

Sample No.	Description	Surface elevation	Sample elevation	Moisture content	Liquid limit	Plastic limit	Plasticity index	Shrinkage limit	Specific gravity	Maximum grain size, in millimeters	Unconfined compression strength, in tons per square foot	Initial void ratio	Compression index
F1-3A	Clay mottled gray to reddish brown	182.6	143	51.9	53.3	14.1	39.3	17.3	2.84	0.002	0.083	1.48	0.41
F1-4B	Mottled gray to brown clay—some gravel	182.6	137	42.1	...	...	...	...	...	...	0.44	1.36	0.21
F3-4	Mottled gray to brown clay—some gravel	181.9	150	54.8	80.3	28.9	51.4	18.1	2.73	0.002	0.59	1.71	0.22
F4-3	Alternate seams of clay, mottled gray to brown	189.5	152	68.0	83.8	38.6	45.2	19.0	...	0.002	0.32	1.62	0.20

Minimum dry unit weights were obtained using different procedures of pouring the sand into the container. Results agreed within 1.5% of the average value of 90 lb per cu ft. The specific gravity of the sand is 2.67.

FOUNDATIONS

A study of the soil explorations and laboratory data indicates that settlement of the foundations may be the result of two well-defined causes: (1) A change in state of the upper layer of sand from loose to dense; and (2) consolidation of the different layers of clay below El. 150, approximately 30 ft below grade.

Settlement because of a change in state of the loose sand may result from vibrations caused by railroad operations and vibrations resulting from the machinery, principally the battery of sixteen 300-hp motors and vacuum pumps in the process building. Settlement because of the consolidation of the clay layers depends on the pressure imposed upon them by the various foundations. Because the footings for most of the main buildings have a width of 10 ft (less than one third of the depth to the compressible clay layers) and are subjected to light loads, settlement caused by consolidation is negligible. For example, the average uniform pressure imposed by the process building is 500 lb per sq ft, and the largest footing is 10 ft square. Load conditions are similar for other buildings with the exception of the two main storage buildings. One is a three-hinged arched structure 600 ft long with a 200-ft span and an average floor load of 1,200 lb per sq ft. The second storage building is a four-bin silo, 110 ft high, supported on a rigid raft foundation approximately 100 ft square. The dead load for the second building is 1,100 lb per sq ft, and the dead load plus full live load is 3,300 lb per sq ft. The design of successful spread footings for all but these two structures required (1) compacting the loose sand and (2) keeping the base of the footings as near to the ground surface as possible.

Piles 50 ft to 60 ft in length, with tips reaching the gravelly clay layer (El. 120), were considered for the foundation of the storage buildings. Investigations of the foundation for the silo storage building revealed that the settlement of a pile foundation would exceed that of a raft foundation placed on a compacted sand. Although standard penetration tests indicated high resistance and refusal at El. 120, it was not certain that this resistance would be obtained during the driving of piles. As noted previously, these lower deposits are a conglomerate of hard and soft clay formations; hence, the piles would act as friction piles rather than bearing piles. The pressure imposed on the clay layers by the frictional forces of the piles would result in consolidation of the clay layers and, therefore, surface settlement. The pile load would, in turn, be gradually transferred to the tip of the piles, and the increased pressure would result in further settlement.

Short, point-bearing piles driven to refusal into the sandy matrix to by-pass the loose-sand deposits offered no advantage. The transfer of load to the pile tips imposes a greater soil pressure on the underlying clay layers than would spread footings near the surface; hence, larger settlements would occur. Apparently, it would have been difficult to drive piles to El. 120 and to penetrate the sandy matrix without "jetting."

It was concluded that successful spread footings and raft foundations could be designed if the loose sand were compacted. To compact the sand, the vibroflotation process was selected. In this process[6] a 15-in.-diameter tube is vibrated by a rotating eccentric weight mounted within the tube. The vibration and movements of the sand particles produced by the vibroflot are sufficient, under saturated conditions, to cause adequate compaction of the sand within a radius of 4 ft.

PRELIMINARY COMPACTION TESTS

As noted previously, the dry unit weight of the sands near Bartow ranged from a minimum of 90 lb per cu ft to a maximum of 110 lb per cu ft (obtained by vibration of the container). The specific gravity of the sand is 2.67. From the definition of D, the relative density,

$$D = \frac{e_L - e_N}{e_L - e_D} \quad \text{(1)}$$

it can be shown that

$$D = 5.50 - \frac{495}{\gamma_N} \quad \text{(2)}$$

in which e_L is the loose void ratio, e_D denotes the dense void ratio, e_N represents the natural void ratio, and γ_N is the natural dry unit weight (in pounds per cubic foot).

TABLE 2.—AVERAGE RESULTS OF VIBROFLOTATION COMPACTION TESTS FOR TEST PATTERNS SHOWN IN FIG. 7

Test pattern No.	Point	Relative density, in percentage	Distance from point to nearest vibroflot hole, in feet	Distance between vibroflot holes, in feet	Sum of influence coefficients
1[a]	1	59	5.4	7.3	4
	2	63	4.0	7.3	6
	3	93	2.0	7.3	16
2[a]	1	87	1.9	8.0	16
	2	65	3.9	8.0	9
	3	57	5.7	8.0	4
3[a]	1	62	4.0	8.0	12
	2	59	4.6	8.0	10
4[a]	1	86	3.0	6.0	20
	2	92	2.8	6.0	22
	3	70	4.3	6.0	18
5[b]	1	80	3.8	7.5	18
	2	73	2.3	7.5	14
	3	88	1.3	7.5	26
	4	68	4.3	7.5	12

[a] Results are averages from samples taken at depths of 4 ft, 6 ft, and 8 ft. [b] Results are averages from samples taken at depths of 3 ft, 6 ft, and 9 ft.

A sand with a relative density of 70% or greater was selected as the criterion for adequate compaction. This selection was based on the experience of previous investigators.[8,10] A sand with a relative density greater than 70% would be a suitable foundation material because the settlements caused by the compaction of the sand from vibrations and sudden shocks would be negligible. Hence, the compaction process had to be conducted so as to increase the dry unit weight of the soil to a minimum of 103 lb per cu ft. To do this by vibroflotation, the most effective pattern and spacing of the vibroflot had to be established.

Three patterns were studied—the line, square, and triangle—with different

---

[10] "The Importance and Practical Use of Relative Density in Soil Mechanics," by D. M. Burmister, A.S.T.M., Vol. 48, 1948, pp. 1249–1268.

spacings between points of compaction. The test patterns are shown in Fig. 7. The test results are given in Table 2. In each pattern the vibroflot was withdrawn (after maximum compaction had been obtained) in 1-ft lifts. The sand added to each hole averaged $2\frac{1}{4}$ cu yd.

A 6-in. Shelby tube equipped with a driving head was used for the field-density tests. The points at which the tests were made are shown in Fig. 7. Each compacted area was excavated, following which field-density tests were made at various depths below the ground surface. Each of the relative-density values given in Table 2 is an average of at least three tests. For pattern 2 the relative density at point 1 is an average of twelve tests.

It is reasonable to assume that the effectiveness of the process will decrease as the distance from the center of compaction is increased. The effect will decrease rapidly at first, then more slowly, as the distance from the vibroflot increases (as in an exponential type of variation). A plot of the test results in Fig. 8 shows this variation.

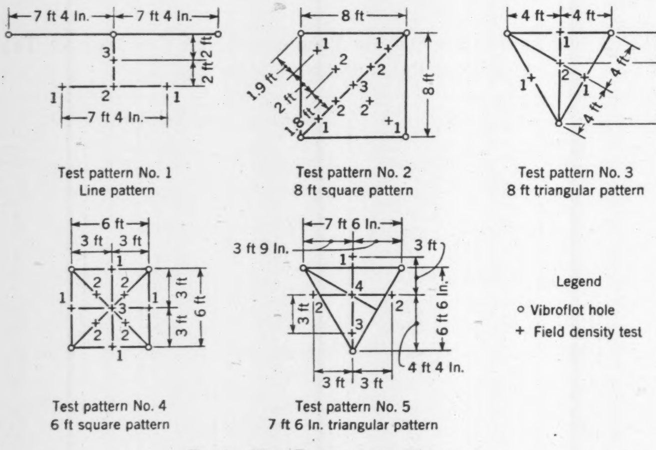
7 ft 4 In.
7 ft 4 In.
3
2 ft
2 ft
1
2
1
7 ft 4 In.
Test pattern No. 1
Line pattern
8 ft
1
1
2
2
3
2
2
1
1
1.9 ft
2 ft
1.8 ft
8 ft
Test pattern No. 2
8 ft square pattern
4 ft
4 ft
1
2
1
1
4 ft
4 ft
2.3 ft
4.6 ft
Test pattern No. 3
8 ft triangular pattern
6 ft
3 ft
3 ft
1
2
2
1
3
1
2
2
1
3 ft
3 ft
6 ft
Test pattern No. 4
6 ft square pattern
7 ft 6 In.
3 ft 9 In.
3 ft
1
4
2
2
3
3 ft
6 ft 6 In.
4 ft 4 In.
3 ft
3 ft
Test pattern No. 5
7 ft 6 In. triangular pattern
Legend
○ Vibroflot hole
+ Field density test

Fig. 7.—Test Patterns for Vibroflot

The greatest increase in density was obtained with the spacing of pattern 4. The overlapping effect of each vibroflot was pronounced, and relative densities of 70% or greater were obtained throughout the compacted area.

The results of the line pattern with a 7-ft 4-in. spacing between compactions, and of the square and triangular patterns with 8-ft 0-in. spacings, were approximately the same. For distances of 2 ft 6 in. and less from the center of the vibroflot, shorter spacings improved the compaction. At distances greater than 2 ft 6 in., the effects of changes in pattern and spacing were not noticeable.

From these preliminary tests it is concluded that:

1. The compaction of a single vibroflot does not increase the relative density above 70% at points greater than 3 ft from the vibroflot.

2. The overlapping effect of the vibroflot when used at intervals greater than 8 ft is small.

3. The effect of compactions can be superimposed.

4. The spacing of the vibroflot at 6 ft or less gives relative densities of 70% or greater throughout the compacted area.

The difference between a square or triangular pattern does not appear to be significant. The triangular pattern is preferred because it has the greatest overlapping of compaction effort.

DESIGN

From the foregoing results, a procedure for determining a suitable spacing of the vibroflot was developed. In Fig. 8 is shown how the compaction decreases with increased distance from the vibroflot; an arbitrary measure is needed to describe this variation. Conveniently, a number or an influence coefficient is used to denote the degree of compaction at each 1-ft interval from the center of a single vibroflot compaction. The dashed curve in Fig. 8 is assumed to be the compaction caused by a single vibroflot. It should (and does) follow the lower field curve.

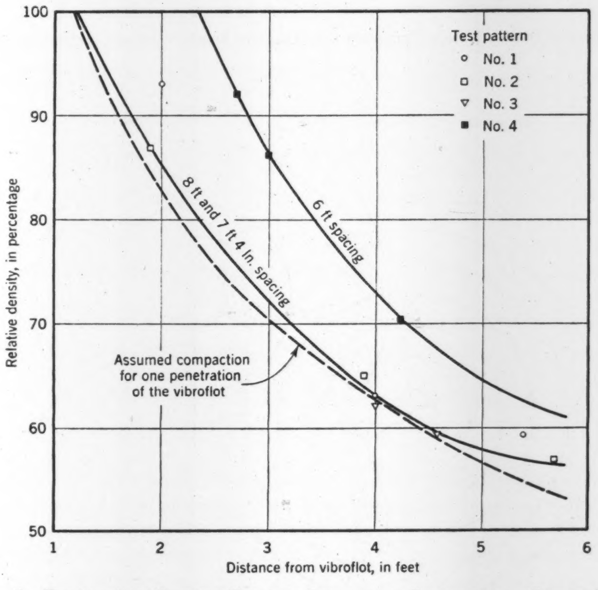

FIG. 8.—RELATIONSHIP BETWEEN RELATIVE DENSITY AND DISTANCE FROM VIBROFLOT

Arbitrarily, the influence coefficient at a distance of 6 ft from the vibroflot is chosen as unity. The coefficient at each 1-ft interval toward the vibroflot is

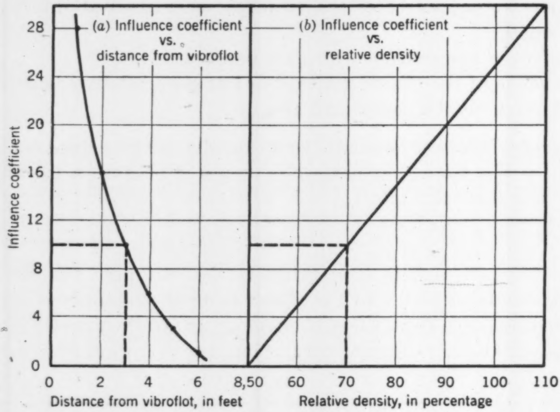

FIG. 9.—EFFECT OF DISTANCE FROM VIBROFLOT AND RELATIVE DENSITY ON THE INFLUENCE COEFFICIENT

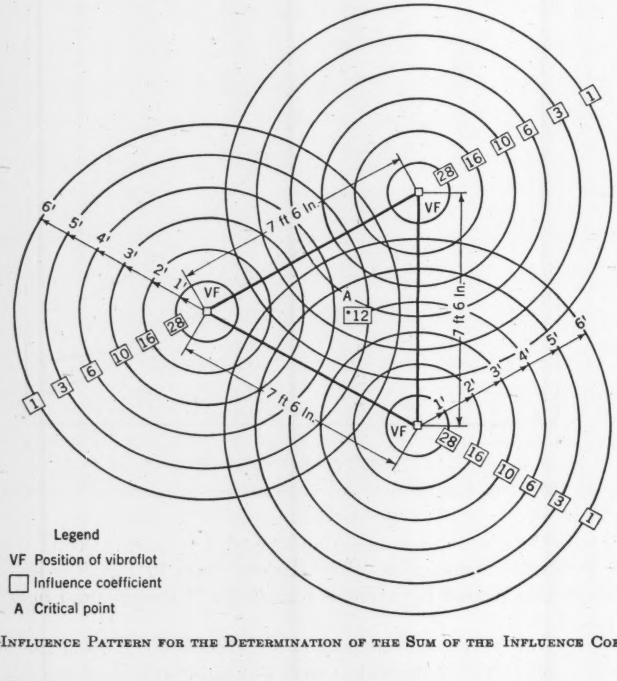
VF
VF
VF
7 ft 6 In.
7 ft 6 In.
7 ft 6 In.
1'
2'
3'
4'
5'
6'
28
16
10
6
3
1
A
12
Legend
VF Position of vibroflot
Influence coefficient
A Critical point

FIG. 10.—INFLUENCE PATTERN FOR THE DETERMINATION OF THE SUM OF THE INFLUENCE COEFFICIENTS

then scaled as the ordinate to the dashed curve in Fig. 8. The plot of the influence coefficient against the distance from the center of the vibroflot is shown in Fig. 9(*a*). From Fig. 8 one can also readily plot the relationship between influence coefficient and relative density, as in Fig. 9(*b*). For design it is then assumed that, if at any point in a pattern of vibroflot compactions the sum of the influence coefficients is greater than 10, a relative density of 70% is obtained. To check this assumption, a triangular pattern with 7-ft 6-in. spacings, as shown in Fig. 10, was tested. From the design curves in Fig. 9 the sum of the influence coefficients at the critical point A is found to be 12. A relative density greater than 70% should, therefore, be found throughout the area enclosed by the sides of the triangle.

The results of the field-density tests conducted in an excavated pit at 3 ft, 6 ft, and 9 ft below ground surface are summarized in Table 2. The field data are in good agreement with the design curves in Fig. 9.

FIELD TESTS

The soil was compacted at the site in a triangular pattern with 7-ft 6-in. spacings of the vibroflot. Approximately 3.5 acres (shaded area in Fig. 1) were compacted to an average depth of 12 ft. Field control of the compaction was maintained by density tests taken in ten test pits dug to an average depth of 10 ft. Tests were conducted at 3-ft intervals from the ground surface. In addition, field-density tests were made at the bottom of the excavation of almost all major footings.

In Fig. 11 are the results of random field-density tests made at the bottom of the excavations for the footings of the process building (building number 2). The soil was tested at points of weakest compaction. The curve in Fig. 11(*a*) is typical of the test results obtained from the other foundation areas. A total of 142 field-density tests were made to determine the sand compaction. In Fig. 12 there is shown the wall of a 9-ft-deep excavation in a compacted area. The white regions denote the core of compacted white sand that was added. It is interesting to note that the surcharge caused by the crane located approximately 5 ft from the edge of the cut did not cause a failure of the vertical sand face.

SETTLEMENT

Bench marks placed solidly in the soil were located throughout the area. Settlement readings of the walls and footings of the various buildings were read during and after construction. The data presented in Fig. 13 are for the large silo storage bin (building number 3). This structure has a raft foundation approximately 100 ft square. Placed on this mat are circular bins 40 ft in diameter. The average uniform dead load is 1,100 lb per sq ft. The maximum dead load plus live load is 3,300 lb per sq ft. Because of their functions, it was quite likely that the bins would be full about three quarters of the time. Hence, settlement computations based on two values of uniform pressure were made to "box-in" the estimated settlement.

Boring STS–B3 (Fig. 3) shows the compressible layers beneath the silo storage building. It was estimated that the total thickness of compressible material between El. 152 and El. 118 was 15 ft; the remainder was neglected in

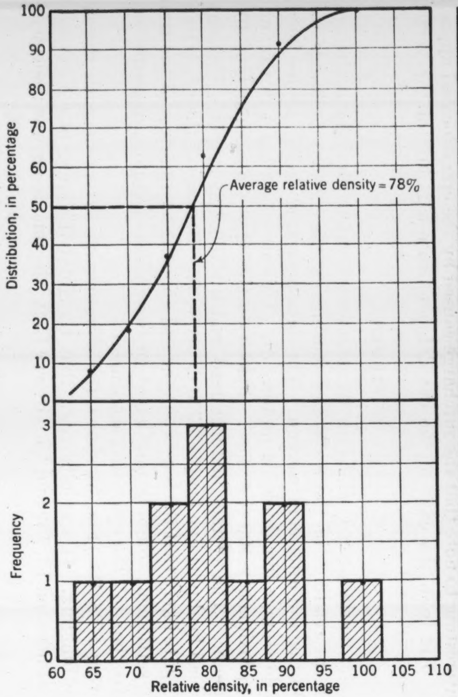

FIG. 11.—FIELD-DENSITY TESTS FOR BUILDING NUMBER 2

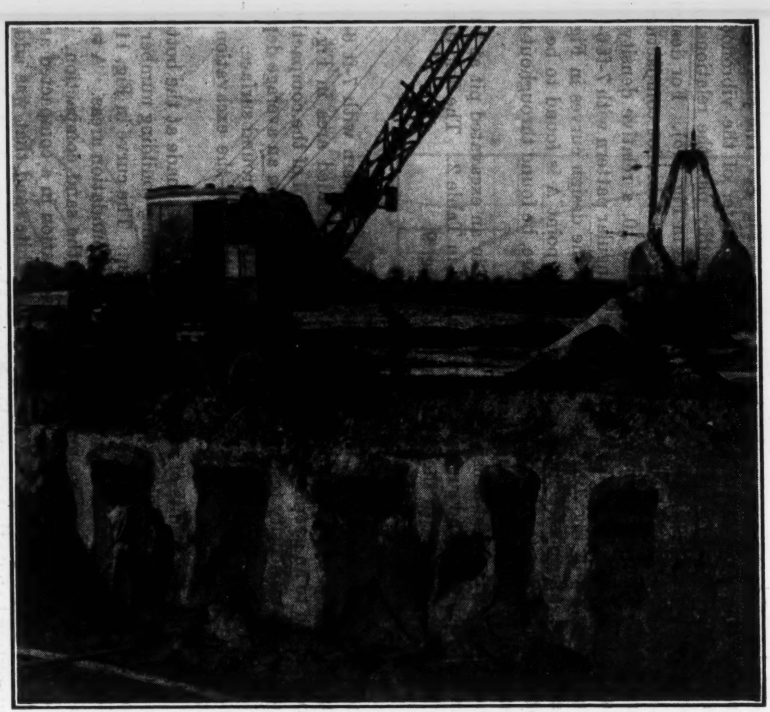

FIG. 12.—EXCAVATION IN A COMPACTED AREA

the settlement computations. The boring showed that the clay and sand deposits were in alternate layers—1 in. to 2 in. thick. Soil explorations also indicated a clay layer 3 ft thick between El. 152 and El. 148. The undisturbed, 3-in., Shelby-tube soil sample, 12 in. thick, which was removed from El. 150 was a gray clay with soil properties as shown in Table 1 for soil sample F3–4. It was assumed that this and similar samples from the other borings were representative of the 15 ft of compressible soil.

The results of classification and consolidation tests are shown in Table 1. Based on these tests, an average value of

$$\frac{C_c}{1 + e_0} = 0.103 \qquad \text{(3)}$$

was used in the settlement computations. In Eq. 3, C_c is the compression index and e_0 is the initial void ratio. The estimate of the dead-load settlement was 1.43 in., and the dead-load plus full live-load settlement was 3.96 in.

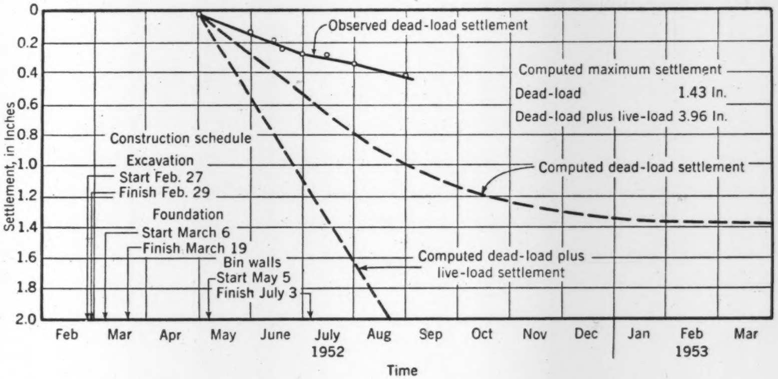

FIG. 13.—RELATIONSHIP BETWEEN SETTLEMENT AND TIME FOR SILO STORAGE BUILDING

If the compressible clay layer were continuous and had drainage top and bottom, approximately 650 days would be required for 90% consolidation. However, because of the alternate layers of clay and sand, it was estimated that approximately 200 days would be required for 90% consolidation.

The computed settlement-time curves for dead load and dead load plus live load are shown in Fig. 13. Settlement readings were taken at twelve points on the periphery of the foundation. The record was begun in May, 1952, just prior to the construction of the walls of the bins. The solid line in Fig. 13 shows the average of the twelve points of observation extending over a period of 131 days. The observed settlement is less than the computed settlement for dead load by approximately 50%.

Settlement observations will be continued for a period of several years (subsequent to 1954) to determine the movement of the building because of the changes in load and the level of the water table during the rainy season.

Conclusions

The loose sands at the plant site were compacted adequately with a vibroflot spaced in a 7-ft 6-in. triangular pattern. Relative densities of 70% were found at points of weakest compaction, and the effectiveness of the vibroflotation process was established. Design curves for the compaction of clean, uniform sands similar to those in the vicinity of Bartow were developed.

Settlement records were obtained for the various buildings during and after construction. Observations of the movement of the foundation for the silo storage building show a settlement that was 50% less than the computed dead-load settlement.

Acknowledgments

The Rust Engineering Company of Pittsburgh, Pa., supervised the engineering and construction of the phosphate plant. Sergey Steuerman, M. ASCE, performed the sand compaction. The writers are indebted to Joseph Kelvington of the Rust Engineering Company for reviewing the field data and assisting in the preparation of the drawings.

AMERICAN SOCIETY OF CIVIL ENGINEERS
Founded November 5, 1852
TRANSACTIONS

Paper No. 2731

WIND VELOCITIES DURING HURRICANES

BY ROBERT C. GENTRY[1]

SYNOPSIS

The structure of hurricanes, the duration of hurricane-force winds, and the distribution of wind velocity in hurricanes are investigated in the paper. The variation of wind velocity with height and the probability of hurricane occurrence are also examined. The author presents examples of the highest measured velocities and estimates of the highest velocity winds ever observed in the United States.

NOTATION

Technical terms used herein are defined in Appendix I. The letter symbols adopted for use in this paper are defined where they first appear and are arranged alphabetically, for convenience of reference, in Appendix II.

INTRODUCTION

In the long battle of man against hurricanes, one of the courses of action followed to reduce accident rates, death rates, and property losses has been the building of "hurricane-proof" structures. The paper gives the design engineer information as to the strength of the winds and gusts in hurricanes. There is presented a description of the type of storm which is termed a hurricane. Data concerning the observed velocity of winds in some of the more violent hurricanes in the United States are offered. There are also included data concerning gusts that have been experienced in hurricanes. In so far as practical, records obtained by the Weather Bureau, United States Department of Commerce (USWB), were consulted for the data.

STRUCTURE OF HURRICANES

The surface winds of a hurricane blow around and, at the same time, spiral in toward the center until they approach the inner wall of the storm. At the inner wall are located the strongest winds and the worst weather. The converging air currents ascend in this area to cause tall cloud formations, torrential

---

NOTE.—Published, essentially as printed here, in July, 1953, as *Proceedings-Separate No. 218.* Positions and titles given are those in effect when the paper was received for publication.

[1] Meteorologist, Weather Bureau, U. S. Dept. of Commerce, Miami, Fla.

rain, and many strong eddies. Inside the inner wall, at the center of the storm, is the eye of the hurricane. Passing into the eye, one would note a sudden decrease in the wind velocity and a cessation of most or all the rain, and one might see clear skies.

The hurricane is a warm-core storm; that is, the air in the eye is warmer than either the air in the surrounding circulation or the air surrounding the entire hurricane. This warm air is believed to be pulled down into the eye by subsiding air currents. The air is warmed during this descent because it is being compressed. The eye extends to the top of the storm; however, the walls and the axis of the eye are not necessarily vertical. Although the air in the lower layers of the storm is moving along a spiral, the radius of the spiral is so great that an observer at any one fixed point would not be able to detect the curvature in the trajectory of the air. Hurricanes vary in height just as they vary in intensity. Being a warm-core storm, the difference in the pressure gradient from the center to the outer edge of the storm must decrease with height. Although there are other factors which may partly compensate for this, the decrease will cause the storm's intensity to begin to diminish with increased height at some level above the surface. This level will vary from storm to storm but will usually be from 4,000 ft to 25,000 ft.

Diameters of hurricanes range from a few miles to hundreds of miles; the size of the eye also varies. Storms have been reported in which the eye was as small as 3 miles in diameter or as large as 50 miles (sometimes even larger in decaying, dispersing storms). Concerning the hurricane of October, 1950, in Florida, Grady Norton reported[2] that the area of destructive winds was only 14 miles wide and that the eye was only 5 miles wide at the time the storm passed over Miami. The maximum wind velocity observed at a land station in this storm was 97 miles per hr, and the extreme velocity was 122 miles per hr. By contrast, the hurricane of September 10, 1947, to September 19, 1947, had hurricane-force winds over an area 240 miles in diameter at the time it crossed the Florida coast. In contrast, typhoons are frequently observed in the Pacific Ocean in which winds with velocities greater than 75 miles per hr cover an area of more than 500 miles in diameter.

The maximum velocity of the winds in a storm is not necessarily highly correlated with either the size of the hurricane or with the central pressure. The maximum velocity is, however, directly related to the maximum intensity of the pressure gradients within the storm and with the distance from the center at which these maximum pressure gradients occur.

Duration of Winds Within a Hurricane

Once a hurricane has formed, it will almost always persist until one of three things happens: (1) The hurricane moves over rough terrain and is dissipated. (2) Cold air enters the wind system. (This seldom happens until the storm has moved into the northern latitudes.) (3) Dry air enters the circulation. Therefore, after a hurricane has formed in the tropic zone, it is probable that the winds will remain of destructive intensity for many days. As to the duration of winds of hurricane force at any one point, there are two factors to be considered: (a) The area of destructive winds in the hurricane; and (b) the speed with which the hurricane is moving. In the Atlantic Ocean, the diameter of the destructive-wind area will usually be from 15 miles to 300 miles. The average movement of the hurricane will usually be approximately 15 miles per hr. Thus, a hurricane should pass a point in from 1 hr to 20 hr; however, hurricanes seldom follow the averages. Some hurricanes move much more quickly than 15 miles per hr, and others stagnate in an area and move very little for several days. Fortunately, most of these latter hurricanes (prior to 1954) have occurred over water with no land nearby; however, there is no reason why a large hurricane could not stagnate close to a coast and cause hurricane-force winds at some city for 72 hr or more.

---

[2] "Hurricanes of the 1950 Season," by Grady Norton, *Monthly Weather Review*, January, 1951, p. 14.

FORCES ACTING ON WINDS IN HURRICANES

Exclusive of the frictional drags, there are three forces acting on air particles in a hurricane. The hurricane is a low-pressure system; that is, the atmospheric pressure in the center of the storm is lower than the pressure on the outer edge of the storm. Thus, there is a pressure force acting to move the air toward the center of the storm. This force gives the wind an acceleration proportional to the ratio of the pressure gradient and the density of the air, $\frac{1}{\rho}\frac{dp}{dn}$, in which ρ is the density of the air and $\frac{dp}{dn}$ is the rate of change of pressure, p, measured along the normal vector, n. The path of the air has two horizontal deflective forces because of its velocity: (1) A force caused by the air moving over a rotating sphere, the earth; and (2) a force caused by the air moving in a curved path. Following the derivation offered[3] by W. J. Humphreys, acceleration from the first force is $2\,\omega\,V\sin\phi$, in which ω is the angular velocity of the earth, V denotes the velocity of the air, and ϕ is the latitude of the point under investigation. Acceleration from the second horizontal deflective force is V^2/r, in which r is the radius of curvature of the air path. When the winds become approximately steady, the deflective forces balance the pressure gradient and

$$\frac{1}{\rho}\frac{dp}{dn} = 2\,\omega\,V\sin\phi + \frac{V^2}{r} \qquad (1)$$

Solving Eq. 1 for V results in

$$V = \sqrt{\frac{r}{\rho}\frac{dp}{dn} + (r\,\omega\sin\phi)^2} - r\,\omega\sin\phi \qquad (2)$$

Eq. 2 is the equation of the gradient wind. This is the theoretical velocity of the wind in a hurricane above the layer of frictional influence if there are no accelerations. In low latitudes, $\sin\phi$ is much less than 1, and, with hurricane-force winds, V is much less than V^2. Therefore, approximate expressions are

$$\frac{1}{\rho}\frac{dp}{dn} = \frac{V^2}{r} \qquad (3)$$

---

[3] "Physics of the Air," by W. J. Humphreys, McGraw-Hill Book Co., Inc., New York, N. Y., 1940, pp. 119–120.

and

$$V = \sqrt{\frac{r}{\rho}\frac{dp}{dn}} \quad \ldots\ldots\ldots\ldots\ldots\ldots\ldots\ldots \quad (4)$$

Thus, there is a physical basis for the direct relationship between the velocities and the pressure gradients of a storm. Data are available which give the variation of $\frac{1}{\rho}\frac{dp}{dn}$ with height in several hurricanes. R. W. James analyzed[4] data from Tampa (Fla.) obtained during the hurricane of October 19, 1944, and found that this ratio remained relatively constant up to 10,000 ft and then decreased in value with greater altitudes. For the typhoon which passed over Tokyo (Japan) on August 31, 1949, Mr. James found that the ratio remained relatively constant for heights up to approximately 27,000 ft; at higher levels, the ratio decreased in value. From averages computed[5] by E. J. Schacht for several hurricanes, Mr. James also found that the ratio remained relatively constant in the lower levels of the atmosphere. Therefore, to the extent that balanced flow prevails in a hurricane, the velocity of winds in a hurricane remains almost constant in the lower levels of the atmosphere (at least below 3,000 ft) above the layer of frictional influence (approximately 1,000 ft). The few data that are available (as of 1954) indicate that balanced flow is only a rough description of what takes place in a hurricane, and, once data are available, it may be found that the velocity varies with height. Until more data are available, however, an assumption of constant velocity in the layer from 1,000 ft to 3,000 ft (and to considerably higher levels in mature, intense storms) appears to be reasonable.

DISTRIBUTION OF WIND VELOCITY IN HURRICANES

Although every hurricane has its individual characteristics, winds usually increase in velocity toward the center of the hurricane until the radius of maximum velocity is reached. This radius is relatively small. As the first approximation of the horizontal velocity profile of a hurricane, George P. Cressman assumed[6] that solid rotation exists from the edge of the hurricane eye out to a distance r_1, where a maximum value of $r\,\Omega$ is found. In this expression r is the radius of curvature of the trajectory of the air particle, and Ω is the angular velocity of the air particle. Mr. Cressman further assumed that from r_1 to r_{ob} a (Vr^k)-vortex exists in which r_{ob} is the radius of the outer boundary of the vortical circulation of the hurricane. According to Mr. Cressman,[6] various studies made by W. F. McDonald,[7] by USWB forecasters,[8] and by Mr. James[9] have shown that k varies from values of slightly greater than 1 for small immature systems to values near ½ for large mature typhoons.

---

[4] "A Note on the Vertical Structure of a Typhoon," by R. W. James, *Monthly Weather Review*, November, 1951, pp. 205–207.

[5] "A Mean Hurricane Sounding for the Caribbean Area," by E. J. Schacht, *Bulletin*, Am. Meteorological Soc., Vol. 27, 1946, pp. 324–327.

[6] "The Development and Motion of Typhoon 'Doris' 1950," by George P. Cressman, *ibid.*, Vol. 32, 1951, p. 332.

[7] "On a Hypothesis Concerning the Normal Development and Disintegration of Tropical Hurricanes," by W. F. McDonald, *Monthly Weather Review*, January, 1942, pp. 1–6.

[8] "Hurricane Notes," *Weather Bureau Training Paper No. 1*, Weather Bureau, U. S. Dept. of Commerce, Washington, D. C., 1948.

[9] "On the Evolution of Tropical Cyclones," by R. W. James, *Journal of Meteorology*, February, 1951, pp. 17–24.

Data from individual storms show that there are many variations from this idealized profile. Usually, the right-front quadrant (when facing the direction toward which the storm is moving) will have stronger winds than the other quadrants, and one of the left quadrants will have the weakest winds; however, there are exceptions. Some storms have their strongest winds to the left of the center, and others have the strongest behind the center. Although, in general, the strongest winds are near the boundary of the eye, sometimes they are far removed. This is particularly true in the cases of immature, developing storms and of mature storms which have become distorted while passing over land.

DATA

Hurricane data have been collected and recorded by the USWB since it was organized in the latter part of the nineteenth century. The *Monthly Weather Review* of the USWB contains an annual summary of the season's hurricane activity, in which are included (1) a description of each storm, (2) maximum and extreme observed winds, and (3) the resulting damage. Ivan Ray Tannehill has summarized[10] most of these data and has collected many more which extend back to 1494. From all these data one might think it would be easy to obtain an accurate estimate of the highest wind velocities that can be expected in hurricanes. However, the problem is complicated by the fact that wind instruments may not be exposed at the proper location to measure the highest winds. As noted previously, the highest velocities may cover only a relatively small area. If this most intense part of the storm does not pass over a weather station at or near the coastline, no measurement is secured of the highest velocity because the storm decreases in intensity soon after passing over land.

The hurricane over the Florida Keys in September, 1935, set a new record for the lowest atmospheric pressure ever measured at sea level over land and undoubtedly had the highest wind velocities of any hurricane (as of 1954) to affect the United States since records have been kept. The hurricane, however, did not pass close to an anemometer during the time it was at its peak intensity, and there exist only estimates of its maximum and extreme velocities. Securing measurements of the highest velocities ever experienced in hurricanes is further complicated by the fact that anemometers often fail when the wind velocity exceeds 100 miles per hr. Mr. Tannehill has stated:[10]

> "One very serious problem in designing wind-measuring devices arises from the requirement that the instrument be sufficiently sensitive to respond to variations at moderate velocities and yet be sturdy enough to withstand the winds of the hurricane. In many violent hurricanes, the wind instruments have been damaged or blown away before the highest storm winds were experienced. In some instances, the steel towers which supported the anemometers have been wrecked. In other cases, the buildings on which the instruments were exposed have been destroyed or unroofed."

As will be noted subsequently, the highest maximum velocity measurement of hurricane winds secured in the United States was made by an anemometer just before it became inoperative and probably before the highest velocities had been experienced.

Any attempt to obtain an estimate of the gust factor, the gust ratio, or the variation of the various velocity measurements with height is also complicated by the lack of proper instruments in the right place at the right time. Indeed, it would be expensive to set up a station to obtain data concerning variation of velocity with height under proper controls, as was noted[11] by R. H. Sherlock, M. ASCE. Even if cost were immaterial, one would have to be extremely fortunate to secure the data in a reasonable length of time. For example, the probability of hurricane occurrence along the southeast coast of Florida is as high as anywhere else in the United States. From 1900 to 1926, however, no hurricane-force winds were observed in Miami.

---

[10] "Hurricanes," by Ivan Ray Tannehill, Princeton University Press, Princeton, N. J. 1945.

Most of the USWB stations and other cooperating weather services make wind measurements with either a three-cup anemometer or a four-cup anemometer. Some of the anemometers are connected with a register which records the passage of each mile of wind on a revolving drum which is driven by a clock. From these records, it is easy to obtain the extreme velocity and also the maximum velocity, but it is not feasible to make any estimate of the gust velocity. In some of these stations a buzzer is connected to the anemometer which buzzes at every sixtieth of a mile. By counting the number of buzzes per minute, one can obtain directly the velocity in miles per hour. By this method, a careful observer can measure the maximum and extreme velocities, but estimates of the gust velocities are unsatisfactory when the winds are greater than 100 miles per hr. At other stations, the anemometer is connected to a direct-reading dial which gives the instantaneous wind velocity (within the limits measured by the anemometer). From this arrangement, a careful observer can obtain a satisfactory estimate of the gust velocity and an acceptable estimate of the extreme velocity (fastest mile). Some offices without registers do not make measurements of the maximum velocity (the highest average velocity for five consecutive minutes). Therefore, most of the available data are in two groups: (1) Data from stations where extreme-velocity measurements and maximum-velocity measurements were made, and (2) data from stations where gust-velocity measurements and extreme-velocity measurement were made.

EXAMPLES OF HIGH VELOCITIES

All previous records of hurricane winds were exceeded at San Juan, Puerto Rico, on September 13, 1928, when at 11:44 a.m. the anemometer at the USWB office lost one of its cups immediately after recording a maximum velocity of 135 miles per hr and an extreme velocity of 144 miles per hr. At this time, the storm center was approximately 30 miles away. According to Oliver L. Fassig,[12]

> "* * * the storm increased in intensity for 3 hours after the record * * * was made. Most of the damage to the property on the Weather Bureau Reservation occurred between 2:30 and 3:30 P.M. * * *. With only two cups the anemometer still recorded about 75 mph. The second cup disappeared at 12:47 P.M. The arms and the shaft of the anemometer with one cup still attached were blown away at 1:33 P.M.; these parts were later found * * * a third of a mile to the southwest * * *."

---

[11] "Variation of Wind Velocity and Gusts with Height," by R. H. Sherlock, *Transactions*, ASCE, Vol. 118, 1953, p. 463.

[12] "San Felipe—The Hurricane of September 13, 1928, at San Juan, P. R.," by Oliver L. Fassig, *Monthly Weather Review*, September, 1928, p. 351.

In the hurricane over the northeastern part of the United States in September, 1938, a maximum velocity of 121 miles per hr was observed at the Blue Hill Observatory in Milton, Mass.; a velocity of 186 miles per hr was observed for a shorter period. This velocity probably exceeds any other velocity measured for hurricanes, but its representativeness is open to doubt. The observatory is on top of a hill, and some of the velocity may have been caused by the orographic effect; that is, winds in the hurricane flowing over level ground may not have been so strong as indicated. An extreme velocity of 155 miles per hr was measured at the Hillsboro Lighthouse near Fort Lauderdale, Fla., on September 17, 1947. The maximum velocity for the same storm at that station was 121 miles per hr. The anemometer at the Hillsboro Lighthouse is 146 ft above the ground.

During the hurricane of August, 1949, a maximum velocity of 132 miles per hr was measured at the Jupiter Lighthouse near West Palm Beach, Fla., before the instrument failed; this is believed to be the highest maximum velocity measured during a hurricane in the United States. The extreme velocity for this hurricane was 153 miles per hr. The observer at the Jupiter Lighthouse (where the anemometer is 106 ft above the ground) reported that winds became stronger after the instrument failed, but he felt unable to make a reliable estimate of the extreme velocity.

The hurricane which passed over Lower Matecumbe Key, Fla., on September 2, 1935, undoubtedly had stronger winds than any that have been measured. The lowest atmospheric pressure was measured as equivalent to that of 26.35 in. of mercury which is the lowest recorded sea-level reading at a land station (as of 1954); lower readings have been made at sea. When the August, 1949, hurricane crossed the coastline of Florida, its minimum-pressure reading was only 28.17 in. of mercury. Furthermore, the diameter of the storm of September, 1935, was much less than that of the storm of August, 1949; thus, the difference in pressure gradients would be even greater than the difference in the minimum pressures. (The pressure gradients would have been at least twice as strong in the 1935 storm as the pressure outside each storm would have been about 29.90 in.) Because the strength of the winds is closely related to the pressure gradients, it is obvious that the winds should have been much stronger in the September, 1935, storm than in the August, 1949, storm. It is quite possible that these winds reached or exceeded a velocity of 200 miles per hr.

In addition to the high winds regularly observed in hurricanes, several tornadoes have occurred in Florida along the northern periphery of hurricanes. No measurement has ever been made of the winds in these tornadoes as they usually affect a relatively small area, and none has passed over a weather station. However these winds are believed to exceed considerably 200 miles per hr.

GUST FACTOR AND GUST RATIO

Data from nine hurricanes during the period from 1944 through 1950 were analyzed to obtain an estimate of the gust factor (V_i/V_5, in which V_i is the gust velocity and V_5 is the maximum velocity); only data from stations having hurricane-force winds were used. The stations were divided into two groups—

(1) four stations with instruments at levels of 146 ft to 226 ft and (2) all the other stations with instruments at lower levels. The range of elevation of instruments in the second group was from 30 ft to 110 ft. In the first group, data were available to compute only the ratio of the extreme velocity to the maximum velocity (V_m/V_5). Mean ratios, maximum ratios, minimum ratios for the two groups, and the number of cases used to compute the mean ratios, are given in Table 1. There was no difference in the ratio of V_m/V_5 for the two groups of stations; therefore, it is not possible to give any variation in the gust ratio or gust factor with height.

For the stations with lower elevations, values are given in Table 1 for the gust factor. For stations equipped only with the mile register and the sixtieth-of-a-mile buzzer, however, it is difficult to obtain an accurate estimate of the gust velocity when winds are strong. Because

$$\frac{V_i}{V_m}\frac{V_m}{V_5} = \frac{V_i}{V_5} \qquad (5)$$

it is believed that a more accurate estimate of the gust factor is obtained by computing the product of the first two ratios in Eq. 5. In this case, the gust factor in Table 1 would be 1.4 rather than the value of 1.3 which was indicated by the actual estimates made by the observers.

TABLE 1.—THE EFFECT OF HEIGHT ABOVE GROUND ON VARIOUS RATIOS

Height above ground, in feet	VALUE OF V_i/V_m			VALUE OF V_i/V_5			VALUE OF V_m/V_5		
	Mean	Max	Min	Mean	Max	Min	Mean	Max	Min
30 to 110	1.2[a]	1.6	1.1	1.3[b]	1.7	1.1	1.2[c]	1.8	1.0
146 to 226							1.2[a]	1.3	1.0

[a] Mean value determined from twelve cases.
[b] Mean value determined from thirteen cases.
[c] Mean value determined from thirty-three cases.

TABLE 2.—THE EFFECT OF HEIGHT ABOVE GROUND ON THE VALUE OF m

Height above ground, in feet	VALUE OF m	
	For maximum velocities	For extreme velocities
40	3.4	3.4
160	5.2	5.8
220	6.8	7.5
280	5.8	4.1
350	6.4	6.8

The hurricane of August, 1949, passed over several wind-measuring stations on Lake Okeechobee in southern Florida. These stations were equipped with pressure-tube anemometers (which should measure gusts more accurately than the cup anemometers used at most stations) and multiple-pen recorders. Meteorologists in the Hydrometeorological Section of the USWB abstracted from the recorder traces the average speed and the strongest gust for each 10-min period. For the times when the 10-min mean wind was from 75 miles per hr to 80 miles per hr, the ratios of the maximum gust to the mean wind speed for the same 10-min period averaged slightly more than 1.4. This value (1.4) compares closely with the values obtained in a study of non-hurricane winds performed with special instrumentation on specially constructed towers. Mr. Sherlock has found[11] that at levels from 25 ft to 150 ft, the gust factor in a winter storm averaged from 1.3 to 1.4.

In the period from 1945 to 1946, the Daniel Guggenheim Airship Institute Division of the University of Akron at Akron, Ohio, conducted an investigation to determine (1) the variation of wind velocity with height, (2) the ratio of extreme gust velocities to average wind velocities, and (3) the variation of the gust ratio with height. The results reported (but not published) by P. O. Huss show that the mean gust factor at levels of 40 ft, 100 ft, and 160 ft were 1.6, 1.4, and 1.4, respectively, with individual values at those levels ranging from 1.9 to 1.2. The gust ratios for the same three levels were 1.5, 1.3, and 1.3, which are all higher than the value (1.2) given in Table 1 for hurricane-force winds.

The data collected for the hurricanes from 1944 through 1950 were also examined to determine if there were any correlation between the gust factor and the speed of the wind. No significant correlation was found in the available data.

VARIATION OF VELOCITY WITH HEIGHT ABOVE GROUND

From the available hurricane data (as of 1954), it is impossible to make any satisfactory deductions concerning the variation of the wind with height in the more violent parts of the storm. To do this it would be necessary to have data from two or more wind-measuring instruments installed at the same station at different heights. The velocities of winds in a hurricane vary so greatly within even short distances that it is not feasible to compare readings at two neighboring stations and to attribute all the differences between the velocities to the difference in heights of the anemometers.

During the study at the University of Akron this problem of variation with height was investigated. Mr. Huss reported that the variation of velocity with height could be represented by the equation,

$$\frac{V_h}{V_0} = \left(\frac{h}{h_0}\right)^{1/m} \quad \dots\dots\dots\dots\dots\dots\dots\dots \quad (6)$$

in which V_0 is the velocity at height h_0 equal to 100 ft and V_h is the corresponding velocity at any height h which is not to exceed 350 ft. This limitation to the value of h is made only for the observation. Limited extrapolation of the results beyond 350 ft may be reliable. The value of m was found to vary with height and with the type of velocities considered, such as V_i, V_m, or V_5. Mean values of m at each level for the maximum and extreme velocities are given in Table 2. The values of m in Table 2 agree with those obtained in investigations made prior to 1946. G. Hellman obtained[13] an expression similar to Eq. 6 and found values of m equal to 8 for h greater than 16 m (52.4 ft) and m equal to 5 for h greater than 32 m (104.8 ft).

Working with later data, Mr. Sherlock[11] independently concluded that Eq. 6 with m equal to 7 gives good results. As all these investigators arrived at similar conclusions, it is believed that it would be satisfactory to use the values for m furnished by Mr. Sherlock for levels up to 1,000 ft until sufficient data become available to determine m more accurately. For higher levels a constant velocity should be assumed (in accordance with the previous information) up to at least 3,000 ft.

---

[13] "Über die Bewegung der luft in den untersten Schickten der Atmosphere," by G. Hellman, *Meteorologische Zeitschrift*, Vol. 34, 1917, p. 273.

PROBABILITY OF OCCURRENCE OF HURRICANE–FORCE WINDS

All the states in the United States along the Gulf of Mexico coastline and the Atlantic Ocean coastline occasionally experience hurricanes. The frequency of occurrence, however, is much higher in some areas than in others. In Table 3 are indicated the number of tropical storms with hurricane-force winds in various areas from 1900 through 1951.

The information in Table 3 reveals that the number of hurricanes was slightly greater in the extreme southern part of Florida (greater Miami and Cape Sable southward through the Florida Keys) than for any other equal length of coastline. Texas ranked second in frequency with northwestern Florida and Alabama (Apalachee Bay area west to Mississippi), third. The areas listed in Table 3 are in the order of descending frequency per unit length of coastline. The total number of hurricanes shown for each area is significant only when compared with those for other sections of similar size. For example, Texas experienced 23 hurricanes, and the extreme south of Florida had 18 hurricanes; however, Texas represents a longer length of coastline. The high frequency for North Carolina is largely caused by the exposed position of Cape Hatteras which juts out into the Atlantic Ocean near the path of many storms. Actually, the frequency of hurricanes in sections of North Carolina other than the sparsely settled area near Cape Hatteras is low. The information in Table 3 was prepared[14] by the writer, P. L. Moore, and A. M. Marshall, and it is emphasized that the statistics are based on only 52 yr of data. The frequency of occurrence of subsequent hurricanes may be quite different.

TABLE 3.—NUMBER OF HURRICANES EXPERIENCED BY SEVERAL AREAS FROM 1900 THROUGH 1951

Area[a]	No.
Extreme South Florida (Miami-Cape Sable southward through the Florida Keys)	18
Texas	23
Alabama and Northwest Florida (Apalachee Bay area to Mississippi)	18
Florida West Coast (south of Apalachee Bay and north of Cape Sable)	13
Louisiana and Mississippi	16
North Carolina	10
Eastern Florida (north of greater Miami)	16
Georgia	3
South Carolina	3
Virginia	5
Maryland, Delaware, and New Jersey	4
New York and New England	5

[a] In order of descending frequency per unit length of coastline.

TABLE 4.—CHANCES OF SEVERAL CITIES IN FLORIDA EXPERIENCING HURRICANE-FORCE WINDS IN ANY GIVEN YEAR

City	Chances[a]
Jacksonville	1 in 50
Daytona Beach	1 in 30
Melbourne-Vero Beach	1 in 20
Tampa-St. Petersburg	1 in 20
Apalachicola-St. Marks	1 in 15
Fort Myers	1 in 12
Palm Beach	1 in 10
Pensacola	1 in 10
Key West	1 in 7
Miami	1 in 7

[a] Weighted averages based on available records.

---

[14] "Hoist Hurricane Warnings," by R. C. Gentry, P. L. Moore, and A. M. Marshall, Weather Vane Publications, Miami Springs, Fla., 1950.

Mr. Norton has studied all available records and prepared some data[15] indicating the chance of Florida cities having hurricane winds. He states that Table 4 indicates (approximately) the chances for a city in Florida to experience a hurricane. Table 4 is based on a record of from only 63 yr to 75 yr (1874 to 1949), and it should be realized that this is too short a time to indicate the expectancy with any high degree of accuracy. The records of the period from 1929 to 1949 materially changed the expectancy, and subsequent records may further alter it.

Conclusions

A few hurricanes can be expected to give extreme velocities of 150 miles per hr at a height of 100 ft above ground. In the period from 1879 to 1954, there was one hurricane with an estimated extreme velocity of approximately 200 miles per hr. Gusts in hurricanes average about 20% higher than the extreme velocities, and there is little or no correlation between the extreme velocity and the gust ratio. In the absence of proper data for establishing a definite relationship, the "one-seventh-power law" (Eq. 6) should be used to approximate the variation of the wind velocity with heights up to 1,000 ft, above which a constant velocity should be used. The limited data available (as of 1954) indicate little or no variation of gust factors with height.

APPENDIX I. DEFINITIONS

Eddy.—A group of air parcels with components of motion transverse to the general stream.

Eye of Hurricane.—Central area of the storm in which the winds are relatively light.

Extreme Velocity.—Average velocity during the time the fastest mile of wind passes a point during the storm (V_m).

Gradient Wind.—Wind vector above the layer influenced by ground friction under assumed conditions of no accelerations.

Gust.—A high, localized wind velocity lasting a short time.

Gust Factor.—Ratio of the highest gust velocity to the maximum velocity (at a station) for the same storm, but not necessarily measured during the same 5-min period (V_i/V_5).

Gust Ratio.—Ratio of the highest gust velocity to the extreme velocity at a station for the same storm, but not necessarily measured during the same period (V_i/V_m).

Gust Velocity.—Instantaneous velocity, as measured by either a three-cup anemometer or a four-cup anemometer, unless otherwise indicated (V_i).

Hurricane.—A storm of tropical origin with winds of hurricane force revolving (counter-clockwise in the northern hemisphere) around a central area that is relatively calm. The atmospheric pressure inside the center is less than that outside the circulation. The same type of storm is also known by such names as typhoons, tropical cyclones, willy-willies, and baguios.

---

[15] "Florida Hurricanes," by Richard W. Gray, U. S. Govt. Printing Office, Washington, D. C., 1949, p. 1 (revised by Grady Norton).

Hurricane-Force Winds.—Winds greater than 75 miles per hr.

Isobar.—Locus of points of equal atmospheric pressure.

Maximum Velocity.—Highest average velocity during five consecutive minutes of any storm (V_5).

Pressure Gradient.—Rate of change of atmospheric pressure per unit distance. The pressure gradient is shown graphically on a weather map by the spacing of the isobars; that is, isobars that are close together indicate a strong gradient, and isobars with relatively large spaces between them indicate a weak gradient.

Surface Wind.—Wind vector in the layers near the ground—usually at the height of the wind instruments, which in most cases are erected at heights of from 30 ft to 150 ft above the ground.

Wind Velocity.—Speed (in miles per hour) and direction of air movements with respect to the ground.

APPENDIX II. NOTATION

The following symbols, adopted for use in this paper and for the guidance of discussers, conform essentially with "American Standard Letter Symbols for Structural Analysis" (ASA Z10.8–1949), prepared by a Committee of the American Standards Association with ASCE representation, and approved by the Association in 1949:

h = height;
h_0 = specific height;
m = exponent in Eq. 6;
n = normal vector;
p = pressure;
r = radius of curvature of the air path;
r_{ob} = radius of curvature of the outer boundary of the vertical circulation of the hurricane;
V = velocity of the air:
    V_h = velocity at any height, h;
    V_i = gust velocity;
    V_m = extreme velocity;
    V_0 = velocity at height of 100 ft;
    V_5 = maximum velocity;
ρ = density of the air;
ϕ = latitude;
ω = angular velocity of the earth; and
Ω = angular velocity of an air particle.

AMERICAN SOCIETY OF CIVIL ENGINEERS
Founded November 5, 1852
TRANSACTIONS

Paper No. 2732

INELASTIC BEHAVIOR OF REINFORCED CONCRETE MEMBERS

By Lawrence H. N. Lee,[1] A. M. ASCE

With Discussion by Messrs. Boris Bresler, Alfred J. Ashdown, and Lawrence H. N. Lee

Synopsis

An experimentally determined stress-strain relationship for concrete in compression (as a result of flexure) is developed herein. A theory of inelastic flexure based on this relationship is formulated to explain the behavior of reinforced concrete members and to predict ultimate loads. Close agreement is found between the theoretical results and experimental data. A method for determining the collapse loads of statically indeterminate beams is given and is used in checking the test results obtained for three such beams.

Notation

The letter symbols adopted for use in this paper are defined where they first appear, in the illustrations or in the text, and are arranged alphabetically, for convenience of reference, in the Appendix.

Introduction

In the analysis of reinforced concrete members, one of the factors which is difficult to account for is plastic flow. The stress-strain relationship for concrete is affected by time, previous history of stress and strain, and the restraining conditions. This uncertainty explains why modern (1954) inelastic theories are in a semi-empirical form.

In order that a continuous frame may fail simultaneously at many places, its design must be based not only on the ultimate strengths of individual sections but also on the moment-deformation relationships along the axis of the frame. By use of the theory of elasticity, the distribution of moments in the

---

Note.—Published, essentially as printed here, in September, 1953, as *Proceedings-Separate No. 286*. Positions and titles given are those in effect when the paper or discussion was received for publication.

[1] Asst. Prof. of Eng. Mechanics, Univ. of Notre Dame, Notre Dame, Ind.

structure can be determined for the design load; because of the nonlinear characteristics of the material, this theory cannot be used to determine the collapse load of the structure. Hence, the factor of safety based on ultimate loads is uncertain.

To derive the moment-deformation relationship, the stress-strain relationship should be established first. This relationship has been formulated on the basis of various tests of compression cylinders and of beams subjected to short-time static loads. In both cases, the uncertainty resulting from plastic flow is eliminated.

CONCRETE IN COMPRESSION

It is universally recognized that the typical stress-strain curve for concrete tested in a short-time, static, standard compression test, up to maximum stress, is a part of a parabola which is oriented with its axis vertical and its vertex upward. The standard cylinder test does not determine the shape of the stress-strain curve beyond the point of maximum stress. However, there has been research to determine the shape of the curve beyond the maximum stress.[2,3,4,5] The results of tests reported[6,7] by the Bureau of Reclamation, United States Department of the Interior (USBR), show that the curve appears to be close to a second-degree parabolic curve up to a strain of approximately $1\frac{1}{2}$ times the strain corresponding to the maximum stress.

The stress-strain relationships for concrete in compression resulting from flexure has been discussed considerably. Methods have been developed[8,9,10] to determine the complete stress-strain relationship directly from the beam tests. By use of a small pressure cell, direct measurements of the stresses occurring in a concrete beam were obtained[11] by the USBR. The results showed that, although the strains were linear up to failure, the distribution of compressive stresses were curvilinear. Also significant was the fact that the measured ultimate stress was equal to the cylinder strength. Similar results were found by the use of the other methods, and it has been concluded that the stress-strain relationship for concrete in compression resulting from flexure is essentially similar to that obtained for concrete in direct compression.[12] In

---

[2] "Der Beiwert n," by F. V. Emperger, *Beton und Eisen*, Vol. 35, No. 19, 1936, pp. 324–332.

[3] "Bruchzustand und Sicherheit im Eisenbetonbalken," by R. Saliger, *ibid.*, pp. 317–320 and No. 20, pp. 339–346.

[4] "A Comparison of Physical Properties of Concrete Made of Three Varieties of Coarse Aggregate," by Oscar E. Kiendly and Joe A. Maldari, thesis presented to the University of Wisconsin, Madison, Wis., in 1938, in partial fulfilment of the requirement for the degree of Bachelor of Science in Civil Engineering.

[5] "A Modified Plastic Theory of Reinforced Concrete," by Paul Anderson and Hwa-Ni Lee, *Bulletin No. 33*, Univ. of Minnesota Eng. Experiment Station, Minneapolis, Minn., 1951.

[6] "Stress-Strain Curves for Concrete Strained Beyond the Ultimate Load," by D. Ramalay and D. McHenry, *Laboratory Report No. SP-12*, Bureau of Reclamation, U. S. Dept. of the Interior, Washington, D. C., March, 1947.

[7] "Plastic Flow of Concrete Relieves High Load Stress Concentrations," by R. F. Blanks and D. McHenry, *Civil Engineering*, Vol. 19, 1949, pp. 320–322.

[8] "Studies of Compressive Stress Distribution in Simply Reinforced Concrete near the Point of Failure," by Lester A. Herr and L. E. Vandergrift, *Bulletin No. 144*, The Ohio State Univ. Eng. Experiment Station, Columbus, Ohio, 1951.

[9] "The Distribution of Concrete Stress in Reinforced and Prestressed Concrete Beams When Tested to Destruction by a Pure Bending Moment," by J. M. Prentis, *Magazine of Concrete Research*, London, England, January, 1951, pp. 73–77.

[10] "Recent Research in Reinforced Concrete, and Its Application to Design," by A. L. C. Baker, *Journal*, Inst. of C. E., London, England, Vol. 35–36, February, 1951, pp. 262–329.

[11] Discussion by A. L. Parme, on "Review of Research on Ultimate Strength of Reinforced Concrete Members," by C. P. Siess, *Journal*, A. C. I., Vol. 23, No. 10, 1952, pp. 862–864.

[12] "Inelastic Deformation of Reinforced Concrete in Relation to Ultimate Strength," by H. J. Cowan *Engineering*, London, England, Vol. 174, No. 4518, August, 1952, pp. 276–278.

order to confirm this matter further, tests on three beams were performed, and a method similar to the methods developed by A. Nadai[13] and J. M. Prentis[9] was used to analyze the test results.

Assumptions.—The derivation of the method is based on the following assumptions:

1. The plane sections of the members remain plane throughout the entire range of flexure. In certain restricted regions these sections undoubtedly become warped by shear, but—in general—this assumption is confirmed by many investigators to be substantially true.

2. There is no creep of the concrete during the test period. This assumption is considered valid only if the entire test is performed continuously within approximately 20 min, and if the duration of the test at high loads, from 60% to 100% of the ultimate load, is limited to 5 min. It has been found[14] that the short-time creep of concrete in a cylinder test is small with lower loads, but that the creep is large with higher loads. However, because of the restraining effect of the concrete close to the neutral axis, the creep of the concrete in a beam test is less.

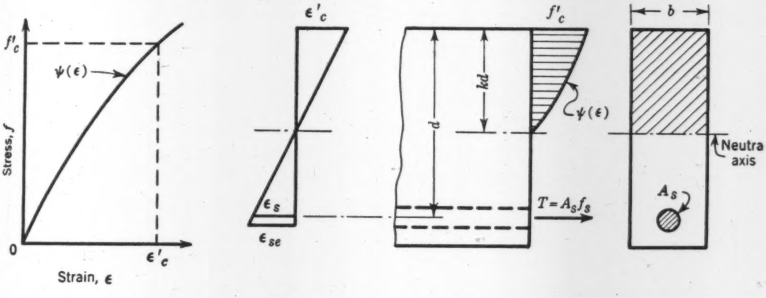

(*a*) Stress-strain relationship

(*b*) Strain distribution

(*c*) Stress distribution

(*d*) Cross section

FIG. 1.—CONCRETE IN BENDING

3. The tensile stress in concrete is negligible. This assumption is not valid if the value of the tensile strain in the extreme fiber is lower than the value of the ultimate tensile strain of concrete. When the value of the tensile strain reaches the value of the ultimate tensile strain of concrete—which varies from 1×10^{-4} to 2×10^{-4}—fine cracks are formed.[12] Because of the brittle characteristics of concrete in tension and the accompanying stress concentrations, the cracks will propagate toward the neutral axis; once the cracks approach the neutral axis, the assumption is good.

For the rectangular beam reinforced with an intermediate grade of structural steel in Fig. 1, the general stress-strain relationship for the concrete can be expressed as

---

[13] "Theory of Flow and Fracture of Solids," by A. Nadai, McGraw-Hill Book Co., Inc., New York, N. Y., 1950, Section 22-2, p. 356.

[14] "Short-time Creep Tests of Concrete in Compression," by R. S. Jensen and F. E. Richart, *Proceedings*, A.S.T.M., Vol. 38, 1938, pp. 410–417.

$$f = \psi(\epsilon) \ldots\ldots\ldots\ldots\ldots\ldots (1)$$

in which f denotes stress and ϵ is strain. The condition of equilibrium of horizontal forces requires that

$$\frac{k\,b\,d}{\epsilon'_c}\int_0^{\epsilon'_c}\psi(\epsilon)\,d\epsilon = A_s\,E_s\,\epsilon_s \ldots\ldots\ldots\ldots\ldots\ldots (2)$$

for $0 < \epsilon_s < \epsilon_{sy}$. In Eq. 2 ϵ'_c is the compressive strain in the concrete, E_s denotes the modulus of elasticity of steel in tension, ϵ_s is the tensile strain in the steel, and ϵ_{sy} represents the yield-point tensile strain for the steel. Differentiating both sides of Eq. 2 with respect to ϵ'_c and rearranging, there results

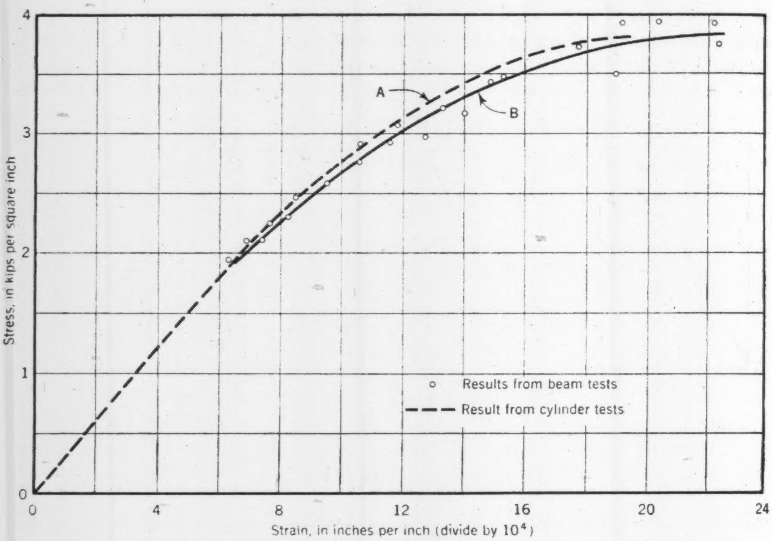

Fig. 2.—Stress-Strain Relationship from Bending Tests

$$f'_c = p\,E_s\left(\epsilon'_c\,\frac{d\epsilon_s}{d\epsilon'_c} + 2\epsilon_s\,\frac{d\epsilon_s}{d\epsilon'_c} + \epsilon_s\right) \ldots\ldots\ldots\ldots\ldots\ldots (3)$$

for $0 < \epsilon_s < \epsilon_{sy}$. In Eq. 3, f'_c is the compressive stress in the concrete and

$$p = \frac{A_s}{b\,d} \ldots\ldots\ldots\ldots\ldots\ldots (4)$$

If the strain in the steel has reached the yield-point strain ϵ_{sy}, the extreme fiber compressive stress, f'_c, of the concrete can be found similarly from

$$f'_c = p\,f_{sy}\left(1 + \frac{d\epsilon_s}{d\epsilon'_c}\right) \ldots\ldots\ldots\ldots\ldots\ldots (5)$$

for $\epsilon_{sy} < \epsilon_s < \epsilon_{wh}$. In Eq. 5, f_{sy} is the yield-point tensile stress of steel and ϵ_{wh} denotes the strain at which the work-hardening effect of steel begins.

These relationships (Eqs. 2 through 5) are not restricted to a section subjected only to pure bending; they can be used at any section if the condition that the plane section remains plane is justified. In Fig. 2, curve A is the average stress-strain curve obtained in the four standard cylinder tests, and curve B is the average stress-strain curve derived from the three beam tests by utilizing Eqs. 3 and 5. The beams and cylinders were made of the same concrete mix. The tests and sample computations are described subsequently. As shown in Fig. 2, the average maximum stress for the beams, 3,810 lb per sq in., is close to the average cylinder strength of 3,800 lb per sq in. There is a discrepancy between the strains corresponding to these stresses—2,240 × 10^{-6} and 1,920 × 10^{-6}, respectively—because the time interval for the beam test was greater than that for the cylinder test. The stress-strain relationship beyond the point of maximum stress was not determined because the strains changed swiftly at that stage, and it was difficult to obtain any significant measurements without the aid of automatic devices. However, it is believed

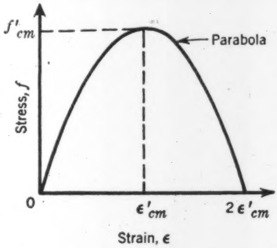

FIG. 3.—IDEALIZED STRESS-STRAIN RELATIONSHIP FOR CONCRETE SUBJECTED TO SHORT-TIME STATIC LOAD

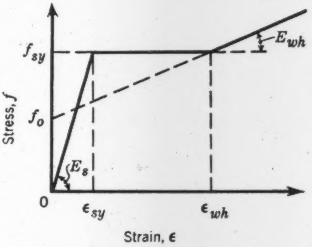

FIG. 4.—IDEALIZED STRESS-STRAIN DIAGRAM FOR STEEL

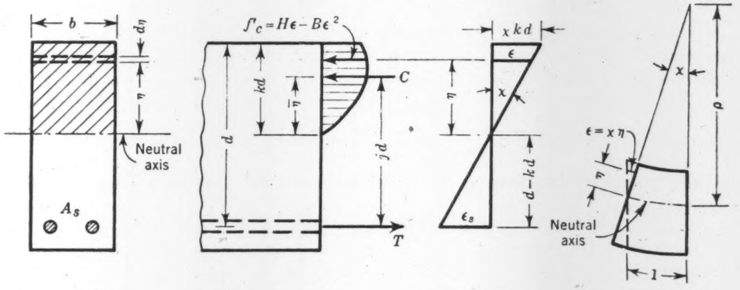

(a) Cross section (b) Stress distribution (c) Strain distribution (d) Strain-curvature relation

FIG. 5.—RECTANGULAR SECTION IN BENDING

that the stress-strain relationship for concrete in compression caused by flexure is essentially similar to that obtained in direct compression.

DEVELOPMENT OF THEORY

Basic Assumptions.—Additional assumptions to those previously cited are as follows:

1. The stress-strain relationship for concrete in compression as a result of flexure is assumed to be expressed by

$$f'_c = H\,\epsilon - B\,\epsilon^2 \dots\dots\dots\dots (6)$$

for $0 < \epsilon < 2\,\epsilon'_{cm}$. In Eq. 6

$$H = \frac{2\,f'_{cm}}{\epsilon'_{cm}} \dots\dots\dots\dots (7a)$$

and

$$B = \frac{f'_{cm}}{(\epsilon'_{cm})^2} \dots\dots\dots\dots (7b)$$

In Eq. 7, f'_{cm} is the maximum compressive stress in the concrete and ϵ'_{cm} is the corresponding strain (Fig. 3).

2. The concrete is homogeneous and isotropic.

3. The members are designed so as to prevent all failures except flexural failure.

4. The stress-strain relationship for the intermediate grade steel is of the form shown in Fig. 4.

Based on these assumptions, formulas can be developed with the concurrent use of the equilibrium and compatibility equations.

Rectangular Beams Reinforced for Tension Only.—On the assumption that plane sections remain plane during bending, it is found that the strain ϵ at a distance η from the neutral axis of a rectangular beam (as shown in Fig. 5) is

$$\epsilon = \frac{\eta}{\rho} = \chi\,\eta \dots\dots\dots\dots (8)$$

in which χ is the curvature and ρ is the radius of curvature. Thus, Eq. 6 can be written as:

$$f'_c = H\,\chi\,\eta - B\,\chi^2\,\eta^2 \dots\dots\dots\dots (9)$$

By the use of Eq. 9 and the condition of horizontal equilibrium, it is found that

$$k^2\left(\frac{H}{2} - \frac{B\,\chi\,k\,d}{3}\right) = p\,E_s\,(1 - k) \dots\dots\dots\dots (10a)$$

for $0 < \epsilon_s < \epsilon_{sy}$,

$$\chi\,k^2\,d\left(\frac{H}{2} - \frac{B\,\chi\,k\,d}{3}\right) = p\,f_{sy} \dots\dots\dots\dots (10b)$$

for $\epsilon_{sy} < \epsilon_s < \epsilon_{wh}$, and

$$\chi\,k^2\,d\left(\frac{H}{2} - \frac{B\,\chi\,k\,d}{3}\right) = p\,[f_o + E_{wh}\,d(1 - k)\,\chi] \dots\dots (10c)$$

for $\epsilon_s > \epsilon_{wh}$. The resisting moment of the beam section is

$$M_r = b\,d^3\,k^2\,\chi\left[\frac{H}{6}(3-k) - \frac{B}{12}\chi\,k\,d(4-k)\right]\ldots\ldots\ldots(11)$$

From Eq. 11 it can be seen that the resisting moment of the section is a function of two variables, the curvature χ and the ratio k. For the case in which the bending moment at the section is known, the values of χ and k associated with this moment can be found by solving Eqs. 10 and 11 simultaneously. The stress distribution caused by this moment can be determined by substituting χ into Eq. 9.

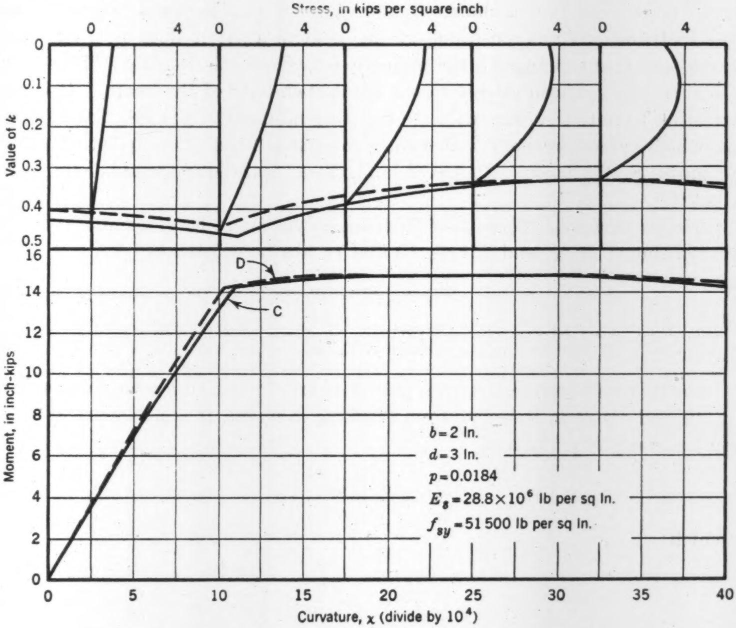

FIG. 6.—MOMENT-CURVATURE RELATIONSHIPS AND STRESS DISTRIBUTIONS

The experimental method of determining the moment-curvature relationship is simple. The bending moment at any section of a simply supported beam can be computed from the loads. The corresponding curvature at the section can be found by

$$\chi = \frac{\epsilon'_c + \epsilon_s}{d_g}\ldots\ldots\ldots\ldots\ldots\ldots\ldots\ldots(12)$$

in which ϵ_s and ϵ'_c are the measured strains at the surface of the tensile steel and at the compression side of the concrete, respectively; the quantity d_g is the distance between these two gages. However, it is not so simple to determine the stress distribution experimentally. The method previously presented can be used to determine the stress distribution if the concrete is assumed to be homogeneous and isotropic.

Theoretical moment-curvature relationships and stress distributions for a rectangular beam are given in Fig. 6. The curves were obtained by substituting the respective values from the data for the beam into Eqs. 9, 10, and 11. For comparison, two sets of curves (with $f'_{cm} = 3{,}810$ lb per sq in.) are plotted in Fig. 6. One set, curve C, with a value of $\epsilon'_{cm} = 2{,}240 \times 10^{-6}$ obtained in flexure tests, is shown by solid lines. Another set, curve D, with a value of $\epsilon'_{cm} = 1{,}920 \times 10^{-6}$ obtained in cylinder tests, is shown by dashed lines. These curves show that a change in the value of ϵ'_{cm} causes a change in the stress distributions and positions of the neutral axis; it does not, however, cause a significant change in the moment-curvature relationship. These theoretical results conform closely to the actual behavior of the beam. It is also interesting to note that the ultimate resisting moment of the beam is 14.7 in.-kips, which agrees precisely with values computed from (1) a "plastic theory" by Charles S. Whitney,[15] M. ASCE, and (2) a "parabolic formula" by A. N. Talbot.[16,17]

Ultimate Resisting Moments of Rectangular Beams.—To determine the relationship among M, χ, and k, Eqs. 10 and 11 can be written as

$$\zeta\,(\chi, k) = 0 \quad\ldots\ldots\ldots\ldots\ldots\ldots (13a)$$

and

$$M_r = \lambda\,(\chi, k) \quad\ldots\ldots\ldots\ldots\ldots\ldots (13b)$$

In order to determine a certain pair of values for χ and k which will satisfy Eqs. 10 and result in the maximum resisting moment, it is necessary to solve simultaneously Eq. 13a and

$$\frac{\partial M_r}{\partial \chi} + \frac{\partial M_r}{\partial k}\frac{dk}{d\chi} = 0 \quad\ldots\ldots\ldots\ldots\ldots\ldots (14)$$

in which

$$\frac{dk}{d\chi} = -\frac{\dfrac{\partial \zeta}{\partial \chi}}{\dfrac{\partial \zeta}{\partial k}} \quad\ldots\ldots\ldots\ldots\ldots\ldots (15)$$

Exact solution of Eqs. 13a and 14 is tedious; however, using the fact that k is a slowly varying function of χ (Fig. 6), one obtains an approximate solution by setting $dk/d\chi$ equal to 0. Consequently

$$\frac{\partial M_r}{\partial \chi} = 0 \quad\ldots\ldots\ldots\ldots\ldots\ldots (16a)$$

---

[15] "Plastic Theory of Reinforced Concrete Design," by Charles S. Whitney, *Transactions*, ASCE, Vol. 107, 1942, pp. 215–326.

[16] "Tests of Reinforced Concrete Beams," by A. N. Talbot, *Bulletin No. 1*, Univ. of Illinois Eng. Experiment Station, Urbana, Ill., September, 1904.

[17] "Tests of Reinforced Concrete Beams of Series 1905," by A. N. Talbot, *Bulletin No. 4*, Univ. of Illinois Eng. Experiment Station, Urbana, Ill., April, 1906.

and

$$\chi = \frac{2\,\epsilon'_{cm}\,(3 - k)}{k\,d(4 - k)} \quad \text{.................... (16}b\text{)}$$

Substituting the value for χ from Eq. 16*b* into Eq. 11 results in the ultimate resisting moment

$$M_{ru} = \frac{k\,(3 - k)^2}{3\,(4 - k)} f'_{cm}\,b\,d^2 \quad \text{.................. (17)}$$

The corresponding value for k which indicates the position of the neutral axis at the ultimate stage can be obtained by eliminating χ from Eqs. 10 and 16*b*. After simplification, it is found that

$$\frac{k^2\,(6 - k)}{6\,(4 - k)\,(1 - k)} = \frac{p\,E_s\,\epsilon'_{cm}}{2\,f'_{cm}} \quad \text{............... (18}a\text{)}$$

for $0 < \epsilon_s < \epsilon_{sy}$,

$$k = \frac{4}{3}\frac{f_{sy}\,p}{f'_{cm}} \quad \text{...................... (18}b\text{)}$$

for $\epsilon_{sy} < \epsilon_s < \epsilon_{wh}$, and

$$k^2 - \left(\frac{4}{3}\frac{f_o}{f'_c} - \frac{2\,E_{wh}\,\epsilon'_{cm}}{f'_c}\right) p\,k - \frac{2\,E_{wh}\,\epsilon'_{cm}}{f'_{cm}}\,p = 0 \quad \text{........ (18}c\text{)}$$

for $\epsilon_s > \epsilon_{wh}$.

The critical steel percentage, defined conventionally as the percentage for which the yield-point stress of steel will be reached at the ultimate resisting moment, is determined by

$$p_{sy} = \frac{3}{4}\frac{f'_{cm}}{f_{sy}}\left(2 - \sqrt{\frac{4\,\epsilon_{sy} + 2\,\epsilon'_{cm}}{\epsilon_{sy} + \epsilon'_{cm}}}\right) \quad \text{.............. (19)}$$

A comparison of the results of two hundred and eighteen beam tests with the ultimate resisting moments computed by Eqs. 17 and 18 is shown in Fig. 7. No attempt was made to compare all the beam tests; only four well-controlled series were included.[18,19,20,21] In the reports concerning these four series of tests, the values of the cylinder strength f'_{cm} were given, but values of corresponding strain were not given. In the present analysis, the values of ϵ'_{cm} are required: therefore, it was assumed that

$$\epsilon'_{cm} = 1{,}220 + \frac{1}{6} f'_{cm} \quad \text{.................... (20)}$$

in which f'_{cm} is in pounds per square inch and ϵ'_{cm} is in microinches per inch.

---

[18] "Compressive Strength of Concrete in Flexure As Determined from Tests of Reinforced Beams," by W. A. Slater and I. Lyse, *Proceedings*, A.C.I., Vol. 26, 1930, pp. 831–874.

[19] "Tests of Reinforced Concrete Beams with Recommendations for Attaining Balanced Design," by K. C. Cox, *ibid*, Vol. 38, 1941, pp. 65–80.

[20] "The Ultimate Strength of Reinforced Concrete Beams," by S. D. Lash and F. W. Brison, *ibid*, Vol. 46, 1950, pp. 457–472.

[21] "High Yield Point Steel as Tension Reinforcement in Beams," by B. Johnston and K. C. Cox, *ibid*, Vol. 36, 1939, pp. 65–80.

The tests by B. Johnston, M. ASCE, and K. C. Cox,[21] A. M. ASCE, were made on thirty-two beams reinforced with low percentages of steel. In this series both ultimate loads and yield-point loads were recorded; it is believed that the steel was stretched into the work-hardening range at the ultimate loads. Because there is insufficient information concerning the properties of steel in the work-hardening range, the recorded yield-point moments were compared with the moments computed by Eqs. 17 and 18.

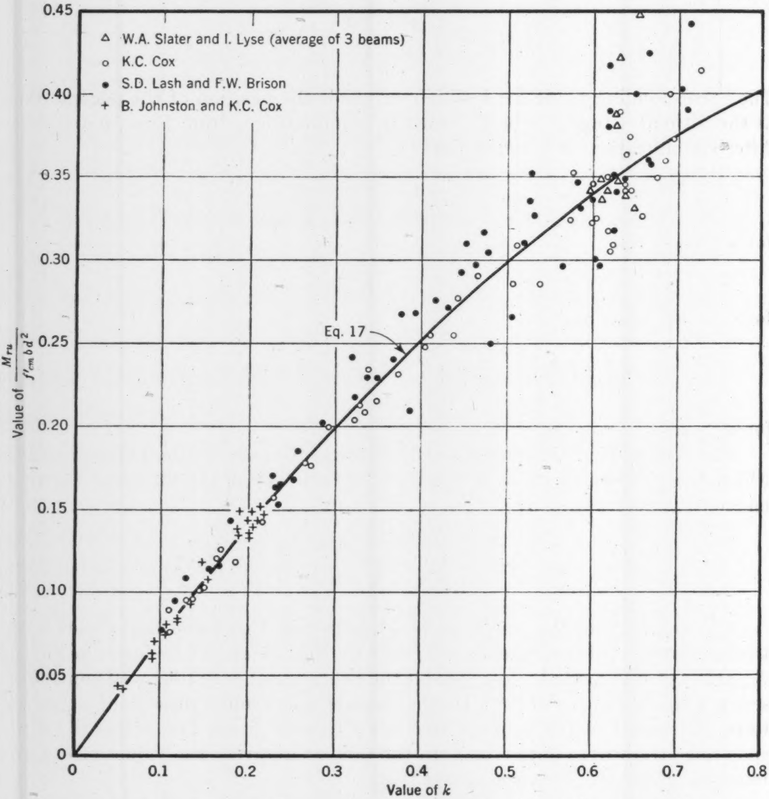

FIG. 7.—COMPARISON OF THEORETICAL ULTIMATE MOMENT AND RESULTS REPORETD BY SEVERAL INVESTIGATORS FOR CONCRETE BEAMS

The average ratio of recorded to predicted ultimate resisting moments for the four series of beams was 1.00, the standard deviation of the ratio being ±0.062.

ECCENTRICALLY LOADED COLUMNS

Load-Curvature Relationship for Rectangular Sections.—A rectangular section (with reinforcement at opposite faces) loaded in the plane of symmetry is shown

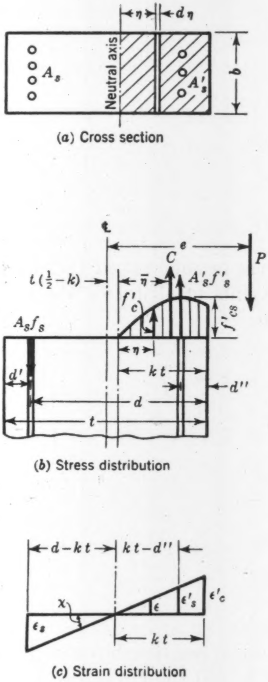
η
dη
A_s
Neutral axis
A'_s
b
(a) Cross section
℄
e
C
P
t (½ − k)
η̄
A'_s f'_s
f'_c
f'_cs
A_s f_s
η
kt
d'
d''
d
t
(b) Stress distribution
d − kt
kt − d''
χ
ε
ε'_s
ε'_c
ε_s
kt
(c) Strain distribution

FIG. 8.—RECTANGULAR SECTION SUBJECTED TO COMBINED AXIAL LOAD AND BENDING

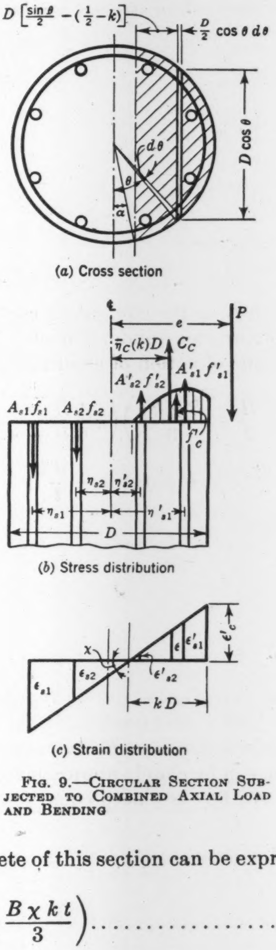
D [sin θ/2 − (½ − k)]
D/2 cos θ dθ
D cos θ
dθ
θ
α
(a) Cross section
℄
e
P
η̄_C(k)D
C_C
A'_s2 f'_s2
A'_s1 f'_s1
A_s1 f_s1
A_s2 f_s2
f'_c
η_s2
η'_s2
η_s1
η'_s1
D
(b) Stress distribution
χ
ε_s2
ε_s1
ε
ε'_s1
ε'_s2
ε'_c
kD
(c) Strain distribution

FIG. 9.—CIRCULAR SECTION SUBJECTED TO COMBINED AXIAL LOAD AND BENDING

in Fig. 8. The total compression in the concrete of this section can be expressed as

$$C = b\,\chi\,k^2\,t^2\left(\frac{H}{2} - \frac{B\,\chi\,k\,t}{3}\right)\ldots\ldots\ldots\ldots\ldots\ldots(21)$$

for $0 < k < 1$. Projecting all the forces in Fig. 8 on a vertical line results in

$$P = b\,\chi\,k^2\,t^2\left(\frac{H}{2} - \frac{B\,\chi\,k\,t}{3}\right) + A'_s\,(f'_s - f_{cs}) - A_s\,f_s\ldots\ldots(22)$$

An examination of Fig. 8 shows that the strains are given by

$$\epsilon'_s = \chi\,(k\,t - d'')\ldots\ldots\ldots\ldots\ldots\ldots\ldots(23a)$$

and

$$\epsilon_s = \chi\,(d - k\,t)\ldots\ldots\ldots\ldots\ldots\ldots\ldots(23b)$$

The corresponding stresses can be found from the stress-strain relationships:

$$f'_s = E'_s\, \epsilon'_s \quad \text{(24a)}$$

for $\epsilon'_s < \epsilon'_{sy}$,

$$f'_s = f'_{sy} \quad \text{(24b)}$$

for $\epsilon'_s > \epsilon'_{sy}$,

$$f_s = E_s\, \epsilon_s \quad \text{(24c)}$$

for $\epsilon_s < \epsilon_{sy}$,

$$f_s = f_{sy} \quad \text{(24d)}$$

for $\epsilon_s > \epsilon_{sy}$, and

$$f_{cs} = H\, \epsilon'_s - B\, (\epsilon'_s)^2 \quad \text{(24e)}$$

in which f_{cs} is the equivalent compressive stress in concrete at the position of the compression reinforcement. Taking moments of all forces about an axis at the line of action of external load results in

$$\chi\, k^2\, t \left(\frac{H}{2} - \frac{B\, \chi\, k\, t}{3}\right)\left(k\, \frac{4\,H - 3\,B\,\chi\,k\,t}{6\,H - 4\,B\,\chi\,k\,t} + \tfrac{1}{2} - k - \frac{e}{t}\right)$$
$$+ p_c\, f_s \left(\tfrac{1}{2} - \frac{d'}{t} + \frac{e}{t}\right) + p'_c\, (f'_s - f_{cs}) \left(\tfrac{1}{2} - \frac{d''}{t} - \frac{e}{t}\right) = 0 \quad \text{(25)}$$

in which

$$p_c = \frac{A_s}{b\, t} \quad \text{(26a)}$$

and

$$p'_c = \frac{A'_s}{b\, t} \quad \text{(26b)}$$

Eqs. 22, 23, 24, and 25 represent a theoretical relationship among the external load P, the position of the neutral axis k, and the curvature χ.

Ultimate Loads on Rectangular Sections.—The ultimate load for a rectangular section can be closely approximated if Eq. 21 is differentiated with respect to χ, the derivative is placed equal to zero, and χ is determined as follows:

$$\frac{\partial C}{\partial \chi} = 0 \quad \text{(27a)}$$

and

$$\chi = \frac{1.5}{k\, t}\, \epsilon'_{cm} \quad \text{(27b)}$$

for $0 < k < 1$. Substituting Eq. 27*b* into Eq. 22 results in

$$P = \tfrac{3}{4} f'_{cm}\, k\, b\, t + A'_s\, (f'_s - f_{cs}) - A_s\, f_s \quad \text{(28)}$$

The corresponding value of k can be obtained by solving

$$k^2 + \frac{12}{5}\left(\frac{e}{t} - \tfrac{1}{2}\right) k + \frac{16}{5\, f'_{cm}} \left[p'_c\, (f'_s - f_{cs}) \left(\frac{e}{t} - \tfrac{1}{2}\right.\right.$$
$$\left.\left. + \frac{d''}{t}\right) - p\, f_s \left(\frac{e}{t} + \tfrac{1}{2} - \frac{d'}{t}\right)\right] = 0 \quad \text{(29)}$$

The respective stresses can be determined by finding the corresponding strains,

$$\epsilon'_s = 1.5\,\epsilon'_{cm}\left(1 - \frac{d''}{k\,t}\right) \ldots\ldots\ldots\ldots\ldots\ldots (30a)$$

and

$$\epsilon_s = 1.5\,\epsilon'_{cm}\left(\frac{d}{k\,t} - 1\right) \ldots\ldots\ldots\ldots\ldots\ldots (30b)$$

The total eccentricity e in Eqs. 25 and 29 is the sum of the original eccentricity and the maximum deflection δ of a column. The value of δ can be found by determining the moment-curvature relationship for the column and the restraining conditions at the ends. For the case in which the characteristics of the deflection curve are known, the value of δ can be obtained by an approximate method. For example, the deflection curve of a column hinged at both ends is very close to a sine wave, as was shown[22] experimentally by E. Hognestad, A. M. ASCE. The curvature of the sine wave at midheight of the column of length l is

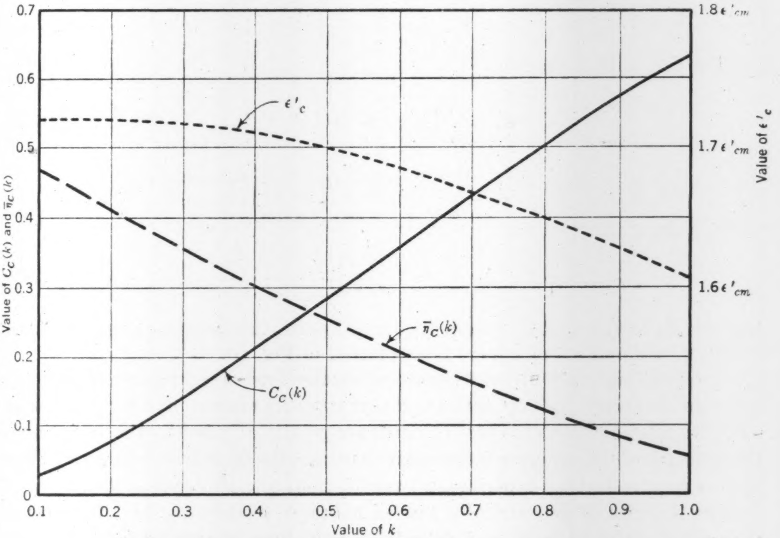

FIG. 10.—FUNCTIONS OF k FOR ANALYSIS OF CIRCULAR SECTIONS

$$\frac{d^2y}{dx^2} = \frac{\delta\pi^2}{l^2} \ldots\ldots\ldots\ldots\ldots\ldots\ldots\ldots (31)$$

Equating Eqs. 27*b* and 31 results in the maximum deflection of a rectangular column

$$\delta = \frac{1.5\,\epsilon'_{cm}\,l^2}{\pi^2\,k\,t} \ldots\ldots\ldots\ldots\ldots\ldots\ldots\ldots (32)$$

---

[22] "A Study of Combined Bending and Axial Load in Reinforced Concrete Members," by E. Hognestad, *Bulletin No. 399*, Univ. of Illinois Eng. Experiment Station, Urbana, Ill., November, 1951.

for the case in which the neutral axis lies within the section at the ultimate load.

Ultimate Loads of Cylindrical, Spiral Columns.—The moment-curvature relationships and the equations for the ultimate loads of eccentrically loaded cylindrical spiral columns can be derived on the basis of the general assumptions presented. With reference to Fig. 9, the following equations for the ultimate loading can be formulated:

Ultimate Load.—

$$P = C_C(k)\, f'_{cm}\, D^2 + \Sigma\, A'_s\, (f'_s - f_{cs}) - \Sigma\, f_s\, A_s \tag{33}$$

and

$$C_C(k)\, f'_{cm}\, D^2 \left[e - \bar{\eta}_C(k)\, D\right] + \Sigma\, A'_s\, (f'_s - f_{cs}) (e - \eta'_s) - \Sigma\, A_s\, f_s\, (e + \eta_s) = 0 \tag{34}$$

for $0 < k < 1$.

Compatibility Equations.—

$$\epsilon'_s = \frac{\epsilon'_c}{k\, D} \left[\eta'_s - D(\tfrac{1}{2} - k)\right] \tag{35a}$$

and

$$\epsilon_s = \frac{\epsilon'_c}{k\, D} \left[\eta_s + D(\tfrac{1}{2} - k)\right] \tag{35b}$$

Deflection.—

$$\delta = \frac{l^2}{\pi^2} \frac{\epsilon'_c}{k\, D} \tag{36}$$

In order to facilitate the numerical computations, the dimensionless functions, $C_C(k)$, $\bar{\eta}_C(k)$, and ϵ'_c, of k have been plotted in Fig. 10.

The behavior and ultimate loads of axially loaded columns and columns subjected to eccentric loads with small eccentricities are not investigated herein. The ultimate capacities of these columns are greatly affected by the variation of the strength of the concrete,[23] the strain rate, and the plastic instability. These factors require further experimental verifications and theoretical studies.

For a series of eccentrically loaded columns tested[22] by Mr. Hognestad, theoretical ultimate loads and deflections have been computed using Eqs. 28, 29, 30, 32, 33, 34, 35, and 36. The average of the ratios of the actual ultimate load to the computed ultimate load for ninety-five square and cylindrical columns was 0.976, the standard deviation being ±0.062. The actual ultimate loads were generally lower than the theoretical values, and the actual deformations were generally higher except the group of square columns having large eccentricity. This is partly a result of the time interval necessary for the tests.

ANGLE CHANGES AND DEFLECTIONS

In determining the angle changes and the deflections, the deformation caused by shear stress is neglected as being small compared to that stress produced by bending. The variation in position of the neutral axis (Fig. 6) is also neglected as being small compared to the radius of curvature at all points.

---

[23] "Effect of Size and Shape of Test Specimens on Compressive Strength of Concrete," by H. F. Gonnerman, *Proceedings*, A.S.T.M., Vol. 25, 1925, pp. 237–250.

Under conditions of short-time static loads, the curvature χ is a definite function of the external bending moment M_e, which is in turn a function of the variable x which defines the position of the section being considered. Thus,

$$\frac{d^2y}{dx^2} = \chi\,[M_e(x)] \ldots\ldots\ldots\ldots\ldots\ldots\ldots (37)$$

The integrations of Eq. 37 result in the angle change and the deflection y as functions of x. Because of the complexity of nonlinear characteristics of reinforced concrete members, it would—in many cases—be more practical to perform the integrations by semigraphical methods.

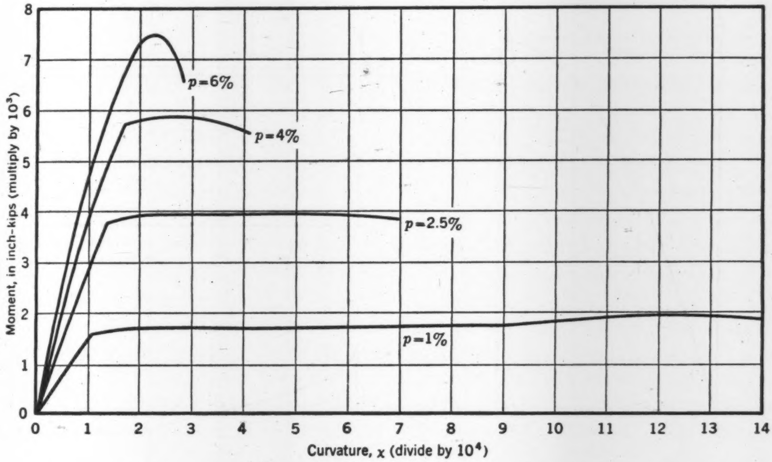

Fig. 11.—The Effect of Varying the Steel Percentage on the Moment–Curvature Relationship for Rectangular Beams

COLLAPSE LOADS OF REINFORCED CONCRETE STRUCTURES

It has been realized that the actual distribution of moments in a reinforced concrete structure at the limiting state is different from that determined by elastic theory. The plastic behavior of the structure allows a redistribution of moments which causes an increase in the load-carrying capacity of the structure. The increase varies from a small percentage to approximately 30% more than the ultimate load obtained by conventional analysis. Test results on the destruction of continuous two-span beams reported by F. B. Kazinczy[24] showed that the increase is much greater in under-reinforced beams than in over-reinforced beams. These results were also cited by W. H. Glanville and F. G. Thomas,[25] and A. L. L. Baker.[26,10]

---

[24] "Die Plastizitat des Eisenbetons," by F. B. Kazinczy, *Beton und Eisen*, Vol. 32, No. 5, 1933, pp. 74–80.

The test results of three single-span, under-reinforced beams, which were fixed at the ends and tested to destruction, are presented subsequently. The collapse loads of these beams were approximately 30% higher than the ultimate loads obtained by elastic theory.

For a more efficient use of the materials, it is necessary to determine the collapse loads and corresponding distributions of moments for structures. In determining the limiting states, the moment-curvature relationships for all members concerned are derived, and the expressions for the deflections and angle changes are then developed. Following the determination of the moment-deflection relationships and the moment-angle change relationships, the determination of the distributions of moments can be carried out in the conventional manner—that is, by solving simultaneous equations which involve angle changes and deflections as prescribed by the conditions of restraint.

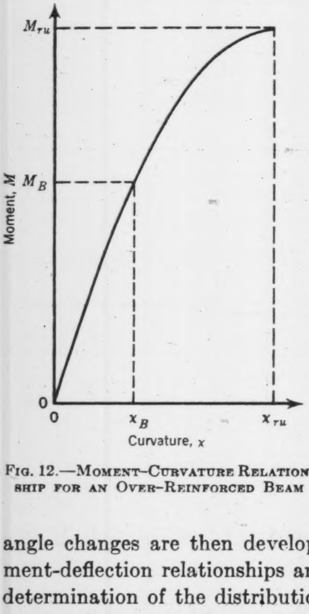

FIG. 12.—MOMENT-CURVATURE RELATIONSHIP FOR AN OVER-REINFORCED BEAM

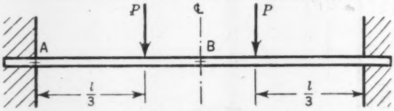

(a) Beam diagram

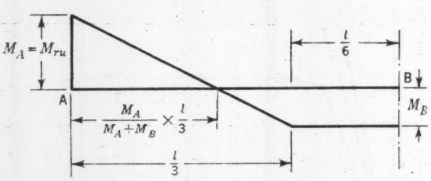

(b) Moment distribution

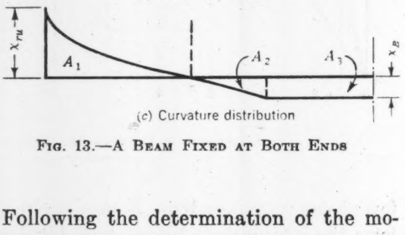

(c) Curvature distribution

FIG. 13.—A BEAM FIXED AT BOTH ENDS

The moment-curvature relationship of a beam depends on many factors, but the characteristics of the relationship are greatly influenced by the steel percentage. For example, the moment-curvature relationships of four beams of the same size and the same concrete mix, but with four different steel percentages, were determined by Eqs. 10 and 11. The physical properties of the beams are as follows:

---

[25] "Studies in Reinforced Concrete. V; Moment Redistribution in Reinforced Concrete," by W. H. Glanville and F. G. Thomas, *Technical Paper No. 22*, Great Britain Dept. of Scientific and Industrial Research, Building Research Board, London, England, May, 1939.

[26] "A Plastic Theory of Design for Ordinary Reinforced and Pre-stressed Concrete Including Moment-Redistribution in Continuous Members," by A. L. L. Baker, *Magazine of Concrete Research*, London, England, Vol. 1, No. 2, 1949, pp. 57–66.

Item	Value
b, in inches	10
d, in inches	20
E_s, in pounds per square inch	30×10^6
E_{wh}, in pounds per square inch	8×10^5
f_{sy}, in pounds per square inch	45,000
ϵ_{wh}, in percentage	1.5
f'_c, in pounds per square inch	5,210
ϵ'_{cm}, in percentage	0.208
H, in pounds per square inch	5×10^6
B, in pounds per square inch	1.2×10^9
p_{sy}, in percentage	5.81

The moment-curvature relationships are shown in Fig. 11. The curves terminate at the points where the extreme fiber strains reached the value of $2\,\epsilon'_{cm}$. From Fig. 11 it can be seen that the moment-curvature relationship for the beam with a low steel percentage resembles the yielding characteristics of steel, and the moment-curvature relationship of the over-reinforced beam resembles the brittle characteristics of concrete.

Example.—The moment-curvature relationship for an over-reinforced beam, which is reinforced equally for both positive and negative bending, is assumed to be a parabola, as shown in Fig. 12. The beam is absolutely fixed at both ends and is subjected to loads at the third points, as shown in Fig. 13(*a*). In order to determine the collapse load, it is necessary first to determine the distribution of moments in the beam at incipient failure.

To satisfy the static conditions, the distribution of moments must be as shown in Fig. 13(*b*). The moment, M_A, at the fixed end can, under no condition, exceed the value of the ultimate resisting moment, M_{ru}; in the limiting state, $M_A = M_{ru}$. In this case, the value of M_B is the only unknown, and the distribution of curvature is as shown in Fig. 13(*c*). The angle change of point B with respect to point A is zero; hence,

$$\phi_{BA} = \int_A^B \chi\,[M_e(x)]\,dx = 0 \qquad (38)$$

By solving Eq. 38, it is found that

$$M_B = 0.58\,M_{ru} \qquad (39)$$

and the corresponding collapse load is

$$P_{CO} = \frac{4.74\,M_{ru}}{l} \qquad (40)$$

Eq. 40 illustrates the fact that the collapse load for the over-reinforced beam subjected to the loads shown is 5.4% higher than the ultimate load determined by the elastic theory. The result agrees closely with the findings of previous investigators.

TEST RESULTS

The tests were made with three beam specimens as shown in Fig. 14. The beams were designed to use the available testing equipment and to prevent any kind of failure except failure in flexure. The ends of the beams were fixed as shown in Fig. 14. The total time required to test each beam was approximately 25 min.

The extreme fiber stresses with respect to the corresponding measured strains were computed by the use of Eqs. 3 and 5. Computations for the stresses and moments for the specimen PB3 at Section 1 are illustrated in Table 1. The average stress-strain curve is plotted in Fig. 2. The moment-curvature relationships for the two sections were computed by Eqs. 10 and 11. In the computations, the values of f'_{cm} and ϵ'_{cm} obtained from the average stress-strain curve were used. The moments at the sections corresponding to the measured curvatures were obtained from the theoretical moment-curvature relationships. The variations of the moments at the six sections are shown in Fig. 15, in which

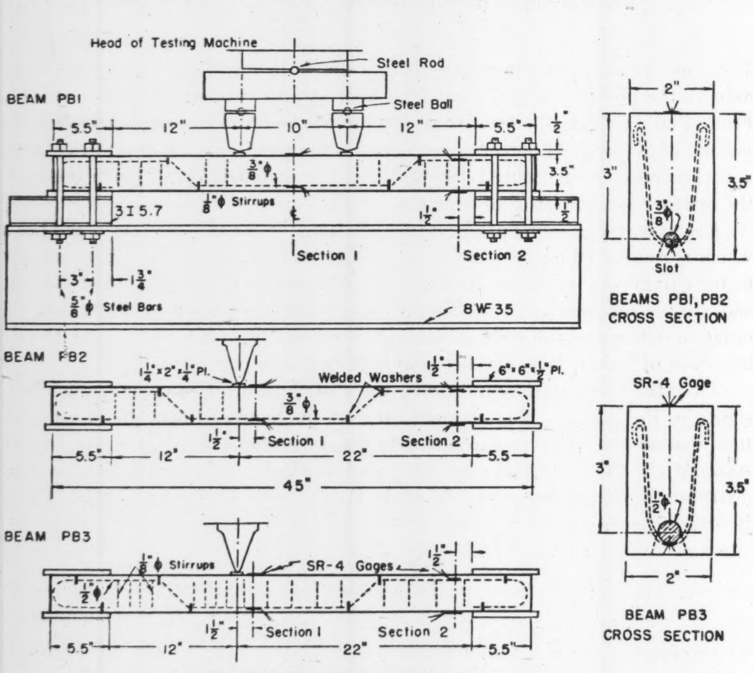
Head of Testing Machine
Steel Rod
BEAM PB1
Steel Ball
5.5"
12"
10"
12"
5.5"
1/2"
3/8" ϕ
3.5"
1/8" ϕ Stirrups
3I5.7
1 1/2"
1/2"
℄
Section 1
Section 2
3"
1 3/4"
5/8" ϕ Steel Bars
8WF35
2"
3"
3.5"
3/8" ϕ
Slot
BEAMS PB1, PB2 CROSS SECTION
BEAM PB2
1 1/4" x 2" x 1/4" Pl.
Welded Washers
1 1/2"
6" x 6" x 1/2" Pl.
3/8" ϕ
1 1/2"
Section 1
Section 2
5.5"
12"
22"
5.5
45"
SR-4 Gage
3"
3.5"
1/2" ϕ
2"
BEAM PB3 CROSS SECTION
BEAM PB3
1/8" ϕ Stirrups
SR-4 Gages
1 1/2"
1/2" ϕ
1 1/2"
Section 1
Section 2
5.5"
12"
22"
5.5"

FIG. 14.—TEST BEAMS AND ARRANGEMENT

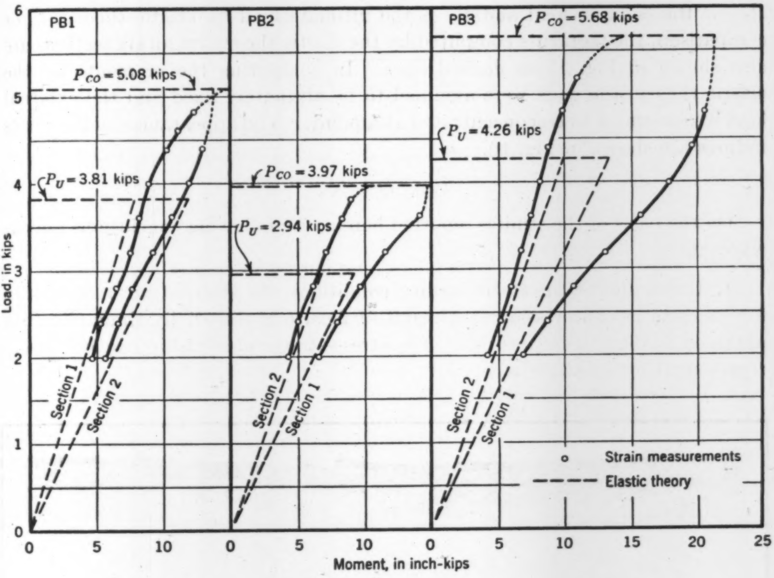

FIG. 15.—TEST RESULTS

TABLE 1.—TEST RESULTS AND COMPUTATIONS FOR SECTION 1, PB3[a]

Load (1)[b]	ϵ'_c (2)[c]	ϵ_s (3)[c]	$\Sigma \epsilon$ (4)[c,d]	f'_s (5)[e]	χ (6)[c,f]	M (7)[g]
0	0	0	....	0	0	0
2,000	586	512	....	....	365	7,010
2,200	658	569	1,991	1,875	407	7,800
2,400	745	638	2,240	2,110	459	8,780
2,600	833	706	2,442	2,300	510	9,700
2,800	940	788	2,716	2,555	573	10,800
3,000	1,060	875	2,911	2,740	642	11,970
3,200	1,188	968	3,236	3,040	715	13,220
3,400	1,335	1,067	3,403	3,210	798	14,550
3,600	1,481	1,162	3,640	3,420	879	15,790
3,800	1,625	1,250	3,771	3,540	945	16,800
4,000	1,779	1,340	3,945	3,720	1,038	18,080
4,200	1,921	1,422	4,174	3,930	1,110	18,920
4,400	2,042	1,487	4,183	3,940	1,170	19,650
4,600	2,144	1,542	4,365	4,110	1,227	20,350
4,800	2,230	1,583	4,156	3,910	1,265	20,650
5,680	Collapse load		Collapse load		Collapse load	

[a] $E_s = 28.7 \times 10^6$ lb per sq in.; $p = 0.0328$; and f_y = 46,400 lb per sq in. [b] In pounds. [c] Multiply by 10^{-6}. [d] $\Sigma \epsilon = \epsilon'_c (\Delta \epsilon_s / \Delta \epsilon'_c) + 2 \epsilon_s (\Delta \epsilon_s / \Delta \epsilon'_c) + \epsilon_s$. [e] In pounds per square inch. $f'_s = p E_s \Sigma \epsilon$. [f] $\chi = (\epsilon'_c + \epsilon_s)/3$. [g] In inch-pounds.

P_{CO} is the collapse load and P_U is the ultimate load by elastic theory. For comparison, the moments computed by the elastic theory for all six sections are also shown in Fig. 15 as dashed lines. In computing the moments by the elastic theory, the ends were assumed to be absolutely fixed and the external load was assumed to be concentrated at a point. The appearances of the beam failures are shown in Fig. 16.

CONCLUSIONS

On the basis of the studies reported herein, the following conclusions appear warranted:

1. Under short-time static loading conditions, the stress-strain relationship for concrete in compression as a result of flexure is essentially similar to that obtained in direct compression. The stress-strain relationship can be closely represented by a parabola.

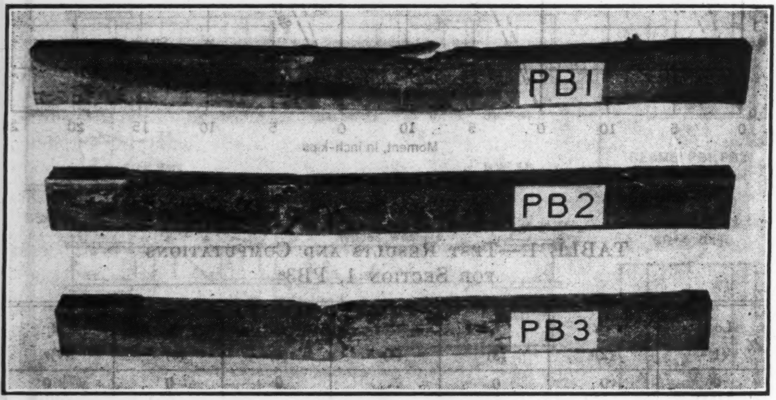

FIG. 16.—TEST BEAMS AFTER FAILURE

2. The proposed inelastic theory gives satisfactory predictions of the ultimate loads for reinforced concrete beams and columns.
3. Within the scope of its assumptions, the theory provides a rigorous method of determining a complete picture of stress and deformation in statically indeterminate or determinate reinforced concrete members.

ACKNOWLEDGMENTS

The tests described herein were performed in the laboratories of the Civil Engineering and Engineering Mechanics departments of the University of Notre Dame at Notre Dame, Ind. The equipment, materials, and facilities were provided by the university. F. M. Kobayashi and S. S. Hsu assisted in the experimental work, and M. O. Peach reviewed the paper.

APPENDIX I. NOTATION

The following symbols, adopted for use in the paper and for the guidance of discussers, conform essentially with "American Standard Symbols for Structural Analysis" (ASA Z10.8-1949) prepared by a committee of the American Standards Association with ASCE representation, and approved by the Association in 1949:

A = area:
  A_s = area of tensile reinforcing steel;
  A'_s = area of compressive reinforcing steel;
  A_1, A_2, and A_3 = areas in Fig. 13(*c*);
B = term defined in Eq. 7*b*;
b = width of a beam;
C = force on area of concrete in compression in a rectangular member;
C_C = force on area of concrete in compression in a circular member;
D = diameter of a circular member;
d = distance from top of beam to tensile reinforcing steel:
  d' = distance from tensile reinforcing steel to bottom of beam;
  d'' = distance from top of beam to compressive reinforcing steel;
  d_g = distance between gages;
E_s = modulus of elasticity for steel in tension:
  E'_s = modulus of elasticity for steel in compression;
  E_{wh} = modulus of elasticity for steel in the work-hardening range;
e = eccentricity of load;
f = stress:
  f'_c = compressive stress in concrete;
  f'_{cm} = maximum compressive stress in concrete;
  f'_{cs} = equivalent compressive stress in concrete at the position of the compression reinforcement;
  f_o = stress in steel defined in Fig. 4;
  f_s = tensile stress in steel;
  f'_s = compressive stress in steel;
  f_{sy} = yield-point tensile stress in steel;
  f'_{sy} = yield-point compressive stress in steel;
H = term defined in Eq. 7*a*;
j = term defined in Fig. 5(*b*);
k = term defined in Fig. 1(*c*);
l = length;
M = bending moment:
  M_A = bending moment at point A in Fig. 13(*a*);
  M_B = bending moment at point B in Fig. 13(*a*);
  M_e = external bending moment;
  M_r = resisting moment of the section;
  M_{ru} = ultimate resisting moment of the section;

P = load:
  P_{CO} = collapse load;
  P_U = ultimate load;
p = percentage of steel defined in Eq. 4:
  p_c = percentage of steel defined in Eq. 26*a*;
  p'_c = percentage of steel defined in Eq. 26*b*;
  p_{sy} = percentage of steel defined in Eq. 19;
T = force of tensile reinforcing steel;
t = total depth of a member;
x = distance which defines the section under consideration;
y = deflection at section defined by x;
α = angle defined in Fig. 9(*a*);
δ = maximum deflection;
ϵ = strain:
  ϵ'_c = compressive strain in concrete;
  ϵ'_{cm} = compressive strain corresponding to the maximum compressive stress in concrete;
  ϵ_s = tensile strain in steel;
  ϵ'_s = compressive strain in steel;
  ϵ_{se} = tensile strain on extreme steel fiber;
  ϵ_{sy} = yield-point tensile strain in steel;
  ϵ'_{sy} = yield-point compressive strain in steel;
  ϵ_{wh} = threshold strain of work-hardening range of steel;
η = distance from neutral axis:
  $\bar{\eta}$ = distance defined in Fig. 5 and Fig. 8;
  η_C = distance defined in Fig. 9;
θ = angle defined in Fig. 9(*a*);
ρ = radius of curvature;
ϕ_{BA} = angle change of point B with respect to point A in Fig. 13(*a*);
χ = curvature:
  χ_B = curvature at point B in Fig. 13(*a*); and
  χ_{ru} = curvature of member when member is subjected to the ultimate resisting moment.

DISCUSSION

Boris Bresler,[27] A. M. ASCE.—The application of the inelastic-flexure theory to reinforced concrete members is a valuable addition to the literature. An interesting feature offered by Mr. Lee is the assumption of a parabolic stress-strain relationship for concrete in flexure and the verification of this assumption by beam tests. In deriving the relationship between concrete stress and observed strains (Eq. 3), the author has assumed the idealized stress-strain relationship for steel that is shown in Fig. 4. For steel stresses between the proportional limit and the yield point this assumption may introduce significant errors if the actual stress-strain diagram for the steel varies appreciably from the assumed relationship.

The importance of the actual shape of the stress-strain diagram for the steel becomes apparent if values of the concrete stress corresponding to the yield strain for steel are computed from both Eqs. 3 and 5. As the data in Table 1 are limited to steel strains that are just less than the yield-point strain, the following estimated values will be used to illustrate the discrepancy between Eqs. 3 and 5: $\epsilon_{sy} = 1{,}615 \times 10^{-6}$; $\epsilon'_c = 2{,}310 \times 10^{-6}$; and $(d\epsilon_{sy}/d\epsilon'_c) = 0.40$. Using these values in Eq. 3 results in a value of 3,600 lb per sq in. for f'_c. The same values used in Eq. 5 result in a value of 2,130 lb per sq in. for f'_c. The discrepancy between these values of f'_c indicates that at strains approaching the yield point Eqs. 3 and 5 are not valid.

Eq. 2 can be rewritten—in terms of the steel stress—as follows:

$$\int_0^{\epsilon'_c} f\,d\epsilon = \frac{A_s\,E_s\,\epsilon_s\,\epsilon'_c}{k\,b\,d} = \frac{p\,f_s\,\epsilon'_c}{k} \dots\dots\dots\dots\dots (41)$$

Substituting k in terms of ϵ_s and ϵ'_c into Eq. 41 and differentiating both sides with respect to ϵ'_c results in

$$f'_c = p\left[f_s\left(1 + \frac{d\epsilon_s}{d\epsilon'_c}\right) + \frac{df_s}{d\epsilon'_c}(\epsilon_s + \epsilon'_c)\right] \dots\dots\dots\dots (42)$$

Eq. 42 is the general expression for f'_c, and Eqs. 3 and 5 can be derived from Eq. 42 for the assumed shape of the stress-strain diagram for steel.

The flexural stress-strain curve for concrete can be obtained from beam-test data by the use of either Eq. 41 or Eq. 42. Differentiation of Eq. 41 with respect to the concrete strain determines the value of the extreme fiber stress f'_c corresponding to the extreme fiber strain ϵ'_c—

$$\frac{d}{d\epsilon}\int_0^{\epsilon'_c} f\,d\epsilon = f'_c = \frac{d}{d\epsilon}\left(\frac{p\,f_s\,\epsilon'_c}{k}\right) \dots\dots\dots\dots\dots (43)$$

The stress-strain relationship for a given range of strain can be determined from Eq. 43 by the use of graphical or numerical differentiation.

---

[27] Associate Prof. of Civ. Eng., Univ. of California, Berkeley, Calif.

An experimental investigation of the flexural stress-strain relationship based on Eq. 43 was performed[28] at the University of California at Berkeley. Three reinforced concrete beams, 11 ft 6 in. long, having various concrete strengths, cross-sectional dimensions, and percentages of reinforcement, were subjected to loading at the third points and were tested to failure. Strains were measured at three levels in the concrete and also in the steel reinforcement.

Stress-strain relationships for the three beams were determined from Eq. 43 by the use of a numerical-differentiation procedure. Three 6-in. by 12-in. cylinders were cast with each beam and were tested to determine the stress-strain relationship in compression. In Fig. 17 the flexural stress-strain relationship obtained from one of the beams is compared with the average of three compressive stress-strain curves obtained from the cylinder tests. It can be seen that the flexural stress-strain diagram varies considerably from the cylinder stress-strain curve in the region of high stress.

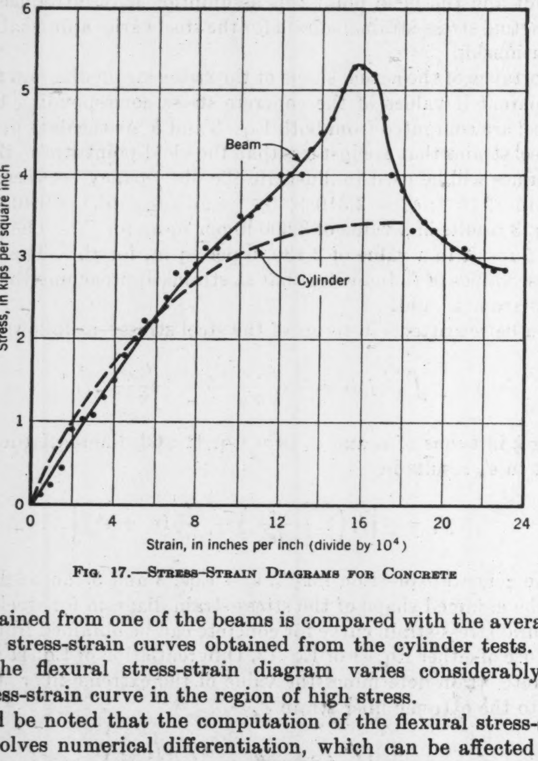

FIG. 17.—STRESS-STRAIN DIAGRAMS FOR CONCRETE

It should be noted that the computation of the flexural stress-strain relationship involves numerical differentiation, which can be affected by the accuracy of the experimental measurements. The experimental accuracy obtained in the tests[27] is sufficient to allow the type of analysis proposed; therefore, the curve shown in Fig. 17 is a reliable representation of the test data. Although the test results described herein seem to indicate that the flexural stress-strain relationship for concrete may differ considerably from that obtained in compression, the results of this limited investigation cannot be considered to be conclusive. Furthermore, it is considered that the precise shape of the flexural stress-strain curve is primarily of academic interest because the effects of plastic flow, shrinkage, size, previous history of stress and strain, state of stress, and stress gradient have been neglected.

---

[28] "Flexural Behavior of Reinforced Concrete Beams," by Stuart H. Bartholomew, thesis presented to the University of California, at Berkeley, Calif., in October, 1952, in partial fulfilment of the requirement for the degree of Master of Science.

Mr. Lee's assumption of a parabolic stress-strain diagram allows one to predict—in a relatively simple manner—theoretical values for the strength and deformation of reinforced concrete members under short-duration static loads. Additional experimental evidence is needed, however, to establish the validity of the parabolic stress-strain relationship, particularly when it is used to predict the deformations of beams at loads approximating the ultimate strength.

ALFRED J. ASHDOWN[29].—The concrete stresses which have been estimated by Mr. Lee would certainly be erroneous if they were obtained for an ordinary reinforced beam because the interaction of the steel with the concrete is not as ordinarily assumed. The curve of stress obtained[9] by Mr. Prentis was for a nongrouted prestressed beam and therefore was more nearly representative of the actual stress distribution.

It would seem that the correct manner in which to determine stress distribution in the concrete is to perform tests on beams reinforced with bars that are anchored at the ends and free to move in holes. The beams should also have stirrups passing around the holes to prevent shear failures. Even if these conditions are met, the results would represent only the stress history of the top fiber. It is significant that the author's readings (Table 1) stopped at 84½% of the collapse load; in the remaining 15½% considerable strain would have developed with a loss of extreme fiber stress, thereby causing more stress in the fibers below the top.

If the fundamental parts of Mr. Lee's paper are invalidated, the complicated formulas produced are unwarranted because many engineers desire simple expressions with which to work.

LAWRENCE H. N. LEE,[30] A. M. ASCE.—The view expressed by Mr. Bresler that the precise shape of the flexural stress-strain curve for concrete is primarily of academic interest is correct because variations in the properties of concrete are large. There is no doubt, however, that a certain stress-strain relationship representing the average properties of concrete is needed—a relationship that can be mathematically expressed and manipulated. For the study of the behavior of statically indeterminate structures, buckling of columns, and other problems the strength-deformation relationships are required; hence, the stress-strain relationship should be established.

It has been determined that the stress-strain curve for concrete tested in a standard compression-cylinder test is a parabolic curve.[15,16,17] It is also known that the state of stress on the compression side of a beam is identical to the state of stress at a point inside a compression cylinder. The stress-strain relationships of two elements made of identical material and subjected to the same state of stress for the same duration obviously cannot be different. It has also been observed[16] that

---

[29] Research Officer, Concrete Technology, Civ. Eng. Dept., Imperial College, London, England.

[30] Asst. Prof. of Eng. Mechanics, Univ. of Notre Dame, Notre Dame, Ind.

> "Various curves have been proposed to represent the stress-deformation relation for concrete, but the parabola is the most satisfactory general representation. Frequently, the parabola expresses the relation almost exactly and in nearly every case the parabolic relation will fit the stress-deformation diagrams very closely through the part which is ordinarily developed in beams."

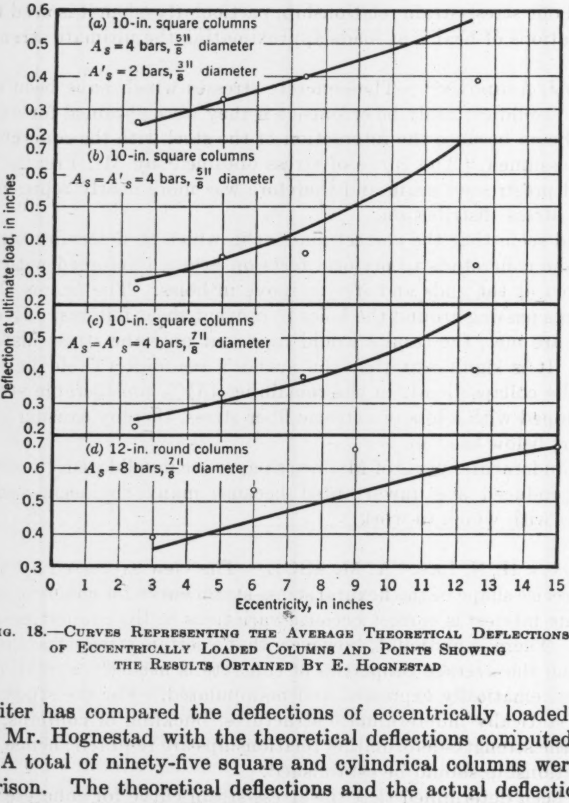

FIG. 18.—CURVES REPRESENTING THE AVERAGE THEORETICAL DEFLECTIONS OF ECCENTRICALLY LOADED COLUMNS AND POINTS SHOWING THE RESULTS OBTAINED BY E. HOGNESTAD

The writer has compared the deflections of eccentrically loaded columns tested[22] by Mr. Hognestad with the theoretical deflections computed by Eqs. 20 to 36. A total of ninety-five square and cylindrical columns were used in the comparison. The theoretical deflections and the actual deflections agree reasonably well, as shown in Fig. 18.

The reinforcing bars used in the writer's experiments were made of mild steel having a sharp yield-point characteristic; this type of steel is commonly used in construction. The stress-strain curve of the steel is almost exactly represented by the idealized stress-strain curve shown in Fig. 4. In this case, the proportional limit and the yield point are very close to each other.

Mr. Bresler's use of Eqs. 3 and 5 is not correct; Eq. 3 is for the range of $0 < \epsilon_s < \epsilon_{sy}$, and Eq. 5 is for the range of $\epsilon_{sy} < \epsilon_s < \epsilon_{wh}$. The point $\epsilon_s = \epsilon_{sy}$ is a point of discontinuity in the first derivative. The values of $(d\epsilon_s/d\epsilon'_c)$ for the left side of the yield point are not the same as those for the right side of the yield point. Eq. 42 is useful for the range when steel stresses are between the proportional limit and the yield point.

It is correct that computation of the flexural stress-strain relationship involves numerical differentiation that may be affected by the accuracy of the experimental measurements, as noted by Mr. Bresler. It has been the experience of the writer that tests should be performed with uniform increment of load in uniform time interval. The total time of testing should be short, and special attention is needed at the ultimate-load stage. It has also been the writer's experience that use of a simply supported beam will not give a stress-strain relationship for a large range of strain because the rapid collapse of the beam after it has absorbed a maximum strain energy prevents the taking of an adequate number of accurate readings.

It should be realized that the test results with strains less than 6×10^{-4} shown in Fig. 17 are not valid because the assumption of no tensile stress in concrete is not valid in that range.

The method of obtaining the flexural stress-strain relationship suggested by Mr. Ashdown is questionable because under the suggested condition there is no way to preserve the condition that a plane remains plane after bending—a basic assumption in forming the stress-strain relationship.

The readings shown in Table 1 do not exceed 98% of the yielding moment of the section and 84½% of the collapse load of the restrained beam, as shown in Fig. 15. The strains beyond that load were not obtained because the strains changed swiftly at that stage. The distribution of stresses as estimated by Mr. Ashdown is shown in Fig. 6.

To overcome Mr. Ashdown's apparent objection to the complicated formulas one could place the results in tabular and graphical form.

AMERICAN SOCIETY OF CIVIL ENGINEERS
Founded November 5, 1852
TRANSACTIONS

Paper No. 2733

ERECTION OF MAIN RIVER SPAN, PASSAIC RIVER BRIDGE

By Jonathan Jones,[1] Hon. M. ASCE

Synopsis

From the erection of the first of the five main spans of the Passaic River Bridge to the final swinging required a period of 70 days. This time interval is short in comparison with the time that is usually required to erect bridges of comparable size. Engineering studies made prior to the beginning of erection accounted for the positions of equipment, delivery of material, and sequences of operations. These studies did much to reduce the time of erection. Of great concern to the erectors were the deflections that the structure would undergo during the erection procedures. These movements, although small to the casual observer, are of considerable importance to the engineer because the members which are fabricated in the shop must, on being lifted into position, fit exactly with the joining members. These studies and other construction problems involved in the erection of the main river span of the Passaic River Bridge are described in great detail.

Passaic River Bridge

The total length of the Passaic River Bridge (New Jersey) between the embankments is 6,955 ft.[2,3] At the lower right (or southern end) of Fig. 1 the structure is seen to cross over US 1 and then under an arch of the Pulaski Skyway, these being, respectively, the principal truck route and the principal passenger car route in New Jersey to the Holland Tunnel (between New Jersey and New York). Toward the top left of Fig. 1 is shown the main crossing of the Passaic River, whence the structure descends to an embankment approach.

A transverse section of the deck structure is shown in Fig. 2. The deck is composed of two 3-lane roadways of 36 ft, a 6-ft center mall, and two 3-ft safety

---

Note.—Presented at the Centennial Convocation, Chicago, Ill., September, 1952. Published, essentially as printed here, in November, 1953, as *Proceedings-Separate No. 321*. Positions and titles given are those in effect when the paper was received for publication.

[1] Bethlehem, Pa.

[2] "Hackensack and Passaic River Bridges: Deck Plate Girders of Record Span Adopted," by O. H. Ammann, *Civil Engineering*, January, 1952, p. 60.

[3] "Hackensack and Passaic River Bridges: Design, Fabrication and Erection Complicated by Size of Members," by Ellis E. Paul, *ibid.*, p. 66.

walks. This deck is carried on longitudinal beam stringers, thence by plate-girder floor beams and floor beam overhangs to a pair of main girders approximately 48 ft on centers.

Approaches.—Almost without exception the approach girders were designed as simple spans resting on concrete piers composed of two simple shafts and a top cross member. A typical pier and a representation of the soil profile prevalent at the site of the Passaic River Bridge are shown in Fig. 3. Span lengths were as great as 174 ft, and girder weights were as much as 125 tons.

FIG. 1.—AERIAL VIEW OF THE PASSAIC RIVER BRIDGE (NEW JERSEY)

There were many points of interest in the erection of these approaches such as work in close quarters, over main-line tracks, and under high-tension wires. The erection procedures (except for the purely repetitive operations) were completely planned in the erection engineering office; dimensioned drawings, showing the positions of equipment, the delivery of material, loads, reaches, sequences, and every type of precaution to be observed, were supplied to the resident erection engineer and were scrupulously followed.

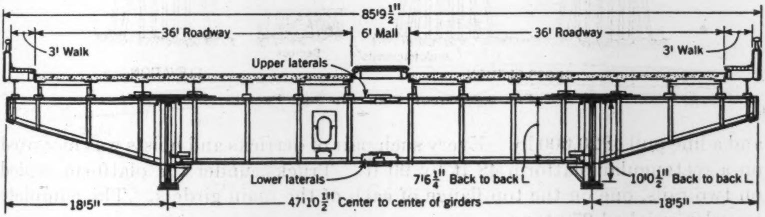

FIG. 2.—TRANSVERSE SECTION OF THE PASSAIC RIVER BRIDGE (NEW JERSEY)

Erection Equipment.—Speed and flexibility of erection were both important under the terms of the contract. It was therefore decided that the two twin-boom travelers (shown in Fig. 4) would give greater production than would single-boom travelers with the boom capacity required to handle the heaviest girders. The capacities specified in purchasing new travelers were, accordingly:

Capacity of each boom, in tons	Reach, in feet	Length of boom, in feet
115	65	85
100	75	115
70	96	115
45	110	115
15	135	Flat, on 20-ft jib

Thus, two of the exceptionally heavy girders could be picked up by two booms (Fig. 4) in little more time than a single heavier boom could have set one girder.

Each traveler was composed of two stiffleg derricks, having a three-drum-and-swinger, torque-converter, air-controlled gasoline hoist of 195-hp capacity, and a line pull of 20,000 lb. Every such pair of derricks and hoists was mounted on a rectangular platform 48 ft by 90 ft. Trucks, under the platform, rolled on two rails, one on the top flange of each of the main girders. The complete traveler weighed 270 tons.

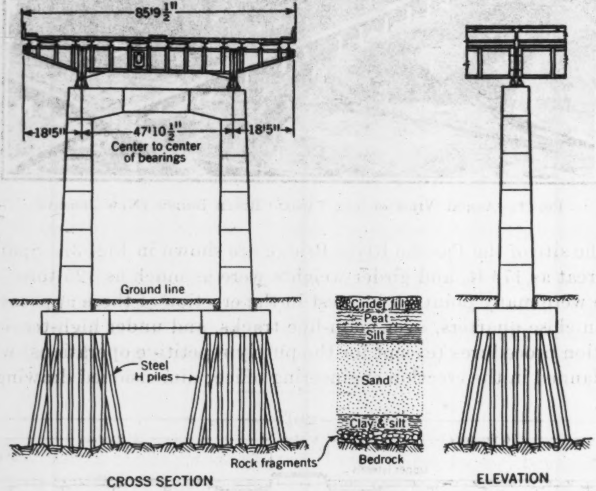
85'9½"
18'5"
47'10½"
Center to center of bearings
18'5"
Ground line
Steel H piles
Cinder fill
Peat
Silt
Sand
Clay & silt
Rock fragments
Bedrock
CROSS SECTION
ELEVATION

FIG. 3.—BRIDGE PIER AND SOIL PROFILE

MAIN SPANS OF THE RIVER CROSSING

The five main spans of the river crossing, as broken down by field splices for fabrication and erection, are shown in Fig. 5. From Fig. 5 the following can be seen: (1) The main span is 375 ft, or longer than any plate-girder span built in the United States prior to 1952. (2) This span rests on a fixed shoe at each end, thus requiring concrete piers 1N and 1S to flex during the changes of steel length caused by a change in live load and temperature. (3) The flanking and continuous spans of 275 ft cantilever an additional 31 ft 3 in. to receive an end of the last approach span, making the total length of continuous girders 987 ft 6 in. (4) The vertical curve over this crossing is unsymmetrical, which approximately doubled the time and cost of many elements of the drawings, the engineering computations, and the fabrication.

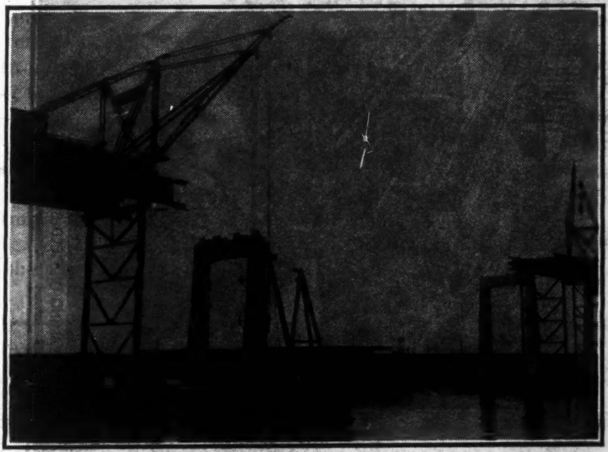

FIG. 4.—TWIN-BOOM TRAVELERS IN OPERATION

Haunched Girders.—In Fig. 5 there are shown the division of the span, by field splices, into pieces of practical dimension and weight for shipment and raising, and the system of reference numbering. In general, the girders have parallel flanges and are 14 ft deep. Over the two main piers, however, the girder depths are increased to $22\frac{1}{2}$ ft to resist the maximum moments. To facilitate shipping, sections 1N and 1S required the horizontal splices shown by the dotted lines in Fig. 5. These horizontal splices were connected on the

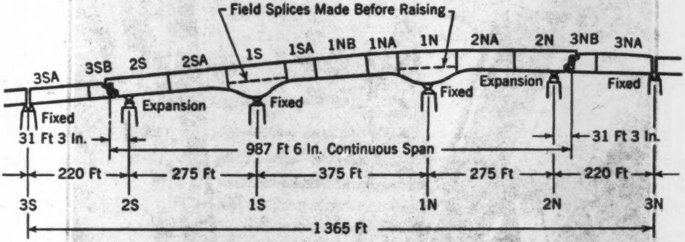
Field Splices Made Before Raising
3SA
3SB
2S
2SA
1S
1SA
1NB
1NA
1N
2NA
2N
3NB
3NA
Fixed
Expansion
Fixed
Fixed
Expansion
Fixed
31 Ft 3 In.
987 Ft 6 In. Continuous Span
31 Ft 3 In.
220 Ft
275 Ft
375 Ft
275 Ft
220 Ft
3S
2S
1S
1N
2N
3N
1 365 Ft

FIG. 5.—MAIN SPAN OVER THE PASSAIC RIVER AND SHORES (NEW JERSEY)

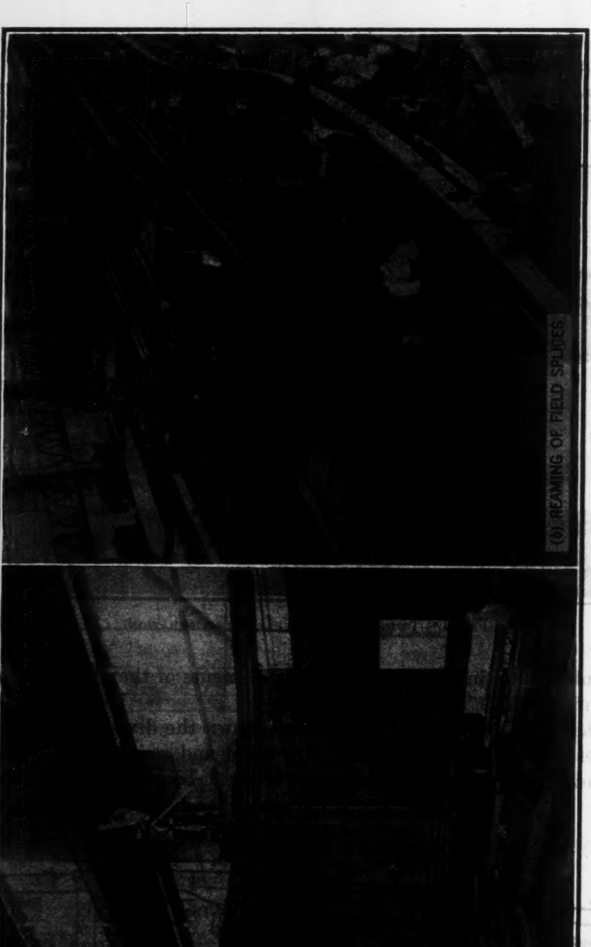
(b) REAMING OF FIELD SPLICES
(c) ASSEMBLED

FIG. 6.—HAUNCHED GIRDER

transport barges, making a lift of 173 tons for each haunched girder. The raising of one of these pieces is shown in Fig. 4.

In preparation for fabrication, each girder was "laid out" on heavy paper on the floor of the templet room in sections of full size with all rivet holes and other details exactly located. The divisions that included the four haunched sections over the main piers were each approximately 175 ft long. From these layouts, smaller templets were made for marking the individual angles and plates of steel. In most of the constituent pieces occasional bolt holes were sub-drilled according to the templets, but in those pieces which would be on the inner side of the fabricated girder all the holes were sub-drilled as guides.

In Fig. 6(*a*) the 22-ft-deep haunched girder is shown assembled in the shop. This girder was laid on its side, all the holes were drilled (full size) through the guide holes, and the girder was riveted. Perfection of its dimensions, and circular form for its rivet holes, were thus assured.

In Fig. 6(*b*) the haunched section is shown being assembled at its ends to some of the parallel-sided girders for reaming of the field splices. At this stage the cambered outline of the girder was carefully checked by transit and tape; also measured were several triangles determined by the most important working points. In this position all remaining shop rivets were driven, and the field-splice material was riveted—in so far as was practical—to one of the shipping pieces.

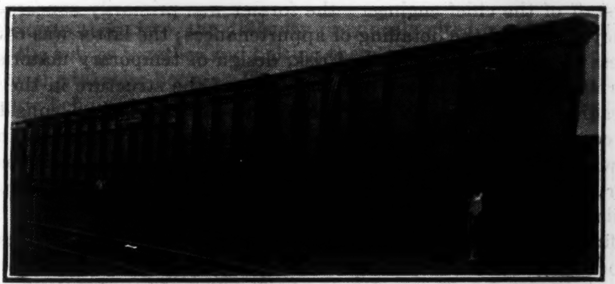

FIG. 7.—SHIPMENT OF GIRDER

Shipment of the Girders.—In Fig. 7 there is shown the shipment of a 124-ft length of one of the side-span girders (2S), the 14-ft depth of which was too great to allow for railroad clearance on flat cars. The girder was accordingly mounted on the trucks to constitute a "car" in itself and was provided with a special drawbar and a standard coupling. Fig. 7 shows the stiffeners and cross-bracing connections over pier 2S and the links from which the suspended girder 3S is hung.

An interesting feature affecting these links is that, because the roadway at this point is on a horizontal curve, there is a small angle, in plan, between the two girders. To allow for this curve, the upper and lower parts of the link plates are planed on opposite tapers in thickness and are bored normal to the resulting outer surfaces; the pins are therefore at the requisite angle in plan, one with the other.

ERECTION OF SPANS

Engineering Studies.—The successful determination of the deformations and the proper choice of manipulations form two of the most interesting, and at times rewarding, experiences of the structural engineer. The changes of size and shape of a large steel bridge, although imperceptible to the casual observer, are in reality matters of inches and are of prime importance to the erector. If a group of rivet holes in a given piece does not come into the intended exact alinement with the same group in the connecting piece (even by a quarter of an inch) and cannot be put there by available and safe manipulations, there is going to be grief. However, when by predetermined forces the inertia of the structure is overcome, and the mass of steel moves responsively through the precomputed movements into the intended relation with its neighboring member, the planners feel the natural satisfaction which is the result of a job well done.

The engineering studies for the erection of the main river spans of the Passaic River Bridge were a joint enterprise between the erection department and the staff of the chief engineer—the former was primarily concerned with expediency, cost, and the detailing of appurtenances; the latter was concerned with stress computations, degrees of risk, design of temporary materials, and the deformations and necessary manipulations of the structure in the various stages leading to its completion. These functions overlapped considerably; through cooperation they resulted, after consideration of many ideas, in a final scheme which involved the positions of the field splices, the positions of the temporary supports, practical traveler positions, delivery route for materials, and similar general decisions.

The first step in the erection studies was the computation of the elastic constants for the girders. This computation was made for small increments of length because of the rapid and substantial variations in section. Similar data determined by the consulting engineers in checking their continuous design provided a useful check but had to be independently repeated so that the chosen increments of length would fit the field-splice positions and the positions of the temporary supports.

From the prescribed vertical contour of the completed bridge hypothetical deflections were determined which corresponded to the removal of all weight. The resulting contour (higher at the middle of the main span and in other places lower than the final or "normal" contour) was the "cambered" or "no-load" outline. This outline was that to which the girders were placed when they were on their sides (in the shop) for the reaming of splices and for riveting.

Girders thus dimensioned—if they could be erected as completed pieces and allowed to deflect first under their own weight and then under the weight of the concrete roadway—should conform exactly to the intended normal contour. Because, unfortunately, each girder had to be erected in nine pieces and, because their own weight plus that of the floor steel was great enough to cause considerable deformations, their tendency was to deflect to different angles, one piece with the next, from the angles at which the splices had been reamed.

This meant that splices would stand open at the top when closed at the bottom, or vice versa.

The last two splices to be made, as the erection proceeded simultaneously from each end, were those at the ends of the center piece, 1NB (Fig. 5). At all splices prior to these two, the difficulty previously cited could be overcome by bringing the splices together and bolting them while the forward piece was still carried by the traveler boom. The piece would then be lowered to its support with elastic bending at the splices. However, for the last two splices (which were made simultaneously at the two ends of the final section) it was necessary to bring up the ends of the two receiving sections (then cantilevered from piers 1N and 1S and naturally drooping) to such elevation and angle that, when the final section was connected and released from the traveler falls, the final

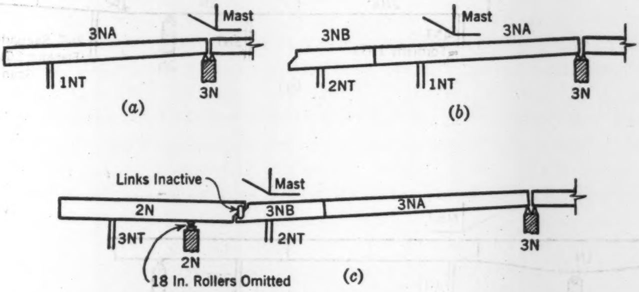
Mast
3NA
1NT
3N
(a)
Mast
3NB
3NA
2NT
1NT
3N
(b)
Links Inactive
Mast
2N
3NB
3NA
3NT
2NT
2N
3N
18 In. Rollers Omitted
(c)

FIG. 8.—ERECTION SEQUENCES

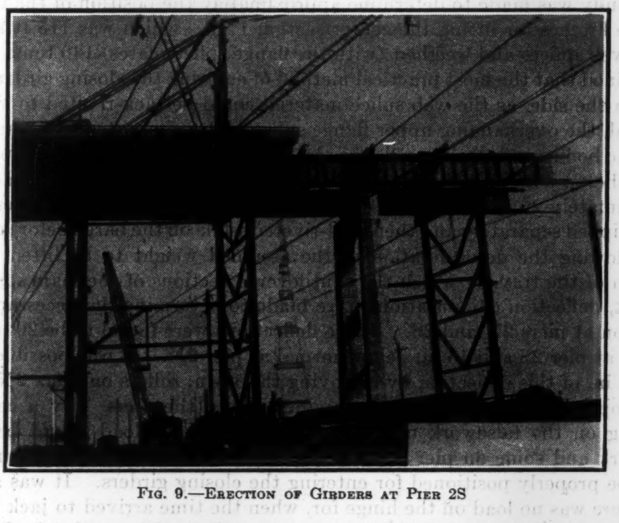

FIG. 9.—ERECTION OF GIRDERS AT PIER 2S

section would assume the proper contour for the condition of dead load less the floor slab. To assure this condition, it was necessary to control, or manipulate, the placement and support of each of the four previously placed pieces coming in from each end. Thus, the geometry of the closing position dictated a forced geometry for the prior stages.

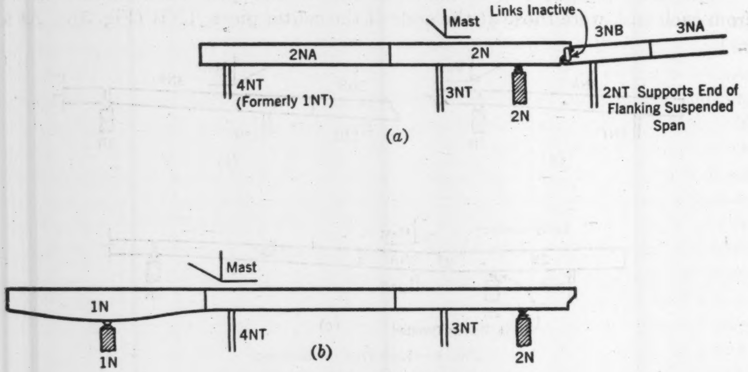

FIG. 10.—ERECTION OF SPAN 2

A study was made to determine approximately the position of the travelers and the hitches for lifting the center section 1NB—which was 115 ft long between web splices and weighed (with the flange splice plates) 146 tons. It was determined that the most practical method of entering the closing girders would be from the side, as the web splice material could be tack-riveted to the main material, the overhanging upper-flange splice plates supported by a runner line from the boom, and the lower-flange plates allowed to droop and then pulled up by long bolts. Because the flange splice plates of the closing girders would extend approximately 26 ft beyond the center line of the web splice at each end, they were shipped separately and then field-riveted while on the barge before erection.

Following the determination of the assumed weight to be lifted and the position of the traveler which the cantilevered sections of the main span could support, deflection computations were made to determine the necessary girder elevation at piers 2N and 2S. These deflections were found to be 20 in. below normal at pier 2S and 15 in. below normal at pier 2N. It was possible to provide 17 in. of this deflection by removing the 18-in. rollers on piers 2N and 2S and dropping the anchor bolts temporarily into the piers. By a controlled lowering on the falsework near pier 2S so that some load would be on the falsework and some on pier 2S, it was found that the ends of the cantilevers could be properly positioned for entering the closing girders. It was assumed that there was no load on the hinge for, when the time arrived to jack up span 2 to replace the rollers, the computations indicated that the girder in span 2 could not carry the reaction of the suspended span on the cantilevered length of over 70 ft from the falsework bent to the link. Carrying the load of the suspended span on an independent bent would keep the loads on each of the two bents close to that required in the earlier stages of erection. In order, therefore, to prevent transfer of stress at the hinge point, the holes in the upper ends of the links were slotted vertically 3 in. and the suspended span held 1½ in. high, with the erector checking after each major lift to see that the pin stayed in the middle third of the slotted hole.

Erection Sequences.—Although the computations relative to the erection proceeded from midspan backward and might be mistaken for plans to take the bridge down rather than put it up, the field operations are best described in their actual sequence. In Figs. 8(*a*) and 8(*b*) there is shown the successive erection of sections 3NA and 3NB with the traveler in the respective positions noted as "Mast"; their erection required two temporary erection bents 1NT and 2NT. Together they constitute girder 3N, which is the 190-ft simple span designed to be supported on pier 3N at its outer end and on a pin link at its inner end.

In Fig. 8(*c*) section 2N has been erected with the traveler standing over forward bent 2NT; the rearward bent 1NT has been taken out for re-use. The connection of the suspended span (3N) to the cantilever arm has been made at the link, but no load is being transferred through it. The (exaggerated) droop of the profile shows that a nest of 18-in. rollers has been omitted from the bearing of girder 2N on pier 2N, in order that, using the shoe on pier 1N as a fulcrum, the steel in the main span may be given an upward inclination.

FIG. 11.—BRACING FOR STABILITY

Fig. 9 illustrates the foregoing situation at pier 2S on the opposite side of the Passaic River. The original temporary bent 1ST is being taken out by a crane;

temporary bents 2ST and 3ST are in place. The traveler has just erected girder sections 2S and is filling in the floor steel. It can be seen that there are no rollers under the steel shoe on pier 2S. The pin link is evident, and the floor break is indicated by the double brackets.

In Fig. 10(*a*) span 2N is completed in the customary fashion; section 2NA overhangs the falsework bent 4NT, which was originally used in position 1NT.

No shear is being passed through the links between spans 2N and 3N. Across their top flanges there has been installed an adjustable connection which stabilizes the structure longitudinally to the fixed shoe back at pier 3N. This connection can be manipulated to secure fair holes between the girders and their fixed shoes when pier 1N is reached.

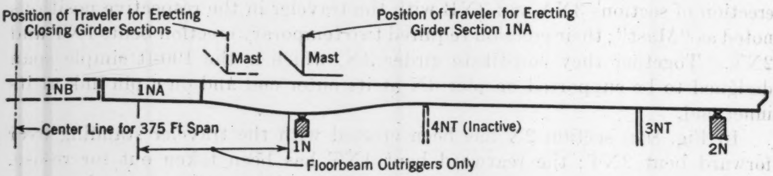
Position of Traveler for Erecting Closing Girder Sections
Position of Traveler for Erecting Girder Section 1NA
Mast
Mast
1NB
1NA
Center Line for 375 Ft Span
1N
4NT (Inactive)
3NT
2N
Floorbeam Outriggers Only

FIG. 12.—ERECTION OF THE CLOSING GIRDERS

In Fig. 10(*b*) the main span has been reached, and section 1N has been raised. The raising of haunched section 1N off the barge, with the load taken on two booms, is shown in Fig. 4. Fig. 10 exaggerates the degree to which section 1N is forced to slope upward because of the omission of the rollers on pier 2N.

In Fig. 11 there is shown one section 1N raised onto its shoe, this section being the first of the pair. Because of its great depth, the section would have been unstable if both booms had simply released it to raise the companion piece. A splice was therefore introduced into the permanent transverse frame, and approximately one fourth of its total length (Fig. 11) was used as a temporary brace between the top of the girder first erected and the pier.

In Fig. 12 the traveler standing over the main river pier 1N has erected the 65-ft section 1NA and has advanced to a position 50 ft from the main pier, where it will erect, with its opposite number, the 115-ft, 146-ton closing section 1NB. From the pier to the end of section 1A, all floor steel not required for stability or convenience was omitted to reduce the cantilevered weight. In exaggerated fashion, Fig. 12 indicates that the projecting end has been raised to the point desired.

In Fig. 13 the two closing girders have been brought in on cars and a car float and are being hoisted simultaneously, with no cross connection and at somewhat less than their final center-to-center distance. This simultaneous lift had been decided on because (1) the effect of warping the span from unsymmetrical lifts would be eliminated, (2) equipment and man power would be available, and (3) the channel would be blocked only once.

Fig. 14 illustrates the difficulty of making the final splices. It is obvious that the splice material was so long that a sidewise entry was imperative. Each flange at this point included a side plate on each side of the main web, four angles forming an "H," and additional plates over the vertical legs of each angle pair. The clearance between these latter plates and the inner horizontal

Fig. 13.—Lifting the Closing Girders

surfaces of the outstanding legs of the flange angles between which they lay was so small that a slight error in the angular position of the cantilevered girders would have made the entry of this material impossible. This angular position

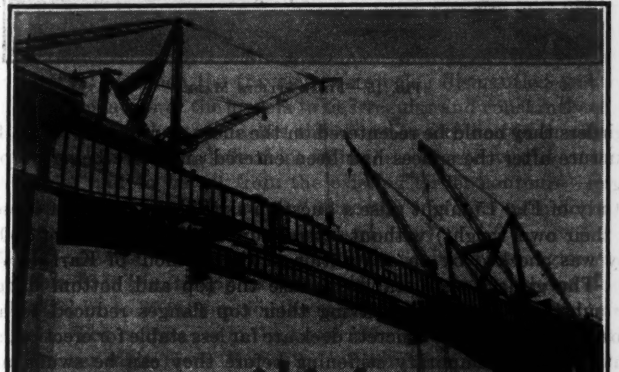

Fig. 14.—Entering the Closing Girders

had, however, been brought under control by the provisions made for raising or lowering the falsework in the flanking spans (spans 2) to cause the main-span cantilevers to rotate about piers 1. The existing positions were instrumentally checked, and entry into the splices was determined to be feasible before the two closing sections were picked off the barge.

In Fig. 5 it is indicated that the main 375-ft span is fixed to the piers at both ends. In order that one pair of girders might be retracted (at main pier 1S) so that the final entry could be made, longitudinal motion was provided for at the top of the shoe, where a plane surface adaptable for sliding existed in the design, and where jacking brackets could be attached readily to the girders. Of the jacking force to be exerted, all except that resulting from friction on the sliding surface would obviously react against the concrete pier and deflect it. The engineers limited this to a deflection corresponding to a thrust of 250-kips per shoe. To design the jacks and brackets, 10% of the vertical load was added, and 200-ton jacks were selected. The sliding surfaces were machined particularly smooth and were well greased, thus justifying the friction coefficient of 10%. Jacks in opposing pairs were provided so that after the final splicing of the girders they could be recentered on the shoes as required. Fig. 15 shows the structure after the splices had been entered and were being prepared for riveting.

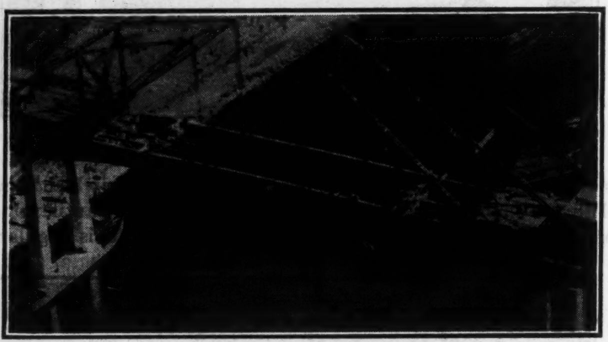

Fig. 15.—Final Splices Made

A study of Fig. 15 might raise a question as to the stability of these girders (under their own weight) without lateral support for a length of 250 ft; this stability was checked by an adaptation of the method[4] of Karl de Vries, M. ASCE. The girders were stable because the top and bottom flanges were equally substantial. Girders having their top flanges reduced to allow for "composite action" with a concrete deck are far less stable for erection, and they frequently require temporary stiffening before they can be swung as simple spans.

As the closing girders were entered, the splices at the north or fixed end were contacted, then pinned and bolted for the lower third. At the south end the cantilever girders were pushed into contact by jacking horizontally at pier 1S the east girder $2\frac{1}{4}$ in. (which closely approximated the computed movement) and the west girder 3 in., the jack loads being 192,000 lb, and 288,000 lb, respectively. The motion over the shoe never exceeded the gain at the splice by ½ in. which indicated that there was no excess deflection of the pier top. Both south splices came approximately 70% fair, and, as soon as the lower third of the splice was pinned and bolted, the load in the falls was gently lowered "to fair" the remaining holes. The northeast splice was made by the time all the load in the south falls and north falls had been released; the northwest splice was still only 70% fair. It was necessary to lift the west part of the falsework bent 3NT 2 in. to make the top chord holes in the northwest splice.

---

[4] "Strength of Beams As Determined by Lateral Buckling," by Karl de Vries, *Transactions*, ASCE, Vol. 112, 1947, pp. 1245–1271.

As the floor steel was subsequently being placed, it was noted that the bottom flange holes in the girder at pier 1S were approaching the holes in the top shoe. When the distances between holes had diminished to ⅜ in. for the east girder and ⅞ in. for the west girder, the horizontal jacks were used to aline the holes, and permanent stop plates were placed against the shoes and were riveted. This jacking indicated (approximately) a friction coefficient of 0.03.

Because falsework bents 4T were inactive after the traveler moved beyond piers 1, the girders were raised over piers 2 by raising the jacks under falsework bents 3T. Simultaneously the girders were raised enough on falsework bents 2T, under the suspended spans, to keep the pins in the center of the slotted holes and thus avoid loading the links. The omitted rollers were then slid laterally into position at piers 2. This jacking on falsework bents 3T was, of course, against the elastic resistance of the completed continuous structure. Bents 3T were then lowered to load the rollers on piers 2; falsework bents 2T were lowered to move the end reaction of spans 3 onto the links; the steel was then completely "swung."

Roadway.—The grade of the concrete roadway slabs was determined, throughout the bridge, by screed angles riveted to the floor steel along the slab edges. Concreting on the five main spans had to proceed from the two ends during an interval in which the travelers were being dismantled and lowered, which caused the contour of the girders to be irregular and constantly changing. Therefore, whereas on the approaches the screed angles had been adjusted on the basis of the precomputed deflections from the concrete weight, on the main spans the angles had to be set from the existing girder contours—for it was anticipated that these would be correct when the travelers were down. This expedient subsequently proved to be adequate.

Details of the Design.—The back-to-back distance between angles varies for the girders from 10 ft ½ in. to approximately 11 ft 9 in. for suspended side spans and from 13 ft 3½ in. to 21 ft 6½ in. for the main river spans. The main material is silicon steel. The web varies in thickness from $\frac{9}{16}$ in. to ¾ in. and is stiffened longitudinally over main piers 1S and 2S. Each flange is composed of 26-in.-wide cover plates, side plates under four 8-in. by 8-in. by 1⅛-in. angles, and, at places, additional side plates over the web legs and between the outstanding legs of the angles.

An unusual feature for a through plate-girder bridge is the provision made at each floor beam for expansion of the pair of floor stringers adjacent to the main girders. This feature was introduced to prevent large lateral bending moments from developing in the floor beam flanges. The stress deformation of the flange or chord while the stringers remain of practically unchanged length is a great problem in the erection of long-span bridges, especially with regard to the stringer closest to the girder or truss. During cantilever erection this differential is, of course, much larger than normal, but it is frequently a problem under changes of stress in the permanent structure. This problem was eliminated by the expansion detail which was used.

Erection Details.—The girders have expansion shoes at pier 2; therefore, during erection it was necessary to provide longitudinal stability at the hinge points close to the pier. This stabilizing force not only had to be flexible in a vertical direction to allow for relative deflections, but also had to be adjustable longitudinally to allow for matching the holes in the fixed shoes at pier 1N at any expected erection temperature and for possible shop and field errors. The change in depth of the girders at the hinge point made it possible to provide a link detail which connected to a 3-in.-diameter eyebolt fastened to the top flange of the shallower suspended girder. The bending stress was eliminated from the eyebolt by clip angles with slotted holes over the end of the pin through the eyebolt. This detail was also complicated by the necessity of running the traveler over it as the erection proceeded.

At the hinge point it was also necessary to (1) leave the bracing connections loose, (2) leave all interlocking material loose, and (3) raise the steel mall and curb sections of the main spans high enough to clear the adjacent sections. This raising was done to allow sufficient longitudinal clearance with the girders in their lowered position at pier 2. Enough permanent clearance was available between the girders at the hinge so that no change in the girders themselves was necessary. Because of the different vertical curvatures at the two link locations, it was determined that the clearance between girders 3 and 2 would be reduced less at the south end than at the north end when rotation would be introduced about pier 1. This is why the shoe at pier 1S was made the temporary expansion shoe for closing the main span, whereas the permanent connection of the girder to the shoe at pier 1N was made when first erected.

At pier 2 the requirements were that (1) the girder should be not more than 17 in. low; (2) free longitudinal movement should be permitted; (3) transverse motion should be prevented; and (4) it should be possible to erect the rollers on the piers adjacent to the shoes at the same time the shoes were erected and to skid them sideways into place after the girders had been made continuous. In order to insert the rollers by skidding them sideways, the girders had to be jacked 6 in. above normal to clear the toothbars.

Final deflection computations proved that there would be sufficient latitude for all conceivable errors by erecting the shoe and girder 16½ in. low, loading the falsework bents 3T, and varying the angle of the ends of the main-span cantilevers by jacking up or lowering on falsework bents 3T to match the ends of the closing girder. Omission of the 18-in. rollers left room to replace them with a greased plate, grooved top and bottom. The greasing allowed longitudinal motion, and the grooving engaged the ridges on the top shoe casting and on the base plate which normally prevent transverse motion of the rollers. Computations were also made to ensure that, with the girders finally continuous, there would be sufficient jack capacity at bents 3 to raise the girders 6 in. above normal at pier 2 without overstressing the girders.

The elevations of bents 2, 3, and 4 were so set that, with the bearing at pier 2 set 16½ in. low, the camber position of the girder at pier 1 would be 1 in. high. This was done to allow for girder deflections and settlement, if any, of bent 4 under maximum load when raising girder section 1 (Fig. 10). With this 1-in. allowance it was thought that, when girder section 1 rested on pier 1, the splice just ahead of falsework bent 4 would be exactly alined or the bottom splice holes would be fair with the top of the splice open, thus requiring jacking down at bents 3 and 4 to make the splice. Three of the four splices were made without jacking; the one that had to be jacked, however, was raised.

The positions of the cantilever ends of the girders were determined for the condition which would exist immediately prior to lifting the closing girders, and after lifting the closing girders (as the derricks were standing on these cantilever arms). It was hoped that a check on this could be obtained in the field. As a minimum, it was prescribed that readings should be taken before picking up the girders to determine if the openings both top and bottom would be sufficient and the relative elevations of the girders be approximately correct. However, only the minimum readings were made; even that was with the booms of the north derrick working, with the load on both the anchor span and the cantilever increased to expedite erection, and with the falsework at bent 3N approximately 3 in. low. Comparing these measurements with the computed theoretical measurement for similar loadings, it was apparent that the closing girders could be entered and that bent 3N could be jacked up, if necessary, to close the splices. The reason for taking only the minimum readings was to speed erection so that the girders could be erected on the day planned; conditions were nearly perfect, with the sky cloudy, temperature close to normal, and no wind. This last was important as there were few days at this time of the year (October, 1951) that had not been windy.

Construction Roadway.—Both time and money were saved on the construction of the approaches to the Passaic River Bridge by the requirement in the foundation contract that the contractor build a specified construction roadway. This roadway was called for under thirty-four of the approach spans, with a total length of approximately 4,400 ft. These spans were over meadowland which is under water most of the time. By specifying a satisfactory construction roadway—in this case approximately 113 ft wide—each of the superstructure contractors knew at the time of bidding just what the site conditions would be and how materials could be delivered. With a road of that width, deliveries could be made simultaneously to the foundation contractor and to the steel erector without causing delays to either. Both contractors had a suitable working platform for unloading and sorting their materials. Subsequently, the roadway-slab contractor delivered his forms directly to the spans as required and concrete to hoist-towers spaced along the edge of the superstructure, without interfering with steel erection. Later the painting contractor used the construction roadway. This roadway should prove useful throughout the life of the superstructure.

Omission of the construction roadway from the foundation contract would have meant that: (*a*) The foundation contractor would have included in the bid the cost of a minimum road. Not knowing whether the road could be used by the steel contractor, no allowance could have been made for any salvage value. (*b*) The steel contractor, knowing the foundation contractor might demand an exorbitant price for the use of his road, would probably have decided on running the 13,000 tons of steel out over the top. This is a slow and costly method, which also delays the slab contractor. (*c*) The slab and painting contractors would have also included additional delivery costs in their estimates. The sum of all these individual allowances would, in all probability, be greater than the actual cost of the construction roadway without making any allowance for the time saved in completing the contract for a structure financed by revenue bonds.

ACKNOWLEDGMENTS

Fabrication and erection of the Passaic River Bridge were performed by the division of Fabricated Steel Construction of the Bethlehem Steel Company, at Bethlehem, Pa. The advance engineering was directed by the writer, assisted particularly by W. H. Jameson, M. ASCE, and George L. Gray, A. M. ASCE. Erection was in charge of J. H. Wagner, through E. L. Durkee, M. ASCE, and George P. Adair.

AMERICAN SOCIETY OF CIVIL ENGINEERS
Founded November 5, 1852
TRANSACTIONS

Paper No. 2734

THE IMPORTANCE OF SHORAN SURVEYING

By CARL I. ASLAKSON,[1] M. ASCE

SYNOPSIS

During World War II many electronic devices were developed which were used subsequently in various fields of endeavor. One such device was shoran, a transceiver-transponder system by which radio-wave travel time is measured. Shoran has since been developed further and is a surveying instrument by which inaccessible terrain can be surveyed by combining shoran with photogrammetry with an accuracy comparable to third-order control. Horizontal control by the use of shoran is quite accurate, but vertical control leaves much to be desired; continued work in this direction is needed.

Shoran and photogrammetry are especially applicable to inaccessible terrains such as those which exist in the Southern Hemisphere. This application is needed because it has been found that the improvement of an area closely follows the surveying in that area.

INTRODUCTION

In 1944 the surveying and mapping engineer began to make strange additions to his vocabulary. Such words as "shoran," "raydist," "decca," "irrad," "moran," "geodimeter," and "electronic position indicator" have become common to the engineer. This is only a partial list; the surveyor is also concerned with "radio altimetry," "profile recorders," the "refractometer," the "dielectric constant of air," the "velocity of radio waves," and similar subjects. These additions to the engineer's vocabulary have been made necessary by the rapid development of electronic surveying, a method which is having a profound effect on the future of surveying and mapping.

Geodetic control on a unified continental datum is being established (as of 1954) throughout the island areas of the Antilles and in vast areas of the Canadian wilderness. Other important geodetic ties are being made throughout the world.

Many papers concerned with electronic surveying and related subjects have been published, and several of these are listed in the Appendix. The

---

NOTE.—Published essentially as printed here, in November, 1953, as *Proceedings-Separate No. 353*. Positions and titles given are those in effect when the paper was received for publication.

[1] Comdr., Coast and Geodetic Survey (U. S. Dept. of Commerce), and Air Force Missile Test Center Geodetic Officer, Patrick Air Force Base, Cocoa, Fla.

subsequent material is related, however, to a single instrument and its use. That instrument is shoran, a blind-bombing instrument (developed during World War II), which has been modified and adapted to surveying. Shoran is described because it is in more extensive practical use (as of 1954) than any other system. In restricting the investigation to shoran, it is not implied that similar instruments cannot be used to accomplish the same purpose after they have undergone extensive trials. Long-distance trilateration by shoran combined with shoran-controlled photography is of greater importance to South America, Mexico, Central America, and the Antilles than electronic-surveying instruments designed to compete with the conventional type. This greater importance exists because shoran will span the oceans for great distances, map difficult—and even inaccessible—terrain, and enable all of these maps to be placed on a single datum.

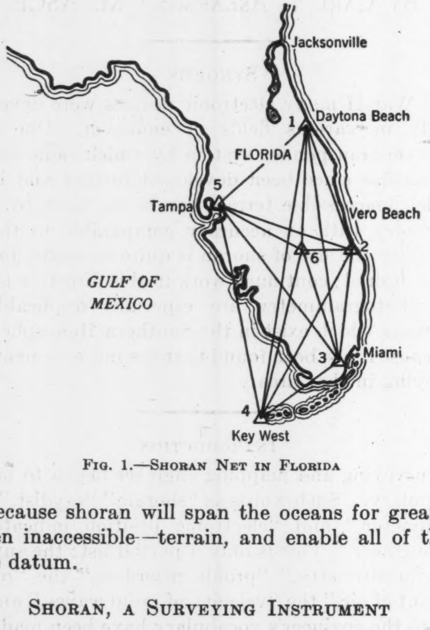

FIG. 1.—SHORAN NET IN FLORIDA

SHORAN, A SURVEYING INSTRUMENT

Detailed descriptions of shoran design and operations are available (1).[2] Briefly, shoran is a transceiver-transponder system by which radio-wave travel time is accurately measured from an airplane to each of two antennas located at ground stations. This time measurement is translated directly into distance which is either read on dials or automatically recorded. These air-ground distances can then be reduced to geodetic distances by the application of corrections which involve certain instrumental corrections, meteorological factors, and the respective altitudes of the aircraft and ground stations.

Test of Shoran Accuracy.—Reports on tests of the accuracy of shoran have generally been classified, and only the results of that test performed in 1950

---

[2] Numerals in parentheses, thus (1), refer to corresponding items in the Bibliography (see Appendix).

(2) (3) will be presented. This test was performed in Florida (Fig. 1), where a total of fifteen distances were measured by shoran, and the results were compared with the distances obtained from conventional first-order triangulation. The distances varied in length from approximately 40 miles to 320 miles. Results of this test are given in Table 1. The maximum discrepancy with a surveyed distance was approximately one part in 40,000; the average discrepancy was 0.0012 mile, or approximately 6 ft.

TABLE 1.—SHORAN RESULTS IN FLORIDA TEST

Line[a] (1)	Geodetic distance, in miles[b] (2)	Adjusted shoran distance, in miles (3)	Col. 2 minus Col. 3, in miles (4)	Proportional discrepancy, in parts per million (5)
2–6	40.6131	40.6123	+0.0008	19.7
3–4	96.7171	96.7147	+0.0024	24.8
5–6	100.3098	100.3105	−0.0007	7.0
1–5	118.9953	118.9951	+0.0002	1.7
1–6	133.0113	133.0122	−0.0009	6.8
2–3	134.9698	134.9685	+0.0013	9.6
2–5	139.1225	139.1250	−0.0025	18.0
3–6	145.8427	145.8420	+0.0007	4.8
1–2	145.8884	145.8913	−0.0029	19.9
4–6	190.5047	190.5060	−0.0013	6.8
2–4	199.1914	199.1912	+0.0002	1.0
3–5	226.9903	226.9893	+0.0010	4.4
4–5	235.5264	235.5241	+0.0023	9.8
1–3	277.0569	277.0572	−0.0003	1.1
1–4	320.1519	320.1521	−0.0002	0.6
Average			0.00118	9.1

[a] Points which are the ends of these lines are located in Fig. 1. [b] Results of first-order triangulation.

One of the most convincing results of this project was the discovery of a local surveying error (4) at Key West, Florida. In that instance, five shoran measurements were made to this station from other shoran stations (Fig. 1), the shortest measurement being approximately 96 miles and the longest 320 miles (Table 1). On the basis of a computation which used the shoran-measured distances, it was predicted that a local surveying error of 35.4 ft having an azimuth of 39¾° was present. Several months later, triangulation by the

TABLE 2.—VELOCITY OF LIGHT, IN KILOMETERS PER SECOND

Investigator	Year	Method	Velocity of light, in kilometers per second
C. I. Aslakson........................	1949	Shoran	299,792.4 ±2.4
W. W. Hanson and K. Bol............	1950	Cavity resonator	299,789.3 ±1.2
L. Essen..................................	1950	Cavity resonator	299,792.5 ±4.5[a]
C. I. Aslakson........................	1950	Shoran	299,794.2 ±1.4
E. Bergstrand..........................	1951	Geodimeter	299,793.1 ±0.3
K. D. Froome..........................	1952	Microwave interferometer	299,792.6 ±0.7
J. W. M. DuMond and E. R. Cohen....	1952	Statistical[b]	299,792.9 ±0.8

[a] This probable error was assigned by J. W. M. DuMond and E. R. Cohen. L. Essen's limit of maximum possible error was 3 km per sec with a probable error of ±1 km per sec. [b] Based on a least-square adjustment of atomic constants.

Coast and Geodetic Survey, United States Department of Commerce, revealed that the error actually was 36.4 ft in an azimuth of 37°.

A second convincing proof of the accuracy of shoran lies in the fact that measurements made by this method (2)(5)(6)(7)(8)(9)(10)(11)(12) have been accepted by physicists as a new and accurate determination of *c*, the velocity of light. Almost from the outset of research (1944), indications were found that the statistical value for *c* of 299,776 km per sec, determined by R. T. Birge (13) in 1941, was too low. The writer published (2)(3), in 1949 and 1951, two values for the velocity of light of 299,792.4 km per sec and 299,794.2 km per sec, based on shoran measurements in Florida. Other measurements of the velocity of light are given in Table 2. Clearly, shoran measurements agree closely with the statistical value obtained by J. W. M. DuMond and E. R. Cohen.

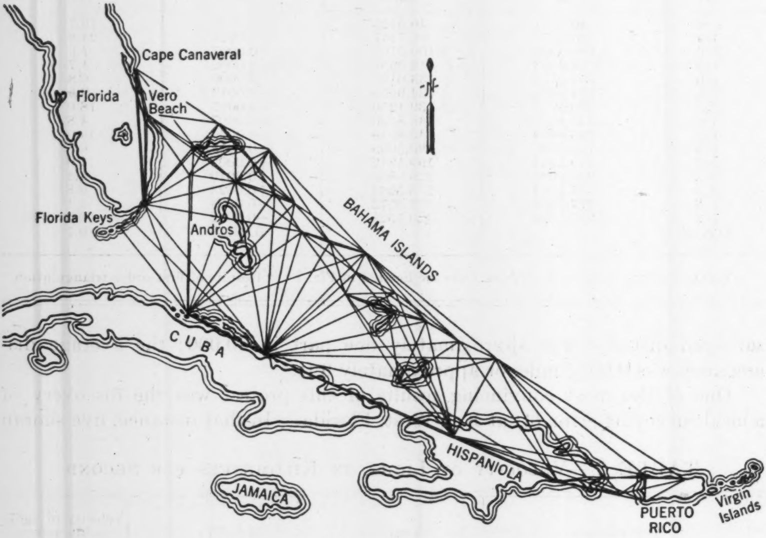

FIG. 2.—SHORAN NET OF AIR FORCE MISSILE RANGE

What Shoran Can Accomplish.—The advantages of the shoran method of electronic surveying can be enumerated as follows:

1. Geodetic accuracy can be obtained over distances as great as 500 miles.
2. Errors are a function of time and therefore do not increase perceptibly with an increase in distance.
3. Aerial photography can be controlled by shoran distances, permitting accurate mapping of all areas within the range of the shoran ground stations.
4. Navigational devices, utilizing the shoran distance readings, permit flight-line navigation of great accuracy.

5. Shoran photographic techniques permit the establishment of control points of low accuracy without anyone touching the ground.

6. Vertical control of various degrees of accuracy are possible by shoran-photographic-radio-altimeter methods.

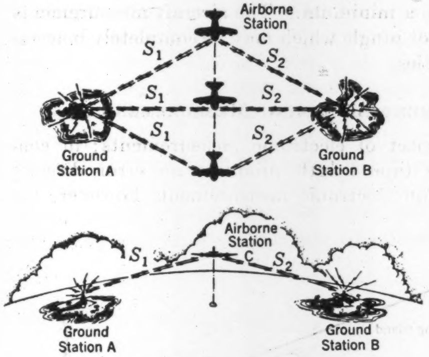
Airborne Station C
S_1
S_2
S_1
S_2
S_1
S_2
Ground Station A
Ground Station B
Airborne Station
S_1
C
S_2
Ground Station A
Ground Station B

FIG. 3.—SHORAN LINE CROSSING

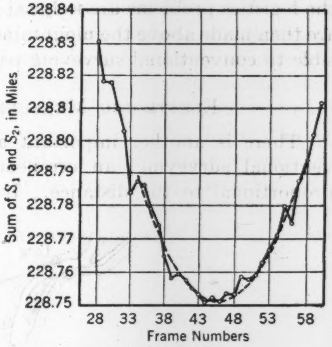

FIG. 4.—DETERMINATION OF MINIMUM SUM DISTANCE

Shoran Geodetic Surveying.—The survey of the United States Air Force Missile Test Center Range from Florida to Puerto Rico (shown in Fig. 2) is an excellent example of the use of shoran. Without these techniques, all the islands now (1954) being surveyed would remain geodetically isolated.

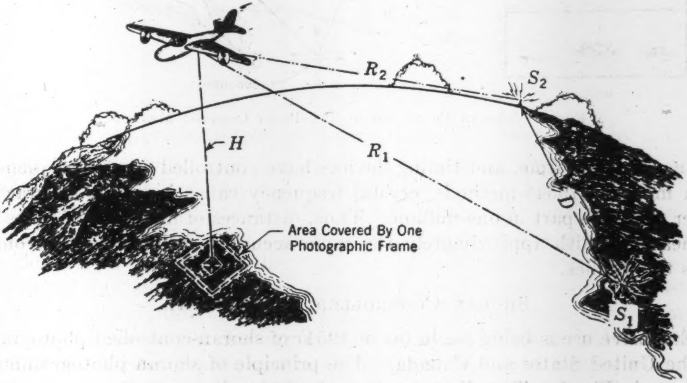
R_2
S_2
H
R_1
D
Area Covered By One Photographic Frame
S_1

FIG. 5.—SHORAN-CONTROLLED PHOTOGRAPHY

By use of shoran, however, the Bahama Islands, Cuba, Hispaniola, and Puerto Rico will all have a unified datum. The distance measurements are accomplished by flying across the line joining two ground stations and making an analytical computation of the minimum sum of the distance from each

station. This minimum is then reduced by the corrective terms to the geodetic distance (Figs. 3 and 4).

An important feature of shoran geodetic control is that, in general, the schemes can be situated so as to span mountain ranges or jungle areas. The ground stations may be situated in plains areas or on accessible rivers where the logistics problems are reduced to a minimum. The aircraft measurements are then made above the mountains or jungle which may be completely inaccessible to conventional surveying parties.

ELECTRONIC MEASUREMENT AS TIMING MEASUREMENT

There is another important aspect of electronic measurements; in conventional surveying, an erroneous tape length produces an error directly proportional to the distance. In an electronic measurement, however, the unit measured is time, and timing devices have controlled crystal frequencies. With modern (1954) methods, crystal frequency can achieve an accuracy of better than one part in one million. Thus, distances of hundreds of miles can be measured with approximately the same accuracy as distances of from 25 miles to 50 miles.

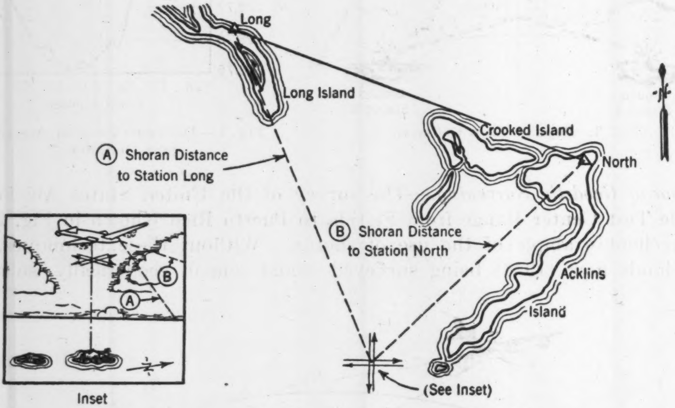
Long
Long Island
N
Crooked Island
North
Ⓐ Shoran Distance to Station Long
Ⓑ Shoran Distance to Station North
Acklins Island
(See Inset)
Ⓑ
Ⓐ
Inset

FIG. 6.—SHORAN PHOTOGRAPHIC PIN-POINT CONTROL METHOD

SHORAN-CONTROLLED PHOTOGRAPHY

Extensive use is being made (as of 1954) of shoran-controlled photography by the United States and Canada. The principle of shoran photogrammetry is shown in Fig. 5. Two distances to each of two shoran stations are recorded simultaneously with the exposure of the picture. Several methods of photographic analysis have been developed to utilize these distances in controlling the compilation of maps. It has been concluded that 1:500,000 maps can be produced in this manner without other horizontal ground control. The efficiency of a combined shoran and geodetic-photogrammetric operation is therefore obvious. Geodetic measurements can be made under conditions—darkness, fog, or extensive cloud coverage—which prevent photography. Therefore, the higher priority can be allotted to photography, and the combined process can be operated very efficiently by utilizing the unfavorable weather to measure the distances for geodetic control.

Flight-Line Navigation.—At least four different flight-line navigational instruments have been developed in the United States, Canada, and Australia which utilize the shoran distance measurements to control the aircraft navigation. These instruments are simple in principle and highly successful; they make possible airplane navigation over unmapped terrain so accurate that gaps between adjacent flight lines are almost nonexistent. This makes shoran flight-line navigation most economical for side-lap can be kept to a minimum.

Secondary Photographic Control.—Main-scheme trilateration furnishes first-order control; shoran-controlled photography can be considered to be third-order control. If, then, it is desired to establish other points of n intermediate accuracy (second-order control), this operation can be performed by a shoran-photographic method.

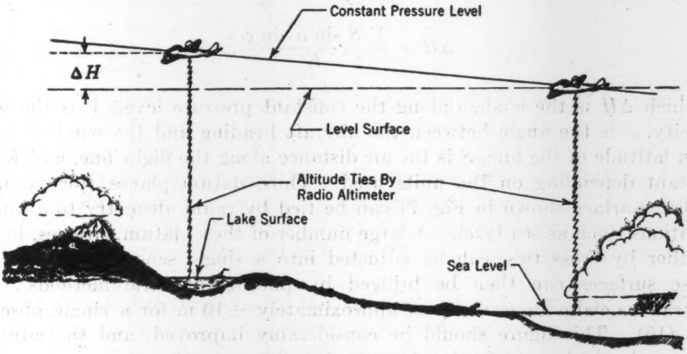

FIG. 7.—ESTABLISHMENT OF DATUM PLANES

In Fig. 6, there is shown an example of the method for establishing these intermediate-control points on two islands where no main-scheme shoran station is placed. Repeated flights in four directions (as shown in Fig. 6) with the camera operating at the minimum exposure interval—and with simultaneous pairs of shoran distances recorded for each picture—will furnish the data necessary to obtain the ground coordinates for a selected point, using any one of several methods of photogrammetric analysis. This procedure has been tested in the United States and in Canada and was used extensively in the Florida-Puerto Rico survey. It is concluded that a ground point can be positioned with an accuracy of from ±100 ft to ±25 ft relative to the two shoran stations used. This accuracy is dependent on the method of analysis and whether or not any local horizontal control exists in the area photographed. The important feature of this technique is that a geodetic position can be obtained in this manner in an inaccessible area without setting foot on the ground.

Vertical Control.—Radio altimetry has not kept pace with horizontal control developments, but some success has been attained. It has been reported (14) that vertical control with a relative accuracy of ±10 ft has been attained with a Canadian profile recorder. Certain narrow-beam radio altimeters have been developed in the United States, but their application has not been completely explored. The British have made tests with an instrument similar to shoran and with one of their radio altimeters from which it was concluded that an accuracy of ±10 m was possible (15).

A promising technique has been tested by Australia, Canada, and the United States. This process consists of the establishment of datum planes as shown in Fig. 7. If an airplane flies along a constant pressure level at a sufficient height so that the winds are geostrophic (winds caused solely by the rotation of the earth), the differential height between the constant pressure surface and a level surface can be computed from certain readily observable data when shoran navigation is used. This height difference is shown as ΔH in Fig. 7. The expression for ΔH is a simple one:

$$\Delta H = \frac{V\, S \sin \alpha \sin \phi}{K} \quad \ldots\ldots\ldots\ldots\ldots\ldots\ldots (1)$$

in which ΔH is the change along the constant pressure level, V is the wind velocity, α is the angle between the aircraft heading and the wind, ϕ is the mean latitude of the line, S is the air distance along the flight line, and K is a constant depending on the units used. Thus, datum planes (for example, the lake surface shown in Fig. 7) can be tied by radio altimetry to a known elevation—such as sea level. A large number of these datum surfaces, locked together by cross ties, can be adjusted into a single scheme of elevations. These surfaces can then be bridged by photogrammetric methods. The Australians claim an accuracy of approximately ±10 m for a single observation (16). This figure should be considerably improved, and the adjusted datums should be still further improved.

CONCLUSION

The applications of shoran mapping have been described. Vast areas exist throughout the equatorial belt and in the Southern Hemisphere where only navigational charts exist, and many of these are of questionable accuracy because no unified datums are in existence. By this method of mapping large-scale maps can be rapidly produced, and these maps can all be compiled on a single datum. In the establishment of a datum for South America, a complete network of shoran trilateration can be established which covers the entire continent. This network can then be tied to existing triangulation. These ties serve a dual purpose: (1) They determine the scale for the shoran scheme and thus obviate any necessity for an exact knowledge of the velocity of propagation of radio waves. (2) They are controlled by Laplace azimuths and thus serve to control the shoran network in azimuth. Now, if astronomic positions are observed at all shoran stations, a least-square solution will determine a datum which will be the best fit for the entire continent. The practical and scientific value of such a project can hardly be overestimated.

A project such as previously outlined would require the cooperation of all the governments of South America and their surveying agencies. If this cooperation were secured, the individual cost to each nation would not be excessive. With efficient preparation the entire project could be consummated in from one year to three years.

History has proved that development follows good mapping. The small financial outlay required for this project would return its initial cost many times over in increased utilization of the natural resources of the cooperating nations.

APPENDIX. BIBLIOGRAPHY

(1) **"Shoran for Surveying,"** by W. F. Kroemmelbein, *Electronics*, March, 1948.

(2) **"Velocity of Electromagnetic Waves,"** by Carl I. Aslakson, *Nature*, October 22, 1949, pp. 711–712.

(3) **"A New Measurement of the Velocity of Radio Waves,"** by Carl I. Aslakson, *ibid.*, September 22, 1951, pp. 505–508.

(4) **"Use of Shoran to Detect Surveying Error,"** by Carl I. Aslakson, *The Military Engineer*, Vol. 43, No. 296, November–December, 1951, pp. 436–437.

(5) **"The Velocity of Propagation of Electromagnetic Waves Derived from the Resonant Frequencies of a Cylindrical Resonator,"** by L. Essen, *Proceedings*, Royal Soc. of London, Series A, Vol. 204, 1950, pp. 260–277.

(6) **"The Velocity of Light and of Radio Waves,"** by L. Essen, *Nature*, April 15, 1950, pp. 582–583.

(7) **"A Check Determination of the Velocity of Light,"** by Erik Bergstrand, *Arkiv för Fysik*, Kungs. Svenska Vetenskapas-akademien, Vol. 3, No. 26, February 14, 1951, pp. 479–490.

(8) **"The Velocity of Light,"** by L. Essen, *Science Progress*, January, 1952, pp. 54–70.

(9) **"New Determination of the Velocity of Radio Waves,"** by Carl I. Aslakson, *Transactions*, Am. Geophysical Union, Vol. 32, No. 6, December, 1951, pp. 813–821.

(10) **"Some Recent Determinations of the Velocity of Light,"** by Joseph F. Mulligan, *American Journal of Physics*, March, 1952, pp. 165–172.

(11) **"Determination of the Velocity of Short Electromagnetic Waves by Interferometry,"** by K. D. Froome, *Proceedings*, Royal Soc. of London, Series A, Vol. 213, 1952, p. 123.

(12) **"Least-Squares Adjusted Values of the Atomic Constants,"** by J. W. M. DuMond and E. R. Cohen, *Special Technical Report No. 1*, Atomic Energy Commission, California Inst. of Technology, 1952.

(13) **"The General Physical Constants,"** by R. T. Birge, *Proceedings*, The Physical Soc., London, England, Vol. VIII, 1941, pp. 90–134.

(14) **"Something New in Aerial Surveying,"** by C. E. Bush, Jr., *Petroleum Engineer*, October, 1949, p. 623.

(15) **"Surveying from Air Photographs Fixed from Remote Radar Control,"** by C. A. Harte, Royal Soc. of London, Empire Science Conference, Directorate of Military Survey, July, 1946, p. 14.

(16) **"The Accurate Determination of Aircraft Altitude,"** by J. Warner, *Journal*, Inst. of Nav., Vol. 2, 1949, p. 159.

(17) **"The Accurate Determination of Aircraft Altitude,"** by J. Warner, *ibid.*, April, 1949.

(18) **"Microwave Measurements of the Dielectric Properties of Gases,"** by George Birnbaum, S. J. Kryder, and H. Lyons, *Journal of Applied Physics*, January, 1951, pp. 95–102.

(19) **"Dielectric Constant and Refractive Index of Air and Its Principal Constituents at 24,000 mc/s,"** by L. Essen and K. D. Froome, *Nature*, March 31, 1951, p. 512.

(20) **"The Use of Shoran in Geodetic Control,"** by Carl I. Aslakson and D. A. Rice, *Transactions*, Am. Geophysical Union, Vol. 27, No. 4, August, 1946, pp. 459–463.

(21) **"Measurement of Distances by High Frequency Light Signalling,"** by Erik Bergstrand, *Bulletin Géodesique*, Vol. 11, March, 1949, pp. 81–92.

(22) **"The Influence of Electronics on Surveying and Mapping,"** by Carl I. Aslakson, *Surveying and Mapping*, Vol. 10., No. 3, 1950, pp. 163–174.

(23) **"Shoran, Application to Geodetic Triangulation,"** by J. E. R. Ross, *The Canadian Surveyor*, Vol. 10, No. 3, January, 1950, pp. 9–18.

(24) **"Some Aspects of Electronic Surveying,"** by Carl I. Aslakson, *Transactions*, ASCE, Vol. 117, 1952, p. 1.

(25) **"The Use of Electronic Surveying in Establishing Control for Mapping Large Areas,"** by Carl I. Aslakson, *Proceedings*, Fourth Annual Surveying and Mapping Conference, Florida Eng. and Industrial Experiment Station, Gainesville, Fla., Vol. VI, No. 3, November, 1951, pp. 5–15.

(26) **"The Use of Electronics in Surveying and Mapping,"** by Carl I. Aslakson, Third National Surveying-Teachers Conference, ASCE Committee 8, August, 1952.

(27) **"Electronics in Surveying,"** by Carl I. Aslakson, *Proceedings-Separate* No. 284, ASCE, September, 1953.

(28) **"The Effect of Meteorological Conditions on the Measurement of Long Distances by Electronics,"** by Carl I. Aslakson and Omar O. Fickeissen, *Transactions*, Am. Geophysical Union, Vol. 31, No. 6, December, 1950, pp. 816–826.

(29) **"A Recording Microwave Refractometer,"** by George Birnbaum, *Review of Scientific Instruments*, February, 1950, pp 169–176.

(30) **"Reduction Procedures in Shoran Geodetic Measurements,"** *Report No. ERA-143*, National Research Council of Canada, Ottawa, Canada.

(31) **"A Rigorous Method of Computing Distance from Shoran Observations,"** by Cedric W. Kroll, *Transactions*, Am. Geophysical Union, Vol. 30, No. 1, February, 1949, pp. 1–4.

(32) **"Can the Velocity of Propagation of Radio Waves be Measured by Shoran?"** by Carl I. Aslakson, *ibid.*, No. 4, August, 1949, pp. 475–487.

AMERICAN SOCIETY OF CIVIL ENGINEERS
Founded November 5, 1852
TRANSACTIONS

Paper No. 2735

STRUCTURAL WELDING INSPECTION

By John L. Beaton,[1] A. M. ASCE, and Paul G. Jonas[2]

Synopsis

The authors examine the status of fabrication inspection in the welding industry and find a need for emphasizing certain phases of such inspection. They recommend particularly that inspectors discuss all jobs with the fabricator before work begins and recommend (as of 1953) new specifications related to welded steel fabrication.

Introduction

The rapid progress of the welding industry coupled with a large program for welded steel construction has required the California State Division of Highways to restudy its methods of inspecting and testing fabrication. This study has re-emphasized the need for fully qualified, visual inspection and has also emphasized the proper function of radiography in bridge weldment inspection.

In 1935, the California Division of Highways first used welding as a major connecting medium in bridge work, using bare electrodes for the welding of all minor connections throughout a structural steel trestle, Bradley Overhead, near Merced, Calif. (Fig. 1). Since that time the progress of the welding industry has given an impetus to more extensive use of welding (Fig. 2). However, it was not until 1951 that welding in California began to be used extensively. During the two-year period following 1951 contracts were let by the California Division of Highways for approximately 15,000 tons of welded structural steel. The factors influencing this trend and the fabrication of one of the large contracts have been well described in two articles on the Division Street Interchange.[3,4]

In order to take advantage of the economies of a rapidly rising industry, it was necessary to project bridge designs during this period of growth beyond

---

Note.—Published, essentially as printed here in August, 1953, as *Proceedings-Separate No. 243*. Positions and titles given are those in effect when the paper was received for publication.

[1] Superv. Highway Engr., California State Div. of Highways, Sacramento, Calif.

[2] Welding Engr., Materials and Research Dept., California State Div. of Highways, Sacramento, Calif.

[3] "California's All-Welded Viaduct Points Way to Improved Design," by L. C. Hollister, *Civil Engineering*, September, 1952, p. 180.

[4] "Sequence and Continuity Mark Modern Welding Practice," by R. W. Binder, *ibid.*, p. 187.

the limits of standards and specifications which were then published. It also has been necessary to readjust procedures, techniques, and policies covering the inspection and testing of such work. It is these latter adjustments that will be explained in the paper.

During the past several years the inspection of structural welding became somewhat standardized. Welders, procedures, and materials were qualified, and close supervision was maintained by a qualified inspector. When the California Division of Highways began using welding as a major joining method, it was decided that, in addition to the usual procedure, a supplemental method of post-inspection should be used; such a method was absolutely necessary to satisfy the exacting safety requirements necessary for public transportation. Therefore, a study was made of all proven methods of nondestructive structural weldment inspection. As the result of this investigation, visual inspection was augmented by the use of penetrant dye, trepanning, and hardness testing during fabrication, followed by radiographic inspection of the completed weldment.

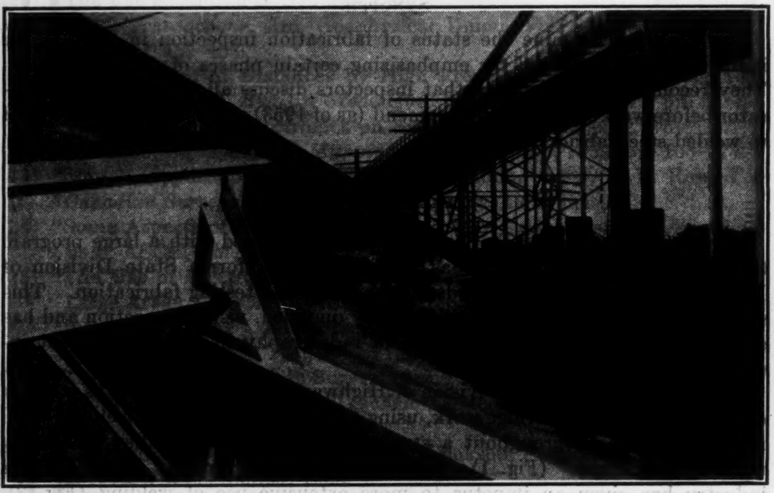

FIG. 1.—1935—BRADLEY OVERHEAD, NEAR MERCED, CALIF.

Preheating, where required, is controlled through the use of temperature-sensitive crayons and surface contact pyrometers. When there is need to determine the metallurgical structure, special investigations are made by the use of microphotographs and macrophotographs.

SPECIFICATIONS

The specifications that control the welded structural steel fabrication of the California Division of Highways are contained in the latest edition of the American Welding Society's (AWS) specifications for highway and railway bridges,[5] supplemented by the following special provisions:

---

[5] "Standard Specifications for Welded Highway and Railway Bridges," (D2.0-47), Am. Welding Soc., 1947.

Special Provisions.—The special provisions of the California Division of Highways now (1954) control all steel subject to welding by the use of the American Society for Testing Materials (ASTM) specification for weldable steel A 373.[6]

In addition to the special materials needed for welding, it has been the writers' experience that the use of preheat and controlled cooling in the fabrication of heavy structures is essential to assure crack-free welds; therefore, the special provisions for California bridge construction usually contain the following paragraph:

FIG. 2.—1952—BAYSHORE FREEWAY, NEAR SAN FRANCISCO, CALIF.

> "If necessary, the contiguous areas about the welding operations shall be preheated and held at a temperature of not to exceed 400°F during the welding operation. Also, if necessary, the lighter parts shall be postheated, keeping the temperature of contiguous parts substantially equal while the weld is cooling."

---

[6] "Tentative Specification for Weldable Structural Steel," A.S.T.M., adopted March 31, 1954.

This statement allows for judgment on the part of the engineer and fabricator to determine the proper preheat. Such latitude is essential as the preheat requirement will vary considerably with the relative masses and positions of the various components.

MATERIALS

Following the standard ASTM procedure, base metal is tested and inspected at the mill. Welding electrode material is sampled in the shop and tested in the Sacramento (Calif.) Laboratory. It is routine to check each lot of welding electrodes by the fillet-weld test and low-hydrogen electrodes additionally for moisture content. Complete ASTM tests are made only when the classification of the rod is apparently not correct. Deviation from the manufacturers' ratings is seldom found.

QUALIFICATION

The AWS test is followed for qualifying welders employed to do manual welding both in the shop and in the field. However, such qualification tests are expensive and, in the writers' judgment, are necessary only when a man is first qualified for a particular project to do manual welding. The simple fillet-weld break test should be used more extensively because: (*a*) If a welder cannot pass this simple test, it is not economical to subject him to the complete AWS qualification test; (*b*) the fillet-weld test is economical in checking the continuing skill of a manual operator.

For qualifying the operators of semiautomatic or automatic equipment, the procedure is slightly modified. The work of the California Division of Highways usually requires a procedure qualification; thus, the procedures are examined and the operators are qualified simultaneously. As this automatic welding is always run with the steel in flat and horizontal positions, for the welding of butt welds and fillet welds the welder is qualified for work in these positions only. The test plates are then tested according to the standard AWS procedure qualification requirements. It is found that an X-ray of the test plates before beginning the standard tests is helpful. If the X-ray indicates excessive defects, there is no value in completing the test. X-ray plates of this type cost approximately $6.00 (1954); they not only save the expense of completing the tests but also show the results immediately. A nick break test is usually used to check the continuing skill of the operators of this type of equipment.

The procedure for automatic welding is prequalified by making trial runs on small sections composed of material of the same sizes and shapes and subject to the same welding conditions to be used during the fabrication. After this trial run is made, the weldment is cut into sections for examination. Inspection is made of the depth of penetration, the size and shape of the weld bead, slag inclusion, porosity, cracks, and the structure of the weld metal. Hardness tests are also made of the metal in the fusion zone and heat-affected area, and of the unaffected parent metal.

For welding long members, "run-over" tabs are used on the ends of the members. These tabs serve two purposes: (1) They insure continuity of the weld to the end of the member and (2) they are cut into sections for testing so that a true representation of the welding in the structure is observed.

VISUAL INSPECTION

Visual inspection can be divided into five important steps : (1) The selection of the inspector; (2) the prefabrication review of planned procedure and sequence; (3) the inspection prior to welding; (4) the inspection during welding; and (5) The inspection after welding.

The welding inspector must not only know and understand the principles of inspection but he must also be so familiar with welding fabrication that he could actually do the job. He must be able to anticipate difficulties and possess the ability to communicate his thoughts clearly to the shop personnel. He also must have the ability to understand the capabilities of each welder. Most important is that he know the causes of all defects—especially the hidden defects that can occur during welding.

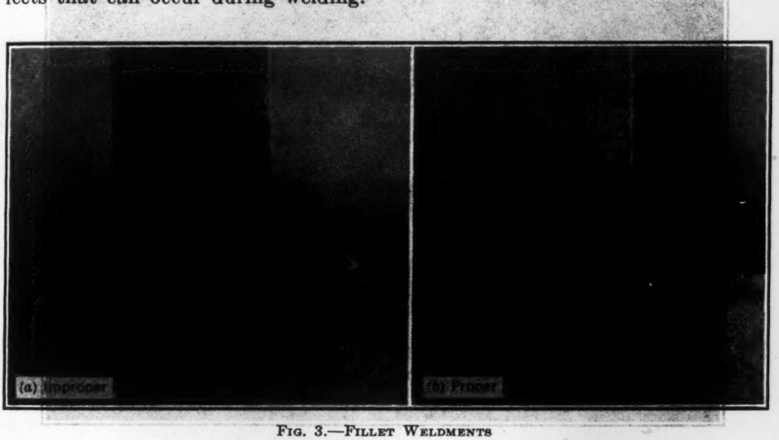

FIG. 3.—FILLET WELDMENTS

Step two is the first duty of the welding inspector when starting a new job. It is important that he discuss with the engineer and the fabricator the general procedures and sequences to be followed during fabrication. At this time any anticipated difficulties can be discussed, and the inspector can plan his work to fit the job. It is at this time that a harmonious working relationship is developed between the inspector and fabricating personnel.

The third step includes inspecting the shop equipment for its adequacy to handle the fabrication; checking the base metal against the test reports; inspecting the welding electrodes; and inspecting the fitting-up procedures and joint preparation, and proposed jigs.

The next step is the inspection during the welding operation. The inspector may have several welding operators working under his surveillance at any one time; it is necessary that he be alert. He must observe not only the fusion and penetration being obtained but also the formation of the welded bead, the burn-off rate of the electrodes, and the sound of the arc. The qualified welding inspector should be able to tell from any one of these indications whether or not the proper procedure is being used and the proper results are being achieved.

The last step—the post-inspection of the welding—can be misleading when performed alone, but when worked into a complete program it is very valuable. The surface defects—such as undercutting, overlay, major cracking, and surface porosity—are obvious. To the experienced inspector, the size and shape of the weld can also indicate the location of craters, slag inclusions, and subsurface porosity. However, even the most competent inspector cannot always determine subsurface defects by post-inspection alone.

In Fig. 3 it is shown how welding can be affected by the angle of the electrode in relation to the plate of the fillet to be welded: Fig. 3(*a*) indicates that, if the electrode is allowed to burn off on the weld and not in the crater, lack of fusion and slag inclusion at the root of the weld will result; Fig. 3(*b*) shows a joint welded with the electrode at the proper angle.

Fig. 4.—Fillet Weldment Being Tested with Penetrant Dye

Certain aids to visual inspection are valuable. The penetrant dye method is useful not only to detect cracks but also to determine the limits of subsurface defects during repair. The penetrant dye method is especially useful in connection with the automatic welding process in which the welds are smooth enough to check without grinding—especially for small surface defects. When the run-over tab of a weldment shows internal defects, the inspector may have the weld ground and, with the penetrant dye, check for the defect and establish its limits.

Fig. 4 shows a defective fillet weldment being checked with penetrant dye, which shows surface defects. The white surface on the weld is the developer, and the dark lines in the middle of the weld are caused by the penetrant dye as it bleeds out of the defects onto the white surface.

The California Division of Highways uses trepanning primarily to inspect fillet welds for the determination of penetration. The trepan tool is also used to obtain cores for microphotographs (Fig. 5). Because the work involves heavy sections, it does not lend itself to magnetic-particle inspection.

A portable Brinell hardness testing machine is used in the shop and field for determining the hardness of the affected areas of the weldment. This type of hardness testing is not so accurate as laboratory testing, but it does serve as a guide to be supplemented by laboratory tests on end-tab specimens. The portable hardness tester is useful for supervision purposes.

FIG. 5.—TREPANNING DRILL

FABRICATION

The writers wish to describe only those matters of common concern to all fabrication shops.

For automatic and semiautomatic welding, oxyacetylene cutting is used for joint preparation in most cases and also for the cutting of sections for fabrication. The cut-out pieces have their flame-cut edges ground before welding. The grinding overlaps the sides slightly so as to remove all oxidation slag, rust, and mill scale. In automatic welding, foreign matter tends to be trapped during the welding process because it cannot be removed by manipulation (as in manual welding). Slag inclusion may occur in the weldment as a globular defect (Fig. 3), or it may cause cracking. Circular cuts made where stress will be involved must be smooth; therefore, after cutting, grinding is usually necessary in order to meet specifications.

Manual welding requires the use of open joints during fabrication; in automatic work, the edges are held tightly together. Automatic equipment requires such high amperage that, if a tight fit is not obtained, the electrode will burn through. Small tack welds are usually used for holding work together while it is being automatically welded.

The majority of welded highway structures on the California highway system are made of long, heavy stringers or grinders. Automatic welding lends itself well to this type of fabrication; however, care must be exercised to control warpage and distortion and to eliminate shrinkage cracks, such as the one shown in Fig. 6. Cracking of this type often occurs when a pear-shaped weld is made. The center cools more slowly than the remainder, and the shrinkage of the outside area causes a tear at the center. Preheating to 400°F, combined with a balanced program of controlled heating and cooling, will usually result in a weldment that is within the tolerances for structural shapes specified by the American Institute of Steel Construction (AISC). As a secondary benefit, tests indicate that the metallurgical condition of the weldment can be expected to be improved by such preheating.

FIG. 6.—SHRINKAGE CRACKING

RADIOGRAPHIC INSPECTION

An important problem is when and where to radiograph. It is unnecessary and uneconomical to make radiographic plates showing 100% of the welding. The present (1954) practice of the California Division of Highways is to radiograph at least 80% of all butt welds of tension flanges. In addition, if continuing defects are observed in the tensile butt welds, they are radiographed 100%

as are also the butt weldments; otherwise, only one of every four compression-flange butt weldments is so pictured. In so far as fillet welding is concerned, the writers' opinion is that, after the procedure for fillet welding has been regulated, there is little value from radiographic inspection. In so far as fillet welding is concerned, radiography should be resorted to only if it is desired to prove the presence of an already suspected defect. An experienced radiographic technician can show most serious defects in a butt weldment. However, experience indicates that extreme care must be taken in order to picture the defects in fillet weldments, especially if a relatively thin web is being welded to a thick flange. A typical record of radiographic inspection appears in Fig. 7.

An acceptable weldment must be free from any form of cracking in the weld and welding area; however, it may contain slight oxide or slag inclusions or small gas pockets, providing they are within the tolerances indicated by the AWS specifications. Such standards necessarily must be arbitrary. However, as the use of radiography evolves, procedures can be developed that will permit a closer correlation between defects and the stresses or other uses of the joint.

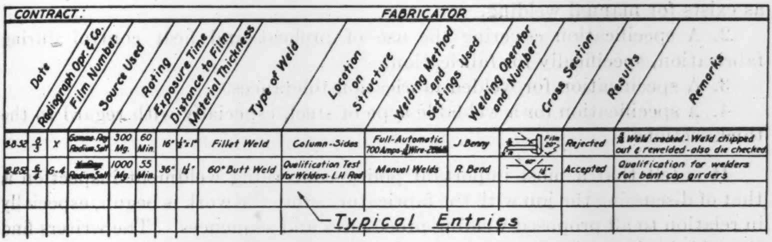

CONTRACT:									FABRICATOR					
Date	Radiograph Opr. & Co.	Film Number	Source Used	Rating	Exposure Time	Distance to Film	Material Thickness	Type of Weld	Location on Structure	Welding Method and Settings Used	Welding Operator and Number	Cross Section	Results	Remarks
9-8-52	6/3	X	Gamma Ray Radium Salt	300 Mg.	60 Min.	16"	1/2"x1"	Fillet Weld	Column-Sides	Full-Automatic 700 Amps-[illegible] Wire-[illegible]	J Benny	Film 20"	Rejected	3/8 Weld cracked - Weld chipped out & rewelded - also die checked
12-12-52	6/4	6-4	~~X-Ray~~ Radium Salt	1000 Mg.	55 Min.	36"	1¼"	60° Butt Weld	Qualification Test for Welders - L.H Rod	Manual Welds	R. Bend	60° 1¼"	Accepted	Qualification for welders for bent cap girders

FIG. 7.—FORM USED IN RADIOGRAPHIC INSPECTION

From the standpoint of inspection, the experience of the writers has indicated that the four most important points to consider in the administration of radiography are: (1) Careful and experienced selection of the welded areas to be radiographed; (2) careful selection of experienced radiographic personnel; (3) careful and experienced interpretation of the radiographic film; and (4) consultation with the management and shop personnel on the results of the radiographic inspection.

Although the prime purpose of radiographic inspection is to determine the adequacy of the weld, several secondary benefits are just as valuable: Radiographic inspection tends to induce the welding operator to exercise additional care; by seeing the defects on the film, and by discussing the cause, most welders improve their work habits. During the past two years, radiographic work for the California Division of Highways has been done by both X-ray and gamma-ray with the gamma-ray source usually being Cobalt 60. Inspections are recorded on film either 4.5 in. by 17 in. or 3.5 in. by 16 in. in size. The history of the division's costs from 1951 through 1954 is interesting. In the beginning they cost approximately $26 per radiographic plate, this cost reflecting a lack of experience combined with lower sources of radiation than are now available. At the present time, costs are averaging $7.50 per plate, the lowest cost thus far (1954) attained being $2.00 per plate under ideal conditions.

On an over-all basis, radiographic inspection from 1951 through 1954 has averaged approximately $0.16 per ton of welded steel construction, varying somewhat with the size and design of each job. Experience indicates that, under the safety requirements of the structures of the California Division of Highways, radiography is well worth while.

CONCLUSION

The welding of structural steel is a rapidly advancing branch of technology. Therefore, it is not ready to be tethered by completely objective specifications in all its areas of operation. However, certain factors should be clarified by the development of specifications for over-all use. As of 1953 these are as follows:

1. A specification for automatic welding and semi-automatic welding, such as exists for manual welding.
2. A specification covering the use of preheat and heat control during fabrication, specifically for fabrication.
3. A specification for welded fabrication tolerances.
4. A specification for a weldable type of steel, especially with regard to the thick sections.

It is felt that a most important policy concerning weldment inspection is that of discussing the job with the fabricator before the work is begun, especially in relation to all proposed welding procedures and sequences. The writers find that this leads to a harmonious cooperation between the inspection force and the fabricator, resulting in structures of which all can be proud.

AMERICAN SOCIETY OF CIVIL ENGINEERS
Founded November 5, 1852
TRANSACTIONS

Paper No. 2736

CHESAPEAKE BAY BRIDGE

By Ethan F. Ball,[1] M. ASCE

Synopsis

When the Chesapeake Bay Bridge in Maryland was opened to traffic on July 30, 1952, it became an important link in the highway system of the United States. The fabrication and construction problems that were encountered in this project are outlined herein. Because of the unusually high elevation of some of the trusses and the great depth of water, the contractor had to adopt a unique erection scheme. This scheme combined a floating derrick, an erection dock with adjustable falsework, and controlled barges.

Introduction

In Fig. 1 there is shown a simplified elevation of the superstructure of the Chesapeake Bay Bridge in Maryland. The length from the west abutment to

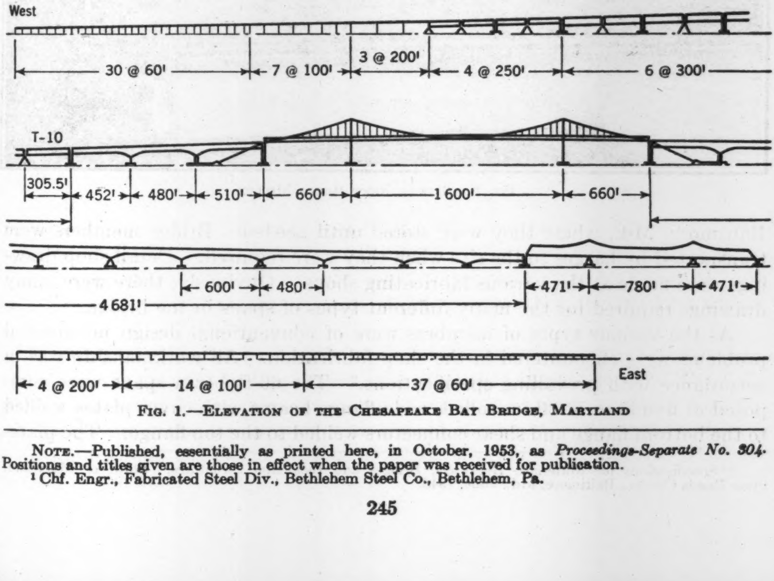

Fig. 1.—Elevation of the Chesapeake Bay Bridge, Maryland

Note.—Published, essentially as printed here, in October, 1953, as *Proceedings-Separate No. 304*. Positions and titles given are those in effect when the paper was received for publication.

[1] Chf. Engr., Fabricated Steel Div., Bethlehem Steel Co., Bethlehem, Pa.

the east abutment is approximately 4 miles. The number and length of the various spans are shown in Fig. 1.

SHOP FABRICATION

Shop fabrication of the steelwork was done in three locations. Beam spans were of all-welded construction and were fabricated in Bethlehem, Pa. Riveted plate-girder spans were fabricated in Rankin, Pa., as were the simple-truss spans and the through-cantilever span. The deck-cantilever spans and their supports and the structural-steel parts for the suspension bridge were fabricated in Pottstown, Pa.

The material was rolled at various mills and was shipped by rail to the fabricating shops. After fabrication the parts were shipped by rail to a yard in Baltimore, Md., where they were stored until needed. Bridge members were transported by barges to the site when they were required. Detail shop drawings were made at the various fabricating shops. Obviously, there were many drawings required for the many different types of spans in the bridge.

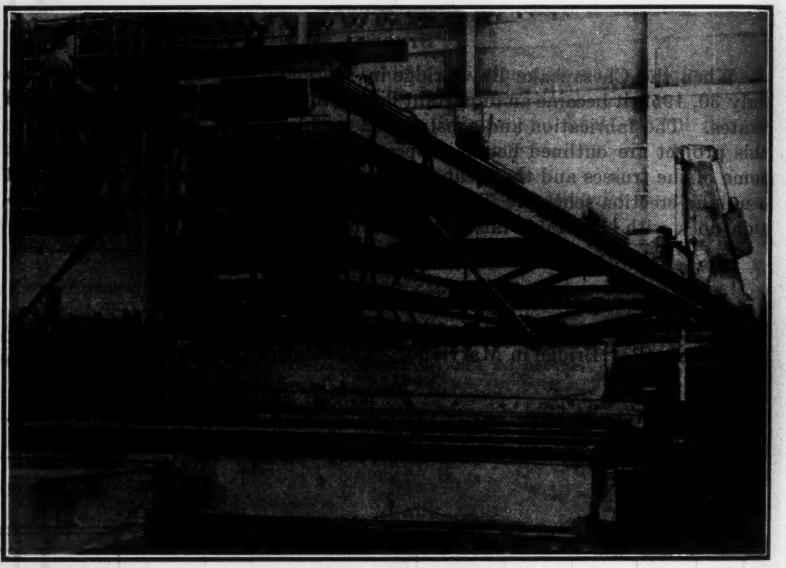

FIG. 2.—TOWER BENT BEING MILLED

As the various types of members were of conventional design no unusual problems were encountered in the shop fabrication. All workmanship was in accordance with prevailing specifications.[2] The 60-ft beam spans were composed of five lines of 30-in. rolled, wide-flange beams with cover plates welded to the bottom flange and shear connectors welded to the top flange. The plate-girder spans were of standard riveted construction except that shear connectors were welded or riveted on the top flange so as to result in composite action with the concrete slab.

---

[2] "Specifications for Materials, Highways, Bridges and Incidental Structures," State of Maryland, State Roads Comm., Baltimore, Md., June, 1948.

The trusses, bents, and towers were of normal riveted construction. Chords and web members for the long spans were designed with perforated cover plates in accordance with prevailing practice.

Towers.—The pyramidal towers presented some problems in the fabricating shop because it was necessary that all angles be correct. Two of the four faces of each tower were assembled in the shop; projecting gusset plates were provided to receive (in the field) the members which constituted the trussing of the other two faces. One of these tower bents is shown in Fig. 2, blocked up on a slope in front of a milling machine so as to produce a smooth bearing in an inclined plane across the upper ends of the two columns.

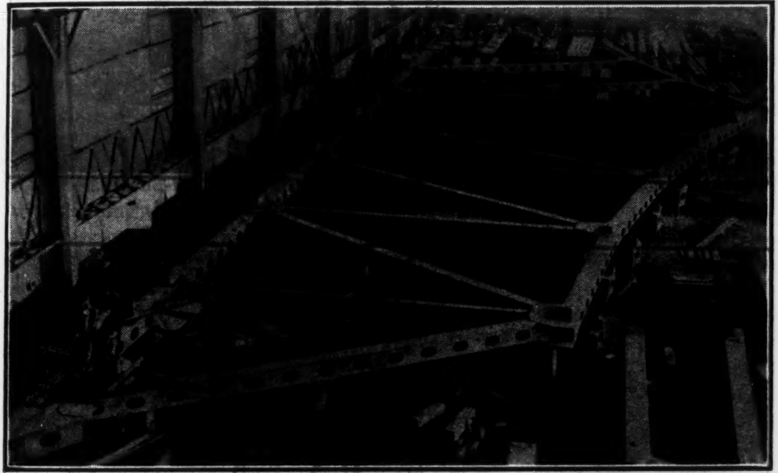

FIG. 3.—DECK-CANTILEVER TRUSS ASSEMBLED FOR REAMING

Spans.—The 480-ft deck-cantilever spans required unusually accurate fabrication in order to assure proper fitting during erection. The curved bottom chords were assembled for the full length of the span, end to end, in order that the splices between the sections could be properly fitted and reamed. At this stage the over-all dimensions and shape were carefully checked by transit and tape.

Through the deepest part of the deck-cantilever trusses, over the supports, the work was thought to be sufficiently critical that the entire truss was completely assembled for reaming, as shown in Fig. 3. At other locations, the web members were reamed separately with the aid of metal templets that were also used for reaming the chord gussets to which the web members would be attached in the field.

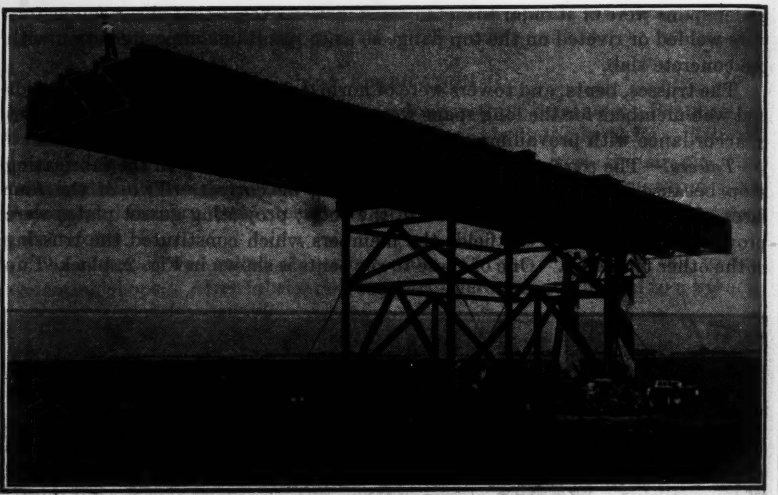

FIG. 4.—FLOATING THE SPAN

FIG. 5.—DERRICK ERECTING SPAN T 10

There were no other features of special interest in the shop fabrication, but there were many unusual and interesting schemes developed to erect the various spans in the field.

FIELD ERECTION

The 60-ft beam spans and 100-ft girder spans were erected in a conventional manner from barges by a tower derrick boat. Most other spans, except the cable suspension bridge, were floated into position, either high or low, beginning with the 200-ft girder spans.

These 200-ft girder spans were divided into 50-ft end sections and a 100-ft central section. Over a 100-ft gap left in the approach, the right-hand 50-ft section, which cantilevered into the opening, was erected. The 100-ft central section was then placed so that its left end was over a support on the left-hand beam span. The final 50-ft section was then added over the beam span. The 200-ft span thus completed was ready for floating into final position. The span was floated on two barges with falsework, as shown in Fig. 4. The barges were partly submerged to the proper elevation and were then floated under the girder span and lifted by pumping the water out. The barges were 32 ft wide, 128 ft long, and 9½ ft deep. They contained four watertight bulkheads forming two end-buoyancy chambers and three flooding compartments equipped with flooding valves, pumps, and depth gages.

Truss spans of the type used in the Chesapeake Bay Bridge would usually be erected by driving groups of falsework piles under each span to support the superstructure on temporary steel bents until the complete span became self-supporting. However, in this case, the bottom was so deep and soft that a different system had to be adopted.

Only one set of falsework was used—an erection "dock" on steel piles erected next to truss span T 10, which was the highest of the 300-ft deck-truss spans and was located 1 mile from the west shore. The tower derrick boat was used to drive 100-ft steel H-piles and to construct the falsework dock. Four steel pile clusters were driven, and grillage was placed over them. The tower derrick boat was then used to erect one of the 200-ft plate-girder spans with a 25-ft special section spliced to each end. On top of these girders two falsework towers were constructed. In Fig. 5 the derrick is shown erecting parts of span T 10.

After span T 10 was completely erected, including the hinged supporting bent at the right end, two pairs of partly submerged flotation barges were brought in under the girder span and were blocked against its underside. The barges were pumped out so that the entire span and upper falsework were lifted off the piling supports. The barges were then moved laterally to place the span in its permanent position on the center line of the bridge. The barges were flooded, causing the falsework to be lowered. They were then moved back to their original positions on the pile clusters, as shown in Fig. 6.

On top of span T 10, there were then erected two stiff-leg derrick travelers. The travelers moved back and forth along the deck of truss T 10 and erected succeeding spans on the falsework. Each span was moved from the dock with cables from engines on the barges to anchors. The span was then towed to its

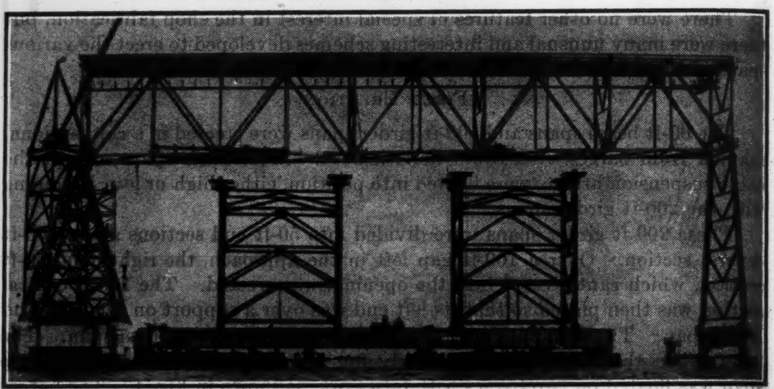

Fig. 6.—Falsework and Span T 10

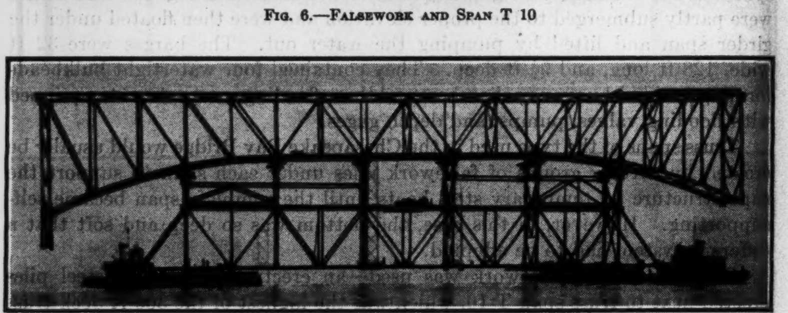

Fig. 7.—Moving a 480-Ft Anchor Span

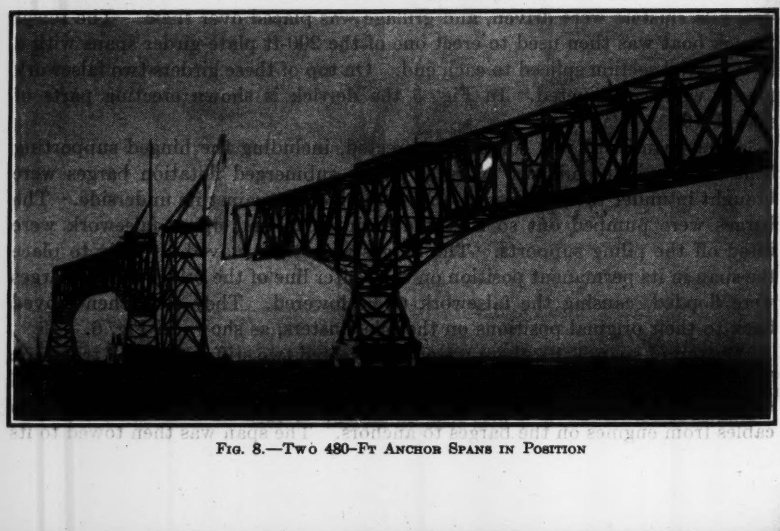

Fig. 8.—Two 480-Ft Anchor Spans in Position

permanent location by tugboats. In Fig. 7 there is shown one of the 480-ft anchor spans being moved to its permanent location. The plate-girder falsework had to be replaced by the truss span because of the great length and height of these deck-cantilever spans. The spans were erected on the dock and were floated just above their final elevation in order to clear anchor bolts for the shoes. When the spans were opposite their piers, they were moved into position by cables.

In Fig. 8 two of the 480-ft anchor spans are shown in position. The 600-ft intervening cantilever span is being filled in by two pieces of equipment. At the left end, a light stiff-leg derrick traveler running on the top deck is building out the cantilever arm and half of the simple span. At the right end, the tower derrick boat is performing the same operation; its work is much further advanced. In this phase the 600-ft span, carrying its own weight only—with no floor slab or live load—was cantilevered 300 ft from each end to meet in the middle. By the manipulation of hydraulic jacks in the truss chords the two halves were then connected so that when the jacks were unloaded there was a 300-ft simple span in the center, supported at each end on a 150-ft cantilever arm.

FIG. 9.—ATTACHING A CABLE BAND

The anchor arms for the through-cantilever span were erected and floated at a high level in a similar manner. The cantilever arms and their supported simple span were erected by cantilevering, as were the deck-cantilever spans. It was found impractical to float three of the truss spans at high level—the two spans at the ends of the suspension bridge and one span at the west end of the through-cantilever span. These spans were each erected on a car float and were floated to the site at low level. They were then raised by four sets of lifting tackle and hoisted to their final elevation.

Suspension Bridge.—The suspension bridge over the main navigation channel was erected by conventional methods. The two main shafts in each of the main-span towers were composed of four rectangular plate-and-angle sections which, when assembled, formed a cruciform cross section containing five interior squares just large enough for the passage of workmen. The first six tiers of each shaft were erected by the derrick boat. The derrick boat then erected a "Chicago boom" on one shaft. This boom erected the seventh tier of the other shaft and then a second Chicago boom. The two Chicago booms then stepped up alternately to complete the tower, which was 347 ft high.

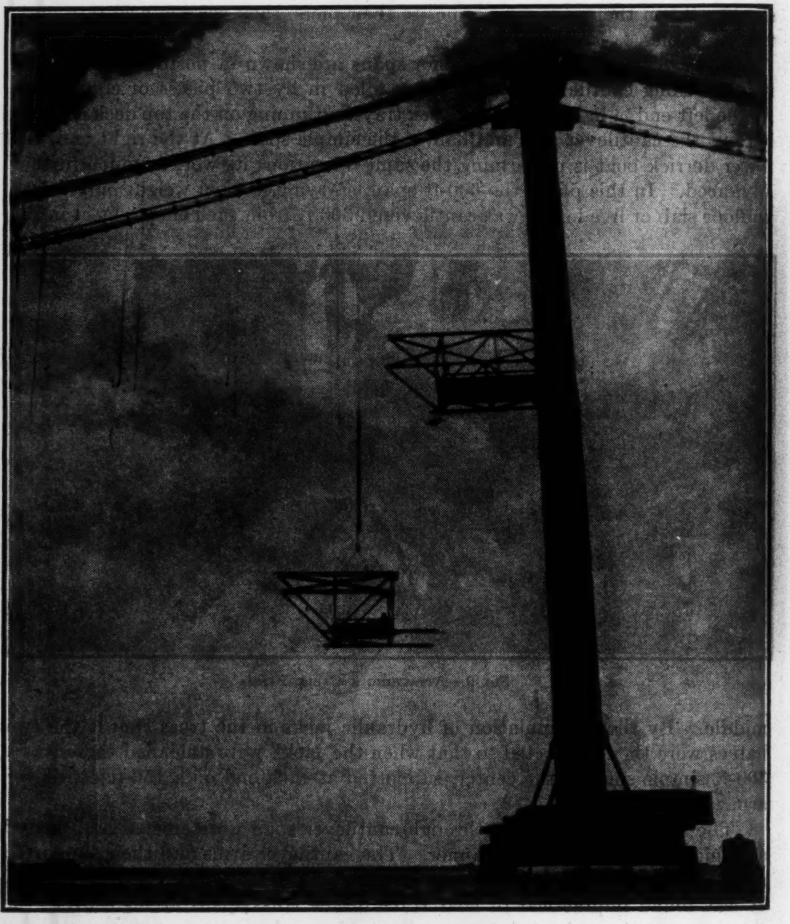

FIG. 10.—RAISING A TRUSS SECTION

Each of the two cables was composed of fifty-five prestressed strands of

1 11/16-in. diameter and six strands of 29/32-in. diameter, arranged in an approximate circle. The cables were rounded with extruded aluminum fillers and wrapped with No. 9 soft galvanized wire to produce a finished diameter of approximately 14 in.

To erect the cables, footwalks were first constructed from anchorage to anchorage across the tower tops. The footwalks were supported on wire ropes strung across the channel by tugs and barges and were lifted into position by derricks on top of the two main towers.

Bridge strands of 1 11/16-in. diameter were pulled across the span by an endless hauling rope. The strands were measured in the shop and were socketed. They were also marked to indicate where they were to be placed in the saddles on the towers in order to result in a span of proper length and sag. The strands were "spun" during the day but were adjusted at night to take advantage of more uniform temperatures and less wind.

FIG. 11.—AERIAL VIEW OF THE CHESAPEAKE BAY BRIDGE, MARYLAND

After the strands were compacted into as tight a cable as possible, cable bands were carried out on a light falls from the tramway rope and were attached at intervals of 41 ft in order to support the suspender ropes. In Fig. 9 there is shown a cable band being attached. The bands were composed of welded steel plates bent into cylindrical form, with interior zinc liners cast to the same shape as the exterior of the strand group. The bands were clamped around the cables with highly torqued, high-strength bolts to prevent slipping. The suspenders were 1½-in., high-strength wire strands.

The floor system, comprised of stiffening trusses, floorbeams, stringers, and bracing, was preassembled on barges, mostly in two-panel lengths, and was towed to the site. The floor sections were hoisted into place from the barges by falls attached to special supports temporarily clamped to the cables. In Fig.

10 there is shown the method in which the truss sections were assembled to avoid interference between top and bottom chords as they were raised into place. The floor sections were raised and hung on the suspenders on the basis of a predetermined schedule. Many studies and computations were necessary to determine a sequence which avoided too-great distortions in the shape of the highly flexible cable. The maximum vertical movement during erection was from 23 ft above normal to 10 ft below normal—a range of 33 ft. Concrete deck, asphalt paving, and railing construction proceeded simultaneously from the east and west abutments. The final operations in the construction were the cable wrapping and the finish painting.

CONCLUSION

In Fig. 11 there is shown the completed structure. The Chesapeake Bay Bridge was opened to traffic on July 30, 1952, and added an important link to the highway system along the Atlantic coast of the United States.

ACKNOWLEDGMENTS

The superstructure for the Chesapeake Bay Bridge was constructed and erected by the Bethlehem Steel Company of Bethlehem. The engineering was done by the J. E. Greiner Company of Baltimore, Md. Fabrication and erection were performed under the general supervision of F. A. Strouce. The advance engineering was directed by Jonathan Jones, Hon. M. ASCE, and the writer. Erection was supervised by J. H. Wagner, E. L. Durkee, M. ASCE, and G. P. Bullard, M. ASCE.

AMERICAN SOCIETY OF CIVIL ENGINEERS
Founded November 5, 1852
TRANSACTIONS

Paper No. 2737

OPEN CHANNELS WITH NONUNIFORM DISCHARGE

By Wen-Hsiung Li,[1] A. M. ASCE

With Discussion by Turgut Sarpkaya, and Wen-Hsiung Li

Synopsis

Steady flows in an open channel with the addition of water along the course of flow are encountered frequently in engineering practice. Examples of this condition are the wash-water troughs in filters, the effluent channels around sewage-treatment tanks, and side-channel spillways. An equation based on the principle of conservation of momentum is derived in this paper. For cases in which the loss of energy because of friction is of secondary importance, solutions are obtained for prismatic channels of various cross sections and slopes. The hydraulic behavior of the flow is described with nondimensional quantities, and the validity of the theory is verified by tests on model channels.

Notation

The letter symbols adopted for use in this paper are defined where they first appear, in the illustrations or in the text, and are arranged alphabetically, for convenience of reference, in the Appendix.

Introduction

The hydraulic behavior of an open channel with the addition of water along the course of flow is quite different from that of a channel with uniform discharge. During uniform discharge, energy is lost entirely because of frictional and form resistance. During nonuniform discharge an appreciable part of the loss of energy results from the impact between the added water and the water flowing in the channel. In many cases, the energy loss because of impact is of primary importance.

Note.—Published, essentially as printed here, in January, 1954, as *Proceedings-Separate No. 381*. Positions and titles given are those in effect when the paper or discussion was received for publication.

[1] Asst. Prof. of Civ. Eng., The Johns Hopkins Univ., Baltimore, Md.

THE MOMENTUM EQUATION

Because the loss of energy as a result of impact in channels with nonuniform discharge is not known, an equation based on the conservation of energy is not useful in this case. The principle of conservation of momentum, however, is applicable. The momentum equation has been used successfully in the study of hydraulic jumps in straight channels having a moderate slope.

In order to obtain a relatively simple momentum equation, the following must be assumed:

1. The flow is considered to be uni-directional, but actually there are strong cross currents in the case of a side-channel spillway. However, in investigating the flow along the channel, the lateral unevenness of the water surface, as a result of cross currents, can be neglected.
2. The velocity in the direction of flow is uniformly distributed across each cross section.
3. The pressure in the flow is considered to be hydrostatic. This assumption is valid except for a short distance near the outlet end of the channel where the curvature of the water surface can be appreciable.
4. The average shearing stress at the channel walls is considered to be identical, at the same depth, as the stress for the same discharge in uniform flow.

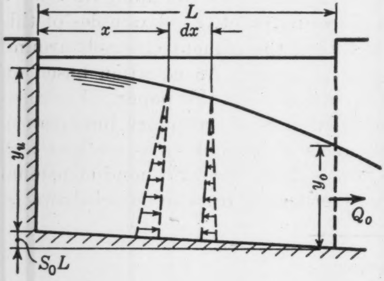

FIG. 1.—OPEN CHANNEL WITH NONUNIFORM DISCHARGE

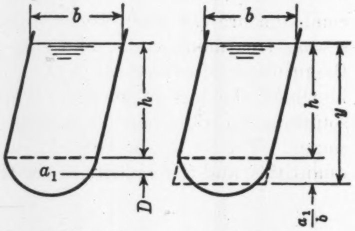

(a) IRREGULAR BOTTOM

(b) EQUIVALENT SECTION

FIG. 2.—CHANNEL WITH PARALLEL SIDE WALLS

A volume of water bounded by two sections a distance dx apart is shown in Fig. 1. The rate of momentum, in the direction of the flow, supplied to this volume is the sum of $\frac{\rho Q^2}{A}$ and $\rho q v' dx$. The rate of momentum emitted from this volume is $\frac{\rho (Q + dQ)^2}{A + dA}$. The difference between these two rates of momentum is equal to the force acting on the volume in the direction of the flow. Thus, neglecting the small effect of the slope on the pressure, and that of the entrained air on the volume of flow,

$$\rho g \bar{y} A - \rho g (\bar{y} + d\bar{y}) (A + dA) + \rho g A S_0 dx - \frac{\rho g Q^2 P}{A^2 C^2} dx$$

$$= \frac{\rho (Q + dQ)^2}{A + dA} - \frac{\rho Q^2}{A} - \rho q v' dx \quad (1)$$

in which ρ is the mass per unit volume of the water, g denotes gravitational acceleration, $\bar{y}$ is the vertical distance from the centroid of the water cross section to the water surface, A represents the area of the cross section, S_0 is the slope of the channel, Q denotes the rate of discharge, P is the wetted perimeter, C is the Chezy coefficient, q represents the additional discharge per unit length of the channel, and v' is the component of the velocity of the added water in the direction of the channel flow.

For cases in which the frictional loss is of secondary importance, the shearing force at the channel walls can be considered to be balanced by the momentum of the added water. Then,

$$\rho\, g\, \bar{y}\, A - \rho\, g\, (\bar{y} + d\bar{y})\, (A + dA) + \rho\, g\, A\, S_0\, dx = \frac{\rho\, (Q + dQ)^2}{A + dA} - \frac{\rho\, Q^2}{A} \quad \text{(2)}$$

When water is added uniformly along the channel,

$$Q = \frac{Q_o\, x}{L} \quad \text{(3a)}$$

and

$$(Q + dQ) = \frac{Q_o\, (x + dx)}{L} \quad \text{(3b)}$$

With the Froude number $\mathbf{F}_o$ defined as

$$\mathbf{F}^2{}_o = \frac{Q^2{}_o\, b_o}{g\, A^3{}_o} \quad \text{(3c)}$$

Eq. 2 can be reduced to

$$-\, \bar{y}\, A^2\, dA - A^3\, d\bar{y} + A^3\, S_0\, dx = \frac{2\, \mathbf{F}^2{}_o\, A^3{}_o\, A\, x\, dx}{b_o\, L^2} - \frac{\mathbf{F}^2{}_o\, A^3{}_o\, x^2\, dA}{b_o\, L^2} \quad \text{(3d)}$$

in which b is the width of the water surface in the channel. The subscripts o, u, and c are used to signify values in the channel at the outlet end, the upstream end, and the section with critical flow, respectively.

Eqs. 1, 2, and 3*d* are differential equations from which a closed-form solution cannot be obtained in the general case. However, for a particular channel flow, the profile of the water surface in the channel can be obtained by numerical integration. Eq. 3*d* will be used subsequently for investigating channels with parallel side walls and channels with side walls set at a constant slope (triangular and trapezoidal sections). The results presented will enable engineers to design channels without the tedious process of numerical integration.

CHANNELS WITH PARALLEL SIDE WALLS

Channels are to be considered as having uniform slope, along which water is to be added uniformly, and in which the energy loss resulting from friction is negligible. Fig. 2(*a*) represents a channel having parallel sides and a bottom of arbitrary shape. The centroid of the area a_1 is located as shown, and the water surface is considered to lie above this area.

In Fig. 2(*a*),

$$A = b\,h + a_1 \tag{4a}$$

and

$$A\,\bar{y} = \tfrac{1}{2}\,b\,h^2 + a_1\,(h + D) \tag{4b}$$

from which

$$\bar{y} = \frac{A}{2\,b} + \frac{1}{A}\left(a_1\,D - \frac{a_1^2}{2\,b}\right) \tag{5a}$$

and

$$d\bar{y} = \left[\frac{1}{2\,b} - \frac{1}{A^2}\left(a_1\,D - \frac{a_1^2}{2\,b}\right)\right] dA \tag{5b}$$

Substituting Eqs. 4 and 5 into Eq. 3*d* and simplifying,

$$\left[\mathsf{F}^2_o\left(\frac{x}{L}\right)^2 - \left(\frac{A}{A_o}\right)^3\right] d\left(\frac{A}{A_o}\right) = \left[2\,\mathsf{F}^2_o\left(\frac{A}{A_o}\right)\left(\frac{x}{L}\right) - \left(\frac{A}{A_o}\right)^3 \frac{S_0\,L}{\left(\dfrac{A_o}{b}\right)}\right] d\left(\frac{x}{L}\right) \tag{6}$$

Reducing the channel section to a flat-bottomed section of equal area, and letting *y* denote the depth of flow measured from the resulting flat bottom (Fig. 2(*b*)),

$$\frac{A}{A_o} = \frac{b\,y}{b\,y_o} = \frac{y}{y_o} \tag{7a}$$

and

$$\left[\mathsf{F}^2_o\left(\frac{x}{L}\right)^2 - \left(\frac{y}{y_o}\right)^3\right] d\left(\frac{y}{y_o}\right) = \left[2\,\mathsf{F}^2_o\left(\frac{y}{y_o}\right)\left(\frac{x}{L}\right) - G\left(\frac{y}{y_o}\right)^3\right] d\left(\frac{x}{L}\right) \tag{7b}$$

in which G is defined as $S_0\,L/(A_o/b_o)$ and in this case is equal to $S_0\,L/y_o$.

Channels with Level Bottom.—For a level-bottomed channel, S_0 equals zero and Eq. 7*b* reduces to

$$\frac{d\left(\dfrac{x}{L}\right)^2}{d\left(\dfrac{y}{y_o}\right)} - \frac{\left(\dfrac{x}{L}\right)^2}{\dfrac{y}{y_o}} = -\frac{\left(\dfrac{y}{y_o}\right)^2}{\mathsf{F}^2_o} \tag{8}$$

With the boundary conditions y/y_o and x/L both equal to unity at the outlet end of the channel, the solution of Eq. 8 is

$$2\,\mathsf{F}^2_o\left(\frac{x}{L}\right)^2 = (2\,\mathsf{F}^2_o + 1)\,\frac{y}{y_o} - \left(\frac{y}{y_o}\right)^3 \tag{9a}$$

At the upstream end of the channel (where $x = 0$),

$$\frac{y_u}{y_o} = \sqrt{2\,\mathsf{F}^2_o + 1} \tag{9b}$$

By the use of Eq. 9*a* the entire profile of the water surface in the channel can be determined from the flow condition at the outlet end. When free fall occurs at the outlet end, the flow is critical, and therefore $\mathbf{F}_o = 1$. The depth y_o can be computed through the knowledge of Q_o. When the outlet end is submerged y_o is fixed by the downstream surface elevation, and $\mathbf{F}_o$ can be computed by knowing y_o and Q_o. There are two real positive solutions for y/y_o from Eq. 9*a* for each value of x/L. Because the energy of a water particle must decrease as it proceeds downstream, only the values of $y/y_o \geqq 1$ are true solutions for the problem of level channels.

To demonstrate the validity of the momentum equation, a 9-in.-wide rectangular channel with a flat bottom was used. The length of the channel was varied from 7.50 ft to 4.38 ft. Water was added to the channel over the level tops of the two side walls. The outlet end of the channel was connected to a similar channel 6 ft long, and no water was added to this part of the flow. The value of $\mathbf{F}_o$ at the outlet end of the upper channel was computed by observing Q_o and y_o and was found to be 0.64 for all rates of discharge. The observed surface profiles in the upper channel at various rates of discharge are shown in Table 1 with the values computed from Eq. 9*a* shown in parentheses. Thus, the corresponding observed and computed values are in agree-

TABLE 1.—DEPTH OF FLOW IN LEVEL RECTANGULAR CHANNELS[a]

Channel length, in feet	Discharge, in cubic feet per second	VALUE OF x/L				
		0.033	0.266	0.444	0.633	0.772
7.50	3.06	1.40(1.46)	1.39(1.44)	1.35(1.41)	1.31(1.35)	1.18(1.28)
	2.52	1.25(1.28)	1.25(1.27)	1.20(1.24)	1.14(1.18)	1.05(1.12)
	2.26	1.19(1.19)	1.18(1.18)	1.14(1.15)	1.07(1.10)	1.02(1.05)
	2.14	1.11(1.15)	1.11(1.13)	1.07(1.11)	1.03(1.06)	0.94(1.01)
	1.85	1.05(1.04)	1.04(1.03)	1.01(1.01)	0.95(0.96)	0.89(0.91)
	1.60	0.98(0.95)	0.98(0.94)	0.95(0.91)	0.91(0.88)	0.85(0.83)
	1.25	0.82(0.81)	0.79(0.80)	0.79(0.78)	0.75(0.74)	0.70(0.71)
		VALUE OF x/L				
		0.022	0.258	0.510	0.701	
5.63	2.15	1.10(1.15)	1.11(1.14)	1.07(1.10)	1.01(1.04)	
	1.64	0.98(0.96)	0.98(0.95)	0.99(0.92)	0.94(0.87)	
	1.39	0.88(0.86)	0.87(0.85)	0.84(0.82)	0.80(0.78)	
	0.88	0.62(0.63)	0.61(0.63)	0.62(0.60)	0.58(0.57)	
		VALUE OF x/L				
		0.048	0.372	0.623		
4.38	2.50	1.25(1.27)	1.24(1.24)	1.18(1.18)		
	2.47	1.27(1.27)	1.22(1.23)	1.11(1.17)		
	1.90	1.11(1.06)	1.02(1.04)	1.01(0.99)		
	1.87	1.05(1.05)	1.02(1.03)	0.99(0.98)		
	1.52	0.88(0.91)	0.89(0.89)	0.82(0.85)		
	1.50	0.90(0.91)	0.90(0.89)	0.85(0.84)		
	1.06	0.69(0.72)	0.71(0.70)	0.65(0.67)		

[a] Values shown in parentheses represent depths computed from Eq. 9*a*. Other values represent experimentally observed depths in feet.

ment. The application of the momentum equation to this case is therefore acceptable.

Channels with Bottom at a Uniform Slope.—For channels with a sloping bottom, a closed-form solution of Eq. 7*b* cannot be obtained. Except for cases with a hydraulic jump in the channel, the surface profile can be obtained from a known depth of flow by numerical integration. For cases with $\mathbf{F}_o \leqq 1$, values of y_u/y_o have been obtained from the known condition that y/y_o equals unity at x/L equal to one, and are shown as solid lines in Fig. 3. The values of y_u/y_o are shown because the water surface slopes downward in a downstream direction and only the value of y_u is of interest in determining the dimensions of the channel.

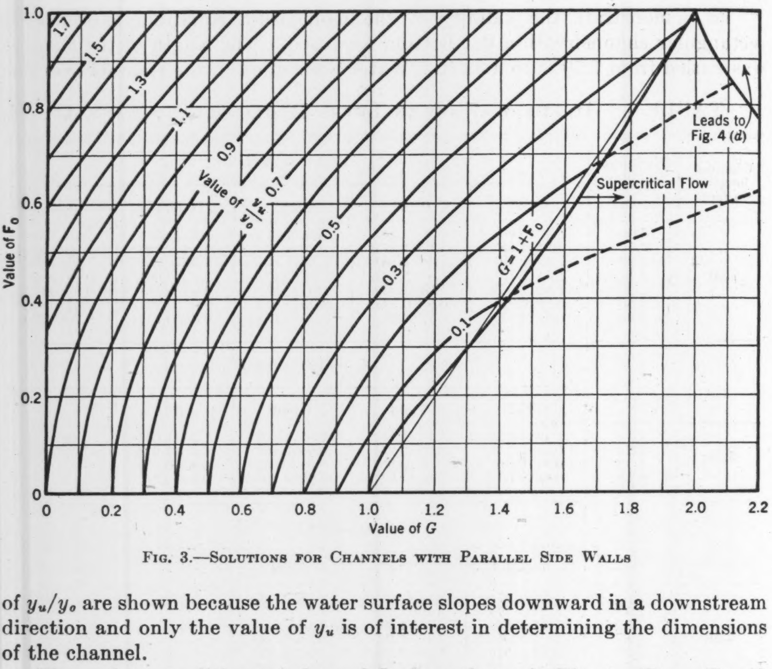

FIG. 3.—SOLUTIONS FOR CHANNELS WITH PARALLEL SIDE WALLS

The various conditions of channel flow are shown in Fig. 4. From Eq. 7*b* it can be seen that, if G is less than $\frac{2}{3}(1 + 2\,\mathbf{F}^2_o)$, then $d\mathbf{F}/dx$ exceeds zero—that is, the value of $\mathbf{F}$ increases as the flow proceeds downstream as shown in Fig. 4(*a*). The dashed lines in Figs. 4(*a*), 4(*b*), 4(*c*), and 4(*d*) indicate the depths at which $\mathbf{F}$ is equal to unity.

When G is greater than $\frac{2}{3}(1 + 2\,\mathbf{F}^2_o)$ but less than approximately $(1 + \mathbf{F}_o)$, the value of $\mathbf{F}$ first increases as the flow proceeds downstream to reach a maximum value; then $\mathbf{F}$ decreases, as shown in Fig. 4(*b*). The line dividing regions B and C in Fig. 4(*e*) (corresponding to Fig. 4(*b*) and 4(*c*), respectively) includes all the cases in which the maximum value of $\mathbf{F}$ in the channel is equal to unity. This line can be represented approximately by the equation, $G = 1 + \mathbf{F}_o$.

When G is greater than approximately $(1 + \mathbf{F}_o)$, there is supercritical flow in a part of the channel. If the outlet is sufficiently submerged, a hydraulic jump will form as shown in Fig. 4(*c*). In this case, the control point is shifted into the channel, and the elevation of the water surface at the outlet does not affect the entire profile in the channel. Thus, the surface profile above the hydraulic jump cannot be determined from the value of y_o.

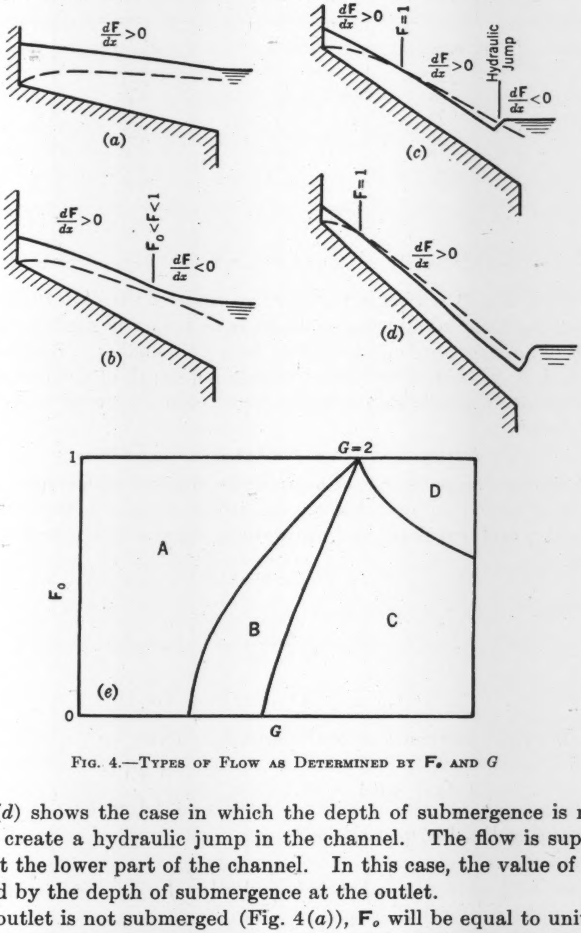
$\frac{dF}{dx} > 0$
(a)
$\frac{dF}{dx} > 0$
$F_o < F < 1$
$\frac{dF}{dx} < 0$
(b)
$\frac{dF}{dx} > 0$
F = 1
$\frac{dF}{dx} > 0$
Hydraulic Jump
$\frac{dF}{dx} < 0$
(c)
F = 1
$\frac{dF}{dx} > 0$
(d)
G = 2
1
0
F_o
G
A
B
C
D
(e)

FIG. 4.—TYPES OF FLOW AS DETERMINED BY $\mathbf{F}_o$ AND G

Fig. 4(*d*) shows the case in which the depth of submergence is not great enough to create a hydraulic jump in the channel. The flow is supercritical throughout the lower part of the channel. In this case, the value of $\mathbf{F}_o$ is not determined by the depth of submergence at the outlet.

If the outlet is not submerged (Fig. 4(*a*)), $\mathbf{F}_o$ will be equal to unity if G is less than, or equal to, 2. When G is greater than 2, the flow is supercritical at the lower part of the channel. Cases involving supercritical flow will be investigated subsequently.

To verify the theory for sloping channels, a model rectangular channel, 3 in. wide and 4 ft 6 in. long, with S_0 equal to 13% was used. Water was added uniformly along the flow over a weir on one side of the channel. The outlet end was free so that F_o was equal to unity when G was less than 2. The depths y_u and y_o were measured at various rates of discharge. The results obtained are shown in Table 2. The observed values of y_u/y_o and

TABLE 2.—DEPTHS OF FLOW IN SLOPING RECTANGULAR CHANNEL

y_o, in inches	y_u, in inches	Value of G	Value of $\frac{y_u}{y_o}$	Value of $\frac{S_0 L}{y_o} + \frac{y_u}{y_o}$
5.00	2.75	1.40	0.55	1.95
4.88	2.00	1.44	0.41	1.85
4.50	1.50	1.56	0.33	1.89
4.25	1.25	1.65	0.30	1.95
4.00	1.25	1.75	0.31	2.06
3.75	1.12	1.87	0.30	2.17
3.62	1.00	1.93	0.28	2.21
3.50	1.00	2.00	0.29	2.29

$\frac{S_0 L}{y_o} + \frac{y_u}{y_o}$ are approximately 20% and 5%, respectively, lower than the values obtained from Fig. 3. This is probably caused by the fact that, at such a steep slope, the term involving v' in Eq. 1 is no longer negligible. At a lesser slope, the difference can be expected to be much smaller. Because it is the value of $S_0 L + y_u$ that determines the required depth of channel at the outlet, the verification is considered satisfactory. The results presented will lead to a safe design.

CHANNELS WITH SLOPING SIDE WALLS

Fig. 5 shows a cross section of a prismatic channel with sloping side walls. The water is added to the channel uniformly along the flow, the channel bottom is at a uniform slope, and the water surface is above area a_2.

In Fig. 5,

$$A = \tfrac{1}{2} k h^2 - a_2 \qquad (10a)$$

from which

$$h = \sqrt{\frac{2 (A + a_2)}{k}} \qquad (10b)$$

Also,

$$A \bar{y} = \tfrac{1}{6} k h^3 - a_2 (h - D) \qquad (10c)$$

in which D locates the centroid of the area a_2. Thus,

$$A\, d\bar{y} + \bar{y}\, dA = d(A \bar{y}) = \frac{A\, dA}{\sqrt{2 k (A + a_2)}} \qquad (10d)$$

Substituting Eq. 10*d* into Eq. 3*d*,

$$- \sqrt{\frac{1 + B^2}{\frac{A}{A_o} + B^2}} \left(\frac{A}{A_o}\right)^3 d\left(\frac{A}{A_o}\right) + G \left(\frac{A}{A_o}\right)^3 d\left(\frac{x}{L}\right)$$
$$= 2\, \mathsf{F}^2{}_o \left(\frac{A}{A_o}\right)\left(\frac{x}{L}\right) d\left(\frac{x}{L}\right) - \mathsf{F}^2{}_0 \left(\frac{x}{L}\right)^2 d\left(\frac{A}{A_o}\right) \qquad (11)$$

in which B denotes $\sqrt{\frac{a_2}{A_o}}$, and G is equal to $\frac{S_0 L \sqrt{2 k (A_o + a_2)}}{A_o}$ in this case.

Level Triangular Channels.—For level triangular channels, B and G are equal to zero. Because

$$\frac{A}{A_o} = \left(\frac{y}{A_o}\right)^2 \qquad (12a)$$

and

$$d\left(\frac{A}{A_o}\right) = 2\left(\frac{y}{y_o}\right) d\left(\frac{y}{y_o}\right) \qquad (12b)$$

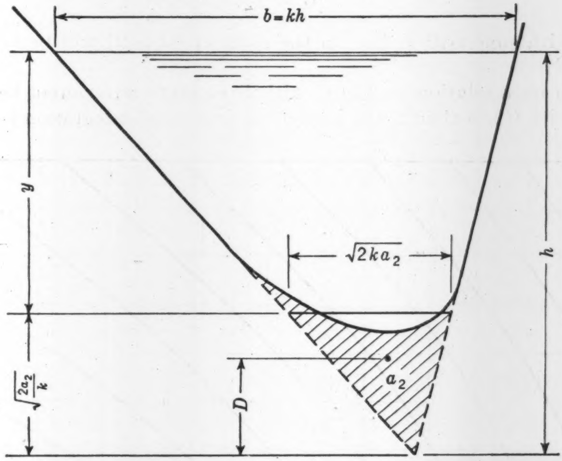

FIG. 5.—CHANNEL WITH SLOPING SIDE WALLS

Eq. 11 can be reduced to

$$\frac{d\left(\frac{x}{L}\right)^2}{d\left(\frac{y}{y_o}\right)} - \frac{2}{\frac{y}{y_o}}\left(\frac{x}{L}\right)^2 = -\frac{2}{\mathsf{F}^2_o}\left(\frac{y}{y_o}\right)^4 \qquad (13a)$$

With the boundary condition y/y_o equals one at x/L equal to one, the solution of Eq. 13a is

$$3\,\mathsf{F}^2_o\left(\frac{x}{L}\right)^2 = (3\,\mathsf{F}^2_o + 2)\left(\frac{y}{y_o}\right)^2 - 2\left(\frac{y}{y_o}\right)^5 \qquad (13b)$$

There are two real positive solutions for y/y_o for each value of x/L. Because of energy considerations, only the values of y/y_o greater than unity are the true solutions. At the upstream end of the channel, where $x = 0$,

$$\frac{y_u}{y_o} = \sqrt[3]{\tfrac{3}{2}\,\mathsf{F}^2_o + 1} \qquad (14)$$

Sloping Triangular Channels.—For triangular channels with a uniform bottom slope, the various types of flow occurring in the channel are similar to those shown in Fig. 4. In this case, it can be seen from Eq. 11 that the equation for the line between regions A and B is

$$G = \tfrac{4}{5}\left(1 + \tfrac{3}{2}\,\mathbf{F}^2_o\right) \qquad (15a)$$

and for the line between regions B and C,

$$G = 2 \qquad (15b)$$

The case with supercritical flow in the channel ($G > 2$) will be investigated subsequently.

A closed-form solution for Eq. 11 with B^2 equal to zero cannot be obtained. For cases with G less than 2, the method of numerical integration is used, and the resulting values of y_u/y_o for various values of $\mathbf{F}_o$ and G are presented as solid lines in Fig. 6. It should be noted that, in this case, $G = \dfrac{2\,S_0\,L}{y_o}$.

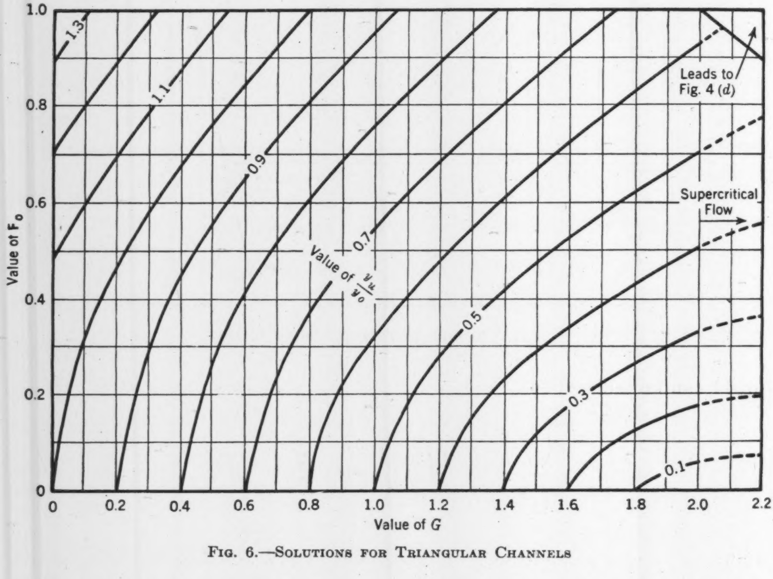

FIG. 6.—SOLUTIONS FOR TRIANGULAR CHANNELS

Level Channels with Sloping Side Walls.—With G equal to zero, Eq. 11 can be reduced to

$$\frac{d\left(\dfrac{x}{L}\right)^2}{d\left(\dfrac{A}{A_o}\right)} - \frac{\left(\dfrac{x}{L}\right)^2}{\dfrac{A}{A_o}} = -\,\frac{\sqrt{1+B^2}}{\mathbf{F}^2_o}\,\frac{\left(\dfrac{A}{A_o}\right)^2}{\sqrt{\dfrac{A}{A_o}+B^2}} \qquad (16)$$

With the boundary condition that A/A_o equals one at x/L equal to one, the solution of Eq. 16 is

$$\left(\frac{x}{L}\right)^2 = \frac{A}{A_o}\left\{1 + \frac{2\sqrt{1+B^2}}{3\,\mathsf{F}^2_o} \times \left[(1+B^2)^{3/2} - \left(\frac{A}{A_o} + B^2\right)^{3/2}\right] - \frac{2B\sqrt{1+B^2}}{\mathsf{F}^2_o} \times \left[(1+B^2)^{1/2} - \left(\frac{A}{A_o} + B^2\right)^{1/2}\right]\right\} \quad (17)$$

Eq. 17 yields the surface profile in the channel.

At the upstream end of the channel (where x equals zero) the value of A_u/A_o can be obtained from

$$1 + \frac{2\sqrt{1+B^2}}{3\,\mathsf{F}^2_o}\left[(1+B^2)^{3/2} - \left(\frac{A_u}{A_o} + B^2\right)^{3/2}\right] - \frac{2B\sqrt{1+B^2}}{\mathsf{F}^2_o}\left[(1+B^2)^{1/2} - \left(\frac{A_u}{A_o} + B^2\right)^{1/2}\right] = 0 \quad (18)$$

If the depth y is measured from the bottom of an equivalent trapezoidal section, as shown in Fig. 5, y_u/y_o can be determined from

$$\frac{y_u}{y_o} = \frac{\sqrt{\frac{A_u}{A_o} + B^2} - B}{\sqrt{1+B^2} - B} \quad (19)$$

This process of obtaining a solution for y_u/y_o is tedious. A suggested empirical formula giving results to within 1% of those obtained by use of Eq. 19 is

$$\frac{y_u}{y_o} = \left(\frac{y_u}{y_o}\right)_r - \left(\frac{1}{3}\right)^B\left[\left(\frac{y_u}{y_o}\right)_r - \left(\frac{y_u}{y_o}\right)_t\right] \quad (20)$$

in which $(y_u/y_o)_r$ is the value of y_u/y_o for a rectangular section having the same F_o as given by Eq. 9*b*, and $(y_u/y_o)_t$ is the value of y_u/y_o for a triangular section, by Eq. 14.

Sloping Channels with Sloping Side Walls.—The various types of flow that will occur in a sloping channel with sloping side walls are similar to those shown in Fig. 4. In this case, the line between regions B and C is represented approximately by the expression:

$$G = 2 - 2\,(1 - \mathsf{F}_o)\,(\sqrt{B^2\,(1+B^2)} - B^2) \quad (21)$$

For actual values of G greater than those determined from Eq. 21 there will be supercritical flow in the channel.

For cases not involving supercritical flow, the profile of the water surface in the channel for given values of F_o, G, and B^2 can be obtained from Eq. 11 by numerical integration. A close approximation for y_u/y_o can be obtained from Fig. 3 for a rectangular channel by use of the given values of F_o and

G; the same can then be done for a triangular channel from Fig. 6. The value of y_u/y_o for the channel in question can be obtained from Eq. 20.

CHANNELS WITH SUPERCRITICAL FLOW

It has been stated that when the actual value of G exceeds the value determined by Eq. 21, there will be supercritical flow in the channel. Also, if the outlet end is sufficiently submerged, a hydraulic jump will form. It should be noted that Eq. 21 will change to $G > 1 + \mathsf{F}_o$ and $G > 2$ for channels with parallel walls and for triangular channels, respectively. When free fall occurs at the outlet, F_o is equal to one if G is equal to or less than 2, and F_o exceeds unity if G exceeds 2 for all channels.

Flow Above Critical Section.—If x_c locates the section with critical flow, and because

$$\frac{Q_c}{Q_o} = \frac{x_c}{L} \tag{22a}$$

and

$$\mathsf{F}^2_c = \frac{Q^2_c\, b_c}{g\, A^3_c} = 1 \tag{22b}$$

then

$$\frac{Q^2_o\, b_c}{g\, A^3_c} \left(\frac{x_c}{L}\right)^2 = 1 \tag{23}$$

If the upper part of the channel is considered as a separate channel of length x_c, $G_c = \dfrac{S_0\, x_c}{A_c/b_c}$ by definition. Because F_c is equal to unity, G_c cannot be greater than 2. However, G_c cannot be smaller than 2 because this would make $\dfrac{S_0\, x}{A/b}$ less than 2 at the sections immediately downstream, and the flow there would be subcritical. Therefore,

$$\frac{S_0\, x_c}{\dfrac{A_c}{b_c}} = 2 \tag{24a}$$

or

$$\frac{x_c}{L} = \frac{2\, A_c}{S_0\, L\, b_c} \tag{24b}$$

Substituting Eqs. 24 into Eq. 23,

$$A_c\, b_c = \left(\frac{2\, Q_o}{\sqrt{g}\, S_0\, L}\right)^2 \tag{25}$$

From Eq. 25 y_c can be determined. The value of y_c being known, x_c can be computed from Eq. 24*b*. According to Figs. 3 and 6 and Eq. 20, the value of y_u is given by

$$\frac{y_u}{y_c} = 0.31 - \left(\frac{1}{3}\right)^E (0.31 - 0.63) \tag{26}$$

in which E is equal to $\sqrt{a_2/A_c}$.

Flow Below Critical Section—Without Hydraulic Jump.—For a steep channel without a hydraulic jump (Fig. 4(*d*)) the outlet condition is independent of the depth of submergence at the outlet. The surface profile below the section with critical flow can be obtained by numerical integration. For this purpose, Eq. 3*d* can be reduced to

$$\left[\left(\frac{x}{x_c}\right)^2 - \sqrt{\frac{1+E^2}{\frac{A}{A_c}+E^2}}\left(\frac{A}{A_c}\right)^3\right] d\left(\frac{A}{A_c}\right) = 2\left[\frac{x}{x_c}\frac{A}{A_c} - \left(\frac{A}{A_c}\right)^3\right] d\left(\frac{x}{x_c}\right) \quad ..(27)$$

The boundary condition is A/A_c equals one at x/x_c equal to one. The values of A/A_c at various (x/x_c)-values have been computed and are shown in Fig. 7.

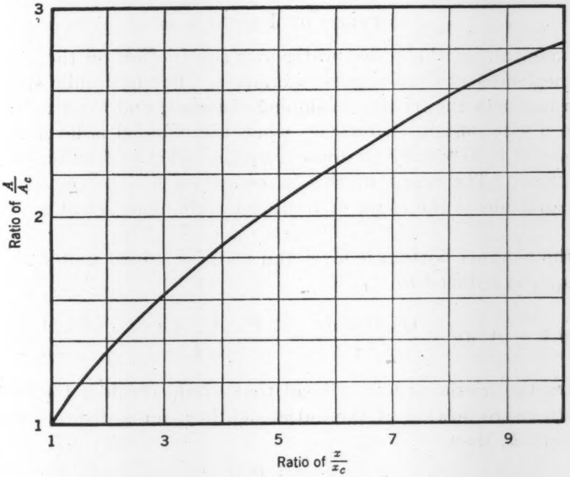

FIG. 7.—SURFACE PROFILE IN SUPERCRITICAL SECTIONS

It should be noted that the values of A/A_c are practically the same for various values of E^2. To determine the outlet condition for a given channel flow, x_c/L is computed from Eq. 24*b*, and the value for A_o/A_c is equal to the value of A/A_c at $x/x_c = L/x_c$. The values of y_o and F_o can then be computed from the value of A_o.

Flow Below Critical Section with Hydraulic Jump.—For a steep channel with a hydraulic jump (Fig. 4(*c*)) the profile of the water surface in the supercritical sections can be determined from Fig. 7. At the outlet the minimum depth of submergence required to produce a hydraulic jump is equal to the conjugate depth for the values of F_o and y_o applicable to the case without the jump. The values of F_o and G computed from this minimum depth of submergence form the line dividing region C and the region leading to the situation shown in Fig. 4(*d*). A depth of submergence greater than this minimum depth will move the hydraulic jump upstream.

When there is a hydraulic jump in the channel, the values of F_o, G, and y_o are determined by the depth of submergence at the outlet. A convenient expression for finding y_u can be obtained by combining Eqs. 25 and 26. Thus, for channels with parallel side walls,

$$\frac{y_u}{y_o} = 1.24 \left(\frac{\mathsf{F}_o}{G}\right)^2 \qquad (28a)$$

and for triangular channels,

$$\frac{y_u}{y_o} = \left(\frac{\mathsf{F}_o}{G}\right)^{\frac{2}{3}} \qquad (28b)$$

Eqs. 28 have been plotted as dashed lines in Figs. 3 and 6.

Effect of Friction

The momentum of the added water and the friction on the channel walls have been neglected in the foregoing examples. For hydraulic structures the momentum balances the friction in sloping channels, and the results presented will lead to a safe design. However, when the channel is level or at a very gradual slope, it is necessary to investigate the effect of friction on the depth of channel flow. The result of this investigation will serve to indicate the order of magnitude of the effect of friction for channels set at a very gradual slope.

When the channel bottom is level and water is added uniformly along the channel, Eq. 1 is reduced to

$$-\bar{y}\, A^2\, dA - A^3\, d\bar{y} - \frac{Q^2{}_o\, P\, x^2\, dx}{C^2\, L^2} = \frac{2\, \mathsf{F}^2{}_o\, A^3{}_o\, A\, x\, dx}{b_o\, L^2} - \frac{\mathsf{F}^2{}_o\, A^3{}_o\, x^2\, dA}{b_o\, L^2} \qquad (29)$$

If h_f denotes the frictional loss of head that would result if the total channel discharge, Q_o, were flowing at the outlet depth y_o for a distance equal to the channel length L, then

$$h_f = \frac{Q^2{}_o\, P_o\, L}{C^2{}_o\, A^3{}_o} \qquad (30)$$

according to the Chezy formula. With the approximation that $C = C_o$, Eq. 30 can be rewritten as

$$-\bar{y}\, A^2\, dA - A^3\, d\bar{y} - \frac{h_f\, A^3{}_o\, P\, x^2\, dx}{P_o\, L^3} = \frac{2\, \mathsf{F}^2{}_o\, A^3{}_o\, A\, x\, dx}{b_o\, L^2} - \frac{\mathsf{F}^2{}_o\, A^3{}_o\, x^2\, dA}{b_o\, L^2} \qquad (31)$$

Level Channels with Parallel Side Walls.—For level channels with parallel side walls, Eq. 31 can be reduced to

$$\left(1 + \tfrac{1}{2}\, \frac{h_f}{\mathsf{F}^2{}_o\, y_o}\, \frac{P}{P_o \sqrt{\dfrac{y}{y_o}}}\, \frac{\dfrac{x}{L}}{\sqrt{\dfrac{y}{y_o}}}\right) \frac{d\left(\dfrac{x}{L}\right)^2}{d\left(\dfrac{y}{y_o}\right)} - \frac{\left(\dfrac{x}{L}\right)^2}{\dfrac{y}{y_o}} = -\frac{\left(\dfrac{y}{y_o}\right)^2}{\mathsf{F}^2{}_o} \qquad (32)$$

This nonlinear differential equation should be solved by successive approximations. The first approximation is obtained for frictionless flow by neglecting the term involving h_f; this results in Eq. 9*a*. From Eq. 9*a*, the following can be obtained—

$$\frac{\dfrac{x}{L}}{\sqrt{\dfrac{y}{y_o}}} = \sqrt{1 - \frac{1}{2\,\mathsf{F}^2_o}\left[\left(\frac{y}{y_o}\right)^2 - 1\right]} \tag{33}$$

The value of $(y/y_o)^2$ changes along the channel, is equal to unity at the outlet, and is equal to $(2\,\mathsf{F}^2_o + 1)$ at the upstream end, according to Eq. 9*b*. Thus the value of $(x/L)/\sqrt{y/y_o}$ varies from zero at the upstream end to unity at the outlet. To find y_u (for practical purposes), a constant value of $\frac{1}{2}$ can be used for $(x/L)/\sqrt{y/y_o}$ throughout the channel. It can also be shown that the value of $(P/P_o)\sqrt{y/y_o}$ remains very close to unity throughout a channel of reasonable proportion. Thus, Eq. 32 can be linearized for finding y_u:

$$\left(1 + \frac{1}{4}\,\frac{h_f}{\mathsf{F}^2_o\, y_o}\right)\frac{d\left(\dfrac{x}{L}\right)^2}{d\left(\dfrac{y}{y_o}\right)} - \frac{\left(\dfrac{x}{L}\right)^2}{\dfrac{y}{y_o}} = -\,\frac{\left(\dfrac{y}{y_o}\right)^2}{\mathsf{F}^2_o} \tag{34}$$

The solution of Eq. 34 gives the following value of y_u at the upstream end:

$$\frac{y_u}{y_o} = \left(1 + \frac{8 + 3\,\alpha}{4}\,\mathsf{F}^2_o\right)^I \tag{35}$$

in which α denotes $\dfrac{h_f}{\mathsf{F}^2_o\, y_o}$ and I equals $\dfrac{4 + \alpha}{8 + 3\,\alpha}$. With h_f equal to zero for frictionless flow, Eq. 35 is identical to Eq. 9*b*.

The percentage increase of y_u because of friction, obtained by comparing Eqs. 9*b* and 35, is shown in Fig. 8. It can be verified that for wash-water troughs and side-channel spillways the increase of y_u as a result of friction is usually negligible. For effluent channels around sewage-treatment tanks, the value of $\dfrac{h_f}{\mathsf{F}^2_o\, y_o}$ can be as high as 2, and the increase of y_u caused by friction can become as large as 10%.

Level Channels with Sloping Side Walls.—With the same approximation as was applied to the case of channels with parallel side walls, Eq. 31 yields the following result for level triangular channels:

$$\frac{y_u}{y_o} = \left(1 + \frac{6 + 5\,\alpha}{4}\,\mathsf{F}^2_o\right)^J \tag{36}$$

in which $J = \dfrac{2 + \alpha}{6 + 5\,\alpha}$. With h_f equal to zero for frictionless flow, Eq. 36 reduces to Eq. 14.

The percentage increase of y_u caused by friction has been computed from Eqs. 14 and 36 and is found to be accurately represented by Fig. 8. Thus, Fig. 8 is applicable to triangular channels and to channels with parallel side walls. Furthermore, because these two channel shapes are the two extreme cases of channels with sloping side walls, Fig. 8 can be applied safely to all channel shapes.

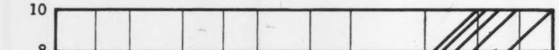

FIG. 8.—INCREASE OF y_u AS A RESULT OF FRICTION IN LEVEL CHANNELS

EXAMPLES OF APPLICATION

The application of the preceding results will be illustrated by several examples.

Example 1.—If it is required to design a rectangular wash-water trough 20 ft long to discharge 5 cu ft per sec with a free fall at the outlet end, the channel requiring the least material for construction must be found.

With a free fall at the outlet end, $\mathbf{F}_o$ will be equal to unity if G is less than or equal to 2. For a given value of y_o, the area of the two side walls is equal to $\left(\frac{2\,y_u}{y_o} + G\right) y_o\,L$. Because y_u/y_o depends on G for a given value of $\mathbf{F}_o$, the area of the side walls depends on the choice of G. By examining Fig. 3 it can be found that, for $\mathbf{F}_o$ equal to unity, $\left(2\,\frac{y_u}{y_o} + G\right)$ is a minimum at G equal to 1.7. For this value of G, y_u/y_o equals 0.45. Thus, the area of the side walls is equal to $(2 \times 0.45 + 1.7)\,y_o\,L$ or $2.6\,y_o\,L$.

The depth y_o at the outlet end depends on width b of the channel, $\mathbf{F}_o$

being equal to unity. By definition,

$$y_o = \left(\frac{Q_o}{\sqrt{g}\,\mathbf{F}_o\, b} \right)^{\frac{2}{3}} = \frac{0.92}{b^{\frac{2}{3}}} \qquad (37)$$

Neglecting the end wall, the total wall and bottom area A_t of the channel is

$$A_t = 2.6 \times 0.92 \times \frac{L}{b^{\frac{2}{3}}} + b\,L \qquad (38)$$

If the bottom and side walls are of the same thickness, the material required for construction will be proportional to A_t. To find the condition for the least value of A_t let dA_t/db equal zero—

$$\frac{dA_t}{db} = -\,2.6 \times 0.92 \times L \times \tfrac{2}{3}\, b^{-5/3} + L = 0 \qquad (39a)$$

$$b = 1.32 \text{ ft} \qquad (39b)$$

$$y_o = \frac{0.92}{b^{\frac{2}{3}}} = 0.76 \text{ ft} \qquad (39c)$$

$$S_0 = \frac{G\,y_o}{L} = \frac{1.7 \times 0.76}{20} = 0.065 = 6.5\% \qquad (39d)$$

$$y_u = 0.45\, y_o = 0.34 \text{ ft} \qquad (39e)$$

$$\text{depth of channel at outlet end} = y_u + S_0\,L = 1.64 \text{ ft} \qquad (39f)$$

and

$$A_t = 2.6\, y_o\, L + b\,L = 66.2 \text{ sq ft} \qquad (39g)$$

Example 2.—If it is required to design a level rectangular trough with a free fall at the outlet (for the same conditions as in Example 1), then $\mathbf{F}_o$ equals unity, and from Eq. 9*b*,

$$y_u = \sqrt{2\,\mathbf{F}^2{}_o + 1} \qquad (40a)$$

and

$$y_o = 1.73\, y_o \qquad (40b)$$

By the use of Eq. 37,

$$y_u = 1.73 \times \frac{0.92}{b^{\frac{2}{3}}} \qquad (40c)$$

The total area A_t of the side walls and bottom is

$$A_t = 2\,y_u\,L + b\,L = 2 \times 1.73 \times \frac{0.92}{b^{\frac{2}{3}}} \times L + b\,L = \frac{3.18}{b^{\frac{2}{3}}} + b\,L \qquad (40d)$$

For a minimum A_t, dA_t/db equals zero:

$$-3.18 \times \tfrac{2}{3} \times L \times b^{-5/3} + L = 0 \qquad (41a)$$

$$b = 1.57 \text{ ft} \qquad (41b)$$

$$y_o = \frac{0.92}{b^{2/3}} = 0.68 \text{ ft} \qquad (41c)$$

$$\text{depth of channel} = y_u = 1.73\, y_o = 1.18 \text{ ft} \qquad (41d)$$

and

$$A_t = 2\, y_u\, L + b\, L = 78.6 \text{ sq ft} \qquad (41e)$$

On comparing the results with those in Example 1, these facts become apparent: (*a*) The required depth of channel at the outlet end is less for a level channel than for a sloping channel. When the available head is limited, a level channel should be used. (*b*) A sloping channel requires slightly less material for construction. The cost of construction, however, may be lower for a level channel because of its simpler layout.

It is apparent that there is nothing to be gained by using sloping channels for wash-water troughs and effluent channels around sewage-treatment tanks. A level channel consumes less hydraulic head, and the cost is comparable to that of a sloping channel.

Example 3.—This example will show the method of determining the performance of a trapezoidal channel of a side-channel spillway 400 ft long, discharging 16,000 cu ft per sec. The bottom slope of the channel is 15%, the bottom width is 10 ft, side slopes are 2:1 (the area a_2 being equal to 50 sq ft). The outlet end of the channel is connected to a channel of similar cross section at a supercritical slope.

Because the downstream channel is at supercritical slope, the outlet end of the side channel is not submerged. The value of F_o can be greater than or equal to unity depending on whether the value G is greater or less than 2. If F_o equals unity, then (from Eq. 3*c*) y_o equals 28 ft, making $G = 3.4$. Therefore, F_o is greater than unity, y_o is less than 28 ft, G exceeds 3.4, and there will be supercritical flow in the channel.

From Eq. 25, y_c equals 17.3 ft when A_c is equal to 323 sq ft and b_c equals 27.3 ft. From Eq. 24*b* the critical depth occurs at x_c equal to 158 ft. From Eq. 26, y_u equals 10.0 ft. At the outlet L/x_c is equal to 2.53. From Fig. 7, A_o/A_c equals 1.50, or A_o is equal to 485 sq ft, resulting in y_o equal to 22.7 ft. These results can be compared with those obtained for a similar channel.[2]

Example 4.—This example illustrates the method of designing the channel of a side-channel spillway 400 ft long discharging 16,000 cu ft per sec. The maximum allowable side slope is 2:1, and the outlet end of the side channel is connected to a channel of similar cross section at a supercritical slope. The cost of construction is affected by the amount of earthwork and lining. For channels on sloping hillsides, it is usually more economical to use steep side slopes and small bottom widths.[2]

---

[2] "Side Channel Spillways: Hydraulic Theory, Economic Factors, and Experimental Determination of Losses," by Julian Hinds, *Transactions*, ASCE, Vol. 89, 1926, p. 881.

Let it be decided to use the maximum allowable side slope (2:1). A bottom width of 10 ft is chosen for trial. This choice makes the area a_2 equal 50 sq ft. The choice of bottom slope is guided by the empirical expression,

$$\sqrt{2\,\mathbf{F}^2_o + 1} < G < 2 \qquad (42)$$

Because the outlet end is not submerged and G is chosen to be less than 2, for example, 1.8, the value of $\mathbf{F}_o$ is equal to unity. From Eq. 3*c*, y_o equals 28 ft when A_o is equal to 672 sq ft and b_o equals 38 ft. Thus, $S_0 = \dfrac{G\,A_o}{L\,b_o} = 8\%$.

To find y_u, Eq. 20 is used. For $\mathbf{F}_o$ equal to unity and G equal to 1.8, $(y_u/y_o)_r$ equals 0.40 from Fig. 3, and $(y_u/y_o)_t$ equals 0.67 from Fig. 6. With B^2 equal to 0.0745, Eq. 20 results in y_u/y_o equal to 0.60 and y_u equal to 16.8 ft. With y_u and S_0 determined, the cost of construction can be estimated.

Several bottom widths and G-values should be tried in order to obtain the most economical channel. It can be shown that the channel determined in this example with its gradual bottom slope involves only about two thirds as much earthwork as the channel described in Example 3.

SUMMARY

A differential equation based on the principle of the conservation of momentum has been derived for channels with nonuniform discharge. Straight prismatic channels with water added uniformly along the flow have been investigated.

The effect of friction on the channel flow has been investigated, and the result is shown in Fig. 8. In many cases the effect of friction can be neglected; the hydraulic behavior of the flow depends only on three dimensionless quantities which describe the outlet condition, the cross-sectional shape, and the slope of the channel. The various types of channel flow are shown in Fig. 4.

The solutions for channels with parallel side walls are given in Fig. 3, and those for triangular channels are given in Fig. 6. For channels with sloping side walls Eq. 20 is suggested. With the actual value of G exceeding the value determined from Eq. 21, there will be supercritical flow in part of the channel. Under these conditions, the solution can be obtained from Eqs. 24*b*, 25, and 26. The surface profile in the supercritical sections is shown in Fig. 7.

Experimental verification of the theory has been successfully performed with model channels. Several examples are presented to illustrate the methods of design.

APPENDIX. NOTATION

The following symbols, adopted for use in this paper and for the guidance of discussers, conform essentially with American Standard Letter Symbols for Hydraulics (ASA Z10.2—1942), prepared by a committee of the American Standards Association, with ASCE representation and approved by the Association in 1942:

A = cross-sectional area;
A_t = total wall and bottom area;
a_1 = area (Fig. 2);
a_2 = imaginary area (Fig. 5);
$B = \sqrt{a_2/A_o}$;
b = width of the water surface;
C = Chezy coefficient;
c = subscript used to denote the section with critical flow;
D = distance used to locate the centroid of areas a_1 and a_2;
$E = \sqrt{a_2/A_c}$;
F = Froude number $= \sqrt{\frac{Q^2\, b}{g\, A^3}}$;
$G = \frac{S_0\, L}{\frac{A_o}{b_o}}$;
h = height (Figs. 2 and 5);
$I = \frac{4 + \alpha}{8 + 3\,\alpha}$;
$J = \frac{2 + \alpha}{6 + 5\,\alpha}$;
k = ratio of the width to the height of the channel shown in Fig. 5;
L = length of the channel;
o = subscript denoting the outlet end of the channel;
P = wetted perimeter;
Q = rate of discharge;
q = the additional discharge per unity length;
r = subscript denoting a rectangular section;
S_0 = slope of the channel bed;
t = subscript denoting a triangular section;
u = subscript denoting the upstream end of the channel;
v' = component of the velocity of the added water in the direction of the channel flow;
x = distance from the upstream end of the channel;
y = depth of flow (Figs. 2 and 5);
$\bar{y}$ = vertical distance from the centroid of water cross section to the water surface;
$\alpha = \frac{h_f}{\mathsf{F}^2_o\, y_o}$; and
ρ = mass per unit volume of water.

DISCUSSION

TURGUT SARPKAYA,[3] J. M. ASCE.—Flow in open channels with nonuniform discharge has been studied extensively by investigators such as H. Favre,[4] Julian Hinds,[2] and Thomas R. Camp,[5] M. ASCE. Unfortunately, except for the pioneering work of Mr. Hinds, their important works appear to have escaped the attention of the author. Mr. Li's contribution, however, does revive interest in this elusive problem and is a concise presentation of the material in a useful and practicable manner.

The energy loss caused by the impact between the added water and the flowing water is (as noted in the "Introduction") of primary importance. However, the impact of the added water does not appear in Mr. Li's analysis except that a momentum term is introduced—as it was also in Mr. Favre's analysis—by assuming a velocity component in the direction of flow (v'). In the horizontal plane this velocity component is zero for the majority of hydraulic and sanitary engineering works. If, however, the channel receives the water from another channel or from a reservoir in which there is an approach velocity (as for some dam spillways), the component of velocity along the channel should be considered. In such instances, the added discharge may also be nonuniform—complicating the problem still further.

The water which is added to the channel over the weir entrains air, thus generally disturbing the water flowing in the channel. The total resistance to the flow is therefore significantly greater than the resistance to flow at the same rate without the impact. Evidently, the free fall of the added water increases along the channel because of the bottom slope and the decreasing elevation of the water surface in the conduit. Consequently, the greater the slope of the channel bottom, the greater the impact of the added water on the flow along the flume. The drawdown between the upstream section and the downstream section is equal to twice the velocity head at the downstream section, as can be seen by an examination of Eq. 9*b*. The discrepancy between the experimental and the theoretical results probably is caused by the effect of this increasing impact on the resistance rather than by a neglect of the term involving v' in Eq. 1, as stated by the author. In connection with Eqs. 1 and 2, Mr. Li considered the shearing force at the channel walls to be balanced by the momentum of the added water. As has been shown[5] by Mr. Camp, the frictional loss is of little importance in short channels and need not be considered in most cases.

The studies of the nonuniform runoff resulting from rainfall on impervious surfaces are relevant to the present problem. In several studies,[6,7] runoff from a given drainage area was observed to increase markedly just after the rain ceased and before the runoff decreased gradually to zero. This apparent paradox results from the established fact that the resistance to flow during rainfall is significantly greater than the resistance to flow at the same rate of runoff after rainfall has ceased. Consequently, the surface detention in the equilibrium stage during rainfall is greater than that necessary to maintain the same rate of total runoff after the rain has ceased. The increase in runoff is thus the discharge of the excessive amount of water in detention.

---

[3] Research Assistant, Iowa Inst. of Hydr. Research, Iowa City, Iowa.

[4] "Contribution à l'Étude des Eaux Courants," by H. Favre, Rascher & Cie., Zurich, Leipzig, and Stuttgart, 1933.

[5] "Lateral Spillway Channels," by Thomas R. Camp, *Transactions*, ASCE, Vol. 105, 1940, pp. 606–617.

[6] "Miscellanées," *La Houille Blanche*, No. 4, 1950, pp 498–500.

[7] *Ibid.*, No. 1, 1951, pp. 72–75.

The author's introduction of the dimensionless parameter, G, makes possible a more significant presentation than those made by previous investigators. The parameters used by Mr. Li, however, could have been obtained by a dimensional analysis of the problem in the following form:

$$\frac{y_u}{y_o} = f(\mathsf{F}, G) \qquad (43)$$

For various types of cross sections, Eq. 43 has been presented graphically (Figs. 3 and 6). Although Mr. Li considered channels of various cross sections, he included only channels of constant width. This unnecessary restriction, particularly for large structures, makes impossible the achievement of economy in construction material. If both the width of the channel and the slope of the weir crest are varied, an increase in capacity and a resulting economy in material can be obtained.

Because the discharge is proportional to the $\frac{3}{2}$ power of the head on the weir, the equation of momentum (using the notation shown in Fig. 9) can be written as

$$\begin{aligned} &- \rho\, g\, (\beta\, x + b_u)\, y\, \Delta y - \rho\, g\, \beta\, \frac{y^2}{2}\, \Delta x + \rho\, g\, y\, (\beta\, x + b_u)\, S_o\, \Delta x \\ &- \rho\, g\, f\, \frac{Q^2{}_x}{A^2{}_x} \frac{1}{8\, g} \frac{b_x\, y}{R_x}\, \Delta x = 2\, \delta\, \gamma\, \frac{[(\epsilon\, x + H_u)^{\frac{5}{2}} - H^{\frac{5}{2}}{}_u] H^{\frac{3}{2}}{}_x}{y(\beta\, x + b_u)} \\ &\times \left(1 - \frac{\Delta y}{y} - \frac{\beta\, \Delta x}{\beta\, x + b_u}\right) \Delta x \qquad (44) \end{aligned}$$

in which f is the Darcy-Weisbach resistance coefficient, R_x denotes the hydraulic radius of the cross section,

$$\beta = \frac{b_o - b_u}{L} \qquad (45a)$$

$$\gamma = \frac{2}{3}\, C\, \sqrt{2\, g} \qquad (45b)$$

$$\delta = \frac{2}{5} \frac{\gamma}{\epsilon} \qquad (45c)$$

and

$$\epsilon\, \alpha = \frac{H_o - H_u}{L} \qquad (45d)$$

The existing relationships are

$$H_x = \epsilon\, x + H_u \qquad (46a)$$

$$b_x = \beta\, x + b_u \qquad (46b)$$

$$A_x = y(\beta\, x + b_u) \qquad (46c)$$

$$R = \frac{y(\beta\, x + b_u)}{2\, y + \beta\, x + b_u} \qquad (46d)$$

$$q = \Delta Q = \gamma\, H^{3/2}{}_x \qquad (46e)$$

$$Q_x = \gamma \int_0^x (\epsilon\, x + H_u)^{3/2}{}_{dx} = \delta[(\epsilon\, x + H_u)^{5/2} - H^{5/2}{}_u] \qquad (46f)$$

and

$$Q_o = \delta(H^{5/2}{}_o - H^{5/2}{}_u) \qquad (46g)$$

The surface profile can be obtained from a known depth of flow by numerical integration. In this manner the free fall of the nappe near the outlet is decreased. Because the rate of inflow and the distance of free fall have opposing effects, the net amount of impact cannot be predicted. Nevertheless, considerable economy in construction material can be attained.

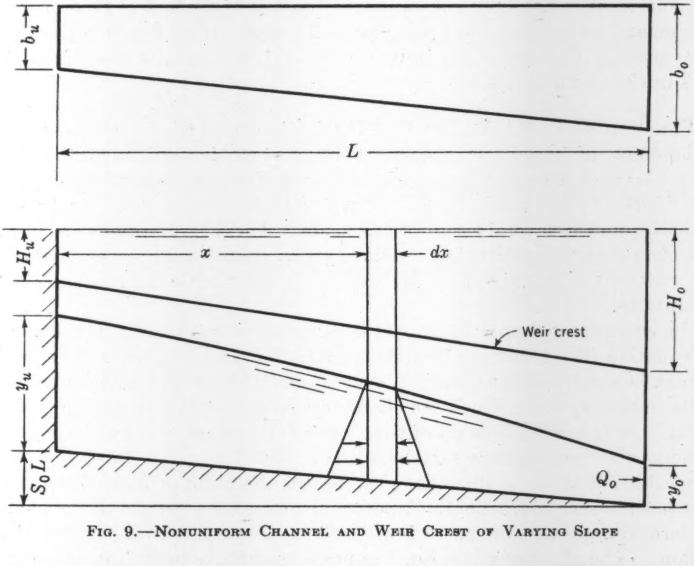

FIG. 9.—NONUNIFORM CHANNEL AND WEIR CREST OF VARYING SLOPE

Pertinent to this discussion are comments on the uncertainties of the control sections and on the experimental results. The author states (under the heading, "Channels with Parallel Side Walls: Channels with Level Bottom") that:

> "When free fall occurs at the outlet end, the flow is critical, and therefore, $\mathbf{F}_o = 1$. The depth y_o can be computed through the knowledge of Q_o."

This is not quite precise; actually, the depth at the rim of the fall is considerably less than the critical depth ($0.655\, y_c$ to $0.715\, y_c$).[8,9] The distance between the location of the critical depth and the rim of the fall has been found[8] to be approximately $11.6\, y_c$. However, the uncertainty of the control sections should be remembered—not only in the case of a free fall—but also in all the other cases cited by Mr. Li.

The experiments made by the author to demonstrate the validity of his results are remarkable. Unfortunately, no mention was made as to the method whereby this highly disturbed, wavy, air-entrained water surface was measured in order to obtain such precise results. It is stated (under the heading, "Channels with Parallel Side Walls: Channels with Level Bottom"):

> "Thus, the corresponding observed and computed values are in agreement. The application of the momentum equation to this case is therefore acceptable."

This statement is not fully substantiated because of the lack of theoretical and experimental knowledge concerning several important factors involved in the phenomenon. Compensating factors may tend to minimize the effect of the errors in the assumptions.

WEN-HSIUNG LI,[10] A.M. ASCE.—The fundamental relationship used in the development of the basic theory is Euler's momentum theorem.[11] This theorem is exact as long as it is possible to apply Newton's laws of motion and to treat fluids as continuous media. Eq. 1 follows immediately for prismatic channels from the several assumptions made. These assumptions are justified by the fact that the results thus obtained are substantiated by experiments; the main part of the discussion by Mr. Sarpkaya deals with the exactness of the assumptions.

The energy loss caused by impact does not appear explicitly in the momentum equation (Eq. 1) but has been included in the various terms in the equation. This can be seen from the fact that, even when frictional loss is neglected, Eq. 1 results in flow systems which are characterized by a decrease in energy downstream. As in the application of the momentum equation to hydraulic jumps, no energy-loss term is necessary in Eq. 1.

In addition to the component v' along the direction of flow, the incoming water has another component, v'', perpendicular to the bottom of the channel. The term v'' does not appear in Eq. 1 because it is written for the direction of the flow. The effect of v'' on Eq. 1 appears as changes in (1) the velocity distribution over each cross section and (2) the wall friction in the direction of the flow. Such changes can be accounted for in Eq. 1 by using the proper velocity distribution and frictional coefficient, which, unfortunately, are unknown (as of 1954). By making assumptions 2 and 4 (under the heading, "The Momentum Equation") in obtaining Eq. 1, it was implied that the effect of v'' is only secondary in the flow systems that were cited. That these assumptions are justified can be seen from the test results listed in Table 1. In these tests, the magnitude of v'', although varying along the channel in each test and varying also from test to test, did not affect the validity of Eq. 9. This investigation of the effect of v'' is interesting but does not affect the validity of the results presented; they have been obtained by neglecting the frictional resistance. That this resistance can be neglected in practical cases has been demonstrated quantitatively in Fig. 8.

---

[8] "Handbook of Hydraulics," by H. W. King, McGraw-Hill Co., Inc., New York, N. Y., 3d Ed., 1939, pp. 389-390.

[9] "Fluid Mechanics for Hydraulic Engineers," by H. Rouse, McGraw-Hill Book Co., Inc., New York, N. Y., 1938, p. 323.

[10] Asst. Prof. of Civ. Eng., The Johns Hopkins Univ., Baltimore, Md.

[11] "Theoretical Hydrodynamics," by L. M. Milne-Thomson, The Macmillan Co., New York, N. Y., 1950, p. 74.

The critical depth is the depth of flow with minimum specific energy which has physical meaning only when the pressure distribution is hydrostatic. In the analysis of flow in open channels, the pressure distribution, for simplicity, is usually assumed to be hydrostatic with the inherent result that the depth at a free drop is equal to the critical depth. The well-known discrepancy between this result and the experimental observations is caused by the curvature of the water surface which causes the pressure distribution to depart from the hydrostatic distribution. This effect of surface curvature has been mentioned in assumption 3 in the derivation of Eq. 1. The departure of the depth at a free outlet from the critical depth depends on the flow and the geometry of the structure; in this problem the depth and geometry are different from those which occur in flat channels with uniform flow, for which Mr. Sarpkaya has cited several values. The critical depth has been used for the free outlet of channels with $G \leq 2$ in order to be consistent with assumption 3. When applied, this approximation does not change the result appreciably. For cases with critical depth in the channel, the surface curvature at the critical section is very small, and the error caused by using this assumption is always negligible.

These assumptions were made so as to obtain practicable results for a large variety of channel sections in terms of three simple dimensionless parameters. Without these justifiable assumptions, these practicable, simple results would not have been possible.

Prismatic channels with uniform bottom slope and uniform addition of water have been investigated. These channels were chosen because they are the most commonly used channels. By citing these channels, the writer does not rule out the possibility of other types of channels. Eq. 1 is completely applicable to prismatic channels with nonuniform slope and nonuniform addition of water. Mr. Sarpkaya uses Eq. 1 in deriving Eq. 44 with the omission of the term involving v'. He also seems to have neglected the component of the pressure force on the tapered walls in the direction of the flow. The channel with a sloping weir crest (as suggested by Mr. Sarpkaya) may result in a less expensive structure, but the economic advisability of the arrangement for spillways is questioned because the storage volume of the reservoir below the weir crest is reduced with a sloping weir crest—even though the same high water level in the reservoir during the design flood is maintained.

In the experiments reported by the writer, the water-surface elevation was measured with a point gage. Each of the depths listed in Table 1 and Table 2 is the average of ten readings. In these experiments, a phenomenon of practical interest was observed which the writer did not cite in order to maintain continuity in the presentation. It was observed that the weir can be drowned to a depth of approximately $H/2$ without decreasing its capacity. Thus, the required depth of channel at the upstream end is only $(y_u - \frac{1}{2} H)$. A margin of safety will be provided if a depth equal to y_u is used.

One might question the method in which Eq. 43 was obtained through dimensional analysis of a problem involving so many variables. Eq. 43 should involve the dimensionless parameter B. Without examining the differential equations and their results, the advisabiltiy of using the parameters $\mathbf{F}_o$, G, and B for various cross-sectional shapes could not have been ascertained. Because the functional relationship must be obtained by integrating the differential equations, dimensional analysis is not useful in this case.

To Mr Sarpkaya's list of previous investigators one might add C. N. Miller[12,13] and M. F. Stein.[14]

---

[12] "An Approximate Formula for Calculating the Discharge Capacity of Rapid Sand Filter Wash Water Troughs," by C. N. Miller, Appendix B, in "Water Purification," by J. W. Ellm, McGraw-Hill Book Co., Inc. New York, N. Y., 1928.

[13] "Diagram for the Design of Wash Water Gutters," by C. N. Miller, *Engineering News-Record*, Vol. 90, 1923, p. 882.

[14] "The Design of Wash Water Troughs for Rapid Sand Filters," by M. F. Stein, *Journal*, A.W.W.A. Vol. 13, 1925, p. 411.

AMERICAN SOCIETY OF CIVIL ENGINEERS
Founded November 5, 1852
TRANSACTIONS

Paper No. 2738

CORRECTION OF LANDSLIDES AND SLIPOUTS

By Arthur W. Root,[1] A. M. ASCE

Synopsis

Correction of landslides and slipouts has been a major problem in highway construction and maintenance in California. The author presents measures for the corrective treatment of landslides which have been found to be successful in California. It should be realized, however, that treatment is determined for each location after exploration and analysis of the slide. There is no universal method for correcting all landslides; each slide must be studied as an individual problem.

Introduction

Property damage, interruption in and interference with transportation and communication, and even loss of life are a few of the consequences of landslides. In California—a state which has a wide variety of geologic, topographic, and climatic conditions—landslides constitute a serious problem in highway design, construction, and maintenance. Corrective treatment of landslides affecting California highways requires an average annual expenditure of several hundred thousand dollars.

Landslide Classification

Corrective treatment of landslides cannot be planned intelligently without some knowledge of the types, causes, and mechanics of landslides. According to Karl Terzaghi,[2] Hon. M. ASCE,

> "The term landslide refers to a rapid displacement of a mass of rock, residual soil, or sediments adjoining a slope, in which the center of gravity of the moving mass advances in a downward and outward direction."

Slipout.—One type of landslide most troublesome to highway engineers is the slipout—a landslide occurring at or below roadway grade. During a slipout

---

Note.—Published, essentially as printed here, in August, 1953, as *Proceedings-Separate No. 235.* Positions and titles given are those in effect when the paper was received for publication.

[1] Superv. Materials and Research Engr., Materials and Research Dept., State Div. of Highways, Sacramento, Calif.

[2] "Mechanism of Landslides," by Karl Terzaghi, from "Application of Geology to Engineering Practice," a symposium, Geological Soc. of America, Berkey volume, 1950, pp. 88–123.

part or all of the roadbed moves downward and outward. Slipouts generally occur where the roadbed is partly on an embankment; a typical slipout does not extend above the roadway grade. If, however, the surface of rupture is deep, the head of the slipout may be within the cut slope above the road.

There are many types of landslides which can be classified[3] according to rate of movement, type of soil, ground-water and moisture conditions, geological structure, and other variables.

Slump Slide.—The most common and most troublesome landslide is of the slump type—in which a large mass of soil moves with relatively little deformation along an internal slip surface (or surface of rupture). The trace of the surface of rupture on a vertical plane along the axis of the slide commonly (although not necessarily) approximates a circular arc. At the toe of a slump slide there is often a "push-up" or upheaval. Roadway slipouts are generally slump slides. Ground water is an important factor in causing slump slides.

Rock Slide.—Another type of slide, the rock slide, which is fairly common and sometimes of considerable magnitude, is more readily recognizable than most other types, and its causes are more apparent. The movement is frequently controlled by zones of weakness such as contact planes between weak strata or weak bedding planes. The general group of rock slides includes "bedding-plane" slides and slides of talus or detritus. Ground water is seldom the primary cause of these movements. Numerous other types of landslides could be listed, but most of the slides to which corrective treatment has been applied in California have been slump slides.

LANDSLIDE CORRECTION

Regardless of the type of landslide, the slide movement occurs when the driving force exceeds the resisting force. The driving force consists of gravitational force and sometimes seepage forces or hydrostatic pressure; the resisting force is the shearing resistance of the soil mass. Prevention and correction of slides involve either reduction of the driving force or increase in the resisting force, or perhaps a combination of the two. These corrective measures can be accomplished by a number of different methods.

Investigation.—The first and one of the important steps in the correction of a landslide is the exploration and analysis of the slide. Seldom can the most economical and successful treatment be determined from a superficial inspection of the slide. A contour map of the slide and the adjacent terrain is of help in analyzing the problem; a geologic study should be made to determine the bedding, structure, and nature of the rock. Borings are essential for locating the rupture surface, determining ground-water conditions, and—where necessary—obtaining undisturbed soil samples for laboratory tests. With this information the slide can be analyzed, its causes can be determined, and various kinds of corrective treatment can be compared in order to determine the most economical treatment which will provide reasonable assurance of stability. In most cases there are several possible alternate methods of correction, and the choice must be based on costs, with proper consideration of the probable effectiveness of the alternate treatments. In addition to all the studies and computations, the final design will necessarily be influenced by experience, judgment, and perhaps some intuition on the part of the engineer.

---

[3] "Landslides and Related Phenomena," by C. F. Stewart Sharpe, Columbia University Press, New York, N. Y., 1938, p. 10.

The preliminary investigation is essentially the same for the roadway slipout and the slide above grade. Although corrective treatment for the two may differ somewhat, the differences are not sufficient to warrant separate examination herein. The various slide treatments with which engineers in California have had experience will be described subsequently, with comments on their applicability to the two types of land movement.

Drainage.—Frequent reference will be made subsequently to ground water and subdrainage. Thus, it seems important to comment on the effect of ground water so that the importance of drainage will be clearly understood. The popular concept of moisture causing slides by lubrication of the soil is considered to be fallacious. Ground water acts in two ways to induce slide movement: (*a*) The weight of a soil mass increases appreciably as the soil becomes wet, thus adding to the driving force tending to cause movement; and (*b*) the presence of water results in a reduction of the shear strength of the soil. If the soil is not cohesive, a rise in the water table results in a lowering of the effective soil weight, with a corresponding reduction in the available shearing strength. In the case of cohesive soils the cohesion decreases with increasing moisture content. If excess hydrostatic pressures develop, the normal forces contributing to the frictional resistance of the soil may become nil; the soil then possesses little or no internal friction. In addition to these two factors, ground-water movement may result in seepage forces within the soil mass, thus adding to forces inducing slide movement. Water is undoubtedly the most important single factor contributing to slide movement.

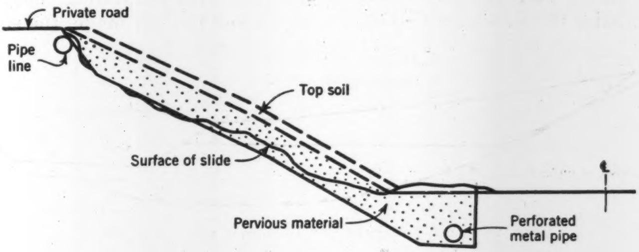

FIG. 1.—SLIDE TREATMENT BY PERVIOUS BLANKET AND UNDERDRAIN

Seepage may cause failures of cut slopes even though major landslides do not develop. In 1948, shortly after the construction of a project in Monterey County (California), a small slide developed in one of the cut slopes and progressed so far that a private road and gas line above the cut slope were jeopardized. In Fig. 1 there is shown a typical cross section of this slide. The slide action appeared to be caused by ground water and seepage and was successfully treated by placing a blanket of pervious material on the face of the cut and installing an underdrain along the gutter line. This type of treatment—with various modifications—has been applied successfully in several cases where the slope failures were the result of progressive weakening of the cut slope rather than being true landslides in which large masses of soil had moved.

Change of Alinement.—The most obvious method of correcting a slide is to avoid it by changing the alinement of the highway. Occasionally the highway can be shifted into stable ground at slight cost and without impairing the alinement. Such a possibility, although infrequent, should not be overlooked.

There have been instances in California where, as a result of slide movement in adjacent cut slopes, the roadway was raised, causing objectionable distortion and humps in the grade line. In at least two such cases it was feasible to raise the grade line through the slide area; by the placement of approximately 10 ft of embankment over the push-up areas, the slides were stabilized as a result of the added surcharge weight at the toe of the slide.

This type of corrective treatment is illustrated in Fig. 2, which shows a typical cross section through a roadway in San Diego County (California). In this case a slide and push-up of the roadbed occurred during construction (1949). After the slide area had been mapped and borings made, the slide was analyzed by the techniques of conventional soil mechanics. These studies indicated that the removal of any reasonable amount of slide material would not affect the desired stability. However, by constructing a strut fill at the toe of the slide and by removing a small quantity of material near the head of the slide, the factor of safety would be increased from 0.8 to approximately 2.0. Accordingly, the roadway grade through the cut was raised 8 ft, and the material for constructing the embankment required by the higher grade line was obtained by benching the cut slope, as depicted in Fig. 2.

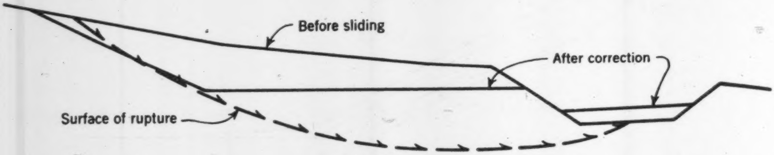

FIG. 2.—SLIDE TREATMENT BY BENCHING AND STRUT FILL

The majority of slides cannot be corrected by line or grade changes; therefore, some method must be found to improve one of the two basic factors affecting stability—that is, either the driving force must be reduced or the shear resistance must be increased.

SLUMP SLIDES

In the case of a slump slide in which the cut slope or natural ground above the roadway slides onto or across the roadbed, two types of treatment have been used successfully in California: (*a*) Reduction of the driving forces by removing weight at the head of the slide, or by benching or flattening the slope; (*b*) subdrainage, either by horizontal drains or by drainage trenches. If the slide is shallow and the transverse slope is relatively flat, the first method is often most economical. If the slide is large, and especially if the transverse slope of the terrain is steep, it is often uneconomical to remove sufficient material to stabilize the slide by this method alone. In such cases horizontal drains have proved most effective; only in very shallow slides are drainage trenches normally feasible.

The unloading of a slide must be carefully planned as removal of material from the wrong area may reduce stability rather than improve it. It has been the experience of engineers in California that benches are essential, both to provide surface drainage and to intercept the seepage that usually occurs in this type of slide; the benches also prevent rocks or mud from falling on the traveled way. The design of excavation slopes and location of benches are based on the data obtained in the preliminary investigation of the slide.

Horizontal Drains.—Increased incidence and severity of landslides are a result of the increasingly large cuts and fills necessitated by continuous improvements in the geometric standards of highways in California. Realizing the importance of adequate subdrainage in the prevention and correction of landslides, California highway engineers attempted to devise more effective and economical methods of drainage. Although the idea of installing perforated drainpipes in drilled horizontal holes did not originate in California, the California State Division of Highways (hereafter referred to as the Division of Highways) pioneered the development of practicable methods and equipment for installing horizontal drains. These methods—or modifications of them—have been used by several other agencies. The first installation of horizontal drains by the Division of Highways was made in 1939; since then (as of 1953) an aggregate of approximately 200,000 lin ft of drains have been installed at approximately one hundred slide locations in California. Although slide movement has continued at a few of these locations, the vast majority of the horizontal-drain installations have effectively stabilized the slides or reduced the slide activity to a negligible amount. The largest single installation of horizontal drains by the Division of Highways was at the Orinda slide in Contra Costa County where approximately 12,000 lin ft of drains were installed.[4]

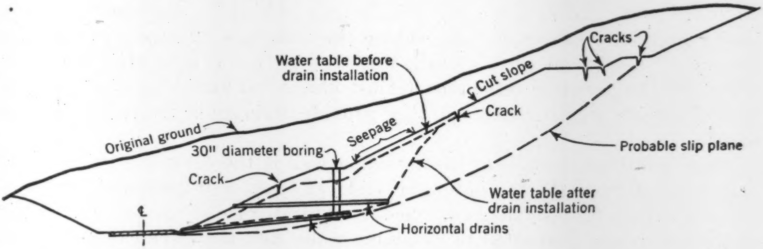

Fig. 3.—Slide Treatment by Horizontal Drain

A typical example of slide correction by the use of horizontal drains is a roadway cut in San Luis Obispo County (California) where a large slide occurred during construction. In Fig. 3 there is shown a typical cross section of this slide. The water table dropped rapidly after the drains were installed, and no further slide movement has occurred (as of 1953).

---

[4] "Orinda Slide," by E. W. Herlinger and Gifford Stafford, *California Highways and Public Works*, Div. of Highways, State of California Dept. of Public Works, Sacramento, Calif., January-February, 1952, p. 45.

When horizontal drains are to be installed, the slide is first resloped to improve surface runoff, and benches are constructed at the levels from which the drains are to be installed. Vertical exploratory borings are helpful in locating the water-bearing layers; these borings serve as a guide in fixing the location and gradient of the drains and also provide observation wells for recording the effect of the drains on the ground-water level.

Piles, Bulkheads, and Retaining Walls.—A commonly suggested method of combating slide movement is the use of piles, bulkheads, or retaining walls. It has been the experience of engineers in California that such treatment is successful only in exceptional cases; the forces involved in a large landslide are of such magnitude that in most cases the added restraint furnished by piles or walls is insufficient to produce stability, and as a result the retaining structure is sheared or displaced. Walls and bulkheads, however, have been used successfully in certain cases where the slide was relatively shallow and the rate of movement slow. These walls act in two ways to stabilize slides: They provide increased resistance against movement and, when the walls are backfilled with pervious material, they provide drainage at the toe of the slide mass.

One useful application of the retaining wall is the control of talus slides. Any excavation at the toe of a talus slide will induce movement which continues until the talus slope has reached its natural angle of repose. Movement at the toe can be prevented by retaining walls, and the slope can thereby be stabilized. The forces exerted by the talus slide are small in comparison to those exerted by the slump slide.

A few slides in California have been corrected by a modification of the retaining-wall principle. Where the slip surface is above roadway level the usual retaining wall would sometimes be founded on an unsound foundation or, if extended down to firm footing, the total height would be excessive. At one location where this condition existed, a wall of nominal height was constructed in the slope at the surface of rupture, with heavy reinforced concrete struts extending down the slope to a footing below roadway grade. To prevent uplift of the wall as a result of the thrust of the slide pressure, cast-in-place concrete piles were tied to the bottom of the retaining wall. This type of slide treatment has limited application; it is cited as an example of treatment especially designed for a particular slide.

ROCK SLIDES

Most of the treatments cited previously refer exclusively to the slump slides—the most frequent and at the same time the most difficult to analyze and correct. Rock slides especially of the bedding-plane type are common, but the choice of corrective treatment is rather limited. From a geologic study the rock formation, dip and strike, and competency are determined; thus, corrective treatment can be devised. This treatment usually consists of excavating sufficient material to prevent further slide movement along the bedding planes or zones of weakness within the rock formation.

SLIPOUTS

All the slide-correction methods cited previously have been for landslides in slopes above roadway grade. Although large volumes of earth are excavated annually from such slides and considerable money is expended in their correction, roadway slipouts cause greater interference to the free movement of traffic and are often more costly and more difficult to correct. The very nature of a slipout prevents the application of some of the treatments used in stabilizing slides in roadway cuts. In a slipout the soil mass which comprises the driving weight consists of the embankment and roadbed; therefore, the removal of weight from the head of the slide is not feasible. The slipout may be corrected by three general methods: (*a*) Drainage, either by horizontal drains or by stabilization trenches; (*b*) construction of a toe support or strut fills at the toe of the slipout; or (*c*) an increase of the shearing resistance by constructing buttresses at the toe. The last method, although to some extent a preventive treatment, has been applied infrequently as corrective treatment.

Several large slipouts have been corrected by excavating a system of stabilization trenches, placing filter material on the bottoms and slopes of the trenches, and then restoring the embankment.[5] When this method is applied, the stabilization trenches are excavated down to firm material below the slip surface, thus contributing a considerable increment of shear strength in addition to providing subdrainage. If the slipout is small, one such transverse trench may be sufficient; however, a large slipout may require an extensive system of drainage trenches, frequently in a herringbone pattern. This method of slipout correction has been very successful; however, it is costly and, if the embankment is high and the slide is deep, the cost of correction by this method is sometimes prohibitive.

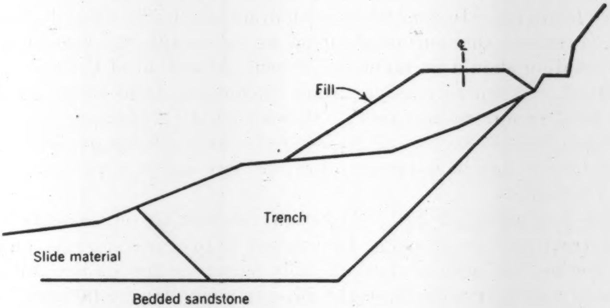

FIG. 4.—CORRECTION OF A SLIPOUT BY TRENCHING

A large slipout on the Redwood Highway in Humboldt County (California) was corrected by stabilization trenches. Approximately two years after construction, a large embankment slipped out necessitating construction of a detour to permit the movement of traffic. Borings and geologic study showed that the slipout was caused by seepage forces in a mantle of disintegrated shale and sandstone which was underlain by firm sandstone. Various methods of correcting the slipout, including realinement of the road, were compared. The adopted treatment, which consisted of stabilization trenches, is depicted in Fig. 4.

---

[5] "Problem of Slipouts Studies by State Highway Engineers," by A. W. Root, *California Highways and Public Works*, Div. of Highways, State of California Dept. of Public Works, Sacramento, Calif., March, 1938, p. 18.

Horizontal Drains.—Installation of horizontal drains is often the most economical method of correcting roadway slipouts. The drains are usually installed from the toe of the embankment and—if necessary—from one or more benches on the fill slope. The location, number, length, and gradient of the drains are estimated from boring data but are modified according to conditions observed during the progress of the work.

A slipout which occurred on the Redwood Highway in Humboldt County is a typical example of treatment by the installation of horizontal drains. The entire outer shoulder had slipped out, and there was serious settlement of one traffic lane. Borings revealed that ground water was causing the slipout, and study of the slide indicated that horizontal drains would be the most economical corrective treatment. After the drains were installed the embankment was restored, and the pavement was built up to the original grade. There has been no subsequent slide movement (as of 1953).

Surface Drainage.—In connection with drainage of slipouts and other slides, it should be realized that surface drainage as well as subdrainage is important. Every precaution should be taken to prevent saturation of the slide mass by surface runoff. When necessary, surface ditches should be constructed above the slide to intercept storm runoff. Slopes should be reshaped, and benches or ditches constructed to carry off surface water as rapidly as possible. Paving of surface ditches may be required to prevent percolation of surface water into the slide material.

Strut or Counterweight Fill.—Although subdrainage of some type is the corrective treatment most frequently applied to roadway slipouts, an entirely different method has been used successfully where the terrain is suitable—that is, the use of a strut or counterweight fill. In a circular-arc failure of a slump slide, the soil at the toe tends to move outward and upward. The application of a surcharge weight at the proper location adds to the forces resisting slide movement and will tend to stabilize the slide. This principle is often applied to the design of embankments over unstable foundation soil, by placing toe support fills outside the normal slope lines. If the toe of a slipout is on level terrain, or if there is a stable bank or stable ascending slope just outside the toe of the slipout, the construction of a strut fill may provide sufficient resistance to produce stability. However, the slide must be carefully analyzed to assure that the toe support fill itself will not be unstable, and that the added fill weight is placed where it will be most effective.

Combination of Methods.—In 1952, one year after completion of a California freeway, a roadway slipout near San Francisco, Calif., caused loss of one traffic lane and jeopardized the remaining lanes. Because of the heavy volume of traffic it was imperative that the slipout be corrected quickly and with a minimum of interference to traffic. After borings were made to determine the depth of the slide and to locate ground water, the corrective treatment was determined. A transverse stabilization trench was excavated along the axis of the slide, a drainage trench was constructed along the toe of the slipout, horizontal drains were installed, and a toe support fill was constructed. In Fig. 5 there is shown a typical cross section of the slipout.

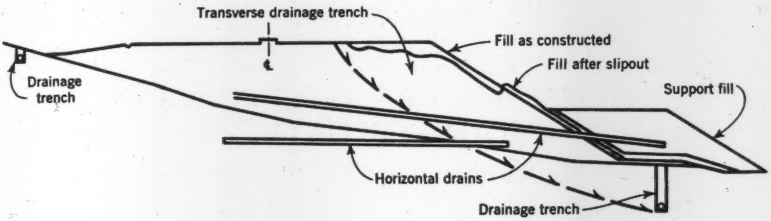

Fig. 5.—Slipout Treatment by a Combination of Methods

CONCLUSIONS

Correction of landslides and slipouts has been a major problem in highway construction and maintenance in California. Numerous methods of correction have been applied. The corrective treatment is determined for each location after exploration and analysis of the slide; there is no simple universal method of correcting all landslides. It is much easier and cheaper to prevent a landslide than to correct it. Too often, much money is expended in the correction of a landslide or slipout that could have been prevented by relatively inexpensive treatment during construction.

ACKNOWLEDGEMENT

The material on which the illustrative material was based was obtained from the Materials and Research Department of the Division of Highways. T. W. Smith, A. M. ASCE, assisted in compiling these data, and H. R. Cedergren, A. M. ASCE, made many constructive and helpful comments.

AMERICAN SOCIETY OF CIVIL ENGINEERS
Founded November 5, 1852
TRANSACTIONS

Paper No. 2739

DISCHARGE CHARACTERISTICS OF TAINTER GATES

BY ARTHUR TOCH,[1] J. M. ASCE

SYNOPSIS

Although Tainter gates are widely used to control the flow of water, little has been known about their discharge characteristics. Two methods that can be used to describe these characteristics are presented. The discharge coefficients of the Tainter gate for free flow and submerged flow are shown in their relationships to parameters expressing the geometry of the gate. With the aid of a simplified theoretical analysis, the energy loss occurring during submerged flow is depicted in a similar manner. The methods that are applied to Tainter gates should be applicable to other gate shapes.

INTRODUCTION

Prediction of the efflux characteristics of Tainter gates in the course of their design has been possible until now (1953) only through specific model studies. Therefore, general methods are required for the evaluation of these characteristics; these evaluations should prove to be of use in the design and operation of gates.

Previous Studies.—Tainter gates are in the general class of devices for the control of water which also includes sluice gates and roller gates. A short survey of previous studies of these devices is presented to indicate the extent of their applicability.

Efflux from two-dimensional slots has sometimes been related to efflux from gates. Thus, the coefficient of contraction for slots—that is, the ratio of limiting jet thickness to slot height—derived[2] by R. von Mises has been considered applicable to sluice gates. Mr. von Mises' analysis contains the usual assumptions of the free-streamline theory of hydrodynamics—constant velocity along the free streamline and constant pressure across the jet at infinity. The com-

---

NOTE.—Published, essentially as printed here, in October, 1953, as *Proceedings-Separate No. 295.* Positions and titles given are those in effect when the paper was received for publication.

[1] Research Associate, Iowa Inst. of Hydr. Research, State Univ. of Iowa, Iowa City, Iowa.

[2] "Berechnung von Ausfluss- und Überflusszahlen," by R. von Mises, *Zeitschrift,* Vereines deutscher Ingenieure, 1917, p. 47.

puted contraction coefficient varies widely with the ratio of gate opening to headwater depth. The extent to which this analysis applies to the actual gate efflux can only be determined by comparison with experimental data.

A mathematical treatment of sluice-gate efflux has been presented[3] by G. Pajer. In this analysis the velocity along the free streamline was assumed to vary with elevation. This premise contains, implicitly, the concept of hydrostatic pressure distribution in the sections of uniform flow. Variation of the coefficient of contraction with the ratio of gate opening to headwater depth is small in comparison to the large variation obtained for slots. Mr. Pajer has shown that the analytically derived jet profiles agree with experimental measurements. The values of the contraction coefficient determined from actual flow are, of course, always larger than the corresponding computed values for irrotational flow because the jet geometry is modified by the decelerative action of the boundary shear. Moreover, contraction coefficients derived from this analysis are based on the section of uniform flow at infinity whereas continued boundary resistance causes the actual vena contracta to be located only a short distance from the gate.

Mr. Pajer's mathematical treatment of efflux from a sluice gate can only be applied to the limiting condition of a Tainter gate with infinite radius and 90° lip angle. Application of the free-streamline theory to the curved surface of the Tainter gate is, unfortunately, not feasible because of the mathematical difficulties usually involved in treating any boundaries other than straight, solid boundaries. Hydrodynamic theory in the form of the relaxation method[4] can be used to obtain theoretical solutions for the curved Tainter gate. This method is extremely tedious, however, and each solution is applicable only to the particular geometric proportions chosen.

Because of the limitations imposed by the assumptions of irrotationality[5] any such application of hydrodynamic theory must be confined to free-jet efflux, for which the tailwater does not interfere with the jet emanating from the gate. Under conditions of submerged efflux, for which the tailwater depth is greater than the sequent depth at which the jet would form a hydraulic jump, an approximation of the actual flow can be computed by using the continuity and impulse-momentum equations and by a modification of the Bernoulli equation; this method will be presented subsequently. Similar derivations have been published[6] but not in readily applicable form.

R. E. Horton has proposed[7] another method of determining the free-jet efflux from Tainter gates. Recurrent references indicate the advisability of including it in this review. In this method a constant multiplier was used to convert "theoretical" to actual discharge coefficients. The multiplier was devised by comparing a limited number of experimentally determined discharge coefficients with the corresponding "theoretical" coefficients. The experimental coefficients were apparently obtained by using a sluice gate having a beveled lip. The equation by which the "theoretical" discharge coefficients are computed was determined[8] by A. Koch and M. Carstanjen for contraction coefficients and was based on several approximations which are far removed from actual flow conditions. Any agreement between coefficients derived from actual Tainter-gate discharge and the "theoretical" coefficients is therefore fortuitous.

---

[3] "Über den Strömungsvorgang an einer unterströmten scharfkantigen Planschütze," by G. Pajer, *Zeitschrift für angewandte Mathematik und Mechanik*, Vol. 17, No. 5, 1937, p. 259.

[4] "Applications of the Relaxation Technique in Fluid Mechanics," by J. S. McNown, E. Y. Hsu, and C. S. Yih, *Transactions*, ASCE, Vol. 120, 1955.

[5] "Hydrodynamics," by G. Birkhoff, Princeton University Press, Princeton, N. J., 1950.

[6] "Technische Hydraulik," by C. Jaeger, Birkhäuser, Basel, Switzerland, 1949, p. 146.

[7] "Discharge Coefficients for Tainter Gates," by R. E. Horton, *Engineering News-Record*, January 4, 1934, p. 10.

The amount of experimental study of the Tainter gate is considerable. Many small-scale tests have been made, often on models for particular projects. The usual efflux equation was generally used, and an attempt was made to find that definition of head which would give minimum variation of the discharge coefficient. Agreement has not yet (1953) been reached as to which definition of head—total depth, depth to midheight of opening, or another depth—should be used for the best results. This disagreement can be resolved by noting that all such definitions are in simple geometric relationship to each other and that no one of them is significant for the entire geometric range.

The lack of coordinated knowledge prompted this study, in which a systematic graphical representation of the relationships between the pertinent variables will be presented subsequently. An approximate analysis, based on several assumptions, permits the energy changes for submerged efflux to be assessed.

EXPERIMENTAL PROCEDURE

To permit generalization from the variety of field installations of Tainter gates that exist, laboratory studies were made on simply designed models at the Iowa Institute of Hydraulic Research in Iowa City. The first of these models consisted of a gate and pier simulating a specific project.[9,10] The gate had a radius of 2.17 ft and a fixed trunnion height of 1.42 ft. The gate opening of the model was adjustable, as was that of the prototype. In the second model the pier was eliminated, but the trunnion height of the gate was adjustable.[11] The radius of this gate was 1 ft. Both models were located in laboratory flumes of rectangular cross section with level floors, 30 in. and 12 in. wide, respectively.

Water was supplied from the circulation system of the laboratory, and the flow was measured by calibrated elbow meters and air-water manometers. The depths of flow upstream and downstream from the gates were measured by point gages and by manometers connected to piezometric openings in the floors of the flumes.

Both series of experiments were made according to the following system: For a given gate opening and discharge, the tailwater elevation was varied and the headwater was free to reach a corresponding depth. In the first series several gate openings, each with a number of discharges, were tested in this manner. Similar runs were made in the second series of experiments, in which the trunnion height was also varied.

---

[8] "Bewegung des Wassers und dabei auftretende Kräfte," by A. Koch and M. Carstanjen, Julius Springer, Berlin, Germany, 1926.

[9] "A Model Study of Tainter-Gate Operations," by Donald E. Metzler, thesis presented to the State Univ. of Iowa, at Iowa City, in 1948, in partial fulfilment of the requirements for the degree of Master of Science.

[10] "Model Studies Aid in Design of Brazilian Hydro-Project," by Emmett M. Laursen, *Civil Engineering*, January, 1951, p. 44.

[11] "The Effect of Lip Angle upon Flow under a Tainter Gate," by Arthur Toch, thesis presented to the State Univ. of Iowa, at Iowa City, in 1952, in partial fulfilment of the requirements for the degree of Master of Science.

EXPERIMENTAL RESULTS

General Considerations.—As previously noted, two different states of efflux, free-jet flow and submerged flow, can occur in the flow of water through a gate. In the case of free-jet flow, loss of energy in passage through the gate opening is small. In the case of submerged efflux, a considerable part of the kinetic energy of the flow is dissipated in diffusion directly downstream from the gate. The transition from free-jet flow to submerged flow can be idealized as a hydraulic jump which is approaching the gate from downstream. The characteristics of the free-jet efflux will exist until the toe of the jump reaches the gate.

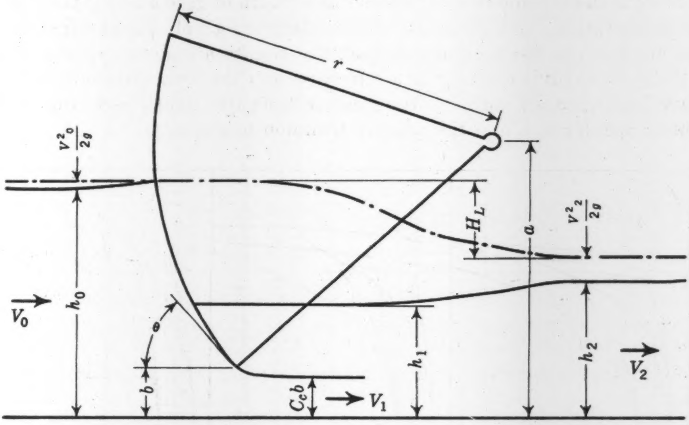

FIG. 1.—DEFINITION SKETCH

As soon as this position is reached, an increase in the headwater depth occurs for a constant rate of flow. The headwater depth continues to increase as the tailwater level rises, and the water surface just below the gate also changes. From the state of turbulent aeration of the jump at initial submergence, the flow attains a progressively smoother and more level surface as the depth of flow increases until aeration becomes negligible and the surface elevation at the gate is only slightly lower than the subsequent level of the tailwater. These visible changes are evidently accompanied by a modification of the form of diffusion. As the depth of submergence increases and aeration becomes less noticeable, the energy of the jet is dissipated with decreasing production of surface waves.

The over-all problem of gate efflux can be considered to be a function of the geometry of the gate alone despite the fact that the complex mechanism of diffusion is involved. Two distinct methods of describing the efflux in terms of the geometric proportions of the gate and the flow are presented subsequently.

In Fig. 1, a definition sketch, there are shown the variables which are of primary importance in the study of the Tainter gate. It should be noted that the loss of head in the uniform flow sections upstream and downstream from the gate is ignored. Also, only two-dimensional flow will be considered herein, with the exception of the contraction coefficients that were obtained from the first model study.

Systematized Characteristics.—Donald E. Metzler has shown[12] that a discharge coefficient for the Tainter gate can be graphically related to the ratios of various pertinent boundary lengths. The coefficient of discharge C_d was defined as

$$C_d = \frac{q}{b\sqrt{2\,g\,h_0}} \qquad (1)$$

in which q is the volume rate of flow per unit width of gate and g is the gravitational acceleration. An extension of Mr. Metzler's graph was obtained by the writer by varying the trunnion height; the results are shown in Fig. 2. In Fig. 2 the gate radius r is used as a reference, and the basic parameters are the relative headwater depth h_0/r, the relative tailwater depth h_2/r, the relative height of opening b/r, and the relative trunnion height a/r.

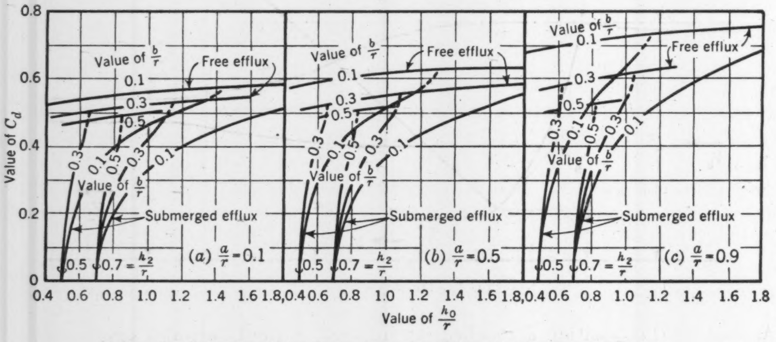

FIG. 2.—COEFFICIENT OF DISCHARGE FOR FREE AND SUBMERGED FLOW

In Fig. 2 the curves rising from the axis of $C_d = 0$ pertain to submerged efflux. The limiting curves on the upper parts of Fig. 2 pertain to free efflux. Fig. 2 contains the curves for three ratios of a/r and for several values of the other parameters. It is evident that for free-jet efflux the changes which occur in the magnitude of the discharge coeffiicent are relatively small, although the relative headwater depth is widely varied. In the case of submerged flow, however, a wide variation in C_d occurs for the same change in h_0/r. The influence of the other parameters is also apparent in Fig. 2. In order to obtain the discharge corresponding to given numerical values of the geometric variables, the appropriate ratios can be formed and C_d can be found from Fig. 2.; Eq. 1 can then be used to compute the discharge to be expected.

---

[12] "Engineering Hydraulics," edited by Hunter Rouse, John Wiley & Sons, Inc., New York, N. Y., 1950, p. 540.

Free Efflux.—An essential part of the discharge analysis is the evaluation of the effect of the lip angle on the jet contraction. In the case of free efflux the lip angle can be seen (Fig. 3) to affect the coefficient of contraction C_c considerably. As is to be expected, C_c increases with decreasing lip angle because the free streamline leaves the lip of the gate in a more nearly horizontal direction. The scatter of the experimental points, which is partly the result of the difficulty of measuring accurately the depth of the jet, is undoubtedly also caused by the effect of b/h_0. That at least some variation of C_c with b/h_0 should occur can be deduced from the variation in the contraction coefficient obtained[3] by Mr. Pajer for the sluice gate. The lack of experimental evidence is not surprising because the variation is presumably no more pronounced for the Tainter gate than for the sluice gate.

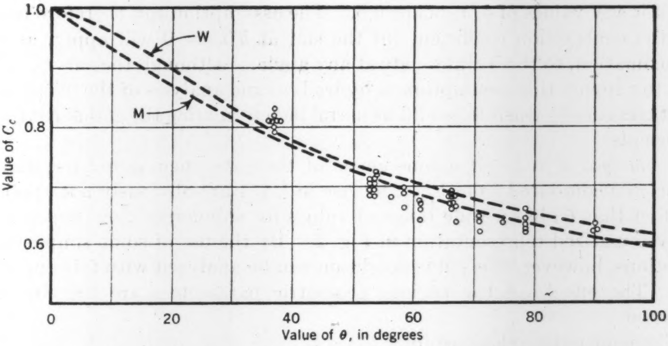

FIG. 3.—EFFECT OF LIP ANGLE ON THE COEFFICIENT OF CONTRACTION

If the discharge coefficient defined by Eq. 1 is to be evaluated from the coefficient of contraction, recourse must be had to the equations of continuity and energy. The resulting relationship,

$$C_d = \frac{C_c}{\sqrt{1 + C_c \dfrac{b}{h_0}}} \quad \text{.......................} \quad (2)$$

if correct, should yield values of C_d in agreement with those obtained from Eq. 1. Corresponding values obtained from Eq. 2 using representative values from the plotted points in Fig. 3 indicate a maximum variation of approximately 10% in C_d for the writer's data. If the relationship between C_c and b/h_0 can be clearly determined, the agreement should be closer. Some difference will always exist because the assumption of constant energy implicit in Eq. 2, although approximately correct, is not exactly satisfied in real flow.

For reasons cited previously, analytical values for the contraction coefficients of Tainter gates are not available. Two curves for somewhat different flow conditions are therefore plotted in Fig. 3 for comparison. Curve M is the locus of the contraction coefficients computed by Mr. von Mises for a slot with straight inclined walls at $b/h_0 = 0$. Curve W similarly locates experimental contraction coefficients determined by J. Weisbach for efflux from a slot at presumably very small (b/h_0)-values. The data for curves M and W were obtained from Mr. von Mises' work[2] on discharge coefficients.

If the axis of symmetry of these slots is assumed to be replaced by a solid surface, there results a boundary geometry comparable to that of a gate. At $\theta = 90°$ the gate would be equivalent to a sluice gate, and at any angle it could be considered to be a Tainter gate with infinite radius. Mr. Pajer has shown[3] that the theoretical coefficient of contraction of the sluice gate is approximately 0.611 for any values of b/h_0 below 0.5. The assumption can therefore be made that the contraction coefficient for the slot at $b/h_0 = 0$ will apply, as a first approximation, to the Tainter gate at any angle. Although the curves in Fig. 3 seem to support this assumption, a hydrodynamic analysis of the Tainter gate, if mathematically feasible, would be useful in determining the actual contraction coefficients.

Submerged Efflux.—If submergence of the gate opening occurs, discharge coefficients computed from Eq. 2 for use in Eq. 1 are obviously not applicable. The fact that C_d has a wide range of values for submerged flow was shown by the systematized representation in Fig. 2. By the use of some simplifying assumptions, however, this efflux condition can be analyzed with fair approximation. The effects of the various geometric parameters are thereby clearly indicated.

The continuity relationships,

$$q = V_0 h_0 = V_1 C_c b = V_2 h_2 \quad \text{.................. (3)}$$

the energy equations,

$$\frac{V^2_0}{2g} + h_0 = \frac{V^2_1}{2g} + h_1 = \frac{V^2_2}{2g} + h_2 + H_L \quad \text{............ (4)}$$

and the momentum equation,

$$\tfrac{1}{2} g \left(h^2_2 - h^2_1\right) = q \left(V_1 - V_2\right) \quad \text{.................. (5)}$$

can be combined to obtain theoretical relationships for the gate efflux. Eqs. 3 express the premise of continuity of flow. Eqs. 4 are based on the assumption that all loss of head occurs in the zone of diffusion between sections 1 and 2 (Fig. 1). In Eqs. 4 and 5 it is assumed that hydrostatic pressure distribution prevails not only in the tranquil-flow sections but also at section 1 immediately downstream from the gate. Furthermore, Eqs. 3, 4, and 5 are written in terms of mean velocities, which implies that the velocity is constant across each section. Eqs. 3 and 4 can be solved simultaneously for the discharge to result in

$$q = h_2 \sqrt{\frac{2g\left(h_0 - h_2\right)}{\psi + 1 - \left(\frac{h_2}{h_0}\right)^2}} \quad \text{.................. (6)}$$

in which ψ is the head-loss parameter and can be represented as

$$\psi = \frac{H_L}{\frac{V^2_2}{2\,g}} \qquad (7)$$

To obtain an expression for the commonly used discharge coefficient C_d, the discharge q is eliminated from Eqs. 1 and 6 so that

$$C_d = \frac{h_2}{b}\sqrt{\frac{\frac{h_0 - h_2}{h_0}}{\psi + 1 - \left(\frac{h_2}{h_0}\right)^2}} \qquad (8)$$

For free efflux $h_2 = C_c\,b$, and, if $H_L = 0$, Eq. 8 reduces to Eq. 2.

If Eqs. 3, 4, and 5 are solved simultaneously, an expression for the head-loss parameter can be obtained—

$$\begin{aligned} \psi = {} & \left(\frac{1}{\beta}\right)^2 - 1 \\ & + \frac{\gamma^2\,(\beta - 1)}{\gamma\,\beta - 2\,(\alpha - 1) \pm \sqrt{[2\,(\alpha - 1) - \gamma\,\beta]^2 - \gamma^2\,(\beta^2 - 1)}} \qquad (9) \end{aligned}$$

In Eq. 9

$$\alpha = \frac{h_2}{C_c\,b} \qquad (10a)$$

$$\beta = \frac{h_0}{h_2} \qquad (10b)$$

and

$$\gamma = \left(\frac{h_2}{C_c\,b}\right)^2 - \left(\frac{h_2}{h_0}\right)^2 \qquad (10c)$$

A plot of Eq. 9 is shown in Fig. 4(*a*) as dashed curves. For various values of h_2/h_0 these curves can be seen to branch off from a common base line, the locus of

$$\frac{H_L}{\frac{V^2}{2\,g}} = \left(\frac{y_2}{y_1}\right)^2 - 4\,\frac{\frac{y_2}{y_1}\left(\frac{y_2}{y_1 - 1}\right)}{\frac{y_2}{y_1 + 1}} - 1 \qquad (11)$$

which pertains to the hydraulic jump. Eq. 11 is derived in a manner similar to Eq. 9. The depths y_1 and y_2 are equivalent to the depths $C_c\,b$ and h_2, respectively, for the Tainter gate if the jump occurs at the vena contracta.

Data obtained in the second series of experiments were analyzed in the manner indicated by the theoretical development, and the results were plotted in Fig. 4(*a*) as points connected by solid curves. Because the geometry of the submerged jet could not be directly determined, the coefficient of contraction

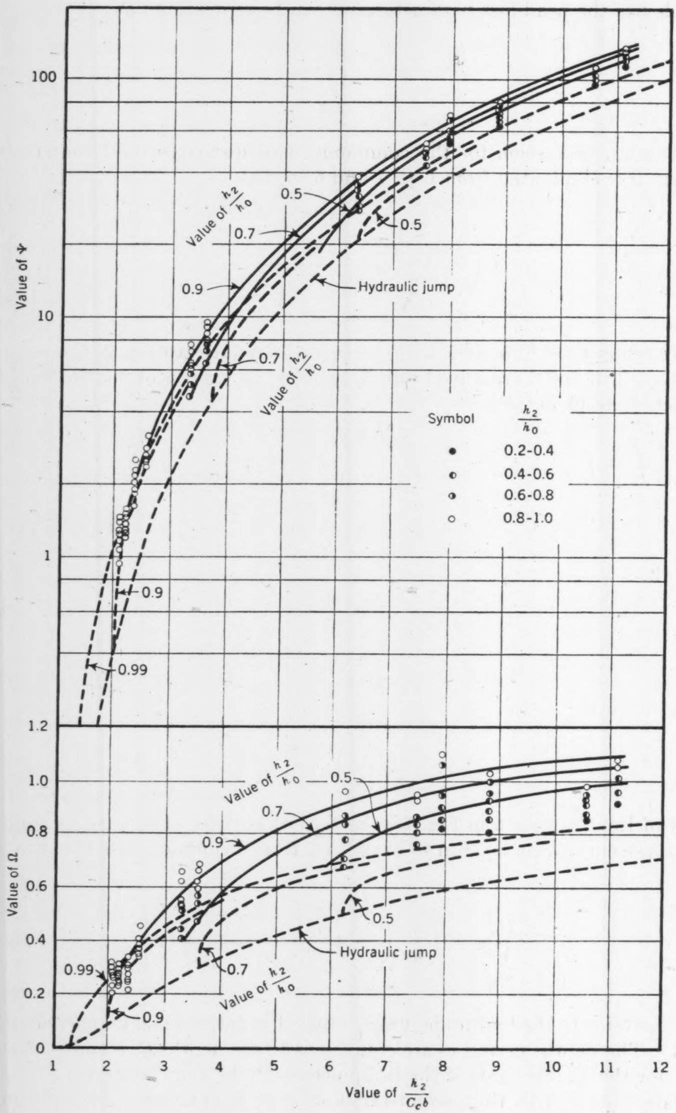

FIG. 4.—HEAD-LOSS PARAMETERS Ω AND Ψ FOR SUBMERGED EFFLUX

was assumed to be the same as that for free efflux, although this assumption is not completely correct. For a known lip angle, C_c was obtained from a mean curve through the plotted points in Fig. 3. All other values are based on directly measured quantities for submerged flow. The similarity in trend between the analytic and experimental curves is evident as is the difference in their respective locations. For a clearer comparison of the simplified analysis with experimental data, Fig. 4(*b*) is presented. The difference between Figs. 4(*a*) and 4(*b*) is the use of the jet-velocity head instead of the downstream velocity head in the head-loss parameter,

$$\Omega = \frac{H_L}{\frac{V^2_1}{2\,g}} \qquad (12)$$

This change, easily accomplished numerically by multiplication of ψ by $(C_c\, b/h_2)^2$, makes the plot more significant principally because the new head-loss parameter shows the energy loss as a decimal fraction of the energy of the jet. The dashed lines in Fig. 4(*b*), which are analytic results, show the theoretically necessary tendency toward a limit of $\Omega = 1$ at large values of $h_2/(C_c\, b)$. For the experimental points and the curves derived from them, the same general shape can be noted, but the limit does not apply.

The lack of agreement in location between the analytically determined curves and those derived from experimental data results from Eqs. 4 and 5. In these equations some assumptions were made which are known to be merely approximations of the actual efflux from gates but which were desirable because of the resultant mathematical simplicity. Therefore, the square of the mean velocity was used as an indication of the kinetic energy in each section although the mean of the squares of the actual velocity distribution may be considerably larger. The effect of boundary shear was completely ignored as were the complex flow conditions existing at section 1. The assumption of hydrostatic pressure distribution and the use of the mean velocity of the jet may be only rough approximations of the mechanics of diffusion and of the roller above the jet. Eqs. 4 and 5 should therefore be expressed as integrals[13] if a more accurate solution is required. For the purpose of this study the simplified analysis is sufficient, however, because the important parameters are easily discernible and the functional trend of the equations, as shown in Fig. 4, would not be greatly changed by the refinements mentioned.

CONCLUSIONS

Discharge characteristics of Tainter gates, which until now (1953) were usually determined only for individual gates, can be functionally represented for both free efflux and submerged efflux. The systematic graphs[9] of the relationship between the discharge coefficient and the geometry of the gate and flow as presented by Mr. Metzler have been extended to include the effect of a variable trunnion height. Further extension of these graphs would permit representation of any desired geometry including those of piers and sills. Such an extension would not affect the simplicity of computing the discharge.

---

[13] "Elementary Mechanics of Fluids," by Hunter Rouse, John Wiley & Sons, Inc., New York, N. Y., 1946, pp. 111–113.

Although a complete theoretical analysis of the discharge characteristics does not seem possible at present (1953), the existing theoretical tools can be applied to ascertain the important parameters and the functional trends among them. Under conditions of free efflux, Mr. von Mises' contraction coefficient[2] for slots with inclined walls has been shown to approximate the variation with the lip angle of the coefficient of actual Tainter gates. The effect of the ratio of gate opening to headwater depth is indicated, moreover, by Mr. Pajer's analysis[3] of the sluice gate.

Similarly, a one-dimensional analysis of the flow not only results in the parameters pertinent to the effects of submergence but also indicates the nature of the functional relationships among them. In essence, in this analysis the effects of submergence are separated from those of contraction. The latter must be assumed, at present, to be the same for submerged efflux as for free efflux. A single family of curves should be sufficient, however, to determine the head-loss parameters for all jet geometries, without regard to gate geometry.

The results of the model studies presented herein are directly applicable to Tainter-gate installations on level floors. Their reliability, of course, would be enhanced by comparison with prototype data, because the effect of lip shape and of viscous forces were not determined in the models. The general methods of analysis of these data are applicable to other types of gates.

ACKNOWLEDGMENTS

Gratitude is expressed for the encouragement and advice given by Hunter Rouse, M. ASCE, and Emmett M. Laursen, A.M. ASCE. Mr. Metzler, who was the writer's adviser on the thesis on which the present study is based, is thanked for permission to use the data he had collected in his investigation.

AMERICAN SOCIETY OF CIVIL ENGINEERS
Founded November 5, 1852
TRANSACTIONS

Paper No. 2740

CONSTRAINED CIRCULAR BEAMS ON ELASTIC FOUNDATIONS

BY ENRICO VOLTERRA,[1] M. ASCE, AND RANDALL CHUNG[2]

SYNOPSIS

The problem of a circular beam resting on an elastic foundation, loaded by concentrated symmetric forces, and constrained in such a way that the sections where the vertical loads are applied cannot rotate is solved in explicit form.

Tables for the deflections, angles of twist, and bending and twisting moments are presented.

NOTATION

The letter symbols in this paper are defined where they first appear, in the text or by diagram, and are assembled alphabetically in Appendix III.

INTRODUCTION

In earlier papers (1) (2) (3)[3] the problem of the deflections of a circular beam resting on an elastic foundation and loaded by symmetric or antisymmetric forces has been studied. The beam was assumed free to rotate where the loads were applied.

R. D. Mindlin, A. M. ASCE, of Columbia University (New York, N. Y.) commented during the discussion which followed the presentation of one of the papers (1) that frequently the vertical concentrated loads are transmitted to the circular beam through structural members that are rigidly connected to the beam. These structural members restrain the beam at the points of application of the concentrated loads from rotating about the center line of the beam (Fig. 1).

The purpose of this paper is to analyze deflections of circular beams under such conditions of restraint and to express their deflections, angles of twist, and bending and twisting moments in explicit forms as functions of the externally applied forces P, the section characteristics $E\ I_x$ of the beam, the

---

NOTE.—Published, essentially as printed here, in July, 1953, as *Proceedings-Separate No. 205*. Positions and titles given are those in effect when the paper was received for publication.

[1] Prof., Dept. of Mechanics, Rensselaer Polytechnic Inst., Troy, N. Y.

[2] Structural Engr., Dominion Bridge Co., Montreal, Que., Canada.

[3] Numerals in parentheses, thus: (1), refer to corresponding numbers in the bibliography (Appendix II).

elastic constant k of the foundation, and the angular distance 2γ between the forces. For particular values of the angles 2γ—namely, $2\gamma = 120°, 90°, 60°, 45°$, and $30°$, tables giving the values of the deflections, angles of twist, and bending and twisting moments are presented subsequently.

The following assumptions are made: (*a*) The beam has constant section characteristics $E I_x$, and its axis is a circle of radius R. (*b*) At equidistant points, equal concentrated forces P are applied, the angular distance between the forces being indicated by 2γ (Fig. 1). (*c*) The sections where the loads are applied are not free to rotate. (*d*) The foundation reacts following the Winkler-Zimmermann hypothesis—that is, the reactive forces exerted by the foundation material are proportional at every point to the deflection of the beam at that point (4) (5) (6).

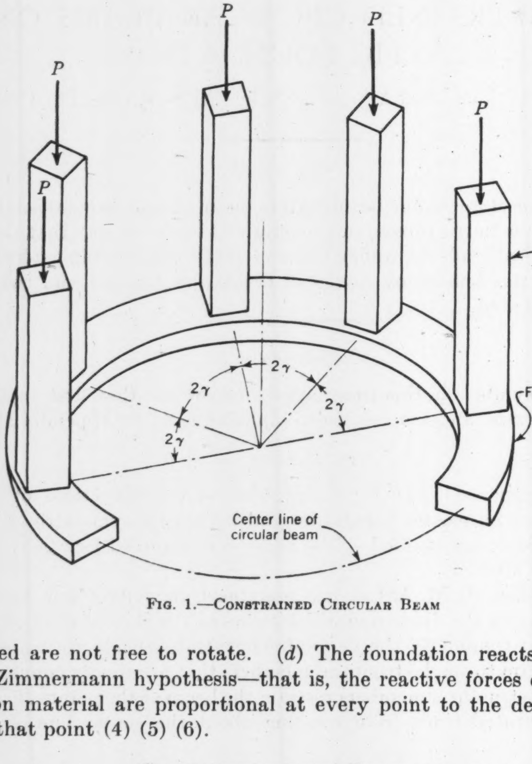

Fig. 1.—Constrained Circular Beam

Statement of the Problem

The beam is referred to a system of rectangular coordinates, O x y z, being the origin O at the centroid of the cross section, the axes x and y coinciding with the principal axes of inertia of the cross section, and the axis z, with the tangent to the center line at O (Fig. 2). If v is the displacement of the centroid O in the direction of the y-axis, s the arc length along the center line, β the angle of twist of the cross section about the z-axis, M_x and M_z the moments acting on the cross section at point O about the x-axis and z-axis, $E I_x$ the flexural rigidity, K the torsional rigidity, and $1/R$ the initial curvature of the center line of the bar—the two following equations will be verified (1) (3) (7) (8) (9):

$$\left.\begin{aligned} E\,I_x\left(\frac{\beta}{R}-\frac{d^2v}{ds^2}\right) &= M_x \\ K\,\theta = K\left(\frac{d\beta}{ds}+\frac{1}{R}\frac{dv}{ds}\right) &= M_z \end{aligned}\right\}\dots\dots\dots\dots\dots\dots(1)$$

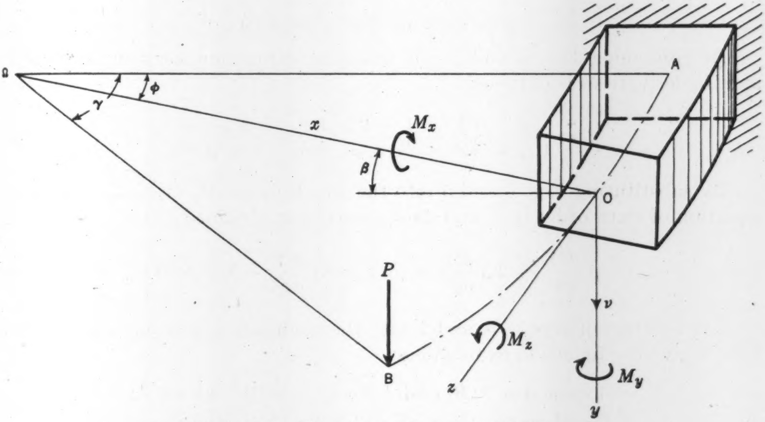

Fig. 2.—Beam Referred to Coordinate System

If k is the elastic constant of the foundation, P the external concentrated force, and $2\,\gamma$ the angular distance between the points of application of the external forces (Figs. 1 and 2), $Y = \frac{v}{R}$; $a = \frac{E\,I_x}{R}$; $\mu = \frac{K}{E\,I_x}$; $\nu = \frac{P\,R^2}{E\,I_x}$; and $\lambda = \frac{k\,R^4}{E\,I_x}$. Eqs. 1 become

$$\left.\begin{aligned} a\left(\beta-\frac{d^2Y}{d\phi^2}\right) &= M_x \\ \mu\,a\left(\frac{d\beta}{d\phi}+\frac{dY}{d\phi}\right) &= M_z \end{aligned}\right\}\dots\dots\dots\dots\dots\dots(2)$$

The conditions of equilibrium are

$$\left.\begin{aligned} \frac{dM_z}{d\phi}-M_x &= 0 \\ \frac{d^2M_x}{d\phi^2}+\frac{dM_z}{d\phi}-a\,\lambda\,Y &= 0 \end{aligned}\right\}\dots\dots\dots\dots\dots\dots(3)$$

and the boundary conditions in this case are

$$\left.\begin{aligned} \beta\,(\gamma) = \beta\,(-\,\gamma) &= 0 \\ Y\,(\gamma) = Y\,(-\,\gamma) & \end{aligned}\right\}\dots\dots\dots\dots\dots\dots(4a)$$

$$\left.\begin{aligned}\frac{dY(\gamma)}{d\phi} &= \frac{dY(-\gamma)}{d\phi}\\ \frac{d^2Y(\gamma)}{d\phi^2} &= \frac{d^2Y(-\gamma)}{d\phi^2}\end{aligned}\right\}\dots\dots\dots\dots\dots\dots\dots\dots(4b)$$

and

$$\frac{dM_x(\gamma)}{d\phi} - \frac{dM_x(-\gamma)}{d\phi} = a\,\nu\dots\dots\dots\dots\dots\dots\dots(4c)$$

SOLUTION OF THE PROBLEM

By combining Eqs. 2 and 3, the following expression for β in terms of Y and its derivatives is obtained:

$$\beta = \frac{\mu}{1+\mu}\frac{d^4Y}{d\phi^4} + \frac{1+2\mu}{1+\mu}\frac{d^2Y}{d\phi^2} + \frac{\lambda\mu}{1+\mu}\frac{dY}{d\phi}\dots\dots\dots\dots(5)$$

By substituting Eqs. 3 and 5 into the equation for M_z (Eqs. 2), the linear equation of sixth order in Y and its derivatives is obtained:

$$\mu\frac{d^6Y}{d\phi^6} + 2\mu\frac{d^4Y}{d\phi^4} + \mu(1+\lambda)\frac{d^2Y}{d\phi^2} - \lambda Y = 0\dots\dots\dots\dots(6)$$

The solution of Eqs. 6, 5, and 2 with the boundary conditions expressed by Eqs. 4 give the following expressions:

$$\left.\begin{aligned}Y &= A\cosh m\phi + B_1\cosh r\phi\cos t\phi + B_2\sinh r\phi\sin t\phi\\ \beta &= C\cosh m\phi + D_1\cosh r\phi\cos t\phi + D_2\sinh r\phi\sin t\phi\\ M_x &= (F\cosh m\phi + G_1\cosh r\phi\cos t\phi + G_2\sinh r\phi\sin t\phi)\,a\\ &\text{and}\\ M_z &= (H\sinh m\phi + J_1\sinh r\phi\cos t\phi + J_2\cosh r\phi\sin t\phi)\,a\end{aligned}\right\}\dots(7)$$

in which m, r, and t are determined from the formulas:

$$\left.\begin{aligned}m &= \sqrt{\xi + \eta - \frac{2}{3}}\\ r &= \frac{1}{2}\sqrt{\frac{2}{m}\left(\frac{\lambda}{\mu}\right)^{\frac{1}{3}} - m^2 - 2}\\ &\text{and}\\ t &= \frac{1}{2}\sqrt{\frac{2}{m}\left(\frac{\lambda}{\mu}\right)^{\frac{1}{3}} + m^2 + 2}\end{aligned}\right\}\dots\dots\dots\dots\dots\dots(8a)$$

In the expression for m,

$$\left.\begin{aligned}\xi &= \frac{1}{3}\sqrt[3]{9\lambda + 1 + \frac{27\lambda}{2\mu} + \left[27\lambda(\lambda+1)^2 + \frac{9\lambda+1}{\mu} + \frac{27\lambda}{4\mu^2}\right]^{\frac{1}{2}}}\\ &\text{and}\\ \eta &= \frac{1}{3}\sqrt[3]{9\lambda + 1 + \frac{27\lambda}{2\mu} - \left[27\lambda(\lambda+1)^2 + \frac{9\lambda+1}{\mu} + \frac{27\lambda}{4\mu^2}\right]^{\frac{1}{2}}}\end{aligned}\right\}\dots(8b)$$

The constants are expressed as follows:

$$\left.\begin{aligned}
A &= \frac{\nu\,(r\,Q_1 + t\,Q_2)}{2\,m\left(r\,S_1 + t\,S_2 - \dfrac{2\,r\,t}{1+\mu}\,T\sqrt{\dfrac{\lambda}{\mu}}\right)} \\
B_1 &= -\,\frac{\nu\left[\mu\,m\,U\sinh m\,\gamma + \left(m^2 + \dfrac{\lambda}{m^2} - \mu\right)X\cosh m\,\gamma\right]}{2\,\mu\,m\left(r\,S_1 + t\,S_2 - \dfrac{2\,r\,t}{1+\mu}\,T\sqrt{\dfrac{\lambda}{\mu}}\right)} \\
&\text{and} \\
B_2 &= -\,\frac{\nu\left[\mu\,m\,V\sinh m\,\gamma - \left(m^2 + \dfrac{\lambda}{m^2} - \mu\right)Z\cosh m\,\gamma\right]}{2\,\mu\,m\left(r\,S_1 + t\,S_2 - \dfrac{2\,r\,t}{1+\mu}\,T\sqrt{\dfrac{\lambda}{\mu}}\right)}
\end{aligned}\right\}\ldots\ldots(9)$$

in which

$$Q_1 = (m^2+1)^2\left(-1 + \frac{m}{\sqrt{\lambda\,\mu}}\right)\sin t\,\gamma\cos t\,\gamma \ldots\ldots\ldots (10a)$$

$$Q_2 = -\,(m^2+1)^2\left(1 + \frac{m}{\sqrt{\lambda\,\mu}}\right)\sinh r\,\gamma\cosh r\,\gamma \ldots\ldots\ldots (10b)$$

$$S_1 = (m^2+1)\left[\lambda\left(\frac{1}{\mu\,m^2} - 2\right) + \frac{2\,m^2+1}{m}\sqrt{\frac{\lambda}{\mu}}\right]\sinh m\,\gamma\sin t\,\gamma\cos t\,\gamma \ldots (10c)$$

$$S_2 = (m^2+1)\left[\lambda\left(\frac{1}{\mu\,m^2} - 2\right) - \frac{2\,m^2+1}{m}\sqrt{\frac{\lambda}{\mu}}\right] \times \sinh m\,\gamma\sinh r\,\gamma\cosh r\,\gamma \ldots (10d)$$

$$T = \frac{1+m^2}{m^2}\left(m^2 + \frac{\lambda}{m^2} - \mu\right)\cosh m\,\gamma\,(\sinh^2 r\,\gamma\cos^2 t\,\gamma + \cosh^2 r\,\gamma\sin^2 t\,\gamma) \ldots (10e)$$

$$U = \left[\frac{1}{2}\left(m^2 + \frac{1}{\mu}\right)(m^2+2) + 1\right]\sinh r\,\gamma\sin t\,\gamma + 2\,r\,t\left(m^2 - \frac{1}{\mu}\right) \times \cosh r\,\gamma\cos t\,\gamma \ldots (10f)$$

$$V = -\left[\frac{1}{2}\left(m^2 + \frac{1}{\mu}\right)(m^2+2) + 1\right]\cosh r\,\gamma\cos t\,\gamma + 2\,r\,t \times \left(m^2 - \frac{1}{\mu}\right)\sinh r\,\gamma\sin t\,\gamma \ldots (10g)$$

$$X = r\cosh r\,\gamma\sin t\,\gamma + t\sinh r\,\gamma\cos t\,\gamma \ldots\ldots\ldots\ldots (10h)$$

and

$$Z = r\sinh r\,\gamma\cos t\,\gamma - t\cosh r\,\gamma\sin t\,\gamma \ldots\ldots\ldots\ldots (10i)$$

Likewise,

$$F = \frac{A\,\mu}{1+\mu}\left(\frac{\lambda}{\mu\,m^2} - m^2 - 1\right) \ldots\ldots\ldots\ldots\ldots\ldots (11a)$$

$$\left.\begin{aligned} G_1 &= -\frac{\mu}{2\,(1+\mu)}\,(1+m^2)\,(m^2\,B_1 + 4\,r\,t\,B_2) \\ \text{and} \qquad & \\ G_2 &= -\frac{\mu}{2\,(1+\mu)}\,(1+m^2)\,(m^2\,B_2 - 4\,r\,t\,B_1) \end{aligned}\right\}\ldots\ldots\ldots(11b)$$

$$H = \frac{F}{m}\ldots\ldots\ldots\ldots\ldots\ldots\ldots\ldots\ldots(11c)$$

$$\left.\begin{aligned} J_1 &= m\,\sqrt{\frac{\mu}{\lambda}}\,(r\,G_1 - t\,G_2) \\ \text{and} \qquad & \\ J_2 &= m\,\sqrt{\frac{\mu}{\lambda}}\,(r\,G_2 + t\,G_1) \end{aligned}\right\}\ldots\ldots\ldots\ldots\ldots(11d)$$

NUMERICAL TABLES

The values of the functions β/ν, Y/ν, $M_x/(a\,\gamma)$, and $M_s/(a\,\gamma)$ are given in Tables 1, 2, and 3 for the following values of the parameters:

$$\lambda = 60, \quad \mu = 0.7; \quad \lambda = 100, \quad \mu = 0.7$$
$$\lambda = 60, \quad \mu = 1.0; \quad \lambda = 100, \quad \mu = 1.0.$$

TABLE 1.—DEFLECTIONS, ANGLES OF TWIST, AND BENDING AND TWISTING MOMENTS

DIMENSIONLESS PARAMETERS		ϕ, in degrees	Ratio, $\frac{Y}{\nu}$	Ratio, $\frac{\beta}{\nu}$, in radians	$\frac{M_x}{a\,\nu}$	$\frac{M_s}{a\,\nu}$
λ	μ					
			$2\,\gamma = 120°$			
60	0.7	0	0.000765	0.025504	−0.027786	0
		10	0.001570	0.024198	−0.026544	−0.004780
		20	0.003902	0.020025	−0.021398	−0.009044
		30	0.007469	0.013813	−0.008300	−0.011791
		40	0.011673	0.006654	0.018768	−0.011130
		50	0.015458	0.000806	0.066487	−0.004035
		60	0.017188	0.000000	0.140059	0.013592
60	1.0	0	0.000835	0.023236	−0.029301	0
		10	0.001629	0.021999	−0.027973	−0.005039
		20	0.003929	0.018414	−0.022594	−0.009534
		30	0.007454	0.012936	−0.009176	−0.012463
		40	0.011614	0.006579	0.018209	−0.011926
		50	0.015370	0.001232	0.066157	−0.004908
		60	0.017092	0.000000	0.139811	0.012671
100	0.7	0	−0.000520	0.019018	−0.016618	0
		10	0.000021	0.018112	−0.017019	−0.002927
		20	0.001627	0.015406	−0.016567	−0.005897
		30	0.004188	0.011042	−0.010423	−0.008384
		40	0.007367	0.005655	0.008925	−0.008770
		50	0.010391	0.000981	0.050354	−0.003982
		60	0.011843	0.000000	0.121438	0.010543
100	1.0	0	−0.000482	0.017425	−0.017854	0
		10	0.000054	0.016615	−0.018180	−0.003138
		20	0.001644	0.014201	−0.017521	−0.006295
		30	0.004182	0.010318	−0.011092	−0.008924
		40	0.007337	0.005515	0.008543	−0.009401
		50	0.010344	0.001175	0.050182	−0.004660
		60	0.011791	0.000000	0.121342	0.009844

TABLE 1.—(*Continued*)

DIMENSIONLESS PARAMETERS		ϕ, in degrees	Ratio, $\frac{Y}{\nu}$	Ratio, $\frac{\beta}{\nu}$, in radians	$\frac{M_x}{a\nu}$	$\frac{M_z}{a\nu}$
λ	μ					
$2\gamma = 90°$						
60	0.7	0	0.006335	0.017598	−0.043027	0
		10	0.007237	0.015783	−0.036459	−0.007130
		20	0.009686	0.010887	−0.015351	−0.011885
		30	0.012885	0.004640	0.024001	−0.011429
		40	0.015440	0.000163	0.086021	−0.002185
		45	0.015869	0.000000	0.126474	0.007040
60	1.0	0	0.006379	0.016396	−0.044266	0
		10	0.007267	0.013850	−0.037641	−0.007343
		20	0.009680	0.009670	−0.016389	−0.012293
		30	0.012837	0.004292	0.023126	−0.012003
		40	0.015367	0.000305	0.085252	−0.002901
		45	0.015702	0.000000	0.125720	0.006258
100	0.7	0	0.002662	0.015340	−0.035777	0
		10	0.003385	0.013815	−0.031054	−0.005974
		20	0.005479	0.009650	−0.014760	−0.010174
		30	0.008269	0.004207	0.018815	−0.010124
		40	0.010556	0.000177	0.076825	−0.002181
		45	0.010948	0.000000	0.116707	0.006209
100	1.0	0	0.002659	0.013451	−0.036951	0
		10	0.003411	0.012148	−0.032157	−0.006174
		20	0.005478	0.008579	−0.015681	−0.010552
		30	0.008238	0.003885	0.018099	−0.010645
		40	0.010504	0.000296	0.076243	−0.002813
		45	0.010894	0.000000	0.116143	0.005527

TABLE 2.—DEFLECTIONS, ANGLES OF TWIST, AND BENDING AND TWISTING MOMENTS FOR $2\gamma = 60°$

DIMENSIONLESS PARAMETERS		ϕ, in degrees	Ratio, $\frac{Y}{\nu}$	Ratio, $\frac{\beta}{\nu}$, in radians	$\frac{M_x}{a\nu}$	$\frac{M_z}{a\nu}$
λ	μ					
60	0.7	0	0.014517	0.006623	−0.039032	0
		5	0.014689	0.006242	−0.035562	−0.003305
		10	0.015174	0.005168	−0.025103	−0.006004
		15	0.015884	0.003601	−0.007514	−0.007479
		20	0.016675	0.001879	0.017388	−0.007102
		25	0.017342	0.000476	0.049767	−0.004227
		30	0.017631	0.000000	0.089673	0.001803
60	1.0	0	0.014523	0.005613	−0.039559	0
		5	0.014692	0.005295	−0.036086	−0.003351
		10	0.015172	0.004396	−0.025617	−0.006095
		15	0.015876	0.003083	−0.008017	−0.007615
		20	0.016659	0.001634	0.016897	−0.007281
		25	0.017322	0.000439	0.049285	−0.004448
		30	0.017608	0.000000	0.089193	0.001540
100	0.7	0	0.008175	0.006418	−0.037538	0
		5	0.008340	0.006052	−0.034274	−0.003181
		10	0.008807	0.005016	−0.024382	−0.005789
		15	0.009494	0.003503	−0.007583	−0.007236
		20	0.010261	0.001833	0.016495	−0.006902
		25	0.010911	0.000466	0.048254	−0.004133
		30	0.011193	0.000000	0.087927	0.001751
100	1.0	0	0.008183	0.005441	−0.038063	0
		5	0.008346	0.005135	−0.034794	−0.003227
		10	0.008809	0.004268	−0.024889	−0.005880
		15	0.009489	0.002999	−0.008076	−0.007370
		20	0.010249	0.001599	0.016026	−0.007077
		25	0.010895	0.000430	0.047799	−0.004349
		30	0.011175	0.000000	0.087476	0.001495

TABLE 3.—DEFLECTIONS, ANGLES OF TWIST, AND BENDING AND TWISTING MOMENTS

Dimensionless Parameters		ϕ, in degrees	Ratio, $\frac{Y}{\nu}$	Ratio, $\frac{\beta}{\nu}$, in radians	$\frac{M_x}{a\,\nu}$	$\frac{M_t}{a\,\nu}$
λ	μ					
			$2\gamma = 45°$			
60	0.7	0	0.020635	0.002941	−0.031173	0
		5	0.020762	0.002649	−0.026338	−0.002580
		10	0.021102	0.001865	−0.011814	−0.004315
		15	0.021541	0.000864	0.012440	−0.004359
		20	0.021886	0.000101	0.046432	−0.001860
		22.5	0.021943	0.000000	0.006753	0.000607
60	1.0	0	0.020634	0.002463	−0.031422	0
		5	0.020760	0.002220	−0.026586	−0.002601
		10	0.021099	0.001569	−0.012060	−0.004358
		15	0.021535	0.000734	0.012196	−0.004423
		20	0.021878	0.000091	0.046190	−0.001946
		22.5	0.021935	0.000000	0.066811	0.000510
100	0.7	0	0.012143	0.002912	−0.030794	0
		5	0.012268	0.002623	−0.026048	−0.002549
		10	0.012605	0.001848	−0.011754	−0.004269
		15	0.013039	0.000857	0.012230	−0.004319
		20	0.013381	0.000100	0.046038	−0.001848
		22.5	0.013438	0.000000	0.066633	0.000601
100	1.0	0	0.012144	0.002438	−0.031043	0
		5	0.012268	0.002199	−0.026296	−0.002571
		10	0.012603	0.001555	−0.011998	−0.004312
		15	0.013035	0.000728	0.011989	−0.004383
		20	0.013375	0.000091	0.045800	−0.001933
		22.5	0.013432	0.000000	0.066395	0.000506
			$2\gamma = 30°$			
60	0.7	0	0.031661	0.000894	−0.021441	0
		5	0.031741	0.000704	−0.014127	−0.001658
		10	0.031925	0.000270	0.007792	−0.002041
		15	0.032042	0.000000	0.044227	0.000124
60	1.0	0	0.031660	0.000742	−0.021521	0
		5	0.031740	0.000585	−0.014207	−0.001665
		10	0.031923	0.000225	0.007712	−0.002055
		15	0.032040	0.000000	0.044148	0.000103
100	0.7	0	0.018925	0.000893	−0.021390	0
		5	0.019006	0.000703	−0.014102	−0.001655
		10	0.019189	0.000269	0.007765	−0.002037
		15	0.019306	0.000000	0.044173	0.000124
100	1.0	0	0.018925	0.000741	−0.021470	0
		5	0.019005	0.000584	−0.014182	−0.001662
		10	0.019188	0.000225	0.007686	−0.002051
		15	0.019306	0.000000	0.044090	0.000103

ACKNOWLEDGMENTS

The numerical computations involved in the preparation of these tables are laborious. At first the writers had prepared tables with four decimal places. However, for engineering use it is advisable to have tables accurate to a greater number of decimal places; it is not practical to prepare them without the use of proper computing machines. The tables presented, with six decimal places, were computed at the Istituto per le Applicazioni del Calcolo of the Italian Consiglio Nazionale delle Ricerche in Rome. The writers want to express their appreciation to the director of the Istituto per le Applicazione del Calcolo, Mauro Picone, for his generous help.

APPENDIX I. NUMERICAL EXAMPLE

A reinforced concrete circular beam, having a radius, R, of 25 ft and a square cross section of 30 in. by 30 in., is acted upon by eight vertical loads of 75 tons each, equally spaced at $2\gamma = 45°$. The modulus of elasticity of concrete is assumed to be 3×10^6 lb per sq in., and the elastic constant of the foundation is supposed to be 1,500 lb per in. per in.

It follows that $I_x = 6.75 \times 10^4$ in.^{4}; $\lambda = 60$; $\mu = 0.7$; $\gamma = 0.0666$; $a = 28{,}125$ ft-tons; and $a\gamma = 1{,}873.12$ ft-tons.

The results obtained for this particular case (from Table 3) are given in Table 4(*a*) whereas in Table 4(*b*) are listed the results for a beam that has the same characteristics and is under the same loads but is free to rotate. The results in Table 4(*b*) are taken from an earlier paper by the writer (1).

TABLE 4.—RESULTS

Beam type	ϕ (degrees)	$\beta \times 10^2$ (radians)	v (inches)	M_x (foot-tons)	M_z (foot-tons)
(*a*) Constrained	0	0.1959	0.4122	−58.391	0
	5	0.1764	0.4148	−49.334	−4.833
	10	0.1242	0.4216	−22.129	−8.082
	15	0.0575	0.4304	23.301	−8.165
	20	0.00673	0.4373	86.973	−3.484
	22.5	0	0.4384	125.598	1.137
(*b*) Free to rotate	0	0.0966	0.4122	−61.288	0
	5	0.0766	0.4146	−52.222	−5.076
	10	0.0229	0.4216	−25.025	−8.579
	15	0.0466	0.4304	20.398	−8.916
	20	0.1033	0.4372	84.084	−4.495
	22.5	0.1106	0.4384	122.708	0

If one compares the results given in Table 4, one sees that the values in the β-columns are completely different for the two types of beam and that the values for v are practically the same, whereas the values of M_x and M_z are close.

APPENDIX II. BIBLIOGRAPHY

(1) **"Bending of a Circular Beam Resting on an Elastic Foundation,"** by Enrico Volterra, *Journal of Applied Mechanics*, March, 1952, pp. 1–4.

(2) **"Deflections of Circular Beams Resting on Elastic Foundations under Symmetric or Antisymmetric Loading,"** by Enrico Volterra. *Proceedings*, Eighth International Cong. of Theoretical and Applied Mechanics, Istanbul, Turkey, August, 1952.

(3) **"Deflections of Circular Beams Resting on Elastic Foundations Obtained by Methods of Harmonic Analysis,"** by Enrico Volterra, *Journal of Applied Mechanics*, June, 1953, pp. 227–232.

(4) **"Die Lehre von der Elastizität und Festigkeit,"** by E. Winkler, Prague, Czechoslovakia, 1867, p. 182.

(5) **"Die Berechnung des Eisenbahnoberbaues,"** by H. Zimmermann, Berlin, Germany, 2d Ed., 1930.

(6) **"Beams on Elastic Foundation,"** by M. Hetényi, The University of Michigan Press, Ann Arbor, Mich., 1946.

(7) **"Mémoire sur le calcul de la résistance et de la flexion des pièces solides à simple ou à double courbure, en prenant simultanément en consideration les divers éfforts auxquels elles peuvent être soumises dans tous les sens,"** by Barré de Saint-Venant, *Comptes Rendus*, l'Academie des Sciences de Paris, Vol. XVII, 1843, pp. 942–954 and pp. 1020–1031.
(8) **"The Mathematical Theory of Elasticity,"** by A. E. H. Love, Dover Publications, New York, N. Y., 4th Ed., 1944.
(9) **"Strength of Materials—Advanced Theory and Problems,"** Pt. II, by S. Timoshenko, The Macmillan Co., New York, N. Y., 1936, pp. 467–473.

APPENDIX III. NOTATION

The following symbols, adopted for use in the paper, and for the guidance of discussers, conform essentially with American Standard Letter Symbols for Structural Analysis (ASA Z10.8—1949), prepared by a committee of the American Standards Association, with ASCE representation, and approved by the Association in 1949:

$A, B_1, B_2, F, G_1, G_2, H, J_1, J_2$ = constants;
$a = \dfrac{E\,I_x}{R}$;
E = the Young modulus;
I_x = the moment of inertia of the cross section of the beam with respect to the x-axis;
K = the torsional rigidity of the beam;
k = the elastic constant of the foundation;
M_x = bending moment;
M_z = twisting moment;
m, r, t = terms defined by Eqs. 8*a*;
P = the concentrated force;
$Q_1, Q_2, S_1, S_2, T, U, V, X, Z$ = terms defined by Eqs. 10;
s = arc length;
v = displacement of the axis of the beam in a direction perpendicular to the plane of the beam;
x, y, z = rectangular coordinates;
$Y = \dfrac{v}{R}$;
$1/R$ = the initial curvature of the center line of the beam;
β = the angle of twist;
$2\,\gamma$ = angular distance between points of application of external forces;
θ = the unit angle of twist;
$\lambda = \dfrac{k\,R^4}{E\,I_x}$;
$\mu = \dfrac{K}{E\,I_x}$;
$\nu = \dfrac{P\,R^2}{E\,I_x}$;
ξ, η = terms defined by Eqs. 8*b*; and
ϕ = the angle subtended by a specified length of the beam.

AMERICAN SOCIETY OF CIVIL ENGINEERS
Founded November 5, 1852
TRANSACTIONS

Paper No. 2741

DEAD-LOAD-STRESS MEASUREMENT IN A LONG SPAN BRIDGE

By Lawrence T. Wyly,[1] M. ASCE, Maurice B. Lagaard,[2] M. ASCE, Ralph W. Kluge,[3] A. M. ASCE, Kenneth H. Lenzen,[4] A. M. ASCE, Edward W. Larson, Jr.,[5] J. M. ASCE, and Lewis B. McCammon, Jr.,[6] A. M. ASCE

With Discussion by Messrs. Almon H. Fuller; and Lawrence T. Wyly, Maurice B. Lagaard, Ralph W. Kluge, Kenneth H. Lenzen, Edward W. Larson, Jr., and Lewis B. McCammon, Jr.

Synopsis

The paper is a report of dead-load-stress measurements made on several members of the East St. Louis Veterans Memorial Bridge. The purpose of the measurements was to study the actual stress distributions to be expected in the members of large bridges of modern design and construction. The work was performed while the bridge was under construction, during the summer of 1949 and the winter and fall of 1950.

The measured stresses were less than the computed dead-load stresses by approximately 1,000 lb per sq in. Large strain and stress concentrations were measured locally in the truss splices. It was found that the engineers and contractors had been successful in eliminating large secondary stresses in the chord members near the channel piers. Stresses probably caused by differential temperatures and other erection conditions were found to be approximately 3,000 lb per sq in. in both the horizontal plane and the vertical plane.

Note.—Published essentially as printed here, in July, 1953, as *Proceedings-Separate No. 219*. Positions and titles given are those in effect when the paper or discussion was received for publication.

[1] Research Prof. and Head of Structural Eng. Dept., Purdue Univ., Lafayette, Ind.

[2] Associate Prof. and Chairman of Eng. Drawing Dept., Northwestern Univ., Evanston, Ill.

[3] Head of Civ. Eng. Dept., Univ. of Florida, Gainesville, Fla.; formerly Associate Prof. of Structural Eng., Purdue Univ., Lafayette, Ind.

[4] Research Associate and Instructor in Structural Eng., Purdue Univ., Lafayette, Ind.

[5] Test Engr., Hughes Tool Co., Culver City, Calif.; formerly Research Associate and Instructor in Civ. Eng., Northwestern Univ., Evanston, Ill.

[6] Associate Prof. of Civ. Eng., Northwestern Univ., Evanston, Ill.; formerly Research Associate and Instructor in Structural Eng., Purdue Univ., Lafayette, Ind.

INTRODUCTION

The construction of the Veterans Memorial Bridge across the Mississippi River at East St. Louis, Ill., offered an opportunity to obtain information concerning the actual distribution of stress in the members of a large highway bridge which was fabricated and erected under the best conditions of modern (1950) practice. The dead-load stresses are approximately 75% of the design stresses for the large members. The test models were full scale, and the testing machine was the structure itself. The results obtained from these measurements provide an index of the effectiveness of the procedures which were used in the design and construction of this bridge. Because of the importance and scarcity of information of this type, members of the staffs of Purdue University at Lafayette, Ind., and Northwestern University at Evanston, Ill., proposed a program for measuring the stresses in this bridge and comparing the computed stresses with the stresses measured at several critical sections.

PURPOSE

The purpose of the investigation was to obtain information on the following: (1) The actual dead-load stresses at selected sections of the main members entering the lower-chord joint above the shoe at a channel pier; (2) measurements of the closing of the milled butt joints and measurements of the stresses in the splice plates of both shop splices and field splices in some main members under dead loads; (3) the efficacy of the practice of attempting to eliminate the secondary stresses in the main chords by inducing a reversed bending during construction; and (4) any stresses which might be residual in the members as a result of the construction or erection conditions.

It was desired to ascertain the stress distribution across the members at sections free from the local stresses caused by rivets in gussets and splices, and also at sections through the center of the cover-plate perforations.

Computations showed that large secondary stresses in the bottom chords (approximately 65% of the primary stresses) would be expected to occur in the lower chords adjacent to the river piers if no corrective measures were taken. An attempt to eliminate these stresses was made by inducing reversed bending through the shop and field operations.

DESCRIPTION OF BRIDGE

The Memorial Bridge connecting St. Louis, Mo., and East St. Louis consists of a cantilever structure with a main center span of 964 ft including a 324-ft suspended span and two anchor spans of 470 ft each, as shown in Fig. 1. The structure provides a 40-ft roadway to carry H-20 loading.[7] The design and construction of this bridge were conceived by George A. Maney, with Lawrence T. Wyly, M. ASCE, as principal assistant. The project has been described by Craig P. Hazelet,[8] M. ASCE, and A. L. R. Sanders,[9] M. ASCE.

---

[7] "Standard Specifications for Highway Bridges," A.A.S.H.O., 1944, pp. 127–128.

[8] "$10,000,000 Toll Bridge Over Mississippi River Financed by East St. Louis, Ill.," by Craig P. Hazelet, *Civil Engineering*, March, 1950, p. 34.

[9] "East St. Louis Veterans Memorial Bridge," by A. L. R. Sanders, *Transactions*, ASCE, Vol. 118, 1953, pp. 838–848.

FABRICATION AND ERECTION PROCEDURES

The trusses were cambered so that the entire bottom chord is a straight level line under full dead load. The lengths of all members were corrected in the shop so as to produce this cambered condition. Assembly reaming of the chord splices in the shop was performed with the chords in their geometric positions, the web members being shifted accordingly. This practice had been previously used on other large structures.[10] During erection, if the members were connected in the field at the proper length, reverse bending would be caused—particularly in the lower-chord truss members. Thus (theoretically), when the span had been swung and was carrying full dead load, the members would have no bending stress.

Erection, beginning at the anchor piers and proceeding to the center of the main opening, was accomplished by use of a traveler operating at deck level. In the anchor spans only four falsework bents were used. These were at panel points L_2, L_4, L_6, and L_{10}, with L_0 at Pier Nos. 8 and 11 and the numbers increasing to the center of main span (Fig. 1). During erection, adjustment to line and level was accomplished by the use of wedge jacks located at the base of the steel falsework columns and a short distance above the river level. No falsework was used in the main span.

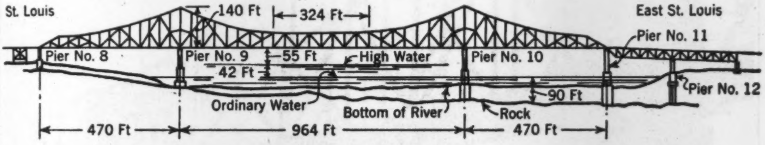

FIG. 1.—PROFILE VIEW OF EAST ST. LOUIS VETERANS MEMORIAL BRIDGE, EAST ST. LOUIS, ILL.

Unequal temperatures of the lower chords during erection created a problem because the bridge axis is east and west. During the period of closing the anchor span, the lower chords of the south truss were exposed to the sun's rays while those of the north truss were shaded by the adjacent stringers and other members. This condition caused the span to warp northward, out of line in a horizontal plane. This warping necessitated corrective measures to bring the span back into line at panel point L_{14} at Pier Nos. 9 and 10. At this stage the falsework bent at panel point L_{10} was the only one in action. The correction was accomplished by lowering the jack situated at the bottom of the bent under the south falsework column at panel point L_{10}, thus producing rotation of the entire falsework bent (in its own plane) about the north jack as a pivot. This rotation moved the entire bridge horizontally southward and also lowered the south truss.

Another factor which permanently affected the stresses was the erection method used in connecting points M_{13} and M_{15} on the anchor and cantilever spans, respectively, to the middle of the main post U_{14}–L_{14}. It was necessary that these secondary bracing members would be in action as the erection proceeded over the pier. Such connecting members, however, restrain the natural tendency of these points (M_{13} and M_{15}) to deflect downward and horizontally away from the pier as erection proceeds. If left as originally connected, the connecting members would cause a permanent redistribution of stress quite different from the state of stress contemplated by the designer.

---

[10] "Investigation of Dead-Load and Live-Load Stresses in a 350 Ft. Truss Span on the A T & S F System," *Bulletin* A.R.E.A., June-July, 1953, p. 41.

The logical solution would have been to cut both bracing members free from the main post at panel point M_{14} after the structure had been completed and after all dead loads, including the floor slab, were in place. This cutting would allow the structure to deflect to its normal position and would free the main post from the members tending to pull it out of line. After the structure had thus been allowed to assume its normal position, the bracing members could then be permanently reconnected to the post at panel point M_{14}. Where the main post is too slender to carry safely the full dead load without any bracing at the midpoint, an alternative solution, consisting of cutting only one member free and leaving the other member permanently connected, is sometimes adopted. This alternative solution was used on this structure, the vertical post being cut free from the cantilever span but left permanently connected to the anchor span.

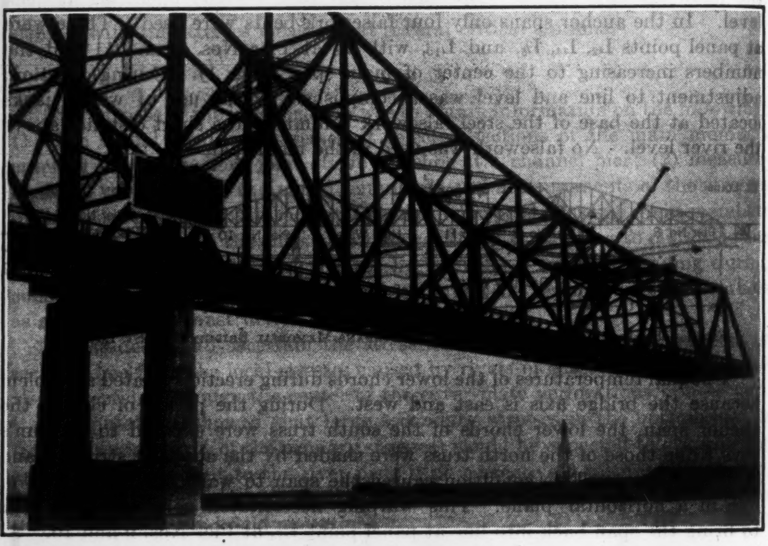

FIG. 2.—BRIDGE AT CANTILEVER STAGE

GENERAL PROGRAM

The program of the investigation was primarily a field study. However, it was supplemented by laboratory work to solve problems encountered as the work progressed and to calibrate various instruments used in the tests. In an effort to measure the stresses which (1) might develop in the process of erection and (2) might be caused by the application of the dead load as the bridge was built, readings were taken at three different stages: (*a*) No load—members on skids in the shop; (*b*) dead load—steel only, cantilever stage of construction; (*c*) full dead load—span swung and ready for traffic.

The first series of measurements was taken while the fabricated members were resting on wooden supports in the shop of the fabricating plant. Because of the massiveness of the members and the method of support (blocks under the points where the test gage lines were located), any bending which occurred while the members were supported in the shop was found, by computation, to be negligible. These shop readings were considered to be the initial readings. A second set of readings was taken in the field when the bridge was in the cantilever stage (Fig. 2) to determine the strains that had developed and also to substantiate the accuracy of the method of taking the readings. Final readings were taken after the bridge was completed (including the concrete floor), but before the bridge was open to traffic.

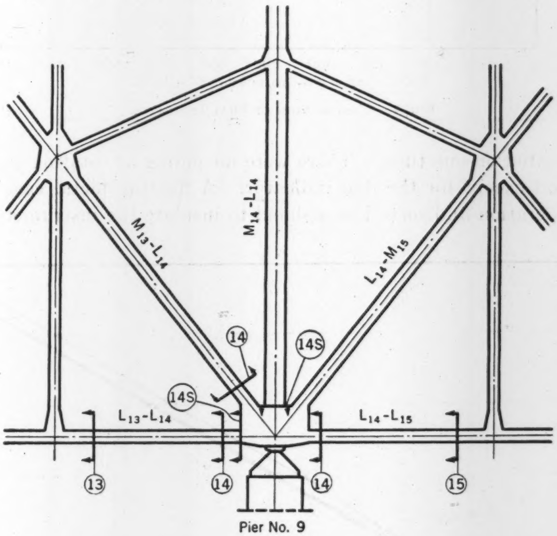

FIG. 3.—SECTIONS INVESTIGATED

Readings were taken on the members of both trusses framing into the lower joints at Pier No. 9 (Fig. 3). Two of the sections were through splices; the other five sections were taken through the perforations in the cover plates.

DESCRIPTION OF STRAIN-MEASURING INSTRUMENTS

Strain measurements were made with Whittemore strain gages having gage lengths of 2 in., 5 in., and 10 in. The instruments consisted of two tubes, one of steel and one of invar, one telescoped within the other and articulated through plate fulcrums—each carrying a conical point which was inserted into a small hole in the steel member. Movement of these points relative to each other was registered by a linear measuring dial indicator, graduated to 1/10,000 in. and mounted on one tube. There were no sliding or rotating parts and no magnification except for the dial indicator. A floating metal case permitted one-hand operation and served as a shield to insulate the instrument from the heat of the hand. This instrument had the advantage of being equally accurate for reading in any position—upsidedown, sidewise, horizontally, or vertically—the only requirement being that a reasonably consistent pressure be applied by the operator in all positions.

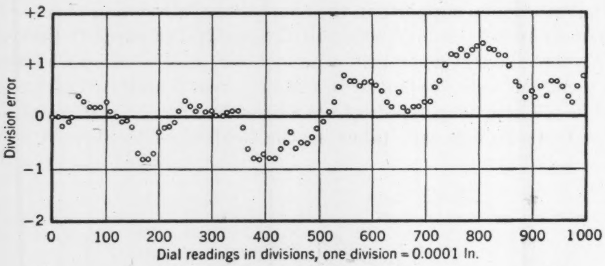

Fig. 4.—Calibration of Dial Indicator

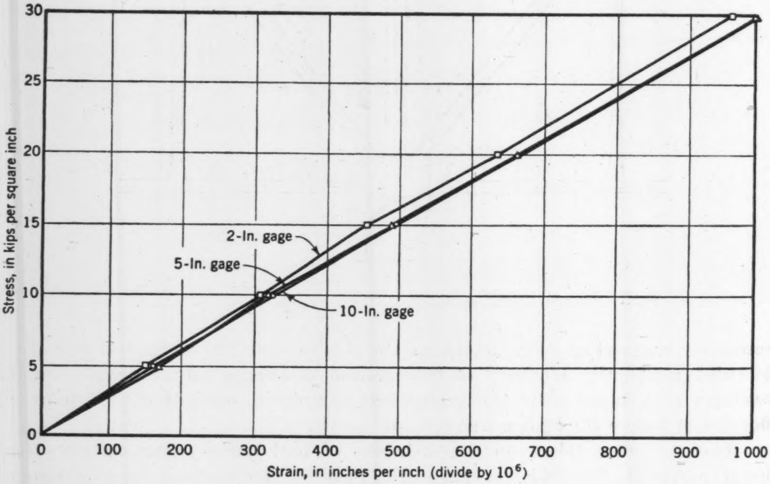

Fig. 5.—Calibration of Strain Gages

SPECIAL STUDIES

The calibration of one of the dial indicators used on the instruments is shown in Fig. 4. The average range of the dial in reading a gage line and in comparing the reading with the standard bar was approximately fifty dial divisions, and the maximum range encountered was one hundred dial divisions.

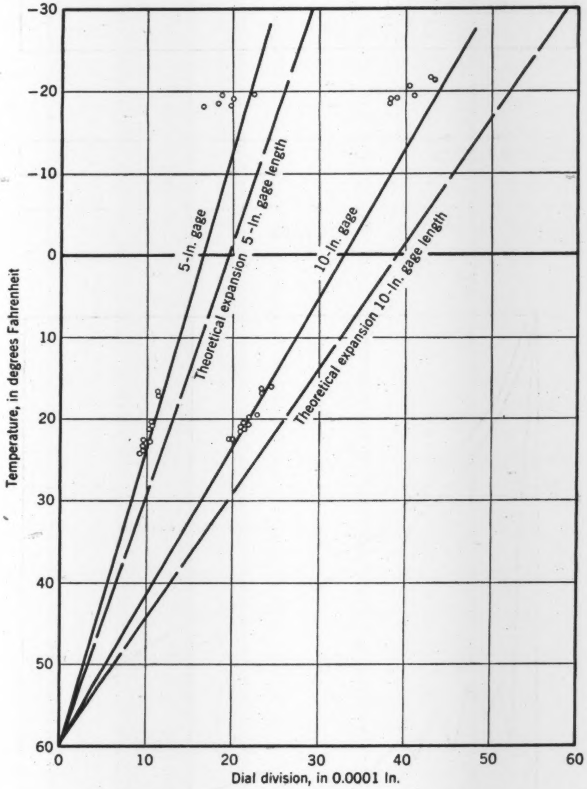

FIG. 6.—EFFECT OF TEMPERATURE ON READINGS ON STANDARD BAR

Hence, it is evident that errors caused by the dial may have been as large as one division.

These gages were calibrated with reference to each other by taking readings on a steel bar under tensile loads and obtaining a stress-strain curve with each gage, as shown in Fig. 5. The instruments with gage lengths of 5 in. and 10 in. showed good agreement, and readings for the 2-in. gage were approximately 4% lower.

A check was also made on the effect of temperature on the gages and standard bars. Readings were taken in a variable-temperature room, thermocouples being mounted on strain gages and standard bars, both of which were at approximately the same temperatures. Fig. 6 shows the effect of a wide range of temperature, from 20° F to 60° F, on the readings. Because at no time in this investigation did the temperature of the gage or the standard bar differ by more than 1° F, it was not necessary to make any correction for this relationship.

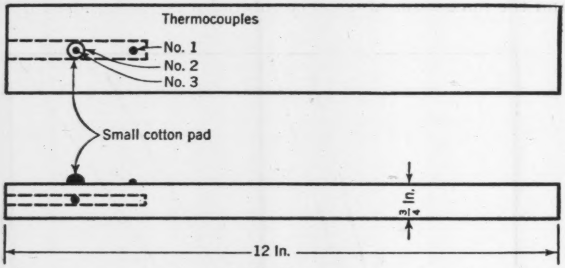

(a) Steel bar

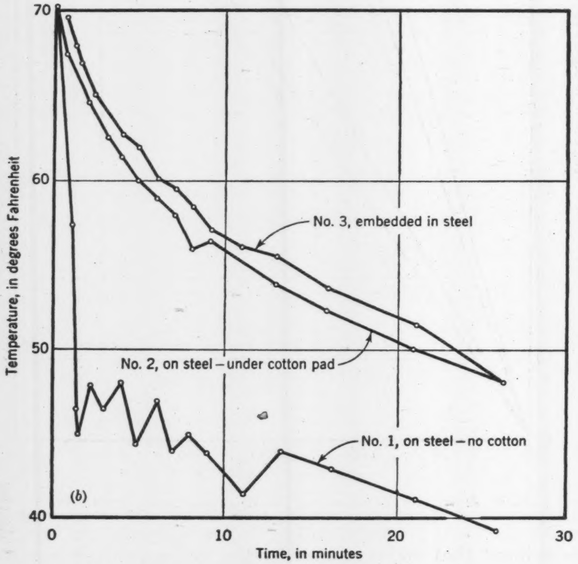

FIG. 7.—METHODS OF MEASURING TEMPERATURE OF STEEL

All strain-gage readings in the field were referred to standard bars; two such bars were used for each instrument. One bar consisted of a section of structural silicon steel from the same lot of material as used in the bridge, with small hardened inserts for the gage holes so as to minimize wear. The other bar, which was furnished by the manufacturer of the gage, consisted of mild steel. Each instrument was cross-checked with the standard bars at frequent intervals during the tests. Each standard bar was calibrated with respect to all others.

Fig. 7 shows the results of a study of the method of measuring steel temperatures. In the study initial readings on the mild steel bar were taken by the copper constantan thermocouple with the bar at a room temperature of 70.5° F. The bar was then placed in cooler air, and readings were taken for a period of 26 min. This study demonstrated that, unless a small pad of cotton is placed on top of the thermocouple used to measure the temperature of the steel, the indicated temperature will be not that of the steel, but a compromise between the temperature of the steel and that of the air. Accordingly, the cotton pad was used on all thermocouple installations.

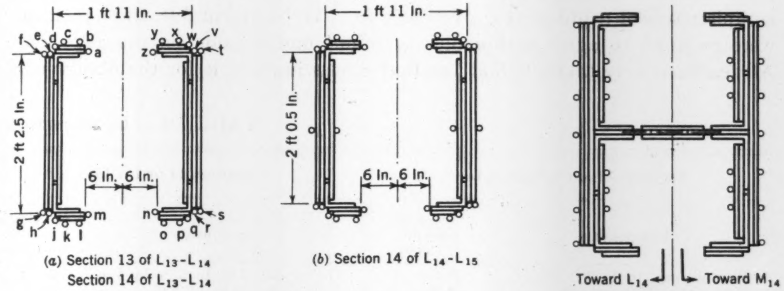

(a) Section 13 of L_{13}-L_{14}
Section 14 of L_{13}-L_{14}

(b) Section 14 of L_{14}-L_{15}

(c) Section 14S of L_{14}-M_{14}

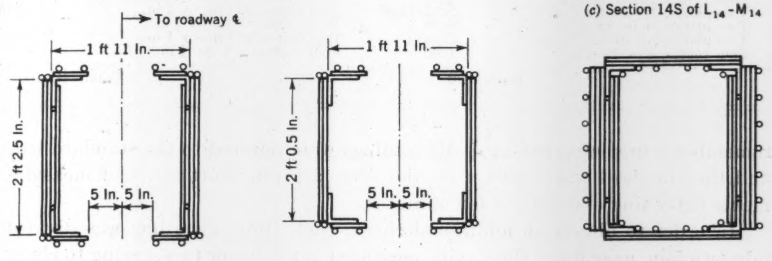

(d) Section 15 of L_{14}-L_{15}

(e) Section 14 of M_{13}-L_{14}

(f) Section 14S of L_{13}-L_{14}

FIG. 8.—LOCATION OF GAGE LINES AT TEST SECTIONS

LOCATION OF THE GAGE LINES

The location of the gage lines at the test sections is shown in Fig. 8. The composition of the members at these sections is given in Table 1.

TESTING PROCEDURE

The most difficult problem in the project was the securing of satisfactory holes at the gage lines. This is particularly difficult in silicon steel which is, by nature, hard. Errors in readings will obviously result (1) if the surface of the metal is not perfectly smooth and flat, (2) if the surface of the metal and the axis of the hole are not normal to each other, (3) if the holes are not truly circular, (4) if the holes are too shallow, or (5) if the axes of the two holes are not parallel.

Strain readings were obtained by three groups, each composed of two men. Each man acted alternately as observer and recorder, and, in addition, one or more assistants obtained thermocouple readings. Each man took two or more complete sets of readings at a given section. To be acceptable, these readings were required to agree within plus or minus one division on the gage dial. All readings were taken "blind" so that it was impossible for the observer to remember a previous reading. All readings were referred to the standard bar, and the standard was read before and after a given short series of measurements extending over only a few minutes.

TABLE 1.—COMPOSITION OF

SECTIONS 13 AND 14 OF L_{13}–L_{14}		SECTION 14 OF L_{14}–L_{15}	
Components	Area, in square inches	Components	Area, in square inches
Four angles, 5 in. by 5 in. by ⅝ in.	23.44	Four angles, 5 in. by 5 in. by ⅝ in.	23.44
Four plates, 26 in. by ¾ in.	78.00	Four plates, 26 in. by ¾ in.	78.00
Two plates, 22½ in. by ⅝ in.	28.12–15.00	Two plates, 22½ in. by ⅝ in.	28.12–15.00
Two plates, 16 in. by ⅝ in.	20.00	Two plates, 16 in. by ⅝ in.	20.00
Two plates, 23½ in. by 9/16 in.	26.44	Two plates, 23½ in. by ½ in.	23.50
Four plates, 4 in. by ⅜ in.	6.00	Four plates, 4 in. by ⅜ in.	6.00
Total	167.00	Total	164.06

In order to obtain an additional check, each 10-in. gage line was divided into two 5-in. gage lines, the strains measured in the latter two serving to check the strain obtained in the other. Thus, in effect, there were four independent checks on the strain observation.

To minimize the effect of temperature, all shop readings were taken under cover and only on cloudy days or at night. All field readings were taken at night. Temperatures of the air, the standard bars, and the steel members were taken by thermocouples, and a continuous record was kept during the strain-reading periods.

As a 1° F difference in temperature will give the same strain as 200 lb per sq. in., it was decided that corrections for temperature would not be made for less than 1° F. The maximum recorded difference in temperature between the standard bar and the steel was 2° F; this occurred only in a very few cases. This favorable temperature situation was probably caused by the fact that readings were taken at night.

Fig. 9 shows the lower chord and staging. The regular perforations are 10 in. wide and 20 in. long. The members are large enough to permit the observer to go inside and take readings on the inside as well as the outside of the sections. The reinforced perforations near the panel points are 12 in. wide and 24 in. long.

Probable Errors in Readings

The most common cause of error in readings taken with mechanical gages is poor gage holes. The silicon steel of which the bridge members are made is hard, particularly in certain spots, and it was not always possible to get perfect holes. In some cases holes were redrilled. Even so, a few of the holes were found to be unsatisfactory; this fact was noted in the records, and readings at these holes were discarded. Considering all probable sources of error, it is believed that the readings were in error by not more than ±1,000 lb per sq in. and that in most cases the error did not exceed half of this value.

Members at Test Sections

Section 15 of L_{14}–L_{15}		Section 14 of M_{14}–L_{14}	
Components	Area, in square inches	Components	Area, in square inches
Four angles, 5 in. by 5 in. by ⅝ in.	23.44	Four angles, 5 in. by 5 in. by ¾ in.	27.76
Four plates, 26 in. by ¾ in.	78.00	Two plates, 24 in. by ¾ in.	36.00
Two plates, 22½ in. by ⅝ in.	28.12–12.50	Two plates, 24 in. by 13⁄16 in.	39.00
Two plates, 16 in. by ⅝ in.	20.00	Two plates, 22½ in. by ⅝ in.	28.12–12.50
Two plates, 23½ in. by ½ in.	23.50		
Total	160.56	Total	118.38

Test Results: Measured Strains and Stresses

Table 2 illustrates how the final stresses were computed from the field record sheets. The measured stresses for both the cantilever stage of construction and for the final, full-dead-load stage are shown for section 15 of L_{14}–L_{15} in Fig. 10. A comparison between computed stresses and measured stresses for this section is given in Table 3. The measured closing movements of the shop-riveted butt joints in chords L_{13}–L_{14} are shown for the cantilever stage of construction in Fig. 15. Comparisons of the measured and computed bending stresses in the vertical planes are given in Figs. 16 and 17 for the cantilever and final stages, respectively. Measured bending stresses in the horizontal plane are also given in Figs. 16 and 17.

The detailed values of the average measured unit stresses at all gage lines at section 15 of L_{14}–L_{15} for the cantilever stage of loading are given in Figs. 10(*a*) and 10(*b*) in which the stresses are also plotted to scale. In Figs. 10(*c*) and 10(*d*) the full-dead-load stresses are plotted to scale, but the detailed values are not shown. The modulus of elasticity was 30,000,000 lb per sq in. Similar information for the other sections studied is shown in Figs. 11 through 14. In Table 3 there are listed for all sections: Computed unit stress, average measured

TABLE 2.—DETERMINATION OF DEAD-LOAD STRESS FOR SECTION 15 OF L_{14}–L_{15} IN THE NORTH TRUSS

Observer	Gage length, in inches	Initial reading	Steel Loads, Cantilever				Full Dead Load			
			Reading	Difference	Strain, in inches per inch	Stress, in pounds per square inch	Reading	Difference	Strain, in inches per inch	Stress, in pounds per square inch
1	5	+589	+385	−204	−0.000408	−12,240	+305	−284	−0.000568	−17,040
	5	−708	−893	−185	−0.000370	−11,100	−990	−282	−0.000564	−16,920
	10	−151	−569	−418	−0.000418	−12,540	−700	−549	−0.000549	−16,470
2	5	−701	−903	−202	−0.000404	−12,120	−989	−288	−0.000576	−17,280
	5	+587	+377	−210	−0.000420	−12,600	−312	−275	−0.000550	−16,500
	10	−152	−580	−428	−0.000428	−12,840	−691	−539	−0.000539	−16,170
Mean		•				−12,240				16,730

TABLE 3.—STRESSES AT VARIOUS SECTIONS

Load	Truss	Gross area, in square inches	Computed stress, in kips per square inch	Average measured stress, in kips per square inch	Measured Unit Bending Stress, in Kips per Square Inch	
					Vertical plane	Horizontal plane
Section 15 of L_{14}–L_{15}						
Cantilever	North	160.56	9.05	6.81	2.86	1.81
	South	160.56	9.05	8.18	0.42	2.10
Full dead	North	160.56	12.83	11.06	3.44	1.78
	South	160.56	12.83	11.38	0.04	2.06
Section 14 of L_{14}–L_{15}						
Cantilever	North	164.06	8.84	8.27	3.00	0.21
	South	164.06	8.84	8.49	1.60	2.70
Full dead	North	164.06	12.55	11.78	1.12	0.58
	South	164.06	12.55	12.20	0.10	2.61
Section 14 of M_{13}–L_{14}						
Cantilever	North	118.38	3.94	3.74	1.92	2.06
	South	118.38	3.94	2.73	1.39	1.17
Full dead	North	118.38	7.75	7.37	1.25	1.80
	South	118.38	7.75	6.25	1.16	1.32
Section 14 of L_{13}–L_{14}						
Cantilever	North	167.00	8.74	7.83	0.22	2.82
	South	167.00	8.74	7.70	4.23	3.41
Full dead	North	167.00	11.82	10.03	0.68	3.07
	South	167.00	11.80	10.83	2.71	2.80
Section 13 of L_{13}–L_{14}						
Cantilever	North	167.00	8.74	8.14	0.50	3.12
	South	167.00	8.74	8.19	0.25	1.96
Full dead	North	167.00	11.80	10.34	1.32	2.98
	South	167.00	11.80	11.16	0.92	1.76

unit stress, and measured unit bending stress at extreme fiber in both vertical and horizontal planes.

Because the sections studied were far enough from the truss panel points to be free from the local stress-raising effects of the rivets in the gussets and splices, it is to be expected that the stress distribution across the members would be rather linear. So far as the main components (the four angles and the main web plates) were concerned, this linearity was found to exist in some cases and not in others. The cover plates obviously tend to act more or less independently of the rest of the member; that is, the average stress in the cover plate is induced by the stress in the main angles to which it is connected. However, the cover tends to act like any other plate with a series of perforations down

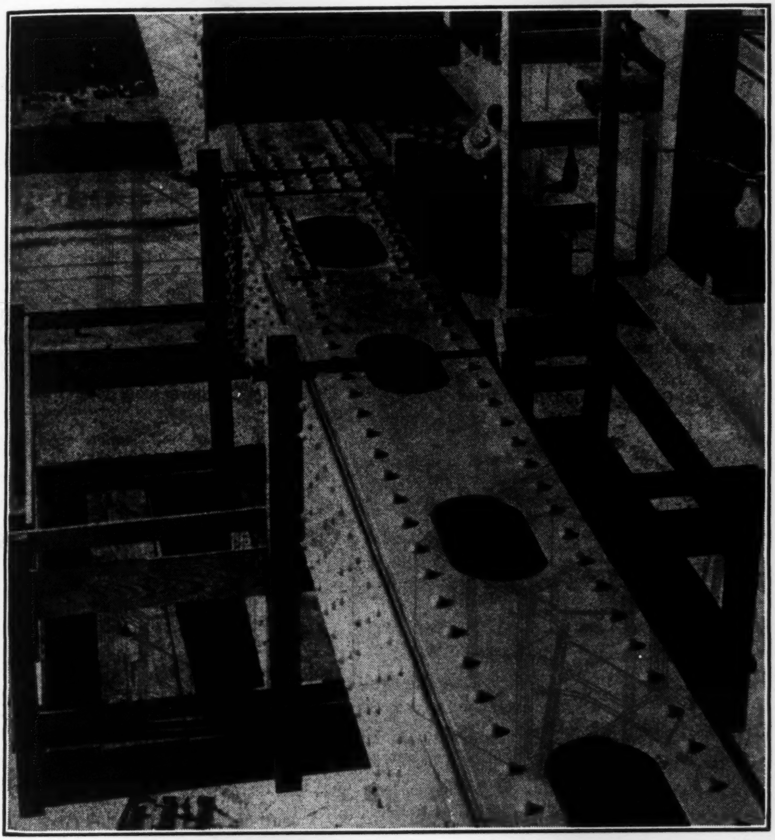

FIG. 9.—LOWER CHORD MEMBER AND STAGING

its center except in so far as it is restrained by the flange angles. Hence, it has seemed logical to consider the "average measured stress" (Table 3) to be the average of the stress at the four corners of the section, and the stress at each corner has been taken as the average of the readings on the edges of the two webs at that corner. The "measured unit bending stress" (Table 3) in the vertical plane has been considered accordingly to be the difference between the average measured unit stress and the average of the measured unit stresses at the top corners of the webs or at the bottom corners of the webs. Similarly, the measured unit bending stress in the horizontal plane has been

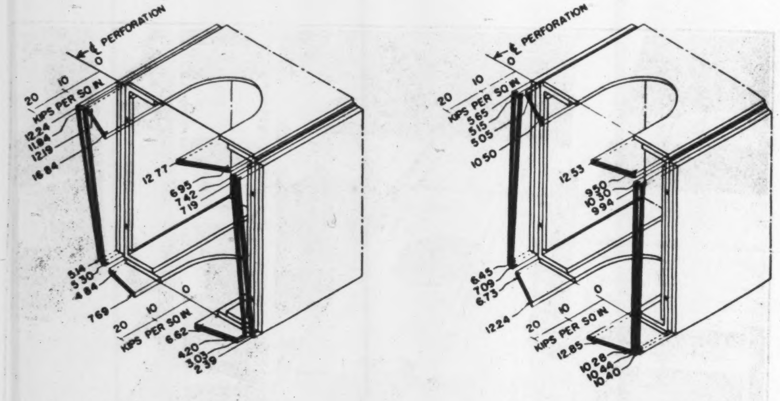
℄ PERFORATION
0
10
20
KIPS PER SQ IN
12.24
11.94
12.19
16.84
12.77
6.95
7.42
7.19
5.14
5.30
4.84
7.69
0
10
20
KIPS PER SQ IN
6.62
4.20
3.03
2.39
℄ PERFORATION
0
10
20
KIPS PER SQ IN
5.65
5.15
5.05
10.50
12.53
9.50
10.30
9.94
6.45
7.09
6.73
12.24
0
10
20
KIPS PER SQ IN
12.85
10.28
10.44
10.40

(*a*) Cantilever load, north truss

(*b*) Cantilever load, south truss

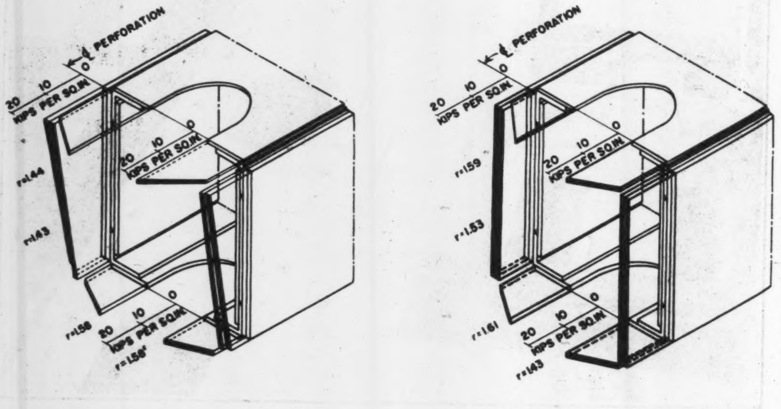
℄ PERFORATION
0
10
20
KIPS PER SQ IN
r=1.44
r=1.43
0
10
20
KIPS PER SQ IN
0
10
20
KIPS PER SQ IN
r=1.58
r=1.58
℄ PERFORATION
0
10
20
KIPS PER SQ IN
r=1.59
r=1.53
0
10
20
KIPS PER SQ IN
0
10
20
KIPS PER SQ IN
r=1.61
r=1.43

(*c*) Full dead load, north truss

(*d*) Full dead load, south truss

FIG. 10.—STRESSES AT SECTION 15 OF L_{14}–L_{15}

taken as the difference between the average measured unit stress and the average of the measured unit stresses at the two corners of the webs on the north side of the member or on the south side of the member.

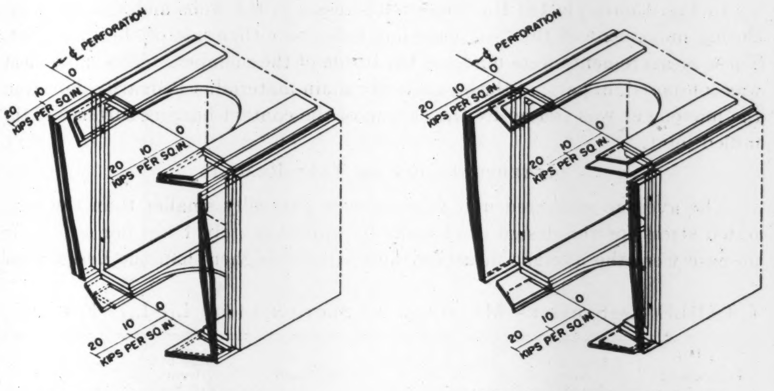
℄ PERFORATION
0
10
20
KIPS PER SQ. IN.
0
10
20
KIPS PER SQ. IN.
0
10
20
KIPS PER SQ. IN.
℄ PERFORATION
0
10
20
KIPS PER SQ. IN.
0
10
20
KIPS PER SQ. IN.
0
10
20
KIPS PER SQ. IN.

(*a*) Cantilever load, north truss (*b*) Cantilever load, south truss

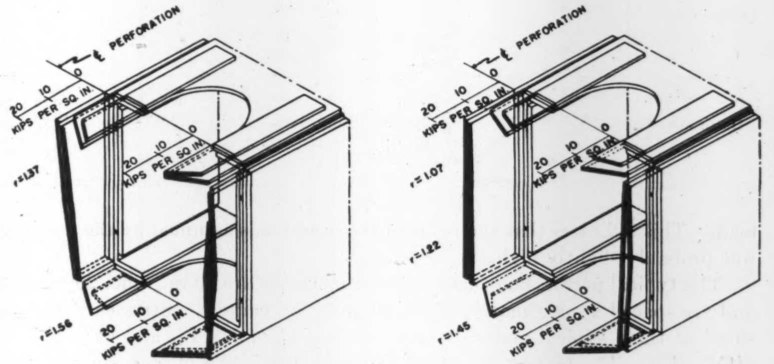
℄ PERFORATION
0
10
20
KIPS PER SQ. IN.
r=1.37
0
10
20
KIPS PER SQ. IN.
r=1.56
0
10
20
KIPS PER SQ. IN.
r=1.59
℄ PERFORATION
0
10
20
KIPS PER SQ. IN.
r=1.07
0
10
20
KIPS PER SQ. IN.
r=1.22
r=1.45
0
10
20
KIPS PER SQ. IN.
r=1.52

(*c*) Full dead load, north truss (*d*) Full dead load, south truss

FIG. 11.—STRESSES AT SECTION 14 OF L_{14}–L_{15}

The following information is shown in Fig. 18 and Table 4 for section 14 of L_{13}–L_{14} in the south truss for the full-dead-load stage:

1. Measured unit stresses at all gage lines (Table 4).

2. Average measured unit stresses at the four corners of the webs and on central planes (Table 4 and Fig. 18(*b*)).

3. Measured unit bending stresses in both vertical and horizontal planes (Fig. 18(*b*)).

4. Computations of the ratios of the stress at the inside of the cover plate perforations to the stress obtained by interpolation between the measured stresses in the adjacent web plates (Figs. 18(*a*) and 18(*c*)).

In Fig. 15 are plotted the measured stresses in the webs and also the total closing movement of the 2-in. gage-line holes on either side of the butt joint. These measurements were made on the inside of the member. This movement was composed, in part, of the strain in the main material. Primarily, however, the movement was caused by the closing of the contact bearing surfaces of the milled joint.

INTERPRETATION OF TEST RESULTS

The average measured unit stresses were generally smaller than the computed stress for the design dead loads by approximately 1 kip per sq in. In no case were the average measured unit stresses higher than the design dead load. This indicates that the value of the dead loads assumed by the designers was probably slightly high.

TABLE 4.—STRESSES MEASURED AT SECTION 14 OF L_{13}–L_{14} (FIG. 18)

Component	Gage line from Fig. 8(*a*)	Measured stress, in kips per square inch	Component	Gage line from Fig. 8(*a*)	Measured stress, in kips per square inch
Cover plates	a	19.60	Bars	b	17.80
	d	14.00		c	12.50
	z	19.90		x	14.55
	w	12.20		y	20.20
	m	13.85		k	7.42
	j	6.15		l	11.00
	n	14.80		o	12.38
	q	9.43		p	9.20
North webs	v	17.05	South webs	e	10.40
	t	16.30		f	10.38
	Average	16.68		Average	10.39
	r	9.86		g	5.56
	s	11.28		h	5.71
	Average	10.57		Average	5.64

The typical perforations used in these members are 10 in. wide, 20 in. long, and are spaced approximately 47 in. to 50 in. on centers. Stresses were measured at these typical perforations at section 15 of L_{14}–L_{15} and at section 14 of M_{13}–L_{14}. The highest measured stress on the inside of such a perforation was at section 15 of the north truss and was 22.2 kips per sq in. This value was twice the average measured unit stress for the member at this section. A more representative relationship would probably be the ratio between the stress at the inside of the perforation and the value obtained by interpolating between the measured stresses at the adjacent webs. Such ratios, designated as r, have been computed for all the measured stresses at the insides of the perforations. These ratios vary from approximately 1.4 to 1.6 for section 15 (Fig. 10).

Reduction of Stress Concentration.—A plate having a single elliptical perforation of the proportions used in the Memorial Bridge, with supported edges and carrying an axial load, would be expected to have a stress at the inside of the perforation somewhat higher than the axial stress. Two factors act to reduce this stress concentration:

1. The perforations are spaced close together; thus, the section of the plate which is in line with the perforations and is located between them will carry a low stress, which in turn reduces the stress at the sides of the perforations. A direct measurement of this action has been obtained.[11,12] Increasing the distance between perforations would probably result in raising the stress in the cover plate at the inside of the perforations.

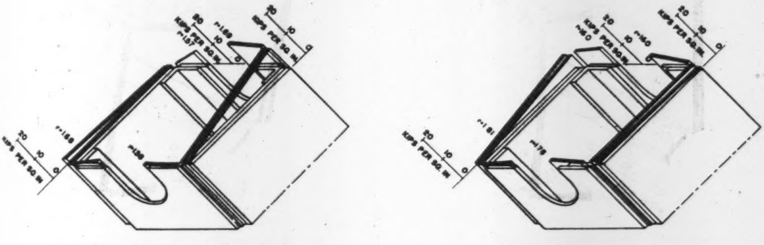

(a) Cantilever load, north truss

(b) Cantilever load, south truss

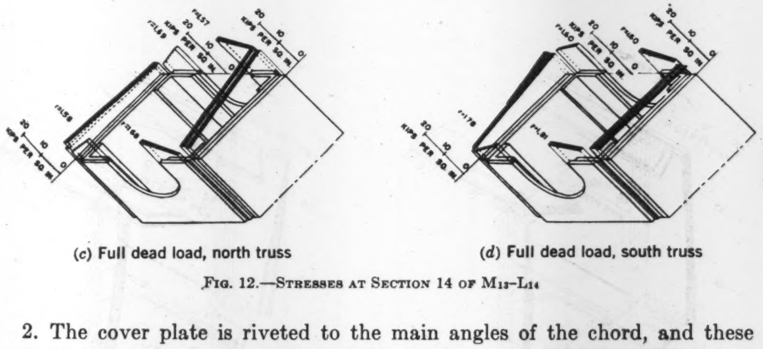

(c) Full dead load, north truss

(d) Full dead load, south truss

FIG. 12.—STRESSES AT SECTION 14 OF M_{13}–L_{14}

2. The cover plate is riveted to the main angles of the chord, and these angles restrain the elastic yielding of the cover plate at the sides. It should be noted, however, that the edge distance of the cover plate from the rivet line is 3 in. For bending in a horizontal plane, the rivet line is placed near the neutral axis of the strip of the cover plate outside the perforation. In consequence, the stress at the outside of the cover plate through the perforations is frequently very different from that in the adjacent main webs. Reducing this edge distance would probably result in reducing the stress in the cover plate at the inside of the hole.

---

[11] "Investigation of Dead-Load and Live-Load Stresses in a 350 Ft. Truss on the A T & S F System," *Bulletin*, A.R.E.A., June–July, 1953, p. 97, Fig. 34.

[12] *Ibid.*, p. 99, Fig. 36.

It is to be noted that the highest stress occurs in the plate at section 15 (Figs. 10(*c*) and 10(*d*)) which is taken at a typical perforation. It should also be noted that the reinforcing bars which were added to the cover plate at the sides of the perforations were apparently under-riveted as most of them have a lower stress than the plate they are intended to support.

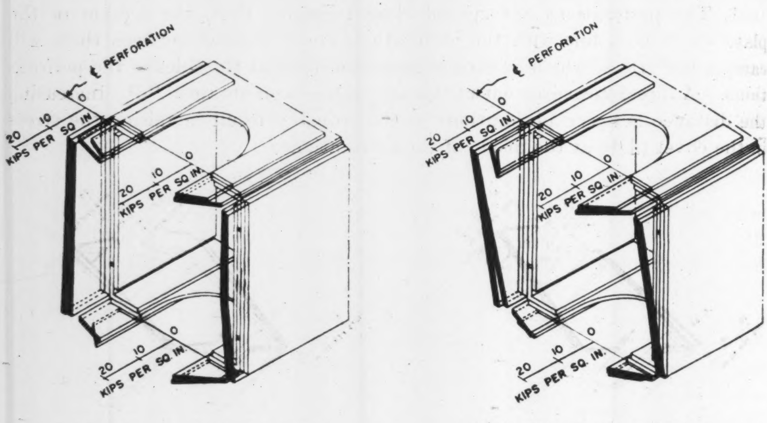
℄ PERFORATION
0
10
20
KIPS PER SQ. IN.
℄ PERFORATION
0
10
20
KIPS PER SQ. IN.

(*a*) Cantilever load, north truss

(*b*) Cantilever load, south truss

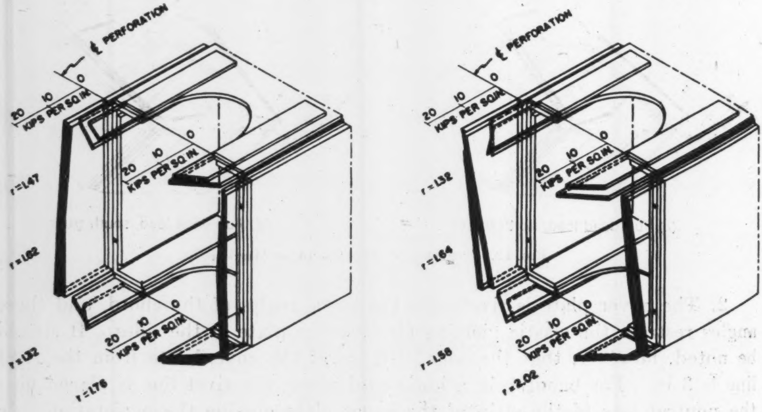
℄ PERFORATION
0
10
20
KIPS PER SQ. IN.
r = 1.47
r = 1.62
r = 1.32
r = 1.76
℄ PERFORATION
r = 1.32
r = 1.64
r = 1.58
r = 2.02

(*c*) Full dead load, north truss

(*d*) Full dead load, south truss

FIG. 13.—STRESSES AT SECTION 14 OF L_{13}–L_{14}

The measurements indicated the stress to be approximately linear at sections 13 and 15 of the north truss, at section 14 of L_{13}–L_{14} and L_{14}–L_{15}, and at section 15 of the south truss. At the other sections the members appeared to have undergone some warping. It should be noted that the stresses were measured at the middle of the width of the vertical webs (Fig. 8(*b*)) for both sections 14 of the lower chords. These measurements showed a stress distribu-

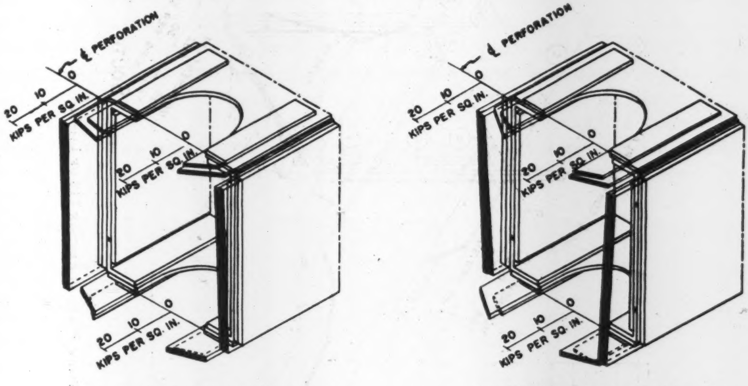
℄ PERFORATION
20
10
0
KIPS PER SQ. IN.
20
10
0
KIPS PER SQ. IN.
20
10
0
KIPS PER SQ. IN.
℄ PERFORATION
20
10
0
KIPS PER SQ. IN.
20
10
0
KIPS PER SQ. IN.
20
10
0
KIPS PER SQ. IN.

(*a*) Cantilever load, north truss

(*b*) Cantilever load, south truss

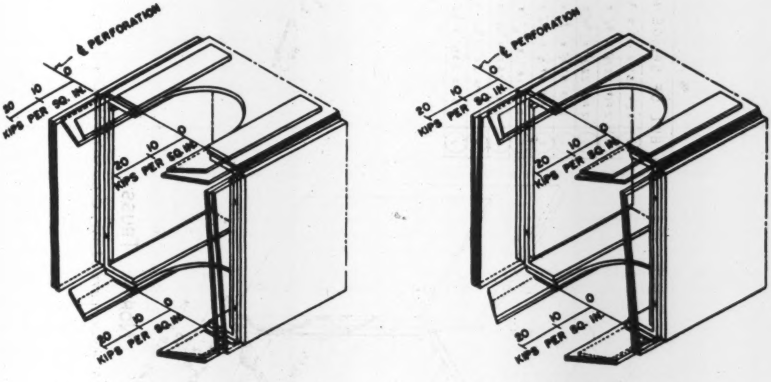
℄ PERFORATION
20
10
0
KIPS PER SQ. IN.
20
10
0
KIPS PER SQ. IN.
20
10
0
KIPS PER SQ. IN.
℄ PERFORATION
20
10
0
KIPS PER SQ. IN.
20
10
0
KIPS PER SQ. IN.
20
10
0
KIPS PER SQ. IN.

(*c*) Full dead load, north truss

(*d*) Full dead load, south truss

FIG. 14.—STRESSES AT SECTION 13 OF L_{13}–L_{14}

tion in each web that was approximately linear across the width of the plate—that is, across the vertical face.

If the stress distribution across the member had been measured at sections adjacent to the gussets or splice plates, it is highly probable that the measurements would have indicated high local stress concentrations delivered from the rivet loads to the member by the gusset or splice plates.

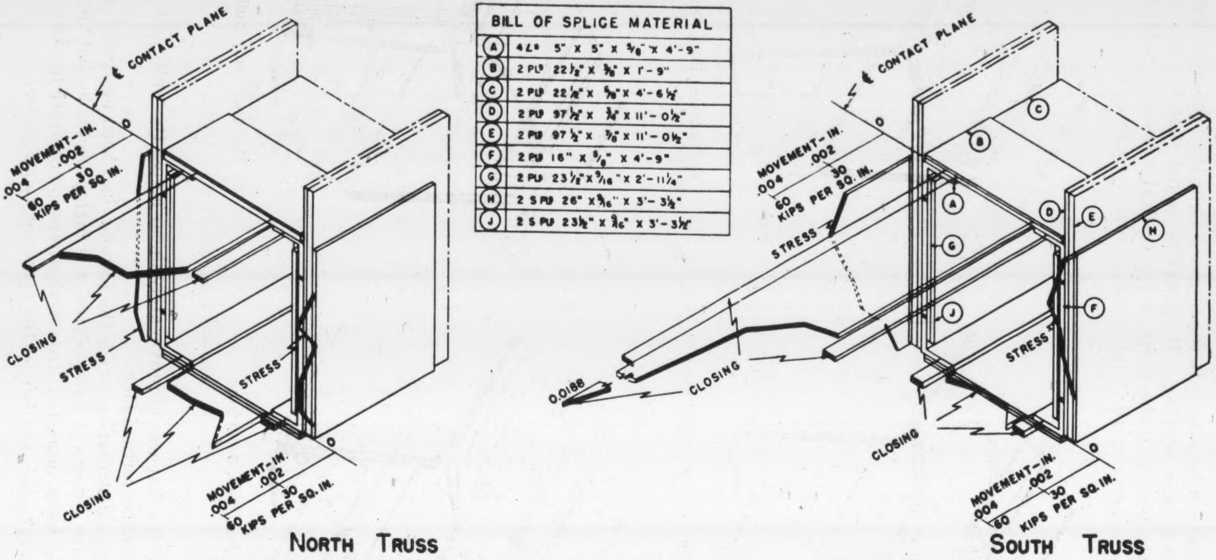
℄ CONTACT PLANE
MOVEMENT-IN.
.004
.002
0
60
30
KIPS PER SQ. IN.
STRESS
CLOSING
NORTH TRUSS
A
B
C
D
E
F
G
H
J
0.0188
SOUTH TRUSS

BILL OF SPLICE MATERIAL	
Ⓐ	4∠s 5" × 5" × 5/8" × 4'-9"
Ⓑ	2 PLs 22½" × 3/8" × 1'-9"
Ⓒ	2 PLs 22½" × 5/8" × 4'-6½"
Ⓓ	2 PLs 97½" × 3/4" × 11'-0½"
Ⓔ	2 PLs 97½" × 7/8" × 11'-0½"
Ⓕ	2 PLs 16" × 5/8" × 4'-9"
Ⓖ	2 PLs 23½" × 9/16" × 2'-11¼"
Ⓗ	2 S PLs 26" × 9/16" × 3'-3½"
Ⓙ	2 S PLs 23½" × 9/16" × 3'-3½"

FIG. 15.—CANTILEVER LOAD, CLOSING OF MILLED JOINT, AND STRESSES IN PLATE AT SECTION 14S OF L_{13}–L_{14}

Movement at a Shop Splice.—In Fig. 15 are plotted measurements taken at the shop-riveted splice at section 14S in the lower chord. This splice was designated to carry 50% of the stress in the chord, the other 50% to be taken in bearing at the milled-joint surfaces. In the vertical planes, splice plates were provided both inside and outside of each main web or rib section. In the horizontal planes, splice plates were placed on the outside surfaces only. It was thus possible to take readings on 2-in. gage lines located at 90° to the plane of the milled joint and centered on it, on the horizontal legs of the main angles, and on the inside faces of the top and bottom cover plates (Fig. 8(*f*)). The readings on these gage lines inside the member at this splice were a measure of the movement of the contact surfaces of the material plus any shortening of the material caused by a stress change. Readings on the 2-in. gage lines located at 90° to the plane of the milled joint and centered on it on the outside splice plates, in both the horizontal plane and the vertical plane, were a measure of the shortening of these plates caused by the stress.

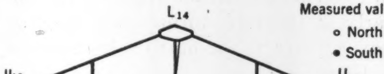
Measured values shown
○ North truss
● South truss
L14
U12
U16
0.2
0.4
1.6
4.2
3.0
2.9
L12
L14
L16
3.1
2.8
0.2
1.8
Secondary stresses, in plane of lower chords
2.1
2.0
3.0
2.7

FIG. 16.—COMPARISON OF MEASURED AND COMPUTED BENDING STRESSES (IN KIPS PER SQUARE INCH) AT THE CANTILEVER STAGE

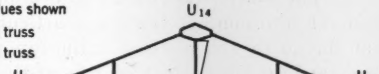
U14
U12
U16
6.6
9.3
3.2
2.7
3.4
3.5
L12
L14
L16
3.0
3.1
0.6
1.8
Secondary stresses, in plane of lower chords
2.1
1.8
2.8
2.6

FIG. 17.—COMPARISON OF MEASURED AND COMPUTED BENDING STRESSES (IN KIPS PER SQUARE INCH) AT FINAL FULL LOAD STAGE

The measurements plotted in the horizontal inside planes in Fig. 15 represent principally the movement of the contact surfaces toward each other, and the measurements plotted on all outside planes represent strains and stresses in the outside splice plates. It should be noted that both of these readings have been plotted to the same equivalent scale.

The following observations are noteworthy:

1. The measurements show a closing of the joints to a magnitude of approximately 0.019 in. at the north top corner of the south-truss chord and somewhat less at the same corner of the north-truss chord (Fig. 15).

2. For both truss splices little or no stress is measured in the horizontal splice plates placed outside the butt joint. For the north-truss splice a reasonable stress is measured in the north-outside splice plates, but for the south-truss splice the measured unit stress in the north-outside plates is approximately equal to the elastic limit of the material; also, the stress variation across the width of the splice plates in the vertical plane is great. In both trusses little or no stress was measured in the outside south plates.

3. Measurements taken at these shop splices at the full-dead-load stage showed no appreciable change in readings over the cantilever-stage readings; these data indicate that the joint had been almost completely closed on all four sides at the cantilever stage.

The circumstances cited may possibly be explained by the following:

a. The south web plates and bottom cover plates of each truss chord were brought into contact bearing (particularly at the top) during shop riveting, but the north web plates and the top cover plates at the north sides were not brought into full contact bearing at this time.

b. During the loading for the cantilever stage, the butt joint closed to full bearing; thereafter, little stress was added to the splice plates.

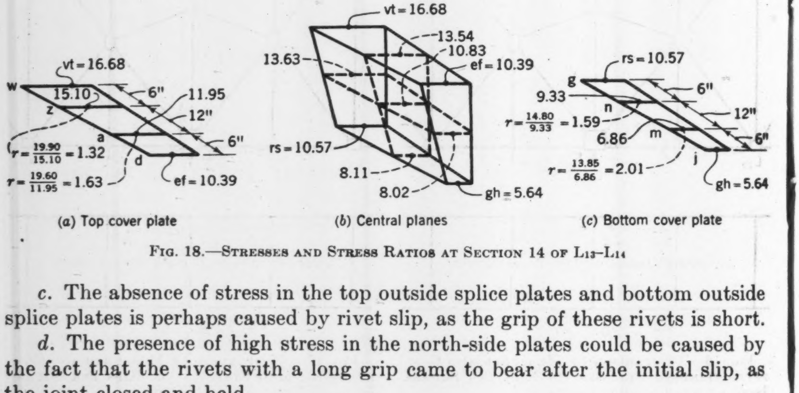

(*a*) Top cover plate (*b*) Central planes (*c*) Bottom cover plate

FIG. 18.—STRESSES AND STRESS RATIOS AT SECTION 14 OF L_{13}–L_{14}

c. The absence of stress in the top outside splice plates and bottom outside splice plates is perhaps caused by rivet slip, as the grip of these rivets is short.

d. The presence of high stress in the north-side plates could be caused by the fact that the rivets with a long grip came to bear after the initial slip, as the joint closed and held.

e. The greater stress in the splice plates of the south truss may easily have been caused by the fact that the movement measured in closing the joint was greater than in the north truss.

The implications of these measurements on the shop-riveted butt joint (designed to carry a considerable part of the load in direct bearing) are:

(1) If the material is not in complete and full bearing at the time of riveting (a condition not easily attained), slip of the rivets and serious readjustment of the stress distribution among the elements of the splice will probably occur at an early stage of loading.

(2) The material in such a connection is likely to be stressed to above the elastic limit at any time, depending entirely on the fit of the metal in the original connection and the load subsequently placed on the joint.

Stress Measurements at a Field Splice.—Complete sets of readings were taken on the gage lines of the field splice at section 14S of M_{14}–L_{14} at all stages of construction (Fig. 8(*c*)). The readings were checked by a second group of two men, and close agreement was found between the results by all observers at a given stage. In this case, also, readings were taken on the outside of the splice plates. All measured stresses were in tension, and some were in the elastic-limit region. The explanation may be as follows:

1. Initial readings in the shop were taken when the splice plates were riveted only to joint L_{14}.
2. A large part of the dead-load stress was placed on the joint in the field, thus bringing the contact surfaces to firm bearing before the field riveting was done. Therefore, only a small part of the compressive deformation was caused in the splice plates by the additional load in the vertical member U_{14}–L_{14}.
3. All splice plates at the joint may have been bent outward, perhaps by the shop riveting or perhaps by accident, prior to the taking of initial readings. The pulling of these plates into tight contact with the vertical member during field riveting could then produce a large tensile stress on the outside faces of the plates.
4. It also seems probable that the heavy clamping of the hot-driven rivets may have caused large stresses in the material adjacent to the rivets.

The implication of these measurements is that detail material in such a splice is likely to be highly stressed.

Several construction operations can be expected to affect the final dead-load stresses in the structure. During erection the structure was held to proper level and alinement. As has been noted, it was intended to induce reverse bending in the lower-chord truss members adjacent to the channel pier so as to neutralize the secondary stresses caused by the dead load. To accomplish this, the proper web members were shortened in length so that the chords would be pulled up in erection.

Two other construction operations, both cited previously, may be expected to affect the final dead-load stresses in some of the members. The first is the cutting loose of the bracing member M_{14}–M_{15} from the post U_{14}–L_{14} at joint M_{14}. The second is the manner of closing the anchor span at the channel pier when unequal temperatures were obtained in the lower chords of the north and south trusses. The success attained in all these operations can be seen in the residual stresses in the structure at its completion.

Secondary Stresses.—In Fig. 16 are plotted: (1) Computed bending stresses in a vertical plane resulting from the dead-load secondary stresses at the cantilever stage, including the effect of cutting M_{14}–M_{15} loose from joint M_{15}; (2) measured unit bending stresses in the vertical plane at the sections under study; and (3) measured unit bending stresses in the horizontal plane for the lower-chord members.

In Fig. 17 are plotted the same stresses for the final full-dead-load stage of construction. The effect on the secondary stresses of large truss joints such as that at L_{14} of this bridge is considerable. This effect was taken into account by a rational and expeditious method of analysis which has been presented and checked[13] against measured stresses for a large bridge.

The following comments are pertinent:

1. Computed secondary stresses at the edge of the gusset of member L_{14} (made on the assumption of no corrective measures having been taken) were approximately 9.3 kips per sq in. or 72% of the computed dead-load stress on the river side, and were approximately 6.6 kips per sq in. or 55% of the computed dead-load stress on the shore side. These values include the effect of the brace M_{13}–M_{14} in pulling U_{14}–L_{14} out of line toward the shore.

2. The attempt to avoid the high secondary stresses in the lower chords was completely successful for L_{13}–L_{14} in the north truss and for L_{14}–L_{15} in the south truss. In L_{13}–L_{14} for the south truss at section 14 the bending stress was reduced to approximately 2.7 kips per sq in. or 23% of the dead-loss stress. In L_{14}–L_{15} the bending stress was reduced to a negligible value at section 14 and reached a value of 3.4 kips per sq in. or 26% of the dead-load stress at section 15.

3. In two cases the residual bending stresses were opposite in sign to the computed secondary stresses, suggesting that correction was carried beyond the intended value.

4. The marked nonlinear variation of stress in M_{13}–L_{14} at section 14 could have been caused during riveting if all pins and bolts had been removed from one side of the member while it was carrying substantial stress.

5. The influence of the counterclockwise rotation of joint L_{14}, because of the pull of M_{13}–M_{14} on the vertical, is seen in the measured stress pattern for all members entering this joint. If this brace could be cut free and then reconnected, an improved stress condition would result.

6. The lower-chord bending stresses of 3.1 kips per sq in. in the horizontal plane for L_{13}–L_{14} at section 14 on the north truss and of slightly less stress in the other members may have been caused by the unequal temperature conditions. They may also have been a result of slippage in the plates in the splices on either side of joint L_{14}.

CONCLUSIONS

From the results of the investigation the following conclusions are warranted:

1. When properly conducted, dead-load-stress measurements made under field conditions are entirely reliable and trustworthy. However, errors as large as 1,000 lb per sq in. may be expected.

2. It is desirable to study further the action of perforated cover plate columns, particularly for ultimate loads.

3. It should be recognized that, in joints carrying load partly by riveted splice plates and partly by milled joints in bearing, differential local slippage is likely to occur and the splice plates are likely to be stressed into, and perhaps above, the yield-stress range.

---

[13] "Rigid Frame Analysis for Members of Variable Moment of Inertia," Pts. 1 and 2, by L. T. Wyly and K. H. Lenzen, *Bulletin No. 502*, A.R.E.A., June–July, 1952, pp. 1–64.

4. It is entirely practicable and possible to reduce the dead-load secondary bending in the plane of the trusses by changing the lengths of the members, but, unless unusual precautions are taken and supervision is provided, there is no assurance that success will attend the effort.

5. Bending in the horizontal plane caused perhaps by conditions of temperature during erection or perhaps by slippage in splices designed for bearing may be expected to exist to the extent of approximately 25% of the axial dead-load stress.

6. Where fabrication and erection processes do not attain the standards used on the construction of the East St. Louis Veterans Memorial Bridge, the bending stresses in both planes will probably be considerably larger.

ACKNOWLEDGMENTS

The writers are indebted to many persons for assistance in conducting this investigation. The officials of the Bethlehem Steel Company of Bethlehem, Pa., permitted the tests to be made, allowed initial readings to be taken in their shops, furnished field-office space, and built substantial stagings and walkways on the job. The executive officers of G. A. Maney and Associates in Chicago, Ill., assisted in arranging the project and helped in its execution. N. J. Law, M. ASCE, and his assistant, L. D. Urbain, cooperated in the field. Purdue University and Northwestern University supported the project financially (as did the Research Corporation of America) and permitted the staff members to perform the necessary work. A number of former graduate students at Purdue University and at Northwestern University assisted in the investigation. A. D. M. Lewis, J. M. ASCE, planned the thermocouple layout. Leonard Duane Pyle, J. M. ASCE, J. P. McCalley and Za Lee Moh, J. M. ASCE, did much of the work in computing secondary stresses. John Aberson, A. Andros, William Rux, J. M. ASCE, Philip Swanberg, Henry W. Swanson, J. M. ASCE, and A. A. Thorup assisted in the field and laboratory investigations. Valuable advice and suggestions were received from Jonathan Jones, Hon. M. ASCE, E. J. Ruble, M. ASCE, and Frank Baron, M. ASCE.

DISCUSSION

Almon H. Fuller,[14] M. ASCE.—The six conclusions offered by the authors suggest a careful analysis of the results of a well-prepared and ably performed investigation of this interesting bridge; the results command confidence. The recognized error of 1,000 lb per sq in. is in accord with other field investigations of stresses and strains.

In the "Synopsis," two values are given which are not included in the "Conclusions." The stresses caused by temperature and erection effects (3,000 lb per sq in.) are noted differently in item 5 in the "Conclusions." The statement, that the measured stresses were lower than the computed dead-load stresses by approximately 1,000 lb per sq in. is given as a statement of fact without corroborating data. This point is of great interest as some of the available results of field investigations prior to 1954 show that between the observed stresses and the computed stresses there are differences of various magnitudes which are, however, primarily in the same direction. Among the reasons for such differences are (*a*) the retarding effect of deflection because of the bending of the members (secondary stresses), and (*b*) the fact that the deformation of a steel member under stress is dependent (even if to an unmeasured extent) on the length of time under stress. Physicists maintain that steel is not 100% elastic and that, therefore, its deformation is dependent on time.

There is reason to believe that the retarding effect of the bending of members in a trussed structure is within 5% of the total deflection; therefore, the direct stresses are reduced by approximately the same amount. The reduced observed stresses, reported as approximately 1,000 lb per sq in., are near 10% of the highest reported stresses. Therefore, in the few members under consideration, more than 5% of the difference between observed and computed stresses remains unaccounted for.

The writer, in 1925, made some field observations on strains and stresses during the erection of the Equitable Building in Des Moines, Iowa. Observed stresses[15,16,17] exceeded the computed stresses by considerably more than 10%. In 1928, Clyde T. Morris, M. ASCE, made similar observations during the erection of the American Insurance Union Building in Columbus, Ohio, and found that the results were comparatively the same. In his report,[18] Mr. Morris included a discussion of the writer's data. Mr. Morris represented the relationship between the computed stress and the observed strain in the form of a "modulus of elasticity." This modulus represented the relationship of stress and strain in large built-up columns over a number of weeks. The modulus varied from less than 20,000,000 lb per sq in. to more than 24,000,000 lb per sq in. with the average unit stresses varying from approximately 6,000 lb per sq in. to 9,000 lb per sq in. The duration of time is not recorded but extends over a number of weeks.

---

[14] Prof. of Civ. Eng., Iowa State College, Ames, Iowa.

[15] "Measurement of Stresses in Four Steel Columns of the Equitable Building, Des Moines, Iowa," by Almon H. Fuller, *Bulletin No. 72*, Iowa Eng. Experiment Station, Iowa State College, Ames, Iowa, August, 1924.

[16] "Measured Stresses in Columns of 18-Story Building," *Engineering News-Record*, October 2, 1924, p. 540.

[17] "Stress Measurements in Buildings," *ibid.*, October 23, 1924, p. 655.

[18] "Dead Load Stresses in the Columns of a Tall Building", by Clyde T. Morris, *Bulletin No. 40*, Eng. Experiment Station, The Ohio State Univ., Columbus, Ohio, 1928.

The writer does not find in this paper, or in some other reports of field investigations,[18] any indication of continued deformation under stress. Nevertheless, it is believed to exist, even if it is so small as to be accepted as a part of the inevitable lack of precision. This is one phase where current (1954) methods of computation charge the structure with greater stresses than it will be required to carry. This point might well be remembered when it becomes economical to design with more refinement than is required by present specifications.

Lawrence T. Wyly,[19] M. ASCE, Maurice B. Lagaard,[20] M. ASCE, Ralph W. Kluge,[21] A. M. ASCE, Kenneth H. Lenzen,[22] A. M. ASCE, Edward W. Larson, Jr.,[23] A. M. ASCE, and Lewis B. McCammon, Jr.,[24] A. M. ASCE.—The care that Mr. Fuller has evidently used in studying this paper is appreciated. His comments are concerned mostly with the fact that the measured dead-load stresses were approximately 1,000 lb per sq in. lower than were the computed dead-load stresses. Mr. Fuller also discusses (1) the effect of secondary stresses in the plane of the main trusses in reducing the axial stresses in these truss members and (2) the problem of creep or flow in steel at stresses well below the elastic limit as a function of time.

The effect of secondary bending stresses in the plane of the main trusses in reducing the axial stresses in the truss members is usually negligible; computations have shown[25] these reductions to be 0.3% for a bottom chord and 0.5% for a top chord in a 160-ft span. This reduction of axial stresses can be expected to vary approximately with the depth-to-length ratios of the members. Because this ratio is approximately the same for the lower chords of the Veterans Memorial Bridge as it is for the 160-ft span (that is, 0.029) it appears reasonable to believe that the reduction in axial stresses in the former would be less than 1%. The secondary stresses computed on the assumption that no corrective measures had been taken are quite small in the trusses of the Veterans Memorial Bridge, except at joint L_{14} at the main piers. However, it should be noted that the shop-assembly reaming and the erection operations were adopted to eliminate the secondary stresses in the chord members; the stress measurements show that this was largely accomplished at the points adjacent to the L_{14} points.

---

[19] Research Prof. and Head of Structural Eng. Dept., Purdue Univ., Lafayette, Ind.

[20] Associate Prof. and Chairman of Eng. Drawing Dept., Northwestern Univ., Evanston, Ill.

[21] Head of Civ. Eng. Dept., Univ. of Florida, Gainesville, Fla.; formerly Associate Prof. of Structural Eng., Purdue Univ., Lafayette, Ind.

[22] Research Associate and Instructor in Structural Eng., Purdue Univ., Lafayette, Ind.

[23] Test Engr., Hughes Tool Co., Culver City, Calif.; formerly Research Associate and Instructor in Civ. Eng., Northwestern Univ., Evanston, Ill.

[24] Associate Prof. of Civ. Eng., Northwestern Univ., Evanston, Ill.; formerly Research Associate and Instructor in Structural Eng., Purdue Univ., Lafayette, Ind.

[25] "Modern Framed Structures," by J. B. Johnson, C. W. Bryan, and F. E. Turneaure, John Wiley & Sons, Inc., New York, N. Y., 10th Ed., 1929, Pt. II, pp. 460–463, Paragraph 327.

In view of these considerations it would seem that the estimated 5% reduction in axial stresses caused by secondary bending is much too high.

Regarding possible flow or creep in the steel at atmospheric temperatures, the writers reviewed the literature on various phenomena which might affect the time-strain relationship. The results[26] of the work of many laboratories showed that a creep of 0.01% was measured at a stress varying from 12,000 lb per sq in. to 13,000 lb per sq in. after the load had been applied for 1,000 hr at a temperature of 800° F. This result is for a steel similar in composition to the steel used in the Veterans Memorial Bridge. No evidence has been found of any significant creep or flow in this grade of steel at atmospheric temperatures at stresses well below the elastic limit.

The problem of flow or creep was also referred to the steel supplier for the bridge. In the report the typical chemical composition and mechanical properties for the silicon steel produced by this company were given as follows:

Chemical composition—

Carbon, in percentage	0.30
Manganese, in percentage	0.90
Silicon, in percentage	0.25
Phosphorus, in percentage	0.02
Sulfur, in percentage	0.03

Mechanical properties—

Yield point, in pounds per square inch	50,000
Tensile strength, in pounds per square inch	86,000
Elongation in 8 in., in percentage	23

The supplier's metallurgical engineer reported that creep (being associated with a permanent form of physical change in steel) would be so small at room temperature or ambient temperatures as to be immeasurable.

According to this engineer there is no way of measuring creep at room temperature as this term has no meaning. The metallurgical engineer further stated that he had no information on creep in silicon steel. He explained that the stress-strain curve for silicon steel is similar to that for carbon steel and has a straight line variation below the yield point. There is no reason (so far as he knew) to believe that silicon steel will show a definite measurable strain under constant load for a long time. Once it reaches elastic deformation under this load it should continue to hold the load without strain. If there are local stresses (or locked-up stresses) higher than the yield point, the metal will have a local permanent set, and the high local stresses will be relieved; this is true for carbon steel or silicon steel. In other words, concluded the engineer, there was no creep effect for silicon steel peculiar to that grade of steel.

The writers are familiar with the stress investigations on large steel buildings[15,18] reported by Mr. Fuller; these studies are valuable additions to the science of structural engineering. There are certain differences, however, between the results obtained in these investigations and those obtained in the bridge investigation. First, the discrepancy between computed and measured dead-load stresses is more than twice as great in the case of Mr. Fuller's report,[15] averaging approximately 2,200 lb per sq in. rather than 1,000 lb per sq in. Secondly, in the case of the measurements on buildings reported by Messrs. Fuller and Morris, the measured values were found to be larger than the computed values by from 20% to 35% whereas the measured dead-load stresses in the bridge were lower than the computed dead-load stresses by approximately 10%. It is obvious that a theory of creep or flow in steel under stress would have to be reversed to explain the difference between measured and computed stresses in the case of the Veterans Memorial Bridge—that is, the steel would have to lengthen as a function of time under compression.

---

[26] "Compilation of Available High Temperature Creep Characteristics of Metals and Alloys," by the Creep Data Section, Joint Research Committee of the ASME and ASTM on the Effect of Temperature on the Properties of Metals, 1938, p. 15, Fig. 13A.

AMERICAN SOCIETY OF CIVIL ENGINEERS
Founded November 5, 1852
TRANSACTIONS

Paper No. 2742

ISSUES IN HIGHWAY ENGINEERING EDUCATION

By Harmer E. Davis[1] and Ralph A. Moyer,[2]
Associate Members, ASCE

Synopsis

The problem of supplying the required manpower to solve the many highway-transportation difficulties facing highway administrators is crucial and complex The approach must be a composite one; no single program of action will result in a real solution. The problems that exist in engineering education have been reviewed many times. A program that was adopted in California in 1947 is cited as comprehensive; it begins with the undergraduate education of the prospective engineer and is continued with extension courses and in-service training.

Introduction

Nationwide attention has been directed (1954) in many ways to the seriousness of the highway situation. The nature of the situation was ably summarized[3] by Dwight D. Eisenhower, President of the United States:

> "The obsolescence of the nation's highways presents an appalling problem of waste, danger and death. Next to manufacturing of the most modern implements of war as a guarantee of peace through strength, a network of modern roads is as necessary to defense as it is to our National economy and personal safety. We have fallen far behind in this task—until today there is hardly a city of any size without almost hopeless congestion within its boundaries and stalled traffic blocking roads leading beyond these boundaries."

President Eisenhower stated that a solution can be found through the joint planning of federal, state, and local governments.

There are many factors which have contributed to the seriousness of the predicament: (1) Vehicle registration and usage increased rapidly following World War II causing unexpected overcrowding of highways. (2) Unusual population

---

Note.—Published, essentially as printed here, in August, 1953, as *Proceedings-Separate No. 236*. Positions and titles given are those in effect when the paper was received for publication.

[1] Director and Prof. of Civ. Eng., Inst. of Transportation and Traffic Eng., Univ. of California, Berkeley, Calif.

[2] Research Engr. and Prof. of Civ. Eng., Inst. of Transportation and Traffic Eng., Univ. of California, Berkeley, Calif.

[3] *Road Builders' News*, Vol. 29, November–December, 1952, p. 7.

growth and increasing decentralization in urban areas contributed to daily traffic jams in both cities and towns. (3) Inflation cut the value of the appropriated money in half. (4) Wartime neglect contributed to a rapid deterioration of roads. (5) There was a shortage of trained engineering personnel. In many states, the existence of the following conditions compounded the difficulties of providing adequate highway systems: (*a*) Legislative bodies and public officials did not provide the necessary legislation to finance urgently needed highway improvements. (*b*) There were excessive diversion and dispersion of highway funds. (*c*) Employment in some highway departments was relatively unattractive to professionally trained engineers; the pay was poor, and political influences unduly affected appointments and promotions as well as technical operations.

The blame for this critical highway situation cannot be placed on particular agencies, organizations, and professions. Highway transportation and traffic problems are so intimately interwoven with the daily activities of all persons as to make highways and traffic the responsibility of many public and private groups. As might be expected with so great a division of responsibility, certain important phases of highway engineering have suffered from lack of coordinated attention and planning. One of these phases—the acquisition, education, and professional development of personnel—is particularly in need of attention at the present time (1954).

Highway and traffic engineering are important segments of civil engineering; a major responsibility for solving highway and traffic problems has thus been placed on civil engineers, and consequently a share of responsibility also falls on the engineering educators and research staffs of the colleges. Practicing civil engineers, educators, and research staffs have contributed in countless ways to improve highway transportation, but there is considerable evidence that "we have fallen far behind in this task* * *." Furthermore, highway and traffic problems are becoming increasingly complex; their solution presents greater challenge than at any previous time. Some universities have recognized the need for broader and more intensive highway engineering education programs to meet the challenge created by the critical traffic situation, and some unusual programs have been introduced.

CRITICAL PROBLEMS IN ENGINEERING EDUCATION

Many engineering educators are alarmed about the present (1954) shortage of engineers, the greater shortage in prospect, and the increasing demands for the engineers' services resulting from rapid advances in science and technology. Also, there is great concern as to whether the programs of engineering education will satisfy future demands for engineers. It should be recognized that engineering progress depends, to a great extent, on engineering education and on the extent to which promising high school graduates can be attracted to the study of engineering.

Solomon C. Hollister, M. ASCE, has clearly set forth[4] the need for studying the engineering profession and engineering educational programs in view of the shortage of engineers. The increasing demands for engineering services accentuate the need for immediate appraisal. Mr. Hollister reported that surveys indicated that approximately 80,000 engineers would be needed whereas the number of engineering graduates for 1952 and for the subsequent years was 20,000 or less per year. Because of the inadequate number of graduate engineers and because of the existing military program, it is evident that the present (1954) shortage of engineers will continue for some time.

---

[4] "A Goal for American Engineering Education," by Solomon C. Hollister, *The Journal of Engineering Education*, Vol. 43, No. 1, September, 1952, p. 7.

Even if the number of engineers called into military service is reduced, there still remains the continually increasing need for engineers because of the rapidly accelerating technological development of the era. The following statistics are significant: According to the census, in 1890 there was one engineer to approximately 300 workmen employed in industry; in 1950 there was one engineer to approximately 50 workmen employed in industry. Mr. Hollister noted[4] that

> "* * * this increase is not going to continue, since the number of freshmen normally entering engineering is a fixed percentage of the age population, and this percentage is not likely to increase. Thus the increase of engineers as a percent of the population has reached a stopping point."

Therefore, there is the problem of an increasing demand for engineers with relatively fewer engineers from year to year to meet these demands. This situation is almost certain to require a revision of objectives in engineering education, a possible reorganization of the professional function, and a revision of engineering curricula.

In 1952 the American Society for Engineering Education (ASEE) formed a committee on the evaluation of engineering education. This committee was organized on a nationwide basis to establish the needs of the profession and of the United States. As an indication of the importance of the work of this committee, the Engineers' Council for Professional Development (ECPD), which is responsible for accrediting engineering curricula at all the engineering schools in the United States, announced that there would be no inspection of new curricula in engineering until adequate criteria had been established, based, in part, on the findings of this ASEE committee.

It is evident that, in planning a highway engineering education program, the limitations imposed by the engineering manpower situation must be considered. Furthermore, consideration should be given to plans which will provide for the most effective use of the engineer's time, both as a student and later as a practicing engineer.

HISTORICAL BACKGROUND

The early engineer was trained by apprenticeship whereby he had the advantage of being trained while doing productive work. Under a good master, an apprentice received excellent training. The in-service training programs widely used (1954) in industry and in large engineering organizations are a form of apprenticeship. The earlier apprenticeship practices, however, did not lend themselves to training large numbers of engineers. As the demand for engineers increased, engineering schools evolved. The first of these was organized in France in 1747 by J. R. Perronet. Mr. Perronet was given the job of building a system of national highways; recognizing the importance of good technical training, he organized his staff into a school which became the famous École des Ponts et Chausées in 1775. Mr. Perronet has been called the father of engineering education and because he trained men to build highways he may also be considered to be the father of highway engineering education.[5,6]

By 1852 there were five engineering schools in the United States. Emphasis was placed on a fairly broad education. Subjects in the basic sciences, such as mathematics, chemistry, physics, and mechanics, were included whereas only limited instruction was given in practical engineering. During the next four decades there was an increasing public interest in science and engineering. There also occurred transitions in educational patterns from general to practical and finally to a balance between scientific and professional instruction. In 1862 the first Morrill Act[7] resulted in the creation of many land grant colleges of agriculture and "mechanic arts." By 1893 engineering instruction was given in more than one hundred schools in the United States; it was a natural development at this time that the Society for the Promotion of Engineering Education (SPEE) was organized. Although previously the subject of engineering education had not lacked its appraisers and commentators, the SPEE became the vehicle for a number of later notable studies of engineering education.

By the end of the nineteenth century there had evolved the four-year undergraduate engineering curriculum, the first two years of which were comprised largely of studies of mathematics and physical sciences, and the last two years of which included instruction of more or less professional character in the major field of specialization. It is of interest to realize that, in spite of much investigation and examination of curricula, there has since been no profound change in philosophy or pattern of formal undergraduate engineering education (as of 1954).

INVESTIGATIONS OF ENGINEERING EDUCATION

The first comprehensive study of engineering education was made[8] by C. R. Mann during the period from 1914 to 1918. In the study of the curricula of one hundred and twenty-five schools, the division of time was found to be 20% for the humanities and cultural subjects, 30% for mathematics and basic sciences, and 50% for technical subjects. The most significant finding of Mr. Mann's study was based on a questionnaire sent to members of the national technical societies who were asked to express their opinions of the characteristics essential to an engineer's success. The returns from more than 7,000 members gave the following, in order of importance: (1) Character, integrity, resourcefulness, and initiative; (2) judgment, common sense, scientific attitude, and perspective;

---

[5] "A Comparative Study of Engineering Education in the United States and in Europe," by William E. Wickenden, from "Report of the Investigation of Engineering Education, 1923–1929," Vol. 1, Univ. of Pittsburgh, Pittsburgh, Pa., 1930, p. 758.

[6] "History of Engineering Education," by F. T. Mavis, *The Journal of Engineering Education*, Vol. 43, No. 4, December, 1952, pp. 217–218.

[7] *U. S. Statutes at Large*, Vol. 12, Chapter CXXX, July 2, 1862, pp. 503–505.

[8] "A Study of Engineering Education," by C. R. Mann, a report prepared for the Joint Committee on Eng. Education of the National Eng. Societies, New York, N. Y., and The Carnegie Foundation for the Advancement of Teaching, *Bulletin No. 11*, 1918.

(3) efficiency, thoroughness, accuracy, and industry; (4) understanding of men and executive ability; (5) knowledge of fundamentals; and (6) techniques of practice and business. This survey provided some unexpected results by placing personal traits of character, initiative, and common sense at the top of the list and technical competence at the bottom. Mr. Mann concluded[8] that the survey clearly indicated that "* * * the professional demand identified the aim of engineering education with the aim of all education, namely, the development of men of character and of practical ability." It is fair to conclude that this report has had a large influence on engineering education. It discouraged overspecialization (at the undergraduate level) along technological lines in a period of spectacular scientific discoveries and great technological advances. It encouraged educators to hold to the ideals of a broad education in engineering whereby some humanistic-social studies are integrated with the studies in science and technology. It set a pattern of investigation of the engineering profession and engineering education which has been followed repeatedly.

During the period from 1920 to 1954, engineering education and the curricula have been the subject of almost continual study. The report made[9] by William E. Wickenden and Harry Parker Hammond constitutes a monumental treatise on every phase of engineering education in the United States and in Europe. This investigation contributed immeasurably toward the achievement of its objective, "to develop, broaden and enrich Engineering Education." It is significant that in all the major investigations of engineering education and engineering curricula there has been remarkable agreement among the findings. The recommendations[10] made by the SPEE in 1940 can be considered to be representative of the findings in all the reports. The general objectives and scope of engineering education outlined in this report have been widely accepted by professional engineers and engineering educators. One might expect that, as a result of the general acceptance of the committee recommendations, engineering curricula would be standardized. The various investigating committees recognized this possibility and strongly advised against it. Each committee reaffirmed the need for careful experimentation with engineering education programs if progress were to be made. Thus, whereas the general pattern of engineering education is the same at almost all engineering schools, there are wide differences in the details of the pattern at each school. This was clearly shown in the results of the study[11] of civil engineering curricula at one hundred and fourteen engineering schools. The civil engineering content of the curricula at these schools varied from 15% to 42% of the total units required for graduation; the mathematics content from 6% to 17%; the content of the physical sciences (physics, chemistry, and geology) from 9% to 22%; the content in basic mechanics from 6% to 15%; and the content in humanistic-social studies from 7% to 28%.

---

[9] "Report of the Investigation of Engineering Education, 1923–1929," by William E. Wickenden and Harry Parker Hammond, Office of the Secretary, Society for The Promotion of Eng. Education, Univ. of Pittsburgh, Pittsburgh, Pa., Vol. I, 1930; Vol. II, 1934.

[10] "Report of Committee on Aims and Scope of Engineering Curricula," by Harry Parker Hammond, *The Journal of Engineering Education*, Vol. 30, No. 7, March, 1940, pp. 563–566.

[11] "Engineering Education: Progress Report of the Society's Professional Committee on Engineering Education, for 1944 and 1945," *Proceedings*, ASCE, Vol. 72, 1946, p. 375.

In commenting on this study Harold E. Wessman, M. ASCE, stated[12] that

> "Every one of the 114 schools will argue earnestly that they are doing a good job in engineering education. It is obviously very difficult to evaluate quantitatively any particular type of educational plan. Every school in the country has outstanding graduates who have made notable records in the practice of engineering and to whom the school will point with pride as evidence of the quality of its education."

HIGHWAY ENGINEERING EDUCATION PROGRAM

The important phases and significant trends in engineering education have been presented because it is felt that they provide the basis for developing a sound over-all program in highway engineering education. Because highway engineering is one of the major fields in civil engineering, the program in highway engineering should be coordinated and integrated with the civil engineering program. It follows also that education in highway engineering as well as engineering education in general should be responsive to the changing technology and needs of the times. As noted previously, there are unprecedented needs in highway engineering which will require expanded programs in highway engineering education. However, it should be obvious from the trends in the pattern of undergraduate engineering education that, in spite of some variation in emphasis in the undergraduate curricula, little further professional specialization can be expected. Thus, if needs are to be met, an approach other than the introduction of a new set of undergraduate courses is necessary.

The California Program.—In 1947 an act[13] was passed in California which provided for the establishment of an Institute of Transportation and Traffic Engineering at the University of California at Berkeley. In passing this act the legislature was primarily concerned with establishing an institute which would give attention to the requirements for training highway engineering personnel at the university and on the job and to a continuing program of fundamental research aimed at the improvement and further development of highway transportation in California. It should be noted, however, that the institute was established to make studies of the whole field of transportation and that its activities were, therefore, not restricted to highway transportation but were intended to include all forms of transportation.

The Undergraduate Program.—At the undergraduate level, the institute cooperates with the civil engineering staff in offering the transportation option within the civil engineering curriculum to provide a selection of courses related to transportation engineering. The present (1954) program provides for a course in highway engineering required of all civil engineering students. The option courses which civil engineering students majoring in transportation may elect include route surveying, soil mechanics laboratory, asphalt laboratory, traffic engineering, and railroad engineering. In addition, civil engineering students may elect one or two courses from a wide variety of courses such as photogrammetry, airphoto interpretation, economics of transportation, and statistics.

---

[12] "Broadening of Curricula in Engineering Education," by Harold E. Wessman, *Civil Engineering*, April, 1949, p. 35.

[13] *California Laws, Statutes.* Chapter 1573, July 19, 1947.

The use of undergraduate options in engineering curricula has been debated for many years. The arguments opposing options most commonly advanced are: (*a*) A four-year program does not allow sufficient time to introduce courses in specialized professional training; (*b*) the time devoted to options can be used more effectively in an expanded program of basic and applied sciences and socio-humanistic courses; and (*c*) results of placement studies are cited which show that up to 50% of the engineers trained in one field of engineering eventually find employment in another field of engineering or in a non-engineering field. It should be noted, however, that this tendency generally applies to engineers in industry and does not apply to civil engineers because only a small percentage of the latter are employed in industry.

Many of the large universities are continuing (as of 1954) the use of options in civil engineering for the following reasons: (1) In the professional or specialized engineering courses the student is introduced to the engineering method of thought and analysis which has been a distinctive feature of engineering education over many decades; (2) in these courses the student is motivated, and in many cases he finds that they have contributed to his success in college and after graduation; (3) the socio-humanistic courses at many engineering schools are poorly coordinated and superficial and under these conditions are of doubtful value in attaining the desired objective of a broad and liberal engineering education; and (4) the placement studies[14] made by Mr. Wickenden in 1925 indicated that less than 30% of the graduate civil engineers obtained employment in another field of engineering or in non-engineering work. This last fact was most evident in the placement of recent graduates where the percentage in another field of engineering or in non-engineering work was less than 15%, as was shown in the 1925 report by Mr. Wickenden[14] and also in the report of a study made in 1954 at the University of California.[15]

Therefore, it is evident that no clear-cut decision in regard to options has been reached (as of 1954). Of course, it is true that the option plan is suitable for use only at the larger colleges and universities and is not practicable in engineering schools with a small enrollment in civil engineering. Such a plan requires many sections, and the cost of instruction per student would be prohibitive at the smaller schools.

An important question in the planning of undergraduate civil engineering curricula relates to the effect which advances in science and technology, such as in nuclear physics, electronics, thermodynamics, optics, and engineering mechanics and materials, will have on the civil engineering curricula. In general, the widest application of the advances in science will be in fields of engineering other than civil engineering. The applications in civil engineering will at first be introduced in courses at the graduate level. In time, however, certain applications will be assimilated in undergraduate courses and will replace outmoded material.

---

[14] "Report of the Investigation of Engineering Education, 1923-1929," by William W. Wickenden and Harry Parker Hammond, Office of the Secretary, Society for the Promotion of Eng. Education, Univ. of Pittsburgh, Pittsburgh, Pa., Vol. I, 1930, p. 231.

[15] "Placement of Civil Engineering Graduates: Classes of 1947 through 1953 at the University of California, Berkeley," by H. S. Lapin and R. A. Moyer, Inst. of Transportation and Traffic Eng., Univ. of California, Berkeley, Calif., 1954 (unpublished).

It is therefore recommended that: (*a*) A basic four-year civil engineering program be established conforming to the general pattern of basic sciences, applied science, applied engineering, and some socio-humanistic studies. The socio-humanistic studies should be integrated with the scientific and technologic subjects and studied concurrently. (*b*) A general course in highway engineering be required of all civil engineering students, consisting of a three-unit or four-unit course for one semester, covering the fundamental principles, theories, and practices in highway engineering and including such topics as highway finance, economics of highway location, highway capacity, geometric design, channelization, mechanics of traffic operations, highway drainage, grading operations, soil stabilization, design and construction of flexible and rigid pavements, and economic selection of pavements. (*c*) Provision be made through options or free electives for a limited amount of specialization in highway engineering by civil engineering students selecting transportation as their major subject.

The Graduate Program.—The graduate program in highway engineering at the University of California is administered by the Division of Transportation Engineering. The program provides for the professional education of advanced engineering students in the field of transportation engineering. Candidates for advanced degrees must take work in one or more of the following areas of study: Statistics, business administration, public administration, and city planning. The graduate program provides professional training for a selected group of students with the required qualifications for advanced study and research. In general, the graduate courses are of a highly technical and specialized nature. The graduate program provides for a systematic study of a large body of technical knowledge in transportation not readily available to these students in any other form or place, such as through job experience or in an in-service training program. Although it is desirable that graduate students have realistic contact with practice, there is an increasing trend to take graduate work as a fifth year of study directly after graduation from a four-year program. Generally, once the graduate is established in a job to his liking, he will not resign or request a leave of absence to return to a college or university for graduate work.

An important feature of the graduate program is the close coordination of instruction with the research program in which the teaching and research staffs are engaged. Graduate study, to be most effective, should provide opportunity for training in the creative and practical phases of engineering design and development through the use of the project method. Individual and group research have been recognized as distinctive features of graduate work which make this work of professional caliber. Many outstanding contributions to engineering knowledge have been made through graduate student research, and for this reason it offers the greatest opportunity for doing productive work in the engineering education program.

The Research Program.—It has been indicated that a successful graduate program requires a parallel program of research. In addition to serving its direct purposes of developing new knowledge and contributing to education, the research program yields two important by-products: (*a*) It serves to stimulate the thinking of staff members, and (*b*) it provides a cooperative link between the university and other agencies.

The Extension Program.—An extension program is an extremely important phase of educational activity. The objective of the extension program should be to make available to personnel engaged in highway and other transportation fields opportunities for extending their fundamental education, for reviewing and exchanging information, and for keeping abreast of new technical developments. The function of the university should be to identify needs, devise programs to meet them, develop instructional materials, and provide instructors.

The identification of needs is established largely by an extensive program of direct contact by the extension representative, as well as by other staff members, with the many individuals and agencies working in the transportation field. It is felt that only through close contact of this kind can the program be adjusted to actual needs and be coordinated with the activities of other agencies. Staff members should explore the problems of road officials of the counties, cities, and state highway districts. In addition, direct liaison must be established with other appropriate state agencies and numerous non-governmental groups. The mediums for conducting the extension program may be broadly classified as conferences, short courses, and regular extension courses. Conferences, ranging from one-half-day to three-day meetings, are generally conducted in major population centers on subjects of major interest and are addressed to large numbers of transportation engineers. Short courses have been conducted by the University of California in (1) various geographic areas of the state in the form of one-evening or two-evening, or weekend, sessions dealing with some specific technical problem and (2) a single area each year in the form of various one-week to two-week, full-time courses dealing with related problems.

ORGANIZATIONAL IN–SERVICE TRAINING

A survey[16] made by the Bureau of Public Roads, United States Department of Commerce (USBPR), indicated that there were 273,300 state and federal employees engaged on highway projects in 1950, of which 52,200 were state employees in engineering, supervisory, and administrative positions. California had 4,000 state employees working on highway projects with 3,000 in the professional grade of junior engineer or higher. The turnover in personnel is very high, especially in the lower grades, where many young men must perform military service. Not only, then, is the need for well-trained and well-informed highway engineers greater than ever before (as of 1954), but a real need exists for continuously developing personnel on the job for increasingly effective discharge of duties and for expanding responsibilities. A program of personnel development also gives promise of reducing turnover through stimulating employee interest and job attractiveness.

The USBPR and certain state highway departments have adopted student training programs which provide in-service, summertime experience for civil engineering students on highway projects with good pay and other inducements.

---

[16] "Highway Facts," Automotive Safety Foundation, Washington, D. C., 1952, p. 67.

This program is an excellent method not only of training men but of attracting them after graduation to full-time engineering employment. Another form of in-service training program used by the USBPR and some state highway departments to attract engineering graduates into highway engineering and to make best use of professional and subprofessional personnel work is the use of a rotation plan whereby the young trainee is given a variety of experience within an allotted time. In the usual plan, the trainee is given experience in each phase of highway work, such as road design, traffic, soils, construction, materials testing, and maintenance, for a period of from two months to six months.

The present (1954) shortage of engineering graduates for the increasing demand for engineering services is almost certain to continue for many years to come. By properly coordinating the university-extension type program with the rotation-type, in-service training program, the efficiency and effectiveness of the work of the young engineers in highway departments can be greatly increased. Also, the young engineer can more quickly find the job most suitable to his aptitudes. This general type of program, if supported by a reasonably competitive salary scale, opportunities for promotion, and other inducements, should attract promising young engineers into the highway field, promote progressive professional development, and help alleviate the effects of the shortage of engineers. However, to satisfy fully all the needs for highway engineering personnel, it seems almost certain that it will be necessary to develop training programs for subprofessional employees who can assist in survey work, routine work on road plans, inspection, and similar subprofessional work. The men assigned to this type of work could be high school graduates or men who have had only a year or two of college. It is not intended that these men should necessarily later qualify for work in the professional grades, although—if they have the promise and the desire to do so, and if they qualify themselves by subsequent education or experience—one can expect to find a significant fraction of them taking competitive examinations for positions in the professional grades.

CONCLUSIONS

Even a cursory examination of highway-transportation problems indicates a continuing demand for a wide range of technologic and engineering services, including those of the very highest and broadest professional type. The problem of supplying the required manpower—both as to quantity and quality—is crucial and complex. It is felt that the approach must be a composite one. No single, isolated program of action, such as a recruitment campaign or specialized undergraduate training program, will result in a solution. Rather, the training and education of highway personnel, recruitment, retention, and professional development of highway engineers are interrelated problems which require the cooperative and coordinated attention of highway administrators and educators.

Post-graduate education must and should be a recognized and calculated part of professional development. The post-graduate work can, however, take a variety of forms. For some individuals a year or two of graduate study may be advantageous. For others, a combination of job rotation and in-service training during the early period of employment may be preferable. For many others, a carefully planned program of study through extension services can be most valuable.

In view of a probable limit on the number of professional engineers available to serve the needs of the nation and the consequent necessity for efficient use of the limited supply, consideration should be given to the segregation of tasks which can be performed by technician-operators who can be more rapidly trained for these specific occupations.

Apparently, educational developments such as have been described are taking shape (as of 1954) in various parts of the United States. One must hope that they will be made continuously more effective by the cooperative effort of engineer-administrators and engineer-educators. Finally, there must be an attitude, a philosophy, and an avenue which can lead to the development of highway engineers who have a broad grasp of the problems of their profession and who can eventually take their places as top administrators. This, of course, is an attitude which must extend throughout the profession, and to which college education can only contribute the incentive and initial drive.

AMERICAN SOCIETY OF CIVIL ENGINEERS
Founded November 5, 1852
TRANSACTIONS

Paper No. 2743

SEWAGE AERATION PRACTICE IN CHICAGO

By Norval E. Anderson,[1] M. ASCE

Synopsis

Complete sewage treatment is necessary in The Sanitary District of Chicago (Ill.); the activated-sludge process is used in its major plants. In this paper the original design data relative to sewage aeration in these plants are reviewed, changes made since original construction of the plants are explained, and actual operating data are compared with the original design factors.

Introduction

Complete treatment is required for the sewage of The Sanitary District of Chicago (subsequently referred to herein as the Sanitary District), which in 1953 averaged 1,112 mgd and was derived from a human population of 4,500,000 and an industrial equivalent of 2,800,000—a total equivalent population of 7,300,000.

Complete treatment is required because the effluent and other drainage are conducted by the Chicago Sanitary and Ship Canal down the Illinois Waterway. Dilution in this waterway is limited by a decree of the United States Supreme Court, issued April 21, 1930, which provided that the annual average diversion from Lake Michigan into the Illinois Waterway at Chicago should be reduced from 8,500 cu ft per sec to 1,500 cu ft per sec by December 31, 1938.

The authorized diversion of 1,500 cu ft per sec does not provide adequate dilution for nominally complete treatment, which is 90% to 95%. The Sanitary District's continued pleas for an increase in diversion were still unsuccessful as of 1954. Langdon Pearse, M. ASCE, has summarized[2] the 1940–1941 testimony before the Supreme Court on the subject of this increase.

The activated-sludge process was selected by the Sanitary District for its major sewage treatment plants because it was most economical for the degree of treatment required. Each plant was studied separately at the time of

---

Note.—Published, essentially as printed here, in October, 1953, as *Proceedings-Separate No. 310*. Positions and titles given are those in effect when the paper was received for publication.

[1] Engr. of Treatment Plant Design, The Sanitary Dist. of Chicago, Chicago, Ill.

[2] "Illinois Water Litigation, 1940–1941," by Langdon Pearse, *Transactions*, ASCE, Vol. 109, 1944, p. 799.

TABLE 1.—PHYSICAL CHARACTERISTICS OF MAJOR ACTIVATED-SLUDGE PLANTS OF THE SANITARY DISTRICT OF CHICAGO (ILL.)

Description	SEWAGE TREATMENT WORKS		
	North Side	Calumet	West–Southwest
Operations begun	1928	1935	1939
Alterations or additions completed	1937	1951	1945, 1949
Designed capacity (average)[a]	250	136	900
Sewage treated in 1952 (average)[a]	223	88	802
Tributary, human, 1950[b]	1,080,000	440,000	2,820,000
Treated, human plus industrial equivalent, 1950[b]	1,049,000	416,700	5,856,000
PRELIMINARY TREATMENT			
Grit-chamber velocity, in feet per second	0.75 to 1.0	None	None
Clear openings in the bar screens, in inches	3/4	5/8	2
Average detention of the settling tanks, in minutes	23	20	34[c]
AERATION TANKS			
Design detention period (sewage basis), in hours	5.25	6.25	4.0
Number of tanks (all spiral flow)	36	21	24
Width of the flow channel, in feet	16.17[d]	33.25[e]	32.75
Length of the flow channel, in feet	420	425	1,736
Water depth, in feet	15.5	15.5	15.5
Water depth over the diffusers, in feet	15.0	15.0	15.0
Overhang of the top baffles, in feet	3.25	3.17	3.13
Angle between top baffles and the horizontal[f]	38.17	40.13	40.5
AERATION-TANK DIFFUSER SYSTEM[g]			
Number of diffusers (12 in. by 12 in.) per tank	1,440	720	(16) 2,820[h] (8) 4,728
Ratio, number of diffusers per square foot of tank area	1/9.5	1/19.6	(16) 1/20[h] (8) 1/12
Width of the diffusion band, in feet	3.75	3.54	(16) 3.00[h] (8) 6.21
Distance from center of band to face of wall[i]	3.44	3.60	(16) 3.08[h] (8) 5.09
FINAL SETTLING TANKS[j,g]			
Number of tanks	42	16	72
Size of tanks, in feet:			
Square	(30) 77 by 77	91 by 91	
Circular	(12) 75		126
Side-water depth, in feet	(30) 13.0 (12) 12.0	12.0	(32) 11.0 (40) 13.75
Influent arrangement	(30) OS[k] (12) center	center	center
Effluent weir arrangement	(30) grid (12) peripheral	peripheral	(32) peripheral (40) AT[l]
Design rate of weirs, gallons per foot per day	16,000[m]	26,000	24,400[n]
Design overflow rate, gallons per square foot per day	960	1,040	1,000
Point of sludge draw-off	center	center	center

[a] In millions of gallons per day. [b] Population figures. [c] This time is for Southwest sewage, at 400 mgd. West Side sewage receives approximately 1.5 hours settling in Imhoff tanks. [d] One tank has a 33.5-ft-wide channel. [e] One tank has a 67.5-ft-wide channel. [f] In degrees. [g] Numbers in parentheses are the number of tanks to which the figures apply. [h] In battery A, experimental diffuser arrangements are in use (1954), for which these figures vary. [i] In feet. [j] All final settling tanks are equipped with Dorr mechanisms. [k] On two opposite sides. [l] Annular troughs. [m] Thirty tanks at 14,500 gal per ft per day; twelve tanks at 22,500 gal per ft per day. [n] Thirty-two tanks at 32,500 gal per ft per day; forty tanks at 20,000 gal per ft per day.

planning. The studies were based on economic aspects of the individual sites as applied to data obtained from the Sanitary District's earlier treatment plants and experimental installations.

MAJOR ACTIVATED-SLUDGE PLANTS

Physical Data.—Physical data on the three major activated-sludge plants of the Sanitary District are given in Table 1. The relatively large size of the plants (136 mgd, 250 mgd, and 900 mgd, totaling 1,286 mgd average capacity) resulted from considerations of the relative costs of intercepting sewers, pumping stations, and treatment works, as applied to the topography of the area.

A brief consideration of the design of each plant and an explanation of the variations in some of the tabular data follow:

North Side Sewage Treatment Works.—The design of the original North Side Sewage Treatment Works was adopted on the recommendation of a commission of consulting engineers—Harrison P. Eddy, George W. Fuller, and T. Chalkley Hatton—after an exhaustive study of data and preliminary designs prepared by the Sanitary District. The commission made its report on February 27, 1922, the first contract was awarded in August, 1923, and the plant was placed in operation in October, 1928, with a design capacity of 175 mgd.

The aeration plant is divided into three batteries of aeration and final settling tanks with an operating gallery between the aeration tanks and final tanks of each battery. Each battery consists of twelve aeration tanks, each 33 ft by 420 ft. Each tank has a dividing wall which makes two parallel 16-ft flow channels, except for one tank that has a 33-ft channel. The aeration tanks have remained unchanged (1954).

Originally there were ten final settling tanks in each battery, each 77 ft square, equipped with Dorr mechanisms (diagonal scrapers on radial arms which move solids to the center as the mechanism slowly revolves) with extension arms to sweep the corner areas. The influent is introduced over weirs on two opposite sides of the tanks, and the effluent is removed by a grid of weir troughs suspended in the tank. These tanks are still in service (1954). In 1937, four additional final settling tanks were added to each battery. The latter tanks are of 75-ft diameter; they utilize center feed, peripheral effluent weirs, and Dorr mechanisms.

The addition of the twelve final tanks increased the capacity of the plant from 175 mgd to 250 mgd average flow. This increase was possible because, although the commission of consulting engineers had recommended 6-hr detention in the aeration tanks on the mixed-liquor basis, the hydraulics of the three batteries was designed for an average flow of 250 mgd in the event that the aeration-tank design might be too conservative.

Calumet Sewage Treatment Works.—The aeration system of the Calumet plant has remained nearly as it was designed because the tributary flow has not yet (1954) reached the design capacity. In this plant the hydraulic capacity was made 20% greater than the nominal treatment capacity in the event that the tank design might be too conservative.

The aeration plant is divided into two batteries of aeration tanks and final settling tanks with operating galleries between them—a layout similar to that of the North Side plant. The aeration tanks are 33.25 ft by 425 ft, except for one tank which is 66.5 ft wide. There are eleven tanks in one battery and ten in the other. All tanks are single-pass tanks; the flow channels are the same width as the tanks. Each battery contains eight final settling tanks, each 91 ft square and equipped with Dorr mechanisms having extension arms that sweep the corner areas. The influent is received through the center pier, and the effluent is removed over peripheral weirs.

The plant additions begun in 1949 and completed in 1951 consisted of four preliminary settling tanks; these additions increased the original settling period from 10 min to 20 min. The sixteenth final tank was also completed. This tank had omitted from the original construction in order to try a multiple-tray tank in its place. The use of the tray tanks was abandoned before the final tank was built. At the same time the traction-drive final tank mechanisms were converted to center-drive mechanisms.

West–Southwest Sewage Treatment Works.—The original aeration plant of the West–Southwest Sewage Treatment Works was designed for 400 mgd of Southwest sewage and consisted of two batteries (A and B), each battery having eight aeration tanks, sixteen final settling tanks, and operating galleries between the two sets of tanks.

The aeration tanks are 136 ft by 434 ft and are divided into four passes, with flow channels 33.25 ft wide and 1,736 ft long; both the influent and the

TABLE 2.—CHANGES AT WEST–SOUTHWEST AERATION PLANT

Design factors at average design flow	1939, Original	1945, 1st Addition	1949, 2d Addition
Average design flow, in millions of gallons per day	400	500	900
AERATION TANKS			
Number of tanks, 136 ft by 434 ft	16	16	24
Detention time, sewage basis, in hours	6.0	4.8	4.0
Detention time, mixed-liquor basis, in hours	5.0	3.7	3.1
Sludge return, percentages	20	30	30
Diffuser ratio, number of plates per square foot[a]:			
Batteries A and B	1/20	1/20[b]	1/20[b]
Battery C			1/12
FINAL SETTLING TANKS			
Number of tanks, 126 ft in diameter	32	48	72
Side-water depth, in feet:			
Original	11.0	11.0	11.0
Added tanks		13.75	13.75
Effluent weirs per tank, in feet:			
Original	381	381	381
Added tanks		615	615
Detention time, mixed-liquor basis, in hours	2.0	2.2	1.9
Overflow rate, in gallons per square foot per day	1,000	833	1,000
Weir rate, in gallons per square foot per day:			
Original	32,800	27,300	32,800
Added tanks		17,000	20,300

[a] Of tank area. [b] Variations in tanks of battery A due to experimental diffuser arrangements still in use.

effluent are at the same end. The original thirty-two final settling tanks—sixteen per battery—are 126 ft in diameter, utilizing center feed, having peripheral effluent weirs, and equipped with 4-arm center-drive Dorr mechanisms.

In 1945, sixteen final settling tanks—eight per battery—were added to the original two batteries of tanks, and the rated capacity was increased to 500 mgd. These tanks differ from the original tanks in that the sludge mechanisms have two arms instead of four, and the effluent weirs are on the two sides of a 4-ft-wide concrete trough cantilevered from the tank wall 14 ft toward the center.

In 1949, a third battery of final settling tanks was added to the plant, and the rated capacity was raised to 900 mgd. Battery C is similar in layout to batteries A and B, having eight aeration tanks of the same dimensions and twenty-four final tanks nearly the same as the 1945 additions to batteries A and B. The 1949 addition also provided for bringing the West Side Imhoff-tank effluent into the aeration plant for final treatment. The West Side sewage, approximately 60% of the total 900 mgd, receives an average of 1.35 hr of settling, and the Southwest sewage is retained only 35 min in the preliminary tanks—an average of 63 min preliminary settling for the mixed West-Southwest sewage at design flow. In Table 2 are shown the major design changes in the West–Southwest aeration plant.

Operating Data.—Average operating results for the aeration process of the three major plants are given in Table 3. Data for recent representative periods have been given in each case: From 1946 through 1950 for the North Side Treatment Works (because of irregular operation in 1951 while new diffusers were being installed); from 1946 through 1950 for the Calumet Treatment Works (because of irregular operations in 1951 while additional preliminary tanks were being installed); and in 1951 and 1952 for the West–Southwest Treatment Works since the third battery of tanks has been in operation.

Some of the factors given in Table 3 are not ordinarily reported in operating results because they are not of direct concern to the operator. However, they may have significance for the designer and are defined as follows:

a. The "sludge age" (used by R. H. Gould, M. ASCE), given in days, is the number of pounds of mixed-liquor suspended solids in the aeration tanks divided by the number of pounds of suspended solids added to the aeration system per day.

b. The "solids aeration period" (used in the Sanitary District studies), given in hours, is the number of pounds of mixed-liquor suspended solids in the aeration tanks divided by the number of pounds of suspended solids removed from the sewage per hour.

Terms *a* and *b* are similar and useful indices for the designer and also for the operator as a general guide to the proper quantity of mixed-liquor solids to be carried in the system. However, the Sanitary District does not use either of these criteria in routine operation control.

c. The "solids rate" for final settling tanks, in pounds per square foot per day, is the quantity of mixed-liquor suspended solids that settles from the

TABLE 3.—AVERAGE OPERATING DATA OF MAJOR ACTIVATED-SLUDGE PLANTS OF THE SANITARY DISTRICT OF CHICAGO, ILL.

Description	SEWAGE TREATMENT WORKS		
	North Side	Calumet	West-Southwest
Number of years (inclusive) represented	1946–1950	1946–1950	1951–1952
Sewage treated, in millions of gallons per day	213	77	794
Raw sewage:			
Suspended solids, in parts per million	135	146	185
5-day B.O.D., in parts per million	102	109	143
Preliminary settling:			
Detention period, in minutes	27	18	71[a]
Suspended solids removed, in percentages	35	28	43
5-day B.O.D. removed, in percentages	25	20	32
Aeration period, in hours:			
Sewage basis	6.0	6.1	4.6
Total-flow basis	4.9	4.9	3.3
Sludge return, in percentages	22.7	24.4	38.5
Mixed liquor:			
Suspended solids, in parts per million	2,000	2,230	2,330
Solids aeration period, in hours	152	150	118
Sludge age (R. H. Gould), in days	5.7	5.4	4.2
B.O.D. loading[b]	19	19	32
Air used:			
Cubic feet per gallon of sewage	0.48	0.48	0.68
Cubic feet per pound of 5-day B.O.D. removed:			
Raw sewage	600	590	600
Settled sewage	800	740	905
Final settling:			
Detention period, in hours	2.1[c]	2.3	2.1[d]
Overflow rate[e]	925	810	885
Weir rate[f]	13,500[g]	18,700	21,600[h]
Solids rate[i]	15.4	15.7	17.2
Sludge index (F. W. Mohlman)	89	8	81
Sludge index (W. Donaldson)	1.12	51.72	1.23
Final effluent, in parts per million:			
Suspended solids	9	14	15
5-day B.O.D	6	11	7
Removal from preliminary effluent:			
Suspended solids, in percentages	88.5	87.0	86.0
5-day B.O.D., in percentages	92.5	87.5	92.0
Removal from raw sewage:			
Suspended solids, in percentages	93.5	91.8	92.0
5-day B.O.D., in percentages	94.0	90.0	94.7

[a] In West Side Imhoff tanks, 468 mgd at 93 min, and in Southwest preliminary tanks 326 mgd at 39 min, the average being 71 min. [b] In pounds per thousand cubic feet of aeration-tank volume. [c] Thirty final tanks at 2.7 hr, and twelve final tanks at 1.8 hr, the average being 2.6 hr. [d] Thirty-two final tanks at 1.9 hr, sixteen at 2.2 hr, and twenty four at 2.4 hr, the average being 2.1 hr. [e] In gallons per square foot per day. [f] In gallons per foot of weir per day. [g] Thirty final tanks at 12,400 gal per ft per day, and twelve final tanks at 19,200 gal per ft per day, the average being 13,500 gal per ft per day. [h] Forty final tanks at 17,900 gal per ft per day, and thirty-two final tanks at 28,900 gal per ft per day, the average being 21,600 gal per ft per day. [i] In pounds per square foot per day. This refers to mixed-liquor solids settled from the overflow.

final tank overflow. This rate, suggested by H. R. King, M. ASCE, of the Sanitary District, is an additional criterion for final tank design and is believed to have an important influence on settling-tank performance.

Operating results are, of course, affected by the type of sewage treated as well as by the design characteristics of the treatment works. Even for three arge plants in the same metropolitan area, the types of sewage are different.

North Side sewage is predominantly domestic, relative weak—having a B.O.D. of approximately 102 ppm—and yields readily to treatment. Calumet sewage is a little more concentrated, its B.O.D. being approximately 109 ppm; although it is largely domestic, it contains many troublesome industrial wastes, such as pickling liquor, which adds an average of approximately 7 ppm of iron, paint wastes which sometimes give unusual color effects, and oily wastes. West–Southwest sewage is the strongest—having a B.O.D. of 143 ppm—and has the highest percentage of industrial wastes, including those from the stockyards and the large meat-packing plants.

Operating results for the activated-sludge plants of the Sanitary District are among the best reported. However, yearly average results always seem disappointing to those responsible for the design and operation of the plants. After having noted final-effluent B.O.D.'s and suspended-solids results of from 3 ppm to 5 ppm for several weeks, it is surprising that there are enough bad periods to bring the yearly averages up to 10 ppm or 15 ppm.

Bases for Design

The Sanitary District is one of the pioneers in the activated-sludge process; some of the earliest data were developed under the direction of Mr. Pearse and Floyd W. Mohlman. Experimental sewage-testing stations were built and operated: At the Thirty-Ninth Street Pumping Station, on domestic sewage, from 1908 to 1911; at the stockyards, on packinghouse wastes, from 1912 to 1918; along the North Branch, on tannery wastes, from 1919 to 1922; at a corn-products company, on the corn-products refinery wastes, from 1920 to 1926; and at a paint company plant, from 1926 to 1928. The Des Plaines River Sewage Treatment Works,[3] an activated-sludge plant having a capacity of 4.5 mgd, was operated on a semi-experimental basis from 1922 to 1931. The old Calumet Sewage Treatment Works included two experimental activated-sludge units[4] of approximately 1.5-mgd capacity each, which were operated in various ways from 1923 to 1935. Each of the major plants has been operated on an experimental basis, in whole or in part, at various periods to test ideas or to obtain specific data.

Design criteria for the Sanitary District's aeration plants have been obtained from such experiments, with due consideration given to the experimental and operating data of other plants. The bases for the major design factors are summarized herein.

Preliminary Treatment.—Evaluation of the desirable degree of preliminary treatment has fluctuated with the passage of time and has been influenced by its effect on ultimate sludge disposal as much as by consideration of economy in the aeration process.

In the original design of the North Side Works, mechanically cleaned, fine screens with $\frac{1}{16}$-in. openings were considered in accordance with previous practice. However, before these were built, comparative studies showed that 30-min preliminary settling would remove five or six times as much coarse solid material at the same or a lower cost; this procedure was adopted.

The Calumet Works were originally built with only 10-min preliminary settling because it was thought that this period would give the most advantageous sludge mixture for vacuum filtering and heat drying of waste sludge. Operating experience showed that a greater preliminary-tank volume was desirable for flexibility in handling peak flows. In 1951, the capacity of the preliminary settling tank was doubled to give 20-min detention at design flow.

---

[3] "The Des Plaines River Activated Sludge Plant," by Langdon Pearse, *Engineering News-Record*, December 9, 1920, p. 1134.

[4] "Activated Sludge Experiments at the Calumet Sewage Treatment Works," by Floyd W. Mohlman and C. E. Wheeler, *Sewage Works Journal*, October, 1930, p. 528.

At the West–Southwest Works, preliminary settling of 34 min for a flow of 400 mgd is provided for Southwest sewage. The average preliminary settling of more than one hour of the West–Southwest Works is the result of the continued use of the Imhoff tanks for preliminary treatment of West Side sewage.

In the consideration of the effect of preliminary treatment, it appears that air requirements are not reduced in proportion to the removal of suspended solids or B.O.D. prior to aeration. This is probably due to a slower rate of oxidation for the coarse solids removed in the preliminary process.

Aeration Tank Type and Proportions.—Spiral-flow aeration tanks are almost universally used in the United States, as opposed to the ridge-and-furrow type still favored considerably in Great Britain.

Plans for the North Side aeration tanks were changed from ridge-and-furrow tanks to spiral-flow tanks just before construction, after tests at the Des Plaines River Plant had demonstrated the superiority of the spiral-flow type. The advantages of spiral flow are greater air economy, lower construction cost, and more accessible location of diffusers for maintenance.

Numerous velocity traverses measured with current meters on the Sanitary District's spiral-flow aeration tanks have failed to show any dead zone or core in the cross section, contrary to frequent theorizing on that condition. Therefore, the Sanitary District has never used either baffles or cross-aeration to break up the core.

The Sanitary District has standardized the water depth of aeration tanks to 15 ft above the diffusers, although a theoretical study[5] by the writer in 1934 indicated that different depths probably could be used with little if any loss in power economy if site conditions made shallower or deeper tanks advantageous.

An aeration channel width of approximately 33 ft has been used because comparative operating tests at the North Side Works demonstrated that the 33.5-ft-wide tank gave results equal to those of the 16-ft channels of the other tanks. At the Calumet Works, one aeration tank was 67.5 ft wide but had two rows of air-diffuser plates on each side of the tank; that tank apparently gives results equal to those of the 33-ft channels. Channel width does not appear to be critical and is selected so as to give the best layout of units. Wider channels, of course, have smaller construction costs.

Aeration-tank lengths—especially in the range required for large plants—do not appear to affect operating results and are selected to fit layout conditions. At the North Side Works and the Calumet Works, aeration tanks are approximately 420 ft long with the influent at one end and the effluent at the other. At the West–Southwest Works, the aeration tanks are 434 ft long, but each tank is divided into 4 passes of 33.75–ft width so that the flow length of each tank is 1,736 ft with the influent and effluent at the same end.

---

[5] Discussion by Norval E. Anderson of "Aeration Tanks for Activated Sludge," by S. W. Freese, *Transactions*, ASCE, Vol. 103, 1938, p. 1641.

Baffles with an overhang of approximately 3.2 ft and at an angle of approximately 40° from the horizontal have been provided in all cases at the tops of aeration-tank walls. At battery C of the West–Southwest Works, the baffles have a 3-ft-radius fillet where they intersect the wall; all others are straight. In tests at the Des Plaines River Works in 1924 with baffles at 35°, 40°, 50°, and 60° from the horizontal small differences were shown in resulting velocities. In tests at the North Side Works in 1935, in which 4-ft-radius baffles and straight baffles were compared, little difference was shown in velocity of circulation. Since 1950, the Sanitary District has been questioning the value of any kind of baffles that increase circulating velocity because increased velocities decrease the bubble contact period and thereby reduce absorption of oxygen from the bubbles, which normally provide much more oxygen than does surface aeration. Limited tests on a model-sized tank seem to confirm this. This principle would not apply to the treatment of weak sewage if the air requirements were not sufficient to maintain the minimum velocity needed to prevent settling without the aid of baffles.

Air Diffusers.—The Sanitary District uses standard 12-in. by 12-in. porous diffuser plates of 80 permeability in all its major plants. The decision to continue the use of plates in the latest design was based on comprehensive comparative tests started in 1941 and reported[6] by the writer in 1949. These tests were begun at a time when the problem of clogging of plate diffusers at the West–Southwest Works had become extremely critical. The major test was a comparison of the eight aeration tanks of battery A at the West–Southwest Works, each equipped with a different diffuser system; the systems were operated in parallel. The diffuser systems tested included plates of various permeabilities and arrangements, slotted brass tubes, fixed porous tubes, and porous tubes and "precision tubes" on "swing diffusers."

Economic studies based on the test results led to the adoption, at the West–Southwest Works, of the diffuser design for battery C, which has a capacity of 300 mgd and which was completed in 1949. The salient features of this diffuser system are: A new air-filtering system consisting of bag filters with loose asbestos-fiber lining for primary filtering followed by automatic electronic filters; diffuser plates of 80-permeability rating, cemented into 6-plate precast concrete holders; plate holders set normal to the tank wall and connected into 4-in. headers 34 ft long, with 6-in.-diameter feeders at the center of each header; 4,728 plates per tank—an average diffuser ratio of $\frac{1}{12}$ and an average air rate of 3.0 cu ft per min per plate; a 27% greater concentration of plates in the influent half of the tank than in the effluent half for the purpose of securing a more uniform rate of diffuser clogging, not for "tapered aeration."

Tests[7] by Mr. King, in which the oxygen absorption rating of diffusers was measured, provided a long-needed test of diffuser pore size to supplement the permeability specification in the purchase of diffusers.

---

[6] "Tests and Studies on Air Diffusers for Activated Sludge," by Norval E. Anderson, *Sewage and Industrial Wastes*, April, 1950, p. 461.

[7] "Tests to Determine Oxygen Absorption Rating of Porous Plate Air Diffusers," by H. R. King, *ibid.*, July, 1952, p. 826.

Aeration Period.—On the basis of experiments and operating data the aeration period has been gradually reduced from the conservative 6.25-hr period (mixed-liquor basis) used in the original design of the North Side Works in 1925, to the latest figure (1953) for the West–Southwest Works of 3.1 hr on the mixed-liquor basis or 4.0 hr on the basis of sewage only. It should be noted that this is for complete treatment without sludge re-aeration.

A large-scale experiment at the North Side Works, in which one battery of tanks was operated for two years (1934–1935) at an average aeration period of from 3.0 hr to 3.5 hr (mixed-liquor basis) without increased air per gallon of sewage or sacrifice in quality of effluent, demonstrated that the shorter period could be used for aerating North Side sewage.

A 0.6 mgd experimental plant[8] operated in 1938 on West Side Imhoff-tank effluent gave 89% removal of B.O.D. for raw sewage having a B.O.D. of from 78 ppm to 101 ppm, with aeration periods of 1.6 hr to 2.3 hr, on the sewage basis, using from 0.18 to 0.26 cu ft of air per gal of sewage.

TABLE 4.—RATE OF SLUDGE RETURN: DESIGN ALLOWANCE AND OPERATING PRACTICE

Treatment works	Design average, in percentages	DESIGN RANGE, IN MILLIONS OF GALLONS PER DAY		RANGE OF YEARLY AVERAGES, IN MILLIONS OF GALLONS PER DAY	
		Minimum	Maximum	Minimum	Maximum
North Side	20	25	100	40	50
Calumet	20	15	55	16	24
West–Southwest	30	100	360	250	300

Air Use.—Design estimates of air requirements for the various plants have proved to be somewhat inaccurate. For the North Side Works, the design provided for an average of 0.8 cu ft of free air per gal of sewage whereas the actual yearly averages have ranged from 0.35 cu ft to 0.68 cu ft of air per gal. The Calumet Works was designed for 0.5 cu ft of air per gal, and the yearly averages range from 0.36 cu ft to 0.52 cu ft. The West–Southwest Works was designed for 0.55 cu ft of air per gal, and the yearly averages range from 0.58 cu ft to 0.69 cu ft of air per gal of sewage.

Sludge Return.—The rate of sludge return is determined by the solids concentration to be carried in the mixed liquor and by the settling characteristics of the sludge. The practice of the Sanitary District has been to allow a generous range of capacity after selecting a nominal percentage of average sewage flow for the sludge return. Table 4 compares the design allowances with data obtained from operating practice.

Two 16-in.-diameter air lifts for each final tank are used for sludge return at the West–Southwest Works. These lifts have proved desirable for flexibility and ease of control in addition to the savings in construction cost of a pumping station and conduits. Air lifts were used in the early small plants and experimental installations, but centrifugal pumps are used at the North Side Works and the Calumet Works.

---

[8] "Experimental Work in Progress at the West Side Sewage Treatment Works of the Sanitary District of Chicago," by T. L. Herrick, *Sewage Works Journal*, March, 1938, p. 276.

Final Settling Tanks.—The latest final settling tank design of the Sanitary District is that for battery C at the West–Southwest Works, which was completed in 1949. These tanks are 126 ft in diameter; they have 13.75-ft sidewater depth and 17.58-ft center depth and receive influent up through the center pier; they also have sludge draw-off at the center bottom. The effluent weirs are on both sides of a 4-ft-wide concrete effluent trough placed concentrically in the tank so that the distance from the tank wall to the center of the trough is 14 ft. The trough is supported on concrete cantilever brackets extending from the tank wall.

In addition to their favorable operating characteristics, circular tanks are economical to construct. Alternate bids received in 1941 on rectangular and circular tanks resulted in a low bid for rectangular tanks, being 30% greater ($320,325.50) than the low bid for circular tanks. In the design of these alternates (sixteen tanks for addition to batteries A and B at the West–Southwest Works), all the tanks had the same volume, the same minimum depth, and the same length of effluent weir.

The hydraulic design of the final settling tanks was adopted as a result of comprehensive tests begun in 1940 and reported[9] by the writer in 1944. The tests included velocity measurements in final tanks at Cleveland, Ohio, Columbus, Ohio, and New York, N. Y., and at many trial installations in Chicago's Southwest Works. Also, the Sanitary District had made many tests of rectangular tanks at the old Des Plaines River Works and at the North Side Works in 1931.

Some of the conclusions drawn from the test data were the following: Tank depths should be not less than 10 ft nor more than 12 ft if weirs are placed near the upturn of the density current; no baffling arrangement of the influent has an appreciable effect on the effluent; the greatest influent improvement is low velocity; effluent weirs should preferably be located away from the upturn-of-density current; the overflow rate for effluent weirs should not exceed approximately 20,000 gal per day per ft of weir nor 15,000 gal per day per ft if weirs are located at the upturn-of-density current; the sludge draw-off should be near the influent.

Step-Aeration and Re-Aeration.—Neither step-aeration nor any other form of re-aeration has been adopted by the Sanitary District because studies of available data prior to 1955 have indicated that, for the high degree of treatment required by the Sanitary District, there would be comparatively little saving in over-all costs and a probable sacrifice in the quality of the effluent. However, the possibility of converting to some form of re-aeration has been considered in case it should become necessary to increase the capacity of a plant under conditions in which an increase in tank capacities would not be feasible.

The potential economy of re-aeration is the reduction in the tank volume necessary to maintain the same sludge aeration period, or sludge age, and the same sewage aeration period. However, this economy would be partly offset by the cost of more conduits and controls and a more elaborate air-diffusion system, and by an increase in the operating costs of supplying more air. For best results with re-aeration, it is believed that the rate of air supplied in the re-aeration step should be much higher than for a conventional aeration tank and that, in order to provide a comparable effluent, the over-all air requirement will be greater.

---

[9] "Design of Final Settling Tanks for Activated Sludge," by Norval E. Anderson, *Sewage Works Journal*, January, 1945, p. 50.

The writer doubts that an equal degree of treatment would be obtained because, with the reduction in tank volume necessary for economy in a sludge re-aeration process, the ratio of sludge-return solids to sewage solids would be much smaller; also, the contact period of sewage solids with the returned sludge would be shorter. These factors are important in producing a good effluent, but more data are necessary to evaluate them properly.

Experiments on sludge re-aeration were conducted by the Sanitary District at the tannery testing station in 1920 and at the Des Plaines River Works from 1923 to 1931, with no apparent merit indicated. Better comparative tests were made at the North Side Works in 1934 and 1935 by A. J. Beck, when the necessity for a high rate of air supply to the return sludge was beginning to be recognized. Mr. Beck's conclusion from the latter test was that, "A saving in aeration tanks could be made by aeration of return sludge. However, more air would be required and the final effluent may be slightly poorer quality than with the present method of operation." There is need for more carefully controlled experimental work in the field of sludge re-aeration.

Operating Control

Weekly plant control meetings at the West–Southwest Works (1954) have proved valuable in maintaining successful operation. The meetings, conducted by Mr. Mohlman, are attended by engineers and chemists representing the operating staff and engineers representing the design staff, with a total of ten to fifteen people usually present. Operating results of the past week are discussed, and operation is planned for the week ahead. Also, opportunity is afforded for informal discussion or problems and ideas by the operators and the designers.

All the usual determinations of B.O.D., dissolved oxygen, suspended solids, volatile solids (percentages), and sludge index—together with readings of sewage flow, air used, sludge return, and their computed relationships—are recorded and considered for the control of the aeration process. The two factors that receive attention on every shift are the suspended solids in the aeration tanks and the dissolved oxygen at the effluent end of the aeration tanks.

Samples of mixed liquor are taken at 4-hr intervals and composited for a suspended-solids determination on every 8-hr shift. The amount of suspended solids carried in the aeration tanks yields a Gould sludge age of from 4 days to 6 days, which results in a high degree of treatment. However, sludge age is not considered in the daily control of the plant because it is a less sensitive factor than the parts per million of suspended solids in the aeration tanks.

Dissolved-oxygen determinations are made at 4-hr intervals from samples taken at the effluent ends of the aeration tanks. It has been found desirable to maintain a minimum of approximately 2 ppm of dissolved oxygen at the effluent end of the aeration tanks in order to be sure of healthy aerobic bacteria in the return sludge.

The ash content of the sewage solids is a subject of frequent discussion because of its effect on the sludge index and on the fertilizer value of dried sludge. The Mohlman sludge index[10] of settleability is used by the Sanitary District because it seems easier to visualize a figure that is small for a concentrated sludge and large for a bulking sludge.

CONCLUSIONS

Aeration practice is believed to be best for the requirements of the Sanitary District, according to present (1954) knowledge. Different conditions would of course, require modifications. The engineering staff of the Sanitary District continues to investigate and experiment in quest of improvements in the sewage treatment processes. Although no new sewage treatment plants are contemplated (1954) for the Sanitary District within the foreseeable future, it is expected that major additions will be required at the West–Southwest and North Side Works before 1960 in order to handle the increasing human and industrial wastes.

ACKNOWLEDGMENTS

Acknowledgment is given to Mr. King, senior civil engineer, and Norman Dawson, assistant engineer of treatment plant design, for their assistance in assembling and checking the data presented.

---

[10] "The Sludge Index," by F. W. Mohlman, *Sewage Works Journal*, January, 1934, p. 119.

AMERICAN SOCIETY OF CIVIL ENGINEERS
Founded November 5, 1852
TRANSACTIONS

Paper No. 2744

TRAFFIC AT AN INTERNATIONAL AIRPORT

By Walther Prokosch[1]

Synopsis

An important objective in the design of the Puerto Rico International Airport was the simplification of all types of traffic—that of passengers in the terminal, that of taxiing aircraft, and that of vehicles of all types. Studies were made to determine the character as well as the volume of existing and anticipated air-carrier traffic. Based on this information, the number of aircraft-loading positions (inbound, outbound, and in-transit) was determined, and these were related to an economical aircraft-taxiing pattern. Finally, a passenger-terminal plan was evolved having direct lines of circulation and providing a distinct separation of inbound and outbound passengers.

Introduction

In the design of an airport or an airport terminal all forms of traffic are important and interrelated and must be considered. This traffic can be divided into (*a*) air traffic in the immediate vicinity of the airport, (*b*) ground traffic of airplanes on the airfield, (*c*) passenger traffic moving within the airport terminal, (*d*) cargo traffic moving through the cargo terminal, and (*e*) vehicular traffic that serves the airport. It appears most advantageous to a study of traffic to examine an actual "case history" of the design of the Puerto Rico International Airport. A short review of the traffic forecasts and an exposition of the relationship of these forecasts to the actual design of the installation are included.

Much information is available on the subject of forecasting air traffic, and airport planners have varying ideas as to the best method of preparing these forecasts. The significant phase of any airport planner's work is the interpretation of statistics so as to determine the best organization of buildings, traffic, and other facilities for a given airport.

Traffic Forecasts

In August, 1950, the Puerto Rico Transportation Authority requested that a survey of design requirements be prepared for the Puerto Rico International

---

Note.—Published, essentially as printed here, in August, 1953, as *Proceedings-Separate No. 255*. Positions and titles given are those in effect when the paper was received for publication.

[1] Associate in Charge of Airport Planning, Knappen-Tippetts-Abbett-McCarthy, New York, N. Y.

Airport at San Juan. The authority showed an understanding of the interdependence of traffic forecasting and building requirements in requesting that the survey produce, as its end result, a schedule of requirements for airplane parking and building space.

Every community or area has local characteristics that must be explored and evaluated in the preparation of a traffic forecast—for vehicular, air, or any other kind of traffic. The geographic location and topographic limitations of Puerto Rico had a strong influence on the evaluation of future traffic. An island supporting approximately three million people (as of 1954) and situated 1,000 miles from the United States—to which it is tied politically and economically—will obviously need air traffic. Furthermore, an island on which almost every arable square foot of land is already exploited for agriculture must turn to industrialization to support an expanding population, which again increases the demand for air transportation.

The pattern of economic development which had occurred and which appeared to be continuing was investigated; population was the first subject of this study. Investigations were then made of employment in Puerto Rico, automobile use, imports and exports, agriculture, the use of radio and telephone, per capita income, and various business indices including data on migrant labor, agricultural employment, electric power production, cement production, and building-permit value. The plotting of graphs for all these factors resulted in a generally rising curve, indicating that Puerto Rico would experience a considerable economic growth as well as population growth.

The pattern of migration was then studied; it was found that the net migration loss had been increasing steadily from 1928 to 1954. Despite improving economic conditions in Puerto Rico, it was estimated that the net migration loss would continue to increase gradually. Temporary migration, which includes migration of agricultural workers who labor under contract for the harvesting season in the United States, was also studied. Although this activity had been under way for only three years prior to the preparation of the survey, enough evidence was obtained to indicate that temporary agricultural workers would continue to migrate to the mainland by air in ever-increasing numbers.

Another characteristic of Puerto Rico which has a considerable bearing on anticipated air traffic is the close tie between the homeland of Puerto Rico and the many Puerto Ricans living in the United States—particularly in New York, N. Y. Sizable traffic can be attributed to the location of the latter, for members of a family are induced to visit each other during the course of a year; this traffic is expected to expand.

Tourist trade was also considered. It is obvious that the efforts of the government of Puerto Rico to attract additional tourist trade have been and will be successful. This will also generate increased air traffic.

Additional factors studied in this traffic survey were the travel of students, businessmen, and others between Puerto Rico and the United States or other countries in which many Puerto Ricans have close relationships (such as Spain) and the traffic to and from the Virgin Islands and other Caribbean islands, most of which goes through Puerto Rico. There also exists considerable traffic between the various parts of Puerto Rico; this traffic is expected to increase as airport facilities in other parts of the island are improved.

The in-transit passenger traffic at San Juan was also investigated; the conclusion was reached that this was the only traffic that would not increase. The future pattern of traffic between the United States and South America will call for a greater number of long-range through flights that will not include stops at San Juan.

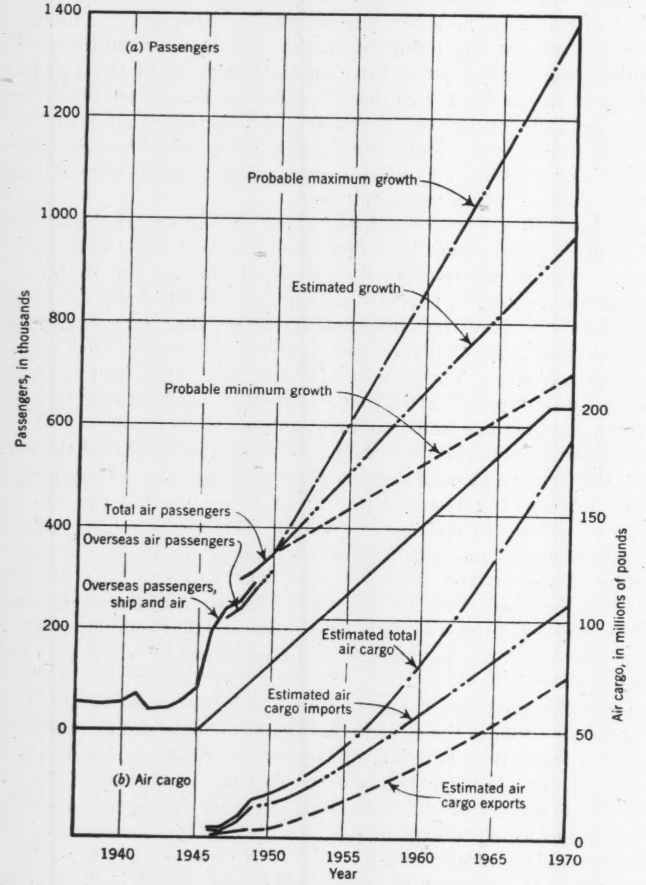

FIG. 1.—ACTUAL AND PREDICTED TRAFFIC AT PUERTO RICO INTERNATIONAL AIRPORT

The anticipated traffic in each of these categories was forecast separately, and all of them were totaled. As a matter of record, the traffic estimate which was prepared in 1950 anticipated an increase from approximately 300,000 passengers in 1950 to 508,000 passengers in 1955 and 968,000 in 1970. Actually, during 1952 there were more than 500,000 passengers, and, therefore, the estimates will be low—as have been almost all the air traffic forecasts that have ever been made (Fig. 1(*a*)). It may be well to note that estimates of future traffic must necessarily be conservative to justify sound financial procedures.

Forecasts of air-mail traffic were then made, based—in general—on the economic data examined for passenger traffic. The air-cargo potential was also investigated. It was found that there will probably be a substantial volume of air cargo because of the continuing necessity for importing various foodstuffs and manufactured goods. The increased industrialization of the island will also contribute to the increase in this category of traffic. The total air-cargo traffic estimated for San Juan in 1970 is almost 1,000,000 tons (Fig. 1(*b*)).

AIRPLANE PARKING POSITIONS

This information about traffic was used in determining the number of airplane parking positions required at the terminal because this number is the basis for planning a terminal. This number, together with the anticipated annual passenger volume, will enable the airport planner to begin to develop the basic design of the terminal building. The same process is applied to the cargo terminal.

In addition to these fundamental requirements, the planner should try to determine the following significant characteristics:

1. The Proportion of Long-Haul Traffic to Local Traffic.—This proportion is important because it gives a forecast of types and sizes of aircraft and also because it has an effect on the utilization of airplane parking positions on the terminal apron.

2. The Proportion of Terminating Flights to Through or In-Transit Flights.—This proportion affects the utilization of airplane parking positions both in terms of time and pattern; it may also have a profound influence on the design of the terminal building. A terminating flight spends less time on the apron than one which is passing through and requires extensive servicing while on the ground. The pattern of operation of an airport terminal building having primarily through flights differs greatly from that of a terminal having principally terminating and originating flights, as will be shown subsequently. This characteristic also affects requirements for short-term aircraft parking space away from the terminal building.

At San Juan it was found that the proportion of long-haul traffic to local traffic was high and also that most flights were terminating or originating flights, rather than in-transit flights.

After these determinations were made, the number of airplane parking positions required for the passenger terminal and the cargo terminal were estimated; the following steps were taken:

(*a*) The peak-hour traffic was estimated first by using the factor of 0.0043% of annual traffic which was developed by the Civil Aeronautics Administration, United States Department of Commerce, as a result of a survey made by that agency at San Juan in 1950. A second method was to relate peak-hourly traffic to peak-daily traffic and peak-monthly traffic. The first method was used for design purposes because it appeared to be more accurate scientifically. However, it resulted in a peak-hourly traffic forecast for 1955 of only 215 passengers, which is probably too low. Actually, the traffic at San Juan reached this peak on several occasions in 1953.

TABLE 1.—ESTIMATED PASSENGER AIRPLANE CAPACITY

Airplane type	Seating capacity	Relative frequency of operation	Total
DC-4	60	3	180
DC-6	60	2	120
Constellation	50	2	100
C-240	40	5	200
B-377	70	1	70
C-46	60	1	60
		14	730

Average size = (730 ÷ 14) (0.55) = 29

TABLE 2.—GATE UTILIZATION BY PASSENGERS

Operation	Elapsed time at gate, in minutes	Relative frequency of operation	Total time, in minutes
Arrival—all types	20	43	860
Departure—local	20	10	200
Departure—foreign	40	33	1,320
Arrival—in-transit	30	7	210
Departure—in-transit	30	7	210
		100	2,800

Average time = 2,800 ÷ 100 = 28 minutes

(*b*) The estimated average airplane seating capacity for a given future year was forecast (Table 1) by predicting the types of aircraft which would be in service in that year with their seating capacities; by estimating the relative frequency of operation of such planes; and by applying to the average product of the two former figures an estimated load factor.

TABLE 3.—SUMMARY OF BUILDING REQUIREMENTS AND PERSONNEL ESTIMATES

Component part[a]	EXISTING, 1950		ESTIMATED, 1960		ESTIMATED, 1970	
	Area, in square feet	Personnel	Area, in square feet	Personnel	Area, in square feet	Personnel
Airlines	16,937	131	35,400	250	47,750	340
Government agencies	13,401	74	31,800	166	40,500	219
Public space	36,833		60,200		82,300	
Services	3,246	86	8,000	222	12,000	333
Concession and rental areas	16,130	50	34,400	114	42,900	143
Government offices	9.960	68	18,000	92	19,750	102
Total for passenger terminal	96,507	429	187,800	852	245,200	1,149
Auto parking	310		780		1,030	

[a] For a detailed breakdown of each of the component parts, see "Airport Traffic and the Puerto Rico International Airport," by Walther Prokosch, *Proceedings-Separate No. 255*, ASCE, Vol. 79, p. 13, Fig. 5.

(*c*) The utilization of airplane parking positions at the terminal (or time during which an airplane occupies its parking position) was estimated (Table 2); for this estimation the relative frequency of terminating or originating flights versus in-transit flights was the important consideration.

(*d*) The peak-hour traffic was divided by the average seating capacity to show the number of flight operations per hour.

(*e*) The number of operations per hour was divided by a utilization factor for the airplane parking positions. This value gave the number of airplane parking positions required. The estimate for 1960 was ten airplane parking positions and, for 1970, fourteen positions.

A somewhat similar process was performed to estimate the number of parking positions required for cargo airplanes, substituting potential payload for seating capacity. Four positions were thus estimated to be necessary in 1960 and nine in 1970.

The last part of the survey consisted of tabulating all the space then (1950) used in the passenger and cargo terminals and the number of personnel working in the terminals. In Table 3 there are presented these figures, together with building requirements and personnel estimates for 1960 and 1970.

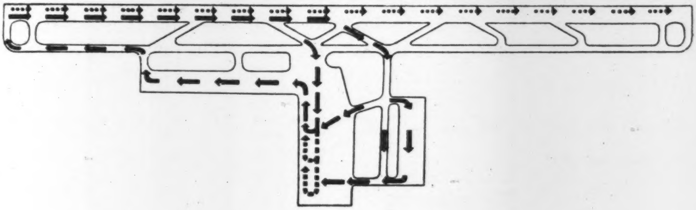

FIG. 2.—BASIC AIRPLANE TAXI PATTERN

APPLICATION OF FORECASTS TO DESIGN

When the statistical phase of the design was completed, aircraft traffic on the ground was studied. In Fig. 2 there is illustrated the relative simplicity of runway traffic that can be obtained in San Juan because of the monodirectional characteristics of the trade winds. The Puerto Rico Transportation Authority had previously computed the landing-roll requirements of anticipated aircraft and had determined optimum exit points from the runway ends; high-speed diagonal taxiways were installed at those points. A one-way system of traffic was evolved which resulted in the shortest possible taxi distances for arriving and departing aircraft. The problem of relating cargo operations to passenger operations was also studied. It was decided that these two types of traffic should be adjacent to, but not directly touching, each other so that either one might expand as required. The taxi pattern was also studied to permit a smooth flow of traffic to and from the cargo terminal.

The determination of a logical taxiway traffic pattern permitted planning for the disposition of airplane parking positions in the terminal area. In Fig. 3 it can be seen that terminating traffic is brought to a given position where passengers can be discharged. From there the aircraft can be towed to a short-term parking space if it is departing in a relatively short time, or to near-by hangars for maintenance. In-transit flights or short turn-around flights are docked at corner positions where they are accessible to both the unloading and loading parts of the building. This location also permits aircraft to operate in the continuous one-way traffic pattern. Outbound airplane parking positions are placed in a row, facing the runway and close to its take-off end, so that departing aircraft have the shortest possible taxi distance. It should be noted that this pattern of airplane parking positions was achieved only because the air carriers serving Puerto Rico agreed to share parking positions.

Terminal Building.—Studies were next initiated dealing with the plan of the terminal building itself. The placing of the airplane parking positions around a corner so as to produce the proper relationship of terminating to in-transit to departing aircraft immediately suggested certain locations for the principal features of the building. These features are concourses or areas for processing departing and arriving passengers. At San Juan it became possible to separate these because of the high percentage of terminating versus in-transit flights.

It has been noted in various studies that the interests of the departing passenger are different from those of the arriving one. The departing or in-transit passenger spends time wandering around the building and patronizing its concessions, whereas the arriving passenger is principally interested in reaching his destination—hotel, home, or other. This is true for any form of transportation. Therefore, it is desirable to permit the terminating passenger to get to his baggage and transportation as quickly as possible and to make concessions more accessible to the departing or in-transit passenger. As well as giving proper emphasis to concessions, such a differentiation permits the simplification of circulation in the building by diverting passengers to separate entrance and exit points. At San Juan the problem was more complex because all passengers (with the exception of a small number of intra-island travelers) are subjected to some kind of government inspection. If the government-inspection rooms can be placed in one block and all such traffic closely related to that block, the building itself becomes simpler. Also, it is obvious that the proper location for airline ticket counters is related to the outbound passenger rather than the inbound passenger. It was, therefore, determined to have an outbound concourse be the principal room in the building, to place in that room all the ticket counters, and to place in or close to it most of the concessions. This room was related to the outbound airplane parking positions, and the block of government offices was related to the inbound airplane parking positions.

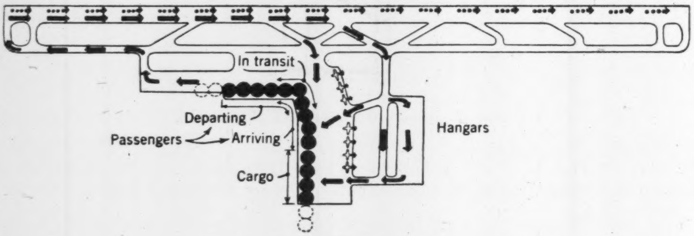

FIG. 3.—AIRPLANE PARKING POSITIONS

The outbound concourse was raised to a second-floor level, which was desirable not only to segregate outbound passengers from other traffic but also to permit the future installation of mechanical airplane-loading devices.

Also, baggage is most easily handled if gravity can be used for flow from one level to another. The airlines operators prefer to have their operations offices closely related to their ticket counters; therefore, the offices were located directly below the outbound concourse, and the ticket-counter areas were connected to them by stairways for personnel.

Another area which serves as a general distribution point for all passengers was added to the final building plan at a half level between the second-fioor outbound concourse and the ground-floor inbound government-process area.

The processing of an aircraft for a terminating or originating flight is different from that for a through flight. This difference has a definite effect on apron services and service-pit requirements. A segregation according to type may result in considerable reduction of necessary apron services, such as air conditioning and, therefore, in savings of construction costs.

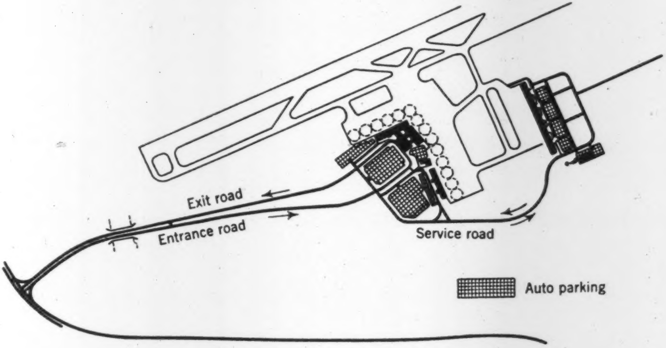

Fig. 4.—Roadway Arrangement

Vehicular Traffic.—Vehicular traffic to the terminal was divided in such a manner that only traffic directly related to departing passengers and taxis for incoming passengers use the main entrance ramp (Fig. 4). Service traffic is diverted before it gets to the ramp as is the traffic going to the parking lots. The major parking lot is connected to the terminal by a short pedestrian underpass. Limousine traffic for arriving passengers is located in such a manner as to be accessible but not to add to the traffic on the main entrance road. This plan was based on the assumption that the most critical vehicular time is the last few minutes before plane departure; anything that can be done to make it easier for the passenger to catch a plane will probably be appreciated.

Cargo Terminal.—For the cargo terminal an analysis was made similar to that for the passenger terminal. Because inanimate objects are easier to handle than people, the design of a cargo terminal is an easier problem—it was possible to evolve a simple building and a simple ground-traffic pattern.

CONCLUSIONS

The contribution which the Puerto Rico International Airport passenger terminal may make to the planning of such structures lies in the fact that it is the first concrete demonstration of the practicability and advantages of segregating inbound traffic from outbound traffic.[2] These advantages include (*a*) simplified airplane traffic circulation on the ground, (*b*) simplified passenger circulation within the building, (*c*) less expensive pit installations in the apron because air-conditioning pits and other services can be eliminated from terminating positions, and (*d*) a more functional relationship of concessions to potential buyers.

---

[2] "Airport Terminal Design—A Selective Method of Planning," by Walther Prokosch, *Journal*, S.A.E., Vol. 56, December, 1948, p. 55–57.

AMERICAN SOCIETY OF CIVIL ENGINEERS
Founded November 5, 1852
TRANSACTIONS

Paper No. 2745

FLOW IN ROUGH CONDUITS

By Henry M. Morris, Jr.,[1] A. M. ASCE

With Discussion by Messrs. Victor L. Streeter, Walter Rand, Harry H. Ambrose, and Henry M. Morris, Jr.

Synopsis

A new concept of flow over rough pipe and channel surfaces is presented. The concept is based particularly on the effect of the longitudinal spacing of surface-roughness elements and their associated vorticity streams. Three basic flow types have been denoted as isolated-roughness flow, wake-interference flow, and quasi-smooth (or skimming) flow.

The friction-factor equations derived for these three types of flow appear to be substantiated by data obtained by many experimenters on all types of roughnesses in both pipes and open channels. The equations can be extended to surfaces of variable roughness so that reasonably accurate predictions of the friction factor can be made for all types of conduit surfaces. The concept is physically reasonable and relatively simple; it bears promise of becoming a useful and rational method for the hydraulic design of conduits.

Notation

The letter symbols adopted for use in this paper are defined where they first appear, in the illustrations or in the text, and are arranged alphabetically, for convenience of reference, in the Appendix.

Introduction

A general concept of flow in rough conduits is developed subsequently. This concept is intended to make possible the prediction of friction factors for any type of conduit surface.

The equation for head loss in a conduit is

$$H_f = f \frac{L}{D} \frac{V^2}{2g} \qquad (1)$$

Note.—Published, essentially as printed here, in January, 1954, as *Proceedings-Separate No. 390.* Positions and titles given are those in effect when the paper or discussion was received for publication.

[1] Prof. and Head, Dept. of Civ. Eng., Southwestern Louisiana Inst., Lafayette, La.

in which H_f represents the head loss as a result of friction in a length L of the conduit, f represents the friction factor, D is the equivalent diameter of the conduit, and V denotes the average velocity of flow across any section. The friction factor is a dimensionless coefficient which can be shown—by dimensional analysis—to be a function of the Reynolds number of the flow and of several dimensionless geometric ratios:

$$f = \phi\left(\mathbf{R}_c, \frac{h}{D}, \frac{\lambda}{D}, \frac{s}{D}, \cdots\right) \qquad (2)$$

in which $\mathbf{R}_c$ is the conduit Reynolds number (and is equal to $D\,V/\nu$ where ν represents the kinematic viscosity of the fluid), h is the radial height of the wall-roughness projections, λ denotes the spacing of the wall-roughness elements in the direction of flow, and s is the clear peripheral spacing between elements. If other dimensions are necessary to describe the roughness elements, more dimensionless geometric terms can be included in Eq. 2.

The velocity-distribution relationship for pipes with rough walls has been found experimentally, especially by J. Nikuradse,[2] to be represented by

$$\frac{v}{v_s} = d + B \log_{10} \frac{y}{r_o} \qquad (3)$$

in which v is the velocity of flow at any point in the cross section, v_s denotes the shear velocity, d is a dimensionless parameter depending on the type of roughness, y represents the radial distance from the roughness crests to any point in the cross section, and r_o is the pipe radius measured to the crests of the roughness elements. The term B is equal to 5.75 which is obtained from

$$B = \frac{\log_e 10}{k} \qquad (4)$$

in which k is the universal turbulence constant developed[3] by T. von Kármán, Hon. M. ASCE. The turbulence constant has been shown to be applicable to the interior turbulence of smooth conduits and rough-walled conduits alike and to have an approximate experimental value of 0.40. The velocity traverses obtained by Mr. Nikuradse in sand-coated pipes are usually described by

$$\frac{v}{v_s} = 8.5 + 5.75\left(\log_{10} \frac{y}{e}\right) \qquad (5)$$

in which e is the diameter of the uniform sand grains which coated the pipe walls. The corresponding equation for the friction factor is

$$\frac{1}{\sqrt{f}} = 2 \log_{10} \frac{r_o}{e} + 1.74 \qquad (6)$$

Eq. 6 obviously implies that f is independent of $\mathbf{R}_c$ and is solely a function of the relative roughness e/r_o. Thus, this type of flow, commonly termed rough-pipe flow, can be represented by the quadratic resistance law, with the head loss proportional to the square of the velocity.

---

[2] "Strömungsgesetze in rauhen Rohren," by J. Nikuradse, *Forschungsheft No. 361*, 1933.

[3] "Turbulence and Skin Friction," by T. von Kármán, *Journal of the Aeronautic Sciences*, Vol. 2, 1934.

However, Mr. Nikuradse also showed that flow in rough pipes normally will have a brief regime of smooth-pipe flow at low Reynolds numbers before the roughness projections begin to have a material effect on the turbulence. A transition-flow regime is then established between smooth-pipe flow and rough-pipe flow. In this regime the friction factor first decreases, then increases, and finally becomes constant as R_c increases.

It has often been assumed that all types of conduit surfaces would also result in a constant friction factor at sufficiently high values of R_c. However, most tests of commercial pipe have yielded descending (f-R_c)-curves; some tests gave horizontal characteristics and, very infrequently, rising characteristics.

The practice of using the equivalent sand-grain diameter, K_s, developed by Mr. Nikuradse as a measure of surface roughness has been increasing among engineers (as of 1954). This term is defined as the sand-grain diameter which would give the same value of friction factor as the actual pipe and is obtained by solving Eq. 6 for K_s equal to e. However, because most (f-R_c)-curves for commercial pipes have been found to have descending characteristics throughout the experimental range, the formula developed[4] by C. F. Colebrook and C. M. White is often used to determine the value of K_s, or at least to define the transition regime for the surface being tested.

$$\frac{1}{\sqrt{f}} = 2\log_{10}\frac{r_o}{K_s} + 1.74 - 2\log_{10}\left(1 + \frac{\dfrac{18.7}{\mathsf{R}_c\sqrt{f}}}{\dfrac{r_o}{K_s}}\right) \ldots\ldots\ldots (7)$$

Eq. 7 results in a (f-R_c)-curve which is asymptotic to both the smooth-pipe curve and rough-pipe curve developed by Mr. Nikuradse. The parameter $(1/\sqrt{f}) - 2\log_{10}(r_o/K_s)$ has been termed[5] by L. Prandtl as the generalized resistance function and is represented by κ_g; the parameter $(\mathsf{R}_c\sqrt{f})/(r_o/K_s)$ can be shown to be a wall Reynolds number which is equal to $[(V_* K_s)/\nu]\sqrt{32}$ and is represented by R_w. Thus, Eq. 7 can also be represented by

$$\kappa_g = 1.74 - 2\log_{10}\left(1 + \frac{18.7}{\mathsf{R}_w}\right) \ldots\ldots\ldots\ldots\ldots\ldots (8)$$

The use of Eqs. 6 and 8, together with the design methods based thereon, undoubtedly represents a substantial improvement in design methodology. There exist, however, several important deficiencies in this method which the subsequent material should overcome.

Probably the most important defect lies in the inapplicability of Eq. 8 to conduit surfaces which cause either horizontal or rising (f-R_c)-curves. The tests performed[6] by Charles W. Harris, M. ASCE, on surfaces of "random" roughness resulted in (f-$\mathbf{R}_c$)-curves which were essentially horizontal after departing from the smooth-pipe curve. Tests[7] at the St. Anthony Falls Hydraulic Laboratory, University of Minnesota, at Minneapolis, on commercial, corrugated-metal culvert pipes revealed a definitely rising characteristic for the (f-$\mathbf{R}_c$)-relationship.

---

[4] "Experiments with Fluid Friction in Roughened Pipes," by C. F. Colebrook and C. M. White, *Proceedings*, Roy. Soc. of London, Vol. 161, 1937.

[5] "Mechanics of Turbulent Flow," by B. A. Bakhmeteff, Princeton University Press, Princeton, N. J., 1936.

Furthermore, even for pipes which cause the usual falling characteristic, experimental values of K_s are not always a function of only the type of surface. Tests[8,9] on concrete pipes at the St. Anthony Falls Hydraulic Laboratory have implied that K_s, as computed from Eq. 7, varies with both $\mathbf{R}_c$ and r_o.

Finally, it is apparent that K_s has no definite physical significance so far as the roughness elements on the surface are concerned, with the exception of uniform sand-coated surfaces. The use of K_s, however, has often seemed to imply that it is being associated with the height of projection h of the elements. There is no reason, of course, for h and K_s to be equal to (or even to be correlated with) each other as other roughness dimensions will obviously exert a material effect on the friction factor.

It is thus desirable (if possible) to develop a concept of rough-conduit flow which will include a physically realistic measure of surface roughness, which can be used to explain and predict the different forms of (f-$\mathbf{R}_c$)-curves, and which can be used to predict friction factors for any surface of known roughness dimensions and for any value of the Reynolds number.

FORM DRAG AND ROUGHNESS SPACING

The chief source of friction loss in a fluid flowing over a rough surface is evidently the generation, spreading, and subsequent dissipation of vortices from the wake and separation zones behind each roughness element. Each element is thus a source of vorticity, and the longitudinal frequency with which such sources of vorticity occur is therefore of significance in controlling the turbulence structure and energy-dissipation phenomena. This fact strongly suggests that the longitudinal spacing of the roughness elements is the roughness dimension that is of greatest importance in rough-conduit flow and would thus offer the most likely basis of correlating friction-loss data in such conduits.

Therefore, two parameters involving the roughness spacing λ should be defined for subsequent use. The roughness index is defined as λ/h, the ratio of the roughness-element spacing to the radial height of the projections. The relative-roughness spacing is defined as r_o/λ, the ratio of radius to spacing of the roughness elements. This latter term is similar to, but should not be confused with, the ratio usually defined as the relative roughness, r_o/h. The radius r_o, as well as other radial dimensions such as y, is measured with reference to a datum through the crests of the roughness elements. This is the best choice of datum because the wake and vortex-generating zone at each roughness element originates at or near the crest of the element.

---

[6] "An Engineering Concept of Flow in Pipes," by Charles W. Harris, *Transactions*, ASCE, Vol. 115, 1950, p. 909.

[7] "Hydraulic Tests on Corrugated Metal Culvert Pipes," by L. G. Straub and Henry M. Morris, Jr., *Technical Paper No. 5, Series B*, St. Anthony Falls Hydr. Lab., Univ. of Minnesota, Minneapolis, Minn., 1950.

[8] "Hydraulic Data Comparison of Concrete and Corrugated Metal Culvert Pipes," by L. G. Straub and Henry M. Morris, Jr., *Technical Paper No. 3, Series B*, St. Anthony Falls Hydr. Lab., Univ. of Minnesota, Minneapolis, Minn., 1950.

[9] "Hydraulic Tests on Concrete Culvert Pipes," by L. G. Straub and Henry M. Morris, Jr., *Technical Paper No. 4, Series B*, St. Anthony Falls Hydr. Lab., Univ. of Minnesota, Minneapolis, Minn., 1950.

BASIC TYPES OF FLOW

Realizing the fundamental significance of the roughness-element spacing in the expenditure of flow energy, it thus becomes apparent that three different types of flow phenomena may occur near the wall; the type which occurs in a given situation will depend primarily on the value of λ for the given roughness.

If the wall-roughness elements are far apart, the individual elements will act as isolated bodies on which are exerted drag forces by the flowing fluid. The wake zone and vortex-generating zone at each element are completely developed and dissipated before the next element is reached. The apparent friction factor would therefore result from the form drag on the roughness elements in addition to the friction drag on the wall surface between elements. The form drag on any one element would depend primarily on the height of the projection h of the element; the total form drag in a given length of conduit would depend on λ. Thus, the roughness index λ/h could be expected to be a significant correlating parameter for this type of flow, which can be designated as isolated-roughness flow.

The second type of flow results when the roughness elements are placed sufficiently close together so that the zones of separation and vortex generation and dissipation associated with each element are not completely developed before the next element is encountered. This type of flow can be termed wake-interference flow, involving as it does the interference by the wake of each element with the vortex spreading and dissipation from the preceding element. The friction drag of the wall is obliterated, and the entire region near the wall is replete with intense and complex vorticity and turbulent mixing. The height h of the element is relatively unimportant in this type of flow, but the spacing λ is obviously of major importance. Also, the size of the pipe will control in part the radial extent of this wall region of abnormal turbulence. For wake-interference flow, therefore, the relative-roughness spacing r_o/λ will be an important correlating parameter.

Another type of flow results when the roughness elements are so close together that the flow essentially skims the crests of the elements. In the grooves between the elements there will be regions of dead water containing stable vortices. The bulk of the flow will be over a pseudo-wall composed of the roughness crests and the upper limbs of the groove vortices. Large roughness projections will be absent from this pseudo-wall; the flow will thus be similar to smooth-conduit flow. This type of flow might be termed either quasi-smooth flow or skimming flow. Much of the energy loss in such flow can probably be attributed to the maintenance of the groove vortices, the size of which are controlled by the width or the depth of the groove, whichever is the smaller; the number of such vortices depends on λ. The roughness index, expressed either as λ/h or λ/j (in which j is the groove width) can thus be expected to be a significant parameter influencing the apparent friction factor in skimming flow.

WAKE-INTERFERENCE FLOW

The phenomena of wake-interference flow will be considered first primarily because the sand-coated pipes[2] seem to have produced this type of flow.

For the purpose of developing general equations descriptive of wake-interference flow, one should consider a section of circular pipe that is sufficiently removed from the entrance or other irregularity to permit full development of the turbulent boundary layer. At each roughness element there will be formed a wake from which vortices will be shed toward the pipe center. The forward velocity of flow will wash the vortices downstream where they will join the vortices from the next roughness wake. Thus, a relatively distinct wall zone of flow will result in which a comparatively high intensity of turbulent mixing will prevail.

In the central region of the pipe, normal turbulence—characterized by the turbulence constant k—will prevail. The boundary between the central region and wall region will be at a distance from the wall which is probably primarily dependent on the spacing of the elements as it is this parameter which controls (1) the frequency of vorticity sources and (2) the spread angle of vortices toward the central region. Accordingly, the distance from the wall of the boundary between the wall zone and the central zone will be $c\,\lambda$, in which the term c can probably be expected to vary with the wall Reynolds number and with the relative-roughness spacing.

The general dimensionless equation of velocity distribution in the central region is therefore

$$\frac{v}{v_s} = a + \frac{1}{k}\left(\log_e \frac{y}{c\,\lambda}\right) = A + \frac{1}{k}\left(\log_e \frac{y}{\lambda}\right) \qquad (9)$$

The dimensionless term a is the value of v/v_s at the boundary between the two regions at y equal to $c\,\lambda$, and the term A is the value of v/v_s at the distance y equal to λ. One should note that

$$A = a - \frac{1}{k}\log_e c \qquad (10)$$

Because of the higher relative intensity of turbulent mixing in the wall region, the velocity distribution would be expected to be more nearly uniform in this region than would the velocity distribution which corresponds to the constant k. The equation for the velocity distributions in this wall zone is not known, of course, but it might reasonably be assumed to be of the same general form as Eq. 9, with a different turbulence parameter replacing k.

Accordingly, the velocity-distribution equation for the wall zone is

$$\frac{v}{v_s} = a + \psi \log_e \frac{y}{c\,\lambda} = A_w + \psi \log_e \frac{y}{\lambda} \qquad (11)$$

in which A_w is the value of v/v_s at y equals λ. The parameter ψ corresponds to $1/k$ in Eq. 9. If v/v_s is plotted against $\log_e (y/\lambda)$ for a given pipe section, $1/k$ is the slope of the curve for the central region and ψ is the slope in the wall region. In general, the value of $1/k$ must equal or exceed the value of ψ because of the abnormal turbulence in the wall zone; a more nearly uniform velocity distribution (when plotted on a semi-logarithmic basis) will therefore result in the wall zone.

The parameter ψ is evidently not a constant as it depends on the wake and vortex-spreading phenomena in the wall region, which, in turn, depend on the form and dimensions of the roughness elements (especially their longitudinal spacing) and on the fluid velocity and viscosity. For a given wall roughness it is probable that ψ will be a function of the wall Reynolds number, defined as $(\mathsf{R}_c\sqrt{f})/(r_o/\lambda)$, and of the cross-sectional form of the individual roughness elements, and that, for a given form of element, ψ will approach $1/k$ as the wall Reynolds number, R_w, increases. It is assumed that ψ does not vary significantly with y. This assumption ignores at least a small transition zone—both near the wall and near the central core zone—but the use of a constant average value of ψ throughout the wall zone will materially simplify the ensuing analysis and will not significantly affect the results. It should be noted that in the wall Reynolds number as defined here the roughness spacing has replaced the equivalent sand diameter as the length parameter because the former has more direct physical effect on the wall turbulence phenomena than does the latter.

It is desirable to obtain an expression for the average velocity of flow throughout the entire cross section. This can be done by integrating the elements of discharge across the section, then dividing by the total area—

$$\frac{V}{v_*} = \frac{\int v\,dA}{A\,v_*} = \frac{2\,\pi\int v\,r\,dr}{A\,v_*} = \frac{2}{r^2_o}\left[\int_0^{c\lambda}(r_o - y)\left(a + \psi\log_e\frac{y}{c\,\lambda}\right)dy + \int_{c\lambda}^{r_o}(r_o - y)\left(a + \frac{1}{k}\log_e\frac{y}{c\,\lambda}\right)dy\right] \quad (12a)$$

Eq. 12*a* can be reduced to

$$\frac{V}{v_*} = \left(A - \frac{3}{2\,k}\right) + \left(\frac{1}{k} - \psi\right)\left[2\left(\frac{c\,\lambda}{r_o}\right) - \frac{1}{2}\left(\frac{c\,\lambda}{r_o}\right)^2\right] + \frac{1}{k}\log_e\frac{r_o}{\lambda} \quad (12b)$$

Replacing V/v_* by its equivalent, $\sqrt{8/f}$, there results

$$\frac{1}{\sqrt{f}} - \frac{1}{k\sqrt{8}}\log_e\frac{r_o}{\lambda} = \frac{1}{\sqrt{8}}\left(A - \frac{3}{2\,k}\right) + \frac{1}{\sqrt{8}}\left(\frac{1}{k} - \psi\right)\left[2\left(\frac{c\,\lambda}{r_o}\right) - \frac{1}{2}\left(\frac{c\,\lambda}{r_o}\right)^2\right] \quad (13)$$

Eq. 13 can be described as the general resistance equation for axial wake-interference flow.

An equation similar to Eq. 13 can be derived for two-dimensional, wake-interference flow in an analogous manner—the final equation being

$$\frac{1}{\sqrt{f}} - \frac{1}{k\sqrt{8}}\log_e\frac{b}{\lambda} = \frac{1}{\sqrt{8}}\left(A - \frac{1}{k}\right) + \frac{1}{\sqrt{8}}\left(\frac{1}{k} - \psi\right)\left(\frac{c\,\lambda}{b}\right) \quad (14)$$

in which b is the distance from the roughness crests to the channel center.

The left members of Eqs. 12 and 14 are referred to as the resistance functions and will be represented by κ_a and κ_t, respectively. The first term in the right member is the lower limiting value of the resistance function. The second term in the right member is the corrective term which approaches—and eventually reaches—zero at high values of the wall Reynolds number because ψ approaches $1/k$ and because c decreases as $\mathbf{R}_w$ increases.

The universal turbulence constant k is usually assumed to be approximately 0.40, although there is considerable evidence that a more generally accurate value would be 0.37 or 0.38. If 0.40 is used, the resistance function κ_a simplifies to $(1/\sqrt{f}) - 2 \log_{10} (r_o/\lambda)$, and κ_t to $(1/\sqrt{f}) - 2 \log_{10} (b/\lambda)$.

The term A also appears to be a universal constant related to the wall-zone turbulence. This fact has not been recognized heretofore and will be seen to have significant consequences. It is obvious that A is constant for a given conduit and roughness type as it is merely the value of v/v_s in the core velocity distribution at y equal to λ and as v/v_s (at any constant value of y) is independent of $\mathbf{R}_c$ and $\mathbf{R}_w$. The magnitude of A can be scaled from any dimensionless plot of the core-velocity distribution at the ordinate y equal to λ.

If a conduit having some other arbitrary roughness—with the same value of λ as the first roughness but having different dimensions and shape—is subjected to a flow velocity so adjusted that the phenomena of separation on the roughness elements are mechanically similar to the corresponding phenomena for flow at some given value of $\mathbf{R}_c$ of $\mathbf{R}_w$ on the first roughness, a different value of $\mathbf{R}_w$ than that used for the first roughness would be required. It is apparent, however, that such a similar condition could be produced. The location of the separation point on the roughness elements can be adjusted by adjusting $\mathbf{R}_c$. The turbulence phenomena in the wall zone (beyond the roughness crests, of course) depend primarily and directly on the character of the wakes rather than on the form of the elements producing the wakes.

Assuming then that the wake and wall-turbulence phenomena at some value of $\mathbf{R}_w$ for the second roughness are made mechanically similar to those for the first roughness at some other value of $\mathbf{R}_w$, the (v/v_s)-distributions for the two situations must be similar in the wall zone. The values of ψ, c, and A_w would therefore be equal in the two situations, and this would also mean that the (v/v_s)-distributions in the core would be the same—that is, the plots of $\log (y/\lambda)$ versus v/v_s for the two situations would coincide. Therefore, the value of A can be made the same for the two roughnesses but, because A is constant for any one roughness, it must therefore have the same constant value for both roughnesses. A similar argument could be developed for roughnesses having different λ-values.

The implication, therefore, is that the term A is independent of surface roughness. Its magnitude may be determined by scaling v/v_s from any curve of the distribution of the core velocity at a distance y equal to λ from the roughness crests.

Therefore, the limiting value of the resistance function, $\dfrac{1}{\sqrt{8}}\left(A - \dfrac{3}{2\,k}\right)$, is also a universal constant which is independent of surface roughness. The magnitude of this limiting value, as well as the magnitude of A, will be determined subsequently from the available experimental data.

First, however, the implications of the additive term in Eqs. 13 and 14 should be noted. In the regime in which the corrective term has not yet vanished its magnitude continuously decreases as the wall Reynolds number increases. An analysis of Eqs. 13 and 14 will show that this means that, for wake-interference flow in any given type, the friction factor must increase with increasing Reynolds number, becoming and remaining constant when the corrective term vanishes.

The corrective term in the case of axial flow may conveniently be simplified to $\frac{2}{\sqrt{8}}\left(\frac{1}{k} - \psi\right)\left(\frac{c\,\lambda}{r_o}\right)$ as the term $\frac{1}{2}\left(\frac{c\,\lambda}{r_o}\right)^2$ would almost always be negligible compared to the term $2\,c\,\lambda/r_o$. For a given value of the wall Reynolds number, the expression $1/k - \psi$ will depend only on the form of the roughness element. The term $c\,\lambda/r_o$ is a ratio of two radial dimensions, the distances from the roughness crests to the break in the velocity-distribution curves and to the pipe center. It is reasonable to assume that these dimensions would be geometrically similar for a given roughness form and that their ratio would be independent of the relative-roughness spacing r_o/λ.

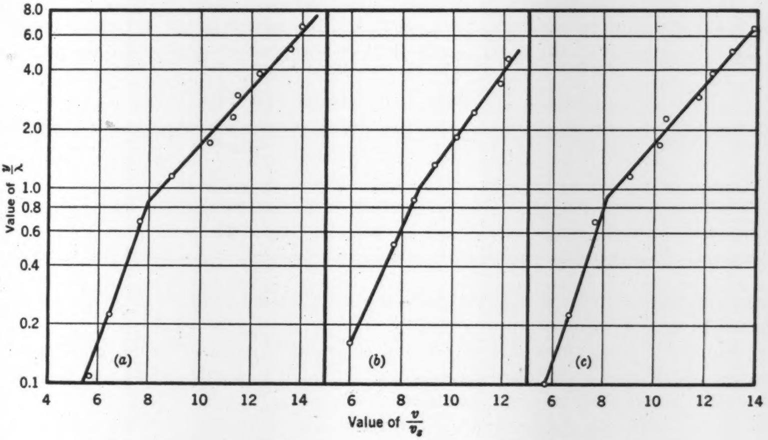

FIG. 1.—TYPICAL VELOCITY-DISTRIBUTION CURVES IN CORRUGATED METAL PIPES

Consequently, the corrective term can be considered to be primarily a function of the wall Reynolds number $\mathbf{R}_w$ and the cross-sectional form of the roughness elements. That is, if the resistance function, κ_a, is plotted against the wall Reynolds number, $\mathbf{R}_w$, a single curve should result for each form of roughness element. Furthermore, the curves for all forms of roughness will approach and reach the same limiting value of the resistance function $\frac{1}{\sqrt{8}}\left(A - \frac{3}{2\,k}\right)$. The value of $\mathbf{R}_w$ at which the corrective term vanishes would be expected to depend on the form of the roughness elements.

Velocity-Distribution Data.—Several sets of experimental velocity-distribution data on conduits having regular surface-roughness patterns are available. However, most of these test conduits were of small size.

The only available applicable velocity-distribution data on large pipes are those from a series of measurements[10] made at the St. Anthony Falls Hydraulic Laboratory on corrugated metal pipes having diameters of 24 in. and 36 in.; the two pipes were each 193 ft long. In all, some fifteen velocity-distribution curves were obtained at sections at which the turbulent boundary layer was fully developed. Three typical curves are shown in Fig. 1; the corresponding values are given in Table 1. When plotted with v/v_* as the abscissa and $\log_{10} (y/y\lambda)$ as the ordinate, these curves all indicated a definite break between the distribution curves for the wall velocity and core velocity. From these plots, the values of k, ψ, and A were measured and plotted with the wall Reynolds number as the common abscissa.

The value of A was found to vary only slightly from its average value of 8.70, the range of values being from 8.4 to 9.3, and the standard deviation being 0.24. Because of all the possible causes of data dispersion, this small deviation appears to demonstrate satisfactorily the essential constancy of A for corrugated pipe at a value of approximately 8.70.

TABLE 1.—TEST CONDITIONS FOR FIG. 1

Item	Fig. 1(*a*)	Fig. 1(*b*)	Fig. 1(*c*)
r_o/λ	6.75	4.50	6.75
$\mathsf{R}_c \times 10^{-3}$	874	745	1,262
$\mathsf{R}_w \times 10^{-3}$	35.2	67.0	51.9
v_*, in feet per second	0.271	0.375	0.384
λ, in inches	$2\frac{2}{3}$	$2\frac{2}{3}$	$2\frac{2}{3}$

Similarly, the values of k were found to be fairly constant, with an average value of 0.36 and a standard deviation of 0.03. The scatter of values of both A and k about their means was essentially random.

It was evident, however, that the parameter ψ increased with increasing values of R_w. The scatter of the data was such that any curvilinear relationship could not be detected. The straight-line regression equation for this relationship was

$$\psi = 1.00 + \frac{\mathsf{R}_c \sqrt{f}}{155{,}000 \frac{r_o}{\lambda}} \qquad (15)$$

It is probable that the assumed straight line represented by Eq. 15 would curve over at high values so as to become tangent to the line $\psi = 1/k$. The minimum value of R_w at which this would occur could be computed by extrapolation of Eq. 15 to the value of $\psi = 1/0.36 = 2.77$. This computation yields the very high value of 274,000 for the smallest value of R_w at which the limiting resistance function might be reached. As the maximum experimental value attained for the latter was 67,000, it is obvious that very high velocities would have to be reached before a constant condition could be established. Thus, it can be seen that the friction factor must continue to increase as the Reynolds number increases to very high values of the latter for corrugated surfaces. It will be seen subsequently that experimental results of friction tests on these pipes confirm this implication.

---

[10] "A New Concept of Flow in Rough Conduits," by Henry M. Morris, Jr., thesis presented to the University of Minnesota, Minneapolis, Minn., in 1950, in partial fulfilment of the requirements for the degree of Doctor of Philosophy.

Supplementary Data.—The tests[2] of Mr. Nikuradse on pipes roughened by densely-packed, uniform sand grains have hitherto been interpreted in terms of the relative roughness, r_o/h. It is evident, however, that the relative-roughness spacing r_o/λ was numerically equal to r_o/h in these pipes so that either parameter could be used without affecting any of the numerical results. The rough-pipe, velocity-distribution equation[2] can therefore be written:

$$\frac{v}{v_s} = 8.5 + \frac{1}{k} \log_e \frac{y}{\lambda} \ldots\ldots\ldots\ldots\ldots\ldots (16)$$

The value of A for surfaces that are densely packed with uniform sand grains is therefore approximately 8.5. Thus, two pipe surfaces as radically different in character as corrugated metal and sand give approximately identical results for the generalized velocity-distribution equations. This agreement is strong confirmation of the significance of the roughness spacing in the flow structure. No such correlation as this is at all possible on the basis of the roughness height.

The tests[11] performed by H. Schlichting included many different types of roughness elements that were installed on test plates which were arranged to form one side of a rectangular conduit in which two-dimensional flow was obtained near the transverse center of the plate. Most of these test plates caused isolated-roughness flow and will be cited subsequently. Three plates, however, evidently produced wake-interference flow. One of these was a plate coated with dense, uniform-grain sand, 0.135 cm in diameter. Another was a plate to which were attached spheres 0.41 cm in diameter and with a spacing of 0.60 cm in both directions. The third plate had angles extending transversely throughout the plate width, 0.30 cm high and spaced at 2.00-cm intervals.

Mr. Schlichting published velocity-distribution curves for all the roughnesses.[11] Although the tests were made at high values of $\mathbf{R}_w$, making the break point in the velocity-distribution curves difficult to determine closely, the latter all revealed a definite decrease in slope in the wall zone. After correcting Mr. Schlichting's data and curves to a datum at the roughness crests and determining A as the value of v/v_s at y equal to λ, it was found that the sand-roughness plate and sphere-roughness plate resulted in a value of 7.8 for A; the plate with long angles resulted in 8.2 for A. These values are not so different from the A-values obtained by Mr. Nikuradse[2] or the writer.[10] The values are consistently lower, however, and probably reflect the two-dimensional structure of the flow.

---

[11] "Experimentelle Untersuchungen zum Rauhigkeitsproblem," by H. Schlichting, *Ingenieur-Archiv*, Vol. VII, No. I, 1936.

The velocity-distribution data obtained[12] by Vito A. Vanoni, M. ASCE, were obtained in a rectangular open channel having a bottom surface composed of densely packed sand, 0.88 mm in diameter. The velocity profiles were taken at the center line where the flow was two-dimensional. Those which are pertinent to this investigation consist of the three runs made with clear water. The boundary between the center zone and the wall zone was quite distinct, occurring at a distance of y equal to approximately 10 λ. This large value of c (c was of the order of magnitude of unity for the corrugated metal pipes[10] and the conduits[11]) appears merely to confirm the deduction that c should be large for small values of λ/r_o.

The A-values for the three curves determined by Mr. Vanoni are found to be approximately 8.0, 6.8, and 7.7, with 7.5 as an average. This value is very near the values of A in two-dimensional flow found by Mr. Schlichting, the slight difference perhaps being attributable to free-surface effects.

The available velocity-distribution data, although limited, thus seem to support the previous theoretical inference that the term A should be a universal constant, independent of the type of wall surface. A small difference caused by cross-sectional form seems to exist, however. For axial flow, A is approximately 8.7 and for two-dimensional flow it is approximately 7.8.

Numerical values of A and k can thus be inserted into the generalized resistance equations (Eqs. 13 and 14). If k is assumed to be 0.40, for simplicity, and A is taken as 8.7 and 7.8 for axial and two-dimensional flow, respectively, these equations become

$$\kappa_a = \frac{1}{\sqrt{f}} - 2 \log_{10} \frac{r_o}{\lambda} = 1.75 + \frac{\sqrt{2}}{2} \left(\frac{c\,\lambda}{r_o} \right) (2.5 - \psi) \ldots\ldots (17a)$$

and

$$\kappa_t = \frac{1}{\sqrt{f}} - 2 \log_{10} \frac{b}{\lambda} = 1.75 + \frac{\sqrt{2}}{4} \left(\frac{c\,\lambda}{b} \right) (2.5 - \psi) \ldots\ldots (17b)$$

It is very interesting, although probably fortuitous, that the limiting value of the resistance function in both axial flow and two-dimensional flow is 1.75. Because most other cross-sectional shapes could probably be referred to a circular section through the use of the hydraulic radius ($r_o = 2\,R$), the value of 1.75 appears to be a most remarkable universal constant, independent of both surface roughness and cross-sectional form.

Experimental Verification.—It has been shown that the velocity-distribution data that are available for wake-interference flow support the general theoretical relations developed previously. These data are limited, however, and much stronger confirmation of the theory can be obtained from the available (as of 1954) friction-loss data in conduits with surface patterns of roughness producing this type of flow.

Eqs. 17 indicate that, for wake-interference flow, the resistance function decreases from some maximum value to a minimum value of 1.75 as $\mathbf{R}_w$ increases. This transition would be expected to have a form depending on the form of the roughness elements, but the limiting value of 1.75 would be applicable to all types of roughness elements. The maximum possible value of the resistance function could be estimated by assuming a value of ψ of zero, and a value for $c\,\lambda/r_o$ of unity. These values would result in 3.52 as the maximum possible value of the resistance function (2.64 for two-dimensional flow). The maximum value for any particular type of roughness may be less than this; it cannot be greater. From Eqs. 17 it can also be seen that the friction factor will increase as the Reynolds number increases—for any given value of r_o/λ. Also, for a given Reynolds number, the friction factor increases as r_o/λ decreases.

---

[12] "Transportation of Suspended Sediment by Water," by Vito A. Vanoni, *Transactions*, ASCE, Vol. 111, 1946, p. 67.

The foregoing description of the transitional zone and limits for wake-interference flow comprises a rigorous set of specifications which experimental data must fulfil. It will be seen, however, that every feature of these specifications is supported by a great variety of data obtained by many different experimenters, working under many different conditions and with many types of conduits—including both pipes and open channels.

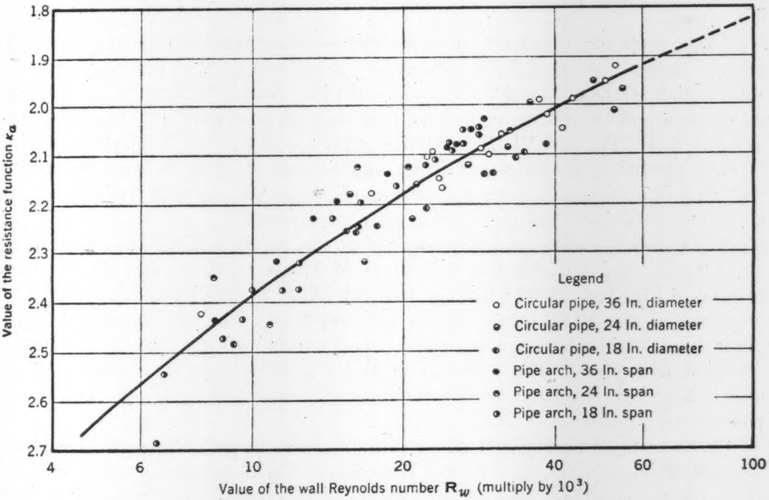

FIG. 2.—THE RELATIONSHIP BETWEEN THE RESISTANCE FUNCTION AND THE WALL REYNOLDS NUMBER FOR CORRUGATED METAL PIPES

These data can best be analyzed when plotted with the resistance function as the ordinate and the wall Reynolds number as the abscissa. A logarithmic scale is used for the latter because of the large range of values involved. The ordinates are plotted increasing downward to emphasize the similar appearance of this type of plot to the more familiar (f-$\mathbf{R}_e$)-plotting.

Tests on several commercial, corrugated metal pipes have been performed at the St. Anthony Falls Hydraulic Laboratory[7,8] on circular pipes having diameters of 18 in., 24 in., and 36 in. and on flattened pipe-arch sections having perimeters equal to those for 18-in., 24-in., and 36-in. circular pipes. The corrugations had a spacing, λ, of $2\frac{2}{3}$ in. and a height, h, of $\frac{1}{2}$ in.

These data strikingly exhibit the phenomena associated with wake-interference flow. In Fig. 2 there is shown the resistance function plotted against the wall Reynolds number for these tests. The strong conformity of the data from all pipes to form one curve is evident. The resistance function is seen to decrease gradually from approximately 2.7 to approximately 1.9 over a range of $\mathbf{R}_w$ from approximately 7,000 to 60,000. The limiting value of 1.75 was not reached, but the curve gives every indication of a tangential approach to this limit at a value of $\mathbf{R}_w$ of approximately 350,000. This is essentially the same inference deduced from the $(\psi\text{-}\mathbf{R}_w)$-curve for the corrugated-pipe velocity distributions cited previously. The friction data for partly full flow in these pipes were also found to lie on the same curve although with somewhat more dispersion.

There are a few other sets of experiments on corrugated pipe surfaces that are of interest. A. H. Gibson made tests[13] on a 2-in. copper pipe having sine-wave corrugations of $\lambda = 0.4$ in. and $h = 0.1$ in. Victor L. Streeter, M. ASCE, made tests[14] on two corrugation-type roughnesses, numbered IV ($\lambda = 0.043$ in. and $h = 0.012$ in.) and VI ($\lambda = 0.087$ in. and $h = 0.016$ in.). The tabulations of data published by Messrs. Gibson and Streeter had to be recomputed on the basis of a datum at the roughness crests, and this was also true of most of the other published data on other types of roughness.

The combined data from the results[10] at the St. Anthony Falls Laboratory ($\lambda = 2.7$ in. and $h = 0.5$ in.) and those of Messrs. Gibson and Streeter are plotted in Fig. 3(*a*), in which the notation S. A. F. is used to signify the results obtained at the St. Anthony Falls Laboratory.[10] The curves in Fig. 3(*a*) define almost the complete transition curve from smooth-pipe flow to quadratic-law turbulent flow. The curve is valid for a wide range of values of λ, h, and r_o for both circular and deformed sections and for both pipe and open-channel tranquil flow.

Other tests on corrugated metal pipes, such as those performed[15] by D. L. Yarnell, F. A. Nagler, and S. M. Woodward, did not include measurements of water temperature, making it impossible to compute accurate values for $\mathbf{R}_c$ or $\mathbf{R}_w$. However, the range in resistance function was about the same as in the corrugated-pipe tests.[10]

In Fig. 3(*b*) there are shown resistance-function data based on experiments on surfaces containing uniform spot-roughness elements. These data include the sand roughness tested by Mr. Nikuradse,[2] the sand roughness and spherical roughness tested by Mr. Schlichting,[11] and two roughnesses tested in an open channel by H. Bazin[16] and discussed by G. H. Keulegan.[17] One of these rough-

---

[13] "The Flow of Water in a Corrugated Pipe," by A. H. Gibson, *The Philosophical Magazine*, Vol. 50, 1925.

[14] "Frictional Resistance in Artificially Roughened Pipes," by Victor L. Streeter, *Transactions*, ASCE, Vol. 101, 1936, p. 681.

[15] "The Flow of Water through Culverts," by D. L. Yarnell, F. A. Nagler, and S. M. Woodward, *Bulletin 1*, Univ. of Iowa Studies in Eng., Iowa City, Iowa, 1926.

[16] "Recherches Hydrauliques," by H. Bazin, *Mémoires divers savants, Scientifique Mathématique et Physique*, Vol. 19, Paris, France, 1865.

[17] "Laws of Turbulent Flow in Open Channels," by G. H. Keulegan, *Research Paper 1151*, National Bureau of Standards, Washington, D. C., 1938.

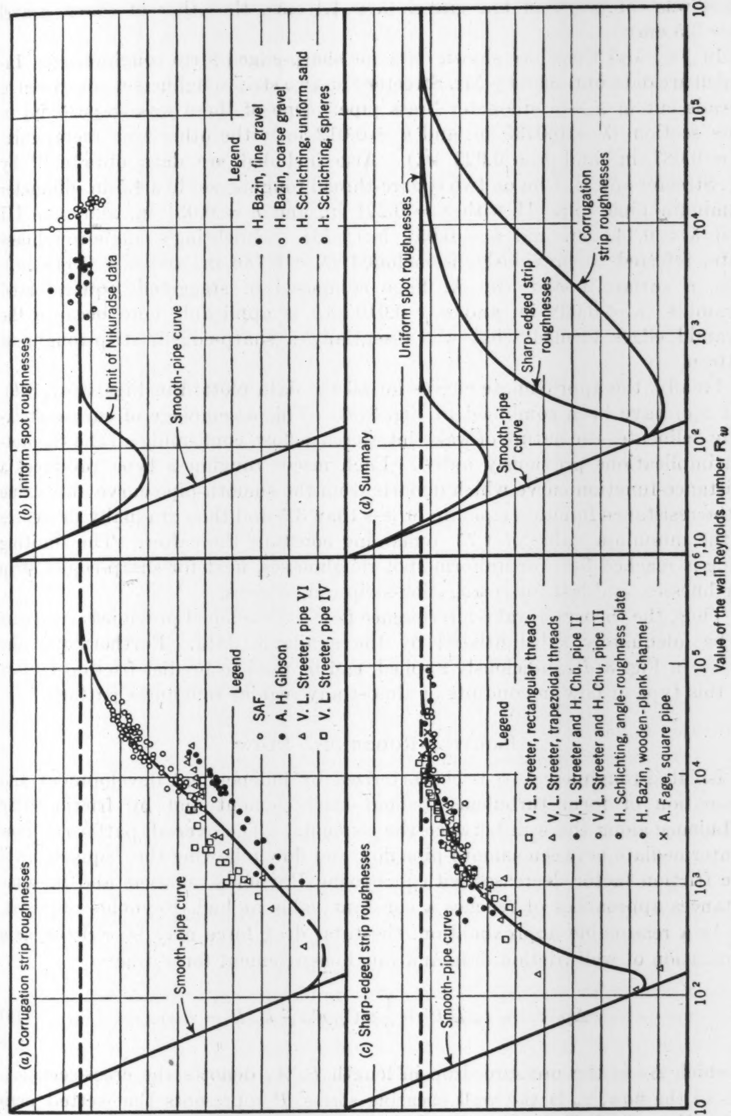

FIG. 3.—THE RELATIONSHIP BETWEEN THE RESISTANCE FUNCTION AND THE WALL REYNOLDS NUMBER FOR WAKE-INTERFERENCE FLOW

nesses was composed of fine gravel ($\lambda = 1.1$ cm), the other of coarse gravel ($\lambda = 3.5$ cm).

In Fig. 3(*c*) there are shown data for sharp-edged strip roughnesses. Included are data obtained by Mr. Streeter[14] on two strip roughnesses composed of threads cut in a 2-in.-diameter brass pipe. One of these was trapezoidal in cross section ($\lambda = 0.0435$ in. and $h = 0.012$ in.); the other was rectangular ($\lambda = 0.087$ in. and $h = 0.022$ in.). Also included are data obtained[18] by Mr. Streeter and H. Chu on two square-thread roughnesses in a 4.5-in.-diameter aluminum pipe (pipe II with $\lambda = 0.221$ in. and $h = 0.051$ in. and pipe III with $\lambda = 0.443$ in. and $h = 0.051$ in.); Mr. Schlichting's angle-roughness plate, referred to previously, is included ($\lambda = 0.786$ in. and $h = 0.118$ in.). Also, a surface tested[19] by A. Fage composed of staggered, square-based pyramids ($\lambda = 0.038$ in. and $h = 0.019$ in.) is applicable here because the pyramid edges formed what was essentially a sharp-edged, strip-roughness pattern.

Finally, the approximate curves for all the data plotted in Figs. 3(*a*), 3(*b*), and 3(*c*) have been combined in Fig. 3(*d*). This assemblage of curves strikingly delineates the nature of wake-interference flow, confirming all the theoretical implications previously noted. Each major roughness type produces a resistance-function curve which departs from the smooth-pipe curve at a value of the resistance function equal to or less than 3.5 and then gradually decreases to the minimum value of 1.75, remaining constant thereafter. The limiting value is reached first for uniform spot roughnesses, next for sharp-edged strip roughnesses, and last for corrugation-strip roughnesses.

Thus, the theory of wake-interference flow as developed previously, appears to be adequately substantiated by the available data. Furthermore, the curves in Fig. 3(*d*), judiciously applied, can be used to predict friction factors for this type of flow in conduits of almost any regular roughness pattern.

ISOLATED-ROUGHNESS FLOW

Isolated-roughness flow is characterized by independent development and dissipation of form turbulence behind each element and by friction-drag turbulence along the wall between the elements. The over-all pattern of flow is intermediate between smooth-pipe flow and flow following the "square law." The friction factor decreases with increasing Reynolds numbers and in some instances approaches or reaches a constant value at high Reynolds numbers.

As a reasonable approximation, the total drag force may be written as a summation of wall-friction drag and roughness-element form drag—

$$\Delta p \, A_f = \tau_w \, L \, P + \frac{1}{2} \rho \, C_D \, v^2_w \frac{L}{\lambda} h \, (P - n \, s) \ldots\ldots\ldots\ldots (18)$$

in which Δp is the pressure drop in length L, A_f denotes the cross-sectional area of the flow, τ_w is the wall shearing stress, P represents the wetted perimeter, ρ is the fluid density, C_D signifies the drag coefficient for the element, n is the number of individual elements in a periphery, and v_w represents the flow velocity at the roughness crests.

---

[18] "Fluid Flow and Heat Transfer in Artificially Roughened Pipes," by Victor L. Streeter and H. Chu, *Project 4918*, Armour Research Foundation, Chicago, Ill., 1949.

[19] "Fluid Flow in Rough Pipes," by A. Fage, *Reports and Memoranda No. 1585*, Aeronautical Research Comm., His Majesty's Stationery Office, London, England, 1934.

If f is the bulk friction factor and f_w is the friction factor for the wall surface only, Eq. 18 can be reduced to

$$f = f_w + \frac{4\,C_D}{\frac{\lambda}{h}}\left(\frac{v_w}{V}\right)^2\left(1 - \frac{n\,s}{P}\right) \ldots\ldots\ldots\ldots\ldots (19)$$

Assuming the wall surface to be essentially smooth, it has been shown by Mr. Nikuradse that

$$\left(\frac{v_w}{V}\right)^2 = 16.8\,f_w \ldots\ldots\ldots\ldots\ldots\ldots\ldots\ldots (20)$$

As an approximation, Eq. 20 can be introduced into Eq. 19 to result in

$$f = f_s\left[1 + \frac{67.2\,C_D}{\frac{\lambda}{h}}\left(1 - \frac{n\,s}{P}\right)\right] \ldots\ldots\ldots\ldots\ldots (21)$$

in which f_s is the smooth-conduit friction factor. From Eq. 21 the nature of isolated-roughness flow can be determined. The friction factor is obtained by multiplying the smooth-pipe friction factor by a coefficient greater than unity, the excess depending on the roughness index λ/h, the drag coefficient C_D, and the proportion of normal wall length intervening between roughness elements around the periphery to the total wetted perimeter, $n\,s/P$; for strip roughnesses, $n\,s$ is equal to zero.

As a general check on the validity of Eq. 21, various test roughnesses used by Mr. Schlichting[11] will be cited. These roughnesses included spheres (two sizes), spherical segments, cones, short angles, and long angles—each tested for various values of λ and s. These plates, with four exceptions, produced isolated-roughness flow. Three of them produced wake-interference flow and have previously been cited; one produced skimming flow. The measured friction factors on the plates that caused isolated-roughness flow agree satisfactorily with friction factors computed from Eq. 21.

Considering also this type of flow in open channels, reference may be made particularly to the data obtained by Ralph W. Powell,[20] M. ASCE, who tested flows over various arrangements of ¼-in. and ⅛-in. square battens on the bottom and sides of a rectangular flume. Again a comparison of measured friction factors with values computed from Eq. 21 indicates excellent agreement. It is interesting that this agreement is obtained for both tranquil and rapid (although not "ultra-rapid") flows. The detailed tabulations of these computed and observed values of f are available elsewhere.[10] It is believed, therefore, that the concept of isolated-roughness flow harmonizes with the data obtained by Messrs. Schlichting and Powell and that Eq. 21 gives a good representation of this type of flow.

---

[20] "Flow in a Channel of Definite Roughness," by Ralph W. Powell, *Transactions*, ASCE, Vol. 111, 1946, p. 531.

QUASI-SMOOTH FLOW

For surfaces with very low roughness indices, the flow will more or less "skip" over the crests of the roughness elements. Between the elements there will be regions of dead water, with stable vortices established in these regions by the fluid moving above the elements. The combination of the roughness crests and the still water in the interstices serves as a pseudo-wall, probably somewhat wavy in character but without large roughness projections. Consequently, this type of flow has been termed quasi-smooth flow or skimming flow.

Vortex generation at the hypothetical smooth wall is the predominant source of turbulence in the bulk flow. However, maintenance of the stationary eddies between the elements probably requires expenditure of more of the available energy. As an approximation to the energy balance involved, it can reasonably be assumed that the total energy consumed is equal to the energy that would be required to maintain flow in a smooth pipe plus that required to maintain the groove eddies.

These eddies can be regarded as essentially rectilinear, circular vortices, having diameters equal to j, the width of groove or h (whichever is smaller) and lengths equal to the conduit perimeter P. The velocity at the vortex perimeter is equal to a coefficient c_w times the wall velocity of flow v_w. The angular velocity ω is constant at any radius.

The energy of flow dE per unit time through any concentric cylindrical shell of the vortex is

$$\begin{aligned} dE &= \tfrac{1}{2}\, v^2_r\, dm = \tfrac{1}{2}\, \rho\, P\, v^3_r\, dr \\ &= \frac{1}{2}\, \rho\, P\, (\omega\, r)^3\, dr = \frac{1}{2}\, \rho\, P\, \frac{(c_w\, v_w)^3}{\left(\frac{j}{2}\right)^3}\, r^3\, dr \qquad \text{(22)} \end{aligned}$$

in which dm is the mass of fluid flowing through the shell of thickness dr at radius r per unit time, v_r represents the tangential velocity in the groove vortex, and r is the distance from the flow axis to any point in the cross section. The total vortex energy is

$$E = 2 \int_0^{j/2} \frac{\rho\, P\, (c_w\, v_w)^3\, 8\, r^3}{2\, j^3}\, dr = \frac{\rho\, P\, j\, (c_w\, v_w)^3}{8} \qquad \text{(23)}$$

The head expended in a length of pipe L as a result of these groove vortices is therefore

$$H_v = \frac{\rho\, P\, j\, (c_w\, v_w)^3}{8}\, \frac{1}{A\, v\, \gamma}\, \frac{L}{\lambda} = \frac{L}{4\, R}\, \frac{V^2}{2\, g}\, \frac{j}{\lambda} \left(\frac{c_w\, v_w}{V}\right)^3 \qquad \text{(24)}$$

in which $A\,v\,\gamma$ is the weight of fluid flowing per unit time. Adding the head loss in a smooth pipe and simplifying, the resulting bulk friction factor is

$$f = f_s + \frac{\left(\dfrac{c_w\,v_w}{V}\right)^3}{\dfrac{\lambda}{j,\,h}} \quad\ldots\ldots\ldots\ldots\ldots\ldots\ldots (25)$$

In the roughness-index term, λ/h or λ/j would be used depending on whether h or j were smaller. The coefficient c_w would have to be somewhat smaller than unity, perhaps of the order of magnitude of $\frac{1}{2}$. The ratio v_w/V would also be of this general order of magnitude.

In many cases the additive term in Eq. 25 would be practically constant, and the (f-R_c)-curve would be roughly parallel to that for smooth pipes (apparently diverging somewhat if plotted on a logarithmic scale). On the other hand, if there is a slight increase in v_w/V with increasing R_c, as seems possible, the additive term will be increased materially because of the cubing operation required. Consequently, for many roughnesses, the friction-factor curve in skimming flow may be expected to diverge somewhat from the smooth-pipe curve at high Reynolds numbers.

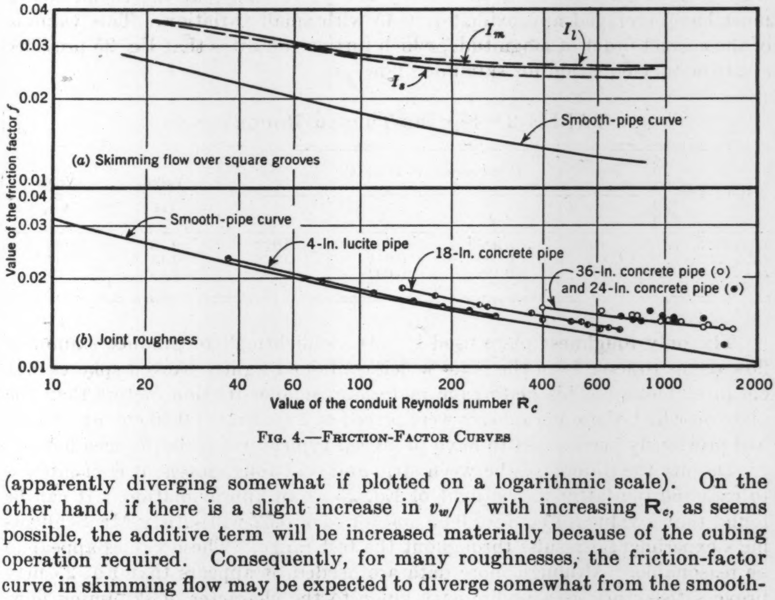

FIG. 4.—FRICTION-FACTOR CURVES

The best available (as of 1954) experimental data on skimming flow appear to be those obtained[18] under the direction of Mr. Streeter. Measurements of friction loss and velocity distribution were made on three geometrically similar square-thread roughnesses cut into a $4\frac{1}{2}$-in.-diameter pipe. The results of the investigation are shown in Fig. 4(a), and the pertinent dimensions are given in Table 2.

It should be noted that the roughness index was the same for all three roughnesses, although the relative roughness was made to vary considerably.

From Eq. 25 it can be seen that the friction factor should be independent of the relative roughness but should depend on the roughness index. In Fig. 4(*a*) the curves are essentially coincident, as implied in Eq. 25. The curves also follow the indicated trend of more or less paralleling the smooth-pipe curve, diverging from it, and becoming essentially horizontal.

The marked difference between the curves of Fig. 4(*a*) and those for the other two roughnesses investigated by Messrs. Streeter and Chu[18] (Fig. 3(*c*)) should be noted. The roughness elements for the latter two roughnesses were identical in every way with roughnesses I_m with the sole exception of the spacing λ, which was large enough to develop wake-interference flow with its typical rising friction-factor characteristic.

The tabulated velocity-distribution data[18] for roughnesses I_l, I_m, and I_s seem to indicate that v_w/V fluctuated randomly from approximately 0.62 to 0.67, with an average value of 0.65. Insertion of this value in Eq. 25, together with various corresponding values of f and f_s, reveals that the coefficient c_w must have averaged approximately 0.45 with small variation. This value is of the correct order of magnitude, which further indicates that Eq. 25 provides a satisfactory equation for skimming flow.

TABLE 2.—SQUARE-THREAD ROUGHNESSES

Roughness	Dimensions, in Inches				Value of λ/h	Value of h/r_o
	λ	j	h	r_o		
I_s	0.0555	0.0282	0.0255	2.273	2.18	1/89
I_m	0.111	0.056	0.051	2.273	2.18	1/44.5
I_l	0.200	0.101	0.092	2.269	2.18	1/24.7

The only roughness plate used by Mr. Schlichting[11] to produce skimming flow seems to have been the plate which contained tightly packed spheres 0.41 cm in diameter. This plate gave materially smaller friction factors than the plate on which the same spheres were placed at a spacing of 0.60 cm, and which had previously been noted to have produced typical wake-interference flow.

Despite the differences between strip and spot roughnesses, it is of interest to examine the latter in the light of Eq. 25 as an approximation. It can be found that a value for v_w/V of 0.65 and for c_w of 0.52 will satisfy Mr. Schlichting's experimental results throughout the test range. These values appear to be reasonable. Although more data are needed, it appears that Eq. 25 may prove satisfactory as a preliminary guide to the character of skimming flow.

JOINT ROUGHNESS

Special cases of isolated-roughness flow and skimming flow may be caused by the introduction of small-scale vorticity at the pipe or flume joints. If the joint causes a peripheral protrusion into the flow, Eq. 21 is applicable; if the joint causes a separation between adjacent conduit sections, Eq. 25 would be applicable. Both conditions would result in a descending (f-$\mathbf{R}_e$)-curve, approximately parallel to the smooth-pipe curve.

This phenomenon is illustrated in two sets of experiments conducted at the St. Anthony Falls Hydraulic Laboratory. One experiment was performed on a 4-in.-diameter lucite pipe, with joints at 4.37-ft intervals,[21] and the other, on three large concrete pipes with diameters of 18 in., 24 in., and 36 in., each with a joint spacing of 6 ft.[9] The joints on the 18-in.-diameter pipe were considerably smoother and fitted more snugly than on the pipes having diameters of 24 in. and 36 in.

All the pipes were smooth-walled; the concrete pipes had been manufactured by a cast-and-vibrated process which produces a glossy-smooth surface. The (f-$\mathbf{R}_e$)-curves for these pipes are shown in Fig. 4(*b*); in each case they are slightly above and essentially parallel with the smooth-pipe curve.

The joint characteristics of the concrete pipes can be seen from the (f-$\mathbf{R}_e$)-curves in Fig. 4(*b*). The 18-in. pipe has the lowermost curve, indicating the best joints. The 24-in. and 36-in. pipe curves were essentially identical and at an approximately constant increment of friction factor above the 18-in. pipe curve. If the turbulence were being determined by the wall surface, as indicated by Eqs. 6 and 7, the 18-in. pipe curve should be the highest of the three.

CRITERIA FOR FLOW TYPES

Equations have been developed for each of the three basic flow types, but adequate criteria are still needed to determine which flow type will prevail in a given situation.

The boundary between wake-interference flow and isolated-roughness flow can be denoted by equating the resistance functions for the two types of flow—

$$\frac{1}{\sqrt{f_s\left[1+\dfrac{67.2\,C_D}{\dfrac{\lambda}{h}}\left(1-\dfrac{n\,s}{P}\right)\right]}}-2\log\frac{r_o}{\lambda}=1.75+\frac{1}{\sqrt{2}}\left(\frac{1}{k}-\psi\right)\frac{c\,\lambda}{r_o}\;..\;(26)$$

If the criterion is applied for a Reynolds number of, for example, 2,500,000, for which f_s is equal to 0.01, and if the additive term in the right member is assumed to be negligibly small, Eq. 26 simplifies to

$$\frac{\dfrac{\lambda}{h}}{C_D\left(1-\dfrac{n\,s}{P}\right)}=\frac{67.2}{\dfrac{100}{\left(2\log\dfrac{r_o}{\lambda}+1.75\right)^2}-1}\;\ldots\ldots\ldots\ldots(27)$$

Eq. 27 would probably prove sufficiently accurate as a discriminating criterion in most cases. The left member involves the roughness-element characteristics, and the right member, the relative-roughness spacing. For a given type of roughness element and a given radius, Eq. 27 can be solved by trial and error for the critical value of the spacing, λ, which will mark the boundary between isolated-roughness flow and wake-interference flow. For example, solution of

---

[21] "Preliminary Flow Tests on a Model Culvert," by Henry M. Morris, Jr., *Project Report No. 7*, St. Anthony Falls Hydr. Lab., Univ. of Minnesota, Minneapolis, Minn., 1948.

Eq. 27 for Mr. Schlichting's long angle roughnesses will be found to yield a critical value for λ of 1.85 cm. The experimental data[11] indicated that wake-interference flow was obtained when this type of roughness had a value of λ equal to 2.0 cm, but isolated-roughness flow occurred at higher values of λ.

The spherical roughnesses used by Mr. Schlichting resulted in a wake-interference flow for a spacing of 0.60 cm and an isolated-roughness flow at higher values. Eq. 27 indicates the limiting value to be 0.70 cm. It can be shown[10] that the trends implied by the other available data on various types of roughness elements are all in substantial accord with the implications of Eq. 27, which seems, therefore, to serve fairly satisfactorily as a discriminating criterion between isolated-roughness flow and wake-interference flow. It can also be noted that, for all parameters except λ held fixed, the friction factor increases as λ decreases in isolated-roughness flow. However, when wake-interference flow is established, a further decrease in λ results in a decrease in the friction factor.

The criterion for differentiating between wake-interference flow and quasi-smooth flow cannot be set up in a similar manner because the resistance function for quasi-smooth flow does not approach that for wake-interference flow as the λ-value approaches the critical value between the two flow types but rather moves away from it. The evident implication is that there is a sudden, rather than gradual, change from skimming flow to wake-interference flow. This sudden change evidently occurs when the stable vortex in the groove gives way to the typical flow-separation phenomenon of a continual succession of vortices growing and washing downstream.

It appears likely that this change will occur when the groove width j becomes significantly larger than the depth h. The vortex occupies the entire width of the groove as long as h is larger than j and therefore can remain stable. However, if j is much larger than h, the vortex will adhere to the upstream face of the groove and the stream will flow over and down the vortex against the opposite groove face; this is essentially a typical flow-separation action, and the vortex must rapidly become unstable.

This inference appears to be confirmed by the available data on skimming flow. All three roughnesses which produced skimming flow[18] had (j/h)-ratios slightly larger than unity. The same was true of Mr. Schlichting's spherical-roughness plate which resulted in skimming flow.[11]

Flow over Variable-Roughness Surfaces.—In the equations previously developed, a regular distribution of roughness elements of identical dimensions has been assumed. A rational analysis is much more difficult when the several parameters are permitted to vary. However, the three basic types of flow must still exist and will occur when the roughness patterns satisfy the appropriate criteria. In many cases the best manner in which to estimate friction factors for varied-roughness patterns would probably be to use simple statistical averages of the parameters which vary.

Not many data are available (as of 1954) with which to check this assumption. However, the plank roughnesses studied by Mr. Bazin[16] can be considered as special types of roughness with a repeating pair of λ-values. These planks were equally spaced but were much wider than their depth; therefore, a wake would be produced at both the upstream and downstream edges of each plank so that the average spacing of wakes was one half the plank spacing. Mr. Bazin's widely spaced plank roughness consisted of 2.7-cm by 1-cm planks on 7.7-cm centers. This roughness produced the rising (f-$\mathbf{R}_c$)-curve characteristic of wake-interference flow, and the limiting resistance function, as computed for the mean spacing, is approximately 1.78. Similar results can be shown to apply for certain plank roughnesses[22] used by Joe William Johnson, M. ASCE, which evidently produced wake-interference flow. The inference, therefore, is that an average value of λ can be used for nonuniformly spaced roughness elements in the wake-interference flow equations.

Spot-roughness elements usually tend to produce isolated-roughness flow, except when they are packed quite closely. Thus, each element acts independently, and the friction factor could presumably be determined by summation of appropriate drag forces on all the individual elements. When the roughness elements are closely packed, however, wake-interference flow is developed. If the roughness elements are predominantly of one size and only occasionally have larger elements, the wake-interference phenomena will be controlled by the smaller elements, with isolated-roughness drag forces being added by the larger elements.

These features are illustrated by the data obtained by Messrs. Colebrook and White[4] who tested various combinations of two sizes of sand coated on a pipe surface, the small grains being densely packed and the large grains in various isolated-roughness patterns. The small grains alone produced a (f-$\mathbf{R}_c$)-curve with the typical dip and rise (obtained by Mr. Nikuradse[2]) which implies wake-interference flow. The large grains alone gave the typical, isolated roughness, descending (f-$\mathbf{R}_c$)-curve.

The (f-$\mathbf{R}_c$)-curves for the various combinations seem to demonstrate that the isolated-roughness effects of the large grains controlled at low Reynolds numbers until the smaller grains became effective. Then wake-interference flow was produced, the bulk phenomenon resulting in a friction factor approximately equal to the friction factor for the densely-packed small grains plus the isolated-roughness value for the large grains.

It can be seen from the curves offered by Messrs. Colebrook and White[4] that, although wake-interference flow was evidently produced, the dip and rise was considerably flattened by virtue of the isolated-roughness effect of the large grains. It seems likely that this effect would be enhanced by having more than one size of large grain interspersed among the small grains. The inference is that, for densely packed spot-roughness elements with a random size distribution, wake-interference flow would be produced but that the dip and rise would be sensibly eliminated, and that the (f-$\mathbf{R}_c$)-curve would become and remain horizontal soon after leaving the smooth-pipe curve. This is, in fact, exactly the result obtained by Mr. Harris[23] in tests on pipes coated with stainless steel spray, the resulting surfaces of which were similar to surfaces of densely packed sand grains of randomly varying sizes.

---

[22] "Rectangular Artificial Roughness in Open Channels," by Joe William Johnson, *Transactions*, Am. Geophysical Union, Pt. VI, May, 1945.

[23] "The Influence of Random Roughness on Flow in Pipes," by Charles W. Harris, *Bulletin No. 115*, Univ. of Washington Eng. Experiment Station, Seattle, Wash., 1949.

Flow over Commercial Conduit Surfaces.—It appears probable that the principles that have been delineated for flow over artificial-roughness patterns can be extended to give a rational explanation of the flow and resistance phenomena experimentally obtained on commercial pipe and channel surfaces. By far the majority of such pipes exhibit a decreasing friction-factor curve, gradually diverging from the smooth-pipe curve.

In many cases this is attributable to joint roughness, as in the concrete pipes tested at the St. Anthony Falls Laboratory. Most commercial pipe surfaces, however, probably contain typical isolated-roughness elements such as rivets or projecting pieces of aggregate. Friction factors for such surfaces should be predictable by Eq. 21, or in some cases by Eq. 25, when the main roughness consists of a joint depression.

Some pipes with very rough surfaces may produce wake-interference flow. In such cases, the typical dip and rise of the friction-factor curves and the resistance-function curves will depend on the form and degree of uniformity of the roughness elements. Uniform, rounded elements such as corrugations will result in a deep dip and a long, gradual rise. Closely packed, random-roughness elements, however, will produce fully turbulent wake-interference flow almost as soon as the elements begin to pierce the laminar film so that the friction-factor curve will become and remain horizontal soon after leaving the smooth-pipe curve.

In various tests concrete surfaces have been found to cause dropping, horizontal, and even rising $(f\text{-}\mathbf{R}_c)$-curves. This variation obviously results from the wide variation of textures on different concrete surfaces.

CONCLUSIONS

The concept of flow over rough-conduit surfaces is based on the assumption that the loss of energy in turbulent flow over such surfaces is attributable largely to the formation of wakes behind each roughness element. The frequency of such vorticity sources in the direction of flow will determine, to a large extent, the character of the turbulence and energy-dissipation phenomena in the flow. Therefore, the longitudinal spacing of the roughness elements is the roughness dimension of paramount importance in rough-conduit flow. Under this concept, there must exist three basic types of flow over rough surfaces. They are isolated-roughness flow, wake-interference flow, and quasi-smooth (or skimming) flow. Eqs. 17, 21, and 25, respectively, can be used to determine friction factors for the three types of flow for surfaces having regular roughness patterns.

The concept can also be extended to surfaces of variable roughness, usually by using average values of the roughness dimensions which vary. If the surface has roughness elements of such variety that more than one of the basic flow types would be produced simultaneously, the friction factors for each flow type can be added to give the apparent friction factor for the surface as a whole.

In general, the expanded concept of rough-conduit flow appears to be adequately substantiated by experimental data from many different sources. Because it is both comprehensive in scope and physically reasonable—as well as relatively simple analytically—it is hoped that it may serve as a stimulus to research and to the development of more rational, practical engineering design methods in this field. It is suggested that, if the general concept and methods presented herein are adopted by the profession, useful corollary studies could be directed toward the development of devices and methods for making rapid physical measurements of surface-roughness characteristics and toward the preparation of design charts or tables based on the various equations presented in the paper.

ACKNOWLEDGMENTS

Lorenz G. Straub, M. ASCE, was the writer's adviser during the preparation of the thesis[10] on which the paper is based. Mr. Streeter kindly made available to the writer unpublished data obtained under his direction. Alvin G. Anderson, Edward Silberman, and Richard Whittington, Associate Members, ASCE, and Thomas Timar contributed many valuable suggestions.

APPENDIX. NOTATION

The following symbols, adopted for use in the paper and for the guidance of discussers, conform essentially with "American Standard Letter Symbols for Hydraulics" (ASA Z10.2—1942), prepared by a committee of the American Standards Association with ASCE representation, and approved by the Association in 1942:

A = value of v/v_* for core-velocity distribution at $y = \lambda$;
A_f = cross-sectional area of flow;
A_w = value of v/v_* for wall-velocity distribution at $y = \lambda$;
a = value of v/v_* at the boundary between the central and wall zones at $y = c\,\lambda$;
B = term defined in Eq. 4;
b = distance from the roughness crests to the channel center, in two-dimensional flow;
C_D = drag coefficient;
c = coefficient such that the distance $y = c\,\lambda$ locates the break point between the core and wall velocity distributions;
c_w = a coefficient which when multiplied by v_w is equal to the velocity at the vortex perimeter;
D = equivalent diameter of the conduit;
d = dimensionless parameter depending on the type of roughness;
E = energy;
e = diameter of the uniform sand grains;
f = friction factor:
    f_s = friction factor for the smooth conduit;
    f_w = friction factor for the wall surface;
H_f = head loss as a result of friction;
H_v = head loss caused by the groove vortices;
h = radial height of the wall-roughness projections;

j = groove width;
K_s = equivalent sand-grain diameter;
k = universal turbulence constant;
L = length of the conduit;
m = fluid mass;
n = number of individual elements in a periphery;
P = wetted perimeter;
R = hydraulic radius;
R_c = conduit Reynolds number;
R_w = wall Reynolds number;
r = distance from the flow axis to any point in the cross section;
r_o = pipe radius measured to the crests of the roughness elements;
s = clear peripheral spacing between elements;
V = average velocity of flow;
v = velocity of flow at any point in the cross section:
    v_r = tangential velocity in the groove vortex;
    v_s = shear velocity;
    v_w = flow velocity at the roughness crests;
y = radial distance from the roughness crests to any point in the cross section;
γ = specific weight of the fluid;
Δp = pressure drop;
κ = resistance function:
    κ_a = resistance function for axial flow;
    κ_g = generalized resistance function;
    κ_t = resistance function for two-dimensional flow;
λ = spacing of the wall-roughness elements in the direction of flow;
ν = kinematic viscosity;
ρ = fluid density;
τ_w = wall shearing stress;
ψ = slope of the curve of v/v_s versus $\log_e (y/\lambda)$ in the wall region; and
ω = angular velocity of the groove vortex.

DISCUSSION

VICTOR L. STREETER,[24] M. ASCE.—For his attempt to solve the difficult problem of classifying both artificial and natural roughness in terms of the resistance function and wall Reynolds number, the author is to be strongly commended. Lack of adequate experimental results does not (as of 1954) permit complete evaluation of the new concepts.

In Mr. Morris' analysis of quasi-smooth flow there is the tacit assumption that the kinetic energy per unit time flowing past a section through a vortex is the energy consumption of the vortex. However, there is probably a very slow mixing of the flow of the main stream with the fluid contained within the vortices as the rapid shedding of vorticity would result in greater energy losses in the pipe flow.

It is reasonable to assume that the rate of energy conversion to heat within a vortex in a unit of time depends on the energy of the vortex. The expression for the kinetic energy of a forced vortex ring can be computed, and the vortex energy per unit weight of fluid flowing can be developed. From this expression and the experiments[18] on square-thread roughnesses, conclusions as to energy dissipation within a ring vortex can be made.

The kinetic energy contained in a ring vortex of circumference πD and of filament radius $j/2$, with angular velocity ω, is

$$\int \frac{1}{2} v^2\, dm = \int_0^{j/2} \frac{1}{2}\, 2\,\pi\, r\, dr\, \rho\, \pi\, D (\omega\, r)^2 = \pi^2\, \rho\, D\, c^2_w\, v^2_w\, \frac{j^2}{16} \ldots\ldots (28)$$

The number of vortex rings per unit length of pipe is $1/(2\,j)$ for square-groove roughness with land thickness equal to groove width. The weight of the flow through the pipe per unit time is $\rho\, g\, V\, \pi\, D^2/4$. The kinetic energy in the vortex rings per unit weight of fluid flowing per unit length of pipe is $j\ (\pi\, c^2_w\, v^2_w)/(8\, g\, D\, V)$. As v_w/V should not vary substantially, the energy in the vortices per unit length per unit time is proportional to $(j\, V)/(g\, D)$.

Three sizes of square-groove roughness were tested[18] by the writer with dimensions varying in the ratios 1:2:4. The test data shown in Fig. 4(*a*) indicate that the friction factor is sensibly the same for the three roughnesses, despite the large variation in roughness and despite the fact that the friction factors are constant for Reynolds numbers larger than 200,000. The energy in the vortices per unit weight of flowing fluid varies directly as the size j of the vortex and the average flow velocity or wall velocity. If the fractional part of the energy converted into heat per unit time within the vortices is designated as t, there results

$$\frac{F\, V\, j\, t}{g\, D} = \frac{\kappa_v}{D}\, \frac{V^2.}{2\, g} \ldots\ldots\ldots\ldots\ldots\ldots (29)$$

in which F is a proportionality factor and κ_v, the resistance coefficient caused by the vortices. Solving for κ_v results in

$$\kappa_v \sim \frac{j\, t}{V} \ldots\ldots\ldots\ldots\ldots\ldots\ldots\ldots (30)$$

---

[24] Prof. of Hydraulics, Civ. Eng. Dept., Univ. of Michigan, Ann Arbor, Mich.

From Eq. 30 it can be seen that t must vary inversely as j and directly as V for a constant value of κ_v. Hence, the larger the vortex cross section (with correspondingly lower angular velocity), the less will be the rate of energy dissipation per unit of energy available in the vortex. Similarly, the proportion of energy dissipated per unit of energy in the vortex increases directly as the wall velocity.

Walter Rand,[25] A.M. ASCE.—The attempt made by Mr. Morris to analyze flow over rough surfaces by considering the roughness characteristics h, λ, and s demonstrates the complexity of the problem and the difficulty of deriving equations that reflect all the aspects of the flow. The writer has analyzed several of the equations related to wake-interference flow so as to find additional methods of interpretation and to reveal the significance of the numerical coefficients that were involved.

The logarithmic velocity distribution adopted by the author as the basis for analysis (Eqs. 3 and 5) can be expressed as

$$\frac{v}{v_s} = \frac{1}{k} \log_e \frac{y}{y'} \qquad (31)$$

in which y' is the value of y at which the logarithmic curve intersects the y-axis. In some handbooks[26] y' is given by

$$y' = \frac{\nu}{9.05\, v_s} = \frac{r_o}{1.6\, \mathsf{R}_c \sqrt{f}} \qquad (32a)$$

for smooth-pipe flow, and by

$$y' = \frac{h}{m} \qquad (32b)$$

for rough-pipe flow, with m equal to 30 for Mr. Nikuradse's sand roughness. Introduction of these values of y' into Eq. 1 will give the equations developed[3] by Mr. von Kármán for v/v_s and $1/\sqrt{f}$ (Eqs. 5 and 6). Analogous equations involving the longitudinal spacing λ can be derived for rough-pipe flow by assuming that y' is proportional to λ:

$$\lambda = n\, y' \qquad (33)$$

An alternative form of Eq. 9 would then be

$$\frac{v}{v_s} = \frac{1}{k} \log_e n + \frac{1}{k} \log_e \frac{y}{\lambda} \qquad (34a)$$

in which

$$A = \frac{1}{k} \log_e n \qquad (34b)$$

The assumption made by Mr. Morris that A is a universal constant means, in this case, that the ratio λ/y' should be a constant for all types of roughness

---

[25] Asst. Prof. of Fluid Mechanics, New York Univ., New York, N. Y.

[26] "Engineering Hydraulics," edited by Hunter Rouse, John Wiley & Sons, Inc., New York, N. Y., 1950.

(provided that k is constant). However, as the roughness height h seems to be insufficient to characterize the roughness fully, it is difficult to believe that λ alone could be sufficient.

In fact, the author gave A-values ranging from 6.8 to 9.3. The corresponding values of n then range from 15.2 to 41.6. Such a scatter does not appear to warrant the assumption of a constant value for A. It would seem that A is rather a function of all the roughness characteristics (h, λ, s, and the cross-sectional form of roughness elements) and could be constant for geometrically similar roughnesses. This indicates that the coefficient 1.75 in Eqs. 17 does not have a general validity and that the value of the resistance function for fully rough wake-interference flow (high $\mathbf{R}$) should be written, in the general form, as

$$\frac{1}{\sqrt{f}} - \frac{1}{k\sqrt{8}} \log_e \frac{r_o}{\lambda} = \frac{1}{\sqrt{8}} \left(\frac{1}{k} \log_e n - \frac{3}{2\,k} \right) \ldots\ldots\ldots\ldots (35a)$$

for pipes, and

$$\frac{1}{\sqrt{f}} - \frac{1}{k\sqrt{8}} \log_e \frac{r_o}{\lambda} = \frac{1}{\sqrt{8}} \left(\frac{1}{k} \log_e n - \frac{1}{k} \right) \ldots\ldots\ldots\ldots (35b)$$

for two-dimensional flow.

The author has assumed that k is a constant ($k = 0.40$) for the total cross section of the flow in the case of fully rough flow as c is equal to zero at high values of the wall Reynolds number. In hydraulics, the coefficient k is also accepted as 0.40 in the case of smooth flow when the laminar sublayer covers the roughness elements. If k were also the same for the transition zone between smooth flow and fully rough flow, the conclusion would be that a variable n in Eqs. 35 could lead to the law for the resistance function in this zone. Relying, however, on the results of velocity measurements (Fig. 1), Mr. Morris has adopted a variable k ($1/k = \psi$) for the wall zone (Eq. 11) to derive Eqs. 13 and 14. These equations reflect the correct trend of the resistance function for the transition zone for the case of uniform roughness. However, the logarithmic velocity-distribution curves (Fig. 1) exhibit a tendency for a more pronounced slope near the boundary; this tendency is artificially stressed by measuring y arbitrarily from a datum through the crests of the roughness elements. The choice of this datum is inconsistent with the assumption made by Mr. Morris that at high values of $\mathbf{R}_w$ the coefficient k is valid for the total velocity profile ($c = 0$). This assumption requires that the velocity be zero at the finite distance y' over the crest roughness—a condition that does not correspond to reality. In fact, various investigators[2,11] have found that for fully rough flow a sensibly straight-line velocity distribution can be plotted on a logarithmic scale by choosing a datum considerably below the crest of the roughness elements—somewhere near the center line of the elements. Of course, the values of c and ψ will depend on the choice of the datum from which y is measured. The fact that the actual k-value can be different from 0.40 (in Fig. 1 the values of k are 0.33, 0.42, and 0.35) makes the use of Eqs. 13, 14, and 17 rather difficult.

Mr. Morris used Eqs. 17 to derive the limiting values of the resistance function (3.52 and 2.64). However, for the large value of c, when $c\,\lambda = r_o$, Eqs.

13 and 14 should be used. The value of the resistance function for $\psi = 0$ and $c\,\lambda/r_o = 1$ is then $A/\sqrt{8}$ for both pipe flow and two-dimensional flow. For a value of A equal to 8.5 the value of the resistance function is 3. However, the limit $A/\sqrt{8}$ with the value of A determined for fully rough flow can have no significance because a velocity distribution with ψ equal to zero over the total cross section is not physically possible. The flow which results in the maximum value (or limit) of the resistance function is very near to smooth-pipe flow, and $\psi = 1/k$ and $c = 0$ would be more realistic assumptions, even if they are not consistent with Eqs. 13 and 14. Moreover, the transition from smooth flow to fully rough flow possibly depends as much on the ratio h/δ' (in which δ' is the thickness of the laminar sublayer) as on the ratio λ/δ', and a wall Reynolds number $(\mathbf{R}_c \sqrt{f})/(r_o/h)$ could be more relevant than $(\mathbf{R}_c \sqrt{f})/(r_o/\lambda)$ in determining the variation of the resistance function in the transition zone.

It is hoped that the considerations that have been offered are further illustrations of the problems encountered in the study of flow over rough surfaces.

HARRY H. AMBROSE,[27] A. M. ASCE.—A review of Mr. Morris' data for small commercial pipe and artificially-roughened pipes and data[28] for large conduits supplies convincing evidence of the fact that the effect of surface-roughness characteristics on resistance to turbulent flow in conduits is an exceedingly complex phenomenon. The author is to be commended for his presentation of a concept of this phenomenon which helps clarify many of its peculiarities—particularly that of the rising resistance-coefficient curves associated with wake-interference flow. The characteristics of the three basic types of flow are well defined and appear to satisfy the trends of the available (1954) data.

Mr. Morris has concluded that wake-interference flow, with its tendency toward constant resistance coefficients for moderate to high Reynolds numbers, is experienced infrequently in commercial pipes and that isolated-roughness flow or skimming flow is more likely to occur, with attendant dependence of the resistance coefficient on the viscous characteristics of flow for moderate or even high Reynolds numbers. One might anticipate a vigorous reaction to these conclusions but there is much substantiating evidence. The existence of data showing resistance curves closely paralleling the smooth-pipe curve has been rather summarily dismissed, and the surfaces yielding such resistance curves have been characterized as "wavy." This description appears hardly adequate because of the similarity of results obtained from such widely varying surfaces as towing planes coated with ship-bottom paints,[29] large steel penstocks,[30] and nominally smooth pipes with artificial depression-type roughnesses. It is apparent that more serious consideration must be given to isolated-roughness flow and skimming flow.

---

[27] Associate Prof., Civ. Eng. Dept., Univ. of Tennessee, Knoxville, Tenn.

[28] "Friction Factors for Large Conduits Flowing Full," by J. N. Bradley and L. R. Thompson, *Engineering Monographs No. 7*, Bureau of Reclamation, U. S. Dept. of the Interior, Washington, D. C., 1951.

[29] "Resistance of Anti-Fouling Ship-Bottom Paints," by R. B. Couch, *Report No. 789*, David Taylor Model Basin, Washington, D. C., 1951.

[30] "High Velocity Tests in a Penstock," by Maxwell F. Burke, *Transactions*, ASCE, Vol. 120, 1955.

Although the writer finds phenomenological satisfaction in the three basic types of flow, certain details of the relationships developed by Mr. Morris are questioned. Every investigator of flow in rough pipes has had the problem of deciding on the correct diameter to be used in computing the resistance coefficient and the Reynolds number and as a reference for velocity distributions. The choice is important both in relating velocity distributions at wall distances within the magnitude of the roughness dimensions and in determining the resistance coefficient—the value of which varies directly as the fifth power of the diameter. The author has chosen to measure the diameter between the crests of the roughness elements at the opposite walls. This choice appears logical for closely-spaced elements. It is suggested, however, that the correct diameter depends on the type of roughness—particularly on whether flow in the space between the roughness elements can be considered as part of the main flow. As an extreme, Mr. Morris' method would most certainly be incorrect when applied to large-scale, isolated roughness consisting of protruding gaskets at flanged joints. The choice of diameter is also of particular significance in testing to determine whether resistance effects of nonuniform elements are additive.

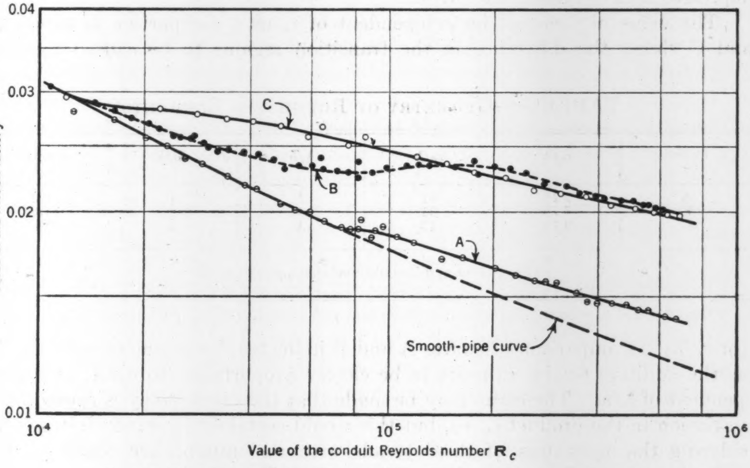

Fig. 5.—Transitions from Smooth-Pipe Flow to Skimming Flow

To be completely general, the resistance equations must allow for transition from smooth-pipe flow to each of the three basic types of rough-pipe flow and also for transition, whether abrupt or gradual, between the three basic rough-pipe flows. The author has not considered transition from smooth-pipe flow to isolated-roughness flow or skimming flow although this is at least as important as the wake-interference transition. Tests performed by the writer on roughness elements consisting of cylindrical depressions in a surface that was otherwise smooth have yielded well-defined transitions from smooth-pipe flow to skimming flow. Three such transitions are shown in Fig. 5. It is of interest to note the appearance of the transition of curve B, which gives every indication of the approach to a constant resistance coefficient too often assumed for rough pipes. The marked downward trend of f for higher values of $\mathbf{R}_c$, however, is very closely parallel to the smooth-pipe curve; thus the transitional nature of the preceding part of the curve is revealed.

The implication of Eq. 25 that for skimming flow the $(f-\mathbf{R}_c)$-relationship is independent of the relative-roughness height and the relative-roughness spacing is not supported by the data in Fig. 5. Values for the roughness element geometry for the three curves in Fig. 5 are given in Table 3. In Table 3, d_d represents the diameter of the depression, and a_d/A_s is the net ratio of depressed area to total surface area.

The value of f cannot be independent of r_o as a comparison of curves B and C shows the difference in the transition regions to be caused by r_o/h (or r_o/λ). Comparison of curves A and B indicates disagreement with Eq. 25 as the additive f-value appears to be closely proportional to a_d/A_s and independent of λ/h. The claim may be made that the discrepancy is caused by a variation in the product $c_w\ v_w$, but this would certainly appear fortuitous considering the agreement of these trends with the unpublished results of the writer's tests on fourteen other surfaces of similar roughness characteristics.

TABLE 3.—GEOMETRY OF ROUGHNESS ELEMENTS[a]

Curve	r_o/λ	r_o/h	λ/h	d_d/h	a_d/A_s
A	7.75	31	4	1	0.047
B	7.75	31	4	2	0.189
C	3.75	15	4	2	0.181

[a] Peripheral and longitudinal spacings are equal.

For wake-interference flow, two distinct regions of velocity distribution are defined—the central or core region and the wall region. Mr. Morris has assumed velocity distributions for each region in the development of the resistance equations; certain discrepancies are to be noted. As Eq. 16 is independent of the Reynolds number of the mean flow it can be valid only for the range proposed by Mr. Nikuradse—that of "completely-turbulent" flow. Similarly, it is not obvious that A is a constant and independent of both $\mathbf{R}_c$ and $\mathbf{R}_w$ unless the resistance equation follows the quadratic law. Despite these facts, the velocity distribution determined from Eq. 16 is assumed to apply to the core region over the entire transition from smooth-pipe flow to rough-pipe flow.

If, as asserted by the author, the value of A is constant, the core distribution of velocity will be governed only by the relative-roughness spacing, whereas the wall distribution will be a function of both the type of roughness and the wall Reynolds number. For the assumed velocity distributions to apply over the entire transition range, therefore, the wall region must contain all the viscous effects. Because the entire velocity distribution for a smooth pipe is dominated by the Reynolds number the following condition results:

At the smooth-pipe end of the transition range the wall region encompasses the entire turbulent flow, the velocity distribution being governed by the wall Reynolds number and being independent of the roughness characteristics. As the Reynolds number is increased there appears a core distribution at the center of the pipe that is governed solely by the relative-roughness spacing, although the wall-velocity distribution enclosing the roughness elements is still primarily a function of the wall Reynolds number. Further increase of the Reynolds number causes the wall region to shrink and at the same time to be governed increasingly by the roughness characteristics rather than by the viscous effects. Finally, the wall region disappears and completely turbulent flow ensues. In brief, if A is constant, the effect of the roughness elements must begin at the pipe center and radiate toward the wall as the Reynolds number increases.

It does appear reasonable, however, that the velocity distribution should be divided into distinct zones that indicate the relative extent of influence on the distribution of each governing quantity. As a matter of fact, Donald Ross has shown[31] this division to be necessary for the more simple case of turbulent flow over smooth surfaces. Mr. Ross divided the entire turbulent zone into an "inner turbulent" region governed by a universal "law of the wall," an "outer turbulent" region governed by the spatial history of the turbulence, and a "blending" region which separates the inner and outer regions. Analogically, a more satisfying concept of the velocity distribution for transitional flow would be (*a*) smooth-pipe velocity distribution as long as a laminar sublayer persists, (*b*) with sufficient increase in the Reynolds number, generation by the roughness elements of eddies which initially would be weak and whose influence would be confined to the wall or inner turbulent region, and (*c*) with further increase in the Reynolds number, an increase in strength and extent of the eddies until finally the entire turbulent velocity distribution is dominated by the roughness elements. The influence of the surface roughness must extend from the boundary toward the center rather than the converse.

The foregoing criticisms do not imply lack of appreciation of the general aspects of the concept of turbulent flow in rough pipes—namely, that three basic types of flow are possible, and that the spacing of the roughness elements is the controlling factor as to which type of flow will prevail in a given case. It is believed that one would do well to reanalyze existing (1954) data in the light of this concept and to use this concept as a guide in future research on the subject.

---

[31] **"Study of Incompressible Turbulent Boundary Layers," by Donald Ross, thesis presented to Harvard University, at Cambridge, Mass., in June, 1953, in partial fulfilment of the requirements for the degree of Doctor of Philosophy.**

Henry M. Morris, Jr.,[32] **A.M. ASCE.**—In view of the rather sharp departure from established concepts in a field of wide interest to hydraulic engineers, it has been surprising that there has been relatively little adverse criticism of the paper. It is hoped that this fact indicates that the concept will prove generally acceptable and useful to the profession. The comments and suggestions of Messrs. Streeter, Rand, and Ambrose are greatly appreciated.

Mr. Streeter suggested an alternative analysis of friction factors for quasi-smooth flow which indicates that the proportion of groove vortex energy actually being converted into heat varies inversely as the groove width and directly as the flow velocity, assuming a constant friction factor.

It appears, however, that there is a dimensional inconsistency in this analysis. Mr. Streeter has derived Eq. 28 for the total kinetic energy (in foot-pounds) contained in the groove vortex and has divided the result by the weight-rate of flow (in pounds per second). The resulting expression, which Mr. Streeter terms the kinetic energy in the vortex rings per unit weight of fluid flowing per unit length of pipe, is actually the vortex energy for each pound per second for a unit length of pipe. The dimensions for this expression are therefore foot-seconds per foot, and the quantity seems to have no pertinent physical significance as it stands. Also, it is questionable whether the entire friction factor for flow as measured in the square-thread tests[18] can be attributed to the energy of the vortex. A substantial part of the energy consumption of the flow is caused by the normal smooth-pipe action whereby vorticity is generated and shed into the main flow at the pseudo-wall consisting of the land areas of the threads and the upper limbs of the groove vortices. It is only the additional energy loss above the normal smooth-pipe loss that is attributable to the groove vortices.

It seems reasonable to assume, as in the derivation of Eq. 24, that the entire vortex energy per unit time is being continuously converted into heat (under equilibrium conditions). However, the vortex itself is not dissipated because it continually receives an equivalent supply of power through attrition of the bulk flow with its upper limb.

Mr. Rand criticized the theory of wake-interference flow, but it is believed that the theory—in its essentials—is adequate to describe this type of flow, especially because it appears to be substantiated—in general—by the available experimental data. The phenomena are quite complex, and the theory and derived equations involve a number of simplifying assumptions; nevertheless these equations appear more satisfactory for explaining the phenomena involved than do previous methods.

The roughness-element spacing seems more reasonable as a physical measure of the roughness than does the roughness height, especially in wake-interference flow, in which the turbulence phenomena originate at or near the crests of the elements and thus can be affected very little by the height of the elements. This location of the origin of the turbulence also is sufficient argument for taking the datum (from which radial distances are measured) at the crests of the elements rather than at some altogether arbitrary datum selected so as to make the same logarithmic velocity-distribution slope apply throughout the pipe. Both physical considerations and experimental measurements have shown that these slopes are not the same in the wall and central zones; there must be a greater relative intensity of turbulent mixing in the wall zone than in the central zone. The fact that this procedure does not account for a small transition zone near the wall does not make it as physically unrealistic as would the arbitrary extension of the central-zone velocity-distribution equation through the wall zone of abnormal turbulence and into the dead-water regions between the elements, as is true of the methods cited by Mr. Rand. The concept and procedure offered by the writer, unlike the established procedures, also provide at least a partial explanation for the peculiar characteristics of the friction-factor curves and resistance-function curves for this type of flow and provide an effective basis for the correlation of data from many types of roughnesses.

---

[32] Prof. and Head, Dept. of Civ. Eng., Southwestern Louisiana Inst., Lafayette, La.

Mr. Rand has also criticized the assumptions made in determining the maximum possible value of the resistance function. It is recognized, of course, that these assumptions are extreme and actually represent physical impossibilities. However, they are quite reasonable as limiting conditions and actually come close to being realized for low wall Reynolds numbers. Both measurements and physical considerations indicate that ψ approaches $1/k$ and c approaches zero at high values of $\mathbf{R}_w$, rather than at the point of initiation of wake-interference flow.

The problem of the location of the datum for computing radial dimensions is also discussed by Mr. Ambrose. He emphasizes correctly the importance of this problem—that it has a great effect on the friction factor and on velocity distribution. It seems evident that the roughness crests provide the best datum in the cases of skimming flow and wake-interference flow. The remarkable correlations of experimental data from many different sources and on many types of roughnesses, as cited previously, are possible only when the datum is chosen in this manner.

However, Mr. Ambrose is correct in noting that isolated-roughness flow, particularly when the roughness elements are widely separated and when they have large radial heights, should be described in terms of the wall-to-wall diameter. The problem of the transition region between isolated-roughness flow and wake-interference flow and the associated problem of the correct datum need further investigation.

The data on skimming flow obtained by Mr. Ambrose are interesting and provide a welcome extension to the data on this type of flow. An item of interest is that the $(f\text{-}\mathbf{R}_e)$-curves for the strip-type roughness elements[18] departed from the smooth-pipe curve at much lower values of the Reynolds number than did the curves for Mr. Ambrose's spot-type roughness elements. The inference is that, in skimming flow, the larger the ratio of wall area to depression area the larger will be the value of $\mathbf{R}_e$ at which the depression vortex begins to contribute substantially to the friction factor.

The statement that in isolated-roughness flow and skimming flow the friction factor was independent of the radius was not, of course, intended to exclude the effect of the Reynolds number, which was explicity stated to be functionally related to f. It was intended to indicate that the friction factor was independent of the relative roughness and the relative-roughness spacing for these types of flow. Apparent variations of friction factor with relative roughness, as obtained on commercial-pipe tests, can probably be attributed to an incorrect choice of radius for computing the friction factor. This has, in fact, been suggested[33] by R. J. S. Piggott, who noted in his extensive studies of commercial-pipe, friction-factor data that the (f–R_e)-curves for a given roughness type can usually be made to coincide (even for pipes of different radii) provided that the proper datum is chosen. Except for the unusual conditions cited previously, this datum is probably the one through the crests of the roughness elements.

The cylindrical-depression, spot-type roughness elements tested by Mr. Ambrose are unique (to the writer's knowledge); it is difficult to classify them. Curve A in Fig. 5, for which the ratio d/h (corresponding to j/h) was unity, seems to follow the trends indicated in Eq. 25 for skimming flow. However, Eq. 25 was derived primarily for a groove-type depression extending around the pipe periphery and reflects the energy expenditure in maintaining a stable ring vortex. This is a somewhat different condition from that in which vortices are formed in cylindrical spot depressions. Furthermore, the roughnesses represented in curves B and C of Fig. 5 had (d/h)-values of 2 and, as indicated by the writer, it is doubtful whether the depression vortices are stable entities when the groove width becomes materially greater than its depth.

Consequently, it is doubtful that skimming flow was produced on roughnesses B and C in Fig. 5. The typical form-drag phenomenon of a continued generation of vortices in the wake would certainly extract more flow energy than would the phenomenon of the stable vortices of skimming flow. This condition probably accounts for the increase in friction factor between roughnesses A and B, rather than the greater proportion of depression area to wall area, as suggested by Mr. Ambrose.

It is therefore likely that, whereas roughness A produced skimming flow, roughnesses B and C produced either wake-interference flow or isolated-roughness flow, with wakes being produced at both extremities of each depression. In view of the peculiar character of curve B, there is the possibility that roughness B tends to produce wake-interference flow at low Reynolds numbers and changes to isolated-roughness flow at higher Reynolds numbers, with the result that curves B and C essentially coincide thereafter—as is indicated by Eq. 21 for isolated-roughness flow. Mr. Ambrose cited other experimental data that he has obtained. It is hoped that when these are published they will help to solve these problems.

It is believed that in Mr. Ambrose's discussion of velocity-distribution equations in wake-interference flow the full significance of the wall region of abnormal turbulence is not recognized. It is not strictly correct to refer to this type of flow as being transitional between smooth-pipe flow and rough-pipe flow, or to speak of the latter as being characterized by complete turbulence, because such terminology implies that this transitional flow is not itself fully turbulent but is partly controlled by boundary-layer effects remaining from smooth-pipe action. Actually, the energy losses in this type of flow are proportional to a power of the velocity greater than 2, as shown by the rising (f–$\mathbf{R}_c$)-curve; thus the turbulence in the wall region should be described as abnormal turbulence, as distinct from the normal turbulence characterized by the quadratic resistance law and the constant k. There is, of course, a short transition from smooth-pipe phenomena to phenomena of abnormal turbulence; this transition is represented by the part of the (κ–$\mathbf{R}_w$)-curve which gradually diverges from the smooth-pipe curve and becomes horizontal. The long rise in the curve which then follows and which finally becomes horizontal again is the zone of abnormal wall turbulence.

---

[33] "The Flow of Fluids in Closed Conduits," by R. J. S. Piggott, *Mechanical Engineering*, Vol. 55, 1933, p. 497.

The wake-interference-flow theory and equations deal, of course, only with the part of these phenomena represented by the rising and ultimately horizontal (f–$\mathbf{R}_c$)-curve. Isolated-roughness flow occurs at lower Reynolds numbers; it is represented by that part of the transition curve from the point of departure from the smooth-pipe curve to the low point in the dip. When wake-interference flow is initiated, the (f–$\mathbf{R}_c$)-curve begins to rise. This rise reflects the fact that the wall zone has been transformed from one which has been controlled primarily by phenomena in the laminar boundary layer (which by then has vanished) to one of abnormal turbulence caused by the wake-interference phenomenon. The velocity distribution near the wall in smooth-pipe flow is characterized by a slope corresponding to a number greater than $1/k$; the wall-velocity distribution in wake-interference flow has a slope ψ which is less than $1/k$, caused by the abnormal intensity of turbulence in that region.

It has been found and it is generally accepted that the dimensionless velocity-distribution equations in the central region of the pipe have the same slope (corresponding to k) regardless of the Reynolds number and for both smooth and rough walls. This is the zone denoted[31] by Mr. Ross as the outer turbulent zone, governed by the spatial history of the turbulence. In this zone, the vorticity generated at the wall or elsewhere (by whatever means—whether by a laminar boundary film or by wake vorticity) has been broken down by mutual attrition and momentum transfer to "normal" turbulence. It is a reasonable assumption that the central-zone turbulence is also "normal" during the transition throughout the full range of wake-interference flow.

As soon as the transition from smooth flow to the quadratic-law flow is complete (indicated by the low point of the dip on the (f–$\mathbf{R}_c$)-curves), true wake-interference flow begins. After this point, the wall-zone turbulence is governed entirely by the roughness elements (more precisely by the element spacing and by the form of the wakes behind them; the latter is a function of the geometric form of the elements throughout the transition). It seems logical that for this regime the terms A and k should be constant. Reasons for this were cited in the paper, and experimental evidence was offered to support this claim.

It appears that most of Mr. Ambrose's discussion of the phenomena of transition from smooth-pipe flow to rough-pipe flow is correctly applicable to the first stage in the transition but not to the second stage. At the initiation of the second stage, the influence of the wall roughness has already extended to the center of the pipe, and the boundary constant A has become established as a characteristic of the core-velocity distribution, although only in the central pipe zone has the wall turbulence been reduced to the normal turbulence characterized by k. As the Reynolds number increases, the central zone extends toward the wall, both by shifting of the boundary of the two zones toward the wall and by more rapid reduction of the abnormal wall turbulence to normal turbulence even in the wall zone, as evidenced by the approach of the velocity-distribution slope in the wall zone to $1/k$, the slope of the core-velocity distribution.

There is no doubt that the phenomena of flow in rough pipes are many and complex. Additional investigation is needed, especially for the various boundary zones. It is hoped that the concepts presented herein will help to clarify at least some of these phenomena and will point the way to further research, and at the same time will prove useful in practical design procedures.

AMERICAN SOCIETY OF CIVIL ENGINEERS
Founded November 5, 1852
TRANSACTIONS

Paper No. 2746

INDUSTRIAL DEVELOPMENT IN THE SOUTH

BY CARL O. HOYER[1]

WITH DISCUSSION BY MR. ROLAND A. KAMPMEIER

SYNOPSIS

Since the beginning of the twentieth century the southern states of the United States have undergone an industrial development which has made this area one of great importance. The industries that have had the most impressive growth have been the chemical and allied industries and manufacturing. This industrial development, with special emphasis on the chemical industry, is traced in the paper. It is concluded that, because of the many advantages in the location of industry in the South, this area of the United States will achieve an economic stability between agriculture and industry.

INTRODUCTION

In this paper the term "South" is used to indicate the following thirteen states of the United States: Alabama, Arkansas, Florida, Georgia, Kentucky, Louisiana, Mississippi, North Carolina, South Carolina, Tennessee, Texas, Virginia, and West Virginia.

It has long been axiomatic that the terms "agriculture" and "the South" are practically synonymous. Having good soil, a fairly abundant rainfall, and a long growing season, the early settlers regarded the South with great favor. With an economy based on the fruits of this apparently inexhaustible soil, the people of the South were content to allow industry to develop almost exclusively in the northern states.

With continued farming, however, it became increasingly difficult to maintain a high level of production, and it was apparent that stable prosperity could be achieved only by broadening the base of the area's production. Agriculture alone was not enough because the northern industrialist controlled the market and reaped the major share of the profits both on the purchase of southern produce and on the sale of the manufactured goods derived from such

---

NOTE.—Published, essentially as printed here, in July, 1953, as *Proceedings-Separate No. 226*. Positions and titles given are those in effect when the paper was received for publication.

[1] Director of Eng., The Chemstrand Corp., Decatur, Ala.

produce. In addition, the southern consumer paid two freight bills—one to haul the raw materials northward and the other to transport the finished article to the South. Diversification in both agriculture and industry was the key to the future development of the South.

Because cotton was the most important product and the basis of the economic structure in the South, it was logical that it should be selected as the raw material for the first large venture into industry. For many years cotton had been exported to the New England states for spinning, weaving, and conversion into finished cloth. At the beginning of the twentieth century, 70% of the industry's facilities were located in New England, but the shift to the South had begun in earnest. At present (1953), 77% of the spindles are located in the eight-hundred mills in the South.

Paralleling this development—but at a somewhat later date—was the rise of the chemical industry in the South. Begun in the early 1930's and expanding rapidly during World War II, the chemical industry in the South today compares favorably with that in the northern states. More than 50% of the expansion in the chemical-manufacturing facilities since 1950 has been located in the South (as of 1954).

Recent (1952) surveys of industry in the United States show that the maximum projected plant expenditures will occur in 1955. In general, manufacturers plan to increase capacity 7% during 1954 and another 9% by 1956; no industry in any category is expected to remain static. Expansion in the chemical industry is expected to be divided into 70% for new spending and 30% for modernization. Manufacturing, in general, normally allots 43% to expansion and 57% to modernization. It is evident, therefore, that, for the chemical industry, expansion predominates and is considerably above the industrial average. Therein is the opportunity for the South. If the trends of the ten years from 1944 to 1954 continue, the South—with some effort—can capture much of the new money for chemical and allied industries. It can continue to exploit its many industrial advantages.

The South has not always been receptive to changes in the pattern of its historic past. This area has watched with alarm the rise of the synthetic-fiber industry because it seemed to challenge one of the South's chief commodities, cotton. As time passed, however, the new industries—chemical and synthetic fibers—have been accepted as important industrial assets which greatly diversify the over-all business and manufacturing activities. What is more, this new industry supplements the accepted, historic, agricultural asset.

It may be asked why the chemical industry and other industries have turned to the South. The answer is evident from a study of the specific factors that must be considered in selecting a region for the development of a new industry. Land suitable for plant sites must be available; there must be people to manage and operate the new installation; raw materials must be available; water of good quality is required; adequate transportation facilities must be available; fuel and power are needed in large amounts and at reasonable rates; certain financial facilities are required; and markets must be accessible. These factors are the base upon which industry is built. The

South will be surveyed subsequently with respect to these factors in order to measure the contribution of each to this rapidly growing industrial empire.

Land and People

Of paramount importance in evaluating any region for industrial purposes is a study of the land—its natural advantages and resources—and the people inhabiting the land. The area which is termed the "South" contains 540,000,000 acres of land, equivalent to 28½% of the United States; historically, geographically, and climatically it can be regarded as a single region.

Of this area 43% is forest, 30% crop land, and 18% pasture and range lands. Good plant sites can be readily located in almost every section. This fact, coupled with the desire of the people to replace their declining agricultural potential with other sources of income, has induced the southern states to extend every possible encouragement to industry. The mild climate of the area has made it possible for many industries to dispense more or less completely with the buildings required for plant operation in other sections of the country. Several of the chemical plants constructed in the South have been built entirely in the open, with consequent large savings in expenditures.

The South has a population of approximately 40,000,000, equivalent to 29% of the total population of the country. As this figure is close to 28½%—the South's share of the total land area of the United States—the density of population is approximately the same as the average in the remainder of the country. The population is increasing at a rapid rate, the number of persons in the South in 1950 being equivalent to the total population of the United States in 1870.

The greatest resource of the South is its people. The southern migration of industry at an accelerating rate during the period from 1944 to 1954 has been caused partly by the ample supply of intelligent, willing, and capable workers who are available for the management and operation of new industrial enterprises. Nowhere has this been more pronounced than in the chemical industry, where a high standard of skill and competence is required for successful operation.

In this connection, it is well to note that the once-prevalent opinion that skilled industrial workers are available only in areas having a long industrial history has been proved to be erroneous. During World War II, it was found that the chemical plants in the South almost invariably had better operating records than similar plants in other sections of the United States. Labor in the South has proved its ability to conduct the most intricate industrial processes and to produce at a rate equal to that of any other section of the United States.

Mineral Resources

The chemical industry has encouraging prospects with regard to mineral resources in the South. This area has a wide variety of minerals, and many are available in substantial amounts. The total value of all minerals produced in the South in 1950 was $4,500,000,000, or 44% of the nation's total. More than half of this amount was produced in Texas, with petroleum accounting for 78% of the area's total. Coal and petroleum amounted to 90% of the over-all southern mineral production.

The total southern production of petroleum, the most important mineral resource, was 1.7×10^9 bbl in 1951. Proven reserves of oil in the United States amount to approximately 32×10^9 bbl, of which the South has approximately 70%. Based on the present (1954) rate of consumption (which has been rising steadily and rapidly), proven reserves of oil are sufficient for thirteen years. To offset this, new reserves are constantly being discovered, and during the period from 1934 to 1954 proven reserves have increased steadily.

The production of natural gas in the South now (1954) amounts to 6×10^{12} cu ft per yr, or 75% of the total production of the United States. In monetary value, natural gas is the South's second most important mineral. Known reserves will last for twenty-five years at predicted rates of consumption, and approximately 80% of the reserves are located in the South.

There has been an enormous increase in the consumption of petroleum and natural gas occasioned to a considerable extent by the substitution of these commodities for coal. Also of importance to the South is the fact that oil and gas are increasingly important basic raw materials for the production of many chemicals such as synthetic rubber and synthetic fibers. More than 85% of the total petrochemical industry in the United States is concentrated along the coast of the Gulf of Mexico within a 200-mile radius of Houston, Tex. Finally, oil and gas are of vital importance to the southwestern part of the United States, which lacks coal and water power and would be severely handicapped if these basic sources of power should become exhausted.

One of the most significant trends during 1951 was the continuing expansion in the field of petrochemicals, which comprises the chemicals derived from oil and natural gas. In fact, many authorities state that the spectacular growth of the petrochemical industry is one of the most important developments of the period from 1929 to 1954. Petrochemicals account for 25% of all the chemicals being produced in the United States (as of 1953); it is predicted that this figure will increase to 50% by 1964. These are rapid strides for an industry established in the 1920's, and substantially all this industry is located in the South.

A measure of the growing importance of this chemical industry is to consider its growth since 1944. The petrochemical industry had an estimated capital investment of $350,000,000 and a production rate of 4×10^9 lb of chemicals per yr in 1940. In 1954, the capital investment increased to $2,000,000,000, and the production rate was 16×10^9 lb per yr. An idea of the magnitude of the raw-material requirements for this industry may be had by considering that more than 3×10^6 tons of liquid gas feed stocks were required in one branch of the petrochemical industry in 1951.

Despite these huge demands, it is estimated that only 1% of the petroleum and only 5% of the natural gas produced in the United States are used in the manufacture of petrochemicals. The industry rests on a firm and secure base; the petroleum industry developed 5.1×10^9 bbl of reserves in 1951, surpassing the highest previous record by nearly 1×10^9 bbl. As petroleum production (withdrawals from reserves) amounted to 2.5×10^9 bbl, the over-all reserves were increased by 2.6×10^9 bbl—that is, for every barrel of crude oil withdrawn from the ground in 1951 two new ones were found. As previously noted, proven reserves now (1954) stand at 32.2×10^9 bbl (the highest on record) and 2½ times the 1936 reserves of 13×10^9 bbl.

The concentration of petrochemical plants in the southwestern part of the United States—more than fifty of which are located along the Gulf of Mexico in Texas and Louisiana—is such as to justify the classification of the petrochemical industry as a southern industry. Because petrochemicals are admirable "building blocks," the majority of the synthetic chemical industries are located in the South. More than 80% of the synthetic rubber industry is located in the South, and more than 50% of the synthetic ammonia production is in the same area. Approximately three quarters of the expansion in the production of ammonia will be located in the South. The synthetic-fiber industry is almost wholly a southern industry.

By 1950 the South had 25% of the chemical-manufacturing plants in the United States; 32.5% of all persons engaged in the chemical industry; 31.6% of chemical income, payrolls, and profits; and 32% of the chemical sales. Substantially, every large chemical company now has one or more Southern plants. As a clear indication of the trend, the world's largest chemical company has nearly half of its total investments and inventories in the South. This is not all: More than 50% of the chemical industry's initial plant expansion for 1951, covered by certificates of necessity and amounting to $600,000,000, was also southern.

The natural gas reserves of the United States now amount to 193.8×10^{12} cu ft. The net gain during 1954 was 8.2×10^{12} cu ft, the second largest on record despite a record-breaking production of 8×10^{12} cu ft. The production of natural gas in the South is 75% of the total for the United States; approximately 80% of the reserves are located in the South.

Coal, the South's third most important mineral, is available in sufficient quantities to last almost indefinitely. The production in 1950 was valued at slightly more than $500,000,000, 22% of the total produced in the United States; approximately 20% of the coal reserve of the United States is in the South.

The South has ample supplies of iron ore and produces 8% of the total mined in the United States. The reserves are estimated at 2×10^9 tons, or nearly 40% of the nation's reserves. The area has 40% of the phosphate rock in the country and accounts for more than 90% of the annual production. The South has all the reserves of bauxite and native sulfur that can be used under normal conditions.

Despite this favorable outlook, one is compelled to view the situation with sobriety. The southwestern part of the United States possesses no alternative fuel. The continuing expansion of the chemical industry in the South is largely dependent on an assured supply of petroleum and natural gas hydrocarbons. Transportation of these petroleum products to other sections of the United States plays a vital role in furthering the chemical industry in the South.

WATER RESOURCES

The high annual rainfall in the South, coupled with a long coast line and many rivers, gives the area an abundance of water resources—a necessity for virtually all chemical-plant operations. The rivers are important as transportation routes, as a source of power, and as a source of water required by chemical-plant operations.

Water is still (as of 1954) the least expensive method of transportation; no other section of the United States has such extensive facilities. Approximately 60% of the navigable waterways of the United States are located in the South. Nine of the states reach tidewater, and five are served by the Mississippi River and its major tributaries.

The potential water power available in the southern states is estimated at 30×10^9 kw-hr, which is more than a third of all the potential water power east of the Rocky Mountains. The total electrical output from all sources in the South in 1950 was almost 100×10^9 kw-hr, which represented almost a fourfold increase since 1939.

OTHER RESOURCES

The South has other important resources. Of the total land area 43% is wooded. This lumber accounts for 36% of the United States' income from this source—in excess of $2,000,000,000 in 1950. The naval-stores industry accounted for $135,000,000 in 1950. The principal products of this industry—turpentine and rosin—are used as raw materials in many chemical industries (for example, soap and detergent manufacture). This area also has 28% of the railroad mileage and 29% of the highway mileage in the United States.

THE CHANGING PATTERN OF AGRICULTURE, INDUSTRY, AND INCOME

Next to mining, southern agriculture is the most important source of raw materials for chemical-plant operations in the South. Any change in this basic activity will have a profound effect on the chemical industry because agriculture is also a large and important market for chemical products.

The South's share in the manufacturing industry of the United States has been increasing steadily. In 1947, this region had 17.7% of all the production workers. At the present time (1954), the textile industry is the most important, followed by food manufacturing, industries based on petroleum and coal, and the chemical industry.

The southern states are receiving a major part of the new industrial facilities under the decentralization trend of the accelerated depreciation program. The South's share has been a widely diversified group of industries including the chemical, aluminum, gasoline product, paper, aircraft, nonferrous metal, and some steel. In aluminum, for example, the South has two thirds of the new installations, or $235,000,000 worth out of a total of $350,000,000. The South is also receiving gasoline plants valued at $254,000,000 out of a total award of $487,000,000 and more than 50% of the approved $600,000,000 chemical plant installations. In all other manufacturing plant allocations the South received 45%.

An economic revolution is (1954) sweeping the South, thus making it the fastest growing industrial area in the United States. An average of seven new plants have opened in the South during every working day in the period from 1944 to 1954. These new plants have created more than 1,250,000 new jobs in southern industry. During 1951, the South added one multimillion-dollar industrial plant each working day, or more than three hundred major plants —representing a capital investment in excess of $3,000,000,000 in twelve months.

The South has made substantial gains in income—with an increase from 47% of the nonsouthern average income in 1929 to 65% in 1947. The source of income also has changed considerably. The proportion of income from agriculture has decreased 18% since 1929 whereas the proportion of income from manufacturing has increased by 20%. In 1929, income from agriculture was about 65% greater than income from manufacturing. At the present time (1954), income from industry is slightly greater than income from agriculture. The South's income is approximately 20% of the total income of the United States and is increasing 150% as fast as the national average. Despite the changes in agricultural income, the production of agricultural chemicals continues to be a lucrative field. Shrinking acreages and the increasing cost of farm labor make it imperative that maximum yields per acre be obtained. This condition creates a larger total market for fertilizers, insecticides, and other agricultural chemicals. At the same time, the growth of southern industry provides a ready market for a large number of industrial chemicals. The South is rapidly becoming its own best customer, and southern goods and produce need no longer look elsewhere for their best markets.

Synthetic Fibers

The 1930's saw the rise of the synthetic organic chemical industry in the United States whereas the next decade witnessed equally impressive developments in synthetic rubber and plastics. The present decade (1950 to 1960) should be one in which synthetic fibers will play an outstanding role. At the present time (1954) the synthetic-fiber industry exceeds all other branches of the chemical industry in rapidity of growth and has great possibilities for the future. Until late in the nineteenth century, the fibers available for the covering, warmth, and adornment of mankind were only four in number—cotton, wool, silk, and linen. From the earliest times these fine fibers so generously provided by nature were sufficient to meet all of man's needs. However, with the further development of the machine age, with its emphasis on productivity and the large-scale manufacture of what had once been regarded as luxury items, an appetite for more and better textiles was created. The feminine wardrobe, which had been restricted to the commoner fibers for all but a few, demanded increasing quantities of costly and exotic garments.

Plant Location

Choosing the best sites for new plants is one of the most difficult problems faced by any company. It is an especially difficult one for the chemical and allied industries. The pitfalls that may be encountered are many, and the disadvantages resulting from choosing a wrong site can be catastrophic. The locating of new plants must be approached most carefully, and a new site must be selected only after the most thorough study and review of all factors and requirements. Therefore, the selection for an industrial location must be made with an attendant evaluation of intangibles which can be accomplished only by exercising good judgment.

There is no fixed formula that will provide a universal approach to the problem, and the factors involved are usually too numerous and too complex to permit the use of standard or stereotyped methods. However, with the trend from individually managed and owned enterprises toward large integrated (although physically dispersed) businesses, close attention must be given to as complete an evaluation of these factors as possible. With increasing competition, management must determine and thoroughly analyze all cost factors in plant-site location. In the period from 1944 to 1954 some basic information and a number of methods for approaching the problem have emerged.

TABLE 1.—PLANT-LOCATION STUDY BASED ON COST, IN DOLLARS, PER 100 LB OF PRODUCT

	COST PER 100 LB OF PRODUCT							TOTAL DIFFERENCE IN COST					
Area	Steam	Power	Water	Labor	Total freight	Taxes	Total	$1,000 per yr before federal income taxes	$1,000 per yr after federal income taxes	per 100 lb of product	Difference in cost of steam	Difference in taxes	Water transportation
1	2.15	0.79	0.75	5.03	3.31	1.16	13.19	0	0	0.00	0.00	0.00	None
2	3.70	0.72	0.73	5.03	3.19	1.97	15.34	215	133	2.15	1.55	0.81	Possible
3	3.77	0.49	0.73	5.03	3.32	2.26	15.60	241	150	2.41	1.62	1.10	Possible
4	3.52	0.87	0.75	5.83	3.78	1.68	16.43	324	200	3.24	1.37	0.52	Possible
5	4.42	0.89	0.75	4.27	3.11	3.06	16.50	331	205	3.31	2.27	1.90	None
6	4.64	0.79	0.73	4.27	3.27	3.06	16.76	357	220	3.57	2.49	1.90	Possible
7	3.94	0.89	0.73	4.70	3.58	3.07	16.91	372	230	3.72	1.79	1.91	None
8	4.64	0.79	0.73	4.38	3.34	3.61	17.49	430	265	4.30	2.49	2.45	None
Maximum difference	2.49	0.40	0.02	1.56	0.67	2.45	4.30	...	...	...	...	...	...

A simple, yet inclusive and concrete, method of showing the effect of all the factors on the ultimate cost is to set up the various costs in chart form as the cost per 100 lb of a product. One such chart is shown in Table 1. In this table factual data for the items that constitute the major costs are consolidated; what the conclusion should be is clearly shown from an economic standpoint. Once these factors are tabulated, intangibles can be given consideration.

As an example of the application of Table 1, under the heading, "Steam," there is involved the cost per ton of the solid fuel (or per barrel of oil) plus its transportation to the site. From computations made previously as to the amount of steam required per 100 lb of product, the cost of steam is determined from the cost of fuel, transportation, potable water used, amortization of the investment or capital cost, and indirect charges such as insurance.

Computations for power are made similarly; from the rates that have been obtained in a survey, a specific cost is fixed to include transportation with an addition made to cover amortization of the capital investment. This cost applies whether power is purchased or generated. It is the over-all power cost that must appear on the manufacturing cost sheets.

The charge for water used for cooling and processing includes pumping charges, amortization on the distribution system, and any charges involved in treating water if this should be necessary.

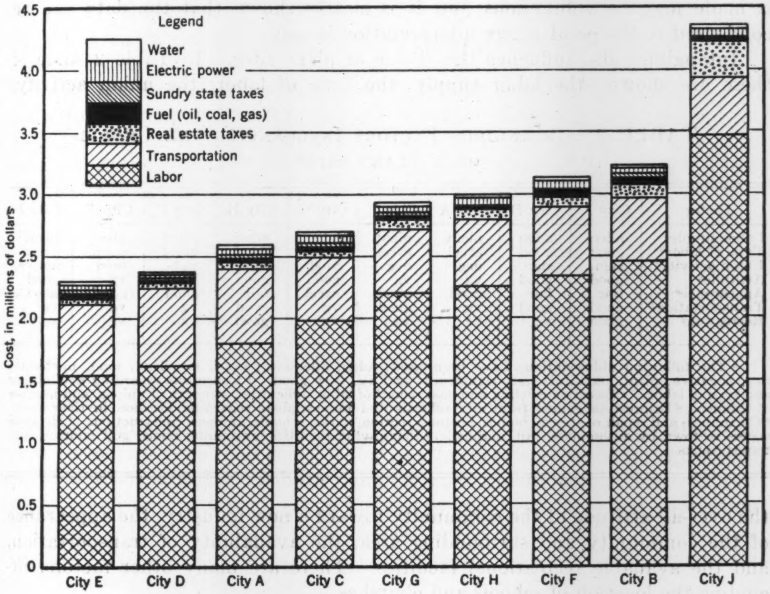

FIG. 1.—SUMMARY OF PLANT-LOCATION SURVEY

The labor factor analysis is made, based on a complete organization chart, which shows the type and number of personnel required to perform the operation. Labor rates for the area are reviewed from job descriptions; those which apply are established. With the applicable number and the wage brackets, the annual cost can be derived, and the cost per 100 lb of product is easily determined.

Raw materials and finished goods must be transported. Raw materials may come from many sources. The annual transportation charge is established, and along with this, transportation on finished goods is computed to make up a total annual charge for transportation from which the cost per 100 lb of product is fixed.

Taxes are an important part of costs. They must be examined specifically and carefully because there is wide variation in the effect of taxes on an operation. The information is available, and once assembled, the annual charge can be reasonably fixed so that the cost per 100 lb of product can be determined. The eight cases in Table 1 were developed in this way. Subsequently, other intangible factors were studied, and a selection was made.

In Fig. 1, a summary of a plant-location survey,[2] another method of presentation, is shown. In Fig. 1 various costs are shown in bar-chart form on an annual basis. In effect, the data, in brief and specific form, make possible a conclusion for selecting the site. The supporting data from which the chart is made may be voluminous, but it is clearly shown that the data can be condensed to the point where interpretation is easy.

Intangibles also influence the choice of plant sites. In Table 2 some of these are shown—the labor supply, the type of labor, the union activity, the over-all attitude of the community toward a new industry, the appearance of the community and surrounding area, the availability of transportation, and the available recreational facilities. There are many other factors, including the location of schools and churches.

TABLE 2.—INTANGIBLE FACTORS INFLUENCING THE CHOICE OF A PLANT SITE[a]

Factor	City E	City D	City A	City C	City G	City H	City F	City B	City J
Labor supply[b]	adeq	adeq	plent	plent	adeq	adeq	plent	plent	plent
Type of labor[b]	good	good	excel	excel	excel	excel	excel	excel	excel
Union activity[c]	sign	sign	neg	neg	mod	sign	sign	mod	active
Attitude[d]	good	good	vg	vg	good	good	vg	vg	good
Appearance[e]	fair	fair	good	good	excel	fair	good	good	good
Transportation[f]	good	good	vg	good	vg	good	vg	vg	vg
Recreation[g]	good	vg	vg	vg	vg	good	vg	vg	vg

[a] The following abbreviations have been used: adeq, adequate; excel, excellent; mod, moderate; neg, negative; plent, plentiful; sign, significant; and vg, very good. [b] Consensus regarding availability and type of labor. [c] Based on existing and past record of labor difficulties, strength of unions, and number of unions. [d] Impression gained from city officials and industrialists regarding location in their town. [e] Cleanliness and repair of streets, homes, business section, parks, schools, and new construction. [f] Relative access to town by automobile, rail, and air. [g] Playground facilities, swimming pools, golf courses, and tennis courts.

A study of Tables 1 and 2 and Fig. 1 provides an almost immediate understanding of the reasons for the South's status as a favorite area for the expansion of the chemical and allied industries. For example, there is the item of fuel. It has been stated that coal is the South's third most important mineral and that, in 1950, 22% of the total coal mined in the United States came from this area. Availability is excellent; as a result, the cost of steam and power from steam can be low compared to other areas where coal is less favorably distributed. Oil is also available in quantity, transported by rail or by water. Moreover, there is a complex network of gas lines. Compared to other areas, the South is in a favorable position as far as all types of fuel are concerned.

---

[2] "Techniques of Plant Location," by Malcolm C. Neuhoff, *Studies in Business Policy, No. 61*, National Industrial Conference Board, New York, N. Y., 1953.

The cost of power is favorable to the South. The water power potential available to the South is large, but even without water power, public utilities can generate power to sell at low rates because fuel is cheap and water abundant.

The freight cost includes both incoming freight (raw materials) and outgoing freight (finished products). Because the South is in a strategic position between abundant raw materials and the markets for finished goods, the balance between incoming and outgoing freight costs is most favorable. The net cost for freight per pound of product will therefore be in a range which will be highly competitive.

The importance of the labor factor is evident from a study of Table 1 and Fig. 1. Viewed with respect to the scarcity of labor (as of 1954) in many of the larger cities in the northern United States, it is easy to understand why a company would settle in the South; in almost any community labor is available, it is intelligent, and can be easily trained, and is generally cooperative in making maximum use of the productive tools provided by management.

Taxes on industry in the South are not as heavy as they are in many other regions. Because of an eagerness to industrialize, a liberal attitude is the rule. Few southern communities want to impose unfair taxes on industry.

In some places, special inducements, such as tax abatement for a period of years, is offered; moratoriums, too, are sometimes offered. In some localities, facilities are built to fit the needs of the operation. However, industry should not give too much weight to these cost depressors because such contributions must be repayed as taxes by someone; industry should carry its just tax load for public purposes.

CONCLUSIONS

With all the assets that have been enumerated—land, people, and mineral resources available to industry (including such versatile and myriad raw materials as petroleum and coal), water as a basic raw material for processing and as a transportation medium, agriculture as an industry source of raw material, and an increasingly large market by reason of increased population catalyzed because of influx of basic industry—the South should look forward to a continuing growth and to an economic stability with good balance between agriculture and industry.

DISCUSSION

Roland A. Kampmeier,[3] **M. ASCE.**—A most commendable and informative presentation has been made by Mr. Hoyer. He has offered a clear picture, not only of the industrial growth of the South but also of the diversified resources on which the industrial development of the region is based. The author has performed a useful service in bringing together brief outlines of some of the South's important resources and also in illustrating how these resources affect the selection of plant locations.

The importance of a well-rounded resource base is apparent. If a region or a particular locality is to be attractive to an industry, all the qualifications necessary for the successful establishment of that industry should be present. Many of these qualifications are the same for a wide variety of industries: Abundant water of good quality, ample low-cost power, efficient transportation, satisfactory labor supply, and an attractive community environment. If an area is to provide suitable locations for industrial development, it is not enough that it should have cheap labor or provide tax incentives. Its land and water resources should be developed as completely and on as well-integrated a basis as possible.

Mr. Hoyer has made an appropriate choice of words in referring to petrochemicals as "building blocks." The South produces "building blocks" of several kinds, including other chemicals, light metals, and the greatly expanded supply of electric energy. Industry in the South has provided the northern states with the raw materials for other industries—not always to the advantage of the South. It seems reasonable to hope that the light metals and synthetic fibers which the South produces will gradually lead to the development in the South of industries which will use these "building blocks" to produce finished consumer goods. This trend will accelerate as the South provides a better market for consumer goods. Conversely, the employment of southern labor in such industries will provide labor with the wages which will make the South a better market.

The paper contains a lesson for any area—it should study the resources in which it is strong and recognize those in which it is weak. It should work toward the sound and well-balanced development of its latent resources so that they can be utilized for the establishment and growth of a diversified industrial economy. The South should note the importance (emphasized by the author) of community attitudes toward industry and of the facilities available in the community for the education, recreation, and comfort of an industry's employees.

The northern states should recognize that, although the South has improved its industrial development, it still has a long way to go. The South lags behind the northern states in industrial development and in income levels (as of 1954). The expansion of southern industry means better business for the northern states, and a stronger South means a stronger United States. As Mr. Hoyer noted, the South as a producer of cotton has been fearful of the development of synthetic fibers; likewise, the coal industry has feared hydroelectric developments. Time has proved such fears to be groundless; wise utilization of resources will benefit, in due course, not only the local region most directly affected, but the entire nation as well.

---

[3] Asst. Mgr. of Power, Tennessee Valley Authority, Chattanooga, Tenn.

AMERICAN SOCIETY OF CIVIL ENGINEERS
Founded November 5, 1852
TRANSACTIONS

Paper No. 2747

CONSTRUCTION OF THE ELIZABETH RIVER TUNNEL

By Joseph Peraino,[1] A. M. ASCE

Synopsis

When the two-lane vehicular tunnel under the Elizabeth River in Virginia was opened to traffic on May 25, 1953, the idea of providing a direct highway link between Norfolk and Portsmouth was brought to fruition. Some of the problems encountered during the construction of the fifth trench-type vehicular underwater crossing to be built in the United States are outlined, and the method of solving these problems is presented. Of particular interest is the method of constructing, floating, and placing the 300-ft, double-shelled, steel casings for the underwater part of the tunnel. It is concluded that the trench-type tunnel was the most economical to build.

Introduction

In 1942 the Commonwealth of Virginia created the Elizabeth River Tunnel Commission to implement long-discussed plans for a quick vehicular route between the cities of Norfolk and Portsmouth, which had previously been connected only by a ferry. After many delays, construction of a bridge-tunnel expressway was initiated in February, 1950. Work on the approaches and bridge naturally entailed special problems, but none matched those involved in exactly positioning the seven 300-ft-long, double-shelled, steel tubes that were used in constructing the 2,100-ft underwater link of the 3,400-ft tunnel.

The Tunnel

On the Shipways.—For the construction of the underwater section, seven double-shelled steel casings, each approximately 300 ft long, were used. The sections were built on a shipway at Sparrows Point, Md., where approximately 650 tons of prefabricated steel were used in the all-welded construction of each of the tubes. Each tube had an outer, octagonal-shaped shell, which was 35 ft 4 in. wide. This outer shell, fabricated of ¼-in. plate, encircled a

---

Note.—Published, essentially as printed here, in November, 1953, as *Proceedings-Separate No. 348.* Positions and titles given are those in effect when the paper was received for publication.

[1] Chf. Engr., New York Marine and Heavy Constr. Div., Merritt-Chapman & Scott Corp., New York, N. Y.

circular inner shell of $\frac{5}{16}$-in. plate with a diameter of 31 ft 4 in. The outer shell was connected to the inner shell by transverse frames, spaced 12 ft on centers. Because the upper quadrant of the section between the shells was to be capped with structural concrete, the top plate was eliminated from the octagonal-shaped shell.

The main body of each double-shelled section was approximately 292 ft long and was faced at each end by a rectangular dam plate of $\frac{5}{8}$-in. plate, $35\frac{1}{2}$ ft wide and 36 ft high. The interior face of the dam plate, which served as a bulkhead, was reinforced with wide-flange beams. A 4-ft 3-in. collar was welded to its outer face as an extension of the inner shell.

During construction on the shipways, a webbing of reinforcing steel was welded to the interior face of the circular shell, exclusive of the part that extended beyond the dam plate. This reduced to a minimum the handling of reinforcing steel at the job site.

In the Water.—Fitted with a temporary launching bow and ballasted with approximately 1,000 tons of concrete placed in the "keel" between the outer and inner shells, the tube was then sent down the ways like any ship. Drawing approximately 8 ft 6 in. of water, the section was then taken in tow by a tug for the 185-mile trip down the Chesapeake Bay (Maryland) to the "shape-up" dock at the tunnel side. On arrival, the section was warped into position alongside a pair of finger piers. While the section was still afloat, it was first necessary to fit it with an 18-in.-thick inner ring of concrete and a 14-in.-thick stretch of roadway slab, 22 ft wide.

Concreting.—Concrete was batched and mixed in a floating concrete plant moored adjacent to the pier. From there, concrete was fed to a pumpcrete plant ashore and was then sent out over the piers and into the tube through 8-in. lines. Concrete was placed in the tube by elephant trunks through six rectangular hatchways spaced along the top of the inner shell.

Because the tunnel section was afloat throughout this operation, care had to be maintained to insure stability. This was achieved by carefully balancing the successive steps followed in building the inner ring of concrete over the webbing of reinforcing steel. In each case, the entire stretch of invert was built first by screeding it in place. Next to be built were the roadway haunches —which encased water mains and drains—the roadway slab, side walls, and arch.

The greatest problem in each of the four successive concreting operations following construction of the invert was to avoid any excessive strain on the steel casing. This problem was solved by using a specially designed system of four traveling forms. The forms were devised so that they could be lowered sectionally through the 3-ft 7-in. by 5-ft 7-in. hatchways in the top of the inner shell; once inside the tube, they were assembled in four $37\frac{1}{2}$-ft sections.

To keep the section in trim, each successive concreting operation within the tube was started simultaneously at the quarter points of the interior section, with two forms teamed on each side to concrete a 75-ft length. When this first pour was completed, two forms were moved toward the center and two toward each end, thereby keeping the tube in trim. Following the construction of the haunches, forms were dismantled; using the same travelers, other forms were installed to construct the roadway slab. The same procedure was successively followed in placing the sidewalls and arch. During placement of the arch, two hatchways were left open to permit the final removal of the dismantled forms. Concreting was then completed by the use of suspended wooden forms, after which all hatches atop the tube were sealed by welded plates.

With all interior concrete in place and the shell completely sealed, the next step was to place sufficient tremie concrete in the "side pockets" between the inner and outer casings. This was done so that the casing would be stable before the structural concrete which formed the cap along the upper quadrant of the section was placed.

As this shape-up concreting progressed, the tube, which had once been extremely buoyant, sank deeper in the water. When the concrete cap was in place the section drew approximately 33 ft, with only 2½ ft of freeboard. The tube was then towed out to a point on the river exactly above its final position in the trench, which meanwhile had been dredged across the river bed.

Sinking.—Preparatory to the sinking operation, tall target masts were fitted atop each end of the tube. Two floating derricks were stationed at either end, their slings hooked into plate shackles built into the top of the tube. A third derrick was used to maneuver the hopper through which additional tremie concrete was placed in the open spaces still remaining in the side pockets that ran the length of the section.

Sinking deeper with each additional ton of concrete, the tube gradually reached the point of negative buoyancy. If weighed in the dry at that time, it would have weighed approximately 9,100 tons—650 tons of which would have been steel and 8,450 tons, built-in concrete. Concreting continued until the section, having lost all buoyancy, weighed approximately 100 tons under water. The two derricks then gently lowered the tube until it came to rest on the blanket of sand, which had been screeded to proper grade and had been prepared for it on the trench bottom. As it went down, the transitmen on shore kept the target constantly in their sights to insure perfect alinement and grade.

The screeding device used to bring the trench to final grade was suspended by cables from a steam-powered car traveling on inclined tracks mounted on a barge at an angle that paralleled the grade of the trench. As the car moved back and forth, the drag brought the trench to exact grade. Once the stretch of trench beneath the barge was screeded to the correct elevation, the barge was moved ahead and, after the length of the drag's cables was adjusted, the operation was repeated.

The first of the seven sections was sunk on the Norfolk side of the Elizabeth River. After underwater examination by divers to insure exact placement, additional tremie concrete was added to keep the section from refloating as a result of possible changes in the specific gravity of the water.

Joining.—Following the same procedure, Tube 2 was then sunk into position and locked to Tube 1. Half-circle, 18-in.-long hood plates projected beyond the collars of each section. On one end they were on the top of the collar; on the other, at the bottom. At each end of the half-circle, the hooded plates were fitted with a slotted flange. As each tube section was positioned next to the other on the river bottom, the hood plates formed a complete circle, bringing the slotted flanges into alinement. After an inspection of the river bottom to insure exact placement, divers drove 5-in.-long pins through the slotted flanges, thus bolting the sections together. The divers then further locked the sections together by tightening five pairs of steamboat ratchets fitted around the circumference of the collars.

Tube 3 was similarly placed and locked into position. That done, a collar of tremie concrete was placed around the joint between Tubes 1 and 2. Backfill was then placed over the first two tubes, with care being exercised to see that the backfill did not cover either the shoreside end of Tube 1 or the joint between Tubes 2 and 3. This procedure was repeated as Tubes 4 and 5 were positioned.

As a first step in planning the construction of the tube joints, continuous strips of steel sheet-piling interlock were welded to the vertical edges of the dam plates. As each tube was set and locked to its neighbor, a half-circle of ¼-in.-thick plate, 37 ft high and edged with steel sheet-piling interlock, was fitted into the interlocks along one side of both dam plates and was lowered to the river bottom. Another was similarly slotted into position between the dam plates on the other side of the tube. This design provided vertical closures that acted in tension as the tremie collar was placed around the joint. The fact that the Elizabeth River crossing is a very dry tunnel is the result of the careful planning that went into construction of the tube joints.

In order to complete the placing of the tubes with ease, it was decided to make a subaqueous juncture between the shore end of Tube 7 and the 625-ft, cut-and-cover section on the Portsmouth side. Whereas Tubes 1 through 5 had been placed in sequence from the Norfolk side, Tube 7, which was to be positioned in a wet trench leading to the cut-and-cover approach, had to be placed before Tube 6. If Tube 6 were already in place, there would be no room to maneuver Tube 7 into the wet trench.

First, a 50-ft-wide trench was excavated for the cut-and-cover section and was begun at a point approximately 225 ft inshore. The sides of the trench, which ranged from 30 ft to 60 ft in depth, were sheeted with master piles and wood lagging, shored throughout; deep well pumps controlled seepage. Before construction of the trench could be started, a 106-ft railroad bridge had to be built to provide uninterrupted service for the Seaboard Airline Railroad, whose railroad tracks crossed the cut-and-cover section diagonally.

A transition joint, consisting of a bulkheaded telescopic tube that matched the diameter of the collar of Tube 7, was erected in the dry at the river end of the cut-and-cover section. The rim of the telescopic tube was fitted with a channel section to receive the collar of tube 7 and was rigged with steamboat ratchets and lugs similar to those on the tube section.

While the cut-and-cover section was under construction, a wet trench was dredged between the shore and a dike which was left to protect the outboard end of the cut-and-cover section. The wet trench, which was 202 ft long, was approximately 70 ft deep at the river end and approximately 60 ft deep at the inshore end. To support its sides, 36-in., wide-flange beams were driven on approximately 31-in. centers. There were then driven between the webs of the 36-in., wide-flange beams individual 30-in., wide-flange beams, thus forming solid retaining walls of steel. This sheeting was braced by two sets of transverse shores, one above water, the other beneath the surface. Four 60-ft-diameter cells and a steel sheet-pile bulkhead were driven at the outer end of the trench to protect adjacent shoreside installations. The outboard face of the deepest cell was in approximately 70 ft of water. After the trench had been constructed, the cut-and-cover section was backfilled inshore of the transition joint. The original dike was then removed, providing a continuous wet trench between Tube 5 and the transition joint.

Tube 7 was then maneuvered so that its inboard end faced the wet trench, and tremie concrete was placed so that the tube reached the point of negative buoyancy. With a land crane pulling by a cable on the inboard end and a floating derrick maneuvering the outboard end, the tube was then carefully warped into the trench. Because the lower set of trensverse shores provided only 5 ft of vertical clearance, extreme care had to be maintained to keep the tube at the exact grade. There was always the danger that the sides of the wet trench would collapse if the tube hit and seriously damaged one of the shores.

Once Tube 7 was locked to the transition joint, Tube 6 was lowered into place and locked to Tube 5. With the telescopic transition joint providing some leeway, Tube 7 was then pulled back approximately 1 ft 6 in. and was locked to Tube 6. With all joints concreted and backfill placed over the tubes, the subaqueous phase of the project was completed.

Meanwhile work had been going forward to effect a juncture between the inboard end of Tube 1 and the 610-ft-long, cut-and-cover section on the Norfolk side. By placing a dam across Tube 1 and dewatering the inboard area, this operation was performed in the dry. Actually, the holing-through operation was begun on the Norfolk side after the fifth tube had been positioned. It should be noted that early work on the Norfolk cut-and-cover section involved erection of a railroad trestle and bridge to permit uninterrupted service by the Norfolk and Southern Railroad.

As indicated previously, an 8-ft 6-in. space existed between the dam plates at each joint. This space within the collar was filled with water, which had to be removed before the bulkheads were holed through. Advance provision for dewatering had been made by installing two valves—one at the top of the bulkhead as an air-relief valve, the other at the bottom for drainage; once drained the two bulkheads were removed. The dismantled bulkheads were put into service as temporary bridges between the stretches of roadway which previously had been built within each section. The joint was then sealed from the inside by welding a closure plate across two T's flanking the joint. An annular space was thus formed, which was then grouted under pressure. This procedure provided maximum assurance against seepage.

Finishing.—Reinforcing steel was then placed around the circumference of the collar and was embedded in 18 in. of concrete to bring the inner face of the joint flush with the rest of the tube section. After the collar concrete had set, the temporary bridging was removed and forms were installed for placing the stretch of roadway slab across the joint.

While this work was going on, other crews—working their way in from the portal—were feeding utility lines through ducts in the sidewalls and were placing concrete for the walkway and curbs. Still other crews were preparing the walls to receive the tile and electrical fixtures and were installing hangers for the suspended ceiling, which provides a minimum vertical clearance of 14 ft. As the interior work moved forward from the Norfolk side, other crews began working from the Portsmouth end. The last bulkhead removed was the one at the outboard end of Tube 7.

At the same time, erection of the ventilation building, located on the Portsmouth side, had been progressing. From the time the first bulkhead was holed through, a constant supply of fresh air was maintained in the tunnel for the construction crews by means of a temporary system of exhaust fans located under the roadway slab. The permanent ventilation system is comprised of four large fans which exhaust air from the tunnel through the spaces above the suspended ceiling and beneath the roadway slab. Fresh air enters the tunnel through the portals at atmospheric pressure.

The roadway wearing surface, a layer of macadam varying from $2\frac{1}{2}$ in. to 5 in. in depth, was placed last in the construction of the tunnel—after the various forms and scaffoldings used in other interior work had been removed.

Conclusions

Placed in actual construction on September 15, 1950, the tunnel was opened for traffic on May 23, 1952; the time which had elapsed was 20 months and 8 days.

A review such as has been presented can contain only the outstanding features of the construction. The review would not be complete, however, if the construction economy, both in money and time, achieved by a trench-type tunnel as compared with a shield-driven tunnel were not noted.

Perhaps the simplest way for one to realize this comparative economy is to note that there would be no tunnel under the Elizabeth River if it had not been possible to construct it by the trench-type method. Had the shield-driven technique been used, the cost of the project—which was financed by revenue bonds—would have been prohibitive.

Acknowledgments

Parsons, Brinckerhoff, Hall, & Macdonald of New York, N. Y., were the consulting engineers for the tunnel phase of the project. The Merritt-Chapman & Scott Corporation of New York built the tunnel. The steel casings were fabricated on the shipways of the Bethlehem Steel Company at Bethlehem, Pa.

AMERICAN SOCIETY OF CIVIL ENGINEERS
Founded November 5, 1852
TRANSACTIONS

Paper No. 2748

BACKWATER FUNCTIONS BY NUMERICAL INTEGRATION

By CLINT J. KEIFER,[1] A. M. ASCE, AND
HENRY HSIEN CHU[2]

WITH DISCUSSION BY MESSRS. FRANCIS F. ESCOFFIER; HENRY J. MILES; RICHARD SILVESTER; AND CLINT J. KEIFER AND HENRY HSIEN CHU

SYNOPSIS

Because of the importance of nonuniform flow and the particular difficulties in computing backwater curves in closed conduits, the authors have devised new procedures facilitating backwater computations. Complete derivations of equations for computing backwater functions are presented, and adaptations of the step method are suggested as additional aids in this field.

NOTATION

The letter symbols introduced in this paper are defined where they first appear, in the text or by illustration, and are assembled alphabetically in the Appendix for convenience of reference.

INTRODUCTION

Hydraulics engineers are repeatedly required to compute backwater curves. In a natural water course, the shape of the cross section may vary greatly among sections. This necessitates the use of one of the many step methods. If the channel is uniform, the computations may be minimized through the integration method appropriate for the particular problem. For channels that are wide in comparison to the depth of flow, for example, one may choose the Bresse backwater functions. The method most applicable to various shapes of open channel was devised by Boris A. Bakhmeteff,[3] Hon. M. ASCE, and supplemented to include velocity head by M. E. Von Seggern,[4] A.M. ASCE.

NOTE.—Published, essentially as printed here, in January, 1954, as *Proceedings-Separate No. 383*. Positions and titles given are those in effect when the paper or discussion was received for publication.

[1] Asst. Engr. of Sewer Design, Dept. of Public Works, Bureau of Eng., Chicago, Ill.

[2] Senior Asst. Sewer Designer, Dept. of Public Works, Bureau of Eng., Chicago, Ill.

[3] "Hydraulics of Open Channels," by Boris A. Bakhmeteff, McGraw-Hill Book Co., Inc., New York, N. Y., 1932.

[4] "Integrating the Equation of Nonuniform Flow," by M. E. Von Seggern, *Transactions*, ASCE, Vol. 115, 1950, p. 71.

These methods cannot be applied accurately to closed conduits when flow is near the top. The writers propose a method for separating many of the involved factors in the nonuniform flow equation so that it can be integrated numerically with respect to the relative depth of flow, y/D, in which y represents the depth of flow and D is the diameter of the conduit. Circular sections have been taken as examples, and tables corresponding to the Bresse function for shallow rectangular sections have been prepared. The application of this circular section is limited, but the same principle and procedure can be applied to any type of conduit or channel.

Numerical Integration

Equation for Nonuniform Steady Flow.—The equation for nonuniform steady flow can be written in the following form:

$$S = \frac{dy}{dx} + \frac{d}{dx}\left(\frac{V^2}{2\,g}\right) + S_0 \ldots\ldots\ldots\ldots\ldots\ldots\ldots (1)$$

in which S is the energy gradient, x represents distance (measured upstream), V is the average velocity at a section, g is the acceleration produced by gravity, and S_0 denotes the slope of the invert or bed. This equation indicates that the slope of the energy gradient is equal to the change in the depth of flow plus the velocity head, with respect to a unit length (dx) plus the bottom slope.

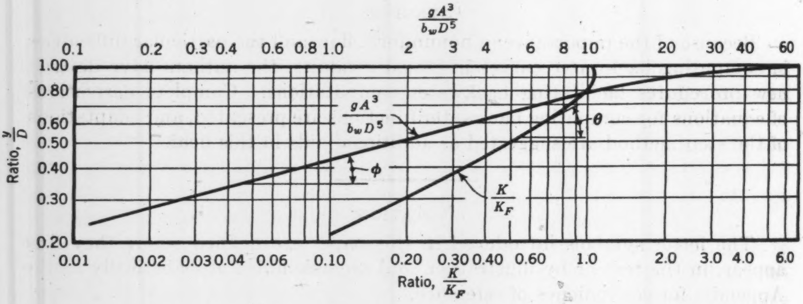

FIG. 1.—DERIVATION OF EXPONENTS i AND m IN CIRCULAR CONDUITS

Substituting Q^2/A^2 for V^2 (Q representing discharge and A being the cross-sectional area of the flow) $S = \frac{dy}{dx} + \frac{d}{dx}\left(\frac{Q^2}{2\,g\,A^2}\right) + S_0$. By differentiation,

$$S = \frac{dy}{dx} - \frac{Q^2}{g\,A^3}\frac{dA}{dy}\frac{dy}{dx} + S_0 \ldots\ldots\ldots\ldots\ldots\ldots\ldots (2)$$

Since the top width of water surface $b_w = \frac{dA}{dy}$,

$$dx = \left(\frac{1 - \frac{Q^2\,b_w}{g\,A^3}}{S - S_0}\right) dy \ldots\ldots\ldots\ldots\ldots\ldots\ldots (3)$$

Eq. 3 is the general differential equation, taking S_0 positive when it is inclined downstream and x is measured upstream. Because the expression between the parentheses in Eq. 3 is a function of depth, this equation may be written:

$$dx = f(y)\, dy \quad \text{.........................} \quad (4)$$

In this form it may be integrated graphically if the size and shape of the conduit or channel, the invert slope, and the discharge are held constant. Each time one of the parameters is changed, the graphical integration must be performed again.

Eq. 3 has not been completely evaluated mathematically without approximations. Mr. Bakhmeteff has integrated Eq. 3 by assuming that the square of the conveyance at any depth of a channel varies as the ith power of the depth so that, if k is the conveyance and i any positive number, $k^2 \propto y^i$. He also neglected the effect of the change in velocity head. This procedure necessitates the use of short steps so that the change in velocity head within each step would not be too great. Mr. Von Seggern makes the same assumptions as Mr. Bakhmeteff and introduces another approximation, $A^3/b_w \propto y^m$, which takes account of the velocity-head changes, m being any positive number.

TABLE 1.—VARIATION OF i AND m IN CIRCULAR CONDUITS

y/D	0.30	0.40	0.50	0.60	0.65	0.70	0.75	0.80	0.85	0.90	0.94	0.95
i	3.93	3.68	3.40	3.12	3.01	2.80	2.47	1.93	1.20	0.85	0	−0.54
m	3.87	3.87	3.87	3.87	3.89	3.99	4.01	4.14	4.42	4.92	5.98	6.50

These assumptions enabled both writers to integrate Eq. 3 analytically and to obtain approximate solutions for most types of open channels. The closed conduit presents a different situation in which the values of i and m, instead of being constant, vary rapidly when the water depth approaches the crown—thus rendering the basic assumption inapplicable. Fig. 1 shows curves describing this variation. The subscript F indicates a full section. The expressions for the exponents i and m are

$$\left.\begin{aligned} i &= 2 \cot \theta = 2\, \frac{d\left(\log_e \dfrac{k}{k_F}\right)}{d\left(\log \dfrac{y}{D}\right)} \\ \text{and} \qquad m &= \cot \phi = \frac{d\left(\log \dfrac{g\, A^3}{b_w\, D^5}\right)}{d\left(\log \dfrac{y}{D}\right)} \end{aligned}\right\} \quad \text{..................} \quad (5)$$

in which θ and ϕ are slopes of the curves in Fig. 1. Values thus determined appear in Table 1. Four parameters are present in the integrand of Eq. 4. A method has been devised for removing two of the parameters from under the integral sign so that for a specified conduit shape the numerical integration must be performed only over the range of one remaining parameter. The following derivation thus required no approximations.

If a particular shape of conduit is chosen—such as a circular section—and the dimensionless ratios y/D and x/D are used to express depth of flow and length along the channel, then Eq. 3 becomes

$$d\left(\frac{x}{D}\right) = \left(\frac{1 - \dfrac{Q^2\, b_w}{g\, A^3}}{S - S_0}\right) d\left(\frac{y}{D}\right) \qquad (6)$$

The flow,

$$\left.\begin{aligned} Q_{\text{cap}} &= k_F \sqrt{S_0} \\ \text{and} \qquad Q = k\sqrt{S} &= k_F \sqrt{S_F} = k_o \sqrt{S_0} \end{aligned}\right\} \qquad (7)$$

in which Q_{cap} represents the capacity of the conduit flowing full and having the energy gradient equal to the bottom slope, the subscript zero indicates the channel bottom, and the subscript 0 indicates normal depth.

Therefore,

$$S = S_F \left(\frac{k_F}{k}\right)^2 = S_0 \left(\frac{Q}{Q_{\text{cap}}}\right)^2 \left(\frac{k_F}{k}\right)^2 \qquad (8)$$

Observing that $(k_F/k)^2$ is a function only of y/D (designated $f_1(y/D)$) and replacing Q/Q_{cap} by α for convenience, it is concluded that

$$S = S_0\, \alpha^2 f_1\left(\frac{y}{D}\right) \qquad (9)$$

In Eq. 6, the value of $\frac{b_w}{g\, A^3}$, after multiplying by D^5, is also a function of the proportional depth y/D—written as

$$\frac{g\, A^3}{b_w\, D^5} = f_2\left(\frac{y}{D}\right) \qquad (10a)$$

Also,

$$f_2\left(\frac{y}{D}\right) = \frac{Q^2{}_c}{D^5} \qquad (10b)$$

in which the subscript c corresponds to conditions at critical depth. The graphs of $f_1(y/D)$ and $f_2(y/D)$ for circular conduits are shown in Fig. 2. Substituting Eqs. 9 and 10a in Eq. 6,

$$d\left(\frac{x}{D}\right) = \frac{1}{S_0}\left[\frac{1 - \dfrac{Q^2}{D^5 f_2\left(\dfrac{y}{D}\right)}}{\alpha^2 f_1\left(\dfrac{y}{D}\right) - 1}\right] d\left(\frac{y}{D}\right) \qquad (11a)$$

and

$$x\Big|_{y=y_1}^{y=y_2} = \frac{D}{S_0}\int_{\frac{y_1}{D}}^{\frac{y_2}{D}} \frac{d\left(\frac{y}{D}\right)}{\left[\alpha^2 f_1\left(\frac{y}{D}\right) - 1\right]}$$

$$- \frac{Q^2}{S_0\, D^4}\int_{\frac{y_1}{D}}^{\frac{y_2}{D}} \frac{d\left(\frac{y}{D}\right)}{f_2\left(\frac{y}{D}\right)\left[\alpha^2 f_1\left(\frac{y}{D}\right) - 1\right]} \quad \text{. . (11b)}$$

in which y_1 and y_2 represent flow depths at two consecutive specified sections.

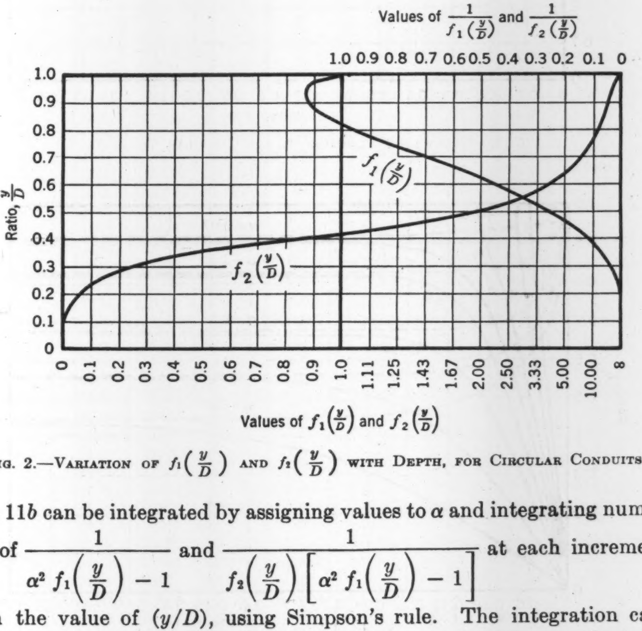

FIG. 2.—VARIATION OF $f_1\left(\frac{y}{D}\right)$ AND $f_2\left(\frac{y}{D}\right)$ WITH DEPTH, FOR CIRCULAR CONDUITS

Eq. 11*b* can be integrated by assigning values to α and integrating numerical values of $\frac{1}{\alpha^2 f_1\left(\frac{y}{D}\right) - 1}$ and $\frac{1}{f_2\left(\frac{y}{D}\right)\left[\alpha^2 f_1\left(\frac{y}{D}\right) - 1\right]}$ at each increment of 0.01 in the value of (y/D), using Simpson's rule. The integration can be started at any reference value of (y/D), such as zero or any convenient depth. Designating members of Eq. 11*b* by

$$\Phi\left(\frac{y}{D}, \alpha\right) = \int_0^{\frac{y}{D}} \frac{d\left(\frac{y}{D}\right)}{\alpha^2 f_1\left(\frac{y}{D}\right) - 1}$$

and

$$\Psi\left(\frac{y}{D}, \alpha\right) = \int_0^{\frac{y}{D}} \frac{d\left(\frac{y}{D}\right)}{f_2\left(\frac{y}{D}\right)\left[\alpha^2 f_1\left(\frac{y}{D}\right) - 1\right]}$$

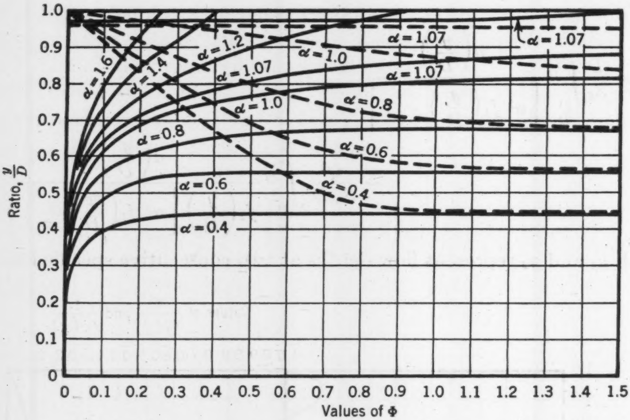

FIG. 3.—BACKWATER FUNCTION Φ, FOR CIRCULAR CONDUITS

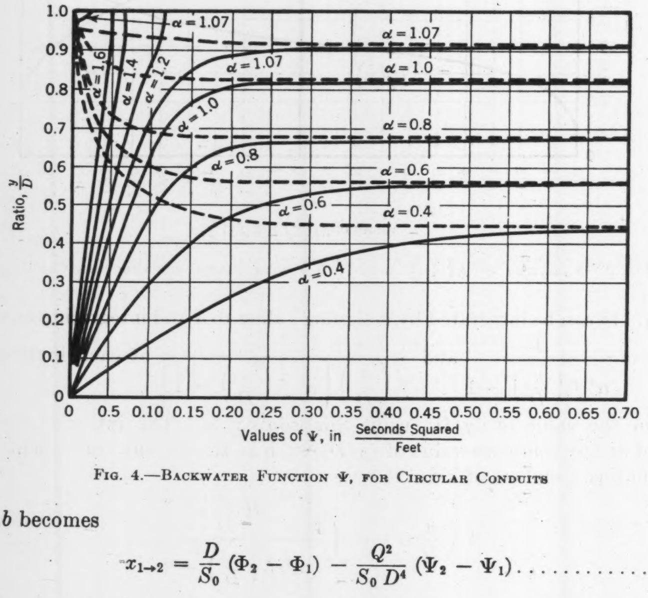

FIG. 4.—BACKWATER FUNCTION Ψ, FOR CIRCULAR CONDUITS

Eq. 11*b* becomes

$$x_{1\rightarrow 2} = \frac{D}{S_0}(\Phi_2 - \Phi_1) - \frac{Q^2}{S_0 D^4}(\Psi_2 - \Psi_1) \ldots\ldots\ldots\ldots (12)$$

For a certain shape of section, the values of Φ and Ψ are functions only of the proportional depth and α. They shall be called backwater functions. These functions have been computed for circular conduits and are exhibited in both graphical and tabular form in Figs. 3 and 4 and in Tables 2 and 3.

Referring to Eqs. 7, when flow is at normal depth,

$$\alpha^2 f_1\left(\frac{y_o}{D}\right) = \left(\frac{Q}{Q_{\text{cap}}}\right)^2 \frac{S_0}{S_F} = 1 \ldots\ldots\ldots\ldots\ldots\ldots (13)$$

Therefore, $\alpha^2 f_1(y_o/D) - 1 = 0$, and the integrand in Eq. 11*a* becomes infinity. Infinite length is required to make any change in normal water depth, meaning that the backwater curve approaches the normal depth asymptotically. Eq. 10*b* indicates that, when flow is at critical depth, the numerator in Eq. 11*a* vanishes. This indicates the length of backwater curve to be zero for any change in water depth.

TABLE 2.—BACKWATER FUNCTION Φ FOR CIRCULAR SECTIONS

Ratio, $\frac{y}{D}$	Values of α									
	0.40	0.60	0.70	0.80	0.90	1.00	1.07	1.20	1.40	1.60
1.00	0	0	0	0	0		1.161	0.9166	0.4075	0.2543
0.98	0.0235	0.0299	0.0368	0.0495	0.0817	0.1085	0.760	0.8567	0.3830	0.2397
0.96	0.0468	0.0592	0.0720	0.0954	0.1517	0.2777	0	0.7822	0.3555	0.2238
0.94	0.0700	0.0883	0.1067	0.1403	0.2188	0.4277	2.872	0.7016	0.3269	0.2074
0.92	0.0932	0.1173	0.1415	0.1851	0.2857	0.5763	5.052	0.6203	0.2982	0.1909
0.90	0.1165	0.1465	0.1764	0.2305	0.3541	0.7345	2.7491	0.5427	0.2701	0.1748
0.88	0.1398	0.1759	0.2119	0.2769	0.4257	0.9160	1.4754	0.4714	0.2432	0.1591
0.86	0.1632	0.2057	0.2481	0.3250	0.5023	1.1459	1.0082	0.4076	0.2178	0.1441
0.84	0.1868	0.2360	0.2852	0.3754	0.5868	1.5020	0.7486	0.3515	0.1942	0.1299
0.82	0.2105	0.2668	0.3236	0.4389	0.6835	2.5439	0.5803	0.3025	0.1724	0.1166
0.80	0.2344	0.2985	0.3637	0.4868	0.8002	0.8911	0.4619	0.2600	0.1524	0.1043
0.78	0.2585	0.3311	0.4059	0.5508	0.9552	0.6046	0.3740	0.2233	0.1343	0.0928
0.76	0.2830	0.3649	0.4509	0.6237	1.2090	0.4518	0.3065	0.1916	0.1179	0.0823
0.74	0.3077	0.4002	0.4997	0.7110	1.5967	0.3521	0.2533	0.1643	0.1031	0.0727
0.72	0.3329	0.4374	0.5536	0.8239	0.5844	0.2810	0.2105	0.1407	0.0899	0.0639
0.70	0.3585	0.4770	0.6151	0.9955	0.4016	0.2275	0.1765	0.1202	0.0781	0.0560
0.68	0.3848	0.5199	0.6885	1.5361	0.3001	0.1858	0.1465	0.1026	0.0676	0.0488
0.66	0.4117	0.5674	0.7831	0.5102	0.2329	0.1527	0.1228	0.0873	0.0583	0.0424
0.64	0.4394	0.6215	0.9263	0.3311	0.1845	0.1259	0.1023	0.0741	0.0500	0.0366
0.62	0.4683	0.6860	1.3682	0.2403	0.1479	0.1039	0.0857	0.0627	0.0428	0.0315
0.60	0.4985	0.7699	0.4083	0.1825	0.1196	0.0858	0.0713	0.0529	0.0364	0.0269
0.58	0.5304	0.8986	0.2596	0.1416	0.0970	0.0708	0.0593	0.0444	0.0308	0.0229
0.56	0.5647		0.1851	0.1113	0.0789	0.0583	0.0492	0.0371	0.0259	0.0193
0.54	0.6022	0.3114	0.1380	0.0882	0.0640	0.0478	0.0406	0.0309	0.0217	0.0163
0.52	0.6446	0.1971	0.1051	0.0701	0.0512	0.0391	0.0334	0.0255	0.0180	0.0136
0.50	0.6947	0.1385	0.0811	0.0557	0.0410	0.0318	0.0274	0.0210	0.0149	0.0112
0.48	0.7591	0.1014	0.0628	0.0442	0.0331	0.0257	0.0221	0.0171	0.0122	0.0092
0.46	0.8585	0.0756	0.0487	0.0347	0.0265	0.0206	0.0178	0.0138	0.0099	0.0075
0.44	3.3677	0.0569	0.0377	0.0273	0.0210	0.0164	0.0142	0.0110	0.0080	0.0061
0.42	0.1837	0.0430	0.0291	0.0212	0.0164	0.0130	0.0113	0.0088	0.0063	0.0048
0.40	0.1107	0.0324	0.0223	0.0165	0.0127	0.0101	0.0088	0.0069	0.0050	0.0038
0.35	0.0419	0.0155	0.0110	0.0082	0.0064	0.0052	0.0045	0.0035	0.0026	0.0020
0.30	0.0169	0.0068	0.0049	0.0038	0.0029	0.0024	0.0021	0.0016	0.0012	0.0009
0.25	0.0062	0.0027	0.0019	0.0015	0.0012	0.0009	0.0009	0.0006	0.0005	0.0004
0.20	0.0019	0.0008	0.0006	0.0005	0.0004	0.0003	0.0003	0.0002	0.0002	0.0001
0.15	0.0004	0.0002	0.0001	0.0001	0.0001	0.0001	0.0001	—	—	—
0	0	0	0	0	0	0	0	0	0	0

The heavy lines in Tables 2 and 3 show the location of normal depth. The tabulated values can be interpolated for intermediate values of Φ and Ψ, but not across the heavy lines because a backwater can never pass through the normal depth. The bottom, $y/D = 0$, cannot be used as a starting point of integration in evaluating Φ and Ψ for depth above the normal depth. The zero value of Φ and Ψ in Tables 2 and 3 shows where the integration has been begun in each case.

TABLE 3.—BACKWATER FUNCTION Ψ FOR CIRCULAR SECTIONS

Ratio, $\frac{y}{D}$	VALUES OF α									
	0.40	0.60	0.70	0.80	0.90	1.00	1.07	1.20	1.40	1.60
1.00	0	0	0	0	0		0.0245	0.1128	0.0680	0.0482
0.98	0.0003	0.0003	0.0004	0.0006	0.0009	0.0016	0.0186	0.1120	0.0677	0.0479
0.96	0.0008	0.0010	0.0012	0.0015	0.0024	0.0053	0	0.1105	0.0671	0.0477
0.94	0.0015	0.0019	0.0023	0.0028	0.0043	0.0098	0.0824	0.1079	0.0663	0.0470
0.92	0.0023	0.0029	0.0036	0.0045	0.0067	0.0150	0.1614	0.1051	0.0652	0.0466
0.90	0.0034	0.0042	0.0050	0.0063	0.0096	0.0215	0.2500	0.1028	0.0641	0.0458
0.88	0.0044	0.0055	0.0067	0.0086	0.0132	0.0303	0.1852	0.0983	0.0627	0.0452
0.86	0.0058	0.0072	0.0087	0.0112	0.0175	0.0438	0.1604	0.0950	0.0613	0.0444
0.84	0.0071	0.0090	0.0110	0.0143	0.0230	0.0667	0.1439	0.0913	0.0598	0.0435
0.82	0.0087	0.0112	0.0136	0.0180	0.0299		0.1321	0.0879	0.0583	0.0426
0.80	0.0106	0.0136	0.0166	0.0225	0.0389	0.1806	0.1230	0.0847	0.0568	0.0416
0.78	0.0128	0.0164	0.0204	0.0282	0.0524	0.1546	0.1153	0.0816	0.0552	0.0405
0.76	0.0150	0.0196	0.0247	0.0349	0.0768	0.1394	0.1088	0.0784	0.0537	0.0396
0.74	0.0177	0.0236	0.0300	0.0440	1.8457	0.1288	0.1032	0.0755	0.0521	0.0384
0.72	0.0206	0.0278	0.0361	0.0571	0.1950	0.1200	0.0980	0.0727	0.0505	0.0375
0.70	0.0240	0.0333	0.0443	0.0817	0.1650	0.1130	0.0933	0.0699	0.0489	0.0363
0.68	0.0280	0.0395	0.0556	0.1747	0.1465	0.1066	0.0891	0.0673	0.0473	0.0354
0.66	0.0324	0.0475	0.0724	0.2320	0.1352	0.1011	0.0851	0.0648	0.0458	0.0343
0.64	0.0377	0.0576	0.0978	0.1882	0.1263	0.0960	0.0813	0.0622	0.0442	0.0332
0.62	0.0438	0.0721	0.2500	0.1680	0.1189	0.0916	0.0777	0.0599	0.0426	0.0322
0.60	0.0511	0.0915	0.2780	0.1545	0.1120	0.0870	0.0743	0.0575	0.0411	0.0310
0.58	0.0600	0.1290	0.2265	0.1437	0.1054	0.0830	0.0710	0.0550	0.0396	0.0299
0.56	0.0705	0.3909	0.2006	0.1343	0.0997	0.0790	0.0678	0.0529	0.0381	0.0288
0.54	0.0840	0.3080	0.1828	0.1260	0.0944	0.0753	0.0647	0.0506	0.0365	0.0278
0.52	0.1014	0.2580	0.1686	0.1186	0.0895	0.0717	0.0618	0.0485	0.0351	0.0266
0.50	0.1253	0.2293	0.1562	0.1117	0.0850	0.0682	0.0588	0.0463	0.0336	0.0256
0.48	0.1609	0.2085	0.1452	0.1054	0.0803	0.0648	0.0561	0.0441	0.0321	0.0244
0.46	0.2235	0.1912	0.1350	0.0993	0.0761	0.0616	0.0533	0.0420	0.0306	0.0233
0.44	1.4143	0.1770	0.1256	0.0935	0.0718	0.0582	0.0505	0.0399	0.0291	0.0221
0.42	0.5000	0.1643	0.1170	0.0880	0.0680	0.0552	0.0478	0.0378	0.0276	0.0210
0.40	0.4116	0.1528	0.1090	0.0826	0.0641	0.0519	0.0451	0.0357	0.0261	0.0199
0.35	0.3090	0.1271	0.0917	0.0700	0.0546	0.0444	0.0386	0.0306	0.0224	0.0171
0.30	0.2432	0.1038	0.0755	0.0580	0.0454	0.0370	0.0321	0.0255	0.0188	0.0143
0.25	0.1903	0.0825	0.0607	0.0466	0.0366	0.0297	0.0258	0.0205	0.0151	0.0114
0.20	0.1425	0.0627	0.0462	0.0356	0.0281	0.0227	0.0197	0.0157	0.0115	0.0088
0.15	0.1000	0.0442	0.0327	0.0250	0.0197	0.0158	0.0138	0.0110	0.0081	0.0062
0	0	0	0	0	0	0	0	0	0	0

Eq. 12 indicates that the backwater functions Φ and Ψ will apply to all cases, regardless of the diameter and discharge values. The use of these functions, however, must be restricted to conduits having bottom slopes in the direction of flow either steeper or milder than the critical slope. If the bottom is horizontal, $S_0 = 0, \alpha = \infty$, and Eq. 9 becomes meaningless. In the case with adverse slope, S_0 is negative, and

$$Q^2_{\text{cap}} = k^2_F\, S_0 \qquad \text{(14)}$$

Therefore, $\alpha^2 = (Q/Q_{cap})^2$ is also negative. The integration process must be repeated, using these expressions to determine values of Φ or Ψ for the adverse slope.

In the case of an open channel, any convenient linear measure (for example, the bottom width) can be used instead of the full depth of closed conduits. The remaining expressions can be derived in the same manner as for closed conduits.

The preparing of the tables for backwater functions for one type of section is laborious—but justified—if the section will be used frequently and if many backwater curves must be computed. The step method may be preferred, however, for hydraulic investigation of conduits having other cross sections that will not be used so often.

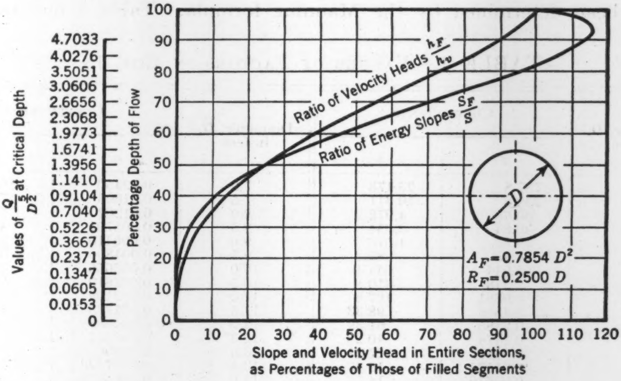

FIG. 5.—ENERGY SLOPE AND VELOCITY HEAD IN CIRCULAR CONDUITS FLOWING PARTLY FULL

BACKWATER CURVES IN UNIFORM CHANNELS BY THE STEP METHOD

The step method for computing backwater curves has certain advantages over the integration method. It provides a complete profile of the water surface, values of the velocity at each section, and many other required factors.

In the step method, Eq. 3 is

$$\Delta x = \frac{\Delta\left(y + \frac{V^2}{2\,g}\right)}{S_{av} - S_0} = \frac{y_2 - y_1 + \frac{V^2{}_2}{2\,g} - \frac{V^2{}_1}{2\,g}}{S_{av} - S_0} \quad \ldots\ldots\ldots\ldots (15)$$

in which S_{av} is the average value of the slope of the energy gradient at the two ends of a reach. For computing the energy slope and velocity head, many laborious steps are involved in commonly used forms of backwater computation. To save this labor, the writers have devised two new approaches which are supplementary to the integration method.

In the first of these, from Eq. 8,

$$\frac{S_F}{S} = \frac{1}{f_1\left(\frac{y}{D}\right)} \quad \ldots\ldots\ldots\ldots\ldots\ldots\ldots\ldots (16)$$

Because S_F can be computed from given values of the discharge Q, and the diameter or size D, values of S for any given water depth can be determined from Eq. 16. Also, for given values of discharge and diameter the velocity head can be computed from the relationship,

$$\frac{\frac{V^2}{2\,g}\,(\text{full})}{\frac{V^2}{2\,g}} = \frac{h_F}{h_v} = f_3\left(\frac{y}{D}\right) \qquad \text{(17)}$$

in which h_v is the velocity head, and h_F is the velocity head of a full section.

Eqs. 16 and 17 are represented graphically in Fig. 5 for circular sections, S_F having been determined by the Manning formula. Table 4 facilitates the computations of slope when full and velocity head flowing full, as expressed in the following equations:

TABLE 4.—VALUES OF FACTORS IN EQS. 18

Diameter, D, in feet	Coefficients	
	a	b
1.0	787.8	25,173
1.25	239.8	10,311
1.5	90.68	4,972
1.75	39.84	2,684
2.0	19.55	1,573
2.25	10.43	982.2
2.5	5.944	644.4
3.0	2.248	310.8
3.5	0.9881	167.8
4.0	0.4846	98.33
4.5	0.2585	61.39
5.0	0.1474	40.28
5.5	0.08867	27.51
6.0	0.05575	19.42
6.5	0.03636	14.10
7.0	0.02450	10.48
7.5	0.01696	7.956
8.0	0.01202	6.146
8.5	0.008701	4.822
9.0	0.006410	3.837
9.5	0.004806	3.091
10.0	0.003656	2.517
10.5	0.002819	2.072
11.0	0.002199	1.719
11.5	0.001735	1.439
12.0	0.001383	1.214
12.5	0.001112	1.031
13.0	0.0009023	0.8814
13.5	0.0007376	0.7578
14.0	0.0006079	0.6553

$$\left.\begin{aligned} S_F &= a\left(\frac{Q}{1{,}000}\right)^2, \quad n = 0.013 \\ h_F &= b\left(\frac{Q}{1{,}000}\right)^2 \end{aligned}\right\} \qquad \text{(18)}$$

in which a and b are quantities evaluated in Table 4. Fig. 5 provides a scale to aid in computing the critical depth, a more complete version of which has been published elsewhere.[5] Detailed computation procedure is shown in Table 5.

Another method used for obtaining the energy slope and velocity head is the preparation of charts such as Fig. 6 for circular conduits. In Fig. 6, the heavy broken lines with arrowheads show the operations when the size, discharge, and depth of flow are specified. Backwater curves can be computed by the procedure shown in the following example (Table 5).

---

[5] "Hydraulics of Steady Flow in Open Channels," by Sherman M. Woodward and Chesley J. Posey, John Wiley & Sons, Inc., New York, N. Y., 1949, p. 42.

TABLE 5.—BACKWATER COMPUTATIONS BY THE STEP METHODS FOR A PIPE OF 72-IN. DIAMETER [a]

Method	Depth, y, in feet (1)	Ratio, $\frac{y}{D}$ (2)	Ratio, $\frac{h_F}{h_v}$ (3)	h_v, in feet (4)	$y + h_v$, in feet (5)	Ratio, $\frac{S_F}{S}$ (6)	Slope, $S \times 10^5$ (7)	Average $S \times 10^5$ (8)	$(S_{av.} - S_0)$ 10^5 (9)	Change in $y + h_v$ (10)	Δx in feet (11)	Station in feet (12)
First Step Method, Using Fig. 5	3.45[b]	0.575	0.352	1.412	4.862	0.395	362					
	3.55	0.592	0.378	1.314	4.864	0.433	330	346	246	0.002	0.8	0.8
	3.65	0.609	0.405	1.227	4.877	0.474	302	316	216	0.013	6.0	6.8
	3.75	0.625	0.431	1.152	4.902	0.511	280	291	191	0.025	13.1	19.9
	3.85	0.642	0.457	1.088	4.938	0.553	259	269	169	0.036	21.3	41.2
	4.00	0.667	0.498	0.997	4.997	0.618	231	245	145	0.059	40.7	81.9
	4.25	0.708	0.570	0.871	5.121	0.730	196	213	113	0.124	110	192
	4.50	0.750	0.642	0.773	5.273	0.833	172	184	84	0.152	181	373
	4.75	0.792	0.714	0.695	5.445	0.935	153	162	62	0.172	277	650
	5.00	0.833	0.790	0.628	5.628	1.025	140	147	47	0.183	389	1,039
	5.25	0.875	0.863	0.575	5.825	1.098	130	135	35	0.197	563	1,602
	5.50	0.917	0.923	0.538	6.038	1.150	124	127	27	0.213	790	2,392
	5.75	0.958	0.970	0.512	6.262	1.151	124	124	24	0.224	933	3,325
	Full	1.000	1.000	0.497	6.497	1.000	143	133	33	0.235	713	4,038
Second Step Method, Using Fig. 6	3.45[b]			1.40	4.85		355					
	3.60			1.27	4.87		320	337	237	0.02	8	8
	3.70			1.20	4.90		280	300	200	0.03	15	23
	3.80			1.13	4.93		270	275	175	0.03	17	40
	3.90			1.06	4.96		240	255	155	0.03	19	59
	4.00			1.00	5.00		230	235	135	0.04	30	89
	4.25			0.87	5.12		195	213	113	0.12	106	195
	4.50			0.76	5.26		170	183	83	0.14	169	364
	4.75			0.68	5.43		150	160	60	0.17	283	647
	5.00			0.62	5.62		140	145	45	0.19	422	1,069
	5.25			0.58	5.83		130	135	35	0.21	600	1,669
	5.50			0.55	6.05		125	127	27	0.22	814	2,483
	5.75			0.52	6.27		125	125	25	0.22	880	3,363
	Full			0.50	6.50		145	135	35	0.23	658	4,021

[a] In this example, $Q = 160$ cu ft per sec, and $S_0 = 0.001$. As computed from Eqs. 18 for use in the first step method, $S_F = 0.00143$, and $h_F = 0.497$. [b] Critical depth.

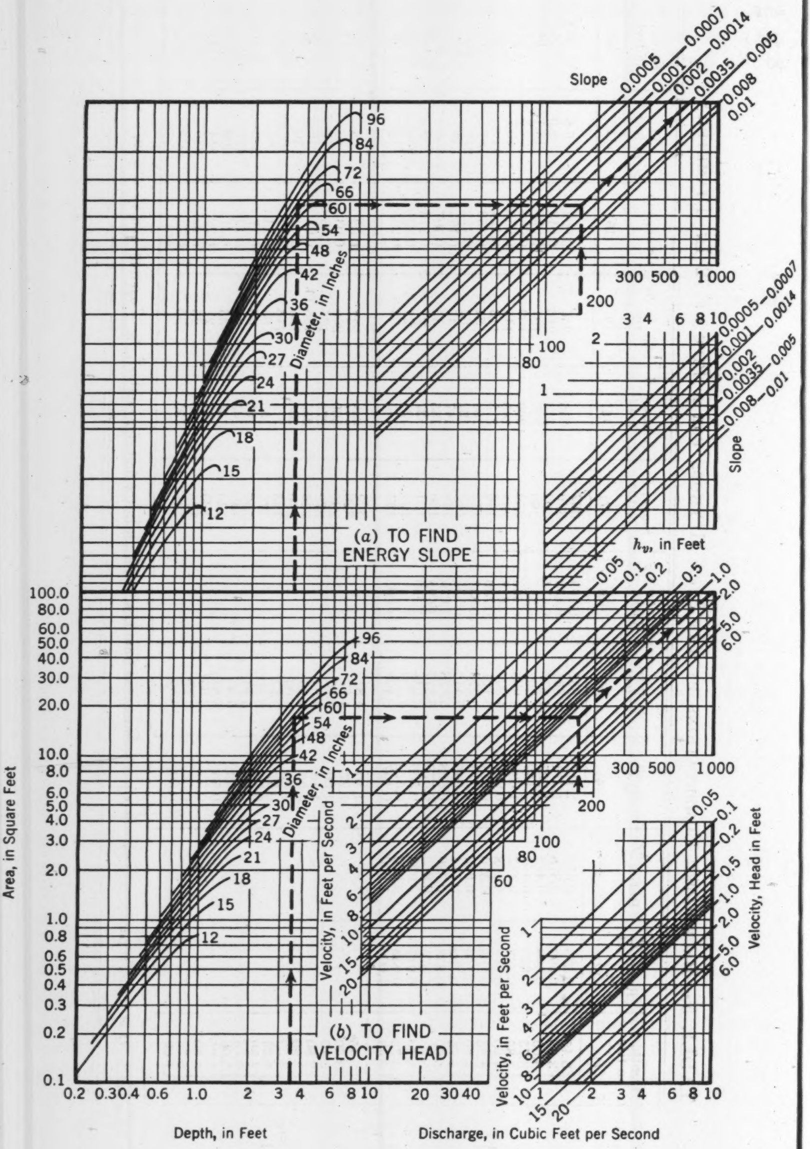

Fig. 6.—Elements of Flow in Circular Conduits Flowing Partly Full

ILLUSTRATIVE EXAMPLE

A circular conduit of 72-in. diameter has a discharge of 160 cu ft per sec, a bottom slope of 1 ft per 1,000 ft and a Manning friction factor of $n = 0.013$. The distance is to be determined between the control section at critical depth and the section at which the conduit becomes full. The discharge capacity Q_{cap} equals $\frac{1.486}{n} A_F R^{2/3}_F S^{1/2}_0$ or 134 cu ft per sec (with R_F denoting the hydraulic radius of full section). Since $Q/D^{5/2} = 1.82$, the critical depth is obtained from Fig. 5 as $\frac{y_c}{D} = 0.575$, or $y_c = 3.45$. The type of backwater curve is M_2 in which the water depth y is less than y_o but greater than y_c.

Integration Method.—From Eq. 12, $x_{1\rightarrow 2} = \frac{D}{S_0} (\Phi_2 - \Phi_1) - \frac{Q^2}{S_0 D^4} (\Psi_2 - \Psi_1)$. Also, $\alpha = \frac{160}{134} = 1.2$, $\frac{D}{S_0} = 6{,}000$ ft, and $\frac{Q^2}{S_0 D^4} = 19{,}960 \frac{\text{ft}^2}{\text{sec}^2}$. Thus, $x_{1\rightarrow 2} = 5{,}245 - 1{,}166 = 4{,}079$ ft.

Step Methods.—The computations using the first step method are shown in Table 5 with the aid of Fig. 5. The distance is $x_{1\rightarrow 2} = 4{,}038$ ft. The computations using the second step method appear in Table 5 with the aid of Fig. 6. This procedure yields a value of $x_{1\rightarrow 2}$ equal to 4,021 ft.

CONCLUSIONS

1. Most natural or artificial channels contain nonuniform flow. Uniform flow, which is usually assumed in making hydraulic computations, is actually rare. New methods are presented for solving nonunifiorm flow in prismatic channels, and the almost universal presence of nonuniform flow is emphasized.

2. Tables of backwater functions Φ and Ψ for circular conduits are presented in this paper. The computation of backwater curves is considerably shortened by the use of these tables, as demonstrated by the example. Tables could be prepared as needed for any other types of conduits.

3. The time-consuming step method computations of the energy gradient and the velocity head can be simplified by the two devices suggested in this paper. The writers believe these to have been heretofore unpublished. Both procedures require the preparation of charts beforehand. Fig. 5 will yield more accurate results than Fig. 6 although values in Fig. 5 are expressed as a percentage of those of the entire section, and one step of conversion is needed to determine the actual values. Furthermore, more labor is required in preparing Fig. 6 than Fig. 5. Therefore, the first method seems preferable. Charts similar to those used with the first method can also be prepared for open-channel sections; any convenient linear measure may be substituted for depth when full in closed conduits (for example, bottom width).

ACKNOWLEDGMENTS

The writers wish to express their grateful appreciation to A. L. Tholin, M. ASCE, chief sewer engineer, Bureau of Engineering, Chicago, Ill., for

his interest and suggestions, and to Nello DiGiusto and Leonard Wichmann for their valuable help in preparing this paper.

APPENDIX. NOTATION

The following symbols, adopted for use in the paper, and for the guidance of discussers, conform essentially to American Standard Letter Symbols for Hydraulics (ASA—Z10.2—1942), prepared by a Committee of the American Standards Association, with ASCE representation, and approved by the Association in 1942:

A = the area of the cross section, in square feet;
b_w = the top width of the water surface, in feet;
D = diameter of the conduit, in feet;
g = acceleration produced by gravity;
h_F = the velocity head when flowing full, in feet;
h_v = the velocity head, in feet;
i,m = numerical exponents;
$k = \frac{1.486}{n} A R^{\frac{2}{3}}$, the conveyance of a cross section:
    k_F = the conveyance at a full section;
    k_o = the conveyance at normal depth;
n = Manning's coefficient of roughness;
Q = discharge, in cubic feet per second;
    Q_c = discharge when flow is at critical depth;
    Q_{cap} = capacity of conduit flowing full, with the slope of the energy gradient equal to the bottom slope;
R = the hydraulic radius;
S = the slope of the energy gradient:
    S_F = the slope of the energy gradient when the discharge is flowing through a full section;
    S_{av} = the average value of the slope of the energy gradient at the two ends of a reach;
    S_0 = slope of the invert or bottom;
V = the average velocity in a section, in feet per second;
x = the distance, in feet, measured upstream;
$x_{1\rightarrow 2}$ = a specific reach;
y = the depth of flow, in feet:
    y_o = the depth of normal flow, in feet;
    y_1, y_2 = flow depths at specific sections;
    y_c = critical depth;
α = the ratio of the discharge to the capacity of a conduit flowing full; and
Φ, Ψ = backwater functions.

DISCUSSION

Francis F. Escoffier,[6] A. M. ASCE.—The computation of water-surface profiles in circular conduits has always been difficult and laborious. The authors have prepared tables of functions that will greatly facilitate these computations. However, the use of these functions in the manner outlined in the paper involves the disadvantage that it is necessary to begin with a known or assumed depth and to solve for the reach length. Usually, in engineering practice, the length is given and the depth is to be computed, and therefore several trials are ordinarily required before a solution can be obtained. Such a disadvantage is readily overcome by means of the graphical construction shown in Fig. 7. In this diagram, the function Ψ has been plotted as the ordinate. The function Φ is the abscissa in the left-hand part of the diagram, and the depth variable $J = y/D$ is the abscissa in the right-hand part.

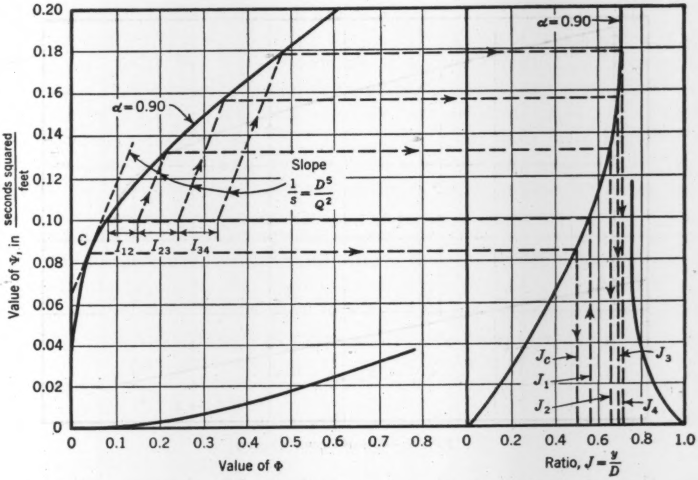

Fig. 7.—Graphical Construction

The graphical solution included in the diagram is that for the drop-down curve shown in Fig. 8. To understand the solution it is only necessary to consider that, if Eq. 12 is multiplied through by S_0/D, there is obtained the result—

$$I = \Phi_2 - \Phi_1 - s\,(\Psi_2 - \Psi_1) \ldots\ldots\ldots\ldots\ldots (19a)$$

in which

$$I = \frac{S_0\, x_{1 \to 2}}{D} \ldots\ldots\ldots\ldots\ldots\ldots\ldots\ldots (19b)$$

and

$$s = \frac{Q^2}{D^5} \ldots\ldots\ldots\ldots\ldots\ldots\ldots\ldots (19c)$$

---

[6] Hydr. Engr., Corps of Engrs., U. S. Dept. of the Army, Mobile, Ala.

For the purposes of this discussion, Eq. 19*a* is rearranged in the form:

$$I = (\Phi_2 - s\,\Psi_2) - (\Phi_1 - s\,\Psi_1) \qquad (20)$$

A given value of $\Phi - s\,\Psi$ appears in the left-hand part of the diagram as a line having a slope $1/s$; Eq. 20 indicates that the horizontal distance between the two successive lines there represented is equal to I. It is believed that the procedure is self-explanatory. Critical depth occurs at the point where the tangent to the curve has a slope equal to $1/s$.

The statement made by the authors (under the heading, "Numerical Integration: Equation for Nonuniform Steady Flow") that the backwater functions Φ and Ψ cannot be used in a conduit with a slope equal to the critical slope is not correct. The only difficulty is that, as the water-surface profile passes through normal depth (and simultaneously through critical depth), it is necessary to pass from the asymptote of one curve to that of the other. This inconvenience could be liminated by displacing the two curves vertically so as to make their asymptotes coincide.

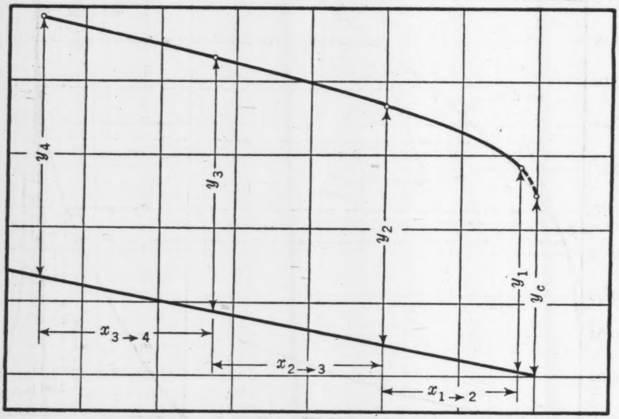

FIG. 8.—DROP-DOWN CURVE

HENRY J. MILES,[7] A. M. ASCE.—The writer was particularly interested in the first part of the paper which is concerned with numerical integration because he had used a similar method in his doctoral dissertation.[8] Referring to Eq. 12, the writer expressed the functions Φ and Ψ in terms of S_F

---

[7] Prof. of Hydr. Eng., Agri. and Mech. College of Texas, College Station, Tex.

[8] "New Methods of Analyzing Steady Flow in Open Channels," by Henry J. Miles, thesis presented to Rutgers University, New Brunswick, N. J., in 1950, in partial fulfilment of the requirements for the degree of Doctor of Philosophy.

instead of S_0, obtaining

$$x_{1\rightarrow 2} = \frac{D}{S_F}\,(A_2 - A_1) - \frac{V^2}{2\,g}\,(\text{full})\,(B_2 - B_1) \quad \text{.........} \quad (21a)$$

which reduces to

$$x_{1\rightarrow 2} = \frac{D}{S_F}\,(A_2 - A_1) - \frac{Q^2}{S_F\,D^4}\,(B_2 - B_1)\,\frac{16}{\pi^2\,2\,g} \quad \text{........} \quad (21b)$$

in which $A = f_1\left(\frac{y}{D}, \frac{S_0}{S_F}\right)$ and $B = f_2\left(\frac{y}{D}, \frac{S_0}{S_F}, \frac{V^2/2\,g}{V^2\,(\text{full})/2\,g}\right)$, which are the reciprocals of those functions shown in Fig. 5. As far as could be determined when the writer first presented these ratios, their use was novel. The authors' statement (under the heading, "Backwater Curves in Uniform Channels by the Step Method") that they had "devised two new approaches" was an interesting confirmation of the writer's opinion.

After developing this method for circular pipes, the writer applied it also to rectangular channels. This procedure was supplemented by a graphical solution to aid in the application of the backwater function.

The authors are to be complimented for making a valuable tool available to the engineering profession. The writer can appreciate from his own experience the immense volume of work involved in preparing a table of functions as complete as the unabridged versions of the authors' backwater functions.

RICHARD SILVESTER.[9]—Graphs and a nomograph which are helpful in computing water-surface profiles with nonuniform flow for various channel shapes, including circular channels and U-shaped channels, have been published elsewhere by the writer.[10,11] Values of $K = 1.486\ AR^{2/3}$ were graphed against depth, y, for certain channel shapes with various bottom widths. Similarly, values of $M = \sqrt{A^3/b_w}$ were plotted on the same graphs for substitution in the nonuniform equation,

$$\frac{dy}{dx} = \frac{S_0 - \left(\frac{Q\,n}{K}\right)^2}{1 - \frac{Q^2}{g\,M^2}} = \frac{S_0 - S}{1 - S_v} \quad \text{...............} \quad (22)$$

in which S_v is the velocity component $Q^2/(g\,M^2)$. Eq. 22 and Eq. 3 are similar except for sign convention. In Eq. 22, dx is positive measured downstream and dy is positive for an increase in depth downstream (negative for a decrease).

The graph of K and M for circular channels and U-shaped channels is shown in Fig. 9. Numerals on the curves of Fig. 9 indicate U-values and D-values, in feet. Solution of the terms $(Q\,n/K)^2$ and $Q^2/(g\,M^2)$ is facilitated by a nomograph (Fig. 10). Figs. 9 and 10 are intended for use with step computations. It is recommended that, when the limits of the profile have been determined, the stage variation be divided into a number of increments which are variable, the

---

[9] Lecturer in Civ. Eng., The Univ. of Western Australia, Nedlands, Australia.

[10] "Flow in Open Channels," by Richard Silvester, *Journal*, Inst. of Engrs., Australia, Vol. 25, 1953, p. 155.

[11] "New Graphs Aid Open Channel Calculations," by Richard Silvester, *Water Power*, September, 1954, p. 338.

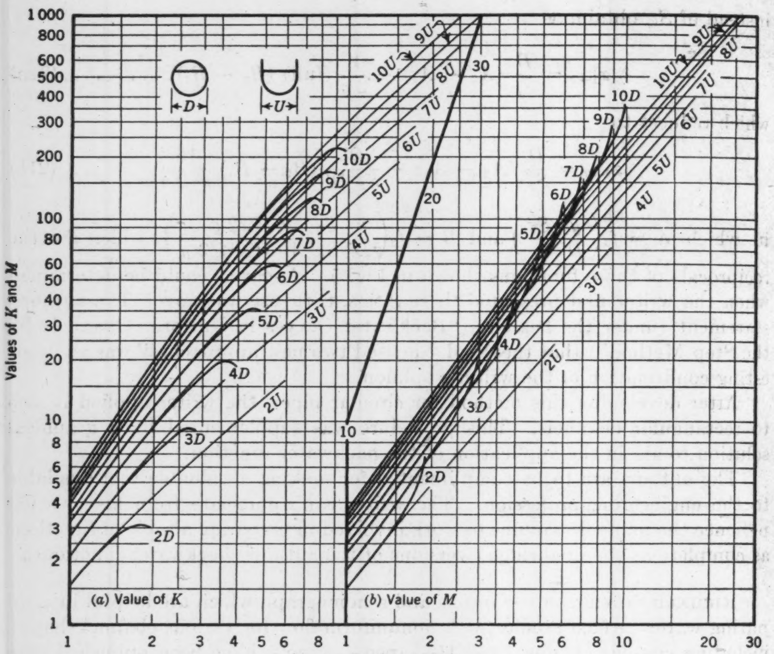

FIG. 9.—VALUES OF K AND M

smallest being near the critical depth. The writer's solution of the "Illustrative Example" is as follows:

As $M_c = Q/\sqrt{g} = 28.2$, $y_c = 3.45$ ft (Fig. 9). From Table 6 (commencing the computations at a depth of 3.6 ft), the total length is 3,841 ft. This resulting length is less than that given by the authors. By using smaller increments in y, this discrepancy would be reduced. The negative sign obtained for dy/dx in Table 6 indicates a decrease in depth downstream as required by the M_2-curve.

TABLE 6.—BACKWATER COMPUTATIONS

Depth, y, in feet	Increment, dy, in feet	Conveyance, K	M	Slope, S	Slope, S_v	$S_0 - S$	$-\frac{dy}{dx}$	Increment, dx, in feet
3.6	0.1	36.3	31	0.0033	0.89	0.0023	0.0209	5
3.7	0.1	38	33	0.003	0.82	0.002	0.0111	9
3.8	0.1	39.7	35	0.0027	0.7	0.0017	0.00567	35
4.0	0.2	44	38	0.0023	0.62	0.0013	0.00342	59
4.2	0.2	46	41	0.0021	0.51	0.0011	0.00225	89
4.4	0.2	49	45	0.0018	0.43	0.0008	0.0014	143
4.6	0.2	51	49	0.00163	0.38	0.00063	0.00102	196
4.8	0.2	54	54	0.00147	0.31	0.00047	0.00068	294
5.0	0.25	57	60	0.0013	0.24	0.0003	0.000395	633
5.25	0.25	58	69	0.00128	0.19	0.00028	0.000346	722
5.5	0.25	59	78	0.00125	0.15	0.00025	0.000294	850
5.75	0.25	58	97	0.00128	0.095	0.00028	0.00031	806

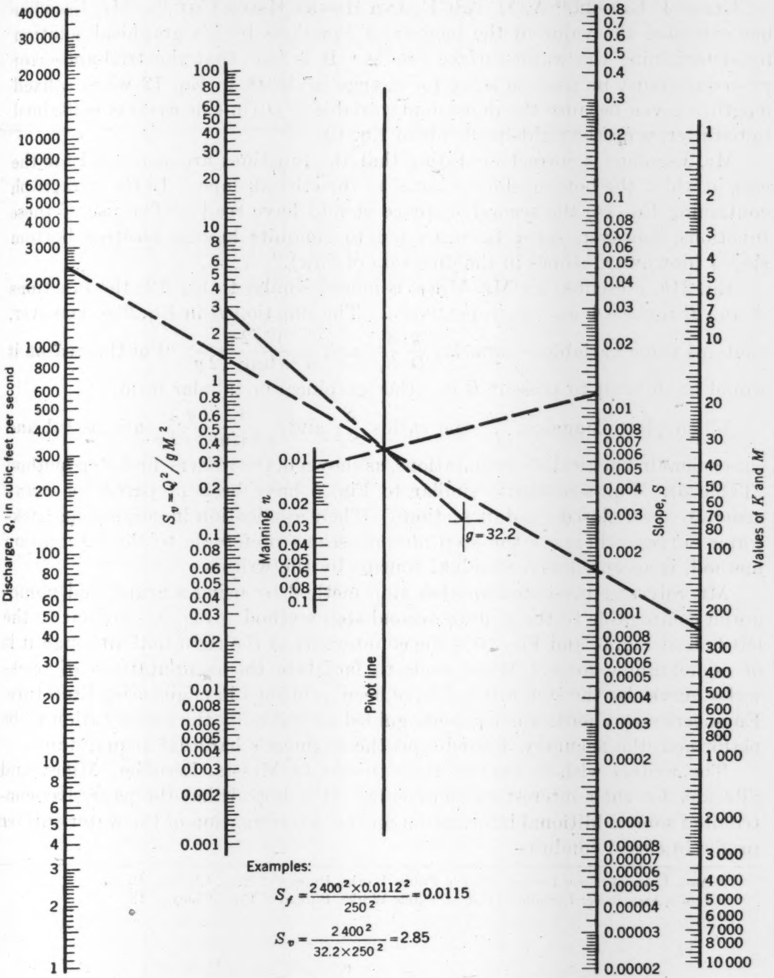

FIG. 10.—NOMOGRAPH FOR BACKWATER CURVES

Although the writer's procedure may require a little more time than substitutions into the authors' graphs and tables, the former gives a better over-all representation of the profile. One can see at a glance the depth at any distance along the curve. The long distances occurring near the normal depth for small increases or decreases of depth are at once apparent; results for design purposes are thus more easily modified.

Clint J. Keifer,[12] A. M. ASCE, and **Henry Hsien Chu**.[13]—Mr. Escoffier has extended the value of the backwater functions by his graphical solution for determining the water-surface profile. It is true that the trial-and-error procedure must be used to solve for change in depth in Eq. 12 when a fixed length is given because the dependent variable y/D (in this case) is contained in both terms on the right-hand side of Eq. 12.

Mr. Escoffier is correct in stating that the functions are also valid for the case in which the bottom slope is equal to the critical slope. In the paragraph containing Eq. 14, the second sentence should have read—"The use of these functions, however, must be restricted to conduits having positive bottom slopes (downward slopes in the direction of flow)."

Eq. 21*b*, presented by Mr. Miles, is indeed similar to Eq. 12; the functions A and B replace Φ and Ψ, respectively. The function B in Eq. 21*b*, however, contains three variables—namely, $\frac{y}{D}$, $\frac{S_0}{S_F}$, and $\frac{V^2/2\,g}{V^2\,(\text{full})\,/2\,g}$. For this reason it would be difficult to present B in either graphical or tabular form.

When plotted against $\frac{y}{D}$, the ratios $\frac{S}{S_F}$ and $\frac{V^2/2\,g}{V^2\,(\text{full})\,/2\,g}$ are useful and convenient in backwater computations, as shown in the writers' first step method (Table 5). Full-size charts similar to Fig. 5 have been prepared for many generally used closed conduit sections. Their application in computing backwater curves, whenever the step method seems preferable to the integration method, is accepted as a standard routine by the writers.

Mr. Silvester presented another step method by using a graph and nomograph comparable to the writers' second step method. Fig. 9 is similar to the left half of Fig. 6, and Fig. 10 is the counterpart of the right half although it is of nomographic form. Many tools to facilitate the computations of backwater curves by the step method have been published in engineering literature. Engineers may choose among them, guided probably by the computation to be performed, the accuracy desired, and the engineer's habitual acquaintance.

The writers wish to express their thanks to Messrs. Escoffier, Miles, and Silvester for their interesting comments. It is hoped that the paper has contributed some additional information on the determination of the water-surface profile in closed conduits.

---

[12] Asst. Engr. of Sewer Design, Dept of Public Works, Bureau of Eng., Chicago, Ill.

[13] Senior Asst. Sewer Designer, Dept. of Public Works, Bureau of Eng., Chicago, Ill.

AMERICAN SOCIETY OF CIVIL ENGINEERS
Founded November 5, 1852
TRANSACTIONS

Paper No. 2749

COMMUNITY AND NEIGHBORHOOD DEVELOPMENT

By Russell H. Riley,[1] M. ASCE

Synopsis

With West Palm Beach, Fla., as an example, it is shown how an existing city can be expanded and improved in a logical manner. This expansion is facilitated by the development of neighborhoods—the basic units of urban life. The requirements for a residential neighborhood are reviewed; how an old area can be improved within its existing framework is shown. Existing planned communities are cited; the experience gained from their planning was used as a basis for the plan to improve West Palm Beach.

Introduction

Communities are as old as civilization itself. From the time when men were forced to band together for mutual protection against their common enemies, people have adapted themselves to living together in cities, towns, and hamlets.

There are many people who state and sincerely believe that the majority of communities are unplanned. This is true in the sense that their physical development has not been directed by an official or accepted master plan. However, these communities actually have grown in accordance with a multiplicity of plans produced by individuals, corporations, and public agencies—each of which was primarily concerned with finding a solution for its particular problem, not with the effect of the solution on the rest of the community.

In relatively few instances the efforts of a dynamic individual have been used to create the complete physical form of a community at the outset of its development, as was the case at Miami Beach, Fla. However, no one could have foreseen the economic changes and technological developments in the United States that have made it possible for thousands of people to enjoy the attractions of this resort; the original conception of the city as a winter refuge for relatively few persons is completely altered. Coral Gables, Fla., is a

---

Note.—Published, essentially as printed here, in September, 1953, as *Proceedings-Separate No. 285.* Positions and titles given are those in effect when the paper was received for publication.

[1] Partner, Harland Bartholomew & Associates, St. Louis, Mo.

similar example of a preplanned community. In contrast, Miami, Fla., has grown haphazardly by the accretion of hundreds of real estate subdivisions.

THE NEIGHBORHOOD CONCEPT

The relationship of neighborhoods to a community might be compared to the relationship of a room to a house. No one would envision building a house without some kind of a plan which allocates space within the structure to various functional uses, such as sleeping, eating, lounging, and homemaking activities. The arrangement of the individual rooms is similar to the selection of locations for schools, parks, shopping centers, churches, and the other physical adjuncts of a residential neighborhood. Although this comparison may be an oversimplification, it may explain the significance of neighborhoods in community planning.

It should be emphasized that the neighborhood concept is based on physical planning rather than on social planning. The concept includes the planning of schools, parks, streets, and shopping areas that will improve the livability and usefulness of the neighborhood.

Realization of the importance of planning the neighborhood is of more recent origin than that of over-all planning for a city, region, county, or other political subdivision. When the regional plan for New York, N. Y., was prepared[2,3] (1922–1929) a special study of the problems of neighborhood development was included as an important part of the survey. The theories of neighborhood planning and the practical applications developed in this study were well expressed.

It is generally understood that in planning cities the term, "neighborhood," denotes a village or local community in a metropolitan area or a smaller residential unit within a city. However, there are also planned industrial districts or industrial neighborhoods that must be properly fitted into the over-all community plan just as residential neighborhoods must be integrated with the larger urban area. These industrial areas are found in many cities—for example, the Fairfax industrial district in Kansas City, Kans.; the rapidly growing Trinity River industrial district in Dallas, Tex.; and several other successful developments in Chicago, Ill. These districts are effective in meeting the requirements of modern industrial development and in preserving usefulness and values over a long period of time.

Regional shopping centers have also been developed in many parts of the United States. Confronted with serious deficiencies in parking space within cities and with the relocation of many potential customers to the suburbs, promoters of these enterprises have built carefully planned store groups surrounded by large parking fields in the country. Several of these commercial developments are being operated successfully; others are under construction, and plans are being prepared for still more (as of 1954). This type of development constitutes a special kind of neighborhood for purposes of planning; the effect on the established street and highway pattern in the vicinity sometimes creates difficult traffic problems.

---

[2] "Regional Survey," by the Committee on Plan of New York and Its Environs, New York, N. Y., 1927–1931, Vols. 1 to 8.

[3] "Regional Plan," by the Committee on Plan of New York and Its Environs, New York, N. Y., 1929–1931, Vols. 1 and 2.

Basic Requirements of Residential Neighborhoods

A residential neighborhood is usually that part of a community which is served by an elementary school. This is a logical definition for almost everyone has a deep interest in the schools attended by their children. The school thus becomes a focal point of the neighborhood—in fact, it is usually the place where neighborhood meetings are held. To be completely self-contained, each neighborhood should also include a park (which preferably should adjoin the school ground), churches, a community center, and a shopping center.

The plan of the city's main thoroughfares to a large extent determines the geometric shape of the neighborhood, and the population density influences its size. The residential neighborhood should be bounded by major streets. For maximum convenience and protection for the residences these streets should carry large volumes of through traffic and fast-moving local traffic and the interior streets should carry local traffic. In single-family districts elementary schools normally serve an area of 1 sq mile; therefore, the major streets should be 1 mile apart. Such spacing is frequently encountered in the outlying sections. Toward the center of the city the major streets are closer together, and the neighborhood may be bisected by a thoroughfare. Although it does not result in maximum advantages, this street plan does not create an impossible condition. Furthermore, population densities invariably increase toward the center of the city, and therefore a smaller neighborhood area will be served by each elementary school. The possibilities of creating homogeneous neighborhoods should be a dominant consideration in major-street planning because the streets divide the city into cells which are the basis of the neighborhoods.

It should be noted that the shapes of some cities prevent the creation of sound residential neighborhoods. For example, several cities along Florida's east coast have developed as long narrow urban strips parallel to the Atlantic Ocean. Because the predominant traffic movement is in a north–south direction, almost all the north–south streets carry large volumes of traffic. Therefore, too much residential property is close to the major streets, and several heavily used streets must be crossed by children to reach elementary schools. The major relief that can be provided for these communities is the development of by-pass routes around areas which carry through traffic, especially large trucks.

The physical form of cities has been profoundly affected by the extraordinary growth and use of the automobile. The concentration of heavy traffic on major city streets has undoubtedly been the greatest influence that has stimulated interest and activity in neighborhood planning. The construction of highways and expressways in urban areas has made possible the expansion of communities to a degree undreamed of in the era of street-railway transportation. Communities have grown enormous; it is not uncommon for people to drive 15 miles or more from their homes to their places of employment. The term, "urban sprawl," has been used to describe the unplanned confusion of urban expansion. It is within the suburbs of these areas that the most effective results can be obtained in neighborhood planning.

Some desirable requirements for good residential neighborhoods not previously mentioned include uniformity in the type of land use and in the general character of improvements. Some persons have advocated intermingling different types of residences in a single neighborhood—primarily to encourage democratic practices. This objective is important, but experience does not indicate that intermingling will maintain value and character satisfactorily or facilitate the planning of the many physical facilities necessary to serve the residences.

The adoption and enforcement of sound zoning regulations best assure the proper land-use pattern, and private-deed restrictions can be used to secure and maintain a uniform character of improvements. There should also be an influential neighborhood association whose membership should include all residents of the area and whose activities and responsibilities should be assumed by duly elected officers.

Possible Improvements in Older Neighborhoods

As previously indicated, the best results in neighborhood planning can be accomplished in new developments. However, substantial parts of larger cities contain residential developments that are depreciating in character and value; these areas exert a major influence on the future welfare of the entire city.

There are many remedial measures that can be applied to restore or improve "in town" neighborhoods, but, at best, it is a slow and difficult task to correct mistakes in land use and to revive formerly attractive residential environments. A major problem is that, although many residences are structurally sound, they are obsolete from the standpoints of size and modern requirements. Some remedies that can be applied in these older areas include:

1. Revising the zoning ordinances to give more protection to established homes. This can sometimes be done by reducing the area of commercial zones or multiple-dwelling zones to coincide more nearly with actual conditions and requirements.
2. Adopting and enforcing minimum housing standards that require either rehabilitation or removal of unsanitary, substandard homes.
3. Modernizing elementary schools and providing adequate playground and recreational space designed and landscaped in such a manner as to add to the attractiveness of the neighborhood.
4. Discouraging the use of residential streets by through traffic by making them discontinuous and narrow. Conversely, one might attract traffic to the main thoroughfares adjoining the neighborhood by improving these main routes.
5. Requiring the provision of off-street parking space near all new structures.
6. Encouraging the formation of neighborhood protective associations for the purpose of persuading each owner to maintain his property.

In neighborhoods where deterioration and obsolesence have resulted in slum conditions, nothing short of complete replanning and rebuilding will suffice. This, of course, is a complicated and difficult procedure. In addition to the serious problems encountered in relocating displaced families in the area, there are many legal and financial problems to be overcome.

Fortunately, Title I of the United States Housing Act of 1949[4] provides a workable solution to these problems. Under the terms of this law a local agency can be created to select areas to be redeveloped, plan for their future use, and receive financial aid from the federal government for rebuilding. This aid is usually in the form of loans and grants, which are designed to make possible a re-use value attractive enough to induce private enterprises to acquire land from the public agency and rebuild it in accordance with approved plans. Many communities throughout the United States are engaged in these urban redevelopment projects.

EXAMPLES OF NEIGHBORHOOD PLANNING

The neighborhood concept is old enough so that many examples of its benefits and advantages can be found. Almost all large cities have residential areas that are twenty years old, in which the houses are still in good condition and are desirable to present or prospective owners.

Probably one of the most outstanding examples of large-scale neighborhood development is one in Kansas City. The original area was known as the "country club district"; the development has since expanded over extensive areas in both Missouri and Kansas. The important features of this neighborhood development are its excellent system of major streets and parkways, its parks, school grounds, and neighborhood shopping centers. In addition, minor streets are well planned for residential service, all areas are protected by comprehensive deed restrictions, and there are active neighborhood associations. The character and value of these developments attest to the potentialities of sound neighborhood planning.

Several entirely new communities have been developed in which special attention was given to neighborhood design. Some of these were government projects, such as the experimental "Greenbelt Towns" developed during the 1930's and the communities made necessary by World War II. Other new communities have been developed by industries and private corporations. Among those that have attracted much attention is the suburban community of Park Forest in Chicago. By conforming to sound standards, the value and usefulness of these communities should be maintained over a long period of time.

There are many examples of sound neighborhood planning and development in the Miami area. As is usually the case, most of these are suburban communities. One good example is the community of Coral Gables, which is recognized for its good residential character. The design of the major-street system and the many restrictions controlling the type and character of residential development have been prime factors in maintaining its desirability. Another community of excellent residential character is Bal Harbor, Fla., which is north of Miami Beach.

Although Miami Beach is long and narrow, it contains extensive residential sections (particularly on the many islands) which are well protected and outstanding in character. Most of these sections are smaller than the theoretical standard and, although they are not always near schools, their excellent

---

[4] *Public Law 171*, **81st Cong., 1st Session, Chapter 338, Section 1070.**

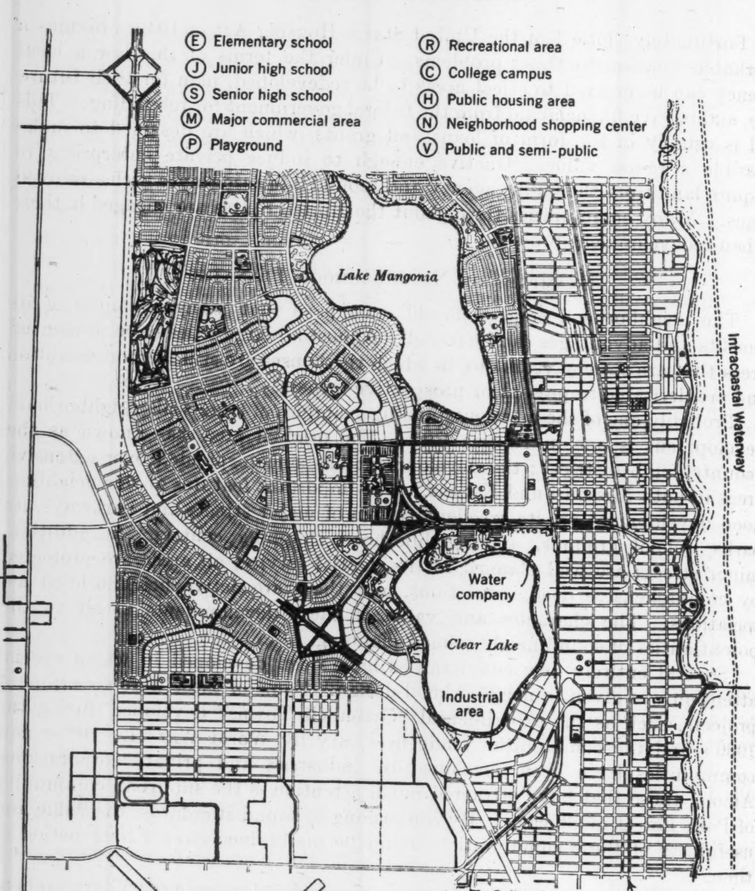
Ⓔ Elementary school
Ⓙ Junior high school
Ⓢ Senior high school
Ⓜ Major commercial area
Ⓟ Playground
Ⓡ Recreational area
Ⓒ College campus
Ⓗ Public housing area
Ⓝ Neighborhood shopping center
Ⓥ Public and semi-public
Lake Mangonia
Intracoastal Waterway
Water company
Clear Lake
Industrial area
Railroad
Railroad
Palm Beach International Airport

FIG. 1.—WESTWARD EXPANSION OF WEST PALM BEACH, FLA.

character reflects the important advantages of protection from through traffic and from other adverse influences. These areas show that many benefits can be realized even though all the requirements for a good neighborhood are not obtainable.

NEIGHBORHOODS IN A FLORIDA CITY

It has been noted that difficult problems are encountered in providing sound residential neighborhoods in some cities along the east coast of Florida because they have long, narrow, urban patterns. Such a community, West Palm Beach, is shown in Fig. 1.

Urban development within the corporate limits of West Palm Beach extends for approximately 8 miles in the north–south direction whereas in the east–west direction it varies in width from ¾ mile to 1⅓ miles. US 1 traverses the city in a north–south direction, and therefore much through traffic—both truck traffic and passenger-vehicle traffic—traverses the area, especially during the winter season. As a result, most continuous north–south streets are used as major thoroughfares and carry large volumes of through traffic and local traffic. Another problem is caused by the fact that most streets have narrow right of ways; widening of streets is expensive, and so one-way traffic movement has been established along certain routes.

This narrow area is traversed and bounded by two important railroads; industrial development adjoins a substantial part of the railroad right of ways.

It is immediately obvious that there is little or no opportunity to develop modern single-family neighborhoods in this area. There are too many major streets, and the industrial development scattered along the railroads establishes barriers or wedges in residential sections. Many children are forced to cross heavily traveled streets or railroads to reach school facilities. Even with these adverse conditions, many residential developments have maintained a satisfactory character. This may be partly the result of the importance of West Palm Beach as a resort community and also the result of its rapid growth.

In 1951 the community was confronted with an unusual opportunity to develop a vacant tract of more than 4,500 acres, the nearest part of which is only 1,600 ft from the central business district. This large area is located northwest of the urban development and is immediately adjacent thereto. It is primarily owned by a water company which acquired its holdings to protect the surface water supply in two lakes, Lake Mangonia and Clear Lake. A small part of the area is owned by the City of West Balm Beach. Subsequent and contemplated projects of the Central Southern Flood Control District have assured an adequate supply of surface water so that the area could be intensively developed (subject to the requirements for the improvement and protection of the lakes for storage purposes). The city and the water company agreed to finance studies for designing the development of this area.

The proposed plan is shown in Fig. 1. Of particular importance is the proximity of the area to, and the integration with, the existing urban patterns. An important improvement will be the relationship of the by-pass expressway (US 1) to the project and to the remainder of the community. This expressway should afford substantial relief to the street pattern in the city.

The proposed major-street pattern in the new area will provide space for large, compact residential areas, within which minor streets have been designed to discourage through traffic and other large movements of vehicular traffic. Although major streets are not always 1 mile apart, it must be remembered that this area is close to the central business district.

The proposed school sites are large areas that will actually serve as combined school grounds and neighborhood parks. Furthermore, these sites are removed from the heavily traveled streets; in only a few instances will elementary-school children be required to cross major throughfares.

The area between the two lakes is proposed for intensive development because of its proximity to the central business district. Here would be located apartment buildings and other forms of multiple dwellings, resort hotels, and a large shopping center conforming to modern standards. There are also provisions for recreational facilities that would be of interest and value to the entire urban area.

Of course, many problems in the dredging, filling, drainage, and installation of other physical improvements were encountered. The important facts are that the problems can be solved and that the estimated costs indicate that the entire project is financially practicable.

The water company, which has the largest land holding, has decided (as of 1954) not to initiate the improvements but has instead offered to sell its entire properties (including the land) to West Palm Beach, Palm Beach, or both, or to sell only the water treatment and distribution facilities. The offer is also extended to any legally established governmental agency in the area affected, and steps are being taken (as of 1954) to have the legislature create a new water district. In the event that neither of the communities nor any official agency accept the offer, the company has announced its desire to sell all its local holdings, including the land, to any private corporation. Thus, consummation of the project seems entirely probable, and there is no reason why the project cannot conform to modern standards and prove of inestimable value to the existing urban area.

CONCLUSIONS

Neighborhoods are the core around which cities exist. These neighborhoods are normally centered about the elementary schools; for this reason schools should be located so that they are easily accessible to the children who attend them. Neighborhoods are therefore normally delineated by major thoroughfares. Of course, it is a relatively easy problem to plan and develop new communities, but the planning for the improvement of existing cities is a challenging task. One must investigate not only the basic requirements of a neighborhood but also the possible (and impossible) improvements.

AMERICAN SOCIETY OF CIVIL ENGINEERS
Founded November 5, 1852
TRANSACTIONS

Paper No. 2750

TOTAL SEDIMENT LOAD MEASURED IN TURBULENCE FLUME

BY PAUL C. BENEDICT[1] AND MAURICE L. ALBERTSON,[2]
MEMBERS, ASCE, AND DONALD Q. MATEJKA,[3]
J. M. ASCE

WITH DISCUSSION BY MESSRS. W. H. CORBETT, O. C. HANSEN, AND W. M. BORLAND; AND PAUL C. BENEDICT, MAURICE L. ALBERTSON, AND DONALD Q. MATEJKA

SYNOPSIS

The results of significant model tests in a glass-walled flume and prototype tests of a turbulence flume are presented. The velocity of flow and the transportation of the total sediment load in suspension were observed under varying conditions of flow. Also noted was the resistance to flow caused by vertical baffles, which were fastened to the floor of the flume. The prototype tests consisted of observations at the measuring sill of velocity and sediment concentration for all flows. For normal flows observations were made upstream and downstream from the flume. Samples of total sediment load and bed material were analyzed for particle size. Minor studies of dune movement in model and prototype were also included.

NOTATION

The letter symbols adopted for use in this paper are defined where they first appear, in the illustrations or in the text, and are arranged alphabetically for convenience of reference in the Appendix.

INTRODUCTION

The proper development of river-control structures, particularly those constructed in alluvial channels, requires data on the total sediment discharge of streams. The suspended load for most streams can be readily determined with

---

NOTE.—Published, essentially as printed here, in August, 1953, as *Proceedings-Separate No. 230.* Positions and titles given are those in effect when the paper or discussion was received for publication.

[1] Regional Engr., Geological Survey, U. S. Dept. of the Interior, Lincoln, Nebr.

[2] Prof. of Civ. Eng. and Head of Fluid Mech. Research, Colorado Agri. and Mech. College, Fort Collins, Colo.

[3] Hydr. Engr., Geological Survey, U. S. Dept. of the Interior, Lincoln, Nebr.

standard sampling equipment, except where the debris load prevents the water-sediment mixture from entering the intake nozzle at stream velocity. The bed load, or remainder of the total load, however, cannot be measured satisfactorily with available (1954) sampling equipment. The concentration and particle-size distribution in the vertical section (from point-integrated, suspended-sediment samples) are factors in bed-load movement, but the rate of movement cannot be determined with assurance from this qualitative information. The deficiency of information on rates of bed-load movement in natural streams became acute in 1948 in connection with the sedimentation investigations in the Loup River basin in Nebraska (Fig. 1). Construction of the flume was begun in October, 1948; the flume was finished in May, 1949; and the recording-gage installation was completed in August, 1949. Basic data were first collected on June 4, 1949.

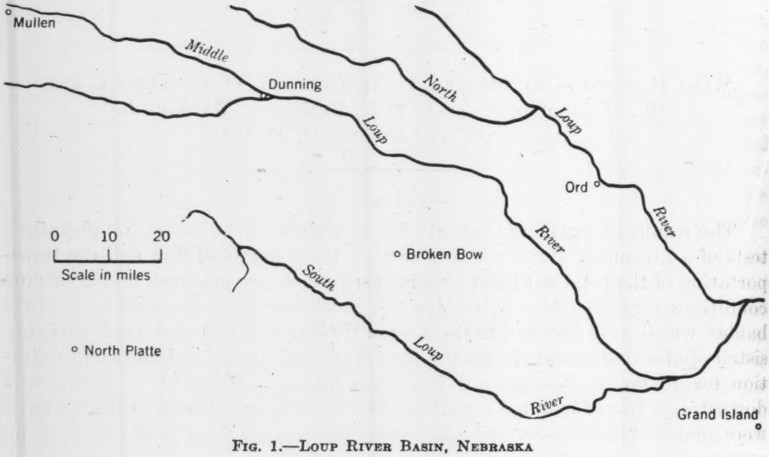

FIG. 1.—LOUP RIVER BASIN, NEBRASKA

A convenient site for the flume was found in a reach of the Middle Loup River at Dunning, Nebr. This site was considered satisfactory for the following reasons:

1. The flume site was downstream from a proposed reservoir and upstream from a proposed diversion structure.
2. The stream characteristics were considered to be rather typical of the sand-hill area (Fig. 2).
3. The stream flow was uniform and had no sharp peaks caused by precipitation or snow melt.
4. The stream was flowing on a sand bed of considerable depth.
5. The sediment in transport consisted principally of medium to fine sand.
6. The information to be obtained could be used as a basis for studies of the total sediment load at other sediment-measuring stations in the Loup River basin and in other areas where similar conditions existed.
7. The operation costs and construction costs were at a minimum.

There are few stream channels in the sand-hill area of Nebraska because the infiltration rate is high. The drainage area of the Middle Loup River at Dunning is 1,760 sq miles; however, only approximately 80 sq miles contribute directly to the surface runoff. The stream flow comes from ground-water sources and is uniform except during periods of high precipitation. The maximum daily water discharge during the period of record (1945 to 1950) was 821 cu ft per sec; the minimum discharge was 220 cu ft per sec. The stage-discharge relationship is very unstable as the stream bed is composed of erodible material. A typical particle-size distribution of bed material is shown in Fig. 3 as a dashed curve.

DESIGN AND MODEL STUDIES

The most comprehensive laboratory studies of bed-load movement were described by G. K. Gilbert[4] in 1914. Following Mr. Gilbert's report, investigations by M. P. O'Brien,[5] L. G. Straub,[6] Hans Kramer,[7] H. A. Einstein,[8] Members, ASCE, Herbert D. Vogel and John Paul Dean,[9] and European engineers[10,11,12] have added much information to the problem of bed-load movement.

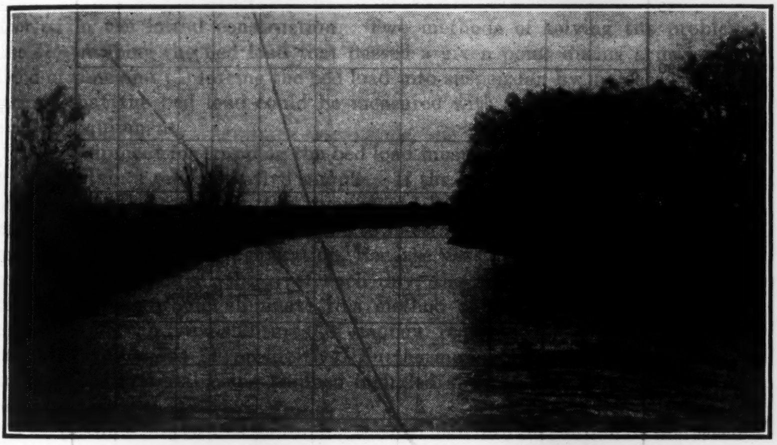

FIG. 2.—MIDDLE LOUP RIVER AT DUNNING, NEBRASKA

---

[4] "Transportation of Debris by Running Water," by G. K. Gilbert, *Professional Paper No. 86*, Geological Survey, U. S. Dept. of the Interior, Washington, D. C., 1914.

[5] "Review of the Theory of Turbulent Flow and its Relation to Sediment Transportation," by M. P. O'Brien, *Transactions*, Am. Geophysical Union, Vol. 14, 1933, p. 487.

[6] "Some Observations of Sorting of River-Sediments," by L. G. Straub, *ibid.*, Vol. 16, 1935, p. 463.

[7] "Sand Mixtures and Sand Movement in Fluvial Models," by Hans Kramer, *Transactions*, ASCE, Vol. 100, 1935, p. 798.

[8] "Calibrating the Bed-Load Trap as Used in the Rhine," by H. A. Einstein, *Schweizerische Bauzeitung*, Vol. 110, No. 14, October 2, 1937, p. 29.

[9] "Geometric versus Hydraulic Similitude," by Herbert D. Vogel and John Paul Dean, *Civil Engineering*, August, 1932, p. 467.

[10] "Le Rhône et les rivières a lit affouillable," by P. Du Boys, *Annales des Ponts et Chaussées*, Series 5, Vol. 18, 1879, pp. 141–195.

[11] "Equilibrium of Grains on Bed of Stream," by C. M. White, *Proceedings*, Royal Soc. of London, Vol. 174A, 1940, pp. 322–334.

[12] "Neuere versuchsresultate uber den Geschiebetrieb," by E. Meyer-Peter, H. Favre, and H. A. Einstein, *Schweizerische Bauzeitung*, Vol. 103, No. 12, 1934, p. 147.

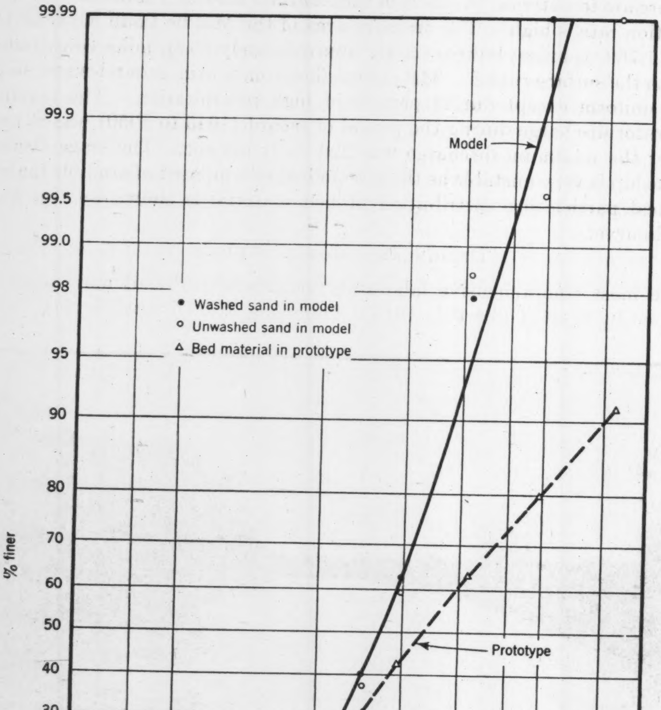

FIG. 3.—PARTICLE-SIZE DISTRIBUTION

These investigations, although limited to studies of the fundamental laws governing bed-load movement, were of material assistance in developing an apparatus whereby the bed load could be transported temporarily in suspension and measured as suspended load. Specific studies by Joe W. Johnson[13] and Ralph W. Powell,[14] Members, ASCE; field investigations by the Geological Survey, United States Department of the Interior (USGS)[15] in the Boise River basin in Idaho; and the cooperative study[16] conducted at the State University of Iowa, at Iowa City, and at the University of Minnesota, at Minneapolis, added more information significant to the problem.

Analysis of the Problem.—As noted previously, a method was needed for measuring the bed load, which is that part of the total load not measured by standard suspended-sediment samplers,[16] such as the US D-43 sampler or the US DH-48 sampler. Any method that was developed had to be readily adaptable for use on the Middle Loup River with a minimum of effort and time expended in actually making the measurements and a minimum of expense involved in the initial construction. Two methods of solving the problem were (1) trapping the bed load that passed a given point during a measured period of time and (2) forcing the bed load into suspension by increased turbulence so that the bed load could be measured with standard suspended-load sampling equipment.

Any equipment for trapping the bed load must be operated continuously in order to obtain a representative sample. If the equipment were not operated continuously, the regime in the river would be changed when operation did begin, and the operating time required to re-establish equilibrium would be too great to permit practicable operation. Because vast quantities of bed material pass a given section in the river each day, the size of equipment for continuous trapping would eliminate this method of solving the problem; the excessive time and expenditures of money required for construction and operation would also be prohibitive. Furthermore, there would be no assurance that the material being trapped included all, and only, the unmeasured load.

Two possible procedures for forcing the bed load into suspension by increased turbulence are: (1) The use of the turbulence created by energy from some external source, such as mixing devices or jets of air or water, and (2) the use of the turbulence originating from the energy of the river itself—such as the installation of baffles to increase the turbulent energy of the flow at the expense of the potential energy of the stream.

The latter method, that of utilizing a part of the energy of the stream to create the turbulence necessary for bed-load suspension, was adopted as the more practical. This method permits continuous operation of the system so that measurements of total load can be made at any desired time.

---

[13] "Rectangular Artificial Roughness in Open Channels," by Joe W. Johnson, *Transactions*, Am. Geophysical Union, Vol. 25, 1944, p. 906.

[14] "Flow in a Channel of Definite Roughness," by Ralph W. Powell, *Transactions*, ASCE, Vol. 111, 1946, p. 531.

[15] "Discharge and Sediment Loads in the Boise River Drainage Basin, Idaho, 1939–40," by S. K. Love and P. C. Benedict, *Water-Supply Paper No. 1048*, Geological Survey, U. S. Dept. of the Interior, Washington, D. C., 1948.

[16] "A Study of Methods Used in Measurement and Analysis of Sediment Loads in Streams," Subcommittee on Sedimentation, Federal Inter-Agency River Basin Committee, *Reports Nos. 1–10*, 1941–1953, Corps. of Engrs., U. S. Dept. of the Army, St. Paul District, St. Paul, Minn.

From the work of Mr. Johnson[13] and Mr. Powell,[14] it was evident that baffles could be used to cause large energy losses in a stream. Therefore, preliminary tests were made with continuous baffles across the floor of the model. These tests disclosed, however, that the bed-load material, which moves downstream in the form of dunes, increased the elevation of the stream bed and completely covered each baffle as the dunes progressed downstream. Because of this situation, it was decided to use a system of individual baffles so that the remainder of each dune could move between adjacent baffles until sufficient turbulence had been created by flow past subsequent baffles to force all the material into suspension. As a result of the need for creating the maximum turbulent energy, baffle plates (Fig. 4) were chosen rather than rectangular battens as used by Mr. Powell.[14] Furthermore, the separation zone, or wake, downstream from each baffle plate was more stable and less dependent on the Reynolds number—a matter of prime importance in model studies that involve free-surface flow.

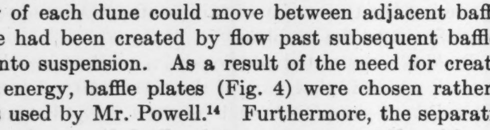

(a) Plan

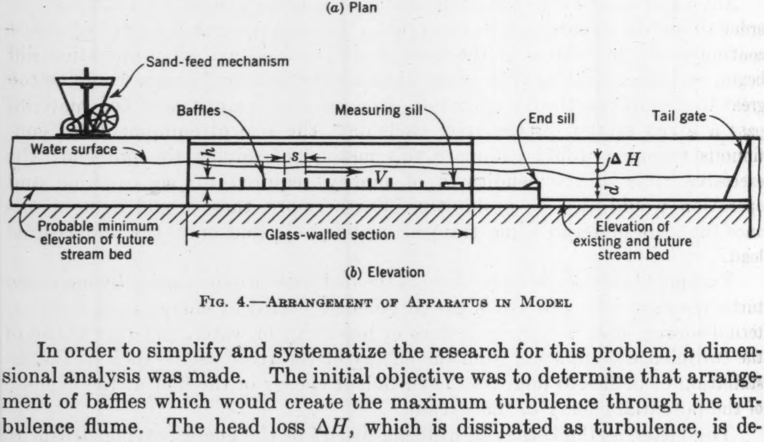

(b) Elevation

FIG. 4.—ARRANGEMENT OF APPARATUS IN MODEL

In order to simplify and systematize the research for this problem, a dimensional analysis was made. The initial objective was to determine that arrangement of baffles which would create the maximum turbulence through the turbulence flume. The head loss ΔH, which is dissipated as turbulence, is dependent on the size and arrangement of the baffles, the characteristics of the flow and sediment, and the properties of the water. This dependence can be expressed in general functional form as

$$\Delta H = \phi_1(h, s, x, b, V, d, c, \omega, \sigma_s, \rho_s, \rho, \mu, \Delta\gamma) \ldots\ldots\ldots\ldots (1)$$

in which ΔH is the drop in water-surface elevation through the flume or through the roughness section used for the studies, h denotes the height of the baffles, s is the longitudinal spacing between the rows of baffles, x represents the open distance laterally between adjacent baffles in a row, b is the width of a baffle, V signifies the mean velocity of the water in an undisturbed section of the stream, d is the mean depth of the water in an undisturbed section of the stream, c denotes the concentration of sediment being transported by the stream, ω is the mean terminal-fall velocity or settling velocity of the sediment in the stream, σ_s represents the standard deviation of the fall velocity of the sediment and is a measure of the size gradation, ρ_s is the density of the sediment, ρ signifies the density of the water, μ is the dynamic viscosity of the water, and $\Delta\gamma$ denotes the difference between the specific weights of the water and air. Eq. 1 can be stated dimensionlessly as

$$\frac{\Delta H}{h} = \phi_2\left(\frac{b}{h}, \frac{x}{h}, \frac{s}{h}, \frac{d}{h}, c, \mathsf{F}, \mathsf{R}, \frac{\omega}{V}, \frac{\sigma_s}{\omega}, \frac{\rho_s}{\rho}\right) \ldots\ldots\ldots\ldots\ldots (2)$$

in which **F** is the Froude number and **R** is the Reynolds number.

A complete investigation of Eq. 2 was obviously impossible in the allotted time; thus, various parameters either were held constant or were eliminated as

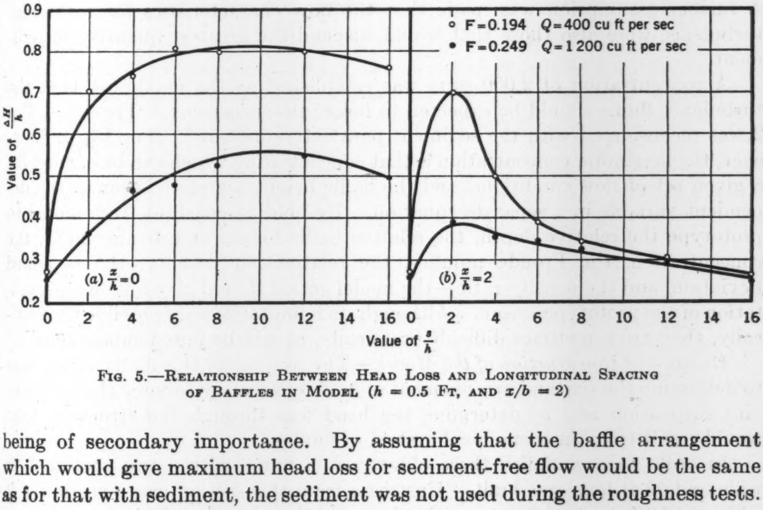

FIG. 5.—RELATIONSHIP BETWEEN HEAD LOSS AND LONGITUDINAL SPACING OF BAFFLES IN MODEL ($h = 0.5$ FT, AND $x/b = 2$)

being of secondary importance. By assuming that the baffle arrangement which would give maximum head loss for sediment-free flow would be the same as for that with sediment, the sediment was not used during the roughness tests. Because the turbulence was great and all separation zones were stable, the Reynolds number was considered to be of little importance. By maintaining the Froude number and relative depth, d/h, constant from model to prototype, Eq. 2 becomes

$$\frac{\Delta H}{h} = \phi_3\left(\frac{b}{h}, \frac{x}{h}, \frac{s}{h}\right) \ldots\ldots\ldots\ldots\ldots\ldots\ldots (3)$$

Eq. 3 is sufficiently simple to be studied systematically.

In order to determine whether baffles have the same characteristics as the battens used by Mr. Powell,[14] a test was made with continuous baffles. The results shown in Fig. 5(a) illustrate that the loss is maximum at a value of

$s/h = 10$, which is approximately the same as that value found by Mr. Powell. The individual baffles required adequate lateral spacing to permit the passage of dunes. To meet this requirement, a density factor of $x/b = 2$ was assumed as the most desirable. With this arrangement, the maximum head loss over the 6-ft length of test section was found to be at $s/h = 2$, as shown in Fig. 5(*b*). The arrangement of baffles, measuring sill, and end sill in the preliminary model tests are shown in Fig. 4.

On the basis of the foregoing analysis and other preliminary tests, it was decided to use a density factor of $x/b = 2$. A prototype baffle height, h, of 0.5 ft was selected as the initial size for model investigations with sediment. If the maximum loss were to be obtained with this height, it would be necessary to space the rows of baffles 1 ft apart longitudinally. Because this spacing required such a large number of baffles, a spacing of 2 ft was chosen for the preliminary value of s. The flow characteristics for maximum head loss were assumed to be the most desirable for the suspension of total load because the energy dissipated is first converted into turbulent energy and then into heat. A further assumption was made that the flow characteristics for maximum turbulence were also those that would suspend the greatest quantity of sediment.

A concentration of 2,000 ppm was established as the maximum that the turbulence flume should be expected to force into suspension. Therefore, Eq. 2 was reconsidered with the sediment parameters included. For Eq. 2, however, the maximum concentration is that concentration which can be carried for a given set of flow conditions, and the baffle height therefore becomes the dependent variable in a separate equation. By holding constant from model to prototype the relative depth, the relative baffle height and arrangement, the concentration, the Froude number, the relative-fall velocity, the standard deviation, and the density ratio—the model action should give a true representation of the prototype action. Although such limitations are possible theoretically, they are sometimes difficult practically, as will be noted subsequently.

Design and Construction of the Model.—The purpose of this model study was to determine the size and arrangement of baffles necessary to force the bed load into suspension and to determine the head loss through the structure that would result from an economical system of baffles.

In order to accomplish these objectives, a flume with a test section 2 ft wide and 13 ft long was built. Upstream from this section was a section 4 ft wide and 10 ft long with a transition between the sections. This arrangement permitted a relatively unmodified boundary layer to develop along the floor of the flume, whereas the boundary layer along the walls was contracted at the transition and was thereby reduced in effectiveness. This measure was taken in order to cause a flow that was as nearly two-dimensional as possible.

A model scale of 1 to 4 was selected after preliminary tests disclosed that a ratio of 1 to 8 was unsatisfactory. Therefore, the 2-ft test section represented a prototype width of 8 ft, which was approximately a quarter of the span between piers of the bridge at Dunning. The 0.5-ft-high baffles required model baffles $1\frac{1}{2}$ in. high. These baffles were made of No. 20-gage, galvanized sheet metal and had a $\frac{1}{2}$-in. flange at the base so that each baffle could be secured in place with thumb tacks. The base of the model was made of exterior plywood, and the measuring sill and end sill were made of white pine.

The discharge in the model was determined by the Froude criterion and by the limits of 250 cu ft per sec and 800 cu ft per sec for which a concentration of 2,000 ppm must be transported in suspension across the measuring sill. Therefore, tests were run at model discharges that simulated 250 cu ft per sec, 400 cu ft per sec, and 800 cu ft per sec. An attempt was made to obtain sand of the proper size to have the velocity ratio, ω/V, the same in the model as in the prototype. The small size of sediment required for the model made it difficult to find material with the proper fall velocity. The velocity ratios for the prototype and the model were as follows:

Discharge, in cubic feet per second	ω/V for the prototype	ω/V for the model
200	0.098	0.160
400	0.072	0.120
800	0.051	0.084

Although it was not possible to obtain sufficient quantities of sand small enough to make the (ω/V)-ratio a constant, the deviation was in a safe direction. If it is possible to force into suspension sand of a given fall velocity, it should be possible to force into suspension the same concentration of a smaller sand that has a lower fall velocity.

The sand used in the model studies was obtained near Fort Collins, Colo. It was passed through a 30-mesh screen and was then washed. The size analysis before and after washing is given in Fig. 3 with the composite result shown by a solid-line curve.

Preliminary tests demonstrated that it would not be possible to obtain a sufficiently high velocity through the structure without constricting the flow by raising the floor above the bed of the stream. In fact, it was necessary for the flow over the measuring sill to approach the critical velocity for all discharges.

Operation of the Model.—The preliminary experiments demonstrated that, if continuous baffles were used, the advancing sand dunes would cover each baffle in turn as the dunes progressed downstream. Individual baffle plates 0.5 ft high and 2 ft long were then tested, and it was found that only for a rather low concentration of sediment was it possible to prevent the advancing dunes from covering first the baffles and eventually the measuring sill. Therefore, all the final experiments were run with the baffles at least 1.0 ft high.

After considerable difficulty, a sand-feed mechanism was devised that would feed the sand into the model at a continuous rate. It was composed of a reciprocating plate which moved at the base of a hopper. A vibrator was mounted on the side of the hopper to keep the sand in a "fluid" state so that it would flow freely. The relative position of the model and the sand-feed mechanism is shown in Fig. 4(*b*). The sand was introduced at a sufficient distance upstream to insure adequate time of fall for the particles to reach the bed of the stream from 10 ft to 20 ft (prototype scale) upstream from the first row of baffles.

Each test was run until equilibrium had been established and a proper evaluation of the design could be made. This procedure sometimes required several hours although generally the time necessary was less than one hour. A point gage mounted on a carriage, which bridged the channel, was used to determine the water-surface profile and the head loss through the flume. The sand was trapped in a 4-ft by 8-ft weir box at the end of the flume.

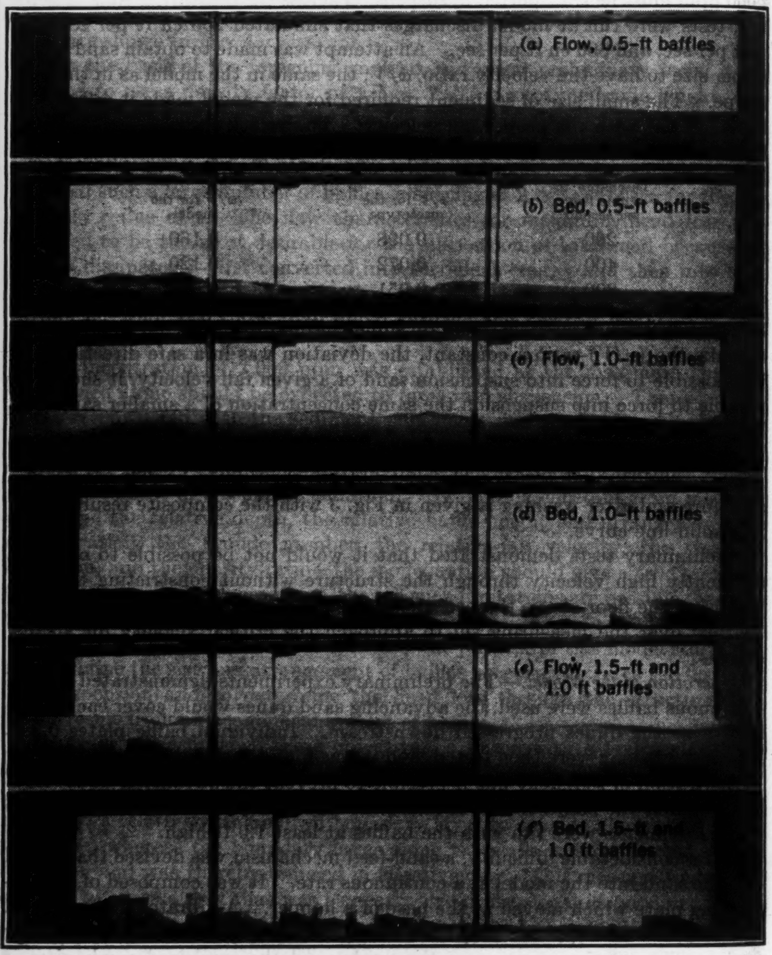
(a) Flow, 0.5-ft baffles
(b) Bed, 0.5-ft baffles
(c) Flow, 1.0-ft baffles
(d) Bed, 1.0-ft baffles
(e) Flow, 1.5-ft and 1.0 ft baffles
(f) Bed, 1.5-ft and 1.0 ft baffles

FIG. 6.—FLOW OVER BAFFLES AND FINAL BED CONFIGURATION IN MODEL FOR PROTOTYPE FLOW OF 400 CU FT PER SEC

Photographs were taken both before and after each test to show the flow pattern of the water and the patterns of the dunes and deposits of sand.

Results of the Model Tests.—The data from the model studies were obtained by measuring or observing (*a*) head loss through the flume; (*b*) flow pattern past the baffles and across the measuring sill; (*c*) dune pattern upstream from and in the flume; (*d*) dunes, deposits, and bed load moving over and near the measuring sill; and (*e*) action immediately downstream from the end sill in regard both to water and to sand movement.

When the baffles were only 0.5 ft high, the sand could not be forced into suspension. Instead the advancing sand covered each of the baffles as it progressed downstream. This is shown in Figs. 6(*a*) and 6(*b*), in which none of the baffles can be seen either during or after operation. At a discharge of 250 cu ft per sec, the measuring sill was approximately half covered with a sand dune, and the tops of several baffle plates were exposed. At a flow of 400 cu ft per sec, however, the measuring sill was completely covered, and only one or two baffles could be located. When a discharge of 800 cu ft per sec was flowing through the flume, the sand bed was nearly smooth, and there was no visible evidence of either the measuring sill or the baffle plates. The head losses through the flume for the three discharges were 0.73 ft, 0.19 ft, and 0.21 ft, respectively.

Because this operation with the 0.5-ft baffles was unsatisfactory, the height of the baffles was increased to 1.0 ft; the location and arrangement remained the same. As can be seen in Figs. 6(*c*) and 6(*d*), the measuring sill remained uncovered regardless of the discharge; deposits were found immediately downstream from each baffle. Furthermore, the upstream baffles were periodically covered almost completely as a result of dunes advancing on the baffles. As the dune proceeded downstream, the baffle would again be at least partly uncovered. The head losses were 0.82 ft, 0.48 ft, and 0.33 ft for discharges of 250 cu ft per sec, 400 cu ft per sec, and 800 cu ft per sec, respectively. The water surface, having waves 0.5 ft high, was irregular for a discharge of 250 cu ft per sec; but, as the discharge was increased to 800 cu ft per sec (as was the depth), the water surface became rather smooth.

The 1.0-ft baffles created sufficient turbulence to transport the entire concentration of 2,000 ppm in suspension over the end sill regardless of the discharge. However, the margin of safety was narrow enough (considering the unprecedented nature of such a model-prototype experiment) so that tests were also made with the two upstream rows of baffles 1.5 ft high and the remainder 1.0 ft high. Figs. 6(*e*) and 6(*f*) show clearly that, although a small deposit remains downstream from each baffle, the measuring sill is clear and there is no tendency for any of the baffles to become completely covered with the advancing dunes. The irregularities of the water surface were somewhat increased, and the head losses were 0.86 ft, 0.53 ft, and 0.42 ft for discharges of 250 cu ft per sec, 400 cu ft per sec, and 800 cu ft per sec, respectively. The end sill operated satisfactorily for all flows that had no tendency to undermine the structure.

Therefore, both the 1.0-ft baffles and the 1.5-ft baffles satisfactorily forced the bed load into suspension. However, the 1.5-ft baffles accomplished this purpose with a greater margin of safety but with greater surface disturbance and a slightly increased head loss.

The concentration of suspended sediment that passed over the measuring sill was determined by sampling with a nozzle made of $\frac{3}{16}$-in. (inside diameter) brass tubing. A siphon tube was attached to the nozzle and arranged so that the velocity of flow within the tube was the same as that outside the tube. By this method, point-integrated samples were obtained at nine depths at the center line of the flume. Samples were also taken at the quarter points, as shown in Fig. 7. The mean concentration was 710 ppm in the center vertical and 690 ppm and 720 ppm at the right and left quarter points, respectively. As would be expected, the distribution of sediment shows a smaller concentration near the water surface than near the sill. The average concentration of the total load in the model was 710 ppm for a discharge equivalent to 360 cu ft per sec in the prototype.

The sand dunes were measured as they approached the model. Although the dunes were irregular in size and shape, an attempt was made to determine the average size and velocity of movement of the dunes by photographing the dunes at the glass wall at 5-min intervals. This system of measurement, of course, included an error that was caused by the effect of the glass wall, but it was the only system that was readily adaptable. Visual observation indicated that the error was not significant.

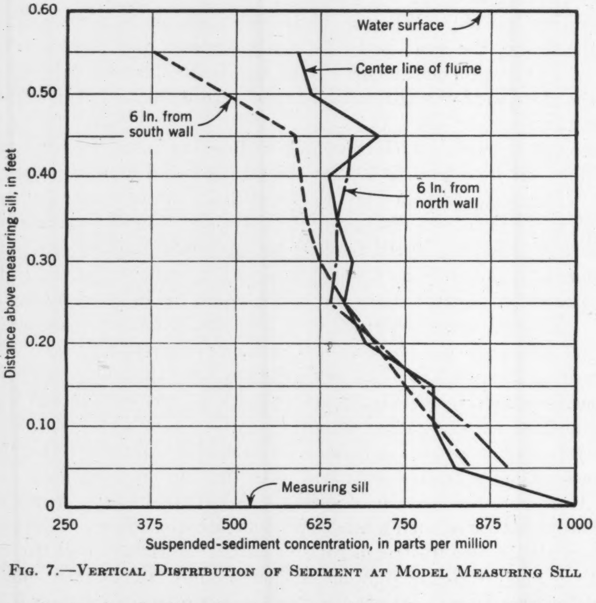

FIG. 7.—VERTICAL DISTRIBUTION OF SEDIMENT AT MODEL MEASURING SILL

From seventy measurements, the average velocity of movement of the dunes in the model was found to be 4.5 ft per hr with a standard deviation of 2.2 ft per hr. The height of the dunes varied considerably, but the average height was approximately 0.12 ft. By using the average height and velocity of the dunes, the measurements indicated that the concentration of material moving as dunes was approximately 160 ppm.

Measurements of the concentration of suspended sediment were taken upstream from the model structure by depth integration. The average concentration was 430 ppm. If the total load at the sill is taken as 710 ppm and the suspended load upstream as 430 ppm, apparently 280 ppm move as bed load or unmeasured load. Based on the measurements of the dunes, 160 ppm of the 280 ppm were moving as dunes and 120 ppm were therefore moving as unmeasured suspended or saltation load and bed load not reflected in the dunes.

Samples were collected from the surface of the stream bed with a withdrawal pipette. The air pressure used was sufficient to withdraw the sediment sample without disturbing the surface of the bed. The mean size of samples collected in this manner was 0.359 mm. The mean size of sediment in the bed of the model was 0.305 mm when tests were begun.

Recommended Design of Prototype Structure.—In view of the previously outlined tests and observations, it was recommended that:

1. The prototype be constructed with nine rows of removable baffle plates 1.0 ft high and 2 ft wide with a lateral spacing of 6 ft and a longitudinal spacing of 2 ft from center to center.
2. A continuous baffle 0.5 ft high be placed 24 in. downstream from the last row of baffles and 28 in. upstream from the 6-in. by 16-in. measuring sill.
3. The end sill be placed 56 in. downstream from the measuring sill.
4. Sheet piling be used both upstream and downstream to reduce the hazards of piping and possible failure of the structure.

The baffle plates were designed to be long enough to withstand reasonable impacts from floating debris yet short enough to prevent significant irregularities in the sediment discharge over the measuring sill. The purpose of the continuous 6-in. baffle was to help in obtaining a uniform lateral distribution of sediment. When the ratio s/h is equal to 2 (Fig. 5(b)) the maximum head loss is produced for a density ratio x/b equal to 2. The arrangement of the roughness baffles can be altered if additional data indicate that a different spacing would be more efficient.

THE PROTOTYPE FLUME

The turbulence flume is a structure for inducing turbulence sufficient to suspend substantially the total sediment load of a stream. The flume consists of a series of 1-ft by 2-ft movable baffles, one continuous 0.5-ft permanent baffle, and a 6-in. by 16-in. wooden baffle (measuring sill) attached to a reinforced-concrete slab 82 ft wide and 38 ft long. The 1-ft by 2-ft baffles are galvanized steel sheets supported by two round rods inserted in pipe sockets embedded in the concrete slab. The permanent baffle, a 6-in. by 4-in. angle, and the wooden measuring sill are bolted to the concrete slab.

The concrete slab, which is the floor of the flume, is supported at each end by interlocking sheet-steel piling driven to a depth of 10 ft. The top of the slab is just below the average elevation of the stream bed at a discharge of approximately 400 cu ft per sec. The wooden end sill, which is bolted to the downstream end of the slab, was designed to produce a reverse roller to prevent scour of the stream bed immediately downstream from the flume.

A gage well and recorder shelter are located on the left bank 25 ft upstream from the flume. The well is equipped with two 3-in. intake pipes with static tubes to eliminate drawdown. A continuous record of the elevation of the water surface is obtained with an automatic water-stage recorder. The elevation of the water surface at the downstream end of the flume is obtained from a staff gage attached to the downstream wing wall of the right bridge abutment. Walkways were installed immediately below the upstream edge of the slab and immediately downstream from the measuring sill to simplify the collection of depth-integrated sediment samples. In Fig. 8 there is shown a skeleton model of the prototype flume with the bridge deck removed. Details of the prototype flume and baffle arrangement are given in Fig. 9. An upstream view of the prototype (with no flow) is shown in Fig. 10.

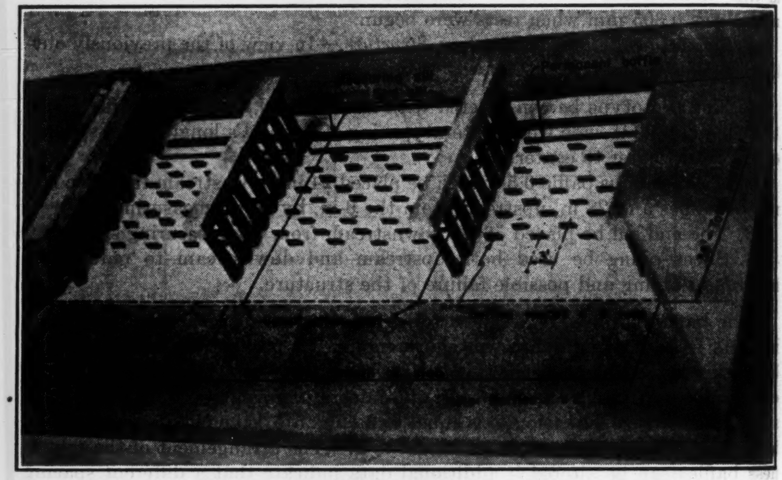

FIG. 8.—SKELETON MODEL OF PROTOTYPE FLUME

OPERATION OF PROTOTYPE FLUME

The initial investigations of the efficiency of the flume consisted of concurrent determinations of water-surface slope, stream velocity, suspended-sediment concentration, and size of sediment in transport.

Sampling Procedure and Analysis.—The quantity and distribution of the sediment were obtained from samples collected biweekly with the US DH-48 and US P-46 samplers[17,18] at representative points in the cross section at the measuring sill. Several sets of instantaneous samples were also collected with the Tait-Binckley sampler.[19]

---

[17] "A Study of Methods Used in Measurement and Analysis of Sediment Loads in Streams," Subcommittee on Sedimentation, Federal Inter-Agency River Basin Committee, *Report No. 6*, Corps of Engrs., U. S. Dept. of the Army, St. Paul District, St. Paul, Minn., 1952, p. 61.

[18] *Ibid.*, *Report No. 8*, 1948, p. 74.

[19] "Discharge and Sediment Loads in the Boise River Drainage Basin, Idaho, 1939–40," by S. K. Love and P. C. Benedict, *Water-Supply Paper No. 1048*, Geological Survey, U. S. Dept. of the Interior, Washington, D. C., 1948, p. 26, Plate 5.

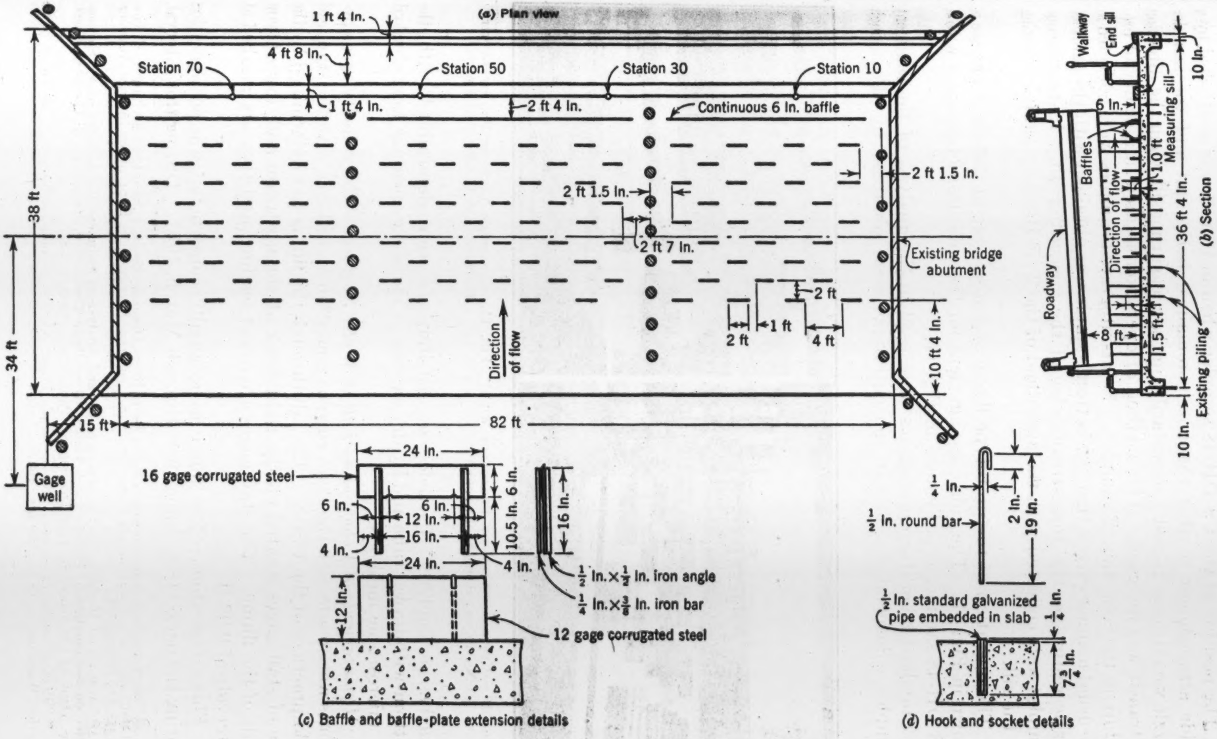
1 ft 4 In.
4 ft 8 In.
Station 70
Station 50
Station 30
Station 10
1 ft 4 In.
2 ft 4 In.
Continuous 6 In. baffle
2 ft 1.5 In.
2 ft 1.5 In.
2 ft 7 In.
Existing bridge abutment
2 ft
1 ft
2 ft
4 ft
10 ft 4 In.
Direction of flow
38 ft
34 ft
15 ft
82 ft
Gage well
Walkway
End sill
10 In.
6 In.
Measuring sill
Baffles
1.0 ft
Direction of flow
36 ft 4 In.
Roadway
8 ft
1.5 ft
Existing piling
10 In.
16 gage corrugated steel
24 In.
6 In.
6 In.
12 In.
16 In.
4 In.
4 In.
10.5 In.
6 In.
16 In.
24 In.
12 In.
½ In.×½ In. iron angle
¼ In.×⅜ In. iron bar
12 gage corrugated steel
¼ In.
½ In. round bar
2 In.
19 In.
½ In. standard galvanized pipe embedded in slab
¼ In.
7¾ In.

(a) Plan view

(b) Section

(c) Baffle and baffle-plate extension details

(d) Hook and socket details

FIG. 9.—PROTOTYPE FLUME

The position of the US DH-48 sampler when in transit was controlled by a guide arrangement so that the nozzle remained horizontal and the sampler nozzle would come to rest momentarily on the measuring sill when the direction of transit was reversed. This method of operation assured uniformity of procedure in the collection of samples. Point-integrated samples were collected in the usual manner except that the bottom sample was obtained with the sampler nozzle resting on the downstream edge of the measuring sill. Instantaneous samples were collected with the upper end of the Tait-Binckley sampler resting on the sill.

The operation of the prototype flume at a discharge of 350 cu ft per sec is shown in Fig. 11. The guide arrangement for the collection of samples with a US DH-48 sampler is not shown in Fig. 11.

Standard laboratory procedures were used in the analysis of the sediment samples. Suspended-sediment concentrations were obtained by the Gooch crucible method.[20,21] Particle-size distributions were determined with the bottom-withdrawal tube and by dry sieving. The sieve openings were checked by microscopic methods.

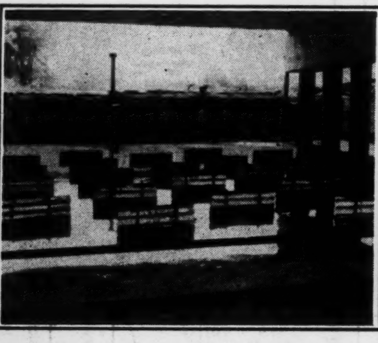

FIG. 10.—UPSTREAM VIEW OF PROTOTYPE WITH NO FLOW, BAFFLES EXPOSED

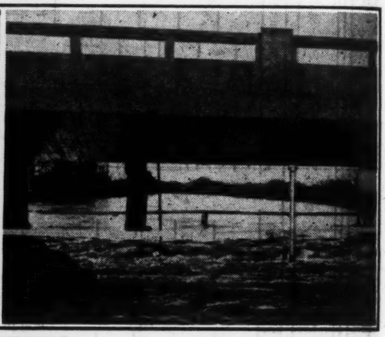

FIG. 11.—UPSTREAM VIEW OF PROTOTYPE WITH FLOW OF 350 CU FT PER SEC

Measurements of Velocity and Fall in Water Surface.—The velocity measurements were made with the Price current meter[22] in accordance with the standard field practices of the USGS. The fall through the flume was determined by the use of staff gages located on the right bank at the upstream and downstream ends of the flume. The staff gages are direct reading, and they are marked at intervals of 0.02 ft.

Flume Operation.—The flume as originally constructed was in operation during the period from June, 1949, through March, 1951. During this interval,

---

[20] "Discharge and Sediment Loads in the Boise River Drainage Basin, Idaho, 1939–40," by S. K. Love and P. C. Benedict, *Water Supply Paper No. 1048*, Geological Survey, U. S. Dept. of the Interior, Washington, D. C., 1948, p. 24.

[21] "A Study of Methods Used in Measurement and Analysis of Sediment Loads in Streams," Subcommittee on Sedimentation, Federal Inter-Agency River Basin Committee, *Report No. 4*, Corps of Engrs., U. S. Dept. of the Army, St. Paul District, St. Paul, Minn., 1941, p. 185.

[22] "Stream-Gaging Procedure," *Water-Supply Paper No. 888*, Geological Survey, U. S. Dept. of the Interior, Washington, D. C., 1943, p. 168.

deposition in the left end of the flume and on the left end of the measuring sill was intermittent. Downstream from the bridge the stream channel has a 10° bend to the right. This change in direction and the presence of brush growth on the left bank, particularly that immediately downstream from the flume, reduced the velocity in the left end of the flume. Sediment was also deposited downstream from each bridge piling. In the original design, it was planned to enclose the bridge piling that comprises each pier, but this was not done because later observations indicated that the effect of the piers on the distribution at the measuring sill was negligible.

The flume operation during the test period was considered satisfactory except for the intermittent deposition of sand on the measuring sill. This deposition indicated that the turbulent energy was insufficient to suspend the total sediment load during maximum dune movement through the flume. On the basis of the results of the model studies, the first two rows of baffles at the upstream end of the flume were raised 0.5 ft (Fig. 9(*c*)) on March 29, 1951. Since that date, the flume and measuring sill have remained clean except when debris becomes lodged in the flume and when there is backwater from ice during winter periods.

Vertical Distributions of Velocity, Concentration, and Size of Sediment.—The turbulence created in passing each successive baffle plate should progressively suspend greater quantities of the total amount of sediment that is passing through the flume until the turbulence created by flow in passing the last baffle (1 ft by 2 ft) is sufficient to suspend the remainder of the total quantity of sediment. When all the sediment is in suspension, the capacity of the flow to transport sediment in suspension must at least be equal to the quantity of sediment available for transport. With its capacity at least equal to the concentration of the total sediment load, the flow should suspend its load of sediment throughout its depth with respect to both concentration and size of the suspended sediment.

Typical vertical distributions of velocity, concentration, and size of total sediment load are shown in Figs. 12 and 13. The curves indicate that the turbulence is sufficiently great to suspend at the surface the coarsest fraction of the load in transport. The size-distribution curves of Figs. 12 and 13 show the percentages of material coarser than 0.25 mm (material that is not found in appreciable quantities at normal sections upstream from the flume) that was sampled at the several elevations above the measuring sill. If the material coarser than 0.25 mm (coarse sand) was uniformly distributed throughout the depth, the total sediment load should be in suspension; therefore, the percentage coarser than 0.25 mm was selected as the reference size. Normally, the vertical distributions of concentration and size of total sediment load would show an appreciable decrease of both concentration and size with increased distance above the bed of an alluvial stream.

The turbulence flume has a measuring sill that will allow a standard sediment sampler to integrate the concentration of the total sediment load (in suspension) throughout the entire depth of flow. Samples thus obtained are samples of the total sediment load, provided the bed load moves at stream velocity and does not form deposits on the measuring sill.

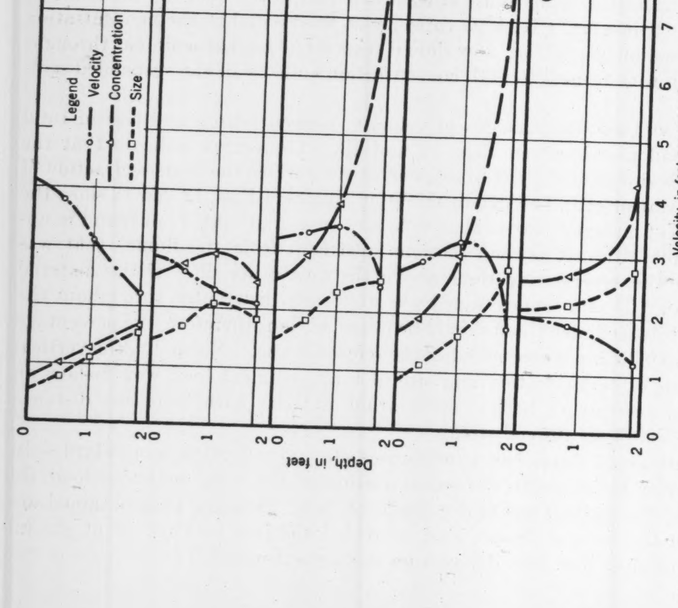

FIG. 12.—VERTICAL DISTRIBUTION OF VELOCITY AND SEDIMENT AT PROTOTPYE MEASURING SILL, 1-FT BAFFLES (AUGUST 27, 1950)

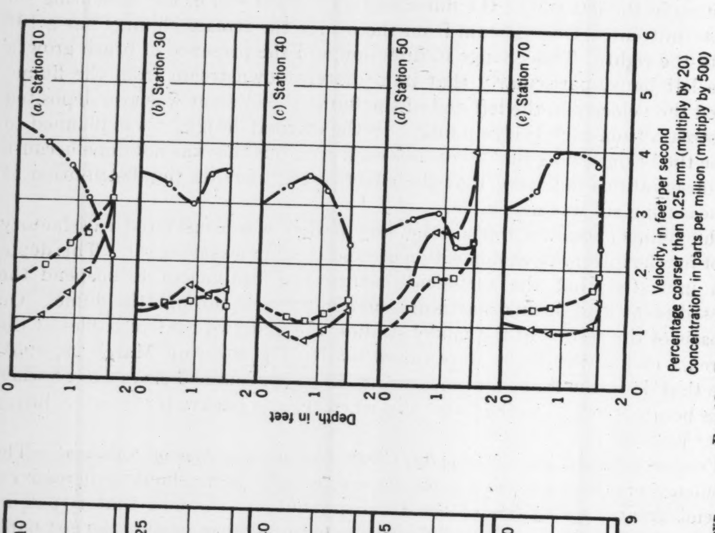

FIG. 13.—VERTICAL DISTRIBUTION OF VELOCITY AND SEDIMENT AT PROTOTYPE MEASURING SILL, 1.5-FT AND 1.0-FT BAFFLES (AUGUST 30, 1951)

At the time the data shown in Fig. 12 were collected, all baffles were 1.0 ft high, and the vertical distributions for station 10, station 25, and station 70 showed that both concentration and size of suspended sediment were relatively uniform with respect to depth. This indicates that the turbulence at these stations is sufficiently great to suspend the coarser fractions throughout the depth of flow. The data for station 40 and station 55 (Figs. 12(*c*) and 12(*d*)) show an appreciable increase in concentration with depth and a noticeable increase in size of suspended sediment with depth. This pattern indicates either that turbulent mixing had not developed at station 40 and station 55 to the extent to which it had at other stations, or that the concentration of sediment was so great that it approximated the capacity of the flume.

The vertical-distribution curves in Fig. 13 indicate a higher degree of turbulent mixing for the entire cross section than do the curves in Fig. 12. All flow characteristics were the same for the two sets of curves, except that the baffles in the two upstream rows were higher for Fig. 13. Fig. 12 represents transport before, and Fig. 13 represents transport after, the height of the upstream baffles was increased. As shown in Fig. 6, the capacity of the flume to suspend the sediment bed load was increased when the first two rows of baffles were raised to a height of 1.5 ft. A comparison of the curves of Fig. 12 and Fig. 13 shows that a change in the distribution curves has taken place. Although the distribution curves are more irregular with the higher baffles, they also show a smaller range in magnitude, which indicates increased mixing as a result of the increased turbulence. As would be expected, the condition at station 70 was changed considerably, but at station 10 the condition was changed only slightly. The zone around station 50 was carrying the heaviest load for both arrangements of baffles.

Fig. 14 shows the vertical distributions of concentration and size of suspended sediment as obtained by an instantaneous Tait-Binckley sampler. These data supplement those obtained with the US P-46 sampler.

Lateral Distributions of Velocity, Concentration, and Size of Sediment.—From Fig. 9(*a*) it can be seen that the baffle arrangement is such that, if a quantity of sediment were released at the center of one of the farthest upstream baffles, the resulting water-sediment mixture should theoretically be distributed over a 49-ft width at the measuring sill. Actually, the turbulence created in passing through the flume appears to carry suspended sediment past the measuring sill in large-scale eddies of high concentration. The data presented in Fig. 15 illustrate this fluctuation of suspended-sediment concentration with time. These measurements were taken on June 27, 1951, after the height of the two upstream rows of baffles had been increased. The data shown are for depth-integrated samples collected at 5-min intervals over a 4-hr period at the four daily sampling verticals above the measuring sill of the flume. A statistical analysis of the data indicates that a single sample collected at any one vertical at any given time might vary by 83.5% from the true mean for the vertical. The standard deviation of the variations at station 30 is 267 ppm which, if the normal error distribution is assumed (for study), means that the variation will be less than ±83.5% for 99.94% of the time. The normal error distribution also indicates that the variation will be less than ±73.1% for 99.7% of the time, less than ±48.8% for 95.5% of the time, and less than ±24.4% for 68.3% of the time. Such a variation is the greatest computed and occurs only about the mean of station 30. For station 10, the variation about the mean will be less than ±23.8% for 95.5% of the time; for station 50, it will be less than ±22.0% for 95.5% of the time; and for station 70, it will be less than ±29.2% for 95.5% of the time.

The variation of the mean concentration for the cross section (Fig. 15(*e*)) during the 4-hr period is less than ±24.8% for 95.5% of the time. In order to determine the increased accuracy resulting from two sets of samples, the average concentrations for successive 5-min intervals were computed and analyzed. By making this comparison, the accuracy can be increased so that the variation will be within ±18.6% for 95.5% of the time.

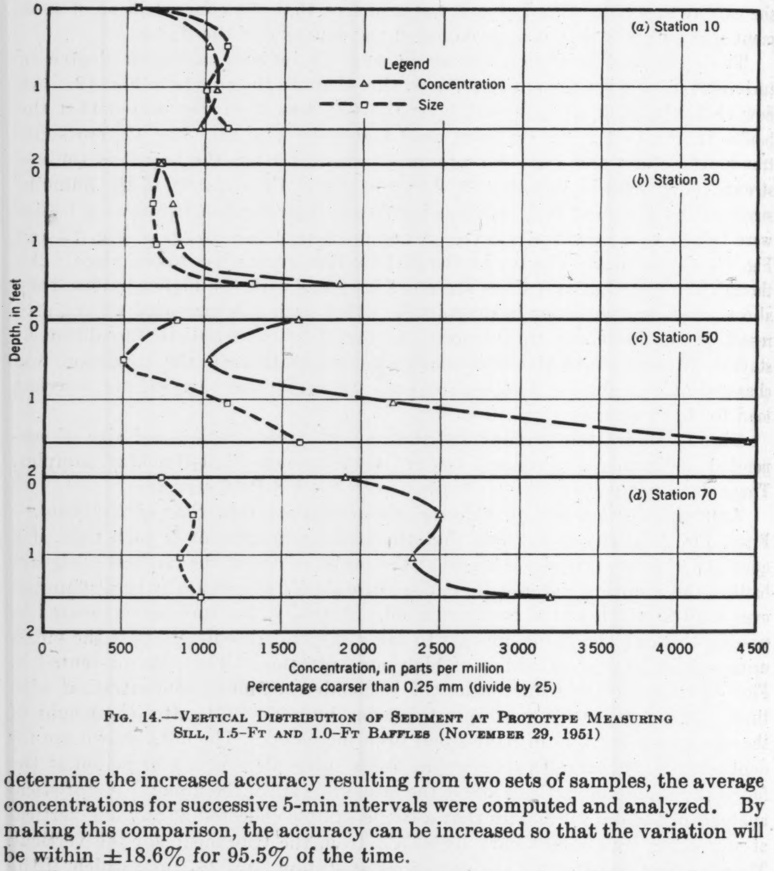

FIG. 14.—VERTICAL DISTRIBUTION OF SEDIMENT AT PROTOTYPE MEASURING SILL, 1.5-FT AND 1.0-FT BAFFLES (NOVEMBER 29, 1951)

These statistical analyses show that, for one set of random samples (one bottle) at the four sampling stations, the maximum deviation from the average concentration may vary as much as ±25%. For two consecutive sets of samples, the maximum deviation from the mean may be as great as ±19%.

In the routine collection of samples the probable deviation from the mean will vary from zero to these maximum percentages based on this statistical study. This rather large deviation is probably caused by the approach and passage of extremely large dunes through the flume. If the dunes were not present, the fluctuations in the concentration would be correspondingly less.

To eliminate, in part, the possibility of obtaining a sample of high concentration from one of the eddies over the measuring sill, a $\frac{3}{16}$-in.-diameter sampler nozzle was used. This nozzle permitted a slower filling rate, and the sample was obtained over a longer period of time than with the $\frac{1}{4}$-in. nozzle. The relatively longer sampling "thread" tended to minimize the effect of momentary periods of high and low concentration.

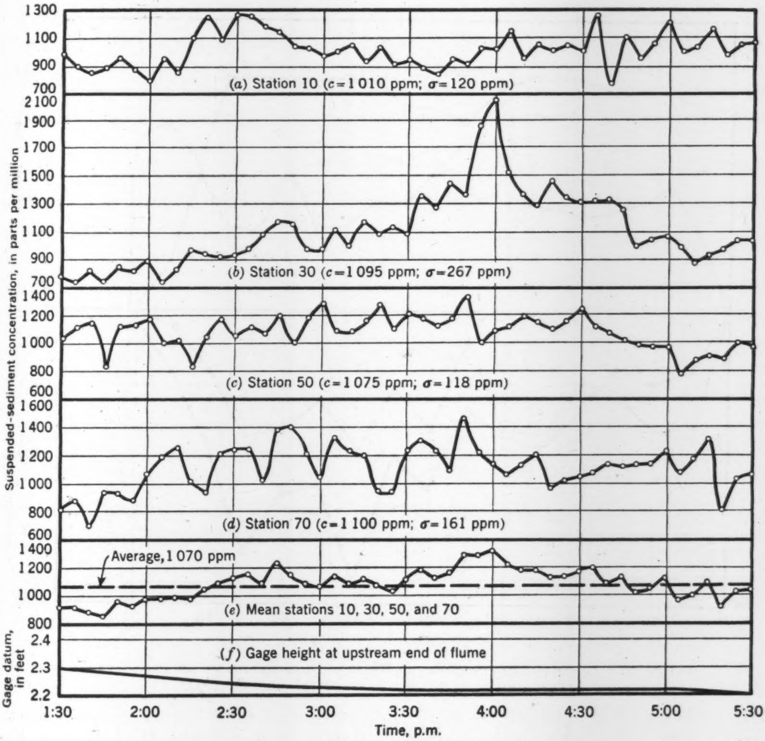

FIG. 15.—FLUCTUATION OF PROTOTYPE SUSPENDED-SEDIMENT CONCENTRATION WITH TIME, 1.5-FT AND 1.0-FT BAFFLES (JUNE 27, 1951)

A study of all samples collected during the period from July 15, 1949, to November 30, 1950, indicated that the concentration of the suspended sediment at any one sampling vertical on the measuring sill varied considerably from the mean, and that some of the verticals in the cross section were subject to wider variations than others. Therefore, a study was made to determine which combination of sampling verticals would define the representative concentration of the cross section.

Twenty suspended-sediment discharge measurements collected at the measuring sill of the turbulence flume were analyzed to determine the proper sampling verticals that would define the true concentration of the cross section. Several combinations of verticals were inspected to find the combination that would best define the concentration of flow. It was found that station 10, station 30, station 50, and station 70, which were being used as the daily sampling verticals at the time of this study, provided the most desirable results. The average ratio of the true sediment concentration in the cross section to the sediment concentration at the daily stations for the twenty samples analyzed was 1.002, and the maximum deviation of the twenty measurements was 28%. Such results were considered satisfactory.

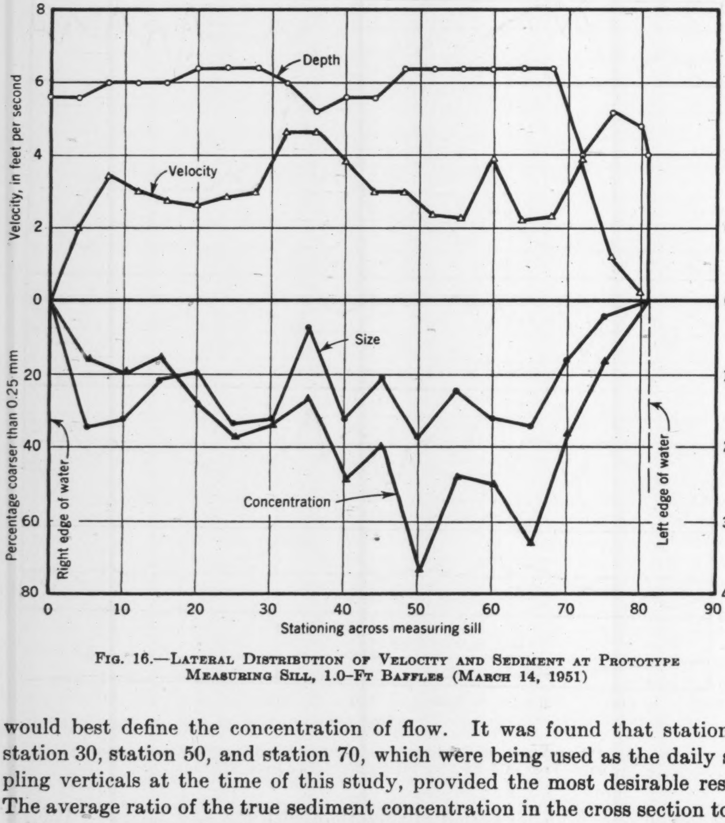

FIG. 16.—LATERAL DISTRIBUTION OF VELOCITY AND SEDIMENT AT PROTOTYPE MEASURING SILL, 1.0-FT BAFFLES (MARCH 14, 1951)

Fig. 16 shows typical lateral distributions of the velocity, concentration, and size of suspended sediment at the measuring sill. Samples collected at 1-ft intervals at the measuring sill indicated that the 1-ft by 2-ft baffles had little if any effect on the lateral distribution of sediment.

Dune Action Upstream from and Through the Flume.—Material comprising the bed load is transported in the form of dunes of irregular size and shape. The bed load does not move in the form of dunes for all cross sections as many of the wider sections of the Loup River transport their bed load in sheet movement. Field data were collected in the reach directly upstream from the turbulence flume to determine the nature of the movement of bed-load material—as to both quantity and rate—and to analyze the nature of the changes in the configuration of the bed.

A grid system was established in the reach directly upstream from the flume by stringing ropes at 5-ft intervals from the catwalk at the measuring sill to a tagline spanning the river approximately 90 ft upstream. Flags were tied to the longitudinal ropes at intervals of 5 ft. The data were then collected by reading the elevation of the stream bed with levels and by noting the depth of flow directly from the level rod. Care was taken to disturb the bed as little as possible, but the dunes were found to re-form almost immediately when disturbed. By collecting a complete set of soundings in the reach at 1-hr intervals, it was possible to chart the average rate, direction, and quantity of movement of some of the major dunes that retained their approximate dimensions as they approached the turbulence flume. Soundings were taken in the upstream end of the flume to determine the configurations of the stream bed as

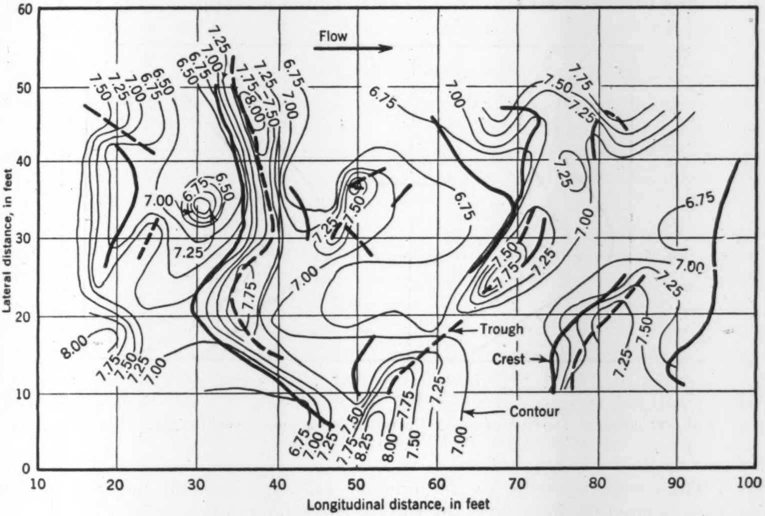

FIG. 17.—CONFIGURATION OF STREAM BED UPSTREAM FROM PROTOTYPE, 1.5-FT AND 1.0-FT BAFFLES (SEPTEMBER 20, 1951, AT 12:30 P.M.)

the initial turbulence induced by the flume began to suspend the bed-load material.

In Fig. 17 there is shown the configuration of the dunes over the entire bed. In Fig. 18(*a*) is shown a dune's crest and trough. In Fig. 18(*b*) the same dune is shown 1 hr later. Contour lines were plotted directly from level notes, and thus maximum readings represent minimum stream-bed elevations. Computations from these data indicated that the height of the sand dunes varied from approximately 0.2 ft to 1.6 ft; the average was approximately 0.7 ft.

The velocity of movement of the dunes was considered to be the average of the velocity of the crest and the velocity of the trough. An entire trough-crest combination was studied over a period of time, and the average velocity of the crest and trough was determined. The velocity of the crest varied from 1.2 ft per hr to 15.6 ft per hr, and the velocity of the trough varied from 4.1 ft per hr to 13.0 ft per hr. The average velocity of the dune was approximately 7.3 ft per hr. These measurements are, of necessity, only approximate, but they do give an indication of the order of magnitude of the velocity of the dune movement in this particular river. By assuming that the average height of the dunes was 0.7 ft and that the average velocity of movement of the dunes was 7.3 ft per hr, the concentration of sediment that moved as dunes was approximately equivalent to 310 ppm.

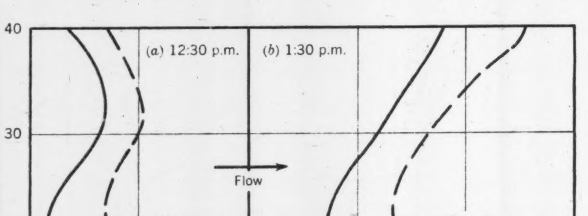

Fig. 18.—Typical Dune Movement Upstream from Prototype During 1-Hr Period, 1.5-Ft and 1.0-Ft Baffles (September 20, 1951)

In walking along the river, it was noticed that certain areas of the dunes were stable and that other areas of the dunes were fluid. Those areas that were the most fluid were forming and moving most rapidly. Although the predominant direction of movement of the dunes was parallel to the direction of flow, many of the dunes had a tendency to move diagonally to the left or to the right.

The crests of the large dunes when approaching the flume would, at times, be at an elevation higher than the top of the baffle plates in the flume. As these dunes moved toward the upstream baffle plate, it appeared that the baffle would be covered. However, when each dune reached a point within 1 ft of the baffle plate, the downstream side of the dune would begin to be carried into suspension; in this manner, most of the dunes were prevented from covering the baffles. Occasionally, however, the dunes were sufficiently large to cover the upstream baffle and move on to the second baffle. In moving from the upstream baffle to the second baffle, a higher percentage of such a dune was carried into suspension so that the dune was never able to cover completely any of the baffles in the second row. As the dune moved downstream, the upstream baffle slowly emerged through the top of the dune. The dune was rapidly forced into suspension by the increased turbulence and was carried downstream.

By the time the dunes had traveled past the first four rows of baffles, only a small quantity of the material was being transported as bed load along the floor of the flume. Deposits on the downstream side of each of the baffle plates were relatively stable and changed little in size or shape with the passage of time. Samples taken from these deposits on the downstream side of the baffles indicated that the deposited material was coarser for the downstream baffles than it was for the upstream baffles. Coarse material with a maximum diameter of $1\frac{1}{4}$ in. along the principal axis was occasionally found on the upstream side of the 6-in. baffle and the measuring sill. Such material was apparently being carried over the measuring sill as bed load. Because the quantity of this material was so small in comparison with the total load carried over the sill in suspension, it was considered negligible.

Increased Turbulence Through Flume.—The quantity of head loss in flow through the flume is a measure of the energy dissipated as turbulence. The length of the flume is 38 ft. For average discharges the fall through the flume was approximately 0.35 ft. The normal slope of the river reach adjacent to the flume averages 7 ft per mile, or 0.00133 ft per ft. When multiplied by the length of the flume, this slope would indicate a normal fall of 0.051 ft. The fall differs by approximately 0.3 ft from the measured fall of the water surface through the flume and is approximately the head loss that is caused by the dissipation of energy by turbulence.

COMPARISON OF MODEL AND PROTOTYPE

Although it was hoped that an accurate comparison of the behavior of the model and the behavior of the prototype structure could be made, there were several reasons why the model could not be operated under conditions dynamically similar to the prototype. In view of this situation, the data from the model cannot be expected to compare exactly with the data from the prototype.

The model was arranged so that the floor was horizontal, and the upstream reach of the model channel, of necessity, could not be exactly similar to that of the prototype. Furthermore, a section of the river and structure was taken so that the side effects and the boundary layer developed along the glass wall were different from those found in the prototype. The sand used in the model was somewhat larger than that which would have been dynamically similar to the sand in the prototype. Therefore, only an approximate comparison regarding the scour is possible. The exact sediment concentration and water discharge for the prototype could not be anticipated when the initial model studies were made; therefore, the model was tested at probable concentrations and probable rates of discharge.

Despite these differences, several interesting and significant comparisons can be made. The model studies indicated that, if all the baffles were at least 1.0 ft high, the measuring sill would be clear. In the prototype, this was found to be true except for the region in which peculiar flow patterns existed and caused deposition. Two of the irregularities were an interference of the flow pattern caused by deposits of debris upstream and downstream from the north section and a slight change in alinement of the river. Because of these peculiarities in the prototype, it was necessary to increase the height of the two upstream rows of baffles to 1.5 ft. By this alteration, the measuring sill was kept clear throughout its length, and none of the baffles was covered permanently.

Observations of the model indicated that the dunes formed a certain pattern as they approached the first baffle. As they passed the succeeding baffles, the turbulence forced the dunes into suspension. Similarly, observations of the prototype showed that the same type of dune pattern was developed and that the dunes moved down among the baffles in approximately the same manner as in the model. In some parts of the prototype flume, the dunes were forced completely into suspension farther upstream than in the model, and in other parts of the prototype the dunes were forced completely into suspension farther downstream than in the model. These differences can be explained, at least in part, by the peculiar situation that caused a three-dimensional and unsymmetrical flow pattern in the prototype.

The concentration of sediment moving over the measuring sill and the variation of this concentration, both vertically and horizontally in the prototype, are somewhat different from those found in the model. In the model, the concentration distribution was uniform in the lateral direction, and the vertical distribution showed a gradual decrease in concentration with height above the sill. In the prototype, however, these distributions were rather irregular. However, most of these irregularities appear to be associated with the peculiarities of the prototype structure caused by the shape and nature of the river channel upstream and downstream from the structure.

The total concentration of sediment carried in suspension upstream from the flume, the concentration carried as bed load in the form of dunes, and the concentration carried in the form of saltation (unmeasured suspended load) and bed load that is not moving as dunes in the model seemed to compare well with the same concentrations measured in the prototype. In the model, 62% of the total concentration was transported as suspended load at an alluvial section, 22% was traveling as dunes, and 16% was traveling as unmeasured suspended load and bed load. In the prototype, the comparable percentages would be 53%, 29%, and 18%, respectively.

The height of the dunes that approached the prototype averaged approximately 0.7 ft, whereas the model indicated that the height of these dunes would be approximately 0.35 ft. Thus, a twofold difference exists in the size of the dunes and can be explained, at least in part, by the fact that the concentration in the prototype was approximately twice that in the model. The velocity of the dunes was approximately 7.2 ft per sec in the prototype, and the model indicated that the velocity of these dunes would be 7.8 ft per sec. This comparison, in view of the approximate nature of the measurements made, is regarded as remarkably similar. It is to be expected, however, that the velocity of the dunes would be approximately the same in the prototype as is indicated by the model because the rate of movement of bed load (hence, the dunes) is proportional to the velocity of the stream.

CONCLUSIONS

This investigation, including both model studies and prototype studies, indicates that it is generally possible to determine in advance, by the use of a model, an approximate quantitative measure of the action of a prototype structure that involves the transportation of sediment. Such a comparison is possible because the turbulence causes the forces of inertia to be predominant over the forces of viscosity in connection with the development of the boundary layer. The predominance of the forces of inertia over the forces of viscosity reduces, or almost eliminates, the importance of the Reynolds number. Furthermore, the sediment is characterized by its settling velocity as the material in the model was dynamically similar to that in the prototype.

It is of interest to note that, where the Reynolds number is involved in the fall velocity of the sediment particles, the influence of viscosity is taken into account and is reflected by the fall velocity of the particles. Therefore, the Reynolds number and viscosity pertain only indirectly to the problem.

The information available (as of 1954) is not sufficient to determine positively whether the model would be able to give an exact indication of the quantitative action of the prototype if it were geometrically and dynamically similar to the prototype.

The studies of the prototype indicate that the available roughness is sufficient to introduce the turbulence required to transport the total sediment load in suspension for the concentration and flow encountered.

ACKNOWLEDGMENTS

The development and construction of the turbulence flume for the measurement of total sediment load in the Middle Loup River were under the general supervision of the Geological Survey in cooperation with the Bureau of Reclamation (USBR) both of the United States Department of the Interior. Permission to build the flume at the highway bridge at Dunning was granted by the Department of Roads and Irrigation, State of Nebraska.

The hydraulic design was made and the laboratory model studies were conducted by the Civil Engineering Department through the Research Foundation of Colorado Agricultural and Mechnical College at Fort Collins. Preliminary plans were sent to the USGS in June, 1948, and a final report was issued in July, 1948. The structural design and the construction plans and specifications of the prototype were prepared by the USGS.

In conducting this investigation, assistance has been received from Thomas Maddock and E. W. Lane, Members, ASCE, W. M. Borland, A. M. ASCE, J. H. Honnold (USBR); D. S. Jones, H. G. Schlitt, M. ASCE (Nebraska); and N. A. Christensen, M. ASCE (Colorado Agricultural and Mechanical College).

Appreciation is due also to the following: Earle Chamness, David Navon, J. M. ASCE, and Pavel Novak for their assistance in the model studies and analysis of data; R. E. Oltman, A. M. ASCE (USGS), for preparing the construction plans for the prototype flume and for supervising a major part of the construction work; and R. B. Vice, M. ASCE (USGS), for supervising the completion of the installation and the collection of the basic data.

APPENDIX. NOTATION

The following symbols, adopted for use in the paper and for the guidance of discussers, conform essentially with "American Standard Letter Symbols for Hydraulics" (ASA Z10.2-1942) prepared by a committee of the American Standards Association with ASCE representation, and approved by the Association in 1942:

b = width of a baffle;
c = concentration of sediment being transported by the stream;
d = mean depth of the water in an undisturbed section of the stream;
F = Froude number;
ΔH = head loss;
h = height of the baffles;
R = Reynolds number;
s = longitudinal spacing between the rows of baffles;
V = mean velocity of the water in an undisturbed section of the stream;
x = open distance between adjacent baffles in a row;
$\Delta\gamma$ = difference between the specific weights of water and air;
μ = dynamic viscosity of the water;
ρ = density of the water;
ρ_s = density of the sediment;
σ_s = standard deviation of the fall velocity of the sediment; and
ω = mean settling velocity of the sediment in the stream.

DISCUSSION

W. H. Corbett,[23] O. C. Hansen,[24] and W. M. Borland,[25] A. M. ASCE.—An interesting presentation has been made of the design and operation of the turbulence flume on the Middle Loup River. The information resulting from the operation of the turbulence flume is valuable to the development of water resources in the area.

The streams of this area are alluvial and are relatively wide and shallow with moderately steep slopes (7.0 ft per mile). The flow of the streams is usually constant with an extremely low probability of having either high discharge or low discharge. The stream flows originate primarily as ground water, seeping either directly to the main-stem streams or to the tributaries. A small part of the total drainage area contributes surface runoff to the streams. This condition exists because the topography is Aeolian and because the infiltration rate of the soil is high. The surface materials are the residuals from the Aeolian action. The area is known locally as "The Sand Hills," and (in a geological sense) considerable movement is taking place (as of 1954) even though the area is covered with grass. The sediment carried by the streams therefore originates principally from the stream bed and the banks. Sand movement and deposition along the stream banks by wind action assure a plentiful supply of sedimentary material.

The use of this stream water for irrigation purposes necessitates some provision for handling the sediments. A visual inspection of these streams will show considerable sand movement. Because of the investigations in the Lower Platte River area (in Nebraska) for the potential irrigation of approximately 1,700,000 acres of land, the USBR is vitally interested in the sediment loads of these streams. The necessity for attention to this subject is forcibly demonstrated by the existing (1954) sediment-disposal pile of the Loup River power district at the Genoa Diversion Dam (near Genoa, Nebr.).

Engineers responsible for the planning or operation of a diversion dam or storage reservoir in this area are immediately confronted with the problem of the costs that must be allocated to the storage of sediment in reservoirs or to the annual maintenance and operation of sediment handling. In the case of a storage reservoir, the problem is the cost of providing additional storage space for the sediment produced by the drainage area during the contemplated life of the structure. In the case of a diversion structure, the problem is that of the annual cost of handling the sediments by a mechanical or hydraulic disposal method. The water-resources plan for the development of these steady-flowing streams includes more diversion dams than on-channel storage reservoirs. Therefore, it is of prime importance that the estimates of the cost of handling the sediment be consistent with the estimates of costs of the other features of the project in determining the potential benefits. This requirement necessitated the construction of some type of field installation which would make possible the measurement of the total sediment load at a particular point. This installation was also needed to establish a correlation with other sampling sites where the total sediment load cannot be found from a study of the data provided by the standard sampling procedures.

---

[23] Civ. Engr., Area Office, Bureau of Reclamation, U. S. Dept. of the Interior, Grand Island, Nebr.
[24] Hydr. Engr., Region 7, Bureau of Reclamation, U. S. Dept. of the Interior, Denver, Colo.
[25] Head, Sedimentation Sect., Bureau of Reclamation, U. S. Dept. of the Interior, Denver Colo.

It was observed that a considerable quantity of the material appeared to move close to the bed of the stream. This raised a question as to the validity of the ordinary sediment-sampling methods for determining the total sediment load. The turbulence flume at Dunning was jointly conceived by those interested in sediment in this area, and it was primarily developed to evaluate the effectiveness of the ordinary sampling procedures. It was expected that the information gained from studying the flume data could be used in evaluating the sampling on the other streams in the area. The problem of the adequacy of the ordinary sampling procedures can be further illustrated by a comparison of the sediment-transport characteristics of these streams and the results provided by the present (1954) sampling procedures and equipment.

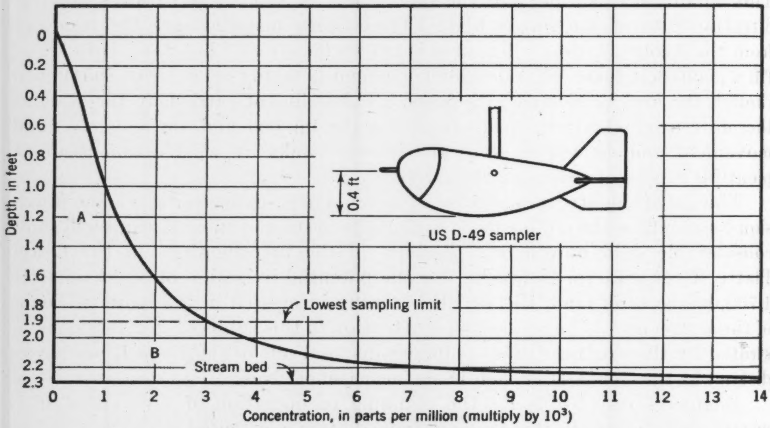

FIG. 19.—VERTICAL SEDIMENT-DISTRIBUTION CURVE

A typical cross section of a sand-hill stream is shallow and wide. For example, eight observations which were made at one section on the Middle Loup River for an average discharge of 362 cu ft per sec indicated an average depth of 1.1 ft and an average width of 153 ft. The average velocity was 2.14 ft per sec. Although the average depth was 1.1 ft, the extremes varied between a few tenths of a foot and slightly more than 2.0 ft. The sediment-sampling equipment in use (1954) at most stations includes the US DH–48 sampler and the US D–49 sampler—both of which are of the depth-integrating type. The US DH–48 sampler is adapted for use by wading, and the US D–49 sampler is adapted for cable-suspension use. The intake nozzle for these samplers, because of the construction and operation of the latter, is located so that a sample can only be integrated to within 0.4 ft of the stream bed. Therefore, if a stream is wide and shallow, a considerable part of even the normal suspended load can be missed by such a sampler. In Fig. 19 there is shown a typical vertical sediment-distribution curve obtained on a sand-hill-type stream. Also shown in Fig. 19 is a sketch of a US D–49 sampler showing the location of the nozzle with respect to its lowest extremity. The vertical sediment-distribution curve was obtained in a stream having a depth of 2.3 ft, as can be noted by the vertical ordinate. The sampler, therefore, will only obtain a sample to a depth, in this case, of 1.9 ft. The sampler will integrate, with respect to depth and velocity, that part of the curve designated as A. The common method of converting the concentration represented by the integrated part A to sediment movement, in tons, is to multiply the concentration by the water discharge. The water discharge is that volume of water moving in the total section—including that area represented by B. The establishment of a true value for the suspended-sediment concentration would require an integration of the total vertical distance including both areas A and B. The magnitude of the error depends on the depth of the section and the shape of the vertical distribution curve. The characteristics of the sand-hill streams are such that both the depth and vertical distribution tend to give a sizable error.

The intensive sampling studies conducted at Dunning and at other locations in the surrounding area have shown the importance of good sampling technique. When the shape of the vertical sediment-distribution curve is such that the concentrations become greater as the stream bed is approached, the magnitude of the error increases. It becomes imperative that each sampling station be intensively studied to determine the probable accuracy of the sampling results. This opinion is further substantiated by the fact that the percentage of unmeasured sediment varied from 20% to 60% for the various experimental sections, which were located above and below the turbulence flume.

One point which the authors failed to emphasize is that the limited size of the material available for suspension makes it possible to sample the total load at the turbulence flume. In the conception of the turbulence flume, the following important factors were considered:

1. The material size was limited to that which could be accommodated by the range of nozzle sizes available for use in the standard samplers.
2. The kinetic energy which was developed or produced by the stream was sufficient to place in suspension the maximum size of sedimentary material contributed by the drainage area or stream bed.

The material from the drainage area is predominantly sand, the major part falling in the fine-sand bracket. A size analysis of the bed material of the Middle Loup River shows that approximately 90% is finer than 1 mm, and approximately 98% is finer than 4 mm. This analysis actually defines a material that is coarser than the average of the bed materials from which it originates because a sorting action has taken place which causes the coarser material to be residual on the stream bed.

The authors refer to the altered vertical distribution of the sediment load which results from the induced turbulence created by the baffle plates of the flume placing in suspension all the sediment carried by the stream. This condition is generally true, as was noted in the operation of the flume. However, it has been noted on several occasions that the vertical distribution of the sediments, particularly in the coarser-sand fractions, increases measurably toward the bottom of the vertical section. The use of the sill downstream from the baffle plates makes it possible to place the sampling nozzle directly on the lip of the sill and thereby to sample the entire vertical sediment load. To assure that this is done for each sample, a set of guides has been constructed whereby the sampler is guided in its vertical movement. Careless or indiscriminate sampling techniques, even in conjunction with the flume, still cannot be used to measure total load at times.

As noted by the authors, the turbulence flume, as tested in the laboratory and as built and operated in the field, is capable of suspending the total sediment load so that it can be measured with existing sampling equipment. However, there is still a need (as of 1954) for further study of the hydraulic characteristics of the channel transporting the load—characteristics such as the depth, velocity, roughness, and slope. Such study will lead to a relationship which can be applied to standard measurements to develop estimates of the total load so that engineers can make more accurate estimates of the sediment at other sites.

PAUL C. BENEDICT[26] and MAURICE L. ALBERTSON,[27] MEMBERS, ASCE, and DONALD Q. MATEJKA,[28] J.M. ASCE.—Appreciation is expressed for the interest taken by Messrs. Corbett, Hansen, and Borland in presenting additional information and constructive criticism. As noted in the discussion, the measurement of total sediment load in alluvial streams is fundamental in the development of river-control works and diversion works. The total load, together with a determination of the specific weight, is of particular significance in planning the capacity of a storage reservoir. Similarly, information regarding the quantities and size distributions of sediment transported by a stream is required for the design of efficient sediment-disposal works. In Fig. 20 is shown part of the desilting works of the Loup River Public Power District, near Genoa.

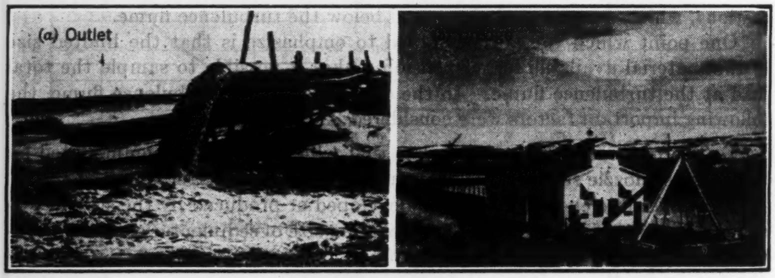

FIG. 20.—DESILTING WORKS (GENOA, NEBR.)

---

[26] Regional Engr., Geological Survey, U. S. Dept. of the Interior, Lincoln, Nebr.

[27] Prof. of Civ. Eng. and Head of Fluid Mechanics Research, Colorado Agri. and Mech. College, Fort Collins, Colo.

[28] Hydr. Engr., Geological Survey, U. S. Dept. of the Interior, Lincoln, Nebr.

In this district it was found that approximately 450 acre-ft of sediment were added annually to the disposal area in the period from 1946 to 1952.

The Middle Loup River provided a site for the turbulence flume where 98% of the bed material ranged from 0.062 mm to 4 mm. The range of material available for transport eliminates the possibility of any appreciable error that might result from the size of the intake nozzle of the US DH-48 sampler. Measurements with a $\frac{3}{16}$-in.-diameter nozzle gave results not distinguishable from results obtained with a $\frac{1}{4}$-in. nozzle. Therefore, the $\frac{3}{16}$-in. nozzle was used because of the longer sampling interval.

The US D-43, US DH-48, and US D-49 samplers were designed to sample within 0.38 ft, 0.29 ft, and 0.34 ft of the stream bed, respectively. In actual practice the accuracy of collecting sediment samples depends on the stream-channel characteristics, sampling equipment, and sampling techniques.[16,29,30,31]

The writers wish to emphasize further the suggestions made by the discussers. The data obtained at the turbulence flume are adequate to define the sediment in transport at Dunning. However, these data must be correlated with the hydraulic characteristics and the sedimentary characteristics of the stream in order to develop satisfactory methods of obtaining reasonably accurate estimates of the total load at other sections or in other streams. Studies should also be made of the relationship between the secondary circulation (transverse flow) within the stream and the shape, orientation, and movement of the dunes.

---

[29] "Measurement and Analysis of Suspended Sediment Loads in Streams," by Martin E. Nelson and Paul C. Benedict, *Transactions*, ASCE, Vol. 116, 1951, p. 891.

[30] "The Efficiency of Depth-Integrating Suspended-Sediment Sampling Equipment," by Ning Chien, *Transactions*, Am. Geophysical Union, Vol. 33, 1952, p. 693.

[31] Discussion by R. F. Kreiss and B. R. Colby, and by Ning Chien of "The Efficiency of Depth-Integrating Suspended-Sediment Sampling Equipment," by Ning Chien, *ibid.*, Vol. 34, 1953, p. 796.

AMERICAN SOCIETY OF CIVIL ENGINEERS
Founded November 5, 1852
TRANSACTIONS

Paper No. 2751

STATUTORY CONTROL OF GROUND WATER IN THE WESTERN UNITED STATES

BY S. T. HARDING,[1] M. ASCE

SYNOPSIS

The increasing importance of the use of ground water in the western states of the United States together with the overdraft that occurs in many areas makes it essential that methods be found to enable individual users to secure an equitable share of the available supply and to limit draft to the safe yield in order that the use of ground water may be permanent and stable. The delay in the accomplishment of these results has been caused as much by lack of agreement on what should be done as it has by the search for legal means for this accomplishment. Conditions in some areas are such that the need for control outweighs the difficulties of its enforcement.

INTRODUCTION

The rapid increase in the use of ground water in several of the western states of the United States has resulted in overdrafts in numerous areas; these overdrafts are the cause of widespread concern. Although high crop prices (as of 1954) have enabled the costs of irrigation pumping to be met, sooner or later the increasing lift will reach a point where pumping will no longer be profitable. This economic limit, rather than the complete physical depletion of the ground-water resource, is the main problem in the majority of such areas. There is a public interest in such conditions because the abandonment of any substantial amount of development affects the economy of the adjacent area and of the state as a whole.

Prevention of such conditions is the best remedy. Much consideration has been given to the methods by which public control may be exercised to restrict overdraft and maintain a stable economy. To meet the overdrafts on their natural ground-water supplies, some areas have been able to secure supplemental water. Such artificial ground waters may be the result of the so-called "spreading" of flood waters on nonproductive absorbent areas or they may be

---

NOTE.—Published, essentially as printed here, in November, 1953, as *Proceedings-Separate No. 346*. Positions and titles given are those in effect when the paper was received for publication.

[1] Cons. Engr., Berkeley, Calif.

the by-products of surface irrigation. These artificial ground waters involve additional questions of title to their use and control.

Statutory control of ground water alone does not solve the entire problem. Securing the factual material required for the administration of any system of ground-water regulation in each ground-water area will be as difficult as selecting the principles of control to be used.

The following material is an attempt to describe the basis on which the control of natural and artificial ground waters may be established in the interests of both the individual users and the general public. The larger part of the references are to conditions in California. Natural and artificial ground waters are discussed separately.

Occurrence of Ground Water

Nearly all ground waters percolate slowly through the generally porous underground materials. Occasionally ground water occurs and moves in definable channels. Use from such subterranean streams follows the same rules as use from surface streams. Ground waters are assumed to be percolating unless a defined channel can be proven.

Percolating water may occur as the result of the saturation of an underground material that is either unconfined or between confining beds. Confined percolating water is usually under some pressure; where the pressure exceeds the depth of the confining materials, flowing wells can be secured. Confined percolating waters are generally referred to as artesian basins, both where the pressure produces surface flow and where the ground water rises only partly to the ground surface.

Pressure areas have confining top strata and, usually, confining lateral boundaries so that such areas are definable ground-water basins. Although unconfined percolating ground waters may have definite lateral boundaries, the saturated material may blend into tighter formations. Unconfined ground waters may occur under conditions which permit defining separate ground-water areas.

The ability to define the margins of ground-water basins has been used as the basis for the separate control of percolating water in basins where similar control of generally diffused ground water has not been undertaken. Ground-water control in New Mexico is limited to water in definable basins. A common interest among the owners of the overlying land is more easily recognizable in a ground-water basin than in vagrant percolating waters.

General Basis for the Control of Ground Water

When conditions arise under which it is essential that new points of law be established or more detailed definition of principles be made, the controlling influence is the public interest. Where they are not bound by established precedents, courts and legislatures seek the basis that will best meet the public needs. Although changes cannot be made in established principles which would result in the equivalent of taking property without compensation, in new fields the legislatures and the courts have much latitude in determining what may best serve the public interest. There has been (as of 1954) an increasing emphasis on the public interest in the conservation of all natural resources. The police powers can be used to secure regulation short of an actual taking of the property being regulated.

NATURAL GROUND WATERS

Title to Natural Ground Waters.—The basis of the title to the use of ground water is not uniform in the various states. There are three separately recognizable standards of title with additional variations.

The earliest basis of title to ground water is the English common law of complete ownership by the overlying owner. Under the English law the ownership of all underground material, including water, is in the ownership of the surface. A landowner under the English common law cannot cause legal injury to a neighbor by any ground-water draft he may make. This rule does not recognize that ground water moves and may be a common source of supply to many owners. The English system of title is sometimes referred to as the right of capture as any overlying owner may capture whatever ground water he can secure from within his land.

Extensive ground-water draft resulted in inequities under the English common law. This led the courts of many states to recognize various degrees of correlative rights among the overlying owners and to permit some form of proportional use.

Some western states have applied the appropriation system used on surface streams to their ground waters.

Although the elements of one or more of these three systems of title have been adopted in each of the western states, variations in their application make it difficult to classify some of these states as following any one of these systems for all ground waters.

Control of Ground Water.—The right to control waste of ground water is well established. Such waste is usually limited to loss from uncapped artesian wells. In some cases control of such waste has been based on the prevention of surface nuisances or the protection of public health. Control can also be based on the general power to prevent waste of a natural resource.

For percolating ground water not under sufficient pressure to rise to the ground surface, the cost of pumping usually controls the waste of the water pumped. Ground-water movement from under one owner's land to another's land may result in a loss in opportunity to secure a ground-water supply but is not a loss or waste of the supply itself.

Control to prevent depletion of a ground-water supply or deterioration of quality or to secure economical conditions of draft represent different practices than the prevention of wasteful flow from an artesian well. Such controls must be justified by a broader interpretation of the public interest under the police power. Overdraft on a ground-water supply may be detrimental to the interests of the overlying owners using the draft and indirectly detrimental to the general public, but such overdraft is generally used without waste.

Requirements of Beneficial Use.—All western states have authority to limit use to reasonable standards of beneficial use. In California the constitutional amendment of 1928[2] limits all users to reasonable quantities and methods of use. Limitations to beneficial use go far beyond the prevention of waste. A use may produce a benefit and still not be reasonable in relation to other uses which may be made of the same water supply. Because of the increasing demands for water in the arid areas, there is a continuing trend toward a stricter interpretation of the standards of beneficial use.

---

[2] **Constitution of the State of California, Article XIV, Section 3.**

A county ordinance which prohibits use for purposes of limited benefit when that use depletes the supply available for other uses was upheld in California.[3] The western states either have, or can secure by proper legislative action, authority to require a reasonably high standard of beneficial use of their ground waters.

Regulation among Individual Users.—Control of ground-water draft by statutory authority is inconsistent with the basis of the English common law. The English common law of ground water is now (1954) in effect in only a few areas having problems of overdraft.

Under systems of correlative rights, control of draft can be established for the purpose of securing to each user his share of the available supply. A determination of the individual shares is required as a basis for such a control. Control can be exercised by an organization of the overlying owners, by a court in the enforcement of its decree, or by a state administrative agency. A state agency can function either under its own determination of the rights or by appointment of the court.

Where the appropriation system is used, the administration of ground waters is similar to that for surface streams when the extent and priority of the rights have been defined. Control consists in limiting the total draft to the safe yield of the supply.

Artificial Ground Waters.—The general law of ground water was developed to apply to the use of naturally available ground-water supplies. Such supplies are frequently less than the demands. In some areas where surface storage may not be available, surplus surface supplies can be placed underground as a supplement to the ground-water supply. When this is done, the title to the use of the artificial supply may rest on different principles than those applicable to the natural ground waters.

Spreading surplus surface waters on absorbent areas to replenish ground-water supplies was recognized as a beneficial use in California in 1919[4] when storing of water underground was declared to be a use for which an appropriation could be made. In some areas temporarily available surplus waters have been purchased for replenishment of underground supplies. Other artificial sources of ground water are the by-products of surface irrigation where the conveyance losses and percolation from the lands served augment the local natural ground waters. Importation of water from outside drainage areas for both supplemental surface irrigation and ground-water recharge is the basic justification for the Central Valley Project of California.

CONTROL OF ARTIFICIAL GROUND WATER

The right to recover artificial additions to the ground water may be vested in the individual landowners, in organizations of overlying landowners, in a nonlandowning agency, or in the state.

---

[3] Ex parte Maas, 27 Pac (2d) 373, 1933.

[4] *California Water Code*, 1919, Section 1242.

When no separate claims of ownership of artificial ground waters are made by the agency responsible for their occurrence, the artificial supply becomes the equivalent of abandoned water in surface streams. Such abandoned ground water combines with the natural supply and is subject to the same basis of title as the natural supply.

Such abandonment occurs in many irrigation systems when the organization providing the supply for surface irrigation makes no further claim to the canal seepage or deep percolation which joins the natural ground-water supply under the irrigated lands. The agency providing the surface supply may be liable if the increment of artificial ground water causes damage, and some forms of such agencies supplying surface irrigation are responsible for providing any needed drainage of the lands served.

Any efforts to restrict ground-water use by individual overlying owners to their natural ground water, thus leaving the artificial supply as a separate source available for other use, will face physical problems more difficult than the legal issues which may be involved. Identification of the artificial supply separately from the natural supply would be a first requirement in any attempt to establish separate title to use of the artificial supply.

The physical works required to provide artificial ground-water supplies usually involve costs which exceed the resources of individual owners. As a result, an organization of the landowners benefited may be formed. An organization may also be needed to act for all owners when conflicts with outside users arise.

This need was recognized in 1913 in California where there was established a form of county water district having authority to sue in behalf of its included landowners for the protection of their ground-water rights even though the district itself does not claim the ownership of the natural ground waters in the district.[5] Such county water districts are also given powers to restrict use by its landowners. The landowners are bound by the results of suits brought by the district and can be taxed for their costs.[6]

Comments of the court in the Coachella case[6] can be interpeted to imply similar powers in California irrigation districts. In Los Angeles vs. Glendale,[7] the case of Stevens vs. Oakdale Irrigation District[8] was cited on the right of an irrigation district to recover surface waters and was used to support the recovery of percolating water.

California also has acts available for the creation of water-conservation districts which have powers in relation to ground waters similar to those of the previously cited form of county water district.[9,10]

Some organizations that store ground water do not own or represent the owners of the lands under which the artificial ground waters are stored. Examples are the claims of the Bureau of Reclamation, United States Department of the Interior (USBR), to the right to waste and seepage waters resulting from the use of project water delivered to contracting units. There are also some areas in California where the ground waters stored are used on both overlying and distant lands.

---

[5] *California Water Code*, Division 12, 1913.

[6] Coachella Valley Co. Water District v. Stevens, 206 Cal. 400, 1929.

[7] 23 Cal. (2d) 68, 1943.

[8] 13 Cal. (2d) 343, 1939.

[9] Water Conservation Act of 1927, 1927:91:160; D.A. 9127a.

[10] Water Conservation Act of 1931, 1931:1020:2045; D.A. 9127c.

It has been the usual practice of the USBR to include a clause reserving to the United States the right to all return flows and waste from the contracting areas. This right of recovery has been sustained for surface return flows.[11] Similar clauses have been inserted in some of the water purchase contracts being made with units of the Central Valley Project where any resulting escaping water will be outward percolating ground water rather then surface waste.

The extent to which a water-supplying agency, such as the USBR, may establish a claim to artificial ground waters having their source in percolation from the conveyance and surface use of the purchased water supply has been and is a very active question in the areas of the Central Valley Project. A large part of the water to be purchased by the local units is to be delivered outside of the time of irrigation demand and placed in ground-water storage within the area of the contracting unit. This further complicates a situation which would be complicated enough if only surface uses were involved.

Any attempt by the supplying agency to claim seepage and waste from the water provided by the project while such ground water is in the area of the contracting unit involves both legal and physical problems. Such ground waters are not wastes while within the lands contracting for service because the water supplies for nearly all lands in the contracting units of the Central Valley Project are based on recovery and use of the available natural and artificial ground waters. In no unit is it planned to acquire sufficient project water to result in high ground water and surface return flows. An application of the recovery clauses in the USBR contracts appears to be limited to waters escaping from the contracting units and found under lands not under contract with the USBR. When the physical difficulty of identification is added to the legal uncertainty of the right to enter noncontracting areas to recover these waters, such claimed rights of recovery appear to have only limited prospect of realization.

In the Central Valley Project, there has also been the attempt to control the size of ownership by restrictions on the delivery of project service; this is the acreage limitation of the reclamation law.[12] Where project service is entirely by surface delivery, physical controls on delivery can be readily enforced. Where project service is by ground-water recharge (to which every landowner has access through works entirely in his ownership and control), no effective method has (as of 1954) been suggested for preventing ground-water draft on excess acreages. These acreage issues are now (1954) before the California courts in cases for which final answers may eventually be secured.

In the City of Los Angeles vs. Glendale,[7] the California court held that Owens River water brought to the San Fernando Valley and either sold for use there or spread for ground-water storage remains the property of Los Angeles. The water spread for ground-water recharge was held to be commingled water en route to the point of recovery and use. Percolation from the use of water sold by the city was given a similar status. This decision may not be controlling in areas of general percolating water—the comments of the court indicate that it considered the ground waters involved to be a part of the general subflow of the Los Angeles River which becomes part of the river flow within the pueblo right of Los Angeles.

---

[11] Ide v. United States, 263 U.S. 497, 1924.

[12] Reclamation Act of June 17, 1902 (32 Stat. 389), Sec. 5.

The unappropriated waters in the western states are owned by the state or are under its control. In states recognizing the appropriation system for ground water, state control of its appropriation follows logically from the similar control of surface streams. The state can also exercise police-power control over ground water in the interest of the public. Such police powers can be used for the prevention of waste and damage.

If a state should undertake to acquire water and to place it underground as an addition to the natural ground waters without owning the lands under which the artificial ground waters would spread, it would act in a proprietory capacity and be subject to the same rules as any other nonlandowning agency seeking the same results.

The state also acts in a judiciary capacity in defining titles to the use of ground water. In California the state engineer may act as referee for the court in ground-water suits. As referee, he investigates the facts and makes recommendations to the court on the issues. After adjudication of the individual ground-water rights in a ground-water area, the state engineer may act as the watermaster for the enforcement of the decree.

CONTROL OF OIL AND GAS

The early law of oil and gas was based on the law of minerals in place. Each landowner could capture whatever oil and gas he could secure from underneath his land. This principle led to competitive drilling, offset wells, and production in excess of the market demand.

In recent years there has been a general recognition of the need for conserving natural resources such as oil and gas. The right of a state to prevent waste of these resources has been recognized since the United States Supreme Court, in 1900,[13] upheld an Indiana statute prohibiting the waste of gas merely to provide pressure for oil production. The court recognized that oil and gas move underground and that all owners have a joint interest in the common supply.

Oil and gas are classified as nonreplaceable minerals which, once taken, are not replaced by natural processes within the time periods recognized by law. Recycling of gas or water is not a contradiction of this classification as such operations are for the purpose of increasing the production of the oil already in the ground and do not create new supplies.

Statutory methods have been found for securing increased recovery and for preventing wasteful production and excessive drilling. These methods have required changes in the former conceptions of the rights of overlying landowners and have demanded recognition that oil and gas occur in definable fields and that all owners in a field have a common interest in its best development.

Interstate Control.—The Interstate Oil Compact[14] was approved in 1935; the Interstate Oil Compact Commission was established to administer interstate matters and provide leadership in the educational activities necessary to secure consistent policies among the oil-producing states. More than twenty states are now (1954) members of this compact commission, which has functioned successfully in its field. This interstate compact and its administration are a good example of the ability of the states to function in interstate matters without requiring federal control. Where interstate ground waters need joint action by the states concerned, similar use can be made of the compact method.

---

[13] Ohio Oil Co. v. Indiana, 177 U.S. 910, 1900.

[14] Resolution of Congress of August 27, 1935, c. 781, 49 Stat 939-941.

Unit Operation.—A major step in the control of oil and gas production has been the recognition of each oil field as a unit in which all landowners have a mutual interest. Earlier unit-operation plans were based on the voluntary action of the landowners. When all owners consent, such voluntary plans meet the needs. When complete consent cannot be secured, demands arise for various degrees of compulsory unit operation. Some states have provided for compulsory unitization and have created state agencies for its administration. In other states the initiation of the procedure for the unit operation of each oil field requires a petition of the majority of the affected owners. When carefully drawn, the unitization statutes have been upheld as a proper exercise of state authority over its natural resources and the prevention of their waste.

CONCLUSIONS

The increasing importance of the use of ground water in the western United States and the overdraft that exists in many areas make it essential that means be found to enable individual users to secure their equitable share of the available supply and to limit draft to the safe yield in order to secure permanent and economical use. The delay in the accomplishment of these results has been due as much to the lack of agreement on the methods to be used as it has been to the finding of legal means for this accomplishment.

Restricting the draft to the average recharge is a natural objective in the apportionment of ground-water supplies among individual owners in areas following correlative rights. In areas following priority of appropriation, such restrictions can be supported on the basis that the average rate of recharge is the measure of the supply subject to appropriation.

The statutory basis for ground-water control has not (as of 1954) been fully developed. Care is required in differentiating between regulation in the public interest under the police powers and the taking of property without due process. However, the legal status of rights to the use of ground water has not been so rigidly defined that means cannot be found, short of an actual taking of property, by which the public interest can be served.

In California it may be considered that the 1928 amendment[2] is not broad enough to support limitations on ground-water draft where all use is reasonable but the total draft exceeds the available supply. An additional constitutional amendment may be needed to authorize control of the draft under such conditions; this can be supported on the basis of the general welfare so that those entitled to use such supplies can be protected in their use and overdraft can be prevented. With such constitutional support for the applicable principle, the state legislature can provide statutes for its enforcement.

There does not appear to be a need for separate statutory control of artificial ground waters. When abandoned and combined with the natural supplies, the artificial sources become part of the natural supplies and thus are subject to the same controls. If the artificial supplies are provided under conditions in which title to their use is retained separately from the natural supply, the terms and conditions under which such title is established should enable the use of the artificial supplies to be controlled in the interest of the agency having such separate title.

Conditions in the western United States vary; it is not to be expected that any one method will give the best results in all states. Each state should work out the solution which best fits its legal background and physical conditions.

Similarly, conditions within a state vary; the various areas may need different degrees of control enforced at different stages in their development. Such variations can be secured by general-authorization laws dependent on local initiative for placing them in effect. Although there is a general state interest in the best use of ground water as a natural resource and in preventing general losses resulting from abandonment of badly overdrawn ground-water supplies, the landowners in the ground-water areas are the principal parties of interest and should have a major voice in the selection of the extent of the control and the time and form of its enforcement.

To represent the landowners in a ground-water area it is desirable to have some form of district organization whose initiation rests with the landowners and whose powers include a right to tax the included lands and to act for the area in matters affecting its ground-water supply. Such public agencies are available in some states including California and can be provided in other states whenever demand for them arises. Preferably, such districts should include all the land in a ground-water basin. Where distinctions in control in various parts of the basin are needed, provision for subdivisions, such as those in the Texas Water Control and Improvement District Act,[15] can be used. Such districts are the equivalent of the unit fields in oil and gas control.

The control of the use of ground water that has been outlined does not represent so wide a departure from past practices as those that have occurred in recent years in the control of oil and gas. Both fields began with the complete independence of the overlying owner; in both, material changes have been made in this ownership. To date (1954) the extent of the changes has been greater for oil and gas because the actual need for change and the agreement regarding this need and how to meet it have been greater than in the field of ground water.

In order to meet existing problems resulting from ground-water overdrafts, no effective method of statutory control can avoid the necessity for the enforcement of limitations on individual wells. As there may be several thousand wells operating in a ground-water area, the mechanical problem of securing the records essential to the enforcement of controls has discouraged efforts to establish control. Similarly, the engineering difficulties in determining the draft that can be maintained without depletion have discouraged all those faced with the administration of any ground-water control. Such physical difficulties are inherent in the nature of ground-water supplies and cannot be avoided. Conditions in some areas have reached or are approaching the point where the demand for some form of control will outweigh the difficulties of its application.

---

[15] Texas Laws, 1949, Ch 306, amending Laws 1925, Ch. 25 to include 3c (Vernon's Ann. Civ. Stats. art. 7880-3c).

AMERICAN SOCIETY OF CIVIL ENGINEERS
Founded November 5, 1852
TRANSACTIONS

Paper No. 2752

IMPULSIVE MOTION OF ELASTO-PLASTIC BEAMS

BY HANS H. BLEICH[1] AND MARIO G. SALVADORI,[2]
MEMBERS, ASCE

WITH DISCUSSION BY MESSRS. P. S. SYMONDS; AND HANS H. BLEICH AND MARIO G. SALVADORI

SYNOPSIS

A general analysis is made of the vibrations of elasto-plastic structures. This analysis is applied to free-free beams moving under dynamic forces. The motion during the successive elastic and elasto-plastic stages is expressed in terms of the normal modes of the structure; the maximum plastic angle is evaluated. The case of impulsive loads (initial velocities), which is of practical interest, is considered specifically; by using simplifying assumptions, upper and (often) lower bounds of the plastic angle can be determined.

GENERAL THEORY

When an ideally elasto-plastic body capable of vibrating elastically in a single infinity of normalized, orthogonal, vectorial modes, $\phi_i(P)$—in which $i = 0, 1, 2, \cdots$—is subjected to a system of external forces varying with time, symbolically represented by $F(t)$, the vectorial elastic displacement $u_e(P)$ of one of its points P can be expanded into a series of modes

$$u_e(P) = \sum_{i=0}^{\infty} q_i(t)\, \phi_i(P) \qquad \text{(1)}$$

In Eq. 1 the generalized coordinates q_i, in the absence of damping, satisfy the Lagrangian equations,

$$\frac{d}{dt}\left(\frac{\partial T}{\partial \dot{q}_i}\right) + \frac{\partial V}{\partial q_i} = Q_i \qquad (i = 0, 1, 2, \cdots) \qquad \text{(2)}$$

NOTE.—Published, essentially as printed here, in September, 1953, as *Proceedings-Separate No. 287*. Positions and titles given are those in effect when the paper or discussion was received for publication.

[1] Prof. of Civ. Eng., Columbia Univ., New York, N. Y.

[2] Prof. of Civ. Eng., Columbia Univ., New York, N. Y.

In Eq. 2, T is the kinetic energy, V is the potential energy of the elastic body, and the Q_i are the generalized forces corresponding to the system of external forces F.

At time t equal to t_0 a plastic state of stress σ_0 is reached (as shown in Fig. 1) in a region of area A_0 about the point P_0, while at all other points the stresses remain elastic. For t greater than t_0, the constant force F_0 equal to $\sigma_0 A_0$ can be considered to be an external force applied to the same body, in which the continuity is destroyed on the area A_0 so far as the strain ϵ corresponding to σ is concerned. Indicating the normalized modes of this new relaxed body by $\psi_i(P)$, its generalized coordinates by $p_i(t)$, and the generalized force corresponding to $F(t) + F_0$ by P_i, the vectorial elasto-plastic displacement $u_p(P)$ can be expanded into a series,

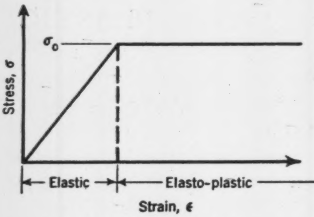

Fig. 1.—Elastic and Elasto-Plastic States of Stress

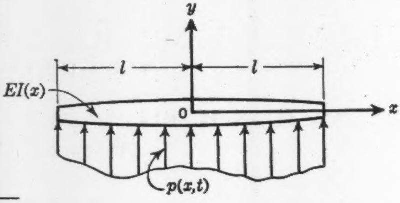

Fig. 2.—Free-Free Beam Under Dynamic Forces

$$u_p(P) = \sum_{i=0}^{\infty} p_i(t)\, \psi_i(P) \qquad (3)$$

in which the functions p_i satisfy the Lagrangian equations,

$$\frac{d}{dt}\left(\frac{\partial T}{\partial \dot{p}_i}\right) + \frac{\partial V}{\partial p_i} = P_i \qquad (4)$$

The modes ψ_i of the relaxed body may be conveniently obtained, in many cases, by the method of "complementary systems."[3] The continuity of the displacement u and of the velocity $\dot{u}$ at t equal to t_0 requires that

$$u_e(P)\,|_{t=t_0} = u_p(P)\,|_{t=t_0} \qquad (5a)$$

and

$$\dot{u}_e(P)\,|_{t=t_0} = \dot{u}_p(P)\,|_{t=t_0} \qquad (5b)$$

or

$$\sum_{i=0}^{\infty} q_i(t_0)\, \phi_i(P) = \sum_{i=0}^{\infty} p_i(t_0)\, \psi_i(P) \qquad (6a)$$

and

$$\sum_{i=0}^{\infty} \dot{q}_i(t_0)\, \phi_i(P) = \sum_{i=0}^{\infty} \dot{p}_i(t_0)\, \psi_i(P) \qquad (6b)$$

---

[3] "Frequency Analysis of Beam and Girder Floors," by Hans H. Bleich, *Transactions*, ASCE, Vol. 115, 1950, p. 1023.

Multiplying Eqs. 6 by ψ_k, integrating over the entire mass of the body, and noting the orthogonality conditions of the modes ψ_i,

$$\int \psi_i \, \psi_k \, dm = 0 \qquad (i \neq k) \tag{7a}$$

and

$$\int \psi_i \, \psi_k \, dm = 1 \qquad (i = k) \tag{7b}$$

shows that the initial conditions for the functions p_i reduce to

$$p_k(t_0) = \sum_{i=0}^{\infty} b_{ki} \, q_i(t_0) \tag{8a}$$

and

$$\dot{p}_k(t_0) = \sum_{i=0}^{\infty} b_{ki} \, \dot{q}_i(t_0) \tag{8b}$$

in which

$$b_{ki} = \int \phi_i \, \psi_k \, dm \tag{9}$$

Similar relaxations will give the equations of motion when other areas of the body become successively plastic, provided the plastic areas do not change shape or location.

The elasto-plastic motion defined by Eq. 3 will continue until the stresses in the plastic area A_0 revert to the elastic range. If this reversal takes place at a time t_1, the displacement $\bar{u}_e(P)$ for t greater than t_1 is given again by Eq. 1 with new generalized coordinates $\bar{q}_i$ satisfying Eqs. 2 and the initial conditions of continuity,

$$u_p(P)\,|_{t=t_1} = \bar{u}_e(P)\,|_{t=t_1} \tag{10a}$$

and

$$\dot{u}_p(P)\,|_{t=t_1} = \dot{u}_e(P)\,|_{t=t_1} \tag{10b}$$

or

$$\sum_{i=0}^{\infty} p_i(t_1) \, \psi_i(P) = \sum_{i=0}^{\infty} \bar{q}_i(t_1) \, \phi_i(P) \tag{11a}$$

and

$$\sum_{i=0}^{\infty} \dot{p}_i(t_1) \, \psi_i(P) = \sum_{i=0}^{\infty} \dot{\bar{q}}_i(t_1) \, \phi_i(P) \tag{11b}$$

Multiplying Eqs. 11 by $\phi_k(P)$ and integrating over the entire mass of the body, the initial conditions for the functions $\bar{q}_i$ become—because of the orthogonality of the modes ϕ_i—

$$\bar{q}_k(t_1) = \sum_{i=0}^{\infty} \bar{b}_{ki} \, p_i(t_1) \tag{12a}$$

and

$$\dot{\bar{q}}_k(t_1) = \sum_{i=0}^{\infty} \bar{b}_{ki}\, \bar{p}_i(t_1) \qquad (12b)$$

in which

$$\bar{b}_{ki} = b_{ik} \qquad (13)$$

A sequence of changes from the elastic range to the plastic range, and vice versa, allows the description of the elasto-plastic forced vibrations of the body at any time t.

Under particular circumstances, one or more of the plastic regions A can change either shape or location or both before a reversal of stress, or before additional plastic regions appear. In these cases (which will not be considered herein), new and more complicated equations of motion must be formulated; their integration may have to be performed by approximate, step-by-step methods.

Elasto–Plastic Vibrations of Free–Free Beams

As a typical example of the application of the general theory, one may consider the forced vibrations of a free-free beam of length $2\,l$, variable flexural rigidity $E\,I$, and variable mass per unit length m (Fig. 2).

The free vibrations of such a beam are governed by the differential system:

$$(E\,I\,y'')'' + m\,\ddot{y} = 0 \qquad (14)$$

$$y''(\pm\, l, t) = y'''(\pm\, l, t) = 0 \qquad (15)$$

$$y(x, 0) = y_0(x) \qquad (16)$$

and

$$\dot{y}(x, 0) = \dot{y}_0(x) \qquad (17)$$

in which the primes denote differentiation with respect to the variable x measured along the centroidal axis of the beam with the origin at its middle, and dots denote differentiation with respect to time.

The substitution of

$$y(x, t) = \phi(x)\, q(t) \qquad (18)$$

into Eqs. 14, 15, 16, and 17 shows that the beam can vibrate in an infinite number of modes ϕ_i, satisfying the equations,

$$(E\,I\,\phi''_i)'' - \omega^2_i\, m\,\phi_i = 0 \qquad (i = 0, 1, 2, \cdots) \qquad (19)$$

and the boundary conditions,

$$\phi''_i\,(\pm\, l) = \phi'''_i\,(\pm\, l) = 0 \qquad (20)$$

The modes ϕ_i are orthogonal and can be normalized so that

$$\int_{-l}^{l} \phi_i(x)\, \phi_j(x)\, dm = 0 \qquad (i \neq j) \qquad (21a)$$

and

$$\int_{-l}^{l} \phi_i(x)\, \phi_j(x)\, dm = 1 \qquad (i = j) \quad \ldots\ldots\ldots\ldots\ldots (21b)$$

It is convenient to indicate by the subscript i the number of nodes in the ith mode. Thus, i equal to zero represents the rigid translation of the beam, i equal to unity, its rigid rotation; i equal to 2, its first elastic mode; and so forth.

Indicating the general integral of Eq. 19 by

$$\phi_i = c_1 z_1 + c_2 z_2 + c_3 z_3 + c_4 z_4 \quad \ldots\ldots\ldots\ldots\ldots (22)$$

and substituting this value of ϕ_i into Eqs. 20, there results a homogeneous system of four linear algebraic equations in the constants c_1 to c_4, whose determinant, when set equal to zero, determines the frequency ω_i of the ith mode. The modes ϕ_i can be evaluated rigorously from the differential system (Eqs. 19 and 20)—or, if this is impossible or inconvenient, they can be obtained by approximate numerical or experimental methods.

The forced elastic deflections $y_e(x, t)$ of a free-free beam caused by an external, time-varying pressure $p(x, t)$ per unit length can be expanded in an infinite series of modes,

$$y_e(x, t) = \sum_{i=0}^{\infty} \phi_i(x)\, q_i(t) \quad \ldots\ldots\ldots\ldots\ldots (23)$$

Substitution of Eq. 23 into Eqs. 2 and into the initial conditions represented by Eqs. 16 and 17 shows that the generalized coordinates q_i satisfy the equations,

$$\ddot{q}_i + \omega^2{}_i\, q_i = Q_i \quad \ldots\ldots\ldots\ldots\ldots (24)$$

and the initial conditions,

$$\sum_{i=0}^{\infty} \phi_i(x)\, q_i(0) = y_0(x) \quad \ldots\ldots\ldots\ldots\ldots (25a)$$

and

$$\sum_{i=0}^{\infty} \phi_i(x)\, \dot{q}_i(0) = \dot{y}_0(x) \quad \ldots\ldots\ldots\ldots\ldots (25b)$$

The generalized forces Q_i corresponding to the load $p(x, t)$ are given by the integrals,

$$Q_i(t) = \int_{-l}^{l} p(x, t)\, \phi_i(x)\, dx \quad \ldots\ldots\ldots\ldots\ldots (26)$$

Multiplication of Eqs. 25 by $\phi_j\, dm$ and integration over the length of the beam gives the initial conditions for the functions q_i:

$$q_i(0) = \int_{-l}^{l} y_0(x)\, \phi_i(x)\, dm \quad \ldots\ldots\ldots\ldots\ldots (27a)$$

and

$$\dot{q}_i(0) = \int_{-l}^{l} \dot{y}_0(x)\, \phi_i(x)\, dm \qquad (27b)$$

At any time t, during the elastic stage of the vibrations, the bending moment at a section x is obtained by double differentiation of the deflection,

$$M(x, t) = -E\, I\, y''_e = -E\, I \sum_{i=0}^{\infty} \phi''_i(x)\, q_i(t) \qquad (28)$$

Under the assumption of an ideal elasto-plastic material, the elastic stage of the vibrations ends at the smallest value of the time t—say, t_0—at which the moment M reaches the plastic capacity value M_0 anywhere in the beam. If the moment M reaches the capacity value first at a section x equal to $\bar{x}$, the elastic stage of the vibrations ends when

$$|M(\bar{x}, t_0)| = \left| -E\, I \sum_{i=0}^{\infty} \phi''_i(\bar{x})\, q_i(t_0) \right| = M_0(\bar{x}) \qquad (29)$$

in which $M_0(\bar{x})$ is the capacity moment of the beam at the section x equal to $\bar{x}$. If, at least for a time, the capacity moment is not reached at any other section, the moment $M(\bar{x}, t_0)$ will remain constant and equal to $M_0(\bar{x})$. The elasto-plastic vibrations of the beam are then identical to the vibrations of another beam equal to the beam considered, but with a hinge at x equal to $\bar{x}$; this beam is acted upon by the same load $p(x, t)$ and by two external, equal, and opposite moments $M_0(\bar{x})$ at the hinge.

Indicating by $\psi_i(x)$ the orthonormal modes of the hinged beam, the elasto-plastic vibrations of the original beam can be expanded into a series,

$$y_p(x, t) = \sum_{i=0}^{\infty} \psi_i(x)\, p_i(t) \qquad (30)$$

in which the new generalized coordinates p_i satisfy the differential equations:

$$\ddot{p}_i + \Omega^2_i\, p_i = P_i \qquad (31)$$

in which Ω_i is the frequency of the ith mode of the hinged beam and P_i represents the generalized forces caused by the load p and the moments $M_0(\bar{x})$. The generalized force P_i is thus given by

$$P_i(t) = \int_{-l}^{l} p(x, t)\, \psi_i(x)\, dx + M_0(\bar{x})\, [\psi'_i(\bar{x} + 0) - \psi'_i(\bar{x} - 0)] \qquad (32)$$

The conditions of continuity of displacements and velocities at t equal to t_0 require that

$$y_e(x, t_0) = y_p(x, t_0) \qquad (33a)$$

and

$$\dot{y}_e(x, t_0) = \dot{y}_p(x, t_0) \qquad (33b)$$

Substitution of Eqs. 23 and 30 into Eqs. 33, multiplication by $\psi_k(x)\, dm$, and integration over the entire beam reduce these equations to the form:

$$p_k(t_0) = \sum_{i=0}^{\infty} b_{ki}\, q_i(t_0) \qquad (34a)$$

and

$$\dot{p}_k(t_0) = \sum_{i=0}^{\infty} b_{ki}\, \dot{q}_i(t_0) \qquad (34b)$$

in which the constants b_{ki} are given by Eqs. 9.

When a beam has its mass symmetrically distributed about its middle point, and when the pressure $p(x, t)$ is also symmetrical and such that the first hinge will develop at the midpoint, the modes ψ_i of the hinged beam are obtained by noting that there is no force transmitted through the hinge and that each part of the beam vibrates as a free-free beam of length l. The modes ψ_i are therefore the modes of the two half-beams normalized over the entire beam.

While the moment at x equal to $\bar{x}$ remains constant, a plastic angle $\theta(t)$ develops at this section; its value equals the discontinuity of the slope of the elasto-plastic deflection at x equal to $\bar{x}$:

$$\theta(t) = y'_p(\bar{x} + 0, t) - y'_p(\bar{x} - 0, t)$$
$$= \sum_{i=0}^{\infty} [\psi'_i(\bar{x} + 0) - \psi'_i(\bar{x} - 0)]\, p_i(t) \qquad (35)$$

At the time—say, t_1—when this angle reaches a maximum value, the relative motion of the two parts of the beam is reversed, and the moment at x equal to $\bar{x}$ becomes elastic again. Under the assumption of small plastic deflections and of elastic stresses at all sections of the beam except at x equal to $\bar{x}$, the beam deflections are given again by the series in Eq. 23 with new general-coordinates $\bar{q}_i$ satisfying Eqs. 24 and conditions of continuity at t equal to t_1. As the actual computations for a specific problem cannot be performed with more than the first few terms of the series expansions in Eqs. 23 and 30 (three to five terms are usually sufficient), conditions of continuity on the displacements y and on the velocities $\dot{y}$ at t equal to t_1 do not necessarily make the accelerations continuous at that time and hence may give a numerical discrepancy in the values of the moment $M(\bar{x}, t_1)$ computed by inertia forces in the elasto-plastic range and according to Eq. 28 in the elastic range. It is therefore often advisable to obtain the initial values of the functions $\bar{q}$ by imposing conditions of continuity on the velocities and on the accelerations in order to obtain continuous stresses at t equal to t_1. These conditions require that

$$\dot{y}_p(x, t_1) = \dot{\bar{y}}_e(x, t_1) \qquad (36a)$$

and

$$\ddot{y}_p(x, t_1) = \ddot{\bar{y}}_e(x, t_1) \qquad (36b)$$

By the use of Eqs. 23, 30, and 21, Eqs. 36 reduce to

$$\dot{\bar{q}}_k(t_1) = \sum_{i=0}^{\infty} \bar{b}_{ki}\, \dot{p}_i(t_1) \qquad (37a)$$

and

$$\ddot{\bar{q}}_k(t_1) = \sum_{i=0}^{\infty} \bar{b}_{ki}\, \ddot{\bar{p}}_i(t_1) \qquad (37b)$$

in which

$$\bar{b}_{ki} = \int \phi_k \psi_i \, dm = b_{ik} \qquad (38)$$

On the basis of the assumptions made, the stresses in the beam can be evaluated at any time t in terms of successive elastic and elasto-plastic deformations of the type given by Eqs. 23 and 30. In some cases the successive development of plastic hinges at more than one section must be considered, but the new hinges can be treated as shown previously with the introduction of no essential difficulty in the solution. In other cases, one or more of the successive hinges may shift their location continuously so that a whole part of the beam becomes plastic.[4,5] These wandering hinges introduce essential difficulties into the integration of the problem, which then can be solved, for example, step by step by using numerical-integration methods. Alternatively, such cases can be treated approximately by assuming that the beam has one or more "weak" points in the plastic region; all plastic deformations then occur at these weak points, and moments slightly in excess of M_0 are tolerated outside these points.

IMPULSIVE MOTION OF FREE–FREE BEAMS WITH CONSTANT FLEXURAL RIGIDITY

The Elastic Stage.—The impulsive motion of a beam resulting from forces of high intensity and short duration is equivalent, in the limit, to the motion caused by a sudden initial velocity. As an illustration of the theory presented previously, there shall be derived subsequently the formulas governing the elasto-plastic motion of a free-free beam of length $2l$ and constant flexural

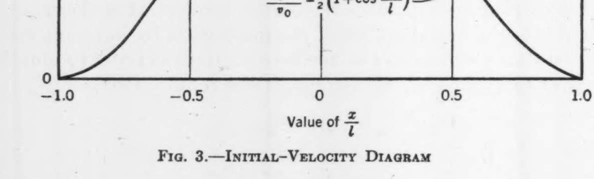

FIG. 3.—INITIAL–VELOCITY DIAGRAM

---

[4] "Large Plastic Deformations of Beams under Transverse Inpact," by E. H. Lee and P. S. Symonds, *Transactions*, ASME, Vol. 74, 1952, p. 308.

[5] "On the Development of Plastic Hinges in Rigid-Plastic Beams," by Mario G. Salvadori and F. DiMaggio, *Quarterly of Applied Mathematics*, July, 1953, p. 223 ff.

rigidity $E\,I$, whose initial velocity $v_0(x)$ is given by the symmetrical distribution (Fig. 3):

$$\dot{y}_0(x) = \frac{v_0}{2}\left(1 + \cos\frac{\pi}{l}\,x\right) \qquad (39)$$

The elastic orthonormal modes of such a beam are given by[6]

$$\phi_0 = \frac{1}{\sqrt{2\,m\,l}} \qquad (40a)$$

$$\phi_1 = \frac{\sqrt{3}}{\sqrt{2\,m\,l}}\,\frac{x}{l} \qquad (40b)$$

$$\phi_i = \frac{1}{\sqrt{2\,m\,l}}\left(\frac{\cos k_i\,x}{\cos k_i\,l} + \frac{\cosh k_i\,x}{\cosh k_i\,l}\right) \qquad (i = 2\,r;\ r = 1, 2, \cdots) \qquad (40c)$$

and

$$\phi_i = \frac{1}{\sqrt{2\,m\,l}}\left(\frac{\sin k_i\,x}{\sin k_i\,l} + \frac{\sinh k_i\,x}{\sinh k_i\,l}\right) \qquad (i = 2\,r + 1;\ r = 1, 2, \cdots) \qquad (40d)$$

The corresponding frequencies are given by

Value of i	Value of $2\,k_i\,l$
0	0
1	0
2	4.730
3	7.853
4	10.996
5	14.137
6	17.279

with

$$(k_i\,l)^4 = \frac{m\,l^4}{E\,I}\,\omega^2{}_i \qquad (41)$$

in which $k_i\,l$ are the roots of the transcendental equation,

$$\cos 2\,k\,l \cosh 2\,k\,l = 1 \qquad (42)$$

The roots of Eq. 42 approach asymptotically the values $(i - \frac{1}{2})\,\pi$ as i approaches infinity.

The generalized coordinates q_i, in the absence of the external pressure $p(x, t)$, satisfy the homogeneous equations,

$$\ddot{q}_i + \omega^2{}_i\,q_i = 0 \qquad (43)$$

As $y_0(x)$ is assumed equal to zero, the initial conditions (Eqs. 27) become

$$q_i(0) = \int_{-l}^{l} y_0(x)\,\phi_i(x)\,dm = 0 \qquad (i = 2\,r) \qquad (44a)$$

---

[6] "Vibration Problems in Engineering," by S. Timoshenko, D. Van Nostrand Co., Inc., New York, N. Y., 2d Ed., p. 342 ff.

and

$$\dot{q}_i(0) = \int_{-l}^{l} \dot{y}_0(x)\,\phi_i(x)\,dm \qquad (i = 2\,r) \ldots\ldots\ldots\ldots (44b)$$

Hence, the functions q_i are given by

$$q_0(t) = \dot{q}_0(0)\,t = \left(\frac{v_0}{2}\sqrt{2\,m\,l}\right) t \ldots\ldots\ldots\ldots (45a)$$

and

$$q_i(t) = q_i(0)\cos\omega_i\,t + \left[\frac{\dot{q}_i(0)}{\omega_i}\right]\sin\omega_i\,t$$

$$= \left[\frac{\dot{q}_i(0)}{\omega_i}\right]\sin\omega_i\,t \qquad (i = 2\,r) \ldots (45b)$$

The First Elasto-Plastic Stage.—The symmetrical initial velocity (Eq. 39) excites only the even modes of the elastic beam and creates a bending-moment diagram $M(x, t)$ with a maximum value at x equal to zero, at least in the neighborhood of t equal to zero. Hence, the section first reaching plasticity is the section x equal to zero. The "initial plasticity time" t_0 at which the first plastic hinge occurs is determined by

$$\left|\sum_{r=0}^{\infty} \phi''_{2r}(0)\; q_{2r}(t_0)\right| = \frac{M_0(0)}{E\,I} \ldots\ldots\ldots\ldots (46)$$

The modes ψ of the hinged beam are obtained by noting that each half-beam vibrates in a manner similar to a free-free beam and that their common end must have the same deflection. Hence, each half-beam has modes that can be obtained from Eqs. 40 by changing l to $l/2$ and by normalizing the new modes over the entire length, $2\,l$, of the beam. Both the symmetrical and the antisymmetrical modes of the half-beams must be considered; the corresponding frequencies are obtained from the previous tabulation of frequencies by changing $k\,l$ to $k\,l/2$. Thus, the modes, referred to the midpoint of the half-beams, become

$$\psi_0 = \frac{1}{\sqrt{2\,m\,l}} \ldots\ldots\ldots\ldots (47a)$$

$$\psi_2 = \frac{\sqrt{3}}{\sqrt{2\,m\,l}}\,\frac{2\,x'}{l} \ldots\ldots\ldots\ldots (47b)$$

$$\psi_{2i} = \frac{1}{\sqrt{2\,m\,l}}\left(\frac{\cos 2\,k_i\,x'}{\cos k_i\,l} + \frac{\cosh 2\,k_i\,x'}{\cosh k_i\,l}\right) (i = 2\,r) \ldots\ldots (47c)$$

and

$$\psi_{2i} = \frac{1}{\sqrt{2\,m\,l}}\left(\frac{\sin 2\,k_i\,x'}{\sin k_i\,l} + \frac{\sinh 2\,k_i\,x'}{\sinh k_i\,l}\right) (i = 2\,r + 1) \ldots\ldots (47d)$$

in which $-\frac{l}{2} \leqq x' \leqq \frac{l}{2}$, the k_i are taken from the frequency tabulation, and $x' = x - l/2$.

The elasto-plastic generalized coordinates p_i satisfy the nonhomogeneous equations:

$$\ddot{p}_{2i} + \Omega^2_{2i}\, p_{2i} = P_{2i} \qquad (48a)$$

with

$$\Omega^2_{2i} = 2^4\, \omega^2_i \qquad (48b)$$

and the initial conditions (Eqs. 34), in which the constants b_{ik} are computed by substituting the values of ϕ_i and ψ_k of Eqs. 40 and 47 into Eq. 9. The generalized forces P_i caused by the moments $M_0(0)$ are given by

$$P_{2i} = M_0(0)\, \theta_{2i} \qquad (49)$$

in which the angle θ_{2i} equals the slope discontinuity of the ith mode:

$$\theta_{2i} = \psi'_{2i}(0^+) - \psi'_{2i}(0^-) = 2\,\psi'_{2i}(0) \qquad (50)$$

Hence, the generalized coordinates p_i take the form:

$$p_{2i}(t) = \frac{P_{2i}(t - t_0)^2}{2} + \dot{p}_{2i}(t_0)\,(t - t_0) + p_{2i}(t_0) \qquad (i = 0, 1) \ldots (51a)$$

and

$$p_{2i}(t) = A_{2i}\cos\Omega_{2i}\, t + B_{2i}\sin\Omega_{2i}\, t + \frac{P_{2i}}{\Omega^2_{2i}} \qquad (i = 2, 3, \cdots) \ldots (51b)$$

In Eqs. 51

$$A_{2i} = \left[p_{2i}(t_0) - \frac{P_{2i}}{\Omega^2_{2i}}\right]\cos\Omega_{2i}\, t_0 - \frac{\dot{p}_{2i}(t_0)}{\Omega_{2i}}\sin\Omega_{2i}\, t_0 \qquad (52a)$$

and

$$B_{2i} = \left[p_{2i}(t_0) - \frac{P_{2i}}{\Omega^2_{2i}}\right]\sin\Omega_{2i}\, t_0 + \frac{\dot{p}_{2i}(t_0)}{\Omega_{2i}}\cos\Omega_{2i}\, t_0 \qquad (52b)$$

The elasto-plastic displacements of the beam are computed by substitution of the ψ_{2i} (from Eqs. 47) and the p_{2i} (from Eqs. 51) into Eq. 30. The plastic angle at x equal to 0 is computed from Eq. 35, which becomes in this case

$$\theta(t) = 2\sum_{i=0}^{\infty} \psi'_{2i}(0)\, p_{2i}(t) \qquad (53)$$

The maximum absolute value $|\theta|_{\max}$ of the plastic angle θ is of practical importance both because it determines the amount of energy, $M_0(x)\,\theta_{\max}$, spent in plastic flow and because the time—say, t_1—of its occurrence establishes the transition from the elasto-plastic stage to the elastic stage. The time t_1 is determined by setting equal to zero the derivative of $\theta(t)$, as given by Eq. 53; that is, by the equation,

$$\sum_{i=0}^{\infty} \psi'_{2i}(0)\, \dot{p}_{2i}(t_1) = 0 \qquad (54)$$

An upper bound for $|\theta|_{\max}$ can be obtained by assuming that the available energy of impact which is not transformed into translational energy goes entirely into plastic flow. By allowing that part of the energy which would actually be spent in elastic vibrations to be available for plastic work, the computed value of $|\theta|_{\max}$ is made larger than the true value. Hence, the upper bound for $|\theta|_{\max}$ is computed from Eq. 53 by considering only the rigid rotation mode, ψ_2. The plastic hinge occurs at t_0 equal to 0, at which time the total energy in the system is its kinetic energy. Considering the beam as having a plastic hinge at the center but otherwise being rigid, the amount of energy available for deformation will be the kinetic energy at t equal to 0 reduced by the kinetic energy of translation. Placing all the remaining energy as kinetic energy in the second mode, therefore, results in an upper bound for $\theta(t)$. Thus, with

$$p_2(0) = \int_{-l}^{l} y_0(x)\,\psi_2(x)\,dm = 0 \qquad (55a)$$

and

$$\tfrac{1}{2}\,[p_2(0)]^2 = m\int^{l}[v(x)]^2\,dx - \tfrac{1}{2}\,[p_0(0)]^2 \qquad (55b)$$

one can obtain an upper bound $\theta_u(t)$ for $\theta(t)$—

$$\theta_u(t) = 2\,\psi'_2(0)\left[\frac{P_2\,t^2}{2} + p_2(0)\,t\right] \qquad (56)$$

The maximum absolute value of the upper bound $\theta_u(t)$ occurs at a time,

$$t_1 = -\,\frac{p_2(0)}{P_2} \qquad (57)$$

and is given by

$$|\theta_u|_{\max} = \frac{\psi'_2(0)}{P_2}\,[p_2(0)]^2 > |\theta|_{\max} \qquad (58)$$

in which $p_2(0)$ is given by Eq. 55*b* and P_2 is found from Eqs. 49 and 50.

The value $|\theta_u|_{\max}$ is a good approximation to the true value $|\theta|_{\max}$ whenever the initial velocity $v_0(x)$ is so large that the maximum bending moment which would develop at 0 if the beam never became plastic is several times larger than the capacity moment. Thus, even if the impact time is short, the maximum plastic angle may be well approximated by the rigid-plastic approach although the time history of the angle is incorrect as a result of the assumption of a plasticity time t_0 equal to zero.

Another approximation θ_l of θ, which gives a more correct time history and is often a lower bound, can be obtained by "freezing" the beam into a rigid plastic body at t equal to t_0 rather than at t equal to zero. In this case, θ is obtained from Eq. 53 by considering only the rigid rotation mode ψ_2 after t equal to t_0—

$$\theta_l(t) = 2\,\psi'_2(0)\,P_2(t) = 2\,\psi'_2(0)\left[\frac{P_2}{2}\,(t-t_0)^2 + p_2(t_0)\,(t-t_0) + p_2(t_0)\right] \qquad (59)$$

The absolute value of θ_l becomes maximum at a time

$$t_1 = t_0 - \frac{\dot{p}_2(t_0)}{P_2} \qquad (60)$$

and is given by

$$|\theta_l|_{\max} = \frac{\psi'_2(0)}{P_2}\left\{[\dot{p}_2(t_0)]^2 - 2\,P_2\,p_2(t_0)\right\} \qquad (61)$$

in which $\dot{p}_2(t_0)$ and $p_2(t_0)$ are determined from Eqs. 34.

It is seen that, as $\dot{y}_0(x)$ increases and as t_0 approaches zero, $|\theta_l|_{\max}$ approaches $|\theta_u|_{\max}$. Hence, $|\theta_l|_{\max}$ is also a good approximation of $|\theta|_{\max}$ for values of $v_0(x)$ which cause elastic moments $M(0)$ several times larger than the capacity moment $M_0(0)$.

Successive Elastic and Elasto-Plastic Stages.—From t equal to t_1 on, the deflections become elastic again; they are computed by the elastic modes (Eqs. 40) and generalized coordinates $\bar{q}_i$ which satisfy the initial conditions in Eqs. 37—

$$\bar{q}_i(t) = A_i \cos \omega_i\, t + B_i \sin \omega_i\, t \qquad (i = 2\,r) \qquad (62)$$

in which

$$A_i = -\frac{1}{\omega^2_i}\left[\ddot{\bar{q}}_i(t_1) \cos \omega_i\, t_1 + \omega_i\, \dot{\bar{q}}_i(t_1) \sin \omega_i\, t_1\right] \qquad (63a)$$

$$B_i = \frac{1}{\omega^2_i}\left[\omega_i\, \dot{\bar{q}}_i(t_1) \cos \omega_i\, t_1 - \ddot{\bar{q}}_i(t_1) \sin \omega_i\, t_1\right] \qquad (63b)$$

$$\dot{\bar{q}}_k(t_1) = \sum_{i=0}^{\infty} \bar{b}_{ki}\, \dot{p}_i(t_1) \qquad (63c)$$

and

$$\ddot{\bar{q}}_k(t_1) = \sum_{i=1}^{\infty} \bar{b}_{ki}\, \ddot{p}_i(t_1) \qquad (63d)$$

The functions p_k are obtained from Eqs. 51 and the $\bar{b}_{ki}$ from Eq. 13.

In many cases of impulsive motion the consideration of further elasto-plastic stages is unnecessary because of the energy spent in plastic flow. However, successive elasto-plastic stages and elastic stages can be determined, whenever needed, by equations analogous to Eqs. 34 and 37.

NUMERICAL EXAMPLE

In order to illustrate its main features the theory previously presented will be applied to a specific beam. The results of this application, in which the first three terms of the series were taken into account, are given graphically.

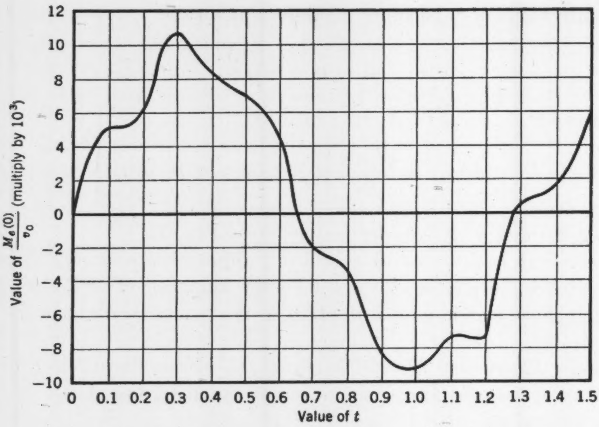

FIG. 4.—ELASTIC MOMENT AT THE CENTER OF THE BEAM VS TIME

The beam considered has the following characteristics in a consistent system of units:

Item	Value
Length, $2\,l$	320
Flexural rigidity, $E\,I$	3.58×10^8
Mass per unit of length, m	0.800
Capacity moment, $M_0(0)$	6.69×10^4
Fundamental period of the beam, T	1.36

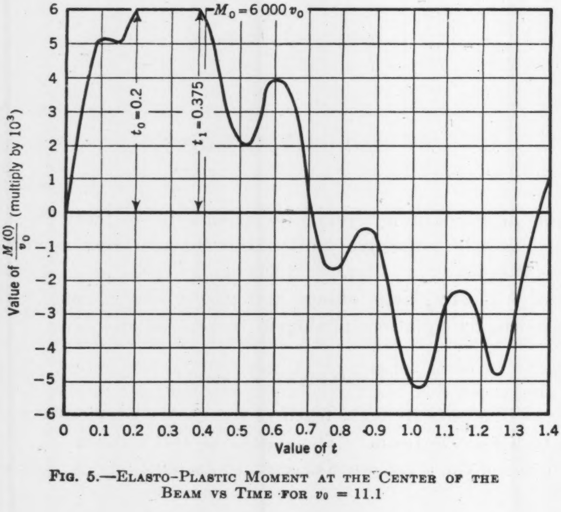

FIG. 5.—ELASTO-PLASTIC MOMENT AT THE CENTER OF THE BEAM VS TIME FOR $v_0 = 11.1$

Two values of the initial-velocity parameter v_0 were used—11.1 and 67.4. The initial plasticity time t_0, evaluated from Eq. 46, was found to be

$$t_0 = 0.2 \qquad \text{for} \quad v_0 = 11.1$$

and

$$t_0 = 0.016 \qquad \text{for} \quad v_0 = 67.4$$

In Fig. 4 there is shown the graph of the elastic moment at x equal to zero for a full period of the fundamental mode of the beam, under the assumption of an infinitely large capacity moment throughout the beam. In Fig. 5 is shown the graph of the elasto-plastic moment at x equal to zero for v_0 equal to 11.1 and for a full period of the fundamental elastic mode of the beam. It can be seen from Figs. 4 and 5 that the maximum elastic moment $M(0)$ would be about twice the capacity moment. The moment becomes elastic again at time t_1 equal to 0.375 (Eq. 54) and does not revert to its plastic value within the time considered.

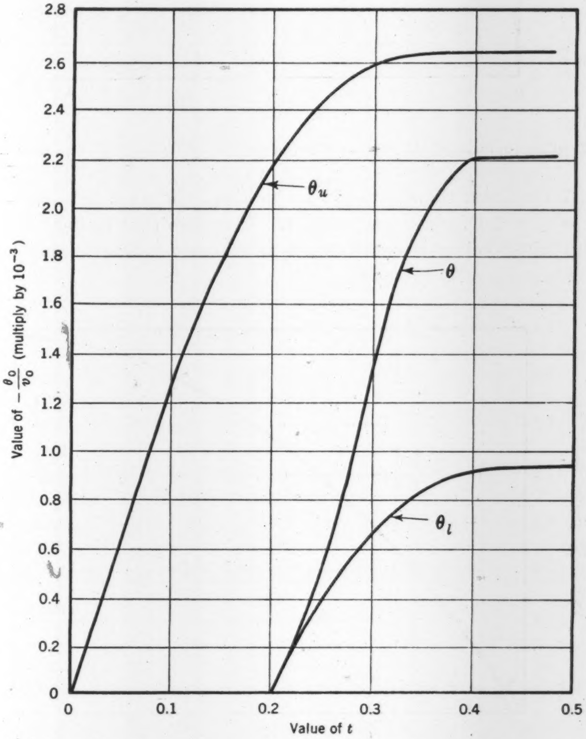

FIG. 6.—PLASTIC ANGLE RESULTING FROM A COSINE IMPULSE FOR $v_0 = 11.1$

In Fig. 6 there is shown the plastic angle at x equal to zero (Eq. 53) together with the upper bound θ_u of Eq. 56 and the bound θ_l of Eq. 59, which—in this case—is a lower bound. For the low value (11.1) of the impact velocity, the lower bound for $\theta_{\max}$ has an error of -56%, and the upper bound has an error of $+22\%$. The time at which the moment becomes elastic again (t_1 equal to 0.375) is approximated by 0.406 from Eq. 60 (derived from the lower bound) and by 0.346 from Eq. 57 (derived from the upper bound). It is thus seen that for low values of the impact velocity the elasto-plastic theory is needed to predict the behavior of the beam.

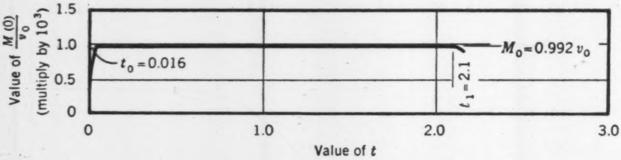

FIG. 7.—ELASTO-PLASTIC MOMENT AT CENTER OF THE BEAM VS TIME FOR $v_0 = 67.4$

In Fig. 7 is shown the elasto-plastic moment diagram between t equal to zero and $t = t_1 = 2.1$ for v_0 equal to 67.4. It is seen that in this case the high value of the initial velocity would create an elastic bending moment ten times the value of the capacity moment.

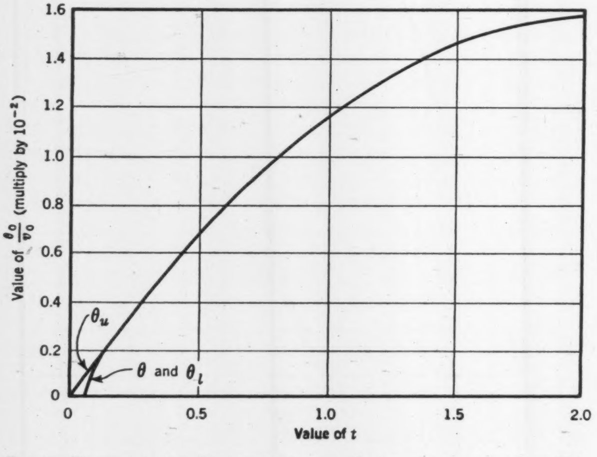

FIG. 8.—PLASTIC ANGLE RESULTING FROM A COSINE IMPULSE FOR $v_0 = 67.4$

In Fig. 8 there is shown the plastic angle θ together with its upper and lower bounds; for the high value (67.4) of the initial velocity parameter, the upper and lower bounds are identical within the accuracy of the graphs except for the interval between t equal to 0 and t_0 equal to 0.016.

CONCLUSIONS

It can thus be seen that in the case of impulsive motion the approximate solutions based on rigid-plastic behavior become acceptable whenever the maximum theoretical bending moment caused by impact is much larger—five or more times larger—than the capacity moment, whereas elasto-plastic solutions are required in all other cases.

ACKNOWLEDGMENTS

In this paper are presented the results of research supported by the Office of Naval Research under Contract Nonr 266-(08).

DISCUSSION

P. S. SYMONDS.[7]—A valuable contribution has been made by the authors in showing how the normal-mode analysis of elastic structures can be extended to problems where plastic flow must be considered in the transient response to a dynamic load. There is no doubt that the problems which involve beams and frames in the plastic range as a result of dynamic loading are difficult ones. Therefore, the assumptions made by the authors are necessary to render the problems tractable to an analysis of moderate length and complexity. These basic assumptions concern the physical properties of the beam; they can be summarized by stating that the moment-curvature relationship has the same shape as the stress-strain diagram in Fig. 1. That is, it is assumed that the diagram consists of two straight lines—one at the elastic angle with slope $E\,I$, and the other parallel to the curvature axis and lying a distance M_0 above this axis. When the capacity moment, M_0, is maintained at a particular section, curvatures of arbitrarily large magnitudes can occur there, and plastic-hinge action can take place.

Even with these assumptions, the analytical and numerical work is often lengthy, and shorter approximate methods become highly desirable. The authors' methods for obtaining an upper bound and a lower bound are examples of such approximate methods.

The writer has been concerned with applications of the rigid-plastic analysis of dynamical problems of structures. This analysis contains the basic simplification that deformations of elastic magnitude are altogether neglected. This type of analysis should give satisfactory results for the final deformations when the work done in plastic deformation is considerably greater than the maximum elastic energy that could be stored in the beam. On this basis, solutions for a variety of dynamical problems have been found—in most cases with relative ease: Problems of impact, impulsive motion (initial velocities), and various types of specified force-time curves have been solved for beams; a problem of a circular ring under concentrated side load has been treated; and certain problems of transverse bending of circular plates have been solved.

The authors' solution for the upper bound is obtained on the assumption that deformation occurs only at a hinge at the midpoint of the beam. This assumption does not give the correct solution according to the rigid-plastic hypothesis. Such a solution for the upper bound would be the correct rigid-plastic solution only for a beam strengthened in the interior of each half so that no deformation could occur except at the midpoint where the capacity moment is M_0. The true rigid-plastic analysis for the uniform beam accounts for the plastic flow which occurs at sections other than that at the midpoint.[8] The results for the central angle for the authors' "Numerical Example" are shown in Table 1. It can be seen that the final value of θ_{rp} from the rigid-plastic analysis is considerably less than the final value of θ and of θ_u.

---

[7] Prof. of Eng., Brown Univ., Providence, R. I.

[8] "Plastic-Rigid Analysis of a Beam under a Symmetric Impulsive Loading," by B. A. Cotter and P. S. Symonds, *Technical Report No. A11-104*, Brown Univ., Providence, R. I., to Office of Naval Research, N7onr-35801, April, 1954.

Similarly, in the elasto-plastic solution for the uniform beam, the authors have taken proper account of plastic flow at the midpoint of the beam but have not considered possible violations of the yield condition at other points. Again, the final computed deformations would be correct only, in general, for a beam strengthened in the interior of each of its halves so that plastic flow could occur only at the midsection; hence, the values for the central angle are, in general, too high. Although the authors state (under the heading, "Elasto-Plastic Vibrations of Free-Free Beams") that the solution for the elasto-plastic motion in terms of normal-mode vibrations could be performed for cases other than that in which a single stationary hinge occurs, it would appear that the practical numerical difficulties would be great. This perhaps explains, in view of the limitations of space, why methods were omitted for examining all cross sections of the beam to ensure that the capacity moment was not exceeded.

TABLE 1.—FINAL ANGLE AT MIDPOINT OF FREE-FREE BEAM

	(a) $v_0 = 11.1$					(b) $v_0 = 67.4$	
Time, t	$\frac{\theta_{rp}}{v_0}$	$\frac{\theta_u}{v_0}$	$\frac{\theta}{v_0}$	$\frac{\theta_l}{v_0}$	Time, t	$\frac{\theta_{rp}}{v_0}$	$\frac{\theta_u}{v_0}, \frac{\theta}{v_0}, \frac{\theta_l}{v_0}$
	Multiply by 10^{-3}					Multiply by 10^{-2}	
0.00	0.00	0.00	0.00	0.00	0.00	0.00	0.00
0.05	0.00	0.66	0.00	0.00	0.25	0.00	0.36
0.10	0.45	1.30	0.00	0.00	0.75	0.42	0.93
0.15	0.93	1.80	0.00	0.00	1.00	0.64	1.16
0.20	1.31	2.18	0.00	0.00	1.25	0.82	1.32
0.25	1.57	2.44	0.54	0.40	1.50	0.95	1.46
0.30	1.72	2.57	1.38	0.68	1.75	1.04	1.53
0.35	1.77	2.63	1.97	0.84	2.00	1.07	1.56
0.40	1.77	2.63	2.20	0.93	2.25	1.08	1.58
0.45	1.77	2.63	2.20	0.95	2.50	1.08	1.58

Messrs. Bleich and Salvadori have compared their single-hinge, elasto-plastic solution with the single-hinge, rigid-plastic solution and find that for the value v_0 equal to 11.1 the final angle values differ by 22%, whereas for the high value ($v_0 = 67.4$) the final results are identical. As both their solutions assume plastic flow localized at a single hinge, the conclusions do not seem justified; no comparison was made between a true rigid-plastic analysis and the elasto-plastic solution. Also, as the single-hinge, rigid-plastic solution appears to be in error, the observed agreement between the final angle computed by the upper-bound method and that given by the elasto-plastic analysis indicates that the elasto-plastic solution is also in error. The agreement between the two solutions for large initial velocities is to be expected because both apply to fictitious beams strengthened in such a way that plastic flow occurs only at the midsection. Hence, this comparison gives no indication of the correctness of either solution, and, although the elasto-plastic solution gives correct results at low velocities, both this and the upper-bound solution are in error at large velocities.

The complete rigid-plastic solution obtained[8] by B. A. Cotter and the writer can be expected to be correct at sufficiently high initial velocities. According to the criterion proposed[9] by E. H. Lee and the writer, the results obtained by the rigid-plastic analysis should be good approximations if the work done in plastic deformation greatly exceeds the maximum possible elastic strain energy that could be stored in the beam. The ratio of these two energies is approximately one in the case in which v_0 is equal to 11.1, and approximately thirty six for the case in which v_0 is equal to 67.4. Because valid elasto-plastic solutions for a uniform-beam problem have not yet been obtained (as of 1954), one cannot say how large this ratio must be in order for the rigid-plastic analysis to give satisfactory results. Comparisons[10] have been made, however, for simple mass-spring systems. It has been shown that, when the energy ratio is higher than twenty, the rigid-plastic analysis gives results accurate to within 5% for an initial-velocity problem. From this result it seems fairly probable that the rigid-plastic solution obtained[8] by Miss Cotter and the writer for the initial velocity of 67.4 is reasonably accurate.

Hans H. Bleich[11] **and Mario G. Salvadori**,[12] **Members, ASCE.**—The objections raised by Mr. Symonds are based on supposed discrepancies between the numerical results obtained by use of Miss Cotter's rigid-plastic analysis[8] and the results of the writers' elasto-plastic analysis; they do not refer to the theoretical part of the work.

Miss Cotter found that the deformation of the bar, according to her rigid-plastic analysis, is of the type shown in Fig. 9, but that the total permanent deformation θ_1 near the center of the bar consists of two parts—a kink at the center and a bend distributed over a length of approximately $l/6$. In presenting Miss Cotter's results, Mr. Symonds referred only to the value of the kink-angle at the center, which differs substantially from the angle obtained by the writers on the basis of a single central hinge. However, if the value of the distributed bend in the vicinity of the center (also obtained by Miss Cotter) is added to the kink-angle, the total angles found by Miss Cotter and by the writers are practically equal:

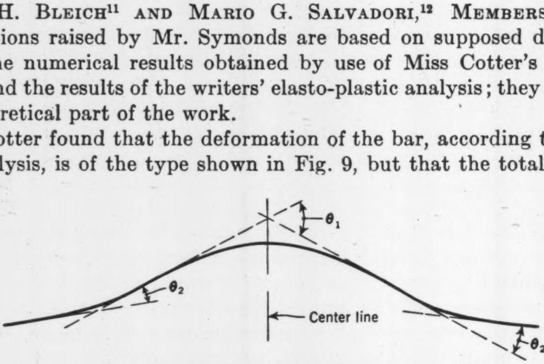

FIG. 9.—PERMANENT DEFORMATION OF BEAM

Initial velocity, v_0..........	11.1	67.4
θ_1 by Miss Cotter..........	$2.64\, v_0\, 10^{-3}$	$1.60\, v_0\, 10^{-2}$
θ_1 by the writers...........	$2.67\, v_0\, 10^{-3}$	$1.61\, v_0\, 10^{-2}$

---

[9] "Large Plastic Deformations of Beams under Transverse Impact," by E. H. Lee and P. S. Symonds, *Journal of Applied Mechanics*, Vol. 19, No. 3, 1952, pp. 308-315.

[10] "The Response of Simple Structures to Dynamic Loads," by Nancy Brazell Brooks and N. M. Newmark, technical report of the Univ. of Illinois, Urbana, Ill., to Office of Naval Research, N6ori-071 (06), *Structural Research Series No. 51*, April, 1953.

[11] Prof. of Civ. Eng., Columbia Univ., New York, N. Y.

[12] Prof. of Civ. Eng., Columbia Univ., New York, N. Y.

The higher value of θ_1 given by the writers differs from the value given by Miss Cotter only in that some of the deformation is distributed over a short distance rather than concentrated as a kink.

The physically important result is obviously the total angle. This angle is closely approximated by the writers' theory even when compared with the results of Miss Cotter's analysis. Therefore, there is no basis for the contention that the elasto-plastic analysis and the conclusions therefrom must be wrong because the single-hinge analysis was used.

It is, of course, inherent in the single-hinge analysis that no information on the division of the total angle between kink and distributed bend can be obtained. It appears that for the two cases studied this information also cannot be obtained from Miss Cotter's rigid-plastic analysis. For the low-velocity case, in which $v_0 = 11.1$, the criterion quoted by Mr. Symonds eliminates the rigid-plastic analysis. For the case in which $v_0 = 67.4$, this criterion seems satisfied; however, because the criterion (as shown subsequently) is necessary but not sufficient, Miss Cotter's rigid-plastic result does not approximate the actual elasto-plastic case.

To assure good agreement between rigid-plastic solutions and elasto-plastic solutions in an initial-velocity problem, a second criterion must also be satisfied. One might consider the response of the elastic beam prior to the plastic stage and the time history of the bending moments. For sufficiently small values of t, the displacements are given by

$$y(x, t) = t\,\dot{y}_0(x) \qquad (64)$$

and the bending moments become, for small values of t,

$$M(x, t) \approx -E\,I\,\dot{y}''_0(x)t \qquad (65)$$

For the velocity distribution under consideration, Eq. 65 indicates that the largest moments of opposite signs occur at $x = 0$ and $x = \pm l$. However, the points $x = \pm l$ are at the ends of the beam where the moments must necessarily vanish; Eq. 65 therefore does not apply, even for small values of t, if $l - |x|$ is small. One can, however, visualize the actual bending moments to be the sum of Eq. 65 and of the moment caused by the correcting stress waves originating at $x = \pm l$ such that the condition,

$$M(\pm l, t) = 0 \qquad (66)$$

remains satisfied for the total moment. (To be consistent, the beam should be deemed to have rotatory inertia and to be infinitely rigid in shear because Eq. 65 does not visualize shear deformations.) This suggests that Eq. 65 will apply at points near the ends $x = \pm l$ only if t is smaller than the time required for a stress wave to travel the distance $l - |x|$. In this case these stress waves will decrease all moments near the ends but will increase those at the center of the beam. When the time t is larger than l/c, the time required by the waves to travel through the entire beam, Eq. 65 becomes inapplicable for all values of x, and the bending moments will be redistributed in a manner which need not be similar to the original curve $\dot{y}''_0(x)$. If first yield takes place at a time $t_0 > l/c$, the sign of the bending moments at yield and the direction of the permanent curvature will no longer be governed by the sign of $\dot{y}''_0(x)$.

The reasoning for the foregoing is physically incomplete because shear deformations have been neglected; for sufficiently small values of time t this is not permissible. It is not difficult, however, to reason similarly for the case of a Timoshenko beam allowing for shear deformations. Excluding cases in which yield in shear occurs (which are not contemplated herein), one finds again that the yield pattern is governed by the sign of $\dot{y}''_0(x)$ only if the time at yield is small in comparison to l/c, thus confirming the conclusion found without shear effects.

From Miss Cotter's rigid-plastic analysis, the location and direction of yielding are obtained from the values of $\dot{y}''_0(x)$; one must conclude that this analysis cannot be relied on when the time to yield in the elasto-plastic structure is of the order of l/c or larger because in such a case the actual yield pattern is quite different from the one assumed. The examples presented by the writers may be interpreted as applying to steel beams by selecting a suitable set of units (that is, feet, seconds, and kips). The times to first yield, 0.2 sec and 0.016 sec, respectively, are not small in comparison to l/c (which is equal to 0.01 sec); hence, Miss Cotter's rigid-plastic solution is not applicable in either case. It should be clear that the time to yield would have to be considerably smaller than l/c to make the rigid-plastic solution applicable.

It may be useful to emphasize the type of problem which should and can be treated by normal-mode methods in general, with or without plasticity. If one desires to treat a problem in which accurate information at many points is required, normal-mode methods are impractical even in the elastic case. On the other hand, if one is seeking approximate, yet physically reasonable results, mode methods are useful because one can restrict the computations to a small number of modes. Such a restriction results in a loss of detail. In problems of elasto-plastic beams it would be absurd to consider minor motion of hinges or areas which are becoming plastic; any conclusions as to such matters on the basis of a few terms of an expression would be quite unrealistic. It is consistent with the limited accuracy obtainable to place a yield hinge only in a suitably selected, strategic position, or in several positions if necessary; one will still obtain useful and meaningful results. This is the reason for the selection of a yield hinge at only the center in the examples treated; such a selection represents the essential physical effects.

Therefore, both elasto-plastic methods and rigid-plastic methods have their usefulness. The elasto-plastic approach is necessary in the important practical cases in which the loads exceed the elastic capacity by only a modest amount because a rigid-plastic analysis (which is necessarily simpler) is inapplicable to such cases. Moreover, it should be noted that in cases of initial velocities the additional time-to-yield criterion must be satisfied in order for the rigid-plastic solution to be valid.

AMERICAN SOCIETY OF CIVIL ENGINEERS
Founded November 5, 1852
TRANSACTIONS

Paper No. 2753

TRANSIT LINING OF HIGH-SPEED TRACK

By Neil R. Berndt,[1] J. M. ASCE

With Discussion by Mr. Harry Rubey

Synopsis

Many methods of transit-lining high-speed track are unsatisfactory because of the lack of a simplified, standard procedure. A simplified method of transit-lining high-speed track is presented herein; this method was developed following an investigation of surveying geometry and has been made possible by improved computational devices. The suggested procedure is such that tangent track can be established from a graph of the existing conditions, curve data can be computed in the office, and the throw of the track can be limited but still selected with a definite, corrective relationship to a proposed center line.

Introduction

The usual methods of transit-lining high-speed track must be clarified for the instrumentman because too often he is called on to use his own initiative and judgment as to methods of transit-lining curves. Therefore, it is essential that a simplified, standard procedure of establishing alinement be developed. The purposes of such a standard procedure should be to expedite good alinement and to reduce the costs of track lining and engineering.

There is developed subsequently a method for the transit lining of high-speed track—both tangent and curved. The procedure is such that throws can be limited but still selected with a definite corrective relationship to the proposed center line of track.

Tangent Track

The principal difficulty in alining tangent track is in the determination of that straight line which will cause the least throw and still maintain standard track centers. The first inclination would be to run a line between two points

---

Note.—Published, essentially as printed here, in September, 1953, as *Proceedings-Separate No. 271*. Positions and titles given are those in effect when the paper or discussion was received for publication.

[1] City Engr., St. Joseph, Mich.

chosen from rather uniform straight track with standard track centers. In many cases, if the line so chosen is long, excessive throws and substandard track centers result or, if the line is projected into a curve, a distorted point of intersection is formed.

Random Tangent Line.—A better method of secting a tangent line would be to obtain a true record of the tracks as they lie on the roadbed. This record can be obtained by projecting long random lines from curve to curve, from knoll to knoll, or from crossing to crossing. The tangent line is established between random control points on the center line of track, and transverse offset measurements are then taken at 100-ft intervals from the random line to the gage of one rail of the track that is to be lined. It is sometimes desirable, for ease and accuracy in field work, to project the random-line control points to locations on the track shoulder. Track-center measurements and clearances to any limiting facilities, such as bridge piers and signals, are also required to complete the information; graphs of the offset and track-center measurements represent the true conditions. By adjusting the random line on a graph, track throws can be minimized, kinks can be hidden, and track centers can be planned. Also, on curves, the point of intersection—determined by the projection of the tangent lines—is more likely to coincide with the original point.

It is apparent that extreme care and accuracy in the establishment of the random tangent line is essential. Experience has shown that the best lines can be established in the early morning or early evening hours during the summer months—otherwise heat waves may cause image distortion. Under satisfactory conditions, successful results have been attained with lines as long as 2 miles. The longest possible line should always be used, and the work should be suspended when adverse conditions (such as heat waves and wind) are encountered.

Field Party and Work.—A field party of four, consisting of a transitman, a rodman, and two tackmen is suggested. After choosing the extremities or control points of the random line, the transitman sights on the distant rodman and signals for an intermediate target to be set on line by the tackman at a point approximately 2,000 ft ahead of the transit. This target becomes the foresight for this part of line, and tacks are set in track ties at 100-ft stations over the 2,000-ft interval. The transit is then moved to the target point, and the process is repeated until the initial distant point is reached.

Tangent Example.—In Fig. 1 there is shown an example of a ½-mile random line between two curves: There is demonstrated (1) the minimizing of throw through the crossover and street crossing, (2) the provision of standard track clearances to the overhead road bridge, and (3) the determination of centers to the eastward main track.

In order to compose Fig. 1(*b*) and Fig. 1(*d*), field distances (random line to the rail of track to be lined and track centers before lining) were plotted, and the points of limited throw were specifically noted. If random line AB were accepted, the proposed throw would be as shown in Fig. 1(*b*). By adjusting line AB to the new position CD, the throws are reduced as shown in Fig. 1(*b*).

In the choice of line CD, consideration is given to (*a*) balancing the throw for economical lining procedure; (*b*) points of limited throw involving track clearances, track centers, and crossings; and (*c*) providing future control for lining adjacent tracks.

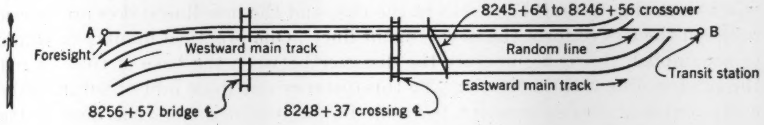
A
Foresight
Westward main track
8245+64 to 8246+56 crossover
B
Random line
Transit station
Eastward main track
8256+57 bridge ℄
8248+37 crossing ℄

(*a*) Track diagram

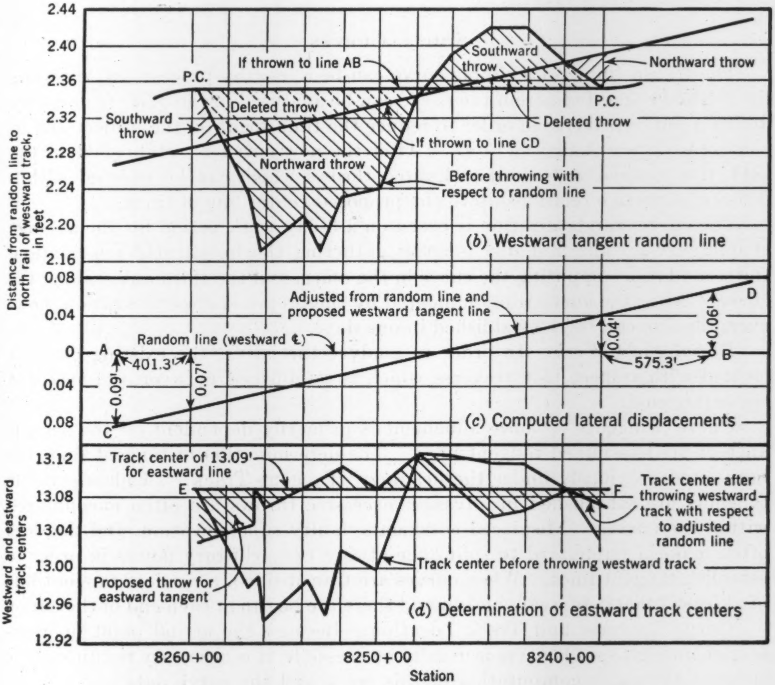

FIG. 1.—DETERMINATION OF THROWS AND TRACK CENTERS

This last item is illustrated in Fig. 1(*d*). The proposed throws related to the adjusted line CD are superimposed on the plotted track centers, and a new line EF is developed. Line EF is determined in the same manner as line CD and with the same degree of flexibility. Therefore, there results an independent line which has a definite relationship to line CD.

When a satisfactory determination of lines CD and EF has been made, the lateral displacements from the initial random line can then be scaled directly for use in adjusting the line in the field. The ease of this operation is illustrated in Fig. 1(*c*). The new tangent is therefore ready for staking.

Staking the New Tangent Line.—The computed displacements are laterally offset from the random-line tacks in the ties, and the new line stakes are driven between the ties to form the new tangent line. One practical manner in which to accomplish this is to measure the distance between the base of the rail and the random-line tack in the tie. To this distance one must add or subtract the computed lateral displacement to result in the distance from the base of the rail to the new tangent line. By using the base of the rail as a parallel straight edge and transferring the latter distance, the stake is set in the adjacent tie crib to form the new tangent line.

Simple Curves

The transit lining of a simple curve can be a lengthy process, but by using the method suggested herein the curve can be analyzed in the office from a preliminary curve traverse in order to reduce the time spent on the project and to achieve a better quality of work. After the new curve is established in the field, this method will result in limited throws which can be selected with a definite corrective relationship to the proposed center line of track.

The curve standardization is based on a 3-day work period for the average simple curve. The first day is spent gathering the initial field information, the second day computing the curve in the office, and the third day staking the curve. After the curve is monumented by the proposed standardization, however, the line can be re-established in one day.

Initial Field Work.—In order to analyze the curve, the existing curve is located with respect to a traverse which is established between the accepted curve tangents.

Curve Tangents.—Curve alinement is primarily dependent on the acceptance of predetermined tangent lines. The determination of tangent lines has been cited previously under the heading, "Tangent Track." Unless suitable tangents are established in advance, excessive throws are often encountered within the curves. Misplaced easements, faulty superelevation, and dog legs often make it haphazard to split gage at any two arbitrary points in order to establish tangent lines. When curves are transit-lined, a random tangent line of at least 2,000 ft (if available) should therefore be run at each end of the curve.

Curve Traverse and Track Location.—Because the actual point of intersection on high-speed curves is usually inaccessible, it is necessary to run a curve traverse to enable computation of this point and the curve data.

In Fig. 2(*a*) there is shown an example of a traverse of a simple curve. The procedure for obtaining the illustrated field data is as follows:

1. Primary hubs of the traverse are conveniently located on the outside shoulders of the roadbed and at distances which permit line and chainage to fall within the roadbed limits. In the example illustrated it was possible to use corrected random-line tangent points A and B because they fulfil this requirement.

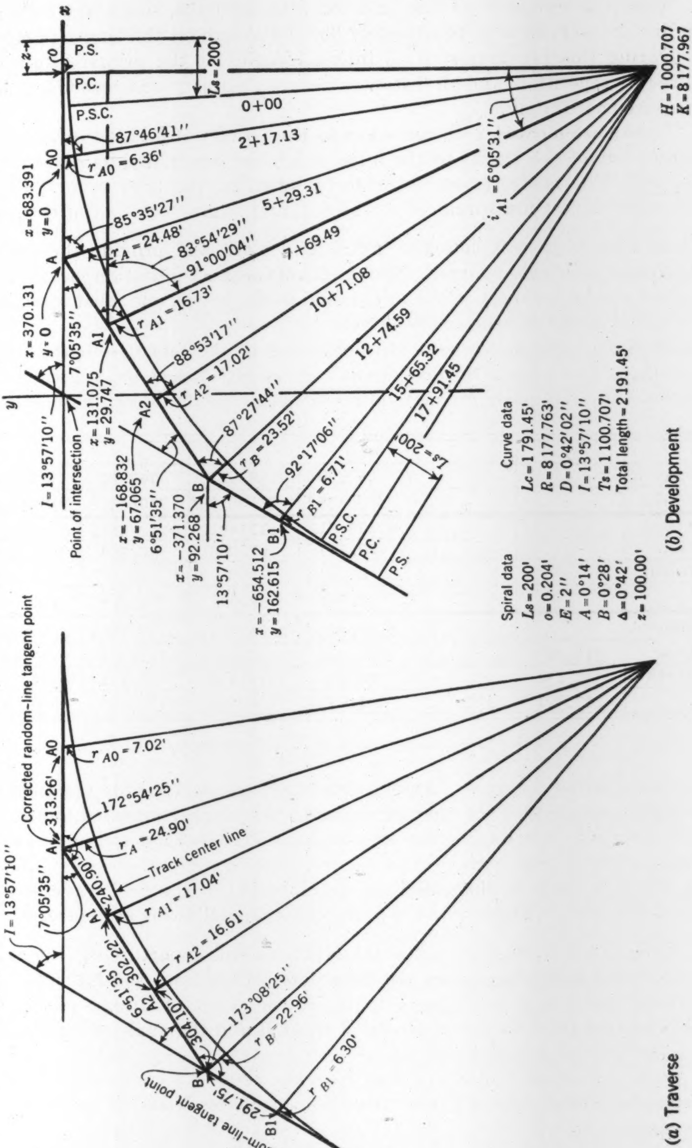
(a) Traverse
I = 13°57'10''
7°05'35''
313.26'
Corrected random-line tangent point
A0
r A0 = 7.02'
A
172°54'25''
r A = 24.90'
Track center line
240.90'
A1
r A1 = 17.04'
302.22'
6°51'35''
A2
r A2 = 16.61'
304.10'
173°08'25''
B
r B = 22.96'
291.75'
B1
r B1 = 6.30'
Corrected random-line tangent point
(b) Development
x
y
O
z
P.S.
P.C.
P.S.C.
Ls = 200'
0+00
87°46'41''
2+17.13
A0
r A0 = 6.36'
x = 683.391
y = 0
85°35'27''
5+29.31
r A = 24.48'
83°54'29''
91°00'04''
7+69.49
A
x = 370.131
y = 0
7°05'35''
r A1 = 16.73'
A1
10+71.08
88°53'17''
r A2 = 17.02'
x = 131.075
y = 29.747
A2
I = 13°57'10''
Point of intersection
i A1 = 6°05'31''
12+74.59
87°27'44''
15+65.32
17+91.45
r B = 23.52'
x = −168.832
y = 67.065
6°51'35''
x = −371.370
y = 92.268
B
92°17'06''
r B1 = 6.71'
13°57'10''
x = −654.512
y = 162.615
B1
P.S.C.
P.C.
P.S.
Ls = 200'
H = 1 000.707
K = 8 177.967
Curve data
Lc = 1 791.45'
R = 8 177.763'
D = 0°42'02''
I = 13°57'10''
Ts = 1 100.707'
Total length = 2 191.45'
Spiral data
Ls = 200'
o = 0.204'
E = 2''
A = 0°14'
B = 0°28'
Δ = 0°42'
z = 100.00'

FIG. 2.—A SIMPLE CURVE

2. When the transit is on line between primary hubs, secondary hubs are set on line at intervals of approximately 300 ft throughout the length of curve.

3. During this previous step all internal angles at the primary hubs are measured by repetition, and all distances between primary and secondary hubs are measured accurately.

4. Tracks are located with reference to the traverse by radial offsets from the center line of the tracks to the hubs which are designated as r_{A0}, r_A, r_{A1}, and so on. The measurement is made by swinging the tape from the hub, reading the smallest measurement to the rail, and adding one half of the gage.

These four steps complete the initial field work and provide the control for staking the computed curve. The results of these computations are entirely dependent on the accuracy of the initial field work; hence, one must take great care in chaining and measuring the angles.

Office Work.—All curve data are developed in the office from the initial field work. Whereas curve development is usually based on trigonometric principles, this trial-and-error method requires the use of a coordinate system, which has many advantages. Among those that are most readily apparent are the complete analysis of the characteristics of the curve, controlled alinement, and the simplicity which facilitates standardization of method and preservation of data.

POINT	AO	A	A1	A2	B	B1
FIELD DIST			240.90	543.12	747.22	291.75
BEARING ∠			7°05'35"	7° 05'35"	7°05'35"	13°57'10"
SIN BEARING			0.1234812	0.1234812	0.1234812	0.2411221
LATITUDE			29.747	67.065	92.268	70.347
ADJUSTMENT			0	0	0	92.268
Py			29.747	67.065	92.268	162.615
COS. BEARING			0.9923469	0.9923469	0.9923469	0.9704948
DEPARTURE	313.26		-239.056	-538.963	-741.501	-283.142
ADJUSTMENT	370.131		370.131	370.131	370.131	-371.370
Px	683.391	370.131	131.075	-168.832	-371.370	-654.512

FORM 1.—DETERMINATIONS OF HUB COORDINATES

In Fig. 2(*b*) there is illustrated the development of the field traverse data shown in Fig. 2(*a*). These data are processed in the following sequence:

1. Using Form 1, one computes[2] the latitudes and departures of the curve traverse. The hub coordinates are then determined from the latitudes and departures; the origin is assumed to be at the point of intersection. The y-axis is located from the y-coordinate of point B and the angle of intersection I.

2. In trial 1, using Forms 2(*a*) and 2(*b*), one chooses a curve radius and its corresponding spiral data and computes the coordinates H and K for the center of the curve.

---

[2] "Natural Sines and Cosines to Eight Decimal Places," *Special Publication No. 231*, U. S. Govt. Printing Office, Washington 25, D. C., 1942.

The choice of the radius is made from previous records or knowledge of the curve. The y-coordinate K of the center of a simple spiraled curve is equal to $R + o$ and the x-coordinate H is equal to $(R + o) \tan (I/2)$ or $K \tan (I/2)$.

3. Using Form 3(a), trial 1, one substitutes the values of H, K, and R derived from the previous step and computes the throw for hub A1. This hub is used because of its proximity to the center of the curve. Then, by use of

$$R + r_{A1} = [(H - A1_x)^2 + (K - A1_y)^2]^{\frac{1}{2}} \ldots\ldots\ldots\ldots\ldots (1)$$

one subtracts the radius R from $R + r_{A1}$ to determine the computed radial

(a) Trial curve data

TRIAL		1	2	3	4
CURVE DATA	I	13°57'10"	13°57'10"	13°57'10"	
	1/2	6°58'35"	6°58'35"	6°58'35"	
	R	8,124.000	8,218.086	8,177.763	
	D			0° 42.038'	
SPIRAL DATA	E	2"	2"	2"	
	Ls	200	200	200	
	o	0.205	0.203	0.204	
	z	100	100	100	
	A			0° 14.013'	
	B			0° 28.025'	
	Δ			0° 42.038'	
T				1,000.707	
Ts				1,100.707	
Lpc-pc				1,991.452	
Lpsc-psc				1,791.452	
Lps-ps				2,191.452	

(b) Tangent distances

R	8,124.000	8,218.086	8,177.763	
o	0.205	0.203	0.204	
K	8,124.205	8,218.289	8,177.967	
Tan I/2	0.1223663	0.1223663	0.1223663	
H	994.129	1,005.641	1,000.707	
z			100.000	
Ts			1,100.707	

(c) Radius correction

± Throw	0.70	-0.30		
Exsec. I/2	0.00744	0.00744		
R Corr.	94.086	-40.323		
Old R	8,124.000	8,218.086		
New R	8,218.086	8,177.763		

FORM 2

(*a*) Throw

TRIAL	1	2						3					
POINT	A1	A1	A0	A	A2	B	B1	A1	A0	A	A2	B	B1
H	994.129	1,005.641	1,005.641	1,005.641	1,005.641	1,005.641	1,005.641	1,000.707	1,000.707	1,000.707	1,000.707	1,000.707	1,000.707
-Px	-131.075	-131.075	-683.341	-370.131	168.832	371.370	654.512	-131,075	-683.391	-370.131	168.832	371.370	654.512
H-Px	863.054	874.566	322.250	635.510	1,174.473	1,377.011	1,660.153	869.632	317.316	630.576	1,169.539	1,372.077	1,655.219
K	8,124.205	8,218.289	8,218.289	8,218.289	8,218.289	8,218.289	8,218.289	8,177.967	8,177.967	8,177.967	8,177.967	8,177.967	8,177.967
-Py	-29.747	-29.747	0.000	0.000	-67.065	-92.268	-162.615	-29.747	0.000	0.000	-67.065	-92.268	-162.615
K-Py	8,094.458	8,188.542	8,218.289	8,218.289	8,151.224	8,126.021	8,055.674	8,148.220	8,177.967	8,177.967	8,110.902	8,085.699	8,015.352
-(R±r)	-8,140.338	-8,235.112	-8,224.604	-8,242.824	-8,235.401	8,241.867	8,224.961	-8,194.495	-8,184.120	-8,202.241	-8,194.788	-8,201.287	-8,184.474
+R	+8,124.000	+8,218.086	+8,218.086	+8,218.086	+8,218.086	+8,218.086	+8,218.086	+8,177.763	+8,177.763	+8,177.763	+8,177.763	+8,177.763	+8,177.763
r computed	-16.338	-17.026	-6.518	-24.738	-17.315	-23.781	-6.875	-16.732	-6.357	-24.478	-17.025	-23.524	-6.711
r measured	+17.04	+17.04	+7.02	+24.90	+16.61	+22.96	+6.30	+17.04	+7.02	+24.90	+16.61	+22.96	+6.30
THROW	+0.70	+0.01	+0.50	+0.16	-0.70	-0.82	-0.57	+0.31	+0.66	+0.42	-0.42	-0.56	-0.41

(*b*) Radius and hub angle

H-Px								869.632	317.316	630.576	1,169.539	1,372.077	1,655.219
R±r								8,194.495	8,184.120	8,202.241	8,194.788	8,201.287	8,184.474
Sin i or Cos (90°-i)								0.10612393	0.03877216	0.07687850	0.14271742	0.16730021	0.20223890
i								6°05'31"	2°13'19"	4°24'33"	8°12'18"	9°37'51"	11°40'04"
90°-i								83 54'29"	87°46'41"	85°35'27"	81°47'42"	80°22'09"	78°19'56"
Bearing								7°05'35"	0°00'00"	0°00'00"	7°05'35"	7°05'35"	13°57'10"
R HUB ∠								91°00'04"	87°46'41"	85°35'27"	88°53'17"	87°27'44"	92°17'06"

(*c*) Station

i								6.091 944	2,221 945	4,409 167	8,205 000	9,630 834	11,667 778
D								0.700 633	0.700 633	0.700 633	0.700 633	0.700 633	0.700 633
L1								869.49	317.13	629.31	1,171.08	1,374.59	1,665.32
Adjustment								100.00	100.00	100.00	100.00	100.00	100.00
STATION								769.49	217.13	529.31	1,071.08	1,274.59	1,565.32

FORM 3

offset r_{A1}. The difference between the computed and the measured radial offset is the computed throw.

4. In all probability the radius of curvature in trial 1 will result in a large throw; therefore, another attempt at approximating the field condition is required. Using Form 2(*c*), one substitutes the value of the throw at hub A1 for the plus or minus throw under trial 1.

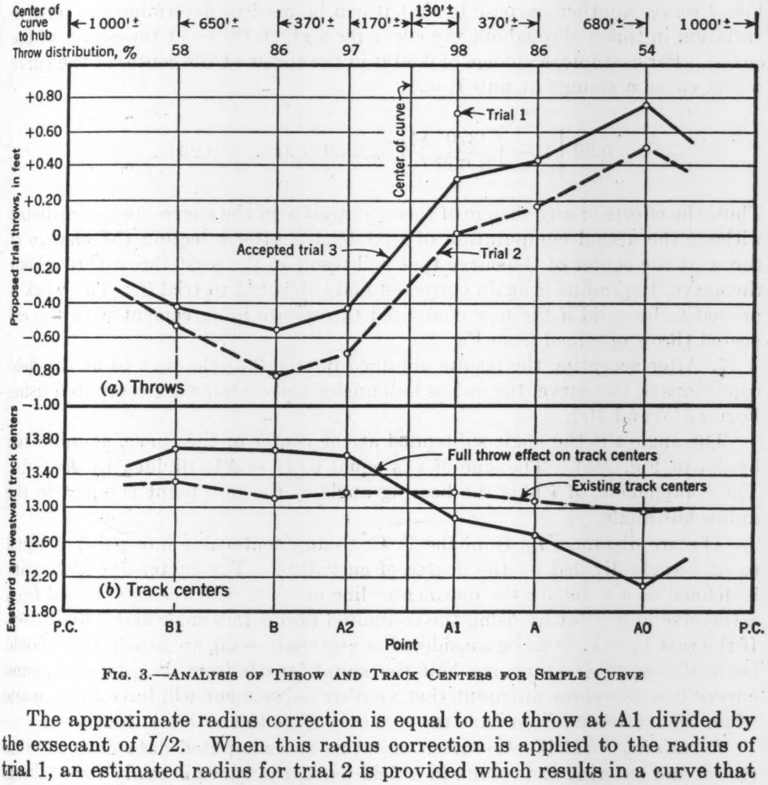

FIG. 3.—ANALYSIS OF THROW AND TRACK CENTERS FOR SIMPLE CURVE

The approximate radius correction is equal to the throw at A1 divided by the exsecant of $I/2$. When this radius correction is applied to the radius of trial 1, an estimated radius for trial 2 is provided which results in a curve that should pass through hub A1 with little or no throw.

5. Substituting the corrected radius into trial 2, one repeats the process described under steps 2 and 3. In addition, one must compute the throws at all hub points.

6. By applying the data from trial 2 to Fig. 3, the throws and resulting track centers are analyzed to determine the characteristics of the curve.

In Fig. 3 approximate horizontal scale distances are used for the location of the hubs and points of curve with relation to the center of the curve. Trial 2 throws are then plotted at the hub points. In Fig. 3, it is clearly shown whether the curve should be solved as a simple curve or as a compound curve in order to conserve throw. In this example, a simple-curve solution was used.

In Fig. 3 the throw distribution, in percentage, is determined from

$$100\left[1-\left(\frac{\text{center of curve to hub}}{\text{center of curve to P. C.}}\right)^2\right].$$

Fig. 3 serves another purpose in that it can be used to determine the relative variation in throw throughout the curve for a given throw at the center of the curve. For example, a change of 0.30 ft in the throw at the center of the curve would cause a change at hub B of

$$0.30\left[1-\left(\frac{370}{1{,}000}\right)^2\right]=0.30\times 0.86=0.26\text{ ft}.$$

Thus, the effects of any change of throw in trial 3 on the curve can be predicted without the actual computation of that trial. After selecting the change of throw at the center of the curve that will result in the least throw throughout the curve, the radius is again corrected and subjected to trial 3. The work is proved to be valid if the new computed throws are in agreement with the expected throw obtained from Fig. 3.

7. After accepting the results obtained in trial 3 as the best to fit the field conditions of the curve, the radius hub angles and stations are computed using Forms 3(*b*) and 3(*c*).

The angle i is the angle subtended at the center of the curve, as indicated by i_{A1} in Fig. 2(*b*). The sine of i is equal to $H - \mathrm{A1}_x$ divided by $R \pm r_{A1}$. The complement of i plus the bearing angle of the hub point is equal to the radius hub angle.

The arc distance, L_i, from the P. C. to any center-line hub point is equal to its i-angle divided by the degree of curvature. The center-line hub point is defined as a point for the new center line of track which is established from a traverse hub point by using the computed radius hub angle and radial offset. If the east P. S. C. is to be considered as station 0 + 00, an adjustment should be made by subtracting one half the spiral length from L_i. In compound curves it will become apparent that another adjustment will have to be made when the stationing from one degree of curvature to another is continued.

Remaining Field Work.—After accepting the computed data derived from trial 3 and entering the results in a field book, the curve is ready for staking.

Staking the Curve.—The curve can be staked by two methods, the choice of which depends on the condition of the present line and on the maximum allowable throw. The ideal procedure is to stake the proposed center line; often this is impossible because of excessive throws, a shortage of manpower, and the necessity of keeping the track on a previously prepared tamp.

A satisfactory alternative method is to stake an alternate center line which minimizes throw, meets points of limited throw, and still retains a relationship to the actual proposed center line. Graphs are made of actual proposed throws, and alternate throws are developed as shown in Fig. 4.

After a few years of corrective lining by the method shown in Fig. 4, most curves can eventually be lined to their proposed center lines. Therefore, this graphing procedure tends to produce a standard curve. However, if a curve possesses good riding qualities, it does not have to be completely lined to its theoretical center line.

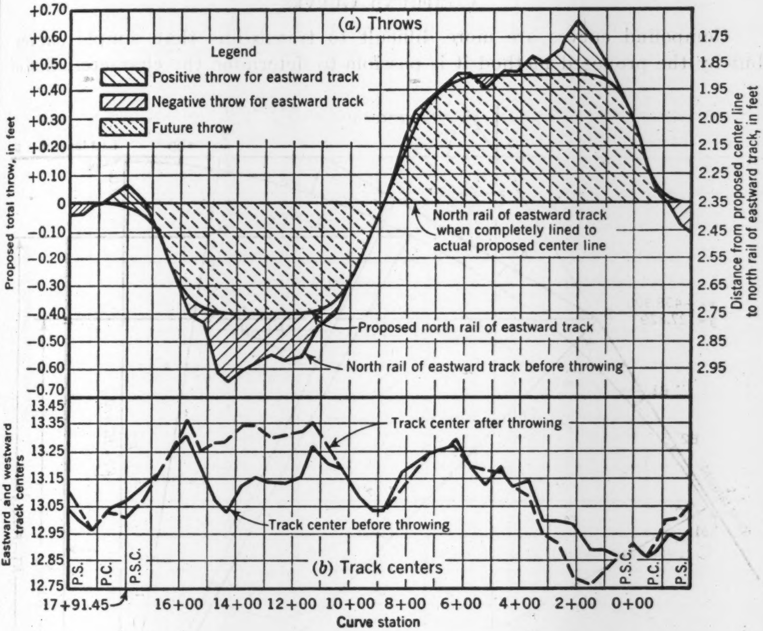

FIG. 4.—PROPOSED THROWS AND TRACK CENTERS

In either method the center-line hubs are established by turning off the computed radius angles from the traverse hub points and laying off the distances equal to the radial offsets obtained in trial 3. By using the established center-line hubs as curve transit stations the curve can be laid out by the use of deflection angles. A check of the work is provided when the total deflected angle at any center-line hub, turned between its two adjacent hubs, is in agreement with its theoretical deflection.

Monumenting the Control Points.—To avoid duplication of the preliminary work in future years, all control points should be monumented with iron pins. These iron pins may be placed on the center line of the track every 1,000 ft to 2,000 ft on tangents and 300 ft to 400 ft on curves so as to facilitate the reestablishment of future line. Some instrumentmen may prefer to place iron pins at the traverse hub points rather than on the center line of curves. This preference may have an advantage in that the pins are less likely to be disturbed if properly placed, but it has the disadvantage of necessitating the establishment of center-line hubs during each transit lining of the curve. As well as monumenting the control points, one must place concrete markers on the roadbed shoulder to designate the location of spirals and points of compound curvature, the degree of curvature, the number of the curve, and the superelevation.

COMPOUND CURVES

Compound curves are more difficult to transit-line than simple curves, but by the proposed method it is possible to determine the characteristics of

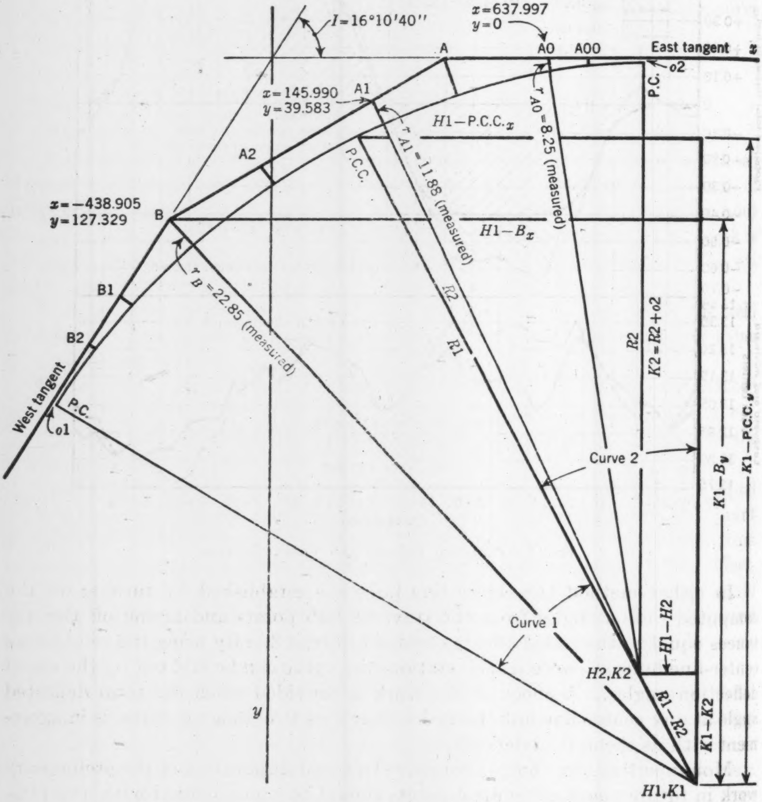

I = 16°10′40″
x = 637.997
y = 0
A
A0
A00
East tangent
x
o2
P.C.
x = 145.990
y = 39.583
A1
H1 − P.C.C.x
r A0 = 8.25 (measured)
A2
P.C.C.
r A1 = 11.88 (measured)
x = −438.905
y = 127.329
B
H1 − Bx
R2
B1
r B = 22.85 (measured)
R1
R2
K2 = R2 + o2
B2
West tangent
P.C.
o1
Curve 2
K1 − By
K1 − P.C.C.y
Curve 1
H1 − H2
H2,K2
R1 − R2
K1 − K2
y
H1,K1

FIG. 5.—A COMPOUND CURVE

the curve and locate the points of change in degree of curvature. By substituting data on three accepted field conditions in the corresponding analytic geometry formulas and by solving these equations simultaneously, the coordinates of the center of the respective curve and the radius of that particular trial can be computed. These values should then be placed in Form 3 and computed in the same manner as a simple curve.

A typical compound curve is illustrated in Figs. 5 and 6. Following a study of this example and its combination of analytic geometry formulas, one should be able to solve any compound curve by the use of the same principles.

In treating this example as a simple curve, it is shown in "Trial 2 simple curve" in Fig. 6 that excessive throws are encountered. Therefore, to minimize throws it is necessary to compound the curve.

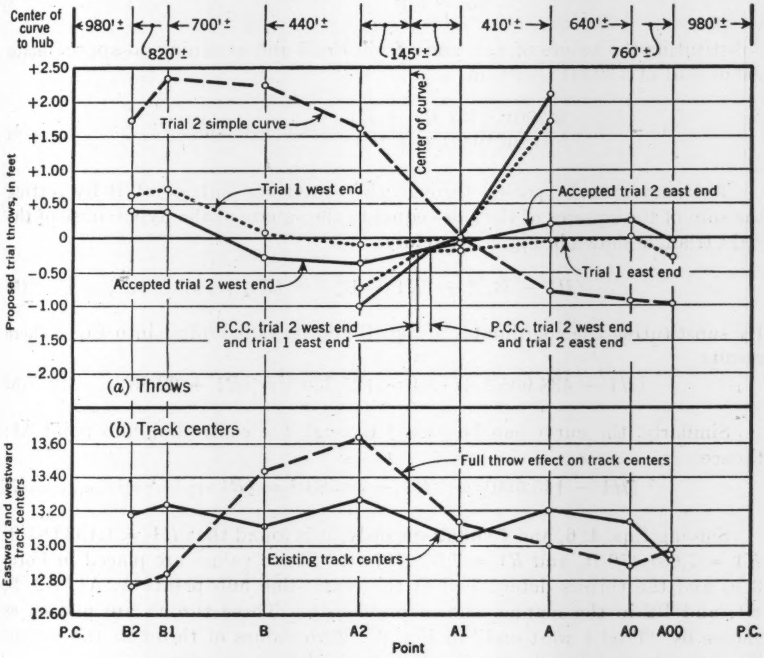

FIG. 6.—ANALYSIS OF THROW AND TRACK CENTER

Trial 1, West End.—This trial is developed from the west end of the curve as indicated by curve 1 in Fig. 5. It is necessary to formulate three simultaneous equations to solve for the three unknowns *H*1, *K*1, and *R*1. The first equation is dependent on the fact that the curve will be tangent at an *o*1-offset to the west tangent line. The second and third equations allow the curve to pass through two points in the existing curve, center-line hub points B and A1. Points B and A1 are chosen because of their location relative to the west end of the curve. It is suggested that the distances be made approximately equal between the three equation points so that the curve will be more representative of the existing conditions.

The distance from the west tangent line to the center of the curve ($H1$, $K1$) can be found in the following manner:

The normal equation of the west tangent line is

$$0.290106311\ H1 + K1 = 0 \quad \text{(2)}$$

Reducing Eq. 2 to the normal form results in

$$\frac{a_{H1} + b_{K1} + c}{(a^2 + b^2)^{\frac{1}{2}}} = R1 + o1 \quad \text{(3)}$$

Substituting the values of a, b, and c from Eq. 3 and assuming an approximate value of $o1$ of 0.335 ft results in

$$\frac{0.290106311\ H1 + K1}{(0.290106311^2 + 1^2)^{\frac{1}{2}}} = R1 + 0.335 \quad \text{(4)}$$

The curve can be passed through the center-line hub point B by setting the sum of the squares of the sides equal to the square of the hypotenuse of the right triangle shown in Fig. 5; therefore,

$$(H1 - B_x)^2 + (K1 - B_y)^2 = (R1 + r_B)^2 \quad \text{(5)}$$

By substituting the coordinates of hub B and its radial offset into Eq. 5 there results

$$(H1 - 438.905)^2 + (K1 - 127.329)^2 = (R1 + 22.85)^2 \quad \text{(6)}$$

Similarly, the curve can be passed through the center-line hub point A1; thence,

$$(H1 - 145.990)^2 + (K1 - 39.583)^2 = (R1 + 11.88)^2 \quad \text{(7)}$$

Solving Eqs. 4, 6, and 7 simultaneously, it is found that $H1 = 1{,}133.681$ ft, $K1 = 7{,}657.479$ ft, and $R1 = 7{,}669.787$ ft. These values are placed in Form 3(*a*) and the throws determined at the center-line hub points A, A1, A2, B, B1, and B2 in the manner shown previously. These throws are plotted as shown by "Trial 1 west end" in Fig. 6. Zero values of throw at the center-line hubs A1 and B indicate a partial check of the computations.

Accepted Trial 2, West End.—To reduce the throw at the center-line hub points B1 and B2, a negative 0.35-ft throw is introduced at center-line hub point B for the proposed "Trial 2 west end." This adjustment will not appreciably change the three equations used in trial 1.

The only possible change in Eq. 4 is a new value of $o1$. To obtain the new distance of $o1$ for trial 2, the $o1$-distance from trial 1 should be corrected by using the radius computed in that trial. If the new $o1$-distance is in close agreement with the one initially assumed, as it was in this case, it does not have to be corrected. Therefore, Eq. 4 of trial 1 remains the same in trial 2. The difference between the assumed and theoretical o-distances will be explained subsequently.

The only revision in Eq. 6 is the change in the value of the radial offset r_B to accommodate the proposed negative 0.35-ft throw at the center-line hub point B. When Eq. 6 is thus revised—

$$(H1 - 438.905)^2 + (K1 - 127.329)^2 = (R1 + 23.20)^2 \tag{8}$$

Eq. 7 remains the same because there is no proposed throw at center-line hub point A1.

When Eqs. 4, 7, and 8 are solved simultaneously, there results $H1 = 1{,}158.170$ ft, $K1 = 7{,}774.707$ ft, and $R1 = 7{,}789.195$ ft. The new throws are computed and plotted as shown by "Trial 2 west end" in Fig. 6. This trial was accepted because the throws were not excessive and were reasonably balanced.

Trial 1, East End.—The first trial for the east end was developed from the east end of curve 1 and was continued to the east tangent line as shown by curve 2 in Fig. 5. The first of the necessary three equations determines the point of compound, the second passes the curve through the existing center-line hub A0, and the third makes the curve tangent at an $o2$-offset to the east tangent line.

The two curves may be compounded by determining an equation involving their center coordinates and radii. In Fig. 5 it is seen that a right triangle exists which is used to determine a relationship between these common properties—

$$(H1 - H2)^2 + (K1 - K2)^2 = (R1 - R2)^2 \tag{9}$$

By substituting the center coordinates and radius of curve 1, there results

$$(1{,}158.169853 - H2) + (7{,}774.706960 - K2)^2 = (7{,}789.195423 - R2)^2 \tag{10}$$

If the difference between the degrees of curvature of the two curves were large enough to require an internal spiral, Eq. 10 would be revised to

$$(H1 - H2)^2 + (K1 - K2)^2 = [(R1 - o) - R2]^2 \tag{11}$$

The internal spiral o-distance may be assumed for the initial trial and then corrected for subsequent trials by using the initial trial radius.

When the curve is passed through the center-line hub A0,

$$(H2 - 637.997)^2 + (K2 - 0)^2 = (R2 + 8.25)^2 \tag{12}$$

The distance from the east tangent line to the center of the curve ($H2$, $K2$) is

$$K2 = R2 + o2 \tag{13}$$

Assuming an approximate value of 0.349 ft for $o2$, one obtains

$$K2 = R2 + 0.349 \tag{14}$$

Solving Eqs. 10, 12, and 14 simultaneously, one finds $H2 = 956.344$ ft, $K2 = 6{,}409.461$ ft, and $R2 = 6{,}409.112$ ft. The throws are determined and plotted as shown by "Trial 1 east end" in Fig. 6.

Accepted Trial 2, East End.—To obtain a better balance between positive and negative throws, a positive 0.25-ft throw is introduced at center-line hub point A0 for the proposed "Trial 2 east end." This adjustment will not change Eq. 10 but will slightly alter Eqs. 12 and 14.

A change in the value of the radial offset r_{A0} to accommodate the proposed positive 0.25-ft throw at the center-line hub point A0 results in

$$(H2 - 637.997)^2 + (K2 - 0)^2 = (R2 + 8.00)^2 \tag{15}$$

Using the corrected value of 0.377 ft for $o2$, Eq. 14 becomes

$$K2 = R2 + 0.377 \tag{16}$$

The simultaneous solution of Eqs. 10, 15, and 16 results in $H2 = 947.903$ ft, $K2 = 6{,}295.268$ ft, and $R2 = 6{,}294.891$ ft. The "Trial 2 east end" throws are developed in the manner given previously and are accepted as indicated in Fig. 6.

Determination of the Point of Compound.—The point of compound can be computed by the use of similar triangles. It can be seen in Fig. 5 that

$$\frac{H1 - H2}{H1 - (\text{P.C.C.})_x} = \frac{R1 - R2}{R1} \tag{17}$$

A substitution of the known values leads to

$$\frac{1{,}158.169853 - 947.903123}{1{,}158.169853 - (\text{P.C.C.})_x} = \frac{7{,}789.195423 - 6{,}294.891455}{7{,}789.195423} \tag{18}$$

Then

$$(\text{P.C.C.})_x = 62.135 \tag{19}$$

and, similarly,

$$(\text{P.C.C.})_y = 62.999 \tag{20}$$

Spiral Adjustments.—In order to avoid making an extra trial to recorrect the assumed *o*-distance exactly, the length of the spiral can reasonably be altered to fit the assumed *o*-distance. For example, a standard east spiral length for the curve that was investigated previously would be 240 ft, and its theoretical *o*-distance would be 0.381 ft; by changing the spiral length to 239 ft, the theoretical *o*-distance changes to 0.378 ft as compared to 0.377 ft assumed in the computations. Because this discrepancy is small the spiral distance is assumed to be 239 ft.

Radius Hub Angles and Stationing.—The radius hub angles and stationing for compound curves are determined in the same manner as for simple curves. In this example the curve stationing is carried from the east P.S.C. to the west P.S.C. in the direction of valuation stationing. When computing the station at the P.C.C. of curve 1, it is apparent that a new stationing adjustment must be determined to keep the stationing of curve 1 in agreement with the stationing of curve 2. The angle i at the P.C.C. is divided by the degree of curvature of curve 1 to obtain L_{i1}. The difference between L_{i2} and L_{i1} plus one half of the east spiral distance is the new stationing adjustment for the stationing of curve 1.

ADVANTAGES AND DISADVANTAGES

The advantages of the proposed method of transit-lining high-speed track are as follows:

1. Absolute control is provided in establishing tangent track, and the most economical lining procedure is advocated.

2. Curves are computed in the office so that field crews are free to do other work, which reduces the cost of transit-lining curves.

3. In most instances the quality of the office computations is superior to that of field computations, and the computations can be more quickly completed.

4. A curve can be established from a traverse at intervals of approximately 300 ft, thus providing a center line of track which is accurate and easily located.

5. By graphing the actual throws, an alternate center line can be proposed which minimizes throw, meets points of limited throw, and still retains a relationship to the actual proposed center line. Also, the flexibility obtained by graphing allows larger initial throws to be proposed, which tends to discourage an excessive number of degrees of curvature and hence facilitates standardization.

The disadvantages of this method are:

1. Because this method is comprehensive, it can become involved.

2. It is necessary to have a computing machine available for office computations.

CONCLUSIONS

Some other methods of transit-lining curves are closely related to string-lining. By these methods, the curve is arbitrarily divided into segments of different degrees of curvature without regard to standardization of the curve as a whole. The only satisfaction derived from these methods is the probable limitation of throw. The method suggested herein introduces a control which tends to discourage an excessive number of degrees of curvature and facilitates standardization.

It is acknowledged that this method is intricate; however, it is no more complicated than most engineering design work. The most complex part of the method is the solution of compound curves by simultaneous equations. Familiarity with the method and use of the proposed forms will greatly increase the speed of the office computations.

In the event of any major main-line track changes, such as a program of widening track centers, this method could be adapted exceptionally well. Therefore, engineering and track-lining costs might be reduced greatly through the use of this method of transit lining.

DISCUSSION

Harry Rubey,[3] M. ASCE.—The work presented by Mr. Berndt is important not only because it presents an ingenious application of surveying and is a well-developed study for improving track alinement, but also because it promotes the use of the increasingly necessary transit lining of railway curves, which will result in better alinement standards. Because increasing speeds and track standards are essential for meeting the competition of other forms of transportation, railways must improve curve alinement. Many maintenance engineers will prefer transit lining for a considerable part of their programs. It is therefore urgent that this subject be thoroughly investigated and that alternative methods for transit lining be made a part of the discussion.

String lining became popular during the 1930's and during World War II, partly on its merits and partly because of the scarcity of engineering personnel. Following this period, engineering personnel became involved in management with increasing frequency, and the resultant shortage of engineers for transit lining tended further to popularize string lining. String lining, which is of undoubted value for smoothing curves, has frequently been used where transit lining would be better. As the author implies, important track should be lined correctively toward a perfect transit curve rather than in the makeshift manner that is encouraged by string lining. Actually, string lining may be used under certain conditions and transit lining under others.

Mr. Berndt's paper presents a valuable analysis and helpful suggestions for alining the tangents, improving the clearance on multiple track, gradual corrective lining of the curves toward an ultimately optimum alinement, and monumenting the control points. Fortunately, his analysis may be applied to other methods of lining the curves.

The ingenious coordinate method used on the curve appears to be practical except for the fact that for many railways too much specialized surveying skill, too much time, too much travel, too much office work, and too much selection by office personnel of the optimum alinement are required. The factors influencing the alinement decision can be evaluated equally well or better in the field. Mr. Berndt's method would appear suitable where (1) heavy traffic prevails, (2) a highly organized division office exists, (3) engineering personnel is abundant and relatively stable, and (4) engineering standards are high.

A simpler alternative method of transit realinement is available. This method[4] was developed to permit complete staking of a relatively simple curve in one day of field work; tables and diagrams are included which speed the work in the field—without them the time lost by the field party while computations were being made would be prohibitive. It is thought to be a simple, easy, quick, and inexpensive method with the added advantage of selecting the optimum curve in the field, where all influencing factors can be properly weighed.

Unless an economical method for transit lining receives wide recognition, string lining will continue to be used even where transit lining is preferable.

---

[3] Chairman of Civ. Eng. Dept., Univ. of Missouri, Columbia, Mo.

[4] "A New Transit Method for Realigning Railway Curves and Spirals," by Harry Rubey, *Bulletin No. 34*, Eng. Experiment Station, Univ. of Missouri, Columbia, Mo., 1946.

AMERICAN SOCIETY OF CIVIL ENGINEERS
Founded November 5, 1852
TRANSACTIONS

Paper No. 2754

MODERNIZATION OF THE HALES BAR PLANT

By Adolf A. Meyer,[1] M. ASCE

With Discussion by Messrs. George R. Rich, Clarence E. Blee,
George A. Jessop, and Adolf A. Meyer

Synopsis

The Hales Bar Hydroelectric Plant on the Tennessee River was built between 1905 and 1914. In 1941 a comprehensive program of improvements and additions was begun which was intended to improve the safety of some of the original structures, to facilitate navigation, to increase the power capacity and output of the station, and at the same time to simplify operation.

History and Description of Initial Project

A study of additions and improvements to a hydroelectric plant demands familiarity with the project as it was originally built. In the case of the Hales Bar plant this introductory information is especially interesting because the plant is one of the pioneer hydroelectric plants in the United States.

Just below Chattanooga (Tenn.), the Tennessee River departs from the direction it follows from Kingston (Tenn.) and turns in a westerly direction to cut through Walden's Ridge. For thirty miles it passes through a narrow gorge, with a total drop of 30 ft. This gorge, called The Narrows, was once a dangerous reach for river navigation. In 1890, the lower river and middle river were joined for navigation by the opening of the Muscle Shoals Canal in Alabama. There naturally followed agitation for improvements in the navigation conditions of The Narrows, the dangerous stretch separating the middle river from the upper reaches. At approximately the same time, the first transmission of electric energy over moderate distances was accomplished. Therefore, the two goals—better navigation and an electric power supply for the City of Chattanooga—were combined. Following promotions by citizens of Chattanooga, the Congress of the United States passed an act[2] in 1904 that

---

Note.—Published, essentially as printed here, in October, 1953, as *Proceedings-Separate No. 294*. Positions and titles given are those in effect when the paper or discussion was received for publication.

[1] Head Civ. Engr., Tennessee Valley Authority, Knoxville, Tenn.

[2] *Public Act 165*, Chapter 1605, 58th Cong., approved April 26, 1904.

authorized the Secretary of War to grant permission to the City of Chattanooga to build a dam in The Narrows. If Chattanooga failed to apply for permission within four months after the passage of this act, permission could be granted to a private corporation or to individuals. The total cost of the project, except the plans, equipment, and gates at the lock, was to be paid by the contracting party. The deed for the property on which the lock, dam, and reservoir were to be located was to be transferred to the federal government. In return, the act granted a ninety-nine-year right to generate power.

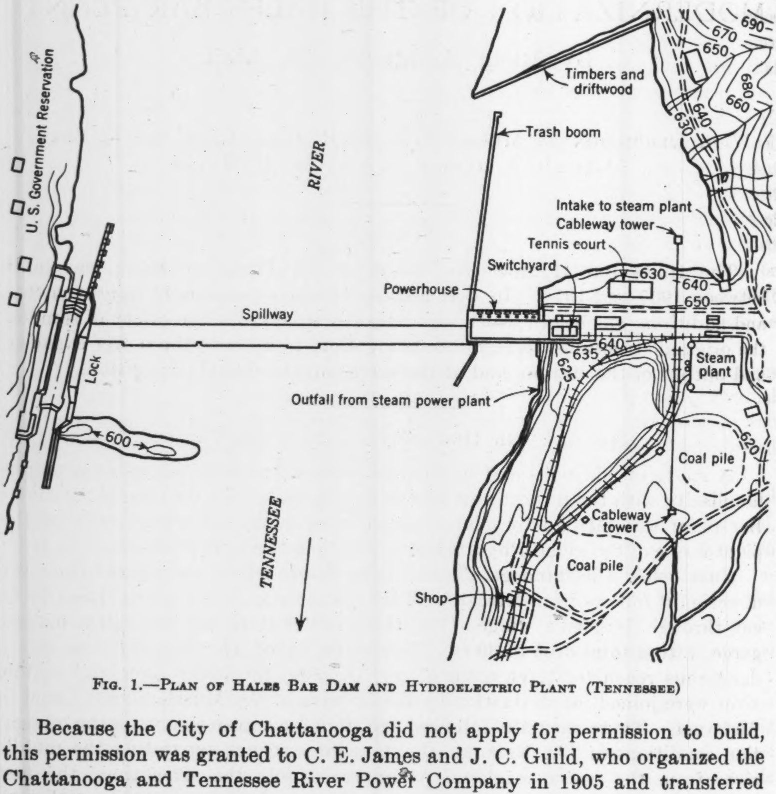
U. S. Government Reservation
RIVER
Timbers and driftwood
Trash boom
690
670
650
680
660
640
630
Intake to steam plant
Cableway tower
Tennis court
Switchyard
Powerhouse
630
640
650
Spillway
640
635
625
Steam plant
Lock
Outfall from steam power plant
600
620
Coal pile
Cableway tower
Coal pile
TENNESSEE
Shop

FIG. 1.—PLAN OF HALES BAR DAM AND HYDROELECTRIC PLANT (TENNESSEE)

Because the City of Chattanooga did not apply for permission to build, this permission was granted to C. E. James and J. C. Guild, who organized the Chattanooga and Tennessee River Power Company in 1905 and transferred their rights to that company.

By the fall of 1905, the final site for the dam had been selected, and designs had been prepared; construction work was ready to begin. The costs were estimated at $3,000,000; the time required for completion of the project was assumed to be two years.

In the project layout (Fig. 1), the navigation lock is located at one side of the river, the powerhouse at the other, and a straight overfall spillway between.

An earth embankment forms a barrier over the low flood plain between the powerhouse and the left shore. The total length of the barrier from shore to shore is approximately 2,350 ft. The general arrangement of the structures at Hales Bar closely resembles the arrangements used thirty years later for the neighboring projects at Chickamauga (Tenn.) and Guntersville (Ala.)

At the selected site, rock is outcropping across the entire channel width. The formation is Mississippian limestone, having nearly horizontal bedding. At that time the accepted geological theory was that no solution channels would form in rock below the ground-water level. This erroneous concept concerning the foundation rock caused a long series of disappointments. Many interconnecting solution channels honeycomb the formation as far as 100 ft below the surface. As the cofferdams were advanced over this honeycombed rock, unwatering became increasingly difficult. By the time that approximately half the spillway was built, unwatering by means of cofferdams became impossible, and pneumatic-caisson foundations became necessary. The continuous fight against leakage delayed construction so that it was April, 1914, eight and a half years after the beginning of construction, when the plant was finally ready for commercial operation. Correspondingly, the project costs, originally estimated as $3,000,000, rose to $11,300,000.

The useful head created by the dam was 37 ft at low flow, which could be increased by approximately 3 ft by placing flashboards on the spillway crest. The navigation lock has a main chamber 60 ft wide with a clear length of 265 ft. It is designed to provide a 9-ft navigation depth. Little attention was given to the safety and ease with which vessels could approach and leave the lockin chamber.

The basic layout of the powerhouse substructure is of surprising simplicity. Eight buttress walls, each 10 ft thick, 97 ft long, and 94 ft high, form seven flumes, each 19 ft wide, that are separated from the forebay by a low concrete sill and a head gate approximately 30 ft high. In each of these flumes two units are mounted. The original eight units are vertical triple-runner Francis wheels; the six units installed in 1915 and 1916 are single-runner Francis wheels. The runner diameters vary between 61 in. and 82 in.; their operating speeds are 112.5 rpm and 100 rpm. The total capacity of the fourteen units is 51,000 kw.

The arrangement for the initial units with six runners within one flume required great ingenuity, as illustrated by Fig. 2. The various passageways are separated by concrete walls and steel draft-tube liners. The hydraulic efficiency of this complicated setting was necessarily low.

The fourteen generators are housed in a well-built concrete superstructure. At the shore, a large indoor switching station adjoins the generating station. This switch house enclosed all the transformers and the 115,000-volt switching equipment. A 46,000-volt switching station was built on the roof of the building. A railroad track extends the full length of the switch house and generator room. The small turbine runners required narrow spacing of the rack bars—consequently, much trash handling had to be anticipated. To ease this situation, the forebay upstream from the intake was fully enclosed, with a floating trash boom on its river side.

Measured by the standards of hydroelectric developments at the time of its inception, the Hales Bar power plant was well built and adequately equipped when it was put in operation. However, the foundation leakage that had upset construction so extensively continued to cause trouble. In spite of the fact that the dam foundation had been lowered 30 ft below the original rock line and that much drilling and grouting had been performed in the solution zones, the filling of the reservoir produced seepage boils in the tailwater below the dam. These boils gradually increased in number. Attempts to stop the leakage by plugging the suction inlets within the reservoir failed. Between 1919 and 1921 a program of asphalt grouting was executed. More than 6,000 lin ft of $2\frac{3}{4}$-in.-diameter holes were drilled from the inspection gallery of the dam, and more than 75,000 cu ft of asphalt were injected into these holes. This operation appeared to be successful—the leakage was reduced to an insignificant rate. However, by 1931 the leakage had increased to 200 cu ft per sec and by 1939 it had reached 1,650 cu ft per sec.

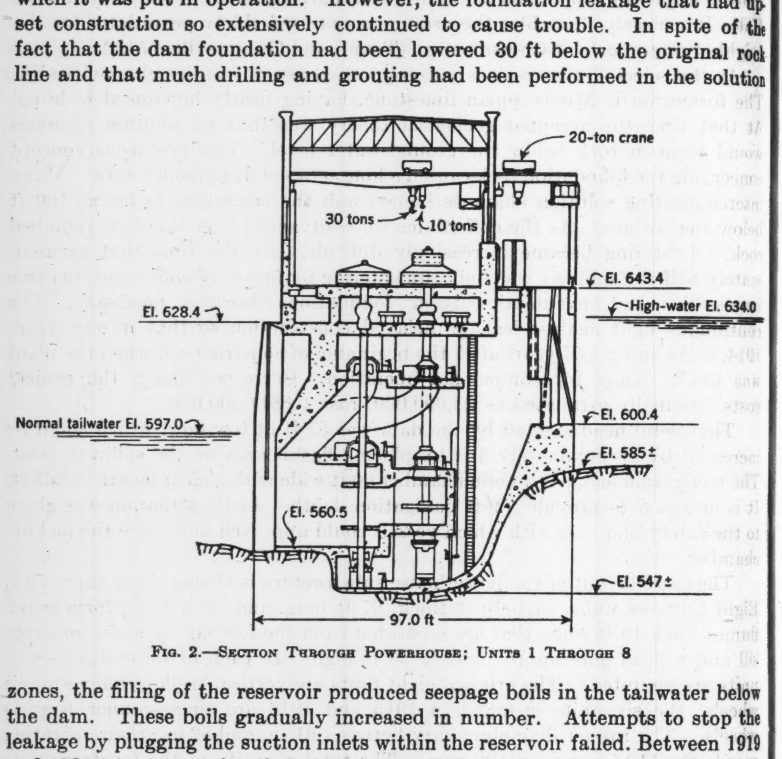

Fig. 2.—Section Through Powerhouse; Units 1 Through 8

In 1922, the Hales Bar Dam property was acquired by the Tennessee Electric Power Company. In 1924, this new owner built a steam plant of 40,000-kw capacity adjacent to the hydroelectric station. In 1939, the Tennessee Valley Authority (TVA) acquired the Hales Bar hydroelectric and steam plants.

Arresting Leakage Under Dam

In 1939, the water passing under the dam represented a yearly loss of more than 20,000,000 kw-hr of energy. Furthermore, the continuous undermining of the foundation rock made questionable the ultimate safety of the structure. Immediately following the acquisition of the dam, the TVA began to study means by which the leakage might be stopped. These studies indicated that permanent correction would require construction of a cutoff wall penetrating solid rock below all the honeycombed areas. To build such a wall without lowering the reservoir was an unprecedented feat. The wall was built by drilling a system of overlapping holes, 18 in. in diameter. The drill holes were lined with asbestos cement pipe and filled with concrete. The foundation was then extensively consolidated downstream of the cutoff wall. This work was accomplished between 1941 and 1944 and has been described in detail in a paper[3] by L. A. Schmidt, Jr., M. ASCE.

NAVIGATION ADJUSTMENTS

The next project was the adjustment of the river reach at Hales Bar to the requirements of the improved Tennessee River navigation channel. Below Hales Bar, the TVA had already built the Guntersville Dam. Its headwaters provided a channel of 9-ft depth to the Hales Bar lock, a little dredging being required at a few gravel bars. On the upstream side, Chickamauga Dam had been built 7 miles upstream from Chattanooga. In this 7-mile reach between Chattanooga and the Chickamauga lock, the depth was insufficient for navigation during low-flow periods—only 4 ft in some sections. When the Chickamauga site was selected, improvement of this reach either by dredging or by raising the Hales Bar pool was contemplated. Comparative estimates indicated that raising the minimum headwater from El. 626.25 to El. 632.00 combined with a small amount of channel dredging offered the most economical solution. In order to raise the pool, piers and gates had to be installed. Space had to be provided for an additional lock to be built when the existing lock, which is of substandard length, becomes inadequate for river traffic; space also was needed for an extension of the powerhouse. In order to build these additions economically, parts of the old spillway had to be allotted for the future structures. These allotments, including 224 ft assigned to the future lock and 188 ft assigned to the powerhouse extension, shortened the spillway (originally 1,200 ft long) to an over-all length of 788 ft. To compensate for the flood discharge capacity lost by this change in length it was necessary to lower the crest. With seventeen gate openings and piers 6 ft thick, the new crest had to be set at El. 616—10.25 ft below the original crest. The gates are of the radial type, with their tops at El. 635. The reservoir level may vary between El. 632 and El. 634, leaving a 1-ft freeboard on the gates at maximum pool.

Because the stability of the dam was adequate for the increased head, the design of the spillway changes did not offer any unusual problems. The piers were anchored into the old weir by reinforcing bars set in drill holes 12 ft deep. The concrete for the new crest was made between 2 ft and 3 ft thick; careful bonding with the old concrete was specified, and the reinforcement was anchored to the old concrete by dowels 5 ft on centers. The piers support an operating deck at a level that provides clearance for all flood conditions. Two traveling hoists can be moved along this deck for raising and lowering the gates. The adjustment to the transverse joints in the old dam was made with great care; it was difficult because the joints were distributed in a most irregular pattern and because some of the joints were active contraction joints whereas others were obviously "frozen." Because there had been a moderate amount of scouring below the old dam, tests were made in the hydraulic laboratory to find a form of apron that would prevent further scour. The tests showed that by filling the existing apron to El. 588 a stable condition for nearly all flows could be obtained. The same tests were used to establish the minimum length and height of the training walls at each end of the spillway. The wall at the powerhouse side was designed as a bulkhead to withstand full water load while it formed a part of the cofferdam for the powerhouse extension.

---

[3] "Flowing Water in Underground Channels, Hales Bar Dam, Tennessee," by L. A. Schmidt, Jr., *Transactions*, ASCE, Vol. 110, 1945, p. 965.

All the spillway alterations had to be constructed without lowering the level of the reservoir. To do this economically, extensive use was made of structural-steel bulkheads that could be used again in many alternate positions. For the large amount of line drilling involved, special "jumbos" were devised. The construction methods have been described elsewhere.[4]

The raising of the reservoir level solved the navigation problems in the upper reach of the Hales Bar pool, but to satisfy reasonable demands of traffic safety and efficiency the lock had to be improved. Because the locks at Wilson Dam are also of substandard length, the short lock chamber at the Hales Bar Dam will not be a serious impediment until improvements have been made at Wilson Dam. Therefore, it was decided to improve the existing lock and allot space for a new lock to be built when river traffic demands it. The primary objectives of the changes were the improvement of the approach conditions both downstream and upstream, a reduction of navigation interruptions during flood stages, the betterment of the mooring and towing facilities in the lock chamber, and miscellaneous equipment modernizations. At the lower end of the downstream guard wall, troublesome eddies frequently hindered safe navigation. Tests in the hydraulic laboratory indicated that good approach conditions would exist if the wall were lengthened by 560 ft. To build this wall without unwatering, fifteen sheet-pile cells, 27 ft in diameter and filled with tremie concrete, were constructed with their tops projecting above low-water level. On top of these cells a continuous concrete wall 29 ft high was placed. The old guard wall was raised to the same elevation. The old and new walls together form a guard wall 750 ft long, with the top at El. 625. The wall will be visible at all flows less than 300,000 cu ft per sec. On the land side, three mooring cells were built to guide traffic into the lock chamber. Similar improvements were made on the upstream approach. Along the rocky cliff on the land side, which previously was unprotected, a guide wall 425 ft long was built. An inverted U-shaped concrete box is supported on two rows of precast concrete piles that are anchored in the rock. Traffic impacts are transferred by the horizontal girder to articulated concrete struts which are connected to anchors on the rock bluff. The old upstream guard wall was improved by the addition of curtain walls between the piers to stop troublesome side currents in the approach bay.

---

[4] "Hales Bar Dam: Rebuilt and Ready for More Power," by A. H. Weber, *Engineering News-Record*, October 19, 1950, p. 37.

Although the dam was strong enough to withstand the increased head according to normal design criteria, an analysis of the river wall of the dock chamber indicated tensions at the base produced by the raised level of the pool. A triangular block of concrete was added on the river side in order to obtain a wider base. To make sure that this block would actually buttress the old concrete, a grouting plane was formed near the base of the block on a slope perpendicular to the principal stress. During the cold-weather season and with the lock chamber empty, grout under pressure of 30 lb per sq in. was introduced into this sealed-off joint. In this manner, a permanent prestress was established in the new block (Fig. 3). In the lock chamber itself, three floating mooring bitts and a towing unit for barges were installed. New valves were placed in the filling culverts, and the miter-gate operating mechanism was rearranged and its capacity increased. In Fig. 4 there are shown plans of the old locks and the improved locks side by side.

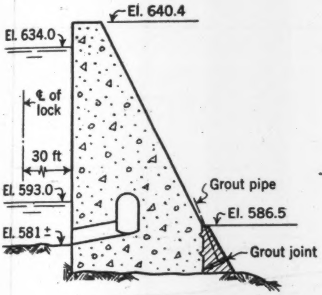

FIG. 3.—STRENGTHENING OF THE RIVER WALL OF THE LOCK

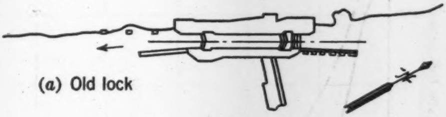

(*a*) Old lock

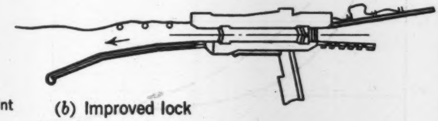

(*b*) Improved lock

FIG. 4.—HALES BAR LOCK (TENNESSEE)

The raising of the pool level necessitated some adjustments in the reservoir. Additional land had to be bought, additional clearing had to be done, and at Chattanooga some sewer outfalls had to be raised.

Construction on the improvements to the dam and the lock was begun in 1946 and completed in 1950.

ADDITIONS AND IMPROVEMENTS TO THE POWER FACILITIES

The third step of the improvement program at Hales Bar concerns the power installation. When the Hales Bar Dam was built, there was no flow regulation within its 21,800-sq-mile drainage area. The variations in flow were very large, varying between an extreme low flow of 3,300 cu ft per sec and a maximum flow of 460,000 cu ft per sec. There are now many reservoirs upstream of Hales Bar Dam, which have a combined useful storage volume of almost 10,000,000 acre-ft. The flow characteristics of the river have changed markedly, as indicated by the duration curves for natural and regulated flow shown in Fig. 5.

The useful storage capacity of the Hales Bar pool, with only 2 ft of fluctuation, is limited—only 13,100 acre-ft. The adjoining reservoir on the upstream side, the Chickamauga pool, has a useful storage capacity of 329,000 acre-ft. In order to utilize the regulation made possible by the large reservoir at Chickamauga, it was desirable to have the draft of the turbines at Hales Bar at least equal to the draft of the turbines at Chickamauga. The four units at Chickamauga draw approximately 38,400 cu ft per sec. The corresponding draft for the old station at Hales Bar is 19,200 cu ft per sec. A new turbine installation with draft almost equal to that of the old station was therefore selected. It consists of two Kaplan wheels with nominal ratings of 24,300 kw each at 36-ft head and with maximum discharge capacities of 22,000 cu ft per sec. The addition of these wheels increases the station output, which had amounted to 238 × 10^6 kw-hr during the average year of unregulated flow and 369 × 10^6 kw-hr during the average year of regulated flow, to 594 × 10^6 kw-hr.

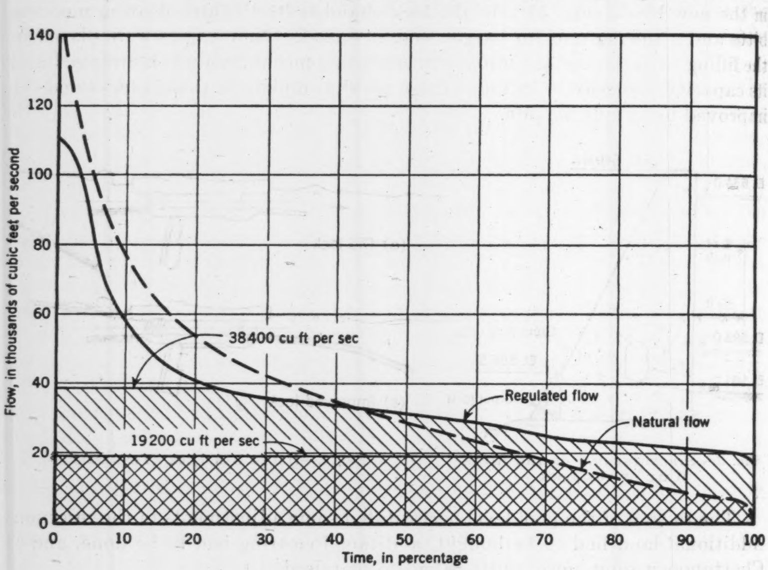

Fig. 5.—Duration Curves

The construction of these two units necessitated further changes in the power facilities as follows:

The 62,100-kva capacity of the new units made the existing transmission facilities inadequate. New 161-kv system ties were provided to replace the existing 115-kv tie line.

New step-up transformers and switching equipment installed outdoors were provided to replace the existing indoor equipment. A serious fire hazard was thus removed from the building, and valuable building space was made available for operating facilities that would otherwise have been provided as part of the new control building.

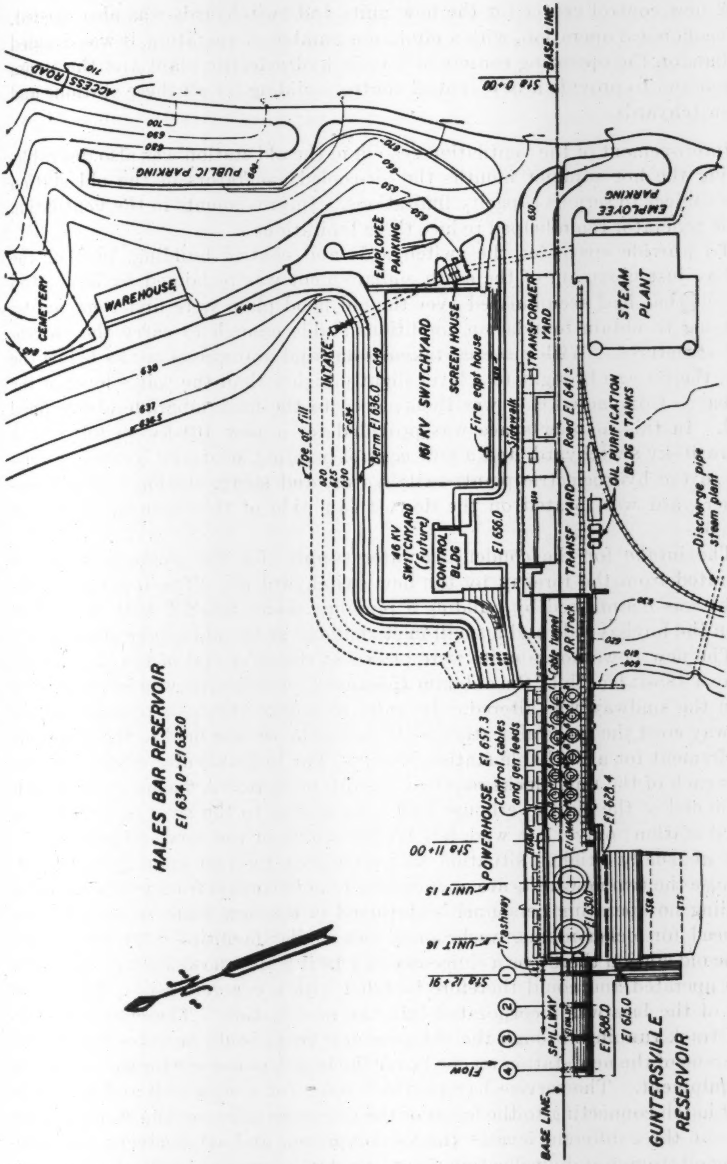
HALES BAR RESERVOIR
El 634.0-El 632.0
GUNTERSVILLE RESERVOIR
BASE LINE
Sta 0+00
ACCESS ROAD
710
700
690
680
670
660
650
640
639
637
636.5
634
630
625
620
PUBLIC PARKING
EMPLOYEE PARKING
CEMETERY
WAREHOUSE
INTAKE
SCREEN HOUSE
Fire eqpt house
Sidewalk
161 KV SWITCHYARD
Berm El 636.0
Toe of fill
46 KV SWITCHYARD (Future)
CONTROL BLDG
El 656.0
TRANSFORMER YARD
TRANSF YARD
Road El 641±
STEAM PLANT
EMPLOYEE PARKING
OIL PURIFICATION BLDG & TANKS
Discharge pipe steam plant
RR track
Cable tunnel
POWERHOUSE
El 657.3
Control cables and gen leads
El 628.4
El 630.0
Trashway
UNIT 15
UNIT 16
Sta 11+00
Sta 12+91
SPILLWAY
El 588.0
El 615.0
Flow
1
2
3
4

Fig. 6.—Plan of Powerhouse and Transformer Yard

A new control center for the new units and switchyards was also needed. For economical operation, with a minimum number of operators, it was decided to abandon the operating centers of the old hydroelectric plant and the steam station and to provide a new central control building for all these stations and the switchyards.

Improvement of the ventilation system in the old station was also desirable. During the hot summer months the air-cooled generators of the old station were subject to serious capacity limitations. Improvements in the ventilation of the generator room helped reduce these limitations.

To provide space for the switchyards and control building, part of the forebay just upstream of the earth embankment was reclaimed by fill. Mud and silt that had accumulated over the old flood plain were first removed by dredging to obtain foundation conditions stable enough to carry the switchyard structures. With material taken from sand and gravel banks below the dam, the fill was brought to a level slightly higher than the water level of the forebay. Compacted clay was then placed to the final subgrade above flood level. In this manner space was provided for a new 161-kv switchyard, a future 46-kv switchyard, and a new control building, centrally located in relation to the hydroelectric plant, switchyards, and steam station. The transformer yard was located on the downstream side of the earth embankment (Fig. 6).

The intake for the condensing-water supply for the steam station was separated from the forebay by the new switchyard fill. The function of the intake was maintained by building a pipe line under this fill, with a drop inlet on the forebay side and a small inlet chamber at the old intake structure.

The new powerhouse units were placed at the river end of the old station, where a 188-ft length of the old dam (previously mentioned) was left in reserve when the spillway was altered. In order to reduce the costs of lowering the spillway crest the space allocation for the powerhouse was held to the minimum requirement for a workable station layout. For hydraulically efficient waterways each of the unit blocks required a width of 78 ft. A trashway 15 ft wide at the end of the old powerhouse had to be moved to the river end of the enlarged station; only 17 ft were left for the width of the service bay (Fig. 7). This unusually "tight" situation was alleviated by two circumstances: (1) Because the two new units are operated by remote control from the new control building no operating personnel is stationed in the new plant so that there is no need for locker-rooms, washrooms, and similar facilities. (2) At the end of the old station there was a sluiceway bay 18 ft wide; the sluiceway had never been operated and could therefore be filled with a concrete plug. The upper part of the bay was incorporated into the new station. Therefore, the railroad track running through the old generator room could be extended so that the crane of the new station reached over the length of one car for the unloading of equipment. The service bay provided room for a stair well and an equipment hatch connecting to the levels of the two main galleries, the station sump, and—on three different levels—the air compressor and air receivers, the lubricating oil storage and purification plant, the station service electrical equipment, and the carbon-dioxide storage area.

In developing the unit blocks, great effort was made to provide efficient waterways, compact arrangement of the main equipment, and good communications. At the intake side, the upstream face is alined with the face of the old station intake. The new deck forms a continuation of the old deck and is of equal width. Water enters the bellmouthed intake, which is subdivided into three passageways for each unit, through trashracks mounted on the upstream face. If emergency unwatering is required, stoplogs can be set into the trashrack guides. Each opening is 46 ft high and 23 ft wide; a velocity of 3 ft per sec results for the gross area at the entrance. The upper lip of the bellmouth is 9 ft below the lowest normal reservoir level. The intake gate openings just downstream from the bellmouth are 37 ft high. To close the openings, one set of intake gates is provided. Each gate is composed of two leaves. The gates for two openings are slide gates, and the gate for the third opening is of the fixed-wheel type. Stoplogs for unwatering one intake opening are kept on hand. The gate leaves are kept in storage pits in the intake deck, and the stoplogs are stored in the upper part of the trashrack slots. A gantry crane of 30-ton capacity is used to handle the gates, stoplogs, and trashracks.

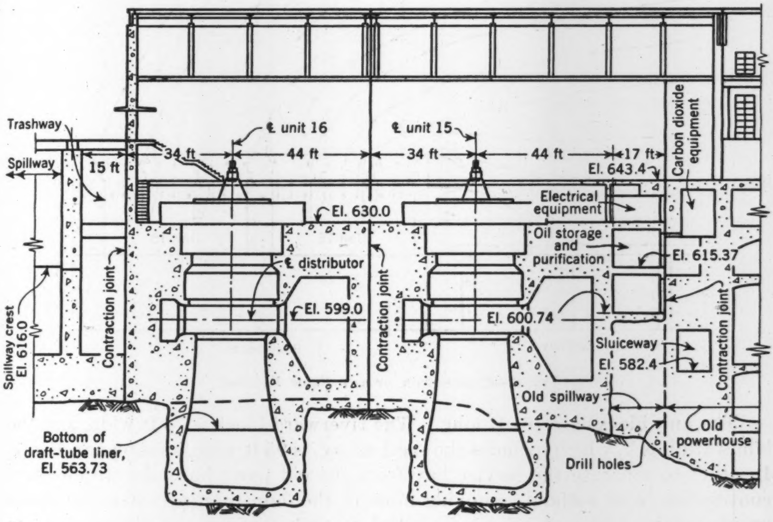
Trashway
Spillway
15 ft
34 ft
℄ unit 16
44 ft
℄ unit 15
34 ft
44 ft
17 ft
El. 643.4
Carbon dioxide equipment
Electrical equipment
El. 630.0
Oil storage and purification
El. 615.37
℄ distributor
El. 599.0
El. 600.74
Spillway crest El. 616.0
Contraction joint
Contraction joint
Contraction joint
Sluiceway
El. 582.4
Old spillway
Old powerhouse
Drill holes
Bottom of draft-tube liner, El. 563.73

FIG. 7.—SECTION TAKEN THROUGH THE NEW POWERHOUSE UNITS

An unusual complication developed from alining the new intake with the old one. This arrangement made it necessary to locate the face of the intake 49 ft upstream from the face of the dam; the deep corner pocket tended to produce eddy flows. Hydraulic laboratory tests showed that eddies affected the flow pattern in the intake in a particularly unfavorable way. At the river side unit, the flow into the passageway adjacent to the dam was almost nil. It was estimated that the resulting turbulence in the intake would cause a power loss of 1,500,000 kw-hr per yr. Various types of flow guides to correct the flow pattern at the intake were tested in the laboratory. Two guides selected on the basis of the test results were installed, one at the river end of the units and one between the two units. They are shown shaded in Fig. 8. Because there was not enough space for the guides to be built "in the dry" while the cofferdam was in place, they had to be precast and lowered into slots after the cofferdam was removed. They were made of hollow concrete sections, one on top of the other; the hollow spaces were filled with gravel to make the guides more stable.

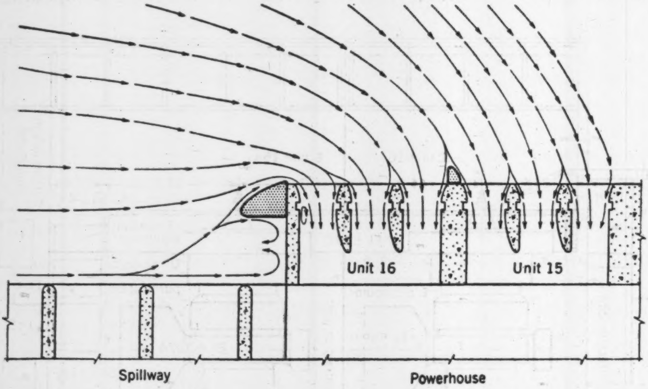

Fig. 8.—Correction of the Flow Pattern

The unit blocks are 161 ft long. The riverward block is 78 ft wide, and the landward block, which includes the service bay, is 95 ft wide, as shown in Fig. 7. In order to separate the service bay from the old powerhouse by an effective contraction joint without removing more of the dam than necessary for space requirements, a line of holes was drilled to rock through the old concrete to establish a plane of weakness. The center line of the unit is 99 ft from the draft-tube exit (Fig. 9). The area at the exit (Fig. 10) is 1,515 sq ft (which results in an exit velocity of 6.3 ft per sec at maximum discharge). The center line of the distributor is at El. 599, 6 ft above minimum tailwater. This position made possible the establishment of the generator-room floor at El. 630, 13.4 ft below the floor of the generator room of the old station. To provide unloading facilities for the track extension on the level of the old generator room, a balcony was provided at that level in the service bay (Fig. 9). This balcony also provides space for the rotor erection. It is connected to another balcony that extends the full length of the new station. At the river end, a stairway leads up to a balcony at the level of the spillway deck, with a door in the river wall connecting to the deck. A shelter for the operators of the spillway cranes is provided inside this door.

Because the outside diameter of the generator, which operates at 69.2 rpm, was 46 ft 6 in. and because erection space for the runner and the bearing bracket

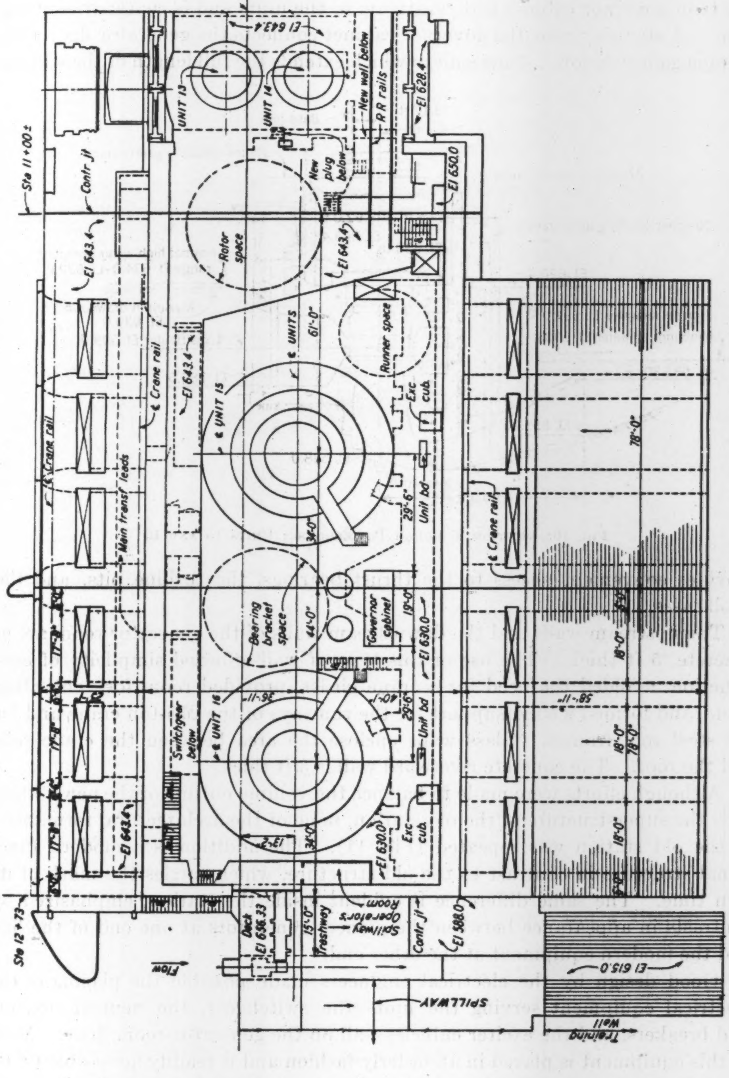
BASE LINE
El 643.4
UNIT 13
UNIT 14
New wall below
R R rails
El 628.4
Sta 11+00±
Contr jt
New plug below
El 650.0
El 643.4
Rotor space
El 643.4
℄ UNITS
61'-0"
Runner space
Exc cub.
℄ UNIT 15
℄ Crane rail
El 643.4
℄ Crane rail
Main transf leads
36'-0"
29'-6"
Unit bd
78'-0"
℄ Crane rail
Bearing bracket space
44'-0"
Governor cabinet
19'-0"
El 630.0
8'-0"
18'-0"
36'-11"
40'-1"
29'-6"
58'-11"
Unit bd
18'-0"
78'-0"
℄ UNIT 16
Switchgear below
El 643.4
17'-8"
Exc cub.
34'-0"
El 630.0
18'-0"
Sta 12+73
Deck El 656.33
Trashway
15'-0"
Spillway Operators Room
Contr jt
El 588.0
El 615.0
Flow
SPILLWAY
Training Wall

FIG. 9.—PLAN OF NEW POWERHOUSE

was required on the generator-room floor, the new station had to be wider than the old station (Fig. 9). It was necessary to offset the downstream wall by 10 ft 6 in. However, the roof could be kept on the level of the old station roof. The twin governor cabinet is downstream of the units and is centered between them. A stairway near the governor cabinet connects the generator floor with the pipe gallery below. This gallery which extends the full length of the station provides convenient access to the thrust bearings, the turbine pits, and the scroll cases.

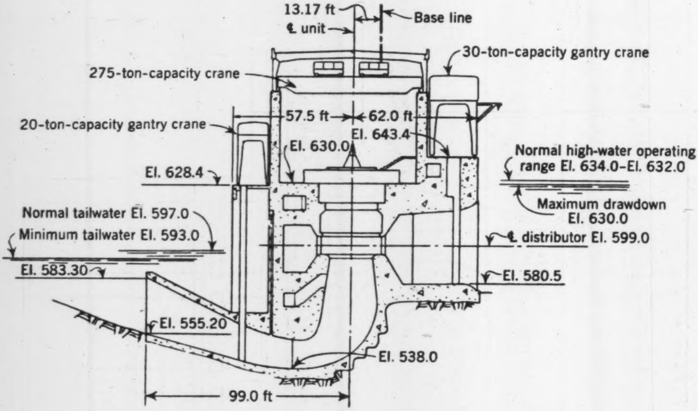
13.17 ft
℄ unit
Base line
30-ton-capacity gantry crane
275-ton-capacity crane
20-ton-capacity gantry crane
57.5 ft
62.0 ft
El. 643.4
El. 630.0
Normal high-water operating range El. 634.0-El. 632.0
El. 628.4
Maximum drawdown El. 630.0
Normal tailwater El. 597.0
Minimum tailwater El. 593.0
℄ distributor El. 599.0
El. 583.30
El. 580.5
El. 555.20
El. 538.0
99.0 ft

FIG. 10.—SECTION THROUGH POWERHOUSE; UNITS 15 AND 16

The upstream walls and the downstream walls of the generator room are of concrete, 5 ft thick. The use of this type of wall afforded simplicity of construction, avoided the need for a crane girder, provided room for ventilating ducts, and formed a solid support for the runways of the 275-ton crane and for the steel roof frames. Glass walls enclose the area between the crane rails and the roof. The concrete riverward wall is 3 ft thick.

Although efforts were made to balance the volume outline of the new station with the superstructure of the old station, none of the architectural formalities of the old station was repeated (Fig. 11). The addition is a modern functional structure in contrast to the old structure, which carries the mark of its own time. The same difference is evident inside the station, emphasized by contrasts in appearance between the pioneer generators at one end of the hall and the modern equipment at the other end.

Good design by the electrical engineers made possible the placing of the electrical equipment serving the unit—the switchgear, the neutral reactors and breakers, and the exciter cubicles—all on the generator-room floor. Most of this equipment is placed in an orderly fashion and is readily accessible under the balcony along the upstream wall (Fig. 9). The oil-pressure, pipe-line type cables for the generator leads pass from the switchgear through the upstream wall to the cable tunnel under the new intake deck. This tunnel, which also houses the control cables, terminates in a pulling chamber at the junction of the new deck and the old deck. From there to a pulling chamber at the shore end of the old deck, station service power and control cables enclosed in heavy-wall transite pipes, together with the steel pipes containing the generator cables, are exposed along the upstream wall of the old station. A new cable tunnel built into the earth embankment along the old switch building then takes the generator leads and control cables from the new station and the old station to the transformers and the new control building, respectively.

FIG. 11.—ARCHITECTURAL COMPARISON, OLD AND NEW POWERHOUSES

The control building is located next to the switchyard on ground reclaimed from the forebay (Fig. 6). It is an L-shaped building covering an area of approximately 5,400 sq ft. The substructure is a monolithic concrete box; the superstructure consists of steel framing with brick and tile walls. In addition to the main control room, the building houses the relay room, the communication room, and the battery room. It also contains facilities for the operators—a fileroom, a locker-room, a washroom, and a kitchen. The building is air-conditioned. It serves as the central control room for the old hydroelectric station and the new one, for the steam station, and for the switchyards. The new hydroelectric units are operated by remote control whereas the old station requires the presence of one operator on the floor. By combining the controls into one building, the operating force could be reduced by five men per shift.

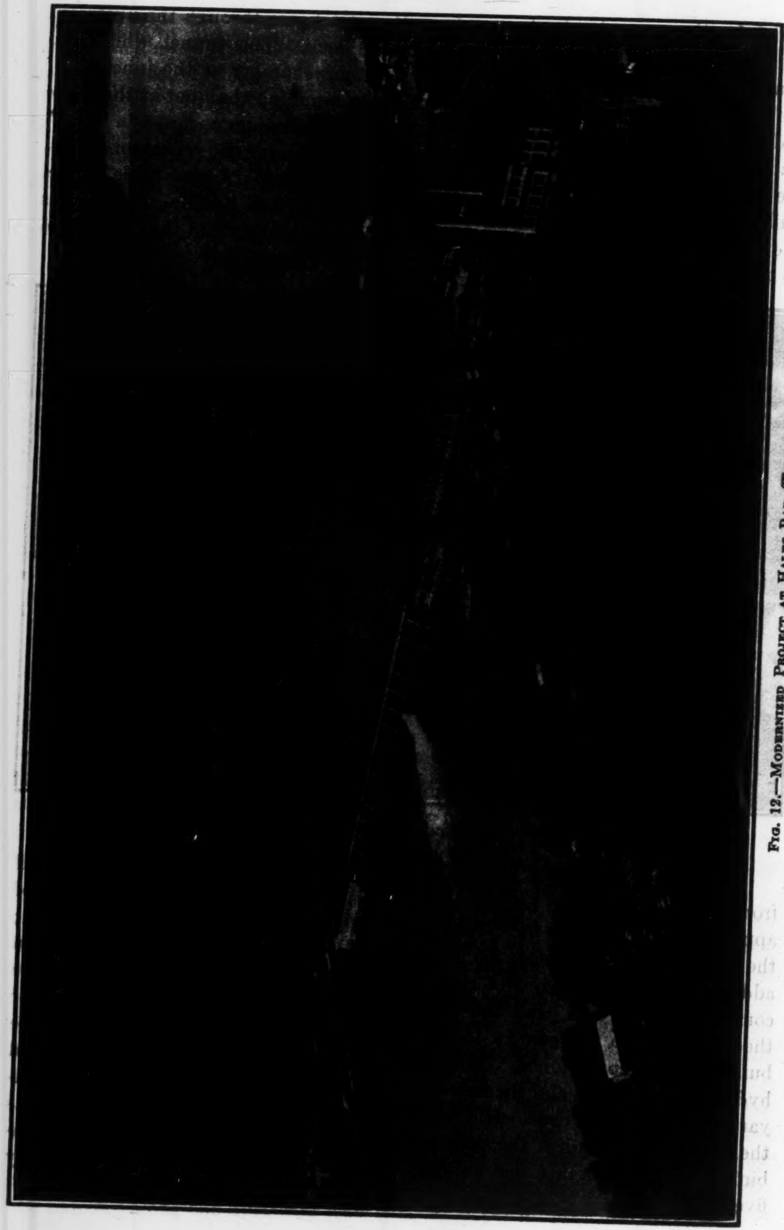

FIG. 12.—MODERNIZED PROJECT AT HALES BAR (TENNESSEE)

Because the high-tension equipment and the old control room were removed from the switch building, much space became available there. The building was altered to provide some urgently needed facilities for plant operation. These facilities include office space for the superintendent and his assistant and for clerical personnel, a test room, a first-aid room, and a large assembly room. A new machine shop and storage rooms were also provided. For visitors, washrooms and a lobby overlooking the generator room have been provided. Adjacent to the switchyard there was room for a large parking area for operators. On the hillside along the access road, a parking area for the numerous visitors has been established. This area offers a good view of the plant layout.

The construction of the two units necessitated the solution of some unusual problems. Because the forebay level had to be maintained at all times the upstream cofferdam temporarily replaced the concrete dam, and therefore its design required a high degree of safety. Normally, the cofferdam had to withstand a head of 50 ft. Steel sheet-pile cells 70 ft in diameter were used. Special templates[5] were developed for driving these cells.

The downstream cofferdam also presented a peculiar problem. It was U-shaped in plan to enclose the area of excavation for the units and the tailrace. Rock excavation 45 ft deep was necessary at the low point of the draft tube. The west side of the cofferdam was formed by the new spillway training wall; the opposite side was formed by cells along the old tailrace connecting with the old station. Because there were horizontal bedding joints in the rock and clay present in some of these joints, it was feared that the rock supporting the cofferdam, especially the narrow shelf between the old tailrace and the new tailrace, might slide into the new excavation after the rock inside the cofferdam was removed. After a study of various schemes for the prevention of sliding, a system requiring step-by-step excavation was adopted. In the first step, excavation was extended only 62.5 ft downstream from the center line of the units. After the unit blocks were built to El. 569, they acted as struts, and the remainder of the draft-tube area was excavated. When the draft tubes had been built and the contraction joint between the units along the top slab had been grouted, this slab acted as a strut, and the tailrace was excavated. By proceeding in this manner, the shear in the cofferdam foundation was limited at all times to approximately 15 lb per sq. in.

Actual construction work on the powerhouse additions and improvements was begun in 1951. The new units were put in commercial operation during July and during December, 1952. The improvements had been essentially completed by the end of 1953.

SUMMARY

The costs of the changes, additions, and improvements at Hales Bar Dam are as follows:

---

[5] "Templates Take Trouble Out of Driving 70-foot Cofferdam Cells," by O. R. Bengston, *Engineering News-Record*, January 17, 1952, p. 34.

Item		Cost, in dollars
Foundation treatment		2,730,000
Increasing the reservoir level:		
Dam	2,309,000	
Lock	1,307,000	
Reservoir	1,026,000	
Miscellaneous	128,000	
Total		4,770,000
Installation of units 15 and 16 and improvements of power facilities		15,000,000
Total		22,500,000

The writer has described the gains obtained from these expenditures—greater safety of the structures, better navigation facilities at the lock and in the river channel, and substantially increased power output with more economical and dependable operation. The modernized project is shown in Fig. 12.

ACKNOWLEDGMENTS

All engineering and construction work for the TVA is under the direction of Clarence E. Blee, M. ASCE, chief engineer. The planning is the responsibility of James S. Bowman, M. ASCE, chief water control planning engineer; designs of structures, as well as specifications and inspection of equipment, are under the direction of Robert A. Monroe, M. ASCE, chief design engineer. George K. Leonard, M. ASCE, is chief construction engineer.

DISCUSSION

George R. Rich,[6] M. ASCE.—An excellent account of the redevelopment of one of the pioneer multipurpose projects has been presented. From a historical standpoint the original construction provides an outstanding example of the need for careful subsurface exploration and expert interpretation of the findings prior to design. In the light of more recent knowledge the earlier notion that solution channels cannot cause damage to foundation rock below the ground-water level appears curious, but a moral concerning the acceptance of theories unsubstantiated by actual exploration is made evident. It is the writer's impression that the turbine waterways in the original substructure (described in detail by Mr. Meyer) were designed by one of the most eminent hydraulic engineers of that time, Clemens Herschel, the inventor of the venturi meter.

The striking feature of the over-all design of the redevelopment is its cleanness; the power-station architecture is simple, functional, and effective. The design shown for the power-station substructure is highly efficient. In Kaplan-turbine installations, the ratio of wheel diameter to head is always such that the combined mass of the intake and draft tube can be utilized to sustain the hydrostatic loading from the reservoir. Because of the low entrance velocities it is proper that the intake be comparatively short; because of the necessity for regaining a high percentage of the energy in the velocity of exit from the turbine, the draft tube is relatively long. The structure is necessarily cellular; the main piers constitute the principal elements of structural stability. These piers are made liberally thick, not only to facilitate final load delivery to the foundation rock but also to provide adequate space for the workmen putting concrete around the reinforcement. The heavy roof slab of the scroll case serves as a horizontal girder which transmits the top reactions of the intermediate piers of the intake to the main piers. It will also be noted that the contraction joints in the main piers form a single unbroken plane through the entire cross section.

On the basis of the cost data furnished by the author it is interesting to apply a few approximate checks on the economy of design of the redevelopment. The point of diminishing returns with respect to installed generating capacity is frequently in the vicinity of 20% of the regulated flow-duration curve. The Hales Bar redevelopment, which has a turbine discharge of 40,000 cu ft per sec, appears to satisfy this criterion.

One can check the economic justification for the power part of the redevelopment by either of two criteria. One can use the values of energy and capacity and the corresponding fixed charges from the annual TVA report, or one can adopt the energy rates and capacity rates with the corresponding fixed charges from any representative private-utility system. In the cases tested approximately by the writer there appears to be a suitable margin of return on the investment by either method.

With respect to the investment in navigation facilities, the TVA annual reports show that the TVA system between Paducah, Ky., and Knoxville,

---

[6] Director and Partner, Chas. T. Main, Inc., Boston, Mass.

Tenn., (600 miles) carries 600,000,000 ton-miles of freight annually at an estimated saving to the consumer of $7,000,000 per year. From the exploratory computations of the writer, improvement of low-flow draft from 4 ft to 9 ft between Hales Bar and Chickamauga (approximately 7 miles) appears to warrant the expenditure for navigation given in Mr. Meyer's tabulation.

Clarence E. Blee,[7] **M. ASCE.**—An extensive alteration of an old power plant such as that at Hales Bar always presents more problems, both from the standpoint of design and of construction, than would the building of a completely new plant of similar size. It also offers greater opportunities to develop unique arrangement in design and ingenious methods in construction. The Hales Bar plant is of particular interest because it is one of the pioneer hydroelectric plants of the United States.

In the paper are described the difficulties in constructing the original dam caused by its foundations—how the time and cost greatly exceeded the estimates, and how it was finally necessary to resort to pneumatic caissons to extend the foundations to apparently sufficiently sound rock. After completion, leakage developed under the dam, which greatly impaired the usefulness and safety of the structure.

The writer does not believe that the foundation rock at the Hales Bar site was worse than that at the Chickamauga Dam, 40 miles upstream, or at the Fort Loudoun Dam. Both these dams were constructed by the TVA, using open-cofferdam methods and also extensive grouting and other foundation treatments. The difference was that, in the early 1900's, engineers did not have the experience and techniques that were developed later and that have made possible the utilization of sites which would have been considered impossible even in the 1920's.

Also, engineers did not have the advantages of extensive subsurface exploration, so they did not know what they were "up against." The hypothesis that disintegration of the rock would not occur below the permanent groundwater level was a comforting one but unfortunately was not founded on facts. The cavitation of limestone rock below water level is not a process of erosion but one of solution, which only requires a gradient sufficient to keep the water that is in contact with the rock constantly moving.

The failure of the asphalt grout to stop leakage permanently was apparently not due to any deterioration of this material but rather to the fact that the openings through the rock were not entirely filled. The high-velocity leakage water gradually washed out the disintegrated rock, thus enlarging the water passages. During the subsequent drilling work, deposits of asphalt were frequently encountered by the drills and appeared to be sound and resilient.

In making the additions, the construction personnel developed several ingenious devices to overcome difficult situations and to take advantage of repetitive operations. In lowering the elevation of the spillway crest, a slot just wide enough to accommodate the forming and pouring of the pier was first cut in the concrete at each pier location. In order to carry this work down below water level a steel box-shaped caisson with rubber contact strips was fastened against the upstream face of the dam and was pumped out. As soon as the concrete of the pier was brought above water level the caisson was moved to the next location. A great amount of line drilling and drilling of blast holes and holes for anchor rods had to be done from the rollway of the dam. As mentioned in the paper, a jumbo on which were mounted the drifter drills was built on the site, equipped with adjustable, telescopic legs on the downstream side so that the working platform remained level as the jumbo was moved down the face of the dam. Floating equipment, such as cranes, barges, and a floating mixing plant, was used extensively.

---

[7] Chf. Engr., Tennessee Valley Authority, Knoxville, Tenn.

The outstanding feature from the viewpoint of construction was the upstream cofferdam which was needed to permit the removal of the nonoverflow section of the dam next to the old powerhouse. This cofferdam was constructed of 70-ft-diameter steel sheet-piling cells to withstand a normal head of 50 ft. The writer has learned to be careful about claiming world records for the size of construction features; it was fortunate that it was not done in this case for it was learned later that two 76-ft-diameter cells had been used at the Hadley Falls Station of the Holyoke (Mass.) Water-Power Company. However, for the conditions existing at the Hales Bar site, it is the writer's opinion that the height and diameter of the cofferdam cells approached the safe limit. The river bottom was an irregular rock surface that afforded no penetration for the piling. When the cofferdam was unwatered, exposing the downstream surface of the cells, the piling was found to have been pulled out of the interlocks in several places, and the entire shell gave the general impression of being rather highly stressed. Steel plates were welded across the places where the interlocks were weakened, and a low concrete "kicking block" with a gutter to conduct leakage water was poured against the toe of the shell and dowelled into the rock. The constructors were glad when the concrete work which replaced the dam section rose above reservoir level. Any failure of the cofferdam while the main dam was breached would, of course, have been disastrous.

An interesting observation in connection with the addition of the new units is that, although the fourteen old units are decidedly obsolete and of low efficiency, studies showed that the scrapping of these units could not be justified. They are of value for carrying peak loads of short duration and for operating when excess water is available—situations in which efficiency is not of prime importance. It is probably true that the scrapping of hydroelectric equipment is unjustified if the equipment will produce power.

George A. Jessop,[8] M. ASCE.—The building of the Hales Bar hydroelectric plant from the original construction in 1905 until the more recent extension described by the author covers a period of almost half a century; the development of the art and science of turbine design and construction is strikingly demonstrated. During this period, turbines of four different designs have been installed, and wheels of three of these types are now in service.

It is necessary to select the type and size of the power-producing equipment before the design of the powerhouse is completed; in 1904 and 1905 there were available turbines of "standard" design only. It was customary at that time to build turbine units with multiple runners on one shaft to increase the speed and reduce the cost of the generator. Usually the shaft was horizontal and the runners arranged in pairs—with the discharge of the runners being in opposite directions to balance the thrust. The selection of multiple-runner vertical units at Hales Bar was somewhat novel. It corresponded to a trend developing at the time.

---

[8] Formerly Consultant to S. Morgan Smith Co., York, Pa. (Mr. Jessop died on September 24, 1954.)

The order for the turbines was placed in 1907, but because of unexpected construction difficulties the plant was not placed in operation until 1914. During this period great advances were made in the hydraulic and mechanical design of turbines. By the time the plant was placed in operation, the power-producing equipment and the water passages to and from the turbines were outmoded and of obsolete design. This was unfortunate but beyond the control of the engineers who conceived and built the project.

Originally, the plant contained ten triple-runner units, two in each of five bays. As shown in Fig. 2, each unit consisted of two standard wheels, 72 in. in diameter, one discharging downward and one upward to balance the thrust, and one standard wheel of 63-in. diameter mounted above the pair and used as a "booster" when the head was low and the flow ample. These wheels had the "inside-type" gate-operating mechanism customary at the time. The rated capacity of the two lower wheels was approximately 4,950 hp at 37 ft of head.

In 1915 and 1916, six units of single-runner vertical wheels, each in a concrete spiral case and with a concrete elbow draft tube, were installed—two units in each of three flumes. The two units are necessarily on the same transverse center line but are on different longitudinal center lines, one being further downstream than the other. The upstream wheel is placed lower than the downstream wheel so that the spiral cases and draft tubes are separate and distinct water passages. Two of these turbines replaced two of the original triplex turbines and were connected with the old generators operating at 112.5 rpm. The four other units were placed in two unused bays and had generators operating at 100 rpm (Fig. 13).

These turbines are essentially modern in design and construction, having efficiencies that compare favorably with the best that can be obtained today (1954) in new power plants. The rated horsepower, however, is 4,150 at a head of 37 ft—considerably less than the capacity of the original units. The size of these turbines was limited by the original width of the bays.

The weight of the revolving element of each original unit and the downward thrust of the booster wheel were carried by an oil-pressure thrust bearing. Two of these thrust bearings were also used for two of the newer single-runner, spiral-case turbines. The bearings proved unsatisfactory and were replaced by oil-bath bearings in which the oil surrounded and covered the bearing at atmospheric pressure. Oil-bath bearings of satisfactory design and performance first became available about 1913, a year before the turbines were placed in operation but many years after the turbines were selected and designed. The triplex units (units 1 through 8) have Gibbs bearings, and the single-runner units (units 9 through 14) have Kingsbury bearings. All these bearings have been giving excellent service for many years.

In 1925, a program was initiated to replace the eight remaining original turbines with turbines having improved mechanical construction, higher efficiency, and the maximum capacity possible, as governed by the existing discharge passages or draft tubes. More efficient runners were used; the new distributors, or wheel cases, had cast-iron stay rings and gates with integral stems supported in bronze-bushed sockets in the head covers and bottom rings, with levers keyed to the upper end of the stems and connected by links to the gate-operating rings. These distributors, although submerged, had essentially "outside-type," modern gate-operating mechanisms—thus eliminating the original inside-type mechanisms. The internal flanges on the draft tubes were cut in the field so that runners with the largest possible discharge diameters and greatest possible capacities could be installed. The rated output of the

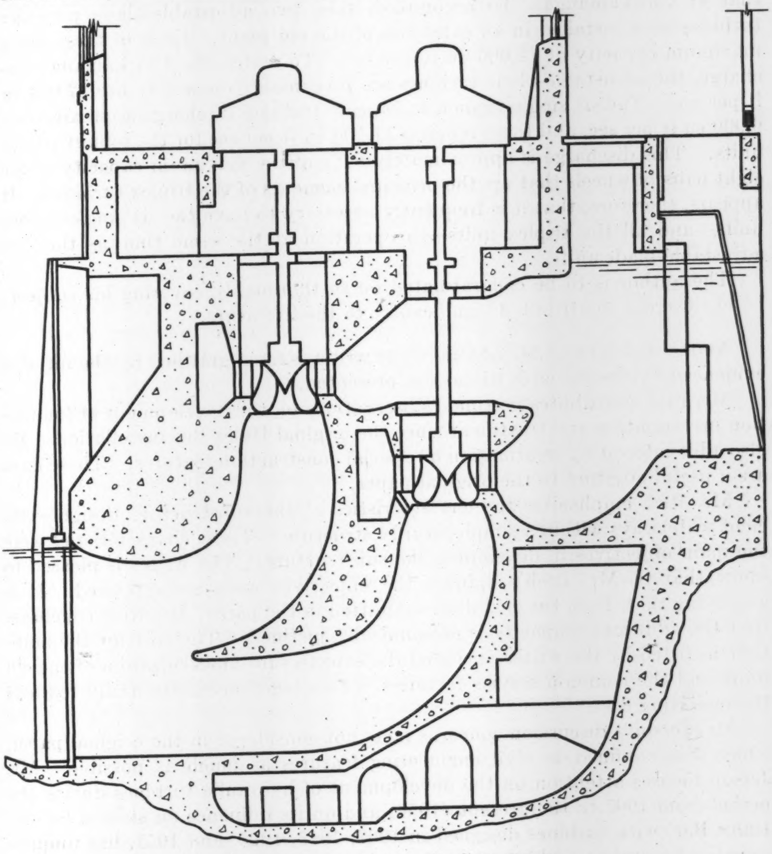

FIG. 13.—SINGLE-RUNNER VERTICAL UNITS

two lower wheels was increased to approximately 5,530 hp. The last of the original turbines were replaced in the summer of 1946.

Upstream of Hales Bar is the Chickamauga plant, which has ample storage capacity and a discharge capacity of 40,000 cu ft per sec. As explained by the author, it is advantageous to have the discharge at Hales Bar at least equal to that at Chickamauga. To accomplish this, two adjustable-blade propeller turbines were installed in an extension of the old plant. Each of these has a maximum capacity of 11,000 cu ft per sec. To match the Chickamauga discharge, the adjustable-blade turbines are presumably opened to use 22,000 cu ft per sec. The six single-runner, spiral-case turbines discharge approximately 6,900 cu ft per sec, and there remains 11,100 cu ft per sec for the rebuilt triplex units. This discharge is approximately 84% of the maximum capacity of the eight pairs of wheels that are the principal elements of the triplex turbines. It appears, therefore, that it is frequently necessary to have the six single-runner units—and all the triplex units—in operation at the same time as the new adjustable-blade units.

The author is to be congratulated on so thoroughly covering his subject; he has thereby contributed significantly to the literature.

ADOLF A. MEYER,[9] M. ASCE.—The writer is most gratified by the interest evidenced by the valuable discussion presented.

Mr. Blee contributes pertinent observations on the development of foundation investigation and treatment since the original Hales Bar installation. He also adds interesting information on special construction features. These data are a useful addition to the original paper.

Mr. Rich emphasizes the characteristics of the substructure design—efficient waterways within a simple, sturdy structure. These characteristics were the main objectives in developing the substructure. The writer is pleased to know that in Mr. Rich's opinion the objectives were accomplished. It is gratifying that, from the cost data submitted in the paper, Mr. Rich concludes that the additional capacity is economically justified. The cost for the addition, as listed by the writer, included the expenses for modernization of the old units and the common service facilities, which together substantially reduced the operating cost.

Mr. Jessop's discussion concerns facts not considered in the original paper, which was confined to civil engineering features as much as possible. Mr. Jessop focuses attention on the development of hydraulic turbines during the period from 1907 to the present (1954) and on its influence on station layout. Hales Bar, with turbines designed in 1907, 1915, 1925, and 1951, has unquestionably become something of a prize exhibit on the history of turbine design. Two of these designs, those of 1907 and 1951, were integrated designs—that is, both the waterways and the turbine itself were developed together. In the 1915 design, of which Mr. Jessop added an exhibit (Fig. 13), the development of the waterways was limited by the existence of the turbine bay in the old powerhouse. The 1925 design was strictly mechanical redesign without any change in the waterways. Turbines of the 1915, 1925, and 1951 designs all operate together now (1954). Mr. Jessop's discussion adds measurably to the value of the paper.

---

[9] Head Civ. Engr., Tennessee Valley Authority, Knoxville, Tenn.

AMERICAN SOCIETY OF CIVIL ENGINEERS
Founded November 5, 1852
TRANSACTIONS

Paper No. 2755

EFFECT OF WELL SCREENS ON FLOW INTO WELLS

By Jack S. Petersen,[1] Carl Rohwer,[2] M. ASCE,
and Maurice L. Albertson,[3] J. M. ASCE

With Discussion by Messrs. Wen-Hsiung Li; Arthur L. Collins; Mohammad Nazir and Nazir Ahmad; Matthew I. Rorabaugh; Dean F. Peterson, Jr.; G. Cohen de Lara; Gérard Tison, Jr.; and Jack S. Petersen, Carl Rohwer, and Maurice L. Albertson

Synopsis

The hydraulics of wells involves flow (1) in the surrounding aquifer, (2) through the well screen, and (3) inside the well. This paper is concerned with the flow through the screen and inside the well. A theoretical development is presented which relates the loss of head to the characteristics of the well screen. To support the theoretical development, a laboratory investigation of well screens was made.

The objective of the investigation was to establish criteria which could be used to aid in the selection of well screens to meet the varied conditions found throughout the United States. To do this, screen coefficients (permitting the use of a theoretical equation for design purposes) were determined for specific well screens.

Introduction

The increasing demand for domestic, industrial, and irrigation water in the United States has made necessary the development of ground-water resources to supplement surface supplies. The importance of wells is not limited to water supply, however, since wells have been found to be an effective aid in solving drainage problems. The essential feature of ground-water development (whether for water supply or for drainage) is the installation of ground-water

---

Note.—Published, essentially as printed here, in December, 1953, as *Proceedings-Separate No. 365.* Positions and titles given are those in effect when the paper or discussion was received for publication.

[1] Graduate Student, Univ. of Missouri, Columbia, Mo.

[2] Senior Irrig. Engr., Div. of Irrig. and Water Conservation, SCS, U. S. Dept. of Agriculture, Fort Collins, Colo.

[3] Prof. of Civ. Eng. and Head of Fluid Mechanics Research, Colorado Agri. and Mech. College, Fort Collins, Colo.

wells. Installing a well consists of digging a hole into a water-bearing formation, placing a casing or screen in the hole to support the surrounding aquifer, and setting the pump. The quantity of water that can be obtained from a well depends primarily on the characteristics of the underground reservoir which cannot be changed by the engineer. For any specific location, however, the quantity and cost of water depend on the efficiency of the well system and the pumping plant. Since these efficiencies are determined by factors over which the engineer has some control, research dealing with such factors is important in the establishment of better design criteria and development methods.

Although many elements are involved in the construction of wells, one of the difficulties encountered is the selection of the well screen to meet the specific needs and conditions found at the well site. The basic requirements for any well screen are that it (1) be resistant to corrosion and deterioration, (2) be structurally strong enough to prevent collapse, (3) prevent excessive movement of sand into the well, and (4) have a minimum resistance to the flow of water into the well. An efficient screen must represent a compromise of several desirable characteristics. For example, a screen with a large percentage of open area will provide a lower resistance to flow into the well, but it will have less structural strength and will permit more pumping of sand than a screen with a smaller percentage of open area. The characteristics of the well screen and the characteristics of the surrounding media influence the pattern of inflow and the losses. The importance of each characteristic must be evaluated for the particular field conditions existing at the location of the well.

The investigation reported on herein has been confined to the hydraulic characteristics of various types of well screens and the porous media immediately surrounding the screens. From such an investigation it is possible to design for the basic requirement of minimum head loss. Although this study was confined to water wells, the theoretical analysis is general for any liquid, and the results obtained should be applicable to other liquids of low viscosity.

Since there are few investigations of well screens, the selection of a proper screen is usually a matter of engineering judgment and experience. A criterion proposed by E. W. Bennison is that a velocity of less than from 0.1 ft per sec to 0.25 ft per sec through the individual screen openings will keep sand movement and head losses to a minimum.[4] A significant observation was made by G. L. Corey concerning the percentage of open area of a screen.[5] Mr. Corey stated that there is a critical percentage of open area above which the head losses are no longer a function of the open area. Criteria for drainage wells have been established by the Corps of Engineers, United States Department of the Army.[6] These criteria provide a relationship—between the gravel in the gravel envelope and the size of the particles in the surrounding formation—which will meet the permeability and stability requirements. Relationships were also determined for the size of screen openings to be used with a specific size of gravel filter.

---

[4] "Ground Water," by E. W. Bennison, Edward E. Johnson, Inc., St. Paul, Minn., 1947, p. 509.

[5] "Hydraulic Properties of Well Screens," by G. L. Corey, thesis presented to Colorado Agri. and Mech. College, at Fort Collins, Colo., in 1949, in partial fulfilment of the requirement for the degree of Master of Science.

[6] "Field and Laboratory Investigations of Design Criteria for Drainage Wells," *Technical Memorandum No. 195-1*, U. S. Waterways Experiment Station, Vicksburg, Miss., 1942, p. 78.

A satisfactory study of the head losses resulting from flow into a well must include experimental work conducted in the laboratory or in the field. As in most problems in hydraulics, however, a theoretical analysis of the problem is desirable as a guide to experimental work. Some phases of the experimental work can be shortened (with adequate analysis) to that which is necessary to validate the theory; the investigation described herein was conducted with this idea in mind. The various factors involved in the flow into and through a screen were related theoretically. Tests were performed on idealized well screens to establish the validity of the theory; then commercial well screens were tested to determine screen coefficients that would permit the use of theoretical equations for the determination of head loss to be expected (in the field) when a given combination of screen and gravel envelope was used.

THEORETICAL DEVELOPMENT

The problem of flow into and through well screens can be considered to be one of flow through a series of orifice openings as the water enters the screen and flow within a pipe manifold as it moves along the axis of the screen. As the water enters the screen through the openings, a conversion of potential energy to kinetic energy is necessary to develop the jet velocity. A dissipation of the jet energy, which can be assumed to be complete, then occurs. That is, the kinetic energy of the jet is not recovered as either potential or kinetic energy. The water then accelerates in a direction parallel to the center line of the screen. The acceleration results in a change of the momentum flux.

The theoretical analysis will be made for a screen contained in a large body of liquid where the flow inside the screen is downward. A definition sketch is shown in Fig. 1, in which the origin or zero length is at the top of the perforated section. As a first approach to a solution, an analysis will be made for a screen surrounded only by a liquid—the effect of the surrounding gravel being eliminated from consideration.

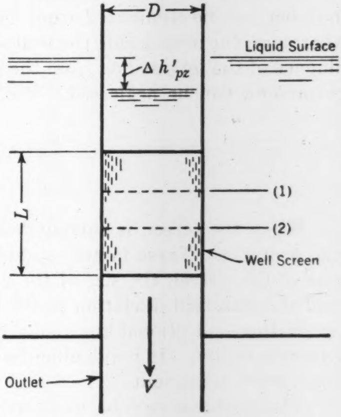

FIG. 1.—DEFINITION SKETCH

The loss of head caused by flow through a well screen depends on the characteristics of the screen geometry, the fluid, and the flow. The variables of greatest importance involved in the problem are: (1) The screen length, L; (2) the screen diameter, D; (3) the percentage of open area, A_p; (4) the coefficient of contraction for the openings, C_c; (5) the internal roughness of the well screen, k; (6) the difference in pressure between the inside and the outside of the screen, Δp; (7) the velocity of the liquid in the well screen, V; (8) the mass density of the fluid, ρ; and (9) the coefficient of dynamic viscosity, μ. The variables can be expressed in the following relationship:

$$f_1(L, D, \Delta p, k, \rho, \mu, V, A_p, C_c) = 0 \ldots\ldots\ldots\ldots\ldots\ldots (1)$$

If D, ρ, and V are chosen as repeating variables, a dimensional analysis will yield the function,

$$f_2\left(\frac{L}{D}, \frac{k}{D}, A_p, C_c, \frac{\Delta p}{\rho\, V^2}, \frac{V\, D\, \rho}{\mu}\right) = 0 \ldots\ldots\ldots\ldots\ldots\ldots (2)$$

The parameter $\frac{\Delta p}{\rho\, V^2}$ can be arranged in the form of $\frac{\Delta h_{ps}}{V^2/g}$ by multiplying by γ/γ, in which γ is the specific weight of the fluid and Δh_{ps} is the difference in piezometric head between the pressure inside and the pressure outside the screen. This is justified if the pressure drop is assumed to take place between two points at the same elevation. The function can be written in the form,

$$\frac{\Delta h_{pz}}{\frac{V^2}{g}} = f_3\left(C_c, A_p, \frac{L}{D}, \frac{k}{D}, \frac{V\, D\, \rho}{\mu}\right) \ldots\ldots\ldots\ldots\ldots\ldots (3)$$

Because the effects of viscosity are of secondary importance, the Reynolds number can be eliminated from consideration as a first approximation. Furthermore, the drag inside the well screen is almost entirely the result of the influence of the jets issuing from the screen openings, and therefore the roughness parameter can be neglected. With these simplifications, Eq. 3 reduces to

$$\frac{\Delta h_{pz}}{\frac{V^2}{g}} = f_4\left(C_c, A_p, \frac{L}{D}\right) \ldots\ldots\ldots\ldots\ldots\ldots (4)$$

When the screen is surrounded by gravel, several additional factors enter the problem. These factors include the size of the openings in relation to the size of the gravel, the size of the gravel relative to the diameter of the screen, and the standard deviation of the gravel.

Without additional knowledge of the phenomenon, Eq. 4 must be evaluated experimentally. It is possible, however, to analyze the problem further by a theoretical treatment.

The problem can be analyzed by applying the principles of continuity, energy, and momentum. The usual forms for these relationships, assuming (1) no acceleration normal to the direction of flow, (2) no variation in the velocity across the sections considered, and (3) no resistance to flow, are

$$Q = V_1\, A_1 = V_2\, A_2 \ldots\ldots\ldots\ldots\ldots\ldots (5a)$$

$$\frac{V^2{}_1}{2\,g} + \frac{P_1}{\gamma} + z_1 = \frac{V^2{}_2}{2\,g} + \frac{P_2}{\gamma} + z_2 \ldots\ldots\ldots\ldots\ldots\ldots (5b)$$

and

$$F_y = \rho\, (Q_1\, V_1 - Q_2\, V_2)_y \ldots\ldots\ldots\ldots\ldots\ldots (5c)$$

in which Q is the rate of flow parallel to the screen axis, A denotes the cross-sectional area of the well screen, g is the gravitational acceleration, P/γ denotes the hydrostatic head, ρ is the density, z is the distance from a datum, F_y denotes the change in momentum along axis of screen between the indicated points, and the subscripts 1 and 2 correspond to the sections shown in Fig. 1.

The increment of discharge dQ, through an increment of length dL, can be shown by the energy and continuity equations to be

$$dQ = C_c\, A_p\, \pi\, D \sqrt{2\, g\, \Delta h_{pz}}\, dL \ldots\ldots\ldots\ldots (6)$$

By integrating Eq. 6 the total discharge into the screen is

$$Q = C_c\, A_p\, \pi\, D \sqrt{2\, g} \int_0 \sqrt{\Delta h_{pz}}\, dL \ldots\ldots\ldots\ldots (7)$$

in which Δh_{pz} is the difference in head between the inside and the outside of the screen in the increment of length dL.

The momentum equation can be applied to the flow within the pipe (between sections 1 and 2) to give the equation,

$$A\, \gamma\, (h_{pz,1} - h_{pz,2}) = -\, \rho\, (Q_1\, V_1 - Q_2\, V_2) \ldots\ldots\ldots\ldots (8a)$$

which can be written in differential form as

$$-\, A^2\, g\, dh_{pz} = d(Q^2) \ldots\ldots\ldots\ldots (8b)$$

in which h_{pz} is the piezometric head within the screen. If the piezometric head on the entire outside surface is constant,

$$\Delta h_{pz} = \text{a constant} - h_{pz} \ldots\ldots\ldots\ldots (9a)$$

and

$$d(\Delta h_{pz}) = -\, dh_{pz} \ldots\ldots\ldots\ldots (9b)$$

This permits Eq. 8b to be written as

$$d(Q^2) = A_2\, g\, d(\Delta h_{pz}) \ldots\ldots\ldots\ldots (10a)$$

Integrating Eq. 10a results in

$$Q^2 = A^2\, g\, \Delta h_{pz} + C_1 \ldots\ldots\ldots\ldots (10b)$$

Since Δh_{pz} is equal to $\Delta h'_{pz}$ when Q equals zero,

$$C_1 = -\, A^2\, g\, \Delta h'_{pz} \ldots\ldots\ldots\ldots (11)$$

in which $\Delta h'_{pz}$ is the difference in piezometric head between the inside and the outside of the screen at the point where L equals zero. Eq. 10b can be written as

$$Q^2 = A^2\, g\, (\Delta h_{pz} - \Delta h'_{pz}) \ldots\ldots\ldots\ldots (12)$$

Differentiating Eq. 12 with respect to the length L results in

$$\frac{dQ}{dL} = \frac{A^2\, g}{2\, Q}\, \frac{d(\Delta h_{pz})}{dL} \ldots\ldots\ldots\ldots (13)$$

When Eqs. 6, 12, and 13 are combined into the dimensionless relationship,

$$\frac{2\,C_c\,A_p\,\pi\,D\,\sqrt{2\,g}\,dL}{\sqrt{g\,A^2}} = \frac{d(\Delta h_{pz})}{\sqrt{(\Delta h_{pz})^2 - \Delta h_{pz}\,\Delta h'_{pz}}} \quad \text{(14a)}$$

or

$$\frac{C}{D}\,dL = \frac{d(\Delta h_{pz})}{\sqrt{(\Delta h_{pz})^2 - \Delta h_{pz}\,\Delta h'_{pz}}} \quad \text{(14b)}$$

integration of Eq. 14*b* yields

$$C\,\frac{L}{D} = \cosh^{-1}\left(\frac{2\,\Delta h_{pz} - \Delta h'_{pz}}{\Delta h'_{pz}}\right) + C_2 \quad \text{(14c)}$$

in which

$$C = 11.31\,C_c\,A_p \quad \text{(14d)}$$

The constant of integration C_2 equals zero since Δh_{pz} equals $\Delta h'_{pz}$ when L is equal to zero. Replacing $\Delta h'_{pz}$ with its value from Eq. 12, Eq. 14*c* can be reduced to the form:

$$\frac{\Delta h_{pz}}{\dfrac{Q^2}{A^2\,g}} = \frac{\cosh\dfrac{C\,L}{D} + 1}{\cosh\dfrac{C\,L}{D} - 1} \quad \text{(15)}$$

or in terms of the velocity

$$\frac{\Delta h_{pz}}{\dfrac{V^2}{2\,g}} = 2\,\frac{\cosh\dfrac{C\,L}{D} + 1}{\cosh\dfrac{C\,L}{D} - 1} \quad \text{(16)}$$

Eq. 15 is a specific relationship that combines the dimensionless parameters C_c, A_p, and L/D into a single variable.

A laboratory investigation of the problem can be made with Eq. 15 as a basis for the study. The experimental results would be expected to follow this theoretical equation in some manner. Deviations would exist where the effect of the variables eliminated from Eq. 3 become important—that is, when the effect of the Reynolds number and the roughness parameter become significant. Additional deviations could occur as a result of the assumptions made in deriving Eq. 15. The more important of these assumptions are as follows:

1. The velocity variation is small across any section inside the screen.
2. The piezometric head on the outside of the screen is constant over the entire outside surface of the screen.
3. The kinetic energy of the jet entering the screen is not recovered as either potential energy or usable kinetic energy.

The two dimensionless numbers involved in Eq. 15 $\left(\dfrac{\Delta h_{pz}}{Q^2/(A^2\,g)} \text{ and } \dfrac{C\,L}{D}\right)$ can be plotted to give the theoretical curve shown in Fig. 2. As shown by the theoretical curve, the loss coefficient $\left(\dfrac{\Delta h_{pz}}{Q^2/(A^2\,g)}\right)$ becomes nearly constant

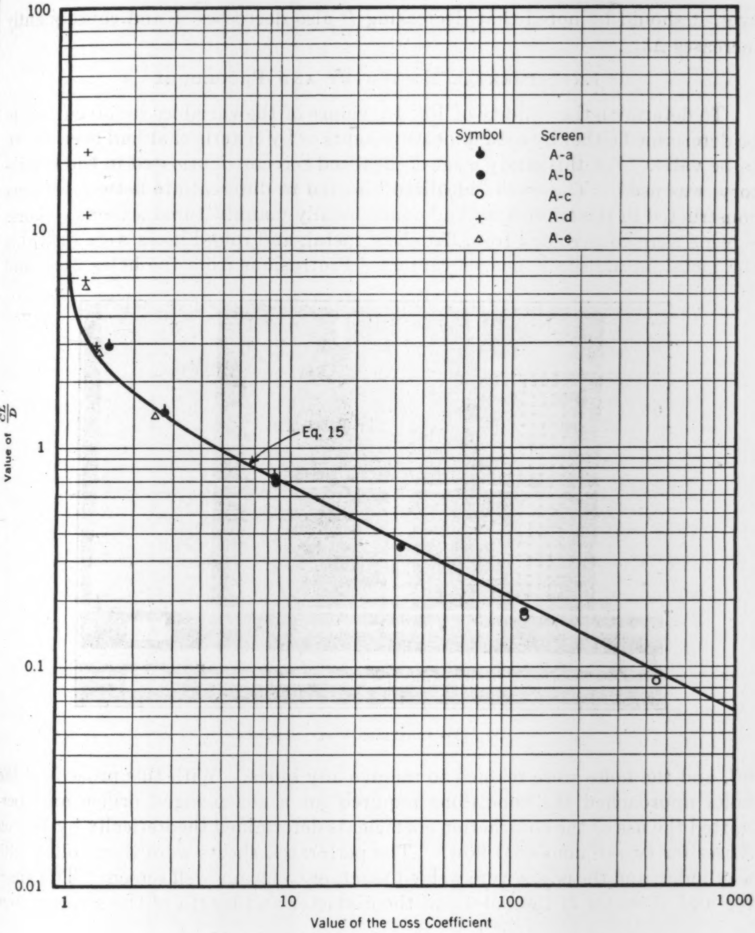

FIG. 2.—LOSS COEFFICIENT AS A FUNCTION OF $\frac{C\,L}{D}$ FOR TYPE A SCREENS

when the hyperbolic cosine of $(C\ L)/D$ is large, so that the plus or minus 1 is insignificant. The curve becomes asymptotic to a loss coefficient equal to unity, but for practical purposes the loss coefficient equals unity for all values of $(C\ L)/D$ greater than 6. Since the loss coefficient is a measure of the loss, the loss is a minimum when the parameter is a minimum. The value of $(C\ L)/D$ can be made larger than the critical value of 6 by increasing C_c, A_p, and L, or by decreasing D—that is, the percentage of open area of the screen for the head loss to be a minimum depends on the length and diameter of the screen. However, it should be noted that decreasing D also decreases A and consequently increases Δh_{pz}.

EXPERIMENTAL EQUIPMENT AND PROCEDURE

To determine the validity of Eq. 15, values of the variables involved had to be determined either by actual measurements or by criteria that had been shown to be valid. For this study a set of idealized screens, fabricated in the laboratory, was used. The word "idealized" is used to differentiate between screens constructed in the laboratory and commercially manufactured screens. These screens were constructed from flat sheet metal, and round holes were drilled in the metal on uniformly spaced centers. Protrusions from the holes were filed off, and the holes were reamed to remove any burrs. With this procedure the holes approached the conditions required for a sharp-edged orifice and permitted the use of the contraction coefficients determined theoretically by R. von Mises for two-dimensional flow.[7] The perforated sheets were then rolled into a cylinder, and the edges were welded together to form a well screen. The spacing and diameter of the holes and the diameter and length of the screens were determined by (1) the $\left(\frac{CL}{D}\right)$-ratio necessary to cover the practical range of the theoretical curve and (2) the desirability of having data on these screens for conditions comparable to those of the commercial screens that were tested. These screens designated type A screens are shown in Fig. 3. Dimensions of the screens are presented in Table 1.

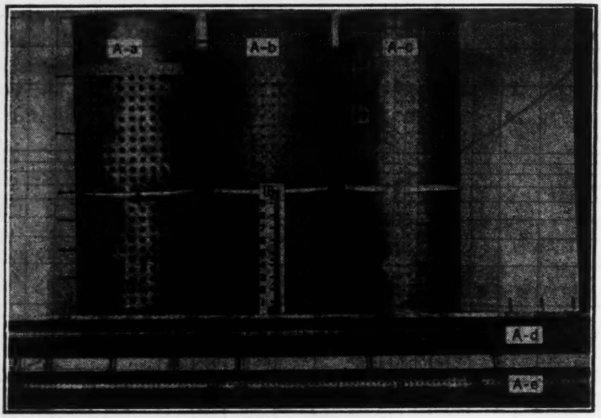

FIG. 3.—IDEALIZED WELL SCREENS

The commercial screens tested were representative of the types commonly used in actual wells. For identification these screens were designated types B, C, D, E, and F. These screens are shown in Fig. 4; the important dimensions are given in Table 2.

---

[7] "Elementary Mechanics of Fluids," by Hunter Rouse, John Wiley & Sons, Inc., New York, N. Y., 1946.

TABLE 1.—DIMENSIONS OF IDEALIZED SCREENS

Screen	Screen diameter, in feet	Hole diameter, in inches	Screen length, in feet	Hole spacing on centers, in inches	Percentage of open area	Screen thickness, in inches
A-a	1.008	½	2.00	1	19.63	0.045
A-b	1.008	¼	2.00	1	4.93	0.045
A-c	1.008	⅛	2.00	1	1.23	0.020
A-d	0.252	⅛	4.00	¼	19.71	0.020
A-e	0.252	⅛	4.00	½	4.93	0.020

All the gravel used in these tests was river-bed material which had been subjected to stream action long enough for the sharp edges to be eroded away. Each size of gravel was screened so that the particles passed through a screen of one size and were retained on a screen of a smaller size. The five sizes of gravel used and the results of the sieve analyses are shown in Fig. 5. The 50% size of the gravel (as shown by the sieve analysis) was used as the representative size required for the analysis of test data.

TABLE 2.—DIMENSIONS OF COMMERCIAL SCREENS

Screen	Screen diameter, in feet	Slot width, in inches	Screen length, in feet	Percentage of open area	Screen thickness, in inches
B-a	0.9804	1/16	2.07	3.46	0.080
B-b	0.9804	1/8	2.02	7.15	0.080
B-c	0.9804	3/16	2.09	11.23	0.080
B-d	0.9804	1/4	2.09	14.62	0.080
C-a	0.9054	0.020	2.03	18.18	9/64
C-b	0.9054	0.040	2.00	30.76	9/64
C-c	0.9054	0.100	2.01	52.63	9/64
C-d	0.9054	0.200	2.03	68.96	9/64
D-a	0.9804	1/8	2.00	4.77	0.080
E-a	0.8419	1/2	2.00	14.75	11/32
F-a	0.9231	0.145	2.00	33.64	1/4

The laboratory apparatus (shown in Fig. 6) used for testing the well screens consisted of a cylindrical steel tank installed in a recirculating system. The steel testing tank was 7.5 ft in diameter and 6 ft deep. Water entered the tank through a diffusion ring which distributed the water equally around the periphery near the bottom of the tank. The water level in the tank was maintained at a constant depth of 5 ft by two overflow pipes installed in the inside of the tank. Flow through the screen was controlled by a valve on the pipe carrying the water from the tank to the weir box. To hold the gravel envelope in place a heavy wire screen 30 in. in diameter and 6 ft long was placed around the well screen. The water was pumped from a sump through an 8-in.-diameter pipe to the tank. From the tank the water passed (by gravity flow) through the test screens located at the center of the tank and then downward through an outlet pipe to a weir box. From the weir box the water spilled into a return channel connected to the sump of the pump.

The differences in piezometric head were determined by hook gages set in stilling wells. The hook-gage readings could be made to one-thousandth of a

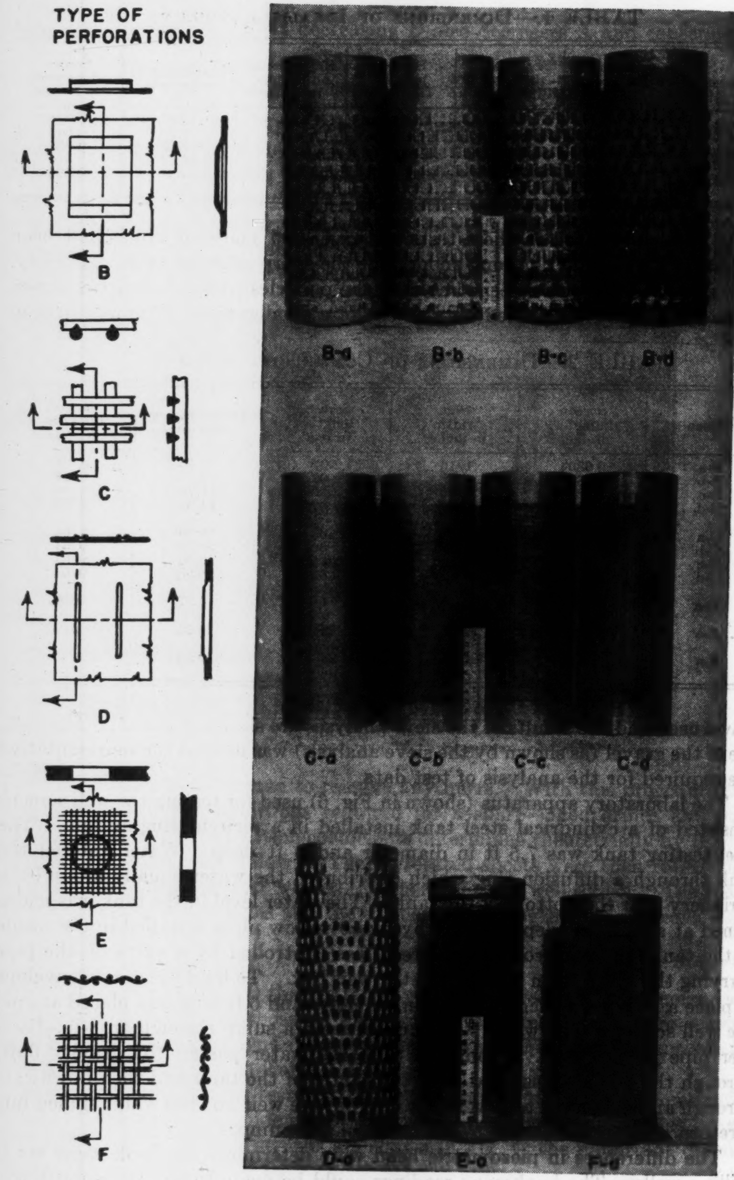
TYPE OF PERFORATIONS
B
C
D
E
F
B-a
B-b
B-c
B-d
C-a
C-b
C-c
C-d
D-a
E-a
F-a

FIG. 4.—COMMERCIAL WELL SCREENS

foot, and it was possible to estimate the readings to the nearest five ten-thousandths of a foot.

Extensions to the screens were made by joining an unperforated length of casing to each end of the screen. The extensions on the upper end were made to permit a substantial loss of head through the screen and yet maintain submerged flow through the openings. The extensions on the bottom end of the screen were made to bring the perforated area to the desired level above the bottom of the tank. For the 1-ft-diameter screen the openings began approximately 1 ft from the bottom of the tank, and 2 in. from the bottom of the tank for the 3-in.-diameter screens. Several of the commercial screens tested were extended in length by adding a section of 10-in.-diameter pipe. For the commercial screens a correction had to be made for the difference in piezometric head to account for the change in velocity head inside the pipe resulting from the reduction in diameter.

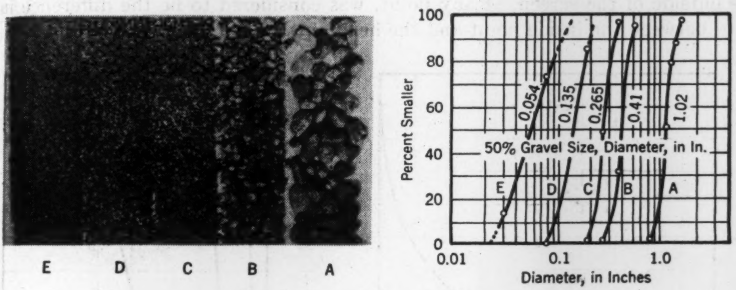

Fig. 5.—Gravel Used in Tests

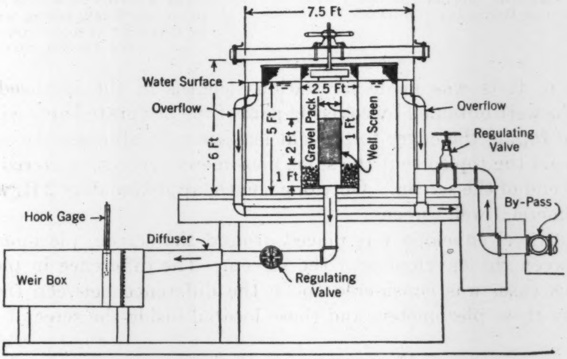
7.5 Ft
Water Surface
Overflow
2.5 Ft
5 Ft
2 Ft
1 Ft
Gravel Pack
1 Ft
Well Screen
Overflow
Regulating Valve
6 Ft
By-Pass
Hook Gage
Diffuser
Weir Box
Regulating Valve

Fig. 6.—Test Apparatus

The testing procedure consisted primarily of measuring the difference of piezometric head between the inside and the outside of the well screen at a number of points for various discharges. Discharges of from $\frac{1}{8}$ cu ft per sec to

2 cu ft per sec for the 12-in.-diameter screens and from $\frac{1}{32}$ cu ft per sec to $\frac{1}{8}$ cu ft per sec for the 3-in.-diameter screens were obtained by adjusting the outlet valve. Continuous readings of the gages were taken until only normal fluctuations in the water level existed. This condition was considered to exist when five consecutive readings were consistent. The average of these five readings was used for the analysis. The difference in piezometric head between the inside and the outside of the screen, at any point, was considered to be the difference in head between the inside point and the head outside the 30-in.-diameter screen.

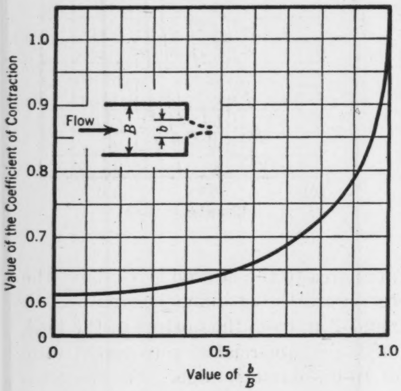

FIG. 7.—COEFFICIENT OF CONTRACTION AS A FUNCTION OF THE BOUNDARY GEOMETRY

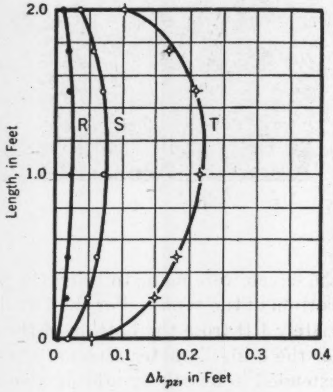

FIG. 8.—DIFFERENCE IN PIEZOMETRIC HEAD BETWEEN INSIDE AND OUTSIDE OF GRAVEL ENVELOPE FOR SCREEN A-b AND GRAVEL SIZE C

A series of tests was made for various lengths of the idealized screens. These lengths were obtained by covering part of the perforated area with plastic sheeting and taping the edges to prevent leakage. In all cases the screen was shortened from the top so that the same piezometer always registered the head at the lower end of the screen. Only one length, approximately 2 ft, was tested for the commercial well screens.

When a gravel envelope was placed around the screen, piezometers were located between the envelope and the screen. The difference in piezometric head, in this case, was considered to be the difference between the reading registered by these piezometers and those located inside the screen.

DISCUSSION OF RESULTS

In Fig. 2, there are shown the theoretical curves obtained from Eq. 15 and the experimental data obtained from the idealized screens when not surrounded by gravel. It should be recalled that these data were taken for the purpose of establishing the validity of Eq. 15. The data were computed from direct measurements. Values used for C_c were determined[7] from Fig. 7. .

A satisfactory agreement of the experimental data with the theoretical development is apparent for a large part of the range investigated (Fig. 2).

Deviations from the theoretical curve do exist, however, especially at each end of the range—that is, for large values of $(C\,L)/D$ the loss coefficient becomes asymptotic to a value of approximately 1.2 rather than the theoretical value of unity, and for small values of $(C\,L)/D$ the experimental data fall below the theoretical curve. As would be expected, if these deviations are a result of the assumptions used in the theoretical development, an analysis of the assumed conditions might provide an explanation for the deviations and permit the making of corrections.

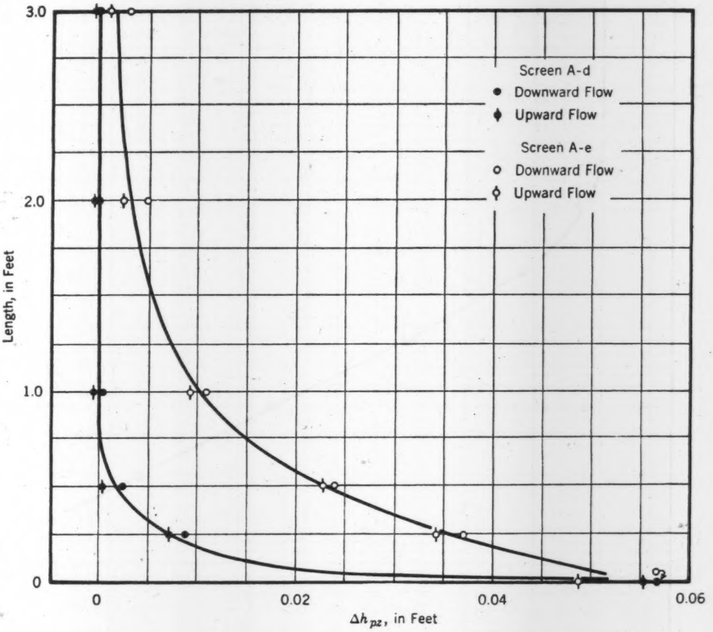

Fig. 9.—Comparison of Differential Head Distribution for Upward and Downward Flow, Screens A-d and A-e

The assumptions most probably in error are that: (1) The piezometric head on the outside surface of the screen is the same at every point; (2) the coeffi-

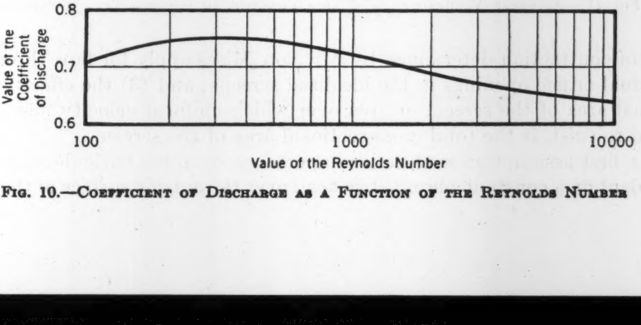

Fig. 10.—Coefficient of Discharge as a Function of the Reynolds Number

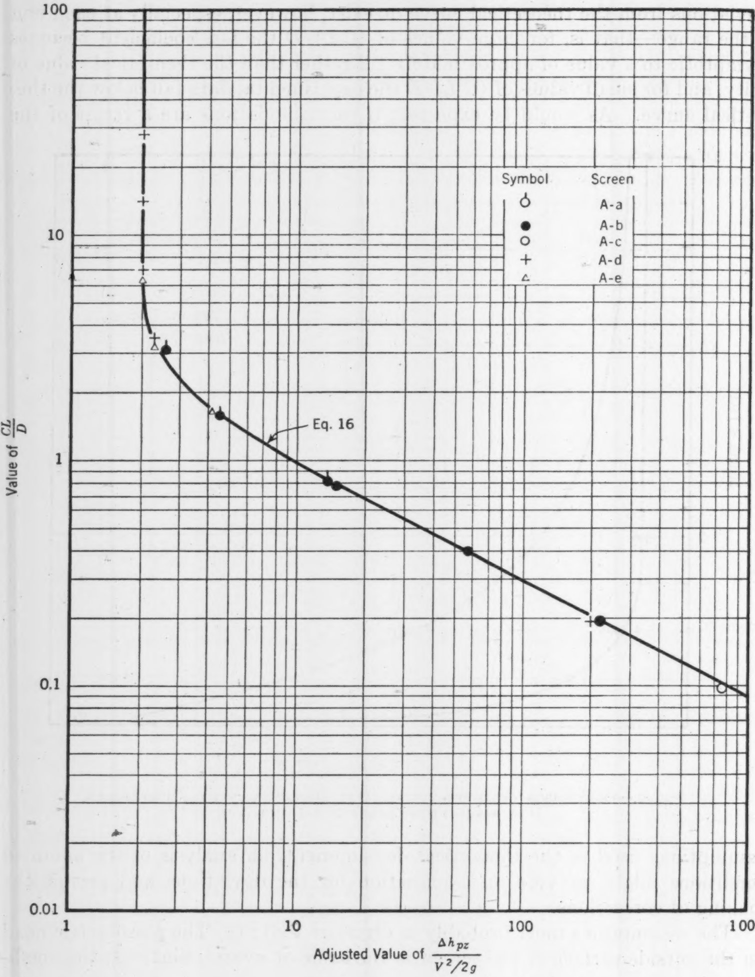

FIG. 11.—ADJUSTED VALUES OF $\frac{\Delta h_{pz}}{V^2/2g}$ AS A FUNCTION OF $\frac{CL}{D}$ FOR TYPE A SCREENS

cients of contraction determined by Mr. von Mises apply for flow through the individual orifice openings in the idealized screens; and (3) the effective cross-sectional area of the screen, or area over which uniform velocity may be considered to exist, is the total cross-sectional area of the screen.

The first assumption is of major importance since the basic development is dependent on a constant piezometric head over the outside surface of the screen.

The variation of this head was not sufficiently great to permit measurement in the laboratory for screens tested without a gravel envelope. However, a variation (illustrated by Fig. 8) did exist when the screens were surrounded with gravel. In Fig. 8 curve R is drawn for a discharge of 0.248 cu ft per sec, curve S is drawn for a discharge of 0.501 cu ft per sec, and curve T is drawn for a flow of 1.001 cu ft per sec. Curves presented by H. E. Babbitt indicate that this variation is a minor factor for relatively small drawdown in a well.[8] Although conclusive evidence is not available to establish the accuracy of this assumption, the status of the investigation does not warrant the use of a correction for the variation.

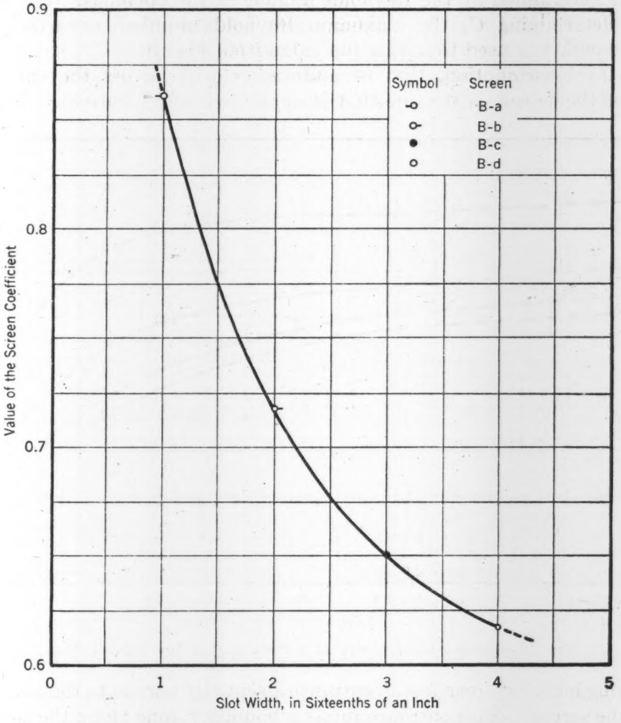

FIG. 12.—SCREEN COEFFICIENT AS A FUNCTION OF THE SLOT SIZE FOR TYPE B SCREENS WITH NO GRAVEL ENVELOPE

It should be noted that the direction of flow (whether upward or downward) is not a factor in causing the deviations from the theoretical curve. Tests (with $Q = 0.0616$ cu ft per sec) made on two of the idealized screens are shown in Fig. 9. Fig. 9 shows that the differential head distribution is the same for either direction of flow.

---

[8] "The Free Surface Around, and Interference Between, Gravity Wells," by H. E. Babbitt and D. H. Caldwell. *Bulletin No. 374*, Illinois Experiment Station, Univ. of Illinois, Urbana, Ill., 1948, p. 60.

The use of the coefficients developed by Mr. von Mises would be exact only if the contraction of the jet and the discharge through the openings are independent of the Reynolds number—that is, if the viscous effects of the fluid are insignificant. Many investigations have shown this to be true for high Reynolds numbers, but for low Reynolds numbers the viscous effects do become important.[9] Although a change in C_c (or more accurately C_q) of 0.1 is probably the largest variation that will occur, it was decided to use a coefficient of discharge as determined by the Reynolds number of the openings. For the purpose of determining C_q the maximum Reynolds number, occurring at the discharge end, was used to obtain the value from Fig. 10.

The third assumption, that of uniform velocity across the entire cross section of the screen, is the one that is most obviously incorrect. The water discharging into the screen has an entrance essentially normal to the longitudinal axis of the screen. This entrance forms a boundary zone along the side of the screen where the flow is normal—rather than parallel—to the longitudinal axis, and in effect reduces the cross-sectional area of the screen. According to one of the writers, the distance from the efflux section of a jet (at which point complete mixing with the surrounding fluid takes place) is a function of the jet diameter.[10] This statement applied to the well screen would mean that the thickness of the boundary zone would be a function of the size of openings. Other factors (such as the Reynolds number of the screen) would also affect the thickness of the zone. No attempt was made to determine a relationship be-

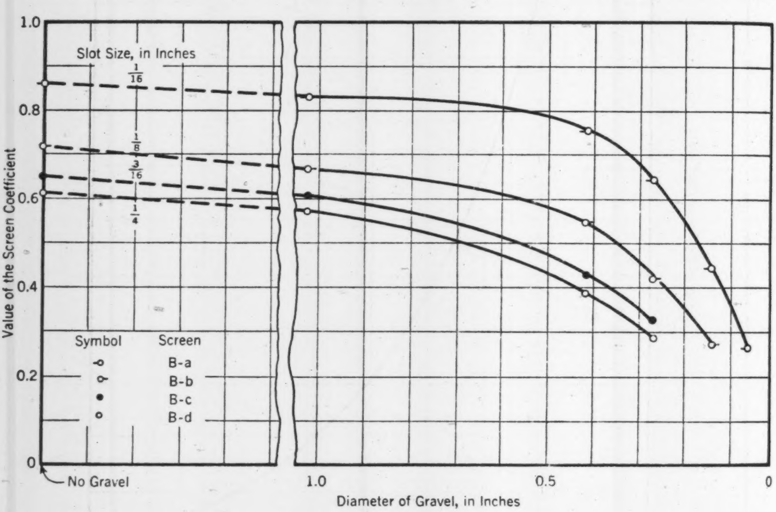

FIG. 13.—SCREEN COEFFICIENT AS A FUNCTION OF THE GRAVEL SIZE

tween the effective diameter of the screen and the several influencing factors. By a trial-and-error method, however, the use of an effective diameter equal to 0.96% of the true diameter was found to give an accurate correction for the screens tested. When the test data were corrected for viscous effects and boundary-zone conditions, the data followed the theoretical curve over the entire range investigated. These corrected data (which indicate that the theoretical development is basically sound) are shown in Fig. 11.

---

[9] "Elementary Mechanics of Fluids," by Hunter Rouse, John Wiley & Sons, Inc., New York, N. Y., 1946, p. 168.

[10] "Diffusion of Submerged Jets," by M. L. Albertson, Y. B. Dai, R. A. Jensen, and Hunter Rouse, *Transactions*, ASCE, Vol. 115, 1950, pp. 639–697.

It can reasonably be assumed that Eq. 15 can be used to determine approximate losses for flow into and through commercial well screens. The application of Eq. 15 to commercial screens, however, introduces factors that must be evaluated experimentally for the individual screens. The coefficient of discharge for the openings and the reduction in open area caused by the surrounding aquifer are variables that cannot be measured by direct methods. A screen coefficient, C_s, to account for these factors can be obtained by determining a loss coefficient for the screen from the experimental data, obtaining the $\left(\frac{C\,L}{D}\right)$-value from the theoretical curve shown in Fig. 2, and solving for C_s. This coefficient changes Eq. 14*d* to

$$C = 11.31\,A_p\,C_s \ldots\ldots\ldots\ldots\ldots\ldots\ldots\ldots (17)$$

in which C_s replaces C_c and includes the reduction factor for A_p which is necessary when gravel surrounds the screen.

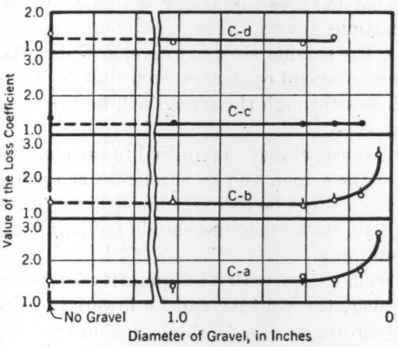

FIG. 14.—LOSS COEFFICIENT AS A FUNCTION OF THE GRAVEL SIZE FOR TYPE C SCREENS

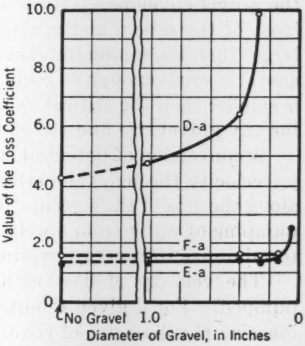

FIG. 15.—LOSS COEFFICIENT AS A FUNCTION OF THE GRAVEL SIZE FOR SCREENS OF TYPES D, E, AND F

Values of C_s for one set of screens (type B) when not surrounded by gravel are shown in Fig. 12. The curve shows that the coefficient becomes large for small widths of openings—approaching short tube effect—and becomes small for larger widths of openings—approaching the values for a sharp-edged orifice. This variation of C_s could be anticipated from work presented by J. S. McNown, M. ASCE, on screen tests in wind tunnels where the coefficient of contraction was shown to vary with screen thickness and amount of rounding of the upstream edges of the holes.[11]

This same method was used to determine C_s for the screens when the screens were surrounded by different gravel sizes. However, the difference in piezometric head at any point inside the screen was considered to be the difference in readings between the piezometer at the point and the piezometer at the center of the screen located between the screen and gravel envelope. These coefficients (shown in Fig. 13) can be applied to Eq. 15 to determine the approximate losses caused by flow into screens. For a particular opening of the type B screens and a specific gravel size in the gravel envelope, a value of C_s can be obtained from the curve which should apply to any length and diameter of screen.

Figs. 14 and 15 show the loss coefficient plotted against the size of gravel in the gravel envelope. It can be seen that the loss coefficient is a constant for most of the screen and gravel combinations tested. The coefficient becomes larger than the minimum value only for the smaller sizes of gravel. Unless the gravel is small enough to reduce the percentage of open area such that $(C\ L)/D$ is smaller than the critical value, the losses through the screen will be the same for any gravel size and screen opening.

A conversion of potential energy to kinetic energy is required to develop the jet velocity through the perforations of the screen and to accelerate the water along the axis of the screen. This energy cannot be recovered or utilized in the pumping of water from a well. Therefore, both velocities should be kept small to minimize the energy required for pumping.

The velocity of flow within the well varies with the quantity of water pumped. For a given quantity, however, the velocity can be lowered by increasing the diameter of the well. According to Eq. 15 the loss of head (nonusable kinetic energy) varies with several factors, but is at a minimum when $(C\ L)/D$ is greater than 6. For these conditions the velocity head within the well is approximately equal to the velocity head of the jets. Although increasing the diameter decreases the value of $(C\ L)/D$, the actual head losses vary directly with V^2; that is, $(C\ L)/D$ varies inversely with D while the actual head losses vary inversely with D^4. Increasing the diameter may change $(C\ L)/D$ so that the losses are no longer a minimum for that particular diameter, but they will still be less than the losses resulting from a screen with a smaller diameter.

Mr. Bennison stated that the losses can be decreased by increasing the amount of open area, the length of the screen, or the diameter of the screen.[4] The theory developed by the writer is strictly in accord with these ideas, with the exception that there is a limit to the amount of reduction in loss of head. This has been shown by Mr. Corey with laboratory tests on well screens of a fixed diameter and length.[5] Mr. Corey found that, for a fixed length and diameter of screen, there is a limiting percentage of open area above which the losses become constant. An examination of Eq. 15 shows that this limit—above which the loss coefficient is constant—could also be reached by changing the other variables. The theory would apply at any point along the screen length, but since a discharge at these points could not be measured, the data used to check Eq. 15 were for the total screen length. According to the theory, the differential head would vary over the length of the screen. This variation is shown in Fig. 16 for 4-ft lengths of screens A-d and A-e. The test on screen A-d was made with $Q = 0.125$ cu ft per sec and the test on screen A-e was made with $Q = 0.126$ cu ft per sec. The value for Δh_{pz} is greatest at the discharge end and decreases with an increase in distance from this end. Since the dis-

---

[11] "Exploratory Tests on Flow Through Screens," by J. S. McNown and M. L. Albertson with D. R. Bianco, P. G. Hubbard, and E. G. Peterson, *Report No. 15*, Iowa Inst. of Hydr. Research, State Univ. of Iowa, Iowa City, Iowa, 1947.

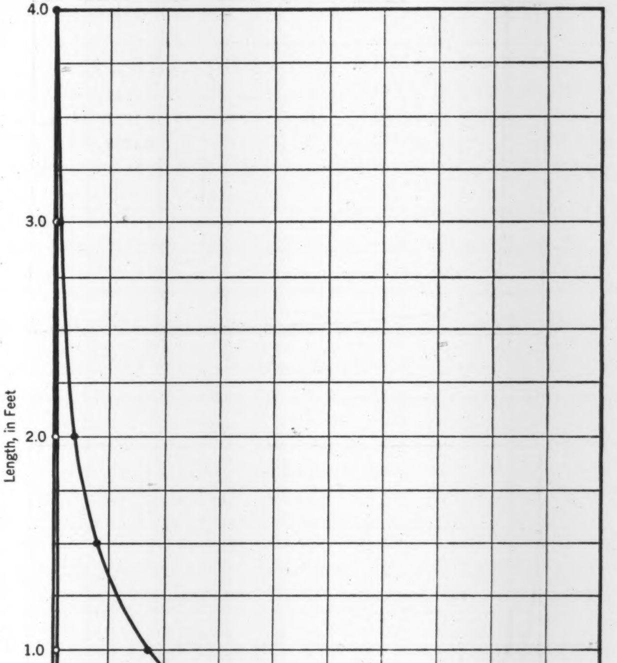

Fig. 16.—Difference in Piezometric Head Between the Inside and the Outside of Screens A-d and A-e

charge through the individual openings varies with $\sqrt{\Delta h_{pz}}$ the same type of distribution exists for the discharge into the screen as exists for Δh_{pz}. For a 4-ft length of screen A-d, the value of $(C\,L)/D$ is greater than the critical value of 6 for lengths greater than 1 ft. Therefore (for screen A-d), the loss coefficient

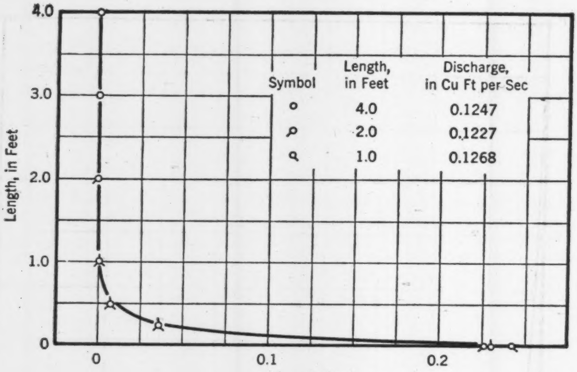

FIG. 17.—DIFFERENTIAL HEAD DISTRIBUTION FOR VARIOUS LENGTHS OF SCREEN A-d

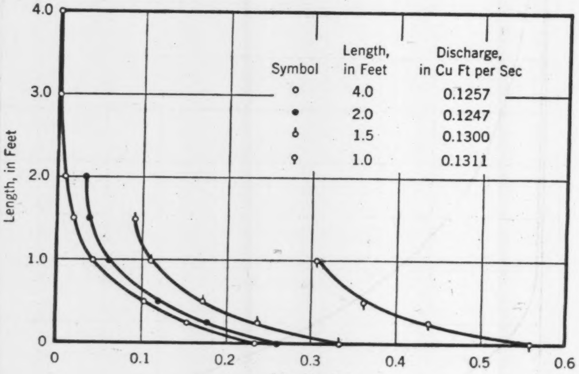

FIG. 18.—DIFFERENTIAL HEAD DISTRIBUTION FOR VARIOUS LENGTHS OF SCREEN A-e

which is proportional to Δh_{pz} is independent of $(C\,L)/D$ for any length of screen greater than 1 ft.

In Fig. 17 this independence is shown to be true since the curves plotted for total screen lengths of 4 ft, 2 ft, and 1 ft are approximately the same. Fig. 16 shows that the screen A-e must not be less than 4 ft long to be in the constant value range for the loss coefficient. If the length is decreased, the loss coefficient increases as is shown by the curves in Fig. 18.

PRACTICAL APPLICATION

Choosing a well screen for a particular installation is greatly simplified when adequate design criteria are available. It is believed that, with Eq. 15 as a basis, the logical selection of a screen can be made. It can be seen that the major criterion for minimum losses (or drawdown in a well) is that $(C\,L)/D$ be equal to or greater than 6. The conditions existing in the field are so variable that a set procedure cannot be specified.

Items to be considered in installing a well are (in addition to those listed under the heading, "Theoretical Development") (1) the depth of the water-bearing formation; (2) the size of the openings in the screen; (3) the size of the gravel in the gravel envelope or surrounding formation; (4) the type of pump and location of pump bowl and suction pipe inlet; and (5) the approximate lift or proposed maximum drawdown in the well. Many of these variables are predetermined by factors such as (*a*) existing geological conditions, (*b*) availability of equipment and material, or (*c*) economic considerations. The length of the screen is usually determined by these factors. The diameter may or may not be predetermined; in either case, the effective diameter would depend on the location of the pump bowl. If the bowl is located near the bottom of the well, the diameter must be corrected to account for the reduction in cross-sectional area caused by the riser pipe. If the bowl is located above the perforated section, however, a correction is not necessary unless the suction pipe extends into the perforated section. With the diameter and length of the screen determined, a specific screen can be checked to see if it meets the established criteria. For this check the percentage of open area must be known and a C_s-value for the screen and gravel size must be obtained from a curve such as is shown in Fig. 13. The possibility exists that a specific type of screen must be used to control sand movement or to support the surrounding formation. In this case the diameter of the well—or possibly the length of the screen—could be varied to obtain a value of $(C\,L)/D$ of 6 or greater.

Eq. 15 also provides a method of checking the head losses incurred by flow through the screen and in the well. This loss might be a major design factor, especially for wells of small diameter.

The variation of discharge into the well can have important significance in certain installations. The laboratory tests indicate that practically all the flow into the well takes place only through the length of screen, from the discharging end, necessary to obtain a value of 6 for $(C\,L)/D$. Although this test result may not prove completely accurate in the field, the same pattern should exist. Better screens could thus be used at the discharge end of the well (the discharge end would depend on the location of the pump bowl and the end of the suction pipe). The use of screens of different material in the well would be of great importance where corrosion is likely to occur, and cost considerations do not permit installation of corrosion resistant screens for the entire length. Since the maximum difference in head occurs at the suction-pipe intake, the velocity through the screen in this region will be greatest, and, consequently, excessive movement of sand is liable to occur there. This fact must be realized when choosing the well screen.

CONCLUSIONS

Design criteria resulting from Eq. 15 can be summarized as follows:

1. For minimum screen losses, $(C\ L)/D$ must be greater than 6.
2. If $(C\ L)/D$ is greater than 6, the losses through the screen are independent of gravel size. Therefore, the size of gravel in the gravel envelope can be selected on the basis of sand-flow control.
3. When $(C\ L)/D$ is greater than 6, the actual head loss for a given discharge depends only on the diameter of the screen. This loss can be determined from Eq. 15 and kept to an allowable value by increasing the screen diameter. Increasing the diameter may reduce the value of $(C\ L)/D$ below 6; in this case the loss will no longer be a minimum, but when this occurs $(C\ L)/D$ can be increased by using a longer screen.
4. The greater part of the flow into a well takes place over the length of screen (measured from the discharging end) required to obtain a value of 6 for $(C\ L)/D$. The quality of this section of screen is therefore of greater importance than that of the remainder of the screen.

Available screen coefficients are limited to a few selected screen and gravel size combinations. For the criteria to be of greatest practical value to the well driller, a large extension of the available coefficients is necessary. The principal value of this study, however, is that it calls attention to hydraulic properties of well screens which are not generally known, but which must be given consideration if the best results are to be obtained.

ACKNOWLEDGMENT

The experimental investigation was conducted in the Hydraulic Laboratory of Colorado Agricultural and Mechanical College at Fort Collins. This paper covers part of a comprehensive investigation of well screens sponsored by the Colorado Agricultural Experiment Station of the college and the Division of Irrigation of the Soil Conservation Service, United States Department of Agriculture, in cooperation with well screen manufacturers and well drilling companies.

APPENDIX

The following symbols, adopted for use in this paper and for the guidance of discussers, conform essentially with "American Standard Letter Symbols for Hydraulics" (ASA Z10.2—1942), prepared by a committee of the American Standards Association with ASCE representation, and approved by the Association in 1942:

A = cross-sectional area;
A_p = percentage of the total area of a well screen that is open area;
C = coefficient defined by Eq. 14d;
  C_c = coefficient of contraction;
  C_q = coefficient of discharge;
  C_s = well screen coefficient depending on the screen and the gravel envelope;

D = diameter of the well screen;
F_y = difference in momentum;
g = acceleration of gravity;
h_{pz} = piezometric head inside the well screen;
Δh_{pz} = difference in piezometric head between inside and outside of a well screen;
$\Delta h'_{pz}$ = difference in piezometric head between the inside and the outside of a well screen at the end through which no flow passes;
k = roughness factor for the inside walls of the well screen;
L = length of the perforated section of the well screen;
P = hydrostatic pressure;
Δp = difference in pressure between the inside and the outside of a well screen at a point of the well screen;
Q = quantity of flow, parallel to the screen axis, past a given section inside the well screen;
V = average velocity parallel to the longitudinal axis inside a well screen;
v = velocity of flow through the openings;
z = distance from a datum;
γ = specific weight;
μ = coefficient of dynamic viscosity; and
ρ = density.

DISCUSSION

Wen-Hsiung Li,[12] A. M. ASCE.—The authors have conducted a systematic investigation. A simple dimensionless quantity $(C\,L)/D$ was found for determining the hydraulic properties of well screens.

The equation of continuity, Eq. 5*a*, is incorrect as the discharge Q in the well changes along the direction of flow. The energy equation, Eq. 5*b*, is also incorrect because, even when frictional loss can be neglected, energy is lost as a result of the impact of the incoming water on the water flowing in the well. That there is a loss of energy caused by impact can be seen from Eq. 12. According to the definition of h_{pz} and Eq. 12,

$$\frac{v^2}{2\,g} + \frac{P}{\gamma} + z = \frac{Q^2}{2\,g\,A^2} + h_{pz} = \tfrac{1}{2}\,(\Delta h_{pz} - \Delta h'_{pz}) + (h_o - \Delta h_{pz}) \quad . . (18)$$

in which h_o is the piezometric head just outside the screen. The total head varies with Δh_{pz} along the flow in the well. Fortunately, Eqs. 5*a* and 5*b* were not used in the investigation. With the assumption that the piezometric head h_o was constant, Eq. 15 was derived; Eq. 15 agrees with observations on screens surrounded by free water (Figs. 2 and 11). The validity of the momentum equation, Eq. 5*c*, and the orifice equation, Eq. 6, is therefore well demonstrated. However, one might question the validity of the result for screens surrounded by soil in an aquifer. By assuming a constant value for h_o, the authors have obtained a solution which shows that the discharge through the screen is concentrated near the discharge end of the well. If the screen were put in an aquifer, such concentration of flow would necessitate a decrease of piezometric head h_o toward the discharging end, as shown in Fig. 19. The magnitude of the variation of h_o depends on the permeability of the soil among other factors. The higher the permeability of the soil, the less the

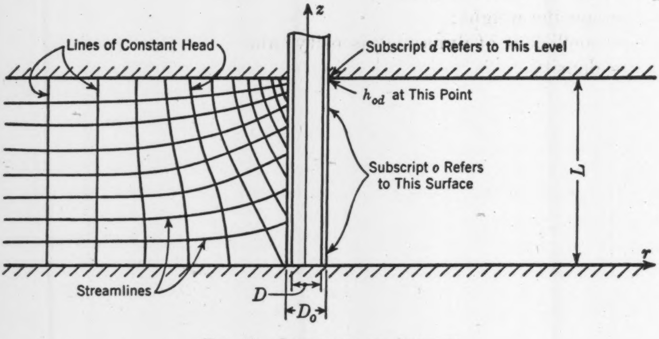
z
Lines of Constant Head
Subscript d Refers to This Level
h_{od} at This Point
Subscript o Refers to This Surface
L
r
Streamlines
D
D_o

Fig. 19.—Screen in an Aquifer

---

[12] Asst. Prof. of Civ. Eng., The Johns Hopkins Univ., Baltimore, Md.

variation of h_o along the screen. In the tests reported by the authors, the free water surrounding the screen is equivalent to a soil with infinite permeability; therefore, h_o is sensibly constant as assumed. When the screen is surrounded by soil of lower permeability, h_o cannot be assumed to be constant.

In the analysis of flow into a well, one must account for the permeability of the soil in the aquifer. If h is the piezometric head at any point in the aquifer, and C_p is the coefficient of permeability of the soil (as defined by the equation for seepage in isotropic, porous materials),

$$q_r = - C_p \frac{\partial h}{\partial r} \quad \text{(19a)}$$

and

$$q_z = - C_p \frac{\partial h}{\partial z} \quad \text{(19b)}$$

in which q_r and q_z are the volumes of flow per unit time per unit cross section of soil in the r-direction and z-direction, respectively (Fig. 19). Both C_p and q have the dimensions of length per unit time. As a result of the continuity of flow in the aquifer,

$$\frac{\partial^2 h}{\partial r^2} + \frac{1}{r}\frac{\partial h}{\partial r} + \frac{\partial^2 h}{\partial z^2} = 0 \quad \text{(20)}$$

must be satisfied for axial-symmetric flow.[13] To solve Eq. 20, the conditions at the boundaries of the aquifer must be known. For the case of a screen fully penetrating a confined aquifer (Fig. 19), $\partial h/\partial z$ must be zero at the top and bottom of the aquifer as q_z must vanish there. At great distances from the well, $\partial h/\partial z$ must also be zero as the flow there is radial.

The condition at the remaining boundary (just outside the screen) depends on the flow in the well. If h_d and Q_d are h_{pz} and Q, respectively, at the discharging end of the screen ($z = L$), the momentum equation, according to Eq. 8a, results in

$$h_{pz} = h_d + \frac{Q^2{}_d}{A^2 g} - \frac{Q^2}{A^2 g} \quad \text{(21)}$$

in which the subscript d refers to the discharge end of the screen. From a consideration of the continuity of flow across the screen,

$$\frac{dQ}{dz} = \pi D_o C_p \left(\frac{\partial h}{\partial r}\right)_o \quad \text{(22)}$$

in which D_o is the outside diameter of the screen, $(\partial h/\partial r)_o$ is $\partial h/\partial r$ at $r = D_o/2$ and the subscript o refers to the outside surface of the screen. From a consideration of the continuity of flow in the well, the discharge Q at any point z is

$$Q = Q_d - \int_z^L \frac{dQ}{dz}\, dz = Q_d - \pi D_o C_p \int_z^L \left(\frac{\partial h}{\partial r}\right)_o dz \quad \text{(23)}$$

---

[13] "The Flow of Homogeneous Fluids Through Porous Media," by Morris Muskat, McGraw-Hill Book Co., Inc., New York, N. Y., 1937, p. 141.

Substituting the value of Q from Eq. 23 into Eq. 21 results in

$$h_{pz} = h_d + 2\pi \frac{Q_d D_o C_p}{A^2 g} \int_z^L \left(\frac{\partial h}{\partial r}\right)_o dz - \frac{(\pi D_o C_p)^2}{A^2 g} \left[\int_z^L \left(\frac{\partial h}{\partial r}\right)_o dz\right]^2 \text{..(24)}$$

To relate h_{pz} to the variable h_o along the outside surface of the screen, the use of the orifice equation, Eq. 6, leads to

$$\frac{C_c A_p \pi D}{\sqrt{2g(h_o - h_{pz})}} = \frac{dQ}{dz} \text{.....................(25)}$$

Substituting Eqs. 14*d*, 22, and 24 into Eq. 25 and simplifying,

$$h_o - h_d - \frac{2\pi Q_d D_o C_p}{A^2 g} \int_z^L \left(\frac{\partial h}{\partial r}\right)_o dz + \frac{(\pi D_o C_p)^2}{A^2 g} \times \left[\int_z^L \left(\frac{\partial h}{\partial r}\right)_o dz\right]^2 - \frac{(8 D_o C_p)^2}{g C^2 D^2} \left(\frac{\partial h}{\partial r}\right)_o^2 = 0 \text{..(26)}$$

Eq. 26 must be satisfied by the values of h and $\partial h/\partial r$ from Eq. 20 just outside the screen. The solution of Eq. 20 satisfying the boundary condition specified by Eq. 26 can be obtained by relaxation methods.[14] However, some characteristics of the flow can be determined without actual numerical computation.

If h_{od} is the piezometric head in the soil at the discharge end just outside the screen, and $\delta = h_{od} - h_d$ (that is, Δh_{pz} at the discharging end), one must let $\phi = h/\delta$, $R = r/L$, and $Z = z/L$ in order to study the problem in dimensionless form. Eq. 20 can therefore be reduced to

$$\frac{\partial^2 \phi}{\partial R^2} + \frac{1}{R}\frac{\partial \phi}{\partial R} + \frac{\partial^2 \phi}{\partial Z^2} = 0 \text{..................(27)}$$

Eq. 27 must be solved to satisfy the boundary condition at the screen as specified by Eq. 26. Eq. 26 can be rewritten as

$$\phi_o - \phi_{od} + 1 - 2\pi \frac{Q_d D_o C_p}{A^2 g} \int_Z^1 \left(\frac{\partial \phi}{\partial R}\right)_o dZ + \pi^2 \left(\frac{Q_d D_o C_p}{A^2 g}\right)^2 \frac{\delta}{\frac{Q^2_d}{A^2 g}} \times \left[\int_Z^1 \left(\frac{\partial \phi}{\partial R}\right)_o dZ\right]^2 - 4\pi^2 \left(\frac{D}{C L}\right)^2 \left(\frac{Q_d D_o C_p}{A^2 g}\right)^2 \frac{\delta}{\frac{Q^2_d}{A^2 g}} \left(\frac{\partial \phi}{\partial R}\right)_o^2 = 0 \text{..(28)}$$

in which the subscript *od* refers to the discharge end just outside the screen. It can be seen that, given the geometrical shape of the aquifer (that is, D_o/L) and given the coefficients in Eq. 28, a unique solution of Eq. 28 can be obtained. That is, the loss coefficient equals

$$\frac{\delta}{\frac{Q^2_d}{A^2 g}} = f\left(\frac{C L}{D}, \frac{Q_d D_o C_p}{A^2 g}, \frac{L}{D_o}\right) \text{................(29)}$$

---

[14] "Relaxation Methods in Theoretical Physics," by R. V. Southwell, Oxford University Press, Oxford, England. 1946.

The actual value of ϕ_{od} is immaterial as it represents a constant head for the entire aquifer. In order to have some insight into the effect of C_p on the loss coefficient in Eq. 29, let

$$m \frac{Q_d}{L} = \pi D_o C_p \left(\frac{\partial h}{\partial r} \right)_o \dots\dots\dots\dots\dots\dots (30)$$

in which m is the ratio of the rate of flow through the screen at any point to the mean rate of flow through the screen. With this coefficient m, Eq. 26 can be reduced to

$$\frac{h_o - h_{od}}{\dfrac{Q^2{}_d}{A^2 g}} + \frac{\delta}{\dfrac{Q^2{}_d}{A^2 g}} - 2 \int_Z^1 m \, dZ + \left(\int_Z^1 m \, dZ \right)^2 - 4 \left(\frac{D}{C L} \right)^2 m^2 = 0 \,.\,. (31)$$

At the discharging end of the screen, $Z = 1$, $h_o = h_{od}$, and $m = m_o$. Thus,

$$\frac{\delta}{\dfrac{Q^2{}_d}{A^2 g}} = 4 \left(\frac{D}{C L} \right)^2 m^2{}_o \dots\dots\dots\dots\dots\dots (32)$$

Thus, the loss coefficient is dependent on $\dfrac{D\, m_o}{C L}$, in which m_o is the value of m at the discharging end of the screen. The value of m_o depends, of course, on the independent variables in Eq. 29. In the case of a fully penetrating well, the two extreme values of m_o are obtained from the case of constant h_o and the case of uniform discharge through the screen. Both of these cases are never realized in the field, but they serve as the limits to the actual cases. A sensibly constant h_o is obtained with very permeable soils which offer almost no resistance to the concentration of the discharge at the discharge end of the screen; the authors' result is an approximate solution for such cases. On the other hand, an approximately uniform distribution of discharge through the screen is obtained with soils of low permeability which offer high resistance to the concentration of the discharge. An approximate solution for such cases can be obtained by setting m_o equal to unity. Thus, for small values of $\dfrac{Q_d\, D_o\, C_p}{A^2 g}$, the loss coefficient can be approximated as

$$\frac{\delta}{\dfrac{Q^2{}_d}{A^2 g}} = 4 \left(\frac{D}{C L} \right)^2 \dots\dots\dots\dots\dots\dots (33)$$

When Eqs. 15 and 33 are plotted in Fig. 20, it can be seen that the two curves coincide for $(C L)/D$ less than unity. This means that, for all cases in which $(C L)/D$ is less than unity, both h_o and the discharge through the screen are approximately constant. For $(C L)/D$ larger than unity, the curve for a given screen may lie anywhere between these two curves. The value of $(C L)/D$ for a minimum value of the loss coefficient must be larger than 6, and the minimum loss coefficient must be less than unity.

Additional factors may also influence the value of m_o, and therefore the magnitude of the loss coefficient. For partly penetrating wells, there is a tendency for the discharge to concentrate near the bottom of the screen,[15] thus reducing the value of m_o. When the screen is surrounded by gravel, the analysis previously presented must be modified as Eq. 22 is not true when there is a redistribution of the discharge through the gravel layer. The actual problem is complicated. The authors' result gives a loss through the screen which is the greatest loss that can possibly occur and is, therefore, of great practical value.

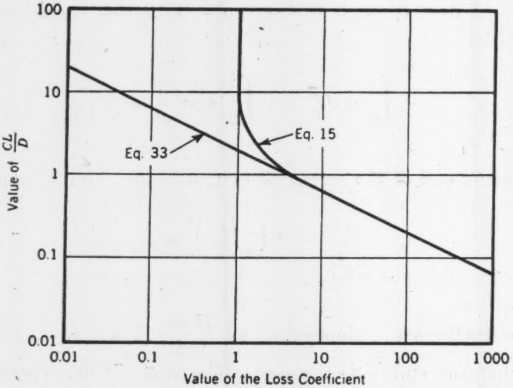

FIG. 20.—THE RELATIONSHIP BETWEEN $(CL)/D$ AND THE LOSS COEFFICIENT

Another point of interest in this subject should also be mentioned. The condition of constant h_o or uniform distribution of discharge through the screen is never realized in nature. Thus, even for fully penetrating wells, the flow in the aquifer can never be truly radial. This fact is not generally recognized in the study of flow into wells.

ARTHUR L. COLLINS,[16] A. M. ASCE.—In the "Synopsis" it is stated:

> "The objective of the investigation was to establish criteria which could be used to aid in the selection of well screens to meet the varied conditions found throughout the United States."

Another interesting statement is contained in the "Conclusions": "For the criteria to be of greatest practical value to the well driller, a large extension of the available coefficients is necessary." It would be of interest to know to what extent the laboratory tests should be extended. Also, what value should the well driller place on the test information?

In their investigation the authors have anticipated the construction of the gravel-packed well. This type of construction necessitates the boring of a large-diameter well which is protected temporarily by a large casing and then by the installation of a smaller casing with perforations. This installation is followed by the placing of selected gravel between the casings and finally by the removal of the outside casing.

---

[15] "The Flow of Homogeneous Fluids Through Porous Media," by Morris Muskat, McGraw-Hill Book Co., Inc., New York, N. Y., 1937, p. 269.

[16] Cons. Engr., Berkeley, Calif.

The reasoning behind the gravel-packed well is correct, but in practice this type of construction is unreasonably expensive. In contrast, the well driller who is familiar with the substrata in which he is drilling has probably learned to construct a well which will satisfy the requirements of the user at a fraction of the cost of the made-to-order well with packed gravel. For example, the many wells constructed for irrigation purposes are principally located in the alluvial fills of valleys and are not founded in extensive rock formation. There must also be present a clay or hardpan stratum on top of the sand and gravel through which the water must pass. It is believed that the average well and the large-quantity well have clear-water pockets which exist at the top of the sand stratum and are bridged by a clay roof. The well, if normal, will have part of the perforations entirely unobstructed. As a result of this unobstructed condition, there is insufficient outside pressure to cause the water to flow through the partly obstructed perforations.

The well driller uses the factory-perforated casing, or he makes the perforations at the proper depth after the casing is in place with a perforating instrument. By the use of these methods he is able to make a well which is equal to, or perhaps superior to, the gravel-packed well at a fraction of the cost.

In order to explain the water-pocket theory, a description of a well system without any perforations will be presented. The well with large perforations made after the casing is in place and opposite the assumed pocket is virtually a screenless well.

There are many localities where wells can be constructed without the use of screens. Such a location would be one where there are thick clay deposits separated by sand and gravel strata of a few feet in thickness. The clay cap must be compact enough to bridge the sand if a part of the sand is removed. Also, the strata must be below the water level in the well at all times. A well that will pump sand to any extent can be assumed to contain a pool in which the clear water collects.

The subject of well development first interested the writer in 1910 when he learned that in California ample irrigating water could be obtained from bored wells or augered wells. It was also at this time that the deep-well turbine became available. This turbine provided the solution to the problem of drawing the water from a deep well without providing deep pits for the centrifugal pump or for other cumbersome equipment.

The substrata of the valley floor from Bakersfield to Corning in the San Joaquin and Sacramento valleys of California (a distance of approximately 400 miles) follows this general pattern (clay deposits separated by sand and gravel strata). In this area there has been little change in the type of well and casing that has been used from 1910 to 1954. Both the slotted section made in the shop and the slots made in the field after the well is constructed are used. From 1910 until welding equipment became available in the field the drillers favored 4-ft-long, double-casing sections. The sections, having slightly different diameters, were telescoped with the joints made at the midsection. The pipe presently used (1954) is the 4-ft section of heavy-gage steel with welded collars.

The strainerless well was patented by the writer on April 28, 1914. The idea originated from a clue discovered in a locality where an unusually large supply of water could be obtained from a few feet of sand and gravel. In these wells the contractor ended the casing some distance above the gravel stratum and used no strainer. Elaborating on this idea and applying it to other areas where the sands were finer, it was observed that, when the well was pumped heavily, sand would be emitted and afterward the water would become clear. This action results because the water itself flushes out a percolating area until there is a balance between the water velocity and the sand. It was also assumed that the percolating space extended radially along the roof of the sand stratum from the well to form a sheet of thin depth.

Therefore, if the casing is extended to the floor of the sand stratum, the sand will be moved downward by gravity, and the void area of the well will be increased. This increase, however, results from the removal of too much sand. If the strainer is opposite the sand, the well is improved by heavily perforating the casing near the top of the sand stratum. The strainer adds little to the well efficiency.

After reaching these conclusions concerning the open-bottom well, the writer conceived the idea of constructing a well with a 12-in. casing or a 14-in. casing which was terminated at the first sand stratum. Then a second string of 10-in. casings was extended into the second stratum. The 10-in. casing was then cut off near the end of the first stratum—thus leaving an annular space through which the water from the first stratum was taken into the casing to join the water from the lower stratum. In this way it was possible to extend the open-bottom-well principle to several strata in the well.

It is of interest to note that the writer was a supervising engineer and not an experienced well driller when the theory of the open-bottom well was deduced. However, not long after the patent was granted, a professional well driller sought a license to use the patent. Prior to that date the well driller had constructed fifty wells according to this principle, and only when he applied for a patent did he learn that one had been previously obtained.

As a check on the work of this well driller, an agent for a manufacturer who furnished most of the well casing for several drillers operating in the area observed the wells made by this particular driller. The agent concluded that the driller's wells produced 50% more water (with no sand pumping) than did other wells.

Because of the sight-unseen conditions in a well and the methods of construction which differ among well drillers, it will always be difficult to obtain data—such as the size of the casing, the area of the perforations, and the size of the sand grains—which will enable the engineer to predetermine the performance of a well.

Mohammad Nazir[17] **and Nazir Ahmad.**[18]—A solution to the problem of excessive head loss through screens (which are in general use (1954) in the Punjab Province of Pakistan) has been presented by the authors. Since the inception of the use of ground water, engineers in the Punjab Province have used a screen made of $\frac{1}{8}$-in.-thick brass sheets in which horizontal slits, 1 in. long and of varying widths (from 0.010 in. to 0.014 in.) are cut. These slits are sharp on the outside and expand toward the inside at an angle of approximately 30°. The distance between adjacent slits is $\frac{1}{8}$ in. In order to maintain sufficient strength in the strainer, a $\frac{3}{4}$-in. space is left between two sets of 1-in. slits. Thus, the open area of these screens is from 6% to 10% of the total surface area.

The prevalent aquifer formation in a part of the Punjab Province is composed of medium sand; therefore, the coarsest formation has a mean size of between 0.30 mm and 0.45 mm. The screens are usually placed in medium sand which has a mean diameter of between 0.25 mm and 0.45 mm and an effective size of between 0.15 mm and 0.25 mm. The sand has a high coefficient of uniformity—between 1.6 to 2.5—and the usual diameter of the brass screen is between $7\frac{1}{2}$ in. and 9 in. A length of approximately 150 ft is considered sufficient to pump 2 cu ft per sec. In order to exclude the low-yield region and any saline water, a blind pipe with a length of from 40 ft to 100 ft is normally installed below the natural surface.

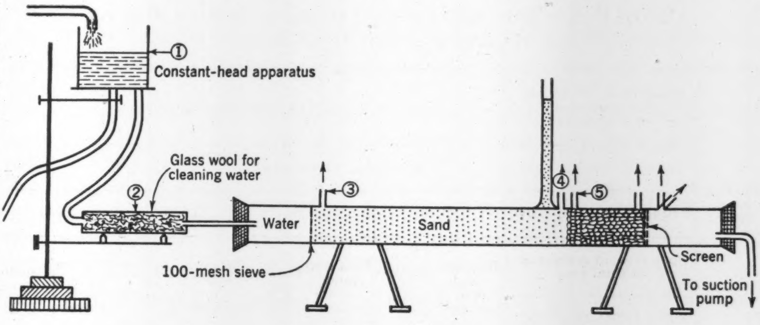

Fig. 21.—Test Setup

Several pumping tests have been performed in regions where the water table lies from 3 ft to 10 ft below the natural surface. A study has also been made of the accompanying lowering of the water table. It has been noted that, even at a distance of 2 ft from a well screen, the lowering of the water table has seldom exceeded 20% of the pumping level in the well. The lowering observed at a distance of 1,000 ft from the well has measured from $\frac{1}{2}$ ft to 1 ft. This small lowering has been attributed to: (1) The formation of free surface; (2) the head loss from the formation into the shrouding which envelopes the screen; and (3) the head loss between the gravel shrouding and the screen.

---

[17] Director, Irrig. Research Inst., Lahore, Pakistan.

[18] Head, Physics Dept., Irrig. Research Inst., Punjab, Lahore, Pakistan.

If this lowering is attributed to the concept of a free surface, the existence of a long blind pipe and the absence of a discharge face are arguments against this concept. It can be argued that the small lowering is caused by the greater yield of the formation. However, the pumping level in the well contradicts this argument.

Some laboratory experiments have been performed to study the head loss between the formation and the gravel and that between the gravel and the screen. Assuming the flow in the screen region to be horizontal, the experimental arrangement shown in Fig. 21 was devised. A supply of air-free and filtered water was made available on the inflow side, and on the exit side suction up to 20 ft was applied. Small outlets were provided at points 1, 2, 3, 4, and 5 to record pressure by mercury manometers. The screen studied had four different slit sizes—0.014 in., 0.020 in., 0.030 in., and 0.040 in.—with open areas equal to 7.65%, 11.0%, 13.4%, and 19.3% of the total surface area, respectively. The head losses between the gravel and the screen and between the sand and the gravel and the observed discharge are shown in Table 3.

TABLE 3.—THE EFFECTS OF INCREASE OF SLIT SIZE ON DISCHARGE AND HEAD LOSS

Suction head, in feet	DISCHARGE, IN CUBIC CENTIMETERS PER MINUTE				HEAD LOSS, IN FEET							
	SLIT SIZE, IN INCHES											
	0.014	0.020	0.030	0.040	0.014		0.020		0.030		0.040	
	Open area, in percentage of total area				Between sand and gravel	Caused by screen	Between sand and gravel	Caused by screen	Between sand and gravel	Caused by screen	Between sand and gravel	Caused by screen
	7.65	11.01	13.4	19.3								
5	224	238	260	266	0.62	0.17	0.58	0.17	0.46	0.09	0.37	0.08
7	302	318	346	354	1.22	0.20	0.94	0.20	0.76	0.12	0.64	0.10
10	421	436	476	485	1.82	0.23	1.60	0.23	1.40	0.16	1.26	0.15
12	504	519	560	568	2.18	0.26	2.00	0.25	1.88	0.20	1.70	0.18
15	636	640	692	710	2.65	0.28	2.45	0.28	2.50	0.15	2.32	0.30
17	720	722	784	808	2.90	0.30	2.70	0.30	2.81	0.31	2.74	0.30

A study of Table 3 reveals that the head loss between the screen and the gravel is nearly constant, the variation being from 0.1 ft to 0.3 ft with suction head varying from 5 ft to 17 ft. The head loss between the formation and the gravel is, however, significant, as it is approximately ten times as great as that between the gravel and the screen. Similarly, the discharge with a given suction head was the highest for the screen with the widest slits. Experiments with wider slits and open area greater than 20% are in progress (1954), but the preliminary observations have shown that screens with slits wider than 0.040 in. may not increase the discharge under a given suction head.

Although there is no question about the mathematical derivation of Eq. 15, it does seem that in the authors' range of application, laminar flow should exist and there should be no movement of particles. Therefore, the effect of viscosity cannot be eliminated. Similarly, the statement that the factor $(C\ L)/D$ should always be greater than 6 to reduce the screen loss to a minimum seems difficult to comprehend. From the writers' experience in Pakistan, D does not exceed 9.0 in., L can be as great as 150 ft, and the value of C (from Eq. 14*d*) can be much greater than 30. Therefore, the factor $(C\ L)/D$ will always be greater than 6, and the loss will be minimum regardless of the water pumped out. However, a consideration of this point does not explain the high pumping level, high yield, and attendant slight lowering of the water table in Pakistan.

MATTHEW I. RORABAUGH,[19] A. M. ASCE.—The experimental data presented by Messrs. Petersen, Rohwer, and Albertson are a valuable contribution to the hydraulics of wells. Much speculation and many claims have been made concerning the magnitude of head losses through well screens. The data presented should do much toward clarifying some of the problems involved in screen design and in the selection of well screens.

The authors are to be complimented on their work considering the difficulties inherent in such a study. The economical construction of a suitable model which will be hydraulically equivalent to the prototype is particularly difficult. Small-scale models of screens are costly items. Other items also add to the cost of research and to the sensitivity of the necessary physical observations.

One of the basic assumptions in the theoretical development is that the piezometric head on the outside of the screen is constant over the entire outside surface of the screen. In the case of a gravel envelope, this condition was not met, as is implied in Fig. 8. The authors considered this variation to be relatively small and concluded that the status of the investigation did not warrant the use of a correction for the variation. The effects shown in Fig. 8 result, in part, from the fact that the screen (2 ft long) does not fully penetrate the saturated thickness (5 ft). Flow enters the gravel pack over this 5-ft length and travels through the gravel to discharge through the 2-ft screen. Flow lines converge radially in the horizontal plane and also converge in the vertical plane. The head losses in Fig. 8 are taken horizontally through the gravel pack. The shape of the curves in Fig. 8 is partly controlled by the position of the screen in relation to the boundaries—the bottom of the tank and the water surface in the tank.

The effects of the boundary conditions on flow toward the screen in the laboratory structure are related to the data in Figs. 16, 17, and 18. From reference to the test apparatus shown in Fig. 6 and to the tests on screens without a surrounding grave pack, it should be evident that, as A_p approaches 100%, the horizontal component of velocity at the screen varies from approximately zero at the water surface to a maximum near the base of the screen. This generalization can be visualized easily by considering the flow net that would be developed between the overflow rim and the outflow pipe shown in Fig. 6. That is, for the condition of no screen or screens having a low friction loss, head-distribution curves similar in shape to those in Figs. 16, 17, and 18 would result. These curves would be based on the flow pattern in the tank and would be controlled by the tank boundaries and the position of the inflow and outflow pipes. Item 4 in the "Conclusions," apparently based on those data in Fig. 17, applies to the test apparatus used. However, considering the effects of boundary conditions and of the partial penetration introduced by the addition of a gravel pack 9 in. thick (as demonstrated in Fig. 8), it is doubtful whether this conclusion can be applied to prototype structures.

---

[19] Dist. Engr., Geological Survey, U. S. Dept. of the Interior, Ground Water Branch, Louisville, Ky.

The investigation deals with head losses in a very small zone in and near the screen. This is only a small part of the problem of total drawdown in a well. Before the screen data are used to form conclusions for general well design, it would be desirable to consider comprehensively the head distribution in and about the pumping well.

If an artesian gravel bed, 4 ft thick, having a permeability of 2,500 gal per day per sq ft and a storage coefficient of 0.003, is fully penetrated by a 4-ft-long, 3-in.-diameter, A-d-type, well screen, and if pumping is conducted at rate of 0.125 cu ft per sec, the conditions approximate those shown in Fig. 17. For a pumping time of 1 hr the drawdown in the well, computed by the nonequilibrium formula developed[20] by C. V. Theis, is approximately 10 ft, if turbulent losses in the aquifer are not considered.[21] According to this conclusion (item 4) the most efficient well screen would have to penetrate only 1 ft of the 4-ft aquifer (Fig. 17). Using the Kozeny[22] equation for partial penetration, the drawdown at the well is approximately 15 ft rather than 10 ft. A plot of head distribution about a partly penetrating well is given by M. Muskat.[23] Thus, the selection of an efficient well screen for this example (by use of item 4 in the "Conclusions") results in a crowding of the flow lines outside the well and inefficient use of the aquifer. Although the head loss for the 1-ft screen and the 4-ft screen will be almost the same when tested in a tank, the drawdown will differ by approximately 5 ft when installed in an aquifer of the type used in the example.

The permeability of the aquifer is an important item in examining the various factors influencing well design. In an aquifer having a very high permeability, the aquifer losses will be small, and attention to a modified form of item 4 in the "Conclusions" could be justified by a consideration of the head distribution in the aquifer. However, in most of the unconsolidated aquifers tested in the United States, the usual operating head loss is measured in feet and in tens of feet. For these wells, a screen loss of a few tenths of a foot is small in proportion to the total loss, and item 4 in the "Conclusions" would not form an important part of the economies in the entire flow system.

It is noted that the rates of flow used in the studies were, in general, higher than those in most producing wells. Rates in the tests, for example, were 0.125 cu ft per sec through 1 ft of a 3-in. screen and 1 cu ft per sec through 2 ft of a 12-in. screen. With these rates, only a few tenths of a foot of head loss was measured. In a field installation, using 20 ft of a 12-in. screen and producing 500 gal per min, losses through the screen become small when compared to other losses.

---

[20] "The Relation Between the Lowering of the Piezometric Surface and the Rate and Duration of Discharge of a Well Using Ground-Water Storage," by C. V. Theis, *Transactions*, Am. Geophysical Union, Vol. 16, 1935, p. 520.

[21] "Graphical and Theoretical Analysis of Step-Drawdown Test of Artesian Well," by M. I. Rorabaugh, *Proceedings-Separate No. 362*, ASCE, December, 1953.

[22] "The Flow of Homogeneous Fluids Through Porous Media," by M. Muskat, J. W. Edwards, Inc., Ann Arbor, Mich., 1946, p. 274.

[23] *Ibid.*, p. 270.

This investigation should do much to clear up misunderstandings between owners, drilling contractors, and screen manufacturers as to the extent of the head losses of screens. The data demonstrate that losses in most commercial screens are small, and that the screen manufacturers have done well in designing efficient screens.

DEAN F. PETERSON, JR.,[24] M. ASCE.—A most interesting experimental verification of a theoretical hypothesis in fluid mechanics has been presented; experimental results are seldom as satisfactory as in this case. The authors are to be complimented on their application of the basic laws of hydrodynamics to the development of this hypothesis and the manner in which they organized their experimental program to check it.

In the tests that omitted a gravel pack, the outside piezometric head was essentially constant. This constancy could not be true of a well in a sand formation or in a gravel formation. The screen phenomenon would undoubtedly cause the streamlines approaching the well to converge near the discharge end of the screen and would thus cause pressures outside the casing to be lowest near the discharge end. This would tend to overcome, to some extent, the effects of the screen which were reported by the authors. The foregoing effect would certainly be secondary, and it is expected that the authors' analysis will still give useful quantitative results.

Most welcome would be a solution to the problem of the hydraulics of a well in an aquifer which would take into account the screen effects suggested by the authors. All solutions of the problem of well hydraulics, such as that offered by Jules Dupuit,[25] are based on the assumption of equal piezometric head throughout the length of the well.

Another interesting problem is the effect of a pump intake located within the length of the screen. The velocities inside the screen would converge from both directions toward the pump intake. One would thus infer that, by proper placement of the pump intake, a "double effective" length of screen might be developed—one length above the intake and one below. For the most effective operation, it would appear that the pump intake would need to be set above the bottom of the screen a distance such that $(C\,L)/D$ is greater than 6 in order that the screen might be unrestricted by pump bowls and columns throughout the effective length. In addition, there would be an effective distance above the pump intake of $(C\,L)/D$ equal to 6. For this latter case, D would need to be corrected to allow for the area occupied by the pipe columns and bowls. Experiments on an effective screen length using actual pump installations would be enlightening; perhaps this might be done by the use of a small-scale pump and screen.

---

[24] Prof. and Head of Civ. Eng., Colorado Agri. and Mech. College, Fort Collins, Colo.

[25] "Études théoretiques et pratiques sur le mouvement des eaux," by Jules Dupuit, Paris, France, 2d Ed., 1863.

G. COHEN DE LARA.[26]—The development of ground-water resources in Algeria and Tunisia necessitated a general study of friction losses in well screens and in the surrounding aquifer. This study, begun in 1949, resembles in part that performed by Messrs. Petersen, Rohwer, and Albertson. On the whole, these results agree with those of the authors, but some of their conclusions appear to be incomplete.

The problem was approached by determining the theoretical laws of continuous flow through screens, with and without porous material surrounding them. In order to support the theory, air-flow tests (without surrounding material) were performed according to the Reynolds similarity. The tests with surrounding material were conducted with water on the semicircular model shown in Fig. 22. The results of these latter tests have not been published (as of 1954). The purpose of these tests is similar to the purpose of those performed by the authors, although different methods were used.

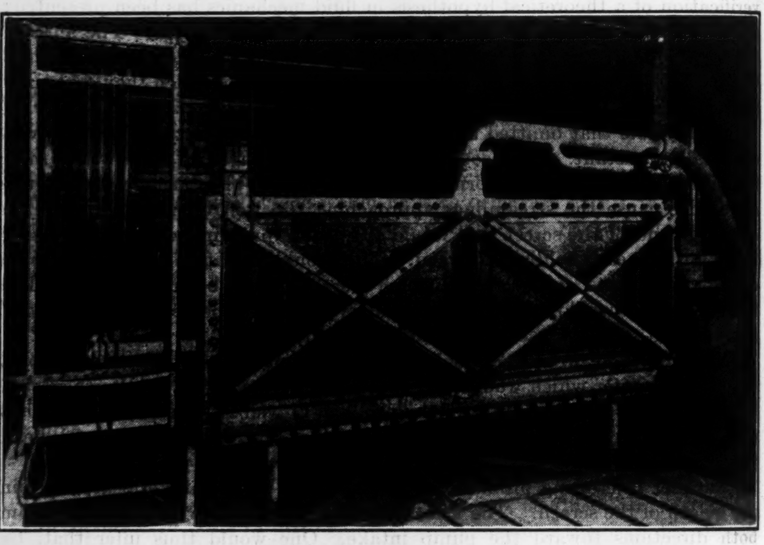

FIG. 22.—SEMICIRCULAR MODEL

Theoretical Computation and Experimental Research for a Screen Surrounded Only by a Liquid.—The theoretical computation is similar to that offered[27] by P. Arnaud, and the experimental measurements accurately confirm the basic assumptions. It is agreed that the experimental determination of a coefficient C_s (which varies according to the type of commercial screen used) allows one to apply the theoretical computation to commercial screens, to which the basic assumptions used in the computation do not always apply.

---

[26] Engr., Laboratoire Dauphinois d'Hydraulique, Grenoble, France.

[27] "Pertes de Charge dans les Crépines de Puits de Pompage," by P. Arnaud, *Troisième Journées de l'Hydraulique*, Paris, France, 1954.

Well Screen Surrounded by Gravel.—During the tests on a circular model, it was found (as also by the authors) that the pressure on the exterior wall of the screen was not constant. For a louvre-type screen (200 mm in diameter and 70 cm in length) with high discharges, there resulted curves similar to those shown in Fig. 8. It is not known whether the trend of these curves is maintained for small discharges as the resulting pressure differences were too small to be measured.

In the theoretical computation, it is supposed that the pressure on the exterior wall is constant. The authors have tried to avoid the difficulty by determining a coefficient, C_s, similar to the one used for commercial screens surrounded only by liquid. The head loss, Δh, entering in the dimensionless number, $\Delta h \Big/ \frac{V^2}{2\,g}$, was taken as the difference in pressure between the static pressure intake in the interior of the screen and the static pressure intake half way along the screen, between the gravel and the screen—that is, where there is a minimum static pressure for the given discharge. Based on this definition, the authors determined several values for C_s, which appears as a function of the opening dimensions and size of gravel used for a given type of screen. It is implied by the authors that C_s is applicable regardless of the voids ratio of the surrounding soil and of the thickness of the gravel. This result seems incomplete as a change in the surrounding soil thickness or of its voids ratio will entail a variation of Δh—therefore of C_s—even for the same discharge using the same apparatus.

Furthermore, a second theoretical computation has been established[27] by Mr. Arnaud for a screen surrounded by gravel in which head losses are assumed to be laminar. This computation has been verified by tests on the semicircular model. The results of this theoretical and experimental work show that the minimum length, L, of the screen—beyond which $\Delta H \Big/ \frac{V^2}{2\,g}$ remains constant regardless of further increase of the screen length—depends on the permeability, K, and the thickness of the surrounding material. The resulting formula is

$$\frac{\Delta H}{\frac{V^2}{2\,g}} = f\left(\frac{L\,K}{\log \frac{t}{r}}\,\frac{\sqrt{h}}{C_{qs}}\right) \ldots\ldots\ldots\ldots\ldots\ldots (34)$$

in which ΔH is the drop in head across the screen; K denotes the permeability of the soil; t is the thickness of the surrounding soil; r represents the screen radius; h is the total head loss through the screen, gravel, and aquifer; and C_{qs} denotes the discharge coefficient for the screen slots. The surrounding material also changes the contraction coefficient for the openings and the percentage of open area of the screen. These two changes depend on the relative dimensions of screen openings and gravel. The over-all effect of the surrounding gravel on the screen, characterized by the discharge coefficient, C_{qs} (Eq. 34), was determined by a comparison—at constant discharge—of head losses in a screen and filter of given thickness obtained in the two following cases: (1) A well screen surrounded by fine wire gauze, with a percentage of open area higher than that of the surrounding material, and (2) an ordinary well screen, without wire gauze. The discharge coefficient, C_{qs}, could thus be experimentally determined as a function of the mean diameter of the surrounding grains.

The values of C_s determined by Messrs. Petersen, Rohwer, and Albertson therefore apply only to the conditions on their model—that is, for the filter thickness and voids ratio used by them.

TABLE 4.—RELATIONSHIP AMONG SCREEN COEFFICIENT, GRAVEL SIZE, AND SLOT WIDTH[a]

Screen coefficient (1)	Mean diameter of gravel, in inches (2)	Slot width, in inches (3)	Col. 2 ÷ Col. 3 (4)	Mean value of Col. 4 (5)
0.3	0.075	$\frac{1}{16}$	1.2	1.23
	0.16	$\frac{1}{8}$	1.28	
	0.23	$\frac{3}{16}$	1.23	
	0.3	$\frac{1}{4}$	1.2	
0.4	0.12	$\frac{1}{16}$	1.92	1.9
	0.24	$\frac{1}{8}$	1.92	
	0.36	$\frac{3}{16}$	1.92	
	0.44	$\frac{1}{4}$	1.75	
0.5	0.17	$\frac{1}{16}$	2.71	2.75
	0.34	$\frac{1}{8}$	2.71	
	0.55	$\frac{3}{16}$	2.94	
	0.68	$\frac{1}{4}$	2.71	
0.6	0.24	$\frac{1}{16}$	3.84	4.7
	0.55	$\frac{1}{8}$	4.9	
	0.95	$\frac{3}{16}$	4.9	

[a] Values obtained from Fig. 13.

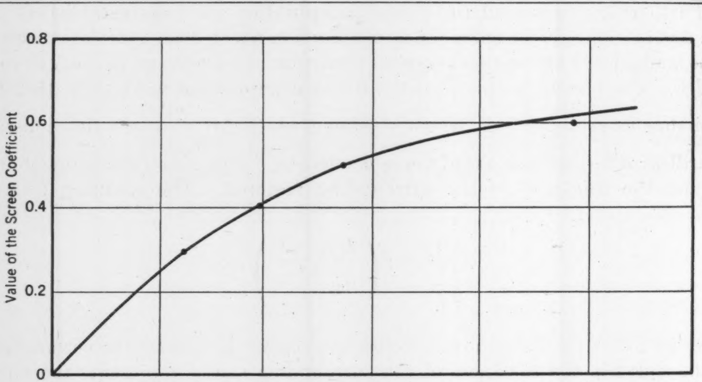

FIG. 23.—VARIATION OF SCREEN COEFFICIENT WITH GRAVEL SIZE AND SLOT WIDTH

The Variation of the Value of the Screen Coefficient.—Fig. 13 represents the variation of C_s as a function of the size of surrounding gravel for different widths of type B screen openings. It appears from Fig. 13 that a geometric similitude does not exist and that different values of C_s can be found for a given ratio of *d* (diameter of gravel) to *s* (slot size). Using the authors' results, it was possible to see that all the curves of Fig. 13 can be reduced to a single curve, with the variation of C_s considered to be a function of d/s (Table 4 and Fig. 23). Geometric similitude is thus obtained for type B screens. It would be interesting to make the same observations for screens of other types.

Practical Application.—The practical application of the results obtained in this study requires a knowledge of the hydro-geologic variables entering into Eq. 34 and of the permeability of the surrounding aquifer. The composition of a natural or artificial filter, intended to prevent sand particles from entering the well and to diminish the loss of head in the immediate vicinity of the well, complicates the problem. The minimum length that can be given to a screen will depend on the thickness of the natural or artificial filter, the hydro-geologic conditions, and the permeability of the filter and aquifer. If it were possible to determine C_s as a function of these variables and to determine the effect of C_s on C, it would be possible to apply Conclusion 1 of the paper.

In view of the difficulties that must be overcome, it can be seen how much knowledge and intuition are needed to determine accurately the minimum length of a well screen. Nevertheless, an examination of the combination of screen and soil shows that a great part of the head loss occurs in the immediate vicinity of the screen because of the convergence of flow. It is then possible to determine an "effective radius of influence," which can be defined as the radius of the zone within which 95% of the total head loss in the combination screen-aquifer occurs. Knowing the soil composition and assuming maximum consolidation, it is possible to determine the minimum economical length of the screen to be installed in a well.

GÉRARD TISON, JR.[28].—At the hydraulic laboratory of the University of Ghent in Belgium, some investigations have been made concerning the resistance to a flow of water through a special type of well screen. The screen was made of steel with large elongated holes and was surrounded by an envelope (of gravel or sand) 14 mm (0.55 in.) thick. The grains of this sand or gravel were bound by plastic matter which was kept to a minimum so that the permeability of the envelope was held as nearly as possible to the natural permeability. The grain size of the sand used in the test sample ranged from 0.7 mm to 1.2 mm (from 0.028 in. to 0.047 in.).

The methods of investigation were slightly different from those used by the authors. A well-screen element 0.86 m (2.62 ft) long and with a 0.076-m (1.93 in.) inside diameter was placed along the horizontal axis of a steel cylindrical tank the diameter of which was 0.90 m (2.74 ft) and the length of which was 1.25 m (3.81 ft). This cylindrical tank (Fig. 24) was closed at its two ends by steel sheets. A 2-in.-diameter pipe which was fitted into one of the end plates of the cylinder was the outlet for the flow through the screen.

The cylindrical tank was connected with a water supply. The pressure in the tank was maintained at a constant magnitude by a valve on the supply pipe. Under the effect of that pressure the water flowed through the well screen. Outside the well screen there was hydrostatic pressure. Inside the well screen the value of the pressure was a maximum at the closed end and a minimum at the outlet pipe.

---

[28] Civ. Engr., Hydr. Lab., Univ. of Ghent, Ghent, Belgium.

Investigations concerning filtration have shown that movement is laminar so long as

$$\mathsf{R} = \frac{V_f\, d}{\nu} < 5 \qquad (35)$$

in which V_f, the filtration velocity, is

$$V_f = \frac{Q}{A_f} \qquad (36)$$

R represents the Reynolds number, d is the effective grain size, ν denotes the kinematic viscosity, and A_f is the area of the filtration surface.

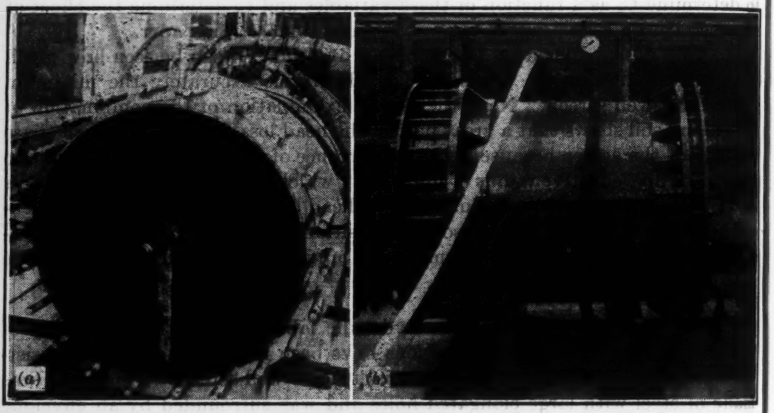

FIG. 24.—HORIZONTAL EXPERIMENTAL WELL SCREEN

Several of the investigations at the University of Ghent satisfied the condition represented by Eq. 35. It is known that in this case the discharge is proportional to the difference of piezometric head between the inside and the outside of the screen. Applying the momentum equation to the flow within the pipe between the closed section (0) through which no flow passes and any section (1) of that pipe,

$$A\gamma\,(h_{pz,0} - h_{pz,1}) = \frac{\rho\, Q^2}{A} \qquad (37)$$

As the piezometric head is constant outside the well screen, Eq. 37 can be written as

$$Q^2 = g\, A^2\,(\Delta h_{pz} - \Delta h'_{pz}) \qquad (38)$$

Differentiating Eq. 38 with respect to the length L results in

$$\frac{dQ}{dL} = \frac{A^2\, g}{2\, Q}\;\frac{d(\Delta h_{pz})}{dL} = \frac{A\,\sqrt{g}}{2\sqrt{\Delta h_{pz} - \Delta h'_{pz}}}\;\frac{d(\Delta h_{pz})}{dL} \qquad (39)$$

However, the increment of discharge dQ into the screen corresponding with an increment of length dL is

$$dQ = K \frac{\pi D}{e} \Delta h_{pz}\, dL \ldots\ldots\ldots\ldots\ldots\ldots\ldots (40)$$

in which e is the thickness of the gravel envelope.

Combining Eqs. 39 and 40 results in

$$dL = \frac{\sqrt{g}\, e\, D}{8\, K} \frac{d(\Delta h_{pz})}{\Delta h_{pz} \sqrt{\Delta h_{pz} - \Delta h'_{pz}}} \ldots\ldots\ldots\ldots\ldots\ldots (41)$$

Integration of Eq. 41 yields

$$L = \frac{\sqrt{g}}{4} \frac{e\, D}{4} \frac{1}{\sqrt{\Delta h'_{pz}}} \text{ arc tan } \sqrt{\frac{\Delta h_{pz} - \Delta h'_{pz}}{\Delta h'_{pz}}} \ldots\ldots\ldots (42)$$

in which the constant of integration equals zero. The value of K for the envelope was found to be 0.00525 m per sec. With **R** equal to 5, it was possible to measure Δh_{pz} in certain sections inside the screen well by using a pitot tube. The results of these measurements (and a comparison of the measured values with those obtained from Eq. 6) are as follows:

Distance between closed end of drain and section, in centimeters	Value of Δh_{pz} from Eq. 42, in meters	Measured value of Δh_{pz}, in meters
0	0.0166	
38	0.0182	0.018
46	0.019	0.019
51	0.0195	0.0195
56	0.0202	0.02
61	0.0215	0.0215
66	0.0229	0.023
71	0.0246	0.025
76	0.0262	0.0265
80	0.0275	0.028
81	0.0278	0.03
82	0.028	0.05

The previously tabulated discrepancies in the value of Δh_{pz} are negligible except for the last sections close to the outlet tube. The discrepancy can be explained by the contraction of flow in the vicinity of the outlet. This contraction increases the velocity and decreases the head inside the tube. Assuming for Δh_{pz} the value 0.0275 m (the last measurement on which the contraction has no influence), it is found from Eq. 40 that $Q = 0.00148$ cu m per sec. The measured discharge was 0.001495 cu m per sec.

When **R** is greater than 5, laboratory tests have shown that the filtration movement is no longer laminar. The discharge is then proportional to $(\Delta h_{pz})^n$ with n having values between 1 and $\frac{1}{2}$. Hence, integration of Eq. 41 becomes impossible.

Jack S. Petersen,[29] **Carl Rohwer,**[30] **and Maurice L. Albertson,**[31] **Members, ASCE.**—Certain interesting ideas worthy of serious consideration have been advanced by Mr. Li. Contrary to Mr. Li's statement, Eqs. 5*a* and 5*b* are correct because they are given simply as the "usual forms." Unfortunately, it was not made clear that, when Eqs. 5*a* and 5*b* are used, the subscripts do not correspond with those in Fig. 1. When applied to the flow approaching and passing through the screen opening and to the jet issuing from the opening, the subscripts must be changed accordingly. Furthermore, the energy which is lost is that of the jet, not that of the longitudinal flow, as implied by Mr. Li. Therefore, Eqs. 5*a* and 5*b* were used in deriving the orifice equation, Eq. 6, which was used to obtain Eq. 14*a*.

Mr. Li states that "* * * one might question the validity of the result for screens surrounded by soil in an aquifer." It is true that the higher the viscosity of the fluid and the lower the permeability of the aquifer, the greater the variation of the piezometric head along the outside of the screen. However, for simplicity in deriving the theoretical equations, this variation was assumed to be of secondary importance. The data (shown in Fig. 11) clearly demonstrate that this assumption was justified.

Within the aquifer at a substantial distance from the screen the flow is undoubtedly laminar, as it must be if Eqs. 19*a* and 19*b* are to be applicable. However, it is possible that for certain conditions the Reynolds number within the gravel envelope is sufficiently high to cause transition flow or even turbulent flow, in which case Eqs. 19*a* and 19*b* are not applicable. If the Reynolds number is greater than 1.0, the flow is no longer laminar; in computing the Reynolds number, D is the grain diameter and V is computed from the bulk area.

Eq. 29, as derived by Mr. Li, is an excellent contribution to the investigation. As in the case of Eq. 16, however, such a derivation is no stronger than its weakest assumption. The final test is its comparison with the data. Therefore, experimental data are necessary to establish the exact influence of each of the parameters in Eq. 29.

In Eq. 32, m is assumed to be independent of the loss coefficient and the screen coefficient, and Eq. 33 further depends on m being equal to unity—all of which are not necessarily true. The writers have evaluated all the data at their disposal (including experiments they have made using a gravel envelope), and in no case is the loss coefficient less than 1.0. Therefore, despite the ingenious derivation of Eq. 33 and the desire of the writers to utilize it, it must be concluded that either the limiting assumptions make it invalid or the range of experimental data is not sufficiently wide to include this special case.

Although the open-bottom wells described by Mr. Collins are used successfully in coping with the problem of sand pumping when suitable clay or rock strata cover the aquifer, there are many areas where these strata are not strong enough to support the overlying material. Where this condition exists other methods of constructing wells have to be adopted. Other types of wells may sometimes develop large cavities similar to those produced in open-bottom wells; this condition is dangerous because collapse of the roof over the cavity may ruin the well. One reason for the use of gravel-packed wells is that the gravel tends to prevent the formation of these cavities.

---

[29] Instructor, Univ. of Missouri, Columbia, Mo.

[30] Fort Collins, Colo.

[31] Prof. of Civ. Eng. and Head of Fluid Mechanics Research, Colorado Agri. and Mech. College, Fort Collins, Colo.

It was not the intention of the writers to recommend the construction of any one type of well but, because wells with screens (with or without gravel envelopes) are most common, a study of the hydraulic principles governing the flow of water into such wells seemed desirable.

As to the questions raised by Mr. Collins regarding the tests, it is believed that well drillers should take account of the facts established by the laboratory experiments. The writers, however, are aware that field confirmation of the proposed theory of flow is desirable even though the laboratory tests were in remarkably good agreement with the theory.

The writers are interested in the experiments on the loss of head through screens and gravel packs reported by Messrs. Nazir and Ahmad. The report on the results of loss-of-head tests on screens with larger percentages of openings should be most valuable. Although the results reported in Table 3 show, in general, that the head losses through the screens decrease as the percentage of open area increases, the tests on the screens with larger openings should demonstrate that the losses become constant. The data on the loss of head through the gravel for a constant suction head indicate that the loss decreases as the discharge increases for the larger slit openings. It is difficult to understand why this decrease should occur unless fine material was being washed out of the gravel.

Although the wells in Pakistan have values of $(C\,L)/D$ greater than 30, it does not necessarily follow that all of the screen in the well is effective in decreasing the loss of head. If the writers' analysis is valid, only that part of the screen which will make $(C\,L)/D = 6$ will be utilized (Fig. 17). However, it was not their intention to imply that the loss of head would be the same minimum regardless of the discharge. For each discharge there is a minimum loss which an increase in the length of screen or the percentage of openings will not reduce.

Mr. Peterson's suggestion that a "double effective" length might be developed in a well by properly locating the suction inlet seems reasonable. This phase of the problem was not investigated, but the flow from above the suction inlet—as well as the flow from below the suction inlet—should follow the criterion presented by the writers.

The experiments performed at the University of Ghent, as reported by Mr. Tison, take into account the effect of a special gravel envelope on the head losses through the screen. Although the equipment and the analysis differed from those used by the writers, the head losses follow the pattern reported by them, as shown in Figs. 16, 17, and 18. Unfortunately, the percentage of openings and the coefficient of discharge are unknown for this type of screen. Otherwise it would have been possible to compute the length of screen required to reach the limiting value of $(C\,L)/D = 6$.

The writers are of the opinion that, if the (Δh_{ps})-values for distances of 82 cm (32.3 in.) and 86 cm (33.8 in.) between the closed end of the drain and the section had been measured, still larger head losses would have been observed. It is also believed that the observed losses reported by Mr. Tison may be more nearly correct than the computed losses.

Problems involving many variables can be approached in many ways; different investigators may derive formulas of different form for the solution of the same problem by using a different approach. Eq. 34 reported by Mr. de Lara, provides for the thickness and permeability of the gravel envelope whereas Eq. 15 takes account of the gravel envelope in so far as it affects the value of C by changing the orifice coefficient and the effective open area of the screen. As shown in Figs. 14 and 15, the loss through the screen is independent of the gravel envelope except when the percentage of open area in the screen is inadequate and the size of the gravel is small.

An important relationship based on Fig. 13 is shown by Mr. de Lara in Table 4 and Fig. 23. Fig. 23 shows that the curves for the different slot openings in Fig. 13 can be combined into a single curve by substituting the ratio d/s for the gravel size. However, when d/s is less than 1, the gravel particles would not be held back effectively by the screen, and an unstable condition would result. For this reason the part of the curve for d/s less than 1 should either be eliminated from Fig. 23 or be shown as a broken line. No doubt the screen coefficients for the type C screens could also be plotted theoretically on a single curve because of the geometrical similitude of the slots in these screens. However, these screens have a relatively large percentage of open area, and as a result most of the tests were in the range in which the head losses were a minimum—that is, $(C\,L)/D$ greater than 6. Consequently, sufficient data are not available for the analysis because the effective length of the screen is unknown.

The writers recognize that the conclusions stated in the paper require confirmation by field tests. Their primary purpose was to call attention to the peculiarities of flow into wells that had not been previously reported.

As noted by Mr. Rorabaugh, the data are based on tests of screens that do not penetrate the aquifer completely. The original plan for the tests included the installation of flexible disks in the gravel at the top and bottom of the perforated area of the screens so that all the water would approach the screen radially and horizontally. This plan was not satisfactory because the disks moved as the gravel settled. The disks also produced a plane of different permeability at the top and bottom of the screen. For these reasons the disks were not used.

It should be noted that complete penetration of the screen would not have eliminated the converging flow lines because the tests showed that most of the water entered the screen at the discharging end. This condition tends to concentrate the flow lines at the discharge end. The same effect is shown by the tests reported by Mr. Tison and by Mr. Li in Fig. 19.

The head loss through the screen and the gravel pack is a small fraction of the total drawdown because most of the head loss occurs in the aquifer. The loss in the aquifer depends on the discharge and the characteristics of the aquifer and not on the screen or the gravel pack.

In Mr. Rorabaugh's analysis of the drawdown in a well in an artesian aquifer under conditions of full and partial penetration it is shown that the drawdown decreases as the depth of penetration increases. No doubt this is true under certain conditions, but the writers believe that it may not be true if the length of screen required to make the value of $(C\,L)/D$ equal to 6 is less than the depth of penetration. So far as is known, these two conditions have never been checked by actual tests. Such a test is possible and would certainly yield useful results.

The writers appreciate the interest shown by all those who have contributed discussions. It is hoped that this work will lead others to investigate the problem by conducting field tests wherever conditions are favorable.

AMERICAN SOCIETY OF CIVIL ENGINEERS
Founded November 5, 1852
TRANSACTIONS

Paper No. 2756

THE TRAINING OF CITY PLANNERS

BY HOWARD K. MENHINICK [1]

WITH DISCUSSION BY MR. JORMA J. SALOVAARA

SYNOPSIS

Following a review of the trends that affect instruction in city planning, the contents of a graduate curriculum in city planning are outlined. Such a curriculum should contain seminars that include (1) the major aspects of urban community development, (2) illustrations of the required integration between the various professions, and (3) an investigation of the sociological and psychological techniques in city planning. Students should also be shown the place of planning in local government.

TRENDS AFFECTING INSTRUCTION IN CITY PLANNING

Cities are aware of the need for planning their future growth and development. The problems caused by suburban migration—(1) a dispersed and scattered population which must receive customary governmental services, (2) downtown traffic congestion and lack of adequate parking spaces, (3) public transit systems whose services are declining at a time when they should be increasing, (4) slum areas that are developing more rapidly than they can possibly be cleared and redeveloped, and (5) antiquated zoning ordinances that have long since ceased to be useful for guiding the utilization of urban land—are tangible evidences that the business of building and running a city, as any other enterprise, cannot be accomplished satisfactorily without adequate long-range planning. If these evidences were not enough, the increasing costs of public services and the inadequate yields of the sources of tax revenue that are available to cities are compelling arguments for the most efficient possible development and operation of these cities.

The result of the rapidly increasing utilization of planning to help solve the pressing problems that are facing cities is an acute shortage of well-trained city

---

NOTE.—Published, essentially as printed here, in March, 1954, as *Proceedings-Separate No. 423*. Positions and titles are those given when the paper or discussion was received for publication.

[1] Regents' Prof. of City Planning, Georgia Inst. of Technology, Atlanta, Ga.

planners. This shortage appears likely to continue (as of 1954) because too few first-rate men are being trained for the profession. This is largely a result of the fact that college students are not made aware of the challenging needs and opportunities afforded by the rapidly developing profession of city planning. Too much city planning is being done by well-meaning but incompetent persons; there does not exist the necessary competition for jobs that would weed out those who are not qualified. Cities suffer, and the prestige of city planning as an important function of government is lowered. Consequently, colleges and universities should endeavor to train competent city planners in order to perform a greatly needed service.

Not only are increasing numbers of cities recognizing the need for city planning, but the very nature of planning is changing. At one time, city planning was conceived of primarily as an engineering blueprint—a master plan which incorporated a planner's knowledge of how streets, parks, railroads, and other physical facilities should be located and designed, all in proper relation to each other. There was also a time when planning was considered a "one-shot" enterprise with the master-plan blueprint as its objective. Although a significant number of isolated accomplishments can be credited to the best of these plans, many of them have wound up on library shelves rather than as accomplishments in brick and steel.

The master plan is certainly a key tool in the planning process, but it is only one of a number of important tools and is most certainly not the end product of planning. The plan's usefulness is limited by the fact that many public agencies and thousands of individuals daily make decisions regarding city planning and development. If these many daily decisions are to be influenced, guided, and brought into harmony to produce a well-planned and well-developed city, planning must proceed not as an effort made once in a decade but as a daily operation. The objective should be not a "planned city" but a "planning city." This objective requires a different kind of training than was needed to produce a master-plan blueprinter.

In this connection, it is significant that in an increasing number of cities planning is an accepted function of government. These cities are establishing adequately staffed departments of city planning which coordinate their work with other city departments and are headed by a planning director reporting directly to the city's chief administrative officer. Specialists as well as directors are needed for these staffs. The object of the training of city planners should thus be to produce graduates who can soon make worthwhile planning contributions, particularly in the fields in which they have had their undergraduate training. The graduates should also be trained broadly enough so that they can eventually perform the planning coordinating function that is the unique contribution of the city planning profession.

It is generally recognized that many of the problems of city development are so complex that they cannot be solved, except superficially, by the efforts of any one man or, indeed, any one profession. A team is usually required. Less argument is offered now (1954) than previously as to whether planning is the appropriate province of the architect, the landscape architect, or the civil engineer. All three professions and many others have important contributions to make. Most people are convinced that the involved problems of urban development require the participation and collaboration of many different professions and disciplines—civil engineering, architecture, landscape architecture, sociology, economics, psychology, geography, and public administration. At the same time, city planning—as a discipline—has principles and techniques which are its particular contribution. There is an opportunity and a need for those who are primarily planning specialists in one of the long-established professions or disciplines. There is also a need for planners with general knowledge who are capable of performing the essential coordinating functions. Both those with a general background and those with special knowledge require a broad understanding of the problems of urban development—the one, to contribute his specialty properly to the total picture and the other, to perform competently the coordinating function. In addition, those who have a general understanding of planning require executive and leadership ability to enable them to serve as directors of planning undertakings.

In the light of these developments in the profession of city planning, a graduate school should admit as candidates outstanding persons who have a degree in one of the previously cited disciplines or in the humanities. Men with training in these various fields can make unique contributions to city planning. In working together as a team in the solution of city planning problems, a group of students with diverse backgrounds gains valuable first-hand knowledge of the techniques and of the possible contributions of the various professions. They develop early a habit of interdisciplinary collaboration which will be of value to them throughout their subsequent professional careers. It is also advantageous to have a number of students from those countries that have developed planning to a high degree. These men are able to contribute a knowledge of the planning policies and techniques that are in use in their countries and, in turn, gain an understanding of the planning experience of the cities in the United States.

The Planning Curriculum

The core of a graduate city planning program should be a series of interrelated seminars and studies of drafting room and field problems covering the major aspects of urban community development—streets, transit, railroads, ports, airports, and utilities; schools and other public buildings; parks, playgrounds, and other public open spaces; and residential, business, and industrial districts. Various devices for effecting a plan, such as zoning ordinances, land-subdivision regulations, mapped-street acts, urban-redevelopment programs, and capital-expenditure budgets, should also be included.

Seminars which provide a basis for field problems should include instruction in urban sanitary facilities and urban transportation systems such as highways, railways, waterways, ports, and airports, given especially for the graduate city planning students by the civil engineering department. The objective should be to give enough instruction so that the student who is not a civil engineer will understand the important aspects of these subjects.

Seminar instruction should also include problems in the preparation of land-use surveys, land-use plans, and urban-redevelopment projects. The social sciences make important contributions to these problems. For example, simultaneously with a field problem in urban redevelopment, the students might participate in a seminar which would deal, in part, with the solution of the human and governmental problems encountered in an urban-redevelopment project. It is obvious that, unless the human, governmental, and political problems can be satisfactorily resolved, the planner will have no opportunity to solve the physical problems. In this same course, the students might attend, observe, and criticize group conferences seeking to resolve issues, such as controversial meetings of various zoning boards. This particular instruction should be given on the theory that basic policy decisions in planning, as opposed to technical decisions, should be made by the citizens of a community through the various democratic processes that are available to them. It is therefore important that the planner learn how to conduct hearings and conferences in a manner that will effectively elicit the viewpoints of the participants as an important step in the process of making democratic planning decisions.

Because city planning is basically a governmental function, students in a governmental seminar should learn the place of planning not only in the nominal structure and functioning of local government but also in the less readily discernible community power structure. In still another seminar, students should gain an insight into the nature of the economic resources of communities, techniques for at least roughly measuring these resources so that plans prepared for a community may bear a proper relation to the community's ability to pay, and an understanding of the effects of various kinds of planning decisions on a community's economic base.

In their daily work, planners are required to write clear, convincing reports and to explain and defend their recommendations at public meetings. There should be required a course in speaking and writing on planning subjects; the students might give a public talk and prepare a manuscript suitable for publication on some aspect of planning. Statistics is another field in which students should gain reasonable competence.

The curriculum should aim to provide enough training in the skills and special techniques of the profession so that graduates will be able to take their places as immediately useful members of the staffs of planning agencies and of planning consultants. At the same time, the program must give the students a broad understanding of cities—their functioning, their planning limitations, and their planning opportunities—so that in the ensuing years of the students' professional careers they may rise to positions of planning leadership where they can make important contributions to the improvement of the urban environment in which increasing numbers of the people of the world are destined to live, work, and play.

Cooperative Program

A significant development is a cooperative program of city planning instruction, research, and service in the South whose joint participators are the Georgia Institute of Technology, at Atlanta, the University of North Carolina, at Chapel Hill, the University of Oklahoma, at Norman, and the Southern

Regional Education Board, at Atlanta. Other interested institutions and agencies of the fourteen southern states of the United States joined with these three institutions and the board in a Southern Regional Congress on City Planning held in 1952 at Roanoke, Va. The participants in the congress identified the principal city planning problems of the South and jointly recommended programs of instruction, research, and service that would contribute to the solution of these problems. The recommendations are in the process (as of 1954) of being implemented.

Additional universities which propose to develop strong programs in the field of city planning will be invited to become members of the cooperative program. States that decide to concentrate their university resources on programs in other fields for which they consider themselves especially well-equipped have the privilege of sending their residents who wish to study city planning to one of the cooperating institutions that has elected to develop strength in the field of city planning.

Conclusions

City planning is rapidly becoming a profession in its own right. It incorporates the skills and resources of many professions. The training program that is devised for city planners must therefore be arranged so that all who enter will be shown the necessity of correlating the knowledge of city planning with other basic training. Only by such studied planning of a curriculum can the graduate of the program be expected to assume his logical role in the community.

DISCUSSION

Jorma J. Salovaara,[2] A. M. ASCE.—In his analysis under the heading, "Trends Affecting Instruction in City Planning," Mr. Menhinick in commenting on master plans states that:

> "The plan's usefulness is limited by the fact that many public agencies and thousands of individuals daily make decisions regarding city planning and development."

This fact, far from limiting the usefulness of a master plan, makes imperative the need for this "key tool." Whereas the master plan is "most certainly not the end product of planning," some such guide—which contains an over-all approach, is realistically conceived and sufficiently flexible to permit changes or variations in even its principal recommendations, and is capable of widespread dissemination—is needed if a proper coordination of the many diverse activities and community interests is to be achieved and directed toward the planning and building of a better city. That "many of them [master plans] have wound up on library shelves rather than as accomplishments in brick and steel" is not a failure inherent in the so-called blueprint but is rather the result of a failure to promote and sell the concept underlying a "planning city" as differentiated from the "planned city." More often than not, good solutions to city planning problems have gone begging for want of the ability or technique to promote and sell them to those who must implement them.

In presenting the content of a planning program (under the heading, "The Planning Curriculum") the author notes that:

> "It is * * * important that the planner learn how to conduct hearings and conferences in a manner that will effectively elicit the viewpoints of the participants as an important step in the process of making democratic planning decisions."

It is even more vital that planners understand generally why such a procedure is necessary and, specifically, the fundamental importance of active citizen participation in both the formulation of the master plan and in the continuing planning process if they are ever to realize the adoption of even a limited number of the proposals and solutions recommended.

Just as the planner must understand and deal with a community's economic, political, and social problems before he can hope to present solutions to its physical problems, so must the recommended solutions be understood and sold to those who will actually implement the proposals of the master plan. The careful selection of a citizens' committee and the well-planned organization of its task force teams for surveying individual or technical aspects requiring consideration will prove invaluable to the city planner and his staff. Such a procedure is indispensable if a general understanding of the continuing nature of planning and the specific acceptance of a master plan are to be had. Truly representative bodies, comprised of key citizens each with either (*a*) interests that are technically involved, (*b*) interests as taxpayers, and (*c*) interests as government administrators should be selected. With due concern given to a geographical and a political distribution and to the selection of women as well as men, such a representative body should assure consideration and treatment of all the underlying problems and permit a satisfactory compromise to be reached for most of the conflicts present. In any event, such participation by the citizens concerned will serve to negate a frequent charge that the plan is that of a special group or interest, or that it was conceived by an outside expert. Such participants form a corps of salesmen prepared to explain and defend the decisions made, to promote and sell the proposals and recommendations of the master plan, and to secure compliance and enforcement of its provisions through building and zoning regulations should such action become desirable or necessary.

---

[2] Executive Secy., Schuylkill County Branch, Pennsylvania Economy League, Inc., Pottsville, Pa.

The best-made master plan will go astray if its dissemination is restricted because too few copies at too high a price were included in the budget, if the mass media of information—newspapers, local magazines, radio, and television—are not utilized, or if its promotion among the school children of the community was overlooked. Inculcation as to the benefits obtainable from a systematic planning for the growth of a city and the orderly revision of such plans in the face of changing needs cannot be undertaken too early in the lives of its future active citizens.

AMERICAN SOCIETY OF CIVIL ENGINEERS
Founded November 5, 1852
TRANSACTIONS

Paper No. 2757

ANALYSIS AND TESTS OF A CYLINDRICAL SHELL ROOF MODEL

By Bruno Thürlimann[1] and Bruce G. Johnston,[2] M. ASCE

With Discussion by Messrs. G. C. Ernst; Charles S. Whitney; Boyd G. Anderson; and Bruno Thürlimann and Bruce G. Johnston

Synopsis

Analytical expressions for the effective width of cylindrical shells are presented herein. These formulas are used for the analysis of a cylindrical shell roof acted upon by horizontal longitudinal forces. Also studied are the influences of foundation movements, temperature changes, and shrinkage.

A comparison is made between theoretical results and experimental measurements obtained from a model of an actual cylindrical shell roof constructed in the approximate ratio of 1 to 30. It is established that there is satisfactory agreement between the theoretical analysis and the test results.

Notation

The letter symbols adopted for use in this paper are defined where they first appear, in the illustrations or in the text, and are arranged alphabetically for convenience of reference in Appendix I.

Introduction

It is a common misconception that the use of shells as structural elements is a development of the twentieth century. Two thousand years ago, the Romans constructed the Pantheon, which was covered by a spherical shell with a diameter of approximately 145 ft. The cupolas of the cathedral in Florence (Italy) and St. Peter's Basilica in Rome (Italy), built during the fifteenth and sixteenth centuries, respectively, and having diameters of approximately 140 ft, are examples of remarkable craftmanship, based only on

---

Note.—Presented at the Centennial Convocation, Chicago, Ill., September, 1952. Published, essentially as printed here, in April, 1954, as *Proceedings-Separate No. 434*. Positions and titles given are those in effect when the paper or discussion was received for publication.

[1] Research Asst. Prof., Fritz Eng. Lab., Lehigh Univ., Bethlehem, Pa.

[2] Prof. of Structural Eng., Civ. Eng. Dept., Univ. of Michigan, Ann Arbor, Mich.; formerly Director of Fritz Eng. Lab., Lehigh Univ., Bethlehem, Pa.

experience and intuition. The contribution of the twentieth century to this type of construction consists in the development of a rational analysis which can be used to predict the state of stress in the shell.

The development of the shell theory was initiated by A. E. H. Love (1)[3] who derived the differential equations for curved plates. E. Meissner (2) (3) succeeded in integrating these equations for spherical and conical shells. F. Bauersfeld (4), U. Finsterwalder (5), and F. Dischinger (6) made possible the application of the theory to the analysis of actual structures. Several reinforced concrete shells were built in Europe immediately following World War I, and there were concurrent theoretical contributions.

The arena in Hershey, Pa., built in 1936 (7), was the first modern cylindrical shell roof constructed in the United States. In the years that followed, and especially during and subsequent to World War II, a number of shell roofs were built—to be used as storage houses, factory buildings, airplane hangars, sport arenas, and armories—covering a total of 10,000,000 sq ft.

At present (1953) the largest span for a cylindrical shell roof is 340 ft (the hangars at Rapid City, S. Dak. (8) and at Limestone, Me. (9)). These large-span structures accentuated certain problems which were of secondary importance in the previously built smaller structures. Because there is a tendency toward increasing the span of shell structures, a careful analysis of the pertinent problems is mandatory.

The supporting ribs in cylindrical shell roofs can be designed as T-sections to include the additional effective section provided by the shell. A study (10) of the interaction between the ribs and shell shows that an "effective width" of the shell can be determined and the combined section used in a relatively simple arch analysis of the rib structure.

Lateral horizontal forces, caused by wind action on the front and back doors of large-span cylindrical shell roofs, can reach a considerable magnitude. The influence of these forces on the structure cannot be considered secondary. A difference of temperature inside and outside the building can produce relatively high thermal stresses. Shrinkage and plastic flow greatly affect the stability of the structure. These are a few of the problems to be considered in the analysis of large shell roofs.

During the period from January 1, 1949, to February 15, 1951, a research program on shell arch roofs was conducted at the Fritz Engineering Laboratory of Lehigh University at Bethlehem, Pa., with special emphasis on the previously cited problems. A careful theoretical study of the problems was made, and the results were checked experimentally on the model of a cylindrical shell roof shown in Fig. 1. This paper presents three contributions to the analysis of shell roofs made during the course of the research program. It will be shown that the model tests were in excellent agreement with the theory.

EFFECTIVE WIDTH OF CYLINDRICAL SHELLS

The stress distribution in the flange of a T-beam with a straight axis, subjected to bending in the plane of the rib, is not constant over the width of the

---

[3] **Numerals in parentheses—thus, (1)—refer to corresponding items in the Bibliography (see Appendix II).**

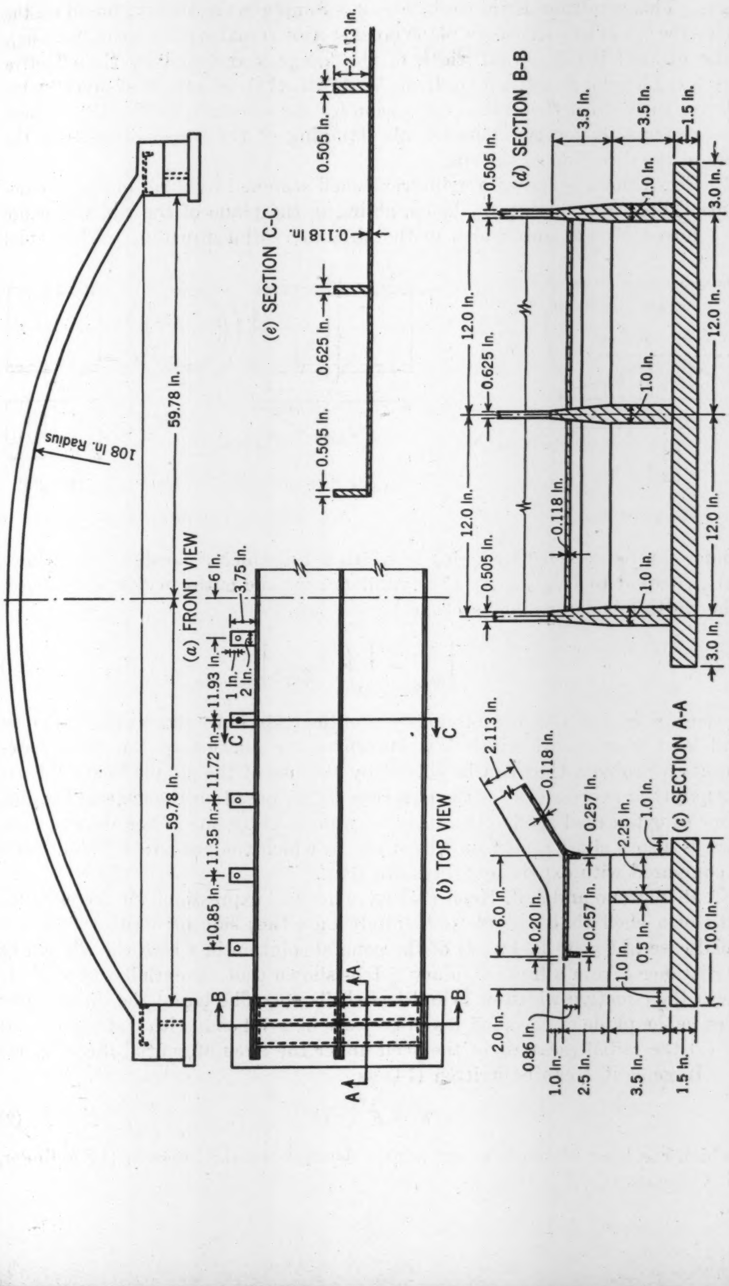
108 In. Radius
59.78 In.
59.78 In.
(a) FRONT VIEW
6 In.
3.75 In.
10.85 In.
11.35 In.
11.72 In.
11.93 In.
1 In.
2 In.
C
C
B
B
A
A
(b) TOP VIEW
(e) SECTION C-C
0.505 In.
0.625 In.
0.505 In.
0.118 In.
2.113 In.
(d) SECTION B-B
0.505 In.
0.625 In.
0.505 In.
12.0 In.
12.0 In.
0.118 In.
1.0 In.
1.0 In.
1.0 In.
3.5 In.
3.5 In.
1.5 In.
3.0 In.
12.0 In.
12.0 In.
3.0 In.
(c) SECTION A-A
2.113 In.
0.118 In.
0.257 In.
0.257 In.
6.0 In.
0.20 In.
2.0 In.
0.86 In.
2.25 In.
1.0 In.
1.0 In.
0.5 In.
10.0 In.
1.0 In.
2.5 In.
3.5 In.
1.5 In.

FIG. 1.—SHELL ROOF MODEL

flange. This condition is shown in Fig. 2. Simple beam theory, based on the Navier-Bernoulli hypothesis (a plane cross section remains plane after bending), can be utilized if the actual width of the flange is replaced by the effective width b. Theodor von Kármán, Hon. M. ASCE (11), was the first investigator to derive the correct theoretical expression for this effective width (12). Shear lag is responsible for the considerable damping of the direct stresses in the flange in the direction of the rib.

In Fig. 3 there is shown a cylindrical shell stiffened by a rib in the circumferential direction. Arbitrary loads, acting in the plane of the rib, will cause direct forces N_ϕ per unit width in the circumferential direction. The actual cylinder can be replaced by a ring of width b, for which a constant direct force $(N_\phi)_{x=0}$ (equal to $(N_\phi)_{x=0}$ for the cylinder) over the entire width is assumed. If the width b is determined so that

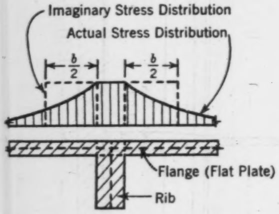

Fig. 2.—T-Beam

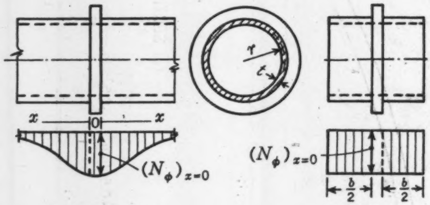

(a) CYLINDER (b) RING

Fig. 3.—Cylindrical Shell

$$\left[b(N_\phi)_{x=0}\right]_{\text{Ring}} = \left[\int N_\phi \, dx\right]_{\text{Cylinder}} \quad \ldots\ldots\ldots\ldots\ldots (1)$$

the stresses in the ribs are obviously identical for both structures under an equal load system. If width b is known, determination of the rib stresses becomes a problem that can be solved by the use of the simple beam theory.

Analytical expressions for the effective width, based on the general bending theory of cylindrical shells (13), have been derived by one of the writers (14). There is also a short report on this study in which the analytical values for b are compared with experimental results (10).

C. B. Biezeno and J. J. Koch (15) have derived expressions for the effective width of a shell that extends indefinitely on either side of a rib. This is a special case ($\beta l = \infty$ in Fig. 4) of the general solution in which the rib can be any distance l from a free boundary. It is shown that, essentially, two effects govern the effective width of cylindrical shells: (a) The lag of the direct shear forces in the plane of the shell (as in the case of a T-beam with a straight axis) and (b) the radial escaping of the shell under the circumferential direct forces N_ϕ. In general, b can be written (14) as

$$b = K \sqrt{r\,t} \quad \ldots\ldots\ldots\ldots\ldots\ldots\ldots\ldots (2)$$

in which r is the radius of the cylinder, t denotes the thickness of the cylinder, and K equals $f(\lambda, \beta l)$ (Fig. 4).

The parameter λ (Fig. 4) takes into account the influence of the direct shear forces on the effective width

$$\lambda = n\sqrt{\frac{t}{r}} \quad \text{(3)}$$

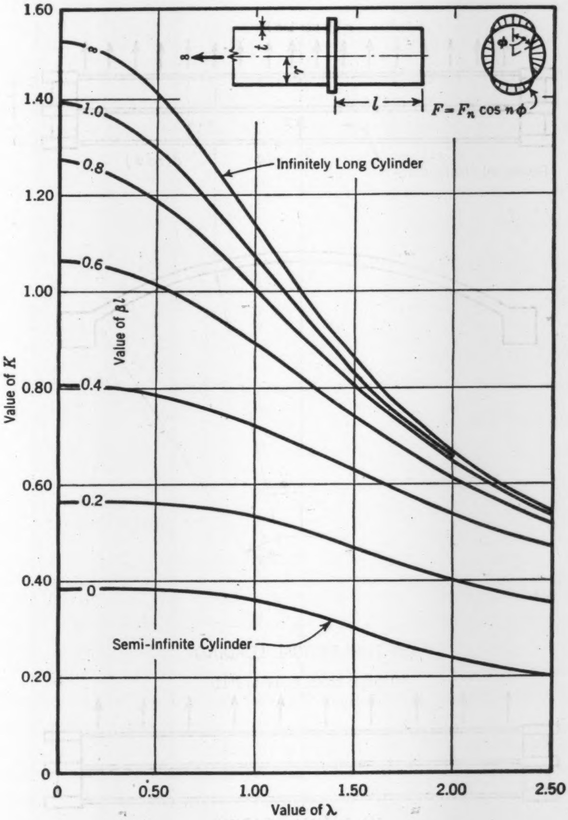

FIG. 4.—THE RELATION AMONG K, λ, AND β

in which n depends on the variation of the stresses in the circumferential direction and is the number of complete waves made by a harmonic function around the circumference of the cylinder (Fig. 4). For n equal to zero, the stress distribution has axial symmetry, and the effective width has its maximum value. The parameter $\beta\, l$ is dependent on the length of the overhang of the shell l and on the shell constant (13a)

$$\beta = \frac{\sqrt[4]{3}}{\sqrt{r\, t}} \quad \text{(4)}$$

As shown in Fig. 4, the shell is assumed to extend infinitely on the left side. This can be assumed safely if the product βs exceeds 2.4, in which s is the distance of the left end from the rib (14*a*).

Taking the effective width b as the flange and the rib as the web of a T-section, the Bernoulli-Navier hypothesis leads to the correct values for the rib stresses. Also, denoting the circumferential stress along the connecting line of rib and shell by σ_a, the total direct force F in the shell is the integral of all direct forces ($N_\phi = \sigma_\phi t$) over the entire length of the shell or is equal to the product of the stress σ_a, the thickness t, and the effective width b. Thus,

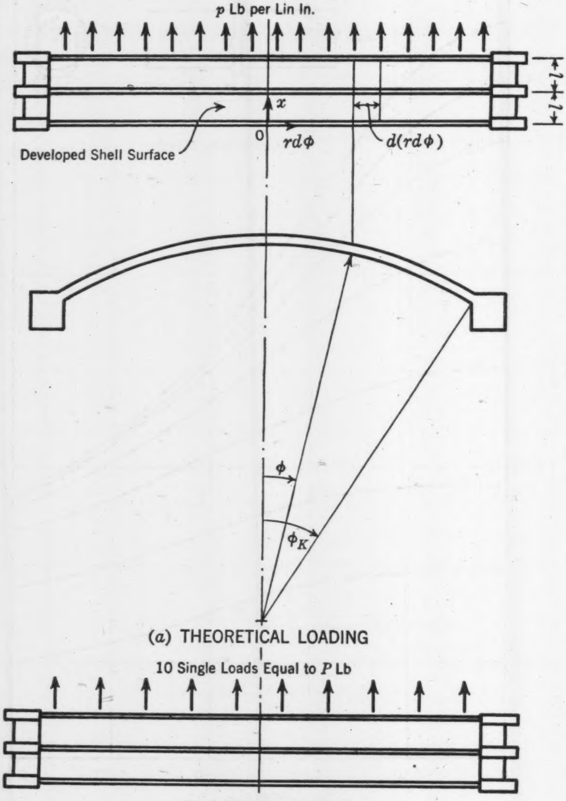

(*a*) THEORETICAL LOADING

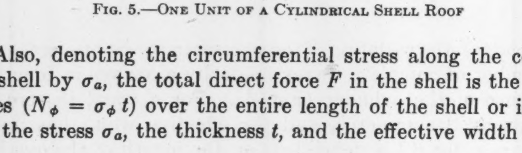

(*b*) ACTUAL LOADING

FIG. 5.—ONE UNIT OF A CYLINDRICAL SHELL ROOF

$$F = \int N_\phi \, dx = \sigma_a \, t \, b \qquad (5)$$

For a given value of F and a given set of boundary conditions, all forces and moments in the shell can be determined. Tables and graphs which reduce these computations to a minimum are available (14).

Knowledge of the effective width of a cylindrical shell simplifies an involved problem of elasticity to a common problem of the ordinary beam theory. This effective width will be used subsequently in the analysis of shell roofs.

THE EFFECT OF HORIZONTAL LONGITUDINAL FORCES

The action of the wind on the front and back doors of cylindrical shell roofs produces considerable horizontal forces. This type of loading will be analyzed, and numerical results will then be compared to test results obtained on a model.

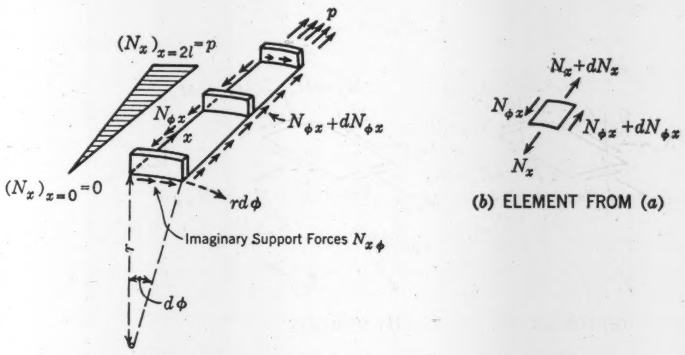

(a) INFINITESIMAL WIDTH

(b) ELEMENT FROM (a)

FIG. 6.—PART OF A SHELL ROOF

During construction, the roof is erected in units in order to re-use the forms and to provide expansion joints. One unit of a cylindrical shell roof is shown in Fig. 5; it is subjected to horizontal forces in the direction of the axis. On a cross section a shear force V, a bending moment M_B, and a twisting moment M_T are acting. It is necessary to find the stress distribution resulting from these forces and moments.

In Fig. 6 there is shown a part of a cylindrical shell of infinitesimal width $r\,d\phi$. The forces and moments acting on the shell element are defined in Fig. 7. The direct force N_x in the axial direction is equal to the applied uniformly distributed load p at the rib $x = 2\,l$. The force N_x equals zero at the rib $x = 0$. Assuming a linear variation of N_x along the x-axis, then

$$N_x = \frac{x\,p}{2\,l} \quad \text{(6a)}$$

and

$$\frac{\partial N_x}{\partial x} = \frac{p}{2\,l} \quad \text{(6b)}$$

The assumption of a linear variation of N_x is especially true for shell roofs whose width is relatively small in comparison to the span L. The equilibrium of an infinitesimal shell element $dx\, r\, d\phi$ in the x-direction (Fig. 6) results in

$$\frac{\partial N_x}{\partial x}\, dx\, r\, d\phi + \frac{\partial N_{\phi x}}{\partial \phi}\, d\phi\, dx = 0 \ldots\ldots\ldots\ldots\ldots\ldots (7a)$$

Replacing $\partial N_x/\partial x$ by its value from Eq. 6*b* results in

$$\frac{\partial N_{\phi x}}{\partial \phi} = -\frac{r\, p}{2\, l} \ldots\ldots\ldots\ldots\ldots\ldots (7b)$$

By integrating Eq. 7*b* and considering the fact that, because of symmetry, the shear force $N_{x\phi}$ is zero at the center of the span, $N_{\phi x}$ becomes

$$N_{\phi x} = -\frac{r\, p\, \phi}{2\, l} \ldots\ldots\ldots\ldots\ldots\ldots (8)$$

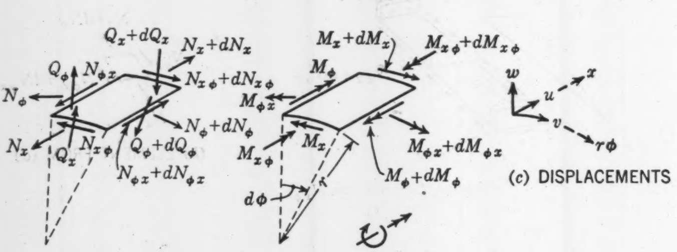

(*a*) FORCES (*b*) MOMENTS

FIG. 7.—FORCES AND MOMENTS ACTING ON THE SHELL ELEMENT

It follows that $N_{\phi x}$ is constant for a section in which ϕ is a constant and varies in proportion to the angle ϕ along the span of the shell. From the equality of the shearing stresses ($\tau_{\phi x} = \tau_{x\phi}$) the direct shear forces, $N_{x\phi}$, in a radial direction can be considered equal to the direct shear forces $N_{\phi x}$. Thus,

$$N_{x\phi} \cong N_{\phi x} = -\frac{r\, p\, \phi}{2\, l} \ldots\ldots\ldots\ldots\ldots\ldots (9)$$

Eq. 9 is a reasonable approximation, but it should be realized that $N_{x\phi}$ is not exactly equal to $N_{\phi x}$ as a result of the curvature of the shell (16).

If imaginary support forces $N_{x\phi}$ acting along the outer ribs ($x = 0$ and $x = 2\, l$) are assumed, the shell is in equilibrium under the load p and is subjected only to shear forces $N_{x\phi}$ and $N_{\phi x}$ and to direct forces N_x. Actually these imaginary forces are not acting. Introducing the shear forces $-N_{x\phi}$ along the connecting line of the shell and the ribs, the imaginary forces $N_{x\phi}$ are eliminated. This procedure is similar to the method of moment distribution. In that method, the joints are locked by imaginary moments which afterward are eliminated by introducing moments in the opposite direction. The interaction between the rib and the shell is accounted for by considering the effective width of the shell as a flange of the rib. This effective section, consisting of the rib and the effective width, is used in analyzing the arches.

Analysis of the Ribs.—The rib at $x = 2\,l$ is acted upon by shear loads, $N_{x\phi}$ per unit length, along the connecting line of the rib and the shell. The loads are considered positive as shown in Fig. 8. On the rib x equal to zero, the positive $N_{x\phi}$-forces are acting in the opposite sense. Fig. 6 shows the sign convention for the forces $N_{x\phi}$. The distance from the loads $N_{x\phi}$ to the centroidal axis of the effective section is equal to z_A. The rib is an elastically restrained arch, having only two redundants as a result of the symmetry of the structure and the load with respect to the center line. In Fig. 8 one half of one rib is shown with the horizontal thrust H_c and the bending moment M_c as redundants at the center. The two geometrical conditions furnishing the two equations for the determination of H_c and M_c are a known horizontal movement δ_K of the foundation and a known rotation θ_K. For a fully restrained rib the conditions are

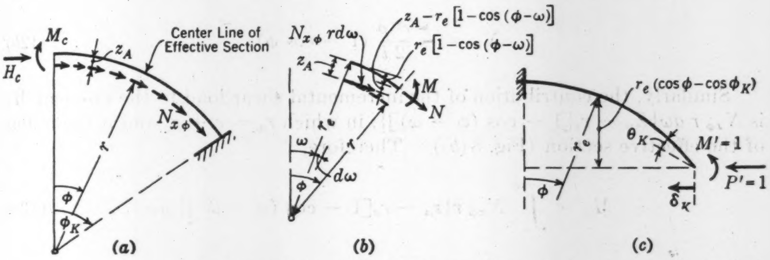

FIG. 8.—SHEAR LOADS UPON THE ROOF SHELL

$$\left.\begin{aligned} \phi = \phi_K : \delta_K &= 0 \\ \theta_K &= 0 \end{aligned}\right\} \ldots\ldots\ldots\ldots\ldots\ldots\ldots\ldots (10)$$

In the case of an elastically restrained arch, with known measured foundation movements, the conditions are

$$\left.\begin{aligned} \phi = \phi_K : \delta_K &= (\delta_K)_{\text{meas}} \\ \text{and} \qquad \theta_K &= (\theta_K)_{\text{meas}} - \kappa\, M_K \end{aligned}\right\} \ldots\ldots\ldots\ldots\ldots\ldots\ldots (11)$$

The terms $(\delta_K)_{\text{meas}}$ and $(\theta_K)_{\text{meas}}$ are the measured horizontal displacement and rotation of the abutment, respectively. The symbol κ is the coefficient of elastic restraint, and the product $-\kappa\, M_K$, in which M_K is the restraining moment, represents the elastic end rotation of the rib.

In general, the shape of the center line of the rib and the variation of the moment of inertia I of the effective section require a numerical procedure for the determination of the two redundants H_c and M_c. For the special case of a circular center line and a constant moment of inertia, the quantities H_c and M_c can be computed by direct integration. Extension can be made to other cases, such as a parabolic shape of the rib and I equal to $I_c/\cos\phi$, or to a numerical solution.

For the statically determinate system shown in Fig. 8, the normal force N_o and the bending moment M_o, caused by the shear load $N_{x\phi}$, can be obtained by integrating the contribution of the distributed shear load. If ϕ is the angle at which N_o and M_o are determined, then $N_{x\phi}\, r\, d\omega$ represents the shear load applied over an infinitesimal rib length $r\, d\omega$ at any angle ω between zero and ϕ. Then from Fig. 8(*b*),

$$N_o = -\int_o^{\phi} N_{x\phi}\, r \cos(\phi - \omega)\, d\omega \quad \text{(12a)}$$

Substituting from Eq. 9 and integrating Eq. 12*a* results in

$$N_o = -\frac{r^2 p}{2\, l}(1 - \cos\phi) \quad \text{(12b)}$$

Similarly, the contribution of the incremental shear load to the moment M_o is $N_{x\phi}\, r\, d\omega\{Z_a - r_e[1 - \cos(\phi - \omega)]\}$, in which $r_e = r + z_a$ and is the radius of the effective section (Fig. 8(*b*)). Therefore,

$$M_o = \int_0^{\phi} N_{x\phi}\, r\{z_a - r_e[1 - \cos(\phi - \omega)]\}\, d\omega \quad \text{(13a)}$$

Substituting from Eq. 9 and integrating Eq. 13*a* results in

$$M_o = \frac{r^2 r_e p}{2\, l}\left[\left(1 - \frac{z_a}{r_e}\right)\frac{\phi^2}{2} - 1 + \cos\phi\right] \quad \text{(13b)}$$

The total normal force N and the total bending moment M are (Fig. 8(*a*))

$$N = N_o - H_c \cos\phi \quad \text{(14)}$$

and

$$M = M_o + H_c r_e (1 - \cos\phi) + M_c \quad \text{(15)}$$

In order to compute H_c and M_c, the horizontal displacement δ_K and the rotation of the abutment θ_K must be determined. Choosing a virtual load system as shown in Fig. 8(*c*), P' equal to unity at the abutment produces a virtual normal force N' and a virtual bending moment M' at an angle ϕ in the rib. These qualities are related by

$$P' = 1:\; N' = -\cos\phi \quad \text{(16)}$$

and

$$M' = -r_e(\cos\phi - \cos\phi_K) \quad \text{(17)}$$

By use of the work equation, the displacement δ_K of the actual system is expressed as the work done by the virtual load ($P' = 1$):

$$\delta_K = \int \frac{M'\, M\, ds}{E\, I} + \int \frac{N'\, N\, ds}{E\, A} \quad \text{(18a)}$$

in which

$$ds = r_e\, d\phi \quad \text{(18b)}$$

and A is the cross-sectional area. The influence of the normal force N on the displacement is extremely small and therefore can be safely disregarded. Assuming that the product $E\,I$ is a constant and replacing M' and M by their values from Eqs. 17 and 15, respectively, Eq. 18*a* becomes

$$\delta_K = \frac{1}{E\,I} \int_0^{\phi_K} [-\,r_e\,(\cos\phi - \cos\phi_K)] \\ \times [M_o + H_c\,r_e\,(1 - \cos\phi) + M_c]\,r_e\,d\phi \quad \text{..(19)}$$

Replacing M_o by its value from Eq. 13*b* and integrating Eq. 19,

$$-\,\delta_K \frac{E\,I}{r^2_e} = M_c\,(\sin\phi_K - \phi_K\cos\phi_K) + H_c\,r_e\,(\sin\phi_K + \tfrac{1}{4}\sin 2\,\phi_K \\ -\tfrac{1}{2}\,\phi_K - \phi_K\cos\phi_K) + \frac{r^2\,p}{2\,l}\,r_e \left\{\left(1 - \frac{z_a}{r_e}\right)\left[\phi_K\cos\phi_K \right.\right. \\ \left. + \left(\frac{\phi^2{}_K}{2} - 1\right)\sin\phi_K - \frac{\phi^3{}_K}{b}\cos\phi_K\right] \\ \left. -\sin\phi_K - \tfrac{1}{4}\sin 2\,\phi_K + \tfrac{1}{2}\,\phi_K + \phi_K\cos\phi_K\right\} \quad \text{.............(20)}$$

The rotation θ_K of the abutment is determined by the same procedure. The virtual moment M'_K equal to unity of Fig. 8(*c*) produces a bending moment M' equal to unity for any angle ϕ such that

$$M'_K = 1:\; M' = 1 \quad \text{.....................(21)}$$

Inserting Eqs. 21 and 15 into the work equation,

$$\theta_K = \int \frac{M'\,M\,ds}{E\,I} \quad \text{.....................(22)}$$

results in

$$\theta_K = \frac{1}{E\,I} \int_0^{\phi_K} [M_o + H_c\,r_e\,(1 - \cos\phi) + M_c]\,r_e\,d\phi \quad \text{......(23)}$$

If M_o is substituted by its value from Eq. 13*b*, the integration of Eq. 23 leads to

$$\theta_K \frac{E\,I}{r_e} = M_c\,\phi_K + H_c\,r_e\,(\phi_K - \sin\phi_K) \\ + \frac{r^2\,p}{2\,l}\,r_e \left[\left(1 - \frac{z_a}{r}\right)\frac{\phi^3{}_K}{6} - \phi_K + \sin\phi_K\right] \quad \text{..(24)}$$

Eqs. 20 and 24 each have the two unknowns, H_c and M_c. The normal force N and the bending moment M for any angle ϕ are determined from Eqs. 14 and 15 following the solution for the redundants. The stresses in the ribs are determined from

$$\sigma = \frac{N}{A} \pm \frac{M\,z}{I} \quad \text{.....................(25)}$$

in which A and I are, respectively, the cross-sectional area and the moment of inertia of the effective section, consisting of the rib as a web and the effective width of the shell as a flange. The symbol z represents the distance of a fiber from the centroidal axis of the effective section.

Coefficient of Elastic Restraint.—In Eq. 11 a coefficient of elastic restraint κ was introduced. In arch bridges this coefficient provides for the elasticity of the soil and the abutment. In general, the arch cannot be considered fully restrained at the springing line.

During the tests performed on the model shown in Fig. 1 another consideration led to the introduction of κ. The section A–A in Fig. 1 gives a typical construction detail at the springing line of the rib and the shell. The latter is supported by a relatively flexible edge member. The rib, however, terminates in a very heavy end wall and can be regarded to be fully restrained. There are two extreme cases that can be considered: (1) The shell is held rigidly along the edge member and (2) the shell has a free edge. In the first case the N_ϕ-forces of the shell will be resisted by the support, and the effective width is sensibly constant down to the edge member as in Fig. 9(*a*). If there is no support, the effective width must be reduced to zero at the springing line, as in Fig. 9(*b*). The actual condition lies between these two cases. Because this disturbance of the effective width of the shell has only a local effect, the reduction of the moment of inertia of the effective section can be accounted for by considering the value of I as being constant to the springing line and by assuming an elastic restraint for the rib. The higher flexibility of the effective section in the end zone is therefore concentrated at the springing line.

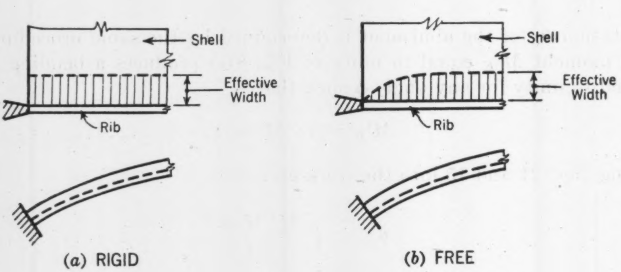

(*a*) RIGID (*b*) FREE

FIG. 9.—EXTREME CONDITIONS OF SHELL SUPPORT

It is obvious that the magnitude of the coefficient of elastic restraint depends on the effectiveness of the edge member in supporting the shell. No theoretical analysis was made of κ during the investigations.

Determination of the Shell Forces.—The stress along the connecting line of the rib and shell σ_a is computed by use of Eq. 25, following the determination of the normal force N and the bending moment M of the effective section. The total circumferential direct force F of the shell is given by Eq. 5.

The problem consists of finding the forces and moments in the shell for a given value of F and a given set of boundary conditions. In the present case the boundary condition for the shell at the ribs $x = 0$ and $x = 2\,l$ is

$$M_x = 0 \ldots\ldots\ldots\ldots\ldots\ldots\ldots\ldots (26)$$

in which M_x is the bending moment of the shell in the axial direction. The condition given in Eq. 26 presupposes the neglect of the torsional stiffness of the rib. The influence of the middle rib on the stress distribution can be disregarded, the forces and moments being rapidly damped with increasing distance from the end ribs. The actual computations for these forces and moments are readily made by use of tables (14).

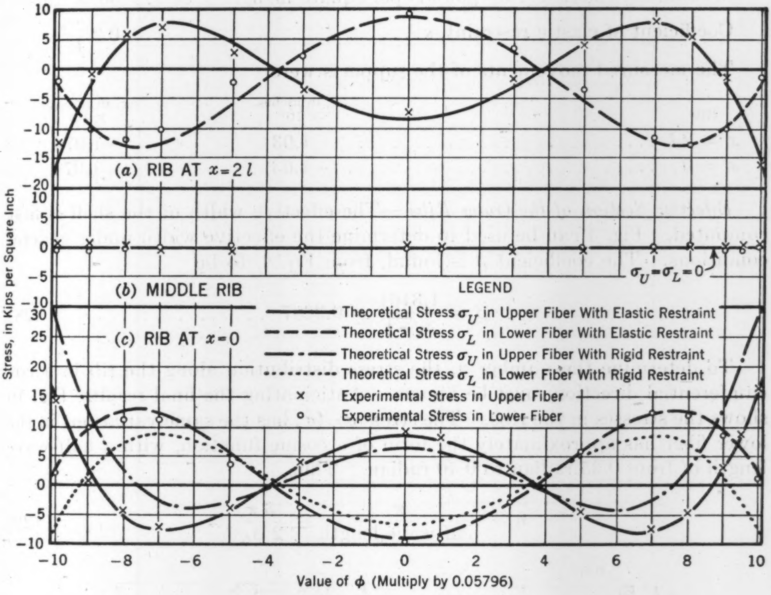

FIG. 10.—FIBER STRESSES IN THE RIBS WHEN THE MODEL IS SUBJECTED TO TEN LOADS OF 1,687.5 LB EACH ON THE EDGE AT $x = 21$

Deflections of the Rib.—Knowing the area A and the moment of inertia I of the effective section, the normal force N, and the bending moment M for any angle ϕ along the rib, the deflection of the rib is readily determined from the work equation. Placing an imaginary load P' equal to unity at the point at which the deflection is desired, the work of this unit load as a result of the deformations caused by the actual load system is equal to the deflection under consideration, or

$$\delta = \int \frac{M'\,M\,ds}{E\,I} + \int \frac{N'\,N\,ds}{E\,A} \ldots\ldots\ldots\ldots (27)$$

in which N' and M' are caused by the imaginary load, and M and N are a result of the actual loads.

Numerical Example.—The foregoing theory will be applied to the analytical solution of a model of a shell roof. Fig. 1 gives the dimensions of the model of the hangar at Rapid City built to the scale of 1 to 30. Structural steel was chosen as material for the model, the dimensions (a shell thickness of approximately $\frac{1}{8}$ in.) leaving no other choice. The dimensions and properties not shown in Fig. 1 are as follows:

Item	Value
ϕ_K for outer ribs (radians)	0.5866
Load, p (pounds per linear inch)	140.62
Modulus of elasticity, E (pounds per square inch)	30×10^6
Coefficient of elastic restraint, κ	$0.2 \frac{r_e}{E\,I}$

The measured movements of the supports were

Rib	δ_K, in inches $\times 10^2$	ϕ_K, in radians $\times 10^3$
$x = 2\,l$	1.03	−1.074
$x = 0$	−1.03	1.074

Effective Section of the Outer Ribs.—The effective width of the shell is first computed. Fig. 4 can be used to determine the effective width under general conditions. The coefficient β is found, from Eq. 4, to be

$$\beta = \frac{1.3161}{\sqrt{r\,t}} = 0.3687 \qquad (28)$$

To determine the number n, the stress distribution along the rib in a circumferential direction must be known. Anticipating the final results, Fig. 10 shows the stresses in the ribs. The stress σ_L (σ_a has the same variation) in the lower fiber has approximately the form of a cosine function, with a half-wave length of from 0.35 radian to 0.40 radian. Thus,

$$n = \frac{\pi}{\text{half-wave length}} \cong \frac{3\,\pi}{2\,\phi_K} \qquad (29)$$

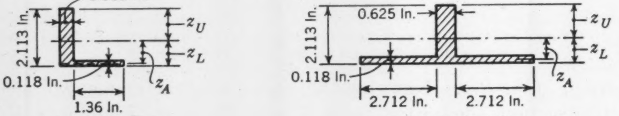

(*a*) OUTER RIB (*b*) MIDDLE RIB

FIG. 11.—EFFECTIVE SECTION OF THE RIBS

The right side of Eq. 29 is an approximate expression for n in terms of the angle ϕ_K (shown in Fig. 8) and holds for this particular case only. Another load would produce another variation of the stress σ_L. Substituting the numerical value for ϕ_K into Eq. 29 results in n equal to 8.03. The coefficient λ is found, from Eq. 3, to equal 0.26.

The two outer ribs have no overhang, and the distance to the middle rib can be considered to be infinite. Entering the chart in Fig. 4 with the values

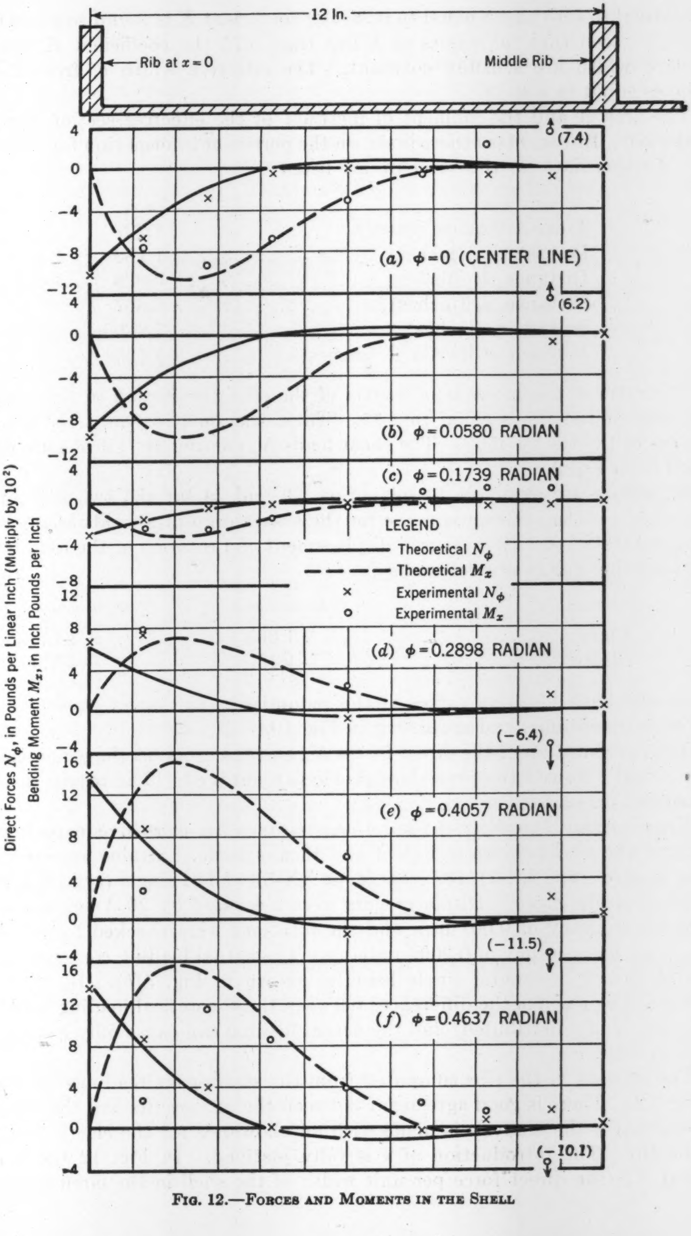

FIG. 12.—FORCES AND MOMENTS IN THE SHELL

of βl equal to zero and λ equal to 0.26, the coefficient K is found to equal 0.38. It can be seen that for values of λ less than 0.75 the coefficient K and the effective width are sensibly constant. The effective width b, from Eq. 2, becomes equal to 1.36 in.

The area A and the moment of inertia I of the effective section are then computed. In Fig. 11 (*a*) there is shown the pertinent information for the outer rib. Further data for the outer rib are listed:

Item	Value
Area, A (square inches)	1.227
Distance, z_u (inches)	1.186
Distance, $z\sigma$ (inches)	0.926
Distance, z_a (inches)	0.867
Radius, r_s (inches)	108.926
Moment of inertia, I (inches^4)	0.536

The ratio of the moment of inertia of the effective section to the moment of inertia of the rib is equal to 1.35. Thus, the shell increases the bending stiffness of the rib by 35%. The shear loads $N_{x\phi}$ acting on the ribs are determined from Eq. 9.

All values are available to solve Eqs. 20 and 24 for the two redundants H_c and M_c. The solution is made for the assumption of a rigid restraint and an elastic restraint with measured displacement and rotation of the foundation. The following values are determined:

Restraint	H_c, in pounds	M_c, in inch-pounds
Rigid	−1,068	+3,156
Elastic	−1,457	+4,371

On the basis of these values of the redundants, the direct stresses in the ribs were determined and are shown in Fig. 10.

The computation of the direct forces N_ϕ and the cross bending moment M_x in the shell followed the procedure previously outlined. The results are presented in Fig. 12.

Experimental Investigation and Comparison.—An extensive experimental study on the model shown in Figs. 1 and 13 was made. Strains were recorded by 44 rosette (type AR-1), 137 cross (type AX-5), and 81 single (type A-5) SR-4 electrical strain gages. Displacements were measured by 20 Ames dial gages (with an accuracy of 0.001 in.), and the rotations were checked by two level bars (with an accuracy of 0.0002 radian). The actual loading consisted of ten equally spaced horizontal single loads as shown in Fig. 5(*b*). By virtue of St. Venant's principle the differences between the theoretical loading (assumed to be uniformly distributed) and the actual loading can cause only local differences in behavior.

The stresses in the ribs computed from the strain-gage readings are shown in Fig. 10. There is good agreement between the test results and the theoretical analysis if the analysis is made with an allowance for the elastic restraint of the rib. The introduction of κ is fully justified. In Fig. 12 the experimental N_ϕ (the direct force per unit width of the shell in the circumferential direction) and M_x (the bending moment per unit width in the axial direction) of the shell are plotted.

The agreement between the analytical and the theoretical results is quite close. It is of interest to note that the stress distribution is perfectly antisymmetric with respect to the middle rib. The middle rib is unstressed and therefore does not add to the strength of the structure under the present loading condition. The rib at x equal to $2\,l$ has exactly the opposite stresses of the rib at x equal to zero. This fact is also demonstrated in Fig. 14 in which the measured vertical deflections of both outer ribs are plotted.

FIG. 13.—ROOF SHELL IN THE LABORATORY

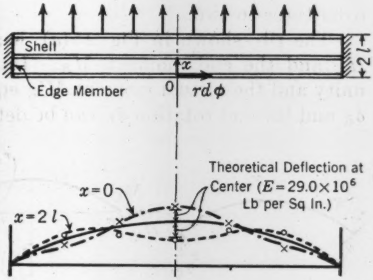

FIG. 14.—EXPERIMENTAL VERTICAL DEFLECTIONS OF THE OUTER RIBS FOR LATERAL LOADS

Conclusions Concerning Horizontal Longitudinal Forces.—

1. The analysis of the effect of horizontal lateral wind loads on cylindrical shell roofs was fully confirmed by the experimental investigations on the model.
2. For actual shell roofs of the type constructed at Rapid City, the wind pressure on the front door (as prescribed by building codes) is from 30 lb per sq ft to 35 lb per sq ft, or approximately 1,000 lb per lin ft of the rib. This results in maximum rib stresses of approximately 400 lb per sq in. Obviously, a stress of this magnitude cannot be considered a secondary one. By combining a number of shell units, these stresses can be lowered considerably.

FOUNDATION MOVEMENTS

The horizontal thrust of long-span shell roofs are of sufficient magnitude to offer serious foundation problems. In certain cases, tension ties have been found necessary to balance the horizontal thrust acting on the abutments (8a). It is usually impossible to prevent any foundation movements, except by special devices such as the artificial stressing of the tension ties between the abutments.

The general procedure for the computation of the forces in arches subjected to foundation movements can be used if the interaction occurring between the ribs and the shell is taken into account. This will be done by taking as a cross section of the rib the effective cross section formed by the rib and the effective width of the shell.

Analysis of the Ribs.—The horizontal displacement δ_K and the symmetrical rotations θ_K of the two abutments are considered. Unequal rotations θ_{Kl} and θ_{Kr} of the left and right abutments can be solved by superimposing symmetrical rotations,

$$\theta_{K1} = \tfrac{1}{2}\,(\theta_{Kl} + \theta_{Kr}) \qquad (30)$$

and antisymmetrical rotations,

$$\theta_{K2} = \pm\,\tfrac{1}{2}\,(\theta_{Kl} - \theta_{Kr}) \qquad (31)$$

The advantage of this procedure is that the number of redundants is reduced from three to two.

The rib, shown in Fig. 15(*a*), has two redundants—the horizontal thrust H_K and the end moment M_K. Introducing the virtual load H'_K equal to unity and the virtual moment M'_K equal to unity, the horizontal displacement δ_K and the end rotation θ_K can be determined by use of the work equation.

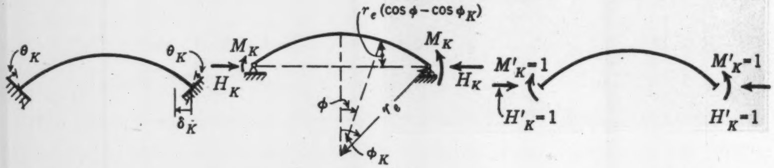

(*a*) ACTUAL SYSTEM (*b*) BASE SYSTEM (*c*) VIRTUAL LOAD SYSTEM

FIG. 15.—LOADS ON THE RIB

The actual normal force N and bending moment M (Fig. 15(*a*)) are

$$N = -\,H_e \cos\phi \qquad (32)$$

and

$$M = M_K - H_K\, r_e\,(\cos\phi - \cos\phi_K) \qquad (33)$$

Because H'_K is equal to unity (Fig. 15(*c*)),

$$N' = -\cos\phi \qquad (34)$$

and

$$M' = -\,r_e\,(\cos\phi - \cos\phi_K) \qquad (35)$$

Hence,

$$\delta_K = \int_{-\phi_K}^{+\phi_K} \frac{M'\,M\,ds}{E\,I} + \int_{-\phi_K}^{+\phi_K} \frac{N'\,N\,ds}{E\,A} \qquad (36)$$

Assuming the products $E\,I$ and $E\,A$ to be constant, inserting Eqs. 32, 33, 34, and 35 into Eq. 36, and integrating leads to

$$\delta_K \frac{E\,I}{2\,r^2_e} = M_K\,(\phi_K \cos\phi_K - \sin\phi_K) + H_K\, r_e \Big[\phi_K\,(\tfrac{1}{2} + \cos^2\phi_K) - \tfrac{3}{4}\sin 2\,\phi_K + \frac{I}{A\,r^2_e}\,(\tfrac{1}{2}\,\phi_K + \tfrac{1}{4}\sin 2\,\phi_K)\Big] \qquad (37)$$

If M'_K and M' are made equal to unity and N' is made equal to zero, the work equation provides the end rotation θ_K. The reduction of the effective width in the edge-member zone is accounted for by a coefficient of elastic restraint κ. Thus the product of the external moment (M'_K equal to unity) of the virtual load system times the rotation ($-\kappa\, M_K$) caused by the elastic restraint under the actual load system gives a contribution to the external work:

$$\theta_K - \kappa\, M_K = \int_0^{\phi_K} \frac{M'\, M\, ds}{E\, I} + \int_0^{\phi_K} \frac{N'\, N\, ds}{E\, A} \dots\dots\dots\dots (38)$$

Substitution of Eqs. 32 and 33 into Eq. 38 and integrating yields

$$\theta_K \frac{E\, I}{r_e} = M_K\, (\phi_K + \bar{\kappa}) + H_K\, r_e\, (\phi_K \cos \phi_K - \sin \phi_K) \dots\dots (39)$$

in which

$$\bar{\kappa} = \frac{E\, I}{r_e}\, \kappa \dots\dots\dots\dots\dots\dots\dots\dots (40)$$

For any given values of δ_K and θ_K, the two redundants H_K and M_K are determined by Eqs. 37 and 39. The direct stresses in the ribs are determined by use of Eq. 25.

Determination of the Shell Forces.—The procedure for determining the shell forces resulting from foundation movements follows the steps used in the case of horizontal longitudinal forces. For the two outer ribs and the middle rib, the corresponding F-forces are computed from Eq. 5 following the determination of the stress σ_a along the connecting line of the rib and shell (from Eq. 25). Knowing the boundary conditions for the shell and the F-forces, the stress distribution in the shell can be determined. This analysis can be found elsewhere (14).

Numerical Example.—The model shown in Fig. 1 is analyzed for a given horizontal displacement δ_K and end rotation θ_K. The effective width of the ribs must first be computed. In order to know the number n, used in Fig. 4 to determine the effective width, the stress distribution along the rib must be known. Fig. 16 shows that, as a first approximation, the variation of the stress σ_L in the lower fiber of the middle and outer ribs is a cosine function with a half-wave length of approximately 0.75 radian. Hence,

$$n = \frac{\pi}{0.75} \cong \frac{3\, \pi}{4\, \phi_K} \dots\dots\dots\dots\dots\dots\dots (41)$$

This value of n is a first approximation if symmetrical foundation movements are considered. Inserting the value of ϕ_K (0.5866 radian) into Eq. 41 results in n being equal to 4.14. From Eq. 3, λ is found to equal 0.14. Thus, for the middle rib $\beta\, l$ is equal to 4.42 (greater than 2.4) and for the outer ribs $\beta\, l$ is equal to zero.

From Fig. 4 it is obvious that the values of K for (*a*) $\lambda = 0$, $\beta\, l = \infty$ in case of the middle rib and (*b*) $\lambda = 0$, $\beta\, l = 0$ in case of the outer ribs are sufficiently accurate for the determination of the effective width. Thus, for the middle rib K is equal to 1.52 in. and b is equal to 5.43 in. For the outer rib K is equal to 0.38 in. and b equals 1.36 in.

The following is a list of values for the effective section of the middle rib

Item	Value
Area, A (square inches)	1.961
Distance, z_u (inches)	−1.382
Distance, z_L (inches)	0.731
Distance, z_a (inches)	0.672
Radius, r_e (inches)	108.731
Moment of inertia, I (inches^4)	0.921

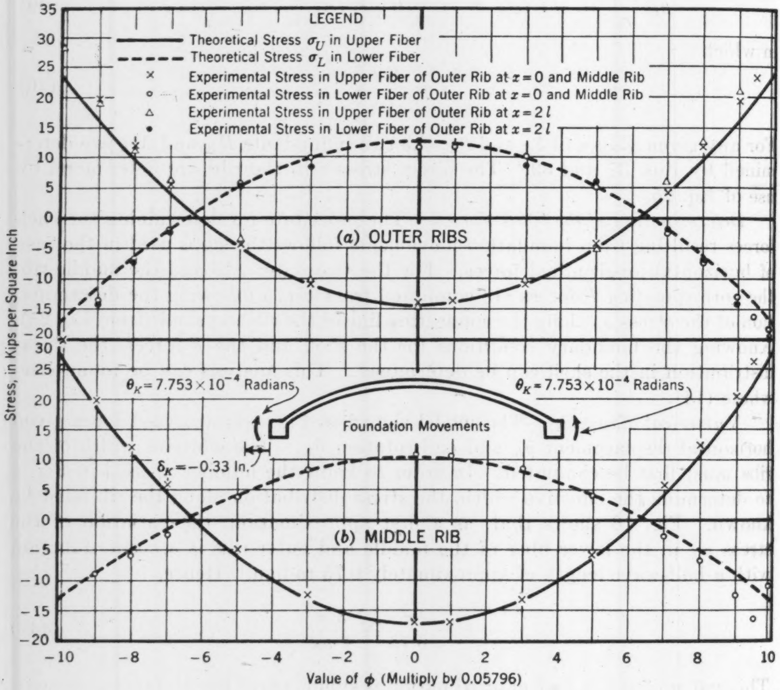

FIG. 16.—THEORETICAL AND EXPERIMENTAL STRESSES IN THE MODEL AS A RESULT OF FOUNDATION MOVEMENTS

The ratio of the moment of inertia of the effective section to the moment of inertia of the rib is equal to 1.84. The considerable increase (84%) of the bending stiffness of the middle rib as a result of including the effective width of the shell is especially noteworthy.

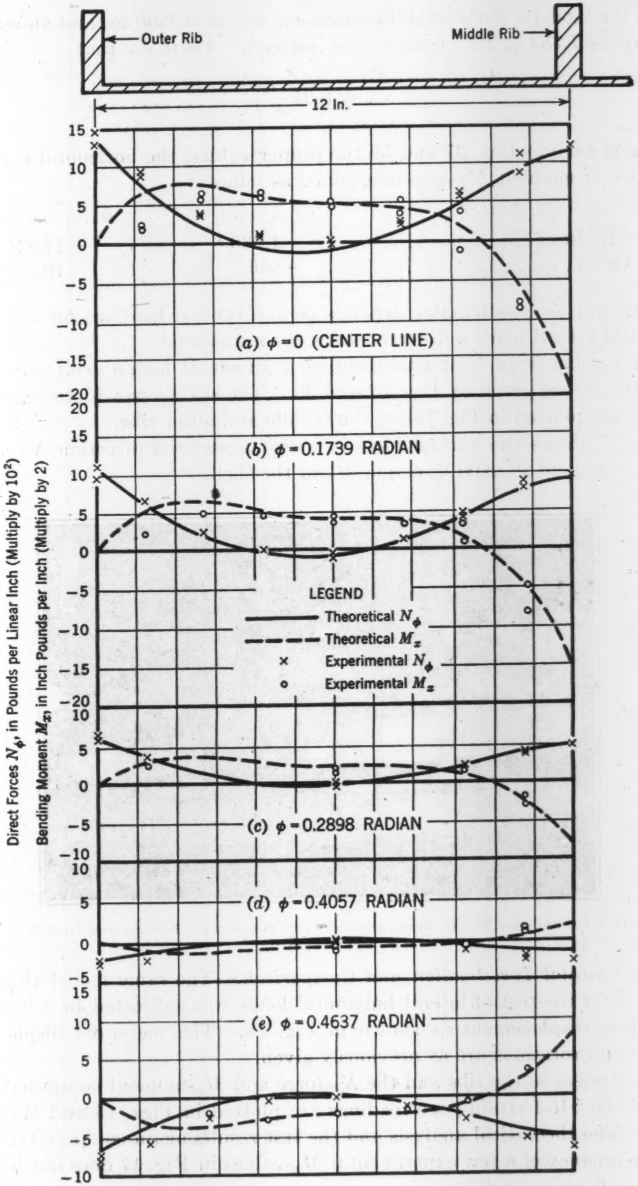

FIG. 17.— NORMAL FORCE IN A CIRCUMFERENTIAL DIRECTION AND BENDING MOMENT IN THE AXIAL DIRECTION

On the model a horizontal displacement, δ_K, of 0.3300 in. and an end rotation, ϕ_K, of 7.753×10^{-4} radian were induced. Assuming that

$$\kappa = 0.05 \frac{r_e}{E\,I} \qquad (42)$$

and inserting into Eqs. 37 and 39 the proper values, the horizontal thrust H_K and the end moment M_K are determined as follows:

Rib	H_K, in pounds	M_K, in inch pounds
Middle	−1,636	−17,850
Outer	−946	−10,350

It should be noted that κ depends on the type of loading; for the case of horizontal lateral loads a different value for κ was used.

The normal force N and the bending moment M for an arbitrary angle ϕ along the rib are given by Eqs. 32 and 33. The rib stresses (determined from Eq. 25) are plotted in Fig. 16 for the middle and outer ribs.

Fig. 17 shows the normal force in a circumferential direction N_ϕ and the bending moment in axial direction M_x of the shell.

FIG. 18.—LABORATORY MODEL BEING SUBJECTED TO HORIZONTAL FOUNDATION DISPLACEMENT

Experimental Investigation and Comparison.—The same model (Fig. 1) as was used for the test of lateral horizontal loads was subjected to a horizontal foundation displacement as shown in Fig. 18. The measured displacement and the end rotations are as previously given.

The stresses in the ribs and the N_ϕ-force and M_x-moment computed on the basis of the SR-4 strain-gage readings are plotted in Figs. 16 and 17, respectively. The theoretical analysis and the test results again compare favorably. The discrepancy of a few experimental M_x-values in Fig. 17 does not influence the over-all agreement.

Conclusions Concerning Foundation Movements.—

1. By taking as the effective width of the shell the flange of a T-section (the web of which is the rib), the analysis of the ribs for foundation movements can be accomplished by use of the simple arch theory. Following the determination of the stresses in the ribs, the stress distribution in the shell can also be computed. Experimental results on the model support the theoretical analysis.

2. Eqs. 37 and 39 show that, for given foundation movements δ_K and ϕ_K, the moment M_K and the horizontal thrust H_K are proportional to the moment of inertia I of the effective section of the rib. Neglecting the influence of the normal force on the deformations, which is completely negligible,

$$N = f_1(\phi)\, I \quad \text{(43a)}$$

and

$$M = f_2(\phi)\, I \quad \text{(43b)}$$

in which $f_1(\phi)$ and $f_2(\phi)$ are functions of ϕ.

The stress in the rib becomes, from Eq. 25,

$$\sigma = \frac{f_1\, I}{A} \pm \frac{f_2\, I\, z}{I} = \frac{f_1\, I}{A} \pm f_2\, z \quad \text{(44)}$$

Thus, σ is approximately proportional to the distance z of the fiber from the centroidal axis of the cross section because the first term of the right side of Eq. 44 is relatively small. The importance of these derivations will be explained subsequently.

SOME SPECIAL PROBLEMS

Uniform Temperature Change and Shrinkage of the Concrete.—Suppose a shell roof undergoes a uniform temperature change of $\Delta t°$. If the whole structure were supported as a simple beam, this temperature change would cause an increase ΔL of the span L:

$$\Delta L = \alpha\, \Delta t°\, L \quad \text{(45)}$$

in which α is the coefficient of thermal expansion. Actually, this increase (ΔL) is impossible because the abutments are restrained. Therefore, the original span L must be restored by diminishing the new span $(L + \Delta L)$ by ΔL. The latter is equal to a horizontal displacement, δ_K, previously investigated under the heading, "Foundation Movements." By substituting into Eqs. 37 and 39 the values,

$$\delta_K = \alpha\, \Delta t°\, L \quad \text{(46a)}$$

and

$$\theta_K = 0 \quad \text{(46b)}$$

the horizontal thrust H_K and the end moment M_K caused by a temperature rise $\Delta t°$ can be determined.

It is usual to consider the effect of shrinkage of the concrete as equivalent to a fall in temperature of a specified $\Delta t°$. Hence, the stress caused by shrinkage can also be determined by the same procedure.

Differential Temperature Change Between Ribs and Shell.—If there is a temperature difference between the outside and inside air of a shell roof structure, the ribs, exposed mostly to the outside air, will have a different average temperature than the shell. The difference in temperature between the shell and the rib can be considered to be $\Delta t°$. Obviously, stresses will be produced in the structure.

An analysis of this case indicated thermal stresses as great as 100 lb per sq in. for a temperature difference of 10° F in a hangar of the type built at Rapid City (340-ft span).

The actual temperature distribution will be somewhat different from the assumed one because the temperature will vary continuously. Temperature measurements should be made on an actual structure to determine the variation.

Stability of the Structure.—The thickness t of the shell is mainly governed by stability considerations. For a certain spacing of the ribs, l a radius r of the shell, and a given distributed load, a minimum thickness t of the shell is required (13) (16). The resulting membrane stresses reach only a fraction of the allowable concrete stresses in compression. It is of interest to note that the ratio of the thickness to the radius of modern shell roofs is smaller than the corresponding ratio for an egg shell. This fact illustrates the perfection to which these structures have been developed.

The ribs, reinforcing the shell at regular intervals l, increase the buckling stiffness of the shell panel. Furthermore, the ribs are indispensable for carrying a one-sided live load (such as snow) acting on the structure. To provide sufficient buckling safety for the entire structure, the ribs must have a specific minimum stiffness. The buckling load is proportional to the moment of inertia of the effective section. Previous considerations concerning the stresses caused by a volume change led to a stiffness of the rib that was as small as possible. Obviously, the stiffness should be kept at the minimum required for stability and bending strength so that the stresses caused by a volume change do not become excessive.

Consequently, the factor of safety against buckling of the ribs is important. A smaller factor of safety will require less stiffness, and therefore smaller stresses will be set up by volume changes. Plastic flow of the concrete affects the geometrical shape of the structure and thus the forces—in a dangerous manner if the factor of safety is decreased excessively. In addition, the secondary moments caused by deformations of the structure can be correlated to the factor of safety against buckling (17) (18).

Location of the Shell with Respect to the Rib.—The idea of placing the shell in the middle of the rib was advocated by C. S. Whitney, M. ASCE, in 1950 (19). Considering the stresses caused by a volume change, Mr. Whitney concluded that the stiffness of the ribs should be minimum. By placing the shell in the middle of the rib the stiffness of the effective section is diminished to a great extent, as shown in Fig. 19. The same decrease can be obtained, however, by taking a smaller rib, with the shell at one edge of the rib. To illustrate this decrease, the sections shown in Fig. 19 must be considered. Sections 1 and 2 are identical except for the location of the rib. Placing the shell in the middle of the rib reduces the moment of inertia by 47%. Section 3 has a moment of inertia approximately equal to section 2 as a result of the reduction in the height of the rib. The normal force and bending moment caused by the volume changes are proportional to the moment of inertia of the effective section, as can be seen by comparing Eqs. 37, 39, and 43. The fiber stresses, however, are approximately proportional to the distance z of the fiber from the neutral axis (Eq. 44). The ratio of the corresponding stresses of the two sections is thus equal to the ratio of the corresponding distances z. Therefore, for the upper fibers,

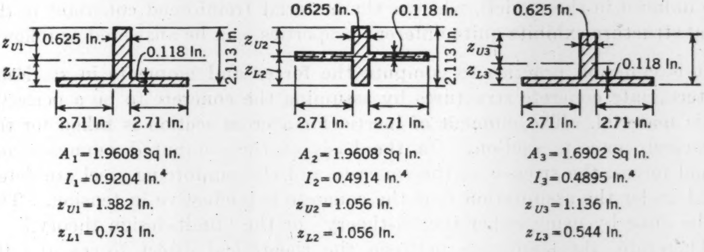
0.625 In.
0.118 In.
2.113 In.
z_{U1}
z_{L1}
2.71 In.
2.71 In.
$A_1 = 1.9608$ Sq In.
$I_1 = 0.9204$ In.^{4}
$z_{U1} = 1.382$ In.
$z_{L1} = 0.731$ In.
0.625 In.
0.118 In.
2.113 In.
z_{U2}
z_{L2}
2.71 In.
2.71 In.
$A_2 = 1.9608$ Sq In.
$I_2 = 0.4914$ In.^{4}
$z_{U2} = 1.056$ In.
$z_{L2} = 1.056$ In.
0.625 In.
0.118 In.
1.680 In.
z_{U3}
z_{L3}
2.71 In.
2.71 In.
$A_3 = 1.6902$ Sq In.
$I_3 = 0.4895$ In.^{4}
$z_{U3} = 1.136$ In.
$z_{L3} = 0.544$ In.

(a) SECTION 1 (b) SECTION 2 (c) SECTION 3

FIG. 19.—VARIATIONS OF THE RIB SECTION

$$\frac{\sigma_{U3}}{\sigma_{U2}} = \frac{z_{U3}}{z_{U2}} = \frac{1.136}{1.056} = 1.08 \ldots\ldots\ldots\ldots\ldots\ldots \quad (47a)$$

and for the lower fiber,

$$\frac{\sigma_{L3}}{\sigma_{L2}} = \frac{z_{L3}}{z_{L2}} = \frac{0.544}{1.056} = 0.52 \ldots\ldots\ldots\ldots\ldots\ldots \quad (47b)$$

Section 3 has in the upper fiber a stress 8% higher and in the lower fiber a stress 48% lower than the stresses in section 2. The objection that in section 3 important cross bending stresses σ_x are set up can be rejected, for in the most extreme case σ_x is 1.73 times the lower fiber stress of the rib (14*b*). Therefore,

$$\frac{\sigma_x}{\sigma_{L2}} = 1.73 \times 0.52 = 0.90 \ldots\ldots\ldots\ldots\ldots\ldots \quad (48)$$

from which it can be seen that the cross bending stress σ_x is 10% smaller than σ_{L2}. Furthermore, the cross bending is concentrated over a very short length.

Therefore, for section 3 with a 21% lighter rib than section 2, the bending moment and normal force caused by volume changes are identical. Neglecting the influence of the normal force, the stresses of section 3 are +8% and −48% of the stresses of section 2. Cross bending stresses σ_x are 10% lower than the maximum stress in section 2 and of local importance. These stresses have the form of a strongly damped oscillation beginning at the rib. Thus, from theoretical considerations, section 2 does not have any advantage over section 3. Contrarily, 21% of the dead weight of the rib can be saved by using section 3. **Therefore, it can be concluded that it is not only ineffective but wasteful to place the shell at the center of the rib.**

CONCLUSIONS

Theoretical solutions for some problems encountered in designing long-span cylindrical shell roofs have been presented. Tests on a steel model in the scale of 1 to 30 of an actual structure built of reinforced concrete (the hangar in Rapid City) confirmed the theoretical analysis. Possible objection to the fact that the test results were obtained from a perfectly elastic model (only elastic strains were induced in the model), whereas the material (reinforced concrete) in the actual structure exhibits quite different properties, can be answered as follows:

It is common practice to compute the forces and moments in statically indeterminate concrete structures by assuming the concrete to be a perfectly elastic material. The moment of inertia for a cross section is taken for the uncracked concrete section. On the basis of the computed moments and normal forces, the stresses in the concrete and the reinforcing steel are determined under the assumption that the concrete is ineffective in tension. This can be done by using either the "*n*-theory" or the "limit-design theory."

Therefore, the similitude between the theoretical direct forces and the bending moment in the steel model and the concrete structure can be made. These values were checked by results of the tests performed on the model, built of a nearly perfectly elastic material. Between the stresses in the model and those in the actual structure no such direct relationships can be derived. It is an established fact (proved by many tests), however, that reinforced concrete structures, analyzed as elastic structures and reinforced according to the computed moments and normal forces, behave essentially as predicted.

Many tests, not reported herein, were made during the course of the investigation. Similar procedures of analysis, based on the use of the effective width, were found to be adequate in checking test results to a close approximation in all cases.

It was found satisfactory to estimate roughly the value of n because the effective width for the proportions of structures tested and the type of stress variation induced by usual loads put n in a region where variations caused little or no change in the effective width. Other engineering uncertainties are of much greater magnitude. In applying this analysis to different problems, it may be necessary to perform analyses by use of a Fourier series representation of the stress variation along the juncture of the rib and shell. In such cases effective widths and stresses could be determined for each of the significant terms of the Fourier series, and the actual stress at any point could be determined by superposition.

ACKNOWLEDGMENTS

This paper presents the results of part of the theoretical and experimental studies made during the course of a two-year research program on shell arch roofs performed at the Fritz Engineering Laboratory. K. R. Harpel, foreman of the laboratory, gave valuable assistance throughout the experimental investigation.

The Roberts and Schaefer Company of Chicago, Ill., was the sponsor of the research program. Thanks are extended to J. E. Kalinka, Robert Zaborowski,

A. M. ASCE, Anton Tedesko, M. ASCE, Otto Gruenwald, W. A. Renner, A. M. ASCE, and Paul Rongved, M. ASCE—all of the Roberts and Schaefer Company.

APPENDIX I. NOTATION

The following symbols adopted for use in the paper and for the guidance of discussers, conform essentially with "American Standard Symbols for Structural Analysis" (ASA-Z 10.8–1949), prepared by a committee of the American Standards Association with ASCE representation, and approved by the Association in 1949:

A = cross-sectional area;
b = effective width of the shell;
E = modulus of elasticity;
F = total direct force defined in Eq. 5;
H_c = horizontal thrust at the center of a rib shown in Fig. 8(*a*);
  H_K = horizontal thrust on rib shown in Fig. 15(*a*);
  H'_K = virtual horizontal thrust;
I = moment of inertia;
I_c = moment of inertia at the center of a rib;
K = a function of λ and βl, graphically represented in Fig. 4;
L = span of the roof;
l = overhang distance;
M = total bending moment:
  M' = virtual bending moment;
  M_B = bending moment on a unit;
  M_c = bending moment at the center of a rib shown in Fig. 8(*a*);
  M_K = restraining moment;
  M'_K = virtual restraining moment;
  M_o = bending moment of rib in statically determinate system;
  M_T = twisting moment;
N = total normal force:
  N' = virtual normal force;
  N_o = normal force of rib in statically determinate system;
  N_x = direct force per unit width of shell in the axial direction;
  N_ϕ = direct force per unit width of shell in the circumferential direction;
  $N_{\phi x}$ and $N_{x\phi}$ = direct shear forces per unit width of shell in circumferential and axial direction, respectively;
n = number of complete waves made by a harmonic function around the circumference of a cylinder;
P' = virtual load;
p = applied uniformly distributed load;
r = radius of the cylinder;
r_e = radius of the effective rib section;

s = distance;
t = thickness of the cylinder;
V = shear force on a unit;
x = coordinate in axial direction of shell;
z = distance of a fiber from the centroidal axis of the effective section;
z_A = distance from the loads $N_{\phi x}$ to the centroid of the effective section;
α = coefficient of thermal expansion;
β = shell constant defined in Eq. 4;
δ_K = known horizontal movement;
θ_K = known rotation of the abutment;
θ_{Kl} = rotation of the left abutment;
θ_{Kr} = rotation of the right abutment;
κ = coefficient of elastic restraint;
λ = parameter defined by Eq. 3;
σ_a = circumferential stress along the connecting line of rib and shell;
σ_L = circumferential stress in the lower fiber;
σ_x = cross bending stress;
$\tau_{\phi x}$ and $\tau_{x\phi}$ = shearing stresses;
ϕ = angle defined in Figs. 5 and 8;
ϕ_K = angle defined in Figs. 5 and 8; and
ω = angle defined in Fig. 8(*b*).

APPENDIX II. BIBLIOGRAPHY

(1) **"Elasticity,"** by A. E. H. Love, Cambridge University Press, Cambridge, England, 4th Ed., 1927.

(2) **"Das Elastizitätsproblem für dünne Schalen,"** by E. Meissner, *Physikalische Zeitschrift,* Vol. 14, 1913, p. 343.

(3) **"Ueber Elastizität und Festigkeit dünner Schalen,"** by E. Meissner, *Vierteljahrsschrift,* Naturforschenden Gesellschaft, Zürich, Switzerland, Vol. 60, 1915, p. 23.

(4) **"Handbuch für Eisenbeton-Bau,"** Wilhelm Ernst und Sohn, Vol. VI, 4th Ed., 1928, p. 269.

(5) **"Die querversteiften zylindrischen Schalengewölbe mit kreissegmentförmigem Querschnitt,"** by U. Finsterwalder, *Ingenieur Archiv,* Vol. 4, 1933, p. 43.

(6) **"Die strenge Theorie der Kreiszylinderschale und ihre Anwendung auf die Z. D. Schalen,"** by F. Dischinger, *Beton und Eisen,* Vol. 34, 1935.

(7) **"Principles of Concrete Shell Dome Design,"** by E. C. Molke and J. E. Kalinka, *Proceedings,* A. C. I., Vol. 9, 1938, p. 649.

(8) **"Thin Concrete Arch Roof Provides 340 Ft. Clear Span For Bomber Hangar,"** by L. W. Prentiss, *Civil Engineering,* Vol. 19, 1949, p. 86. (*a*) p. 87.

(9) **"Construction of Long-Span Concrete Arch Hangar at Limestone Air Force Base,"** by J. E. Allen, *Proceedings,* A. C. I., Vol. 21, 1950, p. 405.

(10) **"The Effective Width of a Circular Cylindrical Shell Adjacent to a Circumferential Reinforcing Rib,"** by B. Thürlimann, R. Bereuter, and B. G. Johnston, *Proceedings,* The First National Cong. for Applied Mechanics, published by the ASME, 1952, p. 347.

(11) **"Die mittragende Breite,"** by T. von Kármán, *Festschrift August Föppls,* J. Springer, Berlin, Germany, 1924, p. 114.

(12) **"The Determination of the Effective Width of Wide-Flanged Beams,"** by W. Raithel, *Technical Report No. 61,* Ordnance Research and Development Div., U. S. Dept. of Army, Washington, D. C., 1949.

(13) **"Theory of Plates and Shells,"** by S. Timoshenko, McGraw-Hill Book Co., Inc., New York, N. Y., 1940, p. 433. (*a*) p. 392.

(14) **"The Effective Width of Circular Cylindrical Shells Reinforced by Ribs,"** by B. Thürlimann, dissertation presented to Lehigh Univ., at Bethlehem, Pa., in partial fulfilment of the requirements for the degree of Doctor of Philosophy, 1950, (*a*) p. 25. (*b*) p. 42.

(15) **"The Effective Width of Cylinders Periodically Stiffened by Circular Rings,"** by C. B. Biezeno and J. J. Koch, *Proceedings,* Koninklijke Nederlandsche Academie, Van Weten-Schappen, Vol. XLVIII, 1945, p. 147.

(16) **"Statik und Dynamik der Schalen,"** by W. Flügge, J. Springer, Berlin, Germany, 1934, p. 112.

(17) **"Untersuchungen über die Knicksicherheit,"** by F. Dischinger, *Bau-Ingenieur,* Vol. 18, 1937, p. 487.

(18) **"Elastische und plastische Verformungen,"** by F. Dischinger, *ibid.,* Vol. 20, 1939, p. 53.

(19) **"Cost of Long-Span Concrete Shell Roofs,"** by C. S. Whitney, *Proceedings,* A. C. I., Vol. 21, 1950, p. 765.

(20) **"Inelastic Buckling of Plain and Reinforced Concrete Columns, Plates, and Shells,"** by G. C. Ernst, J. J. Hromadik, and A. R. Riveland, *Bulletin No. 3,* Univ. of Nebraska Eng. Experiment Station, Lincoln, Nebr., August, 1953.

(21) **"Stability of Thin-Shelled Structures,"** by G. C. Ernst, *Journal,* A.C.I., December, 1952, p. 277.

(22) **Discussion** by Herbert A. Sawyer, Jr., of **"Stability of Thin-Shelled Structures,"**by G. C. Ernst, *ibid.,* December, 1953, p. 292–1.

(23) **"Plain and Reinforced Concrete Arches,"** Report of Committee 312, *Proceedings,* A.C.I., Vol. 22, 1951, p. 681.

(24) **Discussion of "Long Span Concrete Arch Hangar at Limestone Air Force Base,"** by Anton Tedesko, *ibid.,* December, 1950, p. 416.

DISCUSSION

G. C. Ernst,[4] M. ASCE.—The problems met in obtaining experimental verification of shell theory, particularly for reinforced concrete shells, are numerous and not easily solved. Aside from the difficulty of interpreting the results of tests in the light of a relatively complex theory, tests on shells are costly and time-consuming. The authors are to be commended for the sustained care demonstrated in the performance of their tests and in the interpretation and presentation of the results of their investigation. In view of a possible objection to the use of a steel model to represent the elastic action of a reinforced concrete structure, data are presented herein from tests on small reinforced concrete shells made at the University of Nebraska at Lincoln. Although the tests were on long shells rather than short ones, the linear relationship between deflection and load prior to initial cracking provides justification for the authors' use of an elastic material such as steel.

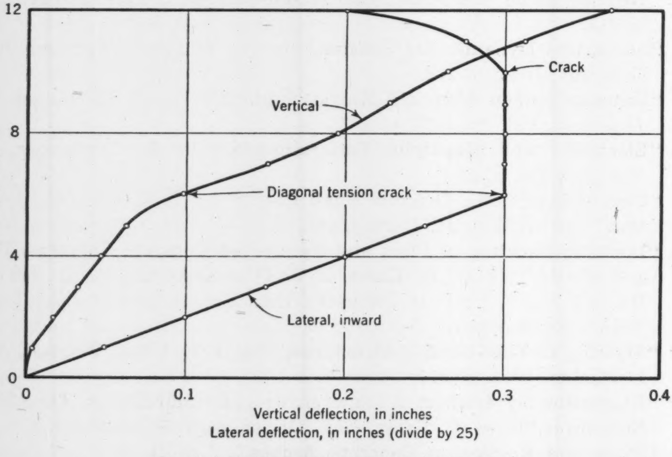

Fig. 20.—Experimental Deflection Curves

The tests performed at the University of Nebraska were made on three long cylindrical shells of reinforced Portland cement mortar, of such size as to permit testing under the controlled loading of a testing machine. The shells were simply supported at the corners, with a longitudinal span of 60 in. and a tranverse span of 40 in. Each shell had an inside radius of 30 in.; the thickness was uniform longitudinally but varied transversely from $\frac{3}{8}$ in. at the crown to $\frac{5}{8}$ in. at the edge beams. The reinforcement in the shell consisted of a double layer of 1-in. by 1-in. by 15-gage welded wire mesh in the central 36 in. and a single layer of the same mesh in the outer 12 in. of each end. The double layer in the central part served as over-reinforcement against transverse-bending failure in the regions of greatest shear difference. This shear was developed under vertical loads uniformly distributed in the transverse direction at the third points by specially constructed, multiple-spring loading heads. The primary purpose of the tests was an investigation of the action of long shells at ultimate loads producing high shearing stresses. The longitudinal steel in the edge beams differed for each shell. Data taken on each shell were directed toward ultimate-load analysis, but only that pertinent to the authors' subject is presented herein.

---

[4] Prof. and Chairman, Dept. of Civ. Eng., Univ. of Nebraska, Lincoln, Nebr.

Fig. 20 provides information on the range of virtually elastic action of reinforced concrete shells. The lateral deflections of the shells were entirely consistent (in direction and order of magnitude) with elastic theory, up to the load at which initial diagonal-tension cracking developed. The average vertical deflection at the center of the two edge beams showed a similar characteristic, with the customary early lag in deflection prior to tensile cracking at the level of the longitudinal steel in the edge beams.

With regard to the stability of the structure, two basic approaches must be considered. Design should be based either on (*a*) structural proportions that will assure the full development of the concrete in compression under longitudinal and transverse thrusts at the ultimate capacity of the structure, or (*b*) the use of design stresses that are a conservative reduction from the values obtained from the inelastic buckling theory (20)(21)(22).

CHARLES S. WHITNEY,[5] M. ASCE.—That there is satisfactory agreement between model-test results and theoretical analysis based on the elastic theory has been clearly demonstrated by the authors. That being true, the authors' investigation has added nothing new to the knowledge of the behavior of cylindrical shells stiffened by arch ribs.

Messrs. Thürlimann and Johnston have, however, chosen as part of their report to draw conclusions which are not warranted either on the basis of the tests or the elastic theory. These conclusions relate to the effects of volume changes which were discussed by the writer in 1950 (19). The comments made under the heading, "Some Special Problems," seem to indicate a lack of understanding of the total effects of the different factors involved. This understanding can only be obtained by performing complete designs on a comparative basis. For this reason, these statements regarding the effects of the various factors are misleading.

Under the heading, "Foundation Movements: Conclusions Concerning Foundation Movements," it is stated that for given movements the moments and thrusts in the rib are proportional to the moment of inertia of the effective section of the rib and, further, that the stress in the rib is approximately proportional to the distance from the neutral axis to the fiber being considered. These statements are true according to the elastic theory and were verified by tests on the steel model. The first statement is probably substantially true regarding a concrete structure, but the actual stress condition is completely different when the shell slab is on the tension side of the neutral axis. Concrete arches must be designed for reversals of moments, and tension in the concrete must be ignored when computing the strength of the section.

---

[5] Partner, Ammann & Whitney, Cons. Engrs., Milwaukee, Wis.

Therefore—assuming the same depth of the rib—moving the slab from the center of the rib to the top or bottom approximately doubles the moment of inertia and the moments resulting from abutment rotation without increasing the strength of the section.

Furthermore—a point neglected by the authors—the increased moments caused by the increased stiffness have an important effect on the cost of the foundations, which must be designed for greater eccentricity of thrust.

The same condition exists in regard to volume changes resulting from temperature changes and shrinkage. Bending moments are proportional to the effective stiffness, but the rib strength is not increased by using a T-section when the T-flange is on the tension side.

It is also obvious that, in the case of a difference in temperature between the rib and the shell, higher bending stresses will be produced in the rib if the shell is at the top or bottom rather than at the center of the rib.

The suggestion made by Messrs. Thürlimann and Johnston that the effect of increased stiffness which results from placing the shell at the bottom of the rib can be offset by using a shallower rib to reduce volume-change stresses is impractical because the strength of the rib would at the same time be reduced below that required to carry critical combinations of dead loads and live loads together with the effects of volume changes, abutment movements, and deflection stresses. Deflection stresses are easily controlled without excessive stiffness.

The writer challenges the accuracy of the authors' statements regarding cross bending stress which lead to Eq. 48. The writer has shown (19) that the cross bending moments in the shell produced by placing the shell at the bottom of the rib instead of at the center can be of the same magnitude as those produced by both dead loads and live loads. Their importance cannot be rejected.

To summarize, moving the shell from the bottom of the rib to the center reduces its stiffness by approximately one half and greatly reduces the total bending moments without reducing its strength to resist moments which produce tension at the bottom of the rib. Conversely, placing the shell at the bottom of the rib instead of at the center approximately doubles the rib stiffness and consequently doubles the moments caused by volume change and abutment deflection without any corresponding increase in strength. Placing the shell at the bottom of the rib materially increases the costs of the structure if the structure is consistently designed. The importance of the various factors can be judged only by considering simultaneously their total effect rather than by attempting a separate analysis of their individual effects as the authors have done.

Boyd G. Anderson.[6]—The comments made by the authors under the heading, "Some Special Problems: Location of the Shell with Respect to the Rib," are based on the assumption of an elastic section and are restricted to a comparison of rib sections in which the area of the rib is determined solely from the stiffness of the member. Mr. Whitney has also dealt with the effect of rib stiffness but he has included the characteristics of the concrete members and considered the other interrelated factors occurring under actual design conditions (19)(23).

---

[6] Cons. Engr., Ammann & Whitney, New York, N. Y.

Long-span arch members are subject to stresses caused by a combination of external loads, volumetric effects, and deflections. The member in all cases must be strong enough to resist all these applied forces. The forces will be at a minimum if the arch rib is flexible enough to limit stresses caused by volume changes, yet stiff enough to limit deflection stresses. As these two conditions are opposing design requirements, they must be balanced so as to yield the minimum possible thrust and moments on the rib.

Even if stiffness were the sole consideration governing the size of the rib, as indicated by Messrs. Thürlimann and Johnston, it would be difficult to predict an effectiveness of the shell flange that would be neither too large (which would result in underestimation of the deflection stresses) nor too small (which would result in underestimation of the volumetric stresses). Furthermore, in this prediction of rib stiffness one would have to consider that the flange is subject to tension over part of its length and to compression over the remainder and that these areas of opposite moment sign would change under different loading combinations.

Rib stiffness, however, is only one of the many factors that determine the total moment and thrust that must be carried by the arch rib. The capacity of the rib to resist these forces is not independent of the sectional area and the lever arm, as was assumed by the authors. Instead, for any given concrete strength the capacity of the member will depend directly on the area of the member, the lever arm of the steel, and the percentage of reinforcing steel. The practical areas of reinforcement will in turn depend (in general) on the area of the rib and (in particular) on the width of the rib. The flange adds little to the capacity of the rectangular section in any case because of limitations in the amount of reinforcement that can be crowded into a rib; it adds nothing at all to the capacity in the part of the arch length where the flanged side is in tension. Because of a possible variation in moment sign, tension in the flange can occur anywhere along the length of the arch.

The authors also state that cross bending of the shell will not be critical because the neutral axis will be near the flange—thus resulting in a low fiber stress in the flange and consequently in a low cross bending effect in the shell. However, although the distribution of moments can be approximated by elastic analysis, the stress in the extreme fibers of reinforced concrete members cannot be determined from the section modulus, as indicated by the authors. If the member is designed efficiently, the concrete in the flange will be at the maximum stress. Cross bending in the shell (which is a function of this fiber stress in the rib) accordingly will usually be an important design consideration.

It is impossible to substitute a small-flanged member for a larger rectangular member and expect that the strength of the smaller section of presumed equal stiffness will be equal to the strength of the larger unflanged section. For any particular section of a long-span arch a certain rib of specific area, reinforcement, and lever arm will be required to carry internal moments and thrust which will vary in sign and magnitude. Moving the flange to the edge of this rib will not appreciably increase the strength of the member and so will not permit a substantial reduction in size. Moving the flange to the edge, however, will materially increase the stiffness, as noted by Messrs. Thürlimann and Johnston, and it will also increase the volumetric moments and the required strength.

BRUNO THÜRLIMANN[7] AND BRUCE G. JOHNSTON,[8] M. ASCE.—In Fig. 20 Mr. Ernst has shown that thin-shell models made of cement mortar behave elastically up to the cracking load.

The comments of Mr. Anderson and Mr. Whitney are critical of the same points and thus might logically be considered together. Mr. Anderson repeats the statement made under the heading, "Some Special Problems: Stability of the Structure," that the ribs present two opposing design requirements. On the one hand, the stiffness should be large enough to minimize the secondary bending moments that are caused by the deformations under load. Some additional stiffness is required because plastic flow increases these deformations; this important problem has been discussed previously (17) (18). On the other hand, an increase in stiffness has the undesirable effect of increasing the moments caused by volumetric changes resulting from foundation movement, temperature change, or shrinkage. The purpose of the design should be to keep the stiffness at the minimum value required by considerations of stability, secondary moments produced by deformations, and plastic flow under load. It was demonstrated by the tests that, for an elastic material, stiffness and strength of a T-section are both improved when the shell is placed at the edge of the rib. Such a rib may be considerably reduced in size as compared with a rib of equivalent stiffness and strength with the shell attached at the mid-height of the rib. It is true that reinforced concrete sections present a somewhat different problem. Both Mr. Anderson and Mr. Whitney agree that placing the shell either at the top or bottom of the rib increases the stiffness. Stiffness is required all along the ribs to provide sufficient stability. However, there are only a few places—such as at the springing line—where the full strength is needed. The strength of the section required to carry a normal force and bending moment increases only if the shell is in compression. Where then should this shell be attached? It is agreed that the total cost of comparative designs is the final answer to the problem. From this point of view Mr. Whitney is convinced that attaching the shell to the middle is the proper solution (19). However, a review of the discussions of his paper (19) and of another (24) will reveal that quite a few other engineers disagree with this conclusion. The writers have not made cost analyses and therefore they cannot enter into this discussion.

Mr. Whitney contends that "* * * the authors' investigation has added nothing new to the knowledge of the behavior of cylindrical shells stiffened by arch ribs."

---

[7] Research Asst. Prof., Fritz Eng. Lab., Lehigh Univ., Bethlehem, Pa.

[8] Prof. of Structural Eng., Civ. Eng. Dept., Univ. of Michigan, Ann Arbor, Mich.; formerly Director of Fritz Eng. Lab., Lehigh Univ., Bethlehem, Pa.

It is true that the primary contribution is one of experimental confirmation of the theory. However, in Fig. 4 is provided a simple, practical procedure by which engineers can determine the effective width of shell that can be assumed to act as part of the arch rib. The tests confirm the use of this effective width; this information was not previously available in such simple form.

Mr. Whitney questions the accuracy of the statements which lead to Eq. 48. As far as elastic behavior is concerned, one can easily prove the statements that confirm Eq. 48. Because Mr. Whitney offered no computations to substantiate his disbelief, such proof is not offered herewith. The conclusion, however, follows from the fact that, under the most extreme conditions, the stress σ_x produced by cross-bending is never more than 173% of the lower fiber stress of the rib. The test results fully confirm this fact which was also derived from theoretical considerations. A short computation made by use of the experimental results for N_ϕ and M_x from Fig. 17, or from other test results (14), will verify this statement.

AMERICAN SOCIETY OF CIVIL ENGINEERS
Founded November 5, 1852
TRANSACTIONS

Paper No. 2758

APPLICATIONS OF THE RELAXATION TECHNIQUE IN FLUID MECHANICS

By John S. McNown,[1] M. ASCE, En-Yun Hsu,[2] A. M. ASCE, and Chia-Shun Yih[3]

With Discussion by Messrs. Fred W. Blaisdell; Henry M. Paynter and Ronald F. Scott; Mladen Boreli; Turgut Sarpkaya; and John S. McNown, En-Yun Hsu, and Chia-Shun Yih

Synopsis

Problems in fluid mechanics of essentially irrotational flow are often so complex that numerical methods must be used in their resolution. A simple, yet generally useful method is the relaxation process, which is based on a network of values of the required function determined by means of the finite-difference theory. The numerical process is simple, and techniques are available for satisfying various types of boundary conditions. The computations are useful in solving problems of efflux and seepage and in analyzing flow through transitions or around submerged bodies. Examples of these various types have been solved, and the results are presented as illustrations of the process.

Introduction

Relaxation, a numerical method of integration, can be used to obtain solutions for a wide variety of problems which cannot be solved by standard methods. In using this method, a network of values is assumed for the function sought; the network is then systematically corrected as the errors are "relaxed." Based on the calculus of finite differences, this method was brought to fruition in England by R. V. Southwell and his associates[4]; it has been used in solving a variety of problems dealing with elasticity, heat transfer, and fluid mechanics.

Note.—Published, essentially as printed here, in July, 1953, as *Proceedings-Separate No. 223.* Positions and titles given are those in effect when the paper was received for publication.

[1] Associate Director, Iowa Inst. of Hydr. Research, State Univ. of Iowa, Iowa City, Iowa.

[2] Research Engr., Hydrodynamics Lab., California Inst. of Technology, Pasadena, Calif.

[3] Research Engr., Iowa Inst. of Hydr. Research, State Univ. of Iowa, Iowa City, Iowa.

[4] "Relaxation Methods in Theoretical Physics," by R. V. Southwell, Oxford Press, 1946.

Although only particular solutions can be obtained by such methods and although the computations are time consuming, relaxation methods are effective in cases for which general solutions cannot be obtained by direct methods.

Partial differential equations such as the Laplacian, the Poisson, and the biharmonic can be integrated by using the relaxation procedure. These equations are often encountered in engineering, and numerous general solutions have been obtained for simple boundary conditions. However, general solutions are usually unobtainable if the boundary conditions are complex. It is in such cases that numerical solutions are particularly valuable because in their application a complex boundary condition can be fulfilled almost as easily as a simple one. There is presented herein the method of solving only the Laplace equation, the one most frequently encountered in the analysis of fluid flow. Although this is the simplest of the several equations, the manner of solving it is nonetheless indicative of the general method. Applications of this differential equation are restricted to potential flows such as seepage, flow through boundary contractions, efflux through slots or orifices, certain types of wave motion, and flow over weirs. Only for two-dimensional flow patterns and axisymmetric flow patterns is it feasible to obtain solutions.

Resolution of any significant problem by the relaxation process will require at least many hours and perhaps several months, yet the individual steps in the process are few and easily mastered. These steps are presented subsequently in some detail, from the initially assumed network of values, through the elimination of residual errors and the advances to successively finer nets, to the eventual satisfaction of both the differential equation and the assigned boundary conditions. A number of applications are cited, the analyses having been conducted at the Iowa Institute of Hydraulic Research, State University of Iowa, at Iowa City.

FINITE DIFFERENCE THEORY

Essential Elements.—The goal in applying the relaxation method is to attain a network of values of a function which satisfies a given partial differential equation at each point of a discrete network covering the region and which also satisfies a given set of boundary conditions. The number of points must be large enough (or the mesh fine enough) to make the assumption of a linear variation of the function between adjacent points justifiable. For such a network, the theory of finite differences can be successfully used.

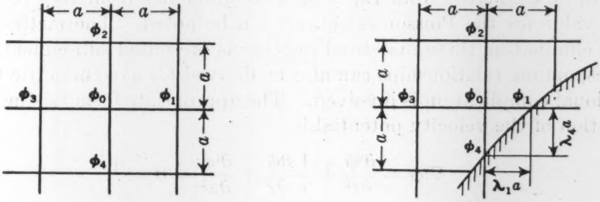

(*a*) Regular (*b*) Irregular

FIG. 1.—PATTERN OF FUNCTION VALUES

An algebraic expression for the Laplacian of a particular function, such as the velocity potential ϕ, can be obtained quite simply. For example, in Fig. 1 (*a*), the approximate value of

$$\nabla^2 \phi = \frac{\partial^2\phi}{\partial x^2} + \frac{\partial^2\phi}{\partial y^2} \qquad (1)$$

is sought for the central point in terms of the several values of ϕ in the immediate vicinity, the mesh being square and the lines spaced a distance a apart. If the coordinates of the central point are designated as x_0 and y_0, at the points $(x_0 + a/2, y_0)$ and $(x_0 - a/2, y_0)$,

$$\frac{\partial\phi}{\partial x} \approx \frac{\phi_1 - \phi_0}{a} \qquad (2a)$$

and

$$\frac{\partial\phi}{\partial x} \approx \frac{\phi_0 - \phi_3}{a} \qquad (2b)$$

respectively. The second partial derivative of ϕ can be obtained in a similar manner—

$$\frac{\partial^2\phi}{\partial x^2} \approx \frac{\dfrac{\phi_1 - \phi_0}{a} - \dfrac{\phi_0 - \phi_3}{a}}{a} = \frac{\phi_1 + \phi_3 - 2\,\phi_0}{a^2} \qquad (3a)$$

In the same way, one can obtain an expression for the second partial derivative with respect to y—

$$\frac{\partial^2\phi}{\partial y^2} \approx \frac{\phi_2 + \phi_4 - 2\,\phi_0}{a^2} \qquad (3b)$$

Finally, the equivalent form for Eq. 1 expressed in finite-difference form is

$$a^2\,\nabla^2\phi \approx \phi_1 + \phi_2 + \phi_3 + \phi_4 - 4\,\phi_0 \qquad (4)$$

Although Eq. 4 is an approximation, equality is closely approached as the spacing is reduced. For a given set of ϕ-values, either known or assumed, $a^2\,\nabla^2\,\phi$ can be evaluated from Eq. 4, and its difference from zero (or another assigned value for the Poisson equation) can be noted. The method of successively eliminating these undesired residues is presented subsequently.

Corresponding relationships can also be derived for axisymmetric flow, but an additional complication is involved. The appropriate form for the differential equation of the velocity potential is

$$\nabla^2\phi = \frac{\partial^2\phi}{\partial r^2} + \frac{1}{r}\frac{\partial\phi}{\partial r} + \frac{\partial^2\phi}{\partial x^2} = 0 \qquad (5)$$

in which x is measured parallel to the axis of symmetry and r at right angles to it. Although both the velocity potential and the stream function ψ for two-dimensional flow satisfy the same equation, the Stokes stream function, for axisymmetric flow, satisfies an equation similar to Eq. 5 but differing in the sign of the first-order term—

$$\frac{\partial^2\psi}{\partial r^2} - \frac{1}{r}\frac{\partial\psi}{\partial r} + \frac{\partial^2\psi}{\partial x^2} = 0 \qquad (6)$$

For the point (x_0, r_0), the value of $\partial\phi/\partial x$ is unchanged from the two-dimensional case (Fig. 1 (a)); in addition,

$$\frac{\partial\phi}{\partial r} \approx \frac{\phi_2 - \phi_4}{2\,a} \ldots\ldots\ldots\ldots\ldots\ldots\ldots\ldots (7)$$

If this value is substituted into Eq. 5, together with the finite-difference equivalents of the second partial derivatives,

$$a^2\,\nabla^2\,\phi = \phi_1 + \phi_2 + \phi_3 + \phi_4 - 4\,\phi_0 + \frac{1}{2\,n}\,(\phi_2 - \phi_4) = 0 \ldots\ldots (8)$$

The corresponding form for ψ is

$$\psi_1 + \psi_2 + \psi_3 + \psi_4 - 4\,\psi_0 - \frac{1}{2\,n}\,(\psi_2 - \psi_4) = 0 \ldots\ldots\ldots\ldots (9)$$

in which n is the number of subdivisions between the axis of symmetry and the point (x_0, r_0) and is denoted by r_0/a.

If the four neighboring points are not equidistant from a given point, such as a point near an irregular boundary, the forms of Eqs. 4, 8, and 9 must be modified. As shown in Fig. 1 (b), the lengths of two of the legs on the star may be less than a. If these lengths are designated as $\lambda_1\,a$ and $\lambda_4\,a$, in which $0 < \lambda < 1$, the appropriate form for the Laplacian operator for two-dimensional flow is

$$a^2\,\nabla^2\,\phi \approx \frac{\phi_1}{\lambda_1} + \phi_2 + \phi_3 + \frac{\phi_4}{\lambda_4} - \phi_0\left(2 + \frac{1}{\lambda_1} + \frac{1}{\lambda_4}\right) \ldots\ldots\ldots (10)$$

and for axisymmetric flow is

$$a^2\,\nabla^2\,\phi \approx \frac{\phi_1}{\lambda_1} + \phi_2 + \phi_3 + \frac{\phi_4}{\lambda_4} - \phi_0\left(2 + \frac{1}{\lambda_1} + \frac{1}{\lambda_4}\right) + \frac{\phi_2 - \phi_4}{n\,(1 + \lambda_4)} \ldots (11)$$

For some problems it is preferable to use a reverse method in which the dependent and independent variables are interchanged. In two-dimensional potential flow, if ϕ and ψ are considered to be the independent variables, x and y satisfy the Reimann-Cauchy equations,

$$\frac{\partial x}{\partial\phi} = \frac{\partial y}{\partial\psi} \ldots\ldots\ldots\ldots\ldots\ldots\ldots\ldots (12a)$$

and

$$\frac{\partial x}{\partial\psi} = -\,\frac{\partial y}{\partial\phi} \ldots\ldots\ldots\ldots\ldots\ldots\ldots\ldots (12b)$$

from which follow the inverse Laplace equations,

$$\frac{\partial^2 x}{\partial\phi^2} + \frac{\partial^2 x}{\partial\psi^2} = 0 \ \ldots\ldots\ldots\ldots\ldots\ldots\ldots\ldots (13a)$$

and

$$\frac{\partial^2 y}{\partial\phi^2} + \frac{\partial^2 y}{\partial\psi^2} = 0 \ldots\ldots\ldots\ldots\ldots\ldots\ldots\ldots (13b)$$

Eqs. 13 can, of course, be expressed in terms of finite differences in the aforementioned manner.

Because the region of interest in fluid flow can always be bounded by a pair of potential lines (on which ϕ is constant) and a pair of streamlines (on which ψ is constant), no irregular stars will be encountered if the $(\phi-\psi)$-plane is chosen for computation. This advantage sometimes compensates for the drawback that the values of x and y along some boundary are unknown (although related) functions of ϕ. As will be illustrated subsequently, the use of ϕ and ψ as independent variables is particularly advantageous if, as in free-jet problems, the boundary streamlines are not fixed a priori but are determined by trial from a double boundary condition.

RELAXATION TECHNIQUE

The relaxation process can be described as a method of systematic refinement of an assumed variation of a function. In addition to the special techniques for satisfying various boundary conditions, two principal procedures are required: (*a*) The reduction of the residues and (*b*) the subdivision of the network wherever the assumption of linear variation is found to be inaccurate.

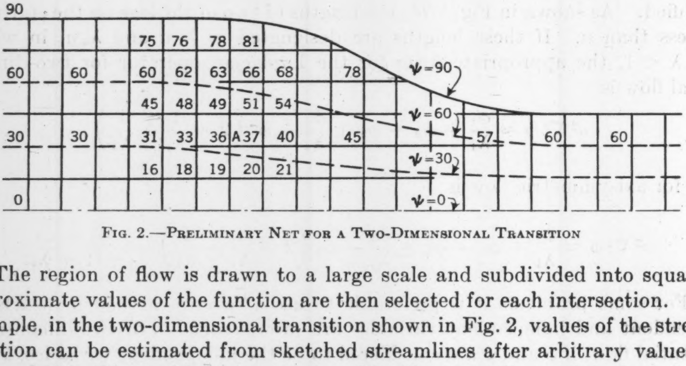

FIG. 2.—PRELIMINARY NET FOR A TWO-DIMENSIONAL TRANSITION

The region of flow is drawn to a large scale and subdivided into squares; approximate values of the function are then selected for each intersection. For example, in the two-dimensional transition shown in Fig. 2, values of the stream function can be estimated from sketched streamlines after arbitrary values of ψ (0 and 90 in this case) have been assigned for the center line and the boundary. The numerical values can be selected at will because the results are to be presented dimensionlessly in terms of the flow characteristics either upstream or downstream from the transition.

Using Eqs. 4 and 10, one can compute from the assumed values of the function the value of the residue for each of the intersections. For example, near point A in Fig. 2 the values could be as shown in Fig. 3, and the residues as recorded to the right of the intersections of the lines. At point A,

$$a^2 \nabla^2 \psi = R = 37 + 49 + 33 + 19 - 4(36) = -6.$$

The other values are similarly computed. In order to reduce the residues it is necessary to adjust repeatedly the many values of ψ.

For a regular star, one for which all four legs are equal in length, a unit increase of ψ at a given point will result in a decrease of 4 in the corresponding residue, as is apparent from Eqs. 4, 8, or 9. Thus, if ψ_A for Figs. 3 or 4 is decreased by 1, the residue is reduced from -6 to -2, as can be seen by referring to Eq. 4. In the same adjustment, the residues for each of the neighboring points are also decreased by 1 because ψ_A becomes ψ_4 in the computation of the residue at the point above, and so forth. The process is therefore continued in accordance with the simple star pattern shown at the left of Fig. 4(*a*) for the several possible cases. Because each change in ψ affects four other ψ-values directly and still others indirectly, the various values will have to be corrected many times. Large residues are first reduced without attempting to make them extremely small, refinement being sought only after all large discrepancies have been eliminated. In less than an hour of computation, one can obtain a familiarity with the simple process and a feeling for various short cuts, such as overcorrection and regional or block relaxation, for which simple formulas can be derived. In Fig. 5 there is shown a stage of computation following single operations at each of points A to D (in alphabetical order). The original ψ-values were obtained from Fig. 3, the values having been multiplied by 10 to avoid the use of decimals.

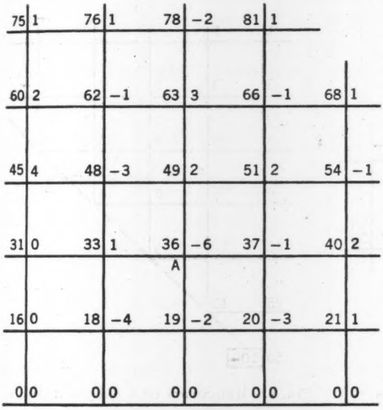
75 1
76 1
78 −2
81 1
60 2
62 −1
63 3
66 −1
68 1
45 4
48 −3
49 2
51 2
54 −1
31 0
33 1
36 −6
A
37 −1
40 2
16 0
18 −4
19 −2
20 −3
21 1
0 0
0 0
0 0
0 0
0 0

FIG. 3.—COMPUTATION OF INITIAL RESIDUES

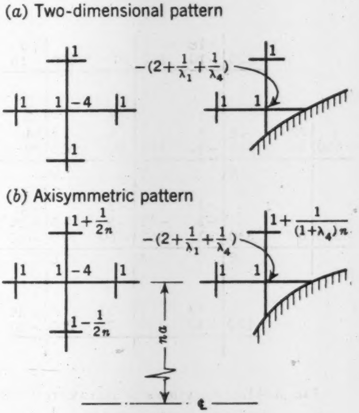
(a) Two-dimensional pattern
1
1
1 −4
1
1
$-(2+\frac{1}{\lambda_1}+\frac{1}{\lambda_4})$
1
1
1
(b) Axisymmetric pattern
$1+\frac{1}{2n}$
1
1 −4
1
$1-\frac{1}{2n}$
$-(2+\frac{1}{\lambda_1}+\frac{1}{\lambda_4})$
$1+\frac{1}{(1+\lambda_4)n}$
1
1
na
℄

FIG. 4.—PATTERNS FOR RELAXATION

Reduction of the residues to a negligible value on a coarse net, such as that shown in Fig. 2, is usually not sufficient because errors are likely to be made in the many numerical processes and because the net is too coarse for the assumption of linearity to apply. The errors can be found by recomputing all the residues from the corrected values of the function; a difference between the recomputed value and that obtained from the successive alteration indicates an error in computation. Thus, for point A in Fig. 5,

$$364 + 490 + 330 + 190 - 4(345) = -6$$

based on the revised values constitutes a check on several of the preceding computations.

Such errors once found can usually be eliminated rather rapidly; hence they cause no particular trouble unless residues are checked too infrequently. If they occur at a distance from the boundary in a two-dimensional flow pattern, corrections can be made directly in accordance with a predetermined pattern (Fig. 6). In the preparation of Fig. 6, it was assumed that a residue (or error) of 100 was found for point A and that those residues (or errors) for all other points in the vicinity of point A were negligible. In reducing R_A to zero, one hundred and twenty-eight neighboring values of the function were found to be affected by at least as much as 1% of R_A. Of course, for local residues other than 100, proportional values can be used. The correction at any point is determined directly in terms of the coordinates of the points; that is, at a point three squares to the left and two squares below the point at which the error was made, the correction indicated in Fig. 6 would be 6% of the anomalous residue.

Because the initial grid is deliberately made coarse for simplicity, the variation of ψ in some regions is probably not linear. The existence of this undesirable condition can be easily ascertained once the relaxation of the initial network has been satisfactorily completed. In a given region, a value of ψ can be obtained for the center of a square by averaging the four values at the corners (points A, C, D, and F in Fig. 5). If this is done for each of four squares with a common vertex, the four new values then can be averaged to give a second value for the common point. If this value—ψ'_A—differs significantly from ψ_A, a smaller spacing should be used. The necessary step, termed an advance to a finer net, need be taken only in the region for which nonlinearity is evident from such computations. If successively finer nets are used only as required, the work is kept to a minimum. Fortunately, the check for nonlinearity and the first step in an advance are the same. As the work progresses, it is desirable to add one or more zeros to each of the numbers, thereby permitting further reduction of the residues without resorting to decimals. Once again, some experience is required to attain an insight into the proper concepts for balancing the merits of additional refinements on a coarse net against those of an advance to a finer one.

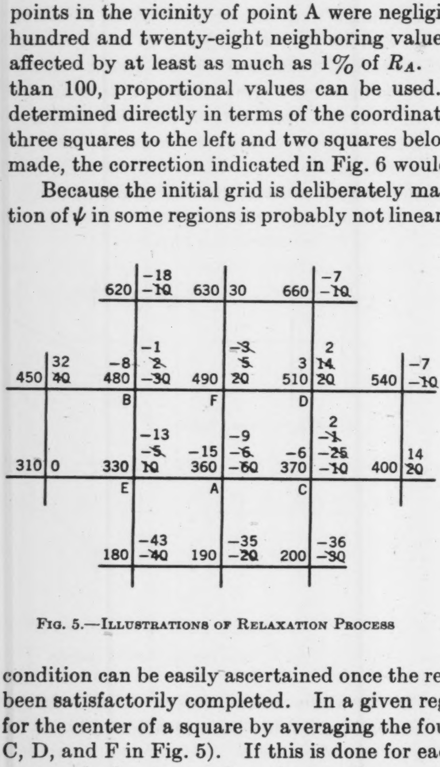

FIG. 5.—ILLUSTRATIONS OF RELAXATION PROCESS

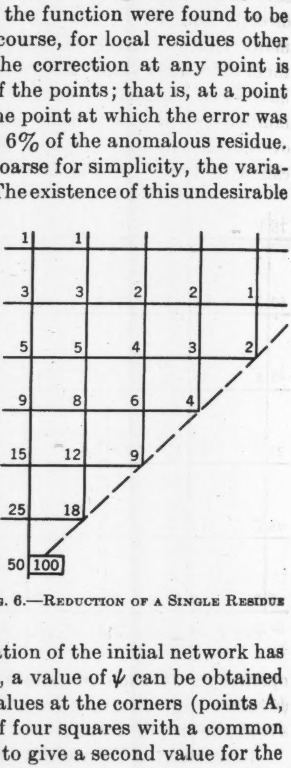

FIG. 6.—REDUCTION OF A SINGLE RESIDUE

Naturally, the relaxation technique that has been described also applies if ϕ and ψ are used as independent variables.

The accuracy of a given result can be judged only by computing velocity or pressure distributions along a boundary line or another arbitrarily selected line and determining whether they are both systematic and comparatively insensitive to further refinement. For this reason, it is desirable to make such computations at various stages. It may be known that a small region of nonlinearity remains; however, if further advance does not appreciably alter the computed distribution nearby, there is no need to continue.

BOUNDARY CONDITIONS

Little mention has been made of the method of satisfying a given set of boundary conditions because the procedure is actually a separate part of the problem and because a variety of techniques is required. For the transition in Fig. 2, no difficulty exists; the values of ψ along the solid boundary and center line are fixed, and the net is simply, if laboriously, extended to the right and left until the condition of constant velocity ($\psi = k\,y$) is satisfactorily approached. For other problems, however, special procedures are required.

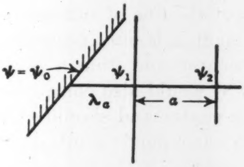

FIG. 7.—COMPUTATION OF $\partial\psi/\partial x$ AT A BOUNDARY

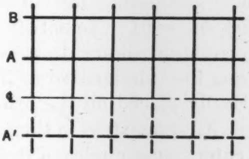

FIG. 8.—INDICATION OF REFLECTION PRINCIPLE

Among such conditions are those specifying (*a*) symmetry at the boundary, (*b*) free streamlines with or without gravitational effects, (*c*) the free surface in a seepage problem, and (*d*) the special condition for the inverse method. In some cases, the velocity at the boundary must be evaluated before the boundary condition can be assessed.

Along a solid boundary, the function ϕ is a variable and ψ is a constant. If ϕ is used, the velocity v can be computed directly for the midpoint of each interval along the boundary from

$$v = -\frac{\partial \phi}{\partial s} \approx -\frac{\phi_1 - \phi_4}{a\sqrt{\lambda^2_1 + \lambda^2_2}} \quad \ldots\ldots\ldots\ldots\ldots\ldots (14)$$

in which s represents distance along a streamline and ϕ_1 and ϕ_4 are adjacent values along the boundary as shown in Fig. 1(*b*). If ψ is used, the normal gradient $\partial\psi/\partial n$ must be determined from $\partial\psi/\partial x$ (or $\partial\psi/\partial y$), which in turn is estimated from two values, one on the boundary and the other near the boundary. In such a case (Fig. 7),

$$v_y = \frac{\partial \psi}{\partial x} \approx \frac{\psi_1 - \psi_4}{\lambda_1\, a} \quad \ldots\ldots\ldots\ldots\ldots\ldots (15)$$

yields an approximation of the y-component of the velocity at a point which is a distance $\lambda_1 a/2$ away from the boundary. Even though the assumption of local linearity approaches the actual conditions, better results are obtained by using a finite-difference formula for the derivative at the boundary based on three ψ-values as illustrated in Fig. 7—

$$\frac{\partial\psi}{\partial x} \approx \frac{1+\lambda}{\lambda}\,\frac{\psi_1-\psi_0}{a} - \frac{\lambda}{1+\lambda}\,\frac{\psi_2-\psi_0}{a} \qquad (16)$$

Inclusion of more than three terms is unnecessary, the increased complexity of the computation not being accompanied by a significant increase in accuracy. Curvilinear extrapolation of this kind might seem unwarranted in a method which is based on the assumption of locally linear variation, but the resulting increased accuracy can obviate an advance to a finer net.

In the event that a flow pattern is symmetrical with respect to a center line, only one of the two halves need be determined, the line of symmetry being a streamline (as in Fig. 3). If ψ is used, the corresponding boundary condition is automatically fixed as it is for a solid boundary, and residues which would be transferred to points on such a boundary are ignored. If, however, the velocity potential is used, the boundary values are not known but are subject to the condition that lines of constant ϕ must intersect the line of symmetry at right angles ($\partial\phi/\partial n = 0$). To satisfy this requirement it is only necessary to note that any residue coming to a point on the center line from a point on the neighboring line (designated as line A in Fig. 8) would also come from line A′ symmetrically placed on the other side of the center and should therefore be doubled. All other steps in the process remain unchanged; points on line B and on the center line are relaxed in the usual manner.

In the analysis of the patterns of flow occurring for various types of efflux, the free streamlines which are encountered necessitate special procedures. Along a free streamline the pressure is constant; thus, for irrotational flow the velocity is either constant (if gravitational effects are ignored) or proportional to the square root of the vertical distance below the line of total head (if gravitational effects are included). Initially the location of the free streamline is not known and it consequently must be assumed. The corresponding flow pattern is next determined by use of the relaxation process, and the velocities along the free streamlines are computed. Because the values obtained will not, in general, satisfy the specified boundary condition for the velocity, the assumed location of the free streamline must be changed and the process repeated. Because ψ is used in the direct method for this type of problem, the aforementioned method of evaluating $\partial\psi/\partial n$ by curvilinear extrapolation is extremely useful.

In the analysis of unconfined seepage through a porous medium, a somewhat different type of free streamline is encountered. Because the piezometric head (velocity potential) is generally used, two conditions are required: (*a*) At every point along the free streamline the pressure must be zero and (*b*) the normal component of velocity must be zero. Accordingly, after a trial curve has been drawn for the streamline bounding the flow, values can be assigned for ϕ which automatically satisfy the condition that $p = 0$—that is, that ϕ is equal to the elevation. After the corresponding complete network has been obtained, the second boundary condition can be checked, and a revised bounding line drawn as required. Once again, this process can be repeated, entirely or in part, until an acceptably correct result is obtained.

To check the imposed boundary condition or to evaluate the velocity along a curved or irregular boundary, $\partial\psi/\partial n$ is evaluated from $\partial\psi/\partial x$ or $\partial\psi/\partial y$. With reference to Fig. 7, $\partial\psi/\partial x$ is determined from Eq. 16 for the point on the bounding streamline. The value of $\partial\psi/\partial n$ is then determined from

$$v = \frac{\partial\psi}{\partial n} = \frac{1}{\sin\theta}\frac{\partial\psi}{\partial x} = \frac{1}{\cos\theta}\frac{\partial\psi}{\partial y} \qquad (17)$$

in which θ is the angle between the bounding streamline and the x-axis. For axisymmetric flow, the corresponding expression is

$$v = \frac{1}{r}\frac{\partial\psi}{\partial n} = \frac{1}{r\sin\theta}\frac{\partial\psi}{\partial x} = \frac{1}{r\cos\theta}\frac{\partial\psi}{\partial y} \qquad (18)$$

It should be noted that no sign convention need be defined because the direction of the velocity is never in question.

The treatment of the boundary condition—if ϕ and ψ are used as independent variables—can best be explained by an example. On the surface of a jet issuing from a two-dimensional nozzle, the pressure and magnitude of the velocity are constants; this condition will determine the shape of the jet. With reference to Fig. 9, it is sufficient to consider the region ABCDE, where line AE and line CD are comparatively far away from the contraction. Along line CD, ϕ can be assumed to be a constant, such as zero. The corresponding value for x can be taken from Fig. 9 and is denoted by X. Taking $\psi = 0$ along line ED, $\psi = -q/2$ along line ABC, q being the discharge per unit width of the nozzle. The value of ϕ along line AE can be taken to be a constant K large enough so that the flow upstream from line AE is essentially uniform; it should be remembered, however, that so far the corresponding value of x (denoted by X') has not been determined. Except for the somewhat complicated boundary conditions for x and y along line ABC, the conditions at the boundaries are

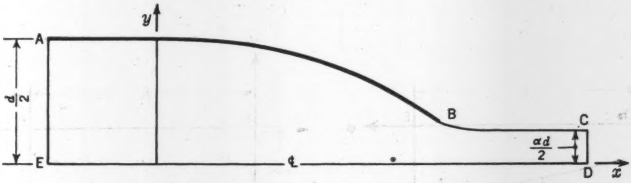

FIG. 9.—SCHEMATIC DIAGRAM FOR REVERSE METHOD

$$\text{for } \phi = 0:\ x = X \text{ (known)},\quad y = -\alpha\psi\frac{d}{q}$$

$$\text{for } \phi = K:\ x = X' \text{ (unknown)},\quad y = -\psi\frac{d}{q}$$

$$\text{and}\quad \text{for } \psi = 0:\ \frac{\partial x}{\partial\psi} = 0,\quad y = 0$$

in which d is the width of the nozzle at point A.

Along line AB it would be possible to translate the condition $\partial\phi/\partial n = 0$ (n being measured in a direction normal to line AB) into one involving x or y as the unknowns, but the result would be extremely unwieldy. Instead, one requires the satisfaction of one of the Riemann-Cauchy equations (Eq. 12*a*), and that

$$x = x(\phi) \qquad \text{(19a)}$$

and

$$y = y(\phi) \qquad \text{(19b)}$$

must be equivalent to

$$y = f(x) \qquad \text{(20)}$$

which describes the boundary AB.

The condition along line BC can be similarly formulated. One again demands the satisfaction of one of the relationships from Eqs. 12 along $\psi = -q/2$. However, instead of Eqs. 19, one requires that

$$\left(\frac{\partial x}{\partial \phi}\right)^2 + \left(\frac{\partial y}{\partial \phi}\right)^2 = \left(\frac{\alpha d}{q}\right)^2 \qquad \text{(21)}$$

in which α is the ratio of the ultimate width of the jet to d.

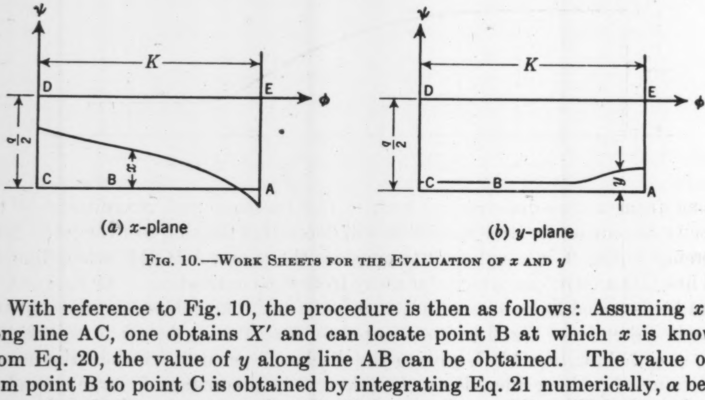

(*a*) *x*-plane (*b*) *y*-plane

FIG. 10.—WORK SHEETS FOR THE EVALUATION OF x AND y

With reference to Fig. 10, the procedure is then as follows: Assuming $x(\phi)$ along line AC, one obtains X' and can locate point B at which x is known. From Eq. 20, the value of y along line AB can be obtained. The value of y from point B to point C is obtained by integrating Eq. 21 numerically, α being assumed such that y computed at C will be equal to $\alpha\, d/2$. With the value of y at point C given, the boundary condition for y at $\phi = 0$ is determined from the linear relationship between y and ψ along line CD.

After the relaxation procedure for y is completed, the result is checked against one of Eqs. 12. If this equation is not satisfied, $x(\phi)$ is corrected accordingly. The process is repeated until the equation is satisfied. Finally, x can be computed either by one relaxation process, or directly by using Eqs. 12.

In the assumption of $x(\phi)$ along line AC, it should be noted that $x(\phi)$ is asymptotically linear. At $\phi = 0$, $\partial x/\partial\phi$ is approximately equal to $-\alpha\, d/q$ and y is approximately equal to $\alpha\, d/2$. At $\phi = K$, $\partial x/\partial\phi$ is approximately equal to $-d/q$, and y is approximately equal to $d/2$. The final result of a computation for the two-dimensional nozzle with the boundary geometry given in Fig. 9 is presented subsequently.

After the various steps in the relaxation process have been completed, any required results can be obtained. The shape of a free streamline is established in the process, the pressure and velocity distributions can be determined throughout space with reference to the pressure and velocity in a region of uniform flow, comparative quantities of seepage can be evaluated, and coefficients of discharge can be computed. The one remaining question is the degree of accuracy obtained—a difficult question to answer.

There is no direct way to assess the accuracy other than to make determinations, for example, of velocity distributions from each of the various nets prepared. If the change in this result following a particular refinement is comparatively small, one can conclude that the result is satisfactory. Various methods of partly resolving this troublesome matter will become evident in each problem. It is a significant fact that no two regions are entirely equivalent. In one region several subdivisions may be required; in another, none. Furthermore, even sizable errors in the pattern at one point may have a very small effect at another. As the entire process is time consuming, special care should be taken to assess the reliability of the results at each stage of the computation.

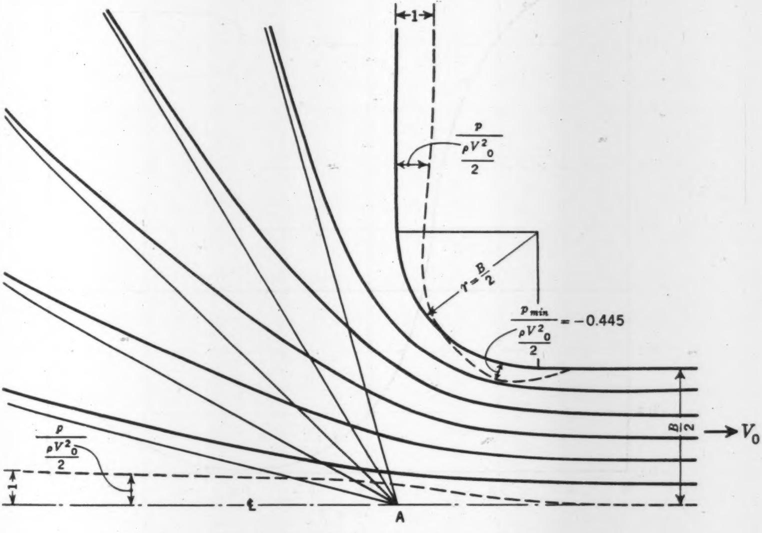
1
$\frac{p}{\frac{\rho V_0^2}{2}}$
$r = \frac{B}{2}$
$\frac{p_{min}}{\frac{\rho V_0^2}{2}} = -0.445$
$\frac{B}{2}$
V_0
$\frac{p}{\frac{\rho V_0^2}{2}}$
1
℄
A

FIG. 11.—TWO-DIMENSIONAL CURVED INLET

APPLICATIONS

The importance of the relaxation method is best indicated by its diversity of application. This diversity is evident from the following series of examples for flow through boundary transitions, flow with a free surface, and seepage. The patterns are two-dimensional or axisymmetric. Because the details of the computation procedure for the interior are similar in all problems, only in the satisfying of the boundary conditions do the problems differ significantly.

The results of computation of the flow through a two-dimensional inlet transition between a reservoir and a conduit are shown in Fig. 11; in this case the radius of rounding is equal to half the conduit width. The distribution of pressure along the boundary is indicated, and representative streamlines are shown together with the radial lines which they approach asymptotically. The pattern of the flow some distance upstream of the inlet is identical to that for flow toward a sink at point A—the intersection of the projection of the vertical boundary and the axis of symmetry. The result has been found to conform closely with that obtained from a different type of analysis and with that from an experiment.[5]

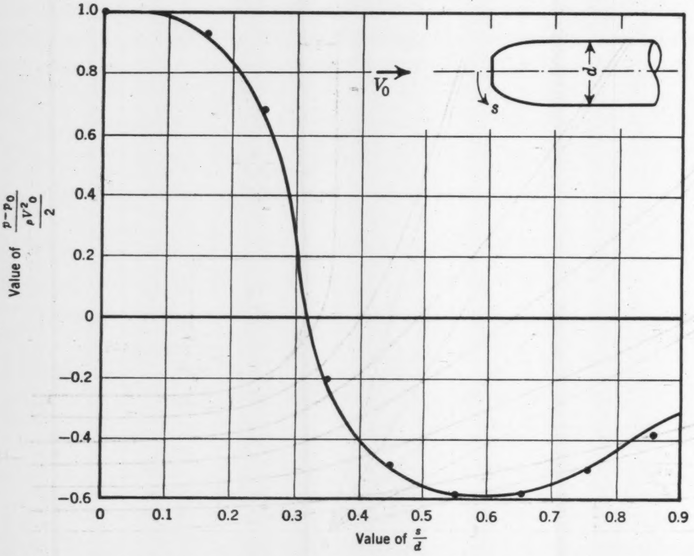

FIG. 12.—PRESSURE DISTRIBUTION FOR AXISYMMETRIC FLOW PAST A MODIFIED ELLIPSOIDAL HEAD FORM

A second example is an internal boundary transition in axisymmetric flow. In a study of a series of head forms,[6] the pressure distribution was determined for a modified ellipsoidal form as indicated in Fig. 12. In this study a comparison was made of the results obtained from the water tunnel with those computed numerically. The correspondence is good from the point of stagnation to a point somewhat beyond the region of minimum pressure. The dimensionless value for the minimum pressure is -0.57, which can be compared with a value of -0.74 for a hemispherical nose form. The significance of this comparison is that a body with the modified nose form could move at higher velocities without producing cavitation than could one with the hemispherical form. The effects of the boundary layer in this region are evidently very small.

---

[5] "Pressure Distribution from Theoretical Approximations of the Flow Pattern," by John S. McNown and En-Yun Hsu, *Proceedings*, Heat Transfer and Fluid Mechanics Inst., 1949, pp. 65–76.

[6] "Cavitation and Pressure Distribution—Head Forms at Zero Angle of Yaw," by Hunter Rouse and John S. McNown, *Studies in Engineering Bulletin 32, No. 420*, State Univ. of Iowa, Iowa City, Iowa, 1948

Applications of the relaxation technique to the determination of flow patterns involving a free surface include problems of efflux, overflow, jet impingement, and steady cavity flow. Each of these is characterized by the existence of a boundary along which the pressure is constant. These problems have been the subjects of several computations, which serve as further illustrations of the method.

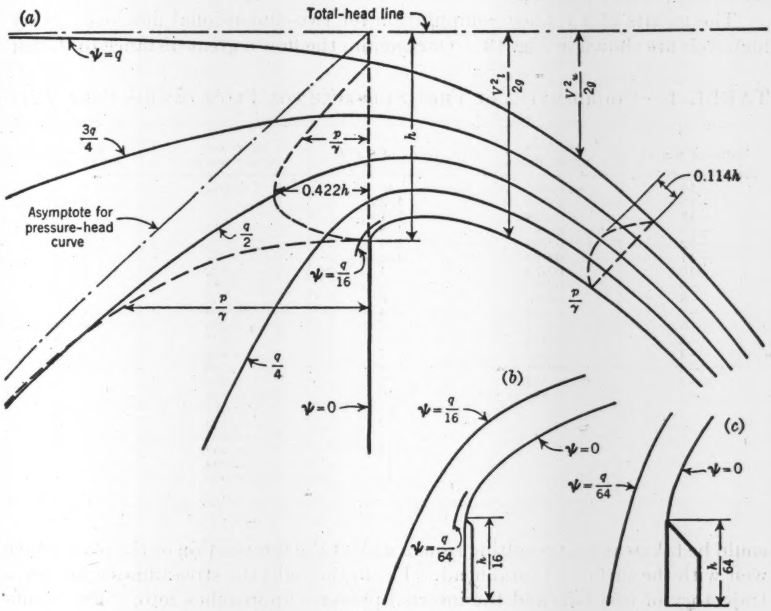
(a)
Total-head line
ψ=q
$\frac{3q}{4}$
$\frac{V_1^2}{2g}$
$\frac{V_u^2}{2g}$
h
$\frac{p}{\gamma}$
0.422h
0.114h
Asymptote for pressure-head curve
$\frac{q}{2}$
$\psi=\frac{q}{16}$
$\frac{p}{\gamma}$
$\frac{p}{\gamma}$
$\frac{q}{4}$
ψ=0
(b)
$\psi=\frac{q}{16}$
ψ=0
$\psi=\frac{q}{64}$
$\frac{h}{16}$
(c)
ψ=0
$\psi=\frac{q}{64}$
$\frac{h}{64}$

FIG. 13.—PATTERN OF FLOW OVER A VERY HIGH WEIR

From extensive computations, Hunter Rouse, M. ASCE, and A. H. Abul-Fetouh have presented[7] detailed information for efflux through an orifice symmetrically placed at the end of a circular conduit. The shape of the free jet, the pressure distribution along the solid boundary, and the coefficient of contraction were presented for various ratios of the diameter of the orifice to the diameter of the conduit. A comparison of the results with those for similar two-dimensional flows revealed remarkably close correspondence for the values of the contraction coefficient. Furthermore, the coefficients available from various experiments were found to follow essentially the same trend.

---

[7] "Characteristics of Irrotational Flow Through Axially Symmetric Orifices," by Hunter Rouse and A. H. Abul-Fetouh, *Journal of Applied Mechanics*, Vol. 17, No. 4, 1950, pp. 421–426.

Overflow problems are indeterminable by ordinary methods of hydrodynamics because of the paramount importance of gravity. That is, surfaces of constant pressure are not, for these flows, also surfaces of constant velocity. Thus, even the classical method of the free-streamline theory is not applicable. Mr. Southwell has presented[4] a computation for the free overfall. D. Citrini has published[8] the results of a computation for a circular weir which are applicable to the design of a morning-glory spillway; Mr. Citrini obtained the pattern for the case in which the (horizontal) radius of curvature of the weir was ten times the total head on the weir.

The results of a refined computation for two-dimensional flow over a very high weir are shown in Fig. 13. Once again, the flow a great distance to the left could be taken as that resulting from a sink at the intersection of the plane of the weir with the surface of total head. Far to the right the streamlines approach a trajectory of free fall, and the internal pressure approaches zero. The significant region near the crest of the weir is shown at three different scales in the various parts of Fig. 13. The coefficient of discharge C_d in the conventional equation,

$$Q = C_d \sqrt{2\,g}\,L\,H^{3/2} \qquad (22)$$

was found to be 0.408. This value, as it should be, is somewhat more than the value of 0.388 found by Mr. Citrini for the curved weir. Both free surfaces and representative internal streamlines are shown in Fig. 13. Because the shape of the former is significant in the design of spillways, coordinates of the two bounding curves in their ratio to the head are given in Table 1.

TABLE 1.—COORDINATES OF FREE SURFACES FOR FLOW OVER A HIGH WEIR

Value of 8 x/H	y/H for upper nappe	Value of 8 x/H	y/H for upper nappe	y/H for lower nappe
−16	0.991	0	0.855	0
−15	0.989	1/32	....	0.013
−14	0.988	1/16	....	0.020
−13	0.985	1/8	....	0.031
−12	0.983	1/4	....	0.047
−11	0.979	1/2	....	0.068
−10	0.973	1	0.822	0.091
−9	0.969	2	0.781	0.113
−8	0.965	3	0.733	0.101
−7	0.959	4	0.678	0.065
−6	0.951	5	0.609	0.010
−5	0.943	6	0.531	−0.058
−4	0.932	7	0.442	−0.135
−3	0.921	8	0.340	−0.222
−2	0.903	9	0.230	−0.323
−1	0.880	10	0.114	−0.432
		11	−0.011	−0.561
		12	−0.149	−0.705
		13	−0.305	−0.866
		14	−0.491	−1.043
		15	−0.694	
		16	−0.910	

---

[8] "Un'esperienza di calcolo numerico; Lo stramazzo a pianta circulare," by D. Citrini, Rendicont Seminario Matematico e Fisico di Milano, Vol. XXI, 1951, pp. 125–147.

Perhaps the longest of all the computations described herein was that for axisymmetric flow with an internal boundary which was partly fixed and partly a steady-state cavity. Once again, this computation duplicated part of the experiments conducted in the water tunnel at the Iowa Institute[6] for cavitating flow around a hemispherical head form mounted on a shaft of equal diameter. The cavitation index for this case was 0.2, a value that was so low that a large vapor cavity formed. The pressure distribution observed in the experiments[6] was imposed as an internal boundary condition, and the corresponding shape of the vapor cavity was determined by successive approximation.

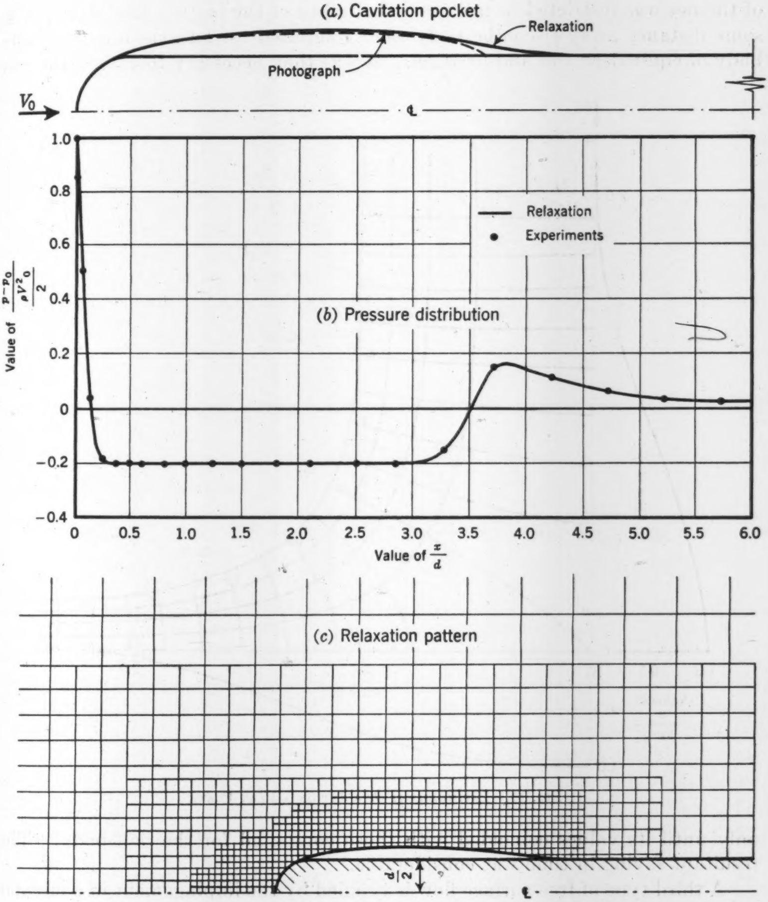

FIG. 14.—FLOW WITH CAVITATION FOR A HEMISPHERICAL HEAD FORM

In Fig. 14 there are shown (*a*) the observed and computed cavity profiles, (*b*) the pressure distribution, and (*c*) the pattern used for computation. Further details of the computation are available,[9] including the ψ-values at each of the intersections in Fig. 14(*c*). The conditions far upstream or far downstream were, of course, those for parallel flow. By use of an artifice, the radial extent of the net was restricted to ten times the radius of the body. The values of ψ some distance away from the body were computed for an axisymmetric half-body of equivalent size and location. It was then necessary to extend the net only until its values coincided with those computed for the half-body. The resultant saving in time was considerable.

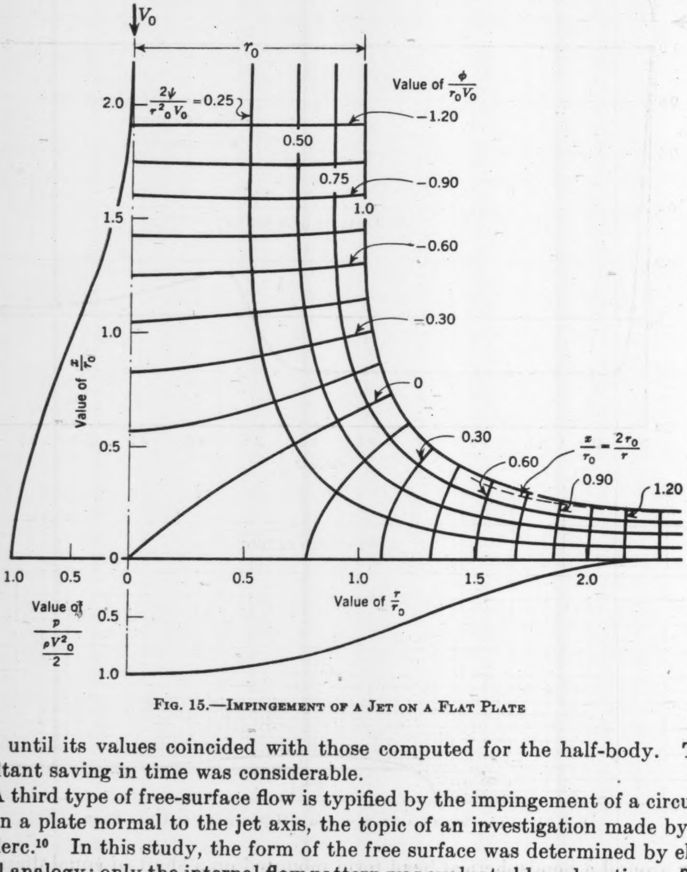

FIG. 15.—IMPINGEMENT OF A JET ON A FLAT PLATE

A third type of free-surface flow is typified by the impingement of a circular jet on a plate normal to the jet axis, the topic of an investigation made by A. LeClerc.[10] In this study, the form of the free surface was determined by electrical analogy; only the internal flow pattern was evaluated by relaxation. The velocity was assumed to be sufficiently high that the effect of gravity as well as that of viscosity could be neglected. The shape of the jet and representative streamlines, the variation of the pressure along the axis and along the plate, and the limiting curve for the free surface are shown in Fig. 15.

---

[9] "Approximate Analyses Interrelating Pressure Distribution and Axisymmetric Body Form," by En-Yun Hsu, thesis presented to the State University of Iowa, at Iowa City, in 1950, in partial fulfilment of the requirements for the degree of Doctor of Philosophy.

[10] "Déviation d'un jet liquide par une plaque normale à son axe," by A. LeClerc, *La Houille Blanche*, Vol. 5, 1950, pp. 816–821.

A characteristic application of the inverse method is shown in Fig. 16. The pattern of efflux from a curved two-dimensional nozzle is that which was also used in explaining the techniques. An arbitrary parabolic curve at the end of a parallel approach reduces the normal section at the region of efflux to one third of that of the approach. The curve is defined by

$$\frac{y}{b} = 3 - \frac{(x/b)^2}{18} \quad \text{.......................} (23)$$

The contraction coefficient was found to be 0.75. It is of importance to note, once again, that regular stars are used throughout this computation even though both the solid boundary and the free boundary are curved.

Problems of seepage comprise a third group to which the methods of relaxation are applicable. As is well known, a consequence of the Darcy law is the applicability of potential theory to problems of laminar seepage. The pressure or the piezometric head acquires the role of the velocity potential, and the Laplace equation is hence applicable. Several examples of the application of the relaxation procedure to various types of seepage flows have been published; results of simply bounded structures have been presented for two-dimensional horizontal seepage through a monolith[11] and for various patterns of two-dimensional seepage into an excavation which is partly protected by impervious sheet piling.[12]

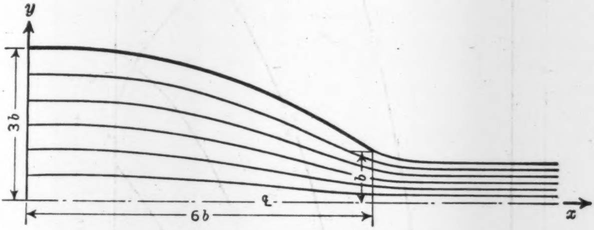

FIG. 16.—EFFLUX FROM A CURVED NOZZLE

Applications to the more complex case of seepage with a free surface have been presented elsewhere[4,11], a refined version being presented in Fig. 17. These are cases for which, once again, the bounding streamline is initially unknown and can be determined only by trial and error. The two boundary conditions for the free surface are as follows: (*a*) The direction of the resultant velocity must coincide with that of the free streamline. (*b*) The free surface must be one of constant pressure. (That is, the piezometric head, which is ϕ, is equal to the elevation h.) The second of these conditions was assumed for a trial curve, and a relaxation of the interior was completed. Adjustment of the free surface was then made on the basis of the shortcomings with regard to the first condition. Because the ϕ-function was used throughout, the boundary condition for the horizontal bottom line was that of orthogonality (or symmetry) and was fulfilled by the application of double residues as previously described. The value of ϕ is a constant on the upstream face but is equal to the elevation on the downstream face.

---

[11] Discussion by John S. McNown of "The Significance of Pore Pressure in Hydraulic Structures," by L. F. Harza, *Transactions*, ASCE, Vol. 114, 1949, p. 245.

[12] "Seepage into Sheeted Excavation," by J. McNamee, *Geotechnique*, London, England, Vol. 4, December, 1949, pp. 227–241.

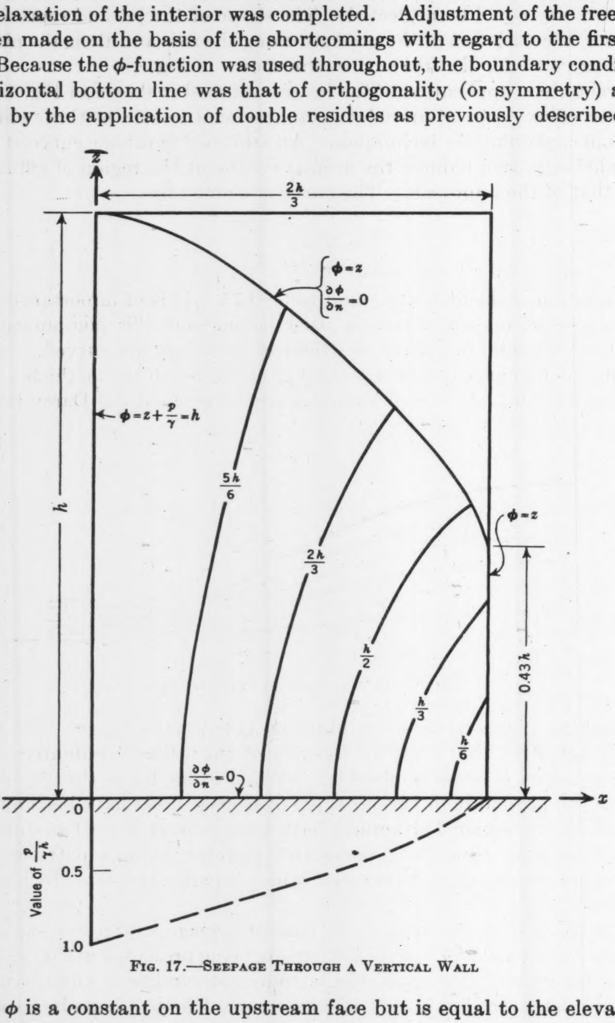
z
$\frac{2h}{3}$
$\phi = z$
$\frac{\partial\phi}{\partial n} = 0$
$\phi = z + \frac{p}{\gamma} = h$
$\frac{5h}{6}$
h
$\frac{2h}{3}$
$\phi = z$
$\frac{h}{2}$
$0.43h$
$\frac{h}{3}$
$\frac{h}{6}$
$\frac{\partial\phi}{\partial n} = 0$
0
x
Value of $\frac{p}{\gamma h}$
0.5
1.0

FIG. 17.—SEEPAGE THROUGH A VERTICAL WALL

Although many problems of seepage in two dimensions can be obtained more satisfactorily by use of classical methods, only such a method as relaxation can be used for complex or curved boundaries. In addition, axisymmetric flows—such as flow of ground water to a well—or the axisymmetric counterpart of the problem of seepage into an excavation[12] are beyond the scope of ordinary methods.

CONCLUSIONS

In the presentation both of the relaxation method and of examples in which it is utilized, the utility and flexibility of the process have been amply demonstrated. Fortunately, the technique can be quickly mastered, containing as it does only two basic parts. The mechanism of the internal reduction of residues is simple and extremely repetitive. The various boundary conditions are either assigned initially or met indirectly as a part of the process. An advantage of the method is that absolute accuracy is not a requirement; an occasional error once made will be caught and need not cause an excessive loss of time. Although the method is simple, it is not completely mechanical, so that the exercise of judgment and the introduction of suitable modifications of a given routine can greatly reduce the time required.

The method is restricted to the resolution of problems of essentially irrotational flows or flows for which the Reynolds number is quite small. It will not be and should not be considered as a replacement for the well-known analytical solutions characterizing classical hydrodynamics. Although still restricted to flows which are essentially two-dimensional or axially symmetric, its utility lies in the fact that within these limitations the relaxation process can be used regardless of the complexity of the boundary conditions. A small change in boundary form that might preclude the solving of an otherwise classical problem by standard methods presents no difficulty in its resolution by numerical methods. Because the engineering profession is constantly discovering many new applications for analyses of potential flows, the relaxation technique is recommended as a powerful adjunct to standard methods. The flow patterns presented herein are both useful in themselves and representative of the variety of problems which can be solved by relaxation.

ACKNOWLEDGMENTS

Much of the work described herein was supported by the Office of Naval Research, Department of the Navy, under contract N8onr-500. Among those who assisted in the computations are S. Ince, J. M. ASCE (Fig. 11), W. Hsieh (Fig. 12), S. C. Liu (Fig. 13), Mr. Leclerc (Fig. 15), Turgut Sarpkaya, J. M. ASCE (Fig. 16), and Y. C. Soong, of the State University of Iowa. Mr. Rouse suggested or directed several of the studies.

DISCUSSION

Fred W. Blaisdell,[13] M. ASCE.—In describing the relaxation technique together with its advantages and its limitations, the authors have provided a distinct service to those who might consider the use of this "tool." The examples of the application of the relaxation technique are most interesting, and the comparisons with experimental data, where presented, show good agreement.

The writer has conducted a study of experimental data[14] on the form of the nappe emitting from a vertical, sharp-crested, suppressed weir. A general equation was obtained for that part of the nappe which was free-falling. This conforms to the region defined by the authors (under the heading, "Applications") where "Far to the right the streamlines approach a trajectory of free fall, and the internal pressure approaches zero."

TABLE 2.—Comparison of Nappe Surface Coordinates

Value of $8\,x/H$	Lower Nappe				Upper Nappe				Value of T/H
	y/H		Eq. 25		y/H		Eq. 25		
	FWB[a]	MHY[b]	FWB[a]	MHY[b]	FWB[a]	MHY[b]	FWB[a]	MHY[b]	
4	+0.071	+0.065	...	...	+0.630	+0.678	...	...	...
5	+0.018	+0.010	−0.832	−0.832	+0.577	+0.609	−0.832	−0.576	...
6	−0.048	−0.058	−0.832	−0.576	+0.511	+0.531	−0.832	−0.704	...
7	−0.127	−0.135	−0.896	−0.640	+0.432	+0.442	−0.896	−0.832	0.577
8	−0.220	−0.222	−0.832	−0.896	+0.339	+0.340	−0.832	−0.512	0.562
9	−0.326	−0.323	−0.832	−0.512	+0.233	+0.230	−0.832	−0.384	0.553
10	−0.445	−0.432	−0.896	−1.280	+0.114	+0.114	−0.896	−0.576	0.546
11	−0.578	−0.561	−0.832	−0.960	−0.019	−0.011	−0.832	−0.832	0.550
12	−0.724	−0.705	−0.832	−1.088	−0.165	−0.149	−0.832	−1.152	0.556
13	−0.883	−0.866	−0.832	−1.024	−0.324	−0.305	−0.832	−1.920	0.561
14	−1.055	−1.043	−0.896	...	−0.496	−0.491	−0.896	−1.088	0.552
15	−1.241	...	−0.832	...	−0.682	−0.694	−0.832	−0.832	...
16	−1.440	...	...	...	−0.881	−0.910	...	...	...
Average			−0.849	−0.868			−0.849	−0.855	0.557 0.559[a]

[a] The writer, Fred W. Blaisdell. [b] The authors, Messrs. McNown, Hsu, and Yih.

The data available to the writer indicate the free-fall region to include values of x/H in excess of 0.5. Therefore, the writer's results and Table 1 should yield comparable results when $x/H \geqq 0.5$; the comparison is made in Table 2. For the lower nappe there seems to be some trend to the differences between the writer's results and the authors' results. For the upper nappe, the differences are erratic and no trend can be detected.

A second comparison and test can also be applied. The general equation developed by the writer has the form:

$$\frac{y}{H} = C + \tan\theta\,\frac{x}{H} + \frac{S}{2}\left(\frac{x}{H}\right)^2 + \frac{T}{H} \qquad (24)$$

---

[13] Project Supervisor, Agri. Research Service, U. S. Dept. of Agriculture, St. Anthony Falls Hydr. Lab., Minneapolis, Minn.

[14] "Equation of the Free-Falling Nappe," by Fred W. Blaisdell, *Proceedings-Separate No. 482*, ASCE, August, 1954.

The second differential of Eq. 24 is

$$\frac{d^2\left(\frac{y}{H}\right)}{d\left(\frac{x}{H}\right)^2} = S \qquad (25)$$

Eq. 25 indicates that the second differences should be constant; these differences are given in Table 2. The lack of absolute constancy in the writer's second differences is caused by the fact that the nappe coordinates were recorded to only three significant figures. The writer's value for S is 0.850; there seems to be considerable variation in the second differences derived from the authors' data.

Still a third comparison and test can be applied to the data. The term T in Eq. 24 represents the vertical thickness of the nappe. This dimension is a constant because the horizontal velocity is constant where the nappe is free-falling. (For the lower nappe the term T is zero.) The nappe thickness in terms of H computed from the authors' data is given in Table 2. This nappe thickness can be compared with 0.559, the nappe thickness derived by the writer for the authors' boundary conditions.

The validity of comparing (y/H)-values is perhaps open to some question because either method of analysis could yield valid results from the basic data and assumptions, and one could not choose which method would give the most accurate values. However, the comparison within each group of data of nappe thickness and, more particularly, of the second differences should yield some information on the precision of the results. Based on the authors' presentation, it would seem that the relaxation technique should give identical nappe thicknesses for each value of x/H and identical second differences if the network were sufficiently subdivided. This does not seem to be completely substantiated by the writer's tests of the data.

HENRY M. PAYNTER,[15] J. M. ASCE, AND RONALD F. SCOTT.[16]—The definition of relaxation methods given by the authors does not appear to be complete. Rather than merely being techniques of numerical integration, relaxation methods are a mode of attack on any problem or set of relationships, be they graphic, algebraic, or numerical. Such methods constitute much the same approaches which have come to be termed "Hardy Cross" methods in the United States.[17] Essentially these methods involve the prior determination of the mutual influence patterns among the variables, followed by a systematic successive application of this pattern (stylus or matrix) to each and every equation of the system until the unbalances (residuals) are reduced to within the required tolerances.

---

[15] Asst. Prof. of Hydr. Eng., Massachusetts Inst. of Technology, Cambridge, Mass.

[16] Research Associate, Massachusetts Inst. of Technology, Cambridge, Mass.

[17] "The Relation of Analysis to Structural Design," by Hardy Cross, *Transactions*, ASCE, Vol. 101, 1936, p. 1363.

The general philosophy behind all such methods has been discussed fully.[18,19] Besides the treatise[4] cited by the authors, further details and special manipulations have been investigated by Mario G. Salvadori, M. ASCE, and Melvin L. Baron,[20] J. M. ASCE, J. B. Scarborough,[21] W. E. Milne,[22] and F. S. Shaw.[23]

The relaxation principle differs from simple iteration in that the personal judgment and insight of the individual can be exercised at each step of the process. Relaxation methods reduce to purely iterative procedures if this judgment factor is removed; this point is clearly brought out in the work of H. W. Emmons.[19]

It is also important to distinguish between steady-state solutions and transient solutions as they affect the applicability of different numerical approaches. The diffusion equation,

$$\frac{\partial \phi}{\partial t} = a \nabla^2 \phi \qquad (26)$$

reduces to the Laplace equation,

$$\nabla^2 \phi = 0 \qquad (27)$$

under steady conditions ($\partial \phi / \partial t = 0$). If, for example, it were desired to find the values of seepage flow through a dam during a drawdown of the reservoir or the values of the hydrostatic excess pore-water pressure during a soil-consolidation process, relaxation methods would not be appropriate. In these cases, iterative techniques, such as those used for thermal diffusion or soil-consolidation problems,[19,22,24,25] become useful.

In a similar manner, when the Poisson equation,

$$\nabla^2 \phi = f(x, y, z) \qquad (28)$$

is to be solved, there are certain cases in which, with the proper choice of grid and symmetry conditions, direct numerical solutions are often possible. The senior writer has studied such a case involving the cooling of a chemical reactor in which heat was generated uniformly and removed by a grillage of cooling tubes. In this case, a hexagonal grid was used, making maximum use of symmetry; the heat flow could be summed directly by computing outward from the tubes.

It is regretted that the authors did not "tie down" all the interesting features and consequences of the potential-flow solutions according to the manner in which the height of the seepage face is located—as 0.43 h, for example, in

---

[18] "Numerical Methods of Analysis in Engineering," arranged by L. E. Grinter, Macmillan Co., New York, N. Y., 1949.

[19] "The Numerical Solution of Partial Differential Equations," by H. W. Emmons, *Quarterly of Applied Mathematics*, Vol. II, No. 3, October, 1944, p. 173.

[20] "Numerical Methods in Engineering," by Mario G. Salvadori and Melvin L. Baron, Prentice-Hall, New York, N. Y., 1952.

[21] "Numerical Mathematical Analysis," by J. B. Scarborough, 2d Ed., Johns Hopkins Press, Baltimore, Md., 1950.

[22] "Numerical Solution of Differential Equations," by W. E. Milne, John Wiley & Sons, Inc., New York, N. Y., 1953.

[23] "An Introduction to Relaxation Methods," by F. S. Shaw, Dover Publications, Inc., New York, N. Y., 1953.

[24] "Numerical Solution of Some Problems in the Consolidation of Clay," by R. E. Gibson and P. Lumb, *Proceedings*, Inst. of C. E., London, England, Pt. I, Vol. 2, No. 2, March, 1953.

[25] "Numerical Analysis of Consolidation Problems," by R. F. Scott, thesis presented to Massachusetts Inst. of Technology, Cambridge, Mass., in 1953, in partial fulfilment of the requirements for the degree of Master of Science.

Fig. 17. However, even in this case the phreatic line (free-surface curve) can be located only very crudely by a graphical procedure. Moreover, it would be most helpful to soils engineers and hydraulic engineers to have the effective conductance G of this wall expressed numerically—that is, a numerical value for the coefficient G in the expression,

$$Q = G\,k\,(L\,h)\,\frac{h}{b} = G\left(k\,\frac{L}{b}\right)h^2 \qquad (29)$$

in which L is the length of the wall and k is the permeability.

Perhaps it is not realized at the time the solutions are performed that these results are the very answers engineers are seeking, and that such numbers can be obtained with precision only from the original computation sheets. For this reason many of those in the numerical-computation field prefer to publish the numerical values of the potential (or stream) function as determined at each point in the grid, together with the final unbalanced residual at each such point.

TABLE 3.—WEIR DISCHARGE PROFILE

UPPER NAPPE				LOWER NAPPE			
Value of $8\,x/H$	Relaxation MHY[a]	Experiment USBR[b]	Difference	Value of $8\,x/H$	Relaxation MHY[a]	Experiment USBR[b]	Difference
−16	0.991	0.979	0.012	0	0	0	0
−12	0.983	0.972	0.011	½	0.068	0.066	0.002
− 8	0.965	0.958	0.007	1	0.091	0.096	0.005
− 4	0.932	0.921	0.011	2	0.113	0.112	0.001
0	0.855	0.845	0.010	3	0.101	0.102	0.001
4	0.678	0.670	0.008	4	0.065	0.070	0.005
8	0.340	0.344	0.004	5	0.010	0.021	0.011
16	−0.910	−0.905	0.005	6	−0.058	−0.046	0.012
				7	−0.135	−0.122	0.013
				8	−0.222	−0.214	0.008
				12	−0.705	−0.724	0.019

[a] The authors, Messrs. McNown, Hsu, and Yih. [b] From reference 27.

However, it should be noted that the authors and their co-workers have done a great service to the profession in publishing, for example, the table (Table 1) of coordinates of the upper and lower nappes corresponding to the relaxation solution for the free overflow from a high, sharp-crested, vertical weir. In Table 3 the values from Table 1 are compared with values derived from experimental data obtained by the Bureau of Reclamation, United States Department of the Interior (USBR), and others.[26] Over the range of values compared the fit is impressive; if the free surface of the relaxation solution was obtained (or at least refined) independently of this experimental information, the result constitutes a remarkable testimonial to the value of potential-flow methods in general, and relaxation procedures in particular, in obtaining basic design information for free-surface flow where viscous effects are not significant.

---

[26] "Studies of Crests for Overfall Dams," by J. N. Bradley, *Bulletin No. 3*, Pt. VI, Bureau of Reclamation, U. S. Dept. of the Interior, Washington, D. C., 1948.

The writers believe this point might be stressed to the advantage of analytical procedures.

The authors have restricted their attention to the use of uniform square grids or meshes. Whereas this may be justified because of space limitations, it may leave one with the incorrect impression that such a grid is to be preferred in most cases. Several other mesh systems are preferable for particular instances; a few, among others, are (*a*) nonuniform rectangular, (*b*) oblique, (*c*) triangular, and (*d*) hexagonal.

In connection with analog studies, R. H. MacNeal[27,28] has treated the problem in which completely nonuniform grids are used as shown in Fig. 18(*a*). It was proved by Mr. MacNeal that the best general values of distribution coefficients for such cases can be obtained by constructing what hydrologists would term a "Thiessen Polygon Network" of tributary influence areas around each node,[29] such as is shown in Fig. 18(*b*). From the sides of these polygons and from the distances between nodes, as indicated in Fig. 18(*c*), Mr. MacNeal has shown that influence coefficients can be determined. These coefficients might be termed λ_{ab} which is equal to d_{ab}/l_{12}. Thus, the expression equivalent to Eq. 8 becomes

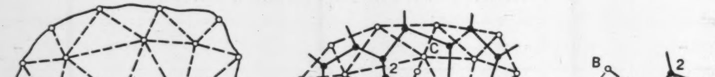

(*a*) (*b*) (*c*)

FIG. 18.—IRREGULAR MESHES

$$\frac{\phi_B}{\lambda_{ab}} + \frac{\phi_C}{\lambda_{ac}} + \frac{\phi_D}{\lambda_{ad}} + \frac{\phi_E}{\lambda_{ae}} + \frac{\phi_F}{\lambda_{af}} - \phi_A \left(\frac{1}{\lambda_{ab}} + \frac{1}{\lambda_{ac}} + \frac{1}{\lambda_{ad}} + \frac{1}{\lambda_{ae}} + \frac{1}{\lambda_{af}} \right) = 0 \,.\,. \quad (30)$$

For the special case of square nets, the four λ-values are all unity, and Eq. 28 reduces to Eq. 8.

The foregoing techniques can be used to good advantage for all types of solutions, particularly where irregular boundaries or irregular symmetry conditions are involved. Mr. MacNeal has noted that all radial angles must be acute if negative resistance is to be avoided in passive electrical-resistor networks.

---

[27] "The Solution of Partial Differential Equations by Means of Electrical Networks," by R. H. MacNeal, thesis presented to California Inst. of Technology at Pasadena, Calif., in 1949, in partial fulfilment of the requirements for the degree of Doctor of Science.

[28] "An Asymmetrical Finite Difference Network," by R. H. MacNeal, *Quarterly of Applied Mathematics*, Vol. XI, No. 3, October, 1953.

[29] "Engineering Hydraulics," edited by Hunter Rouse, John Wiley & Sons, Inc., New York, N. Y., 1950, p. 276.

Iteration and relaxation methods demonstrate, as intermediate or end results, the solution at every point in the net and give a complete picture of heat or fluid flow or potential function distribution in the region considered. However, in many cases engineers are concerned only with the conditions at one or two points, and the distribution of the solution throughout the remainder of the area is not a matter of prime importance. In such cases, satisfactory solutions using these two methods consume considerable time in relation to the information desired, and some other approach would prove valuable.

Such an approach is offered by the Monte Carlo method,[22] or solution by random walks, in which a method of statistics is applied to the solution of partial differential equations.

Monte Carlo Method.—In order to illustrate the Monte Carlo method of estimating the stream function or potential function at a point in a fluid flowing irrotationally, a rectangular, two-dimensional bend is shown in Fig. 19(*a*). At a distance on each side of the corner equal to the width of the section, the flow was assumed to be uniform, and convenient values were assigned to the streamlines. It will be seen from the solution of the problem that the actual position at which uniform flow is assumed has little effect on the result.

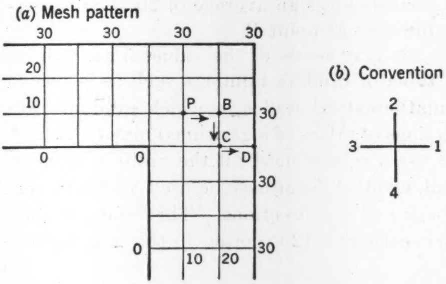

(c) Table

Boundary	Arrivals	Total	Count
30	𝍸 𝍸 𝍸 𝍸 𝍸 𝍸 𝍸 𝍸 |||	43	1 290
20	—	—	—
10			1	10
0	𝍸 𝍸 𝍸 𝍸	20	—
	Total	64	1 300
	Average		20.31

FIG. 19.—MONTE CARLO METHOD

The section under investigation is covered with a square meshwork of some appropriate size. It will be obvious that the work required for a solution depends on the size of the mesh chosen; no method is known for determining the optimum size for a particular problem. The convention sketch in Fig. 19(*b*) is drawn beside the main diagram (Fig. 19(*a*)) to indicate the direction of travel assigned to each number from 1 to 4. The point P at which the stream function, in this case, is desired is then chosen (it may be noted that the position of this point may influence the original choice of the net) and can be considered the origin of all movement; a pencil point is placed there.

Briefly, the method proceeds as follows: A wooden prism of square cross section is obtained, and the four long sides are marked 1, 2, 3, and 4. The prism, as if it were a die, is then tossed onto a flat surface, and the number turning up is noted in order that the pencil may move from point P according to the convention in Fig. 19(*b*). Assuming that the number 1 turns up, the pencil is moved to point B. The prism is cast again, and 4 appears; the pencil is moved to point C. Another throw, and 1 appears once more; the pencil is now at point D, a point on the boundary, of value 30 units. Consequently, in the column marked 30 in the accompanying table, a check or tally is placed, and the pencil is returned to point P. The entire procedure is carried through again until a boundary is again reached, and the value is noted.

Eventually, for example, a total of from fifty to one hundred values are recorded. A count is made of the number of units from the column corresponding to each boundary point, and these counts are totaled. Division by the number of times the boundaries were encountered gives the desired value of the stream function at point P.

In the example demonstrated, it is seen that, out of a total of sixty-four boundary arrivals, forty three were on the outer boundary of value 30 units. Only one reached the 10-unit interpolated point; twenty reached the inner 0 boundary. In this case, the value of the stream function at point P would be

$$(43 \times 30) + (1 \times 10) + (20 \times 0) = 1{,}300$$

arrival units which for sixty-four arrivals gives an average of 20.31 units, representing the value of the stream function at point P.

Instead of a prepared prism, a die may be used, the values 5 and 6 being disregarded; one may also use a table of random numbers such as is used in statistical work. Any book of mathematical tables in which random digits can occur (for example, certain sections of tables of logarithms) may be utilized. Of course, it is not necessary to use a square mesh; if the problem seems to demand it, a triangular, hexagonal, or other form may be used, and a suitable convention adopted for the numbering of the directions. This stratagem may be warranted, for example, if a 60° corner or 120° corner in the boundaries is encountered.

If a three-dimensional problem is to be solved and a cubical mesh used, the new directions can be assigned the numbers 5 and 6; a tabular system of coordinates can be set up, with the values of the various boundaries being noted. It would then be necessary to check coordinates of each point arrived at to see if it coincided with a boundary.

From the example presented, it will be seen that the principal contributions to the final result are the values on the two boundaries immediately adjacent to the point and that the assumptions of parallel flow at a section some distance away from the bend play a very small part in the computations; this section could be pushed indefinitely outward without materially affecting the labor of solution.

Mr. Milne has stated[22] that the error (correct solution minus approximate solution) in a solution of this sort varies as $1/\sqrt{n}$ in which n is the number of arrivals at boundaries; this fact can be utilized in extrapolating to better solutions. To the writers' knowledge, not enough work has been done to correlate the optimum number of arrivals at boundary points with mesh dimensions in order to obtain reasonably accurate solutions. Further investigation of a mathematical nature, however, may give a correct indication.

Mladen Boreli.[30]—As indicated by the variety of results obtained by the authors, the relaxation method is a powerful tool for solving engineering problems. Because the method is essentially one of successive approximations —so that the process involved is, of necessity, rather laborious—it is of great importance to explore all possibilities for reducing the necessary time to attain a certain specified accuracy. From the experience gained by use of the relaxation method to compute free-surface flow toward partly penetrating wells—a project which the writer undertook at the Polytechnic Institute of the University of Grenoble (France)—it is believed that the fineness of the mesh and hence the labor involved depend to a great extent on the treatment of the irregular stars and the singular points.

There are three ways in which irregular stars can occur: (*a*) They appear in the region where a finer mesh matches with a coarser one; (*b*) they appear at a fixed or free boundary; or (*c*) they are simply chosen under favorable conditions as a matter of preference. Wherever irregular stars are encountered, it is necessary to have a formula to determine residues. For an irregular star having legs of different lengths, as shown in Fig. 20, one can obtain from Eq. 10

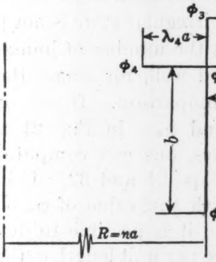

FIG. 20.—IRREGULAR STAR

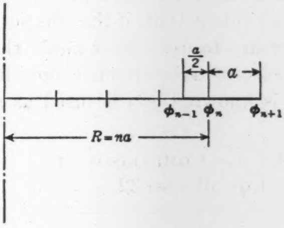

FIG. 21.—AXISYMMETRIC FLOW

$$a^2 \nabla^2 \phi = (\phi_2 - \phi_0) + \frac{\phi_4 - \phi_0}{\lambda_4} + \frac{\phi_2 - \phi_4}{n(1 + \lambda_4)} + \frac{a}{b}\left[(\phi_1 - \phi_0) + \frac{\phi_3 - \phi_0}{\lambda_3}\right] \quad (31)$$

for the residue. On the other hand, using a Taylor expansion, there results

$$a^2 \nabla^2 \phi = \frac{1}{1 + \lambda_4}\left[(\phi_2 - \phi_0)\left(2 + \frac{\lambda_4}{n}\right) + \frac{\phi_4 - \phi_0}{\lambda_4}\left(2 - \frac{1}{n}\right)\right] + \frac{a^2}{b^2}\,\frac{2}{1 + \lambda_3}\cdot\left[(\phi_1 - \phi_0) + \frac{\phi_3 - \phi_0}{\lambda_3}\right] \quad (32)$$

which, in spite of its apparently more complicated form, is no more difficult to apply than Eq. 31. A comparison of Eqs. 31 and 32, in connection with the ways in which irregular stars can occur, will show their relative merits.

---

[30] Assistant, Fluid Mech. Lab., Polytechnic Inst., Univ. of Grenoble, Grenoble, France; on leave from Hydrotechnic Inst., Serbian Academy of Sciences, Beograd, Yugoslavia.

Transition from a Coarser to a Finer Mesh.—For axisymmetric flow, the formula for the residue at the center of a regular star is

$$a^2 \nabla^2 \phi = \phi_1 + \phi_2 + \phi_3 + \phi_4 - 4\,\phi_0 + \frac{a}{2\,r}(\phi_2 - \phi_4) - 2\sum_{n=2}^{\infty}\frac{a^{2n}}{2\,n!} \times \left(\frac{\partial^{2n}\phi}{\partial r^{2n}} + \frac{\partial^{2n}\phi}{\partial z^{2n}}\right) - \frac{a}{r}\sum_{n=2}^{\infty}\frac{a^{2n-1}}{(2\,n-1)!}\,\frac{\partial^{2n-1}\phi}{\partial r^{2n-1}} \quad (33)$$

The quantities on the right side of Eq. 33 which involve the derivatives of y can be denoted by ΔE. It is immediately clear that, if these derivatives are large and r is small, ΔE is not necessarily small. Thus, the greater the variation of the function ϕ and the smaller the values of r, the finer the mesh must be. This seems to have been universally recognized for the authors have shown that the fineness of the actual mesh used varies from region to region. Because the transition from a fine mesh to a coarser one is effected by irregular stars, it is evident that, if the computation for the irregular stars is not precise, it is necessary to use a finer mesh, thus increasing the number of joints.

The case of axisymmetric flow into a confined well, for which the exact solution is known,[31] can be used as a basis for comparison. If one supposes that ϕ_{n-1} and ϕ_{n+1} in Fig. 21 are the correct values, one can compute ϕ_n according to Eqs. 31 and 33. Using ϕ_{n-1} and ϕ_{n+1} with the value of ϕ_n obtained in each case, it is possible to determine the discharge per unit length q_1 through a cylindrical surface of radius $(n - \frac{1}{2})a$, and q_2 through a cylindrical surface of radius $(n + \frac{1}{2})a$. These discharges, in general, differ from the correct value q. The absolute values of the deviations of q_1 and q_2 as determined from Eq. 31 are denoted by Δq_1 and Δq_2, and their mean value is denoted by $\Delta q''$; the corresponding quantity computed from Eq. 32 is denoted by $\Delta q'$. Table 4 shows that for a specified accuracy the value of n corresponding to Eq. 31 is larger than that corresponding to Eq. 32, so that the latter equation is preferable to the former.

TABLE 4.—COMPARISON OF EQS. 31 AND 32

n	$100\,\Delta q/q$	$100\,\Delta q'/q$	$\Delta q'/\Delta q$
1	11.2	11.2	1.00
2	6.01	2.65	0.440
3	4.07	1.20	0.298
4	3.11	0.72	0.232
5	2.40	0.43	0.179
6	2.01	0.33	0.164

Boundary Conditions.—Irregular stars usually occur at the boundary, which may be fixed or free. For a free surface the boundary conditions can be checked only after all the residues have been eliminated. If the expressions for the residue are not correct, the free-surface position will not be correctly determined.

To make a further comparison of Eqs. 31 and 32, one may consider the region near the free surface in seepage flow. In addition to satisfying the Laplace equation, the potential function ϕ has to adhere to the conditions that at the free surface $\phi = z$ and $\partial\phi/\partial n = 0$, in which z is the elevation of the free surface and n is measured in a direction normal to the free surface. Because $\partial\phi/\partial n = 0$, it is possible to consider point A′ rather than point A (Fig. 22), thus eliminating one irregular leg and leaving only one leg of irregular length. Eq. 31 thus results in

---

[31] "The Flow of Homogeneous Fluids Through Porous Media," by M. Muskat, 2d Ed., McGraw-Hill Book Co., Inc., New York, N. Y., 1946, p. 151.

$$a^2 \nabla^2 \phi = \phi_2 + \phi_4 - 2\,\phi_0 + \frac{\phi_2 - \phi_4}{2\,n} + \phi_1 - \phi_0 + \frac{\phi_3 - \phi_0}{\lambda_3} \ldots\ldots (34)$$

which becomes

$$a^2 \nabla^2 \phi = \phi_2 + \phi_4 - 2\,\phi_0 + \frac{\phi_2 - \phi_4}{2\,n} + \phi_1 - \phi_0 + a \sin^2 \alpha \ldots\ldots (35)$$

because

$$\frac{\phi_3 - \phi_0}{\lambda_3} = a \sin^2 \alpha \ldots\ldots\ldots\ldots\ldots\ldots\ldots\ldots (36)$$

Similarly, Eq. 32 results in

$$a^2 \nabla^2 \phi = \phi_2 + \phi_4 - 2\,\phi_0 + \frac{\phi_2 - \phi_4}{2\,n} + \frac{2}{1 + \lambda_3} (\phi_1 - \phi_0 + a \sin^2 \alpha) \ldots (37)$$

To make a cursory comparison of Eqs. 35 and 37, one can let $\lambda_3 \rightarrow 0$ and $\sin \alpha \rightarrow 0$. In the limit, Eqs. 35 and 37 should lead to the formula for the residue at a joint located on a horizontal impermeable bed. This is the case with Eq. 37 but not with Eq. 35. The coefficient 2 appearing in the left side of Eq. 37 shows that the direction normal to the free surface is a privileged one—a property which is not displayed in Eq. 35. Because Eq. 35 is derived from Eq. 31 and Eq. 37 from Eq. 32, it is indicated that Eq. 32 is again preferable to Eq. 31.

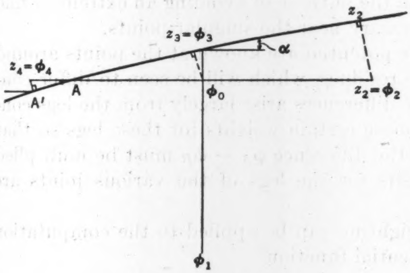

FIG. 22.—ELIMINATING AN IRREGULAR LEG

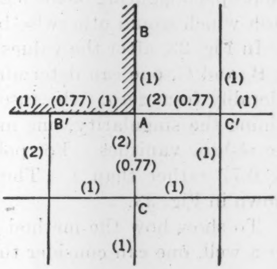

FIG. 23.—WEIGHTING THE LEGS

The method of reflection used in Fig. 22 is not always convenient. One may use the ratio 2 to 1 for the lengths of the legs. If the joint is located on the surface, Eq. 32 leads to

$$a^2 \nabla^2 \phi = 2 \left(\phi_1 + \phi_2 - 2\,\phi_0 + a \sin^2 \alpha - a \sin \alpha \cos \alpha + \frac{a \sin \alpha \cos \alpha}{2\,n} \right) \ldots (38)$$

whereas Eq. 31 results in

$$a^2\,\nabla^2\phi = \phi_1 + \phi_2 - 2\,\phi_0 + a\sin^2\alpha - a\sin\alpha\cos\alpha + \frac{\phi_2 - \phi_0}{n} \ldots\ldots (39)$$

Because the numerators of the fractions are approximately equal, the residue determined from Eq. 38 is twice that computed from Eq. 39.

Rectangular Meshes.—If the gradient of the unknown function can be judged a priori to be considerably larger in one direction than in the other, rectangular meshes can be used advantageously, with the long legs in the direction along which the gradient is small. Sometimes the number of joints involved can thus be reduced by from 30% to 40%. Evidently a more exact formula for the residue will be of considerable importance.

If, under favorable conditions, the mesh is made rectangular, with the longer legs twice as long as the shorter ones, Eq. 32 results in

$$a^2\,\nabla^2\phi = \phi_2 + \phi_4 - 2\,\phi_0 + \tfrac{1}{4}(\phi_1 + \phi_3 - 2\,\phi_0) + \frac{\phi_2 - \phi_4}{2\,n} \ldots\ldots (40)$$

whereas the left side of the corresponding formula given by Eq. 32 is only half as great. Consequently, the difference is large.

On the basis of the foregoing comments on the formulas for the residue at the joint of an irregular star, it is of interest to note a method of treating the singular points in some detail. The method involved consists, essentially, in the proper weighting of the legs, with the purpose of avoiding an extremely fine mesh which would otherwise be necessary near the singular points.

In Fig. 23, after the values of the potential are known at the points around A, B, and C, one can determine the residues, which will be seen to differ considerably from zero. Because these differences arise largely from the legs containing the singularity, one may choose certain weights for these legs so that the residue vanishes. For point B the difference $\phi_A - \phi_B$ must be multiplied by 0.77 rather than 1. The weights for the legs of the various joints are shown in Fig. 23.

To show how the method of weighting can be applied to the computation for a well, one can consider the potential function

$$\phi = L\,r^2 + M\log r + N \ldots\ldots\ldots\ldots (41)$$

For this case

$$a^2\,\nabla^2\phi = 4\,L\,a^2 = (\phi_2 - \phi_0)\,\frac{a^2}{r^2}\,\frac{4}{k - m\,l} - (\phi_0 - \phi_4)\,\frac{a^2}{r^2} \cdot \frac{4\,l}{k - m\,l} = (\phi_2 - \phi_0)\,A_l - (\phi_0 - \phi_4)\,B_l \ldots (42)$$

in which

$$k = \left(\frac{r_2}{r_0}\right)^2 - 1 \ldots\ldots\ldots\ldots (43a)$$

$$m = 1 - \left(\frac{r_4}{r_0}\right)^2 \ldots\ldots\ldots\ldots (43b)$$

and

$$l = \frac{\log r_2 - \log r_0}{\log r_0 - \log r_4} \quad (43c)$$

For the case shown in Fig. 21, one can obtain the following coefficients:

Value of n	Value of A_l	Value of B_l
1	1.7778	1.7778
2	1.5788	2.2255
3	1.5031	2.3716
4	1.4628	2.4443

It can be seen, therefore, that in each of the three cases in which irregular stars can occur Eq. 32 is preferable to Eq. 31. Moreover, by the use of proper weights considerable economy in labor can also be achieved in the vicinity of a singular point.

TURGUT SARPKAYA,[32] J. M. ASCE.—The engineering profession is indebted to the authors for their informative presentation of the relaxation technique as it is applied to problems in fluid mechanics. The numerous examples of a practical nature are most valuable. It should be emphasized that both the direct and reverse relaxation methods, although by nature approximate and relatively time consuming, have distinct advantages over such approximate methods as the source-sink method[5] and the flow-net method.[33] Also of interest are (*a*) the applicability of the reverse method, (*b*) the application of the direct method to wave problems, (*c*) the accuracy of results, and (*d*) the treatment of sharp corners and singularities.

As was emphasized by the authors, the application of the direct relaxation method (using the $(x\ y)$-plane) to the problems in which some part of the boundary is exposed to constant pressure is not a rational approach because it is difficult to estimate to what extent the boundary should be changed between successive trials. However, the application of the reverse method, especially to free-jet problems, does provide a rational approach to the solution. The reverse method, as it is presented by the authors, has the advantage that the assumption of the variation of the potential with distance—that is, the assumption of an $x(\phi)$-curve—is made only once. The relaxation procedure for y is then completed, the results are checked against one of the Cauchy-Riemann equations, and a new $x(\phi)$-curve is obtained. This procedure eliminates the necessity of assuming another entirely arbitrary $x(\phi)$-relationship. It is recommended that the x-values for the final trial be computed with a relaxation similar to that for the y-values rather than determined directly from Cauchy-Riemann conditions.

The authors note that the relaxation method is applicable to certain types of wave motion. An example, the case of irrotational standing waves in a channel of constant depth and variable width, will be offered after the general procedure is explained. Many types of wave motion are essentially irrotational, and the motion can therefore be defined in terms of a velocity potential—

---

[32] Research Engr., Hydrodynamics Lab., Massachusetts Inst. of Technology, Cambridge, Mass.

[33] "Fluid Mechanics for Hydraulic Engineers," by Hunter Rouse, McGraw-Hill Book Co., Inc., New York, N. Y., 1938, p. 54.

$$\phi = \psi(x, y) \cos \frac{2\pi t}{T} \cosh [k(h - z)] \qquad (44)$$

in which ϕ satisfies the Laplacian equation,

$$\nabla^2 \phi = 0 \qquad (45)$$

Also, if the amplitude of the motion is small, the condition for the free surface is

$$\frac{\partial^2 \phi}{\partial t^2} + g \frac{\partial \phi}{\partial z} = 0 \qquad (46)$$

in which z is taken as positive in the upward vertical direction. If the value of ϕ from Eq. 44 is substituted into Eq. 45, $\psi(x, y)$ is found to satisfy the criterion,

$$\psi_{xx} + \psi_{yy} + k^2 \psi = 0 \qquad (47)$$

Also, if Eq. 46 is to be satisfied,

$$\left(\frac{2\pi}{T}\right)^2 - k\, g \tanh k\, h = 0 \qquad (48)$$

These two relationships, Eqs. 47 and 48, are fundamental to this study as well as to studies of other physical problems. The goal of the analysis is the attainment of a solution that satisfies Eq. 47 and the boundary condition $\partial\phi/\partial n = 0$. Eq. 38 represents the relationship between the period of the wave, the depth of the water, and the parameter k. Eq. 47 can be written in the usual finite-difference form as

$$\sum_{i=1}^{4} \left(\frac{\psi_i}{x_i}\right) + \left[k^2 - \sum_{i=1}^{4} \left(\frac{1}{x_i}\right)\right] \psi_0 = R \qquad (49)$$

Hence, with k taken from Eq. 48 by trial, arbitrary ψ-values assigned, and $\sum_{i=1}^{4} \left(\frac{1}{x_i}\right)$-values computed, the relaxation process can be performed. After it is completed, the elevation η of the free surface is obtained from

$$\eta = \frac{2\pi}{g\, t} \cosh \psi_i\, (x, y) \qquad (50)$$

The troughs and crests of succeeding waves are obtained by connecting, respectively, locally maximum and minimum η-values.

An application of this result is shown in Fig. 24. A parabolic transition reduces the width of a rectangular, constant-depth channel to one fourth of its original width, as shown. The assumptions made were that the depth of the still water in the channel was 0.6 ft, k was equal to π ft^{-1}, and the period was 0.64 sec. In Fig. 24 there is shown the instantaneous pattern of the crests of standing waves in the channel. The amplitude of the wave, also indicated in Fig. 24, was found to be inversely proportional to the square root of the width, in accordance with Green's law.[34] If constant depth can be assumed, the relaxation method can be applied in the analysis of seiche in irregularly shaped harbors, for which standard methods of analysis fail.

The authors caution that the accuracy of a given result can only be judged by computing the velocity or pressure distribution along a boundary or other arbitrarily selected lines. However, the computation of velocities on a free boundary even from a fine mesh—if the mesh size near the boundary is of the order of magnitude of the radius of curvature of the boundary—will not lead to an absolute check because of the variation of λ-values in the star. If a star with a very small λ-value is to be considered, a formula for curvilinear extrapolation must be used.

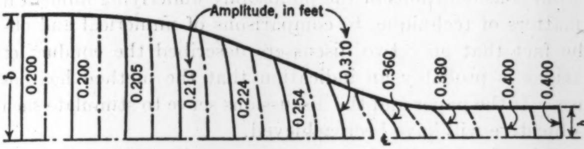

Fig. 24.—Trough and Crest Lines for Standing Waves

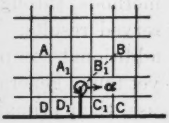

Fig. 25.—Sharp Corner

The solution of certain practical problems may present difficult boundary conditions such as sharp corners which give rise to singularities of various types. Special treatment is essential if the function approaches infinite values near the corner. This difficulty can be overcome by the application of a somewhat more complicated method.

The solution of Eq. 45 can be expressed by the series,

$$\phi = \sum_{-\infty}^{+\infty} A_k\, r^n \cos n\,\theta \ldots\ldots\ldots\ldots\ldots\ldots\ldots\ldots (51)$$

in which $n = \pi\, k/\alpha$, ($k = 0, \pm 1, \pm 2, \ldots$), and α is the angle of the sharp corner as is shown in Fig. 25. For $\alpha = 2\,\pi$, ϕ takes the form:

$$\phi = A_0 + A_1 r^{\frac{1}{2}} \cos\frac{\theta}{2} + A_2\, r \cos\theta + A_3 r^{\frac{3}{2}} \cos\frac{3}{2}\theta + \;\ldots\quad \ldots\ldots (52)$$

In Eq. 52 only the first four terms need be retained. The units of r can be so chosen that $r = 1$ at points A, B, C, and D. In terms of ϕ_A, ϕ_B, ϕ_C, and ϕ_D, which are known, one obtains the coefficients A_0, A_1, A_2, and A_3. Using these coefficients ϕ_{A1}, ϕ_{B1}, ϕ_{C1}, and ϕ_{D1} can be expressed in terms of ϕ_A, ϕ_B, ϕ_C, and ϕ_D as follows:

$$\left.\begin{aligned}
\phi_{A1} &= 0.4572\,\phi_A + 0.2351\,\phi_B + 0.2093\,\phi_C + 0.0992\,\phi_D \\
\phi_{B1} &= 0.2351\,\phi_A + 0.5930\,\phi_B + 0.0992\,\phi_C + 0.0728\,\phi_D \\
\phi_{C1} &= 0.2093\,\phi_A + 0.0992\,\phi_B + 0.4572\,\phi_C + 0.2351\,\phi_D \\
\phi_{D1} &= 0.0992\,\phi_A + 0.0728\,\phi_B + 0.2351\,\phi_C + 0.5930\,\phi_D
\end{aligned}\right\}\ldots\ldots (53)$$

---

[34] "Engineering Hydraulics," edited by Hunter Rouse, John Wiley & Sons, Inc., New York, N. Y., 1950, Chapter X, p. 738.

The mathematical analysis for this method is available.[19,35] Eqs. 53 are used at singular points; the relaxation procedure is performed in the usual manner, observing that Eqs. 53 hold at singular points.

John S. McNown,[36] M. ASCE, En-Yun Hsu,[37] A. M. ASCE, and Chia-Shun Yih.[38]—In the several discussions submitted, contributions have been made which range from considerations of the philosophy underlying numerical methods, through matters of technique, to comparisons of numerical and observed results. The fact that only two discussers described the conduct of additional computations is probably an indication that the method has not yet found general use. If the paper and the discussions serve to stimulate such use, their primary objective will have been achieved.

Mr. Blaisdell considered primarily the accuracy, or rather the consistency, of the numerical results for flow over a weir. The results obtained from Eq. 24 and the relaxation method are remarkably close together. Although Mr. Blaisdell characterized a part of the correspondence as erratic, Messrs. Paynter and Scott apparently found the general agreement between the results observed by the USBR[26] and those of the relaxation almost perfect. Actually, these data[26] came to the writers' attention after the manuscript had been completed. Had they been used, reference would, of course, have been made to them. In communications to the writers, Frank B. Campbell, M. ASCE, informed the writers of the existence of these data, and J. N. Bradley, A. M. ASCE, submitted a comparison similar to that of Messrs. Paynter and Scott.

A comparison between second differences can be misleading, particularly if one set is computed from a quadratic equation for which the second differences are inherently constant. Because their order of magnitude in this computation is approximately $H/100$, presentation of the second differences as three-digit and four-digit numbers by Mr. Blaisdell is misleading. Even for Eq. 24, the rounding-off process results in a sizable change.

The trend of the values for the thickness of the jet is more significant. However, the value of 4 for $8\,x/H$ is not large enough for the internal pressure to be ignored, as is clearly indicated in Fig. 13. For $8\,x/H \approx 8$, the internal pressure head is still more than $H/10$. Thus, the conditions of free fall assumed by Mr. Blaisdell are only approximately valid. The fact that the observed thickness differs from the mean of the computed thicknesses by less than 1% seems quite remarkable.

Messrs. Paynter and Scott have objected to the absence of both a broader statement of the underlying philosophy of numerical methods and fuller numerical detail. In their comment, "Rather than merely being techniques of numerical integration * * *," the word "merely" is the discussers' and not the

---

[35] "Relaxation Methods Applied to Engineering Problems," by D. W. de G. Allen, D. G. Christopherson, L. Fox, J. R. Green, H. Motz, F. S. Shaw, and R. V. Southwell, *Philosophical Transactions*, Royal Soc. of London (A), 1945, pp. 239, 367–385, 519–537.

[36] Associate Director, Iowa Inst. of Hydr. Research, State Univ. of Iowa, Iowa City, Iowa.

[37] Research Engr., Hydrodynamics Lab., California Inst. of Technology, Pasadena, Calif.

[38] Research Engr., Iowa Inst. of Hydr. Research, State Univ. of Iowa, Iowa City, Iowa.

writers'; their more general interpretation of the method is in accord with the writers' views.

Numerical details were included in the original paper more as illustrations of what can be done than as exhaustive solutions to practical problems. In this connection the computations for weir flow (Fig. 13) and for seepage (Fig. 17) are hardly comparable in significance. The former is a classic problem of considerable practical importance; the latter is an isolated example which is only illustrative of an infinite variety of boundary configurations. Furthermore, difficulties inherent in the presentation of the numerical results will be obvious to the reader. In the cavity flow (Fig. 14), for example, more than 1,300 values of the stream function were determined. To have elaborated in either of the somewhat opposing directions proposed by Messrs. Paynter and Scott would have unduly extended the paper.

Messrs. Boreli and Paynter and Scott described methods and conditions for which a mesh other than square is used. Some of these were also discussed in Mr. Southwell's work.[4] Aside from the square mesh, however, only the rectangular mesh which Mr. Boreli used to advantage in computing seepage toward wells is likely to be applicable to problems of fluid flow. The distantly related Monte Carlo method is interesting and perhaps useful for isolated applications.

Mr. Boreli's contention that Eq. 32 obtained by a Taylor expansion for the residue is often preferable to Eq. 31 is readily conceded. In fact, in using the relaxation technique to determine the cavity shape (Fig. 14), the formula from a Taylor expansion was used. It must be noted, however, that, if the second and higher derivatives of the unknown function are large and if the net is comparatively coarse, the superiority of Eq. 32 to Eq. 31 cannot be established, because Eq. 32 is then only a rough approximation. All one can say is that, as the net becomes finer, the accuracy of Eq. 32 is increased more rapidly than that of Eq. 31.

Mr. Boreli proposed a treatment of singular points by properly weighting the neighboring legs. Unfortunately, it was not mentioned how the weighting is to be determined. The treatment presented by Mr. Sarpkaya for the same purpose is simple and systematic and is a welcome contribution to this troublesome aspect of the relaxation technique.

Although it was stated (under the heading, "Introduction") that application of the relaxation method is feasible only for two-dimensional flows or axisymmetric flows, some studies[39,40] have included analyses of problems for which variations in all three dimensions are significant. S. K. Roy obtained[39] a rough approximation for flow through a transition from a reservoir to a rectangular conduit, and D. N. de G. Allen and S. C. R. Dennis demonstrated[40] a useful technique which is particularly well suited to problems for which the third dimension is small compared to the others. A solution of acceptable accuracy for a three-dimensional flow with a free surface, as an extreme example, remains an exorbitant undertaking.

---

[39] "Development of Three Dimensional Relaxation Processes for a Systematic Approach to Flow Analysis in Hydraulic Structures," by S. K. Roy, (in three parts), *Irrigation and Power*, Govt. of India Press, Simla, Vol. 9, No. 1, January, 1952.

[40] "The Application of Relaxation Methods to the Solution of Differential Equations in Three Dimensions," by D. N. de G. Allen and S. C. R. Dennis, I. Boundary Value Problems, *Quarterly Journal of Mechanics and Applied Mathematics*, Vol. IV, Pt. 2, June, 1951, pp. 199–208.

The discussers indicated that they share the writers' convictions as to the applicability and versatility of the relaxation technique. Mr. Sarpkaya's application of the method to problems of wave motion is additional evidence of its adaptability to a wide variety of potential flows. By their contributions, the discussers have expanded and reinforced various phases of the study.

AMERICAN SOCIETY OF CIVIL ENGINEERS
Founded November 5, 1852
TRANSACTIONS

Paper No. 2759

SEDIMENT SAMPLING IN TIDAL WATERWAYS

BY EDWARD A. SCHULTZ,[1] A. M. ASCE

SYNOPSIS

Many studies of the problem of shoaling in tidal waterways have been performed. These studies have included data relative to the suspended sediment in the waterways, but occasionally the results were of little value because they were not representative and were not obtained with an awareness of their subsequent use. There is described herein a series of studies made in the Charleston (S. C.) harbor for the purpose of determining (1) the accuracy of sediment-sampling procedures and (2) the value of performing only a few—rather than many—operations. It is concluded that the considerable variation in the suspended-sediment concentration that exists in tidal waterways makes it impractical, if not impossible, to measure accurately the quantity of sediment discharge. However, estimates or approximations from direct measurements have their value because they can be used to locate and establish the significance of the source of the shoaling and therefore to determine the feasibility of remedial measures.

INTRODUCTION

Large quantities of public and private funds are expended annually for maintenance dredging of navigation channels in tidal waterways and in adjacent berthing areas. It is only natural that, as a consequence, small-scale hydraulic-model investigations and prototype field investigations have been performed to study methods for eliminating or mitigating the shoaling problem and—in the process—to determine the nature and causes of the shoaling and the sources of the material which forms the shoals. To this end some of the field programs have included the collection of samples (in both limited and extensive quantities) of suspended sediment from the tidal waterways. On occasion, the field investigations have been entered into without benefit of competent advice, and extensive sampling has been performed without the investigator recognizing how representative the results might be or how the results would be used. The subsequent material is devoted to that aspect of prototype investigations concerned with sampling of suspended sediment in

---

NOTE.—Published, essentially as printed here, in March, 1954, as *Proceedings-Separate No. 427*. Positions and titles given are those in effect when the paper was received for publication.

[1] Hydr. Engr., Corps of Engrs., U. S. Dept. of the Army, Charleston Dist., Charleston, S. C.

tidal waterways and dealing specifically with (1) the question of accuracy of measurements of total sediment discharge in given cross sections of an estuary and (2) the value of a few well-planned and well-executed operations to provide information about the hydraulic and sediment characteristics of the waterway.

FLUCTUATION IN THE QUANTITY OF SEDIMENT

In some cases the investigator may feel that solution of the shoaling problem requires knowledge of the total discharge of sediment in an estuary. It should be recognized, however, that the procurement of such information by direct observation is a difficult task. It is impractical, if not impossible, to obtain as accurate and reliable results as are obtained from similar measurements in an upland stream where the flow is unidirectional and sensibly constant and where the density of the water is homogeneous. This conclusion was reached in a study of the problems associated with the measurements of the sediment load transported by tidal waterways and was generally concurred in by many of the forty-five organizations and individuals provided with the opportunity of reviewing and commenting on a brief of the problem.[2]

The many unique characteristics of an estuary which complicate the problem of measuring the total sediment discharge are listed in this brief as follows:

> "1. The discharge is rapidly variable.
>
> "2. Velocity distribution varies in the vertical and the horizontal independently of the discharge variation.
>
> "3. The complex regimen existing for the flow in one direction is discarded every six hours (approximately) and an equally complex regimen, but of different characteristics, is set up for flow in the opposite direction.
>
> "4. Successive 'cycles' are not identical—in fact, are frequently quite different.
>
> "5. The water in some reach of every estuary is not of homogeneous density, nor is the difference constant."

The brief further states,

> "It is readily apparent that a determination of the suspended sediment content made at the surface of an estuary at hour 1200 is not comparable with an observation at the bottom at hour 1215. The discharge might have changed 25% in 15 minutes. Likewise, a sample taken at 1215 at the bottom at a given location along the cross-section line can be related logically to one taken at the bottom somewhere else along the line in this respect only: they both contain water and sediment taken from the same estuary."

The instantaneous fluctuation of the current velocity is another factor that affects the results. It has been demonstrated that successive short-time observations with a current meter—of the order of 40 sec to 70 sec—at intervals of 1 min and 2 min over a period of several minutes will produce velocities that vary as much as 20%.

All these factors contribute materially to the difficulties of accurately measuring the quantity of sediment discharge in tidal waterways. However, research by the Charleston (S. C.) District of the Corps of Engineers, United

---

[2] "Sediment Discharge Measurements in Tidal Waterways," by C. F. Wicker, *Technical Bulletin No. 1*, Committee on Tidal Hydraulics, Corps of Engrs., U. S. Dept. of the Army, May, 1954.

States Department of the Army, has revealed that there is still another contributing factor as important as, or more important than, the ever-changing tidal flow and density currents. This factor is the considerable variation in concentration of the suspended sediment both temporally and spatially in tidal waterways. The research has indicated that variations in sediment concentrations can be expected to range up to 1,000% or more for samples taken only a few feet or a few minutes apart. A considerable quantity of the sediment, no doubt, moves in slugs—a phenomenon which has frequently been observed in the surface of the harbor both under natural conditions and in connection with maintenance-dredging operations. The sediment is not mixed and distributed throughout the tidal water so uniformly as might be supposed. Unquestionably, the variations in tidal flow are largely responsible for the variations in sediment concentration, and the two phenomena cannot be disassociated from each other. Apparently, however, the order of variation of sediment concentration is greater and, because sediment load is the product of the sediment concentration and the discharge, it has more influence on the computation results. In order to clarify the several significant conclusions which are to be drawn from this revelation, it is of importance to describe briefly some of the sampling operations which were conducted in the Charleston harbor and the objectives of these operations.

Charleston Harbor

From 1948 through 1953, the Charleston District conducted extensive investigations of the harbor, both in the prototype and on a small-scale hydraulic model, to determine the causes and remedial measures for the greatly increased rate of shoaling in the inner-harbor navigation channels. Of these investigations only the suspended-sediment sampling and related operations in the lower salt-water reaches of the harbor are within the scope of this subject matter. The operations in the lower harbor were conducted to learn as much as possible about the hydraulic, saline, and sedimentation characteristics of the harbor; to determine the nature, mechanics, and causes of the shoaling phenomena; and to identify, if possible, the sources of shoaling material and their significance. These objectives involved, among other things, determination of the quantity of sediment load in transport throughout the harbor; this, in turn, involved observations of tidal heights, magnitudes and directions of current velocities, and procurement of samples of suspended sediment.

Advisers on the studies cautioned against a series of disconnected comprehensive sampling operations which would be performed on different days and on various ranges throughout the harbor and would use a number of samplers simultaneously in each cross section. Instead, they suggested a program of correlated operations, in which five or six ranges would be occupied and worked simultaneously but only one sampler would be in each cross section—either located at the centroid of discharge or at two centroids (one each for ebb and flood)—if required. However, it was difficult to select these control stations from an examination of only the plotted cross sections, and it was even more difficult to determine the probable locations of representative sediment concentrations and sediment discharges. Therefore, the original plan of sampling each cross section separately and comprehensively for one condition of tide was adopted. It was hoped that these operations would provide the data required to select the centroids of sediment discharge, after which the recommended plan would be followed and repeated for several different tidal conditions.

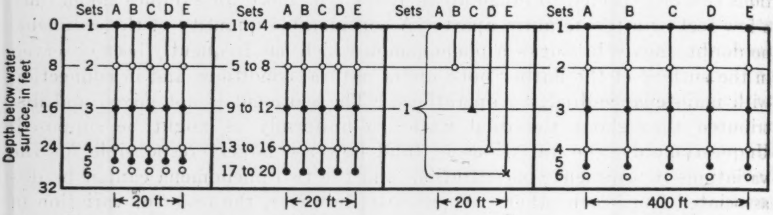

(*a*) Step 1 (*b*) Step 2 (*c*) Step 3 (*d*) Step 4

FIG. 1.—ARRANGEMENT OF SUSPENDED-SEDIMENT SAMPLERS IN SPECIAL RESEARCH OPERATION

These operations were conducted as follows: Each cross section was investigated throughout a complete tidal cycle. From three to five US P-46 point-integrating, suspended-sediment samplers were distributed across the range and operated simultaneously—first at the surface, then at various increments of depth in succession to the bottom. Before obtaining each sample, the velocity required both for computing the water discharge and sediment discharge and for determining the filling rate of the sampler was measured. From 15 min to 20 min were required to explore and sample the entire cross section in this fashion, and the process was repeated hourly during the tidal cycle, with extra observations on the half hour of only the velocities. The sediment discharge was then computed from these field measurements and the laboratory analyses of the samples.

Examination of these data showed that the sediment concentration was very erratic (with respect to both depth and width) and caused concern over the validity of the measurements. It was reasonable to assume that, if different

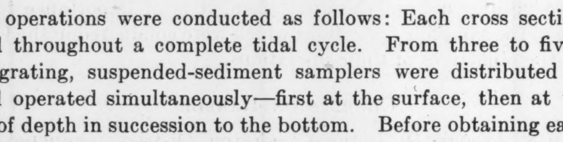

FIG. 2.—TYPICAL LAYOUT OF CROSS SECTION AND FIVE SAMPLERS FOR REGULAR SAMPLING OPERATIONS

stations on the range had been used, different values for sediment concentration and consequently for sediment discharge would have been obtained. Thus, the sampling of a half-dozen verticals in a cross section would not provide an accurate representation of the sediment load passing that cross section.

Special Research

A special research operation was therefore planned and conducted with the aim of collecting sediment data which would establish the validity of this assumption and be useful in evaluating the suspended-load measurements by the methods being used. The technique used in this special operation is illustrated in Fig. 1. In Fig. 2, for comparison, is a typical layout of a cross section and five samplers for a regular suspended-load measuring operation. In step 1 (Fig. 1(*a*)) one bateau complete with sampler, current meter, and other appurtenant gear was anchored over a cross section on one of the established stations, and four other bateaux, similarly equipped, were brought alongside and anchored—all touching each other. This placed the samplers as close together as the widths of the bateaux would permit, the distance between outside samplers being 20 ft. In all steps of the operation, five samplers, making up a set, were obtained simultaneously with US P-46 samplers. The velocity of the current was measured immediately before obtaining each set of samples in order to determine the filling rate of the samplers. In step 1, sets of samples were obtained at 4-min intervals, the first set at the surface and successive sets below the surface at 8-ft depth increments; the last two sets were obtained 2 ft and 1 ft above the bottom. The procedure was then repeated two more times, for a total of three runs. The objective in this case was to determine the variation of the sediment concentration with respect to lateral distance. In step 2 (Fig. 1(*b*)) sets of samples were obtained at 3-min intervals,

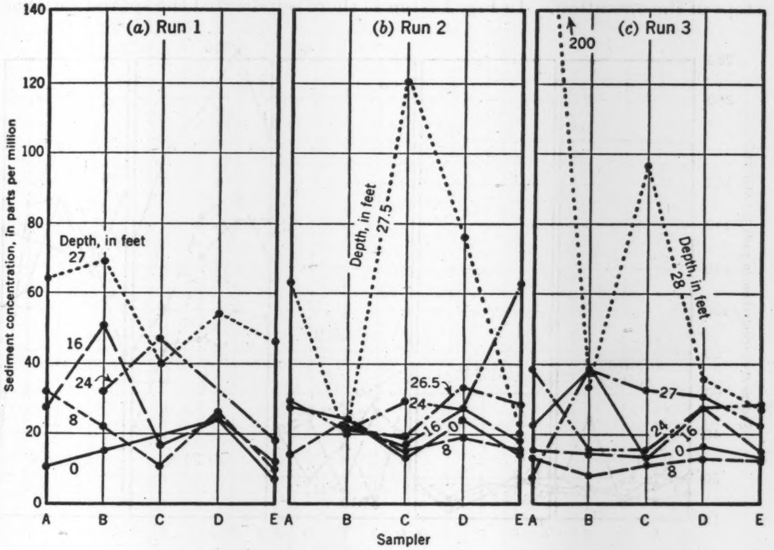

FIG. 3.—STEP 1

and the sequence was different from that in step 1. Four successive sets of samples were obtained at the same depth, after which four more sets were obtained at the next depth. The depths sampled were at the surface and 8 ft, 16 ft, 24 ft, and 28 ft below the surface. The objective in this case was to determine the variation of the sediment concentration with respect to time. Step 3 (Fig. 1(*c*)) differed from the others in that single samples were obtained simultaneously at five different depths; sets were taken at 5-min intervals and ten runs were made. The objective was to determine variation in sediment concentration with respect to both depth and time. Step 4 (Fig. 1(*d*)) was the same as step 1, except that the lateral spacing of individual samplers was increased from 5 ft to 100 ft.

Figs. 3 to 6 contain the suspended-sediment results for each of the four steps of the operation. In Fig. 3 (step 1) there is indicated the spatial variation in sediment concentration which existed. Each of the three runs shows five different results at each depth for each of the five points spaced 5 ft apart. The least variation was found in the upper stratum where concentrations were of the order of 8 ppm to 38 ppm; maximum deviations from the low to the high values at the surface and at a depth of 8 ft ranged from 50% to 220%. The maximum variation was found at a depth 1 ft from the bottom where concentrations were of the order of 20 ppm to 200 ppm; in the third run, the high value was 640% greater than the low value.

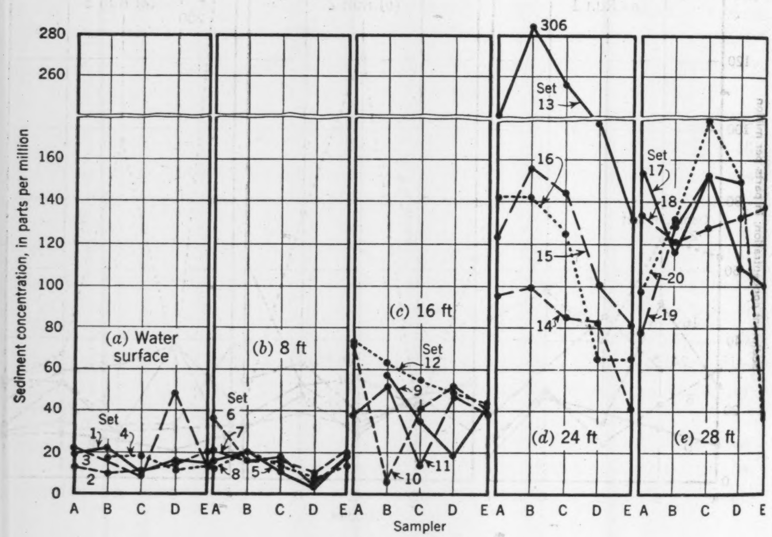

FIG. 4.—STEP 2

In Fig. 4 (step 2) there is indicated the temporal variation in sediment concentration which existed. Although successive values for four of the samplers in the surface were in fair agreement, sampler D produced values ranging from 11 ppm to 48 ppm (or a deviation from the low value to the high value of 340%) within a period of 3 min. As in the case of step 1, maximum variations were found near the bottom. At the 24-ft depth, sampler B produced values ranging from 98 ppm to 306 ppm, and at the 28-ft depth sampler E produced values ranging from 38 ppm to 138 ppm, within a period of 3 min. The former results in a deviation from the low to the high value of 210%, and the latter, of 260%. These deviations are increased to 670% and 370%, respectively, if the maximum and minimum values are considered at each depth, regardless of the particular samplers which produced the results. This is a reasonable consideration because, from a practicable standpoint, the close spacing of the samplers, in effect, puts them in the same vertical line; the 3-min sampling interval, in effect, makes successive samples approximately instantaneous; and the five samplers are supposed to be equally accurate.

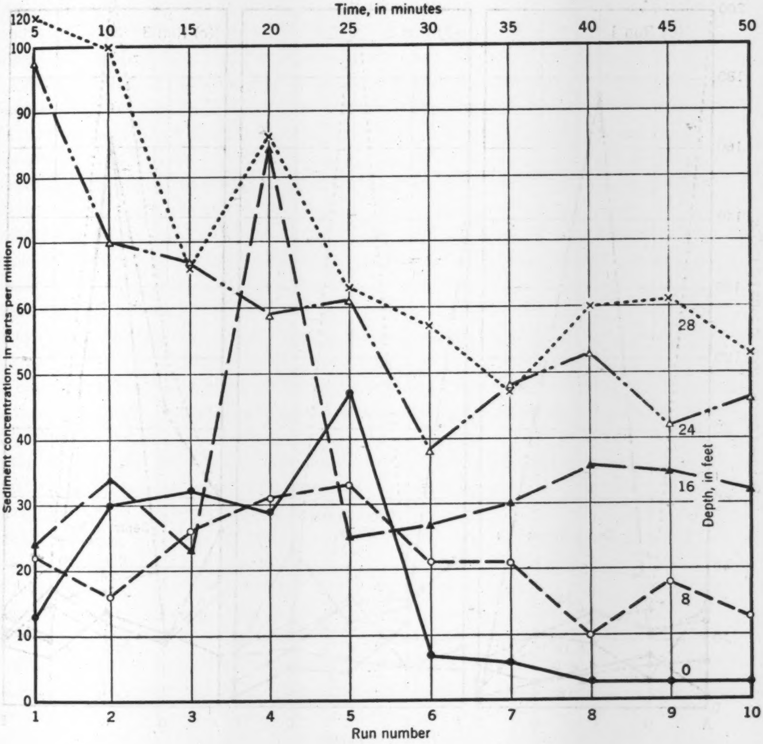

FIG. 5.—STEP 3

The results from steps 3 and 4 (Figs. 5 and 6) show the same trends as do the results from the first two steps. Step 4, with a sampler spacing of 100 ft, like step 1, with a sampler spacing of 5 ft, indicates the spatial variation in sediment concentration which existed. However, the order of variation—particularly in the very lowest stratum—was greater. At a depth 1 ft from the bottom the values ranged from 8 ppm to 6,085 ppm, 17 ppm to 335 ppm, and 28 ppm to 347 ppm, for runs 1, 2, and 3, respectively. Overlooking the results for run 1 (which seem to be out of line), the corresponding deviations from the low to the high values for runs 2 and 3 are 1,870% and 1,140%, respectively. It has been suggested that the excessive variation shown could possibly be attributed to the fact that the samplers were resting in the soft bottom of the estuary. However, the investigators are reasonably certain that this was not the case; under these circumstances the sampler would have come up empty.

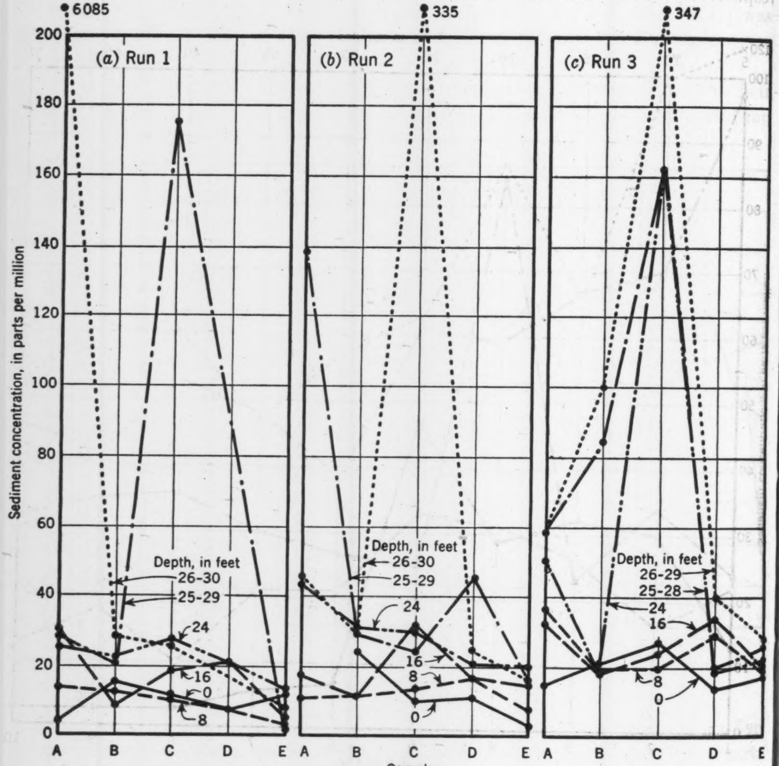

FIG. 6.—STEP 4

As a result of the findings described herein, it is concluded that the considerable variation in the sediment concentration which exists in tidal waterways—especially in those cases where the material is predominantly silt and clay particles—makes it impracticable, if not impossible, to measure accurately the quantity of sediment discharge. This, of course, is the same conclusion reached by others,[2] based on the ever-changing tidal flow, density currents, and other factors cited previously.

The question arises as to whether knowledge of the total discharge of sediment in an estuary by direct observation is worth the effort. Estimates or approximations of the sediment load have their value; thus, direct observations made in this connection are worth both the cost and the effort if the shoaling problem is important enough, if other needed information can be obtained as a result of, or in conjunction with, these sediment-sampling discharge-measuring operations, and if the number of operations are kept within reasonable bounds.

After the investigator has completed a few exploratory operations and learned the mechanics of sediment transport in the tidal waterway with which he is concerned, he will have to decide whether knowledge of the sediment load is necessary and, if so, whether accurate answers are necessary or whether reasonable approximations will suffice for his problem. The main point is that he recognize the limitations of the data. If he decides that information on the sediment load is desirable, he should limit the number of cross sections to be explored and work these for several conditions of tidal-water flow and fresh-water flow in order to obtain more representative data and establish that the resulting trends of the operations are in line with one another. The implications of the variations in sediment concentration were recognized early in the course of the Charleston harbor investigation. Nevertheless, it was decided to conduct a limited number of suspended-load operations because it was felt that approximate determination of the quantity of material in transport would help supply some of the answers to the problems. For example, the three main tributaries to Charleston harbor are tidal throughout most of their lengths; thus, it was out of the question to measure their sediment loads above the head of tide. Nevertheless, measurements at the mouths of the tributaries provided data to support the conclusion that one tributary is a significant source of potential shoaling material and the other two are not. These types of measurements also showed that the net transfer of material in a cross section may be seaward whereas the net transfer at the bottom may be inland, and the measurements gave some idea of the quantities moving in the upper and lower zones. Furthermore, these operations provided information which was helpful to an understanding of the mechanics of sediment transport in the harbor. For example, it was learned that the suspended sediment in a tidal waterway, unlike that in a river (where the sediment stays in suspension most of the time), alternately goes to the bottom with the slackening current and rises to the higher strata with the accelerating current. Finally, because other observations were made concurrently with the sampling, these operations were the means by which much was learned about the hydraulic and saline characteristics of the harbor.

CONCLUSIONS

Notwithstanding the foregoing, the implications of the variations in sediment concentration in tidal waterways should be recognized. It appears that there are sufficient grounds for questioning the validity of the procedure of measuring the sediment discharge in a cross section by operating one sampler in a single vertical which has been previously rated, as in stream-gaging operations; it appears also that not much better answers can be obtained from the "shuttle" procedure in which one vertical is continuously occupied and others are occupied discontinuously by shuttling back and forth between them. Finally, good correlation is probably impossible between data obtained simultaneously on several ranges distributed through the saline part of the tidal waterway. The variation in sediment eliminates the "control-net" scheme for correlating sampling results, in which one or two centroids or control verticals are established on each range and then occupied in subsequent operations calling for simultaneous measurements on perhaps five or six ranges. Strictly valid comparisons cannot be made of data obtained simultaneously on two wide ranges defining a given reach of a channel where, for example, three, four, or five verticals on each range are explored. These types of operations have their value, of course; however, if the sediment variation were not recognized, erroneous conclusions could be formed on such matters as the net movement of sediment load or the pick-up or deposition in various reaches of the channel.

AMERICAN SOCIETY OF CIVIL ENGINEERS
Founded November 5, 1852
TRANSACTIONS

Paper No. 2760

PRESSURE SURGES IN PUMP INSTALLATIONS

By John Parmakian,[1] M. ASCE

With Discussion by Messrs. Carroll E. Withers, Peter Linton,
and John Parmakian

Synopsis

There is described herein the method of water-hammer analysis and control used in the design for the condition of power failure at the pump motors of the Tracy Pumping Plant near Tracy, Calif. A summary of the major features of this installation is included, and a comparison between the observed and computed transient effects is made. Useful charts for obtaining the approximate water-hammer effects caused by a power failure in any pump discharge line without control valves are also presented.

Notation

The letter symbols adopted for use in this paper are defined where they first appear, in the illustrations or in the text, and are arranged alphabetically, for convenience of reference, in the Appendix.

Introduction

The Tracy Pumping Plant is located in the Central Valley Project near Tracy, Calif. The plant's function is to pump water from the lower delta region of the Sacramento River to the Delta Mendota Canal. The canal is located along the west side of the San Joaquin Valley for a distance of more than 100 miles, and the water is used to supply an extensive irrigation system. The basic data for this plant are presented in Table 1; the general arrangement is shown in Fig. 1. Briefly, the plant consists of six large pumping units with each pair of pumps connecting through a wye branch to a 15-ft-diameter, reinforced concrete pipe which extends approximately 1 mile to the upper canal. Each pump is driven by a 22,500-hp motor and delivers water at the rate of

---

Note.—Published, essentially as printed here, in December, 1953, as *Proceedings-Separate No. 361*. Positions and titles given are those in effect when the paper or discussion was received for publication.

[1] Head, Technical Eng. Analysis Section, Design Div., Bureau of Reclamation, U. S. Dept. of the Interior, Denver, Colo.

767 cu ft per sec to the canal under a rated head of 197 ft. On the discharge side of each pump there is a butterfly valve which closes at a variable rate under the action of a servomotor when a power failure occurs at the pump motors.

TRANSIENT CONDITIONS CAUSED BY POWER FAILURE

There are several operating conditions at the Tracy Pumping Plant that can cause substantial pressure changes in the discharge lines. The most serious of these operating conditions is the sudden stoppage of the motors as a result of a power failure. In Fig. 2 there is shown the time history of the pressure, flow, and speed changes at the pumping plant caused by a simultaneous power failure at the motors of two pumps on the same discharge line. The transient phenomena are as follows: When the power supply to the pump motors is suddenly cut off, the only energy that is left to drive each pump in the forward direction is the kinetic energy of the rotating elements of the motor and pump and the entrained water in the pump. Because this energy is small when compared to that required to maintain the flow against the discharge head, the reduction in pump speed is rapid. As the pump speed is reduced, the flow of water in the discharge line adjacent to the pump is also reduced. As a result of these rapid flow changes at the pump, water-hammer waves of subnormal pressure are formed in the discharge line at the pump. These subnormal pressure waves move rapidly up the discharge line to the discharge outlet where a wave reflection occurs. The speed of the pump is then reduced to a point at which no water can be delivered against the existing head and the flow through the pump reverses, although the pump may be still rotating in the forward direction. The pump speed thus is reduced more rapidly, and soon the pump reverses in rotation. However, it is prevented from reaching maximum runaway speed in reverse by the closure of the butterfly valve, which restricts the

TABLE 1.—BASIC DATA FOR TRACY PUMPING PLANT (CALIFORNIA)

ITEM	DATA
Type of pump	**double volute**
Number of pumps in pumping plant	**6**
Number of pumps on each discharge line	**2**
Number of pump discharge lines	**3**
Warranted pump discharge at rated head, in cubic feet per second	**767**
Rated pumping head, in feet	**197**
Range of pumping head, in feet	**174 to 204**
Length of pump discharge lines, in feet	**5,130**
Water-hammer wave travel time in each discharge line, in seconds	**1.75**
Diameter of discharge line, in feet	**15**
Pipe-line constant ρ (Eq. 15)	**2.0 (for two-pump operation)**
Type of discharge conduit	**buried reinforced concrete pipe**
Motor horsepower rating	**22,500**
Motor speed, in revolutions per minute	**180**
Motor λ, in pound-feet squared	**3,500,000**
λ of pump and entrained water, in pound-feet squared	**540,000**
Pump and motor inertia constant K_1 (Eq. 6)	**0.120**
Type of control valve at each pump	**butterfly valve**
Open area of butterfly valve, in square feet	**47.9**
Closing rate of butterfly-valve leaf, in seconds:	
First 55°	**14**
Remaining 27°	**46**
Type of discharge outlet	**siphon, interrupted by power failure**
Date pump units placed in operation	**1951**

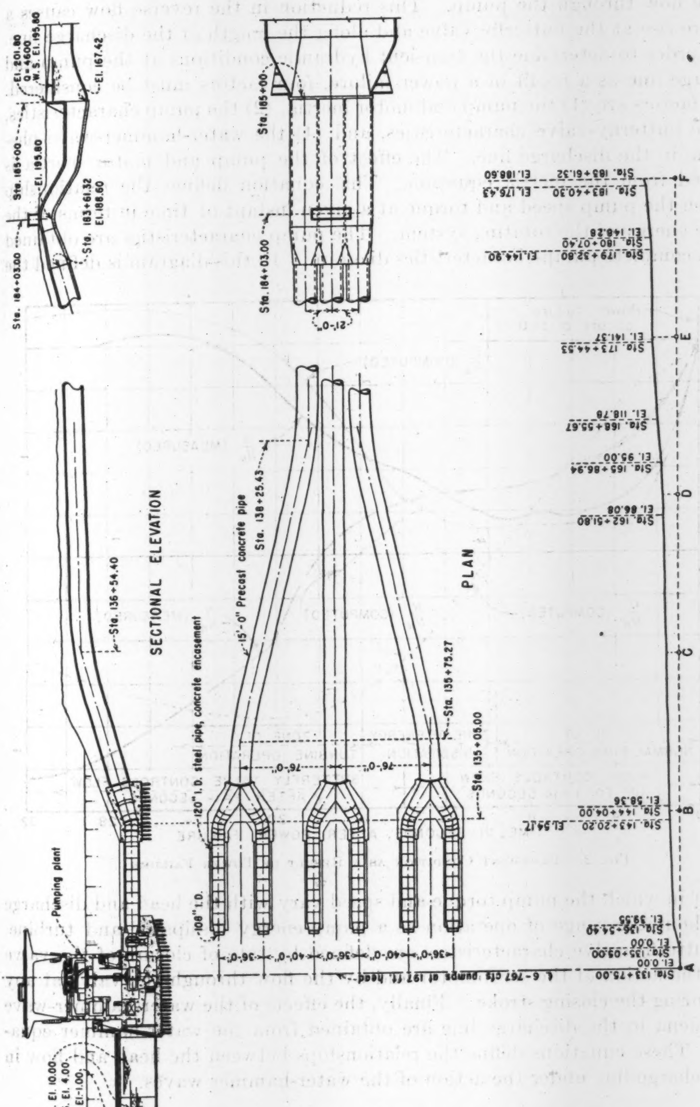
El. 201.80
Q = 4600
W.S. El. 195.80
El. 167.42
Sta. 185+00
El. 195.80
Sta. 183+61.32
El. 188.60
Sta. 184+03.00
Sta. 185+00
Sta. 184+03.00
21'-0"
SECTIONAL ELEVATION
Sta. 136+54.40
15'-0" Precast concrete pipe
Sta. 138+25.43
120" I.D. steel pipe, concrete encasement
Sta. 135+73.27
Sta. 135+05.00
PLAN
76'-0"
76'-0"
108" I.D.
Pumping plant
36'-0"
40'-0"
36'-0"
40'-0"
36'-0"
℄ 6-767 cfs pumps at 197 ft. head
Max. W.S. El. 10.00
Mean W.S. El. 4.00
Min. W.S. El. -1.00
DISCHARGE LINE PROFILE
A
B
C
D
E
F
Sta. 133+75.00
El. 0.00
Sta. 135+05.00
El. 0.00
Sta. 136+54.40
El. 39.55
Sta. 143+20.20
El. 54.12
Sta. 144+04.00
El. 58.36
Sta. 162+51.80
El. 86.08
Sta. 165+86.94
El. 95.00
Sta. 168+55.67
El. 118.78
Sta. 173+44.53
El. 141.37
Sta. 179+32.80
El. 144.90
Sta. 180+07.40
El. 146.26
Sta. 183+40.30
El. 176.43
Sta. 185+61.32
El. 188.60

FIG. 1.—TRACY PUMPING PLANT (CALIFORNIA) AND DISCHARGE LINES

reverse flow through the pump. This reduction in the reverse flow causes a pressure rise at the butterfly valve and along the length of the discharge line.

In order to determine the transient hydraulic conditions at the pump and discharge line as a result of a power failure, four factors must be considered. These factors are (1) the pump and motor inertia, (2) the pump characteristics, (3) the butterfly-valve characteristics, and (4) the water-hammer-wave phenomena in the discharge line. The effect of the pump and motor inertia is obtained from the inertia equation. This equation defines the relationship between the pump speed and torque at a given instant of time in terms of the kinetic energy of the rotating system. The pump characteristics are obtained from a complete pump-characteristics diagram. In this diagram is defined the manner in which the pump torque and speed vary with the head and discharge throughout the range of operation as a pump energy dissipator and turbine. The butterfly-valve characteristics are defined by rate of closure of the valve under the action of the servomotor and by the flow through the valve at any time during the closing stroke. Finally, the effects of the water-hammer-wave phenomena in the discharge line are obtained from the water-hammer equations. These equations define the relationships between the head and flow in the discharge line under the action of the water-hammer waves.

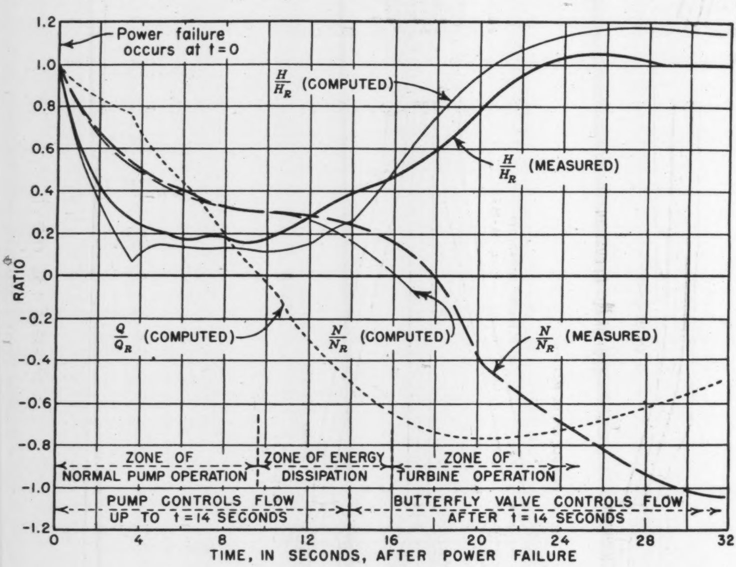

FIG. 2.—TRANSIENT CONDITION AS A RESULT OF POWER FAILURE

INERTIA EQUATION

When the power to the pump motor is suddenly cut off, the deceleration of the pump at any instant depends on the flywheel effect of the rotating parts of

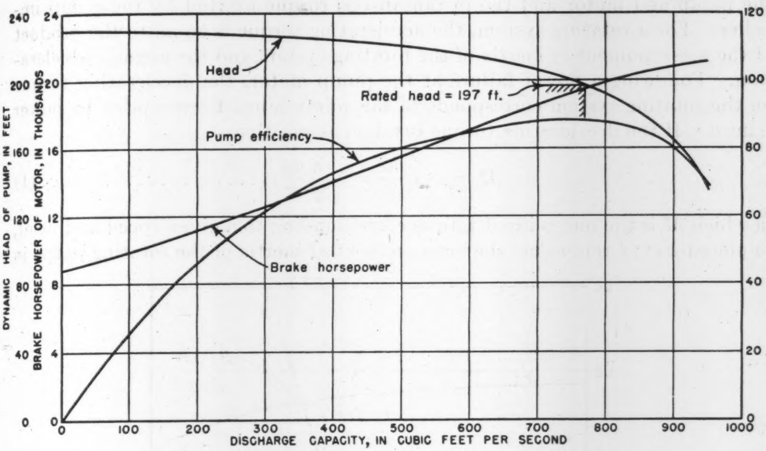

FIG. 3.—PUMP-PERFORMANCE CURVES

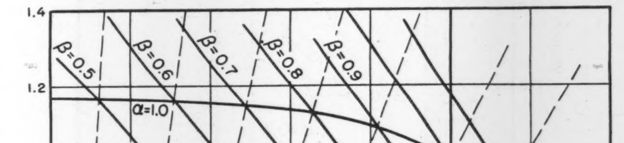

FIG. 4.—CHARACTERISTIC DIAGRAM FOR REGION OF NORMAL PUMP OPERATION

the pump and motor and the instantaneous torque exerted by the pump impeller. For a rotating system, the accelerating torque is equal to the product of the mass moment of inertia of the rotating system and the angular acceleration. Following a power failure at the pump motor, the decelerating torque on the rotating system corresponds to the pump-input torque prior to power failure. If the decelerating torque is taken as positive,

$$M = - I \frac{d\omega}{dt} = - \frac{\lambda}{g} \frac{d\omega}{dt} \quad \ldots\ldots\ldots\ldots\ldots\ldots\ldots (1)$$

in which M is the pump input torque corresponding to a given speed and head, in pound-feet; I represents the mass moment of inertia of the rotating parts, in

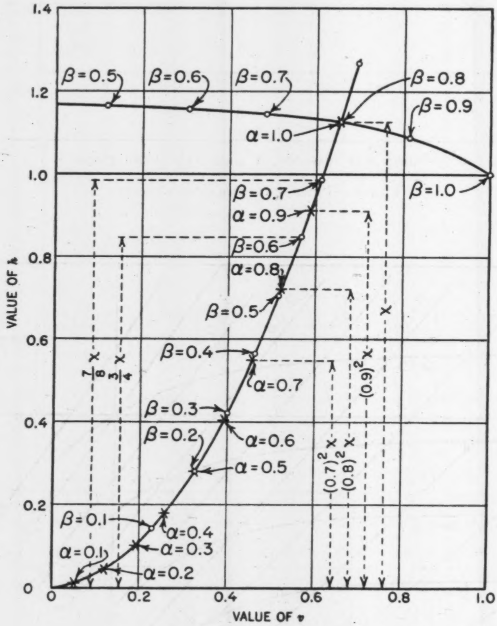

FIG. 5.—CONSTRUCTION OF CHARACTERISTIC DIAGRAM

pound-feet seconds squared; ω is the angular velocity of pump and motor shaft, in radians per second; t denotes time, in seconds; λ is the flywheel effect, or moment of inertia in terms of the weight of the rotating parts of the motor, pump, and entrained water, in pound-feet squared; and g represents the gravitational acceleration, in feet per second squared. Because the pump torque varies with the speed, Eq. 1 is applicable for specific instants of time only. For a small time interval ($\Delta t = t_2 - t_1$), Eq. 1 is written approximately as

$$\frac{M_1 + M_2}{2} = - \frac{\lambda}{g} \frac{\omega_2 - \omega_1}{\Delta t} = \frac{2 \pi \lambda}{60 \, g} \frac{N_1 - N_2}{\Delta t} \quad \ldots\ldots\ldots\ldots (2)$$

in which N is the pump speed, in revolutions per minute. Eq. 2 can be written as

$$\alpha_1 - \alpha_2 = \frac{15\, g\, M_R}{\pi\, \lambda\, N_R}\, (\beta_1 + \beta_2)\, \Delta t \quad \text{(3)}$$

in which $\alpha = N/N_R$, $\beta = M/M_R$, and the subscript R is used to denote rated conditions. The decelerating torque at the rated head and speed of the pump is

$$M_R = \frac{60\, \gamma\, H_R\, Q_R}{2\, \pi\, N_R\, \eta_R} \quad \text{(4)}$$

in which γ is the specific weight of water, in pounds per cubic foot; H represents the pressure head for surge conditions measured above the pump-intake water-surface elevation, in feet; Q is the pump discharge, in cubic feet per second; and η denotes the pump efficiency. Then

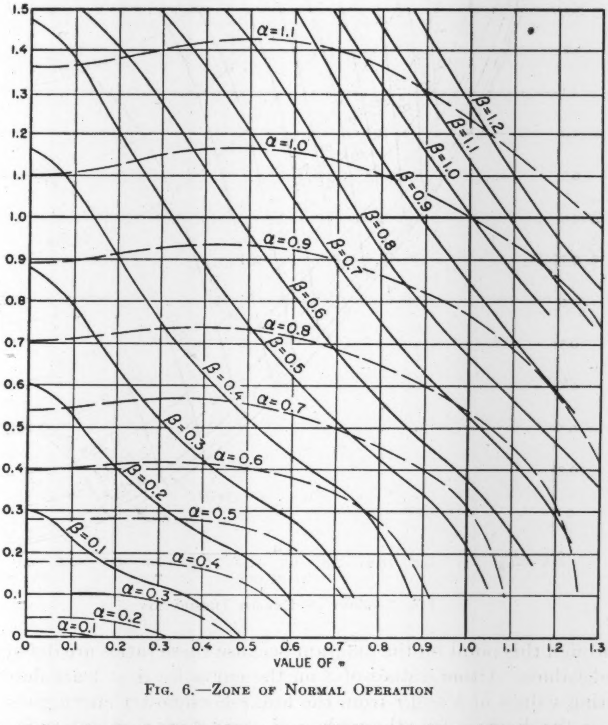

Fig. 6.—Zone of Normal Operation

$$\alpha_1 - \alpha_2 = K_1\, (\beta_1 + \beta_2)\, \Delta t \quad \text{(5)}$$

in which

$$K_1 = \frac{450\, g\, \gamma\, H_R\, Q_R}{\pi^2\, \lambda\, \eta_R\, N^2_R} = \frac{91{,}600\, H_R\, Q_R}{\lambda\, \eta_R\, N^2_R} \quad \text{(6)}$$

Pump Characteristics

The pump-performance data supplied by the manufacturer of the Tracy pumps are shown in Fig. 3 and include the head, brake horsepower, and efficiency plotted against the pump discharge. These data are converted to a family of torque and speed curves on an *hv*-diagram—$h = H/H_R$ and $v = V/V_0 = Q/Q_0$ (in which V is velocity of flow)—in the following manner: Referring to Fig. 4, the point corresponding to the rated head and discharge of the pump has the coordinates $h = 1$, $v = 1$. The curves for $\alpha = 1$ and $\beta = 1$ also pass through this point on the diagram because these ratios are defined in terms of rated values. Other values of β on the curve for $\alpha = 1$ are determined by computing values of h and v from the brake-horsepower curve given in Fig. 3. Points on the diagram for other values of α and β are then determined from the laws of homologous pump operation.[2] For example, for a given pump, H and M vary with N^2 whereas N and $H^{\frac{1}{2}}$ vary with Q. To use these relationships on the *hv*-diagram a parabola of the type $h = K_2 v^2$ is passed through a known point on the diagram such as that shown in Fig. 5 at $\alpha = 1.0$, $\beta = 0.8$. The vertical

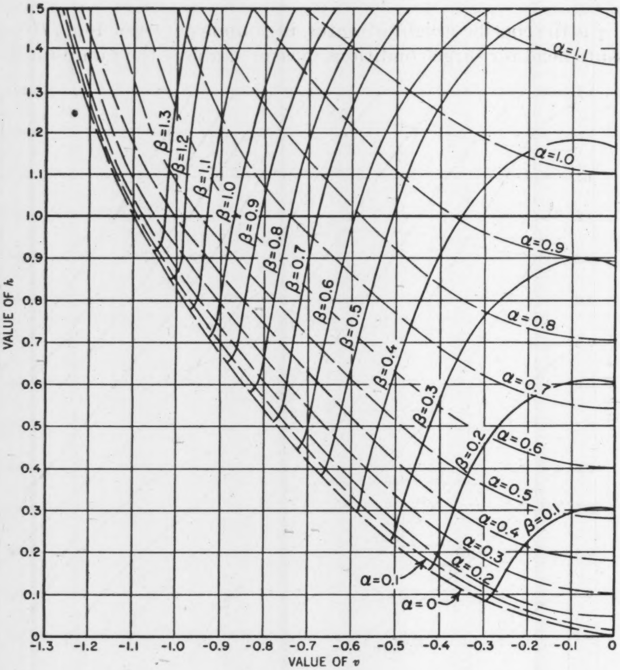

Fig. 7.—Zone of Energy Dissipation

---

[2] "Centrifugal and Axial Flow Pumps," by A. J. Stepanoff, John Wiley & Sons, Inc., New York, N. Y., 1948.

distance $h = 1.12$ at this point is denoted as χ and is then divided into eight equal parts, and the points corresponding to $\beta = 0.7, 0.6, \cdots$ are located on the parabola at ordinate values of $h = \frac{7}{8}(1.12), \frac{3}{4}(1.12), \cdots$. Similarly, points corresponding to $\alpha = 0.9, 0.8$ are located on the same parabola at values of $h = 1.12(0.9)^2, 1.12(0.8)^2, \cdots$. A smooth curve is then drawn through the points on the various parabolas corresponding to each value of α and β. In Fig. 4 there are shown families of torque and speed curves which were constructed in this manner.

The pump characteristics shown in Fig. 4 define the manner in which the pump torque and speed vary with the head and discharge for the zone of normal pump operation. For the condition of power failure at the pump motors, these characteristics are sufficient for determining the minimum transient pressures and the likelihood of water-column separation at all points in the discharge line. However, after the flow is reversed through the pump (and prior to the control of the reverse flow by the butterfly valve), additional pump characteristics are required in (*a*) the zone of energy dissipation in which the pump is running in the forward direction with the flow through the pump in reverse and (*b*) the zone of turbine operation in which the flow through the pump and the pump rotation are both in reverse. The characteristics of the Tracy pumps

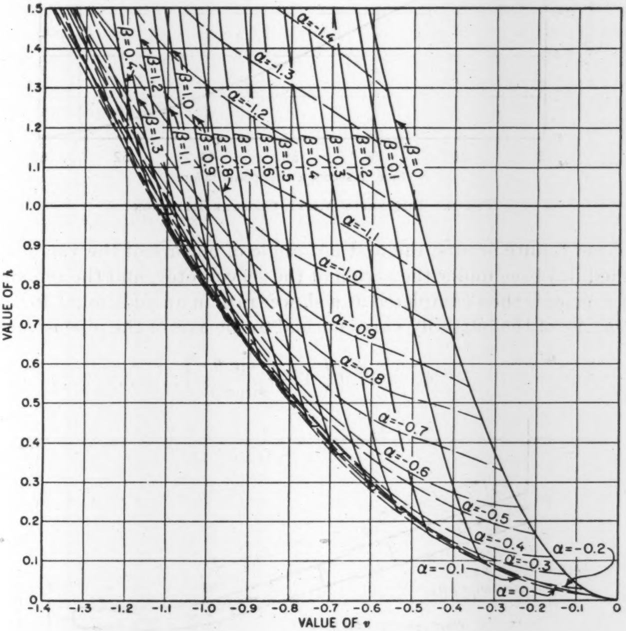

FIG. 8.—ZONE OF TURBINE OPERATION

for these two zones of abnormal operation were not available but were estimated from the complete pump characteristics shown in Figs. 6, 7, and 8 for another double volute pump.

CHARACTERISTICS OF THE BUTTERFLY VALVE

The butterfly valves used at the Tracy Pumping Plant have a wide open area of approximately 47.9 sq ft and an 82° angle of rotation of the valve leaf.

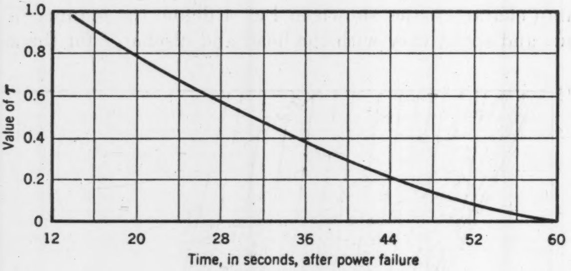

FIG. 9.—BUTTERFLY-VALVE CLOSURE RELATION

When power failure occurs, the first 55° angle of closure of the valve leaf is accomplished in 14 sec under the action of the servomotor, and the remaining 27° angle of closure is then completed at a slower rate in an additional 46 sec. The open area, A_v, of the butterfly valve normal to the axis of the pipe is very nearly

$$A_v = 47.9 \left(1 - \frac{\sin \theta}{\sin 82°} \right) \text{.....................} (7)$$

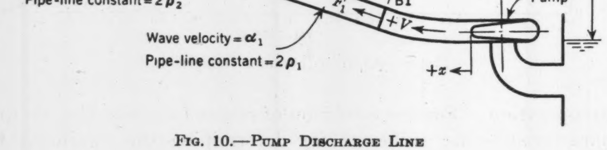

FIG. 10.—PUMP DISCHARGE LINE

in which θ is the angle between the axis of the discharge line and the butterfly-valve leaf, in degrees. The flow through the butterfly valve is

$$Q = C_d \, A_v \sqrt{2 \, g \, H} \text{........................} (8)$$

in which C_d is the coefficient of discharge of the butterfly valve. When the variable rate of closure is considered and a coefficient of discharge of 0.7 is used, the flow ratio is defined by

$$v = \tau \sqrt{h} \quad \text{(9)}$$

in which τ, a function of time, is related to t in Fig. 9.

WATER-HAMMER EQUATIONS

The water-hammer equations for the pump discharge line shown in Fig. 10 are

$$h_{B1, t1} - h_{C1, t2} = - 2 \rho_1 (v_{B1, t1} - v_{C1, t2}) \quad \text{(10)}$$

and

$$h_{C2, t3} - h_{B2, t4} = + 2 \rho_2 (v_{C2, t3} - v_{B2, t4}) \quad \text{(11)}$$

In Eqs. 10 and 11 the time $(t_2 - t_1)$ is the travel time for the wave between B1 and C1 for an F-type pressure wave, and $(t_4 - t_3)$ is the wave travel time between C2 and B2 for an f-type pressure wave. For a uniform discharge line, the pipe-line constant is given by

$$2 \rho = \frac{a V_0}{g H_0} \quad \text{(12)}$$

Because the Tracy Pumping Plant discharge line consists of a number of lengths of uniform pipe which have the length, area, and pressure-wave velocity characteristics that are denoted by L_1, A_1, and a_1, in series, the discharge line is considered to be the same hydraulically as an equivalent uniform pipe line of characteristics L, A, and a, by making the following substitution:

$$\frac{L}{A} = \Sigma \left(\frac{L_n}{A_n}\right) = \frac{L_1}{A_1} + \frac{L_2}{A_2} + \frac{L_3}{A_3} + \cdots + \frac{L_n}{A_n} \quad \text{(13)}$$

$$\frac{L}{a} = \Sigma \left(\frac{L_n}{a_n}\right) = \frac{L_1}{a_1} + \frac{L_2}{a_2} + \frac{L_3}{a_3} + \cdots + \frac{L_n}{a_n} \quad \text{(14)}$$

and

$$2 \rho = \frac{Q_0 \Sigma \left(\frac{L_n}{A_n}\right)}{g H_0 \Sigma \left(\frac{L_n}{a_n}\right)} \quad \text{(15)}$$

Eqs. 10 and 11 define the relationships between the head and velocity ratios during the transient water-hammer phenomena. On a coordinate system of h and v these equations are represented by straight lines which have a slope of $\pm 2 \rho$ as shown in Fig. 11. Each water-hammer equation gives one relationship between the value of h and v at a point in a uniform section of the discharge line in terms of h and v which are known at another point in the line. In order to determine h and v explicitly, a second independent relationship is required. When the pump is controlling the flow, the second independent relationship is obtained from the pump-inertia equation with the use of the pump-characteristics diagram. When the butterfly valve has closed sufficiently so that it is controlling the reverse flow through the pump, the second independent relationship is obtained from the head-flow ratios at the butterfly valve as defined by

Eq. 9. These flow relationships at the butterfly valve are represented by parabolas on the *hv*-diagram.

EFFECT OF PIPE-LINE FRICTION

When two pumps are delivering water to the same discharge line, the friction loss in the pipe line is at a maximum and is estimated at approximately 5.6 ft for pump operation at the rated head. Because this head loss is a small percentage of the pumping head, its effect is approximated in the water-hammer solution by locating a hypothetical obstruction at the discharge outlet of the pump. This hypothetical obstruction is assumed to have the same head loss as the entire friction loss for the pipe line. This obstruction is represented on a coordinate system of h and v by a head-loss curve (Fig. 12) in which—for forward flow in the zone of normal pump operation—the head ratio at the pump discharge outlet at F is

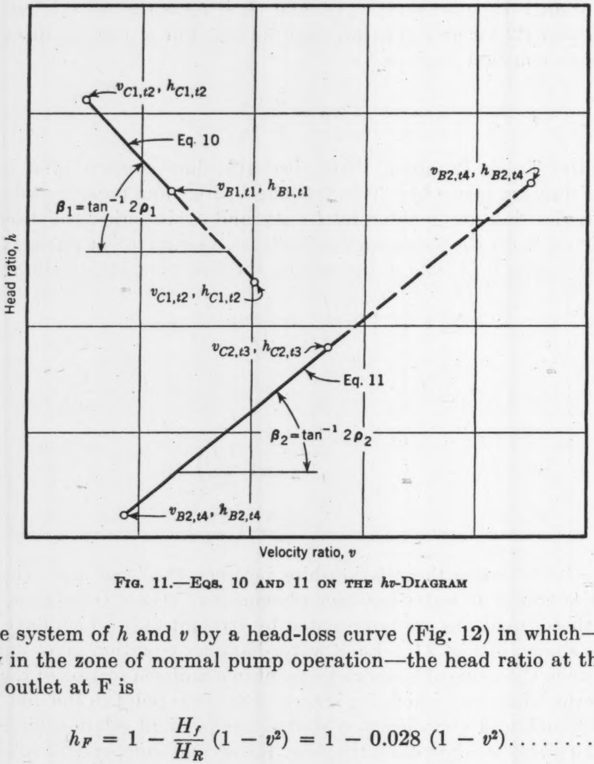

$v_{C1,t2}$, $h_{C1,t2}$
Eq. 10
$v_{B1,t1}$, $h_{B1,t1}$
$\beta_1 = \tan^{-1} 2\rho_1$
$v_{B2,t4}$, $h_{B2,t4}$
$v_{C1,t2}$, $h_{C1,t2}$
$v_{C2,t3}$, $h_{C2,t3}$
Eq. 11
$\beta_2 = \tan^{-1} 2\rho_2$
$v_{B2,t4}$, $h_{B2,t4}$
Head ratio, h
Velocity ratio, v

FIG. 11.—EQS. 10 AND 11 ON THE *hv*-DIAGRAM

$$h_F = 1 - \frac{H_f}{H_R}(1 - v^2) = 1 - 0.028\,(1 - v^2) \qquad (16a)$$

in which H_f is the head loss as a result of friction, and—for reverse flow through the pump—

$$h_F = 1 - 0.028\,(1 + v^2) \qquad (16b)$$

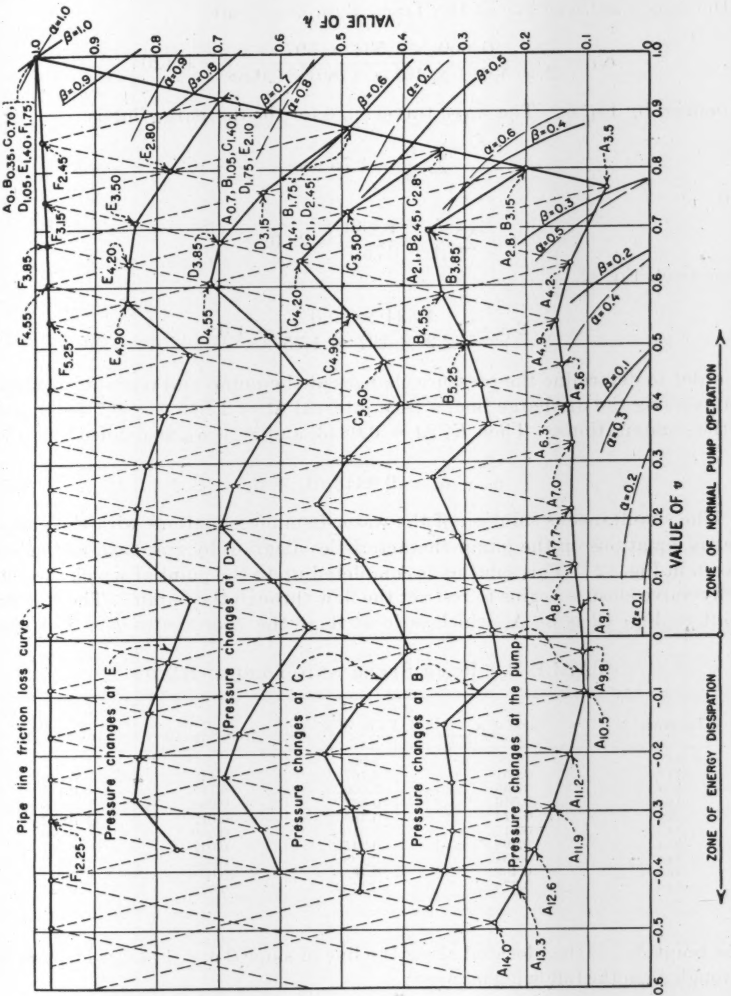

FIG. 12.—PRESSURE CHANGES IN THE DISCHARGE LINE

GRAPHICAL WATER-HAMMER ANALYSIS

For a power failure at the motors of two pumps which are supplying water to the same discharge line at the Tracy Pumping Plant,

$$K_1 = \frac{91{,}600 \times 1{,}534 \times 197}{2 \times 4.040 \times 10^6 \times (180)^2 \times 0.88} = 0.1204,$$

as defined by Eq. 6. The wave travel time for the discharge line is

$$\sum \frac{L}{a} = 1.75 \text{ sec}$$

and

$$\sum \frac{L}{A} = \frac{5{,}130}{176.7} = 29.0.$$

Then from Eq. 15,

$$2\,\rho = \frac{1{,}534 \times 29.0}{32.2 \times 197 \times 1.75} = 4.0.$$

In order to determine the pressure changes at the pump and four intermediate points along the discharge line, a time interval $\Delta t = 2\,L/5\,a = 0.7$ sec is used in the computations. Then $K_1\,\Delta t = 0.0843$, and $\alpha_1 - \alpha_2$, as defined by Eq. 5, is

$$\alpha_1 - \alpha_2 = 0.0843\,(\beta_1 + \beta_2) \qquad (17)$$

The simultaneous solution of the water-hammer equations with the pump-inertia equations on the pump-characteristics diagram by graphical methods is shown in Fig. 12. This solution is completed up to the point at which the butterfly-valve closure begins to restrict the flow through the pump. The starting point in Fig. 12 is at A_0 which is located at the coordinates $h = 1$, $v = 1$.

TABLE 2.—PUMP SPEED AND TORQUE RATIOS

Location	Value of α	Value of β	$\alpha_1 - \alpha_2$ from Fig. 12	$\alpha_1 - \alpha_2$ from Eq. 17
A_0	1.000	1.000	0	0
$A_{0.7}$	0.851	0.767	0.149	0.149
$A_{1.4}$	0.736	0.600	0.115	0.115
$A_{2.1}$	0.646	0.467	0.090	0.090
$A_{2.8}$	0.574	0.385	0.072	0.072
$A_{3.5}$	0.515	0.310	0.059	0.059
$A_{4.2}$	0.468	0.245	0.047	0.047
$A_{4.9}$	0.431	0.198	0.037	0.037
$A_{5.6}$	0.400	0.165	0.031	0.031
$A_{6.3}$	0.374	0.140	0.026	0.026

The point $A_{0.7}$ is then located along the line of slope $2\,\rho = +\,4.0$, which passes through A_0 in the following manner:

The location of $A_{0.7}$ is first estimated. Values of α_2 and β_2 at the estimated position of $A_{0.7}$ are then read from the pump-characteristics curves. This value of β_2 is used in Eq. 17 to compute α_2. If the computed value of α_2 does not agree with the value of α_2 read from the pump-characteristics curves, the point for $A_{0.7}$ is shifted up or down along the line $2\,\rho = 4.0$ until these values of

α_2 agree. This particular point is located at a value of $\beta = 0.767$ and $\alpha = 0.851$. Other points for $A_{1.4}$, $A_{2.1}$, · · · are determined in a similar manner. The values for several of these points are shown in Table 2, and the graphical water-hammer solution is completed (Fig. 12) up to $t = 14.0$ sec, at which point the butterfly closure begins to restrict the flow.

Parabolas corresponding to the flow through the butterfly valve, as defined by Eq. 9, are shown in Fig. 13 for each 3.5-sec time interval. The intersection of the lines of $(\pm 2\rho)$ slope with the pertinent parabolas and the head-loss curve (Fig. 13) completes the solution of the water-hammer problem caused by the butterfly-valve closure.

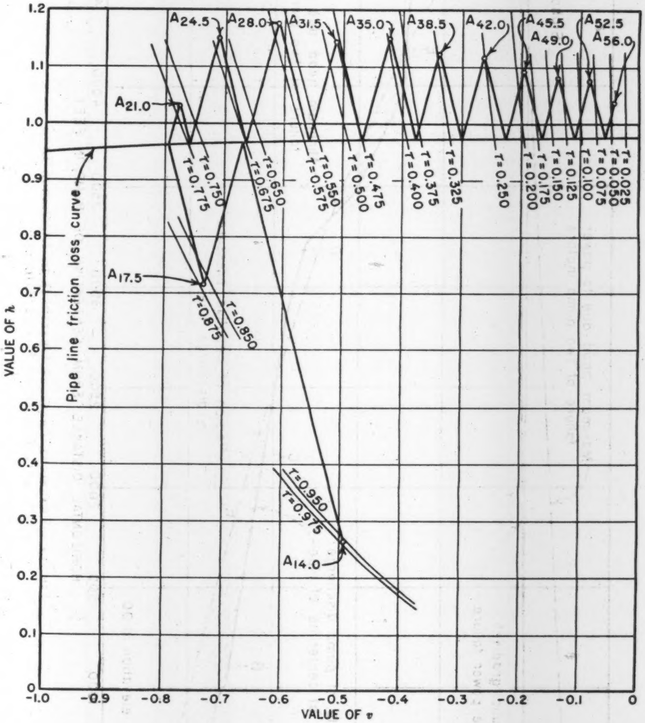

FIG. 13.—PARABOLAS FOR FLOW THROUGH THE BUTTERFLY VALVE

A time history of the head, flow, and speed changes as obtained from the graphical water-hammer solution is shown in Fig. 2. In addition to the time history, the following limiting values are also obtained from the graphical solution: (*a*) Maximum drop in head at the pump = 0.93 H_R; (*b*) maximum drop in head at point B = 0.80 H_R; (*c*) maximum drop in head at point C = 0.67 H_R; (*d*) maximum drop in head at point D = 0.51 H_R; (*e*) maximum drop

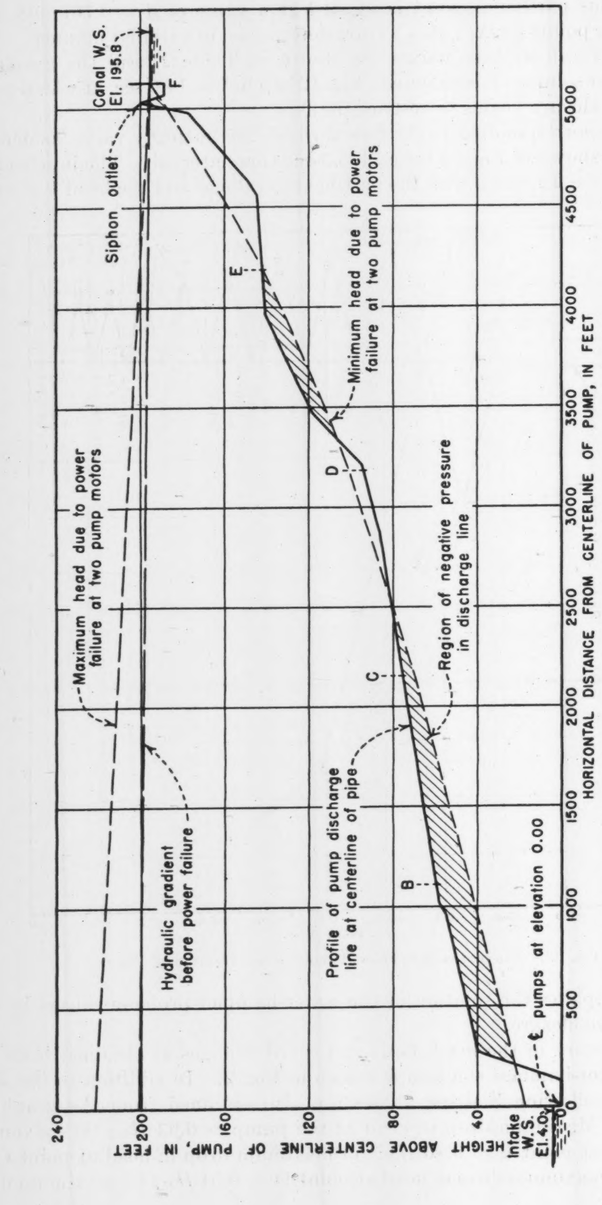

FIG. 14.—TRANSIENT PRESSURE GRADIENTS IN DISCHARGE LINE AS A RESULT OF POWER FAILURE

n head at point E = 0.30 H_R; and (*f*) maximum head rise at the butterfly valve = 0.17 H_R.

WATER–COLUMN SEPARATION

The maximum positive and negative pressures obtained from the graphical water-hammer solution are plotted on the discharge-line profile in Fig. 14 to show the limiting pressures which are exerted on the discharge line as a result of a power failure at the two pump motors. If the minimum pressure at any point in the pipe line had reached the vapor pressure of water, or 33.4 ft below atmospheric pressure, the water-hammer solution would no longer have been valid and water-column separation in the discharge line would have been a possibility. Water-column separation sometimes occurs during the initial negative surge waves on long pump-discharge lines at high points which are near the hydraulic gradient. Whenever possible, this condition should be avoided because of the heavy surge pressures that are sometimes created when the separated water columns rejoin. At the Tracy Pumping Plant the computed minimum pressure at the center line of the discharge line is 17 ft below atmospheric pressure, and, hence, water-column separation is improbable.

OBSERVED AND COMPUTED RESULTS

Pressure-surge tests were conducted at the Tracy Pumping Plant for the condition of power failure at the pump motors to check the adequacy of the pumps, discharge lines, and pressure-control equipment, and also to check the accuracy of the water-hammer analyses. The tests included the following conditions of operation:

1. Two pumps supplying water to the same discharge line when a power failure occurred at both pump motors.
2. Two pumps supplying water to the same discharge line when a power failure occurred at only one pump motor.
3. One pump supplying water to the discharge line when a power failure occurred at the pump motor.

In general, agreement between the computed and observed results was satisfactory. Moreover, there was no evidence of water-column separation in the discharge line. A comparison between the observed and computed results for a power failure at two pump motors is shown in Fig. 2.

WATER–HAMMER CHARTS

In obtaining the graphical water-hammer solution for a pump installation subsequent to a power failure at the motors, two independent parameters are used with the complete pump characteristics. These are 2 ρ, the pipe-line constant, and K_1 2 L/a, a constant which includes the effect of the pump and motor inertia and the water-hammer wave travel time of the discharge line. For a given set of pump characteristics, the results of a large number of water-hammer solutions can be shown on charts as indicated in Fig. 15. These charts furnish a convenient method for estimating the transient effects caused by a power failure at the pump motors when no control valves are present at the pump. Although the charts were obtained by using the complete characteristics of a particular pump operating at the rated head prior to power failure, they are useful for obtaining the approximate water-hammer effects in any pump discharge line.

USE OF SURGE TANKS AND AIR CHAMBERS AT THE TRACY PUMPING PLANT

During the initial design studies of the Tracy Pumping Plant, surge tanks or air chambers were considered necessary for preventing water-column separation and for reducing the water-hammer effects in the discharge line caused by a power failure at the pump motors. In the final designs it was ascertained that, because water-column separation was improbable, surge tanks or air chambers would not be required.

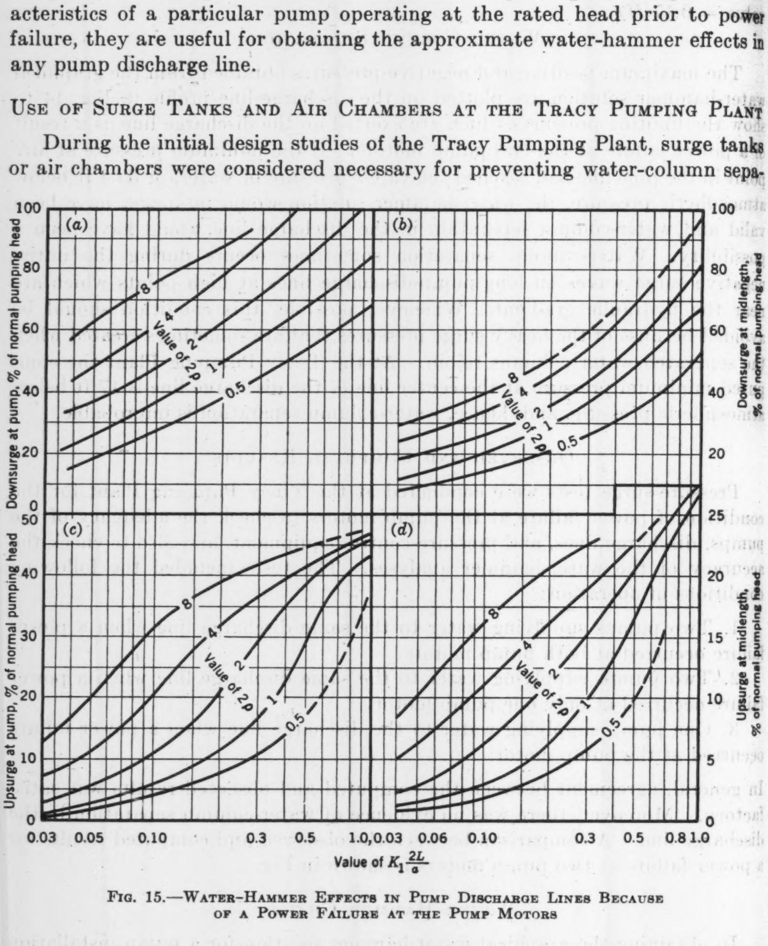

FIG. 15.—WATER-HAMMER EFFECTS IN PUMP DISCHARGE LINES BECAUSE OF A POWER FAILURE AT THE PUMP MOTORS

CONCLUSIONS

Pressure surges in pump discharge lines subsequent to a power failure at the pump motors can be determined with satisfactory accuracy if the complete characteristics of the pump and control valves are known. At the Tracy plant only the pump characteristics for the zone of normal operation were obtainable from the pump-performance data supplied by the manufacturer. This permitted an accurate determination of the water-hammer effects in the discharge line up to the point at which the flow reversed through the pump. However, these data were sufficient for determining the possibility of water-column separation in the discharge line. Pump characteristics for abnormal operation and the characteristics of the butterfly valve were then estimated for the remainder of the water-hammer solution. This type of water-hammer analysis afforded a large monetary savings for the Tracy Pumping Plant by the elimination of expensive surge tanks or air chambers which were initially considered necessary for pressure control.

ACKNOWLEDGMENTS

Assistance was received from F. E. Cornwell, C. C. Crawford, and W. E. Evans during the original water-hammer analyses at the Tracy Pumping Plant and during the preparation of the water-hammer charts. F. W. Taylor assisted during the water-hammer tests, and R. H. Williams aided in the preparation of the illustrative material.

APPENDIX

The following symbols, adopted for use in the paper and for the guidance of discussers, conform essentially with "American Standard Symbols for Hydraulics" (ASA Z10.2–1942) prepared by a committee of the American Standards Association, with ASCE representation, and approved by the Association in 1942:

A = cross-sectional area of the pipe;
A_v = open area through the butterfly valve;
a = velocity of the water-hammer pressure wave;
C_d = coefficient of discharge of the butterfly valve;
g = gravitational acceleration;
H = pressure head for surge conditions measured above the pump-intake water-surface elevation;
H_f = head loss in discharge line as a result of friction;
h = ratio of pressure head for surge conditions to rated pumping head;
I = mass moment of inertia of the rotating parts;
K_1 = term defined in Eq. 6;
L = length of pipe;
M = pump input torque corresponding to a given speed and head;
N = pump speed at any time;
Q = pump discharge at any time;
R = subscript denoting rated conditions;
t = time at the instant under consideration;
V = velocity of the water in the discharge line for surge conditions at any time;

v = ratio of velocity of water for surge conditions to that for initial conditions;

α = ratio of pump speed at any time to rated pump speed;

β = ratio of pump input torque for any given speed to pump input torque at rated speed and head;

γ = specific weight of water;

η = pump efficiency;

θ = angle between axis of discharge line and the butterfly valve leaf;

λ = flywheel effect, or moment of inertia in terms of the weight of the rotating parts of the motor, pump, and entrained water;

ρ = a pipe-line constant;

τ = function of time, equal to flow through the butterfly valve divided by Q_0; and

ω = angular velocity of pump and motor shaft.

DISCUSSION

CARROLL E. WITHERS.[3]—In citing the pump characteristics of the Tracy plant, Mr. Parmakian has stated that the pump-performance data necessary for investigating the transient hydraulic conditions in the zone of energy dissipation and the zone of turbine operation were not available and had to be estimated from the curves of another double volute pump. Because of the expense involved in making the necessary tests, no pump manufacturer will obtain this information unless it is required (and paid for) by the purchaser. The lack of this information means that, in most cases, when investigating the transient hydraulic conditions in a pump-discharge system, the pump characteristics in these regions must be estimated from the known curves of the few pumps that have been tested. It would be of interest to know whether the error induced in making such assumptions is of sufficient consequence to require the necessary testing.

Comparison of the transient hydraulic conditions in the Tracy pumping system, as designed, with those of the system without any valves is interesting. Neglecting friction—which in this case will not induce appreciable error—and using the values of $2\,\rho$, K_1, and $2\,L/a$ given by Mr. Parmakian, it is found that the pressure rise at the pump would have been $1.40\,H_R$. This value indicates an increase of approximately 20% over the pressure rise obtained with the valve. This computation shows how effective a valve of this type can be when properly operated. The pressure drop at the pump will be the same as that which would result with the valve and will occur in 3.5 sec after power failure to the pump motors; a complete reversal of flow in the pump discharge line will follow in approximately 10 sec. Therefore, valves with a slow time of closure can be of no value in the control of transient hydraulic conditions because the maximum pressure rise, the maximum drop, and the reversal of flow in the pump discharge line occur within a short period. Further comments relative to the proper valve closure time would be of great interest.

It would also be desirable to know the maximum reverse speed of a pump and to have a complete time history of the transient hydraulic conditions in a pump system after power to the pump motors fails.

PETER LINTON.[4]—A valuable service has been performed by Mr. Parmakian in reporting these full-scale tests on pressure surges after power failure. This information unfortunately is published in only a few cases. The tests illustrate the value of a full analysis of transient conditions in leading to savings in surge-control devices, such as surge tanks and control valves.

The time history of the pressure surge (Fig. 2) is most interesting and clearly illustrates the results of the pressure-surge diagrams (Figs. 12 and 13).

---

[3] Engr., Bureau of Reclamation, U. S. Dept. of the Interior, Denver, Colo.

[4] Research Engr., British Hydromechanics Research Assn., Harlow, England.

Comparison between the measured and computed curves shows good agreement as far as the general shape is concerned; the lowest pressure reached is approximately 17 ft higher than the computed pressure, and the subsequent pressure rise is 26 ft less than that computed. In both cases the measured pressures are more favorable than the computed ones, and the author's tests therefore confirm the fact that a careful analysis of the pressure surges leads to a a somewhat conservative result. This difference between computed and measured results might be valuable as an additional margin of safety if it could be relied on in all cases; it is therefore important to investigate some of the possible causes.

It can, of course, be assumed that the instruments used could have followed accurately the fast pressure oscillations which were expected; no details were given of the instruments. It would be of interest to learn the type of instrument used and its probable accuracy under the actual conditions.

The theoretical minimum pressure depends, to some extent, on the assumptions implicit in the surge diagram (Fig. 12). As noted by Mr. Parmakian, the actual pipe line, which consists of a number of different pipes in series, has been replaced by the equivalent uniform pipe line determined by Eqs. 13 and 14. This replacement may have contributed to the low value of the minimum pressure because, in a complete diagram, the line A_0 $A_{3.5}$ (Fig. 12) would be replaced by a series of lines staggered either to the right or to the left. It would be interesting to know whether an attempt has been made to draw a complete pressure-surge diagram to include all or at least most of the changes in the pipe line and whether that diagram has given a value closer to the measured one.

From Fig. 12 it is also clear that the position of point $A_{3.5}$ and the minimum pump pressure are determined primarily by the shape of the pump head-flow characteristic in this region. A comparison with Fig. 4 shows that these characteristics in Fig. 12 represent a considerable extrapolation beyond the design point, well past the end of the pump characteristic given in Fig. 3. The method by which this extrapolation was performed should be noted as well as whether the curves in Fig. 6 were used in this connection. It would also be important to know whether this part of the pump characteristic is likely to vary from one machine to another, particularly when the pump does not cavitate as in the present case.

Additional and highly important results appear to have been obtained by Mr. Parmakian in another test at the Tracy Pumping Plant when only one pump of a pair discharging into a common pipe line was stopped. To the writer's knowledge, no such experiments have been reported on an installation of this type, in which reverse flow through the pump occurs during slowing down before the butterfly valve has been closed. It would be valuable to have a comparison between computed and measured pressures for this case also—if the author has made such an investigation—together with some indication of the method by which the distribution of flow between the running pump and the one slowing down has been determined.

John Parmakian,[5] M. ASCE.—The discussions by Messrs. Withers and Linton have emphasized the ever-present question confronting pumping-plant designers: What will be the operating characteristics of the pumps to be furnished for this installation? Mr. Withers notes that the pump-characteristic diagrams are not available for most pumps, especially in the zones of energy dissipation and turbine operation. Therefore, it is necessary to compare the characteristics of the pump studied in the region of normal operation with available diagrams. This comparison can be made by the use of homologous relationships and the pump-performance curves supplied by the manufacturer. In most cases it is not necessary to construct a characteristics diagram. Instead, the complete characteristics diagram used is one for the same type of pump having approximately the same specific speed as the pump being studied. Experience has shown this method to be satisfactory for most engineering purposes.

In the study at the Tracy Pumping Plant the characteristics in the normal region of operation, as determined by homologous relationships, agreed fairly well with those given[6] by R. T. Knapp, M. ASCE. Therefore, the complete characteristics diagram obtained by Mr. Knapp was used. Since it is likely that the characteristics in the region of point $A_{3.5}$ could vary from one machine to the next, as suggested by Mr. Linton, the use of Mr. Knapp's diagram could have caused the minor difference between the test and the computed values.

It is perhaps unfortunate that for the actual solution the extrapolated point $A_{3.5}$ is the lowest point and represents the minimum head. The error which is introduced by extrapolation would have been reduced further if the minimum head had occurred at some later time. Any error introduced at point $A_{3.5}$ has little effect on the value of the maximum computed head. The minor difference between the test and computed minimum values is probably caused by the use of a pump-characteristic diagram which is not truly representative of the pumps. The use of the equivalent line had little effect on the computed values because the (L/A)-values of the wye branches are small when compared to the total (L/A)-value for the line.

Another reason for the difference between the test and computed minimum heads is the operation of the siphon outlet. The vacuum-breaker valve on the siphon outlet opens immediately when the power is interrupted. This action increases the head at the discharge end of the line as much as 15 ft. This increase causes a higher minimum head to occur than was determined because the effect of the siphon was neglected in the computed solution.

The minor difference between the computed and observed maximum heads is believed to be caused primarily by the draining of the line away from the siphon. During the time of the transient, the level at the discharge end of the line drops from 15 ft to 20 ft. This drop lowers the maximum head below the computed head. However, it should be noted that the head rise is only slightly affected by the pump characteristics because the valve does most of the controlling in the region of negative flow.

---

[5] Head, Technical Eng. Analysis Section, Design Div., Bureau of Reclamation, U. S. Dept. of the Interior, Denver, Colo.

[6] "Centrifugal Pump Performance as Affected by Design Features," by R. T. Knapp, *Transactions*, ASME, Vol. 63, 1941, pp. 251–260.

Mr. Linton suggests that the differences between the computed and test heads be used as an additional factor of safety if the computed values can be depended on to be conservative. This condition does not always exist because there are so many parameters involved whose true values are unknown.

The instruments used in this series of tests were Statham pressure transmitters, Brush strain gage amplifiers, and direct writing oscillographs. The instruments followed the pressure oscillations accurately up to a frequency of 100 cycles per sec and were adjusted to read pressure changes with an accuracy of less than 1 ft of head.

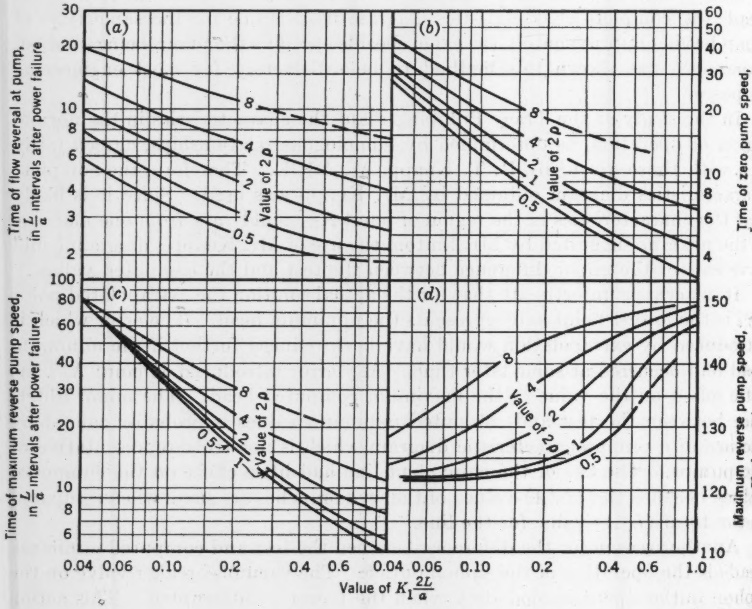

FIG. 16.—ADDITIONAL WATER-HAMMER EFFECTS IN PUMP DISCHARGE LINES DUE TO A POWER FAILURE AT THE PUMP MOTORS

Mr. Withers states that the head rise at the pump would have been greater if there were no valve in the line or if the valve had closed slowly. This is true for the subject installation. However, in some cases it is possible to have a higher head rise as a result of a valve closing too fast or with its fast rate of closure occurring at a time when reverse flow takes place. It is also possible that a valve properly operated to keep the head rise to a minimum when two or more pumps fail might give a higher head rise when only one pump fails. The curves from which the maximum reverse speed and the time history of the transient hydraulic conditions can be estimated for an installation without control valves are presented in Fig. 16.

AMERICAN SOCIETY OF CIVIL ENGINEERS
Founded November 5, 1852
TRANSACTIONS

Paper No. 2761

AERODYNAMIC STABILITY OF SUSPENSION BRIDGES

1952 REPORT OF THE ADVISORY BOARD ON THE INVESTIGATION OF SUSPENSION BRIDGES

PREFACE

The Advisory Board on the Investigation of Suspension Bridges was organized in 1942 by Thomas H. MacDonald, Hon. M., ASCE, Commissioner of Public Roads, at the request of a representative group of engineers concerned with the problems of suspension bridge design. A list of the sponsor organizations and their representatives is given in Sect. 25.

The purpose of the Advisory Board is to coordinate research dealing with suspension bridges with particular regard to their aerodynamic stability. It has acted in an advisory capacity with respect to the following projects and many of the specific investigations made have been initiated at the suggestion of the Board:

1. Cooperation of the Washington Toll Bridge Authority, the University of Washington and the Bureau of Public Roads in a study of the effect of aerodynamic forces on models of suspension bridges and a theoretical and experimental study of means for predicting the aerodynamic behavior of actual suspension bridges.

Numerous progress reports have been submitted to the Board and a final report (3)[1] in five parts has been prepared. The studies are continuing.

NOTE.—Published, essentially as printed here, in August, 1952, as *Proceedings-Separate No. 144A–144B.* Positions and titles given are those in effect when the paper was received for publication in 1952.

[1] Numerals in parentheses, thus: (3), denote corresponding items in the list of references, Appendix I.

2. Cooperation of the American Institute of Steel Construction and the Bureau of Public Roads in theoretical analyses of the action of suspension bridges when subjected to aerodynamic forces.

Twelve reports by the late Friedrich Bleich, M. ASCE, have been submitted to the board and incorporated in two subsequent publications (1) (11) (See item 7).

3. Cooperation of the Golden Gate Bridge and Highway District and the Bureau of Public Roads in making observations of the movements of the Golden Gate Bridge. Progress reports have been submitted to the Board. Brief news items concerning these investigations have been published.

4. A study of the damping characteristics of structural steel members in the laboratory of the Bureau of Public Roads. Reports have been submitted to the Board and the test results have been published (17).

5. Cooperation of the Oregon State Highway Commission and the Bureau of Public Roads in static model tests to verify Friedrich Bleich's Linearized Deflection Theory, particularly adapted for evaluating the effect of diagonal tower stays and mid-span cable ties on the behavior of the bridge under static loading. A report has been printed (1) (See item 7).

6. Publication by the Agricultural and Mechanical College of Texas in cooperation with the Bureau of Public Roads of a reprint of the three original official reports of the failure of the Tacoma Narrows Bridge. In 1941, shortly before the organization of the Advisory Board, there was also published (25) by the Agricultural and Mechanical College of Texas in cooperation with the Bureau of Public Roads, "A History of Suspension Bridges in Bibliographical Form," by A. A. Jakkula.

7. Cooperation of the Oregon State Highway Commission and the Bureau of Public Roads in the preparation of the manuscript (1) for "The Mathematical Theory of Vibration of Suspension Bridges" which has been printed by the Bureau of Public Roads.

The Board has cooperated, through the exchange of information, with the National Physical Laboratory of Great Britain, which has made wind tunnel studies for the proposed suspension bridge over the Severn River near Bristol, England.

Although the investigations have not been completed, it is possible now to incorporate certain findings and tentative recommendations in a preliminary report. In addition to the above listed projects, the Board has drawn upon the reports of other investigations and the published writings of others in this field.

This report was prepared for the Advisory Board on the Investigation of Suspension Bridges by George S. Vincent, M. ASCE, Principal Highway Bridge Engineer, Bureau of Public Roads, and has been reviewed, amended and officially approved by the Board. Because of his close association with the investigations with which the Board has been concerned and his intimate knowledge of the subject, Mr. Vincent was well qualified for this task.

SYNOPSIS

The aerodynamic forces which act upon a bridge in the wind depend only upon the velocity and direction of the wind and the size, shape, and motion of the bridge. The occurrence of resonance involving these wind forces with the motion of the bridge depends upon the same factors. The amplitude of oscillation which may be built up depends upon the strength of the wind forces (including their variation with amplitude) the energy storage capacity of the structure, the structural damping and the duration of a wind capable of exciting motion.

The wind velocity and direction (including vertical angle) can be determined by extended observations at the site. They can be approximated with reasonable conservatism on the basis of a few local observations and extended study of more general data. The choice of the wind conditions for which a given bridge should be designed may always be largely a matter of judgment.

The size and shape of the bridge are, of course, known. Its motion, consisting essentially of natural modes of vibration, is determined completely by its mass, mass distribution, and elastic properties, from which the motion and energy storage capacity can be computed by reliable methods.

The only unknown element is that factor relating the wind to the bridge section and its motion. This is a highly individual factor which can not at present be generalized but is subject to reliable determination in each case. Properties of the bridge including its elastic forces and its mass and motions (determining its inertial forces) can be computed and reduced to model scale, and wind conditions bracketing all probable conditions at the site can be imposed upon a section model. The motions of such a dynamic section model in the properly scaled wind will duplicate reliably the motions of a convenient unit length of the bridge. The wind forces and the rate at which they can build up energy of oscillation respond to the changing amplitude of the motion, and the rate of energy change can be measured and plotted against amplitude. Thus the section model test measures the one unknown factor which can then be applied by calculation to the variable amplitude of motion along the bridge to predict the full behavior of the structure under the specific wind conditions of the test. These predictions are not precise but are about as accurate as some other features of the design analysis.

As stated, this factor, relating bridge movement to wind conditions, is highly individual; therefore, detailed criteria for the design of favorable bridge sections can not be written until a large mass of individual data has been accumulated. However, it can be stated that:

(1) In general, a truss-stiffened section is more favorable than a girder-stiffened section.

(2) Deck slots and other devices which tend to break up the uniformity of wind action are likely to be favorable.

(3) The use of two planes of lateral system to form a four-sided truss can materially increase the frequency of any torsional motion. Such design strongly inhibits flutter and also raises the critical velocity of a pure torsional motion.

(4) For a given section a high natural frequency of vibration is usually favorable—
  (a) For short to moderate spans a useful increase in frequency, if needed, can be attained by increased truss stiffness. (Although not closely defined, the term "moderate spans" may be regarded as including lengths to about 1800 ft.)
  (b) For long spans it is not economically feasible to obtain any material increase in natural frequency of vertical modes above that inherent in the span and sag of the cable.
  (c) The possibility should be considered that for longer spans in the future, with their unavoidable low natural frequencies, oscillations due to any unfavorable aerodynamic characteristics of the cross section may be more prevalent than in the case of bridges of moderate span.

(5) It appears probable that at most bridge sites the wind is broken up—that is, non-uniform across the site, unsteady and turbulent so that a condition which could cause serious oscillation does not continue long enough to build up an objectionable amplitude. However,
  (a) There are undoubtedly sites where the winds from certain quarters are unusually steady and uniform.
  (b) There are bridge sections on which any wind over a wide range of velocity will continue to build up some mode of oscillation.

(6) An increase in stiffness arising from increased weight increases the energy storage capacity of the structure without increasing the rate at which the wind can contribute energy, and thereby increases the time required to build up an objectionable amplitude. This may have a beneficial effect much greater than is suggested by the percentage increase in weight because of the sharply reduced probability of the wind continuing unchanged for the greater length of time. Increased stiffness may give added structural damping and other favorable results.

Although more specific design criteria than the above cannot be given, it is possible to design a suspension bridge with a high degree of security against aerodynamic forces. This involves the calculation of natural modes of motion of the proposed structure, the performance of dynamic section model tests to determine the factors of behavior, and the application of these factors to the prototype by suitable analysis. This analysis is not more complicated than that commonly applied to the design of the structure for static loading although at present it is less familiar.

If the analysis forecasts an unfavorable aerodynamic behavior it will also suggest the general line of modification which is likely to result in improvement at least expense. The modified design must then be investigated. This procedure is similar to that by which the most economical and satisfactory of several alternate designs is usually established.

INTRODUCTION

The Advisory Board recognizes the obligation to make this preliminary report as concise as possible consistent with clear presentation. However, this relatively new subject (aerodynamic vibration of suspension bridges) in the literature of civil engineering must be presented without presuming on the reader's familiarity with the background and fundamentals. The intent is to cover all phases of the problem but not to burden the text with detailed proof or analysis, using instead citations to specific references in Appendix I, elaborating the statements made so that the reader can satisfy himself as to each point in question. The list of references is not complete but has been selected for conciseness.

The nature of wind action and of the behavior of the bridge in response to it are discussed in Part I. It is hoped that this will throw light on the mechanics of the phenomenon, give an appreciation of the relative influence of the many factors involved, give clues to the design features which can be manipulated to improve the stability of a bridge and suggest the type of investigation required to determine its probable behavior.

In Part II are discussed the means by which the aerodynamic characteristics of a design may be improved and a statement is given of tentative criteria for making a bridge safe against objectionable oscillation in the wind. An analytical and test procedure for confirming the adequacy of the design is presented.

Part III reviews the facts which have been established and points out the features which yet remain to be investigated before a fully satisfactory basis can be established for designing suspension bridges against objectionable oscillation under wind action.

I.—THE NATURE OF WIND ACTION AND OF THE BRIDGE RESPONSE

1. WIND PRESSURE

(A) *Static Forces.*—The principal force exerted on a bridge by a steady wind is a substantially constant pressure acting in the general direction of the wind. This constitutes the conventional wind loading taken into account in bridge design. The intensity of this pressure increases as the square of the velocity and is expressed by the formula (see any reference book on fluid mechanics):

$$p = C \frac{\rho}{2} V^2 \dots\dots\dots\dots\dots\dots\dots\dots (1)$$

in which p is in pounds per square foot, ρ is the mass density of the air (0.00238 slugs per cubic foot at sea level and 15° C.), V is the velocity in feet per second and C is a constant depending upon the shape and size of the obstruction. The term, $\rho \frac{V^2}{2}$, is known as the "dynamic pressure." Constant C is less for wide than for narrow members and less for streamlined than for blunt surfaces.

NOTE.—Written comments are invited for publication; the last discussion should be submitted by February 1, 1953.

The resultant of the steady wind force usually does not act exactly in the direction of the wind but is deflected, often to a considerable extent, by a force component which acts at right angles to the direction of the wind. In the field of aerodynamics this is known as the lift. The component in the direction of the wind is known as the drag.

As a rough, preliminary conception, the varying pressures over the surface of a body in a wind stream may be regarded as the forces which must by applied to the windstream to change its direction, acting in general toward the center of curvature of the streamline. Since the air pressure within the undisturbed mass of the wind stream remains constant the added force causing the curvature is supplied by the body as an added pressure at the leading edge, deflecting the stream away from it and contributing to the drag, and a reduced pressure where the curvature must be reversed in order for the wind element to follow the surface of the body thus contributing to the lift (see Fig. 1).

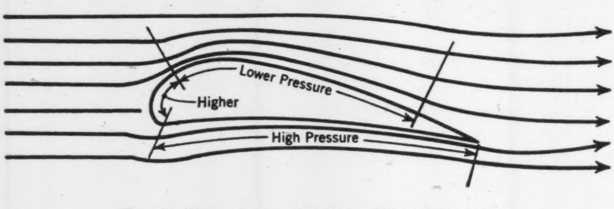

FIG. 1.—STREAMLINES AROUND A WING SECTION

Actually the situation is not so simple as conceived above due to the action of viscous frictional forces which retard a layer of wind near the surface, known as the boundary layer. A discussion of the boundary layer and its effects on the flow and forces can be found in any reference book on aerodynamics. It suffices here to state that it is only in the boundary layer that viscous effects are important.

The velocity varies from point to point in accordance with the streamline pattern associated with the displacement of the flow by the body and its boundary layer and wake. Outside the boundary layer and wake, the pressure and velocity are related by Bernoulli's law, which states that the difference in pressure between two points in a fluid is proportional to the difference in the squares of the velocities at the two points, the direction being such that an increase in velocity means a decrease in pressure. Obviously the shape and position with reference to the direction of the wind are very important in determining the relative amounts of lift and drag. In general the higher velocities and lower pressures tend to occur along the streamlines following the longer paths around the body unless they involve too sharp changes in direction. Fig. 1, which will be recognized as a wing section, is an example of a body producing high lift and low drag. Due to the shape and angle of attack the pressure over the upper surface is much lower than that over the lower surface. Lift may be obtained on objects of less regular shape and may, of course, be up or down. The resultant force is likely to fall to one side of the center of gravity of the object and of its support, resulting in a torque tending to produce rotation.

If the curvature of the surface is excessive, boundary-layer effects cause the air near the surface to move from a higher pressure region to a lower one, and at times even reverse direction, causing the growth of eddies or vortices which break away periodically producing a highly turbulent wake. These phenomena are usually associated with a loss of lift and an increase of drag.

Of course a blunt, angular bridge structure has little of the smooth curved surface of an airplane wing, and turbulence is the dominant characteristic of the wind stream around a bridge. Nevertheless, there is a pattern of flow curvature and of moderate velocity and pressure differentials characteristic of an envelope of significant parts of the bridge cross section, supplemented by similar but more pronounced effects over limited areas where stronger and smoother flow occurs locally. These forces would have little influence on vibration of the bridge but for the fact that they have a periodic fluctuation or pulsation which can be in resonance with a natural mode of vibration of the bridge and thus accumulate energy and build up the amplitude. It is startling to discover how small a periodic force can be (of the order of 1 lb per ft of bridge) and still be capable of causing a substantial amplitude of vibration (1a).[1]

It has been pointed out that the pattern of streamlines about a body is determined, not only by the shape and attitude of the body, but also by the presence of the boundary layer and wake. Because of this fact the viscosity can have an important influence on the velocity and pressure field and hence on the forces. Associated with this effect is what is commonly called scale effect, which arises from the fact that the inertial or pressure forces are proportional to the square of the velocity while the viscous forces are proportional to the first power of the velocity and inversely proportional to the linear dimensions of the body so that the ratio of inertial forces to viscous forces will not be the same on a scale model as on its prototype (both in the same fluid) unless the velocity scale is distorted. The type of section, nature of the phenomenon under investigation and the model scale determine whether or not such distortion is desirable, permissable or practicable.

The ratio of the inertial forces to the viscous forces depends upon density, viscosity, velocity and length, and is expressed by a dimensionless scale parameter known as the Reynolds number denoted by R. Thus

$$R = \frac{V\,L}{\nu} \qquad \text{.........................(2)}$$

where V is the velocity, L is a convenient linear dimension of the body and ν is the ratio of viscosity to density called the kinematic viscosity $\left(\frac{1}{\nu} = 6380\,\frac{\text{Sec}}{\text{ft}^2} \text{ at } 15°\text{ C and sea level}\right)$.

Two geometrically similar bodies will in general have different force coefficients (such as C in Eq. 1) if the Reynolds number is different. In other words they are geometrically similar but dynamically dissimilar. "Dynamic" refers here to the air and not to the model. This is an important consideration in model testing, for the model must show what the prototype will do. If a model is made geometrically similar to the prototype in all external detail and the Reynolds number under test conditions is made equal to the Reynolds number of the prototype, then both geometrical and dynamical similarity of the windstream exist. According to the foregoing considerations the model test should then give the force coefficients of the prototype. However, the turbulence in the air stream of most wind tunnels also has an effect like Reynolds number. Fortunately it has been found that wind-tunnel-turbulence effects are small when the Reynolds-number effect is small. It therefore becomes necessary to conduct a test over a range of Reynolds numbers to determine the effect of Reynolds number.

---

[1] Numerals in parentheses, thus: (1a), denote corresponding items in the list of references, Appendix I.

In the case of flow over blunt and comparatively sharp-edged objects like bridge sections, Reynolds-number effects are not encountered to any significant degree, as proved by comparative model tests at different scales and velocities, and illustrated by smoke stream studies of the paths of the wind (2a) (3c) (3d) (3f).

It is apparent that above some large value of the Reynolds number (that is, the ratio of inertial force to viscous force) the viscous forces may have small effect and a further increase in R results in no change in force coefficients. In the case of flow around blunt and sharp-edged objects, even though the Reynolds number may be low, the relative influence of the viscous forces may be subordinated by the turbulence and resultant loss of energy.

Naturally, the lift forces vary when the wind is angled upward or downward from the horizontal. Usually an upward angled wind (positive angle of attack) has a greater positive lift than occurs in a horizontal or downward angled wind. However, there are many shapes of an obstruction which show, paradoxically, a reduction in the lift when the wind has an upward vertical component, even to the degree that the upward moving wind may exert a net downward force (negative lift) on the obstruction. The reverse also can occur, a downward angled wind (negative angle of attack) causing a net upward force

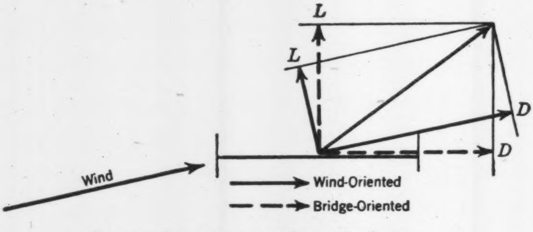

FIG. 2.—ORIENTATION OF LIFT AND DRAG

(positive lift). It will be recognized from the foregoing discussion that this can occur if the velocities are the greater across the surface more directly approached by the angled wind, especially if excessive turbulence destroys the lift action on the opposite surface.

When a model of a section having the characteristics described in the preceding paragraph is tested in a wind tunnel and the measured lift at different angles of attack is plotted against angle of attack the curve shows a negative slope, with lift decreasing for increasing angle over a certain range of angle of attack and with positive slope over other parts of the curve (2b) (3g). The practice is to plot the coefficient of lift C_L (corresponding to C in Eq. 1) rather than actual lift. Also, for the study of bridge sections the measured values should be corrected to orient them to the horizontal axis of the bridge rather than to the direction of the wind (See Fig. 2). Curves of this type are shown subsequently in Fig. 6. This negative slope of the lift curve is the basis for one hypothesis explaining in part, the oscillation of suspension bridges in the wind. The action is described in clear detail by J. P. Den Hartog as an explanation of the "galloping" of transmission lines (4a). For want of a better name it is referred to as the "Negative Slope Theory." Its application to the oscillation of a bridge is discussed in Art. 6.

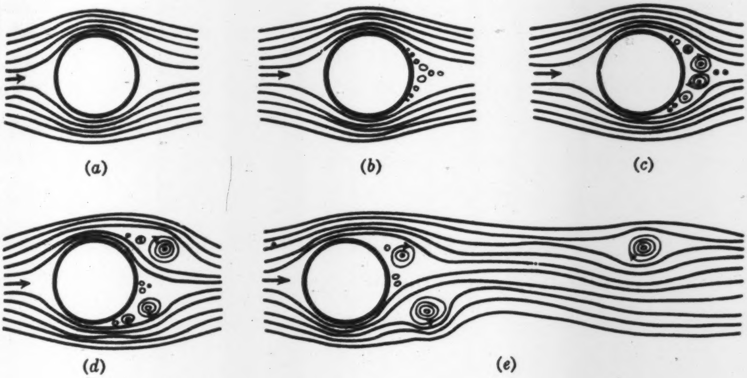

FIG. 3.—VORTEX DEVELOPMENT

(B) *Vorticity.*—In an earlier paragraph mention was made of the formation of eddies or vortices due to the flow of the fluid (liquid or gas) in response to the pressure gradient along the surface of the obstruction. It will be profitable to examine this phenomenon further.

It is to be expected that a difference in pressure along a surface will cause a flow of fluid from the higher toward the lower pressure area (unless the surface is so well streamlined that the viscous or turbulent stresses in the boundary layer prevent the flow) and this is borne out by a series of photographs made by L. Prandtl showing the streamlines around a cylinder which was moving at a uniform velocity through the fluid (5a). Immediately after the start the streamlines show the theoretical "potential flow," smooth curving lines with dead spots or "stagnation points" centered on the leading and trailing edges (Fig. 3a). This condition continues at the leading edge but the photographs show that a moment later a mass of turbulent fluid accumulates at the center of the trailing edge (Fig. 3b) and subsequent photographs show this mass growing and spreading and crowding the streamlines farther away from the trailing edge as shown in Fig. 3c. At the same time this mass of fluid is seen to take on twin whirling motions due to the viscous drag from the passing windstream. Finally the enlarging eddy itself becomes a major obstruction to the flow and is torn away by the forces acting upon it (Fig. 3d) and carried away in the fluid stream, moving at a velocity somewhat less than that of the fluid (Fig. 3e). (Fig. 3 illustrates the development of the flow around a cylinder. It occurs in modified form around any shape of obstruction except one that is perfectly "streamlined.")

It is to be expected that the time required to build up and discharge a vortex will increase with the diameter, d, of the cylinder but will be reduced by an increase in the velocity, V. This is indeed the case as verified by tests which show the time interval between vortex discharges may be expressed as a function of the ratio, $\frac{d}{V}$. V. Strouhal, who first determined this relationship in 1878 expressed the frequency of the discharge as

$$N = \frac{S\,V}{d} \qquad (3)$$

in which S is known as the Strouhal number and is about 0.2 for a cylinder. It varies considerably with the shape of the obstruction (between approximate limits 0.14 to 0.30) and for streamlined or partially streamlined obstructions it is influenced by the Reynolds number (3c) (6) (7).

Not only may one anticipate a regular time interval between these vortex discharges, but one may expect also that if one vortex is whipped off by one side of the fluid stream the next vortex, already forming, will accumulate and be discharged from the other side, rotating in the opposite direction, and that thereafter the vortices will be discharged alternately as shown in Fig. 3e. This also has been demonstrated by tests, and Mr. von Kármán has formulated the mathematical theory for the vortex path, frequency, spacing, and velocity and the forces acting on them and on the obstruction (5b) (9). The pattern of alternating vortex discharge in the wake of the obstruction is known as the Kármán trail.

The fluid motion which causes the alternating vortex discharge also causes inertial forces to react against the obstruction thus subjecting it to alternating pressures. The strength, point of application, direction and frequency of these forces are determined by the stream velocity and the form of the obstruction. They may cause major fluctuations in the lift and relatively smaller variations in the drag. Clearly, these can be a cause of oscillatory motion of a body such as a paddle drawn through the water or a suspension bridge in the wind. This explanation, referred to as the "Vortex Theory," will be discussed in Art. 7.

It is well to note a distinction between two types of vortex discharge—(a) the starting vortex which is initiated following any new wind condition (velocity or direction) and is discharged after a distinctive period of time during which the potential flow is modified while the first vortex builds up, and (b) the Kármán vortices which follow the starting vortex in rhythmic alternation (5c).

2. NATURAL VIBRATIONS OF A SUSPENSION BRIDGE

Suspension bridges, in common with all elastic structures, vibrate at definite frequencies determined by the ratio, $\sqrt{\frac{k}{m}}$, in which k is the spring constant and m is the mass, both expressed in consistent units. In common with all beams they have an infinite number of degrees of freedom and can vibrate in an infinite number of displacement forms, each at its own distinctive frequency. The bridge can oscillate in a pure vertical motion or a rotation about a longitudinal axis and with a single loop over the entire span (the fundamental mode) or with any number of loops although the designer is seldom concerned with modes with more than three of four loops in the main span. (The original Tacoma Narrows Bridge and its full model in the wind tunnel vibrated (2c) (3h) with as many as nine loops but these higher modes were rare and their amplitudes were small.) Fig. 4 shows the forms of several modes of vibration of the original Tacoma Narrows Bridge and its full model. (The broken lines and numerals in parentheses, in Fig. 4, represent the modified condition with the mid-point of the main cable tied to the suspended structure.) Similar forms have been observed on other models (3i) (3j).

If the mode has an even number of loops one of the stationary or node points is at mid-span and the wave form is asymmetrical about this point. Also the waves are balanced vertically about the normal position which makes it possible for the main span to vibrate while the side spans are still. On the other hand, the fundamental mode cannot occur unless the side spans move symmetrically and in the opposite direction to the main span movement (except for the small amplitudes which can be permitted by the stretching of the cables). This is generally true of all the symmetrical modes (with odd numbered loops) except that as the number of loops increases it becomes possible for their lengths to vary so that the areas under the loops above and below the normal position are nearly equal and the motion is approximately balanced on the main span and therefore only slight motion of the side span is necessary, as illustrated by mode type 8 of Fig. 4.

Most of the spring constant (that is, the stiffness) of a suspension bridge is due to the resistance of the loaded cable. The stiffening truss, added to reduce local bending under concentrated loads, adds only moderately to the overall stiffness and to the frequency of vibration. Its influence increases for the higher modes with their sharper curvature. For example, the 33-ft truss of the new Tacoma Narrows Bridge contributes about 20% to the frequencies of the fundamental mode and the first asymmetric mode (two loops) but (3k) doubling the truss stiffness would increase the frequencies of these modes only about 12%. For the second symmetric mode (two nodes and three loops on the main span) the truss stiffness contributes 30% to the frequency and doubling it would increase the frequency another 20%. Making the stiffening truss continuous at the towers would increase the frequency only slightly (1b).

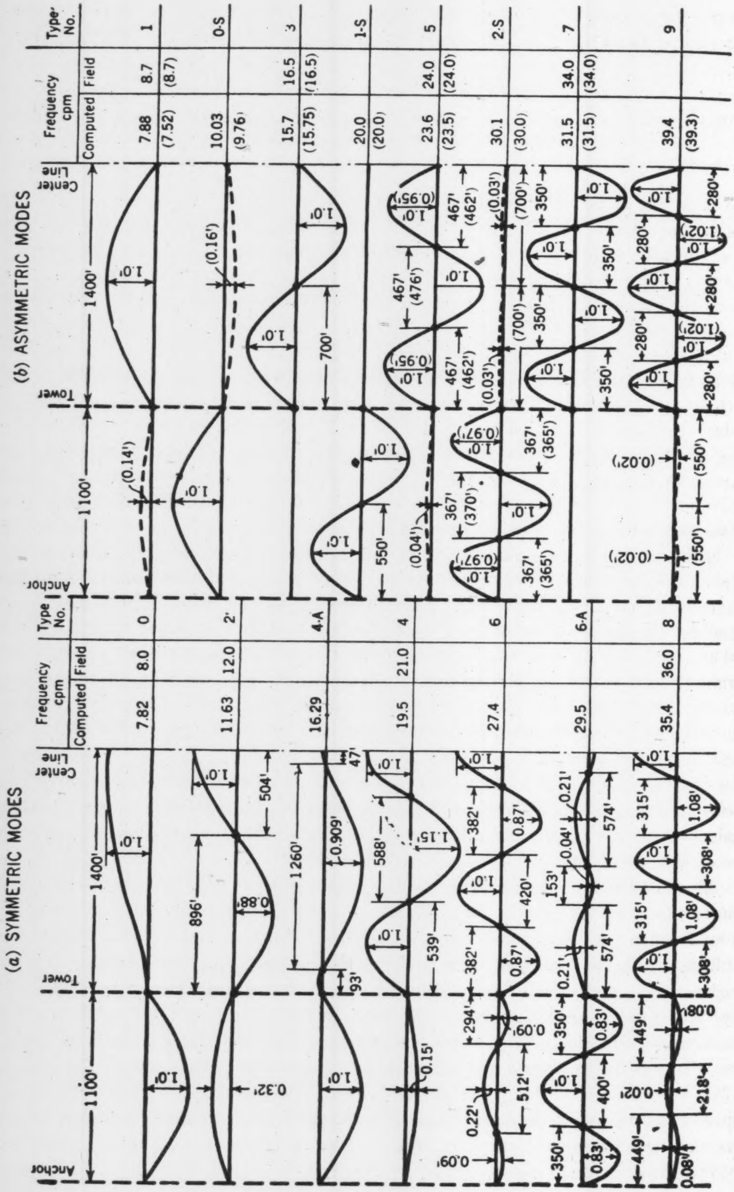
(a) SYMMETRIC MODES
(b) ASYMMETRIC MODES
Anchor
Tower
Center Line
1100'
1400'
Frequency cpm
Computed
Field
Type No.
0
7.82
8.0
2
11.63
12.0
4-A
16.29
4
19.5
21.0
6
27.4
6-A
29.5
8
35.4
36.0
1
7.88
(7.52)
8.7
(8.7)
0-S
10.03
(9.76)
3
15.7
(15.75)
16.5
(16.5)
1-S
20.0
(20.0)
5
23.6
(23.5)
24.0
(24.0)
2-S
30.1
(30.0)
7
31.5
(31.5)
34.0
(34.0)
9
39.4
(39.3)
1.0'
0.32'
0.88'
896'
504'
1260'
93'
47'
0.909'
0.15'
539'
588'
1.15'
0.09'
0.22'
512'
294'
382'
420'
0.87'
350'
400'
0.83'
0.21'
153'
0.04'
574'
449'
218'
0.02'
0.08'
308'
315'
1.08'
(0.14')
(0.16')
550'
700'
(0.04')
367'
(370')
(365')
(0.97')
467'
(476')
(462')
(0.95')
(0.03')
(700')
(0.02')
(550')
280'
(1.02')

Fig. 4.—Modes of Vibration, Original Tacoma Narrows Bridge

For torsional oscillation the motion is substantially the same as for the corresponding vertical mode except that the two sides of the bridge move in opposite directions—that is in opposite phase. The cable and truss offer the same resistance to the torsional as to the vertical displacement and the equivalent spring constant, k, is the same. However, the effective mass is less for the torsional than for the vertical motion, being that mass which, if concentrated at the center line of the truss, would have the same mass moment of inertia about the axis of rotation as does the actual structure. Thus if m is the mass of the cables, plus the mass of the suspended structure, b is the width center to center of trusses, and r is the radius of gyration of the entire structure, then the effective mass is

$$m' = m\left(\frac{2\,r}{b}\right)^2 \ldots\ldots\ldots\ldots\ldots\ldots\ldots\ldots (4)$$

For most suspension bridges the torsional frequencies are approximately 25% greater than the corresponding vertical frequencies.

The foregoing statement is based on the assumption that there is only one plane of lateral bracing. With lateral systems in the planes of both the top and bottom chords, the resistance of the structure to torsional motion is completely changed. The four-sided system of trusses behaves as a tube under torsion and its resistance depends upon the depths of the four trusses and the areas of their diagonals instead of the depth of the vertical trusses and the areas of their chords. The high torsional rigidity of such a four-sided truss system contributes the major resistance of the span to torsional displacement and thus increases materially the frequencies of the torsional modes. For example, in the new Tacoma Narrows Bridge, the addition of the second plane of laterals (in the plane of the bottom chord) increased the frequency of the first and second symmetric torsional modes by 128% and 176% respectively (1c).

In most suspension bridges the tower offers comparatively little resistance to a force at the tower top tending to cause bending parallel to the bridge axis and therefore has little effect on the vertical modes of vibration. In the case of a symmetric torsional mode, however, the tops of the two columns of each tower move in opposite directions because the two cables move in opposite phase and thus the tower is subjected to torsion. The torsional rigidity of modern bridge towers of box or cellular section with substantial bracing is considerable and does influence the frequency as well as the wave form of the symmetric torsional modes (1d) (31).

In the first asymmetric mode the cable tends to straighten over one half span and take on greater curvature over the other half. This causes the midpoint of the cable to move back and forth in a longitudinal direction. If a shear tie is introduced between the truss and the midpoint of the cable then the entire suspended structure must participate in this longitudinal movement and the frequency will be reduced due to the additional mass moved. If, with the center tie, the suspended structure is anchored at one tower the first asymmetric mode will be inhibited unless the tower tops and side spans also oscillate as shown in Fig. 4 (Type O-S). The first asymmetric torsional mode will be inhibited even without end anchorage because the two cables will pull in opposite directions on the suspended structure. (The couple resulting from these opposing forces at opposite sides of the roadway tends to produce a reversed bending of the suspended structure in the horizontal plane but usually this tendency is slight.)

The bridge offers considerable resistance to a lateral oscillation and there is little evidence that the wind tends to cause such motion (a strong wind does cause a non-oscillating horizontal deflection). A small lateral oscillation accompanies torsional oscillation if the axis of rotation is raised above the deck by some means such as diagonal stays across the roadway between each cable and the opposite truss (with a strut between cables at the points of connection of the stays). This causes the cables and suspended structure to oscillate laterally in opposite directions and tends to increase the frequency.

For a suspension bridge the formula for frequency—

$$N = \frac{1}{2\pi}\sqrt{\frac{k}{m}} \qquad (5)$$

—becomes somewhat complicated. Considering a bridge with a negligible stiffening girder, the spring constant comes entirely from the resistance of the loaded cable to displacement from its dead load position. This resistance is of course, proportional to the dead-load tension in the cable which in turn is proportional to the dead load. Thus it is that an addition to the dead load which increases m causes a proportionate increase in k so that the frequency remains unchanged by the additional weight. (This statement is not precise since the stretch of the cable permits a yield, usually small, in addition to the effect of cable displacement.)

The dead-load tension in the cable is also inversely proportional to the sag. Therefore the spring constant varies inversely with the sag and the frequency varies inversely with the square root of the sag.

If a substantial stiffening truss is added then an addition to the spring constant is made which is independent of the mass, and the frequency becomes more responsive to a change in the mass. The loaded cable and the truss both offer increased resistance to multiple loop distortion (per unit displacement) and therefore the frequency increases by steps for the higher modes.

If two springs act in parallel to carry a load, then each carries but a part of it and the deflection will be less than if either sustained the load alone. Their resistances are additive and the combined spring constant is the sum of the individual spring constants. On the other hand, if they act in series the total load acts on each of them and their yielding is additive. With series loading the reciprocal of the combined spring constant is the sum of the reciprocals of the individual spring constants; that is, the combined spring constant is less than either individually. It is apparent from the frequency formula, then, that if an elastic element is added to the bridge in such a way as to increase the resistance to displacement it will tend to increase the frequency whereas if it is added in such a way as to increase the yielding under loading it will tend to reduce the frequency. Thus the addition of a stiffening truss increases the frequency whereas increasing the sag increases the yielding and reduces the frequency. This simple principle makes it easy to form a qualitative judgment of the influence of almost any elastic element of the structure.

3. FACTORS AFFECTING NATURAL VIBRATIONS

With the preceding article as a background the principal factors which influence the natural vibrations of suspension bridges may be summarized. (It will be seen in the next article that it is desirable to keep the frequency as high as economically feasible.)

(A) *Sag.*—The frequencies of all the modes vary inversely as the square root of the sag. If other resisting elements are so weak that the spring constant is determined by the cable force alone then the frequencies of the asymmetric modes depend only on the sag (substitute the value of μ given by F. C. Smith and G. S. Vincent (3m), Members, ASCE, and solve for ω) and those of the symmetric modes on only the sag and the ratio of the side span to main span length (1e) (3n). (Except the symmetric mode shown in Fig. 4, Type 4-A, which can occur only by virtue of cable stretch (3 o).)

(B) *Side Span Length.*—The asymmetric modes are not affected by side span length. Shortening the side spans increases the frequencies of the symmetric modes and also distorts their form. If the side spans are unequal in length, the perfect symmetry of the symmetric modes will be destroyed but the modes will not be inhibited.

(C) *Unloaded Back Stays.*—Unloaded back stays represent the ultimate reached in shortening the side spans. The effects are described above, though more pronounced.

(D) *Moment of Inertia.*—An increase in the moment of inertia increases the frequency and alters the wave form, although the effect is only moderate within practical limits. On longer spans increasing the moment of inertia several-fold beyond the requirements for limiting grade change produces only a small increase in frequency (1f).

(E) *Torsional Rigidity of Suspended Span.*—If the lateral resistance to the horizontal wind force is provided by two lateral systems in the planes of the top and bottom chords rather than concentrated in a single system in one plane, the resulting four-sided truss system will have a torsional rigidity which will double or treble the torsional frequency (1g). (This double system does present an added design problem for certain positions of the live load.)

(F) *Weight.*—Adding weight has little effect on frequencies, except where the truss contributes a large part of the total stiffness (1h). However, an increase in weight increases the total energy of vibration at any given amplitude without affecting the aerodynamic forces exciting motion and therefore reduces the relative effectiveness of these forces. This will be further discussed in Part II of this report.

(G) *Center Ties.*—Center ties are quite effective for preventing the first asymmetric torsional mode (which destroyed the original Tacoma Narrows Bridge). If combined with longitudinal restraint of the stiffening truss at one tower they will strongly oppose the first asymmetric vertical mode but will produce heavy stresses under asymmetric live loading. They have no effect on symmetric modes because these involve no relative longitudinal movement of the suspended structure and the midpoint of the cable.

(H) *Diagonal Stays.*—Diagonal stays from the tower tops to intermediate points on the truss tend to inhibit a mode unless the point of attachment to the truss happens to be at a node point. If a mode is forced in spite of the stays, they increase the frequency moderately due to their added resistance. In wind tunnel tests a single system of stays (from each tower top to one point on the side span and one point on the main span) delayed the excitation of the mode until a higher velocity was reached after which the stays had little noticeable effect, except to alter the frequency (3d) (3p) (10a). Multiple stays are more generally effective. These, however, make the structure highly indeterminate and susceptible to alteration in elastic properties when affected by temperature change. Stays from the tower at about deck level to points on the cables out on the span have similar dynamic effects but their temperature influence is greater because the stays oppose the main cables.

(I) *Cross Road Stays.*—Stays extending from each cable diagonally across the roadway to the opposite truss and supplemented by struts between the cables at the point of attachment of the stays have a strong effect on torsional modes unless they are near the node point. They do not prevent the motion but move the center of rotation upward so that the cable must move laterally in one direction while the truss moves in the opposite direction and the frequency is considerably increased due to the added resistance thus encountered (3d) (10a).

(J) *Towers.*—The towers must be flexible or hinged to permit longitudinal motion under changing live load, and therefore offer very little resistance to the vertical modes; however, their torsional rigidity is considerable and they have a very noticeable effect on symmetric torsional modes (1d) (3e). Nevertheless, only a small additional benefit is gained by even a considerable increase in the metal necessary to provide for the stability of the tower itself.

(K) *Hangers.*—The hangers act in series with the cables to sustain the loading and therefore their stretch increases the yield and tends to reduce the frequency but the effect is negligible.

(L) *Cable Stretch.*—Cable stretch makes possible one peculiar vertical and a similar torsional mode on almost any bridge and completely controls its frequency and wave form (3o). Cable stretch also has a modifying effect on other symmetric modes, particularly if the back stays are not loaded. If the displacement form of the mode is approximately balanced about the normal position, then the additional stress due to vibration is small and the effect of cable stretch is negligible.

(M) *Lateral Stiffness.*—Lateral stiffness does not appear to be involved in the aerodynamic vibration of suspension bridges except in combination with cross road stays which force lateral displacement of the structure. This is not to deny the possibility that a bridge may be designed with such lateral flexibility as to bring about objectionable oscillation.

4. General Behavior of a Bridge in the Wind

(A) *Constant* $\frac{V}{N\,b}$ *-Ratio.*—The dominant characteristic of the behavior of a bridge in the wind is the presistent and consistent relation between the frequency (N, cycles per second) of the vibration of the structure and the velocity (V, feet per second) of the wind which causes it. It is convenient to divide this ratio by b, the width of the bridge in feet (a constant for any given bridge) because this makes the ratio non-dimensional and therefore applicable without alteration to a bridge or any scale model of the bridge. The significance of this ratio is further revealed by the fact that it shows up as one of the most important parameters in theoretical analyses dealing with the forces and motions involved in aerodynamic vibration (see any reference on aeroplane or suspension bridge vibration (11)).

It is helpful to examine this ratio for its physical interpretations. First, $\frac{b}{V}$ equals the time required for an element of the wind stream to cross the bridge and $\frac{1}{N}$ is the period in seconds of a cycle of the bridge vibration; therefore $\frac{V}{N\,b}$ is the ratio of the period of vibration to the time required for a particle in the wind to cross the bridge. Similarly, $\frac{V}{N}$ is the distance a particle in the wind travels during one cycle of the vibration and $\frac{V}{N\,b}$ is the ratio of this distance to the width of the structure. Again $N\,b$ is the velocity at which a particle must move to cross the bridge in one cycle and $\frac{V}{N\,b}$ is the ratio of the wind velocity to that velocity. The ratio $\frac{V}{N\,b}$ expresses the wind velocity with b as the unit of distance and the period, $1/N$ as the unit of time. In all of these conceptions the $\frac{V}{N\,b}$ -ratio relates the motion of the bridge in any of its modes to any periodic phenomena which occur in the wind stream such as the Kármán vortex discharge.

(B) *Character of Motion.*—Any form of wind-actuated oscillation of a bridge can be classified as restricted or catastrophic. Oscillations of restricted character will start at a definite wind velocity and will increase in amplitude as the velocity increases until a maximum is reached (2d) (3c) (3d) (3e) (10b). With further increase of velocity the amplitude decreases and, at a slightly higher velocity the motion ceases. The $\frac{V}{N\,b}$ -ratio at which the motion starts is known as the lower critical; that at which the motion ceases, as the upper critical. Each of these has a substantially constant value for all vertical modes and a different value, also approximately constant, for all torsional modes. However there are often weak appearances of a mode at approximately a submultiple of the $\frac{V}{N\,b}$ -ratio which characterizes its principal appearance.

In the case of any catastrophic motion, the oscillation begins at a definite critical $\frac{V}{N\,b}$-ratio but with increased velocity (or in some cases without increase in velocity) the oscillation builds up rapidly and there is no upper critical velocity.

Factors which influence the critical $\frac{V}{N\,b}$-ratio can be listed as follows (3c) (3d) (3e) (11):

(a) The shape is perhaps the most important factor.

(b) The angle of attack alters the path of the wind with respect to the section and modifies the $\frac{V}{N\,b}$-ratio.

(c) The type of motion whether vertical or torsional.

(d) For truss-stiffened bridges and flat plates placed horizontally in the wind, the wind-forced motion is usually a combination or "coupling" of the vertical and torsional types of motion which are forced to a common frequency by the action of the wind. This occurs at a distinctive $\frac{V}{N\,b}$-ratio.

(e) Damping increases the critical ratio of a catastrophic oscillation and tends to increase the lower and decrease the upper ratios of a restricted motion.

(C) *Behavior of a Girder-Stiffened Section.*—In all tests of oscillating models of girder-stiffened sections except extremely shallow girders the motion has been either a pure vertical mode or a pure torsional mode at substantially the natural frequency of vibration (3c) (3e). For such a section the $\frac{V}{N\,b}$-ratios and the character of oscillation (restricted or catastrophic) are influenced primarily by the ratio, d/b, of the depth of the girder to the width of the bridge. Details such as girder flanges, stringers, and curbs, and the position of the deck with reference to the girders also have important modifying influences. This influence of details is not always predictable.

It is characteristic of girder sections that they may oscillate at restricted amplitudes at moderate wind velocities and with a variety of successive modes and corresponding frequencies as the velocity changes. In general, depending upon the shape, both vertical and torsional modes may reappear at higher velocities (but at their characteristic frequencies), and some of these may be catastrophic.

As the $\frac{d}{b}$-ratio decreases below about 1/7 the girder-stiffened section shows increasing evidence of the coupled type of oscillation described in the next paragraph.

(D) *Behavior of Truss-Stiffened Sections.*—All oscillations that have been observed on models of truss-stiffened bridges and the observed small motion of the Golden Gate Bridge as well have been of the coupled type (3d) (3e) (11). Often the mode appears to be almost a pure torsion but the frequency is reduced toward that of the corresponding vertical mode. In many cases (including all of the catastrophic motions observed), the vertical mode component has sufficient amplitude to shift the axis of rotation considerably to the windward from the center line of the structure. In some cases the axis of rotation has been practically at the windward truss or even well beyond it. It appears very probable that the oscillation which damaged the Menai Straits Bridge (3q) in 1839 was coupled since the leeward side of the bridge deck was largely destroyed while the windward carriage-way was only moderately damaged. Also the destructive oscillation of the Brighton Chain Pier was described as consisting of both "an undulatory motion along the road" and "oscillating motion across the roadway (3q)."

It is characteristic that coupled types of oscillation occur at considerably higher velocities than do the pure vertical and torsional types of the girder sections. It is apparent also that the aerodynamic forces on the truss-stiffened section are determined primarily by the deck and truss members adjacent thereto. In model tests the removal of the bottom chord and web members of a deck truss section has affected the motion only slightly. These members are beneficial aerodynamically in that they add a little to the aerodynamic damping.

Since coupled motion requires a blending of vertical and torsional motions in a manner to be mutually exciting under wind action, it depends upon the elastic factors affecting the relative frequencies of the vertical and torsional modes (11). The use of two planes of laterals as described in the preceding article increases the torsional stiffness and thus throws the vertical and torsional frequencies of corresponding modes so far apart in many cases that the critical velocity of coupling and flutter is increased beyond any probable wind velocity.

5. Value of Theories

The facts summarized in the preceding articles have shown how the bridge oscillation problem is related to other, more familiar problems and have suggested theories explaining what happens. It is helpful to state these theories, even with their limitations, because they help to give a clearer conception of causes and effects and possible cures. Moreover a theory is essential to any purely mathematical solution of the problem.

6. Negative Slope Theory (3r) (4a) (10) (12)

If, from any cause, a bridge is moving downward while a horizontal wind is blowing the resultant wind with reference to the bridge is angled upward (positive angle of attack) as illustrated by Fig. 5.

If the lift coefficient, C_L, as measured in static tests shows a variation such as illustrated by curve A in Fig. 6 then, for moderate amplitudes, there is a wind force acting downward on the bridge while the bridge is moving downward. The bridge will therefore move to a greater amplitude than it would without this wind force. However, the motion will be halted and reversed by the action of the elastic forces, whereupon the vertical component of the wind reverses, the angle of attack becomes negative and the lift becomes positive tending to increase the amplitude of the rebound. As the bridge oscillates with increasing amplitude its vertical velocity, v, also increases and therefore the maximum positive and negative values of α increase until a part of the motion occurs in the angle range where the lift opposes the motion—that is, where the slope of the lift coefficient is positive. Finally an amplitude is reached at which the net energy derived from the wind action in a cycle is just sufficient to offset the energy loss per cycle caused by frictional or damping forces. Thereafter, the wind velocity remaining constant, the bridge oscillates at a steady state amplitude. If, now, the wind velocity, V, is increased then (see Fig. 5) a corresponding increase in the velocity of vibration, v, must take place if the maximum range of α is maintained at its steady state value. This increase in v for a given mode of vibration can take place only if the amplitude of vibration increases since the frequency remains constant. Thus it is seen that with an increasing velocity the amplitude will increase indefinitely or until the bridge is destroyed.

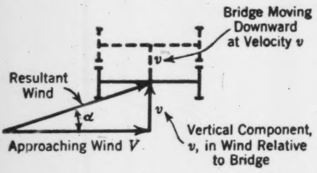
Bridge Moving Downward at Velocity v
v
Resultant Wind
α
v
Approaching Wind V
Vertical Component, v, in Wind Relative to Bridge

FIG. 5.—ANGLE OF ATTACK, α, INDUCED BY BRIDGE MOTION

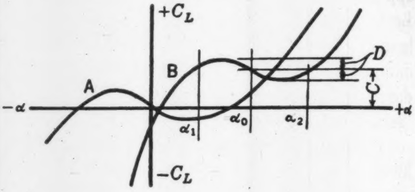

FIG. 6.—TYPES OF LIFT CURVE

If the region of negative slope occurs elsewhere on the graph than at the origin (see curve B in Fig. 6) the situation is only slightly altered. If horizontal and vertical lines are drawn through the approximate midpoint of the region of negative slope the lift acting on the stationary bridge will be C if the windstream is turned upward at an angle, α_0, from the horizontal. If the bridge oscillates the effective angle of attack will range, say, from α_1 to α_2 and the bridge will be acted upon by the steady lift, C, plus or minus a varying lift, D. The steady lift will oppose the downward motion and assist the upward motion and its net energy contribution will be zero. However, during the downward motion the effective angle of attack will be increased as previously described and the force D will be negative and will assist the motion. Also as the bridge moves upward and the effective angle is diminished, D becomes positive and assists the upward movement. For the lift graph shown as A, Fig. 6, the maximum effect occurs in a horizontal wind. For that marked B the action is the same except that the maximum effect occurs in a wind angled upward an angle α_0.

A similar though more complicated situation may occur with respect to a torsional or twisting motion of the bridge. If the resultant wind force acts eccentrically with respect to the elastic and inertial forces acting on the bridge it tends to rotate the structure about its longitudinal axis. There are sections of such shape that, with the change in angle of attack resulting from this rotation, there is an increase in the torque tending to cause the rotation. In such cases static tests reveal a characteristic reversal in the slope of the curve for the moment coefficient, C_M, when plotted against angle of attack. (The actual sign of the slope depends upon the sign convention for moment and angle.) The action is complicated, however, by the fact that in the case of torsional oscillation, the instantaneous angle of attack is a function of both the instantaneous position of the section and its instantaneous velocity. Also the velocity varies from zero at the axis of rotation to its maximum value at the edges and its direction is opposite at the two sides of the structure.

The negative slope theory is not in full agreement with the observed behavior of bridges and models, the most important defects being:

(a) It does not explain the fact that an oscillation of a given frequency may begin at a certain wind velocity and increase in amplitude as the velocity increases but be stopped by the action of the windstream if the velocity increases further. In such a case the rate of decay is more rapid than in still air.

(b) It does not explain the excitation of structures for which the slopes of the lift and moment coefficients are found to be positive (10b).

(c) It leaves to chance the initial motion which gives rise to the initial change in effective angle of attack. This is not a serious deficiency since this initial displacement, perhaps on only a small part of the bridge, can be explained by wind gusts.

7. VORTEX THEORY

The vortex theory attributes the aerodynamic excitation of a suspension bridge to the action of periodic forces having a certain degree of resonance with a natural mode of vibration of the bridge. The alternating vortices, moving across the bridge with a rolling motion at about 80% to 85% of the speed of the wind (7) give rise to moving zones in which the wind velocity adjacent to one surface of the bridge is materially reduced, in contrast to the increased velocity next to the opposite surface. (Mr. von Kármán found 0.86 for a circular cylinder and 0.80 for a flatplate normal to the wind (9).) By Bernoulli's Theorem the pressure is the greater over the zone of reduced velocity. This is the source of the periodic force. The frequency of the vortex discharge is bound to the wind velocity by the Strouhal number. The wind velocity therefore determines the degree of resonance.

The action described above has been visualized through the use of smoke streams over a model in the windstream (3c). With the wind velocity a little above the critical and the model at rest, a weak pattern of alternating vortex discharge can be seen with a frequency, perhaps some multiple 2 to 4, of the frequency of the vibration of the model which is about to begin. These are Kármán vortices and their frequency corresponds to a reasonable value of Strouhal number (about 0.145 to 0.186) for a horizontal girder section (3c). The vortex forces, applied at a multiple of the natural frequency of the bridge, could not build up the motion of the latter if both the forces and the bridge motion were of simple harmonic variation. The forces would add energy to the bridge oscillation during part of the cycle and remove an equal amount of energy during the remainder. However, there is ample evidence that these forces are nonlinear in relation to the bridge movement. With nonlinear forces the slower bridge oscillation is built up by sub-harmonic excitation (4b).

As soon as the oscillation becomes distinct it is observed that the vortex action alters and only two vortices are discharged per cycle. One leaves the upper edge of the windward girder when the model starts down and the pressure zone of this vortex moves across the deck while the downward movement continues. The other leaves the lower windward edge when the model starts up and causes a similar upward acting pressure zone during the upward movement. These vortices are distinct, of large diameter and vigorous. They are regarded as "starting vortices," (3c) each being initiated by the change in angle of attack caused by the reversal of the motion of the model. They are enlarged due to the receding of the edge from which they are shed as well as the increasing effective angle of attack. The time required for their formation also seems to increase. This enlargement and slowing of the vortex discharge when oscillation of the obstruction occurs has been noted by previous investigators who found that the frequency decreased with increasing amplitude (7) (8). Thus when the increased velocity is "paced" more or less by increasing amplitude there is a limited velocity range within which the vortices can retain their frequency of two vortices per cycle of bridge oscillation. As the upper critical velocity is approached, however, they move across the section more rapidly until they act only during a small part of the half cycle and abruptly lose their effectiveness. Then the amplitude decays, the motion of the bridge "loses control" of the vortex action and the Kármán vortices reappear at the higher frequency dictated by the increased wind velocity. At that point the frequency of vortex discharge may have increased approaching resonance (usually subharmonic) with a higher natural mode of the bridge so that the higher mode is built up displacing the original. This process continues while the wind velocity increases and the bridge oscillation progresses through higher and higher modes, both vertical and torsional, with one definite value of critical $\frac{V}{N\,b}$-ratio applying to all the vertical modes and a different value to the torsional modes. If, however, the bridge is subject to catastrophic oscillation one of the lower modes will reappear in catastrophic form at a higher $\frac{V}{N\,b}$-ratio (a multiple or nearly so of its earlier appearance). Section model tests of some sections at very low damping reveal a weak appearance of a mode at a lower velocity also. Some of these may be in resonance (not sub-harmonic) with the rate of the Kármán vortex discharge (3c).

It is seen that the vortex theory does account for the initial small amplitude of a given mode and also explains the selective action which limits each mode to a definite velocity range consistent with the observed $\frac{V}{N\,b}$-ratio.

8. FLUTTER THEORY

When the first full model of the proposed design for the new Tacoma Narrows Bridge with solid deck and one lateral system was first tested in the wind tunnel late in 1943 a torsional oscillation developed but its frequency was 6% to 8% less than the natural torsional frequency of the model when excited in the same mode by hand (3d). Also the leeward side of the model had a greater amplitude of motion than did the windward so that the axis of rotation was not on the longitudinal center line but upwind from it. In effect the oscillation was a combination of both the torsional and vertical modes of the same form and the frequency was intermediate between those of the two pure modes.

When this behavior was brought to the attention of Friedrich Bleich, M. ASCE, he suggested that it indicated flutter as experienced with the wings and other elements of aeroplanes, and applied to the suspension bridge the general theory previously applied to the aeroplane by Theodore Theodorsen and others. His theoretical analysis (1) was first submitted in a report to the Advisory Board in 1945. In a later report it was modified to take into account the additional effect of vortex forces. It was published (11) in October 1948. A similar analysis was later made (12) by D. B. Steinman, M. ASCE.

The pure mathematical theory of flutter applies to an infinitely thin flat plate placed horizontally in a horizontal wind. Such a plate is "stable" in the sense that it does not shed the disturbing Kármán vortex trail.

The mechanism of flutter depends upon the fact that the plate is supported so that it can move elastically in a vertical direction and in torsion about a longitudinal axis. The wind force causes a lift which acts eccentrically and therefore also induces a twisting moment. The resulting torsional movement alters the angle of attack so that the lift is increased which also increases the twisting moment. This chain action quickly becomes catastrophic provided the vertical and torsional motions can take place at the same coupled frequency and at an appropriate phase relation. This necessary condition is brought about through the influence of the wind. If such a plate is oscillated by external means while in a wind stream the frequency of the natural vibration is altered progressively by an increase in the wind velocity which reduces the frequency of the torsional mode and increases that of the vertical until, at some critical velocity, they have a common frequency. At this wind velocity any slight movement of the plate, whether vertical or torsional or mixed, takes on this common frequency thus satisfying the conditions for flutter, and develops rapidly into the coupled type of oscillation, the action being catastrophic, almost explosive.

The ideal, theoretical condition is never fully realized. The plate has a finite thickness and may have a blunt edge; and it does shed a vortex trail, which is accentuated if there is an angle of attack of a few degrees. The effect of this vortex action is to bring on vibration at a lower velocity than the critical velocity of flutter. This logical effect has been demonstrated by tests made on oscillating flat plates at the University of Washington for the purpose of verifying Friedrich Bleich's application of the flutter theory (3e) (11a). This vortex effect—that is, the reduction in critical velocity—becomes more pronounced if the thickness is increased. At the same time however, the flutter, brought in at a lower velocity, is less explosive and may require an increase in velocity before it becomes catastrophic.

Tests on oscillating section models of several truss-stiffened sections and of very shallow girder-stiffened sections show that such sections have the characteristic flutter behavior of a flat plate modified by the vortex discharge of the blunt edges. One truss-stiffened section showed (3d) a coupled oscillation, with a weak vertical component and a frequency only a little less than that of the natural torsional mode, coming in at a velocity far below the critical value predicted by the flutter theory. This oscillation was vigorous but became catastrophic only after a considerable increase in velocity. As the velocity was gradually increased, approaching the computed critical velocity, the relative amplitude of the vertical mode component increased, shifting the axis of rotation to the windward. Also the frequency gradually fell farther below the natural frequency of the torsional mode. The computed critical velocity for flutter of an ideal flat plate having the mass and elastic properties of this model could not be reached in the wind tunnel but at the maximum velocity attainable the frequency was near the predicted value and the flutter was violently explosive; in fact, when the model was released at this velocity it was necessary to seize it again so quickly that an accurate measurement of the frequency was impossible.

9. Summary of Theories

It appears well established that both the vortex theory and the flutter theory apply to the behavior of suspension bridges in the wind and with many sections their effects are combined.

With a truss-stiffened section flutter is dominant but modified noticeably, often considerably, by the vortex action caused by the blunt edges (reduced critical velocity, less violent response). The flutter characteristics are controlled by the mass and elastic properties of the structure as a whole and the dimensions of the deck. The modifying vortex action is controlled by the thickness of the deck structure, as well as those truss members adjacent thereto. The positions of abrupt corners of curbs and stringers near the windward edge influence the degree of vortex action as does also the angle of attack. The influence of angle of attack is not symmetrical for plus and minus angles, probably because of the stringers and other unsymmetrical elements. There is little evidence that chords and web members at a distance from the deck have any but a damping effect. It is conceivable, however, that a section may have such dimensions and properties that the vortex discharge from a remote chord synchronizes with the motions caused by the dominant forces. Such a chance condition might result in unexpected activity of a bridge thought to be entirely safe on the basis of generalized design criteria. (However a condition of this kind could be readily detected by a simple series of tests on an oscillating section model of the adopted design.)

With a girder-stiffened section the vortex action is dominant. For all except unusually shallow girder sections the coupling of modes and alteration of frequency which characterize flutter cannot be detected or are very slight (3c) (3e) (11a).

The "negative slope theory" may possibly explain the excitation of the catastrophic vibration of a girder-stiffened section in the moderate to high velocity range in which the Kármán vortices in a cycle of bridge oscillation are so numerous and move so rapidly that the bridge cannot respond to their individual effects but does respond to the slower pressure changes controlled by the changing angle of attack. This pressure pattern includes the combined or statistical effect of the stream of vortices traversing the portions of the bridge lying downstream from the sharp edge from which the vortices are discharged.

10. ENERGY AND DAMPING

The picture of what happens when a suspension bridge oscillates in a windstream remains hazy unless the transfer, storage and absorption of energy are clearly understood. The oscillating bridge is a machine and as such its energy relationships are of major importance; the forces are of interest only if they become great enough (through the accumulation of energy) to threaten local failure. As in all complicated problems in vibration the analysis is made most easily by the energy method.

(A) *Nature of Damping Action.*—The total energy of vibration is proportional to the square of the product of the frequency and the amplitude. It is all in the form of kinetic energy at the instant when all parts of the structure pass at maximum velocity through their normal rest positions. At the instants of maximum displacement the structure is stationary and all the energy is stored as elastic energy in the strained cables and stiffening members and gravitational energy due to the changed elevation of the parts of the structure. Energy is lost due to air resistance, hysteresis loss in the strained material and friction between moving parts. If the wind forces are such as to cause oscillation of the bridge the net effect of the air is to add energy to the vibration. This effect can be treated mathematically as "negative damping." If this negative damping adds the same amount of energy per cycle that is lost due to hysteresis and friction then the energy of the vibrating system remains constant and the amplitude is maintained at its "steady state." The effect of a net loss or gain in energy is measured by a change in amplitude from one cycle to the next since there is no appreciable change in frequency.

The strength of a damping action is conveniently expressed by the "logarithmic decrement," δ, which is defined as the natural logarithm of the ratio of the amplitudes of two successive vibrations. For small damping the numerical value of δ is very nearly the ratio of the change in amplitude in one cycle to the amplitude of that cycle and twice this ratio, that is, $2\,\delta$, expresses the proportion of the energy of vibration, ψ, lost or gained per cycle. Instruments are available for measuring and recording conveniently the amplitude under any condition of positive damping or of excitation making it possible to determine the value of δ continuously. This indicates for a given vibration the rate of input or of dissipation of energy per cycle at all amplitudes and thus measures quantitatively the net work performed by all forces acting and obviates the necessity of determining the strength and lines of action of these forces and their detailed variation throughout the cycle. With these quantitative values determined under different conditions the individual effects of structural damping, still air damping and wind (positive or negative damping) can be computed for either model or prototype.

The various forms of damping differ widely in their effect on the rate of change of energy and amplitude and it is necessary to recognize their characteristics when studying the influence of design features upon the magnitude of structural damping or studying the mechanism and quantitative effect of wind excitation. An analysis of these characteristics, as they bear on the study of wind-excited oscillation of suspension bridges, is assembled in Appendix II.

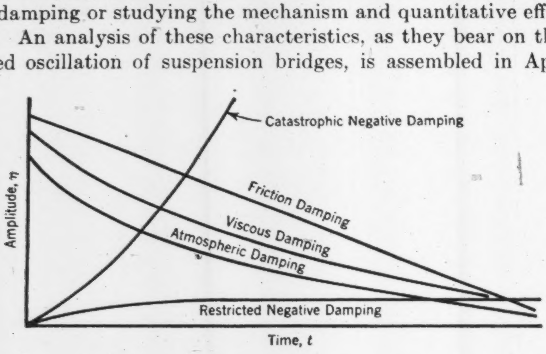

FIG. 7.—CHARACTERISTIC FORMS OF AMPLITUDE DECAY

The differences are illustrated to some extent in Fig. 7 which shows the rates of decay of amplitude with time and in Fig. 8 which shows the variation of the logarithmic decrement, δ, and the rate of change of energy, ψ, with the amplitude η.

(B) *Structural Damping.*—Varied information is available concerning structural damping. Hysteresis damping is quite low for steel (13) (14). Different investigators get different results depending upon the methods and type of specimen. The more rigorous tests generally indicate the lower values.

The structural damping of machines and structures varies widely. There is much and varied data available concerning bridges—usually simple spans (15) (16). However, none of this has much application to a suspension bridge because the stiffening members have neither the concentrated end reactions and accompanying frictional movements which provide most of the damping of beam or truss spans nor stress sufficiently high to produce material hysteresis effects. Friedrich Bleich has made a theoretical study of the sources of damping in a suspension bridge and correlated this with the results of damping tests on beams and trusses made by the Bureau of Public Roads (1i) (17). He has indicated the damping effect of sliding friction devices at the ends of the span and has also demonstrated how damping may be increased by designing to exploit sliding friction at the bearings of stringers on floorbeams.

It is hardly possible to secure quantitative data on the structural damping of a suspension bridge by means of model tests because the model details cannot be fabricated to reproduce the damping of the actual structure. This information must be obtained by tests on actual bridges representing various proportions of cable, truss and deck contribution to the damping. Preliminary studies to this end have been made by the University of Washington and the Bureau of Public Roads (3e). Tests have been made on a number of girder-stiffened bridges in Norway (26) and more tests are planned. It may be hoped that the results of these and a few additional tests can be correlated with Friedrich Bleich's theoretical studies to give the needed information.

(C) *Atmospheric Damping.*—On the other hand, the atmospheric damping can be reasonably determined by tests on a properly scaled oscillating section model (3e). Its shape must, of course, be accurately scaled because, to a large degree, this determines the air forces. The mass must be to proper scale if the measured δ is to be applicable since mass affects δ and ψ as is seen in Eqs. 14, 17, 19, and 20 in Appendix II. For this particular test there is an advantage in making the mass low in a known ratio because the measured δ will then be high in the same ratio and more easily measured. The correct value can be found by applying the corrective ratio. The tests show that the damping capacity and logarithmic decrement for atmospheric damping increase with amplitude and approach zero at low amplitudes as illustrated in Fig. 8. The damping can be regarded as composed of a small and negligible viscous damping (constant with η) shown by the dashed line (curve 5a, Fig. 8) plus a much greater component due to a force that is proportional to the square of the velocity which makes the logarithmic decrement proportional to η (Eq. (20) in Appendix II). For torsional motion the increase with amplitude is even more pronounced.

It is seen that plotting the logarithmic decrement against amplitude does much to reveal the nature of the damping or exciting forces. Further than that, these curves can be used to compute for all amplitudes the rates of energy transfer to and from the vibrating structure caused by the different damping and exciting forces, and their effects can be combined to determine the development of the vibration without the necessity of determining in detail the actual varying forces or pressures (3e).

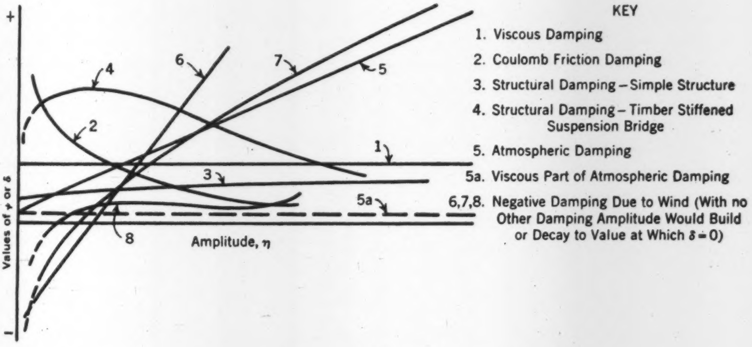

Fig. 8.—Typical Curves for δ or ψ

11. Model Testing

Much of the present knowledge of the wind-actuated oscillation of suspension bridges has been acquired through model tests and additional testing is recommended in the further pursuit of the problem. It is pertinent, therefore, to state briefly the methods of model testing and the conditions which must be fulfilled if the model indications are to be reliable.

(A) *Static Model.*—A static model must be correctly scaled as to form so that the wind paths, velocities and pressures will correspond to those of the prototype. The model, representing a section of the bridge, must be long enough so the distortion due to the flow of air around the ends will be negligible or it must have "end plates" to prevent such end flow. It is mounted in the wind tunnel with supporting elements attached to scales outside the tunnel in such manner that the vertical and horizontal components of the total force exerted by the wind can be weighed separately and that the moment of the resultant wind force about some convenient axis can be determined. Tests are run at various measured wind velocities and a wide range of angles of attack (3c) (3d) (3e).

(B) *Aerodynamic Model.*—The static model tests supply information concerning wind actuated oscillation of the structure to the extent that the negative slope theory applies but an aerodynamic model capable of performing the essential motion of the prototype is necessary for a full investigation. Whereas force and moment represent the significant wind effects upon a stationary bridge, energy becomes the more important factor in the case of oscillation. Furthermore, time enters the picture in a dominant way and as a result inertia, acceleration, mass, and moment of inertia, as well as elastic and damping forces take on definite significance and must be properly scaled or accounted for. Also such factors as frequency, resonance and phase—entirely absent from the static model tests—become controlling elements. It is true that these factors are subject to treatment on a theoretical basis but this requires additional mathematical steps in the processing of test data and, therefore, increased occasion for deviation between actual and predicted behavior. Moreover, the static tests yield only the steady forces, averaging out, but not revealing, the periodic variation in pressure occasioned by the passage across the section of the vortex discharged from its leading elements. The phase treatment of the variation of the steady force with angle of attack leaves out the effect of these small but resonant variations. On the other hand, if all the properties of an aerodynamic model of the entire bridge are properly scaled from the prototype, the model will move in the same manner as would the prototype under the same conditions and its wave form, distortion, velocity, frequency, acceleration and inertial and elastic forces will represent those of the prototype to appropriate scales. A section model, mounted on springs and oscillating at the same frequency as the full model, is subjected to the same gravitational, elastic, inertial and wind forces that act upon a short length of the full model at the same amplitude.

The studies on the Tacoma Narrows Bridge and also those on the proposed Severn River Bridge in England (22) (23) have been carried on by means of both full and sectional aerodynamic (oscillating) models.

(C) *Scales of Aerodynamic Model.*—It is not difficult to determine the scales of all of the controlling elements of the aerodynamic model. These are fixed by simple laws of geometry and mechanics and three governing conditions which must be satisfied. These conditions are (3s):

(a) The wind forces are inertial; the viscous forces are not significant and can be disregarded (see Art. 1).

(b) The acceleration of gravity, g, acts alike on model and prototype and its scale, $\frac{g_m}{g_p}$, must be unity. (Subscripts, m and p, refer to the model and prototype, respectively. The other symbols are defined in the text.) If the inertial forces are to be proportional to the gravitational forces then the scale of any acceleration, $\frac{a_m}{a_p}$, must likewise be unity.

(c) Natural air acts upon the model and the prototype alike so that the scale of mass density, $\frac{\rho_m}{\rho_p}$, is unity for air and must likewise be unity for all parts so that all dynamic forces will be reproduced to proper scale.

Simple geometry dictates the scales of length, area, volume, and area moment of inertia as n, n^2, n^3, and n^4 respectively, n being the ratio of a length on the model to the corresponding length on the prototype.

With the scale of acceleration fixed as unity it is possible to determine the scale of time from the simple relation, $a = L/t^2$, L being distance and t being time. In other words:

$$t = \sqrt{\frac{L}{a}} \qquad (6)$$

The scale of time can be expressed:

$$\frac{t_m}{t_p} = \sqrt{\frac{L_m/a_m}{L_p/a_p}} = \sqrt{\frac{L_m}{L_p}} = \sqrt{n} \qquad (7a)$$

—remembering that $a_m = a_p$. The scale of velocity follows from those of distance and time:

$$\frac{V_m}{V_p} = \frac{L_m/t_m}{L_p/t_p} = \frac{L_m\,t_p}{L_p\,t_m} = \frac{n}{\sqrt{n}} = \sqrt{n} \qquad (7b)$$

If the scale of mass density is unity then the scale of mass (which is density times volume) must be n^3, the same as the scale of volume. Also weight, $m\,g$, will have the scale, n^3, since the scale of g is 1. Furthermore the inertial forces, $m\,a$, will have the same scale, n^3, since a also is the same on model and prototype. Naturally, all other forces acting on or within the structure must be proportional to the weight and inertial forces and must have the same scale, n^3.

The scale of unit stress is the scale of $\frac{\text{force}}{\text{area}}\left(\text{that is, } \frac{n^3}{n^2} = n\right)$ which is therefore also the scale of modulus of elasticity, E.

Any of the scales can be modified by any convenient ratio provided compensating adjustments of other scales can be made without violating the proper scales of any essential properties. For example, the mass density scale, $n = 1$, can be disregarded for a given truss member or a concrete floor slab provided the outside dimensions are kept true to the linear scale, n, and its weight is kept to the force scale, n^3, by suitable interior loading or hollowing out or choice of material. It is, of course, necessary that the combined weights be correct to the scale, n^3, and that the weight distribution be correct so that the mass moment of inertia and radius of gyration will be correct to their scales of n^5 (mass times distance squared) and n, respectively.

It is difficult to find material for the essential structural elements of the model (cable and stiffening girder) which meets the scale requirement $\frac{E_p}{E_m} = n$, and has the proper value for other essential properties such as damping capacity (non-dimensional). This difficulty can be avoided by appropriate scale adjustment as shown by the following analysis.

The modulus of elasticity, E, affects the cable stretch and girder deflection which, being linear dimensions, must have the scale, n. Thus the stretch, $\Delta L = \frac{F\ L}{A\ E}$ has the dimensions $\frac{n^3\ n}{n^2\ n} = n$. If E is made the same on model and prototype the necessary condition can still be filled if the scale of $A\ E$ is maintained as n^3 by applying the scale n^3 to stress-carrying area. This has been done on the model of the Tacoma Narrows Bridge. A piano wire with area reduced by the scale n^3 carries the stress; the correct mass and exposed area are provided by sectional steel sleeves strung on the wire with a snug fit at the middle of each section so that they do not slip or make contact, one with the other (3c).

Similarly, a bending deflection, $\frac{F\ L^3}{C(E\ I)}$, having the scale, $\frac{n^3\ n^3}{n\ n^4} = n$, can be kept to correct scale by scaling E at unity and I at n^5, the distorted scale of I applying only to the moment-resisting section. The equivalent of this is done by introducing properly designed springs in series with truss members, which would otherwise be excessively strong, or by carrying the bending stress in a weak beam which is masked by the normally scaled beam, the latter being cut to relieve it of stress (3c) (3d).

While such details as girder flanges do not appear to affect the Strouhal number (Art. 1B) model tests show that they do affect the lift, drag and moment and the oscillation; it is not permissable to omit them on the model. Stringers under the deck of an otherwise fully symmetrical section cause a very noticeable difference in behavior in upward or downward angled winds of the same degree. Curbs may have a similar effect. All edges should be true and their corners should be sharp unless distinctly rounded on the prototype. Small mesh openings as in gratings cannot be scaled down because they then block the wind as does a veil and give the effect of solid panels on the model. (This is an effect of viscosity.) Such a grating can be represented by a grid of coarser mesh than a truly scaled one but with the same solidity ratio. The model should be carefully detailed to keep damping to a minimum to make sure it will reveal any possible behavior of the prototype.

The form of a section model must be built to correct scale, and the mass radius of gyration must be correct. The mass can be reduced in order to get more sensitive readings of the damping as noted in Art. 10C. The model must be rigid so that it will not be appreciably distorted during testing. It is supported by springs designed to permit both vertical and torsional motion or to confine the motion to either type. For investigating flutter the frequencies of the vertical and torsional components can be adjusted separately as needed (3c) (3e). The aspect ratio, length over width, should preferably be not less than 4.5 or 5.0 or end plates should be used to prevent distorted results due to the flow of air over the ends.

(D) *Choice of Model Type.*—An aerodynamic section model will reveal the velocity at which a catastrophic oscillation of any type will occur under damping conditions similar to those applicable to the model. This is all the information needed concerning such motion. In most oscillations the air forces and the motion of the structure both bear a constant relation to the amplitude so that all forces acting on a unit length of the section model are identical to those acting on a unit length of a full model moving at the same frequency and amplitude. For such oscillations the behavior of the prototype can be calculated from section model tests. There are phenomena, however, which require full models if they are to be investigated only by model tests. Examples are:

(a) The possible effect of gusts of wind blowing nearly parallel to the bridge. Tests at the National Physical Laborabory of the Department of Scientific and Industrial Research of Great Britain on a full model of an early design for the proposed Severn Bridge failed to reveal any synchronized oscillation set up by periodic gusts but did show irregular motions caused by random gusts.

(b) A full model is preferable for investigating or verifying the effects of stays of all types. However, the effect of a simple system of stays can be quite well evaluated by means of section model tests together with the analysis developed by Friedrich Bleich for predicting the effect of stays on frequency and wave form (1m).

(c) The possibility of flutter, coupling any pair of the calculated vertical and torsional modes of the proposed structure can be investigated with a section model designed for the correct vertical and torsional frequencies; however, if the coupled modes have not the same wave form, then their relative amplitudes and phase will not be constant along the span. A full model is best for determining the amplitude of a restricted oscillation of this type. However, it would appear that a fair approximation of it could be computed from the decrement curves for a section model by applying a correction based on Mr. Bleich's factor, *D* using it (11b) in accordance with its influence on the aerodynamic damping terms, positive or negative (11c). It is improbable that two modes of markedly different form can combine to produce a flutter of serious vigor even though their frequencies may be nearly equal. In any case the tendency to flutter in coupled modes of different form can be no worse than indicated by the section model.

(E) *Instrumentation.*—There are several methods of measuring satisfactorily the wind velocity. For this type of model testing they must be suitable for low to moderate velocities. Pitot tubes are satisfactory for the higher velocities used. Instruments which use a weak calibrated spring to balance the pressure over a rather large opening or those based on the change in electrical resistance of an electrically heated fine wire when cooled by the wind stream are satisfactory for velocities below the sensitivity of the manometers used with the pitot tubes (3c). The vertical angle of the wind can be measured by noting the angle of a smoke stream or silk fiber in the jet or by means of a "pitchmeter," a horizontal cylinder having two holes about 84° apart in its cylindrical surfaces, these being connected to the opposite sides of a manometer. A graduated scale measures the pitch angle, the angle to which the cylinder must be rotated in order to balance the manometer (3c). The model motions can be picked up by means of small accelerometers or by devices utilizing bonded or unbonded wire resistance strain gages, and recorded on an oscillograph, or by other means (3c).

12. LESSONS FROM BRIDGE PERFORMANCE

The investigation of the aerodynamic stability of suspension bridges and of means for achieving satisfactory designs would be incomplete without a study of the records of actual bridges. In the nineteenth century a number of relatively light suspension bridges in Europe and the United States were destroyed or severely damaged by wind action. These were either unstiffened, except for continuity of the floor system, or stiffened by heavy railings or light trusses. Almost invariably the record describes the wind as of hurricane intensity (3q). After an interval of some 80 yr the twentieth century has recorded the collapse of the Tacoma Narrows Bridge, the damage and seriously threatened safety of the Deer Isle Bridge as originally built, and moderate oscillation of the Bronx-Whitestone, Fykesund (Norway) and Thousand Islands Bridges (3a) (20) (21). During 1950 a 580-ft girder stiffened bridge at Beauharnois, Quebec, showed considerable activity. In addition to the foregoing girder-stiffened bridges moderately severe oscillations have been observed on certain truss-stiffened bridges (Golden Gate and the Peace and Liard River bridges on the Alaska Highway). Data concerning these bridges are given in Table I and more information concerning some of them will be found in Appendix III.

Within the scope of the observations the behavior of actual bridges tends to verify the indications of model tests and of theory on three important points.

(1) The motions of the girder-stiffened bridges are either purely vertical or purely torsional, whereas those of the truss-stiffened bridges or bridges stiffened only by the deck structure are coupled vertical and torsional motions (see Art. 4(D)).

(2) Destructive oscillation of truss-stiffened bridges occurs only at very high velocities, whereas such oscillations can occur on girder-stiffened bridges at quite moderate velocities (42 mi per hr on the original Tacoma Narrows Bridge).

(3) Moderate oscillations at low wind velocities have been observed on some girder-stiffened bridges, whereas higher velocities are needed to cause moderate oscillation of truss-stiffened or unstiffened bridges.

The use of diagonal stays or an increase in vertical stiffness has reduced the amplitudes of the oscillations of a number of bridges (for example, stays on

TABLE 1.—MODERN SUSPENSION BRIDGES SUBJECT TO AERODYNAMIC OSCILLATION

(a) DESCRIPTION AND IDENTIFICATION, WITH REMARKS

Item	Bridge	Remarks	Reference[a]
1	Tacoma Narrows, Tacoma, Wash.	Original structure: Several vertical modes at low to moderate velocity; catastrophic torsion above 30 mi per hr; destroyed December 7, 1940.	(3a)(3b)(3c)
2	Thousand Islands, St. Lawrence River, New York to Ontario, Canada	Before stays were added: 24-in. maximum double amplitude in the fundamental vertical mode; with center ties added, the maximum was 15 in. at the main-span quarter point and 12 in. at the center of the side span in one node vertical mode.	(21)
3	Deer Isle, Me.	Early movements of 6 in. to 10 in. reported in the first asymmetric vertical mode; after the initial installation of stays, 12.5 ft single amplitude in the first symmetric vertical mode developed in a wind of 72 mi per hr on December 2, 1942; a more complete stay system was installed later.	(10c)(21)
4	Bronx Whitestone, East River, New York, N. Y.	Original condition: First asymmetric vertical mode only; maximum observed double amplitude 30 in., more or less; the greatest activity occurred in a quartering wind.	Appendix III
5	Fykesund, Norway	Vertical oscillation with one, two and three nodes; maximum double amplitude, 5.25 ft; no torsion; wind not measured; no movement was reported since stays were installed in 1945.	Appendix III
6	Beauharnois, Quebec	Symmetrical vertical oscillation in a quartering wind across the lake; maximum double amplitude, 13 in.; no oscillation in a normal wind (possibly turbulent); no asymmetric mode.	Appendix III
7	Golden Gate, San Francisco, Calif.	Symmetrical torsional oscillation in winds stronger than about 30 mi per hr normal to the bridge; maximum double amplitude, 45 in.; damped by downward wind approaching the north side span over a hill; first asymmetric mixed torsional and vertical modes, single amplitudes 4 ft to 6 ft on Dec. 1, 1951, in wind reaching 70 mi per hr.	Appendix III (2)
8	George Washington, Hudson River, New York, N. Y.	Original condition: Mild vertical and slight torsional movements.	Appendix III
9	Lions Gates, Vancouver, B. C., Can.	About 3 in. amplitude in the first symmetric mode, in wind estimated at 50 to 60 mi per hr; the heaviest in 15 yr.	Appendix III
10	Peace River, Alaska Highway, B. C., Can.	Alaska Highway: Small motion in a moderate wind; symmetric torsion, estimated 10° double amplitude in a wind of 40 to 50 mi per hr.	
11	Liard River, Alaska Highway, B. C., Can.	With temporary timber deck: Small motion in a moderate wind; torsional motion enough to cause noticeable relative motion between adjacent longitudinal floor planks in a wind estimated at 35 to 40 mi per hr.	Appendix III

(b) DIMENSIONS AND CHARACTERISTICS

Item[b]	SPAN (FT)		Sag (ft)	Cables[c] (ft)	Weight (lb per ft)	STIFFENING MEMBER			Stiffness Index[d]
	Main	Side				Type	Depth (ft)	Total I (in.^{2}–ft^2)	
(1)	*(2)*	*(3)*	*(4)*	*(5)*	*(6)*	*(7)*	*(8)*	*(9)*	*(10)*
1	2800	1100	232	39	5,700	plate girder	8	2,566	160
2	800	350	...	30.5	3,200	plate girder	6	...	350
3	1080	484	108	23.5	2,400	plate girder	6.54	828	190
4	2300	735	200	74	10,940	plate girder	11	5,300	400
5	755	...[e]	95.5	23.6	3,100	I-beam	17.7[f]	36[g]	230
6	580	...[e]	58	30	3,430	plate girder	7.5	1,800	2400
7	4200	1125	470	90	21,300	truss	25	88,000	347
8	3500	610[h]	316	106	31,590	none	...	...	600
9	1550	614	150	40	4,600	truss	15	10,500	400
10	930	465	93	30	4,500	truss	13	10,400	1560
11	542.8	232.7	54.28	30	3,040	truss	8	2,000	2700

[a] See Appendix III, or the reference cited by number in Appendix I. [b] For name and further description, see Table 1(a). [c] Distance, center to center, in feet. [d] "Stiffness Index" developed by O. H. Ammann (not published) is: $8.2\ w/f + 2(0.07\ I/l^4)$ multiplied by a factor for side-span effect, ranging from 0.95 to 0.67. In this equation: w denotes dead weight per foot of bridge, in pounds; f is the sag of the main span, in feet; I is the moment of inertia of both trusses, in in.^{2}–ft^2; and l is the length of the main span in units of 1000 ft. [e] Side spans not loaded. [f] This depth is in inches. [g] Includes the equivalent in steel of longitudinally reinforced concrete deck. [h] Side spans 610 ft and 650 ft.

Deer Isle, Thousand Islands, Bronx-Whitestone bridges; stiffening on Menai Straits, and Bronx-Whitestone bridges). The behavior of stays is in general agreement with the indications of tests and theory (that is they can inhibit or modify certain modes of motion which may occur on a given bridge). They have undesirable features (see Art. 3 and Art. 15) and are generally recommended more for remedial than for original design.

It was natural that the failure of the Tacoma Narrows Bridge should have been attributed initially to the rather extreme flexibility of the structure. Several investigators pursuing studies along this line found a correlation between the stiffness and reported behavior of a number of suspension bridges. Mr. Steinman (10d) used the basic stiffness terms $\frac{H}{l^2}$ and $\frac{E\,I}{l^4}$ multiplied by the weight per foot and divided by the square of the width of the suspended structure. Louis Balog (10e) made different use of the same basic stiffness terms plotted against the main span length, l. Shortridge Hardesty, M. ASCE, plotted the deflection under a half span load of 200 lb per ft against the length of the main span (not published). O. H. Ammann, M. ASCE, computed a "stiffness index," the half-span load per foot necessary to cause a deflection of one foot at the quarter point of the main span (not published). Each of these studies as applied to existing bridges showed a rather consistent relation between the stiffness and the tendency to oscillate. However, the model studies and theoretical analyses made to date have failed to indicate that increased stiffness is an important factor in preventing oscillation, and therefore afford little information for the evaluation of the proposed indices. Obviously, indices of such nature, if they could be firmly established, and their scope and limitations determined, would be of great value to designers.

One modern truss-stiffened bridge sometimes regarded as questionable—the Golden Gate Bridge—is among the more flexible bridges of this type. It is quite exposed to wind from the sea. In fact, it would probably oscillate a great deal more if the uniformity of the west wind approaching it were not disturbed by the hill shielding the north span.

The truss-stiffened suspension bridges over the Peace River and the Liard River on the Alaska Highway exhibit small oscillations in moderate winds up to 30 mi per hr. However, rather large motions have been observed on each during infrequent strong winds. The "stiffness index" proposed by Mr. Ammann exceeds 1500 and 2500 for the Peace River and Liard River bridges, respectively. These two bridges have open-strand cable construction. The vibration of individual strands between cable clamps (27) should not be confused with the oscillation of the bridges as a whole.

The Beauharnois Bridge provides a recent addition to this record of data on actual bridge behavior. It shows that an extremely rigid girder-stiffened bridge can be oscillated if the required wind conditions occur. This particular section with a $\frac{d}{b}$-ratio of 0.25 and one outside sidewalk has not been investigated by dynamic section model tests. However, if its behavior may be estimated from such tests on models with $\frac{d}{b}$-ratios of 0.24 and 0.2875 the bridge might be expected to show restricted vertical oscillation in very moderate winds and a possibility of severe vertical and torsional oscillation at high velocities. The bridge has remained stable in quite high normal winds, yet oscillates (in the first symmetric mode) in moderate quartering winds. From the model tests it appears that the oscillation could be caused by the normal component of the quartering wind which approaches across Lake St. Louis, and may be uniform and quite steady. The normal wind of high velocity may be turbulent or may be deflected by the local topography and building (also there may be a question about its actual velocity and direction; see Appendix III). Longitudinal components of gust action, referred to in connection with the Bronx-Whitestone Bridge, cannot be considered as an explanation because the asymmetric mode which such action can excite has not been observed here. The behavior of this bridge is discussed in some detail in Appendix III.

The behavior of this stiff bridge supports, in a striking way, the indications of tests on the Tacoma Narrows and Severn Bridge Models as cited in Paragraph (c), Art. 18 (B); that is, that increased vertical stiffness alone is not always to be relied upon to eliminate a seriously objectionable oscillation.

Of the three relatively stiff short-span bridges listed in Table I the girder-stiffened Beauharnois Bridge has shown objectionable motion, while the two truss-stiffened bridges on the Alaska Highway have indicated the possibility that they may develop objectionable motion. On the other hand the truss-stiffened Lion's Gate Bridge of relatively low stiffness has shown negligible motion under severe exposure to wind. Some ten other bridges of relatively low to moderate stiffness not listed in Table I (Mount Hope in Rhode Island, St. John across the Willamette river at St. Johns, Ore., Ambassador at Detroit, Mich., Mid-Hudson at Poughkeepsie, N. Y., Ile d'Orleans across the St. Lawrence river at Quebec, Can., Transbay between San Francisco and Oakland, Calif., Brooklyn and Triborough over the East river at New York, and several Scandinavian bridges of relatively short span) are not known to have experienced motions under wind action. While no records of wind intensity and direction at the sites of these bridges are available, it must be assumed that most of them at times have been subjected to severe wind action during the 15 yr to 68 yr of their lives.

Table I and Appendix III describe only those modern bridges which are known to have oscillated under wind action. The recorded behavior of a much larger number of suspension bridges of a wide variety of structural characteristics and range of span length leads to the conclusion that only a very small proportion of suspension bridges have oscillated significantly due to wind action, although many of them must have been subjected to winds of high velocity.

Most of the modern girder-stiffened bridges and the narrow, essentially unstiffened early bridges built principally in England and the United States, are characterized by low stiffness. Among these bridges a relatively large porportion have experienced oscillations under wind action. Of the stiffer girder-stiffened structures the Beauharnois Bridge has developed oscillations, whereas the Toledo Bridge has not. The long-span extremely heavy and unstiffened George Washington Bridge has experienced insignificant motions.

The interpretation of the history of suspension bridge behavior is necessarily dependent upon what other knowledge is taken into account and opinions differ with the weight given to various findings. Statistically, the record may be interpreted as evidence that stiffness has a determining influence on the stability of suspension bridges against motion under wind action and some regard stiffness as the dominant factor. Others do not accept this appraisal; first, because model tests show a marked susceptibility to oscillation of the girder-type sections regardless of stiffness and, second, because rational analysis indicates only moderate benefits from stiffness unless it may give rise to a considerable increase in damping. More information is needed before these views can be reconciled.

There is general agreement that natural winds usually lack the degree of uniformity and steadiness required to build up oscillation and that some bridges which do not move might do so at other sites where the wind is steadier and more uniform.

Nonuniformity of wind action over the length of the structure is likely to be of relatively greater influence on long spans than on short ones. This may account for the susceptibility to motion of the relatively stiff short-span bridges listed in Table I, while none of the large number of stiff bridges of medium and long span have experienced motion.

Very little has so far been observed and recorded on the characteristics of the wind acting on existing suspension bridges.

II.—DESIGN CRITERIA AND METHODS

13. The Problem

Engineering experience, in general, has developed many problems of vibration and their solutions. Objectionable vibration must be dealt with in almost every machine or dynamic mechanism. The solutions are found in three general methods of attack; redesign to (a) weaken or eliminate the source of vibration, (b) break up resonance, and (c) introduce damping. Road surfaces and tires are improved to reduce the shocks applied to an automobile; the springs, wheel-base and weight distribution are manipulated to minimize the objectionable resonance of the car with the unavoidable road shocks and, finally, shock absorbers remove energy built up in vibration and thus limit the amplitude and the disagreeable acceleration felt by the passengers.

The problem of suspension bridge oscillation is not unique but resembles other vibration problems and can be solved by (1) fundamental changes in form which greatly modify the wind action causing the oscillation, (2) altering the frequency of the wind force by less drastic changes in form or altering the natural frequency of the bridge by changes in stiffness, in order to avoid resonance of the exciting force with the bridge motion and (3) damping out of the remaining, less potent vibration.

14. Means Available to the Designer

The latitude within which the designer can act to prevent objectionable oscillation is determined by the degree to which he can control the physical properties of the bridge. His control of various properties is limited by the physical characteristics of materials, the live loading and also by economics, as follows:

(a) Span length, side span-main span ratio, and sag ratio can be manipulated within rather narrow limits without disproportionate increase in cost.

(b) Dead load mass can be reduced in preparing the design specifications by sacrificing load capacity or discounting future development and can be controlled within restricted limits without such sacrifice through some choice of materials of differing weight, efficiency and cost. It can be increased materially only at corresponding increase in cost.

(c) Stiffness can be increased by reducing the sag or increasing the moment of inertia. The former may range from, say 1/9 to 1/12 of the span. Moment of inertia can be greatly varied by using girders or trusses, which provides a considerable range of overall stiffness on spans under 1000 ft but a much smaller practical range for spans over 2000 ft. Torsional stiffness can be greatly increased by using both top and bottom laterals. Towers become increasingly flexible as the span increases and cannot be economically stiffened in bending enough to influence behavior though their torsional resistance can be increased to some extent.

(d) A great range of shapes is possible through the choices of girder or truss stiffening, deck, through or half-through construction, outside or inside sidewalks, solid, grated or slotted decking, etc.

(e) Friction can be considerably increased through design details or special mechanisms.

15. AVOIDING SOURCES OF EXCITATION

(A) *Girder Versus Truss Types of Stiffening Member.*—When a designer chooses between the girder and truss types of stiffening member he determines the type of wind action to which the bridge may be subjected, that is, predominantly vortex action (and possibly "negative slope" action) on the girder section, or flutter on the truss or extremely shallow girder section. In the former case, a tendency to restricted or catastrophic oscillation (torsional or vertical or both) may be expected at moderate velocities in a steady, uniform wind. In the latter, the response, if any, will probably occur at higher velocities but is likely to be catastrophic unless modified by means described below.

(B) *Stability of Girder Sections.*—Although girder sections are subject to oscillation over a considerable range of velocities, it will probably be found that they can be proportioned to avoid serious wind action within the expected velocity range. Certainly the $\frac{d}{b}$-ratio has a strong influence. Mr. Steinman and F. J. Maher have predicted their behavior from static model tests and indicate certain ranges of the $\frac{d}{b}$-ratio in which catastrophic vertical or torsional motion is not expected to occur (18). These indications should not be fully relied upon until verified by dynamic section model tests. (One such verification has been made at the University of Washington where it was confirmed that the vertical oscillation is catastrophic for d/b greater than 0.24 but is restricted for smaller $\frac{d}{b}$-values (3c).

The behavior of air flow around various types of sections suggests that girder-stiffened bridges might be stabilized by outside sidewalks or fins. Messrs. Steinman and Maher found this to be critical in static model tests and it appears that only certain ratios of fin width to girder depth may be favorable. A limited series of tests, on dynamic section models at the University of Washington showed little or no benefit from the fins. In fact they were unfavorable with one deck combination (3c).

It may be expected that roadway or sidewalk openings can be arranged to improve the stability of girder sections; however, the University of Washington tests showed definitely that girder sections with open roadway or open sidewalks or even a completely open deck gave torsional activity at a lower wind velocity than was found with the solid deck (3t).

(C) *Stability of Truss Sections.*—Many details of truss-stiffened sections have only a secondary damping effect in the wind although leading edge details near the plane of the deck have more positive influence. On the other hand, a system of slots definitely changed a catastrophic flutter of a proposed Tacoma Narrows design (with single lateral system) to a weak restricted oscillation easily damped out (3d). It does not follow that the identical system will be equally effective on a truss section of distinctly different form. It is quite likely that a completely open deck (that is grating) would weaken or prevent flutter of a truss-stiffened section. A beneficial effect which is dependent upon special minor details which may be altered within the life of the bridge should not be relied upon.

16. Avoiding Resonance

(A) *Alteration of Wind Action.*—With a knowledge of the $\frac{V}{N\,b}$-ratio obtained through section model tests and of the natural modes of motion of the bridge calculated from the mass and elastic properties of the proposed design, a study can be made to determine whether or not the critical velocity of an objectionable oscillation which may be present can be pushed up beyond probable occurrence. In general, high frequency is an advantage but in many cases the increased frequency obtained by even costly stiffening will not be adequate to avoid objectionable oscillation. In such cases the other methods must be relied upon such as altering the wind action through a major change in shape or (if the motion is not catastrophic) increasing the damping.

(B) *Adjustment of Frequency.*—In the case of flutter, frequency adjustment can be readily used to throw the vertical and torsional components out of resonance (1j) (11). The use of top and bottom laterals can accomplish this in almost any case. It appears that if the torsional frequency is $2\frac{1}{2}$ or possibly 2 times that of the corresponding vertical mode, flutter is highly improbable within any likely wind range (3e). If the stiffening system is too shallow to make effective use of top and bottom laterals, the torsional frequency can be increased by using several cross frames made up of struts between the cables with diagonal stays from each cable to the opposite girder, provided these can be located away from the node points of the torsional modes which must be modified (3d). (This treatment is undesirable in original design but may be used to improve an existing bridge (21).)

(C) *Center Ties and Diagonal Tower Stays.*—Center ties and diagonal tower stays can be used to break up resonance in the sense that they tend to inhibit certain modes (3a) (3c) (3d). Center ties, for example, effectively prevent the first asymmetric torsional mode (unless the towers are very weak in torsion). Diagonal stays, if attached to the truss near points of maximum amplitude inhibit the early development of a mode though single sets of stays may not always prevent its ultimate development if the excitation is vigorous (3d) (19).

In using ties and stays, certain design problems must be faced. Unyielding center ties restrict the normal deformation of the main span under certain possible though improbable asymmetric live loadings. They and the lateral truss must be made strong enough to sustain the resulting stresses (a difficult thing) or, preferably, relieving devices should be introduced so that they may gradually relax as the loading condition develops. Center ties with hydraulic relieving links are used on the new Tacoma Narrows Bridge. They yield under heavy slowly applied traffic loads but resist the briefly applied longitudinal forces which result from oscillatory wind action.

Diagonal stays must be designed for the static loading to which they will be subjected and their effects throughout the design temperature range should be considered. For example, stays from the tower upward toward the cable near the quarter-point act against the main cables and therefore a drop in temperature doubly increases their tension. Stays must have considerable initial tension in order to be effective which requires adjustment of the hanger loads at adjacent panels to prevent distortion of the gradeline.

17. INCREASING DAMPING CAPACITY

Model tests have shown that a catastrophic oscillation may be reduced to a mild restricted form by modifying the wind forces through alteration of the shape and the flow pattern or by control of resonance by increasing torsional stiffness without changing vertical stiffness. The milder oscillation would probably not damage the structure but might be objectionable from a psychological standpoint. In such a case, a moderate increase in the structural damping is sufficient to reduce the oscillation to negligible proportions. For example, it was found in full model tests of the tentative design for the Tacoma Narrows Bridge with one lateral system that the restricted torsional oscillation which remained after slots were provided in the deck to eliminate the catastrophic flutter could be completely prevented (3d) by damping having a total logarithmic decrement of 0.05.

Mr. Bleich has shown (1i), as previously discussed, how the normal damping of a bridge can be increased, possibly doubled, at low amplitudes by effectively designing to develop friction. Methods suggested are:

(a) Designing all stringers for bearing on the floorbeam, using an extended spacing of deck expansion joints and bracing the floorbeams laterally so that the relative movement will cause sliding instead of horizontal deflection of the floorbeam.

(b) Placing the deck near the plane of the top or bottom chord and using stiff connections so that the floor slab participates in the chord strains and thereby stores energy in the slab where the structural damping is presumably higher than in the truss.

(c) Providing end friction. This is done in the design of the new Tacoma Narrows bridge by introducing hydraulic cylinders between the truss and the tower with the apertures designed for slow release of pressure. Similar units are provided in the center cable ties (24). Such units give a considerable damping effect in addition to their function of slowly yielding to gradual stress changes. Mechanical friction "tongues" were used at the towers of the Bronx-Whitestone bridge to brake longitudinal motion of the suspended structure (19).

(d) If the structural damping of the truss or girder is found to be greater than that of the cable (not clearly established at the present time) the overall damping can be increased by increasing the proportion of the total energy that is stored in the stiffening member. This can be accomplished to some extent by increasing the cable sag and the moment of inertia of the stiffening member.

18. Effect of Weight and Stiffness

In the foregoing application of the three primary methods of preventing vibration no direct reference is made to weight and vertical stiffness for the reason that their influence is complex and requires special consideration.

(A) *Weight.*—Weight influences the wind forces and the possibility of their resonance with bridge motion only through its effect on the motion. If all of the stiffness is due to the loaded cable an increase in weight has no effect upon the frequency. With a substantial girder or truss increased weight reduces the frequency, usually an unfavorable effect (see the last paragraphs of Art. 2 and paragraph F of Art. 3).

An increase in weight without reduction in frequency tends to reduce the structural damping by increasing m in Eq. 17 and 19 in Appendix II. There will also be a tendency for the increased stress or cross sectional area to increase the constants in these equations in partial compensation for the increase in m but this will not affect damping due to truss action which is not stressed by dead load, only by deflection. On the other hand, if the truss stiffness is sufficient to influence the frequency an increase in weight will reduce ω^2 in Eqs. 17 and 19 which also tends to offset the increase in m. Summing up, an increase in weight cannot be expected to make a significant change in structural damping.

The greatest influence of an increase in weight lies in the fact that it increases the energy storage in the same ratio and thereby decreases by the square root of that ratio the amplitude which can be built by a given input of energy from an outside source. It also increases the time required for a given rate of energy input to build up a given amplitude.

(B) *Vertical Stiffness.*—An increase in vertical stiffness in a certain ratio increases the frequency by the square root of that ratio except when the increased stiffness results from increased weight which increases both spring constant and mass and so has only a slight secondary effect upon frequency (as noted in the preceding paragraph and in Arts. 2 and 3).

For longer spans the degree to which the frequency may be increased by increasing the vertical stiffness is quite limited but there are other benefits derived from stiffness as follows:

(a) Model tests and some field data suggest that sizeable amplitudes in the first asymmetric vertical mode can be caused by the action of eddies or random gusts of wind acting nearly parallel to the bridge axis. The oscillation in this case does not arise from the gradual input of energy but develops as a result of the momentary displacement when the bridge yields to the direct pressure of the gust (a force several times the magnitude of the alternating components of pressure which, due to resonance, gradually build up motion in a cross wind). The initial displacement under this direct wind pressure is inversely proportional to the first power of the stiffness (in contrast to a frequency increase proportional to the square root of the ratio of stiffness increase). Thus an increase in stiffness which can cause only a moderate increase in frequency may be sufficient to inhibit oscillation resulting from longitudinal or quartering gusts (see "1. Bronx-Whitestone Bridge," Appendix III).

(b) The energy storage at a given amplitude increases in direct proportion with the overall stiffness and the limiting amplitude for a given energy input is decreased as the square root of the ratio of increase in stiffness.

(c) An increase in vertical stiffness brought about by increased weight increases the denominator of Eq. 20, which interprets the general character of negative aerodynamic damping, and so reduces ψ and δ. Using this reduced value of δ in Eq. 12b necessarily increases the time, t, required to bring about a given change in the amplitude, η, since weight generally has only a small effect upon frequency (N,ω).

An increase in truss stiffness, on the other hand, if effective at all, increases the frequency, ω, and does not change ψ and δ in Eq. 20. Therefore if δ is unchanged and ω is increased in Eq. 12b the time required will be reduced. Actually such an effect of increased truss stiffness may not occur because the negative atmospheric damping in a wind stream is not quite as simple as expressed by Eq. 20 for the positive damping. For example, its variation with the amplitude, η, is more complicated as shown in Fig. 8.

Any factor which increases the time required for a motion to build up in the wind may have a beneficial effect much greater than is suggested by the percentage increase because of the sharply reduced probability of the wind continuing within the required range of conditions (velocity, direction, and uniformity) for the additional length of time.

This benefit will vary in individual cases depending upon the wind required to excite motion of the section. For example, each vertical mode of the original Tacoma Narrows Bridge was excited only in a limited range of velocity; if the velocity changed beyond this range the mode was damped out and a different mode might begin in its place. The field records show this continuous changing of modes without serious amplitudes being built up in any one. On the other hand, after the center stays were disabled the torsional mode by which the bridge was destroyed could be built up continuously at any velocity above 20 mi per hr (3a) (3c).

The indication of model tests is that increased vertical stiffness alone is not always to be relied upon to eliminate a seriously objectionable oscillation. Tests were made on the full model of the new Tacoma Narrows Bridge with solid deck and one lateral system but with the truss replaced by a 12-ft plate girder to give the $\frac{d}{b}$-ratio, 0.2, of the original bridge (3e). However, the stiffness of the basic model skeleton was excessive for any girder, being equivalent to that of 12-ft girders having 200 sq in. of metal in each flange and more than ten times the stiffness of the girders of the original bridge. Notwithstanding this additional stiffness the model showed the general behavior of the original bridge and its full model. Also despite the stiffness of the 25-ft trusses of an early proposed design of the Severn Bridge, the full model thereof when masked by paper to give the general shape of a girder section, showed the typical behavior of the original Tacoma Narrows Bridge.

The same point is demonstrated by a bridge built in 1949 at Beauharnois, Quebec, with a span of only 580 ft, unloaded back stays and stiffening girders 7.5 ft deep which, though very stiff, has oscillated with a double amplitude of 13 in. in a moderate wind.

19. Design Procedure

At the present time the aerodynamic phase of the design of a suspension bridge must be accepted as analogous to the static analysis of an indeterminate structure. The individual effects of various factors of shape, mass and stiffness, are known in a general way and may be incorporated in the design but it is necessary to investigate the overall design to determine what will be the actual behavior of the structure. Just as there are methods for analyzing an indeterminate structure to determine the stresses after the sections have been assumed, so methods have been developed for predicting with more or less reliability the aerodynamic behavior of a suspension bridge after its various design factors have been selected.

20. Predicting Probable Behavior

(A) *Preliminary Investigation for Flutter.*—If the structure is stiffened by a truss or by an extremely shallow girder and therefore has the characteristics of a flat plate, a very good indication of its probable behavior can be obtained by applying the flutter analysis developed by Mr. Bleich (1) (11). If this indicates flutter within the possible wind velocity range, one can be quite positive that a drastic change is needed. Moreover, it can be expected that, if flutter is indicated by the calculations, restricted oscillations of undesirable amplitude may be expected at a somewhat lower velocity.

A dynamic section model should be constructed and tested in a wind tunnel. This will supply data for use in Mr. Bleich's analysis to determine the modifying effect of vortex action (11d). A few further tests will provide directly the $\frac{V}{N\,b}$-ratio of the resulting oscillation in the ideal horizontal wind and in vertically angled winds of any degree which might be expected (3e). If the section model shows a catastrophic motion it is only necessary to note its critical velocity (prototype) and decide whether the wind at the site can reach that velocity.

(B) *Prediction of Severity of Restricted Oscillation.*—A moderate extension of the section model tests on either girder-stiffened or truss-stiffened sections will supply information from which the probable severity of restricted oscillations can be determined. This extended technique consists simply of testing the model at various velocities and recording the rate of increase or decay of oscillation, from which the logarithmic decrement can be computed and plotted against the amplitude. Associated with these tests are similar determinations in still air from which the aerodynamic damping of the model (and of the prototype as well) and the structural damping of the model set-up can be measured separately.

The frequency and wave forms of any probable modes can be readily calculated from the geometric, elastic, and mass properties of the proposed design and the energy of vibration of any mode can likewise be calculated. Knowing the rate of energy transfer per unit length of bridge at any amplitude (from the section model tests and the curves for logarithmic decrement) the rate of energy transfer to the prototype can be calculated by a single process of integration for the known variation of amplitude over the length of the structure (3e).

It is estimated that the probable amplitude of a restricted oscillation of the proposed bridge can be determined by this procedure to about the same degree of precision that applies to the calculation of stress in many phases of conventional design provided a reasonably accurate figure for the structural damping of the prototype is available.

21. WIND EXPOSURE PROBABILITY

Knowledge concerning the wind conditions upon which the aerodynamic solution must be predicated is comparable to the uncertainty concerning stream flow conditions for which a bridge must be designed. Tests show that a wind of steady velocity uniformly distributed over the bridge will be more severe than a variable or non-uniformly distributed wind. Also for each design there is a certain angle of attack which causes greatest excitation. Common experience and a few special field observations give some idea as to the degree to which these unfavorable conditions may occur.

No general discount ratio can be assumed but observations at a given site may establish quite definite limitations on the severity of wind conditions which must be provided for. For example, tests on a section model of the Golden Gate bridge showed that vigorous oscillation is to be expected in a normal wind of moderate intensity approaching at an upward angle of a few degrees. Considerable excitation was also indicated in a horizontal wind (3d) (11e). Nevertheless, detailed measurements of the movement of this bridge over a period of years have shown that much of its motion in the wind is more or less random. Even when the double amplitude reached 20 in. to 45 in. in the dominant symmetric mode, large amplitudes were maintained for only a few cycles in immediate response to a wind gust. The very probable reason for the failure of symmetric modes to build up steadily stands out quite clearly. The 1,000-ft hill just northwest of the bridge causes any normal wind to be deflected sharply before it strikes the north side span. The prevailing westerly wind is turned down perhaps 30° and the rare east wind is turned up correspondingly. (Full model tests of the first design for the new Tacoma Narrows bridge with solid deck showed that a vigorous oscillation set up by a wind stream can be quickly brought to rest by simply turning sharply downward the wind which strikes one side span (3d).) On December 1, 1951, in a wind which reached 69.5 miles per hour at the mid-point of the main span of the Golden Gate Bridge and probably exceeded that velocity elsewhere on the bridge, the motion was primarily a one-node coupled torsional and vertical oscillation which reached double amplitudes of about 12 ft and 8 ft, respectively, at the southeast and southwest quarter-points (2.5° to 12.8° double amplitude in torsion depending on the phase of the coupled modes). This asymmetric motion can occur without participation of the side spans. Hence it was not impeded by the distorted wind action on the side spans to the degree which would be expected for the symmetric modes which require side-span participation. However, there was considerable oscillation of the side spans and the interference may have exerted a moderating influence.

A program of section model tests is under way for determining the behavior of certain existing bridges under laboratory controlled wind conditions. It is expected that the comparison of these indications with the actual observed behavior of the bridges will give a general idea as to the extent to which idealized predictions may be discounted for field conditions.

While considering the difference between actual response and idealized predictions of the behavior of existing bridges it is pertinent to speculate, perhaps, as to what these bridges might do at other, less favorable sites. For example, a bridge similar to the Golden Gate Bridge, if located in flat terrain and subject to hurricane winds, very likely would develop serious oscillation. It is hardly to be expected, furthermore, that of all modern bridges, this is the only one which might show such behavior at a less favorable site.

22. TOLERANCE

It yet remains to be determined what amplitude of oscillation may be tolerated in a suspension bridge. Due to their flexibility, amplitudes of several feet in the lower modes will have no serious structural effect on the larger suspension bridges but it is probable that any oscillation which becomes noticeable to the public should be considered objectionable. In the case of vertical oscillation this probably hinges largely on the acceleration, which produces the sensation of movement and which in turn, is a function of the span and the amplitude so that the permissible amplitude might be expressed as a rather simple function of the span after the necessary experimental constants have been determined. (However, the visual sensation of the large vertical movements of the original Tacoma Narrows Bridge was more objectionable than the acceleration.) If the bridge is used by pedestrians, a very small amplitude in torsion can be detected by sighting from one sidewalk across the opposite rail.

It was observed on the Bronx-Whitestone Bridge as originally built that double amplitudes appreciably over 12 in. in the first asymmetric vertical mode (frequency about 8.5 cpm) were sufficiently perceptible to cause discomfort and possible panicky feeling in some people (unpublished report by Mr. Ammann). This represents $\frac{1}{1150}$ of the wave length and an acceleration of less than one ft per sec^2.

III.—SUMMARY OF CRITERIA AND ADDITIONAL DATA REQUIRED

23. CRITERIA

There are some rather definite criteria for designing suspension bridges to avoid objectionable oscillation but the influence of some factors cannot be stated quantitatively at the present time with any degree of precision except after tests of the particular section involved. The criteria may be summarized as follows:

A. *Selection of Stiffening Member.*—The use of a truss instead of a girder for the stiffening member will probably avoid the frequent annoying oscillation in moderate winds such as occurred on the original Tacoma Narrows Bridge although the behavior of the Golden Gate Bridge shows that a truss-stiffened bridge may also be, to a lesser degree, subject to such oscillation.

B. *Truss Sections.*—Flutter of a truss-stiffened section can, in all probability, be avoided by using both top and bottom lateral systems or by a suitable system of openings in the deck. With present knowledge it is advisable to verify their effect on a proposed design by analysis and by wind tunnel tests of a dynamic section model.

C. *Girder Sections.*—It is quite probable that girder stiffened sections can be used safely by using a favorable $\frac{d}{b}$-ratio or some favorable form combination such as outside sidewalks, slots or fairing but at the present time such remedies should be relied upon for a given design only if their value is confirmed by aerodynamic tests of a section model of the particular design. If tests indicate that a moderate increase in frequency is desirable to raise the critical velocity above the probable velocity at the site this may sometimes be accomplished by a practicable increase in stiffness (most effectively through a reduction in sag). Damping can be increased if necessary at moderate cost by attention to ordinary design details and by introducing frictional devices.

D. *Analysis and Model Tests.*—By mathematical analysis and dynamic section model tests the aerodynamic stability of a given design under idealized wind conditions can be adequately determined. Until more specific knowledge accrues, it is advisable to make such investigations of any important suspension bridge unless it closely resembles a bridge known to be stable under the conditions at the proposed site.

24. FURTHER RESEARCH NEEDED

A. *Character of Natural Winds.*—A very important requirement is to determine the characteristics of natural winds including the constancy of wind velocities and angle of attack and the uniformity of wind across a bridge site. These investigations should indicate the degree of uniformity to be expected from various types of storms in certain regions as well as the modifying influence of topographic and cultural features. Recording instruments showing velocity, wind direction and vertical angle at different locations adjacent to actual bridges should contribute materially to the accumulation of this necessary information. These observations should be closely correlated with the behavior of the bridge. The probable behavior of the bridge in idealized winds should be determined by mathematical analysis and aerodynamic section model tests to provide a basis for comparison to indicate the relative effectiveness of the actual wind.

B. *Structural Damping of Suspension Bridges.*—Data should be obtained as the structural damping to be expected in various types of suspension bridges. Theoretical analysis may go a long way toward indicating the probable values but it is believed tests on at least a number of actual bridges will be necessary. These tests need to cover a reasonable range of distribution of the energy of vibration between the cable and the truss, and should give some indication of the damping with different types of floor system since the latter may very likely provide a large share of the total damping. Usual methods of oscillating a structure by means of eccentric weights, etc., can hardly be used because of the extremely slow vibration of suspension bridges. Some preliminary tests have been made on small bridges. Methods have been studied for making measurements on major bridges (3e).

C. *Catalogue of Characteristics of Bridge Sections.*—A series of section model tests is needed, first to determine in a broad way the effects of various shape factors $\left(\frac{d}{b}\text{-ratio, fins, slots, deck or through construction, etc.}\right)$ and second to build up eventually a catalogue of quantitative data on the aerodynamic characteristics of various bridge sections. Such tests will confirm or modify various theories as to the behavior of sections and in time may establish certain rather broad limitations within which a type of design may be used without detailed tests.

D. *Improvement of Methods for Predicting Behavior.*—Correlation studies of full model and section model tests show discrepancies in critical velocities which can be as much as 20%. Part of this can be attributed to the limited precision of controls and measurements but part may be due to the influence on the $\frac{V}{N\,b}$-ratio of some factors which are not fully understood. Further investigation should clear up this uncertainty and increase the precision and reliability of the predictions. It may be expected also that the method of making predictions can be simplified.

E. *Effect of Weight and Stiffness.*—There is evidence that weight and stiffness beyond the minimum requirements to meet static conditions may have more beneficial effects than can be rationally explained at this time. The effect of weight and stiffness should be the subject of further investigation.

F. *Camber, Stays and Longitudinal Forces.*—There are a number of subsidiary questions, many of which should be cleared up in connection with the above listed investigations. The use of a full model will facilitate the further investigation of such features as camber, stays, and logitudinal forces although they can be treated analytically also.

25. MEMBERSHIP ROSTER

Chairman: E. F. Kelley
Vice Chairman: Raymond Archibald

Agricultural and Mechanical College of Texas.—
A. A. Jakkula, M. ASCE, Executive Director, Texas A. & M. Research Foundation

American Association of State Highway Officials.—
Raymond Archibald, M. ASCE, Chairman, Committee on Bridges and Structures
C. B. McCullough, M. ASCE, Assistant Chief Engineer, Oregon State Highway Commission*
G. S. Paxson, M. ASCE, Bridge Engineer, Oregon State Highway Commission

American Institute of Steel Construction.—
F. H. Frankland, M. ASCE, Counsulting Engineer
C. F. Goodrich, M. ASCE, Chief Engineer, American Bridge Company†
Jonathan Jones, H. M., ASCE, Chief Engineer, Fabricated Steel Construction, Bethlehem Steel Company
C. Earl Webb, M. ASCE, Chief Engineer, American Bridge Company

American Society of Civil Engineers.—
Russell G. Cone, M. ASCE, General Manager, Silas Mason Company
Shortridge Hardesty, M. ASCE, Consulting Engineer
Charles M. Spofford, M. ASCE, Professor of Civil Engineering, Emeritus, Massachusetts Institute of Technology; Consulting Engineer

Bureau of Public Roads, U. S. Department of Commerce.—
O. L. Grover, Principal Highway Bridge Engineer†
E. F. Kelley, Chief, Physical Research Branch
R. B. McMinn, Senior Highway Bridge Engineer, Division 8
Leon S. Moisseiff, M. ASCE, Research Consultant*

California Department of Public Works.—
C. H. Purcell, Hon. M. ASCE, Director of Public Works*‡
Norman C. Raab, M. ASCE, Projects Engineer, Division of San Francisco Bay Toll Crossings
George D. Whittle, M. ASCE, Division of San Francisco Bay Toll Crossings

---

* Deceased. † Retired. ‡Resigned.

California Institute of Technology.—
Theodor von Karman, H. M. ASCE, Director, Daniel Guggenheim Aeronautical Laboratories
Delaware River Joint Commission.—
Frank M. Masters, M. ASCE, Consulting Engineer
Engineering Institute of Canada.—
P. L. Pratley, M. ASCE, Consulting Engineer
Golden Gate Bridge and Highway District.—
John G. Little, M. ASCE, Consulting Engineer
Leon H. Nishkian, M. ASCE, Consulting Engineer*
Highway Research Board.—
R. W. Crum, M. ASCE, Director*
Franklin N. Wray, M. ASCE, Engineer of Design
John A. Roebling's Sons Company.—
Chas. C. Sunderland, Chief Engineer, Bridge Department
National Bureau of Standards, U. S. Department of Commerce.—
H. L. Dryden, Chief, Division of Mechanics and Sound‡
G. B. Schubauer, Chief, Aerodynamics Section
Port of New York Authority.—
O. H. Ammann, M. ASCE, Consulting Engineer
Princeton University.—
Elmer K. Timby, M. ASCE, Consulting Engineer
Triborough Bridge Authority.—
Emil H. Praeger, M. ASCE, Chief Engineer, Madigan-Hyland
University of Washington.—
F. B. Farquharson, M. ASCE, Director, Engineering Experiment Station
Washington Toll Bridge Authority.—
Charles E. Andrew, M. ASCE, Principal Consulting Engineer
Glenn B. Woodruff, M. ASCE, Consulting Engineer
Yale University.—
Hardy Cross, H. M. ASCE, Professor of Civil Engineering

January, 1952

APPENDIX I.—LIST OF REFERENCES

Numbers in parentheses in the text of this report refer to the following reading references:

1. "Mathematical Theory of Vibration in Suspension Bridges," by Friedrich Bleich, C. B. McCullough, Richard Rosecrans and George S. Vincent, Bureau of Public Roads, U. S. Department of Commerce, Government Printing Office: (a) Fig. 19; (b) Art. 8, Chapter 4 and Tables 8, 9 and 10; (c) page 156; (d) Chapter 5, Parts 2 and 3; (e) Fig. 15; (f) Fig. 17 and Tables 2 and 5; (g) Chapter 5, Part I; (h) Fig. 16 and Table 6; (i) Chapter 6; (j) Chapter 7; (k) Eq. 6.20; (l) Fig. 73; (m) Chapter 5, Part 4.
2. "The Failure of the Tacoma Narrows Bridge; A Report to the Federal Works Agency," by O. H. Ammann, Theodore von Kármán and Glenn B.

---

* Deceased. ‡ Resigned.

Woodruff, March 28, 1941: (a) Fig. 25; (b) Figs. VIII–18 to VIII–21, Appendix VIII; (c) Chapter I, Appendix VI and drawings 4 and 5; and, (d) Chapter IV.

3. "Aerodynamic Stability of Suspension Bridges with Special Reference to the Tacoma Narrows Bridge," University of Washington Engineering Experiment Station Bulletin No. 116:
   (a) Part I, "Investigations Prior to October, 1941," by F. B. Farquharson;
   (b) Part II, "Mathematical Analyses," by Frederick C. Smith and George S. Vincent;
   (c) Part III, "The Investigation of Models of the Original Tacoma Narrows Bridge Under the Action of Wind," by F. B. Farquharson, June, 1952;
   (d) Part IV, "The Investigation of Models of the New Tacoma Narrows Bridge Under the Action of Wind," by F. B. Farquharson, April, 1954.
   (e) Part V, "Amplitude Predictions, Damping Tests, and General Investigations," by George S. Vincent June, 1954.

   Supplementary text references—(f) see Part I, Chapter VIII; (g) see Part I, Figs. 24 and 26 and Chapter VII; (h) see Part I, Chapter III and Appendix III; (i) See Part I, Figs. 9 and 10; (j) see Part II, Figs. 5, 6, 7 and 9; (k) see Part II, Fig. 8; (l) see Part II, Chapter VI and Appendix V; (m) see Part II, Eq. 2.9 and the expression for μ in Art. 6; (n) see Part II, Eq. 2.8 and the expression for μ in Art. 6; (o) see Part II, Eq. 3.5 and Art. 15; (p) see Part I, tables IX and X; (q) see Part I, Appendix I; (r) see Part I, Chapter IV; (s) see Part I, Chapter V; (t) see Part III, Table V; and, (u) see Part II, Chapter VII.
4. "Mechanical Vibrations," by J. P. Den Hartog, McGraw-Hill Book Co., New York, Third Ed., 1947: (a) Art. 59; (b) Art. 75; (c) Art. 32; and (d) Art. 13.
5. "Applied Hydro- and Aeromechanics," based on lectures of L. Prandtl, by O. Tietjens, McGraw-Hill Book Co., Inc., New York, 1934: (a) Plates 1 to 4; (b) Art. 82; (c) Art. 99.
6. "The Frequency of the Eddies Generated by the Motion of Circular Cylinders Through a Fluid," by E. F. Relf and L. F. G. Simmons, Reports and Memoranda No. 917, June 1924, Technical Report of Aeronautical Research Committee for 1924–25 (London).
7. "Problems of Aerodynamic and Hydrodynamic Stability," by D. B. Steinman, Proceedings of the Third Hydraulics Conference, Bulletin 31, University of Iowa Studies in Engineering.
8. "Vibration and Drag of Towing Cables in a Uniform Stream," by L. Landweber. Memorandum, David Taylor Model Basin, Jan. 13, 1945.
9. Note IV, "Mechanism of Fluid Resistance," by Theodore von Kármán and H. Rubach, U. S. National Advisory Committee for Aeronautics Technical Reports 24–50, 1918. Government Printing Office (Translation from paper in Physikasische Zeitschriff, January 15, 1912).

10. "Rigidity and Aerodynamic Stability of Suspension Bridges," by D. B. Steinman, Transactions ASCE, Vol. 110 (1945), p. 439 and: (a) Part 4; (b) discussion by F. B. Farquharson on p. 492; (c) p. 544; (d) closing discussion, p. 532; and, (e) discussion by Louis Balog, p. 522.
11. "Dynamic Instability of Truss-Stiffened Suspension Bridges Under Wind Action," by Friedrich Bleich, Transactions, ASCE, Vol. 114 (1949), p. 1177 and: (a) Discussion beginning p. 1225; (b) Eq. 45; (c) as indicated in Eqs. 46; (d) Part 6; and, (e) p. 1214.
12. "Aerodynamic Theory of Bridge Oscillations," by D. B. Steinman, Transactions, ASCE, Vol. 115 (1950), p. 1180.
13. "Practical Importance of Damping Capacity of Metals, Especially Steels," O. Foppl, Iron and Steel Institute Journal, Advance Paper No. 2, September, 1936.
14. "The Damping Capacity of Steel and Its Measurement," by G. P. Contractor and F. C. Thompson, Paper No. 1/1940 of the Alloy Steels Research Committee, Iron and Steel Institute Journal, 1941.
15. "Impact in Steel Railway Bridges of Simple Span," by J. B. Hunley, AREA Bulletin, Vol. 37, No. 380, October, 1935.
16. "Investigation of Bridge Impacts with a Mechanical Oscillator," by Committee 30—Impact and Bridge Stresses, A.R.E.A. Bulletin, Vol. 49, No. 467, June–July, 1947.
17. "Structural Damping in Suspension Bridges," by Friedrich Bleich and L. W. Teller, Transactions, ASCE, Vol. 117, 1952 p. 165.
18. "Wind Tunnel Tests of Suspension Bridge Section Models," by F. J. Maher, D. Frederick and E. R. Estes and by D. B. Steinman, Bulletin No. 69, Engineering Experiment Station Series, Virginia Polytechnic Institute.
19. "Stays and Brakes Check Oscillations of Whitestone Bridge," Engineering News-Record, Vol. 125, No. 23, p. 750, Dec. 5, 1940.
20. "Additional Stiffening of Bronx-Whitestone Bridge," by O. H. Ammann, Civil Engineering, Vol. 16, No. 3, March, 1946, p. 101.
21. "Two Recent Bridges Stabilized by Stays," Engineering News-Record, Vol. 125, No. 23, p. 752, Dec. 5, 1940.
22. "The Severn Bridge Aerodynamic Research," by R. A. Frazer (National Physical Laboratory, London) Nature, Vol. 163, p. 7, Jan. 1, 1949.
23. "An Experimental Investigation of the Aerodynamic Stability of Suspension Bridges," by C. Scruton (National Physical Laboratory, London) Preliminary Publication of the Third Congress, International Association for Bridge and Structural Engineering, 1948.
24. "Unusual Design Problems—Second Tacoma Narrows Bridge," by Chas. E. Andrew, ASCE Transactions, Vol. 114 (1949), p. 955.
25. "A History of Suspension Bridges in Bibliographical Form," by A. A. Jakkula, Texas Agricultural and Mechanical College, Engineering Experiment Station, Series No. 57, Fourth Series, Vol. 12, No. 7, July 1, 1941.
26. "Dampening Effect in Suspension Bridges" by Arne Selberg, Vol. X, Publications of the International Association for Bridge and Structural Engineering.
27. Engineering News-Record, September 2, 1948.

APPENDIX II.—ENERGY AND DAMPING

The total energy of vibration of the bridge is expressed by the equation (to be found in most books on vibration (3u)(4c)):

$$U = \frac{w\,\omega^2}{2\,g}\int_L \eta^2\,dx \ldots\ldots\ldots\ldots\ldots\ldots\ldots (8)$$

in which: U is the total energy of vibration; w is the weight per foot of the structure; g is the acceleration of gravity; ω is the circular frequency (that is, $2\,\pi\,N$); and, η is the amplitude at any point, x, along the span. The integration over the length of the bridge is necessary in arriving at the total because η varies along the span but can be expressed as a function of x.

If the bridge oscillates at a steady state, neither increasing nor decreasing in amplitude the total energy remains constant regardless of the instantaneous position. The total energy, U, is the sum of the instantaneous values of the kinetic energy, T, and the potential energy, V. The kinetic energy, $T = \frac{m\,v^2}{2}$, has the maximum value given by Eq. 8 which occurs at the instant all parts of the bridge pass at maximum velocity through their normal dead-load positions. At that instant the potential energy is zero. At maximum displacement the bridge is momentarily at rest and has no kinetic energy, all of the energy being stored as potential energy due to the position of the mass and the elastic strain in the bridge members. It will be noted that the energy of vibration increases with the square of the amplitude.

Considering, for simplicity, a unit length of the structure having a mass, m, and vibrating at the frequency, ω, and the amplitude η, then (see Eq. 8):

$$U = \frac{m\,\omega^2\,\eta^2}{2} \ldots\ldots\ldots\ldots\ldots\ldots\ldots (9a)$$

If, due to the action of damping or frictional forces, the amplitude is reduced in one cycle to $\eta - \Delta\eta$ then the energy is reduced to

$$U = \frac{m\,\omega^2}{2}\,[\eta^2 - 2\,\eta\,\Delta\eta + (\Delta\eta)^2] \ldots\ldots\ldots\ldots (9b)$$

and by subtracting Eq. 9b from Eq. 9a the energy loss is

$$\Delta U = \frac{m\,\omega^2}{2}\,[2\,\eta\,\Delta\eta - (\Delta\eta)^2] = m\,\omega^2\,\eta\,\Delta\eta\left(1 - \frac{\Delta\eta}{2\,\eta}\right) \ldots\ldots (10)$$

and the proportion of the energy lost in one cycle, known as damping capacity, is

$$\psi = \frac{\Delta U}{U} = \frac{m\,\omega^2\,\eta\,\Delta\eta}{m\,\omega^2\,\eta^2/2}\left(1 - \frac{\Delta\eta}{2\,\eta}\right) = \frac{2\,\Delta\eta}{\eta}\left(1 - \frac{\Delta\eta}{\eta}\right) \ldots\ldots (11)$$

Equation (11) also expresses the proportion of energy gained if exciting forces cause an increase of $\Delta\eta$ in the amplitude.

The damping forces can be conveniently classed as (a) structural (mechanical hysteresis, bearing and rivet friction, plastic yielding of deck and other elements, etc.) and (b) atmospheric (opposing inertial and viscous forces from still or moving air). It is the combined effect of all damping forces which causes any observed decay in the amplitude. In order to understand the damping action, therefore, it is necessary first to consider the character of viscous, hysteresis, friction and atmospheric damping.

(A) *Viscous Damping.*—If a damping force is directly proportional to the velocity of the vibrating system (as is true of viscous forces in a fluid) the curve representing the decay of amplitude will be the exponential curve (given in any book on vibration (4d)):

$$\eta = \eta_0 \, e^{-cgt/(2w)} \ldots\ldots\ldots\ldots\ldots\ldots\ldots\ldots (12a)$$

in which: η_0 is the initial amplitude; η is the amplitude at the end of a period of time, t; c is the damping force per unit velocity; g is the acceleration of gravity; and, w is the weight of the system which vibrates at the amplitude, η. Eq. 12a can also be expressed:

$$\eta = \eta_0 \, e^{-\delta N t} = \eta_0 \, e^{-\delta \omega t/(2\pi)} \ldots\ldots\ldots\ldots\ldots\ldots (12b)$$

in which $\delta = \frac{c\,g}{2\,w\,N} = \frac{\pi\,c}{m\,\omega}$, N being the frequency in cycles per second and $\omega = 2\,\pi\,N$ being the circular frequency in radians per second. Symbol δ is called the "logarithmic decrement" and for viscous damping, is constant for all amplitudes during a given vibration but is reduced if the frequency, ω, is increased without changing c or m. If $t = \frac{2\,\pi}{\omega}$, the length of one cycle, then $N\,t = 1$ and Eq. 12b expresses the ratio of two successive amplitudes:

$$\frac{\eta_1}{\eta_0} = e^{-\delta} \ldots\ldots\ldots\ldots\ldots\ldots\ldots\ldots\ldots (13)$$

Thus $-\delta = \log_e \frac{\eta_1}{\eta_0}$ or $\delta = \log_e \frac{\eta_0}{\eta_1}$.

It is difficult to measure accurately the change in amplitude in one cycle but the change in, say, ten cycles can be measured with satisfactory precision. If Eq. 12b is written for the time, $t = 10 \times \frac{2\,\pi}{\omega}$, it gives the ratio, $\frac{\eta_{10}}{\eta_0} = e^{-10\delta}$; and, $\delta = \frac{1}{10} \log_e \frac{\eta_0}{\eta_{10}}$. Thus the viscous damping force can be easily evaluated by measuring its effect on the amplitude.

The instantaneous position of a mass that is vibrating at a frequency, ω, and an amplitude, η, in simple harmonic motion may be expressed $\bar{\eta} = \eta \sin \omega\,t$. Its velocity $\frac{d\bar{\eta}}{dx} = \omega\,\eta \cos \omega\,t$, the maximum velocity being $\omega\,\eta$. A viscous damping force varying with the velocity may be expressed $F \cos \omega\,t = c\,\omega\,\eta \cos \omega\,t$ where c is the force at unit velocity. This force acts in phase with the velocity and in one cycle it performs work equal to $F\,\pi\,\eta = c\,\pi\,\omega\,\eta^2$ provided the damping is low so that the motion is essentially simple harmonic.

(While acting through the distance, $d\bar{\eta}$, the force performs work, $F \cos \omega t \, d\bar{\eta}$; $d\bar{\eta} = \frac{d\bar{\eta}}{dt} dt = \omega \eta \cos \omega t \, dt$; and, the work performed is $(F \cos \omega t) \, \omega \eta \cos \omega t \, dt$. In one cycle t ranges from 0 to $\frac{2\pi}{\omega}$; hence the work per cycle is $\Delta U = F \omega \eta \int_0^{2\pi/\omega} \cos^2 \omega t \, dt = F \omega \eta \int_0^{2\pi} \frac{1}{\omega} \cos^2 \omega t \, d(\omega t) = F \pi \eta$.) The relative decrease in energy is

$$\psi = \frac{c \pi \omega \eta^2}{m \omega^2 \eta^2/2} = \frac{2 \pi c}{m \omega} \qquad (14)$$

It will be noted that this energy ratio is just twice the value of δ as used in Eq. 12b. The same relationship can be derived by expressing

$$-\delta = \log \frac{\eta}{\eta_0}$$

—by the first two terms of the series for natural logarithms

$$\frac{\eta_1}{\eta_0} = \frac{\eta_0 - \Delta\eta}{\eta_0} = 1 - \frac{\Delta\eta}{\eta_0}$$

$$-\delta = \log_e \left(1 - \frac{\Delta\eta}{\eta_0}\right) = -\frac{\Delta\eta}{\eta_0} - \frac{1}{2}\left(\frac{\Delta\eta}{\eta_0}\right)^2 = -\frac{\Delta\eta}{\eta_0}\left(1 + \frac{\Delta\eta}{2\,\eta_0}\right);$$

and,

$$\delta = \frac{\Delta\eta}{\eta_0}\left(1 + \frac{\Delta\eta}{2\,\eta_0}\right) \qquad (15)$$

Comparing Eq. 15 with Eq. 11 and noting that both η and η_0 as used represent the higher of two successive amplitudes it is seen that, very nearly,

$$\psi = 2\,\delta \, \frac{1 - \delta/2}{1 + \delta/2} \qquad (16)$$

If δ is small, say less than 0.05, the error in using $\psi = 2\,\delta$ is not serious but for larger values of δ the damped vibration differs from simple harmonic motion enough to require the corrective term. If δ exceeds 0.40 a still more refined correction is needed.

(B) *Hysteresis Damping.*—Hysteresis damping arises from the absorption of energy due to the imperfectly elastic behavior of the stressed element (1i). The stress-strain curve is not perfectly straight and is slightly different for descending than for ascending loads as shown by Fig. 9 which may represent the behavior of a simple spring, such as a wire supporting a weight.

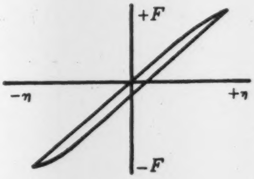

FIG. 9.—HYSTERESIS LOOP

The area enclosed within the stress-strain curves for a complete, closed cycle represents force times distance and indicates the energy lost per cycle. Both the stress and the strain vary directly with the amplitude of the displacement. Therefore, the energy loss is some constant times η^2. For this reason authorities usually consider the energy loss arising from hysteresis as the work done by a damping force which is proportional to the amplitude and in phase with velocity (that is, equal to $C\,\eta \cos \omega t$) and the work it performs in a cycle is $C\,\pi\,\eta^2$ C being a constant, the damping force per unit amplitude, to be determined experimentally. The damping capacity then is

$$\psi = \frac{C\,\pi\,\eta^2}{m\,\omega^2\,\eta^2/2} = \frac{2\,\pi\,C}{m\,\omega^2} \qquad (17)$$

It would appear by comparing Eqs. 14 and 17 that hysteresis damping is even more sensitive to the frequency, ω, than is viscous damping but this is not the case because the hysteresis damping represented by C in the numerator all arises from the action of the spring which also determines the value of ω^2 in the denominator. This can be shown as follows:

If k is the spring constant and η the displacement, then the force on the spring is $k\,\eta$ and the stress may be expressed as $C_1\,k\,\eta$, C_1 being the constant of proportionality relating the spring force and the stress in the particular spring. The damping force, proportional to the stress, is $C_1\,C_2\,k\,\eta$, C_2 being a constant of proportionality. The damping force per unit amplitude, then, is $C_1\,C_2\,k$ which can be substituted for C in Eq. 17. Then

$$\psi = \frac{2\,\pi\,C_1\,C_2\,k}{m\,\omega^2} \qquad (18)$$

The natural frequency of a spring is $\omega = \sqrt{\frac{k}{m}}$; hence $k = m\,\omega^2$. If the frequency is changed without affecting m then, automatically, k must change in the same ratio as ω^2 and ψ is unchanged; ω^2 can also be altered without affecting k by changing m in the inverse ratio but the product, $m\,\omega^2$, will then be unchanged and ψ remains constant. In fact, k cancels $m\,\omega^2$ and $\psi = 2\,\pi\,C_1\,C_2$—that is, it depends only on the hysteresis curve of the material (which determines C_2) and the design of the spring (which determines C_1). Carried still further, it is independent of the spring design because both the damping force (which absorbs energy) and the elastic force (which stores energy) are proportional to C_1 which cancels out in expressing the ratio of the absorbed to stored energy. In the last analysis the hysteresis damping capacity is a function of the hysteresis curve only.

While Eq. 17 indicates ψ to be independent of the amplitude, η, tests show that it increases slowly with amplitude and stress, which means that the damping force actually increases as some fractional power of η a little greater than 1.

(C) *Coulomb Friction Damping.*—The friction force is constant and does not depend upon the amplitude or frequency and the work it does in a cycle may be expressed as some constant, C_3, times η. The damping capacity, proportion of energy of vibration damped out per cycle, then is

$$\psi = \frac{C_3\,\eta}{m\,\omega^2\,\eta^2/2} = \frac{2\,C_3}{m\,\omega^2\,\eta} \qquad (19)$$

For such damping the logarithmic decrement decreases as the amplitude increases. The curve of the decay of amplitude, plotted against time is a straight line rather than the exponential curve in Eq. 12b.

Notwithstanding the general statement above, Mr. Bleich has shown that under certain conditions the movement of a frictional force may be proportional to the square of the movement of the oscillating mass so that its work varies as η^2 and it then has the character of hysteresis damping. However, this second type of friction damping is small (1k).

(D) *Structural Damping.*—The character of the structural damping of a complicated structure depends upon the relative proportions and character of its hysteresis and friction components. The damping capacity may increase or decrease with amplitude or be nearly constant. Some field tests on light suspension bridges have shown it increasing up to a certain amplitude and then decreasing (3e). This form of curve may be attributed to the gradual increase in sources of friction as the increasing stress (due to increasing amplitude) overcomes the static friction and causes motion to begin progressively at various contacting surfaces. This increase in sources of friction causes a progressive increase in the overall frictional force. When the amplitude increases further after all sources of friction are working, the damping capacity decreases and the curve approaches the hyperbolic form characteristic of simple friction damping. The possibility of this type of damping was anticipated by Mr. Bleich in his theoretical studies (1l).

(E) *Atmospheric Damping.*—The atmospheric damping forces arise from the relative movement of the air and the vibrating body and may be viscous or inertial. In the case of bridge structures the flow is essentially turbulent and the forces are mostly inertial—that is, the force varies as the square of the velocity as stated by Eq. 1. In still air the velocity is entirely due to the vibration and is equal to $\omega\,\eta \cos \omega\, t$. The force is then proportional to $\omega^2\,\eta^2$ and its work is proportional to $\omega^2\,\eta^3$ and the damping capacity may be stated,

$$\psi = \frac{C_4\,\omega^2\,\eta^3}{m\,\omega^2\,\eta^2/2} = \frac{2\,C_4\,\eta}{m} \qquad \text{.....................(20)}$$

which is independent of frequency and increases with amplitude. In Eq. 20, C_4 is an experimental constant.

In a wind stream the relative velocity is determined by both the wind and the motion of the body. The resulting forces and the work they perform in a cycle do not bear the simple relation to ω and η such as represented by Eqs. 14, 17, 19 and 20. In fact, at certain velocities their sign or phase may change with respect to the motion and they may develop resonance and tend to increase the amplitude—that is, they may excite motion. Under these circumstances their energy is a contribution to, rather than a dissipation of, the energy of vibration. Mathematically their effect can be treated simply as a negative damping whose effect on the vibration can be measured by a negative logarithmic decrement.

APPENDIX III.—BEHAVIOR OF EXISTING BRIDGES

1. BRONX–WHITESTONE

The data concerning movement of the bridge as indicated in Table I are taken from an unpublished "Report to the Triborough Bridge Authority on

Behavior of the Bronx-Whitestone Bridge under Wind Action and on Provisions Made to Stiffen the Bridge" by O. H. Ammann, dated July 23, 1945. This report includes a chart of daily measurements of bridge movement and of maximum wind velocities measured either at the bridge site or in lower Manhattan and describes the center cable ties, end frictional devices and diagonal tower stays which were installed to restrain the oscillation. Center ties and frictional devices were installed early, proved fairly effective and were progressively increased in size and effectiveness. Of stay ropes the report states:

> "While the stay ropes have had a considerable stiffening effect insofar as the ordinary moderate oscillations are concerned and in this respect confirm the conclusions derived from the model tests (dynamic tests in still air at Princeton University) it is evident that their effect has not been sufficient to prevent nor apparently reduce the exceptional oscillations of larger amplitude."

This observation is in agreement with the results of wind tunnel tests at the University of Washington (see Art. 3H).

The report indicates that the severest motions occurred most frequently during northwest winds (approximately 30° to 45° from the axis of the bridge) and that strong upward wind currents have been noticed outside of and through openings in the bridge floor. It states the early conclusion "that the motions were principally the result of longitudinal wind pressure acting from below on the pockets formed by the floor structure," and suggests also the explanation that the prevailing strong gusty winds come from the northwest. The severe oscillations occurred on days when the wind velocity was low or moderate but not high. The report was prepared prior to the widening of the roadway and the addition of the truss. Motion is reported to be negligible since this work was done.

2. Fykesund, Norway

The data concerning this bridge are taken from plans furnished by Mr. Selberg, and his letter of January 24, 1947, to Mr. Farquharson from which the following is quoted:

> "The Fykesund bridge has shown vertical oscillations with 1, 2, or 3 nodes and amplitudes about ±0.8 *m*. Positive reports of torsional oscillations are never received.
>
> "The Fykesund bridge lies in a very stormy place, and the wind direction is frequently varying, both vertically and horizontally. The oscillations have mainly occurred for wind directions in or out the fiord.
>
> "The wind velocity has never been measured; we had no occasion for it during the war. Since the erection of stays in 1945 the bridge has shown no oscillations, however, we have arranged for measuring eventual oscillations, and wind velocities."

The map shows the bridge about one and a half miles from the mouth of Fykesund with a fetch of about five miles across the main fiord for a normal wind from the southeast. The stays mentioned are attached to the deck at points approximately 100 ft and 145 ft from each tower and extend downward to the piers at angles of about 60° and 68° respectively to the vertical.

3. BEAUHARNOIS, QUEBEC, CANADA

Data concerning this bridge and its movements have been given by D. B. Armstrong, of the Dominion Bridge Company, Limited, in correspondence with G. S. Vincent, M. ASCE.

Inasmuch as this bridge represents a new addition to the record of modern bridge movements it is desirable to present here data concerning its characteristics as tabulated below:

Span, in feet	580
Sag, in feet	58
Horizontal length of unloaded backstays, in feet	178.75
Distance between centers of cables and girders, in feet	30.0
Roadway width, in feet	28
Sidewalk width (one walk along outside north girder), in feet	4
Weight, in pounds per foot per cable—	
Dead load	1715
Cable only	100
Depth of plate girders, back to back of angles, in feet	7.5
Average moment of inertia per girder (including a moderate allowance for the stiffness of the deck), in in.^{2}–ft^2	1000
Net area of one cable (thirty-seven $1\frac{1}{8}$-in. strands), in square inches.	27.71
Top of roadway 3.5 ft below top of girder	...
Deck, 3-in. I-beam Lok filled with concrete	...
Curbs, 9-in. concrete (sealed to girder web by $\frac{1}{4}$-in. plate)	...
Stringers—	
Roadway, seven lines 16-in. WF beams at 45 lb	...
Sidewalk, one 10-in. 15.3-lb channel	...

The center cable bands are connected to the stiffening girders by means of rigid diagonal struts, designed to prevent relative longitudinal motion between the cable and girders. The laterals are located in the plane of the bottom flanges of the floor beams and the floorgrid is, in turn, welded to the tops of the stringers and floor beams. This constitutes a closed section having the depth of the floor beam and providing effective torsional resistance.

Mr. Armstrong furnished a copy of a report on observations made by engineers of Beauharnois Light, Heat and Power, Consolidated and a print showing temporary stays installed in 1950 extending from the tower tops to points on the span 40 ft and 80 ft from the towers. He also stated:

> "The bridge runs East and West, close to the shore of Lake St. Louis which provides an uninterrupted sweep of 12 miles for wind from the Northeast. On the South side the power house, 120 feet high above lake level and over 2000 ft long, parallels the bridge at a distance of about 900 feet and shields it fairly well from critical South westerly winds.
>
> "When being designed the stiffness of the bridge was checked by both the Ammann and Steinman formulas and appeared to have twice the stiffness required. However, under a steady moderate diagonal wind it rises and falls with a constant frequency of 33 cycles per minute, with both cables in phase and no sign of a longitudinal wave action.
>
> "It has been suggested that the topography of the site, the unbalanced sidewalk to the North side and the elasticity of the single strand hangers may all have something to do with it.
>
> "Since the diagonal stays were installed, there have been no winds of sufficient velocity to test their effectiveness but a close watch is being kept

> on the bridge by the engineers of Beauharnois, Light, Heat & Power Company. It may be of interest to know that previously, without stays, the bridge remained motionless under normal steady winds of up to 50 mph and that oscillations only occurred under diagonal wind."

The tabulation of observed motions of the bridge indicates that only the first symmetric vertical mode has been observed (see Fig. 10a). Its observed frequency was thirty-three cycles per minute; the computed frequency is 32.8. The computed wave form indicates that the amplitude at the quarter point is about one-eighth of that at the center line. This probably accounts for the fact that there is only one observation of an amplitude at the quarter point and that is only ¼ in.

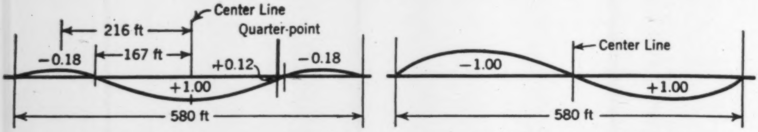

(*a*) FIRST SYMMETRIC VERTICAL

$\mu_2 = 4.22$ $\mu_0 = 6.51$
$\omega = 3.43$ $N = 32.8$ cpm

(*b*) FIRST ASYMMETRIC MODE

Center Free
$\mu_2 = 3.1416$ $\mu_0 = 4.17$
$\omega = 2.20$ $N = 21.0$ cpm

Center Tied
$\mu_2 = 3.01$ $\mu_0 = 3.92$
$\omega = 2.07$ $N = 19.8$ cpm

FIG. 10.—COMPUTED WAVE FORMS

The asymmetric mode appears to be inhibited by the center cable ties and the added damping which they cause by forcing a longitudinal sway of the suspended structure with accompanying end friction.

4. GOLDEN GATE

Data concerning the movements of the Golden Gate Bridge have been taken from the records of the cooperative research project of the Golden Gate Bridge and Highway District and the Bureau of Public Roads. A complete report on this project is to be published.

5. LIONS GATE

The following is quoted from a letter of June 3, 1943, addressed to Mr. Ammann by P. L. Pratley, M. ASCE:

> "On April 23rd a very severe gale of short duration was experienced in the Burrard Inlet across which the Lion's Gate Bridge is built. This gale is supposed to have been the heaviest in the neighborhood for some 15 years and is therefore the most severe the bridge has experienced. I was in Vancouver on inspection of the structure at the time and am therefore well acquainted with the situation. The wind blew very strongly, and in heavy gusts from the east at about 7 AM and reversed itself entirely to become a west wind of about equal intensity by about 7:30 AM and persisted in this direction and at about this strength for about 1 hour. The direction was maintained but the force was reduced for the next three hours and then again just before noon, a very heavy 'blow,' lasting for some 15 or 20 minutes, and almost equal in intensity with the heaviest wind experienced

in the early morning, completed the gale. I have no official figures of the wind velocity but would imagine it was between 50 and 60 miles an hour as I saw people literally blown off their feet on the main east and west streets of Vancouver and from information given me by the naval personnel no one could possibly walk out on the structure except by holding on to the fence which these officials were compelled to do. The gale was apparently quite unexpected and being of such short duration we had no opportunity of setting up instruments for scientific measurement.

"In the early morning I am assured that some vertical vibration was perceptible from the Signal bridge which is an observation and control structure built across the roadway at the center of the main span from which the marine and naval authorities command a perfect view up and down the narrows. The officer in charge told me that he could detect vertical movement by sighting one or more of the suspender sockets against the railway structures on the north shore. The sockets in question would be 300 or 400 feet from the Signal Bridge and the railway span referred to is about 1800 ft from the same Signal Bridge. His impression was that the structure was vibrating slightly with a maximum amplitude of about 3 inches, this occurring at the center of the main span so that the 1550 ft would be oscillating without nodes.

"I further learned that one of the maintenance staff was below the structure at the time and he also felt quite sure that he could detect a slight vertical vibration which appeared to arise with the heavy gusts and then to quickly dampen down. He ventured no figures as to the amplitude but agreed that the 3″ mentioned by the signal officer would be a perfectly safe maximum figure. He also suggested that this vibration arose 3 or 4 times during the gale and fell away to nothing as each heavy gust subsided.

"Both officials stated definitely that there was no indication of lateral movement and this is substantiated by my own observations just before noon when the final heavy gust occurred. I was then on the structure and from the South Main Tower I sighted, with the naked eye, the Signal Bridge cabins against the toll houses at the north end, the intercept being 775 feet from me to the Signal Bridge and about 4200 feet from the Signal Bridge to the toll house. For a period of several minutes I could detect no vibration and no restitutional movement.

"As to frequency, I of course have no reliable figures but the signal officer illustrated to me the approximate frequency by the movement of his hands and these indications would suggest something of the order of 12 or 15 cycles per minute. Also, at noon I could detect no vertical vibration whatsoever either by standing on the approach spans or by standing on the suspended span. At the same time I feel that there must have been some very minute vertical movement, and that its repercussions finally reached the bearings at the extreme south end of the south side suspended span because during my examination of these bearings before noon 'blow' had completely ceased I thought I could detect very small vertical movements of the steel sliding plates in the bronze guides as the grease seemed to be alternately sucked in and exuded. Such movements would be in the nature of a few thousandths of an inch only and in half an hour's time they had disappeared.

"I also immediately inspected the main sliding and rotating devices on the towers and found perfectly normal movements and nothing beyond normal movements had taken place at the shear bearings where wind reaction is transmitted to the tower. Furthermore, I examined the north backstay cables which, although unsupported for over 400 feet, had certainly not swayed sufficiently in any plane to touch the viaduct steel which they normally clear by about 1 inch.

> "Where these cables depart from the saddles on the North Cable Bents nothing more than the usual hair crack in the red lead paste, which acts as caulking from cable to saddle seat, could be detected. Up on the top of the towers, over the main saddles, there was absolutely no indication of such hair cracks having been caused and as those points have been consistently examined year after year I regard this as very sound evidence that the structure has sufficient rigidity in lateral as well as vertical planes.
>
> "On the whole, I am thus very well satisfied that the span stood up to this heavy wind condition without suffering in any particular and without experiencing any noticeable or abnormal movements objectionable or unobjectionable."

6. Peace River

The following is quoted from a letter from Raymond Archibald, M. ASCE, who was in charge of the design and construction of this bridge and describes his observations during opening ceremonies in July, 1943:

> "The Peace River Bridge was dedicated and opened to traffic in July 1943. I was seated in the stand located at the center of the main span and a strong steady wind was blowing from an upstream direction normal to the bridge. It is my estimate that this wind reached a velocity of 40 or 50 miles per hour at times and held this high velocity for periods from 3 to 5 minutes in length. When the wind was steady and of high velocity, the bridge definitely moved. My observations were made by sighting the positions of the truss with respect to the horizon. This movement reached proportions which gave me a slight sensation of sea-sickness. I believe it was primarily a torsional motion."

Targets and an anemometer were placed on this bridge and a transit was set up to observe its motion in the wind over a period of two weeks in July, 1947. During this period the wind velocity generally ranged up to about twenty-five miles an hour, rarely reaching the latter figure, and the observed double amplitude never exceeded one inch. These smaller motions appeared to be essentially vertical and had a period of about 3.5 seconds. (The computed period for the first symmetric vertical mode is 3.8 seconds; the observed period being shorter than this suggests that the motion was coupled, with the frequency shifted somewhat toward that of the torsional mode, that is toward a shorter period.)

Joe Trca, living near the Peace River Bridge, has described his observations during a windstorm late in September, 1947, during which velocities of 70 mi per hr were reported by radio. He estimated the maximum at 50 mi per hr during his observations. He found difficulty in walking due to the motion of the deck and discomfort and uneasiness when he sat on the curb to note the torsional motion.

7. Liard River

Transit and anemometer readings were made on this bridge for two weeks in August, 1947, during which time the wind reached a velocity of 35 mi per hr. The maximum double amplitude (2 in.) was observed in a wind of 20 mi per hr to 25 mi per hr. It was specifically noted that the higher winds were turbulent and gusty and motion only built up after the gust died down to a steady wind of about 20 mi per hr. Frequently it was observed by noting the movements of the trees that a high wind was limited to a small area. Such winds had little effect upon the bridge.

This bridge is subject to much greater movements at other seasons when higher winds are more frequent. The following is quoted from the report (unpublished) on the observations made in 1947:

> "Greater wind and motion have been observed by others at Liard River Bridge also. Again, no attempt has been made to give the amplitude, but Lieutenant Baldock (Bridge Engineer, Northwest Highway System) reported he had been on this bridge when the motion of individual longitudinal planking of the deck could be observed. This could not have happened except with much greater amplitude than noted during the present series of observations, and it appears quite likely that a considerable torsional motion must have been involved."

AMERICAN SOCIETY OF CIVIL ENGINEERS
Founded November 5, 1852
TRANSACTIONS

Paper No. 2762

ASEISMIC DESIGN OF FIRMLY FOUNDED ELASTIC STRUCTURES

By Lawrence E. Goodman,[1] A. M. ASCE, Emilio Rosenblueth,[2] J. M. ASCE, and Nathan M. Newmark,[3] M. ASCE

Synopsis

A rational basis for the design of earthquake-resistant structures is developed. Structures designed on this basis will have uniform strength in the sense that each element will have an equal probability of successfully withstanding strong-motion earthquakes of the general type recorded by the Coast and Geodetic Survey, United States Department of Commerce, on the North American continent. The theory is based on inferences drawn from accelerograms of strong-motion earthquakes and on the theory of probability. Although the general method of approach is capable of wider extension, the conclusions of the present study are limited to elastic structures founded on ground having a stiffness comparable to that of the sites at which reliable earthquake accelerograms have been recorded.

Introduction

There is an important branch of engineering seismology concerned with the analysis of structures subjected to earth tremors. In recent years impetus has been given to this work by the availability of reliable accelerograms of fourteen strong-motion earthquakes recorded by the Coast and Geodetic Survey, United States Department of Commerce (USCGS). The complexity of the recorded ground motions, however, has been a handicap to analysis and (even more) to design. Details of future ground motions can hardly be anticipated by the designer. Progress in analysis has depended heavily on the construction—by means of the torsion pendulum (1)[4] or digital and electronic-analog computing machinery (2)—of "response spectra,"

Note.—Published, essentially as printed here, in November, 1953, as *Proceedings-Separate No. 349*. Positions and titles given are those in effect when the paper was received for publication.

[1] Prof., Mechanics and Materials, Univ. of Minnesota, Minneapolis, Minn.

[2] Cons. Engr., Mexico, D. F. Mexico.

[3] Research Prof. of Structural Eng., Univ. of Illinois, Urbana, Ill.

[4] Numbers in parentheses—thus: (1)—refer to corresponding numbers in the Bibliography (see Appendix).

giving the maximum response (stress, velocity, or displacement) of a single-degree-of-freedom structure as a function of its natural period. Somewhat idealized spectrum diagrams have been proposed as a basis for structural design (3) (4).

An entirely different approach to the design problem is suggested by the discovery made by G. W. Housner, A.M. ASCE (5), that, so far as their effects on structures are concerned, destructive earthquakes may be regarded as successions of perfectly random motions. The writers refer to local effects at surface sites near the epicenter and not to disturbances recorded seismographically after having been propagated over long distances. The latter, of course, have been studied extensively. Local effects, on the other hand, determine whether or not a particular structure will fail. They are influenced in a complex way by local geological and topographical conditions. The discovery that perfectly random pulse sequences produce spectra that do not differ significantly from those of recorded accelerograms opens the way to a systematic analysis of the probable effects of such motions on structures.

The chief advantage of the approach advanced by the writers is that it provides a means of establishing a basis for design in which every part of a structure will have an equal probability of successfully withstanding ground motion. What that probability ought to be—that is, the intensity of earthquake for which a structure should be designed—is a problem the answer to which will always depend on engineering judgment based on: (*a*) Accumulated experience of seismic destructiveness in various regions of the world, (*b*) the importance of structural integrity to public safety, and (*c*) economic considerations. In this respect, aseismic design resembles the design of dams to resist flood contingencies. The writers' approach based on the theory of probability also makes possible the prediction, in a statistical sense, of the relative magnitudes of earthquake effects in different existing structures and in different parts of any one structure.

Consideration has been limited in the present work to structures whose behavior can be idealized as elastic or to structures which are subject to viscous damping. The conclusions presented are applicable only to structures that rest on formations having a considerable stiffness, comparable to that of the ground where reliable accelerograms have been recorded. Although the method of analysis has been extended to structures resting on soft formations, the somewhat different response of such structures and the additional assumptions that are required indicate the desirability of a separate treatment.

STRUCTURAL RESPONSES

For convenience of reference, certain relationships used in connection with the motion of structures are stated in this section. Developments of the theorems have been published in textbooks dealing with the theory of structural vibrations (6) (7).

Fig. 1 is a schematic representation of any linearly elastic structure having a single degree of freedom. If the system is started from rest at time $t = 0$ and the support undergoes a motion $x_g(t)$, the displacement, x, of the mass relative to the support is, at time t—

$$x = x_s - x_g = -\frac{1}{p}\int_0^t \ddot{x}_g(\tau)\sin p(t-\tau)\,d\tau \qquad (1a)$$

in which superscript dots indicate differentiations with respect to t; x_s equals absolute displacement of the mass; p equals $\sqrt{k/m}$, the natural (circular) frequency of the system; k equals the static force required to produce unit relative displacement of the mass and its support; and m equals the mass of the system. The natural period of the system is

$$T = \frac{2\pi}{p} \qquad (1b)$$

The dimensional units in which these quantities are measured must, of course, be mutually consistent. In the English system of units, for example, x_s, x_g, and x would be measured in inches; p, in radians per second; k, in pounds per inch; m, in pound-seconds^2 per inch; $\ddot{x}_g$, in inches per second per second; and t and T, in seconds. The dummy variable, τ, disappears on integration.

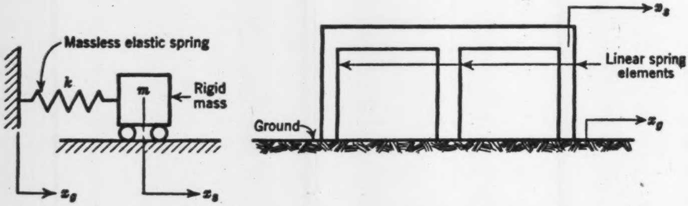

(a) Schematic representation of simple structure

(b) Frame idealizable as a simple structure

FIG. 1.—STRUCTURE HAVING A SINGLE DEGREE OF FREEDOM

Eq. 1*a* can be used for a study of actual structures if the effects of damping, ground coupling, and higher modes of vibration can be neglected. Under these circumstances the support in Fig. 1 represents the foundation of the structure; the spring represents a group of flexible elements; and the concentrated mass stands for the mass of the structure and of the loads that it supports.

Ideal elastic systems having a single degree of freedom and no energy losses are referred to as simple structures throughout this analysis.

Engineers agree that in general several modes of vibration of structures are transiently excited by earthquakes (8). To take account of additional degrees of freedom, the natural modes can be treated separately as individual simple structures. Total responses—either the stresses or deformations at any point—are, at any given time, the algebraic sums of those responses associated with the several natural modes considered. For example, the displacement x relative to the ground at any point of a structure can be computed by means of the expression:

$$x = \sum_{i=1}^{N} -\frac{a_i}{p_i}\int_0^t \ddot{x}_g(\tau)\sin p_i(t-\tau)\,d\tau \qquad (2)$$

in which N equals the number of degrees of freedom of the structure, which in turn equals the number of modes considered. Also, p_i equals the natural (circular) frequency of the ith mode; a_i is a dimensionless number, the excitation coefficient of the mode; and the symbol $\sum_{i=1}^{N}$ indicates that the sum of terms of this kind for all the modes $i = 1, 2, \ldots N$ is to be taken. This equation can be written in the form:

$$x = \int_0^t \ddot{x}_g(\tau)\,\phi(t-\tau)\,d\tau \quad \text{(3a)}$$

in which ϕ is a convenient shorthand symbol for the sum of several sine functions:

$$\phi(t-\tau) = \sum_{i=1}^{N} -\frac{a_i}{p_i}\sin p_i(t-\tau)\,d\tau \quad \text{(3b)}$$

The first part of the integrand of Eq. 3a, $\ddot{x}_g$, involves only the nature of the ground motion and is independent of the structure, whereas the second part, $\phi(t-\tau)$, depends only on the properties of the structure and not on the particulars of the earthquake.

The function ϕ may or may not be periodic. In some instances—for example, the shear deformations of tall, uniform structures—the frequencies of all higher modes are integral multiples of the fundamental frequency. In this case ϕ is periodic and its period is the same as the fundamental period of the structure.

When $\ddot{x}_g(t) = 0$ for all values of t greater than, say, t', Eq. 3a can be written as

$$x(t) = \int_0^{t'} \ddot{x}_g(\tau)\,\phi(t-\tau)\,d\tau,\ t \geq t' \quad \text{(3c)}$$

whereupon, integrating by parts and recalling that the structure is started from rest, one finds, for $t \geq t'$:

$$x(t) = \dot{x}_g(t')\,\phi(t-t') - \int_0^{t'} \dot{x}_g(\tau)\,\frac{d\phi}{d\tau}\,d\tau \quad \text{(3d)}$$

Setting $\dot{x}_g(t')$ equal to 1 and letting t' approach zero, one can see that the displacement response, $x(t)$, to an instantaneous unit increment in ground velocity occurring at $t = 0$ is numerically identical with $\phi(t)$. Sudden changes of ground velocity will be referred to as acceleration pulses.

In addition to structural deformations, stresses and bending moments can be determined from the usual relationships between displacements and stresses in terms of linear combinations of displacements measured relative to the ground. Expressions similar to Eq. 3a can be established for any of these types of response or for their first derivatives with respect to time. The functions ϕ that appear in these expressions will, of course, differ for different kinds of response.

Similar relationships can be derived for systems subject to viscous damping. For example, the function ϕ governing relative displacement in a structure having a single degree of freedom is, under these conditions,

$$\phi(t - \tau) = -\frac{1}{p'}\, e^{-c(t-\tau)} \sin p'(t - \tau) \qquad (3e)$$

in which

$$p' = \sqrt{\frac{k}{m - c^2}} \qquad (3f)$$

and the damping force is $2\,m\,c\,\dot{x}$. Expressions of the form of Eq. 3*a* also hold for elastic structures coupled to the ground, provided the ground can be treated as an elastic body (which may have internal viscous damping).

In all cases, the amount that any individual acceleration pulse, $\ddot{x}_g\,dt$, contributes to the relative displacement $x(t)$, is independent of the remainder of the ground motion. For a ground motion consisting of a sequence of such pulses, $x(t)$ can therefore be obtained by adding the products of all the pulses multiplied by a function ϕ whose value is independent of the ground motion. The conclusion follows from Eq. 3*a*; it is true also regarding stresses, bending moments, and shears in the general types of structure under consideration.

RESPONSE OF STRUCTURES TO IDEALLY RANDOM GROUND MOTIONS

Prediction of Response at Any Time.—As a first approximation to true earthquakes the writers consider motions consisting of random arrays of concentrated acceleration pulses. There are a number of aspects of the pulses that may be made random. Many of these different ways of specifying random pulses lead to approximately the same final results and at least one of them has been studied previously (5*a*). Because the final velocity of the ground after an earthquake is zero, it is reasonable to idealize earthquake motions as sets of pulses selected subject to the condition that their sum be zero. The pulses are assumed to be distributed in time in a random order, either at small, uniformly spaced intervals, or at randomly spaced instants of time. In either case, the number of pulses is large, and the magnitude of the largest pulse is small in comparison with the sum of the absolute magnitudes of all the pulses. This appears to be true for all reliable strong-motion accelerograms of destructive earthquakes. Therefore, the probability theory of large numbers may be applied to structures affected by them without introducing excessive errors.

Displacements relative to the ground are given by Eq. 3*a*. Therefore, when the ground motion consists of a series of pulses of magnitude—

$$u_i = \int_{t_i-\epsilon}^{t_i+\epsilon} \ddot{x}_g\, d\tau \qquad (4a)$$

in which $2\,\epsilon$ is the duration of the pulse; the relative displacement at time t is

$$x = \sum_i \phi(t - t_i)\, u_i \qquad (4b)$$

In Eq. 4*b*, t_i denotes the instant at which the pulse u_i occurs. The theorem follows from Eq. 3*d* and the linear relationship between static forces and displacements assumed to be valid for the class of structures under study.

All individual terms of the type $\phi(t - t_i)\, u_i$ are small in comparison with $\sum_i |\phi(t - t_i)\, u_i|$. If the fundamental period of the structure is small compared with t, every such element has nearly random sign. The elements $\phi(t - t_i)\, u_i$ can be likened to the random errors that arise in a series of independent measurements. The response x would correspond to the sum of a large number of such errors. (6)

In the foregoing paragraph, and throughout this paper, vertical lines in a mathematical expression indicate that the quantity enclosed is to be taken as positive, only its magnitude being of interest—that is, $|-3| = 3$.

According to the theory of probability (9) (10), the probability distribution of a quantity x determined by a series of random events is given by

$$P(x_1, x_2) = \int_{x_1}^{x_2} \frac{e^{-n}}{\sigma \sqrt{2\pi}}\, dx \ldots\ldots\ldots\ldots (5a)$$

in which $P(x_1, x_2)$ is the probability that x lies between the values x_1 and x_2, n is equal to $x^2/2\,\sigma^2$, and σ is the standard deviation of values of x from the mean. In this case, the mean is zero, motions in either direction being equally probable. The quantity σ is a measure of the dispersion or variability of the quantity x from its mean value.

From a structural viewpoint, however, one is more interested in the average value of $|x|$ resulting from a large number of determinations of x. This quantity is designated as the "expected" value of $|x|$, $E|x|$. In a similar way one may also think of the expected value of x^2, $E(x^2)$. This last is related to the standard deviations, σ:

$$\sigma^2 = E(x^2) \ldots\ldots\ldots\ldots (5b)$$

It can also be shown (9*a*) (10*a*) that

$$E(x) = \int_{-\infty}^{\infty} \frac{x\, e^{-n}}{\sigma \sqrt{2\pi}}\, dx \ldots\ldots\ldots\ldots (5c)$$

Because $-E(-x) = E(+x)$,

$$E|x| = 2\,E(+x) = \sqrt{\frac{2}{\pi\,\sigma^2}} \int_0^{\infty} x\, e^{-n}\, dx = \sigma \sqrt{\frac{2}{\pi}} \ldots\ldots (5d)$$

the integral being equal to σ^2. From Eqs. 5*b* and 5*d*,

$$E|x| = \sqrt{\frac{2\,E(x^2)}{\pi}} \ldots\ldots\ldots\ldots (6)$$

A quantity that is the product of independent variables can be shown to have an expected value equal to the product of the expected values of the individual variables (10*b*). Because the acceleration pulses that constitute the motions under examination are independent of ϕ, Eqs. 3*a* and 4*a* imply that

$$E(x^2) = E(\sum_i u^2_i)\, E(\phi^2) \ldots\ldots\ldots\ldots \tag{7a}$$

The number of pulses that have occurred at time t is independent of u_i. Denoting this number by N_t, a further separation of variables is possible, yielding

$$E(x^2) = E(N_t)\, E(u^2)\, E(\phi^2) \ldots\ldots\ldots\ldots \tag{7b}$$

If there are a great many of these pulses, or if they occur at randomly spaced instants, one can write

$$E(\phi^2) = \frac{1}{t}\int_0^t [\phi(t-\tau)]^2\, d\tau \ldots\ldots\ldots\ldots \tag{8}$$

It follows from Eqs. 6 and 7*a* that

$$E|x| = \left\{\frac{2\, E(N_t)\, E(u^2)}{\pi\, t}\int_0^t [\phi(t-\tau)]^2\, d\tau\right\}^{\frac{1}{2}} \ldots\ldots\ldots \tag{9a}$$

This equation expresses the expected magnitude of the displacement as a function of time.

The quantity $2\, E(N_t)\, E(u^2)/\pi$ does not depend on the structure but on the nature of the earthquake motion. This quantity may be denoted by the symbol K^2. Eq. 9*a* then becomes

$$E|x| = \left\{\frac{K^2}{t}\int_0^t [\phi(t-\tau)]^2\, d\tau\right\}^{\frac{1}{2}} \ldots\ldots\ldots \tag{9b}$$

The term K^2/t in Eq. 9*b* may be seen to be directly related to the average number of pulses occurring in time t. Because the pulses u_i occur at closely spaced instants, this average number is relatively constant and independent of time t. Therefore, the factor K^2/t in Eq. 9*b* depends solely on the magnitudes of the pulses that comprise the motion. It can be evaluated, for example, by computing the responses of a structure subjected to numerous motions consisting of a set of acceleration pulses rearranged in different orders and then computing the average of the (slightly) different responses.

In particular, if the structure is such that the function ϕ is periodic and its period, T, is small compared with the times t in which one is interested, Eq. 9*b* can be expressed in the form:

$$E|x| = \left\{\frac{K^2}{T}\int_0^T [\phi(\tau)]^2\, d\tau\right\}^{\frac{1}{2}} \ldots\ldots\ldots \tag{9c}$$

Knowledge of the expected magnitude of displacement is useful in establishing a basis for a uniformly safe design. Knowledge of the deviation from the "expected" value which may be anticipated is also useful in this connection as well as for comparing the effects of random motions with those of true strong-motion earthquakes. The dispersion (squared standard deviation) of $|x|$ can be obtained by means of the relationship (10c):

$$(\sigma|x|)^2 = E(x^2) - (E|x|)^2 \qquad (10)$$

From Eq. 6 it follows that

$$(\sigma|x|)^2 = \left(\frac{\pi}{2} - 1\right)(E|x|)^2 = 0.571\ (E|x|)^2 \qquad (11)$$

Thus far in this paper the structural response—primarily the expected magnitude of the displacement—has been considered as a function of time; that is, relationships such as Eqs. 7, 8, and 9 refer to the response at a specified instant. These quantities are of no interest in themselves for design purposes. What is wanted is the probable maximum numerical value reached by these responses.

MAXIMUM RESPONSE

At present (1954) no completely general solution is available for computing the value of maximum response as a function of ϕ. Approximate conclusions are developed herein for ϕ-functions that characterize two classes of structures. Qualitative conclusions are reached for other cases.

If ϕ is periodic, the maximum $|x|$ in response to a specified ground motion can be selected in two operations. The first consists of dividing the time interval between the first and the last acceleration pulse into portions of duration T, the period of ϕ—at most, only the last portion need have a duration different from T—and then finding the response at all division points and selecting the maximum numerical value. This maximum may be denoted by $|x_T|_{\max}$. The ratio, $E|x_T|_{\max}/E|x(s)|$, in which $x(s)$ is the response that occurs at the end of the ground motion of duration s when $t = t_s$, is designated by the symbol C_1:

$$C_1 = \frac{E|x_T|_{\max}}{E|x(s)|} \qquad (12a)$$

The second operation consists of introducing a phase shift, θ, smaller than T and then selecting that value of θ which maximizes $|x_T|_{\max}$. The largest value of $|x_T|_{\max}$ found in this operation is evidently the absolute maximum, $|x|_{\max}$, of response to the motion. For simplicity, $|x|_{\max}$ will be designated by the symbol X. Symbols C_2 and C are further defined by

$$C_2 = \frac{E(X)}{E|x_T|_{\max}} \qquad (12b)$$

and

$$C = C_1\,C_2 = \frac{E(X)}{E|x(s)|} \qquad (12c)$$

As noted in the "Introduction," a graph giving values of X as ordinates and values of the period T as abscissas can be designated a "displacement spectrum." Instead of plotting values of $|x|_{\max}$ as ordinates, one can plot $|\dot{x}|_{\max}$. The resulting graph is known as a "velocity spectrum." It can be shown that the ordinates in a graph of $p\,X\,T$ have the same probability distributions as those in a velocity spectrum. This relationship is useful in studying the characteristics of destructive earthquakes because the important characteristics of the graph are more noticeable in velocity spectra than in displacement spectra.

When $|\phi|$ has a period $T/2$, or is symmetric at intervals of $T/2$, the first operation may consist of dividing the earthquake duration s into intervals of duration $T/2$ instead of T. Under these circumstances, the phase shift θ introduced in the second step need only vary between zero and $T/2$. This is true for the sinusoidal and square-wave functions ϕ considered subsequently.

The quantity C_1 can be determined by reference to the theory of probability. It is analogous to the probable maximum amount held by a player in a game of chance at any one of a number of instants during the game, divided by his probable final holdings. Proceeding along the lines suggested by the theory of probability, it is possible to show that, if structural periods are small compared with the duration of the temblor ($T \ll s$), C_1 is nearly constant, independent of ϕ, and equal to $\pi/2$. The dispersion of $|x_T|_{\max}$ is found to be $0.17\ (E|x_T|_{\max})^2$.

The value of C_2 can be computed for sinusoidal functions ϕ by means of a simple trigonometric transformation. Eq. 1*a* can take the form (11) (5*b*):

$$x = \frac{1}{p}\left\{\left[\int_0^t \ddot{x}_g(\tau)\sin p\,\tau\,d\tau\right]^2 + \left[\int_0^t \ddot{x}_g(\tau)\cos p\,\tau\,d\tau\right]^2\right\}^{\frac{1}{2}} \sin\,(p\,t - \alpha) \quad \text{..(13a)}$$

in which α is a phase angle. If $\ddot{x}_g$ is assumed to be zero in the interval from t to $t + T/2$, the maximum x-value during this interval is obtained when $\sin(p\,t - \alpha) = 1$. If the period of the structure is small compared with the duration of the temblor ($T \ll s$), neglecting the acceleration pulses falling within any one interval of duration $T/2$ does not cause appreciable error. Confining attention to a single interval, it can be seen that C_2 is very nearly equal to the ratio between the expected value of $|x|$ computed from Eq. 13*b*:

$$x = \frac{1}{p}\left\{\left[\int_0^t \ddot{x}_g(\tau)\sin p\,\tau\,d\tau\right]^2 + \left[\int_0^t \ddot{x}_g(\tau)\cos p\,\tau\,d\tau\right]^2\right\}^{\frac{1}{2}} \quad \text{....(13b)}$$

and the value computed from Eq. 9*b*. From Eq. 6,

$$E|x| = \sqrt{\frac{2\,E(x^2)}{\pi}} \quad \text{.....................(14a)}$$

and from Eq. 13*b*,

$$E|x| = \frac{1}{p}\left[\frac{K^2}{T}\left(\int_0^T \sin^2 p\,\tau\,d\tau + \int_0^T \cos^2 p\,\tau\,d\tau\right)\right]^{\frac{1}{2}} = \frac{K}{p} \quad \text{....(14b)}$$

The denominator as obtained from Eq. 9*c* is

$$E|x| = \frac{1}{p}\left(\frac{K^2}{T}\int_0^T \sin^2 p\,\tau\,d\tau\right)^{\frac{1}{2}} = \frac{K}{p\sqrt{2}} \qquad (14c)$$

Taking the ratio of the expressions from Eqs. 14*b* and 14*c*,

$$C_2 = \frac{K/p}{K/p\,\sqrt{2}} = \sqrt{2} \qquad (15a)$$

whence

$$C = \frac{\pi}{\sqrt{2}} = 2.22 \qquad (15b)$$

In connection with tall buildings of relatively uniform cross section, ϕ-functions having a square-wave shape are of special interest (Fig. 2(*a*)). For these ϕ-functions, a somewhat greater value of C_2 is found than in the case of sinusoidal ϕ-functions. In this case, $C_1 = C_2 = \pi/2$ and $C = \pi^2/4 = 2.47$.

Another ϕ-function that occurs in the analysis of tall buildings is shown in Fig. 2(*b*). It coincides with a square wave over some range of its period—say, t_1, and is equal to zero elsewhere. Although in this case C_1 is still approximately equal to $\pi/2$—C_2 may be greater than in the case of the functions previously considered. The difference in C_2-values is caused by the fact that, ϕ being zero part of the time, certain pulses affect the x_T-values and others do not. The phase shift θ, which is greater than t_1, may introduce sets of pulses which had not previously entered the computation. The sharper the function ϕ, the more pronounced will be the effect of the phase-shift operation. In other words, C_2 (and, hence, C) increases as the interval of time during which ϕ differs from zero decreases.

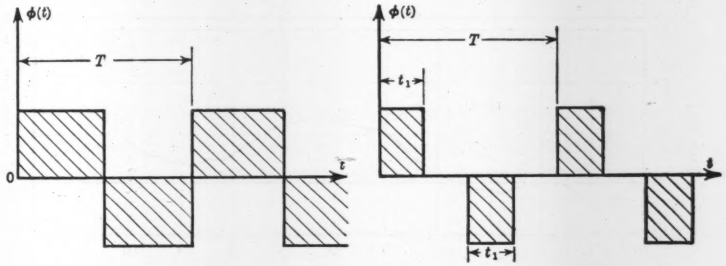

(*a*) At base of structure

(*b*) Intermediate height

FIG. 2.—STRUCTURAL-RESPONSE FUNCTIONS FOR TALL UNIFORM BUILDINGS

The estimates of C and, hence, of the ratio of the probable absolute maximum displacement or stress to the probable final displacement or stress—derived from theoretical considerations based on the theory of probability—have been confirmed by empirical studies. For this purpose, several motions having pulses of random sign were created. The results of these studies were in good agreement with the conclusions previously presented herein. However, in order to interpret the results of this and similar investigations it is necessary to take account of the limited number of acceleration pulses used. It is generally impractical to investigate fictitious motions having a large number of acceleration pulses; the computational labor is great even for a structure of only moderate complexity. Values of C_1, C_2, and therefore C determined in this way are and ought to be slightly smaller than the predicted values previously given, which are based on a theory in which a large number of closely spaced pulses is presumed. Actually, within a considerable range of moderately large numbers of pulses, C_1 was found to be approximately 1.41 for both sine and square-wave ϕ-functions as compared with the theoretical estimate of 1.57 in both these cases. The ratio C_2 was also found to be approximately 1.41 as compared with theoretical estimates of $\sqrt{2}$ in the case of sine-wave functions and a slightly greater value in the case of square-wave functions. The value of C found in this way was 2.00 for both cases as compared with estimates of 2.22 and a somewhat greater value. The check on the estimates of maximum response so obtained appears to be satisfactory. It should be remembered that estimates of the probable maximum response are being obtained and that these will not agree precisely with calculations based on a particular motion or motions.

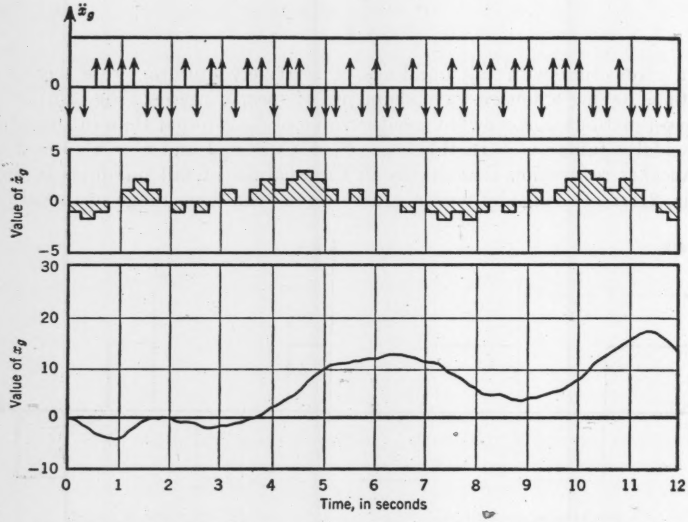

FIG. 3.—MOTION GENERATED BY A 48-UNIT ACCELERATION PULSE OF RANDOM SIGN

The dispersion of $\dot{X}$ in the case of a sinusoidal function is of some interest in comparisons of structural effects of true earthquakes with those predicted by possible "substitute" motions, including the class examined herein. Because a complete analytical solution was not available, the dispersion was investigated by computing the response of a structure having a sinusoidal ϕ-function ($\phi = - p^{-1} \sin p\, t$) to motions of the type shown in Fig. 3. This motion consists of 48 unit pulses, equally spaced at intervals of 0.25 sec, and having random sign. Responses to this motion were computed by means of a graphical procedure (12). The maximum numerical values of these responses

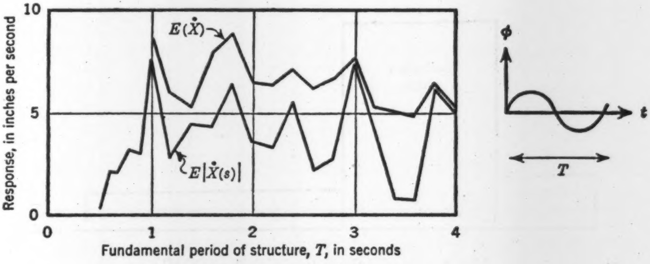

Fig. 4.—Velocity Spectrum of the Motion of Fig. 3

($p\,X$-spectrum and $\dot{X}$-spectrum) are shown in Fig. 4. The dispersion was found to be $[\sigma\,(p^2\,X^2)]^2 = 0.043\,p^2\,\bar{X}^2$ in which $\bar{X}$ is the average value of X for all periods investigated.

Response of Structures to True Earthquakes

The random motions treated in the foregoing sections differ from true earthquakes in several respects. The three principal differences are considered herein.

1. In reality, acceleration pulses cannot be instantaneous. This would imply accelerations of infinite magnitude lasting for infinitesimal intervals of time. Actually, ground accelerations are finite as are also the durations of seismic waves. A method of correcting the computed expected spectrum ordinates to account for this effect is presented under the heading, "Correction for Finite-Wave Duration." The correction, in general, is not large.

2. The various kinds of seismic waves have different velocities. Because of this situation there are three distinct phases or segments in recorded accelerograms. The first or "primary" phase contains the waves of shortest period. The secondary phase includes the waves having the largest average amplitude. Finally, the tertiary or standing-wave phase includes the ground motions having the longest period and smallest average amplitude of seismic waves. As an approximation to the variation of seismic intensity with time, it is reasonable to assume a sequence of three regimes, each having uniform intensity (Fig. 5).

A quantity that is the sum of variables having a Gaussian probability distribution with respect to time will itself have a Gaussian distribution with respect to time. Conclusions previously drawn herein referring to responses at specified instants have been inferred from the Gaussian distribution of these responses. Because the contribution of any one phase to the total structural response has this distribution, these conclusions are not affected by the existence of distinct phases.

3. The accelerograms of strong-motion earthquakes published by the USCGS indicate that in destructive earthquakes the ground acceleration oscillates rapidly from positive values to negative values. If ground motions were truly random, one might expect intervals of single-signed pulses. The theory of perfectly random motion is therefore not completely justified even within each phase of an earthquake. The importance of this and other departures from perfect randomness as they affect structural responses can be assessed by comparing the predicted structural responses with those calculated in actual earthquakes.

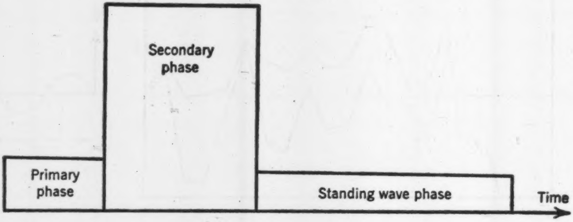

FIG. 5.—IDEALIZATION OF SEISMIC INTENSITY

The ten velocity spectra studied by Mr. Housner (5c) have been selected for comparison with the spectra predicted by the foregoing random-motion theory. According to Eq. 14b, for simple structures,

$$E(X) = E|x(s)|C_1 C_2 = \frac{C_1 C_2}{p} \frac{K}{\sqrt{2}} \ldots\ldots\ldots\ldots\ldots (16)$$

It follows that $p\,E(X)$ and consequently $E(\dot{X})$ ought not to show consistent variation with T, at least so long as T/s is small. This is indeed the case for the spectra of actual earthquakes. Furthermore, if the ten spectra computed by Mr. Housner from actual earthquake accelerograms are averaged, the mean is very nearly a horizontal line within the range of structural periods for which the spectra have been obtained (approximately 0.2 sec to 3.0 sec). This average should exhibit, approximately, the characteristics of the expected or probable spectrum ordinates. The agreement between spectra of actual earthquakes and "expected" spectra generated by random motions is highly satisfactory.

On the other hand, the dispersions in velocity spectrums of actual earthquakes have been found to be approximately 0.125 $p^2\,\bar{X}^2$, compared with a value of 0.043 $p^2\,\bar{X}^2$ for purely random motions, as discussed previously. In Fig. 6 is shown the way in which the relative dispersion $[\sigma\ (p^2\,X^2)]^2/E(p^2\,X^2)$ varies with the sharpness of the variation in X, in ϕ, or in the product $C_1\,C_2$. The comparison between responses to actual recorded earthquakes and to random-acceleration pulses has indicated a good agreement in expected responses but a discrepancy in expected deviations from the average. From this comparison it seems justified to conclude that the expected responses at specified instants are practically unaffected by the lack of perfect randomness in actual earthquakes; this lack does have an influence on the ratio C, tending to reduce it. Any increase in C is attributable to the possibility of selecting between independent sets of pulses; therefore, it may be concluded that C is actually more nearly a constant for true earthquakes than it is if the pulses have perfect randomness.

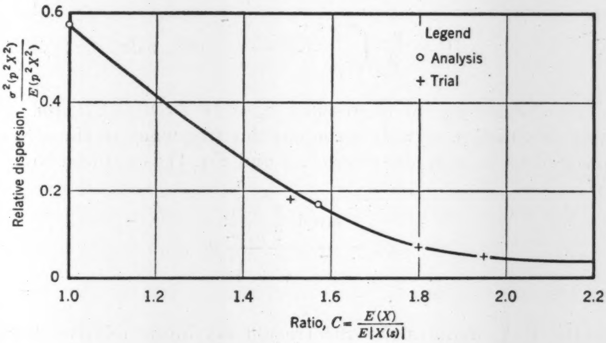

FIG. 6.—DEPENDENCE OF DISPERSION ON THE RATIO OF THE EXPECTED MAXIMUM RESPONSE TO THE EXPECTED FINAL RESPONSE

CORRECTION FOR FINITE-WAVE DURATION

The velocity spectra of true earthquakes computed by Mr. Housner (*5c*) permit an estimate of the effect that the finite duration of seismic waves has on structural responses. From what has been stated about the agreement between these computations and the spectra predicted by a random-motion theory using infinitely sharp pulses, it may be concluded that, in the case of simple structures, the effect is negligible—at least for all structures having natural periods greater than 0.2 sec. For natural periods less than this, the available information is insufficient to permit definite conclusions. Such small fundamental periods, however, are not of much structural interest. In the case of structures that are not simple there is some value in correcting for the effect of finite duration of seismic waves.

It has been suggested (*5d*) (*5e*) that, as an approximation to true earthquakes, concentrated pulses be replaced by half sine waves. The general appearance of accelerograms discloses important deviations from sinusoidal shape. For this reason other wave shapes, such as square and triangular, have been investigated. In this way it has been possible to assess the importance of the wave shape in addition to the duration.

The effect of changing concentrated pulses into finite pulses can be taken into account by replacing the function ϕ with a "corrected" function ϕ_c. The latter must be such that the effects of a concentrated pulse on a structure characterized by the function ϕ_c are the same as the effects of a finite pulse on the structure characterized by ϕ. The area under the acceleration-time graph for a finite pulse must, of course, be equal to the magnitude of the instantaneous pulse.

In accordance with the foregoing specification, the corrected function for half sine waves of duration t_o is

$$\phi_c(t) = \frac{p_o}{2} \int_{-t_o/2}^{+t_o/2} \phi(t - \tau) \cos p_o \tau \, d\tau \ldots\ldots\ldots\ldots (17a)$$

in which t_o is defined by the expression: $\ddot{x}_g = (\pi/2\, t_o) \cos \pi/t_o$ for $-t_o/2 < t < t_o/2$; and in which $p_o = \pi/t_o$ is the circular frequency of the seismic wave. For simple structures, ϕ is also sinusoidal and Eq. 17 is reduced to

$$\phi_c = \frac{\cos\left(\frac{\pi}{2}\frac{p}{p_o}\right)}{1 - \left(\frac{p}{p_o}\right)^2} \phi \ldots\ldots\ldots\ldots (17b)$$

Consequently, if X_o denotes the uncorrected maximum relative displacement of a simple structure,

$$\frac{E(X)}{E(X_o)} = \left| \frac{\cos\left(\frac{\pi}{2}\frac{p}{p_o}\right)}{1 - \left(\frac{p}{p_o}\right)^2} \right| \ldots\ldots\ldots\ldots (18a)$$

Proceeding in a like manner for triangular waves,

$$\frac{E(X)}{E(X_o)} = \frac{8}{\pi^2}\left(\frac{p_o}{p}\right)^2 \left| 1 - \cos\left(\frac{\pi}{2}\frac{p}{p_o}\right) \right| \ldots\ldots\ldots\ldots (18b)$$

Similarly, for simple structures, square waves give

$$\frac{E(X)}{E(X_o)} = \frac{2}{\pi}\frac{p_o}{p} \left| \sin\left(\frac{\pi}{2}\frac{p}{p_o}\right) \right| \ldots\ldots\ldots\ldots (18c)$$

The principal error associated with Eqs. 18 arises from the tacit assumption that t_o is a constant. Alternatively, a frequency distribution of t_o such as that shown in Fig. 7 could be investigated. In Fig. 7, t'_o represents the duration of any seismic wave; the ordinates F are proportional to the corresponding amplitudes multiplied by the number of times that a wave of duration t'_o occurs before the maximum response; and t_o is thus the weighted average of t'_o using the ordinates F as weighting factors. Because, for any value of t'_o, the response at a specified instant, $|x(t)|$, has a Gaussian probability distribution, the square of $E|x|$ is proportional to $E(x^2)$. Therefore, in the case of variable t'_o, $E|x|$ is equal to the square root of the weighted average of the squares of $E|x|$ that correspond to each t'_o-value. The weighting factors are again the ordinates F in the frequency curve.

As will be explained subsequently, it is justifiable to assume that $E(X)$ is proportional to $E|x|$. Therefore, the square of the ratio $E(X)/E(X_o)$ can be obtained by averaging the squares of the ratios given by Eq. 18*a* and using as weighting factors the ordinates in Fig. 7.

In Fig. 8 is shown the value of $E(X)/E(X_o)$ as a function of the ratio of the period of the structure to the duration of seismic waves, T/t_o. Curves have been plotted for half sine-wave, triangular-shaped, and square-wave pulses of constant duration and for half sine-wave pulses having a distribution of durations as shown in Fig. 7. For structures having a fundamental period greater than six times the duration of the seismic wave, the ratio between the corrected and uncorrected expected maximum responses is nearly unity for all the wave shapes investigated.

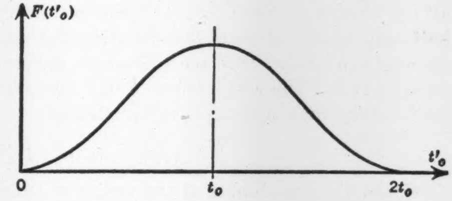

FIG. 7.—ASSUMED DISTRIBUTION OF WAVE DURATIONS

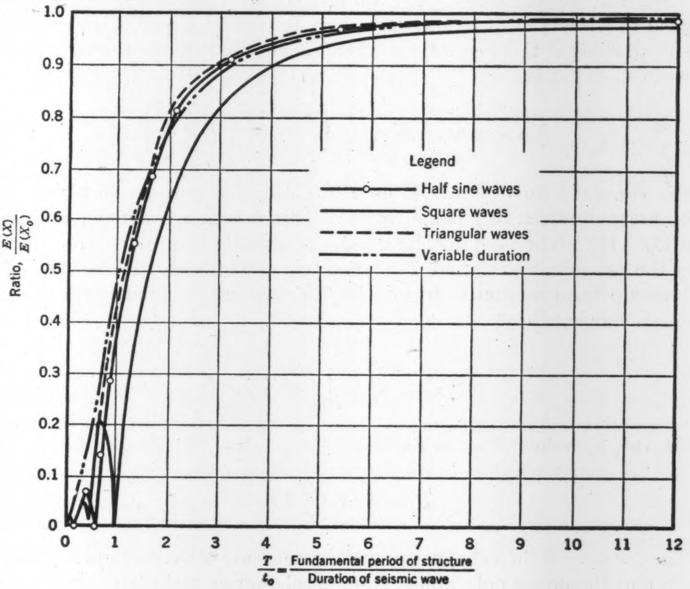

FIG. 8.—CORRECTION FACTOR FOR FINITE-WAVE DURATIONS

Judging from published strong-motion accelerograms and velocity spectra, a reasonable design value of t_o seems to be between 0.05 sec and 0.10 sec. The former value is conservative and may be adopted in the absence of accurate computations based on measured accelerograms. Preferably, t_o should be deduced from the ordinates of velocity spectra within the range of from 0 sec to 0.20 sec when these spectra are available. The value of t_o to be used in design can then be obtained by adjusting the time scale in Fig. 8 so that the best possible agreement with average spectra will result.

As may be inferred from Fig. 8, the wave shape selected for this purpose is not critical. If the time scales of the curves in Fig. 8 are properly adjusted, all the curves can be made to agree within 3% with the one corresponding to half sine waves of constant duration, for natural periods T not less than t_o, or approximately 0.05 sec. Shorter natural periods have little structural significance. The assumption of half sine-wave shapes of constant duration is satisfactory for engineering applications.

APPLICATION TO DESIGN

From the standpoint of the designer, interest centers in the displacements or forces which the structure under consideration must withstand. The point of view adopted in this paper is that of one who is designing for certain displacements; if the structure yields elastically, however, displacements and stresses are proportional and can be converted to equivalent static forces. Denoting the displacement (X_D) that a point of the structure should be designed to withstand, it follows from Eqs. 9*a* and 9*b* that X_D is given by the right-hand sides of these equations when t is chosen to make the terms as large as possible. That is,

$$X_D = \max_t \left\{ K \sqrt{\frac{1}{t} \int_0^t [\phi_c(t - \tau)]^2 \, d\tau} \right\} \qquad (19a)$$

The corrected function, ϕ_c, is used in place of ϕ in order to take account of the finite duration of seismic waves. This function is defined in terms of ϕ by Eq. 17*b*. When ϕ (and, hence, ϕ_c) is periodic and, as is often the case, when the fundamental period T is small compared with the duration of the earthquake, the criterion expressed by Eq. 19*a* can be written in a simpler form. Following Eq. 9*c*,

$$X_D = K \sqrt{\frac{1}{T} \int_0^t [\phi_c(\tau)]^2 \, d\tau} \qquad (19b)$$

In Eq. 19*b*, K is defined as in Eq. 9*a*:

$$K^2 = E(N_t) \frac{2}{\pi} E(u^2) \qquad (20)$$

The quantity K (in inches per second) is a measure of the earthquake intensity. It can and should be determined from accelerogram records of strong-motion earthquakes such as those obtained by the USCGS.

It may be noted that the function ϕ depends on the natural frequencies and mode shapes of the structure. In practice this means that the preliminary design must be sufficiently refined so that the frequencies of the structure can be estimated before the design deflections, X_D, are determined. This awkwardness is common to structural design in general. Even a simple truss subjected to static loads cannot be designed until its dead weight is known. This information in turn can be obtained only from a preliminary design or the examination of similar structures.

In designing for the displacement X_D or for the corresponding equivalent static forces, a factor of safety appropriate to the uncertainty in the material properties and static loadings is to be included. In addition, the earthquake intensity factor, K, should contain a further factor of safety. As noted in the "Introduction," the intensity of earthquake for which a structure should be designed depends on the seismic record of its site, the public importance of the structure, and economic considerations. When this choice has been made, however, design based on Eqs. 19 insures a uniform strength in the sense that no part of the structure is overdesigned or underdesigned. All parts have an equal probability of successfully resisting ground motion. By selecting a design intensity, K, corresponding to an intense temblor, that probability may be made very high.

The sine functions whose sum yields the ϕ_c of Eq. 19*b* may be regarded as the Fourier expansion of ϕ_c. The integrals of the products of different terms cancel over an interval T. Eq. 20 can therefore be written in the form:

$$X_D = \sqrt{\sum_{i=1}^{N} X^2_{Di}} \qquad (21)$$

in which X^2_{Di} denotes the square of the design displacement that the point under consideration would have (with respect to the ground) if the structure vibrated in the *i*th mode alone. The symbol $\sum_{i=1}^{N}$ indicates that these quantities are to be summed for all the modes of the structure that are to be considered.

Eqs. 19*b* and 21 are applicable to structures whose fundamental periods are short compared with the earthquake duration. Although this restriction still includes the majority of structural cases, the use of these equations—if T is large or ϕ is markedly aperiodic—may result in error on the unsafe side. In this case, Eq. 19*a* must be used. The use of this equation is somewhat hampered by the present lack of quantitative data concerning the time variation of $E(u^2)$ which enters into the evaluation of K. It is possible, however, to find an upper limit for the design response. Fig. 5 constitutes a good approximation to the variation of $E(u^2)$ with time. It is conservative to neglect the first and third phases of earthquakes and to assume a constant intensity for the secondary phase which is the most severe. This assumption tends to lead to the prediction of proportionately greater responses for structures in which T/s is large. If the duration of the secondary phase in destructive earthquakes (estimated at 10 sec) is designated as t_2, these simplifications yield as an estimate for design purposes—

$$X_D = \max_t \left[K \sqrt{\frac{1}{t_2} \int_0^{t_2} \phi_c(t - \tau)\, d\tau} \right] \qquad (22)$$

in which t, in seconds, is selected so as to maximize the radical.

Eqs. 19, 21, and 22 have been derived from Eq. 1*a* for displacements relative to the ground. Because expressions similar to Eq. 1*a* can be established for stresses, bending moments, and equivalent statical forces, the design values of responses of these types can be obtained from Eqs. 19, 21, and 22 by substituting the required response for X_D. It is, of course, necessary to substitute the corresponding function ϕ_c in the right members.

Conclusions

This work has led to a basis for the design of earthquake-resistant structures. The scope of the material developed herein is limited to structures whose design distortions are small enough so that the behavior of the structure is essentially elastic and to structures found on firm ground. The structures may have any number of degrees of freedom. Both structure and ground may have internal viscous damping. Under these conditions, structural responses (at any time t) can be obtained from expressions of the form:

$$R(t) = \int_0^t \ddot{x}_g(\tau)\,\phi(t-\tau)\,d\tau \qquad (23)$$

in which the response R can be a displacement relative to the ground, a stress, or a bending moment; $\ddot{x}_g$ is the ground motion; and ϕ is a function of the structure, independent of the ground motion and equal to the response generated by a sudden unit change of ground velocity.

Considering the origin and properties of earthquake motions, it has been concluded that they can be replaced, for purposes of structural design, by nearly random motions. This conclusion has been substantiated by comparing the spectra predicted by a random-motion theory with those of actual, destructive, strong-motion earthquakes recorded by the USCGS.

By means of the theory of probability, a method for computing design values of responses has been developed. Structures designed to withstand these responses will be of uniform strength in the sense that all parts will have equal probability of successfully withstanding a temblor. Different parts of a structure will not be relatively overdesigned or underdesigned. When the ratio T/s (T is the fundamental period of the structure and s is the earthquake duration) is small, the design value of R is (from Eqs. 9*c* and 19*b*) $R_D = K\sqrt{\frac{1}{T}\int_0^t [\phi_c(t)]^2\,dt}$, in which K (in inches per second) is a measure of the earthquake intensity and ϕ_c is given, approximately, by

$$\phi_c(t) = \tfrac{1}{2}\,p_o \int_{-t_o/2}^{+t_o/2} \phi\,(t-\tau)\cos p_o\,\tau\,d\tau \qquad (24)$$

In Eq. 24, t_o is the average seismic-wave duration, and $p_o = \pi/t_o$.

The foregoing design value for R can take the form of Eq. 21: $R_D = \sqrt{\sum_{i=1}^{N} R^2_{Di}}$ in which R_{Di} is the design response associated with the *i*th natural mode and N is the number of degrees of freedom of the structure.

These expressions usually provide satisfactory results. However, when T/s is not small they err on the unsafe side. As in Eq. 22, an upper limit to the design value can be computed from the expression: $R_D = \max_t \times \left[K\sqrt{\frac{1}{t_2}\int_0^{t_2} \phi_c(t - \tau)\,d\tau}\right]$, in which t_2 (equal to approximately 10 sec) is the duration of the second phase of the earthquake motion and t is selected to maximize the right-hand side.

ACKNOWLEDGMENT

The preparation of this work has been supported in part by the Office of Naval Research, Mechanics Branch. This paper is based on the doctoral dissertation of Mr. Rosenblueth presented to the Department of Civil Engineering of the University of Illinois at Urbana.

APPENDIX. BIBLIOGRAPHY ON ENGINEERING SEISMOLOGY

(1) **"A Mechanical Analyzer for the Prediction of Earthquake Stresses,"** by M. A. Biot, *Bulletin*, Seismological Soc. of America, Vol. 31, 1941, pp. 151–171.

(2) **"Computations on the Response of One-Mass Undamped Structures to the El Centro Accelerograph Record,"** by E. C. Robison, Watson Scientific Computing Lab., Columbia Univ., New York, N. Y., 1949.

(3) **"The Physical Evaluation of Seismic Destructiveness,"** by H. Benioff, *Bulletin*, Seismological Soc. of America, Vol. 24, 1934, pp. 398–403.

(4) **"Lateral Forces of Earthquake and Wind,"** by a Joint Committee of the San Francisco (Calif.) Section, ASCE, and the Structural Engrs. Assn. of Northern California, *Transactions*, ASCE, Vol. 117, 1952, p. 716.

(5) **"Characteristics of Strong-Motion Earthquakes,"** by G. W. Housner, *Bulletin*, Seismological Soc. of America, Vol. 37, 1947, pp. 19–31. (*a*) p. 20. (*b*) p. 21. (*c*) pp. 23–28. (*d*) p. 22. (*e*) p. 30.

(6) **"Vibration Problems in Engineering,"** by S. Timoshenko, D. Van Nostrand Co., Inc., New York, N. Y., 1928.

(7) **"Theory of Sound,"** by Lord Rayleigh, Macmillan, London, England, 2d Ed., 1894.

(8) **Discussion by N. J. Hoff of "Analytical and Experimental Methods in Engineering Seismology,"** by M. A. Biot, *Transactions*, ASCE, Vol. 108, 1943, pp. 389–390.

(9) **"Probability and Its Engineering Uses,"** by T. C. Fry, D. Van Nostrand Co., Inc., New York, N. Y., 1928, pp. 206–213. (*a*) pp. 184–185.

(10) **"Introduction to Mathematical Probability,"** by J. V. Uspensky, McGraw-Hill Book Co., Inc., New York, N. Y., 1937, pp. 243–245. (*a*) pp. 161–162. (*b*) pp. 170–171. (*c*) pp. 172–173.

(11) **"A Method of Calculating the Dynamic Force on a Building During an Earthquake,"** by M. P. White, *Bulletin*, Seismological Soc. of America, Vol. 32, July, 1942, pp. 194–195.

(12) **"Influence of Ductility on the Response of Simple Structures to Earthquake Motions,"** by S. L. Pan, L. E. Goodman, and N. M. Newmark, Technical Report to the Office of Naval Research (1951), N6ori-71, Task Order VI, Project NR–035–183, *Structural Research Series, No. 11*, Dept. of Civ. Eng., Univ. of Illinois, Urbana, Ill.

AMERICAN SOCIETY OF CIVIL ENGINEERS
Founded November 5, 1852
TRANSACTIONS

Paper No. 2763

REDUCTION IN SOIL STRENGTH WITH INCREASE IN DENSITY

BY CHARLES R. FOSTER,[1] A. M. ASCE

WITH DISCUSSION BY EDWARD S. BARBER, GEORGE R. HALTON, AND CHARLES R. FOSTER

SYNOPSIS

Laboratory and field data are presented which show that, for certain given moisture contents, increases in density result in increases in strength as measured by the California Bearing Ratio (CBR) up to a certain density, after which increases in density result in a decrease in CBR. Confirmation of the decrease in strength is presented as field observations of the behavior of a silty clay soil in accelerated traffic tests. The decrease in strength is believed to be the result of the development of pressure in the void phase of the soil structure. As long as the combination of moisture and density is such that no pore pressures develop, increases in strength occur with increase in density. When pore pressures develop, further increases in density produce decreases in strength.

INTRODUCTION

The usual concept of the relationship between soil density and strength is that an increase in density will result in an increase in strength. Whereas this is generally true, the strength can decrease with an increase in density under certain moisture conditions. When California Bearing Ratio (CBR) tests[2] are made on samples compacted at a given water content, *w*, over a range of densities, the CBR increases with an increase in density up to a certain point. Further increases in density result in decreases in the CBR; similar behavior has been noted during accelerated traffic tests. This behavior has been noted in a wide range of soil types but is most prevalent in silty materials.

NOTE.—Published, essentially as printed here, in July, 1953, as *Proceedings-Separate No. 228*. Positions and titles given are those in effect when the paper or discussion was received for publication.

[1] Engr., Chf. of Flexible Pavement Branch, Soils Div., U. S. Waterways Experiment Station, Corps of Engrs., Vicksburg, Miss.

[2] "The Preparation of Subgrades," by O. J. Porter, *Proceedings*, Highway Research Board, National Research Council, Washington, D. C., Part II, December, 1938.

Laboratory and field data illustrating this type of behavior in the silty clay native to the grounds of the Waterways Experiment Station (Vicksburg, Miss.) are presented herein.

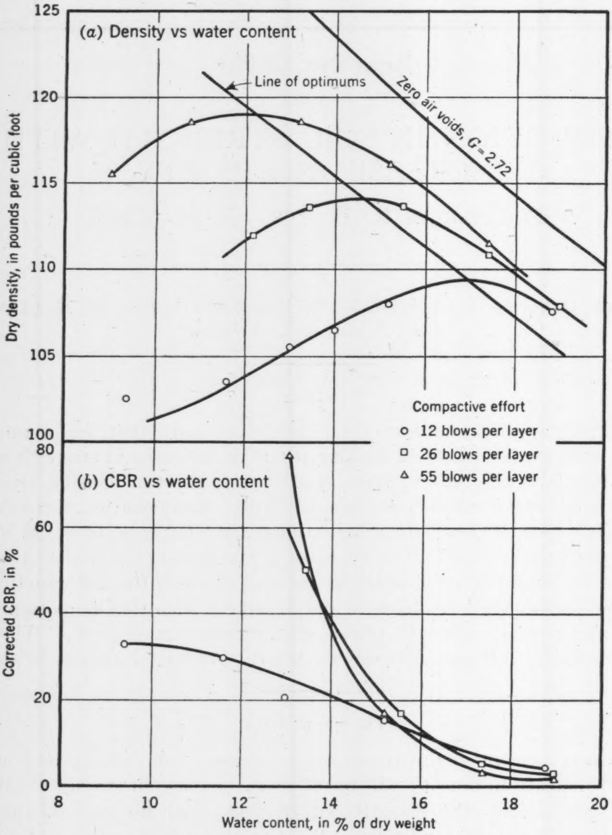

Fig. 1.—The Effect of Water Content on Density and CBR for Various Laboratory Compactive Efforts

Laboratory Tests

Soil.—The soil used in these studies was obtained from the weathered zone of the loess found at Vicksburg. It is a silty clay with a liquid limit of approximately 38 and a plasticity index of approximately 13. The soil is classified as ML–CL according to the United States Department of the Army Unified Soil Classification System.[3]

---

[3] "The Unified Soil Classification System," *Technical Memorandum No. 3-357*, Waterways Experiment Station, Vicksburg, Miss., March, 1953.

Laboratory CBR Tests.—In Fig. 1 there are shown the relationships between density and water content and CBR and water content for samples of the silty clay compacted in the laboratory at three compactive efforts. The samples were compacted in five equal layers (approximately 1 in. thick) in 6-in.-diameter molds with the modified American Association of State Highway Officials (AASHO) compaction hammer (10-lb, 18-in. drop). New material was used for each test. In Fig. 1(*a*) there are shown density-water content curves for the three compactive efforts, and in Fig. 1(*b*) there are shown CBR-water content curves obtained by performing CBR tests on each of the compacted specimens; the CBR tests were made on the as-molded specimens without soaking. The curves in Fig. 2 illustrate the same data shown in Fig. 1 interpolated to show families of CBR-density curves for equal water contents. The points plotted in Fig. 2 are not basic test data but are interpolated from Figs. 1(*a*) and 1(*b*). This method of showing the results of CBR tests was developed in connection with the initial program of laboratory investigations of the CBR test[4] conducted at the Waterways Experiment Station and has been used in connection

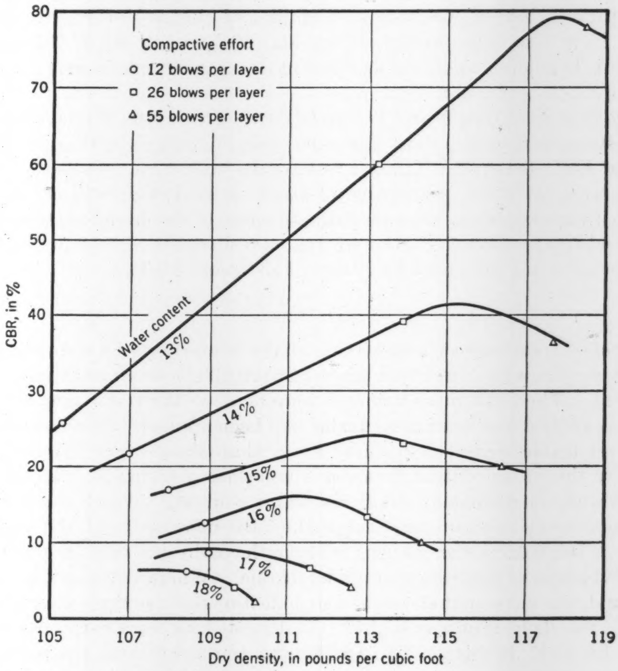

FIG. 2.—THE RELATIONSHIP BETWEEN CBR AND DENSITY FOR VARIOUS LABORATORY WATER CONTENTS

with CBR testing. This method is required by the Corps of Engineers, United States Department of the Army, in the design of flexible pavements.[5]

---

[4] "The California Bearing Ratio Test as Applied to the Design of Flexible Pavements for Airports," *Technical Memorandum 213-1*, U. S. Waterways Experiment Station, Vicksburg, Miss., July, 1945.

It will be noted in Fig. 2 that the strength increases with an increase in density up to a certain point; further increases in density result in decreases in strength. This condition occurs commonly in laboratory CBR tests, and numerous families of curves showing this phenomenon are available.[6,7,8,9] In 1945 J. B. Eustis and J. L. McRae, Associate Members, ASCE, obtained (but did not publish) families of CBR-density curves for equal water contents. They called attention to the fact that the CBR decreased with an increase in density for high densities; however, they did not discuss the subject in detail nor did they include a conclusion. Families of curves showing this type of behavior have also been presented[10] by Mr. McRae and W. J. Turnbull, M. ASCE, but the phenomenon of a decrease in strength with an increase in density has received little attention.

Unconfined Compression and Triaxial Tests.—The results of unconfined compressive-strength tests will show also a decrease in strength with an increase in density at high densities. Triaxial test results will show this behavior if the deviator stress at a low percentage of strain is used; they will not show this behavior if the maximum value or ultimate value of the deviator stress is used. Unconfined compressive strength and triaxial test results plotted in this manner are available[4,6] and were used by Messrs. Eustis and McRae.

FIELD TESTS

General.—Accelerated traffic testing at the Waterways Experiment Station on a test section with a test cart loaded to 120,000 lb produced similar results in the field. The CBR measurements were made in the traffic lane before any traffic was applied and again after traffic had been applied. The measurements made after traffic were substantially lower than those made before traffic in areas were the water content was above a certain percentage. This behavior occurred with no significant change in water content. Where the water content was below this certain percentage, the CBR increased with the application of traffic. In all cases, the changes in strength conditions were accompanied by visible evidence in the behavior under traffic. Where decreases in strength were found, the pavement showed large deflections or weaving; where increases occurred, the deflection was slight.[8] Pertinent data were extracted and presented[11] by J. F. Redus, A. M. ASCE, and the writer and are not repeated herein.

---

[5] "Engineering Manual for Military Construction," Corps of Engrs., U. S. Dept. of the Army, Washington, D. C., Part XII, Chapter 2, Appendix B, July, 1951.

[6] "Soil Compaction Investigation," *Technical Memorandum 3-271*, U. S. Waterways Experiment Station, Vicksburg, Miss.: Report No. 1, April, 1949; Report No. 2, July, 1949; Report No. 3, October, 1949; Report No. 4, February, 1950; and Report No. 5, June, 1950.

[7] "Investigation of the Design and Control of Asphalt Paving Mixtures," *Technical Memorandum 3-254*, U. S. Waterways Experiment Station, Vicksburg, Miss., May, 1948.

[8] "Investigation of Effects of Traffic with High-pressure Tires on Asphalt Pavements," *Technical Memorandum 3-312*, U. S. Waterways Experiment Station, Vicksburg, Miss., May, 1950.

[9] "Airplane Landing Mat Investigation, Engineering Tests on Steel, Pierced Type, M8 and Aluminum, Pierced Type, M9," *Technical Memorandum 3-324*, U. S. Waterways Experiment Station, Vicksburg, Miss., May, 1951.

[10] "Soil Tests Shown Graphically," by W. J. Turnbull and J. L. McRae, *Engineering News-Record*, May 25, 1950, pp. 38–39.

[11] "Moisture Conditions Under Flexible Airfield Pavements," by J. F. Redus and Charles R. Foster, from "Frost Action in Soils," A Symposium, *Special Report No. 2*, Highway Research Board, National Research Council, Washington, D. C., 1952.

Unfortunately, the full importance of the developing conditions was not realized, and the density was not obtained for every case. As a result, development of a clear concept of the relationships between the behavior in the laboratory and in the field was not possible.

Subsequent to the tests described previously, reductions in the CBR have been noted in several of the accelerated traffic tests. In one particular series made in connection with investigations of landing mats, rather comprehensive measurements were made of the CBR, water content, and density following construction and at intervals during traffic. The purpose of these accelerated traffic tests was to determine if the landing mats would carry certain airplane wheel loads on a subgrade with a CBR of approximately 15%; detailed results are available[9] and pertinent data are given subsequently.

Test Sections.—The test sections were constructed of the silty clay soil in such a manner as to provide a 24-in. depth of soil in as uniform a condition as possible. The soil was moistened or dried to obtain the desired water content, placed in 6-in. lifts, and compacted with a heavy sheepsfoot roller. After the subgrade was constructed, the test area was surfaced with M6 (light steel), M8 (heavy steel), and M9 (aluminum) landing mats. The test sections were constructed under a hangar for protection from rainfall. The water table was at depths in excess of 100 ft and was not a factor. The sections were covered with tarpaulins, except during the period that they were subjected to traffic so as to minimize evaporation.

Traffic.—Traffic was applied to the test sections with the load test cart equipped with airplane tires operated in a manner that simulated taxiway traffic. The cart traveled back and forth along the test section and was shifted laterally to produce uniform coverage across the traffic lane. One application of the tire over every spot in a traffic lane constituted one coverage. Traffic was continued until failure occurred or until 1,000 coverages had been applied. Observations of behavior were made throughout the period of traffic; tests of the CBR, water content, and density were made at pertinent intervals, particularly when significant distress occurred. Distress usually was evidenced by large deflections and weaving under traffic. Sections were said to have failed when a condition of mat breakage and surface roughness developed that was considered to be hazardous to aircraft operation. Failure was caused primarily by shear deformation (plastic movement) of the soil under the repetitive loads. In Table 1 there are summarized the CBR, water content, and density data and the behavior observations.

Effect of Water Content.—In the first group of tests (sections 1, 3, 4, and 5) it was intended to process the soil to an average water content in the range of 16.5% to 17.0%; the results of these tests made both before and during traffic averaged 16.9%. As noted in Table 1, the CBR during traffic was generally below the intended value of 15%, and failures occurred well before the anticipated life of 1,000 coverages. In the second series of tests (sections 6, 7, and 8) the soil was processed to a drier water content to avoid the large reductions in the CBR values that occurred in the first group of tests. The results of tests of the water content made in these three sections before and during traffic averaged 14.7%; it can be seen in Table 1 that, instead of reductions in the CBR, fairly large increases in the CBR occurred. In the third group of tests

TABLE 1.—RESULTS OF TESTS AND OBSERVATIONS

				BEFORE TRAFFIC			AFTER TRAFFIC							
Test load (1)	Section (2)	Type of mat (3)	Depth, in inches (4)	CBR, in % (5)	w, in % (6)	Density[a] (7)	Subsection (8)	Coverages (9)	Depth, in inches (10)	CBR, in % (11)	w, in % (12)	Density[a] (13)	CBR change (14)	Behavior (15)
80,000-lb dual wheels, inflation pressure of 165 lb per sq in.	1	M9	1	6	17.9	108.4	1A	12	3	14	17.0	112.5	+	Traffic stopped at 12 coverages.
			5	12	17.5	109.0			8	6	17.2	112.9	−	
			13	11	16.1	112.7								
	3	M6	1	8	18.2	108.9	3A	108	2	8	15.9	115.5	−	Distress began at 40 to 50 coverages; failure occurred by 108 coverages.
			5	21	16.5	109.8			10	7	16.3	114.7	−	
			10	17	16.5	110.2			19	5	17.5	111.8	−	
			13	17	17.0	111.6								
			17	11	17.8	109.8								
	4	M8	1½	6	18.3	109.3	4B	192	3	9	15.9	115.7	−	Distress began at approximately 60 coverages; failure occurred at 192 coverages.
			6	24	16.4	108.2			10	7	16.2	114.9	−	
			10	22	16.1	...								
			13	11	16.9	110.6	4A	204	2	15	15.2	117.5	+	Distress began at 120 coverages; traffic was stopped at 204; failure estimated at 230 coverages.
									9	13	15.8	115.9	−	
									19	14	16.5	115.1	+	
	5	M9	2	7	17.8	109.1	5B	48	2	6	18.1	111.5	−	Distress began at approximately 50 coverages; failure occurred at 136 coverages.
			8	14	16.8	112.1			9	3	17.6	111.8	−	
			15	10	17.9	111.7								
							5A	192	1	11	16.4	113.9	+	Distress began at approximately 50 coverages; failure occurred at 192 coverages.
									6	6	16.5	115.2	−	
									16	3	18.0	111.2	−	
	6	M6	1	19	14.4	107.0	6A	1,000	2½	67	14.6	114.8	+	Satisfactory at end of 1,000 coverages.
			8	24	14.7	107.3			10½	46	14.3	109.6	+	
			17	26	13.6	108.1			19	24	15.8	111.7	−	
	7	M8	2	14	14.1	107.2	7B	1,000	2	55	13.8	114.7	+	Satisfactory at end of 1,000 coverages.
			10	14	14.5	107.2			10	28	14.7	109.3	+	
			18	21	14.6	113.6			18	23	15.2	116.1	+	
	8	M9	3	17	14.4	106.9	8B	1,000	3	48	14.5	116.4	+	Satisfactory at end of 1,000 coverages.
			11	13	15.1	103.9			11	34	15.6	112.4	+	
			19	13	14.0	109.1			19	18	16.4	113.1	+	

50,000-lb single wheel, inflation pressure of 200 lb per sq in.	9	M6	2 9 16	22 25 25	14.9 14.5 15.3	110.8 110.8 110.7	9B	250	4 11 18	12 9 15	14.8 15.8 15.5	118.3 116.3 115.8	– – –	Distress began at approximately 100 coverages; failure occurred at 250 coverages.
							9A	276	4 9 16	14 10 27	14.5 15.4 15.2	118.9 116.5 116.4	– – +	Distress began at approximately 100 coverages; failure occurred at 276 coverages.
	10	M8	3 10 17	21 20 19	15.1 16.5 15.2	114.2 113.2 113.3	10B	276	3 10 17	13 12 14	14.9 15.4 16.4	118.5 117.2 115.7	– – –	Large deflections at 276 coverages.
								532	4 11 17	15 8 18	14.5 15.8 15.5	117.1 116.3 115.7	– – –	Considered failed.
							10A[b]	276	3 9 16	32 21 17	14.7 15.4 15.8	116.6 115.6 115.1	+ + –	Satisfactory.
								686	3 9 16	20 16 20	14.6 15.1 16.2	118.9 117.4 114.1	– – +	Satisfactory.
								1,000	3 13 18	18 11 13	14.5 15.9 16.0	119.5 116.5 116.0	– – –	Satisfactory almost to 1,000 coverages but distress apparent during last few coverages.
							10A[c]	1,000	3 10 17	51 43 30	15.5 14.5 15.1	117.0 116.2 113.7	+ + +	Satisfactory.
	11	M9	3 9 18	27 25 20	14.3 15.3 16.0	112.7 111.9 110.2	11B	276	3 9 18	29 37 28	14.5 14.9 15.8	118.2 111.0 110.3	+ + +	Satisfactory.
								670	3 9 16	68 29 25	13.5 15.1 16.2	119.3 117.1 113.7	+ – –	Satisfactory.
								950	3 10 17	19 10 21	14.3 15.5 15.9	118.3 117.2 114.8	– – –	Failed after 750 coverages.
								1,000[d]	3 10 17	89 25 21	13.0 15.4 15.9	119.2 114.3 116.6	+ – –	Satisfactory.
							11A	900	3 10 17	15 9 14	14.2 15.8 15.9	118.9 116.4 116.2	– – –	Satisfactory to 750 coverages; distress apparent between 750 and 850 coverages; failed at 850 to 900 coverages.

---

[a] In pounds per cubic foot. [b] West half. [c] East half. [d] Small area.

(sections 9, 10, and 11), which were actually made for a different wheel assembly, advantage was taken of this previously noted behavior, and the soil was processed at a water content between the two values of 14.7% and 16.9%. The results of the water content tests made before and during traffic averaged 15.2%. In this group of tests, the CBR during traffic was generally in the desired range, and the tests were successful in that all parts of the lane carried substantial traffic and some parts carried traffic for the intended life of 1,000 coverages. A detailed description of the behavior in section 10 is given subsequently as being typical of the observations of behavior in all the sections.

Behavior of Typical Section During Traffic.—Section 10 was 34 ft long and was divided into two subsections, 10A and 10B, to accommodate slight differences in the manufacture of locking lugs of the M8 mat used for surfacing. These differences in manufacture did not affect the behavior of the tests; the differences observed in behavior in various parts of the section were caused by slight differences in the water content of the subgrade.

Tests to determine the CBR, water content, and density were made prior to traffic in a pit near the center of subsection 10B; this area was considered reasonably representative of the entire section. From two to five individual tests were made at three successive levels, usually 3 in., 10 in., and 17 in. below the surface of the subgrade. In Table 1 there are shown the values obtained by averaging the individual tests at each level. The average water content prior to traffic throughout the three levels was 15.6%, and the CBR was 20%.

As traffic was applied, it was noted that after 276 coverages large deflections were occurring in subsection 10B; after 532 coverages the subsection was considered to have failed. The water content throughout the entire depth averaged 15.4%—slightly lower than the as-constructed value (probably as a result of evaporation)—and the CBR was generally considerably lower than the as-constructed value of 20%.

During this same period, subsection 10A carried traffic with no distress. In fact, subsection 10A carried traffic for almost the full intended life with no distress. In the west half of the lane of this subsection, relatively large deflections developed during the last few coverages, but there was no sign of distress in the east half. In the west half of the lane, an increase in the CBR was measured at 276 coverages, but after 686 coverages the CBR had returned to approximately the as-constructed value, and after 1,000 coverages the values were considerably below the as-constructed value. By comparison, the CBR in the east half of the lane at the location measured at 1,000 coverages was very high. Average water contents in the east half were 15.0%, 0.4% less than the average of 15.4% in the west half.

Similar observations and test data for the other sections are recorded in Table 1. The next to last column in Table 1 indicates whether or not the CBR decreased during traffic: A minus sign indicates a case in which the CBR was less than the before-traffic value or less than a previous reading in the subsection at the same level; a plus sign is shown for all other cases. Because all the tests were not made at the same levels, it was necessary to plot CBR-depth curves in a few cases and interpolate values for intermediate depths; these curves are not presented herein.

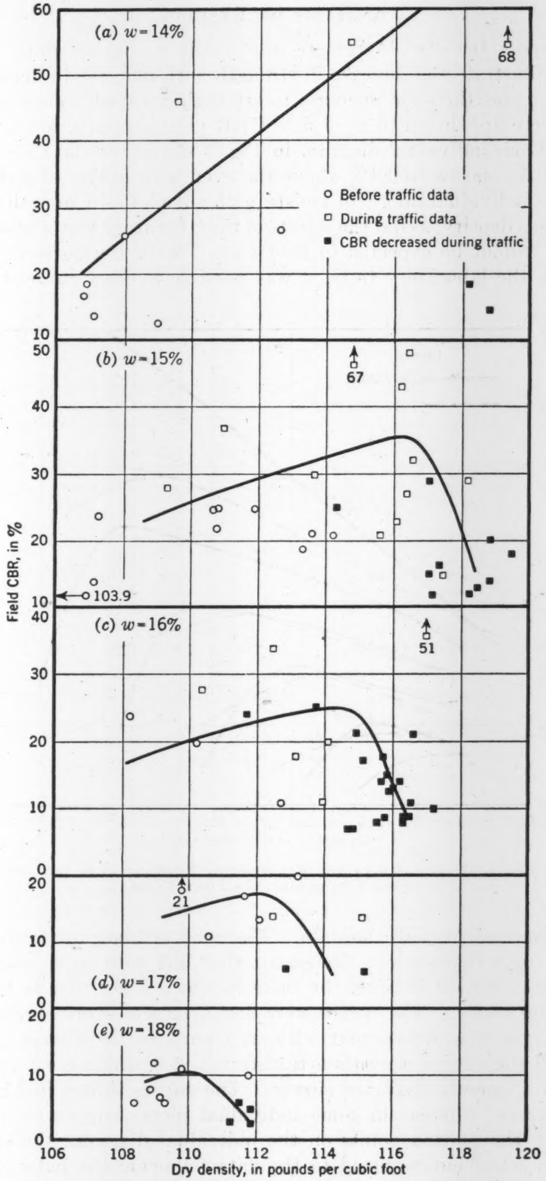

Fig. 3.—The Effect of Water Content on the Relationship Between Field CBR and Density

ANALYSIS OF RESULTS

CBR Versus Density.—Attempts were made to devise plots that would graphically illustrate the increase in strength with increase in density up to a certain point and then the decrease in strength with additional compaction. In Fig. 3 there are shown plots of field CBR versus density for various water contents. Each individual diagram in Fig. 3 shows the data for water contents from 0.5% below to 0.4% above the even percentages of water content. Data for the individual ranges of moisture do not plot as a smooth progression of CBR versus density, as did the results of the laboratory test, but such smooth progression cannot be expected in field tests. With the pattern of behavior known from the laboratory tests, it was possible to draw curves that were in reasonable agreement with the data. The solid symbols are pertinent to the part of the curve that shows a decrease in the CBR with an increase in density because these symbols indicate the cases in which a decrease in the CBR occurred during traffic. The curves were first drawn on work sheets for the individual ranges of water content without regard to the curves in the other ranges. All the curves were then transferred to a single sheet and adjusted to result in a smooth family of curves. The curves shown in Fig. 3 are the adjusted curves; whereas in some individual plots the curves do not agree exactly with the plotted points on the individual diagram, the entire family represents a set of curves fitted to the data following the pattern set by the laboratory tests.

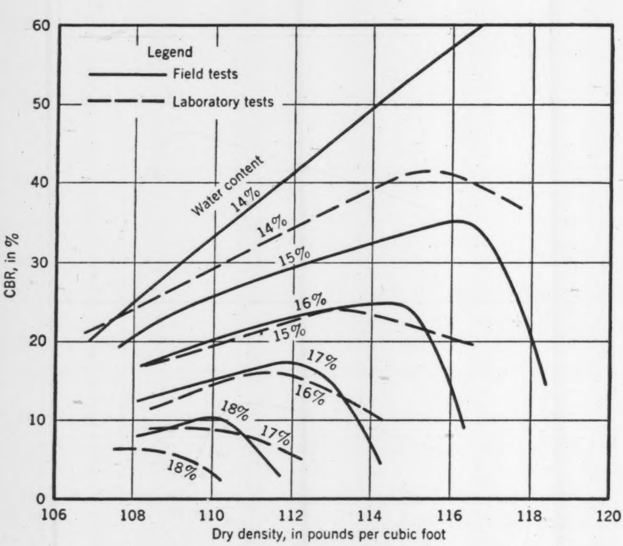

FIG. 4.—COMPARISON OF THE RELATIONSHIP BETWEEN CBR AND DENSITY FROM LABORATORY AND FIELD TESTS

Laboratory versus Field Data.—In Fig. 4 there is shown a comparison of the CBR-density curves from the laboratory and those from field tests. The laboratory test results, shown by the dashed lines, were obtained from Fig. 2; the field results, shown by solid lines, were obtained from Fig. 3. The laboratory tests were made on samples of the silty clay used as the subgrade for the landing-mat test sections. It can be seen that the field-CBR values are consistently higher at equal values of water content and density than the laboratory values. Whether the difference shown in these tests would have remained through periods of moisture adjustment (soaking in the laboratory test and moisture accumulation in the field) is not known definitely because there was not time to allow the subgrade to accumulate moisture in a normal manner. However, data published[11] by Mr. Redus and the writer indicate a fairly close agreement between the laboratory design CBR for a soaked sample and the value obtained in the field for this soil after 5 yr to 7 yr of moisture accumulation.

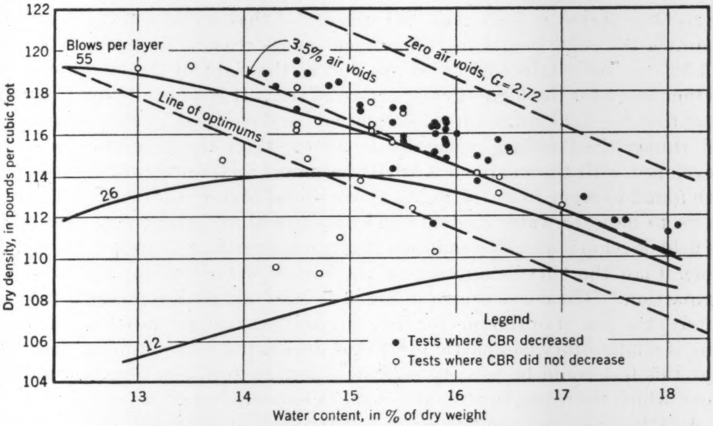

FIG. 5.—THE RELATIONSHIP BETWEEN DENSITY AND WATER CONTENT FOR THE FIELD TESTS

General.—The decrease in strength above certain values of density in both the laboratory tests and field tests is believed to be caused by the development of pressure in the void phase of the soil structure. As long as the combination of moisture and density is such that no significant pore pressures develop, increases in strength occur with increases in density. When pore pressures develop, further increases in density produce decreases in strength.

Attempts have been made to develop procedures to predict the moisture and density conditions under which such a decrease will occur. In the laboratory tests, the density-water content curves, as shown in Fig. 1(*a*), for three compactive efforts are usually arranged so that the peaks of the three curves (point of optimum moisture and maximum density) can be joined by a smooth curve which usually parallels the zero air-voids line; this "line of optimums" is illustrated in Fig. 1(*a*). It has also been found that, generally, the water content-density conditions along this line of optimums represent the points at which decreases in strength are indicated when the test data are plotted as CBR-density curves, as illustrated in Fig. 2. It was first thought that the CBR would decrease in the field at any time the density and water content would fall above and to the right of the line of optimums (Fig. 1(*a*)). Fig. 5 is a plot of the field water content and densities from Table 1. The before-traffic data are not shown in Fig. 5 because they would only cause confusion. Laboratory compaction curves taken from Fig. 1(*a*) are shown in Fig. 5 for comparison.

It is noted (Fig. 5) that, in general, the solid points, which represent cases in which the CBR decreased with traffic, tend to plot in a zone above the laboratory compaction curves, and the open points, which represent cases where an increase occurred during traffic, generally tend to plot below this zone. A few solid points occur below the zone, and a few open circles fall in the zone. The reasons for these inconsistencies are not known, but such inconsistencies are to be expected in field data. It was found that a curve of 3.5% air voids separates the solid points from the open points reasonably well. The curve of 3.5% air voids falls slightly above and to the right of the laboratory compaction curve for the highest compactive effort. It has been found from other tests[6] that the field optimum water content, as developed by sheepsfoot rolling and rubber-tired rolling, generally is wetter than the laboratory optimum (developed with the modified AASHO hammer) and, for this specific soil, has been found to range from 1% to 2% above the laboratory optimum. The curve drawn to indicate water contents and densities above which pore pressures in the field develop is at water contents that are approximately from 1.5% to 1.7% higher than the curve representing the line of optimums for the laboratory compaction. The curve drawn in Fig. 5 at 3.5% air voids represents (approximately) the line of optimums for the compactive effort produced by the traffic. Also, if a laboratory compaction test that duplicated field optimum were available, this test could be used to indicate water content and density conditions above which decreases in strength could be expected to occur in the field.

A rather common occurrence in construction on silty soils is the development of a soft, quaky condition under the traffic of the construction equipment or during rolling operations. The condition can be controlled on fills by drying out the soil, or—as has been demonstrated[12] by Mr. Turnbull—a plastic condition can be produced deliberately where desired by rolling at water contents above optimum. The condition also occurs in subgrades during construction where the water table is high and is often attributed to pumping up of water from the water table. The development of extremely soft conditions in silty subgrades was observed during the construction of Selman Airfield at Monroe, La., and Adams Airfield at Little Rock, Ark. The development of the soft, quaky condition on these airfields was attributed to pumping up of water from the water table. It is believed, however, that the behavior in these two instances, and probably in many more instances, which was attributed to pumping up of water, was nothing more than compaction to the point where the water content and density were above the line of field optimums. Thus, there resulted large reductions in strength.

---

[12] "Utility of Loess as a Construction Material," by W. J. Turnbull, *Proceedings*, Second International Conference on Soil Mechanics and Foundation Engineering, Rotterdam, The Netherlands, June, 1948, Vol. V, pp. 97–103.

Conclusions

Both the laboratory tests and field-CBR tests indicate that a decrease in strength occurs when the water content and density conditions are above certain values. This decrease in strength has been observed in many construction projects and has been confirmed by behavior in traffic tests. The traffic tests described herein emphasize that very small changes in water content were critical because strength increased at certain water contents and decreased at slightly higher values. The water content-density conditions above which the decrease in strength occurs are defined in the laboratory by the line of optimums, a curve drawn through the peaks of the laboratory density-water content curves. The conditions appear to be defined in the field by the line of optimums for field rolling; the field line appears to lie at greater water contents than the laboratory line. A laboratory compaction test which closely duplicates the field line of optimums probably could be used to predict conditions of water content and density above which a decrease in strength would occur.

DISCUSSION

Edward S. Barber,[13] A.M. ASCE.—It is reasonable to expect pore pressures for compaction beyond the line of optimums because the phenomenon of an optimum moisture is caused by pore pressures developed in excess water which cannot move away quickly enough. Conversely, no optimum is obtained for very permeable soils or indeed for any soil under static loading if sufficient oppotrunity for drainage is provided.

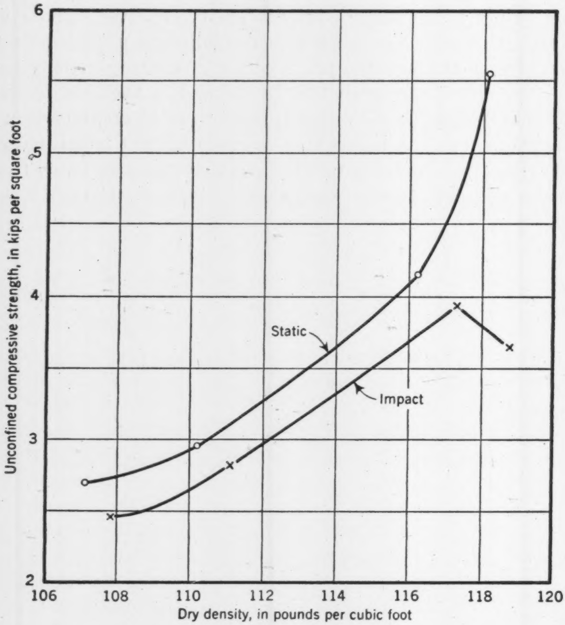

Fig. 6.—The Effect of the Type of Compaction on the Strength of Keyport Silt Loam Having a Liquid Limit of 33, a Plasticity Index of 14%, and a Water Content of 14%

In Fig. 6 the fact that one reduces strength by overcompacting by impact is corroborated; however, the continued increase in strength with density for static compaction indicates that something besides pore pressure is involved. Because shearing is restricted in static compaction, it is suggested that the shearing involved in impact may cause reduced strengths.

To eliminate pore pressure as a factor, tests were made by the writer on dry sand. For a fine sand, with the modified AASHO compaction hammer, an as-compacted CBR value of 5% was obtained whereas compaction to the same density by vibration gave a CBR value of 18%. Similar tests on a coarse sand gave CBR values of 6% and 16%, respectively. Apparently, the reduced density along the shear surfaces as a result of impact is a major factor in reducing strength.

---

[13] Highway Engr., Physical Research Branch, Bureau of Public Roads, U. S. Dept. of Commerce, Washington, D. C.

A clayey sand and gravel, initially compacted by impact to 129 lb per cu ft with $w = 8.8\%$, was subjected to 100,000 repetitions of 4 kips per sq ft producing a density of 130 lb per cu ft and a CBR value of 47%. Repetition of the test with 2% sodium sulfate added to the soil produced a density of 141 lb per cu ft and increased the CBR to 132%. A similar material with a constant water content of 5.7% had a soaked CBR of 90% after twenty-five blows of the hammer; after fifty-five blows the CBR was reduced to 75%. However, with fifty-five blows plus seven thousand repetitions of static load, the CBR was increased to 145%.

Thus, the strength may increase or decrease with increased density depending on the structure produced by the method of compaction.

GEORGE R. HALTON,[14] M. ASCE.—The theme adopted by Mr. Foster is supported by reliable data for the particular type of soil tested. The precautions taken to eliminate contributory variables, as exemplified by the use of new material for each specimen, are commendable. In many respects the author's findings parallel those of an investigation made in 1943 by the California Division of Highways at the Oxnard Flight Strip in Ventura County, California.

It should be noted that the Oxnard base material was coarser than the soil from which the author's data were derived and that the laboratory CBR values at densities equivalent to field conditions at Oxnard did not corroborate the field performance of the relatively coarse material which failed in small areas. Otherwise, Mr. Foster's premise of an inverse strength-density relationship above certain water contents is substantiated by the Oxnard study. Both the Vicksburg and the Oxnard data exhibit perched saturation and freedom from the influence of a high water table.

The Oxnard Flight Strip was one of many built during the early years of World War II under the general supervision of the Public Roads Administration, with detailed investigation and inspection by various state highway departments. The material used in its base and subbase was classified[15] as an A-2 friable to A-2 plastic gravelly sand. It approximated an SC-GF soil in contrast to the ML-CL soil at Vicksburg.

The native subgrade at the Oxnard site was a silty "adobe" clay estimated to require a cover of from 2.5 ft to 3.0 ft of 15% CBR subbase and 30% CBR base material. A buried bank of gravelly sand, discovered 2 miles from the strip, provided the necessary 280,000 cu yd of material which complied with the CBR and other requirements of the specifications.

Relative compaction was specified to be not less than 90% based on the California method[16] and averaged 96% in 118 control tests. The special tests of the investigation averaged approximately 102%. The water content was not specified but was well regulated, averaging 6.6% in place at the time of sampling and 8.8% at optimum. The water content at the time of rolling was probably 1% or 2% higher than when sampled. Only two of the control tests exceeded their respective optimums.

---

[14] Cons. Engr., Newark, N. J.

[15] "Subgrade Soil Constants, Their Significance, and Their Application in Practice," by C. A. Hogentogler, A. M. Wintermyer, and E. A. Willis, *Public Roads*, Vol. 12, No. 4 and No. 5, 1931.

[16] "Procedures for Testing Soils," A.S.T.M., July, 1950, p. 209.

The ratio of 2:118 is equivalent to the areal proportion of several base failures which developed under the trucks hauling bituminous plant-mixed leveling course and surfacing. All but a few of the forty-five spots that failed had received bituminous surface treatment when distress appeared. The defective areas exhibited typical retrogression from an initial slight springiness to a final, pronounced, alligator cracking and rutting.

TABLE 2.—COMPARISON OF TESTS OF FAILURES AND NONFAILURES

Property	Failures			Nonfailures		
	Range	Average	Sample CL-36	Sample CL-39	Average	Range
% passing ¾-in. sieve	94–99	96	95	94	95	94–96
% passing No. 50 sieve	34–53	44	41	43	44	43–46
% passing No. 200 sieve	18–32	23	20	20	21	20–22
% finer than 5 microns	5–9	6	5	5	6	5–7
% finer than 1 micron	1–3	2	1	1	2	1–3
Liquid limit, in %	14–20	16	14	14	14	14–16
Plasticity index, in %	1–6	3	1	1	1	1
Classification[a]	—	A-2 Pl.	A-2 Fr.	A-2 Fr.	A-2 Fr.	—
Field condition:						
Density, in lb per cu ft[b]	129–135	132	131	127	128	122–129
Water content, in %	7.1–9.4	8.4	8.3	8.3	7.0	5.8–7.9
Saturation, in %	74–100	90	87	74	69	58–76
Laboratory equivalent of field condition:						
Density, in lb per cu ft	127–132	130	130	127	127	122–129
Water content, in %	7.8–8.4	8.2	8.4	8.2	7.4	6.1–8.2
4-day soak water content, in %	7.8–8.3	8.0	8.0	8.7	8.9	8.3–9.7
Gain (+) or loss (−)	+0.1 to −0.6	−0.2	−0.4	+0.5	+1.5	+0.5 to +2.2
CBR before soaking, in %	86–154	120	154	112	125	21–196
CBR after soaking, in %	80–110	96	83	78	65	27–92
Expansion, in %	0.0–0.1	0.1	0.1	0.1	0.2	0.1–0.3
Standard Laboratory CBR:						
Density, in lb per cu ft[c]	122–129	124	123	123	124	123–126
Water content, in %	7.8–8.8	8.1	8.8	8.8	8.5	8.4–8.8
CBR, in %[c]	50–87	6	80	69	72	65–85

[a] See reference 15. [b] One failure sample with an apparent denisty of 140 lb per cu ft and a saturation of 127% was omitted. [c] See reference 16.

During the special investigation to determine the cause of failure, twenty samples from the failure areas and six samples from adjacent areas that showed no distress were tested to determine field conditions and laboratory properties. Most of the samples were taken within a few days after damage occurred; several were taken within a few minutes after distress was deliberately induced by truck routing.

Unfortunately neither the equipment nor the precedent for Hveem stabilometer tests[17] of untreated aggregate or for field CBR tests were available. The majority of the samples taken in the special investigation were tested in the laboratory for the CBR at the approximate field condition as well as at the soaked and unsoaked densities achieved under a static load of 2,000 lb per sq in. The results of the special tests are summarized in Table 2.

Infiltration from 0.8 in. of precipitation in the week preceding failure was immediately suspected of being the cause of failure. However, the rainfall was deemed immaterial after field permeability tests of the bituminous-treated upper 3 in. of base material showed an infiltration of only 2×10^{-4} ft per day. Ground-water elevation and capillary action were discarded as causes of failure when the special tests of natural subgrade material showed it to be relatively dry, dense, and stable.

During the repair of the failures the characteristic springiness was observed in only the upper half of the 2.5-ft to 3.0-ft combined thickness of base and subbase materials. Some of the incipient failures that were not immediately repaired subsequently showed no distress when loaded trucks were deliberately routed over them. Elsewhere one or two spot failures were artificially induced by deliberate repetition of truck passes. Following the interruption as a result of repairs, the paving was completed without the recurrence of old failures or the development of new ones; the paved strip was still in good condition in 1947.

The investigation was hampered somewhat by the late fall paving tempo of construction and by the immaturity and divergence of opinions which characterize problems lacking in precedent. The disparity between field behavior and routine or standard CBR values did prompt special tests of laboratory CBR at field conditions; in a final field test three or four weeks after the occurrence of spot failures, the rear tire of a loaded truck was driven within 8 in. of a 6-in.-diameter auger hole filled with water in a rubber bag.[18] This test produced no observable change in water level.

The field and laboratory investigations at Oxnard were made by experienced, expert personnel. Samples from 6-in.-diameter auger holes were weighed in the field to the nearest 0.01 lb, placed in metal containers with sealed covers, and checked for weight in the laboratory. Calibrated sand backfill from moistureproof containers was also weighed to the nearest 0.01 lb in the field, and special depth-density calibrations and techniques assured accurate volume determinations at all horizons in the sample holes. At least 50 lb of additional soil immediately adjacent to the hole were secured from each horizon sampled to provide new material for each laboratory specimen. The entire auger part of each sample was dried at a controlled low temperature, and the test specimens were moistened for 24 hr before the final addition of water required either to match the field condition or to straddle the optimum.

It was concluded in 1943 that the Oxnard failures were the result of excessive saturation in the dense upper half of base and subbase material and that they would have healed or ceased retrogression if left unrepaired for a few weeks.

---

[17] "The Factors Underlying the Rational Design of Pavements," by F. N. Hveem and R. M. Carmany, *Proceedings*, Highway Research Board, Natoinal Research Council, Washington, D. C., Vol. 28, 1948, pp. 130-134.

[18] "Procedures for Testing Soils," A.S.T.M., July, 1950, p. 104.

The slightly greater plasticity of the samples from failed areas was not considered a general cause of failure because ninety-three of ninety-five plasticity-index determinations ranged between 0 and 4 and because the correlation within that narrow spread was inconsistent. The high values of laboratory CBR at equivalent field conditions were attributed to the slow rate of CBR penetration as compared to the deformation under a rolling truck; the CBR loading rate allowed time for the attenuation of excess pore pressures which the truck roll compounded into rupture.

In retrospect these conclusions appear to be sound, but the reported differences in density and saturation of the failures as against the nonfailures suggest that some unknown factor exaggerated the true differences. The abnormal saturation, the unusual rebound, the difficult laboratory duplication of the reported field densities, and the loss of water during the soaking period all suggest that the auger holes in failed areas were subjected to bleeding and constriction during the sampling. The inconsistency of computed field densities on an (*e*-log *p*)-chart verifies these suspicions; the term *e* signifies the void ratio, and *p* is pressure.

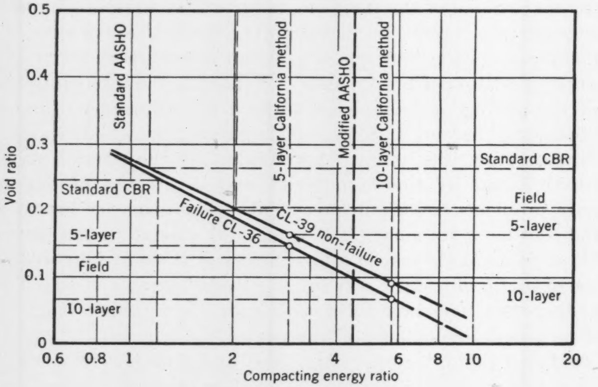

FIG. 7.—RELATIONSHIP BETWEEN VOID RATIO AND COMPACTING ENERGY RATIO

The qualitative relationship of void ratio to pressure is shown in Fig. 7, in which the unit on the (log *p*)-scale is a theoretical energy ratio rather than a numerical quantity of energy per cubic foot (foot-pound per cubic foot-unit pressure). The virgin slopes were determined from densities achieved in the 5-layer and 10-layer variations of the California method. The difference in field densities is inconsistent with the uniform, lapped pattern of many roller passes and the nonuniform, spotty pattern of actual failures.

The spotty pattern of failed areas suggests that individual loads or groups of loads from drier or wetter parts of the pit may have been an antecedent cause. Delayed absorption in coarse particles wetted shortly before or during rolling probably caused pore pressures, which were "built-in" by the roller, to diminish gradually. If the delayed part of absorption was 0.4% by weight (1.0% by volume) and if rolling left 3.0% by volume of air in the voids between particles, the total air voids would be 4.0%. If the pressure trapped in the air in the voids between particles was 4 tons per sq ft, delayed absorption would reduce this to approximately 3 tons per sq ft. Compacted soil which underwent such an internal relief of pore pressure could then withstand an increment of pressure corresponding to 1% of compression.

Soil without delayed particle absorption would lose trapped pressure, but more slowly, through regional diffusion and in proportion with permeabilities and lengths of escape paths. Loads applied before such external relief had become effective could withstand only slight increments of pressure without rupture.

From these considerations, in conjunction with Mr. Foster's data and deductions, it seems logical that the critical volume of air voids, although of the order of 3% on the average, is probably a function of load and loading rate as well as a function of the dimensions, type, and condition of soil. With behavior subject to so many variables, anomalies such as the correlation of field CBR with field strength in one soil and the lack of a similar correlation in another soil are to be expected.

CHARLES R. FOSTER,[19] A. M. ASCE.—The data presented by Mr. Barber form a welcome addition to the information on the effect of different types of compaction. The differences in strength at equal water content and density that he has found with the different types of compaction, particularly between impact and static, are in general agreement with findings at Vicksburg. Mr. Barber's statement that

> "* * * the strength may increase or decrease with increased density depending on the structure produced by the method of compaction"

illustrates that the statements made by the writer were not qualified as to type of compaction. One of the basic purposes, however, was to show the behavior that develops under compaction equipment and to show that similar behavior, which has been noted in samples compacted dynamically, agreed with the field behavior.

The two cases cited by Mr. Barber imply that the reductions in strength noted by the writer could have been caused by differences in structure rather than by the development of pore pressures. The fact that the reduction in strength occurred at a combination of water content and density that resulted in a constant quantity of air voids is considered conclusive evidence that, in the cases cited by the writer, the reduction was related to the development of pore pressure.

With respect to Mr. Halton's interesting observations, it is believed that the failures at Oxnard were definitely caused by the development of pore pressure under the compactive effect of the construction equipment. The "springiness" under traffic is believed to be the same behavior described by the writer

---

[19] Engr., Chf. of Flexible Pavement Branch, Soils Div., U. S. Waterways Experiment Station, Corps. of Engrs., Vicksburg, Miss.

(under the heading, "Field Tests: Traffic") as "large deflections and weaving." Also, air voids computed from the average water content and density given in Table 2 show a value of 2.4% in the failure area and 8.3% in the nonfailure areas indicating that the critical air voids are somewhere between these two percentages. There is little reason to believe that the critical value of 3.5% reported by the writer is applicable to more than a limited range of soils; as suggested by Mr. Halton, the critical value of air voids is probably a complex function of load and loading rate as well as the dimensions, types, and condition of soil.

AMERICAN SOCIETY OF CIVIL ENGINEERS
Founded November 5, 1852
TRANSACTIONS

Paper No. 2764

EVALUATION OF THE PERFORMANCE OF BIOFILTRATION PLANTS

By Renville S. Rankin,[1] M. ASCE

With Discussion by Messrs. Peter Homack, and Renville S. Rankin

Synopsis

High-rate filters are devices for the biological treatment of sewage. However, design data for the average municipal filtering plant have been developed primarily on an empirical basis rather than on a theoretical basis. An analysis of operating data from selected biofiltration plants shows that measures of performance can be defined that are applicable to the economical design of new plants and that allow for predicting results with considerable assurance.

Three methods of evaluating performance are herein applied to several single-stage plants, and the computed results are compared to the actual results; two methods of evaluation are applied to several two-stage plants. The use of single-stage, high-rate filters and two-stage filters is described. An evaluation is made as to when it is more economical to use two-stage treatment. A flowsheet is presented for use in producing an effluent of any condition between that of primary sedimentation and that of single-stage complete treatment.

Introduction

The high-rate filter installations that have been selected for study belong to the group classified as biofiltration plants. The term "biofiltration" is used in reference to those high-rate filter plants which—in a single-stage plant or a two-stage plant—unite some part of the discharge of the filter with the raw-sewage influent of the primary sedimentation tank. For these plants there is a variety of arrangements (or flowsheets), but this study is limited to two typical flowsheets for single-stage plants, two flowsheets for two-stage plants, and one flowsheet for intermediate treatment. Intermediate treatment is

---

Note.—Published, essentially as printed here, in November, 1953, as *Proceedings-Separate No. 336*. Positions and titles given are those in effect when the paper or discussion was received for publication.

[1] Mgr., San. Eng. Div., The Dorr Co., Stamford, Conn.

intended for conditions that require more than primary sedimentation but less than complete treatment. The various flowsheets are shown in Fig. 1.

For biofiltration plants there are considerations which are not necessary for standard-rate, trickling-filter plants. Foremost among these considerations is the permissible load that can be applied to the filter. Other factors are the dosing rate on the filter, the rate of recirculation, the point at which recirculation can be most effectively applied, and the choice of a single-stage or two-stage arrangement of filters. Although some of these factors do concern the designer of standard-rate filters, experience has led to the development of well-established standard designs. The decision to use a high-rate filter is a matter that must be determined by local conditions with particular reference to the receiving body of water.

The reduction of biochemical oxygen demand (B.O.D.) in most biofiltration plants (in fact, in most high-rate filter plants of any type) when dosed in excess of 10^7 gal per acre per day often equals, or even exceeds, reductions in standard-rate filters although there is little if any evidence of nitrification, which is commonly associated with standard-rate filters. Available analyses of biofiltration-plant effluents, however, indicate substantial reductions in the total organic nitrogen. It is a matter for the pollution-control authority to decide whether a nitrified effluent is required of the biologic-treatment step or merely an adequate reduction in B.O.D. The proportion of high-rate filter plants to standard-rate filter plants constructed following World War II indicates that a well-nitrified effluent is not thought to be as essential as it was before World War II. This factor, however, should not be overlooked in the selection of a high-rate filter plant as the method of treatment.

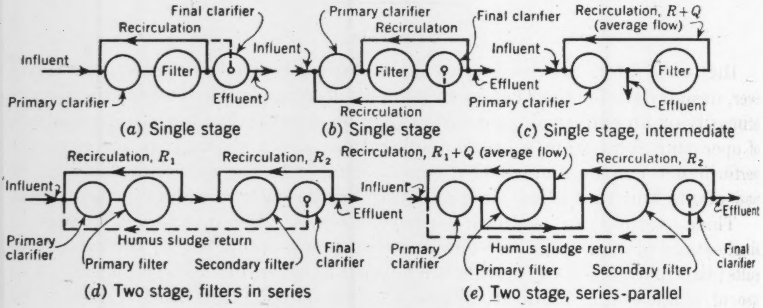
Final clarifier
Recirculation
Influent
Filter
Primary clarifier
Effluent
Primary clarifier
Recirculation
Final clarifier
Influent
Filter
Effluent
Recirculation
Recirculation, $R+Q$ (average flow)
Influent
Filter
Primary clarifier
Effluent
Recirculation, R_1
Recirculation, R_2
Influent
Effluent
Primary clarifier
Humus sludge return
Primary filter
Secondary filter
Final clarifier
Recirculation, R_1+Q (average flow)
Recirculation, R_2
Influent
Effluent
Primary clarifier
Humus sludge return
Primary filter
Secondary filter
Final clarifier

(*a*) Single stage (*b*) Single stage (*c*) Single stage, intermediate

(*d*) Two stage, filters in series (*e*) Two stage, series-parallel

FIG. 1.—TYPICAL BIOFILTRATION FLOWSHEETS

The measure of performance of biofiltration plants is the removal of B.O.D. Generally, in biologic-treatment plants the removal of suspended solids approximates the removal of B.O.D.; if the latter fulfils the requirements, the former is also likely to do so if reasonable care is exercised in operating the plant. This condition appears to be true for biofiltration plants as well; hence, the data on removal of suspended solids from the various plants are not included herein.

B.O.D. REMOVAL BY SEDIMENTATION

There is another problem in evaluating the removal of B.O.D. in the primary tank caused by sedimentation of the raw sewage. In plants with no flow recirculated to the primary tank, there is no problem because merely an analysis of the influent and effluent is necessary. If flow is recirculated to the primary-tank influent, this procedure will not give correct results. Some method is needed to determine that part of the B.O.D. in the raw sewage which passes on to the biologic process. The method used herein is to assume a certain percentage of removal caused solely by sedimentation, based on the overflow rate in the primary sedimentation tank, Q_{op}. The assumed removals and corresponding overflow rates are shown in Fig. 2; these data are essentially those termed[2] "Tentative Standards." The residual B.O.D. in the sewage after subtracting that part removed by sedimentation is considered to be the filter load.

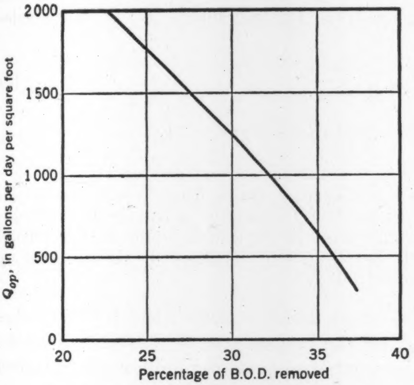

FIG. 2.—ESTIMATED REMOVAL OF B.O.D. BY PRIMARY SEDIMENTATION

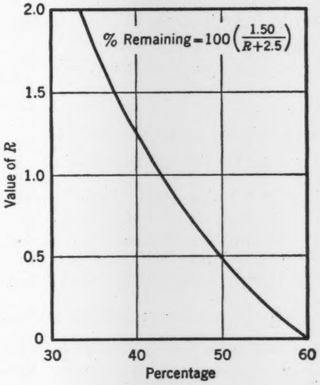

FIG. 3.—REMAINING SETTLED RAW B.O.D. IN EFFLUENT OF SINGLE-STAGE, INTERMEDIATE PLANT

METHODS OF EVALUATING PERFORMANCE

Three methods are used herein to evaluate the performance of the various biofiltration plants; it is necessary to explain each of them.

Tentative Standards.—For the Tentative Standards,[3]

> "Type A (single-stage) filters will be considered where * * * the applied load recirculation included, does not exceed 110 lbs. 5-day BOD per 1000 cu. ft. (4800 lbs. per acre ft.) of filter media per 24-hr. [Also,] * * * the recirculation system shall apply sufficient dilution to the settled sewage so that the BOD of the influent to the filter, recirculation included, shall not exceed three (3) times the BOD of the required settled effluent."

The first statement indicates the maximum permissible loading to which the second statement applies. If the influent load moving toward the filter

---

[2] "Report of Joint Committee of the Upper Mississippi River Board of Public Health Engineers and Great Lakes Board of Public Health Engineers," January, 1951 (available by writing to the various state sanitary engineers).

[3] *Ibid.*, p. 35

(including the recirculation) is not to exceed three times the effluent, it can be concluded that the settled effluent will be one third of the filter influent in a single-stage plant. With B.O.D. values expressed in parts per million and with the assumption that the recirculated flow contains the same number of parts per million as the settled filter effluent, then for a single-stage plant

$$e_s = \frac{c}{2\,R_s + 3} \qquad (1)$$

in which e_s is the B.O.D. of the settled effluent, c represents the B.O.D. of the settled raw sewage, and R_s is the ratio of recirculated flow to raw-sewage flow.

In Figs. 1(*a*) and 1(*b*) the recirculated flow is the filter discharge, settled either in the primary clarifier or in the final clarifier; hence, the value of R is the ratio for the total volume recirculated through the filter and a settling tank. According to the foregoing analysis, the efficiency, E_s, of the single-stage filter is given by

$$E_s = \frac{R_s + 1}{R_s + 1.5} \qquad (2)$$

and is applied to the B.O.D. of the settled raw sewage.

For two-stage filters,[3]

> "* * * the BOD load applied to the second stage filter, recirculation included, shall not exceed two times the BOD expected in the settled effluent. When the effluent of the first stage filter is applied directly to the second stage filter without intermediate settling, the assumed BOD removal by the first stage filter shall not exceed 50%."

In Fig. 1(*d*) there are shown two-stage filters in series; the B.O.D. values are expressed in parts per million, and the recirculated flow from the second stage is assumed to contain the same number of parts per million as the settled effluent. Therefore,

$$e_{t1} = 0.5\,c \qquad (3a)$$

and

$$e_{t2} = \frac{e_{t1}}{R_{t2} + 2} \qquad (3b)$$

in which e_{t1} is the B.O.D. of the effluent in the first stage, e_{t2} denotes the B.O.D. of the effluent in the second stage, and R_{t2} is the ratio of recirculated flow to raw-sewage flow in the second stage.

It should be noted that this method does not account for any variation in the recirculation ratio in the first stage. Operating data from plants using this flowsheet indicate that a recirculation ratio, R_{t1}, of at least 1.0 should be used. According to this analysis, the efficiency, E_t, of a two-stage filter (as in Fig. 1(*d*)) is given by

$$E_t = \frac{R_{t2} + 1.5}{R_{t2} + 2} \qquad (4)$$

which is applied to the B.O.D. of the settled raw sewage.

The only reference in the standards[2] to the rate of application to the filter is the qualification that the dosing rate shall be from 10^7 gal per acre per day to 30 × 10^6 gal per acre per day. The only reference to filter volume is the limitation of the maximum allowable loading for high-rate filters.

National Research Council.—The National Research Council (NRC) Formula,[4] developed from operating data for plants serving military installations during World War II, is

$$E_{sc} = \frac{100}{1 + 0.0085 \sqrt{\dfrac{W}{V\,F_s}}} \quad \text{(5)}$$

in which E_{sc} is the efficiency of B.O.D. removal of the single-stage filter and the accompanying clarifier, in percentage; W represents the applied B.O.D. loading, in pounds per day, of settled raw sewage; V is the volume of filter media, in acre-feet; and F_s is the recirculation factor which is given by

$$F_s = \frac{R + 1}{(0.1\,R + 1)^2} \quad \text{(6)}$$

For two-stage filters, including an intermediate clarifier,

$$E_{t2c} = \frac{100}{1 + 0.0085 \sqrt{\dfrac{W_i}{V_{t2}\,F_{t2}\,(1 - E_{t1})^2}}} \quad \text{(7)}$$

in which E_{t2c} is the efficiency of B.O.D. removal of the second-stage filter and accompanying clarifier, in percentage; W_i denotes the B.O.D., in pounds per day, in the effluent of the intermediate clarifier; V_{t2} is the volume of filter media, in acre-feet, in the second stage; E_{t1} represents efficiency of the first stage which is computed by using Eq. 5; and F_{t2} is the recirculation factor for the second stage and is expressed by

$$F_{t2} = \frac{R_{t2} + 1}{(0.1\,R_{t2} + 1)^2} \quad \text{(8)}$$

Eq. 7 is intended to account for the decreased "treatability" of the sewage entering the second stage.

The over-all efficiency, E_{to}, of a two-stage plant is therefore

$$E_{to} = E_{t1} + E_{t2c} - E_{t1}\,E_{t2c} \quad \text{(9)}$$

In the application of Eq. 9 to the performance of two-stage plants with filters in series, no allowance has been made for the possible omission of the intermediate clarifier. The omission of the intermediate clarifier should result in a lower efficiency than that computed by Eq. 9.

A Basic Law.—Clarence J. Velz, M. ASCE, has presented[5] a logical theory which is applicable to all biologic beds. According to this theory the combined

---

[4] "Report of the Sub-Committee on Military Sewage of the Sanitary Engineering Committee of the National Research Council, May 1946," *Sewage Works Journal*, September, 1946, p. 789.

[5] "A Basic Law for the Performance of Biological Filters," by Clarence J. Velz, *ibid.*, July, 1948, p. 607.

TABLE 1.—OPERATING DATA FOR BIOFILTRATION PLANTS

Description	(a) SINGLE STAGE								(b) TWO STAGE				
	Free-mont, Ohio	Great Neck, N. Y.	Okla-homa City, Okla.[a]	Rich-land, Wash.[b]	Dothan, Ala.	Cen-tralia, Mo.[c]	Storm Lake, Iowa[d]	Alisal, Calif.[e]	Win-chester, Va.	Benton-ville, Ark.	Siloam Springs, Ark.	Liberty, N. Y.	Med-ford, Ore.
FLOW RATES													
Sewage flow, in 10^6 gal/day	1.75	0.52	16.173	2.169	0.548	0.098	1.388	0.588	1.932	0.343	0.255	1.13	4.63
Recirculation ratio:													
R_s	1.5	1.15	1.0	2.76	2.31	0.95	2.14	3.06					
R_{t1}									1.52	1.67	1.41	1.78	1.17
R_{t2}									2.63	2.78	1.54	1.65	1.17
Clarifier-overflow rate, in gal/day/sq ft:													
Primary	1,140	540	620	500	650	197	340	770	1,160	550	390	1,400	1,675
Final	870	157	630	500	280	104	760	2,110	920	810	410	1,160	1,675
FILTER DATA													
									Primary				
Area, in acres	0.231	0.146	1.99	0.238	0.199	0.0222	0.203	0.115	0.282	0.079	0.076	0.115	0.180
Depth, in ft	3.3	4.0	6.0	4.5	3.0	3.0	8.0	3.2	3.0	5.0	5.0	3.0	3.0
Volume, in acre-ft	0.762	0.584	11.94	1.070	0.597	0.0666	1.624	0.370	0.845	0.394	0.380	0.345	0.540
Dosing rate, in 10^6 gal/acre/day	19.0	7.68	16.3	19.6	15.0	8.65	21.5	20.8	17.3	11.6	8.1	27.2	57.0
									Secondary				
Area, in acres									0.282	0.054	0.054	0.115	0.180
Depth, in ft									3.0	5.0	5.0	3.0	3.0
Volume, in acre-ft									0.845	0.268	0.270	0.345	0.540
Dosing rate, in 10^6 gal/acre/day									24.8	24.1	11.8	26.0	57.0

PERFORMANCE BASED ON B.O.D. REMOVAL

B.O.D. of raw sewage, in ppm	134	187	463	173	230	210	690[f]	293	243	335	621	400	215
Estimated removal by settling, in %	30.5	36	35	36	35	36	45[g]	40[g]	30.5	35	36.5	28	26.5
B.O.D. of settled raw sewage,													
in ppm	93	120	303	111	150	134	380	176	169	231	394	288	158
in lb/day	1,360	519	40,680	2,003	685	109	4,390	865	2,720	657	840	2,710	6,100
in lb/acre-ft	1,780	888	3,400	1,900	1,150	1,640	2,700	2,320	1,610	996	1,290	3,920	5,630
B.O.D. of settled effluent,													
in ppm	21	20.2	66	19.5	19	14	61	23.5	20.1	27.5	34	31	21.1
in lb/day	306	88	8,970	353	87	11.5	706	115	323	79	72	292	813
in lb/acre-ft	401	151	750	330	145	173	435	311	191	119	111	423	743
B.O.D. removed from settled raw sewage													
in ppm	72	99.8	237	91.5	131	120	319	152.5	148.9	203.5	360	257	136.9
in lb/acre-ft	1,379	737	2,650	1,570	1,005	1,467	2,265	2,009	1,419	877	1,179	3,597	4,887
Efficiency based on													
settled raw sewage, in %	77.5	83.1	78.0	82.7	87.4	89.4	84.0	86.6	88.1	88.1	91.4	89.3	86.7
raw sewage, in %	84.3	89.2	85.8	88.7	91.7	93.3	91.1	92.0	91.7	91.8	94.5	92.3	90.2

EFFICIENCY OF B.O.D. REMOVAL FROM SETTLED RAW SEWAGE

% Efficiency:													
Actual	77.5	83.1	78.0	82.7	87.4	89.4	84.0	86.6	88.1	88.1	91.4	89.3	86.7
Computed on basis of													
Tentative Standards	83.3	81.1	80.0	88.3	86.9	79.6	86.3	89.0	88.8	89.6	86.0	86.5	84.2
NRC formula	79.4	83.8	72.2	80.5	83.7	78.9	77.0	79.1	90.0	92.3	90.6	83.2	77.8
C. J. Velz formula	85.5	83.8	80.9	83.3	86.1	86.1	80.1	85.5					
Actual ÷ Computed × 100:													
Tentative Standards	93.0	102.3	97.5	93.8	100.5	112.0	97.5	97.4	99.2	98.3	106.0	103.3	103.0
NRC formula	97.6	99.1	108.0	103.0	104.3	113.2	109.2	109.4	97.8	95.5	100.8	107.4	111.4
C. J. Velz formula	90.5	99.1	96.4	99.4	101.3	103.7	104.8	101.3					

EFFICIENCY OF OVER-ALL B.O.D. REMOVAL

% Efficiency:													
Actual	84.3	89.2	85.8	88.7	91.7	93.3	91.1	92.0	91.7	91.8	94.5	92.3	90.2
Computed on basis of													
Tentative Standards	88.4	87.9	86.9	92.7	91.4	87.0	92.5	94.4	92.2	92.8	91.2	90.3	88.4
NRC formula	85.7	89.6	81.9	87.5	89.3	86.5	87.3	87.5	93.0	95.0	94.0	87.9	83.7
C. J. Velz formula	89.9	89.6	87.5	89.3	90.9	91.1	89.1	91.3					
Actual ÷ Computed × 100:													
Tentative Standards	95.4	101.5	98.8	96.0	100.5	107.0	98.5	97.5	99.5	98.9	103.5	102.2	102.0
NRC formula	97.4	99.7	104.8	101.3	102.7	107.8	104.3	105.0	98.6	96.5	100.5	105.2	107.8
C. J. Velz formula	92.8	99.7	98.2	99.4	101.0	102.4	102.3	100.7					

[a] South Side Plant, first stage. [b] Plant II. [c] Fourth test period. [d] First stage. [e] First test period. [f] Weighted average of domestic and industrial wastes.
[g] Includes flocculation of raw sewage.

performance of a filter and the accompanying settling tank is expressed by

$$\frac{L_D}{L} = 10^{-kD} \qquad (10)$$

in which L is the total removable fraction of B.O.D.; D denotes the depth of the filter, in feet; L_D is the corresponding quantity of removable B.O.D. remaining at depth D; and k represents the logarithmic rate of extraction.

For high-rate filters continuously dosed at a hydraulic rate of approximately 20×10^6 gal per acre per day, Mr. Velz has estimated the value of k as 0.1505 and L as 0.784. These values have been used in computing the performance and efficiency of single-stage filters. In this investigation, neither the variations from the dosing rate of 20×10^6 gal per acre per day nor the variations in sewage temperatures have been accounted for, both of which, Mr. Velz has stated, require consideration. This method has not been applied to the determination of the performance of two-stage plants.

SINGLE-STAGE PLANTS

Data from eight representative municipal plants operating according to the flowsheets in Fig. 1(*a*) or Fig. 1(*b*) or minor variations of both are analyzed in Table 1(*a*). Six plants were in routine operation during the period represented by the data, and two—those at Centralia, Mo., and Alisal, Calif.—were engaged in special tests when the data were collected. All had been in operation prior to the time that the data were taken.

Numerous other data from single-stage municipal plants were received, but it was deemed unwise to include them because of the omission of facts essential for accurate evaluation. It was also decided to omit references to those plants serving military or public institutions.

From Fremont, Ohio, the data represent a 1-month average of daily determinations; from Great Neck, N. Y., an average of 24-month operations; from Oklahoma City, Okla., an average of 6-month operations; from Richland, Wash., an average of 7-month operations; and from Dothan, Ala., 3-day tests made by the Alabama Bureau of Sanitation under normal operating conditions. The Centralia data are taken from special tests[6] by the United States Public Health Service; the data from Storm Lake, Iowa, are taken from special tests under normal operating conditions; and the Alisal data are from special tests.[7] In computing the averages given in Table 1(*a*) all data were weighted on the basis of flow.

An examination of the plant locations indicates a variety of climatic conditions. It should not be construed that the data relate to subzero temperatures because most biologic processes are at a minimum or cease altogether at these temperatures. In most cases the data were taken under temperate climatic conditions, which are the most critical conditions that plants are usually required to meet.

---

[6] "Efficiency Study of a Recirculating Sewage Filter at Centralia, Mo.," by W. A. Moore, R. S. Smithland, and C. C. Ruchhoft, *Sewage and Industrial Wastes*, February, 1950, p. 184.

[7] "Recirculation Tests on High Rate Filter," by Clyde C. Kennedy and Walter C. Roberts, *Sewage Works Engineering*, December, 1947, p. 622.

The flow data and filter data show a wide variation in recirculation ratios, clarifier-overflow rates, depths of filters, and filter-dosing rates. This is to be expected because plants are designed according to various theories to meet certain assumed, future conditions in a variety of areas. In Table 1(*a*) there is also shown the B.O.D. at the various plants; again, the loadings per unit of filter volume vary widely although none approaches the upper limit or "breakthrough" level where reductions per unit of filter volume tend to decrease. Data concerning efficiencies of B.O.D. removal are included not only for the settled sewage applied to the filter but also for the raw sewage because the latter B.O.D. removal is the real measure of performance for the plant as a whole.

An interesting fact is that the B.O.D. in the effluents from these single-stage plants are less than 30 ppm, except for two plants with very strong sewage where the first stage of biofiltration is followed by a second stage in which standard-rate filters are used. For the average municipal sewage it appears feasible to produce an effluent of from 20 ppm to 25 ppm from a biofiltration plant.

Efficiency.—By the use of the three methods described, the efficiencies in removing B.O.D. have been computed and compared with the actual operating efficiency. In Table 1(*a*) there are shown the results of these computations together with ratios of actual efficiency to computed efficiency for removals from settled sewage. According to these ratios it is apparent that the method offered by Mr. Velz yields data closest to the actual data; the Tentative Standards method, the next closest; and the NRC formula results in the greatest variation from actual data. In Table 1(*a*) there is also shown a comparison for the efficiency of over-all B.O.D. removals from the raw sewage, which indicates over-all plant performance.

Because of its simplicity and ease of application, the method derived from the Tentative Standards seems most useful. The method offered by Mr. Velz, although most accurate, is somewhat difficult to apply. Also, according to the strict application of the theory presented by Mr. Velz, recirculation ratios could be considerably reduced and the plant would still yield the same effluent; this possibility requires more substantiating evidence than is available. Although the NRC formula yields readily to graphic solution, it is nevertheless unwieldy to apply. A designer needs a method of determining proportions of a plant before it is built rather than a method of checking its actual performance later. The Tentative Standards method seems to serve this purpose in the simplest manner.

TWO-STAGE PLANTS

Filters in Series.—Data from five representative plants were studied which use two stages of filters in series without intermediate settling tanks; the flowsheet is shown in Fig. 1(*d*). All plants were in normal operation during the period represented by the data. Data from Winchester, Va., were collected during an entire year; from Bentonville, Ark., and Siloam Springs, Ark., the data were collected over a period of four and five days (respectively) by the Arkansas State Board of Health during routine plant operation. The data from Liberty, N. Y., were taken during a summer month when conditions were fairly uniform, although operating data are available for this plant for more than 12 yr. The data from Medford, Ore., were collected from a 6-month operation which included the canning season. This plant, which was constructed in 1942, served Camp White, Ore., during World War II and has since been operated by the city; it appears to be hydraulically overloaded. Data from several other plants were reviewed, but unfortunately information essential for this presentation was not included.

An examination of the basic data for two-stage installations in Table 1(*b*) indicates (as for single-stage plants) a variety of conditions of recirculation, clarifier-overflow rates, and filter-dosing rates. In Table 1(*b*) there is also shown the performance of these plants measured by removal of B.O.D. both from settled sewage applied to the filter and from the raw sewage. The over-all efficiencies of all the plants exceed 90%.

A comparison of computed efficiency and actual efficiency of B.O.D. removal from settled raw sewage and from the raw sewage (or over-all efficiency) is given in Table 1(*b*). The efficiencies were computed by using the Tentative Standards method and the NRC formula. In applying the latter, no allowance was made for the omission of the intermediate clarifier, which is normally assumed to be in the flowsheet. However, it should be noted that in three of the plants, actual performance is better than computed performance according to the NRC formula. As in the single-stage plants, the results of the Tentative Standards method of computing performance deviate less from actual performance than do those of the NRC method.

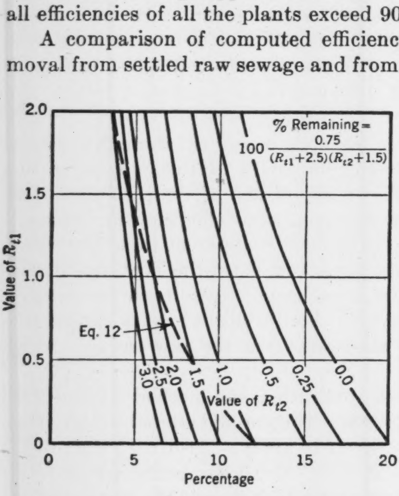

FIG. 4.—REMAINING SETTLED RAW B.O.D. IN EFFLUENT OF TWO-STAGE, SERIES-PARALLEL PLANT

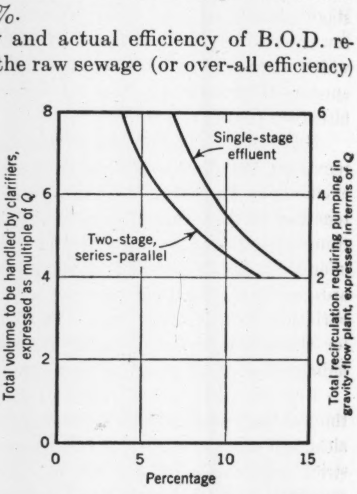

FIG. 5.—PERCENTAGE OF SETTLED RAW B.O.D. REMAINING IN EFFLUENT

The simplicity of the Tentative Standards method makes it the most practical method of predicting the performance of two-stage plants with filters in series. One reservation should be made in applying the Tentative Standards, concerning the recirculation in the first stage. Theoretically, recirculation could be reduced to zero, and the same mathematical efficiency would result.

Practically, however, there are not sufficient data to prove this point, and operation of actual plants indicates an absolute minimum recirculation ratio of 0.5, but preferably of 1.0 or more.

Intermediate Treatment.—Occasion often arises when the stipulated reduction in B.O.D. is somewhat greater than that which can be accomplished by sedimentation alone but somewhat less than that from a complete single-stage plant. Raw-sewage flocculation is occasionally applicable but is frequently inadequate. One solution to this problem is the use of the flowsheet in Fig. 1(*c*), which consists of a clarifier and filter in series, the filter effluent returning to the clarifier influent and the plant effluent withdrawn from the clarifier effluent. This flowsheet is used in a number of plants, principally in the western part of the United States, but unfortunately it was not possible to obtain any useful operating data from these plants.

An analysis of this flowsheet indicates that settled effluent from the clarifier must be passed once through the filter before recirculation can be established. Hence, the flow to the filter Q_f is represented by

$$Q_f = Q + R_s Q \text{......................} (11)$$

in which Q is the average raw-sewage flow. The clarifier must have the capacity to handle the filter effluent in addition to the raw-sewage flow, which results in a total flow into the clarifier equal to $Q\ (R_s + 2)$. This increased capacity of the primary clarifier takes the place of a separate final clarifier in settling the filter effluent. The difference is that this settled filter effluent constantly unites with the settled raw sewage, thus resulting in a substantial reduction in the B.O.D. of the settled raw sewage.

The expected performance of a plant using this flowsheet (Fig. 1(*c*)) is shown in Fig. 3. This performance has been computed, using the Tentative Standards, by assuming repeated passage through the filter of weighted volumes of settled raw sewage and settled filter effluent. The plant effluent is that part of this mixture which is equal to the raw-sewage flow.

Series-Parallel.—A further application of the intermediate plant flowsheet may be made by expanding the flowsheet by the addition of a second stage (Fig. 1(*e*)). This flowsheet has some unusual characteristics. A part of the settled raw sewage constantly passes to the second-stage filter, thus assuring a more even distribution of the initial food supply between the two stages. Thus the second stage can function with the same efficiency as the first stage; the "treatability" of the sewage should be the same for both filters. In a gravity-flow plant using this flowsheet, the two stages of filters can be placed at approximately the same elevation, with pumping requirements equal to $Q\ (R_{t1} + 1)$ in the first stage and $Q\ R_{t2}$ in the second stage.

The performance of plants using this flowsheet (Fig. 1(*e*)) can be evaluated by referring to Fig. 4. Fig. 4 has been devised by comparing the performance of a single-stage filter, using the Tentative Standards method, to the effluent from an intermediate-type plant. In the practical application of this flowsheet it should be observed that, when the same overflow rates are selected for the primary clarifier and the final clarifier, they will be of identical size when

$$R_{t2} = R_{t1} + 1 \text{......................} (12)$$

The filter volume is usually determined by computing the total volume required and dividing the latter equally between the primary filter and the secondary filter.

Operating data from plants using the flowsheet (Fig. 1(*e*)) are meager, although twenty-five to thirty plants, mostly in the western part of the United States, have utilized this flowsheet. It is possible that the limited use of the flowsheet has been caused by an unfamiliarity with it. Two plants widely separated geographically have yielded sufficient data to give some idea of performance; these data are shown in Table 2. The Orlando (Fla.) data were taken from an entire year of operation; it should be noted that the actual flow is only approximately half of the design flow. The data from the Petaluma (Calif.) plant were obtained during a 5-day test period in 1939. The unusual strength of the sewage in this plant was caused by wastes from poultry-packing plants and other similar industries. Because of a greatly increased tributary load, the Petaluma plant (built in 1938) was enlarged in 1953.

TABLE 2.—OPERATING DATA FOR TWO-STAGE PLANTS USING SERIES-PARALLEL FLOWSHEET

Description	Orlando, Fla.	Petaluma, Calif.
Flow, in 10^6 gal/day	3.90	0.505
Recirculation ratio:		
R_{I1}	1.6	1.43
R_{I2}	2.06	2.43
Clarifier-overflow rate, in gal/day/sq. ft:		
Primary	600	880
Final	965	880
Filters:		
Total area, in acres	1.04	0.203
Depth, in ft	5.0	3.0
Volume, in acre-ft	5.20	0.609
Dosing rate, in 10^6 gal/acre/day:		
Primary filter	19.3	12.0
Secondary filter	23.0	17.2
B.O.D. of raw sewage, in ppm	176	576
Estimated removal by settling, in %	30	33
B.O.D. of settled raw sewage		
in ppm	123	385
in lb/day	3,960	1,620
in lb/acre-ft	760	2,660
B.O.D. of final effluent		
in ppm	10.6	14
in lb/day	345	59
in lb/acre-ft	66	97
B.O.D. removed from settled raw sewage		
in ppm	112.4	371
in lb/acre-ft	694	2,563
Efficiency based on		
settled raw sewage, in %	91.4	96.4
raw sewage, in %	94.0	97.6
Computed efficiency based on		
settled raw sewage, in %	94.9	95.1
raw sewage, in %	96.4	97.2

SINGLE-STAGE OR TWO-STAGE FILTERS

Whether to select a single-stage flowsheet or a two-stage flowsheet is a problem that occasionally arises. In the smaller plants, where single filters will suffice and where the strength of the raw sewage is average, there is little doubt that a single-stage plant offers the simplest solution. Where multiple filters are required it is generally possible to provide two stages of treatment at little additional cost. In Fig. 5 there is shown a comparison between the total flow, including recirculation, to be passed through the clarifiers (primary and final) when using single-stage treatment and the same flow when using two-stage treatment. To achieve the same quality of effluent, the two-stage filter requires less tank capacity; conversely, an equal tank capacity yields a better effluent with two-stage treatment than with single-stage treatment. In each case, tank requirements vary with recirculation—the determining factor.

In either single-stage plants or two-stage plants it has been proved essential to remove the humus sludge from the final tank continuously because of its tendency to become septic rather quickly and deplete the oxygen in the effluent. Because continuous removal usually results in a thin sludge, common practice is to pump the humus sludge to the primary tank for consolidation with the raw sludge before the mixture is pumped to the digester. Another method is to utilize this humus-sludge outlet in the final clarifier as a source of recirculating material. Because this sludge is withdrawn from the clarifier bottom, it does not affect the volume overflowing at the tank surface and hence can be disregarded in determining the size of the final clarifier.

CONCLUSIONS

Although these conclusions may appear to be derived from data from a relatively small number of plants, it should be emphasized that, if the data were available, the conclusions would undoubtedly apply to a much greater number of single-stage plants and two-stage plants.

The performance of the plants cited appears to be dependent primarily on one factor—the ratio of recirculation. Dosing rate, loading of the filter, or depth of the filter have no significant effect within the range of values represented by the data.

For the treatment of average municipal sewage in smaller plants where one filter is feasible, single-stage filters appear to be most applicable and at the same time able to produce effluents containing a B.O.D. of from 20 ppm to 25 ppm. For larger plants where multiple filters are necessary or where stronger-than-average sewage is to be treated, a two-stage, series-parallel arrangement o filters should yield better effluent than single-stage filters for the same volume of tanks and filters and for the same volume of recirculation.

ACKNOWLEDGMENT

For data generously contributed, acknowledgment is particularly due to M. H. Klegerman, M. ASCE, Samuel H. Reaves, Grover L. Morris, Arthur N. Beck, M. ASCE, F. L. McDonald, Raymond S. Fish, Luis Ramos Robles, John S. Hess, C. MacCallum, M. ASCE, and Harry Eichenauer.

DISCUSSION

Peter Homack,[8] A. M. ASCE.—The report prepared by Mr. Rankin of the performance of several biofiltration plants is of considerable value in verifying the empirical methods that are used to predict the performance of biofiltration plants. The compilation of operating results and the analysis of these data should make the limitations and effectiveness of recirculation more clearly understood. With the advent of recirculation for trickling filters, many varieties and combinations of recirculation systems have been classified as high-rate filters with various recirculation ratios. For single-stage, high-rate filters, recirculation ratios of 1 to 1 or greater are generally used. The recirculation ratio has been considered to be an important factor in establishing filter efficiency. In analyzing Eqs. 2, 5, and 10 for single-stage filters, it will be noted that (except in Mr. Velz' formula, Eq. 10) the rate of recirculation governs the degree of efficiency.

In the Tentative Standards method (Eq. 2) the recirculation ratio affects the efficiency as follows:

Value of R_s	Value of E_s (%)
0.5	75
1.0	80
2.0	85.7
3.0	88.9

In the NRC formula (Eq. 5) the efficiency for a single-stage filter with a B.O.D. filter load of 2,000 lb per acre-ft is as follows:

Value of R_s	Value of E_s (%)
0	72.5
0.5	75.5
1.0	77.2
2.0	79.2
3.0	80.3

Therefore, an increase in recirculation results in an increase in efficiency in both Eqs. 2 and 5.

The data for the several biofiltration plants analyzed by Mr. Rankin indicate that the recirculation ratio is the governing factor in plant performance. Mr. Rankin concludes that, "Dosing rate, loading of the filter, or depth of the filter have no significant effect within the range of values represented by the data."

Eq. 10 provided results which checked closest to the data presented. It was concluded, however, that Mr. Velz' theory—which implies that recirculation ratios can be considerably reduced without affecting plant performance—requires more substantiating evidence than is available. The necessity for obtaining further data on the subject is evident; Mr. Rankin has presented operating results which form the basis for an initial analysis and comment.

---

[8] San. Engr., Elson T. Killam, Hydr. & San. Cons. Engr., Short Hills, N. J.

The Plainfield Joint Meeting Sewage Treatment Plant, in Plainfield, N. J., a treatment plant which cannot be considered to be a high-rate biofiltration plant—based on applied-loading standards—has been using recirculation (single stage) since 1938. In 1952 and 1953 the plant loads applied to the trickling filters were approximately 600 lb B.O.D. per acre-ft and 5.0×10^6 gal per acre per day for flow application. These loads are slightly smaller than the lowest loads of the plants analyzed by Mr. Rankin. The results of plant performance at Plainfield compare favorably with those reported by Mr. Rankin for that high-rate plant with the lowest applied load (Centralia).

The recirculation ratio has been reduced at Plainfield; the results indicate that the reduced recirculation ratio has not decreased plant efficiency. Consequently, the results of the performance of this plant will be compared for the period from 1950 to 1953 and will also be compared with the data presented by Mr. Rankin. It will be shown that a reduction in recirculation has not reduced the efficiency of plant performance. Dosing of the filters (by fixed nozzles providing a rain-drop application with a rising and falling cycle which will result in unusually uniform distribution), relatively low applied loading (compared to standard biofiltration applications), and possibly filter depth seem to be factors as important as, if not more important than, the recirculation ratio in the zone of "modified biofiltration" as practiced at the Plainfield plant.

History of Recirculation at Plainfield.—Recirculation has been practiced at the Plainfield Joint Meeting plant (serving Plainfield, North Plainfield, and Dunellen, N. J.) since 1938 at recirculation rates and applied loadings far below those generally considered in the design of single-stage biofiltration plants[9]. The plant was designed and placed in operation in 1917 as a standard-rate trickling filter with fixed nozzles.

The reason for the practice of recirculation was not to increase the efficiency of the filters but to provide for continuous sewage application and to prevent a psychoda-fly nuisance. When John R. Downes, plant engineer, was confronted with the psychoda-fly problem, he devised a plan for recirculating part of the final effluent back to the dosing tanks which precede the trickling filters in order to provide continuous sprinkling on the beds and thus prevent the escape of the psychoda fly. For economy, the minimum quantity of final effluent was recirculated. Prior to this recirculation, the psychoda flies had escaped from under the stone in the trickling filters while the beds were "resting" and were carried away by the wind so that a local nuisance was created. By sprinkling the beds continuously, the flies were trapped in the interstices of the trap rock and were eventually washed through the filter bed. In order to distribute the sewage uniformly over the entire bed, a motor-operated butterfly valve was installed in the discharge line from the dosing-siphon chamber so that the spray from the fixed nozzles would rise and fall uniformly with the opening and closing of the valve. As a result, not only was the entire surface area of the filters kept continuously wet, but a relatively uniform distribution of the sewage resulted. This distribution was considered to be at least as uniform as that which is obtained with rotary distributors. Recirculation was found to be so successful in eliminating the psychoda-fly nuisance that this practice of

---

[9] "Why High Rate Filters Work," by John R. Downes, *Water and Sewage Works*, June, 1946, p. 251.

TABLE 3.—Performance of Plainfield Joint Meeting Plant

Month[a]	1950				1951				1952				1953			
	5-Day B.O.D.			% removed	5-Day B.O.D.			% removed	5-Day B.O.D. [a]			%removed	5-Day B.O.D.			% removed
	Loading on filter, in pounds	Final Effluent			Loading on filter, in pounds	Final Effluent			Loading on filter, in pounds	Final Effluent			Loading on filter, in pounds	Final Effluent		
		in pounds	in ppm			in pounds	in ppm			in pounds	in ppm			in pounds	in ppm	
January	9,230	1,810	47	81.4	7,290	1,990	43	62.7	7,994	2,558	48	68.0	6,950	2,140	40	69.2
February	8,840	2,200	46	75.0	7,140	2,205	45	69.0	7,771	2,249	44	71.0	10,260	2,920	56	71.5
March	7,710	1,760	38	77.2	7,270	2,685	57	63.0	8,650	2,740	50	68.4	5,890	1,730	30	70.6
April	6,560	1,400	31	78.7	7,780	2,160	42	72.2	6,595	1,585	31	76.0	6,050	1,800	31	70.2
May	7,120	1,450	33	79.6	5,660	1,075	25	81.0	6,560	1,330	26	79.8	5,390	1,220	21	77.4
June	5,550	780	17	85.9	6,440	1,372	29	78.6	8,160	2,230	38	72.7	7,940	1,250	22	84.2
July	4,675	545	12	88.3	6,640	1,462	32	78.0	9,000	710	12	92.1	4,970	765	14	84.6
August	5,050	637	15	87.4	6,170	1,175	27	81.0	6,110	1,150	21	81.2	5,300	935	18	82.4
September	6,180	1,192	28	80.7	6,070	1,060	22	82.5	8,230	1,830	36	77.8	6,630	1,030	19	84.5
October	7,130	1,292	33	81.8	5,790	627	14	89.2	6,450	820	16	87.3	6,030	1,100	21	81.8
November	5,560	1,152	30	79.2	10,470	2,955	52	71.8	8,550	2,200	46	74.2	6,290	1,650	32	73.8
December	6,730	3,165	70	53.0	9,270	2,375	47	74.4	6,900	1,690	33	75.5	6,330	1,566	30	75.2
Average	6,700	1,450	33	78.4	7,150	1,760	37	75.4	7,570	1,760	33	76.7	6,500	1,505	28	76.8
Average flow, 12 months[b]	5.22				5.73				6.34				6.55			
Average flow, May to October[b]	5.20				5.45				6.50				6.55			
R_s, May to October	0.73				0.65				0.385				0.37			

[a] Continuous recirculation from May through October. [b] In 10^6 gal per day.

limited, controlled recirculation (modified biofiltration) has been continued at the Plainfield plant during the fly season ever since. Recirculation is begun in mid-April of each year and is continued until the first week in November. For the rest of the year, because of the absence of the psychoda fly and for economy, recirculation is not practiced, and the plant operates as a standard-rate trickling filter.

Plant Statistics.—The sewage-treatment plant consists of 1.8 acres of standard-rate trickling filters with fixed nozzles; the beds are 6.0 ft deep. When recirculation was initiated it was varied during the day so as to provide a constant rate of application on the filters totaling 9.0×10^6 gal per day.

The population of the tributary municipalities increased from 50,000 in 1938 to 70,000 in 1953; the average daily raw-sewage flow increased during the same period from 4.5×10^6 gal per day to more than 6.5×10^6 gal per day. The recirculation ratio has thus been reduced over this period of time from 1 to 0.385.

TABLE 4.—SUMMARY OF PLAINFIELD PLANT EFFICIENCY

Year	Recirculation ratio	Flow, in 10^6 gal per day	B.O.D. load on trickling filter, in pounds	B.O.D. of final effluent, in pounds	Efficiency, pounds (%)
ANNUAL AVERAGES					
1950	...	5.22	6,700	1,450	78.4
1951	...	5.73	7,150	1,760	75.4
1952	...	6.34	7,570	1,760	76.7
1953	...	6.55	6,500	1,505	76.8
AVERAGES FROM MAY THROUGH OCTOBER					
1950	0.73	5.20	5,820	980	83.2
1951	0.65	5.45	6,130	1,130	81.6
1952	0.385	6.50	7,420	1,345	81.8
1953	0.37	6.55	6,043	1,050	82.6

Results of Plant Performance.—Average monthly data for trickling-filter performance measured by 5-day B.O.D. tests during 1950, 1951, 1952, and 1953 are shown in Table 3. It will be noted that the efficiencies during the periods of recirculation (May through October) are appreciably greater than those during the months when recirculation is not practiced.

In Table 4 there is shown a summary of plant efficiency between 1950 and 1953 based on annual averages and averages for the periods of recirculation—May through October. It can be noted that during this period the plant flow increased from 5.20×10^6 gal per day to 6.55×10^6 gal per day whereas the recirculation ratio decreased from 0.73 to 0.37. Despite the decrease in recirculation, the efficiency was relatively constant. During this period of recirculation, the efficiency was approximately 6% higher than the average efficiency for the entire year.

From Tables 3 and 4, it can be seen that efficiency increases when recirculation is resumed in the spring. The effect of temperature in increasing biological activity (therefore increasing filter efficiency) is particularly noticeable during July, August, and September.

A program of recirculation which was originally initiated to control the psychoda fly has thus resulted in a simple, relatively inexpensive, and effective method of producing an acceptable final effluent through increased filter efficiency.

TABLE 5.—1953 OPERATING DATA FOR PLAINFIELD PLANT

Description	Value	
FLOW RATES		
Average sewage flow, in 10^6 gal/day	6.55	
Recirculation ratio, R_s	0.37	
Clarifier-overflow rate, in gal/day/sq ft:		
Primary	1,350	
Final	1,290	
FILTER DATA		
Area, in acres	1.78	
Depth, in ft	6.0	
Volume, in acre-ft	10.75	
Dosing rate, in 10^6 gal/acre/day	5.0	
PERFORMANCE BASED ON B.O.D. REMOVAL		
	May through October averages	12-month averages
B.O.D. of raw sewage, in ppm	192	202
Estimated removal by settling, in %	43	41
B.O.D. of settled raw sewage,		
in ppm	110	119
in lb/day	6,043	6,500
in lb/acre-ft	560	603
B.O.D. of settled effluent,		
in ppm	19	28
in lb/day	1,050	1,505
in lb/acre-ft	97	142
B.O.D. removed from settled raw sewage,		
in ppm	82	91
in lb/acre-ft	463	463
Efficiency based on		
settled raw sewage, in %	82.6	76.8
raw sewage, in %	90	86
EFFICIENCY OF B.O.D. REMOVAL FROM SETTLED RAW SEWAGE, MAY THROUGH OCTOBER, 1953		
% Efficiency:		
Actual	82.6	
Computed on basis of		
Tentative Standards	73.5	
N.R.C. formula	84.5	
C. J. Velz formula	80.9	
Actual ÷ Computed × 100:		
Tentative Standards	113	
NRC formula	98	
C. J. Velz formula	102	

Although the recirculation rate in 1953 was below the minimum rate (1 to 1) generally prescribed for single-stage, biofiltration plants, the results of a modified biofiltration plant have been found to be acceptable. Further studies are warranted for the analysis of plants using biofiltration methods but having low recirculation ratios and of existing standard-rate, trickling-filter plants in which increased loading is desired. It would appear from the results obtained at the Plainfield plant that modified biofiltration (reduced recirculation ratios) applied to existing standard-rate filters may be as feasible and desirable in many instances as modified aeration has been in the activated-sludge method of sewage treatment.

Comparison of Performance with Existing Biofiltration Plant Data.—In order to compare basic data for the Plainfield plant with Tables 1 and 2 and to evaluate the actual performance of the Plainfield plant as compared with the three empirical methods, Table 5 has been prepared. It will be noted that, except for the reduced recirculation ratio, the results at the Plainfield plant compare favorably with the results of performance reported for single-stage biofiltration plants.

Although the plant loads do not even approach a dosing rate of 20×10^6 gal per acre per day, the results of the plant operation tend to substantiate the strict application of the theory proposed by Mr. Velz—namely, that recirculation ratios can be considerably reduced and still yield the same quality of effluent.

Renville S. Rankin,[10] M. ASCE.—The value of recirculation of the effluent from a high-rate trickling filter has been amply demonstrated, but there is little information concerning the benefits, if any, of recirculation in low-rate filters or medium-rate filters. Mr. Homack's contribution relative to the experience at the Plainfield plant is instructive not only in establishing the fact that recirculation is beneficial in plants operating below the range of high-rate filters but also in providing a measure of that benefit.

The Plainfield plant is one of the oldest fixed-nozzle types of trickling-filter plants in the United States. Mr. Downes was most adept at solving operating problems with a minimum of expenditure. It is of interest that he used recirculation as a method of controlling the psychoda fly and, at the same time, producing a better effluent from the heavily loaded filters without major plant additions.

The effect of recirculation on trickling-filter performance and the rate of recirculation required are of importance not only to the designer but also to the operator. Recirculation is a continuing expense and hence should be held to the minimum required to attain the desired results. At Plainfield the filter loads were approximately 600 lb of 5-day B.O.D. per acre-ft compared to an average of more than 1,200 lb per acre-ft in the high-rate filter plants cited by the writer. This reduced load required less recirculation to yield an effluent comparable to that from a more heavily loaded filter; the results at Plainfield confirm this fact.

When the performance during that period of the year when recirculation was practiced at Plainfield is evaluated by the three methods used by the writer, Eqs. 5 and 10 give close predictions of the actual performance and Eq. 2 does not, according to Mr. Homack. It was stated that Eq. 10 was applicable where the filters were continuously dosed at a hydraulic rate of approximately 20×10^6 gal per acre per day. At Plainfield, the continuous dosing rate was only 5.0×10^6 gal per acre per day. Hence, because of the close relationship between the actual effluent and the computed effluent it seems possible that the range of application of Eq. 10 may be broader then Mr. Velz realized.

---

[10] Mgr., San. Eng. Div., The Dorr Co., Stamford, Conn.

Evidently Eq. 5 is as applicable as Eq. 10 in predicting performance at Plainfield when recirculation is used. However, it should be emphasized that Eq. 5 was developed primarily from the performance of military plants and was intended to apply to all types of filters, low-rate filters as well as high-rate filters. It is therefore interesting to evaluate the performance of the Plainfield filters by Eq. 5 for that period when recirculation was not being used and when the filters were operating in the usual range of low-rate filters. In Table 3 is contained the average monthly B.O.D. in pounds per day for a 4-yr period. Selecting the year 1953 and the averages for January through April, November, and December, the results for the period of zero recirculation are as follows:

Load on filters............	6,960 lb B.O.D. per day
Effluent..................	1,970 lb B.O.D. per day
Removal..............	4,990 lb B.O.D. per day or 71.7%

By applying Eq. 5 to this B.O.D. load, the resulting removal would be 82.3% or a ratio of actual performance to computed performance of 0.87.

Eq. 2 is obviously not applicable to the conditions at Plainfield. The basis for Eq. 2 is simply that a high-rate filter will remove two thirds of the applied B.O.D. load including recirculation when dosed at rates of 10×10^6 gal per day to 30×10^6 gal per day and when the B.O.D. load is 1,300 lb per acre-ft or more. The filter loads at Plainfield were less than half as great as these and hence are outside the scope of application of Eq. 2.

Therefore, of the three methods of evaluation of high-rate filters studied, the application of Eq. 10 to single-stage filters appears most accurate even in a range of loads below those stipulated by Mr. Velz. Eq. 10 is based on a biological oxidation law, but as for similar laws, certain factors must be derived from experience. Continued research should result in a more accurate determination of these factors so that Mr. Velz' method may ultimately become a more accurate method of predicting performance. However, Eq. 2 presumes a constant rate of biological oxidation for loads between wide limits; this presumption, although not unreasonable, is probably inconsistent with basic principles. A trickling filter, usually constructed with a coarse-rock medium, provides, however, anything but uniform oxidation facilities and actually is a rather crude device. Precise functioning according to a basic law cannot be expected. The object of the investigation was to provide a method whereby a designer could predict the performance of a proposed high-rate filter plant of specific proportions with reasonable assurance. Mr. Homack's useful contribution offers a method of predicting performance in a range well below that of the writer's field of study. In general, all factors considered, Eq. 2 appears to be the simplest and most applicable for high-rate filters within the accepted load range whether the filter is single-stage, two-stage, or a modification thereof.

AMERICAN SOCIETY OF CIVIL ENGINEERS
Founded November 5, 1852
TRANSACTIONS

Paper No. 2765

FINANCING OF SEWAGE WORKS IN PENNSYLVANIA

By Samuel I. Zack,[1] M. ASCE

Synopsis

There are presented herein the experiences of several localities in Pennsylvania with respect to the financing of sewage works by the sale of authority revenue bonds. It is shown that this type of financing is practical when the municipality does not have the capacity or means to finance such projects with general-obligation bonds supported by tax funds. The interest rates of such revenue bonds indicate that the risk is not considered to be excessive. The resulting sewer-rental charges are reasonable; experience of collections of sewer rentals against billings has been satisfactory, and ample revenues have been collected to meet annual operating and fixed expenses.

Municipality Authorities Act

The Municipality Authorities Act of 1945[2] has provided Pennsylvania with a practical method of financing the construction of sewage collection and treatment projects. Practically all the projects completed since 1945 have been constructed with the aid of such financing.

Authorities created under this act have the power—without referendum—(1) to sell bonds to pay for the financing and construction of sewage works and (2) to provide revenue through sewer-rental charges to amortize and pay interest on the bonds and to meet the annual expenses of operating and maintaining the works so constructed.

Although a law[3] has been passed in Pennsylvania that provides for the financing of public works by a municipality through the sale of revenue bonds without a referendum and although its legality has been supported, the law has not been tested (as of 1955) in the courts. Consequently, on the advice of a counsel, bonding firms have not been willing to purchase or expedite the sale of such revenue bonds.

Note.—Published, essentially as printed here, in June, 1954, as *Proceedings-Separate No. 453*. Positions and titles given are those in effect when the paper was received for publication.

[1] Chief of San. Div., Gannett, Fleming, Corddry and Carpenter, Inc., Cons. Engrs., Harrisburg, Pa.

[2] Act of May 2, 1945, *Public Law No. 382*, as amended (Commonwealth of Pennsylvania).

[3] Municipal Borrowing Law of June 25, 1941, *Public Law No. 159* (Commonwealth of Pennsylvania).

Sewage Projects Financed by Authorities

Construction of sewerage systems and sewage treatment plants in Pennsylvania for the boroughs of Mechanicsburg, Lemoyne, Middleburg, and Shippensburg and intercepting sewers and treatment plants for Bloomsburg, Gettysburg, Danville, and Catawissa was financed through the sale of municipal authority bonds. The Bloomsburg project also included an incinerator for burning sludge and refuse. Revenue for annual expenses of operation and fixed charges is derived in each case from sewer-rental charges. Although it is considered possible to finance construction of lateral sewers by front-foot assessments, this method was not used by these municipalities. The 1950 population, design population, sewage flows, scope of the project, total cost of construction contracts, and the bonds issued in each case are presented in Table 1.

TABLE 1.—CONSTRUCTION

Authority	Population		Average sewage flow[a] (design)	Scope of project[b]	Construction contracts (in dollars)	Bonds issued (in dollars)	Date of issue
	1950 census	Design					
Mechanicsburg	6,786	9,800[e]	0.64	SS, CT	1,082,000	1,040,000[f] 250,000[f]	6/1/49 6/1/50
Lemoyne	4,605	7,000	0.53	SS, PT	838,000	880,000[f] 135,000[f]	5/1/49 5/1/50
Middleburg	1,283	1,700	0.16	SS, PT	371,000	475,000[f, g]	4/1/51
Bloomsburg[h]	10,633	43,000[i]	2.10	IS, IT, R&SI	1,030,000	1,250,000[j]	4/1/51
Gettysburg	7,046	8,500	1.00	PTI, AST&RS	415,000	475,000[j]	10/1/51
Danville	6,994	9,300	1.30	IS, PT	410,000	475,000[f, k]	2/1/52
Shippensburg	5,722	9,300	0.93	SS, CT		1,300,000[f]	4/1/52
Catawissa	2,000	2,000	0.20	IS, PT	113,000	150,000[f]	5/15/52

[a] In million gallons per day. [b] The symbols used denote the following: SS, sewerage system; CT, complete treatment; PT, primary treatment; IS, intercepting sewers; IT, intermediate treatment; R&SI, refuse and sludge incineration; and AST&RS, addition of secondary treatment and relief sewers. [c] Allowing for premium or discount on bonds. [d] No adjustment for initial interest from bond issue. [e] Includes industrial wastes B.O.D.

Items of Cost Included in Bond Issues

In addition to the funds required for the construction contracts, bonds were issued by the authority to provide for such items as repayment of engineering costs advanced by the federal government or by the municipality for the preparation of construction plans, engineering costs incurred by the authority before and during construction, real estate and rights of way, local and bond counsel, printing indenture, trustee's initial fees, administrative and operating expenses or working capital for the authority, initial debt-service reserves, interest during construction, and contingencies.

The authority is usually guided by a financial advisor or fiscal agent and bond counsel in the financing and preparation of prospectuses, financial schedules, and indentures. The fiscal agent may be selected to provide for the sale of bonds through public sale, or a fiscal agent may serve in negotiating the purchase price of the bonds at a private sale. With the exception of Bloomsburg and Danville, the bonds were sold at private sale by negotiation. In the case of Danville, where bonds were advertised for public sale, the bond issue also included printing of bonds, financial advisor's fees, printing and mailing of prospectuses, and advertising. The Bloomsburg bonds were first advertised for public sale, but because no formal bids were received the bonds were sold by negotiated private sale.

AWARDING OF CONTRACTS AND SALE OF BONDS

The receiving of bids for construction and the awarding and execution of contracts were timed and coordinated with the private or public sale and delivery of the bonds so that the commitments of the authority with respect to contracts became effective almost simultaneously with the availability of funds through the sale of bonds; therefore, none of the parties concerned was left with commitments that could not be fulfilled.

CONTRACTS AND BOND FINANCING

Interest rate %	Years to maturity of issue	Bond price (in dollars)	Average years total issue	Actual average interest rate (%) (computed)[c]	Total interest during life of bonds (in dollars)	Average annual fixed charges[d] (in dollars)	Fixed charges under indenture (in dollars) (1953)	Fixed charges under indenture 8th year (in dollars)
3¼, 3⅜	40	97.50	26.70	3.515	952,250[e]	61,138	60,100	68,000
3¼	40	97.50	25.22	3.300	203,281[e]			
3¼, 3½	40	100.00	25.90	3.490	794,775	49,348	53,515	55,721
3¾	40	100.00	32.41	3.750	164,163			
2¾, 2⅞	40	100.00	26.02	2.789	344,706	20,492	15,200	23,500
2½	30	99.00	18.44	2.580	588,750[e]	61,292	74,656	74,656
2⅝	40	100.18	24.56	2.606	304,666[e]	19,491	24,200	24,200
1⅞, 2, 3	27	100.08	16.50	2.015	158,083[e]	23,448	32,000	32,000
2½, 2⅝, 2¾, and 2.8	40	99.00	25.99	2.773	927,418[e]	55,685	....	72,300
2¼, 2½	29	100.00	18.45	2.731	75,712	7,783	10,300	10,300

population of 1,800. [f] Lease-back to borough for operation. [g] Borough guarantees $2,500 per year from tax revenue. [h] Refuse and sludge incinerator included. [i] Includes industrial wastes B.O.D. population of 30,000. [j] Operated by authority. [k] Borough guarantees to make up deficits from tax revenue.

The number and price of bonds sold, date of issue and maturity, average interest rate, and total interest on the bonds during the scheduled maturity period are also shown in Table 1. In each case the discount and premium on the bonds were taken into consideration in computing the actual average interest rate of the bonds. Although different for each bond issue, various quantities of bonds were to mature each year. As an entire bond issue approached maturity and interest charges on unretired bonds became less, the principal of the bonds to be retired became greater each year or after a period of several years. The average life of the total principal of each bond issue was computed by weighting the bonds scheduled for retirement each year and the life to maturity of such individual bonds.

TRUST INDENTURES SECURING BOND ISSUE

In each case a trust indenture setting forth the requirements for securing the revenue-bond issue was executed between the authority and a trustee in behalf of the bond purchasers. The indenture required revenues from sewer-rental charges to cover administrative costs, operating and fixed charges, and reserves—with provisions for an increase in rates in the event of inadequate revenue.

In all the municipalities cited herein, except Bloomsburg and Gettysburg, the entire projects were leased to the municipality for operation, maintenance, and collection of revenue. The Bloomsburg and Gettysburg projects were managed and operated by the authority. The lease contract under the indenture between the borough and the authority at Danville guaranteed that the borough's tax revenues would be provided to meet deficits if sewer-rental revenues failed to cover the annual expenses of operation and debt-service requirements. At Middleburg an annual contribution toward operating costs from tax revenue of not less that $2,500 per year was pledged by the borough to lessen the individual sewer-rental charges and to meet any deficit between annual revenue and annual expenses. In all cases the financing was arranged so that the average of anticipated annual receipts from sewer rentals would be greater than the annual operation and maintenance expenses and average annual debt-service and authority expenses by a substantially safe margin.

It is obvious that the anticipated collection of revenue would thus result in accumulation of surplus funds. Such surplus funds were to be available (1) to supplement deficits in revenue needed for annual requirements of debt service, authority expenses, and the costs of operation and maintenance; (2) to establish reserves for debt service, maintenance, and emergency repairs and replacements; and (3) for the bond redemption and improvement fund to retire bonds before maturity or to make improvements and additions to the project. Surplus funds from the sale of bonds not used for initial construction purposes also became available for reserves and for bond redemption and improvement funds. Indentures stipulated the redemption price of longer maturity bonds when redeemed during the initial years of the bond issue.

In each case provisions were included in the indenture for the sale of additional bonds, if required, with means for providing revenue to service and amortize such supplemental bonds. Supplemental bonds totaling $135,000 were sold at Lemoyne and $250,000 at Mechanicsburg to provide for an extension of sewer services, overrun of rock, and other unforeseen contingencies.

SEWER CONNECTION AND RENTAL CHARGES

Each municipality or authority passed an ordinance establishing a schedule of sewer-rental charges and methods of collecting such rentals and permitting the placing of liens against property owners in the event of failure to collect sewer service charges. After taxes such liens have priority over any other claims against the properties involved. Trust indentures required that rental rates be increased whenever the revenues do not meet the requirements of operating costs, debt service, and reserves.

The ordinances that were passed required all property owners to connect their premises with the sewerage system, and rentals or charges were to become effective at the time of such connection. Rental charges for sewerage service were made subject to penalties if not paid within thirty days after they are due, with additional penalties if not paid within sixty days after due. It was further provided that all delinquent bills for rentals or charges could be entered as liens

TABLE 2.—SCHEDULE OF SEWER CONNECTION CHARGES[a] (IN DOLLARS)

Description	Mechanicsburg	Lemoyne	Shippensburg	Middleburg
Residential:				Each initial connection charge, $75. During second year, $105; third year, $110; fourth year, $115; fifth year, $120; sixth year and thereafter, $125.
First, 6 in. or less	30.00	30.00	35.00[b]	
Additional six, 6 in.	15.00	15.00	20.00[b]	
Over six, 6 in.			15.00[b]	
Commercial:				
First, 6 in. or less	40.00	40.00[c]	50.00	
Additional, 6 in.	20.00	20.00[c]	30.00	
First, 8 in.	50.00	75.00[d]	65.00	
Additional, 8 in.	25.00		35.00	
Industrial:				
6 in.	50.00		65.00	
8 in.	75.00	75.00[d]	90.00	
10 in.	100.00	[e]	115.00	
Over 10 in.	[e]	[e]	140.00	
Future connections		[f]		

[a] Per connection. [b] Per family unit. [c] Water meter less than 1 in., with water meter 1 in. or 1½ in.; $50. [d] Water meter 2 in. or larger. [e] As determined by municipality, but not less than $100. [f] Surcharge $10 per yr up to $100.

against property and that such liens were to be filed and collected in a manner provided by law for the filing and collecting of municipal claims.

Where the construction of a complete new sewerage system was involved, as in Mechanicsburg, Lemoyne, Middleburg, and Shippensburg, it was not possible to collect any revenues until the treatment plant was completed, connections of the sanitary facilities of properties were made to the sewer system, and sewer-rental charges became due and payable. In order to provide for initial debt-service requirements, a charge for connecting properties to the sewer system was established and collected as soon as connections were made. Such

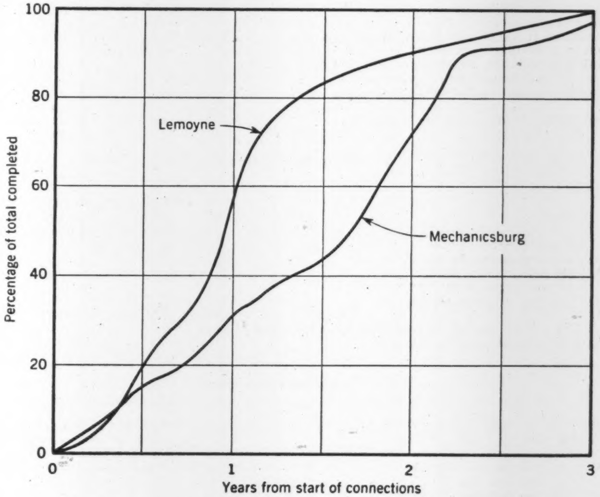

FIG. 1.—ACTUAL RATE OF CONNECTING SEWER SERVICE UNITS

connection charges were to increase after a given period of time so that vacant properties connecting at a later date would have to pay more than those properties connecting initially. The schedules of sewer connection charges adopted at Mechanicsburg, Lemoyne, Middleburg, and Shippensburg are shown in Table 2.

The time taken in connecting properties to the sewer system is dependent on the number of plumbers in a given area, on the willingness of property owners to expedite the work, and on any difficult excavating conditions encountered because of rock. A great deal of rock was encountered at Mechanicsburg and Lemoyne. The originally contemplated number of 2,300 properties at Mechanicsburg and 1,455 at Lemoyne were connected to the sewer system within 3 yr, although a period of from 4 yr to 5 yr had originally been contemplated. At Lemoyne, where the immediate need for connection to the sewer system was

TABLE 3.—SUMMARY

Metered and nonmetered water users	Strength of waste surcharge added to charge, based on metered water or sewage
(*a*) MECHANICSBURG	
Residential and commercial: Based on Table 4 (*a*) Industrial, metered: $25 per 1,000 gal per day of average discharge for week of year of maximum discharge or water use.	0.20% for each part per million suspended solids in excess of 150 ppm, plus 0.10% for each part per million B.O.D. in excess of 200 ppm
(*b*) LEMOYNE	
Metered: Residential and commercial: First 20,000 cu ft, $0.63 per 100 cu ft per quarter 20,000 cu ft to 80,000 cu ft, $0.42 per 100 cu ft per quarter Exceeding 80,000 cu ft, $0.2625 per 100 cu ft per quarter Minimum for residential, $4.50 per quarter Minimum for commercial, $6.00 per quarter Industrial: $0.25 per 100 cu ft of wastes per quarter	0.10% for each part per million suspended solids in excess of 150 ppm, plus 0.10% for each part per million B.O.D. in excess of 200 ppm
(*c*) MIDDLEBURG	
Nonmetered: Based on Table 4 (*b*) Metered: First 3,000 gal per quarter, $2.50 Next 5,000 gal per quarter, $1.50 Next 42,000 gal per quarter, $0.75 Next 50,000 gal per quarter, $0.50 Over 100,000 gal per quarter, $0.30 Industrial: $60 per 1,000 gal per day of average discharge for week of year of maximum discharge or water use.	0.10% for each part per million suspended solids in excess of 150 ppm, plus 0.10% for each part per million B.O.D. in excess of 200 ppm
(*d*) BLOOMSBURG	
Nonmetered: Based on Table 4 (*c*) Metered: First 200,000 gal per quarter, $0.35 Next 400,000 gal per quarter, $0.25 Over 600,000 gal per quarter, $0.15	0.05% for each part per million suspended solids in excess of 250 ppm, plus 0.05% for each part per million B.O.D. in excess of 200 ppm

greater because of difficulties with septic tanks and where more plumbers were available, 60% of the connections were completed in the first year; on the other hand, at Mechanicsburg only 30% were completed by that time. In 1½ yr 82% were completed at Lemoyne and only 42% at Mechanicsburg; in 2 yr it was 90% against 75%. In both municipalities, because of real estate activity, the total numbers of connections exceed those originally contemplated. The rates at which the originally contemplated numbers of connections were made at Mechanicsburg and Lemoyne are shown in Fig. 1.

of Sewer-Rental Rates

Metered and nonmetered water users	Strength of waste surcharge added to charge, based on metered water or sewage
(*e*) Gettysburg	
Metered: First 1,000 cu ft per quarter, $0.30 per cu ft Next 5,000 cu ft per quarter, $0.25 per cu ft Next 44,000 cu ft per quarter, $0.15 per cu ft Next 300,000 cu ft per quarter, $0.09 per cu ft Over 400,000 cu ft per quarter, $0.075 per cu ft Minimum quarter: Domestic—1,000 cu ft, allowance $3.00 Commercial and municipal—2,200 cu ft, allowance $6.00	0.10% for each part per million suspended solids in excess of 150 ppm, plus 0.10% for each part per million B.O.D. in excess of 200 ppm
(*f*) Danville	
Basic rentals: 100% of water charges. Minimum charge of $12.00 per year Metered: Under 100,000 gal per quarter, $0.20 per 1,000 gal Over 100,000 gal per quarter, $0.15 per 1,000 gal Based on credit for metered water not discharged to sewers or metered sewage— Under 100,000 gal per quarter, $0.25 per 1,000 gal Over 100,000 gal per quarter, $0.20 per 1,000 gal	0.10% for each part per million suspended solids in excess of 250 ppm, plus 0.5% for each part per million chlorine demand in excess of 15 ppm
(*g*) Shippensburg	
Basic rentals: 350% of water charges Metered: $0.25 per 1,000 gal per quarter Based on credit for metered water not discharged to sewers or metered sewage— $0.35 per 1,000 gal per quarter	0.05% for each part per million suspended solids in excess of 200 ppm, plus 0.05% for each part per million B.O.D. in excess of 250 ppm
(*h*) Catawissa	
Basic rentals: 100% of water charges Metered: $0.50 per 1,000 gal of industrial wastes or water per quarter with credit for water excluded from sewers.	0.10% for each part per million suspended solids in excess of 250 ppm, plus 0.5% for each part per million chlorine demand in excess of 15 ppm

In anticipation of excessive rock and a limited number of plumbers at Shippensburg, it was planned (for estimating revenue from sewer connections and rentals) that it would take at least 4 yr to complete substantially the sewer connections. Although the connection charge was to be paid when the connection was made, it was assumed that there would be a delay before billings could be made and revenues actually received from sewer rentals. The estimated rate of connecting sewer service billings and the receipt of revenue at Shippensburg are shown in Fig. 2.

Sewer service charges (except for large users) at Mechanicsburg and Bloomsburg were based on fixtures because only partial metering of water existed at Mechanicsburg and no metering of small users existed at Bloomsburg. In

TABLE 4.—QUARTERLY SEWER-RENTAL SCHEDULE BASED ON FIXTURES (IN DOLLARS)

Item	Residential units	Commercial units[a]	Restaurants, clubs, hotels[b]	Public buildings, hospital, railroad station	Garages and service stations
(a) MECHANICSBURG					
First fixture, sink, basin, or toilet	4.00	5.00	10.00	10.00	7.50
Each additional fixture:					
Basin	1.00	1.50	2.00	3.00	3.00
Bath or shower	1.00	1.50	1.50	3.00	1.50
Toilet	1.50	2.00	2.00	4.00	3.00
Urinal	1.50	1.50	2.00	4.00	3.00
Sink or laundry tub, single	1.50	2.00	2.00	10.00	
Sink or laundry tub, double	2.00	2.50	2.50	12.50	
Washing machine and tub	0.50	1.00			
Water motor	0.50	0.50			
Drinking fountain		0.50	0.75	0.75	0.75
Soda fountain or bar drain		3.00		5.00	
Refrigerator drain		0.75	0.75	1.00	0.75
Wash rack					10.00
(b) MIDDLEBURG					
First fixture	7.50	10.00			
Additional fixtures:					
Sink	2.00	2.50			
Bathtub and shower	1.50	2.00			
Lavatories	1.50	2.00			
Toilet or urinals	2.00	2.50			
Laundry tub	2.00				
Cellar or garage drain	1.00	1.50			
(c) BLOOMSBURG					
First outlet (sink, toilet, or basin)	2.50	4.00	6.00		
Each additional unit	1.00	1.50	1.50		
First toilet	1.25				
Each additional unit	0.50				
First basin	1.00	1.25	2.00		
Each additional unit	0.50	0.75[c]	1.50		
First bathtub, shower, or combination	1.00	1.00	2.00		
Each additional unit	0.50	0.75	1.00		
First washing machine	0.50	1.00	1.00		
Each additional unit	0.25	0.75	0.75		
First sink		1.25	2.00		
Each additional unit		0.75	1.50		
First urinal		1.00	2.00		
Each additional unit		0.50	1.50		
First drinking fountain		1.25	1.25		
Each additional unit		0.75			
First dishwasher		1.00	2.00		
Each additional unit		0.75			
Floor drain (also refrigerator and steam)	0.25	0.50[c]	0.75		
Auto wash rack, private		3.00			
Auto wash rack, for revenue		6.00			

[a] For Mechanicsburg this item includes stores, offices, banks, and other commercial establishments and churches; for Bloomsburg, stores, offices, banks, public buildings, railroad station, garages, and service stations. [b] For Mechanicsburg this item includes theaters and recreation halls. [c] $1.00 for garages.

both cases the water utilities were privately owned. At Middleburg, schedules based both on metered water and on fixtures were established because partial metering of water was in effect in that borough. At Lemoyne and Gettysburg the sewer service rates were based entirely on the metered use of water. Arrangements were made with the private water company to do the billing at Lemoyne. The municipal authorities did the billing at Gettysburg and Bloomsburg.

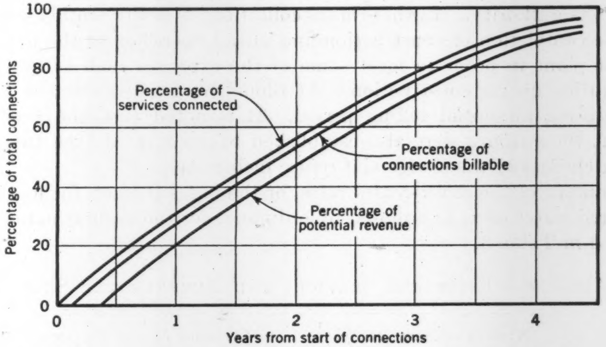

FIG. 2.—RATE OF CONNECTING SEWER SERVICES, BILLINGS, AND REVENUE AT SHIPPENSBURG (ESTIMATED UNITS, 2,000)

At Danville, Catawissa, and Shippensburg—where domestic users were billed on a combination of flat rate, fixtures, and size of home and large users of water were charged on the basis of metered use—the sewer service charge, except for large users of water, was made on the basis of a percentage of the water bill. In the case of Catawissa and Danville this was 100%, and for Shippensburg—where a low water rate existed and construction of a sewerage system as well as a treatment plant was involved—it was 350%.

TABLE 5.—QUARTERLY PER CAPITA SEWER-RENTAL CHARGES FOR SCHOOLS, INDUSTRIES, AND HOSPITALS

Authority	Industrial establishments, minimum per employee (in dollars)	Schools per pupil (in dollars)
Mechanicsburg....	1.50	0.35
Lemoyne..........	1.00	[a]
Middleburg.......		[a]
Bloomsburg.......	0.50	0.30
Gettysburg.......	0.50	[a]
Danville[b].......	0.75	[a]
Shippensburg......	1.50	0.75
Catawissa.........	1.00	0.50

[a] Same as residential. [b] Hospitals are rated at $1.50 per quarter per person occupying premises.

Sewer-rental schedules in all cases provided for a surcharge because of excessive suspended solids, chlorine demand, and 5-day B.O.D. Sewer-rental schedules provided credits for uncontaminated cooling waters and other such waters discharged directly to outlets other than the sewers and included means of charging for water coming from wells or other private water supplies. Rentals for schools were based on a rate per pupil in some cases, and industrial establishments were charged in accordance with the scheduled rates with a minimum rate per employee.

Municipalities which had existing sewerage systems—Bloomsburg, Gettysburg, Danville, and Catawissa—deeded their sewerage systems to their authorities, and at Gettysburg the existing overloaded primary treatment plant was deeded to its authority. In these cases collections of sewer rentals were begun before the completion of construction and initial operation of the new sewage treatment plant in order to meet some of the expenses such as interest and administration during construction. At Bloomsburg a deduction of 50% was allowed during an initial billing period. It is noted that the sewer-rental charges at Bloomsburg were also established to pay annual fixed charges and operating charges of the sludge and refuse incinerator.

A summary of the sewer-rental rates, or the bases thereof, for metered and nonmetered water users as adopted by ordinance for the various municipalities is outlined in Table 3.

TABLE 6.—ESTIMATED SERVICES AND REVENUE PER SERVICE

	NUMBER OF SERVICES		Average revenue per service connection (in dollars)	AVERAGE ANNUAL REVENUE FROM RENTALS		
	Commercial[a]	Residential dwelling units		Per commercial service (in dollars)	Per residential dwelling unit (in dollars)	Percentage from residential
Mechanicsburg	175	2,125	28.00	146.00	30.50	72
Lemoyne	85	1,370	33.00	210.00	31.50	71
Middleburg	58	439	85.00	124.00	50.00	74
Bloomsburg	85	3,368	....	630.00	24.00	60
Gettysburg	317	1,331	....	90.00	17.10	45
Danville	...	2,000[b]	....	....	20.40[b]	76
Shippensburg	190	1,986	31.00	114.00	37.50	78
Catawissa	54	538	....	108.00	23.50	69

[a] Commercial includes industrial, schools, institutions, hospitals, and public buildings. [b] Nonmetered users include small commercial users.

The sewer-rental schedules based on fixtures adopted at Mechanicsburg, Middleburg, and Bloomsburg are shown in Table 4.

The sewer-rental schedules based on fixtures or water use provided that industrial establishments pay a minimum per employee regardless of the rental payments based on fixtures or water use. These minimum rentals ranged from $0.50 to $1.50 per employee. Sewer rentals for schools based on the number of pupils ranged from $0.30 to $0.75 per quarter per pupil at Mechanicsburg, Bloomsburg, Shippensburg, and Catawissa. In the other municipalities schools were charged on the basis of fixtures or metered water use. The quarterly per capita charges for schools, industries, and hospitals are shown in Table 5.

The estimated average annual sewer rentals in those municipalities where complete new sewerage systems had to be built were more than $30.00 per dwelling unit, even though the period to maturity of the bond issue was 40 yr. In the municipalities which already had sewerage systems the sewer rentals were less than $25.00 per dwelling unit per year with bond issues of 30 yr or less. At Gettysburg, where there was an existing sewerage system coupled with a high percentage of commerical and industrial users and with 40-yr bonds, the annual sewer-rental charge was $17.10 per dwelling unit.

The number of commercial, industrial, and other nonresidential sewer services; the number of residential dwelling units; the average revenue per service connection; average annual revenue per commercial service and per residential dwelling unit; and the percentage of revenue from residential units in the various municipalities are shown in Table 6.

INDUSTRIAL WASTE REGULATIONS

Most of the sewer-rental schedules adopted defined industrial establishments as any premise used wholly or in part for the manufacture, processing, cleaning, laundering, or assembly of any products, commodities, or articles. The municipality reserved the right to refuse connection with the sewer system, to compel discontinuance of use of a sewer, or to compel pretreatment of industrial waste by an industrial establishment in order to prevent discharges considered harmful to the sewerage system, sewage treatment plant, or sludge handling processes.

Sewer-rental rates included a surcharge on the strength of waste to be added to the charge based on metered water or sewage, as outlined in Table 3. A representative of the municipality was permitted to have access at all times to the industrial establishments and to any meters used for establishing or determining water consumption, water excluded from the sewer system, or sewage or waste waters discharged into the sewer system.

The strength of waste that establishes the surcharge could be determined by the municipality either (*a*) by suitable sampling and analyses of the wastes at the time of maximum production; (*b*) by relating production and waste strength at the time of sampling to waste strength at maximum production if sampling was not performed at the time of maximum production; (*c*) from estimates; or (*d*) from known relationships between the products and the strength of wastes for those industries if such factors have been established. Any industrial establishment was permitted, under the supervision of a representative of the municipality, to determine or verify the strength of waste for billing purposes by taking samples and making laboratory analyses if the strength of wastes had not been determined by the municipality.

Industries were required to install fine screens to remove husks, hulls, vegetable skins and peelings, thread, lint, grease, and other such nonsettleable and floating solids, or other organic or inorganic substances considered or found by the municipality to overload, impair the efficiency of, or cause difficulties in the operation of the sewage treatment plant or in maintaining the quality of treated effluent.

Requirements for equalization of flow by holding tanks were set up in all cases for plants which discharged 50,000 gal or more of sewage per day to provide uniform discharge over 24 hr, with the provision that peak rates of discharge should not exceed by more than 50% the average 24-hr rate estimated or determined for from 3 days to 5 days of maximum production. This provision was instituted to prevent overloading of the treatment plants. In the case of Catawissa, which is one of the smaller plants, equalization of flow and holding

TABLE 7.—FUNDS UNDER INDENTURE FOR FIXED CHARGES AND RESERVES

Item	Mechanicsburg	Lemoyne	Middleburg	Shippensburg	Bloomsburg[a]	Gettysburg[a]	Danville	Catawissa
Date of bond issue	June, 1949[b]	May, 1949[c]	April, 1951	April, 1952	April, 1951	October, 1951	February, 1952	May, 1952
Construction begun	June, 1949	May, 1949	June, 1951	July, 1952	June, 1951	October, 1951	February, 1952	June, 1952
First sewer connection made	August, 1950	June, 1950	February, 1952	April, 1954				
Sewer rentals or operation begun					August, 1953	May, 1953	May, 1953	July, 1953
Bond issue, years to maturity	40	40	40	40	30	40	27	29
Funds from bond issue:								
Interest, years	2½[b]	2[c]	2	2	1		1	¼
Interest, amount, in dollars	98,015	62,594	26,375	70,658	31,250		10,019	1,014
Working capital for authority, in dollars	1,000	1,200[d]	500	7,000	20,000	60,000[e]	1,000	1,000
Debt-service reserve, in dollars		15,000	6,000					
Funds to trustee from sewer rentals, in dollars:								
During first year of bond issue					43,406	24,200[f]	16,000	7,725
second[g]		2,500	5,200	18,500	74,656	24,200	32,000	10,300
third	37,300	20,800	17,800	39,300				
fourth	53,600	29,608	25,300	58,000				
fifth	61,600	55,410	24,000	71,500				
sixth	67,500	57,300	23,500	78,000				
seventh	68,500	56,576	23,500	72,300				
eighth[h]	68,000	55,721[i]	23,500	72,300				
Reserves from funds to trustee, in dollars:								
During first year of bond issue						5,000	14,000	600
second			4,500	17,500	15,000	5,000	12,000	1,700
third		1,000	2,500	2,400	24,000	5,000	12,000	3,900
fourth	15,000	15,000	5,000	21,000	22,000	5,000		3,900
fifth	10,000	17,000	4,000	33,100	17,000	5,000		3,900
sixth[h]	10,000[j]	2,000	2,000					
Total	65,000	35,000	18,000	74,000	78,000	25,000	38,000	14,000
Authority and trustee expense, in dollars	900	900[d]	500	1,500[k]	[l]	[l]	1,500	900[m]

[a] Payment to trustee 1½ times annual debt service. [b] Supplementary bond issue—June, 1950—interest, 1½ yr. [c] Supplementary bond issue—May, 1950—interest, ½ yr. [d] First two years, $1,200 each. [e] $50,000 to capital additions and bond redemption fund. [f] Includes estimated $9,200 per year to capital additions and bond redemption fund. [g] And subsequently for B, G, D, and C. [h] And subsequently. [i] Varies somewhat each thirty-ninth and fortieth year, each $71,600. [j] $10,000 each year until total is reached. [k] First year, $1,000. [l] As may be reasonable. [m] First year, $675.

tank was required for discharges of 25,000 gal per day instead of 50,000 gal per day.

ANNUAL EXPENSE AND REVENUE

In all the municipalities cited herein, revenue had to be sufficient for the annual payments provided for in the indenture for interest, amortization and reserves, and operating expenses (which herein indicate normal maintenance, repairs and replacements, and administrative costs). Fixed payments had to be such that the revenue received during the initial years would be sufficient for the payments as they became due. It was therefore necessary to make estimates of the annual requirements for interest, amortization, reserve funds, and authority expenses under the indenture, as well as of the annual operating costs and the annual revenue which could reasonably be collected. It was not difficult to make these estimates for those municipalities in which the collection of sewer rentals was begun before the operation of the treatment plant was started—that is, in those cases in which sewer systems already existed.

As previously noted, where construction of a new sewer system was involved, the receipt of revenue during the initial years of the bond issue was dependent on the progress of construction of the sewer system and treatment plant—and particularly on the rate of connecting properties to the new sewer system. Usual practice allowed a property from sixty days to ninety days to connect after receipt of notice to do so, thus resulting in a time lag beyond the physical ability to make the connection.

The revenues collected at Mechanicsburg, Lemoyne, Middleburg, and Shippensburg during the early period of operation were more than sufficient to meet requirements for fixed and operating charges. For the Bloomsburg, Gettysburg, Danville, and Catawissa plants, collections of revenues were begun soon after construction was begun, and revenues were more than ample. The dates of (1) bond issue, (2) beginning construction, and (3) operation are shown in Table 7.

Annual expenses which have to be covered by sewer-rental charges are costs of operation (as previously defined) and expenses of administration including insurance (fire, casualty, and payroll), taxes, bookkeeping, billing, office rental, telephone, stationery, supplies, and postage; engineering and legal services; authority expenses including trustee's fees and auditing; and the fixed payments or transfer of funds to the trustee to meet requirements for interest and retirement of bonds and to provide for establishing debt service, maintenance, and other reserve funds.

In those municipalities in which complete new sewerage systems and treatment plants were financed and constructed, interest for at least 2 yr was provided in the bond issue. At Mechanicsburg interest for 2½ yr was provided. When a sewer system was already in existence and the project was limited to constructing a treatment plant and intercepting sewers, it was possible to begin collecting sewer rentals shortly after construction was begun. Consequently, it was only necessary to provide interest for 1 yr in the bond issues at Bloomsburg and Danville. At Catawissa, where collection of sewer rental was begun soon after the bonds were sold and less construction time was involved, interest for only ½ yr was included. Gettysburg had an existing plant, and sewer rentals were in effect before financing and construction of the improvements were begun; therefore, no funds for interest had to be provided out of the bond issue.

Working capital in greater or lesser amounts was provided out of the bond issue for use by the authorities until revenues from sewer rentals could be received. The sum of $50,000 was provided in the bond issue at Gettysburg for construction of relief sewers, miscellaneous repairs, and replacements of existing sewers. Debt-service funds of $15,000 at Lemoyne and $6,000 at Middleburg were provided in the respective bond issues.

Proceeds from the sale of bonds were in all cases deposited with a trustee and paid out for construction upon requisition by the proper official of the authority. Balances in this fund after the completion of construction were transferred to make up deficits in debt-service funds or to various other funds established to provide reserves, bond redemption, or improvements and additions to the project.

Municipalities operating on a lease-back system were required by the indenture to deposit with the trustee, either quarterly or semiannually, a fixed amount of funds taken from sewer-rental revenue for the use of the trustee in paying interest and principal of bonds, for expenses of the authority and trustee, and to establish debt-service reserve and maintenance reserve funds. The funds to be deposited with the trustee were designed to be greater than required for interest, amortization, reserves, and the expenses of the authority and trustee. Surplus funds could be used for additional redemption of bonds, project improvements and additions, or sewer extensions.

For projects requiring construction of a sewer system, the reserve funds were usually not begun until the second, third, or fourth year but were fully established by the fifth or sixth year. When construction did not involve a new sewer system, the reserve funds began to accumulate the first or second year and were complete by the third year at Danville and the fifth year in the other municipalities.

Under the lease-back arrangement the municipality paid the operating expenses (including administration) out of sewer-rental revenues. After making the required fixed payments to the trustee and paying the annual operating expenses, surplus funds had to be deposited with the trustee first to make up deficits in any of the established funds and then for bond redemption, improvements, and extensions.

In the case of Bloomsburg all the sewer-rental revenues had to be deposited with the trustee. Administrative and operating expenses were paid out of a working fund, which was periodically replenished with funds requisitioned from the trustee by the officials of the authority.

At Gettysburg sewer-rental revenues were deposited into a clearing fund, from which administrative and operating expenses were paid and payments were made to the trustee to cover debt service, reserves, and a so-called "capital additions and bond redemption fund" which provided for sewer extensions and replacement to the extent of 2% of the annual gross revenue from sewer rentals.

The funds for interest, working capital, and debt-service reserves which were taken out of the various bond issues, the fixed or estimated annual payments for debt service and reserves which had to be made to the trustee, and the annual fixed authority and trustee expenses are shown in Table 7.

The Mechanicsburg indenture provided for a reduction in fixed-lease rental payments to the trustee of 110% of the costs of interest and principal on bonds and the expenses of the authority and trustee after redeeming bonds totaling $200,000. After issuing the additional bonds at Mechanicsburg and Lemoyne, revenues from sewer rentals had to be sufficient for adminstrative and operating expenses and for 110% of the average annual fixed-lease rental payments to the trustee under existing and additional bond issues.

Middleburg was required to collect sufficient sewer-rental revenue to provide a margin of safety of 10% over the annual-lease rental payments to the trustee and the annual administrative and operating expenses. This municipality was also required to make an annual contribution of not less than $2,500 out of its tax revenue in addition to the sewer rentals collected.

Sewer rentals had to provide for a 5% margin of safety over the annual fixed-lease payments by the municipalities of Shippensburg, Danville, and Catawissa.

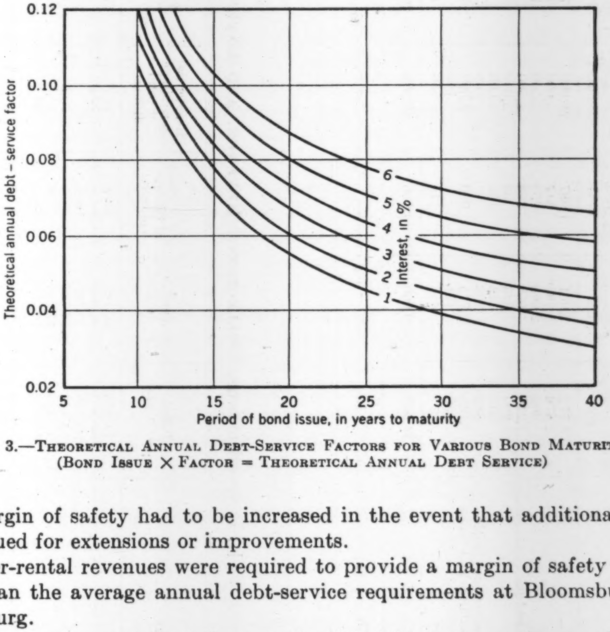

FIG. 3.—THEORETICAL ANNUAL DEBT-SERVICE FACTORS FOR VARIOUS BOND MATURITIES (BOND ISSUE × FACTOR = THEORETICAL ANNUAL DEBT SERVICE)

The margin of safety had to be increased in the event that additional bonds were issued for extensions or improvements.

Sewer-rental revenues were required to provide a margin of safety of 25% more than the average annual debt-service requirements at Bloomsburg and Gettysburg.

The average annual fixed charges of each bond issue, assuming equal annual payments during the full period of the bond issue to cover interest and amortization without any margin, have been determined and are presented in Table 1, along with the fixed charges including the margin of safety and the reserves in 1953 and in the eighth year after issue of bonds. In all the municipalities except Middleburg the fixed payments under the indenture reached a maximum by the eighth year. In Middleburg the annual fixed payments continued to increase. The fixed payments in Shippensburg did not begin until 1954.

TABLE 8.—ANNUAL EXPENDITURES FOR ADMINISTRATION, BILLING, OPERATION, AND MAINTENANCE (IN DOLLARS)

	Mechanicsburg 1952	Lemoyne 1952[a]	Middleburg 1953	Bloomsburg[b] (estimated)	Gettysburg 1953[c]	Danville 1954 budget	Shippensburg (estimated)	Catawissa (estimated)
Salaries and wages	3,772	3,961	1,987	28,000	7,040	6,500	4,900	2,000
Electric power	2,878	1,282[d]	517	5,000	1,842	2,400	3,600	400
Maintenance and repairs	990	2,095	253	2,500	1,890	1,200	500	500
Fuel, light, water, gasoline, and oil	1,248	653	224	2,500		600	400	100
Material and supplies	1,290	343	94	3,000	3,851	2,300	1,350	600
Insurance and taxes	631	145	166	3,000	802	750	600	500
Miscellaneous expenses for autos and trucks	845	298		600	190	2,400	250	200
Administrative and billing salaries and wages	3,136	2,775	900	5,000	3,660	2,475	3,000	1,700
Telephone	150	121		150		200		
Miscellaneous office expenses		417	15	150	1,015	350		
Total	14,940	12,090	4,156	49,900	20,290	19,175	14,600	6,000

[a] Year ending April 30, 1953. [b] Includes incinerating expenses. [c] Year ending September 30, 1953. [d] Includes water.

TABLE 9.—BILLINGS, COLLECTIONS, REVENUE, AND EXPENSES FOR 1953

Authority	Billed (in dollars)	Collected (in dollars)	Percentage of billings collected	Residential percentage of total billings	Total revenue (in dollars)	ANNUAL EXPENSES (IN DOLLARS)		
						Fixed	Operating	Total
Mechanicsburg	71,925	69,187[a]	96.2	70.5	77,317[b]	60,100	14,940	75,040
Lemoyne	66,203	66,822[a]	101.0	70.0	67,142[c]	47,015	12,090	65,605
Middleburg	22,635	22,317[d]	98.6		28,187[e]	15,200	4,156	19,356
Bloomsburg	132,526	124,731	94.0	70.5	124,731[f]	74,656	49,900	124,556
Gettysburg	47,638	47,543	99.8	45.5	47,543	24,200	20,290	44,290
Danville	67,422	66,908	99.2	58.5	66,908	32,000	19,175	51,195

[a] Exclusive of connection charges. [b] Includes connection charges of $8,130. [c] Includes connection charges of $320. [d] Exclusive of connection charges and contribution by the borough. [e] From sewer connection and miscellaneous, $2,721; from borough taxes, $3,125. [f] Surplus available from previous year.

Interest was only paid on bonds which had not been redeemed. The average interest year weighted for the full bond issue has been computed in each case and is also shown in Table 1, together with the amount of bonds issued, years to maturity, and the average and actual fixed payments. The theoretical or average annual debt-service factors for various bond maturities and interest rates are shown in Fig. 3. The bond issue times the debt-service factor equals the average or theoretical annual debt service for each year until maturity of the entire bond issue.

Expenditures such as those for administration, billing, operation, and maintenance for one year for each of the municipalities as spent, estimated, or budgeted are shown in Table 8.

Collection as a percentage of billings for sewer rentals in 1953 ranged from 94% to 101%; the figure of 101% is explained by the fact that Lemoyne had a carryover from the previous year. Some collections were deferred at Bloomsburg until an agreement was made with the state on sewer-rental charges to the normal school and until the canning season, when the strength of wastes in one of the canning establishments could be determined. Payment of a bill for industrial wastes from a milk plant was delayed in Mechanicsburg in 1953 until the volume of wastes not reaching the sewer and the strength of wastes reaching the sewer were established and agreed upon. Sewer-rental billings and collections for six municipalities are shown in Table 9.

There was readily available in five municipalities information about the percentage of billings for sewer services to residential users as compared to total billings to residential, commercial, and industrial users. Compared to the estimated percentage of billings to residential users shown in Table 6, the actual percentages were very close in Mechanicsburg and Gettysburg. Percentages of residential billings were greater at Bloomsburg and less at Danville than estimated, which of course indicates that less revenue from commercial and industrial users at Bloomsburg and more at Danville were being received than anticipated. The high percentage of revenue from commercial and industrial users at Gettysburg is explained by the fact that Gettysburg has a larger number of commercial establishments such as stores, hotels, rooming houses, and restaurants, than the average municipality for the entertainment of large numbers of tourists and visitors and that it also has a sizable college.

A comparison of total revenue and annual fixed, operating, and total expenses in 1953 for the six municipalities in Table 9 indicates that in all cases revenue exceeded expenses that year.

SUBSIDY FROM PENNSYLVANIA

Pennsylvania passed a law[4] under which it will annually pay to municipalities a subsidy of 2% of the construction cost of intercepting sewers and treatment plants which have been built since 1937 or which will be built in the future under the order of the Pennsylvania Sanitary Water Board. A municipality can use the subsidy as income to meet expenses of operation or as additional annual fixed payments toward interest and amortization, in which case the retirement of the total bond issue would be advanced. If not used to speed up retirement of bonds, sewer-rental charges could be reduced.

---

[4] Act of August 20, 1953, *Public Law No. 339* (Commonwealth of Pennsylvania).

In reviewing bond issues from the point of view of financing new projects, bonding firms and bond counsel have considered the subsidy as income over and above any revenue from sewer rentals. Consequently, projects which otherwise were not considered acceptable for sound financing because sewer rentals—to meet annual expenses of operation, fixed charges, and reserves—were considered to be too high became acceptable for such financing when the subsidy was taken into account. The municipalities cited herein were all entitled to receive the subsidy in 1954.

The estimated subsidy in each case, the computed subsidy per dwelling unit, and the estimated percentage of annual operating expenses in 1953 are shown in Table 10.

TABLE 10.—SUBSIDIES AND EXPENSES

	Total	Percentage residential	Percentage of annual operating expenses	Per dwelling unit
Mechanicsburg	8,000	70.5[a]	53.5	2.65
Lemoyne	3,700	70.0[a]	30.5	1.90
Middleburg	3,000	74.0[b]	72.0	5.10
Shippensburg	8,000	78.0[b]	55.0	3.15
Bloomsburg	16,000	70.5[a]	32.0	3.35
Gettysburg	8,000	45.5[a]	38.5	2.75
Danville	8,500	58.5[a]	41.5	2.50
Catawissa	2,500	69.0[b]	41.5	3.20

[a] From 1953 billings. [b] Estimated.

DUTIES OF THE CONSULTING ENGINEER

The trust indenture securing the bond issue provides that the sewage project be constructed in accordance with plans and specifications prepared or revised by a competent consulting engineer and that the authority engage the services of a consulting engineer as long as any bonds are outstanding. The duties of the consulting engineer are clearly defined and affect the security of the bond issue.

When the bonds are issued the engineer must certify that in his opinion the sums to be set aside from the bond issue for construction purposes are sufficient to construct the project for which the bonds are issued and that the income which may reasonably be realized annually under the ordinance establishing sewer-rental rates will be sufficient (1) for the annual operating expenses of the project; (2) for paying the costs of the authority, the trustee, and the principal and interest on the bonds; and (3) for establishing the required reserves.

In the event that additional bonds have to be issued the engineer has to certify (*a*) that the bonds are being issued and are necessary for the cost of completing the project or for extraordinary repairs, renewals or replacement, and extensions or improvements; (*b*) that such construction is required for proper and effective operation of the project and that the funds being provided are estimated to be sufficient; and (*c*) that the annual revenues of the project estimated under the existing schedule of sewer rentals or under a supplementary rental schedule will be sufficient to cover costs of operation, fixed charges, and reserves.

During construction the engineer has to approve and certify all payments to contractors for construction of the project and on completion of the project to certify that it has been completed in accordance with his plans and specifications. No capital additions are permitted without a certification from the engineer that such additions are useful or desirable and that the sewer rentals in effect or to be put into effect are sufficient for operation, fixed charges, and reserves.

The engineer has to certify annually that in his opinion (*a*) the schedule of rates and charges in effect is sufficient for annual costs of operation, fixed expenses, and the required reserves; (*b*) the project is in a proper state of maintenance and repair; (*c*) repairs, renewals, or replacements are needed or not needed for suitable and efficient operation of the project; and (*d*) reasonable amounts of fire and casualty insurance are carried by the authority or municipality. In the event of loss or damage to the project by fire or otherwise, the engineer has to certify to the repairs, renewals, or replacements that have to be made and the payment for them.

The sale or lease of any property of the project must be certified by the engineer. In some cases the engineer is required to make a general inspection of the operating records and policies of the authority and to make recommendations as to operating methods and renewals, replacements, alterations, additions, improvements, or extensions or changes in operating policies.

Subject to certification by the engineer, reserve funds established for maintenance and repairs and as redemption and improvement funds may be used for renewals, replacements, repairs, additions, extensions, or improvements necessary for proper operation, maintenance, or repair of the project when the expense of such work is outside the scope of ordinary maintenance and operation.

If reserve funds for maintenance or improvements are to be used for redeeming bonds, a certificate from the engineer is required to the effect that, in his opinion, money in such funds will not be required for maintenance, repairs, or extensions.

The foregoing outlines the principal duties and responsibilities of the consulting engineer under trust indentures securing bonds issued by authorities, although such duties and responsibilities may vary to some extent from one indenture to another.

CONCLUSIONS

The experiences outlined herein indicate that sufficient money was obtained through the sale of authority revenue bonds to construct the sewerage sytsem intercepting sewers, and pumping stations required. The interest rates, although higher than current (1955) interest rates for general obligation bonds, have not been excessive, indicating that bond purchasers do not consider investment in authority bonds for sewage projects particularly risky.

Sewer-rental rates required to provide for fixed, operating, and reserve funds have not been excessive. Except in rare instances the public has not opposed the required connection to the new sewer system and the payment of sewer-rental charges. Experience with collections as against billings may be considered satisfactory. The revenues collected have been sufficient to meet annual-expense requirements. In most cases there has been no difficulty in meeting annual payments and setting up required reserves. It appears that sewer-rental charges have been more than ample to meet requirements—the charges could be reduced or the retirement of bonds could be expedited. The "cushion" provided by the reserves and revenues over requirements would make it possible to reduce rental rates or to overcome deficiencies in collections during a depression.

As a result of the annual subsidy from Pennsylvania, the security of authority bonds has been greatly enhanced. It is evident that the financing of sewage projects by authority bonds and annual sewer-rental revenues provides practical means for construction and operation of sewage collection and treatment projects when a municipality cannot finance such projects through the sale of general obligation bonds and service these bonds from tax revenues.

AMERICAN SOCIETY OF CIVIL ENGINEERS
Founded November 5, 1852
TRANSACTIONS

Paper No. 2766

HIGH-VELOCITY TESTS IN A PENSTOCK

By Maxwell F. Burke,[1] A. M. ASCE

With Discussion by Messrs. Steponas Kolupaila, Frank B. Campbell, Arthur L. Collins, R. Clifford Youngquist, and Maxwell F. Burke

Synopsis

Flow tests were made at relatively great Reynolds numbers in three coated-steel penstocks at San Gabriel Dam in California. The resulting friction factors seem to extend the confirmation of the smooth-pipe curve of J. Nikuradse and Theodor von Kármán, Hon. M. ASCE, to Reynolds numbers as great as 3.8×10^7. Additional measurements were made of velocity distribution in one penstock, and the results are compared with the velocity-distribution equations of L. Prandtl and Mr. von Kármán.

Introduction

The Los Angeles County Flood Control District (subsequently referred to herein as the "District") owns and operates several dams and reservoirs within the District boundaries in Southern California. The reservoirs, although small for the tributary drainage areas, are operated during the flood season primarily for the control or reduction of flood peaks. During the last few weeks of the flood season the operation of the reservoirs is gradually changed, and more emphasis is given to conservation and storage of runoff for gradual release during the dry summer months.

San Gabriel Dam, formerly San Gabriel Dam No. 1, located just below the main forks of the San Gabriel Canyon, lies twenty-five miles northeast of Los Angeles, Calif. The reservoir has a capacity of 43,825 acre-ft at El. 1453, which is the elevation of the overflow spillway. At this elevation the static head on the outlet valves is from 236 ft to 248 ft. Details of the dam are included in a paper by Paul Baumann,[2] M. ASCE. Further description of

---

Note.—Published, essentially as printed here, in October, 1953, as *Proceedings-Separate No. 297*. Positions and titles given are those in effect when the paper or discussion was received for publication.

[1] Civ. Engr., Los Angeles County Flood Control Dist., Los Angeles, Calif.

[2] "Design and Construction of San Gabriel Dam No. 1," by Paul Baumann, *Transactions*, ASCE, Vol. 107, 1942, p. 1595.

the dam and appurtenances will be limited to those features affecting the tests being reported herein.

Outlet works, consisting of trashracks, penstocks, and needle valves or gate valves, are provided at all District reservoirs for flood and conservation releases. Because of the relative scarcity of water in the southwestern United States and the resultant "water-consciousness" of the inhabitants—and of engineers in particular—and because of the water rights involved, it is necessary to measure accurately the water released from the reservoirs. These data constitute part of the records required to be kept by a public agency. At most of the District reservoirs such outflow records are obtained at weirs or gaging stations in the canyons below the dams. At San Gabriel Dam this procedure was not feasible because the outlets discharge directly into Morris Reservoir, which is part of the Metropolitan Water District system. Consequently, the metering apparatus was installed in the penstocks leading to the needle control valves.

The outlet penstocks for San Gabriel Dam consist of four steel pipes; two have nominal inside diameters of 51 in. and 96 in., and two have 123-in. inside diameters, all branching off from a 30-ft-diameter tunnel. The general arrangement of outlets is shown in Fig. 1. At the inlet to each penstock is a butterfly valve and a vacuum-relief valve, followed by a straight uniform section of pipe approximately 860 ft long on a slope of −0.005, at the far end of which is a venturi meter. Below the venturi meters the pipes extend approximately 300 ft to balanced-pressure needle valves by which the flows are controlled. These needle valves discharge freely into the air, and the jets end 40 ft below in the upper reach of Morris Reservoir.

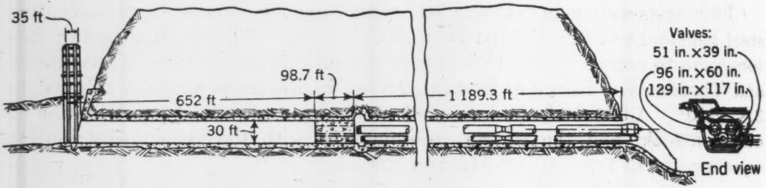

Fig. 1.—Penstock in San Gabriel Dam No. 1 (near Los Angeles, Calif.)

Objectives

The primary problem in this installation was to measure the outflow through each of these pipes at various rates of flow between 100 cu ft per sec and a possible 5,500 cu ft per sec, covering a range of mean velocities from 6 ft per sec to approximately 65 ft per sec. For several design reasons, the throat-to-line diameter ratios of the venturi meters were from 0.82 to 0.93; these ratios are outside the range for which test data were available for determining the venturi coefficients. In order to obtain proper values of the venturi coefficient so that flow-recording apparatus could be designed, the venturi meters had to be rated in place.

It was anticipated that an important result of the rating of the venturi meters would be the determination of the friction factor in the straight run of pipe leading to the venturi meter. Great efforts were made to reduce the friction losses in the penstock by using flush rivets, grinding down welds, and providing a special enamel lining. This lining was applied hot by a centrifugal spinning process in the shop, and an exceptionally smooth surface resulted. Field joints at 40-ft intervals were coated with hot enamel by hand. It was anticipated that experimental values of friction factors could be determined for Reynolds numbers ten times the values for which factors were previously available. Repetition of friction-factor determinations would also indicate the deterioration that might occur in the lining.

Velocity traverses within the pipe, besides affording a measurement of flows, would serve as a means of checking some theoretical velocity-distribution curves at high Reynolds numbers. The possibility of obtaining some data indicating the thickness of the laminar boundary layer was also considered.

GAGING

Because nearly all data derived from the tests were dependent on the basic determinations of flow rates, three different methods of flow determinations were used. These methods consisted of volumetric gaging, color-prism velocity measurement, and pitot-tube velocity measurements. All three methods were used on the 51-in.-diameter line; the volumetric method was successfully used on the 123-in.-diameter line, and the pitot-tube method was used unsuccessfully thereon. No gagings were made on the 96-in.-diameter line because the needle valve had been dismounted from this line, and the line could not be operated at less than full discharge.

Volumetric Gaging, 51-in.-Diameter Line.—The first serious attempts at gaging were made after the wet season of 1938 when conditions in the reservoir were satisfactory for volumetric gaging. Furthermore, discharges could be made within rather broad limitations with respect to rates and durations because of the existing water conditions. Advantage was taken of this opportunity to obtain data for rating the 51-in.-diameter outlet and for incorporating the venturi coefficient in the recording equipment.

Instrument surveys were made of reservoir contours at El. 1380 and El. 1390, and the areas for these two contours were computed. Variations in water surface during the test periods were from El. 1375 to El. 1385. A section of area curve was drawn through these two known points parallel to the original capacity curve, and increments were computed for the range of water-surface elevations during the test period.

During the test period frequent measurements were made of inflow to the reservoir from the two forks of the river. At the end of the test period all dam outlets were closed for a period of sixteen hours, and the total inflow was determined from accurate water-surface elevation changes. Subtracting the gaged inflow from the total inflow gave a figure for the ungaged inflow which was used with the test data.

Tests were made at six rates of flow varying from 143 cu ft per sec to 498 cu ft per sec. The durations of test runs were from one hour to three days and depended principally on the requirements of water rights and storage. Continuous records of water-surface elevation were made by visual observations of two micrometer point gages at different locations in the reservoir. Differential heads on the venturi meter were recorded by a differential-pressure recorder, the calibration of which was checked in place against a water column.

In Table 1 is shown the result of the six volumetric tests on the 51-in.-diameter by 42-in.-diameter venturi meter with the venturi-meter coefficient computed from the standard formula:

$$Q = C \frac{A_1 A_2}{\sqrt{A^2_1 - A^2_2}} \sqrt{2 g H} \quad \ldots\ldots\ldots\ldots\ldots\ldots (1)$$

During test No. 3 a breeze rendered the reservoir gage readings questionable. Omitting that determination, the average coefficient is 0.989.

TABLE 1.—VOLUMETRIC TESTS TO ESTABLISH A VENTURI COEFFICIENT

Test No.	Duration (hr)	Discharge (cu ft per sec)	Line velocity (ft per sec)	Venturi coefficient
		51-IN.-DIAMETER LINE		
1	72	143.1	10.19	0.987
2	48	337.0	23.99	0.992
3	3.5	266.5	18.97	0.974
4	3	319.4	22.74	0.985
5	1	514.2	36.61	0.989
6	72	498.6	35.50	0.991
Average				0.986
		123-IN.-DIAMETER LINE		
1	1.5	3,396	41.33	0.963
2	2	2,636	32.08	0.966
3	4	1,404	17.09	0.968
Average				0.966

Subsequent to the foregoing tests the reservoir surface was dropping, and accumulated debris at the upper end of the reservoir was being carried into the reservoir, changing the area and capacity so much that further volumetric tests were considered to be unproductive.

Volumetric Gaging, 123-in.-Diameter Line.—Rating data are not so numerous for the 123-in.-diameter line as they are for the 51-in.-diameter line. The volumes of water involved in testing the larger outlet are unavailable for extensive testing where water is scarce. However, three volumetric tests were made on the east 123-in.-diameter line in the year following the volumetric tests on the 51-in.-diameter line.

During these tests accurate water-surface elevations were recorded by special open-scale water stage recorders in both the San Gabriel Reservoir from which the water was drawn and the Morris Reservoir into which the water was discharged. Inflow measurements to San Gabriel Reservoir and outflow measurements from Morris Reservoir were made during the test period, and continuous records were maintained. Differential pressures on the 123-in.-diameter by 114-in.-diameter venturi meter were recorded with the same differential-pressure recorder used in tests of the 51-in.-diameter line. It was apparent from an inspection of the reservoir area above San Gabriel Dam, which was dewatered during these tests, that the area and capacity curves surveyed for the tests of the 51-in.-diameter line had greatly changed because of the "migration" of large volumes of debris deposited in the upper reaches of the reservoir. Consequently, data from this reservoir were discarded for test purposes because possible errors (up to 15%) might exist. However, Morris Reservoir had been spared a similar volume of debris accumulation, and its capacity curve was used for the rating.

The results of the three volumetric ratings are listed in Table 1 with the venturi coefficient computed from the data. It is believed that these results are subject to a maximum error of 2% due to possible error in the storage curve of Morris Reservoir. Other errors entering into the volumetric rating are of smaller magnitude.

Color-Prism Gaging.—Although the volumetric ratings apparently produced results that were satisfactory for designing the venturi recording instrument, the volumes of water concerned were such—particularly in the case of the large penstocks—that volumetric calibration tests would be severely limited by availability of water to be used in this way. A gaging system that required only a fraction of the time necessary for the volumetric tests, and hence only a fraction of the water discharged, was desirable; thus, the color-prism method of gaging was attempted.

The 51-in.-diameter line was used to develop the color testing technique with the intention of subsequently applying the technique to the larger line. To date (1953) the only color-prism test data available are on the 51-in.-diameter line.

Preliminary tests indicated that several improvements were necessary on the initial installation before adequate measurements could be made. Potassium permanganate was found to be an unsatisfactory dye because its color could not be readily seen in the outlet jet. Fluorescein was satisfactory and could apparently be easily identified in the jet. Attempts to "bleed off" color samples at various points along the line were not successful because the color change could not be easily identified. In the jet, however, the white envelope caused by air entrainment around the jet changed to a bright green with the passage of the coloring matter. Both ends of the color prism could be followed from the valve outlet into the Morris Reservoir pool 35 ft below. The coloring material was injected a few feet downstream from the butterfly valve. An injection consisted of a pint of fluorescein solution entering the pipe through a $\frac{1}{2}$-in.-diameter, quick-opening cock under a net pressure of 200 lb per sq in. The opening of the cock was evidenced to the timers at the outlet by an electrical contact on the cock handle setting off a photographic flash bulb nearby. Four observers operating 0.1-sec timers recorded the times that both ends of the color prism entered the lower reservoir surface. Timing corrections were made for injection time, acceleration through the venturi meter, length and ecnter of gravity of the color prism (assumed to be a paraboloid), and time in the free jet. The final results of the color-prism tests are listed in Table 2.

Two complete determinations were made at each flow rate, and four observers recorded time. It will be noted that the color-prism determinations agree with the 51-in.-diameter volumetric determinations within 1%, in terms of the venturi coefficients.

Pitot-Tube Gaging.—The third gaging method consisted of making velocity traverses on two diameters of the 51-in.-diameter line by use of the pitot tube. A description of the pitot-tube installation will be given subsequently in connection with a discussion of velocity distribution in the pipe. Fifteen complete sets of gagings were made on flows ranging from 96 cu ft per sec to 424 cu ft per sec; the results are to be found in Table 2.

TABLE 2.—COLOR-PRISM GAGING AND PITOT-TUBE GAGING

Test No.	Discharge (cu ft per sec)	Line velocity (ft per sec)	Venturi coefficient
	COLOR-PRISM GAGING		
6a, 6b	101.8	7.25	0.979
7a, 7b	150.8	10.74	0.977
8a, 8b	198.8	14.15	0.963
9a, 9b	304.0	21.64	0.975
10a, 10b	403.7	28.74	0.982
11a, 11b	445.2	31.69	0.983
Average			0.977
	PITOT-TUBE GAGING		
1	96.2	6.85	0.971
2	114.8	8.17	0.954
3	124.9	8.89	0.929
4	148.3	10.55	0.952
5	161.4	11.49	0.950
6	165.9	11.81	0.949
7	198.8	14.15	0.941
8	238.3	16.96	0.986
9	252.9	18.01	0.970
10	278.5	19.83	0.984
11	298.3	21.24	0.970
12	326.2	23.22	0.978
13	350.1	24.93	0.954
14	376.3	26.79	0.967
15	423.9	30.18	0.964
Average			0.961

In summary, three methods of gaging the discharge through the 51-in.-diameter line yielded the following results in terms of the venturi-meter coefficient:

Method	Coefficient
Volumetric	0.986
Color-prism	0.977
Pitot-tube	0.961
Average	0.974

Attempts to make pitot-tube gagings in the 123-in.-diameter line gave results that were only fragmentary because of mechanical difficulties. Consequently, the three volumetric tests on this line, yielding an average venturimeter coefficient of 0.966, must be relied on for flow determination.

FRICTION TESTS

The penstock installations at San Gabriel Dam offered highly advantageous features for making friction tests. Among the advantages were the 860 ft of straight, uniform pipe section from the butterfly valve to the venturi meter; the exceptionally smooth surface produced by enameling the inside of the pipe; the possibility of rating the venturi meters in place; the permanently installed instruments on the venturi meters for recording flow rates; the control of rates of flow afforded by the needle valves; and the high values of Reynolds numbers to be expected at maximum discharges. Disadvantages were primarily due to the normal scarcity of water for test discharges and the limitations on durations and rates of flow that were set by the District.

Prior to installing the test equipment the pipes were dewatered, and internal diameter measurements were made in place. Each pipe was measured on four diameters at stations 100 ft apart along the pipe axis. Measurements were made with a specially constructed micrometer that was calibrated before and after the measurements. The mean diameters thus determined were 50.748 in., 95.753 in., 122.737 in. (east 123-in.-diameter pipe), and 122.712 in. (west 123-in.-diameter pipe). It is apparent that the desired $\frac{1}{8}$-in. coating was closely approximated.

The reach selected for friction-test purposes lay in the uniform straight reach of the pipes and extended 700 ft upstream from the inlets to the venturi tubes. Pressure taps were installed in each of the four pipes at points 500 ft and 700 ft upstream from the venturi meter and were connected to a common manifold of $\frac{1}{4}$-in.-diameter copper tubing. This manifold was connected to the high-pressure sides of a differential-pressure water manometer and a differential-pressure recorder. The low-pressure sides of these two instruments were connected through a manifold to the upper piezometer rings of the venturi meters. Valves were provided so that the pressure drop in either the 500-ft reach or the 700-ft reach of any of the four penstock pipes might be measured.

Flow was regulated by varying the percentage opening of the needle control valves at the ends of the pipes. No regulation could be effected on the 96-in.-diameter line because the needle valve had been removed. Steps in valve openings were generally in increments of 10% except for the west 123-in.-diameter line for which all steps were in 20% increments. The flow rates were obtained from the venturi-meter recorders, which were tested for recording accuracy immediately preceding the test period.

The results of the two series of test data are tabulated in Table 3 and are shown graphically in Fig. 2. The coefficient n is that found in the Manning formula. The resistance factor, f, equals $\frac{H\,D}{L\,V^2/2\,g}$, in which H is the total head, in feet; D, the diameter; L, the length of reach; V, the mean velocity; and g, the acceleration due to gravity.

TABLE 3.—Pipe-Friction Test Data for San Gabriel Dam (California)

Discharge (cu ft per sec)	Differential Pressure (Ft)		Line velocity (ft per sec)	Roughness coefficient, n	Reynolds number, $\mathbf{R}$	Resistance factor, f
	Recorder	Manometer				
(a) East 123-In.-Diameter Line; 500-Ft Test Length [a,b]						
4,000	11.68		48.68	0.00873	3.449	0.00648
3,975	11.61		48.38	0.00875	3.428	0.00653
3,860	10.82		46.98	0.00870	3.329	0.00645
3,645	9.85		44.36	0.00880	3.143	0.00659
3,395	8.60		41.32	0.00882	2.928	0.00663
3,035	6.99		36.94	0.00890	2.618	0.00674
2,525	5.11		30.73	0.00913	2.178	0.00712
2,535	5.1[illegible]		30.85	0.00918	2.186	0.00718
1,915		3.07	23.31	0.00931	1.652	0.00743
1,260		1.52	15.33	0.00993	1.086	0.00851
490		0.49[c]	5.96	0.01460[c]	0.442	0.01811[c]
(b) East 123-In.-Diameter Line; 500-Ft Test Length [a,d]						
4,040	11.90		49.17	0.00872	3.751	0.0065
4,030	11.83		49.05	0.00871	3.741	0.0065
3,930	11.20		47.83	0.00870	3.648	0.0064
3,750	10.18		45.64	0.00869	3.481	0.0064
3,480	8.97		42.36	0.00879	3.231	0.0066
3,120	7.21		37.97	0.00879	2.896	0.0066
2,565	5.16		31.22	0.00904	2.381	0.0070
2,565	5.31		31.22	0.00918	2.381	0.0072
1,930	3.27		23.49	0.00957	1.792	0.0078
1,320		1.46	16.07	0.00934	1.226	0.0074
600		0.34	7.30	0.00993	0.557	0.0083
(c) East 123-In.-Diameter Line; 700-Ft Test Length [a,b]						
4,040	17.84		49.17	0.00903	3.751	0.0069
4,030	17.67		49.05	0.00900	3.741	0.0069
3,930	16.81		47.83	0.00900	3.648	0.0069
3,750	15.32		45.64	0.00901	3.481	0.0069
3,480	13.33		42.36	0.00905	3.231	0.0070
3,120	10.79		37.97	0.00909	2.896	0.0070
2,565	7.69		31.22	0.00934	2.381	0.0074
2,565	7.32		31.22	0.00911	2.381	0.0071
1,930	4.42		23.49	0.00939	1.792	0.0075
1,320		1.92	16.07	0.00904	1.226	0.0070
600		0.52	7.30	0.01035	0.557	0.0092
(d) West 123-In.-Diameter Line; 500-Ft Test Length [e,d]						
4,100	11.97		49.92	0.00861	3.807	0.0063
3,995	11.30		48.64	0.00858	3.709	0.0063
3,530	8.85		42.98	0.00859	3.278	0.0063
2,585	5.21		31.47	0.00901	2.400	0.0069
1,350		1.49	16.44	0.00922	1.254	0.0073
(e) West 123-In.-Diameter Line; 700-Ft Test Length [e,d]						
4,100	18.32		49.92	0.00899	3.807	0.0069
3,995	17.50		48.64	0.00902	3.709	0.0070
3,530	13.82		42.98	0.00908	3.278	0.0070
2,585	7.92		31.47	0.00938	2.400	0.0075
1,350		2.25	16.44	0.00956	1.254	0.0078

TABLE 3.—(*Continued*)

Discharge (cu ft per sec)	Differential Pressure (Ft)		Line velocity (ft per sec)	Roughness coefficient, n	Reynolds number, R	Resistance factor, f
	Recorder	Manometer				
(*f*) 51-In.-Diameter Line; 500-Ft Test Length [f,b]						
443	19.86		31.54	0.00975	9.52	0.00972
422	18.19		30.04	0.00979	9.07	0.01097
404	16.64		28.76	0.00978	8.68	0.01094
368	13.86		26.20	0.00980	7.91	0.01098
312	10.15		22.21	0.00990	6.70	0.01227
252	6.75		17.94	0.00999	5.42	0.01141
201	4.15		14.31	0.00982	4.32	0.01103
193	3.89		13.74	0.00990	4.15	0.01121
144		2.07	10.25	0.00968	3.09	0.01071
141		1.99	10.04	0.00969	3.03	0.01074
85		0.78	6.03	0.01010	1.82	0.01168
(*g*) 51-In.-Diameter Line; 500-Ft Test Length [d,f]						
505	24.93		35.95	0.00958	11.74	0.01049
492	23.97		35.03	0.00964	11.44	0.01063
482	23.27		34.29	0.00970	11.20	0.01077
455	20.98		32.39	0.00976	10.58	0.01088
425	18.28		30.29	0.00974	9.89	0.01084
351	12.04		24.96	0.00959	8.15	0.01043
276	7.12		19.64	0.00937	6.41	0.01004
234	5.11		16.69	0.00934	5.45	0.00998
173	2.72		12.34	0.00922	4.03	0.00972
99		1.04	7.01	0.01004	2.29	0.01151
(*h*) 51-In.-Diameter Line; 500-Ft Test Length [d,f]						
505	32.8		35.95	0.00929	11.74	0.00986
492	29.9		35.03	0.00910	11.44	0.00947
482	28.8		34.29	0.00912	11.20	0.00952
455	26.24		32.39	0.00922	10.58	0.00972
425	23.92		30.29	0.00941	9.89	0.01013
351	16.72		24.96	0.00955	8.15	0.01035
234	7.17		16.69	0.00935	5.45	0.01000
173	3.77		12.34	0.00917	4.03	0.00963
99		1.36	7.01	0.00970	2.29	0.01074

[a] The measured mean diameter of the line was 10.228 ft. [b] The water temperature was 50.5°F. [c] These data, considered questionable, were not used in Fig. 2. [d] The water temperature was 55.5°F. [e] The measured mean diameter of this line was 10.226 ft. [f] The measured mean diameter of this line was 4.229 ft.

THE MANNING ROUGHNESS COEFFICIENT

The curves relating the Manning n to line velocity for the 51-in.-diameter pipe exhibit a certain peculiarity of shape that is not consistent with the basic assumption of n being a constant for a given quality of surface. Except for the single point on each set of test data that represents the smallest velocity, the general tendency is for the plotted points to form a curve concave downward. However, for designing on the basis of the Manning n, it is believed that the location of the curves is more important than their shape. Omitting the first three points (beginning with the lowest velocity) as being most subject to error because of the small head loss in the test reaches, the average of all other points is 0.00945. Maximum variations from this average are approximately 5%. Within this variation, a design value of 0.0095 should be satisfactory, and a value of 0.010 should be safe. These values correspond with the lower ranges of *n* recommended for brass and glass pipes.

A similar plotting of *n* as related to line velocity for the 123-in.-diameter pipes discloses somewhat the same characteristic for the individual curves, except that each individual test curve shows a general tendency toward a decrease in *n* with an increase in velocity. Again, omitting the two values for velocities of approximately 7 ft per sec, the average of the remaining points is 0.00901 with maximum variations of +10% and −5%.

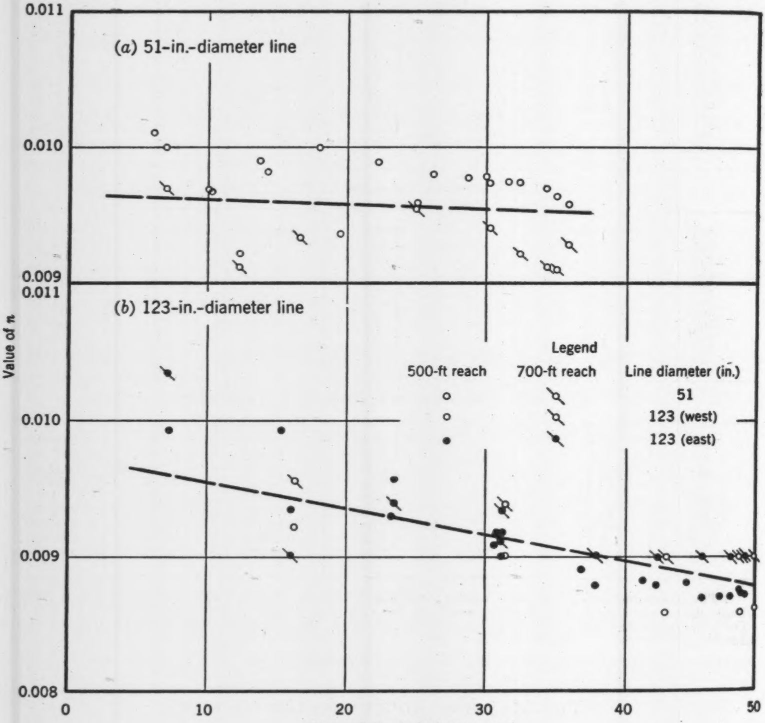

FIG. 2.—RESULTS OF FRICTION TESTS

Because both sets of data plotted in Fig. 2 exhibit a general tendency for a decrease in *n* with an increase in velocity, straight-line curves were computed for both sets of data by the least-squares method; the resulting lines are shown in the graphical presentation. No data for velocities less than 10 ft per sec were used in the computations.

Pipe Friction Factor Related to the Reynolds Number

The equation for the smooth-pipe friction factor obtained by Mr. von Kármán[3] is $f^{-\frac{1}{2}} = A'_f + B_f \log (\mathsf{R} \sqrt{f})$, in which f is the Darcy friction factor, R is the Reynolds number, and A'_f and B_f are constants. This analytically derived equation was verified by the Nikuradse data, the constants having the values $A'_f = -0.8$ and $B_f = 2.0$. In Fig. 3 this equation is plotted on the graph of the test results of this paper.

In Fig. 3 it is shown that, within the range of observational data, the 123-in.-diameter line acts as a "smooth" pipe. This conclusion is based on the general grouping of data points around the smooth-pipe curve developed by Mr. von Kármán.[4] Although the data show spread on both sides of the curve, there is no apparent tendency toward a systematic departure. Hence, a comparison with other pipe-friction data should be limited to the range in which the pipe may be considered smooth.

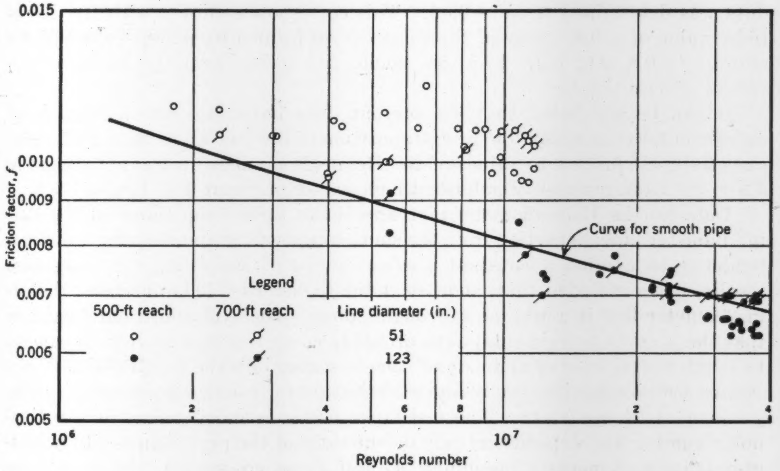

Fig. 3.—Relationship Between f and R

The Nikuradse smooth-pipe data[5] extended from $2.8 < \log (\mathsf{R} \sqrt{f}) < 5.5$ and $4.7 < f^{-\frac{1}{2}} < 10.2$. The present data extend from $5.7 \log < (\mathsf{R} \sqrt{f}) < 6.5$ and $10.4 < f^{-\frac{1}{2}} < 12.6$. It is obvious that the present data cover a range only one third as great in the $\log (\mathsf{R} \sqrt{f})$-direction and a range only four tenths as great in the $f^{-\frac{1}{2}}$-direction; the determination of the constants in the equation from the present data would not be expected to be so accurate as that from the Nikuradse data. However, a least-squares determination was made of the constants, using all the data from the 123-in.-diameter line, and the following equation was determined:

---

[3] "Mechanics of Turbulent Flow," by Boris A. Bakhmeteff, Princeton University Press, Princeton, N. J., 1936, p. 83.

[4] "Turbulence and Skin Friction," by Theodor von Kármán, *Journal of the Aeronautical Sciences*, Vol. 1, 1934, p. 1.

[5] "Fluid Mechanics for Hydraulic Engineers," by Hunter Rouse, McGraw-Hill Book Co., Inc., New York, N. Y., 1938, p. 248, Fig. 121.

$$f^{-\frac{1}{2}} = 0.27 + 1.85 \log (\mathsf{R}\, f^{\frac{1}{2}}) \ldots\ldots\ldots\ldots\ldots\ldots (2)$$

The variation from the Nikuradse constants is $-7\frac{1}{2}\%$ for B_f and $+134\%$ for A'_f. Because the value of B_f is considered to be of the nature of a universal constant for both smooth and rough pipes, because the range of the present data is too small to yield more than an approximation of the value, and because the difference from the Nikuradse data was only $7\frac{1}{2}\%$, the Nikuradse value of 2.0 was considered to give a satisfactory representation of the District's data. Using this value of 2.0 for B_f, the value for A'_f from the present data was determined to be -0.66. This corresponds closely with the Nikuradse value of -0.8. Any of the three curves formed by paired values of A'_f and B_f (-0.8, 2.0; 0.27, 1.85; or -0.66, 2.0) passes near the center of the spread of data points.

It can be concluded that the present data have provided a substantial experimental verification for the extrapolation of the von Kármán or Nikuradse smooth-pipe equation to values of the Reynolds number up to approximately 3.8×10^7 from previously published high values of about 3×10^6.

Data for the 51-in.-diameter pipe apparently differ from those for the 123-in.-diameter pipe, departing from the smooth-pipe curve and showing a distinct tendency to assume a constant f-value (Fig. 3). Following the Nikuradse results, it is concluded that, at least at the higher Reynolds numbers, the 51-in.-diameter line is acting as a "rough" pipe. The Nikuradse data indicate that the present experimental data probably cover the transition from smooth to rough characteristics and extend some distance into the rough region. Mr. Nikuradse[6] obtained as the resistance equation for rough pipes the expression, $f^{-\frac{1}{2}} = A_f + B_f \log (r_o/e)$. The resistance factor is independent of the Reynolds number and depends entirely on the ratio of the pipe radius r_o to height-of-roughness elements e (assuming A_f and B_f as constants). Thus, for one pipe, which necessitates a single value of r_o/e, the friction factor should be constant, provided that the Reynolds number exceeds the minimum value at which the pipe may be considered rough.

Because the paper includes experimental data for only one pipe that acted as a rough pipe it is impossible to determine the values of A_f and B_f from the test data. However, some interesting indications may be noted.

Assuming that throughout the range of tests the 51-in.-diameter pipe consistently acted as a rough pipe, the value of f should be constant, and the most probable value is the mean of the observed values, or 0.01054. If it be further assumed that the Nikuradse rough-pipe equation, $f^{-\frac{1}{2}} = 1.74 + 2.0 \log r_o/e$, holds for the pipe of this experiment, it is possible to determine the value of r_o/e for this mean value of f. This value of r_o/e is 10,100, and because the pipe radius is 2.114 ft the value of e is found to be 0.0025 in. Therefore, the apparent height-of-roughness elements in the 51-in.-diameter pipe, to the scale of the Nikuradse sand-grain roughness, is approximately 0.002 in. The minimum e-value tested by Mr. Nikuradse was 0.0039 in.

---

[6] "Strömungsgesetze in rauhen Rohren," by J. Nikuradse, *Verein Deutscher Ingenieure, Forschungsheft 361*, 1933.

The explanation of why the same pipe can display either smooth or rough characteristics lies in a consideration of the relative dimensions of the roughness-element height and thickness of the zone of laminar flow that exists adjacent to the pipe wall. If the laminar zone is thick enough to cover the tops of the roughness elements, the pipe will act as a smooth pipe. However, if the laminar film becomes thin enough so that the roughness elements project above it, they will add their turbulent effect to the flow, and the pipe will act as a rough pipe.

The thickness of the laminar layer[7] may be assumed to be at the intersection of the velocity-distribution curves in the laminar and turbulent zones. This assumption results in the equation—

$$\delta = \frac{11.6\,\nu}{\sqrt{\tau_o/\rho}} = \frac{11.6\,\nu}{V\,\sqrt{f/8}}, \ldots\ldots\ldots\ldots\ldots\ldots\ldots (3)$$

—in which δ is the thickness of the laminar film, ν is the kinematic viscosity of the fluid, ρ is the density of the fluid, and τ_o is the boundary or wall shear.

For the smallest velocities in the 51-in. pipe and the average value of f, δ equals approximately 0.0064, or $2\frac{1}{2}$ times the apparent height of the roughness elements. According to the concept of rough and smooth pipes previously explained, the pipe should be acting as a smooth pipe at the lowest velocities.

For the maximum velocities and the average value of f, the value of δ is computed to be 0.0012 in., or one half the apparent height of the roughness elements. Therefore, the pipe should act as a rough pipe at these velocities. Somewhere between these extremes of data a zone of transition from smooth to rough characteristics should occur. This is qualitatively substantiated by the trend shown in Fig. 3.

The foregoing computations of e are fictitious because they are based on the relationship between the friction factor and the height of sand-grain roughness elements determined by Mr. Nikuradse. A visual inspection of the pipe lining shows a smooth surface texture with no indication of discrete roughness projections such as would be formed by sand grains. Variations in the surface appear to consist of small gradual changes in pipe diameter that would cause the surface to be characterized as "wavy" rather than rough. In order to obtain direct information on the surface characteristics a series of measurements were made.

A profilometer was constructed which could be used to take a profile of the lining parallel to the pipe axis for a length of 16 in. Measurements along the profile could be read to 0.01 in. Variations of the profile in a direction perpendicular to the pipe wall were measured with a dial indicator reading to 0.001 in. Six sample profiles were taken within the friction-test reach in the 123-in.-diameter line and four, in the 51-in.-diameter line. One profile in each line was taken across the location of a circumferential weld whereas the remaining profiles were representative of the regular surface.

---

[7] "Fluid Mechanics for Hydraulic Engineers," by Hunter Rouse, McGraw-Hill Book Co., Inc., New York, N. Y., 1938, p. 243.

The general shape of the eight regular-surface profiles was a curve rising (or falling) to a single maximum between the ends of the profile. In three of the eight profiles, a second rise began within the gage length. Variations from a smooth curve through these "waves" was not more than 0.002 in. In the 123-in.-diameter line the maximum height of the profile was 0.018 in. above a straight line joining the two ends, and the minimum was 0.004 in., with an average of 0.010 in. for the five profiles. Similar figures for the 51-in.-diameter line were 0.008 in., 0.004 in., and an average of 0.005 in. for the three sections. The profilometer was not long enough to detect any regularity of recurrence of these waves. The average length of the waves was 13.75 in.

In the fabrication of the pipe lines, steel sheets were rolled into cylinders 8 ft long and were welded longitudinally; five cylinders were then butt-welded to make a 40-ft section of pipe. On the inside of the pipe all welds were ground flush before the lining was applied. However, across each circumferential weld there is some variation from a straight line. In the 123-in. line, the profile measured across the weld showed a rise of 0.047 in. above the straight line joining the two ends of the profile. In the 51-in.-diameter line the comparable figure was 0.024 in. The length of pipe influenced by these weld variations is approximately 8 in. or 8% of the pipe length. On the basis of the foregoing measurements, the variations in surface profile in the 123-in.-diameter line are twice those in the 51-in.-diameter line.

Some negative information as to the application of the Nikuradse rough-pipe law to the measurements described herein may be obtained from the following considerations: If it is assumed that the Nikuradse law of roughness applies to the surfaces under consideration, that the constants A_f and B_f in the law are the same as Mr. Nikuradse obtained, and, furthermore, that the 51-in.-diameter pipe is exhibiting rough characteristics through the range of data obtained, then the absolute height e of roughness elements computed for the 51-in.-diameter line is 0.0025 as previously determined. This value is approximately the same as the maximum deviation of the wave profiles from a smooth curve and was found to be the same for both pipes. This value should also be applicable to the 123-in.-diameter pipe. Using this value of e and the known pipe radius, the value of f at which the 123-in. line should act as rough was computed as 0.0090. The fact that the values of f for the 123-in.-diameter line do not "level off" at this value but continue to decrease along the smooth-pipe curve to average values of 0.0067 indicates that all the foregoing assumptions are not fulfilled. If the mean heights of the wave profiles, 0.005 in. and 0.010 in. for the 51-in.-diameter and 123-in.-diameter lines, are used as the effective roughness height e, the computed values at which f should be constant are 0.0119 and 0.0115, respectively. The indications from the foregoing failures to correlate the data from the two lines with the roughness law of Nikuradse are that either the data are inconsistent or the Nikuradse roughness law does not adequately express the roughness relationship exhibited by the two pipes. It is believed that the surfaces reported are primarily of the wavy type rather than the "grainy" or "indented" type prepared by Mr. Nikuradse. In this case it is possible that a change in constants A_f and B_f might be required, a change in form of the law might better fit the wavy surface, or a combination of two laws—one for the microscopic surface texture and one for the macroscopic surface profile—might be required to explain fully this type of surface. However, the available data are insufficient to confirm any of these conjectures.

Conclusions Based on Friction-Test Results

Results of the friction tests indicated that the care taken in fabricating and lining the outlet pipes produced one major desired result—the attainment of a highly favorable value of the Manning *n*. In the 51-in.-diameter line, reliable test values lie between 0.0090 and 0.0098, with 0.0095 as an average. In the 123-in.-diameter line, reliable test values ranged from 0.0086 to 0.0099—an average being 0.0090. These average values are below the best values recommended for the design of coated cast-iron pipe and lie in the low range of values recommended for brass and glass pipes.

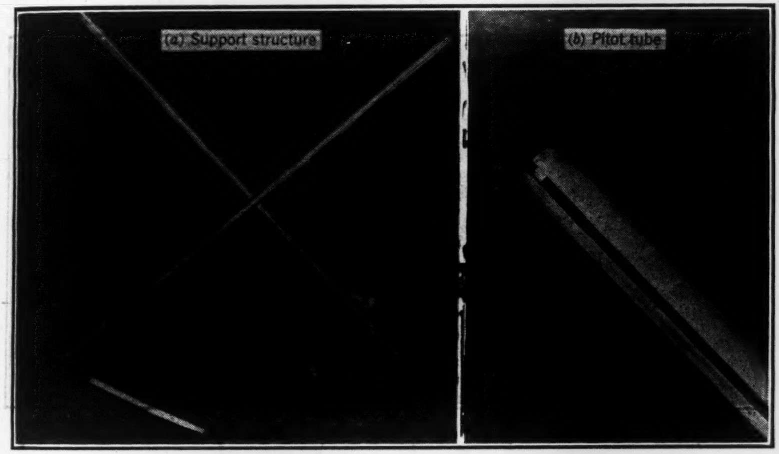

Fig. 4.—Pitot-Tube Installation

In the correlation of friction factors with Reynolds numbers, test results were obtained at values of the Reynolds number ten times as high as in previously published data. The general grouping of data for the 123-in.-diameter pipe about the extrapolated smooth-pipe friction curve verifies the curve beyond previously tested limits. The data for the 51-in.-diameter pipe seem to show that even a very smooth surface will act as a rough surface at sufficiently high values of the Reynolds number.

An analysis of the test data indicates that the surfaces concerned do not conform to the rough-pipe law of Nikuradse and that a change of constants, or possibly a new law, might serve to express the roughness of surface that may be classified as wavy.

Velocity Distribution

The operation of pitot equipment in the 51-in.-diameter line for gaging flows resulted in data sufficient to produce velocity patterns for flows at a limited range of Reynolds numbers. Because some features of the installation and operation may be of special interest, they will be described in some detail.

Pitot-Tube Installation.—Preliminary investigation indicated that an unsupported pitot probe, cantilevered from the pipe wall, would not be entirely satisfactory for operation at the expected velocities exceeding 40 ft per sec. Consequently, a structure was installed in the pipe to support the pitot tubes in their traverses across the pipe. This support structure was in the form of a cross with arms set on pipe diameters 90° apart (Fig. 4(*a*)). The support members were solid rods 1 in. in diameter clamped together where they crossed at the center line of the pipe. Streamlined fairing was brazed to the trailing edge of each support. On the leading edge of each support, a slot was milled to carry and guide the pitot tube and head (Fig. 4(*b*)). The pitot tubes were made of $\frac{3}{16}$-in.-diameter tubing fitted with a square head at the probe end. The square head carried a pitot tip made from a No. 20 hypodermic needle having an outside diameter of 0.043 in. and an interior diameter of 0.023 in., which extended 1 in. upstream of the support members. The square head sliding in the milled slots kept the pitot tip parallel to the axis of the pipe. On the upstream support, the pitot tube could traverse the full pipe diameter, but separate pitot tubes were installed on the downstream support to traverse from the pipe walls to the center.

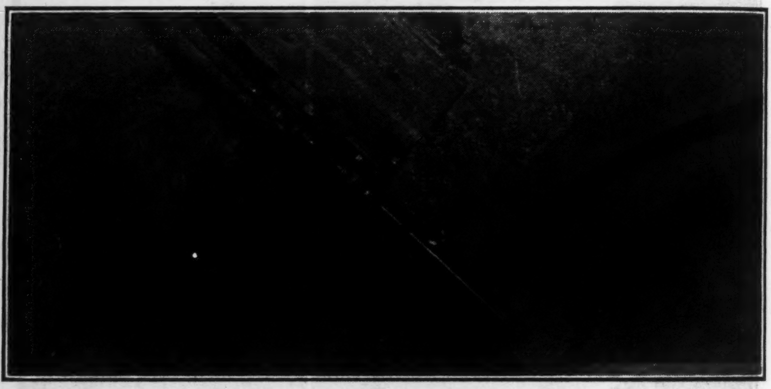

Fig. 5.—Pitot-Tube Installation Outside the Penstock

On the outside of the pipe, the pitot tube extended through a packing gland and was connected through a water trap to a flexible tube (Fig. 5). The entire installation was placed close to a concrete pier supporting the four penstocks, and the pier was used to anchor a steel angle that served as a guide for the pitot tube. A micrometer arrangement was provided to measure the first three inches of travel from the pipe wall, and the remainder of the distance was measured using a steel rule or a tape.

The pressure from the pitot tips to the pressure-measuring equipment was transmitted by gas instead of by the usual water columns. Three advantages were thus obtained: (1) The elimination of a long water column of great inertia which would tend to give surging readings, (2) the elimination of possible air bubbles in the transmission line and of consequent inaccuracies in pressure readings, and (3) the development of a pitot coefficient of 1.00. This unity coefficient had been previously established for this gas-operated type of pitot tube by the National Bureau of Standards (Washington, D. C.) and by the National Advisory Committee for Aeronautics (Washington, D. C.) for velocities up to 60 ft per sec.

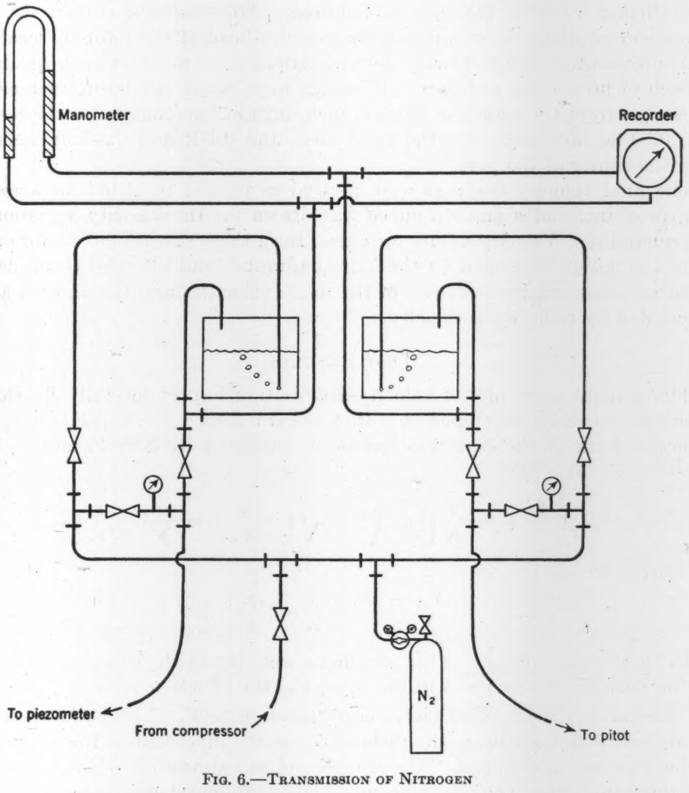

Fig. 6.—Transmission of Nitrogen

Commercial nitrogen was selected for use in the pitot equipment because of its low solubility in water and its safety features. In Fig. 6 is shown the method of gas transmission. The gas is brought, successively, through a pressure regulator, an adjustable needle valve for controlling the gas flow, a sight-feed glass to equalize visually the gas flow in the two legs, and then to the pitot tube or to the piezometer connections. Cross connections were provided so that gas under high pressure could be used to blow the lines clear of any water that might have entered the pressure transmission system. Static pressures from the pipe line were obtained from four wall piezometers connected to a common manifold.

Static pressure from the piezometer and static pressure plus dynamic pressure from the pitot tip were transmitted by the gas to opposite sides of a differential-pressure manometer and differential-pressure recorder—the manometer utilizing water or mercury as required. After suitable corrections, the manometer readings thus indicated the velocity head at the pitot-tip location.

Approximately forty velocity determinations were made in each quadrant for each of fifteen rates of flow. Readings were taken at 0.05-in. increments of distance from the walls for the first inch, 0.20-in. increments for the second inch, 0.50-in. increments for the third inch, and 0.1-ft and 0.2-ft increments on to the center of the pipe.

The final velocity readings were plotted as related to radial distance for each quadrant, and a smooth curve was drawn for the velocity variation in each quadrant. Velocity values were read from these smooth curves for every 2% of the radius (averaged for the four quadrants), and the total Q was determined by summing the products of the mean velocities and the annular areas represented by each mean velocity.

TEST RESULTS

The general form of the velocity-distribution curves for fully developed turbulence has been developed on a theoretical basis by Mr. von Kármán, and a simpler form of the equation has been suggested by Mr. Prandtl.[8] The von Kármán expression is

$$\frac{V_m - V'}{V_*} = -\frac{1}{K}\left[\log_e\left(1 - \sqrt{1 - \frac{y}{r_o}}\right) + \sqrt{1 - \frac{y}{r_o}}\right] \ldots\ldots (4)$$

and that of Prandtl,

$$\frac{V_m - V'}{V_*} = \frac{1}{K}\log_e\frac{r_o}{y} \ldots\ldots\ldots\ldots\ldots\ldots\ldots (5)$$

In these equations, V_m is the maximum velocity at the center of the pipe; V', the velocity at any point in the pipe; V_*, the "friction velocity," equal to $V\sqrt{f/8}$; and f, the friction factor corresponding to V. The point where V' is obtained is defined by y, the distance from the pipe wall to the center line of the pipe along a radius. The dimensionless expressions of Eqs. 4 and 5 give the ratio of the "velocity deficiency" (the difference between the maximum center-line velocity and velocity at any point) to the "friction velocity" in terms of the relative distance from the wall to the center of the pipe. The theoretical equations have been confirmed experimentally by the Nikuradse tests which agree with Eq. 5 as well, if not better than, with Eq. 4.

In fully developed turbulent flow with the 51-in.-diameter pipe acting as a rough pipe, the value of f should be constant and a single curve should contain all the velocity-distribution points. However, because the computed values of f for the tests of the 51-in.-diameter pipe are not all identical, there will be a variation in velocity-distribution curves that can be shown by an enveloping band. In Fig. 7 are shown this band of velocity-distribution points and similar bands computed for the von Kármán equation and the Prandtl equation.

---

[8] "Neue Ergebnisse der Turbulenzforschung," by L. Prandtl, *Zeitschrift des Vereins Deutscher Ingenieure*, *No. 5*, 1933.

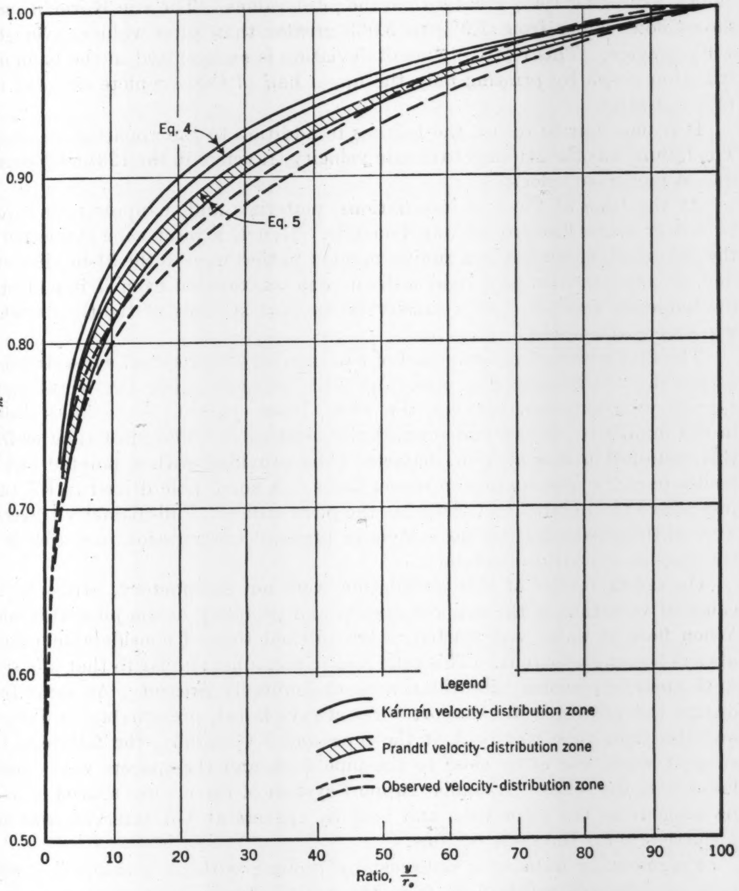

FIG. 7.—VELOCITY DISTRIBUTION IN THE 51-IN.-DIAMETER PIPE

Selection of band limits was made from the observed data by taking the two flow rates that showed the highest and lowest ratios of V'/V_m for any point on the average velocity curves. The Prandtl and von Kármán distributions were then computed from the same flow rates. In the tests on which Fig. 7 is based, **R** varied between 2×10^6 and 9.5×10^6.

The total flow represented by the theoretical curve distributions of Messrs. Prandtl and von Kármán exceeds the flow measured by the pitot tube. This fact is confirmed by comparing the integration of the theoretical curves with the flows computed from the pitot traverses. The Prandtl curve gives flow values from 0.05% less than the pitot values to 3.2% greater than the pitot values, averaging 1.4% greater than the pitot values. The von Kármán curve shows flow values from 1.9% to 5.0% greater than pitot values, averaging 3.3% greater. This relatively small deviation is exaggerated in the band distribution graph by printing only the upper half of the complete range of the (V'/V_m)-ratio.

It is only fair to record the failures in addition to the apparent successes. The failure was the attempt to obtain velocity traverses in the 123-in.-diameter line at moderate velocities.

At the time of the test installations, materials and manpower were controlled or scarce because of war demands. Hence, a pitot tube supported in the 123-in.-diameter line in a similar manner to that used in the 51-in.-diameter line, or supported in any rigid fashion, was unavailable even if it had been mechanically feasible. As a substitute, support systems of tightly stretched wires were attempted.

The first system was comprised of two parallel 12-gage steel wires stretched across the 123-in.-diameter pipe. At 6-in. intervals along the wires, metal spacers were attached between the wires, these spacers having holes drilled in the middle to receive and support the pitot tube. The pitot tube used in this installation was a $\frac{3}{16}$-in.-diameter tube provided with a pointed end to facilitate entry into successive spacer holes. A small hole drilled in the tube just above the pointed end served as the pitot orifice. Full-diameter traverses were anticipated, and the gas system of pressure transmission was used as in the tests of the 51-in.-diameter line.

Operating results of this installation were not satisfactory, primarily because of vibration in the support system and probably in the pitot tube also. When flow of water was started, a low-pitched tone of considerable volume always became apparent. This tone rose in a manner similar to that of a siren until some supersonic vibrations were undoubtedly present. At some time during this sequence the support wires always failed, presumably by fatigue, and the pitot tube was bent at the pipe wall. Generally, the failure of the support wires was at or close to the pipe wall, and the spacers were broken loose from the wires. A similar support system of three wires spaced so as to be tangent to the pitot tube and held by spacers at 1-ft intervals was also unsuccessful for the same reasons.

Fragmentary data were obtained by probing with an unsupported pitot tube to distances within 3 in. from the wall, but even here vibration was so severe that the results were not dependable.

CONCLUSIONS

The foregoing descriptive report was prompted by the desire to make available to the engineering profession the results of a series of tests undertaken over a period of several years. It was believed that the range of test values covered would extend information previously available over a greater range and possibly verify extensions of theoretical curves. Although the test results show a variability that is much greater than would be acceptable under closely controlled laboratory conditions, it is felt that they compare favorably with similar field-type experiments.

ACKNOWLEDGMENTS

Although the writer was in charge of conducting the tests, the enthusiasm and resourcefulness of E. S. Fuller were largely responsible for any success in obtaining test data. The unfailing support of Mr. Baumann aided greatly in initiating the tests and in providing the necessary equipment and time to make the tests possible. All work on this project was under the general direction of H. E. Hedger, M. ASCE, chief engineer of the Los Angeles Flood Control District.

DISCUSSION

Steponas Kolupaila.[9]—The investigations described in this paper are highly valuable because unusually great Reynolds numbers (a maximum of 3.8×10^7) were reached. In the literature there are few examples of such values as great as 1×10^7. In 1936 an extensive summary of Italian data was published,[10] in which the greatest Reynolds number mentioned is 1.08×10^7 for a riveted steel pipe 2.80 m (102 in.) in diameter.

TABLE 4.—Velocities Along Four Radii, in Feet per Second

Distance from wall, in feet	Radii				Average
	A	B	C	D	
0.002	18.12	20.09	18.80	17.07	18.52
0.004	20.17	21.89	20.66	19.89	20.65
0.008	20.80	22.48	21.28	21.37	21.48
0.013	21.82	22.58	21.85	22.27	22.13
0.017	22.22	22.97	22.49	22.74	22.60
0.021	22.60	23.17	23.35	23.12	23.06
0.025	23.15	23.62	23.17	23.30	23.31
0.029	23.35	23 91	23.82	23.86	23.74
0.033	23.62	24.36	24.01	24.04	24.01
0.038	23.99	24.41	24.28	24.21	24.22
0.042	24.25	24.55	24.38	24.21	24.35
0.046	24.45	24.64	24.74	24.74	24.64
0.050	24.60	25.00	24.94	24.83	24.84
0.054	24.77	25.00	25.19	25.00	24.99
0.058	25.03	25.01	25.27	25.26	25.14
0.063	25.20	25.19	25.45	25.26	25.28
0.067	25.25	25.27	25.55	25.51	25.40
0.071	25.28	25.31	25.62	25.81	25.51
0.075	25.70	25.38	25.72	25.92	25.68
0.079	25.61	25.45	25.83	26.09	25.74
0.083	25.86	25.46	26.06	26.20	25.89
0.100	26.26	25.96	26.32	26.40	26.24
0.117	26.41	26.32	26.50	26.88	26.53
0.133	26.89	26.67	27.01	27.10	26.92
0.150	27.20	26.81	27.31	27.34	27.16
0.167	27.42	26.94	27.44	27.64	27.36
0.208	27.54	27.27	28.03	27.85	27.67
0.250	28.05	27.82	28.61	28.05	28.15
0.300	28.55	28.40	29.03	28.78	28.69
0.400	29.14	29.14	29.82	29.47	29.39
0.600	30.36	30.09	30.88	30.57	30.48
0.800	31.12	31.07	31.74	31.62	31.39
1.000	32.00	31.82	32.56	32.25	32.16
1.200	32.58	32.49	33.12	33.13	32.83
1.400	33.11	33.01	33.40	33.47	33.25
1.600	33.80	33.46	34.01	34.00	33.82
1.800	34.04	33.97	34.21	34.19	34.10
2.000	34.14	34.21	34.23	34.20	34.20
2.114	34.33	34.33	34.33	34.33	34.33

Velocity distribution in these unusual conditions is particularly interesting. As the author shows in Fig. 7, his results disagree with the known theoretical laws of velocity distribution. Both the logarithmic law by Mr. Prandtl and the combination of a parabola with a logarithmic curve by Mr. von Kármán give essentially larger values than the observed data. A simple parabolic law,

---

[9] Prof., College of Eng., Univ. of Notre Dame, Notre Dame, Ind.

[10] "Correnti uniformi entro grandi condotte e grande canali," by G. de Marchi, *L'Energia Elettrica*, Vol. 13, No. 8, 1936.

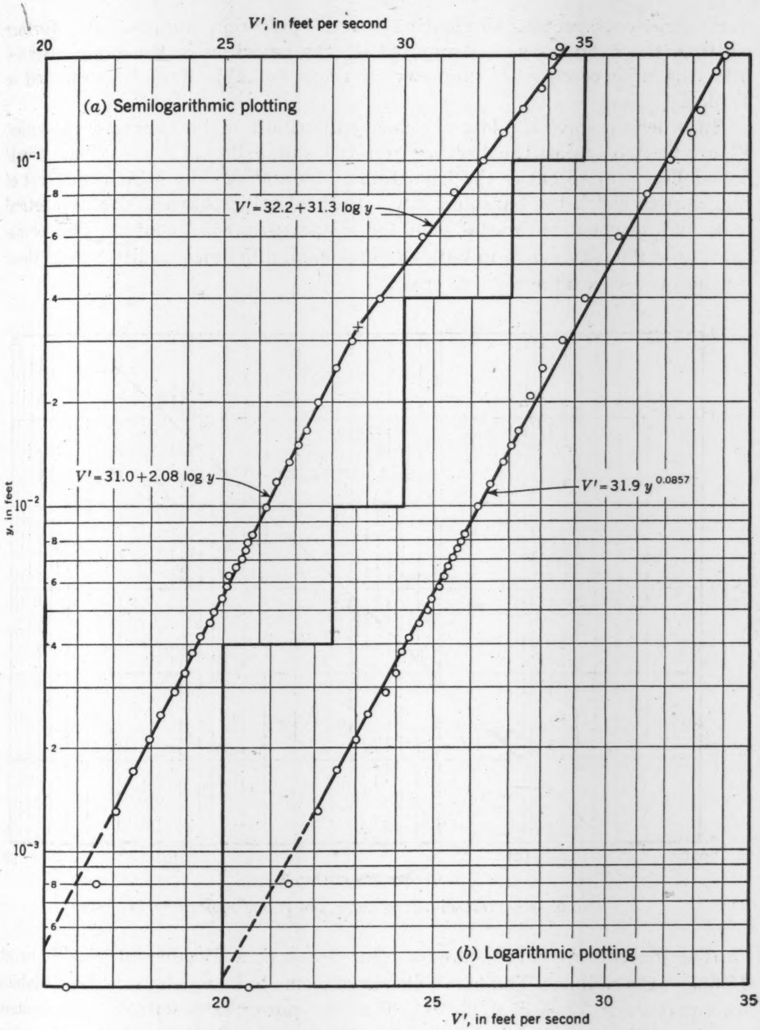

FIG. 8.—AVERAGED VELOCITIES

widely applied by Mr. Nikuradse,[11] $V'/V_m = (y/r_o)^x$, with the power x approximately equal to 0.1, would fit better.

The writer examined the complete results of one representative test, a copy of which he obtained through the courtesy of the author. The original data were slightly corrected, eliminating several pulsation humps. For further plotting, the averages were computed for the velocities in the same distance from the pipe center. A summary of these valuable data is presented in Table 4.

---

[11] "Gesetzmässigkeiten der turbulenten Strömung in glatten Rohren," by J. Nikuradse, *Forschungsheft 356, Verein Deutscher Ingenieure,* 1932.

In order to prove the law of velocity distribution the averaged velocities, V', are plotted against the distance from the wall, y, on (1) the semilogarithmic net of Fig. 8(*a*) to check the logarithmic law and (2) the logarithmic net of Fig. 8(*b*) to check the parabolic law. Both plottings have the same vertical scale and adjusted horizontal scale for nonpartisan conclusions. The points below $y = 0.01$ ft deviate in both cases; a small difference in distance at these y-values causes a large relative error.

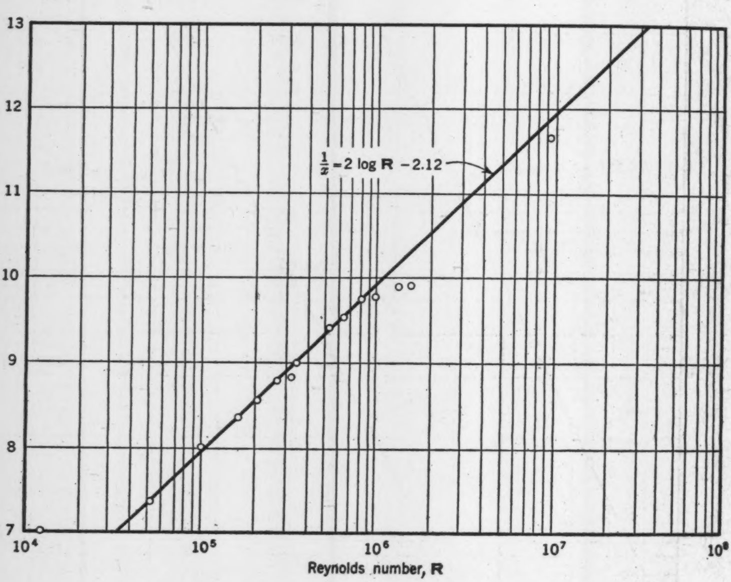

FIG. 9.—RELATIONSHIP BETWEEN x AND R FOR SMOOTH PIPES

The logarithmic curve shows a clear break at a distance of 0.33 ft or at 15.6% of the radius. The parabolic curve seems to be much more dependable; its equation is $V' = 31.9\ y^{0.0857}$. The low power, $x = 0.0857$, corresponds closely to the smooth pipe surface and to the small value of the Manning coefficient $n = 0.0096$. An empirical relationship between the power of the parabola and the Reynolds number (based on earlier European data[12]) $1/x = 2 \log R - 2.12$, although extrapolated far beyond its original data, fits surprisingly well with the author's data, points of which are plotted in Fig. 9.

---

[12] "Widerstand von Platte und Rohr bei hohen Reynoldsschen Zahlen," by L. Schiller and R. Hermann, *Ingenieur-Archiv*, Vol. 1, 1930, No. 4, pp. 391–398.

In this relationship, $V = 30.0$ and d equals 4.229; for water at 55.5°F, the kinematic viscosity is 1.298×10^{-5}, R is 9.78×10^{6}, and log R equals 6.990. Therefore, $1/x = 2 \times 6.990 - 2.12 = 11.86$ and $x = 0.0843$. This power can be further checked by the ratio between the average velocity across the pipe and the velocity at the center, $k = V/V_m = 30.0/34.3 = 0.874$. This value is unusually high.

For the parabolic law $V' = a\,y^x$, integration across the pipe gives the ratio $k = 2/(x + 1)(x + 2)$. Substituting $x = 0.0857$, $k = 0.883$; or substituting $k = 0.874$, $x = 0.0932$. These two results agree closely.

The discharge for these computations was determined graphically by plotting $V'(r_o - y)$ against y and planimetering the area beneath the curve.[13] The area was 67.10 cu ft per sec, and the discharge was $Q = 2\,\pi \times 67.10 = 422$ cu ft per sec, approximately 3.1% less than the recorded 435 cu ft per sec; this difference seems to be too large. From this information, $V = Q/A = 422/14.08 = 30.0$ ft per sec.

The Coriolis coefficient $\alpha = \int (V')^3\, dA/V^3 A$ was determined by plotting $(V')^3(r_o - y)$ against y. The planimetered area was 62,200; $\alpha = 2\,\pi \times 62{,}200/[(30.0)^3 \times 14.08] = 1.035$. This value is in agreement with usual values for smooth pipes.[14]

Frank B. Campbell,[15] M. ASCE.—The test results presented by Mr. Burke are particularly valuable in view of the lack of experimental work on flow in pipes or conduits with large Reynolds numbers. The Reynolds numbers in the 123-in.-diameter line extended to 3.8×10^{7}. Several experiments have been made with R-values somewhat less than 10^{7}. The R-values of the Ontario (Canada) Power Company test[16] reached 3×10^{7}. Tests were made on the outlet works conduit at Denison Dam[17] (in Oklahoma and Texas) at a single Reynolds number of 1.2×10^{8}.

The San Gabriel Dam test results are of special value to the design engineer as they emphasize the low values of the Manning n that occur at high Reynolds numbers. The Denison Dam conduits were of concrete poured against steel forms, and the Manning n determined from the tests was 0.0097. This is a much smaller value than is commonly used for design assumptions and is an indication of the tendency to overdesign for large Reynolds numbers. The Darcy friction factor for the Denison Dam conduit was 0.0064. The von Kármán-Prandtl smooth-pipe equation gives a Darcy f-value of approximately 0.0058 for the same Reynolds number. Thus, the trend of values of the smooth-pipe curve is a more reliable guide to design assumptions for conduits of large Reynolds numbers than is the Manning n.

The grouping of plotted points in Fig. 3 for the 123-in.-diameter pipe reveals an interesting pattern. The friction factors at the higher Reynolds numbers

---

[13] "Wassermessungen bei Wasserkraftanlagen," by L. A. Ott, *Wasserkraft-Jahrbuch*, 1924, pp. 253–282.

[14] "Hidraulika," by S. Kolupaila, J. Penikas, Kempten, Germany, 1947.

[15] Chf., Hydraulics Analysis Branch, Waterways Experiment Station, Corps of Engrs., U. S. Dept. of the Army, Vicksburg, Miss.

[16] "The Flow of Water in Concrete Pipes," by F. C. Scobey, ***Bulletin No. 852***, U. S. Dept. of Agriculture, Washington, D. C., October, 1920.

[17] "Pressure and Air Demand Tests in Flood Control Conduit, Denison Dam," *Miscellaneous Paper No. 2-31*, Waterways Experiment Station, Vicksburg, Miss., April, 1953.

THE UNIVERSITY OF MICHIGAN LIBRARIES

are generally greater for the 700-ft reach than those for the 500-ft reach. A similar phenomenon was observed in the Denison Dam conduit which was equipped with piezometers along the entire length. The pressure gradient was slightly concave upward near the upstream end and exhibited a fairly straight friction slope near the downstream portal. In this case, it was reasoned that the intake, gate slots, and transition generated an intensity of turbulence in excess of that which would be sustained by wall friction alone. It was further believed that the excess turbulence decayed throughout the curved part of the hydraulic gradient and reached a uniform friction slope near the downstream portal.

The pattern of plotted data in Fig. 3 appears to substantiate the interpretation of the Denison Dam tests mentioned in the preceding paragraph. Because the reach lengths were measured from the piezometer ring which was farthest downstream, the 700-ft reach could well have extended into a zone of excess turbulence decay. The smaller f-values from the 500-ft reach are therefore believed to be closer to the true friction factor. Even though the smaller values lie below the smooth-pipe curve, it seems remarkable that an equation based on experiments at substantially lower Reynolds numbers should extrapolate to values so close to the author's results.

The generation of excess turbulence at the pipe entrance is believed to occur only at very large Reynolds numbers. G. H. Keulegan[18] has pointed out that, for laboratory experiments with relatively small Reynolds numbers, the boundary layer begins to form near the entrance and to increase in thickness, leaving a laminar core extending into the pipe. The test points for Reynolds numbers smaller than 2×10^7 exhibit no such pattern as can be found for the test points at greater Reynolds numbers (Fig. 3). It is conceivable that, for the entrance geometry under consideration, a laminar core extends from the entrance for Reynolds numbers less than this value but that excess turbulence is generated near the entrance for greater Reynolds numbers.

This supposition may be verified only if the velocity distribution near the entrance can be measured and compared with that for a section much farther downstream. The development of apparatus which will allow the turbulence spectra for these two locations to be compared may also offer information on the generation of excess turbulence for large Reynolds numbers.

The problem of excess turbulence and its decay is important not only in the proper measurement of the friction factor but also in the evaluation of the entrance-loss coefficient. More information is needed on the intensity of turbulence near the entrance so that methods can be devised to simulate the condition in models of large conduits having high velocities.

ARTHUR L. COLLINS,[19] A. M. ASCE.—The measurements made on the San Gabriel Dam penstocks, having diameters of 51 in., 96 in., and 123 in., have produced data of particular interest because of the velocities on which the data are based. Venturi tubes having unusually large throat ratios of 0.82 and 0.93

---

[18] "Theory of Flow Through Short Tubes with Smooth and Corrugated Surfaces and Square Edged Entrances," by G. H. Keulegan, *Research Report 6B*, Highway Research Board, National Research Council, Washington, D. C., December, 1948, pp. 9–16.

[19] Cons. Engr., Berkeley, Calif.

were calibrated. A careful consideration of the data relating to pipe friction and venturi coefficients shows the need of a code not now (1954) in existence for conducting tests.

The purpose of this discussion is to offer suggestions for improving the methods of making field measurements and not to enter into a discourse on mathematical formulas. The first objective of an exploration is to obtain accurate data. The student can refer the data to the hydraulic charts such as those prepared by Fred C. Scobey, M. ASCE, and published by the United States Department of Agriculture, or to the Hazen and Williams tables, to see where the information fits into the general picture. He can then put the data to practical use.

Pitot Tubes.—The conditions at the San Gabriel Dam were highly favorable for the use of the pitot tube in determining accurate discharges. The use of one pitot-static tube held in one position as an independent unit to serve as a pilot and a multiple-tube system for obtaining the velocity distribution offers certain advantages. The logical tube to use in view of the high velocity is designated as the "standard pitot-static tube," for which the National Advisory Committee for Aeronautics (NACA) is to be given credit. The design of the tube was based on an extensive study of pitot tubes conducted in 1935. Although the tube has been used in the code[20] for testing fans, it has been largely ignored in hydraulic engineering circles.

The ASME Power Test Code.—The American Society of Mechanical Engineers (ASME) has been the principal source of information on water measurements that include use of the pitot tube. The writer considers the 1949 ASME code[21] impractical in the matter of pitot tubes and he believes that the manufacturers of turbines and pumps were partly responsible for this condition. The foregoing statement is not intended as a slur on the integrity of the manufacturers but is meant to call attention to the "hands-off" policy regarding acceptance tests. The attitude of buyers toward such tests would be entirely different if there were (1954) a method of measurement which would never produce errors exceeding 1%.

In the 1949 ASME code the two accepted methods are that of a particular commercial brand and the old method using a single orifice having a tapered tip approximately 3 in. long, attached to a rod. The static piezometer is built into the rod of the former method; in the latter the static pressure must be measured at the pipe wall.[22,23] If testing is complicated by requiring coefficient corrections as great as 3% (as outlined in the ASME code) and if there is no simpler method, there should be no recognized pitot-tube method of measurement. The required tolerance of 1% is obscured when the arbitrary corrections are applied.

The Code of the Hydraulic Institute.—The Hydraulic Institute (New York, N. Y.) is a technical agency supported mostly by pump manufacturers rather

---

[20] "Test Code," National Assn. of Fan Manufacturers, Detroit, Mich., 1941.

[21] "Hydraulic Prime Movers," ASME Power Test Codes, PTC 18, 1949.

[22] "Pitot Tube Practice," by Edward S. Cole, *Transactions*, ASME, Vol. 57, 1935, p. 281.

[23] Discussion of "Pitot Tube Practice," by Edward S. Cole, *ibid.*, Vol. 58, 1936, pp. 147–165.

THE UNIVERSITY OF MICHIGAN LIBRARIES

than the turbine or water-wheel builders. It has its own code which is used, for example, by the Bureau of Reclamation, United States Department of the Interior (USBR). However, the code is principally that of the ASME. It specifies the use of the Gibson method, the Allen salt-velocity method, and the Cole method. The remaining tapered-tip, single-pitot method is self-eliminating because of the controversial factors entering into the data.

The Hydraulic Institute code recommends that the test be conducted by the inventors of the methods, or experts (who are usually the inventors). The manufacturer of the turbine benefits by a small flow measurement whereas the pump manufacturer is favored by a large discharge measurement. It has been (1954) the practice of buyers for several years to avoid the hazards of making an erroneous field measurement by accepting the laboratory test of the prototype.

The Standard Pitot-Static Tube.—In a NACA publication nine pitot tubes which various important agencies were using in 1935 were analyzed.[24] With this information one is able to anticipate the performance of any pitot tube of the conventional bent-tube type. The information, however, does not refer to the pitot cylinder of the capillary tube. Because of this information it has been possible to construct the standard pitot-static tube referred to previously. The tube consists of an outer tube $\frac{5}{16}$-in. in diameter, with a small inner tube. The tip or nose is semispherical; the impact orifice is $\frac{1}{16}$ in. in diameter; the static openings are drilled with a No. 60 drill and are spaced $2\frac{1}{2}$ in. from the tip or nose; and the length is 14 in.[25] The foregoing dimensions permit tolerances. The tube can be attached to a handle or stem, or to a support.

The coefficient is unity and is compensated for in that angularity has little effect on the readings. Coefficients for tubes that are similarly made will agree within ±0.25%. Manufacture of the standard pitot-static tube is not controlled by patent. The design is suggested by the National Bureau of Standards, which will check the calibration for a nominal sum.

Two methods of using the tube are suggested. First, at least ten pitot tubes should be spaced and supported at specified radial distances on a frame across two diameters. This arrangement is the conventional method of dividing the pipe area into annular spaces of equal areas. In the second method there are four conventional pitot tubes which are introduced at four places on the pipe circumference for traversing.

The Aeolian vibrating effect on the tube at the high velocities encountered at San Gabriel is always a problem and must be prevented. This term has been borrowed from the text of a United States patent[26] in which is described a method of measurement using a rod which is suspended from a wall and which emits vibrations.

Plotting of Data.—In any type of tube where a traverse is made, the user is confronted with the difficulty of interpreting the manometer readings taken near the pipe wall. The method of dividing the pipe area into equal annular areas and omitting the reading of the velocity in the area close to the pipe wall has provided highly satisfactory results. The plotting of the data with the velocity measurements as ordinates and the radial distances, squared, as abscissas aids in determining the proper rating when the curve is projected to the wall. The outer annular-area velocity is not eliminated in this method, but the reading within a fraction of an inch of the wall is unnecessary. This outer area is always unstable from turbulence of such a nature that it is practically impossible to tie-in the readings with the tube calibrations.

---

[24] "Comparative Tests of Pitot-Static Tubes," by Kenneth G. Merriam and Ellis R. Spaulding, *Technical Note No. 546*, National Advisory Committee for Aeronautics, Washington, D. C., November, 1935.

[25] "Test Code," National Assn. of Fan Manufacturers, Detroit, Mich., 1941, p. 13.

[26] *U. S. Patent 1,935,445*, November 11, 1932.

Pilot Pitot Tube.—In the planning of tests such as those conducted at San Gabriel Dam it would be of considerable interest to install a pilot tube either of the standard pitot-static type or the pilot-cylinder type at a considerable distance upstream of the venturi meter with the orifices near the mid-diameter. From the general data now accumulating (1954) regarding the velocity distribution in large pipes, it is apparent that the average pipe velocity ratio is approximately 85½, varying between 82 and 89. In the information on ratios, the type of pitot tube is never mentioned. Hence, it is impossible to tell whether the results are comparable within a range of from ±3% to ±4% because of the characteristics of the various tubes.

Although the two major commercially available types of pitot tubes have been in use for many years and serve a useful purpose, it will be found that a velocity traverse made in the same pipe section by these two types of tubes will not show identical curves. Also, it can be observed that, if one of these tubes is inserted into the pipe and is extended entirely across the pipe, it will show a symmetrical curve. If the test is repeated by inserting the tube from each side of the pipe and extending it to the mid-diameter, the two curves will not be identical. The standard pitot-static tube has its orifices far enough away from the supporting stem to avoid interference with the readings—a highly desirable feature.

Consistency.—When the pilot tube is placed in service the pipe velocity coefficient is assumed to be 85½%, with the possibility that the correct value is ±3½% in error. It can be further assumed that the same error will prevail over the entire range of velocities exceeding approximately 2 ft per sec and that the consistency will be less than ±0.50%. If, during the tests for obtaining the venturi coefficient for any other purpose, it is possible to obtain a single accurate check on the assumed values, the pitot tube becomes an accurate metering unit. This is also predicated on the assumption that the velocity distribution curve tends to follow the parabola, except for velocities of 1 ft per sec or 2 ft per sec.

A large water-distribution company began using this method around 1945 and since 1949 has made more than forty pitot-tube installations with recorders on cement-lined pipes from 8 in. to 48 in. in diameter. It was found unnecessary to calibrate the tubes in the field. The tubes forming the metering system are primarily for control purposes, and no serious harm will result if the rating is 3% or 4% in error.

The Venturi-Meter Data.—In the venturi-meter data for the 51-in.-diameter pipe, the average coefficient is 0.961 (with a spread of 4½%), and the readings do not show a tendency to change from high velocity to low velocity. The inference is that the velocity ratio or distribution ratio of the flow of the water in the pipe does not change. Had a pilot tube been installed and had readings been taken simultaneously with the venturi meter, the data could have been analyzed to find the cause of the variations.

It would appear that the reading of greatly depressed manometer deflections up to 0.001 in. is superfluous as compared to the more important details incidental to the over-all accuracy.

Capillary Pitot Tube.—In studying the capillary-tube data obtained from the 51-in.-diameter pipe, it will be interesting and perhaps instructive to plot the original manometer readings without any eliminations. The length of the capillary pitot tube is 1 in., and the tube is supported by a relatively close and large cross member. The support members themselves may have some effect on the readings, particularly the readings taken from the trailing member. The curve should be plotted from the square-root value of the deflections and the square of the radial distance. How closely will the curve approach a straight line? There will be a 1% or 2% area at the wall which must be properly evaluated. In routine testing, using the equal-ring or equal-annular-area method, the outer radius for the last reading is only 5.1% of the radius from the wall. In the 51-in.-diameter pipe this amounts to 1.3 in. It is generally assumed that the continuation of readings at small intervals beyond this distance is not justified. The projection of the curve to the wall is always of interest.

The Dye Method.—The application of the color test for conditions existing at San Gabriel Dam seems to check accurately the results of volumetric gaging. The method should provide consistent readings for the same reasons that are true for the methods involving the venturi-meter and the pitot tube. Again, consistency does not mean accuracy. In a color test, if consistency exists, it is necessary only to apply a correction as is done with the pitot tube in order to obtain accurate data.

A Pitot Tube for Small Pipes.—Although advantages of the standard pitot-static tube have been stressed, its necessarily great length makes it awkward to use in a small pipe. There are 100,000 or more irrigation pumps in California with discharge pipes of from 6 in. to 12 in. in diameter. These pumps should be checked at intervals to determine the pump efficiency and quantity of water pumped. The tolerance accuracy should be within ±2% or ±3%. This can be accomplished by the use of the cylinder pitot tube. This type of tube has been described by J. E. Christiansen, A.M. ASCE, and O. C. French.[27]

Notwithstanding the wide use of the cylinder pitot, the engineering student is led to believe that the weir and the related Parshall flume and orifice plate are the established methods of measuring water in the field. The orifice plate is of course satisfactory where conditions permit. However, in 50,000 tests made on farmers' pumps by a power company, it is doubtful if the weir was ever used where the pipe could be tapped for the pitot tube. Ordinarily, an accurate reading can be made in a few minutes under almost any condition encountered in ordinary pumping plants.

---

[27] "Characteristics of Transverse Tubes," by J. E. Christiansen and O. C. French, *Agricultural Engineering*, January, 1937, pp. 21–24.

R. Clifford Youngquist,[28] A.M. ASCE.—Some interesting test data are provided by the author on flows of abnormally high velocities ranging up to almost 50 ft per sec, with Reynolds numbers as great as 38×10^6. The values of the Manning n and of the Darcy f decrease with an increase in the rate of flow.

At a given date any pipe line not originally lined by present-day techniques will have a certain roughness condition which will become more rough with respect to time. The average slope of a curve representing the observed head losses plotted against the rate of flow, Q, is approximately 1.85, showing that h_f varies as $Q^{1.85}$. Any data on a given size and length of line may vary slightly above or below this exponential expression. Often when the exponent is greater than 1.85, the difference can be traced to velocity disturbances produced by bends or changes in size, the head loss from which may affect the hydraulic and energy gradients as much as 100 diameters downstream.

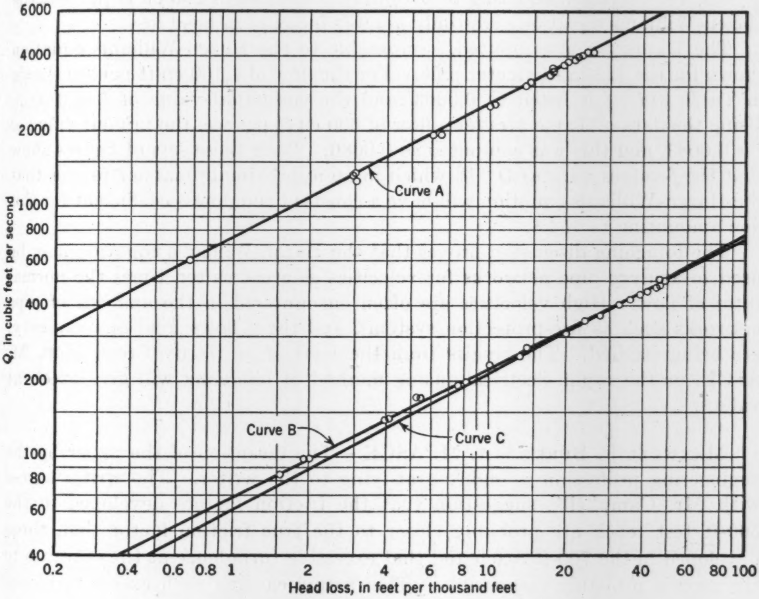

Fig. 10.—Head Losses Related to Flow Rates

The head losses for the data shown in Table 3 were converted to losses per 1,000 ft so that all data could be plotted on one curve. Some of these head losses and the related rates of flow were plotted in Fig. 10, and a line designated "curve A" and having a slope of 1.85 was drawn through points representing the 123-in.-diameter pipe. As explained elsewhere[29] by the writer, if the in-

---

[28] Hydr. Engr., Dept. of Water and Power, City of Los Angeles, Calif.

[29] "Complicated Hydraulic Structures Analyzed by Hazen-Williams Formula," by R. C. Youngquist, *Civil Engineering*, Vol. 21, 1951, p. 411.

THE UNIVERSITY OF MICHIGAN LIBRARIES

terior diameter were 10.227 ft, the Hazen-Williams equation would be $h = 507\ Q^{1.85} \times 10^{-6}$, and the friction coefficient would be 154.8. None of the points departs far from the curve. The 123-in.-diameter pipe was certainly very smooth.

Likewise, points were plotted in Fig. 10 for the 51-in.-diameter line. In these data the trend is toward a steeper slope or exponent of 1.944, showing that for this pipe the head loss varies as $Q^{1.944}$. The second curve (curve B) is based on the Hazen-Williams equation, $h = 277\ Q^{1.944} \times 10^{-4}$, passing through the point where $h_f = 49.86$ ft and $Q = 505$ cu ft per sec. This line has a friction coefficient of 130.6. Curve C represents the expression, $h = 499\ Q^{1.85} \times 10^{-6}$. It is interesting to note that, for a flow of 200 cu ft per sec, the Hazen-Williams equation gives only a 0.9-ft increase in head loss.

The Darcy f was computed, comparable to the Hazen-Williams equation shown for the 123-in.-diameter pipe. For the flow of 4,100 cu ft per sec shown in Table 3(*d*), f is listed as 0.0063, and the computed value of f is 0.0065. Using the data of Table 3(*c*) for a flow of 600 cu ft per sec, the tabular value of f is 0.0083, and this was computed as 0.0086. Both these sets of figures show that the f-values vary as $Q^{-0.15}$, which in an approximate manner proves that the Hazen-Williams equation will have a constant roughness coefficient for this line amounting to 154.8.

The foregoing discussion proves that the Hazen-Williams equation may be used to analyze pipe networks for velocities as great as ten times the normal rates of flow. High velocities are often encountered in the analysis of pipe networks such as fire-protection systems, and these flows, real or imaginary, are being studied. The results from the method of Hardy Cross, Hon. M. ASCE, or the rapid electrical-analog method of modeling will give excellent values.

MAXWELL F. BURKE,[30] A. M. ASCE.—The reception of the paper by the engineering profession is highly gratifying to the writer. The writer agrees with Mr. Campbell's suggestion that the friction factors developed in the 500-ft test reach are probably closer to the true friction factor than those developed in the 700-ft reach and that excessive turbulence at the entrance to the pipe is probably responsible. The factors causing such excess turblence are the transitions from the common 30-ft-diameter tunnel to pipes of smaller diameters, the expansion and contraction around the butterfly valve, the butterfly valve itself, the vacuum-relief valves downstream of the butterfly valve, and the manhole openings in the pipes. The possibility of excess turbulence created by these factors, extending down into the 700-ft test reach, was the primary reason why pressure taps were also installed for a 500-ft reach.

Mr. Collins has raised the question of a standardized code for pitot measurements on which the writer does not feel qualified to comment. However, the information on the standard pitot-static tube is appreciated. The writer was aware of several designs of pitot-static tubes made by competent persons but chose to utilize the design developed by the District for the reasons mentioned in the paper. In addition, the intention was to measure the velocities as close to the wall as possible, and a very small diameter pitot tube seemed the best engineering answer. By extending the velocity observations to a short distance from the wall, the distance the velocity curve must be projected to meet the wall is minimized. Measurements as close as 0.15 in. from the wall invariably conformed to the velocity pattern in the remainder of the pipe, as determined from a logarithmic plotting of velocity versus distance from the wall. Values at lesser distances were smaller than the plotting extension would indicate.

---

[30] Civ. Engr., Los Angeles County Flood Control Dist., Los Angeles, Calif.

The installation of a fixed standard pitot tube at the center of the pipe as a metering or control device is unsuitable for the existing penstocks because they are required to discharge debris of considerable size, sometimes as great as 6 in. in diameter. Any fixed device projecting into the flow would be subject to considerable battering from such debris. Venturi meters escape such treatment.

No influence of the supports on the pitot-tube readings could be discerned from a comparison of the velocities measured on the leading support as against those measured on the trailing support—with the exception of trailing-support readings taken $\frac{1}{4}$ in. from the leading support. Readings in such close proximity to the leading support showed a very small reduction of velocity from the readings taken at the leading support.

TABLE 5.—VELOCITY DISTRIBUTION

Q (pitot)	a	x	V_m	V	V/V_m	k
96.24	7.29	0.0948	7.88	6.85	0.742	0.872
114.8	8.71	0.0976	9.40	8.17	0.869	0.869
124.9	9.49	0.0965	10.26	8.89	0.867	0.870
142.3	11.33	0.0937	12.15	10.55	0.868	0.873
161.4	12.25	0.0956	13.24	11.49	0.868	0.871
165.9	12.70	0.0960	13.61	11.81	0.868	0.871
198.8	15.20	0.0998	16.35	14.15	0.865	0.866
238.3	18.11	0.0980	19.42	16.96	0.873	0.868
252.9	19.20	0.0924	20.52	18.01	0.878	0.875
278.5	21.31	0.0910	22.63	19.83	0.876	0.877
298.3	22.64	0.0889	24.17	21.24	0.879	0.879
326.2	24.76	0.0890	26.56	23.22	0.874	0.879
350.1	26.56	0.0931	28.21	24.93	0.884	0.874
376.3	28.55	0.0944	30.58	26.79	0.876	0.873

The writer is indebted to Mr. Kolupaila for his detailed analysis of the velocity distribtuion for the test data submitted to him. It should be mentioned that the recorded Q of 435 cu ft per sec was merely a label given to this particular set of measurements for identification and was not intended to represent accurately the true flow rate.

Because the velocity distributions obtained in the remainder of the flow tests may be of interest, the test data for the other fourteen tests were plotted on logarithmic paper, and straight lines were fitted to each set of data by eye. The results in Table 5 were obtained for the basic formula $V = a\,y^x$.

The values of K, which were computed from $2/\,(x+1)\,(x+2)$ correspond closely to the ratio V/V_m, as noted by Mr. Kolupaila.

The writer is also indebted to Mr. Youngquist for his analysis of the flow data for the two pipes in terms of the Hazen-Williams pipe formula. The data were analyzed and presented according to what the writer believed were the two best-known flow formulas—the Manning and the Darcy. Other exponential-type formulas have been generally regarded with distrust by the writer because of their lack of dimensional homogeneity. However, the primary reason for submitting the data for publication was to make them available to the profession. If the data are accepted and use can be made of them, the writer's purpose has been accomplished.

AMERICAN SOCIETY OF CIVIL ENGINEERS
Founded November 5, 1852
TRANSACTIONS

Paper No. 2767

STABILIZATION OF MUNICIPAL REFUSE BY COMPOSTING

By Percy H. McGauhey[1] and Harold B. Gotaas,[2]
Members, ASCE

With Discussion by Messrs. Arthur W. Furbank; and
Percy H. McGauhey and Harold B. Gotaas

Synopsis

The essentials of aerobic composting to stabilize municipal refuse, developed during more than two years of research into the practice and fundamentals of composting, are presented. Composting processes used throughout the world are briefly reviewed.

Composting is a natural biological process which proceeds most rapidly under thermophilic aerobic conditions. The principal environmental factors that govern the speed and course of the process are shown to be moisture content, aeration, particle size, and initial carbon-nitrogen ratio. Seeding is shown to be unnecessary, and hydrogen ion concentration proves to be an unimportant factor in composting municipal refuse.

Important steps in composting refuse—such as segregating, grinding, stacking, turning, and remilling—are discussed, as are operating factors and the judging of the condition of a compost on the basis of observations, course of temperature, and control tests. The time required for stabilizing several types of refuse material by various processes is shown, and the merit of finished compost as a fertilizer and soil conditioner is observed. The problems of practical municipal composting are reviewed. It is concluded that composting offers an economical and sound solution to the refuse disposal problems of many communities, at the same time reclaiming organic material of great value to agriculture.

Note.—Published, essentially as printed here, in October, 1953, as *Proceedings-Separate No. 302*. Positions and titles given are those in effect when the paper or discussion was received for publication.

[1] Research Engr., Univ. of California, Richmond Field Station, Richmond, Calif.

[2] Prof. of San. Eng. and Chmn., Civ. Eng. Div., Univ. of California, Berkeley, Calif.

INTRODUCTION

In a broad sense, composting refers to the production from organic matter, through the agency of microorganisms, of a relatively stable humus which may beneficially be used on agricultural soils. For many centuries it has been practiced in a simple form by individuals and village groups wherever vast populations have maintained themselves for long periods on limited areas of tillable land. The processes of composting exist in nature; however, there have been attempts to systematize and commercialize composting in Europe and Asia during the past twenty-five years for the purpose of increasing food production or maintaining soil fertility.

Because of the enormous capacity of the United States to produce food by applying inorganic fertilizers to its relatively virgin soils, interest in composting has, until recently, been confined principally to individual gardeners and to a few entrepreneurs more interested in selling patented processes and devices than in producing and marketing compost. These attempts at selling composting have often been surrounded by mystery and secret formulas and may have actually retarded commercial development and production of useful compost. The present, widespread, serious interest in composting in the United States is the result of a new concept of the process as a device for the disposal of municipal refuse.

The need for a new method of refuse disposal in many municipalities is acute. Some communities that have too long endured the nuisance of open dumps or rudimentary landfills now must solve the problem of financing immediately the offspring of a generation of delayed progress. Other communities have a variety of refuse disposal problems—landfill sites are being overrun by subdivisions; new landfill sites are excessively expensive or nonexistent within economic haul distances; and incinerators are expensive and difficult to locate in the community. Then, too, a new set of considerations are complicating the problem of refuse disposal in many areas. These include the contamination of ground waters by leachings from dumps and fills and the pollution of the air by gases and particulate matter from burning or incineration.

Any new process for disposing of municipal refuse should be free of the health hazards and nuisance aspects of dumps; require a smaller area than the landfill; cost much less to install than an incinerator; and involve a rapid, sanitary, reliable, and economical procedure. The possibility that composting represented such a process created a great interest in it and led to the research into its fundamentals on which this report is based.

COMPOSTING PROCESSES

Composting processes may be divided into two general classes: (*a*) That in which the stabilization achieved is principally the result of anaerobic decomposition of organic matter; and (*b*) that in which aerobic decomposition predominates. Strictly speaking, the latter process is carried out by facultatively aerobic organisms requiring only a modest amount of atmospheric oxygen, but the rapid rate of decomposition, the freedom from odors, and the degree of stabilization achieved are so characteristic of aerobic decomposition that the process is called "aerobic" in contrast with the slow, odorous, and somewhat less complete stabilization characteristic of the "anaerobic" process.

Most of the older traditional composting procedures are anaerobic. The more primitive methods long used in the Orient involve placing miscellaneous organic matter, including night soil and animal manures, in open piles or pits and allowing from eight months to twelve months for composting. This procedure was systematized in India thirty years ago by Sir Albert Howard (1)[3] and was widely used since then in that country as well as in South Africa, during World War II. The practice is to pile on the ground or in pits to a depth of 5 ft or more alternate layers of putrescible materials, such as garbage, animal manures, night soil, sewage sludge, and more stable matter such as leaves and straw. The mass is usually turned twice during a composting period from six months to eight months and drainage liquors may be recirculated. In Africa and Australia, holes are punched in the pile with sharpened sticks in a moderately successful attempt to admit sufficient air to prevent anaerobic conditions inside the pile.

In Europe the refinement of ancient composting practices took the form of mechanization of the process. During the decade 1920–1930, various closed cells were designed and patented. Most important are those developed by Beccari in Italy and by Verdier (2) in France. The Beccari cell incorporates air vents that are opened to afford some minor degree of aeration of a charge of organic matter after it has undergone an initial period of anaerobic decomposition. Mr. Verdier added provision for recirculating gases or drainage liquors.

Both open piles and closed cells have been used in Europe in various composting operations intended to be aerobic. In 1931, Jean Bordas (3) of France patented a batch composter in the form of a silo divided by a grate into an upper and lower section, with provision for introducing air along the walls and through a central pipe. However, there seem to be no reports of its successful operation. In 1932, a refuse disposal company in Holland (4) began what is now the most extensive composting enterprise in the world. This process is essentially an adaptation of the Indore process to the composting of municipal refuse other than garbage. As originally practiced, the Indore process involved dumping refuse in long high piles with no treatment other than periodic sprinkling with recirculated drainage liquor. In a more recent installation refuse is ground in a special mill, then placed in open piles, sprinkled, and turned occasionally during a three-week or four-week composting period. In Denmark and Sweden, refuse is ground by the Dano process before composting in open piles under either anaerobic or aerobic conditions, depending on the subsequent handling of the material.

When composting in the United States began to be taken seriously as a method of refuse disposal, it soon became apparent that practices elsewhere in the world were not readily applicable. The Indore process involved too much hand labor and the use of animal manures; a few installations of the Beccari process had already been constructed in the United States and abandoned because of unsatisfactory performance (in any event, the slow anaerobic processes involved were not well suited to American needs). All methods advocated in the United States involve aerobic decomposition although none of these has yet been put on a commercial basis utilizing mixed refuse on a municipal scale. Of the four methods most seriously considered, one has been described elsewhere by John R. Snell, A. M. ASCE, a second by Eric Eweson (5), a third by R. P. Stovroff (6), and the fourth will be described herein. It is sufficient to state here that the Frazer-Eweson and Earp-Thomas procedures make use of closed cells or digesters, whereas the Compost Corporation of America and the University of California use open piles.

---

[3] **Numerals in parentheses, thus: (1), refer to corresponding items in the Bibliography (see Appendix).**

EXPERIMENTAL INVESTIGATION

In 1950 the Sanitary Engineering Research Laboratory of the University of California (Berkeley) began a study of composting (7) as a possible solution to urgent problems of refuse disposal aggravated by California's sudden growth in population. From a study of the literature it soon became evident that composting did not develop according to a scientific theory and was consequently surrounded by a haze of misconceptions concerning its fundamentals. For example, many processes had been patented that were based on the application of forced air to sustain aerobic decomposition and, simultaneously, on the recirculation of drainage liquors which develop only under anaerobic conditions. Other procedures reported to be essential to successful composting included seeding with manure, inoculation with special organisms, recirculation of liquids or gases, forced aeration, and the addition of enzymes and hormones. Established principles of organic decomposition were found throughout scientific literature, but little significant work had been done on their application to the composting of municipal refuse. It was therefore necessary to conduct research studies to establish the fundamentals of composting before a procedure could be developed.

For convenience, flexibility, and control of variables, experiments were first conducted on a laboratory scale. The knowledge gained and the procedures developed during these studies were then applied to larger-scale pilot studies and field-scale studies in order to adapt these procedures to practical composting.

Laboratory studies of organic material were made in 5-gal jars and 55-gal drums in a high-temperature laboratory. The materials composted included shredded vegetable trimmings, which were composted alone or in various combinations with such materials as straw, horse manure, shredded paper, oyster shell, and garden soil. Pilot-scale studies were conducted on similar materials in bins 40 in. square, holding approximately 1.5 cu yd, and located in an unheated warehouse. Field-scale studies were conducted at the Berkeley refuse disposal site on thirteen different loads, weighing between 2 and 3 tons each, of combined city refuse from eleven different districts of the city. In addition, city refuse was composted in combination with raw sewage sludge, digested sewage sludge, pear wastes, and garden soil. The material was shredded in a hammermill and was composted in open piles.

Basic Considerations.—Because composting is a biological process, environmental factors influencing the activities of microorganisms determine the speed and course of the composting cycle. In general, such factors include seeding, moisture content, aeration, hydrogen ion concentration, temperature, and particle size and initial carbon-nitrogen ratio of the food material.

Seeding.—Many proposals for commercial composting are built around the use of some special inoculum known only to its discoverer, who claims it to be fundamental to successful operation of the process. Others prescribe the use of horse manure in quantities as great as 30% of the total mass, the addition of garden soil, or the recycling of partly composted material to seed the raw refuse. Inasmuch as the success as well as the economy of a process is involved in the matter of seeding, early studies were made to evaluate seeding. Chemical and bacteriological tests were sufficient to show that several commercial preparations were worthless. Other preparations were studied by controlled laboratory experiments and pilot-scale experiments. Several studies were made using various amounts of horse manure as the seeding material. In all cases it was obvious that moisture and aeration were far more important factors. No significant increase in the rate of buildup of bacterial population resulted from the use of 30% horse manure in a typical garbage material.

TABLE 1.—ANALYSIS OF SEEDED AND UNSEEDED COMPOSTS

MATERIAL	Days after start of experiment	Percentage of ash	Percentage of carbon	Carbon-nitrogen ratio	pH
Shredded vegetable trimmings	0 2 8	10.9 14.1 17.8	42.0 21.8 35.5	20.2 11.4 10.8	6.2 5.2 9.1
Shredded vegetable trimmings plus 2% horse manure	0 2 8	10.9 12.9 20.1	42.0 38.4 37.4	20.2 21.2 18.6	6.2 4.6 8.8

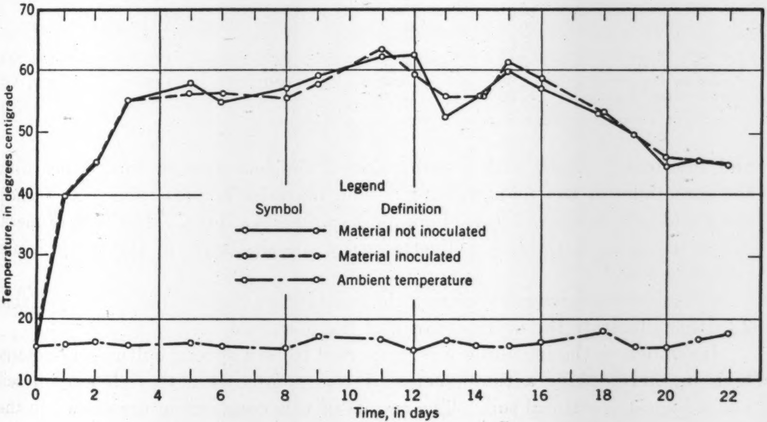

FIG. 1.—TEMPERATURE CURVES SHOWING SIMILARITY OF INOCULATED AND UNINOCULATED AEROBICALLY COMPOSTING MATERIAL

Both seeded and unseeded composts reached temperatures at the top of the mesophilic range within twenty-four hours.

Criteria for the degree of decomposition are an increase in the percentage of ash, a decrease in carbon, and a decrease in the carbon-nitrogen ratio during the composting period. When these criteria were used as indicators of the value of seeding with a reasonable quantity of horse manure, no significant benefits were observed. Table 1 is typical of the results obtained.

Two studies were made using commercial additives. The first study involved a "starter" and was made in the high-temperature laboratory. Two 55-gal drums were filled with identical mixtures of shredded leafy vegetables and dry hay. To one was added the starter in the amount specified by the manufacturer. Both were aerated in the same manner and both produced a satisfactory compost, with no discernible benefit from the additive.

The second investigation made use of a highly promoted secret inoculum. Half-ton portions of identical mixtures of shredded vegetable trimmings and paper were placed in each of two bins. The material in one bin was sprayed and thoroughly mixed with a suspension of the inoculum in accordance with the directions of the manufacturer. The material in both bins was turned daily and both produced a good compost in nineteen days. The lack of merit of the inoculum is strikingly illustrated by the similarity of the temperature curves in Fig. 1.

TABLE 2.—ANALYSIS OF UNINOCULATED AND INOCULATED COMPOSTS

Analysis	Initial	Third Day		Final (Nineteenth Day)	
		Uninoculated	Inoculated	Uninoculated	Inoculated
Ash (%)	10.51	13.8	16.12	29.18	28.86
Moisture (%)	90.18	80.67	79.38	74.74	75.07
Carbon (%)	37.75	38.59	41.67	31.87	31.41
Nitrogen (%)	2.16	2.27	2.30	1.95	1.91
Phosphorus (%)	0.17	0.25	0.31	0.31	0.33
Potassium (%)	1.00	0.93	0.81	1.08	1.10
Carbon-nitrogen ratio	17.50	17.00	18.00	16.20	16.50

Chemical analyses made during the composting period and shown in Table 2 further illustrate the unimportance of the inoculum.

Inasmuch as the inoculum was purported to be a special culture of bacteria high in thermophilic actinomycetes, it was compared with rich garden soil and a poor agricultural soil. The results of this comparison are shown in the following tabulation, in which is listed the comparative number of thermophilic actinomycetes in various materials. (The organism count for horse manure is that reported by S. A. Waksman(8).)

Material	Organism count (number of colonies) per gram of material
Inoculum	15.8×10^7
Rich soil	13.4×10^7
Poor soil	15.8×10^6
Horse manure	15.0×10^7

Other experiments demonstrated that the addition of soil or the recycling of composting material did nothing to alter the speed of decomposition. From these studies and similar results by other observers it was concluded that both mesophilic and thermophilic microorganisms indigenous to refuse are sufficient to carry on the composting process with great rapidity when environmental conditions of moisture and aeration are suitable. Subsequent success with numerous composts confirms the fact that seeding is not an essential part of a practical process for composting municipal refuse.

Hydrogen Ion Concentration.—Inasmuch as hydrogen ion concentration can be an important factor in biological processes, experiments were conducted to determine the benefits which might result from the addition of a calcium-carbonate buffer. Various amounts of calcium carbonate were used. The result was a very slight reduction in the normal pH-sag shown roughly in the final column of Table 1, a slightly greater degree of decomposition as indicated by increase in percentage of ash after correction for the added calcium carbonate, and an improved physical appearance of the final product. On the other hand, a serious loss of nitrogen occurred in samples containing the buffer and composting time was not shortened. The experiments and subsequent experience in composting demonstrated that the addition of calcium carbonate to a compost is of doubtful value and that pH-control is not necessary in the composting of garbage, municipal refuse, and other mixtures studied during the research investigations.

Moisture.—Moisture content is one of the most important factors in aerobic composting. Too low a moisture content deprives microorganisms of the water needed in their metabolism and consequently inhibits bacterial activity. At too great a moisture content water displaces air in the interstices between particles, giving rise to anaerobic conditions with attendent putrefactive odors, foul drainage liquors, and retarded decomposition.

The maximum amount of moisture permissible varies with the nature of the material to be composted—especially with its ability to maintain structural strength when wet. In the laboratory and field studies it was possible, through aeration by daily turning, to compost mixtures of vegetable trimmings and straw having initial moisture contents as great as 85%, but 76% initial moisture was too great when paper was used instead of straw. Municipal refuse was composted at moisture contents of from 30% to 75%, although it was difficult to prevent a small degree of anaerobiosis when moisture exceeded 70%. Under normal conditions, the moisture content of municipal refuse, which has been properly shredded without pulping, may generally be expected to fall within the 40% to 60% range found most suitable for composting.

Excessive moisture may be reduced by additives such as straw, dry soil, or dry sawdust if the quantities necessary do not greatly increase the carbon-nitrogen ratio and thus unduly prolong the composting period. Paper was found to be quite ineffective in controlling moisture. Frequent turning seems to be the most desirable method of moisture control because it promotes loss of moisture by evaporation without disturbing the carbon-nitrogen ratio and at the same time acts as an effective aerating procedure. If the moisture content becomes too low, turning permits effective adding of moisture during the process.

The foregoing considerations concern refuse having a high initial moisture content. There is evidence that material being composted in the open may become excessively wet if rainfall is heavy, necessitating the use of preventative measures such as shed roofs or special shaping of the piles. Observers in both Scotland and South Africa report soaking of compost piles by relatively continuous heavy rainfall, although intermittent heavy rains did no harm. One heavy rain was experienced during the Berkeley field studies. It penetrated open compost piles with rounded tops to a depth of from only $\frac{1}{8}$ in. to $\frac{1}{2}$ in.

Aeration.—As previously noted, the quantity of atmospheric oxygen required to prevent typical anaerobic decomposition from developing is not great. Nevertheless, some air must be supplied if rapid, nuisance-free composting is to be achieved. Methods proposed include periodic turning of the material, forced air, and the use of chimneys or other openings through the pile. Experiments with both bins and open piles showed turning to be most effective. Forced air did not satisfactorily penetrate masses of moist material and, when introduced through adequate diffusers, proved expensive and was apt to cause excessive drying. Water sprayed on the pile to overcome drying did not penetrate to any appreciable extent, and the disturbing of the pile necessary to add moisture constituted in itself adequate aeration. This and other evidence indicates that aeration of material in closed digesters by forced air would be both difficult and expensive. Chimneys and holes penetrating

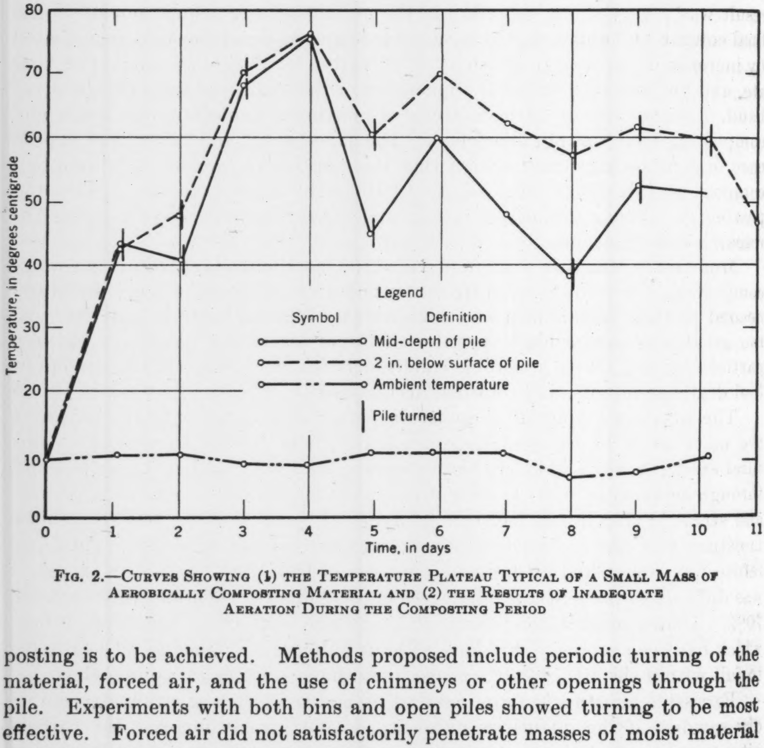

FIG. 2.—CURVES SHOWING (1) THE TEMPERATURE PLATEAU TYPICAL OF A SMALL MASS OF AEROBICALLY COMPOSTING MATERIAL AND (2) THE RESULTS OF INADEQUATE AERATION DURING THE COMPOSTING PERIOD

the composting mass proved totally ineffective, producing at best only a minor local zone of aerated material in a large putrefying mass.

Temperature.—Except for very small masses such as might be used in laboratory experiments, there is no need for temperature control when material is composted in open piles in moderate climates. In cold climates it seems probable that an outer shell between 6 in. and 12 in. thick might remain quite inactive and serve merely to insulate the composting material within the pile. When turned into the interior of the pile, this shell might introduce a thermal shock and result in a lengthening of the compost period.

The temperature variation in an aerobically composting mass follows a typical curve. Consequently, temperature becomes an important control test and an aid to judging the course of a compost. The handling of material involved in placing it in a compost pile brings its temperature close to that of the ambient temperature of the surrounding air. If other environmental conditions such as moisture and aeration remain suitable, mesophilic organisms indigenous to the refuse multiply rapidly, their metabolic processes producing heat that escapes slowly because the pile is to a large degree self-insulating. The result is a rapid rise of temperature to 45° C or 50° C, which represents the upper limit for mesophilic organisms. At this temperature, however, the environment becomes optimum for thermophilic microorganisms and, if moisture and aeration remain proper, their rapid

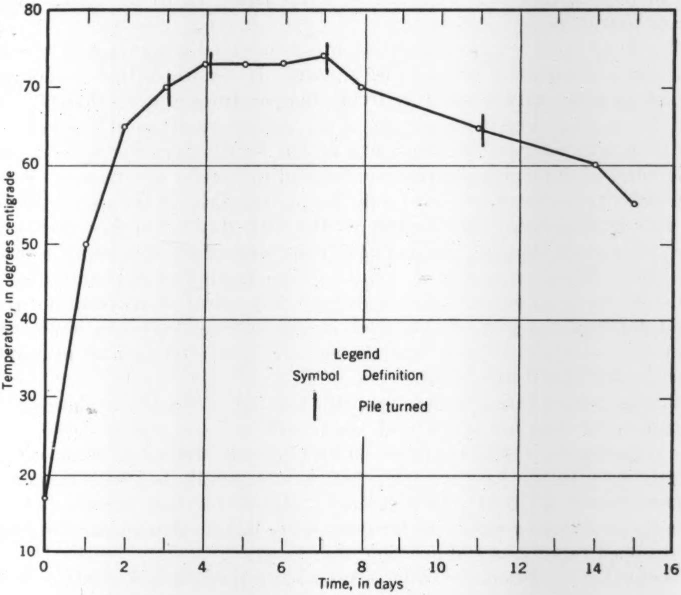

FIG. 3.—TEMPERATURE CURVE TYPICAL OF A LARGE MASS OF AEROBICALLY COMPOSTING MATERIAL

THE UNIVERSITY OF MICHIGAN LIBRARY

growth and activity cause a further rise of temperature to 70° C or 75° C, or to a level at which excess temperature limits bacterial populating. The high temperature then persists until food supply becomes the limiting factor—that is, until the stabilization of the organic matter is well advanced. After that, the temperature of the mass declines and the compost is considered finished in that it may be stored for long periods without any additional generation of heat or appreciable chemical change, although slow bacterial activity may continue for a long time.

In a small mass of composting material there is a typical temperature plateau as the mesophilic bacterial population declines and the thermophilic population develops. Fig. 2 illustrates a typical case of the successive development of populations and rapid rise of temperature to 75° C during the first three or four days.

The study from which Fig. 2 was made involved a compost of vegetable trimmings and straw in a bin 40 in. square. It is notable that, although the ambient air temperature was only 10° C, temperatures of more than 60° C persisted for several days within 2 in. of the exposed surface of the pile. The large decline in temperature beginning on the fourth day illustrates the result of the onset of anaerobic conditions produced by lack of aeration.

A quick recovery of aerobic conditions is signalled by the rise in temperature following aeration by turning on the fifth day. Another decline took place as the material again became anaerobic, recovering once more on turning. Successively lower maxima and a final decline in temperature indicated that stabilization was approaching completion. The lower temperatures recorded at mid-depth of the pile indicate that, in a situation where aeration is critical, bacterial survival is greatest near the surface where diffusion of atmospheric oxygen adds a small increment.

In large piles where heat loss from the interior of the pile is slow, the temperature curve does not hesitate at the transition from mesophilic to thermophilic organisms. Fig. 3 is typical of aerobic composting as observed in the field studies. In this case the temperature rose rapidly to a maximum in four days and slowly declined. In many other studies the high temperature range of the curve remained quite flat for four or five days. After that the temperature dropped rapidly as stabilization progressed.

Carbon-Nitrogen Ratio.—To be economically feasible as a method of refuse disposal, composting must produce a product that can be sold for use on agricultural land. Consequently, the ratio of carbon to nitrogen in the finished product becomes a matter of importance. The carbon-nitrogen ratio of the raw materials is likewise important for the time required for composting organic matter depends on it. From the initial and final values, the change in carbon-nitrogen ratio during the process can be found. This change normally indicates the degree of decomposition and hence is more significant than the absolute value of the final ratio in judging the fitness, for use on growing crops, of a compost made from material having a high content of paper or lignocellulose.

Living organisms utilize about 30 parts of carbon for each part of nitrogen; hence, an initial carbon-nitrogen ratio of 30 would seem most favorable for rapid composting. Various researchers have reported the optimum value as being between 26 and 31. Material with initial carbon-nitrogen ratios of from 20 to 78 was composted in the University of California studies. From the results, an initial carbon-nitrogen ratio of between 30 and 35 can be recommended as optimum for rapid composting of municipal refuse without loss of nitrogen. Above that range, composting time can be expected to increase with carbon-nitrogen ratio; below that range rapid composting is likely to be accompanied by an increasing loss of nitrogen.

The optimum carbon-nitrogen ratio for composting is not, of course, the optimum carbon-nitrogen ratio for the soil. A value of 20 has been widely accepted as the upper limit at which there is no danger of robbing the soil of nitrogen. The availability of the carbon, however, seems the most important factor, and carbon-nitrogen ratios greater than 20 are acceptable when the carbon is not readily usable by bacteria. Humus resulting from composting has often been reported as having a carbon-nitrogen ratio of from 10 to 20. Such values may be obtained by composting garbage alone but may not result from composting mixed municipal refuse even though a high degree of stabilization is achieved.

TABLE 3.—RELATION OF THE INITIAL CARBON-NITROGEN RATIO TO THE TIME REQUIRED FOR STABILIZATION, THE FINAL CARBON-NITROGEN RATIO, AND THE CHANGE IN PERCENTAGE OF NITROGEN

Study No.	Composting time, in days	Initial C/N ratio	Final C/N ratio	Change in percentage of nitrogen	Remarks
1	7	21.0	12.1	+0.60	
2	8	18.5	12.2	+0.53	
3	16	24.9	14.1	+0.80	Became anaerobic
4	10	20.2	10.8	+0.27	
5	10	34.6	26.4	+0.06	
6	14	27.7	20.5	+0.08	
7	16	40.2	20.1	+0.32	
8	17	54.6	22.8	+0.54	High paper content
9	12	19	14	−0.06	
10	14	20	19	−0.11	
11	14	22	19	−0.11	
12	16	28	19	−0.01	
13	14	31	20	+0.11	
14	14	30	19	+0.01	
15	16	32	20	−0.29	
16	14	33	19	+0.44	
17	15	35	24	+0.11	
18	16	50	24	+0.45	High paper content
19	16	51	22.7	+0.33	High paper content
20	21	78	35	+0.36	High paper content

In Table 3 are listed the reductions in carbon-nitrogen ratio achieved in several of the pilot-plant studies and field tests that yielded satisfactory finished compost, together with the accompanying change in percentage of nitrogen. Studies No. 1 to No. 8 were made on vegetable trimmings mixed with various additives, and Studies No. 9 to No. 20 were made on municipal refuse from the City of Berkeley.

The great changes in the carbon-nitrogen ratio observed in Studies No. 8, No. 18, No. 19, and No. 20 and shown in Table 3 represent the conversion to carbon dioxide of readily available carbon in the garbage component of the refuse. The remaining carbon, although sufficient to cause a large carbon-nitrogen ratio, represents material such as paper which is much more resistant to bacterial decomposition.

ESSENTIALS OF COMPOSTING

The process which can be recommended for composting municipal refuse as a result of these studies involves segregating, grinding, stacking, turning, and regrinding the refuse and requires a knowledge of how to control and judge the process on the basis of observations and laboratory tests.

Segregation of Refuse.—An appreciable portion of municipal refuse is material which is not subject to bacterial decomposition and which must be removed during the process before compost is placed on agricultural soils unless it is ground into small particles. The following tabulated physical analysis shows the percentage of various compostable and noncompostable materials found in approximately 30 tons of mixed municipal refuse from all sections of Berkeley:

Type of Material	Percentage
Tin cans	9.8
Bottles and broken glass	11.7
Rags	1.6
Metals	0.9
Inorganic wastes of no value	7.6
Compostable material	68.4

The item "Inorganic wastes of no value" refers to broken ceramics, concrete, plastics, and similar material.

Inasmuch as grinding is an essential step in the composting process some segregation of noncompostable items seems inescapable. Rags and nonferrous metal objects are of sufficient value to justify removing them by hand-picking as the refuse moves along a conveyor belt. Tin cans and ferrous metals may be taken out by use of a magnetic separator. It has been estimated by a commercial concern that in a large-scale operation this material in addition to glass would represent profitable salvage. Ceramic objects are perhaps the greatest nuisance because hand picking is expensive, and devices capable of pulverizing such material while shredding paper and garbage are neither available nor easy to design.

Grinding or Shredding of Refuse.—Grinding or shredding of raw refuse produces several beneficial results which hasten decomposition. The material is rendered more susceptible to bacterial invasion through exposing greater surface to attack and destroying the natural resistence of vegetation to microbial invasion. In addition, the material is rendered homogenous, is given a beneficial initial aeration, and acquires a structure that makes it more responsive to moisture control and aeration and easier to handle.

There is no special size requirement, but the material must not be reduced to pulp lest it become too soggy to compost. The pilot-plant studies were conducted satisfactorily on material chopped into 1-in. pieces by means of a roughage mill. A hammermill was used in the field study on Berkeley refuse. On the basis of that experience, a minimum screen size of 1.5 in. is recommended. Wet grinding has been used to overcome the extreme abrasiveness observed when refuse is ground just as it comes from the collection vehicle, but the resulting mass is too wet for aerobic composting. One of the most serious deterrents to commercial composting at the present time is the lack of grinding equipment especially adapted to shredding refuse.

Stacking Shredded Refuse for Composting.—Shredded refuse to be composted in the open is placed on the ground or on a paved area in piles or windrows. For reasons of space economy and ease of handling, windrows are most convenient. They may be of any appropriate length or width, but the height is somewhat critical. If the pile is too high the material will be compressed by its own weight, losing pore space and becoming anaerobic; thus, there will be required excessive handling costs for aeration by turning and an extended composting period. In some instances the maximum practical height may be governed by the equipment used for stacking or by a tendency of the pile to get excessively hot—exceeding approximately 70° C. If the pile is too shallow, heat loss may be excessive and optimum temperatures for thermophilic organisms may not be achieved. A maximum height of 5 ft or 6 ft and a minimum of 4 ft is recommended for freshly ground municipal refuse. As the pile shrinks during decomposition the desired height can be maintained by reducing the width of windrow at the time it is turned.

For convenience in turning, the initial width of the windrow will probably not exceed 8 ft or 10 ft if the cross section is made trapezoidal. If the top is rounded to shed water, the width may be governed by permissible maximum height. Suitable dimensions of the pile to meet conditions of weather, equipment used in stacking and turning, and daily tonnage processed will, of course, be developed by those with experience in each individual case.

Aeration by Turning.—Conditions necessary for rapid aerobic decomposition of organic matter are maintained by periodically aerating the composting material. The simplest method of aerating a compost pile is by turning it as often as necessary to prevent development of serious anaerobic conditions. An anaerobic condition usually results from a moisture content too great for the normal turning schedule adopted. Excess moisture may be inherent in any particular refuse, or it may result from continual soaking by rain. Anaerobic conditions may develop also as a result of equipment breakdown or other interruption of a normal turning schedule or during a long period of unusually wet weather; whatever the cause, such conditions will disappear if there is frequent aeration of the pile by turning.

The frequency of turning and the total number of turns required during the composting process are governed primarily by the moisture content. Experience at Berkeley indicates that for municipal refuse the following turning schedule is adequate:

1. If initial moisture is more than 70%, the refuse should be turned daily until moisture is reduced to less than 70%. Thereafter, the schedule in Table 4 should be followed.
2. If initial moisture is less than 70%, the first turn should be made on the third day. Thereafter, the schedule in Table 4 should be followed until eleven or twelve days have elapsed.

In following the schedule in Table 4 it is not necessary to determine moisture after the initial analysis. Experience soon teaches the operator to recognize the need for adding moisture or for increasing the frequency of turning. A good "rule of thumb" is to begin a schedule of daily turning if a foul odor is evident when a pile is disturbed either by turning or by digging into it for inspection purposes and continue daily turning until the odor no longer is evident. Inasmuch as turning will reclaim an anaerobic compost it can be omitted on weekends and holidays if additional costs are involved, without permanent injury to the compost.

Uniform decomposition is essential to rapid composting. To insure this, it is necessary that the outer edges be turned into the center of the pile at each turn. Such an inward mixing exposes any fly larvae, pathogens, or insect eggs which might survive at the cooler surface to the lethal temperatures of the interior of the pile. Specialized machinery for accomplishing such turning has not been developed in the United States, but the problem would not be particularly difficult to solve if there were a demand for such a device.

A food company in California uses a modified Barber-Greene self-propelled over-cab loader in turning a compost of manure and straw for use in growing mushrooms.

TABLE 4.—RECOMMENDED SCHEDULE OF TURNING IN RELATION TO INITIAL MOISTURE CONTENT OF MATERIAL

Moisture content (%)	Turning schedule	Approximate total number of turns required
Less than 40%	Moisture should be added, then the following schedule adopted:	
From 40% to 60%	3-day intervals	3 or 4
From 60% to 70%	2-day intervals	4 or 5

A self-propelled machine similar to a modern twin-helix snow plow equipped with a windrow shaping device would seem to have great possibilities for turning a compost stacked in the open.

Judging the Condition of a Compost.—In a compost pile in which aerobic decomposition progresses in a typical manner, the temperature follows the orderly course previously described—a rapid initial rise to between 60° C and 70° C in three or four days, a period of sustained high temperature, and, finally, a temperature recession. Temperature alone, however, is not a sufficient indicator of the situation inside a composting mass because a temperature decline may result from the development of conditions unfavorable to aerobic thermophiles either through excessive heat, an onset of anaerobic conditions, or a lack of sufficient moisture. If a thermal kill is responsible for a decrease in temperature, temperatures appreciably above 70° C will have obtained for some time prior to the decrease. Anaerobic conditions are quite easily detected. A putrefactive odor especially noticeable when the pile is disturbed indicates the need of aeration. In addition, the material inside an anaerobic pile has an easily recognizable pale green, faintly luminescent color that shows little change from day to day, whereas properly developing aerobic compost is characterized by a progressively darkening color. Generally the anaerobic mass is excessively moist, and foul-smelling drainage liquors may appear.

Lack of moisture is likewise easily detected by the human eye. The observer quickly learns to tell by a visual inspection when added moisture is needed.

A declining temperature, which is not due to thermal kill, oxygen shortage, or low moisture and which follows a typical sustained temperature plateau, is a good indication that the compost is finished. Since bacterial die-away is greater than temperature drop would indicate, because of the insulating qualities of the pile, the compost may generally be considered finished when the declining temperature reaches between 55° C and 50° C.

Characteristic changes in odor during the period of composting may aid judgment. Grinding or shredding serves to replace the sour greasy odor of raw garbage with an odor generally associated with freshly cut green vegetation. As temperature increases, cooking odors develop and then disappear as stabilization progresses. A slight odor of ammonia may persist or become quite pronounced in a compost that is losing nitrogen. Finally the material may be free of odor or have a slightly earthy or moldy odor.

TABLE 5.—COMPOSTING TIMES, VARIOUS MATERIALS, AND PROCESSES

MATERIAL	PLACE REPORTING	TIME	CONDITIONS
Mixed municipal refuse	University of California	12 to 21 days	Field
Garbage plus straw	University of California	5 to 9 days	Pilot plant
Garbage plus manure	University of California	5 to 9 days	Pilot plant
Garbage plus sewage sludge	University of California	12 to 16 days	Field
Selected garbage plus sewage sludge	Frazer, N. Y.	7 days	Field
Mixed municipal garbage and other wastes	Dannevirke, New Zealand	20 to 30 weeks	Field
Air-dry refuse, night soil, and other wastes	Ficksburg, South Africa	30 days[a] 4 to 6 weeks[b]	Field
Selected refuse and sewage sludge	Domfriesshire, Great Britain	6 weeks[c] 6 weeks[d]	Field
Grass clippings	University of California	11 to 14 days	Pilot plant
Municipal refuse containing no garbage	Holland	3 to 6 weeks[e] 4 to 6 months[f]	Production

[a] In pit. [b] "Ripening." [c] Composting. [d] Maturation. [e] Summer refuse. [f] Winter refuse containing ashes.

Color is a poor indicator of the condition of a compost which has not become anaerobic inasmuch as the appearance of rich dark soil is achieved long before stabilization has been accomplished. Some processes purported to produce a finished compost in three days or less (9) achieve very little stabilization but produce a material having a good color.

The change in the carbon-nitrogen ratio is a good criterion of the degree of stabilization accomplished by composting, especially when the increase in the percentage of ash is also observed. Unfortunately, this value is not easily determined in the laboratory because of the difficulty of running the necessary test for carbon. New Zealand researchers (9) have suggested an approximate equation:

$$\%\ \text{Carbon} = \frac{100 - \%\ \text{ash}}{1.8}$$

The field studies showed this equation to provide results accurate within from 2% to 10%. It is therefore recommended as sufficiently accurate for practical composting.

Familiarity with the time normally required for composting in general, or in a particular operation, is useful in judging the course of a compost. As the carbon-nitrogen ratio of a material increases, the period required for stabilization increases. The relationship between composting time and carbon-nitrogen ratio observed at Berkeley for mixed municipal refuse having a moisture content less than 70% is as follows:

Initial carbon-nitrogen ratio	Approximate composting time, in days
20	12
20—50	14
78	21

For other materials, the composting time varies with the nature of the material and the composting method.

Some observed composting times for various materials and composting processes are presented in Table 5.

Remilling of Compost.—In the interest of appearance and ease of application of compost to the soil, it is desirable to regrind the finished product. Finished compost is much easier to grind than raw refuse. At Berkeley, finished compost with a moisture content of 55% was reground without any difficulties in the hammermill. A screen with ⅜-in. openings was found to be most satisfactory. The amount of material to be ground after composting is somewhat less than the original weight of refuse. In the field studies, the yield was between 70% and 80%, based on the dry weight of the compostable fraction of municipal refuse, although the loss in volume amounted to 50% or more. The yield from plain vegetable trimmings and straw used in the pilot studies was somewhat lower, averaging between 50% and 60%.

THE VALUE OF COMPOST

The value of compost may be expressed according to its two mutually dependent functions—(1) its intrinsic value to the soil and (2) the price per ton at which it can be sold at a profit to private enterprise or at a loss to the community no greater than the cost of alternate disposal methods.

The value of compost to agricultural soils lies both in fertilizer and trace elements and in the unique ability of humus to (*a*) improve soil structure, thus increasing its water retention capacity and encouraging more extensive development of root systems of plants; (*b*) form a complex with inorganic phosphate, making it more readily available to higher plants; and (*c*) retain nitrogen in the form of bacterial protoplasm, thus preventing its leaching away and making its rate of availability more nearly equal to the rate at which plants can utilize it.

The fertilizer and other constituents of the compost made at Berkeley from various materials are shown in Table 6.

The price per ton at which compost can be produced and sold is a matter of speculation. A careful analysis of the processes advocated in the United States based on such data as are available and on preliminary design estimates indicates that compost might eventually be produced and sold at a modest profit at fifteen dollars per ton of finished compost, provided that: (*a*)

The present cost of collecting refuse and hauling it to the disposal site is not considered a part of the cost of production; (*b*) the profits from salvage accrue to the composting operation; (*c*) the composting operation is on a scale beyond the economic break point (probably 100 tons of raw material per day); (*d*) the yield of compost on a dry-weight basis is from 70% to 80% of the compostable fraction of municipal refuse, as observed at Berkeley; and (*e*) large-scale agriculture will accept the product at such a price, as would seem to be the case in California.

PROBLEMS OF MUNICIPAL COMPOSTING

It seems probable that composting will become an important method of refuse disposal in the United States within a very few years. Private enterprise is increasingly interested in the commercial possibilities of compost, and several companies are undertaking pilot scale work to explore the process. Interest on the part of public officials is considerable, and there is a widespread and growing feeling among citizens that this nation cannot continue to prosper indefinitely without reclaiming its organic wastes and returning them to the soil. As evidence, they point to the experience of older segments of the earth. Realistically, however, it must be recognized that the need for solving refuse disposal problems is acute and immediate in many communities whereas the need for reclamation of organic matter is more speculative.

TABLE 6.—FERTILIZER AND OTHER CONSTITUENTS OF COMPOST MADE FROM VARIOUS MATERIALS

Material	Nitrogen (%)	Phosphorus pentoxide (%)	Potassium oxide (%)	Carbon (%)	Ash (%)	Carbon-nitrogen ratio
Municipal refuse	1.63	0.96	0.87	30.84	29.20	19.0
Municipal refuse	1.44	0.78	1.01	28.75	42.10	19.0
Municipal refuse	1.32	1.20	0.84	32.55	40.84	24.0
Municipal refuse	1.21	1.87	0.84	28.08	51.07	23.0
Municipal refuse	1.24	1.10	0.53	24.43	39.42	19.0
Municipal refuse	1.02	1.36	0.72	29.64	37.59	29.0
Municipal refuse	1.24	1.10	0.53	24.43	39.42	19.0
Municipal refuse	0.90	0.90	0.65	31.90	37.04	35.0
Municipal refuse	0.97	0.73	0.51	23.51	26.64	24.0
Municipal refuse and 4%[a] raw sewage sludge	1.20	0.60	1.39	24.56	38.02	20.3
Municipal refuse and 6%[a] digested sewage sludge	1.10	1.06	1.39	27.30	45.30	22.7
Municipal garbage and 5.5%[a] pear wastes	1.33	1.24	1.06	25.68	45.69	19.0
Municipal garbage plus 10% soil	1.02	1.10	0.94	20.71	63.85	20.0
Grass clippings	1.97	2.29	3.95	28.40	40.68	14.4
Miscellaneous garden and kitchen refuse	1.58	1.37	1.15	26.10	41.32	16.5
Vegetable trimmings and paper	1.32	0.60	1.43	36.59	16.91	26.1
Vegetable trimmings and paper	1.57	1.84	0.96	38.30	20.00	24.4
Vegetable trimmings and paper	1.22	1.28	1.48	30.72	20.86	26.4
Vegetable trimmings and 2% horse manure	2.01	1.88	4.52	37.44	20.12	18.6

[a] Based on dry weight of materials.

Although composting of municipal refuse has not yet been undertaken on a municipal scale in the United States, considerable progress has been made toward the development of an economical process. Straightforward operations involving modern mechanization have been devised by competent engineers; procedures successful in Europe have been modified in such a manner that they seem adaptable to conditions in the United States; and market surveys have been made. These and other developments have all but eliminated the unsound promotional efforts which previously characterized the subject of composting; they were aimed at interesting public officials in untried processes from which a profit to the promoter was to come as process royalties for secret inoculums rather than from the sale of compost.

As a matter of sound public administration, municipal officials must require that any refuse-disposal process adapted shall not involve the city in a program of process experimentation, development of equipment, and marketing of products. It does not seem likely, therefore, that the first composting plants are destined to be municipal undertakings.

Under the existing conditions, city officials would be pleased if private enterprise entered into commercial composting of the city's refuse and would probably grant the long-term right to publicly owned raw materials which industry would need in order to make a composting project profitable. There would seem to be a good field for risk capital in such a venture, although it may well be that some of the cost of development will have to be borne by the public.

There seems little likelihood that composting can be expected to pay the cost of collecting and transporting refuse. In many large cities, for example in New York, it is possible that space requirements and distance from markets for the product might rule out the process altogether. However, there is good reason to believe that a process such as is defined by these studies offers an economical and sound solution to the refuse disposal problems of many communities, at the same time reclaiming a material of immense value to agriculture.

ACKNOWLEDGMENTS

Many staff members of the Sanitary Engineering Research Laboratory of the University of California contributed to the success of the composting studies. C. G. Golueke, mycologist, and Bradley J. Card, J. M. ASCE, sanitary engineer, conducted the principal research work. Linvil Gene Rich, A. M. ASCE, sanitary engineer and biochemist, assisted in carrying out the earlier experiments. J. F. Thomas, chemist, was responsible for the laboratory analyses.

The field studies were conducted at the refuse disposal site of the City of Berkeley with the cooperation of Owen Dyer, director of services of Berkeley.

APPENDIX. BIBLIOGRAPHY OF COMPOSTING

---

(1) **"The Waste Products of Horticulture and Their Utilization as Humus,"** by Albert Howard, *Scientific Horticulture*, Vol. 2, 1935, p. 213.

(2) **"Composting for Disposal of Organic Refuse,"** ***Technical Bulletin No. 1***, **San. Eng. Research Project, Univ. of California, Berkeley, Calif., 1950.**

(3) **"The Treatment of City Wastes by the Beccari Closed-Vessel Method,"** by Jean Bordas, *Bulletin,* Société d'encouragement l'industrie nationale, Vol. 128, 1929, p. 170.

(4) **"The New Dutch Scheme for Refuse Disposal,"** by W. A. G. Weststrate, *Public Cleansing and Salvage,* Vol. XLI, No. 491, July, 1951.

(5) **"Composting of Garbage and Sewage Sludge,"** by Eric Eweson, *Proceedings-Separate No. 312,* ASCE, Vol. 79, October, 1953.

(6) **"Capitalizing on Municipal Wastes by Composting,"** by R. P. Stovroff, *Proceedings-Separate No. 545,* ASCE, Vol. 80, November, 1954.

(7) **"Reclamation of Municipal Refuse by Composting,"** *Technical Bulletin No. 9,* San. Eng. Research Project, Univ. of California, Berkeley, Calif., 1953.

(8) **"Humus,"** by S. A. Waksman, Williams and Wilkins Co., Baltimore, Md., 2d Ed., 1938, p. 118.

(9) **"Second Interim Report of the Inter-departmental Committee on Utilization of Organic Wastes,"** *New Zealand Engineering,* November–December, 1951.

(10) **"An Agricultural Testament,"** by Sir Albert Howard, Oxford University Press, New York, N. Y., 1940. (*a*) p. 45. (*b*) p. 235. (*c*) p. 49. (*d*) p. 44.

(11) **"The Soil and the Microbe,"** by S. A. Waksman and R. L. Starkey, John Wiley & Sons, Inc., New York, N. Y., 1949, p. 213. (*a*) p. 165.

(12) **"Elementary Bacteriology,"** by J. E. Greaves and E. O. Greaves, W. B. Saunders, Philadelphia, Pa., 1947, p. 228. (*a*) p. 230.

DISCUSSION

Arthur W. Furbank.[3]—"Most of the older traditional composting procedures are anaerobic." It is easy to believe that this statement (under the heading, "Composting Processes") is accurate. However, the assertion that Howard "systematized" a practice of this sort is not in accordance with the principles he laid down so definitely in "An Agricultural Testament" (10).

The procedure Howard devised during the years between 1924 and 1931 at the Institute of Plant Industry at Indore, Central India, was known thereafter as the Indore Process. Its outstanding features were first published in 1931; a lecture given in 1938 is reprinted with full descriptions and diagrams (10).

For many years prior to 1938 Howard had devoted study and experimentation to many of the ancient farming practices of the Orient. While doing so he was able to recognize the essential difference between aerobic and anaerobic composting; he must have seen and studied numerous examples of the latter procedure, and it is eloquent testimony that in his writings he always insists on aerobism (10).

Describing the practical details of operation, he states "Abundant aeration is essential during the early stages" (10*a*). Again (10*b*),

> "The process is sanitary throughout, and there is no nuisance of any kind * * *. The manufacture of humus from agricultural and urban wastes by the Indore Process depends on the same principle—an adequate supply of oxygen throughout the conversion."

This insistence on aeration is repeated frequently throughout the book and applies to compost during and—as much as is possible—after its formation; an entire chapter of twenty-seven pages is devoted to the aeration of the soil.

Howard was probably the first agriculturist to preach consistently the doctrine that in composting it is impossible to minimize the loss of nitrogen from organic materials by any act of enclosure. He was able to show that any sealing-off will, on the contrary, have precisely the opposite effect and will bring about conditions that do result in loss. Illustrations of this phenomenon can be found in many places; the Imhoff tank or the ordinary septic tank provides an example of anaerobic conditions causing the disruption of insoluble materials and extensive loss in gaseous form.

In the storage of manure, different rules apply. Preventing the access of air—particularly during the middle and final stages of storage—has the effect of minimizing nitrogen losses. A comment by S. A. Waksman and R. L. Starkey (11) helps to explain this:

> "In order to eliminate the losses of nitrogen through denitrification the manure is so handled as to prevent the formation of nitrate. Since anaerobic conditions prevent nitrate formation, manures are frequently packed tightly * * * to prevent appreciable penetration of air."

---

[3] Cons. Engr., Darien, Conn.

When composted, this manure (now under aerobic conditions) will react under the influence of moisture as well as of air; ideally its carbohydrates are decomposed and its ammoniacal nitrogen is converted into an insoluble form by the microorganisms as they convert it into their cell substance. The speed of these processes is increased by the rise in temperature. If aerobism is maintained as long as possible, most of the original nitrogen will be conserved.

Clearly, the authors are fully in favor of adequate aeration, and the only purpose of the foregoing comments is to give some recognition to the fact that Howard spent a great part of his life in stressing its importance.

In regard to hydrogen ion concentration (as described under the heading, "Experimental Investigation: Hydrogen Ion Concentration"), the experience of the authors seems to be different from that of others. A serious loss of nitrogen is reported in the case of those samples to which calcium carbonate had been added. However, according to Howard's record (10*c*):

> "Soon after the second turn [about 7 or 8 weeks] the ripening process begins. It is during this period that the fixation of atmospheric nitrogen takes place. Under favorable circumstances as much as 25 per cent of additional free Nitrogen may be secured from the atmosphere."

To achieve this result, ample aeration must be provided. The reason for the additions of calcium carbonate which Howard has specified in his description is also clear; it is to maintain the general reaction within (10*d*) "the optimum range (pH 7.0 to 8.0) needed by the micro-organisms which break down cellulose." Two other authorities may be quoted in regard to the aerobic bacterium Azotobacter, which J. E. Greaves and E. O. Greaves describe as "the champion nitrogen fixer" (12), adding later (12*a*) that

> "It has been suggested that the Azotobacter be used as an index of the lime requirements of a soil as they do not tolerate an acidity greater than pH 6."

Messrs. Waksman and Starkey report (11*a*) that

> "In the absence of an abudance of buffering materials in soils, the large amounts of acids which are produced would soon change the reaction to such acidity as to make the soil a medium unfit for the growth of * * * various important soil organisms, especially those that are sensitive to acid conditions, as Azotobacter * * *."

It is of course true that there are acid-loving and anaerobic bacteria which also can fix the atmospheric nitrogen but, because of what must be their relatively limited scope of operation (when the air supply is restricted), their importance for the purpose under discussion can only be comparatively small. It would be interesting to discover whether by further efforts to improve aeration in the middle and later stages of the work described in the paper (as well as in the earlier stages) the aerobic Azotobacter could be induced to remedy by assimilation from the atmosphere the nitrogen loss which is reported.

PERCY H. MCGAUHEY[4] AND HAROLD B. GOTAAS,[5] MEMBERS, ASCE.—Interest in composting as a method of solving municipal waste disposal problems has developed rapidly in the United States, and several composting plants have been built in other countries since the authors originally presented their paper in 1953. A healthy emphasis on producing compost on a commercial scale and deriving a profit from its sale in a competitive market is beginning to replace earlier attempts to profit by selling untried processes and secret inoculums.

There seems to be a general desire for a composting machine that can be sold or purchased as a package unit capable of producing finished compost in a single operation. Several such devices have been suggested, probably because of the obvious commercial possibilities of a one-unit plant. Composting of municipal refuse, however, requires a series of operations which should be designed and engineered for the particular conditions of each individual situation. Facilities must be provided for the following operations: (*a*) Receiving the refuse; (*b*) preparing the refuse for composting (this includes segregating salvageable and noncompostable material and shredding the large particles of the remainder to a size satisfactory for composting); (*c*) stabilizing the shredded material by composting; and (*d*) preparing the compost for marketing by such operations as milling and bagging.

Mechanization is necessary for receiving refuse economically, preparing it for composting, and preparing the final product for marketing. The unit process of composting, however, can be done in piles or windrows in the open, under a shed roof, or in enclosed structures. Economic considerations favor the pile or windrow for large plants because it can be turned for aeration by relatively simple machinery at a low power cost.

This is, therefore, the method most used in present successful composting operations. There is, nevertheless, a considerable interest in developing an enclosed mechanical composter, and several such devices are being used for small installations. The most successful are rotating cylinders, the longest of which require some forced air to displace gases which might otherwise prevent aeration of the mass in the central sections of the cylinder. These devices are expected to produce in a very few days a compost which at best is sufficiently stabilized for marketing, or at least is capable of completion in large piles without further aeration. Vertical silos with mechanical stirring, utilizing a considerable volume of forced air, and various procedures for environmental control are in the experimental stage. The goal is the production of compost in a matter of hours.

One of the most successful mechanical composters appears to be a slowly rotated cylinder placed so that the axis has about a 5° slope from the horizontal. The refuse is injected into one end, and after approximately 5 days active decomposition in the cylinder is discharged from the other end for screening. Air introduced into the cylinder comes into intimate contact with the composting mass during rotation, and aerobic decomposition is maintained. The combined effect of abrasion during rotation and biological decomposition tends to disintegrate the material to form friable particles.

---

[4] Research Engr., Univ. of California, Richmond Field Station, Richmond, Calif.
[5] Prof. of San. Eng. and Director, San. Eng. Research Lab., Univ. of California, Berkeley, Calif.

Obviously a number of large cylinders or other mechanical composting devices would be required to handle the amount of refuse from a large or moderate sized city. Thus, the plant cost per ton of refuse composted is considerably higher for the mechanical composter than for the windrow method. However, because the mechanical composter is enclosed, it will be more aesthetically acceptable than the open windrow; its location in the built-up area of the city might be feasible, especially if any after-handling of the product is done inside buildings on the site, or if the product is transported elsewhere for final processing. It appears that to be competetive with the windrow method for large installations in favorable climates, mechanical composters would have to be placed in several strategic locations in a city so that the added plant costs involved in the method would be offset by a reduction in hauling costs.

At the present time the minimum retention period for a mechanical composter processing mixed municipal refuse from a city in the United States has not been determined. A high-speed composting process poses no technical problems when composting only garbage which has a low carbon-nitrogen ratio, but highly selected garbage of this type might be more economically cooked and fed to hogs. Because of the higher carbon-nitrogen ratio of mixed municipal refuse, it is difficult to produce a compost having a carbon-nitrogen ratio suitable for agricultural use in from 2 to 5 days. In the investigation reported by the writers, leafy green vegetables were composted in less than 5 days and were made to have the appearance of compost in little more than 48 hr. When refuse contains considerable paper and other cellulose and materials more resistant to decomposition, it is unlikely that a good finished compost can be produced in less than from 8 to 10 days. Under such conditions, it is doubtful that the mechanical composter will be economically competetive with open-turning methods using efficient materials-handling techniques. Except for the desire to make the mechanical composter economical, rapid composting (2 days instead of 2 weeks) is not particularly important because the demand for commercial quantities of compost is seasonal. However, because stock-piling of compost is necessary, a small amount of composting could continue in the stock pile provided the material was sufficiently decomposed at the time of piling to be capable of reaching stabilization without further aeration and without becoming anaerobic. Thus, a mechanical composter need not produce a highly stabilized product unless the compost is to be bagged at once, but it is doubtful that normal composting time can be reduced by more than 40% to 50% by taking advantage of stock-pile composting.

Compost is at best a low-value material; to have commercial possibilities, therefore, the process must make use of efficient materials-handling procedures requiring a minimum of machinery and power. For this reason, the writers believe that composting without the aid of mechanical composters or digesters, but with efficient mechanization of the various operations involved, will be the answer to successful commercial composting in large plants in much of the United States. Progress has been made in recent months toward solving the equipment problems mentioned in the paper as well as toward improving the economic aspects through more effective operational procedures and reduction in land-area requirements. Present designs, for example, aim at minimizing initial grinding and facilitating segregation through suitable screening of incoming refuse. With this arrangement, grinding is greatly reduced.

On the basis of equipment designs and flow diagrams completed by competent engineers during 1954, it seems probable that the cost of composting will be much less than originally estimated in the paper. In some places where salvage can be made to pay a share of the cost, composting can be done more cheaply than incineration, not including any value for the compost. It now appears that the plant cost for composting by the windrow method will be from 25% to 35% of the cost of an incinerator for plants with a capacity of more than 200 tons per day; for mechanical composters, the plant cost will be about the same as for incineration. Selling prices of $5 per ton—approximately the price of stable manure and steer manure—are being anticipated by some private concerns seriously considering going into the business of commercial composting using already-completed designs.

AMERICAN SOCIETY OF CIVIL ENGINEERS
Founded November 5, 1852
TRANSACTIONS

Paper No. 2768

MOTION OF PARTICLES ON BED OF A TURBULENT STREAM

BY ARTHUR T. IPPEN,[1] M. ASCE, AND RAMJEE P. VERMA,[2] A. M. ASCE

SYNOPSIS

The principal aim of this study was to reduce the number of parameters involved in sediment transport in streams to the minimum that could be accurately controlled and systematically and independently varied. Flow conditions were determined independently of the sediment—the quantity of which was too small to affect the conditions. The sediment (small spheres) moved without mutual interference; the variables entering the experimental analysis were therefore confined to distinct characteristics of the sediment and the stream.

The bed roughness was described by an effective roughness computed from the von Kármán logarithmic laws rather than by the diameter of the sand grains because irregularities and spacing of the grain affect this roughness. The Shields entrainment function was checked and was found to be untenable for cases in which the bed load and the bed are constituted differently. An entrainment function of more general validity for the range of experimental results was derived.

It should be noted that the scope of this study is limited—only a few pertinent variables have been considered. However, the trend of the results proved that the techniques that were used can be expanded for more comprehensive studies and can thus lead to a more rational analysis of the bed-load problem.

NOTATION

The letter symbols adopted for use in this paper are defined where they first appear, in the illustrations or in the text, and are arranged alphabetically for convenience of reference in the Appendix.

NOTE.—Published, essentially as printed here, in the *Proceedings* of the Minnesota International Hydraulics Convention, September 1–4, 1953, Minneapolis, Minn. Positions and titles given are those in effect when the paper was received for publication.

[1] Prof. of Hydraulics, in charge of Hydrodynamics Lab., Massachusetts Inst. of Technology, Cambridge, Mass.

[2] Principal, Bihar College of Eng., Patna, Bihar, India.

OUTLINE OF THE PROBLEM

Bed-load movement has been extensively investigated by both the experimentalist and the practicing hydraulic engineer because of its important role in the performance of natural and artificial watercourses and related structures. The solution of the problem, however, depends on so many variables that a satisfactory rational explanation for all its complex phases remains remote. Essentially, two main lines of attack have been followed—one by defining in detail the internal mechanics of the occurrences of physical motion and the second by making bulk analyses from measurements and correlating the results into empirical laws on the basis of statistical assumptions. Both approaches have resulted in a clearer concept of the problem but they have not led to a comprehensive solution.[3,4,5,6]

The subsequently described study was deliberately confined to a relatively restricted phase of sediment motion and was designed to explore the roles of as few variables as possible without detracting unduly from the general validity of the results. The study was planned to determine, in detail, the factors producing the entrainment or the initial motion in flowing streams of discrete spherical particles varying in size and specific weight. Because of the small number of particles, the flow characteristics remained essentially unaffected by these particles and the hydraulic behavior was always defined by the bottom roughness, the Reynolds number of the stream, **R**, and the Froude number, **F**. The motion of the particles was one of intermittent rolling and sliding along the bed over the range of hydraulic flows that produced from zero transport to equilibrium transport of the samples of particles used. More specifically, the experimental analysis dealt with the motion of statistical samples of particles having known properties in relation to two-dimensional turbulent flow in a laboratory channel; the hydraulic characteristics of the channel were accurately defined. The subsequent investigation is concerned primarily with the presentation of these experimental findings. Although some theoretical investigations have shown considerable promise, they are not conclusive enough to be included.

FORCES ACTING ON INDIVIDUAL PARTICLES ON A GRANULAR BED

The physical conditions considered in this study are those related to the systematic variation of the dynamic forces that act on individual spherical particles resting on a stream bed of fixed granular roughness, as illustrated in Fig. 1.

The effective body force directed normal to the bed is given by the weight of the sphere relative to the fluid—

$$W_b = \gamma \, (s_s - 1) \frac{\pi}{6} d^3 \quad \ldots\ldots (1)$$

---

[3] "Engineering Hydraulics," by Hunter Rouse, John Wiley & Sons, Inc., New York, N. Y., 1950, Chapters I and XII.

[4] "Movement of Sediment as Bed-Load in Rivers," by A. A. Kalinske, *Transactions*, Am. Geophysical Union, Vol. 28, No. 4, 1947, pp. 615–620.

[5] "Equilibrium of Grains on Bed of Stream," by C. M. White, *Proceedings*, Royal Soc. of London, Vol. 174A, 1940, pp. 322–334.

[6] "Approaches to the Study of the Mechanics of Bed Movement," by L. G. Straub, *Bulletin No. 20*, Proceedings of Hydraulics Conference, Univ. of Iowa Studies in Eng., Iowa City, Iowa, 1940.

in which γ is the specific weight of the water and s_s denotes the specific gravity of the sediment. All other forces are the results of the flow conditions around the particles. These conditions are determined by the effective roughness of the bed and by the parameters governing the flow. The conditions remain unaffected (in this study) by the moving particles, which are so few in number that they are of negligible influence on the flow. In general, a rather steep and almost linear velocity gradient exists near the bed within the height of the particles. Of dominant influence with respect to the dynamic forces exerted is the statistical mean velocity at the top of the particles, or edge velocity $\bar{V}_e$, which therefore was chosen as the reference velocity for the subsequent investigation.

The buoyant weight of the particles is counteracted by the dynamic lift produced by the difference in velocity over the height of the particle. This lift can be expressed as

$$F_L = K_1 \rho \, d^2 \, \bar{V}^2_e \ldots\ldots (2)$$

in which K_1 is a proportionality constant and ρ denotes the density of the water. In addition to the lift, the particle is subject to dynamic forces acting in the direction of flow—a form drag and a skin-friction drag. For the range of particle Reynolds numbers,

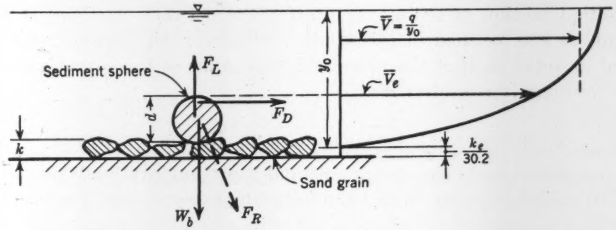

FIG. 1.—DEFINITION SKETCH

$$\mathbf{R}_e = \bar{V}_e \frac{d}{\nu} \ldots\ldots (3)$$

in question, the coefficients of form drag and skin friction are inversely proportional to the square root of $\mathbf{R}_e$ so that the total drag for a constant average viscosity ν and fluid density ρ can be given as

$$F_D = K_2 \, d^{3/2} \, \bar{V}^{3/2}_e \ldots\ldots (4)$$

in which K_2 is another proportionality constant. The resultant of the body forces and dynamic forces acting on a particle will exert a moment about the points of contact between particle and bed; motion may be said to be initiated when the resultant passes through the bearing points or lines, as illustrated in Fig. 1. The exact location of the resultant force is unknown because of the uncertain distribution of lifting pressures and tangential shearing stresses over the surface of the particle, and the geometry of the bed is insufficiently defined in terms of the grain size k; therefore, the critical condition of incipient motion is only approximated by

$$\phi\left(\frac{d+k}{k}\right)=\frac{W_b-F_L}{F_D}\qquad(5)$$

Although the experimental study adhered as closely as possible to these simple concepts, the ultimate analysis of the results had to be different in order to correlate the data.

Several factors are obviously omitted from this summary treatment, particularly the roles of turbulent-velocity fluctuations and turbulent-pressure fluctuations near the bed; an exact definition of the bed-surface geometry also could not be included. The mean fluctuations of the longitudinal velocity components, however, are expected to vary by not more than from 15% to 20% from the mean value of the edge velocity $\bar{V}_e$ and can thus be absorbed into the proportionality constants K_1 and K_2. The "unsteadiness" effect of the turbulent velocity on the forces is also believed to be of secondary order. Nothing is known in detail concerning the turbulent-pressure fluctuations near the bed; however, their role was considerably reduced by making the bed a fixed one. In the actual motion of sediment, interference between particles is naturally important, as was verified in this study. However, this interference was not examined in detail so that the more restricted aims of the investigation might be more thoroughly considered.

Experimental Conditions and Range of Study

The potentialities of the equipment and a preliminary analysis of the variables to be considered determined the following experimental approach:

1. Uniform flow was established for a series of runs under conditions of various slopes, depths, and mean velocities to produce a range of sediment-particle transport from no motion to well-established mean motion.
2. A full series of runs was made on all sediments used for two types of uniform bottom roughness. These roughnesses were obtained by coating the bottom of a rectangular channel with carefully sieved sand particles of widely differing mean diameters.
3. Four types of sediment consisting of small spheres were used in samples of fifty spheres, large enough to define a statistical average motion and small enough so that the flow conditions determined in items 1 and 2 were unaffected. These spheres varied considerably in size from the mean diameter of the sand particles forming the bed.

The experimental flume was 15 ft long, 2 ft wide, and accurately adjustable in slope. The flow entered the flume from a forebay which received the discharge from a constant-head tank. By proper baffles and screens as well as by a roughened transition section with gradually accelerating flow, uniform flow was obtained in a test section 5 ft long at depths generally lower than 3 in. and for the majority of runs averaging only 1 in. Thus, the width-to-depth ratio was always larger than 8, and the effective length of the flume varied from 40 times to more than 200 times the depth. For a given discharge and slope, the depth was adjusted by a tailgate until uniform conditions of flow were obtained (as determined by numerous point-gage readings along and across the channel). The depth was referred to the plane passing through the tops of the sand grains forming the bed. Discharge measurements were made on a triangular 90° weir in a weir box of standard proportions.

The sand used for bed roughness was obtained for the rougher bed by sieving Plum Island (Massachusetts) sand and retaining the grains passing a No. 10 (0.0787 in.) sieve, but collecting on the No. 12 (0.0661 in.) sieve; this material was assumed to be represented by an average diameter of 0.072 in. (0.0060 ft). This sand was rather irregular in shape and texture, having pointed edges, and thus was not ideal for the experiment. The smoother bed was prepared from Ottawa (Ill.) sand, which had better characteristics in that it consisted of nearly uniform, fine particles. A mean diameter of 0.030 in. (0.0025 ft) was obtained as the average of the passing and retaining sieve sizes, No. 20 (0.0328 in.) and No. 25 (0.0276 in.).

The particles used for the movable bed load were plastic and glass spheres so that a wide variation of buoyant weight was obtained. The plastic spheres were 2 mm (0.00655 ft) and $\frac{1}{8}$ in. (0.0104 ft) in diameter, and the glass balls were $\frac{1}{8}$ in. (0.0104 ft) and 4 mm (0.013 ft) in diameter. Micrometer readings taken to select the samples of fifty balls of each type indicated almost truly spherical shapes and no sensible variation in size. Specific gravities were verified as 1.28 for the plastic spheres and 2.38 for the glass spheres. The low value of the latter specific gravity is accounted for by the small air bubbles enclosed in the glass spheres as a result of their manufacture. The fall velocities, w, for these spheres were determined from a standard chart (because they lie well outside the Stokes range) and were also checked by laboratory tests within a few percentage points. Their values are, in feet per second and in the order from the smallest plastic to the largest glass sphere, 0.32, 0.46, 1.15, and 1.25.

Experimental procedures were gradually evolved after considerable preliminary testing. The accurate establishment of uniform flow demanded careful adjustment because of the relatively short flume length. This short length also proved to be a considerable handicap with respect to the establishment of a suitable "race course" for the sediment particles. However, this difficulty was overcome, and it is believed that the final results did not suffer from it after a suitable procedure had been established.

Each experimental run was begun by establishing a fixed slope and a given discharge in the flume. A uniform depth was adjusted by the tailgate and carefully checked. Fifty of the spheres were widely spaced and were lined up in back of a "starter" consisting of several fine wires stretched across the flume near the bottom. The starter was lifted slowly with a minimum of disturbance to the flow. The erratic forward movement of the individual spheres was timed over a length of 5 ft in the lower part of the flume. The average velocity with which the fifty spheres traversed this distance was then determined. The process was repeated for the four types of particles so that each discharge resulted in four runs. Each series of runs was begun with the lowest discharge; the discharge was gradually increased up to the capacity of the supply. From

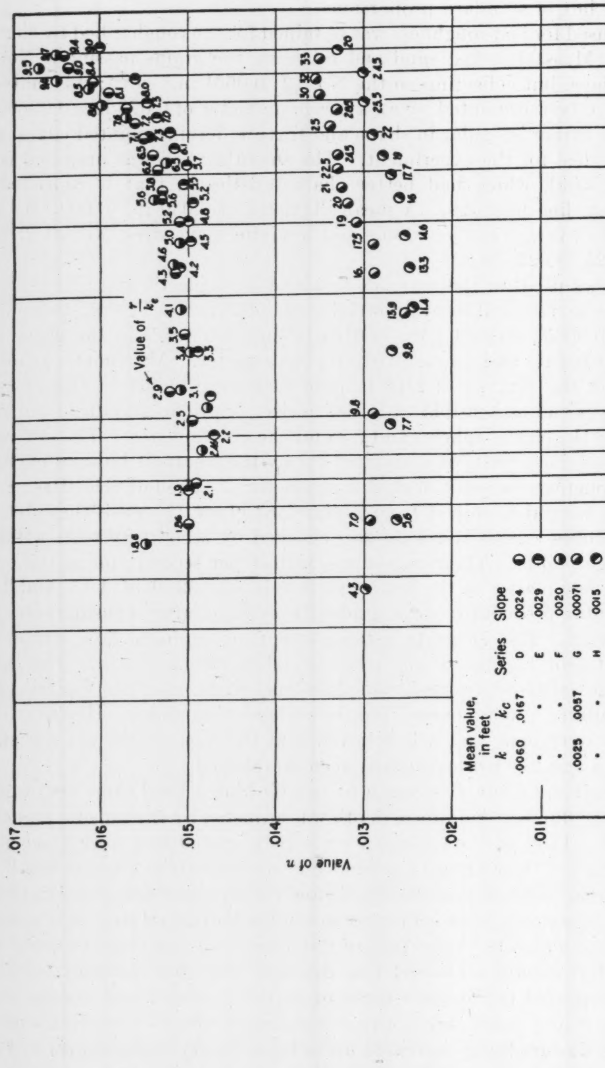

FIG. 2.—VARIATION OF n WITH r/k_c AND R

nine to eighteen runs were thus made to define the average ball velocity, $\bar{V}_b$, in each series. Three such series of runs were made with various slopes for the rougher bottom surface, and two series of runs for the smoother one. In all, more than two hundred and fifty runs form the basis of the experimental results analyzed subsequently.

Accuracy.—In view of some of the shortcomings of the experimental arrangement, a consideration of the accuracy of some of the observations is necessary.

Point-gage readings were taken to the nearest 0.10 mm. At higher velocities the wavy water surface made it difficult to measure the depth accurately. Then the depth was relatively great, however, and by taking a number of readings a satisfactory mean value seems to have been obtained (judging from the consistency of the data). For shallower depths, errors in the readings were reduced by the smoothness of the surface. Uniform flow at lower depths, however, was difficult to establish.

Despite all the precautions taken, a slight unevenness of the bed remained, which at low velocities affected the motion of the balls. The large number of spheres observed, however, is believed to have given representative results. Using fifty spheres also lessened the errors in timing, which increased as the velocities increased and as it became harder to follow the individual spheres. The method of starting the spheres is subject to criticism in that some temporary disturbance was introduced and in that acceleration had to take place before conditions were stable. However, this transition phase was of short duration compared to the total length of travel. Because the channel was short, the initial phase of travel may have been affected by a slight change in the velocity distribution and thus in the turbulence distribution. However, measurements of the turbulence in boundary layers demonstrate the effect to be negligible because the spheres were always well immersed in the boundary layer growing upward from the bottom. Thus, the effective degree of turbulence within several heights of the spheres would not change measurably in the longitudinal direction.

HYDRAULIC CHARACTERISTICS AND BED ROUGHNESS

The quantities defining the stream flow for any run consist essentially of depth and discharge in addition to the conditions (initially set) of slope, roughness, and viscosity. The mean velocity $\bar{V}$ and depth y_0 were plotted as a check for all runs at a given slope against the channel Reynolds number $\mathsf{R} = 4\,r\,\bar{V}/\nu$ (r is the hydraulic radius); a consistent trend was shown throughout. To define the channel roughness, the Manning coefficient n was computed and plotted against R as shown in Fig. 2, which illustrates the effect of R on n for such small laboratory channels. In computing n, side-wall effects were accounted for in the standard manner; corrections were generally small.

A comparison of the experimental results with the Nikuradse pipe-friction curves is given in Fig. 3 for the equivalent Darcy coefficients f and the Reynolds number R. These coefficients are defined by

$$C = \sqrt{\frac{8\,g}{f}} = \frac{1.49\,r^{1/6}}{n} \qquad \text{(6)}$$

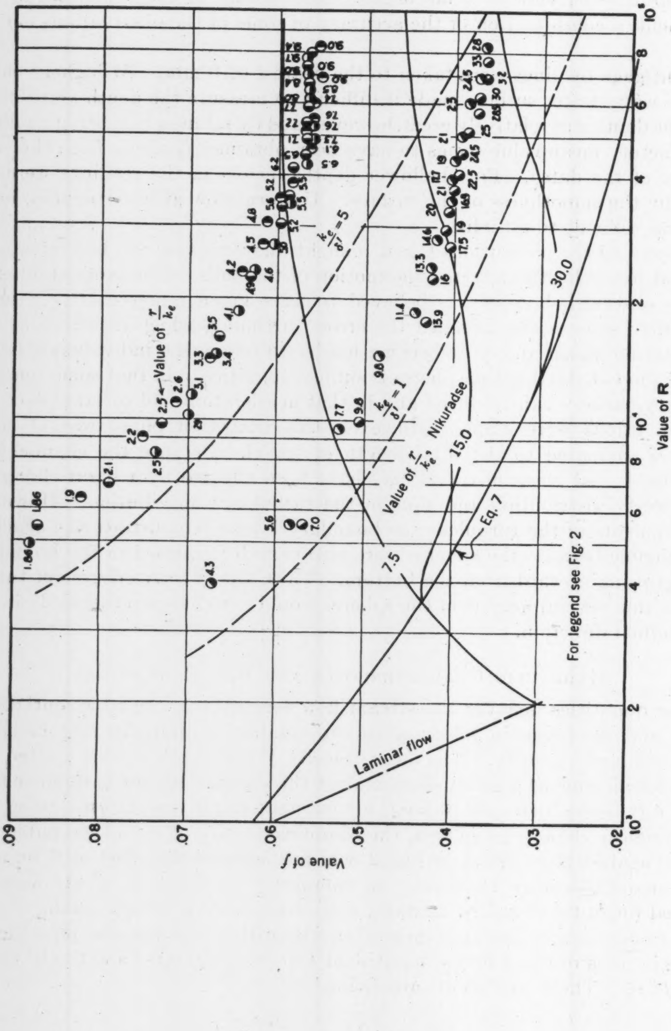

For legend see Fig. 2

FIG. 3.—VARIATION OF f WITH r/k_e AND R

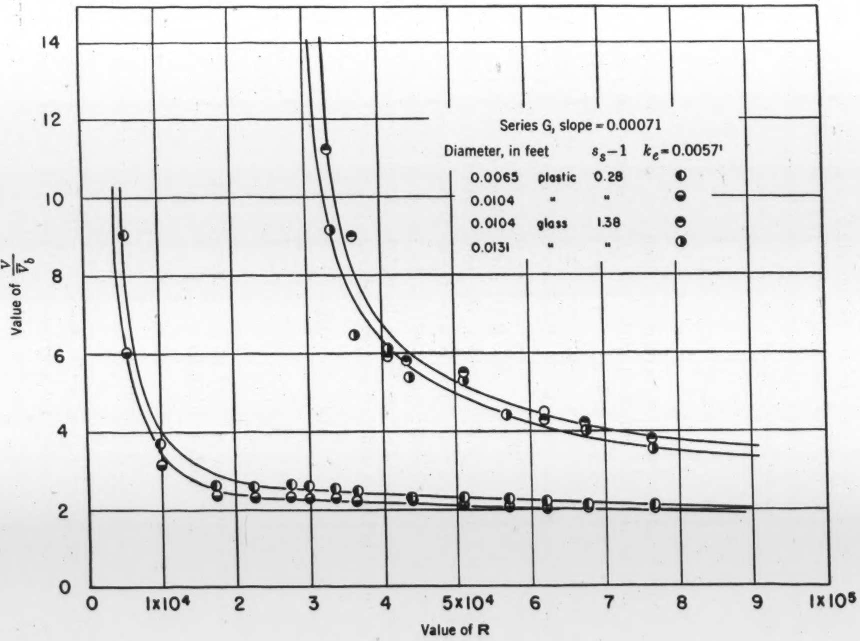

Fig. 4.—Variation of $\overline{V}/\overline{V}_b$ with R

in which g is the gravitational acceleration. Also shown in Fig. 3 is the smooth-pipe curve which satisfies

$$\frac{1}{\sqrt{f}} = -\,0.91 + 2.03 \log_{10} \mathbf{R} \sqrt{f} \tag{7}$$

Although the values of f still seem to vary somewhat with the highest values of $\mathbf{R}$ for the smoother channel, the minimum value of f was used to compute the equivalent sand roughness k_e for each roughness condition according to the von Kármán-Nikuradse law for rough pipes:

$$\frac{1}{\sqrt{f}} = 2.03 \log_{10} \left(12.3 \frac{r}{k_e}\right) \tag{8}$$

The values of r/k_e given for all experimental points show the variation in the relative roughness for this constant value of k_e. Because the relative submergence of the roughness protrusions is of interest, lines of constant values of k_e/δ' (the ratio of k_e to the laminar sublayer thickness δ') are also indicated in Fig. 3. The trend of the experimental values of f for both sand-roughness values is significantly parallel at lower values of $\mathbf{R}$ to the lines of constant values of k_e/δ'. This trend illustrates that, for a given open channel, as the flow or depth and therefore $\mathbf{R}$ decrease, the roughness factor f is ultimately determined by a constant ratio of k_e/δ' and thus attains a condition of "fixed minimum smoothness." This is in contrast to pipes in which the ratio decreases until all surface-roughness effects disappear and smooth-surface flow is obtained. Because the laminar sublayer thickness is given by

$$\delta' = \frac{11.6\,\nu}{\sqrt{\frac{\tau_0}{\rho}}} = \frac{11.6\,\nu}{\sqrt{g\,r\,s}} = \frac{131\,r}{\mathbf{R}\sqrt{f}} \tag{9}$$

(in which τ_0 is the intensity of shear at the channel bottom), a condition of the minimum ratio of k_e/δ' leads readily to

$$\frac{k_e}{\delta'} = \text{constant} = \frac{\mathbf{R}\sqrt{f}}{131}\,\frac{k_e}{r} \tag{10}$$

Accordingly, the relative roughness r/k_e decreases with $\mathbf{R}\sqrt{f}$ after the minimum value of k_e/δ' has been reached for a given roughness. It is also clear that, in accordance with Eq. 8, open channels never exhibit a constant value of f so long as the absolute effective roughness k_e remains the same for a given channel. Instead, with increasing discharge or Reynolds number, f should continually decrease as the relative roughness r/k_e increases.

PARTICLE MOTION ALONG THE BED

In Fig. 4 there is shown a plot typical of the results of the observations for the various sediment samples. For each condition of slope and roughness, the mean velocity of the particles $\bar{V}_b$ was determined for successively increased rates of flow or Reynolds numbers. Each point represents the ratio of the mean velocity $\bar{V}$ of the stream to the ball velocity $\bar{V}_b$ for a given flow. In general, the plastic spheres were moved, as is to be expected, at a relatively low Reynolds number because of their low specific gravity. The range of **R** within which an almost constant ratio of $\bar{V}/\bar{V}_b$ was attained is surprisingly narrow although the glass spheres caused a more gradual decrease in this ratio to its ultimate value. Obviously, greater dynamic forces had to be developed by the stream to move the glass spheres. The relatively minor effect of size, both with respect to the critical Reynolds number of incipient motion and to the final ratio of $\bar{V}/\bar{V}_b$, should also be noted. The transport of the plastic spheres is considerably faster at smaller values of $\bar{V}/\bar{V}_b$ for established motion than that of the glass spheres for identical flow conditions.

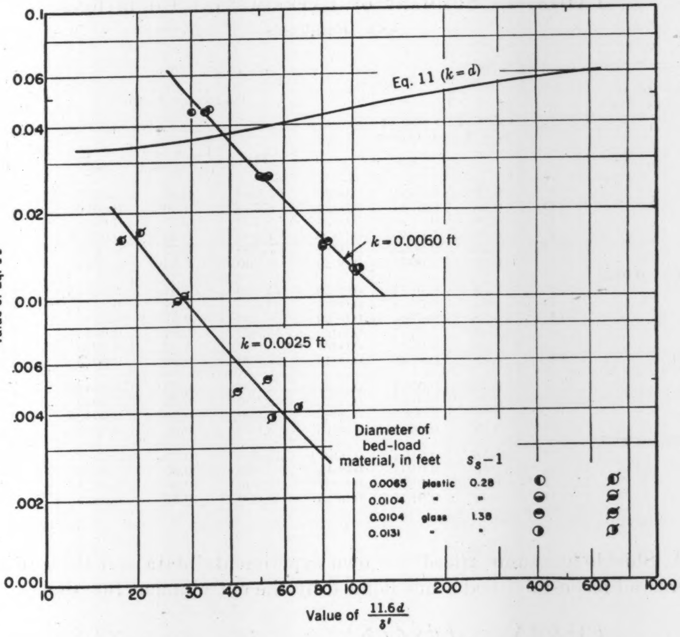

FIG. 5.—THE RELATIONSHIP BETWEEN EQ. 11 AND *d*

Plots similar to those in Fig. 4 were made for the five series of runs from D through H representing the results of runs for the two types of roughness used. A summary of the basic experimental conditions and results derived from these plots is presented in Table 1.

Incipient Particle Motion

The plots for series G given in Fig. 4 show the general trend of all curves obtained with $\bar{V}/\bar{V}_b$ approaching infinity for a particular value of $\mathbf{R}_c$. The value of $\mathbf{R}_c$ derived from these curves is that which defines the beginning of particle motion or the entrainment. The critical condition of incipient motion is thus clearly recognized within narrow limits from the experimental data in contrast to all previous attempts in which incipient motion has been judged entirely by eye.

TABLE 1.—Summary of Experimental Conditions and Results

Sand Roughness, in Feet		Series	Value of $s_s - 1$	Value of d, in feet	Value of S	Incipient Motion			Established Motion
k	k_s					$\mathbf{R}_c$	$\bar{V}_c$, in feet per second	δ', in feet	$\frac{\bar{V}}{\bar{V}_b}$
0.0060	0.0167	F	0.28	0.0104	0.0020	7,000	0.46	0.0024	1.75
		D	0.28	0.0104	0.0024	6,500	0.50	0.0023	1.70
		E	0.28	0.0104	0.0029	5,500	0.51	0.00225	1.70
		F	0.28	0.00655	0.0020	7,500	0.51	0.0025	2.0
		D	0.28	0.00655	0.0024	7,000	0.52	0.0023	1.9
		E	0.28	0.00655	0.0029	6,000	0.53	0.0022	1.8
		F	1.38	0.0104	0.0020	45,000	1.04	0.00145	5.3
		D	1.38	0.0104	0.0024	34,000	1.01	0.0015	4.9
		E	1.38	0.0104	0.0029	26,000	0.97	0.0015	3.9
		F	1.38	0.0131	0.0020	45,000	1.04	0.00145	4.5
		D	1.38	0.0131	0.0024	35,000	1.02	0.0015	4.4
		E	1.38	0.0131	0.0029	27,500	0.99	0.0015	3.5
0.0025	0.0057	G	0.28	0.0104	0.00071	4,500	0.33	0.00445	1.9
		H	0.28	0.0104	0.0015	2,500	0.35	0.0042	1.5
		G	0.28	0.00655	0.00071	5,000	0.35	0.00425	2.0
		H	0.28	0.00655	0.0015	3,000	0.36	0.00375	1.6
		G	1.38	0.0104	0.00071	32,500	0.69	0.0021	3.5
		H	1.38	0.0104	0.0015	9,000	0.55	0.0028	2.7
		G	1.38	0.0131	0.00071	32,500	0.69	0.0021	3.3
		H	1.38	0.0131	0.0015	9,000	0.55	0.0029	2.5

A. Shields has summarized[7] his own experimental data and those of many others and has established a line defined by the entrainment function—

$$\phi\left(\frac{11.6\,d}{\delta'}\right) = \phi\left(\frac{d\sqrt{g\,r\,S}}{\nu}\right) = \frac{\tau_0}{\gamma\,(s_s - 1)\,d} = \frac{\gamma\,r\,S}{\gamma\,(s_s - 1)\,d} \quad \ldots\ldots (11)$$

It should be noted that all the experimental results included in Mr. Shields' analysis concerned the motion of particles on beds composed of the same particles. By contrast, in this investigation the sand forming the bed was different from the sediment spheres in both size and texture. If d is defined as the mean diameter of the moving sediment in Eq. 11, a question arises with respect to the sediment diameter to be used for the present test data when the bed grain diameter k differs from the sediment sphere diameter d. The points for incipient motion obtained from the plots represented by Fig. 4 were compared to the line of Eq. 11 by using d for both parameters in Fig. 5 and also by using k for the parameter containing the bottom shear τ_0 in Fig. 6.

---

[7] "Anwendung der Aenlichkeitsmechanik und der Turbulenzforschung auf die Geschiebebewegung," by A. Shields, *Mitteilungen der Preuss*, Versuchsanstalt fuer Wasserbau und Schiffbau, Berlin, Vol. 26, 1936.

It is seen that consistent plotting results in both cases. The points fall on two well-defined lines distinguished in Fig. 5 solely by the bottom roughness but showing excellent correlation with respect to all other variables. In Fig. 6 the roughness effect is eliminated, and general alinement with the trend of Eq. 11 is accomplished. However, in this case the specific gravity is the factor separating the two groups of points.

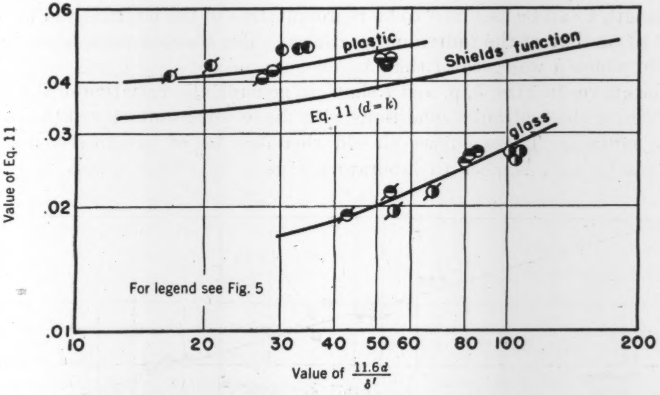

FIG. 6.—THE RELATIONSHIP BETWEEN EQ. 11 AND k

To bring all points to a single curve most closely approximating the line of Eq. 11, the shear-stress parameter was multiplied empirically by 1.5 $(s_s - 1)^{\frac{1}{3}}$ and plotted for all test points against the same abscissa scale with the result given in Fig. 7. The empirical relationship can thus be restated as

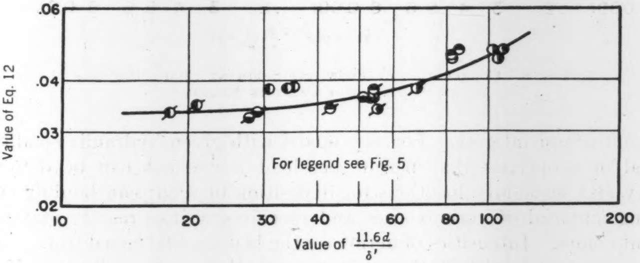

FIG. 7.—EMPIRICAL ENTRAINMENT FUNCTION

$$\frac{1.5 \frac{\tau_0}{\rho}}{g\,(s_s - 1)^{\frac{1}{3}}\,k} = \phi\left(\frac{11.6\,d}{\delta'}\right) \ldots\ldots\ldots\ldots\ldots\ldots\ldots (12)$$

The effect of all the variables involved may be assessed separately with respect to the initiation of sediment transport. The extension beyond Mr. Shields' curve is possible because of a clearer definition of incipient motion and is illustrated by the validity of the curves given for sediment different in size from the sediment forming the bed. For mixtures of bed material, the incipient movement of particles varying in size may be differentiated because the roughness length k can be assumed to be representative of the mixture and the diameter d to be that of the individual particles. The tests covered, however, only cases in which d was greater than k.

The curves in Figs. 5, 6, and 7 show, in general, the variation of the quantities defining the hydraulic conditions with the limiting diameter of the particles set in motion. These curves should therefore be of practical significance, particularly with respect to laboratory studies in which trends of bed-load movement are of interest. For any model with given hydraulic conditions, a material of properties that permit bed-load movement can be determined. Primary and secondary locations for deposition or scour can be differentiated by using material of various sizes and specific gravities readily identified by different colors. Intensities of action on the bed may be gaged from statistical analyses of particle distribution. In general, the great sensitivity of particle motion to even small changes of the hydraulic parameters is emphasized; even variations in water temperature and thus in viscosity were found to be quite important.

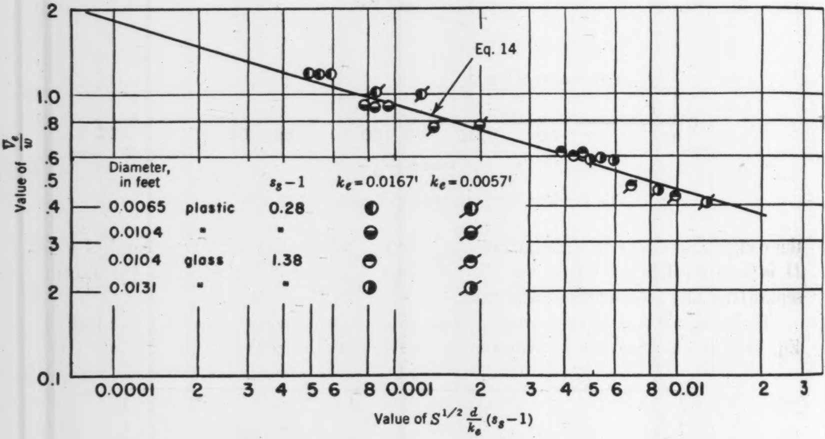

FIG. 8.—CORRELATION OF FLOW AND SEDIMENT CHARACTERISTICS AT BEGINNING OF PARTICLE MOTION

A second approach to incipient motion was based on a consideration of the individual forces acting on particles near the boundary. Of importance is the edge velocity $\bar{V}_e$, to which the upper part of a particle is exposed and which is primarily responsible for the drag and lift forces exerted. The fall velocity w

of a particle indicates the relative magnitude of the body and drag forces. The hydraulically effective roughness k_e and the channel slope S further define the hydraulic conditions. Another functional relationship was therefore investigated of the form,

$$\frac{\bar{V}_c}{w} = \phi\left[(s_s - 1)\frac{d}{k_e}S\right] \qquad (13)$$

This function was plotted in Fig. 8 and gave excellent correlation of all the points described by the empirical equation,

$$\frac{\bar{V}_c}{w} = 0.12\left[(s_s - 1)\frac{d}{k_e}S^{\frac{1}{3}}\right]^{-0.3} \qquad (14)$$

The critical points of incipient motion seem to be defined more closely by Eq. 14 than by Eq. 12 with a clear-cut arrangement of the pertinent variables. This may be caused particularly by the introduction of the fall velocity w, which incorporates an important experimental relationship between the drag coefficient and the sphere Reynolds number. Because the fall velocities lie beyond the Stokes range in the transition zone, their use apparently by-passes analytical difficulties to a considerable extent.

Established Uniform Motion.—In addition to the more accurate definition of incipient particle motion, the experimental results exemplified by Fig. 4 provided some consistent data on the ratio of the mean velocity $\bar{V}$ to the statistical sediment velocity $\bar{V}_b$ after bed-load motion had been established. For all tests this ratio approached a constant ultimate value with respect to the Reynolds number following a transition which was very short for the plastic sphere samples and considerably longer for the glass spheres. This transition range of varying values of $\bar{V}/\bar{V}_b$ has not been analyzed in detail herein, but it is believed to be considerably affected by the action of turbulence near the bottom and by the varying relative magnitude of the dynamic forces cited previously with respect to particle properties. This transitional phase of the motion merits further attention.

The ultimate, nearly constant ratio $\bar{V}/\bar{V}_b$ was assumed to be governed by the following variables defining stream and particle characteristics:

$$\frac{\bar{V}}{\bar{V}_b} = \phi\left[(s_s - 1), \frac{k_e}{d}, \frac{1}{S}\right] \qquad (15)$$

Best results were obtained by plotting the ultimate value of $\bar{V}/\bar{V}_b$ against the product of $(s_s - 1)\ k_e/d\ (1/S)^{\frac{1}{3}}$, which resulted in a simple linear relationship for the range of data (shown in Fig. 9),

$$\frac{\bar{V}}{\bar{V}_b} = 1 + \frac{1}{12}(s_s - 1)\frac{k_e}{d}\frac{1}{S^{\frac{1}{3}}} \qquad (16)$$

Eq. 16 leads to several interesting conclusions with respect to particle motion on a rough bed, even though the tests covered only a relatively narrow range of the variables involved and were restricted to the motion of widely spaced particles. The particle velocity relative to the mean velocity increases as the slope and the particle diameter are increased. This is evidently the result of the increase in the dynamic pressures by higher edge velocities. With larger particles, the rolling resistance will increase at a lower rate with d than the dynamic forces, which are raised not only by the particle size but also by the steeply increasing velocities near the boundary; this seems to be an important factor in the phenomenon of sorting.

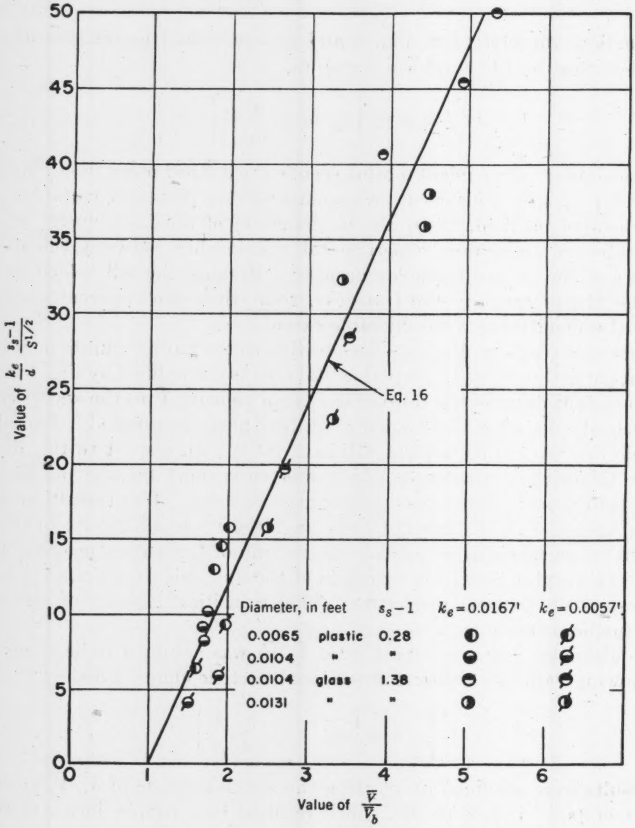

FIG. 9.—CORRELATION OF FLOW AND SEDIMENT CHARACTERISTICS FOR ESTABLISHED UNIFORM PARTICLE MOTION

In Eq. 16 the edge velocity $\bar{V}_e$ might have been used instead of the mean velocity $\bar{V}$. The ratio of these velocities is readily obtained from the logarithmic velocity distribution for two-dimensional turbulent flow, and within the range of these tests the use of this ratio would have resulted only in an adjustment of the constants involved. Eq. 14 is presented primarily as an expression of the special test results analyzed; no general validity should be inferred until further evidence is available.

CONCLUSIONS

The experimental program was restricted to the study of discrete particles on a rough channel bed of fixed characteristics, which are free to move under the influence of the hydrodynamic forces exerted by the flow. Certain pertinent conclusions can be drawn from the analytical and experimental results:

1. Darcy's friction factor f is preferable to Manning's n in analyzing roughness effects in open channels. The pattern of variation with the Reynolds number is consistent with the laws accepted for pipe flow on the basis of the von Kármán-Nikuradse analysis.

2. The change in relative roughness in open channels is continuous with the Reynolds number, and values of f always depend on the absolute roughness k_e. For a given channel, the factor f seems to be governed by a minimum value of K_e/δ', which is reached at low values of the Reynolds number. The line of smooth-surface flow is not approached for roughened open channels as it is in the case of pipes because the relative roughness k_e/r increases rapidly as the Reynolds number decreases.

3. An effective hydraulic roughness k_e or the equivalent sand roughness must be computed to make the von Kármán-Prandtl logarithmic functions applicable. These values of k_e may be appreciably larger than that of the average sand-grain diameter k because of the differences in pattern and texture of the surface coating.

4. A new approach to incipient particle motion has been made on the basis of rational hydrodynamic concepts. This approach extends the analysis of incipient motion to cases in which bed material and the transported material are different, and thus Eq. 11 does not apply.

5. The hydrodynamic effects on rolling particles are such that they produce an average particle velocity, which remains essentially constant in relation to the mean velocity of flow over a wide range of the Reynolds number for the stream.

6. The relative consistency of the results encourages further experiments with the procedure outlined herein and the systematic exploration of the effects of other parameters pertinent to bed-load movement—such as the influence of shape and texture, of mutual interference and number, of local boundary changes, and of secondary currents.

APPENDIX

The following symbols adopted for use in the paper conform essentially with "American Standard Letter Symbols for Hydraulics" (ASA Z10.2-1942), prepared by a committee of the American Standards Association with ASCE representation and approved by the Association in 1942:

d = diameter of sediment sphere;
$\mathbf{F}$ = Froude number;
$\mathbf{F}_D$ = total drag on particle;

F_L = lift on particle;
F_R = resultant force on particle;
f = Darcy coefficient of resistance;
g = acceleration of gravity;
K_1 and K_2 = proportionality constants;
k = average sand-grain diameter;
k_s = effective hydraulic roughness length;
n = Manning's roughness coefficient;
q = discharge of water per unit width of channel;
R = Reynolds number of stream:
  R_c = Reynolds number of stream for incipient motion;
  R_s = Reynolds number of the particles;
r = hydraulic radius;
S = slope of energy gradient;
s_s = specific gravity of sediment;
$\bar{V}$ = mean velocity of flow:
  $\bar{V}_b$ = mean velocity of sediment spheres;
  $\bar{V}_s$ = temporal mean velocity of flow at upper edge of sediment particle;
W_b = buoyant weight of particle;
w = settling velocity of sediment spheres;
y_0 = depth of uniform flow;
γ = specific weight of water;
δ' = thickness of laminar sublayer;
ν = kinematic viscosity in square feet per second;
ρ = density of water; and
τ_0 = intensity of shear at channel bottom.

AMERICAN SOCIETY OF CIVIL ENGINEERS
Founded November 5, 1852
TRANSACTIONS

Paper No. 2769

STRESS MEASUREMENTS, SAN LEANDRO CREEK BRIDGE

By Ray W. Clough[1] and Charles F. Scheffey,[2]
Junior Members, ASCE

Synopsis

Many difficulties are encountered in investigating live-load effects on a bridge in the field. There is presented a description of such a full-scale investigation on the San Leandro Creek Bridge near Oakland, Calif. Among the difficulties are the effects of temperature and localized strain patterns. The use of dummy gages to compensate for temperature changes is described, and the limitations of such compensation are examined.

Introduction

Comparison of the actual stresses developed in highway structures with design stresses which are computed by standard methods of analysis has long interested structural engineers. Advances in the science of experimental stress analysis have greatly simplified the problem of making the large-scale field investigations that are required to determine the actual stresses in full-scale structures. Thus, in order to study methods and develop techniques for performing such large-scale investigations, the Institute of Traffic and Transportation Engineering of the University of California at Berkeley, in the spring of 1950, initiated an extensive program of measurements of strain and deflection in a typical slab and girder highway bridge, in cooperation with the Bureau of Public Roads (USBPR), United States Department of Commerce, and the California Division of Highways.

In addition to the basic purpose of developing techniques for field-stress measurements, the specific objectives of the test program were:

1. To study the manner in which loads applied to the slab were distributed to the main girders.

THE UNIVERSITY OF MICHIGAN LIBRARIES

Note.—Published, essentially as printed here, in August, 1953, as *Proceedings-Separate No. 246* Positions and titles given are those in effect when the paper was received for publication.

[1] Associate Prof. of Civ. Eng., Univ. of California, Berkeley, Calif.

[2] Asst. Prof. of Civ. Eng., Univ. of California, Berkeley, Calif.

2. To evaluate the degree of composite action which existed in a structure in which no special anchoring devices were provided to develop bond between the concrete deck and the steel girders.

3. To obtain data from which the impact stresses—that is, the increase of stress caused by the motion of the vehicle, might be evaluated.

The presentation is divided into two parts: First will be described the design and installation of the instruments used in obtaining the basic records and, next, the methods of reducing these records and some of the difficulties encountered in obtaining reliable data. Analysis and interpretation of the stress information are available elsewhere.[3]

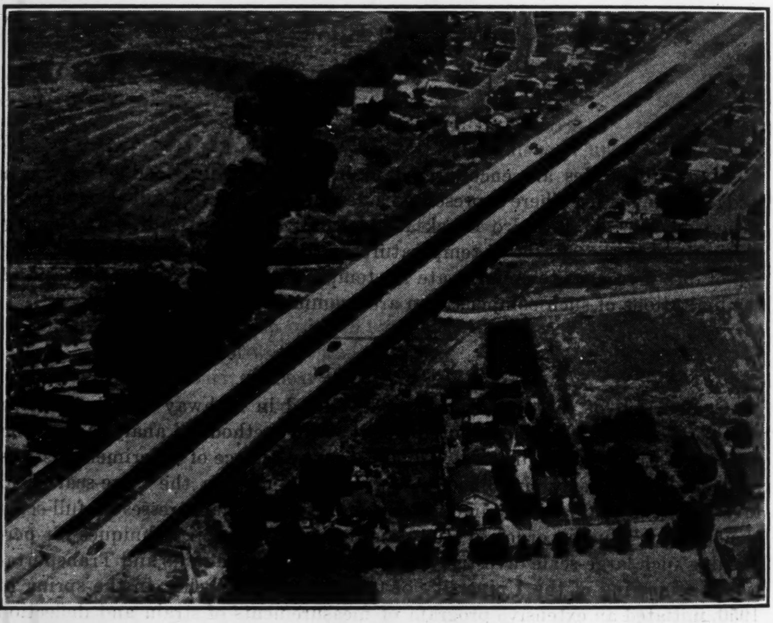

FIG. 1.—AERIAL VIEW OF THE SAN LEANDRO CREEK BRIDGE (CALIFORNIA)

INSTRUMENTATION

The design and installation of the instruments used to obtain the basic records for this project can best be described by making reference to the illustrative material.

Description of the Test Structure.—In Fig. 1 there is shown an aerial view of the structure selected for the test program. It is the San Leandro Creek Bridge, a link in the Eastshore Freeway, located at the southern limits of the City of Oakland, Calif. The bridge consists of two parallel, two-lane structures of twenty-three spans each. Each structure has an 8-in. concrete deck supported by three longitudinal girders on 11-ft centers. Every third span has a suspended section that is hinge-supported on the cantilevered ends of the girders which are continuous over the adjacent two spans. Two representative spans, spans 19 and 20 of the east structure, were selected for testing—19 being a typical suspended span and 20 a typical continuous span.

---

[3] "Investigation of Stresses in the San Leandro Creek Bridge," *Research Report No. 13*, Inst. of Traffic and Transportation Eng., Univ. of California, Berkeley, Calif.

In Fig. 2 there is shown the layout of the test spans. The outer girders are supported directly on the columns, and the middle girder is supported by transverse beams framing into the outer girders. Diaphragms are provided in each span to aid in distributing the load among the girders.

Design of the Instrumentation.—The manner in which load is distributed to the girders by the slab and diaphragms is indicated by the relative magnitudes of the bending moments acting in the three girders at a given cross section.

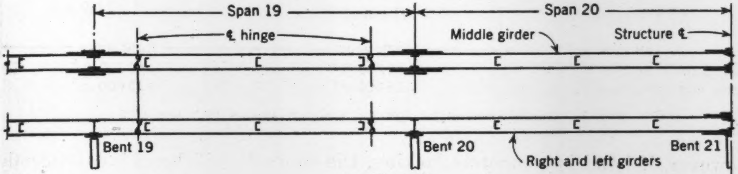
Span 19
Span 20
℄ hinge
Middle girder
Structure ℄
Bent 19
Bent 20
Bent 21
Right and left girders

(*a*) Elevation

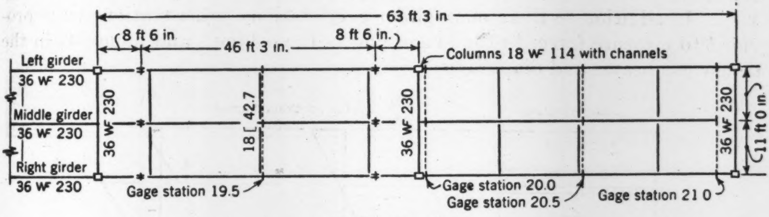
63 ft 3 in
8 ft 6 in
46 ft 3 in.
8 ft 6 in.
Columns 18 WF 114 with channels
Left girder
36 WF 230
Middle girder
36 WF 230
Right girder
36 WF 230
36 WF 230
18 [42.7
36 WF 230
36 WF 230
11 ft 0 in.
Gage station 19.5
Gage station 20.0
Gage station 20.5
Gage station 21.0

(*b*) Framing plan

Fig. 2.—Steel Layout of Test Spans

For the purpose of studying distribution of load, main gage stations were established at four sections in the test spans, as indicated in Fig. 2. In addition, supplementary stations were established at Station 19.7 and Station 20.3.

In Fig. 3 there is shown the location of the strain gages at the midspan gage stations. Carlson strain meters were placed at two levels in the concrete, and SR-4 strain gages were applied to the flanges of the girder. From a knowledge of the properties of the section it is possible to compute the total moment carried by each composite girder from the strain measurements provided by these gages. For the purpose of these computations, the deck was assumed to be divided into three longitudinal strips, each strip being assumed to act with the girder which supported it.

A detail of the arrangement of strain gages at a station adjacent to a girder support is shown in Fig. 4. At these stations, additional gages (rosettes) were provided in the web of the girder, from which shear forces and a check on the

THE UNIVERSITY OF MICHIGAN LIBRARIES

longitudinal strains could be obtained. Fig. 4 also shows how the degree of composite action existing at a given gage station can be evaluated by plotting the strains indicated at the several gage positions across the depth of the girder. If the concrete is effectively bonded to the steel, the composite section will act as a unit and strains will vary linearly through the entire depth (Fig. 4(*b*)). However, if bond is competely lacking, the concrete will bend independently of the steel and the strain diagram will show a discontinuity, as shown in Fig. 4(*c*). In addition to these main-girder gage stations, other stations were provided to measure forces in the hinges and in the columns and moments in the transverse beams and diaphragms.

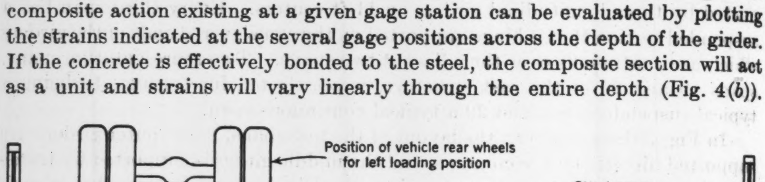
Position of vehicle rear wheels for left loading position
Strain gages
8 in. ± reinforced concrete
36 W= 230
SR-4 strain gages
2 ft 11 in.
2 ft 11 in.
3 ft 0 in.
11 ft 0 in.
11 ft 0 in.
11 ft 0 in.
3 ft 0 in
Left girder
Middle girder
Right girder
I composite = 58 100 in.⁴
I steel only = 15 000 in.⁴
= 44 200 in.⁴
= 15 000 in.⁴
= 49 100 in.⁴
= 15 000 in.⁴

FIG. 3.—CROSS SECTION OF BRIDGE, GAGE STATIONS 19.5 AND 20.5

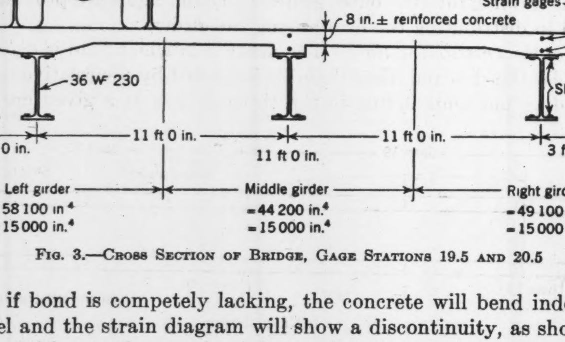
Strain meters
Typical strain diagrams
Rosettes
Neutral axes
(a)
(b)
(c)

(*a*) Gage pattern at stations 20.0 and 21.0 (*b*) Full composite action (*c*) No composite action

FIG. 4.—ARRANGEMENT OF GAGES ADJACENT TO SUPPORT

Installation of Gages.—The principal strain-measuring device used in this project was the SR-4 resistance-wire strain gage. This gage consists of a fine wire sandwiched between pieces of paper so that it can be bonded to the structure. As the structure is strained, the fine wire is strained equally, causing its resistance to change proportionately to the strain. Two types of SR-4 gages were used on the San Leandro Creek Bridge, the A-1 for normal strain measurements and the AR-1 rectangular rosette for measuring both normal and shear strains. The installation of the gage followed the usual laboratory procedure in most respects. The metal was smoothed and cleaned with emery cloth and acetone, and the gages were glued in place with a nitro-cellulose cement.

In Fig. 5 there is shown a typical installation of a rosette and an ordinary SR-4 gage after the lead wires were connected and waterproofing was applied. The gages were waterproofed by coating them thoroughly with an asphaltic compound which had been heated sufficiently to render it quite fluid. The effectiveness of this waterproofing technique is demonstrated by the fact that none of the gages on the structural steel was grounded out at any time during the test program, despite the fact that the structure was thoroughly hosed after the deck was poured in order to wash off the cement which had dripped through the forms.

The temperature-compensating gages or "dummy" gages are also visible in Fig. 5. These additional SR-4 gages are similar to those applied to the structure but mounted on separate pieces of steel and fastened to the girder adjacent to the active gages. The circuit used in measuring strains with the SR-4 gages was so designed that stress-free deformations in the structure as a result of thermal expansion were balanced by the equal thermal strains developed in the dummy gages. Thus, only strains caused by stress (which would not affect the dummy gages) were indicated by the measuring circuit. Separate compensating gages were used in the circuit for every SR-4 gage installed in the structure in order that the temperature compensation be as complete as possible.

FIG. 5.—ACTIVE AND DUMMY GAGES ON A GIRDER

FIG. 6.—ACTIVE AND DUMMY GAGES ON REINFORCING BARS

In addition to those on the girders, SR-4 gages were applied at twenty-eight locations on the reinforcing steel in the deck slab. A typical installation of the SR-4 gages on the reinforcing bars is shown in Fig. 6. The procedure followed in applying these gages had been used with success in previous laboratory tests. The active gages were coated with two layers of asphaltic compound and the dummy gages were coated with the same material and sealed in brass tubes. Despite these precautions, however, very low resistances to ground were measured in many of the circuits, indicating failure of the waterproofing.

For this reason, these gages were considered unreliable and were not used in the test program. The reason for the failure of the waterproofing technique is not known, but it is believed that the failure probably occurred in the zone between the end of the cable sheath and the strain gages.

Strains in the concrete deck were measured with the strain meters (resistance-wire gages operating on essentially the same principle as the SR-4 gage) which are shown in three stages of assembly in Fig. 7. The outer protective shell has been removed from the lowest gage in order to show its internal construction. Strains in the concrete into which the meter is cast cause its end flanges to move relative to each other, thus developing strains in the resistance-wire coils. The flexible brass protective tube is shown in place on the middle gage. The upper gage has been covered with a cloth sleeve which serves to keep the concrete from bonding to the protective shell and thus permits the flanges to strain freely.

These strain gages were installed by fastening them in the proper position, either to the reinforcing steel or to the girders, and then packing the concrete carefully about them so as to avoid disturbing their position, as shown in Fig. 8.

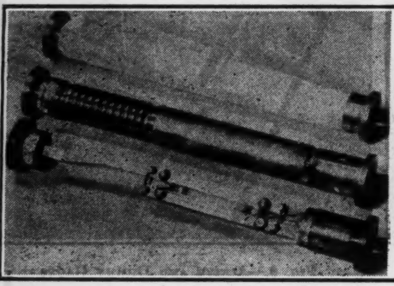

Fig. 7.—Strain Meter in Three Stages of Assembly

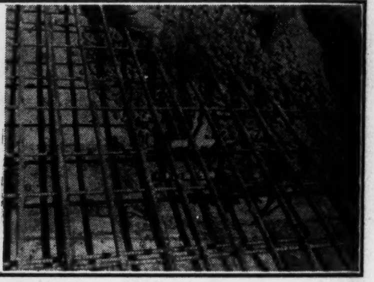

Fig. 8.—Placing Concrete Around Strain Meters

The deflections of the bridge were measured with variable-inductance gages. This type of gage consists of a coil of fine wire mounted in a base which is firmly fastened to the ground and a steel slug attached to the end of a pipe suspended from the lower flange of the girder. As the girder deflects, the steel slug is caused to move up or down in the coil, thus effecting a change in its inductance. By calibration, this change of inductance can be related to the deflection of the girder.

In concluding the description of the gage-installation program, the following statistics are presented. A total of 220 active SR-4 gages and 184 dummy gages were used throughout the structure requiring 129 separate circuits for the SR-4 gage measurements. In addition, 16 strain meters and 8 deflectometers were installed. A separate circuit was required in each of these gages making a total of 153 circuits required for all measurements.

Recording Equipment.—All gages were connected to the recording and indicating equipment by three-lead, shielded, microphone cables having a water-proof outer cover. The lead wires were supported on the lower flanges of the girders and were brought down to an instrument shack located under the structure. In Fig. 9 there is shown the interior of the instrument shack with the lead wires entering through the opening at the upper rear and connecting to three banks of switches. The switches for the SR-4 gage circuits are contained in the large box at the left, the strain-gage switches are seen at the right center, and the deflectometer switch box is mounted on the rear wall. Static readings of the various gages were made by connecting standard SR-4, strain-gage, or deflectometer static-indicating instruments to the corresponding switch boxes and switching the gages into the circuit one at a time.

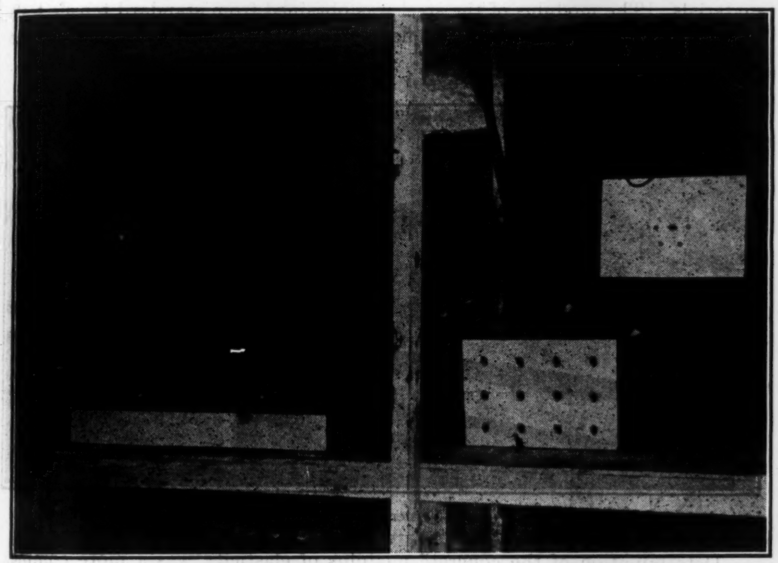

FIG. 9.—SWITCH BOXES IN INSTRUMENT SHACK

For dynamic recordings of strains and deflection, additional leads were connected from the switch boxes to a trailer housing the dynamic recording equipment. Dynamic recording equipment used in this test program included two twelve-channel strain-gage control and amplifier units, 1 twelve-channel gage control unit without amplifiers, and 3 twenty-four-channel oscillographs. With this equipment it was possible to record simultaneously the output of the 8 deflectometers plus only 24 SR-4 or strain-gage circuits. Thus, in order to obtain dynamic records from all the strain gages, it was necessary to repeat the load runs several times with different combinations of strain gages connected to the oscillographs.

Test Vehicle.—The vehicle used for loading the bridge in most of the test work is shown in Fig. 10. It is a standard earth-moving truck loaded with sand and steel ingots to a gross weight of 67,000 lb. Of the total load, approximately 50,000 lb were carried by the rear axle and 17,000 lb by the front axle.

During the moving-load tests, coordination between the truck driver and the oscillograph operators was provided by the test engineer on the bridge deck by use of a field telephone set.

CONTROL TESTS

Concurrently with the placing of the instruments on the structure, a program of control tests was performed to determine the properties of the materials used in the structure. The most important property, from the standpoint of the stress measurements, was the modulus of elasticity of each of the various materials. The modulus of the steel was obtained from standard tensile tests performed on specimens taken from flanges and webs of the girders and from the reinforcing bars.

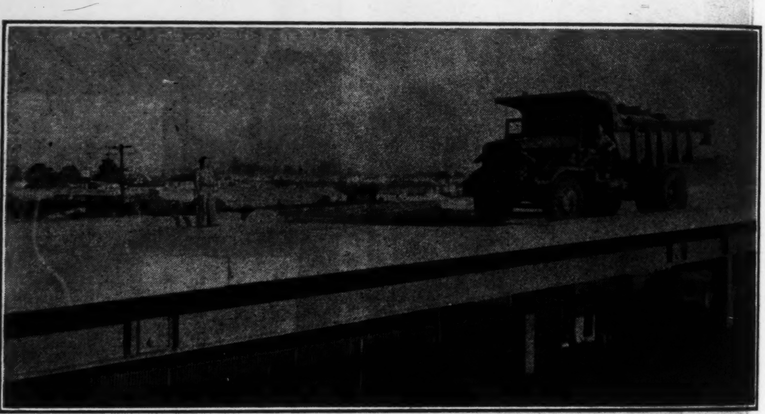

FIG. 10.—TEST VEHICLE OF 67,000 LB ON BRIDGE

Determination of the concrete modulus of elasticity was a more complex problem because its modulus varies with the weather conditions. Thus, it was necessary to devise specimens that would simulate, as closely as possible, conditions within the test slab and to test these specimens continuously during the stress-measurement program. Two types of specimens were used: (1) Standard 6-in. by 12-in. cylinders for the compression tests; and (2) 10-ft-long by 10-in.-wide unreinforced rectangular beams for the flexure tests. All beams were sealed on the sides and exposed to the air at the top surface. Three of the beams were made 8 in. deep and had their bottom surfaces exposed to the air to simulate conditions in the slab between the girders; the other three were made 10 in. deep and were sealed on the bottom to simulate conditions over the girders. The beams were then stored on the deck of the bridge in order to be exposed to the same temperature and moisture conditions as the slab. Strain meters were embedded in the beams at midspan and were used to measure the flexural strains.

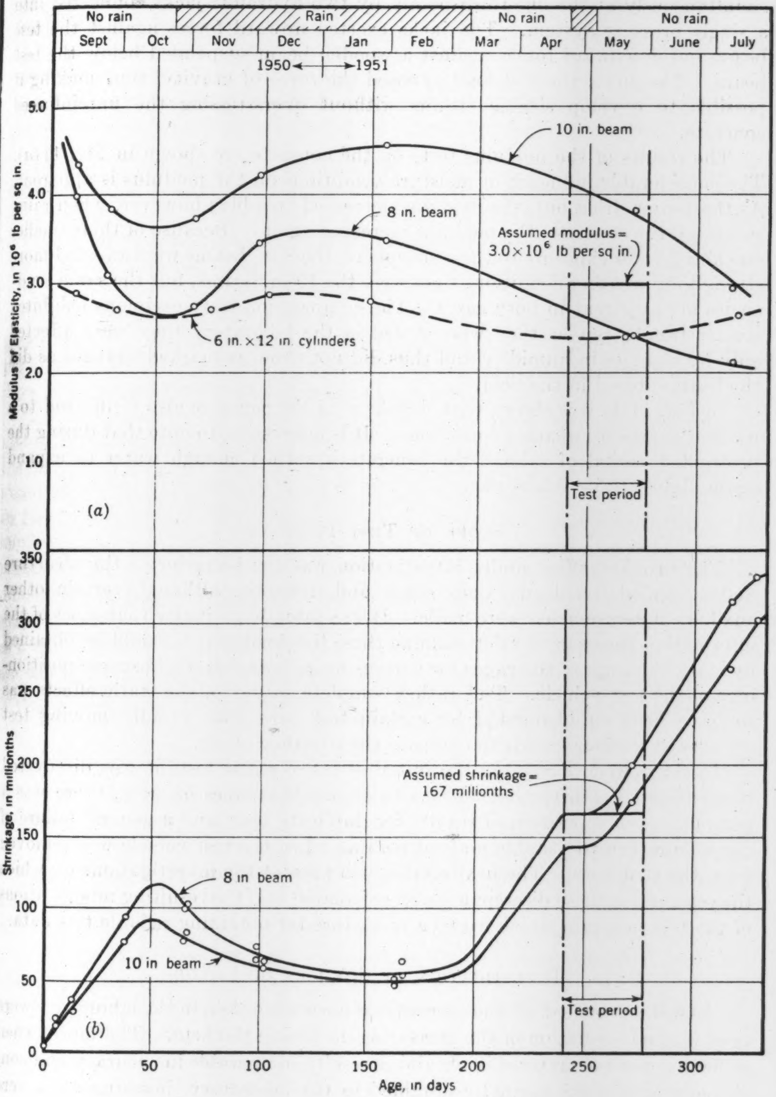

FIG. 11.—MODULUS OF ELASTICITY AND SHRINKAGE OF CONCRETE

In order to determine the flexural properties of the beams, loads were applied simultaneously at the one-third points by two hydraulic jacks connected into a single pressure system. The jacks exerted upward forces against the test beam and downward forces against a wooden beam suspended below the test beam. Therefore, the test load opposed the force of gravity, thus making it possible to develop sizable strains without overstressing the unreinforced concrete.

The results of the modulus tests on the concrete are shown in Fig. 11(*a*). The considerable influence of moisture conditions on the modulus is apparent. As the beams dried out, the modulus decreased steadily; however, when rains saturated the concrete, the modulus increased again. Because of their smaller size and greater exposure to the atmosphere, the 8-in. beams were affected more strongly by weather conditions than were the 10-in. beams, but the same tendencies are apparent in both cases. The compression-test specimens exhibited similar trends, but as they were stored in the laboratory they were affected only by changes in humidity and thus did not show as marked changes as did the beams stored in the field.

In Fig. 11(*b*) it is shown that shrinkage of the concrete also is affected to a marked degree by weather conditions. It is interesting to note that during the protracted period of rainfall the concrete absorbed enough water to expand again almost to its initial size.

SCOPE OF TEST PROGRAM

The primary effect under investigation was the behavior of the structure under applied live loads, both static and dynamic, although certain other auxiliary measurements were made. It was intended initially that most of the information necessary for determining these live-load effects would be obtained by static readings of the gages for various longitudinal and transverse positionings of the test vehicle. This rather complete survey of the static effects was to have been supplemented by certain test runs with rapidly moving test vehicles at various speeds to evaluate the dynamic effect.

In the course of making the initial series of static tests it was discovered that, despite extensive precautions to eliminate sources of error, there was a poor degree of repetition of results for duplicate tests and a general failure of gages to return to a stable no-load reading when the test vehicle was removed from the structure. The next section will present the investigations by which the reasons for these discrepancies were isolated and the resulting modifications of the test program which led to a procedure for obtaining reliable test data.

INVESTIGATION OF SOURCES OF ERROR

As will be recalled, all the precautions normally taken in the laboratory were used in the installation of the measuring devices in the field. Therefore, when difficulty was encountered in obtaining results comparable in accuracy and consistency with those normally obtained in the laboratory, investigations were made of possible new sources of error peculiar to a field-test arrangement. The difficulties were finally traced to three effects:

1. Inadequate temperature compensation as a result of a rapid rise or fall of ambient temperature, and difference in heating and cooling rates for the structure and the dummy gages.
2. Actual stresses in the structure caused by factors other than load, especially those resulting from temperature changes.
3. Actual stresses in the structure caused by highly localized effects in the vicinity of the load which were sensitive to the positioning of the load.

The effectiveness of the temperature compensation at certain locations subject to rapid heating and cooling was checked by obtaining temperatures of the structural steel, the concrete slab, and the dummy-gage strips by the use of resistance thermometers and thermocouples. It was found that during the morning and afternoon hours, when temperature changes of the surroundings were rapid, there was at times a difference of 1° F or 2° F in the temperatures of the dummy gage and the structure at the location of the corresponding active gage. This in itself would account for an apparent strain of from 10 microin. per in. to 12 microin. per in. This effect was particularly troublesome on sunny days, whereas on cloudy days it was not noticeable.

The second source of trouble proved to be the most difficult. A series of no-load readings taken during the course of a single day without any load on the structure indicated changes in the strain at some of the gage locations in excess of what could be accounted for by inadequate temperature compensation. In fact, some of these differences were even larger than those caused by the application of the live load. A continuous record of temperatures at various points on the structure during this same period pointed to the reason for this difficulty. A correlation of the records of no-load strains and temperatures shows that large and rapidly varying actual stresses were set up in the structure as a result of the changes in the ambient conditions. Although these stresses are probably not important from the design standpoint, they certainly must be considered when conducting field-stress measurements. These types of stresses are:

a. The temperature stresses of the type inherent in any indeterminate structure. For example, in this structure where there is a hinge joint between the girder and the supporting columns, there results a bending of the columns and some direct stress in the girders as a result of the changes of girder length with temperature. In addition, if the slab heats faster than the girders, there is a tendency for the two-span continuous beam to lift off the center support, causing a redistribution of the dead-load reactions, with subsequent stresses.

b. Warpage stresses caused by nonsymmetrical heating. In this structure a rapid heating of the lower flange of one of the outside girders, such as is produced by early morning sun, causes this girder to tend to bend downward. It is restrained by the slab and also by the adjacent unheated girders, setting up a further complexity of stresses.

c. Internal stresses which exist even if only a single unrestrained member is considered for there will be actual stresses caused by temperature changes unless the temperature gradient across the cross section is linear. Any nonlinearity of temperatures will produce direct stresses to achieve equilibrium and strain compatibility in the section.

The stresses produced by all these temperature effects are difficult to evaluate or measure. Furthermore, these stresses are not constant but are continuously varying. The successful elimination of the errors of live-load strain caused by this "background" effect of temperature requires that the no-load reading, loaded reading, and check on the no-load reading be made during a time interval short enough that no appreciable changes occur in these background effects during the interval. By actual test it was found that significant changes might occur in intervals greater than 15 min. This imposes a serious limitation on the number of measurements that can be made with a single loading of the structure for, with two experienced operators using the indicating equipment, it was found that 15 gages were all that could be read within this time. In a test program as extensive as this one, in which up to 150 circuits were read for each lateral and longitudinal position of the test load, this would require an unreasonable number of repetitions of the positioning of the live load.

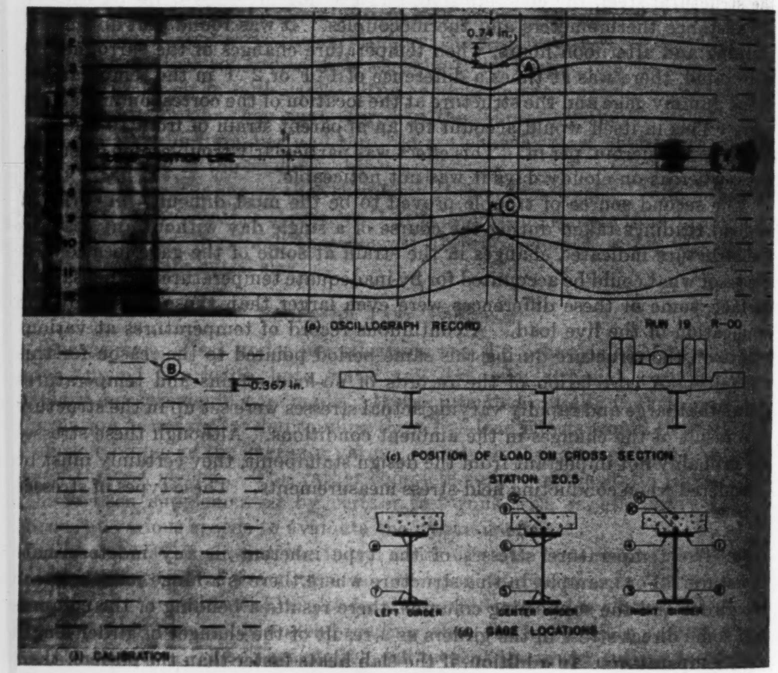

Fig. 12.—Typical Oscillographic Results

This repositioning of the live load is in itself responsible for the third source of error. In some of the gages local strains were produced which were extremely sensitive to a small difference in positioning of the load. This problem will be cited subsequently, after the use of the dynamic recording equipment is explained.

INTERPRETATION OF DYNAMIC RECORDS

A typical oscillograph record is reproduced in Fig. 12(*a*), together with part of the calibration records for this series of runs and necessary identifying information. The procedure for producing such a record begins with the connection of the selected gages to the various channels of the oscillograph and the introduction of electrical elements of resistance and capacitance into this circuit to bring the reading of each channel to the zero position. This operation is accomplished by visual observation of the light spots on the galvanometer scale, after which a photographic record is made by running off a small piece of the sensitized paper. This operation produces the row of short "zero" marks along the left edge of the record. The vehicle is then brought up to proper speed and run across the test spans in the selected lateral position—in this case, close to the right-hand curb. At the same time the sensitized paper is moved at the predetermined speed past the recording aperture of the galvanometers; thus, there results a continuous record of strain in each gage circuit. After the run, a final set of "zeros," which can be seen near the right edge of the record, was obtained. The total time elapsed between initial and final zeros was, in most cases, less than 1 min, so that strain variations as a result of temperature changes were extremely small. That they would be appreciable over longer periods of time can be seen by noting the initial zeros for the next run, particularly channel No. 11, which shows a decided shift. The interpretation of this record for any point on a given channel "trace" requires making two measurements—(1) the value of the strain and (2) the position of the load. The first of these is represented by the excursion of the trace at the point in question from the straight line connecting the initial and final zeros. For example, at point A on the trace of channel No. 2, this excursion is 0.74 in. on the original record. In order to relate this measurement to strain in microinches per inch at the gage point, it is necessary to make a calibration for each series of test runs. Part of the record of such a calibration is reproduced in Fig. 12(*b*). A known resistance is introduced into the circuit for each gage channel in turn, causing a sharp displacement of the trace, indicated as point B. By the known electrical properties of the circuit, this resistance can be converted to an equivalent strain in the gage. In this case, the resistance introduced was equivalent to a strain at the gage of 64.6 microin. per in. The trace at point B measured 0.367 in. on the original; hence, there is a calibration factor of 176 microin. per in. of trace deflection. The strain at point A in the test run is therefore 0.74 × 176 or 130 microin. per in.

The position of the vehicle at the instant at which these strains existed is found by reference to the vehicle-position trace between strain traces No. 6 and No. 7. This circuit was connected to traffic counting-type air switches actuated by the wheels passing over hoses on the deck at Stations 19.0, 20.0, and 21.0. Measurements from the "pips" made by the wheels permit determination of vehicle position and speed.

The examination of these oscillograph records made clear the reason for the erratic behavior which had been noted in some of the slab and top flange girder gages. Trace No. 11 of this record is for a strain gage in the slab over the center of the right girder at Station 20.5, a section of normally positive moment. The trace is distinguished by two sharp pips in the record at point C. This gage shows a normal buildup of compressions as the load approaches the gage point, but these two sharp pips, which indicate a sudden increase in compression, occur as the front and rear wheels pass over the gage location. Inspection of the trace for the bottom gage in the slab (No. 10) at this point shows a similar sudden reduction of compression for the corresponding instant, as does also the trace for each of the gages attached to the adjacent top flange of the girder (traces No. 1 and No. 4). The explanation of this effect is found by a consideration of the localized transverse bending stresses produced in the slab. As the wheels of each axle straddle the gage location, strong transverse bending strains are developed in the slab—tensile on top and compressive at the bottom. Because of the Poisson effect, these transverse strains cause localized longitudinal strains in the slab and top flange of the girder, compressive on top and tensile at the bottom. It is the superposition of these localized strains on the longitudinal bending strain of the composite girder which causes the pips in the records. The localized effects were eliminated in evaluating the records by sketching a smooth curve cutting off the pip from the oscillograph trace.

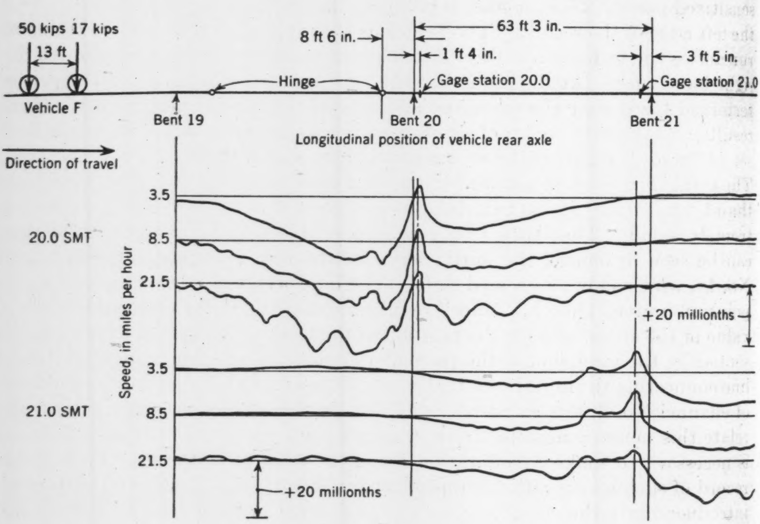

FIG. 13.—TYPICAL DYNAMIC RECORDS

This strain is measured to the smooth line which can be drawn through the actual trace, thus resulting in a value free of oscillations caused by the vibration of the span at its own natural frequency. This value can be shown theoretically to differ—by a small amount—from the strain which would be produced by a static test with the load placed in the same position. The difference between the two is a function of the speed of the vehicle as related to the natural frequency of vibration of the span. For slow speeds, such as this test at 5 miles per hr, the dynamic and static strains are nearly identical, differing theoretically by less than 1%. Thus it is permissible to replace the static tests by low-speed dynamic runs.

Use of the dynamic recording equipment in place of the static indicators has many advantages in large-scale field investigations. First, such use eliminates the many difficulties associated with temperature changes because each test can be completed before appreciable changes in temperature occur; second, considerable time is saved in obtaining the test data; and third, a more complete picture is given of the strains within the structure, thus making possible the detection and elimination of local effects.

It was therefore decided to abandon all static readings and collect all necessary data by slow-speed, moving-load tests using the dynamic recording equipment. Test runs at the higher speeds desired to evaluate the effects of vehicle speed were made in the same series of runs with each of the gage combinations set up for these slow-speed runs. The actual speed of the vehicle was determined by the timing lines on the oscillograph record. These are not visible in Fig. 12 but run completely across the record from top to bottom at intervals of 0.01 sec, thus permitting accurate time measurements.

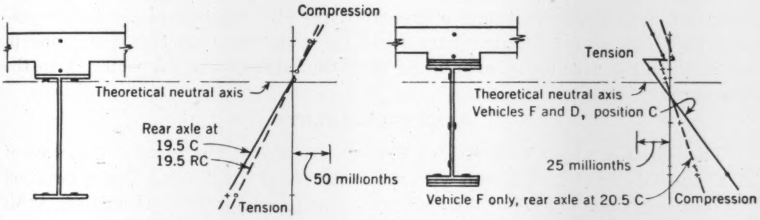

(*a*) Gage station 19.5, middle girder (*b*) Gage station 21.0, middle girder

FIG. 14.—INTERPRETATION OF STRAIN CROSS SECTIONS

A graphic summary of the results of moving-load runs at three different speeds on each of two particular gages is presented in Fig. 13. The oscillograph records in this case have been replotted in order to reduce them all to the same length. This replotting permits direct comparison of effects of the load at any given position for each of the three speeds. It will be noted that the slow-speed run at 3.5 miles per hr caused few oscillations. The sharp loops in the trace in each case are the pips caused by the front and rear wheels of the test vehicle passing over the gage location. It will also be noted that these pips occur in combination with the oscillations caused by vibration in the high-speed runs, requiring careful interpretation of these records.

A typical application of the results to the interpretation of structural behavior is illustrated in Fig. 14. In Fig. 14 it is sought to determine the extent to which composite action between the slab and girder exists at each of two cross sections. At section 19.5, subjected to positive bending moment, the plot of strains across the section shows an essentially linear variation from top to bottom, indicating complete composite action. In the plot of strains for section 21.0, the linearity of strain is in two segments, with a sharp discontinuity at the junction of the slab and girder. Hence, it is obvious that composite action has been destroyed at this section that has been subjected to negative moment.

CONCLUSIONS

1. Investigation of live-load effects on full-scale bridge structures by using standard instruments for static testing presents many difficulties not encountered in the laboratory, unless the number of gages to be read and the number of load positions to be used are small.
2. When available, the use of dynamic-type recording equipment to obtain essentially static-test data by slowly moving loads offers great advantages in eliminating troublesome temperature effects, detecting of localized strain patterns, and saving time.
3. If it is planned from the start of a test program to use such continuous-recording equipment, great simplification is possible in the installation of gages because the importance of long-term stability of gages and of temperature compensation of individual circuits is greatly reduced. It probably would be possible to use a single dummy gage for large numbers of active gages and to use only single wire leads, grounding the other side of the gage circuit to the structure.

ACKNOWLEDGMENTS

The San Leandro Creek Bridge Project was under the general direction of T. Y. Lin, M. ASCE. Liaison with the Institute of Traffic and Transportation Engineering of the University of California was provided by R. Horonjeff, A. M. ASCE. V. A. Plumb, J. M. ASCE, acted as field engineer in charge of loading tests and was later responsible for the reduction of field data.

AMERICAN SOCIETY OF CIVIL ENGINEERS
Founded November 5, 1852
TRANSACTIONS

Paper No. 2770

TRANQUIL FLOW THROUGH OPEN-CHANNEL CONSTRICTIONS

By Carl E. Kindsvater,[1] M. ASCE, and
Rolland W. Carter,[2] A. M. ASCE

With Discussion by Messrs. Emmett M. Laursen and Arthur Toch; Fred W. Blaisdell; Pin-Nam Lin; Carl F. Izzard; Chesley J. Posey; and Carl E. Kindsvater and Rolland W. Carter

Synopsis

Area constrictions in many forms are encountered in both natural and artificial open channels. The hydraulics of transitions, control sections, and bridge piers and piles has been extensively investigated in the field and in the laboratory. It is remarkable, therefore, that most investigations of obstructions in bridge waterways have ignored the fact that the waterway itself is a definitive example of a width constriction in the river channel. The bridge waterway is studied in the basic research described in this paper.

The effect of an area constriction on the hydraulics of steady, open-channel flow depends on the geometry of the flow boundaries, the rate of flow, and the physical properties of the fluid. The resulting flow pattern is not subject to a general analytical solution. A practicable solution of the discharge equation has been achieved by the application of a systematic experimental investigation to an approximate analysis. Experimental data, which extend the solution to a wide variety of boundary conditions, are presented in dimensionless, graphical form. A significant feature is a detailed description of the external and internal characteristics of the flow pattern.

Notation

The letter symbols adopted for use in this paper are defined where they first appear, in the illustrations or in the text, and are arranged alphabetically for convenience of reference in the Appendix.

Note.—Published, essentially as printed here, in August, 1954, as *Proceedings-Separate No. 467*. Positions and titles given are those in effect when the paper or discussion was received for publication.

[1] Prof. of Civ. Eng., Georgia Inst. of Technology, Atlanta, Ga.

[2] Staff Engr., Geological Survey, U. S. Dept. of the Interior, Surface Water Branch, Water Resources Div., Atlanta, Ga.

INTRODUCTION

Purpose of the Investigation.—For several years the Water Resources Division of the Geological Survey, United States Department of the Interior (USGS), has conducted field and office investigations of various "indirect" methods for determining flood discharge. Among these methods was the "contracted-opening" method. Certain unexplained inconsistencies revealed in these investigations resulted in the authorization of a program of fundamental research on the contracted-opening method. The purposes of the research begun in February, 1951, were (1) to acquire a critical knowledge of the mechanics of the flow of water through width constrictions in open channels and (2) to develop, if possible, a practicable method (based on field surveys of flood marks and channel characteristics) for computing the discharge through bridge waterways.

It was immediately recognized that the attainment of the second objective would depend entirely on a preliminary success in accomplishing the first objective. It was also realized that the flow pattern involved was not subject to a general analysis and that the attainment of the first objective would depend largely on a carefully controlled experimental investigation of certain basic boundary forms. It was anticipated that the laboratory study would not only establish the relative influence of the various flow parameters and primary geometric variables, but that a general method of evaluating the discharge function could be developed and subsequently verified by a systematic examination of the influence of additional boundary conditions. Thus, during the first phase of the investigation, the ultimate objective was subordinated to an intensive investigation of the arbitrarily defined fundamental problem of tranquil flow through open-channel constrictions. This part of the research is believed to have general significance as a basic tool in applied fluid mechanics.

Scope of the Investigation.—The flow of water through bridge waterways was the definitive problem in the determination of the scope of the research. Normally, this example of rapidly varied motion involves steady, turbulent flow, entirely in the tranquil range. The submerged parts of the highway embankments, bridge abutments, and piers comprise an abrupt width constriction in the natural channel.

The variety of natural boundary conditions, considering the adjacent channel reaches and the constrictive elements, is almost unlimited. It was therefore necessary to restrict the basic investigation to certain elementary boundary forms which could be easily described and conveniently reproduced in the laboratory. Thus, the constrictions used in the experimental studies were limited to the forms made possible by the use of vertical walls of various lengths, widths, and corner roundings. Limitations on the relative size and location of the constrictions, the range of stream velocities, depths of flow, channel configurations, and channel roughnesses were governed by an arbitrary definition of the normal, single-opening bridge waterway.

The effects of piers and piles, multiple openings, and sloped embankments were not investigated during this phase of the research. By restricting the study to tranquil flows through constrictions simulating bridge waterways, certain problems which are associated with shaped transitions in artificial channels were also excluded. These exclusions were justified, in part, by the fact that other investigations[3,4,5,6,7] had provided satisfactory solutions to many aspects of the problems related to transitions and critical-flow control sections. It is of interest to note that the variety of boundary conditions considered is equal to, if not greater than, that covered by available information on the orifice, which is the closed-conduit counterpart of the problem investigated.

Review of the Literature.—Information (published prior to 1953) on the theory and methods of computing flow through open-channel contrictions is both rare and inconclusive. Ivan E. Houk,[8] M. ASCE, reporting methods of computing flood discharges used by the Miami (Ohio) Conservancy District, was probably the first to describe the contracted-opening method. Mr. Houk credited S. M. Woodward for the procedure used by the District. Mr. Houk showed that the discharge equation underlying Mr. Woodward's analysis was identical with that which described the flow through a venturi tube—that is, a form of the combined energy and continuity equations. The discharge equation offered by Mr. Houk included a coefficient which was primarily a contraction coefficient.

E. W. Lane,[5] M. ASCE, is the first known investigator in the United States to have studied simple width constrictions in the laboratory. However, his work was concerned primarily with higher Froude numbers than are usually involved in natural flow under bridges, and the variety of boundary forms studied by Mr. Lane was extremely limited.

D. L. Yarnell, in his research on flow past bridge piers, made an extensive study of the literature, which is annotated in his report.[9] Mr. Yarnell's experiments ignored the effect of the bridge abutments. For his analysis, Mr. Yarnell selected

> "* * * the bridge-pier formulas most commonly used in the United States * * * d'Aubuisson's, Nagler's, Weisbach's, and Rehbock's."[9]

Mr. Yarnell dismissed as unsound the Weisbach formula, which assumes that the total flow through a constricted section is the sum of an orifice discharge and a weir discharge. This conclusion, which Mr. Houk had previously stated, is generally accepted. The d'Aubuisson formula, in its basic form, is simply the discharge equation which results from a simultaneous solution of the continuity and energy equations. Therefore, the resulting equation is essentially the same as that suggested by Mr. Woodward and should not be

---

[3] "The Hydraulic Design of Flume and Siphon Transitions," by J. Hinds, *Transactions*, ASCE, Vol. 92, 1928, p. 1423.

[4] "The Flow of Water in Flumes," by F. C. Scobey, *Technical Bulletin 393*, U.S.D.A., Washington, D. C., December, 1933.

[5] "Experiments on the Flow of Water Through Contractions in an Open Channel," by E. W. Lane, *Transactions*, ASCE, Vol. 83, 1919–1920, p. 1149.

[6] "High-Velocity Flow in Open Channels: A Symposium," *ibid.*, Vol. 116, 1951, p. 265.

[7] "Channel Transitions and Controls," by Arthur T. Ippen, in "Engineering Hydraulics," edited by H. Rouse, John Wiley and Sons, Inc., New York, N. Y., 1950, Chapter VIII, p. 496.

[8] "Calculation of Flow in Open Channels," by Ivan E. Houk, *Technical Reports*, Miami Conservancy District, Dayton, Ohio, Part IV, 1918.

[9] "Bridge Piers as Channel Obstructions," by David L. Yarnell, *Technical Bulletin 442*, U.S.D.A., Washington, D. C., November, 1934.

termed an empirical "formula." The Nagler and Rehbock equations are essentially forms of the discharge equation which have been adapted specifically to the bridge-pier problem. These equations are more logically termed empirical formulas.

In 1944, the USGS began using a procedure for estimating the flow through area constrictions which was based on a form of the d'Aubuisson equation. The USGS (as a result of Mr. Houk's work and of a limited number of field observations) used values of the coefficient of discharge that were related to the degree of rounding of the upstream edges of the constriction.

Laboratory Arrangement.—Laboratory tests made as a part of the investigation were conducted in the hydraulics laboratory of the Georgia Institute of Technology, at Atlanta, through arrangements with the Georgia Tech Research Institute. The principal item of equipment was a steel flume 18 in. high and 10 ft wide, with a usable, uniform-flow length of approximately 21 ft. Water was supplied from the laboratory's recirculating system. Discharges were measured by use of either a venturi meter or a bend meter, both located in the supply piping. Water levels were measured by manometer-connected floor piezometers, portable static tubes, and point gages. Velocities were determined by a small (Pygmy) current meter and pitot tubes.

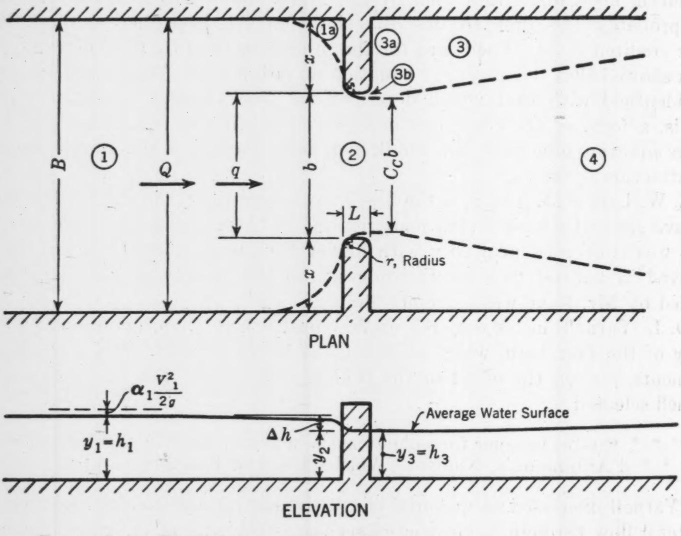

PLAN

ELEVATION

Fig. 1.—Simple Width Constriction in a Horizontal Rectangular Channel

Constrictive elements and false walls were constructed of concrete, aluminum, or exterior-grade plywood. Artificial channel roughness was created by various arrangements of chain-link fencing fastened to the smooth, concrete floor of the flume. Experimentally determined values of Manning's n corresponding to the three degrees of roughness investigated were 0.012 (for the smooth floor), 0.027, and 0.036. Irregular channel cross sections were produced by placing various arrangements of $\frac{1}{2}$-in.-thick, cement-asbestos board on the floor of the flume. Manning's n for the board (smooth side) was determined to be 0.011 within the range of conditions tested.

DESCRIPTION OF THE FLOW PATTERN

General.—There is particular reason for including a detailed examination of the external and internal flow characteristics in an investigation of the open-channel constriction.

Because the experimental investigation must be limited to certain basic boundary conditions, the successful application of the results to practical problems will depend, to a large extent, on a critical knowledge of the internal mechanism of the flow. Equally important, however, is an understanding of the external characteristics of the flow pattern so that the data required for proper application of the results can be determined. There is ample evidence that the failure to recognize the critical variables has accounted for many of the inconsistencies attributed to the contracted-opening method of computing discharge.

The External Picture.—Fig. 1 illustrates certain basic boundary conditions and hydraulic characteristics of flow through simple width constrictions in rectangular open channels. The beginning of acceleration of the central body of water approaching an open-channel constriction is indicated by a slight decrease in water surface level at a distance upstream from the face of the constriction approximately equal to the width of the opening. Deceleration occurs along the outer boundaries, and a separation zone is created in the corner adjacent to the constriction (zone 1a in Fig. 1). The size of the separation zone and the amount by which its surface level differs from the full stagnation level is a function of the upstream channel characteristics and the geometry of the constriction.

Water from the sides enters the opening as a sharply curved and contracting stream, indicating that it is being accelerated in directions both normal and parallel to the streamlines. Just as the longitudinal acceleration and the consequent negative pressure gradient is reflected as a drop in the longitudinal profile, the normal acceleration accounts for a considerable difference in level between the outside filaments of flow and the central filaments of flow. It generally happens that the greater part of the total drop in average surface level occurs very near the upper face of the constriction.

As the water passes through the constriction, the contracted stream reaches a minimum width at section 2 which corresponds to the vena contracta in orifice flow. The flow is bounded here by an eddying body of water in zone 3 which marks a second separation zone. Expansion of the live stream begins at the vena contracta and ends at the section of normal regimen in the full-width channel section 4. The length of channel required for this process depends on the boundary configuration, the roughness of the channel, and the magnitude of the pertinent flow parameters. Hunter Rouse,[10] M. ASCE, working with a two-dimensional orifice discharging into the atmosphere, found that the nominal boundary of the expanding jet would have a slope of 1 on 4 with respect to the longitudinal axis. H. R. Henry,[7,10] working with the two-dimensional discharge below a sluice gate (wherein the expansion is limited by a fixed lower boundary and a free-surface upper boundary), reported a slope of approximately 1 on 6.

---

[10] "Diffusion of Submerged Jets," by M. L. Albertson, Y. B. Dai, R. A. Jensen, and Hunter Rouse, *Transactions*, ASCE, Vol. 115, 1950, p. 639.

The average level of the stream at the vena contracta (section 2) is approximately equal to the level in the downstream separation zone (3). The level of the fully expanded jet at section 4 is usually higher than that in zone 3. The latter relationship is a function of the shape and friction characteristics of the channel between these sections.

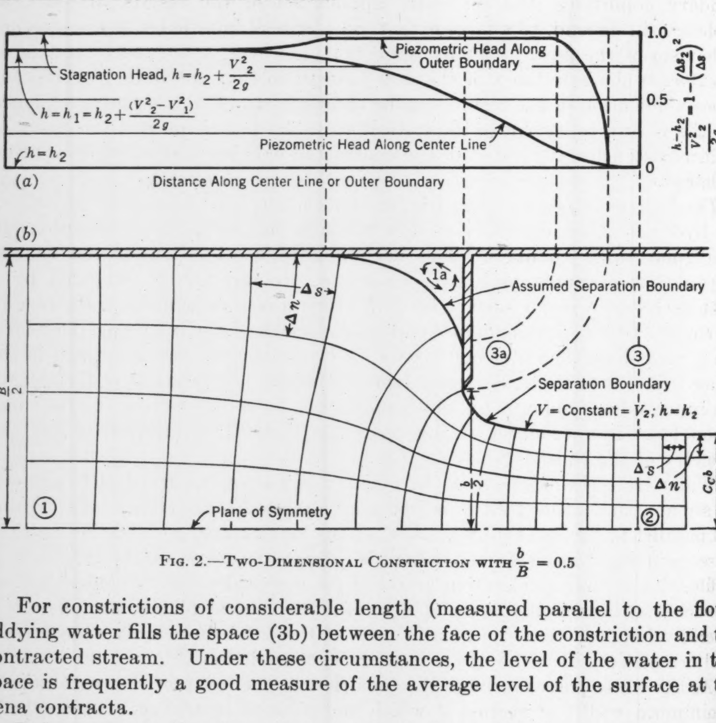
Stagnation Head, $h = h_2 + \frac{V^2_2}{2g}$
$h = h_1 = h_2 + \frac{(V^2_2 - V^2_1)}{2g}$
$h = h_2$
Piezometric Head Along Outer Boundary
Piezometric Head Along Center Line
1.0
0.5
0
$\frac{h-h_2}{\frac{V^2_2}{2g}} = 1 - \left(\frac{\Delta s_2}{\Delta s}\right)^2$
(a)
Distance Along Center Line or Outer Boundary
(b)
Δs
Δn
1a
Assumed Separation Boundary
3a
3
Separation Boundary
V = Constant = V_2; $h = h_2$
$\frac{B}{2}$
$\frac{b}{2}$
Δs
Δn
$C_c \frac{b}{2}$
1
Plane of Symmetry
2

FIG. 2.—TWO-DIMENSIONAL CONSTRICTION WITH $\frac{b}{B} = 0.5$

For constrictions of considerable length (measured parallel to the flow), eddying water fills the space (3b) between the face of the constriction and the contracted stream. Under these circumstances, the level of the water in this space is frequently a good measure of the average level of the surface at the vena contracta.

It is apparent, therefore, that certain factors which have a dominant influence on the flow pattern deserve closer attention. It is of particular importance to examine the effect of the fixed boundaries, the separation boundaries, and the upper, free-surface boundary on the distribution of velocities and surface elevations over the flow pattern. Under similar circumstances, a flow net is frequently utilized. In this case, however, the same restrictions which prohibit the accomplishment of a general analytic solution also prohibit the construction of a flow net. By temporarily ignoring the influence of the free surface, however, an approximate flow net can be drawn on the basis of an analogy with the classic, two-dimensional orifice.

The Orifice Analogy.—Within the specified limits of the investigation, the accelerated motion in the vicinity of an open-channel constriction can be considered to be primarily two-dimensional in the horizontal plane. Subject to obvious theoretical and practical limitations, it follows that the flow pattern can be approximated by a flow net drawn for a two-dimensional constriction.

Fig. 2(*b*) shows a thin-plate orifice, or slot, located symmetrically in—and normal to—parallel boundaries. The fluid flowing is assumed to be incompressible, and it is assumed to fill the space downstream from the orifice. The flow net was constructed by approximate, graphical methods. In its preparation, it was assumed that velocities in the approach section were uniformly distributed between the boundaries, but that separation would occur in the corner upstream from the constriction. These are contradictory assumptions because the first implies irrotationality (corequisite to the assumption of a nonviscous fluid) and the second implies rotationality. Furthermore, the separation boundary shown in Fig. 2(*b*) is an arbitrarily assumed line, the exact location of which is indeterminate. These contradictions, which were required for the purposes of the analogy, are not unusual. The resulting flow net is not expected to be seriously in error for the case of smooth boundaries and high values of the Reynolds number.

It should be emphasized that the purpose of introducing the orifice analogy is to facilitate a qualitative—rather than a quantitative—analysis of the phenomenon under investigation. In fact, the main purpose is to make Fig. 2(*b*) available for the subsequent analysis of the internal flow picture. Fair agreement between the three-dimensional, open-channel flow pattern and the analogous two-dimensional pattern is expected only when the former is restricted to tranquil, turbulent flows in smooth, regular channels, with low to moderate degrees of channel contraction. The investigation of conditions outside this range is benefited indirectly by the analogy.

The Internal Picture.—Two specific occurrences of separation are indicated in Figs. 1 and 2(*b*). In the first instance, separation occurs near the corner formed by the conduit boundary and the upstream face of the constriction. The separation at this point is consistent with the admission that the flow of real fluids is accompanied by the existence of a boundary layer. Thus, the normal deceleration tendencies in the corner immediately adjacent to the boundary (where the limiting boundary-layer velocity is already zero) result in the reverse flow which initiates separation. The separation zone, designated as zone 1a in Fig. 2(*b*), is a region of eddying fluid under an essentially constant piezometric head equivalent to the piezometric head along the bounding streamline. Thus, the separation prevents the occurrence of a full stagnation head in the corner. The separation also influences the piezometric head and the velocity distribution over the adjacent flow pattern. The velocity discontinuity at the separation boundary creates eddies which result in a loss of energy.

The second instance of separation, shown in Figs. 1 and 2(*b*), is marked by the boundary between the contracted stream and the eddying fluid in the corners downstream from the constriction. Unlike the upstream separation zone, this zone is fixed by the boundary conditions and the assumption of irrotationality of the live stream. Thus, the jet outline is assumed to be identical with the free-surface boundary which would exist if the stream were not enclosed by the fluid flowing. Here, also, the piezometric head in the separation zone is essentially constant and equal to the piezometric head on the bounding streamline. From the properties of the flow net, furthermore, it is seen that the piezometric head in the separation zone must be equal to the piezometric head across the vena contracta. This conclusion is substantiated by the observation that, from Newton's second law, a piezometric-head gradient cannot exist across the boundary of the jet where that boundary is a straight line, for in that instance there is zero acceleration normal to the flow. It also follows from this principle that the piezometric head in the zone adjacent to the downstream side of the constriction (zone 3a in Fig. 2(*b*)) is essentially equal to that in zone 3 opposite the vena contracta because of the negligible accelerations which exist between these points.

Expansion of the Contracted Stream.—A description of the internal flow picture is not complete without an explanation of the expansion or diffusion and the resulting deceleration of the contracted stream downstream from the constriction. A knowledge of this process is of little significance in relation to the discharge equation but is prerequisite to an understanding of the energy transformations which occur downstream from the constriction.

In Fig. 2(*b*) the idealized boundary which divides the downstream separation zone from the live stream is not indicative of the disturbed flow which ordinarily characterizes this region. The boundary actually exists as a fairly smooth, steady surface only when a heavy fluid, such as water, discharges into a large space occupied by a relatively light fluid, such as air. When (as is assumed in this case) the fluid discharges into an enclosed space occupied by a fluid of similar density, the extreme velocity gradient at the separation boundary results in shear stresses sufficient to initiate violent eddy action. The end effect is a condition of instability wherein the kinetic energy of the live stream is steadily converted into turbulence energy, which is eventually dissipated through viscous shear.

As shear along the separation boundary results in deceleration of the live stream, the width of the jet increases in the direction of flow in accordance with the continuity relationship. Eddies created along the boundary result in lateral mixing of the two bodies of fluid until eventually the diffused jet occupies the full area of the cross section. Just as the fluid in the jet is decelerated, the fluid originally in the separation zone below the constriction is accelerated, entrained, and carried downstream by the mixing process. For steady flow to be maintained within the fixed boundaries, therefore, equal quantities of fluid must be exchanged across the boundary of the expanding flow. The circulatory flow which occurs in the separation region is thus a consequence of the mixing process and the slight pressure gradient which exists along the conduit boundary between the constriction and the expanded jet.

Distribution of Piezometric Head.—The assumption of irrotationality within the limiting streamlines shown in Fig. 2(*b*) permits the application of the constant-energy principle to all points in the flow. From the properties of the flow net, therefore, an equation can be written which relates the variation in piezometric head to the relative spacing of the streamlines. The piezometric head at any point on the surface of an open-channel flow (in which pressure is hydrostatically distributed) is equivalent to the elevation of that point. This assumption is valid if the accelerations in the vertical direction are relatively small. In this case, the only region in which vertical accelerations might account for minor departures from hydrostatic pressure distribution is in the region of maximum total acceleration, near the upstream corner of the constriction. Thus, the orifice flow net, drawn for purposes of analogy, yields an approximate picture of the variation of surface level in the vicinity of a similar open-channel constriction.

Because it is implied (in the assumption of irrotationality) that the fluid is "frictionless," the energy loss between any upstream section of a particular streamtube and a section at the vena contracta can be ignored. Thus, the Bernoulli equation takes the form,

$$\frac{V^2}{2\,g} + h = \frac{V^2_2}{2\,g} + h_2 \ldots\ldots\ldots\ldots\ldots\ldots\ldots\ldots (1)$$

in which V is the average velocity in the streamtube cross section; h is the piezometric head, defined as the sum of the pressure head and the elevation; and g is the gravitational acceleration. From the principle of continuity, as applied to the two-dimensional streamtube of width Δn,

$$q = V\,\Delta n = \text{a constant} \quad \ldots\ldots\ldots\ldots\ldots\ldots (2)$$

in which q is the unit discharge. From the properties of the flow net, the normal distance between the streamlines, Δn, is equal to the normal distance between the potential lines, Δs, at the same point in the flow. Therefore,

$$\frac{V}{V_2} = \frac{\Delta n_2}{\Delta n} = \frac{\Delta s_2}{\Delta s} \ldots\ldots\ldots\ldots\ldots\ldots\ldots\ldots (3)$$

Combining Eqs. 1 and 3 results in

$$\frac{h - h_2}{\dfrac{V^2_2}{2\,g}} = 1 - \left(\frac{\Delta s_2}{\Delta s}\right)^2 \ldots\ldots\ldots\ldots\ldots\ldots\ldots\ldots (4)$$

in which the term to the left of the equal sign is a dimensionless piezometric-head ratio and the term on the right is determined at every point in the flow pattern by the relative spacing of the streamlines. Because the geometry of the flow net is fixed by the geometry of the limiting streamlines, the piezometric-head ratio is independent of the absolute magnitudes of the reference head, h_2, the reference velocity, V_2, and the size of the orifice. The distribution of the piezometric head along the center line of the conduit and the upstream boundary of the orifice is shown in Fig. 2(*a*). These curves can be assumed to be fair approximations of the variation in the relative surface elevations at corresponding locations at the open-channel constriction. The ordinate scale in Fig. 2(*a*) corresponds to Eq. 4.

SIMPLE CONSTRICTIONS IN RECTANGULAR OPEN CHANNELS

Selection of the Independent Variables.—The flow pattern in the vicinity of an open-channel constriction is influenced by the physical properties of the fluid (assumed to be water throughout this paper), the rate of flow, and the shape and roughness of the constriction and adjacent channel reaches. In this case the influence of surface tension and compressibility can be ignored. In the region of comparatively rapid acceleration near the constriction, the influence of viscosity can be assumed to be relatively insignificant. Thus, the influence of fluid weight is presumed to be dominant among the physical forces which govern the motion pattern. The critical flow parameter, therefore, is the Froude number **F** expressed as

$$\mathbf{F} = \frac{V}{\sqrt{g\,y}} \qquad (5)$$

in which y is a significant depth.

Because only tranquil flows have been considered, the Froude number is always less than unity; because the range of depths is fixed by arbitrarily defined, normal, natural-channel conditions, the velocity and also the unit discharge are limited to comparatively narrow bounds.

The most distinctive influences, therefore, are those which constitute the boundary conditions. Among these influences are many natural boundary characteristics which are not independently expressible in terms of simple mathematical quantities. Others, such as roughness and channel shape, might be incorporated in a uniform-flow equation but they are conveniently omitted from an analysis of the discharge characteristics of the constriction. For purposes of an approximate analysis, therefore, certain boundary conditions which are peculiar to irregular natural channels are excluded. The subsequent examination considers only rectangular, level channels.

It is required to select the variables which play major, independent roles in influencing the motion pattern previously described. As nothing in the mechanical process of dimensional analysis will indicate the omission of critical independent variables, every possible variable must be examined. Certain significant flow characteristics, such as water levels and velocities, are omitted because they are dependent on variables which are more conveniently incorporated in a practical solution. Certain other variables, which are preferred for describing the analogous orifice pattern shown in Fig. 2(*b*), are necessarily replaced by variables better suited to the description of an open-channel flow.

Dimensional Analysis.—The variables selected and illustrated in Fig. 1 are believed to be sufficient to describe the average flow characteristics. The total discharge is denoted by Q; B is the width of the channel; b denotes the width of the opening; and $\Delta h = h_1 - h_2$ is the difference in piezometric heads (or surface levels, assuming hydrostatic pressure distribution) between the approach section (1) and the section of maximum contraction (2). The average depth of flow at section 2 is represented by y_2 (at least one depth must be included, and y_2 is assumed to be best defined as an average); L is the length of the constriction at the opening, parallel to the flow; and r denotes the radius of the rounding of the upstream corners of the constriction. The density ρ is not included as an independent variable because it is contained in the terms Δh and g.

With the selected variables assembled in a functional relationship,

$$f_1\,(Q,\,B,\,b,\,\Delta h,\,y_2,\,L,\,r,\,g) = 0 \ldots\ldots\ldots\ldots\ldots\ldots (6a)$$

they are combined by methods of dimensional analysis into a minimum number of significant ratios,

$$f_2\left(\frac{Q}{b\,y_2\,\sqrt{g\,\Delta h}},\ \frac{Q}{b\,y_2\,\sqrt{g\,y_2}},\ \frac{b}{B},\ \frac{y_2}{b},\ \frac{L}{b},\frac{r}{b}\right) = 0 \ldots\ldots\ldots (6b)$$

The first ratio in Eq. 6*b* is proportional to a coefficient of discharge, C, and the second is equivalent to F for the contracted stream. The other ratios are representative of the principal geometric properties of the boundary.

If Eq. 6*b* is written in the more significant form,

$$C = f_3\left(\mathsf{F},\ \frac{b}{B},\ \frac{y_2}{b},\ \frac{L}{b},\ \frac{r}{b}\right) \ldots\ldots\ldots\ldots\ldots\ldots (6c)$$

it is seen that, for any given form of boundary, the configuration of the free surface is a unique function of the Froude number of the contracted stream. That is, C is a constant for any given boundary and value of the Froude number.

The Discharge Equation.—The form of the discharge function indicated by Eq. 6*c* is approximated by combining the one-dimensional energy equation and the continuity equation between sections 1 and 2 in Fig. 1. It is appropriate, however, to recognize the two major energy losses which occur between the nominal approach section (1) and the section of maximum contraction (2). The least of these losses, designated as h_e, is the eddy loss caused by the turbulence engendered in the upstream separation zone. The greater loss is h_f, the boundary friction loss, which is primarily a function of the channel characteristics.

An additional consequence of recognizing the influence of the channel configuration and roughness is the introduction of factors that account for the nonuniform velocity distribution in the flow cross section. Thus, letting α represent the ratio of the average kinetic energy to the kinetic energy corresponding to the average velocity, the energy equation takes the form,

$$\alpha_1\,\frac{V^2{}_1}{2\,g} + h_1 = \alpha_2\,\frac{V^2{}_2}{2\,g} + h_2 + h_e + h_f \ldots\ldots\ldots\ldots\ldots (7)$$

Introducing C_c, the coefficient of contraction, in the equation of continuity results in

$$Q = B\,y_1\,V_1 = C_c\,b\,y_2\,V_2 \ldots\ldots\ldots\ldots\ldots\ldots\ldots (8)$$

Solving Eqs. 7 and 8 simultaneously for the discharge,

$$Q = \frac{C_c\, b\, y_2}{\sqrt{\alpha_2}} \sqrt{2\, g\, (h_1 - h_2 - h_e - h_f + \alpha_1 \frac{V^2_1}{2\, g}} \quad \text{(9)}$$

The terms h_f and $\alpha_1 \frac{V^2_1}{2\, g}$ are dependent primarily on the resistance characteristics of the approach channel. These terms are relatively independent of the variables which describe the accelerated motion through the constriction. In any practicable computation procedure, therefore, the factors are best evaluated separately for substitution in an equation such as Eq. 9. The terms h_e and α_2, however, are much less dependent on channel shape and roughness than on the geometry of the constriction. Thus, these factors are functions of the variables contained in Eq. 6. Therefore it follows that Eq. 9 can be written as

$$Q = C\, b\, y_2 \sqrt{2\, g \left(h_1 - h_2 - h_f + \alpha_1 \frac{V^2_1}{2\, g} \right)} \quad \text{(10)}$$

in which C incorporates the influence of h_e, C_c, and α_2. If it is assumed that

$$h_e = K_L \frac{V^2_2}{2\, g} \quad \text{(11)}$$

in which K_L is an energy-loss coefficient, from Eqs. 6c and 10, wherein C is a coefficient of discharge in the form indicated by Eq. 6c,

$$C = \frac{C_c}{\sqrt{K_L + \alpha_2}} = f_4 \left(\mathsf{F},\ \frac{b}{B},\ \frac{y_2}{b},\ \frac{L}{b},\ \frac{r}{b} \right) \quad \text{(12)}$$

In the foregoing description of the flow pattern, it was observed that the elevation of the water surface at the downstream side of the constriction (zone 3a in Fig. 1) is essentially equivalent to the elevation of the water surface at the section of maximum contraction (2). Under these conditions, it is possible to compute y_2 as the difference between the average level at 3a and the average bottom elevation at 2. In terms of natural-channel conditions, therefore, y_2 is approximately the difference between the average level of the water surface at the downstream face of the constriction and the average bottom elevation at a corresponding section across the opening. This is not only a very practicable procedure, but for all conditions (except, perhaps, extreme values of L/b) the depth computed in this manner, y_3, is a close approximation for y_2. Eq. 10 thus takes the form,

$$Q = C\, b\, y_3 \sqrt{2\, g \left(\Delta h - h_f + \alpha_1 \frac{V^2_1}{2\, g} \right)} \quad \text{(13)}$$

in which $\Delta h = (h_1 - h_3)$, the difference in water-surface elevations between the nominal approach section (1) and the downstream side of the constriction (3a). The discharge coefficient remains a function of the parameters contained in Eq. 12.

Experimental Verification of the Analysis.—In the preceding development the form of the discharge equation was determined by an approximate energy analysis. The significant parameters that govern the coefficient of discharge were determined from dimensional analysis of the assumed variables. The primary purpose of preliminary laboratory tests which were made in connection with this investigation was to substantiate the form of the discharge function and to establish the relative importance of each of the parameters. The functional relationship for C, expressed by Eq. 12, was assumed to be correct only to the extent that it was a dimensionally correct combination of the selected variables. It was assumed that failure to include all of the pertinent variables would be indicated by the inability to correlate all the experimental data by use of the derived parameters.

The preliminary exploratory tests were made in a laboratory reproduction of the basic boundary conditions shown in Fig. 1. These tests not only substantiated the selection of variables but demonstrated that the test procedure could be simplified by ignoring the influence of certain variables for all or part of the practical range. Thus, of the ratios contained in Eq. 12, it was indicated that the width ratio, b/B, is of major importance, whereas $\mathbf{F}$, L/b, and r/b are of less but appreciable importance in defining the C-function. The ratio y_2/b, a shape factor, appeared to have a negligible influence for the entire range of conditions which were considered to be practical.

With the ratio y_2/b eliminated, the functional relationship for C in Eq. 12 contains four ratios. Not more than two of these ratios can be shown conveniently, together with C, in any single graphical illustration of experimental results. Because of the necessity for developing a practicable computational procedure, the experimental data from the initial tests were examined in detail. After much study, a procedure was adopted which involved an approximation method for determining the complex interrelationships of the principal variables. The method was then substantiated by demonstrating that it would yield results of sufficient accuracy for the entire practical range of all the variables.

An Approximate Solution for Simple Constrictions.—The procedure adopted involved a base curve of the relationship between C, b/B, and L/b, which was first determined for certain arbitrary constant values of $\mathbf{F}$ and r/b. To complement the base curve, average "adjustment" curves were developed from systematic investigations of the separate influences of the latter ratios. In every case, the adequacy of the average curves was checked throughout a reasonable range of all the independent ratios. With these curves derived from the experiments, a straightforward procedure was achieved for computing the essential characteristics of flow through simple constrictions in level, rectangular channels.

SIMPLE CONSTRICTIONS IN IRREGULAR CHANNELS

The General Problem.—An analysis of discharge characteristics and a satisfactory computational procedure have been presented for a definitive, simplified example of an open-channel constriction. For this basic case, the coefficient of discharge was shown to be a function of five independent ratios, one of which was eliminated as a result of a laboratory investigation. One of the remaining ratios is a flow parameter—characteristic of all gravity-controlled phenomena—the Froude number. The other ratios are descriptive of the geometry of the constriction. The geometry of the channel in which the constriction is located is involved, to only a minor extent, in the evaluation of the friction-loss term in the discharge equation.

However, it is necessary to extend the analysis to the more complex boundary conditions involved in the definitive practical problem—the bridge waterway. Outstanding among these complexities are the configuration and roughness of the channel. It is assumed that the friction loss can be computed by use of the Manning formula or a similar open-channel-flow formula. But the influence of a rough, irregular channel on the efflux characteristics of the constriction is a matter which cannot be evaluated by analytic means, nor can it be approximated by analogy with the common orifice. This, then, is the principal objective of an extended analysis.

Additional Variables in the Extended Analysis.—As specified under the heading, "Introduction: Scope of the Investigation," this study is restricted to certain basic boundary conditions. The simplest of these, as illustrated in Fig. 1, were involved in the successful accomplishment of an approximate solution. The extended analysis involves irregular channels of varied roughness patterns and three additional conditions relative to the shape and arrangement of the constriction in the channel.

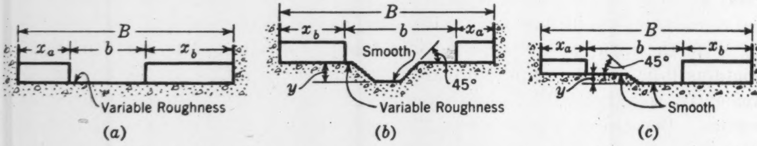

FIG. 3.—VARIATIONS IN SHAPE OF CHANNELS (SEE TABLE 1)

The channel in the vicinity of natural-channel constrictions is irregular in the sense that it is comprised of a main channel and one or two overbank, flood channels. The cross-sectional shapes tested in the laboratory are shown in Fig. 3 and the corresponding dimensions are listed in Table 1. As indicated in Fig. 3 and Table 1, the relative width occupied by the overbank channel was assumed to vary, and the constricted waterway was assumed to include various proportions of main channel and flood channel. It was also assumed that each of the component sections might possess different roughness characteristics. Thus, the roughness patterns tested in the laboratory were composed of various combinations of artificial bottom roughnesses, varying, in terms of Manning's n, from 0.011 to 0.036. It was assumed that the channel would have the same shape and roughness characteristics downstream from the constrictions as upstream. Exploratory tests indicated that major variations in the shape of the downstream channel have no significant effect on the discharge characteristics of the constriction.

Anticipating that the channel shape and roughness characteristics do not have to be included in the array of independent variables involved specifically in the discharge function, only three new boundary parameters need be added to those contained in Eq. 12. These parameters are described as eccentricity, angularity, and entrance guide walls.

Whereas it was previously assumed that the constrictions would be symmetrically located with respect to the longitudinal axis of the channel, in the extended analysis it will be assumed that they might be eccentrically located. The degree of eccentricity, represented by the ratio e, is defined as the ratio of the length of the shorter obstruction to the length of the longer obstruction.

In the initial analysis, it was assumed that the parallel faces of the constrictive element were perpendicular to the parallel boundaries of the channel. Natural-channel boundaries are not necessarily parallel, and the thread of the stream is not necessarily perpendicular to the parallel plane of the constriction. Thus, in the extended analysis, an angle of skew or angularity, ϕ, is defined as the acute angle between the plane of the constriction and a line perpendicular to the thread of the stream.

The third added variable involves the shape of the upstream corners of the constriction. Exploratory tests indicated that rounding the downstream corners has an insignificant effect on the coefficient of discharge. In the initial analysis the upstream corners were taken to be either sharp or rounded to circular arcs. In this analysis it was assumed that the corners might have diagonal, plane faces, simulating vertical guide walls. A single variety of guide walls (set at 45° as indicated in Fig. 9, to be shown subsequently) was investigated. Verification of the approximate solution as applied to this design should be adequate evidence of the validity of the solution. The ratio W/b is a measure of the relative length of the guide wall.

TABLE 1.—VALUES OF THE VARIABLES SHOWN IN FIG. 3.

Figure	B, in feet	b, in feet	$e = \frac{x_a}{x_b}$	y, in feet
3(a)	2.50 to 10.00	1.00 to 8.00	0.00 to 1.00	
3(b)	5.56 to 9.05	1.34 to 5.23	0.79 to 1.00	0.17 to 0.33
3(c)	9.50	2.40	0.73	0.17

The additional boundary conditions impose certain qualifications on the parameters included in Eq. 12. Thus, areas cannot be computed as simple products of depths and widths, velocities cannot be assumed to be uniformly distributed across the channel, and depths cannot be referred to a horizontal bottom datum. The most disturbing consequence, however, is the changed significance of the width ratio, b/B.

The Channel-Contraction Ratio.—The width ratio, b/B, was previously used as a convenient measure of boundary geometry. For rectangular cross sections this ratio is proportional to an area ratio. With a uniform velocity distribution across the section, the ratio is also equivalent to a discharge ratio. If the ratio q/Q is substituted for b/B, however, q/Q is seen to possess a greater significance. As illustrated in Fig. 1, q is that part of the total discharge Q which occupies an area of width b in the total cross section upstream from the constriction. To extend this definition to the general case, q is defined as the normal discharge capacity of a channel having the area characteristics of the opening and the roughness characteristics of the approach channel. As ordinarily defined, the "contraction ratio" is a measure of the relative constriction imposed on a given channel. Therefore, if m is defined as the channel-contraction ratio,

$$m = 1 - \frac{b}{B} = 1 - \frac{q}{Q} = \frac{Q - q}{Q} \quad \text{(14)}$$

A significant physical interpretation of the channel-contraction ratio is suggested by the last term in Eq. 14. That is, m can be interpreted as a measure of that part of the total flow which enters from the sides into the contracted stream.

The particular advantage of this concept in connection with the general bridge-waterway problem is that the channel-contraction ratio for irregular, natural channels can be computed as a ratio of hydraulic conveyances. Thus, even for the most extreme combinations of varied depths, alinements, and roughnesses in the approach channel, m can be evaluated from

$$m = 1 - \frac{q}{Q} = 1 - \frac{K_q}{K_Q} \quad \text{(15)}$$

in which K_q is the conveyance of that part of the approach channel occupied by the discharge q, and K_Q is the conveyance of the total section. Conveyance is defined, in terms of the Manning formula, as

$$K = \frac{1.49}{n} A \, R^{\frac{2}{3}} \quad \text{(16)}$$

in which A is the area, and R is the hydraulic radius of the cross sections under consideration.

The General Discharge Equation.—Substituting the three new boundary parameters in Eq. 12, the functional relationship for the coefficient of discharge in Eq. 13 becomes

$$C = f_5\left(\mathsf{F}, \; m, \; \frac{y_3}{b}, \; \frac{L}{b}, \; \frac{r}{b}, \; e, \; \phi, \; \frac{W}{b}\right) \quad \text{(17)}$$

To account for irregular cross sections at the constriction, the depth, y_3, is defined as the difference between the water-surface elevation at the downstream side of the constriction, adjacent to the contracted stream, and the average bottom elevation across the opening. It should be emphasized that y_3 is assumed to be an adequate substitute for y_2, the depth of the contracted stream at the vena contracta. The difference between these two depths is small for all but the larger values of L/b, and even in the latter instance the difference is a function of the variables contained in Eq. 17. Thus, the experimentally determined values of the coefficient of discharge always contain the effect of this approximation.

VERIFICATION OF THE APPROXIMATE GENERAL SOLUTION

Experimental Procedure.—The verification procedure used for the general solution involved a systematic investigation of the influence of each of the independent variables contained in Eq. 17. Ideally, this procedure would require that the variation of C with each independent variable be measured for a full range of each of the remaining variables. An almost unlimited variety of conditions would be involved. Actually, considering the minor influence of certain variables, the procedure was simplified by analyzing and correlating the test results as the experiments were made. The only conditions tested, therefore, were those required to define a series of curves capable of correlating the significant variables for a practical range of each. This leads to the procedure described previously for the approximate solution of the simple constriction in rectangular channels. In this case, however, many more tests were needed to develop the average adjustment curves required for the approximate computation procedure. The range of variables tested and the process of developing the empirical relationships are described subsequently.

Computation of the Friction Head.—It was considered sufficient to investigate only three channel roughnesses in the laboratory. The smoothest boundary condition resulted when a cement-asbestos board (smooth surface up) was used to create irregular channel cross sections in the flume. The Manning n for this surface, as determined by experiment, was 0.011. The Manning n for the concrete floor of the flume was 0.012, which is not sufficiently different from that for the cement-asbestos board to be considered a distinct degree of roughness. With one layer of 11-gage, 2-in. mesh, chain-link fencing covering the floor, the measured n was equal to 0.027. Maximum roughness was created by use of two layers of chain-link fencing, for which n was equal to 0.036. The net flow area used in computing n for conditions involving the wire fencing was the gross area of the section minus the average cross-sectional area occupied by the wire. The average depth was computed as the ratio of the net area to the top width of the section.

It is recognized that the principal effect of increased channel roughness is an increase in the differential head across the constriction. Thus, as roughness increases, evaluation of the net velocity head at section 2,

$$\frac{V^2_2}{2g} = \Delta h - h_f + \alpha_1 \frac{V^2_1}{2g} \qquad (18)$$

is increasingly dependent on an accurate evaluation of h_f, the loss of head caused by friction between sections 1 and 2. For smooth channels and relatively large values of the channel-contraction ratio, h_f is insignificant relative to the drop in water surface, Δh. For extremely rough channels, especially those that contain considerable amounts of tree growth and brush, the computation of friction losses in the accelerated flow approaching the constriction is subject to errors of judgment as well as errors in method.

The procedure used in computing h_f in the verification tests was the standard method used by the USGS. Briefly, the method consists first of computing the average energy gradients at the nominal approach section (1) and at the constricted section (2). The energy gradient (slope) is computed as the square of the ratio of the discharge to the conveyance of the section under consideration. The total friction loss is then computed as the head loss in the reach between section 1 and the upstream face of the constriction, plus the head loss through the constriction (appreciable only for larger values of L). For the upstream reach, the head loss is defined as the geometric mean of the average gradients at the end sections times the length of the reach. The loss in the constriction is the product of the average gradient at the constricted section and the length of the constriction. Acknowledged weaknesses in this method of computation apparently did not affect its validity for the conditions tested.

Location of the Approach Section.—The approach section is defined as the section which marks the beginning of acceleration of the flow approaching the constriction. Because this is not distinctly defined as a line across the flow pattern, it is more difficult to determine by measurement in the field than it is in the laboratory. For practical purposes in this case, the beginning of acceleration (or beginning of drawdown as it is frequently termed) is of most concern at the boundaries. In terms of high-water marks, it is desirable to be able to determine the beginning of the drawdown on the upstream face of the embankment as well as on the banks of the stream. The error which results from inaccurate determination of this location is reflected in the discharge equation as an error in Δh. When the friction head is small, therefore, this error can be avoided by making a generous estimate of the distance from the constriction to the approach section. When the friction head is appreciable, the assumption of too long an approach section results in a small positive error in the computed value of h_f. This is seldom of significance in the range of conditions considered.

The location of the approach section is influenced primarily by the Froude number and the channel-contraction ratio. Tests were made mainly for the purpose of establishing a rough general rule for locating the nominal approach section. The tests indicate that a convenient and adequate approximation of the length of the approach reach, measured along the center of the channel, is a distance equal to the gross width of the opening, b.

The field conditions for which high-water marks along the upstream face of the embankment may ordinarily comprise the best source of data are those corresponding to larger channel-contraction ratios. In this case, for values of m greater than 0.80, the average water-surface elevation in the approach section may be approximated as the elevation of the water at a point a distance equal to one half the width ($b/2$) from the nearest corner of the opening.

Computation of the Average Kinetic Energy.—An additional effect of the channel shape and the boundary roughness is reflected in the magnitude of the factor α_1 in the kinetic energy term $\alpha_1 \frac{V^2_1}{2g}$. This term and the term h_f in the discharge equation, Eq. 13, are generally of approximately equal magnitude for the conditions considered. Both quantities are ordinarily small in comparison with the total measured drop, Δh. The coefficient α_1 was evaluated on the basis of detailed velocity surveys for several conditions of flow. It was found to vary from 1.06, for relatively large depths of flow in irregular sections, to 1.10 for smaller depths in rectangular channels. These average values were used in the computations. The error involved in estimating α_1 for a natural channel is ordinarily smaller than the error involved in estimating n.

Evaluation of the Discharge Coefficient.—The approximate computation procedure described in connection with the verification of the basic analysis will also be used for the expanded analysis. Previously, this procedure necessitated the determination of a "standard" empirical relationship between the three most critical independent variables contained in the functional equation for C, Eq. 14. The variables selected for this purpose are C, m, and L/b. Ignoring the ratio y_3/b, which was shown by experiment to be insignificant, the standard condition is then defined as that for which the remaining ratios are constant and equal to the following values: $\mathsf{F} = 0.5$; $r/b = 0$, $e = 1$, $\phi = 0°$, and $W/b = 0$. From the experimental data for the standard condition, a family of base curves showing the relationship between C, m, and L/b was constructed. Individual "adjustment" curves were then developed from systematic investigations of the separate influence of the ratios F, r/b, e, ϕ, and W/b. In each case, as for the basic analysis, the adequacy of the average adjustment curves was then tested throughout a reasonable range of all the related ratios.

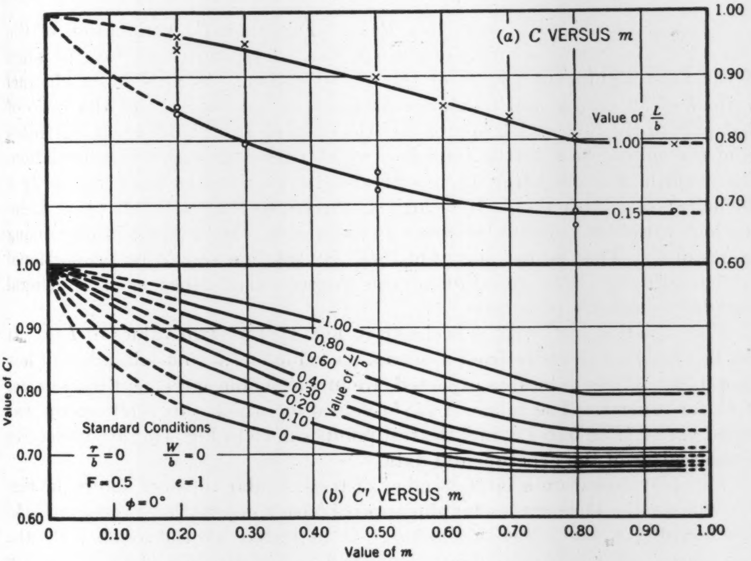

FIG. 4.—VARIATION OF DISCHARGE COEFFICIENT C AND C' WITH m AND L/b

The method of applying the experimentally determined functional relationships to the computation of the coefficient of discharge is as follows: For a given case, C' is equal to the "standard" value of the coefficient of discharge, corresponding to the standard values of F, r/b, e, ϕ, and W/b, and the given values of m and L/b; k_{F} denotes a coefficient which, multiplied by C', will yield a coefficient of discharge adjusted for the effect of the given Froude number, F; k_r is a coefficient similar to k_{F} which adjusts the coefficient of discharge for the given corner-rounding ratio, r/b; k_e represents a coefficient similar to k_{F} which adjusts the coefficient of discharge for the given eccentricity, e; k_ϕ is a coefficient similar to k_{F} which adjusts the coefficient of discharge for the given angularity, ϕ; and k_w denotes a coefficient similar to k_{F} which adjusts the coefficient of discharge for the given guide-wall ratio, W/b (this coefficient cannot exist concurrently with $r/b > 0$). It follows that the adjusted coefficient of discharge can be computed from the equation,

$$C = (k_{\mathsf{F}}\, k_r\, k_e\, k_\phi\, k_w)\, C' \leqq 1.0 \dots\dots\dots\dots\dots (19)$$

Effect of the Channel-Contraction Ratio.—Experimental verification of the concept of the channel-contraction ratio in terms of conveyances (Eq. 15) is one of the most significant results of this investigation. As applied to channel sections of all shapes and roughness patterns, m is a measure of the ratio of that part of the flow which approaches the opening from bank areas upstream from the constriction to the total flow which passes through the constriction. The coefficient of discharge, C, was previously described as being primarily a coefficient of contraction. It is logical, therefore, that with all other independent variables constant, increasing values of m should result in decreasing values of C. That is, the degree of "jet" contraction should be proportional to the ratio m. Substantiation of this concept establishes m as a general boundary-geometry parameter.

The variation of C with m is shown in Fig. 4(*a*) for two values of L/b. It can be seen that C varies from a maximum value of 1.0 to a minimum of less than 0.70. These values, as expected, are in reasonable agreement with values of C_c for orifices. The range of (L/b)-values for which this relationship was tested varied from 0 to 1.0, and the test points shown in Fig. 4(*a*) are indicative of the scatter of the experimental data.

Fig. 4(*b*), based on a large number of tests similar to those shown in Fig. 4(*a*), shows the base curves for the approximate computation procedure. In this figure, the coefficient of discharge is indicated by the symbol C', the 'standard" value, corresponding to specified constant values of the secondary variables, F, r/b, e, ϕ, and W/b. The standard values of the secondary variables for Fig. 4(*b*) are the same as in Fig. 4(*a*).

It is significant that the definition of the curves shown in Fig. 4(*b*) was not only substantiated but was refined by plotting on the original a great many values computed from Eq. 19. Thus, Fig. 4(*b*) represents the composite of experiments made for a wide variety of channel configurations and different, nonstandard values of the secondary variables. The successful correlation of these data constitutes the most critical step in the verification of the approximate solution.

Effect of the Length Ratio.—The variation of C with the length ratio L/b is indicated by the vertical spread of the curves in Fig. 4(*b*). For all the conditions tested, L was measured as the perpendicular distance from the upstream face to the downstream face of the constriction. The width of the opening was measured as the minimum clear width between the vertical faces of the opening.

The primary effect of length, as indicated in Fig. 4(*b*), is to increase the coefficient of discharge by decreasing the contraction of the stream as it passes through the opening. That is, the contraction is suppressed, even at small values of L/b, by the negative pressure gradient which exists between the live stream and the eddying fluid which surrounds it. The existence of the pressure gradient is the result of the entrainment of the eddying fluid and the reduced opportunity for fluid in the downstream separation zone to replace that which is entrained. Thus, as L/b is increased, the area of access for the return flow (at the downstream corner of the opening) is increasingly constricted by the expansion of the stream, and the surface level in zone 3b in Fig. 1 tends to drop further below that at the end of the opening, at zone 3a. Simultaneously, however, this difference in level is decreased by the energy loss which results from the expansion process. As it is the level at zone 3a which is used in computing y_3 in the discharge equation, the effect of the first influence is to increase the apparent coefficient of discharge, and the effect of the head loss is to decrease the coefficient of discharge. The growth of these conflicting influences is indicated by the relative spacing of the curves in Fig. 4(*b*).

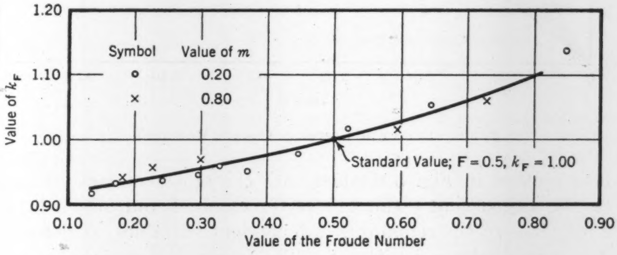

FIG. 5.—EFFECT ON DISCHARGE COEFFICIENT OF THE FROUDE NUMBER

Effect of the Froude Number.—The Froude number can be defined as a ratio of a typical unit inertial reaction to a typical unit weight force involved in a given fluid motion. Thus, a low value of the Froude number at any point in a free-surface flow pattern ordinarily indicates that gravity, or fluid weight, has a large influence on the motion at that point. In this case, the prerequisite of tranquil flow limits the Froude number in the contracted stream to values less than the critical value. Within this low range, however, larger values of **F** for the contracted stream are usually indicative of a relatively large drop in water level, Δh, and a relatively large change in Froude number between the approach section and the constricted section for any given boundary. Furthermore, the effect of gravity on the motion is partly removed by the condition of "submergence" which exists at the downstream side of the opening. Thus, the relative influence of the Froude number is proportional to Δh, which, for any given boundary geometry, increases with increasing values of **F** for the contracted stream.

The effect of the Froude number on the coefficient of discharge is indicated in Fig. 5, the first of the empirical adjustment curves. Here the value of **F** is the Froude number for the contracted stream and is computed from the equation,

$$\mathbf{F} = \frac{Q}{b\, y_3 \sqrt{g\, y_3}} \qquad (20)$$

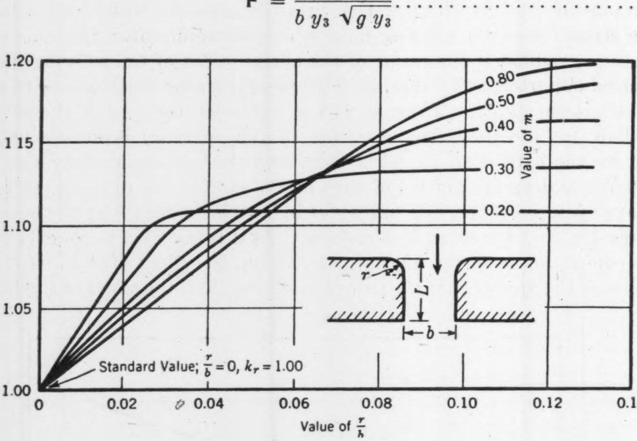

FIG. 6.—EFFECT OF UPSTREAM CORNER ROUNDING

Typical data plotted in Fig. 5 demonstrate the apparent lack of correlation between $k_{\mathbf{F}}$, the adjustment ratio, and m, the channel-contraction ratio. The modifying influence of the remaining independent variables, as determined by check tests, is similarly insignificant. The increasing positive slope of the adjustment curve with larger values of **F** is an indication of the increasing influence of the Froude number as the flow conditions approach the critical.

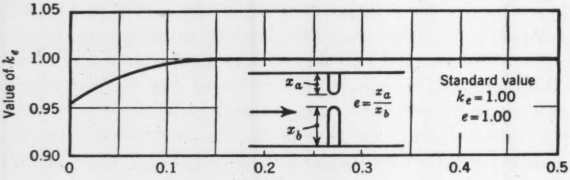

FIG. 7.—EFFECT OF ECCENTRICITY

Effect of Entrance Rounding.—The most common form of "streamlined" entrance for open-channel constrictions is that in which the upstream corners are rounded to circular arcs. Generally, identical forms are used for both the upstream and downstream corners, but the influence of the downstream streamlining is not well established. In this case, the laboratory tests indicated that the effect of rounding the downstream corners was negligible.

THE UNIVERSITY OF MICHIGAN LIBRARIES

The effect of rounding the upstream corners of the constriction was determined from tests covering a practical range of the relative radius of curvature, r/b. The results of these tests are shown in the form of adjustment curves in Fig. 6. It was necessary to include a third variable, m, in order to correlate the results with the standard values of the remaining independent variables.

The obvious effect of rounding is to suppress the contraction and increase the coefficient of discharge. The curves in Fig. 9 show, in general, that C increases at a diminishing rate until it reaches a maximum value. This maximum value of C corresponds to a value of C_c approaching unity. Under these limiting conditions, therefore, the coefficient of discharge reflects the boundary friction loss.

Effect of Eccentricity of Opening.—The opening is described as being eccentrically located when the length of one of the obstructions which comprise the constriction is greater than the other. It would appear that the principal effect of eccentricity would be to change the significance of the channel-contraction ratio in the functional relationship for C. The experiments show that the effect of e on the standard value of C is so small, however, that it can be ignored in most cases. The adjustment curve for the effect of eccentricity is shown in Fig. 7.

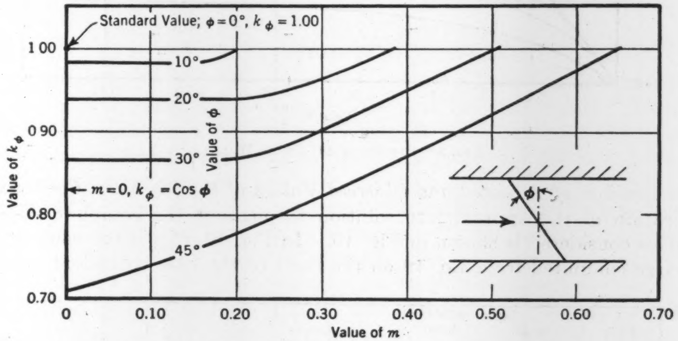

FIG. 8.—EFFECT OF ANGULARITY

Effect of Angularity.—When a constriction is skewed with respect to the main thread of the stream, the effective area of the opening is decreased. It follows that the coefficient of discharge is decreased in proportion to the magnitude of the skew angle, ϕ. In Fig. 8, results of experiments on the effect of ϕ are plotted as an adjustment curve for the standard value of C. The channel-contraction ratio is an important third variable. As indicated in Fig. 8, the limiting value of k_ϕ, corresponding to $m=0$, is equal to the cosine of ϕ. For this condition, of course, the channel is not constricted. It is apparent from Fig. 8 that the effect of angularity is very small for values of ϕ less than 20°.

Effect of Guide Walls.—The influence of diagonal guide walls at the entrance to the constriction is similar to that of streamlining. Only one form of

THE UNIVERSITY OF MICHIGAN LIBRARIES

guide wall was investigated in the laboratory. This involved plane, vertical walls set at an angle of 45° with the face of the constriction. Fig. 9 shows the effect of the guide walls on the standard value of the coefficient of discharge. The shape of the curves in Fig. 9 is logically similar to that shown by the rounding-ratio curves (Fig. 6).

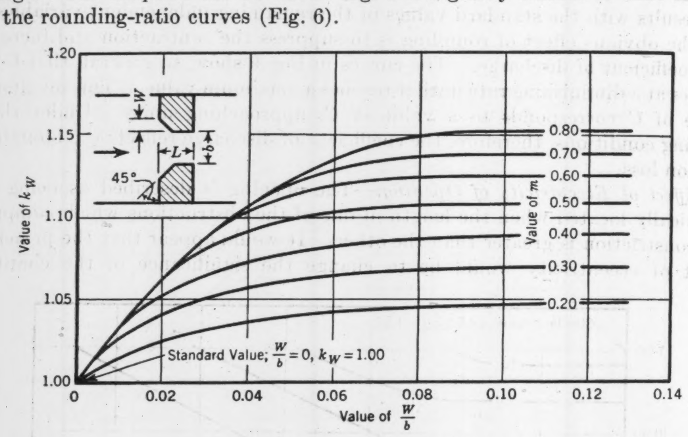

FIG. 9.—EFFECT OF 45° GUIDE WALLS

Comparison of Adjusted and Observed Values of the Discharge Coefficient.—Verification of the approximate solution throughout the complete range of variables considered is shown in Fig. 10. In Fig. 10, C_{adj} is the coefficient of discharge computed from Eq. 19 on the basis of the base coefficient diagram,

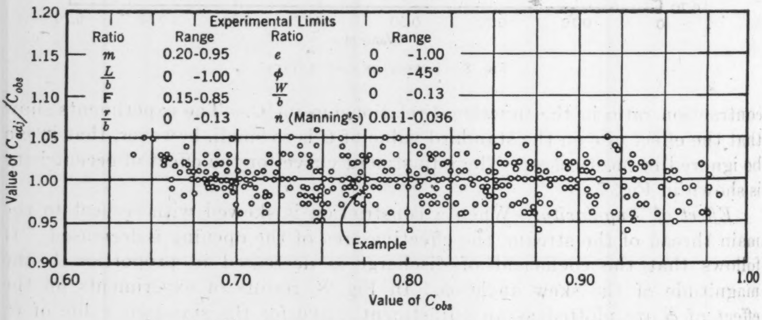

FIG. 10.—COMPARISON OF ADJUSTED AND OBSERVED VALUES OF C

Fig. 4(*b*), and the adjustment curves, Figs. 5 to 9, inclusive. The "observed" value of the coefficient, C_{obs}, is computed directly from Eq. 13 on the basis of the measured values of the primary variables.

The ratio of C_{adj} to C_{obs} is a measure of the relative accuracy of the solution. This ratio is plotted as a function of C_{obs} in Fig. 10. The indicated accuracy is satisfactory within the limits of the conditions tested. These limits are tabulated in Fig. 10.

Illustrative Example.—The recommended procedure for obtaining the adjusted coefficient of discharge from the experimental data is illustrated in the following example: These measured data correspond to a test condition arranged in a smooth, rectangular laboratory flume: $Q = 0.710$ cu ft per sec, $y_1 = 0.305$ ft, $y_3 = 0.255$ ft, $B = 10.0$ ft, $b = 2.00$ ft, $r = 0.083$ ft, $L = 0.81$ ft, $e = 1.00$, and $\phi = 0°$. Computed data are: $\Delta h = 0.050$ ft, $h_f = 0.001$ ft, $\alpha_1 \frac{V_1^2}{2g} = 0.001$ ft, $m = 0.80$, $\frac{r}{b} = 0.042$, $\frac{L}{b} = 0.41$, and $\mathbf{F} = 0.49$. For these conditions, C_{obs} computed from Eq. 13 is 0.774. This example involves only two adjustment ratios, $k_{\mathbf{F}}$ and k_r. Taking these from Figs. 5 and 6, respectively, for the conditions indicated, $k_{\mathbf{F}} = 0.995$ and $k_r = 1.085$. The corresponding standard value of the discharge coefficient is $C' = 0.705$. Thus, the adjusted value of the coefficient is $C_{adj} = k_{\mathbf{F}}\, k_r\, C' = 0.995 \times 1.085 \times 0.705 = 0.761$. The relative accuracy of the adjustment procedure in this case is indicated by the ratio $\frac{0.761}{0.774} = 0.984$, which is plotted in Fig. 10 ("Example").

CONCLUSIONS

A practicable method of solving the discharge equation for the tranquil flow of water through open-channel constrictions is described. The functional relationship between the coefficient of discharge and the principal independent variables is presented in the form of experimental data which were the result of a systematic laboratory investigation. Boundary conditions considered include vertical constrictive elements, channel cross-sectional shapes, and roughness patterns. Within the limits tested, the proposed computation procedure yields satisfactory results.

Applicability of the proposed solution to bridge waterways in natural channels will depend, to large extent, on a critical analysis of the factors controlling the flow pattern. For this reason, a significant part of the paper is devoted to a detailed consideration of the flow pattern.

ACKNOWLEDGMENTS

Much of the credit for the conception and accomplishment of this investigation is due Tate Dalrymple, A.M. ASCE, USGS, Washington, D. C., and M. T. Thomson, A.M. ASCE, District Engineer, USGS, at Atlanta. Preliminary studies of field data which emphasized the need for the present study were made by R. W. Carter and Jack Terry, A.M. ASCE, USGS, Denver, Colo. Engineer personnel of the Atlanta District, USGS, participated in the laboratory investigation.

APPENDIX. NOTATION

The following letter symbols, adopted for use in the paper and the guidance of discussers, conform essentially with American Standard Letter Symbols for Hydraulics (ASA-Z10.2-1942), prepared by a committee of the American Standards Association with ASCE representation, and approved by the Association in 1942:

A = area of channel cross section;
B = width of the channel;
b = width of the opening;
C = coefficient of discharge;
C' = "standard" value of the coefficient of discharge;
C_c = coefficient of contraction;
e = eccentricity ratio;
F = Froude number;
g = acceleration caused by gravity;
h = piezometric head;
  h_e = eddy loss between sections 1 and 2;
  h_f = boundary friction loss;
K = conveyance, from the Manning formula;
K_L = energy loss coefficient;
k = adjustment coefficient—ratio of the adjusted to the standard coefficient of discharge:
  k_e = adjustment coefficient for the effect of eccentricity;
  k_{F} = adjustment coefficient for the effect of the Froude number;
  k_r = adjustment coefficient for the effect of the corner-rounding ratio;
  k_w = adjustment coefficient for the effect of the guide-wall ratio;
  k_ϕ = adjustment coefficient for the effect of angularity;
L = length of the constriction;
m = channel-contraction ratio;
n = distance measured normal to the streamlines or the retardation coefficient in the Manning formula;
p = pressure intensity;
Q = total discharge at a channel cross section;
q = unit discharge in a rectangular section, or a part of the total discharge through a constriction;
R = hydraulic radius;
r = radius of a circular arc;
S = hydraulic slope;
s = distance measured parallel to streamlines;
V = average velocity;
v = velocity at a point;
W = width of the entrance guide walls;
x = linear horizontal distance;
y = depth of flow referred to the average bottom elevation at a cross section;
z = elevation referred to an arbitrary horizontal datum;
α = kinetic energy correction factor;
γ = specific weight of the fluid;
ρ = density of the fluid; and
ϕ = acute angle between the plane of the constriction and a line normal to the thread of the stream.

THE UNIVERSITY OF MICHIGAN LIBRARIES

DISCUSSION

Emmett M. Laursen,[11] A.M. ASCE, and **Arthur Toch**,[12] J.M. ASCE.—Within the limitations of the range of geometries used in the model investigations, the coefficients presented by the authors should aid greatly in the indirect determination of streamflows. The scatter of ± 5% in Fig. 10 indicates a higher degree of accuracy for the discharge coefficient than is likely to be obtained for Δh and m in the field. Because the limitations recognized by the originators of such solutions as this are too often misunderstood or ignored, two major limitations on the applicability of this method of determining stream discharges should be mentioned.

If the stream banks between zones 2 and 3 are covered with brush and trees, the water-surface elevation on the downstream side of the constriction may not be equal to that in the constriction. Depending on the density of the vegetal screen, the elevation of the water surface in zone 3 may rather more nearly approximate that elevation in zone 4. Although laboratory experiments with screens of known solidity ratio could determine this effect, in practice the difficulty of determining the density of a brush and tree cover would still remain. The companion work[13] to the paper might be used to obtain Δh in this case, but in using the curves therein, it is suggested that m be determined from the downstream discharge ratio. Because the slopes of the main channel and the flood plain would not be the same, the conveyance ratio should not be used.

If the bed of the stream is erodible, scour in the constriction may occur during a flood and the scour hole may be completely or partly refilled by the time the elevation of the bed of the stream is determined. Considerable error could thus, of course, be caused in the estimation of the depth of flow. An approximate indication of the order of magnitude of this effect has been made[14] by the writers.

The writers wish to express their admiration for the careful experimental work which forms the basis of this paper. It is agreed that the analysis, admittedly empirical, is the only one feasible; much more information is needed about the fundamentals of turbulent flow before a more rational analysis can be practicable.

Fred W. Blaisdell,[15] M. ASCE.—When the results of a comprehensive series of generalized tests are summarized in the few curves presented by Messrs. Kindsvater and Carter, it is difficult to realize the tremendous effort and large number of tests that are required to obtain these results. The writer and Charles A. Donnelly completed (in 1950) a generalized study of the capacity of the box inlet drop spillway;[16] the methods of analysis and presentation closely parallel those used by the authors. Because of this experience, the writer can fully appreciate what is meant by the statement (under the heading, "Simple Constrictions in Rectangular Open Channels: Experimental Verification of the Analysis") that "After much study, a procedure was adopted * * *." The benefit is well worth the effort for, in presenting their results, the authors have done much of the work required for the practical application of the results of their research.

---

[11] Research Engr., Iowa Inst. of Hydr. Research, State Univ. of Iowa, Iowa City, Iowa.

[12] Research Associate, Iowa Inst. of Hydr. Research, State Univ. of Iowa, Iowa City, Iowa.

[13] "Backwater Effects of Open-Channel Constrictions," by Hubert J. Tracy and Rolland W. Carter, *Transactions*, ASCE, Vol. 120, 1955, p. 993.

[14] Discussion by Emmett M. Laursen and Arthur Toch of "River-Bed Scour During Floods," by E. W. Lane and W. M. Borland, *ibid.*, Vol. 119, 1954, p. 1084.

[15] Project Supervisor, U. S. Dept. of Agriculture, Agri. Research Service, St. Anthony Falls Hydr. Lab., Univ. of Minnesota, Minneapolis, Minn.

As noted by Messrs. Kindsvater and Carter, the discovery that variations in the geometrical shape of the channel cross section can be expressed in terms of conveyances is certainly an interesting and valuable contribution. It is to be regretted that values of m less than 0.20 were not included in the test schedule. It would have involved only a little more work and would have eliminated questions that always arise when curves are extrapolated beyond the range of the tests. It may be that these low values of m are assumed to be outside the range of practical application. However, there may arise practical situations in which values of m will be less than 0.20. It has been the writer's practice to extend the range of laboratory tests well beyond the "practical" limits set by those experienced in the actual design of structures. Even so, subsequent practical applications outside this extended range of test variables have been frequent.

Tests at values of m less than 0.20 would have been particularly helpful in defining the effects of angularity, corner rounding, and guide walls. In the case of the adjustment curves for angularity, a large part of the curvature is at values of m less than 0.20. Although the curves are shown to be solid in Fig. 8, one must assume (according to the table in Fig. 10) that they must have been drawn without the benefit of experimentally determined points.

The comparison of the adjusted and observed values of C presented in Fig. 10 provides a crucial test of the analytical methods. The agreement shown is excellent. Although it is undoubtedly possible to obtain less spread in the data for individual curves, greater spread must be expected as adjustments are added. Compensating benefits include an expanded range of application and an increased reliability resulting from the greater volume of data required to define the coefficient and adjustment curves.

PIN-NAM LIN.[17]—The discharge coefficient has been virtually defined by Messrs. Kindsvater and Carter in two ways. It is defined in one case by the first dimensionless group in Eq. 6*b* and in the other by Eq. 10. Because h_f and $\alpha_1 V^2{}_1/2\,g$ in Eq. 10 have opposite signs it is possible that in many cases the two values of C are approximately the same. In general, the two definitions will yield different values of C; the case of channels having considerable tree growth and brush, cited by the authors, is an example. The apparent discrepancy, however, appears to be the result of an error in presentation because, if the first definition were to be considered, Eq. 6*a* should have included the coefficient α_1 as well as a variable to indicate the roughness of the channel. For a given boundary geometry at a given locality, Δh will vary not only with Q and y_2 but also with the channel roughness and the velocity distribution upstream of the constriction. When C is defined by Eq. 10, it is reasonable that C will be expressed by Eq. 12 or Eq. 17.

---

[16] "Hydraulic Design of the Box Inlet Drop Spillway," by Fred W. Blaisdell and Charles A. Donnelly, *Technical Paper No. 8-B*, St. Anthony Falls Hydr. Lab., Univ. of Minnesota, Minneapolis, Minn., January, 1951.

[17] Asst. Prof., Dept. of Civ. Eng., Colorado Agri. & Mech. College, Fort Collins, Colo.

Flow through channel constrictions at high values of m is accompanied by considerable surface curvature. As a result of the surface curvature, the acceleration in a vertical plane may be considerable. Analysis of a flow that is no longer "gradually varied" was first conducted by Boussinesq.[18,19] Because the pressure distribution is no longer hydrostatic in the section where the surface curvature is pronounced, coefficients should also be introduced to account for the effect of pressure distribution on the static-head terms in the energy and momentum equations. Because the surface curvature at section 2 may be considerable, it would be more appropriate to write Eq. 7 as

$$\alpha_1 \frac{V^2_1}{2\,g} + h_1 = \alpha_2 \frac{V^2_2}{2\,g} + \beta\, y_2 + h_e + h_f \ldots\ldots\ldots\ldots\ldots (21)$$

in which

$$\beta = \frac{1}{Q\, y_2} \int\!\!\int_{A_2} \left(\frac{p}{w} + z\right) dQ \ldots\ldots\ldots\ldots\ldots\ldots (22)$$

In tranquil flow, the static head above the bottom of the channel is usually the major part of the specific head so that—depending on the surface curvature—β may be an important coefficient. In fact, because the flow at section 2 is markedly convergent the velocity distribution in this section should be approximately uniform, and thus α_2 probably does not differ greatly from unity; that is, α_2 is often of secondary importance. From Eq. 21, one would be inclined to include the coefficient β in Eq. 9. It is believed that this step is probably not necessary in the present case, in which the main objective is to compute the discharge on the basis of experimental coefficients of discharge. One may consider Eq. 10 or Eq. 13 as a formula defining C, which is expressed by Eq. 12 or Eq. 17; the effect of surface curvature is included in Eqs. 12 and 17.

If, however, Eqs. 9 and 10 are regarded as rational deductions from the equations of energy and continuity (that is, Eqs. 7 and 8), the coefficient β should be included in the energy equation as indicated by Eq. 21. Boussinesq assumed[20] that the curvature in a vertical section varies linearly from the surface to the bed and obtained, for the case of uniform velocity distribution in a vertical direction, the formula:

$$\frac{p}{w} = y - z + \frac{V^2}{g\, y} \frac{d^2y}{dx^2} \left[y\,(y - z) - \frac{(y - z)^2}{2} \right] \ldots\ldots\ldots (23)$$

---

[18] "Steady Flow in Open Channels: The Problem of Boussinesq," by C. Jaeger, *Journal*, Inst. of C. E., London, England, February, 1948, pp. 339–349.

[19] "Fluid Mechanics for Hydraulic Engineers," by H. Rouse, McGraw-Hill Book Co., Inc., New York, N. Y., 1938, pp. 301–307.

[20] "Technische Hydraulik," by C. Jaeger, Birkhäuser, Basel, Switzerland, 1949, pp. 116–122.

THE UNIVERSITY OF MICHIGAN LIBRARIES

Assuming further that the velocity distribution is uniform in section 2, there results

$$\beta = \frac{1}{Q\,y_2}\int\!\!\int_{A_2}\left(\frac{p}{w}+z\right)dQ$$

$$= \frac{C_c\,b}{Q\,y_2}\int_0^{y_2}\left(\frac{p}{w}-z\right)V_2\,dz$$

$$= \frac{1}{y^2_2}\int_0^{y_2}\left\{y_2 - \frac{V^2_2}{g\,y_2}\left(\frac{d^2y}{dx^2}\right)_2\left[y_2\,(y_2-z)-\frac{(y_2-z)^2}{2}\right]\right\}dz$$

$$= 1+\frac{1}{3}\,\frac{V^2_2}{g\,y_2}\left(y\,\frac{d^2y}{dx^2}\right)_2 \quad\text{.............................(24)}$$

In general, C. Fawer[21] showed that, by assuming the curvature at any level to be given by $(z/y)^n\,d^2y/dx^2$, Eq. 24 could be extended to yield

$$\beta = 1+\frac{1}{n+1}\,\frac{V^2_2}{g\,y_2}\left(y\,\frac{d^2y}{dx^2}\right)_2 \quad\text{..................(25)}$$

Naturally, both Eqs. 24 and 25 are far from exact. These expressions are, nevertheless, at least qualitatively correct. Because the surface at section 2 is concave d^2y/dx^2 is positive, and therefore $\beta > 1$. This result may be anticipated if it is noted that the centrifugal effect of flow at section 2 is to increase the local pressure beyond that predicted by the hydrostatic pressure distribution. For a given value of m, different cases of flow through a given type of constriction should be geometrically similar. As a result, corresponding to a given value of m, the dimensionless parameter $y(d^2y/dx^2)$ should be approximately constant. On the basis of Eqs. 24 and 25, several qualitative observations can thus be made concerning β for flow through a given type of constriction: (1) Even if m is kept constant, β still increases with the Froude number. (2) Regardless of the magnitude of m, β approaches unity as the Froude number approaches zero. (3) The term β increases with m. These observations indicate clearly that the magnitude of β depends not only on the surface curvature of flow but also on the Froude number.

In order to gain some idea regarding the influence of the coefficient β, the possible effect of β on the ratio $(y_1 - y_4)/\Delta h$ will be cited briefly. Because the value of β at section 2 is greater than unity, the total energy per unit volume of water at section 2 is greater than that indicated by $(y_2 + \alpha_2\,V^2_2/2\,g)$. The value of Δh computed by the energy equation without taking β into account will therefore be less than the actual value of Δh. The effect of β is thus to increase the value of Δh. However, the quantity $(y_1 - y_4)$, being governed essentially by conditions in sections 1 and 4, may be considered independent of β. Therefore, the resultant effect of β is to reduce the ratio $(y_1 - y_4)/\Delta h$. In the light of the three observations previously made regarding β, the following remarks concerning $(y_1 - y_4)/\Delta h$ can be made:

---

[21] "Étude de quelques écoulements permanents à filets courbes," by C. Fawer, La Concorde, Lausanne, Switzerland, 1937.

a. For a given value of m, $(y_1 - y_4)/\Delta h$ decreases as the Froude number increases.

b. For a given value of the Froude number, the decrease in $(y_1 - y_4)/\Delta h$ is greater as m increases.

Both of these trends appear to be supported by experimental data.[22] Consequently, within the range of data presented by Messrs. Kindsvater and Carter, it seems certain that a more rational analysis of the problem should include a consideration of β.

Carl F. Izzard,[23] **A.M. ASCE.**—The placing of a constriction in an open channel inevitably results in an increase in the upstream stage over the stage which existed for the same discharge in the unconstricted channel. In Fig. 11 there is illustrated the change in profile from flow at a uniform depth y_n to a typical backwater flow. Also shown are the lines of total head obtained by plotting the velocity head above the free water surface, assuming that one can estimate the kinetic energy in the flow. The depth y_1 is the increased depth which Messrs. Kindsvater and Carter have measured at a section a distance b upstream from the upper edge of a constriction whose width normal to the direction of flow is b. To generalize the analysis, the channel is shown to have a slope S_0 which actually was zero in the authors' experiments.

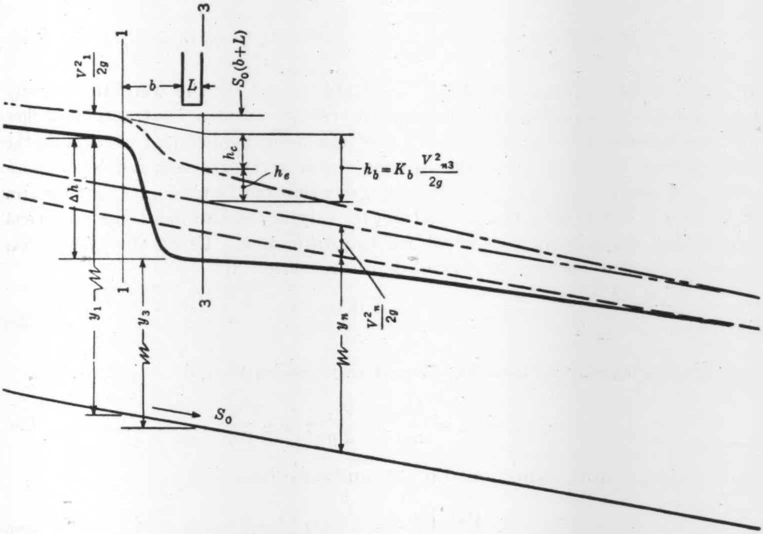

FIG. 11.—DEFINITION SKETCH OF BACKWATER

---

[22] "Backwater Effects of Open-Channel Constrictions," by Hubert J. Tracy and Rolland W. Carter, *Transactions*, ASCE, Vol. 120, 1955, p. 1001, Fig. 4.

[23] Chf., Hydr. Research Branch, Bureau of Public Roads, U. S. Dept. of Commerce, Washington, D ·C

THE UNIVERSITY OF MICHIGAN LIBRARIES

Using the nomenclature adopted by the authors, section 3 is taken at the downstream edge of the constriction. The drop in the total-head line from section 1 to section 3 can be considered to be equal to the normal resistance loss plus the loss h_c caused by the contraction of flow and is probably small compared to the total loss. This flow, however, has to expand, and in so doing additional energy is released that is represented by the difference h_e between the total head at section 3 and the total head with uniform flow. The sum,

$$h_c + h_e = h_b \qquad (26)$$

thus represents the total energy loss in excess of the normal friction loss between section 1 and a section downstream where the flow is again at normal depth. From Fig. 11 it is apparent that h_b is also equal to the change in total head at section 1.

The energy equation between section 1 and section 3 then becomes

$$S_0\,(b + L) + y_1 + \frac{V^2{}_1}{2\,g} = y_n\,\frac{V^2{}_n}{2\,g} + h_b + S_0\,(b + L) \qquad (27)$$

Where a cross section is irregular, a suitable value for the weighted velocity head should be substituted. Because h_b results from a contraction of flow one can assume that it is a function of the velocity head at section 3; the experiments, however, have shown that the water surface is not level transversely at section 3. To avoid this complication one can assume that the area at section 3 is taken at the normal depth, relying on the head-loss coefficient determined empirically to correct for the difference. Using the symbol V_{n3} to designate the velocity at normal depth in section 3,

$$h_b = K_b\,\frac{V^2{}_{n3}}{2\,g} \qquad (28)$$

Substituting this value into Eq. 27 and transposing terms,

$$y_1 - y_n = \frac{V^2{}_n}{2\,g} - \frac{V^2{}_1}{2\,g} + K_b\,\frac{V^2{}_{n3}}{2\,g} \qquad (29)$$

From the continuity equation, Eq. 29 can be expressed as

$$y_1 - y_n = \frac{V^2{}_{n3}}{2\,g}\left[\left(\frac{A_{n3}}{A_n}\right)^2 - \left(\frac{A_{n3}}{A_1}\right)^2 + K_b\right] \qquad (30)$$

from which

$$K_b = \frac{y_1 - y_n}{\dfrac{V^2{}_{n3}}{2\,g}} - \left(\frac{A_{n3}}{A_n}\right)^2\left[1 - \left(\frac{A_n}{A_1}\right)^2\right] \qquad (31)$$

If A_n/A_1 approaches unity as it will for relatively small quantities of backwater, an approximate equation for K_b is

$$K_b = \frac{y_1 - y_n}{\dfrac{V^2{}_{n3}}{2\,g}} \qquad (32)$$

Backwater can then be estimated as

$$y_1 - y_n = K_b \frac{V^2_{n3}}{2\,g} \qquad (33)$$

provided values of K_b for a given type of constriction are known. After a trial value of y_1 is determined from Eq. 33, a more accurate value can be obtained using Eq. 30 because a close approximation of A_1 will then be known.

Experiments have been described[13] from which it has been possible to test the applicability of Eqs. 29 to 33. In those tests steady flow was first established with no constriction, and an equivalent of normal depth was recorded. The flume used had a level floor, but the change in depth between section 1 and section 3 was usually very small in relation to the change in depth between the same sections with the constriction in place. The most extensive data were for a vertical constriction with a symmetrically placed rectangular opening. In Fig. 12 it is shown that K_b varies systematically with the contraction ratio m and to a lesser extent with the parameter $V^2_{n3}/(2\,g\,y_n)$. In Fig. 12 only tests made with $L = 0.02$ ft and $n = 0.012$ are shown. The correlation is good except for a few tests in which the surface profile for flow with no constriction appeared to be irregular. A more significant plot of the data is shown in Fig. 13(*a*) which is derived from the curves drawn in Fig. 12. In Fig. 13(*a*) it is indicated clearly that K_b is primarily a function of m, the variation with the velocity-head parameter being of minor importance; similar and slightly lower curves could be drawn for other values of L. Roughness of channel ap-

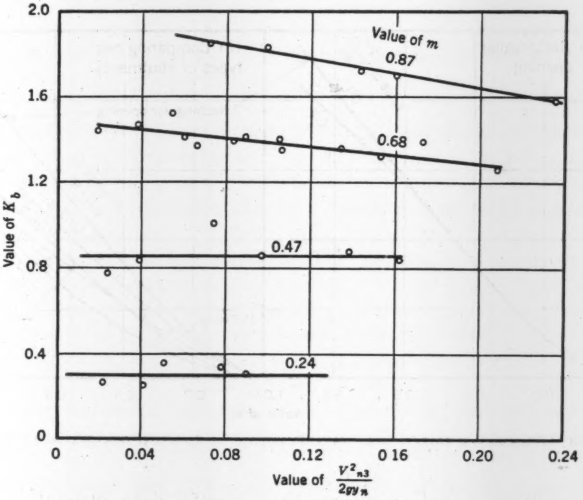

FIG. 12.—BACKWATER COEFFICIENT AS A FUNCTION OF VELOCITY HEAD RELATIVE TO NORMAL DEPTH ($n = 0.012$, $L = 0.02$ ft)

pears to affect K_b slightly, but this difference may be the result of the increased head required to obtain flow on a level floor.

A few runs were made with other types of constrictions. The computed values of K_b for two types are shown in Fig. 13(*b*) in comparison with the curve for the rectangular opening. The 45° wing wall had a constant dimension of $w = 0.25$ ft so that w/b was variable with the value of b and therefore with m; this accounts for the tendency of the curves for the wing-wall type to approach the curve for a rectangular opening when w is relatively small and to approach the curves for the rounded embankment for the case in which w is relatively large. The radius at the toe of the 1 on 1 rounded embankment was not constant, this radius varying from one third to one half of the distance across the constriction between the toe of the slope on each side.

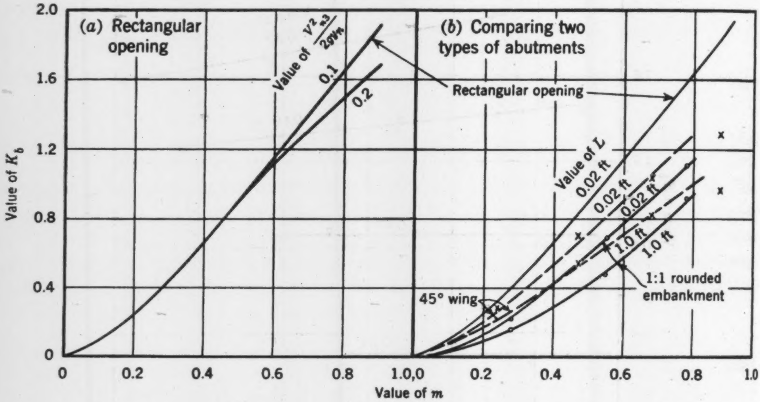

FIG. 13.—BACKWATER COEFFICIENT AS A FUNCTION OF CONTRACTION RATIO ($n = 0.012$)

These analyses, based on meager experimental data, strongly suggest the possibility—using a tilting flume—of determining values of K_b that would be applicable to standard types of bridges and that would be independent of channel roughness. If so, backwater could be computed by using Eq. 33. By applying this method the contracted depth y_3 at the downstream side of the abutment would not be given, but this value is not important to the bridge designer. Actually $y_n - y_3$ is a function of $V^2_{n3}/2\,g$ similar to Eq. 33.

The foregoing discussion has been directed at the problem of estimating backwater caused by constricting a channel carrying a known flow at normal depth, which is the problem of the highway engineer. Messrs. Kindsvater and Carter, however, were confronted with the reverse problem of estimating discharge from measurement of water levels in the vicinity of a channel constriction. Because the depth y_3 is sensitive to small changes in geometry, it was necessary to devise a system which would reflect these changes; this they have done with remarkable ingenuity.

THE UNIVERSITY OF MICHIGAN LIBRARIES

Performing the tests in a channel with a level floor greatly simplified the experimental procedure but left some question as to the applicability of the discharge coefficient to flow in a sloping channel, particularly when h_f is large in comparison to Δh. The basic equation defining C (Eq. 13) includes a term for head loss in the approach reach computed by the geometric mean of the energy slopes at sections 1 and 3 and the energy slope through the contracted reach. The evaluation of C would have been simpler if h_f had been computed solely for the friction loss in the unobstructed channel over the length $b + L$. All the energy losses attributable to the geometry of the constriction would thereby be included in the discharge coefficient. Thus, one would avoid the question as to whether or not the friction loss is correctly evaluated by the geometric mean of the energy slopes for the case in which the transition is not gradual but abrupt.

In computing discharge for an actual bridge, the normal friction loss could be checked against the energy slope in an unobstructed reach of the same cross section and should be approximately equal to the average bed slope. Thus, the uncertainties involved in estimating the Manning n—required to compute the friction loss—would be avoided. It would still be necessary to use n in estimating the contraction ratio but, because n appears in both numerator and denominator, the effect of error would be minimized. Consequently, the evaluation of C in Eq. 13, using h_f as the normal friction loss, would simplify computation in the field. Further simplification could be attained by defining m as K_q/K_Q instead of $1 - K_q/K_Q$. The obvious term for m would then be "conveyance ratio."

The problem of estimating discharge from field measurements requires that the elevations h_1 and h_3 must be measured at certain points to determine Δh. In estimating backwater $y_1 - y_n$, it is not necessary to compute y_3 if K_b in Eq. 33 is known from experimental data. The computation is simple and gives results which appear to be as consistent, if not more so, than those obtained by computing Δh from Eq. 13 and then applying corrections[13] to get $y_1 - y_n$.

In a discussion[24] the writer demonstrated that y_1/y_n was a function of $V^2_{n3}/(2\, g\, \bar{y}_n)$ and the parameter m for a given type of constriction. By subtracting unity from the ordinate scale and multiplying both scales by y_n, these quantities take the form of Eq. 33 in which K_b becomes the slope of a straight line approximating the curved lines. The reason for the consistency of the data in relation to the velocity-head parameter based on normal depth in the contracted opening is that the total head loss caused by the contraction h_b (as defined in Fig. 11) is referred to total energy at normal depth.

The use of Eq. 33 together with charts similar to Fig. 13(*b*) is believed preferable to the use of another chart[25] because Eq. 33 gives the increment in depth and not a depth relative to a normal depth which might prove difficult to define for irregular channels. More experimental data are needed, preferably from a sloping flume, to define K_b for standard types of bridges

---

[24] Discussion by Carl F. Izzard of "Backwater Effects of Open-Channel Constrictions," by Hubert J. Tracy and Rolland W. Carter, *Transactions*, ASCE, Vol. 120, 1955, p. 1008.

[25] *Ibid.*, Fig. 9.

THE UNIVERSITY OF MICHIGAN LIBRARIES

Chesley J. Posey,[26] **M. ASCE.**—The work of Messrs. Kindsvater and Carter should do much to clarify the thinking of engineers on a problem that has often proved puzzling. The tests reported not only provide useful information but also point the way for future experimentation that will be even more valuable.

The authors properly emphasize the importance of accounting for the contraction of the jet. They omitted one factor, however, that can have a considerable effect on the contraction—friction along the upstream face of the obstruction; the corresponding orifice effect is recorded in standard text books on hydraulics.[27] Messrs. Kindsvater and Carter should have included some tests with variable roughness in this location inasmuch as they did vary the bed roughnesses.

In their future tests, the authors should give special attention to the contraction to be expected under various conditions. The right of way along the fill section approaching a bridge is apt to be kept cleared whereas the flood-plain bottom beyond the right-of-way lines is often overgrown with underbrush and trees. Hence, the flow parallel to the fill approaching the bridge will attain a higher velocity than it would under the flow-net assumption of equal (or nonexistent) friction throughout the approach area. Entering the main flow transversely just above the bridge opening, this current of high velocity will cause more contraction than would otherwise exist. Not only is this condition almost universal but it is often accentuated by the presence of borrow pits or large ditches along the side of the fill.

The designation of some formulas as "rational" and others as "empirical" seems unfortunate. Because all formulas representing physical phenomena are empirical, what is probably meant is that some have more claim to rationality than others.[28] The rationality of the Weisbach formula is not at all appealing but, because it includes two terms with different exponents (and hence is similar to a power series), it can be fitted more closely to the experimental data than can other formulas that have a more logical basis but only one term.[5] A close examination of the Nagler formula[9] shows that it has at least as good a claim to "rationality" as has, for example, the application of the flow net to open-channel problems. The authors' introduction of the concept of contraction in the study of open-channel flow is not new[8,29] but, when correlated with systematic experimental studies, it seems to bring order out of chaos. One wonders whether Messrs. Kindsvater and Carter could predict the experimental results obtained[5] by Mr. Lane by an a priori evaluation. Perhaps their suggestion that the degree of jet contraction should be proportional to the ratio m can be provided with "adjustments" to take into account the existence and relative elevations of side borrow pits, ditches, or cleared right of ways.

---

[26] Prof. of Hydraulics and Structural Eng. and Head, Dept. of Civ. Eng., State Univ. of Iowa, Iowa City, Iowa.

[27] "Hydraulics," by H. W. King and C. O. Wisler, John Wiley & Sons, Inc., New York, N. Y., 3d Ed., 1933, p. 101.

[28] "The Science of Mechanics," by Ernst Mach, Open Court Publishing Co., Chicago, Ill., 5th Ed., 1942.

[29] "An Experimental Study of the Flow of Water through Transitions in Rectangular Open Channels," by George B. Lyon, thesis presented to the State University of Iowa, Iowa City, Iowa, in February, 1942, in partial fulfilment of the requirements for the degree of Master of Science.

CARL E. KINDSVATER,[30] M. ASCE, AND ROLLAND W. CARTER,[31] A. M. ASCE.—The subject of this paper was the first phase of a comprehensive investigation of the flow of water through bridge openings. Since the delivery of the paper at New Orleans, La., in 1952, two additional reports on related research have been published. In the first of these[32] the study of discharge characteristics is extended to include additional boundary conditions; the second[13] deals with the flow pattern downstream from the constriction. As the basis for these and other investigations still in progress, the writers' paper is appropriately complemented by the excellent discussions submitted by Messrs. Laursen and Toch, Blaisdell, Lin, Izzard, and Posey.

Messrs. Laursen and Toch refer to certain limitations on the applicability of the writers' solution. They observe correctly that the relationship between the level of the water in zone 3 and that in zone 2 depends somewhat on the density and distribution of the vegetal cover on the banks of the stream. It should be emphasized, however, that the experimental coefficients are based on measurements made at zone *3a*. In terms of natural-channel conditions, this zone is on the downstream face near the waterway end of the embankment. It is unlikely that the influence of trees and brush between this point and zone 2 would ordinarily be significant.

Mr. Lin's remarks concerning contradictory definitions of C appear to based on a misunderstanding of the purpose of the dimensional analysis leading to Eq. 6*b*. In the section entitled "Simple Constrictions in Rectangular Open Channels: Selection of the Independent Variables," the resistance characteristics of the upstream channel are recognized, but they are omitted from the dimensional analysis in anticipation of their subsequent treatment in the discharge equation. Thus, the second dimensionless group in Eq. 6*b* is described as a ratio that is "proportional to a coefficient of discharge." It is, in fact, simply an indication of the existence of a general parameter having the form of a Euler number. It was the purpose of the section following Eq. 6 to formulate the coefficient of discharge expressed by Eqs. 10 and 12. A brief justification of the writers' method of accounting for h_f and $\alpha_1 V^2_1/2\,g$ is contained in the paragraph following Eq. 9.

Mr. Lin describes some of the complications that result from the application of the one-dimensional energy and momentum equations to a section in which the pressure is nonhydrostatically distributed. It is usually possible to avoid these complications by applying the equations to zones of parallel flow; that is, to sections in which the normal acceleration—and, therefore, the normal piezometric-head gradient—is zero. This was accomplished in the writers' study by defining section 2 quite arbitrarily as the vena contracta. Actually, of course, this qualification is largely academic. Regardless of where section 2 is located, both α_2 and β_2 ordinarily will be functions of the independent variables on which the experimentally determined values of C depend. It follows that the influence of a nonhydrostatic pressure distribution, in addition to the influence of a nonuniform velocity distribution in the constricted section, is contained in the coefficient of discharge defined by Eq. 13.

---

[30] Prof. of Civ. Eng., Georgia Inst. of Technology, Atlanta, Ga.

[31] Hydr. Engr., Geological Survey, U. S. Dept. of the Interior, Atlanta, Ga.

[32] "Computation of Peak Discharge at Contractions," by Carl E. Kindsvater, Rolland W. Carter, and Hubert J. Tracy, *Circular No. 284*, Geological Survey, U. S. Dept. of the Interior, Washington, D. C., 1953.

The writers are grateful for Mr. Blasidell's recognition of the large amount of work and the many tests required to establish empirical solutions for complex fluid phenomena. Problems involving open channels, particularly natural channels, typically depend on many independent variables. It is seldom possible to consider all the variables in a laboratory investigation. The decision to limit the experiments to values of m greater than 0.20 was one of the consequences of the necessity to restrict the scope of the study to the conditions most frequently encountered in practice. Nevertheless, it should be recognized that the tests were conducted at a relatively small scale, and therefore that values of m less than 0.20 would result in very small changes in water-surface level and quantities such as Δh would be subject to large experimental errors. The writers agree with Mr. Blaisdell that, from the viewpoint of the researcher, so-called "practical" limits are often frustrating.

Much of Mr. Izzard's discussion is concerned with the determination of the backwater due to an open-channel constriction. This is one of the objectives of the comprehensive investigation in which the writers are engaged. An analysis and much additional experimental data pertaining specifically to that problem are therefore contained in a subsequent paper.[13]

Mr. Izzard is concerned about the fact that, in all the writers' tests, the bottom of the experimental flume was horizontal. The significance of this limitation is that a small part of the change in depth in a level flume is due to the acceleration which results from the unbalanced boundary resistance force. For the conditions of this investigation the influence of bottom slope is believed to be insignificant. Mr. Izzard also proposes a simplification in the method of computing h_f. In his words, "All the energy losses attributable to the geometry of the constriction would thereby be included in the discharge coefficient." Actually, he would be adding one variable, the conveyance of the constricted waterway, to those already involved in the evaluation of the discharge coefficient. That this variable has been effectively removed in the writers' solution is demonstrated by the lack of correlation between C and n throughout the full range of tests reported. In connection with both Mr. Izzard's criticisms, it should be observed that the contracted-opening method of determining the discharge in natural channels is not feasible when the boundary resistance loss, h_f, is a large part of Δh.

Mr. Posey deplores the omission of certain natural-channel variables, including constriction roughness as well as borrow pit, drainage ditch, and right-of-way characteristics. In a subsequent report[32] many variables were considered in addition to those involved in the present study. These variables, all concerned with natural bridge waterways, resulted from sloping embankments, a variety of abutment forms, piles and piers, and partial bridge submergence. Thus, of the "almost unlimited" number of variables acknowledged in the "Introduction," a large number have been considered. It is possible that experience in the application of the proposed computation procedure will indicate the necessity for experiments involving additional variables. In the meantime, growing evidence of the successful application of the writers' data to the computation of flood flows in natural waterways is encouraging.

THE UNIVERSITY OF MICHIGAN LIBRARIES

AMERICAN SOCIETY OF CIVIL ENGINEERS
Founded November 5, 1852
TRANSACTIONS

Paper No. 2771

BACKWATER EFFECTS OF OPEN-CHANNEL CONSTRICTIONS

By Hubert J. Tracy[1] and Rolland W. Carter,[2]
A. M. ASCE

With Discussion by Messrs. Paul V. Hodges; Carl F. Izzard; Harold R. Henry; and Hubert J. Tracy and Rolland W. Carter

Synopsis

A method of computing the nominal backwater due to open-channel constrictions was sought. A practicable solution, based on an empirical discharge coefficient and a laboratory investigation of the influence of channel roughness, has been reached. Also investigated as a part of the laboratory tests were the effects of channel shape and constriction geometry. The solution involves the computation of water-surface drop through the constriction and the determination of a factor which is the ratio of backwater to water-surface drop. This ratio is shown to be a function of channel roughness, percentage of channel contraction, and constriction geometry.

Notation

The letter symbols adopted for use in the paper are defined where they first appear, in the illustrations or in the text, and are arranged alphabetically for convenience of reference in the Appendix.

Introduction

It is generally recognized that the introduction of a constriction in an open channel causes local, and in some instances, far-reaching changes in the water-surface profile. Evaluation of this "backwater" effect is of interest to those concerned with the location of artifical obstructions in natural channels. Highway departments have found such information desirable as a part of hydraulic studies made at proposed bridge sites.

Note.—Published, essentially as printed here, in February, 1954, as *Proceedings-Separate No. 413*. Positions and titles given are those in effect when the paper was received for publication.

[1] Hydr. Engr., Geological Survey, U. S. Dept. of the Interior, Atlanta, Ga.

[2] Hydr. Engr., Geological Survey, U. S. Dept. of the Interior, Atlanta, Ga.

This study was undertaken as an extension of an investigation[3,4] completed in 1953 by the Geological Survey, United States Department of the Interior (USGS), which was specifically concerned with the discharge characteristics of the constriction. Experimental data and certain computation procedures developed are directly applicable to this study.

Object and Scope of the Investigation.—The object of this investigation was to study, by theoretical as well as by experimental methods, the backwater effect of width constrictions in open channels. The ultimate objective was a practicable method of computation adapted to the evaluation of this effect.

This study was limited to an investigation of single-opening constrictions and to steady, tranquil flows. The hydraulic characteristics of the channel were assumed to be uniform throughout the backwater reach. Thus, in the laboratory, the channels upstream and downstream from the constriction were made identical with respect to bed roughness, shape, and width. Variables in the laboratory investigation were the discharge, depth of flow, channel roughness, and a limited variety of constriction geometries and channel shapes.

Description of the Problem

It is pertinent to a study of the backwater problem to compare the backwater condition with the normal, friction-controlled flow in the same channel reach without the constriction.

The backwater effect due to a constriction in a channel of mild slope is first manifested upstream from the constriction by a backwater profile of the M-1 variety[5] in which the velocities—and consequently the rate of loss of flow energy—are less than normal. The beginning of this reach is designated as section 0 in Fig. 1. Near the constriction, at section 1 in Fig. 1(*a*), the central body of water begins to be accelerated, whereas deceleration occurs along the outer boundaries, and a separation zone is formed in the corners upstream from the constriction. (In Fig. 1(*b*) the horizontal scale has been distorted.)

At the constriction, the flow is characterized by rapid acceleration in directions both parallel and normal to the streamlines. The average longitudinal water-surface profile falls rapidly in this region. Within the constriction, the "live" stream contracts to a width somewhat less than the gross width of the opening, and the spaces between the live stream and the constriction boundaries are occupied by eddying water. The extent of the contraction and consequent separation depends on the rate of flow, constriction and boundary geometry, and roughness.

Immediately downstream from the section of minimum live-stream width (the vena contracta, section 2) the expansion process begins; it continues until the normal regime of flow has been re-established in the full-width channel downstream (section 4). The reach from section 2 to section 4 is one of decelerated flow in which the average velocities and energy losses are greater than normal because of the turbulence engendered by the expansion process. The length required to establish the normal regime downstream from the constriction is not

---

[3] "Tranquil Flow Through Open-Channel Constrictions," by Carl E. Kindsvater and Rolland W. Carter, *Transactions*, ASCE, Vol. 120, 1955, p. 955.

[4] "Computation of Peak Discharge at Contractions," by Carl E. Kindsvater, Rolland W. Carter, and H. J. Tracy, *Circular No. 284*, Geological Survey, U. S. Dept. of the Interior, Washington, D. C., 1953.

[5] "Gradually Varied Channel Flow," by C. J. Posey, Chapter IX in "Engineering Hydraulics," edited by H. Rouse, John Wiley & Sons, Inc., New York, N. Y., 1950, p. 610.

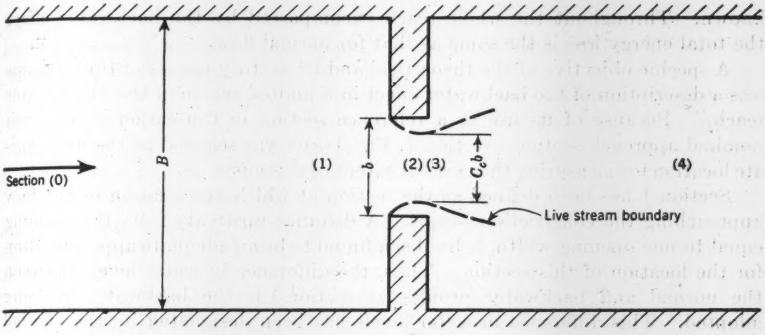
Section (0)
B
(1)
b
(2) (3)
$C_c b$
(4)
Live stream boundary

(*a*) Plan

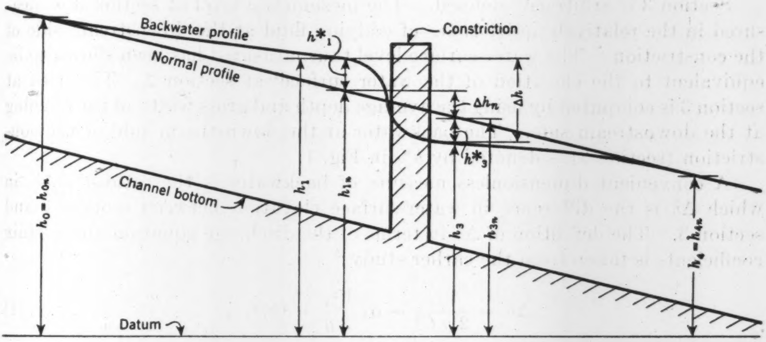
Backwater profile
Constriction
h^*_1
Normal profile
Δh_n
Δh
h^*_3
Channel bottom
$h_0 = h_{0n}$
h_1
h_{1n}
h_3
h_{3n}
$h_4 = h_{4n}$
Datum

(*b*) Elevation

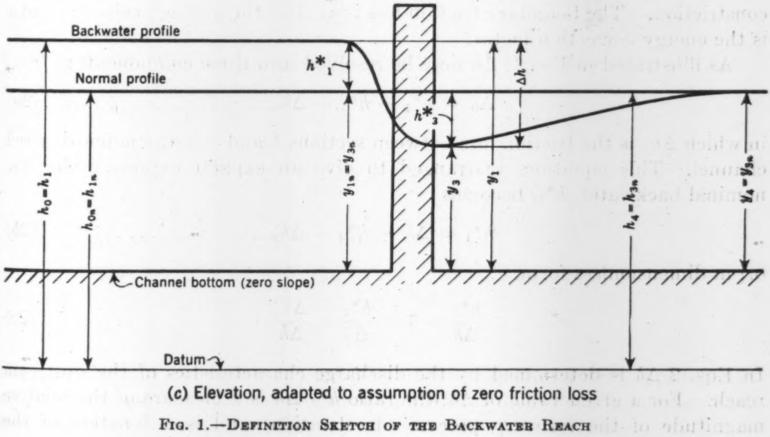
Backwater profile
h^*_1
Normal profile
Δh
h^*_3
$h_0 = h_1$
$h_{0n} = h_{1n}$
$y_{1n} = y_{3n}$
y_3
y_1
$h_4 = h_{3n}$
$y_4 = y_{3n}$
Channel bottom (zero slope)
Datum

(*c*) Elevation, adapted to assumption of zero friction loss

FIG. 1.—DEFINITION SKETCH OF THE BACKWATER REACH

known. Throughout the whole reach encompassed by the backwater effect the total energy loss is the same as that for normal flow.

A specific objective of the theoretical and laboratory phases of this analysis was a description of the backwater effect in a limited region of the "backwater reach." Because of its use as a reference section in the earlier study,[3] the nominal approach section—section 1, Fig. 1(*a*)—was selected as the appropriate location for measuring the vertical extent of this effect.

Section 1 has been defined as the section at which acceleration of the flow approaching the constriction begins. A distance upstream from the opening equal to one opening width, b, has been found to be an adequate approximation for the location of this section. Thus, the difference in water levels between the normal and backwater profiles at section 1 is the backwater measure adopted. This difference in water levels has been designated by the symbol h^*_1 in Fig. 1.

Section 3 is arbitrarily defined. The piezometric level at section 3 is measured in the relatively quiet zones of eddying fluid at the downstream side of the constriction. The water-surface level thus measured has been shown to be equivalent to the elevation of the water surface[3] at section 2. The area at section 3 is computed by using the average depth and gross width of the opening at the downstream side. The backwater at the downstream side of the constriction (section 3) is denoted by h^*_3 in Fig. 1.

A convenient dimensionless measure of backwater is the ratio $h^*_1/\Delta h$, in which Δh is the difference in water-surface elevation between section 1 and section 3. The definition of Δh in terms of the discharge equation and certain coefficients is taken from the earlier study:[3]

$$\Delta h = \frac{V^2_3}{2\,g\,C^2} - \alpha_1 \frac{V^2_1}{2\,g} + (h_f)_{1-3} \qquad (1)$$

in which C, the coefficient of discharge, is a function of shape and roughness of the approach channel, an appropriate Froude number, and the geometry of the constriction. The boundary friction loss is h_f, V is the average velocity, and α is the energy correction factor.

As illustrated in Fig. 1, Δh may be resolved into three components:

$$\Delta h = h^*_1 + h^*_3 + \Delta h_n \qquad (2a)$$

in which Δh_n is the friction loss between sections 1 and 3 in the nonobstructed channel. This equation, rearranged to give an explicit expression for the nominal backwater, h^*_1, becomes

$$h^*_1 = \Delta h - h^*_3 - \Delta h_n \qquad (2b)$$

or, in dimensionless form,

$$\frac{h^*_1}{\Delta h} = 1 - \frac{h^*_3}{\Delta h} - \frac{\Delta h_n}{\Delta h} \qquad (2c)$$

In Eqs. 2 Δh is determined by the discharge characteristics of the upstream reach. For a given value of Δh, the ratio $h^*_3/\Delta h$ is a measure of the relative magnitude of the recovery process (deceleration) and is a function of the hydraulic characteristics of the downstream channel reach. The term $\Delta h_n/\Delta h$ represents the role played by friction in producing Δh as compared with the influence of acceleration.

The assumption is frequently made that the water surface immediately downstream from the constriction is the normal elevation; hence, if friction losses are neglected, the backwater h^*_1 is equal to the drop, Δh. Accordingly, the backwater ratio $h^*_1/\Delta h$ would always have a value of 1.0. Eq. 2c is useful in demonstrating that this assumption may be erroneous. The backwater ratio is equal to unity only if the normal friction loss and the downstream recovery of energy are small in comparison with Δh.

APPROXIMATE SOLUTION FOR THE BACKWATER RATIO

An approximate analytical solution for the backwater ratio can be obtained if it is assumed that normal boundary friction losses are zero. In this development of the approximate solution it is also assumed that the channel is horizontal, the velocities in the live stream at section 2 are essentially constant, and the piezometric head at section 3 is equivalent to the level at section 2, as shown in the earlier study (Fig. 1(*b*)).[3]

If V_2 is the average velocity of the live stream at section 2 and V_3 the average velocity at section 3 based on the gross area at section 3, the continuity relationships are

$$Q = V_1 B y_1 = V_2 C_c b y_2 = V_3 b y_3 = V_4 B y_4 \dots\dots\dots\dots (3)$$

From the momentum equation,

$$\frac{\gamma b y^2_2}{2} + \frac{\gamma (B - b) y^2_2}{2} - \frac{\gamma B y^2_4}{2} = Q \rho (V_4 - V_2) \dots\dots\dots (4)$$

in which ρ denotes density and γ the specific weight. From the energy equation,

$$y_1 + \frac{V^2_1}{2g} = y_2 + \frac{V^2_2}{2g} \dots\dots\dots\dots\dots\dots\dots\dots (5)$$

Using the equality $y_2 = y_3$, and introducing the Froude number $\mathbf{F}_3 = V_3/\sqrt{g\, y_3}$, Eqs. 3 and 4 may be combined to yield

$$\left(\frac{y_3}{y_4}\right)^3 - \frac{1 + 2\frac{b}{B}\frac{\mathbf{F}^2_3}{C_c}}{2\left(\frac{b}{B}\right)^2 \mathbf{F}^2_3}\left(\frac{y_3}{y_4}\right)^2 + \frac{1}{2\left(\frac{b}{B}\right)^2 \mathbf{F}^2_3} = 0 \dots\dots\dots\dots (6)$$

Solved simultaneously, Eqs. 3 and 5 yield

$$\left(\frac{y_1}{y_3}\right)^3 - \frac{2 + \left(\frac{\mathbf{F}_3}{C_c}\right)^2}{2}\frac{y_1}{y_3} + \frac{\mathbf{F}^2_3\left(\frac{b}{B}\right)^2}{2} = 0 \dots\dots\dots\dots\dots (7)$$

In Eqs. 6 and 7 y_3/y_4 and y_1/y_3 are described implicitly for this approximate solution in terms of the channel-contraction ratio b/B, a Froude number, and the coefficient of contraction, C_c.

From these solutions for y_1/y_3 and y_3/y_4, the backwater ratio for this approximate solution may be computed. For the frictionless condition, and with no bottom slope, $y_{1n} = y_4$. Hence,

$$\frac{\frac{y_1}{y_3}\frac{y_3}{y_4} - 1}{\frac{y_1}{y_3}\frac{y_3}{y_4} - \frac{y_3}{y_4}} = \frac{y_1 - y_4}{y_1 - y_3} = \frac{h^*_1}{\Delta h} \quad \text{.................... (8)}$$

In the development[3] of an empirical expression for the coefficient of discharge, C, that coefficient was shown to be primarily a coefficient of contraction. A comparison of the expression for C with an equation derived theoretically for the discharge through a constriction leads to the relationship:

$$C = C_c \left(K_L + \alpha_2\right)^{-\frac{1}{2}} \quad \text{........................ (9)}$$

in which K_L is used to describe eddy losses in the upstream separation zone, which are normally small. The velocity distribution coefficient α_2 is commonly assumed to be unity. From dimensional analysis[3] C can be shown to depend on a Froude number, the geometry of the upstream channel and of the constriction, and on an appropriate depth.

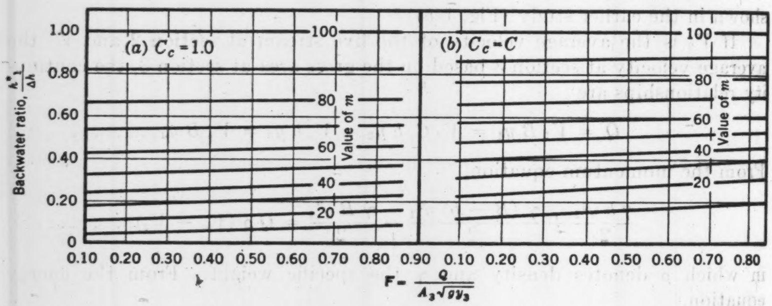

FIG. 2.—APPROXIMATE SOLUTION FOR BACKWATER RATIO

Thus, C_c may be represented by the coefficient C in Eqs. 6 and 7. The variation of C with the previously named variables has been shown graphically by Carl E. Kindsvater, M. ASCE, and the writers[4] who have defined C for several practical constriction types.

Two solutions for the backwater ratio are shown in Fig. 2. For the first of these solutions, Eqs. 6 and 7 were solved for y_3/y_4 and y_1/y_3 (Fig. 2(*a*)) by choosing constriction and channel geometries for which $C = 1.00$ for a full range of values of F and b/B. A similar solution (Fig. 2(*b*)) was made by selecting C for constriction geometries having minimum contraction coefficients —those for vertical-faced constrictions with square-edged entrances.

In Fig. 2, the description of the degree of channel contraction has been modified to be expressed as $m = (1 - b/B)\ 100$ instead of the (b/B)-ratio indicated in Eqs. 6 and 7.

For this special solution it will be noted from Fig. 2 that the Froude number has little effect on the ratio $h^*_1/\Delta h$ and that this ratio depends primarily on m, with C_c exerting a secondary influence. The effect of a decrease in C_c is to increase $h^*_1/\Delta h$ but, even when C_c is varied through its maximum practical range, as it was in the two solutions, its effect is rather small.

THE LABORATORY INVESTIGATION

Exploratory tests in the initial phase of this study were made in the hydraulics laboratory of the Georgia Institute of Technology at Atlanta. These tests established the relative importance of the variables involved and indicated the desirability of conducting further tests in a flume of greater length than that used for the exploratory tests.

Test Equipment.—Thus, arrangements were made for the use of a flume in the A. N. Talbot Hydraulics Laboratory of the University of Illinois at Urbana. This flume is rectangular in cross section, 164 ft long, 5 ft wide, and 4.75 ft deep. The floor of the flume is level. A maximum discharge of 14 cu ft per sec is provided by the laboratory's recirculating system. Discharges are measured by means of a 12-in. bend meter in the supply pipe. Baffles are used to obtain uniform velocities downstream from the supply entrance.

The beginning of the test reach in the flume was approximately 15 ft from the supply-pipe outlet. The depth of flow in the flume was regulated by means of an adjustable tail gate 148 ft downstream from the beginning of the test section. Except in the vicinity of the constriction, water-surface elevations were measured at 10-ft intervals along the length of the flume by fixed point gages set over the center of the flume. At the constriction, water-surface levels were measured by a movable point gage that traversed both the width and the length of the flume. Constrictive elements were of aluminum plate and plywood. For all tests, the constriction was 55 ft downstream from the beginning of the test section.

Boundary roughness was created by means of various arrangements of chain-link fencing and expanded metal. The cross-sectional shape of the test section was altered by false floors of smooth transite sheets and redwood lumber.

Methods of Testing.—The general test procedure for backwater measurements consisted of making surface-level observations over the full length of the test section. This was done, first, with the constriction in place and, second, with the constriction removed.

Tests on the rectangular flume were made with four degrees of channel roughness. The concrete floor and sides of the basic flume provided a condition of minimum roughness corresponding to a Manning n of 0.012, which was constant over the range of depths tested. A second degree of roughness was created by covering the flume floor uniformly with 2-in., chain-link, diamond-mesh, wire fencing. The resulting n as determined in the laboratory was 0.023. By adding expanded-metal sections that projected 2.5 in. above the chain-link fence, a value of n of 0.050 was measured at a flow depth of 1 ft. For this condition of roughness, n decreased slightly at greater depths and was considerably greater at depths less than 1 ft.

For testing the effect of a change in shape of channel cross section, a false bottom was built into the flume. The dimensions of this alternate arrangement are shown in Fig. 3. A limited number of tests were made in this flume for which the Manning n was computed as 0.010.

ANALYSIS OF EXPERIMENTAL DATA

The laboratory phase of the investigation was first concerned with the measurement of the backwater ratio, $h^*_1/\Delta h$, in a uniform rectangular flume at various degrees of bed roughness, using vertical-faced constrictions with square-edged abutments (entrances). Using the curves defined by these data as base (standard) values, other constriction shapes and channel geometries were tested, and the variation of the backwater ratio was then determined as a departure from these base values.

The Backwater Ratio for the Basic Condition.—Sufficient tests were made to describe the backwater ratio for vertical-faced constrictions with square-edged abutments in the rectangular flume for three degrees of channel roughness, ranging from smooth to fairly rough. The results, plotted separately for each of the three roughness conditions, are shown in Fig. 4, in which $m = (1 - b/B)\,100$. For convenience, these three curves in Fig. 4 have been summarized in Fig. 5, omitting the Froude number as a variable because of its minor effect. Also shown in Fig. 5 are curves resulting from the approximate analysis. The approximate solution is an aid in describing the shape and limits of the experimental curves.

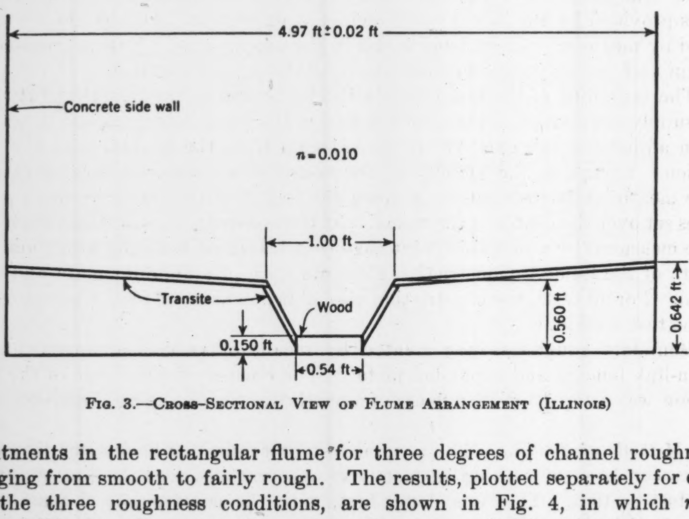

FIG. 3.—CROSS-SECTIONAL VIEW OF FLUME ARRANGEMENT (ILLINOIS)

Important during this series were tests made to isolate the influences of (1) the depth of flow, y_3/b, and (2) the constriction length, L/b. With all other variables held constant, a variation of these parameters between tests proved to have no effect on the backwater ratio.

The width ratio, b/B (or $1 - b/B$), is sufficient to describe the percentage of channel contraction in the rectangular channels of uniform roughness.

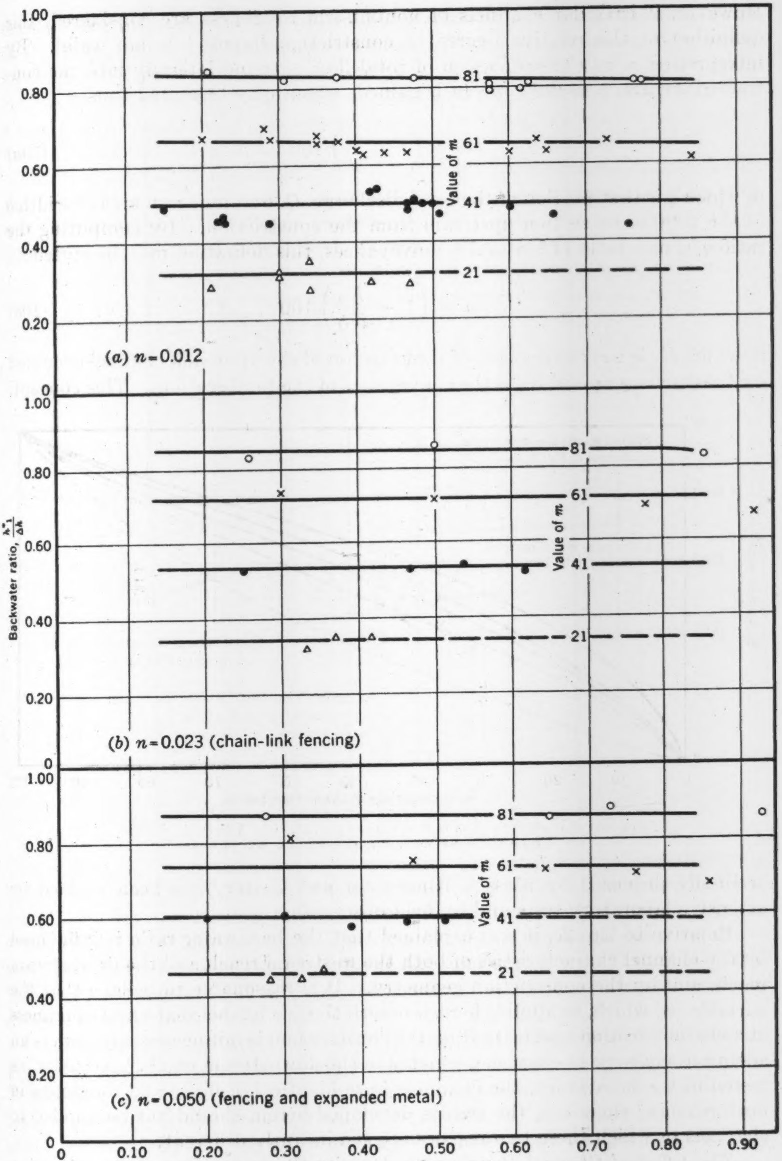

FIG. 4.—MEASURED VALUES OF THE BACKWATER RATIO

However, if irregular channels of nonuniform roughness are considered, this definition of the relative degree of constriction imposed is not valid. By interpreting m as the proportion of total flow entering laterally into the contracted stream, a useful concept is gained, which may be stated thus—

$$m = \left(1 - \frac{q}{Q}\right) 100 \quad \text{(10a)}$$

in which q is that portion of the total discharge, Q, occupying an area of width b in the total cross section upstream from the constriction. By computing the ratio q/Q as a ratio of hydraulic conveyances, this definition may be stated:

$$m = \left(1 - \frac{K_q}{K_Q}\right) 100 \quad \text{(10b)}$$

in which K_q is the conveyance of that portion of the approach channel occupied by the discharge q and K_Q is the conveyance of the total section. This concept, originally proposed by Messrs. Kindsvater and Carter,[3] has been verified by extensive laboratory tests and by field observation.

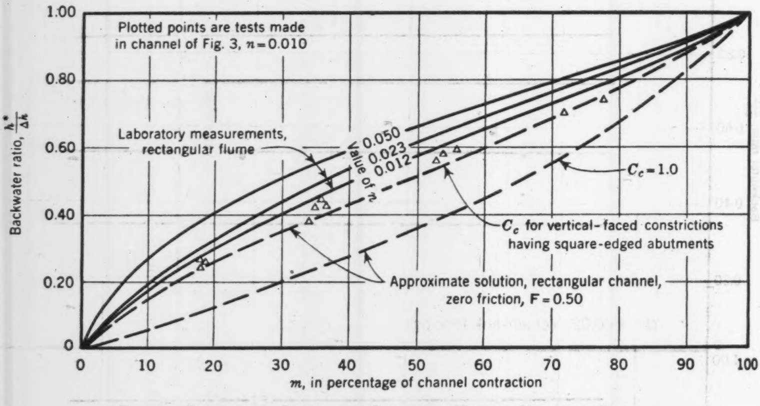

FIG. 5.—BACKWATER RATIO FOR CHANNELS HAVING VERTICAL-FACED CONSTRICTIONS WITH SQUARE-EDGED ABUTMENTS

Relative to Eq. $2c$, it was explained that the backwater ratio is influenced by the channel characteristics of both the upstream reach and the downstream reach, and by the constriction geometry. It is reasonable to believe that the variable, m, which, as applied here, is descriptive of channel shape and roughness at a channel section upstream from the constriction, is not necessarily always an adequate measure of channel geometry in the downstream reach. Actually, as tested in the laboratory, the channels were identical in shape and roughness in both reaches; therefore, the results developed herein should not be applied to channels in which these two reaches are significantly different.

The Effect of Channel Roughness.—Despite the limitations of the Manning n as a measure of channel roughness, its use in this study is not a serious shortcoming primarily because roughness is relatively unimportant as a factor in the determination of the backwater ratio. This is shown in Fig. 6, which is an alternative presentation of the data shown in Fig. 5, replotted to show more clearly the variation of $h^*_1/\Delta h$ with n. In Fig. 6 it is indicated that at an n of about 0.050, the limit of the change in the backwater ratio due to channel roughness has been reached.

An examination of Eq. 1 and Fig. 6 shows that h^*_1 increases as n is increased. Eq. 1 indicates an increase in Δh with n. In Fig. 6 an increase in $h^*_1/\Delta h$ with n is demonstrated. It is thus evident that h^*_1 must also increase with n. Similiarly, it may be shown that h^*_3 decreases as n increases.

The Effect of Channel Shape.—Twelve tests were made using the flume shown in Fig. 3 to determine the effect on the backwater ratio of a single variety of complex channel cross section. Vertical-faced constrictions with square-edged abutments were used to permit these tests to be compared directly with those made in the rectangular channel using the same type of constriction. The Manning n for this channel was computed to be 0.010. These twelve tests are plotted on the curves developed for the rectangular channel in Fig. 5. Considering the differences in channel roughness, the agreement between these tests and those made in the concrete rectangular flume ($n = 0.012$) is close. This fact has been taken as further evidence that the influence of cross-sectional shape is incorporated in the variable, m.

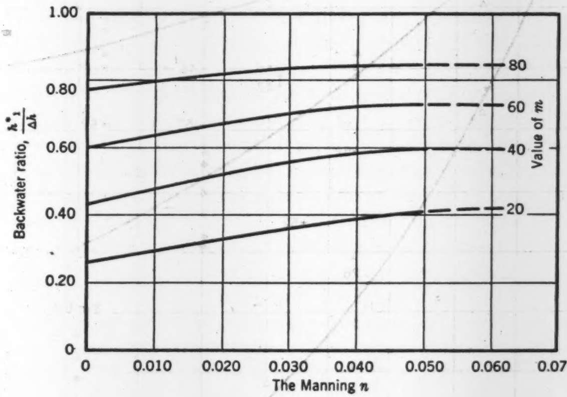

FIG. 6.—THE EFFECT OF CHANNEL ROUGHNESS ON THE BACKWATER RATIO FOR VERTICAL-FACED CONSTRICTIONS WITH SQUARE-EDGED ABUTMENTS

The Effect of Constriction Geometry.—The backwater ratio is defined in Fig. 5 for the basic constriction type (vertical face, square-edged abutments). To determine the variation in the backwater ratio due to constriction geometry, tests were made in the smooth, rectangular, concrete flume using constrictions which differed from the basic type. These included both vertical and sloping-face constrictions, with both rounded and wing wall entrances. These tests invariably gave lower backwater ratios than those for the basic condition. It is reasonable to assume that these variations from the basic condition may be related to the coefficient of discharge C because C is primarily also a function of constriction geometry.

Accordingly, by dividing the backwater ratios for the latter tests by the backwater ratios appropriate to the basic condition, a measure of the variation of backwater due to constriction geometry is obtained. This factor is designated k_c. Then, in a similar manner, a ratio of the coefficients of discharge C/C_{base} may be used to describe the effective change in constriction geometry which caused the variation in backwater measured by k_c.

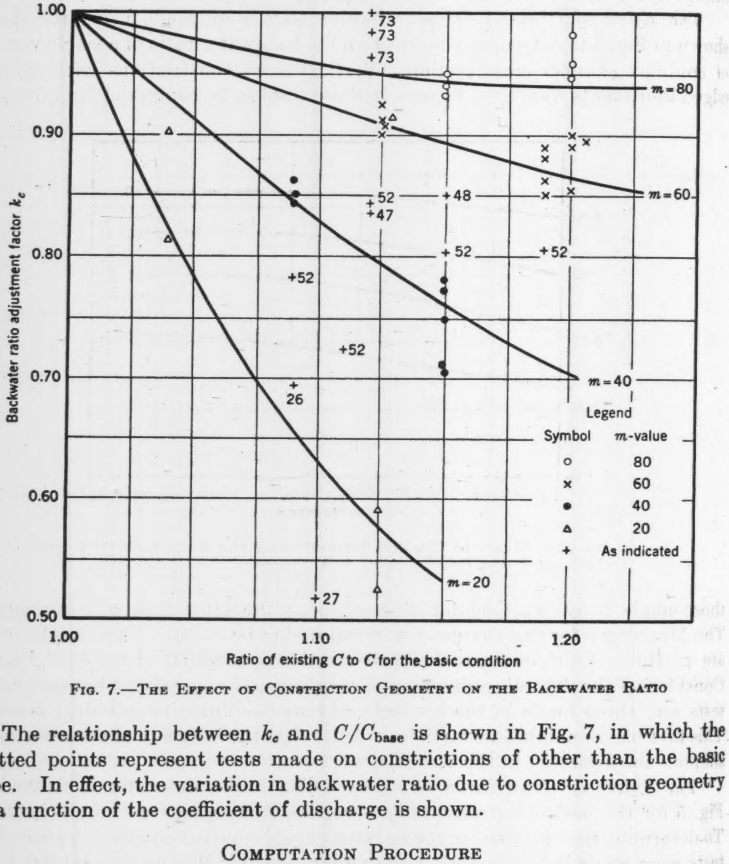

Fig. 7.—The Effect of Constriction Geometry on the Backwater Ratio

The relationship between k_c and C/C_{base} is shown in Fig. 7, in which the plotted points represent tests made on constrictions of other than the basic type. In effect, the variation in backwater ratio due to constriction geometry as a function of the coefficient of discharge is shown.

Computation Procedure

In this study a nominal backwater produced by open-channel constrictions, which has been referred to as h^*_1 (Fig. 1), has been defined. This backwater is the difference between the water-surface profile of the normal channel and that of the constricted channel at an arbitrarily chosen section (section 1). This backwater index has been divided by a known quantity, Δh, to yield a dimensionless measure of the backwater effect.

When integrated with an earlier study in which the discharge characteristics of open-channel constrictions were investigated, and using the concepts and charts developed during that study,[3,4] the results of the present analysis may be used to predict h^*_1 for constricted natural channels, within the scope of this study.

The backwater, h^*_1, is computed as the product of $h^*_1/\Delta h$ and h. The difference in piezometric heads between section 1 and section 3 for the constricted channel, Δh, may be computed from Eq. 1. The solution of this equation depends on a knowledge of the channel properties at section 1 and section 3 and on the evaluation of the coefficient C.

The backwater ratio itself, $h^*_1/\Delta h$, has been shown by laboratory data to be a function primarily of the percentage of channel contraction. The influences of bed roughness and constriction geometry are secondary. Variables characteristic of the flow, such as the Froude number and the depth, are largely unimportant in their effect on this ratio.

In application, $h^*_1/\Delta h$ appropriate to the bed roughness and percentage of channel contraction is selected from Fig. 5. Compatible with the conditions under which the laboratory tests were made, this roughness must represent an average in the channel reaches both upstream and downstream from the constriction. Some latitude is tolerable in the precision of the selection because of the relative insenstivity of $h^*_1/\Delta h$ to the Manning n. Computation of m for a channel of nonuniform roughness is described elsewhere.[4]

After $h^*_1/\Delta h$ of the previous step has been chosen, it is adjusted for a constriction-geometry effect by the factor k_c obtained from Fig. 7. This correction factor is a function of C/C_{base} (the computation of which has been outlined) and the percentage of contraction, m. The adjusted backwater ratio may then be multiplied by Δh to yield the value of h^*_1.

ACKNOWLEDGMENTS

This investigation was conducted as a part of the research program of the Surface Water Branch of the Water Resources Division, USGS. Mr. Kindsvater of the Georgia Institute of Technology, as consultant to this program, made many helpful suggestions during the course of the study.

The writers wish to express their appreciation of the cooperation afforded by Wallace M. Lansford, M. ASCE, and other faculty members of the Department of Theoretical and Applied Mechanics of the University of Illinois, and to William D. Mitchell, M. ASCE, and J. H. Morgan of the Champaign (Ill.) office of the USGS.

APPENDIX. NOTATION

The following letter symbols, adopted for use in the paper and for the guidance of discussers, conform essentially with American Standard Letter Symbols for Hydraulics (ASA-Z10.2), prepared by a committee of the American Standards Association with ASCE representation, and approved by the Association in 1942:

A = area of channel cross section;
B = width of channel;
b = width of opening;
C = coefficient of discharge:
  C_{base} = discharge coefficient for the vertical-faced, square-edged constriction;
  C_c = coefficient of contraction, ratio of area of contracted stream to area of opening;
$\mathbf{F}$ = Froude number, a dimensionless flow parameter for gravity-controlled phenomena;
g = acceleration due to gravity;
h = piezometric head, sum of elevation and pressure heads;
h_f = boundary friction loss;
h^* = a difference in piezometric heads involving normal and constricted channel flow;
K = conveyance, the quantity $\frac{1.49}{n} A R^{\frac{2}{3}}$ in Manning's formula for open-channel flow;
K_L = energy loss coefficient;
k_c = an adjustment coefficient relating the backwater ratio to the backwater ratio for the basic condition;
L = length of constriction, measured parallel to flow;
m = channel contraction ratio;
n = roughness coefficient in the Manning formula for open-channel flow (also used as a subscript to denote "normal");
Q = volume rate of flow, which is the total discharge at a channel cross section;
V = average velocity, ratio of total discharge to total area of a cross section;
y = depth of flow referred to average bottom elevation of cross section;
α = kinetic energy correction factor;
γ = specific weight or weight per unit volume;
Δ = a symbol denoting "change" or "difference"; and
ρ = density or mass per unit volume.

DISCUSSION

Paul V. Hodges,[6] M. ASCE.—A useful and simple method for determining backwater effects caused by different types of channel contractions is presented in the paper. The base curves and coefficients have been defined elsewhere.[4] When the drop in water surface, Δh, for a particular contraction has been determined by field observation, the actual backwater, h^*_1, caused by the contraction can then be determined from base curves similar to those of the authors in Fig. 5, which would give the backwater ratio $h^*_1/\Delta h$ for various percentages of contraction.

According to the tests made in the investigation, the variation of L/b has no effect on the backwater ratio. Elsewhere[4] the coefficient C is shown to vary with L/b, and in Fig. 7 the backwater ratio is shown to vary with coefficient C. Consequently, it appears that the backwater ratio should also vary with L/b.

The basic condition is defined as a vertical-faced constriction with square-edged abutments; the curves in Fig. 5 evidently refer only to this condition. It is inferred that the relationship between $h^*_1/\Delta h$ and m would be different for each type of constriction.

By assuming different values of Δh and y_3 for a particular type and size of bridge opening, the discharge Q can be computed by an equation published previously,[4]

$$Q = 8.02\, C\, A_3 \sqrt{\frac{\Delta h}{1 - \alpha\, C^2 \left(\frac{A_3}{A_1}\right)^2 + 2\, g\, C^2 \left(\frac{A_3}{K_3}\right)^2 \left(L + L_w \frac{K_3}{K_1}\right)}} \quad \ldots (11)$$

in which L_w is the distance upstream from the constriction to section 1 and is assumed equal to the width of opening, b. Thus the relationship between backwater h^*_1 and the discharge can be determined to fit the assumed conditions. Under actual conditions of flow, however, the relative values of Δh and y_3 would be governed by channel characteristics, both upstream and downstream from the contraction, and consequently the discharge could be computed only after the actual determination of Δh and y_3.

The method presented by the authors could often be used to compute the backwater from channel obstructions caused by bridge piers. Backwater formulas, based on many tests, have been derived for the computation of backwater effects of bridge piers; the formula presented by F. A. Nagler appears to be the most satisfactory.[7,8,9] Using the authors' notations, the Nagler formula is

$$Q = 8.02\, K_n\, b \left(y_4 - \frac{\theta\, V^2_4}{2\, g}\right) \left(h^*_1 + \frac{\beta\, V^2_1}{2\, g}\right)^{\frac{1}{2}} \quad \ldots\ldots\ldots\ldots (12)$$

---

[6] Denver, Colo.

[7] "Obstruction of Bridge Piers to the Flow of Water," by F. A. Nagler, *Transactions*, ASCE, Vol. 82, 1918, p. 334.

[8] "Bridge Piers as Channel Obstructions," by D. J. Yarnell, *Technical Bulletin No. 442*, U. S. Dept. of Agriculture, Washington, D. C., 1934.

[9] "Hydraulics of Steady Flow in Open Channels," by S. M. Woodward and C. J. Posey, John Wiley & Sons, Inc., New York, N. Y., 1941, Chapter X, p. 127.

in which K_n is the Nagler coefficient. The values of coefficients θ and β have been given by Mr. Nagler[7,9] and D. J. Yarnell.[8,9]

The relationships among drop in water surface Δh, backwater h^*_1, degree of contraction m, and discharge as computed for a certain type and size of bridge opening are given in Table 1. This table shows the computed value of K_n, which, when used in the Nagler formula, will yield values of the backwater h^*_1.

TABLE 1.—Relationships Among Contraction, Backwater, Discharge for a Vertical–Faced Constriction Having Square–Edged Abutments[a]

m, in percentage	Δh, in feet	Ratio, $h^*_1/\Delta h$	h^*_1, in feet	Coefficient, K_n	Q, in cubic feet per second[b]
20	1	0.34	0.34	0.886	12,900
20	2	0.34	0.68	0.916	19,100
30	1	0.45	0.45	0.861	10,900
30	2	0.45	0.90	0.884	15,900
40	1	0.54	0.54	0.840	9,470
40	2	0.54	1.08	0.860	13,800
50	1	0.62	0.62	0.810	8,510
50	2	0.62	1.24	0.822	12,400

[a] This table is based on the following relationships: $b = 90$ ft, $L = 30$ ft, $y_3 = 15$ ft, $A_3 = 1,350$ sq ft, $n = 0.025$, $y_1 = y_3 + \Delta h$, $y_4 = y_3 + \Delta h - h^*_1$, $L/b = 0.333$, and $y_3/b = 0.167$. [b] Discharge was computed by means of Eq. 11.

The authors indicate that the backwater ratio is not influenced by a variation in the parameters, y_3/b and L/b, but only by the degree of contraction, m. Under these conditions, the method presented in the paper would have wide and easy application compared to earlier methods that are much more complicated and that involve discharge formulas.

•

Carl F. Izzard,[10] A. M. ASCE.—In this paper, as well as in the companion paper by Carl E. Kindsvater, M. ASCE, and Mr. Carter,[3] is reported the first comprehensive effort to obtain experimental model data from which to develop a method for computing backwater caused by a channel constriction such as a bridge. The contribution reflects the judgment of the USGS that small-scale hydraulic model tests offer a sound means of exploring the significance of the many variables involved in the problem of indirect measurement of discharge by the contracted-opening method. The research has been intelligently organized and aggressively conducted. The reports published to date (including the paper) have been confined to conclusions drawn from the experimental data. Although not stated in the paper, the USGS is making field measurements of backwater and discharge as rapidly as possible in order to verify the results of the model tests.

One of the outstanding results of the work is the knowledge of where to take significant measurements of contracted flow. The verification of the laboratory results by prototype measurements will be followed with great interest not only by engineers who want to compute discharge for a known backwater but also by engineers who must estimate backwater for a proposed bridge or other constriction of an open channel.

---

[10] Chief, Hydr. Research Branch, Bureau of Public Roads, U. S. Dept. of Commerce, Washington, D. C.

Viewpoint of the Highway Engineer.—This entire discussion will be limited primarily to the problem from the viewpoint of the highway engineer. His objective is to build a structure that will safely handle the vehicular traffic at a minimum annual cost. That cost should include not only capital investment and maintenance cost but also costs for less tangible items such as flood risk (defined as flood-damage cost multiplied by the probability of flood occurrence). The flood-damage cost is directly related to the backwater both with respect to the damage to abutting property, which sometimes entails litigation, and to the destruction of parts of the highway itself. The frequency of a flood that overtaxes the highway structure determines the period of time over which the probable damage must be charged off as flood-risk cost. Depending on the nature of traffic and the average daily count, the flood-risk cost may also include substantial charges for interruption to, or interference with, movement of traffic. If approach roadways are designed to be subject to overflow, the expected backwater and flood duration are important in addition to the frequency.

The following distinction between the objectives of the hydrologic engineer and those of the highway designer is important: The former is expected to achieve a fairly high standard of accuracy in his estimate of the flood discharge as computed from backwater, and that estimate is the end result. The highway designer, however, reverses the computation and wants to know approximately how much backwater can be expected for floods of various frequencies whose peak discharges can probably be estimated no more accurately than ±20% (unless a gaging station having a long record happens to exist nearby). Obviously, then, the highway engineer does not have to work to the close tolerances expected of the engineer who is gaging streams. This distinction is explained in order to avoid creating the impression that the writer is unduly simplifying a complex problem or casting reflections on the USGS for being too meticulous. At this stage of development the research must be as thorough as possible.

The following analysis was possible only because of the cooperation of the authors who made available all the basic data from the tests conducted at the A. N. Talbot Laboratory of the University of Illinois.

Analysis of Data for the Basic Condition.—A constriction placed in an open channel requires that the velocity in the constricted section be greater than that in the normal section. The forces producing this change in momentum—neglecting forces to overcome normal resistance—are the unbalanced forces represented by the total pressure at some upstream section, minus the total pressure against the embankment constricting the flow and the hydrostatic pressure within the contracted jet. Because the water elevations against the embankment cannot be determined precisely, and because they are decreasing where the flow is accelerating, an exact mathematical analysis in this reach is impracticable, although it is fairly practicable in the case of the decelerating reach below the constriction, as demonstrated in the paper.

This concept leads to a hypothesis that the depth in the approach section relative to the normal depth of flow should correlate with the change in momentum. The change in momentum obviously depends on the conveyance of the constricted section relative to the conveyance of the approach section, which is essentially the same as $(1 - m)$. A convenient form of plotting the experimental data as a means of testing this hypothesis is shown in Fig. 8, in which the ordinate is the depth ratio y_1/y_n previously mentioned, and the abscissa is the velocity head in the constricted section relative to the "normal" depth. "Normal" depth in Fig. 8 is taken as the depth of flow in the unconstricted channel at section 3. This depth is considered to be the same as "normal" depth at section 1 in the unconstricted channel although there actually is a slight difference due to the nonuniform flow caused by the level bed of the flume. The velocity head at the constricted section is based on the area at the "normal" depth, and the mean "normal" depth $\bar{y}_n$ is this same area divided by the top width of the water surface. The ordinate in Fig. 8 is the backwater depth y_1 relative to y_n, rather than to the mean value.

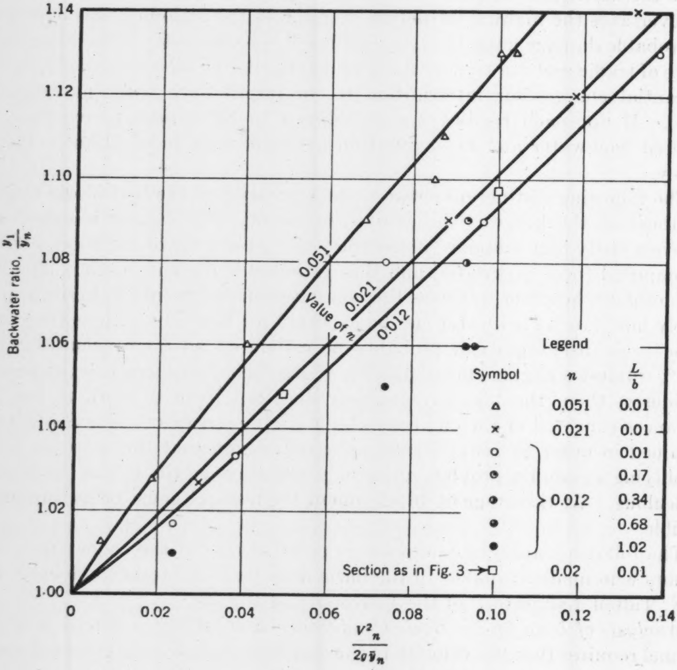

FIG. 8.—BACKWATER DEPTH RELATIVE TO NORMAL DEPTH FOR VERTICAL-FACED CONSTRICTIONS HAVING SQUARE-EDGED ABUTMENTS ($b = 2.95$ ft, $m = 40$)

The experimental data for a vertical-faced constriction with a square-edged abutment of one particular size (basic condition) define three curves for three values of roughness. The maximum difference between extreme values of n is of the order of 2.5% of the normal depth and is therefore not important from the highway engineer's viewpoint. Also, the length of constriction, L, measured along the flow, has little effect so long as L is less than one third of the width of the opening, b. The curves also apply reasonably well to the nonrectangular section (Fig. 3) for a comparable value of m, as shown by the two points so designated in Fig. 8.

For other values of b, the change in momentum for a particular normal flow would be different. In Fig. 9 are shown curves for values of m of 0.21, 0.41, 0.61, and 0.81; no ordinate scale is indicated because the object is to show the relative position of the curves and not to provide a working chart. The curve for m = 0.41 corresponds to an intermediate roughness value in Fig. 8.

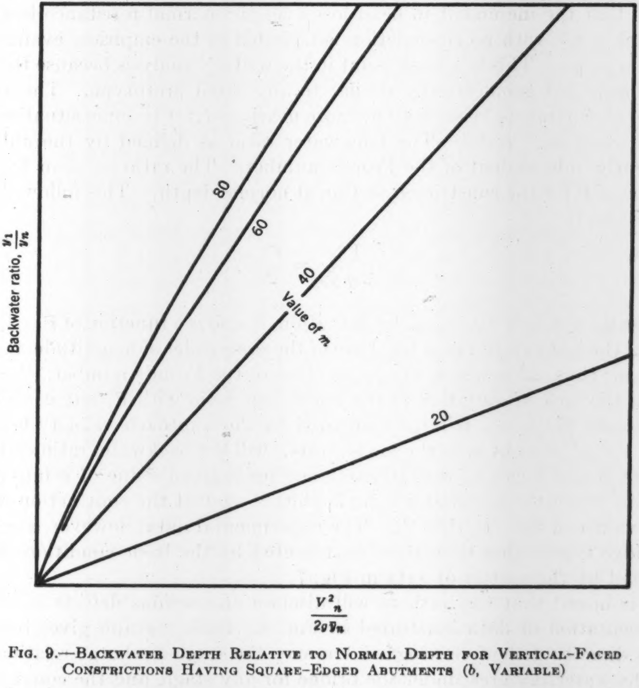

FIG. 9.—BACKWATER DEPTH RELATIVE TO NORMAL DEPTH FOR VERTICAL-FACED CONSTRICTIONS HAVING SQUARE-EDGED ABUTMENTS (b, VARIABLE)

Application of Analysis.—The apparent correlations obtained from analyzing the data from the scale model are encouraging but not conclusive. The indications are that a graph such as Fig. 9 might be used as a simple means of estimating the relative backwater caused by bridges of different length. A separate set of curves might be developed for each of the commonly-used bridge types. Adjustment factors for skew, eccentricity, and piers might be computed.

Comparisons of backwater depths computed by this "short-cut" method and by the procedure recommended by the authors for certain hypothetical cases have shown reasonably close agreement. The agreement is closer for irregular cross sections if the depth ratio at the upstream point is considered to apply to the mean depth at the section rather than to the depth above the stream bed at a particular point.

The validity of any computational method based on the model tests cannot be firmly established until prototype measurements of backwater and discharge are available for verification. Actual stream crossings will rarely involve depths of flow as great (relative to the flow width) as those used in the model test.

Although the use of a level flume simplified testing at both laboratories, the effect of stream slope on backwater is obscured. It seems reasonable to assume that the increment in head loss over the normal resistance loss in the approach reach with no constriction is included in the empirical evaluation of the ratio y_1/y_n. This is a weak point in the writer's analysis because the model is obviously not geometrically similar to any usual prototype. The authors' method of separating losses may be more nearly correct in some situations.

The Backwater Ratio.—The backwater ratio as defined by the authors is apparently independent of the Froude number. The ratio y_1/y_n in Fig. 8 is a function of F for the constricted section at normal depth. This follows because the abscissa is

$$\frac{V^2_n}{2\,g\,\bar{y}_n} = \frac{\mathsf{F}^2}{2} \qquad (13)$$

Because $y_n + h^*_1 = (y_1/y_n)y_n$ by definition, it also is a function of F. Furthermore, if the last two terms in Eq. 1 are of the same order of magnitude, they tend to cancel; thus, Δh is also a simple function of the Froude number. This may explain the lack of variation in the backwater ratio with F, but it also raises a question: If $(h_f)_{1-3}$ is large compared to the approach velocity-head term in Eq. 1 (and it is not so in the model tests), will the backwater ratio still apply?

Figs. 5 and 7 can be readily combined for a given value of n into a single graph in which the backwater ratio is plotted against the contraction ratio for equal values of the variable C_c. The experimental data, however, are meager for bridge types other than those represented by the basic condition, which is indicated by the scatter of data in Fig. 7.

It is hoped that the authors will disclose any serious defects in the form of presentation of data illustrated in Fig. 9. Such a graph gives backwater values directly if the following are known—the stage-discharge relation at the site, the waterway area under the bridge for any stage, and the conveyance of the bridge section in relation to the conveyance of the approach section. It does not give a measure of the depth y_3, which is the depth in the eddy area at the downstream side of the abutment and which is usually less than the normal depth of the unconstricted stream. Although important for indirect discharge measurements, this depth seems to have no engineering significance in bridge design. The model tests indicate that water-surface elevations at other points along section 3 will be slightly higher than elevation h_3.

Anyone experienced in measuring velocities and depths of flow at bridges will know that the bed as a whole (not considering localized scour around piers) may be lower during high stages of flow if the stream bed is alluvial and especially if it is noncohesive. This increase in area apparently would reduce the required velocity, but what would be the effect on backwater values? This is one of the many problems that still must be investigated and may justify use of admittedly approximate solutions of the backwater depth at the present juncture.

HAROLD R. HENRY,[11] J.M. ASCE.—An orderly experimental approach to a long-neglected problem has been presented by the authors in a paper that should eliminate the practice of computing bridge backwater profiles by assuming that the elevation of the water surface at the most contracted stream section is the same as the elevation of the surface downstream from the diffusion reach. This assumption is equivalent to stating that the efficiency of diffusion is zero.

The problem of determining the required bridge clearance or waterway area depends on two principal factors—namely, the hydrology of the contributing drainage area from which the magnitude of the design flood will be derived and the hydraulics of the bridge site after construction of the bridge. The paper is a great step forward in the proper evaluation of the latter.

In order to use the data presented by the authors, the stage of the design flood in the natural channel must also be known. Then the problem of determining the correct clearance becomes one principally of evaluating the backwater caused by the bridge. Although Fig. 5 yields the backwater ratio for a given percentage of contraction, the actual evaluation of the water-surface elevation at section 1 (Fig. 1) must involve a trial-and-error solution for Δh which is defined by Eq. 1. A first-trial assumption for Δh will give first trials for water-surface elevations at sections 1 and 3, which in turn may be used to revise Δh, and so on. A graphical solution based on the use of the curves of specific energy and momentum indicates the possibility of eliminating this trial-and-error computation.

It is significant that the backwater ratio is shown to be almost independent of the Froude number (Fig. 4) and to vary but little with roughness (Fig. 6). However, the presentation of all the data in terms of this ratio tends to obscure the fact that the actual magnitude of the backwater increases considerably with the Froude number and tends to convey the impression without sufficient proof that the role of roughness in determining the magnitude of backwater is minor. The graphical solution referred to previously brings these facts to the fore and is amenable to inclusion of the effect of roughness and energy loss.

In any analytical approach—graphical or otherwise—section 4, downstream from the diffusion reach, is the control section. The depth at this section for bridge conditions is the same as that for natural conditions and must be used as a starting point for the computations of all other depths or surface elevations. This fact is shown in Fig. 1. However, an exception occurs in the case when the percentage of contraction is equal to or greater than the value necessary to cause flow at critical depth in the contracted stream. In this case, the control is at section 2, where critical depth occurs, and the solution must proceed from this known fact. The graphical solution allows rapid determination of the position of the control.

---

[11] Asst. Prof. of Civ. Eng., Michigan State College, East Lansing, Mich.

In the following discussion of the construction of the momentum curves and specific-energy curves necessary for the backwater solution, Eqs. 4 and 5 have been generalized to apply to flow in a channel of arbitrary cross section; it is required, however, that the channel sides be approximately vertical at the elevations for which the water-surface variations are considered. For purposes of discussion it is also assumed that the natural channel is approximately constant in cross section between sections 1 and 4.

Eq. 4 is based on the premise that the pressure force plus the flux of momentum at section 2 are equal to the same sum at section 4. This is true if the resistance force exerted by the channel walls and bottom on the fluid between the two sections is neglected. Expressing this fact with depths placed in ratio to $\bar{y}_c$, the critical mean depth in the natural channel, the following is obtained:

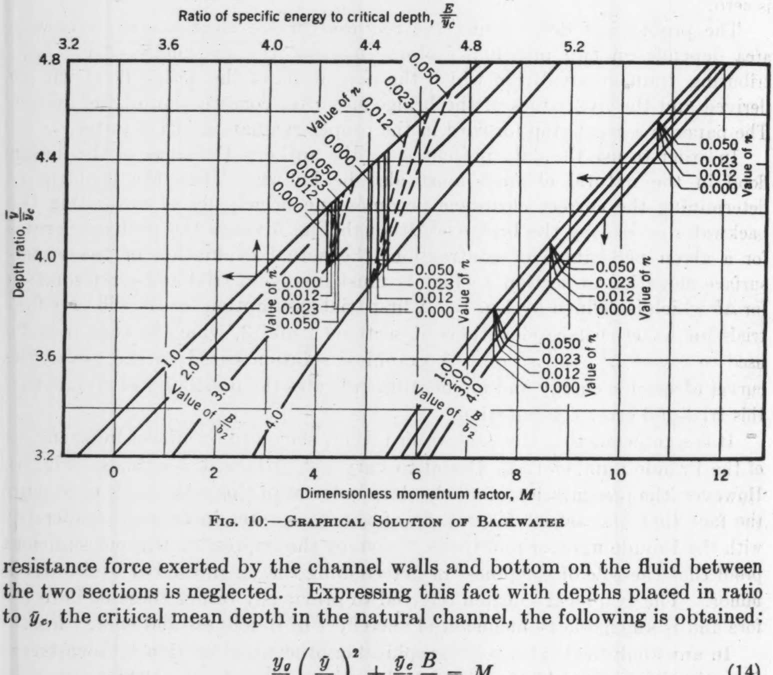

FIG. 10.—GRAPHICAL SOLUTION OF BACKWATER

$$\frac{y_g}{\bar{y}}\left(\frac{\bar{y}}{\bar{y}_c}\right)^2 + \frac{\bar{y}_c}{\bar{y}}\,\frac{B}{b_2} = M \qquad \text{(14)}$$

in which y_g is the distance from the surface to the centroid of the flow section, $\bar{y}$ is the mean depth defined by the ratio of the area to the top width, B is the top width of the flow section in the natural channel, b_2 is the width of contracted stream, and M is the dimensionless momentum factor which is approximately equal at sections 2 and 4. The ratio of y_g to the mean depth is characteristic of the shape of the channel. Its value is 0.5 for a rectangle, 0.542 for a semicircle, 0.6 for a parabola, and 0.667 for a symmetrical vee.

For the example presented herein the value 0.5 is used. The right-hand group of curves in Fig. 10 shows M plotted as the abscissa against a limited practical range of the depth ratio for contraction ratios B/b_2 of 1, 2, 3, and 4. The surface elevation at section 2 may be estimated by dropping a vertical line from the point on the uppermost curve that represents the depth at section 4 to the curve representing the contraction ratio of the live stream at section 2.

The equation of specific energy (Eq. 5) is based on the assumption of no energy loss between sections 1 and 2. The dimensionless expression for the arbitrary channel assumed herein is

$$\frac{\bar{y}}{\bar{y}_c} + \frac{1}{2}\left(\frac{\bar{y}_c}{\bar{y}}\right)^2\left(\frac{B}{b}\right)^2 = \frac{E}{\bar{y}_c} \qquad (15)$$

in which E is the specific energy, which is approximately the same at sections 1 and 2. The left-hand group of curves in Fig. 10 shows specific energy plotted as the abscissa against the depth ratio for contraction ratios of 1, 2, 3, and 4. The surface elevation at section 1 is determined by locating the depth at section 2 (previously found from the momentum curves) on the specific-energy curve representing the contraction ratio of the live jet and projecting vertically to the uppermost curve, which represents conditions at section 1. This solution is the same as that yielded by the upper dashed line in Fig. 5, except that the writer's solution gives the values of water-surface elevations at sections 2 and 1, thus eliminating the need for trial-and-error computations.

A brief inspection of Fig. 10 shows that the magnitude of the backwater, defined as the difference in water-surface elevation at section 1 before and after the construction of the bridge, increases considerably with an increase in the Froude number (a decrease in the depth ratio). However, accompanying this increase in backwater is a decrease in surface elevation at section 2 which keeps the backwater ratio nearly constant, as is indicated by the authors' measurements.

Using the data given in Fig. 5 for the increase in the backwater ratio with the increase in n, the probable effects of roughness on the magnitude of the backwater can be evaluated from Fig. 10. An approximation of the true phenomenon is obtained by assuming that the effect of roughness occurs solely because of a decrease in momentum occasioned by boundary resistance between sections 2 and 4. This assumption is indicated in Fig. 10 for three selected depth ratios at section 4—namely, 4.58, 4.08, and 3.80. The loss in momentum between sections 2 and 4 necessary to yield the increased backwater ratios for $n = 0.012$, 0.023, and 0.050 is shown by the slanting solid lines. For the conditions of the downstream depth ratio of 4.08 and the contraction ratios of 3 and 4, the magnitude of the backwater is shown by the vertical solid lines cutting the specific-energy curves. The increase in the backwater ratio as roughness increases is affected by a decrease in the depression of the water surface at section 2 as well as by an increase in the elevation of the water surface at section 1.

For purposes of comparison with the foregoing assumption, it is assumed that the increase in backwater ratio with roughness as given in Fig. 5 is caused solely by a loss of energy between sections 1 and 2. For the selected downstream depth ratio of 4.08 and contraction ratios of 3 and 4, the slanting broken lines cutting the specific-energy curves yield the magnitude of the backwater. Under this assumption the depression of the water surface at section 2 does not change with n; hence, to yield the authors' values of backwater ratio, the elevation of the water surface at section 1 must be greater than it was under the former assumption.

An indication of the proper solution for the magnitude of backwater, which lies somewhere between the two foregoing assumptions, may be obtained by approximating the actual energy loss between sections 1 and 2 by the method commonly used and given in the paper by Mr. Kindsvater and the authors.[4] In this method the total decrease in energy is taken as the sum of the loss in the approach section and the loss through the bridge. The loss in the approach section is computed from the geometric mean of the friction slopes at sections 1 and 3. The following is a modification of the equation used by Mr. Kindsvater and the authors[12] to yield a dimensionless expression for the head loss between sections 1 and 2 with the added assumptions that the approach length and the length of the abutments are the same as the opening width b and that the hydraulic radius may be approximated by the mean depth:

$$\frac{h_f}{\bar{y}_c} = 14.6\,\frac{B}{\bar{y}_c}\left(\frac{\bar{y}_c}{\bar{y}_2}\right)^{5/3}\frac{n^2}{\bar{y}^{1/3}{}_c}\left[\left(\frac{\bar{y}_c}{\bar{y}_3}\right)^{5/3}\frac{B}{b}+\left(\frac{\bar{y}_c}{\bar{y}_1}\right)^{5/3}\right] \quad \text{........(16)}$$

Preliminary computations with Eq. 16 yield such small values for the dimensionless head loss that they strengthen the validity of the assumption that the increase in backwater with roughness is caused primarily by a decrease in momentum between sections 2 and 4. It is interesting to note the relative roughness ratio appearing in Eq. 16. Although the absolute roughness is usually sufficient for open-channel computations, the role of relative roughness is more pronounced for large n-values and shallow depths, as indicated by the variations of n with depth in the authors' measurements for $n = 0.050$.

The solid lines cutting the momentum curves in Fig. 10 suggest that an empirical law for the loss of momentum might be derived from original data. A guide for determining the loss in momentum is obtained by considering the boundary resistance in uniform flow, which for a unit channel length is $\gamma\, A\, S$, in which S is the channel slope. This expression embodies the fact that the boundary resistance is equal in magnitude to the force of gravity in the direction of flow. For uniform or nonuniform flow the shearing stress exerted on the water by the sides and bottom of the channel depends on the velocity gradient at the boundary in addition to the channel roughness. For uniform flow, the effect of velocity and roughness may be considered by substituting for S its equivalent from the Manning formula, yielding $\gamma\, A\, (Q/K)^2$ for the boundary resistance per unit length. As a first approximation, it is assumed that the mechanism of the boundary shearing stress in the expansion reach downstream from the bridge is such that it may be determined by the latter expression using the conveyance, K, of the active stream section only. Such an assumption leads to the following dimensionless expression for the total boundary force on the body of water between sections 2 and 4:

---

[12] "Computation of Peak Discharge at Contractions," by Carl E. Kindsvater, Rolland W. Carter, and H. J. Tracy, *Circular No. 284*, Geological Survey, U. S. Dept. of the Interior, Washington, D. C., 1953, p. 5, Eq. 3.

$$P = 14.6 \frac{n^2}{\bar{y}^{1/3}{}_c} \frac{B}{\bar{y}_c} \int_0^{a/b_2} \left(\frac{\bar{y}_c}{\bar{y}}\right) \frac{b_2}{b'} \, d\left(\frac{X}{b_2}\right) \ldots\ldots\ldots\ldots (17)$$

in which P is the dimensionless force to be added directly to the dimensionless momentum factor M; a is the distance downstream from the bridge within which the diffusion process occurs; X is the coordinate along the channel with origin at section 2; and b' is the variable width of the expanding stream. The foregoing integral, which embodies a statement of the characteristics of the size of the active stream during the diffusion process, is probably a function of roughness and could be evaluated by laboratory measurements of the jet expansion. Computations assuming that the integral is not a function of n—that is, that P varies only as n^2 with other factors remaining constant—yield values of loss in momentum greater than those indicated by the authors' measurements. The relative roughness appears in Eq. 16 again, showing the importance of this quantity.

It is hoped that the original experimental data of the authors or other data can be used to evaluate more accurately the loss in momentum between sections 2 and 4, facilitating the use of a chart similar to Fig. 10 in solving directly for the magnitude of the backwater.

In the graphical approach it is also possible to consider an appreciable change in the elevation of the mean bottom between sections 1 and 2. Such a change is accompanied by a corresponding negative change of like magnitude in the specific energy. This change may be easily taken into account in the use of Fig. 10. Also, a slight modification of the curves would permit rapid solution of the problem when the average surface width between section 1 and the bridge is decidedly different from the average surface width between sections 2 and 4.

HUBERT J. TRACY[13] AND ROLLAND W. CARTER,[14] A. M. ASCE.—Mr. Henry has provided a thoughtful and stimulating discussion by adapting the momentum and energy statements of Eqs. 4 and 5 to arrive at a direct theoretical solution for the water-level changes at sections 1 and 3. He has shown that this solution may be modified to include the measured friction effects in order to permit its application to nonfrictionless flow.

As Mr. Henry points out, section 4 is no longer the control section when the flow in the contracted stream is critical. The water-surface elevation at section 1 is then independent of the reach downstream from section 3, and its determination may proceed from the recognition of this fact.

It is pertinent at this point to reiterate that the scope of the laboratory investigation was limited to tranquil flow and that, in addition, the Froude number that was used was defined in terms of the total flow area within the constriction and hence is meaningless as a critical flow criterion. It should also be noted that a reliable definition of critical flow for any channel other than a rectangular one is not known.

---

[13] Hydr. Engr., Geological Survey, U. S. Dept. of the Interior, Atlanta, Ga.

[14] Hydr. Engr., Geological Survey, U. S. Dept. of the Interior, Atlanta, Ga.

The direct solution proposed by Mr. Izzard may also be used if an approximation for the backwater is sufficient to fulfill the requirements of the user. The mean-depth relationship becomes less exact for channel shapes that are not rectangular.

Mr. Izzard's comparison of the magnitude of $(h_f)_{1.3}$ with the corresponding size of $\alpha \, V^2{}_1/2 \, g$ as a test of the applicability of the backwater ratio does not seem warranted to the writers. It was concluded from the laboratory tests that, at an n-value of approximately 0.050, the limit of the change in the backwater ratio due to channel roughness had been reached. If this conclusion is valid, the relative size of the two terms is unimportant. An important point has been made however. In applying the results of this study to the computation of the backwater at a specific constriction, the use of Eq. 1 requires the computation of $(h_f)_{1.3}$ from the Manning formula (in the laboratory, both $h^*{}_1$ and Δh were measured directly). If $(h_f)_{1.3}$ is a large part of Δh, the results obtained from Eq. 1 may be approximate.

The writers disagree with the transformation of the Nagler formula made by Mr. Hodges to conform to the notation of the paper. The Nagler formula may be derived from the energy equation by assuming a frictionless rectangular channel and approximating the constricted depth at section 3 by the depth at section 4 minus some multiple, θ, of the velocity head at section 4. This requires that H_3, as derived by Mr. Nagler,[9] be the total fall, $\Delta \, h$, between sections 1 and 3 and not $h^*{}_1$ as shown in the adaptation. The writers were unable to check the computations in Mr. Hodges' table.

The coefficient θ defined by Mr. Yarnell[9] for use in the Nagler formula appears to be unrealistic for any except very small degrees of contraction. Using the laboratory data of this study to compute values of θ, this coefficient was found to vary primarily with m, ranging from zero at a value of $m = 0$ to a value in excess of 10.0 at $m = 0.80$. (Mr. Yarnell's value was a constant, 0.3.)

In this study, the coefficient C has been used as an index to describe the geometry of the constriction in order to relate the change in constriction geometry to the corresponding variation in the backwater ratio. Mr. Hodges questions the conclusion that the backwater ratio can be independent of the length-width ratio L/b of the constriction because C varies with L/b. The invariance of the backwater ratio with L/b merely indicates that the ratio of $h^*{}_1$ to Δh (although both vary with L/b) remains reasonably constant as L/b is independently varied. This, however, is not characteristic of the effect of other geometry features. Thus, as the constriction parameters (other than L/b) varied, $h^*{}_1/\Delta h$ was found to vary. This variation was related to the coefficient C, and the results are shown in Fig. 7.

The writers appreciate the interest shown by Messrs. Henry, Izzard, and Hodges in presenting their alternate solutions and their comparisons with other data.

AMERICAN SOCIETY OF CIVIL ENGINEERS
Founded November 5, 1852
TRANSACTIONS

Paper No. 2772

PLASTIC STRENGTH OF STRUCTURAL MEMBERS

A SYMPOSIUM

PAGE

Foreword

By the Committee of the Engineering Mechanics Division on Plasticity Related to Design 1020

Plastic Deformation of Wide-Flange Beam-Columns

By Robert L. Ketter and Edmund L. Kaminsky, Junior Members, ASCE, and Lynn S. Beedle, A.M. ASCE 1028

Eccentrically Loaded, End-Restrained Columns

By Paul P. Bijlaard, M. ASCE, Gordon P. Fisher, A.M. ASCE, and George Winter, M. ASCE 1070

Eccentrically Loaded Aluminum Columns

By John W. Clark, J.M. ASCE 1116

Investigation and Limit Analysis of Net Area in Tension

By W. Gordon Brady and Daniel C. Drucker, A.M. ASCE..... 1133

FOREWORD

The papers in this Symposium relate to specific problems wherein plastic deformations are a determining factor in evaluating the strength of a structural member. Actually, the role of plasticity in design extends much further. Plasticity underlies current (1955) design specifications to an extent not usually realized and, in addition, offers promise of greater economy in construction. It is the purpose of this foreword to note some of the present and future uses of plasticity in relation to structural design; this, indeed, is the primary objective of the Committee on Plasticity. Attention is called to the fact that the research reported on in three of the papers was sponsored by the Column Research Council of the Engineering Foundation.

STRUCTURAL STRENGTH

A bridge or building—or any other engineering structure—is structurally satisfactory if during its useful life it carries (without excessive deflection) the intended loads with a minimum of initial and operating costs. The ability to carry load can be termed "structural strength" and can be determined by any one of the following four modes of behavior:

1. Buckling, which may be either elastic or plastic, or a combination of the two. The buckling may be localized or general.
2. Endurance strength—that is, the capacity of the structure to carry repetitions of load without a fatigue-type fracture.
3. Brittle fracture under static load, usually resulting from a combination of adverse factors that may include low temperature, combined tensile stress, poor material, and local faults in material, design, or fabrication processing.
4. Large deflections concurrent with plastic yield and increasing load. The structural strength in this case can be computed by a "plastic" analysis.

Engineers are becoming increasingly aware of the importance of this fourth criterion of behavior and of the fact that it can logically be used as a basis for design for those cases in which failure is not caused by the other three possibilities listed.

The idea that initial permanent deflection rather than plastic strength should be the basis for structural design was fostered by the early development of the theory of elasticity; in this theory the assumption of proportionality between stress and strain is basic. S. Timoshenko has stated,[1] with regard to Navier's work of 1826:

> "Navier, from the very beginning, states that it is very important to know the limit up to which structures behave perfectly elastically and suffer no permanent set. Within the elastic range, deformation can be assumed proportional to force and comparatively simple formulas can be established for calculating these quantities. Beyond the elastic limit the relation between forces and deformations becomes very complicated and no simple

---

[1] "History of Strength of Materials," by S. Timoshenko, McGraw-Hill Book Co., Inc., New York, N. Y., 1953, p. 74.

formulas can be derived for estimating ultimate loads. Navier suggests that the formulas derived for the elastic condition should be applied to existing structures, which had proved to be sufficiently strong, so that safe stresses for various materials could be determined which later could be used in selecting proper dimensions for new structures."

In considering this statement by Mr. Timoshenko, it is to be noted that both expediency and simplicity of stress analysis were influential in directing engineers to adopt the foregoing safe basis for strength analyses. Thus, the development of mathematical procedures for stress analysis has not been without its drawbacks; it has tended to overemphasize the importance of stress—rather than strength—as a guide in engineering design. At present (1955) the rules of plastic analysis are better understood and thus permit a return, on a rational basis, to plastic strength as a valid, although not exclusive, basis for determining structural acceptability.

Design procedures based on plastic strength have been included under the broader terms, "limit design" or "collapse-load design." Actually the plastic or ductile behavior of steel used in structural members and frames is important both to elastic design and plastic design. In both concepts, too, the inherent ductility of steel is relied on to provide an intangible factor of safety against the possibility of sudden brittle fracture. There is no intrinsic logic in the argument that stress in a steel structure should not go beyond the elastic range. If such an argument were sound, much current design practice would have to be abandoned. Both for buildings and bridges, specifications allow the designer to use stresses caused by bending, shear, and bearing that result in actual local yielding. Such yielding occurs in pins and rivets and at local points. This local yield results from stress concentrations that are neglected in the simple design formulas. Plastic action is thus depended on to assure the safety of steel structures, and experience has shown that average or nominal maximum stresses form a satisfactory basis for design. Structural members also experience yield while being straightened in the mill, fabricated in a shop, or forced into position during erection. It is actually during these operations that ductility beyond the yield point of steel is utilized to the greatest degree. Having permitted such yielding in the mill, shop, and field, there is no valid basis to prohibit it thereafter, provided such yield has no adverse effect on the structure.

In the earliest days of the art, the engineer intuitively designed structures that, as a result of his experience and feeling for structural behavior, had the strength and durability that was needed. Although theoretical analysis is part of most design procedures, experience is probably still one of the major factors in the writing of specifications. As the engineer learned analytical methods of elastic stress analysis and coupled these with results of laboratory tests on the strength of materials and structural members, his attention was more and more drawn to the individual member, rather than to the whole structure. At present (1955) the trend in analysis and in the laboratory has returned to a consideration of the complete structure rather than the individual structural component.

Plastic Strength in Design Practice

Whether strength is determined by buckling, repeated load, brittle fracture, or plastic behavior, the usual or conventional basis for structural design has been stress analysis rather than strength analysis. Nevertheless, there has been implied a consideration of maximum plastic strength, on the basis of experience, that has found its expression in a permitted variation in the maximum allowable stress under various structural conditions. The knowledge that plastic strength is at least indirectly a part of design practice should offer some encouragement to those who feel it should be more directly accepted as a rational basis for structural design. Two examples, out of the many that might be chosen, will be used to indicate how the evaluation of strength in the plastic range may be utilized to justify allowable unit stresses that are permitted in

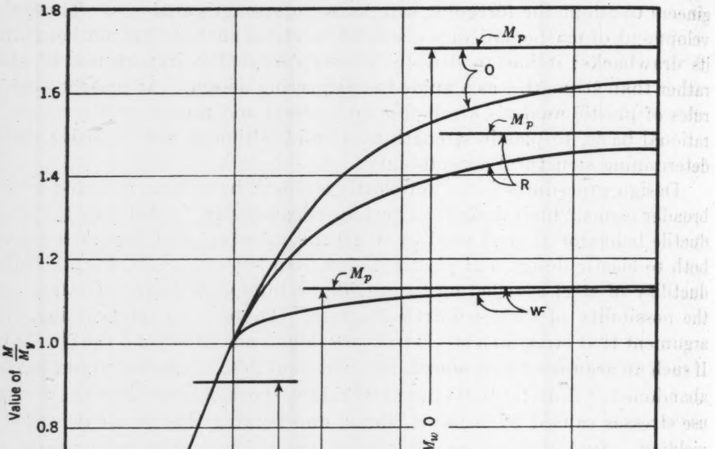

Fig. 1.—Moment Angle Change Relationship

conventional design practice. The first example is concerned with the design of a simple beam (involving local plastic flow), and the second, with a continuous beam (involving distributed plastic flow).

It is well known that when the maximum direct stress caused by bending of a simple beam reaches the yield point failure may or may not be imminent. In some cases—even for a simply supported beam (depending on the shape of the cross section)—much additional load can be carried without excessive deflections. The methods for computing the inelastic relation between bending moment and rate of change of slope per unit length in a beam have long been established. Fig. 1 shows illustrative cases plotted nondimensionally wherein the ratio of bending moment M to bending moment at initial yield M_y is plotted as the ordinate, and the ratio of angle change per unit length ϕ to ϕ_y at initial yield is plotted horizontally. Curves for three cross sections are shown—that of the wide-flange structural shape (denoted by WF), the rectangular beam (denoted by R), and the solid circular section (denoted by O). The greatest "reserve" strength is shown by the solid circular section, in which a moment of 1.70 times M_y is approached after the elastic range is exceeded. Such a section is said to have a "shape factor" (μ) of 1.70. These curves are determined from a simplified stress-strain curve for structural steel that is assumed to consist of two straight lines, one a line with a slope E for the elastic range, and the second a horizontal (plastic-range) line at the yield point for which strain is assumed to proceed with no increase in stress—a reasonable approximation in the case of structural steel. The rectangular steel beam has a value of $\mu = 1.5$; the particular wide-flange structural shape (21WF42) selected for this comparison has a value of $\mu = 1.13$ and the maximum moment is approached in the early states of inelastic bending. In Fig. 1 there are compared the design moments M_w recommended by the American Institute of Steel Construction (AISC) which permit a maximum stress[2] of 20 kips per sq in. when a laterally supported structural shape is used as a beam. This moment is 0.61 times the moment M_y at the yield stress[3] of 33 kips per sq in. that is the minimum for structural steel. Thus, the ratio between the plastic moment M_p for the 21WF142 beam and M_w is 1.86, as indicated in Fig. 1. This is the true factor of safety if the steel beam does not buckle, fracture, or fail by fatigue. In the design of a round steel pin in bending, the same AISC specification permits an allowable stress of 30 kips per sq in. The ratio of M_p to M_w is 1.86—exactly the same as for the particular wide-flange section cited as an example. The agreement between the true factors of safety with respect to ultimate strength in the two cases, although somewhat of a coincidence, is indicative of the influence of experience on the part of engineers, resulting in different permitted working stresses for various practical conditions. Probably no such analysis as the foregoing influenced the choice of different unit stresses that gave identical factors of safety with various sections; nevertheless, the choice of such stresses may be justified on this basis. When years of experience have led to certain empirical practices, these practices can usually be justified on a scientific basis.

---

[2] "Steel Construction Manual," A.I.S.C., 1951, p. 286.

[3] "Standard Specifications for Steel for Bridges and Buildings" *ASTM A7-46*, A.S.T.M., 1946.

Fig. 2 presents a second example of the influence of plastic strength on the choice of permissible unit stresses in design practice. In this case the approach is directly related to the trend to utilize the plastic-strength capacity of a continuous beam or frame as compared to a design based on initial yield. The AISC has adopted[2] an allowable direct stress due to bending for continuous beams of 24 kips per sq in. at the interior supports. The dimensionless curves in Fig. 2 show, as the ordinate, the ratio of the total load per span W to the load causing initial yield W_y. The computations apply to any span of an indefinite number of spans, the results also being applicable to a single span with fully clamped ends. As the abscissa in Fig. 2 there is plotted the ratio of the deflection at the center of a particular span Δ to the deflection at the center at initial yield Δ_y. Including both the shape-factor effect, as previously cited, and the redistribution of bending moment that occurs after initial yielding takes place over the supports of a continuous beam, the indicated increased strength of the continuous beam in the early stages of plastic deflection as compared to the strength of a simple beam seems well worth considering in structural

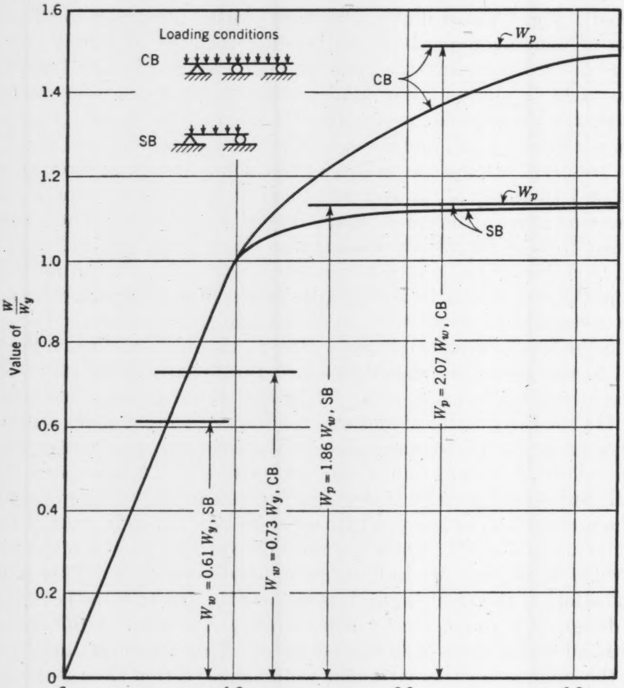

FIG. 2.—UNIFORM LOAD-DEFLECTION RELATIONSHIP

design. The general shape of the load-deflection curve is not much different from that of a simple beam in bending. The full plastic load carried by the continuous beam is 2.07 times the load at initial yield whereas (as previously) the full plastic load for the simple beam is 1.86 times the design load. If 20 kips per sq in. had been used instead of 24 kips per sq in. in conventional design, the strength factor of safety would have been 2.49. Thus, plastic design is already being applied on a limited basis by an approach that adheres to the conventional use of a permissible unit stress rather than a more rational approach based on the computation of maximum structural strength. It might be argued that the unit-stress approach is best because it has already been accepted and that in the further application of plastic-strength analysis to structural design one should simply use different permissible stresses for different shapes, structures, and load conditions. This would require a tremendously complex cataloging of cases and would reduce the procedure to a more or less empirical rather than rational one.

The limited use of plastic design for continuous beams, as permitted by the AISC, has been cited as a recent development in the United States. However, such application of plastic analysis to structural design is by no means new. Plastic analysis, when applied to tier-building design for wind loads, may result in frames quite similar to those arrived at by a so-called elastic analysis. These usually have assumed points of contraflexure in columns at half-story heights. Wherever this assumption has been in error, there has been an actual moment (under the assumed loads) at one floor level greater than that computed and acceptable only because the possibility of plastic action was acceptable. Earlier and more direct application of plastic design has been made in other countries, as will be cited subsequently.

DEVELOPMENT OF PLASTIC ANALYSIS IN DESIGN

The application of plastic analysis to structural design appears to have been initiated by Gabor Kazinczy.[4] Mr. Kazinczy also suggested analytical procedures in which the plastic-hinge concept was utilized for the first time; that is, when a maximum moment occurs at a particular point in a beam there is assumed to develop a plastic hinge. Then, as the bending moment approaches the limiting plastic moment with increasing localized bending, increments of bending moment approach zero and adjacent beam segments rotate with respect to each other more or less as rigid links—thus acting in this load range as two parts connected by a hinge.

Early tests in Germany were made by H. Maier-Leibnitz[5] who showed that the ultimate capacity was not affected by settlement of supports of continuous beams. In so doing he corroborated the procedures previously developed by others for the computation of the maximum-load capacity. The efforts of J. A. Van den Broek[6] and J. F. Baker,[7] A. M. ASCE, to utilize the plastic reserve strength as an actual design criterion are well known. Progress in the theory of plastic structural analysis has been summarized[8] by P. S. Symonds and B. G. Neal. A survey of design trends by George Winter,[9] M. ASCE, considers briefly many of the factors germane to plastic design.

---

[4] "Experiments with Clamped Beams," by Gabor Kazinczy, *Betonszemle*, Vol. 2, 1914, pp. 68, 83, and 101.

[5] "Contribution to the Problem of Ultimate Carrying Capacity of Simple and Continuous Beams of Structural Steel and Timber," by H. Maier-Leibnitz, *Die Bautechnick*, Vol. 1, 1917, p. 6.

[6] "Theory of Limit Design," by J. A. Van den Broek, John Wiley & Sons, Inc., New York, N. Y., 1948.

[7] "A Review of Recent Investigations into the Behavior of Steel Frames in the Plastic Range," by J. F. Baker, *Journal*, Inst. of C. E., London, England, Vol. 3, 1949, pp. 185–240.

Progress toward directly utilizing the plastic strength of steel structures as a design criterion can best be made by a full recognition and study of all the various factors that affect the behavior of structures above the elastic limit.

Much experimental, analytical, and design work has been performed at Lehigh University (Bethlehem, Pa.) under the continuing sponsorship of the Welding Research Council with emphasis both on the limitation and potentialities of the method.[10]

Plastic design is now (1955) permitted in England; the designer is allowed to use the "load-factor" design method as long as account is taken of deformations and accurate methods of analysis are used. The British specification states, in part:[11]

> "* * * For the purpose of such design accurate methods of structural analysis shall be employed leading to a load factor of 2, based on the calculated or otherwise ascertained failure load of the structure or any of its parts, and due regard shall be paid to the accompanying deformations under working loads, so that deflections and other movements are not in excess of the limits implied in this British Standard."

The application to actual portal-frame design is given in some detail in a British publication.[12] Apparently, one of the first uses of this specification was in the construction of the gabled continuous welded frames for the laboratory of the British Welding Research Association at Abington, England.[13] The design of this frame showed a weight reduction of approximately 45% in comparison with truss-and-cantilever-column design and 17% in comparison with elastic design of a similar welded continuous frame. One reason cited for the small difference is the fact that greater load factors are required in the specification for plastic design as compared with those for elastic design. On the other hand, it is noted that no lighter frame could have been used because of prohibitive deflections.

The goal in structural design is to provide a safe and enduring structure that incorporates maximum possible economy. If plastic analysis can be applied to design to realize this goal, it will be so applied to a greater and greater extent in the future. Progress in the application of new concepts is slow because the final test is in the actual structure and not in the designer's theory.

---

[8] "Recent Progress in the Plastic Methods of Structural Analysis," by P. S. Symonds and B. G. Neal, *Journal*, Franklin Inst., Vol. 252, 1951, pp. 383-407 and 469-492.

[9] "Trends in Steel Design and Research," by George Winter, *Proceedings*, Building Research Cong., Div. 1, Pt. II, 1951, London, England, pp. 81-88.

[10] "An Evaluation of Plastic Analysis as Applied to Structural Design," by B. G. Johnston, C. H. Yang, and Lynn S. Beedle, *Research Supplement, The Welding Journal*, Vol. 32, 1953, pp. 224s-239s.

[11] "The Use of Structural Steel in Buildings," *British Standard Specification BSS449*, Section 29c, 1948.

[12] "The Collapse Method of Design," *BCSA Publication No. 5*, British Constructional Steelwork Assn., London, England, 1952.

[13] "Developments of Design and Fabrication in Recent British Structures," by W. S. Atkins and E. M. Lewis, *Transactions*, Inst. of Welding, Vol. 14, 1951, pp. 74-84.

Respectfully submitted,

Lynn S. Beedle	Eugene E. Lundquist
William H. Munse	George Winter
John D. Griffiths	Daniel C. Drucker
Frank Baron	P. S. Symonds
R. L. James	Eivind Hognestad

Bruce G. Johnston, *Chairman*

Committee of the Engineering Mechanics Division on Plasticity Related to Design

PLASTIC DEFORMATION OF WIDE-FLANGE BEAM-COLUMNS

BY ROBERT L. KETTER[1] AND EDMUND L. KAMINSKY,[2]
JUNIOR MEMBERS, ASCE, AND LYNN S.
BEEDLE,[3] A. M. ASCE

WITH DISCUSSION BY MESSRS. GEORGE WINTER; AND ROBERT L. KETTER, EDMUND L. KAMINSKY, AND LYNN S. BEEDLE

SYNOPSIS

The results of an analytical and experimental study of the inelastic deformations of wide-flange steel beam-columns are presented. Emphasis has been placed on the influence of axial thrust on the moment-curvature relationship when stresses exceed the elastic limit. The analysis is extended to include the influence of residual stresses; thus, the moment-curvature relationship is developed as a function of axial thrust and residual stress. Buckling loads are then determined for eccentrically loaded steel columns of wide-flange shape, the necessity for an assumed "shape factor" being eliminated. These derived moment-curvature relationships are also applied to determine end rotations and midheight deflections for columns.

Two sizes of wide-flange shapes are considered, and in the experimental studies tests were performed on as-delivered structural sections.

NOTATION

The letter symbols adopted for use in this paper are defined where they first appear, in the illustrations or in the text, and are arranged alphabetically, for convenience of reference, in the Appendix.

INTRODUCTION

When extending the methods of analysis used in engineering mechanics to include the case of elastic-plastic bending, the relationship of applied moments, axial thrust, and resulting curvature for the case where stresses exceed the elastic limit is basic in importance. This relationship is important because it is the integrated effect of the curvature that determines the deflections and rotations. The moment-deflection data are valuable primarily because the data allow for the determination of true maximum loads and the deflection at those loads. Moment-rotation data are also valuable because one can evaluate performance relating to energy absorption. Furthermore, such data indicate the rotation that a member can sustain at near-maximum moments.

NOTE.—Published, essentially as printed here, in November, 1953, as *Proceedings-Separate No. 330.* Positions and titles given are those in effect when the paper or discussion was received for publication.

[1] Research Instructor, Fritz Eng. Lab., Lehigh Univ., Bethlehem, Pa.

[2] Research Engr., David Taylor Model Basin, Washington, D. C.; formerly Research Assistant, Fritz Eng. Lab., Lehigh Univ., Bethlehem, Pa.

[3] Asst. Director, Fritz Eng. Lab., Lehigh Univ., Bethlehem, Pa.

For flexure in the elastic range,

$$\phi = \frac{M}{E\,I} \qquad (1)$$

in which ϕ is the curvature, M denotes the bending moment at the section in question, E is the modulus of elasticity, and I represents the moment of inertia of the cross section about the axis perpendicular to the plane of the applied moments.

Eq. 1 can be extended (neglecting certain higher order terms) in the form of the differential equation:

$$\frac{d^2y}{dx^2} = \frac{M}{E\,I} \qquad (2)$$

in which x is the distance along the member and y denotes lateral deflection. By direct integration, Eq. 2 defines all the various load-deformation relationships.

Above the elastic limit, however, an easy solution does not exist because stress is no longer a linear function of strain and, therefore, ϕ does not vary linearily with M; the problem of determining M-ϕ relationships in the plastic range has been solved for the condition of pure bending.[4] Because in the problem of pure bending the neutral axis of strain coincides with the geometrical center of the section, relatively simple expressions were developed relating M and ϕ. If, however, axial load is applied in addition to the imposed moment, such a strain condition does not exist.

Influence of Axial Thrust.—The determination of M-ϕ curves, including the effect of axial load, has been developed by S. Timoshenko[5] for rectangular sections. For the case of wide-flange shapes, discontinuities of the cross section make direct computation troublesome, and a "point-by-point" method of computing M-ϕ curves for rolled shapes is presented subsequently. It is similar to the method used for the pure-bending case[4] but also includes the influence of axial thrust.

An important assumption made in this derivation is that the Bernoulli-Navier hypothesis (bending strain is proportional to the distance from the neutral axis) can be extended to include the case of plastic deformations. Actually this assumption is an idealization for steel members. As has been described previously,[6] the only requirements are that the strain be proportional to the distance from the neutral axis in the elastic range and that the stress be equal to the lower yield-point stress in the plastic range. Thus, the curvature at any section is a function of the part of the cross section which remains elastic. These requirements are cited subsequently. If the strain-hardening range is considered, it is once again necessary to make an assumption with regard to strain distribution in the inelastic range. Strain hardening, however, is not considered herein.

---

[4] "Plastic Behavior of Wide Flange Beams: Progress Report No. 1," by William W. Luxion and Bruce G. Johnston, *Research Supplement, The Welding Journal*, Vol. 27, 1948, pp. 538s–554s.

[5] "Theory of Elastic Stability," by S. Timoshenko, McGraw-Hill Book Co., Inc., New York, N. Y., 1936, pp. 51–54.

[6] "The Plastic Behavior of Steel Beams," by Ching Huan Yang, thesis presented to Lehigh Univ., at Bethlehem, Pa., in January, 1951, in partial fulfilment of the requirements for the degree of Doctor of Philosophy.

Using the Bernoulli-Navier hypothesis, together with assumptions regarding the properties of the material, there is outlined and illustrated herein a method whereby a relationship of axial load, bending moment, and curvature can be obtained even though stresses exceed the elastic limit.

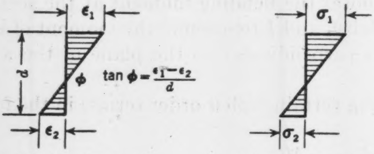

(a) Strain diagram (b) Stress diagram

FIG. 1.—ELASTIC STRESS AND STRAIN DISTRIBUTION

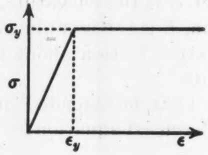

FIG. 2.—IDEALIZED STRESS-STRAIN DIAGRAM

The curvature ϕ is a function of the strain ϵ developed at a section; the moment M and the axial thrust P are functions of the resultant stress distribution, as shown in Fig. 1. Then,

$$P = \int_A \sigma \, dA \quad \text{(3)}$$

$$M = \int_A \sigma y \, dA \quad \text{(4)}$$

and

$$\phi = \frac{\epsilon_1 - \epsilon_2}{d} \quad \text{(5)}$$

in which A is the cross-sectional area, σ is the normal stress, and d denotes the depth. For the case of elastic strains illustrated in Fig. 1 (that is, when $\epsilon_1 < \epsilon_y$ and $\epsilon_2 < \epsilon_y$—in which ϵ_y is the strain corresponding to the initial yield-point stress, as shown in Fig. 2) the distribution of strain and the distribution of stress are similar, σ_1 being equal to $E\,\epsilon_1$, and so forth. When yielding occurs, however, this linear relationship is no longer valid; instead, there results a stress distribution composed of segments of various straight lines or curves depending on the stress-strain properties of the material in question.

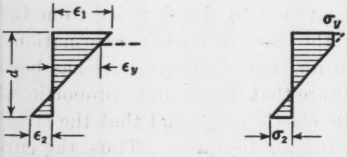

(a) Strain diagram (b) Stress diagram

FIG. 3.—DISTRIBUTION PATTERNS WHEN STRAIN EXCEEDS THE ELASTIC LIMIT

In this analysis the idealized stress-strain curve shown in Fig. 2 is assumed. This curve closely approximates the experimental stress-strain diagram of mild structural steel in the elastic and plastic ranges, but strain hardening is neglected. Fig. 3 is typical of the resultant distribution curves for stress and strain when strains exceed the elastic limit. The stress is equal to the yield-point value when $\epsilon > \epsilon_y$. As would be expected, the moment corresponding to a given value of ϕ would be less than that predicted by using the straight-line relationship of the elastic solution. However, by assuming a given stress pattern, it is possible to compute directly the corresponding value of ϕ; P and M can be determined similarly. This determination can be made for various stress patterns, and curves can be plotted which relate the three variables P, M, and ϕ. For the rectangular section it is not necessary to resort to graphical representation of the interrelation between Eqs. 3, 4, and 5 because analytic expressions connecting these three variables are readily available.[7,8]

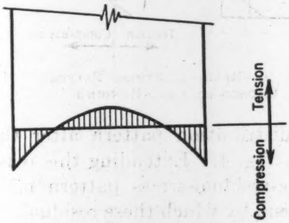

FIG. 4.—HYPOTHETICAL COOLING RESIDUAL-STRESS PATTERN FOR A FLAT PLATE

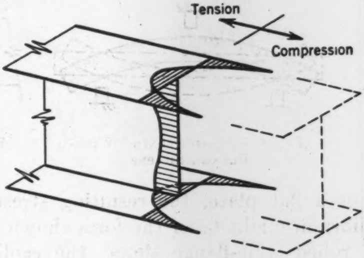

FIG. 5.—TYPICAL COOLING RESIDUAL-STRESS PATTERN FOR A WIDE-FLANGE SECTION

Residual Stresses.—The behavior of structural members may be modified considerably by the presence of residual stresses. Residual stresses are of two basic types: Those caused by differential cooling of the member during and after the rolling process and those that result from cold-bending of the specimen while being straightened or during fabrication.

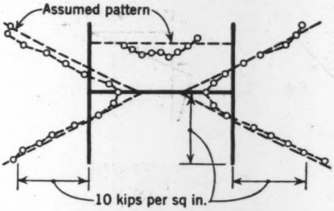

FIG. 6.—MEASURED RESIDUAL STRESS PATTERN FOR THE 8WF31 SECTION

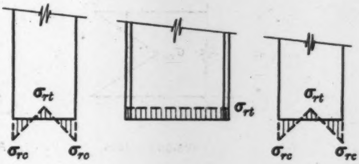

FIG. 7.—ASSUMED COOLING RESIDUAL-STRESS PATTERNS FOR THE WIDE-FLANGE SECTION

Cooling Residual Stress.—When the ingot is originally placed in the rolling mill, the temperature is essentially constant throughout the material.

---

[7] "The Buckling Strength of Metal Structures," by F. Bleich, McGraw-Hill Book Co., Inc., New York, N. Y., 1st Ed., 1952, pp. 37–39.

[8] 'Buckling of Compressed Steel Members," by George Wastlund and Sven G. Bergstrom, *Transactions*, Royal Inst. of Technology, Stockholm, Sweden, 1949, p. 54.

However, as it travels through the various rolls (each reducing the thickness of the different parts of the section), and later on the cooling bed, a differential in temperature develops. As a result of this differential and the subsequent plastic deformation of various parts of the cross section at high temperature, the parts that cool the fastest are usually found to be in residual compression while the slower cooling parts contain tensile residuals.

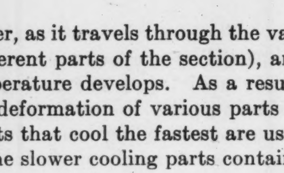

FIG. 8.—STRAIGHTENING WIDE-FLANGE SHAPES

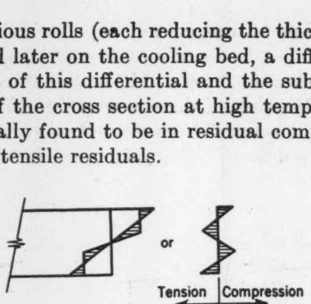
or
Tension
Compression

FIG. 9.—RESIDUAL STRESS PATTERN CAUSED BY COLD-BENDING

For a flat plate, the resulting stress-distribution pattern after thermal equilibrium might be of the form shown in Fig. 4. Extending this reasoning to a rolled wide-flange shape, the cooling-residual-stress pattern might be similar to that shown in Fig. 5; the mechanism by which these residual stresses are formed has been described.[9,10] The influence of cooling residual stresses on axially-loaded specimens has also been described.[11]

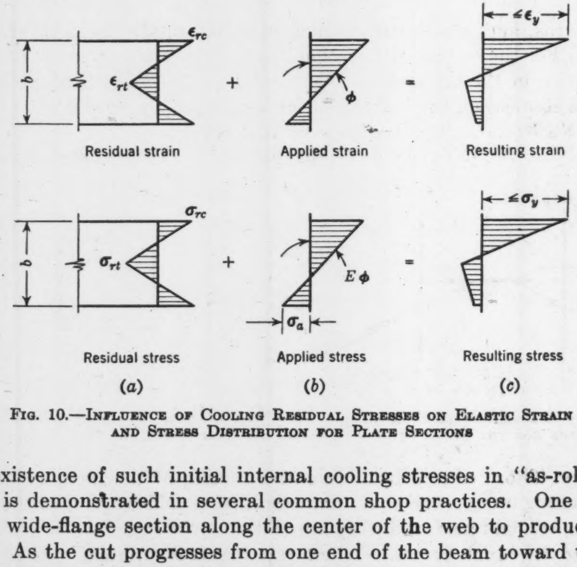
$\le \epsilon_y$
ϵ_{rc}
b
ϵ_{rt}
+
ϕ
=
Residual strain
Applied strain
Resulting strain
$\le \sigma_y$
σ_{rc}
b
σ_{rt}
+
$E\phi$
=
σ_a
Residual stress
Applied stress
Resulting stress
(a)
(b)
(c)

FIG. 10.—INFLUENCE OF COOLING RESIDUAL STRESSES ON ELASTIC STRAIN AND STRESS DISTRIBUTION FOR PLATE SECTIONS

The existence of such initial internal cooling stresses in "as-rolled" steel members is demonstrated in several common shop practices. One is that of cutting a wide-flange section along the center of the web to produce two T-sections. As the cut progresses from one end of the beam toward the other,

---

[9] "Welding Handbook," Am. Welding Soc., 3d Ed., 1950.

[10] "Residual Stress and the Yield Strength of Steel Beams: Progress Report No. 5," by Ching Huan Yang, Lynn S. Beedle, and Bruce G. Johnston, *Research Supplement, The Welding Journal*, Vol. 31, 1952, pp. 205s–229s.

[11] "Residual Stress and the Compressive Properties of Steel," by Alfons W. Huber and Lynn S. Beedle, *ibid.*, Vol. 33, 1954, p. 589s.

the individual T's deform—curving away from or toward each other, depending on the distribution of residual stresses.

As a basis for making an assumption with regard to the magnitude and distribution of residual stress, in Fig. 6 there is shown a typical plot of measured residual stresses in the flanges and web for one of the sections considered in this investigation. The experimental points could be approximated either by parabolas or by straight lines. The latter have been chosen to facilitate computations and have been shown[11] to be a reasonable approximation for the shape studied.

In Fig. 7 it is assumed that residual stress decreases linearly from a maximum compressive residual stress σ_{rc} at the flange edge to a tensile residual stress σ_{rt} at the web junction. Furthermore, it is assumed that this tensile stress is constant across the web. It is required that σ_{rc} and σ_{rt} be chosen in such proportions that static equilibrium of the cross section is maintained. This condition is assured if

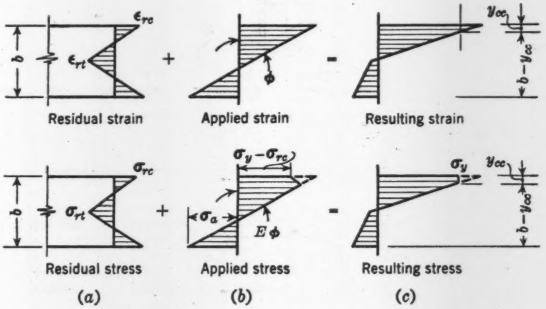

FIG. 11.—INFLUENCE OF COOLING RESIDUAL STRESSES ON STRESS AND STRAIN DISTRIBUTION IN PLATE SECTIONS WHEN STRAINS EXCEED THE ELASTIC LIMIT

$$\frac{\sigma_{rt}}{\sigma_{rc}} = \frac{b\,t}{b\,t + w(d - 2\,t)} = \frac{R_t}{R_c} \qquad \text{. . . . .} \quad (6)$$

in which b is the flange width, t denotes the flange thickness, w is the web thickness, R_t is equal to σ_{rt}/σ_y, and R_c is equal to σ_{rc}/σ_y.

Residual Stresses Caused by Cold-Bending.—After the member passes through the last rolling mill and is cut into lengths suitable for handling, it is placed on the cooling bed. During cooling the member tends to deform because of uneven support and other factors and, when cold, is no longer straight. Therefore, to obtain a straight finished product each member must be cold-bent. The conventional straightening method is to place the member in a "gag" and plastically deform the curved part in the opposite direction to the original curvature. This gag is shown diagrammatically in Fig. 8.

A member enters the gag bent as shown by the solid lines in Fig. 8. By applying a load, it is forced to the position indicated by the dashed lines. If on releasing this load the member is to have the straight form (shown by the dash-dot position), yielding must occur to enable the permanent set to compensate for the original curvature. Because yielding has taken place, the strains in certain fibers have exceeded the elastic limit of the material and will therefore not return to their original positions on removal of the load. The balancing of these strains across the section produces cold-bending residual strains. There is available[10] a discussion of the magnitude and distribution of residual stresses formed as a result of cold-bending. In Fig. 9 there is shown a cold-bending, residual-stress pattern for rectangular members (or wide-flange sections deformed about their weak axis).

Because plastic deformation is localized at points of application of the load in the gag, it would appear that cold-bending residual stresses are also local in nature. It is thus considered that these initial stresses do not have as pronounced an effect on column behavior as do cooling stresses, which are distributed rather uniformly along the length of the member. Therefore, a detailed consideration of the influence of cold-bending residual stresses will not be made, emphasis being directed instead toward the cooling type of initial "locked-in" stresses.

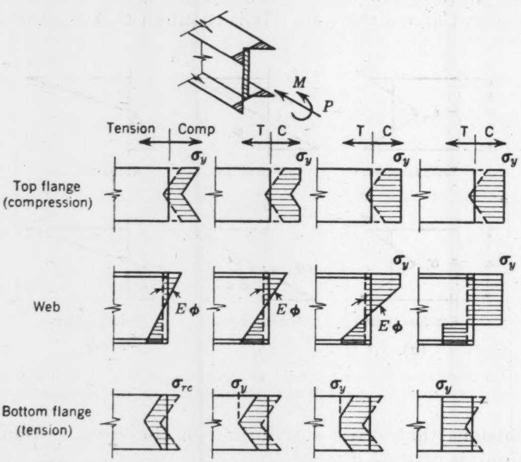

Compression flange	At yield point	Partial yield	Complete yield	Complete yield
Tension flange	Below yield point	At yield point	Partial yield	Complete yield
	(*a*)	(*b*)	(*c*)	(*d*)

FIG. 12.—INFLUENCE OF COOLING RESIDUAL STRESS ON STRESS DISTRIBUTION FOR STRONG-AXIS BENDING OF WIDE-FLANGE SECTIONS

Stress Distribution Beyond the Elastic Limit.—Although the determination of stress distribution and resulting moments and loads from an assumed yield condition is straightforward for members without residual stress, the superposition of load-carrying strains and residual strains requires special attention for members that do contain residual stresses.

In Fig. 10(*a*) there is shown a rectangular section which contains a certain residual strain (and stress) pattern. To this pattern of initial strain one superimposes the strain pattern of an externally applied bending moment and thrust (defined by the applied strain pattern of Fig. 10(*b*)). If the total strains resulting from this superposition (as shown at the top of Fig. 10(*c*)) are within the elastic limit, the applied stress and applied strain patterns are similar across the entire section. Because ϕ is a function of strain whereas M is a function of stress, it is clear that Eq. 1 is applicable to this bending problem. When the combined strains exceed the elastic limit (top of Fig. 11(*c*)), ϕ is no longer a linear function of M. Similarity between stress distribution and strain distribution exists only in those regions in which the combined strains are less than the yield point ($b - y_{cc}$ in Fig. 11(*b*)). The resulting stress pattern (Fig. 11(*c*)) is determined directly from the corresponding strain pattern. The applied stress pattern (Fig. 11(*b*)) is obtained by subtracting the initial residual-stress pattern from the resulting-stress pattern. This description is also applicable to a wide-flange column bent about the weak axis—as long as the web is neglected.

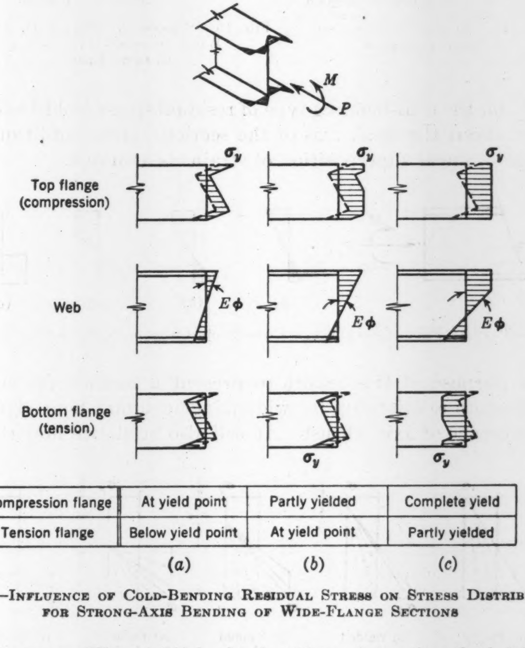

Compression flange	At yield point	Partly yielded	Complete yield
Tension flange	Below yield point	At yield point	Partly yielded
	(*a*)	(*b*)	(*c*)

FIG. 13.—INFLUENCE OF COLD-BENDING RESIDUAL STRESS ON STRESS DISTRIBUTION FOR STRONG-AXIS BENDING OF WIDE-FLANGE SECTIONS

Extending this reasoning to the case of flexure of a wide-flange shape bent about its strong axis, the result of the addition of residual strains and load-carrying strains is illustrated in Fig. 12. On the basis that plane sections before bending remain plane after bending, the applied stress patterns shown in Fig. 12 may be determined by the subtraction process previously described. Under the applied moment and axial load shown diagrammatically, the stress distribution for Fig. 12(*a*) (solid line) is at the instant of first yielding of the compression flange. In Fig. 12(*b*) this flange is partly plastic, and the tension flange has just reached the yield stress. When the compression flange is completely plastic (Fig. 12(*c*)), the tension flange is still partly plastic. In Fig. 12(*d*) the member is completely plastic. A description of the *P-M* relationship at this fully plastic condition is available.[12]

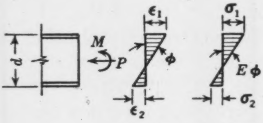

(*a*) Strain diagram (*b*) Stress diagram

FIG. 14.—ELASTIC STRESS AND STRAIN DIAGRAMS

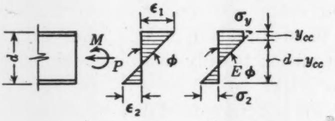

(*a*) Strain diagram (*b*) Stress diagram

FIG. 15.—STRESS AND STRAIN DIAGRAMS WHEN STRAINS EXCEED THE ELASTIC LIMIT

Similarly, for the cold-bending type of residual stress (cold-bending assumed to have been about the weak axis of the section), stress addition is shown in Fig. 13. Again, linear superposition of strains is assumed.

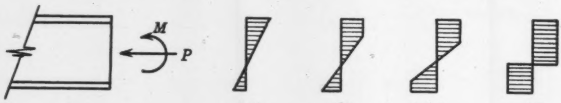

FIG. 16.—TYPICAL PROGRESSIVE YIELD CONDITIONS CAUSED BY BEAM-COLUMN LOADING

It is the purpose of this report to present a method for computing the moment-curvature relationship for wide-flange columns bent about either axis and in the presence of axial thrust. It will also be shown how the presence of residual stress modifies the M-ϕ relationship. Correlation with tests will be shown, and the results will be used to predict the strength of as-delivered columns loaded with equal eccentricities. In the theory, the possibility of local instability and lateral-torsional instability is not considered.

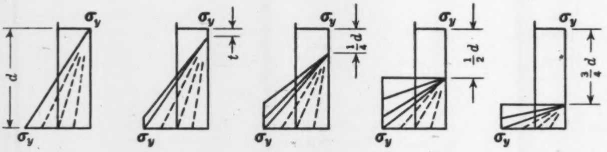

(*a*) Elastic limit (*b*) Yielded through flange (*c*) Yielded $\frac{1}{4}d$ (*d*) Yielded $\frac{1}{2}d$ (*e*) Yielded $\frac{3}{4}d$

FIG. 17.—SAMPLE SET OF ASSUMED YIELD-PENETRATION CONDITIONS FOR DETERMINATION OF AUXILIARY CURVES

---

[12] "Column Strength Under Combined Bending and Thrust: Progress Report No. 6," by Robert L. Ketter, Lynn S. Beedle, and Bruce G. Johnston, *Research Supplement, The Welding Journal*, Vol. 31, 1952, pp. 607s–622s.

MOMENT-CURVATURE RELATIONSHIP

Members Without Residual Stress.—When a member is loaded within the elastic range by combined bending and thrust, stress diagrams and strain diagrams similar to those shown in Fig. 14 result. Because the strains are small in comparison to the depth of the section,

$$\phi = \frac{\epsilon_1 - \epsilon_2}{d} = \frac{\sigma_1 - \sigma_2}{E\,d} \quad \text{(7)}$$

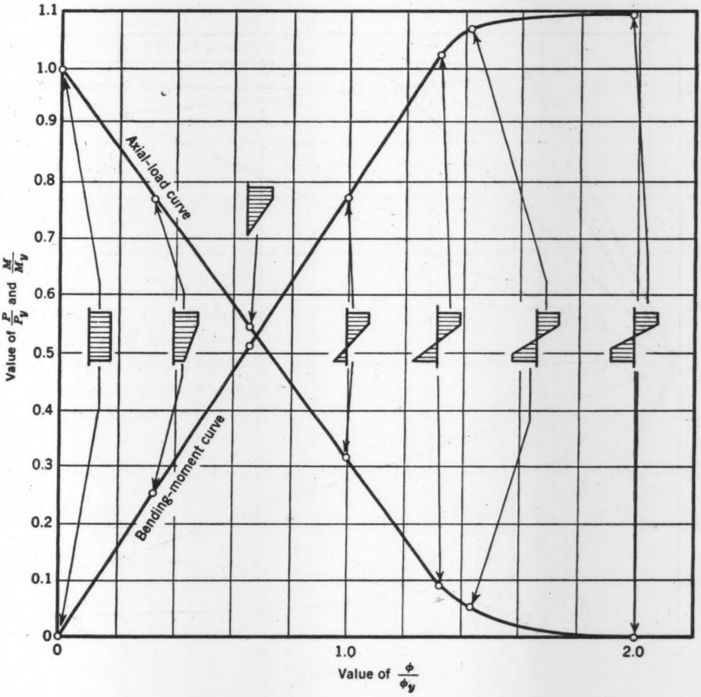

FIG. 18.—AUXILIARY CURVES FOR AN ASSUMED YIELD PENETRATION OF 1/4 *d*

For members loaded beyond the elastic limit (Fig. 15),

$$\phi = \frac{\epsilon_1 - \epsilon_2}{d} = \frac{\epsilon_y - \epsilon_2}{d - y_{cc}} \quad \text{(8a)}$$

or

$$\phi = \frac{\sigma_y - \sigma_2}{E(d - y_{cc})} \quad \text{(8b)}$$

It is thus possible to compute ϕ directly from a stress diagram by considering only that part of the section which remains elastic.

From a stress diagram it is also possible to determine both the moment acting on the section and the applied thrust.[5] By using Eqs. 3, 4, and 8 it is possible to determine M, P, and ϕ for any given stress distribution.

As loads are increased under a given loading condition, it is likely that successive stress distributions will be similar to those shown in Fig. 16. Yielding will first occur at the extreme fiber on the compression side of the specimen. As the loading is increased, yielding will penetrate through the flange on the compression side. Eventually, yielding occurs on the tension side (Fig. 16(c)), and the full plastic condition is typified in Fig. 16(d).

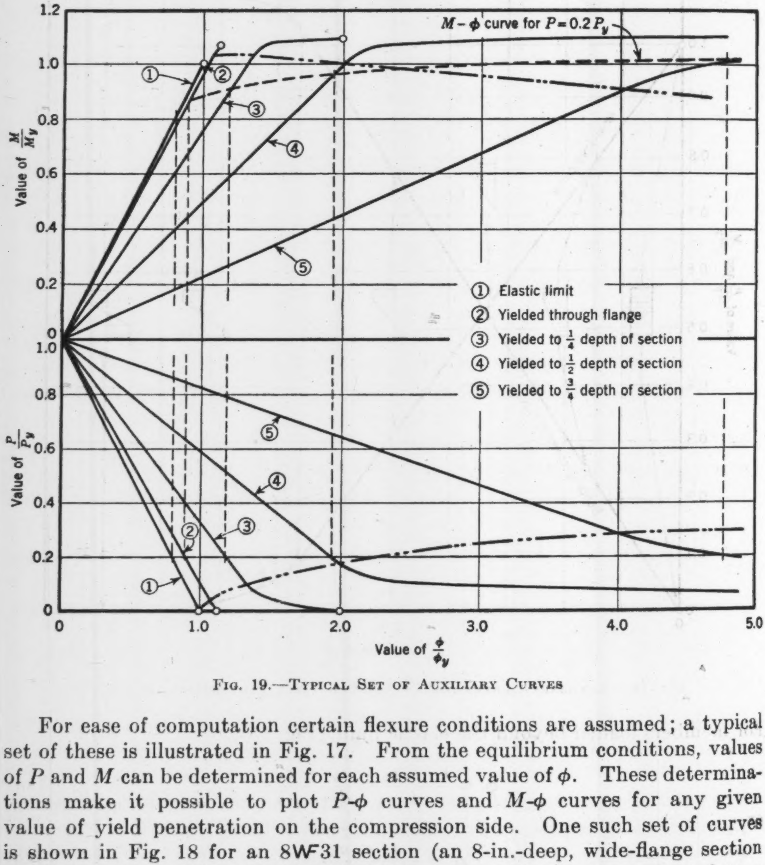

FIG. 19.—TYPICAL SET OF AUXILIARY CURVES

For ease of computation certain flexure conditions are assumed; a typical set of these is illustrated in Fig. 17. From the equilibrium conditions, values of P and M can be determined for each assumed value of ϕ. These determinations make it possible to plot P-ϕ curves and M-ϕ curves for any given value of yield penetration on the compression side. One such set of curves is shown in Fig. 18 for an 8WF31 section (an 8-in.-deep, wide-flange section weighing 31 lb per ft) where yielding was assumed to have penetrated to a depth of $\frac{1}{4}$ d from one side (Fig. 17(c)). These curves have been made nondimensional by plotting P/P_y and ϕ/ϕ_y and M/M_y and ϕ/ϕ_y. For all points plotted, the corresponding stress-distribution diagrams have been shown.

Curves similar to those in Fig. 18 have been computed for each of these assumed values of yield penetration for the 8WF31 section and are presented in Fig. 19. Because the straight-line part of each of these curves is that corresponding to an elastic stress condition on the tension (convex) side of the section, only the limiting cases (in which σ_a is the yield-point stress in compression and tension) need be investigated to define that part of each curve. The limit of this range has been shown as a dash-dot line.

The method of using these "auxiliary curves" (Fig. 19) is to select a value of P/P_y for which an M-ϕ curve is desired. As an example, the value $P = 0.2\ P_y$ is chosen. With this value of P/P_y there is drawn a horizontal line cutting the various auxiliary P-ϕ curves. At these points of intersection, verticals are projected until they intersect the corresponding M-ϕ auxiliary diagrams. Connecting these points gives the desired M-ϕ curve including the effect of an axial thrust of $0.2\ P_y$. This process is indicated in Fig. 19 by dashed lines. Fig. 20 shows the desired curve with the auxiliary construction lines removed.

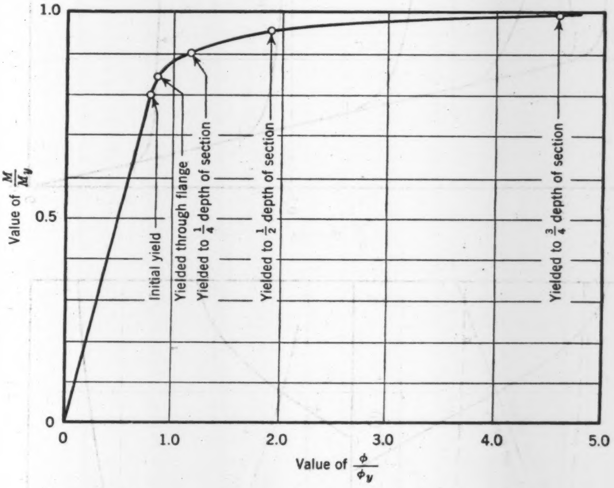

FIG. 20.—MOMENT-CURVATURE RELATIONSHIP FOR $P = 0.2\ P_y$

The curved parts of Fig. 19 have been plotted to a larger scale in Fig. 21 to facilitate greater accuracy in this graphical method. In Fig. 21 M-ϕ curves for several different values of P/P_y have been shown as dashed lines.

The influence of varying axial load for a range of P/P_y is illustrated in Fig. 22. As indicated by the dashed line, only when P is relatively small will the tension flange be plastic. For the range in which the flange remains elastic, only the straight-line part of each auxiliary curve need be considered to obtain the desired M-ϕ curve.

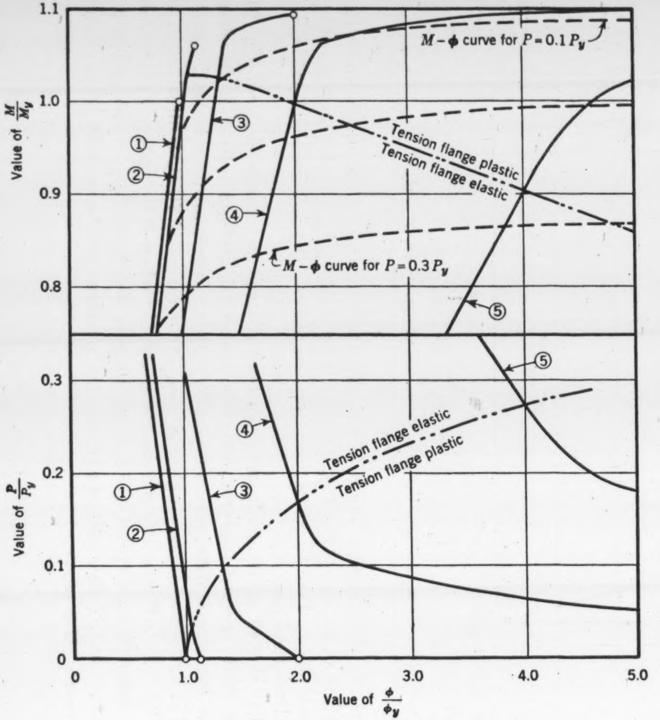

FIG. 21.—ENLARGED AUXILIARY CURVES

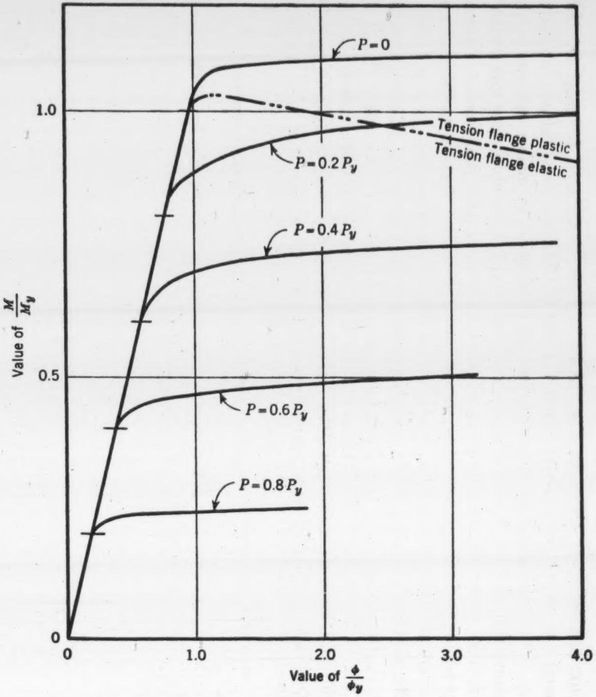

FIG. 22.—MOMENT-CURVATURE RELATIONSHIP FOR THE 8WF31 SECTION (STRONG-AXIS BENDING)

TABLE 1.—SUMMARY OF IMPORTANT EQUATIONS FOR STRONG-AXIS BENDING OF WIDE-FLANGE SECTION (NEGLECTING RESIDUAL STRESSES)

TOP FLANGE (Compression) WEB BOTTOM FLANGE (Tension)	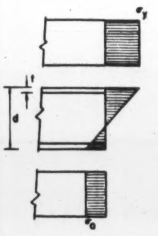 $R_a = \frac{\sigma_a}{\sigma_y}$ CASE 1	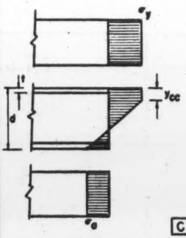 $R_a = \frac{\sigma_a}{\sigma_y}$ $\alpha = \frac{y_{cc}}{d}$ CASE 2	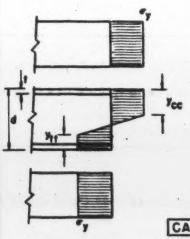 $\alpha = \frac{y_{cc}}{d}$ $\beta = \frac{y_{tt}}{d}$ CASE 3
LIMITS	$-1 \le R_a \le +1$	$\frac{t}{d} \le \alpha \le (1-\frac{t}{d})$ $-1 \le R_a \le 1$	$\frac{t}{d} \le \alpha \le (1-\frac{t}{d})$ $\frac{t}{d} \le \beta \le \alpha$
AXIAL THRUST	$\frac{P}{\sigma_y} = \frac{1-R_a}{2}\left[2bt + w(d-2t)\right]$	$\frac{P}{\sigma_y} = (1-R\ )\left[bt-wt\right] + \frac{(1+R_a)}{2d(1-\alpha)}\left[bt^2 - wd^2(1-\alpha)^2 - wt^2\right]$ $+ wd$	$\frac{P}{\sigma_y} = wd(\alpha-\beta)$
MOMENT	$\frac{M}{\sigma_y} = \frac{1+R_a}{12d}\left[2bt(3d^2-6dt+4t^2) + w(d-2t)^3\right]$	$\frac{M}{\sigma_y} = \frac{(1+R_a)}{12d(1-\alpha)}\left[w\{d(1-\alpha-\frac{t}{d})\}^3\{d(1-2\alpha)-4t\}\right.$ $\left.6d(1-\alpha)(d-t) - 3dt + 4t^2\right]$	$\frac{M}{\sigma_y} = bt(d-t) + \frac{wd^2}{6}\left[6(\beta-\frac{t}{d})(1-\beta-\frac{t}{d})\right.$ $\left.+ (1-\alpha-\beta)(1+2\alpha-4\beta)\right]$
CURVATURE	$\frac{\phi}{\phi_y} = \frac{1+R_a}{2}$	$\frac{\phi}{\phi_y} = \frac{1+R_a}{2(1-\alpha)}$	$\frac{\phi}{\phi_y} = \frac{1}{1-\alpha-\beta}$

TABLE 2.—SUMMARY OF IMPORTANT EQUATIONS FOR STRONG-AXIS BENDING OF WIDE-FLANGE SECTION (INCLUDING RESIDUAL STRESSES)

TOP FLANGE (Compression) WEB BOTTOM FLANGE (Tension)	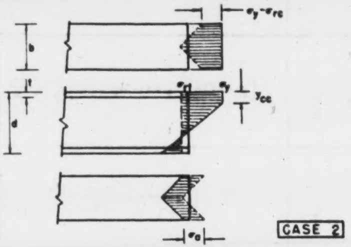 b t d $\sigma_y - \sigma_{rc}$ σ_{rt} σ_y y_{cc} σ_a $R_a = \frac{\sigma_a}{\sigma_y}$ $\alpha = \frac{y_{cc}}{d}$ CASE 2	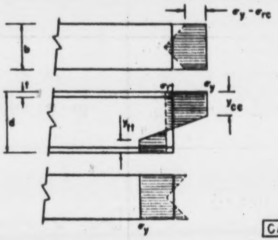 b t d $\sigma_y - \sigma_{rc}$ σ_{rt} σ_y y_{cc} y_{tt} σ_y $\alpha = \frac{y_{cc}}{d}$ $\beta = \frac{y_{tt}}{d}$ CASE 3
LIMITS	$\frac{t}{d} \le \alpha \le (1-\frac{t}{d})$ $-(1-R_c) \le R_a \le +(1-R_t)$	$\frac{t}{d} \le \beta \le (1-\alpha)\frac{R_c+R_t}{2+R_c+R_t}, \quad \beta \le (1-\alpha)$ $\frac{t}{d} \le \alpha \le (1-\frac{t}{d})$
AXIAL THRUST	$\frac{P}{\sigma_y} = \frac{bt}{2}\left[2-R_c+R_t-2R_a+(\frac{t}{d})\frac{1+R_t+R_a}{1-\alpha}\right]+wd\left[(1+R_t)\left\{1-2\frac{t}{d} - \frac{1}{2}(1-\alpha-\frac{t}{d})(1-\frac{t}{d(1-\alpha)})\right\}-\frac{R_a}{2}(1-\alpha-\frac{t}{d})(1-\frac{t}{d(1-\alpha)})\right]$	$\frac{P}{\sigma_y} = bt(R_t+R_c)+w(d-2t)R_t+wd(\alpha-\beta)$
MOMENT	$\frac{M}{\sigma_y} = \frac{bt}{12}\left[3(d-t)(2-R_c+R_t+2R_a)-(3d-4t)(\frac{t}{d})\left\{\frac{1+R_a+R_t}{1-\alpha}\right\}\right] + \frac{wd}{12(1-\alpha)}\left[(1-\alpha)-\frac{t}{d}\right]\left[1-\frac{4t}{d}+2\alpha \quad (1+R_a+R_t)(d\{1-\alpha\}-t)\right]$	$\frac{M}{\sigma_y} = t(d-t)(b-w)+\frac{wd^2}{6}\left[1+\alpha+\beta-2\alpha^2+2\alpha\beta-2\beta^2\right]$
CURVATURE	$\frac{\phi}{\phi_y} = \frac{1+R_a+R_t}{2(1-\alpha)}$	$\frac{\phi}{\phi_y} = \frac{1}{(1-\alpha-\beta)}$

In Table 1 there are contained equations necessary for plotting critical points on the auxiliary curves (Fig. 19 or Fig. 21). It will be noted that the computation is time-consuming, and a tabular solution is appropriate.

No tests using annealed material were conducted as part of this investigation, and consequently comparison between the theory and test is not made herein. However, control tests on axially loaded columns were performed on the 8WF31 material as part of another study.[11]

Members Containing Residual Stress.—By a process analogous to that previously described, expressions for P, M, and ϕ can be developed for assumed yield conditions for sections containing residual stresses; one should examine Fig. 12 for flexure about the strong axis or Fig. 11 for weak-axis bending. The equations for flexure about the strong axis are presented in Table 2 and those for flexure about the weak axis are given in Table 3. In the derivation of these "weak-axis" equations the web was neglected, and the section was considered as two equivalent rectangles. In reality, then, these expressions of M, P, and ϕ apply strictly to the rectangular section. In these equations $R_a = \sigma_a/\sigma_y$, $\alpha = y_{cc}/d$, and $\beta = y_{tt}/d$. The equations, sum-

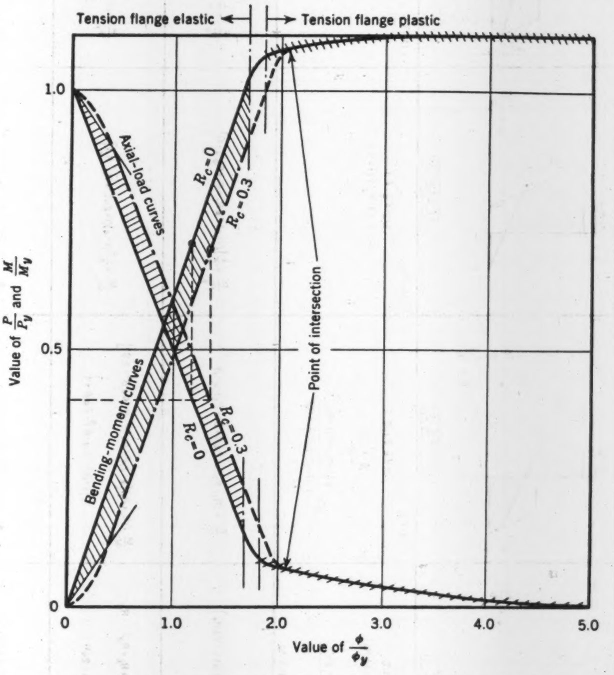

FIG. 23.—AUXILIARY CURVES INCLUDING THE INFLUENCE OF RESIDUAL STRESS ($\alpha = 0.4$ AND $R_c = 0.3$ FOR 8WF31 SECTION)

TABLE 3.—SUMMARY OF IMPORTANT EQUATIONS FOR WEAK-AXIS BENDING OF WIDE-FLANGE SECTION (INCLUDING RESIDUAL STRESSES)

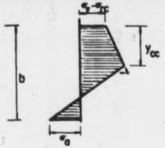 $\alpha = \frac{y_{cc}}{b}$ σ_a positive as shown **CASE 1**	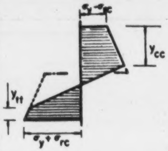 $\sigma_y-\sigma_{rc}$ y_{cc} y_{tt} $\sigma_y+\sigma_{rc}$ $\alpha = \frac{y_{cc}}{b}$ $\beta = \frac{y_{tt}}{b}$ **CASE 2**	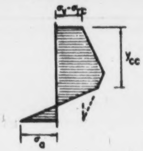 $\alpha = \frac{y_{cc}}{b}$ **CASE 3**	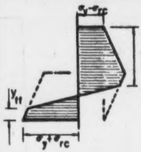 $\sigma_y-\sigma_{rc}$ y_{cc} y_{tt} $\sigma_y+\sigma_{rc}$ $\alpha = \frac{y_{cc}}{b}$ $\beta = \frac{y_{tt}}{b}$ **CASE 4**
LIMITS: $0 \le \alpha \le 1/2$ $-(1-R_c) \le R_a \le (1+R_c)$ - or - $R_a^* \le \frac{R_c(\alpha-1)+(\alpha+1)+2\alpha R_t}{1-\alpha}$ * Condition for Pure Bending	LIMITS $0 \le \alpha \le 1/2$ $\beta = 1/2$ - or - $\beta^* \le \frac{\alpha(1+R_c+R_t)-R_c}{1-(1-2\alpha)(R_c+R_t)}$	LIMITS: $1/2 \le \alpha \le 1$ $-(1-R_c) \le R_a \le (1+R_c)$	LIMITS $1/2 \le \alpha \le 1$ $\beta \le (1-\alpha)$
$\frac{P}{P_y} = \frac{1}{2}\left[(R_c+R_a)(\alpha-1)+(\alpha+1)+2\alpha R_t\right]$	$\frac{P}{P_y} = (R_c+R_t)(\alpha-2\alpha\beta+\beta)-R_c+\alpha-\beta$	$\frac{P}{P_y} = \frac{1}{2}\left[(1+\alpha)-\alpha R_c+R_t+R_a(\alpha-1)\right]$	$\frac{P}{P_y} = \frac{1}{2}(R_t-R_c)+\alpha-\beta$
$\frac{M}{M_y} = \frac{1}{2}(1+\alpha-2\alpha^2)(1+R_c+R_a) - R_c$ $+ R_t(\alpha-2\alpha^2)$	$\frac{M}{M_y} = (R_c+R_t)\left[\alpha-2\alpha^2+4\alpha^2\beta-\beta-4\alpha\beta^2+2\beta^2\right]$ $+(\alpha+\beta)-2(\alpha-\beta)^3-2\alpha\beta+1$	$\frac{M}{M_y} = \frac{1}{2}\left[(1-\alpha)(1+2\alpha)(1+R_a-R_c)\right]$	$\frac{M}{M_y} = (1-\alpha-\beta)(1+2\alpha-4\beta)+6\beta(1-\beta)$
$\frac{\phi}{\phi_y} = \frac{1-R_c(1-2\alpha)+R_a+2\alpha R_t}{2(1-\alpha)}$	$\frac{\phi}{\phi_y} = \frac{1+(\alpha-\beta)(R_c+R_t)}{1-\alpha-\beta}$	$\frac{\phi}{\phi_y} = \frac{1+R_c(1-2\alpha)+R_a+2R_t(1-\alpha)}{2(1-\alpha)}$	$\frac{\phi}{\phi_y} = \frac{1+(R_c+R_t)(1-\alpha-\beta)}{1-\alpha-\beta}$

marized in Table 2, reduce to those shown in Table 1 for annealed material when the residual stress is zero ($R_c = R_t = 0$).

Auxiliary P-ϕ curves and M-ϕ curves are shown in Fig. 23 for one "alpha" condition ($\alpha = 0.4$ indicates that yielding has penetrated to 0.4 of the depth of the member). The assumed residual-stress function ($R_c = 0.3$) is consistent with actual residual-stress measurements. Also shown in Fig. 23 are the auxiliary curves for material free from residual stress. These curves have also been made nondimensional by plotting P/P_y and ϕ/ϕ_y and M/M_y and ϕ/ϕ_y. The parts which are crosshatched correspond to regions covered by the equations in Tables 1 and 2. Where shading is missing, the member has partly yielded in the tension flange, and the equations for this short region are not presented.

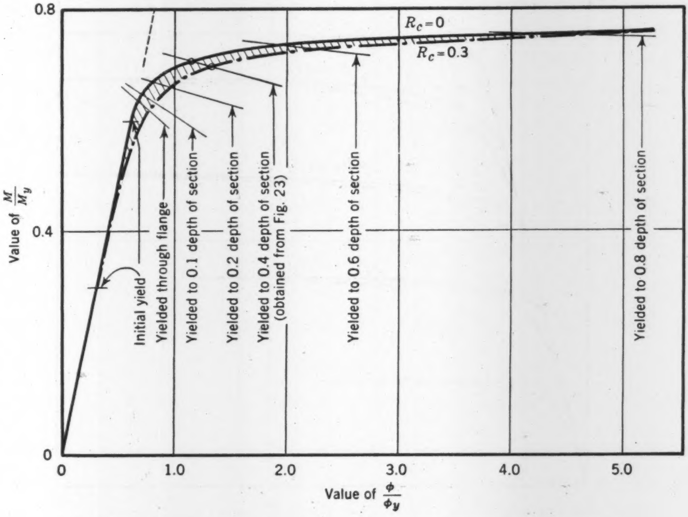

FIG. 24.—MOMENT-CURVATURE RELATIONSHIP INCLUDING THE INFLUENCE OF RESIDUAL STRESS FOR $P = 0.4\ P_y$

In Fig. 23 the point of intersection between the curves for R_c equal to zero and 0.3 is determined by either

$$\beta = (1 - \alpha)\frac{R_c + R_t}{2 + R_c + R_t} \tag{9a}$$

or

$$\beta = \frac{t}{d} \tag{9b}$$

whichever gives the larger value of β. Eq. 9a corresponds to

$$\frac{\phi}{\phi_y} = \frac{2 + R_c + R_t}{2\,(1 - \alpha)} \tag{10}$$

This method of assuming a penetration of yielding on the compression side of the section and then determining curves of P and ϕ and M and ϕ can be performed for any value of yield penetration. Six different values were assumed to obtain the curves presented herein. For each value, a set of curves similar to those in Fig. 23 was plotted preparatory to plotting the M-ϕ curves. The latter are obtained for a given axial load by drawing a horizontal line cutting the various auxiliary P-ϕ curves at the assumed axial-load value; the value $P/P_y = 0.4$ has been chosen for illustration. At these points of intersection, one projects verticals until they intersect the corresponding M-ϕ auxiliary diagrams (circled in Fig. 23). Plotting the values obtained from each of the separate auxiliary curves and connecting the corresponding points gives the desired curves. These curves are plotted in Fig. 24, the points obtained from Fig. 23 being circled for illustration.

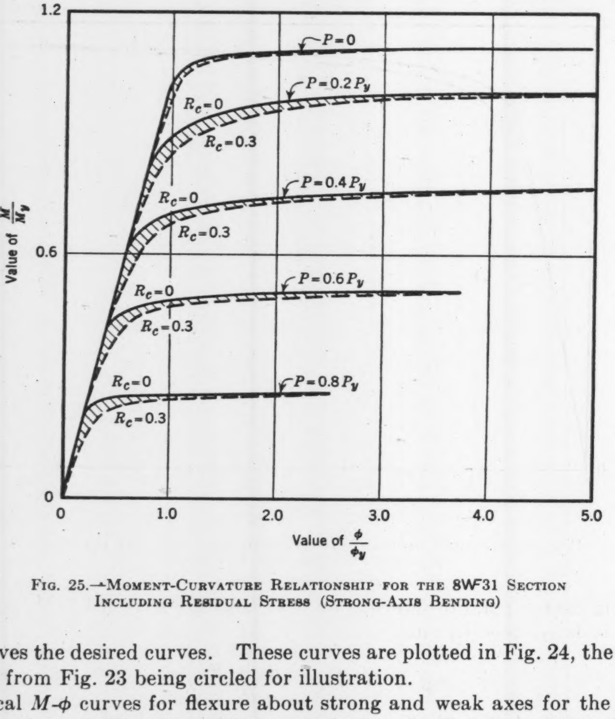

FIG. 25.—MOMENT-CURVATURE RELATIONSHIP FOR THE 8WF31 SECTION INCLUDING RESIDUAL STRESS (STRONG-AXIS BENDING)

Typical M-ϕ curves for flexure about strong and weak axes for the 8WF31 section are shown in Figs. 25 and 26, respectively. In Figs. 25 and 26, solutions neglecting the influence of residual stress are shown by solid lines whereas those including this variable are indicated by dashed lines. As expected, the influence of residual stress on M-ϕ curves is more pronounced for flexure about the weak axis.

Measurements.—In Figs. 27 and 28 there are plotted the M-ϕ relationships obtained in the course of testing sixteen different columns; in Table 4 is summarized the pertinent loading information for each of the tests reported. In Table 4 there is also indicated the observed mode of failure for each specimen. All specimens were tested in the as-delivered condition, and two sizes were used (8WF31 and 4WF13) in a range of L/r from 21 to 111. Details of the test apparatus and procedure have been described;[13] the behavior of some of the specimens tested has been summarized.[12]

The curvature ϕ at any section is a measure of the variation in strain differences across the section. SR-4 strain gages were placed symmetrically about the center line of the section at a known distance from one another, this distance being such that ϕ-measurements could be made relatively far into the inelastic range. They were placed as close as practicable to the section at which the maximum moment was expected.

Moment values at "ϕ-sections" were determined as the sum of applied end moments and the product of applied axial thrust and measured deflections.

TABLE 4.—SUMMARY OF TEST CONDITIONS

Test No.	Loading conditions (Fig. 29)	Section	$\frac{P}{P_y}$	$\frac{L}{r}$	Type of failure
T-3	*b*	8WF31	0.49	55	Bending and twist
T-4	*b*	8WF31	0.12	55	Local buckling
T-7	*b*	4WF13	0.27	111	Bending and twist
T-9	*b*	4WF13	0.10	111	Bending and twist
T-10	*b*	4WF13	0.51	111	Bending and twist
T-12	*c*	8WF31	0.12	55	Bending and twist
T-13	*d*	8WF31	0.12	55	Local buckling
T-14	*a*	8WF31	0.12	55	Was not carried to failure
T-16	*c*	8WF31	0.12	41	Bending, twist, and local buckling
T-17	*b*	4WF13	0.12	55	Local buckling
T-19	*c*	8WF31	0.12	27	Bending and twist
T-20	*c*	4WF13	0.12	55	Bending and twist
T-21	*b*	4WF13	0.50	55	Local buckling
T-23	*d*	4WF13	0.12	84	Bending and twist
T-24	*b*	4WF13	0.12	84	Bending, twist, and local buckling
T-26	*c*	4WF13	0.12	84	Bending and twist

In Figs. 27 and 28 both experimental and analytical M-ϕ curves are presented. The section and material properties for the two sections investigated are presented in Table 5. With each set of curves is shown the loading condition with the column in its deflected configuration. The arrows in Fig. 29 denote the location of the section at which ϕ was measured. The auxiliary sketches in Figs. 27 and 28 are interaction curves,[12] which show the maximum values of axial thrust and end bending moment at collapse as well as the path followed in obtaining that loading.

The theoretical M-ϕ solutions neglecting residual stress are shown by dashed lines. For an assumed residual stress at the flange tip equal to 0.3 of the yield stress, the theoretical curve is shown by a dash-dot line. The experimental curves are shown as solid lines. Initial yield as determined by flaking of the mill scale coated with whitewash is shown for each test by the open arrows.

---

[13] "Tests of Columns Under Combined Thrust and Moment: Progress Report No. 2," by Lynn S. Beedle, Joseph A. Ready, and Bruce G. Johnston, *Proceedings*, Soc. for Experimental Stress Analysis, Vol. VIII, 1950, p. 109.

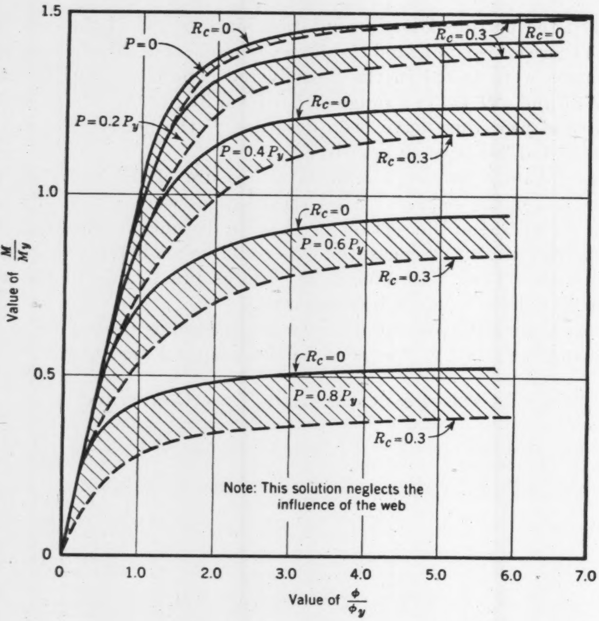

FIG. 26.—MOMENT-CURVATURE RELATIONSHIP FOR THE 8WF31 SECTION INCLUDING RESIDUAL STRESS (WEAK-AXIS BENDING)

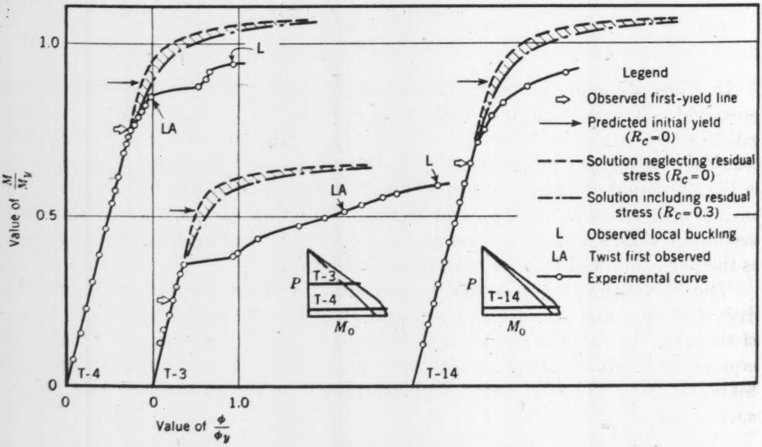

FIG. 27.—EXPERIMENTAL AND THEORETICAL MOMENT-CURVATURE RELATIONSHIPS FOR THREE TEST COLUMNS

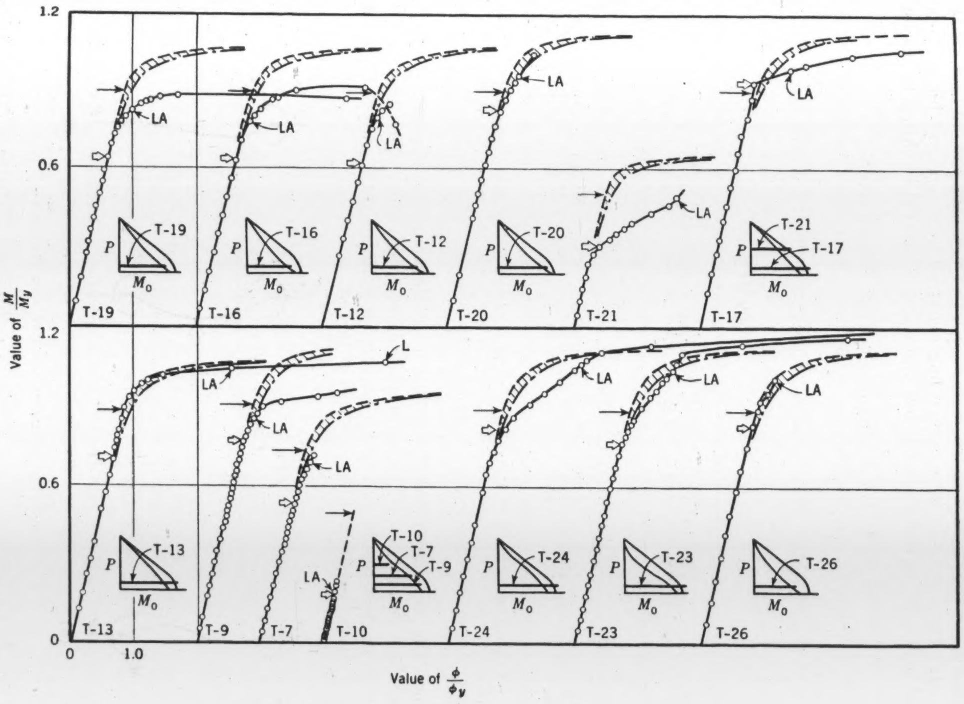

FIG. 28.—EXPERIMENTAL AND THEORETICAL MOMENT-CURVATURE RELATIONSHIPS FOR THIRTEEN TEST COLUMNS (LEGEND THE SAME AS IN FIG. 27)

In Figs. 27 and 28 the symbol LA denotes lateral buckling as observed with the aid of dial gages and SR-4 gages; the symbol L indicates observed local buckling. Point LA was well defined by the measurements made. The mode of failure shown in Table 4 is an effort to show how the column finally collapsed. In each case, lateral buckling occurred at a moment higher than the first observed inelastic action, but the onset of lateral buckling is in most cases not the maximum observed moment. Rather, it is a point at which deformations commence to increase at a more rapid rate. For most of the specimens the test results are in fair agreement with the theory up to the point at which lateral-torsional buckling was observed.

TABLE 5.—AVERAGE SECTION PROPERTIES

	d, in inches	b, in inches	w, in inches	t, in inches	Area, in square inches	I_x, in inches^4	S_x, in inches^3	r_x, in inches
				8WF31[a]				
Measured	8.069	8.032	0.299	0.427	9.177	111.356	27.60	3.483
Handbook	8.00	8.000	0.288	0.433	9.12	109.7	27.4	3.47
Variation, in %	0.86	0.40	3.82	1.39	0.63	1.51	0.73	0.39
				4WF13[b]				
Measured	4.139	4.140	0.258	0.337	3.759	11.215	5.419	1.727
Handbook	4.16	4.06	0.28	0.345	3.82	11.3	5.45	1.72
Variation, in %	5.05	4.93	7.86	2.32	1.59	0.75	0.57	0.41

[a] $\sigma_y = 40.0$ kips per sq in.; $E = 29.9 \times 10^6$ lb per sq in. [b] $\sigma_y = 39.5$ kips per sq in.; $E = 29.2 \times 10^6$ lb per sq in.

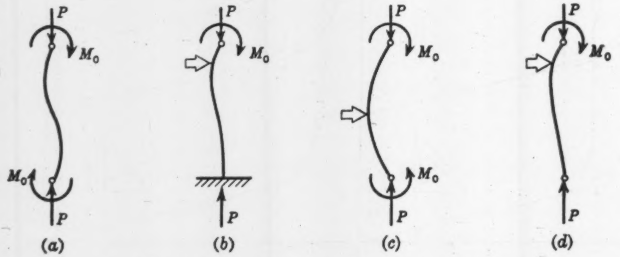

FIG. 29.—METHOD OF LOADING THE COLUMNS

In Fig. 28 the location of the open arrows for T-19, T-16, and T-12 suggests that the residual-stress level was about the same in each of these specimens ($R_c = 0.26$). This is interesting because two different rollings from the same ingot were involved. Furthermore, because lateral buckling (LA) was observed for each of these condition c tests at about the same moment and because the slenderness ratios are different (L/r varies from 27 to 55), inelastic lateral buckling in this range appears to be a function of maximum moment and is not greatly affected by the length.

The behavior of T-13 is different from the rest of the 8-in. specimens, the curve closely approaching that for a member without residual stress. A possible explanation is that the member might have been cold-bent in the region at which ϕ was measured, thus negating cooling residual stresses.

Also in Fig. 28, the open arrows for the 4-in. members indicate that this material had a lower level of residual stress than did the 8-in. material. The average value for all 4-in. specimens tested was $R_c = 0.1$ whereas that for the 8-in. specimens was $R_c = 0.24$.

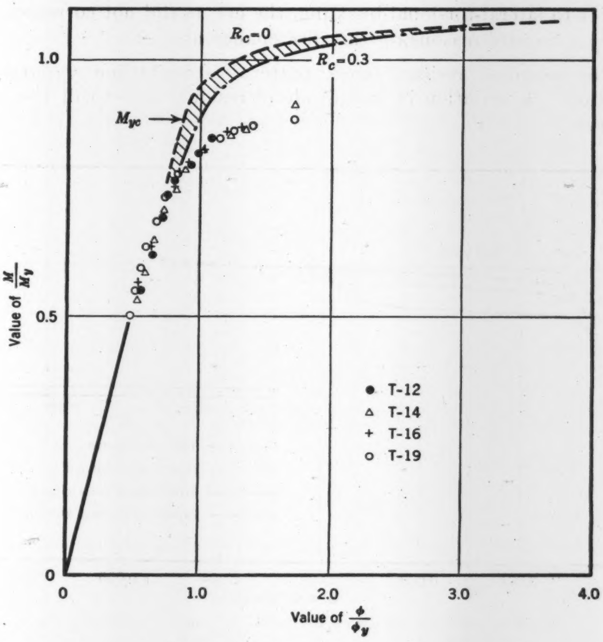

FIG. 30.—SUMMARY OF EXPERIMENTAL AND THEORETICAL MOMENT-CURVATURE RELATIONSHIPS FOR 8WF31 SECTION WITH $P = 0.12\ P_y$

Specimens T-3 and T-21 were identical except for the size of the member. The measured M-ϕ curves are also similar, deviating markedly from the theoretical curve. This behavior seems to be characteristic when a relatively greater axial load is applied to the member. Also, owing to the fact that the column is effectively restrained by the loading (Fig. 29(*b*)), lateral buckling is not observed until considerable plastic deformation has occurred. Incidentally, the reduction in strength of the theoretical curves to T-21 below those of T-17 and T-20 indicates the influence of axial thrust summarized in Fig. 25.

Good correlation between theory and the tests is observed in T-7 and T-9 for 4-in. material even though two different rollings from the same ingot are involved.

In Fig. 30 there are plotted M-ϕ curves for several different tests. It is seen that the experimental results are consistent.

Examining the individual curves for T-12, T-14, T-16, and T-19, the M-ϕ behavior is relatively consistent for these 8WF31 specimens below the point at which twisting of the specimen was noted. The theory is not expected to apply beyond the point at which this type of buckling occurred. However, even prior to lateral-torsional buckling, the curves did not correspond exactly to theory. Several reasons for this discrepancy are:

1. The assumed residual-stress pattern (straight-line variation) is an idealization. A variation in magnitude of residual stress will also affect the M-ϕ curve.

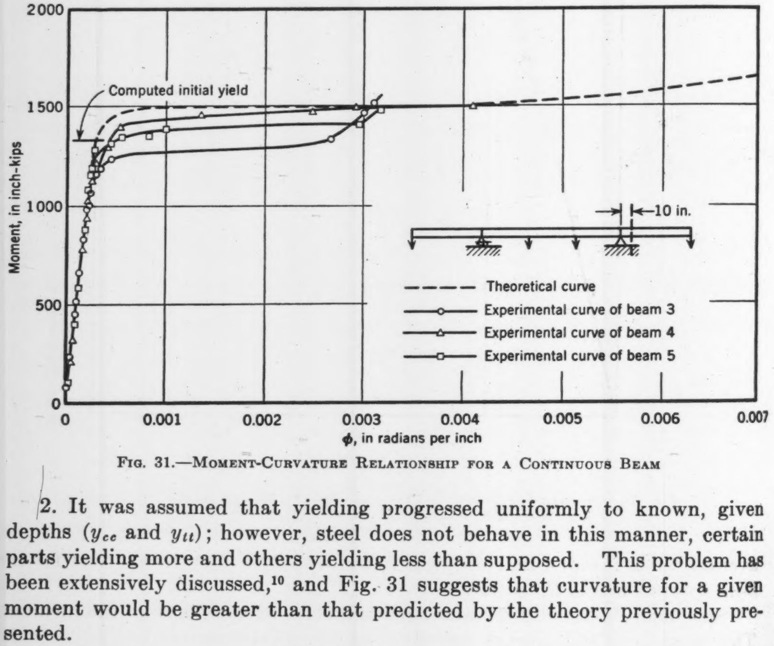

FIG. 31.—MOMENT-CURVATURE RELATIONSHIP FOR A CONTINUOUS BEAM

2. It was assumed that yielding progressed uniformly to known, given depths (y_{cc} and y_{tt}); however, steel does not behave in this manner, certain parts yielding more and others yielding less than supposed. This problem has been extensively discussed,[10] and Fig. 31 suggests that curvature for a given moment would be greater than that predicted by the theory previously presented.

COLUMN STRENGTH

The foregoing results will be applied to a consideration of the eccentrically loaded member shown in Fig. 32. This single-curvature loading condition is essentially the same as loading condition c (Fig. 29). The member is assumed to be initially straight, of uniform cross section, and free from accidental eccentricities. For wide-flange shapes it is of interest to determine (a) the ultimate strength of the eccentrically loaded column, (*b*) the load-deflection relationship for columns with equal eccentricities, and (*c*) the end rotation of columns in the plastic range. Knowledge of the M-ϕ relationship makes possible a solution of these problems—including also the influence of residual stresses.

The strength of the eccentrically loaded column has been considered by F. Bleich,[7] who reviewed the work done up to that time. As Mr. Bleich noted, a determination of true column strength depends on a knowledge of the load-deflection relationship. End rotations are possibly of academic interest in the case of columns loaded with equal eccentricities; such members collapse quickly after reaching the maximum load. They have little "rotation capacity"—that is, the capacity to deform through considerable angle changes at near-maximum loads. On the other hand, columns bent in double curvature may show considerable rotation capacity, and indeed this is required if structural members are to meet the assumption implicit in plastic analysis and design.[14]

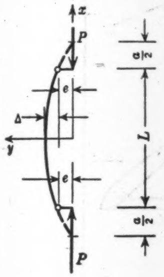

FIG. 32.—ECCENTRICALLY LOADED COLUMN

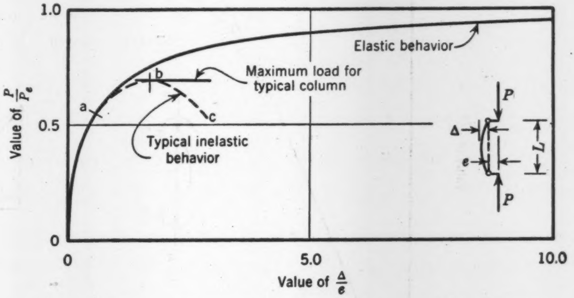

FIG. 33.—LOAD-DEFLECTION RELATIONSHIP FOR AN ECCENTRICALLY LOADED COLUMN

Load-Deflection Relationship.—The difference between the elastic and the plastic load-deflection relationships is shown in Fig. 33. The equation of the elastic curve is

$$\frac{\Delta}{e} = \frac{1 - \cos u}{\cos u} \quad \ldots\ldots\ldots\ldots\ldots\ldots\ldots (11)$$

in which $u = k\,L/2$, e is the end eccentricity of the load, Δ denotes the center-line deflection, and $k = \sqrt{P/E\,I}$.

Even with large eccentricities, the maximum elastic strength approaches the Euler buckling load. However, as the load increases, the stress in the outermost fibers at the center section of the column increases at a faster rate because of the bending moment which is increasing as the product of P and the quantity $\Delta + e$ (Fig. 32). Therefore, columns of the proportions used in engineering structures begin to yield—for example, at some point a in Fig. 33. As the compressive force P is increased beyond this initial-yield value, plastic flow spreads from the edges toward the center of the section and along the bar, thereby reducing its flexural rigidity. Consequently, the deflection *y* (and, hence, the moment of the external forces) increases at a higher rate than it does for the elastic case. Finally, a point is reached at which further increase in load is impossible and collapse occurs. This maximum load would correspond to point b, the part b c representing the inelastic, unstable, load-deflection relationship.

---

[14] "An Evaluation of Plastic Analysis as Applied to Structural Design: Progress Report No. 8," by Bruce G. Johnston, Ching Huan Yang, and Lynn S. Beedle, ***Research Supplement, The Welding Journal,*** Vol. 32, 1953, p. 224 s.

The load-deflection curve is determined by integrating ϕ-values. However, ϕ is dependent on the bending moment which in turn is dependent on the deflection. A numerical-integration procedure[15] is suitable in problems of this type. A deflected shape is assumed and moments are computed; ϕ-values are obtained as outlined previously and these are integrated to obtain a new deflected shape. If the assumed curve is correct, the deflection values obtained will be identical with the assumed deflected shape. This method was applied to the members studied in the program; Fig. 34 shows typical, resulting curves. The solid curve is the experimental result, and the theoretical curves obtained by the numerical method are shown by dot-dash lines for zero residual stress and for residuals estimated at 30% of the yield-point stress. Agreement is reasonable up to the point at which the member begins to twist.

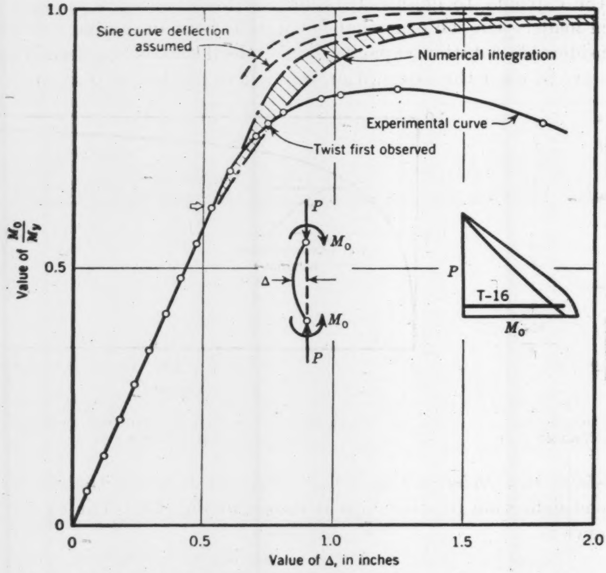

FIG. 34.—TYPICAL END MOMENT VERSUS DEFLECTION CURVES FOR T-16

---

[15] "Numerical Procedure for Computing Deflections, Moments, and Buckling Loads," by N. M. Newmark, *Transactions*, ASCE, Vol. 108, 1943, pp. 1161–1234.

Even though the exact deflected configuration is that which results in the lowest potential energy of the system, the magnitude of the critical load is relatively insensitive to changes in the assumed deflection curve—providing the deflection patterns conform to the geometric boundary conditions of the member. Mr. Bleich described[7] the use of an assumed sine curve by K. Jezek and an assumed partial cosine curve by W. R. Osgood, M. ASCE, and H. M. Westergaard. These two assumptions have also been used in the following study for determining column-buckling loads in the inelastic range.

Assuming that the column bends in a sine curve (Fig. 34),

$$y = \Delta \sin \frac{\pi x}{L} \qquad (12)$$

in which L denotes the length of the column. The section at midheight is subjected to the greatest deformation, and ϕ at this section is

$$\phi = \left.\frac{d^2y}{dx^2}\right|_{x=L/2} = \frac{\pi^2}{L^2} \Delta \qquad (13)$$

The moment at this same section for the eccentrically loaded column is given by

$$M = P (\Delta + e) \qquad (14)$$

and for the condition c loaded column by

$$M = M_0 + P \Delta \qquad (15)$$

From Eq. 13, Eq. 14, or Eq. 15 and the M-ϕ plot for this section, load-deformation curves can be obtained. A typical resulting curve is shown in Fig. 34 by dotted lines for the two material conditions (annealed and as-delivered). The predicted maximum end moment, for this example, agrees with the numerical method within 1%.

Referring to Fig. 32, the deflection expressions for a partial cosine curve is given by

$$y = (\Delta + e) \cos \frac{\pi x}{L + a} \qquad (16)$$

Then, by using the first two terms of a cosine series,

$$\phi = \frac{8.0}{L^2} \Delta \qquad (17)$$

In this case the resulting end moment-deflection curve coincides almost exactly with the numerical-integration curve of Fig. 34 and therefore has not been shown.

The detailed steps which were followed in obtaining these approximate load-deflection curves are reviewed as follows:

1. Assume a center-line deflection, Δ.
2. Using either Eq. 13 or Eq. 17, compute ϕ.

3. Enter the appropriate M-ϕ curves with the value of ϕ/ϕ_y and read off the corresponding (M/M_y)-ratio.

4. Compute M_0 or P from either Eq. 14 or Eq. 15.

Strength of Eccentric Columns.—The ordinary column curve presents strength as a function of the slenderness ratio L/r. By using the sine-curve assumption and the M-ϕ curves of Figs. 25 and 26, column curves are obtained as presented in Fig. 35. Data are shown on a nondimensional basis, the maximum load being divided by P_y as determined from the product of yield-point stress and cross-sectional area. The curves indicate the influence of end eccentricity and of residual stresses. Three curves are shown for each eccentricity ratio $(e\,c/r^2)$: The maximum strength of annealed members, the maximum strength of as-delivered columns containing residual stresses, and the initial-yield (secant) solution. The shaded part of each eccentricity shows the influence of residual stress on collapse strength. Curves of allowable load according to a specification[16] are also given.

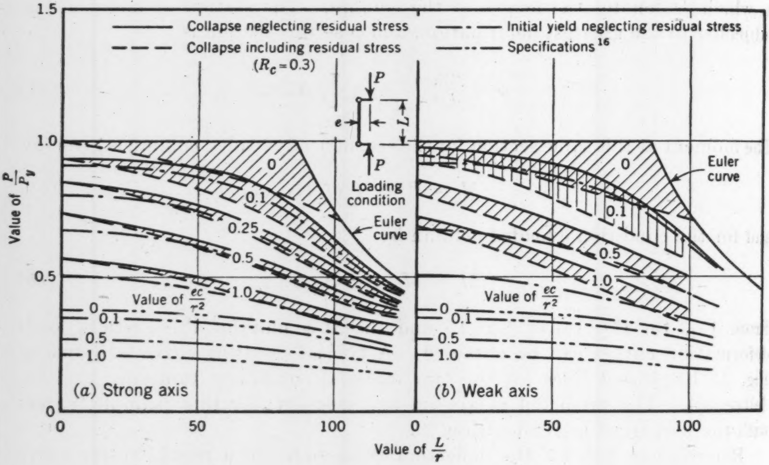

FIG. 35.—COLUMN CURVES INCLUDING THE INFLUENCE OF RESIDUAL STRESSES FOR 8WF31 SECTION

The curves indicate that the secant solution is on the unsafe side for intermediate-length columns with small eccentricities and that it is too conservative for short members—the latter being particularly true for large eccentricities. For small eccentricities, columns will collapse at loads considerably less than those predicted by the initial-yield condition. At zero eccentricity the considerable reduction caused by residual stress has been confirmed by tests.[11]

Fig. 36 is a cross-curve of Fig. 35(a) (strong-axis bending) at $L/r = 55$. In addition to the various theoretical solutions, the results of three tests are shown. The collapse strength for each of these test members is less than the theoretical solution that includes the influence of residual stress. This is in part caused by flexural-torsional buckling of columns bent about the major axis—the mode of failure observed for each of these tests.

---

[16] "Specification for Highway Bridges," A.A.S.H.O., 1949.

The collapse curves in Figs. 35 and 36 are based on the assumption that the section deforms only in the plane of the applied moments and that during this deformation it maintains its original cross-sectional form. Although this assumption is satisfactory for weak-axis bending, lateral-torsional buckling occurs when flexure is forced about the strong axis of the section; a solution for this problem is necessary.

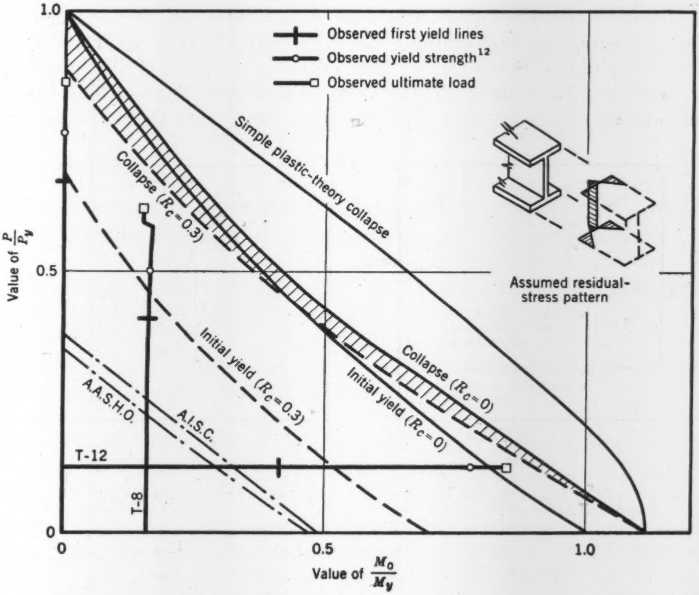

FIG. 36.—INTERACTION CURVES FOR 8WF31 SECTION (LOADING CONDITION SHOWN IN FIG. 29(c))

An opportunity to compare the theory with the results of tests on annealed columns is afforded by experiments performed[17] at Cornell University at Ithaca, N. Y. In that investigation, restrained columns were allowed to bend about the weak axis. In Fig. 37 the theoretical solution, which makes use of a considerable part of the analysis presented in the Cornell studies, and the results of the experiment (circles) are compared. The theoretical curve is obtained by making a cross-curve of Fig. 35(*b*) at a value of L/r of 50, the I-shape being approximate by two equivalent rectangles. It is seen that the agreement is satisfactory. As-delivered specimens were also tested, but—

---

[17] "Eccentrically Loaded, End-Restrained Columns," by Paul P. Bijlaard, Gordon P. Fisher, and George Winter, *Transactions*, ASCE, Vol. 120, 1955, p. 1070.

because the level of residual stress was not known—the corresponding test points and the theoretical curve have not been plotted although a rough approximation to a possible residual-stress pattern yields a fair correlation between test and theory.

Moment-Rotation Relationship.—Typical end moment-end rotation curves are shown in Fig. 38. The theoretical curves obtained by the method of numerical integration are shown by dashed lines; the test result is shown by the solid line. For the theory that takes into account residual stresses, and in the region prior to twisting of the cross section, agreement with the test is excellent.

SUMMARY

Moment-Curvature Relationship with Axial Thrust Present.—A method has been presented for determining the influence of axial load on the M-ϕ relationship in the plastic range. Simultaneous values of thrust, moment, and curvature are determined (Table 1) for different yield conditions, and from these are constructed auxiliary curves (Fig. 19). Once these auxiliary curves are plotted for a particular wide-flange shape, the M-ϕ relationship can be obtained conveniently for any desired value of axial load (Fig. 22). A significant reduction in moment-carrying capacity at a given cross section is to be expected in the presence of axial thrust (Fig. 22).

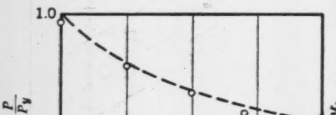

FIG. 37.—COMPARING CORNELL TESTS AND THEORETICAL ANALYSIS

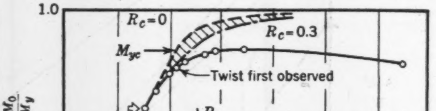

FIG. 38.—TYPICAL END MOMENT-END ROTATION CURVES (T-16)

Previous solutions were limited to rectangular shapes. This semigraphical method extends the solution to wide-flange and other symmetrical shapes. Because all rolled shapes contain some residual stresses, the solution has practical application in that it may be extended to members containing such locked-in stresses.

Influence of Residual Stress.—The method can be applied to members containing residual stresses after a distribution pattern for such stresses has been assumed (Figs. 6 and 7). For flexure about the strong and weak axis, equations are developed (Tables 2 and 3) for the construction of auxiliary curves Fig. (23), from which M-ϕ curves can be obtained by graphical construction (Figs. 25 and 26).

For a given axial thrust, residual stresses increase the deformation in such a way that it appears as though the moment strength were reduced. If straining can be continued sufficiently without column buckling, the effect of residual stress is eliminated, and the strength reaches the predicted value (Fig. 25). Tests and theory show that column collapse may occur in the region in which residual stress is of influence (Fig. 28).

The influence of residual stress is more pronounced for members bent about the weak axis than for those bent about the strong axis (Fig. 26 compared with Fig. 25).

Test results, in general, confirm the theory up to the point at which lateral deformation commences for members bent about the strong axis.

Column Behavior.—Applying the M-ϕ data as derived in this report to compute load-deflection curves for eccentrically loaded columns (by numerical integration) gives a reasonable correlation with the test results up to the point of twisting (Fig. 34).

Excellent correlation between theory and test (up to the point of twisting) is obtained for the relationship of end bending moment to end rotation of the column (Fig. 38).

The ultimate strength of eccentrically loaded columns may be determined by the maximum point of a load-deflection curve. The results obtained using such a procedure are summarized in the column curves of Fig. 35 and show the maximum strength of annealed members and of members containing residuals and the yield-stress (secant) solution. The reduction in collapse strength as a result of residual stress (shaded) at $L/r = 85$ ranges from 22% for $e\,c/r^2 = 0$ to 4% for each $e\,c/r^2 = 1.0$ for the strong axis. Similarly, columns which collapse because of bending about the weak axis suffer theoretical strength reductions of 26% at zero eccentricity to 6% at $e\,c/r^2 = 1.0$.

The initial-yield solution (secant) is generally on the unsafe side for intermediate-length members with small eccentricities and is too conservative for short members. Fair correlation between theory and test is established in Fig. 36 for a few columns which were bent about the strong axis and which eventually collapsed by lateral-torsional buckling.

Final failure for all members tested was caused either by lateral-torsional buckling or by local buckling (Table 4). However, all the theoretical curves derived and presented herein assume that failure is caused by simple-column bending. A consideration of test results (Fig. 38, for example) suggests that the influence of residual stress might be more than the initiation of yielding at low loads with the subsequent loss in buckling strength shown in the theoretical curves. This early yielding caused by residual stresses may aggravate the tendency toward lateral or local buckling.

Considerable computation and plotting are involved in obtaining these results; simplified expressions are required which will sufficiently describe the behavior of these columns. The results are beginning to be applied to columns under different loading conditions and with end restraints. The column strengths reported herein represent a "worst case." Higher strengths will be expected for other loading conditions and end restraints.[17]

Whatever column analysis is made, the basic relationship is that of moment to curvature. The results presented herein are dependent on an assumed magnitude and distribution of residual stress. The assumption seems reasonable in the light of measurements that have been made (as of 1955). Eventually, when more data are collected, design rules may be re-examined to provide more economical structures consistent with adequate safety.

ACKNOWLEDGMENTS

Contributions have been made in the investigation by Chien-Huo Chen' Jan M. Ruzek, and Donall L. McCullough, J. M. ASCE. This work has been performed as part of an investigation sponsored jointly by the Welding Research Council and the United States Department of the Navy with funds furnished by the following organizations: American Institute of Steel Construction, American Iron and Steel Institute, Column Research Council (Advisory), Office of Naval Research (Contract No. onr-39303), Bureau of Ships, and Bureau of Yards and Docks. The helpful criticisms of members of the Welding Research Council, Lehigh Project Subcommittee (T. R. Higgins, M. ASCE, chairman), and the Column Research Council Research Committee D (Nathan M. Newmark, M. ASCE, chairman, and N. J. Hoff, M. ASCE, co-chairman) are sincerely appreciated. This program was performed in the Fritz Engineering Laboratory of Lehigh University at Bethlehem, Pa., of which William J. Eney, M. ASCE, is the director.

APPENDIX. NOTATION

The following symbols, adopted for use in the paper and for the guidance of discussers, conform essentially with "American Standard Letter Symbols for Structural Analysis" (ASA Z10.8–1949), prepared by a committee of the American Standards Association with ASCE representation, and approved by the Association in 1949:

A = area of cross section;
b = flange width;
d = depth of wide-flange section;
E = modulus of elasticity;
e = eccentricity of load;
I = moment of inertia;
L = length of column;
M = moment:

  M_0 = moment applied at the end of a member;
  M_y = moment at which yield point is reached in flexure;
  M_{yc} = moment at which initial outer-fiber yielding occurs when axial thrust is present;

P = concentric axial thrust on a column;
P_y = axial load corresponding to yield-stress level over entire section;

R = stress ratio:

R_a = ratio of the normal stress on the tension side to the yield-stress level;

R_c = ratio of the maximum compressive residual stress to the yield-stress level;

R_t = ratio of the maximum tension residual stress to the yield-stress level;

r = radius of gyration;

S = section modulus;

t = flange thickness;

w = web thickness;

y = depth:

y_{cc} = depth of yield penetration in compression;

y_{ct} = distance from yield penetration in compression to extreme fiber in tension;

y_{tt} = depth of yield penetration in tension;

Z = plastic modulus;

α = ratio of the depth of yield penetration in compression to the total depth of the section;

β = ratio of the depth of yield penetration in tension to the total depth of the section;

Δ = center-line deflection of a beam-column loaded to produce single curvature;

ϵ = strain:

ϵ_{rc} = maximum residual compressive strain;

ϵ_{rt} = maximum residual tensile strain;

ϵ_y = strain corresponding to initial yield-point stress;

σ = normal stress:

σ_a = variable normal stress on tension side of specimen (positive when in tension);

σ_{rc} = maximum residual compressive stress;

σ_{rt} = maximum residual tensile stress;

σ_y = lower yield-point stress;

ϕ = curvature at a section;

ϕ_y = curvature corresponding to initial outer-fiber yielding ($P = 0$); and

θ_A = column end rotation (at end A).

DISCUSSION

GEORGE WINTER,[18] M. ASCE.—The numerical-integration procedure developed by the authors for analyzing the behavior of beam-columns in the plastic range represents an ingenious further development of the general approach originated by Theodor von Kármán,[19] Hon. M. ASCE, E. Chwalla,[20] Mr. Jezek,[21] and others. Although this procedure is too laborious for direct, practical application, it may be a powerful tool for research work on which design methods can be based. The original manner in which the influence of residual stresses has been included in the analysis should be valuable for further investigations of this troublesome feature.

The authors' theoretical curves in Figs. 25 to 28 seem to indicate that the influence of the assumed pattern of residual stress on the moment-curvature relationship is relatively minor for strong-axis bending but is significant for weak-axis bending, for which no tests were made. With regard to column strength, Fig. 35 again seems to indicate that these residual stresses for strong-axis bending have a relatively minor weakening effect, except for small or zero eccentricities; the effect is larger, however, for weak-axis bending.

Tests Influenced by Twist.—It is unfortunate that the experimental evidence cannot be regarded as a corroboration of the analytical method in view of the fact that failure by a combination of bending and twisting interfered in almost all the tests. This is seen from Figs. 27 and 28 in which the occurrence of twist is indicated by LA. This interference was to be anticipated because during the eccentric-column tests performed[22] in 1942 (also at Lehigh University) the same torsional-flexural behavior was exhibited in nearly all the tests of columns bent about the strong axis. Mr. Bleich has already noted this feature of those tests.[23]

These and the present tests indicate that, for columns bent about the strong axis, failure which involves twist in addition to bending is of considerable practical consequence. To the writer this evidence of the importance of twist is one of the chief values of the authors' tests. Thus, it is somewhat disquieting to learn from Figs. 34 and 38 that the weakening influence of twist is sizable even for slenderness ratios as low as $L/r = 41$—amounting in this case to a reduction of moment capacity of approximately 15%. The quoted test results seem to indicate that this feature may prove to be of far greater consequence in reducing the strength of such members than the influence of residual stresses and that further investigations of flexural-torsional failure of steel columns in the plastic range are urgently needed.

---

[18] Prof. and Head, Dept. of Structural Eng., Cornell Univ., Ithaca, N. Y.

[19] "Die Knickfestigkeit gerader Stäbe," by Theodor von Kármán, *Physikalische Zeitschrift*, Vol. 9, 1908, p. 136.

[20] "Die Theorie des aussermittig gedrückten Stäbes aus Baustahl," by E. Chwalla, *Der Stahlbau*, Vol. 7, 1934, p. 161.

[21] "Die Festigkeit von Druckstäben aus Stahl," by K. Jezek, Julius Springer, Vienna, 1937.

[22] "Steel Columns of Rolled Wide Flange Section: Progress Report No. 2," by Bruce G. Johnston and L. Cheney, A.I.S.C., 1942.

[23] "The Buckling Strength of Metal Structures," by F. Bleich, McGraw-Hill Book Co., Inc., New York, N.Y., 1952, p. 47.

Residual Stresses May Have Different Patterns.—With regard to residual stresses, the authors base their analytical findings on an assumed residual-stress pattern (Fig. 7) which follows closely the measured stress distribution obtained on an 8WF31 section (Fig. 6). All computed curves, such as those in Figs. 25, 26, and 35, specifically refer to this particular section; the authors do not claim general validity for other shapes. It should be noted, however, that the residual-stress pattern of Figs. 6 and 7, although undoubtedly valid for the investigated section, may not be typical for rolled I-shaped sections in general. The authors' pattern results in an average residual compression stress in the flanges and an average residual tension stress in the web—the former being essentially the cause of the weakening influence of these stresses. There is some evidence that average residual cooling stresses of exactly the opposite distribution have been observed. Average residual tension stresses rather than compression stresses in flanges of 9JB7.5 and 7JB5.5 (junior beams) beams ranging from 2,500 lb per sq in. to 19,000 lb per sq in. have been reported.[24] In German wide-flange sections, 42.5 cm deep (approximately 17 in.), residual average compression stresses rather than tension stresses of approximately 24,000 lb per sq in. have been measured in the web.[25] It would seem that the pattern of the cooling stresses depends primarily on the details of the distribution of material in flanges and web which, of course, affect the nature of the cooling process. It is possible that the authors' results—obtained on a section having a depth equal to its width and with relatively little difference between the thickness of the web and the flanges—may not be representative of sections whose depth is considerably larger than the width and whose flange thickness exceeds that of the web by a considerably larger percentage than for an 8WF31 section. Cooling stresses are always so distributed that the part which cools first shows residual compression stresses. It seems likely that, in relatively deep and narrow sections with relatively thick flanges, the web would cool first, resulting in a pattern of average residual stresses in web and flanges substantially the reverse of that of the authors.

Before practical conclusions are drawn regarding the influence of residual cooling stresses on the strength and performance of beam-columns, a more complete investigation of the distribution of these stresses in the more common sections may be advisable.

Although neither the authors nor the writer has made any theoretical or experimental determination of the influence on column strength of a pattern of average residual stress substantially opposite to that used by the authors, one may assume that such a stress pattern would not weaken and might even strengthen the member in eccentric compression. Because the evidence previously cited makes it appear that in as-rolled sections patterns of either kind will probably be found, the explicit inclusion of the influence of residual stress in design procedures may prove to be an extremely involved undertaking in view of the variety of probable stress patterns.

---

[24] "Tests of Continuous Right I-Beam Bridges," by C P. Siess and I. M. Viest, *Bulletin No. 416*, Univ. of Illinois Experiment Station, Urbana, Ill., 1953.

[25] "Die Tragfähigkeit Metallischer Baukörper," by K. H. Rühl, Wilhelm Ernst und Sohn, Berlin, Germany, 1952, p. 66.

Cornell Tests.—Because the results of most of the authors' tests were influenced by premature twisting, they have attempted in Fig. 37 to correlate their theory with tests performed at Cornell University. These latter tests were performed with eccentric bending produced about the minor axis for the purpose of eliminating twist. The tests represent part of an extensive analytical and experimental investigation by Paul P. Bijlaard, M. ASCE, Gordon P. Fisher, A. M. ASCE, and the writer.[17]

The investigation at Cornell University was concerned with columns elastically restrained at the ends whereas the authors' theory was developed for pin-ended columns. This attempt to reconcile two different situations has caused some misunderstandings which make Fig. 37 invalid. The tests used by the authors in Fig. 37 are available.[26]

In the theoretical part of that paper[17] it is shown that elastically restrained, eccentrically loaded columns of slenderness ratio L/r and eccentricity e can be analyzed by replacing them by an equivalent hinged column of slenderness $c\, L/r$ and eccentricity e_e. The methods for determining these two quantities are stated therein.

For the restrained columns of Fig. 37 the actual slenderness ratio (between knife edges) was approximately $L/r = 80$, and the actual eccentricity ratios e/r were as indicated in Fig. 37. For the equivalent hinged column (according to the Cornell paper[17]), the effective slenderness was $c\, L/r = 50.2$, in close agreement with the value of 50 indicated by the authors. However, the equivalent eccentricity ratio according to that theory was $e_e/r = 0.256\ (e/r)$. The authors did not take account of this fact in plotting e/r. Hence, Fig. 37 refers in part to the equivalent hinged column ($c\, L/r$) and in part to the real, restrained column (e/r) and is therefore contradictory in itself. The apparently good agreement between test and theory shown in Fig. 37 is caused by an accidental arithmetical oversight which happened to compensate almost exactly for the error introduced by using the wrong kind of eccentricity. This error was found independently by the authors and by the writer in an attempt to analyze Fig. 37.

It is hoped that the authors will present a revised evaluation of these tests, based on an application of their theory to the concept of replacing a restrained column by an equivalent hinged column as developed[17] by the writer and his collaborators. If such a correct evaluation showed good correlation between theory and tests, it would represent a confirmation not only of the authors, analytical method for hinged columns but also of the approach to the analysis of restrained, eccentric columns as adopted at Cornell University.

It may be of interest to note that part of the tests at Cornell University was made on annealed specimens in order to eliminate residual stresses whereas part was made on as-rolled specimens. The stress-strain curve[27] for the unannealed I-sections—if compared with that of the annealed I-sections—indicates by its rounded knee that residual stresses must have been present. The theory given[17] does not explicitly account for the influence of residual stresses. It merely assumes that the compressive yield point as obtained by testing the entire section (rather than coupons cut from the section) reflects, in some measure, the influence of these residual stresses. Although this assumption is known to be approximate, the agreement between the theory and tests developed at Cornell University is equally good for the annealed and for the unannealed sections, at least in the tested range.

---

[26] "Eccentrically Loaded, End-Restrained Columns," by Paul P. Bijlaard, Gordon P. Fisher, and George Winter, *Transactions*, ASCE, Vol. 120, 1955, p. 1091, Fig. 14(*a*).

[27] *Ibid.*, p. 1087, Fig. 12.

In addition, the 4I9.5 section used in the Cornell tests is extremely stocky as compared to the authors' wide and thin-walled 8WF31. In view of what has been noted previously about residual-stress patterns, it may be assumed that the residual stresses in the I-section were considerably smaller than those in the wide-flange section and also that their distribution pattern was different from that in the authors' section. The authors' statement (under the heading, "Column Strength: Load-Deflection Relationship") relative to the possible influence of residual stress on the Cornell tests is, therefore, viewed with some reservation.

Summary.—

a. The authors' analytical method seems to represent a valuable research tool for the investigation of beam-columns with and without residual stresses.

b. It would be desirable to have this theory confirmed by tests which would specifically exclude the influence of twist. This influence, which is not included in the authors' analysis—but which affected almost all their tests—makes it impossible to establish a firm correlation between theory and tests, within the scope of the tests.

c. The experimental evidence, together with that of the earlier Lehigh tests,[22] indicates the sizable weakening effect of twist even for relatively short columns bent about the strong axis. This influence seems to be of considerably greater importance than that of residual stress. The performance and particularly the strength of columns bent about the strong axis will be understood only when an adequate theory of flexural-torsional behavior in the plastic range becomes available.

d. In rolled sections, there is some evidence that patterns of average residual stress in web and flanges may occur which are different from, and possibly even substantially opposite to, the particular pattern measured by the authors for an 8WF31 section and assumed in their analysis. The details of the pattern seem to depend on the details of the cross-sectional dimensions. In view of this great variety of possible residual-stress patterns, attempts to account for them rationally in design procedures may prove to be complex.

Robert L. Ketter[28] and Edmund L. Kaminsky,[29] Junior Members, ASCE, and Lynn S. Beedle,[30] A. M. ASCE.—Several points of importance have been noted by Mr. Winter. First of all, each of the members tested as part of the experimental study was loaded with a combination of axial thrust and end moments applied about the stronger principal axis of the section. Moreover, knife edges were located at each end of the specimens in a manner which allowed rotation about an axis perpendicular to the web but which restrained it in the direction of the web. This was done because it was considered that strong-axis bending is that condition most frequently encountered in practice.

---

[28] Research Instructor, Fritz Eng. Lab, Lehigh Univ., Bethlehem, Pa.

[29] Research Engr., David Taylor Model Basin, Washington, D. C.; formerly Research Assistant, Fritz Eng. Lab., Lehigh Univ., Bethlehem, Pa.

[30] Asst. Director, Fritz Eng. Lab., Lehigh Univ., Bethlehem, Pa.

From the previous Lehigh study[22] it is possible to compare the predicted strength of columns with the results of pin-end tests in which the possibility of twist was eliminated. In Fig. 39 there is shown the correlation between the predicted strength curve (Fig. 35(*b*), $e\,c/r^2 = 1.0$) and a set of weak-axis tests (315.7). The collapse solution, neglecting residual stress, has been used even though the members were tested in the as-delivered condition. This solution was used because the pure axial test of the same section indicated that relatively small cooling residual stresses were present in the specimen. Agreement between the predicted and observed values is reasonable.

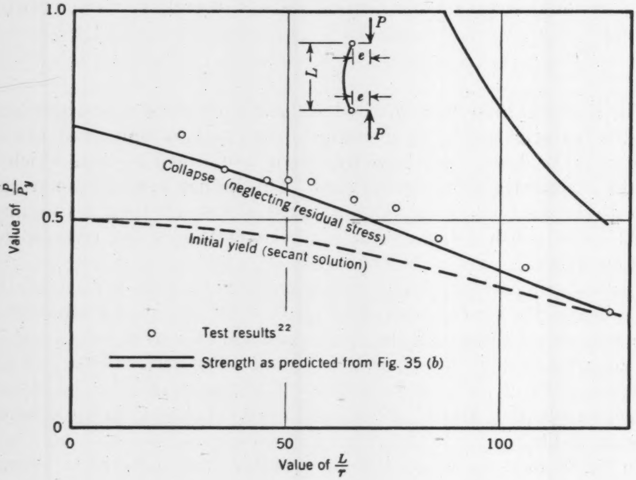

Fig. 39.—Correlation Between Previous Lehigh Tests[22] and Theoretical Collapse Analysis for Weak-Axis Bending of a 315.7 Section

A few weak-axis tests have been made by the writers on columns having an 8WF31 shape; the results are in excellent agreement with the theory.

The second point raised by Mr. Winter was that of the generality of the assumed cooling residual-stress pattern (Fig. 7). Although the actual magnitude and pattern of residual stress present in any given cross section are influenced by the geometric proportions of the section, stresses observed in the flanges of column-type sections actually do not vary as much as might be expected.

In Fig. 40 there is plotted the distribution of residual stresses in four different wide-flange columns. These plots indicate that the assumption made by the writers was not unreasonable. All these shapes have compressive residual stresses at the flange edges. Other measurements made on still other wide-flange shapes (12WF50, 12WF65, 6WF15.5, and 14WF43) show a similar result.

Because this investigation is primarily concerned with columns and not beams, shapes with flanges that are narrow in comparison with beam depth are not of prime interest. Furthermore, the 8WF31 shape is rolled in greater quantities than most other columns. Finally, because the flanges provide the majority of the bending stiffness, the magnitude and pattern of residual stress present in the web of the specimen are of relatively minor importance.

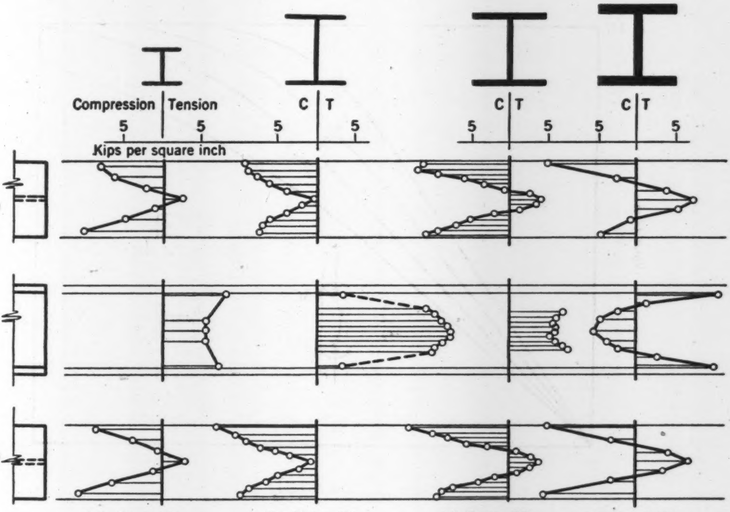

(*a*) 4 WF 13 (*b*) 8 WF 24 (*c*) 8 WF 31 (*d*) 8 WF 67

FIG. 40.—MEASURED RESIDUAL STRESSES

Mr. Winter states:

> "The quoted test results seem to indicate that this feature [influence of twist] may prove to be of far greater consequence in reducing the strength of such members than the influence of residual stresses * * *."

Such a separation of the influence of twist from that of residual stress may be misleading. Torsional stiffness is composed of essentially two parts: (*a*) A St. Venant type[31] of torsional stiffness and (*b*) a cross-bending type of stiffness. Discounting the first factor for the present (its influence will decrease as length decreases), the second factor—cross-bending stiffness—is markedly affected by residual stress. If, for example, a flange had yielded—because of residual stresses and applied stress—to a distance equal to one quarter of the width of the flange from each side, the cross-bending stiffness of that flange containing residual stresses would be one eighth as large as the stiffness of the same kind of flange not having such initial stress imperfections. It is true that the inelastic lateral-torsional problem has not been solved (as of 1955), and a solution is urgently needed. This solution, however, must include the influence of residual stresses if the problem that exists in practice is to be resolved.

---

[31] "Theory of Elasticity," by S. Timoshenko, McGraw-Hill Book Co., Inc., New York, N. Y., 1934, p. 224.

The final point concerns the correlation with the restrained column tests performed at Cornell University (Fig. 37). As was discovered (independently) by both the writers and Mr. Winter, the implied application of the theory to this particular problem does not lead to the correct solution. Instead, the proper procedure is as follows:[32]

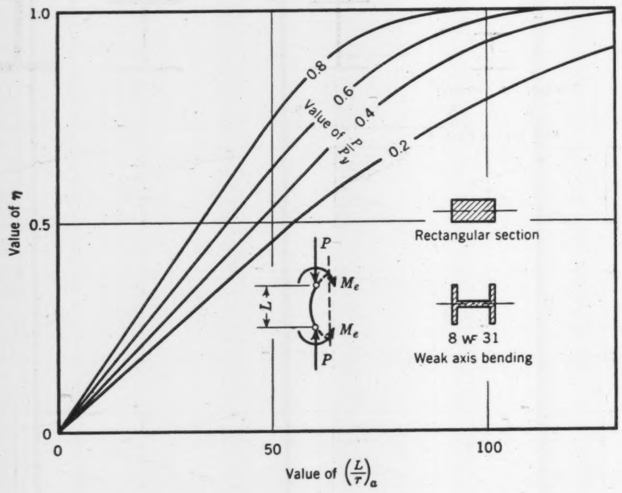

FIG. 41.—PLASTIC REDUCTION FACTOR FOR WEAK-AXIS BENDING OF AN 8WF31 SECTION

1. Given the spring constant β_0, assume an effective length for various values of P/P_y.

2. Determine η from Fig. 41 knowing P/P_y and $c\,L/r$. The term η is the secant to the $\frac{M}{M_y} - \frac{\phi}{\phi_y}$ curve at the point corresponding to collapse of the member in question. This information was available from the computations leading to Fig. 35. In Fig. 41,

$$\left(\frac{L}{r}\right)_a = \frac{L}{r}\sqrt{\frac{\sigma_y}{40.0}} \qquad (18)$$

3. Check c by using[33] the curves of $\beta_0/(\eta\, E\, K)$ versus c.

---

[32] Discussion by Robert L. Ketter and Lynn S. Beedle of "Eccentrically Loaded, End-Restrained Columns," by Paul P. Bijlaard, Gordon P. Fisher, and George Winter, *Transactions*, ASCE, Vol. 120, 1955, p. 1097.

[33] "Buckling of Trusses and Rigid Frames," by George Winter, P. T. Hsu, B. Koo, and M. H. Loh, *Bulletin No. 36*, Cornell Univ. Eng. Experiment Station, Ithaca, N. Y., April, 1948.

4. Repeat steps 1, and 2, and 3 until the assumed c-values agree with those computed.

5. Using the correct η-values corresponding to each assumed value of P/P_y, determine the relationship between e_e and e from the Cornell report.[34]

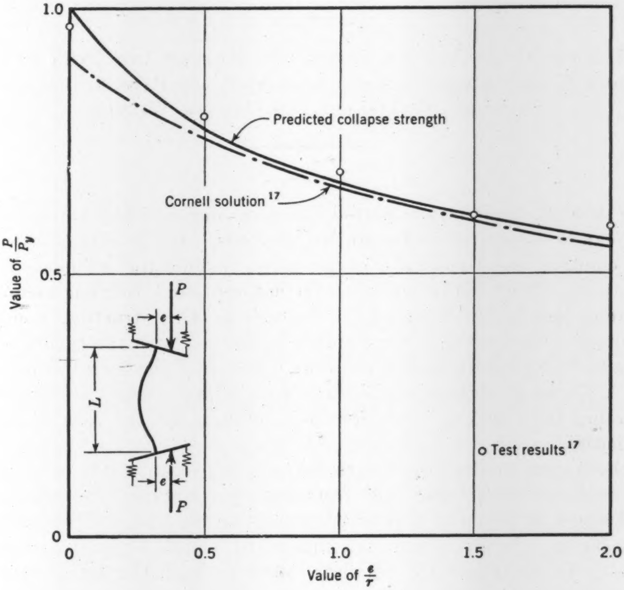

FIG. 42.—CORRELATION BETWEEN CORNELL TESTS[17] AND THEORETICAL ANALYSIS FOR WEAK-AXIS BENDING OF 4I9.5 ANNEALED MEMBERS

6. Determine P/P_y and e_e/r for the corresponding values of $c\,L/r$ from Fig. 35(b).

7. Obtain values of e/r versus P/P_y by multiplying the results of steps 5 and 6.

The corrected curve is shown in Fig. 42. It is in reasonable agreement with both the test results and the Cornell analytical solution.

---

[34] "Eccentrically Loaded, End-Restrained Columns," by Paul P. Bijlaard, Gordon P. Fisher, and George Winter, *Transactions*, ASCE, Vol. 120, 1955, p. 1080, Eq. 12.

ECCENTRICALLY LOADED, END-RESTRAINED COLUMNS

BY PAUL P. BIJLAARD,[1] M. ASCE, GORDON P. FISHER,[2]
A. M. ASCE, AND GEORGE WINTER,[3] M. ASCE

WITH DISCUSSION BY MESSRS. ROBERT L. KETTER AND LYNN S. BEEDLE;
JOHN F. BAKER AND MICHAEL R. HORNE; AND PAUL P. BIJLAARD,
GORDON P. FISHER, AND GEORGE WINTER

SYNOPSIS

The strength of simply supported columns, concentrically and eccentrically loaded, can be computed by recognized methods. In the case of eccentrically loaded columns these methods, of necessity, include the influence of plastic deformation. Most actual columns do not represent isolated members but are more or less rigidly connected at the ends to other structural components. To approach this condition, the paper is concerned with the theory and tests relating to eccentrically loaded columns with equal elastic restraints at both ends. A precise analytical method and a simplified method are presented for determining the buckling loads for such columns for the case of equal end eccentricities.

In the former method the length between inflection points of eccentrically loaded columns with equal end restraints was obtained by assuming the buckled shape to be a sine wave with respect to the pressure line of the compressive forces. In this manner an equivalent, simply supported column was obtained. To determine the column's ultimate load, the actual rather than the approximate deflected shape was used. This shape depends on the stress-strain diagram of the material.

The simplified method reduces the problem to that of analyzing an equivalent, simply supported, eccentrically loaded column. Use is made of an "effective eccentricity," and general formulas are presented which greatly reduce the computation necessary for determining these buckling loads; torsional buckling is not considered. The ultimate buckling loads may be as much as 100% higher than those which cause first yielding in the outer fiber, provided local failure by flange buckling does not occur. Specifications in building codes for columns are generally based on those loads which cause incipient yielding rather than on the ultimate loads.

Tests are reported on eighteen columns, half on square bars and the others on I-sections. To investigate the influence of residual stresses, half the specimens were annealed. The columns were tested with fixed degrees of

---

NOTE.—Published, essentially as printed here, in October, 1953, as *Proceedings-Separate 292.* Positions and titles given are those in effect when the paper or discussion was received for publication.

[1] Prof. of Structural Eng., Cornell Univ., Ithaca, N. Y.

[2] Associate Prof. of Structural Eng., Cornell Univ., Ithaca, N. Y.

[3] Head of Dept. of Structural Eng., Cornell Univ., Ithaca, N. Y.

elastic restraint and with various eccentricities. Ultimate loads were determined as well as loads which caused first local yielding. Stress-strain tests in tension and compression were made on the column material. Experimental ultimate loads and loads which caused first yielding are compared with the values predicted by the theory; satisfactory agreement is obtained.

NOTATION

The letter symbols adopted for use in the paper are defined where they first appear, in the illustrations or in the text, and are arranged alphabetically for convenience of reference in the Appendix.

INTRODUCTION

The performance of isolated columns, both concentrically and eccentrically loaded, is well understood; their carrying capacities can be computed if the stress-strain relationship of the material is known. Most compression members, however, are connected at their ends to other parts of the structure. If they are loaded concentrically, methods are available to compute their buckling loads.[4] In reality most columns are subject to eccentric compression—either from eccentricities caused by imperfection, as in the case of many trusses, or from end moments transmitted by abutting members. F. Bleich has stated:[5]

> "An elaborate study of eccentrically loaded columns with end restraints must be considered as the first step in an investigation of the behavior of columns as part of a rigid frame or in estimating the effect of secondary stresses in trusses upon the buckling strength of its compression members."

As part of such a study, the writers have prepared an analytical and experimental investigation of columns with equal elastic restraints and with equal eccentricities at both ends.

An exact analysis of this type, including plastic deformation of the column, is exceedingly cumbersome; the only exact work on this problem appears to have been done by E. Chwalla.[6] However, Mr. Chwalla's analysis cannot be generalized for practical use. It is a laborious grapho-analytical method which was applied only to eccentric buckling stresses of 21,300 lb per sq in.

A general method for analyzing this type of column will be developed subsequently. This method serves as a check for the development of a simplified, approximate method, which is based on the concept of the equivalent, eccentrically loaded, simply supported column, as used[7] by Annabel Yuen-Wai Lee for computing the load at which yielding begins in the outer fibers of eccentrically loaded, end-restrained columns. Similar methods have been developed for eccentrically loaded columns with any degree of end restraint, equal or unequal, and with any amount of end eccentricity, equal or unequal.[8,9]

---

[4] "Buckling of Trusses and Rigid Frames," by G. Winter, P. T. Hsu, B. Koo, and M. H. Loh, *Bulletin No. 36*, Eng. Experiment Station, Cornell Univ., Ithaca, N. Y., April, 1948.

[5] "Buckling Strength of Metal Structures," by F. Bleich, McGraw-Hill Book Co., Inc., New York, N. Y., 1952, p. 51.

[6] "Aussermittig gedrückte Baustahlstäbe mit elastisch eingespannten Enden und verschieden grossen Angriffshebeln," by E. Chwalla, *Der Stahlbau*, Nos. 7 and 8, 1937, pp. 49–52 and pp. 57–60.

[7] "A Study on Column Analysis," by Annabel Yuen-Wai Lee, thesis presented to Cornell Univ. at Ithaca, N. Y., in June, 1949, in partial fulfilment of the requirements for the degree of Doctor of Philosophy.

ANALYTICAL METHOD

An exact determination of the eccentric buckling stress of simply supported and elastically restrained columns is excessively laborious because eccentric buckling always occurs in the plastic region. In Fig. 1(*a*) there is shown the stress-strain curve (in tension and compression) of the eccentrically loaded column in Fig. 1(*b*). With increasing bending moments, $P\,y$, the strains in the outer fibers in the central part of the column, where moments are large, surpass the strain at the proportional limit, ϵ_p. Consequently, near failure and at failure the stress distribution over a cross section near midlength is the plastic distribution shown in Fig. 1(*c*); near the ends, where moments are small, the elastic distribution shown in Fig. 1(*d*) will usually prevail.

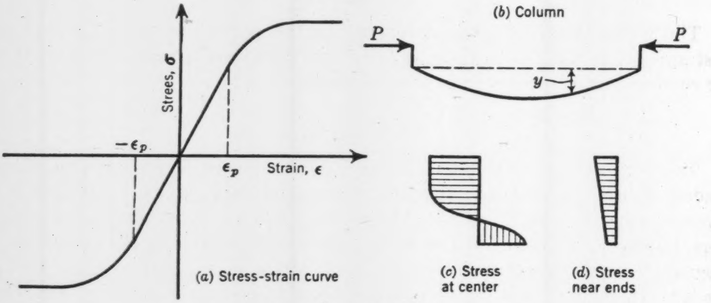

(*a*) Stress-strain curve (*c*) Stress at center (*d*) Stress near ends

FIG. 1.—AN ECCENTRICALLY LOADED COLUMN

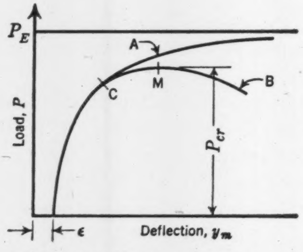

FIG. 2.—LOAD-DEFLECTION DIAGRAM

As long as only elastic deformations occur, the load P required to hold the column in equilibrium will increase and asymptotically approach the Euler load, P_E, as indicated by curve A in Fig. 2. Only when plastic deformations

---

[8] "Second Progress Report on Investigation of Buckling of Rigid Joint Structures," by P. P. Bijlaard, Cornell Univ., Ithaca, N. Y., June, 1951.

[9] "Buckling of Columns with Equal and Unequal End Eccentricities and Equal and Unequal End Restraints," by P. P. Bijlaard, *Proceedings*, 2d U. S. National Cong. of Applied Mechanics, Ann Arbor, Mich., 1954.

begin to occur (thus decreasing the effective flexural deformation modulus of the column) will the load-deflection diagram of the column deviate from curve A (at point C in Fig. 2); it will follow the lower curve B. Because, in most cases, the effective modulus of the material decreases gradually with increasing curvature, curve B will deviate more and more from curve A and at a certain point M it will attain a maximum value,

$$P_{cr} = A\,\sigma_{cr} \quad \text{.........................} (1)$$

in which A is the cross-sectional area of the column. The value, P_{cr}, is the critical or buckling load of the column and σ_{cr} is the maximum average stress (or eccentric buckling stress) it can sustain.

In the case of a simply supported, eccentrically loaded column, for example, the condition of equal internal and external moments requires that (as shown in Fig. 3)

$$-\eta\, E\, I\, \frac{d^2y}{dx^2} = P\, y \quad \text{.......................} (2)$$

in which the x-axis is taken along the axis of thrust. In Eq. 2, η is the reduction factor for plasticity and is unity in the elastic domain, E represents

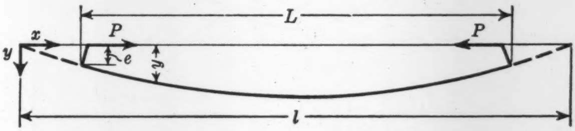

FIG. 3.—SIMPLY SUPPORTED, ECCENTRICALLY LOADED COLUMN

the modulus of elasticity of the column material, and I is the moment of inertia of the column section. In the plastic domain and for infinitely small deflections (as in the case of concentric buckling), this reduction factor can safely (and with sufficient accuracy) be assumed equal to E_t/E, in which E_t is the tangent modulus.[10] It is invariant with x, and η is thus a constant in Eq. 2 which is consequently satisfied by a sine wave.

If, however, the deflections are finite, such as for eccentric buckling and for deflections of concentrically loaded columns subsequent to buckling, η is not independent of x. In Fig. 3, for example, η is smaller in the center of the column, where the curvature is the greatest, and is larger at the ends. Hence, the curvature of the column at the center will be larger than that of a sine wave of equal maximum deflection whereas near the ends it will be smaller.

An exact determination of eccentric buckling stresses of simply supported, as well as elastically restrained, columns is laborious because in the plastic domain the deflection curve is no longer the branch of a sine wave. These facts were taken into account by Mr. Chwalla in his computations, which were concerned with eccentrically loaded and simply supported columns and the equilibrium load of concentrically loaded columns with finite post-buckling deflections.[11,12] For eccentrically loaded and elastically restrained columns, however, this method does not lead to directly applicable results.

---

[10] "Inelastic Column Theory," by F. R. Shanley, *Journal of the Aeronautical Sciences*, Vol. 14, No. 5, 1947, pp. 261–268.

In Figs. 4(*a*) and 4(*d*) there are shown two cases of elastically restrained columns. For the case shown in Fig. 4(*a*), the form of the deflected column is shown in Fig. 4(*b*) in which points G and H are inflection points. Because the moments are zero at these points, the line of thrust of force P passes through G and H. The distance between the inflection points, which is termed the equivalent length, will decrease with increasing external force P whereas the amplitude y_m will increase. This follows from the fact that the compressive resistance is equal to that of the hinged column G H with length l and deflection y_m. For a hinged column with constant length, the resistance in the elastic range remains sensibly constant with increasing deflection y_m.

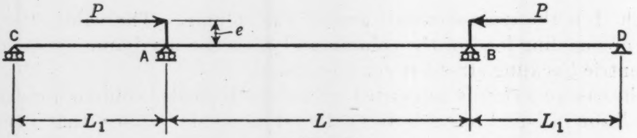

(*a*) Case I

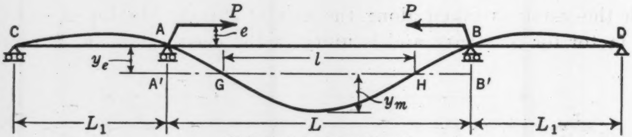

(*b*) Deflected column, Case I

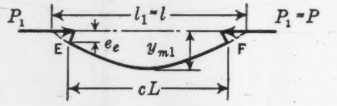

(*c*) Effective column

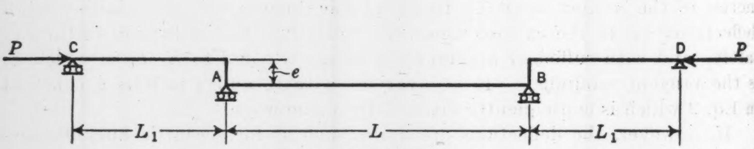

(*d*) Case II

FIG. 4.—ELASTICALLY RESTRAINED COLUMNS

---

[11] "Theorie des aussermittig gedrückten Stabes aus Baustahl," by E. Chwalla, *Der Stahlbau*, Nos. 21–23, 1934, pp. 161–165 and 173–176.

[12] "Discussion of Questions I₁ and I₂," by E. Chwalla, *Final Report*, International Assn. for Bridge and Structural Eng., 1st Cong., Paris, France, 1932, pp. 53–63.

In the plastic range the resistance of a hinged column decreases with increasing y_m because, in this case, the effective plastic-deformation modulus decreases. Hence, the only way for the elastically restrained column to resist an increasing load P is for its equivalent length l to diminish so that its equilibrium load can still increase as its equivalent length decreases. In the elastic range this behavior can be demonstrated by use of an equation[13] by letting the load P increase to and beyond the Euler load and computing the distance between inflection points. In the plastic range the progressive decrease in equivalent length is further accelerated by the plastification of the column. Finally, however, the decrease of the equivalent length l can no longer cancel the decrease of the effective modulus ηE, and the equilibrium load will begin to decrease after having reached an extreme value of P_{cr} (Fig. 2).

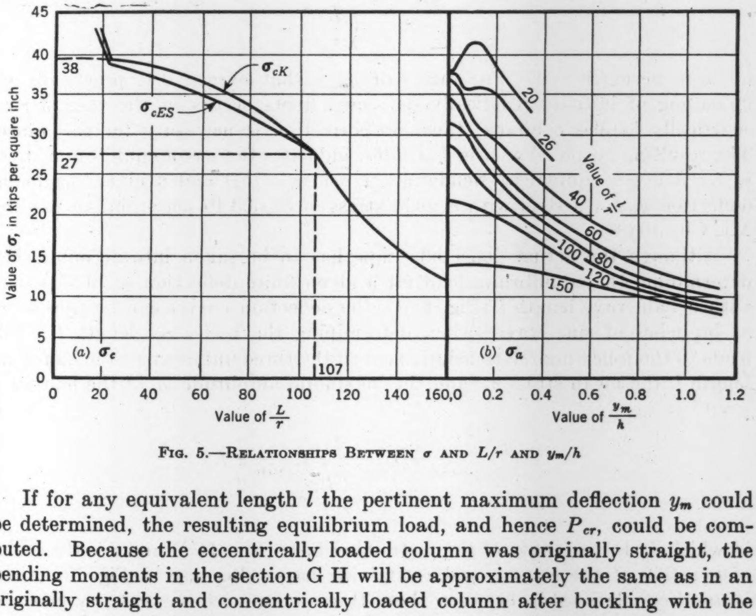

FIG. 5.—RELATIONSHIPS BETWEEN σ AND L/r AND y_m/h

If for any equivalent length l the pertinent maximum deflection y_m could be determined, the resulting equilibrium load, and hence P_{cr}, could be computed. Because the eccentrically loaded column was originally straight, the bending moments in the section G H will be approximately the same as in an originally straight and concentrically loaded column after buckling with the same maximum deflection y_m. A graph of the relationship between resistance and deflection of originally straight, simply supported, rectangular columns after buckling has been determined[12] by the use of the method of double integration[14] for a steel with a yield stress of 38,000 lb per sq in. and an elastic limit of 27,000 lb per sq in. The relationship between slenderness and buckling stress for concentric buckling of columns of the same steel is shown in Fig. 5(a), in which σ_c is the buckling stress, σ_{cES} denotes the buckling stress according to[10] F. Engesser and F. R. Shanley, and σ_{cK} is the buckling stress according to[14] Theodor von Kármán, Hon. M. ASCE.

---

[13] "Buckling of Trusses and Rigid Frames," by G. Winter, P. T. Hsu, B. Koo, and M. H. Loh, *Bulletin No. 36*, Eng. Experiment Station, Cornell Univ., Ithaca, N. Y., April, 1948, p. 9, Eq. 7.

[14] "Untersuchungen über Knickfestigkeit," by Theodor von Kármán, *Mitteilungen und Forschungsarb*, Verein Deutscher Ingenieure, H. 81, Berlin, Germany, 1910.

The graph for the relationship between resistance and deflection of an originally straight column, previously cited, had to be corrected for ratios of y_m/h smaller than 0.1 (in which h is the thickness of the column in the direction of buckling) because the curves were based on the von Kármán theory[14] of unloading fibers that were originally plastically compressed. In the case of eccentric compression, where the compressive force and the bending moments increase simultaneously, such unloading is nonexistent or negligible so that in any section the stress distribution is determined by the original stress-strain diagram of the material (Fig. 1(*c*)). Accordingly, there results

$$\sigma_{cES} = \frac{\pi^2 E_t}{\left(\frac{L}{r}\right)^2} \quad \text{(3)}$$

for zero eccentricity.[10] For ratios of y_m/h that exceed 0.1, practically no unloading of initially plastically deformed fibers occurs in the case of concentrically loaded columns; thus, no correction is necessary for this range. The resulting graph, shown in Fig. 5(*b*), indicates the mean equilibrium stress σ_a for a given equivalent slenderness l/r (Fig. 4(*b*)) and a given maximum deflection y_m for a steel with a yield stress of 38,000 lb per sq in., as used by Mr. Chwalla.[12]

Although the actual deflected shape has to be taken into account when determining the equilibrium load for a given finite deflection y_m of a column with a half-wave length l (Fig. 4(*b*)), the deflection curves can be considered as branches of sine waves when determining the half-wave length l. This leads to the following relationship between the three unknowns—the half-wave length l, the mean stress σ_a, and the maximum amplitude y_m of the half-wave length l:

$$y_m = \frac{e}{\cos \frac{\pi}{2} \frac{L}{l} + \frac{3\,\pi\,E}{\frac{l}{r}\frac{L_1}{r}\,\sigma_a} \sin \frac{\pi}{2} \frac{L}{l}} \quad \text{(4)}$$

in which L_1 is the length of the restraining bars (Fig. 4(*a*)) and r is the radius of gyration of the column and restraining bars. Because in Fig. 5(*b*) there is another relationship between these three unknowns, one can, by choosing several values of l, find the corresponding values of y_m and σ_a from Eq. 4 and Fig. 5(*b*) by trial and error. These values can be then plotted so as to obtain a graph such as C B in Fig. 2, in which

$$P = A\,\sigma_a \quad \text{(5)}$$

The maximum value of P is the critical load of the eccentrically loaded column. For example, for the case shown in Fig. 4(*a*) exact data are available[6] for $L/r = 119.6$, $L_1/r = 50$, and $e/r = 2$ or $e/h = 0.578$, leading to the exact result, $\sigma_a = 21{,}300$ lb per sq in. From Eq. 4 (which is approximate) and Fig. 5(*b*), one can obtain the following values, which represent associated pairs of values of y_m and σ_a (in pounds per square inch) near point M of a curve such as C M B in Fig. 2.

$\frac{l}{r}$	$\frac{y_m}{h}$	σ_a
95	0.253	21,080
90	0.265	21,160
85	0.286	21,160
80	0.310	20,860

Hence, the maximum stress reached is the eccentric buckling stress and is found to be $\sigma_{cr} = 21{,}160$ lb per sq in., which is in good agreement with the exact value of 21,300 lb per sq in. Comparisons such as this illustrate the adequacy of the method based on Eq. 4 and Fig. 5(*b*).

SIMPLIFIED METHOD

To arrive at a simpler approximate-design procedure, Miss Lee's method[7] for determining the load at which yielding of the outer fiber begins in eccentrically compressed, elastically restrained columns was extended to eccentric buckling. According to Miss Lee, the outer fiber stress in column A B (Fig. 4(*b*)) will reach the yield stress at approximately the same load as it will in a simply supported column with a length equal to the effective length $c\,L$ of the concentrically loaded column A B and with an effective eccentricity e_e (Fig. 4(*c*)). To determine e_e the external moments $P\,e$ (Figs. 4(*a*) and 4(*d*)) are distributed to the members A B and to the elastic restraints, with the compressive force in the restraining members neglected.

As stated in connection with Figs. 1 and 2, eccentric buckling always occurs in the plastic region. Hence, it can be assumed that this method can also be used to determine the eccentric buckling stress if—for determining the effective length $c\,L$ and the effective eccentricity e_e of the corresponding simply supported column—a proper plastic reduction factor η is used to account for the decrease of the flexural rigidity $E\,I$ of the buckling member A B (Fig. 4).

The simplified-method procedure, consequently, is as follows: (1) By means of the proper reduction factor η one determines the effective length for concentric buckling ($c\,L$ in Fig. 4(*c*)) of the simply supported column equivalent to the restrained column of Fig. 4(*b*). (2) The concentric buckling stress σ_{cES} of this equivalent column is then determined from Eq. 3. (3) Again using η, the effective eccentricity e_e of the simple column (Fig. 4(*c*)) is found to correspond to the real eccentricity e of the restrained column (Fig. 4(*b*)). (4) Next, the eccentric buckling stress σ_a (which, of course, is smaller than the critical stress for concentric buckling, σ_{cES}) can be found for the equivalent simple column from

$$\sigma_{cr} = \frac{\sigma_{cES}}{\gamma} \qquad (6)$$

in which γ is a division factor larger than one. This division factor depends on the effective eccentricity ratio e_e/k_c (in which k_c is the core radius r^2/c_s)

and the effective slenderness $c\,L/r$. The factor γ is a quantity similar to β used by Mr. Bleich.[15]

The determination of the various quantities which are used in the simplified method was possible only by fitting expressions to the results of the few and limited exact determinations available in the literature, to the analytical method discussed previously, and to the test results reported hereafter.

Determination of the Reduction Factor for Plasticity of Steel.—The reduction factor η was determined by comparison with (1) the exact computations[6] for some cases, (2) the semi-exact analytical method, and (3) the test results described subsequently. The exact computations[6] refer to the case shown in Fig. 4(*a*) and to a steel with a yield stress of 38,000 lb per sq in. (for which the relationship between the slenderness ratio L/r and the concentric buckling stresses σ_{cK} and σ_{cES} is determined from Fig. 5(*a*)). The buckling stress σ_{cES} is given by Eq. 3 and

$$\sigma_{cK} = \frac{\pi^2\,E_r}{\left(\frac{L}{r}\right)^2} \quad \text{(7)}$$

in which E_r is the reduced modulus. Previously[6] Eq. 7 was used, but, as Mr. Shanley showed,[10] Eq. 3 should be used.

It can be expected that the reduction factor η will vary with the buckling stress as well as with the slenderness. It will differ from the reduction factors E_t/E or E_r/E which, from Eqs. 3 and 7, are

$$\frac{E_t}{E} = \frac{\sigma_{cES}\left(\frac{L}{r}\right)^2}{\pi^2\,E} \quad \text{(8a)}$$

and

$$\frac{E_r}{E} = \frac{\sigma_{cK}\left(\frac{L}{r}\right)^2}{\pi^2\,E} \quad \text{(8b)}$$

The moduli E_t and E_r differ considerably for a given value of the buckling stress because (from Fig. 5(*a*)) for a given buckling stress the abscissa L/r, which appears to the second power in Eqs. 8, differs considerably for the two curves. However, for a given abscissa L/r (from Fig. 5(*a*)) the ordinates σ_{cES} and σ_{cK} of the two curves, which appear to the first power only in Eqs. 8, differ very little so that E_t and E_r from Eqs. 8 will differ slightly. This suggests that one can express η as a function of the effective slenderness $c\,L/r$ rather than of the eccentric buckling stress. This is fortunate because the available exact data[6] are all for the same eccentric buckling stress of 21,300 lb per sq in. The case investigated[6] by Mr. Chwalla is that shown in Fig. 4(*a*) where members C A, A B, and D B have the same rectangular cross sections. The numerical values of the parameters e/r, L_1/r, and L/r used by Mr. Chwalla are assembled in Table 1, which also includes values of σ_{cK} for concentric loading. The significance of the columns headed e_e/k_c, γ', and σ_{cr} will be explained subsequently. From the data in Table 1 a provisional value η' for the reduction factor η to be used in the simplified method can be determined so as to lead to the proper eccentric buckling stress of 21,300 lb per sq in.

---

[15] "Buckling Strength of Metal Structures," by F. Bleich, McGraw-Hill Book Co., Inc., New York, N. Y., 1952, p. 41.

The problem is to reduce the elastically restrained column with eccentricity e (Fig. 4(a)) to a simply supported column of length $c\,L$ and with eccentricity e_e (Fig. 4(c)). For the latter case the pertinent reduction factor,

$$\gamma' = \frac{\sigma_{cK}}{\sigma_{cr}} \qquad (9)$$

is known.[12] By adjusting η so that, for a simply supported column of length $c\,L$ and effective eccentricity e_e, the correct buckling stress (21,300 lb per sq in. for the case in Table 1) is obtained, the provisional value η' is found.

TABLE 1.—DATA FOR TEN CASES INVESTIGATED BY E. CHWALLA

Case	e/r	L_1/r	L/r	$c\,L/r$	e_e/k_c	σ_{cK}[a]	γ'	σ_{cr}[a]
1	0.25	200	123.8	99	0.224	28.95	1.41	20.51
2	0.25	100	156.5	105	0.13	27.69	1.31	21.15
3	0.25	50	188.9	110	0.065	25.48	1.20	21.21
4	0.25	19.1	217.0	115	0.024	23.52	1.08	21.72
5	0.25	0	241.2	121	0	21.30	1	21.30
6	2	200	48.1	35	1.35	37.56	1.79	21.01
7	2	100	77.2	51	0.97	36.49	1.74	21.01
8	2	50	119.6	71	0.59	34.20	1.63	21.01
9	2	19.1	176.2	94.5	0.23	29.95	1.41	21.30
10	2	0	241.2	121	0	21.30	1	21.30

[a] In kips per square inch.

First the actual spring constant β of the elastic restraints given by the adjacent members C A and B D is computed—

$$\beta = \frac{3\,E\,I}{L_1} \qquad (10)$$

Then the effective length $c\,L$ for concentric buckling of column A B can be found from a graph[16] in which $\beta/(E\,K)$ has to be replaced by $\beta/(\eta\,E\,K)$, and K is equal to I/L. Hence, from Eq. 10,

$$\frac{\beta}{\eta\,E\,K} = \frac{\dfrac{3\,L}{L_1}}{\eta} \qquad (11)$$

in which η is still an unknown function of $c\,L/r$. If, at first, the ratio $c\,L/r$ is estimated, η can be determined. Then, with $\beta/(\eta\,E\,K)$ determined from Eq. 11, from the graph[16] the factor c and hence $c\,L/r$ can be found. This value must be equal to the value originally estimated. Thus, c is found by trial and error, and $c\,L/r$ has been entered in Table 1. Then the equivalent eccentricity e_e is determined by distributing the external moments $P\,e$, the influence of the axial forces in all members being neglected. Hence, from Fig. 4(*a*),

---

[16] "Buckling of Trusses and Rigid Frames," by G. Winter, P. T. Hsu, B. Koo, and M. H. Loh, *Bulletin No. 36*, Eng. Experiment Station, Cornell Univ., Ithaca, N. Y., April, 1948, p. 57, Graph II.

$$e_e = \frac{2\,\eta\,E\,K}{2\,\eta\,E\,K + \beta}\,e \qquad (12)$$

With the values of $c\,L/r$ and e_e/k_c so obtained the eccentric buckling stress of the column is found from Eq. 9 in which σ_{cK} can be determined from Fig. 5(*a*) for the known ratio $c\,L/r$. The reduction factor γ' for eccentrically loaded and simply supported columns is found from a table[17] and has been entered in Table 1. It appears that a good approximation of the actual

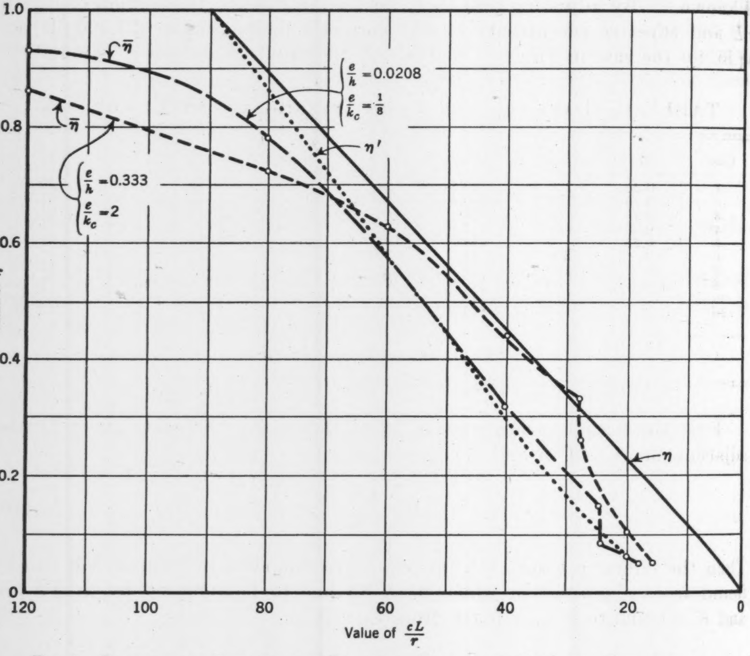

FIG. 6.—RELATIONSHIP BETWEEN THE REDUCTION FACTOR AND EFFECTIVE SLENDERNESS

buckling stress of 21,300 lb per sq in. is obtained if it is assumed that η' (the provisional value) is given by the following relationships:

for $\frac{c\,L}{r} > 90$: $$\eta' = 1 \qquad (13a)$$

for $90 > \frac{c\,L}{r} > 30$: $$\eta' = 0.014\,\frac{c\,L}{r} - 0.26 \qquad (13b)$$

and for $30 > \frac{c\,L}{r} > 20$: $$\eta' = 0.16\left(\frac{c\,L}{30\,r}\right)^2 \qquad (13c)$$

---

[17] "Discussion of Questions I₁ and I₂," by E. Chwalla, *Final Report*, International Assn. for Bridge and Structural Eng., 1st Cong., Paris, France, 1932, p. 59.

Eqs. 13 have been plotted in Fig. 6 and have been used to find $c\,L/r$ and e_e/k_c in Table 1 as explained previously. The values of γ' correspond to the respective values of e_e/k_c; the column (Table 1) of the eccentric buckling stress is seen to be in excellent agreement with Mr. Chwalla's exact value of 21,300 lb per sq in.

These determinations refer only to one specific value of the buckling stress, 21,300 lb per sq in. To obtain an idea of the variation of η with the buckling stress, one should examine two figures prepared by Mr. Chwalla.[18] These figures show the relationship between computed loads and deflections y_{om} of the type shown in Fig. 7 for simply supported, eccentrically loaded columns (Fig. 8) for a range of buckling stresses from 9,450 lb per sq in. to 40,000 lb per sq in. The figures are for eccentricity ratios, e/k_c, of 1/8 and 2 (that is, e/h equal to 0.0208 and 0.333) and several slenderness ratios. From the values σ_{cr} and y_{om} at the point (Fig. 7) of maximum load M, the equivalent bending modulus $\bar{\eta}\,E$ can be computed.

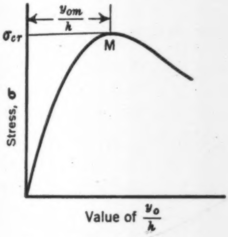

FIG. 7.—STRESS VS. y_o/h

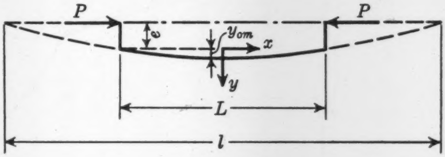

FIG. 8.—COLUMN, SIMPLY SUPPORTED AND ECCENTRICALLY LOADED

Assuming $\bar{\eta}$, the reduction factor for plasticity in the simply supported column, to be independent of x (Fig. 8)—the equality between external and internal moments yields

$$P_{cr}(e + y) = -\,\bar{\eta}\,E\,I\,\frac{d^2(e + y)}{dx^2} \qquad (14)$$

so that

$$(e + y) = (e + y_{om})\cos\frac{\pi}{l}\,x \qquad (15)$$

Insertion of Eq. 15 into both sides of Eq. 14 results in

$$\bar{\eta} = \frac{P_{cr}\,l^2}{\pi^2\,E\,I} \qquad (16)$$

The boundary conditions at $x = \pm\,L/2$ require that

$$(e + y_{om})\cos\frac{\pi}{l}\frac{L}{2} = e \qquad (17a)$$

or

$$\frac{\pi}{l}\frac{L}{2} = \cos^{-1}\frac{e}{e + y_{om}} \qquad (17b)$$

---

[18] "Discussion of Questions I₁ and I₂," by E. Chwalla, *Final Report*, International Assn. for Bridge and Structural Eng., 1st Cong., Paris, France, 1932, pp. 55–56, Figs. 2 and 3.

From Eqs. 16 and 17, using $I = A\,r^2$,

$$\bar{\eta} = \frac{P_{cr}}{E\,I}\,\frac{L^2}{4\left(\cos^{-1}\dfrac{e}{e + y_{om}}\right)^2} = \frac{\sigma_{cr}}{E}\,\frac{L^2}{r^2}\,\frac{1}{4\left(\cos^{-1}\dfrac{e}{e + y_{om}}\right)^2} \quad \text{.....(18)}$$

Values obtained from Eq. 18 are plotted in Fig. 6 for the ratios e/k_c equal to 1/8 and 2 as functions of the effective slenderness $c\,L/r$, which in the present case (Fig. 8) is equal to L/r.

Thus from η' and $\bar{\eta}$ in Fig. 6 and from a comparison of the results of the previously described semi-exact method and the test results, it was concluded that the straight line (as shown in Fig. 6) through the origin and a point $c\,L/r = 90$, $\eta = 1$ gives conservative values for the entire range and is a good approximation for η. In this connection it should be noted that this straight line leads to safe buckling stresses because a higher value of η leads to lower critical stresses. Hence, for a steel with a yield stress of 38,000 lb per sq in.,

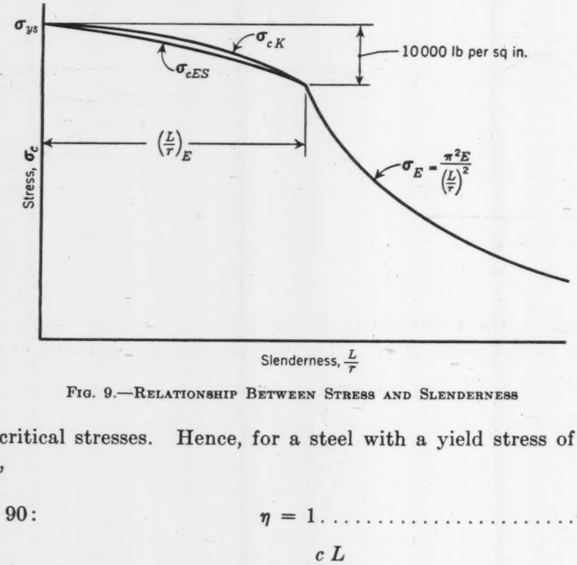

FIG. 9.—RELATIONSHIP BETWEEN STRESS AND SLENDERNESS

for $\dfrac{c\,L}{r} > 90$: $\quad \eta = 1$ ....(19a)

and for $90 > \dfrac{c\,L}{r} > 20$: $\quad \eta = \dfrac{\frac{c\,L}{r}}{90}$ ....(19b)

These determinations refer only to the specific steel ($\sigma_{ys} = 38{,}000$ lb per sq in.) used by Mr. Chwalla. To develop a method which is applicable to mild steel having any yield point it is necessary to generalize this information.

Approximate Formulas for Steels with an Arbitrary Yield Stress.—In order to be able to use the simplified method for steels with an arbitrary yield stress, and using σ_{cES} rather than σ_{cK} for concentric buckling, more general formulas will be developed subsequently.

In order to determine the concentric buckling stress σ_{cES} from Eq. 3 it is necessary to use the proper tangent modulus E_t which varies with stress. Rather than attempting a statistical evaluation of steel stress-strain diagrams, the inverse method of finding an expression for σ_{cES} from known column curves for concentric buckling will be used.[19]

Assuming the proportional limit to be 10,000 lb per sq in. below the yield stress σ_{ys}, the concentric buckling stress for simply supported columns is approximated by the curve in Fig. 9 whose equation is

$$\sigma_{cES} = \sigma_{ys} - 5{,}000 \left\{ \frac{\frac{L}{r}}{\left(\frac{L}{r}\right)_E} + \left[\frac{\frac{L}{r}}{\left(\frac{L}{r}\right)_E} \right]^2 \right\} \qquad (20)$$

as shown by comparison between Fig. 5(*a*) and Fig. 9. In Eq. 20 $(L/r)_E$ is the slenderness, for which the buckling stress is equal to the proportional limit, so that

$$\left(\frac{L}{r}\right)_E = \left(\frac{3 \times 10^8}{\sigma_{ys} - 10{,}000}\right)^{\frac{1}{2}} \qquad (21)$$

To compute the eccentric buckling stress σ_{cr} from Eq. 6, it is necessary to determine the division factor γ for eccentricity.

The division factor γ', which is related to σ_{cK} (Eq. 9) for simply supported columns, is given in a table[17] for a steel with a yield stress of 38,000 lb per sq in. for various ratios of L/r and e/k_c. If γ is the division factor related to σ_{cES} by Eq. 6, it can be seen that

$$\gamma = \gamma' \frac{\sigma_{cES}}{\sigma_{cK}} \qquad (22)$$

in which σ_{cES}/σ_{cK} is determined from Fig. 5(*a*). The ratios so obtained are given in Fig. 10(*a*) by the solid curves and can be approximated

$$\text{for } 200 > \frac{L}{r} > 107 \text{ by:} \qquad \gamma = 1 + \frac{12{,}200 \left(\frac{e}{k_c}\right)^{2/3}}{\left(\frac{L}{r}\right)^2} \qquad (23a)$$

and for $77 > \dfrac{L}{r} > 20$ by:

$$\gamma = 1 + 0.52 \frac{e}{k_c} + \frac{\left(\frac{e}{k_c}\right)^{1/2}}{180} \left(\frac{L}{r} - 20\right) \qquad (23b)$$

One should interpolate between γ_{77} and γ_{107} for $107 > L/r > 77$. Eqs. 23 are applicable only for the steel used[12] by Mr. Chwalla and are believed to be better approximations than those given[5] by Mr. Bleich. Eqs. 23 are plotted as dashed lines in Fig. 10(*a*).

---

[17] "Buckling Strength of Metal Structures," by F. Bleich, McGraw-Hill Book Co., Inc., New York, N. Y., 1952, pp. 53–55.

No exact value for steels other than that used[12] by Mr. Chwalla (σ_{ys} = 38,000 lb per sq in.) is available. Approximate data, assuming a steel with a stress-strain diagram that is straight up to the yield stress and horizontal from there on, are available[20] for steels with yield stresses of 34,000 lb per sq in. and 51,000 lb per sq in. Denoting the difference in γ found[20] by K. Jezek for these two steels by $\Delta\gamma$, the values for a steel with a yield stress of 50,000 lb per sq in. were computed with sufficient accuracy as

$$\gamma_{50} = \gamma_{38} + \frac{50{,}000 - 38{,}000}{51{,}000 - 34{,}000}\Delta\gamma \ldots\ldots\ldots\ldots\ldots (24)$$

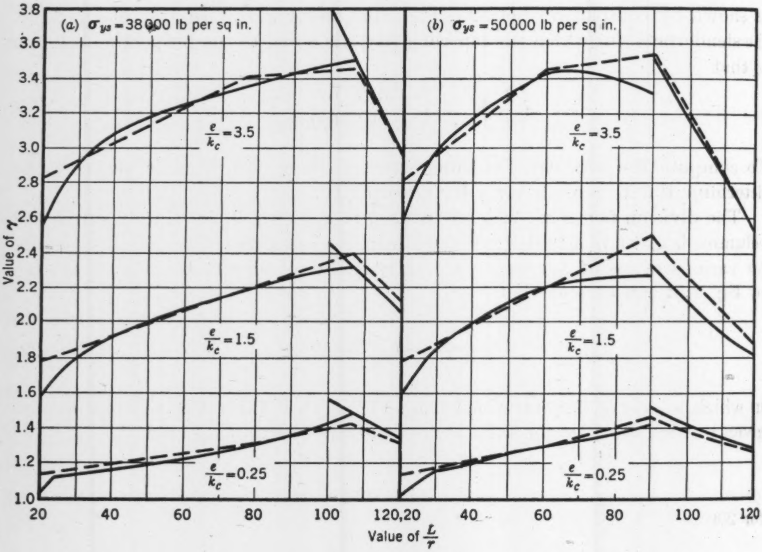

FIG. 10.—RELATIONSHIP BETWEEN THE REDUCTION FACTOR AND SLENDERNESS

In Fig. 10(*b*) there are shown the curves so obtained as solid lines. These curves are approximated fairly well

$$\text{for } 200 > \frac{L}{r} > 90 \text{ by:} \qquad \gamma = 1 + \frac{9{,}500\left(\frac{e}{k_c}\right)^{2/3}}{\left(\frac{L}{r}\right)^2} \ldots\ldots\ldots\ldots\ldots (25a)$$

---

[20] "Die Festigkeit von Druckstäben aus Stahl," by K. Jezek, Julius Springer and Co., Vienna, Austria, 1947.

and for $60 > \dfrac{L}{r} > 20$ by:

$$\gamma = 1 + 0.52\,\frac{e}{k_c} + \frac{\left(\dfrac{e}{k_c}\right)^{1/2}}{120}\left(\frac{L}{r} - 20\right) \qquad (25b)$$

One should interpolate linearly between γ_{60} and γ_{90} for $90 > L/r > 60$. Eqs. 25 are shown as dashed curves in Fig. 10(*b*). Interpolating linearly between Eqs. 23 and 25 one obtains

for $200 > \dfrac{L}{r} > \left(\dfrac{L}{r}\right)_c$:

$$\gamma = 1 + (21{,}000 - 0.23\,\sigma_{ys})\,\frac{\left(\dfrac{e}{k_c}\right)^{2/3}}{\left(\dfrac{L}{r}\right)^2} \qquad (26a)$$

and for $\left(\dfrac{L}{r}\right)_c - 30 > \dfrac{L}{r} > 20$:

$$\gamma = 1 + 0.52\,\frac{e}{k_c} + \frac{\left(\dfrac{e}{k_c}\right)^{1/2}}{370 - 0.005\,\sigma_{ys}}\left(\frac{L}{r} - 20\right) \qquad (26b)$$

For $(L/r)_c > L/r > (L/r)_c - 30$, one should interpolate linearly between γ for $(L/r)_c - 30$ and $(L/r)_c$. In Eqs. 26

$$\left(\frac{L}{r}\right)_c = 157 - 0.0014\,\sigma_{ys} \qquad (27)$$

In order to make the plastic reduction factor η apply for steels of any yield point, it can be observed from Eqs. 19 that, for $\sigma_{ys} = 38{,}000$ lb per sq in., the slenderness ratio $c\,L/r = 90$ is that above which the column can be assumed to act elastically as far as the simplified method is concerned. Because for a given buckling modulus the critical stress is inversely proportional to $(c\,L/r)^2$, the slenderness where plastic action begins to occur is approximately inversely proportional to the square root of the yield stress. Because the limiting value for $\sigma_{ys} = 38{,}000$ lb per sq in. is $c\,L/r = 90$, in general—for steels with other yield stresses—this limiting ratio will be

$$\left(\frac{c\,L}{r}\right)_b = 90\sqrt{\frac{38{,}000}{\sigma_{ys}}} \qquad (28)$$

Thus, in general, from Eq. 19

for $\dfrac{c\,L}{r} > \left(\dfrac{c\,L}{r}\right)_b$:

$$\eta = 1 \qquad (29a)$$

and for $\left(\dfrac{c\,L}{r}\right)_b > \dfrac{c\,L}{r} > 20$:

$$\eta = \frac{\dfrac{c\,L}{r}}{\left(\dfrac{c\,L}{r}\right)_b} \qquad (29b)$$

Shape Factor.—In the preceding investigation, only columns of rectangular cross section have been considered. An extension of the same methods to cross sections of other shapes would require graphs similar to Fig. 5(*b*) and formulas similar to Eqs. 26 for several types of cross sections; also, the reduction factor η from Eq. 29 depends on the shape of the cross section.

A practical method for design, however, is to multiply the equivalent eccentricity e_e by a shape factor which can be determined from Mr. Chwalla's computations[21] and is given in Fig. 11. Fig. 11 differs somewhat from the analogous table prepared[22] by Mr. Bleich.

Summary.—The procedure for determining the buckling stress for symmetrically loaded and symmetrically restrained columns of any cross-sectional shape is therefore as follows for a buckling member A B (Fig. 4(*a*) or Fig. 4(*d*)) having a length L, a moment of inertia I, a radius of gyration r, and a core radius k_c:

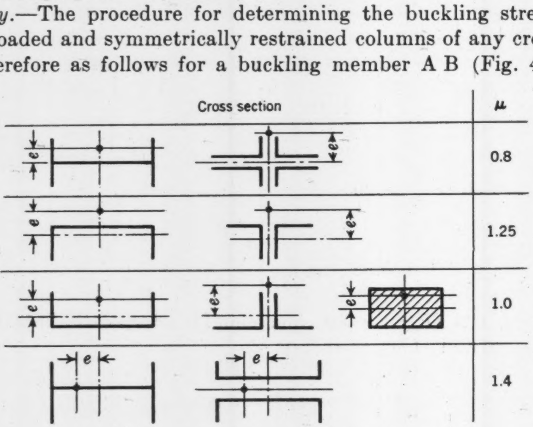

FIG. 11.—SHAPE FACTORS FOR VARIOUS CROSS SECTIONS

1. The spring constant β of the elastic restraints given by the adjacent members to the buckling member is computed, taking account of the axial forces (if any) in these members.[4]

2. The effective length of A B for concentric compression is estimated. For this length, $c\,L$, of the equivalent simply supported column (Fig. 4(*c*)), one must then compute η from Eqs. 29 and $(c\,L/r)_b$ from Eq. 28.

3. The ratio $[\beta/(\eta\,E\,K)]_{AB}$ is then computed, and from it one can find the reduction coefficient c and thus $c\,L$ by means of a graph.[16]

4. The computation for $\beta/(\eta\,E\,K)$ is repeated with the newly found slenderness ratio $c\,L/r$ until this same effective slenderness results from the graph.[16]

5. The equivalent eccentricity e_e is determined by distributing the external moments $P\,e$ without taking account of the axial forces in all members. That is,

$$e_e = \frac{2\,\eta\,E\,K}{2\,\eta\,E\,K + \beta_0}\,e \qquad (30)$$

---

[21] "Der Einfluss der Querschnittsform auf das Tragvermogen aussermittig gedruckter Baustahlstäbe," by E. Chwalla, *Der Stahlbau*, Nos. 25–26, 1935, pp. 193–197 and pp. 204–207.

[22] "Buckling Strength of Metal Structures," by F. Bleich, McGraw Hill Book Co., Inc., New York, N. Y., 1952, p. 45.

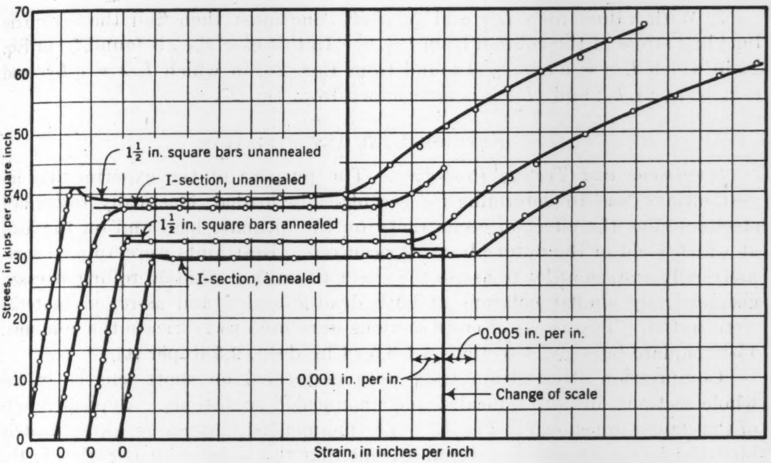

FIG. 12.—STRESS-STRAIN CURVES FOR WHOLE SECTIONS IN COMPRESSION

in which β_0 is the spring constant of the elastic restraints without regard to axial forces.

6. One must then account for the cross-sectional shape by multiplying e_e by the pertinent shape factor μ from Fig. 11.

TABLE 2.—SUMMARY OF ECCENTRIC COLUMN TESTS

Specimen No.[a]	Value of e/r	Value of $c\,L/r$	ULTIMATE MEAN STRESS, IN KIPS PER SQUARE INCH			MEAN STRESS AT YIELD OF OUTER FIBER, IN KIPS PER SQUARE INCH				
			Experimental	Theoretical[b]	Col. 4 ÷ Col. 5	Whitewash	Semiempirical	Theoretical	Col. 7 ÷ Col. 9	Col. 8 ÷ Col. 9
(1)	(2)	(3)	(4)	(5)	(6)	(7)	(8)	(9)	(10)	(11)
7AI	0	50.2	29.00	27.11	1.070	27.20	30.00	30.00	0.907	1.000
6AI	0.5	50.2	24.05	22.65	1.061	23.75	17.88	17.75	1.338	1.006
2AI	1.0	50.2	20.65	20.05	1.030	13.22	13.48	13.29	0.995	1.015
5AI	1.5	50.2	18.40	18.05	1.019	11.98	10.62	10.75	1.114	0.988
3AI	2.0	50.2	17.80[c]	16.45	1.081	10.15	9.21	9.05	1.121	1.018
12UI	0	51.8	34.65	34.25	1.012	30.80	38.00	38.00	0.812	1.000
15UI	0.5	51.8	29.35	27.80	1.056	23.95	21.93	21.77	1.110	1.008
13UI	1.0	51.8	26.00	24.25	1.071	19.90	16.44	16.30	1.220	1.010
16UI	1.5	51.8	21.45	21.70	0.990	15.59	13.10	13.21	1.180	0.992
14UI	2.0	51.8	19.60	19.45	1.007	14.50	11.39	11.13	1.302	1.022
8AS	0	39.6	32.20	29.92	1.076	32.20	32.20	32.20	1.000	1.000
11AS	0.5	39.6	27.00	27.00	1.000	25.55	24.30	23.00	1.110	1.057
10AS	1.0	39.6	24.20	24.93	0.972	21.10	19.77	18.52	1.140	1.066
9AS	2.0	39.6	22.60	21.80	1.037	15.55	14.12	13.53	1.149	1.042
17US	0	40.3	37.78	36.24	1.040	31.10	39.00	39.00	0.797	1.000
20US	0.5	40.3	32.60	32.17	1.013	28.65	27.22	27.40	1.046	0.995
21US	1.0	40.3	30.20	29.55	1.022	24.40	22.55	22.03	1.107	1.022
19US	2.0	40.3	26.00	25.69	1.011	17.10	16.30	16.10	1.062	1.012

[a] A, annealed; U, unannealed; I, I-section; and S, square bar. [b] Computed with shape factor of 0.8 for I-sections and 1.0 for square bars. [c] Ultimate load probably too high—plastic equilibrium not reached.

7. With values for $c\,L/r$ and $(e_e\,\mu)/k_c$, one must then find the eccentric buckling stress of the column from Eq. 6. In this case σ_{cES} is found from Eq. 20 in which $L/r = c\,L/r$; γ is found from Eqs. 26, in which $L/r = c\,L/r$ and $e/k_c = (e_e\,\mu)/k_c$; and $(L/r)_c$ is determined from Eq. 27.

EXPERIMENTAL INVESTIGATION

Specimens and Testing Procedure.—The purpose of the experimental investigations was to determine for eccentrically loaded, elastically restrained steel columns the effect of eccentricity on the ultimate load and on the load at which yield of the outer fiber first occurred. Restraints were applied symmetrically and, in order to assess the effect (if any) of residual rolling stresses, geometrically similar columns of both dead-annealed and as-rolled material were tested. Two types of cross sections were used to fabricate the columns: 1½-in. square bars and I-sections 4 I 9.5 (4 in. deep, 9.5 lb per ft).

Compression stress-strain tests were performed on short lengths of the whole sections, in both annealed and unannealed conditions. Typical results of these tests are shown in Fig. 12. The unannealed material is approximately identical to the annealed material, except that the yield point is higher in the former. A minor effect of residual stress is indicated by the rounded knee of the curve for the unannealed I-sections.

The column specimens had slenderness ratios of approximately 80 based on the total free length between knife edges. The computed effective slenderness ratio ($c\,L/r$) for concentric buckling, in Table 2, is smaller than this free length as a result of the elastic restraints imposed at the ends of the column. Four sets of columns (two annealed and two unannealed) were tested with the value of e/r varying from zero to 2 for each set; the geometric properties are as follows:

Property	1½-in. square bars	I-Sections 4 I 9.5
Clear or flexible length, in inches	27.00	42.00
Distance out-to-out of end blocks, in inches	29.95 ± 0.05	44.95 ± 0.05
Distance between knife edges, in inches	34.95 ± 0.05	49.95 ± 0.05
Nominal cross-sectional area, in square inches	2.25	2.76
Nominal radius of gyration, in inches	0.433	0.580

The general test setup is shown in Fig. 13. The elastic end-restraining fixtures are seen to consist of a pair of channels forming the stationary part (connected to the head or table of the testing machine) and a standard rolled wide-flange section forming the movable part—the two parts being separated by a knife-edge support at their centers and held together elastically at their ends by precompressed springs. An eccentric load applied to the fixture causes a rotation about the knife edge of the wide-flange section relative to the double-channel beam against the resistance afforded by the springs. Each fixture supplied an elastic end restraint of 1,850 kip-in. per radian.

Lateral deflections were measured by dial gages at the center and quarter-points of the columns and at the upper head of the testing machine. Rotations at the stations indicated in Fig. 13 were measured by a portable inclinometer.

Centering Procedure.—The elastic center deflection and end rotations of a given column have unique values for a given load and eccentricity and can be computed by customary elastic analysis.[23,24] They must coincide with measured values of these quantities if the centering of the column is to conform to assumed conditions of support and eccentricity. Each column was located in the testing machine with a predetermined eccentricity, measured from accurately located knife-edge positions; the location so obtained was checked and corrected by centering under load. To assure correct eccentricities at both ends, center deflections and end rotations were measured at selected loads in the elastic range, and centering was adjusted until measurements coincided with precomputed values. The eccentricity at each end had to be checked individually, and it was required that the centering be done by both deflection

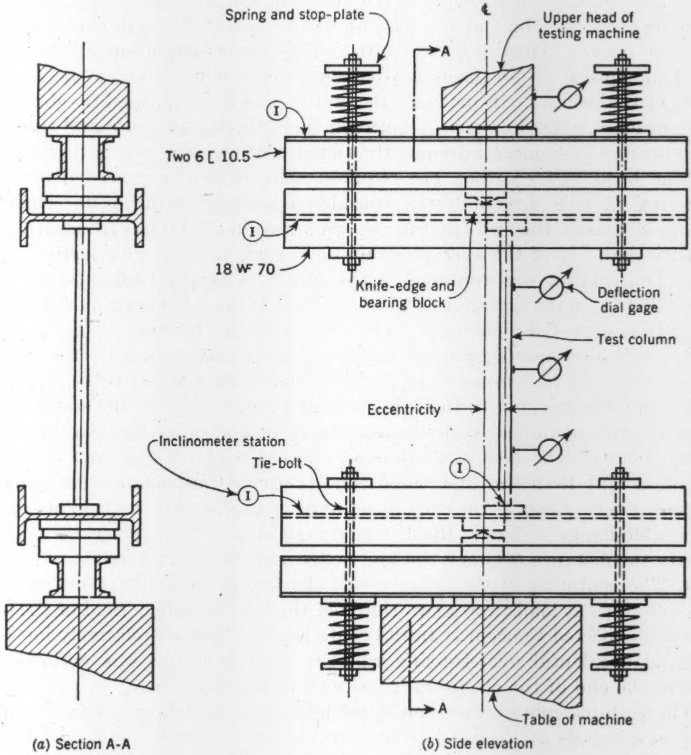
Spring and stop-plate
℄
Upper head of testing machine
A
I
Two 6 [10.5
I
18 W 70
Knife-edge and bearing block
Deflection dial gage
Test column
Eccentricity
Inclinometer station
Tie-bolt
I
I
A
Table of machine

(*a*) Section A-A (*b*) Side elevation

FIG. 13.—SCHEMATIC DIAGRAM FOR TEST ARRANGEMENT

---

[23] "Third Progress Report on Investigation of Flexural Buckling of Rigid Joint Structures," by G. P. Fisher, Cornell Univ., Ithaca, N. Y., June, 1953.

[24] *Ibid.*, Appendix I, by P. P. Bijlaard, pp. 17-20.

and rotation; it is impossible to center by deflection only because a variety of paired values of end eccentricities can result in the same center deflection. Furthermore, the proper combination of center deflection and end rotations cannot be obtained unless the measured end eccentricity is correct, providing a method of adjustment of, and a check on, the predetermined location of the column. The centering procedure was as follows:

1. The column was centered in the direction along the knife edges at a load not more than one third of the load at which yield of the outer fiber was expected to occur. This load was controlled by strain measurements read with four 1-in. optical strain gages located on the extreme fibers at the quarter-points of the column. Equalizing the strains was accomplished by shimming, of the order of 0.005 in., usually between the column base plate and the wide-flange section and, more infrequently, between the elastic-end fixture and the machine head surface when the required shim thickness exceeded 0.005 in. Centering in this direction was considered sufficiently accurate when the average strains on the two opposing column faces did not differ from each other by more than 5% of the average strain on the whole transverse section.
2. The column was centered in the direction perpendicular to the knife edge—that is, in the direction of the eccentricity—at a load not more than one third of the expected yield load. This was controlled in several ways: (*a*) The central deflection had to coincide with its precomputed value; (*b*) the quarter-point deflections had to be equal; (*c*) the end rotations had to be equal, opposite, and coincident with their precomputed value; and (*d*) the strains at the upper quarter-point had to be in reasonable balance with those at the lower quarter-point. The last was intended only as a check and was considered less important than the first three conditions. Adjustments were made by tightening the springs of the elastic-end fixtures to change the initial inclination of the wide-flange section in the direction desired and, if necessary, by changing slightly the distance between the knife edge and the column axis.
3. The centering of the column was checked in both directions as in the previous steps at loads up to two thirds of the load at which yield of the outer fiber was expected to occur. Initial centering was done at relatively low loads to avoid accidental overstressing whereas final centering was performed as close to the end of the elastic range as was considered safe.

The centered column was then tested by measuring deflections and rotations at close intervals at loads up to and beyond the ultimate load. Whitewash was coated on each column before testing to serve as a visual indicator of yielding. Flaking of the whitewash allowed easy and direct observation of initial as well as progressive yielding.

Results.—Experimental and theoretical values of ultimate mean stress and the mean stress at which yield of the outer fiber occurred are presented and compared in Table 2 and in Fig. 14. The mean stress is, in all cases, the axial load on the column divided by the nominal total area of the column. It is noted that, as a direct consequence of higher yield point, the column strength of the unannealed specimens is uniformly higher than that of the annealed specimens. Theoretical values of the ultimate mean stress have been computed by the simplified method.

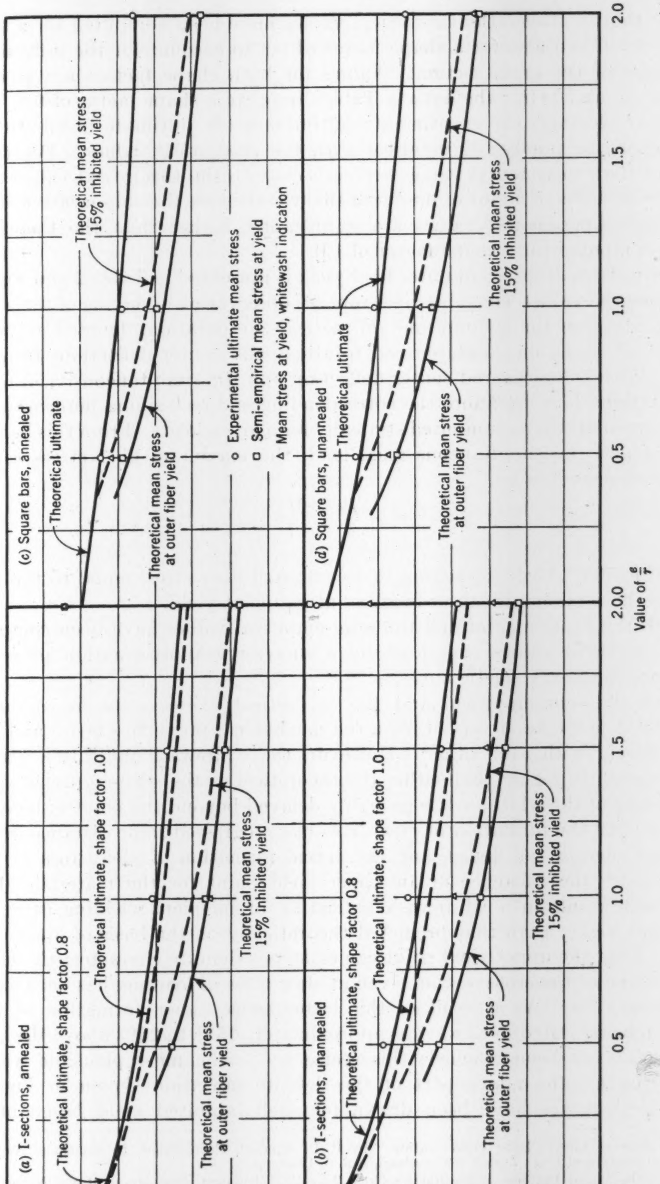

FIG. 14.—TEST RESULTS

For the I-sections, the theoretical values have been computed for a shape factor of 1.0 and also for a shape factor of 0.8 to account for the influence of the shape of the cross section. Values for both shape factors are given in Figs. 14(*a*) and 14(*b*); the data in Table 2 refer to a shape factor of 0.8. For the square sections the experimental ultimate loads (ultimate mean stresses) are seen to be practically identical with the theoretical values. For the I-sections the experimental values are very close to the theoretical values computed with a shape factor of 0.8, with slight scatter on the conservative (high) side. All experimental values are significantly higher than the theoretical values computed for a shape factor of 1.0.

Mean stress at incipient outer fiber yield is presented in Table 2 and Fig. 14. Experimental values were obtained from (*a*) observation of flaking of the whitewash coating on the column and (*b*) statical computation, denoted as "semi-empirical," based on measured end rotations and center deflections from the tests. With the measured center deflection and the simultaneously measured end rotations (and therefore the corresponding end-restraining moments), the center moment can be computed statically for a given load. From this bending moment and the simultaneous axial load, the maximum fiber stress can be computed according to

$$\sigma = \frac{P}{A} + \frac{M\,c}{I} \quad \text{(31)}$$

The value of P/A corresponding to a computed fiber stress equal to the yield point is the semi-empirical mean stress at incipient yield.

Both the experimental and the semi-empirical values have been compared with theoretical values computed by a successive approximation procedure based on customary elastic analysis.[7,23,24]

Both the semi-empirical and the theoretical values were based on the lower yield point (as observed from the mechanical properties tests) and they agree closely with each other. However, the whitewash indication was, in general, slightly higher than either the theoretical or the semi-empirical value. The flaking of the whitewash is probably delayed beyond the point of incipient yielding until the formation of yield lines has progressed some distance inward from the edge of the flange, and the actual formation of yield lines may be inhibited by the existence of an upper yield point for the material. Both effects will result in a whitewash indication of incipient yielding at a load somewhat higher than that predicted theoretically on the basis of lower yield point. That the upper yield point can exist as a definite characteristic related to the shape of the cross section, even at slow rates of loading, has been shown theoretically.[25,26] As a result of this latter cause alone, formation of yield lines can be inhibited until a stress approximately 15% to 20% above the lower yield point has been reached; this seems to be the most plausible way of accounting for the major part of the definite deviation shown in Fig. 14. Theoretical curves have been drawn for such inhibited yield based on an

---

[25] "Theory of Local Plastic Deformations," by P. P. Bijlaard, *Publications*, International Assn. for Bridge and Structural Eng., Zurich, Switzerland, Vol. 6, 1940, pp. 27–40.

[26] "On the Linear Patterns of the Earth's Crust," by P. P. Bijlaard, *Proceedings*, Royal Netherlands Academy of Sciences, Amsterdam, Vol. 51, No. 4, 1948, pp. 450–456.

extreme fiber stress 15% above the lower yield point of the material. The inhibiting of yielding occurs for most of the specimens and is most markedly regular for the unannealed I-sections. The whitewash indication is somewhat erratic for the annealed specimens, presumably as a result of the loosening and irregular shedding of scale during the annealing process.

Typical load-deflection and load-rotation curves are given in Fig. 15(*a*). For small eccentricities, up to $e/r = 1$, deflections at the ultimate (maximum) load are relatively small, generally less than approximately 1/100 of the column length. For larger eccentricities, however, deflections at ultimate loads are significantly larger, of the order of 1/50 of the length.

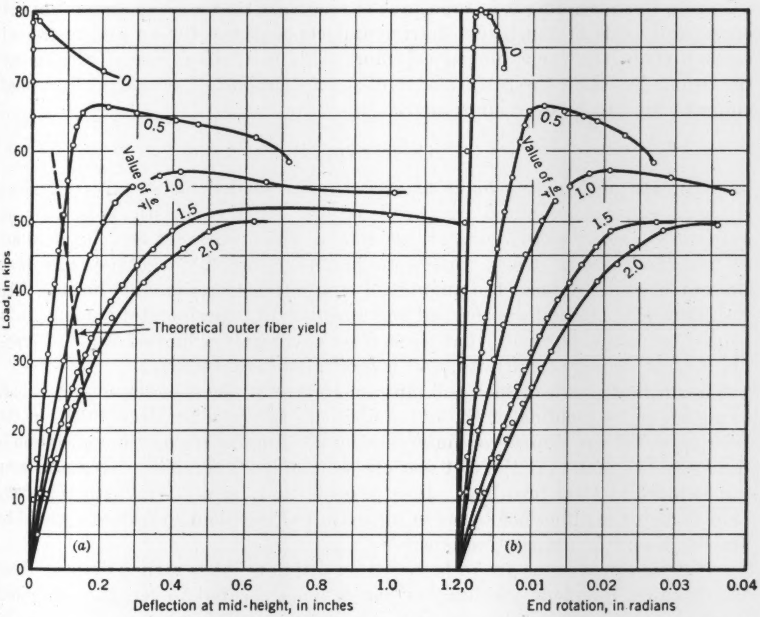

FIG. 15.—DEFORMATION CURVES FOR ANNEALED I-SECTIONS

There may be some doubt that design determinations legitimately should be based on loads accompanied by such large deflections. At loads corresponding to yield of the outer fiber, as shown in Fig. 15(*a*), deflections range between 1/225 and 1/450 of the length, for the largest and smallest non-zero eccentricities. If criteria for limit loads were to be correlated with critera for deflections, the latter might seem permissible whereas the former might not. That is, deflections at ultimate loads may be so large as to impair the usefulness of a structure whereas deflections at loads which produce incipient yielding are of little practical consequence.

The typical load-end rotation curves shown in Fig. 15(*b*) indicate that with increasing load the end rotations increase at a faster rate than do the loads, especially as the ultimate load is approached. The share of the total applied moment $P\,e$ which is resisted by the end restraints is equal to "rotation times spring constant." Hence, this share of the applied moment increases with increasing load so that a progressively smaller part of the applied moment $P\,e$ is resisted by the column. This behavior is easily demonstrated analytically in the elastic range.[27] It is accentuated in the plastic range, as can be seen from Eq. 12. In fact, as the load increases the plastic reduction factor decreases gradually from unity to its final value η so that the effective eccentricity e_e becomes a progressively smaller part of the applied eccentricity e.

From this reasoning it is important to recognize that a given amount of end eccentricity e is of much less detrimental consequence for an end-restrained column than it is for a hinged column. This is another reason why design provisions based on the performance of simply supported, eccentrically loaded columns tend to be overconservative.

CONCLUSIONS

Ultimate or buckling loads of eccentrically loaded, elastically restrained columns can be computed rigorously on the basis of plastic action by an extremely lengthy grapho-analytical method which does not lend itself to use in practical design work. An approximate, simplified method has been presented which reduces the amount of computing to reasonable limits. The results of this method are in good agreement with experimental evidence. It should be noted, however, that these tests cover only a limited range of variables (L/r, degree of restraint, and magnitude of eccentricity).

The ultimate loads of such columns are greatly in excess of those loads which cause incipient yielding of the outer fiber, up to approximately 100% in the tests reported on, depending on eccentricity. In this connection attention is drawn to the fact that the test sections were of very compact shape and were not subject to local buckling. It is possible that for sections with relatively thin flanges the difference between ultimate and incipient yield loads would be smaller than for compact sections.[28,29]

If design provisions are to be based on ultimate loads rather than on those which cause incipient yielding, as has been advocated,[5] even the simplified method may be too cumbersome for practical use. Columns would have to be designed by the use of charts or tables, as is customary in other fields. The methods presented herein may serve as an aid in computing such charts or tables.

In considering the merits of establishing ultimate loads as the basis for design criteria, it should be noted that when ultimate loads are reached column deflections are excessively large, particularly for the larger eccentricities. In contrast, these deflections are of moderate magnitude at those loads which cause incipient yielding.

---

[27] "Buckling of Trusses and Rigid Frames," by G. Winter, P. T. Hsu, G. Koo, and M. H. Loh, *Bulletin No. 36*, Eng. Experiment Station, Cornell Univ., Ithaca, N. Y., April, 1948, pp. 10–11.

[28] "Flange Buckling, a Limitation of Plastic Design of Beams, Frames, and Columns," by G. Winter, *Final Report*, International Assn. for Bridge and Structural Eng., 4th Cong., Cambridge and London, England, 1953, p. 139.

[29] "An Evaluation of Plastic Analysis as Applied to Structural Design," by B. G. Johnston, C. H. Yang, and L. S. Beedle, *Welding Journal*, Vol. 32, May, 1953, p. 224.

In elastically restrained columns a part of the applied end moment $P\,e$ is resisted by the end restraints so that the column resists only the remaining part. The fraction of the total end moment carried by the column decreases with increasing load, both in the elastic and the plastic ranges. It follows that a given amount of end eccentricity is much less detrimental to a restrained column than it would be for the same column without restraints. Design provisions based on simply supported, eccentrically loaded columns, therefore, tend to be overconservative if applied to compression members which are parts of rigid frameworks.

ACKNOWLEDGMENTS

This paper reports on part of the results of a research project on buckling of rigid joint structures at Cornell University (Ithaca, N. Y.) sponsored by the Column Research Council and the Bureau of Public Roads, United States Department of Commerce. The advisory group for the project consists of Committee D of the Council, Nathan M. Newmark, M. ASCE (chairman), N. J. Hoff, M. ASCE (co-chairman), the Bureau being represented by E. L. Erickson and Neil Van Eenam, M. ASCE. The steel for the specimens was donated by the Bethlehem Steel Company (Bethlehem, Pa.).

APPENDIX. NOTATION

The following symbols, adopted for use in the paper and for the guidance of discussers, conform essentially with "American Standard Letter Symbols for Structural Analysis" (ASA Z 10.8—1949), prepared by a committee of the American Standards Association with ASCE representation, and approved by the Association in 1949:

A = cross-sectional area of the column;
c = effective length of the column divided by its actual length;
c_s = distance from centroid to outer fiber of section;
E = modulus of elasticity:
  E_r = reduced modulus;
  E_t = tangent modulus;
e = eccentricity of load;
e_e = effective eccentricity;
h = thickness of the column in the direction of bending;
I = moment of inertia;
K = ratio of the moment of inertia to the length of a column;
k_c = core radius;
L = actual length of the column;
L_1 = length of restraining columns in Fig. 4;
l = length of the equivalent column;

P = point force:
- P_{cr} = critical or buckling load;
- P_E = Euler load;

r = radius of gyration;
x = distance along the axis of thrust;
y = distance perpendicular to the axis of thrust:
- y_m = amplitude;
- y_o = amplitude for simply supported column;
- y_{om} = deflection at point of maximum load;

β = actual spring constant of the elastic restraints;
β_0 = spring constant of the elastic restraints without regard to their axial loads;
γ = division factor for eccentricity;
γ' = division factor for eccentricity related to the von Kármán load;
ϵ = strain;
ϵ_p = strain at the proportional limit;
η = reduction factor for plasticity:
- η' = provisional value of the reduction factor for plasticity;
- $\bar{\eta}$ = reduction factor for plasticity in a simply supported and eccentrically loaded column;

μ = shape factor;
σ = stress:
- σ_a = mean equilibrium stress;
- σ_c = buckling stress;
- σ_{cES} = buckling stress determined by F. Engesser and F. R. Shanley;
- σ_{cK} = buckling stress determined by Theodor von Kármán;
- σ_{cr} = maximum average stress or eccentric buckling stress; and
- σ_{ys} = yield point stress.

DISCUSSION

Robert L. Ketter,[30] J. M. ASCE, and Lynn S. Beedle,[31] A. M. ASCE.—The work performed by Messrs. Bijlaard, Fisher, and Winter is a significant contribution to engineering knowledge. Although most structural compression members are restrained beam-columns, many specifications are based on the strength of the pin-ended member with an estimate made of the effective length caused by end restraint. In order to approach the problem more realistically the authors have developed a solution to the problem of the elastically restrained column by limiting the study to members that do not fail by local or lateral-torsional instability; this solution is basic to subsequent work in this field.

The writers endeavor herein to consider some aspects of the experimental results; to present a precise method of determining the plastic reduction factor, η; to examine the "shape factor" cited by the authors (under the heading, "Simplified Method: Shape Factor"); and to suggest a tentative form for the design curves.

The term c, as used by the authors, is apparently a factor whose value is less than that of the Euler length factor,[32] K (Fig. 4(c)). In an earlier work,[4] however, there is no doubt that c is equal to the Euler length factor. It would seem that comment on this point is necessary.

The use of a square shape is justified for checking theoretical considerations. The testing of a limited number of I-shapes that bend about the weak axis is also justified to confirm the findings because in these cases the variable of lateral-torsional instability is eliminated. Attention should, however, also be directed to the wide-flange shape with flexure forced about the strong axis because most structural columns are loaded in this manner. Lateral-torsional buckling will occur when columns without complete lateral bracing are similarly bent. A lower carrying capacity results.[33] Theoretical studies are being performed (1954) at Lehigh University, at Bethlehem, Pa., in an effort to predict this behavior.

Yielding of Steel.—The use of whitewash as a strain-indicating device is certainly valuable—as noted by Inge Lyse, A. M. ASCE, and Bruce G. Johnston, M. ASCE,[34] and others. R. S. Johnston[35] used a mixture of portland cement and water for the same purpose. The objective, of course, is to reveal more clearly the flaking of mill scale.

The authors introduced a factor of 15% to account for the fact that the indication of first yield by whitewash was consistently above the computed value. The factor was introduced for both the as-delivered and the annealed members. The delayed indication of yielding by whitewash might also be attributed to an irregular mill scale or else to the fact that the flaking might not have been observed when it first developed. Considerable data obtained[36,37,38] at Lehigh University indicate that for typical wide-flange shapes yielding occurs at less than the nominal computed value and is caused by residual stresses. Considering such initial stresses, fair agreement has been obtained between the theoretical yield load and the load at which flaking of whitewash was first observed.[37,38] No issue is taken with the fact that an upper yield-point effect exists, but it is doubtful that this phenomenon can account for any such increase as that shown, for example, in Fig. 14(*b*).

---

[30] Research Instructor, Fritz Eng. Lab., Lehigh Univ., Bethlehem, Pa.

[31] Asst. Director, Fritz Eng. Lab., Lehigh Univ., Bethlehem, Pa.

[32] "The Basic Column Formula," *Technical Memorandum No. 1*, Column Research Council, Bethlehem, Pa., May, 1952.

[33] "Plastic Deformation of Wide-Flange Beam-Columns," by Robert L. Ketter, Edmund L. Kaminsky, and Lynn S. Beedle, *Transactions*, ASCE, Vol. 120, 1955, p. 1028.

[34] "Structural Beams in Torsion," by Inge Lyse and Bruce G. Johnston, *Transactions*, ASCE, Vol. 101, 1936, p. 857.

[35] "Compressive Strength of Column Web Plates and Wide Web Columns," by R. S. Johnston, *Technologic Paper 327*, U. S. Bureau of Standards, Vol. 20, 1926, pp. 33–82.

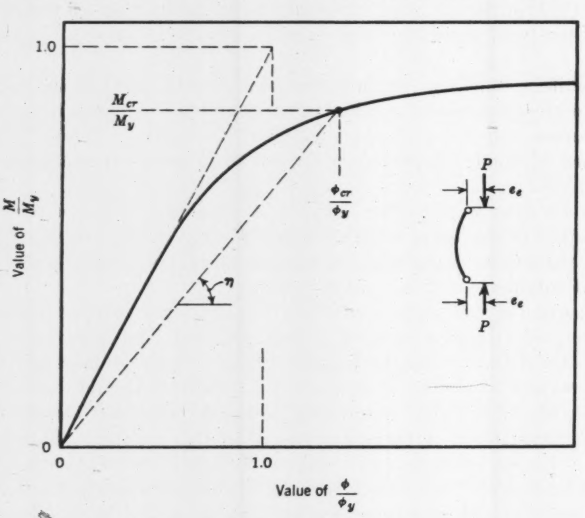

FIG. 16.—TYPICAL MOMENT-CURVATURE RELATIONSHIP

Influence of Residual Stress.—The authors mention (under the heading, "Experimental Investigation: Specimens and Testing Procedure") a "minor effect of residual stress" which is indicated by the rounded knee of the curve in Fig. 12 for the as-delivered I-section. Studies[38] have shown that similar deviations from linearity have a significant effect. From a figure[39] the maximum strength of the as-delivered I-shape column tested by the authors at zero eccentricity is 94 kips, or an average stress of 34 kips per sq in. The yield stress for this as-delivered 4 I 9.5 material is 38.0 kips per sq in. Thus, the reduction in strength is 10% in a region ($c\ L/r = 51.8$) in which a compression

---

[36] "Residual Stress and the Yield Strength of Steel Beams," by C. H. Yang, Lynn S. Beedle, and Bruce G. Johnston, *Research Supplement, The Welding Journal*, Vol. 31, 1952, p. 205s–229s.

[37] "Plastic Deformation of Wide-Flange Beam-Columns," by Robert L. Ketter, Edmund L. Kaminsky, and Lynn S. Beedle, *Transactions*, ASCE, Vol. 120, 1955, pp. 1048–1049, Figs. 27–28.

[38] "Residual Stress and the Compressive Strength of Steel," by A. W. Huber and Lynn S. Beedle, *Research Supplement, The Welding Journal*, Vol. 33, 1954, pp. 589s–613s.

[39] "Third Progress Report on Investigation of Flexural Buckling of Rigid Joint Structures," by G. P. Fisher, Cornell Univ., Ithaca, N. Y., June, 1953, Fig. 22.

member should carry full yield-point stress in the absence of residuals and eccentricities.

It is to be expected that the residuals would be less in the more compact I-shape than in most wide-flange shapes. However, it must also be noted that the stress-strain diagram (Fig. 1) on which the authors base their theory is not unlike the test of the as-delivered I-shape, as presented in Fig. 12. It should also be noted that Mr. Chwalla's work[6] was based on a steel whose stress at the proportional limit, σ_p, was 0.80 times the yield-stress level, σ_{ys}, and that in Fig. 12 $\sigma_p = 0.75\,\sigma_{ys}$. Thus, the influence of residuals had already been taken into account, empirically, in Mr. Chwalla's theory.

Of course, as the eccentricity ratio $e\,c/r^2$ increases, the influence of residuals diminishes rapidly[33] until, for a member subjected to bending alone, there is no influence on the load-carrying capacity.

Plastic Reduction Factor.—The author's solution is based on the premise that, for the given full-length column which is eccentrically loaded and elastically restrained, there corresponds a shorter, hypothetical, pin-ended column subjected to an end eccentricity of load such that it behaves in the same manner as the original member. The solution, therefore, is basically that of determining the equivalent, hypothetical member. With this length and the adjusted eccentricity known, strengths could be predicted based on collapse solutions for pin-ended columns.

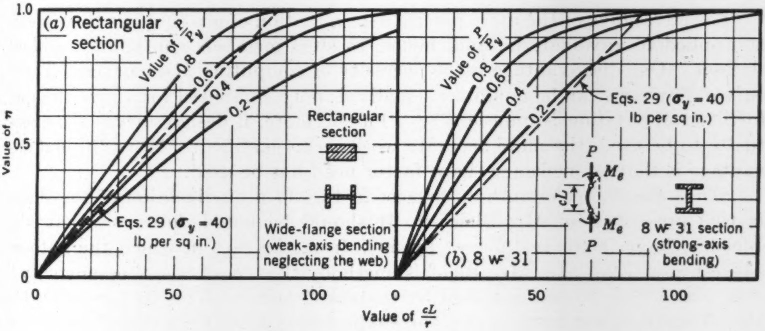

FIG. 17.—PLASTIC REDUCTION FACTOR

Besides the use of the moment-distribution equation (Eq. 12), the most important aspect of the problem is the determination of η, the plastic reduction factor. The authors suggest a straight-line approximation, plotted in Fig. 6, which is given as Eqs. 29. A method for determining a more precise value of η should also be examined—a method that can be applied equally well to any material whose moment-curvature relationship can be obtained.

From Eq. 2 it can be seen that the secant to the moment-curvature curve in the inelastic range is $\eta\,E\,I$. If the M-ϕ curve is nondimensionalized, as shown in Fig. 16, η is the secant to this curve. As noted by the authors, η decreases in value as the load increases until the critical load (or moment) is reached. Thus, the correct value of η is that which exists at the critical load.

A method based on knowledge of the moment-curvature relationship is available for obtaining the critical load for an eccentric column; methods for obtaining the M-ϕ curve which include the influence of axial thrust and other variables are also available.[33] From the computations of the relationship between moment and center-line deflection which leads to another figure,[40] the values of the center line corresponding to critical load can be obtained. Hence, precise η-values can be obtained for a wide-flange shape bent about the weak axis.[41] The determination of η from an M-ϕ curve is illustrated in Fig. 16. These η-values are plotted in Fig. 17 (*a*) as influenced by the axial load and by the slenderness ratio. The curves in Fig. 17 (*b*) are for a wide-flange shape (8WF31) bent about the strong axis.

Throughout the writers' computations, it is assumed that the deflected shape is that of a partial cosine curve. This is a contradiction in fact; however, if the boundary conditions are satisfied, an error in shape has but little influence on the critical load;[33] as a matter of fact, it appears that the authors make the same simplifying assumption (under the heading, "Analytical Method").

The advantage of the more precise determination of η is that the theory can be applied to any material and, hence, to steel members containing residual stresses. One disadvantage is the necessity of computing M-ϕ curves. These curves, however, can be nondimensionalized; once computed for a given shape, further computation is unnecessary. Furthermore, if design curves are eventually to be used, the more accurate work seems justified. An additional advantage is that an arbitrary shape factor need not be used.

Shape Factor.—The authors suggest in Fig. 11 a modification of the shape factors presented by Mr. Bleich.[42] It should be noted, however, that Mr. Bleich's shape factor is different by 50% from the case in which the authors suggest $\mu = 1.25$. In Mr. Bleich's method, the "equivalent eccentricity," κ ($\kappa = e_e\, c/r^2$) is to be multiplied by the shape factor. The authors multiply the effective eccentricity (e_e) by the shape factor μ. Unless c/r^2 of the shape under question is the same as c/r^2 of the rectangle, the two methods are not equivalent. Mr. Bleich has noted[42] that his values of μ

> "* * * must be considered as crude approximations only, since the effect of cross-sectional form upon the buckling strength of eccentrically-loaded columns is by no means cleared up."

One influence of shape can be noted by comparing Fig. 17 (*a*) and Fig. 17 (*b*). Another can be seen by comparison of the two curves[40,43] in Fig. 18. An alternative to the more precise determination of μ, however, is not to use it at all. The procedure suggested previously for determining the plastic reduction factor and the determination of critical loads in eccentric columns[33] make a separate consideration of the shape factor unnecessary. This factor is already inherent in the computations.

---

[40] "Plastic Deformation of Wide-Flange Beam-Columns," by Robert L. Ketter, Edmund L. Kaminsky, and Lynn S. Beedle, *Transactions*, ASCE, Vol. 120, 1955, p. 1058, Fig. 38.

[41] *Ibid.*, p. 1048, Fig. 26.

[42] "Buckling Strength of Metal Structures," by F. Bleich, McGraw-Hill Book Co., Inc., New York, N. Y., 1952, p. 45.

[43] "Plastic Deformation of Wide-Flange Beam-Columns," by Robert L. Ketter, Edmund L. Kaminsky, and Lynn S. Beedle, *Transactions*, ASCE, Vol. 120, 1955, p. 1056, Fig. 35.

In Fig. 19 there is shown the variation in the shape factor for an 8W31 shape bent about the strong axis; Fig. 19 was derived from Fig. 18. It can be seen that μ may not be considered as constant for a given value of L/r or for a given axial load.

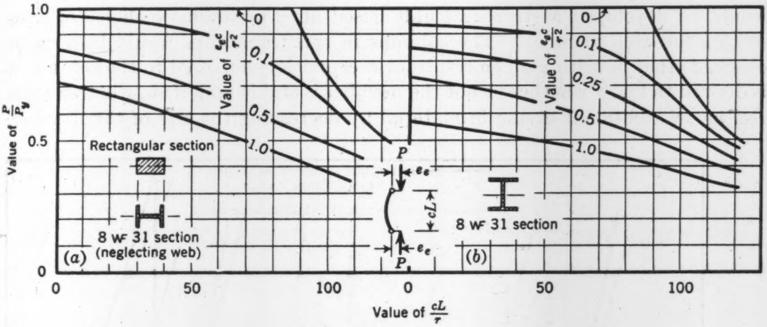

FIG. 18.—MAXIMUM STRENGTH OF PIN-ENDED, ECCENTRICALLY LOADED COLUMNS

Comparison of Methods.—Referring to the seven steps suggested by the authors (under the heading, "Simplified Method: Summary"), the only significant change in the procedure offered by the writers is in step 2 (determination of η) and steps 6 and 7. These steps, in outline, are as follows:

2*a*. Assume effective lengths, $c\,L$, for a range of values of P/P_y.

2*b*. Determine η from Fig. 17(*a*) for the assumed values of P/P_y and $c\,L/r$.

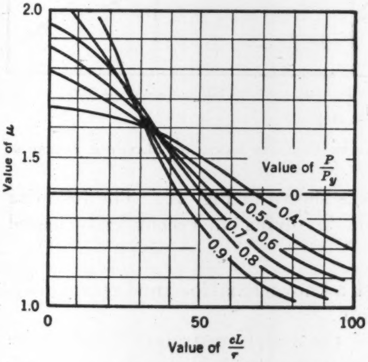

FIG. 19.—SHAPE FACTOR FOR 8W31 SECTION

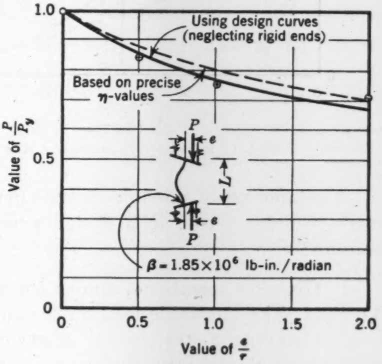

FIG. 20.—MAXIMUM STRENGTH OF SQUARE BARS ($L/r = 80.6$)

7*a*. From Fig. 18 obtain e_e/r for the various values of P/P_y and $c\,L/r$ obtained previously.

7*b*. Multiply the results of steps 5 and 7*a* to obtain values of P/P_y versus e/r.

This alternate procedure has been used for the annealed square bars, and the results are plotted in Fig. 20 together with the data from Fig. 14(*c*). The procedure correlates satisfactorily with the experimental data and with the authors' procedure.

Design Curves.—In the design of a building frame it is expected that there would be developed a structural unit based on a preliminary choice of cross section for each member. The columns in this framework would have to be checked; that is, with a given resultant eccentricity delivered to the column, it is desired to know whether or not the member is stable and, if so, whether there can be an additional saving in material by decreasing the size of the member.

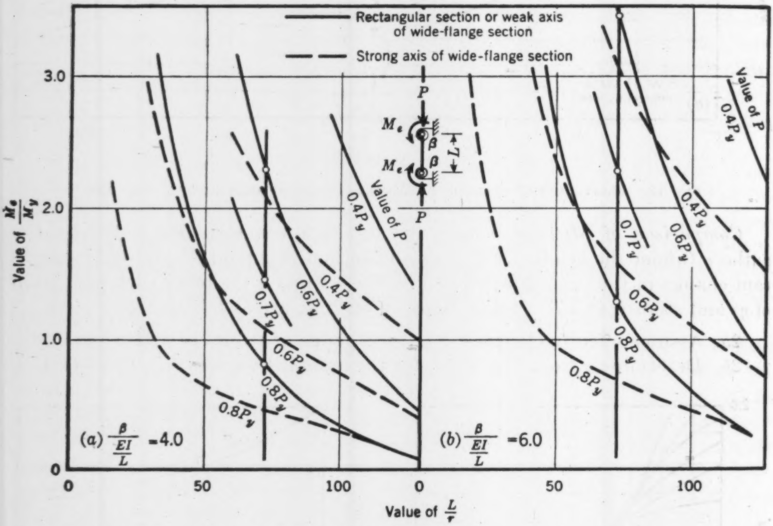

FIG. 21.—DESIGN CURVES FOR ELASTICALLY RESTRAINED COLUMNS BASED ON MAXIMUM STRENGTH

A sample set of possible design curves is shown in Fig. 21. The following steps would be used in a design problem involving an eccentrically loaded column:

1. Given: A member of known L/r with a known axial load and eccentricity. To Find: The allowable load on the column.
2. Compute β, the spring constant of the elastic restraints. This value would be obtained from the analysis of the frame which is already completed.
3. For two values $\beta/(E\ K)$ obtain the allowable load P at the given end moment (or eccentricity).
4. Interpolate (or extrapolate) between the values obtained from the two curves of $\beta/(E\ K)$. Compare the result with the given value of P.
5. Improve the design by increasing or decreasing the section modulus of the member based on the results of step 4. Steps 2, 3, and 4 would be repeated as a check.

What is important about the use of Fig. 21 is that it is unnecessary to consider the plastic reduction factor, η, or the Euler length factor, c. These factors appear only in the computations leading up to Fig. 21. The curves are developed as follows:

(*a*) Select an effective slenderness ratio, $c\,L/r$.

(*b*) Select η from curves such as in Figs. 17.

(*c*) From a suitable $(M/M_y - \phi/\phi_y)$-curve (for example, Fig. 17), determine M/M_y and ϕ/ϕ_y noting that

$$\eta = \frac{M_{cr}/M_y}{\phi/\phi_y} = \frac{M_{cr}}{\phi}\frac{1}{E\,I} \qquad (32)$$

(*d*) From $c\,L/r$ of step (*a*) and P/P_y of step (*b*) obtain the end moment for the pin-ended eccentrically loaded column, $M = P\,e_e$. This may be done either from curves such as those in Fig. 18 or by assuming a cosine curve and making use of step (*c*).

(*e*) Assume $\beta/(E\,K)$ and compute $\beta/(\eta\,E\,K)$.

(*f*) Obtain c and then compute L.

(*g*) Compute e/e_e from Eq. 12 as

$$\frac{e}{e_e} = 1 + \frac{\beta}{2\,\eta\,E\,K} = \frac{M_e}{M_E} \qquad (33)$$

in which M_e is the moment at the end of the elastically restrained column of length L and M_E is the moment at the end of the hypothetical pin-ended member.

(*h*) From step (*d*) and step (*g*) obtain M_e by direct multiplication. This may be expressed as M_e/M_y; there is now known the relationship between the stiffness, $\beta/(E\,K)$, the full length of member, L, the critical axial load, P, and the end eccentricity, e, or end moment, M_e.

One set of curves is needed for each basic shape. The wide-flange section curves shown in Fig. 21 are for the 8WF31 shape. Although there is considerable variation in wide-flange shapes, it is probable that a few typical M-ϕ curves covering groups of wide-flange shapes will prove to be sufficiently accurate.

For any given member, of course, the allowable load at a given eccentricity can be determined quickly from Fig. 21. This has been done for the $1\frac{1}{2}$-in.-square annealed bars; the results are shown in Fig. 20. A length correction,

$$\left(\frac{L}{r}\right)_a = \frac{L}{r}\sqrt{\frac{\sigma_y}{40.0}} \qquad (34)$$

is made as a result of a difference in material properties because Fig. 21 was developed for $\sigma_y = 40$ kips per sq in. The agreement among the results obtained, the tests, and the analysis is most satisfactory.

John F. Baker,[44] **A. M. ASCE, and Michael R. Horne.**[45]—The subject presented by the authors has been studied in Great Britain as part of a series of investigations into the behavior of continuous structures in the elastic-plastic range. A brief review of the investigations of stanchions was presented in 1949;[46] a complete account has been given in a series of reports.[47,48,49,50,51,52,53] Tests were performed on stanchions rigidly connected to beams which provided elastic end restraint. The beams were loaded to bend the stanchions either in single or in double curvature, the single-curvature case corresponding exactly to the problem cited by Messrs. Bijlaard, Fisher, and Winter. Additional direct axial load was applied until complete collapse occurred. An exact theoretical treatment has been presented [52,53] and was found to be in good agreement with test results.[52,53] In the course of this analysis, full account was taken of the exact deflected form of the stanchion over its full length at all stages of loading, and—where necessary—account was also taken of the unloading of plastic zones. The theoretical analysis was based on the assumption of a stress-strain curve for mild steel composed of straight lines—an assumption which has been fully justified by a careful investigation into the theory of bending of beams in the elastic-plastic range.[54]

The authors present a "precise" analysis of the problem, in which they state (under the heading, "Analytical Method") that "* * * the deflection curves can be considered as branches of sine waves when determining the half-wave length l." No justification of this statement is given, and it is difficult to reconcile this assumption with any claim that the analysis is precise.

In the "simplified method," the column is replaced by an equivalent, pin-ended, eccentrically loaded strut. The computation of the equivalent length and equivalent eccentricity is based on a work[7] concerned with the loads at which yield stress is first reached in continuous members. The British investigations show conclusively, however, that there is no consistent relationship between the attainment of yield stress in a continuous stanchion and the load at which that stanchion may be expected to collapse. Although the simplified method may give satisfactory agreement with the authors' test results, it should be regarded as an empirical treatment with little theoretical justification.

---

[44] Prof. of Mechanical Sciences and Head of Dept. of Eng., Cambridge Univ., Cambridge, England.

[45] Asst. Director of Research, Dept. of Eng., Cambridge Univ., Cambridge, England.

[46] "A Review of Recent Investigations into the Behaviour of Steel Frames in the Plastic Range," by by J. F. Baker, *Journal*, Inst. of C. E., London, England, Vol. 31, 1948-1949, p. 188.

[47] "The Behaviour of Stanchions Bent in Single Curvature," by J. F. Baker and J. W. Roderick, *Transactions*, Inst. of Welding, London, England, Vol. 5, 1942, p. 97.

[48] "The Behaviour of Stanchions Bent in Single Curvature," by J. W. Roderick, *Report FE1—5/24*, British Welding Research Assn., 1945.

[49] "The Behaviour of Stanchions Bent in Double Curvature," by J. F. Baker and J. W. Roderick, *Welding Research*, Vol. 2, 1948, p. 2.

[50] "Approximate Methods of Calculating Collapse Loads of Stanchions Bent in Double Curvature," by J. W. Roderick and J. Heyman, *ibid.*, p. 63.

[51] "Further Tests on Stanchions," by J. F. Baker and J. W. Roderick, *ibid.*, p. 110.

[52] "The Behaviour of a Ductile Stanchion Length When Loaded to Collapse," by J. W. Roderick and M. R. Horne, *Report FE1/11*, British Welding Research Assn., 1948.

[53] "The Behaviour of Continuous Stanchions," by J. F. Baker, M. R. Horne, and J. W. Roderick, *Proceedings*, Royal Soc. of London, Series A, Vol. 198, 1949, p. 493.

[54] "Carrying Capacity of Simply Supported Mild Steel Beams," by J. W. Roderick and I. H. Phillipps, *Research, Engineering Structures Supplement*, 1949, p. 49.

In the course of the British investigations, approximate methods have been obtained[48,50] for determining the collapse loads of stanchions bent in single curvature and in double curvature. These approximate methods are in good agreement with test results and appear to be simpler than the method suggested by the authors.

PAUL P. BIJLAARD,[55] M. ASCE, GORDON P. FISHER,[56] A. M. ASCE, AND GEORGE WINTER,[57] M. ASCE.—The valuable contribution made by Messrs. Ketter and Beedle in their discussion is sincerely appreciated. It is gratifying that the investigations performed on different phases of the eccentric-column problem at Lehigh University and at Cornell University complement each other and are in basic agreement. The discussion by Messrs. Baker and Horne was noted with interest.

Clarifications.—The term c is the Euler length factor as ordinarily defined, provided the concentric buckling stress is in the elastic domain, in which case c is a function of $\beta/(E\,K)$; this term is so used in the earlier work[4] which presents only elastic theory. However, if the concentric buckling stress is in the plastic domain, this length factor becomes a function of $\beta/(\eta\,E\,K)$ and is smaller than it would be if the column were elastic. The definition of c is the same in both cases, and the same methods for determining it apply provided $\beta/(\eta\,E\,K)$ is used rather than $\beta/(E\,K)$; this is clearly indicated by step 3 under the heading, "Simplified Method: Summary." However, Fig. 4(*c*) concerns an eccentrically loaded column. The effective length, $c\,L$, of the corresponding concentrically loaded column is smaller than the half-wave length l of the eccentrically loaded column.

In discussing the shape factor, Messrs. Ketter and Beedle maintain that the writers apply this factor only to the eccentricity e_e whereas Mr. Bleich applied it to the eccentricity ratio $e_e\,c/r^2$, thus implying that the writers' method is less general. Apparently they have overlooked step 7 under the heading, "Simplified Method: Summary." Although in step 6 the eccentricity e_e is multiplied by the shape factor μ to account for the cross section—in step 7, $\mu\,e_e$ appears exclusively in the expression $\mu\,e_e/k_c$. Because the core radius k_c is equal to r^2/c_e, the shape factor is seen to have been applied to the eccentricity ratio in the same manner as was done by Mr. Bleich. This can be seen from the following identities:

$$\frac{\mu\,e_e}{k_c} = (\mu\,e_e)\,\frac{c_e}{r^2} = \mu\,\frac{e_e\,c_e}{r^2} \quad\ldots\ldots\ldots\ldots\ldots\ldots\ldots (35)$$

It should be noted that, for unsymmetrical sections, k_c has to be determined by using the distance c_e from the center of gravity to the concave edge of the cross section where the compressive stress is the highest.

It may also be useful to note that Eq. 20 for σ_{cES} applies in the plastic range only—that is, if $c\,L/r$ is smaller than $(L/r)_E$ from Eq. 21. This is shown clearly in Fig. 9. If $c\,L/r$ is larger, of course, Euler's formula has to be used, as is indicated in Fig. 9.

---

[55] Prof. of Structural Eng., Cornell Univ., Ithaca, N. Y.

[56] Associate Prof. of Structural Eng., Cornell Univ., Ithaca, N. Y.

[57] Prof., Head of Dept. of Structural Eng., Cornell Univ., Ithaca, N. Y.

Yielding of Steel.—It was noted that the indication of yielding by flaking of whitewash seemed to be retarded by approximately 15% on the average. Messrs. Ketter and Beedle assert that, at least for wide-flange shapes, yielding occurs at loads less than the nominal computed values, that this is attributable to residual stresses, and that—with this in mind—whitewash flaking was found to be an accurate criterion. The question of whitewash indication is one of experimental technique and will be studied subsequently. The problem of incipient yielding in columns, however, is of primary interest—for example, in connection with fatigue—even though such initial yielding often does not imply failure under static load.

In order to explore this problem, additional tests have been performed with more accurate instrumentation. Unannealed square bars and I-sections of the same sectional properties were used as given under the heading, "Experimental Investigation: Specimens and Testing Procedure." End restraints, however, of 985 kip-in. per radian were used (as compared to 1,850 kip-in. per radian in the original series), and the specimens were more slender, as follows:

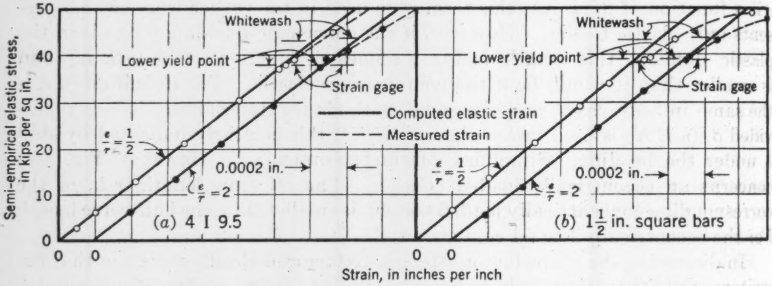

FIG. 22.—SEMI-EMPIRICAL STRESS-STRAIN CURVES FOR EXTREME COMPRESSION FIBER AT MIDHEIGHT OF UNANNEALED SECTIONS

Property	1½-in.-square bars	4 I 9.5
Clear or flexible length, in inches	36.00	56.00
Distance out-to-out of end blocks, in inches	38.90	58.90
Distance between knife edges, in inches	43.90	63.90
Effective slenderness, $c\,L/r$	63.7	81.0

Eccentricities were varied from $e/r = 0$ to $e/r = 2.0$ as in the original tests. Four optical strain gages were mounted at the four corners at midlength, and strain readings were obtained up to loads considerably beyond first yielding.

It is not possible to detect initial yielding by plotting observed strain against load because in eccentric columns this relationship is nonlinear. It is possible, however, to linearize this relationship in the elastic domain in the following manner. For each test load the maximum compression stress at midlength is computed from the observed mid-deflection and the observed end rotations on an elastic basis. If this "semi-empirical" stress is plotted against observed strain, the relationship must be linear as long as all deformations are elastic and must become nonlinear when yielding begins. In Fig. 22 there are shown four sample curves so obtained—two for the I-section and two for the square-bar columns. It is seen that below the yield point the relationship is linear and exactly as computed. It is further seen that strain measurements indicate yielding by deviation from the straight line at stresses almost exactly identical with the yield point as determined from sectional compression tests. In contrast, the whitewash flaking is seen always to occur after considerable delay.

In Fig. 23 there are given the complete test results of these two additional series. It is seen that the ultimate loads of these more slender columns with lesser end restraint are in just as good agreement with the proposed theory as are the earlier tests. It is also seen that yielding, as detected by accurate instrumentation, occurs at loads equal to or almost imperceptibly below the value computed by elastic theory on the basis of the compressive yield point of the material. This is so despite the facts that unannealed material was used and that residual stresses were obviously present, at least in the I-sections. Although this finding is contrary to the situation described by Messrs. Ketter and Beedle, it is quite possible that the distribution of residual stresses in these I-sections is sufficiently different from those in the wide-flange sections tested at Lehigh University to allow both statements to be true.

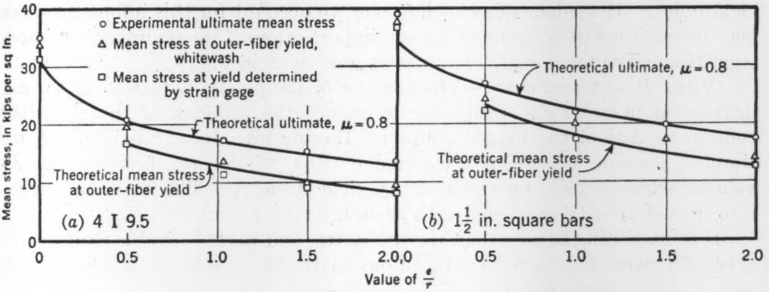

FIG. 23.—TEST RESULTS, $\beta = 985$ KIP-IN. PER RADIAN, UNANNEALED SECTIONS

The foregoing substantiates the writers' opinion that the flaking of the whitewash does not indicate incipient yielding but is caused by the subsequent formation of macroscopic yield lines at loads higher than the initial yield load. This is also indicated by the fact that the flaking occurs discontinuously along typical yield lines of the type observed in polished specimens. It has been shown[25,26] that in relatively thick sections, as used in these tests, the incipient state of stress occurring in these flow lines is not one of pure compression or tension, as in the elastic column, but one of plane strain. Therefore, the axial compressive or tensile stress required to initiate a yield layer is $2/\sqrt{3}$ times the lower yield point, or 15% above the lower yield point; this, therefore, determines the upper yield point. Although there are other circumstances (speed of testing or nucleation) which may influence the upper yield point, the fact that the whitewash flaking occurred at loads approximately 15% greater than the lower yield stress is in good accordance with the foregoing theory. The plastic deformation measured prior to the formation of yield lines may be attributed to localized flow in small, disconnected regions.

Influence of Residual Stress.—The writers and Messrs. Ketter and Beedle are in agreement that some residual stresses were present in the I-sections. They are also in agreement that Fig. 9, on which the theory is based, implicitly accounts for the presence of some residual stress. It is further agreed that this influence on column strength is significant only for completely, or approximately, concentric loading (which case is not the subject of the present investigation). The writers wish to add that they doubt whether this relatively small effect warrants, practically, the rather elaborate methods referred to[33] by Messrs. Ketter and Beedle, particularly in view of the erratic character of residual stresses, both as to magnitude and distribution. This erratic character is illustrated by the preceding observations.

It is not advocated that the influence of residual stress be discounted—this would be identical with assuming the Euler hyperbola to be valid up to the yield point. It seems sufficient, however, to account for this influence, which may be regarded as just one of many "imperfections," by assuming some such transition curve for low (L/r)-values as was given in Fig. 9.

Plastic Reduction Factor.—The concept of the plastic reduction factor was introduced in order to enable one to reduce the problem of the restrained column to that of the hinged column. Having introduced this concept, the simplest possible approximate expression (Eqs. 29) for the factor η was developed which is valid for steels of any yield strength. The prime aim, therefore, was simplicity combined with accuracy rather than with rigor.

It is interesting to note that Messrs. Ketter and Beedle are able to determine a plastic reduction factor by ingenious methods.[33] Whether these methods give a "more precise value of η", is questionable.

Although it is true that in Eq. 2 the quantity $\eta\, E\, I$ is the secant to the moment-curvature curve at one section, it has been noted (under the heading, "Analytical Method") that η varies with x. Furthermore, the reduction factor η serves a double purpose: The term η is used for determining the Euler factor c; it is also used for computing that part of the end moment $P\, e$ which is distributed to the column. For each purpose a different value of η would be needed. However, for practical applications one can find a single value of η that, used for both purposes, leads to the correct buckling loads. Messrs. Ketter and Beedle propose to determine this value of η only at midlength and assume a partial cosine curve for the column shape; the latter is, of course, a crude approximation. In contrast, the writers have not made the assumption of a cosine curve. The expressions for η as given by Eqs. 29 were obtained by adaptation to (1) Mr. Chwalla's "rigorous"—although limited—theory,[6] (2) additional data obtained from the "Analytical Method," and (3) their own tests. Hence, in all sources on which Eqs. 29 are based, the eccentric column (*a*) was elastically restrained and (*b*) was allowed to assume its natural shape rather than that of an imposed cosine curve. The writers' value of η, therefore, represents the integrated effect of a quantity which is actually variable along the column. It could have been termed the "effective plastic reduction factor" except for the awkwardness of such a designation. In contrast, the determination by Messrs. Ketter and Beedle is based on the behavior of only a single section of an eccentric column which is simply supported—not elastically restrained—and whose shape has been approximated by a cosine curve. It is not implied that the determination by Messrs. Ketter and Beedle is necessarily inferior. However, it cannot be regarded as inherently more precise and it is certainly much more complex and laborious. The adequacy of the writers' simple method of determining η seems to be proved by the extensive test confirmation given both in the paper and by the additional tests described in this closure. From these tests it follows that, with the writers' value for η as a function of $c\,L/r$ only, accurate agreement between theoretical and experimental results is obtained for all ratios of P/P_y. This shows that, if in their determination the writers would use a value of η which varies with P/P_y (as is done in Fig. 17), they would obtain discrepancies between analysis and test.

Shape Factor.—As indicated previously, the shape factor μ is applied to the ratio e_e/k_c. Both Mr. Bleich's shape factor and the writers' shape factor are based on Mr. Chwalla's work,[21] in which the correction factor ϕ is applied to the core radius k_c so that

$$\mu \frac{e_e}{k_c} = \frac{e_e}{\phi\, k_c} \qquad \text{(36a)}$$

and

$$\mu = \frac{1}{\phi} \qquad \text{(36b)}$$

It should be noted that for unsymmetrical sections k_c applies to the stress at the concave side of the column. For the case in Fig. 11 in which $\mu = 1.25$, Mr. Chwalla's factor, ϕ, required to obtain the exact eccentric buckling stress for these sections, varies between 0.667 and 1.158 so that μ varies between 1.5 and 0.87. Therefore, the writers used the relatively safe value of 1.25 whereas Mr. Bleich's value of 0.80 is obviously quite unsafe (perhaps caused by interchanging μ with ϕ). The discussers' argument in defining a shape factor is not clear; in particular one cannot see the significance of the restriction that, in order to reduce a wide-flange shape to a rectangular section by use of a shape factor, the yield values P_y and M_y of the two sections must be the same. This restriction seems foreign to the concept of a shape factor. Apparently owing to the misunderstanding of the manner in which the writers' value for μ was determined, the shape factors μ, computed from Fig. 18 and given in Fig. 19, are not correct. For example, from Figs. 18, for $c\,L/r = 20$ and $P/P_y = 0.9$, the required ratio $e\,c_s/r^2$ (equal to e/k_c) for the rectangular sections and wide-flange sections (the latter bent about their strong axis) is 0.19 and 0.135, respectively. Hence, using the computations for rectangular sections, correct results are obtained for the wide-flange section if a ratio $e\,c_s/r^2 = 0.19 = 1.41(0.135)$ is used. Therefore, the shape factor for $c\,L/r = 20$ and $P/P_y = 0.9$ from Fig. 18 is $\mu = 1.41$, which is close to the over-all value of 1.4 adopted by the writers. However, from Fig. 19 it is indicated for this same case that $\mu = 1.85$. This shows that the great spread in the μ-values

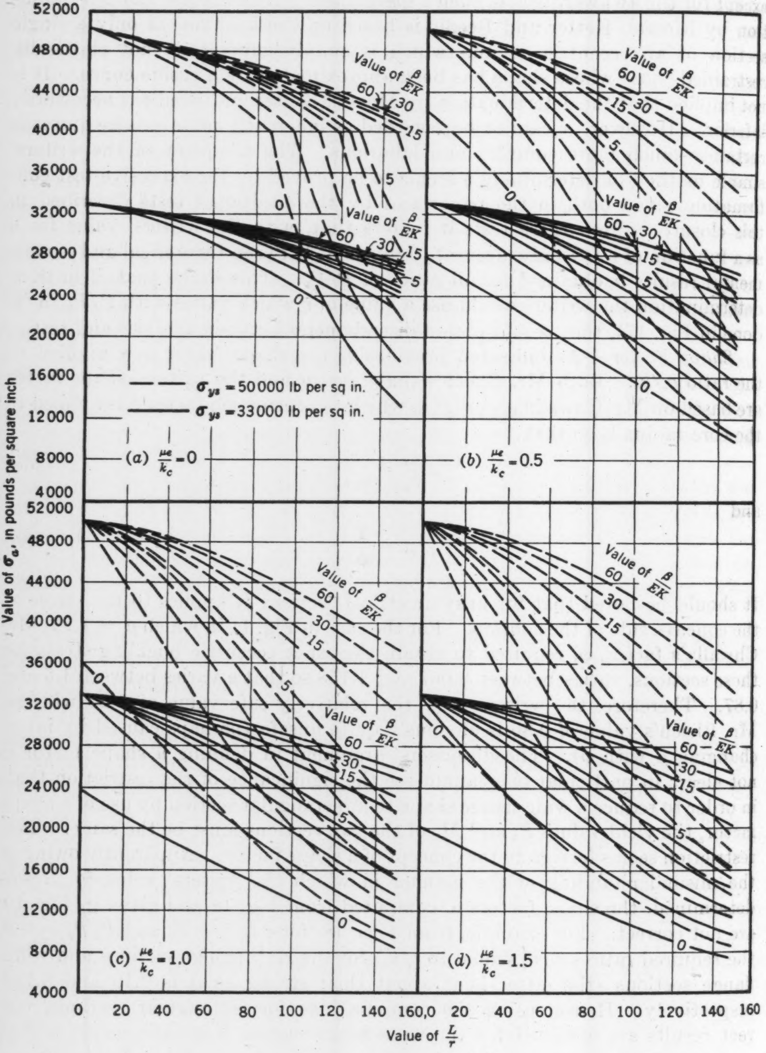

FIG. 24.—DESIGN CURVES

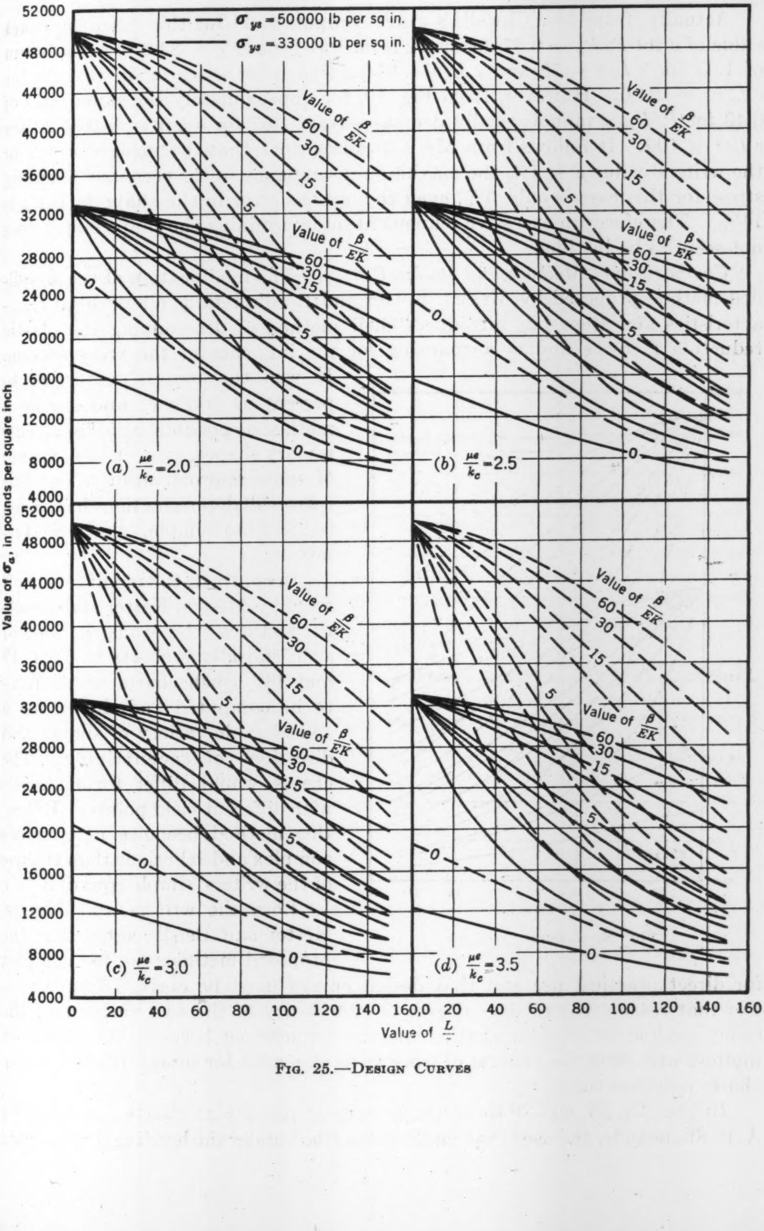

FIG. 25.—DESIGN CURVES

computed by Messrs. Ketter and Beedle is based on a misconception in the method of determining μ.

Actually, from Mr. Chwalla's exact computation[21] for this case, the exact value of μ for $P/P_y = 0.37$ decreases from 1.41 for $c\,L/r = 33.9$ to a minimum of 1.33 for $c\,L/r = 75$ and $c\,L/r = 85$ and then increases again to 1.59 for $c\,L/r = 124.6$. However, from Fig. 19, for approximately the same ratio of 0.40 for P/P_y, μ monotonically decreases from 1.67 for $c\,L/r = 0$ to 1.20 for $c\,L/r = 100$. It follows from Mr. Chwalla's work that, by using $\phi = 0.7$ or the writers' value $\mu = 1.4$, the maximum discrepancy in the eccentric buckling stress for this case is only 3%, even though the error in the shape factor μ is 14%. Therefore, an excessive refinement in determining the shape factor does not seem to be justified.

Comparison of Methods and Design Curves.—The modification of the simplified method proposed by Messrs. Ketter and Beedle retains all essential characteristics and steps but introduces their method of determining the plastic reduction factor η and of accounting for the influence of the cross section. It was the writers' objective to present as compact and simple a method as possible, valid for all customary shapes, even at the expense of some approximation. For this reason all determinations have been reduced to simple, algebraic formulas.

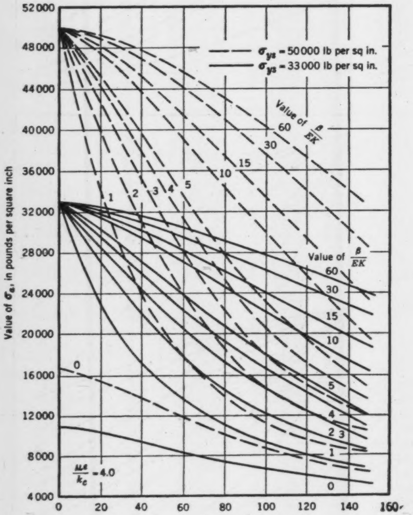

FIG. 26.—DESIGN CURVES

In contrast, the modification offered by Messrs. Ketter and Beedle necessitates the construction of such subsidiary charts as Figs. 17 and 18. Such charts would have to be computed and drawn for a considerable variety of shapes and directions of eccentricity. The charts would differ for materials with different yield points. Hence, this method becomes much more complex and laborious than the use of the writers' simple equations.

Both the writers and Messrs. Ketter and Beedle agree that the proposed methods are too complex for direct practical use and that design curves must be derived from them. For that reason, the relative degree of complexity of the two variants of the same method is of somewhat secondary importance because the choice of method will affect the amount of work to be expended for computing the design charts only one time.

In Figs. 24, 25, and 26 there are presented these design charts computed by A. E. Shabaan by the use of the method described under the heading, "Simplified

Method." In each chart, curves are given for two steels with yield stresses of 33,000 lb per sq in. and 50,000 lb per sq in. In these charts μ is the shape factor from Fig. 11, and

$$\beta = \sum \frac{E\,K_n}{\phi_n} \qquad (37)$$

is the spring constant of elastic end restraint produced by all members framed into the column at an end. In Eq. 37

$$K_n = \frac{I_n}{L_n} \qquad (38)$$

is the rigidity of the nth restraining member. The quantity ϕ_n depends on the axial force in the restraining member and can be found from tables.[58] If axial forces in restraining members are absent or neglected, $\phi_n = 0.333$.

In design work, the values of L, r, c_s, K, E, e, and β are given or they are known from preliminary computations. One determines $k_c = r^2/c_s$, finds the shape factor μ from Fig. 11, and computes $\mu\, e/k_c$, L/r, and $\beta/(E\,K)$. Using these quantities, one reads $\sigma_{cr} = \sigma_a$ from the appropriate chart or determines it by interpolation. Then the ultimate load of the column is

$$P_{\text{ult}} = \sigma_{cr}\,A \qquad (39)$$

Messrs. Ketter and Beedle indicate that the special merit of their sample design charts is that they obviate the necessity of determining the factors η and c; this, of course, is the very purpose of the design charts. It is only the complexity of determining η and c which makes design charts necessary in the first place, and it is the whole point of such charts that η and c are needed only in their original construction—not in their subsequent use.

One practically significant difference between charts of the type in Figs. 24, 25, and 26, and those in Fig. 21 is that in the latter separate curves are needed for the various cross-sectional shapes and the various directions of bending, requiring an elaborate set of design charts to cover all possible combinations. Figs. 24, 25, and 26, on the contrary, are constructed in terms of $\mu\, e/k_c$ and therefore are valid for any shape and any direction of bending because these influences are expressed by the shape factor, μ.

In Figs. 24, 25, and 26 there is also illustrated the last conclusion of the writers (stated under the heading, "Conclusion")—a given eccentricity has an incomparably smaller effect on a restrained column than on a hinged column. Thus, for $\sigma_{ys} = 33{,}000$ lb per sq in., $L/r = 80$, and $\mu\, e/k_c = 3$, a column with a restraint factor as small as $\beta/(E\,K) = 2.0$ is seen to have a buckling stress of approximately 16,500 lb per sq in.—almost twice the buckling stress of approximately 8,700 lb per sq in. which the same column would have if it were hinged.

British Methods.—Messrs. Baker and Horne refer to an exact method and also to a design method.[48, 50, 52, 53] Their exact method was not known previously to the writers but has since been examined. It is a trial-and-error method, which has to be numerically applied to each case separately. Although ingenious, this method is extremely laborious and thus has the same drawback as Mr. Chwalla's exact method in that it represents, exclusively, a research method. In contrast, it was the writers' aim to develop satisfactorily accurate methods which are sufficiently simple so that they can be used in practical design, either directly or by the use of simple charts. Also, for columns in double curvature (equal restraints and equal and opposite eccentricities) the method of Messrs. Baker and Horne does not lead to correct results because they assume that up to and through failure the center of the column does not deflect. Hence, they actually consider a column of length $L/2$ that is elastically restrained and eccentrically loaded at one end and simply supported and concentrically loaded at the other. In fact, however, when the buckling load is reached, the center of the column deflects; this fact is confirmed by their own tests. As explained previously,[8] at the moment of buckling a bifurcation occurs and the column deflects in a superimposed symmetrical deflection. This bifurcation happens after the half-wave length of the deflection curve becomes equal to the half-wave length in which the column would buckle symmetrically, so that with elastic restraints this half-wave will be longer than half the length of the column. Thus, the buckling stress is less than that found by Messrs. Baker and Horne.

---

[58] "Buckling of Trusses and Rigid Frames," by G. Winter, P. T. Hsu, B. Koo, and M. H. Loh, *Bulletin No. 36*, Eng. Experiment Station, Cornell Univ., Ithaca, N. Y., April, 1948, p. 49, Appendix D, Table I; p. 52, Table II.

According to Messrs. Baker and Horne the approximate methods[48,50] are in good agreement with test results. This may be true for their tests on columns with small (L/r)-ratios and large end restraints (large values of β), but these methods certainly cannot be used over the entire range of slendernesses and end restraints. For example, for the case in Fig. 4(*a*) the work[48,51] of Messrs. Baker and Horne leads to the critical load being expressed as

$$P_{cr} = \pi \frac{M^{s}_{p}}{\theta L} \qquad (40)$$

in which M^{s}_{p} is the ultimate bending moment that can be resisted by column AB and θ is the angular rotation of the restraining members CA and BD at A and B, caused by moments $P\,e$ and M^{s}_{p} at A and B, respectively. If the restraint is very small (say, $\beta = 0$), θ will be infinite whereas M^{s}_{p} is finite so that P_{cr} would erroneously be found to be zero. Thus, the proposed formulas are not applicable for small values of the rotational restraints. Furthermore, these methods do not apply for (L/r)-values larger than 50 because for zero eccentricity Eq. 40 yields a buckling stress equal to the yield stress for all slenderness ratios. Evidently for concentric loads and large values of L/r a correct method has to result in the Euler stress rather than the yield stress.

A study of the approximate method[48,50] had been made by the writers before they began their own investigation. The previous conclusions were stated[59] somewhat more elaborately:

---

[59] "Second Progress Report on Investigation of Buckling of Rigid Joint Structures," by P. P. Bijlaard, Cornell Univ., Ithaca, N. Y., June, 1951, p. 93.

> "Unfortunately this study [of the Baker and Roderick method] proved that their approach gives reasonably reliable results only for a very limited range of variables (slenderness, restraints, eccentricity) and cannot be generalized to cover the entire field. It was for this reason that the present elaborate study was found necessary."

The justification for the "precise" analysis, mentioned by the writers (under the heading, "Analytical Method") in connection with Eq. 4 and Fig. 5(*b*), is available and it was shown[8] that for several cases the resulting buckling stresses do not differ by more than 3% from the exact values; this method is termed "precise" in view of this agreement. It is not a mathematically rigorous method such as Mr. Chwalla's. In this method sine waves are used only for determining the half-wave length l; the equilibrium load for these half-wave lengths is found from Fig. 5(*b*) or from a similar graph for other materials, based on the exact form of the deflection curves rather than on a sine wave.

It is agreed that there is no consistent relationship between the attainment of yield stress in a continuous or discontinuous column and the load at which the column collapses. For eccentric, simply supported columns this has been known ever since the classical investigations by Mr. von Kármán. It was one of the main objectives of the writers to confirm this fact for end-restrained columns. What has been done by the simplified method is this: Miss Lee's method, which applies only in the elastic range, has been generalized by use of the plastic reduction factor η. It was thus possible to obtain a relatively simple method for analyzing columns in the post-yield range.

ECCENTRICALLY LOADED ALUMINUM COLUMNS

By John W. Clark,[1] J. M. ASCE

Synopsis

Tests were made on eccentrically loaded aluminum alloy columns that failed by plastic buckling in the plane of the applied bending moment. Measured strains, deflections, and critical loads agreed well with computed values. Comparison of the measured critical loads with various design formulas leads to the recommendation that members of this type be designed on the basis of the same interaction formula that has been found to be applicable to aluminum alloy beam-columns which fail by lateral buckling.

Introduction

If a structural member that is subjected both to a compressive end load and to bending is so proportioned that it does not fail by either lateral-torsional buckling or local buckling, failure will result from the instability caused by plastic yielding of the material. There is described herein an experimental investigation of the latter type of failure, in which the combined loading was obtained by testing specimens as eccentrically loaded columns with simply supported ends.

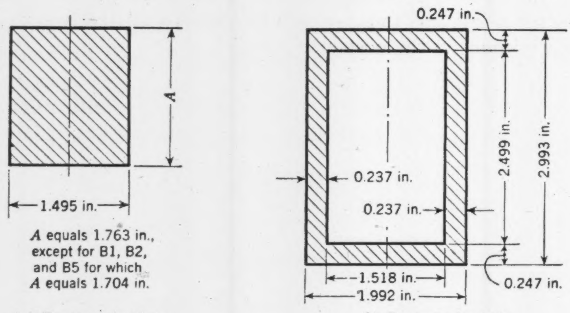

(a) Rectangular bar (b) Rectangular tube

Fig. 1.—Average Cross-Sectional Dimensions of Column Specimens

The principal object of the investigation was to obtain critical values of combined end load and bending moment that could be used to check design formulas for this type of member. An additional objective was to obtain records of the behavior of the test specimens as the critical load was reached and

---

Note.—Published, essentially as printed here, in October, 1953, as *Proceedings-Separate No. 299*. Positions and titles given are those in effect when the paper was received for publication.

[1] Research Engr., Aluminum Research Labs., Aluminum Co. of America, New Kensington, Pa.

passed. For this purpose, continuous measurements of load, deflection, and strain were recorded on a multichannel oscillograph. The results of these measurements were compared with the behavior computed on the basis of the stress-strain characteristics of the material.

DESCRIPTION OF SPECIMENS

The column specimens were made from aluminum alloy 6061-T6 (formerly 61S-T6) rolled rectangular bars and drawn rectangular tubes; the alloy is one that is commonly used for structural applications. The bar was selected to represent a solid section, and the tube was chosen as a section in which resistance to bending was provided primarily by the material in the flanges. Average cross-sectional dimensions are shown in Fig. 1; the dimensions of the individual specimens were all within 1% of the values given in Fig. 1. The areas, A, of the rectangular bars were 2.55 sq in. for specimens B1, B2, and B5 and 2.64 sq in. for the others. The least radius of gyration, r, for all bar specimens was 0.432 in. For the rectangular tube specimens $A = 2.17$ sq in. and $r = 0.757$ in.

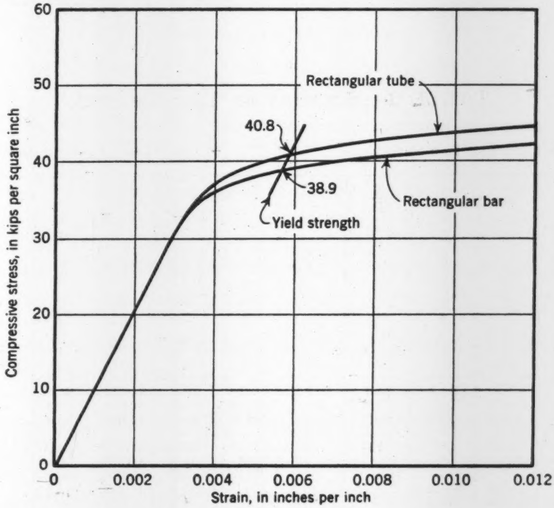

FIG. 2.—COMPRESSIVE STRESS-STRAIN CURVE FOR 6061-T6 ALUMINUM ALLOY COLUMN SPECIMENS

Average mechanical properties in the longitudinal direction for the two types of specimens are given in Table 1. These values are typical of those commonly found in commercial products of this alloy. Values of tensile strength and compressive yield strength for individual specimens were within 1% of the average values, and the variation of the tensile strength from the average given in Table 1 did not exceed 1.2%. Compressive stress-strain curves for the two types of specimens are shown in Fig. 2.

TABLE 1.—MECHANICAL PROPERTIES

Material	Tensile strength, in kips per square inch	Tensile yield strength, in kips per square inch[a]	Percentage elongation in 2-in. gage length	Compressive yield strength, in kips per square inch[a]
Rolled rectangular bar	44.0[b]	40.6[b]	17[b]	38.9[c]
Drawn rectangular tube	46.5[d]	40.8[d]	16[d]	40.8[e]

[a] Set = 0.2%. [b] Determined from standard ½-in.-diameter tension specimens, as given in "Standards," A.S.T.M., 1952, Pt. II, E8-52T, p. 1211, Fig. 7. [c] Determined from ½-in.-diameter compressive specimens, 1.875 in. long. [d] Determined from standard ½-in.-wide rectangular tension specimens, cut from the tube wall and machined to uniform thickness; "Standards," A.S.T.M., *ibid.*, p. 1211, Fig. 6. [e] Determined from ¾-in.-wide, 2.630-in.-long rectangular compressive specimens, cut from the tube wall and machined to uniform thickness (tested in subpress; "Standards," A.S.T.M., *ibid.*, E9-52T, p. 1224, Fig. 3, and p. 1226, Fig. 4a).

TABLE 2.—SUMMARY OF TEST RESULTS

(a) RECTANGULAR BAR SPECIMENS						(b) RECTANGULAR TUBE SPECIMENS					
Specimen	L, in inches	e, in inches	Measured P_f, in kips	Computed[a] P_f, in kips	$\frac{\text{Col. 5} - \text{Col. 4}}{\text{Col. 4}} \times 100$	Specimen	L, in inches	e, in inches	Measured P_f, in kips	Computed[a] P_f, in kips	$\frac{\text{Col. 5} - \text{Col. 4}}{\text{Col. 4}} \times 100$
(1)	(2)	(3)	(4)	(5)	(6)	(1)	(2)	(3)	(4)	(5)	(6)
B16[b]	15.1	0.002	94.4	91.7	−2.9	T16[b]	20 0	0.002	81.5	80.5	−1.2
B15[b]	15.1	0.045	78.5	77.7	−1.0	T14[b]	20.0	0.100	70.5	67.8	−3.8
B17[b]	15.1	0.160	63 5	60.0	−5.5	T15[b]	20.0	0.300	56.6	53.0	−6.4
B20[b]	15.1	0.245	55.0	52.7	−4.2						
B19[b]	15.1	0.330	48.2	47.4	−1.7	T12[b]	35.0	0.003	74.2	70.9	−4.4
B18[b]	14.9	0.425	43.0	42.5	−1.2	T9[b]	35.0	0.095	56.6	54.9	−3.0
						T10[b]	35.0	0.305	43.8	41.5	−5.3
B11[b]	25.1	0.002	75.2	71.1	−5.5	T11[b]	35.0	0.620	33.5	31.9	−4.8
B13[b]	25.1	0.055	55.8	53.7	−3.8						
B12[b]	25.1	0.155	43.8	42.6	−2.7	T8[c]	52.5	0.002	46.8	45.4	−3.0
B14[b]	25.1	0.450	30.5	29.3	−3.9	T5[c]	52.5	0.095	37.7	36.3	−3.7
						T6[c]	52.5	0.290	30.3	29.4	−3.0
B5[c]	37.6	0.005	35.9	34.5	−3.9	T7[c]	52.5	0.545	25.1	24.5	−2.4
B8[c]	37.6	0.045	31.3	31.6	+1.0						
B7[c]	37.6	0.155	26.0	26.1	+0.4	T4[c]	67.5	0.007	27.6	27.7	+0.4
B6[c]	37.6	0.350	22.1	21.7	−1.8	T2[c]	67.5	0.095	25.2	24.9	−1.2
B9[c]	37.6	0.445	19.8	19.5	−1.5	T3[c]	67.5	0.280	22.0	21.4	−2.7
						T1[c]	67.4	0.570	18.8	18.2	−3.2
B1[c]	47.6	0.000	23.2	22.0	−5.2						
B4[c]	47.6	0.035	21.1	21.1	0	T2[d]	65.0	0.915	17.4	16.6	−4.6
B2[c]	47.6	0.175	17.8	17.6	−1.1						
B3[c]	47.6	0.310	16.2	16.1	−0.6						
B4[d]	45.1	0.645	14.6	14.3	−2.1						
Avg					−2.4	Avg					−3.3

[a] Based on Eq. 3. [b] Tested on spherically seated, hydraulically supported platens, with centers of rotation at ends of column. [c] Tested on knife-edge platens with the centers of rotation 1.25 in. beyond the ends of the column. Lengths listed include this extra 2½ in. [d] Tested with knife edge machined on the ends of the column.

The various specimen lengths and eccentricities of loading are presented in Table 2. Values of the slenderness ratio (L/r, in which L is the length) ranged from approximately 35 to 110 for the rectangular bar specimens and from 26 to 89 for the rectangular tubes. The eccentricities, which were determined from the measured strains and deflections as described in Appendix I, varied from zero to slightly less than one half the depth of the cross section. The direction of the eccentricity was normal to the axis of least stiffness in all cases; that is, the specimens were forced to bend about the vertical axes shown in Fig. 1.

Dial-gage measurements (to 0.001 in.) of crookedness, with the specimens supported as beams above a flat surface, indicated that the crookedness—the deviation of the center from a straight line through the ends—was less than 1/1,000 of the length for all specimens.

DESCRIPTION OF TESTS

The columns were tested in a 300,000-lb-capacity testing machine. Loads were increased continuously to failure in all cases. Initial loads were 1 kip for some specimens and 5 kips for others.

Three types of end support were used, as indicated in Table 2. The shorter specimens were tested on hydraulically supported, spherically seated platens[2] (United States Patent No. 2,346,281) as shown in Fig. 3(a). The advantages of these loading fixtures are that they have a large loading capacity combined with a low resistance to rotation and that the centers of rotation are in the faces of the platens. The spherically seated platens were not used with the longer specimens because these platens cannot tip more than 5°. In order to accommodate the end rotations of the longer specimens, it was necessary to use the knife-edge platens shown in Fig. 3(b) which permitted 15° rotation. The centers of rotation of the knife-edge platens were 1.25 in. from the faces of the platens. This factor was accounted for in the analysis of the test data by assuming the length of these specimens to be the distance between the centers of rotation of the knife-edge platens; the error produced by this assumption is negligible.[3]

After the original series of tests, two of the specimens—one bar and one tube—were retested with knife edges machined on the ends of the specimens at a distance of 0.15 in. from one edge. The knife edges were rounded to a radius of $\frac{1}{16}$ in. and were supported in 120° grooves in bearing plates. The purpose of this method of loading was to obtain large deflections without the danger of the specimens slipping off the platens. Although the specimens had received a slight permanent set in their initial loading, their crookedness still did not exceed 1/1,000 of the length.

Two methods were used to measure the lateral deflection of the specimens. For the shorter members, deflection was measured by slender beams supported against the columns of the testing machine as shown in Fig. 3(a). These beams were attached to the column specimens by rods and yokes so that the beams were forced to bend as the columns deflected. Wire strain gages, cemented to the beams and calibrated in terms of lateral deflection of the column specimens

---

[2] "Hydraulically Supported Spherically Seated Compression Testing Machine Platens," by R. L. Templin, *Proceedings*, A.S.T.M., Vol. 42, 1942.

[3] "Corrections for Lengths of Columns Tested Between Knife Edges," by W. R. Osgood, *Journal of the Aeronautical Sciences*, Vol. 11, No. 4, 1944, p. 378.

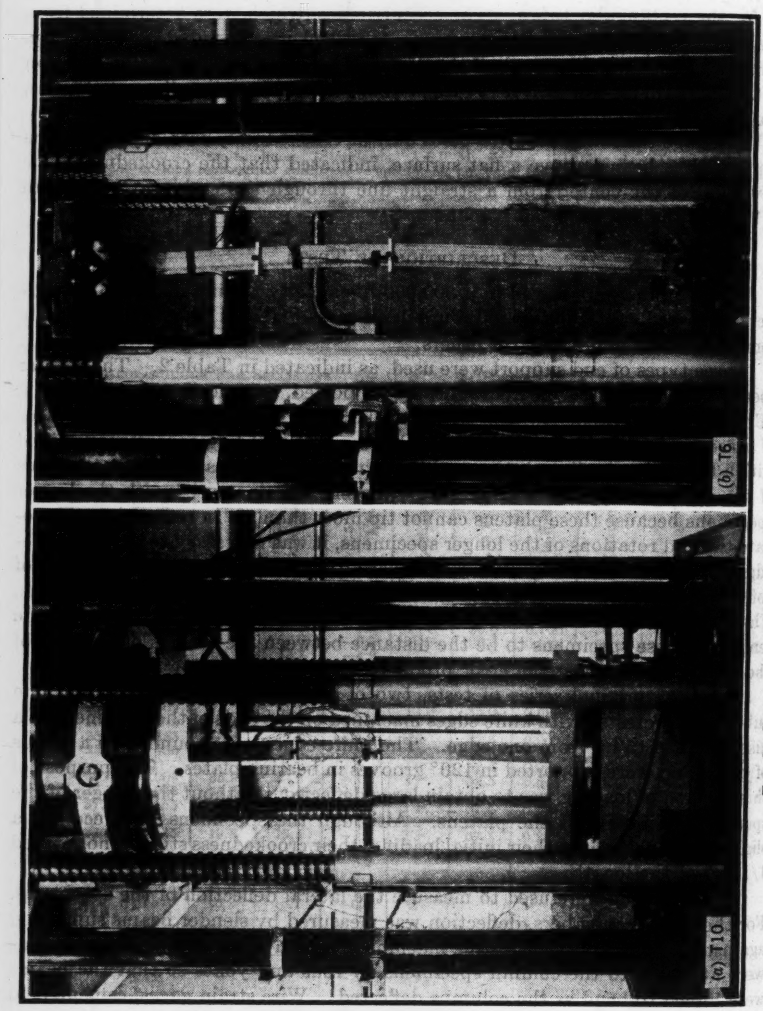

FIG. 3.—RECTANGULAR TUBE COLUMN SPECIMENS AFTER LOADING TO FAILURE

by recording the strain signals for various known values of deflection as measured by a dial gage, indicated the resulting bending strain.

These beams were quite flexible so that the forces they exerted on the column specimens were minimized. Computations revealed that the bending moments induced in the specimens by the lateral forces required to deflect the beams did not exceed 0.01% of the bending moments produced by the end loads on the specimens.

In tests on the longer columns, continuous rotating potentiometers with pulleys were used to indicate deflections. The pulleys were actuated by 0.005-in. wires attached to yokes at the center and at one of the quarter-points of the column specimens. The electrical signal from the potentiometers was calibrated against deflections measured with a 0.001-in. micrometer screw.

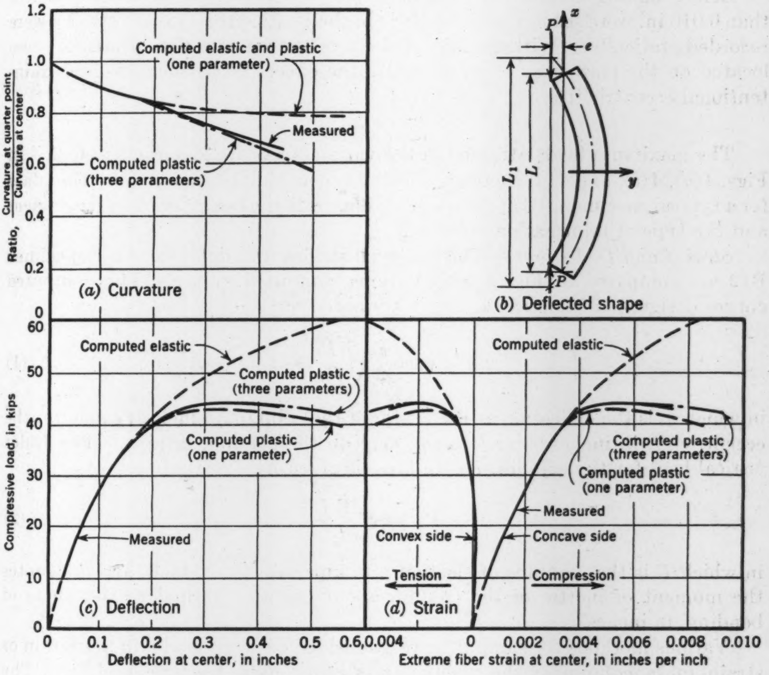

FIG. 4.—CURVATURE, SHAPE, DEFLECTION, AND STRAINS IN B12

The measurement of deflection in the manner described requires that the testing-machine platens do not move in relation to the columns of the machine. This movement was checked by dial-gage measurements and found to be negligible for loads exceeding 10 kips. At lower loads there was some shifting of the platens, and for this reason the "zero" load for the deflection measurements was taken to be 10 kips.

Strains were measured on all four sides of the specimens at the midlength and on two sides at one of the quarter-points.

To indicate load, a fluid pressure cell having a capacity of 5,000 lb per sq in. was connected with the hydraulic circuit of the testing machine. Values of the maximum load were read from the load-indicating dial of the testing machine, which periodic calibrations have shown to be accurate within ±1.0%. These maximum-load values were used to calibrate the signals from the pressure cell. The signals from this cell as well as the strain and deflection signals were recorded on an oscillograph.

Before loading to failure, the specimens for which the eccentricities were less than 0.010 in. were subjected to loadings in the elastic-stress range; strains were recorded statically. With the aid of these measurements the specimens were located on the platens so as to minimize the effects of crookedness and unintentional eccentricities.

RESULTS

The maximum loads attained in the various tests are given in Table 2. In Figs. 4 (*a*), 4 (*c*), and 4 (*d*) there are shown some of the strain and deflection data for a typical specimen, B12; these curves illustrate the behavior of the specimens and the type of information obtained.

Strains and Deflections.—The observed strains and deflections for specimen B12 are compared in Fig. 4 with various computed values. The computed curves designated "elastic" in Fig. 4 are based on[4]

$$y_0 = e \left(\sec \frac{\pi}{2} \sqrt{\frac{P}{P_E}} - 1 \right) \ldots\ldots\ldots\ldots\ldots\ldots (1)$$

in which y_0 is the deflection at the center of the column, in inches; e denotes the eccentricity, in inches; and P is the load on the column, in kips. The Euler critical load for the column, P_E, in kips, is given by

$$P_E = \pi^2 \frac{E\,I}{L^2} \ldots\ldots\ldots\ldots\ldots\ldots\ldots\ldots (2)$$

in which E is the modulus of elasticity, in kips per square inch, and I denotes the moment of inertia of the column about the axis normal to the plane of bending, in inches.

Various methods for computing relationships between load and deflection or strain for a column in the plastic-stress range have been devised.[5,6,7] The methods used herein are described briefly and are presented in more detail in Appendix II.

From the stress-strain curve of a material, one can determine a relationship between the load, moment arm of the load (eccentricity plus deflection), and curvature for a given column cross section. The assumption of a particular shape of the column in the deflected position leads to a second relationship between curvature and moment arm. For a given load, one can find values of the deflection that satisfy both the relationship based on the stress-strain curve and that based on the assumed shape of the column; thus, one can establish the computed deflection of the column at the given load. The two sets of relationships are not satisfied at every point along the length of the column but only at a finite number of points, depending on the number of arbitrary parameters in the mathematical expression assumed for the deflected shape of the column.

---

[4] "Buckling Strength of Metal Structures," by F. Bleich, McGraw-Hill Book Co., Inc., New York, N. Y., 1952, p. 45.

[5] "Strength of Steel Columns," by H. M. Westergaard and W. R. Osgood, *Transactions*, ASME, Vol. 50, 1928, p. 65.

[6] "Inelastic Column Behavior," by J. E. Duberg and T. W. Wilder, III, *Technical Note No. 2267*, National Advisory Committee for Aeronautics, January, 1951.

[7] "Buckling Strength of Metal Structures," by F. Bleich, McGraw-Hill Book Co., Inc., New York, N. Y., 1952, p. 25.

In Fig. 4 (*b*) there is shown a diagrammatic sketch of a column in a deflected position. Expressions which were assumed to represent the deflected shape of the column are:

For one parameter,

$$y = a \cos \frac{\pi x}{L_1} - e \ldots\ldots\ldots\ldots (3)$$

For three parameters,

$$y = a_0 \left(1 - \frac{4 x^2}{L^2}\right) + a_1 \cos \frac{\pi x}{L} + a_2 \cos \frac{3 \pi x}{L} \ldots\ldots\ldots\ldots (4)$$

Eqs. 3 and 4 were used in computing the curves for plastic behavior plotted in Fig. 4.

The cosine relationship (Eq. 3) is the same as that used by H. M. Westergaard and William R. Osgood, M. ASCE, in an analysis of eccentrically loaded steel columns.[5] This curve is the correct one when the stresses are in the elastic-stress range. For stresses in the plastic range, this curve makes possible a relatively simple solution involving only one arbitrary parameter. As can be seen in Figs. 4 (*c*) and 4 (*d*), the strains and deflections at the center of the columns that are computed on the basis of this assumption are not significantly in error. The maximum load indicated by the computed curves is approximately 2.7% less than the measured value.

Better agreement between measured and computed values can be achieved by assuming a more complicated deflection curve which can be made to fit more closely the actual shape of the deflected member. Eq. 4, which incorporates three arbitrary parameters, yielded very close agreement between measured and computed strains and deflections.

A rather sensitive indication of the deflected shape of the column was obtained by comparing the curvatures at the quarter-point and center as indicated by the strain measurements at those points. In Fig. 4 (*a*) there are plotted the measured and computed values of the ratio of curvature at the quarter-point to curvature at the center. The good agreement between measured values and those computed on the basis of Eq. 4 can be observed.

Maximum Loads.—Maximum loads for all specimens were computed with the assumption that the column deflects in a cosine curve (Eq. 3). These maximum loads are listed in Table 2. The computed critical loads averaged 2.4% less than the measured values for the rectangular bar column specimens and 3.3% less than the measured values for the tubes.

These differences are of the same order of magnitude as the difference in maximum loads for the two sets of computed curves in Figs. 4(*c*) and 4(*d*); part of the error in the computed maximum loads in Table 2 was no doubt a result of the approximations involved in using the cosine curve (Eq. 3) to represent the deflected shape of the column in the plastic-stress range.

An additional factor affecting the agreement between measured and computed maximum loads is the end restraint provided by the loading fixtures. This restraint seems to have been appreciable only in the case of specimens loaded with eccentricities less than 0.010 in. Comparison of critical loads for zero eccentricity, determined—as described subsequently—from the test data, with computed critical loads at stresses in the elastic range indicated that the ratio between the effective length and the actual length of the specimens with the smallest eccentricities was approximately 0.985; this ratio is 1.0 for perfectly hinged ends and 0.5 for fixed ends. For the specimens with greater eccentricities, analysis of the measured strains and deflections showed that the ratio of effective length to actual length was even closer to unity and thus that the effect of end restraint was negligible.

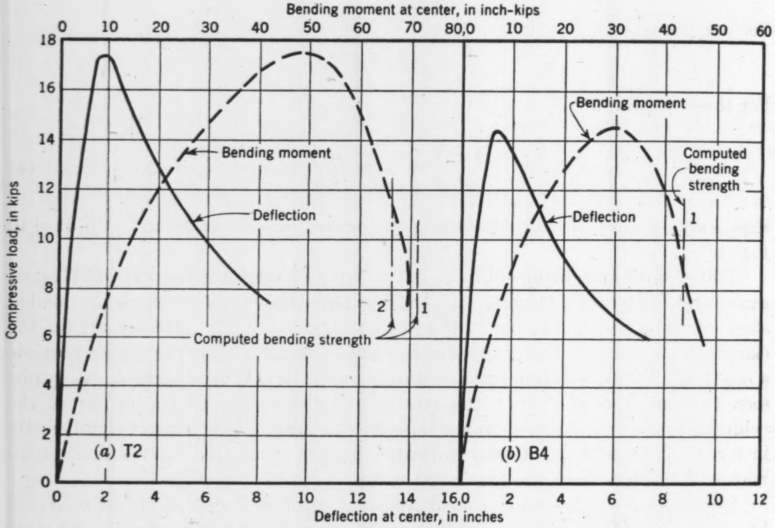

FIG. 5.—DEFLECTION AND BENDING MOMENT IN COLUMN SPECIMENS TESTED WITH KNIFE-EDGE ENDS

Secant Column Formula.—One method of design for members of this type is based on the assumption that failure occurs when the extreme fiber stress reaches some limiting value. The maximum extreme fiber stress is assumed to be the sum of the axial stress plus the bending stress at the center, where the moment arm used in computing the bending stress is the eccentricity plus the center deflection as given by Eq. 1. The resulting expression for maximum stress is termed the secant formula.[4]

On the basis of the test results, this method does not appear to be satisfactory for application to aluminum alloy members. For example, if it is assumed that a member fails when the extreme fiber stress reaches the yield strength, the secant formula results in critical loads for the rectangular tubes that vary from 5% less than the experimental value for specimen T15 to 15% greater than the actual ultimate strength for specimen T12. Critical loads computed in the same manner for the bars are from 7% too high in the case of specimen B16 to 22% too low for specimen B18.

Interaction Formulas.—Another method of predicting the strength of beam-columns for design purposes involves the use of an "interaction" formula. Such a formula expresses a relationship between (*a*) the ratio of axial load on the column to the load that would cause failure under axial compression alone and (*b*) the ratio of bending moment on the member to the moment that would cause failure under bending alone. To investigate these test results from the standpoint of interaction relationships, it was necessary to obtain values of critical axial load and critical bending moment. Values of critical axial load for each length of specimen were obtained by plotting test values of axial stress at failure versus eccentricity for the specimens of that length. The stress at which a curve drawn through the test points crossed the axis of zero eccentricity was taken to be the critical stress for a centrally loaded column of the same length as the test column. The loads corresponding to these critical stresses were from zero to 2.9% higher than the critical loads for the specimens with the smallest eccentricities.

An indication of the strength of these members in pure bending was obtained from the tests of specimens B4 and T2 with knife edges machined on the ends of the specimens. The results of these two tests are plotted in Fig. 5. In addition to curves of load versus center deflection, Fig. 5 shows the relationship between load and bending moment at the center of these specimens. Values of the bending moment were obtained by multiplying the load times the sum of the initial eccentricity and the measured deflection at that load. It can be seen from Fig. 5 that in the case of the rectangular tube the bending moment reached a definite maximum value. At this point the cross section of the tube at the center of the column was visibly distorted, both the tension and compression flanges being bent toward the neutral axis of the tube. The resulting reduction in stiffness of the section was sufficient to prevent any further increase in bending moment. Because at the end of the test the axial stress was relatively low (3.5 kips per sq in.), it was concluded that the value of the maximum bending moment attained was not influenced appreciably by the axial stress. This bending moment, 69.5 in.-kips, was assumed to be the same as the critical value for pure bending.

In Fig. 5 the line for the computed ultimate bending strength that is marked 1 is based on the assumption of a rectangular distribution of stress equal to the tensile strength; the line marked 2 is based on the assumption that the bending stress ($M\,c/I$) reaches the tensile strength at the centroid of the tension flange.

The bending moment for specimen B4 did not reach a maximum value. This is typical of solid sections, which can be given very severe bends without failure resulting. Therefore, it was necessary to choose a value of the critical bending moment for the solid section on a somewhat arbitrary basis. The value of critical bending moment selected was one corresponding to a modulus of failure equal to 150% of the tensile strength of the material—a limiting value that is sometimes used in estimating ultimate strength for design purposes.[8] As indicated in Fig. 5, when a bending moment corresponding to a modulus of failure of 150% of the tensile strength was reached, the deflection of specimen B4 was 4.2 in., or approximately one tenth of the length of the specimen. The axial stress, 3.5 kips per sq in., was low enough so that it was assumed to have relatively little effect on the bending strength.

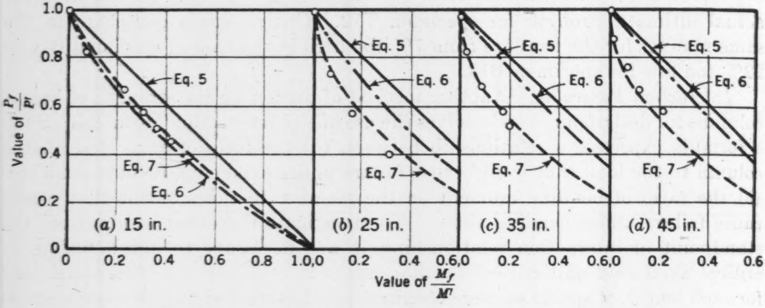

FIG. 6.—INTERACTION CURVES FOR RECTANGULAR BARS TESTED AS ECCENTRICALLY LOADED COLUMNS OF VARIOUS LENGTHS

The test results of this investigation are plotted in interaction form in Figs. 6 and 7. Also plotted in these figures are three different interaction curves that have been suggested as being applicable to the design of beam-columns. The algebraic expressions for these interaction curves are

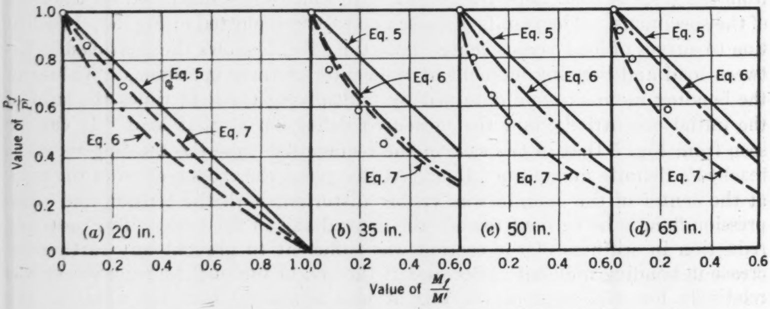

FIG. 7.—INTERACTION DIAGRAMS FOR RECTANGULAR TUBES TESTED AS ECCENTRICALLY LOADED COLUMNS OF VARIOUS LENGTHS

$$\frac{P_f}{P'} + \frac{M_f}{M'} = 1 \qquad (5)$$

$$\frac{P_f}{P'} + \frac{M_f}{M'\left(1 - \frac{P_f\,S}{M'\,A}\right)} = 1 \qquad (6)$$

---

[8] "Designing Aluminum Alloy Members for Combined End Load and Bending," by H. N. Hill, E. C. Hartman, and J. W. Clark, *Proceedings-Separate No. 300*, ASCE, October, 1953.

and

$$\frac{P_f}{P'} + \frac{M_f}{M'\left(1 - \frac{P_f}{P_E}\right)} = 1 \qquad (7)$$

In these interaction equations P_f is the load on the column at failure, in kips; P' denotes the maximum load for axial compression alone, in kips; M_f is the bending moment at failure (for these specimens, end load times initial eccentricity), in inch-kips; M' is the maximum bending moment for bending alone, in inch-kips; and S represents the section modulus of the cross section, in inches.^{3}

Eq. 5 has served as a basis for at least one widely used design formula for steel members subjected to combined loading;[9] it results in a straight diagonal line on the interaction diagram. The fact that all the test points lie below this line in Figs. 6 and 7 indicates that Eq. 5 is not conservative. The critical loads predicted by Eq. 5 were as much as 39% higher than the test values.

Eq. 6 is similar to a design formula that has been used in specifications for aluminum alloy structures.[10,11] Although Eq. 6 is an improvement on the straight-line relationship, it predicts critical loads that are from 10% lower to 31% higher than the measured values for the specimens of this investigation.

Eq. 7 was originally developed for application to aluminum alloy beam-columns that fail by lateral buckling and twisting.[12] It has also been suggested as a possible basis for the design of steel beam-columns.[13] For the column tests described herein, values of ultimate strength predicted by Eq. 7 were within ±10% of the measured maximum loads. This agreement is considerably better than that obtained with either of the other two interaction formulas or with the secant formula.

In view of this agreement, Eq. 7 is recommended for use in the design of eccentrically loaded, aluminum alloy columns that fail by plastic buckling in the direction of the applied bending moment as well as for members that fail by lateral buckling and twisting.

Although these tests were confined to cases in which the bending moment was applied by eccentric loading with equal eccentricities at the two ends, it is believed that the recommended design formula should be satisfactory for any case of a simply supported, aluminum alloy column of uniform section subjected to axial load and bending when the maximum applied bending moment occurs at or near the center of the member and failure is of the type considered herein. Thus, there are included not only columns with equal eccentricities but also columns in which bending is introduced by initial crookedness, by uniformly distributed lateral load, or by concentrated lateral loads distributed about the center in a fairly symmetrical manner.

---

[9] "Steel Construction," A.I.S.C., 5th Ed., 1950, p. 284.

[10] "Specifications for Heavy Duty Structures of High-Strength Aluminum Alloy," Final Report of the Committee of the Structural Division on Design in Lightweight Structural Alloys, *Transactions*, ASCE, Vol. 117, 1952, p. 1258, paragraph *B*-7a.

[11] "Specifications for Structures of a Moderate Strength Aluminum Alloy of High Resistance to Corrosion," Progress Report of the Committee of the Structural Division on Design in Lightweight Structural Alloys, *Proceedings-Separate No. 132*, ASCE, May, 1952, p. 6, paragraph *B*-7a.

[12] "Lateral Buckling of Eccentrically Loaded I- and H-Section Columns," by H. N. Hill and J. W. Clark, *Proceedings*, First National Cong. of Applied Mechanics, 1951, p. 407.

[13] "Investigation of Interaction Formula," by J. Zickel and D. C. Drucker, *Report No. 1*, Column Research Council, Brown Univ., Providence, R. I., April, 1951.

Values of combined end load and bending moment that cause failure of a member are somewhat smaller when the applied bending moment is constant along the length (equal eccentricities) rather than varying from zero at the ends to a maximum near the center, as is the case when the moment is introduced by lateral loading or initial crookedness. Differences in strength corresponding to the various types of loading are relatively small, however, because the relationship between deflection of a member and curvature at the center, which primarily governs the maximum load for a beam-column, is not greatly affected by variations in the shape of the bending-moment diagram. Thus, a design formula that is applicable to eccentrically loaded columns can be expected to give reasonably accurate results—somewhat on the safe side—for the other types of loading.

Evidence in support of this conclusion appears in the work of Messrs. Westergaard and Osgood,[5] who found that a column subjected to a given combination of axial load and bending moment at the center has approximately the same ultimate strength regardless of whether the applied bending moment is introduced by equal eccentricities at the ends or by initial curvature.

CONCLUSIONS

The results of this investigation of beam-column behavior, in which tests were made on eccentrically loaded columns of aluminum alloy 6061-T6 rolled rectangular bars and drawn rectangular tubes, can be summarized as follows:

1. All specimens failed by yielding, resulting in an eventual "falling-off" of the load accompanied by rapidly increasing deflections. This behavior is typified by the curves of measured strain and deflection shown in Fig. 4.
2. Measured strains and deflections in the plastic-stress range were in approximate agreement with values computed on the basis of the assumption made by Messrs. Westergaard and Osgood[5] that the deflected shape of the column is part of a cosine curve (Eq. 3). Maximum loads computed on this basis averaged 2.4% less than the measured critical loads for the rectangular bar specimens and 3.3% less than the test values for the rectangular tubes.
3. Agreement between measured and computed behavior was improved by assuming the shape of the deflection curve to be represented by a parabola and two terms of a sine series (Eq. 4).
4. The assumption that failure occurs when the extreme fiber stress as computed by the secant formula reaches the yield strength of the material resulted in computed critical loads that were from 22% lower to 15% higher than the test values.
5. The straight-line interaction formula (Eq. 5) predicted critical loads that were higher than the test values by as much as 39%.
6. Maximum loads computed from Eq. 6 varied from 10% lower to 31% higher than the measured values.
7. The interaction formula, Eq. 7, gave critical loads that agreed with the test results within ±10%. Eq. 7 is recommended as a basis for the design of eccentrically loaded, aluminum alloy columns that fail by plastic buckling in the plane of the applied bending moment. The formula is believed to be ap-

plicable also to columns in which bending is introduced by initial crookedness or by lateral loads as long as the maximum applied bending moment occurs at or near the center of the member.

APPENDIX I. DETERMINATION OF EFFECTIVE ECCENTRICITIES

The nominal eccentricities used in these tests were, in inches, (*a*) for the bar specimens, 0.00, 0.05, 0.15, 0.25, 0.35, 0.45, and 0.60; and (*b*) for the tubes, 0.0, 0.1, 0.3, 0.6, and 0.85. The last value given in each case is for the member tested with knife edges machined on the ends. Tests of specimens of each given length were not necessarily made at all eccentricities.

The actual effective eccentricities were somewhat modified by the effects of initial crookedness, and for this reason the values of eccentricity used in the analysis of the test data were computed values based on the measured strains and deflections.

In determining the effective eccentricities, use was made of the following relationships (which are based on Eq. 1)—

$$e = \frac{y_0}{\sec \frac{\pi}{2}\sqrt{\frac{P}{P_E}} - 1} \quad \ldots\ldots\ldots\ldots (8)$$

and

$$e = \frac{E\,S\,(\epsilon_1 - \epsilon_2)_0}{2\,P \sec \frac{\pi}{2}\sqrt{\frac{P}{P_E}}} \quad \ldots\ldots\ldots\ldots (9)$$

in which $(\epsilon_1 - \epsilon_2)_0$ is the difference in extreme fiber strains at the center of the column, in inches per inch.

If the numerators are plotted against the denominators in the expressions on the right sides of Eqs. 8 and 9, the resulting slope is the eccentricity. These equations apply, of course, only as long as the stresses are within the elastic range.

For the specimens with eccentricities less than 0.010 in., the values of eccentricity listed in Table 2 were computed from Eq. 9, using the static measurements made while centering these specimens on the platens. These values of eccentricity are given to the nearest 0.001 in.

Most of the other values of eccentricity in Table 2 were computed on the basis of the strain data obtained from the oscillograph records. In the few cases in which the strain data were incomplete (specimens B14, B9, and the two specimens with knife edges machined on the ends), Eq. 8 was used with the measured deflections to determine the eccentricity. Eccentricities computed from oscillograph-record data are given to the nearest 0.005 in.

APPENDIX II. COMPUTATION OF STRAINS AND DEFLECTIONS

The usual assumptions were made that deflections are small relative to the length of the member, shear deformations can be neglected, and plane sections remain plane. It was also assumed that the material adheres to the stress-strain relationships determined in tests under uniaxial tension or compression.

Given values of extreme fiber strain, ϵ_1 and ϵ_2, at a cross section of the column, one can determine the distribution of stress on the section from the stress-strain curve and from this stress distribution compute the axial load and the bending moment on the given cross section. The integration required to compute the load and bending moment can be performed by numerical or graphical methods, or it can be performed analytically by expressing the stress-strain curve in mathematical form. The latter method was used in this case, the mathematical expression used being the one developed by Walter Ramberg and Mr. Osgood[14] and expressed in a modified form by H. N. Hill,[15] M. ASCE.

Dividing the bending moment at the section by the load on the member gives a value of the moment arm; this arm is equal to the sum of the eccentricity plus the deflection at that cross section.

The given values of extreme fiber strain are also used to determine the curvature at the section, the curvature being equal to $(\epsilon_1 - \epsilon_2)/d$, in which d is the depth of the member. If these computations are repeated for a number of different assumed values of extreme fiber strains, the results can be plotted in dimensionless form as a family of curves relating the quantity $(\epsilon_1 - \epsilon_2)$ and the ratio of the moment arm to the depth of section, $(e + y)/d$, for constant values of average stress on the column.

Another relationship between curvature and deflection can be established by setting the second derivative of the assumed deflection curve equal to the curvature. The cosine curve (Eq. 3) has only one arbitrary parameter and thus can be made to satisfy the relationship based on the stress-strain curve at only one point along the length of the column. It is convenient to choose this point as the center of the column, which results in

$$\frac{e + y_0}{d} = \frac{e}{d} \sec \sqrt{\frac{L^2 \, (\epsilon_1 - \epsilon_2)_0}{4 \, d(e + y_0)}} \quad \ldots\ldots\ldots\ldots\ldots (10)$$

Eq. 10 can be plotted as a curve on the chart of $(\epsilon_1 - \epsilon_2)$ versus $(e + y)/d$. Points of intersection of this curve with the previously-drawn family of curves relating $(\epsilon_1 - \epsilon_2)$ and $(e + y)/d$ for constant values of average stress establish the deflections and extreme fiber strains corresponding to the various average stresses.

---

[14] "Description of Stress-Strain Curves by Three Parameters," by Walter Ramberg and W. R. Osgood, *Technical Note No. 902*, National Advisory Committee for Aeronautics, 1943.

[15] "Determination of Stress-Strain Relations from Offset Yield Strength Values," by H. N. Hill, *Technical Note No. 927*, National Advisory Committee for Aeronautics, 1944.

If Eq. 4 is used, the curvature-deflection relationship can be satisfied at three points along the length of the column. The end ($x = L/2$), one-third point ($x = L/6$), and center ($x = 0$) were chosen, resulting in

$$\frac{e + y_{L/2}}{d} = \frac{e}{d} \qquad \text{(11a)}$$

$$\frac{e + y_{L/6}}{d} = \frac{e}{d} + \left(\frac{L}{d}\right)^2 \left[\left(\frac{1}{9} - \frac{1}{\pi^2}\right)(\epsilon_1 - \epsilon_2)_{L/2} + \frac{1}{\pi^2}(\epsilon_1 - \epsilon_2)_{L/6}\right] \qquad \text{(11b)}$$

and

$$\frac{e + y_0}{d} = \frac{e}{d} + \left(\frac{L}{d}\right)^2 \left\{\left[\frac{1}{8} - \frac{1}{\pi^2}\left(\frac{16}{9\sqrt{3}} + \frac{1}{9}\right)\right](\epsilon_1 - \epsilon_2)_{L/2} + \frac{16}{9\sqrt{3}\,\pi^2}(\epsilon_1 - \epsilon_2)_{L/6} + \frac{1}{9\,\pi^2}(\epsilon_1 - \epsilon_2)_0\right\} \qquad \text{(11c)}$$

Each of Eqs. 11 represents a straight line on the chart of $(\epsilon_1 - \epsilon_2)$ versus $(e + y)/d$. For a given value of axial stress on the column, Eq. 11*a* establishes the difference in extreme fiber strains at the end of the column, which is used in Eq. 11*b* to find the difference in extreme fiber strains at the one-third point. Both these values are then substituted into Eq. 11*c* to determine the deflection and strain at the center of the column.

In order to simplify the task of computing the relationship of load, moment arm, and curvature from the stress-strain diagram, it was assumed that no stress reversal occurred at a point after the stress at that point had entered the plastic-stress range. The strain measurements indicated this assumption to be correct for all but the shortest columns tested with the smallest eccentricities. One consequence of this assumption is that the limiting load for zero eccentricity in the plastic-stress range is computed to be the tangent-modulus critical load rather than the somewhat higher value which results if strain reversal is taken into account.[6] An additional assumption used to simplify the computations for the rectangular tube was that all resistance to bending was concentrated at the centroids of the flanges.

APPENDIX III. NOTATION

The following symbols, adopted for use in the paper, conform essentially with "American Standard Letter Symbols for Structural Analysis" (ASA Z10.8-1949), prepared by a committee of the American Standards Association with ASCE representation and approved by the Association in 1949:

A = cross-sectional area of the column;
d = depth of the section;
E = modulus of elasticity;
e = eccentricity of the load;

I = moment of inertia;
L = length of the column;
M = bending moment:
M_f = bending moment at failure;
M' = maximum bending moment;
P = load on the column:
P_E = Euler critical load;
P_f = load at failure;
P' = maximum load for axial compression;
r = radius of gyration;
S = section modulus;
y = deflection; and
ϵ = strain.

INVESTIGATION AND LIMIT ANALYSIS OF NET AREA IN TENSION

BY W. GORDON BRADY[1] AND DANIEL C. DRUCKER,[2] A. M. ASCE

WITH DISCUSSION BY MESSRS. WILLIAM H. MUNSE; PAUL P. BIJLAARD; AND W. GORDON BRADY AND DANIEL C. DRUCKER

SYNOPSIS

The problem of the weakening effect of holes in tension members is reexamined from the viewpoint of plastic action. Using the maximum-shearing-stress yield criterion and the Mises criterion, upper and lower bounds for the limit load are computed for thin sheets with six configurations of staggered rows of holes. Comparisons are made with design specifications and with the results of a number of tests performed on hot-rolled steel and on 61S-T6 aluminum alloy sheet. It is found that the limit loads, as determined by test, confirm the main features of the analysis and lie somewhat above the ranges of load computed with the maximum-shearing-stress criterion. The ($s^2/4\,g$)-design rule is shown to correspond with an approximate upper bound and, as such, may be appreciably on the unsafe side for configurations of open or plugged holes; for riveted tension joints, however, it is probably reasonable.

NOTATION

The letter symbols adopted for use in this paper are defined where they first appear, in the illustrations or in the text, and are arranged alphabetically, for convenience of reference, in the Appendix.

INTRODUCTION

Theorems for limit analysis[3,4] offer an opportunity to check current (1955) design specifications for net area in tension members as well as to determine how closely the limit loads of selected configurations of rows of holes in steel and aluminum alloy sheets—as determined by test—agree with idealized theory. The limit load is herein defined as the force required for unrestricted plastic flow to occur across the entire section and is therefore above the load at which plastic deformation first occurs. At this limiting stage, plastic deformation—either localized or over-all—is considerable, and therefore the limit load may provide a reasonable value on which to base the working load.

NOTE.—Published, essentially as printed here, in October 1953, as *Proceedings-Separate No. 296.* Positions and titles given are those in effect when the paper or discussion was received for publication.

[1] Asst. Engr., Cornell Aeronautical Laboratory, Inc.; formerly Research Assistant in Applied Math., Brown Univ., Providence, R. I.

[2] Chairman, Div. of Eng., Brown Univ., Providence, R. I.

[3] "The Safety Factor of an Elastic-Plastic Body in Plane Strain," by D. C. Drucker, H. J. Greenberg, and W. Prager, *Journal of Applied Mechanics*, Vol. 18, 1951, pp. 371-378.

[4] "Extended Limit Design Theorems for Continuous Media," by D. C. Drucker, W. Prager, and H. J. Greenberg, *Quarterly of Applied Mathematics*, Vol. 9, 1952, pp. 381-389.

Several design specifications have been proposed and used for determining the net area in tension members with staggered rows of holes. In the case of one row of holes normal to the length of the member, subtracting the hole diameters from the gross width of the member is a rational rule for determining the net width if it is assumed that uniform stress exists across the section after plastic flow has occurred. For holes that are staggered across the normal section, the assumption of a uniformity of stress as a result of plastic deformation is not so obvious. For the two staggered holes in Fig. 1 there are two extreme possibilities: (*a*) Taking the net area across each normal section as $b - d$ and (*b*) taking the net area as $b - 2d$. The term b is used to signify the gross width of the piece, and d is the diameter of each hole. Intuitively, the first case would seem to be unsafe and the second too conservative. The correct net width probably lies between these extremes; moreover, it appears likely that the correct net width is a function of the stagger and gage. Stagger is the longitudinal spacing between the centers of adjacent holes, and gage is the transverse spacing between centers of two adjacent holes.

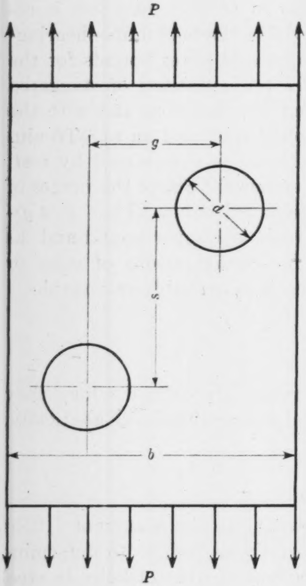

FIG. 1.—TENSION MEMBER

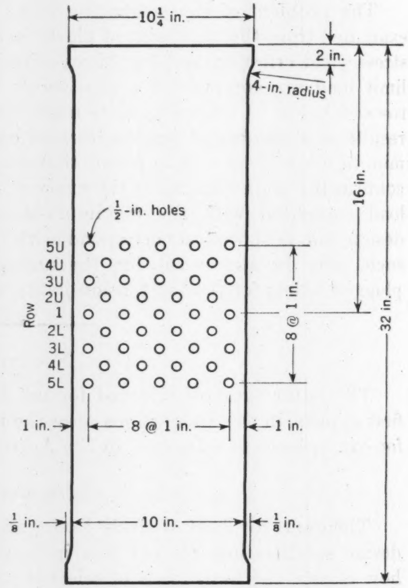

FIG. 2.—TEST PIECE

Many suggestions have been advanced for design rules,[5,6] and in 1915 T. A. Smith,[7] on the basis of the work by Victor H. Cochrane,[6] proposed the

---

[5] "Some Tests Bearing on the Design of Tension Members," by Edward Godfrey, *Engineering News*, Vol. 55, 1906, pp. 488–489.

[6] "Calculating Net Section of Riveted Tension Members, and Fixing Rivet Stagger," by Victor H. Cochrane, *ibid*, Vol. 59, 1908, p. 465.

[7] "Diagram for Net Section of Riveted Tension Members," by T. A. Smith, *ibid*, Vol. 73, 1915, p. 893.

following:

$$x = \frac{g}{d} - \frac{2\,(g^2 + s^2 - d\,\sqrt{g^2 + s^2})}{d(g + \sqrt{g^2 + 4\,s^2})} \ldots\ldots\ldots\ldots\ldots\ldots (1)$$

in which x is the fractional part of a hole to be deducted, g denotes the distance between gage lines, and s is the pitch or stagger.

Other formulas have been suggested as approximations to Eq. 1. One offered by C. R. Young,[8] M. ASCE, is

$$x = 1.50 - 1.25\,\frac{s}{g} \ldots\ldots\ldots\ldots\ldots\ldots (2)$$

Mr. Cochrane proposed[9]

$$r = d - \frac{s^2}{4\,g} \ldots\ldots\ldots\ldots\ldots\ldots (3)$$

in which r is the width of strip to be deducted. Eq. 3 is the formula in general use (as of 1955) and is specified for computing net area for sections with staggered holes by the American Railway Engineering Association (AREA), the American Institute of Steel Construction (AISC), and the American Association of State Highway Officals (AASHO). The following[10] is typical:

> "The net width for any chain of holes extending progressively across the part shall be obtained by deducting from the gross width the sum of the diameters of all the holes in the chain and adding, for each gage space in the chain, the quantity:
>
> $$s^2/4g$$
>
> where s equals the pitch of any two successive holes in the chain, g equals the gage of the same holes.
>
> "The net section of the part is obtained from the chain which gives the least net width."

Tests to failure of drilled steel plates with two and three staggered holes were performed by Mr. Young and W. B. Dunbar,[11] who concluded that Eq. 1 was somewhat too conservative.

Clarence Holleman[12,13] has reported on tests to failure on several aluminum alloys, as well as on SAE X4130 steel.[14] Mr. Holleman recommended the use of a tension efficiency of 90% based on net area for tension members with holes when using aluminum alloys. C. H. Stevenson[15] has reported on tests to failure on sheet specimens of several aluminum alloys with one and two holes drilled in various configurations. Mr. Stevenson noted increasing efficiencies as stagger was increased, but there were wide variations of efficiency—as much as 13% between the alloys tested. In these reports, efficiency of a tension member was defined as the ratio of ultimate strength based on net area to the ultimate strength of a solid tensile specimen, expressed in percentage.

---

[8] "True Net Sections of Riveted Tension Members," by C. R. Young, *Engineering Research Bulletin No. 2*, Univ. of Toronto, Toronto, Ont., Canada, 1921, pp. 233–244.

[9] "Rules for Rivet-Hole Deductions in Tension Members," by Victor H. Cochrane, *Engineering News-Record*, Vol. 89, 1922, pp. 847–848.

[10] "Standard Specifications for Highway Bridges," A.A.S.H.O., 1949, p. 175.

[11] "Net Section of Drilled Plates," by C. R. Young, and W. B. Dunbar, *Engineering Research Bulletin No. 6*, Univ. of Toronto, Toronto, Ont., Canada, 1926, pp. 51–65.

[12] "Tension Joints in Aircraft Structures," by Clarence H. Holleman, *Journal of the Aeronautical Sciences*, Vol. 10, 1943, pp. 295–302.

[13] *Ibid*, p. 310.

[14] "Mechanical Properties of Metals and Alloys," *Circular C447*, National Bureau of Standards, Washington, D. C., December, 1943, p. 164.

[15] "The Effects of Open Holes on the Tensile Strength of Some Aluminum Alloys," by C. H. Stevenson, in the "Symposium on Notch Effects in High-Strength Aluminum Alloys," *Journal of the Aeronautical Sciences*, Vol. 13, 1946, pp. 395–397.

H. N. Hill, M. ASCE, and R. S. Barker[16,17] have reported on tests on specimens cut from aluminum and magnesium alloy sheet, the tests being carried to failure. The specimens were taken at right angles to the direction of rolling. It was reported that the specimens containing two staggered holes showed a reduced efficiency, based on the ($s^2/4\,g$)-rule, the reduction increasing with increasing ratio of pitch to gage up to a ratio of unity. They also reported that the greatest reduction in ultimate strength was found for the most ductile materials. Unfortunately, because none of these reports included limit-load data, no direct comparison can be made with the present tests.

The hole patterns cited herein were chosen so as to give the same least net area for two or more rows of holes as for one row using the ($s^2/4\,g$)-rule (Fig. 2). The configurations were the one-row case (1); the two-row case (1, 2U); the three-row cases (1, 2U, 3U) and (2L, 1, 2U), termed 3S and 3L, respectively; the five-row case (3L, 2L, 1, 2U, 3U); and all nine rows. Thus, on the basis of the ($s^2/4\,g$)-criterion, the sheets with one or more rows should all have the same limit load.

LIMIT-ANALYSIS THEOREMS

The limit-analysis theorems offer a method of determining upper and lower bounds for the limit load of any perfectly plastic material, and therefore the almost impossible exact plastic analyses which would otherwise be required are avoided. The limit theorems will be described as applied to perfectly plastic materials, in a state of plane stress, which obey the maximum-shearing-stress criterion of H. Tresca.[18] According to this criterion, plastic deformation occurs only when the maximum shearing stress has reached a value k, the yield stress in pure shear. Perfect plasticity implies that the maximum shearing stress cannot exceed k. If principal stresses σ_1, σ_2 are used as Cartesian coordinates ($\sigma_3 = 0$), the states of stress with the maximum shearing stress k are represented by the points of the hexagon ABCDEF in Fig. 3.

The principal axes of the plastic-strain rate or increment in a isotropic material coincide with the principal axes of stress. The principal plastic-strain rates are denoted by $\dot{\epsilon}_1$, $\dot{\epsilon}_2$, and $\dot{\epsilon}_3$ and are in the directions of σ_1, σ_2, and σ_3, respectively. If the plastic-strain rate is represented by a vector with principal components ($\dot{\epsilon}_1$, $\dot{\epsilon}_2$) and if strain axes are superposed on the stress axes, this "vector" is outwardly normal to the hexagon representing the state of stress in plastic flow[19,20] (Fig. 3). At the vertices, the direction of the vector represent-

---

[16] "Effect of Open Circular Holes on Tensile Strength and Elongation of Sheet Specimens of Some Aluminum Alloys," by H. N. Hill and R. S. Barker, *Technical Note No. 1974*, National Advisory Committee for Aeronautics, Washington, D. C., 1949.

[17] "Effect of Open Circular Holes on Tensile Strength and Elongation of Sheet Specimens of a Magnesium Alloy," by R. S. Barker, *Technical Note No. 2716*, National Advisory Committee for Aeronautics, Washington D. C., 1952.

[18] "Mémoire sur l'écoulement des corps solides soumis à defortes pressions," by H. Tresca, *Comptes Rendus*, Vol. 59, 1864, pp. 754–758.

[19] "Some Implications of Work-Hardening and Ideal Plasticity," by D. C. Drucker, *Quarterly of Applied Mathematics*, Vol. 7, 1950, pp. 411–418.

[20] "A More Fundamental Approach to Stress-Strain Relations," by D. C. Drucker, *Proceedings*, ASME, First U. S. National Cong. of Applied Mechanics, June, 1951, pp. 487–491.

ing the plastic-strain rate may lie anywhere between (and may include) the directions of the plastic-strain rate determined by the two adjacent sides of the hexagon. It should be noted that the incompressibility condition,

$$\dot{\epsilon}_1 + \dot{\epsilon}_2 + \dot{\epsilon}_3 = 0 \qquad (4)$$

determines $\dot{\epsilon}_3$ when $\dot{\epsilon}_1$ and ϵ_2 are known.

When a tension member with a row of holes is loaded, the strains at first are purely elastic. As the loading is increased, the maximum shearing stress at points on the boundary of the holes becomes equal to k in magnitude, and plastic flow may take place. Further increase in load causes the plastic regions to grow but they are initially completely contained in regions in which the strains are still elastic. The strains in the plastic regions, therefore, will still be of the same order of magnitude as the elastic strains in the surrounding regions. This state, according to W. Prager,[21] M. ASCE, is termed "contained plastic flow." At some load, often after regions of plastic flow have reached completely across the member, the plastic region is no longer constrained by elastic regions. The load at which this occurs is termed the limit load, and the member is now in a state of impending plastic flow. In the cases considered herein, large plastic deformations will then take place at no increase in load.

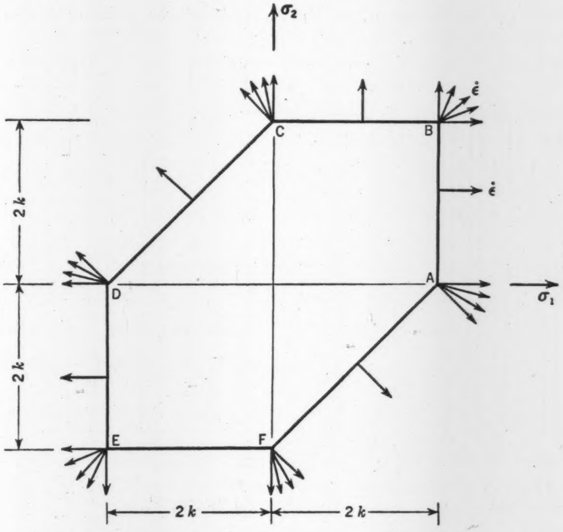

FIG. 3.—MAXIMUM-SHEARING-STRESS CRITERION FOR PLANE STRESS

The first basic limit-analysis theorem[3,4] is that the limit load is the largest load for which a statically admissible stress field can be found. A statically admissible stress field is defined as one which (*a*) satisfies equilibrium everywhere, (*b*) satisfies the stress boundary conditions, and (*c*) does not have a maximum shearing stress that exceeds k. Such a stress field may be discontinuous, as will be shown subsequently.

---

[21] "Plasticity for the Aerodynamicist," by W. Prager, *Journal of the Aeronautical Sciences*, Vol. 15, 1948, pp. 253–262.

The second basic theorem is that the limit load is the lowest load for which a kinematically admissible velocity field can be found. A kinematically admissible velocity field is defined as one in which (*a*) the strain rates are to be considered as plastic only; (*b*) the incompressibility condition is satisfied; and (*c*) the rate at which work is done by the external loads or surface tractions is equal to, or exceeds, the internal rate of dissipation of energy for the whole body under consideration. This theorem remains valid for velocity fields with surfaces of discontinuity through which the velocity component normal to the surfaces varies continuously while the tangential component is discontinuous.

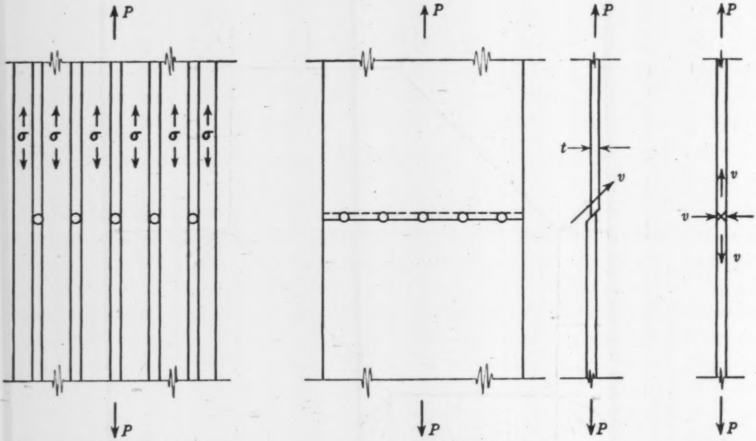

(*a*) Stress field (*b*) Velocity fields (*c*)

FIG. 4.—ONE-ROW CONFIGURATION

These surfaces may be treated as the limiting cases of a transition layer with continuous, but rapidly varying, tangential velocity components.

For plane stress and continuous velocity distributions, the internal rate of dissipation of energy per unit volume, D_{iv}, is expressed by

$$D_{iv} = \sigma_1 \dot{\epsilon}_1 + \sigma_2 \dot{\epsilon}_2 \qquad (5)$$

The value of D_{it}, the internal rate of dissipation of energy for the entire body, is obtained by integrating Eq. 5 over the volume of the body. It should be noted that D_{iv} for plane-stress fields is the scalar product of the vector from the origin to one of the stress points on the hexagon in Fig. 3 and the vector representing the plastic-strain rate. This product can be written as

$$D_{iv} = 2\,k\,|\epsilon|_{\max} \qquad (6)$$

in which $|\dot{\epsilon}|_{\max}$ is the magnitude of the absolutely largest principal component of the plastic-strain rate[22,23] $\dot{\epsilon}_1$, $\dot{\epsilon}_2$, or $\dot{\epsilon}_3$. For a surface of discontinuity, D_{ia} per unit area at any point in the surface is

$$D_{ia} = k\,v \qquad (7)$$

in which v is the change in the tangential velocity component across the surface of discontinuity at the point. The total rate of internal-energy dissipation for the whole surface is obtained by integrating Eq. 7 over the area of the surface.

The rate at which work is done by the external loads or surface tractions can be computed after a velocity field has been determined.

LIMIT LOADS FOR TESTED PATTERNS OF CIRCULAR HOLES

One-Row Configuration of Five Holes.—A stress field consisting of uniaxial tension in strips lying longitudinally between the holes is statically admissible if the tensile stress does not exceed $2\,k$ (Fig. 4(*a*)). In Fig. 4 it should be noted that the end boundary conditions on the sheet are the sheet being pulled by rigid bars rather than being subject to a uniform stress. As the sheet widens at the end, however, the two cases are in fact equivalent. Then,

$$P_l \geqq t\,(b - 5\,d)\,2\,k \qquad (8)$$

in which P_l is the limit load for the sheet, t denotes the thickness of the sheet, and $2\,k$ is the stress in the strips between the holes. As the limit load for a solid sheet would be

$$P_0 = 2\,k\,b\,t \qquad (9)$$

a lower bound for the ratio P_l/P_0 is

$$\frac{P_l}{P_0} = \frac{b - 5\,d}{b} \qquad (10)$$

One kinematically admissible velocity field for the one-row configuration is shown in Fig. 4(*b*), half of the sheet sliding with velocity v along a section through the holes 45° out of the plane of the sheet. In this case,

$$D_{ia} = k\,v \qquad (11)$$

for the entire discontinuity surface, and the total rate of internal energy dissipation is $k\,v$ times the area of the surface. Thus, for very thin sheets, the total internal energy dissipation rate is

$$D_{it} = \sqrt{2}\,t\,(b - 5\,d)\,k\,v \qquad (12)$$

The rate of external work, W_e, done on the sheet by load P is

$$W_e = \frac{P\,v}{\sqrt{2}} \qquad (13)$$

---

[22] "Limit Design of Reinforcements of Cut-Outs in Slabs," by P. G. Hodge, Jr., and W. Prager, *Report B11-2*, Office of Naval Research, Brown Univ., Providence, R. I., 1951.

[23] "The Application of Limit Analysis to Punch Indentation Problems," by R. T. Shield and D. C. Drucker, *Journal of Applied Mechanics*, Vol. 20, 1953, pp. 453–460.

Equating Eqs. 12 and 13 leads to a value of P which in this case is an upper bound for the limit load P_l. Therefore,

$$\frac{P_l}{P_0} \leqq \frac{b - 5\,d}{b} \quad\ldots\ldots\ldots\ldots\ldots\ldots\ldots\ldots (14)$$

The same result is obtained with the symmetric discontinuous velocity pattern in Fig. 4(*c*). As the upper and lower bounds coincide, the solution for the limit load is exact for the maximum-shearing-stress criterion within the assumptions of the theory for very thin sheets, and

$$\frac{P_l}{P_0} = \frac{b - 5\,d}{b} = 0.75 \quad\ldots\ldots\ldots\ldots\ldots\ldots\ldots\ldots (15)$$

for $b = 10$ in. and $d = \frac{1}{2}$ in.

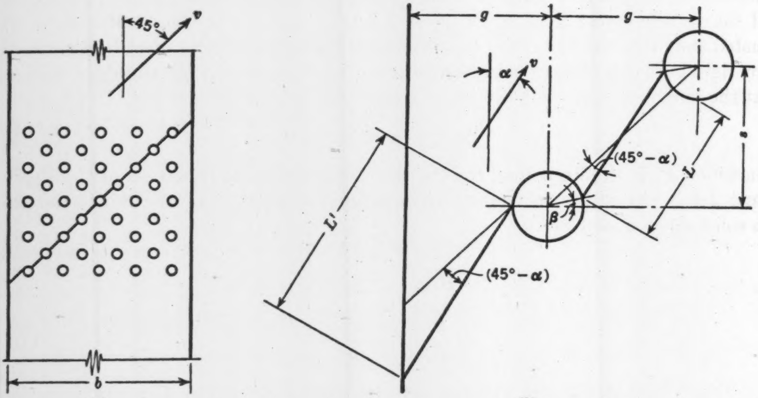

FIG. 5.—VELOCITY FIELDS FOR NINE-ROW CONFIGURATION

The restriction to sheets of thicknesses that are small compared to the hole diameter is clear from Fig. 4. Out-of-plane sliding on a 45° angle would take place on an appreciably larger area than $(b - 5\,d)\,t\,\sqrt{2}$ for thick plates.

Nine-Row Configuration.—A statically admissible stress field, in which all the holes have been taken out and which is similar to that for the one-row configuration, results in

$$P_l \geqq (b - 9\,d)\,2\,k \quad\ldots\ldots\ldots\ldots\ldots\ldots\ldots\ldots (16)$$

and

$$\frac{P_l}{P_0} \geqq \frac{b - 9\,d}{b} = 0.55 \quad\ldots\ldots\ldots\ldots\ldots\ldots\ldots\ldots (17)$$

A simple, kinematically admissible velocity field is obtained by letting one part of the sheet slide on two sets of planes perpendicular to the plane of the sheet and through the nine holes on a 45° plane, as shown in Fig. 5(*a*). Here again, the internal dissipation, D_{it}, is k times the area of the surface of sliding multiplied by the discontinuity velocity, v, or

$$D_{it} = [b\sqrt{2} - (8\,d + \sqrt{2}\,d)]\,t\,k\,v \quad (18)$$

The rate at which work is done by the external force is

$$W_e = \frac{P\,v}{\sqrt{2}} \quad (19)$$

Eqs. 18 and 19 give

$$P_l \leqq k\,t\,[2\,b - (8\sqrt{2} + 2)\,d] \quad (20)$$

or

$$\frac{P_l}{P_0} \leqq 1 - (4\sqrt{2} + 1)\,\frac{d}{b} = 0.67 \quad (21)$$

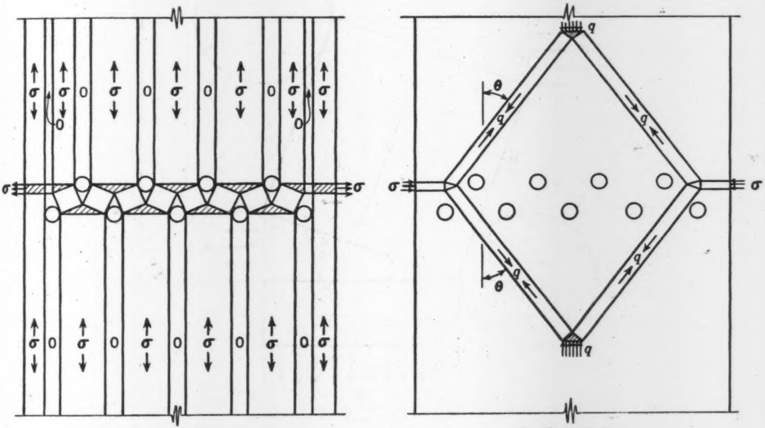

(*a*) Part (*b*) Remainder

FIG. 6.—STRESS FIELD, TWO-ROW CONFIGURATION

This result may be improved by changing the angle of sliding slightly, as shown in Fig. 5(*b*). Although $L' + 4\,L$ is increased, $v \cos \alpha$ likewise becomes larger. An angle $\beta = 28°$, corresponding to $\alpha = 36°$, results in

$$\frac{P_l}{P_0} \leqq 0.63 \quad (22)$$

Two-Row Configuration.—The stress field which was used for the nine-row configuration is statically admissible for the two-row configuration. Also, the velocity field used for the one-row configuration is a kinematically admissible velocity field for the two-row configuration. Thus,

$$0.55 \leqq \frac{P_l}{P_0} \leqq 0.75 \quad (23)$$

In fact, these are bounds for all configurations with two or more rows of holes.

To improve the lower bound, one might consider the stress field which is a superposition of the stress fields shown in Figs. 6(*a*) and 6(*b*). The shaded regions are isotropic stress regions ($\sigma_1 = \sigma_2$). A detail of the manner in which the stress field is taken through the holes is shown in Fig. 7. Fig. 6(*b*) incorporates a discontinuous stress field,[23] the details of which are sketched in Fig. 8(*a*). The maximum shearing stress is not increased when the stress field in Fig. 6(*b*) is superposed on the stress field in Fig. 6(*a*) if the angle $\theta = 35°$ and *c* is made as large as possible (Fig. 8(*a*)). For the present configuration—for $\rho = 19.9°$, which minimizes L'', and for $\theta = 35°$—a lower bound on P_l/P_0 is 0.70. Therefore, for the two-row configuration,

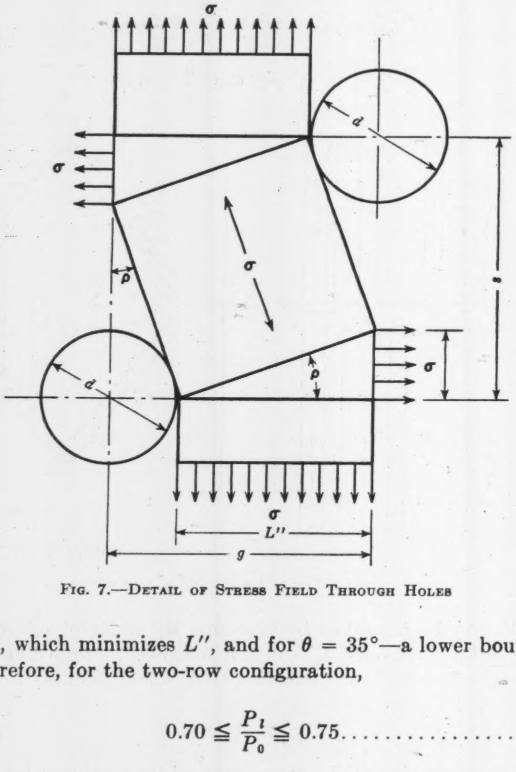

FIG. 7.—DETAIL OF STRESS FIELD THROUGH HOLES

$$0.70 \leqq \frac{P_l}{P_0} \leqq 0.75 \qquad (24)$$

Three-Row Configuration (3S).—For a three-row configuration a stress field similar to that applied to the two-row configuration can be used, as shown in Fig. 8(*b*). The geometry is such that an angle $\theta = 33°$ for the discontinuous part of the stress field is possible without increasing the maximum shear. However, the excess side tensile force is twice as large as that for the two-row configuration; hence, the lower bound of the limit load is correspondingly reduced.

For this configuration,

$$\frac{P_l}{P_0} \geqq 0.66 \ldots\ldots\ldots\ldots\ldots\ldots\ldots\ldots (25)$$

A kinematically admissible, discontinuous velocity field is shown in Fig. 9(*a*). The upper part of the sheet moves up with velocity *v*, the lower part moves down with velocity *v*, and the two wedges, ABC and DEF, move laterally

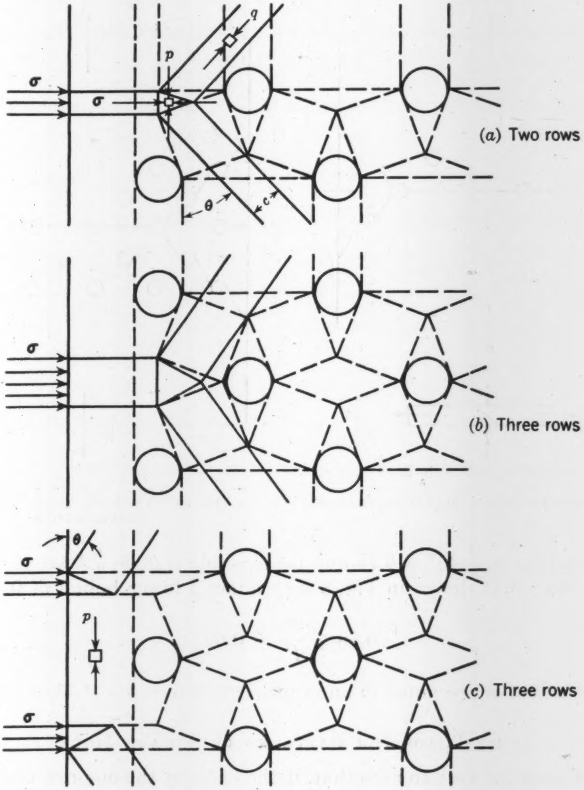

(*a*) Two rows

(*b*) Three rows

(*c*) Three rows

FIG. 8.—DISCONTINUOUS STRESS FIELDS

with velocity $v' = v \tan \alpha$. The details of the velocity field along BD are shown in Fig. 9(*b*). The upper bound on P_l/P for the simplest case of $\alpha = 45°$ is 0.73 and for $\alpha = 36°$ is 0.72; therefore,

$$0.66 \leqq \frac{P_l}{P_0} \leqq 0.72 \ldots\ldots\ldots\ldots\ldots\ldots\ldots\ldots (27)$$

Three-Row Configuration (*3L*).—In Fig. 8(*c*) there is shown a statically admissible field somewhat more elaborate than that for the two-row case which gives

$$\frac{P_l}{P_0} \geqq 0.67 \qquad (28)$$

Five-Row Configuration.—A velocity field of the type applied to the 3S three-row configuration is used for a five-row configuration (Fig. 10). The upper bound for $\alpha = 45°$ is 0.71 and for $\alpha = 36°$ is 0.69. A stress field more elaborate than that shown in Fig. 8 determines a lower bound of 0.58 so that

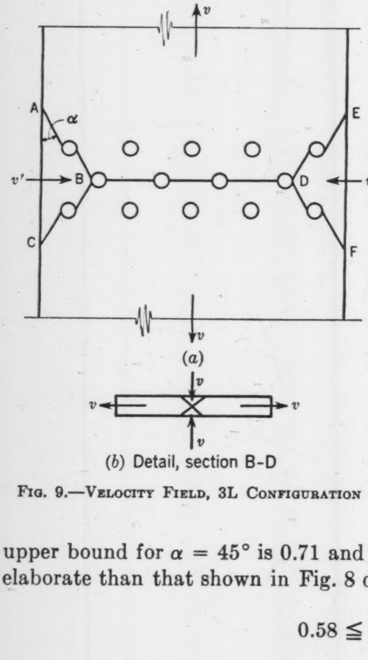

(*a*)

(*b*) Detail, section B-D

FIG. 9.—VELOCITY FIELD, 3L CONFIGURATION

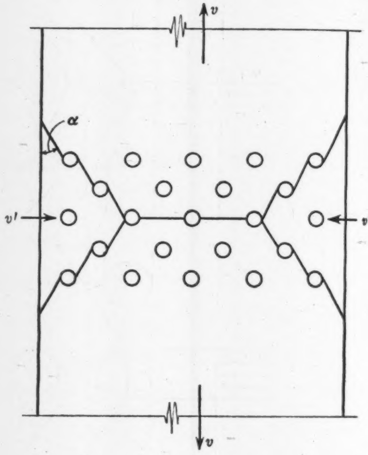

FIG. 10.—VELOCITY FIELD, FIVE-ROW CONFIGURATION

$$0.58 \leqq \frac{P_l}{P_0} \leqq 0.69 \qquad (29)$$

The lower bound is not much of an improvement over the 0.55 of Eq. 17.

LIMIT LOADS FOR PATTERNS OF SQUARE HOLES

It is of some interest to note that, if the holes in the one-row configuration and the nine-row configuration were ½-in. squares, the limit loads would be exactly

$$\frac{P_l}{P_0} = 0.75 \qquad (30)$$

for the one-row configuration, and

$$\frac{P_l}{P_0} = 0.55 \qquad (31)$$

for the nine-row configuration. Fig. 11 shows the symmetric 45° velocity pattern which gives the same result as the simple one-plane slide of the type shown in Fig. 5.

THE ($s^2/4\,g$)-RULE

A load-carrying plate in a riveted joint which is transmitting some or all of its load to cover plates or other members differs essentially from the perforated plates previously described. The rivets do not act simply as plugs but take load out of the plate (Fig. 12). Yielding, in the sense of reaching a limit load, may occur across the first rivet holes or by some combination of first and second holes but generally will not involve additional rows because the loaded rivets interfere. One possible pattern is yielding in zones extending between the holes, as shown in Fig. 13. The lower part of the plate is assumed to move in the direction of P with a velocity v. Each zone inclined at α to the direction of P is then stretched at a speed $v \sin \alpha$ and sheared at $v \cos \alpha$. For a very thin plate, using the maximum-shearing-stress criterion, this is equivalent to stretching at a speed,

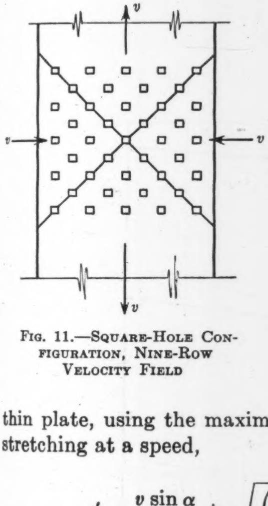

FIG. 11.—SQUARE-HOLE CONFIGURATION, NINE-ROW VELOCITY FIELD

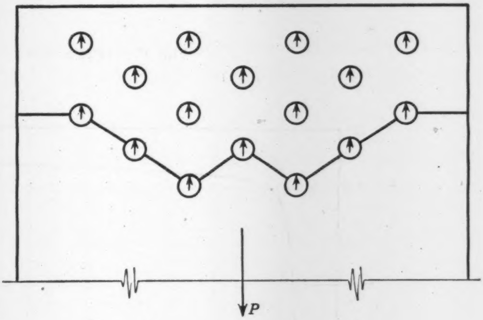

FIG. 12.—RIVETED JOINT

$$v' = \frac{v \sin \alpha}{2} + \sqrt{\left(\frac{v \sin \alpha}{2}\right)^2 + \left(\frac{v \cos \alpha}{2}\right)^2} = \frac{v}{2}\,(\sin \alpha + 1) \qquad (32)$$

in analogy to

$$\epsilon_{\max} = \frac{\epsilon}{2} + \sqrt{\left(\frac{\epsilon}{2}\right)^2 + \left(\frac{\gamma_s}{2}\right)^2} \qquad (33)$$

the expression for maximum strain in terms of the normal strain ϵ and shearing strain γ_s. An upper bound on the contribution to P_{l1} from the length L of the zone of yielding is then obtained from

$$P_{l1}\, v \leqq P_1\, v = 2\, k\, v'\, L\, t \qquad (34)$$

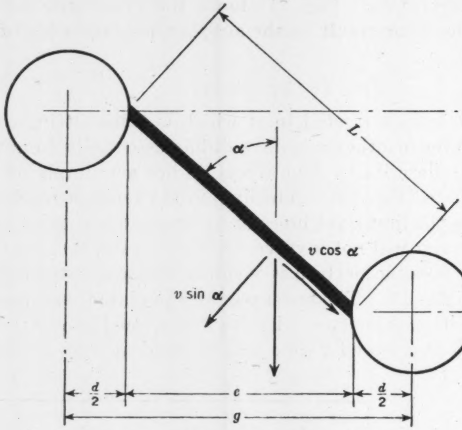
L
α
s
v cos α
v sin α
d/2
c
d/2
g

FIG. 13.—($s^2/4\,g$)-RULE

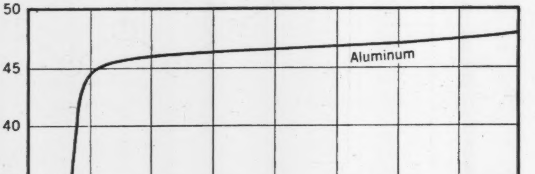

FIG. 14.—STRESS-STRAIN CURVES FOR STEEL AND ALUMINUM SHEETS

Thus,

$$P_{l1} \leqq k\,t\,L\,(1 + \sin\alpha) \ldots\ldots\ldots\ldots\ldots\ldots (35)$$

If, as shown in Fig. 13, the zone of yielding is assumed to extend between the horizontal-diameter extremes at the holes so that

$$L \sin\alpha = e \ldots\ldots\ldots\ldots\ldots\ldots (36)$$

and

$$L^2 = e^2 + s^2 \ldots\ldots\ldots\ldots\ldots\ldots (37)$$

then

$$P_{l1} \leqq k\,t\,(\sqrt{e^2 + s^2} + e) = k\,t\,e\sqrt{\left(1 + \frac{s^2}{e^2} + 1\right)}$$

$$= k\,t\,e\left(2 + \frac{s^2}{2\,e^2} - \cdots\right) = 2\,k\,t\,e\left(1 + \frac{s^2}{4\,e^2} - \cdots\right) \ldots (38)$$

which is, in a sense, an $(s^2/4\,e)$-rule for the range of s which is small compared with e and is close to the $(s^2/4\,g)$-specification. This upper bound can be improved (that is, lowered) by choosing a better value of α. It appears that the $(s^2/4\,g)$-rule is reasonable for riveted joints where the rivets take load out of the plate considered.

CRITERION OF YIELDING

If the Mises criterion is used instead of the maximum-shearing-stress criterion as previously cited, the yield curve is the circumscribing ellipse to the hexagon in Fig. 3. The shearing stress on the planes of sliding discontinuity is then larger in the ratio 2 to $\sqrt{3}$ or 1.155. All computed upper bounds for the perforated plates are therefore increased by a little more than 15%. Lower bounds remain lower bounds, and stress patterns considerably more elaborate would be needed to raise them.

EXPERIMENTAL PROGRAM

Low-carbon, hot-rolled sheet steel was used in the first series of tests because of its flat yield characteristic and because it was hoped that the mechanical properties would be sufficiently uniform so that the tests would not be complicated by local variations of these properties. The variation in yield strength was so large that several additional series of tests were run on hot-rolled sheet steel.

A 61S-T6 aluminum alloy was chosen to check the results with a material which has a much smaller ultimate elongation than hot-rolled steel, and which does not have a truly flat yield characteristic (Fig. 14). All specimens were cut with the long dimension in the direction of rolling from sheets approximately $\frac{1}{16}$ in. thick.

The sheet thickness was measured to ± 0.0002 in. at the intersection points of a 1-in. grid ruled over the central 10-in.-long test section of each sheet. The readings for each sheet were averaged, the average being taken as the sheet thickness. The sheet widths were machined to 10.000 ± 0.005 in., and the 0.500-in.-diameter holes were drilled with a precise jig. Lubricated spherical

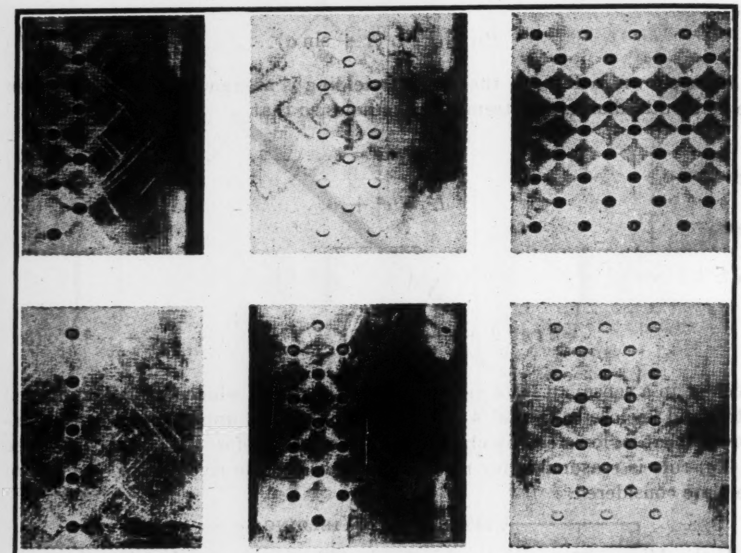

FIG. 16.—YIELD PATTERNS

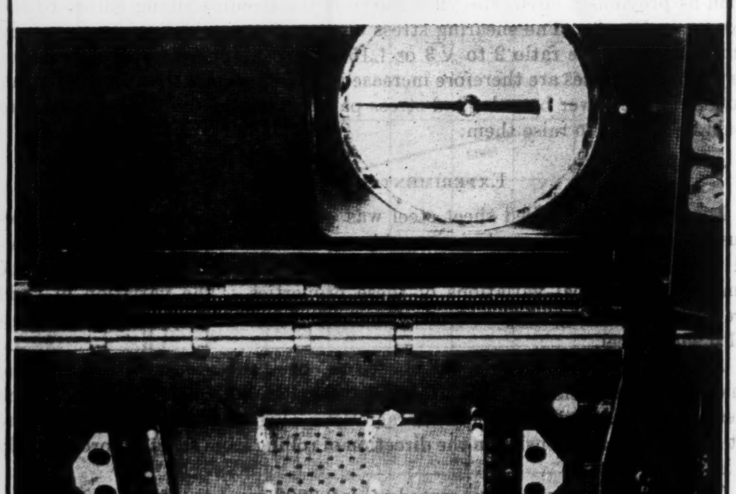

FIG. 15.—TEST ARRANGEMENT

seats and nuts were incorporated in the grip system. Two extensometers, designed for simplicity and ruggedness, were mounted—one on each edge of the sheet—with a 10-in. gage length. As a check on the performance of the grips, a dial gage was used to measure the relative displacement of the heads of the testing machine. The testing machine showed a maximum error of + 0% and − 0.3%. The general test arrangement is shown in Fig. 15.

The test pieces were pulled to a total extension (in the 10-in. gage length) which was sufficient to insure flow across the specimen. They were not purposely carried to fracture.

Originally, it had been hoped that uniformity of mechanical properties (as determined from three test pieces with no holes) would allow the accurate determination of the yield stress of the material in each series. However, uniformity did not exist, and it was necessary to cut tension-test coupons from the test pieces themselves, or to use pieces at each end of each large test piece, for the purpose of determining the yield stress of that particular test piece. Coupons 9.5 in. wide could be obtained from the test specimens because yielding in the 10-in. specimens was confined to the region of the holes. In the computations, the yield stress for each large test piece was taken arbitrarily to be the average obtained from the test coupons from that piece. This point will be cited in more detail subsequently.

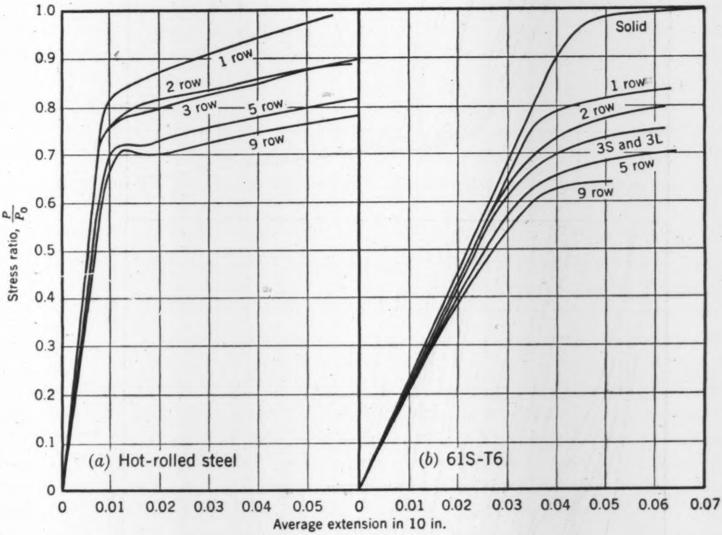

FIG. 17.—STRESS RATIO VERSUS EXTENSION

Photographs of the flaked scale patterns of representative hot-rolled steel test pieces are shown in Fig. 16. It should be noted that Fig. 16 shows the pattern after the tests were completed. However, the patterns are interesting

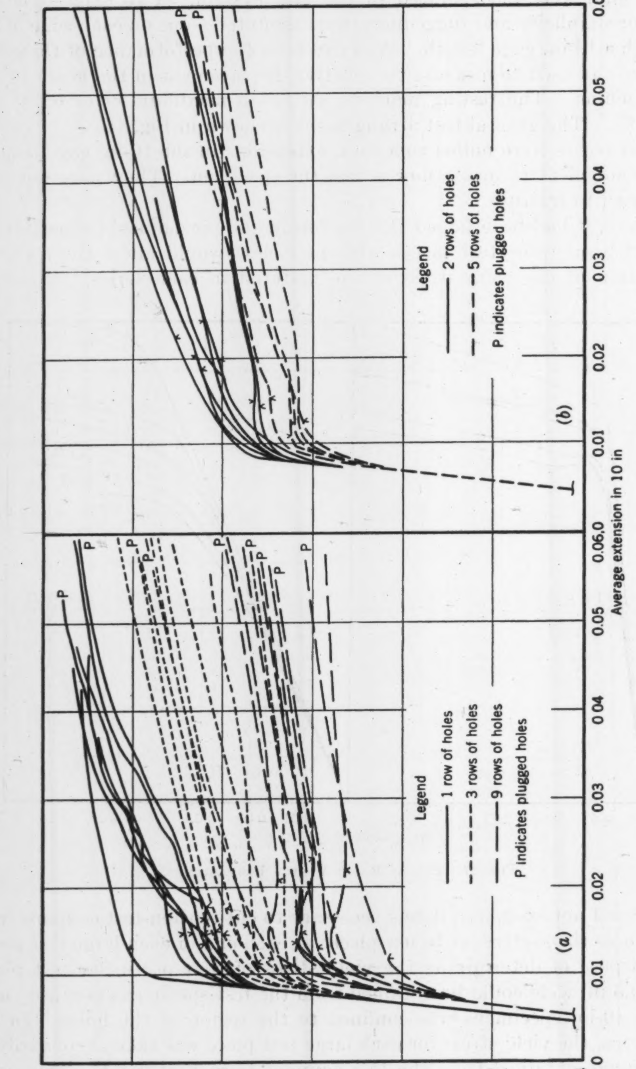

FIG. 18.—SCATTER OF TEST RESULTS

in that the tendency to yield along the diagonal through the holes is clearly shown for configurations with two or more rows of holes. Visual observation of the one-row configuration during tests established that the yield occurred initially along a transverse section through the holes, as had been assumed for the velocity field in the analysis. One sheet was tested with strain gages mounted in the transverse section through the holes to establish the limit load accurately and to demonstrate that large strains occur for a small bend in the over-all load-deformation curve.

A series of curves for specimens from one large sheet of hot-rolled steel is presented in Fig. 17(*a*). The ordinate is made dimensionless by dividing the load P by P_0, the product of the "average" yield stress and the gross area Beginning with the one-row configuration, the limit load is marked by hardly more than an indentation in the curve; the curves then flatten out increasingly at the limit load as the number of rows of holes is increased. For the nine-row configuration, there are marked upper and lower yields. In Fig. 17(*b*) is a similar set for the 61S-T6 specimens which exhibit the same general pattern except, of course, for the absence of an upper yield. Placing plugs in the holes has small effect in any case, except for details of shape.

In Figs. 18(*a*) and 18(*b*) the large scatter which was obtained for the hot-rolled steel sheets is demonstrated. To avoid confusion, the one-row, three-row, and nine-row cases are separated from the two-row and five-row cases. All curves are brought in tangent to the average elastic line by slight displacements left or right to minimize distortion of shape. Each limit load selected is indicated by a small arrowhead because in several cases the choice was quite arbitrary. Despite the scatter, it is clear that there is an appreciable and significant difference between the limit loads for the different configurations of holes.

The questions which should be answered are—why do the data for any one configuration of holes cover so wide a range and which values should agree with the limit-analysis theory. The temptation is to take the average value; if this is done, agreement is obtained, in principle, with the limit-analysis theory although the values are above those computed with the maximum-shearing-stress criterion. Using an average value to compare theory and experiment is proper, however, only if the deviations are caused by haphazard factors such as experimental error. In these tests there would seem to be no possibility of instrumental error of appreciable magnitude compared with the observed variations, so that averaging is suspect.

Some oversimplified examples explain the difficulty and indicate that the lower values of P_l/P_0, the stress ratio, are the ones which should agree with an idealized theory. Suppose, first, that the yield stress is constant across the sheet but varies periodically between 25,000 lb per sq in. and 30,000 lb per sq in. along the length of the sheet. If there are no holes, a yield stress of 25,000 lb per sq in. will be found experimentally because the weakest section will govern. A sheet with one row of transverse holes will exhibit a variation in limit load corresponding to the range of from 25,000 lb per sq in. to 30,000 lb per sq in., or more than 15%, depending on whether the line of holes is located in a weak or a strong region. If a large number of tests are run, the results will scatter as in Fig. 18, and clearly the answer which should agree with theory is the lowest limit load obtained, barring experimental error. On the other hand, if the yield stress varies in the transverse direction but is constant along the length of the sheet, the test result obtained for a specimen without holes will have an average value of 27,500 lb per sq in., and the average of the one-row cases should be compared with theory. In general, the variation in yield stress will not follow either pattern and will tend to be somewhat random. Under these conditions, in most cases there will be some way for the large test coupons, without holes, to yield at approximately 25,000 lb per sq in. whereas the sheets with holes will usually have stronger regions impeding plastic deformation.

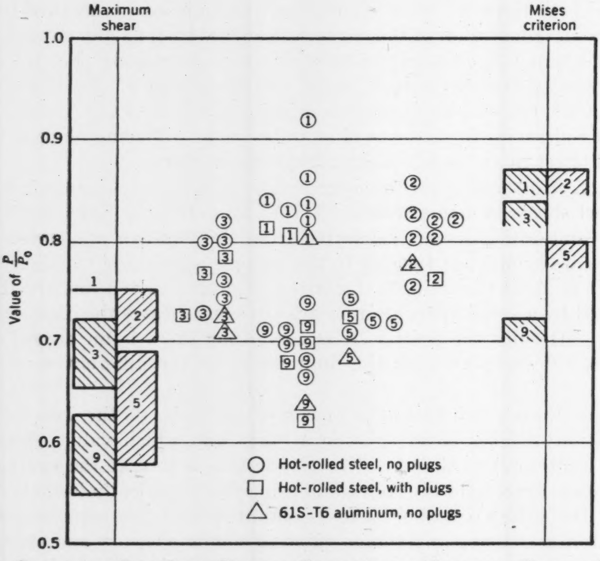

FIG. 19.—SUMMARY OF TEST DATA (NUMBERS DESIGNATE THE NUMBER OF ROWS OF HOLES)

The lower values of limit load, although not necessarily the lowest, should then correspond to the theory.

A variation in thickness has an effect analogous to a variation in yield stress but in the experiments did not exceed 2%, whereas the yield stress determined by small test coupons in one extreme case varied by more than 25% over the entire sheet. An interesting verification of the importance of local variations in yield is provided by comparing the yield stress obtained from the small test coupons (approximately 3 sq in. of sheet) with that of the large test coupons which were twenty to sixty times larger than this area. Several cases of small coupons ranging from 25,000 lb per sq in. to 29,000 lb per sq in. were obtained whereas the large coupons in the same region of the sheet tested between 25,000 lb per sq in. and 26,000 lb per sq in.

A summary of all experimentally determined stress ratios, P_l/P_0 is given in Fig. 19; the points are subject to considerable latitude in their position. Inspection of Figs. 17 and 18 shows that the limit load is not defined precisely in most experiments with a work-hardening material. Nevertheless, all indications are that the answers of the maximum-shear-stress theory are reasonable for an ideal homogeneous material. However, as usual, a compromise between the Mises criteria and the maximum-shear stress criteria will probably be better. The use of a dimensionless plot enables comparison of the data for aluminum and steel. The results for the aluminum specimens are in the low range of the results for steel. Because aluminum has uniform properties, a further confirmation of the influence of variable yield stress in the steel sheet seems to be provided.

CONCLUSIONS

Both the limit analysis and the tests show clearly that the configuration of holes is important in a sheet under tension and that it must be taken into account for an accurate analysis of open or plugged holes. As might be expected, this is not done properly by the $(s^2/4\,g)$-rule for riveted joints. The specification rule is shown to be based conceptually on an upper-bound computation for riveted joints in which the rivets take load out of the sheet being analyzed.

The value of 0.75 for P_l/P_0 is given by the rule for all configurations of holes tested. This is appreciably above many of the test results which range from 0.63 to 0.92, depending on the number of rows of holes and the uniformity of the test specimen.

ACKNOWLEDGMENTS

The results presented in this paper were obtained in the course of research sponsored by the Office of Naval Research under Contract N7onr 35801.

Appreciation is expressed to Robert Carlson and Anthony Gemma for performing many of the check tests, to William Johnson for machining all the specimens, and to C. K. Liu and F. D. Stockton for helpful advice.

APPENDIX

The following symbols, adopted for use in the paper and for the guidance of discussers, conform essentially with "American Standard Letter Symbols for Structural Anslysis" (ASA Z10.8–1949), prepared by a committee of the American Standards Association with ASCE representation, and approved by the Association in 1949:

b = gross width;
c = distance in Fig. 8;

D = rate of dissipation of energy:
  D_e = external rate of dissipation of energy;
  D_i = internal rate of dissipation of energy;
  D_{ia} = internal rate of dissipation of energy per unit area;
  D_{it} = total internal rate of energy dissipation;
  D_{iv} = internal rate of dissipation of energy per unit volume;
d = diameter of the hole;
g = distance between gage lines or gage of rivets;
k = yield stress in pure shear
L = length in Fig. 5(*b*):
  L' = length in Fig. 5(*b*);
  L'' = length in Fig. 7;
P = load:
  P_l = limit load for the entire sheet;
  P_0 = limit load for a solid sheet;
r = width of strip to be deducted;
s = pitch or stagger of rivets;
t = thickness of the sheet;
v = change in the tangential velocity component across the surface;
v' = lateral velocity;
W_e = work done by external force;
x = fractional part of a hole to be deducted;
α = angle in Fig. 5(*b*);
β = angle in Fig. 5(*b*);
γ_s = shearing strain
ϵ = strain;
$|\dot{\epsilon}|_{\max}$ = absolutely largest principal component of the plastic-strain rate;
θ = angle in Fig. 6(*b*);
ρ = angle in Fig. 7; and
σ = stress.

DISCUSSION

WILLIAM H. MUNSE,[24] A. M. ASCE.—It is gratifying to learn a new approach to a problem which engineers have been studying for many years—that of determining the net area of a tension member. It is hoped, however, that the analysis and tests presented by Messrs. Brady and Drucker will not be considered the complete answer but only part of the answer or a starting point from which to build a better answer than is now (1955) available. These tests, as well as many of the previous tests on net sections,[25] have been conducted on flat-plate specimens and then analyzed in terms of design rules which are used for riveted or bolted connections in which the load transfer may differ greatly from that of the flat plate. Engineers need an accurate analysis or analyses for the behavior of tension members but will want to be assured that the theory is applicable to realistic members.

The limit-load theorems presented by the authors provide a new viewpoint in so far as the behavior of tension members is concerned. Consequently, it would have been helpful if the tests had been carried to failure and the relationships between the limit load and ultimate load-carrying capacity of the plates determined. This information would have made possible a comparison—at least in part—of the result of these tests with the many tests reported in the literature.

In some structures, general yielding across an entire member may produce failure of the member or, at least, exceed its limit of serviceability. In other instances initial yielding or, possibly, ultimate load-carrying capacity may be the limiting factor of serviceability and a more reasonable value on which to base the working load. Thus, if the material is to be used efficiently, the mode of failure as well as the limit load must be considered in any determination of working stresses.

As an example, one might consider a long tension member in a bridge. When general yielding occurs in the connections of such a member, this yielding is usually restricted to the first row of fasteners in the connections at either end of the member, which is a relatively small part of the member. The effect of this plastic deformation on the over-all deformation of the entire member may be small and may have little effect on the usefulness of the member. In all probability, it would be a general yielding of the entire member that would be the limiting factor for such a structure rather than the yielding at the connections. However, even after the entire member has been subjected to a general yielding, the member would still retain considerable load-carrying capacity.

In tests[26] conducted at the University of Illinois at Urbana on 18-in. I-sections with ½-in. gusset plates, it was found that the distribution of load in the members was greatly different from that generally obtained in flat plates. This difference in distribution results from the fact that the load is taken out of the member through only the flanges whereas a large percentage of the area of the members is concentrated in the web. However, strain measurements on the webs of the members provided data which can be correlated with the limit-analysis study by the authors. A general indication of the behavior of the members can be obtained from the following tabulation:

---

[24] Research Associate Prof. of Civ. Eng., Univ. of Illinois, Urbana, Ill.

[25] "A Study of the Practical Efficiency Under Static Loading of Riveted Joints Connecting Plates," by W. M. Wilson, William H. Munse, and M. A. Cayci, *Bulletin 402*, Eng. Experiment Station, Univ. of Illinois, Urbana, Ill., 1952.

[26] "A Study of the Behavior of Large I-Section Connections," by J. R. Fuller, T. F. Leahey, and William H. Munse, *Proceedings-Separate No. 659*, ASCE, Vol. 81, April, 1955.

Loading conditions	Average gross stress, in kips per square inch
Initial yielding	15.0
General yielding in joint (critical section)	36.4
General yielding in gross section	37.6
Ultimate strength of member	50.2

From the test data, it was found that general yielding in the joint (when the yield-point strain was attained in the center of the web) occurred when the stress ratio P_l/P_0, or yield-strength efficiency for the member, was 97%. However, the members failed at a test efficiency of approximately 74.5%. It appears that parts of the section may have been strained into the work-hardening range when the center of the web at the critical section reached the yield-point strain. These data suggest that several analyses may be necessary to explain completely the behavior of tension members—an elastic analysis, a limit analysis, and an empirical ultimate-strength relationship.

It is realized that the foregoing raises questions concerning the applicability of limit analysis to tension members. Nevertheless, it is hoped that the authors will find it possible to pursue their study further and to expand it to include actual joints of various types as well as other factors such as variations in pitch, gage, material properties, and the preparation of the fastener holes. By determining the limit loads as well as the ultimate load-carrying capacity it may be possible to evaluate this information in terms of the limit-analysis theorems as well as other concepts based on the ultimate strength or elastic properties of the materials.

PAUL P. BIJLAARD,[27] M. ASCE.—Computations similar to those made by the authors were published (in Dutch) by the writer in 1931, using the maximum-shearing-stress yield criterion[28] as well as the Mises criterion.[29] In these computations the subject is covered in more detail than it is in those of Messrs. Brady and Drucker; a footnote summary (in English) of these computations is available.[30] In addition to his computations, the writer made elaborate experiments.[28] It will be shown subsequently in which situations the authors obtained essentially the same results as those of the writer's earlier investigations and in which cases the two differ.

---

[27] Prof. of Structural Eng., Cornell Univ., Ithaca, N. Y.

[28] "Resistance of a Section of a Plate Between Rivets in an Oblique Row, Calculated from the Mohr Criterion of Plasticity," by P. P. Bijlaard, *de Ingenieur*, The Hague, Holland, Vol. 46, 1931, pp. B.47–B.57.

[29] "Resistance of a Weakened Oblique Section of a Plate Subjected to Tension, Calculated by the Plasticity Criterion of Huber-Hencky," by P. P. Bijlaard, *ibid.*, pp. B.249–B.251.

[30] "Theory of Local Plastic Deformations," by P. P. Bijlaard, *Publications*, International Assn. for Bridge and Structural Eng., Vol. 6, 1940–1941, pp. 27–44, footnote on p. 35.

The writer showed that minor plastic deformations in a weakened section (AB in Fig. 20 or ABB′A′ in Fig. 21) result in a state of stress which produces maximum resistance against deformation before the section fails. This result assumes an elasto-plastic stress-strain diagram of the mild-steel type. This situation applies if the maximum-shearing-stress yield criterion is used, and—at the same time—plastic deformation is assumed to occur by sliding along the planes of maximum shear stress.[28] The situation also applies if the Mises criterion is used; at the same time, plastic deformation is assumed to occur quasi-isotropically—that is, in the same way as the elastic deformation, but with a varying plastic modulus and with a Poisson ratio[29,30] of $\frac{1}{2}$.

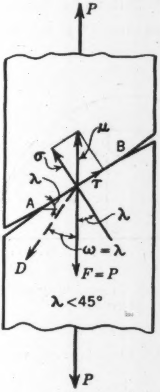

FIG. 20.—OBLIQUE WEAKENED SECTION

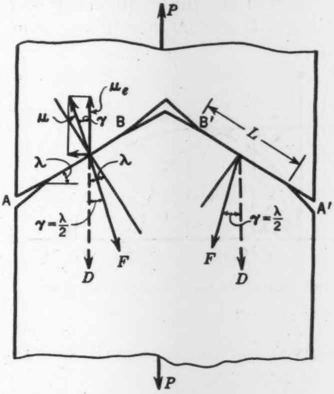

FIG. 21.—SYMMETRICAL WEAKENED SECTION

If the maximum-shearing-stress criterion is used for an oblique section such as that in Fig. 20, one obtains a limit curve for the total stress,

$$\mu = \sqrt{\sigma^2 + \tau^2} \qquad (39)$$

which is given in Fig. 22 for any angle λ. For $\lambda = 0$ the total stress is

$$\mu = \sigma = \sigma_{ys} = 2\,k \qquad (40)$$

in which σ_{ys} is the yield stress in tension. The limit curve consists of a quarter circle with its center at $\sigma = k$ for $\lambda \leqq 45°$ and a straight line $\tau = k$ for $\lambda \geqq 45°$. For $\lambda \geqq 45°$, the state of stress in the oblique section AB at the limit load is given by a circle that touches the line PN at the end point Q of the pertinent vector μ_{AB}, which represents the total stress μ on the weakened section AB (Fig. 22). However, the pure tensile stress assumed by the authors in obtaining Eq. 16 for $\lambda \geqq 45°$ would lead to a limit curve given by the dashed quarter circle NO, which results in much lower limit loads than the limit curve PN.

The writer also showed[28] that—if the plate is subjected to tensile forces P, subsequent to fully plastic deformation in the section AB—the relative movement of the elastic part of the plate below AB with respect to that above AB is given by the dashed arrow D (the direction of yielding). For $\lambda \leqq 45°$ (as in Fig. 20, in which the planes of maximum shear stress are not perpendicular to the middle plane of the plate), the arrow D subtends an angle $\omega = \lambda$ with the axis of the plate. If $\lambda \geqq 45°$ the planes of maximum shear stress are perpendicular to the middle plane of the plate so that the direction of yielding coincides with AB, and

$$\omega = 90° - \lambda \qquad (41)$$

In a symmetrical case (Fig. 21), it is not necessary for the forces F, transferred by the oblique sections AB and A′B′, to be in the direction of the total force P, acting in the axis of the plate. If the forces F deviate by an angle γ from the axis of the plate, they will subtend angles $\lambda - \gamma$ with the normals to the sections AB and A′B′. Then, from Fig. 23, the total stress μ in AB and A′B′ is given by the vector OR, and the effective stress in the direction of the force P is given by

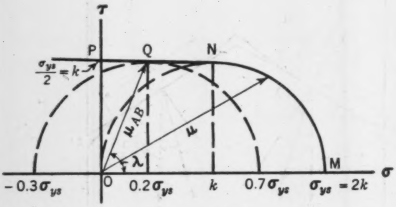

FIG. 22.—LIMIT CURVE, OBLIQUE SECTION

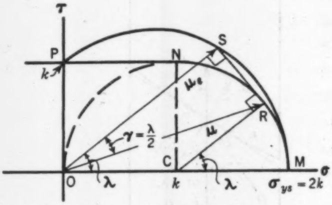

FIG. 23.—LIMIT CURVE, SYMMETRICAL SECTION

$$\mu_e = \mu \cos \gamma \qquad (42)$$

and is shown in Fig. 23 as the vector OS. It follows directly from Fig. 23 that μ_e = OS will be as large as possible if the perpendicular RS to OS is tangent to the limit curve MNP. In that case CR is parallel to OS and

$$\sphericalangle \text{MOR} = \lambda - \gamma = \frac{\lambda}{2} \qquad (43)$$

so that $\gamma = \lambda/2$. Hence, the limit curve for the effective stress μ_e for symmetrical sections is given by the locus MSP of the feet S of the perpendiculars RS—the pedal curve to the curve MNP. From Fig. 23,[28]

$$\mu_e = k\,(1 + \cos \lambda) \qquad (44)$$

so that the maximum force which a section AB or A′B′ in Fig. 21 can take is

$$\frac{P}{2} = k\,t\,L\,(1 + \cos \lambda) \qquad (45)$$

Eq. 35 is identical with Eq. 45 because the angle α is the complement of the angle λ.

Comparison of Figs. 20 and 21 shows why the forces F, acting on each of the sections AB and A′B′, will establish themselves in such a way that $\gamma = \lambda/2$. In that case, the forces F subtend angles as given by Eq. 43 with the normals to the sections AB and A′B′. Hence, from Fig. 20 the directions of yielding D will subtend angles $\omega = \lambda/2$ with the forces F so that from Fig. 21 the vectors D are parallel to the axis of the plate. It is obvious that the directions D must be parallel to each other because the elastic lower part of the plate in Fig. 21 moves in one direction only. Furthermore, from symmetry, D must be parallel to the axis of the plate.

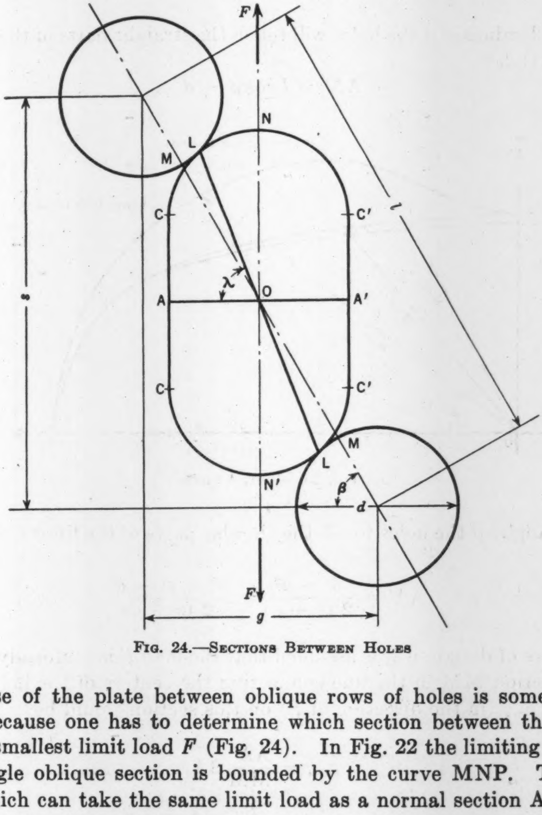

FIG. 24.—SECTIONS BETWEEN HOLES

The case of the plate between oblique rows of holes is somewhat more intricate because one has to determine which section between the holes will fail at the smallest limit load F (Fig. 24). In Fig. 22 the limiting total stress μ for a single oblique section is bounded by the curve MNP. The oblique sections which can take the same limit load as a normal section AA′ (normal to the force F), with cross-sectional area A, must have cross sections $2\,k\,A/\mu$. Using a value of μ from Fig. 22, it follows that all those equivalent oblique sections through point O (Fig. 24) are bounded by the curve ANA′N′, consisting of two straight lines of lengths equal to AA′ and two semicircles with diameters equal to AA′. For example, any oblique section LL, subtending an angle λ

with the section AA′, which is normal to the force F, has the same limit load as the section AA′. Consequently, that section LL between the holes which can take the smallest load is obtained by placing the limit curve ANA′N′ (using an appropriate scale) between the holes so that it touches the perimeters of the holes. Then the section connecting the two tangent points, like LL in Fig. 24, is the weakest section. It has been shown[28] that the line LL must be straight. Hence, in Fig. 24 the limit load for the section between the holes is equal to the limit load for the normal section AA′, or

$$P_l = 2\,k\,\mathrm{AA'}\,t \ldots\ldots\ldots\ldots\ldots\ldots (46)$$

For small values of β the holes will touch the straight parts of the limit curve ANA′N′ so that[28]

$$\mathrm{AA'} = l\cos\beta - d \ldots\ldots\ldots\ldots\ldots\ldots (47)$$

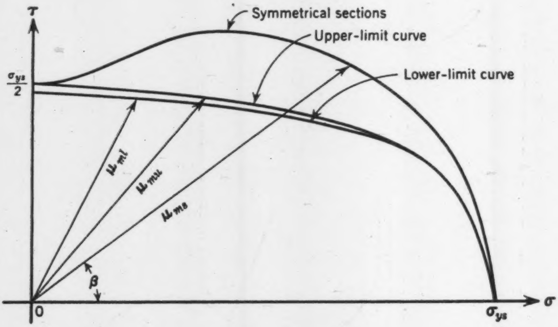

FIG. 25.—LIMIT CURVES

For larger angles β the holes touch the circular parts of the limit curve ANA′N′ so that[28]

$$\mathrm{AA'} = \frac{l^2 - d^2}{2\,(s + d)} = \frac{s^2 + g^2 - d^2}{2\,(s + d)} \ldots\ldots\ldots\ldots\ldots (48)$$

For purposes of design, if it is assumed that the load F is uniformly distributed over the section MM in the line connecting the centers of the holes, the total limit stress μ_{mu} (in the direction of F) on this section would be

$$\mu_{mu} = \frac{\mathrm{AA'}}{\mathrm{MM}}\,2\,k \ldots\ldots\ldots\ldots\ldots\ldots (49)$$

The limit curve for the oblique limit stress μ_{mu} is given graphically in Fig. 25 for the most unfavorable case—when l/d is as small as possible—which was assumed to be $l/d = 3$. This curve was denoted as the upper-limit curve because it was obtained, as shown previously, by assuming the stress distribution in all planes to be as favorable as possible. Obviously these most-favorable stress distributions differ for adjacent sections and therefore cannot always occur simultaneously.

In order to find a lower-limit curve for several values of β (Fig. 24) a body of equal plastic resistance was drawn between the holes, also assuming $l/d = 3$. This body was given such a form that almost everywhere within that body the state of stress (σ_1, σ_2) was at the yield stress and was such that the resistance of its effective section AB to the forces F was as large as possible (Fig. 26). The stress is uniformly distributed over this section AB, which subtends an angle $\lambda = \beta + \delta$ with the normal to the line of action of the forces F. In Fig. 26, the angle $\beta + \delta$ is chosen as $\tan^{-1} 2.5$ so that from Fig. 22, in which μ_{AB} is the total limit stress on AB, the principal stresses are

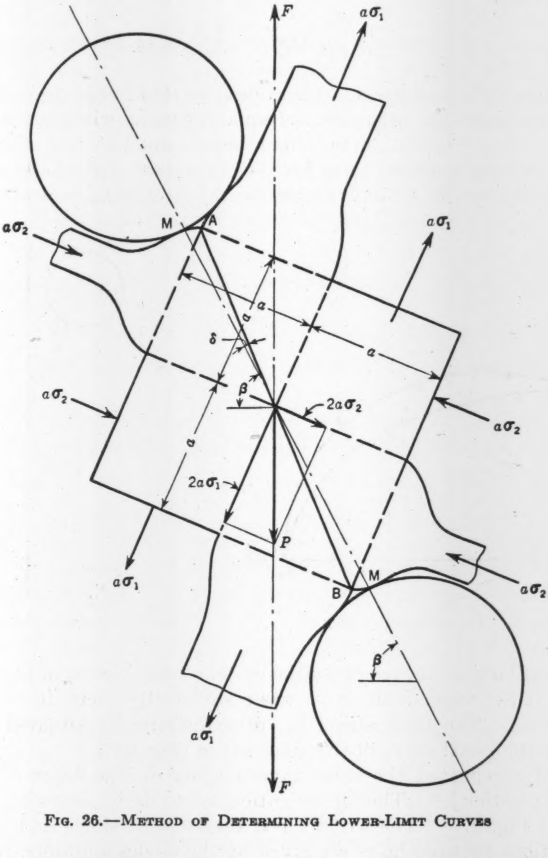
F
$a\sigma_1$
M
A
$a\sigma_2$
$a\sigma_1$
a
a
a
δ
β
$a\sigma_2$
$2a\sigma_2$
$a\sigma_2$
a
$2a\sigma_1$
P
$a\sigma_1$
M
B
$a\sigma_2$
β
$a\sigma_1$
F

FIG. 26.—METHOD OF DETERMINING LOWER-LIMIT CURVES

$$\sigma_1 = 0.7\,\sigma_{ys} \ldots\ldots\ldots\ldots \quad (50a)$$

and

$$\sigma_2 = -0.3\,\sigma_{ys} \tag{50b}$$

The load F that can be transferred between the holes in Fig. 26 is

$$F = \mathrm{AB}\,t\,\mu_{AB} \tag{51}$$

The stress μ_{ml}, assumed to be uniformly distributed over the section MM (Fig. 24), is then[28]

$$\mu_{ml} = \frac{\mathrm{AB}}{\mathrm{MM}}\,\mu_{AB} = \frac{2\,a\,\sqrt{2}}{l - d}\,\mu_{AB} \tag{52}$$

Because a more favorable stress distribution than that in Fig. 26 is possible and because the material outside the body of equal resistance will restrain the plastic deformation, the stresses μ_{ml} determine a lower bound for the stress μ_m. By considering sections between holes for various values of β, the limit curve in Fig. 25 (denoted as a lower-limit curve) for the stresses μ_{ml} was obtained.

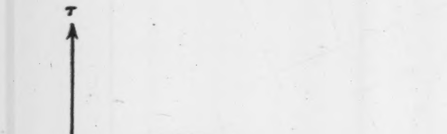

FIG. 27.—EXPERIMENTAL RESULTS

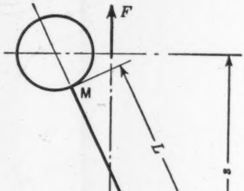

FIG. 28.—SECTION BETWEEN HOLES

In connection with the results of the writer's tests (circles in Fig. 27), it was assumed that the upper-limit curve was a sufficiently accurate bound for the limit stress μ_m. The limit stress μ_{ms} of symmetrically situated sections is bounded by the pedal curve of this limit curve (Fig. 25).

The writer repeated the same investigation on the basis of the Mises criterion of plasticity.[29] This investigation led to limit curves for μ_m and μ_{ms} as shown in Fig. 27.[30] The writer's test results with single and symmetrical oblique sections between holes are given by the circles and dots, respectively. Because the rotation of the forces F through an angle γ may over-stress other sections and because it is too difficult to prescribe where the curve for μ_{ms} can be used, the writer recommended[30] that the limit curve for μ_m be used in all sections. It is an ellipse with the equation:

$$\sigma^2 + 3.3\,\tau^2 = \sigma^2_{ys} \tag{53}$$

Eq. 53 leads to allowable total stresses in the section MM between the holes (Fig. 24) of[30]

$$\mu_m = \frac{\sigma_{\text{all}}}{\sqrt{1 + 2.3 \sin^2 \beta}} \qquad (54)$$

—in which σ_{all} is the allowable stress for pure tension—so that the allowable force F is (Fig. 24)

$$\text{MM}\, t\, \mu_m = (l - d)\, t\, \mu_m \qquad (55)$$

The conditions used by Messrs. Brady and Drucker for obtaining the upper and lower limit loads are essentially identical to those used by the writer[28] and lead to the same results. Because the most unfavorable or the most favorable cases were not considered, the limit loads obtained by the authors are not so close together as those obtained[28] by the writer.

It is not agreed that the ($s^2/4\,g$)-specification is reasonable because, for a section subjected to pure shear (in which $g = 0$), $s^2/4\,g$ would become infinite. Actually, Eq. 38—which is based on their Eq. 35, which is identical with Eq. 45, and which equates $\sqrt{1 + s^2/e^2}$ to $1 + s^2/2\,e^2$—does not hold if s/e is more than approximately unity. If s/e is large so that $\sqrt{1 + s^2/e^2}$ is approximately equal to s/e, from Eq. 38—

$$P_{l1} = k\, t\, e \left(\frac{s}{e} + 1\right) \cong k\, t\, s \qquad (56)$$

Actually for large values of β it is more unfavorable to consider the section MM between the holes (Fig. 28), so that $\lambda = \beta$. If β becomes 90°, then from Eq. 45,

$$F = k\, t\, L\, (1 + \cos \lambda) = k\, t\, L = k\, t\, (s - d) \qquad (57)$$

Therefore, the limit stress for $\beta = 90°$ is k, which also follows from Fig. 23. However, Eq. 54 is recommended for the allowable stress in the sections MM between the holes (Fig. 24), which (in terms of s and g) may be written as

$$\mu_m = \frac{\sigma_{\text{all}}}{\sqrt{1 + 2.3 \dfrac{s^2}{s^2 + g^2}}} \qquad (58)$$

For further details one must refer to the writer's work.[28,29]

W. Gordon Brady[31] and Daniel C. Drucker,[32] A. M. ASCE.—A helpful addition has been made by Mr. Munse who emphasized the limitations of limit analysis. In most, but not all, problems of importance in civil engineering first yielding or purely elastic action is not of great significance. In most cases the limit load will be the maximum load which the engineer would wish to consider, and so he will base his factor of safety on it. As Mr. Munse notes, however, ultimate strength may be of more interest in many problems. As to the example of the I-beam load through the flanges only, it is likely that limit analysis will show an efficiency of the order of 75% rather than 100% because work hardening is not taken into account.

---

[31] Asst. Engr., Cornell Aeronautical Lab., Inc., Buffalo, N. Y.

[32] Chairman, Div. of Eng., Brown Univ., Providence, R. I.

Mr. Bijlaard's contributions to the theory of plasticity and its applications are well known, and it is regretted that no reference was made to his papers on the effect of holes and notches; their presentation in English is most welcome. Mr. Bijlaard demonstrates the fact that an experienced engineer can obtain good answers to the most complicated problems. It should be noted, however, that the upper or lower bounds he describes may not be correct. The limit theorems as given in the paper require that kinematic patterns be used for upper bounds and that equilibrium patterns below yield throughout be used for lower bounds. As reported by the writers, the theory and tests both show clearly that the number of rows of holes has a significant effect. A simplified discussion in terms of what happens in the two-row case is not sufficient. Fig. 26 would have to be extended to the boundaries of the sheet under tension without altering the computed axial pull. This difficult task—and it is a physical as well as a mathematical one—is precisely what causes the lower bounds in the paper to be low. The added effort to narrow the bounds is great and not essential in the majority of applications.

Perhaps the real contribution of limit analysis is in serving as a tool for the inexperienced engineer to produce results which otherwise take a lifetime of learning rather than as an aid to the engineer who knows the practical answers.

AMERICAN SOCIETY OF CIVIL ENGINEERS
Founded November 5, 1852
TRANSACTIONS

Paper No. 2773

LATERAL BUCKLING OF I-BEAMS

By Mario G. Salvadori,[1] M. ASCE

With Discussion by Messrs. Robert V. Whitman, Michael R. Horne, and Mario G. Salvadori

Synopsis

The critical combinations of thrust and unequal end moments for the lateral buckling of I-beams simply supported in the weak plane are derived by the Rayleigh-Ritz method. It is shown that these critical combinations can be used to obtain approximate, safe bounds of the critical combinations for continuous beams and frames.

Introduction

A slender beam, acting as a member of a framed structure, can buckle in a variety of ways, among which the following are of practical interest:

1. In bending under axial thrusts P (Euler buckling);
2. In bending and torsion (lateral buckling) under the action of end moments caused by the continuity of the structure; and
3. In bending and torsion under a combination of axial thrusts and end moments, in which case the moments may be the result either of the continuity of the structure or of known eccentricities of the thrusts.

The solution of the lateral-instability problem in case 3 involves the determination of the critical combination of thrust and moments and hence of "interaction curves" from which the critical value of the moments can be derived for a given thrust or the critical value of the thrust can be determined for given end moments.

Interaction curves for thrust and equal end moments have been determined by S. Timoshenko for beams of rectangular cross section[2] and by B. G. Johns-

---

Note.—Published, essentially as printed here, in October, 1953, as *Proceedings-Separate No. 291*. Positions and titles given are those in effect when the paper or discussion was received for publication.

[1] Prof. of Civ. Eng., Columbia Univ., New York, N. Y.

[2] "Theory of Elastic Stability," by S. Timoshenko, McGraw-Hill Book Co., Inc., New York, N. Y., 1936.

ton, M. ASCE, for I-beams.[3] In both cases the interaction curves take the simple form:

$$\frac{P}{P_{cr}} + \left(\frac{M}{M_{cr}}\right)^2 = 1 \ldots\ldots\ldots\ldots\ldots\ldots\ldots (1)$$

in which P_{cr} is Euler's load and M_{cr} is the critical value of the end moment without thrust.

The critical value of unequal end moments has been computed by the writer for beams of rectangular cross section[4] and by W. E. Thomas for I-beams.[5,6] Interaction curves for beams of rectangular cross section under thrust and unequal end moments have been determined by F. DiMaggio.[6,7]

Interaction curves for I-beams simply supported in the weak plane under thrust and unequal end moments will be determined subsequently by the Rayleigh-Ritz method.

LATERAL-BUCKLING ENERGY OF I-BEAMS

The total energy of an I-beam which has buckled laterally under the action of transverse loads and longitudinal thrusts is given by[2,8,9]

$$V = \frac{B}{2}\int_0^l (u'')^2\, dz + \frac{D\,h^2}{4}\int_0^l (\beta'')^2\, dz + \frac{H}{2}\int_0^l (\beta')^2\, dz + \int_0^l M\,\beta\,u''\, dz - \frac{P}{2}\int_0^l (u')^2\, dz \,.\,.\, (2)$$

in which B is the minimum flexural rigidity of the beam; u denotes the lateral deflection of the beam in the plane of minimum rigidity; l is the beam length; D represents the flexural rigidity of one flange in its own plane; h is the beam depth; β denotes the angular rotation of the section of abscissa z; H is equal to $C - (P\,I_p/A)$ and is the equivalent torsional rigidity of the beam; C denotes the torsional rigidity of the beam; P is the thrust, uniformly distributed on the beam cross section; I_p represents the polar moment of inertia of the beam cross section about its centroid; A is the cross-sectional area of the beam; M denotes the bending moment in the plane of maximum flexural rigidity at the section of abscissa z; and z is the abscissa measured along the beam axis with the origin at one of its ends.

Eq. 2 has been proved[10] by H. H. Bleich to be rigorously correct under the assumption that the thrust P is evenly distributed over the end sections of the beam. Mr. Bleich also showed that Eq. 2 can be used with sufficient accuracy even if P is otherwise distributed—for example, if it is concentrated at the centroid of the section. The equivalent torsional rigidity H accounts for the weakening of the torsional rigidity C as a result of the tendency of a compressed beam to buckle in pure torsion when $P = A\ C/I_p$. In most practical cases H is equal to C. The term in Eq. 2 containing the bending moment $M(z)$ in the plane of the maximum flexural rigidity represents the work of the transverse loads applied to the beam, and its use is limited to beams simply supported or built-in at either end, or to cantilevered beams.

---

[3] "Lateral Buckling of I-Section Columns with Eccentric End Loads in the Plane of the Web," by B. G. Johnston, *Transactions*, ASME, Vol. 63, 1941, p. A-176.

[4] "Lateral Buckling of Beams of Rectangular Cross-Section under Bending and Shear," by Mario G. Salvadori, *Proceedings*, 1st U. S. National Cong. of Applied Mechanics, Chicago, Ill., 1951.

[5] "Lateral Buckling of I-Beams under Unequal End Moments," by W. E. Thomas, thesis presented to Columbia Univ., at New York, N. Y., in May, 1951, in partial fulfilment of the requirements for the degree of Master of Science.

[6] "Lateral Buckling of Beams in Bending and Compression," by F. DiMaggio, A. Gomza, W. E. Thomas, and Mario G. Salvadori, *Journal of the Aeronautical Sciences*, 1952, No. 8.

[7] "Lateral Buckling of Narrow Rectangular Beams under Bending, Shear and Compression," by F. DiMaggio, thesis presented to Columbia Univ., at New York, N. Y., in May, 1951, in partial fulfilment of the requirements for the degree of Master of Science.

[8] "Buckling Strength of Metal Structures," by F. Bleich, McGraw-Hill Book Co., Inc., New York, N. Y., 1951.

[9] "Flexural-Torsional Buckling of Bars of Open Section," by J. N. Goodier, *Bulletin No. 28*, Cornell Univ. Eng. Experiment Station, Ithaca, N. Y., January, 1942.

[10] "Refinement of the Theory of Torsional Buckling of Thin-Walled Columns," by H. H. Bleich, *Proceedings*, 1st Midwestern Conference on Solid Mechanics, June, 1953.

The two differential equations in u and β governing the buckling of the beam can be derived from Eq. 2 by the calculus of variations together with the natural boundary conditions of the problem. However, because the differential equations in u and β are not readily integrable in finite terms, it is more practical to obtain interaction curves by the Rayleigh-Ritz method.

Lateral Buckling of Simply Supported I-Beams

Considering, in particular, simply supported beams whose end sections are free to rotate around their principal axes but are prevented from twisting around the longitudinal beam axis, the boundary conditions for u and β become

$$u(0) = u''(0) = u(l) = u''(l) = 0 \qquad \text{(3a)}$$

and

$$\beta(0) = \beta''(0) = \beta(l) = \beta''(l) = 0 \qquad \text{(3b)}$$

and u and β can be expanded into the sine series:

$$u = \sum_{n=1}^{\infty} a_n \sin \frac{n\,\pi\,z}{l} \qquad \text{(4a)}$$

and

$$\beta = \sum_{n=1}^{\infty} b_n \sin \frac{n\,\pi\,z}{l} \qquad \text{(4b)}$$

Indicating by M_2 the value of $M(z)$ at the end $z = l$ and by M_1 the value of $M(z)$ at the end $z = 0$, and setting $r = M_1/M_2$, the bending moment $M(z)$ becomes, in this case,

$$M(z) = M_2 \left[r + \frac{(1 - r)z}{l} \right] \qquad \text{(5)}$$

Taking into account an increasing number of terms of the series in Eqs. 4, substitution of these values for u and β in Eq. 2 results in a quadratic form in the a_n and b_n. The partial derivatives of this form with respect to the a_n and b_n when equated to zero form a set of homogeneous linear simultaneous equations in the a_n and b_n. The determinant of these equations when set equal to zero determines pairs of critical values for P and M_2 as functions of the parameters r and

$$\frac{l^2}{a^2} = \frac{2\,l^2}{h^2}\frac{H}{D} \qquad \text{(6)}$$

TABLE 1.—VALUES OF K IN TERM

Value of r	Value of p											
	0	0.2	0.4	0.6	0.8	1	0	0.2	0.4	0.6	0.8	1
	(a) $l^2/a^2=0.1$						(b) $l^2/a^2=1$					
1.0	31.40	28.06	24.30	19.84	14.03	0	10.36	9.26	8.02	6.55	4.63	0
0.9	33.80	30.44	26.53	21.79	15.30	0	11.16	10.04	8.75	7.19	5.05	0
0.8	35.75	32.26	28.16	23.15	16.25	0	11.81	10.64	9.29	7.63	5.36	0
0.7	37.53	33.82	29.48	24.22	17.04	0	12.40	11.15	9.73	7.99	5.63	0
0.6	39.35	35.37	30.76	25.21	17.80	0	13.01	11.67	10.15	8.32	5.88	0
0.5	41.40	37.12	32.20	26.33	18.65	0	13.68	12.25	10.63	8.69	6.16	0
0.4	43.82	39.21	33.97	27.74	19.70	0	14.47	12.94	11.22	9.16	6.51	0
0.3	46.69	41.78	36.20	29.57	21.04	0	15.41	13.79	11.95	9.76	6.95	0
0.2	50.07	44.86	38.95	31.89	22.74	0	16.52	14.81	12.86	10.53	7.51	0
0.1	53.95	48.50	42.28	34.77	24.86	0	17.79	16.00	13.95	11.48	8.20	0
0	58.30	52.65	46.16	38.21	27.44	0	19.22	17.37	15.23	12.61	9.05	0
−0.1	63.02	57.25	50.54	42.18	30.51	0	20.77	18.88	16.67	13.92	10.06	0
−0.2	67.99	62.18	55.33	46.63	34.09	0	22.40	20.50	18.24	15.38	11.23	0
−0.3	73.03	67.27	60.38	51.45	38.16	0	24.06	22.17	19.90	16.96	12.57	0
−0.4	77.92	72.31	65.50	56.51	42.71	0	25.67	23.82	21.58	18.62	14.07	0
−0.5	82.39	77.04	70.46	61.63	47.71	0	27.14	25.38	23.21	20.30	15.71	0
−0.6	86.13	81.17	74.99	66.60	53.10	0	28.38	26.74	24.70	21.93	17.49	0
−0.7	88.79	84.33	78.76	71.16	58.82	0	29.26	27.78	25.94	23.44	19.37	0
−0.8	89.97	86.15	81.41	75.04	64.78	0	29.66	28.38	26.83	24.72	21.34	0
−0.9	89.23	86.16	82.53	77.90	70.89	0	29.42	28.40	27.21	25.67	23.37	0
−1.0	86.07	83.90	81.67	79.39	77.03	0	28.40	27.68	26.95	26.19	25.41	0
	(e) $l^2/a^2=10$						(f) $l^2/a^2=16$					
1.0	4.43	3.96	3.43	2.80	1.98	0	4.00	3.57	3.09	2.53	1.79	0
0.9	4.76	4.28	3.73	3.05	2.14	0	4.29	3.85	3.35	2.75	1.93	0
0.8	5.03	4.53	3.95	3.24	2.26	0	4.54	4.08	3.55	2.92	2.04	0
0.7	5.28	4.75	4.14	3.40	2.38	0	4.77	4.28	3.72	3.06	2.15	0
0.6	5.55	4.98	4.34	3.54	2.50	0	5.01	4.49	3.89	3.20	2.25	0
0.5	5.84	5.23	4.54	3.71	2.63	0	5.27	4.72	4.09	3.35	2.37	0
0.4	6.18	5.53	4.79	3.92	2.79	0	5.58	4.99	4.32	3.54	2.51	0
0.3	6.58	5.89	5.11	4.17	2.98	0	5.93	5.32	4.61	3.77	2.69	0
0.2	7.04	6.31	5.49	4.50	3.22	0	6.34	5.70	4.95	4.06	2.90	0
0.1	7.57	6.81	5.94	4.89	3.51	0	6.81	6.14	5.36	4.42	3.16	0
0	8.16	7.37	6.47	5.36	3.86	0	7.33	6.64	5.83	4.83	3.47	0
−0.1	8.80	7.99	7.06	5.90	4.27	0	7.89	7.19	6.35	5.30	3.84	0
−0.2	9.46	8.65	7.70	6.49	4.76	0	8.47	7.77	6.92	5.83	4.26	0
−0.3	10.14	9.33	8.38	7.14	5.30	0	9.07	8.37	7.52	6.40	4.75	0
−0.4	10.80	10.01	9.07	7.83	5.92	0	9.65	8.97	8.13	7.01	5.29	0
−0.5	11.40	10.65	9.74	8.52	6.60	0	10.18	9.53	8.72	7.62	5.90	0
−0.6	11.91	11.21	10.36	9.20	7.34	0	10.64	10.03	9.27	8.23	6.56	0
−0.7	12.29	11.66	10.89	9.84	8.14	0	10.98	10.43	9.74	8.80	7.28	0
−0.8	12.48	11.94	11.28	10.40	8.99	0	11.16	10.68	10.10	9.31	8.05	0
−0.9	12.43	11.99	11.49	10.85	9.88	0	11.13	10.75	10.30	9.72	8.86	0
−1.0	12.07	11.76	11.45	11.13	10.80	0	10.85	10.57	10.29	10.00	9.71	0
	(i) $l^2/a^2=40$						(j) $l^2/a^2=100$					
1.0	3.51	3.14	2.72	2.22	1.57	0	3.29	2.95	2.55	2.08	1.47	0
0.9	3.75	3.37	2.93	2.40	1.68	0	3.50	3.16	2.74	2.24	1.56	0
0.8	3.97	3.57	3.10	2.54	1.78	0	3.70	3.34	2.89	2.37	1.65	0
0.7	4.17	3.75	3.26	2.67	1.87	0	3.89	3.51	3.04	2.49	1.74	0
0.6	4.38	3.93	3.41	2.80	1.97	0	4.10	3.68	3.19	2.61	1.84	0
0.5	4.62	4.14	3.59	2.94	2.08	0	4.33	3.88	3.36	2.75	1.95	0
0.4	4.89	4.38	3.80	3.11	2.21	0	4.59	4.10	3.56	2.91	2.08	0
0.3	5.20	4.66	4.05	3.32	2.36	0	4.87	4.36	3.79	3.11	2.22	0
0.2	5.55	4.98	4.34	3.57	2.55	0	5.20	4.66	4.06	3.34	2.40	0
0.1	5.95	5.35	4.69	3.87	2.78	0	5.55	5.00	4.38	3.61	2.60	0
0	6.38	5.77	5.08	4.22	3.04	0	5.94	5.37	4.73	3.93	2.84	0
−0.1	6.84	6.22	5.52	4.62	3.35	0	6.35	5.77	5.12	4.29	3.12	0
−0.2	7.33	6.71	5.99	5.06	3.70	0	6.77	6.20	5.54	4.68	3.43	0
−0.3	7.82	7.20	6.48	5.53	4.11	0	7.20	6.64	5.98	5.11	3.80	0
−0.4	8.30	7.70	6.99	6.03	4.57	0	7.61	7.08	6.43	5.56	4.21	0
−0.5	8.74	8.17	7.48	6.55	5.08	0	8.00	7.50	6.87	6.02	4.67	0
−0.6	9.12	8.59	7.94	7.06	5.65	0	8.34	7.88	7.29	6.49	5.18	0
−0.7	9.42	8.94	8.35	7.56	6.27	0	8.61	8.19	7.66	6.94	5.75	0
−0.8	9.59	9.18	8.68	8.01	6.94	0	8.78	8.42	7.97	7.36	6.38	0
−0.9	9.61	9.27	8.88	8.39	7.66	0	8.83	8.53	8.18	7.74	7.06	0
−1.0	9.43	9.18	8.94	8.69	8.44	0	8.72	8.49	8.27	8.04	7.81	0

of p AND r FOR VARIOUS VALUES OF l^2/a^2

Value of p												Value of r
0	0.2	0.4	0.6	0.8	1	0	0.2	0.4	0.6	0.8	1	
(c) $l^2/a^2=2$						(d) $l^2/a^2=6$						
7.66	6.85	5.93	4.84	3.42	0	5.11	4.57	3.96	3.23	2.28	0	1.0
8.25	7.42	6.47	5.30	3.72	0	5.50	4.94	4.31	3.53	2.47	0	0.9
8.73	7.86	6.86	5.64	3.95	0	5.82	5.24	4.57	3.75	2.62	0	0.8
9.16	8.24	7.18	5.90	4.15	0	6.11	5.49	4.79	3.92	2.75	0	0.7
9.61	8.62	7.50	6.14	4.34	0	6.41	5.75	5.00	4.09	2.88	0	0.6
10.11	9.05	7.85	6.42	4.55	0	6.75	6.04	5.24	4.28	3.03	0	0.5
10.70	9.56	8.28	6.77	4.81	0	7.14	6.38	5.53	4.52	3.21	0	0.4
11.39	10.19	8.83	7.21	5.14	0	7.60	6.80	5.89	4.81	3.43	0	0.3
12.21	10.94	9.50	7.78	5.54	0	8.14	7.29	6.33	5.19	3.71	0	0.2
13.14	11.82	10.30	8.48	6.07	0	8.75	7.87	6.86	5.65	4.05	0	0.1
14.19	12.82	11.24	9.31	6.69	0	9.44	8.53	7.48	6.20	4.46	0	0
15.33	13.93	12.30	10.27	7.43	0	10.18	9.26	8.17	6.83	4.95	0	−0.1
16.52	15.12	13.45	11.34	8.29	0	10.97	10.08	8.93	7.53	5.51	0	−0.2
17.74	16.35	14.67	12.50	9.27	0	11.76	10.84	9.72	8.30	6.15	0	−0.3
18.92	17.57	15.91	13.72	10.37	0	12.53	11.63	10.53	9.10	6.88	0	−0.4
20.00	18.71	17.11	14.96	11.58	0	13.24	12.38	11.32	9.91	7.67	0	−0.5
20.91	19.71	18.21	16.16	12.89	0	13.84	13.04	12.04	10.70	8.53	0	−0.6
21.56	20.48	19.13	17.27	14.28	0	14.27	13.55	12.66	11.44	9.46	0	−0.7
21.86	20.93	19.78	18.23	15.73	0	14.48	13.86	13.10	12.08	10.43	0	−0.8
21.71	20.96	20.08	18.94	17.24	0	14.40	13.90	13.32	12.58	11.45	0	−0.9
20.98	20.44	19.90	19.34	18.76	0	13.95	13.60	13.24	12.87	12.49	0	−1.0
(g) $l^2/a^2=24$						(h) $l^2/a^2=32$						
3.73	3.34	2.89	2.36	1.67	0	3.59	3.21	2.78	2.27	1.61	0	1.0
4.00	3.59	3.13	2.56	1.79	0	3.84	3.45	3.00	2.46	1.73	0	0.9
4.23	3.80	3.31	2.71	1.90	0	4.06	3.65	3.18	2.61	1.83	0	0.8
4.44	3.99	3.48	2.84	1.99	0	4.27	3.84	3.34	2.74	1.92	0	0.7
4.67	4.18	3.64	2.97	2.10	0	4.49	4.03	3.50	2.87	2.02	0	0.6
4.92	4.40	3.82	3.12	2.21	0	4.73	4.24	3.68	3.01	2.13	0	0.5
5.21	4.65	4.04	3.30	2.35	0	5.01	4.49	3.89	3.18	2.26	0	0.4
5.54	4.95	4.30	3.52	2.51	0	5.33	4.77	4.15	3.39	2.41	0	0.3
5.92	5.31	4.62	3.79	2.71	0	5.69	5.11	4.45	3.65	2.60	0	0.2
6.35	5.71	4.99	4.12	2.95	0	6.10	5.50	4.80	3.96	2.83	0	0.1
6.83	6.17	5.42	4.50	3.24	0	6.55	5.93	5.21	4.32	3.11	0	0
7.34	6.67	5.90	4.94	3.58	0	7.03	6.40	5.66	4.73	3.43	0	−0.1
7.88	7.20	6.42	5.42	3.97	0	7.54	6.90	6.15	5.19	3.80	0	−0.2
8.41	7.75	6.97	5.94	4.41	0	8.04	7.42	6.67	5.69	4.22	0	−0.3
8.94	8.29	7.52	6.50	4.91	0	8.54	7.93	7.19	6.21	4.70	0	−0.4
9.42	8.81	8.07	7.06	5.47	0	9.00	8.42	7.71	6.75	5.23	0	−0.5
9.83	9.27	8.58	7.62	6.08	0	9.40	8.86	8.19	7.28	5.82	0	−0.6
10.13	9.64	9.02	8.15	6.75	0	9.70	9.21	8.61	7.79	6.46	0	−0.7
10.30	9.89	9.36	8.63	7.46	0	9.88	9.45	8.94	8.26	7.14	0	−0.8
10.27	9.97	9.56	9.03	8.22	0	9.89	9.54	9.15	8.64	7.88	0	−0.9
10.01	9.84	9.58	9.31	9.03	0	9.69	9.44	9.19	8.93	8.67	0	−1.0
(k) $l^2/a^2=\infty$												
3.14	2.81	2.43	1.99	1.40	0							1.0
3.31	2.99	2.60	2.13	1.49	0							0.9
3.48	3.16	2.75	2.25	1.58	0							0.8
3.68	3.33	2.89	2.37	1.66	0							0.7
3.89	3.51	3.04	2.49	1.76	0							0.6
4.12	3.70	3.21	2.63	1.86	0							0.5
4.37	3.92	3.40	2.79	1.98	0							0.4
4.64	4.16	3.62	2.97	2.12	0							0.3
4.93	4.44	3.88	3.19	2.28	0							0.2
5.24	4.75	4.16	3.44	2.48	0							0.1
5.56	5.08	4.48	3.73	2.70	0							0
5.90	5.44	4.83	4.05	2.96	0							−0.1
6.25	5.81	5.20	4.40	3.25	0							−0.2
6.61	6.19	5.58	4.78	3.57	0							−0.3
6.97	6.56	5.97	5.18	3.94	0							−0.4
7.32	6.92	6.36	5.59	4.34	0							−0.5
7.66	7.25	6.73	6.00	4.78	0							−0.6
7.96	7.52	7.06	6.41	5.26	0							−0.7
8.19	7.73	7.34	6.80	5.77	0							−0.8
8.25	7.85	7.54	7.14	6.31	0							−0.9
8.03	7.85	7.65	7.44	6.89	0							−1.0

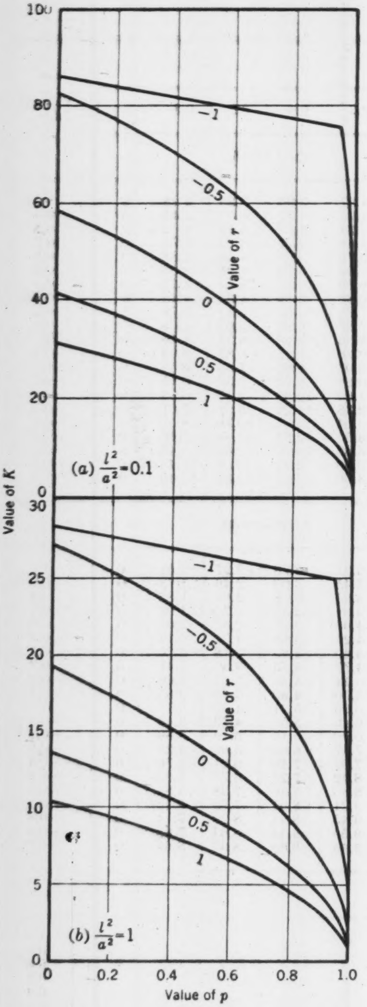

FIG. 1

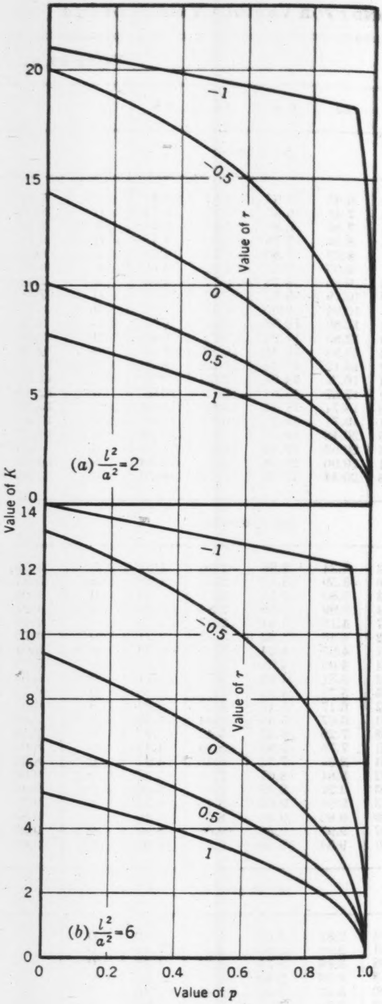

FIG. 2

The results of the computations are presented in Table 1 in terms of the moment coefficient:

$$K = \frac{M_2 \, l}{\sqrt{B \, H}} \quad \text{(7)}$$

and of the nondimensional thrust:

$$p = \frac{P}{P_e} = \frac{P\,l^2}{\pi^2 B} \qquad (8)$$

for various values of r and l^2/a^2.

The cases in which $r = 1$, corresponding to equal end moments, and the cases in which $l^2/a^2 = \infty$, corresponding to beams of rectangular cross section, were taken from the works of Messrs. Timoshenko,[2] Johnston,[3] and DiMaggio.[6,7] The cases in which $p = 0$, corresponding to lack of thrust, were taken from the works of the writer[4] and Mr. Thomas.[5,6]

The values of K for the various values of p were obtained by a solution of the determinantal equation, taking into account one term of each series (Eqs. 4) for $r = 1$, three terms for $r = \frac{1}{2}$, $r = 0$, and $r = -\frac{1}{2}$ (although two terms would have been sufficient for $r = \frac{1}{2}$), and four terms for $r = -1$. The successive approximations indicate that the results are correct within the number of figures given in Table 1. Whatever the number of terms of the series used, it was found that the determinantal equation for $r = -1$ splits into two separate equations whose common root occurs for values of p varying between 0.949 and 0.759 as l^2/a^2 varies from 0.1 to ∞. These results indicate a change of equilibrium configuration at these values of p and required the solution of the determinantal equation for $p = 0.95$ when $r = -1$ in order to obtain greater accuracy in the K-graphs shown in Figs. 1, 2, 3, and 4.

In Table 1 the values of K corresponding to the intermediate values of r, not included among the five values of r shown in Figs. 1, 2, 3, and 4, were obtained by Lagrangian interpolation. The interpolated values have a maximum error of between 1% and 2%.

Figs. 1, 2, 3, and 4 and Table 1 can be used directly when P is given and M_2 is to be determined. To solve for P for a given value of M_2, one computes first an approximate value K' of K by substituting C for H in Eq. 7. With this value of K one determines, from Table 1 or Figs. 1, 2, 3, and 4, the corresponding value of p and hence of P (from Eq. 8), which allows the evaluation of $H = C - P\,I_p/A$ and hence of a more accurate value of K. A new value of p is then derived from Table 1 or Figs. 1, 2, 3, and 4, but it is seldom that this procedure must be iterated.

When the end moments are caused by known eccentricities e_1 and e_2 of the thrust at $z = 0$ and $z = l$, respectively, these can be determined by noting that

$$e_2 = \frac{M_2}{P} \qquad (9a)$$

and

$$e_1 = r\,e_2 \qquad (9b)$$

LOWER BOUNDS OF INTERACTION CURVES FOR CONTINUOUS BEAMS AND FRAMES

The interaction curves can be conveniently used to determine lower (that is, safe) bounds for thrusts and end moments of continuous beams and frames, as shown by the following examples.

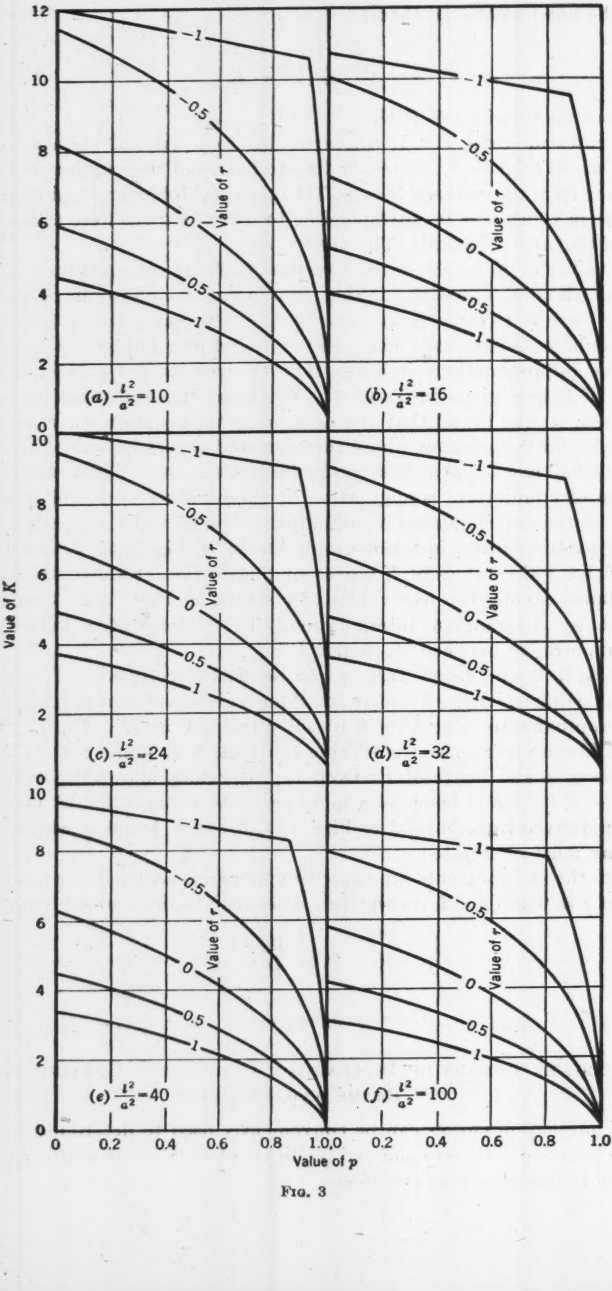
Value of K
Value of p
Value of r
-1
-0.5
0
0.5
1
(a) $\frac{l^2}{a^2}=10$
(b) $\frac{l^2}{a^2}=16$
(c) $\frac{l^2}{a^2}=24$
(d) $\frac{l^2}{a^2}=32$
(e) $\frac{l^2}{a^2}=40$
(f) $\frac{l^2}{a^2}=100$
12
10
8
6
4
2
0
0.2
0.4
0.6
0.8
1.0

FIG. 3

Example 1.—In Fig. 5 there is shown an I-beam with two identical spans of $l^2/a^2 = 6$, which is built-in at the left support and simply supported at the right. This beam is loaded by an eccentric thrust P. In order to determine a lower bound for the eccentricity e when $P/P_e = 0.6$ (in which P_e is Euler's load for each span when the spans are considered to be simply supported), one lets $Pe = M_C$. Two three-moment equations then give

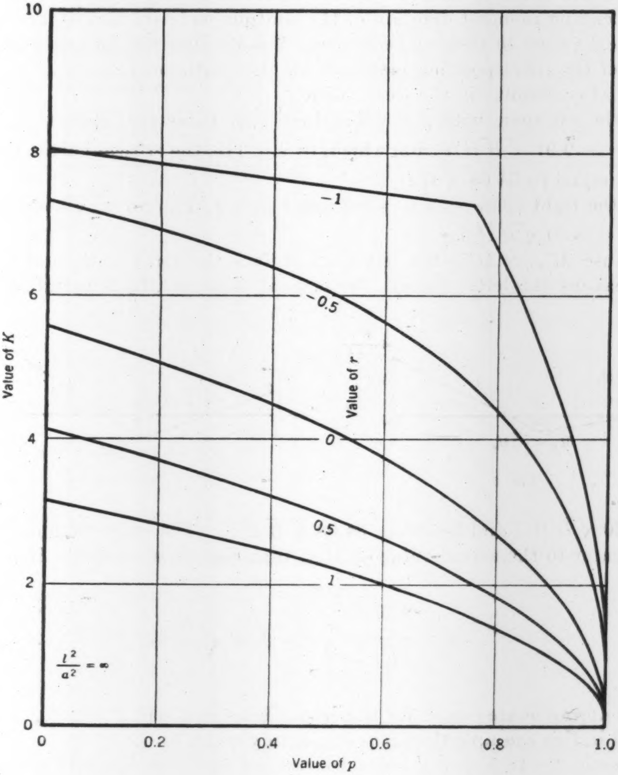

FIG. 4

$$2\,M_A + M_B = 0 \quad (10a)$$

and

$$M_A + 4\,M_B + M_C = 0 \quad (10b)$$

from which

$$M_A = \frac{1}{7}\,M_C \quad (11a)$$

and

$$M_B = -\frac{2}{7} M_C \ldots\ldots\ldots\ldots\ldots\ldots\ldots\ldots (11b)$$

Hence, the ratio r is $r' = -\frac{1}{2}$ for the left span and $r'' = -\frac{2}{7}$ for the right span.

If one now considers each of the two spans as simply supported but loaded by the bending moment diagram of the continuous beam and if one evaluates the critical values of their end moments, these values will be upper and lower bounds of the corresponding moments for the continuous beam, as a result of the lack of continuity in the weak plane.

For the left span, with $p = 0.6$ and $r = -\frac{1}{2}$, Table 1 (d) leads to $K_1 = 9.91$ or $M_B = -9.91 \sqrt{B\,H}/l$ from which, by Eq. 11b, the critical value M'_C of M_C becomes equal to $34.68 \sqrt{B\,H}/l$.

For the right span with $p = 0.6$ and $r = -\frac{2}{7}$, Table 1 (d) gives $K_2 = 8.30$ or $M''_C = 8.30 \sqrt{B\,H}/l$.

Because $M'_C > M''_C$ the left span stiffens the right span, and the right span weakens the left. Hence, the critical value of M_C is certainly greater than $8.30 \sqrt{B\,H}/l$ and less than $34.68 \sqrt{B\,H}/l$. The lower bound is usually much nearer to the actual value of $M_{C_{cr}}$ than the upper bound. Hence,

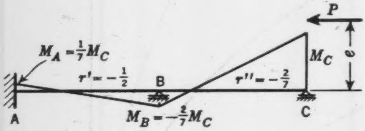

FIG. 5

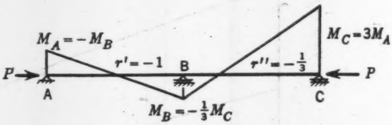

FIG. 6

$$e = \frac{8.30 \dfrac{\sqrt{B\,H}}{l}}{0.6\,\pi^2 \dfrac{B}{l^2}} = 1.40 \sqrt{\frac{H}{B}}\, l \ldots\ldots\ldots\ldots\ldots (12)$$

is a safe approximate bound for the eccentricity of a load $P = 0.6\,P_e$. It was assumed in this example that H is practically equal to C.

Example 2.—In Fig. 6 a beam continuous on three supports is loaded by end moments M_A and $M_C = 3\,M_A$. In order to determine a lower bound for the critical thrust P for

$$\frac{l^2}{a^2} = 10 \ldots\ldots\ldots\ldots\ldots\ldots\ldots\ldots (13a)$$

$$M_A = 3 \frac{\sqrt{B\,H}}{l} \ldots\ldots\ldots\ldots\ldots\ldots\ldots\ldots (13b)$$

and hence for

$$M_C = 9 \frac{\sqrt{B\,H}}{l} \ldots\ldots\ldots\ldots\ldots\ldots\ldots\ldots (13c)$$

one obtains by means of a three-moment equation,

$$M_A = -M_B = \tfrac{1}{3} M_C \ldots\ldots\ldots\ldots\ldots\ldots\ldots\ldots (14)$$

so that the values of r for the left and right span become, respectively, $r' = -1$ and $r'' = -\frac{1}{3}$.

The curve $r = -1$ in Fig. 3(*a*) gives, for $K = 3$, a value of $p \doteq 1$ or a thrust $P = \pi^2 B/l^2$. Fig. 3(*a*) or Table 1(*e*) leads to $p = 0.32$ or a thrust $P = 0.32\,\pi^2 B/l^2$ for $K = 9$ and $r = -0.33$ (interpolating linearly first between $r = -0.3$ and $r = -0.4$ for $p = 0.2$ and $p = 0.4$, and then between $p = 0.2$ and $p = 0.4$ for $r = -0.33$). Once again the left span stiffens the right span, and

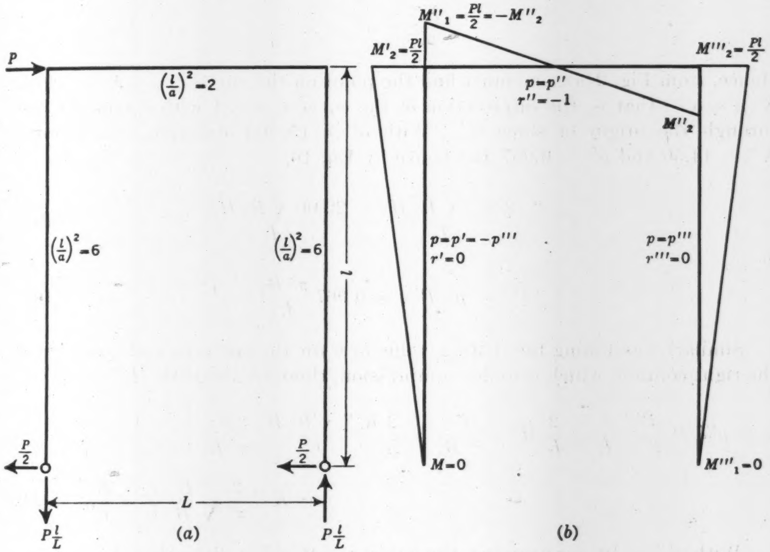
P
$\left(\frac{l}{a}\right)^2 = 2$
$\left(\frac{l}{a}\right)^2 = 6$
$\left(\frac{l}{a}\right)^2 = 6$
l
$\frac{P}{2}$
$\frac{P}{2}$
L
$P\frac{l}{L}$
$P\frac{l}{L}$
(a)
$M''_1 = \frac{Pl}{2} = -M''_2$
$M'_2 = \frac{Pl}{2}$
$M'''_2 = \frac{Pl}{2}$
$p = p''$
$r'' = -1$
M''_2
$p = p' = -p'''$
$r' = 0$
$p = p'''$
$r''' = 0$
$M = 0$
$M'''_1 = 0$
(b)

FIG. 7

$$P_{cr} > 3.16\,\frac{B}{l^2} \ldots\ldots\ldots\ldots\ldots\ldots\ldots\ldots (15)$$

It was assumed in this example that H is practically equal to C.

Example 3.—The frame in Fig. 7(*a*) is loaded by a horizontal force P, and one must determine a lower bound for the critical value of this force, assuming that the frame is prevented from buckling laterally as a whole. The bending-moment diagram in Fig. 7(*b*) shows that the ratio r has the value $r'' = -1$ for the horizontal beam and $r' = r''' = 0$ for the columns.

With $(l/a)^2$ equal to 2 for the horizontal beam and assuming this beam to be simply supported, the critical value of P can be found as follows:

Because $M''_2 = P\,l/2$, the parameter p becomes, in this case,

$$p = p'' = \frac{P''}{P''_e} = \frac{2}{l}\,M''_2\,\frac{L^2}{\pi^2 B_2} = \frac{2}{l}\,\frac{K''\sqrt{B_2 H_2}}{L}\,\frac{L^2}{\pi^2 B_2} = K''\,\frac{2}{\pi^2}\sqrt{\frac{H_2}{B_2}}\,\frac{L}{l} \quad (16)$$

Letting

$$\alpha'' = \frac{\pi^2}{2}\sqrt{\frac{B_2}{H_2}}\,\frac{l}{L} \quad (17)$$

the ratio of K'' to p'' becomes

$$\frac{K''}{p''} = \alpha'' \quad (18)$$

Hence, from Fig. 2(*a*), one must find the point on the curve $r = -1$ for which $K/p = \alpha''$—that is, the intersection of the curve $r = -1$ with a straight line through the origin of slope α''. With $\alpha'' = 15$, for example, one obtains $K'' = 14.50$ and $p'' = 0.967$ and hence by Eq. 16,

$$P'' = \frac{2\,K''\sqrt{B_2 H_2}}{l\,L} = \frac{29.00\sqrt{B_2 H_2}}{l\,L} \quad (19a)$$

or

$$P'' = p''\,P''_e = 0.967\,\frac{\pi^2 B_2}{L^2} \quad (19b)$$

Similarly, assuming for $(l/a)^2$ a value of 6 for the columns and considering the right column, which is under compression, there results with $M'''_2 = P\,l/2$,

$$p = p''' = \frac{P'''}{P'''_e}\,\frac{l}{L} = \frac{2}{L}\,M'''_2\,\frac{l^2}{\pi^2 B_1} = \frac{2}{L}\,\frac{K'''\sqrt{B_1 H_1}}{l}\,\frac{l^2}{\pi^2 B_1}$$

$$= K'''\,\frac{2}{\pi^2}\sqrt{\frac{H_1}{B_1}}\,\frac{l}{L} = \frac{K'''}{\alpha'''} \quad (20)$$

With $\alpha''' = 10$, for example, the curve $r = 0$ in Fig. 2(*b*) gives $K''' = 6.07$ and $p''' = 0.61$. Hence,

$$P''' = \frac{2\,K'''\sqrt{B_1 H_1}}{l\,L} = \frac{12.14\sqrt{B_1 H_1}}{l\,L} \quad (21a)$$

or

$$P''' = p'''\,\frac{L}{l}\,P'''_e = 0.61\,\frac{L}{l}\,\frac{\pi^2 B_1}{l^2} \quad (21b)$$

The smaller of the two loads P'' and P''' is a lower bound for the critical value of P.

CONCLUSIONS

The critical values of thrust and unequal end moments obtained herein allow for an accurate evaluation of buckling stresses for a number of structural elements often encountered in practice. The values should therefore make the design of these elements both safer and more economical.

ACKNOWLEDGMENTS

Table 1 and Figs. 1, 2, 3, and 4 were evaluated numerically by the staff of the Istituto Nazionale per le Applicazioni del Calcolo, the mathematical laboratory of the Italian National Research Council in Rome, directed by M. Picone. The computations were supervised by Domenico Caligo and Maria S. Roma and were performed by Paolo Bellino and Giuseppe Gullotta.

DISCUSSION

Robert V. Whitman,[11] J. M. ASCE.—At approximately the time that the studies described by Mr. Salvadori were being performed, the writer also undertook a brief investigation of the lateral buckling of simply supported, single-span beams loaded by axial thrust and unequal end moments.[12] The Stodola-Vianello method[13] was used in these studies with the deflections u and β represented by two, or in some cases three, terms of a sine series. The solutions, although not performed with the accuracy obtained by the author and for only

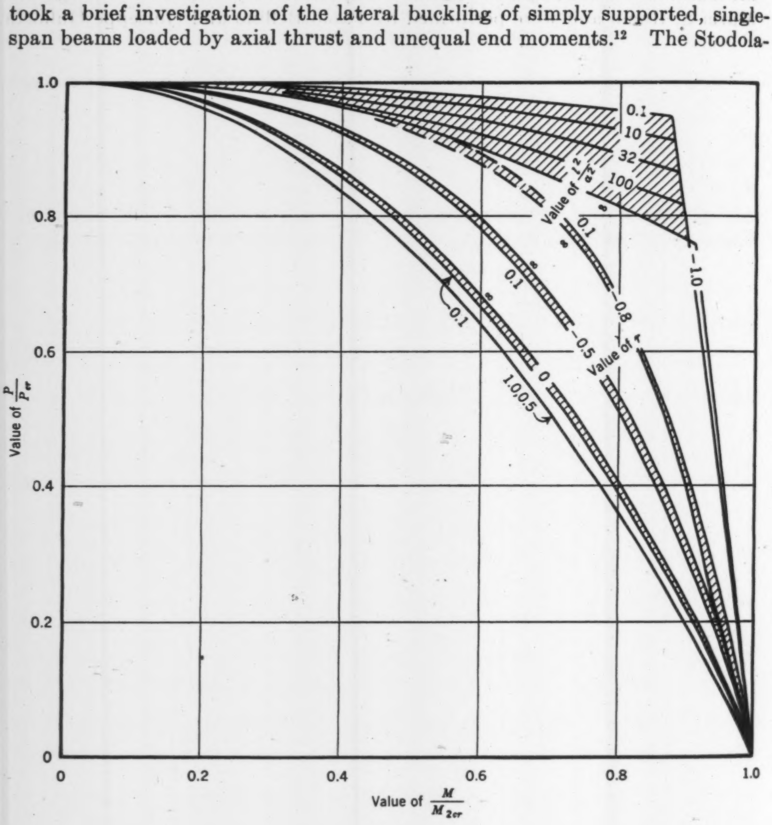

Fig. 8

---

[11] Asst. Prof. of Soil Mechanics, Massachusetts Inst. of Technology, Cambridge, Mass.

[12] "Flexural-Torsional Buckling of Eccentrically Loaded Columns," by Robert V. Whitman, thesis presented in September, 1951, to the Massachusetts Inst. of Technology, Cambridge, Mass., in partial fulfilment of the requirements for the degree of Doctor of Science.

[13] "Numerical Procedure for Computing Deflections, Moments, and Buckling Loads," by N. M. Newmark, *Transactions* ASCE, Vol. 108, 1943, p. 1161.

two values of the parameter l^2/a^2, are in substantial agreement with Mr. Salvadori's results and thus afford a gratifying check.

Figs. 1, 2, 3, and 4 can effectively be combined into a single figure by using a generalization of Eq. 1. In Fig. 8 the author's results have been replotted using the ratio M/M_{2cr} for the abscissa, in which M_{2cr} is the critical value of M_2 when no axial thrust is present. The parts of the curves for $r = -0.8$ that are shown as dotted could not be determined directly from Mr. Salvadori's solutions, and their trend is based on numerical values obtained by the writer during his investigations. Eq. 1, represented by the curve for $r = 1$, is a parabola and, as shown[3] by Mr. Johnston, is independent of the value of the parameter l^2/a^2. The interaction curve for $r = 0.5$ differs so little from that for $r = 1$ that the difference does not appear in Fig. 8; even for $r = 0$ the position of the interaction curve has shifted only slightly. Moreover, for values of r between 1.0 and -0.8, variations of the parameter l^2/a^2 from 0.1 to infinity cause only small shifts in the positions of the interaction curves. In fact, the interaction curves for values of l^2/a^2 between 0.1 and 100 are so similar that their differences cannot be shown. It is only when r approaches -1 that differences in l^2/a^2 cause significant changes in the interaction curves.

The composite set of curves in Fig. 8 shows the effect of unequal end moments on the shape of the interaction curve. It is of interest to note that the curves for values of r between 1 and 0 differ slightly and that the effect of the parameter l^2/a^2 is generally small.

The conditions which lead to the sharp breaks in the interaction curves for $r = -1$ are worthy of comment. The two branches of the curves represent two different modes of buckling. The branches running along the top part of Fig. 8 correspond to solutions in which the deflection u is symmetrical with respect to the midspan and the rotation β is antisymmetrical. The reverse conditions are present in the solutions represented by the branches ascending along the right side of Fig. 8. As might be expected, the solution for the case in which u is symmetrical is critical when thrust is more predominant than bending; the reverse condition is true when the bending movements are predominant. If the ascending branch of the interaction curve for $r = -1$ were to be extended to a value greater than $P/P_{cr} = 1$, it would meet the vertical axis at $P/P_{cr} = 4$, corresponding to the second mode of the Euler buckling condition.

MICHAEL R. HORNE.[14]—Eq. 1 for critical combinations of end thrust P and equal end moments M does not allow for the reduction of torsional rigidity caused by end thrust. The complete solution[8,9,15] is

$$K^2 = \pi^2 \left(1 - \frac{P}{P_E}\right)\left(1 + \frac{\dfrac{\pi^2 a^2}{l^2}}{1 - \dfrac{P\, I_p}{A\, C}}\right) \ldots\ldots\ldots\ldots (22)$$

---

[14] Asst. Director of Research, Dept. of Eng., Univ. of Cambridge, Cambridge, England.

[15] "Lateral Buckling of Eccentrically Loaded I-Section Columns," by H. N. Hall and J. W. Clark, *Transactions*, ASCE, Vol. 116, 1951, p. 1179.

The results given by Mr. Salvadori for the case $r = 1$ should agree with Eq. 22. It will, however, be seen that K cannot be expressed as a function of P/P_E and l^2/a^2 because the term $1 - (P\,I_p)/(A\,C)$ is involved. Investigation of Table 1 shows that this term has been assumed to be equal to unity. As the same term occurs in the interpretation of the symbol K and is not there assumed to have a value of unity, the treatment appears to be incorrect although it does give an answer on the safe side. Results deduced from Table 1 will therefore only be accurate provided $(P\,I_p)/(A\,C)$ is small compared with unity, or provided l^2/a^2 is large compared with π^2.

It is possible to obtain an approximate expression for critical combinations of axial load and unequal end moments, thus avoiding the use of Table 1. It follows from work done by P. M. Worthington[16] that, if M_{cr} is the critical value of the larger end moment when the axial load is zero and P_E is the Euler load for failure about the minor axis, for safe combinations of M_2 and P

$$\left(\frac{M_2}{M_{cr}}\right)^2 = \left(1 - \frac{P}{P_E}\right)\left(1 - \frac{\dfrac{P\,I_p}{A\,C}}{1 + \dfrac{D\,h^2}{2\,C}\dfrac{\pi^2}{l^2}}\right) \ldots\ldots\ldots\ldots (23)$$

The value of M_{cr} depends on the ratio r of the end moments, the torsional rigidity C, and the warping rigidity $D\,h^2/2$. If it were assumed that $D = 0$, the value of M_{cr} would be given by

$$M^2{}_{cr} = F\,\frac{B\,C}{l^2} \ldots\ldots\ldots\ldots\ldots\ldots\ldots\ldots (24)$$

in which F is a function of r only (when $r = 1$, $F = \pi^2$). If $C = 0$, then M_{cr} would be given by

$$M^2{}_{cr} = F'\,\frac{B\,D\,h^2}{2}\,\frac{\pi^2}{l^4} \ldots\ldots\ldots\ldots\ldots\ldots (25)$$

in which F' is also a coefficient depending on r. Mr. Worthington has shown that a safe value of M_{cr} when neither C nor D is zero is given by

$$(M_{cr})^2 = F\,\frac{B\,C}{l^2} + F'\,\frac{B\,D\,h^2}{2}\,\frac{\pi^2}{l^4} \ldots\ldots\ldots\ldots\ldots (26)$$

Hence, Eq. 23 becomes

$$K^2\left(1 - \frac{P\,I_p}{A\,C}\right)\left(1 + \frac{\pi^2\,a^2}{l^2}\right)$$
$$= \left(1 - \frac{P}{P_E}\right)\left(F + F'\,\frac{\pi^2\,a^2}{l^2}\right)\left(1 - \frac{P\,I_p}{A\,C} + \frac{\pi^2\,a^2}{l^2}\right) \ldots (27)$$

---

[16] "The Elastic Stability of Straight I-beams Subjected to Complex Loads," by P. M. Worthington, *Proceedings*, Inst. of C. E., London, England, Pt. 1, Vol. 3, January, 1954, p. 46.

The values of F and F' are given in Table 2. When $r = 1$, $F = F' = \pi^2$ and Eq. 27 becomes identical with Eq. 22. Hence, Eq. 27 gives accurate results for uniform bending about the major axis and conservative results when $-1 \leqq r < 1$.

If the value of $(P\,I_p)/(A\,C)$ is small compared with unity, or if l^2/a^2 is appreciably larger than π^2, Eq. 27 reduces to the simpler form:

$$K^2 = \left(1 - \frac{P}{P_E}\right)\left(F + F'\,\frac{\pi^2\,a^2}{l^2}\right) \qquad \text{(28)}$$

TABLE 2.—THE RELATIONSHIP AMONG r, F, AND F'

Value of r	1.0	0.9	0.8	0.7	0.6	0.5	0.4	0.3	0.2	0.1	0	−0.1	−0.2	−0.3	−0.4	−0.5	−0.6	−0.7	−0.8	−0.9	−1.0
Value of F	9.87	10.96	12.11	13.54	15.13	16.97	19.10	21.53	24.30	27.46	30.9	34.8	39.1	43.7	48.6	53.6	58.7	63.4	67.1	68.1	64.5
Value of F'	9.87	11.44	12.78	14.10	15.50	17.16	19.22	21.82	25.10	29.14	34.0	39.8	44.3	53.4	60.8	67.9	74.3	78.9	81.0	79.7	74.1

The percentages by which K, as obtained from Eq. 28, falls below the values quoted in Table 1 is illustrated in Table 3 in which the results are given to the nearest ½%. It will be seen that Eq. 28 gives results sufficiently accurate for practical purposes when the value of r is positive but not when r is negative.

TABLE 3.—PERCENTAGES BY WHICH THE ESTIMATED K-VALUE IS LESS THAN THE K-VALUE FROM TABLE 1

Value of r	VALUE OF l^2/a^2				
	0.1	1.0	10	100	∞
			$P/P_E = 0$		
1.0	0	0	0	0	0
0.5	0	0	0	0	0
0	0.5	0.5	1.5	1.5	0
−0.5	0.5	1.0	3.5	3.0	0
−1.0	0	0.5	3.0	1.5	0
			$P/P_E = 0.6$		
1.0	0	0	0	0	0
0.5	0.5	0.5	0.5	0.5	0.5
0	3.5	4.0	5.0	6.0	5.5
−0.5	15.5	16.0	18.5	18.5	17.0
−1.0	31.5	32.0	33.5	32.5	31.5

This is caused by the fact that the fundamental modes of lateral deflection, when bending moments act alone and when axial load acts alone, respectively, are similar when r is positive but become increasingly dissimilar as r approaches -1.

MARIO G. SALVADORI,[17] M. ASCE.—The form of interaction curves suggested by Mr. Whitman is enlightening. This form not only allows for a more concise graphical presentation (Fig. 8) of the writer's results but indicates the important physical fact that, for values of the ratio r between zero and unity, the interaction curves are insensitive to the values of the parameter l^2/a^2.

In a paper currently in preparation[18] the writer intends to present in this form additional interaction curves for conditions of support other than simple support in the weaker plane. Of course, Fig. 8 must be used in conjunction with a table of critical values of M_2 for $p = 0$, which should appear, possibly, in a corner of the graphical presentation.

It should be noted, regarding Mr. Horne's contribution, that (1) the advantage of a concise presentation will be available in connection with accurate results when Figs. 1, 2, 3, and 4 are combined as suggested by Mr. Whitman; (2) the approximate results obtained by Mr. Horne are much too conservative when r is less than zero, as shown by his computations; and (3) the weakening of the beam as a result of pure torsional buckling under thrust is of no practical importance as the critical thrust for pure torsional buckling is very high for the type of beams to which the writer's results are to be applied in design. The manner in which one can obtain a more accurate value of the critical moment (that is, the value of K) in those rare cases in which torsional buckling becomes significant was described under the heading, "Lateral Buckling of Simply Supported I-Beams." This simple iteration procedure is always applicable with good results.

---

[17] Prof. of Civ. Eng., Columbia Univ., New York, N. Y.

[18] "Lateral Buckling of Eccentrically Loaded I-Columns," by Mario G. Salvadori, *Proceedings-Separate No. 607*, ASCE. Vol. 81, January, 1955.

AMERICAN SOCIETY OF CIVIL ENGINEERS
Founded November 5, 1852
TRANSACTIONS

Paper No. 2774

MOVEMENTS IN STRUCTURAL CONCRETE IN A POWERHOUSE

By Stanley Moyer[1] and Viggo Hansen,[2] Members, ASCE

With Discussion by Messrs. E. A. Woodhead; Herbert A. Kammer; and Stanley Moyer and Viggo Hansen

Synopsis

After the Conowingo Hydroelectric Plant on the Susquehanna River had been in operation for several years, displacements were observed in the structural concrete. Binding occurred in the butterfly valves, and considerable leakage was noted. A system of plumb points and monuments at vital points was established to study the concrete movements. Laboratory tests of concrete cores were made. Studies are being continued; they indicate that cyclic temperature change may have considerable effect on the concrete movement.

Introduction

The Conowingo Hydroelectric Plant is on the Susquehanna River, approximately four miles above tide water, where US 1 crosses the river on the dam. The Susquehanna River runs from north to south, and the powerhouse is on the west bank.

The entire dam is of concrete masonry construction and was designed as a gravity section. Its total length of 4,648 ft includes the powerhouse headworks —which are 950 ft long—and 2,385 ft of ogee-type, gate-controlled spillway section.

The paper is concerned with the structural movements of the concrete in the powerhouse only. No movements have been observed in the dam.

The powerhouse substructure was extended to a maximum depth of El. −20.5 ft at the hydracone draft tubes of four of the wheels. On the other three wheels, a spreading type of draft tube was used which required excavation to

---

Note.—Published, essentially as printed here, in October, 1953, as *Proceedings-Separate No. 308*. Positions and titles given are those in effect when the paper or discussion was received for publication.

[1] Asst. Mechanical Engr., Philadelphia Electric Co., Philadelphia, Pa.

[2] Engr., in charge of Structural Section, Philadelphia Electric Co., Philadelphia, Pa.

El. −16.5 ft. All elevations are referred to datum of the Coast and Geodetic Survey, United States Department of Commerce (USCGS).

The main powerhouse superstructure of the initial installation includes the generator room, which is approximately 70 ft wide by 75 ft high by 620 ft long. Between the generator room and the headworks is a two-story section approximately 50 ft wide containing the 13,800-volt bus and the switching equipment, above which are located the main transformers. The 220-kv switching station is located on the roof of the generator room. The operating floor of the plant is at El. 46; the generator floor, at El. 60; and the high point of the roof, at El. 121.60.

The initial and present installation of this plant consists of seven 54,000-hp water wheels driving 36,000-kw generators. The wheels operate at 81.8 rpm under a head of 89 ft. Provision for four additional units was made in the initial installation.

A structural-steel pit liner and generator support embedded in concrete is provided for each main unit. It is attached to the speed ring of the water wheel and is designed to support the weight of the generator and the thrust bearing load down to the upper portion of the speed ring, whence the load is transferred through the guide vanes to the lower ring and into the powerhouse substructure. The entrances to the plate-steel riveted scroll cases are controlled by 27-ft-diameter butterfly valves on vertical shafts.

The frame of the powerhouse superstructure is designed of reinforced concrete on structural steel. The concrete roof of the generator room is supported by steel trusses. All loads imposed by the switching station on the roof are transmitted to the substructure through steel columns heavily reinforced with concrete. The loads of the two 150-ton-capacity cranes in the generator room are supported by separate steel columns that are tied to the building columns for lateral support only. The powerhouse structure contains 236,000 cu yd of concrete and 4,600 tons of structural steel.

Construction of this plant was begun in March, 1926. The first concrete was poured in August of that year. The final concrete was poured on December 31, 1927. The first unit was placed in operation on March 1, 1928, and the complete plant was in commercial operation by June 1, 1928.

INITIAL EVIDENCE OF MOVEMENT

By 1940, pronounced structural displacements in the powerhouse were observed. The original installation included several reference points in the powerhouse structure. One of these was on the downstream wall opposite Unit No. 4. It consisted of a bracket on the parapet above the generator-room roof at approximately El. 125 with a brass plug at the roof level and one just above the stop-log gallery at El. 46. Checking both these points with a plumb line gave definite indications of movements throwing the downstream wall out of plumb. Two similar sets of plumb points, one at Unit No. 1 and one at Unit No. 7, were added in 1941, and subsequently the results of movements of the same nature at these locations were observed. The out-of-plumb measurement at Unit No. 4 in 1943 was ½ in.

BINDING OF BUTTERFLY VALVES

At about the same time, difficulty was experienced in operating the butterfly valves. These valves were encased in the substructure concrete up to a plane approximately 2 ft below their horizontal center line; the binding occurred in this area. Operating clearances were maintained for several years by periodic grinding of the bronze seals as long as sufficient metal remained. Meanwhile check points were installed, and it was established that the lower half of the housing was being squeezed out of round by the surrounding concrete. After careful studies to discover the most economical way of correcting this condition, it was decided to free the lower half of the casing from the concrete surrounding it. The work was completed in 1953 on the last two of the seven valves.

Even prior to the concrete removal, there was considerable leakage through the concrete in the valve areas, the most noticeable being at Unit No. 5 which also had the first binding difficulty. This leakage increased as concrete was removed so that it was necessary to repair eroded areas and pressure-grout each of the penstocks. Leakage was reduced considerably, and no appreciable binding has been experienced since completion of these operations.

CONCRETE

In 1943, investigations were begun on the aggregates used in the concrete and on the placing methods. In the course of this investigation, the records revealed that in the first 62,000 yd of concrete placed in the substructure of the powerhouse 60,000 tons of rock from the powerhouse excavation were crushed on the job and used as the coarse aggregate.

A study of construction pictures and reports also indicated that very high-slump concrete was necessary because a chuting system was used for placing concrete throughout the powerhouse area. The areas in which the local stone was employed were determined by studies of the progress reports and of the diamond core borings used to obtain cylinders for testing.

The geological reports of the stone in the area involved were also carefully studied, and recently acquired geological knowledge indicated that the igneous and metamorphic rocks at the Conowingo site probably contained materials which when used as aggregate in concrete might chemically react with deleterious effects.

The study of the record showed that the crusher plant on the project was shut down after production of 60,000 cu yd of aggregate because excessive quantities of fines were produced in the operation. The washing required to make this stone suitable for use in the concrete proved less economical than the importation of coarse aggregate.

The areas in which the suspicious material was used were plotted on typical cross sections of the plant, and the possible effects were studied. It became evident that any change in volume of the concrete prepared with this stone must have a significant effect principally on the downstream and superstructure parts of the powerhouse.

There are no expansion joints in the substructure, but there are two expansion joints in the superstructure (above El. 46), one between Units No. 1 and 2 and one between Units No. 5 and 6.

TESTS ON CONCRETE

Concrete cylinders were cored out of the monolith in the inspection tunnel to provide substructure specimens, and similar cores from the transformer-court wall provided superstructure specimens. The Portland Cement Association was engaged to make tests on these cores, 6 in. in diameter by from 12 in. to 32 in. long the length being determined by the breakage of the core during the drilling. They were shipped to the Chicago (Ill.) Research Laboratory of the Portland Cement Association in special containers and there prepared for compression tests, thermal-coefficient tests, absorption tests, and specific-gravity tests; in addition, specimens were prepared for autoclave soundness tests, petrographic refractive indexing, and X-ray refraction studies.

Compression tests of the substructure concrete showed a variation of 20% from the average, but all tested more than double the design strength of 1,600 lb per sq in. The lateral modulus of elasticity as determined by the sonic method was approximately 4.5×10^6 lb per sq in. The tests for thermal expansion in the dry state were consistent with usual results, which in many cases show a slight decrease in volume. In contrast with this, wet specimens exposed to recurrent changes in temperature varying from 20° F to 85° F showed a cyclic change with a net increase in length.

Microscopic examination of polished and broken sections of the cores disclosed some evidence of alkali-aggregate reaction in the substructure concrete. The apparent specific gravity of the concrete was found to be from 2.2 to 2.4. Absorption values appear to be reasonable for this class of concrete. Autoclaving of prisms (cut from cores) showed a low percentage of expansion, thus indicating that all the cement had been hydrated. Some special laboratory specimens made with a high-alkali cement and fragments of the broken cores showed a relatively high expansion. Long-range tests for a period of eighteen months or more in the laboratory on two cores stored in air over water at 110° F registered 0.019% and 0.043% increases in length. Similar tests of laboratory-made prisms showed an increase in length of 0.012% for those containing low-alkali cement, 0.046% for those of high-alkali cement, and 0.082% for those of high-alkali cement with 1% sodium hydroxide added.

Cores of the substructure concrete that were immersed in water and alternately heated and cooled so that they received a daily cycle of temperature change from 90° F to 40° F were measured and after 50 cycles showed a 0.070% increase at 90° F and a 0.043% increase at 40° F. Similar tests on cores taken from the headworks showed increases of 0.057% and 0.026%, for the same temperatures.

SURVEY SYSTEM

In 1943, it was also decided to install a complete system of check points to measure movements of the structure. Ten east-and-west lines were establishedwhich are identified as follows: The R-line is on the stop-log gallery at El. 46.0 and is the base line for all north-and-south movements. The three monuments controlling this line are carefully located sufficiently far back from the banks of the river, with two of the monuments on the west bank. All monuments are constructed according to standards of the USCGS and extend to bed rock. Another line on El. 46 is designated as the A-line and is approximately 16 ft north of the R-line. A third line on El. 46, designated as the B-line, is north of the generators and is approximately on the center line of the butterfly valves. A fourth line at this elevation is at the north wall of the generator room and is noted BW. Another line is on El. 80 in the headworks wall and is accessible from the transformer transfer court. At El. 60.0, two lines were established, the B-line being directly over the B-line on El. 46 and the AB-line on the walkway around the generator. One series of measurements is referred to the B-line at El. 60 and is taken on a plug on each arm of the generator-supporting frame in order to determine whether these frames are remaining in a horizontal plane and to indicate any misalinement of the supporting barrel and the turbine shaft. There are two lines on El. 35, one being immediately below the A-line at El. 46 and another line as far north as possible, which is designated as the AB-line, being south of the B-line at El. 46. Another line is in the inspection tunnel below the intakes at El. 1. Each of these lines was installed parallel to the R-line and each has one or two points per main unit. The base line for east-and-west movements is controlled by two monuments downstream from the plant, safely far back from the west bank, the northerly one of which is used for the vertical datum. This line projected northward enters the turbine room at El. 46 and intersects the R-line, the A-line, and the B-line at that elevation, with plugs at each intersection. Most of the points for this survey system consist of a bronze plug carefully anchored and grouted into the concrete. A very small center-punch mark was made in each plug; this became the zero (initial) reading. A few control points on thes teel trusses of the turbine-hall roof determine whether any movement occurs in the north-and-south direction, but this movement has proved to be negligible during the past ten years. Plumb lines from the B-line at El. 46 are used for measurements around the butterfly-valve housings.

All instruments and methods used in this work conform to specifications of the USCGS for first-order surveying.

SURVEY RESULTS

Readings taken on these several lines have shown a rather variable pattern, but the net result has been a southward displacement with the magnitude increasing from the headworks to the downstream extremities of the plant. The variations are not directly proportional and are not equal in the areas of each of the seven units. The southward displacement is the least at Unit No. 1; it increases toward Unit No. 4; then decreases slightly at Unit No. 5; increases again so that it is approximately the same at Unit No. 6 as at Unit No. 4; and becomes considerably less at Unit No. 7, which is the east end of the existing powerhouse.

In the area of Unit No. 1 the southward movement is restrained by the keying of the west abutment into the rock and by the concrete retaining wall in the tailrace. At the east end there is no restraint, but a large portion of the monolith adjacent to the future unit section is not exposed to intake water on both sides and a considerable portion is exposed to the atmosphere above the tailrace surface at El. 20. Laboratory test results indicate that in these relatively dry surroundings the growth of the concrete is reduced. Near Units No. 4, No. 5, and No. 6, large areas of concrete are exposed to the intake waters; furthermore, the leakage around the intakes and into the inspection tunnel developed first in the area of Unit No. 5, indicating a gradual saturation of the concrete in the area.

The east-and-west movements are small, probably because of the restriction by the rock on the west bank and the dam on the east end of the powerhouse.

The difference in movement is confirmed by visible cracks at El. 46 and El. 60 with the largest crack, open approximately ¾ in., located at El. 60 just south of the B-line, or at the junction of the circular walkway around Unit No. 4 with the main floor system. A second large crack approximately ⅝ in. wide has occurred near Unit No. 6 at the connection of the floor and the down-river wall at El. 46.

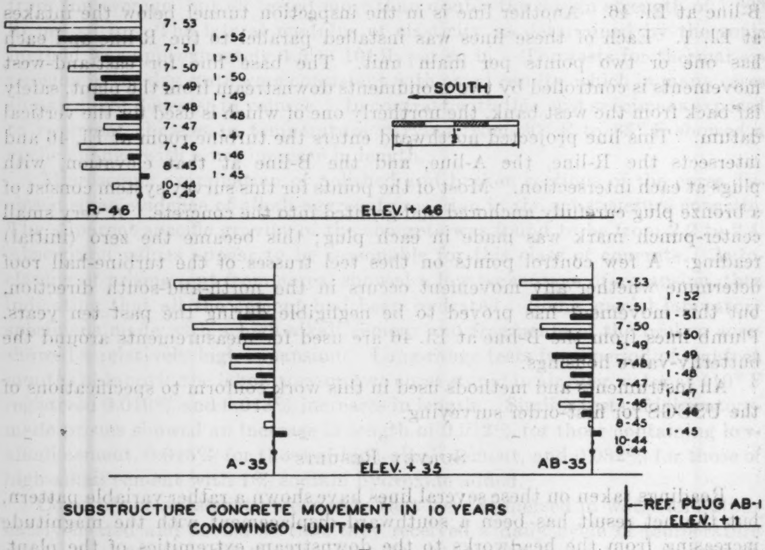

SUBSTRUCTURE CONCRETE MOVEMENT IN 10 YEARS
CONOWINGO - UNIT Nº 1

Fig. 1

The maximum southward movement recorded at El. 46 from 1944 to 1953 is approximately ¾ in. at Units No. 4 and No. 6. The movement at Unit No. 1 in the same period of time was ⅜ in. and at Unit No. 7 was ½ in.

The east-and-west movement of nearly all the points have varied in direction, sometimes showing an easterly movement and sometimes a westerly movement with the net movements being easterly and not more than ¼ in. The largest vertical movement is ¼ in., and all vertical movements are rather uniformly upward.

The measurements on the generator supporting frame have not indicated any appreciable change in the plane of the supports, and as of 1955 there has been no evidence of concrete movements affecting the vertical alinement of the units.

During the first few years, readings were taken over the survey points each winter and summer without very careful control as to their exact timing. Studies of the results of these early surveys indicated a need for closer scheduling in order to reduce to a minimum the variables in the problem. Examination also indicated that surveys at 18-month intervals instead of 6-month intervals would provide sufficient data to measure and plot the movements accurately and would continue to indicate the effect of the change in water temperature. Measurements have been taken at 18-month intervals during the period of 1951 through 1955.

The results of the surveys have been plotted in Figs. 1, 2, and 3 in the form of bar charts to facilitate study and to determine where and when remedial measures will be necessary. The month and year of each reading appear opposite the appropriate bar.

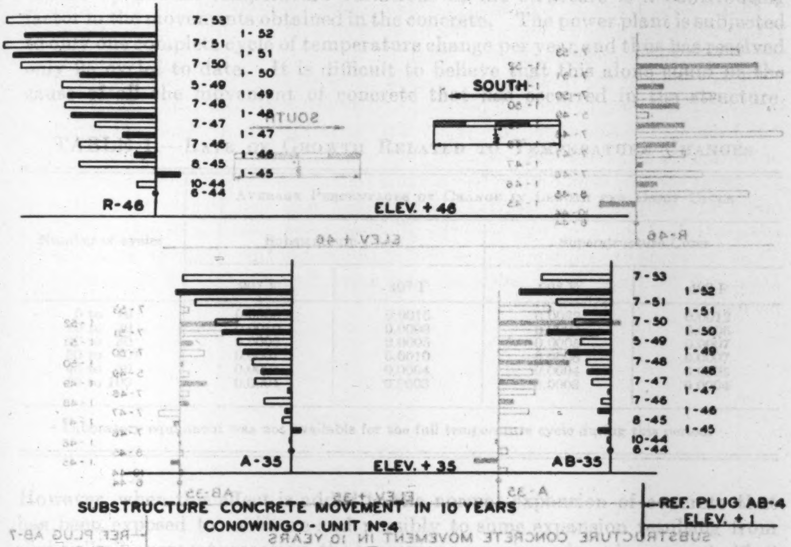

Fig. 2

Effect of Silting

The total movement of the structural concrete of the powerhouse is considered to be the result of two separate actions. The major one is the growth of the concrete, and the other is believed to be the silting in the cracks that occur in the concrete due to temperature changes. A considerable increase in leakage in the lower part of the powerhouse is evidenced each November or early December, reaching a maximum of from three to four times the normal summer leakage. This is undoubtedly due to the contraction of the concrete caused by the drop in temperature of the water, the average difference between the summer temperature and the winter temperature of the water being approximately 50° F. After a storm or other disturbance of the pond, the water carries much fine silt, and as this flows through the several cracks some of it is retained, reducing the leakage very rapidly before the first of the year. During the summer when the concrete expands because of the rise in the water temperature, the silt that was retained in the cracks is compressed and much of it remains permanently in the crack. The actual thickness of this compressed silt has not been and cannot be measured by any means, and its effect cannot be evaluated. Possibly it is rather insignificant because the east-and-west movements are relatively small, as was noted in results of the surveys. Also, the leakage in the butterfly-valve areas has not decreased during the life of the plant except after the previously noted grouting.

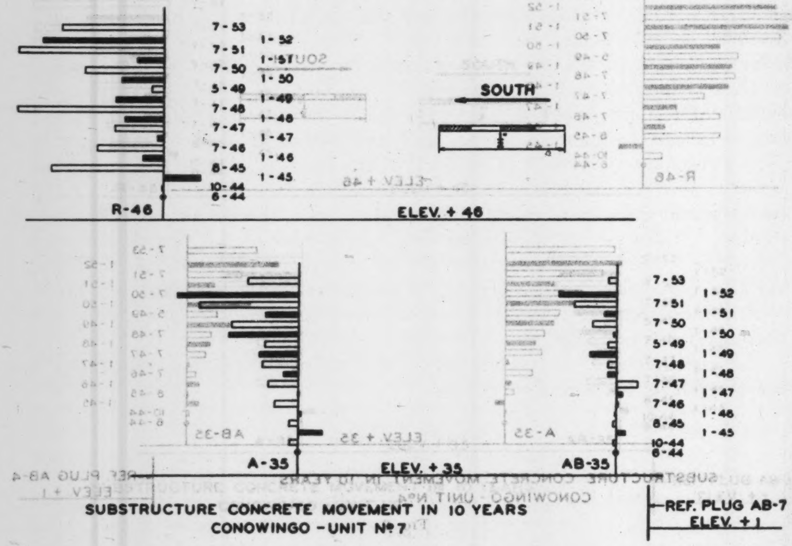

FIG. 3

CONCLUSION

Although this paper should be considered an interim report, certain conclusions have been drawn and future policy determined.

The laboratory tests indicate that there are two unusual characteristics of the concrete which may indicate the cause of the movement which has developed in the structure. These characteristics are (1) the continuing expansion of the concrete cores during exposure to repeated cycles of temperature change and (2) the relatively high expansion of some of the laboratory specimens made either with a high-alkali cement or with this cement plus 1% sodium hydroxide.

Tests for reaction between aggregate and alkalis have not indicated extremely high expansions during the 18-month test period, but some of the expansions are greater than would be expected with normal aggregate, and the trend of some of the curves suggests that there may be some reactivity. At any rate, it is still too early to discount the possibility of alkali-aggregate reaction for such reactions often require a period of years to develop, and some slight evidence of such reaction was found in the examinations of the original concrete cores.

The expansion of the cores subjected to repeated cycles of temperature change (from 40° F to 90° F) is considerably greater than that obtained with the laboratory-made specimens. It may be, therefore, that a similar effect caused by annual temperature variations in the structure is a contributing factor in the movements obtained in the concrete. The power plant is subjected to only one complete cycle of temperature change per year and thus has received only 25 cycles to date. It is difficult to believe that this alone could be the cause of all the movement of concrete that has occurred in the structure. However, when this effect is added to the normal expansion of concrete that has been exposed to moisture and possibly to some expansion resulting from slight alkali-aggregate reaction, the expansions experienced can be accounted for.

TABLE 1.—RATE OF GROWTH RELATED TO TEMPERATURE CHANGES

Number of cycles	AVERAGE PERCENTAGES OF CHANGE IN LENGTH PER DAILY CYCLE			
	Substructure Cores		Superstructure Cores	
	90° F	40° F	90° F	40° F
0 to 10	0.0039	0.0016	0.0032	0.0012
10 to 20	0.0010	0.0008	0.0007	0.0008
20 to 30	0.0005	0.0005	0.0005	0.0007
30 to 40[a]	0.0007	0.0010	0.0008	0.0007
40 to 50	0.0005	0.0004	0.0004	0.0005
50 to 100	0.0004	0.0003	0.0003	0.0004

[a] Laboratory equipment was not available for the full temperature cycle during this period.

It has been explained that the concrete was high in water content and that all the cement had been hydrated, but there is no record of the alkali content of the cements used.

There is nothing in the results to suggest how long the movement of the concrete will continue. However, an analysis of several laboratory tests in which three substructure cores and three superstructure cores were immersed in water and alternately heated and cooled so that they received a daily cyclic change of from 90° F to 40° F does give some encouraging indications of a decrease in the rate of growth as shown in Table 1.

If the movement of ½ in. recorded by the plumb line at Unit No. 4 up to 1943 and the maximum survey reading in 1953 of ¾ in. are considered cumulative, the total measured movement is 1¼ in. In comparison, by taking the width of the plant from the center line of the key in the rock under the headworks to the downstream face of the structure, a distance of 150 ft, and applying the laboratory results to cores from that part of the structure, the computed results would also indicate a movement of 0.105 ft or 1¼ in.

There is no indication of over-all structural weakness in the powerhouse, and there is no concern except to insure the integrity of operation of the equipment.

FUTURE POLICY AND PLANS

Measurements of the survey system are scheduled to be continued at 18-month intervals (in January and July) until an indication of negligible movement is recorded because none of the test results or survey readings can be used to forecast that date.

In general, there is no plan to replace any concrete in the near future. If operating conditions indicate the necessity for local relief, immediate steps will be taken to accomplish such relief.

The cracks at the downstream wall at El. +46 definitely show a separation between the floor and the wall pilasters. The area between Units No. 5 to No. 7 and the wall was designed for "lay-down" area during maintenance operations providing for a 1,000-lb-per-sq-ft live load, and steel beams were installed. Conditions at the pilasters limited the bearing of these steel beams, and the movements are reducing this bearing. As a safety measure, twenty steel columns were installed early in 1955 near the pilasters to support the steel beams fully. These columns are supported directly by the monolithic concrete at El. +35. Data will continue to be collected, and corrective measures will be taken if necessary.

DISCUSSION

E. A. Woodhead.[3]—The Idaho Power Company was made forcibly aware of the phenomenon of concrete growth approximately twenty years ago, when displacement of the concrete in the American Falls plant resulted in the cracking of the downstream concrete walls of the semispiral casings and in the cracking of the cast-iron stay vanes of some of the turbines. Some misalinement of generators also occurred. Repairs were made on the spiral-casing wall of the turbine by means of 1½-in. vertical tie rods recessed into grooves cut in the face of the wall. These rods were prestressed, and then a well-reinforced and anchored facing slab was applied to the wall, as shown in Fig. 4. The turbine stay vanes were repaired by means of plate-steel brackets shaped to fit and studded to the cast iron, as shown in Fig. 5. The misalined generators were reset. These repairs have been satisfactory. A study of the causes that led to this damage has guided design and construction procedure in plants built subsequently. These causes and the remedies or deterrents applied are as follows:

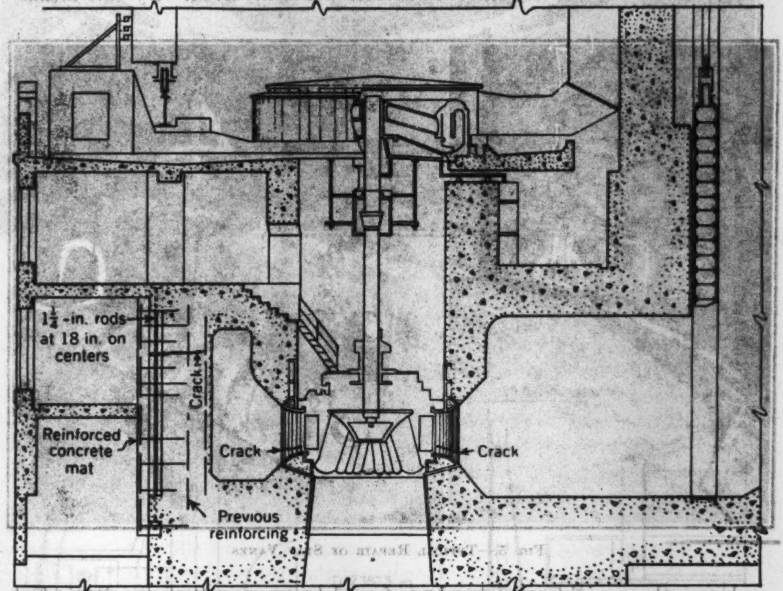

Fig. 4.—Cross Section Showing: (Step No. 1) Tie Rods and Dowels, and (Step No. 2) Reinforced-Concrete Mat and Repair of Stay Vanes

1. **Reactive Aggregates.**—Not much can be done about the presence of reactive aggregates except to select those aggregates that are found by test to be most desirable—or least undesirable.

---

[3] Chf. Cons. Engr., Idaho Power Co., Boise, Idaho.

2. High-Alkali Cement.—The cement most readily available in the company's recent construction work is somewhat alkaline. The company has made a practice, however, of obtaining adequate supplies of a low-alkali cement from a considerable distance to use in certain parts of the work where concrete growth might cause trouble.

3. Directional Expansion.—Concrete growth will manifest itself ordinarily in the direction of least restraint and in proportion to the length of the concrete prism involved in such expansion. This was the primary cause of deformation at American Falls, and it was guarded against in subsequent plants by very heavy reinforcement of the turbine throat ring and by heavy vertical reinforcement of the generator barrel, such reinforcement being of a cross-sectional area proportional to the length of concrete prism involved. By this means, such growth as might occur has been forced to occur in that direction which will cause the minimum of distortion of working clearances or settings. In the cases of the Lower Salmon and Malad plants also, there was some doubt that low-alkali cement would be available in sufficient quantity for requirements, or at all, because of heavy governmental purchases of the most desirable cements at that time (1947), and the generators were therefore ordered with self-equalizing thrust bearings as an additional precaution. However, the company has actually been able to use a low-alkali cement (from 0.4% to 0.5% potassium and sodium oxide equivalent) in all powerhouse substructure work around draft-tube liners, throat rings, and turbine blocks up to the generator foundation level.

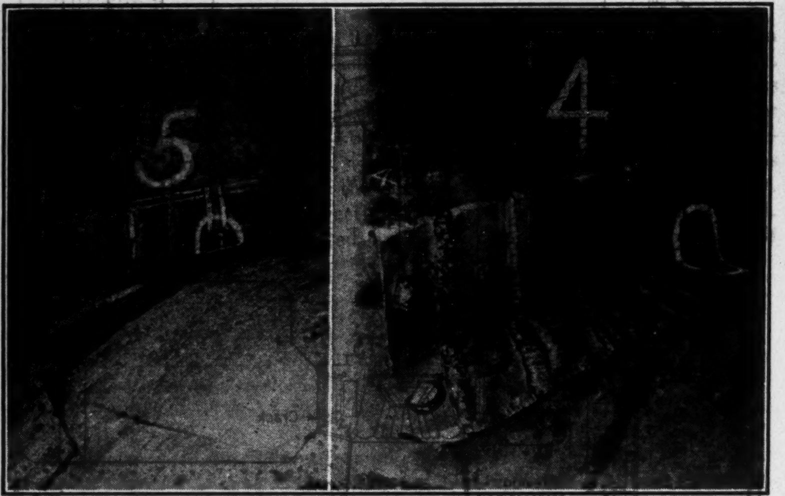

FIG. 5.—TYPICAL REPAIR OF STAY VANES

In the C. J. Strike plant, which was completed early in 1952, the owners were able to use all the experience obtained prior to that time. This plant is

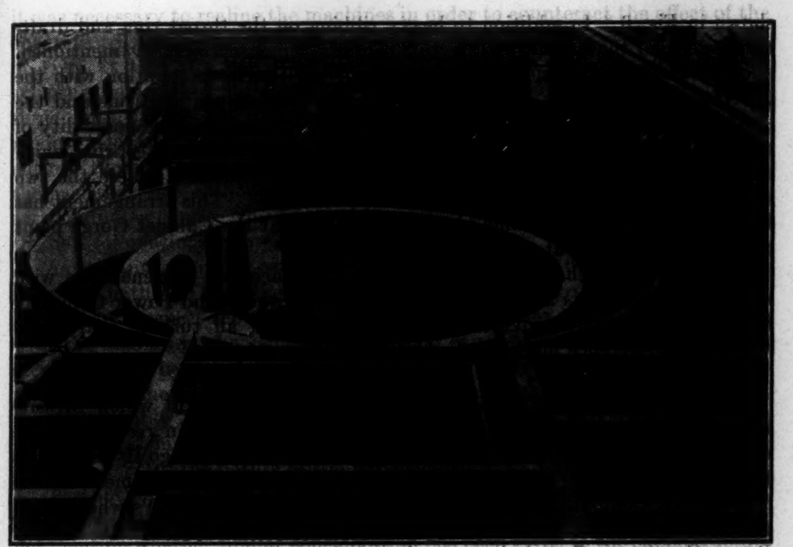

FIG. 6.—THE C. J. STRIKE PLANT

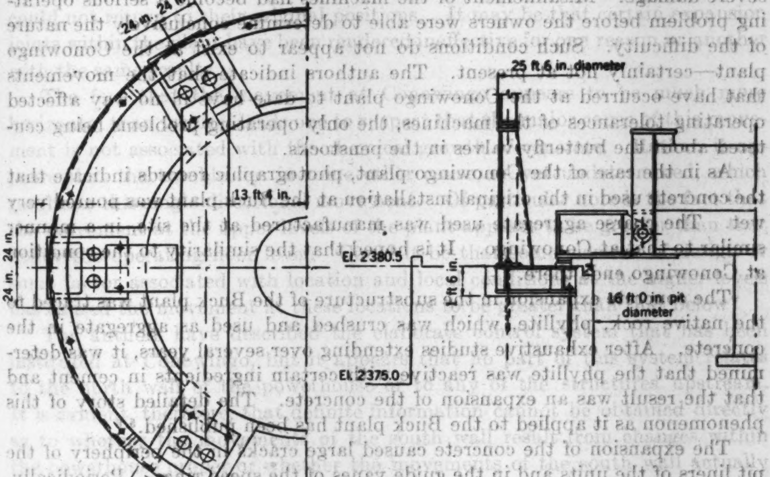
24 in.
24 in.
25 ft 6 in. diameter
13 ft 4 in.
24 in.
24 in.
24 in.
El. 2380.5
1 ft 6 in.
16 ft 0 in. pit diameter
El. 2375.0
24 in.
24 in.

FIG. 7.—GENERATOR BASE RING AND BEARING SUPPORT, C. J. STRIKE DEVELOPMENT

shown in Fig. 6. In addition to heavy ribbing on the throat ring and draft-tube liner and the use of the directional reinforcement previously mentioned, an innovation in the generator design was introduced in cooperation with the generator manufacturer. Instead of having the thrust-bearing arms and the stator yoke supported by concrete at different elevations with the possibility of differential movement, the stator yoke is supported on a heavy steel ring which extends down to the elevation of the thrust-bearing support, where the two elements mentioned are connected as shown in Fig. 7. This arrangement has been successful, and the same idea was later used at the Cabinet Gorge plant of the Washington Water Power Company.

As a means of checking possible vertical displacement of generators with respect to turbines as a result of concrete growth, the Idaho Power Company has for several years provided a reference collar on all turbine shafts and appropriate reference marks on turbine pit walls.

Herbert A. Kammer,[4] A. M. ASCE.—The dilemma in which Messrs. Moyer and Hansen and their associates find themselves, in respect to the movements that have occurred in the structure of the Conowingo Hydroelectric Plant, recalls a similar situation that confronted engineers of the American Gas and Electric Company during the late 1930's and the early 1940's when structural changes in the Buck Hydroelectric Plant of the Appalachian Electric Power Company affected the operation of the three generators at that plant. Actually, the problem at the Buck plant was considerably more severe than that at the Conowingo plant; certain of the machine components had suffered severe damage. Misalinement of the machines had become a serious operating problem before the owners were able to determine conclusively the nature of the difficulty. Such conditions do not appear to exist at the Conowingo plant—certainly not at present. The authors indicate that the movements that have occurred at the Conowingo plant to date have in no way affected operating tolerances of the machines, the only operating problems being centered about the butterfly valves in the penstocks.

As in the case of the Conowingo plant, photographic records indicate that the concrete used in the original installation at the Buck plant was poured very wet. The coarse aggregate used was manufactured at the site, in a manner similar to that at Conowingo. It is hoped that the similarity to the condition at Conowingo ends there.

The concrete expansion in the substructure of the Buck plant was traced to the native rock, phyllite, which was crushed and used as aggregate in the concrete. After exhaustive studies extending over several years, it was determined that the phyllite was reactive with certain ingredients in cement and that the result was an expansion of the concrete. The detailed story of this phenomenon as it applied to the Buck plant has been published.[5,6]

The expansion of the concrete caused large cracks in the periphery of the pit liners of the units and in the guide vanes of the speed rings. Periodically, it was necessary to realine the machines in order to counteract the effect of the concrete growth. The width of the cracks in the pit liners was of the order of 1 in. at the time the Buck plant was shut down and parts of the substructure replaced. A new concrete foundation was installed for each of the three units, using low-alkali cement and sound aggregates and complying with modern techniques of concrete placing. This procedure has proved to be entirely successful to date. The machines have been operating successfully for the past ten years without any alinement troubles in spite of the fact that the surrounding concrete, which was not removed but is physically isolated from the new foundations, continues to grow.

---

[4] Executive Vice-Pres., American Gas and Electric Service Corp., New York, N. Y.

[5] "Repairs to Buck Power House and Dam," by Philip Sporn and H. A. Kammer, *Civil Engineering*, July, 1944, p. 285.

[6] "Investigation of Causes of Delayed Expansion of Concrete in Buck Hydroelectric Plant," by H. A. Kammer and R. W. Carlson, *Journal*, A. C. I., June, 1941 ,pp. 665, 668, and 669.

As the authors point out, it is too early to permit a final conclusion as to the exact nature of the causes of movement at Conowingo. There appears to be reason to suspect the presence of unsound aggregates which, in combination with the alkalies in the cement, are causing expansion of the concrete. This seems to have been the case underlying the troubles that were noted in connection with the operation of the butterfly valves in the penstocks. However, this is probably not the final answer to the problem at Conowingo. The elaborate system of controls that has been established should assist in ascertaining more exactly the nature of the movements.

The authors mention the possibility of silt entrapment within cracks that may exist in the lower sections of the Conowingo concrete. However, they do not mention whether similar consideration has been given to the superstructure of the plant. A check of the condition of the superstructure might show the existence of some cracking into which foreign material has entered at some time during the thermal cycle so that, on contracting, those parts of the plant could not return to their original positions. It may be that certain expansion joints within the plant have been rendered ineffective for one reason or another with the same results.

The fact that the movement at Conowingo appears to be much more horizontal than vertical leads one to suspect that the major cause of this movement is not associated with the chemical growth of concrete. Rather, it appears that the trouble lies in some other cause, as yet undetermined, which results in this single-directional movement. Of particular note is the fact that the movement at the upper levels of the plant appears to be greater than that below the operating floor level. Could it be that some element of design or some factor associated with location and local conditions at the higher levels has caused the movement at these locations to be greater than that below?

The authors have described the elaborate control system that has been instituted at Conowingo, but it appears that no part of this system relates to the north wall of the powerhouse or to any of the structures upstream. It is evident, therefore, that definite information cannot be obtained directly as to whether the movements of the south wall result from changes within the powerhouse proper or whether the movements of the south wall actually reflect movements that occur at or beyond the north wall.

The authors suggest the possibility of over-all expansion of the concrete due to the annual thermal cycle. Corollaries to this reasoning concern the much shorter daily temperature cycle and the intermediate cyclical weather changes of relatively short duration. These conditions may be of particular concern in the roof slab which provides the base for the 220-kv switching station.

The writers hope to receive further reports on the investigations that are in process at Conowingo. It is hoped that the authors and their associates are successful in isolating the causes of the movements at the hydroelectric plant and that they will someday report concerning the causes and the remedies decided on.

Stanley Moyer[7] and Viggo Hansen,[8] Members, ASCE.—One year elapsed between the writing of the paper and this closure. A visual inspection after the increase in leakage late in November, 1954, revealed no definite trend. The first complete survey of the building monuments since the paper was written is being made (early in 1955) according to the schedule given in the paper.

Mr. Kammer had experience with the growth of concrete at the Buck Hydroelectric Plant that was considered to result from to the reactive coarse aggregate, wet concrete, and the probability of high-alkali cement. The writers also are hopeful that solution of their company's problems will not require the serious corrective measures that their contemporaries were compelled to make.

It was apparently fortunate that the change was made to "off-the-site" aggregate after the first 62,000 yd had been used. A total of 236,000 yd was used. In Fig. 8, which shows a cross section of the powerhouse, the area where the "local-stone" concrete was placed is indicated by crosshatching at the lower right corner. This information was not clear in the paper. The survey line referred to under the heading, "Survey System," as "* * * on El. 80 in the headworks wall * * *," can be seen to be close to the upstream part of the powerhouse; it was decided that no line farther north could be accurately surveyed.

Observations indicate that the short cycle of daily temperature change affects only the south wall (downstream) because most of the concrete is not subjected to appreciable daily changes of temperature but is affected by the change in water temperature, which roughly resembles a sine curve for which the year is one complete cycle.

The concrete roof of the turbine hall is supported on steel trusses and purlins, and therefore that concrete would not affect the over-all dimensions; no difficulty has been experienced in the roof structure except that maintenance was required at the two expansion joints.

The only observed leakage at the plant has been in the area where the local aggregate was used—below El. 46. This area is subjected to the full change in water temperature and is vulnerable to the effect of water being applied to the questionable materials in addition to the carrying of silt by water into that part of the powerhouse. The headworks section above the intake has shown no particular distress, and, as previously noted, no leakage has been

---

[7] Asst. Mech. Engr., Philadelphia Electric Co., Philadelphia, Pa.

[8] Engr. in charge of Structural Section, Philadelphia Electric Co., Philadelphia, Pa.

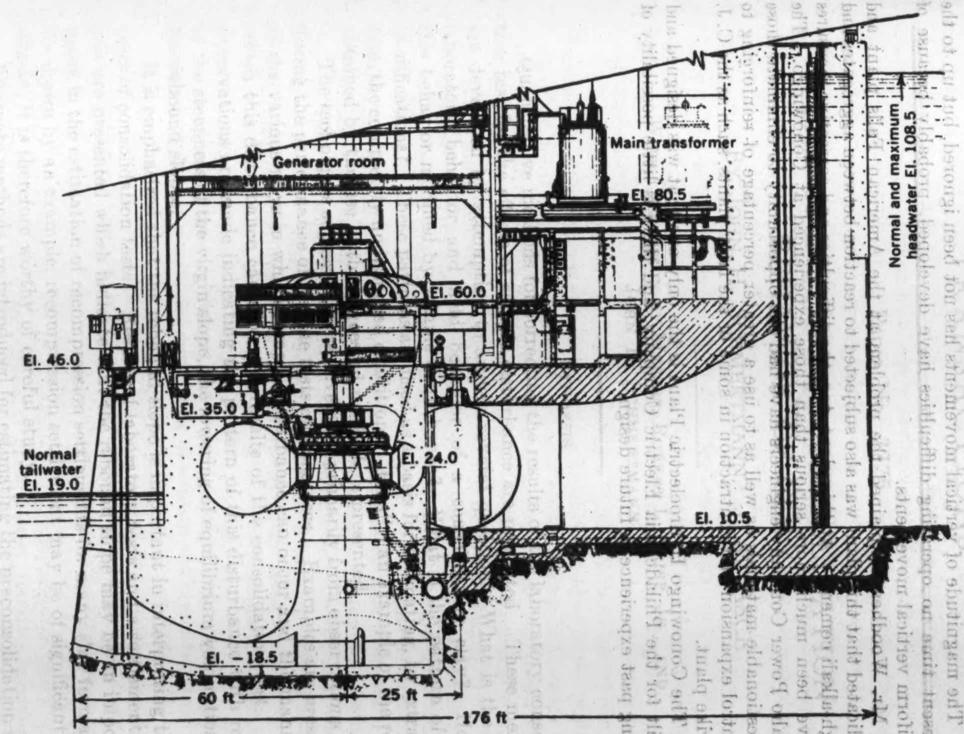
Normal and maximum headwater El. 108.5
Main transformer
El. 80.5
Generator room
El. 60.0
El. 46.0
El. 35.0
El. 24.0
Normal tailwater El. 19.0
El. 10.5
El. −18.5
60 ft
25 ft
176 ft

FIG. 8.—CROSS SECTION, CONOWINGO POWERHOUSE

observed above El. 46. There have been some binding of doors in this section and a few cracks in the walls of the rooms, but the latter do not indicate movements of more that ¼ in. (as noted in the paper).

The magnitude of vertical movements has not been ignored, but up to the present time no operating difficulties have developed, probably because of uniform vertical movements.

Mr. Woodhead explained the problem at the American Falls plant and indicated that this plant was also subjected to reaction between aggregates and high-alkali cement. At this plant, too, the difficulties and corrective measures have been much more serious than those experienced at Conowingo. The Idaho Power Company engineers have had the opportunity to eliminate those questionable materials as well as to use a greater percentage of reinforcing to control expansion and contraction in some of the later plants, such as the C. J. Strike plant.

The Conowingo Hydroelectric Plant is the only one that was designed and built for the Philadelphia Electric Company, and there is little possibility of using past experience in future design.

AMERICAN SOCIETY OF CIVIL ENGINEERS
Founded November 5, 1852
TRANSACTIONS

Paper No. 2775

THE UNDISTURBED CONSOLIDATION BEHAVIOR OF CLAY

By John H. Schmertmann,[1] J. M. ASCE

With Discussion by Messrs. Robert L. Crisp, Jr., and
John H. Schmertmann

Synopsis

Quantitative methods for correcting the results of the laboratory consolidation test for the effects of sample disturbance are presented. These methods are developed by attempting to answer several questions: What is the basic laboratory behavior and field behavior of a consolidating clay? How is this behavior modified by sample disturbance? What is the pattern of such modifications? These patterns are used as a basis for estimating, by extrapolation, the completely undisturbed conditions. Finally, an example of the results obtained by the use of the suggested methods is presented.

The techniques suggested were developed primarily from observations made during the performance of routine tests and analyses. Examples are presented of the various ways in which sample disturbance can occur and the manner in which this disturbance can alter the results of the consolidation test. Some observations are made indicating the pattern of this disturbance with respect to the steepness of the virgin slope, the lowering of equilibrium void ratios, and the rebound slopes.

It is emphasized that the rebound slope is important in interpreting the results of consolidation tests. Results of laboratory tests and a settlement analysis are presented which indicate that the rebound slope may be an important guide in the estimation of recompression settlements for many clay formations. As shown by an example, recompression settlement may be of significant magnitude; it is therefore worthy of careful study.

Alternate methods are introduced for estimating the preconsolidation stress. Because of the manner in which the position of the virgin curve is changed by sample disturbance, the use of a graphical method for determining a minimum

---

Note.—Published, essentially as printed here, in October, 1953, as *Proceedings-Separate No. 311.* Positions and titles given are those in effect when the paper or discussion was received for publication.

[1] **United States Army, Snow, Ice, and Permafrost Research Est., Wilmette, Ill.; formerly Junior Soils Engr., Moran, Proctor, Mueser & Rutledge, New York, N. Y.**

possible preconsolidation stress is suggested. Several examples are presented to show how water-content data can be useful in determining preconsolidation profiles in clay layers having uniform consolidation characteristics. A "void-ratio-reduction-pattern" technique is introduced as another method of determining preconsolidation values.

Sample disturbance in the laboratory is shown to be a contributing cause of too-slow predictions of the rate of settlement of sensitive clays. A time-settlement analysis is presented in which the results of laboratory consolidation tests were corrected for the effects of sample disturbance.

Because of limited data the application of the methods presented is restricted to saturated natural clays of sedimentary or glacial-sedimentary origin.

INTRODUCTION

General Purpose.—The laboratory consolidation test is the basis for computing the settlement of structures overlying compressible clay deposits. This test requires expensive equipment, expert supervision, and considerable time. Each test is therefore a definite technical and financial investment.

Unfortunately, the structure of every test sample is partly altered as a result of the stress changes that occur when the sample is removed from the ground and the distortions that are caused by the sampling operation and subsequent laboratory handling. A certain part of this disturbance has proved unavoidable.[2] Such sample disturbance distorts the results obtained from the laboratory consolidation test. It is therefore technically necessary and economically desirable to be able to correct the results of the laboratory test for the effects of sample disturbance.

It is intended that quantitative methods be presented herein whereby the results of a laboratory consolidation test, modified by the inevitable sample disturbance, can be corrected for the effects of this disturbance and thus be used to better predict the true behavior of the clay in the field.

Scope.—The correction of the results of laboratory consolidation tests is investigated as follows:

1. Examination of the basic behavior of a consolidating clay.
2. Observations of the manner in which this behavior is modified by sample disturbance.
3. Investigation of the pattern of such modifications.
4. The use of such patterns as a basis for estimating, by extrapolation, the completely undisturbed conditions.

There are also included herein investigations of the preconsolidation stress, of recompression settlements and rebound heave, and of the effects of sample disturbance on the laboratory time curves. An example of the results obtained by the use of the suggested methods is presented.

The data and methods introduced are applicable only to natural cohesive soils. The laboratory testing and job experience are limited to saturated organic and inorganic sedimentary clay deposits and to clays deposited as a result of glacial action; therefore, partly saturated and residual clays are excluded from this work.

---

[2] "Subsurface Exploration and Sampling of Soils for Civil Engineering Purposes," by M. J. Hvorslev, Waterways Experiment Station, Vicksburg, Miss., November, 1949, p. 189.

TERMINOLOGY, EQUIPMENT, AND TECHNIQUES

Terminology.—The term "consolidation test" refers to a fixed ring or floating ring, standard, one-dimensional laboratory test. The term "pressure-void ratio diagram" refers to the semilog method of indicating the results of a laboratory consolidation test.

Equipment.—The consolidometer equipment,[3] both floating ring and fixed ring, utilized dead-weight loading at a lever ratio of 10 to 1. The consolidometer ring was 1.00 in. high, with an inside diameter of 2.50 in. All sample compression was measured with dials reading directly to 0.0001 in.

All undisturbed samples were obtained with a thin-walled, fixed-piston sampler. The sampler has a length of 30 in., an inside diameter of 3.0 in., with a wall of No. 16 to No. 20 gage metal. Whenever possible, the sampler was pressed into the soil with a rapid, continuous push.

Techniques.—The consolidation tests were performed using the standard geometric progression of load increments. A continuous time-compression plot (semilog) was kept for each load increment; the subsequent increment was not applied until the increment was determined to be at the stage of secondary compression. The final pressure-void ratio diagrams were computed by adjusting all load-increment compressions for a standard laboratory time interval—that time being one at which all increments were in secondary compression. This time was generally 500 min, 1,000 min, or 1,440 min. Any swelling noted during a load increment was immediately arrested by the application of the next load increment.

A careful determination of the initial height (to 0.0001 in.) and weight (to 0.01 gram) of the test sample was made prior to each consolidation test. A specific-gravity test, using a pycnometer, was also made. This information, in addition to data concerning the final water content of the test sample, permitted an accurate computation of the void ratio and the degree of saturation at the beginning and end of each test. It was therefore possible to make the important cross-check between computed and measured over-all compressions and thus assure that there were no major inaccuracies in the computation of the best results.

EXISTING INFORMATION

The existing (1954) information on the subject of the effects of sample disturbance is largely qualitative in scope. This investigation can be considered to be an attempt to develop this qualitative information and the additional information presented herein into a systematic, quantitative procedure for correcting results of laboratory consolidation tests for the effects of sample disturbance. Perhaps the most comprehensive development of some of the qualitative concepts considered herein has been made[4] by P. C. Rutledge, M. ASCE. A thesis by T. Van Zelst, J.M. ASCE, completed in 1948 at Northwestern University, at Evanston, Ill., included pertinent data and analyses of special significance; Mr. Van Zelst's information is utilized subsequently. Mr. Van Zelst also summarized the available information (as of 1948) on factors that affect the results of laboratory consolidation tests.

---

[3] "Recent Developments in Soil Testing Apparatus," by P. C. Rutledge, *Journal*, Boston Soc. of Civ. Engrs., October, 1935.

[4] "Relation of Undisturbed Sampling to Laboratory Testing," by P. C. Rutledge, *Transactions*, ASCE, Vol. 109, 1944, p. 1155.

BASIC CONSOLIDATION BEHAVIOR

Laboratory.—The basic laboratory behavior of a clay consolidating under the influence of stresses higher than those previously experienced by the sample is such that its void ratio, *e* (or water content, *w*), steadily reduces with increasing intergranular soil pressures. Except in the case of significant long-time secondary consolidation, there is a new equilibrium void ratio for each new effective stress. When several of these points are plotted on a semilog plot, the resulting steep line, with flat curvature, is termed the "virgin consolidation slope."

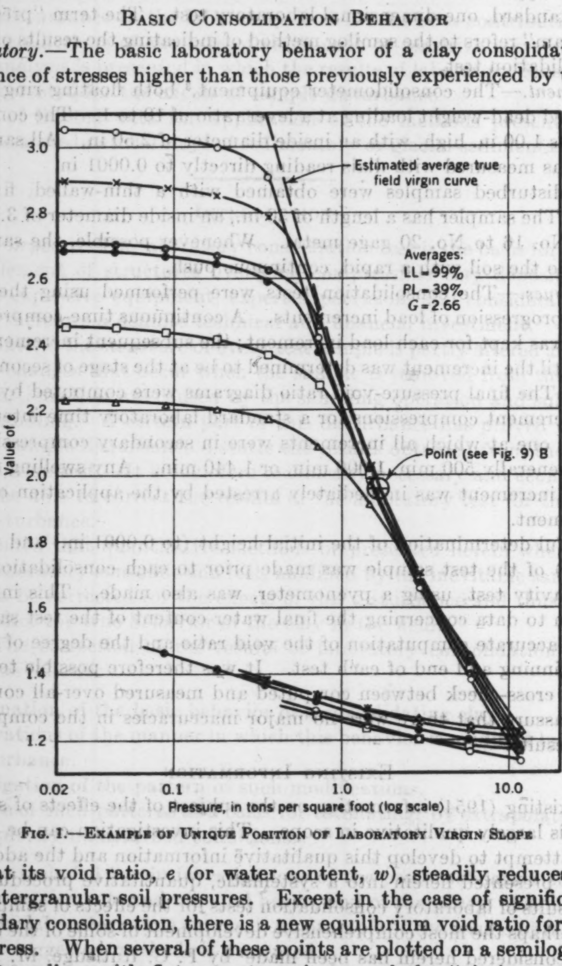

FIG. 1.—EXAMPLE OF UNIQUE POSITION OF LABORATORY VIRGIN SLOPE

In order to demonstrate that, for a given soil, the position of the virgin slope is a unique property of that soil, laboratory test data are presented in Fig. 1.

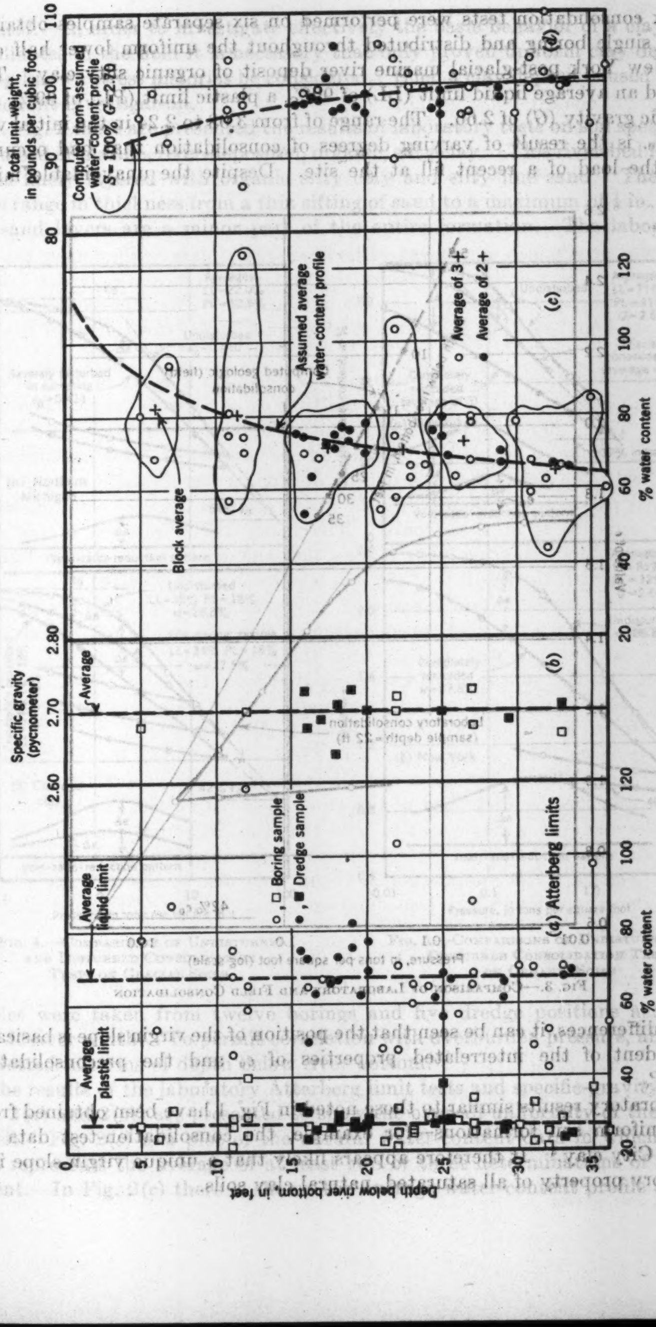

FIG. 2.—LABORATORY TEST DATA FROM RIVER-DEPOSITED, ORGANIC, SILTY CLAY

The six consolidation tests were performed on six separate samples obtained from a single boring and distributed throughout the uniform lower half of a 60-ft New York post-glacial marine river deposit of organic silty clay. This clay had an average liquid limit (LL) of 99%, a plastic limit (PL) of 39%, and a specific gravity (G) of 2.66. The range of from 3.08 to 2.24 in the initial void ratio, e_0, is the result of varying degrees of consolidation that had occurred under the load of a recent fill at the site. Despite the unavoidable minor sample differences, it can be seen that the position of the virgin slope is basically independent of the interrelated properties of e_0 and the preconsolidation stress, P_c.

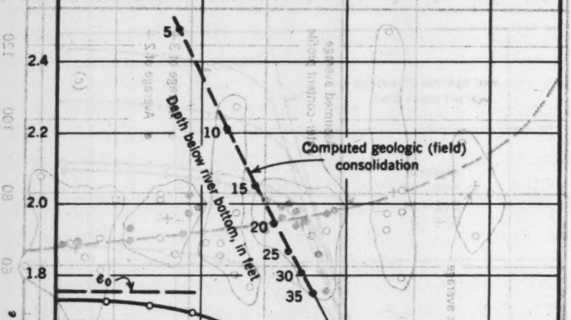

FIG. 3.—COMPARISON OF LABORATORY AND FIELD CONSOLIDATION

Laboratory results similar to those noted in Fig. 1 have been obtained from other uniform soil formations—for example, the consolidation-test data on Mexico City clay.[4] It therefore appears likely that a unique virgin slope is a laboratory property of all saturated, natural clay soils.

Field.—In order to investigate effectively the basic behavior of a clay as it consolidates in the field it is necessary that only proven uniform clay deposits having known stress histories be considered. Such a clay deposit is used in the subsequent investigation.

In Fig. 2 there are presented the results of laboratory tests on soil specimens from a bed of marine, river-deposited, organic, silty clay. This river-bed formation is finely layered with organic silty clay and silty fine sand. The sand layers range in thickness from a thin sifting of sand to a maximum of ⅛ in. The thin sand layers are a minor part of the entire formation. The laboratory samples were taken from twelve borings and five dredge positions across a 4,000-ft river width. To permit correlation with overburden pressure, all data are plotted in terms of depth below river bottom.

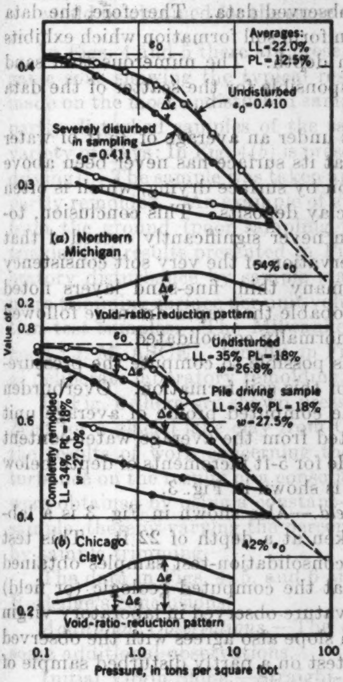

FIG. 4.—COMPARISONS OF UNDISTURBED AND DISTURBED CONSOLIDATION TESTS ON GLACIAL SOILS

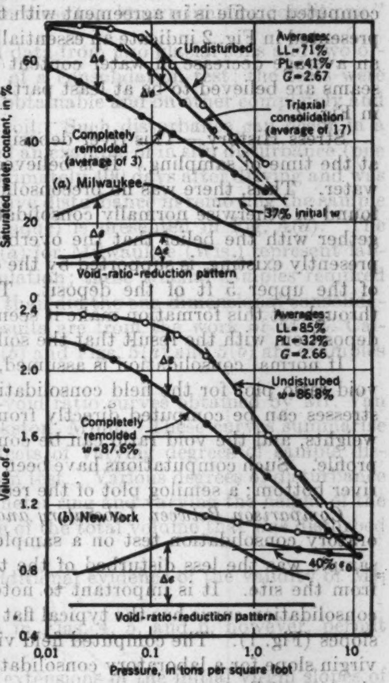

FIG. 5.—COMPARISONS OF UNDISTURBED AND DISTURBED CONSOLIDATION TESTS ON ORGANIC SOILS

The results of the laboratory Atterberg limit tests and specific-gravity tests (Figs 2(*a*) and 2(*b*)) are presented to show the over-all uniformity of the river deposit. Fig. 2(*c*) is a plot of the natural water-content data in which each point represents the average of at least two or three determinations of water content. In Fig. 2(*c*) there is shown the average water-content profile determined on the basis of the most logical curve through block averages of the detailed data. The upper part of the assumed water-content profile is sharply curved because the upper 5 ft of the river formation was reported to be in a "semifluid" condition and could not be sampled. It is probable that this semifluid state results from disturbance of the very soft clay which has a water content much higher than the liquid limit. In Fig. 2(*d*) there are shown the total unit weights determined by weight and volume measurements made on the entire sample before it was removed from the sampler tube, together with a unit-weight profile computed from the assumed water-content profile. The computed profile is in agreement with the observed data. Therefore, the data presented in Fig. 2 indicate an essentially uniform soil formation which exhibits an average decrease in water content with depth. The numerous thin sand seams are believed to be at least partly responsible for the scatter of the data in Fig. 2.

Stress History.—This river deposit was under an average of 35 ft of water at the time of sampling. It is believed that its surface has never been above water. Thus, there was no preconsolidation by surface drying, which is often found in otherwise normally consolidated clay deposits. This conclusion, together with the belief that the overburden never significantly exceeded that presently existing, is supported by the observation of the very soft consistency of the upper 5 ft of the deposit. The many thin, fine-sand layers noted throughout this formation make it seem probable that rapid drainage followed deposition, with the result that the soil is normally consolidated.

If normal consolidation is assumed, it is possible to compute the pressure-void ratio plot for the field consolidation of this soil formation. Overburden stresses can be computed directly from the computed profile of average unit weights, and the void ratio can be computed from the average water-content profile. Such computations have been made for 5-ft increments of depth below river bottom; a semilog plot of the results is shown in Fig. 3.

Comparison Between Laboratory and Field.—Also shown in Fig. 3 is a laboratory consolidation test on a sample taken at a depth of 22 ft. This test sample was the less disturbed of the two consolidation-test samples obtained from the site. It is important to note that the computed geologic (or field) consolidation curve has the typical flat curvature observed in laboratory virgin slopes (Fig. 1). The computed field virgin slope also agrees with the observed virgin slope for a laboratory consolidation test on a partly disturbed sample of the same soil.

The preceding analysis and several others, which include Detroit (Mich.) and Chicago (Ill.) clay formations—but which required more indirect reasoning—have consistently led the writer to the conclusion that many natural clays consolidate in the field along virgin slopes similar, if not identical, to those obtained from a completely undisturbed laboratory consolidation test.

EFFECTS OF SAMPLE DISTURBANCE

Previous Observations.—Mr. Rutledge[5] has summarized the general effects of sample disturbance on the laboratory consolidation test, as follows:

---

[5] "Relation of Undisturbed Sampling to Laboratory Testing," by P. C. Rutledge, *Transactions*, ASCE, Vol. 109, 1944, p. 1164.

"(1) It decreases the void ratio at which the soil will carry any given vertical stress;

"(2) It obscures the previous stress history of the soil and its preconsolidation load; and

"(3) The straight-line portion of the remolded compression curve is displaced downward from the laboratory virgin compression curve, and its slope, or the rate of decrease in void ratio with increasing stress, is less.

"These results show definitely the effects of sample disturbance over the range from the best undisturbed samples which have been obtained for laboratory test to complete remolding. Any intermediate degree of disturbance must result in a compression curve which falls between the curves that would be obtained for the same soil in these two known limiting conditions."

In Figs. 4 and 5 there are presented data from two glacial soils and two organic soils showing the typical results of a consolidation test; the tests were made on the most undisturbed samples obtainable and on other completely and partly disturbed samples of the same soil. Such disturbance can occur in a variety of ways: In Fig. 4(*b*) is presented an example of in situ disturbance (pile driving). The sample was taken approximately 400 days after driving and was partly remolded. An example of excessive disturbance in removing the sample from the ground (poor sampling technique) is presented in Fig. 4(*a*). The triaxial test results presented in Fig. 5(*a*) for Milwaukee (Wis.) represent laboratory disturbance by sample manipulation; these triaxial samples required more trimming surface per unit volume than did the one-dimensional consolidation test samples. The Milwaukee results are from the work of M. L. Calhoon,[6] J. M. ASCE. Finally, in Fig. 4(*b*) and Figs. 5(*a*) and 5(*b*) are examples of deliberate laboratory remolding.

In Fig. 6 there are shown pressure-void ratio curves obtained by Mr. Van Zelst for a glacial lake clay from Crookston, Minn. These curves summarize the results of work concerning the effects of varying degrees of sample disturbance on the results of a consolidation test. Various degrees of disturbance were obtained by using a constant-diameter ring and varying the height of the sample, thereby varying the percentage of the total volume that was disturbed by sample trimming.

The data in Figs. 4, 5, and 6 are additional evidence of the validity of Mr. Rutledge's conclusions.

Additional Observations.—The data in Figs. 4, 5, and 6, however, permit some additional observations.

Initial Virgin Slope.—Straight-line extensions of the initial virgin slopes of consolidation tests on samples disturbed in varying degrees intersect within a narrow range of void ratios. The term, initial virgin slope, is herein defined as the slope of the straight line drawn through the first two laboratory test points which fall on the virgin part of the pressure-void ratio diagram.

In Figs. 3 and 6 it can be seen that the intersection of the field initial virgin slope with the initial virgin slopes of laboratory consolidation tests ranges from 40% to 46% of the initial void ratio of the sample. In Figs. 4, 5, and 14 (to be presented subsequently) the intersection range for undisturbed and more-disturbed samples is between 37% and 60% of e_0. If the unusually dense silty clay shown in Fig. 4(*a*) and the sample disturbed by pile driving 400 days prior to sampling—thereby permitting possible thixotropic action (Fig. 4(*b*))—are excepted, the intersection range becomes from 37% to 46% of e_0.

---

[6] "The Effect of Remolding on the Strength of a Saturated Clay," by M. L. Calhoon, thesis presented to Northwestern University, Evanston, Ill., in 1948 in partial fulfilment of the requirements for the degree of Master of Science.

On the limited basis of these and similar data, it is believed that an initial virgin-slope intersection point at 42% of e_0 would be a good estimate for most clays.

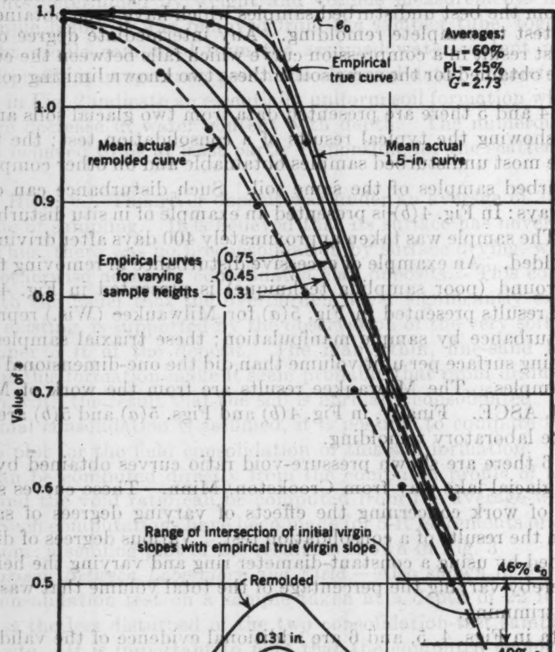

FIG. 6.—EFFECT OF SAMPLE DISTURBANCE ON THE PRESSURE-VOID RATIO DIAGRAM

Void-Ratio-Reduction Pattern.—For each set of comparative consolidation tests there has been plotted a void-ratio-reduction pattern. This term is used herein to describe the curve that shows the pattern of the reduction in void ratio of the disturbed sample test when it is compared to the undisturbed sample test. With respect to the least-disturbed consolidation-test curve, the void-ratio-reduction curves for more-disturbed samples increase symmetrically from a small value at low stresses to a maximum value at or near the preconsolidation stress—and then decrease again along the virgin slope. The data in Fig. 6 indicate that the same pattern may exist between the clay in the field and the laboratory sample.

Rebound Slope.—Finally, disturbance does not appear to alter significantly the rebound slope. Examination of the data from Mr. Van Zelst's thesis and other test data supports this preliminary observation.

Geologic Rebound of a Preconsolidated Clay

Laboratory investigations have shown that it is common to find clays that have been subjected—in their geologic history—to pressures that are greater than those presently existing in the form of overburden; such clay is said to be preconsolidated. During the process of stress release from the preconsolidation stress to that stress now existing, the soil must have swelled or rebounded. One must estimate the magnitude of this rebound when making a complete settlement analysis.

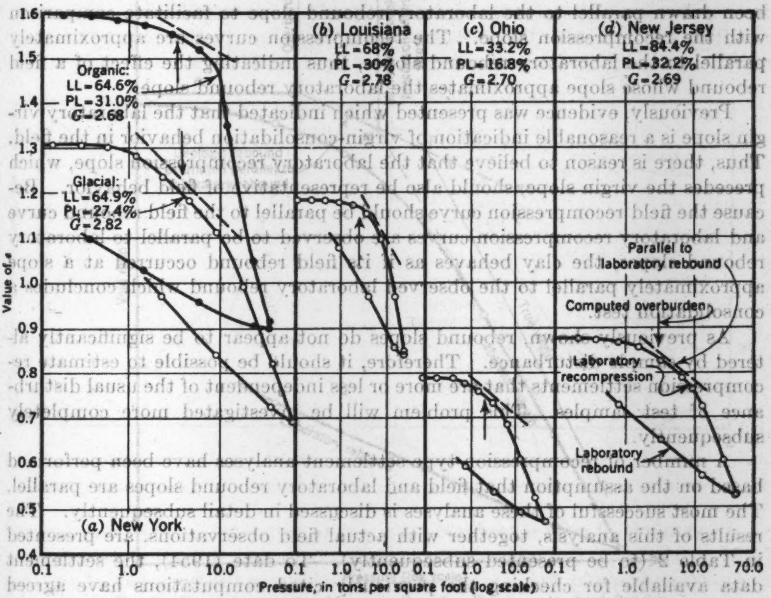

FIG. 7.—COMPARISONS OF LABORATORY RECOMPRESSION AND REBOUND SLOPES

In order to investigate this problem one must imagine a laboratory consolidation test on a highly preconsolidated clay. What would be the shape of the recompression part of the pressure-void ratio diagram? Long rebounds and subsequent recompressions of laboratory samples reveal a shallow hysteresis loop in which the recompression is approximately parallel to and at a slightly higher void ratio than the rebound. If a similar rebound occurred in the field, one would therefore also expect the field recompression curve to be approximately paralled to the field rebound curve, with a shallow loop between the curves.

In Fig. 7 there are shown laboratory consolidation-test results on a variety of highly preconsolidated clays. These results are typical of those of many other tests on such clays. Any swelling under light loads was immediately arrested by the application of the next load increment. The three-slope character of such tests is shown by the approximately constant void-ratio line during the loading interval when swelling was restrained, then by the distinct recompression slope, and finally by the steep virgin slope. For each test there is indicated the computed existing overburden stress, and a dashed line has been drawn parallel to the laboratory rebound slope to facilitate comparison with the recompression slope. The recompression curves are approximately parallel to the laboratory rebound slopes, thus indicating the effect of a field rebound whose slope approximates the laboratory rebound slope.

Previously, evidence was presented which indicated that the laboratory virgin slope is a reasonable indication of virgin-consolidation behavior in the field. Thus, there is reason to believe that the laboratory recompression slope, which precedes the virgin slope, should also be representative of field behavior. Because the field recompression curve should be parallel to the field rebound curve and laboratory recompression curves are observed to be parallel to laboratory rebound slopes, the clay behaves as if its field rebound occurred at a slope approximately parallel to the observed laboratory rebound which concludes a consolidation test.

As previously shown, rebound slopes do not appear to be significantly altered by sample disturbance. Therefore, it should be possible to estimate recompression settlements that are more or less independent of the usual disturbance of test samples. This problem will be investigated more completely subsequently.

A number of recompression-type settlement analyses have been performed based on the assumption that field and laboratory rebound slopes are parallel. The most successful of these analyses is discussed in detail subsequently. The results of this analysis, together with actual field observations, are presented in Table 2 (to be presented subsequently). To date (1954), the settlement data available for checking the previously cited computations have agreed satisfactorily, thus supporting the approximate parallel-relationship hypothesis for the clays at the sites analyzed.

THE PRECONSOLIDATION STRESS

Determination of the preconsolidation stress is very important in estimating the true consolidation behavior of the clay in the field. Unfortunately, distortion of the curvature characteristics of the laboratory consolidation sample, from which the previous stress history of the soil is inferred, is one of the most serious results of sample disturbance. The graphical construction suggested[7] by A. Casagrande, M. ASCE, is the method most commonly used for estimating the value of the preconsolidation stress. In this technique varying degrees of sample disturbance are not completely accounted for. As can be seen by using this construction on the data presented in Figs. 4, 5, 6, and 16, increasing disturbance makes the choice of the minimum radius of curvature quite difficult and generally results in lower determinations of preconsolidation stress.

---

[7] "Determination of the Preconsolidation Load and Its Practical Significance," by A. Casagrande, *Proceedings*, International Conference on Soil Mechanics and Foundation Eng., School of Eng., Harvard Univ., Cambridge, Mass., Vol. III, 1936.

There are presented subsequently several alternate techniques which may also be useful in determining preconsolidation values.

Minimum Possible Preconsolidation Stress.—In Fig. 8 there is illustrated a method that can be used to determine a minimum possible preconsolidation stress. This method was originally suggested by Mr. Rutledge and has been slightly modified herein. In Fig. 8, point E represents the presently existing field overburden and void ratio. Line E–P′ represents the geologic rebound constructed parallel to the laboratory rebound through point E. The laboratory initial virgin slope is extended until it intersects either the initial void-ratio line or geologic rebound line at point m. From the knowledge of the effects of sample disturbance, one knows that the true virgin slope must lie to the right of the laboratory slope. Therefore point m must always be at a lower stress than the true preconsolidation value determined at point P.

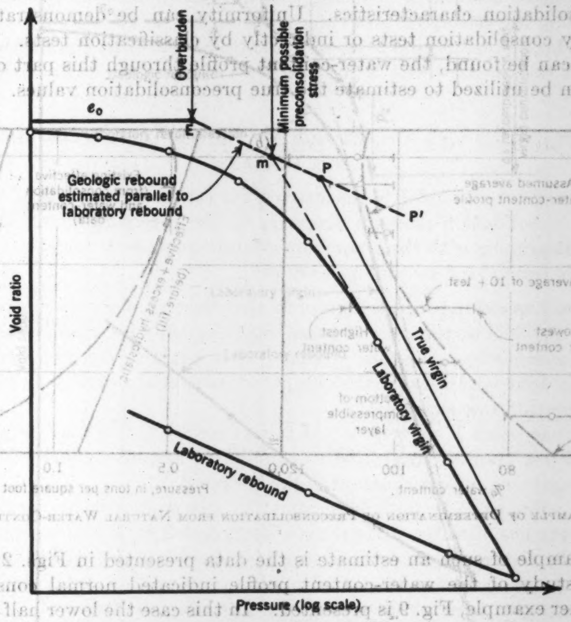
Overburden
Minimum possible preconsolidation stress
e_o
E
m
P
P′
Geologic rebound estimated parallel to laboratory rebound
True virgin
Laboratory virgin
Laboratory rebound
Void ratio
Pressure (log scale)

Fig. 8.—Determination of Minimum Possible Preconsolidation Stress

If it can be stated with a reasonable degree of certainty that the preconsolidation stress cannot be below a certain value, one has established a lower limit that may have engineering significance. If this lower limit is higher than the overburden pressure known to be effective at the sample elevation, one may be reasonably certain that some, if not all, of the consolidation settlement will be recompression. However, if the lower limit is consistently below the computed overburden stress, the analyst then has reason for believing the soil to be normally consolidated and—on rare occasions—under-consolidated.

Water-Content Data.—The water content of a cohesive soil is independent of sample disturbance. Furthermore, it is one of the simplest properties to determine in the laboratory. Information about water content is therefore potentially useful in estimating the undisturbed properties of natural clays.

Although it is rare to find an entire clay layer that is uniform, it is not uncommon to find clay formations with a part of their thickness exhibiting uniform consolidation characteristics. Uniformity can be demonstrated either directly by consolidation tests or indirectly by classification tests. If such a condition can be found, the water-content profile through this part of the formation can be utilized to estimate the true preconsolidation values.

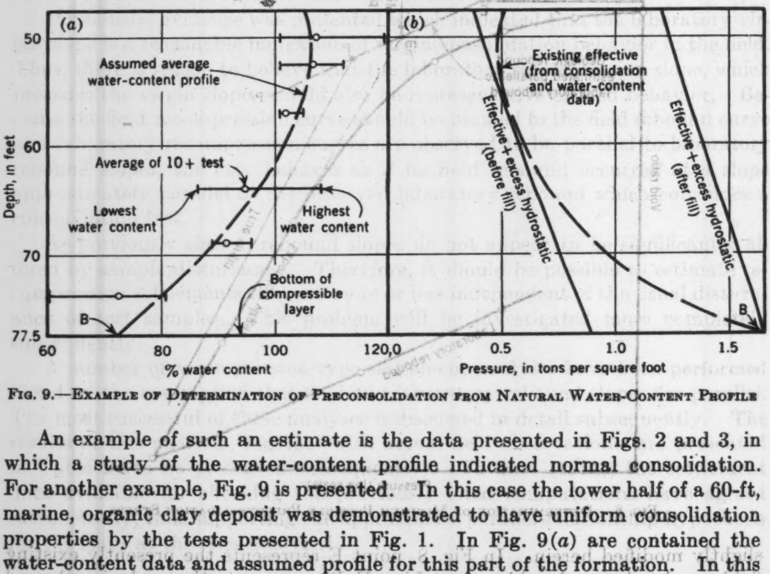

FIG. 9.—EXAMPLE OF DETERMINATION OF PRECONSOLIDATION FROM NATURAL WATER-CONTENT PROFILE

An example of such an estimate is the data presented in Figs. 2 and 3, in which a study of the water-content profile indicated normal consolidation. For another example, Fig. 9 is presented. In this case the lower half of a 60-ft, marine, organic clay deposit was demonstrated to have uniform consolidation properties by the tests presented in Fig. 1. In Fig. 9(*a*) are contained the water-content data and assumed profile for this part of the formation. In this analysis it was possible to establish a direct relationship between water content and effective stress. This correlation was possible because this was a case of double-drainage consolidation under a recent fill. The effective stress at the bottom of the compressible layer was therefore the total stress at that elevation; it could be computed readily. Points B in Fig. 9 indicate the water content and effective stress at the bottom of the layer.

The effective stress-void ratio computation for point B is shown by the circled cross in Fig. 1. This cross represents a point on the true average virgin curve of this soil. The heavy dashed line in Fig. 1, which passes through point

B, is an estimate of the average true field virgin curve over the void-ratio range shown. By converting the water-content profile to void ratio and using the estimated true virgin curve, it is possible to compute the effective-stress profile at the time of sampling.

The results of this computation are shown in Fig. 9(*b*) in relation to the total of effective stresses and excess hydrostatic stresses existing before and after the fill was placed. After the effective-stress distribution was determined for the lower half of the formation, it was relatively easy to estimate the distribution for the upper half. Settlement computations including this complete distribution gave a close agreement with actual observations following the placing of the fill; normal consolidation at the time the fill was placed was assumed.

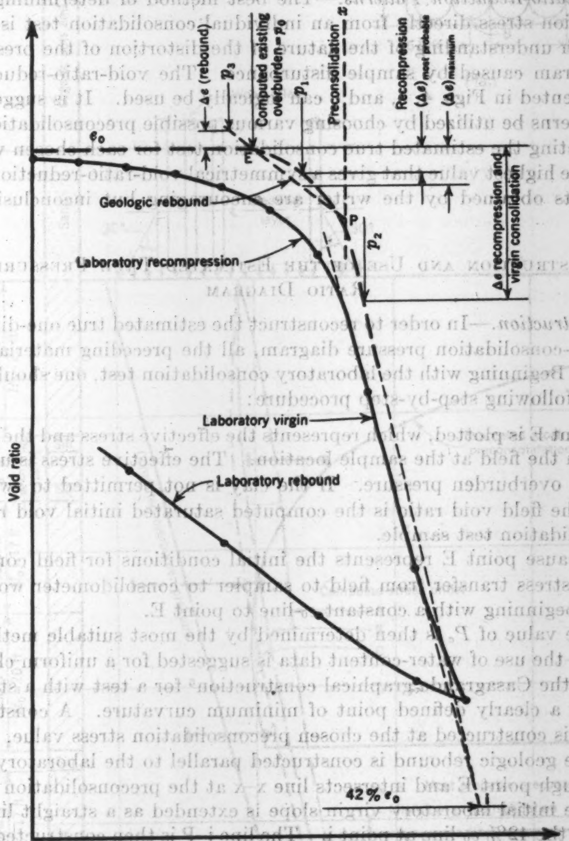

FIG. 10.—RECONSTRUCTION OF TRUE ONE-DIMENSIONAL CONSOLIDATION BEHAVIOR

In cases in which no direct relationship between water content and effective stress can be determined, trial-and-error procedures must be used until the water-content profile checks with an assumed preconsolidation profile.

A method that may permit the successful application of water-content data to the determination of the curvature of the preconsolidation profile involves use of the water content-plasticity ratio.[8]

Void-Ratio-Reduction Patterns.—The best method of determining the preconsolidation stress directly from an individual consolidation test is based on a thorough understanding of the nature of the distortion of the pressure-void ratio diagram caused by sample disturbance. The void-ratio-reduction patterns presented in Figs. 4, 5, and 6 can logically be used. It is suggested that these patterns be utilized by choosing various possible preconsolidation values, reconstructing the estimated true consolidation test for each chosen value, and picking the highest value that gives a symmetrical void-ratio-reduction pattern. The results obtained by the writer are encouraging but inconclusive (as of 1954).

RECONSTRUCTION AND USE OF THE ESTIMATED TRUE PRESSURE-VOID RATIO DIAGRAM

Reconstruction.—In order to reconstruct the estimated true one-dimensional void ratio-consolidation pressure diagram, all the preceding material must be utilized. Beginning with the laboratory consolidation test, one should use Fig. 10 in the following step-by-step procedure:

1. Point E is plotted, which represents the effective stress and the void ratio existing in the field at the sample location. The effective stress is usually the computed overburden pressure. If the clay is not permitted to swell during storage, the field void ratio is the computed saturated initial void ratio, e_0, of the consolidation test sample.

2. Because point E represents the initial conditions for field compression, a perfect stress transfer from field to sampler to consolidometer would result in a test beginning with a constant e_0-line to point E.

3. The value of P_c is then determined by the most suitable method. For example—the use of water-content data is suggested for a uniform clay formation, and the Casagrande graphical construction[6] for a test with a steep virgin slope and a clearly defined point of minimum curvature. A constant stress line, x–x, is constructed at the chosen preconsolidation stress value.

4. The geologic rebound is constructed parallel to the laboratory rebound, goes through point E and intersects line x–x at the preconsolidation point P.

5. The initial laboratory virgin slope is extended as a straight line until it intersects the 42% e_0-line at point i. The line i–P is then constructed; this line represents the position and slope of the upper part of the estimated true virgin curve.

6. A recompression curve is estimated for the geologic rebound line E–P. This curve probably merges with the estimated true initial virgin slope in such a manner that the graphical construction[6] at the point of sharpest curvature will yield the preconsolidation point P.

---

[8] "Application of Soil Mechanics in Designing Building Foundations," by A. Casagrande and R. E. Fadum, *Transactions*, ASCE, Vol. 109, 1944, p. 383.

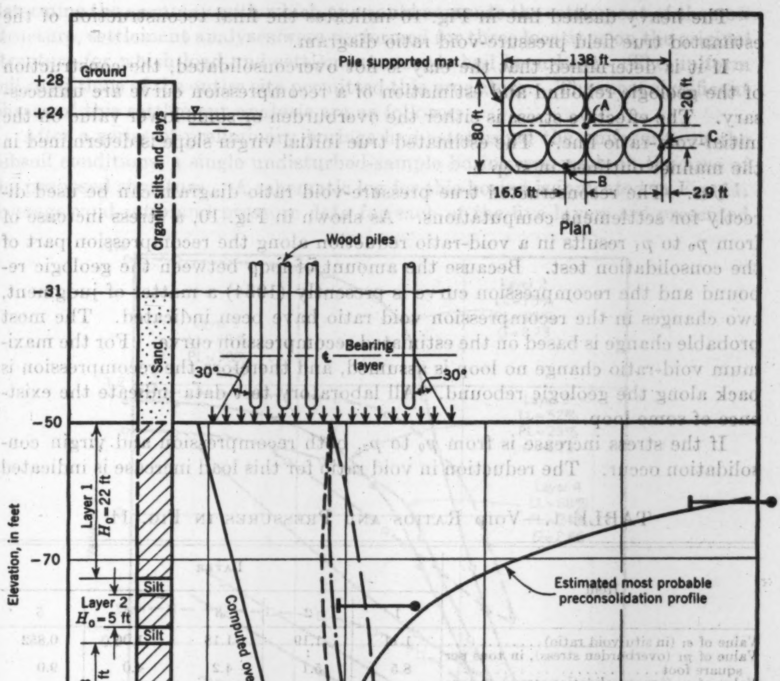

FIG. 11.—STRESS PROFILES UNDER SETTLEMENT POINTS

The heavy dashed line in Fig. 10 indicates the final reconstruction of the estimated true field pressure-void ratio diagram.

If it is determined that the clay is not overconsolidated, the construction of the geologic rebound and estimation of a recompression curve are unnecessary. The effective stress is either the overburden or some lower value on the initial-void-ratio line. The estimated true initial virgin slope is determined in the manner outlined in step 5.

Use.—The reconstructed true pressure-void ratio diagram can be used directly for settlement computations. As shown in Fig. 10, a stress increase of from p_0 to p_1 results in a void-ratio reduction along the recompression part of the consolidation test. Because the amount of loop between the geologic rebound and the recompression curve is presently (1954) a matter of judgment, two changes in the recompression void ratio have been indicated. The most probable change is based on the estimated recompression curve. For the maximum void-ratio change no loop is assumed, and therefore the recompression is back along the geologic rebound. All laboratory test data indicate the existence of some loop.

If the stress increase is from p_0 to p_2, both recompression and virgin consolidation occur. The reduction in void ratio for this load increase is indicated in Fig. 10 and is independent of any assumed recompression curve. Should there be a net decrease in load from p_0 to p_3, the soil would continue to rebound along the established geologic rebound slope and yield the void-ratio increase shown in Fig. 10. Examples of this occurrence can be seen in the consolidation-test results presented in Fig. 7. The glacial lake sample (Fig. 7(*a*)) and the Ohio clay (Fig. 7(*d*)) were both varved. Therefore, the clay in the sampler was able to swell during storage by drawing water from the silt and sand parts of the sample. The relationship between the computed overburden stress and the lower stress at the beginning of the recompression slope indicates that swell occurred. This swell was along the established rebound slope.

TABLE 1.—VOID RATIOS AND PRESSURES IN FIG. 11

Item	LAYER				
	1	2	3	4	5
Value of e_1 (in situ void ratio)	1.11	1.19	1.18	1.06	0.852
Value of p_1 (overburden stress), in tons per square foot	8.5	5.1	4.2	4.0	9.0
Value of p_e (preconsolidation stress), in tons per square foot	2.15	2.56	2.89	3.34	3.97

A SETTLEMENT ANALYSIS

General Approach.—In order to give practical significance to the previously developed theoretical concepts, an interesting settlement analysis will be reviewed which permits the use of some of these concepts.

It was proposed that additional storage facilities be constructed adjacent to a rigid eight-bin silo structure that had been built in 1926. In order to determine the accuracy with which one could compute the settlement of the new structure, settlement analyses were performed for three locations on the original structure for which load and settlement records had been kept. The uniform soil conditions of the entire site permitted this procedure. The most significant phases of this settlement analysis are as follows:

After a series of preliminary borings had established the uniformity of the subsoil conditions, a single undisturbed-sample boring was made in the area of the proposed structure. A schematic log for this boring is indicated in Fig. 11. Average void-ratio and pressure data for each of the five layers are presented

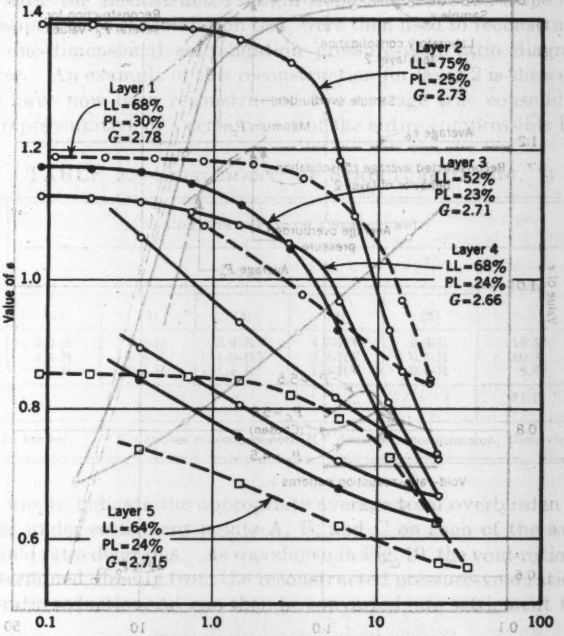

FIG. 12.—LABORATORY CONSOLIDATION-TEST DATA USED IN SETTLEMENT ANALYSIS

in Table 1. In this case the compressible layer causing settlements (shown crosshatched) was a medium to stiff, inorganic, river-deposited, gray-green Pleistocene clay extending from El. −50 to El. −139. This layer contained occasional thin silt lenses and pockets and three silt layers which are indicated on the profile. Numerous water-content tests were performed on undisturbed samples from this compressible layer. On the basis of these tests plus the boring-log information, five settlement layers for computation were established. A consolidation test was performed on an undisturbed sample from each layer in order to determine the consolidation characteristics of each layer and the overall preconsolidation profile. The results of the laboratory consolidation tests are presented in Fig. 12. The elevations of the consolidation-test samples, the minimum and the most probable preconsolidation estimates, and the estimated most probable preconsolidation profile are shown in Fig. 11.

Analysis Techniques.—For this analysis it was decided to use the previously cited void-ratio-reduction-pattern method of estimating the most probable preconsolidation values. An example of this method is shown in Fig. 13. In Fig. 13 various possible preconsolidation values, P_c, were tried, and an estimated true curve was reconstructed for each trial. The resulting void-ratio-reduction patterns for three trials are indicated, as well as the pattern that was chosen.

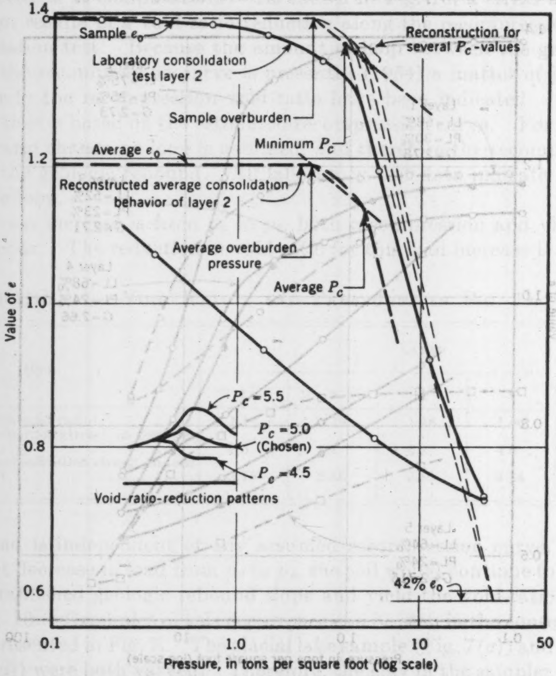

FIG. 13.—TYPICAL UTILIZATION OF LABORATORY PRESSURE-VOID RATIO DIAGRAM

In Fig. 11 there is shown the plan of the foundation mat of the silo structure; included are the locations of the three points for which settlement analyses were performed. The recorded average live load plus computed dead load—which were uniformly distributed over the area of the foundation mat—was 2.23 tons per sq ft. This load was transmitted through wood piles into a 19-ft bearing layer of sand, the top of which was at El. −31. The piles almost penetrate this sand layer. The assumption made to account for the load-distributing action of this bearing layer is shown in Fig. 11. By use of this assumption, the average stress increase at the top of the clay formation was determined as 1.90 tons per sq ft. The Boussinesq elastic stress-distribution charts for rectangular areas were then used to estimate the stress increase under the three settlement points.[9] These stress increases exist in addition to the computed existing overburden pressure and are so plotted in Fig. 11.

The average saturated void ratio for each computational layer was determined from the natural water-content data. The average initial and preconsolidation stresses were determined from the overburden and preconsolidation stress profiles. The values are indicated on the log in Table 1. These values, together with the reconstructed virgin-slope and rebound-slope magnitudes from the appropriate consolidation test, were then used to reconstruct the average true one-dimensional consolidation pressure-void ratio diagram for the entire layer. An example of this reconstruction for layer 2 is shown in Fig. 13.

TABLE 2.—SETTLEMENT[a] OF STRUCTURE IN FIG. 11

Point	Computed (Flexible Structure)						Observed (rigid structure)
	Layer[b]					Total	
	(1)	(2)	(3)	(4)	(5)		
A	5.0-R	1.1-R	3.9-RV	4.7-RV	0.8-R	15.5	12.3
B	4.4-R	0.8-R	1.9-RV	3.3-RV	0.5-R	10.9	11.3
C	4.3-R	0.7-R	1.4-R	1.8-RV	0.4-R	8.6	9.9
Average						11.7	11.2

[a] In inches. [b] R denotes recompression, RV denotes recompression, then virgin.

There have now been reconstructed five average true consolidation tests, each one representative of a certain part of the entire compressible layer. The next step was to indicate the appropriate average total overburden plus structural stress under settlement points A, B, and C on each of the average true pressure-void ratio diagrams. As was shown in Fig. 10, the void-ratio reductions can be determined directly from the reconstructed pressure-void ratio diagrams. The void-ratio reduction, Δe, can then be converted into settlement by

$$\Delta H = H_0 \left(\frac{\Delta e}{1 + e_0} \right) \ldots\ldots\ldots\ldots\ldots\ldots (1)$$

in which ΔH is the change in height or settlement, and H_0 represents initial height of the compressible layer.

Comparison Between Computed and Observed Settlement.—In Table 2 there are shown (1) the results of the settlement computations for each layer, (2) whether the settlements are recompression or both recompression and virgin, and (3) the observed settlement of the rigid structure. Because the time-settlement records indicate that settlements are complete, all computations are for ultimate settlement.

---

[9] "Fundamentals of Soil Mechanics," by D. W. Taylor, John Wiley & Sons, Inc., New York, N. Y., 1948, p. 255.

The observed settlements presented for points B and C are the average of observations made at the four symmetrical locations for each, as noted in Fig. 11. The observed settlement at point A was obtained by adding the measured dishing of the mat to the settlements measured at the edges of the silos.

The correlation between computed settlements and observed settlements indicated in Table 2 is an example of the successful application of the theoretical concepts that have been developed. It is particularly significant that most of the computed settlement was recompression settlement. Hence, this is an example of the successful computation of recompression settlements by a rational method. As shown by this example, such settlements can be of a significant magnitude.

LABORATORY TIME-CONSOLIDATION DATA

Permeability and Sample Disturbance.—One often hears the comment that predicted rates of settlement, based on direct extrapolations from the laboratory time-consolidation curves, are slower than those actually observed in the field. It is usually suggested that this is particularly true for organic soils. The extrapolation is usually based on the height of the test sample and the height of the compressible layer by use of the conventional square relationship.[10] Any discrepancy between prediction and field observation is generally attributed to the existence of unknown drainage layers or two-dimensional or three-dimensional drainage rather than the one-dimensional drainage of the laboratory consolidation test.

These explanations are probably correct in many cases. However, the writer believes that in some instances the discrepancy can be accounted for by the effects of sample disturbance on the laboratory time curves. This opinion is based on the following:

1. Sample permeability should be related to the void structure of the sample. Disturbance may alter any natural interconnected void structure so as to break down this structure and thus reduce permeability.[11]

Fine-grained organic soils generally have a sensitive structure and thus may readily have their permeabilities reduced by sample disturbance. Those who have had experience in classifying organic "silt" will probably agree with this statement. These samples, when in an undisturbed state, break with a vertical face, have a fine-grit surface texture, and often have a surface water sheen—all characteristics of the silt. However, when these samples are remolded to test their plasticity, they lose their original characteristics and behave like organic clays. Thus, these samples often present a field-classification difficulty and—incidentally—provide a striking example of how permeability can be altered by sample disturbance.

2. Several time-settlement predictions, using the H^2-relationship, involving compressible organic soils have come to the attention of the writer. These predictions compared favorably with field observations. The best example is at the site from which the data in Figs. 1 and 9 were obtained. An exten-

---

[10] "Theoretical Soil Mechanics," by K. Terzaghi, John Wiley & Sons, Inc., New York, N. Y., 1943, p. 282.

[11] "The Structure of Inorganic Soil," by T. William Lambe, *Proceedings-Separate No. 315*, ASCE, October, 1953.

sive surface fill, plus the test-proven fact that horizontal permeability and vertical permeability were equal, assured the accuracy of the theoretical drainage pattern. The successful time-settlement computations obtained on this project are believed to be in part the result of using time curves from consolidation-test samples which showed a minimum of sample disturbance.

3. Sensitive organic soils sometimes do not yield suitably undisturbed consolidation-test data. In one such case the writer successfully attempted to correct the time-curve data for the effects of sample disturbance. Some of the details of this investigation are presented subsequently.

Example of Correction for Sample Disturbance.—A 5,500,000-gal oil tank, 140 ft in diameter, was placed on approximately 18 ft of new granular fill overlying a 22-ft layer of compressible, river-deposited, marine, organic silty clay. Settlements became so serious that remedial measures were required. The nature of these remedies depended on the reason for the settlement—whether entirely because of consolidation, or partly because of a bearing-capacity failure. A careful time-settlement analysis was therefore performed to determine whether consolidation alone would account for the recorded time-settlement behavior of the structure.

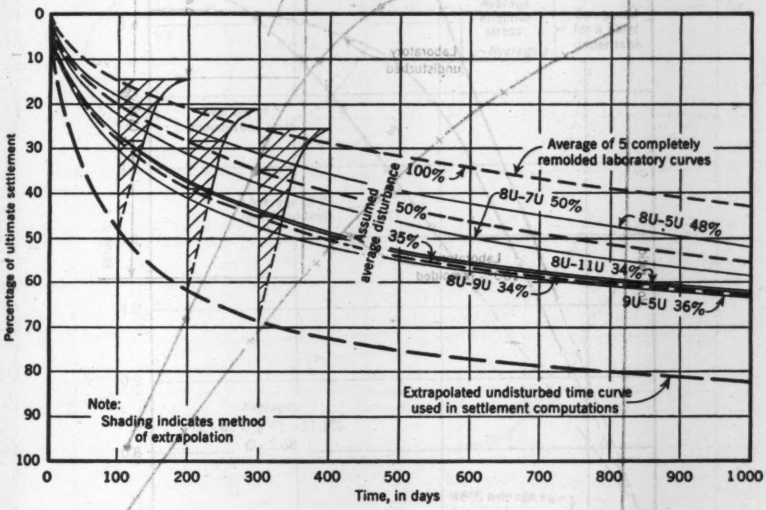

FIG. 14.—EXTRAPOLATION OF UNDISTURBED TIME-SETTLEMENT CURVE FOR 22-FT LAYER FROM DISTURBED LABORATORY CONSOLIDATION TESTS

Fortunately, at this site the drainage pattern was easily determined. Six borings around the circumference of the tank established that no intermediate drainage layers existed within the 22-ft compressible stratum. The borings also established the existence of a silty fine-sand drainage layer under the compressible stratum. The newly placed fill was known to be coarse and clean enough to permit drainage to the surface. The heavy fill blanket and large-diameter tank located over a relatively thin compressible formation assured that the drainage was essentially one-dimensional and of the double-drainage type.

Undisturbed samples obtained at this site proved to be much more disturbed than those from which the data in Fig. 1 were obtained. This finding, together with the observation of a systematic decrease in permeability with increased disturbance, revealed the necessity of attempting to correct the consolidation-test data for the effects of sample disturbance.

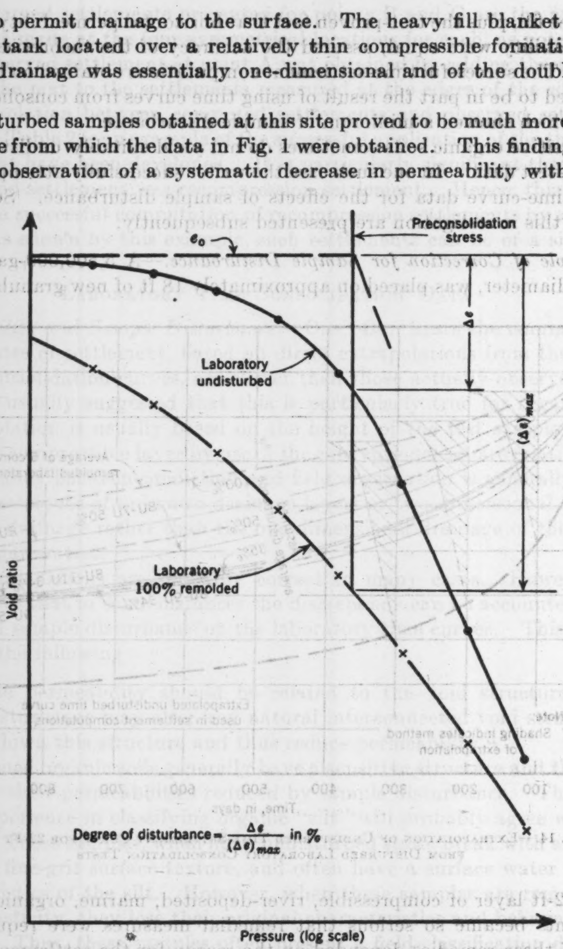
Preconsolidation stress
e_0
Δe
$(\Delta e)_{max}$
Laboratory undisturbed
Laboratory 100% remolded
Void ratio
Degree of disturbance = $\frac{\Delta e}{(\Delta e)_{max}}$ in %
Pressure (log scale)

FIG. 15.—METHOD OF DETERMINING DEGREE OF DISTURBANCE

Five undisturbed-sample tests and two completely remolded-sample consolidation tests were performed on samples from this site. Typical virgin slope-time curves from these tests, adjusted by the conventional square relationship for a 22-ft layer, are plotted with light solid lines in Fig. 14. Each test curve was assigned a degree of disturbance, as shown in Fig. 15, by a method utilizing consolidation-test results. Three groups of time curves were then assigned average disturbance values, and the completely undisturbed-sample time curve shown in Fig. 14 was extrapolated by the method shown in Fig. 15.

In Fig. 16 there are shown the average undisturbed and completely remolded pressure-void ratio diagrams. By utilizing the extrapolated time curve from Fig. 14 and assuming normal consolidation to exist at the time the fill was placed, an average existing effective stress was computed at a specific point under the tank. Based on water-content data, the average existing void ratio at this point was also computed. The result of these computations was the stress-void ratio point indicated by the cross in Fig. 16. This point was assumed to be a point on the field virgin slope. An undisturbed field virgin slope was constructed through this point in Fig. 16.

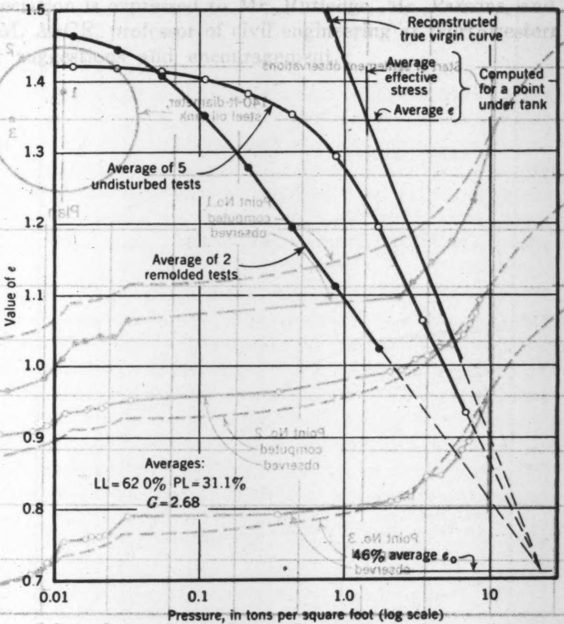

FIG. 16.—DETERMINATION OF TRUE VIRGIN CURVE

By utilizing the undisturbed time-settlement curve in Fig. 14 and the undisturbed virgin curve in Fig. 16, time-settlement computations were made for three points under the tank where settlements have been recorded. In Fig. 17 there are indicated the comparisons of observed and computed time-settlement curves for the three points analyzed. The conclusion, checked by stability analysis and subsequent structure performance, was that the observed settlements at the site were caused entirely by consolidation of the 22-ft organic silty clay stratum.

The favorable time-settlement comparisons indicated in Fig. 17 show that predictions based on uncorrected laboratory test results would have been badly misleading. At this site this error would have resulted in rate predictions that would have been much too low.

CONCLUSIONS

1. Evidence has been presented which indicates that at least some natural clays behave in the field in a manner similar to that predicted by laboratory virgin-slope and rebound-slope data from a consolidation test.

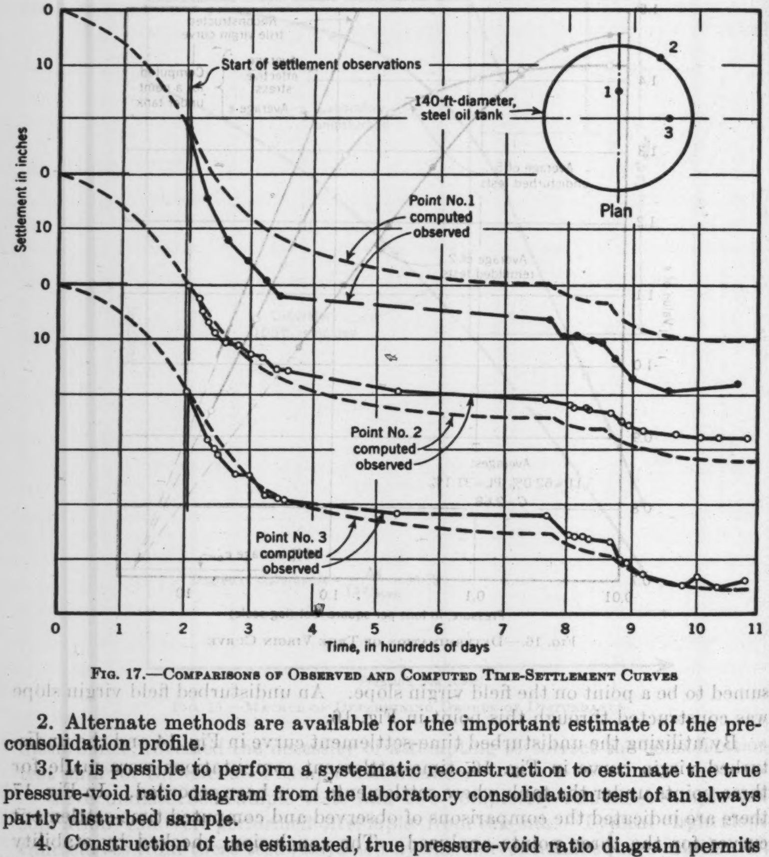

FIG. 17.—COMPARISONS OF OBSERVED AND COMPUTED TIME-SETTLEMENT CURVES

2. Alternate methods are available for the important estimate of the preconsolidation profile.

3. It is possible to perform a systematic reconstruction to estimate the true pressure-void ratio diagram from the laboratory consolidation test of an always partly disturbed sample.

4. Construction of the estimated, true pressure-void ratio diagram permits the simple computation of recompression, as well as virgin void-ratio changes.

5. It may sometimes be necessary to correct the laboratory time-curve data for the effects of sample disturbance.

6. In order to minimize any errors involved in the suggested methods of extrapolation, it is desirable to obtain samples as little disturbed as possible for laboratory use.

ACKNOWLEDGMENTS

The files of Moran, Proctor, Mueser & Rutledge, Consulting Engineers of New York, N. Y., were the source of most of the data contained herein. Their soil mechanics laboratory staff, under the supervision of James D. Parsons, M. ASCE, is responsible for the design of the undisturbed sampler and the quality of the laboratory data used as illustrations in this paper.

Appreciation is expressed to Mr. Rutledge, Mr. Parsons, and J. O. Osterberg, A.M. ASCE, professor of civil engineering at Northwestern University, for their suggestions and encouragement.

DISCUSSION

Robert L. Crisp, Jr.,[12] **J.M. ASCE.**—A valuable contribution to the field of soil mechanics has been made by Mr. Schmertmann. The effects of previous geological history and sample disturbance have been recognized as primary factors in selecting representative compression curves from laboratory consolidation tests.

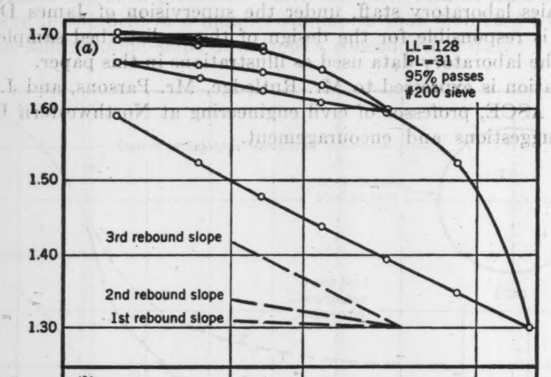

Fig. 18.—Relationship Between Void Ratio and Pressure

With reference to "Geologic Rebound of a Preconsolidated Clay" and "Reconstruction and Use of the Estimated True Pressure-Void Ratio Diagram," it has been the experience of the writer that the slope of the rebound curve of clay soils is a function of the inherent structure of the soil and the consolidation pressure from which rebound begins. Considerable variation in the slope of rebound curves has been noted for samples subjected to repeated cycles of loading and unloading. In general, the slope of the rebound curve tends to increase with an increase in applied stress. Therefore, the rebound curve will have innumerable slopes, each a function of the maximum applied laboratory stress. In Fig. 18 there are shown plots of laboratory test data for samples subjected to cyclic loading. The variation in slope is quite evident in the graphical comparison in each pressure-void ratio diagram.

---

[12] Engr., Soils Mechanics, South Atlantic Div. Lab., Corps of Engrs., U. S. Dept. of the Army, Marietta, Ga.

It is believed that an arbitrary selection of the rebound curve, obtained by reducing the applied stress from the maximum, to approximate geologic rebound can lead to erroneous corrections in locating point P in Fig. 10. The location of this point is critical with respect to settlement computations because the slope of the virgin curve is dependent on the location of point P. In addition, the slope of the recompression curve approximates the slope of the rebound curve only when the rebound curve is very flat. This situation is generally encountered when the applied load is less than the preconsolidation pressure. Therefore, extreme care should be used when reconstructing the recompression part of the true curve from laboratory rebound curves.

John H. Schmertmann,[13] J. M. ASCE.—The validity of the parallel relationship between laboratory recompression and rebound slopes has been questioned by Mr. Crisp. It is agreed that the rebound slope varies with the physical and mineralogical structure of the clay and the void ratio (which is a function of the consolidation pressure) from which the rebound begins. However, an attempt will be made herein to show that this variation is somewhat predictable and that recompression-slope magnitudes (all slopes being measured by Δe over one pressure cycle on a conventional semilog p-e plot) can be estimated without the extreme care that Mr. Crisp believes to be necessary.

Some preliminary work indicates that for many clays the change in the magnitude of the rebound slope with decreasing void ratio may be primarily a function of the rebound slope C_r, and the void ratio at the beginning of the rebound, e_r. This relationship is tentatively expressed as

$$\log \frac{C_{r1}}{C_{r2}} = 2.5 \log \frac{e_{r2} + 1}{e_{r1} + 1} \quad \ldots\ldots\ldots\ldots\ldots\ldots (2)$$

The factor 2.5 is an average value which subsequent work may show to vary predictably with clay structure—perhaps as expressed by Atterberg limits. Laboratory rebound and recompression cycles show that the recompression slope, C_x, can be approximated by 1.15 C_r. Under these conditions it is believed that the best method of plotting available data of comparisons between laboratory recompression and rebound slopes would be a logarithmic plot of $(e_r + 1)/(e_x + 1)$ versus C_x/C_r—in which e_x is the void ratio at the beginning of the rebound that precedes the recompression (the slope of which is C_x) and in which

---

[13] U. S. Army, Snow, Ice, and Permafrost Research Establishment, Wilmette, Ill.; formerly Junior Soils Engr., Moran, Proctor, Mueser & Rutledge, New York, N. Y.

DISCUSSION

Robert L. Crisp, Jr.,[12] J.M. ASCE.—A valuable contribution to the field of soil mechanics has been made by Mr. Schmertmann. The effects of previous geological history and sample disturbance have been recognized as primary factors in selecting representative compression curves from laboratory consolidation tests.

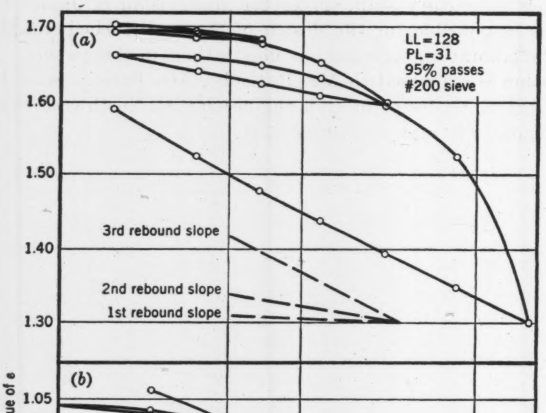

Fig. 18.—Relationship Between Void Ratio and Pressure

With reference to "Geologic Rebound of a Preconsolidated Clay" and "Reconstruction and Use of the Estimated True Pressure-Void Ratio Diagram," it has been the experience of the writer that the slope of the rebound curve of clay soils is a function of the inherent structure of the soil and the consolidation pressure from which rebound begins. Considerable variation in the slope of rebound curves has been noted for samples subjected to repeated cycles of loading and unloading. In general, the slope of the rebound curve tends to increase with an increase in applied stress. Therefore, the rebound curve will have innumerable slopes, each a function of the maximum applied laboratory stress. In Fig. 18 there are shown plots of laboratory test data for samples subjected to cyclic loading. The variation in slope is quite evident in the graphical comparison in each pressure-void ratio diagram.

---

[12] Engr., Soils Mechanics, South Atlantic Div. Lab., Corps of Engrs., U. S. Dept. of the Army, Marietta, Ga.

It is believed that an arbitrary selection of the rebound curve, obtained by reducing the applied stress from the maximum, to approximate geologic rebound can lead to erroneous corrections in locating point P in Fig. 10. The location of this point is critical with respect to settlement computations because the slope of the virgin curve is dependent on the location of point P. In addition, the slope of the recompression curve approximates the slope of the rebound curve only when the rebound curve is very flat. This situation is generally encountered when the applied load is less than the preconsolidation pressure. Therefore, extreme care should be used when reconstructing the recompression part of the true curve from laboratory rebound curves.

John H. Schmertmann,[13] J. M. ASCE.—The validity of the parallel relationship between laboratory recompression and rebound slopes has been questioned by Mr. Crisp. It is agreed that the rebound slope varies with the physical and mineralogical structure of the clay and the void ratio (which is a function of the consolidation pressure) from which the rebound begins. However, an attempt will be made herein to show that this variation is somewhat predictable and that recompression-slope magnitudes (all slopes being measured by Δe over one pressure cycle on a conventional semilog p-e plot) can be estimated without the extreme care that Mr. Crisp believes to be necessary.

Some preliminary work indicates that for many clays the change in the magnitude of the rebound slope with decreasing void ratio may be primarily a function of the rebound slope C_r, and the void ratio at the beginning of the rebound, e_r. This relationship is tentatively expressed as

$$\log \frac{C_{r1}}{C_{r2}} = 2.5 \log \frac{e_{r2} + 1}{e_{r1} + 1} \qquad (2)$$

The factor 2.5 is an average value which subsequent work may show to vary predictably with clay structure—perhaps as expressed by Atterberg limits. Laboratory rebound and recompression cycles show that the recompression slope, C_x, can be approximated by 1.15 C_r. Under these conditions it is believed that the best method of plotting available data of comparisons between laboratory recompression and rebound slopes would be a logarithmic plot of $(e_r + 1)/(e_x + 1)$ versus C_x/C_r—in which e_x is the void ratio at the beginning of the rebound that precedes the recompression (the slope of which is C_x) and in which

---

[13] U. S. Army, Snow, Ice, and Permafrost Research Establishment, Wilmette, Ill.; formerly Junior Soils Engr., Moran, Proctor, Mueser & Rutledge, New York, N. Y.

e_r and C_r refer to the final rebound of the laboratory consolidation test. Such a plot is presented in Fig. 19.

The data in Fig. 19 were obtained from fifty-nine individual consolidation tests on preconsolidated clays showing distinct recompression slopes. Fig. 19 includes only comparisons from samples that were slightly disturbed. As shown by the legend, the type of the symbol denotes geologic origin, and the size of the symbol denotes a qualitative estimate of sample disturbance. These data include forty-nine tests on clays taken from sixteen sites in nine states of the United States and ten tests from five sites in four foreign countries. In nine of the tests an intermediate virgin rebound-reload cycle was performed, and therefore these tests yielded more than one comparison point.

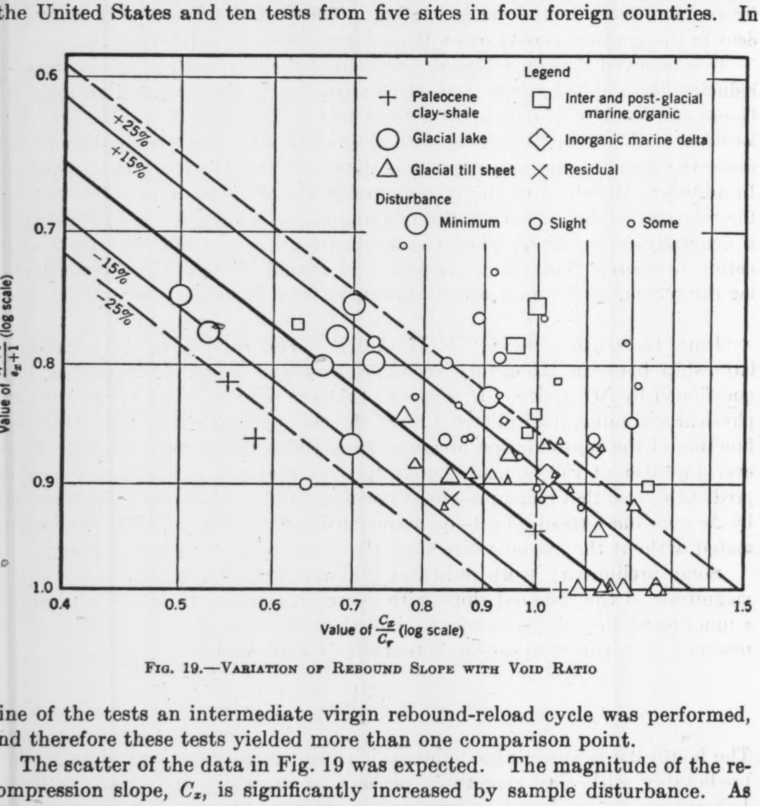

FIG. 19.—VARIATION OF REBOUND SLOPE WITH VOID RATIO

The scatter of the data in Fig. 19 was expected. The magnitude of the recompression slope, C_x, is significantly increased by sample disturbance. As disturbance is known to be variable one should expect scatter. In addition, parameters other than void ratio may be important.

By using a system of weighing individual results according to sample disturbance—minimum, 5; slight, 3; some, 1—the following conclusions can be drawn from the data presented:

The heavy solid line in Fig. 19, the slope of which independently supports the 2.5 factor in Eq. 2, indicates the most probable variation of the recompression slope with void ratio. The light solid lines indicate the ± 15% zone of error about the heavier line. Based on the data presented, one may have 65% confidence that, if one uses the relationship expressed by the heavy line, the error in C_x will not be greater than 15%. The data points within the dashed lines indicate that one may have 80% confidence that the error will not be greater than 25%. The latter error is within the practical accuracy of settlement analyses. The maximum error is approximately 45%. It is therefore believed that the heavy line in Fig. 19 represents a usable empirical relationship.

When using Fig. 19 one must remember that e_x represents the void ratio from which the field rebound began. Unlike e_r, e_x is not definitely known and

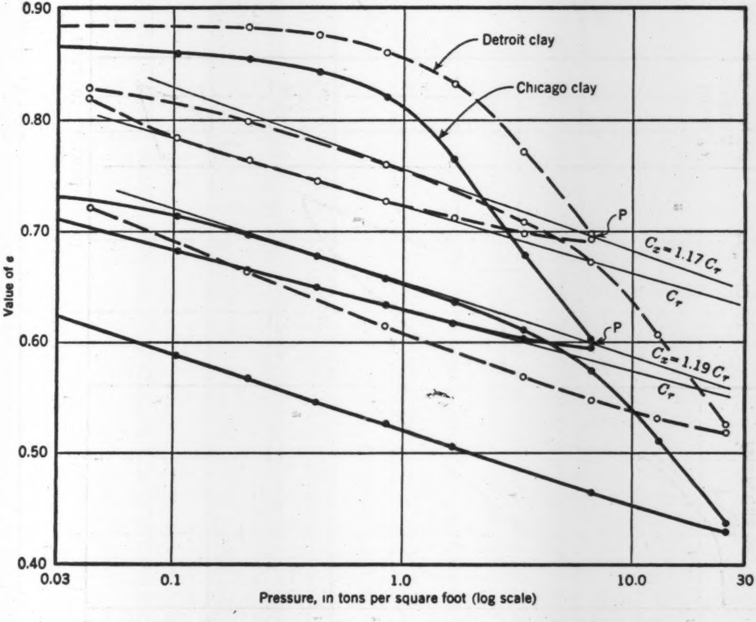

FIG. 20.—TWO COMPARISONS OF REBOUND AND SUBSEQUENT RECOMPRESSION

must be estimated from the pressure-void ratio diagram. As examples, the writer chose the following e_x-values for the tests presented in Fig. 7: (*a*) 1.53 and 1.15, (*b*) 1.06, (*c*) 0.73, and (*d*) 0.77. These e_x-values were easy to estimate because the tests showed a minimum of sample disturbance and the recompression slopes were distinct. In more difficult cases a short, graphical, successive approximation procedure, working back from the in situ pressure (lower pressure if swelling occurred) and the void ratio, will be helpful.

It is interesting to note in Fig. 19 that, for the nine tests presented, a cyclic rebound and recompression procedure (in which $e_x = e_r$) yields an average (C_x/C_r)-value of 1.15, with a range of ± 0.10. Thus, a laboratory rebound

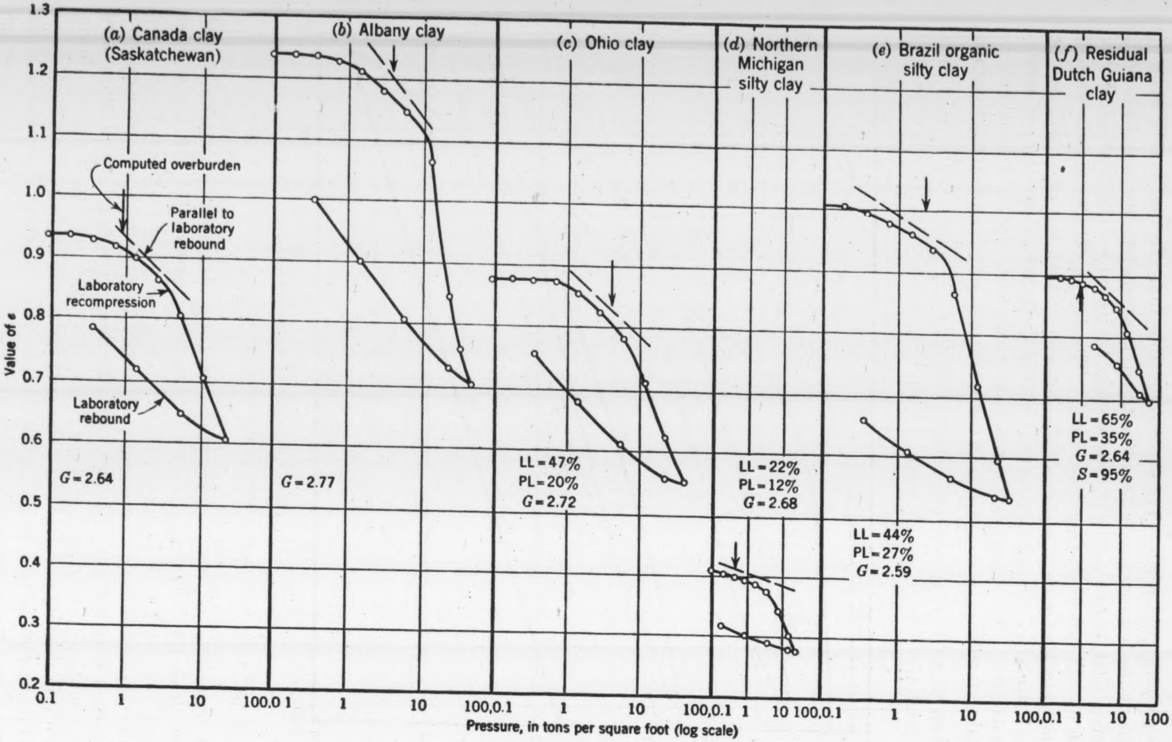

FIG. 21.—SUPPLEMENTARY COMPARISONS OF LABORATORY RECOMPRESSION AND REBOUND SLOPES

slope is approximately 87% of the average slope of the subsequent recompression. The reason for the steeper recompression slope can be seen by comparing the values of C_x and C_r shown in Fig. 20. These laboratory test results were obtained at Northwestern University from two carefully cut, test-pit samples.

The information in Figs. 19 and 20 makes it possible to recommend the following changes in two of the steps listed under the heading, "Reconstruction and Use of the Estimated True Pressure-Void Ratio Diagram":

4. Construct the geologic rebound by estimating the e_x-value and determining the ratio $(e_r + 1)/(e_x + 1)$. The value of C_x/C_r can then be taken as 0.87 C_x.

This geologic rebound is drawn through point E (or the lower stress on the e_0-line if the sample swelled) and intersects line x-x at the preconsolidation point P.

6. Reference to Fig. 20 shows that the C_x-lines, drawn tangent to the average recompression slope, pass closely through the preconsolidation points P. This phenomenon was noted for most of the other cycled tests. Thus, a line with a slope of C_x (determined in step 4) constructed through point P may be useful as an upper-tangent guide line for the reconstruction of the field recompression curve.

If there is no laboratory-test evidence to the contrary, these procedures are recommended as the best empirical relationships presently (1955) available for reconstructing the recompression part of field consolidation behavior.

Mr. Crisp believes that the recompression curve approximates the slope of the rebound curve only in instances where the rebound curve is very flat. Although the rebounds from the test results plotted in Fig. 7 are quite steep, the distinct recompression slopes closely approximate them. Fig. 21 is presented to supplement the data in Fig. 7. According to the data presented in Fig. 18, Mr. Crisp's opinion may be based on a comparison of the final rebound, which begins from the virgin slope, with rebounds beginning at the recompression slope. Because virgin consolidation is believed to be associated with a much more severe change of the clay structure, the two rebound phenomena may not be directly comparable. In this connection it is interesting to note that the upper test in Fig. 18, which Mr. Crisp privately reported to have overburden and preconsolidation pressures of 2.5 tons per sq ft and 6 tons per sq ft, has an over-all recompression slope (upper void-ratio points) that is somewhat steeper than the final rebound slope.

As can be seen in Fig. 10, the reconstructed slope of the upper part of the virgin curve, drawn between points P and i, is not sensitive to the position of point P. A large error in estimating the field rebound slope has a relatively slight influence on the reconstructed virgin slope.

Mr. Crisp is thanked for his thoughtful criticisms and for emphasizing the need to present a more comprehensive review of the laboratory data on comparisons between rebound and recompression slopes.

AMERICAN SOCIETY OF CIVIL ENGINEERS
Founded November 5, 1852
TRANSACTIONS

Paper No. 2776

DESIGN OF STABLE CHANNELS

By Emory W. Lane,[1] M. ASCE

With Discussion by Messrs. Serge Leliavsky; A. Nizery and G. Braudeau; N. K. Bose; José S. Gandolfo; and Emory W. Lane

Synopsis

In 1950 the Bureau of Reclamation, United States Department of the Interior, began an investigation to improve the design of irrigation canals constructed in earth. The results of the preliminary studies are presented herein, and the future investigations are outlined.

The method of designing stable channels which is presented is based on securing a distribution of the tractive force along the sides and bottom of the channels such that the magnitude of this force at all points will be sufficiently large to prevent sediment deposits in objectionable quantities, and at the same time will be small enough to prevent objectionable scour. Limiting values for the tractive force are offered for the various conditions under which a canal may be constructed. The effect of bends, side slope, and transported material on the design is reviewed. Also presented is a method of designing canals having a minimum of excavation and a minimum width in coarse, noncohesive material.

Introduction

In January, 1950, the Bureau of Reclamation, United States Department of the Interior (USBR), began an investigation of the methods for designing unlined canals. Particular emphasis was given to methods of obtaining a rational solution to the problem of sediment movement as it is related to the design of unlined canals.

The results obtained from the investigation (from January, 1950, to June, 1952) are summarized subsequently. In general, the principal progress made in these studies was in three directions: (1) The clarification of the general principles for the design of stable channels; (2) the development of a tentative method for designing unlined earth canals to assure freedom from scour;

Note.—Published, essentially as printed here, in September, 1953, as *Proceedings-Separate No. 280.* Positions and titles given are those in effect when the paper or discussion was received for publication.

[1] Prof. of Civ. Eng., Colorado Agri. Mech. College, Fort Collins, Colo.

and (3) the formulation of a method of analysis for the determination of a channel shape in coarse, noncohesive material which would involve a minimum of excavation. As of June, 1952, it had been impossible to study intensively many important aspects of the general problem, especially those involving the design of canals transporting considerable quantities of coarse sediment. The general principles of a design procedure, however, were developed, and a better understanding of the general problem was achieved.

In studying the principles for the design of stable canals, an intensive study of the literature was made. The subject is a complex one, and a great variety of conditions exists which make the best solution in any one case inapplicable to a situation where other conditions prevail. A complete solution of the problem must, therefore, include an analysis of all these conditions and a determination of the solution applicable to each.

THE DESIGN OF STABLE CHANNELS

Definitions and Principles.—Because the term "stable channels" as used herein has a special meaning, it is desirable to define the term and explain its limitations. A stable channel is an unlined earth channel (*a*) which carries water, (*b*) the banks and bed of which are not scoured objectionably by the moving water, and (*c*) in which objectionable deposits of sediment do not occur. Sediment has been defined[2] as

> "* * * fragmental material transported by, suspended in, or deposited by water or air, or accumulated in beds by other natural agents; any detrital accumulation, such as loess."

This particular investigation is concerned solely with the stability of the channel from the standpoint of the movement or deposition of earth materials by the flowing water. It does not deal with the stability of the banks which slough (or slide) into the canal as this is a problem in soil mechanics for which reasonably satisfactory solutions are available.

Unstable Channels.—There are three classes of unstable channels: (1) Channels in which the banks or bed are scoured without objectionable deposits being formed; (2) channels where objectionable sediment deposits occur without scour being produced; and (3) channels in which scour and objectionable deposits are both present.

When sediment-free water is present in a channel, only the first class of instability can occur. The first class of instability (scour without deposit) can also be caused by water which carries sediment, especially when the amount of sediment carried by the water is small.

The second class of instability (deposit without scour) can only be caused by the sediment brought into the canal with the flowing water or that scoured from the banks and bed of an upstream channel. An example of this case is a lined canal—or a canal cut through a scour-resistant material—into which large quantities of coarse sediment enter with the inflowing water.

The third class of instability (scour and deposit) usually occurs when water containing large quantities of coarse sediment enters a canal, the bank and bed of which are composed of material which has little resistance to scour.

---

[2] "Report of Subcommittee on Sediment Terminology," by E. W. Lane, Chairman, *Transactions*, Am. Geophysical Union, Vol. 28, December, 1947, p. 936.

For prevention of instability of the first class, only an analysis of scouring action is necessary. For prevention of instability of the second class, it usually is necessary to be sure that the sediment brought into the canal at the upstream end is carried out at the downstream end. The basic analysis of this problem must therefore be made on the basis of sediment transportation. The prevention of instability of the third class involves an analysis of the combination of scour and transportation problems.

Sediment Transportation.—Every canal, when flowing at its design discharge, has a definite maximum capacity to carry sediment of a certain size range. If more material of this size range is fed into the canal, deposits will occur. If less than this amount is added, the material will be transported through the canal. In regions where the sediment load carried by the streams is large, canals are frequently supplied with more sediment than they can carry, and harmful deposits result. Where the streams carry light sediment loads, the condition under which canals receive less than they can carry occurs more frequently, and sediment problems are usually of a minor nature. In India and Pakistan, where the sediment loads are usually high, the first condition is encountered. However, in most cases in the United States the second condition exists, and trouble from sediment deposition is not as prevalent as in India and Pakistan.

To understand these conditions, one need but consider a canal which (1) has a uniform slope and cross section, (2) carries a uniform flow of clear water, and (3) has a nonerodible bed and nonerodible banks. If a small quantity of sediment (of a size sufficiently small so that it is readily moved) is fed into the upper end of this canal at a uniform rate, this material will be moved continuously down the canal and out at the lower end (after equilibrium has been attained), at the same rate as it is introduced at the upper end. When this is the case, small patches of the material will form on the bed of the canal. From these patches, particles are alternately moved away or deposited as the velocity fluctuates because of turbulence. If the rate at which the sediment is added is increased, the sediment will be discharged at the lower end of the canal at this new rate, after equilibrium for this new rate is established. Under this condition, there will also be patches of sediment on the bed of the canal, from which the sediment will be alternately picked up and deposited. In this case, however, the area covered by these patches will be greater than in the former case. In both cases, the area will be such that the turbulent currents will move only the amount of material introduced at the upper end. This condition will also exist for further increases in the rate of introduction, until the patches cover the entire bottom of the canal. When this point is reached, the turbulent currents cannot pick up any more sediment and move it along, and the maximum possible amount is carried out at the lower end of the canal. If material is introduced into the upper end of the canal at a still greater rate than this maximum transportation rate, sediment will be deposited in the canal at a rate equal to the difference between the introduction rate and the maximum transportation rate. Therefore, one of the most important problems in the design of stable channels carrying sediment involves the determination of the hydraulic factors for a canal which will have a transporting capacity sufficient to carry the material introduced at the upper end.

Development of Stable-Channel Design.—The science of stable-channel design has been developed over a long period of time, and there is much pertinent literature. Most of the work has been done in India and Pakistan, where the most extensive irrigation works are located. Some work has also been done in Egypt, the United States, and a number of other countries. Some of this literature was not investigated in making this study;[3] however, as only the scour aspects of the problem have been investigated in detail, it was not possible to review thoroughly all the literature dealing with the other cases.

Forces Causing Scour.—The first step in analyzing the problem of eliminating scour in canals appears to be a consideration of the forces causing such scour. Scour on the banks and bed of a canal occurs when the particles composing the sides and bottom are acted on by forces sufficient to cause them to move. As previously reported,[4] when a particle is resting on the level bottom of a canal, the force acting to cause motion is that force caused by the motion of the water past the particle. If scour is to be prevented, this motion must not be rapid enough to produce forces on the particle that are sufficiently large to cause it to move. If a particle is on the sloping side of a canal, it is acted on, not only by the water, but also by the force of gravity which tends to make it roll or slide down this slope. The force causing the downward motion is the component, in the direction of the slope, of the force of gravity acting on the particle. If the resultant of the force caused by the motion of the water and the component of the force of gravity acting on the particle is large enough, the particle will move. For the particles to be moved (where cohesion is present), the forces acting must be sufficient to overcome this cohesion also.

Tractive-Force Distribution.—The movement of material on the banks and bed of a canal where cohesion is not present is dependent on the steepness of the side slope and the velocity and turbulence near the banks and bed. The forces caused by the slope of the sides are easily designated; however, those resulting from the velocity and turbulence near the boundaries are difficult to determine because of the high rate of change of velocity with a change in the distance above the bed and the rapid fluctuations of velocity caused by the turbulence in the flowing water. Another complicating factor is the presence of the boundary layer. Therefore, to reach a satisfactory analysis from a study of the velocities acting on the particles did not seem feasible; instead, the approach from the standpoint of tractive force or shear was adopted.

Briefly, tractive force or shear is the force which the water exerts on the periphery of a channel because of the motion of the water. This force acts in the direction of flow and not normal to the surface as does the static water pressure. Tractive force is not the force on a single particle, but the force exerted over a certain area of the bed or banks. This concept was first introduced by M. P. du Boys.[5]

---

[3] "Progress Report on Results of Studies on Design of Stable Channels," *Hydraulic Laboratory Report No. Hyd.-352*, Bureau of Reclamation, U. S. Dept. of the Interior, Washington, D. C., 1952.

[4] "Stable Channels in Erodible Material," by E. W. Lane, *Transactions*, ASCE, Vol. 102, 1937, p. 134.

[5] "The Rhone and Streams with Movable Beds," by M. P. du Boys, *Annales des Ponts et Chaussées*, Vol. XVIII, 1879.

The shear or tractive force is equal to, and in the opposite direction from, the force which the bed exerts on the flowing water. If no force were exerted by the banks or bed on the water, the water would continue to accelerate as would a frictionless ball rolling down an inclined plane. In a uniform channel (having a constant slope) in which the water is moving in a state of steady, uniform flow, the water is not accelerating because the force tending to prevent motion is equal to the force causing motion. The tractive force under these conditions is therefore equal to the force tending to cause the water to move. This force is the component, in the direction of flow, of the weight of the water. In a channel of infinite width and length with uniform slope, the tractive force exerted by the water on a square foot of area is the component in the direction of flow of the weight of the water above that area. The weight of this water is equal to $w\,y$, in which w is the unit weight of the water and y is the depth of flow. The component of this weight in the direction of flow is the weight multiplied by the sine of the slope or, for ordinary conditions, the tangent of the slope, S_0 or $w\,y\,S_0$. As will be shown subsequently, in most canals of the shape used for irrigation, the tractive force near the middle of the bottom closely approaches that in an infinitely wide channel ($w\,y\,S_0$).

TABLE 1.—LIMITING VELOCITIES AND TRACTIVE FORCES IN COHESIVE MATERIAL[a]

Principal cohesive material of bed	Compactness of Bed							
	Loose		Fairly compact		Compact		Very compact	
	Voids Ratio							
	2.0 to 1.2		1.2 to 0.6		0.6 to 0.3		0.3 to 0.2	
	Velocity[b]	Force[c]	Velocity[b]	Force[c]	Velocity[b]	Force[c]	Velocity[b]	Force[c]
Sandy clays[d]	1.48	0.040	2.95	0.157	4.26	0.327	5.90	0.630
Heavy clayey soils	1.31	0.031	2.79	0.141	4.10	0.305	5.58	0.563
Clays	1.15	0.024	2.62	0.124	3.94	0.281	5.41	0.530
Lean clayey soils	1.05	0.020	2.30	0.096	3.44	0.214	4.43	0.354

[a] From footnote reference 11. [b] Limiting mean velocity, in feet per second. [c] Limiting tractive force, in pounds per square foot. [d] Sand content less than 50%.

In trapezoidal channels such as those commonly used in hydraulic engineering, the tractive force is not uniformly distributed over the bed and banks; therefore, in analyzing scour in canals on the basis of tractive force, it is necessary to determine how this force is distributed. In this study, a condition of similitude of tractive-force distribution in canal cross sections was assumed. For this assumption, in all canals having the same ratio of bed width, b, to y and the same side slopes, the tractive-force distribution will be similar; that is, the tractive force at any point in one cross section will be similar to that at any other point in a corresponding position in a similar section. Thus, if the tractive-force distribution in any canal can be determined, the distribution will be the same in any other canal of similar cross section and roughness distribution. The similarity of distribution is not only true in trapezoidal channels; it can be applied also to other channel shapes.

Tractive Force in Canal Design.—The concept of tractive force or shear has been widely used in fluid mechanics and has been extensively applied to the study of sediment movement. Whereas in the United States this concept has seldom been applied to earth-canal design, in Europe there has been a wider application. A. Schoklitsch suggested the use of tractive force as the basis of canal design,[6] stating that it was not possible to give fixed and definite values for the maximum tractive forces of different soils, but that the following values, in pounds per square foot, could serve as a basis for design: Earth, 0.062; loam, 0.102; sand, 0.082; stony and loamy soil and coarse gravel, 0.205; and very compact soil, 0.256. The use of a shear analysis in canal design has been suggested,[7] but no extensive study of the limiting value for safe design has been made.

Evidence Supporting Tractive-Force Analysis.—One of the advantages of the use of tractive-force analysis rather than the limiting-velocity approach for the design of large canals is that the former indicates why permissible velocities are higher in large canals than in small ones. This fact (that higher velocities can be used in large canals) has long been known. E. A. Moritz, M. ASCE, has stated:[8] "It is a well known fact that small canals erode at a lower mean velocity than large canals." S. Fortier, J. M. ASCE, and F. C. Scobey, M. ASCE, have also indicated this fact and have included a correction for its effect.[9] Ivan E. Houk, M. ASCE, has noted the increase in scouring velocity with depth.[10] In an article,[11] the variation of limiting velocity with depth is given as shown in Tables 1 and 3. The values shown in Tables 1 and 3 agree so closely with those values which would be produced by a constant value of tractive force that it seems probable that the corrections shown in Table 4 were derived from this assumption. A table of canal dimensions, based on the extensive experi-

TABLE 2.—PERMISSIBLE VELOCITIES FOR NONCOHESIVE SOILS[a]

Material	Particle diameter, in millimeters	Mean velocity, in feet per second
	0.005	0.49
Silt		
	0.05	0.66
Fine sand		
	0.25	0.98
Medium sand		
	1.00	1.80
Coarse sand		
	2.50	2.13
Fine gravel		
	5.00	2.62
Medium gravel		
	10.00	3.28
Coarse gravel		
	15.0	3.94
Fine pebbles		
	25.0	4.59
Medium pebbles		
	40.0	5.91
Coarse pebbles		
	75.0	7.87
Large pebbles		
	100.0	8.86
Large pebbles		
	150.0	10.83
Large pebbles		
	200.0	12.80

[a] From footnote reference 11.

---

[6] "Hydraulic Structures," by A. Schoklitsch, ASME, 1937, Vol. II, p. 733.

[7] Correspondence by James Williamson on "Stable Channels in Alluvium," by Gerald Lacey, *Proceedings*, Inst. of C.E., London, England, Vol. 229, 1929–30, Pt. 1, pp. 349–352.

[8] "Working Data for Irrigation Engineers," by E. A. Moritz, John Wiley & Sons, Inc., New York, N. Y., 1915, p. 47.

[9] "Permissible Canal Velocities," by S. Fortier and F. C. Scobey, *Transactions*, ASCE, Vol. 89, 1926, pp. 940–984.

[10] Discussion by Ivan E. Houk of "Permissible Canal Velocities," by S. Fortier and F. C. Scobey, *ibid.*, p. 971.

[11] "Standards for Permissible Non-Eroding Velocities," Bureau of the Methodology of the Hydro-Energo Plan, *Gidrotekhnicheskoye Stroitel'stvo*, Obedinennoe Nauchno-Tekhnicheskoe Isdatel'stvo, Moscow, USSR, May, 1936.

ence of USBR personnel, was formulated for use in the design of earth canals on the Columbia Basin Project in Washington. When studied on the basis of tractive-force analysis, the canals exhibited approximately constant values of tractive force where the conditions were constant. The available (1952) information strongly supports the preference for limiting tractive force, rather than limiting velocity, as a basis for canal design.

TABLE 3.—RECOMMENDED LIMITING VALUES OF THE TRACTIVE FORCE, IN POUNDS PER SQUARE FOOT, FOR CANALS IN FINE, NONCOHESIVE MATERIAL[a]

Median size of material, in millimeters	DESCRIPTION OF WATER		
	Clear water	Light load of fine sediment	Heavy load of fine sediment
0.1	0.025	0.050	0.075
0.2	0.026	0.052	0.078
0.5	0.030	0.055	0.083
1.0	0.040	0.060	0.090
2.0	0.060	0.080	0.110
5.0	0.140	0.165	0.185

[a] From footnote reference 11.

Tractive-Force Distribution from Velocity Distribution.—Studies to determine the distribution of the tractive force or shear on the bottom and sides of canals were made according to two methods. One was based on an analysis of the measured velocity distribution in channels. The other was a mathematical approach, assuming a power law for the velocity distribution. The velocity and shear distributions were developed mathematically for simple cases; for more involved cases the membrane analogy and the method of finite differences were used.

TABLE 4.—CORRECTIONS OF PERMISSIBLE VELOCITY FOR DEPTH[a]

	(a) NONCOHESIVE MATERIAL							
Depth, in meters	0.30	0.60	1.00	1.50	2.00	2.50	3.00	
Depth, in feet	0.98	1.97	3.28	4.92	6.56	8.20	9.84	
Correction factor	0.8	0.9	1.00	1.1	1.15	1.20	1.25	
	(b) COHESIVE MATERIAL							
Depth, in meters	0.3	0.5	0.75	1.0	1.5	2.0	2.5	3.0
Depth, in feet	0.98	1.64	2.46	3.28	4.92	6.56	8.20	9.84
Correction factor	0.8	0.9	0.95	1.0	1.1	1.1	1.2	1.2

[a] From footnote reference 11.

An attempt was made to determine the distribution of shear or tractive force on the perimeter of canals from published data on the velocity distribution in trapezoidal channels. All available data on trapezoidal shapes (including the special cases of rectangular and triangular shapes) were used; the method was probably first developed by J. B. Leighly.[12] Unfortunately, the data available were not sufficiently exact nor of sufficient quantity to provide an adequate solution by this method. The results scattered widely, and, in the range of shapes in which canals ordinarily occur, it was not possible to determine the shear distribution with sufficient certainty to justify the use of the method.

THE ANALYTICAL APPROACH TO SHEAR DISTRIBUTION

An attempt was made to determine the shear distribution by a mathematical process using the logarithmic distribution developed by Theodor von Kármán,[13] Hon. M. ASCE, and the boundary-layer theory, but this was not found to be practicable. It was found possible, however, to develop mathematical solutions for a velocity distribution in which the velocity is proportional to any power of the distance from the bottom.

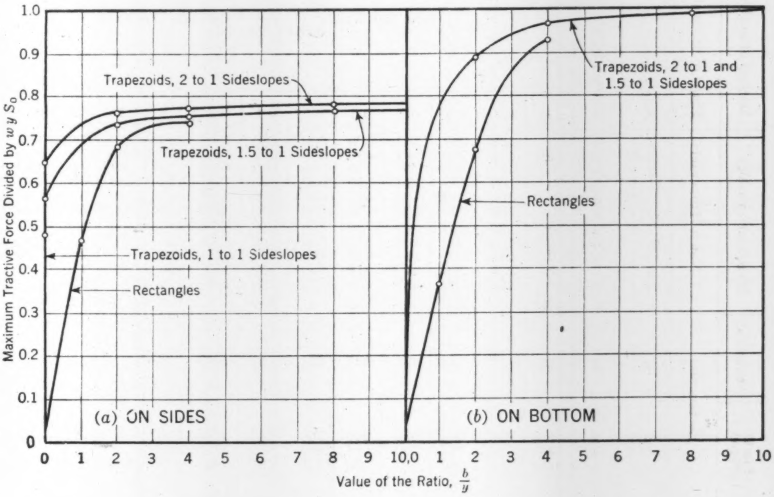

FIG. 1.—MAXIMUM TRACTIVE FORCES IN A CHANNEL

Mathematical solutions were developed for rectangular channels with bed width-to-depth ratios of 2 to 1. The distribution for a bed width-to-depth ratio of 2 to 1 also gave the distribution of a 90° triangular channel. It was not found feasible to use mathematical solutions for the ordinary forms of trapezoidal channels; it was therefore necessary to resort to a membrane analogy. In order to check the reliability of this device, solutions were also made of several of the forms solved by mathematical analysis. Solutions were also made for several cases by use of the method of finite differences; they were checked by comparisons with the mathematical solution.[14] The results of these studies of shear distribution are given in Table 5. In Table 5 the tractive forces at the various points of the perimeter are given in terms of $w\,y\,S_0$. In terms of the maximum shears on the sides (Fig. 1(*a*)) and bottom (Fig. 1(*b*)) of the section, which are the values needed for canal design, the results are given in Fig. 1. The results of these studies give the most reliable information available (as of 1952) on shear distribution. These results indicate that, for trapezodial channels of the shapes ordinarily used in canals, the maximum shear on the bottom would be close to the value, $w\,y\,S_0$, and on the sides the maximum would be close to $0.76\,w\,y\,S_0$.

---

[12] "Toward a Theory of the Morphologic Significance of Turbulence in the Flow of Water in Streams," by J. B. Leighly, *Publications in Geography*, Univ. of California, Berkeley, Calif., Vol. 6, 1932, pp. 1–22.

[13] "Mechanische Ähnlichkeit und Turbulenz," by Theodor von Kármán, *Proceedings*, 3d International Cong. of Applied Mech., Stockholm, Sweden, 1930, Vol. 1, pp. 85–92.

TABLE 5.—DISTRIBUTION OF TRAC

Method of analysis	Shape of channel	Side slope	Bottom width[a]	SIDE BOUNDARY POINTS, VERTICAL DISTANCE ABOVE BOTTOM[a]												
				1.0	0.9	0.8	0.7	0.6	0.5	0.4	0.3	0.2	0.15	0.1	0.05	0.025
Membrane Analogy	Trapezoidal	2:1	2	0	130	250	380	500	600	680	730	760[b]	760	740	670	
		2:1	4	0	130	260	380	490	590	680	740	770[b]	765	750	660	
		2:1	8	0	120	240	360	470	580	660	730	770[b]	760	720	640	
		1½:1	2	0	160	320	450	550	620	690	730	735[b]	720	670	530	
		1½:1	4	0	190	330	450	570	650	710	750[b]	740	710	670	590	
		1½:1	8	0	160	300	420	530	610	690	740	760[b]	710	630	520	
	V-Notch	2:1	0	0	130	260	380	470	550	610	650[b]	640	600	550	440	
		1½:1	0	0	160	290	400	480	530	560	565[b]	520	480	400	290	
		1:1	0	0	230	350	440	470	480[b]	470	440	350		230	130	70
		¾:1	0	0	270	350	375[b]	370	350	320	270	190		110		
		½:1	0	0	275	320	325[b]	305	275	235	190	130		065		
	Rectangular	0:1	2	680[b]		660		620		500		320		180	100	60
Analytical		0:1	2	686[b]	677	654	625	597	566	523	449	335		180		
Finite Difference		0:1	2	686[b]	676	664	636	610	560	510	436	340		200		
		0:1	4	744[b]	740	724	700	664	610	550	476	360		220		
		0:1	1	468[b]		460		435	415	385	342	278	235	180	110	

[a] In terms of depth y. [b] Maximum values.

LIMITING TRACTIVE FORCES FOR NONCOHESIVE MATERIALS

Probably the most important factor in the design of clear-water canals in coarse, noncohesive material is the limiting tractive force which the various types of materials will withstand.

Except for the previously cited suggestions,[7] an extensive search of the pertinent literature disclosed no suggested limiting values for the tractive force to be used in canal design. Information was found, however, on the tractive forces which would start the motion of noncohesive material of various sizes; this information was thoroughly studied and summarized.[3] As will be shown subsequently, the critical tractive force which will start motion is not necessarily the same as the limiting or permissible tractive force which can be used in canal design—especially for the sand-sized materials.

---

[14] "Sedimentation Studies in Open Channels—Boundary Shear and Velocity Distribution by Membrane Analogy, Analytical and Finite Difference Methods," by O. J. Olsen and Q. L. Florey, *Laboratory Report No. Sp. 34*, Bureau of Reclamation, U. S. Dept. of the Interior, Washington, D. C.

Limiting Tractive Forces.—Because the data were meager on limiting tractive forces for coarse, noncohesive material, observations were made on canals in the San Luis Valley of Colorado. Laboratory studies of critical

FORCE IN CHANNELS, DIVIDED BY $w\,y\,S_0 \times 10^{-3}$

BOTTOM BOUNDARY POINTS, HORIZONTAL DISTANCE FROM OUTSIDE EDGE TOWARD CENTER[a]														
0.025	0.05	0.1	0.2	0.3	0.4	0.5	0.6	0.8	1.0	1.2	1.6	2.0	2.4	4.0
		700	770	800	830		870		890[b]					
		730	800	840	870			930		950	960	970[b]		
		720	770	810	840			920			970		980	990[b]
		660	730	780	810		850		890[b]					
		640	740	790	830			910		950	965	970[b]		
		660	730	780	820			910			960		980	990[b]
60	100	180	320		500		620	660	680[b]					
		211	345	436	507	563	605	658	675[b]					
		200	340	436	510	560	610	664	686[b]					
		200	360	470	556	624	684	770	830	870	920	936[b]		
	110	180	275	332	362	372[b]								

[a] In terms of depth y. [b] Maximum values.

tractive force have usually been performed with particles of a small size range; however, the coarse, noncohesive material in which canals are usually constructed contains a large range of sizes. The experiments in the canals of the San Luis Valley provided information from prototype canals and data on the stability of canals built in graded materials.[15]

The canals which were investigated are situated where the Rio Grande leaves the mountains in Colorado and flows out onto an alluvial cone. The material composing this cone decreases in size from the apex outward. Thus, canals in this cone are in a material having a wide range of sizes. The canals are stable, straight, regular in section, and are steep enough to give high velocities and tractive forces. In general, they furnish an unusually complete opportunity for experimentation.

---

[15] "Some Factors Affecting the Stability of Canals Constructed in Coarse Granular Materials," by E. W. Lane and E. J. Carlson, *Proceedings*, Minnesota International Hydr. Convention, International Assn. of Hydr. Research, 1953.

It was expected that the water with high tractive forces, in flowing down these canals, would remove all the material below a certain size; it was also expected that this size would be indicated in the mechanical analysis of the material on the canal beds. This size would be that moved by the tractive force which had acted in these canals. This expectation was not realized, however, as the smaller particles were shielded by the larger ones, and a critical size could not be determined. The tractive forces acting in these canals were therefore compared with the composition of the material through which the canals were constructed. The size used for comparison was that size of which 25% (by weight) of the material was larger. The tractive force used was that resulting from the maximum sustained flow in the canal, as closely as could be determined from the flow records.

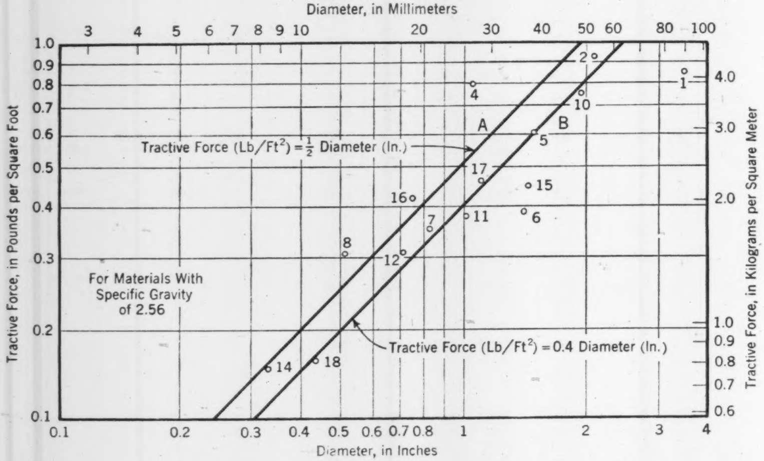

Fig. 2.—Studies on the San Luis Valley Canals, Colorado

Fifteen reaches of canal were used, having discharges ranging from 17 cu ft per sec to 1,500 cu ft per sec and slopes from 4.2 ft per mile to 51 ft per mile. The results of the measurements are summarized in Fig. 2.

Effect of Side Slopes on Limiting Tractive Force

The effect of side slopes on limiting tractive force has been analyzed by a consideration of the forces acting on a particle on the sides of the canal. These forces are: (1) The force of the water tending to move the particle down the canal in the direction of the flow; and (2) the force of gravity tending to move the particle down the sloping side of the canal. By combining the two actions, the effect of the slope of the sides on the critical tractive force necessary to cause motion can be evaluated.

For convenience in design, the effect of side slopes was treated[16] as a factor, K, which is the ratio of the tractive force required to start motion on the sloping sides to that force required, in the same material, to start motion on a level surface.

This ratio involves only the angle of the side slopes of the canal and the angle of repose of the material and is expressed by

$$K = \cos\phi \sqrt{1 - \frac{\tan^2\phi}{\tan^2\theta}} \ldots\ldots\ldots\ldots\ldots\ldots\ldots (1)$$

in which ϕ is the angle (with the horizontal) of the side slope of the canal, and θ represents the angle (with the horizontal) of repose of the material.

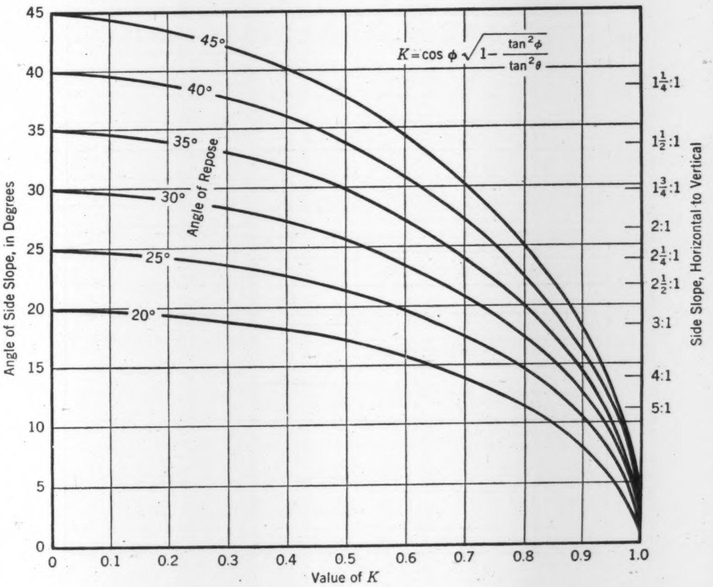

FIG. 3.—RELATIONSHIP BETWEEN SIDE SLOPE AND K

For convenience in solving Eq. 1, Fig. 3 has been prepared. For example, in a material whose angle of repose is 30°, the critical tractive force necessary to move material on the side of a canal with side slopes of 2 to 1 would be 0.44 times that which would cause motion on a level surface.

Angle of Repose of Noncohesive Material.—As previously noted, the stability of the side slopes of a canal in noncohesive material involves the angle of repose of the material. A study was therefore made of this subject, beginning with a thorough review of all available pertinent literature. This review was followed by a limited number of laboratory investigations and observations on a large number of stock piles of various sizes of material at gravel-washing plants.

---

[16] "Critical Tractive Forces on Channel Side Slopes in Coarse, Noncohesive Material," by A. C. Carter, E. J. Carlson, and E. W. Lane, *Hydraulic Laboratory Report No. Hyd.-366*, Bureau of Reclamation, U. S. Dept. of the Interior, Washington, D. C., 1953.

The results of the studies made in the laboratory are given in Fig. 4. These experiments showed that a considerable range of values could be obtained in repetitive tests. Time was not available, however, to make a sufficient number of observations to obtain accurate average values; the determinations made are therefore subject to considerable scatter. The results showed that, for the larger sizes, the angles were not materially different for the various conditions of stacking in air or water, but for the sand sizes these conditions had more effect. The average results of all observations of the angle of repose of stock piles at gravel-washing plants are shown in Fig. 4(*d*). Although these data indicate that the angle of repose increases with both size and angularity, the data scatter widely and are insufficient in number to determine closely any quantitative relations.

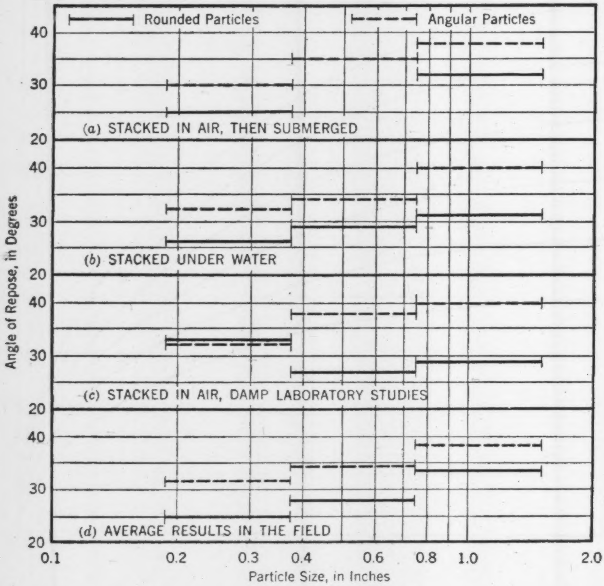

FIG. 4.—OBSERVATIONS OF THE ANGLE OF REPOSE OF COARSE, NONCOHESIVE MATERIAL

For use in design (until more exact relationships can be determined) Fig. 5 is presented, giving values of the angle of repose for material greater than 0.2 in. in diameter for various degrees of roundness. In Fig. 5 the angles of repose have been somewhat arbitrarily limited to a maximum value of 41° for very angular material, and 39° for very rounded material. This limitation was believed necessary to secure conservative designs because of the lack of data on angles of repose of the larger-sized material.

HYDRAULIC ROUGHNESS OF CANALS IN NONCOHESIVE MATERIAL

Measurements of flow of water in channels have demonstrated that the hydraulic roughness of canals in coarse, noncohesive material changes appreciably with the size of material involved. When designing canals in such material, it is therefore important that this fact be considered if correct predictions of the canal-discharge capacity are to be obtained. It is equally important that the slopes be accurately estimated if reliable values of the tractive force which will act on the sides and bottom of the channel are to be

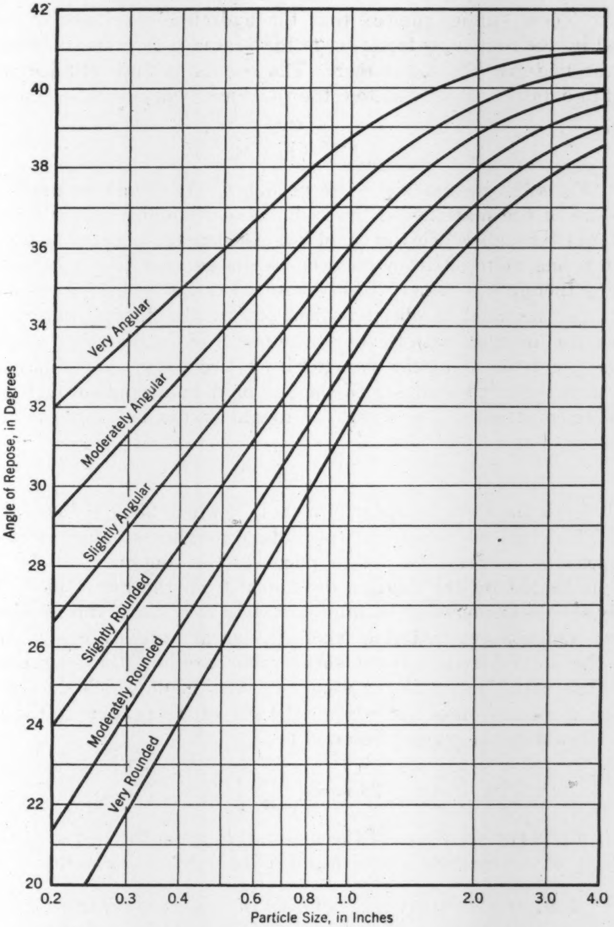

FIG. 5.—ANGLE OF REPOSE OF NONCOHESIVE MATERIAL

obtained. In order to secure a more reliable design for stable channels in such material, a study was made of the relation of hydraulic roughness to the particle size of canal material. The first step in this study consisted of a review of all available pertinent literature. The data from the experiments performed by the USBR on the flow in the San Luis Valley canals were also included. These studies showed that the hydraulic roughness of canals, as expressed by the roughness factor, n, in the Manning formula, increases as the size of the material becomes larger. The results of these studies have been reported in detail.[15] Briefly stated, the roughness values can be expressed as[17]

$$n = \frac{K^{1/6}_{50}}{44.4} \qquad (2)$$

in which K_{50} is the median sieve size in inches. It should be noted that the median size of the material on the bed was considerably larger than that of the material through which the canal was constructed because of the washing out of the fine material from between the larger particles. In designing a canal it is therefore necessary to estimate what the bed composition will be after the fine material has been washed out by the flowing water. Because the value of n increases with the one-sixth power of the diameter, a high degree of accuracy in determining the diameter is not necessary. A comparison of the roughness of the test sections with the size of the material through which the canals were constructed shows that the roughness can be expressed as

$$n = \frac{K^{1/6}_{25}}{39} \qquad (3)$$

in which K_{25} is the sieve diameter in inches, of which 25% of the material was larger. The canal sections from which these roughness values were obtained were especially uniform; for design purposes the roughness in the Manning formula indicated by the relation developed from the San Luis Valley tests probably should be increased by approximately 15%. Eq. 3 is applicable only to coarse, noncohesive material, where the shear values are high enough to remove the fine material. If the shear values are low, the roughness will be smaller than Eq. 3 indicates. A study was also made which showed that the roughness is a function of the ratio of the size of the particle to the hydraulic radius. The data, in general, resulted in

$$26\, n = \left(\frac{K_{35}}{R}\right)^{1/6} \qquad (4)$$

in which K_{35} is the sieve size of the material forming the bed of the canals of which 35% of the material is larger and R is the hydraulic radius.

LIMITING TRACTIVE FORCES FROM LIMITING VELOCITIES

The data for critical tractive forces obtained from laboratory experiments are applicable to the case of coarse, noncohesive material, but experience has shown that canals can resist materially higher values of tractive force than that which would start movement in fine, noncohesive material. For the design of canals in this material, therefore, something more than determinations from laboratory studies is necessary. No laboratory data are available for limiting tractive forces in cohesive material. For both of these cases, it would be desirable if limiting tractive forces could be determined from observations on actual canals. Although studies of this nature are being (as of 1952) conducted by the USBR, sufficient information for this purpose has not yet been accumulated.

---

[17] "Beitrage zur Frage der Geschwindigeckformal und der Rauigkeitszahlen für Strom Kanaele und geschlossene Leitungen," by K. Strickler, *Mitteilungen No. 16*, des Amtes für Wasserwirtshaft, Bern, Switzerland, 1923.

Until field studies of canals in fine, noncohesive and cohesive materials can be made using the tractive-force principle, the only method of determining limiting tractive-force values for such canals is from the limiting velocities which these canals will sustain. Much information concerning such velocities has been accumulated. As velocity is not a completely rational parameter for determining scour, these velocity data are not entirely satisfactory; by an intelligent utilization of them, however, valuable information can be obtained for use in scour analysis by the tractive-force method. An attempt has therefore been made to analyze the data on permissible velocities in canals, as presented in the available publications, and to determine from the values of limiting velocities the values of the tractive force which they represent.

TABLE 6.—COMPARISON OF B. A. ETCHEVERRY'S MAXIMUM ALLOWABLE VELOCITIES WITH VALUES OF THE TRACTIVE FORCE

Material	Value of n	Velocity, in feet per second	Tractive force, in pounds per square foot
Very light pure sand of quicksand character	0.020	0.75 to 1.00	0.006 to 0.011
Very light loose sand	0.020	1.00 to 1.50	0.011 to 0.025
Coarse sand or light sandy soil	0.020	1.50 to 2.00	0.025 to 0.045
Average sandy soil	0.020	2.00 to 2.50	0.045 to 0.070
Sandy loam	0.020	2.50 to 2.75	0.070 to 0.084
Average loam, alluvial soil, volcanic ash	0.020	2.75 to 3.00	0.084 to 0.100
Firm loam, clay loam	0.020	3.00 to 3.75	0.100 to 0.157
Stiff clay soil, ordinary gravel soil	0.025	4.00 to 5.00	0.278 to 0.434
Coarse gravel, cobbles, and shingles	0.030	5.00 to 6.00	0.627 to 0.903
Conglomerate, cemented gravel, soft slate, tough hardpan, soft sedimentary rock	0.025	6.00 to 8.00	0.627 to 1.114

The three sources of systematic data available (as of 1952) on permissible velocities in canals which will be safe against scour are those of B. A. Etcheverry,[18] Messrs. Fortier and Scobey,[9] and the data obtained in Russia[11] which is shown in Tables 1 through 4. The data given by Mr. Etcheverry are shown in Table 6. These data are not related to the size of canals. The data obtained by Messrs. Fortier and Scobey are given in Table 7. These data are for "a depth of 3 feet or less;" Messrs. Fortier and Scobey suggest[9] that, for depths exceeding 3 ft, a mean velocity greater by 0.5 ft per sec may be allowed. They also state that the values are applicable to canals "with long tangents predominating throughout their length," and that for canals in sinuous alinement a reduction of about 25% is recommended. These values are for canals which have been "aged," or brought up to capacity gradually over a considerable period of time. Table 7 also gives values which Messrs. Fortier and Scobey recommended for use when the water transports colloidal silts.

---

[18] "Irrigation Practice and Engineering," by B. A. Etcheverry, McGraw-Hill Book Co., Inc., New York, N. Y., Vol. II, 1915, p. 57.

The Russian data[11] give the permissible values for granular material of various diameters, as shown in Table 2. These values are for a mean depth of 1 m, and for water carrying less than 0.1% of sediment of less than 0.005-mm size. For other mean depths, the values in Table 2 can be multiplied by the factors shown in Table 4(*a*). It is also stated[11] that the permissible velocities of Table 2 can be increased by the following percentages for flows containing from 0.1% to 2.5% of sediment less than 0.005 mm in diameter; from 25% to 65% for sand; from 10% to 45% for gravel; and from 0% to 25% for pebbles. For cohesive material the values given for a 1-m mean depth are as shown in Table 1, and the corrections for other depths are given in Table 4(*b*).

To convert the values of limiting velocity given in the literature[9,11,18] into exactly equivalent values of tractive force, it is necessary to know the size, shape, shear distribution, and energy gradient of the channels to which these values apply. Because these data are not given, it is necessary to make certain assumptions regarding them.

TABLE 7.—COMPARISON OF LIMITING VELOCITIES DETERMINED BY S. FORTIER AND F. C. SCOBEY WITH VALUES OF THE TRACTIVE FORCE FOR STRAIGHT CHANNELS AFTER AGING

Material	Value of *n*	CLEAR WATER		WATER TRANSPORTING COLLOIDAL SILTS	
		Velocity, in feet per second	Tractive force, in pounds per square foot	Velocity, in feet per second	Tractive force, in pounds per square foot
Fine sand, colloidal	0.020	1.50	0.027	2.50	0.075
Sandy loam, noncolloidal	0.020	1.75	0.037	2.50	0.075
Silt loam, noncolloidal	0.020	2.00	0.048	3.00	0.11
Alluvial silts, noncolloidal	0.020	2.00	0.048	3.50	0.15
Ordinary firm loam	0.020	2.50	0.075	3.50	0.15
Volcanic ash	0.020	2.50	0.075	3.50	0.15
Stiff clay, very colloidal	0.025	3.75	0.26	5.00	0.46
Alluvial silts, colloidal	0.025	3.75	0.26	5.00	0.46
Shales and hardpans	0.025	6.00	0.67	6.00	0.67
Fine gravel	0.020	2.50	0.075	5.00	0.32
Graded loam to cobbles when noncolloidal	0.030	3.75	0.38	5.00	0.66
Graded silts to cobbles when colloidal	0.030	4.00	0.43	5.50	0.80
Coarse gravel, noncolloidal	0.025	4.00	0.30	6.00	0.67
Cobbles and shingles	0.035	5.00	0.91	5.50	1.10

Messrs. Fortier and Scobey[9] realized that greater depths permitted higher velocities and specified the depths to which their velocity applied as 3 ft or less. If the tractive-force analysis is sound, a single velocity could not apply to a range of depth from 3 ft to zero. It is believed that most of the canals from which the limiting-velocity data were derived had depths of approximately 3 ft; this depth has therefore been used in the conversion. If the tractive-force principle is correct, the value for a 3-ft depth would vary with the width of the canal and the side slopes. For this conversion, a bottom width of 10 ft and side slopes of 1½ to 1 have been used. These measurements were believed to represent (as closely as can be estimated) a mean of the most probable condition of the canals on which the data were obtained. The energy slope of the canals must also be used; to determine it, use was made (with the

Manning formula) of what was believed to be the most probable value of hydraulic roughness for the nature of the material in which the canal was located. Much of the uncertainty involved in the use of the values of tractive force obtained in this manner is eliminated if the same roughness values and the same formula are used in computing the energy gradient for the canals under study as were used in determining the permissible tractive forces from the permissible velocities. The values of hydraulic roughness used in arriving at the tractive forces are therefore noted. Tractive-force values corresponding to the values used by Messrs. Fortier and Scobey for the limiting velocity, as computed under these assumptions, are given in Table 7. As the use of a single value for the tractive force provides, in a rational manner, a larger velocity for greater depths, no attempt was made to consider the less rational correction proposed by Messrs. Fortier and Scobey for greater depths.

Because Mr. Etcheverry's data[18] included no information on size, shape, or side slope of the channels, the same assumptions were made—somewhat arbitrarily—in converting the data as were made in the case of the data obtained by Messrs. Fortier and Scobey. The values of the tractive force corresponding to the limiting velocities offered by Mr. Etcheverry are also given in Table 6.

The permissible velocities of the Russian data[11] are for an average depth of 1 m. These have been converted into tractive forces by assuming the same bed width-to-depth ratio as is assumed for the data from other authorities. The corrections (Table 4) for other depths are such that practically the same values of tractive force would be obtained if these other depths of flow had been used in estimating the equivalent tractive forces.

MATERIAL IN WHICH CANALS ARE CONSTRUCTED

In designing canals that will be free from scour while carrying relatively clear water, one of the most important factors is the material through which the canal passes. There are three classes of this material, each of which requires a different method of analysis. These three classes are: (1) Coarse, noncohesive material; (2) fine, noncohesive material; and (3) cohesive material.

For the design of canals in coarse, noncohesive material, one must consider not only the limiting tractive force on the bottom but also the action of the particles in rolling down the sloping canal sides. This requires an analysis of the combination of the rolling effect with the longitudinal force of the flowing water, as previously noted, and involves the angle of repose of the material. The distribution of the tractive forces on the perimeter of the canal must also be considered. As the hydraulic roughness of canals in this class varies widely with the size of the particles of the material involved, the roughness factor also is important.

Where the canal is constructed in cohesive material, the particles are prevented from rolling down by cohesion; hence, this part of the analysis is not applicable. The design, therefore, involves only the distribution of the tractive force for the material in which the canal is constructed. In these canals the hydraulic roughness is not a function of the size of the particle but of the surface irregularities on the banks and (usually) of the ripple formations on the bed.

Canals in fine, noncohesive material are intermediate between the other two classes. In this class the effect of small amounts of cohesive sediment in the water, or in the material through which the canal flows, becomes important.

Coarse, Noncohesive Material.—The limiting value of tractive force for use in design of channels in coarse, noncohesive materials is determined from the data obtained at the San Luis Valley canals and from the results of the determinations of limiting tractive force obtained by computation from limiting velocities, as given by Mr. Etcheverry,[18] Messrs. Fortier and Scobey,[9] the Nuernberg Kulturamt, and the Russian article.[11] Of these, the studies made on the canals of the San Luis Valley are most detailed and complete. These latter results are shown in Fig. 2. Line A in Fig. 2 represents the relationship: Tractive force (in pounds per square foot) equals one half the diameter (in inches) of a particle such that 25% of the material in which the canals were constructed is coarser.

As most of the observations fall either above or very close to line A, it is believed that this line probably represents the true value for the limiting tractive force in canals in such material. However, line A does not allow for a sufficient factor of safety for use in design. A value for the limiting tractive force (in pounds per square foot) equal to 0.4 times the diameter (in inches) for the size of which 25% of the material is larger (as shown by line B) is therefore tentatively recommended for design.

For metric units a similar design relationship can be used. This relationship is the tractive force (in kilograms per square meter) equal to 0.8 times the diameter (in centimeters). This relationship differs by only 4% from the one given in English units. As these relationships were determined on straight canals, their use should be limited to such conditions. For curved canals, lower values for the tractive force should be used.

Fig. 2 was developed for material having a specific gravity of 2.56. If used for materials with appreciably different specific gravities, the tractive forces for a given size (as indicated by Fig. 3) must be multiplied by the ratio of the submerged unit weight of the other material to the submerged unit weight of material having a specific gravity of 2.56. In the case of porous material, the saturated unit weight should be used.

The use of a direct relationship between the diameter of the 25% larger size and the tractive force is amply justified by the evidence obtained from investigations of the critical tractive force. These studies show that the general trend of all the data obtained is close to such a relationship.

In canals designed with this relationship (line B, Fig. 2), some of the finer material on the banks and bed (when the canal is first constructed) will be moved downstream, uncovering coarser particles which will protect the bed and banks. If this movement produces undesirable effects, measures to meet the situation will be required. For example, the material moving down a power canal might erode the machinery; steps to prevent this will be necessary until all movable material is washed out and stability is attained.

In canal design, it is necessary to combine the relationships shown by line B, Fig. 2, with the effect of the side slopes and of the tractive-force distribution on the perimeter of the canal. The method of effecting this combination can best be presented in the form of an example: A canal is to be built in slightly angular material, 25% of which is 1 in. or more in diameter, and the canal water section has a 10-ft bottom width, 5-ft depth, and side slopes of 2 to 1. The ratio of bed width-to-depth is therefore 2. The maximum tractive force on the bottom of a trapezoidal canal with $b/y = 2$ and side slopes of 2 to 1 is shown by Fig. 1(*b*) to be 0.89 $w\,y\,S_0$. No motion will occur on the bottom if this value does not exceed the limiting value for the material in which the canal is constructed. This value for the limiting tractive force of material, 25% of which is more than 1 in. in diameter, is shown by Fig. 2 to be 0.40 lb per sq ft. The limiting longitudinal slope for the canal is, therefore, $S_0 = 0.40/(0.89\,w\,y)$, in which w is 62.5 lb per cu ft and y is 5 ft. This limiting slope for movement on the bottom is therefore 0.00144.

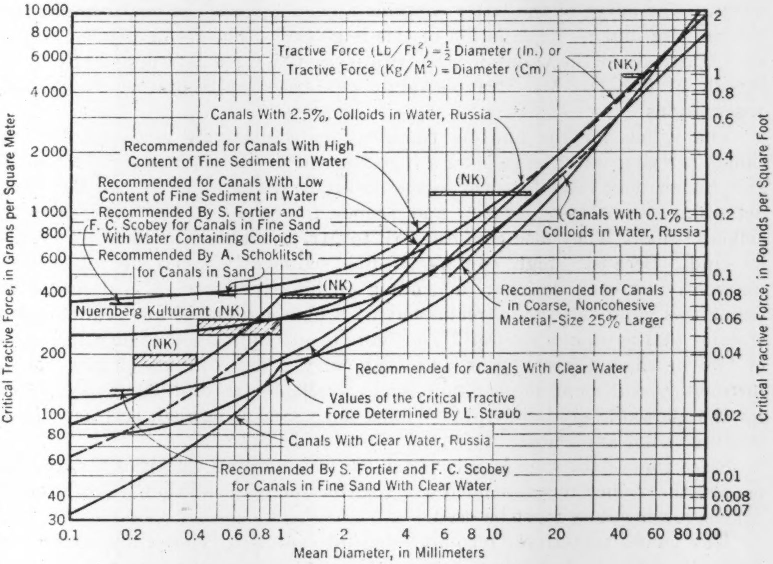

Fig. 6.—Recommended Limiting Tractive Forces for Canals

For the sides of the channel to be stable, the limiting tractive forces must be less than would be safe on a level bottom. The difference must be an amount which depends on the side slope of the canal and the angle of repose of the material. The safe angle of repose for slightly angular material of 1-in. diameter is shown by Fig. 5 to be 36°. For side slopes of 2 to 1 and an angle of repose of 36°, Fig. 3 indicates that the safe tractive force on the side slope would be 0.64 of that on a level bottom, or (for this case) $0.64 \times 0.40 = 0.26$ lb per sq ft. The maximum tractive force on the sides of a trapezoid with $b/y = 2$ and side slopes of 2 to 1 is shown in Fig. 1(*a*) to be 0.76 $w\,y\,S_0$. The longitudinal canal slope required to produce the limiting tractive force on the sides is, therefore, $S_0 = 0.26/(0.76\, w\, y) = 0.00108$. As this limiting longitudinal slope is smaller for the sides than for the bottom, the former would control the design; hence, the canal should not be built with a slope of more than 0.00108.

Fine, Noncohesive Material.—Based on a consideration of all the available data, the best recommendations which can be made for canals constructed in fine, noncohesive material are those given in Table 3. The comparison of these recommendations with most of the data available as of 1952 is shown in Fig. 6.

The recommended values for clear water were selected to agree with the value obtained by Messrs. Fortier and Scobey[9] and conform to the general trend. These values are somewhat higher than the Russian values for clear water. The curve of the latter contains a peculiar break of curvature at the 1.0-mm size, but no explanation of this is given.[11] The recommended values are slightly above the values for the critical tractive force determined[19] by L. G. Straub, M. ASCE. Mr. Straub's values were based on laboratory and stream observations.

The values for the limiting tractive force tentatively recommended for canals carrying water containing a high content of fine sediment are considerably higher than those for clear water, and they are based largely on the value determined by Messrs. Fortier and Scobey for canals in fine sand carrying colloidal silts. They also conform well to Mr. Schoklitsch's value[6] for canals in sand. Because "high content of fine sediment" would be interpreted differently by each designer, depending on his experience, it is desirable to define this more closely. Streams having a high content of fine sediment are streams that contain a load of 2% or more of silt and clay sizes on an average of two or three times a year, but that carry a low content of sand. Unfortunately, sufficient information is not available (as of 1952) to set limits for the allowable sand content. Where much sand is carried, this method of analysis is not applicable.

Since these data were largely obtained from limiting velocities for straight canals, the values recommended are also for such a condition. For crooked canals, lower values must be used.

The values tentatively recommended for canals carrying a low content of fine sediment are intermediate between the values for clear water and those for water with heavy sediment load. The values conform, in general, to the values given by the Nuernberg Kulturamt. A low content of fine sediment is defined as a content of silt and clay sizes reaching 0.2% concentration on the average of two or three times a year. The sand content should be very low.

It will be seen that for canals in fine sand the values tentatively recommended for clear water are much higher than are those indicated by flume tests. The general order of magnitude of the values in the two cases appears to be well established, and some explanation of the difference is therefore needed. This difference is probably caused by the fact that clear water (such as is used in the laboratory) is seldom obtained in natural channels, and that the sand through which the canals pass is rarely as clean as that used in the laboratory, such sand usually containing a little binder material. The growth of minute organisms in the water may also be a factor. However, a slight movement of material in a canal will not make it unstable, as such movement probably will not have objectionable results.

---

[19] *House Document No. 238*, 73d Cong., 2d Session, U. S. Govt. Printing Office, Washington, D. C., p. 1135.

The higher values allowable with fine suspended sediment are usually caused by the cementing effect of this material on the banks and bed of the channel. In the case of high-fine-sediment content there are higher values because, with a silt and clay size content of 2%, some sand would also be carried; this would reduce the effect of the scour on the bed.

The median size, or size of which 50% (by weight) is larger, is specified for the fine, noncohesive material whereas the size specified for the coarse, noncohesive material is the size of which 25% is larger. The median size is used for the fine material because this is the usual criterion for describing such material. In the coarse material, however, only the coarsest remains to protect the bed and banks, and the 25% larger size defines this material better than does the median size. The use of the two systems of description introduces an uncertainty in the vicinity of the 5-mm size, which was somewhat arbitrarily selected as the division between these classifications. For example, a material in which the part larger than 5 mm falls between 25% and 50% would be included in both the coarse and fine classifications. This difficulty can be removed by using whichever classification gives the lower tractive force.

Where very clear water is used, it is probable that the rolling-down effect previously cited will be effective, but information on the angle of repose of such material is meager. For clear water flowing in fine, noncohesive material, flat side slopes are necessary. Where the water carries a low or a high content of fine sediment, and a period of aging occurs before the canal discharge reaches design capacity, the deposits of fine material on the banks will prevent the rolling down. An exception to this occurs where the canal is below the ground-water level, and the water flowing into the canal through the banks prevents the deposition of the fine sediment.

Cohesive Materials.—For the design of canals in cohesive material, the only data on safe tractive forces available (as of 1952) are those obtained by converting limiting velocities (as given by Mr. Etcheverry,[18] Messrs. Fortier and Scobey,[9] and in the Russian article[11]) to the values of the tractive force. Studies are under way (1952) to evaluate the USBR's experience with canals, from which it is hoped more complete information can be obtained; however, a digest and synthesis of the available material into a systematic procedure have not been made. Until this is done, canal designers wishing to use tractive forces will have to select limiting values of tractive force from an examination of the data based on the conversion of limiting velocities to tractive force given in Tables 1, 6, and 7.

In canals in cohesive material the effect of the distribution of tractive forces (shown in Fig. 1) should be considered, but the rolling-down effect is not applicable.

Canals Carrying Heavy Sediment Loads.—Although the USBR has made few quantitative investigations of the case of canals carrying heavy loads of sediment, it is expected that work will be performed in this field. The basic principles involved in the design of such canals, however, have been developed.

Briefly stated, the principles are as follows: If appreciable quantities of sediment are introduced into a canal with the water, the stability of the canal will depend on the fact that this sediment is carried through the canal without deposit. That is, the canal must be able to transport the sediment which is introduced into it. Usually the greatest difficulties are experienced in transporting the sand and coarser sizes of material. Because most of this material travels near the bed, a stable channel must have sufficient shear acting on the bed to transport this load. At the same time, however, the shear on the sides must not be great enough to scour the sides. Also, the shear on the bottom must not be so much greater than that required to transport the sediment that scour of the original material of the bed results.

If large quantities of fine material are carried, the shear throughout the section must be sufficient to keep this material from depositing. The shear, however, must not be of such a magnitude that scouring of the original material will occur. Where large quantities of both fine and coarse material are carried, there must be enough shear on the bed to cause the transportation of the coarse material, and enough shear on the banks to prevent the deposition of the fine material, but not enough to cause scour of the material forming the banks.

It will thus be seen that the laws of transportation of sediment are important in the stable-channel problem. Considerable progress in determining these laws has been made, but much still remains to be accomplished. Probably the most advanced work along this line in recent years is the work of H. A. Einstein,[20] M. ASCE.

EFFECTS OF BENDS

Perhaps the phase of stable-channel design about which least is known is the effect of bends. It has long been evident that sinuous canals scour more easily than do straight ones, but few quantitative studies of this effect are available. Study of the scour at bends, both in the laboratory and in the field, is a part of the program of stable-channel studies being performed (as of 1952) by the USBR.

Canals of the USBR have sometimes been designed to limit the radius of bends to six times the water-surface width. On other canals, a limit of fifteen times the water depth has been used. A number of other suggestions have been made.[21,22] There is a need, however, for more accurate knowledge on which to base design procedures.

The scour in bends can be reduced by lowering the velocity of flow. This reduction can be accomplished by using larger canal areas, but such a procedure results in an increased cost. It will often be more economical to allow scour to begin in canals and stop it by protecting the banks at the points where scour occurs, rather than to use the larger cross sections necessary to insure that no scour will take place. With the present (1952) knowledge, it is impracticable to place protection at the bend in advance, as this would lead—in many cases—to protection where it is not needed.

---

[20] "The Bed-Load Function for Sediment Transportation in Open Channel Flows," by H. A. Einstein, *Technical Bulletin No. 1026*, U. S. Dept. of Agriculture, Washington, D. C., 1950.

[21] "Irrigation Practice and Engineering," by B. A. Etcheverry, McGraw-Hill Book Co., Inc., New York, N. Y., 1915, Vol. II, p. 39.

[22] "Economic Canal Location in Uniform Countries," by Lyman E. Bishop, *Transactions*, ASCE, Vol. LXXIV, 1911, p. 188.

Because the values of limiting tractive force recommended are for straight canals, and many canals are more or less sinuous, a comparison of the velocities and tractive forces in straight canals and canals of different degrees of sinuosity are given in Table 8. In order to define more closely the meaning of these various degrees of sinuosity, the following may be useful: (1) Straight canals have straight—or slightly curved—alinement, as is typical of canals in flat plains. (2) Slightly sinuous canals have a degree of curvature which is typical of slightly undulating topography. (3) Moderately sinuous canals have a degree of sinuosity which is typical of moderately rolling topography. (4) Very sinuous canals have a condition of curvature which is typical of canals in foothills or mountainous topography.

Table 8 compares the permissible tractive forces and velocities in canals having various degrees of curvature with those in straight canals. It will be seen that the tractive-force values have a wider range than the corresponding mean velocities. These values are as close to the true values as is possible with the available data (as of 1952). However, because the values are based on judgment, rather than on observed data, one feels justified in suggesting their use only until more accurate information is obtained.

TABLE 8.—Comparison of Permissible Tractive Forces in Sinuous Canals with Permissible Values in Straight Canals

Degree of sinuousity	Relative limiting tractive force	Corresponding relative limiting velocity
Straight canals	1.00	1.00
Slightly sinuous canals	0.90	0.95
Moderately sinuous canals	0.75	0.87
Very sinuous canals	0.60	0.78

Nonscouring Canals of Minimum Excavation and Width

In studying trapezoidal canals, it was found that limiting tractive forces occurred over only a part of the perimeter. Forces of less magnitude than these acted on most of the perimeter. It was believed that a section on which the limiting tractive force acted over the entire perimeter might have interesting properties; the mathematical requirements of such a section were therefore formulated, and its shape was determined. Study showed that, within the limitations of the approximating assumptions used, this section had other important properties, in addition to the property of impending motion over the entire periphery. Under certain conditions, the utilization of these properties will make possible substantial savings. Further studies were therefore made to refine the accuracy of the determination.

In the section developed, the material on the entire wetted perimeter is in a state of incipient motion, and the side slopes above the water line are at the angle of repose. Under these conditions it was found that this section also has interesting properties for a channel in a coarse, noncohesive material. For material with a given angle of repose and for a given discharge, this section provides not only the channel of minimum excavation, but also the channel of minimum top width, maximum mean velocity, and minimum water area.

The shape of the channel is dictated by the following five assumptions: (1) At and above the water surface, the side slope is at the angle of repose of the material. (2) At points between the center and edge of the channel, the particles are in a state of incipient motion, under the action of the resultant of the gravity component of the particles' submerged weight acting down the side slope and the tractive force of the flowing water. (3) At the center of the channel the side slope is zero, and the tractive force alone is sufficient to cause incipient motion. (4) The particle is held against the bed by the component of the submerged weight of the particle acting normal to the bed. (5) The tractive force on any area is equal to the component of the weight of the water above the area in the direction of flow. Under the first three assumptions, the particles on the entire perimeter of the canal cross section are in a state of impending motion.

For the fifth assumption to be true, there could be no transfer of force horizontally between adjacent currents moving at different velocities in the section. This is, of course, not the case as the faster moving water near the center of the channel tends to carry along the slower moving water near the sides. As part of this study, however, there was a detailed mathematical treatment of the problem which indicated that, for the shape of channel which is likely to be encountered in practice, the departure of the approximate assumption from the true conditions would have little effect on the shape of the section.[3,23]

For a given discharge and longitudinal canal slope in a material of given angle of repose and a known limiting tractive force, the solution provides the shape and dimensions of the channel having the properties previously cited. It is also possible to introduce factors of safety so that the material will have any desired safety factor against motion at all parts of the perimeter of the water and above-water section.

FUTURE STUDIES

The program of studies undertaken by the USBR for the improvement of canal-design procedures is well under way (as of 1952); much work remains to be done.

Additional studies of limiting tractive forces are planned along four lines: (1) Laboratory tests of graded materials are to be made (*a*) to study the shingling effect of the removal of the finer fractions of a graded material, (*b*) to determine safe values of design for such mixtures of sizes, (*c*) to determine the amount of material which must be moved away before stability is obtained, and (*d*) to study the effect of the shape of the particles on the critical tractive force. (2) Studies are to be conducted of available data in the literature, and field observations are to be made to obtain better knowledge of the limiting shear on cohesive material and on the material formed by the deposit of fine sediment carried in suspension by the canals. (3) A field study is to be made of

---

[23] "Stable Channel Profiles," by R. E. Glover and Q. L. Florey, *Hydraulic Laboratory Report No. Hyd.-325*, Bureau of Reclamation, U. S. Dept. of the Interior, Washington, D. C., 1951.

scour in terms of tractive force in USBR-built canals. (4) A study is to be conducted of the scour resistance of clay soil and its relationship to the properties of clay involved in its structural stability.

Further investigations of shear distribution are planned to include both laboratory and field research. The laboratory work should consist of measurements of shear distribution on the periphery of trapezoidal channels and of the corresponding velocity distribution for channels both of equal and unequal roughness on the sides and bottom. Field studies of velocity distribution in similar channels should also be made for comparison with the laboratory studies; thus correlation of model and prototype shear distribution would be obtained. The assumption that the shear distribution on channels of similar cross section will be similar should be checked. Studies—both field and laboratory—are also planned concerning the possibility of measuring the shear at any point on the canal perimeter by measurement of the velocity gradients at these points.

Model studies of trapezoidal channels in coarse, noncohesive material are contemplated to establish the degree of reliability of the analysis of the rolling-down effect on the side slopes. Further studies of the angle of repose of material of various sizes and shapes, and also of graded material of various sizes, are included in the program. Particular attention should be given to the larger sizes of material to allow for removal of the arbitrary limitations suggested herein.

Laboratory and field studies on the laws of sediment transportation should also be performed to determine better methods of estimating the quantity of various sizes of sediment carried by canals. The Hydrology Branch of the USBR is now (1952) conducting such investigations.

A study is also planned to correlate and compare the canal-analysis methods developed in India and Pakistan with the methods developed in this paper, in order to obtain any advantages there might be in a combination of the methods or data.

An investigation, both in the laboratory and in the field, of the effect of bends is included in the program. The laboratory study will consist of experiments with bends of various radii, central angle, bottom width, side slopes, and velocities, in order to study the scouring effects under various conditions. The possibilities of spiraling curves and superelevation of the bed will also be considered. The field study will consist of observations on bends in canals which have produced scour so that data on the conditions which cause trouble in actual cases may be obtained.

A laboratory study is projected to establish the degree of reliability of the analysis of the shape of the channel of impending motion throughout the sides and bottom. It is apparent that it will take a long time to complete this program. The principal purpose in listing these studies is to show what information is still needed to obtain a satisfactory design method.

Conclusion

The methods of design that have been suggested are based on the results of the studies described herein. These methods are largely derived from the writer's interpretation of these results. Because the studies have only recently (1952) been completed, they do not represent experience based on a long period of use in canal design. There has not been sufficient time to secure a thorough discussion of the results from the qualified persons in the USBR, and no formal action on the design proposals has been taken by the USBR. The general reaction to these suggestions seems to be favorable, however, and the use by USBR personnel of tractive force as a parameter of design in place of velocity is rapidly spreading. Some of the processes seem to be well established; others—because of lack of data—are based on less well-established investigations. In all cases, the writer has attempted to indicate the extent of the supporting information. The need for further studies to check and perfect the methods proposed herein is evident. This material should be considered, therefore, to be a progress report. It is believed, however, that the results described and the methods proposed represent progress toward better stable-channel design, and that their use for design in their present form is amply justified until further studies can be made to perfect them.

ACKNOWLEDGMENTS

The studies described in this paper were the work of a large group of men on the staff of L. N. McClellan, M. ASCE, the chief engineer of the USBR. The number of engineers who have taken part in these studies is so large that it is practicable to acknowledge only those who made the more important contributions.

Most of the mathematical work, including the analysis of the most efficient channel and of the shear distribution on the perimeter of canals, was performed by R. E. Glover, M. ASCE, research engineer, assisted by F. E. Swain, R. G. Conard, and Q. L. Florey. The membrane-analogy studies were performed by O. J. Olsen under the direction of D. McHenry, M. ASCE, who also introduced the method of finite-difference analysis. A. C. Carter conducted the studies of shear distribution in canals based on velocity distribution, on limiting tractive forces, angles of repose, and effect of side slopes. O. S. Hanson investigated the hydraulic roughness of canals and angles of repose. E. J. Carlson, M. ASCE, performed most of the studies of the San Luis Canal data, and also studied hydraulic roughness, angles of repose, and the effect of side slopes. C. R. Miller, A. M. ASCE, also worked on the San Luis Valley Canal studies. R. P. Verma, A. M. ASCE, assisted on the velocity-distribution studies. These investigations were largely conducted as a part of the work of the Hydraulic Laboratory Section (USBR) which is under the direction of H. M. Martin, M. ASCE, with C. W. Thomas, M. ASCE, in charge of this part of the work. The staff of the San Luis Valley Project office (USBR) conducted the canal measurements in the valley. Helpful advice was also received from Mr. Glover, D. J. Hebert, C. R. Burky, M. ASCE, I. B. Hosig, M. ASCE, P. W. Terrell, H. G. Curtis, M. ASCE, and N. L. Govinda Rao.

DISCUSSION

Serge Leliavsky,[24] M. ASCE.—A complete summary of the work of the USBR on the problem of scour in canals has been presented by the author. To this summary only minor additions are possible. For example, the fact that in the tests performed by C. M. White concerning scour[25] the angle of repose was used in a more general sense than by Mr. Lane may possibly widen the general outlook on the problems considered by the author. In fact, Mr. Lane introduces the angle-of-repose concept while investigating sideslopes whereas Mr. White introduced the concept by considering both sloping and horizontal bed surfaces and demonstrated, experimentally, that the criterion for scour on such surfaces can be expressed in terms of the angle of repose as for sideslopes.

A paving—consisting of a coarser-grained material than the average—was found by Mr. Lane to have formed naturally on the bed surface of the San Luis Valley canals. It may be of interest to note that the same type of paving was also obtained experimentally[26] by Hunter Rouse, M. ASCE. The significant aspect of this result is that it may explain why the effective size of the grain is larger than the median size. It is therefore desirable to continue these experiments to ascertain the reason for the sudden change in conditions observed by Mr. Lane when the size of the grain was reduced to less than 5 mm.

Mr. Lane has made a genuine attempt to rationalize a design problem which had previously been solved by empirical (or semitheoretical) equations. Therefore, even if some of the author's solutions are not final, he has offered a basis for further, widespread developments of the rational method for designing canals. This aspect of Mr. Lane's work deserves special attention as only that part of the paper entitled "Future Studies" can give rise to differing opinions. The outlined program possibly places too much emphasis on the conventional approach to the tractive-force problem, and canal designers may disagree with the idea of concentrating most of the relevant research in one area. An attempt is therefore made by the writer to outline and substantiate a broader program for future research, which, however, does not imply criticism of the work already done.

The use of the tractive force in Mr. Lane's design method is derived from the following: (*A*) The distribution and local intensities of the tractive forces are determined by either a membrane-analogy method, an analytical method, or the method of finite differences, which are all presumably meant to refer to average values. (*B*) All the tractive forces are assumed to be parallel to the axis. (*C*) The kinetic hydraulic force normal to the surface of the channel is disregarded. (*D*) The loci of permanent (average in time) local accelerations of the flow are ignored. If the foregoing interpretation of the author's design method is wrong or inaccurate, additional explanations on the subject are necessary. In outlining a program for future research each of these items requires individual consideration.

---

[24] Civ. and Hydr. Engr., Cairo, Egypt.

[25] "The Equilibrium of Grains on the Bed of a Stream," by C. M. White, *Proceedings*, Royal Soc. of London, Series A, Vol. 174, p. 331, Experiments 7 and 9, Table 2.

[26] "Criteria for Similarity in the Transportation of Materials," by Hunter Rouse, *Proceedings*, Hydr. Conference, Univ. of Iowa, Iowa City, Iowa, 1940.

With respect to point *A* the author has previously shown[27] that the capacity of the water to dislodge grains of sediment is not a rigid function of the average flow conditions or of the maximum values of the relevant parameters, but that it depends on the entire range of the turbulent pulsations as determined by the Gaussian frequency curve, compounded with the frequency curve of the grain sizes.

Because there is no reference to this point by Mr. Lane in the present paper, it is not clear whether the curves in Figs. 1, 2, 3, and 6 refer to average values, to maximum values of the fluctuating tractive force at a point, or to an "effective" parametrical value thereof chosen in such a manner as to assess the true quantitative scour action.

Had the fluctuations of the local tractive forces at the individual points of the perimeter been insignificant or had they been rigidly correlated with the respective averages, this argument would have been of little concern because the average might have been chosen as the significant parameter. This, however, does not seem to be the case. Mr. White, for example, concludes that in certain cases the maximum tractive force is 2.25 times the average whereas in other cases it is 4.00 times the average.[28,29] Should the range of variation be this high, the quantitative concept of a local tractive force would appear to be vague unless its relation to that range were fully and explicitly defined. This concept must be investigated further.

It is therefore suggested that the program of future studies include the problem of the pulsations of the drag force, in so far as these pulsations affect the stability of the grains forming the channel. The method of performing this study is a matter of discretion, but the use of the ultramicroscope, as in the experiments of A. Fage, should be considered.

Reverting, now, to point *B*—it is noted that, despite all the precautions taken by Vito A. Vanoni, M. ASCE to produce parallel flow in a straight flume, sediment transportation, nevertheless, took place in the form of bands.[30] These bands are symptomatic of the sediment-carrying capacity of well-defined, permanent, regularly arranged, average-in-time, cross currents. This case is only one instance among many which show that the problem is basically three-dimensional. That is, depending on specific circumstances, the diagonal tractive force might (or might not) be more important than parallel forces. Hence, the number and shape of secondary circuits for any given section are another subject for future research. This particular branch of future studies should include the theoretical approach initiated by L. Prandtl[31] and the experimental methods applied by Mr. Lossievsky.[32] In studying this problem, it should not be ignored that Mr. White observed[25] that the granular bed in a diverging flume was extremely active despite the negligible mean drag.

---

[27] "The Relation of Suspended to Bed Material in Rivers," by E. W. Lane and A. A. Kalinske, *Transactions*, Am. Geophysical Union, 1939, p. 637.

[28] "The Equilibrium of Grains on the Bed of a Stream," by C. M. White, *Proceedings*, Royal Soc. of London, Series A, Vol. 174, p. 328.

[29] *Ibid.*, p. 333.

[30] "Transportation of Suspended Sediment by Water," by Vito A. Vanoni, *Transactions*, ASCE, Vol. 111, 1946, p. 67.

[31] "Über die ausgebildete Turbulenz," by L. Prandtl, *Proceedings*, 2nd International Cong. for Applied Mechanics, Zurich, Switzerland, 1927, p. 62.

[32] "Flussbettbewegungen und Geschiebefuhrung," by M. Welikanov, *Proceedings*, 5th Hydr. Conference of Baltic States, Helsinki, Finland, 1936.

To disregard the nonparallelism of the flow does not seem advisable therefore in developing the program for the proposed studies concerning the effect of drag on granular channel materials.

With respect to point *C*, no conclusive proof has been produced that lift should be disregarded and scour analysis should be based exclusively on tangential forces. In fact, lift appears as the center of interest in a number of papers on sediment movement and allied problems. Although some of the investigators[33] quote Mr. White[25] as having demonstrated that life is nonexistent or negligible, the method of this demonstration is subject to considerable doubt. Had there been no vertical component transmitted by the string to the experimental wax grain which was attached to it and placed on the bottom of the experimental flume, this grain would have risen to the surface of the flowing water as a result of the action of buoyancy alone for its specific weight was less than unity. What actually occurred was that any tendency of this grain to rise was prevented by the impact of the water on the string—a design error common to the numerous "tachometers" which (in the seventeenth century) were used in Italy and which impeded the advance of the hydraulic science of the period.[34] Therefore, the fact that the wax grain did not rise to the surface of the flowing water cannot be considered as evidence that lift is negligible—particularly because, according to Mr. White's statement,[29] Mr. Fage's experiments show that lift is at least as great as drag.

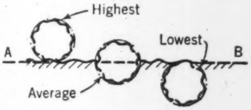

Fig. 7.—Granular Channel Bed

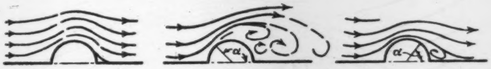

(*a*) LAMINAR (*b*) TURBULENT, WITH LAMINAR BOUNDARY LAYER (*c*) TURBULENT THROUGHOUT

Fig. 8.—Flow Around a Grain

Various mechanical models have been suggested to explain the action of "lift." For example, according to Mr. Einstein[35] and W. W. Rubey,[36] lift is a matter of pulsations whereas H. Jeffreys[37] conceives it as a component of temporal average forces. The trouble with these models is that, although they are clear to the scientist, they are frequently not convincing to a practicing engineer. A force parallel to the direction of the flow is evident, but, unless its nature is clearly demonstrated, a force normal to the flow may appear to be an abstraction. From this standpoint, an elementary—but obvious—model explaining lift is desirable; Fig. 7 may possibly be used as such a model. Taking as a datum the horizontal (or nearly horizontal) plane AB which represents the average surface of a granular channel bed, the relative position of an individual grain belonging to—or forming part of—this surface can then be defined as follows: Highest, when the particle is above the plane and lowest, when it is entirely below the plane. In the average position of the particle, the plane must therefore strike its center. This average position can consequently be assumed to be the starting point for a preliminary "statistical" examination of the problem. The advantage of this approach is that one can thus draw a parallel between the phenomena of scour and sphere-drag and obtain a general idea about the former from the abundant experimental information available about the latter. For example, in Fig. 8, which is based on this analogy and on the principle explained in Fig. 7, a distinction can be made among three possible flow patterns near and around a sediment grain.

---

[33] "Movement of Sediment as Bed Load in Rivers," by A. A. Kalinske, *Transactions*, Am. Geophysical Union, Vol. 28, No. 4, August, 1947, p. 616.

[34] "Historic Development of the Theory of the Flow of Water in Canals and Rivers," by Serge Leliavsky Bey, *The Engineer*, London, England, April 13, 1951, p. 467.

[35] "Formulas for the Transportation of Bed Load," by H. A. Einstein, *Transactions*, ASCE, Vol. 107, 1942, p. 561.

[36] "The Force Required to Move Particles on a Stream Bed," by W. W. Rubey, *Professional Memorandum No. 189-E*, Geological Survey, U. S. Dept. of the Interior, Washington, D. C. 1938.

[37] "On the Transport of Sediment by Streams," by H. Jeffreys, *Proceedings*, Cambridge Philosophical Soc., Vol. 25, 1929, p. 272.

The fact that the flow pattern may vary as shown in Figs. 8(*a*), 8(*b*), and 8(*c*) substantiates the following conclusions: (1) The drag and the lift cannot be represented by one and the same parameter applicable indiscriminately to all the three different phases of flow and to all the possible shapes and arrangements of the grain. (2) Changes from one flow pattern to another are likely to occur suddenly (as they do in experiments with sphere-drag), which furnishes a plausible explanation of the often-disregarded fact that the intensity of the scouring action does not always develop gradually, as must have been the case had the drag criterion been rationally correct. However, when the relevant parameters attain certain critical values, this action undergoes abrupt and apparently anomalous alterations. These alterations can only be caused by sudden changes in the flow patterns for the bulk (in the statistical sense of the term) of the grains, such as the changes from Fig. 8(*a*) to Fig. 8(*b*) and from Fig. 8(*b*) to Fig. 8(*c*). (3) The vertical component of the kinetic force applied to the particle is directed upward, corresponding to the vacuum pressures observed in the sphere-drag experiments. This vertical component is termed lift.

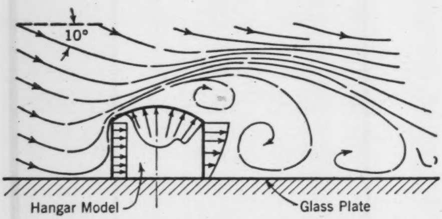

FIG. 9.—MODEL OF AN AIRSHIP HANGAR

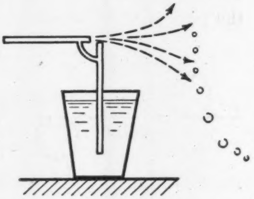

FIG. 10.—A VAPORIZER

To clarify Fig. 8, Fig. 9 is offered. Fig. 9 represents an experiment performed by the writer[38] as early as 1914. The model of an airship hangar was tested in a wind tunnel in order to find the wind forces for its structural design. The experiment showed that, despite the downward inclination of the wind direction to the horizontal (10°), the resultant wind force applied to the building was directed upward, and not downward, as standard specifications imply.

---

[38] "Wind Loads on Tall Buildings," by Serge Leliavsky, Magazine of the Institute of Engineers of Ways of Communication of Emperor Alexander I, St. Petersburg, Russia, 1914 (in Russian).

This result is in complete agreement with the fact that, during severe storms and hurricanes, roofs of buildings are never pressed downward but are frequently lifted from their original positions.

Another diagrammatic application of the same principle is shown in Fig. 10. The vaporizer consists of a combination of two tubes, one vertical and one horizontal, which are held together near the point at which their axes meet. By blowing through the upper pipe, a horizontal air current is created which causes the liquid to rise vertically to the top of the lower pipe, at which point it is diffused in the form of a cloud. It is clear that, here again, the horizontal flow of a liquid (air) produces a "lift" force causing a vertical movement of a heavier substance (water).

These simple examples are irrefutable proof of the very real existence of the lift force, not only as a laboratory experiment, but also, as a matter of practical experience. Moreover, as the horizontal component of the wind pressure acting on the shed (Fig. 9) is obviously a function of the height of the vertical wall whereas the upward component of the force applied to the roof depends on the rise and shape of the latter, it is clear that these two forces cannot be represented by one and the same over-all parameter, applicable to all ratios of height of building to rise of roof. It follows that the lift problem must be envisaged as a self-contained item of research, correlated—but not identified—with the drag problem. It is recommended therefore that the lift force be considered as a desirable problem in the program for future research, in addition to (and parallel with) the drag problem.

The final point must also be considered. Sediment transportation is a composite process consisting of three distinct phases. These phases are: (*a*) The initial period when the particle is picked up and moves—generally at a lesser velocity than the water; (*b*) the transportation period—when both velocities are of the same order of magnitude; and (*c*) the last stage during which the particle is dropped.

It is a debatable (but possibly acceptable) proposition that the tractive force suffices to explain and define sediment behavior in the first period. That it should also be taken as a significant parameter for the second phase is, however, more difficult to accept. Because—with the possible exception of du Boys' concept of a solid mass of granular bed material shifting bodily downstream below the physical bed of the channel[5]—the first phase cannot be conceived without some reference to the second; the specific factors conditioning this second stage are also worthy of attention. Hence, in addition to the erosive power of the stream, its capacity to carry sediment of a certain size range is, possibly, still another indispensable part of a consistent program of research for the silt-carrying capacity of stable canals.

Further research in this connection should be concentrated on the sediment-carrying capacities of individual points in the cross section of a canal, in correlation with its typical pattern of secondary circulation. The concept of uniform flow, as presented in elementary textbooks, is no longer applicable. If one considers the average values of a generally pulsating current, secondary circulation must necessarily cause local foci of permanent, average-in-time accelerations and decelerations, even in the case in which the average velocity for the whole section is constant in every cross section over the length of the investigated reach of the canal.

From the continuity equation it will be found that the acceleration, which usually creates a greater sediment-carrying capacity, must be correlated with convergent currents, whereas deceleration and therefore sediment deposits must coincide with divergent currents.[39] Hence, the form of a stable canal is probably a function of the cross-current pattern. As Mr. Lossievsky[32] has found that this pattern changes with the bed-to-width ratio, there arises an idea of the mechanical processes which cause the tendency of a stream to excavate a channel of a certain given geometrical form. This explanation, preliminary as it may be, may nevertheless be considered as an alternative to the concept of "incipient motion" profile and deserves being investigated in parallel with it.

A. Nizery[40] and G. Braudeau.[41]—The study made by Mr. Lane clearly distinguishes between two basic problems: (1) What is the hydrodynamic force necessary to move a grain of a given material? (2) What channel cross section must be chosen so that the forces applied to the given material are distributed uniformly?

The first problem can be studied in a very wide canal with a horizontal bottom. In this case the force of gravity will have no tangential component, and the tractive force τ will be the only force acting parallel to the wall on the grain. Equilibrium of the grain will be attained if the resultant of the tangential force and the gravitational force lies inside the friction cone defined by the angle of repose ϕ. The tangential force is proportional to τ, to the surface of the grain, and consequently to the square of the diameter d. The weight is proportional to d^3 and to the density of the submerged material γ_s. The equilibrium condition is therefore

$$\frac{A\,\tau\,d^2}{B\,d^3\,\gamma_s} \leqq \tan\phi \ldots\ldots\ldots\ldots\ldots\ldots (5a)$$

from which

$$\frac{A\,\tau}{B} \leqq d\,\gamma_s \tan\phi \ldots\ldots\ldots\ldots\ldots\ldots (5b)$$

and

$$\tau \leqq K\,d\,\gamma_s \tan\phi \ldots\ldots\ldots\ldots\ldots\ldots (5c)$$

in which A is a coefficient which depends on the shape and roughness of the grain and B represents $\pi/6$.

When the grain sizes in the channel lining do not differ greatly, one can use one value for ϕ which is equal to the natural angle of repose of the submerged material. The result in this case is similar to that obtained by use of the formula developed by E. Meyer-Peter.[42] This formula is currently (1954) being used in Europe to study the problems of bed-load transportation. The formula shows that the critical tractive force τ_c is proportional to the diameter and relative density of the grains.

---

[39] Discussion by Serge Leliavsky of "Bank Stabilization by Revetments and Dikes," by Raymond H. Haas and Harrill E. Weller, *Transactions*, ASCE, Vol. 118, 1953, p. 869.

[40] Associate Director of Study and Research, Électricité de France, Paris, France.

[41] Engr., National Hydr. Lab., Électricité de France, Chatou, France.

[42] "Formulas for Bed Load Transport," by E. Meyer-Peter, 2nd Meeting of International Assn. for Hydr. Research, Stockholm, Sweden, 1948.

Mr. Meyer-Peter's formula (which was developed from experimental work) has been applied extensively with good agreement between predicted and experimental results. The agreement improved as the conditions under which the experiments were performed approached the conditions for which this formula had been established. When, however, the grain sizes vary greatly, or when cohesive forces begin to act, the agreement is poor, and it then becomes necessary to resort to a direct measurement of τ_c.

As shown by the author, the best section for a channel will be that section for which the tractive force at each point is equal to the critical force for the material of which the walls are formed. It is such a section that will allow the greatest average velocity for a given rate of flow. This section will therefore be most economical on the basis of the necessary excavation.

If the tractive-force distribution were known for a specific section, it would be possible to determine the equilibrium conditions at each point in a form similar to that indicated previously. It would then be possible to derive the equation for the section which complies with this condition and also—in a general manner—with the five conditions indicated by Mr. Lane. However, the tractive-force distribution depends on the form of section, and the resulting equation is an integral equation. One is therefore compelled to formulate hypotheses and to determine whether these hypotheses are confirmed experimentally.

These questions are now (1954) being analyzed at the National Hydraulic Laboratory at Chatou, France, on a canal having a length of 45 *m* (13.72 ft) and a width of 3.50 *m* (1.07 ft). The form and size of the section, as well as the longitudinal slope, of this canal can be varied easily. Until the present time only the shape of the section has been considered. Therefore, only a uniform sand (3 mm in diameter) has been used in the experiments.

For the study of a given section, the slope is increased while the rate of flow is modified. This procedure results in a uniform regime until the bedload transportation begins to occur at any point of the section. For each regime, velocity measurements are made at many points. In this manner detailed velocity distributions have been obtained for different types of sections, especially for trapezoidal ones. From these velocity distributions, the tractive force at each point has been computed as indicated by Mr. Lane.[43]

It was found, however, that the experimental results did not agree with those predicted by analysis. The bed-load transportation did not begin at the point at which the computation indicated a maximum tangential force. Perhaps this phenomenon occurs when there are secondary flows above the section corners. These secondary flows are indicated by the instability of the velocity measured in these zones.

A section has been determined, however, in which the tangential forces would be uniformly distributed. This section is formed on the hypothesis that the tractive force at any point would be

---

[43] "Principles of Design of Stable Channels in Erodible Material," by E. W. Lane, *Hydraulic Laboratory Report No. Hyd. 295*, Bureau of Reclamation, U. S. Dept. of the Interior, Washington, D. C., 1950.

$$\tau = \gamma\, y_p\, S_w \qquad (6)$$

in which y_p is the depth below the surface of the point under consideration and S_w denotes the slope of the water line.

For such a section, parametrical equations are found of the form:

$$x = y_{\max} \cos \beta \qquad (7)$$

and

$$y_p = \frac{y_{\max}}{\sin \phi} \int_0^{\beta} \sqrt{(1 - \sin^2 \phi \sin^2 \beta)}\, d\beta \qquad (8)$$

in which

$$y_{\max} = \frac{W_g \tan \phi}{K\, \gamma\, g\, S_p} \qquad (9)$$

β is a parameter varying between 0 and π, W_g denotes the weight of a grain, and $y_{\max}$ is the maximum depth.

It is also necessary to add a friction equation correlating $y_{\max}$ and S_w with the rate of flow. Another hypothesis (formulated by R. Koechlin[44]) concerning the manner in which the water acts on the grains results in a section for the canal, the equation of which has the form:

$$y_p = y_{\max} \sin\left(\frac{x}{y_{\max}} \tan \phi\right) \qquad (10)$$

It has been found that the sections determined by either method (Eq. 8 or Eq. 10) for the same regime are similar even though they are computed from different analytical expressions. On such a similar section the same experiments were performed that were performed on trapezoidal sections. It was observed by the writers that the movement of the sediment begins almost simultaneously at all points on the walls and on the bottom. This agreement between test and computation would indicate that the force distribution is correctly represented by Eq. 6, at least in a section that has a height-to-width ratio which is below a certain value; this value has not been determined (as of 1954).

It appears that one can expect from such studies more than the mere development of a rational method for determining the slopes and the sections of canals with alluvial bottoms. The application of these results to natural watercourses may be advantageous. If one considers a meandering river in a high-water bed formed by its own alluvia, observation suggests that the hydrological regime necessitates a certain width, a certain mean depth, and a certain slope for the low-water bed. Thus, there are four variables which do not appear to be independent. For example, the rate of flow determines the values of the three other variables. The mere knowledge of the friction law and of a specific bed-load transportation law (the law relating the solid flow per unit width to the hydraulic conditions relative to an infinite width) does not enable one to account for this occurrence. The width must appear in another relationship. This relationship must express a certain distribution of the tractive forces (uniform or nonuniform as curvature effects arise) necessary for the equilibrium of the transverse profile. This problem is not very different from the problem of stable channel design, although naturally more complex. This complexity is caused by the fact that, although the rates of flow vary, one must consider an equilibrium with bed-load transportation. Considerations similar to those used to study equilibrium without bed-load transportation under a permanent regime may help to solve this problem.

---

[44] "Mécanisme de l'eau et Principes Généraux pour l'établissement d'usines hydro-électriques," by R. Koechlin, Birauger, Paris, France, 1924.

N. K. BOSE.[45]—The introduction of tractive-force analysis into the design of stable channels in alluvium is not a new idea. However, the lines of attack followed by the author are certainly interesting. The basic idea (under the heading, "The Design of Stable Channels: Tractive-Force Distribution") that "* * * in all canals having the same ratio of bed width, b, to y and the same side slopes, the tractive-force distribution will be similar * * *" requires elaboration and proof. Mr. Lane has attempted, by various methods, to determine the tractive-force distribution along the wetted perimeter of a canal section. The membrane-analogy method appears to yield satisfactory solutions and may be of help in design.

The principal difficulty experienced by the various investigators in developing a theory for regime channels, however, has been the correlation of sediment movement with the other hydrodynamic characteristics of channel flow. Whether one uses tractive force or any other hydraulic constant of a canal, such as mean velocity, mean hydraulic radius, wetted perimeter, area of the waterway, or depth of water, the greatest difficulties have been in developing a suitable characteristic of the sediment that the canal carries on the bed or in suspension. The author's analyses do not shed any new light on this aspect of the question. The assumption that either K_{25} or K_{50} is a representative diameter of the sediment has not been justified.

The extensive work performed by the investigators of the Irrigation Research Institute, at Punjab, India, from 1932 to 1942 have shown conclusively that the sediment which a channel carries can greatly influence the determination of the ultimate section and slope which a channel will develop. This fact was most probably in the minds of W. R. Kutter and E. Ganguillet[46] when they tried to modify the Chezy formula by introducing a variable factor n which depends on the rugosity of the channel. In 1895 R. G. Kennedy[47] introduced the idea of silt and turbulence explicitly into the subject and deduced the relationship:

$$V_0 = K\,D^n \quad \text{.......................} (11)$$

in which V_0 is the critical mean velocity, K denotes an arbitrary constant, D is the vertical depth of the channel, and n represents another constant. In 1930, Gerald Lacey[48] revived the subject and proposed a number of relationships involving some of the usual hydraulic constants with a quantity termed the "silt factor" f.

---

[45] Director, River Research Inst., West Bengal, Calcutta, India.

[46] "Flow of Water in Rivers and Other Channels," by W. R. Kutter and E. Ganguillet, John Wiley & Sons, Inc., New York, N. Y., 1889.

[47] "The Prevention of Silting in Irrigation Canals," by R. G. Kennedy, *Minutes of Proceedings*, Inst. of C. E., London, England, Vol. CXIX, 1895, p. 281.

[48] "Stable Channels in Alluvium," by Gerald Lacey, *ibid.*, Vol. 229, 1929–1930, p. 259.

It is known that the principal difficulty in dealing with the problem of the regime channel has been in defining silt. Mr Kennedy proposed an instrument, a siltometer, which (but for some minor defects) would have enabled him to classify silt successfully. Some of these defects have since been removed by A. N. Puri,[49] and the modified siltometer is now (1954) being used extensively in India. The siltometer that has solved the problem of classifying silt and made it possible to proceed with silt investigations was perfected by V. I. Vaidyanathan.[50] The writer has examined,[51,52] the silt data (collected under stable conditions) obtained from a number of regime channels in Punjab. The distribution curves of the silt samples were analyzed and subdivided into different types. These types could not, however, be placed in definite categories; very often they merged, one into the other. Just as the spectrum of a source of light goes from the ultraviolet through the visible part to the infrared, silt curves of a canal also go through these various types if they are analyzed throughout a year. Each of these types indicates a certain condition of equilibrium of a canal, so that the annual frequency distribution of these types of curves for any canal is a reliable indication of the stage of equilibrium of that canal. It was therefore necessary to determine (1) what was the significance of these types, (2) to what stage of the development of the canal they belonged, and (3) what indication they gave of the stability of the canal.

After examining these silt curves and the hydraulic data for a number of stable channels, the writer derived[53] the following relationships:

$$A = 1.15\, Q^{0.85} \qquad (12)$$

$$D = 0.39\, \frac{Q^{0.29}}{S_w^{0.37}} \qquad (13)$$

and

$$S_w \times 10^3 = 2.09\, \frac{m^{0.85}}{Q^{0.21}} \qquad (14)$$

in which A is the area of waterway (in square feet), Q represents the discharge (in cubic feet per second), D is the average depth (in feet), S_w denotes the slope of the water surface, and m is the mean diameter (in millimeters) of the bed sediment. Eqs. 12, 13, and 14 are a sound basis for the design of canals.

In all the analyses performed by the writer, it was not possible to take into account the effect of the quantity of bed movement on the regime equations. Investigators such as Mr. Einstein,[20] A. Shields,[54] and others, however, have introduced this quantity into the regime equations; as yet (1954), no practical solution has been obtained.

---

[49] "A Siltometer for Studying Size Distribution of Silt and Sand," by A. N. Puri, Punjab Irrigation Research Inst., *Research Publication*, Vol. 2, No. 7, 1934.

[50] "An Optical Lever Siltometer," by V. I. Vaidyanathan, *Paper No. 167*, *Proceedings*, Punjab Eng. Cong., Vol. XXI, 1933.

[51] "Silt Movement and Design of Channels," by N. K. Bose, *Proceedings*, Punjab Eng. Cong., 1936.

[52] "An Investigation of the Interrelation of Silt Indices and Discharge Elements for Some Regime Channels in the Punjab," by N. K. Bose, Punjab Irrigation Research Inst., *Research Publication*, Vol. 11, No. 23, 1939.

[53] "Design of Channels in Alluvium," by N. K. Bose, *Proceedings*, Punjab Eng. Cong., 1942.

[54] "Anwedung der Aehnlichkeitsmechanik und der Turbulenzforschung auf die Geschiebebewegung," by A. Shields, *Mitteilungen*, Preussischer Versuchsanstalt für Wasserbau und Schiffbau, Berlin, Germany, No. 26, 1936.

José S. Gandolfo.[55]—An improved application of the tractive-force concept in channels is presented by Mr. Lane. The suggested methods for designing canals in coarse and fine noncohesive material are especially practical.

Many important aspects of these problems need further study and investigation, including those cited by the author under the heading, "Material in Which Canals Are Constructed: Canals Carrying Heavy Sediment Loads." The ensuing discussion is confined to that part of the paper.

When fed by natural streams, a canal will often be required to carry heavy sediment loads, and an unsteady flow is to be expected. If the canal is unlined, the bed will be of the same nature as the heavy load material transported. In the case of variable flow, the concept of a stable channel is not applicable because each flow has a definite mean slope and rate of bed-load movement. Therefore, in periods of lower flood flow, a quantity of bed-load material may be deposited, and the general slope of the bed can be expected to decrease. Conversely, in periods of great flood, the channel bed becomes eroded and rough, and the general slope will increase. Normal flow cannot remove all sizes of coarse bed load; it moves only the small particles not protected in the spaces between coarser particles.

Because the canal configuration is changing continuously, the designer must select a representative flow. Hydraulic needs will be satisfied if the capacity of the canal is designed for maximum flood flow, but to satisfy alluvial requirements the prevailing flow of coarse material must be established.

The product of the flow frequency and the corresponding coarse sediment transported for each discharge in the canal yields data for the coarse sediment frequency curve. Such a curve shows the maximum value of $\Sigma G'$ for a determined flow Q'. The narrow band of flow above and below Q' on the curve is indicative of the flow that transports the largest volume of heavy material. Consequently, the canal slope and alluvial bed configuration will agree well with this value of Q' (in Fig. 11, $Q' = 650$ cu m per sec). F. Schaffernak[56,57] termed Q' "bed generative flow."

In the dike improvement design of the San Juan River (Argentina), the writer found that the mean annual transportation of heavy material was $G'_m = 103$ kg per sec (conversion scales to English units are given in Fig. 11), which corresponds to a flow Q'_m of 538 cu m per sec. The mean annual flow, by comparison, is $Q_m = 521$ cu m per sec. By the bed generative flow concept, the generative coarse sediment transported is computed to be $G' = 175$ kg per sec, which corresponds[58,59] to a flow Q' of 650 cu m per sec. The flood flows

---

[55] Head of Hydraulic Dept. and Prof. of the Universidad Nacional de Eva Peron (Ex La Plata), Buenos Aires, Argentina.

[56] "Die Theorie des Geschiebebetriebes und ihre Anwendung," by F. Schaffernak, *Zeitschrift des österreichischen Ingenieur und Architeken-Vereines*, Vienna, Austria, 1916.

[57] "Neue Grundlagen für die Berechnung der Geschiebe führung in Flussläufen," by F. Schaffernak, Franz Deutike, Leipzig-Vienna, 1922.

[58] "Estimación de la evolución del alveo de los rios," by José S. Gandolfo, *Publication No. 3*, Second Series, Facultad de Ciencias Fisicomatemáticas, Universidad Nacional de Eva Peron (Ex La Plata), Buenos Aires, Argentina, No. 128, 1940, p. 245 et seq.

[59] *Ibid*, Separate, p. 33 et seq.

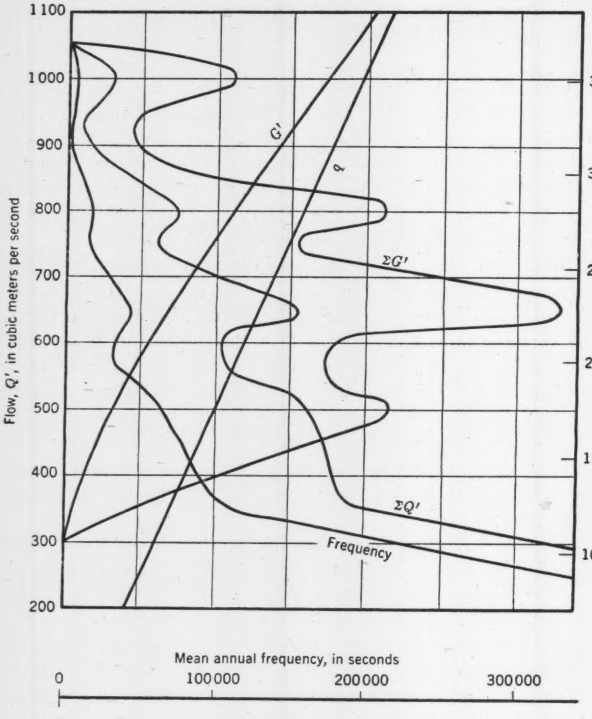

FIG. 11.—COARSE SEDIMENT FREQUENCY CURVE

between 450 cu m per sec and 850 cu m per sec moved 75% of the mean annual load, and $G' = 1.7\ G'_m$.

The Rhine River at Brugg Bridge above Lake Constance[60] showed a mean annual movement G'_m during 1936 of 7.3 kg per sec, which corresponds to a flow Q'_m of 503 cu m per sec; but the observed mean annual flow in that year was actually 457 cu m per sec. Again, by the bed generative flow concept, the generative coarse sediment load G' was determined to be 16.1 kg per sec and the corresponding flow Q', 659 cu m per sec. The flood flows between 520 cu m per sec and 940 cu m per sec moved 62% of the coarse sediment load in 1936; $G' = 2.2\ G'_m$.

The design for the International Rhine regularization from Illmündung to Bodensee was computed using a mean annual heavy material movement G'_m. In the writer's opinion, this is an inadequate dynamic design basis when applied to rivers.[61] When the flood-flow frequency is constant, the mean-annual-load basis will be correct; as illustrated by the preceding examples, however, the movement of heavy bed material increases as flood flows decrease in frequency.

The differences between G'_m and G' will be greater as the number and the distribution of flood periods become more irregular and as intensities and the duration of flood waves become more variable. Consequently, these differences will be greater under the conditions on torrential rivers.

Other conditions remaining constant, the mean-annual-bed-load basis of design produces a flatter slope and a characteristic cross section that is not deep enough. The factor G'_m then encompasses all the material transported—by the lower as well as the higher flood flows—and it is therefore highly variable.

In the generative bed-load concept, G' is a value that is slightly influenced by flood flows with relatively little solid material, even if the frequency is increased. Neither is it modified by extraordinary floods of low frequency, even though they transport great quantities of solid bed material. The generative bed-load flow is confined within the narrow flood-flow zone which, because of its frequency and its capacity for transporting solid bed material, moves the greater volume of coarse sediment and is much less variable then the mean annual flow.

The generative bed-load flow can change from one section to another if there is a difference between the granulometric curve of the bed material, or of the slope, for the two sections. This is true for a varying flow, also, if an adjacent section contains the entrance of a tributary canal, or a diversion structure. Such canals, in which transport conditions vary from section to section, can be designed by the formula:

$$G'_1 = F_1\,[Q'_1, i_1, \phi(h_1), k_1, d_1, \rho_1] \qquad (15)$$

in which Q' is the generative bed-load flow; G' is the coarse material flow rate; d is the mean diameter; ρ is the specific gravity; k is the roughness coefficient; and the dimensions of the geometrical and hydraulic canals are B = width,

---

[60] "Die Internationale Rheinregulierung von der Illmündung zum Bodensee," by F. Nesper, *Schweizerische Bauzeitung*, Zurich, Switzerland, Vol. 110, No. 13, 1937.

[61] "Beitrag zur Berechnung der Geschiebefürung und der Normalprofilbreite von Gebirgsflüssen," by E. Meyer-Peter, H. Favre, and R. Müller, *ibid.*, Vol. 105, No. 10, 1935.

$\phi\ (h)$ = height, and i = inclination, or slope. Numeral subscripts 1, 2, etc., refer to section 1, 2, etc., in the canal under consideration.

If G'_1 is known, and if i_1 is the actual slope (or another slope conveniently selected for design purposes), Eq. 15 can be solved for successive values of $\phi\ (h_1)$. Next, one can compute

$$B_1 = \phi_1\,[Q'_1, i_1, \phi(h_1), k_1] \qquad (16)$$

The best value of B_1 (Eq. 16) can be selected by varying both i_1 and $\phi\ (h_1)$ in Eq. 15.

In the next consecutive section of the canal, the continuity law of heavy material movement for the width of the canal is

$$G'_2 = G'_1 \left(\frac{d_2}{d_1}\right)^3 \pm G_2 \qquad (17)$$

in which $(d_2/d_1)^3$ represents, more or less, the heavy transported bed material, the remainder being abraded and transported as suspended load. When alluvial material is added at the beginning of this stretch, G_2 has a positive value; when coarse material is removed, when the generative bed flow diminishes, or when there is a diversion structure in the section, G_2 has a negative value.

The value of Q'_2 must be investigated in all such cases, but if $G_2 = 0$, it is accurate enough to assume $Q'_2 \cong Q'_1$. If there is any discontinuity in the heavy solid material transported in any stretch of the canal (that is, if $G_r \neq 0$), the corresponding G'_r-values and d_r-values will be the basis for computing G' in the succeeding sections downstream.

In the second canal stretch, the slope i_2 can be solved by

$$f_2\ (i_2) = \frac{G'_2}{Q'_2}\, f_2\,[\phi(h_2), k_2, d_2, \rho_2] \qquad (18)$$

The right-hand function $f_2\ (i_2)$, in Eq. 18, can be determined by assigning values to $\phi\ (h_2)$. On the other hand, it is known that

$$f_2\ (i) = f_2\,[\phi(h_2), k_2, d_2, \rho_2, i] \qquad (19)$$

Assigning values to i, the function $f_2\ (i)$ can be solved and the curve for $[i, f_2(i)]$ drawn. In that curve, the ordinate $f_2\ (i_2)$ gives the slope i_2. Finally,

$$B_2 = \phi_2\,[Q'_2, i_2, \phi(h_2), k_2] \qquad (20)$$

By solving Eq. 20 for successive values of $\phi\ (h_2)$, the best B_2-value can be determined. By solving again for $f_2\ (i)$, a new curve for $[i, f_2(i)]$ can be drawn. Other values of i_2 and B_2 can then be computed immediately.

After the dimensions of the cross section of the canal have been determined for heavy-material transportation, the next step is to compute the hydraulic capacity for maximum project flow.

Elsewhere,[58,59] the writer has presented several characteristic cross sections, determined by applying the (Meyer-Peter, Favre, Müller) formula for heavy, solid-matter transportation. The procedure is general, and can be adapted for the computation of G' by any other formula. The Einstein formula[20] is the most advanced but is more laborious to apply. For the San Juan River dike improvement,[62] the flow of heavy solid material in consecutive stretches was determined by the (Meyer-Peter, Favre, Müller) formula, which was the most generally accepted at that time.

The successive stretches have conjugated slopes, defined by the linear function,

$$i_2 = a\, i_1 - b \qquad (21)$$

in which a and b are coefficients which depend on values of Q'_1, Q'_2, d_1, d_2, ρ_1, ρ_2, B_1, and B_2.

Mr. Lane's paper marks a significant advance in the design of stable channels, offering opportunities for further amplification of the topics listed under the heading, "Future Studies."

Emory W. Lane,[63] M.ASCE.—The receipt of so much valuable information and so many constructive suggestions is most gratifying; the discussers have added materially to the paper.

The information supplied by Mr. Leliavsky regarding Mr. White's tests[25] is valuable because these are apparently the only hydraulic experiments which relate the angle of repose and the transportation of coarse sediments.

Mr. Leliavsky has listed four areas in which uncertainty exists regarding the reliability of assumptions used in the canal-design procedure and has suggested further studies to remove these uncertainties. As Mr. Leliavsky has stated, the values of shear were the average values with respect to time, and not the maximums. At present (1955) the maximums are not known in enough detail to be used in a design method. Further study is necessary to solve the problem of the relationship of the averages of the shear value to the maximum.

Mr. Leliavsky has also made note of secondary currents and has suggested that studies be made of them. The possibility of secondary currents being important is also suggested by Messrs. Nizery and Braudeau. Therefore, this subject might also be added to the list of further studies as knowledge of them is insufficient to include them in a design method.

That lift has its part in sediment transportation is becoming more clearly evident. Here, also, existing knowledge is insufficient to include it in a design method, and further information is therefore desirable. The action producing lift does not always cause an upward force; in coarse, noncohesive material—as a result of the tendency of flat particles to place themselves in a shingle-like position—the force caused by the curvature of the currents may be downward rather than upward.[64]

As Mr. Leliavsky suggests, loci of permanent local accelerations undoubtedly exist in some cases[65] and may be quite important generally. This matter should be studied as well as all other aspects of sediment transportation because the future progress in the improvement of methods for the design of stable channels will be dependent on the rate at which knowledge of the laws of sediment transportation increases.

---

[62] "Estudio de la evolución fluvial que determina el endicamiento del Rio San Juan," by José S. Gandolfo, *Special Publication No. 2*, Facultad de Ciencias Físicomatemáticas, Universidad Nacional de Eva Peron (Ex La Plata) Buenos Aires, Argentina, 1940, No. 126, p. 97.

[63] Hydr. Engr., Fort Collins, Colo.

[64] "Some Observations on the Effect of Particle Shape on the Movement of Coarse Sediments," Emory W. Lane and E. J. Carlson, *Transactions*, Am. Geophysical Union, Vol. 35, June, 1954, p. 458. by

[65] "A New Method of Sediment Transportation," by Emory W. Lane, *ibid.*, Pt. 6, May, 1954, p. 900.

The contribution by Messrs. Nizery and Braudeau regarding the shape of the channel of minimum excavation and width is most valuable. Their discussion supports the use of principles adopted in this study; the writer has been making further studies along these lines. It is hoped that a complete report on the studies of Messrs. Nizery and Braudeau will be forthcoming.

The lack of agreement reported by Messrs. Nizery and Braudeau between the computed tractive-force distribution and the observed results is interesting. This lack of agreement may account for some of the scatter in the results observed when this method was investigated under the writer's direction and supports the decision to use the results of the mathematical and membrane-analogy methods in the proposed design method. It is agreed that secondary currents are probably at least a partial explanation. The suggestions of Messrs. Nizery and Braudeau that the principles of stable-channel design can be used to advantage in the study of regime conditions for natural streams are believed to be fully justified. For some time the writer has been studying the form of natural streams and has found that the principles derived for stable channels are of great help in determining an analysis of this problem.

Mr. Gandolfo's design method shows that many years ago he applied the principle which the writer considers fundamental in designing stable channels which are to carry a heavy sediment load—namely, that for such conditions it is necessary to determine the magnitude of the sediment load and design the canal to carry it. So far as is known, this is the first application of this important principle.

Under the writer's definition of a stable channel, it is not necessary that such a channel always be free from scour or deposit, as Mr. Gandolfo suggests. A stable channel, under the definition, may alternately deposit and scour, provided the scour carries away the deposit before it has accumulated in objectionable quantities and the deposit refills the scoured areas before they scour sufficiently to be objectionable.

Mr. Bose has questioned the reliability of assuming the similarity of tractive-force distribution in channels of similar cross section. The justification of this assumption is that in all but very small channels the Reynolds number is so great that the effect of the viscous forces is negligible. Under these conditions the velocity distribution is similar in geometrically similar sections. The geometrical similarity of velocity distribution from model size to prototype size, where the Reynolds number is sufficiently large, is commonly assumed in making prototype predictions from models. If the similarity holds from model to prototype size, it should hold over a wide range of canal sizes.

Mr. Bose's remarks deal principally with the case in which considerable quantities of sediment are transported by the canals. The studies presented by the writer had not progressed far enough in this area to go much beyond a statement of the fundamental principles that are believed to apply to the design of stable channels under these conditions. These principles are that the canal must be so designed that it will transport substantially all the sediment brought into it, without producing sufficient tractive force on the banks and bed to cause scour. To determine the conditions necessary to transport the required quantity of sediment, use can be made of the formulas developed for the quantity of sediment which will be transported under certain conditions. The greatest need in this field is the measurement of the size and quantity of sediment transported in a considerable number of canals so that the reliability of the various available formulas can be appraised, and, if necessary, new formulas developed.

The writer has not been able to secure a copy of the paper describing the derivation of the formulas for canal design which Mr. Bose has proposed, and therefore he is unable to appraise it. However, the derivation was based on extensive experience and probably considerable data. It is not unlikely that, for the conditions in the canals which were used in developing it, this proposal is a more reliable method of design than one which is based on a computed quantity of sediment transportation. As the laws of sediment transportation become more fully known, however, it is expected that the analysis based on the computed quantity of sediment transportation will eventually become more reliable than Mr. Bose's formulas. For conditions of sediment load differing widely from those in the canals used as data in Mr. Bose's study, it is believed that his formulas and any other design method that neglects the effect of sediment concentration will not give reliable results.

The writer is indebted to Mr. Leliavsky for informing him (in a private communication) that the solution mentioned in the paper for the shape of a channel in coarse, noncohesive material, which would require a minimum excavation and width, was previously determined by Phillip Forchheimer[66] as early as 1930 and perhaps earlier. Mr. Forchheimer included in his analysis not only the effect of the slope of the sides but also the influence of the longitudinal slope of the canal. It is doubtful, however, that this latter effect would ever be significant.

It has also been discovered that the effect of side slopes on the movability of coarse, noncohesive material involving the same basic idea as that presented by the writer—but using velocities rather that tractive forces—was determined by A. Gostev[67] in 1928.

Since preparing the original paper, the writer has been impressed by the importance of the deposits of fine material on the sides of many canals as a stabilizing influence. Because of the cohesive nature of these deposits, the tractive forces which the sides can withstand may be considerably greater when the deposits are present. These deposits may occur naturally in the aging process which takes place when the flows through the canal gradually increase, as more land is irrigated by the canal, but may also be furthered by scientific manipulation of the natural silts. This may be more effectively accomplished by the application of bentonite. A thorough study of these possibilities is being undertaken at Colorado Agricultural and Mechanical

---

[66] "Hydraulik," by Phillip Forchheimer, B. G. Teubner, Leipzig, Germany, 3d Ed., 1930, p. 551. (*Translation No. 47-9*, Research Center, U.S. Waterways Experiment Station, Vicksburg, Miss.)

[67] "On Scouring Velocities," by A. Gostev, *Irrigation News Bulletin*, January, 1928, pp. 65–69. (Translated by Bureau of Reclamation, U. S. Dept. of the Interior, Washington, D. C.)

College at Fort Collins, in conjunction with an extensive investigation of the possibilities of the prevention of seepage out of canals by staunching the bottom and sides of the canal with a bentonite slurry. For canals in fine, noncohesive material—particularly where the presence of a load of sand in the incoming water necessitates a high tractive force to prevent it from depositing—this method, if it can be successfully developed, will greatly improve the form of canal that can be used.

Summary.—Study of stable channels since presentation of the original paper and knowledge gained from the valuable discussions have led to new views and ideas. It is believed that the fundamental principles of stable channels, as originally presented, are very simple and can be readily understood by those having an elementary knowledge of hydraulics. From the definition of a stable channel as one in which neither scour nor deposit in objectionable quantities occurs, it follows that to obtain such a channel all that is necessary is that at all points on the bed and banks of the canal the action of the water be insufficiently severe to cause objectionable scour but sufficiently severe to prevent sediment carried by the water to deposit in objectionable quantities. This statement contains the basis for the proposed method of design. Corollary statements are: (1) If the water entering the canal carries much sediment, to prevent objectionable deposits the inflowing sediment must be transported through the canal without a loss of sediment. (2) On the sides of a canal the force of gravity tends to move sediment particles down the sides toward the bottom, an action which assists the forces resulting from the motion of the flowing water in causing scour on the canal sides. It is believed that these statements are so evident that everyone interested in this subject, after thorough studies, will agree with them.

Because canal stability involves primarily the interaction of the water with the bed and banks of the canal, it seemed that a logical method of approach in devising a method of design for such channels would be a study into the nature of this interaction. It will be noticed that there are two phases of this interaction, a scour phase and a transportation phase. Because knowledge of the science of hydraulics and fluid mechanics is not sufficient to analyze these phases completely, it is not possible to devise a perfect method of design but, by using the best information available, a method can be devised from these principles. Although one does not expect changes in the fundamentals of the method of analysis, it is hoped that some of the assumptions, which it was necessary to make because of the state of knowledge of the science when the methods were adopted, will be improved on when more adequate knowledge is available. However, it is believed that the assumptions made in the design method are the best that it is possible to make.

The design of stable channels for irrigation projects will not wait for the developnent of a perfect method of analysis. For practical purposes all that is required is that the method be complete enough to enable designs to be made by its use, sufficiently simple to be readily understood, logical enough to commend itself to the designing engineer, and more reliable than other available methods; it must not, however, require so much work as to make its application prohibitive. It is believed that for the conditions of small sediment loads in their present (1955) state of development, the proposed methods meet these requirements, although considerable further advance can be made as more knowledge is obtained. For the condition of transporting water containing heavy sediment load, the reliability of the method is less certain because of the lack of knowledge of the reliability of formulas for the transportation of sediment; for very heavy sediment loads the methods are believed to be more reliable than those which do not contain the concentration of sediment as a factor. As knowledge of the science of sediment transportation increases, the reliability of the method in this part of the field will be increased.

Advantages of the writer's method of analysis are that (1) it applies to all cases of stable channels, not only those in self-borne alluvium; (2) it introduces no new empirical coefficients, but deals only in such well-known concepts as shear values and angle of repose; (3) it shows what information is necessary to perfect the method further; and (4) the refinements of new knowledge can be introduced without modifying other aspects of the method. Recent unpublished analysis has shown that the principles developed can be used to explain the shape of cross section which many canals take as the water flows through them.

Acknowledgments.—The assistance of P. N. Lin is gratefully acknowledged in preparing these closing comments.

AMERICAN SOCIETY OF CIVIL ENGINEERS
Founded November 5, 1852
TRANSACTIONS

Paper No. 2777

STRUCTURAL OBSERVATIONS OF THE KERN COUNTY EARTHQUAKE

By Henry J. Degenkolb,[1] M. ASCE

Synopsis

The structural damage that occurred during the Kern County (California) earthquake of July 21, 1952, is reviewed, and the provisions of earthquake-resistant design are examined on the basis of this damage. It is shown that the prevailing scales for measuring damage caused by earthquakes are inadequate. Examination of the buildings in the area of the earthquake revealed that those buildings that were designed to resist earthquakes fared satisfactorily if they were constructed with the same degree of care with which they had been designed. Those buildings that were not designed to resist earthquakes fared poorly, especially if the construction methods were haphazard.

Introduction

On July 21, 1952, an earthquake of considerable magnitude shook a large part of Kern County, California. This earthquake was caused by a sudden displacement along the White Wolf fault extending from Wheeler Ridge, past Arvin, and between Caliente and Tehachapi as indicated on the map shown in Fig. 1.

According to the Gutenberg-Richter scale[2] this earthquake was of the magnitude of $7\frac{1}{2}$, releasing $10^{17.7}$ ft-lb of energy. This can be compared to the Long Beach (Calif.) earthquake of 1933, which had a magnitude of $6\frac{1}{4}$, releasing $10^{15.4}$ ft-lb of energy, and to the San Francisco (Calif.) earthquake of 1906, which had a magnitude of $8\frac{1}{4}$ and released 10^{19} ft-lb of energy. Another commonly used measure of earthquake intensities, the modified Mercali scale,[3] is based on average observed damage and human reactions. On this scale, whereas the San Francisco earthquake was of magnitude X and the Long Beach earthquake

---

Note.—Published, essentially as printed here, in August, 1953, as *Proceedings-Separate No. 244*. Positions and titles given are those in effect when the paper was received for publication.

[1] Chf. Engr., John J. Gould, Cons. Engr., San Francisco, Calif.

[2] "Magnitude Determination for Deep Focus Earthquakes," and earlier articles referred to therein by B. Gutenberg, ***Bulletin***, Seismological Soc. of America, Vol. 35, 1945, pp. 117–130.

[3] "Modified Mercali Intensity Scale of 1931," by Harry O. Wood and Frank Neumann, Vol. 21, 1931, pp. 277–283.

was of magnitude IX, the shock in Kern County was rated at VIII at Tehachapi, Bakersfield, and Arvin with a maximum of XI near Caliente.

Notwithstanding these measures of magnitude, it was the concensus of the engineers familiar with the results of both earthquakes that the effect on buildings in Tehachapi was only approximately 75% as great as that of the Long Beach earthquake on buildings in Long Beach. Some engineers believe that Arvin was shaken as hard or harder than Tehachapi; however, the available evidence is contradictory, and it is therefore difficult to draw any definite conclusions.

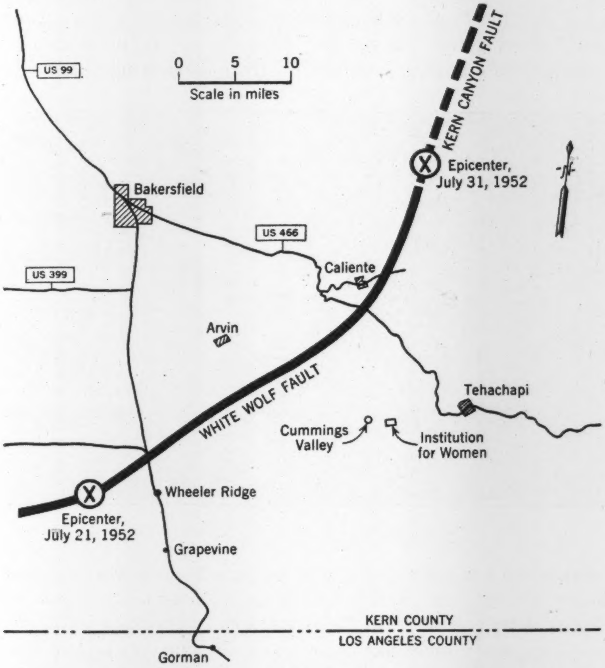
US 99
0
5
10
Scale in miles
KERN CANYON FAULT
Epicenter, July 31, 1952
Bakersfield
US 466
US 399
Caliente
Arvin
Tehachapi
WHITE WOLF FAULT
Cummings Valley
Institution for Women
Wheeler Ridge
Epicenter, July 21, 1952
Grapevine
KERN COUNTY
LOS ANGELES COUNTY
Gorman

Fig. 1.—Kern County Earthquake Fault Line (California)

These inconsistencies emphasize the fact that (as of 1955) there is no adequate engineering scale of intensities for measuring the destructive "force" that causes damage to structures. Although the Gutenberg-Richter scale measures the total energy release, it does not consider the area over which the energy is diffused. A large energy release scattered over a wide area may have less damaging "force" at its maximum intensity than a relatively small energy release if the smaller release is concentrated over a smaller area. On the other hand, the modified Mercali scale is deficient in that it generalizes from the effects on structures with little regard for their construction.

The damage in Tehachapi was greater and much more spectacular than that in Arvin. However, Tehachapi is an older town with many old-style masonry buildings that were particularly vulnerable to earthquake damage whereas Arvin is comparatively young with a higher percentage of newer buildings built by men who had experience in the construction of earthquake-resistant structures. In Caliente, which had only small frame buildings, comparatively little damage was noted despite its high Mercali rating. Thus, a magnitude scale based on observed damage is indefinite, to say the least.

ILLUSTRATIVE EFFECTS

It is not possible to cover herein all the effects of the Kern County earthquake; the following will pertain only to buildings in the areas of maximum damage and to those buildings which illustrate interesting ideas.

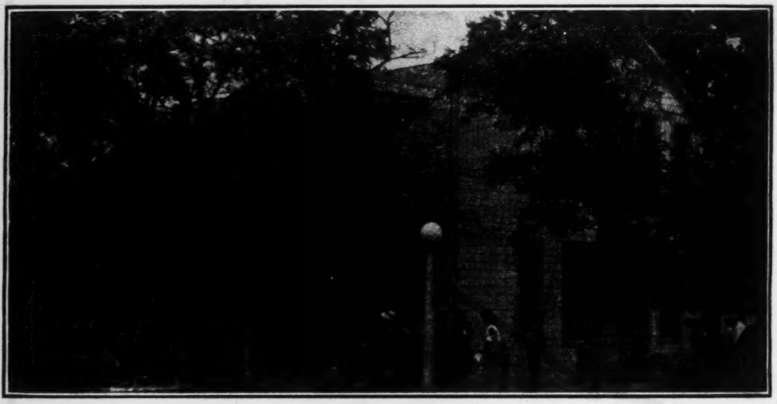

FIG. 2.—FRAME BUILDING, TEHACHAPI, CALIF.

The statement has been made[4] that no new lessons were learned from the Kern County earthquake. If this statement is meant to apply to the spectacular damage that was featured in the newspapers, it is undoubtedly true. The older type of masonry buildings built with poor mortar and not tied together fared badly, as they have in all previous major earthquakes. There is little to learn from such failures although they emphasize to the public how inadequate and unsafe this type of construction is. However, this earthquake "tested" more buildings constructed under the newer codes than did any previous earthquake, and there is much to learn from the behavior of these buildings.

In general, those buildings that were designed and built with conscious thought of lateral-force resistance and that met code requirements in this regard performed very well. Serious damage occurred in those buildings, usually older ones, which were designed with no provisions whatsoever for lateral resistance. It is also interesting to note that, of the newer buildings not adequately designed for lateral forces, less than average damage usually occurred. It is probable that many of the construction techniques that were learned from constructing earthquake-resistant buildings in the general area were unconsciously applied to buildings not specifically so designed.

---

[4] "Tehachapi Quake Left No New Lessons," *Engineering News-Record*, July 31, 1952, p. 26.

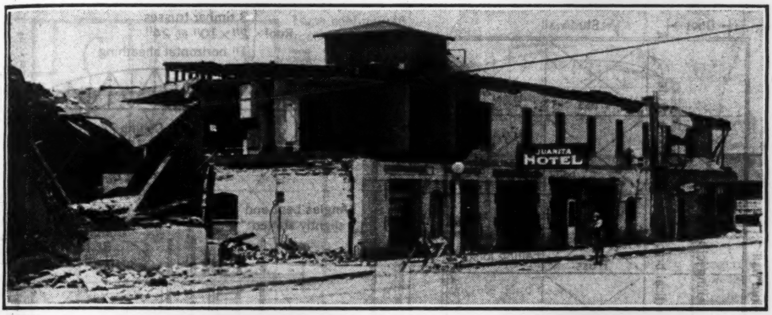

FIG. 3.—MASONRY HOTEL, TEHACHAPI, CALIF.

Before examining in more detail some of the damage, it is well to note one fact that impressed itself on all observers. The construction of buildings must be supervised; many items of damage were caused by inferior materials and workmanship or occurred because the design drawings were not followed. It was often found that damage was either caused or aggravated by the omission of anchors or ties that had been specified by the designer but were omitted in the field. Engineers must realize that clients want to construct buildings—not sets of plans. The safety of the public is not protected by a set of design computations if the intended results are not attained by field construction.

FIG. 4.—WOOD FRAME AND STUCCO MARKET, TEHACHAPI, CALIF.

One approach to studying the performance of structures during an earthquake is the relationship of their performance to rigidity. Certain flexible structures performed satisfactorily despite the fact that they had little or no bracing. Outstanding among this group of buildings were various timber buildings, including warehouses, corrugated iron buildings with wood or steel framing, and steel structures such as service stations. A hotel in Tehachapi (Fig. 2), an old frame board and batten building, was undamaged although in the same block an old masonry hotel (Fig. 3) was badly wrecked and one of its occupants was killed.

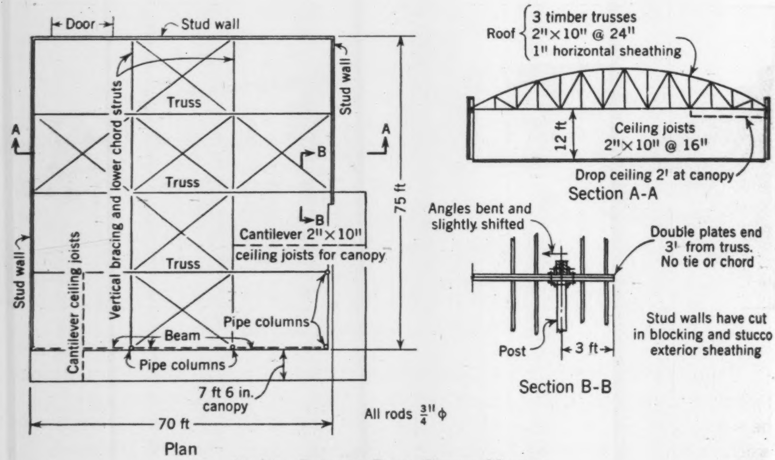
Door
Stud wall
Stud wall
Truss
Truss
Truss
Vertical bracing and lower chord struts
A
A
B
B
Stud wall
Cantilever ceiling joists
Cantilever 2" × 10"
ceiling joists for canopy
Pipe columns
Beam
Pipe columns
75 ft
7 ft 6 in. canopy
70 ft
Plan
All rods 3/4" ϕ
Roof
3 timber trusses
2" × 10" @ 24"
1" horizontal sheathing
12 ft
Ceiling joists
2" × 10" @ 16"
Drop ceiling 2' at canopy
Section A-A
Angles bent and slightly shifted
Double plates end 3' from truss. No tie or chord
Post
3 ft
Stud walls have cut in blocking and stucco exterior sheathing
Section B-B

FIG. 5.—FRAMING PLAN, STUCCO MARKET

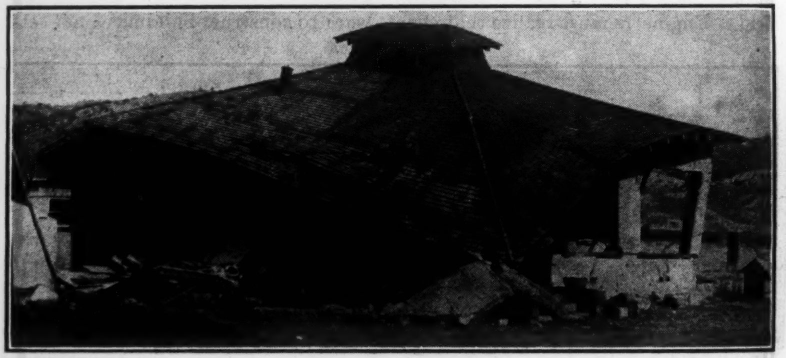

FIG. 6.—CUMMINGS VALLEY SCHOOL

The majority of the timber residences were undamaged. Frame structures such as churches, schools, and stores suffered only minor damage or none at all, even though they were not apparently designed to resist lateral force. The market in Tehachapi shown in Figs. 4 and 5 is a wood frame and stucco building that only lost its plate-glass windows and had minor plaster cracks; except for this, it can be said that the building was essentially undamaged. The store was 75 ft by 70 ft in plan with a ceiling 12 ft high. The building contained three timber trusses with rod bracing at the lower chord and horizontal roof sheathing. When the truss manufacturer designed the rod bracing, it was evidently assumed that there would be resisting elements in the front and rear. However, there was no front resisting element because there were pipe columns and only simple connections to the beams, and therefore there was considerable torsion in the building. As constructed, the market should resist less than 6 lb per sq ft of wind load or approximately 5½% G of dead load only; it is no

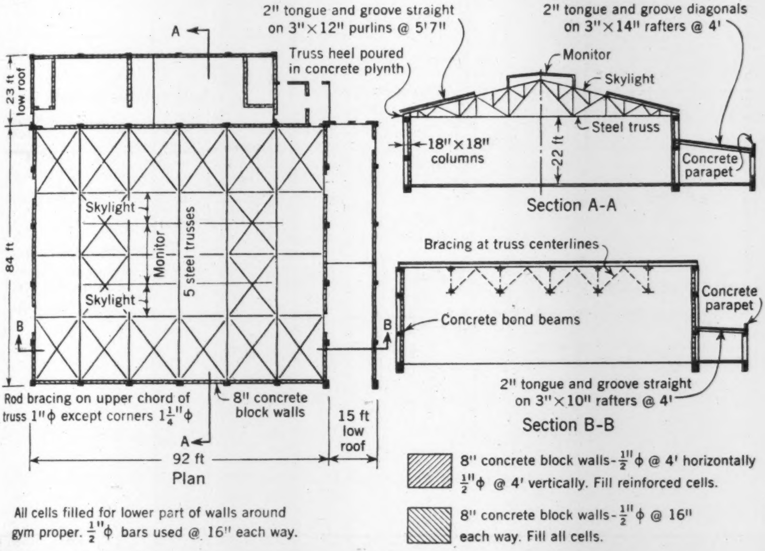

2" tongue and groove straight on 3"×12" purlins @ 5'7"
2" tongue and groove diagonals on 3"×14" rafters @ 4'
A
Truss heel poured in concrete plynth
Monitor
Skylight
23 ft low roof
Steel truss
18"×18" columns
22 ft
Concrete parapet
Section A-A
Skylight
Monitor
5 steel trusses
Skylight
84 ft
Bracing at truss centerlines
Concrete parapet
B
B
Concrete bond beams
2" tongue and groove straight on 3"×10" rafters @ 4'
Section B-B
Rod bracing on upper chord of truss 1"ϕ except corners 1¼"ϕ
8" concrete block walls
A
15 ft low roof
92 ft
Plan
8" concrete block walls-½"ϕ @ 4' horizontally ½"ϕ @ 4' vertically. Fill reinforced cells.
All cells filled for lower part of walls around gym proper. ½"ϕ bars used @ 16" each way.
8" concrete block walls-½"ϕ @ 16" each way. Fill all cells.

FIG. 7.—FRAMING PLAN, TEHACHAPI (CALIF.) VALLEY UNION HIGH SCHOOL

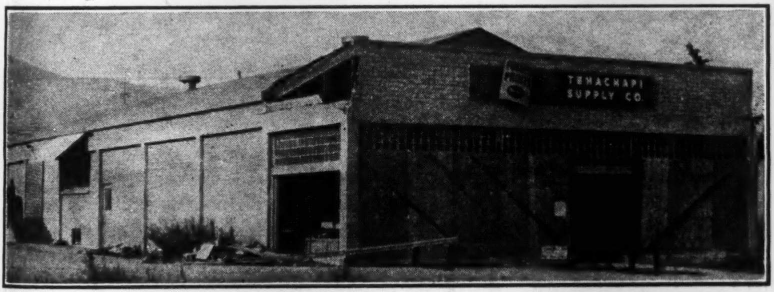

TEHACHAPI SUPPLY CO.

FIG. 8.—CONCRETE-BLOCK BUILDING, TEHACHAPI, CALIF.

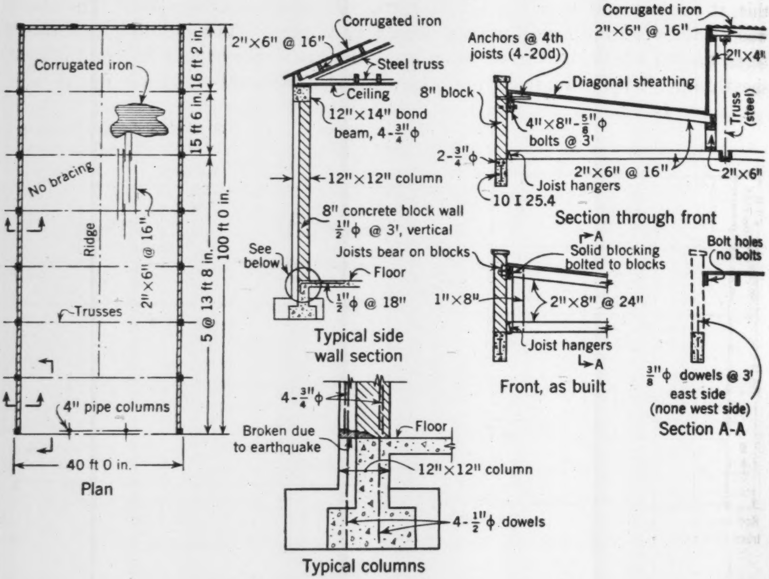
Corrugated iron
No bracing
Ridge
2"×6" @ 16"
Trusses
4" pipe columns
16 ft 2 in.
15 ft 6 in.
5 @ 13 ft 8 in.
100 ft 0 in.
40 ft 0 in.
Plan
Corrugated iron
2"×6" @ 16"
Steel truss
Ceiling
12"×14" bond beam, 4-$\frac{3}{4}$" ϕ
12"×12" column
8" concrete block wall
$\frac{1}{2}$" ϕ @ 3', vertical
See below
Floor
$\frac{1}{2}$" ϕ @ 18"
Typical side wall section
4-$\frac{3}{4}$" ϕ
Broken due to earthquake
Floor
12"×12" column
4-$\frac{1}{2}$" ϕ dowels
Typical columns
Corrugated iron
2"×6" @ 16"
Anchors @ 4th joists (4-20d)
8" block
Diagonal sheathing
2"×4"
4"×8"-$\frac{5}{8}$" ϕ bolts @ 3'
Truss (steel)
2-$\frac{3}{4}$" ϕ
2"×6" @ 16"
2"×6"
Joist hangers
10 I 25.4
Section through front
A
Joists bear on blocks
Solid blocking bolted to blocks
1"×8"
2"×8" @ 24"
Joist hangers
A
Front, as built
Bolt holes no bolts
$\frac{3}{8}$" ϕ dowels @ 3' east side (none west side)
Section A-A

FIG. 9.—FRAMING PLAN, CONCRETE-BLOCK BUILDING

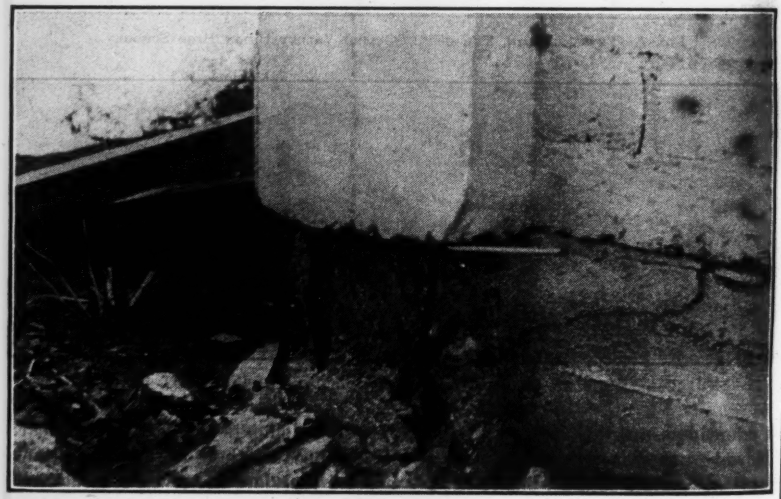

FIG. 10.—FAILURE OF COLUMNS, CONCRETE-BLOCK BUILDING

wonder that the plate-glass windows broke. However, despite the design deficiencies, the store was open for business shortly after the earthquake.

At the other extreme there are heavy, rigid, nonreinforced masonry buildings which often suffer severe damage. Houses constructed of adobe with heavy, weak materials were badly wrecked. The Cummings Valley School (Fig. 1 and Fig. 6), which was built in 1910 of nonreinforced concrete, was destroyed.

The Tehachapi State Prison for Women, built in 1932 and not designed for lateral forces, consists of a group of two-story, reinforced-concrete buildings with steeply pitched tile roofs on wood framing. An exterior view of these buildings indicates little damage except for the loss of some chimneys and some cracking, but the interiors show badly cracked tile partitions and a general shambles of the timber roof framing. By the standards of lateral-force design the timber framing was particularly poor, including inadequate ties or no ties, and it was not at all surprising to see the damage that occurred. Present (1955) codes, however, assign certain shear values for tile partitions and other similarly brittle elements. The shear resistance of many partitions in the top floor would approximately meet many of these code requirements because the partitions were spaced quite closely in order to provide small rooms; these partitions, however, were badly cracked. This observation raises a question as to the adequacy of normal static-shear tests—especially on brittle materials—to establish safe resistance values for earthquake loads. Building codes show an increasing tendency to permit use of brittle materials (such as plaster, plaster substitutes, hollow tile, and weak deck fills) as lateral-force resisting elements by assigning allowable stresses for their use. These values are based on static tests; observations indicate that the performance of these resisting elements may not meet these expectations in actual construction.

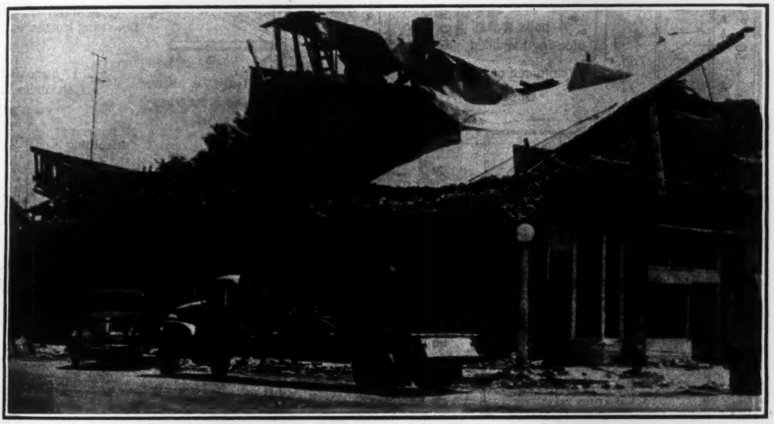

Fig. 11.—Collapse of Second-Floor Auditorium

The performance of these buildings particularly illustrates the necessity of properly tying together various building elements. Where certain key connections are weak, as were the wood-to-concrete connections in the prison, their failure permits a battering action to occur that invariably causes considerable damage. It would have cost little more to make these buildings adequately earthquake resistant by a more judicious choice of construction materials, supervision of field construction, and—most imprtant of all—an adequate engineering design that would have resulted in the building acting as a unit. Without these three necessities, it is doubted that high earthquake coefficients would have appreciably improved the performance of these buildings.

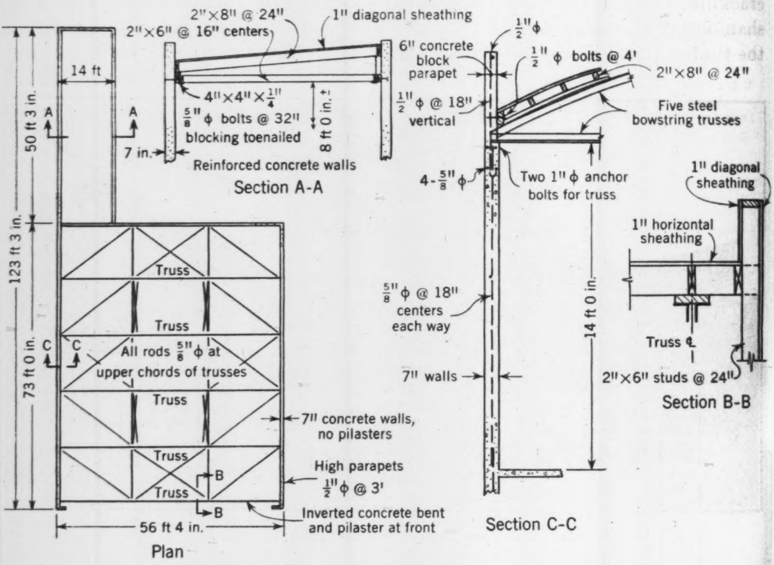
2"×8" @ 24"
2"×6" @ 16" centers
1" diagonal sheathing
14 ft
50 ft 3 in.
A
A
4"×4"×$\frac{1}{4}$"
$\frac{5}{8}$" ϕ bolts @ 32"
blocking toenailed
8 ft 0 in.±
7 in.
Reinforced concrete walls
Section A-A
123 ft 3 in.
Truss
Truss
C
C
All rods $\frac{5}{8}$" ϕ at
upper chords of trusses
73 ft 0 in.
Truss
Truss
Truss
B
B
7" concrete walls,
no pilasters
High parapets
$\frac{1}{2}$" ϕ @ 3'
Inverted concrete bent
and pilaster at front
56 ft 4 in.
Plan
$\frac{1}{2}$" ϕ
6" concrete
block
parapet
$\frac{1}{2}$" ϕ bolts @ 4'
2"×8" @ 24"
$\frac{1}{2}$" ϕ @ 18"
vertical
Five steel
bowstring trusses
4-$\frac{5}{8}$" ϕ
Two 1" ϕ anchor
bolts for truss
$\frac{5}{8}$" ϕ @ 18"
centers
each way
14 ft 0 in.
7" walls
Section C-C
1" diagonal
sheathing
1" horizontal
sheathing
Truss ℄
2"×6" studs @ 24"
Section B-B

FIG. 12.—FRAMING PLAN, BANK IN TEHACHAPI, CALIF.

The Arvin High School is an excellent example of a building that is quite rigid, that met state code requirements[5] for schools, and that, in general, performed excellently. This large school, located comparatively close to the fault line, was evidently shaken quite severely, and one shear wall suffered some damage by cracking. This wall was constructed of grouted brick masonry and according to code standards was not highly stressed. However, field examination and subsequent core samples indicated that the workmanship on this wall was poor, resulting in voids in the grout and inadequate bond to the reinforcing steel. The aftershocks of the earthquake caused this crack to open, and the loss of rigidity then permitted damage to the interior partitions in this part of the building.

---

[5] "California Administrative Code," Title 21, Public Works, Chapter I, Dept. of Public Works, Subchapter 1, Div. of Architecture; Group 3, "Structural Design—Materials and Details of Construction" (formerly Appendix A).

The only other large school structure of recent construction located in the area of greatest damage was the gymnasium of the Tehachapi Valley Union High School (Fig. 7). This was a concrete-block structure with a complete

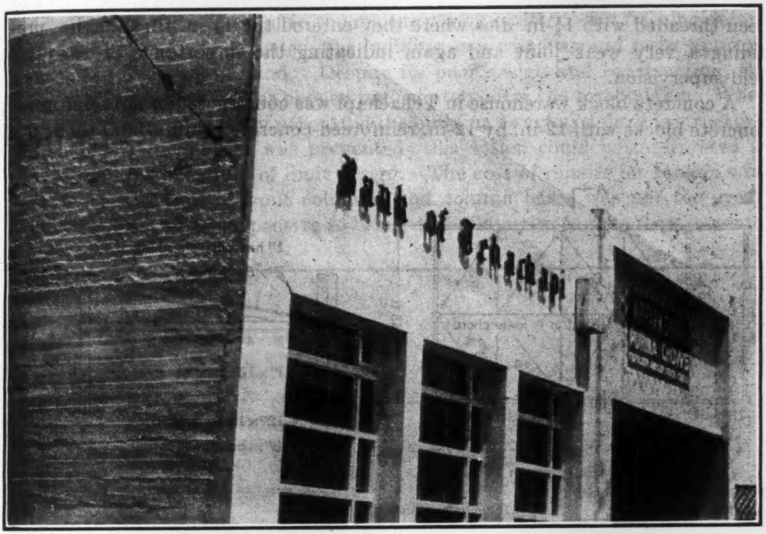

Fig. 13.—Parapet of Bank in Tehachapi, Calif.

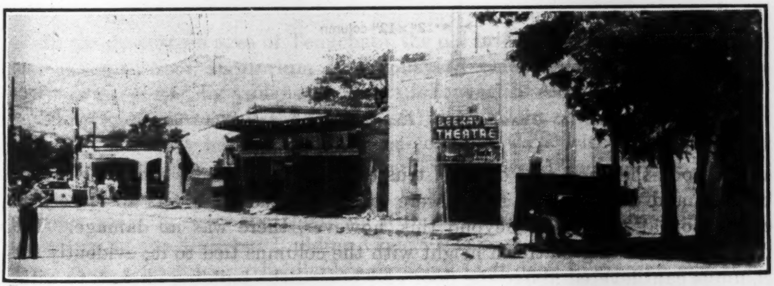

Fig. 14.—Reinforced Concrete Theater, Tehachapi, Calif.

reinforced-concrete frame and a wood roof on steel trusses. This structure was built during World War II and was designed in conformance with the school-building requirements of California.[5] All concrete-block walls were reinforced, and parapets were of reinforced concrete made integral with the bond beams supporting them. Because the roof monitor and the skylights reduced the strength of the roof diaphragm, rod bracing was used at the lower chord of the trusses. The rod bracing was specified to be tightened to 1,000 lb of tension, but this evidently was not done. In general, the rods were 1 in. round except at the corners where 1¼-in.-round bars were used.

The building was essentially undamaged except that the threads were stripped from the 1¼-in. rods. Later examination showed that these rods had been threaded with 1⅛-in. dies where they entered the 1¼-in. turnbuckles, providing a very weak joint and again indicating the importance of adequate field supervision.

A concrete block warehouse in Tehachapi was constructed of nonreinforced-concrete blocks with 12-in. by 12-in. reinforced-concrete columns and tie beams and a wood-sheathed roof on steel trusses. There evidently was no effective bracing, and the end wall gables were thrown out as there was absolutely no connection at the roof. Beyond this, however, there was no damage. The floor was at loading-platform height with the columns tied to it; evidently the columns cantilevered above the floor and braced the building enough to withstand damage from this earthquake. Although this could not be termed a flexible building, the flexibility caused by the bending of the columns undoubtedly reduced the forces exerted on the building.

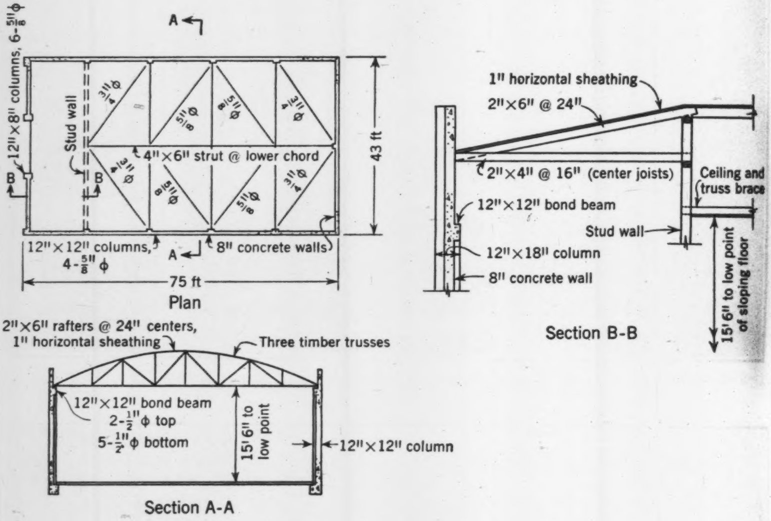
12"×8" columns, 6-5/8" ϕ
A
Stud wall
B
B
3/4" ϕ
5/8" ϕ
5/8" ϕ
3/4" ϕ
4"×6" strut @ lower chord
3/4" ϕ
5/8" ϕ
5/8" ϕ
3/4" ϕ
43 ft
12"×12" columns, 4-5/8" ϕ
A
8" concrete walls
75 ft
Plan
2"×6" rafters @ 24" centers, 1" horizontal sheathing
Three timber trusses
12"×12" bond beam 2-1/2" ϕ top 5-1/2" ϕ bottom
15' 6" to low point
12"×12" column
Section A-A
1" horizontal sheathing
2"×6" @ 24"
2"×4" @ 16" (center joists)
Ceiling and truss brace
12"×12" bond beam
Stud wall
12"×18" column
8" concrete wall
15' 6" to low point of sloping floor
Section B-B

FIG. 15.—FRAMING PLAN, REINFORCED CONCRETE THEATER

The building shown in Figs. 8 and 9 was designed and built in 1946 during material shortages. This building was 40 ft by 100 ft, having concrete-block walls with poured concrete columns and bond beams. Except for the first bay, which was timber, the remainder of the bays were corrugated iron, and there was no bracing as ordinarily understood. Some resistance, however, was developed when the columns cantilevered out of the footings. At the base of the column, the dowels from the footings were $\frac{1}{2}$ in. round although there were $\frac{3}{4}$-in.-round dowels in the column. When the columns acted as cantilevers, they failed at the base (Fig. 10). There was little or no supervision of construction, and changes were made from the design drawings. Dowels to parapets and bolts from the wood roof to the masonry were omitted, and framing details were changed. As constructed, the building as a whole should resist approximately 4% *G* or a 6-lb wind. Despite its poor design and construction, the building was usable and was opened immediately after the earthquake. When the columns shattered, they permitted the building to act as a flexible structure, and thus further damage was prevented; this action could be interpreted as an interesting application of limit design. The cost of repairs for broken windows, parapets, tops of front columns, and column bases was not too great, but it would have been expensive to bring the building up to code requirements.

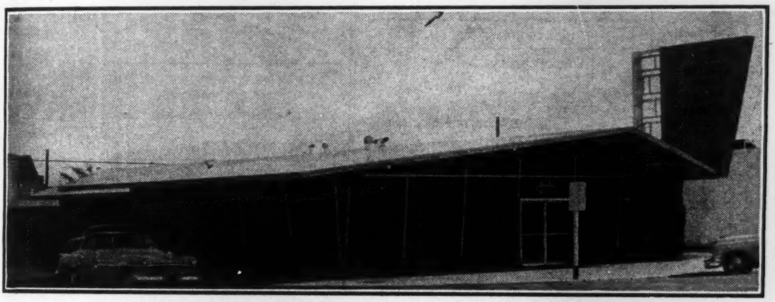

FIG. 16.—WELL-DESIGNED BUILDING, ARVIN, CALIF.

In the downtown area of Tehachapi, the old brick building shown in Fig. 11 had a second-floor auditorium that collapsed completely. The auditorium roof was supported by a piano and seats following its collapse.

There was also a bank (56 ft by 73 ft) with a long low appendage at the rear (Fig. 12). It has 7-in., reinforced-concrete walls with steel bowstring trusses providing a 14-ft ceiling. There was a wood roof having straight sheathing with a rod bracing system. At the rear of the bank this long appendage has a diagonal sheathed roof with no joist anchors. According to the provisions of the Uniform Building Code,[6] this part had a lateral load of 200 lb per ft on a 50-ft span, the diaphragm being 14-ft deep to give an end shear of 360 lb per ft. The front was of wood and stucco with an inverted concrete bent resisting the lateral loads. According to Uniform Building Code provisions, the rods were stressed to 37,000 lb per sq in. with rather inefficient structural details for the rods. There was little damage except to the front and to the parapets, which fell off on one side and were cracked on the other side of the building (Fig. 13). Although the parapet was reinforced with

---

[6] "The Uniform Building Code," Pacific Coast Building Officials Conference, Los Angeles, Calif.

½-in.-round bars at 3 ft 0 in. on centers, there were no dowels for the part of the parapet that broke off.

The theatre shown in Figs. 14 and 15—in the center of the damaged area—was undamaged except for a small crack in the wall on the far side. This building was 43 ft by 75 ft, with 8-in., reinforced-concrete walls between 12-in. by 12-in. columns and bond beams. These columns supported three bowstring timber roof trusses, wood purlins, and straight wood sheathing. It had ⅝-in.-round rod bracing in the plane of the lower chord, but this bracing ended at the lobby stud wall. The plans of this building were inadequate; for such a major building element as this wall there was absolutely no information on the drawings, and the plaster prevented a determination of the construction below the ceiling. Assuming the wall to be an adequate shear-resisting element, the rod bracing could support approximately 11% *G* on dead load only, with a shear in the wall of approximately 350 lb per ft. The computed deflection caused by the rod system is approximately 1 in., assuming tight rods and neglecting such items as bolt slip and deformations in the shear walls. The maximum deflection permitted by one proposed formula is 0.8 in. and must include these effects.

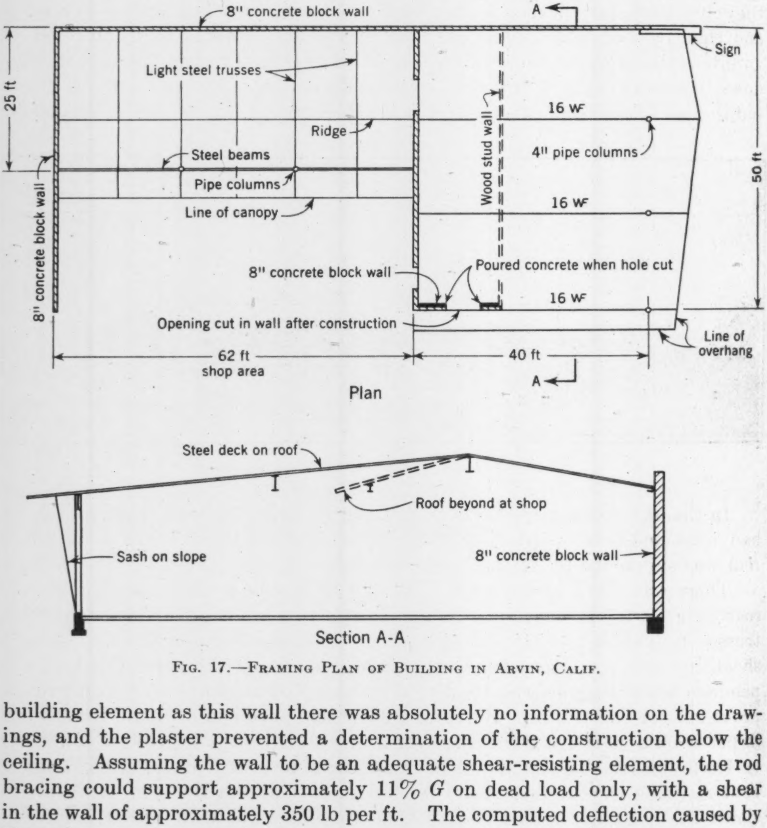
8" concrete block wall
A
Sign
Light steel trusses
25 ft
Ridge
16 WF
Wood stud wall
Steel beams
4" pipe columns
50 ft
Pipe columns
16 WF
Line of canopy
8" concrete block wall
8" concrete block wall
Poured concrete when hole cut
16 WF
Opening cut in wall after construction
Line of overhang
62 ft
shop area
40 ft
A
Plan
Steel deck on roof
Roof beyond at shop
Sash on slope
8" concrete block wall
Section A-A

FIG. 17.—FRAMING PLAN OF BUILDING IN ARVIN, CALIF.

The most interesting building in the earthquake area was the building in Arvin, shown in Figs. 16 and 17. Designed and closely supervised by both an architect and an engineer, the building suffered only the damage of two cracked panels of glass and a small crack in the masonry over the side door. The framing was quite simple—steel beams and columns, a metal roof deck acting as a diaphragm, and reinforced-concrete block walls as resisting elements. However, all the basic elements of lateral-force resistance were present, and the structure was well tied together; the results achieved were outstanding, thus proving that this type of architectural design can be made safe for earthquakes.

CONCLUSIONS

From the variations in damage and response in the various buildings cited, it can be seen that there is one basic reason for the conflicting conclusions of various observers of earthquake damage. Building codes require the same coefficients for all structures regardless of rigidity, the construction materials, or the type of framing. Requirements of analysis and design are given only in the most general terms, many of which are subject to interpretations which differ according to different engineers and also according to different localities. Each engineer views the earthquake damage in the light of his own experience and his individual interpretations of code requirements; it is not surprising to find such a wide divergency of expressed views.

In view of this divergency, it is most surprising to find so much agreement about the final result of structural design among engineers who are familiar with earthquake damage. To the average engineer, a building code is almost a handbook of design which states definite loads, allowable stresses, and required details. The code contains moment coefficients, flat-slab coefficients, hook requirements, minimum nailing, locations of critical shear, and definite formulas for almost everything. This detailed approach is not possible in earthquake design and from a professional viewpoint would not be desirable if it were. In earthquake design, the basic understanding of tying a building together to accommodate an erratic motion is of far greater importance than following detailed code requirements. It is generally found that experienced engineers build very similar final structures as far as lateral bracing is concerned even when they operate under the different coefficients required by various codes; a satisfactory structure is thus attained. For inexperienced engineers following the code as a handbook, the desired results often may not be attained. It has frequently been said, and it is only too true, that a thoroughly unsafe building may meet code requirements entirely, whereas a building that does not meet these requirements may be quite safe. Code requirements should be made to express, as far as possible, the experience derived from actual earthquakes.

From these observations it is possible to draw certain conclusions:

1. To construct earthquake-resistant structures, the primary requirement is to provide for adequate engineering services both in the design and in the field supervision. Neither part of the service is adequate alone. Too many engineers feel that, if the design is adequate, the field construction will take care of itself. Experience has proved that nothing could be further from the truth.

2. It is of great importance that the various components of a structure be adequately tied together so that the structure will act as a unit.

3. A blanket requirement for high earthquake coefficients is not sound. When only the protection of the public is concerned and for certain types of structures (especially the inherently flexible types), rather modest coefficients are adequate and are in the public interest because of the construction savings involved.

4. When expensive finishes or rigid interior partitions must be protected, it may be economical to provide a rigid bracing system with consequently higher earthquake coefficients. This requirement must be clearly differentiated, however, from the requirements that protect the public safety.

5. In the final analysis, the producing of safe earthquake-resistant structures for the public depends basically on the experience and knowledge of the designing engineer rather than on detailed building-code requirements. The engineer who knows the requirements of a project must choose the proper materials for each specific job. He must connect the materials together so as to provide a coherent unit with sufficient lateral resistance to satisfy the particular requirements and yet he must maintain strict economy for his client. The problem is too complex for the provisions of a "handbook" building code that does not discriminate between various materials and so must accommodate its minimum provisions to materials and framing types used in the most unsuitable manner. Inevitably, a large part of the consequent requirements are unjustified, costly, and not in the public interest.

ACKNOWLEDGMENTS

Assistance and cooperation were received from William Cloud, who furnished certain data regarding the fault and magnitudes. Much of the remaining data was gathered from various sources by Gordon Dean and Thomas Wosser, Jr., J. M. ASCE.

AMERICAN SOCIETY OF CIVIL ENGINEERS
Founded November 5, 1852
TRANSACTIONS

Paper No. 2778

HIGH-STRENGTH BOLTS IN STRUCTURAL JOINTS

A SYMPOSIUM

History of the Use of High-Strength Bolts.
By W. C. Stewart 1296

Laboratory Tests of Bolted Joints.
By William H. Munse, D. T. Wright, and Nathan M. Newmark 1299

Comparison of Bolted and Riveted Joints.
By Frank Baron and Edward W. Larson, Jr. 1322

Slip of Joints Under Static Loads.
By R. A. Hechtman, D. R. Young, A. G. Chin, and E. R. Savikko 1335

Fatigue in Riveted and Bolted Single-Lap Joints.
By Jack W. Carter, Kenneth H. Lenzen, and Lawrence T. Wyly 1353

Structural Uses of High-Strength Bolts.
By T. R. Higgins and E. J. Ruble 1389

HISTORY OF THE USE OF HIGH-STRENGTH BOLTS

By W. C. Stewart[1]

Synopsis

Engineers became greatly interested in the use of high-strength bolts after 1938. Extensive research caused rapid increase in the structural application of this type of fastener. The history of the successful development of this bolt has been marked by the contributions of many individuals and organizations.

The history of riveting goes as far back into antiquity as does that of the use of ductile metals. The history of the formal study of riveting and bolting, however, is more recent. A. E. R. deJonge, M. ASCE, in his bibliography on riveted joints[2] dates the first publication on the subject as of the middle of the 19th Century.

Possibly no structural research in recent years has produced so immediate and so extensive a modification of structural practice as has the study of the high-tensile structural bolt. This type of bolt is not new, but its extensive application to structural joints is of recent origin. The bolt is made of accurately controlled, quenched-and-drawn, medium carbon steel. This type of bolt first came into general use shortly after World War I as an aid in the building of automobiles. In applying the bolt to structures, the object is to use a high-tensile bolt torqued to a high tension and supported by hardened washers under the bolt head and the nut. This concept of the bolt and of its effects was not developed at any one time, but gradually, through a process of development and through contributions by many engineers.

Possibly the germ of this idea lay in the early practice of certain fabricators—that of using similar high-strength bolts as "fitting-up" bolts. This provided sufficient clamping power to draw heavy plates tightly against the joint preparatory to riveting.

The first laboratory tests on high-strength bolts in the United States of which the writer is aware were performed by Wilbur Wilson, Hon. M. ASCE, and F. P. Thomas at the University of Illinois at Urbana.[3] They concluded that:

> "The fatigue strength of high-strength bolts, appreciably smaller than the holes in the plates, was as great as that of well-driven rivets if the nuts were screwed up to give a high tension in the bolts."

Note.—Presented at the Centennial Convocation, Chicago, Ill., September, 1952. Published, essentially as printed here, in May, 1954, as *Proceedings-Separate No. 440*. Positions and titles given are those in effect when the paper was received for publication.

[1] Technical Adviser, Industrial Fasteners Inst., Cleveland, Ohio.

[2] "Riveted Joints: A Critical Review of the Literature Covering Their Development, with Bibliography and Abstracts of the Most Important Articles," by A. E. R. deJonge, ASME, New York, N. Y., 1945.

[3] "Fatigue Tests of Riveted Joints," by W. M. Wilson and F. P. Thomas, *Bulletin No. 302*, Eng. Experiment Station, Univ. of Illinois, Urbana, Ill., May 31, 1938.

The joints tested were designed for failure of the bolts rather than of the plates, and the bolt tensions were low in comparison to modern (1954) practice. The tests did establish, however, that the bolts themselves would not fail in fatigue if suitably tightened.

The next step came in 1945, when G. A. Maney prepared drawings for joints of more nearly balanced design. Difficulties were encountered in testing these joints in reverse loading in that the bolt tension was lost because the bolt head and nut indented the structural plate, thereby losing grip. It had not yet been realized that hardened washers were necessary under the bolt head and nut in order to support the high bolt tension. Kenneth H. Lenzen, A. M. ASCE, conducted the tests of these joints. He experimented with various washers—common soft washers, cyanide-hardened washers, deeply carburized washers, washers of quenched-and-drawn medium carbon steel—and on October 23, 1947, he accomplished the first successful test of a balanced joint designed much as it is known today (1954).

The Research Council on Riveted and Bolted Structural Joints was formed on January 15, 1947. Under its sponsorship, Mr. Wilson completed tests of a series of bolted joints designed for failure of the bolts, but having bolt tensions much greater than he had previously used. Again, it was determined that the bolt itself was safe in fatigue when withstanding extremely great tension. Numerous ramifications of the problem of bolted joints have been explored at the University of Illinois and the University of Washington at Seattle. Additional information has also been obtained in connection with another project by Frank Baron, M. ASCE.

Concurrently with these developments, L. T. Wyly, M. ASCE, and J. W. Carter, A. M. ASCE (under the sponsorship of the American Railway Engineering Association (AREA)) were studying the problem of the fatigue failures of floor-beam hangers of railroad bridges. Mr. Wyly advanced the hypothesis that the failures were caused primarily by the high stresses and strains which were induced by rivet bearing. The high-clamping bolt was proposed as a remedy to minimize the effect of this bearing. This explanation, with supporting evidence, was presented to AREA Committee 15, Iron and Steel Structures, on October 19, 1948. This thesis was subsequently verified by Messrs. Wyly and Carter by fatigue tests on single-lap joints connected by rivets, by bolts in bearing without clamping, and by high-clamping bolts. Detailed studies made by Mr. Carter of stress and strain in the vicinity of rivet holes and bolt holes were correlated with the fatigue tests.

The Association of American Railroads became interested in the possibilities of high-strength bolts in the maintenance of bridges and initiated a program of field installations. The first of these installations was made on March 19, 1948, in an ore bridge. The American Society for Testing Materials (ASTM), realizing the importance of these bolts, appointed a committee to prepare specifications to control their quality. These tentative specifications were approved in 1949 and revised in 1951 under the ASTM designation A 325.

The Research Council on Riveted and Bolted Structural Joints (as a result of its research activities and in order to provide industry with suitable control of the assembly of high-tensile bolts) prepared a set of specifications[4] which were approved by the Council in January, 1951.

The high-tensile bolt, in the design required for structural use, was not generally available at the beginning of these investigations, although slightly different products having the same physical properties were widely used. The American Standards Association (ASA), responsible for the standardization of bolt design, considered the problem not only from the viewpoint of American standards but in cooperation with standardizing bodies of Great Britian and Canada. As a result, the ASA, in March, 1952, approved a new standard that increased the availability of the high-tensile bolt for structural use.

The rapid progress made in the study and application of the high-strength bolt has been a remarkable example of cooperative endeavor to provide the profession with a new tool.

---

[4] "Specifications for Assembly of Structural Joints Using High Tensile Steel Bolts," Research Council on Riveted and Bolted Structural Joints of the Engineering Foundation, January, 1951.

LABORATORY TESTS OF BOLTED JOINTS

BY WILLIAM H. MUNSE,[1] A. M. ASCE, D. T. WRIGHT,[2]
AND NATHAN M. NEWMARK,[3] M. ASCE

WITH DISCUSSION BY MESSRS. A. J. FRANCIS; AND WILLIAM H. MUNSE,
D. T. WRIGHT, AND NATHAN M. NEWMARK

SYNOPSIS

The paper summarizes the results of static and fatigue tests on structural joints for which high-strength steel bolts were used as fasteners. The tests indicate that joints of this type are generally superior to similar riveted joints, whether subjected to static loads or fatigue-type loads.

INTRODUCTION

Bolts have long been used in the erection of structures and in some instances have served as the permanent fasteners, although this latter type of application is often restricted by local codes and specifications. Another factor that has limited the use of bolts in structural joints has been the opinion among engineers that the nuts on the bolts might become loose, thereby endangering the structure. However, the results of field and laboratory studies such as those described in the Symposium indicate that the bolts in structural joints remain tight even under extreme loading conditions, providing they are high-strength bolts that have been installed properly. In fact, most of the studies have shown that such joints are superior to similar riveted joints.

To make possible the assembling of a bolted joint, the bolts must be smaller than the bolt holes; as bolts do not expand and fill the holes, it is essential that the bolts be drawn extremely tight to protect the joint against slipping. Hence, the load is transferred across the joint by the friction between the connected parts rather than through shear on the fasteners, except for the case of large static loads.

The frictional forces in a riveted joint, produced by the clamping action of the rivets, determine the ability of the joint to resist slipping at working loads. Nevertheless, the design of riveted joints is invariably based on the premise that the load is transferred from one member to another by means of direct shear on the rivets. By using high-strength bolts as fasteners, one may produce very large clamping forces. This makes possible the design of bolted joints in which the entire working load is resisted by frictional forces.

One of the first studies of the use of high bolt tensions in structural joints was that of W. M. Wilson,[4] Hon. M. ASCE, in connection with some of his

---

NOTE.—Presented at the Centennial Convocation, Chicago, Ill., September, 1952. Published, essentially as printed here, in May, 1954, as *Proceedings-Separate No. 441*. Positions and titles given are those in effect when the paper or discussion was received for publication.

[1] Research Associate Prof. of Civ. Eng., Univ. of Illinois, Urbana, Ill.

[2] Formerly Research Assistant in Civ. Eng., Univ. of Illinois, Urbana, Ill.

[3] Research Prof. of Structural Eng., Univ. of Illinois, Urbana, Ill.

[4] "Fatigue Tests of Riveted Joints," by Wilbur M. Wilson and Frank P. Thomas, *Bulletin No. 302*, Eng. Experiment Station, Univ. of Illinois, Urbana, Ill., May, 1938.

early investigations of structural fatigue. His conclusions, reported in 1938, were among the factors leading to the program of tests reported herein. These tests were planned to determine the strength of structural joints fabricated with high-strength bolts and subjected to both static and fatigue loadings. Numerous individual studies have been made in order to determine the general characteristics of the joints under a variety of conditions.

The bolts, because of their importance in this problem, have been studied separately, as well as in the joints. The bolts have been calibrated and tested in tension and torsion in order to furnish data for their most advantageous use.

TESTS OF BOLTS

The magnitude of the axial bolt tension and the ability of the bolt to maintain this tension are primary factors controlling the functioning of bolted structural joints. In the laboratory, axial tension has been determined with extensometers which are used to measure the change in length of the bolts as they are tightened. This procedure would be impracticable for field use; however, in the laboratory it provides a simple means by which the bolt tensions may be carefully controlled.

TABLE 1.—MECHANICAL PROPERTIES

Bolt diameter[a]	TESTS OF BOLTS[b]		TESTS OF 0.505-IN.-DIAMETER COUPON SPECIMENS			
	Ultimate load, in lb	Tensile strength, in lb per sq in.	Yield strength[c] (tension)	Tensile strength[c]	Elongation, in 2 in.[d]	Reduction in area[d]
¾	39,900 (40,000)	119,500 (120,000)	84,000	113,200	23	63
⅞	66,900 (50,700)	145,000 (110,000)	89,400	118,700	22	59
1	79,200 (66,500)	131,000 (110,000)	101,400	127,100	20	56

[a] In inches. [b] Numbers in parentheses are from ASTM Specification A 325-49 T. [c] In pounds pe square inch. [d] In percentages.

Bolt Materials.—The bolts used in this study were to be of the type furnished under Designation A 325-49 T of the American Society for Testing Materials (ASTM).[5] This provides for medium carbon (0.30% minimum) quenched and tempered steel bolts having a yield strength of about 80,000 lb per sq in. and a tensile strength of about 110,000 lb per sq in. It is not necessary that they be alloy steel bolts.

The ultimate strengths of the test bolts and the mechanical properties of the bolt materials as determined from tests of 0.505-in.-diameter coupon specimens cut from the bolts are summarized in Table 1. The tabulation indicates that the ¾-in. bolts did not have the strength required by the ASTM specification. On close analysis it was found that the ¾-in. bolts were actually hexagon-head cap screws which had an ultimate strength slightly lower than that required and a bolt head which was somewhat smaller than that specified.

---

[5] "Quenched and Tempered Steel Bolts and Studs, (A 325-49 T)," A.S.T.M., 1949.

Load-Elongation Tests.—It was necessary to ascertain the load-elongation characteristics of the bolts for their proper use in the laboratory tests. These characteristics were measured by applying tension to the bolts with a testing machine and simultaneously measuring the change in length of the bolt with an extensometer. Evidently, the load-elongation characteristics for the bolts will vary with the grip and diameter of the bolts. Therefore, the latter factors must be considered in any calibration test.

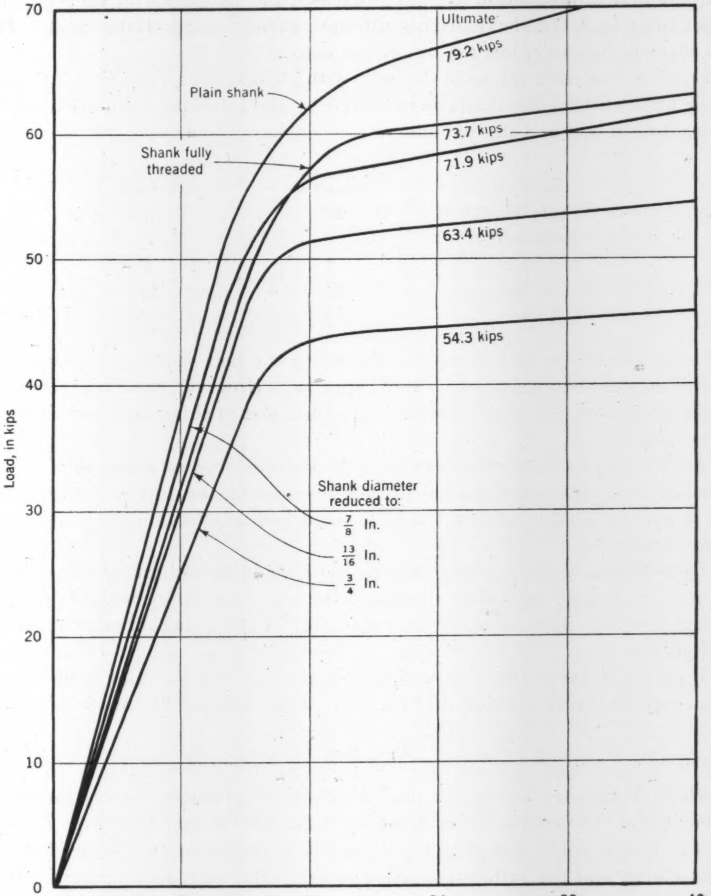

FIG. 1.—TESTS OF BOLTS 1 IN. IN DIAMETER

For maximum bolt efficiency, the total elongation in the bolts, for a given grip and axial bolt tension, should be as high as possible. Consequently, several studies were made in which the bolt elongation, for a given axial tension, was increased by reducing the effective area of the bolt shank. Reduction was accomplished by undercutting or fully threading the shank of the bolt.

The results of the load-elongation tests of 1-in. bolts with various shank conditions are presented in Fig. 1. (The grip was 3.75 in. for all bolts.) It is apparent that the reduction in shank increased the elongation of each bolt for a particular load but decreased its ultimate capacity and elastic limit. The first effect is desirable, but the others are not.

Based on the calibrations of the bolts with plain shanks, the effect of threading or undercutting the shank is indicated by the following tabulation, which applies to the bolt of 1-in. diameter:

Shank condition	% Increase in elongation	% Decrease in ultimate capacity
Fully threaded	20	7
Reduced to:		
$\frac{7}{8}$ in.	11	9
$\frac{13}{16}$ in.	25	20
$\frac{3}{4}$ in.	53	32

It can readily be seen that fully threading the bolt shank gave the largest ratio of increased elongation to loss of capacity. However, the 20% increase in elastic elongation may not be worth the added cost of threading the full shank of the bolt.

Another type of calibration test conducted was that in which the bolt-nut assembly was lubricated. This procedure reduced the torque necessary to obtain a given axial tension in the bolt, but it had no effect on the load-elongation characteristics.

Load-Torque Tests.—Many studies were made to determine the relation between the torque applied to a bolt and the axial tension in the bolt produced by this torque. These studies were made for bolts having different grips and diameters.

Previous investigations[6] have demonstrated the validity (for bolts such as those used in this investigation) of a load-torque relationship of the type:

$$T = K\,D\,P \qquad (1)$$

in which T denotes torque, in pound-inches. The dimensionless torque coefficient is K, the nominal bolt diameter is D, and the bolt tension is P.

The torque coefficient K in Eq. 1 may be expected to vary somewhat with the material and the surface condition of the bolts, nuts, and washers. However, an approximation to the torque may be obtained by using a K-value of 0.20.

Table 2 is a summary of the K-values obtained in bolt tests. The average torque coefficient was found to be 0.221 with a probable error of ±0.016. The variation in the magnitude of the coefficient might be expected because the bolts were all tested in the condition in which they were received.

---

[6] "Predicting Bolt Tension," by G. A. Maney, *Fasteners*, Industrial Fasteners Inst., Vol. 3, No. 5, 1946, p. 16.

Lubrication of the sliding surfaces of the bolt-nut assembly (using a special wax coating) decreased the coefficient of friction and, accordingly, the value of the torque coefficient. When the bolt and nut or the nut alone was waxed, the torque coefficient was found to be 0.15; when the bolt alone was waxed, the torque coefficient was 0.184. These results indicate that treating the nut alone is the more economical and effective means of reducing the torque required to produce a given axial tension in the bolt-nut assembly.

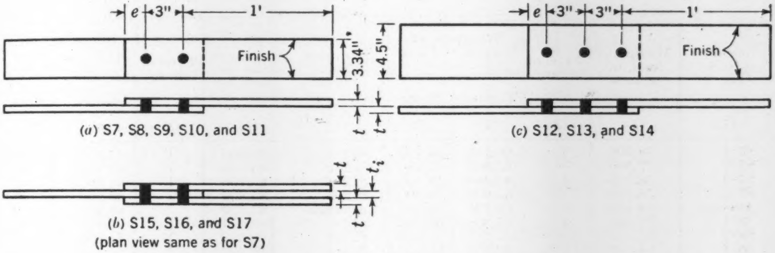

FIG. 2.—DETAILS OF THE SPECIMENS FOR STATIC TESTS

TABLE 2.—SUMMARY, VALUES OF K

Grip, in inches (1)	Specimen No. (2)	BOLT DIAMETER, IN INCHES ¾ (3)	 ⅞ (4)	 1 (5)
3¾	1	0.242	0.210	0.207
	2	0.292	0.196	0.247
	3	0.220	0.231	0.207
	4	0.181	0.206	0.243
2½	5	0.207	0.213	0.208
	6	0.226	0.211	0.224
	7	0.244	0.222	0.208
	8	0.247	0.219	0.196
Averages[a]		0.232	0.213	0.217

[a] Grand average of all tests = 0.221, and probable error = ±0.016

TABLE 3.—SPECIMENS FOR STATIC TESTS

Series No. (1)	Joint type (2)	THICKNESS,[a] IN INCHES t (3)	 t_i (4)	End distance[b] (5)	Tension-shear ratio (6)
S7	Lap	⅜		2	0.75
S8	Lap	½		1½	1.00
S9	Lap	⅝		1¼	1.25
S10	Lap	⅝		1½	1.25
S11	Lap	⅝		1¾	1.25
S12	Lap	⅜		2	0.75
S13	Lap	½		1½	1.00
S14	Lap	⅝		1	1.25
S15	Butt	⅜	⅞	2	0.75
S16	Butt	½	1¼	1½	1.00
S17	Butt	⅝	1½	1½	1.25

[a] Plate thickness. [b] Distance e, in inches.

STATIC TESTS

In the static tests reported in this paper, several factors and their effects on the static strength and "load-slip" relationships have been studied. These variables include (*a*) the ratio of nominal fastener shear to plate tension (shear-tension ratio), (*b*) the type of joint (riveted or bolted), (*c*) the bolt tension, and (*d*) the condition of the faying or contact surfaces.

Description of Specimens and Tests.—The specimens tested in this study were of three general types—two-fastener lap joints, three-fastener lap joints, and two-fastener, butt-type joints. The details and dimensions of the specimens of these three groups are presented in Fig. 2 and Table 3.

The specimens of the first group were lap joints connected by two fasteners in line with the direction of load application. The second group of specimens were similar to the first group except that there were three fasteners in line. The addition of this extra fastener made necessary an increase in the width of the specimen in order that the shear-tension ratios be maintained constant.

TABLE 4.—RESULTS OF STATIC TESTS OF BOLTED JOINTS

Specimen No.[a] (Fig. 2)	Maximum load, in pounds	Type of failure[b]	STRESSES AT MAXIMUM LOAD[c]		Specimen No.[a] (Fig. 2)	Maximum load, in pounds	Type of failure[b]	STRESSES AT MAXIMUM LOAD[c]	
			Tension	Shear				Tension	Shear
(1)	(2)	(3)	(4)	(5)	(1)	(2)	(3)	(4)	(5)
S7-1	58,200	T	66,100	48,400	S12-1	85,300	T	63,100	47,300
S7-2	57,500	T	65,800	47,700	S12-2	85,900	T	64,200	47,500
S7-4	58,200	T	65,400	48,400	S12-4	85,100	T	63,600	47,100
S7-5	58,700	T	65,600	48,800	S12-5	85,800	T	63,900	47,300
Average	58,150		65,720	48,320	Average	85,520		63,700	47,300
S8-1	72,800	T	61,800	60,500	S13-1	118,600	T	66,400	65,700
S8-2	73,400	T	62,200	61,000	S13-2	118,300	T	65,800	65,100
S8-4	74,000	T	62,800	61,500	S13-4	118,200	T	66,400	65,100
S8-5	75,300	T	63,800	62,500	S13-5	120,800	T	67,000	67,000
Average	73,870		62,650	61,370	Average	118,970		66,400	65,720
S9-1	83,600	ET	55,800	69,500	S14-1	149,500	T	67,200	82,700
S9-2	84,700	ET	55,600	70,400	S14-2	144,100	T	64,600	79,500
S9-4	83,700	ET	55,500	69,600	S14-4	152,400	T	68,300	84,000
S9-5	81,200	ET	54,100	76,400	S14-5	152,200	T	68,100	84,400
Average	83,300		55,250	71,470	Average	149,550		67,050	82,650
S10-1	101,000	S	67,200	84,000	S15-1	117,800	T	65,100	48,800
S10-2	103,500	S	68,800	86,000	S15-2	120,300	T	66,000	50,200
S10-3	102,800	S	68,100	85,100	S15-3	116,600	T	64,300	48,200
S10-4	102,600	S	67,900	84,900	S15-4	118,400	T	65,200	48,900
Average	102,470		68,000	85,000	Average	118,270		65,150	49,020
S11-1	102,400	S	67,800	84,800	S16-1	154,700	T	65,100	64,400
S11-2	102,000	T	67,600	84,500	S16-2	155,900	T	65,500	64,800
S11-3	98,400	S	65,200	81,500	S16-3	151,800	S	63,800	63,200
S11-4	102,300	T	67,800	84,800	S16-4	155,000	T	65,100	64,400
Average	101,270		67,350	83,900	Average	154,350		64,870	64,200
					S17-1	179,500	S	59,700	74,600
					S17-2	197,000	S	65,400	81,800
					S17-3	194,700	S	64,800	81,000
					S17-4	198,900	S	66,300	82,200
					Average	192,520		64,050	79,900

[a] Of each group of four specimens, the first and third had zero bolt tension, and the second and fourth had bolt tensions of 35,000 lb. Of each group of four specimens, the first two had dry "mill-scale" faying surfaces, and the third and fourth had lacquered surfaces. [b] The symbol S indicates shear (fastener) failure, T indicates tension (plate) failure, and ET indicates tearing out at the ends of the plates. [c] In pounds per square inch.

The third group of specimens consisted of three series of double-strap, butt-type joints connected by two fasteners in line. These specimens provided joints in which the fasteners were subjected to double shear.

One of the principal relationships studied was that between load and "slip." The slip of the joints (relative movement between the plates) was measured at successively increasing loads by means of a pair of mechanical dial gages mounted on opposite edges of the specimens. This type of measurement does not provide an exact measure of the slip at the fasteners in the joint but does provide a relative measure that can be used to compare similar specimens and to indicate, in a general way, the action of the joints.

Results of Tests.—The results of the static tests of bolted joints are presented in Table 4. This table gives the maximum load carried by the joints and the tensile, shear, and bearing stresses corresponding to this load. Col. 5 of the table indicates, by the letter symbols S, T, and ET, whether the joint failed in the fasteners (shear), in the plate by tearing across the net section (tension), or in the plate by tearing out the ends (end-tearing).

Shear-Tension Ratio.—No bolts failed in shear in the twelve tests of joints having a shear-tension ratio of 0.75; one shear failure was obtained in the twelve tests of bolted joints having a shear-tension ratio of 1.0; and ten shear failures were obtained in the sixteen tests of joints having a shear-tension ratio of 1.25. On the basis of these results, the critical shear-tension ratio is between 1.0 and 1.25; for the lap joints it appears to be approximately 1.25, whereas the value might be somewhat less than 1.25 for the butt-type joints. Consequently, the present (1953) specified[7] shear-tension ratio of 0.75 is conservative for high-strength bolted joints of the type tested in this study.

TABLE 5.—RESULTS OF STATIC TESTS OF RIVETED JOINTS

Specimen No. (1)	Contact surfaces[a] (2)	Maximum load, in lb (3)	Type of failure[b] (5)	STRESSES AT MAXIMUM LOAD	
				Tension, in lb per sq in. (5)	Shear, in lb per sq in. (6)
S7–3	MS	57,800	T	65,000	48,000
S7–6	Lq	58,400	T	65,600	48,700
S8–3	MS	65,200	S	55,600	54,200
S8–6	Lq	68,300	S	57,800	56,800
S9–3	MS	65,600	S	43,400	54,000
S9–6	Lq	69,000	S	45,900	57,300
S12–3	MS	82,500	T	61,200	45,900
S12–6	Lq	84,800	T	62,900	47,200
S13–3	MS	103,400	S	57,200	57,200
S13–6	Lq	108,700	S	60,600	60,000
S14–3	MS	103,100	S	46,100	57,200
S14–6	Lq	106,500	S	47,600	59,000

[a] Dry, "mill-scale" surfaces are indicated by MS, and lacquered surfaces by Lq. [b] A shear (fastener) failure is indicated by S, and a tension (plate) failure by T.

An increase in the shear-tension ratio for joints made with high-strength bolts would have to be accompanied by an increase in the specified safe end distance. However, for the riveted joints the end distance currently (1953) specified[7] was found entirely adequate, as indicated by the results in Table 5.

Type of Joint.—A comparison of the two-fastener lap joints, three-fastener lap joints, and two-fastener butt joints indicates that the type of joint had less effect on the strength of the joints than did the variation in the steel plate used in the various specimens. Specimens S7, S8, and S9 were fabricated on one date, the other specimens on another. A comparison (such as is found in Table 4) indicates a greater variation among the tensile strengths of the two-fastener lap joints than among the averages of the three types of joints, although the variation in strength for the two-bolt joints was small.

When only the joints fabricated from the second set of plates (series S-10 through S17) are considered, one finds that the two-fastener lap joints are slightly stronger than either the three-fastener lap joints or the two-fastener butt joints. These differences, which were apparently the result of variation in joint type, were consistent but small; the maximum difference never exceeded 7%.

---

[7] "Specifications for Iron and Steel Structures," A.R.E.A., 1953.

The greater strength of the two-bolt lap joint might be caused by the shape assumed by the test specimen during testing and the direction of loading resulting from this shape. Because of the eccentricity of load on the lap joints, each specimen deformed into a flattened S-shape during testing. This deformation rotated the direction of principal stress with respect to the original axis of the joint. As a result, the areas resisting the principal stress are slightly greater than the nominal area of the section. An examination of the bolts from those joints that failed in shear clearly illustrates this effect. Each bolt fracture occurring in the lap joints was at a slight angle with the axis of the bolt, whereas each bolt fracture in the butt joints was perpendicular to the bolt axis.

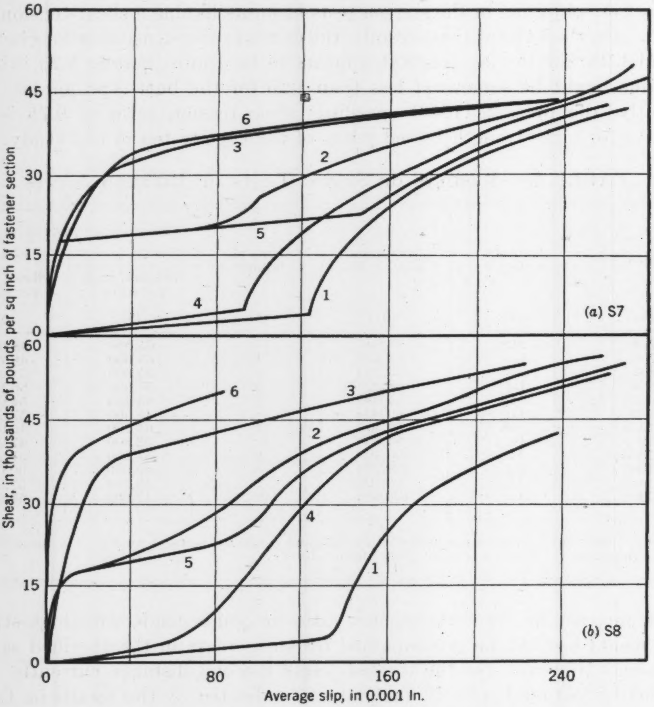

Fig. 3.—Relation Between Load and Slip (Specimen Numbers Appear on Curves)

Bolt Tension.—All the tests reported in Table 4 were conducted with the bolts tightened either "finger tight" or to an axial tension of 35,000 lb in each bolt of $\frac{7}{8}$-in. diameter. A comparison of these specimens indicates that the variation in bolt tension, the surface condition, and the shear-tension ratio did not significantly affect the ultimate strength of the joints.

In general, the bolt tension would have little effect, if any, on the ultimate strength of the joints because loads less than the ultimate load cause the plates to slip sufficiently to produce bearing on the bolts. This action also explains the fact that the contact-surface preparation had little or no effect on the ultimate strengths of the joints.

Surface Preparation.—Although the surface preparation and bolt tension had little or no effect on the ultimate strengths of either the bolted or riveted joints, they had an important effect on the load-slip characteristics of the specimens.

Load-Slip Characteristics.—One of the principal characteristics studied in this program was the relationship between the load and the distance through which the joint slipped. It was found that the condition of the contact surfaces, the type of fastener, and its tension had an important effect on the load-slip relationships, but that the type of joint (lap or butt) and the ratio of the shear stresses to the tensile stresses had little (if any) effect on this relationship.

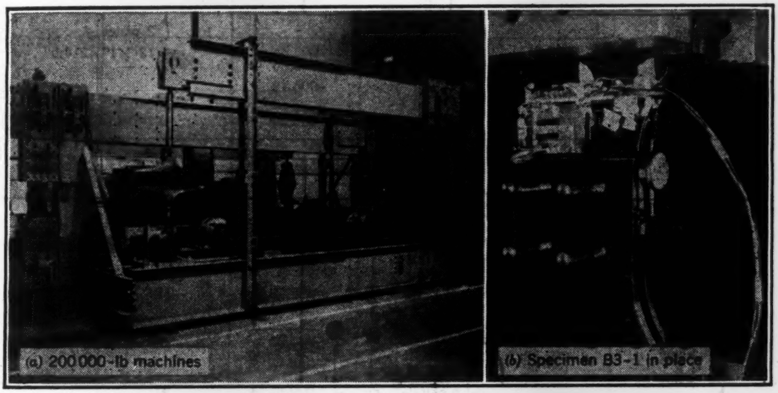
(a) 200 000-lb machines
(b) Specimen B3-1 in place

FIG. 4.—FATIGUE-TESTING APPARATUS

An example of the type of load-slip relationships obtained in these tests is presented in Fig. 3. In this illustration, specimens 1 and 4 were bolted joints in which the bolts had zero tension; specimens 2 and 5 were bolted joints having bolt tensions of 35,000 lb per bolt; and specimens 3 and 6 were riveted joints.

With the bolts finger tight, a slip sufficient to bring the bolts into bearing occurred at a small load. With the bolts tightened to a tensile force of 35,000 lb, the joints resisted an appreciable load with little or no slip by means of friction alone. When this frictional resistance was overcome, the joints slipped markedly with only a slight increase in load, until the bolts were in bearing. For increased loads the load-slip curves for the joints with zero or 35,000-lb bolt tension were quite similar.

A comparison of the load-slip curves for the riveted and bolted joints indicates that, after the joints started to slip, the riveted joints resisted a considerably greater load for a specified value of slip than did the bolted joints. However, after the rivets began to deform plastically, the joint deformation increased rapidly and soon approximated that of the bolted joint. For increased loads thereafter, because of the greater shearing strength of the bolts, the slip-values for the bolted joints were generally less than those for the riveted joints.

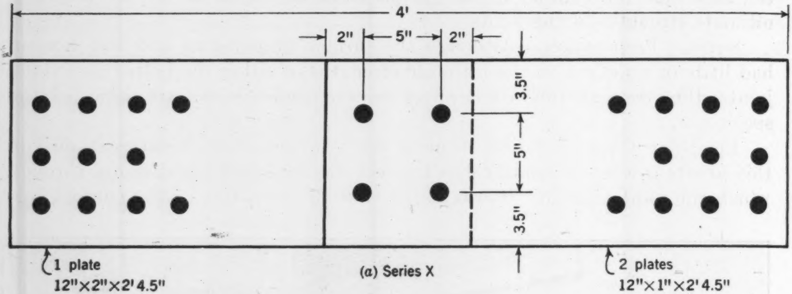
4'
2"
5"
2"
3.5"
5"
3.5"
1 plate
12"×2"×2' 4.5"
2 plates
12"×1"×2' 4.5"

(a) Series X

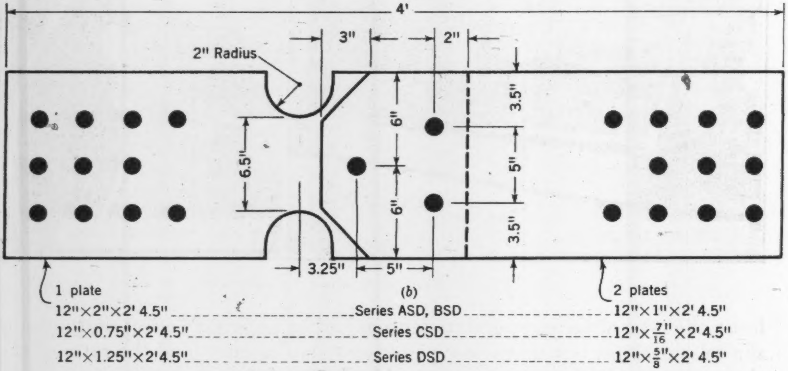
4'
3"
2"
2" Radius
3.5"
6"
6.5"
5"
6"
3.5"
3.25"
5"
1 plate
2 plates
12"×2"×2' 4.5" Series ASD, BSD 12"×1"×2' 4.5"
12"×0.75"×2' 4.5" Series CSD 12"×$\frac{7}{16}$"×2' 4.5"
12"×1.25"×2' 4.5" Series DSD 12"×$\frac{5}{8}$"×2' 4.5"

(b)

Fig. 5.—Specimens for Fatigue Tests of Bolted Structural Joints

Fatigue Tests

The second type of loading included in this program consisted of a fatigue loading that was varied systematically during the test. In these studies both the bolts and the plates were considered.

The use of high-strength bolts is based on the premise that the tension in the bolts is sufficient to transfer the forces between the members by friction and to keep the nuts from loosening. This being true, the plates of a properly functioning joint will slip little or not at all. Consequently, the shear, bearing, or bending in the bolts will be negligible. Variations in bolt stress may result from the Poisson-ratio effect; however, these variations will be small. Therefore, failure was considered unlikely in the bolts of a structural joint fastened with high-strength bolts if this joint were to be subjected to fatigue-type loadings. In addition, because the high clamping force of the bolts tends to distribute the load over a relatively large area, and because the fastener does not bear in the bolt holes, it was thought that the fatigue strength of the plates of the bolted structural joints might be greater than that of the riveted joints.

Description of Tests.—Most of the fatigue tests reported herein made use of machines, shown in Fig. 4(*a*), which are capable of testing large structural components. A specimen in place may be seen at the left end of Fig. 4(*a*). A few of the smaller lap joints were tested in 50,000-lb fatigue machines that are similar in principle to the 200,000-lb machines.

TABLE 6.—RESULTS OF TESTS MADE TO DETERMINE THE FATIGUE STRENGTH OF THE BOLTS IN BUTT-TYPE JOINTS

Specimen No.	Grip, in inches	Bolt tension,[a] in pounds per bolt	STRESS CYCLE, COMPLETE REVERSAL		Thousands of cycles
			Maximum tension and compression[b]	Maximum shear[b]	
X-3	4	45,500	6,250	19,700	4,208.9
X-5	4	65,000	7,230	27,000	3,654.2
ASD1-1	4	21,500	3,140	8,680	886.6
			3,260	9,000	2,203.4
ASD3-1	4	55,500	7,160	19,750	207.7
			8,680	24,000	215.9
			10,200	28,200	198.9
ASD2-A	4	41,500	5,850	16,100	200.9
			7,100	19,600	200.0
			7,960	21,900	200.0
			8,350	23,000	199.8
ASD3-A	4	53,500	4,610	12,700	200.6
			6,920	19,100	200.0
			8,070	22,300	206.6
			9,230	25,300	200.0
			10,400	28,700	207.0
			11,500	31,900	200.0
DSD2-A	2½	35,000	5,210	9,000	200.2
			6,210	10,700	240.8
DSD3-A	2½	50,000	9,240	15,900	204.0
			11,100	19,100	200.1
			12,950	22,300	210.6
			14,800	25,500	206.6
			16,650	28,700	8.6[c]
CSD1-A	1⅝	19,000	4,930	5,100	199.6
			6,160	6,370	200.1
			7,200	7,650	200.1[c]
CSD2-A	1⅝	34,500	9,550	9,880	200.5
			11,580	12,000	200.0
			12,920	13,350	160.7[d]
CSD3-A	1⅝	41,000	12,320	12,750	200.0
			15,400	15,900	200.1
			18,500	19,100	33.7[d]
FSD2-1	2	35,000	17,250	13,400	2,194.9
			20,600	15,600	278.8[d]
FSD3-1	2	50,000	20,600	15,800	1,656.4[d]

[a] On 1-in.-diameter bolts. [b] In pounds per square inch. [c] The joint slipped. [d] A plate failed.

Usually, the specimens were assembled before they were placed in the fatigue machines. After the specimens were placed in the machines, the bolts were tightened to the desired tensions through use of calibrated torque wrenches and elongation gages. Dial gages were then mounted on opposite edges of the specimen to indicate the relative movement between the plates of the joint. A typical joint, complete with slip-measuring dials, is shown in Fig. 4(*b*).

During one of the reversed-load fatigue tests, the eccentricity in the joint was studied. Strain gages, as shown in Fig. 4(*b*), were mounted on the edges and surfaces of the center plate of the joint. This study indicated that the eccentricity of the load in the direction of the plate thickness was approximately

0.01 in. and in the plane of the plate was 0.1 in. In view of the size of the specimen, the size of the machine, and the magnitude of the load (±70,000 lb), this eccentricity was considered to be relatively small and insignificant.

Fatigue Strength of Bolts.—One of the first questions considered in this program was the fatigue strength of the high-strength steel bolts. It was believed that the most severe condition of loading on the bolts would occur when the joints were subjected to a reversed-load stress cycle. Therefore, the plates of the first exploratory test specimens were made extra thick in order that the load on the joints might be large without producing failure in the plates. Details of the first specimens tested are shown in Fig. 5(*a*).

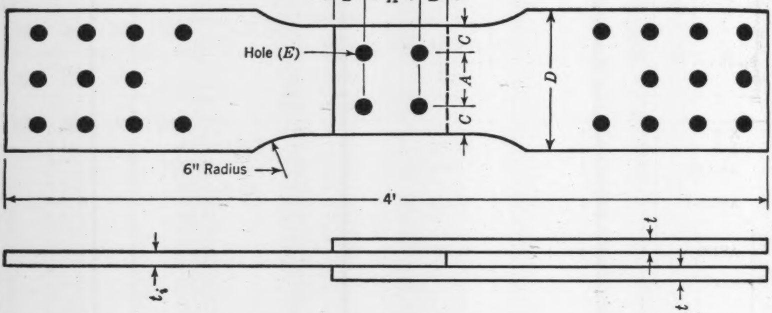

Series	Dimensions, in Inches						
	A	*B*	*C*	*D*	*E*	t_1	t_0
A	$4\frac{1}{2}$	$1\frac{3}{4}$	2	10	$1\frac{1}{16}$	$\frac{3}{4}$	$\frac{1}{2}$
B	$3\frac{1}{2}$	$1\frac{1}{2}$	$1\frac{1}{2}$	9	$\frac{15}{16}$	$\frac{3}{4}$	$\frac{1}{2}$
C	$3\frac{1}{4}$	$1\frac{1}{4}$	$1\frac{3}{8}$	9	$\frac{13}{16}$	$\frac{5}{8}$	$\frac{1}{2}$
D	$2\frac{5}{8}$	$1\frac{1}{8}$	$1\frac{3}{16}$	9	$\frac{11}{16}$	$\frac{1}{2}$	$\frac{1}{2}$
F	$3\frac{1}{2}$	$1\frac{3}{4}$	$1\frac{1}{2}$	9	$1\frac{1}{16}$	1	$\frac{3}{4}$
AG1	$4\frac{1}{2}$	$1\frac{3}{4}$	2	10	$1\frac{1}{16}$	$\frac{3}{4}$	$\frac{3}{4}$
AG2	$4\frac{1}{2}$	$1\frac{3}{4}$	2	10	$1\frac{1}{16}$	$\frac{3}{4}$	1
AG3	$4\frac{1}{2}$	$1\frac{3}{4}$	2	10	$1\frac{1}{16}$	$\frac{3}{4}$	$1\frac{1}{2}$

FIG. 6.—BOLTED FATIGUE TEST SPECIMENS

In order to put high shear loads on the bolts, it was found necessary to reduce the number of bolts to three, as shown in Fig. 5(*b*). The circular notches shown in the center plate were made to facilitate the measurement of the bolt elongation for the center bolt.

The results of the tests made to study the fatigue strength of the bolts in butt-type joints are presented in Table 6. The first specimens tested were those of series X. These specimens were tested under a constant stress cycle throughout the test, and at a nominal shearing stress as high as ±27,000 lb per sq in. on the nominal area of the bolts for a total of 3,654,200 cycles without failure.

From the few specimens tested in the X-series, it was evident that, for a shearing stress as great as ±27,000 lb per sq in., there would be no failures of the bolts providing the joint did not slip. It was observed that the frictional resistance of the joints seemed to increase during each test in spite of the fact that there was a small decrease in the bolt tension. Because of this tendency, several specimens were tested on which the load was increased after each 200,000 cycles of loading. This "coaxing" procedure was continued until the joint started to slip or until failure of the joint occurred.

By the coaxing procedure, it was possible in one test to increase the stress cycle to a shear stress of ±31,900 lb per sq in. before slip of the joint occurred without failure of the bolts. In some of the other joints as the grip was reduced the plates started to fail, or as the bolt tension was lowered the joints slipped. However, in no case was there a bolt failure during the fatigue tests. This result confirms the original assumption that, if there is no slip in the joints, there is little likelihood of failure of the high-strength bolts.

Fatigue Strengths of Plates in Bolted Butt-Type Joints.—The second phase of the fatigue study of structural joints containing high-strength bolts is concerned with the fatigue strength of the plates. In these tests, four specific factors were studied—bolt tension, bolt diameter, length of grip, and fastener type (rivets or bolts).

All the specimens of this group were of so-called "balanced" design; that is, the ratio of the shear stress in the bolts or rivets to the tensile stress in the plates was 0.75. This ratio is proper for the balanced design of a riveted joint but may be too low for a bolted joint. The details of the specimens for the tests included in this study are presented in Fig. 6. High-strength bolts with hardened steel washers were used. In planning this groups of tests, the Project Advisory Committee of the Research Council on Riveted and Bolted Structural Joints established a test cycle of ±18,000 lb per sq in. on the net section of the joint. This, it was thought, would be sufficient to produce failure. However, as may be noted in the results of the test, many of the joints withstood 2,000,000 cycles or more of load application without failure.

Bolt Tension.—The results of the tests in which the bolt tension was varied (specimen numbers A1, A2, A3, and A4) are difficult to interpret because so few of the joints failed, in spite of the large load cycle applied. A summary of the results of these tests is presented in the upper part of Table 7. As shown in Col. 5 of this table, the axial bolt tensions in the bolts of 1-in. diameter were varied between 50% and 138% of the specified elastic proof load. The maximum value was chosen because it is approximately the maximum axial tension that may be developed in the bolts. To produce this high tension, it was necessary to tighten the nuts until the stress in the bolts had considerably exceeded the yield point of the material.

In those instances in which failure was obtained, the fatigue strength corresponding to failure at 2,000,000 cycles was computed from the following expression:

$$F = \frac{S\,N^k}{2{,}000{,}000^k} \qquad (2)$$

in which F is the stress producing failure at 2,000,000 cycles, S is the stress applied to the specimen, N is the number of cycles required for failure at stress S, and k is an experimental constant. A value of k equal to 0.10, as suggested by Mr. Wilson,[4] was used.

When one considers the results of the specimens that failed in the joint, the fatigue strength seems to vary with the bolt tension. However, it is somewhat difficult to distinguish whether this variation in fatigue strength is a result of the variation in bolt tension, or whether the larger slip that usually accompanied the lower bolt tension is the factor that caused the reduction in fatigue strength. Because a decreasing of the bolt tension and an increasing of the slip in the joint usually coincide, the effects of these two variables probably cannot be separated from one another. Nevertheless, for the higher bolt tensions the fatigue strength of failure at 2,000,000 cycles is close to ±20,000 lb per sq in.

TABLE 7.—Effects of Variation in Bolt Tension, Bolt Diameter, and Grip on the Fatigue Strength of Bolted Butt-Type Joints

Specimen No.	Grip, in inches	Bolt diameter, in inches	Bolt Tension		Plate Thickness, in Inches		Fatigue Test		Fatigue strength[d] F
			Force[a]	%EPL[b]	Inside	Outside	Stress cycle[c]	Cycles × 10⁻³	
(1)	(2)	(3)	(4)	(5)	(6)	(7)	(8)	(9)	(10)
A1-1	1¾	1	23,600	50	¾	½	±18,000	924.6	16,700
A1-2								1,499.7	17,500
A1-3								1,469.8	17,450
A2-1	1¾	1	35,400	75	¾	½	±18,000	1,952.4	17,900
A2-2								1,406.4	17,400
A2-3								2,067.1	...
A3-1	1¾	1	47,200	100	¾	½	±18,000	2,046.1	...
A3-2								2,135.8	...
A3-3								2,205.5	...
FSD3-1	2	1	50,000	106	1	½	±20,600	1,656.4	20,200
A4-1	1¾	1	65,000	138	¾	½	±18,000	2,024.5	...
A4-2								2,036.1	...
A4-3								2,029.9	...
B3-1	1¾	⅞	36,000	100	¾	½	±20,000	2,126.7	...
B3-2							±20,000	434.8[e]	
B3-3							±18,000	1,960.3[e]	
B3-4							±20,000	2,068.3	...
B3-5							±18,000	3,883.6	...
C3-1	1⅜	¾	23,700	83.5	⅝	⅜	±18,000	517.4	15,700[f]
C3-2			25,100	88.5			±18,000	2,108.8	18,000+
C3-3			25,500	90			±18,000	1,998.2	18,000
D3-1	1¼	⅝	19,200	100	½	⅜	±18,000	2,083.5	...
D3-2								2,100.0	...
D3-3								5,538.5[g]	18,000+
AG1-1	2¼	1	47,200	100	¾	¾	±18,000	2,236.1[g]	18,000+
AG1-2								3,090.1	...
AG1-3								2,000.5	...
AG2-1	2¾	1	47,200	100	¾	1	±18,000	2,038.3	...
AG2-2								1,619.1[g]	17,600
AG2-3								2,018.5	...
AG3-1	3¾	1	47,200	100	¾	1½	±18,000	2,054.4	...
AG3-2			47,200					2,065.5	...
AG3-3			42,500[h]					817.1[g]	16,450

[a] In pounds per bolt. [b] Percent of the specified elastic proof load. [c] In pounds per square inch. [d] For failure at 2,000,000 cycles in pounds per square inch, from Eq. 2. Three dots indicate that the specimen did not fail. [e] Failed in head. [f] Specimen slipped excessively. After failure, oil was found between the plates. [g] Failed in plate. [h] Bolt tension was accidentally reduced.

This series of tests also provides some further information concerning the fatigue strength of the high-strength bolts. The bolts in specimens A4-1, A4-2, and A4-3 did not fail in more than 2,000,000 cycles of loading, even though they had been elongated approximately 0.02 in. in a grip length of 1¾ in.—an elongation that was due to considerable yielding in the bolts.

Bolt Diameter.—The studies of the effects of bolt-diameter variation (specimen numbers A3, B3, C3, and D3) were conducted using specimens for which the bolt diameter was varied from $\frac{5}{8}$ in. to 1 in. In general, the stress cycles in this study were ±18,000 lb per sq in. However, in three cases a stress cycle of ±20,000 lb per sq in. was used.

Of the specimens reported in Table 7, only three having bolt tensions of approximately 100% of the specified elastic proof load failed in the joint. These three specimens, however, were fabricated with the $\frac{3}{4}$-in.-diameter bolts which, as was previously noted, did not quite meet the specifications then (1949) recommended. In any case, it may be concluded that the fatigue strength of similar joints for failure at 2,000,000 cycles, providing that the joint does not slip and that the bolts meet the specifications, will be at least as great as 18,000 lb per sq in. for a completely reversed stress cycle. Because the range of bolt sizes includes the bolt diameters most commonly used in structural practice, this conclusion is of considerable importance.

TABLE 8.—RELATIVE FATIGUE STRENGTH OF BOLTED AND RIVETED BUTT–TYPE JOINTS[a]

Specimen No. (1)	Fastener[b] (2)	Bolt tension[c] (3)	FATIGUE TEST		SLIP PER CYCLE, IN 0.001 IN.		Remarks (8)
			Stress cycle[d] (4)	Thousands of cycles (5)	Start (6)	Finish (7)	
B3-1	Bolts	36,000	±20,000	2,126.7	0.3	0.2	Did not fail
B3-2	Bolts	36,000	±20,000	434.8	0.4	0.1	Failed in head
B3-3	Bolts	36,000	±18,000	1,960.3	0.0	0.1	Failed in head
B3-4	Bolts	36,000	±20,000	2,068.3	0.2	0.3	Did not fail
B3-5	Bolts	36,000	±18,000	3,883.6	0.2	0.2	Did not fail
B3R-1	Rivets	....	±18,000	713.5	8.5	4.0	Failed, $F_{2,000,000}$ = 16,000
B3R-2	Rivets	....	±18,000	577.8	3.6	3.3	Failed, $F_{2,000,000}$ = 15,900
B3R-3	Rivets	....	±18,000	93.2	15.0	156	Test stopped, excessive slip

[a] All joints had a shear ratio of 0.72 and a grip of $1\frac{3}{4}$ in. [b] All fasteners, bolts and rivets, were of $\frac{7}{8}$-in. nominal diameter. [c] In pounds per bolt. [d] In pounds per square inch.

Grip.—The third factor considered in this study was the effect of the grip (which was varied between $1\frac{3}{4}$ in. and $3\frac{3}{4}$ in.) on the fatigue strength of joints fabricated with high-strength bolts of 1-in. diameter and tested using a stress cycle of ±18,000 lb per sq in. The results of these tests are summarized in Table 7 (specimen numbers A3, AG1, AG2, and AG3).

In view of the three failures obtained in the tests of specimens of series AG' it may be concluded that, in general, the fatigue strength of these specimens is approximately equal to ±18,000 lb per sq in. for failure at 2,000,000 cycles, regardless of the grip.

Relative Strength of Riveted and Bolted Joints.—Three riveted joints of the same dimensions as the specimens of series B shown in Fig. 6 were tested for comparison with the tests on the bolted joints of series B. A summary of the results of these tests is presented in Table 8.

The riveted joints were tested using a stress cycle of ±18,000 lb per sq in.; two of the bolted joints were tested using this same stress cycle, and three were tested using a stress cycle of ±20,000 lb per sq in.

Two of the bolted joints (one at ±18,000 lb per sq in. and one at ±20,000 lb per sq in.) failed in the grip or head end of the specimen but not in the joint. All of the remaining bolted joints, however, withstood between 2,000,000 and 3,000,000 cycles of load application without failure. Thus, the fatigue strength for failure at 2,000,000 cycles appears to be at least equal to 20,000 lb per sq in. in full reversal of stress for the bolted joints.

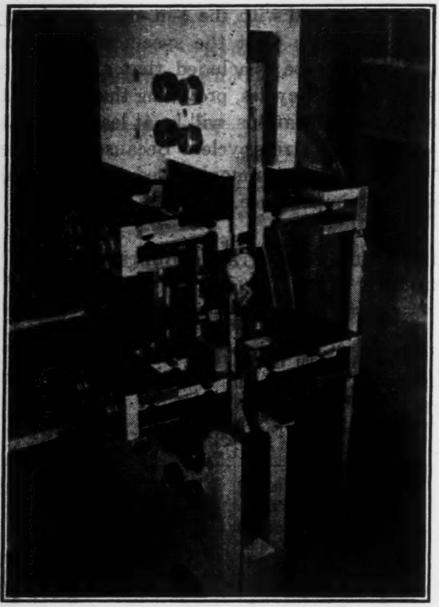

FIG. 7.—SWAY BRACING

The results of the tests on riveted joints were quite different from those on bolted joints. Specimens B3R-1 and B3R-2, each subjected to repeated-stress cycles of ±18,000 lb per sq in., failed after 713,000 and 577,800 cycles, respectively. This is equivalent to a fatigue strength at 2,000,000 cycles of approximately ±16,000 lb per sq in. The third riveted joint, specimen B3R-3, was also subjected to a stress of ±18,000 lb per sq in. However, after 93,000 cycles of load application it was necessary to stop the test because the joint was slipping excessively.

Based on the results of these tests it appears that the riveted joints had a fatigue strength of 16,000 lb per sq in. or less, whereas a similar bolted joint (using high-strength bolts with a bolt tension equal to the elastic proof load) had a fatigue strength greater than 20,000 lb per sq in. This difference indicates that the bolted joints were about 25% stronger in fatigue than were the similar riveted joints.

The relative slip of the riveted and bolted joints is also of interest. The bolted joints exhibited negligible slip at both the start and finish of the fatigue tests. In the case of the riveted joints a considerable slip in the joint was noted at the start of the test. This slip increased rapidly during one of the tests and decreased somewhat during the other tests.

The results observed for specimen B3R-3 are somewhat similar to observations that have been made in the field. In this test, as sometimes occurs in service, the rivets worked loose under repeated loading. This is a type of loading for which bolts of high strength are ideally suited. Although the test results and experience indicate that the bolts will probably not work loose, they may be retightened if necessary; however, if rivets become loose they must be removed and redriven.

Fatigue Tests of Lap Joints

Lap joints are used frequently in engineering structures but have not commonly been tested in fatigue because of the many problems encountered in testing such joints. The principal difficulty results from the eccentricity of loading in lap joints. This difficulty was evident in the writers' preliminary tests of single lap-joint specimens.

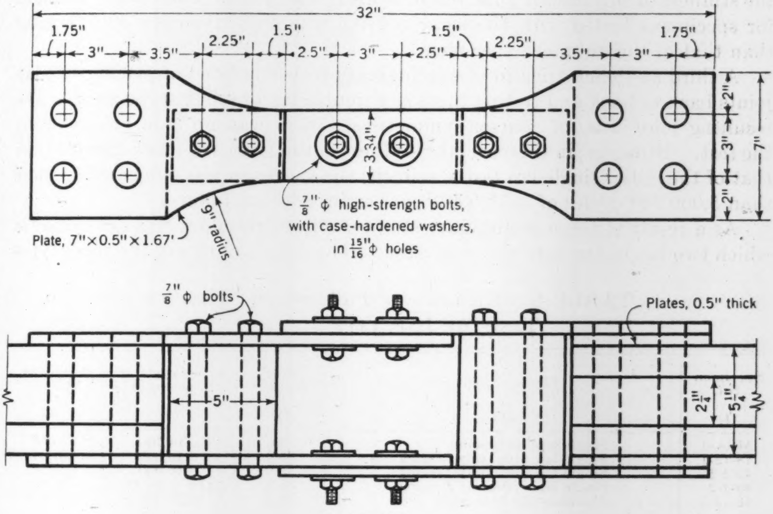
32"
1.75"
3"
3.5"
2.25"
1.5"
2.5"
3"
2.5"
1.5"
2.25"
3.5"
3"
1.75"
2"
3"
7"
2"
3.34"
$\frac{7}{8}$" ϕ high-strength bolts, with case-hardened washers, in $\frac{15}{16}$" ϕ holes
9" radius
Plate, 7"×0.5"×1.67'
$\frac{7}{8}$" ϕ bolts
Plates, 0.5" thick
5"
$2\frac{1}{4}$"
$5\frac{1}{4}$"

(a) Type AMS

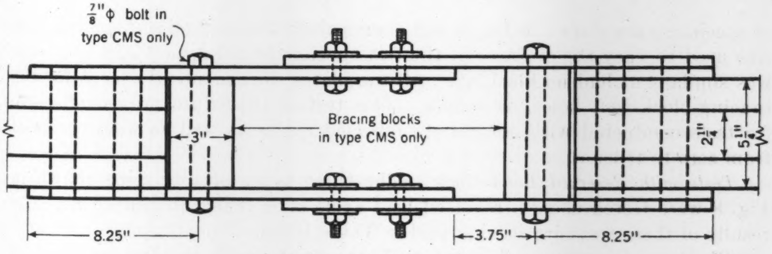
$\frac{7}{8}$" ϕ bolt in type CMS only
Bracing blocks in type CMS only
3"
$2\frac{1}{4}$"
$5\frac{1}{4}$"
8.25"
3.75"
8.25"

(b) Type BMS and type CMS

Fig. 8.—Fatigue Test Specimens

Preliminary Tests.—The results of the preliminary tests of two-bolt, lap-type specimens are presented in Table 9. The first of these specimens, MSA-3, was tested at a stress of ±14,400 lb per sq. in. Failure resulted after 126,600 cycles—a surprisingly small number of cycles.

The next step in the preliminary tests was to provide a system of sway bracing for the lap joints to reduce the side sway of the specimen that resulted from the eccentricity of loading. Fig. 7 shows this bracing, in the 50,000-lb-capacity fatigue-testing machine. Although this bracing eliminated most of the lateral motion of the specimen during the test, the practical significance of the stiffness of this braced joint was difficult to interpret. The fatigue strength for specimens tested with the sway bracing was approximately 50% greater than that of the unbraced specimen.

A third approach tried in the preliminary tests consisted of placing two lap joints back to back and testing them as a double lap or a butt-type joint. The resulting joint was, of course, symmetrical; there was no side sway during the test. However, in this case, the stiffness of the joint was much greater than that of the initial single lap test specimen; the specimen was subjected to more than 5,000,000 cycles of ±16,000 lb per sq in. without failure.

As a result of these preliminary studies, a test procedure was developed in which two lap joints were tested in pairs. The details of two of the three types of specimens are shown in Fig. 8 and demonstrate the method of blocking that was used to vary the stiffness of the test specimens; the type CMS specimen was similar but had no blocking. All the plates were identical except for the bracing-block bolt holes, as shown. This testing procedure proved effective for tests conducted with completely reversed cycles as well as with cycles of from zero to tension.

TABLE 9.—RESULTS OF PRELIMINARY FATIGUE TESTS OF LAP–TYPE JOINTS[a] [b]

Specimen No. (1)	Type of joint (2)	Bolt tension[c] (3)	Stress cycle, in lb per sq in. (4)	Cycles to failure[d] (5)
MSA-3	Single lap, no bracing	35.0	±14,400	126.6
48-12-1	Single lap with sway bracing	35.0	±16,000	1,376.1
49-1-1	Single lap with sway bracing	35.0	±16,000	1,310.0
49-1-2	Single lap with sway bracing	35.0	0 to +24,000	3,078.0
48-12-2	Double-strap butt joint	35.0	±16,000	5,567.0[e]

[a] All joints had shear ratios of unity. [b] All bolts were ⅞ in. in diameter. [c] In kips per bolt. [d] In thousands of cycles. [e] Specimen did not fail.

Tests with Reserved Load Cycle.—The three types of specimens shown in Fig. 8 were tested using a reversed load cycle of ±16,000 lb per sq in. The results of these tests are summarized in Table 10(*a*).

The type C specimens—those with the least restraint—had an average fatigue strength, for failure at 2,000,000 cycles, of approximately 11,400 lb per sq in. This value is not much greater than that obtained for the single-lap-joint specimen in the preliminary tests. The type BMS and AMS specimens, however, had fatigue strengths of 14,000 lb per sq in. and 15,000 lb per sq in., respectively. This increase indicates that the flexibility of the specimens had an important effect on the fatigue strength of the joints.

Slip was measured during these fatigue tests; the slip per cycle was usually less than 0.002 in. at the start of the tests and less than 0.001 in. at the end of

TABLE 10.—FATIGUE STRENGTH OF BOLTED LAP-TYPE JOINTS[a]

Test description (1)	Specimen No. (2)	Stress cycle, in pounds per square inch (3)	Thousands of cycles, to produce failure (4)	$F_{2,000,000}$ (5)	Total cumulative slip, in inches (6)
(*a*) Completely Reversed Load Cycle	AMS-9	±16,000	948.3	14,800	−0.0007
	AMS-12	±16,000	948.3	14,800	+0.0015
	AMS-13	±16,000	983.7	14,900	+0.0012
	AMS-11	±16,000	1,406.6	15,400	+0.0017
	AMS-14	±16,000	1,329.3	15,300	+0.0020
	Average			15,000	+0.0011
	BMS-11	±16,000	524.4	14,000	+0.0008
	BMS-9	±16,000	524.4	14,000	+0.0005
	BMS-14	±16,000	407.1	13,600	−0.0021
	BMS-16	±16,000	447.6	13,800	−0.0014
	BMS-10	±16,000	764.8	14,500	−0.0005
	Average			14,000	−0.0012
	CMS-10	±16,000	137.5	12,200	...
	CMS-12	±16,000	137.5	12,200	...
	CMS-13	±16,000	4.3	8,600	...
	CMS-9	±16,000	152.9	12,400	...
	CMS-16	±16,000	89.2	11,700	...
	Average			11,400	
(*b*) Zero-to-Tension Load Cycle	AMS-4	+24,000	866.5	22,100	0.0040
	AMS-7	+24,000	823.6	22,100	0.0064
	AMS-6	+24,000	1,095.4	22,600	0.0131
	AMS-5	+24,000	1,095.4	22,600	0.0131
	AMS-2	+24,000	1,143.8	22,700	0.0037
	Average			22,400	0.0081
	BMS-1	+24,000	1,660.3	23,600	0.0085
	BMS-7	+24,000	785.9	21,900	0.0019
	BMS-6	+24,000	785.9	21,900	0.0066
	BMS-3	+24,000	1,687.7	23,600	0.0092
	BMS-5	+24,000	2,005.0	24,000	...
	Average			23,000	0.0065
	CMS-4	+19,750	2,708.2	20,400	0.0036
	CMS-8	+24,000	1,046.3	22,500	0.0006
	CMS-5	+24,000	1,183.4	22,800	...
	CMS-6	+24,000	1,090.5	22,600	0.0004
	CMS-18	+24,000	495.1	20,900	...
	Average			21,800	0.0015

[a] All joints had a tension-shear ratio of unity. All bolts were ⅞ in. in diameter.

the tests. As noted in Col. 6 of Table 10, the largest slip accumulated during the tests was 0.0021 in., a value far less than the slip required to bring the bolts into bearing. Because the tests were started with the bolts presumably in the center of the bolt holes, the entire load on the joint was evidently carried by the friction between the plates.

Tests on a Zero-to-Tension Load Cycle.—Five lap joints of each of the three types described herein were subjected to a stress cycle of from zero to tension. The results of these tests are presented in Table 10(*b*). The maximum tensile stress was 24,000 lb per sq in. for all these specimens except CMS-4, for which the maximum stress was only 19,750 lb per sq in.

Comparing the fatigue strengths corresponding to failure at 2,000,000 cycles, one finds that the variation in blocking or in stiffness had no significant effect on the fatigue strength of the specimens listed in Table 10(*b*). This result is contrary to that obtained in the case of the tests conducted using a reversed load cycle in which the stiffness of the specimen had a considerable effect on the fatigue strength of the joints.

The fatigue strengths determined in the tests of the lap-joint specimens are less than those determined in the tests of the butt-type joints. This result is exactly the reverse of the results of static tests, in which the lap joints were found to have a slightly greater strength than the butt-type joints.

Summary of Results, and Conclusions

Static Tests.—Three conclusions may be drawn from the results of the reported tests:

1. The bolt tension seems to have little effect on the ultimate strength of bolted joints. However, the load-slip characteristics of the joints are greatly affected by the axial tension in the bolts. In general, when the bolt tension is at least 85% of the elastic proof load in joints where rivets are replaced by bolts, slip does not occur until stresses in the plates become nearly equal to or slightly greater than normal working stresses.
2. Tests of two-bolt and three-bolt lap joints and two-bolt butt joints indicate that the type of joint has little effect on the ultimate strength.
3. The ultimate tensile strengths determined in the static tests indicate that the permissible shearing stress might be increased to a value approximately 1.25 times the permissible tensile stress in order to obtain a balanced design. However, it will also be necessary to increase the minimum safe end distance now permitted for such joints. Furthermore, slip may occur at loads smaller than normal working loads unless special efforts are made to prevent slip.

Fatigue Tests.—In summary, these tests indicated the following:

1. In no case was there a fatigue failure of the high-strength bolts in the joints, providing there was no slip in the joints during the application of load. This conclusion is true in spite of the fact that the joints were designed so as to subject the bolts to unusually severe loading conditions.
2. It is essential that the bolts be tight, in accordance with the present specifications, to obtain the greatest benefits from the use of high-strength bolts.
3. Tests of duplicate specimens fabricated with rivets and bolts demonstrate that the fatigue strength of bolted joints, properly assembled, is approximately 25% greater than that of similar riveted joints.

These laboratory tests indicate extremely promising results for structural joints made with high-strength bolts under both static and fatigue loadings.

Acknowledgment

The tests described herein constitute a part of a program in the Engineering Experiment Station of the University of Illinois at Urbana sponsored by the Illinois Division of Highways, the Bureau of Public Roads, United States Department of Commerce, and the Research Council on Riveted and Bolted Structural Joints. The tests were conducted using the testing machines of the University of Illinois.

These laboratory studies were conducted by D. T. Wright, M. A. Cayci, F. W. Schutz, Jr., J.M. ASCE, and H. L. Cox, research assistants in civil engineering in the Structural Research Laboratory of the university.

DISCUSSION

A. J. Francis.[8]—In referring to earlier research on the subject of bolted joints it is somewhat surprising that the authors of this interesting paper did not mention the extensive work on mild steel and high-strength steel bolts and bolted joints described in the second and final reports of the Steel Structures Research Committee.[9,10] This work demonstrated for the first time the feasibility of using high-strength bolts, tightened to controlled torques, in steel frame construction.

The writer would be slightly cautious in forming general conclusions on the basis of a somewhat restricted series of tests. A large joint with many bolts may behave quite differently from a one-bolt or two-bolt joint, under either static loading or fatigue loading. The static strength of large joints failing in the rivets or bolts can be considerably less than the aggregate strength of the individual fasteners, as was first demonstrated by tests carried out for the Oakland Bay Bridge (California).[11] It has since been shown, in studies of aluminum-alloy riveted joints,[12] that the reduction in strength depends mainly on the relative ductilities of the material of the fasteners and of the plates or members connected together, the length of the joint, and the number of transverse rows of fasteners. The longer a joint is and the less ductile the fasteners are, the greater will be the loss in shearing strength. One may consider the problem of connecting a member of given material and dimensions to another part of a structure. If high-strength bolting is used, the joint will be shorter and have fewer fasteners than if mild-steel riveting were used. However, the bolts deform less before failure than would rivets; that is, they are less ductile. The two factors of length and ductility have opposite effects on joint strength, and it is not clear without a detailed investigation whether rivets or bolts are more efficient in a particular case. Such an investigation can be made if load-deformation curves for fastener deformation and for sections of connected members between successive rows of fasteners are available. If, as appears likely, strength bolting is to be used in the large joints of truss bridges, extension in this direction of the work described in the paper would seem to be not only desirable but imperative.

The writer does not understand the attitude of the authors to the shear-tension ratio (the ratio of bolt shearing stress to plate tensile stress, mentioned in conclusion 3 under the heading, "Summary of Results, and Conclusions: Static Tests"). Surely in a balanced design this ratio would vary depending on the relative strengths of the bolt material and the plate material, so long as the usual assumptions of conventional design remained applicable.

---

[8] Prof. of Civ. Eng., The Univ. of Melbourne, Melbourne, Australia.

[9] "Investigations on Bolts and Bolted Joints, with Brief Suggestions for the Use of Black Bolts Under Controlled Torque in Steel Frame Construction," by C. Batho and E. H. Bateman, *Second Report*, Steel Structures Research Committee, Her Majesty's Stationery Office, London, England, 1934, p. 138.

[10] "Further Investigations on Bolts and Bolted Joints," by C. Batho and E. H. Bateman, *Third Report*, Steel Structures Research Committee, Her Majesty's Stationery Office, London, England, 1936, p. 394.

[11] "Tension Tests of Large Riveted Joints," by R. E. Davis, G. B. Woodruff, and H. E. Davis, *Transactions*, ASCE, Vol. 105, 1940, p. 1193.

[12] "The Behaviour of Aluminium Alloy Riveted Joints," by A. J. Francis, *Research Report No. 15*, The Aluminium Development Association, London, England, 1953.

Conclusion 3 (under the heading, "Summary of Results, and Conclusions: Fatigue Tests") is hardly justifiable on the basis of tests of three riveted specimens. It would seem safer merely to say that the results suggest that bolted joints of the type tested have a greater fatigue strength than that of similar riveted joints. Even then there is some doubt as to the accuracy of the conclusion because the riveted and bolted joints were of the same dimensions and therefore were not designed to be equally efficient in tension, shear, and bearing.

William H. Munse,[13] A. M. ASCE, D. T. Wright,[14] and Nathan M. Newmark,[15] M. ASCE.—The writers wish to express their appreciation to Mr. Francis for his discussion. Because this paper was part of a symposium the authors did not review the voluminous previous literature, several references to which are given by Mr. Francis. In the opinion of the writers the major impetus toward the use of high-strength bolts in structural connections came from Mr. Wilson's work at the University of Illinois.

Although several pertinent questions have been raised by Mr. Francis, a review of the various papers in this symposium and the perusal of some of the references noted by the writers will show that there is no need for the concern he has expressed. It will be found that since 1947 there has been accumulated a large amount of laboratory and field information concerning the behavior of structural connections that have been assembled with A 325 bolts and hardened washers in accordance with recommended practice.

Bolted connections in A 7 steel assembled in accordance with present specifications contain the same number of A 325 bolts as a similar joint assembled with A 141 rivets—not a smaller number as suggested by Mr. Francis, in spite of the fact that the bolts are nearly twice as strong as the rivets. Even in large long joints it has been found that a high-strength bolted joint is at least as strong as a similar riveted joint whether subjected to static or repeated loads. At a later time it may be desirable to consider the use of greater working stresses for the bolts, but—as noted by the writers—this use might produce connections in which slip would occur at stresses below the working stresses unless special precautions were taken to prevent this slip.

All the studies reported by the writers were conducted on ASTM A 7 steel specimens fastened with ASTM A 325 bolts. Consequently, the statements concerning balanced design were based on the use of these two materials. The use of materials of other strengths, as noted by Mr. Francis, would certainly require a re-evaluation of the shear-tension ratio for balanced design if such a balance were desired. It is important, however, to realize that the behavior of a bolted connection depends on the proportions of the connection and therefore on the shear-tension ratio. For this reason, the selection of design stresses for such connections must be made only after the behavior and the variables affecting this behavior are understood.

Although only three riveted specimens were used in the comparisons of fatigue strengths presented in the paper, it was found that the resistance of these members to repeated loads was typical of the results obtained on many other riveted members. Reference to the voluminous literature on fatigue tests justifies the conclusions that were drawn concerning the superiority of bolted joints subjected to repeated loads. During the fatigue tests of the bolted connections, other observations were made which further demonstrated the superiority of bolted joints, but it was feasible to present only a brief summary in the paper. Nevertheless, all the laboratory studies on connections assembled with A 325 bolts that have been conducted to date by the writers and by other investigators have demonstrated that this method of fabrication produces sound and efficient structures.

---

[13] Research Associate Prof. of Civ. Eng., Univ. of Illinois, Urbana, Ill.

[14] Lecturer in Civ. Eng., Queens College, Ontario, Ont., Canada.

[15] Research Prof. of Structural Eng., Univ. of Illinois, Urbana, Ill.

COMPARISON OF BOLTED AND RIVETED JOINTS

By Frank Baron,[1] M. ASCE, and Edward W. Larson, Jr.,[2] J. M. ASCE

Synopsis

A comparison is made of the behavior of bolted joints and riveted joints subjected to static and fatigue loads. The comparison is based on tests of butt joints having a tension: shear: bearing stress relationship of approximately 1.00:0.75:1.50. The fasteners were hot-driven rivets, cold-driven rivets, and high-strength bolts. Several lengths of grip were considered for each type of fastener. Also considered was a group of butt joints fastened with high-strength rivets and having a tension: shear: bearing relationship of 1.00: 1.26:1.83.

The clamping force of a fastener was one of the most important factors affecting the fatigue strength of a joint. The fatigue strengths of the bolted joints were greater than those of the riveted joints. For static loads, the plate efficiencies were approximately the same, irrespective of the kind of fastener. Efficiencies greater than 80% were realized.

Introduction

The introduction of various kinds of fasteners, high-strength structural steels, and changes in fabrication procedures has raised questions concerning the comparative behavior of riveted joints and bolted joints when subjected to static loads and fatigue loads. Ordinary structural steel rivets (ASTM-A 141)[3] are the most common fasteners used for connecting structural steel members. The use of high-strength structural steels sometimes warrants the use of high-strength rivets. The substitution of high-strength rivets (ASTM-A 195)[4] for ordinary rivets permits a reduction in the number of rivets required in a joint or splice. The ASTM-A 195 rivet has a high strength, but it is frequently difficult to drive because of a low ductility. For ordinary lengths of grip, the high-strength rivet usually has less clamping force than the ordinary steel rivet. Consequently, joints fastened with high-strength rivets may have objectionable slippages and low fatigue strengths.

Driving rivets without heating (cold-driving) has become a standard shop practice with several large fabricators. Frequently, cold-driving makes possible economies in costs and in fabrication time. Cold-driven rivets are

---

Note.—Presented at the Centenniel Convocation, Chicago, Ill., September, 1952. Published essentially as printed here, in August, 1954, as *Proceedings-Separate No. 470.* Positions and titles given are those in effect when the paper was received for publication.

[1] Prof. of Civ. Eng., Northwestern Univ., Evanston, Ill.

[2] Research Associate in Civ. Eng., Northwestern Univ., Evanston, Ill.

[3] "Tentative Specification for Structural Rivet Steel (A 141-52 T)," Book of Standards, A.S.T.M., Pt. 1, 1952, p. 562.

[4] "Tentative Specification for High-Strength Structural Rivet Steel (A 195-52 T)," Book of Standards, A.S.T.M., Pt. 1, 1952, p. 564.

known to have low values of clamping force but are expected to have a good degree of hole-filling. Consequently, the static and fatigue properties of joints fastened with cold-driven rivets may be appreciably different from those of joints with hot-driven rivets.

A procedure commonly used during erection consists of initially bolting together an entire structure or part of a structure and replacing the bolts with rivets. Many engineers have thought that high-strength bolts, tightened to a high initial tension, could be used for a final assembly as well as for the initial assembly of a structure. However, other engineers have believed that bolts would loosen in service, and that the loosening could cause objectionable movements and a decrease in the fatigue strengths of the members.

When the Research Council on Riveted and Bolted Structural Joints (referred to herein as the Research Council) was formed, little was known concerning the properties of joints fastened with cold-driven rivets or with high-strength bolts. The literature dealt principally with the behavior of joints fastened with hot-driven rivets. This literature was extensive and is reviewed in the bibliography prepared by A. E. R. de Jonge,[5] M. ASCE. In 1838, William Fairbairn[6] reported the results of an extensive series of tests of riveted joints. Since then, many investigators have interested themselves in the behavior of riveted joints subjected to static loads. In 1938, W. M. Wilson, Hon. M. ASCE, and F. P. Thomas[7] reported the results of fatigue tests made in connection with the construction of the San Francisco-Oakland Bay Bridge (California). In connection with the same structure, a series of static tension tests of riveted joints was conducted[8] by Raymond E. Davis, M. ASCE, Glenn B. Woodruff, M. ASCE, and Harmer E. Davis, A. M. ASCE. The variables considered in the latter series of tests were: The length and type of joint, the kind of plate steel, the kind of rivet steel, and the rivet pattern. Hot-driven rivets made of carbon steel and of manganese steel were used in fabricating the joints. The behavior in static tension of riveted joints fastened with high-strength rivets was reported in 1942 by Jonathan Jones,[9] Hon. M. ASCE. In 1949, Kenneth H. Lenzen,[10] A. M. ASCE, reported the results of an investigation limited to a comparison of the fatigue strengths of riveted and bolted structural joints having a grip of about 1½ in. At this grip, the fatigue strengths of bolted joints subjected to reversed cycles of loading exceeded those of riveted joints.

In 1947, a project committee of the Research Council was assigned the task of determining the effect of variation in grip on the fatigue strength of riveted and bolted structural joints. Double-butt joints having a tension: shear: bear-

---

[5] "Riveted Joints: A Critical Review of the Literature Covering Their Development, with Bibliography and Abstracts of the Most Important Articles," by A. E. R. de Jonge, ASME, 1945.

[6] "Experimental Inquiry into the Strength of Wrought Iron Plates and Their Riveted Joints as Applied to Ship Building and Vessels Exposed to Severe Strains," by William Fairbairn, *The Philosophical Transactions*, Royal Soc. of London, Vol. 140, 1850, p. 677.

[7] "Fatigue Tests of Riveted Joints," by W. M. Wilson and F. P. Thomas, *Bulletin No. 302*, Eng. Experiment Station, Univ. of Illinois, Urbana, Ill., May 31, 1938.

[8] "Tension Tests of Large Riveted Joints," by Raymond E. Davis, Glenn B. Woodruff, and Harmer E. Davis, *Transactions*, ASCE, Vol. 105, 1940, p. 1193.

[9] "Physical Properties of Driven and Undriven Rivets of High-Strength Structural Steels: Progress Report of the Committee of the Structural Division on Structural Alloys," *Proceedings*, ASCE, May, 1942, pp. 751–773.

[10] "The Effect of Various Fasteners on the Fatigue Strength of a Structural Joint," by Kenneth H. Lenzen, *Bulletin No. 480*, A.R.E.A., Vol. 51, June–July, 1949.

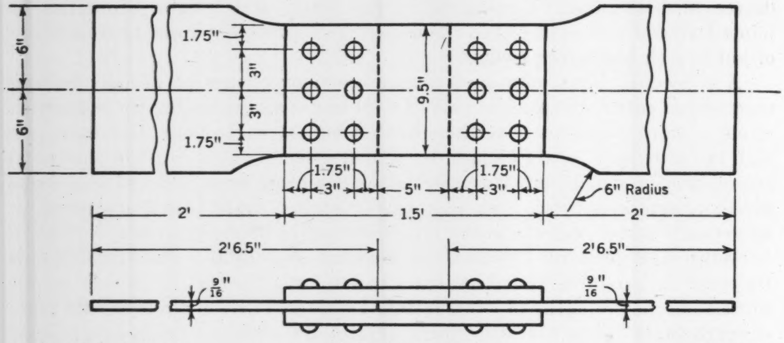
6"
6"
1.75"
3"
3"
1.75"
9.5"
1.75"
3"
5"
1.75"
3"
6" Radius
2'
1.5'
2'
2'6.5"
2'6.5"
9/16"
9/16"

Edge condition – machined

(*a*) Series A and B

Drilled holes

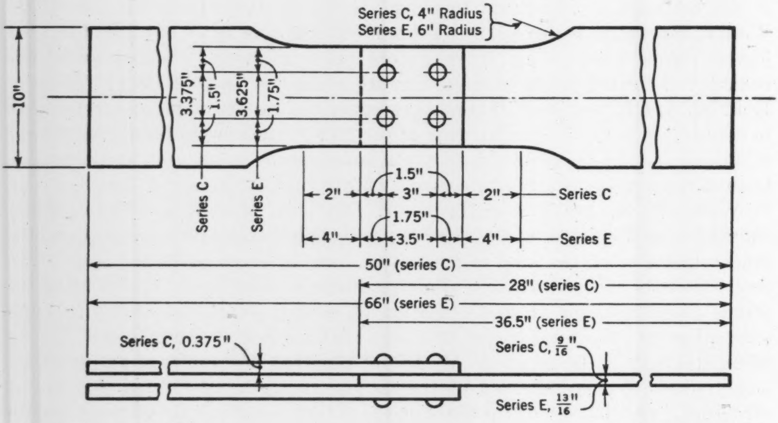
Series C, 4" Radius
Series E, 6" Radius
10"
3.375"
1.5"
3.625"
1.75"
Series C
Series E
1.5"
2"
3"
2"
Series C
1.75"
4"
3.5"
4"
Series E
50" (series C)
28" (series C)
66" (series E)
36.5" (series E)
Series C, 0.375"
Series C, 9/16"
Series E, 13/16"

Edge condition – machine flame cut

(*b*) Series C and E

Series C, punched holes
Series E, drilled holes

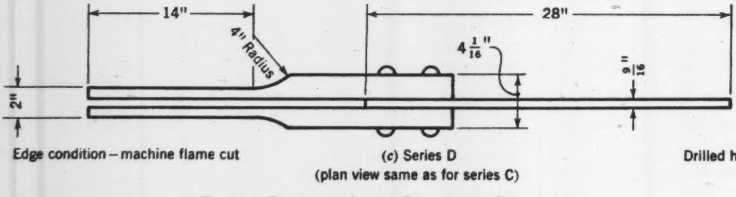
14"
28"
4" Radius
4 1/16"
9/16"
2"

Edge condition – machine flame cut

(*c*) Series D
(plan view same as for series C)

Drilled holes

FIG. 1.—DIMENSIONS AND DETAILS OF SPECIMENS

ing relationship of approximately 1.00:0.75:1.50 were designed for testing in static tension and in fatigue. The fasteners consisted of hot-driven rivets (ASTM–A 141), cold-driven rivets (ASTM–A 141), and high-strength bolts (ASTM–A 325). At about the same time the latter program was begun, an alloy rivet steel meeting the strength requirements of the ASTM–A 195 specification was brought to the attention of the writers. Preliminary tests indicated that rivets of the alloy steel were as easy to drive, were as ductile, and had the same degree of hole-filling as rivets of ordinary ASTM–A 141 rivet steel. In addition, rivets of the alloy steel had a greater clamping force than rivets of ordinary carbon steel. Three series of butt joints were designed to compare the static and fatigue properties of joints fastened with alloy-steel rivets and with ordinary carbon-steel rivets.

TABLE 1.—DESCRIPTION OF SPECIMENS SHOWN IN FIG. 1

Series	Stress relationship, tension: shear: bearing	AREA (Sq In.)			Types of Fasteners[a]	ASTM[b] designation	Grip (In.)
		Tension	Shear	Bearing			
A	1.00:0.75:1.57	3.97	5.30	2.53	High-strength bolts Hot-driven rivets Cold-formed, cold-driven rivets Hot-formed, cold-driven rivets	A 325 A 141 A 141 A 141	$1\frac{3}{16}$, $2\frac{1}{16}$, $3\frac{1}{16}$ $1\frac{3}{16}$, $2\frac{1}{16}$, $3\frac{1}{16}$ $1\frac{3}{16}$, $2\frac{1}{16}$, $3\frac{1}{16}$ $1\frac{3}{16}$, $2\frac{1}{16}$, $3\frac{1}{16}$
B	1.00:0.76:1.59	4.03	5.30	2.53	Hot-formed, cold-driven rivets	A 141	$1\frac{3}{16}$, $2\frac{1}{16}$, $3\frac{1}{16}$
C	1.00:0.75:1.51	2.67	3.54	1.69	Hot-driven rivets	A 141 A 195	$1\frac{3}{16}$ $1\frac{3}{16}$
D	1.00:0.75:1.51	2.67	3.54	1.69	Hot-driven rivets	A 141 A 195	$4\frac{1}{16}$ $4\frac{1}{16}$
E	1.00:1.26:1.83	4.47	3.54	2.44	Hot-driven rivets	A 141 A 195	$1\frac{13}{16}$ $1\frac{13}{16}$, $2\frac{13}{16}$

[a] Nominal diameter of all fasteners, $\frac{3}{4}$ in. Diameter of all holes, $\frac{13}{16}$ in., except Series B, which had $\frac{25}{32}$-in.-diameter holes. [b] Fastener designation.

DESCRIPTION OF SPECIMENS

The dimensions and details of the various specimens tested in static tension and in fatigue are shown in Fig. 1 and in Table 1. Series A was fabricated by a single large fabricating concern and included four types of fasteners. These fasteners were hot-driven rivets, cold-formed cold-driven rivets, hot-formed cold-driven rivets, and high-strength bolts. Series B was fabricated by another large fabricator and included specimens fastened only with hot-formed cold-driven rivets. The lengths of grip considered for both series were $1\frac{3}{16}$ in., $2\frac{1}{16}$ in., and $3\frac{1}{16}$ in. The butt joints of Series A and Series B had a tension:shear: bearing relationship of about 1.00:0.75:1.50. The rivets of both series were of ASTM–A 141 steel. The bolted joints of Series A were assembled in the laboratory with high-strength bolts meeting the requirements of specification ASTM–A 325. The assembly was made in accordance with a tentative specification that was later modified and approved [11] by the Research Council.

---

[11] "Specifications for Assembly of Structural Joints Using High Tensile Bolts," *Bulletin No. 499*, A.R.E.A., Vol. 53, 1952.

In general, the bolts were torqued to a value of 280 lb-ft, as compared to the value of 320 lb-ft now recommended in the specification.

Two kinds of hot-driven rivets were used for the butt joints of Series C, D, and E. The rivets were of ordinary structural steel (ASTM–A 141) and of the alloy rivet steel which met the strength requirements of specification ASTM–A 195. The joints of Series C and Series D had a tension: shear: bearing relationship of 1.00:0.75:1.50 whereas the joints of Series E had a tension: shear: bearing relationship of 1.00:1.26:1.83. The lengths of grip for the joints of Series C and Series D were $1\frac{5}{16}$ in. and $4\frac{1}{16}$ in., respectively. Two lengths of grip—$1\frac{13}{16}$ in. and $2\frac{15}{16}$ in.—were used for the joints of Series E.

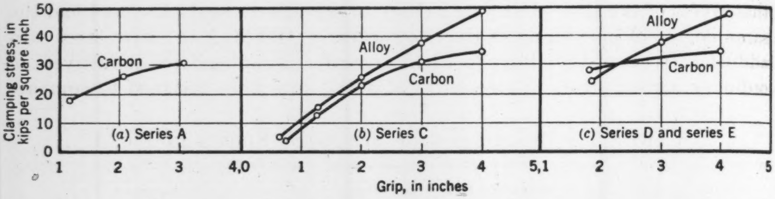

FIG. 2.—AVERAGE CLAMPING STRESSES, HOT-DRIVEN RIVETS

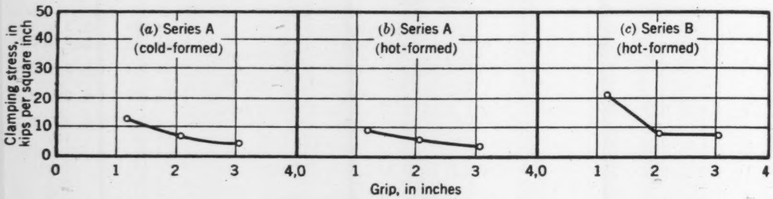

FIG. 3.—AVERAGE CLAMPING STRESSES, COLD-DRIVEN RIVETS

TABLE 2.—AVERAGE PHYSICAL PROPERTIES OF THE MAIN-PLATE MATERIALS

Series	Yield point (lb per sq in.)	Ultimate stress (lb per sq in.)	ELONGATION, in %		Reduction in area (%)
			8 in.	2 in.	
A	37,900	65,900	29.9	54.0	60.2
B	36,400	63,200	27.6	50.8	57.6
C	33,000	63,000	25.5	50.0	56.0
D	36,000	64,200	26.4	49.5	55.6
E	31,900	63,200	32.0	56.2	56.2

The plates of each series were of steel conforming to specification ASTM–A 7 and came from different heats and rollings. The surfaces of the plates of all series, except for those of Series C, were smooth and had the mill scale left intact. The surfaces of Series C were rough and slightly rusty. Average physical properties for the main-plate materials of each series are listed in Table 2.

Clamping stresses for various grips are shown in Figs. 2 and 3 for various types of rivets. These clamping stresses were determined from measurements of the changes in grip caused by removing the plates from between the rivet heads. The clamping stresses of hot-driven rivets increased with the length of grip. As compared to the clamping stresses of ordinary carbon-steel rivets,

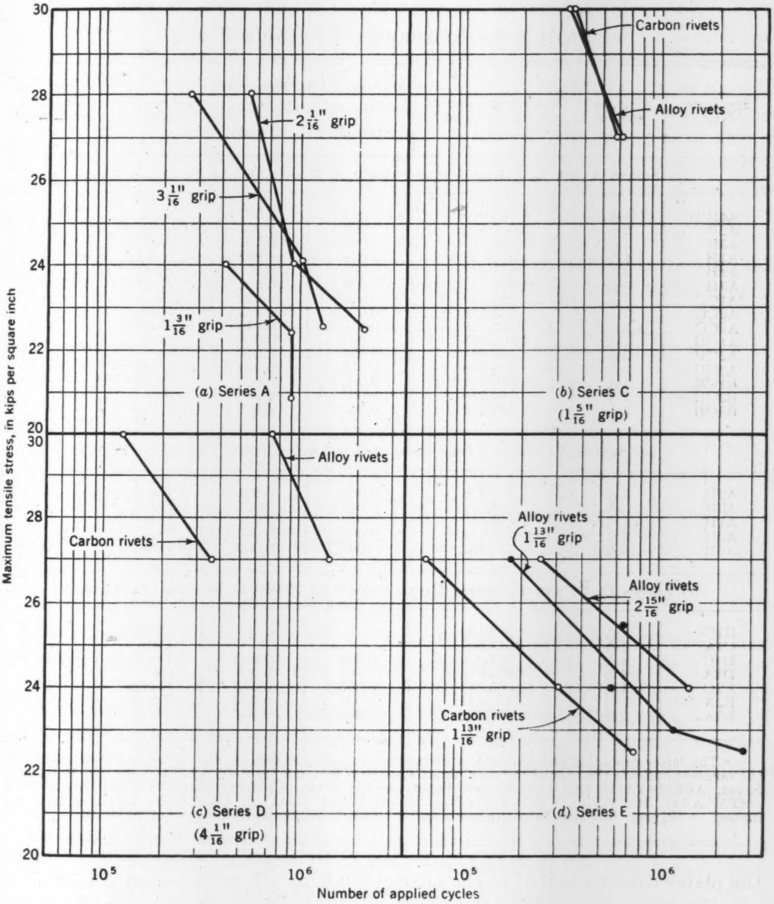

FIG. 4.—RESULTS OF FATIGUE TESTS FOR JOINTS WITH HOT-DRIVEN RIVETS

the clamping stress of the alloy-steel rivets was about the same at a 1-in. grip and was appreciably greater at a 4-in. grip. For the cold-driven rivets, the clamping stresses decreased with the length of grip; these stresses were small except for the specimens of Series B having a $1\frac{3}{16}$-in. grip.

As a result of difficulties encountered in conducting the fatigue tests of the cold-driven specimens of Series A, a survey was made to determine the degree of hole-filling that may exist in joints fabricated with cold-driven rivets. The survey was made of the butt joints of Series A and of sample specimens prepared by four large fabricators. The specimens were sawed through the rivets, and the cut surfaces were ground and polished. The gaps between each rivet and the plates were measured to the nearest 0.001 in. A poor degree of hole-filling was obtained in the butt joints of Series A and in most of the sample specimens. Only one fabricator demonstrated that a good degree of hole-filling can be achieved with cold-driven rivets. Consequently, it was concluded that the butt joints of Series A were representative of usual cold-driving practice. Since the cold-driving procedure of one fabricator resulted in a good degree of hole-filling, this fabricator prepared the specimens for Series B.

TABLE 3.—SUMMARY OF FATIGUE TESTS

Specimen No.[a]	Grip, in inches	Average number of cycles applied	MAXIMUM CYCLICAL SLIP[b]		Main-plate failures[c]	Number of joints tested
			Initial	Final		
(a) SERIES A AND B, STRESS CYCLE FROM 0 TO 24,000 LB PER SQ IN., TENSION						
A1B	$1\frac{3}{16}$	3,123,662[d]	0.001	0.001	None	4
A2B	$2\frac{1}{16}$	3,092,094	0.001	0.002	None	4
A3B	$3\frac{1}{16}$	2,298,120	0.001	0.001	One	4
A1H	$1\frac{3}{16}$	443,446	0.002	0.003	Two	4
A2H	$2\frac{1}{16}$	913,613	0.001	0.001	Three	4
A3H	$3\frac{1}{16}$	1,075,932	0.002	0.002	Three	4
A1CC	$1\frac{3}{16}$	589,819	0.002	0.002	Three	4
A2CC	$2\frac{1}{16}$	927,528	0.006	0.019	Three	4
A3CC	$3\frac{1}{16}$	590,148	0.017	0.040	Rivets[c]	4
A1CH	$1\frac{3}{16}$	1,465,678	0.002	0.006	Four	4
A2CH	$2\frac{1}{16}$	533,824	0.004	0.010	Four	4
A3CH	$3\frac{1}{16}$	908,238	0.015	0.034	Rivets[c]	4
B1CH	$1\frac{3}{16}$	979,411	0.002	0.003	Three	4
B2CH	$2\frac{1}{16}$	954,239	0.002	0.003	Two	2
B3CH	$3\frac{1}{16}$	483,472	0.004	0.009	Rivets[c]	4
(b) SERIES A, STRESS CYCLE FROM +16,000 TO −16,000 LB PER SQ IN.						
A2B	$2\frac{1}{16}$	1,754,738	0.002	0.001	Three	4
A3B	$3\frac{1}{16}$	573,642	0.002	0.002	Three	4
A1H	$1\frac{3}{16}$	1,216,610	0.010	0.022	Two	4
A2H	$2\frac{1}{16}$	722,918	0.002	0.006	Two	4
A3H	$3\frac{1}{16}$	345,481	0.002	0.002	Two	2
(c) SERIES C, D, AND E, STRESS CYCLE FROM 0 TO 27,000 LB PER SQ IN., TENSION						
C1C	$1\frac{5}{16}$	586,940			Three	3
C1A	$1\frac{5}{16}$	617,047			Two	2
D4C	$4\frac{1}{16}$	361,329	0.002	0.003	Two	2
D4A	$4\frac{1}{16}$	1,462,813	0.001	0.001	One	2
E2C	$1\frac{13}{16}$	65,242	0.005	0.005	Rivets[c]	2
E2A	$1\frac{13}{16}$	186,541	0.001	0.002	Rivets[c]	2
E3A	$2\frac{15}{16}$	255,189	0.004	0.004	Three	3

[a] The letter preceding the numeral in each specimen number denotes the series; the letters following the numeral indicate the type of fastener, thus: The letter B stands for Bolt, ASTM–A 395; H, Hot-Driven Rivet, ASTM–A 141; CC, Cold-Driven Rivet, ASTM–A 141, Cold-Formed; CH, Cold-Driven Rivet, ASTM–A 141, Hot-Formed; C, Carbon-Steel Rivet, ASTM–A 141; A, Alloy Rivet, ASTM–A 195. [b] In inches. [c] "Rivets" indicates that the rivets failed. [d] Bolts tightened to a torque of 280 lb-ft.

Comparative Behavior in Fatigue

Fatigue tests were conducted in three machines, two of 250,000-lb capacity and one of 80,000-lb capacity. Each type of joint found in Series A and B was tested at a range of stress of from zero to +24,000 lb per sq in. The results of these tests are summarized in Table 3(*a*). Other ranges of zero-to-tension cycles of loading and a fully reversed cycle of loading were also considered for the various joints of Series A and B. The results for the fully reversed cycle of loading are given in Table 3(*b*). Each type of joint of Series C, D, and E was tested using a range of stress of from 0 to + 27,000 lb per sq in. The results of the latter tests are summarized in Table 3(*c*). The joints of Series C, D, and E were also tested at other ranges of zero-to-tension cycles of loading. Figs. 4 and 5 summarize the results obtained for the riveted joints subjected to the various zero-to-tension cycles of loading. The curves of Fig. 4 are drawn through computed averages. Fig. 5 is divided into two parts based on the type of failure of the joint.

The fatigue strengths of the bolted joints were considerably greater than those of riveted joints. Of the twelve bolted joints tested at a stress range of from 0 to + 24,000 lb per sq in., only one failed before 3,000,000 cycles were applied. For the bolted joints, the average fatigue strength at 2,000,000 cycles of a zero-to-tension loading was slightly greater than 28,000 lb per sq in. The fatigue lives of bolted joints tested at a range of stress of from 0 to + 30,000 lb per sq in. were approximately the same as those of bolted joints tested at a range of stress of ± 16,000 lb per sq in. For each of the latter ranges of stress, the average fatigue lives of the bolted joints decreased with an increase in length of grip. The fatigue fractures of the bolted joints occurred in the main plates and were either across a net section or a gross section as shown in Fig. 6. The fatigue lives of the bolted joints that failed might have been increased if the bolts had been tightened to a greater torque than 280 lb-ft. Two joints for which the bolts were tightened with a torque of 320 lb-ft, as recommended by the Research Council, were tested at a range of stress of from 0 to + 21,500 lb per sq in.; neither failed after 12,275,000 cycles of loading. Four joints for which the bolt tensions exceeded the yield strengths of the bolts were tested at a range of stress of from 0 to + 24,000 lb per sq in.; none of these joints failed after 3,000,000 cycles of loading.

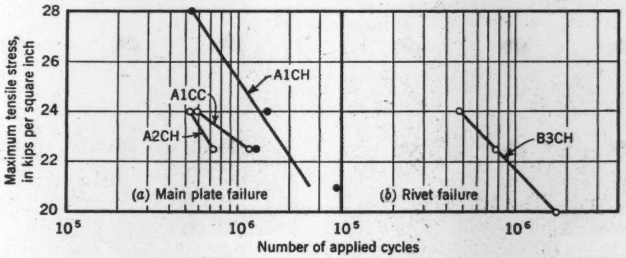

Fig. 5.—Results of Fatigue Tests for Joints with Cold-Driven Rivets

The average clamping force per bolt decreased about 20% during a fatigue test. Loss in clamping force was evidently not caused by the turning of a nut, as no turning of a nut was observed. The relative slip of the plates of a bolted joint during the first application of a desired test load was approximately equal to the specified clearance of the bolt holes. The succeeding cyclical slips of the bolted joints were negligible and did not exceed 0.002 in.

The average fatigue strengths of the joints fastened with hot-driven rivets and tested at zero-to-tension cycles of loading increased with an increase in grip. Strengths for the cyclical tension loadings were in general agreement with the values of the clamping stresses obtained for the various lengths of grip. The average fatigue strengths of the joints with alloy steel rivets having a $1\frac{5}{16}$-in. grip were about the same as those of similar joints fastened with hot-driven rivets of carbon steel. However, with rivets having grips greater than $1\frac{5}{16}$ in., the average fatigue strengths of the joints with alloy-steel rivets were appreciably greater than those of the joints with ordinary carbon-steel rivets. An increase in the ratio of shear to tension in the joints with alloy-steel rivets resulted in a decrease in the fatigue strengths of the joints. The decreases in fatigue strengths caused by the change in the shear-tension ratio were probably influenced by the relative amounts of load that were resisted by the friction between plates and by the bearing of rivets. For the riveted joints of Series A, tested at fully reversed cycles of loading, the average fatigue strengths decreased with an increase in length of grip.

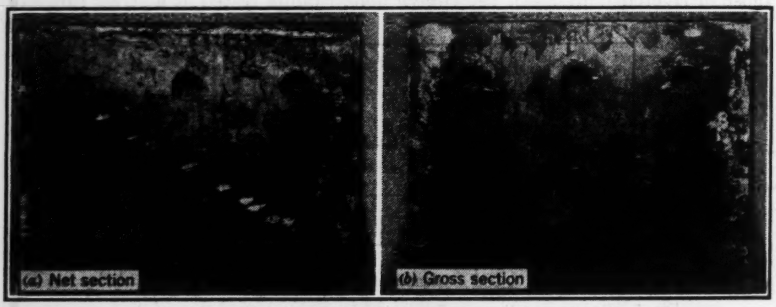

FIG. 6.—TYPICAL FATIGUE FRACTURES

The fatigue fractures of the joints with hot-driven rivets occurred at the net sections of the main plates, except for certain joints of Series E. Broken rivets were obtained in four joints of Series E having a $1\frac{13}{16}$-in. grip and a tension : shear : bearing relationship of 1.00 : 1.26 : 1.83. The cyclical slips for the various series of joints with hot-driven rivets did not exceed 0.005 in. for the zero-to-tension cycles of loading. The cyclical slips of such joints were greater for the reversed cycles of loading than for the zero-to-tension cycles of loading.

The fatigue characteristics of the joints having cold-driven rivets differed from those of the joints with hot-driven rivets. At a $3\frac{1}{16}$-in. grip, the cold-driven rivets of Series A and Series B failed in flexural fatigue for each range of loading considered. The lowest range of loading considered was for stresses from 0 to + 20,000 lb per sq in. on the net section. In many cases, the broken rivets could not be detected until the specimens were cut apart. The fatigue strengths of the cold-driven specimens having a $3\frac{1}{16}$-in. grip were appreciably less than those of the corresponding specimens with hot-driven rivets. The fatigue strengths of the specimens with cold-driven rivets having a $1\frac{3}{16}$-in. grip or a $2\frac{1}{16}$-in. grip depended on the cold-driving procedure and sometimes were as large as those for the corresponding specimens having hot-driven rivets.

The cyclical slips of the cold-driven specimens having a $3\frac{1}{16}$-in. grip were large and for one specimen reached a value of 0.040 in. These slips were so

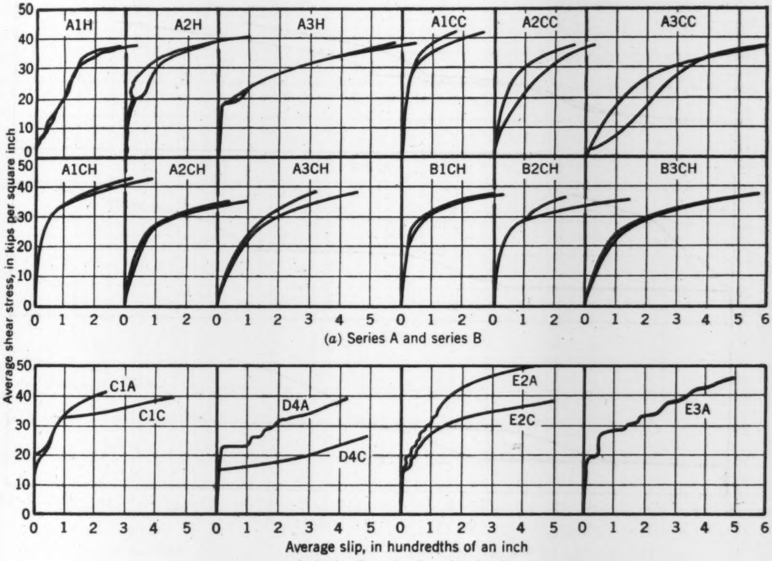

(*a*) Series A and series B

(*b*) Series C, series D and series E

FIG. 7.—SHEAR STRESS RELATED TO SLIP, RIVETED JOINTS TESTED IN STATIC TENSION

large that it was not possible to adjust the machines for the desired loads. The slips in the specimens with cold-driven rivets decreased with a decrease in grip and were, in general, greater than for the corresponding specimens with hot-driven rivets.

COMPARATIVE BEHAVIOR IN STATIC TENSION

The static tension tests of the various types of joints were made to determine the efficiencies, load-slip characteristics, and the shear stresses at which the first major slips occurred. The tests were made in a 1,000,000-lb-capacity Baldwin-Southwark testing machine. The load on a specimen was applied in increments until failure occurred either in the main plate or in the rivets of a joint. If failure first occurred in the rivets, the broken rivets were removed and were replaced with high-tensile bolts. The specimen was then reloaded until failure occurred in the main plate of a joint.

Typical examples of the load-slip relationships for the various joints are shown in Figs. 7 and 8. The plotted values of slip are the averages indicated by two dial gages. One gage on each edge of each joint was placed at a section midway between the rows of fasteners of a joint. For the joints fastened with hot-driven rivets and those fastened with bolts, the load was initially resisted by friction between the plates until the friction was overcome and a sudden slip occurred. When this happened, the fasteners were brought into bearing. For the joints with cold-driven rivets, the fasteners, in general, were in bearing from the beginning of a test.

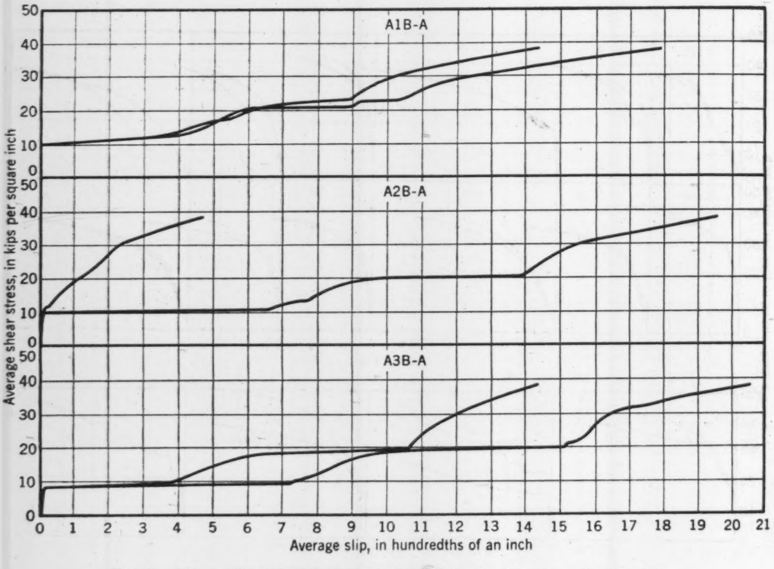

Fig. 8.—Shear Stress Related to Slip, Bolted Joints of Series A, Tested in Static Tension

The shear stress at which the first major slip of a joint occurred depended on the type of fastener and on the length of grip. Average values of the shear stresses at which the first major slips occurred for the joints with hot-driven rivets appear in Table 4. For the bolted joints tested in static tension and in fatigue, the first major slips occurred at a shear stress ranging from between 9,000 lb per sq in. and 16,000 lb per sq in. The values for the bolted joints might have been larger if the bolts had been tightened with a torque greater than 280 lb-ft. The major slips of the bolted joints were of a different order of magnitude from those of the riveted joints because of the difference in the clearances for the driven rivets and for the bolts.

Apparent coefficients of friction were determined for the joints fastened with hot-driven rivets and for the bolted joints. The values of the coefficients for the joints fastened with hot-driven rivets are listed in Table 4 as ratios of the shear stresses at which the first major slips occurred to the initial clamping stresses of the rivets. The ratios for the joints of Series C seem large. However, the plate surfaces of the latter joints were rough and slightly rusty. The values of the ratios for the bolted joints were small (approximately 0.20).

The experimental efficiencies of the joints tested in static tension are summarized in Table 5. For each series of joints, the efficiencies were nearly the same, irrespective of the type of fastener and of the length of grip. In those cases in which broken rivets were replaced with high-strength bolts, the plate efficiencies apparently were not influenced by this substitution. For all joints having drilled holes and a tension : shear : bearing relationship of approximately 1.00:0.75:1.50, the experimental efficiencies were approximately 82%.

TABLE 4.—AVERAGE SHEAR STRESSES AT OCCURRENCE OF FIRST MAJOR SLIP, FOR JOINTS FASTENED WITH HOT-DRIVEN RIVETS

Series	Rivet designation (ASTM)	Grip, in inches	Shear stress,[a] first major slip	Apparent coefficient of friction[b]
A	A 141	$1\frac{3}{16}$	5,800	0.27
		$2\frac{1}{16}$	20,000	0.61
		$3\frac{1}{16}$	19,000	0.54
C	A 141	$1\frac{3}{16}$	21,200	1.22
	A 195	$1\frac{3}{16}$	19,800	1.35
D	A 141	$4\frac{1}{16}$	15,500	0.45
	A 195	$4\frac{1}{16}$	23,000	0.49
E	A 141	$1\frac{11}{16}$	14,500	0.49
	A 195	$1\frac{11}{16}$	18,800	0.81
	A 195	$2\frac{11}{16}$	20,000	0.45

[a] In pounds per square inch. [b] Shear stress at first major slippage, divided by the initial clamping stress.

The theoretical efficiency for the latter group of joints was approximately 75%. The joints of Series C had punched holes and an experimental efficiency of about 71%. The low efficiencies for the joints of Series C were the result of the holes being punched instead of being drilled. The joints having drilled holes and a tension : shear : bearing relationship of 1.00:1.26:1.83 had an experimental efficiency of approximately 86% as compared to a theoretical efficiency of 77%. All the main-plate failures occurred at the first row of fasteners. The fractures were 100% ductile for the joints of Series A to Series D and were 75% ductile for the joints of Series E.

CONCLUSIONS

The following conclusions can be made concerning the comparative behavior of bolted and riveted joints subjected to static and fatigue loads:

1. The fatigue strengths of joints with high-tensile bolts are considerably greater than those of joints with hot-driven or cold-driven rivets. Although

the clamping force of a joint fastened with bolts somewhat decreases during a fatigue test, the nuts do not turn. The cyclical slips of joints fastened with bolts are negligible; however, the slippage during the first application of a load can equal the clearance of the bolt holes. The substitution of high-tensile bolts for rivets does not change the plate efficiencies of a joint subjected to static loads. For joints having a $\frac{1}{16}$-in. clearance for holes, the first major slip of a bolted joint is considerably greater than that of a riveted joint. The shear stress at which the first major slip of a joint occurs is dependent on the clamping force, the degree of hole-filling, and the condition of the contact surfaces of the joint.

2. For zero-to-tension cycles of loading, the fatigue strengths of joints fastened with hot-driven rivets increase with an increase in the length of grip. The fatigue strengths of joints fastened with alloy-steel rivets having larger clamping forces than ordinary steel rivets exceed those of similar joints fastened with ordinary steel rivets. An increase in the stress ratio of shear to tension in a joint fastened with hot-driven rivets can result in a decrease in the fatigue strength of the joint.

TABLE 5.—AVERAGE EFFICIENCIES OF JOINTS TESTED IN STATIC TENSION

Series	Type of fastener	Fastener designation (ASTM)	Plate efficiency, in %
A	Bolts	A 325	82.9
	Hot-driven rivets	A 141	81.5
	Cold-formed, Cold-driven rivets	A 141	81.3
	Hot-formed, Cold-driven rivets	A 141	81.2
B	Hot-formed, Cold-driven rivets	A 141	81.5
C[a]	Hot-driven rivets	A 141	70.8
		A 195	71.3
D	Hot-driven rivets	A 141	83.0
		A 195	82.4
E[b]	Hot-driven rivets	A 141	85.5
		A 195	88.0

[a] Specimens had punched holes. All other specimens had drilled holes. [b] Specimens had a tension: shear: bearing relationship of 1.00:1.26:1.83. All other specimens had a tension: shear: bearing relationship of 1.00:0.75:1.50.

3. The fatigue strengths of a joint fastened with cold-driven rivets having a long grip (such as 3$\frac{1}{16}$ in.) are considerably less than those of similar joints fastened with hot-driven rivets. At this length of grip, the cold-driven rivets will fail in fatigue. The fatigue strength of a joint fastened with cold-driven rivets having a short grip can be as great as that of a similar joint fastened with hot-driven rivets but it is dependent on the cold-driving procedure. For fatigue cycles of loading, large slippages can—and probably will—occur for joints fastened with cold-driven rivets because the degree of hole-filling depends on the cold-driving procedure.

SLIP OF JOINTS UNDER STATIC LOADS

BY R. A. HECHTMAN,[1] A. M. ASCE, D. R. YOUNG,[2] A. G. CHIN,[3]
J. M. ASCE, AND E. R. SAVIKKO,[4] J. M. ASCE

SYNOPSIS

The primary purpose of this investigation has been to determine the slip of structural steel double-lap joints assembled with high-strength steel bolts when subjected to stresses in the design range and somewhat beyond. The joints were subjected to short-time static loading. Although most of the joints were tested in tension, some were tested in compression and in combined compression and torsion. This paper reports the results of seventy-two tests, which are part of a continuing investigation.

Of the principal factors affecting the slip of the joint, those studied included such dimensional properties as the total faying area, the net cross-sectional area, the thickness of the lap-plates, and the number of rows of bolts in the joints. Other properties studied included bolt tension and surface condition of the faying areas. The joints were compared on the basis of the shearing stress on the bolts, the coefficient of friction and the slip (both developed at the first major slip), and the stress on the net cross-sectional area.

INTRODUCTION

The slip of joints assembled with high-strength steel bolts in holes $\frac{1}{16}$ in. larger in diameter than the bolts themselves is resisted initially only by the frictional resistance developed by the normal pressure of the bolts on the faying, or contact, areas between the plates of the joint. In mobilizing this resistance, little slip occurs in a properly designed joint. If the applied load exceeds the initial frictional resistance of the joint, a sudden and appreciable slippage occurs. This point, termed the first major slip, is followed by further slippage of the plates subjected to continued loading until the plates are bearing fully on the bolts.

Three properties are required of a bolted joint designed to resist slip through the frictional resistance developed between the plates:

1. The slip when stresses are within the design range must be small.
2. The slip when stresses are within the design range should not continue to increase during the life of the structure while the joint resists its applied load.
3. A reasonable margin of safety should be present in the joint with respect to the two foregoing properties.

NOTE.—Presented at the Centennial Convocation, Chicago, Ill., September, 1952. Published, essentially as printed here, in September, 1954, as *Proceedings-Separate No. 484*. Positions and titles given are those in effect when the paper was received for publication.

[1] Prof. of Structural Research, Univ. of Washington, Seattle, Wash.

[2] Engr., Boeing Airplane Co., Seattle, Wash.

[3] Engr., Carey and Kramer, Seattle, Wash.

[4] Junior Bridge Engr., State Toll Bridge Authority, Tacoma, Wash.

The first requirement is met if the upper limit of the design range of the joint is less than the stress at the first major slip. To meet the second requirement, it is essential that those properties of a joint which produce frictional resistance are not significantly diminished as time elapses. The proper relation of design stresses to the results of tests of bolted joints assures fulfilment of the third requirement.

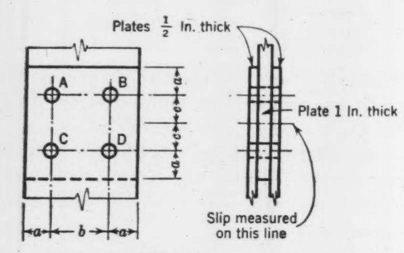
Plates $\frac{1}{2}$ In. thick
A
B
C
D
a
c
c
a
a
b
a
Plate 1 In. thick
Slip measured on this line

(*a*) Type C

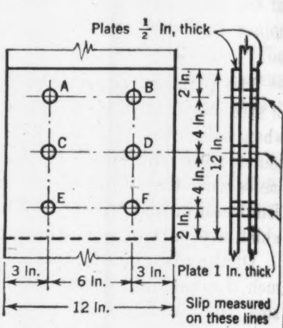
Plates $\frac{1}{2}$ In, thick
A
B
C
D
E
F
2 In.
4 In.
4 In.
2 In.
12 In.
3 In.
6 In.
3 In.
12 In.
Plate 1 In. thick
Slip measured on these lines

(*b*) Type H

Type	Dimension, in inches		
	a	*b*	*c*
C	2	4	2
C1	$1\frac{1}{2}$	3	$1\frac{1}{2}$
C2	$2\frac{1}{2}$	5	$2\frac{1}{2}$
C3	3	6	3
C4	2	4	$1\frac{1}{2}$
C5	$1\frac{7}{16}$	3	$1\frac{1}{2}$
C6	$1\frac{3}{4}$	$3\frac{3}{8}$	$1\frac{11}{16}$
C7	2	4	2

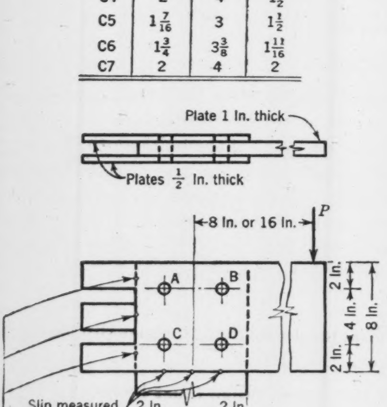
Plate 1 In. thick
Plates $\frac{1}{2}$ In. thick
8 In. or 16 In.
P
A
B
C
D
2 In.
4 In.
2 In.
8 In.
Slip measured at these points
2 In.
2 In.
4 In.
8 In.

(*c*) Type K

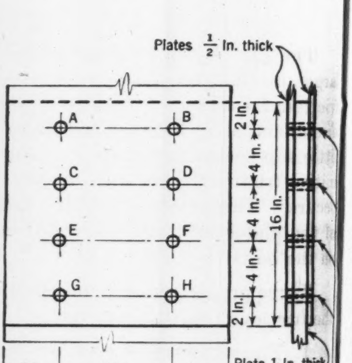
Plates $\frac{1}{2}$ In. thick
A
B
C
D
E
F
G
H
2 In.
4 In.
4 In.
4 In.
2 In.
16 In.
4 In.
8 In.
4 In.
16 In.
Plate 1 In. thick
Slip measured on these lines

(*d*) Type J

FIG. 1.—DETAILS OF JOINT SPECIMENS

The program of tests reported herein was directed toward obtaining data concerning the slip of bolted double-lap structural joints resisting loads up to the load at which the joints slipped into full bearing and at which the bolts began to deform the holes. Special attention was given to the particular shearing stress on the bolts at which the first major slip occurred and to the distance the plates slipped before this point was reached. The phrase "shearing stress on the bolts" is used here in its usual meaning to the structural designer because shear did not actually exist in the bolts until they were bearing on the plates. The average shear on the bolts in these tests was always computed on the basis of the gross cross-sectional area of the bolts. The tension in the bolts was controlled in all tests, the maximum deviation from the desired tension being approximately 3%.

TABLE 1.—PROGRAM OF TESTS

SPECIMEN[a]		LAP PLATES		Surface condition[b]	BOLTS		Faying area (sq in. per bolt)	Nominal bolt tension[d] (kips)	Tension-shear ratio[e]	LOADING	
No. (1)	Type (2)	Thickness (in.) (3)	Net area (sq in.) (4)	(5)	Type[c] (6)	Number in joint (7)	(8)	(9)	(10)	Type[f] (11)	Eccentricity (in.) (12)
10-12B	C1	½	3.91	MS	4140	4	18.0	45.0	1.00:0.62	Te	0
13-15B	C	½	5.91	MS	4140	4	32.0	45.0	1.00:0.94	Te	0
16-18	C2	½	7.91	MS	4140	4	50.0	45.0	1.00:1.26	Te	0
19-21	C3	½	9.91	MS	4140	4	72.0	45.0	1.00:1.58	Te	0
31-33	C4	½	5.91	MS	4140	4	28.0	24.0	1.00:0.94	Te	0
37-39	C	½	5.91	MS	4140	4	32.0	36.0	1.00:0.94	Te	0
48-50	C	½	5.91	RL	4140	4	32.0	45.0	1.00:0.94	Te	0
51-53	C	½	5.91	V	4140	4	32.0	45.0	1.00:0.94	Te	0
54-56	C	½	5.91	S	4140	4	32.0	45.0	1.00:0.94	Te	0
57-59	C4	½	5.91	MS	4140	4	28.0	36.0	1.00:0.94	Te	0
63-65	H	½	9.88	MS	4140	6	48.0	42.5	1.00:1.05	Te	0
66-68	J	½	13.88	MS	4140	8	64.0	42.5	1.00:1.10	Te	0
74-76	C	½	5.91	SPR	4140	4	32.0	45.0	1.00:0.94	Te	0
77-79B	C	½	5.88	MS	4140	4	32.0	42.5	1.00:0.94	Te	0
80-82	C7	5/16	3.67	MS	4140	4	32.0	42.5	1.00:0.59	Te	0
101-103	C	½	5.88	MS	A 325	4	32.0	42.5	1.00:0.94	Te	0
104-106	C	½	5.88	MS	4140	4	32.0	42.5	1.00:0.94	C	0
107-109	C	½	5.88	MS	A 325	4	32.0	52.0	1.00:0.94	Te	0
119-121	K	½	...	MS	4140	4	32.0	42.5	....	To	8
122-124	K	½	...	MS	4140	4	32.0	42.5	....	To	16
128-130	C6	½	4.75	MS	A 325	4	23.6	42.5	1.00:0.75	Te	0
131-133	C5	½	3.75	MS	A 325	4	17.3	42.5	1.00:0.60	Te	0
137-139	C6	½	4.75	MS	A 325	4	23.6	52.0	1.00:0.75	Te	0

[a] Types of specimens are detailed in Fig. 1. [b] Surface conditions are described as follows: MS indicates mill-scale surface, wire-brushed, and cleaned with carbon tetrachloride to dissolve grease and oil. RL indicates wire-brushed, cleaned mill scale, covered with one coat of red lead paint. Paint aged 30 days before assembly. V indicates wire-brushed, cleaned mill scale, covered with one coat of fast-drying varnish. Varnish aged a week before assembly. S indicates that mill scale was completely removed by sandblasting. Surface was cleaned with carbon tetrachloride. SPR indicates that holes in the lap plates were subpunched 11/16 in. in diameter and reamed. Holes in the center plate were drilled 11/16 in. in diameter and reamed. Lap plates were slightly dished around the holes by punching. [c] Bolts that met either Society of Automotive Engineers (SAE) 4140 or American Society for Testing Materials (ASTM) A 325 specifications. [d] Specimen Nos. 107 to 109 and 137 to 139 had bolt tension 10% greater than the elastic proof load. [e] The ratio of the average tensile stress or compressive stress on the net cross-sectional area of the lap plates to the average shearing stress on the gross cross-sectional area of the bolts. [f] The symbol, Te, denotes tension; C, compression; and To, torsion.

DESCRIPTION OF JOINT SPECIMENS AND TEST METHODS

Joint Specimens.—The program of tests is given in Table 1. The details of the joints are shown in Fig. 1. All the specimens were double-lap joints with butt plates 1 in. thick and lap plates ½ in. thick, except for specimen Nos. 80, 81, and 82, which had lap plates 5/16 in. thick. The high-strength steel bolts used were 1 in. in diameter. The clearance in all bolt holes was 1/16 in.

The edges of the joints were milled to the specified width. The plates were then clamped in the same positions in which they were to be tested, and the holes were drilled through all the plates in one operation. This procedure assured alinement of the holes. The surface condition given the faying areas of the joints before assembly is described in Table 1. The burred edges of the drilled holes were smoothed. The plates were then assembled with tight-filling taper pins to aline the holes. The bolts were placed with one washer under the head and one under the nut and were tightened to an elongation corresponding to the desired bolt tension as determined in the calibration test.

The bolt holes in the lap plates of the three specimens with subpunched and reamed holes were punched $\frac{15}{16}$ in. in diameter and reamed to the proper size with the plates assembled in the same manner as the joints with drilled holes. The butt plates of these joints had drilled holes. As the punching slightly "dished" the plates around the holes, the specimens were assembled so that the dished side of one lap plate was bearing on the butt plate, and that of the other lap plate was turned away from it.

TABLE 2.—TENSILE PROPERTIES OF STEEL PLATES

Plate thickness,[a] in inches	Upper yield point, in pounds per square inch	Ultimate strength, in pounds per square inch	Percentage elongation in 8 in.	Reduction of area, in percentage
$\frac{5}{16}$	45,400	68,200	26.5	52.9
$\frac{1}{2}$	36,600 to 40,100	58,100 to 62,100	24.9 to 31.0	49.0 to 57.2
1	32,800 to 36,000	59,600 to 63,600	27.3 to 31.2	44.9 to 56.3

[a] Data from one plate $\frac{5}{16}$ in. thick, six plates $\frac{1}{2}$ in. thick, and three plates 1 in. thick.

Properties of Plates, Bolts, and Washers.—The average tensile properties of the semi-killed, plain-carbon structural steel meeting specification A 7-52T of the American Society for Testing Materials (ASTM),[5] from which the joints were fabricated, are given in Table 2. These properties were determined by testing two standard (ASTM) flat coupons from each plate. If more than one plate of a particular thickness was used, only the maximum and minimum properties are listed in this table.

Two types of bolts were used—a type made of heat-treated steel meeting specification 4140 of the Society of Automotive Engineers (SAE),[6] and a type meeting ASTM specification A 325-52T.[7] Typical load-elongation curves for these two types of bolts are shown in Fig. 2. Every bolt used was individually calibrated in tension at its exact grip to obtain the relation between bolt tension and elongation. As the bolt tensions used in most of the joints were at, or just below, the elastic proof load of an A 325 bolt, the SAE 4140 bolts with a higher proportional limit were used in most of the joints to assure that the bolts would not need to be recalibrated after each test because of any slight overstressing of the bolts during tightening or testing. The A 325 bolts

---

[5] "Specifications for Steel for Bridges and Buildings (A 7-52T)," A.S.T.M., 1952.

[6] "1951 SAE Handbook," Soc. of Automotive Engrs., 1951, p. 42.

[7] "Specifications for Bolts and Studs with Suitable Nuts and Plain Washers, Quenched and Tempered (A 325-52T)," A.S.T.M., 1952.

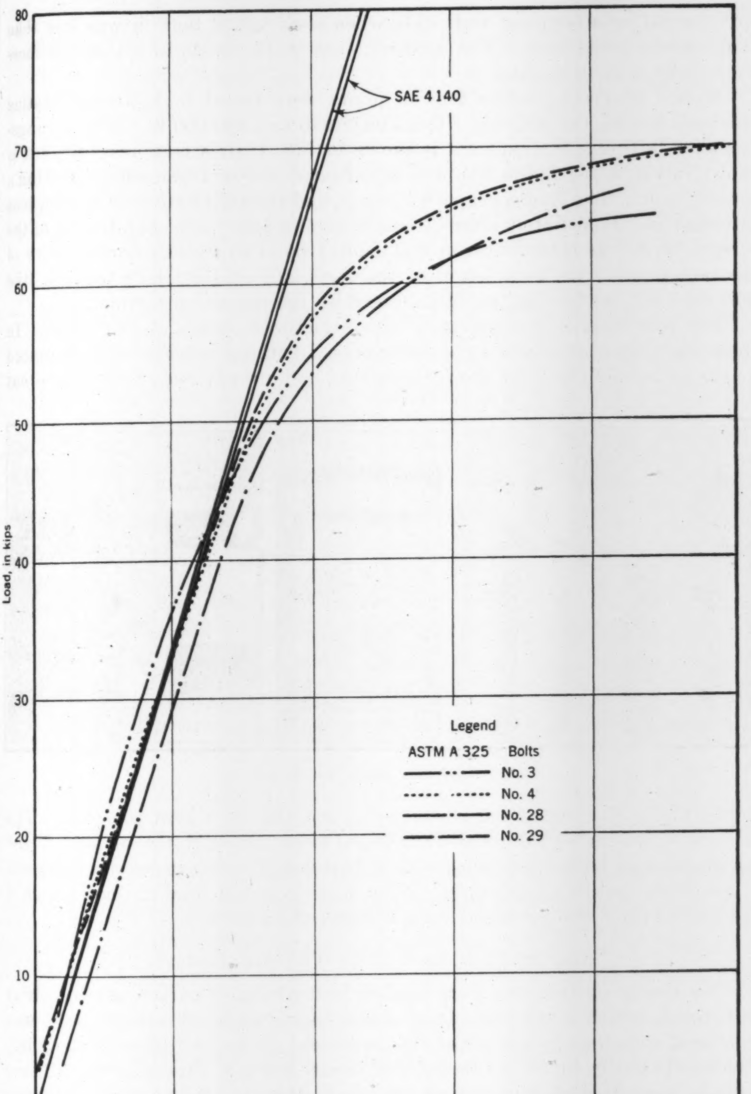

FIG. 2.—LOAD-ELONGATION CURVES FOR TYPICAL BOLTS OF 1-IN. DIAMETER

were reused in subsequent tests only when their initial tension was less than their elastic proof load. The washers were $\frac{3}{16}$ in. thick, and their surfaces were carburized $\frac{1}{32}$ in. deep.

Method of Testing.—The tension joints were tested in hydraulic testing machines having capacities of either 300,000 lb or 2,400,000 lb. The arrangement for testing a tension joint is shown in Fig. 3(*a*); a compression joint is shown in Fig. 3(*b*); and in Fig. 3(*c*) is indicated the arrangement for testing a torsion joint. The load was applied slowly, and the dials were read at frequent intervals and immediately after each sudden slippage. The eccentricity of the torsion joints was measured from the loading point to the center of gravity of the bolt group. On completion of the tests, the residual bolt tension (the bolt tension after testing) was determined by the relaxation method.

The test section of a specimen was sometimes used a second time. In these cases, the lap plates were interchanged without rotation. This placed on the outside of the joint the surfaces that had already been tested, whereas the bolt holes formed by one operation of the drill were kept together. The surfaces of the center plate were thus tested twice, although the surfaces of the lap plates were tested only once. This dual use of test sections did not seem to affect the results significantly. Specimens were not used a second time if the first test had elongated the holes by more than 0.003 in.

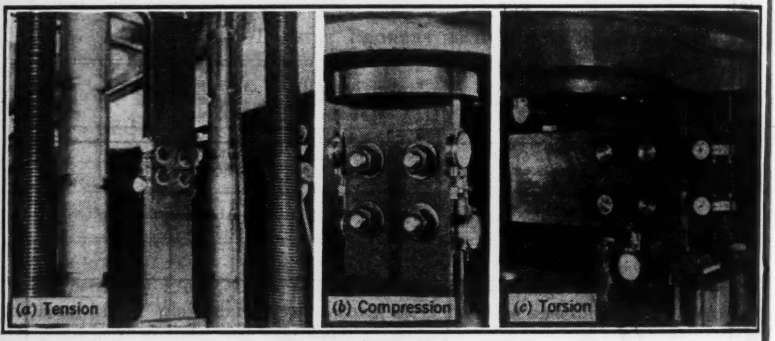

FIG. 3.—JOINTS READY FOR TESTING

SLIP IN TYPICAL BOLTED TENSION JOINTS

The results of each test were plotted in the form of curves relating shear and slip, in which the average shear stress on the gross area of the bolts was compared with the average of the slips measured on the two edges of the joint. Typical shear-slip curves for tension joints are shown in Figs. 4 and 5. These indicate two distinct patterns of behavior—that for joints with mill-scale faying surfaces, and that for joints with painted faying surfaces. Further related information appears in Fig. 1 and Table 1.

Figs. 4, 5(*a*), and 5(*d*) are shear-slip curves for joints with mill-scale faying surfaces. When load was applied to a specimen of this type, there was at first no large slip. A load was eventually reached at which the initial frictional resistance to slip was overcome, and the plates slipped with extreme rapidity. This first large and sudden slip is referred to as the "first major slip" and is so marked in Fig. 4(*a*). As the result of several further cycles of load and slip, the bolts were brought into full bearing on the plates. Thereafter, the increment of load required to produce a given amount of slip was greater than before because the bolts were bearing upon the plates. The test was halted when full bearing was attained.

If a design involves the requirement that slip be held to a minimum in order to maintain moment continuity in a connection or to prevent undesirable deflection of the structure, the part of the shear-slip curves below the point of first major slip would become the operating range of the joint. In other types of connections, slip into full bearing would be entirely permissible. Full bearing in these tests occurred when the average slip was 0.062 in.

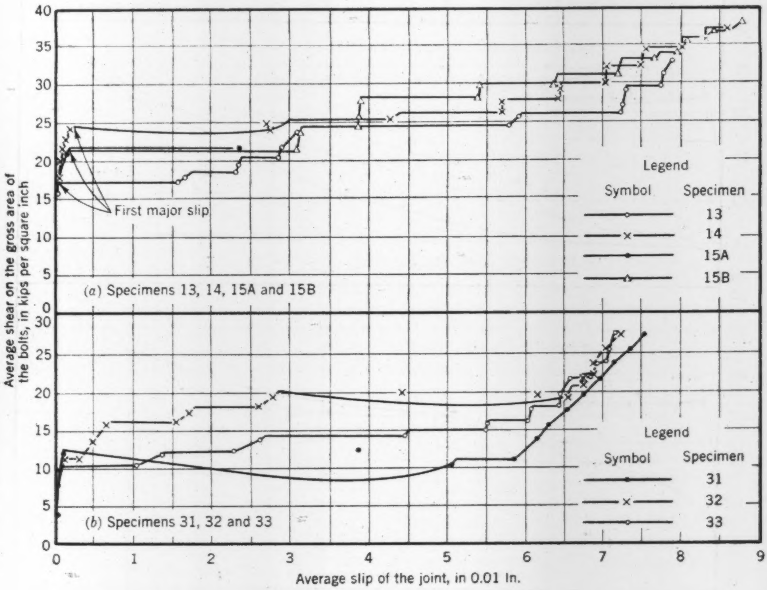

FIG. 4.—COMPARISON OF NOMINAL SHEAR ON THE BOLTS AND AVERAGE SLIP OF THE JOINTS

Specimens with varnish or red lead paint on the faying surfaces had a relationship between shear and slip much different from that of the tests previously described. Instead of slipping suddenly at various increments of load and then maintaining that amount of slip (as did the joints with mill-scale faying areas), the joints with painted faying surfaces slipped slowly and continuously even with small loads. When resisting a constant load, joints of the

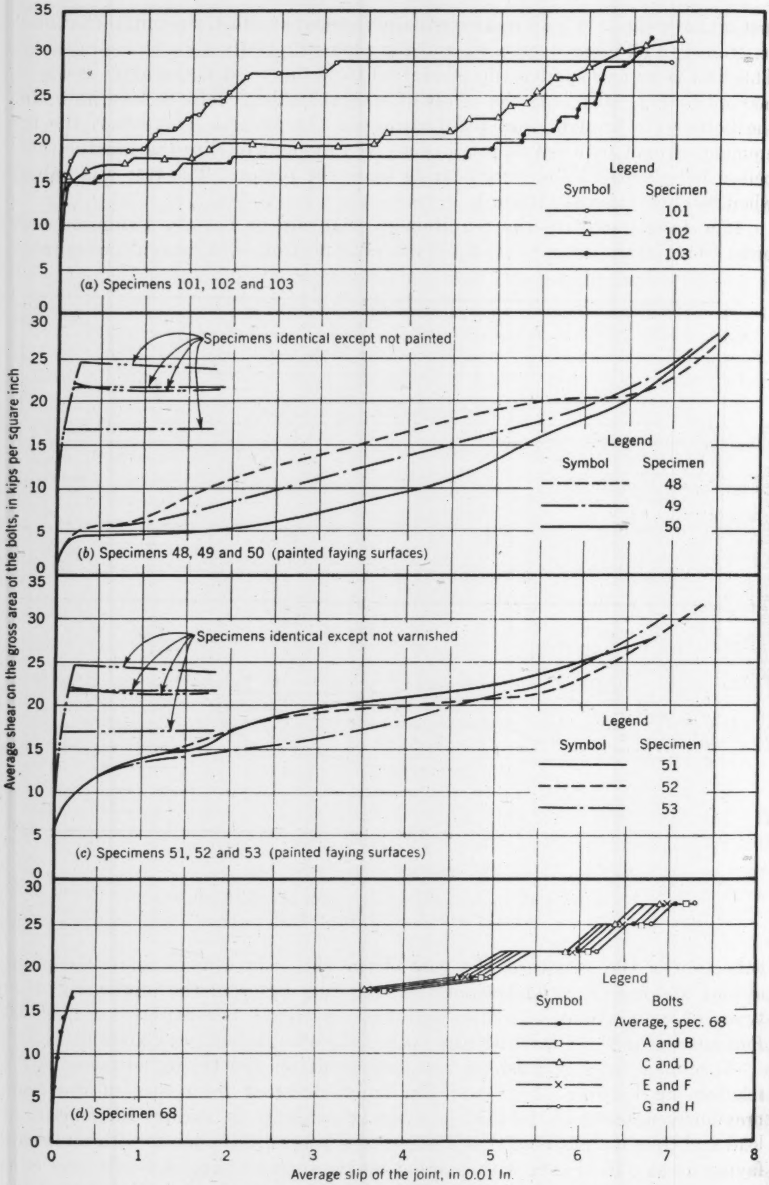

FIG. 5.—COMPARISON OF NOMINAL SHEAR ON THE BOLTS AND AVERAGE SLIP OF THE JOINTS

latter type slipped slowly, the rate of slip decreasing with time. When the time rate of slip at any one load decreased to an average of 0.0001 in. per min in these tests, the slip was read on the dial indicators. This method of slow loading minimized the influence of the operator of the testing machine on the shape of the shear-slip curves and gave a more accurate picture of the behavior of such a joint in a structure.

The more important data of all the tests are summarized in Table 3. The average bolt tension listed in Col. 4 was the average of the measured values. The term "first slip" refers to the first major slip. For torsion specimens, the eccentricity is designated as *e*.

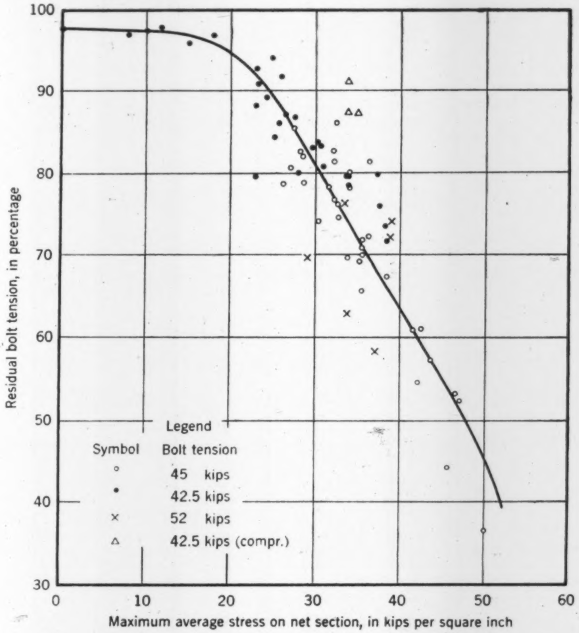

Fig. 6.—Maximum Average Stress on Net Cross-Sectional Area Compared with Residual Bolt Tension

Residual Bolt Tension Related to Joint Stress

A comparison of the maximum average tensile stress (P/A) occurring on the net section of the lap plates during the test and the residual bolt tension after removal of the load from the joint, in percentage of the initial bolt tension, is shown in Fig. 6 for the tension and compression joints. The results indicated that an essentially linear relationship existed between the maximum stress on the net cross section and the residual bolt tension when the former was greater than approximately 20 kips per sq in. As the stress increased from

TABLE 3.—SUMMARY OF TEST RESULTS[a]

SPECIMEN		Surface condition[b]	Average bolt tension, in kips	AVERAGE BOLT SHEAR[c], IN KIPS PER SQUARE INCH		P/A at first slip[d]	Total slip prior to first slip[e]	Coefficient of friction at first slip[f], in %
No.	Type			At first slip	At full bearing			
10	C1	MS	45.1	19.7	25	30.8	9	33
11			44.8	19.4	25	30.2	11	33
12A			45.1	19.2	....	30.0	9	32
12B			45.1	21.9	27	34.3	13	37
Avg				20.1				34
13	C	MS	45.1	17.2	26	17.8	5	29
14			45.3	24.7	28	25.5	22	42
15A			46.0	21.6	....	22.3	10	36
15B			44.8	22.0	31	22.7	13	37
Avg				21.4		22.1		36
16	C2	MS	44.7	23.3	33	17.9	14	40
17			44.6	18.8	32	14.5	10	32
18			44.4	26.4	38	20.3	30	45
Avg				22.8		17.6		39
19	C3	MS	44.9	21.6	33	13.3	17	37
20			44.6	25.2	32	15.5	10	43
21			44.9	24.3	39	14.9	18	41
Avg				23.7		14.6		40
31	C4	MS	24.2	12.5	15	12.9	14	39
32			24.2	11.6	19	12.0	15	37
33			23.8	10.5	19	10.8	6	34
Avg				11.5		11.9		37
37	C	MS	35.7	15.9	24	16.4	21	34
38			36.5	20.2	24	20.7	18	42
39			35.4	16.2	24	16.7	7	35
Avg				17.4		17.9		37
48	C	RL	44.6	....	21	....	....	....
49			44.9	....	....	....	....	....
50			45.0	....	....	....	....	....
51	C	V	44.4	....	....	....	....	....
52			45.5	....	....	....	....	....
53			44.8	....	....	....	....	....
54	C	S	45.6	26.2	25	27.0	16	44
55			44.7	22.5	26	23.2	19	38
56			44.7	34.6	33	35.6	30	59
Avg				27.8		28.6		47
57	C4	MS	35.8	16.9	25	17.4	10	36
58			37.3	18.6	27	19.2	21	38
59			36.8	18.1	25	18.6	12	37
Avg				17.9		18.4		37
63	H	MS	42.4	19.7	27	18.8	35	37
64			42.7	18.9	24	18.0	23	35
65			42.5	21.7	24	20.7	40	40
Avg				20.1		19.2		37
66	J	MS	42.4	18.2	25	16.5	29	34
67			42.4	17.2	23	15.6	29	32
68			42.6	17.3	25	15.7	33	32
Avg				17.6		15.9		33

[a] The term "First Slip," as used in this table, refers to the first major slip. [b] Definitions of code letters are to be found in Table 1. [c] In torsion joints, this is the shear stress on bolts carrying maximum stress. [d] The symbol P represents axial force, and A represents the cross-sectional area. [e] In inches, to be multiplied by 10^{-4}. [f] In torsion joints, this is the coefficient of friction for bolts carrying maximum stress.

TABLE 3.—(*Continued*)

SPECIMEN		Surface condition[b]	Average bolt tension, in kips	AVERAGE BOLT SHEAR[c], IN KIPS PER SQUARE INCH		P/A at first slip[d]	Total slip prior to first slip[e]	Coefficient of friction at first slip[f], in %
No.	Type			At first slip	At full bearing			
74	C	SPR	44.9	20.6	26	21.2	13	35
75			44.6	19.3	30	19.9	9	33
76			45.4	20.1	28	20.7	15	34
Avg				20.0		20.6		34
77	C	MS	42.4	16.7	27	17.9	6	31
78			42.6	17.0	28	18.2	8	31
79A			42.6	21.2	29	22.6	9	39
79B			42.2	17.9	27	18.6	9	33
Avg				18.2		19.3		34
80	C7	MS	42.3	20.0	24	34.3	29	37
81			42.4	15.3	....	26.3	10	29
82			42.6	18.6	26	31.9	11	34
Avg				18.0		30.8		33
101	C	MS	42.2	18.8	29	20.1	15	35
102			42.2	16.5	30	17.6	9	31
103			42.0	15.1	29	16.2	6	28
Avg				16.8		18.0		31
104	C	MS	42.4	20.0	30	21.3	10	37
105			42.2	20.4	30	21.8	12	38
106			42.6	20.4	29	21.8	7	38
Avg				20.3		21.6		38
107	C	MS	52.0	19.9	30	21.2	13	30
108			52.7	18.5	30	19.8	11	28
109			52.0	16.3	28	17.4	11	24
Avg				18.2		19.5		27
119	K $e = 8$ in.	MS	42.5	23.2	....	....	....	43
120			42.5	27.8	....	....	....	51
121			42.2	24.2	34	....	....	45
Avg				25.1				46
122	K $e = 16$ in.	MS	42.8	21.6	28	....	....	40
123			42.8	21.2	33	....	....	39
124			42.3	22.3	30	....	....	41
Avg				21.7				40
128A	C6	MS	41.4	16.6	22	21.9	7	32
128B			42.6	14.1	23	18.6	42	26
129			42.2	13.4	19	17.7	48	24
130			42.3	17.1	18	22.6	10	32
Avg				15.3		20.2		29
131	C5	MS	42.6	17.1	22	28.7	27	32
132			42.3	13.7	23	23.0	9	26
133			43.0	14.8	23	24.7	8	27
Avg				15.2		25.5		28
137	C6	MS	52.1	21.8	29	28.9	36	33
138			52.4	22.3	23	30.3	18	34
139			52.5	21.3	29	28.1	13	33
Avg				21.8		29.1		33

20 kips per sq in. to 50 kips per sq in., the residual bolt tension decreased from 94% to approximately 45% of the original bolt tension. The three compression joints, specimen Nos. 104 through 106, developed residual bolt tensions from 10% to 20% greater than similar joints tested in tension. Overtightening the A 325 bolts to a tension 10% above the elastic proof load of the bolt caused the same proportionate reduction in the residual bolt tension as was found for the 42.5-kip bolt tension.

The residual bolt tension varied little when the maximum tensile stress on the net cross section varied from 0 to 15 kips per sq in.; the residual bolt tension for this range of maximum stress was approximately 97% of the initial value. None of the joints having values of stress on this horizontal part of the curve had reached first major slip; all the joints having values of stress on the sloping part of the curve had undergone their first major slip, and most had slipped into bearing on the bolts.

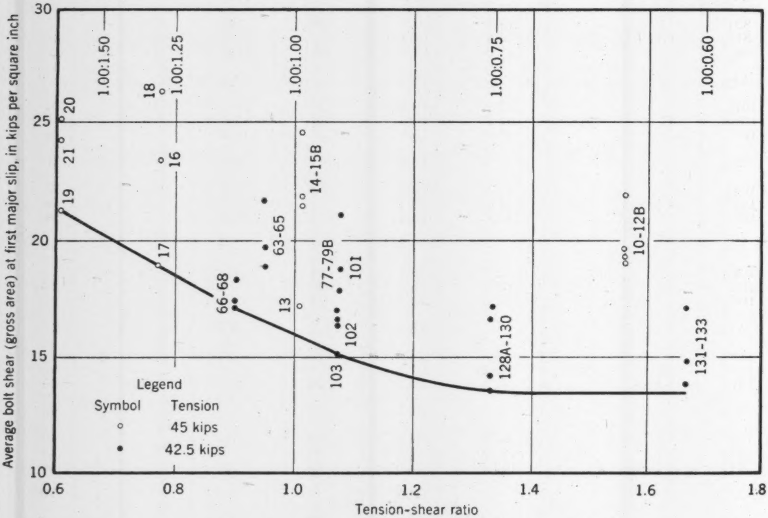

FIG. 7.—COMPARISON BETWEEN AVERAGE BOLT SHEAR AT FIRST MAJOR SLIP AND THE TENSION-SHEAR RATIO

EFFECT OF TENSION-SHEAR RATIO AND FAYING AREA ON AVERAGE BOLT SHEAR

Tension-Shear Ratio.—The data summarized in Table 3 indicate that the tensile stress on the net cross section at the first major slip was often a factor in determining the potential frictional resistance of a tension joint. This fact is indicated in Fig. 7, which is a comparison between the minimum average shear developed on the bolts at first major slip and the tension-shear ratio for tension joints with different net cross-sectional areas. Plotted values in Fig. 7 are identified by the applicable specimen numbers. An increase in the tension-shear ratio corresponds to a decrease in the net cross-sectional areas. As the tension-shear ratio increased, the average shear on the bolts at first major slip decreased sharply. For a tension-shear ratio of 1.33 (or 1.00:0.75, as it is more commonly expressed by the designer), the minimum average shear on the bolts at first major slip was approximately 13,500 lb per sq in.

Because the upper yield point of the plates used in these joints ranged from 32,800 lb per sq in. to 40,000 lb per sq in. and because a stress concentration factor of approximately 3 would exist adjacent to the bolt holes, yielding of the plates in the region of the bolt holes was to be expected when design stress was exerted on the net cross-sectional area. This yielding decreased the thickness of the plates around the bolt holes. The contraction relaxed the tension in the bolts as shown in Fig. 6 and thereby reduced the normal pressure on the faying areas, which produced the frictional resistance.

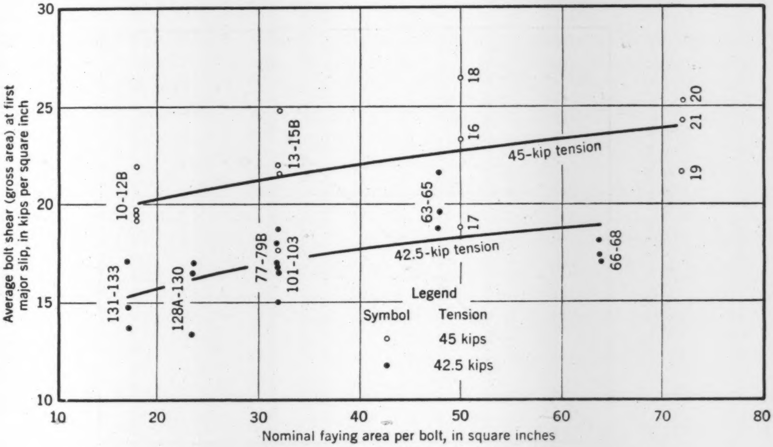

FIG. 8.—COMPARISON BETWEEN AVERAGE BOLT SHEAR AT FIRST MAJOR SLIP AND THE FAYING AREA PER BOLT

Faying Area.—Fig. 8 is a comparison between the average shear on the bolts at first major slip and the nominal faying area per bolt, which is the total faying area of the joint divided by the number of bolts. All these specimens had mill-scale faying areas (prepared as described in the footnote to Table 1). The specimen numbers identify plotted values in Fig. 8. The joints with the larger faying areas developed somewhat higher values of the shear at first major slip than did those with the smaller faying areas. The relationship was not linear, the values of the shear becoming almost constant as the faying area increased. As the joints with the smaller faying areas also had the smaller net cross-sectional areas, the effect of higher stresses in reducing the shear at first major slip (as shown in Fig. 7) must be considered. It seems reasonable to conclude that the size of the faying area alone had no significant effect on the bolt shear developed at first major slip.

Faying area, as previously defined, is the area of overlap between the butt plate and the lap plates. The actual area of contact between the plates was much smaller than the nominal faying area; an examination of the joints after testing showed that the actual areas of contact were concentrated around the immediate vicinity of the bolts.

Effect of Bolt Tension on Average Bolt Shear at First Major Slip

Fig. 9 is a comparison among similar specimens with bolt tensions of 24 kips, 36 kips, 42 kips, 45 kips, and 52 kips per bolt. All the joints in this phase of the investigation had mill-scale surfaces and drilled holes. For the bolt tensions of 24 kips, 36 kips, and 45 kips, only the SAE 4140 bolts were used in the test joints. Both SAE 4140 and A 325 bolts were used for the specimens with the 42.5-kip tension. All bolts with the 52-kip tension were of the A 325 type, tightened to a stress 10% greater than their elastic proof load.

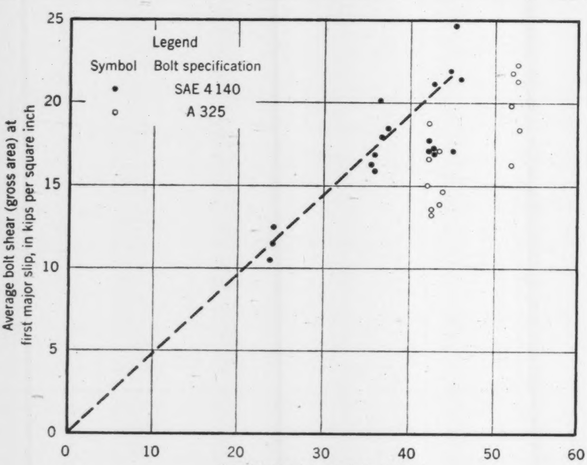

Fig. 9.—Comparison Between the Average Shear on the Bolts at First Major Slip and the Initial Bolt Tension

The results in Fig. 9 showed that the average bolt shear developed at first major slip was linearly related to the bolt tension for values of the bolt tension less than 36 kips. Increasing the bolt tension beyond approximately 36 kips caused no significant increase in the resistance to slip of the bolted joints, so long as the average stress on the net section at first major slip was less than between 16 kips per sq in. and 18 kips per sq in., or less than half the upper yield point of the plate steel. On the contrary, if the minimum stress on the net section at first major slip was greater than between 16 kips per sq in. and

18 kips per sq in., increasing the bolt tension improved the frictional resistance of the joints; the net-section stress for a balanced design with a tension-shear ratio of 1.00:0.75 would be in this higher range.

Effect of the Number of Rows of Bolts on the Average Bolt Shear

The data from specimen Nos. 63 to 68 and specimen Nos. 77 to 79B were used to investigate the effect of the number of rows of bolts in the joint on the slip of the joint. The number of rows of bolts in these joints varied from 2 to 4. The design of these specimens was based on the findings of Fig. 8, which indicated that the average shear on the bolts at first major slip did not appear to depend on the faying area of the joint, providing the tensile stress on the net section was kept constant. It was necessary to increase the net cross-sectional area of these joints as the number of rows of bolts was increased. The test results in Table 3 show that the maximum tensile stress on the net section at first major slip was 22.6 kips per sq in. and the minimum stress was 15.6 kips per sq in.

A shear-slip curve for a typical test from this series is shown in Fig. 5(*d*). When the slip curves of the individual rows of bolts are examined, it may be seen that the first major slip occurred simultaneously on all the bolts.

The plot in Fig. 10(*a*) shows a comparison of the average results obtained from each group of identical joints. Bolts were arranged as shown in Fig. 1. All specimens had mill-scale surfaces. As the number of rows of bolts increased from 2 to 4, the behavior of the joints was essentially the same. For a longer joint, the exterior bolts might slip before the load could be effectively transferred to the interior bolts. Tests of joints with ten and sixteen rows of bolts are being planned (1952).

Effect of the Lap-Plate Thickness on the Average Bolt Shear

The effect of lap-plate thickness on slip was determined by comparing the results obtained from specimen Nos. 80 to 82, which had lap plates $\frac{5}{16}$ in. thick, with those from specimen Nos. 77 to 79B, which had $\frac{1}{2}$-in.-thick lap plates. The average nominal shear on the bolts at first major slip was of the same magnitude for both thicknesses of lap plates; at full bearing the nominal shear on the bolts was less for the joint with the $\frac{5}{16}$-in.-thick lap plates, being 25 kips per sq in. as compared to 28 kips per sq in. for the joints with $\frac{1}{2}$-in.-thick lap plates. The average coefficient of friction at first major slip was 0.33 for the joints with lap plates $\frac{5}{16}$ in. thick and 0.34 for the joints with lap plates $\frac{1}{2}$ in. thick. Thus, for the types of joints tested, there was no apparent difference in the coefficient of friction.

It would seem that the joint with the thinner lap plates would slip at a smaller load because the lap plates would yield at a smaller load. However, it was found that the $\frac{5}{16}$-in.-thick lap plates had an average yield strength of 45.4 kips per sq in. as compared to 38.5 kips per sq in. for the $\frac{1}{2}$-in.-thick plates. Thus, the possible effect of the greater tensile stress on the net section of the $\frac{5}{16}$-in.-thick lap plates was countered in these tests by the higher yield strength of the plate.

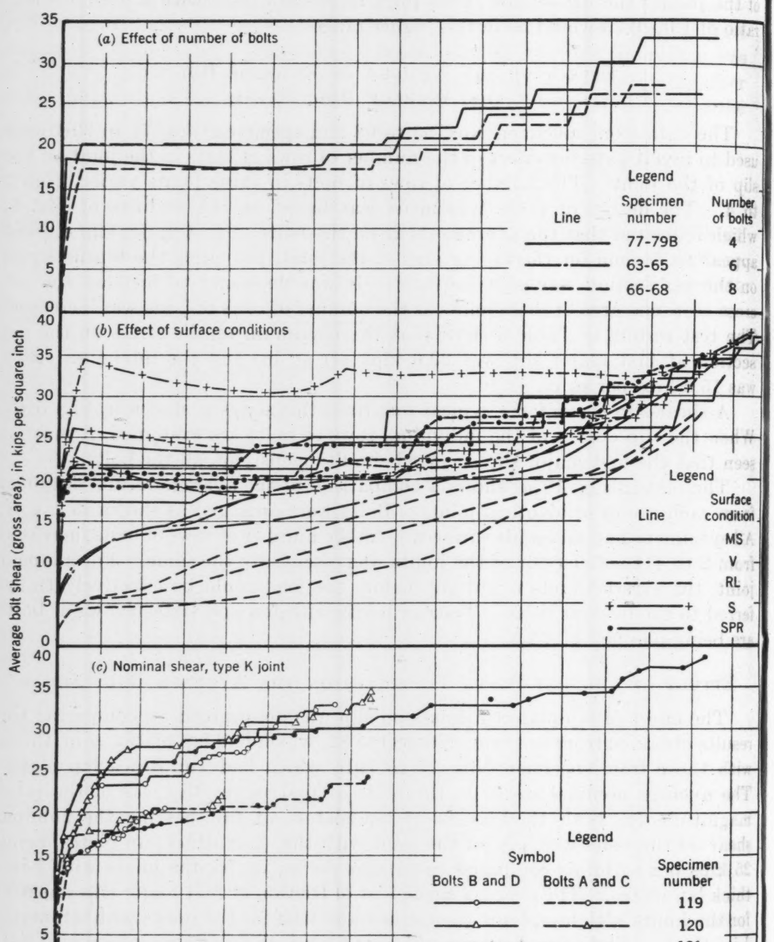

FIG. 10.—RELATION BETWEEN BOLT SHEAR AND SLIP

EFFECT OF THE SURFACE CONDITION OF FAYING AREAS

In tests to determine the effect of the surface condition of faying areas on the slip of bolted joints, type C specimens (Fig. 1) were used exclusively. The tension in the test bolts was approximately 45 kips per bolt. Except as noted in the legend of Fig. 10(*b*), all bolt holes were drilled. The faying surfaces were prepared as previously described (Table 1).

Fig. 10(*b*) shows the shear-slip curves for this series of tests. The different manner in which slip occurred in the joints with painted faying surfaces as compared to those with mill-scale or sandblasted faying surfaces has been described and may also be seen in this figure, which shows the greatly reduced resistance to slip for which these coatings are responsible. Specimens with red lead paint on the faying surfaces developed less resistance to slip than did those with varnish. Because there was no definite point of first major slip and because the distance of slip depended on the period of application of a given load—even for light loads—there was no point even at low values of the bolt shear that could be termed the shear at first major slip.

The average shear stresses developed on the bolts at first major slip were 21.4 kips per sq in., 27.8 kips per sq in., and 20.0 kips per sq in. for specimen Nos. 13 to 15B with mill-scale faying surfaces, specimen Nos. 54 to 56 with sandblasted faying surfaces, and specimen Nos. 74 to 76 with subpunched and reamed holes, respectively. Thus, joints with drilled holes and those with subpunched and reamed holes developed approximately the same shear stress on the bolts at first major slip. Sandblasting the faying areas resulted in an increase in the resistance to slip.

The results of the tests of joints with painted surfaces were so unfavorable that painted faying surfaces are not recommended for bolted joints where slip is undesirable unless the ability of the paint in question to resist shear adequately can be demonstrated. Such a demonstration should subject the test joint to a load sustained for at least four hours to assure that the amount of slip would not increase with time.

A program of tests of joints sustaining loads for long periods of time is in progress (1952). The faying areas of these joints will be coated with various paints and rust preventatives.

SLIP OF BOLTED JOINTS UNDER OTHER TYPES OF LOADING

Compression Joints.—The effect of tensile and compressive loadings on slip was compared in tension specimen Nos. 77 to 79B and compression specimen Nos. 104 to 106. The average shear stress developed on the bolts of the tension joints at first major slip was 18.2 kips per sq in. and on the compression joints was 20.3 kips per sq in. Because of the considerable scatter in the test results of bolted joints, it is reasonable to expect identical joints loaded in either tension or compression to develop approximately equal resistance to slip.

Torsion Joints.—The effect of combined torsional and compressive loading on slip was compared in specimen Nos. 104 to 106, specimen Nos. 119 to 121, and specimen Nos. 122 to 124, in which the eccentricity of the applied load with respect to the center of gravity of the rivet group was 0, 8 in., and 16 in., respectively. Fig. 10(*c*) shows the shear-slip curves for the joints with an eccentricity of the load of 8 in. The nominal shear on the bolts as defined for these tests was computed on the basis of the Gullander method[8] for computing the shear in rivet groups with an eccentric load. The average computed bolt shear stress and the average measured slip used in this plot were those of the two bolts with the maximum computed nominal shear stress and maximum measured slip. The general pattern of behavior in the joints under torsional loading was similar to that in the tension and compression joints. Moreover, on the bolts under maximum shear, the average shear stress at first major slip of 25.1 kips per sq in. for a load eccentricity of 8 in. and 21.7 kips per sq in. for 16 in. compared favorably with the value of 20.3 kips per sq in. in the axially loaded joint. Although insufficient tests were made to establish a definite conclusion, it would appear feasible to apply the Gullander method to the design of eccentrically loaded bolted joints.

CONCLUSIONS

The results of the writers' research seem to justify the following conclusions with respect to the types of bolted joints tested in this investigation:

1. The prevention of appreciable slip by the use of properly tightened high-strength steel bolts is both possible and practicable.
2. For most of the joints, the shear stress on the gross area of the bolts at first major slip for joints with mill-scale faying surfaces was developed when the average stress on the net section of the joint was equal to, or slightly greater than, one half the upper yield-point stress of the plates.
3. Increasing the bolt tension beyond 36 kips caused no significant increase in the resistance to slip of the bolted joints, so long as the average stress on the net cross section at first major slip was less than from 16 kips per sq in. to 18 kips per sq in., or less than half the upper yield point of the plate steel. On the contrary, if the minimum stress on the net cross section at first major slip was greater than from 16 kips per sq in. to 18 kips per sq in., an increase of the bolt tension caused an increase of the frictional resistance of the joints; the stress required for a balanced design, with a tension-shear ratio of 1.00:0.75, would be in this higher range.
4. Properties of the joints such as the lap-plate thickness, the faying area, and the bolt pattern did not appear to have any important effect on the shear developed on the bolts at first major slip.
5. The few tests made of torsion joints indicated that it is feasible to apply the Gullander method to the design of eccentrically loaded joints.
6. Painted faying areas are not recommended for bolted joints unless the ability of the paint in question to resist shear adequately can be demonstrated. Red lead paint and varnish did not give satisfactory performance in these tests.

Further tests (1952) are required before adequate data on bolted joints under static loads will be available.

---

[8] "Structural Design," by H. Sutherland and H. L. Bowman, John Wiley & Sons, Inc., New York, N. Y. 1938, p. 73.

FATIGUE IN RIVETED AND BOLTED SINGLE-LAP JOINTS

BY JACK W. CARTER[1] AND KENNETH H. LENZEN,[2] ASSOCIATE MEMBERS, ASCE, AND LAWRENCE T. WYLY,[3] M. ASCE

WITH DISCUSSION BY MESSRS. GLENN B. WOODRUFF; KARL DE VRIES; HARRY C. PRINCE; AND JACK W. CARTER, KENNETH H. LENZEN, AND LAWRENCE T. WYLY

SYNOPSIS

This paper presents a working hypothesis to explain rationally the cause of, and remedy for, fatigue failures in structural joints and includes supporting evidence. It also presents a correlation of results of a number of fatigue tests of double-lap joints made in the United States and attempts to show that these results are explained by this hypothesis.

INTRODUCTION

When studying new relationships or phenomena that are only imperfectly understood, the scientific procedure is to establish a working hypothesis which will take account of all the known facts and which can be used to assist the investigator in evaluating the relationships between new facts and facts already known and to aid him in planning the search for new facts or relationships. This hypothesis is modified when necessary to conform to these new facts. The writers have followed this procedure in the project described herein.

SURVEY OF FATIGUE FAILURES IN STRUCTURAL MEMBERS

In 1947, at the request of Committee 15 of the American Railway Engineering Association (AREA), the Association of American Railroads (AAR) began an investigation of the causes of and remedies for the fatigue failures in floorbeam hangers in railway bridges. This study has consisted of a survey of the failures, field stress measurements on structures under service loads, laboratory studies under controlled conditions, and theoretical analyses. The following facts yielded by the survey are significant:

1. Some special circumstances or combination of circumstances must cause the failures because only one sixth of the railroads have reported these failures and only a few hangers have developed failures in the structures of a given railroad.

NOTE.—Presented at the Centennial Convocation, Chicago, Ill., September, 1952. Published, essentially as printed here, in August, 1954, as *Proceedings-Separate No. 469.* Positions and titles given are those in effect when the paper or discussion was received for publication.

[1] Senior Engr., The Glenn L. Martin Co., Baltimore, Md.; formerly Asst. Prof. of Structural Eng. and Research Associate, Purdue Univ., Lafayette, Ind.

[2] Instructor in Civ. Eng. and Research Associate, Purdue Univ., Lafayette, Ind.

[3] Research Prof. and Head, Structural Eng. Dept., Purdue Univ., Lafayette, Ind.

2. Although the stress history of the members cannot be established definitely, investigation shows that the number of cycles of heavy loading has probably been less than 100,000 in most cases; axial stresses and bending stresses have not been great (in some cases being quite small); the failures have not occurred at points of greatest computed stress; and the range of stress has been relatively large—from 1 kip per sq in. or 2 kips per sq in. to maximum tension stress.

3. With one or two exceptions, in which vibration seems to have controlled, the failures have all occurred through the lowest rivet holes connecting the members to the gussets.

4. The failure cracks have usually begun at the edge of the rivet hole nearest the toe of the hanger angle or channel at the point where the maximum tensile stress and strain concentration would be computed on the basis of elastic behavior, assuming the load to be delivered to the angle by rivet bearing. The cracks may start in any one of the four angles of the hanger. The cracks usually progress toward the edge of the angle first and subsequently may extend to the back of the angle.

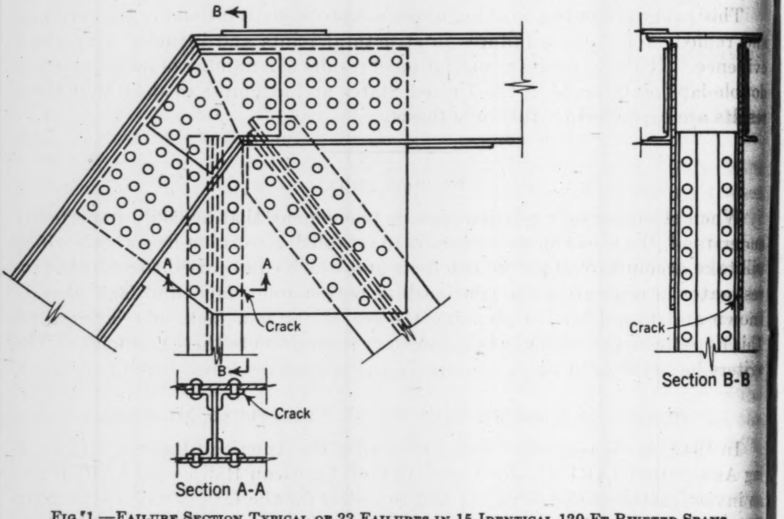

FIG. 1.—FAILURE SECTION TYPICAL OF 22 FAILURES IN 15 IDENTICAL 120-FT RIVETED SPANS

5. Although it is not possible to arrive at any exact knowledge of either the maximum stress or the state of stress preceding a failure crack in a particular member, it is evident that the incidence of failure is increased by the presence of higher unit stresses.

6. These hanger failures have all occurred in single-lap joints (Fig. 1).

7. The working stresses to which these single-lap connections had been subjected and which led to failures were much less than the fatigue strengths of double-lap joint previously reported by W. M. Wilson,[4] Hon. M. ASCE.

---

[4] "Fatigue Strength of Riveted Joints," by W. M. Wilson and F. P. Thomas, *Bulletin No. 302*, Univ. of Illinois Experiment Station, Urbana, Ill., 1938.

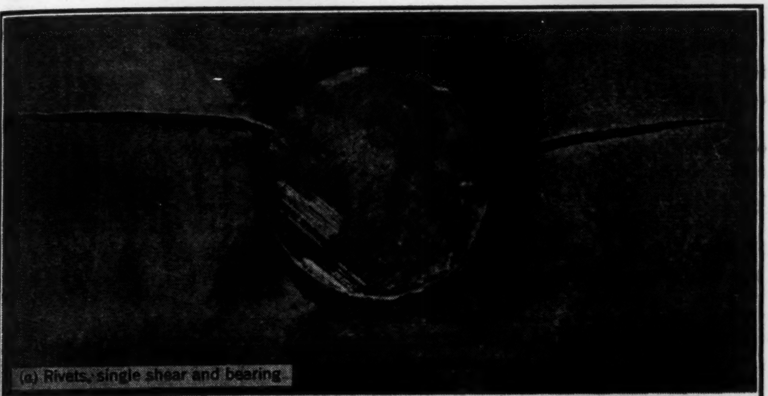

(a) Rivets, single shear and bearing

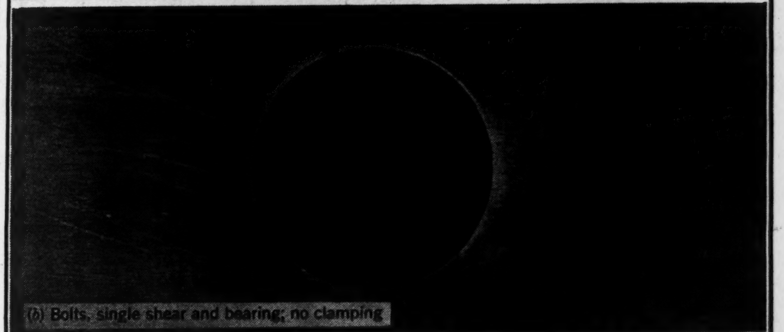

(b) Bolts, single shear and bearing; no clamping

(c) High-strength bolts, no bearing

Fig. 2.—Fatigue Failure in Riveted and Bolted Structural Joints

HYPOTHESIS

Consideration of the foregoing facts led one of the writers to formulate the following working hypothesis explaining the failures and offering a proposed remedy.[5,6]

Working Hypothesis.—It is assumed that the index to the fatigue strength of a structural member is given by the magnitude of the tensile stress concentrations, computed on the elastic basis, and the total tensile strain concentrations to which the member is repeatedly subjected.

The principal source of high stress concentrations and strain concentrations that result in the low fatigue strength of the hangers is the bearing of the rivets nearest the edge of the gussets in the holes at the failure section. These concentrations occur most frequently with rivets that have lost—or never had—high clamping force.

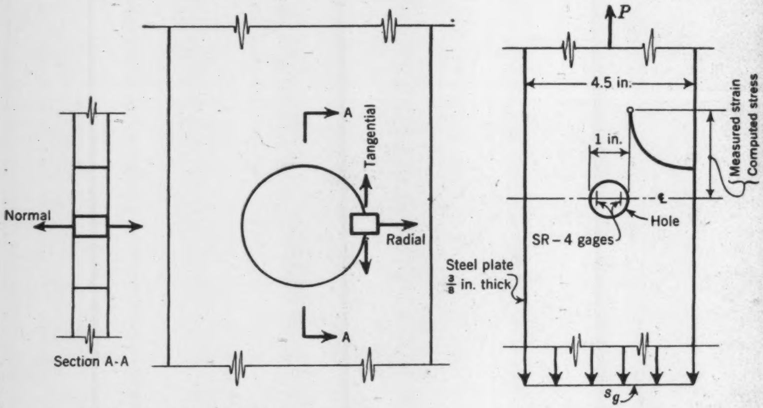

(*a*) Designation of stresses and strains (*b*) Test layout

FIG. 3.—STRESSES AND STRAINS AT THE SIDE OF A HOLE, PLOTTED IN FIGS. 4, 5, AND 6

Proposed Remedy for Fatigue Failures.—This reasoning shows that the remedy must lie in the elimination of bearing in the rivets at the edge of the gussets and the securing of a high clamping force at these holes.

The natural solution for fatigue failures in riveted joints is obtained by replacing the rivets by nonbearing, high-strength, high-clamping-force bolts that will have ample initial clearance in the hole (and therefore will not bear on the plates) and by providing these bolts with a clamping force large enough to (1) prevent slip and (2) provide an initial compression stress and strain at the sides of the holes.

The foregoing explanation was first presented to AREA Committee 15 at Purdue University (Lafayette, Ind.) in November, 1948. Because the writers

---

[5] "Report of Assignment 4. Stress Distribution in Bridge Frames—Floorbeam Hangers," by Lawrence T. Wyly, *Proceedings*, A.R.E.A., Vol. 51, 1950, pp. 498–499.

[6] "Symposium on High Strength Bolts, Part I," by Lawrence T. Wyly, *Proceedings*, AISC Engineering Conference, Chicago, Ill., April 12, 1950, pp. 22–27.

feel that this explanation of the fatigue failures in riveted tension members and the proposed remedy have been verified by studies by others and by themselves and that the same explanation and remedy apply to double-lap joints as well as to the single-lap, tension-member connections and to beams with riveted cover plates, the remainder of the paper will be devoted to developing this thesis. Supporting evidence will be given in detail.

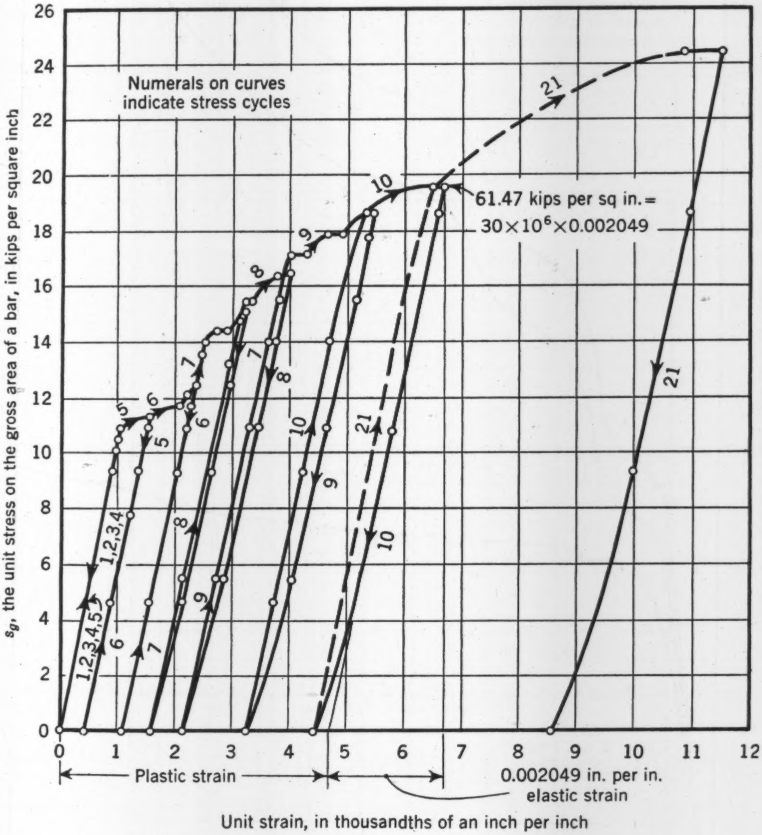

Fig. 4.—Measured Strains at the Sides of a Hole in a Plate Under Increasing Axial Tension (Figs. 3, 4, 5, and 6 To Be Considered Together)

Supporting Evidence

Typical Fatigue Failures in Riveted and Bolted Structural Joints.—Fig. 2 consists of photographs of typical failures in riveted and bolted structural joints. If plates are connected by rivets or bolts acting in single shear and bearing and

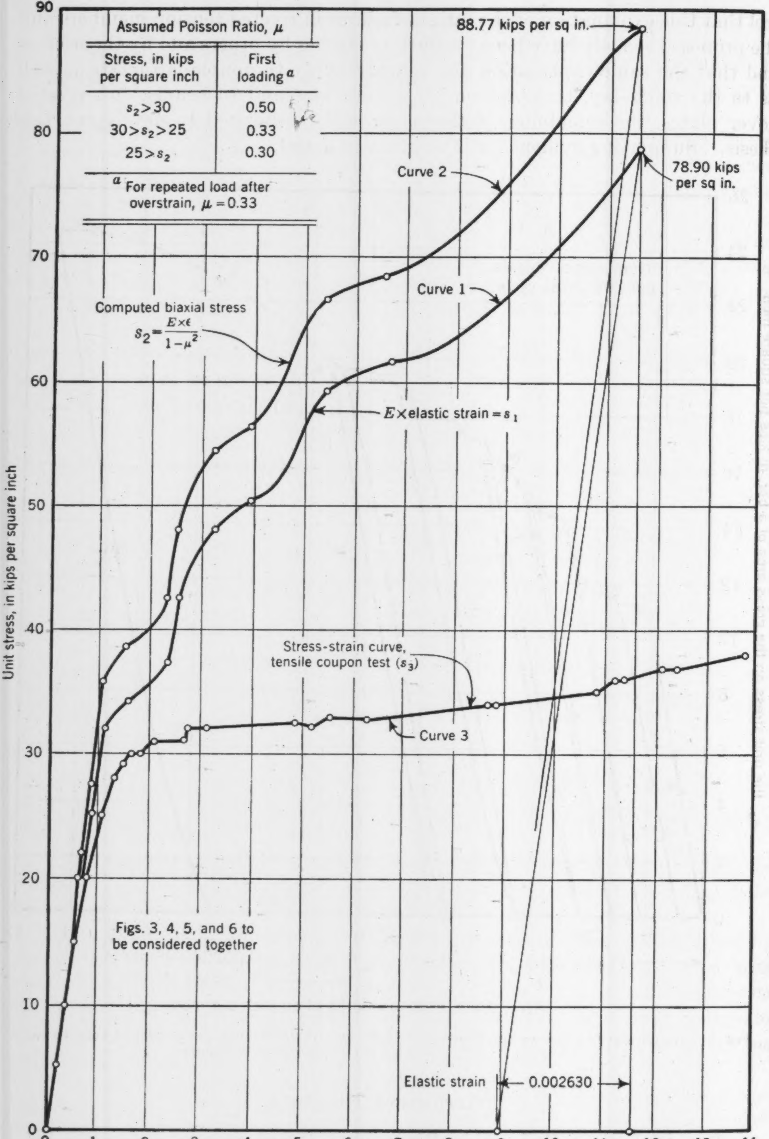

FIG. 5.—COMPARISON OF TENSILE-COUPON TESTS WITH STRESSES AT THE SIDES OF A HOLE IN A PLATE UNDER AXIAL LOAD

exerting little or no clamping force, the type of fatigue failure cracks shown in Fig. 2(*a*) and Fig. 2(*b*) may be expected. If the plates are connected by high-strength bolts having no shear and no bearing and transmitting load by friction which results from high clamping, the type of fatigue cracks shown in Fig. 2(*c*) may be expected. The failures (Fig. 2) were obtained in laboratory tests by two of the writers. Examination of field failures in fatigue of riveted joints usually shows the type of cracks illustrated in Fig. 2(*a*) and Fig. 2(*b*).

Stress and Strain Concentrations.—The stresses and strains at the sides of a rivet hole or bolt hole in a plate under increasing and repeated axial tension have been studied by testing. In Fig. 3 are shown the test layout and the designation of the stresses and strains plotted in Figs. 4, 5, and 6. In Fig. 4 are shown the measured tangential strains for such a test that was performed by two of the writers in 1949. In Fig. 5 are compared the stresses computed for this test on the assumptions of both uniaxial and biaxial stress. A Tuckerman optical strain gage was used for the coupon test. The tangential strain and stress concentration factors, *K*, at the sides of the hole are shown in Fig. 6. For stress,

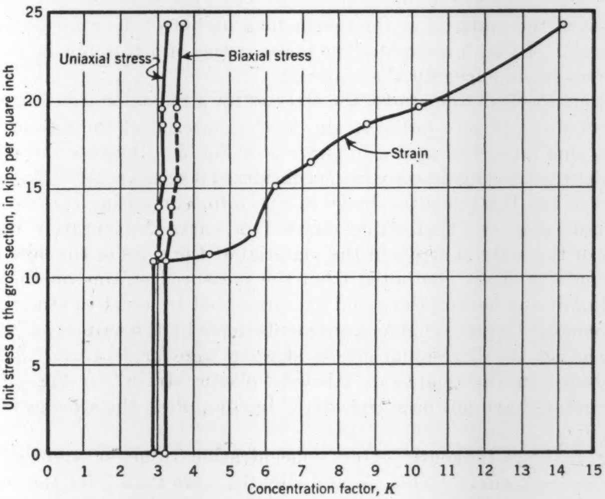

FIG. 6.—CONCENTRATION FACTOR, *K*, FOR STRESS AND STRAIN, CORRESPONDING TO THE TEST OF FIG. 4 (FIGS. 3, 4, 5, AND 6 TO BE CONSIDERED TOGETHER)

$$K = \frac{\text{stress}}{s_g} \quad\text{.........................}\quad (1)$$

in which s_g is the tensile stress on the gross cross section; for strain,

$$K = \frac{\text{strain}}{\dfrac{s_g}{30{,}000{,}000}} \quad\text{.........................}\quad (2)$$

Theoretically, $K = 3.2$ for stresses below the elastic limit.[7] In Figs. 4 and 6 the ordinates are the average stress on the gross area of the bar. The following facts are emphasized by these tests:

1. The graphs of Fig. 4 bear a striking resemblance to the stress-strain graphs for the tensile tests of the material; the proportional limit and yield point are plainly evident. Also present are the plastic flow and strain hardening, overstrain, recovery of elasticity, and the characteristic hysteresis loops.
2. After the material at the sides of the hole had been stressed well into the plastic range and allowed to rest, strain measurements, made by the writers but not published here, showed that the material had recovered its elasticity.
3. Curve 1 of Fig. 5 was computed from the unloading graphs of the hysteresis loops by multiplying the modulus of elasticity, E, of 30,000 kips per sq in. by the elastic strains, ϵ. In the region above the proportional limit, stresses shown by this curve are increasingly larger than the stresses of curve 3 for a coupon test of the material as the tensile load on both is increased.
4. Curve 1 of Fig. 5 resembles the lower stages of a true biaxial or triaxial tensile-stress-strain curve for the material.
5. For comparison and study, the stresses for a biaxial state of stress (that is, for a condition of zero radial strain) in the material at the side of the hole have been computed and shown in curve 2 of Fig. 5. Because the stress and strain under repeated loading are being considered it seems reasonable to assume the values of the Poisson ratio shown in Fig. 5 for computing these stresses.

It is not suggested that either curve 1 or curve 2 accurately represents the stress or the state of stress in the material at the sides of the hole. These graphs represent stress computed from the measured strains on the basis of certain simplifying assumptions and are presented to assist in studying these measurements. Unpublished measurements made by the writers indicate that, after unloading, small residual elastic stresses were present and that elastic strains existed in the quantities labeled "plastic strain" in Fig. 2. These residual stresses have not been considered in computing the stresses for curves 1 and 2.

6. Fig. 6 shows tangential-stress concentration values of approximately 3 for the stresses of curve 1 (Fig. 5) and slightly more than 3 for the stresses of curve 2 in the material at the sides of the hole. This value remains nearly constant as the tension in the bar is increased and the material at the sides of the hole passes into the plastic region. Interestingly, the value of K equal to 3.2 computed from the measured strains for biaxial stress in Fig. 6 agrees with the theoretical value for a specimen of the proportions tested.[8,9] The residual stresses noted previously have not been considered in computing the stress concentrations plotted in Fig. 6. The tangential strain concentrations in the material at the sides of the hole increase rapidly as the axial tension is increased, the maximum value measured in this test being approximately 14. At rupture of the material the value must be very large.

---

[7] "Advanced Mechanics of Materials," by Glenn Murphy, McGraw-Hill Book Co., Inc., New York, N. Y., 1946, p. 98, Fig. 35.

[8] "On the Stresses in the Neighborhood of a Circular Hole in a Strip under Tension," by R. C. J. Howland, *Transactions*, Royal Soc. of London, Vol. 229, Series A, 1929, p. 49.

[9] "Stress Concentration Produced by Holes and Notches," by A. M. Wahl and R. Beeuwkes, *Transactions*, ASME, Vol. 56, 1934, pp. 617–625.

7. Probably tangential stress and strain concentrations at the sides of the hole repeated many times open up and extend the infinitesimal crack in the material (a postulate held in all fatigue-failure theories), and this action undoubtedly increases with the magnitude of the stress and strain concentrations —that is, as the axial tension in the plate increases.

8. It seems likely that the stress and strain concentrations that occur at the root of the above infinitesimal crack develop in the same manner as the strain and stress concentrations measured at the side of the hole in Fig. 2, probably producing a brittle state of stress. When this stress reaches the true tensile strength of the material, the latter pulls apart and crack propagation has begun.

9. The fatigue strength of the plate should vary inversely with stress and strain concentrations and hence inversely with stress on the gross area provided that the stress at the side of the hole does not reach the elastic limit of the material. The fatigue strength of the plate should decrease rapidly as stress in the plate producing tangential stress at the side of the hole is raised above the yield point.

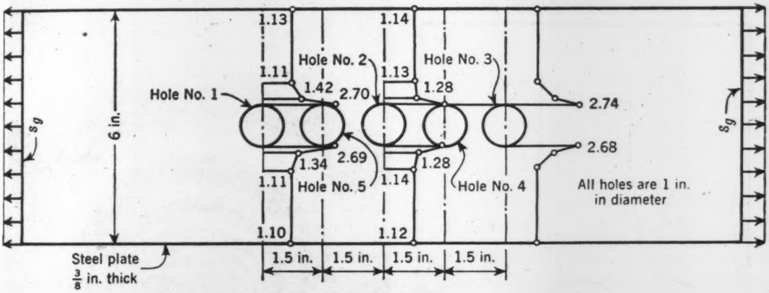

(a) Values of *K*

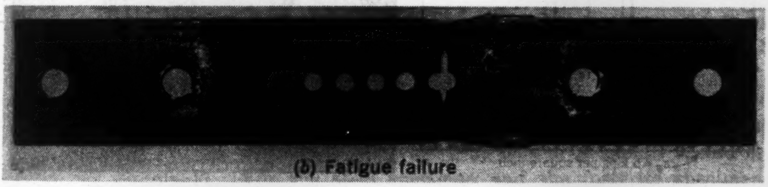

(b) Fatigue failure

FIG. 7.—STRESS CONCENTRATION AS RELATED TO FATIGUE FAILURE

These facts assist in explaining the influence of so-called "stress raisers," such as notches, holes, and corrosion pits, in lowering the fatigue strength of ductile material.

The outstanding feature of the graphs of Fig. 4 is the magnitude of the elastic strain developed for a given total strain in the material at the side of the hole.

The behavior of this material is undoubtedly explained in large part by the reinforcing effect of the material in the plate immediately behind and integral with the thin section that resists the high local stresses. This situation is analogous to the case of a steel beam stressed above the elastic limit on the extreme fiber. Because this overstressed material is reinforced by the adjacent elastic material lying in the direction of the neutral axis, only limited plastic flow occurs. Therefore, no sudden and large deflection will occur until all parts of the cross section of the beam flange have reached the plastic state in bending.

The restraining action of the elastic material of the plate permits only very small increments of strain to occur during a given time in the highly stressed thin section at the side of the hole. When the stress in the thin layer of steel at the side of the hole reaches the yield point, at a strain of approximately 0.001 in. per in., flow occurs (Fig. 4). This flow is limited by the restraint of the next adjacent layer which is still elastic. As additional tension is added to the plate, the next adjacent layer stretches elastically—the first layer resisting no additional stress at this stage; the additional strain measured in the strain gage on the first layer is due to elastic stretch in this second layer. When the yield point in this second layer is reached, it in turn will flow and again will be restrained by the third layer—the strain measured in the gage on the first layer being always influenced by the restraining layers of material.

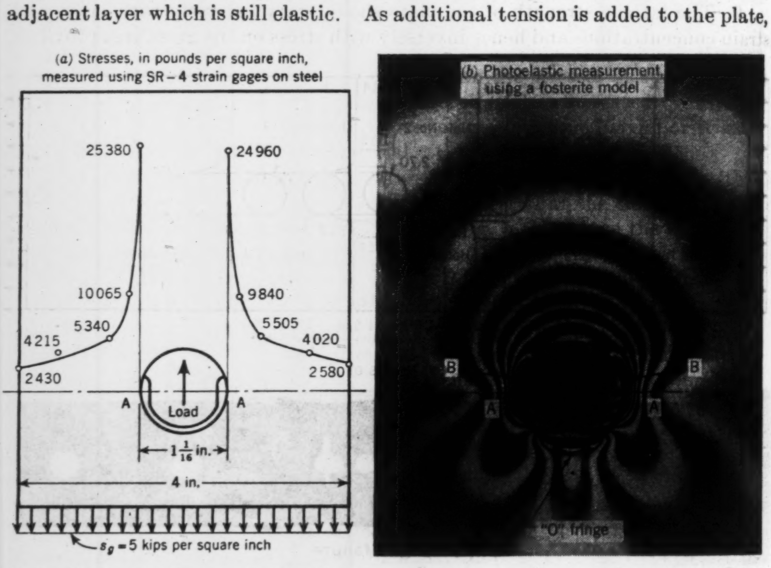
(a) Stresses, in pounds per square inch, measured using SR-4 strain gages on steel

(b) Photoelastic measurement, using a fosterite model

FIG. 8.—CORRELATION BETWEEN STRESSES DETERMINED PHOTOELASTICALLY AND BY USING STRAIN GAGES

It is possible that some radial stress, or some normal stress—or both—may also act on the material in question. The adjacent elastic material may restrict the contraction in a normal direction as the material stretches in a tangential direction.

There is no stress radial to the surface of the material at the sides of the hole. However, at a very small depth below this surface there is such a radial stress in tension, and it is possible that this stress reduces the strains at the sides of the hole. It is also possible that, under these restrained flow conditions, the rise in the Poisson ratio from the elastic value of the order of 0.25 or 0.30 to the plastic value of approximately 0.50 may occur gradually. This condition would also affect relations between stress and observed strains.

Where a notch is substituted for a hole as the strain-and-stress raiser, the increase of the radial tensile stress just below the surface at the root of the notch is quite large and develops quickly. A clear picture of this action has been provided by Maxwell Gensamer.[10] The spreading of the plastic region around the hole in a tension member is clearly described by A. Nadai.[11]

The proportionality between fatigue strength and stress concentrations in the member for values of the latter between zero and approximately 3 has long been recognized. The experimental determination of the stress concentration by comparative fatigue tests for stresses within the elastic limit depends on this proportionality.[12] Fig. 7 also illustrates this relation. The stress concentrations in each of the five holes in line in the steel plate were measured experimentally. The plate was then tested in the fatigue machine, and failure by progressive brittle fracture occurred through one of the end holes where stress concentration was greatest. In Fig. 7, $K = s/s_g$, in which s_{min} was $+ 2$ kips per sq in. and s_{max} was $+ 30$ kips per sq in. The number of cycles, N, was 103,000. High-clamping-force bolts were used to grip the specimen through the large holes shown in Fig. 7(*b*).

Concentrations Due to Rivet Bearing.—When a load is applied to the plate through the bearing of a rivet on the material around the hole, the tangential stress concentrations and strain concentrations are approximately 6, or twice as large as in the former case; and (as shown in Fig. 8) the maximum stress at the side of the hole occurs at a distance equal to about a sixth of the diameter from the center line A–A on the bearing side. The photoelastic measurements by E. O. Stitz and the steel plate measurements by one of the authors of Fig. 8 check and and supplement each other.

In the photoelastic experiment of Fig. 8(*b*), $s = 2\,n\,f/t$, in which n is the the number of fringes, f is the material constant (1.95), and t is the thickness of the model. For the photograph shown, n_a, at section A, equals 9, and n_b, section B, equals 11. For the steel specimen and the fosterite specimen, $d/W = 0.236$. The resulting stresses, in pounds per square inch, were as follows:

Stresses	Fosterite	Steel
s_g	21.1	5,000
s_a	106	25,380
s_b	134	
s_a/s_g	5.03	5.10
s_b/s_g	6.25	

The subscripts *a* and *b* refer to sections A and B.

---

[10] "Strength and Ductility," by Maxwell Gensamer, *Transactions*, Am. Soc. for Metals, 1946, p. 55, Fig. 19.

[11] "Theory of Flow and Fracture of Solids," by A. Nadai, McGraw-Hill Book Co., Inc., New York, N. Y., 2d Ed., 1950, Vol. 1, pp. 289–296, Figs. 18–32 to 18–45.

[12] "Resistance of Materials," by Fred B. Seely, John Wiley & Sons, Inc., New York, N. Y., 3d Ed., 1947, pp. 292–294.

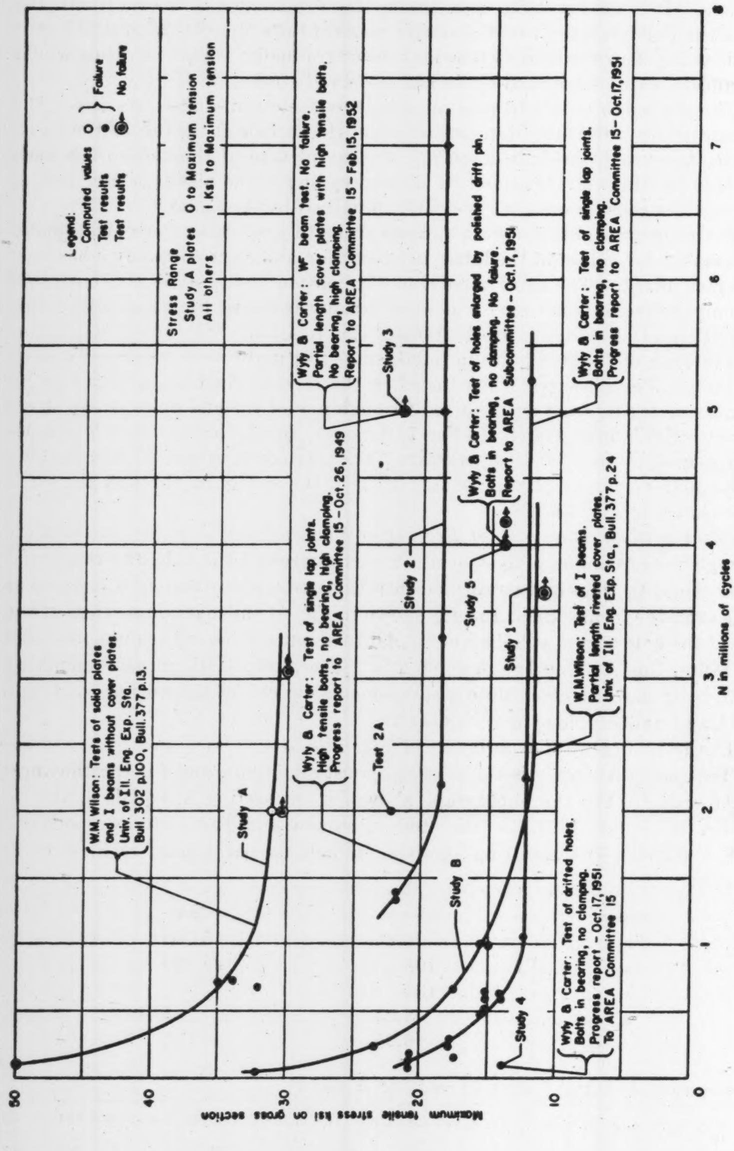

Fig. 9(a).—Fatigue Studies, Riveted and Bolted Single-Lap Joints (Figs. 9 and 10 To Be Considered Together)

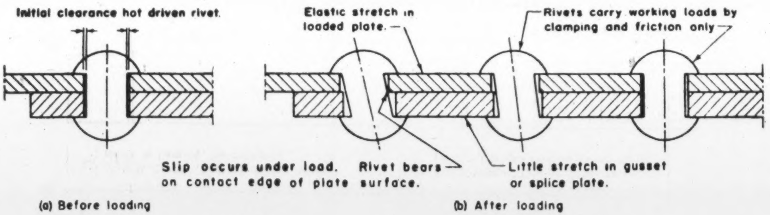
Initial clearance hot driven rivet.
Elastic stretch in loaded plate.
Rivets carry working loads by clamping and friction only
Slip occurs under load. Rivet bears on contact edge of plate surface.
Little stretch in gusset or splice plate.

(a) Before loading

(b) After loading

Eccentric bearing of end rivet on plate in lap joint

CAUSE High stress and strain concentrations at sides of holes due to high rivet bearing plus low clamping

1. Plates slip under working loads, especially at end rivets, and when clamping force is low. End rivets are overloaded. See (b) and Fig. 9.
2. With low clamping large rivet bearing sets up high stress and strain concentrations at sides of holes. For single lap joints these concentrations are very high at the edge of the contact plane of the plate. See (b) and Fig. 12
3. With low clamping force, a range of stress in the member will produce a magnified range of stress and strain at the sides of the holes and will lower the fatigue strength of the member. See Figs. 1,2,3,4,12 and Studies 1, B and A of Fig 7A.

REMEDY Eliminate rivet bearing and provide a high clamping force.

1. Replace rivets by bolts and provide enough clearance so that the bolt will not bear on plate in the hole under service loads. See (e).
2. Provide a high clamping force in the bolt to prevent slip under service loads and to prevent high stress and strain concentrations at the sides of the hole. See Fig. 13(a),(b),(c) and Fig. 15(b).
3. Provide design of washer adequate to reduce tensile stresses and strains in plate from clamping so that fatigue failures in the plate outside the hole will be avoided. See Figs. 13(d) and 14.
4. Avoid local stress and strain raisers in the holes due to drifting or other damage. See Fig. 7A, Study 4. Also avoid notches and other stress raisers in fabrication
5. With the high tensile stress and strain concentrations at the sides of the hole due to the bolt and to rivet bearing eliminated by high clamping, and with the high tensile stress and strain concentrations in the face of the plate under the washer due to high clamping reduced, the fatigue strength of the plate will approach the fatigue strength of a solid plate with no holes. See Fig. 7A, Studies 2,2A,3.

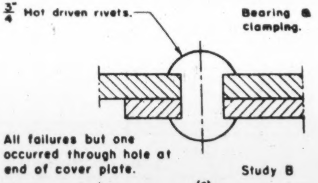
$\frac{3}{4}$" Hot driven rivets.
Bearing & clamping.
All failures but one occurred through hole at end of cover plate.
Study B

(c)

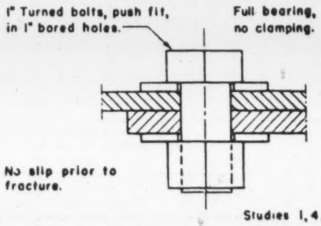
1" Turned bolts, push fit, in 1" bored holes.
Full bearing, no clamping.
No slip prior to fracture.
Studies 1,4,5

(d)

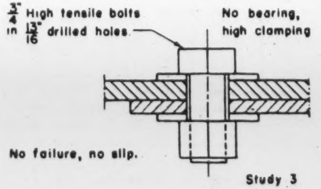
$\frac{3}{4}$" High tensile bolts in $\frac{13}{16}$" drilled holes.
No bearing, high clamping
No failure, no slip.
Study 3

(e)

Note Connections for Studies 2,2A similar except 1" bolts used

FIG. 9(*b*).—CAUSES AND REMEDIES FOR FATIGUE FAILURE (FIGS. 9 AND 10 TO BE CONSIDERED TOGETHER)

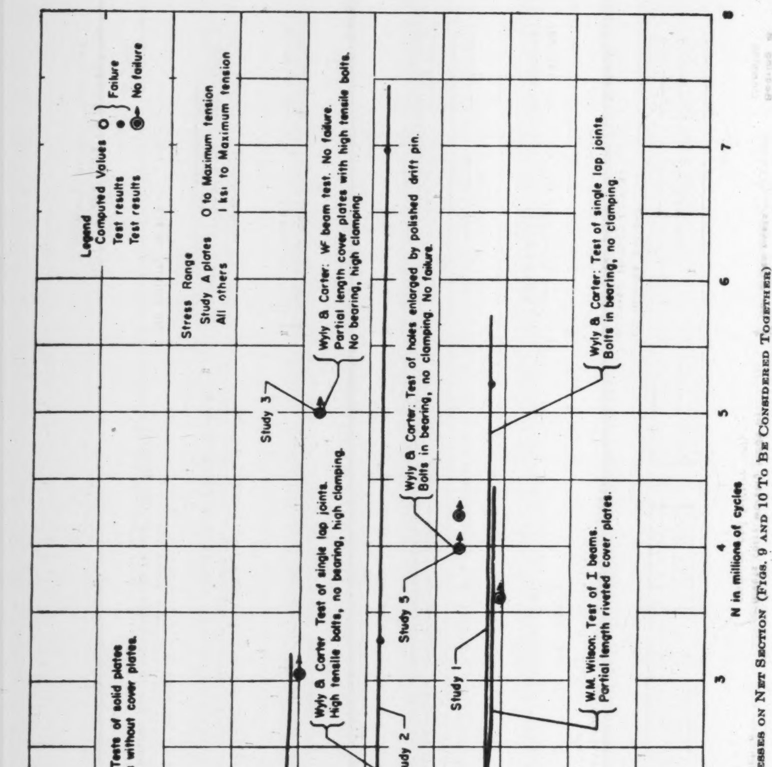

FIG. 10.—STRESSES ON NET SECTION (FIGS. 9 AND 10 TO BE CONSIDERED TOGETHER)

In a single-lap joint, the effect of the bearing of the rivet on the edge of the contact face of the plate when slip occurs, as shown subsequently in Fig. 9(*b*), is to produce a magnification of the stress and strain concentration at the side of the hole.

Overload and Bearing Stress in End Rivets.—In tests on a double-lap tension joint having a single line of rivets, M. B. Scott, A. M. ASCE, J. M. Durfee, and R. M. Stone, J. M. ASCE, have observed that at working loads the rivets at the end of the splice or gusset plates are overloaded 100% or more the inside rivets take very little load, and slip of the end rivets may occur at working loads (Fig. 11, appearing subsequently).[13,14,15] Previous studies by other investigators had demonstrated the same overloading of the end rivets.[16,17]

Exploratory Laboratory Fatigue Tests.—In Fig. 9 are summarized the results of the exploratory fatigue tests made by two of the writers. The tests were made to check the foregoing working hypothesis and proposed remedy. All stress computations are based on the gross section. To the writers this seems to be desirable because it provides a common denominator to use for all cases. However, results of the same tests, showing the stresses on the net section, are presented for comparison in Fig. 10.

For repeated stresses acting in tension only, the results of all fatigue tests of riveted and bolted structural joints for a given grade of steel, when plotted in the form of Figs. 9 and 10, should fall between two boundary curves: (1) The upper curve of study A, representing the fatigue strength of plain structural steel plates having no holes, and (2) the lower curve of study 1, representing the fatigue strength of a single-lap joint connected by bolts having no clamping force and transmitting loads by shear and bearing only. This is tantamount to stating that the most unfavorable stress and strain concentrations at the sides of the holes will be caused by loads delivered through rivet bearing with no clamping present and that the most favorable stress and strain concentrations at the sides of the holes will result if large clamping forces but no bearing stresses are present. Exceptions will occur if lateral bending, poor holes, or other unusual stress-raising factors are present because these may decrease the fatigue strength of the joints represented by the lower curve. Examples of such exceptions are given subsequently. For structural carbon steel, the upper boundary curve (study A, Fig. 9(*a*)) was given by tests on plates without holes[18] and on a standard I-beam without cover plates.[19] For structural steel having a yield point of 32 kips per sq in., a lower boundary curve has been obtained by

---

[13] "Report of Assignment 4. Stress Distribution in Bridge Frames—Floorbeam Hangers," by Lawrence T. Wyly, *Proceedings*, A.R.E.A., Vol. 51, 1950, p. 492, Fig. 23.

[14] "An Investigation of the Effect of Clamping Force on Load Distribution in a Single Line Riveted and Bolted Butt Joint," by J. M. Durfee, thesis presented, in 1950, to Purdue Univ., Lafayette, Ind., in partial fulfilment of the requirements for the degree of Master of Science.

[15] "Investigation of the Load Distribution in a Single Line Riveted and Bolted Butt Joint," by R. M. Stone, thesis presented, in 1950, to Purdue Univ., Lafayette, Ind., in partial fulfilment of the requirements for the degree of Master of Science.

[16] "Tension Tests of Large Riveted Joints," by Raymond E. Davis, Glenn B. Woodruff, and Harmer E. Davis, *Transactions*, ASCE, Vol. 105, 1940, pp. 1222–1225, Fig. 13.

[17] Discussion by H. N. Hill and Marshall Holt of "Work of Rivets in Riveted Joints," by A. Hrennikoff, *ibid.*, Vol. 99, 1934, p. 467, Table 5.

[18] "Fatigue Strength of Riveted Joints," by W. M. Wilson and F. P. Thomas, ***Bulletin No. 302***, Univ. of Illinois Eng. Experiment Station, Urbana, Ill., 1938, p. 100, Table 37.

[19] "Flexural Fatigue Strength of Steel Beams," by W. M. Wilson, ***Bulletin No. 377***, Univ. of Illinois Eng. Experiment Station, Urbana, Ill., January 22, 1948, p. 13, Table 3.

two of the writers and is shown as study No. 1, Fig. 9(*a*).[20,21] In this series the holes were bored and the bolts were turned to a push-fit in the holes. The nuts were turned on by the fingers only and held in place with cotters; no clamping was used. The endurance limit for these conditions was found to be 16 kips per sq in. on the net area or approximately 12.5 kips per sq in. on the gross area. Because the rivets in bearing at the end of a partial-length cover plate should have about the same stress-raising and strain-raising effect on the beam flange as the rivets in bearing at the end of the hanger gusset plate have on the hanger material, the same fatigue strength should be expected of each. Significantly, the curve showing the fatigue strength of standard I-beams with partial-length cover plates (study B, Fig. 9)[22] agrees closely with study 1 for a single-lap joint. The added fatigue strength due to rivet clamping may explain the fact that, for a million cycles of stress or less, the beam tests show slightly greater strength than the bolted joints in study 1. It is equally significant that, with one exception, the failures in the beams tested by Mr. Wilson did not occur at the point of greatest bending stress—that is, at the center of the span and under the load—but through the rivet hole at the end of the cover plate.

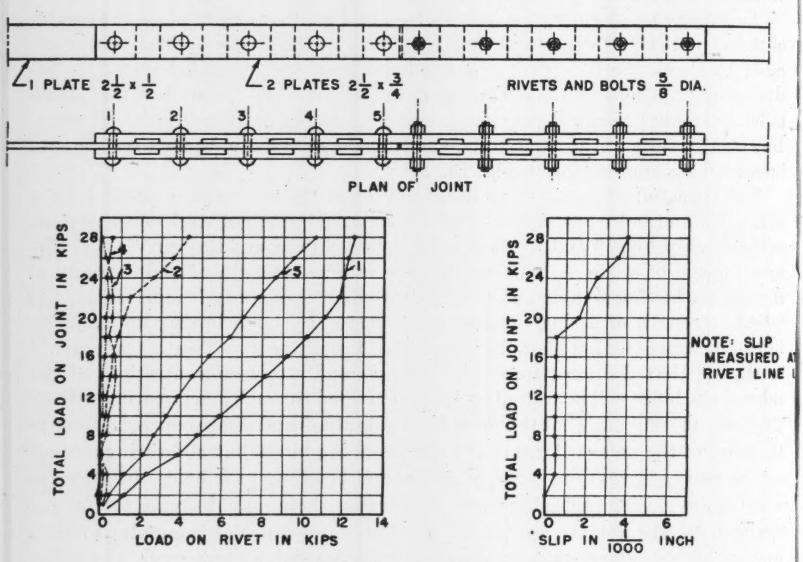

Fig. 11.—Load Distribution in Butt-Riveted Joint

---

[20] Progress Report presented to A.R.E.A. Committee 15, by Lawrence T. Wyly and Jack W. Carter, October 17, 1951.

[21] "Fatigue Tests of Single Lap Joints," by Lawrence T. Wyly and Jack W. Carter, *Bulletin No. 502*, A.R.E.A., June–July, 1952, p. 64, Fig. 23.

[22] "Flexural Fatigue Strength of Steel Beams," by W. M. Wilson, *Bulletin No. 377*, Univ. of Illinois Eng. Experiment Station, January 22, 1948, p. 24, Table 14.

Conversely, when the bearing stress is eliminated and bolts exerting large clamping forces are used instead of rivets, the fatigue strength is increased immediately. The curve of study 2 was obtained by two of the writers for single-lap joints, fastened with high-strength, high-clamping bolts without bearing—using the same steel as for study 1. The endurance limit found in study 2 was 24 kips per sq in. on the net area or approximately 18.7 kips per sq in. on the gross area.[23,24]

In this case, the failure was by brittle progressive fracture, the cracks originating not at the edge of the holes but in the center of the main plate at the edge of the bolt head or nut (under the washer), where the tension at the plate surface due to clamping would be large.[25,26] In these tests, the washers were smaller than those required by the specifications subsequently adopted; they were undoubtedly too thin, resulting in stresses at the point of failure which were higher than desirable or necessary. For the single test labeled 2A, the clamping force was less than that for the tests plotted in the curve of study 2. The 17% increase in fatigue strength is in the right direction. Probably, with the proper design of washers, the (s-N)-curve for the single-lap, non-

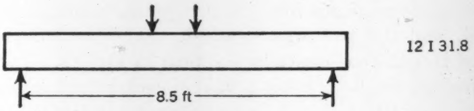

(*a*) Study A

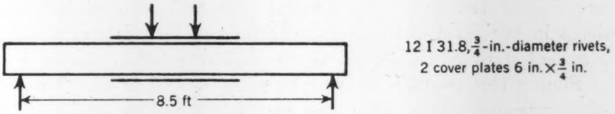

8.5 ft
12 I 31.8, $\frac{3}{4}$-in.-diameter rivets, 2 cover plates 6 in. × $\frac{3}{4}$ in.

(*b*) Study B

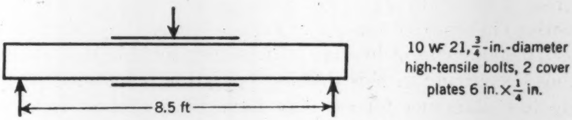

8.5 ft
10 WF 21, $\frac{3}{4}$-in.-diameter high-tensile bolts, 2 cover plates 6 in. × $\frac{1}{4}$ in.

(*c*) Study 3

FIG. 12.—STEEL BEAMS WITH RIVETS AND WITH HIGH-STRENGTH BOLTS FOR STUDIES A, B, AND 3 OF FIG. 9

---

[23] Progress Report to A.R.E.A. Committee 15, by Lawrence T. Wyly and Jack W. Carter, October 26, 1949.

[24] "Report of Assignment 4. Stress Distribution in Bridge Frames—Floorbeam Hangers," by Lawrence T. Wyly, *Proceedings*, A.R.E.A., Vol. 51, 1950, p. 493, Fig. 24.

[25] *Ibid.*, p. 499, paragraph 6.

[26] "Stress Concentrations in Built-up Structural Members," by Jack W. Carter, *Bulletin No. 495*, A.R.E.A., 1951, p. 1.

bearing, high-clamping, bolted joint would be raised still closer to the (s-N)-curve for solid plates without holes (study A). Whether it can be raised as high as the values of study A is still to be determined (1955). In fact, broadly stated, the answer to this question is the main objective of further work in this field.

To demonstrate further the beneficial effect of eliminating rivet bearing and adding large clamping forces and also to demonstrate that the same factors control the fatigue strength both of beams with cover plates and of single-lap joints, a test was made of a 10-in., wide-flange beam with partial-length cover plates connected by high-strength, high-clamping bolts without bearing (Fig. 9, study 3). After the specimen was stressed to an extreme-fiber unit stress of 21,500 lb per sq in. on the gross section or 28,600 lb per sq in. on the net section at the end of the cover plates for 5×10^6 cycles,[27] neither failure nor any slip had occurred, and the test was stopped. Sketches comparing the beams of studies A and B with that of study 3 appear in Fig. 12. In this test, the washers used conformed to the present (1955) specifications recommended by the Research Council on Riveted and Bolted Structural Joints. Again, it seems highly probable that considerably greater stresses could have been produced in this beam with the bolted cover plates without incurring failure.

If severe initial stresses or strains at the rivet holes or initial cracks or other stress-raisers in the steel are present, the fatigue strength of a riveted joint could be expected to be decreased to considerably below the (s-N)-curve of study 1. Such a test result is shown[20] in study 4, Fig. 9(a). The 1-in. bored holes in the plate and gusset were held eccentric by $\frac{1}{32}$ in., and a polished drift pin of the same diameter as the hole, held normal to the plates, was forced through the hole—thus stretching the metal at the sides of the rivet hole. This joint (also containing bolts in bearing, with no clamping) was then tested at a maximum stress of 14,000 lb per sq in. on the gross section (18,000 lb per sq in. on the net section) in repeated tension. Failure occurred by brittle progressive fracture after 70,000 cycles of loading. It seems probable that circumstances similar to those occurring in this drifting operation, combined perhaps with rivets having low clamping forces, may have been present in some of the relatively few floorbeam hangers with riveted connections that have failed in fatigue, but were not present in the many other hangers that have not failed.

A different result was obtained when the polished drift pin of 1-in. diameter was forced through a bored hole of $\frac{31}{32}$-in. diameter in a single plate, thus enlarging its diameter all around. The results of this cold-working operation were as follows: (a) The metal was stretched above its elastic limit in tension around the circumference of the hole, that is, in a tangential direction; (b) simultaneously, the metal was compressed beyond its elastic limit in a direction radial from the center of the hole; and (c) residual compressive tangential stresses were left in the material when the adjacent metal contracted elastically as the pin was removed. Fatigue tests were made on two such identical specimens having bolts in bearing, without clamping. Each was subjected to a tension loading cycle of from 1 kip per sq in. to 18 kips per sq in. on the net section of the plate for more than 4×10^6 repetitions of load. No signs of failure occurred in either case.

---

[27] Progress Report to A.R.E.A. Committee 15 and to Research Council on Riveted and Bolted Structural Joints, by Lawrence T. Wyly and Jack W. Carter, February 15, 1952.

Two factors affected this test. The cold-working of the metal included not only tangential stretching, but also radial compression around the circumference. This operation was thus similar to the refining action of cold-drawing a wire through a die. This operation would not be expected to open existing minute cracks. Secondly, the residual compressive stresses act to hold together any minute cracks in the metal if such exist and also to reduce the magnitude of tensile stresses during later fatigue loading. Both effects have long been recognized as acting to increase fatigue strength of metal. These tests are plotted as study 5 in Fig. 9(*a*).

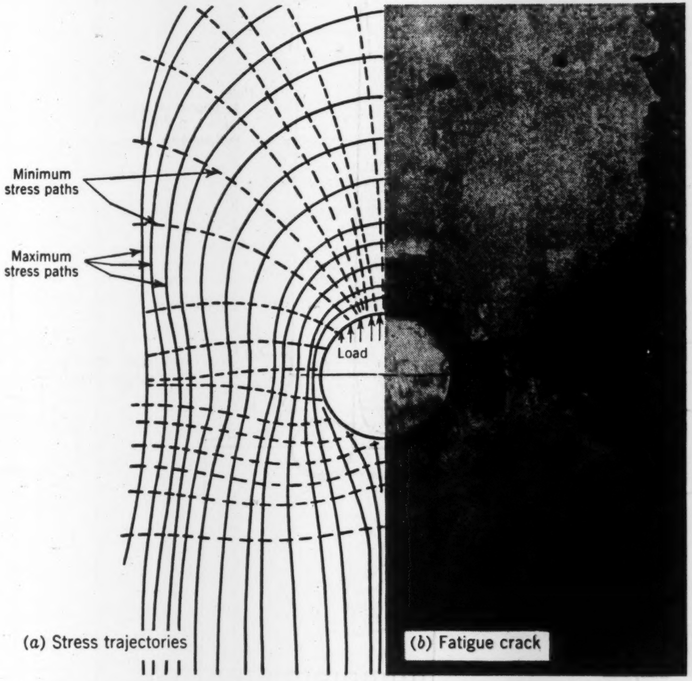

FIG. 13.—CORRELATION OF STRESS VALUES AND DIRECTIONS WITH FATIGUE FAILURE (PIN IN BEARING)

Studies of Stress Concentrations in Riveted and Bolted Joints.—The correlation of stress concentration with fatigue failures in structural members has been investigated by one of the writers by means of photoelastic studies of plastic models of riveted joints and also by strain measurements made on steel models.[28] He found that the failure cracks through the rivet holes, both at points of initation and during subsequent propagation, coincide almost exactly with the maximum tensile-stress locations and paths in the material on a section through the rivet holes as computed on the basis of the elastic behavior and the assumption that the load is delivered to the plate by rivet bearing.[29] This fact is illustrated by Fig. 13. In fact, a fatigue crack of the type shown in Figs. 2(*a*), 2(*b*), and 13(*b*), originating at the side of the rivet or bolt hole at a distance approximately one sixth of the diameter away from the transverse diameter toward the bearing side of the hole, and following the trajectory of the principal tensile stress, may be taken as direct evidence that the crack has been initiated by the bearing of a rivet or bolt.

---

[28] "Stress Concentrations in Built-up Structural Members," by Jack W. Carter, *Bulletin No. 495*, A.R.E.A., 1951.

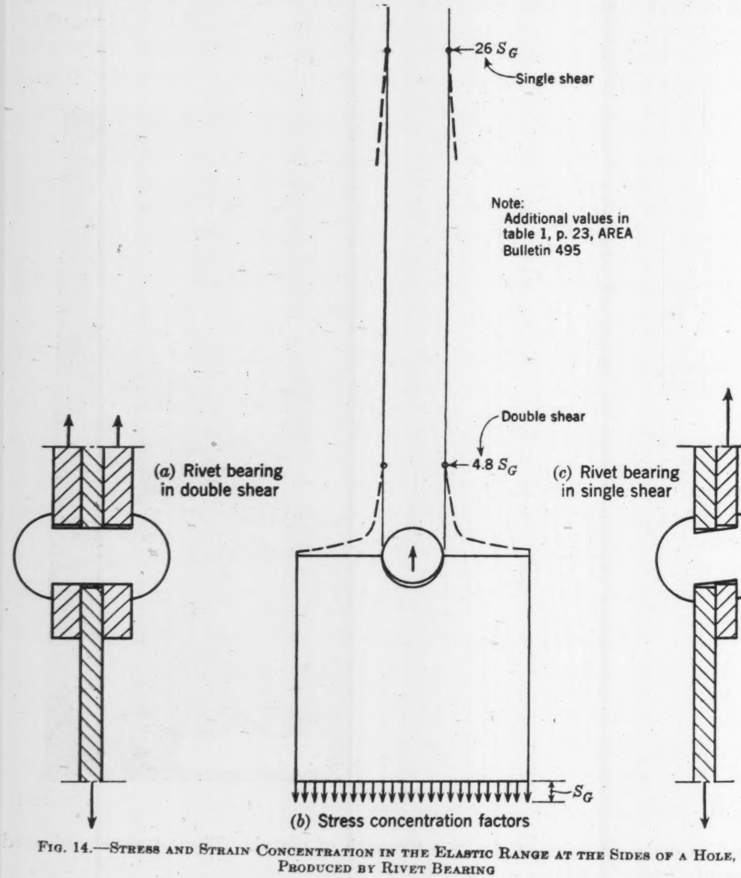

(*a*) Rivet bearing in double shear

(*b*) Stress concentration factors

(*c*) Rivet bearing in single shear

FIG. 14.—STRESS AND STRAIN CONCENTRATION IN THE ELASTIC RANGE AT THE SIDES OF A HOLE, PRODUCED BY RIVET BEARING

---

[29] Progress Report to A.R.E.A. Committee 15, by Jack W. Carter, May 2, 1951.

Using specimens having approximately the proportions of usual riveted joints, one of the writers also studied the stress distributions and measured the critical stresses at the sides of the hole in: (1) A single-lap joint having a rivet in bearing but having no clamping and (2) a plate under clamping without axial load and one under clamping with axial load. He also studied the stress due to clamping at the top of the plate under the washer at the outside edge of the bearing surface of the bolt head, both with and without axial load. These studies are listed in Table 1.

TABLE 1.—PHOTOELASTIC INVESTIGATIONS OF CLAMPING

Line	Joint	Location of measured stresses	Rivet bearing	Clamping force	Axial load	Fig. No.	Section	Page No.[a]
1	Single-lap joint	Sides of hole (Tangential tension)	Full	None	Full	14[b]		22
2	Plate with washers	Sides of hole (Tangential compression)	None	Full	None	15(*a*)	A–A	24
3	Plate with washers	Sides of hole (Normal compression)	None	Full	None	15(*b*)	A–A	25
4	Plate with washers	Top of plate under edge of washer	None	Full	None	16	A–A	25
5	Plate with washers	Section through plate under washer	None	Full	None	17	A–A	27
6	Double-lap joint with washers	Sides of hole (Tangential tension and compression)	None	Full	Full	18	B–B	29
7	Double-lap joint with washers	Top of plate under edge of washer	None	Full	Full	18	A–A	29

[a] From "Stress Concentrations in Built-up Structural Members," by Jack W. Carter, *Bulletin No. 495*, A.R.E.A., 1951. [b] Same as footnote *a*, p. 23, Table 1.

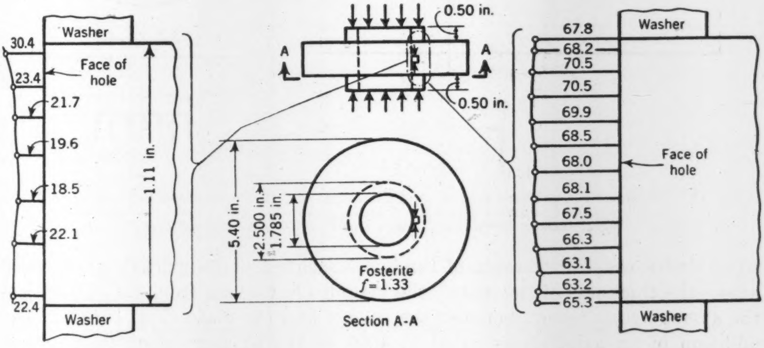

(*a*) Tangential compressive stress (*b*) Specimen (*c*) Normal compressive stress

FIG. 15.—COMPRESSIVE STRESS DISTRIBUTION AT THE SIDES OF THE HOLE, IN POUNDS PER SQUARE INCH, DUE TO CLAMPING (NO AXIAL LOAD; AVERAGE COMPRESSIVE STRESS BETWEEN PLATE AND WASHER = 79.4 LB PER SQ. IN.)

The experiments shown in Figs. 15, 16, 17, and 18 represent the case of a bolt head bearing on a plate without any intervening washer—that is, the proportions of the washers shown in these illustrations correspond to those on the bearing surface of a bolt head, and the load was distributed over the washer as nearly uniformly as was practicable. In these experiments, the computed average stress under the washer due to clamping was about two and a half times the axial stress on the gross section. In the specimen of Fig. 15, the average compressive stress between the washer and the plate was 79.4 lb per sq in. In the specimen of Fig. 16 it was 79 lb per sq in., and in that of Fig. 18 it was 76 lb per sq in. The average axial tensile stress on the gross section of plate No. 1 of Fig. 18 was 31 lb per sq in.

From these measurements it is evident that:

(1) Extremely high tangential tensile-stress concentrations existed at the sides of the holes at the surface of the plate in contact with the gusset in a single-lap joint when rivet bearing without clamping occurred under axial loads (Fig. 14).

(2) With bearing eliminated and clamping added, the nature and magnitude of the stress distribution changed. With no axial load on the specimen, the stress distribution at the side of the hole consisted of tangential compression across the thickness of the plate—the magnitude varying from 22% to 38% of the average compression between the washer and the plate (Fig. 15(*a*)). The addition of an axial stress equal to 40% of the average compressive stress exerted by the washer on the plate reduced this tangential stress at the surface of the plate to nearly zero and changed the stress at the center of the plate to a tension approximately equal to the axial stress (Fig. 18(*b*)). Also, the range of stress at the side of the hole during a loading cycle was greatly reduced.

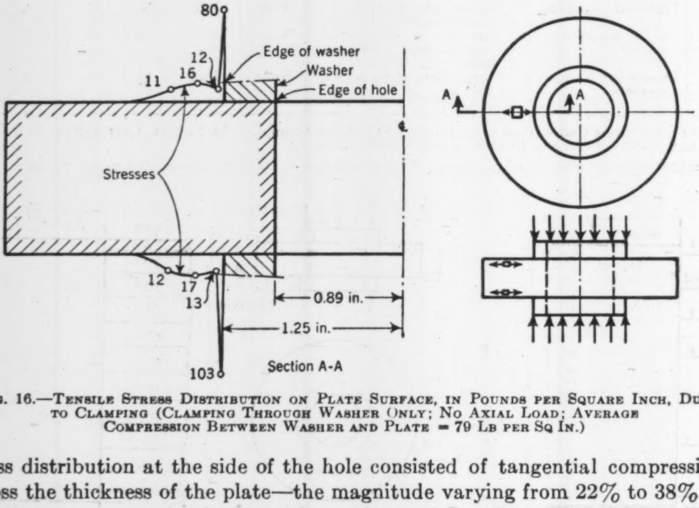

FIG. 16.—TENSILE STRESS DISTRIBUTION ON PLATE SURFACE, IN POUNDS PER SQUARE INCH, DUE TO CLAMPING (CLAMPING THROUGH WASHER ONLY; NO AXIAL LOAD; AVERAGE COMPRESSION BETWEEN WASHER AND PLATE = 79 LB PER SQ IN.)

(3) With clamping present, the tensile-stress concentration at the face of the plate under the carburized washer at the edge of the bearing surface of the bolt head was equal to or greater than the average compression between the washer and the plate; the stress gradient was very sharp at this point (Figs. 15(*c*) and 17). When axial load was added to the specimen, the tensile-stress concentration in the face of the plate at the edge of the washer was increased by an amount approximately equal to the added axial unit stress (Fig. 18(*c*)).

It is believed that these measurements of stress provide a reliable index to the location and magnitude of the stress and strain concentrations at the points in the joint where fatigue failures occur. Furthermore, they show that clamping force has a dual role. It not only builds up frictional resistance to sliding on the contact planes of the joint—a function formerly assigned to rivets in shear—but it is also an indispensable agent whose operation determines the magnitude, range, and nature of the stress and strain concentrations at the bolt holes or rivet holes. It makes all the difference between a connection having rivet-bearing or bolt-bearing, high tangential stress and strain concentrations, and low fatigue strength, and a connection having no rivet-bearing or bolt-bearing, favorable stress and strain distributions and high fatigue strength.

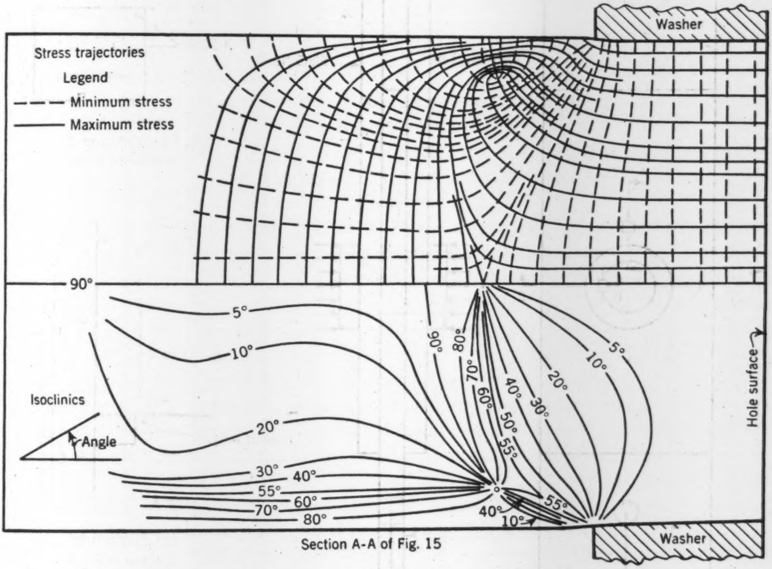

FIG. 17.—STRESS TRAJECTORIES IN SPECIMEN SUBJECT TO CLAMPING ONLY

These measurements also explain the manner of failure of the plates at the joints (fastened with high-strength bolts) where cracks begin at the top of the plate under the edge of the bearing surface of the bolt head. They also suggest that, by proper washer design—that is, by reducing the severe stress and strain concentration and the sharp stress gradient—this type of failure may be controlled.

The measurements in Figs. 16 and 18 also suggest that further studies of the effect of clamping on local stress distribution are desirable. The variables studied should include plate thickness and the possibility of a brittle state of stress resulting. This study should include impact tests.

Slip and Clamping Force.—The critical requirement in the case of the high-strength bolt for structural connections is the capacity of the bolt to develop and hold indefinitely a high clamping force and to resist slip indefinitely.

The first conclusive demonstration that a structural joint—designed to fail in the plates, connected by high-strength bolts, and depending on friction at the contact faces alone to prevent slip—can be used to carry a large number of repetitions of load was made by one of the writers early in 1947. This test program was initiated by the late G. A. Maney and set up by the Industrial Fasteners Institute (formerly the American Institute of Bolt, Nut and Rivet Manufacturers) at Northwestern University (Evanston, Ill.).[30] This series of tests of nine double-lap joints, connected by eight or nine high-strength bolts, carried a reversed stress of from ±15 kips per sq in. to ±20 kips per sq in. on the net section for a total of from 325,000 cycles to 1,600,000 cycles, without slip prior to failure. This series included:

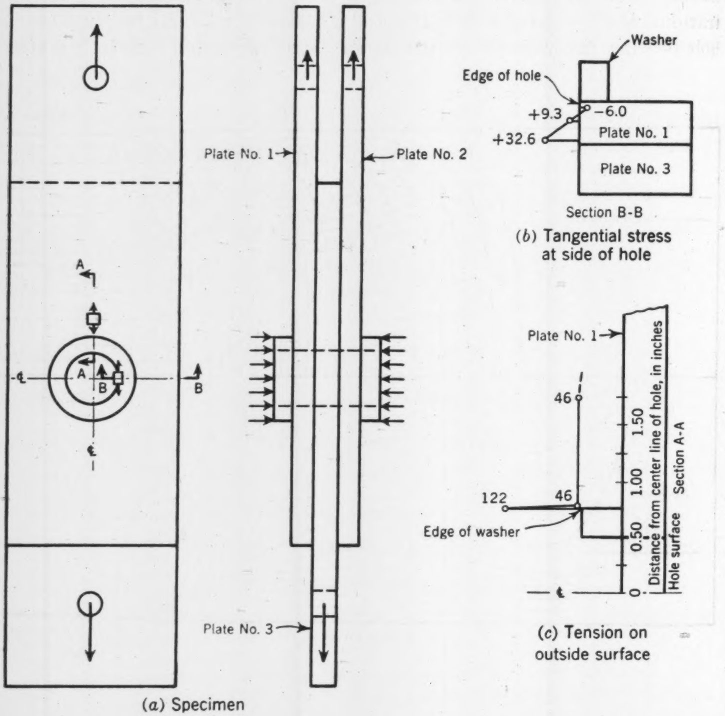
A
A
B
B
℄
℄
Plate No. 1
Plate No. 2
Plate No. 3
Washer
Edge of hole
+9.3
−6.0
+32.6
Plate No. 1
Plate No. 3
Section B-B
Plate No. 1
46
122
46
Edge of washer
℄
0
0.50
1.00
1.50
Distance from center line of hole, in inches
Hole surface
Section A-A

(*a*) Specimen

(*b*) Tangential stress at side of hole

(*c*) Tension on outside surface

FIG. 18.—STRESS DISTRIBUTION, IN POUNDS PER SQUARE INCH, DUE TO AXIAL LOAD PRESENT (AVERAGE COMPRESSIVE STRESS BETWEEN WASHER AND PLATE NO. 1 = 76 LB PER SQ IN.; AVERAGE AXIAL TENSILE STRESS ON GROSS SECTION OF PLATE NO. 1 = 31 LB PER SQ IN.)

---

[30] "The Effect of Various Fasteners on the Fatigue Strength of a Structural Joint," by Kenneth H. Lenzen, *Bulletin No. 480*, A.R.E.A., June–July, 1949.

1. The development of the carburized washer which is necessary to allow large clamping forces to be applied and which has since been standard equipment with the high-strength bolt for structural work.
2. The carrying of the clamping force in the bolts into the yield-strength range without serious loss of clamping.
3. The measurement of normal compressive stress in the metal at the sides of the hole due to clamping with various magnitudes of axial load in the plate.[31]
4. Measurement of the clamping force in the bolts during the test and computation of an average coefficient of friction between the contact surfaces of the plates of 0.35 or 0.36 at the time of the first major slip in the static test.

Mr. Maney had previously measured the axial and shearing stresses in bolts due to "torqueing" and found the latter to be a small percentage of the total stress.[32] In the 1947 tests it was found that when a high-strength bolt is unloaded and reloaded by torqueing, the shear stress rises rapidly due to the galling that occurs in the threads.

In 1949, two of the writers completed the tests in tension of seven single-lap joints connected with high-strength bolts comprising study 2 of Fig. 9. Loading was at the rate of 1,000 cycles per min and the maximum number of cycles carried was 7×10^6. No measurable slip occurred in these tests. These bolts also were torqued to values in the yield stress range.[23]

Fatigue Strength and State of Stress.—One of the writers performed another series of fatigue tests that illustrates the effect of state and magnitude of local stress upon fatigue strength of a riveted and bolted joint.[33] Four double-lap specimens were tested in which the connection consisted of four high-strength bolts spaced equally in each direction, in two transverse rows of two holes each. In the center of the bar, in each row, an open hole was drilled. This arrangement produced four corner holes where the tangential stresses were in initial compression due to the bolt clamping and two open holes where tangential stress and strain concentration due to the presence of the hole would be expected during axial loading. All four joints failed by cracks originating at a transverse diameter of the open hole in the center of the main plate on the most heavily stressed side. These cracks spread to the edges of the plate, passing outside the bolt holes and through the point under the edge of the head or nut of the bolt where the tension and stress gradient in the surface of the plate would be highest; the failure cracks originated at the point of greatest tensile stress and strain concentration (the sides of the open hole) and followed the path of highest tensile stress and strain to the edge of the plate. This is what might be expected from the model study of stress concentration as shown in Figs. 13, 15(*a*), and 18(*b*).

Although the scope of this paper is limited to the study of causes of fatigue failures in riveted and bolted joints directly attributable to the connection details, stress raisers from other sources may markedly reduce the fatigue strength of such members. Tension members in pin-connected spans have been characterized traditionally by ragged cuts and sharp copes near the joints. The axial unit stresses producing failure in the hangers of the pin-connected spans are from 4 kips per sq in. to 6 kips per sq in. lower than the axial unit stresses that produced failures in the riveted spans. This lower fatigue strength may be directly attributed to the presence of these large stress raisers in the pin-connected hangers. Increased severity of the stress raiser is accompanied by decreased fatigue strength.[34]

---

[31] "The Effect of Various Fasteners on the Fatigue Strength of a Structural Joint," by Kenneth H. Lenzen, *Bulletin No. 480*, A.R.E.A., June–July, 1949, Figs. 9 to 12.

[32] "Bolt Stress Measurements by Electrical Strain Gages," by G. A. Maney, *Fasteners*, Industrial Fasteners Inst., 1946, Vol. 2, No. 1, p. 10.

[33] "The Effect of Various Fasteners on the Fatigue Strength of a Structural Joint," by Kenneth H. Lenzen, *Bulletin No. 480*, A.R.E.A., June–July, 1949, p. 23, Fig. 22 and Table 6.

In the previously described series of nine double-lap joints fabricated with cold-driven rivets, two specimens C-6 and C-7 failed through the main plate outside the connection, the cracks in each case resulting from a flaw in the edge of the plate produced by flame-cutting.[35] Also, four of the other joints in this series developed low fatigue strength apparently because of slippage and eccentricities arising from the unequal filling of holes and low clamping strength of the type of connector used.

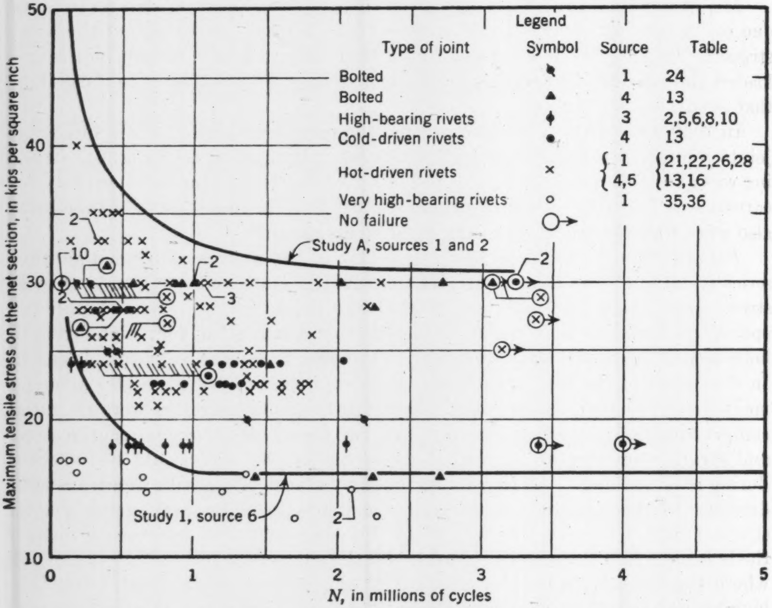

FIG. 19.—CORRELATION OF FATIGUE TEST RESULTS FROM VARIOUS SOURCES—FOR DOUBLE-LAP JOINTS IN TENSION ONLY—TO BE CONSIDERED IN CONNECTION WITH FIG. 9 (THE NUMBER OF IDENTICAL TEST RESULTS IS INDICATED BY A NUMBER ADJACENT TO THE POINT)

It should be borne in mind that the fatigue failures that were studied in the railway-bridge floorbeam hangers and in the tests plotted in studies 1 to 5 in Fig. 9 occurred in members subjected to a minimum of bending due to eccentricity of loading or to lack of lateral bracing. In Fig. 1 are shown the typical make-up and connection of the hangers to the upper gussets where failures most frequently occur. The connection consists of two single-lap joints, one on each flange, the eccentricities of which balance each other. The plates of studies 1, 2, 4, and 5 were tested in stiff holders and likewise suffered little bending from eccentricity or lack of bracing. The cover plates of study 3 were fastened to the beam flange. The effect of the addition of bending due to any cause would logically be to reduce the fatigue strength to less than the results shown in Fig. 9. An example of this action is shown by the report of tests or specimens AMS, BMS, and CMS in the paper (in this Symposium) by William H. Munse, A. M. ASCE, D. T. Wright, and Nathan M. Newmark, M. ASCE. These tests were conducted to study the particular problem of eccentricity.

---

[34] "Report of Assignment 4. Stress Distribution in Bridge Frames—Floorbeam Hangers," by Lawrence T. Wyly, *Proceedings*, A.R.E.A., Vol. 51, 1950, pp. 479 and 494–495, Figs. 17 to 21.

[35] "The Effects of Various Fasteners on the Fatigue Strength of a Structural Joint," by Kenneth H. Lenzen, *Bulletin No. 480*, A.R.E.A., June–July, 1949, Fig. 18, Table 4.

CORRELATION OF FATIGUE TEST RESULTS FROM VARIOUS SOURCES: DOUBLE-LAP JOINTS

The results of approximately 150 fatigue tests from six sources are plotted in Fig. 19 for comparison. These sources are as follows:

No.	Source
1.	"Fatigue Strength of Riveted Joints," by W. M. Wilson and Frank P. Thomas, *Bulletin No. 302*, Univ. of Illinois Eng. Experiment Station, Urbana, Ill., 1938.
2.	"Flexural Fatigue Strength of Steel Beams," by W. M. Wilson, *Bulletin No. 377*, Univ. of Illinois Eng. Experiment Station, Urbana, Ill., 1948.
3.	"Tests of Riveted Joints with High Rivet Bearing, Aug. 1, 1948," *Progress Report*, Committee on Project 1, Research Council for Riveted and Bolted Structural Joints, by W. M. Wilson and William H. Munse.
4.	"Results of Static and Fatigue Tests of Riveted and Bolted Joints Having Different Lengths of Grip, Jan. 2, 1952," conducted at Northwestern Univ. in cooperation with the Research Council for Riveted and Bolted Structural Joints, Project V, by Frank Baron and Edward W. Larson, Jr.
5.	"The Effect of Certain Rivet Patterns on Fatigue and Static Strengths of Joints, Feb. 1, 1952," conducted at Northwestern Univ. in cooperation with the Research Council for Riveted and Bolted Structural Joints, Project VII, by Frank Baron and Edward W. Larson, Jr.
6.	"Fatigue Test of Single Lap Joints," by Lawrence T. Wyly and Jack W. Carter, *Bulletin No. 502*, A.R.E.A., June–July, 1952, p. 64, Fig. 23.

The specimens were all double-lap joints and were tested using fatigue cycles of from zero to maximum tension. Stresses on the net sections are given as shown in the sources. Failures shown are as defined in the reports. The upper and lower boundary curves are those of Fig. 9. Test results not shown are those for (1) specimens that failed in the grips and (2) specimens that did not fail, except for highly-stressed specimens or unusual cases. The individual points for the boundary curves are not plotted here. The outstanding conclusions are:

1. All the test results lie between the upper and lower boundary curves established in Fig. 9 except if the bearing stress of the rivets was five times the tensile stress in the plate, which is the condition referred to in the legend of Fig. 19 as "very high-bearing rivets."

2. The fatigue strength of double-lap riveted joints may be as low as the lower boundary curve, study 1, established for single-lap joints if the rivet bearing stress is high enough. In tests described in source No. 3, rivet bearing was from 2.5 to 3.8 times the tensile stress.[36,37,38,39] When the bearing stress is

---

[36] "Tests of Riveted Joints with High Rivet Bearing, Aug. 1, 1948," *Progress Report*, Committee on Project 1, Research Council for Riveted and Bolted Structural Joints, by W. M. Wilson and William H. Munse, HF 1, Table 2, pp. 22.

[37] *Ibid.*, HGFI, p. 34, Table 5.

[38] *Ibid.*, HGGFI, p. 35, Table 6.

[39] *Ibid.*, HF 2, p. 52, Table 8.

raised to five times the tensile stress, the fatigue strength of such joints is decreased to even less than the lower boundary curve of study 1. This was demonstrated in the tests of source 1, Tables 35 and 36.

3. Under favorable conditions of high clamping, low bearing, and low shear, the double-lap riveted joint may attain a fatigue strength equal to the upper boundary curve of study A (joints B 13–1 and B 14–1 tested at 35,000 lb per sq in. and joint B 14–3 tested at 30,000 lb per sq in., all from source 1, p. 79, Table 22).

4. The fatigue strength of double-lap riveted joints appears to decrease as the bearing increases and to increase as the clamping force increases. Because the clamping force is usually assumed to increase with grip, the high fatigue strength of joints B34, B35, and B36 (source 1, p. 79, Table 22), having a 3-in. grip, even with fairly high bearing, may be explained. However, there is no assurance that a long grip will always develop high clamping force and therefore high fatigue strength. The A3H-joints from source 4, Table 13, tested at 28,000 lb per sq in., approach the lower boundary curve (study 1).

5. The double-lap bolted joints with high clamping force and no bearing may develop a fatigue strength equal to the upper boundary curve (study A). However, only a few of these specimens actually reached this strength. The evidence indicates that the clamping force used in the tests of Table 24, source 1, was low and that the bolts were not made of high-strength steel. In the report for source 4 it is stated that, for most of the specimens, the torques used to obtain clamping force were lower than present specifications require and the bolts were in bearing after the first application of load.

6. The spread of test results for the fatigue tests of the riveted joints is great enough to raise the question of whether rivets should be depended on under repeated loads to develop fatigue strength exceeding the lower boundary curve (study 1).

The results of this correlation tend to support both the working hypothesis and the remedies proposed under the heading, "Supporting Evidence: Exploratory Laboratory Fatigue Tests."

Acknowledgments

The writers are indebted to the AAR and the Research Council on Riveted and Bolted Structural Joints for permission to publish the data in this paper. Thanks are due to the AREA for permission to reproduce Figs. 7, 8, 11, 13, 14, 15, 16, 17, and 18. The specimens and holders for the fatigue tests performed at Purdue University were generously donated by the Wisconsin Bridge and Iron Company of Milwaukee, Wis. The high-strength bolts were donated by the Russell, Burdsall & Ward Bolt Company.

The writers are indebted to Mr. Stitz for valuable advice and suggestions. Mr. Stitz directed the polarized-light studies referred to in Figs. 14 to 18, inclusive, which were made at Purdue University.

The tests reported in Figs. 3, 4, 5, and 6 are part of a research project sponsored by the Research Council on Riveted and Bolted Structural Joints. The other tests reported are part of the floorbeam-hanger project sponsored by the AAR and supervised by a subcommittee of the AREA. Both projects are being conducted at the Purdue University Engineering Experiment Station under the direction of L. T. Wyly.

DISCUSSION

Glenn B. Woodruff,[40] M. ASCE.—The use of high-strength bolts as a substitute for field rivets is increasing rapidly. This change in practice is mainly for economic reasons but, in general, has been justified by the large program of investigation conducted by the Research Council on Riveted and Bolted Structural Joints of which the studies reported by the authors are typical. These investigations, coupled with field experience, have proved that in most applications high-strength bolts are at least the equivalent of rivets. In some applications, especially if vibrations are concerned, the bolts are superior. There are, however, some applications in which the writer believes it has not been demonstrated that high-strength bolts are satisfactory.

The authors' hypothesis fails to explain why the failures have been so few or why they have been confined to hangers since the average unit stresses in the adjacent diagonals are probably of the same order. A crack at the edge of the hole resulting from punching or drilling is a possible explanation; it does not explain why the failures are confined to the hangers. The writer believes that the most obvious explanation is that, for some reason, the stress distribution across the hanger is not uniform.

It has been assumed that, in a material having the ductility of structural steel, these excessive stresses at the edges of a rivet hole would be relieved by plastic flow. However, if a small notch exists at the edge of a hole, the stress concentration will be increased. It is common experience that when a crack starts it continues to lengthen until failure occurs.

The writer does not question the authors' conclusions that a high clamping force reduces the slip and the stress concentration around the hole. However, there are many conditions when comparatively large slips are desirable. In a long riveted splice the design is based on the assumption of equal distribution of shears among all the rivets. It is well known that this never fully occurs and, even as a design assumption, is justified only by the fact that a stress readjustment results from a very considerable slip of the end rivets. Again, measurements of secondary stresses in bridges have indicated that such stresses are less than those calculated. The most plausible explanation is that of a stress readjustment as a result of slip. For these reasons, the writer would hesitate to use high-strength bolts in long-span bridges.

The writer applauds the authors' warning that stress raisers should be avoided in all structures. In addition, the writer suggests that in no case should a structural steel in which the yield point exceeds 60% of the ultimate strength be used.

Karl de Vries,[41] M. ASCE.—The authors, referring to reports on fatigue failures in floorbeam connections of railway bridges, are discussing the more general case of the single-lap joint. They present a hypothesis relating the fatigue strength of a structural member to the magnitude of tensile stress and strain concentrations at the rivet or bolt hole and propose as a remedy for fatigue failure the use of high-strength bolts instead of rivets.

---

[40] Cons. Engr., San Francisco, Calif.

[41] Engr., Bethlehem Steel Co., Fabricated Steel Construction, Bethlehem, Pa.

The authors approach the problem by considering first a hole in a plate subjected to tension and then a hole to which the load is delivered in bearing. The stress concentration factors for these two cases are given in the text as 3 and 6, respectively. They seem to be rather high, particularly to a structural engineer who is accustomed to refer them to the net sections of the plates. If they are referred to the net sections, the concentration factors will be 2.5 and 3.7, respectively, if computed for Figs. 6 and 8(*a*).

The stress concentration factor for tension plus bearing on the contact face of a single-lap joint is given as 26 (Fig. 14), but the rivet shank in that plastic model does not fill the hole, and rivet heads are not used. A similar structural joint would fail if subjected to the smallest loads. Actually, a rivet shank will fill the hole, the rivet heads will be stress-relieving since they supply clamping forces, and, in addition, the rivet heads will be stress participating.

The photoelastic studies of the plastic models shown in Figs. 15, 16, 17, and 18 are to indicate the effect of the clamping force of a bolt without simulating any other forces or their resulting stresses; the force is applied over an area equivalent to that of the bolt head. Actually, a high-strength bolt will have a thin washer which extends considerably beyond the bolt-head area. The clamping force is thus distributed over a larger area and will not cause the high concentrated surface stress at the edge of the washer that is given for the models. Neither should it be assumed that a high-strength bolt supplies a clamping force and that a rivet does not; only the magnitude of their clamping forces differs.

Fig. 11 is given by the authors to indicate the overload on an end rivet of a joint that is provided with five rivets. It should be noted that only two rivets will be required for that joint to have a balanced design and that the part of the total load which was recorded for that end rivet will not necessarily mean an overload for the rivet.

The authors have made a valuable contribution to the knowledge of fatigue behavior of rivets and bolts in single-lap joints. To prove a hypothesis for that case, it seems it is necessary to simulate the actual conditions more closely. The remedy probably is to use high-strength bolts instead of rivets. Nevertheless, it should be stated that rivets are not so unsatisfactory as indicated in the paper.

Harry C. Prince,[43] A. M. ASCE.—The documented results presented in the paper amplify and verify many studies on the use of fasteners for structural steel construction. There are structures in service that have had failures similar to the examples found in railroad floorbeam hangers, but occurring in diagonals of trusses.

These studies have raised the following questions:

1. There have been relatively few failures in floor beam hangers, as stated by the authors. Hence, are the use of riveted details the cause of these failures

---

[43] Designer, American Bridge Div., U. S. Steel Corp., Chicago, Ill.

or are the details and members not designed with proper stress distribution in the members, details, or frame?

2. Are there typical failures only if the thickness of member material is appreciably thinner than the gusset material? Does gusset material fail if it is lighter than the member material? Is there a ratio of member area to gusset area that is important where fatigue is present?

3. If, as the authors have intimated, drifting can cause minute fractures at holes in connections, should members subjected to fatigue stresses be forcibly bent to oppose secondary bending stresses?

4. The indication of plate failure along the edge of the bolt head or washer of high-strength bolts poses the question of load distribution within a large group of such bolts. In riveted joints a load redistribution is possible because of slippage of the joint material at or near the end of the rivet group. High-strength bolts could conceivably restrict such readjustment.

5. What is the effect of high-strength bolts when fatigue and secondary stresses within large joints are present? May they be safely used in such cases?

The writer believes that more extensive research on the effect of high-strength bolts in large joints common in long-span and movable bridges is needed. He agrees with the authors—"* * * that further studies of the effect of clamping upon local stress distribution are desirable * * *"—especially in applying high-strength bolts to large joints.

Jack W. Carter[43] and Kenneth H. Lenzen,[44] Associate Members, ASCE, and Lawrence T. Wyly,[45] M. ASCE.—The writers are grateful to Messrs. Woodruff, de Vries, and Prince for their interest in the paper and for the number of pertinent questions they have asked.

Mr. Woodruff has asked two questions regarding the AAR hanger investigation: (1) Why is the number of hangers that failed so small in comparison to the number that did not fail? (2) Why are no failures reported in the adjacent truss diagonals?

The hanger failures involved were all riveted joints. Mr. Woodruff accepts the writers' conclusions that a high clamping force reduces both the probability of slip and the magnitude of slip—if it occurs—and that it also reduces the concentrations of stress and strain around the rivet hole. It has been quite well established that clamping force may be expected to vary not only with grip but also among rivets within a group in a particular joint in which all have the same grip. Under the heading, "Correlation of Fatigue Test Results from Various Sources: Double-Lap Joints," source 4 shows that, in a group of six hot-driven rivets ($\frac{3}{4}$ in. in diameter and having a grip of $1\frac{3}{16}$ in.), the measured clamping force varied from 3,000 lb to 14,000 lb. The percentage of rivets showing a low clamping force is small as compared with those showing a high clamping force. For rivets having the larger grips the clamping force was higher, and the minimum value of the clamping force was much higher. It has also been established that hot-driven rivets do not fill the holes. Mr. Wilson's measurements (source 1) show clearances between the rivets and the metal at the sides of the holes which vary from 0 in. to 0.035 in. for hot-driven rivets 1 in. in diameter and having 5-in. grips. In general, the rivets of shorter grip may be expected more nearly to fill the holes, and a few of them may be expected to show low clamping force.

---

[43] Senior Engr., The Glen L. Martin Co., Baltimore, Md.; formerly Asst. Prof. of Structural Eng. and Research Associate, Purdue Univ., Lafayette, Ind.

[44] Instructor in Civ. Eng. and Research Associate, Purdue Univ., Lafayette, Ind.

[45] Research Prof. and Head, Structural Eng. Dept., Purdue Univ., Lafayette, Ind.

Because the rivets in most cases may not be expected to fill the holes initially, slip will be necessary to produce a bearing stress. If the clamping force is great, such slip is less likely to occur and, if it does occur, the resulting concentrations of stress and strain are much less severe. The range of stress during a loading cycle is therefore greatly reduced.

The fact that relatively few hangers of the total number in service have been reported as failing is entirely consistent with the foregoing explanation and indeed it is what would be logically expected. It is strong evidence that the great majority of the rivets in the hanger connections have a high clamping force.

The explanation of the lack of failures in the truss diagonals adjacent to the hangers is, in the opinion of the writers, quite direct and logical. They believe that it is due to two factors:

1. The range of stress in the diagonals is more favorable to fatigue strength than it is in the hangers.
2. The number of cycles of maximum stress is much less in the case of the diagonals than in the case of the hangers.

As an illustration, consider the case of a 120-ft through truss span.[46] Twenty-two failures were reported in the hangers in fifteen identical bridges of this design, all at the upper connection of the hangers.

The beneficial effect on fatigue strength of reduction in the stress range is well known. A somewhat simplified picture of this relationship is given by the Goodman-Johnson diagram.[47] In the case of the U_1-L_1 hangers the range of stress is from a minimum (dead load) of approximately 1.5 kips per sq in. to a maximum (dead load plus live load plus impact load) of approximately 19.5 kips per sq in.—each stress being computed at the failure section and including axial stress plus bending due to floorbeam deflection. The range of this stress is thus 18 kips per sq in. for each repetition of maximum loading. The dead load in the adjacent diagonals U_1-L_2 is approximately 16% of the total dead load plus live load plus impact load, and the range of stress is less. Thus, the stress range favors a slightly higher fatigue strength.

The hanger in the aforementioned bridge receives at least two cycles of maximum loading each time an engine or a train crosses the bridge whereas the diagonal receives only one such cycle of maximum loading. Other things being equal, at least twice as much time would be required for fatigue failures to occur in the diagonals as in the hangers. In the cases of structures bearing some of the modern, heavy carloads the hangers may receive many more maximum loading cycles during the passage of a train.

---

[46] "Report of Assignment 4. Stress Distribution in Bridge Frames-Floorbeam Hangers," by Lawrence T. Wyly, *Proceedings*, A.R.E.A., Vol. 51, 1950, p. 474, Fig. 3; p. 476, Fig. 6; p. 482, Fig. 14; and p. 483, Fig. 15.

[47] "Resistance of Materials," by F. B. Seely, John Wiley & Sons, Inc., New York, N. Y., 3d Ed., 1947, p. 298, Fig. 303.

Mr. Woodruff's suggestion—frequently expressed by others—that an unequal stress distribution across the hanger section may be the explanation is not supported by the facts. There are bending stresses in the hanger caused by its rigid connection with the floorbeam and the deflection of the latter under load. The bending stress, however, is at a maximum at the top of the floorbeam and is usually negligible at the failure section at the upper gusset.[48] In the previously cited bridge[46] the bending stress is 21% of the axial stress at the top of the floorbeam and 8% at the failure section at the upper gussets. Also, of the twenty-two failures reported, seven occurred first at the inside angle of the hanger (nearest the center of track) where the bending would reduce the combined stress in the hanger. Furthermore, when all the seventy-nine failures reported in riveted trusses are checked for this bending, it is found that forty-five failed at the inside angles. Also, when the bending due to secondary stress in the plane of the truss is considered, it is found that forty-three failures occurred on the side of the hanger where bending would reduce the combined stress.[49]

Only three hangers failed at the top of the floorbeam, and two of these are attributed to resonant vibration. It is thought that the hangers did not fail at the point of greatest bending because of the fact that a gusset or a reinforcing plate always was extended up the vertical member to engage several rivets above the floorbeam. This probably reduced the tendency of the rivets at the floorbeam connection to slip and come into bearing. In the case of the third failure, which occurred at the top of the floorbeam, such a reinforcing plate did not come up to the section of failure.[50]

Regarding the flow in ductile steel where large local stresses and strains occur, the writers believe that the phenomenon is illustrated by Figs. 3, 4, 5, and 6. Where the yield point of the steel is reached locally the material will flow (Fig. 4), but the stress concentration—that is, the ratio of stress at the side of the hole to stress at the gross section—remains nearly constant from this point on whereas the strain concentration increases as the loading is increased (Fig. 6). It is also important to remember that at any stage of loading the member under conditions such that the steel at the point of consideration (in this case, the side of the hole) is stressed well above the elastic limit, a certain amount of rest or a few cycles of stress to this same prior high value will restore elasticity to the material. This explains why the fatigue cracks are invariably initiated at the point of maximum principal (tensile) stress and their trajectories follow that of the principal stress. All these stresses are computed on an elastic basis (Fig. 13).

The location and path of the fatigue crack are thus direct clues to the source of the stress producing the crack. If the crack begins about one sixth of the diameter above the horizontal center line of the hole on the side on which the rivet bears and follows a curved path (Figs. 2(*a*) and 13), this condition establishes the fact that the principal tensile stress producing the crack is a direct result of rivet bearing. Without such bearing, the crack would begin at the side of the hole on a diameter normal to the axis of the member and would be propagated in a straight line perpendicular to the axial stress, as many tests have shown. In all the cases of actual fatigue failures in this type of connection which the writers had the good fortune to inspect and in which the cracks could be seen, they conformed to the foregoing pattern.

---

[48] "Report of Assignment 4. Stress Distribution in Bridge Frames-Floorbeam Hangers," by Lawrence T. Wyly, *Proceedings*, A.R.E.A., Vol. 51, 1950, p. 482, Fig. 14.

[49] *Ibid.*, p. 472, Table 2.

[50] *Ibid.*, p. 473, Fig. 1; p. 475, Fig. 4; and p. 478, Fig. 11.

It cannot be emphasized enough that attention must be focused on the state of stress and the stress level at the particular local, small spot where the crack begins. It has often been remarked that a doubling of the area of the hangers would cost relatively little and would cure the difficulty. The writers do not believe that this would necessarily have any beneficial effect at all.

Mr. de Vries makes some valuable critical comments on the photoelastic model studied. The plastic rivet did not fill the hole in the plastic plates after load was applied because of elastic yielding. Prior to load application the fit was tight. On the other hand, as already noted, the steel rivet seldom fits the hole as closely as did the plastic model. Many measurements by Mr. Wilson and others have established this fact. The writers have no reason to believe that fatigue cracks are started while high clamping force is present in the rivet. When clamping force is lost, the rivet heads are not stress participating and they are not stress relieving. Although the writers regard the conditions of test of the plastic models as representing a limiting condition, they believe that this limiting condition is approached more closely in practice when failures occur than is generally realized.

The writers do not feel that any significant change in data would have resulted in the plastic model experiments for measuring the stresses in the top of the plate due to the bearing of the head or nut if a washer had been used. The washer, being thin, would have distributed the bearing load outward radially, perhaps over a circular area having a diameter greater than that of the bolt circle by about twice, or less, the washer thickness. One reason for this is that cracks in the plate occurred outside the hole (Fig. 2(*c*)) when the clamping force was high and the washer was thin. Study 2, Fig. 9(*a*), illustrates this case. When the clamping force is decreased (Test 2(A) is representative) or when the washers are made thicker, as in Study 3 (all of Fig. 9(*a*)), the fatigue strength was raised or failure did not occur.

Mr. de Vries questions whether the picture of overloading of the end rivets shown in Fig. 11 is a true one. Similar conclusions—that the end rivets in a row may be overloaded 100%—were arrived at by Raymond E. Davis, M. ASCE, Mr. Woodruff, and Harmer E. Davis, A. M. ASCE, from measurements[51] on large steel joints. They also found some premature failures of rivets in the end holes.[52] Measurements of slip distribution between gussets and the member in a recent experiment tend to support this same thesis.[53] Two large joints representing a wide-flange hanger connected to gussets were tested. The connection consisted of four lines of seven connectors each. In the first joint, rivets were used except that the last two holes at the edge of the gusset in each line were connected with high-strength bolts. In this case, the slip at the end of the connection occurred under smaller loads and was much larger, than the slips at the center of the connection. The other joint was connected entirely by high-strength bolts. First major slips occurred at stresses considerably exceeding the working loads. The same relative slip distributions were observed as for the riveted joint, but the slips near the center of the connection were very small.

---

[51] "Tension Tests of Large Riveted Joints," by Raymond E. Davis, Glenn B. Woodruff and Harmer E. Davis, *Transactions*, ASCE, Vol. 105, 1940, p. 1193.

[52] *Ibid.*, p. 1215, Table 9, Col. 29.

[53] "Comparative Test of a Structural Joint Connected with High-Strength Bolts and a Structural Joint Connected with Rivets and High-Strength Bolts," by Jack W. Carter, J. C. McCalley, and Lawrence T. Wyly, *Bulletin 517*, A.R.E.A., September-October, 1954, pp. 246-249, Figs. 20-23.

Mr. Prince raises five important questions, which the writers will discuss in chronological order. They believe that the question of whether fatigue failures in the hangers are due to inadequate design of the members or to use of riveted connections is answered by the following considerations:

1. At the points of failure the axial stresses plus the bending stresses in the hangers are not large. Even at the points of greatest bending the stresses are not large.
2. At the points of failure little bending stress is present. There is no evidence whatever of high stresses except at the sides of the rivet holes where the cracks occur.

The only exceptions to the foregoing statements are the nine hanger failures in a deck truss bridge.[54] Because of the type of framing, the axial stresses plus the bending stresses in these hangers at the failure sections would amount to about 55 kips per sq in. if computed on an elastic basis. The service life of these hangers was twenty-four years. Three spans were involved.

In the hangers that failed, the ratio of the thickness of the main material to that of the gussets varied from 0.75 to 1.0. In no case were the gussets thinner than the main material. No gusset failures were reported. No results were obtained indicating any significance for any particular ratio of main material to gusset material thickness.

Regarding Mr. Prince's third question, the writers believe, on the basis of Study 4, Fig. 9(*a*), that in members designed for fatigue loading no drifting at all should be permitted (either in the shop or in the field) in holes in the last two transverse rows at the edge of main material or splice material; only light drifting should be permitted near the middle of the connection. They feel that the evidence now available indicates that drifting should not be used to induce stress in members which will carry fatigue loading.

Mr. Woodruff and Mr. Prince are both concerned regarding the magnitude of slip to be expected in bolted joints and whether they will slip enough to allow distribution of load to occur among the various bolts. Tests on large joints reported by various investigators for the Research Council for Riveted and Bolted Structural Joints including two papers in this Symposium,[55,56] and a recent report[57] all show that slip in bolted joints will occur when the relationships between load, clamping force, and coefficient of friction permit it. Also, much more slip can occur in a bolted joint than in a riveted joint because much more clearance is provided between the bolts and the metal at the sides of the holes. Recent experiments by R. A. Hechtman, A. M. ASCE, on the magnitude of total slip to be expected on a long-time test will yield highly valuable information. In the opinion of the writers, more detailed study and experimentation are needed on this subject before a rational basis for the design of a bolted joint is possible. Present results show, however, that the bolts in such a joint will work together and that the ultimate strength of the bolted joint will be much greater than that of the riveted joint.[58]

---

[54] "Report of Assignment 4. Stress Distribution in Bridge Frames-Floorbeam Hangers," by Lawrence T. Wyly, *Proceedings*, A.R.E.A., Vol. 51, 1950, p. 473, Fig. 2; p. 475, Fig. 5; p. 480, Fig. 12; and p. 481, Fig. 13.

[55] "Comparison of Bolted and Riveted Joints," by Frank Baron and Edward W. Larson, Jr., *Transactions*, ASCE, Vol. 120, 1955, p. 1322.

[56] "Slip of Joints Under Static Loads," by R. A. Hechtman, D. R. Young, A. G. Chin, and E. R. Savikko, *ibid*, p. 1335.

In summary, the writers have thus far seen no evidence that is inconsistent with the explanation they have suggested. They agree with Mr. de Vries that many riveted joints are more effective than Study 1, Fig. 9(*a*), would indicate. The specimens tested for this curve had a tension-shear-bearing relationship of approximately 1.00:0.84:1.74, and no clamping. This is probably approximately the lower limit of the (s-N)-curve for single-lap joints in which no clamping is involved, in which the holes have not been damaged, and in which the bearing-tension ratio is not greatly in excess of 1.50 or 1.75. Many riveted joints of these proportions will show greater strength than this—those having high clamping. However, because it is impossible to predict what joints will have high clamping in the rivets—particularly in the rivets at the ends of the connections—the writers feel that greater strength than that indicated by the curve of Study 1 is not to be depended on. For double-lap joints, in which the bearing stress is not too high, a fatigue strength considerably greater than the foregoing may be expected. In any case, some safety factor should be provided. The writers feel that final specifications should be based on a critical examination of the experimentally determined (s-N)-curve, in which each controlling variable is investigated separately.

---

[57] "Comparative Test of a Structural Joint Connected with High-Strength Bolts and a Structural Joint Connected with Rivets and High-Strength Bolts," *Bulletin 517*, A.R.E.A., by Jack W. Carter, J. C. McCalley, and Lawrence T. Wyly, September-October, 1954.

[58] *Ibid.*, p. 223.

STRUCTURAL USES OF HIGH-STRENGTH BOLTS

By T. R. Higgins[1] and E. J. Ruble,[2] Members, ASCE

Synopsis

The use of high-strength bolts as structural fasteners in field connections has increased because of the ease with which the bolts may be installed and because of their superiority to rivets in joints subject to severe fatigue loading.

Of primary interest in this field has been the use of high-strength bolts in joints that transmit shear. Use of high-strength bolts does not involve extensive retraining of personnel or replacement of equipment, and the over-all cost is nearly the same as that for riveted joints. Valuable in the field of industrial fasteners has been the development of several methods for controlling the torque exerted on high-strength bolts by air impact wrenches. This paper describes examples of the use of high-strength bolts in building construction.

Introduction

Although the use of rivets and bolts in joining metal components had been part of the craftsman's art for centuries, engineering concepts concerning the behavior of such joints, by which their strength could be evaluated for the design of structures, were probably first applied by Robert Stevenson during the erection of the Britannia Bridge over Menia Straits and the Conway Bridge over the Conway River, both in Wales, about the middle of the nineteenth century.

Necessarily, these concepts were supported in early days by test data obtained only from very small specimens. Considering the simple and not altogether accurate testing methods, it is remarkable that these data agree as closely as they do with those of more recent investigators.

The contribution to the strength of a joint made by the "friction produced by the cooling of red-hot rivets" was recognized a century ago by at least one writer.[3] He observed that, at working loads, joints acted by friction alone. Nevertheless, the classical concept of a riveted or bolted joint, almost from the beginning, has been that of adjacent plies loaded in opposite directions and held together by the shear strength of the fastener.

Riveted connections are generally assumed to resist applied loading with little if any slip because the forging of the rivet has nearly filled the rivet hole. Likewise, the use of turned bolts in reamed holes is assumed to control the slip between the connected parts within tolerable limits although hole clearances as great as 1/50 in. are permitted in fabrication. In connections where slip is of less consequence, it has long been the practice to place unfinished bolts in holes

---

Note.—Presented at the Centennial Convocation, Chicago, Ill., September, 1952. Published, essentially as printed here, in September, 1954, as *Proceedings-Separate No. 485*. Positions and titles given are those in effect when the paper was received for publication.

[1] Director of Eng., American Inst. of Steel Construction, Inc., New York, N. Y.

[2] Research Engr., Structures, Assn. of American Railroads, Chicago, Ill.

[3] "The Britannia and Conway Tubular Bridges, with General Inquiries on Beams and the Properties of Materials Used in Construction," by Edwin Clark, Day and Son, London, 1850, Vol. 1, p. 392.

which have been punched or drilled to a diameter 1/16 in. greater than that of the bolts themselves.

The accepted use of high-strength bolts, pretensioned sufficiently so that only friction between the connected parts is required to transfer the stress from one structural member to another, has developed only within the past eight years (1948–1955). Several factors have served to stimulate this development.

Hardened washers under the nut and the bolt head made possible clamping forces greatly in excess of any that could be achieved through the shrinkage of hot rivets on cooling. These clamping forces are sustained without significant relaxation even after hundreds of thousands of loading cycles. In the case of bridges and other dynamically loaded structures, the demonstrated superiority of highly prestressed, high-strength bolts in providing a smoother stress path, thus materially improving the fatigue strength of the joint, make high-strength bolt construction distinctly advantageous to riveted construction.

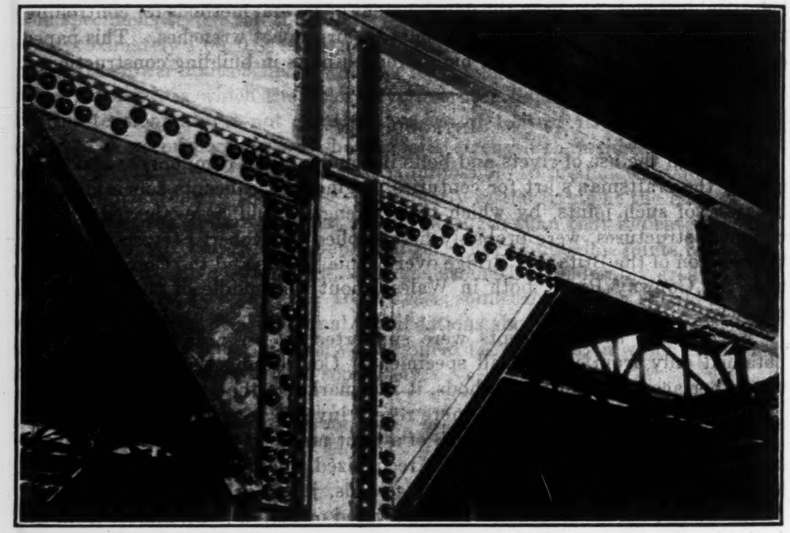

FIG. 1.—HIGH-STRENGTH BOLTS IN A FIELD CONNECTION

High-strength bolts are used primarily at field connections, as shown in Fig. 1. Current (1954) specifications permit their use in joints in which either shear or tension is transmitted across the joint.

The use of high-strength bolts for the field connections of bridges and buildings involves no retraining of draftsmen or fabricating-shop forces nor any replacement or rearrangement of existing shop equipment and fabricating practices.

In respect to cost, high-strength bolt construction competes with riveting. The bolts are much more expensive than undriven rivets, but much (sometimes all) the difference in cost is offset by lower installation costs. Even if this were not so, in many parts of the United States the shortage of riveters which has persisted since the close of World War II would suggest a need for the newer type of fastener, the proper installation of which requires only a short training period for steel workers.

EARLY DEVELOPMENT

During the early stages of the investigation into the use of high-strength bolts by the Research Council on Riveted and Bolted Structural Joints, it was realized that laboratory tests conceivably might not include all the factors affecting the behavior of the bolts in dynamically loaded railroad and highway bridges. The joints of such structures are subject not only to fluctuation in loading but also to concurrent vibrations of varying amplitude and frequency. Accordingly, in 1948, the research staff of the Association of American Railroads arranged with several railroads to replace more than 1,300 existing rivets in joints of fourteen different bridges, where difficulty had been encountered in keeping rivets tight because of excessive vibration and other unusual service conditions. In some of these structures maintenance crews had to redrive several loose rivets each year.

The practice of some railroads had been to replace temporarily, with ordinary unfinished bolts, the rivets that were found by the bridge inspectors to be loose. These bolts would be replaced in turn by new rivets when the accumulated number to be driven was sufficient to justify bringing a compressor and riveting equipment to the site. In the meantime, the temporary bolts often required retightening as they could not retain their initial tension for any extended period under the service conditions.

For each case included in the field-test program, all the rivets in a joint were replaced, one at a time, by high-strength bolts of the same nominal diameter. These bolts have been inspected periodically with the latest inspection during the fall of 1954, and after six years the majority of the bolts still retain their full clamping force. A few of the bolts have shown some loss of clamping action. However, there is some doubt that these bolts were originally tightened to the specified amount because of inadequate clearance for operating the torque wrench. Meanwhile, the rivets in similar joints on the same structures (sometimes at the other end of the same member) have continued to work loose.

In one case in which common washers were originally installed with the high-strength bolts, the bolts did not stay tight. However, since the common washers were replaced with hardened washers in the summer of 1948, the bolts have maintained their initial prestress.

Some bolts were installed in jagged holes that had become enlarged as a result of the frequent backing out of loosened rivets. Wherever two hardened washers were placed under the head and nut of these bolts to prevent washer deflection in the enlarged holes, the bolts retained their full clamping force.

In all these installations, the friction created in the threads by the high initial bolt tension was sufficient to prevent any loosening of the nut. No self-locking type of nut or washer was used, and the threads were not burred after the nuts had been tightened. During inspection of these bolts a torque 15% greater than the minimum required torque was applied without any evidence of the nut turning.

In general the bolts tested in this program were initially tightened to develop a tensile stress on the mean thread area of 72,000 lb per sq in. (equivalent to approximately 85% of the specified yield-point stress). The bolts in several of the joints, however, were deliberately tightened to stresses considerably exceeding the yield-point stress. The excessive prestress did not prove deleterious. These bolts have been functioning satisfactorily since 1948 without exhibiting any visible evidence of damage or impaired clamping force.

One or two bolts from each bridge installation were removed and replaced with new bolts. The old bolts were returned to the laboratory, and a visual inspection indicated there was no rusting of the shank of the bolt after six years in service. One bolt removed from a joint where the holes were enlarged and quite jagged indicated some rusting of the shank.

To study the use of high-strength bolts in cold climates, existing rivets were replaced by such bolts during the fall of 1950 in several floor-beam hangar connections on riveted bridge trusses where the temperatures fall to at least − 40°F. The bolts have now been in place for four winters and have proved entirely satisfactory.

Tightening Procedures

The cost advantage in the use of high-strength bolts on bridge maintenance, as compared with the use of rivets, is apparent. Transportation cost of driving equipment per redriven rivet is high because of the limited number and scattered location of the rivets involved, even when the riveting operation is postponed as long as possible by the temporary substitution of ordinary bolts. However, the required tightening specified for high-strength bolts can be achieved with manually operated wrenches.

Although manual installation is the most economical method when only a few scattered bolts are required at some remote site, it would be unnecessarily expensive for general use on building construction. In this work, the use of air impact wrenches not only reduces the required physical effort to a minimum and saves considerable time but also introduces simple, yet remarkably effective bolt-tightening control.

Pneumatic impact wrenches (Fig. 2) are only slightly heavier than the hand hammers used to drive rivets of the same nominal diameter. They need but a single operator and are about as portable as riveting hammers.

The torque required to spin the nut down and to tighten it to the desired amount is provided by a rapid succession of light blows delivered normal to radial lines passing through the center line of the bolt. The force of any one blow remains approximately constant through a wide range of variation of air pressure. It is small enough so that the reaction which the force produces is absorbed almost entirely by the inertia of the mass of the wrench housing. Because the blows are delivered simultaneously on opposite sides of the bolt center line, their reactions are balanced, and the physical effort required of the operator is considerably less than that involved in driving rivets. Furthermore, this effort needs to be sustained for only a fraction of the time necessary to drive a rivet.

At a normal controlled operating air pressure of, for example, 80 to 90 lb per sq in. at the wrench, less than 5 sec is required after the nut is first seated before it has been turned to the desired tightness. Depending on the size of the bolts being installed, as many as six wrenches can be powered by a single compressor with a capacity of 160 cu ft per min.

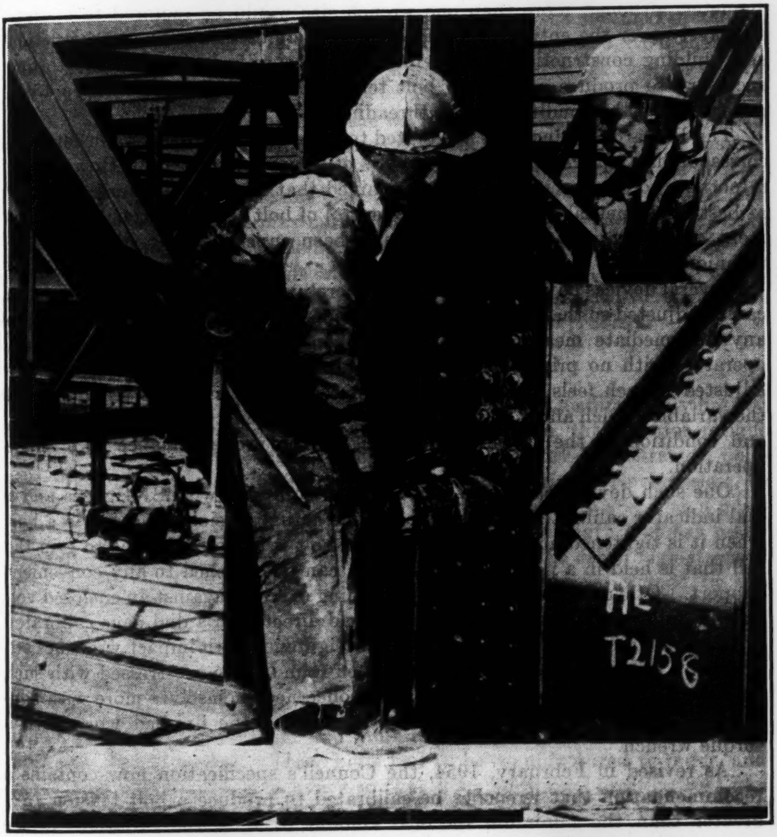

Fig. 2.—Operation of an Impact Wrench

The relationship of air pressure to nut-tightening effort has provided one effective bolt-tension control. By inserting a pressure reducer in the air-supply line to each wrench, the wrench can generally be made to "stall" when the desired bolt tension has been achieved. Naturally, at the reduced pressure, the tightening time is somewhat extended—from perhaps 3 sec to as much as 10 or 15 sec—which places a smaller premium on operator reaction time for the controls. The stalling is indicated by a noticeably heavier vibration in the wrench. At this stage there is little visible turning of the nut, and the tightening socket on the wrench tends to recoil after each blow.

A wrench of given size can be used to tighten bolts of more than one nominal diameter, although more than one wrench size would be required to operate effectively over the entire range of bolt diameters used in bridge construction and building construction. Even for any one specified diameter the torque necessary to produce a specified bolt tension can vary by as much as 15%, depending on the condition of the threading.

The Research Council has attempted to correlate required bolt tension with corresponding equivalent torque for bolts of various diameters.[4] However, in a footnote to the specification it is explained that the torque values given are at best experimental approximations; control of bolt tension through measurement of tightening torque has generally been superseded by more positive techniques.

Several devices have been developed whereby the air pressure at the wrench can be adjusted so that the desired bolt tension is provided without reference to any intermediate measure of torque. When these devices have been used, operators with no prior experience have been able to learn quickly how the adjusted wrench feels at the proper cut-out point. Using this technique, all the variables which affect bolt tightness—wrench capacity, bolt size and length, and condition of the threads—are brought into proper balance in a single operation.

One such device makes use of a load cell equipped with SR4 gages and a dial indicator calibrated to read directly the actual tension produced in a bolt when it is tightened against the cell. The bolt is assembled so as to grip the cell that is held in a portable frame which can be attached to any convenient support. Other devices permit the tightening of a bolt against an enclosed volume of fluid, producing pressure that is read directly on a dial page calibrated in terms of equivalent bolt tension. Bolts tightened with impact wrenches adjusted by means of these devices have been found to be prestressed with such consistent accuracy that inspectors have concerned themselves more with controlling the air pressure than with spot checking the finished work with a torque wrench.

As revised in February, 1954, the Council's specification now contains a recommendation that wrenches be calibrated to produce a bolt tension 15% greater than the minimum specified amount to allow for variations in the actual torque-tension relationship. Although no useful purpose is served when a bolt is strained beyond its elastic proof load, numerous field and laboratory tests have indicated that no damage is sustained by bolts tightened far beyond this point. They remain capable of providing a clamping force limited only by the elastic properties of the bolt. Because the minimum specified breaking strength of the bolts is not reached until there has been applied a tensile force which exceeds 150% of the required minimum tension values given in Table III of the specification, meticulous attention to a close upper prestress limit is unnecessary and only increases the erection cost. In 1954 numerous tests[5] were conducted at the laboratory of the Association of American Railroads in an attempt to relate bolt tension to turn-of-the-nut. It was found that, after the parts of a joint had been brought into contact by means of "fitting up" bolts, high-strength bolts invariably received at least the specified pretension if the nut was given one complete turn from finger tightness. On the other hand, not less than two complete turns were required to break the bolt or strip the thread.

---

[4] "Specifications for Assembly of Structural Joints Using High Tensile Steel Bolts," Research Council on Riveted and Bolted Structural Joints, February, 1954, Table III.

During the short interval when the wrench is spinning the nut into bearing against the hardened washer, the noise from the wrench ordinarily is masked out by the noise incident to other construction operations. In fact, the sharper sound that follows when the nut has been seated is obscured by many common construction noises. The maximum noise level of impact wrenching has been described as approximately one half that of an ordinary riveting hammer. Its duration likewise is only half that required to drive a rivet. It is significant that many early projects in which high-strength bolts were used were additions to hospitals, in which much study was given to the noise problem.

Building Construction

Few building connections are subject to the dynamic loading and vibration characteristic of railway and highway bridges. Hence, the superior fatigue strength which is characteristic of connections made with high-strength bolts loses much of its appeal in ordinary building construction. Nevertheless, to relieve an inadequate supply of trained riveters economically and with a minimum of change in existing practices, use of the high-strength bolt has many advantages. This is evidenced by the rapid growth in the use of high-strength bolts in the short time since their application was first sanctioned by the Council's specification in 1951.

One of the first buildings to be constructed with approximately the same techniques as are recommended by the Research Council was a fourteen-story hospital for the University of Illinois at Urbana. At that time (1951) the American Society for Testing Materials had not adopted the present specifications,[6] and somewhat stronger and more expensive bolts were used in lieu of those now recommended. These bolts had to be manufactured to order, and delays were experienced in delivery so that some additional erection cost was involved. Nevertheless, it has been reported that the bolts cost only between $6.00 and $7.00 more than field rivets would have cost per ton of steel erected.

Included in recent (1952–1954) bolted-construction projects are the first eleven stories of a twenty-one-story addition to the Mayo Clinic at Rochester, Minn., a twenty-one-story building for the Mayo Memorial Medical Center at the University of Minnesota, in Minneapolis, the fifteen-story General Hospital for the University of Oregon Medical School at Eugene, the thirteen-story

---

[5] "Tightening High-Strength Bolts," by F. P. Drew, *Proceedings-Paper No. 786*, August, 1955.

[6] "Quenched and Tempered Steel Bolts and Studs," ASTM Designation A 325-53 T, A.S.T.M. (Revised December 16, 1953).

Johns Hopkins hospital building in Baltimore, Md., the twenty-four-story Mile High Center in Denver, Colo., the twenty-five-story Equitable Life Assurance building in San Francisco, Calif., and a number of large process buildings for the Atomic Energy Commission near Portsmouth, Ohio. Descriptions of some representative early installations (1951) should indicate the immediate popularity of this newest of fastening techniques.

The new plant of the Aluminum Company of America (ALCOA) at Sandow, near Rockdale, Tex.—comprising some twenty-five industrial shed-type buildings—required approximately 100,000 high-strength bolts. The buildings, designed by the engineering department of ALCOA, are one story high. The roof trusses span 60 ft, 80 ft, and 100 ft.

Approximately 10,000 tons of structural steel were required to complete a large jet-engine manufacturing plant for the Chrysler Corporation at Utica, Mich. The project also included a much smaller three-story frame for a powerhouse. All primary connections were fastened with ASTM-A325 bolts. Secondary connections such as purlins and sash angles were fastened with ordinary unfinished bolts as would have been the case had the principal connections been riveted.

The one-story building is so large that considerable planning in organizing the erection forces for the new bolting techniques was justified. The steel was erected with one pin and one "fitting-up" bolt in each connection, in the usual manner. The final bolts were installed by steel workers whose task was completed when these bolts were made snug with an ordinary hand wrench. As there were a great many repetitions of nearly identical connections, each man was assigned the job of placing the bolts in a single type of connection. Tightening gangs, each consisting of two men who did nothing but bring the bolts up to the specified prestress using impact wrenches, followed along immediately behind. Most of the connections could be reached without scaffolding. It was found that three or four men were necessary to keep bolts always in place ahead of a tightening gang. The average production per man, counting all those engaged in the work, was of the order of 150 bolts per day. Two tightening gangs, confining their activities entirely to this one operation, installed a maximum total of 3,100 bolts per working day.

When several bolts are required in a single connection, the tightening of the later bolts often increases the total clamping effect on the connection to such an extent that the first bolts must be retightened. On this project it was found that, in connections with as many as seven holes in a single row, the bolts could be quickly tightened to the proper tension by tightening the center bolt first and then proceeding from the top hole down to the bottom one, thus giving the center bolt a second treatment halfway through the operation.

Some 5,000 high-strength bolts were used in the construction of two sections of a viaduct—one section 550 ft long, and the other approximately 700 ft long—on the freight line of the Union Railroad Company over Turtle Creek in East Pittsburgh, Pa. This viaduct, consisting of four lines of plate girders supporting transverse floor beams 18 in. deep, spaced 2.5 ft on centers, carried track ballast laid on a steel plate deck. The floor beams were connected to the longitudinal girder by high-strength bolts.

More than 150,000 high-strength bolts were required for the primary connections in the General Motors Corporation's huge Buick-Oldsmobile-Pontiac assembly plant at Arlington, Tex. This project, providing 1,250,000 sq ft of floor space, consists principally of bays 45 ft by 45 ft, 45 ft by 90 ft, and 90 ft by 90 ft of one-story truss-and-column framing. Part of the building is two stories high. Overhead traveling cranes are supported on the building frame as is also the case in the ALCOA building at Sandow. In the invitation to bidders, contractors were instructed to quote both on the basis of field riveting and on the basis of high-strength bolts. The successful low bidder submitted the same price for both methods of field fastening.

All of these projects, each using a substantial quantity of high-strength bolts, were begun within a year after the Council first issued its specification. Last year, in one project for the Atomic Energy Commission near Portsmouth, 1,185,000 high-strength bolts were used to erect 79,000 tons of structural steel.

COST

On some of the projects mentioned, costs of the various methods of making field connections were compared. On others, no detailed studies were attempted as some increase in cost would have been tolerated in the interest of expediting construction. Where comparisons have been attempted, any differences that were found usually were so small that they could be verified only by actual performance records on two otherwise identical projects.

A revision in the Council's specification (February, 1954), which has effected some economy in the case of building frames, has removed the earlier blanket prohibition against shop paint at the contact surfaces of connections assembled with high-strength bolts. As in the case of similar provisions usually invoked where connections are to be field-welded, when paint must be omitted in the vicinity of a joint it is necessary to note this fact on the shop drawings. The cost of this drafting room operation, plus the shop expense involved in marking limits for shop painting of the steel parts, and the expense of "touching up" the shop coat in the field after erection can mount up. Under the present provisions of the specification, contact surfaces should be kept free of paint only at joints subject to stress reversal or where stress redistribution due to joint slippage would be undesirable.

RECENT AND ANTICIPATED DEVELOPMENTS

As originally issued, the Council's specification limited the use of high-strength bolts (in lieu of rivets) to joints which transmit their load in shear between the connected parts. Tests which have since been made at the University of Illinois[7] have demonstrated that high-strength bolts loaded cyclically in applied tension have a higher endurance limit than hot-driven rivets of the same nominal diameter, provided the former are properly tightened before being placed in service. Needless to say they have a much greater static tension strength. It was noted that, for any given cyclic loading, the fatigue life was improved as the pretensioning was increased, even in the case where this pretension was as much as 120% of the elastic proof load. The Council's specification now permits the use of high-strength bolts in lieu of rivets for joints subject to tension as well as those loaded in shear.

---

[7] "Bolted Connections—Research," by W. H. Munse, *Proceedings-Separate No. 650*, ASCE, March, 1955.

For those connections in which some slip can be permitted, such as the gradual slip associated with maximum design loads long sustained at painted contact surfaces, the continued use of ordinary unfinished bolts may offer the most practicable solution. However, test data strongly indicate that high-strength bolt shear stresses, considerably larger than those recommended for rivets, might be justified if the resistance to shear of the bolt itself is the only criterion of useful service. When this possibility is studied in the light of present reduced shear values prescribed for unfinished bolts, it is conceivable that there might be an economic justification for using high-strength bolts, even for purposes for which less expensive unfinished bolts have previously been used exclusively—provided that an allowable shear stress for high-strength bolts, in line with their actual shear strength, is adopted.

AMERICAN SOCIETY OF CIVIL ENGINEERS
Founded November 5, 1852
TRANSACTIONS

Paper No. 2779

HYDRAULIC MODEL STUDIES OF MARTIN DAM DRAFT TUBES

By Carl E. Kindsvater,[1] M. ASCE, and
Richard R. Randolph, Jr.[2]

With Discussion by Messrs. Richard S. Woodruff; and Carl E. Kindsvater and Richard R. Randolph, Jr.

Synopsis

Unusual performance characteristics were revealed by turbine acceptance tests made at the Martin Dam power plant in Alabama in 1927. Undesirable characteristics were subsequently shown to be related to flow conditions in the draft tubes. As a result of model tests made in 1928, the draft tubes were modified by installing a half-cone fillet in the heel of each tube. Field tests indicated that this structural modification had corrected the original deficiency. In 1951, however, divers inspected the draft tubes and reported that the fillets installed in 1928 had been destroyed in two of the three original units. In the third unit, the fillet was badly damaged.

Following the report of damage to the remedial structures in the draft tubes, additional model studies were made in the hydraulics laboratory of the Georgia Institute of Technology at Atlanta. It was the purpose of these tests to develop a structural modification that would correct the undesirable turbine characteristics and that could be expected to remain in place for the life of the project.

The problem at Martin Dam is described, the early tests and field experiences are reviewed, and the results of the latest model studies (1951–1952) are presented. The theory underlying draft-tube tests is treated briefly, and significant features of the laboratory apparatus are described.

Background

Description of the Project.—The Martin Dam hydrolectric plant is a medium-head storage project in the Alabama Power Company system. It is located on

---

Note.—Published, essentially as printed here, in January, 1954, as *Proceedings-Separate No. 382*. Positions and titles given are those in effect when the paper or discussion was received for publication.

[1] Prof. of Civ. Eng., Georgia Inst. of Technology, Atlanta, Ga.

[2] Hydr. Engr., Southern Services, Inc., Birmingham, Ala.

the Tallapoosa River, near Tallassee, Ala. The plant began operation in 1926, with an initial installation of three 35,000-kw generating units. A fourth unit was installed in 1951 but is not involved in this discussion.

The hydraulic turbines at Martin Dam are of the conventional American-Francis variety, rated at 45,000 hp, a 145-ft head, and 120 rpm. The three turbines were purchased from two different manufacturers, but the draft tubes for the three units are identical. Fig. 1 shows a typical section through the intake and powerhouse, and in Fig. 2 general details of the original draft tubes are shown.

Turbine Efficiency Tests (*1927*).—In July, 1927, turbine acceptance tests were made on the Martin Dam units. The Gibson method of measuring discharge was used. The results indicated unusual characteristics in all three turbines. Tests on two units (designated Units 2 and 3), furnished by the same manufacturer, showed an abnormal drop in efficiency of about 2% between gate openings of 0.80 and 0.90. Tests on Unit 1, furnished by a different company, indicated a drop in efficiency of approximately 3% at a somewhat smaller gate opening.

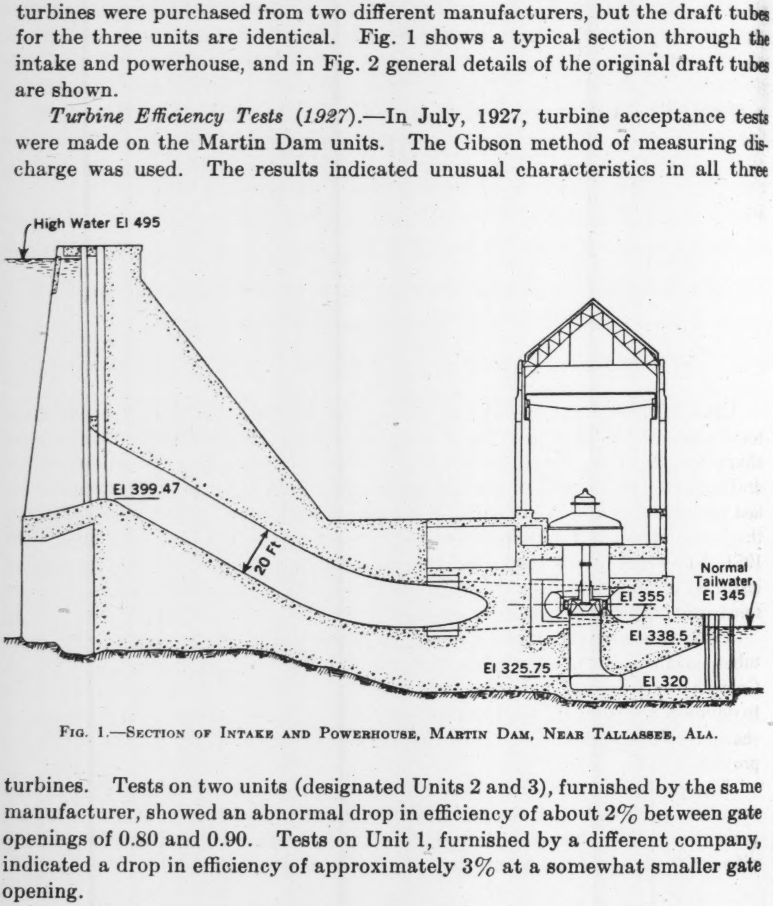

FIG. 1.—SECTION OF INTAKE AND POWERHOUSE, MARTIN DAM, NEAR TALLASSEE, ALA.

Fig. 3(*a*), adapted from the acceptance test report, shows a part of the plant efficiency curve for Unit 2. Fig. 3(*b*) shows a generator output curve based on the same tests. The two curves deviate in a similar manner over a range of loads which would normally include the point of best efficiency. Observers also reported evidence of unit instability, noise, and vibration in all the units when operated between "best gate" and "full load."

Immediately after the acceptance tests the power company, in cooperation with the turbine manufacturers, began an investigation to determine the cause of, and a remedy for, the undesirable performance characteristics revealed by the tests.

Early Model Tests.—The demonstrated similarity in the behavior of the turbines furnished by different manufacturers was evidence that their common troubles could be traced to the water passages leading to or from the turbines. Although the intake was of conventional design, the draft tube was not. Thus, subsequent to the acceptance tests, both turbine manufacturers made laboratory tests in which models of their runners were equipped with scale models of the Martin Dam draft tube. The Alabama Power Company, which at that time maintained a hydraulics laboratory under the direction of I. A. Winter, also made tests on the draft tube. The company model, however, was not equipped with a runner. Previous tests,[3] made on similar models and confirmed by prototype observations, had shown that the relative influence of draft-tube behavior on turbine performance could be predicted on the basis of the hydraulic efficiency of the draft tube.

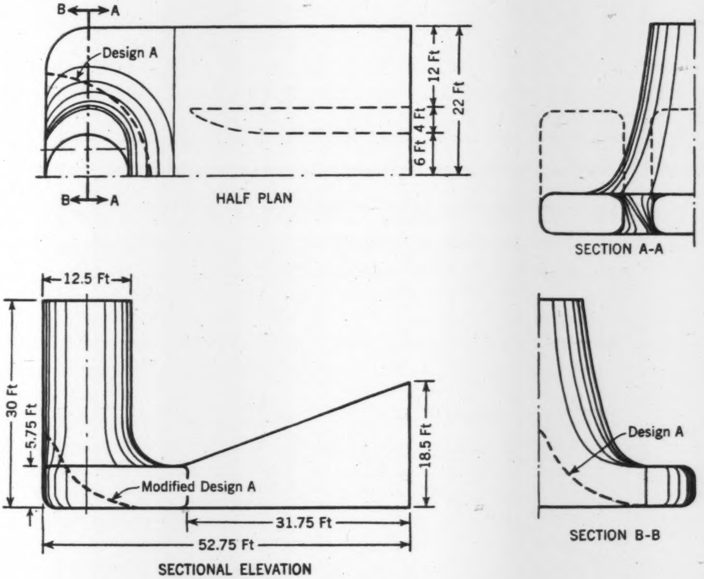

FIG. 2.—GENERAL DETAILS OF ORIGINAL DRAFT TUBE

The model tested by the power company was constructed to a scale of 1:37.5. It consisted of a wooden draft-tube model and an entrance section equivalent to the turbine speed ring or distributor. In order to simulate the effect of whirl in the water discharged from the runner, fixed-position vanes were placed in the distributor. Different degrees of whirl were produced by means of different vane assemblies.

---

[3] "Comparative Tests on Experimental Draft-Tubes," by C. M. Allen and I. A. Winter, *Transactions*, ASCE, Vol. LXXXVII, 1924, p. 893.

All the tests, including those made by the manufacturers on model turbines and those made by the power company, confirmed the conclusion that the draft tubes were responsible for the undesirable characteristics revealed by the Martin Dam turbine acceptance tests. As a result, an economical structural modification which would remedy the apparent deficiency was sought. The alteration finally adopted consisted of placing a concave half-cone fillet in the heel of the original tubes. The outline of the remedial structure is shown by the heavy dashed lines (Design A) in Fig. 2.

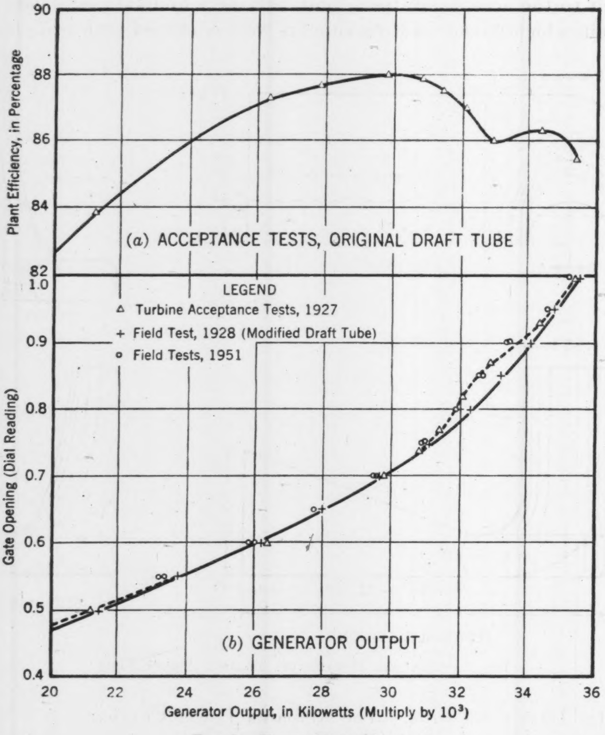

FIG. 3.—TESTS, UNIT NO. 2

The model tests made by the manufacturers, involving model turbines and the original draft tube, did not clearly demonstrate the peculiar irregularity near best gate that had been observed in the acceptance tests. However, they plainly indicated a general increase in efficiency and output with the proposed fillet installed in the draft tube. Tests on the power company's hydraulic model showed that there was a general improvement with the fillet in place and also that the draft-tube efficiency was critically related to the whirl imposed on the flow at the entrance. In fact, tests on the original Martin Dam draft tube showed that the efficiency at zero whirl (axial flow) might be as much as 7% less than that for a whirl resulting from a 15° deflection at the speed ring.

The residual whirl in the discharge from a given turbine is directly related to the discharge and the guide-vane angle. Furthermore, under design conditions of operation, the discharge from an ideal turbine may be presumed to have essentially zero whirl at best gate. Considering the energy involved in the work of the draft tube at Martin Dam, however, the 7% drop in draft-tube efficiency indicated by the hydraulic model tests at zero whirl did not fully explain the abrupt 2% or 3% drop in plant efficiency shown by the acceptance tests at best gate. It was nevertheless apparent that the over-all increase in draft-tube efficiency that would result from the proposed draft-tube modification would justify its installation in the prototype.

Structural Alterations and Field Tests (1928).—In March, 1928, eight months after the turbine acceptance tests, the structural modification developed by the model tests was installed in the Martin Dam draft tubes. The half-cone fillets, the outlines of which are shown in Fig. 2, were formed of ¼-in. steel plate. Each fillet consisted of nine sector-like plate segments, which were assembled and riveted together inside the draft tube as it was installed. Design drawings indicate that the fillets were fastened to the concrete of the original structure by lead cinch anchors. The steel shells were backfilled with concrete.

Immediately after the installation of the draft-tube modification in 1928, field tests were made for comparison with the results of the acceptance tests. As discharges could not be accurately measured without repeating the Gibson tests, the comparison was based on generator output curves instead of efficiency curves. Such a comparison for Unit 2 is shown in Fig. 3(*b*). It is apparent from the curves that the effect of the draft-tube alteration was to remove the irregularity observed previously at the large gate openings. Generator output was increased over the entire range from 0.75-gate to full gate. The maximum increase, about 700 kw, occurred at about 0.85-gate. Thus, the field tests confirmed the indications of the models.

Inspection and Field Tests (1951).—In connection with the installation of a fourth generating unit at Martin Dam in May, 1951, divers were directed to inspect the draft tubes of the three original units. The divers reported that the half-cone fillets in the draft tubes of Units 2 and 3 had completely disintegrated. The main structure of the tubes was not damaged, except where the cinch anchors had been removed. In Unit 1, a large part of the fillet remained, although a part of the steel shell was missing and the concrete backfill had been damaged.

Plant operation records do not show when the draft-tube fillets in Units 2 and 3 were destroyed. It is reasonable to assume, however, that the destruction process was gradual, as indicated by the partial damage discovered in Unit 1.

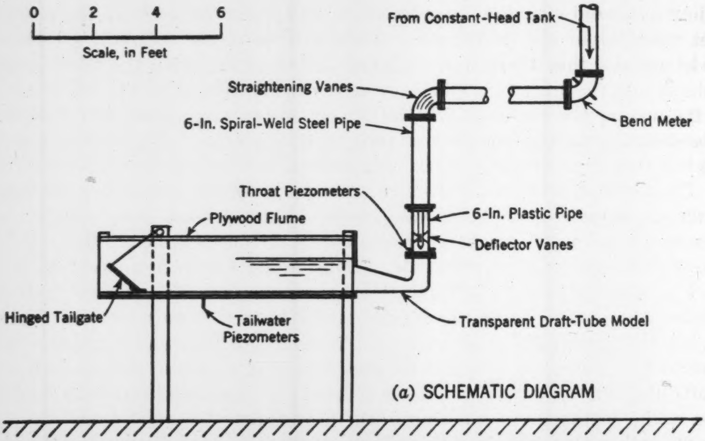
0
2
4
6
Scale, in Feet
From Constant-Head Tank
Straightening Vanes
6-In. Spiral-Weld Steel Pipe
Bend Meter
Throat Piezometers
Plywood Flume
6-In. Plastic Pipe
Deflector Vanes
Hinged Tailgate
Tailwater Piezometers
Transparent Draft-Tube Model

(*a*) SCHEMATIC DIAGRAM

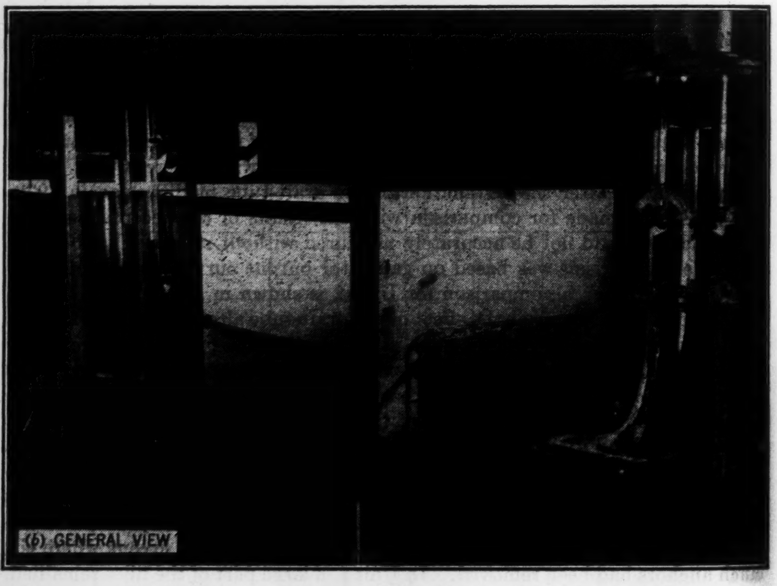

(*b*) GENERAL VIEW

Fig. 4.—Laboratory Setup for Model Tests of Draft Tubes, at Georgia Tech, Atlanta

Following the divers' report concerning the condition of the draft tubes, field tests were again undertaken on Unit 2 for comparison with the tests made immediately before and after the installation of the fillet. The results, shown in Fig. 3(*b*), agree remarkably with the observations made twenty-four years

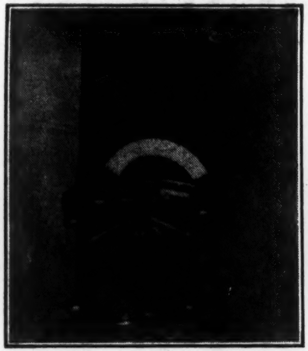

FIG. 5.—VANE SECTION ABOVE THE ENTRANCE TO THE DRAFT TUBE

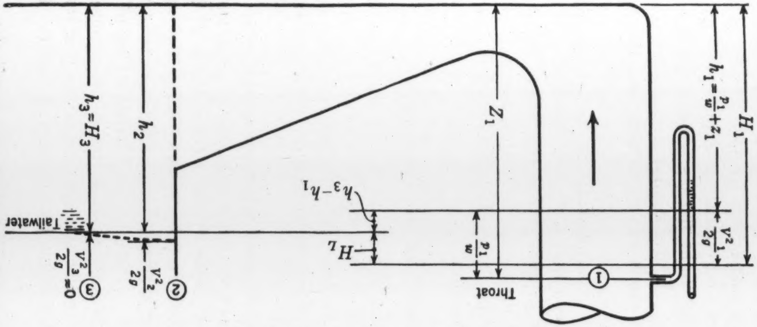
H_1
$h_1 = \frac{p_1}{w} + z_1$
$\frac{V^2_1}{2g}$
Z_1
$\frac{p_1}{w}$
Throat
①
$h_3 - h_1$
H_L
h_2
$\frac{V^2_2}{2g}$
②
$h_3 = H_3$
$\frac{V^2_3}{2g} \approx 0$
③
Tailwater

FIG. 6.—DEFINITION SKETCH OF FLOW IN A DRAFT TUBE

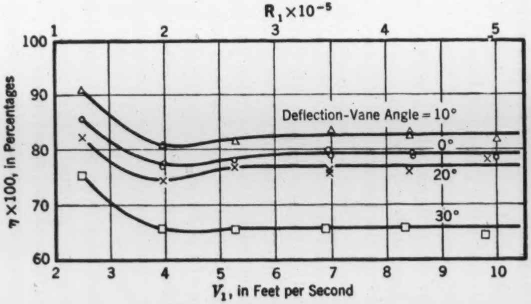

FIG. 7.—INFLUENCE OF R AND V_1 ON η FOR DESIGN A

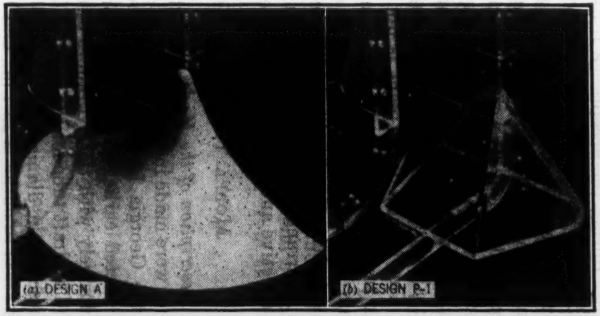
(a) DESIGN A
(b) DESIGN P-1

FIG. 8.—DRAFT-TUBE MODEL, SHOWING MODIFICATIONS IN PLACE

earlier during the acceptance tests. It was also noted at this time that the instability, noise, and vibration reported earlier had been characteristic of performance in recent years. During an inspection by the writers, it was demonstrated that the thundering noises and vibration experienced at the larger gate openings were accompanied by "light flashes" in the tailrace immediately below the end of the draft tube. Under similar circumstances such flashes have been explained[4] as evidence of shock waves; in this case, they were probably generated in the draft tube.

The Martin Dam plant is operated at a comparatively high load factor. The turbines are normally operated between best gate and full load. It was again apparent, therefore (as it had been in 1927), that the loss of efficiency and capacity due to the draft tube would justify investigation and correction. Thus, arrangements were made for additional hydraulic model tests to develop an effective and durable draft-tube modification.

MODEL TESTS AT GEORGIA INSTITUTE OF TECHNOLOGY

Description of the Model.—The latest model tests on the Martin Dam draft tubes were made in the hydraulics laboratory of the School of Civil Engineering of the Georgia Institute of Technology at Atlanta. These tests, like those conducted earlier in the laboratory of the power company, were concerned exclusively with the hydraulics of the draft tube.

The draft tube for the Georgia Tech model was built to a scale of 1:25. At this scale the diameter of the circular throat section is 6 in., the over-all length from heel to outlet is 25.4 in., and the gross inside width at the outlet is 21.2 in. To facilitate study of the flow pattern, the entire tube was constructed of transparent plastic. In order that it could be disassembled easily, the tube was provided with a flanged longitudinal joint. Piers in the horizontal leg of the tube were constructed of wood. At its discharge end it was flange-connected to an open flume with a width equivalent to the unit spacing in the prototype. Tailwater-depth control was provided in the flume by a hinged end gate. Fig. 4 shows the general arrangement.

In the Georgia Tech model, no part of the turbine above the top of the draft tube was reproduced. However, to simulate the effect of runner-discharge whirl, manually adjustable deflection vanes were placed in a short section of 6-in. plastic pipe immediately above the draft tube. An external shift-ring, connected to the vane axles, provided for their simultaneous adjustment to any angle from 0° to 35°, right or left. (This angle is measured with respect to the axis of the tube.) Check tests made repeatedly during the laboratory investigation indicated that the vane settings could be duplicated accurately. Fig. 5 is a photograph of the vane assembly.

Water was supplied to the model from the laboratory's constant-head recirculating system, and discharges were measured by a bend meter in the approach piping. The piezometric-head difference between the draft-tube throat and tailwater level was measured by means of a zero-displacement manometer mounted on a hook-gage staff.

---

[4] "Phenomenon of 'Flashes' at Outlet of Sluices," by Carl E. Kindsvater, *Civil Engineering*, Vol. 15, 1945, p. 565.

Theoretical Considerations.—The draft tube of an hydraulic turbine has two principal functions: (1) It makes possible placing the turbine above normal tailwater level without a corresponding loss of potential energy; and (2) it makes possible the use of relatively small, high-speed turbines without an excessive loss of kinetic energy. The latter function is ordinarily the more important. As an example of a common hydraulic device, the draft tube is a diffuser, the primary duty of which is to convert high velocities to low velocities with a minimum loss of flow energy. It follows that, in general, the best draft tube is the most efficient diffuser.

Fig. 6 is a definitive sketch for a discussion of draft-tube efficiency in terms of the one-dimensional (Bernoulli) energy equation. Under ideal conditions—that is, assuming no loss of energy between Section 1 at the throat and Section 3 in the tailrace—the difference in piezometric heads ($h_3 - h_1$) would be equal to the corresponding difference in velocity heads. Therefore, from the Bernoulli equation and the equation of continuity,

$$h_3 - h_1 = \left[1 - \left(\frac{A_1}{A_3}\right)^2\right] \frac{V_1^2}{2\,g} \dots\dots\dots\dots\dots\dots (1)$$

in which h is as defined in Fig. 6., A is the area of the flow cross section, and V is the average velocity (ratio of total discharge to total cross-sectional area).

When real fluids flow in a real draft tube, however, energy losses result from viscous and turbulent shear. Thus, the left side of Eq. 1 is diminished by an amount equal to H_L, the total energy-head loss. If H_L is assumed to consist of (1) a boundary friction loss designated $H_{f(1-3)}$; (2) an expansion loss in the tube, $H_{x(1-2)}$; and (3) an expansion loss between the end of the tube and the tailrace, $H_{x(2-3)}$ then

$$H_L = H_{f(1-3)} + H_{x(1-2)} + H_{x(2-3)} \dots\dots\dots\dots\dots\dots (2)$$

Each of the terms on the right side of Eq. 2 can be expressed as a function of $\frac{V_1^2}{2\,g}$. Thus, the total loss can be written as

$$H_L = K_L \frac{V_1^2}{2\,g} \dots\dots\dots\dots\dots\dots (3)$$

Eq. 3, when substituted in Eq. 1, gives for real fluids

$$h_3 - h_1 = \left[1 - \left(\frac{A_1}{A_3}\right)^2 - K_L\right] \frac{V_1^2}{2\,g} \dots\dots\dots\dots\dots\dots (4)$$

From dimensional considerations, K_L is a function of the Reynolds number, R, the geometry of the fixed boundaries, and the entrance flow conditions. The Froude number is not involved. Whereas a free surface does exist, namely, between Sections 2 and 3, the effect of gravity on this portion of the flow pattern is largely removed by the condition of submergence. Thus, for any given set of entrance conditions (in this case including the residual whirl of the water leaving the turbine runner), the ratio of the piezometric-head difference to the throat velocity-head is a function of the boundary geometry, including the area ratio, A_1/A_3, and the Reynolds number, or—

$$\frac{h_3 - h_1}{\frac{V^2_1}{2g}} = \phi(\mathbf{R}, \text{geometry}) = \eta \quad (5)$$

in which η is a dimensionaless piezometric-head ratio and a measure of draft-tube efficiency. This relationship is made more apparent by substituting for $(h_3 - h_1)$ the equivalent expression from the Bernoulli equation,

$$\eta = \frac{\frac{V^2_1}{2g} - \frac{V^2_3}{2g} - H_{L(1-3)}}{\frac{V^2_1}{2g}} \quad (6)$$

From Eq. 6, η is the ratio of the energy recovered by the draft tube to the energy available at the throat. The term $\frac{V^2_3}{2g}$ in Eq. 6 approaches zero for small values of the area ratio, which is the case for most draft tubes. For this condition, η is equivalent to both the "pressure efficiency" and the "energy efficiency" as defined elsewhere.[5] Furthermore, as defined by Eq. 5, η is a piezometric-head coefficient proportional to the reciprocal of the Euler number.[6] It follows that η is also proportional to the common discharge coefficient.

Eq. 5 shows that two conditions must be satisfied in order that a draft-tube model indicate correctly the efficiency of the prototype: (1) The model must be geometrically similar to the prototype, and (2) the Reynolds numbers must be identical in the model and prototype. The second condition requires that velocities vary directly with the kinematic viscosity of the fluid and inversely with a suitable length parameter. Thus, in the present instance, involving a model-prototype length scale of 1:25 and a model fluid that is the same as that in the prototype, model velocities would have to be twenty-five times the corresponding velocities in the prototype. As an example of the extremely high velocities involved: Corresponding to a prototype discharge of 2,500 cu ft per sec, the model discharge would be 100 cu ft per sec and the model velocity, in the throat, 510 ft per sec.

Obviously, the second condition for similarity cannot be satisfied under ordinary laboratory conditions. Fortunately, however, it can be anticipated that (as in the case of orifice and venturi-tube coefficients, for example) the efficiency ratio, η, will be independent of the influence of viscosity at the high Reynolds numbers and the fully developed turbulence which characterize flow through draft tubes. Furthermore, on the basis of experimental data[7] on orifices and venturi tubes, it can be assumed that Reynolds numbers obtainable in the laboratory will be high enough to include the range in which the effects of fluid viscosity can be ignored. In any case, the proof of this assumption depends on evidence obtained in the laboratory under the maximum possible range of model discharges. If exploratory tests show that the Reynolds-number influence cannot be ignored, it is customary to attempt an approximate analytical correction to the model test results. An example of this procedure is given by the well-known step-up formulas for turbine model tests. It should be emphasized, however, that the relative effect of experimental changes in certain minor geometric features frequently can be determined on the basis of qualitative model tests run at a constant Reynolds number which is considerably less than that of the prototype.

---

[5] "Effect of Entrance Conditions on Diffuser Flow," by J. M. Robertson and Donald Ross, *Transactions*, ASCE, Vol. 118, 1953, pp. 1068-1091.

[6] "Elementary Mechanics of Fluids," by Hunter Rouse, John Wiley & Sons, Inc., New York, N. Y., 1946, p. 61.

[7] *Ibid.*, p. 256.

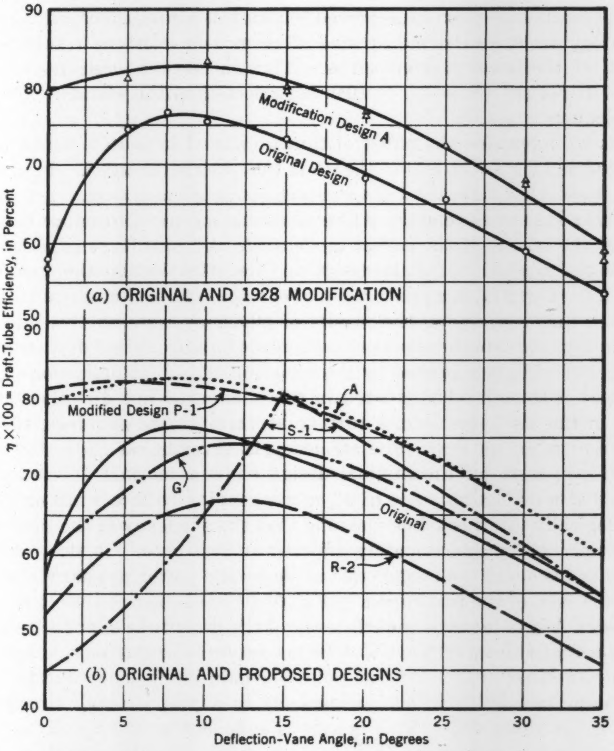

FIG. 9.—COMPARISON OF MODIFICATION DESIGNS ON THE BASIS OF EFFICIENCY

Test Procedure.—An initial step in developing a test procedure for the Martin Dam draft-tube studies was to evaluate the effect of the Reynolds number on the efficiency ratio, η. This was accomplished by making tests at various velocities up to the maximum attainable with the laboratory apparatus. Fig. 7 shows the results of a series of such tests made on modification Design A (1928). A scale of values of the Reynolds number, based on an approximate value of kinematic viscosity equal to 1 × 10^5 sq ft per sec, is shown opposite the scale of velocities. The different curves in Fig. 7 correspond to various deflection-vane positions. (Deflection angles, in degrees, were measured as the acute angles between the vanes and the axis of the tube (Fig. 5).) All the curves in Fig. 7 show a tendency for η to remain constant for all values of **R** exceeding 3×10^5. As was anticipated, the curves have a form similar to those representing the effect of **R** on venturi-tube and orifice coefficients.[7]

The results shown in Fig. 7 indicate that dynamic similarity of model and prototype draft tubes can be achieved without attaining identical values of **R**. Exploratory tests also demonstrated that more consistent results could be obtained at the lower test velocities. Thus, a constant velocity of approximately 7 ft per sec ($\mathbf{R} = 3.5 \times 10^5$) was selected as the standard for most of the subsequent tests.

Tests to determine the effect of tailwater level indicated that η would be unaffected as long as the end of the draft tube was submerged. In all the subsequent tests, therefore, the tailwater was set at normal level.

Another step in developing and evaluating the test procedure consisted of verifying the results of the earlier model tests and prototype experiences with regard to the original draft-tube design and the 1928 modification (modification Design A). Fig. 8(*a*) is a photograph of the disassembled model with Design A in place. Fig. 9(*a*) shows the results of efficiency tests on this setup. Also shown in Fig. 9(*a*) are the results of tests made on the original draft-tube design. The effect of whirl is indicated by the variation of η as the deflection-vane angle is varied. Although whirl created in this manner is not directly comparable to that in the discharge from a turbine at various gate openings, the relative influence of whirl on draft-tube efficiency is nevertheless shown by these results. Thus, tests on the original design show a marked deficiency in performance at a deflection angle of 0°, corresponding to zero whirl or axial flow. This is logically interpreted as meaning that the efficiency of the turbine would be adversely and proportionately affected at best gate. It also confirms the acceptance tests and the model tests made by the power company in 1928.

Comparison of the two curves in Fig. 9(*a*) shows that the effect of modification Design A is to increase the efficiency of the draft tube over the full range of deflection angles, from 0° to 35°. The maximum benefit from this modification occurs at an angle of 0°. At this point the gain in efficiency due to Design A is approximately 22%, which corresponds to a proportional gain in turbine efficiencies of about 2%. This benefit is sufficient to explain the irregularity in the acceptance test curve (Fig. 3(*a*)) and the smoothing effect of the 1928 modification on the capacity curves (Fig. 3(*b*)). It was explained previously that the earlier model tests showed a maximum gain of only 7% efficiency, which was not sufficient to explain the full benefit of the modification as shown by the subsequent field tests. Thus, tests made on the new model were judged to confirm the acceptance tests and the field capacity tests and to compare favorably with the previous model tests.

MODEL TEST RESULTS

Observations on the Flow Pattern.—Distinctive features of the Georgia Tech model included a fully transparent draft tube and other provisions for observing the flow pattern. As shown in Fig. 5, four small stagnation tubes were inserted in the model through glands that permitted the tips of the tubes to be moved to almost any point in the flow cross section. Thus, a dye solution or a stream of air introduced through these tubes could be used to trace the flow throughout the model. As shown in Fig. 4, the bottom of the model was approximately 4 ft above the floor of the laboratory, thereby facilitating observations of the flow pattern.

Observations made during the preliminary tests showed that the unusual flow conditions in the original draft tube were caused by the excessive rate of enlargement of the width of the vertical leg of the tube (Fig. 2). Thus, for axial flow conditions, separation occurs along the side boundaries of the tube and little deceleration takes place until the water strikes the bottom of the tube. Unstable eddies fill parts of the vertical leg and the heel-corner regions of the bottom. High-velocity currents along the bottom are deflected into the two outer passages of the horizontal leg, and dead water fills the upper regions of the center passage. When the deflection vanes impose an initial whirl on the water entering the tube, the resulting normal acceleration causes the live stream to be guided more effectively by the fixed boundaries. For small degrees of whirl, therefore, the flow is caused to decelerate in the vertical leg, the eddy losses resulting from the impact and abrupt enlargement at the bottom are proportionately decreased, and the efficiency of the tube is increased. This apparently accounts for the large difference between efficiencies corresponding to deflection angles of 0° and 7.5°, as indicated by Fig. 9(*a*).

With modification Design A placed in the heel of the tube, the flow is deflected to the front and sides of the vertical leg and into the center passage, in addition to the two outer passages of the horizontal leg. The eddy zones are more stable and are considerably reduced in size. Strangely, the principal benefit from this modification appears to be caused by the "reflection" of the flow off the face of the conical fillet. Subsequent tests on fillets of various shapes and sizes confirmed the observation that no appreciable part of the gain in efficiency shown by the comparison in Fig. 9(*a*) was a result of the constriction imposed on the area of the vertical leg of the tube.

Scope of the Tests.—Verification tests made on the Georgia Tech model confirmed the conclusion based on earlier laboratory and field tests that the draft-tube modification installed in 1928 would correct the principal deficiencies of the original design. Measured efficiencies for the modified design compare well with similar data on good draft tubes of more recent design. Thus, the tests demonstrate that the performance of the Martin Dam draft tubes with modification Design A is as good as could be expected. However, previous experience with this design, as installed in the prototype, has shown that it is not capable of withstanding the destructive forces imposed on it by the turbine discharge. The main object of the new tests, therefore, was to develop a remedial structure that could be expected to remain in place for the life of the project. It was anticipated that this could be accomplished with a design adapted to simpler and cheaper construction details and methods than those required for the 1928 modification.

The designs considered and tested can be roughly classified on the basis of the geometry of the proposed structure: (1) Circular, half-cone fillets located at the center of the heel of the tube; (2) pyramids intended to simulate the effect of the cones but preferred because of structural simplicity; (3) full-width floor wedges located in the heel corners; (4) pedestals located on the floor directly below the vertical leg; and (5) full-width roof wedges and floor wedges in the horizontal legs of the draft tube. Thirty different designs, most of them cones or pyramids, were tested.

Comparison of Results.—It is not necessary to present the results of efficiency tests made on all the thirty different modification designs tested in order to demonstrate the relative merit of the six general varieties listed. In fact, the results can be summarized briefly with these comments on the various proposed designs:

1. The best of seven conical fillets was the original Design A. Tests made on several larger cones, intended to constrict the area of the vertical leg and thereby correct the excessive rate of enlargement in that portion of the draft tube, were not satisfactory.

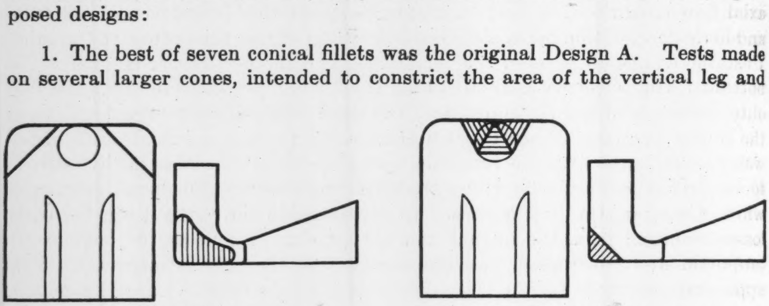

(*a*) DESIGN S-1 (*b*) DESIGN P-1

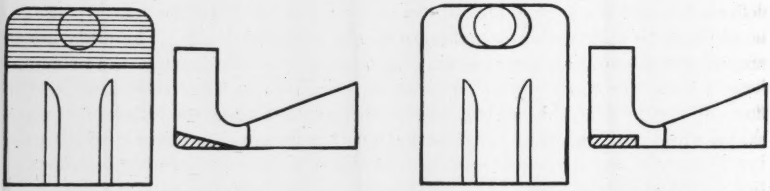

(*c*) DESIGN G (*d*) DESIGN R-2

FIG. 10.—DRAFT-TUBE MODIFICATIONS, FOUR MODEL DESIGNS

2. Tests on only a few examples of the wedges, corner fillets, and pedestals gave sufficient evidence that these structures were either ineffective or, in some cases, actually detrimental in their effect on the performance of the draft tube.
3. Initial tests on pyramids proportioned to simulate the cone of design A showed that this form, preferred because of structural simplicity, was the best of the proposed substitutes for the original modification.

Thus, of the thirty different designs tested, fifteen were pyramids, most of which differed only slightly, but systematically, from the design finally selected as the best. The adopted design, shown as Design P-1 in Fig. 10, is a three-sided pyramid located at the center of the heel of the draft tube. Fig. 8(*b*) is a photograph of Design P-1 in place in the model. Fig. 9(*b*) shows the results of efficiency tests made on this model.

Included in Fig. 10 are three designs in addition to Design P-1. These, included for comparison, are typical of the variety of proposed structures they represent. Design S-1 is representative of the corner fillets; Design G is a heel wedge; and Design R-2 is a medium-height oval pedestal. The results of efficiency tests on these three designs are shown in Fig. 9(*b*). The remarkable ineffectiveness of Designs S-1, G, and R-2 is shown by comparing results of tests on these models with tests on the original design and with those on modification Designs A and P-1.

Fig. 9(*b*) shows clearly that Design P-1 gives results which are generally equivalent to those for Design A. Although the efficiency of Design P-1 is slightly lower than that for Design A at deflection angles between 5° and 25°, its efficiency at 0° is about 2% higher. Thus, the design selected on the basis of these model tests is believed to satisfy the requirements listed in the objectives of the investigation.

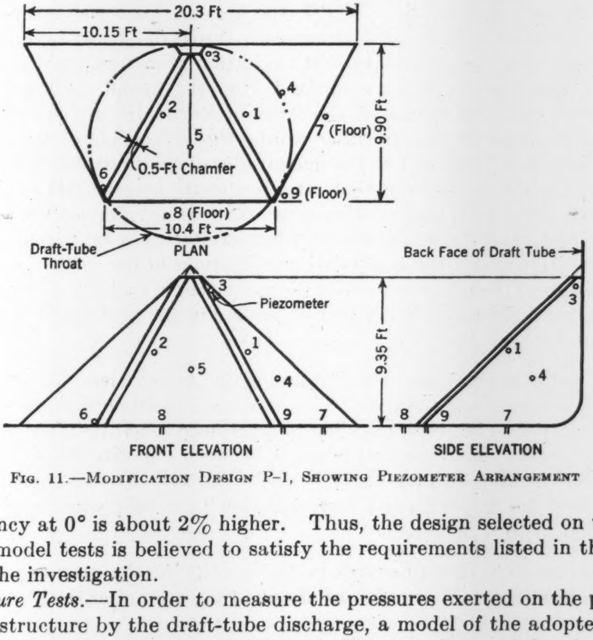

FIG. 11.—MODIFICATION DESIGN P-1, SHOWING PIEZOMETER ARRANGEMENT

Pressure Tests.—In order to measure the pressures exerted on the proposed remedial structure by the draft-tube discharge, a model of the adopted design was equipped with piezometers as shown in Fig. 11. Some of the piezometers were placed at points that would give results indicative of the maximum differential pressure between opposite faces of the pyramid under various conditions of operation. Others were expected to indicate the presence of excessive positive or negative (cavitation) pressures at critical points on or near the pyramid.

Since the pyramid of Design P-1 is symmetrical with respect to the longitudinal center line of the draft tube, piezometers on either of the lateral faces were not duplicated on the opposite face. In order to show the effect of whirl, tests were repeated for equal "right" and "left" deflection angles. The maximum differential pressure between corresponding points on opposite faces was then computed as the algebraic difference of the measurements made on any one piezometer with settings of the deflection vanes of equal angle but opposite sign.

Pressure measurements on the model, like the efficiency tests, were made using a discharge corresponding to a model throat velocity of 7 ft per sec. For analysis, the piezometric head, h, at each of the piezometers was referred to the piezometric head, h_o, at a common reference piezometer. Thus, for each piezometer on the model, a dimensionless pressure ratio was computed as the ratio of the difference in piezometric heads $(h - h_o)$ to the velocity head at the throat, $\frac{V^2_1}{2\,g}$. This ratio, similar in form to the efficiency ratio, Eq. 5, is also a function of the Reynolds number and the entrance flow conditions for any given boundary geometry. Tests made at different Reynolds numbers showed that, like the efficiency test results of Fig. 7, the pressure ratio was independent of the Reynolds number for test velocities at the throat of 7 ft per sec and greater. Thus, disregarding the possibility that cavitation pressures might exist in the prototype, the pressure ratios computed from the model measurements are also expected to be constant over the range of Reynolds numbers relating the model and the prototype. In other words, the magnitude of the computed pressure ratio is independent of the magnitudes of the pressures and velocities that existed in the model, and that ratio is directly transferable to the prototype. Only if the computed prototype pressures at any point are less than the absolute pressure of the water vapor (when cavitation is indicated) will there be any reason to doubt the quantitative indications of the model.

The results of the pressure tests on the model, converted to equivalent values for a maximum discharge of 3,860 cu ft per sec in the prototype, can be summarized as follows:

1. At no point on or near the pyramid is the pressure less than gage zero—that is, all pressures are positive. The maximum positive pressure is approximately 13 lb per sq in., corresponding to a pressure head of 30 ft of water.
2. The maximum differential pressure between opposite faces of the pyramid is at the location of piezometer No. 4 in Fig. 11. At this point the difference is about 4.3 lb per sq in., corresponding to a difference in piezometric heads equal to 10 ft of water.

These results show that pressures in the vicinity of the proposed structure, under the least favorable conditions of operation, are not critical.

CONCLUSIONS

Laboratory tests made on scale models of draft tubes have been confirmed by prototype observations as a means of demonstrating the relative influence of draft-tube flow conditions on turbine performance. The following conclusions are based on field and laboratory investigations of the Martin Dam draft tubes:

1. The efficiency of a draft tube as a flow diffuser can be determined from model tests.

2. The effect of whirl on draft-tube efficiency can be simulated by means of radial deflection vanes placed upstream from the throat.

3. Unusual flow conditions in the original draft tubes at Martin Dam are responsible for the undesirable performance characteristics revealed by acceptance tests on the turbines.

4. A simple remedial structure, installed in the Martin Dam draft tubes, will correct the undesirable flow conditions.

5. At no point on the proposed structure will cavitation pressures occur. Differential pressure forces will not be excessive.

ACKNOWLEDGMENTS

The model tests described in this report were made in the hydraulics laboratory of the Georgia Institute of Technology under an agreement between the Alabama Power Company and the Georgia Tech Research Institute. Coordination with the Alabama Power Company was handled by F. C. Weiss, vice-president in charge of engineering, and E. W. Robinson, vice-president in charge of operations. J. W. Jones and George Schnabel, J.M. ASCE, assisted in making the tests. The plastic draft-tube model was made by Albert H. Smith.

DISCUSSION

Richard S. Woodruff,[8] A. M. ASCE.—Pyramids were installed in the three original draft tubes in September, October, and November, 1952, and were of the dimensions recommended on the basis of the authors' research (Fig. 11). When the draft tubes of Units 2 and 3 were unwatered, large irregular pieces of concrete were found immediately inside the draft-tube exit. The shapes and sizes of these pieces as well as the nature of the broken material indicated that they were from the original half cones. No sections of the ¼-in. steel plate from the surface of the original cones were found in these two tubes. The draft-tube exit of Unit 1 was clear because approximately 75% of the original cone concrete in this tube was still in place. In this tube it was an easy matter to chip out the remains of the old cone because the concrete was of inferior quality and most of the steel plate had washed away. The steel shells of the original cones were filled through a small opening at the top; this was done despite a considerable handicap caused by leakage water from the penstock and the threat of flood-water conditions in the tailrace.

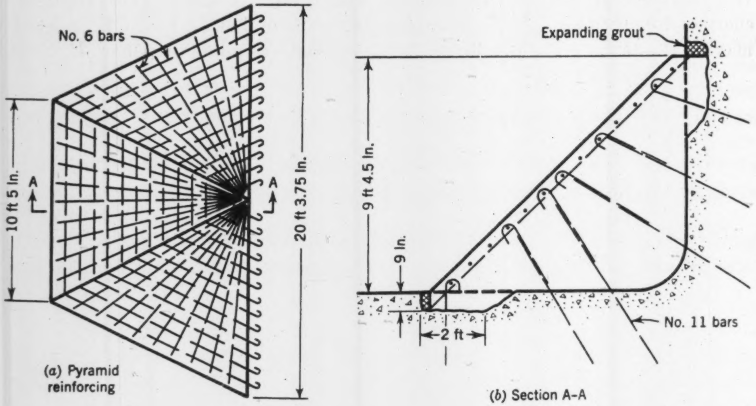

(a) Pyramid reinforcing

(b) Section A-A

Fig. 12.—Diagram Showing Reinforcing Bars

The new pyramids were installed by segregating (with sandbags) and drying the part of the draft tube involved. The original concrete surface was thoroughly cleaned of scum and was carefully chipped to clean, sound material after which No. 11 reinforcing rods were grouted at least 4 ft deep into the old concrete (Fig. 12). Wooden forms were lined with an absorptive form liner ⅜ in. thick in order to produce a smooth, hard, dense surface on the finished pyramid. Forms were not lowered into the draft tube until a few hours before pouring began because of the wet and humid condition. After the forms were assembled, several large light bulbs were installed inside them in order to help keep the absorptive liner dry. Concrete for the pyramids was a seven-sacks-per-cubic-yard design with an air-entraining agent; slump of from 2 in. to 4 in. was specified. The average 28-day strength of concrete test cylinders was 3,800 lb per sq in. A man was inside the form during the pouring process to work the concrete along the face of the forms with a spade as a precaution against honeycombing. A vibrator was used during the pouring, but special care was taken to prevent it from contacting the anchor dowels as the concrete in the bottom of the form had reached its initial set before the pyramid was "topped out." The forms were removed 36 hr after concrete was poured, and the draft tube was flooded a day later. Each pyramid was allowed to cure for 14 days with the unit shut down. From 14 days to 21 days after pouring, the unit was restricted to generation at best gate in order to keep turbulence in the draft tube at a minimum. After 21 days, the unit was released for unrestricted operation.

---

[8] Senior Engr., Alabama Power Co., Birmingham, Ala.

Excellent results were obtained in producing a smooth surface on the pyramid and in using expanding grout around the periphery. The pyramids for all three units were installed at a total cost of approximately $41,000.

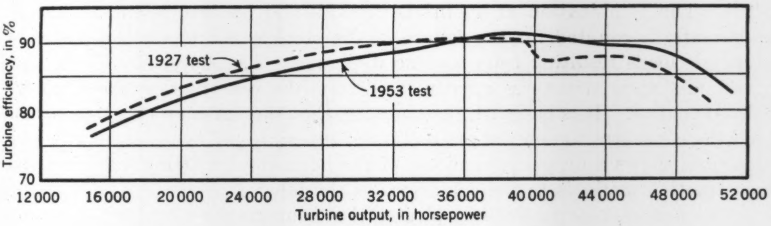

FIG. 13.—TURBINE EFFICIENCY, UNIT 1

In June, 1953, a second Gibson test was performed on Unit 1 for the purpose of comparing the performance of this unit after the pyramid was installed in the draft tube with the 1927 acceptance test. This test disclosed that the maximum turbine output was increased from 50,500 hp to 51,330 hp. This represents a gain of approximately 605 kw in generating capacity, which conformed to the expected results. The efficiency at maximum capacity was increased from 79.5% to 82.2%. Best gate operation was increased from 36,400 hp to 39,000 hp with a corresponding increase in maximum efficiency of from 90.3% to 91.1%. Although the efficiency decreased approximately 0.7% for gate openings producing less than 36,000 hp, its average increase was more than 1% for those producing more than 36,000 hp. Both tests were based on a net head of 145 ft. The increased efficiency is in the range of operation where it will be most beneficial. The "kink," or abnormal drop in efficiency that occurred near 40,000 hp, without the modification, was definitely smoothed out. This is shown by a comparison of the two Gibson-test curves (Fig. 13).

A comparison of the operating characteristics of Units 1, 2, and 3 at Martin Dam results in the following conclusions:

1. An increase in generating capacity and efficiency was obtained by the installation of the half pyramid in the heel of the draft tubes (Fig. 10(*b*)), thus again indicating the value of hydraulic model studies.

2. The installation was economically justifiable because the cost was offset by the value of the increased energy and capacity in approximately one year.

CARL E. KINDSVATER[9] AND RICHARD R. RANDOLPH, JR.,[10] MEMBERS, ASCE. —Mr. Woodruff's discussion is a necessary complement to the writers' description of the events leading to the latest attempt to remedy the undesirable characteristics of the original draft tubes in the Martin Dam power plant. The details of design and the methods used in constructing the remedial structure are of particular interest because they were devised in the light of the unfortunate experiences associated with the modifications made in 1928. The disintegration of the original remedial structures, revealed when the tubes were unwatered, is sufficient evidence of the necessity for the meticulous care with which the latest construction was accomplished.

Mr. Woodruff reports that concrete remnants of the original heel cones were of inferior quality. The poor quality of the concrete used was doubtlessly indirectly related to the difficulty of placing the backfill under the outer steel shell. The combination of an infirm backfill and an insufficient anchorage apparently accounted for the failure of the steel armor under the unsteady dynamic loads resulting from turbine discharge. The simplicity of the new pyramid-shaped structures greatly facilitated the construction described by Mr. Woodruff. It is believed, furthermore, that the omission of a steel armor and the concentration on the production of superior-quality concrete which he describes shows a proper recognition of the necessity for fitting materials and construction methods to the conditions of the job.

The writers were particularly pleased that comparative efficiency tests were made on Unit 1 before and after the remedial construction was completed. Prototype verification of conclusions based on hydraulic model studies is admittedly viewed with considerable relief by the researcher. It is true that the basic principles of similitude are as indisputable as the most fundamental principles of engineering mechanics. Unfortunately, however, the requirements for complete similitude are not always possible to fulfil in the laboratory. It follows that a considerable amount of judgment, based on experience as well as theory, is an important component of every model study. The omniscient Leonardo is quoted as a final warning: "Experiment never errs; only your judgment errs in anticipating results which experience does not confirm."

In connection with Mr. Woodruff's discussion of the prototype tests, it is pertinent to emphasize the impracticality of a direct comparison of the results of the turbine efficiency tests with the results of the hydraulic model tests reported in the paper. Sufficient evidence is believed to be available to substantiate the use of "diffuser efficiency" as an indication of the relative worth of different draft tubes. The writers do not mean to imply, however, that the draft-tube component of the power efficiency of a turbine can be determined from Eq. 5. For this investigation specifically there is little reason to believe that general draft-tube characteristics need be determined from a scale model of the complete machine. Indeed, it was the simplicity of the laboratory apparatus used by the writers that was unique in comparison with previous studies.

---

[9] Prof. of Civ. Eng., Georgia Inst. of Technology, Atlanta, Ga.

[10] Hydr. Engr., Southern Services, Inc., Birmingham, Ala.

It was observed following the derivation of Eq. 5 that η is an adequate measure of the energy efficiency of a diffuser only when the area ratio (A_3/A_1) approaches zero. It should also be acknowledged that the writers' interpretation of Eq. 5 is inadequate as a means of determining the true energy efficiency of any diffuser unless the flow at the end sections is both uniform and axial. It follows that, because the effect of whirl was ignored in evaluating Eq. 5 from the laboratory data, an error of indeterminate magnitude is inherent in certain of the computed efficiency values. This does not of, course, invalidate the procedure used to determine the relative merits of the various draft-tube modifications.

In the derivation of Eq. 5, it was implied that the flow was both uniform and axial. For this condition, the average piezometric head at both Section 1 and Section 3 is represented by the piezometric head at the boundaries. This fact is important, because only at the boundaries are the piezometric heads readily measured. With whirl at Section 1, however, the piezometric head actually varies from a minimum at the center to a maximum at the wall. The magnitude of this variation depends on the magnitude and distribution of the velocity in the cross section. Unfortunately, neither the velocity pattern nor the piezometric-head distribution can be measured by ordinary means. It follows, therefore, that the use of wall piezometers to evaluate h_1 results in an increasing overevaluation as the whirl increases. At Section 3, of course, the residual whirl is usually so small that it has negligible influence on the normal, hydrostatic pressure variation in the section.

The second complication resulting from whirl at Section 1 concerns the denominator of Eq. 5. Thus, when the flow contains a whirl component, V_1 is correctly defined as the vector sum of the axial velocity and the tangential velocity in the section. For a given discharge, therefore, the average kinetic energy at Section 1 increases with increasing whirl. The exact magnitude of this influence is also indeterminate. It was expedient and consistent with the objectives of the investigation, therefore, to evaluate V_1 as the average axial velocity, Q/A_1.

AMERICAN SOCIETY OF CIVIL ENGINEERS
Founded November 5, 1852
TRANSACTIONS

Paper No. 2780

STRENGTH CHARACTERISTICS OF COMPACTED CLAYS

By Gerald A. Leonards,[1] A. M. ASCE

With Discussion by Messrs. Harold J. Gibbs and Jack W. Hilf; James K. Mitchell; Preston T. Bennett and Paul E. Wohlt; and Gerald A. Leonards

Synopsis

The results of a laboratory investigation undertaken to isolate the factors that affect the shearing strength of unsaturated, compacted clays are reported. The primary objective of the study was to establish relationships indicative of the relative importance of the variables involved.

Soils of two types were studied: One was a highly plastic clay, and the other, a clay of low plasticity—a modified loess. Both these soils have been studied extensively by other investigators. Because of large differences in the plasticity characteristics of the two soils, their behavior should exemplify that of many clay-like soils commonly encountered.

Improved techniques were developed for preparing, compacting, and preserving soil samples that resulted in test specimens with essentially duplicate strength and stress-strain characteristics. Measurements of loads, weights, dimensions, and pressures were made with great precision. A special feature of this investigation was the determination of the void ratio for the part of the test specimen that failed.

All triaxial-shear specimens were approximately 1.42 in. in diameter and 2.80 in. high. The apparatus was designed for a maximum of convenience and adaptability in testing and for simplicity of fabrication.

The results show conclusively that, for the two types of soil tested and within the ranges in water content and percentage of saturation considered, the critical factor that reflects the strength of partly saturated, compacted clays is the void ratio at failure. A unique relationship exists between the void ratio at failure (plotted to an arithmetic scale) and the compressive strength (plotted

---

Note.—Published, essentially as printed here, in December, 1953, as *Proceedings-Separate No. 360* Positions and titles given are those in effect when the paper or discussion was received for publication.

[1] Asst. Prof. of Soil Mechanics, School of Civ. Eng., Purdue Univ., Lafayette, Ind.

to a logarithmic scale). It was found that, during the application of shearing stresses on partially saturated clays, changes in void ratio occur that are not accompanied by corresponding changes in water content. The nature of these changes in void ratio depends on the initial conditions, the confining pressure, the preconsolidation pressure, and the quantity of water added to the soil from an external source. On the basis of these facts, some inconsistencies in the theories concerning the strength characteristics of clay-like soils can be resolved.

An important by-product of this investigation was the discovery that, for a given initial water content, a reduction in void ratio achieved by a process of consolidation results in a higher compressive strength than that obtained by a process of compaction. In addition, it was found that swelling in the presence of water, at a specified confining pressure, increases as the amount of compaction increases.

INTRODUCTION

In foundation and earthwork engineering—despite the heralded advances attributed to the science of soil mechanics—experience remains the most important requisite for success. The requirements of the twentieth century are making this fact increasingly disconcerting. Earth dams of unprecedented height and size are being designed and constructed. Highway and airport pavements capable of sustaining repeated loads of ever-increasing magnitude and frequency must be built, and heavy structures are being located in areas formerly considered unsuitable from the standpoint of the supporting power of the underlying soils. Presented with these (and many other) new problems for which suitable precedents are substantially lacking, engineers are finding it increasingly necessary to rely on rational, scientific methods of analysis with correspondingly less emphasis on empirical rules.

Among the principal difficulties in the application of scientific theories to engineering problems dealing with soil are the large number of factors that affect the physical behavior of soils and the great complexity of the interaction of these factors. No matter how intricate and theoretically exact the "stability analysis" of an earth structure may be, its results are usually misleading unless the strength characteristics of the soil, during the entire life of the structure, can be predicted with reasonable certainty. Extensive research (principally during the past thirty years) has resulted in methods for determining within practical limits the shearing strengths of cohesionless soils and of certain saturated, sedimentary clays. However, all compacted soils are initially partly saturated, and little is known of the strength characteristics of these soils. As an illustration of this fact, the following is quoted from a section on the compaction of soils in a leading current textbook on earthwork and foundation engineering (1):[2]

> "At the present time, the relation of moisture content at the time a fill is placed, the degree of compaction, and the physical characteristics of the fill throughout its period of service are still imperfectly understood. The changes in strength, rigidity, and permeability of the fill with age and with

---

[2] Numerals in parentheses—thus, (1)—refer to corresponding items in the Appendix.

changing water content deserve far more attention than they have as yet received. Hence, the remainder of this article contains almost no information concerning the properties of compacted soils. It deals primarily with construction procedures."

In this paper the results of an attempt to contribute to the understanding of the strength characteristics of compacted clays are reported. The development of current knowledge will be traced in some detail, although the review is not meant to be complete. Rather, it is intended to focus attention on the limitations of the present concepts, particularly as they apply to unsaturated, compacted clays. The results of recent research will be presented, and some new concepts regarding the shearing resistance of compacted clays will be suggested. It is hoped that these concepts will provide the basis for a better understanding of the behavior of compacted clays and that they will facilitate more significant field measurements, which may ultimately lead to a more rational basis for the design of compacted earth structures.

DEVELOPMENT OF CURRENT KNOWLEDGE

In 1776, C. A. Coulomb (2) proposed what was probably the first formal hypothesis dealing with the frictional resistance of earth masses. This hypothesis can be expressed algebraically as follows:

$$s = \sigma \tan \phi + c$$

in which s is the maximum shearing resistance; σ denotes the normal stress on any portion of a plane in an earth mass; ϕ indicates the angle of internal friction, a constant for the earth in question; and c is the unit cohesion, also considered to be a constant. In this paper, stresses are in kilograms per square centimeter. For conversion, 1 kg per sq cm equals 14.2234 lb per sq in.

For nearly 150 years after Mr. Coulomb's classic work was published, experimentation was directed principally toward the determination of the values of ϕ and c for a large variety of soils. A typical example of the work done during this early period was reported by M. L. Leygue (3) in 1885, from which it was concluded that the Coulomb equation was "practically verified." The Coulomb equation soon became known as the Coulomb Law. For almost 200 years this "law" has dominated the thinking of engineers and soil technologists; in fact, it is still the basis of all modern theories dealing with the stability of earth masses (4) (5).

In 1910, J. Frontard and M. O. E. Jacquinot (6) conducted experiments on samples taken from an earth dam that had failed because of a considerable lowering of the reservoir level. In so far as the writer could determine, the conclusions from this study (as reported by J. Résal) were the earliest recorded statements of the fact that the unit cohesion was not a constant.

The penetrating researches and keen observations of Karl Terzaghi, Hon. M. ASCE, led to a better understanding of earth action (7) (8) (9) (10) (11) (12) (13). Perhaps the most significant contribution of Mr. Terzaghi's series of researches was the formulation of a theory regarding the stress-deformation-time relationships for saturated, clay-like soils. Regardless of its limitations from the standpoint of predicting the settlement of structures, the theory of consolidation helped explain numerous phenomena encountered in foundation engineering and provided the basis for a more fundamental understanding of the factors accounting for the shearing resistance of soils. The theory drew attention to the significance of the pore-water pressure, the magnitude of which is controlled by the amount of drainage (or degree of consolidation) permitted before and during a shear test. This condition means that the rate of load application has an important bearing on the subsequent shearing resistance of the soil, a fact demonstrated by the researches of A. Casagrande, M. ASCE, and S. G. Albert at the Massachusetts Institute of Technology (M.I.T.), at Cambridge, in 1930, and by the brilliant studies of L. Jürgenson (14) in 1934.

From 1912 to 1916, Swedish railroads experienced a series of disastrous slides in which many lives were lost and property damage was extensive. Although the main objective of the ensuing investigation (15) was to develop reliable methods for analyzing the stability of slopes, the methods proposed by the Swedish Geotechnical Commission have since been widely accepted—a by-product of great significance was the discovery that, when samples from a natural deposit of clay are disturbed, their strength is always reduced, sometimes by as much as 90% of their undisturbed value. The recognition of this simple fact revolutionized the science and art of soil testing (16) (17) (18); it led to a reappraisal of the effects of sampling on test results and to the realization that certain disturbances inherent in the sampling process can never be eliminated (19). The difficulties attending the evaluation of these disturbances have caused the development of equipment for measuring shear strength in place (20). The latter approach promises to open a new chapter in the history of the art of practical soil testing, although the ever-present lack of homogeneity in natural soil deposits will probably limit the usefulness of the procedure as a research tool.

From 1933 to 1936, M. J. Hvorslev, M. ASCE (21) (22), conducted extensive investigations on the conditions for failure of saturated, remolded, cohesive soils, using both a direct shear apparatus and a torsion (or ring shear) device. Among Mr. Hvorslev's conclusions are the following:

1. A cohesive soil will (tend to) undergo, depending on its state of consolidation, either an increase or a decrease in void ratio (during shear).
2. If the rate of load application is sufficiently slow so that at any time the void ratio of the soil can be considered fully adjusted to the prevailing stress conditions, the pore-water pressure will at all times be equal to atmospheric pressure.
3. If the soil tends to reduce in volume under stresses that are applied sufficiently rapidly to prevent full adjustment of the void ratio, the pore-water pressure will be greater than atmospheric; conversely, if the soil tends to increase in volume, the pore-water pressure will be less than atmospheric.
4. The shearing resistance of saturated, remolded, cohesive soils is a function of the effective normal stress and the void ratio at the moment of failure.
5. The "true angle of internal friction" of these soils is a constant, but the cohesion is a function of the void ratio (or water content) at failure.

The first four conclusions were also arrived at independently by L. Rendulic (23) in 1936, using a triaxial compression apparatus.

It is surprising that Mr. Hvorslev's work did not receive the recognition in this country that it so justly deserved because it was the basis for all subsequent research on the shearing resistance of clays. It became clear that a given clay-like soil can exhibit a wide range in the apparent values of c and ϕ, depending on the drainage permitted during a test. Because of this discovery, Mr. Casagrande proposed three types of tests for evaluating the shearing properties of cohesive soils—"quick," "consolidated-quick," and "slow" tests. For saturated soils, the tests automatically impose certain limiting conditions of pore-water pressure, which indirectly control the magnitude of the effective stresses and of the void ratio at failure. For a given project, the particular tests that simulate field pressure and drainage conditions must be used, and the results must be interpreted with due regard to discrepancies between field and laboratory conditions. These conditions demonstrate inherent limitations to the indiscriminate application of the Coulomb Law even if the soil is initially saturated, and these limitations are particularly serious in the case of partly saturated clays.

The tremendous expansion of the work of the Corps of Engineers (United States Department of the Army) immediately before World War II and the lack of knowledge about the physical properties of real soils at that time prompted the Corps of Engineers to authorize a cooperative research program in which (*a*) pertinent seepage data are reviewed, (*b*) research on the triaxial shear method of testing soils is conducted, and (*c*) a soil-pressure cell is investigated. All three programs were begun in 1940. The Waterways Experiment Station was chosen to conduct the seepage and soil-pressure cell studies and was instructed to act as the coordinating agency for a cooperative triaxial-shear research program to be participated in by Harvard University in Cambridge, Mass., the Massachusetts Institute of Technology, and the Waterways Experiment Station in Vicksburg, Miss. The results of the cooperative triaxial-shear research program were presented in seventeen unpublished progress reports between 1940 and 1944. In 1944, P. C. Rutledge, M. ASCE, prepared a critical review (24) of the data from these progress reports. This review contains a wealth of information about the shearing resistance of soils and includes data on apparatus, testing techniques, and test results. In the review cohesive soils are separated into two groups—"homogeneous saturated clays" and "partly saturated clays." The conclusions in the report (24*a*) that are pertinent to this paper are:

> "*Homogeneous saturated clays*
>
> "1. The maximum principal stress difference $[\sigma_1 - \sigma_3]$, called the compressive strength of the clay, depends only on the water content at maximum stress, provided the test specimens have not been pre-consolidated under pressures greater than the test maximum stress and then allowed to rebound to equilibrium under lower pressures. With this one limitation, it is independent of pore-water pressure and of the test method that produces the final water content.
>
> "2. A plot of water content at end of test vs. logarithm of principal stress difference is a curve that begins at the unconfined compressive strength and the natural water content and runs roughly parallel to the semi-

logarithmic pressure-water content curve obtained from a standard consolidation test on the same clay.

"*Partially saturated clays*

"1. Four major variables affect the strength of a soil in this group. These are: the minor principal stress, the dry soil density, the water content, and the degree of saturation.

"2. For compacted soils the method of and the conditions during compaction seem to have independent effects on test strengths.

"3. The relation between compressive strength and water content at end of test varies with the minor principal stress.

"4. The tests in this program were not sufficient to establish the effects of all variables on the strengths of soils in this group."

In Mr. Rutledge's review, the variables affecting shearing resistance were related to the over-all strength; the use of separate components for friction and cohesion was largely abandoned. More recent work done in Europe substantiates the conclusions of Messrs. Hvorslev and Rutledge but deals with friction and cohesion separately (25). Whatever the relative merits of these two approaches may be for the case of saturated clays, the results of the investigation on compacted clays herein described could be analyzed rationally only in terms of the over-all compressive strength.

SOILS STUDIED

The two clay soils selected for study differ widely in their geological origin and physical properties. One is a highly plastic clay from the Fort Union formation, which was obtained at the site of the Garrison Dam near Riverdale, N. Dak. The other is a clay of low plasticity—a modified loess from the Bluff (or Memphis) formation—that was sampled at the Waterways Experiment Station. It is one of several soils that were used by this station for an extensive investigation of soil compaction (26). For convenience and brevity the two soils will be referred to hereafter as Fort Union clay and Mississippi loess.

Fort Union Clay.—The sedimentary rocks of the Fort Union formation were deposited during the Eocene (Tertiary) age; they consist of alternate beds of sandstone, shale, coal, sandy shale, gray clay, and black carbonaceous shale (27). At the site of the Garrison Dam, the formation is approximately 475 ft thick; much of it (approximately 230 ft) is exposed in the bluffs along the valley of the Missouri River, but its top members are extensively covered with glacial drift. The soil samples used in this investigation come from the layers of gray clay taken from the spillway excavation at the east abutment of the dam.

When damp the Fort Union clay has a bluish-gray color that turns light gray when dried. At a moisture content corresponding to the plastic limit the soil is hard and tough. The clay has a particularly high dry strength but a dried sample is slaked by immersion in water. Even at comparatively high water contents the Fort Union clay exhibits an extraordinary affinity for water. Under low confining pressures it continues to absorb water and to swell in a manner characteristic of the action of bentonite. From the standpoint of convenience in testing, the most unsatisfactory feature of the Fort Union clay is its extremely low permeability (approximately 10^{-10} cm per sec, as computed from consolidation-test data). This low permeability not only increases the time required to perform strength tests but also makes the saturation of specimens impracticable.

The writer found that it was not possible to saturate a compacted clay soil by any process that did not disturb the soil structure. However, the degree of saturation of a specimen could be raised more or less uniformly provided that its permeability was not too low. In the case of the Fort Union clay, contact with water under pressure for three weeks resulted merely in a slight increase in water content throughout the lower inch of the specimen. For this reason saturation of the clay was considered impracticable. At first these facts caused the writer considerable consternation, but he later discovered that his experiences had been shared by others (28).

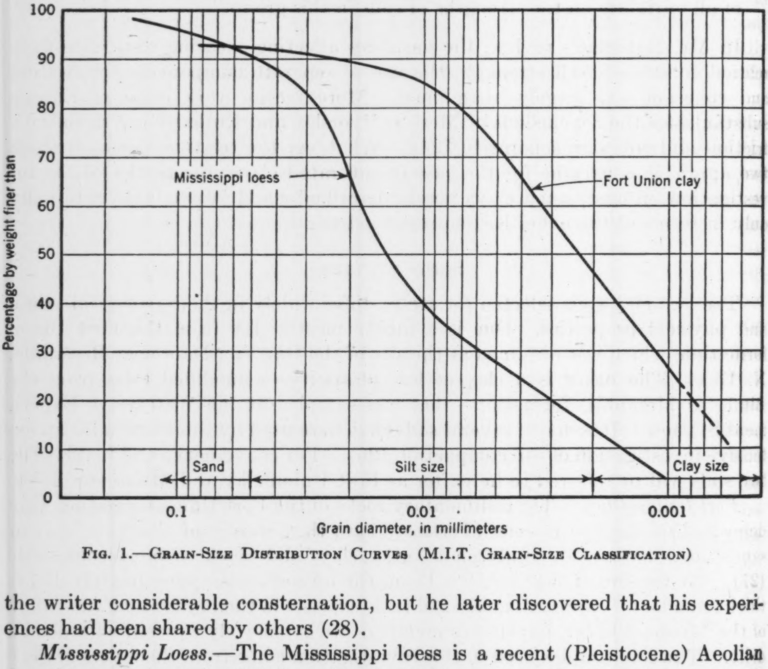

FIG. 1.—GRAIN-SIZE DISTRIBUTION CURVES (M.I.T. GRAIN-SIZE CLASSIFICATION)

Mississippi Loess.—The Mississippi loess is a recent (Pleistocene) Aeolian deposit approximately 40 miles wide that follows approximately the east bank of the Mississippi River for the entire length of the State of Mississippi. The loess is divisible into two parts—(*a*) fine, calcareous, gray to buff-colored, clayey silt, containing lime concretions, iron tubules, and a great variety of fresh-water shells and land shells; (*b*) noncalcareous yellow to brown silty clay, without shells but containing small iron tubules. Near Vicksburg, Natchez (Miss.), and Yazoo City (Miss.) cut slopes in the calcareous part of the loess exhibit a characteristic tendency to stand vertically (29). The soil studied comes from the noncalcareous part of the loess.

In a damp condition the loess has a yellowish brown color and turns light buff when dried. At a moisture content corresponding to the plastic limit, the soil is soft and friable; accordingly, extreme care must be exercised in the preparation of test specimens to prevent spalling and other disturbances. The loess has a moderate-to-high dry strength and is slaked very readily when immersed in water. At higher moisture contents, the soil has little tendency to swell when placed in contact with water. There does, however, seem to be a critical moisture content at which the swelling becomes appreciable. This critical water content is drier than the standard Proctor optimum water content, but its value seems to vary both with the amount and the type of compaction. Under comparable conditions the loess is less compressible and more pervious than the clay. These properties make less time necessary for 100% consolidation of the loess than for that of the clay—approximately one fiftieth as much. For this reason, despite the greater difficulties encountered in shaping test specimens, the loess was studied more extensively than the clay.

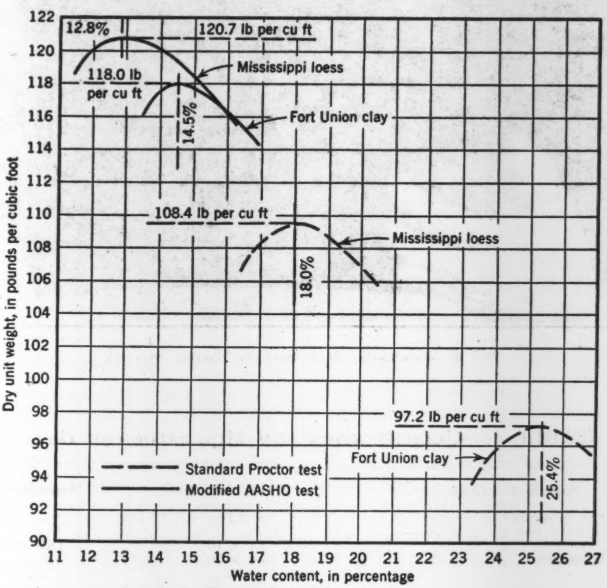

Fig. 2.—Standard Compaction Curves

Classification data and the results of a mineralogical composition determination for the two soils are shown in Table 1; grain-size distribution and standard compaction curves are shown in Figs. 1 and 2, respectively. The curves in Fig. 2 represent results of the standard Proctor test and the modified test specified by the American Association of State Highway Officials (AASHO)

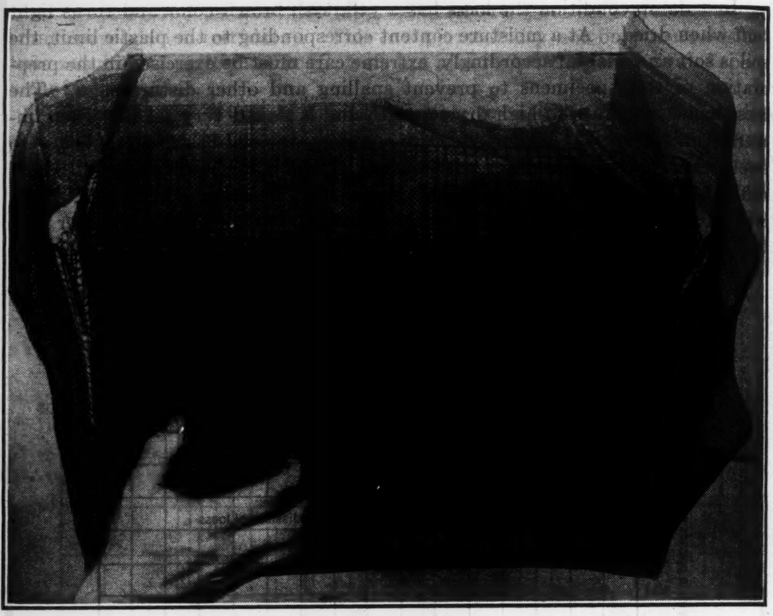

FIG. 3.—PROCESSING RAW SOIL BY FORCED SIEVING

TABLE 1.—CLASSIFICATION AND MINERALOGICAL DATA

Soil characteristic	Fort Union clay		Mississippi loess	
Specific gravity of solids	2.76		2.72	
Grain-Size Distribution[a]:				
D_{60}, in millimeters	34×10^{-4}		180×10^{-4}	
D_{10}, in millimeters	5.4×10^{-4}		15×10^{-4}	
D_{60}/D_{10}	6.3		12.0	
Standard Dynamic Compaction Tests:	Standard Proctor test	Modified AASHO test	Standard Proctor test	Modified AASHO test
Optimum moisture content, in percentage	25.4	14.5	18.0	12.8
Maximum dry unit weight[b]	97.2	118.0	108.4	120.7
Atterberg Limits:				
Liquid limit, in percentage	70		37	
Plastic limit, in percentage	26		23	
Plasticity index	44		14	
Mineralogical Composition[c]:				
Quartz	50–55		85–90	
Calcite	15		5–7	
Montmorillonite	10–15		...	
Kaolinite	10		...	
Illite	5		4–5	
Others	5		1	

[a] The symbol D indicates diameter. [b] In pounds per cubic foot. [c] In approximate percentages.

APPARATUS, TECHNIQUES, AND PROCEDURES

Although the success achieved in the preparation of duplicate test specimens is considered to be an important contribution to further study of the fundamental strength characteristics of soils, only general descriptions of the apparatus and procedures used will be given herein.

Preparation of Raw Soil.—The raw soil was received at the laboratory in a disturbed condition, but most of the natural soil moisture had been retained. The soil was sealed in metal containers and stored in a constant-humidity room (having a relative humidity of 98%) for at least one month in order to obtain a reasonably constant initial water content. All further processing was done in the humid room.

To obtain duplicate soil specimens it is necessary to use a soil that is free of random distribution of coarse particles and that has a uniform water content and structure throughout. Many processes were tried using various types of soil mixers, such as dough mixers and other mixers of special design, and mechanical grinders, such as meat grinders and juice extractors. None of these proved entirely satisfactory for both soils and for the ranges in water contents required. As a final resort, a tedious and time-consuming hand method was adopted.

Enough raw soil was removed from the metal containers to prepare all the specimens for compacting at a particular water content. If water was to be added, it was incorporated by hand-kneading. The soil was then force-sieved, with a large rubber stopper, through a No. 3 sieve and then through a No. 20 sieve. The fine sieve was backed with the coarse sieve for support. All visible coarse particles were removed; the product was a homogeneous material resembling finely ground coffee in appearance (Fig. 3). The yield varied from 2 lb per hr to 8 lb per hr depending on the type of soil and the water content.

The soil processed in this manner was again sealed in metal containers and stored in the humid room. Each box (a 6-in. cube) contained enough soil for one compaction series—approximately 20 lb. The maximum variation in water content between specimens of any one series was 0.2%—for example, (25.0 ± 0.2)%—and the maximum variation between specimens of the several series intended to have the same water content was 0.4%.

Compaction.—In the development of a compaction procedure which was intended to achieve uniformity in the initial value of the dry unit weight, advantage was taken of the experiences of R. I. Mayo, A. M. ASCE (30), and dynamic compaction procedures were not considered. The compaction of individual specimens was first attempted using static pressure in a 3-in.-diameter mold. It was found impossible to eliminate variations in unit weight at the top, center, and bottom of the specimen because of the side friction developed. In addition, the unavoidable variations in structure caused by placing the soil in the mold for each individual specimen caused variations in the resulting stress-strain curves even when the initial conditions of void ratio and water content had been essentially duplicated. Molds of 10-in. diameter were designed to minimize the effects of side friction and to permit simultaneous compaction of all the specimens to be used in a particular test series.

The first 10-in.-diameter mold, designed for the purpose of checking the uniformity of the dry unit weight, water content, and soil structure, consisted

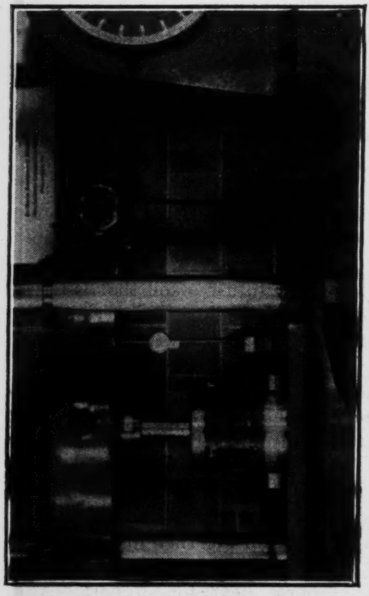

FIG. 5.—COMPACTION EQUIPMENT

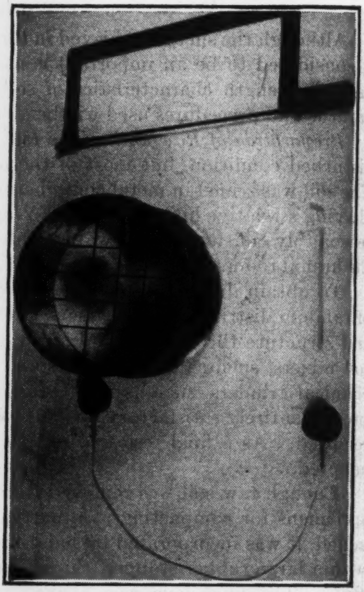

FIG. 6.—MITER-BOX AND CUTTING TOOLS

FIG. 4.—PROCTOR NEEDLE AND PROVING FRAME

of three rings and two collars. After compaction in this mold, the unit weight of the entire sample was determined. Variations in a horizontal direction were evaluated by the use of a Proctor penetration needle attached to a sensitive proving frame (Fig. 4). Water-content determinations were made at each penetration point. The top ring was then removed, the protruding soil was cut off with a wire saw, and the soil surface was carefully screeded with a straight-edge. Again the unit weight, penetration resistances, and water contents were determined. The entire procedure was repeated after the second ring was removed. By successive repetitions of this process a compaction procedure was developed that resulted in essentially uniform conditions of water content, void ratio, and soil structure.

A second 10-in.-diameter mold was designed to yield an "undisturbed" sample approximately 3½ in. high from which twenty-one duplicate specimens could be cut. This mold consisted of a split-ring section and two collars.

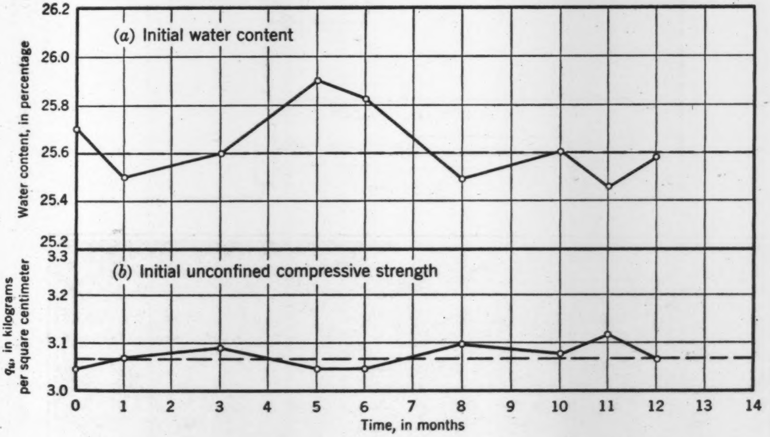

FIG. 7.—UNCONFINED COMPRESSIVE STRENGTH AND WATER CONTENT, RELATED TO TIME

A 10-in.-diameter piston and spacer block (to permit compaction from top and bottom simultaneously) were fabricated to fit this mold with just enough clearance to eliminate friction between them and the sides of the mold, yet not enough to permit the soil to enter the clearance spaces. The split-ring mold is shown assembled in Fig. 5 on the platen of a Southwark-Tate-Emery hydraulic testing machine of 100,000-lb capacity; it is in the process of compacting a test series. The maximum variation in unit weight among the twenty-one samples of a given series was less than 0.5%. This variation is roughly equal to the precision of the measurements used to determine the unit weight.

The compaction process previously described yielded a cake of soil 10 in. in diameter and 3½ in. high. This cake was centered in the base of a circular miter-box (Fig. 6), and the collar (having a diameter slightly larger than 10 in.) was then put in place. Small pins alined the grooves on the collar with those on the base. The soil cake was cut along the mitered grooves either with a

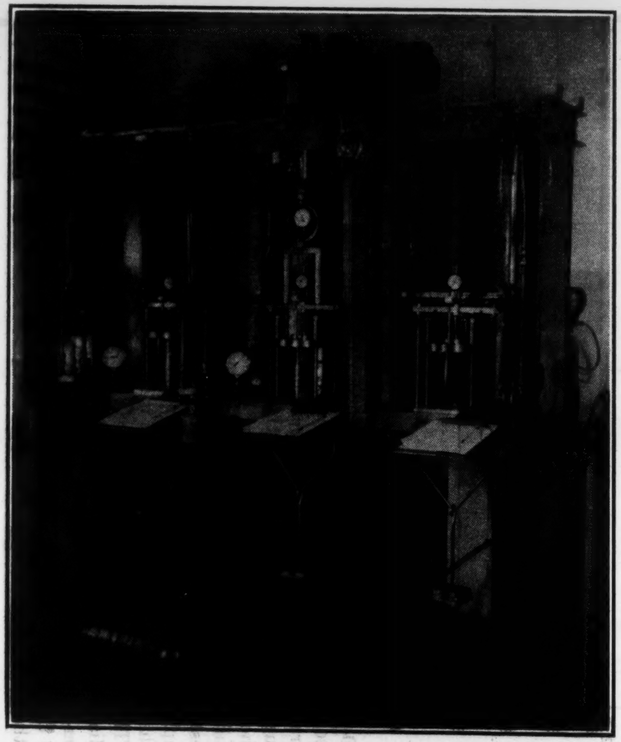

Fig. 8.—Three-Bay Triaxial Testing Apparatus

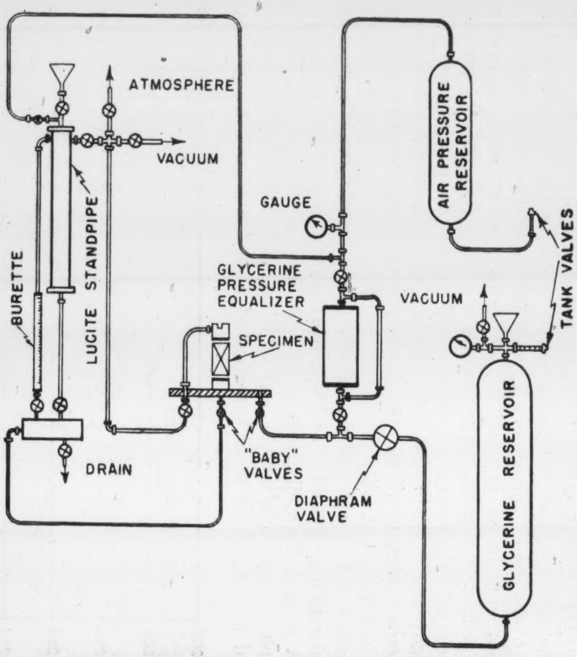

ATMOSPHERE
VACUUM
AIR PRESSURE RESERVOIR
GAUGE
TANK VALVES
BURETTE
LUCITE STANDPIPE
GLYCERINE PRESSURE EQUALIZER
VACUUM
SPECIMEN
DRAIN
"BABY" VALVES
DIAPHRAM VALVE
GLYCERINE RESERVOIR

Fig. 9.—Schematic Piping Diagram for the Triaxial Compression Testing Apparatus of Fig. 8

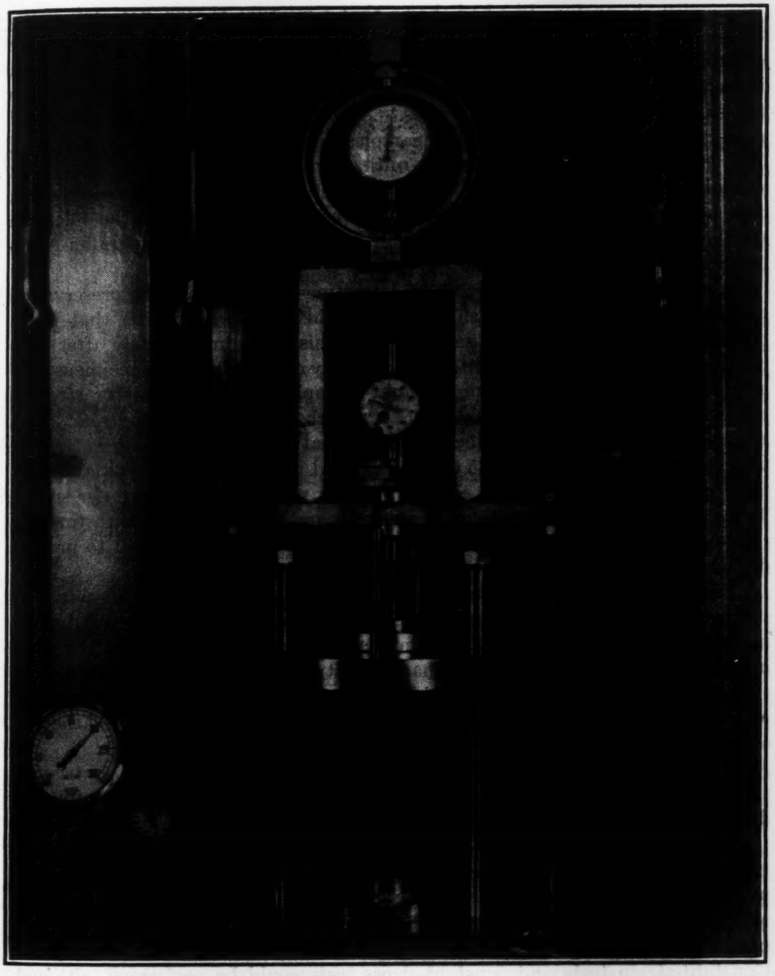

FIG. 10.—ASSEMBLED TRIAXIAL CELL READY FOR SHEAR TESTING

large coping saw or with piano wire; this process was not entirely satisfactory. A thin, continuous, high-speed band saw is considered to be the only satisfactory tool for this purpose.

Preservation of Samples.—Because the anticipated maximum time interval between compaction and shear testing exceeded six months, the use of paraffin alone as a sealing compound was not considered advisable. The work of J. O. Osterberg, A. M. ASCE, and K. H. Tseng done in 1950 at Northwestern

University (Evanston, Ill.) had shown that a mixture of 50% petrolatum and 50% paraffin was satisfactory for a period of a year and that a total thickness of protective coating of from $\frac{1}{2}$ in. to $\frac{3}{4}$ in. was desirable. It was feared that, if such a thick coating were used, the shrinkage of the paraffin might compress the samples having high void ratios. Accordingly, the following method of preservation was adopted: (*a*) The samples were dipped by hand in a mixture of 50% paraffin and 50% petrolatum until a coat of from $\frac{1}{16}$ in. to $\frac{1}{8}$ in. thick was obtained; (*b*) each sample was then carefully wrapped in aluminum foil, care being taken to avoid air spaces between the sample and the foil; and (*c*) the samples were then given another $\frac{1}{8}$-in.-thick coat of the paraffin-petrolatum mixture by hand-dipping.

A control procedure was set up to determine the efficacy of the preservation process and to evaluate the effects of any thixotropic hardening that might occur. Twelve samples were selected from this series immediately after compaction, and their water contents were carefully determined; six specimens were also tested in unconfined compression. Samples were checked for strength and water content approximately once a month for a period of one year. The results are shown in Fig. 7, which indicates that the average initial water content of twelve samples was (25.6 ± 0.3)% and that the average initial unconfined compressive strength, q_u, of six samples was 3.07 ± 0.02 kg per sq cm. These data show that variations in strength and water content with time are random and that they are within the precision of the process used to prepare duplicate specimens.

Preparation of Test Specimens.—The test specimens used in this study were shaped, either wholly or in part, with a power-operated soil lathe. All specimens were approximately 1.42 in. in diameter and 2.80 in. high. In some instances, the spindle of the lathe had to be turned by hand and the specimen shaped by successive cuts with a thin, sharp blade. The specimens prepared in this manner lacked the uniformity in shape achieved when the lathe was operated mechanically, but they were considerably less disturbed.

Triaxial-Shear Testing.—Fig. 8 is a general view of the three-bay triaxial-shear apparatus used in this study. The apparatus was patterned after one designed and built at the soil mechanics laboratory of Northwestern University (31); certain modifications were incorporated that provided increased convenience and adaptability in testing and greater simplicity in fabrication. The unit was designed to provide an axial load of 500 kg and a confining pressure of 10 kg per sq cm at any one of the bays, each bay being completely independent with respect to confining pressure, drainage, and saturation controls. Constant-strain tests and constant-stress tests could be performed, although none of the latter were used in this study.

A control panel (one for each bay) contained all the necessary valves and controls for evacuating, saturating, and measuring the volume change of saturated specimens. A schematic piping diagram is shown in Fig. 9. The line from the air-pressure cylinder permitted saturation of clay specimens by placing the water entering the bottom of the specimen under a known pressure while the top of the specimen was being subjected to a vacuum. In this manner, saturation under pressure, consolidation, and shear testing could be conducted without making or breaking a single connection. After the initial difficulties with piping leaks and alinement were overcome, the precision, convenience, and adaptability of this equipment proved outstanding.

The effects of membrane restraint were essentially eliminated by the use of thin rubber membranes (prophylactics). These membranes are easily ruptured and frequently contain local imperfections that may cause leakage. Because of difficulties attending the proper calibration for membrane restraint at various confining pressures and because of the importance of this effect (24), thin membranes were used for the entire study and occasional membrane failures were tolerated.

"Quick" tests were performed with the valves leading from the top and bottom of the specimen both open and closed. Tests were also run on partly consolidated specimens. When saturation was desired, the water was brought to the base of the specimen and the lower valve was closed prior to the application of the confining pressure; it was kept closed for the entire consolidation period, leaving only the top of the specimen subject to atmospheric pressure. Although the period for consolidation was increased, this procedure was necessary to prevent the air expelled during the application of the confining pressure from forming a large bubble between the water and the specimen and thereby effectively preventing the subsequent flow of water. The formation of an air bubble would also have prevented any attempts to saturate the specimen simultaneously with the application of the confining pressure. The water pressure used varied from 20% to 30% of the confining pressure; higher pressures either caused a disturbance of the soil structure or resulted in flow between the specimen and the rubber membrane.

As previously stated under the heading, "Soils Studied: Fort Union Clay," saturation of the Fort Union clay was found to be impractical. Saturation periods of from four to fourteen days for the Mississippi loess yielded approximately identical results, although in no case did the final degree of saturation exceed approximately 97%. A close-up of the assembled triaxial cell ready for shear testing is shown in Fig. 10.

Determination of Void Ratio at Failure.—In testing soil specimens that had been loosely compacted, it was observed that comparatively large volume changes continued to occur during the application of the deviator stress. Previous to this, all attempted correlations between strength and the initial or consolidated values of void ratio or water content—or even with the final water content—had failed. When further exhaustive tests (in which the measurements of dimensions, weights, pressures, and loads were as precise as possible for soil specimens) failed to yield significant correlations, it was decided to attempt to measure the void ratio at maximum stress. This later proved to be a vital decision which provided the solution for overcoming the difficulties and misunderstandings previously encountered.

The critical measurement in the determination of the void ratio at failure is the bulk volume of the sample. This determination was made by suspending the portion of the specimen within which failure had occurred from a very thin nylon thread (which had negligible weight and surface-tension effects) and weighing it in air. The sample was then coated with a thin layer of paraffin by hand-dipping, after which it was weighed in air and then weighed when submerged in distilled water. The specific gravity of the paraffin being known,

TABLE 2.—Triaxial Compressio

No. and Type	Initial Condition of Specimen							Consolidation			Time^b Allow	
	Diameter, in centimeters	Height, in centimeters	Height-diameter ratio	Water content, in percentage	Void ratio	Dry unit weight^d	Degree of saturation^e	Increments	Maximum consolidation pressure	Void ratio after consolidation	Preliminary consolidation^f	Total preliminary consolidation
(1)	(2)	(3)	(4)	(5)	(6)	(7)	(8)	(9)	(10)	(11)	(12)	(13)
												Seri
2—U^g	3.58	7.11	1.99	25.8	0.818	94.8	86.5	....	....	....	....	....
4—Qc	3.60	7.11	1.97	25.4	0.814	94.9	86.0	1	2.11	0.759	1,680	1,680
5—Qc	3.60	7.11	1.97	25.7	0.828	94.2	85.7	1	1.06	0.790	1,230	1,230
12—Qc	3.59	7.11	1.98	25.3	0.815	94.8	85.7	1	3.52	0.752	1,170	1,170
13—Qc	3.60	7.11	1.97	25.5	0.826	94.3	85.1	1	3.52	0.768	1,020	1,020
14—Qc	3.61	7.11	1.97	25.5	0.825	94.4	85.5	1	2.11	0.777	960	960
15—Qc	3.59	7.11	1.98	25.5	0.812	95.0	86.7	1	1.06	0.785	990	990
16—Qc	3.58	7.11	1.99	25.5	0.824	94.4	85.3	1	0.70	0.790	1,080	1,080
17—Qc	3.60	7.11	1.97	25.6	0.826	94.3	85.6	1	0.35	0.807	1,290	1,290
20—U^g	3.60	7.11	1.97	25.6	0.824	94.4	85.5	....	....	....	....	....
												Seri
1—Qc	3.60	7.11	1.97	25.4	0.770	97.4	91.2	1	0.35	0.750	1,500	1,500
2—Qc	3.60	7.11	1.97	25.7	0.781	96.8	90.7	1	0.70	0.759	1,440	1,440
3—U^g	3.60	7.11	1.97	25.9	0.781	96.8	91.4	....	....	....	....	....
5—Qc	3.60	7.11	1.97	25.4	0.772	97.2	90.8	1	2.81	0.730	1,200	1,200
6—Qc	3.60	7.11	1.97	25.7	0.783	96.6	90.5	1	5.63	0.712	1,170	1,170
7—U	3.60	7.11	1.97	25.4	0.776	96.9	90.4	....	....	....	....	....
8—Qc	3.60	7.11	1.97	25.5	0.776	97.0	90.6	1	2.11	0.741	1,110	1,110
9—Qc	3.63	7.11	1.96	25.6	0.780	96.8	90.4	1	0.35	0.760	1,140	1,140
10—Qc	3.59	7.11	1.98	25.6	0.776	97.0	90.8	1	0.14	0.760	1,080	1,080
11—Qc	3.59	7.11	1.98	25.4	0.777	97.0	90.1	1	2.81	0.725	1,590	1,590
12—Qc	3.60	7.11	1.97	25.4	0.776	97.0	90.2	1	1.41	0.746	1,560	1,560
13—Qc	3.59	7.11	1.98	25.5	0.775	97.0	90.9	1	7.04	0.680	2,880	2,880
14—Q	3.60	7.11	1.97	25.6	0.776	97.0	91.0	1	1.41	0.761	10	10
15—Qc	3.60	7.11	1.97	25.6	0.772	97.2	91.2	1	5.63	0.694	2,700	2,700
13A—Qc	3.60	7.11	1.97	25.4	0.776	97.0	90.4	1	2.81	0.693	7,140	7,140
												Seri
1—U^g	3.60	7.11	1.97	25.6	0.746	98.7	94.7	....	....	....	....	....
2—Qc	3.60	7.11	1.97	25.6	0.747	98.6	94.6	1	0.21	0.727	1,470	1,470
3—Qc	3.60	7.11	1.97	25.5	0.747	98.6	94.3	1	0.70	0.718	1,500	1,500
4—Qc	3.60	7.11	1.97	25.5	0.743	98.8	94.5	1	2.81	0.709	1,470	1,470
5—U	3.60	7.11	1.97	25.5	0.743	98.8	94.6	....	....	....	....	....
6—Q	3.60	7.11	1.97	25.4	0.740	99.0	94.7	1	7.04	0.696	10	10
7—Qc	3.60	7.11	1.97	25.4	0.740	99.0	94.7	1	1.41	0.701	2,880	2,880
8—Qc	3.60	7.11	1.97	25.6	0.746	98.7	94.5	1	5.63	0.683	1,380	1,380
9—Q	3.60	7.11	1.97	25.4	0.743	98.8	94.4	1	1.41	0.727	10	10
10—Q	3.60	7.11	1.97	25.5	0.744	98.8	94.5	1	2.81	0.727	10	10
11—Qc	3.60	7.11	1.97	25.7	0.744	98.8	95.3	1	4.22	0.678	5,760	5,760
12—Qc	3.60	7.11	1.97	25.4	0.744	98.8	94.3	1	2.81	0.666	6,780	6,780
11A—Qc	3.60	7.11	1.97	25.2	0.744	98.8	93.7	1	5.63	0.677	3,180	3,180
11B—Qc	3.60	7.11	1.97	25.5	0.747	98.7	94.5	1	2.81	0.618	15	000

[a] Tests were made using constant-strain, piston-type equipment, with glycerine as the pressure fluid. Membranes 0.0025 in. thick were used, and no membrane-strength correction was made. [b] In minutes. [c] In kilogram per square centimeter (1 kg per sq cm equals 14.2234 lb per sq in.); the major principal stress is designated

TESTS ON FORT UNION CLAY[a]

FOR:		CONDITIONS AT END OF TEST						COMPRESSIVE STRESSES[c]			STIFFNESS[c]		
Application, Axial Load													
To maximum $(\sigma_1 - \sigma_3)$ (14)	To ultimate $(\sigma_1 - \sigma_3)$ (15)	Strain[e] at maximum $(\sigma_1 - \sigma_3)$ (16)	Strain[e] at end of test (17)	Water content[e] (18)	Void ratio (19)	Dry unit weight[d] (20)	Degree of saturation[e] (21)	Minor principal stress, σ_1 (22)	Strength, max. $(\sigma_1 - \sigma_3)$ (23)	Maximum major principal stress (24)	Initial modulus of deformation (25)	Modulus of deformation, zero to max. $(\sigma_1 - \sigma_3)$ (26)	No. and Type (1)
No. 1													
3.5	5.0	6.0	9.0	25.6	....	....	....	0.00	2.28	2.28	90	38.0	2—U[g]
10.0	10.0	20.0	22.1	24.5	0.736	99.2	93.6	2.11	3.72	5.83	250	18.6	4—Qc
11.8	11.8	20.0	19.6	24.9	0.758	98.1	90.9	1.06	3.35	4.41	215	16.7	5—Qc
10.1	12.0	16.8	19.9	24.5	0.743	98.8	92.9	3.52	3.63	7.15	345	21.6	12—Qc
10.0	13.2	16.0	21.9	25.7	0.750	98.4	94.1	3.52	3.43	6.95	340	21.4	13—Qc
11.3	13.0	18.4	21.1	25.2	0.755	98.2	91.5	2.11	3.37	5.48	250	18.3	14—Qc
13.2	13.2	20.0	21.8	25.3	0.763	97.7	91.4	1.06	3.30	4.36	240	16.5	15—Qc
12.0	12.9	19.5	21.0	25.0	0.771	97.3	89.5	0.70	3.23	3.93	235	16.5	16—Qc
7.4	12.6	12.0	20.5	25.2	0.788	96.4	88.2	0.35	2.93	3.28	220	24.4	17—Qc
3.6	4.6	5.8	7.4	25.3	....	....	....	0.00	2.15	2.15	95	37.1	20—U[g]
No. 2													
5.8	12.9	10.0	20.8	25.1	0.746	98.6	92.7	0.35	3.32	3.67	430	33.2	1—Qc
7.2	13.0	11.8	21.3	25.1	0.740	98.9	93.4	0.70	3.36	4.06	435	28.5	2—Qc
5.8	6.5	7.0	10.4	25.9	....	....	....	0.00	2.65	2.65	125	37.9	3—U[g]
8.7	12.4	14.3	20.1	25.1	0.723	99.9	95.9	2.81	3.76	6.57	580	26.3	5—Qc
10.0	12.6	16.2	20.4	25.2	0.718	100.3	97.3	5.63	3.86	9.49	600	23.8	6—Qc
4.2	6.9	6.8	11.1	25.5	0.780	96.8	90.3	0.00	2.58	2.58	125	38 0	7—U
9.7	12.6	15.7	20.4	25.2	0.734	99.4	95.0	2.11	3.50	5.61	440	22.3	8—Qc
7.1	11.5	11.5	18.5	25.3	0.756	98.0	91.9	0.35	3.22	3.57	380	28.0	9—Qc
6.2	10.4	10.0	16.8	25.4	0.770	97.2	90.8	0.14	3.00	3.14	300	30.0	10—Qc
10.2	12.7	16.5	20.6	24.8	0.723	99.9	94.4	2.81	3.77	6.58	440	22.8	11—Qc
8.2	12.9	13.2	20.8	24.9	0.729	99.5	94.3	1.41	3.67	5.08	430	27.8	12—Qc
6.8	10.6	11.1	17.3	24.4	0.693	101.7	97.2	7.04	4.41	11.45	900	39.8	13—Qc
8.2	8.2	10.0	10.0	25.6	0.752	98.3	94.0	1.41	3.29	4.70	415	32.9	14—Q
8.1	11.6	13.1	18.9	24.6	0.704	101.0	96.4	5.63	4.12	9.75	660	31.5	15—Qc
10.0	11.8	16.0	19.6	23.5	0.674	102.8	96.2	2.81	5.00	7.81	905	31.2	13A—Qc
No. 4													
10.2	12.4	15.2	20.0	25.6	....	....	....	0.00	2.79	2.79	110	18.3	1—U[g]
5.3	10.8	9.5	17.4	25.0	0.722	100.0	95.4	0.21	3.46	3.67	350	36.4	2—Qc
7.8	11.6	11.8	18.7	24.8	0.711	100.6	96.1	0.70	3.64	4.34	570	30.9	3—Qc
7.9	12.2	11.9	19.8	24.8	0.708	100.9	96.8	2.81	3.67	6.48	570	30.8	4—Qc
9.8	11.7	15.5	18.8	25.5	0.744	98.8	94.8	0.00	2.80	2.80	115	18.4	5—U
7.1	11.7	11.5	19.0	25.3	0.714	100.4	97.7	7.04	3.55	10.59	570	30.9	6—Q
5.8	12.0	9.5	19.5	24.3	0.692	101.8	96.9	1.41	4.05	5.46	630	42.5	7—Qc
6.1	13.0	9.9	21.2	24.9	0.697	101.5	98.6	5.63	3.83	9.46	770	38.7	8—Qc
7.6	7.6	12.2	12.3	25.3	0.727	99.7	96.1	1.41	3.31	4.72	330	27.2	9—Q
7.7	8.0	12.0	12.9	25.4	0.725	99.8	96.4	2.81	3.32	6.13	325	27.7	10—Q
7.0	10.9	11.4	17.7	24.6	0.689	102.0	98.5	4.22	4.16	8.38	850	36.5	11—Qc
9.5	9.6	15.5	15.6	23.4	0.665	103.5	97.3	2.81	5.00	7.81	900	30.7	12—Qc
6.4	10.7	11.0	17.2	24.7	0.688	102.0	98.7	5.63	4.23	9.86	850	38.4	11A—Qc
7.5	11.7	11.8	18.7	21.5	0.607	107.2	97.8	2.81	7.82	10.63	1,400	66.2	11B—Qc

and the minor principal stress, σ_3. [d] In pounds per cubic foot. [e] In percentage. [f] Average per increment.
[g] Because of excessive cracking, no final void ratios were determined for these specimens.

TABLE 3.—Triaxial Compressio Tes

No. and Type	Initial Condition of Specimen							Consolidation			Time[b] Allow		for: App Axi
	Diameter, in centimeters	Height, in centimeters	Height-diameter ratio	Water content, in percentage	Void ratio	Dry unit weight[d]	Degree of saturation[e]	Increments	Maximum consolidation pressure	Void ratio after consolidation	Preliminary consolidation[f]	Total preliminary consolidation	To maximum $(\sigma_1 - \sigma_3)$
(1)	(2)	(3)	(4)	(5)	(6)	(7)	(8)	(9)	(10)	(11)	(12)	(13)	(14)
												Seri	No.
2—U^g	3.59	7.11	1.98	18.7	1.003	84.6	50.9	....	....	....	....	....	1.6
3—U^g	3.60	7.11	1.97	18.6	0.989	85.3	51.2	....	....	....	....	....	1.4
4—Q	3.59	7.11	1.98	18.5	0.996	85.0	50.5	1	0.35	0.965	10	10	11.7
6—Qc	3.59	7.11	1.98	18.4	0.987	85.4	50.6	1	1.41	0.916	3,180	3,180	12.0
7—Qc	3.59	7.11	1.98	18.4	0.988	85.4	50.7	1	2.81	0.842	2,880	2,880	11.6
8—Qc	3.59	7.11	1.98	18.4	0.983	85.6	51.1	1	5.63	0.716	2,700	2,700	11.9
9—Qc	3.58	7.11	1.99	18.4	1.003	84.6	49.9	1	0.35	1.000	1,740	1,740	12.3
10—Qc	3.59	7.11	1.98	18.4	1.010	84.4	49.5	1	0.70	1.005	1,350	1,350	12.3
11—Qc	3.60	7.11	1.97	18.4	0.990	85.3	50.7	1	0.21	0.981	10	10	12.2
												Seri	No. 2
1—U^g	3.60	7.11	1.97	18.6	0.740	97.5	68.3	....	....	....	....	....	3.1
2—U^g	3.59	7.11	1.98	18.5	0.742	97.3	67.6	....	....	....	....	....	3.2
3—Qc	3.59	7.11	1.98	18.1	0.730	98.1	67.2	1	0.70	0.703	1,320	1,320	11.1
4—Qc	3.59	7.11	1.98	18.1	0.739	97.6	66.6	1	1.41	0.707	1,200	1,200	11.9
5—Qc	3.59	7.11	1.98	18.0	0.735	97.8	66.6	1	2.81	0.699	720	720	11.8
6—Q	3.59	7.11	1.98	18.1	0.730	98.1	67.4	1	0.35	0.715	10	10	7.5
7—Qc	3.59	7.11	1.98	18.1	0.733	98.0	67.2	1	5.63	0.654	150	150	11.6
9—Qc	3.59	7.11	1.98	18.1	0.734	97.9	66.9	1	0.85	0.713	240	240	12.2
												Seri	No. 3
1—U	3.61	7.11	1.97	18.5	0.580	107.2	86.6	....	....	....	....	....	5.8
2—U^g	3.61	7.11	1.97	18.5	0.579	107.2	86.3	....	....	....	....	....	5.2
3—Qc	3.61	7.11	1.97	18.0	0.568	108.2	86.3	1	2.81	0.547	540	540	11.3
4—Qc	3.61	7.11	1.97	18.2	0.567	108.4	87.0	1	1.41	0.566	360	360	9.9
5—Qc	3.61	7.11	1.97	18.0	0.568	108.3	86.4	1	0.70	0.569	240	240	8.3
6—Qc	3.60	7.11	1.98	18.3	0.576	107.7	86.2	1	1.41	0.557	480	480	10.5
7—Qc	3.60	7.11	1.98	18.3	0.575	107.9	86.6	1	5.63	0.520	120	120	12.0
9—Qc	3.61	7.11	1.97	18.2	0.571	108.0	86.7	1	7.04	0.509	180	180	11.8
10—Qc^h	3.59	7.11	1.98	18.1	0.564	108.5	87.2	1	1.41	0.540	300	300	11.7
11—Qc^h	3.60	7.11	1.98	17.9	0.562	108.6	86.6	1	0.70	0.554	120	120	11.4
												Seri	No. 5
1—U^g	3.61	7.11	1.97	22.7	0.738	97.7	84.0	....	....	....	....	....	6.0
2—U^g	3.59	7.11	1.98	22.8	0.739	97.6	83.9	....	....	....	....	....	6.4
3—Qc	3.59	7.11	1.98	22.8	0.741	97.5	83.5	1	0.70	0.716	1,020	1,020	12.4
4—Qc	3.59	7.11	1.98	22.8	0.737	97.7	84.0	1	1.41	0.704	1,080	1,080	11.7
5—Qc	3.60	7.11	1.98	22.9	0.744	97.3	83.5	1	2.81	0.682	900	900	11.9
6—Qc	3.59	7.11	1.98	22.8	0.737	97.7	84.1	1	1.06	0.709	760	760	12.1
7—Qc	3.58	7.11	1.99	22.8	0.747	97.2	83.0	1	2.11	0.699	660	660	11.8
8—Qc	3.59	7.11	1.98	22.8	0.745	97.3	83.2	1	5.63	0.653	480	480	11.0
9—Qc	3.59	7.11	1.98	22.9	0.748	97.1	83.1	1	7.04	0.634	420	420	11.5
10—Qc	3.60	7.11	1.98	22.7	0.746	97.2	82.8	1	4.22	0.667	1,020	1,020	11.4
11—Q	3.60	7.11	1.98	22.9	0.746	97.2	83.5	....	....	....	....	....	12.1
12—Qc^h	3.59	7.11	1.98	22.8	0.745	97.2	83.2	1	1.06	0.714	600	600	11.5
13—Qc^h	3.59	7.11	1.98	22.8	0.739	97.6	83.7	1	2.11	0.700	480	480	11.8
14—Qc^h	3.57	7.11	1.99	22.9	0.744	97.3	83.7	1	4.22	0.667	440	440	11.8
15—Qc^i	3.58	7.11	1.99	22.7	0.740	97.6	83.4	2	4.22 1.41	0.661 0.700	630	1,260	11.4

[a] Tests were made using piston-type equipment, with glycerine as the pressure fluid. Membranes 0.0025 in thick were used, and no membrane-strength correction was made. [b] In minutes. [c] In kilograms per squa centimeter (1 kg per sq cm equals 14.2234 lb per sq in.); the major principal stress is designated σ_1, and th minor principal stress, σ_3. [d] In pounds per cubic foot. [e] In percentage. [f] Average per increment. [g] Becau

of exce
specim
from 4
pressur

TESTS ON MISSISSIPPI LOESS[a]

FOR:		CONDITIONS AT END OF TEST						COMPRESSIVE STRESSES[c]			STIFFNESS[c]		
Application, Axial Load													
To maximum ($\sigma_1 - \sigma_3$) (14)	To ultimate ($\sigma_1 - \sigma_3$) (15)	Strain[e] at maximum ($\sigma_1 - \sigma_3$) (16)	Strain[e] at end of test (17)	Water content[e] (18)	Void ratio (19)	Dry unit weight[d] (20)	Degree of saturation[e] (21)	Minor principal stress, σ_3 (22)	Strength, max. ($\sigma_1 - \sigma_3$) (23)	Maximum major principal stress (24)	Initial modulus of deformation (25)	Modulus of deformation, zero to max. ($\sigma_1 - \sigma_3$) (26)	No. and Type (1)
No. 1													
1.6	2.8	2.6	4.5	18.7	....	....	....	0.00	0.49	0.49	31	18.9	2—U[g]
1.4	2.2	2.3	3.5	18.6	....	....	....	0.00	0.51	0.51	33	22.2	3—U[g]
11.7	11.7	20.0	18.9	18.5	0.870	90.5	57.8	0.35	1.43	1.78	150	7.1	4—Q
12.0	12.0	20.0	19.5	18.4	0.672	101.9	74.8	1.41	3.60	5.01	325	18.0	6—Qc
11.6	11.6	20.0	19.1	18.1	0.585	107.2	84.8	2.81	5.46	8.27	600	27.3	7—Qc
11.9	11.9	20.0	20.1	18.0	0.565	109.5	86.8	5.63	6.90	12.53	1,600	34.5	8—Qc
12.3	12.3	20.0	19.8	18.1	0.867	90.8	56.6	0.35	1.45	1.80	180	7.2	9—Qc
12.3	12.3	20.0	19.3	18.7	0.753	96.8	67.6	0.70	2.26	2.96	220	11.3	10—Qc
12.2	12.2	20.0	19.7	18.6	0.899	89.4	56.2	0.21	1.18	1.39	80	5.9	11—Q
No. 2													
3.1	4.2	5.0	6.8	....	....	....	....	0.00	1.32	1.32	60	26.4	1—U[g]
3.2	4.3	4.8	6.4	....	....	....	....	0.00	1.29	1.29	70	26.8	2—U[g]
11.1	12.6	18.0	20.4	17.5	0.674	101.2	70.0	0.70	3.05	3.75	380	17.0	3—Qc
11.9	12.5	20.0	20.1	17.5	0.615	104.8	77.5	1.41	4.20	5.61	480	21.0	4—Qc
11.8	11.8	20.0	19.1	17.8	0.581	107.3	82.8	2.81	5.24	8.05	1,100	26.2	5—Qc
7.5	10.8	12.0	17.4	18.1	0.713	99.0	69.1	0.35	2.26	2.61	170	18.8	6—Q
11.6	11.6	20.0	18.9	17.9	0.565	108.8	86.4	5.63	6.02	11.65	1,450	30.1	7—Qc
12.2	12.2	20.0	19.7	17.9	0.647	103.3	75.4	0.85	3.37	4.22	270	16.9	9—Qc
No. 3													
5.8	6.7	9.5	11.1	18.4	....	....	....	0.00	2.77	2.77	80	29.2	1—U[g]
5.2	6.0	8.5	9.7	18.4	....	....	....	0.00	3.00	3.00	90	35.2	2—U[g]
11.3	11.3	20.0	18.4	17.9	0.552	109.4	88.1	2.81	7.05	9.86	650	35.3	3—Qc
9.9	12.3	16.0	19.9	17.9	0.567	108.4	86.5	1.41	5.54	6.95	350	34.5	4—Qc
8.3	8.3	14.0	14.0	18.1	0.578	107.4	84.0	0.70	4.40	5.10	220	31.4	5—Qc
10.5	12.4	17.0	20.1	18.0	0.571	108.0	85.5	1.41	5.39	6.80	350	31.7	6—Qc
12.0	12.0	20.0	19.9	17.9	0.539	110.3	90.4	5.63	8.94	14.57	1,350	44.1	7—Qc
11.8	11.8	20.0	19.3	17.7	0.531	110.8	90.5	7.04	10.49	17.53	4,400	52.5	9—Qc
11.7	11.7	20.0	19.0	19.1	0.577	107.5	90.1	1.41	4.68	6.09	90	23.4	10—Qc[h]
11.4	11.4	20.0	18.6	19.4	0.587	106.8	90.0	0.70	3.62	4.32	120	18.1	11—Qc[h]
No. 5													
6.0	9.5	9.6	15.3	22.9	....	....	....	0.00	0.86	0.86	70	9.0	1—U[g]
6.4	9.0	10.4	14.5	22.9	....	....	....	0.00	0.85	0.85	70	8.2	2—U[g]
12.4	12.5	20.0	20.1	23.4	0.709	99.3	89.7	0.70	1.32	2.02	230	6.6	3—Qc
11.7	11.7	20.0	18.9	22.4	0.671	101.6	90.9	1.41	1.94	3.35	540	9.7	4—Qc
11.9	11.9	20.0	19.4	21.5	0.640	103.5	91.4	2.81	2.89	5.70	850	14.5	5—Qc
12.1	12.1	20.0	19.6	22.8	0.688	100.6	90.1	1.06	1.62	2.68	330	8.1	6—Qc
11.8	11.8	20.0	19.1	21.9	0.657	102.4	90.7	2.11	2.32	4.43	550	11.6	7—Qc
11.0	11.0	20.0	18.6	20.7	0.603	105.8	93.1	5.63	4.71	10.34	1,100	23.6	8—Qc
11.5	11.5	20.0	19.5	19.9	0.585	107.1	92.6	7.04	5.55	12.59	1,350	27.8	9—Qc
11.4	11.3	20.0	19.0	21.0	0.616	105.0	92.4	4.22	3.72	7.94	950	18.6	10—Qc
12.1	12.1	20.0	19.6	22.5	0.676	101.3	90.7	2.81	1.82	4.63	300	9.1	11—Q
11.5	11.5	20.0	18.7	23.5	0.710	99.2	90.0	1.06	1.34	2.40	400	6.7	12—Qc[h]
11.8	11.8	20.0	19.4	22.7	0.676	101.3	91.3	2.11	1.91	4.02	850	9.6	13—Qc[h]
11.8	11.8	20.0	19.8	20.9	0.620	104.8	91.7	4.22	3.62	7.84	1,100	18.1	14—Qc[h]
11.4	11.4	20.0	18.9	21.0	0.634	103.9	90.2	1.41	2.98	4.39	700	14.9	15—Qc[i]

---

of excessive cracking, no final void ratios were determined for these specimens. [h] After consolidation of these specimens, full confining pressure was maintained, and each sample was subjected to water under pressure for from 4 to 14 days. [i] This sample was preconsolidated, then allowed to rebound fully, subject to lower confining pressure.

the bulk volume of the soil could be computed by use of the Archimedes principle.

After the bulk volume was determined, the water content of the portion of the specimen that had failed was determined. The total weight, the total volume, the water content, and the specific gravity of solids being known, the void ratio at failure could be computed. The process was time-consuming and involved numerous difficulties; considerable practice was required in order to perfect the technique. In spite of this, the method was satisfactory whenever the samples failed by bulging.

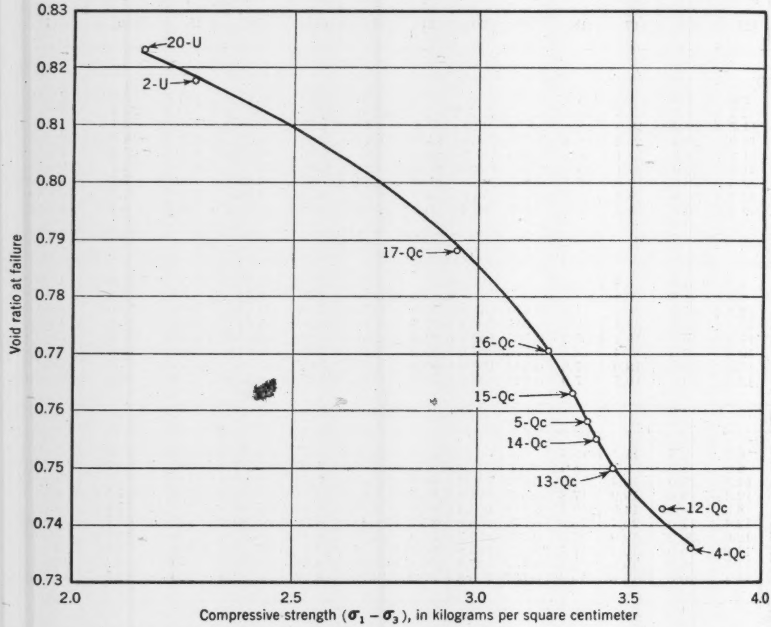

FIG. 11.—FORT UNION CLAY, SERIES NO. 1 (AVERAGE INITIAL CONDITIONS SHOWN IN TABLE 4)

When the test specimen exhibited only one well-defined failure plane, it was separated along this plane and the volume of each half was determined. This procedure reduced the precision of the measurement because of the smaller size of the samples and because of irregularities along the failure plane. When examination of the specimen indicated more than one failure plane, the determination of the void ratio at failure by the foregoing method was not possible; fortunately, this occurred only in the unconfined compression tests, in which cases the initial void ratio was used as an approximation. To remedy this situation a device to measure bulk volume was designed. This apparatus, although sound in principle, remains to be perfected.

RESULTS

Table 2 and Table 3 are summary sheets which present the essential test results pertaining to the Fort Union clay and the Mississippi loess, respectively; they contain the information from which the subsequent curves and diagrams were plotted and from which the final conclusions were drawn. The following abbreviated notations are used:

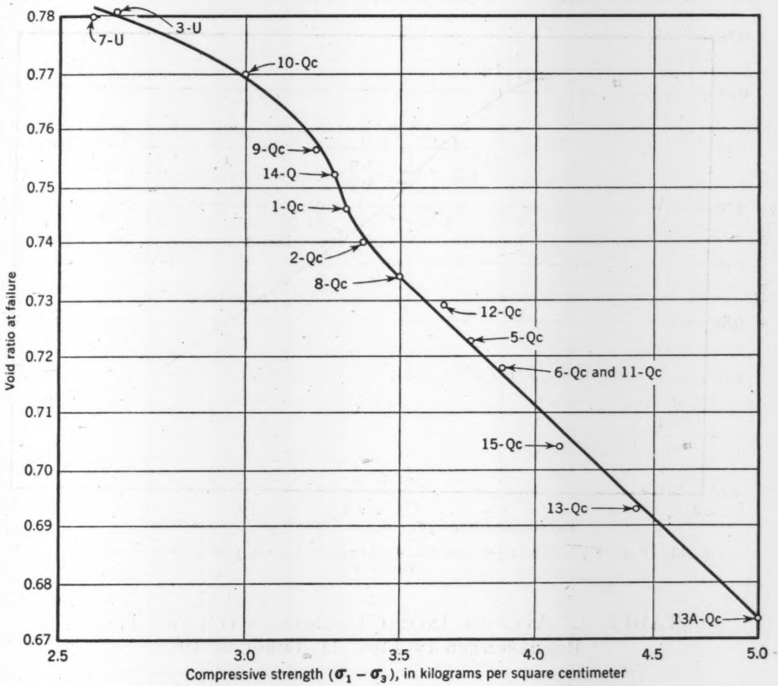

FIG. 12.—FORT UNION CLAY, SERIES NO. 2 (AVERAGE INITIAL CONDITIONS SHOWN IN TABLE 4)

Abbreviation	Type of test
U	Unconfined—Quick
Q	Confined—Quick
Qc′	Partly Consolidated—Quick
Qc	Consolidated—Quick

The principal relationships obtained from the results of this study are shown in Figs. 11 through 14 for the Fort Union clay and in Figs. 15 through 19 for the Mississippi loess. The average initial conditions for the tests represented by Figs. 11 through 19 appear in Table 4. These relationships are plots of the void ratio at failure (arithmetic scale) against compressive strength (logarithmic scale); no consistent relationships were found between compressive strength and any other physical characteristic of the soil. It is important to note that, for a given set of initial conditions, the relationship between compressive strength and void ratio at failure is unique, regardless of the confining pressure, the quantity of drainage permitted, the water content, or the degree of saturation. This statement is certainly valid for the two soils tested, within the limits listed in Table 5. The statement is based on the results of more than one hundred carefully conducted tests in which the drainage permitted varied (through a number of intermediate stages) from no drainage to full drainage under confining pressures of from 0 kg per sq cm to more than 7 kg per sq cm.

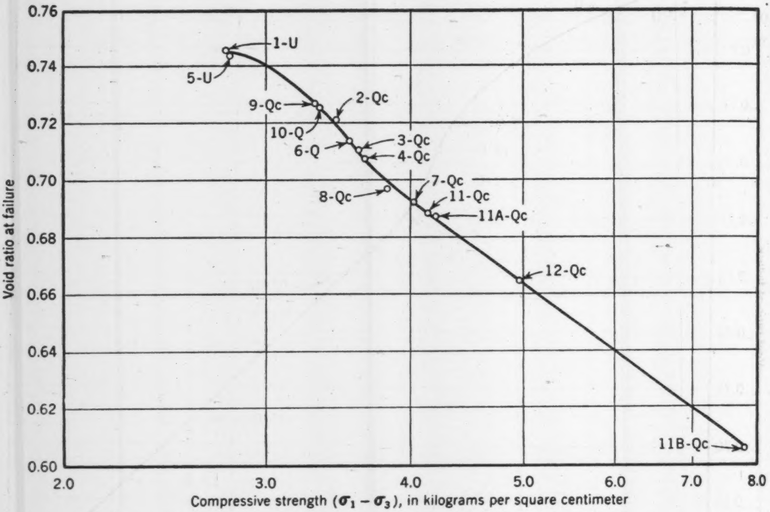

FIG. 13.—FORT UNION CLAY, SERIES NO. 4 (AVERAGE INITIAL CONDITIONS SHOWN IN TABLE 4)

TABLE 4.—AVERAGE INITIAL CONDITIONS FOR THE TESTS REPRESENTED IN FIGS. 11 THROUGH 19

Test series	FORT UNION CLAY			MODIFIED MISSISSIPPI LOESS		
	Void ratio	Water content[a]	Degree of saturation[a]	Void ratio	Water content[a]	Degree of saturation[a]
1	0.82 ± 0.01	25.5 ± 0.3	85.8 ± 0.8	0.99 ± 0.01	18.5 ± 0.2	50.6 ± 0.8
2	0.777 ± 0.004	25.6 ± 0.2	90.7 ± 0.6	0.734 ± 0.008	18.1 ± 0.0	67.0 ± 0.5
3				0.576 ± 0.008	18.3 ± 0.2	86.6 ± 0.5
4	0.744 ± 0.003	25.5 ± 0.1	94.6 ± 0.3	0.545 ± 0.007	18.0 ± 0.1	90.0 ± 0.6
5				0.742 ± 0.005	22.8 ± 0.1	83.5 ± 0.5

[a] In percentage.

Seven specimens of the Mississippi loess were placed in contact with water under a pressure of approximately 25% of the confining pressure for periods of time varying from 4 days to 14 days. The results of all but one of these tests plotted almost exactly on the original curves. These data strongly indicate that the relationship between compressive strength and void ratio at failure is unique even when the degree of saturation is increased by the addition of water from an external source. One specimen (15—Qc) was preconsolidated at a confining pressure that exceeded its compressive strength and sheared after

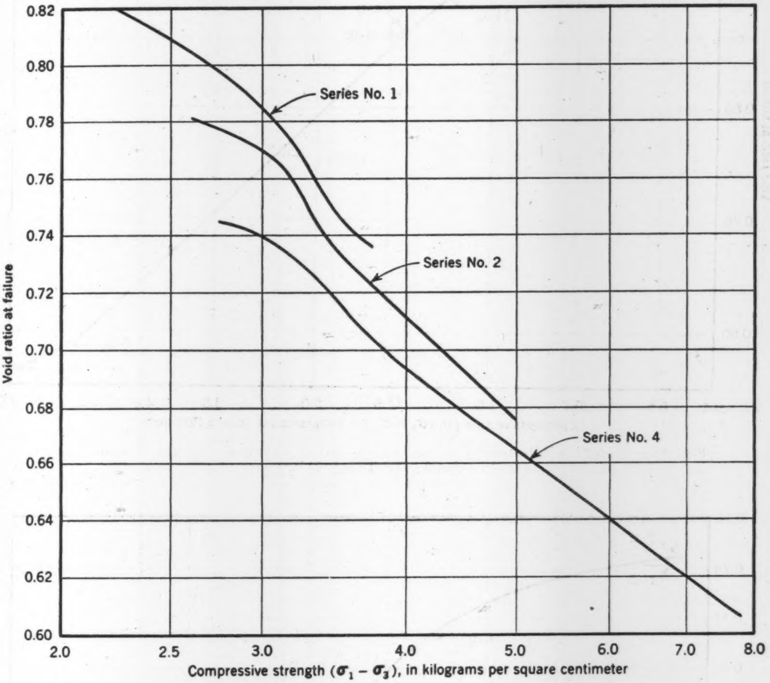

FIG. 14.—SUMMARY FOR FORT UNION CLAY, BASED ON TABLES 2, 3, AND 4 (1 KG PER SQ CM EQUALS 14.2234 LB PER SQ IN.)

TABLE 5.—LIMITS OF SOIL CHARACTERISTICS

Soil type	Water Content (%)		Void Ratio		Degree of Saturation (%)	
	Minimum	Maximum	Minimum	Maximum	Minimum	Maximum
Fort Union clay	21.5	25.7	0.61	0.83	85.6	97.8
Mississippi loess	17.5	23.4	0.51	1.01	51.0	93.1

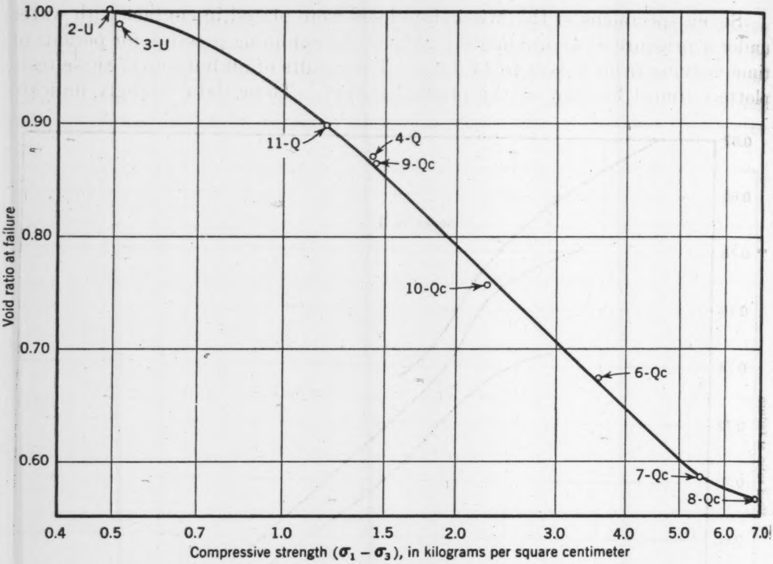

FIG. 15.—MODIFIED MISSISSIPPI LOESS, SERIES NO. 1 (AVERAGE INITIAL CONDITIONS SHOWN IN TABLE 4)

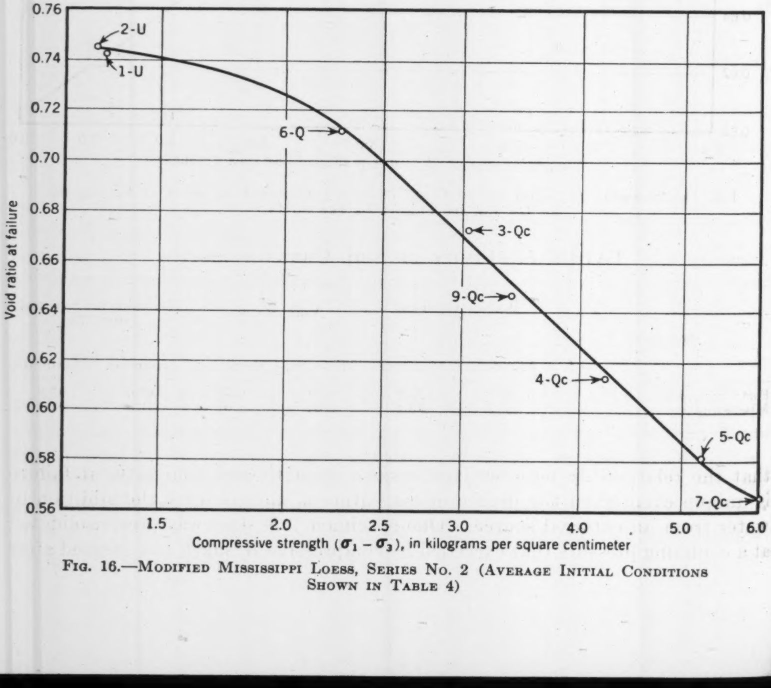

FIG. 16.—MODIFIED MISSISSIPPI LOESS, SERIES NO. 2 (AVERAGE INITIAL CONDITIONS SHOWN IN TABLE 4)

full rebound had been permitted at a lower confining pressure. The results of this test also plotted on the original curve.

No consistent relationships were found between stiffness (as measured either by the initial value of the Young modulus or by the secant modulus to maximum stress) and any other soil property—although, in general, the strain at failure was found to increase with the confining pressure. Typical stress-strain curves for one test series are shown in Fig. 20. It is believed, however, that stress-strain data are likely to be misleading as long as strains must be computed from the total deformation of the sample. A device for evaluating more closely the true strains in soils is greatly needed.

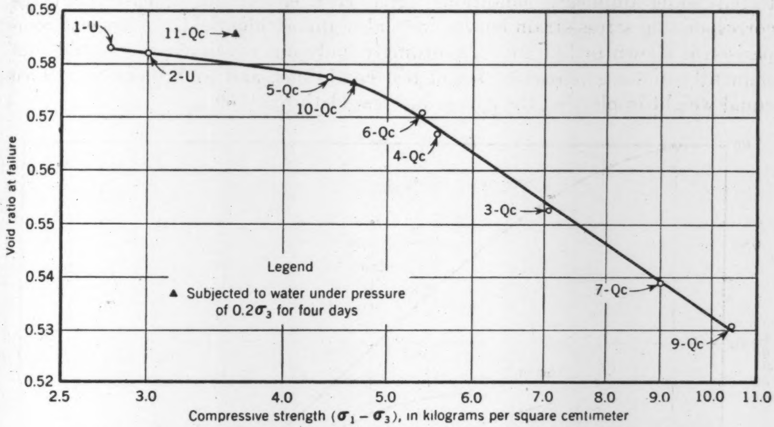

FIG. 17.—MODIFIED MISSISSIPPI LOESS, SERIES NO. 3 (AVERAGE INITIAL CONDITIONS SHOWN IN TABLE 4)

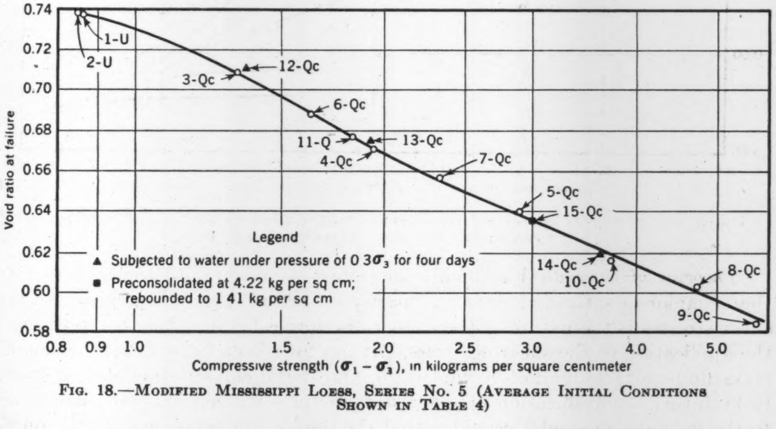

FIG. 18.—MODIFIED MISSISSIPPI LOESS, SERIES NO. 5 (AVERAGE INITIAL CONDITIONS SHOWN IN TABLE 4)

DISCUSSION OF RESULTS

In the early stages of the testing program two specimens were used for each set of test conditions; it was intended to conduct still another test if the results of the first two tests differed substantially. It was soon found that not only did the compressive strength and the void ratio at failure for two samples tested under duplicate conditions agree very closely in all cases, but the corresponding stress-strain curves were also almost identical. A typical comparison is shown in Fig. 21. Accordingly, only one specimen was tested subsequently under a particular set of test conditions, and each point was given equal weight in plotting the curves in Figs. 11 through 19.

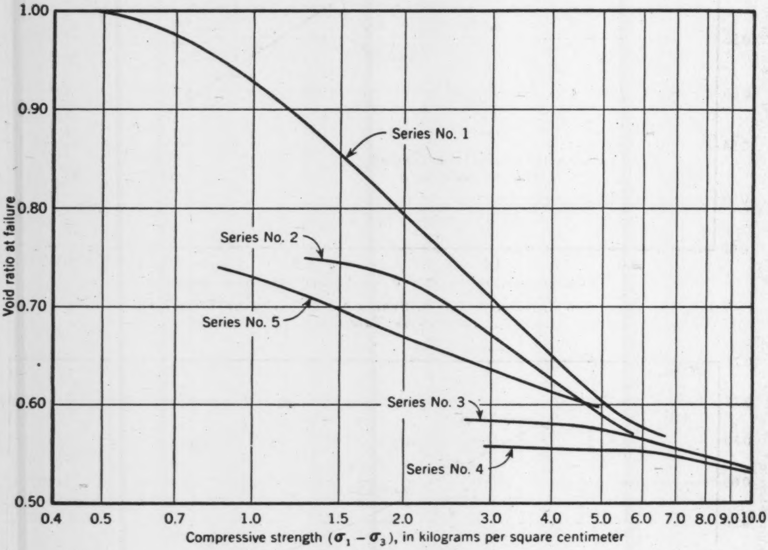

FIG. 19.—SUMMARY FOR MODIFIED MISSISSIPPI LOESS (1 KG PER SQ CM EQUALS 14.2234 LB PER SQ IN.) BASED ON TABLES 2, 3, AND 4

Theories of Strength Variation.—The most significant difference between the behavior of saturated clays and partly saturated clays when subjected to shear stresses is the nature of the changes in void ratio that may occur during the application of the shearing stress. It has long been known (23) that loose clays undergo a reduction in void ratio, and dense clays an increase in void ratio during the application of shear stresses (in a manner entirely analogous to the behavior of sands) provided that the pore-water pressure is at all times maintained equal to atmospheric pressure. When saturated clays are subjected to quick tests or consolidated-quick tests, the change in void ratio during the application of the deviator stress is negligible; any tendency toward a decrease in void ratio is counteracted by an increase in pore-water pressure and, conversely, any tendency toward an increase in void ratio is counteracted by a reduction in pore-water pressure. In the case of partly saturated clays, the change in void ratio during the application of the deviator stress may not only be comparatively large but has been found to depend on the degree of compaction and the confining pressure (Fig. 22). On the basis of these simple facts, the conflicting views regarding the strength characteristics of clay-like soils can be readily reconciled.

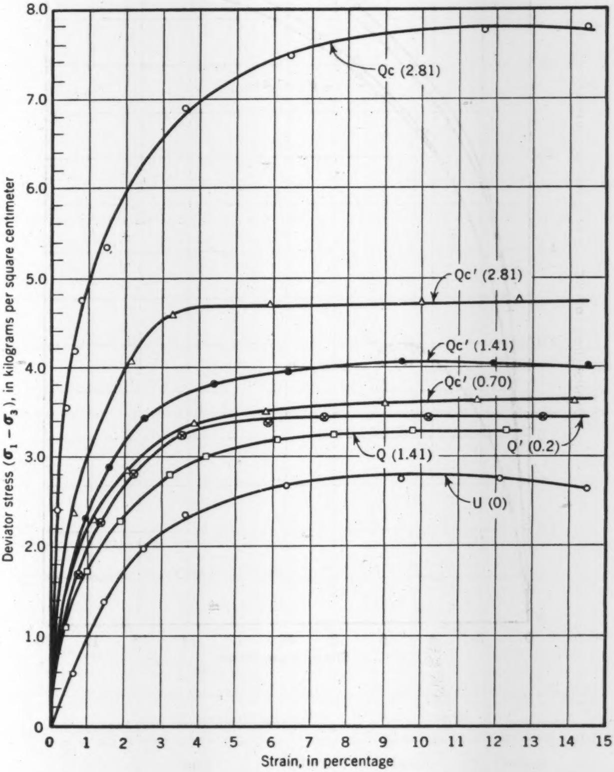

FIG. 20.—STRESS-STRAIN CURVES: FORT UNION CLAY, SERIES NO. 4 (VALUES IN PARENTHESES ARE CONFINING PRESSURES, IN KILOGRAMS PER SQUARE CENTIMETER)

This study has shown that, for a particular set of initial conditions, a change in compressive strength must be accompanied by a change in void ratio at failure and that the relationship is essentially independent of the method used to produce this change in void ratio. Thus, if a clay-like soil is initially saturated, a change in strength must be accompanied by a change in water content at failure, and the relationship between water content and compressive strength should be independent of the method used to produce the change in water

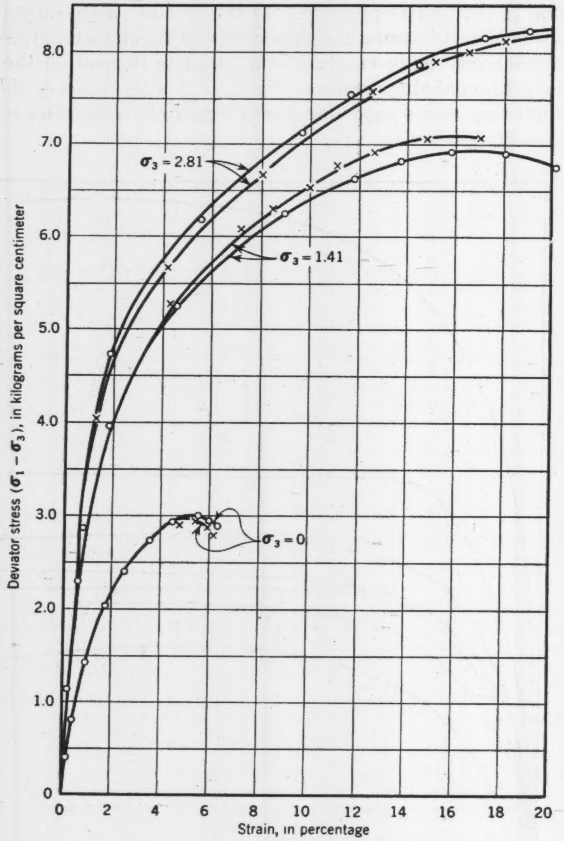

Confining pressure[a], σ_3	Void Ratio		Water Content[b]		Maximum[a] $(\sigma_1 - \sigma_3)$	Strain at failure, in percentage
	Initial	Final	Initial	Final		
0	0.546	....	18.4	18.2	3.02	5.4
	0.548	....	18.3	18.0	2.99	5.2
1.41	0.539	0.546	17.9	17.9	7.08	16.1
	0.545	0.547	18.0	17.9	6.94	17.0
2.81	0.547	0.539	17.9	18.0	8.26	20.0
	0.546	0.538	17.9	18.1	8.20	20.0

[a] In kilograms per square centimeter. [b] In percentage.

FIG. 21.—COMPARISON OF STRESS-STRAIN CURVES FOR SPECIMENS TESTED UNDER DUPLICATE CONDITIONS

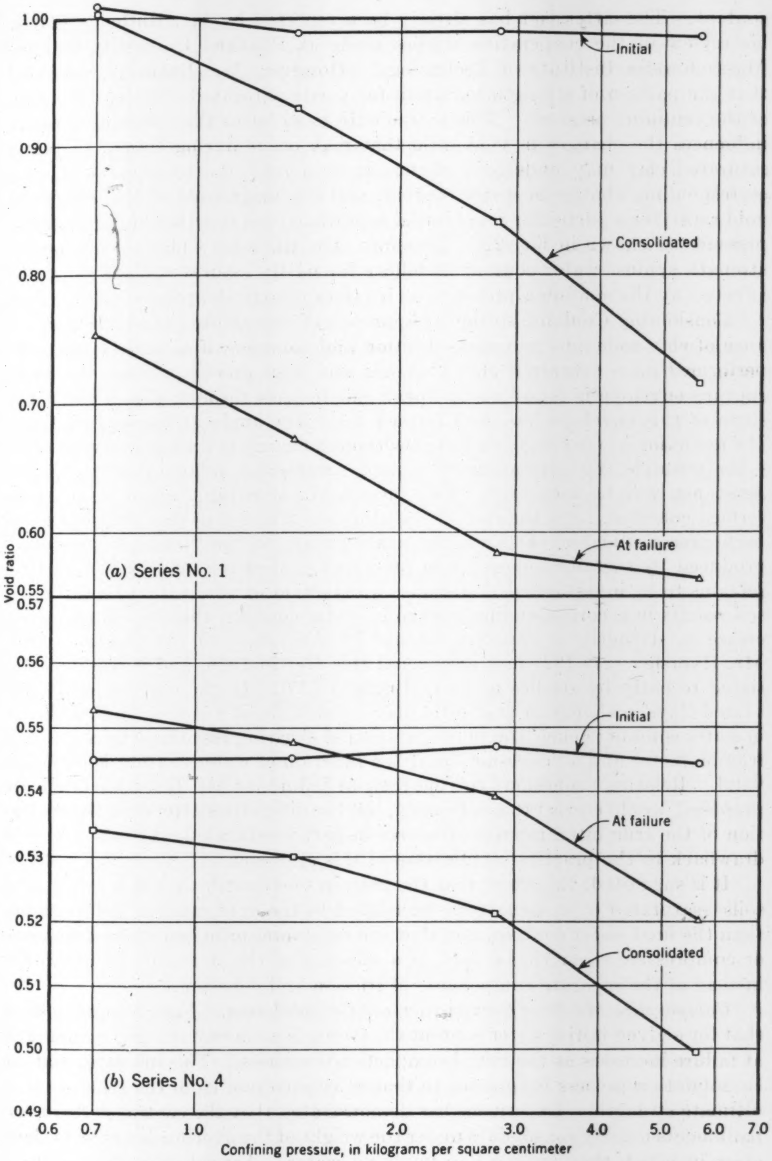

FIG. 22.—EFFECT OF CONFINING PRESSURE ON VOID RATIO AT FAILURE—MISSISSIPPI LOES

content. The latter fact has already been reported by Mr. Rutledge (24) in his review of the cooperative studies made at Harvard University and the Massachusetts Institute of Technology. However, Mr. Rutledge concluded that the pattern of strength variation for partly saturated clays is a function of the confining pressure. This is true only in so far as the confining pressure influences the changes in void ratio that may occur during shear. A partly saturated clay may undergo a change in void ratio during shear without a corresponding change in water content, and the magnitude of this change in void ratio (for a particular set of initial conditions) is a function of the confining pressure, as shown in Fig. 22. Therefore, Mr. Rutledge's plot of compressive strength against water content at failure for partly saturated clays should be affected by the confining pressure, as his data clearly showed.

Considering Coulomb's original approach of separating the shearing resistance of clay soils into two parts, friction and cohesion, if slow shear tests are performed on a saturated clay that has not been precompressed, the Mohr rupture envelope is found to be linear and to pass through the origin. The slope of this envelope has been termed the "true angle of internal friction." If a reduction in void ratio is effected without a change in intergranular pressure—for example, by preconsolidation and subsequent rebound—the shearing resistance will be increased. This increase in shearing resistance has been termed cohesion. (In the case of cohesion in a stratum of clay that has never been preconsolidated (4) (19), the exact nature of the "intrinsic pressures" produced by sustained overburden pressures applied for long periods of time remains to be investigated.) Because a reduction in void ratio of a saturated soil results in a corresponding change in water content, the accompanying increase in strength, or cohesion, should be a function of the water content. Mr. Hvorslev (21) (22) first discovered this fact in 1936, and it was substantiated recently by studies made in England (25). In the case of partly saturated clays, a change in void ratio may occur without a corresponding change in water content; hence, the representation of shearing resistance by a constant friction factor and a "cohesion" that is a function of water content is no longer valid. Relating "cohesion" to void ratio at failure, as Mr. Hvorslev originally proposed, would correct this deficiency, but the difficulties attending the evaluation of the true intergranular pressures in partly saturated clays are a serious drawback to the practical application of this approach.

It is suggested, therefore, that the pattern of strength variation of cohesive soils—saturated or unsaturated—be related to the void ratio at failure rather than the final water content, and that the maximum principal stress difference, or compressive strength, be used as a measure of the strength characteristics instead of the separate components of friction and cohesion.

Comparative Merits of Compaction and Consolidation.—Figs. 14 and 19 show that for a given initial water content the strength acquired at a given void ratio at failure increases as the initial compaction decreases. This indicates that the consolidation process is superior to that of compaction from the standpoint of ultimate strength. Experience has demonstrated that the central parts of embankments usually consolidate under the weight of the overburden even in those cases in which they are used to impound water. Accordingly, the results of this study indicate that in the construction of earth embankments greater advantage can be taken of the beneficial effects of consolidation than has been done in the past. Although this factor may be of considerable engineering importance, the reasons for the apparent superiority of the consolidation process over the compaction process are not immediately evident.

It has been demonstrated that the amount of swelling of a compacted clay soil in the presence of water increases as the initial degree of compaction increases and as the confining pressure decreases (32). Because a large reduction in strength may result from moderate swelling (resulting from the corresponding increase in void ratio), swelling is a critical factor for compacted earth structures in which the confining pressures are small. Subgrades for highway and airport pavements are typical structures of this type. It is entirely possible that high compaction and subsequent swelling (after the pavement is in place) may result in a subgrade inferior to one only moderately compacted but in which subsequent swelling would be negligible.

The apparent advantages of consolidation over compaction in the construction of embankments and the possibilities of "overcompaction" in the case of highway and airport subgrades warrant a careful review of current trends toward higher and higher compaction for the purpose of stabilizing these common earth structures.

Further Research Needed.—Further research is needed to substantiate the uniqueness of the relationship between compressive strength and void ratio at failure for a variety of other soils, particularly when the degree of saturation is increased by the addition of water from an external source. The effects of wider ranges in the value of the initial water content and of consolidation under principal stresses, the ratios of which are other than unity, are curently being studied. The effects of preconsolidation and of other external features, such as frost action, still need to be thoroughly investigated.

From a practical standpoint there is an urgent need for a comprehensive field study to provide information as to how the void ratio at failure can be predicted from the initial compacted conditions, the confining pressures, and the amount of drainage (or increase in the degree of saturation) that actually occurs over extended periods of time. This information would make possible the prediction of the strength of compacted clay soils under any combination of variable external conditions. When this information has been accumulated it will be possible to formulate compaction specifications for a given job on a rational basis. In this connection, a thorough investigation of the effects of various processes of compaction is mandatory because the strength of a compacted soil at a given set of initial conditions depends on the method as well as the degree of compaction (26).

CONCLUSIONS

1. For the two soils tested and within the ranges of water content, void ratio, and degree of saturation used, the pattern of strength variation for partly saturated, compacted clays can be represented by a relationship between the void ratio at failure (plotted to an arithmetic scale) and the maximum value of the principal stress difference, or compressive strength (plotted to a logarithmic scale). For a specified set of initial conditions this relationship is independent of the confining pressure, the amount of drainage permitted, the water content, and the degree of saturation. It is indicated that the relationship is unique even if the degree of saturation (or water content) is increased by the addition of water from an external source, and there is a possibility that this uniqueness

will exist even after the soil has been preconsolidated and then allowed to rebound fully at a lower confining pressure.

2. A principal reason for the difference in behavior between saturated and partly saturated clays subjected to shear stresses is that in the former a change in void ratio must be accompanied by a change in water content, whereas in the latter changes in void ratio can occur freely without corresponding alterations in the water content. For this reason the pattern of strength variation for saturated clays is reflected either by the water content or by the void ratio at failure, whereas the strength variation of partly saturated clays can be related only to the void ratio at failure. On the basis of this fact, current conflicting views regarding the strength characteristics of clay-like soils can be reconciled.

3. For a specified initial water content, a reduction in void ratio achieved through the process of consolidation produces a higher compressive strength than that obtained by a process of compaction. In addition, swelling in the presence of water, at a specified confining pressure, increases approximately in direct proportion to the compactive effort. A critical review of the current trends toward increasingly higher compaction for the purpose of stabilizing clay-like soils is therefore warranted.

4. There is a need for a comprehensive field study that will provide information on the basis of which the void ratio at failure can be predicted from the initial compacted conditions, the confining pressure, the drainage conditions, and the method of compaction. This information will make it possible to formulate specifications for a particular job on a rational basis.

APPENDIX. LIST OF REFERENCES

(1) **"Soil Mechanics in Engineering Practice,"** by Karl Terzaghi and R. B. Peck, John Wiley & Sons, Inc., New York, N. Y., 1948.

(2) **"Essai sur une application des régles de maximis et minimis à quelques problems de statiques,"** by C. A. Coulomb, *Mémoirs Académie Royale des Sciences*, Vol. 3, Paris, France, 1776, pp. 38–44.

(3) **"Nouvelle recherche sur la poussée des terres,"** by M. L. Leygue, *Annales des Ponts et Chaussées*, Pt. 2, 1885, p. 788.

(4) **"Fundamentals of Soil Mechanics,"** by D. W. Taylor, John Wiley & Sons, Inc., New York, N. Y., 1948.

(5) **"Theoretical Soil Mechanics,"** by Karl Terzaghi, John Wiley & Sons, Inc., New York, N. Y., 1943.

(6) **"La Poussée des Terres, Deuxième Partie: Theorie des Terres Coherentes,"** by J. Résal, Beranger, Paris, France, 1910, p. 327.

(7) **"Erdbaumechanic auf bodenphysikalischer Grundlage,"** by Karl Terzaghi, Franz Deuticke, Vienna, Austria, 1925.

(8) **"Principles of Final Soil Classification,"** by Karl Terzaghi, *Public Roads*, Vol. 8, No. 3, 1927, pp. 41–53.

(9) **"The Science of Foundations—Its Present and Future,"** by Karl Terzaghi, *Transactions*, ASCE, Vol. 93, 1929, pp. 270–405.

(10) **"The Mechanics of Shear Failures on Clay Slopes and the Creep of Retaining Walls,"** by Karl Terzaghi, *Public Roads*, Vol. 10, No. 10, 1929, pp. 177–192.

(11) **"Critical Height and Factor of Safety of Slopes Against Sliding,"** by Karl Terzaghi, *Proceedings*, First International Conference on Soil

Mechanics and Foundation Eng., Cambridge, Mass., Vol. 1, 1936, pp. 156–161.

(12) **"The Shearing Resistance of Saturated Soils and the Angle Between the Planes of Shear,"** by Karl Terzaghi, *ibid.*, pp. 54–56.

(13) **"A Fundamental Fallacy in Earth Pressure Computations,"** by Karl Terzaghi, *Journal*, Boston Soc. of Civ. Engrs., Vol. 23, 1936, pp. 71–78.

(14) **"The Shearing Resistance of Soils,"** by L. Jürgenson, *ibid.*, Vol. 21, No. 3, 1934, pp. 242–283.

(15) **"Statens Järnvägars Geotekniska Kommission, Slutbetände,"** a report of the Swedish Geotechnical Commission, Stockholm, Sweden, 1922. English abstract and comments by Karl Terzaghi, filed in the Carnegie Library, Pittsburgh, Pa.

(16) **"Subsurface Exploration and Sampling of Soils for Civil Engineering Purposes,"** by M. J. Hvorslev, U. S. Waterways Experiment Station, Vicksburg, Miss., 1949.

(17) **"Soil Testing for Engineers,"** by T. W. Lambe, John Wiley & Sons, Inc., New York, N. Y., 1951.

(18) **"The Structure of Clay and Its Importance in Foundation Engineering,"** by A. Casagrande, *Journal*, Boston Soc. of Civ. Engrs., Vol. 19, No. 4, 1932, pp. 168–221.

(19) **"Relation of Undisturbed Sampling to Laboratory Testing,"** by P. C. Rutledge, *Transactions*, ASCE, Vol. 109, 1944, pp. 1155–1216.

(20) **"The Vane Borer, An Apparatus for Determining the Shearing Resistance of Clay Soils Directly in the Ground,"** by L. Calding and S. Odenstad, *Proceedings*, Royal Swedish Geotechnical Inst., Stockholm, Sweden, 1950, No. 2.

(21) **"Conditions of Failure for Remoulded Cohesive Soils,"** by M. J. Hvorslev, *Proceedings*, First International Conference on Soil Mechanics and Foundation Eng., Cambridge, Mass., Vol. 3, 1936, pp. 51–53.

(22) **"Über die Festigkeitseigenschaften gestörter bindiger Boden,"** by M. J. Hvorslev, *Ingeniorvidenskabelige Skrifter*, A. No. 35, 1937.

(23) **"Relation Between Void Ratio and Effective Principle Stresses for a Remoulded, Silty Clay,"** by L. Rendulic, *Proceedings*, First International Conference on Soil Mechanics and Foundation Eng., Cambridge, Mass., Vol. 3, 1936, pp. 48–51.

(24) **"Soil Mechanics Fact Finding Survey, Progress Report: Triaxial Shear Research,"** U. S. Waterways Experiment Station, Vicksburg, Miss., April, 1947. (*a*) pp. 21 and 27.

(25) **"Proceedings of the Conference on the Measurement of the Shear Strength of Soils in Relation to Practice,"** *Geotechnique*, Vol. 2, Nos. 2 and 3, 1951.

(26) **"Compaction Studies on Silty Clay: Soil Compaction Investigation,"** *Report No. 2*, U. S. Waterways Experiment Station, Vicksburg, Miss., 1949.

(27) **"Geology and Coal Resources of the Minot Region—North Dakota, 1939,"** *Geological Survey Bulletin No. 906-B*, Geological Survey, U. S. Dept. of the Interior, Washington, D. C., 1939.

(28) **"The Effects of Internal Hydrostatic Pressure on the Shearing Strength of Soils,"** by L. W. Hamilton, *Proceedings*, A.S.T.M., Vol. 39, 1939, pp. 1100–1121.

(29) **"Geology and Mineral Resources of Mississippi,"** by A. F. Crider, *Bulletin No. 238*, Geological Survey, U. S. Dept. of the Interior, Washington, D. C., 1906.

(30) **"Compression Tests on Stabilized Soil Mixtures,"** by R. I. Mayo, thesis presented to Purdue University, Lafayette, Ind., in 1939, in partial fulfilment of the requirements for the degree of Master of Science in Civil Engineering.

(31) **"Testing Equipment and Research Activities of the Soil Mechanics Laboratory, Northwestern University,"** by J. O. Osterberg, Northwestern Univ., Evanston, Ill., 1948.

(32) **"The Compressibility of Two Compacted Clays,"** by H. C. Woodsum, thesis presented to Purdue University, Lafayette, Ind., in 1951, in partial fulfilment of the requirements for the degree of Master of Science in Civil Engineering.

(33) **"Shear Characteristics of Remolded Earth Materials,"** by A. A. Wagner, *Special Publication No. 106*, A.S.T.M., 1950, pp. 192–227.

(34) **"The Use of the Maximum Principal Stress Ratio as the Failure Criterion in Evaluating Triaxial Shear Tests on Earth Materials,"** by W. G. Holtz, *Proceedings*, A.S.T.M., Vol. 47, 1947, p. 1067.

(35) **"Estimating Construction Pore Pressures in Rolled Earth Dams,"** by J. W. Hilf, *Proceedings*, Second International Conference on Soil Mechanics and Foundation Eng., Rotterdam, The Netherlands, Vol. 3, 1948, p. 234.

(36) **"Engineering Properties of Expansive Clays,"** by W. G. Holtz and H. J. Gibbs, *Proceedings-Separate No. 516*, ASCE, October, 1954.

(37) **"The California Bearing Ratio Test as Applied to the Design of Flexible Pavements for Airports,"** *Technical Memorandum No. 213–1*, U. S. Waterways Experiment Station, Vicksburg, Miss., 1945.

(38) **"Stress-Strain Characteristics of Compacted Soil Systems,"** by Joseph B. Eustis and John L. McRae, presented at the Annual Meeting, ASCE, 1945.

(39) **"A Study of Structure in Compacted Soils,"** by Shou-I Tsien, thesis presented to the Massachusetts Institute of Technology in Cambridge, Mass., in 1946, in partial fulfilment of the requirement for the degree of Doctor of Science.

(40) **"Small Soil Compaction Apparatus Duplicates Field Results Closely,"** by Stanley D. Wilson, *Engineering News-Record*, November 2, 1950.

(41) **"The Structure of Inorganic Soil,"** by T. William Lambe, *Proceedings-Separate No. 315*, ASCE, October, 1953.

(42) **"Fundamental Considerations on the Shear Strength of Soil,"** by L. Bjerrum, *Geotechnique*, Vol. 2, No. 3, 1951 p. 209.

(43) **"Experimental Determination of the True Cohesion and True Angle of Internal Friction in Clays,** by R. E. Gibson, *Proceedings*, Third International Conference on Soil Mechanics and Foundation Eng., Zurich, Vol. 1, 1953, p. 126.

DISCUSSION

Harold J. Gibbs[3] and Jack W. Hilf,[4] Associate Members, ASCE.—The author has presented a relationship between volume change and strength of unsaturated remolded clays which is of value in analyzing triaxial-shear test results, but which the writers believe is not a satisfactory substitute for the Mohr strength envelope. Furthermore, the implications in the paper that it may be desirable to reduce the compactive effort on clay soils in earth dam embankments in order to obtain greater strength are substantiated neither by theory nor by tests made by the Bureau of Reclamation, United States Department of the Interior (USBR).

The plot of void ratio at failure for a given initial void ratio, as the ordinate, against the logarithm of maximum deviator stress, as the abscissa, is essentially a diagram relating shearing strength to volume strain—which shows the important role of volume change during shear. The decrease in volume of soil, during shear or otherwise, depends on effective normal compressive stresses which, in turn, are functions of the applied stresses, the compressibility of the pore fluid, and the amount of drainage permitted. For the past fifteen years the USBR has been using the relationship between shearing strength and effective stress in interpreting triaxial-shear tests on unsaturated impervious soils and applying these interpretations to the design of earth dams and canal embankments. A Mohr strength envelope is obtained from sealed tests in which effective normal stresses are determined by subtracting measured pore pressures from the applied normal stresses. In order to compare the two types of plots—the author's and that of the USBR—the writers will analyze data from tests reported in 1950 (33). The particular test series were selected because they contain results pertinent to the question of compaction versus consolidation.

The soil used in these tests was a lean clay from the vicinity of Vallecito Dam in Colorado. It had the following properties:

Property	Value
Specific gravity of grains	2.739
Liquid limit, in percentage	26.6
Plasticity index, in percentage	7.3
Gradation:	
Maximum size, in inches	$\frac{1}{4}$
Percentage larger than No. 200 sieve	27
Percentage smaller than 0.005 mm	23
Proctor Compaction (USBR Standard):	
Maximum dry density, in pounds per cubic foot	116.0
Optimum moisture content, in percentage	13.4
Permeability at Proctor maximum dry density, in feet per year	0.06

The results of triaxial-shear tests of this soil, made under the six different conditions listed in Table 6, appear in Fig. 23 (33). Fig. 24 is a combined plot

---

[3] Engr., Bureau of Reclamation, U. S. Dept. of the Interior, Denver, Colo.

[4] Engr., Bureau of Reclamation, U. S. Dept. of the Interior, Denver, Colo.

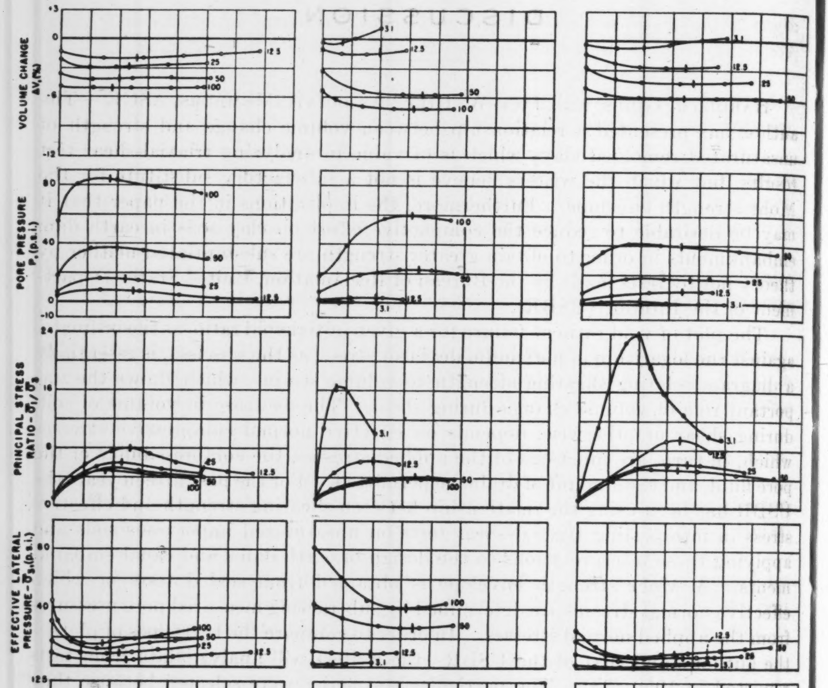

FIG. 23.—TRIAXIAL-SHEAR TEST, TYPICAL

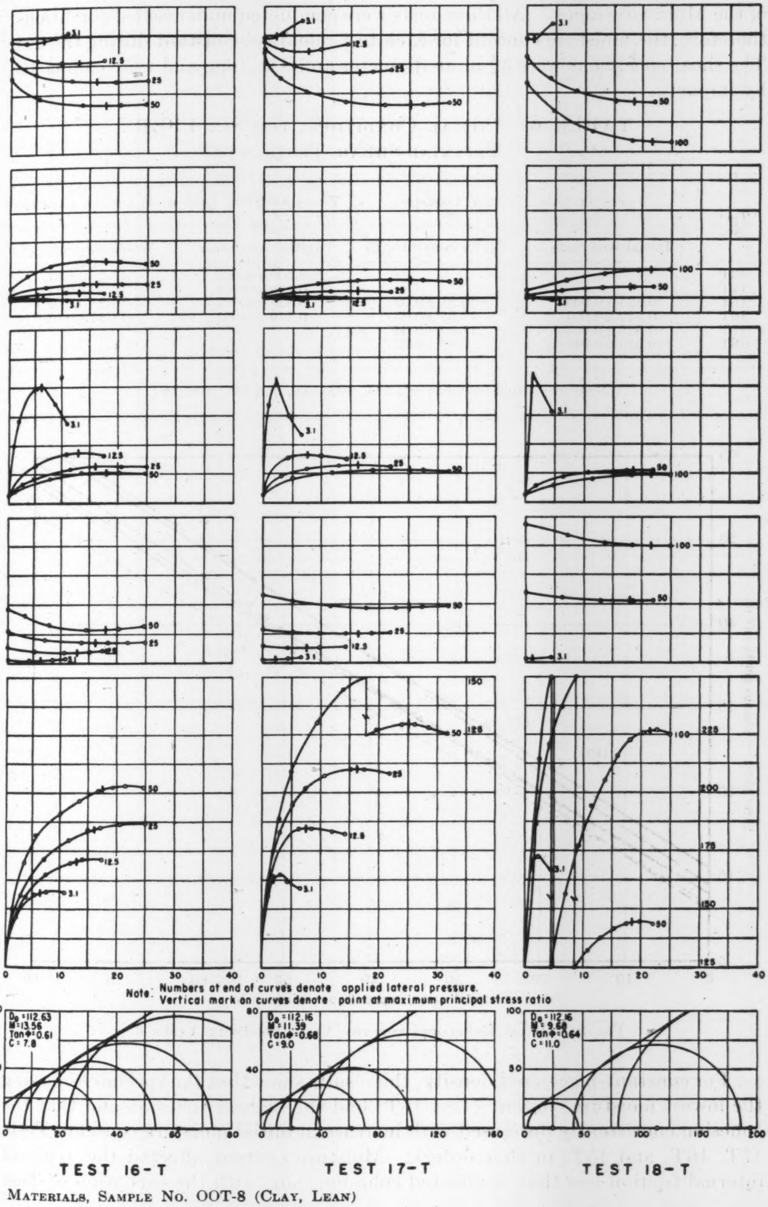

MATERIALS, SAMPLE NO. OOT-8 (CLAY, LEAN) of the Mohr envelopes. All these tests were conducted under sealed conditions; therefore, the moisture content for each test remained constant during the test. The shear specimens were $3\frac{1}{4}$ in. in diameter and 9 in. long and were compacted by impact.

TABLE 6.—INITIAL CONDITIONS FOR SIX USBR TRIAXIAL-SHEAR TESTS

Test No.	TESTS AT SAME INITIAL DENSITY		TESTS AT SAME INITIAL MOISTURE CONTENT[a]	
	Initial void ratio	Water content (%)	Initial void ratio	Water content (%)
13T			0.500 ±0.003	15.25 ±0.07
14T			0.499 ±0.004	13.50 ±0.11
15T	0.525 ±0.003	15.21 ±0.02	0.525 ±0.003	15.21 ±0.02
16T	0.519 ±0.001	13.55 ±0.03	0.519 ±0.001	13.55 ±0.03
17T	0.525 ±0.003	11.39 ±0.04		
18T	0.525 ±0.001	9.67 ±0.02		

[a] Tests are paired as indicated: 13T with 15T, and 14T with 16T.

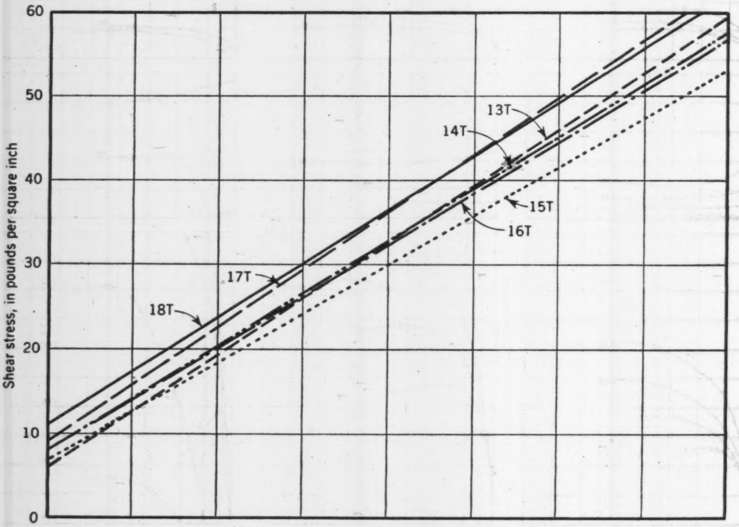

FIG. 24.—MOHR ENVELOPES FOR THE TESTS LISTED IN TABLE 6

For constant-placement density, the results show that the specimens having the lowest moisture content (Test 18T) had the highest cohesion and that the cohesion consistently decreased with increase in initial moisture content (Tests 17T, 16T, and 15T, in that order). Moisture content affected the angle of internal friction less than it affected cohesion, but, with the exception of Test

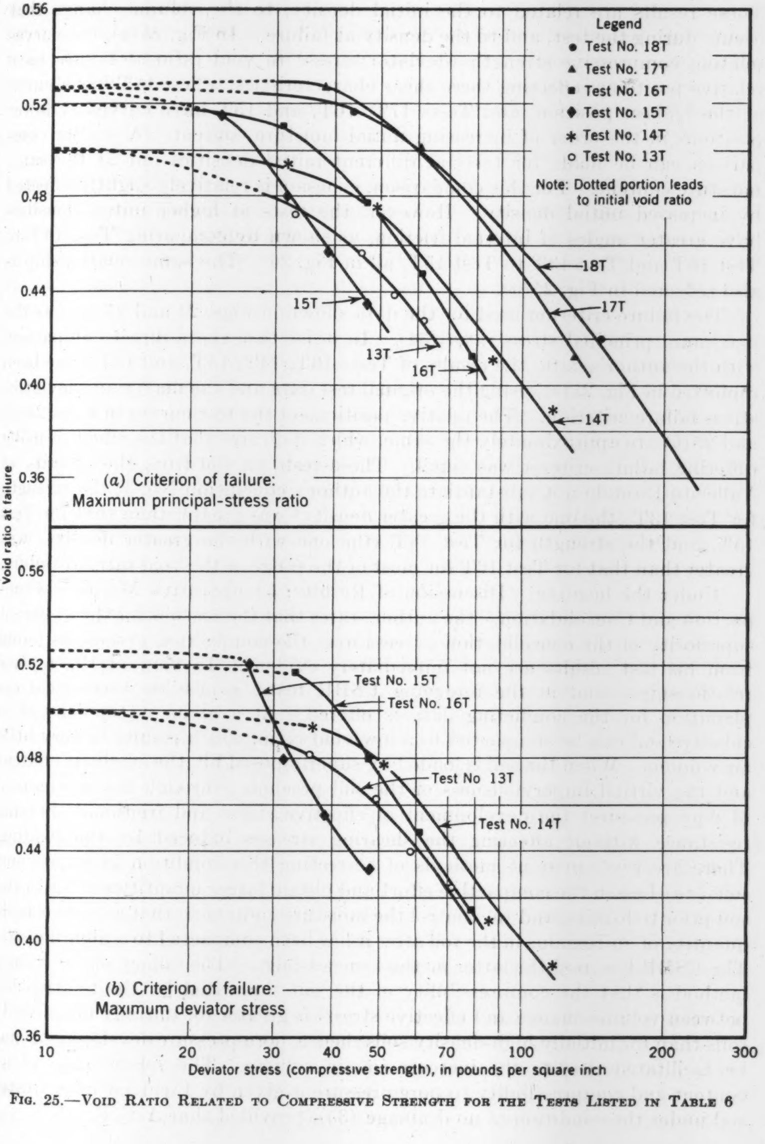

FIG. 25.—VOID RATIO RELATED TO COMPRESSIVE STRENGTH FOR THE TESTS LISTED IN TABLE 6

17T, this angle also became smaller as initial moisture content increased. These results are related to the initial density, to the volume change that occurs during the test, and to the density at failure. In Fig. 25(*a*), the curves relating compressive strength (deviator stress) to void ratio at failure have relative positions reflecting these shear characteristics. Test 18T has a curve at the highest position, and Tests 17T, 16T, and 15T have curves at lower positions in the order of increasing initial moisture content. A similar comparison can be made for tests at different initial densities but at the same moisture content. For this comparison, cohesion is relatively slightly affected by increased initial density. However, the tests at higher initial densities have greater angles of internal friction, as shown by comparing Test 14T to Test 16T and Test 13T to Test 15T, all in Fig. 24. The same relationship is also reflected in Fig. 25(*a*).

The failure criterion used for the data shown in Figs. 24 and 25(*a*) was the maximum principal stress ratio (34). In order to make a direct comparison with the author's data, the results of Tests 13T, 14T, 15T, and 16T have been replotted in Fig. 25(*b*), using the original test data and the maximum-deviator-stress failure criterion. The relative positions of the test curves in Figs. 25(*a*) and 25(*b*) are approximately the same, which indicates that the effect of using differing failure criteria was small. These tests on soil from the vicinity of Vallecito Dam do not substantiate the author's conclusion No. 3; the strength for Test 13T (the one with the greater density) was greater than that for Test 15T, and the strength for Test 14T (the one with the greater density) was greater than that for Test 16T for most of the range of the void ratio at failure.

Under the heading, "Discussion of Results: Comparative Merits of Compaction and Consolidation," the author states that the reasons for the apparent superiority of the consolidation process over the compaction process as found from his test results are not immediately evident. In view of the reverse relationship found in the foregoing USBR tests, a possible theoretical explanation for the conflicting data is offered. At a given water content, a cohesive soil can be compacted to a low void ratio, which results in very little air volume. When the soil is loaded by superimposed fill, the small air content and the virtual imperviousness of the soil preclude (through the mechanism of pore pressure) the development of effective stress and frictional shearing resistance without affecting the shearing stresses induced by the loading. There are two apparent methods of correcting this condition in impervious soils: (*a*) Lessen the compactive effort and obtain larger quantities of air in the soil prior to loading and (*b*) control the moisture content so that an appreciable quantity of air remains in the soil after it has been compacted to a high density. The USBR has used the latter method successfully. The fallacy of the former method is that the compressibility of the soil (indicated by the relationship between volume change and effective stress) is greater for initially low-density soils than for initially high-density soils; hence, pore-pressure development may be facilitated despite the increase in air volume. The relationship of air content and compressibility to pore pressure is given by Eq. 1 for unsaturated soil under the condition of no drainage (35), provided that $\Delta \leqq V_a$:

$$u = \frac{u_a \, \Delta}{V_a + h \, V_w - \Delta} \quad \text{(1)}$$

in which u_a is the initial pore pressure (usually considered as atmospheric pressure); V_w denotes the volume of water in the soil, in percentage of initial total soil volume; h indicates the capacity of water to dissolve air by volume, from Henry's law (0.02 at 20° C); V_a is the initial volume of free air in the soil mass, in percentage of total initial volume; Δ denotes the volume change, in percentage of total initial soil volume (compression is considered positive); and u is the developed pore pressure (gage pressure).

Eq. 1 shows that the pore pressure of an impervious soil at a constant water content increases as compressibility increases and as the air content decreases. Decrease in density of some soils at a constant water content may result in sufficient air to overcompensate for their increased compressibility, which would account for strength results similar to those obtained by the author. In most soils used for dam embankments, the increase in compressibility would be most significant; pore pressures would increase and strength would decrease, which would account for the test results on the soil from the vicinity of Vallecito Dam. However, for the virtually sealed condition that exists in the impervious core of a rolled-earth dam during construction, the pore-pressure formula strongly indicates the desirability of controlling the water content and of using heavy compaction to obtain both appreciable air content and low-volume compressibility of the placed soil. The treatment of expansive clays in the subgrades of lightly loaded structures must be clearly distinguished from the placing of nonexpansive clays in earth dams where the confining stresses are high. The possibility of reducing compaction in the former case has been considered by the USBR to reduce swell under canal linings (36).

The method of triaxial-shear testing and interpreting test results described in a paper (33) by A. A. Wagner is based on effective stresses; pore pressures are measured, and a true angle of internal friction is determined from the Mohr strength envelope. This method requires estimating pore pressures in the prototype in order to determine the stability of rolled-earth dams. The pore pressures are obtained from the flow net for the steady-state seepage condition and are estimated by the use of Boyle's law and Henry's law and by consolidometer tests for the construction condition (35). Although it is based on assumptions which only approximate field conditions, this procedure is both simple and practicable. Improvements in testing techniques and in analysis are progressing. On the other hand, practical application of the author's proposal stated in his conclusion No. 4 seems to demand too much of theoretical soil mechanics. Prediction of the void ratio at failure in an unsaturated clay embankment from given placement conditions appears to require a solution of the stress distribution in the embankment in addition to a prediction of the variation of pore pressures with time and space.

Despite the relationship shown by the author, satisfactory interpretation and application of the results of triaxial-shear tests on unsaturated cohesive soils cannot be made without considering the stresses in the pore fluid of the soil mass. The effective Mohr strength envelope and its inclination, the true angle of internal friction, satisfactorily explain the mechanism of shear failure in all unsaturated soils. This information can be obtained by proper test procedures and is relatively easy to apply in design. Although the author's plot of void ratio at failure against shearing strength can be used in conjunction with the Mohr envelope as an additional check on test results, it is not a satisfactory substitute for the envelope.

JAMES K. MITCHELL,[5] J. M. ASCE.—The author is to be complimented on his detailed investigation and well-written paper. The author's conclusion No. 1,

> "* * * the pattern of strength variation for partly saturated, compacted clays can be represented by a relationship between the void ratio at failure * * * and the * * * compressive strength * * * [for] a specified set of initial conditions * * *"

is not entirely correct. Because the test results reported are for partly saturated, compacted, and then consolidated clays, the actual strength characteristics of a compacted clay as such are not apparent. The author has found—not only with specified initial conditions but also with a specified manner of obtaining the initial conditions—that the logarithm of the strength varies with the void ratio at failure for a consolidated soil. This relationship has been known to be true for saturated soils for many years, and more recent investigations have indicated that it probably holds true for partly saturated soils as well. The author's results serve as further evidence that it does. In each test series all samples were consolidated from the same initial void ratio and water content, as obtained by static compaction. The initial structures of all samples in a particular series were therefore the same, and the test results (Figs. 11 through 19) represent the effect of consolidation on strength—not that of compaction—because, in reality, the compaction only served to impart a certain initial undisturbed structure to the soil.

The actual relationships between the strength of compacted soils and the method of compaction, the density, and the molding water content cannot be drawn from the author's tests. With the exception of the samples in test series No. 5 on the modified Mississippi loess, all samples were compacted with a static load at the optimum water content for standard Proctor compaction. Thus, the location of these samples on a static compaction curve corresponding to the static compactive effort used is not known. The method of compaction, the density, and the molding water content all determine the particle-to-particle relationships, or structure, of the soil.

The importance of the influence of soil structure on the strength has not been mentioned by the author; however, it has been found of primary importance by other investigators. The superiority of consolidation over compaction in increasing strength by decreasing void ratio as shown in Fig. 14 and Fig. 19 can be explained in terms of soil structure. More specifically, in this case the effect of duration of load is probably most important; in a consolidating system the load acts continuously, and there is greater opportunity for close particle approach at a given void ratio than when the load acts for only a short time.

---

[5] Research Assistant, Soil Stabilization Lab., Dept. of Civ. and San. Eng., Massachusetts Inst. of Technology, Cambridge, Mass.

Structural effects in compacted soils were noted at the Waterways Experiment Station (37) (38); it was concluded that structure is significant enough to warrant listing among the primary variables. Shou-I Tsien, A. M. ASCE (39), investigated structure in detail and found, as did the Waterways Experiment Station, that not only does a "dry-side" sample (compacted at a water content less than optimum) have a high strength explainable only in terms of an "additional structural strength," but also—if a dry-side sample is soaked to a water content equal to that of a "wet-side" sample (compacted at a water content greater than optimum) at the same void ratio—that it still has a higher strength than the wet-side sample. Mr. Tsien found that a dynamically compacted, soaked sample has approximately 1.25 times the strength of a statically compacted, soaked sample at the same void ratio; Joseph B. Eustis and John L. McRae, Associate Members, ASCE (38), found the strength of dynamically compacted, soaked samples to be 2.5 times that of statically compacted, soaked samples. Thus, there can be little question that the method of compaction influences strength. This fact did not emerge in the author's investigation because all samples were compacted statically at a particular water content. It is felt, however, that a description of the compaction method should be included with the "given initial conditions" when curves of the nature of those in Figs. 11 through 19 are considered.

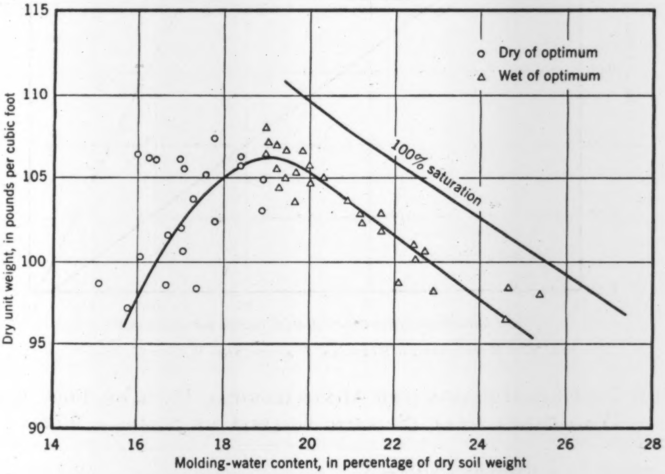

Fig. 26.—Harvard Miniature Compaction Data

Data showing the effect of structure on strength have been obtained by the writer and are given in Table 8 and Figs. 26, 27, and 28. For these tests a sandy clay from Fort Belvoir, Va., was used; properties of this soil (based on the No. 10 sieve fraction) are listed in Table 7. Samples were compacted by means of the Harvard Miniature Compaction Apparatus (kneading compaction), developed by Stanley D. Wilson, A. M. ASCE (40). They were extruded and tested immediately in unconfined compression. Fig. 26 relates density to molding water content. Fig. 27, in which compressive strength is plotted against molding water content, shows decreasing strength of the clay with increasing water content. Although no good correlation exists between axial strain at failure and either water content or strength, the data in Table 8 indicate a tendency toward an increase of the axial strain at failure with increasing water content and decreasing strength.

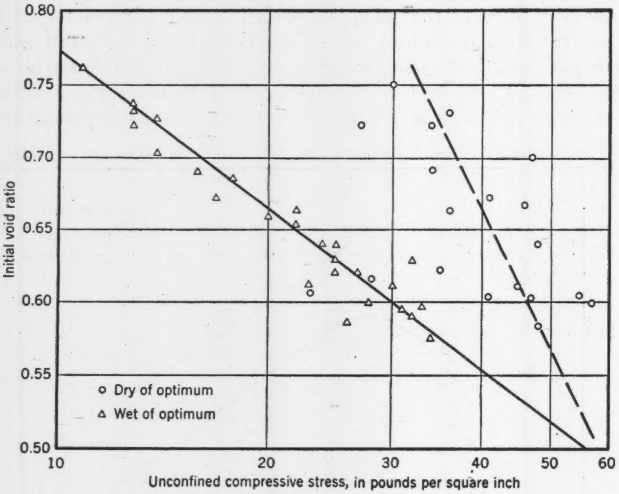

FIG. 27.—RELATIONSHIP BETWEEN STRETCH AND WATER CONTENT

TABLE 7.—CLASSIFICATION AND MINERALOGICAL DATA ON FORT BELVOIR (VA.) SANDY CLAY (SPECIFIC GRAVITY OF SOLIDS = 2.72)

Grain-size distribution		HARVARD MINIATURE COMPACTION		Atterberg limits[a]		Mineralogical composition[a,b]	
		Optimum moisture content[a]	Maximum dry unit weight[c]				
D_{60}	0.20 mm			Liquid limit	45	Kaolinite	35[d]
D_{10}	0.02 mm			Plastic limit	21	Hydrous mica	9
$\frac{D_{60}}{D_{10}}$	10			Plasticity index	24	Montmorillonite	9
		19.0	106			Quartz	40
						Free iron oxide	3

[a] In percentage. [b] No. 140 sieve fraction equals 50% of total. [c] In pounds per cubic foot. [d] Random stratification.

In Fig. 28, in which initial void ratio is plotted against the logarithm of unconfined compressive strength, a very interesting relationship may be noted. (Values determined from samples compacted at, or at wetter than, optimum water content are represented by triangles, and values for samples compacted when drier than optimum moisture content, by circles.) Fig. 28 shows a linear relationship between the initial void ratio and the logarithm of unconfined compressive strength for samples molded above optimum water content. No such relationship exists for those samples molded below an optimum water content. The scatter of dry-side points is probably the result of minor variations in compaction procedure because, in these and other tests, dry-side samples have been noted to be very sensitive to procedure when the Harvard Miniature Compaction Apparatus is used. Even so, there is little reason to expect a direct correlation between void ratio and strength or between water content and strength for dry-side samples because structure cannot, at this time, be expressed by any single parameter. Concepts suggested by T. William Lambe, A. M. ASCE (41), and current investigation at the Massachusetts Institute of Technology lead to the conclusion that structure in a given soil is a function of capillary tensions, water-adsorption characteristics, the nature of adsorbed cations, particle orientation, and interparticle spacing. It is most likely that at wetter than optimum water contents the amount of water present leads to appreciable pore pressures during compaction and a marked reduction in capillary tensions with the result that orientation tends to become somewhat constant, and particle spacing (which can be conveniently expressed by void ratio) becomes the controlling variable.

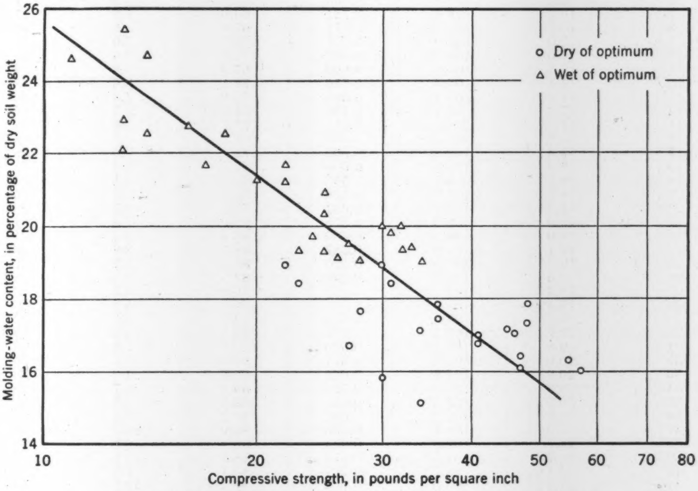

FIG. 28.—RELATIONSHIP BETWEEN STRENGTH AND VOID RATIO

In all probability, if the data in Fig. 28 had been plotted against void ratio at failure, the scatter would have been reduced. It has long been recognized that the failure void ratio has much more theoretical justification than the initial void ratio in all strength studies; however, failure void ratio is a particularly difficult property to measure. The consolidation pressure or the initial void ratio must be used in most investigations. Although the procedure developed by the author for a volume measurement at failure (described under the heading, "Apparatus, Techniques, and Procedures: Determination of Void Ratio at Failure") was satisfactory for his tests, such a procedure would not be possible for the dry-side samples reported in Fig. 28, the failures of which were accompanied by splitting and crumbling of the samples. Initial and final void ratios were probably approximately equal for the dry-side samples as strain at failure was small.

TABLE 8.—SUMMARY OF TEST RESULTS, FORT BELVOIR (VA.) SANDY CLAY

Test No.	Molding water (%)	Dry density[a]	Initial void ratio	Saturation (%)	Axial strain (%)	Compressive strength[b]
1	15.1	98.7	0.721	59.1	2.0	34
2	15.8	97.2	0.750	57.4	1.4	30
3	16.0	106.4	0.599	72.6	4.1	57
4	16.1	100.1	0.700	62.6	2.3	47
5	16.3	106.1	0.604	73.5	4.6	55
6	16.4	106.1	0.603	74.0	3.9	47
7	16.7	98.6	0.721	63.0	1.8	27
8	16.7	101.6	0.671	67.6	2.8	41
9	17.0	102.0	0.667	69.3	3.0	46
10	17.0	106.0	0.603	76.6	3.9	41
11	17.1	100.5	0.690	67.5	2.8	34
12	17.1	105.5	0.610	76.1	3.6	45
13	17.3	103.7	0.640	73.0	4.3	48
14	17.4	98.4	0.730	64.9	2.7	36
15	17.6	105.1	0.615	77.7	4.8	28
16	17.8	107.4	0.583	83.5	6.0	48
17	17.8	102.2	0.662	72.1	3.0	36
18	18.4	105.9	0.606	82.5	4.3	23
19	18.4	106.1	0.599	83.4	4.1	31
20	18.9	104.9	0.620	82.9	3.2	35
21	18.9	102.9	0.654	78.5	4.3	22
22	19.0	108.0	0.575	90.0	7.8	34
23	19.0	106.3	0.600	86.4	6.4	28
24	19.1	107.0	0.587	88.3	8.9	26
25	19.3	106.9	0.590	89.0	5.7	32
26	19.3	104.3	0.629	83.5	5.0	25
27	19.3	105.5	0.611	86.0	5.7	23
28	19.4	106.7	0.595	89.0	6.0	33
29	19.5	104.9	0.620	85.3	8.5	27
30	19.7	103.5	0.640	83.6	12.8	24
31	19.8	106.6	0.595	90.5	7.8	31
32	20.0	105.6	0.611	89.0	7.1	30
33	20.0	104.6	0.629	86.8	4.3	32
34	20.3	105.0	0.620	89.1	10.7	25
35	20.9	103.5	0.640	88.5	10.7	25
36	21.2	102.2	0.663	87.2	10.3	22
37	21.2	102.7	0.658	88.0	10.7	20
38	21.7	102.8	0.654	90.3	10.0	22
39	21.7	101.7	0.671	88.0	12.8	17
40	22.1	98.7	0.721	83.1	7.5	13
41	22.5	100.0	0.703	87.3	12.1	14
42	22.5	101.0	0.685	89.5	12.8	18
43	22.7	100.7	0.690	89.9	9.2	16
44	22.9	98.2	0.732	85.4	11.4	13
45	24.6	96.5	0.761	87.9	10.7	11
46	24.7	98.5	0.727	92.5	12.8	14
47	25.4	98.0	0.737	94.0	12.8	13

[a] In pounds per cubic foot. [b] In pounds per square inch.

The results in Fig. 28 agree with Mr. Tsien's findings and show that there is additional structural strength present in dry-side samples that cannot be explained on the basis of the initial or final void ratio, the water content, or the degree of saturation. At the present time only general, qualitative explanations can be given for this phenomenon, but it is hoped that, as more information about the fundamental nature of soil becomes available, quantitative explanations will be possible.

The following suggestions are made:

1. The author's paper be viewed as concerning the strength properties of compacted and then consolidated soil, with conditions prior to consolidation strictly defined.
2. The effect of structure on the strength of compacted soils not be neglected. Structure, which is a function of soil composition, adsorbed water characteristics, adsorbed cation types, water content, particle orientation, and particle spacing, is much more important in dry-side samples than in wet-side samples.
3. A more accessible property than failure void ratio be sought for the purpose of correlating strength results.

PRESTON T. BENNETT,[6] M. ASCE, AND PAUL E. WOHLT,[7] A. M. ASCE.—The test data presented in this paper constitute a significant contribution to knowledge of the shearing strength of clays. However, the conclusions that have been drawn from the tests may be questioned by those who prefer to interpret the data in terms of the Coulomb hypothesis and the Terzaghi theory of consolidation. It is the purpose of this discussion to show how at least part of the data can be analyzed in accordance with those basic ideas. Series No. 4 has been chosen for this discussion because in this series four different specimens were consolidated under confining pressures for widely varying periods of time prior to the shear test. A plot of the change in void ratio against time is shown in Fig. 29. By geometrical methods, an exponential curve has been fitted to these four points to obtain an estimate of 0.191 as the ultimate change in void ratio which would correspond to full consolidation under the load increment of 2.81 kg per sq cm. No attempt has been made to fit the initial air-void compression to the Terzaghi theory, but it has been assumed that the average rate of change of void ratio, after initial rapid compression, is proportional to the remaining consolidation. This simple assumption agrees closely with the Terzaghi theory for values of average consolidation in excess of 20% (7).

After determining in this manner the change in void ratio corresponding to an intergranular stress increment of 2.81 kg per sq cm, the next step is to estimate intergranular stresses for the intermediate void ratios at which these four shear tests were begun. The assumption of a linear relationship between void ratio and pressure, although customarily used to simplify consolidation theories, would not be consistent with the extremely precise tests methods used. Mr. Rutledge (24) has shown that the curve relating void ratio (or moisture content) to the logarithm of shearing strength is parallel to the consolidation curve for saturated clays. An assumption similar to Mr. Rutledge's finding was made in this case, which is equivalent to the Coulomb hypothesis of a constant ratio between normal and shearing stresses at failure.

---

[6] Chief, Soils, Geology and Materials Branch, Missouri River Div., Corps of Engrs., U. S. Dept. of the Army, Omaha, Nebr.

[7] Civ. Engr., Missouri River Div., Corps of Engrs., U. S. Dept. of the Army, Omaha, Nebr.

It is impossible to construct a semilogarithmic curve relating pressure and void ratio and having zero pressure as the lower limit of the 2.81-kg-per-sq-cm increment under consideration. There are two alternatives for avoiding this impasse. One is to use linear plots (Fig. 30), shaping the synthetic curve in such a manner that its slope is everywhere proportional to that of the observed void ratio-compressive strength curve. In Fig. 30, Curve A represents the relationship between the effective intergranular stress and the change in void ratio, Δe, and Curve B, the relationship between the compressive strength and Δe. The second method is to accept the hypothesis that effective intergranular stresses consist of two parts, one of which depends on the past consolidation or compaction history of the material and the other being a function of the applied external load and its duration. This hypothesis is wholly equivalent to the concept of cohesion. Computation readily shows that the addition of an intrinsic effective stress of 0.97 kg per sq cm to the applied stress increment of 2.81 kg per sq cm yields a synthetic consolidation curve parallel to the curve which relates void ratio and compressive strength. The computation for Fig. 31 is as follows: $\frac{2.81 + \sigma_o}{0 + \sigma_o} = \frac{11.20}{2.88} = 3.89$; hence, $\sigma_o = \frac{2.81}{3.89 - 1} = 0.97$. The values 11.20 and 2.88 are taken by extrapolation from the relationship between the void ratio and shear strength (Curve I, Fig. 31). The synthetic curve relating void ratio and effective pressure is shown by Curve II. As previously

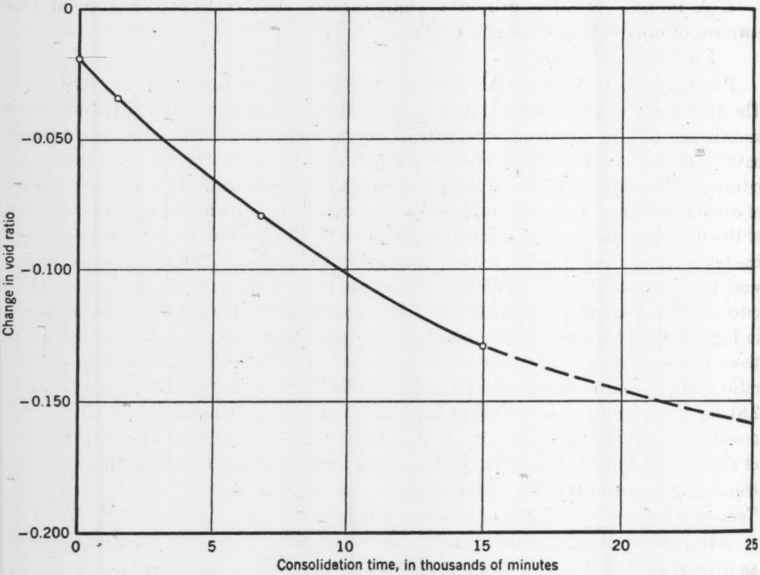

FIG. 29.—CHANGE IN VOID RATIO WITH TIME FOR SERIES NO. 4, FORT UNION CLAY (σ_3 = 2.81 KG PER SQ CM)

stated, the method used in constructing Curve II is mathematically analogous to the a priori assumption that the Coulomb hypothesis is applicable. For any void ratio, Curve II defines $(\sigma_o + \sigma_{III})$, the effective minor stress, and Curve I defines $(\sigma_1 - \sigma_3)/2$, the maximum shear stress at failure. In these expressions, σ_1 and σ_3 are the total externally applied stresses, and σ_{III} represents that part of σ_3 which has become effective through consolidation. Assuming no change in effective stress during the quick-shear test, Fig. 31 indicates a constant ratio between the effective minor stress and the maximum shear stress: $\frac{\sigma_o + \sigma_{III}}{(\sigma_1 - \sigma_3)/2} = 0.675$. This ratio, which does not vary with void ratio, determines ϕ as follows:

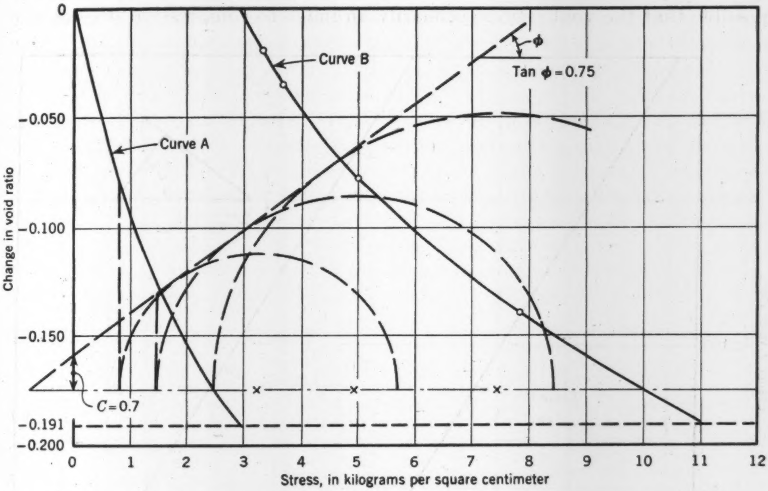

Fig. 30.—Arithmetic Plots for Estimating Effective Intergranular Stresses, Series No. 4, Fort Union Clay (σ_3 = 2.81 Kg per Sq Cm)

$$\sin\phi = \frac{(\sigma_1 - \sigma_3)/2}{\frac{\sigma_1 - \sigma_3}{2} + \sigma_o + \sigma_{III}} =$$

$$\frac{1}{1 + 2\,\frac{\sigma_o + \sigma_{III}}{\sigma_1 - \sigma_3}} = 0.596$$

$$\tan\phi = 0.74.$$

The numerical value of cohesion is determined as follows: $c = \sigma_o \tan\phi = 0.72$ kg per sq cm.

Nearly identical results are obtained if the synthetic relationship between pressure and void ratio is determined by the first of the foregoing methods.

If that procedure is used, c and $\tan\phi$ can be determined by constructing the Mohr diagram (Fig. 30) without the predetermination of σ_o, the hypothetical built-in stress.

The purpose of this discussion has not been to evaluate c and ϕ numerically but to illustrate what is considered to be the physical significance of the relationship between void ratio and shearing strength. It is believed that void ratio is simply an index to the effective intergranular stresses in the soil structure at any time. For the materials and test methods of Table 2, it appears possible that the void ratio is primarily an index to compressive stresses, and that the shearing stresses were of such short duration that they had little effect on the void ratio or on the normal stresses acting on the planes of maximum shear. Furthermore, it seems that the time rate of change of void ratio and effective stress is consistent with the principles of the Terzaghi theory of consolidation, if not with its quantitative details. Considering the fact that several approximations are justifiably introduced into the consolidation theory for the purpose of simplifying its mathematical aspects, one should not expect quantitative agreement.

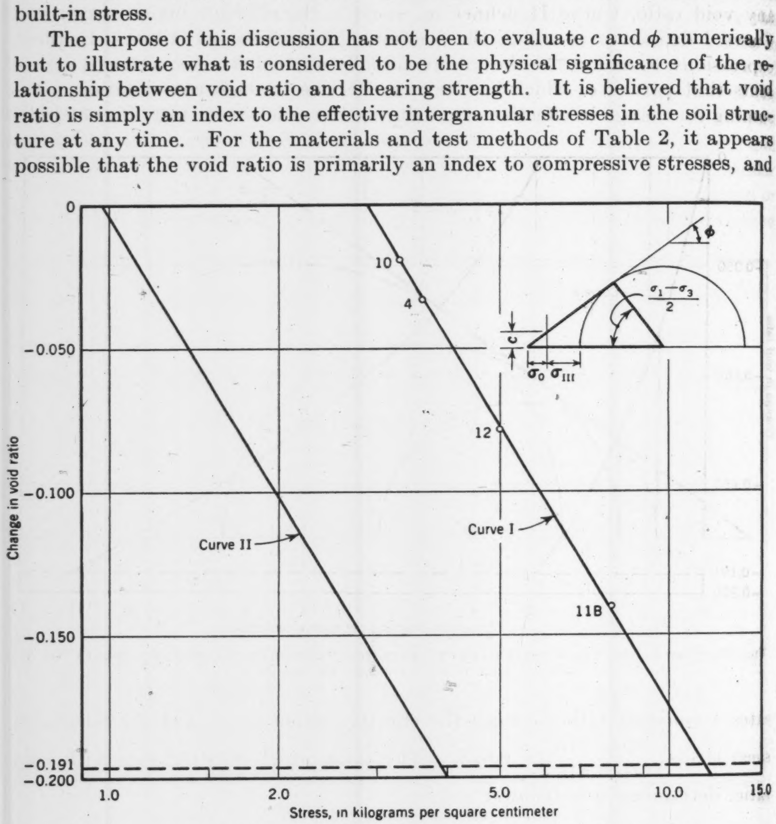

Fig. 31.—Semilogarithmic Plots for Estimating Effective Intergranular Stresses, Series No. 4, Fort Union Clay ($\sigma_3 = 2.8$ Kg per Sq Cm)

Mr. Leonards' unique relationship between void ratio and shearing strength is thus a logical consequence of the retention of the Coulomb hypothesis, modified to account for effective stresses rather than applied stresses. Mr. Rutledge's correlation between moisture content and compressive strength for saturated clays seems also to follow from the Coulomb hypothesis. There is nothing original or unique in these opinions, which only reflect two classic ideas of soil mechanics.

As for the numerical aspects of the writers' interpretation of the tests, it is admitted that numerical precison is lacking. Only in Series No. 4 of Table 2 are there sufficient differences in the duration of consolidation to permit an approximate evaluation of intergranular pressures at the end of the period of partial consolidation. Most of the tests on Fort Union clay are considered to be close approximations of "Q" tests, notwithstanding their "Qc" label. By coincidence, this series is also one in which the shearing of the specimens caused little or no change in void ratio. In this connection it is noted that the author's "void ratio at failure" is actually the void ratio after failure and after removal of all externally applied loads. In the case of the Fort Union material in Series 4, it appears probable that actual void ratio in the failure zone during shear failure was not significantly different from the void ratio after partial consolidation and also after failure and unloading. This probability suggests that void ratio in this particular series of tests may be regarded as a sort of "strain gage" for measuring compressive stresses during shear. For other materials and for other rates of application of the shearing stresses, it is very doubtful that such a simple assumption is valid. For example, one would expect the void ratio of the Mississippi loess specimens of Series No. 1 and No. 2 in Table 3 to respond fairly rapidly to any change in stress conditions because of their relatively large air-void ratios. As another example, one might expect the void ratio of the Fort Union material in Series No. 4 to be responsive to loads applied during shear testing if the rate of application were sufficiently slow. Thus, in the general case, the relationship among compressive stress, shearing stress, void ratio, and time may not be fully represented by the simple diagram of Fig. 31.

TABLE 9.—SUGGESTED TEST PROGRAM

APPLIED TOTAL STRESSES, IN KILOGRAMS PER SQUARE CENTIMETER				Time, in minutes, for systematic determination of the void ratio				
σ_1	$\sigma_2 = \sigma_3$	Mean compressive stress	Shear stress					
3.0	3.0	3.0	0.0	0	1,440	2,880	5,760	→ To at least 90% consolidation
3.4	2.8	3.0	0.3	0	1,440	2,880	5,760	
3.8	2.6	3.0	0.6	0	1,440	2,880	5,760	
4.2	2.4	3.0	0.9	0	1,440	2,880	5,760	
			↓ To failure					

It is believed that these relationships could be successfully investigated using Mr. Leonards' laboratory techniques. One might begin with a series of initially identical specimens, carefully prepared according to the author's techniques, and slowly trace the void-ratio changes due to triaxial compression—

experimentally determining these changes in terms of applied stress, time, and effective stress as derived from consolidation theory. Following this calibration of void ratio as a "strain gage" for measurement of pure compressive stresses, a second series of tests could be performed into which shearing stresses would be introduced while retaining the same mean applied compressive stresses in successive comparative series. As a more specific example, a unit group of tests on a material such as the Fort Union clay in Series A is suggested in Table 9. Although such a group of tests obviously entails an enormous amount of work corresponding to a single value of mean compressive stress, it should be worth the effort as it might positively indicate whether shearing strength can rationally be predicted on the basis of the Coulomb and Terzaghi theories.

Mr. Leonards' tests certainly established a relationship between maximum shearing stress and void ratio after the failure and unloading of the sample. The writers would emphasize, however, that void ratio is the result, not a cause, of stresses. Fig. 32 illustrates this viewpoint. It is a schematic curve relating pressure and void ratio for two materials identical in composition and moisture content in the loose state prior to compaction by static load. Pressures are partial effective intergranular stresses, as distinguished from applied pressures. The term "partial" here excludes any hypothetical effective stresses locked into the material by prior load applications. Specimen A is subjected to an unknown consolidation for an unknown period of time, resulting in an effective pressure and void ratio indicated in Fig. 32 by the point (p_a, e_{a1}). The load is removed, and the material rebounds to zero applied load and void ratio, e_{a2}. Specimen B is subjected to similar treatment, except that the intensity and duration of the static compaction load result in a lower void ratio after rebound, e_{b2}, as indicated in Fig. 32.

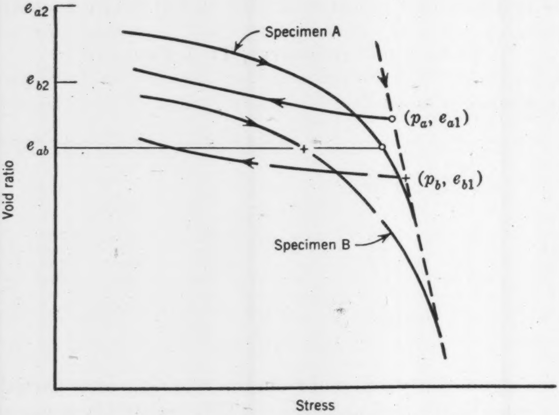

Fig. 32.—Schematic Curve Relating Pressure and Void Ratio

The two specimens are next consolidated by an appropriate combination of load intensity and duration to an identical void ratio, e_{ab}, shown in Fig. 32. Obviously, the effective applied stress necessary to achieve this common void ratio is ordinarily greater for specimen A than for specimen B. Consequently, if the concept of friction is retained, the frictional component of the strength of specimen A would be expected to be greater than that of specimen B. Similarly, because the frictional component with respect to effective intergranular stresses tends to be much greater than the "cohesion" component, one would also expect the total strength of specimen A to be greater than that of specimen B at the same void ratio. Finally, the effective stresses on the two specimens approach equality as the selected common void ratio is lowered, and the two recompression curves approach the common virgin consolidation curve. Referring to Figs. 14 and 19, it is seen that the tendency toward convergence of the curves relating strength and void ratio is apparent as the void ratio is decreased and as the effective confinement of the test specimen is increased.

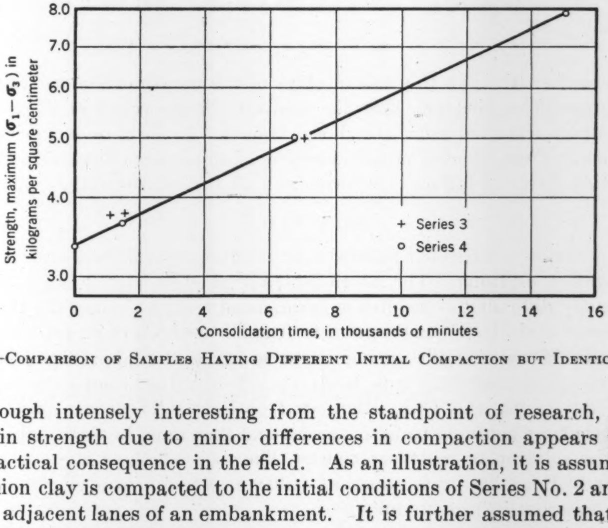

FIG. 33.—COMPARISON OF SAMPLES HAVING DIFFERENT INITIAL COMPACTION BUT IDENTICAL LOADS

Although intensely interesting from the standpoint of research, the difference in strength due to minor differences in compaction appears to be of little practical consequence in the field. As an illustration, it is assumed that Fort Union clay is compacted to the initial conditions of Series No. 2 and Series No. 4 in adjacent lanes of an embankment. It is further assumed that, as the embankment is raised, the two lanes are subjected simultaneously to identical applied loads, which impose shearing stresses and compressive stresses in the field in the same manner as the stresses were imposed in the laboratory in those tests in which the confining pressure was 2.81 kg per sq cm. To the extent that laboratory tests are applicable to field conditions, Fig. 33 shows what may be expected. The potential shearing strength is increased with time as the two materials are consolidated and effective stresses are increased. At any time that the consolidation process is interrupted by shearing failure, the strength is nearly identical for the two materials. If, during construction of the hypothetical embankment, the contractor were paid additional money to obtain a dry density of 99 lb per cu ft instead of 97 lb per cu ft, this would be a case of economic overcompaction. If the two densities were obtained at the same price, there would be no cause for alarm.

In summary, profound admiration must be paid to the precise laboratory methods used in the investigation. At the same time, it is necessary to express disagreement with nearly all the conclusions and implications drawn by Mr. Leonards. It is believed that the correlation among void ratio, moisture content, and similar variables has been overemphasized in the paper and by other investigators.

The maximum shearing stress of a soil can be closely approximated by the expression,

$$s = c + n \tan \phi \qquad (2)$$

in which c is a function of the entire past stress-strain-time history of the material, n is a function of time and the total stresses externally applied to the material, and $\tan \phi$ is a variable with such a small range of values that it can be considered a constant. It is also believed that the void ratio can be defined approximately by

$$e = F_1 (\sigma_1, \sigma_2, \sigma_3, t) \qquad (3)$$

with some reservations in the case of clays of the montmorillonite type. The latter expression implies only that the void ratio is the result of all stress conditions that have existed prior to a chosen time, t. If the chosen time coincides with failure in shear, there is clearly a relationship between void ratio at failure and shearing stress at failure. It happens that the relationship,

$$s_{\text{max}} = F_2 (e_f) \qquad (4)$$

in which e_f is the void ratio at failure, can readily be established experimentally under certain conditions. The relationships implied by Eqs. 2 and 3, however, are extremely difficult to establish experimentally, even though the theories of Mr. Coulomb and Mr. Terzaghi point to fruitful methods of investigation. In the majority of cases, as the author seems to agree, the laboratory solution of Eq. 4, although undoubtedly true, is of no practical value because the important variables σ_1, σ_2, σ_3, and t are eliminated entirely. These are precisely the variables that are common to Eqs. 2 and 3 and that must be dealt with in some form in the solution of most problems. The true worth of the experimental evaluation of Eq. 4 lies in its apparent utility as a tool in studying the difficult problems inherent in Eqs. 2 and 3.

GERALD A. LEONARDS,[8] A. M. ASCE.—The writer is indebted to Mr. Mitchell for directing attention to the important effects of soil structure on the strength characteristics of compacted clays. It was not intended to minimize the significance of soil structure. On the other hand, the variables that can profitably be investigated in any one study are limited in number. Accordingly, it was decided to consider the effects of applied stresses—with or without precompression—and the effects of adding water from an external source. For this purpose accurate duplication of initial water content, void ratio, and soil structure was required; when this was accomplished, the samples were said to have a "given set of initial conditions." Because the data presented cover a broad range of drainage conditions and stress history, the results are considered to be generally valid provided that the initial conditions were duplicated.

---

[8] Associate Prof. of Soil Mechanics, School of Civ. Eng., Purdue Univ., Lafayette, Ind.

Mr. Mitchell suggested that a more accessible property than the failure void ratio be sought for the purpose of correlating strength results. At the present time the only alternative seems to be the determination of pore pressures. The relative "accessibility" of the two types of measurements is largely a matter of the investigator's personal preference.

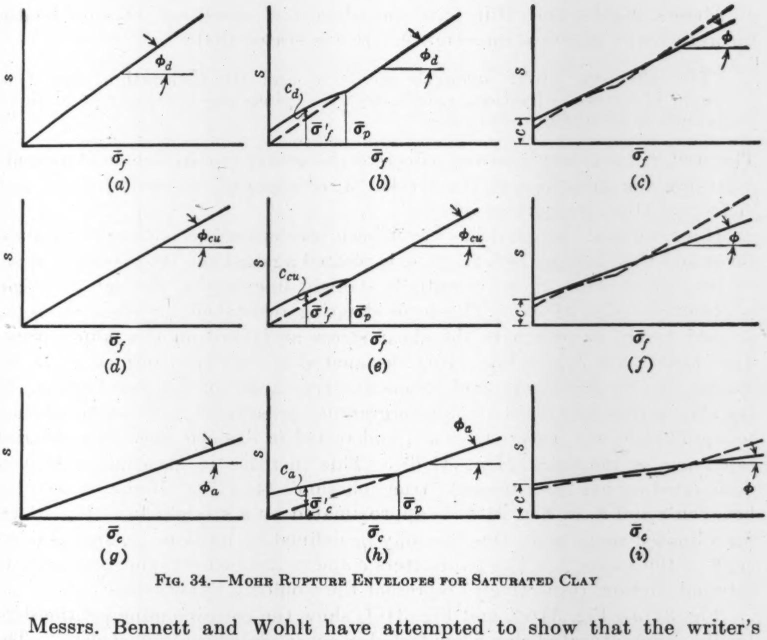

FIG. 34.—MOHR RUPTURE ENVELOPES FOR SATURATED CLAY

Messrs. Bennett and Wohlt have attempted to show that the writer's data could be interpreted in the light of the Coulomb hypothesis and the Terzaghi theory of consolidation. In their discussion it was assumed that (*a*) volume changes do not occur during shear testing, (*b*) the Terzaghi theory of consolidation is valid for unsaturated soils, and (*c*) the curves relating void ratio and compressive strength are parallel to the consolidation curves. Fig. 22 shows that important volume changes do occur even in "undrained" shear, and, although actual relationships were not plotted, the writer's data do not show the compressive strength curves to be parallel to the consolidation curves. Furthermore, if the degree of saturation is less than approximately 90%, the Terzaghi theory of consolidation no longer reflects—even approximately—the pore pressures in the soil mass. Thus, although the interpretations suggested by Messrs. Bennett and Wohlt may be satisfactory for Series No. 4 of the tests of the Fort Union clay (for which the initial degree of saturation was approximately 95%), the general validity of their approach is seriously questioned.

Messrs. Bennett and Wohlt are correct in explaining that the failure void ratios reported are actually the void ratios after failure and removal of all externally applied loads. Were it possible to measure the void ratios in the failure zone prior to removing the applied stresses, the absolute position of the curves presented would undoubtedly be altered—particularly in the region of high confining pressures—but this fact detracts little from the validity of the stated conclusion.

Messrs. Gibbs and Hilf have raised several questions of considerable theoretical and practical importance. It was stated that:

> "The effective Mohr strength envelope and its inclination, the true angle of internal friction, satisfactorily explain the mechanism of shear failure in all unsaturated soils."

The writer disagrees; however, effective discussion requires some statements regarding the meanings of the terms, "true angle of internal friction" and "effective Mohr strength envelope."

If a saturated clay that has never been precompressed is tested in drained shear and the shearing resistance, *s*, is plotted against the intergranular stress on the failure plane, $\bar{\sigma}_f$, an essentially straight line passing through the origin is obtained (Fig. 34(*a*)). The term shearing resistance (or shear strength) is used herein to designate the shear stress at failure on the failure plane. The slope of the line in Fig. 34(*a*), designated ϕ_d, has been termed by D. W. Taylor, A. M. ASCE (4), and others the true angle of internal friction. If the clay is precompressed at an intergranular pressure $\bar{\sigma}_p$, allowed to rebound to equilibrium at a lower stress $\bar{\sigma}'_f$, and tested in drained shear, the shearing resistance is increased (Fig. 34(*b*)). This increase in shearing resistance, designated c_d, has been termed "true cohesion" (4) (17). If the relationship between s and $\bar{\sigma}_f$ in Fig. 34(*b*) is approximated by a straight line (Fig. 34(*c*)) for a limited range of $\bar{\sigma}_f$, this line may be defined by its slope, ϕ, and its intercept on the s-axis, c. The parameters c and ϕ (termed cohesion and angle of internal friction, respectively) represent the Coulomb hypothesis.

Fig. 34(*d*), Fig. 34(*e*), and Fig. 34(*f*) show the corresponding relationships for the same saturated clay when tested in consolidated-undrained shear. The slope of the straight-line part of the Mohr envelope is designated ϕ_{cu}, and the increase in shearing resistance due to precompression, c_{cu}. Because pore-pressure measurements are required to define these envelopes, few reliable data of this kind are actually available. It has not been established that ϕ_d equals ϕ_{cu} or that c_d equals c_{cu}, but it is evident that the Coulomb values of c and ϕ are not equivalent to either of the other parameters. In their discussion, Messrs. Gibbs and Hilf have termed ϕ_{cu} the true angle of internal friction, but the Coulomb c-value was called cohesion. Although this approach lacks consistency, it will be shown later that it has considerable practical utility. One fact should be emphasized at this point: ϕ_{cu} is not a constant for a compacted soil but varies widely with the degree of compaction and the molding-water content. The selected data presented by Messrs. Gibbs and Hilf do not reflect the wide variation in ϕ_{cu} usually encountered (33).

Fig. 34(*g*), Fig. 34(*h*), and Fig. 34(*i*) show the corresponding Mohr rupture envelopes for the same saturated clay that was tested in consolidated-undrained shear, but the shearing resistance s is plotted against $\bar{\sigma}_c$, the normal intergranular stress on the failure plane prior to shear testing. Pore-pressure measurements are not required to define these envelopes. The angle ϕ_a has been termed the "apparent angle of internal friction" (3) and is invariably less than ϕ_d. The "apparent cohesion" c_a, however, is often larger than c_d; thus, the undrained shearing resistance of a highly precompressed soil may be greater than the drained shear strength for low values of $\bar{\sigma}_c$. Finally, for low values of $\bar{\sigma}_c$ compared to $\bar{\sigma}_p$, the Coulomb ϕ-value approaches zero, and the undrained shearing resistance can be approximated by one half the unconfined compressive strength regardless of the magnitude of the externally applied stresses. It is clear that the Coulomb values of c and ϕ are merely convenient coefficients suitable for defining strength characteristics for an arbitrary set of stress and drainage conditions. If the stress history and drainage conditions are not specified, the Coulomb coefficients can be more misleading than helpful.

From a series of classic tests on saturated, remolded, normally consolidated clays, Mr. Hvorslev (22) concluded that, for a constant void ratio at failure, the rate of change of shearing resistance with respect to intergranular pressure on the failure plane was essentially a constant. Thus,

$$\left.\frac{ds}{d\bar{\sigma}_f}\right|_{e_f\,=\,\text{constant}} = \tan\phi_t$$

and ϕ_t was termed the "true angle of internal friction." The remainder of the shearing resistance, termed the "true cohesion" c_d, was found to depend only on the void ratio (or water content) at failure. The angle ϕ_t is smaller than ϕ_d—often considerably smaller. Using Mr. Hvorslev's criterion, the drained shearing resistance would be composed of two parts: $\bar{\sigma}_f \tan\phi_t$ (true friction) and c_t (true cohesion).

When a clay soil is brought to a state of failure in a cylindrical compression test, slip planes are often observed. If at the instant of failure the shearing resistance is the same on all planes through a point in the soil mass, failure would occur along planes of maximum applied shear stress (45° to the major principal plane). If the shearing resistance, s, varies with the effective normal stress, Mr. Terzaghi (12) has shown that for isotropic soils the failure planes should be inclined at $45° + \phi_r/2$ to the major principal plane in which $\tan \phi_r$ is $ds/d\bar{\sigma}_f$. Because the void ratio is the same on all planes through a given point at failure, ϕ_r should equal ϕ_t. By measuring the inclination of the failure planes in undrained compression tests, Mr. Hvorslev (22) demonstrated that this was very nearly the case. The Hvorslev criterion has since been substantiated by a number of investigators, notably L. Bjerrum (42) and R. E. Gibson (43). Mr. Gibson showed that the criterion was also valid for several undisturbed clays. By applying an energy correction to account for the work done by volume changes in the soil mass and by measuring the direction of the slip planes when they first appeared, ϕ_r was found to equal ϕ_t with a high degree of precision. It was also shown that ϕ_t was nearly a constant, decreasing only slightly with increasing water content.

Each of the approaches previously described offers specific advantages depending on the nature of the problem being investigated, and arguments to the effect that any one approach is more fundamental than the others are fruitless. However, in the interest of consistency, the following terminology is suggested:

c = the Coulomb c-value;
c_a = the apparent cohesion;
c_{cu} = the consolidated-undrained shear cohesion;
c_d = the drained shear cohesion;
c_t = the true cohesion;
ϕ = the Coulomb ϕ-value;
ϕ_a = the apparent angle of internal friction;
ϕ_{cu} = the angle of shearing resistance in consolidated-undrained shear;
ϕ_d = the angle of shearing resistance in drained shear; and
ϕ_t = the true angle of internal friction.

The behavior of unsaturated clays is considerably different from that of saturated clays. Although H. C. Woodsum (32) showed that compaction produces an effect similar to precompression in so far as consolidation characteristics are concerned, the data presented by Messrs. Gibbs and Hilf indicate that a comparable curvature in the Mohr rupture envelope does not develop. Studies made at the Norwegian Geotechnical Institute under the direction of Mr. Bjerrum confirm this phenomenon.

According to Mr. Bjerrum, the shearing resistance of clays compacted to a given set of initial conditions can be expressed by

$$s = c + \bar{\sigma}_f \tan \phi$$

in which c and ϕ are constants (approximately) regardless of whether the shear tests are drained or undrained, whether the samples are previously consolidated or not, and whether consolidation is applied isotropically or anisotropically. It is further claimed that, if the sample is consolidated anisotropically, the pore pressures that will develop will be similar to those measured in the field. These statements, if substantiated, will be of outstanding engineering importance because they indicate that the stability of a compacted earthen embankment could be evaluated at all times by means of field pore-pressure measurements.

Investigators in this country may also be interested in learning that the Norwegians have been using the following simple procedure for saturating specimens of compacted clay with considerable success: If it is desired to saturate the sample and to consolidate it at a confining pressure of, for example, 2 kg per sq cm, a chamber pressure of 12 kg per sq cm is applied in the triaxial cell, and simultaneously the water pressure in both porous end plates is raised to 10 kg per sq cm. For such high pressures in the pore water the air is compressed and dissolved until virtually 100% saturation is achieved.

In the writer's opinion, the reliability of pore-pressure measurements obtained during laboratory shear tests on unsaturated clays is open to question. For this reason an important objective of the paper was to demonstrate experimentally that the over-all effects are reflected uniquely in terms of the void ratio at failure (conclusion No. 1). For the test data reported by Messrs. Gibbs and Hilf the degree of saturation ranges between 50% and 90%, and the measured pore pressures agree closely with the values computed from the theoretical equation. Because of their great practical importance, it would be helpful if other investigators could corroborate these results.

The data presented in Fig. 25(*a*) by Messrs. Gibbs and Hilf do not substantiate the writer's third conclusion. The discrepancy may be explained by the fact that in Fig. 25(*a*) the average void ratio at failure is plotted—not the void ratio in the failure zone—or it might be accounted for by the difference between soil structures developed by static compaction and dynamic compaction. Pending further research, it is suggested that this conclusion be viewed with caution.

The strength characteristics of clays are determined by the forces developed between soil particles, between adsorbed atoms and ions, and between solid-liquid-gas interfaces in unsaturated soils. Although the future may look promising, it is still necessary to express the manifestation of these forces in terms of "macroscopic" effects with the result that the properties of clays appear to be complex. A partial list of phenomena, the imperfect understanding of which exemplifies this complexity, is as follows: The changes in strength properties effected by incorporating small amounts of chemicals; the variation of undrained shear strength with the rate of shear; the "threshold" shear strength; peak and "ultimate" shear strengths and their interrelation; deformation rates at constant effective stress (creep); electro-osmotic and electro-chemical hardening effects; and the changes in strength produced by "frost action." Accordingly, the statement that the effective Mohr strength envelope and its inclination satisfactorily explain the mechanism of shear failure in all soils is untenable. Much work remains to be done before any claim to a satisfactory understanding can be made.

AMERICAN SOCIETY OF CIVIL ENGINEERS
Founded November 5, 1852
TRANSACTIONS

Paper No. 2781

SOME ECONOMIC ASPECTS OF WATERWAY PROJECTS

BY HAYWOOD R. FAISON,[1] M. ASCE

WITH DISCUSSION BY MESSRS. DUANE ORR; L. PERRY COOKINGHAM; MARVIN B. MARSH; OWEN G. STANLEY; HERMAN W. SCHULL, JR.; NELS C. MAGNUSON; BRAXTON B. CARR; CYRIL E. CHILDE; FRANCIS J. WILSON AND NEWTON R. GRAHAM; CHARLES L. HALL; JAMES WARREN DAVIS; AND HAYWOOD R. FAISON

SYNOPSIS

The problem of economic feasibility of waterway projects in the United States is studied in this paper, and many of the allegations of malpractice of the Corps of Engineers (United States Department of the Army) are refuted. Evidence is presented to show that the development of inland waterways in this country has in general resulted in traffic increases that more than justify the improvements and that criticism of such development has frequently been founded on unreliable information. Rate-making and other competitive practices among the several forms of transportation are explored in their bearing on waterways economics, and conclusions are drawn. The paper was presented before the Society in 1952.

INTRODUCTION

In 1852, when the Society was founded, inland waterways that had served to open the interior of the country to development were in the heyday of their dominance over the transportation field. However, they were soon to encounter the feeble beginnings of a type of competition that, fostered by liberal financial support and freedom from effective regulation, was to constitute the first successful challenge to their supremacy as avenues of commerce. The railroads, which began as feeders to the waterways, found the easy gradients along the banks of main rivers ideally suited to their extension and interconnec-

---

NOTE.—Presented, essentially as printed here, at the Centennial Convocation, Chicago, Ill., September, 1952, and published in October, 1953, as *Proceedings-Separate No. 318*. Positions and titles given are those in effect when the paper was presented, or when discussions were received for publication.

[1] Arlington, Va.; formerly Chf. Engr.-Economist, Board of Engrs. for Rivers and Harbors, U. S. Dept. of the Army, Washington, D. C.

tion to form trunk lines of their own. The inherent superiority and wider accessibility of rail service was already beginning to make inroads into the high-class passenger and freight commerce of the packet boats. The freedom to practice unlimited discrimination in charging for their services among shippers and localities in competition with the boat lines was laying the foundation for the subsequent annihilation of river transportation and was incidently establishing the inequities of the freight-rate structure that have endured in considerable measure to this day. It was not until thirty-five years later that the first practical steps were taken to protect national commerce in the United States against unrestricted exploitation by the carriers, through establishment of the Interstate Commerce Commission (ICC).

However, federal improvement of the inland rivers for navigation continued to receive legislative sanction on a moderate scale for an additional fifteen years with apparently more consideration being accorded the political than the economic aspects of the projects. It was not until 1902 that Congress[2] created the Board of Engineers for Rivers and Harbors (hereafter referred to as the Board of Engineers) with independent power and obligation to review all examination and survey reports on navigation projects—

> "* * * having in view the amount and character of commerce existing or reasonably prospective which will be benefited by the improvement; the relation of the ultimate cost, both as to construction and maintenance to the public commercial interests involved; the public necessity for the work and the propriety of its construction, continuance or maintenance at the expense of the United States."

The responsibility of the civil engineer does not end with the design and erection of structures which will not fall down, wash out, or cave in. It requires planning and performance to provide for the best, the most efficient, and the most economical use of available capital. If the engineer in public service is to avoid the fixation of public money in nonproductive projects, he must answer satisfactorily not only the question—"will it stand up" but also "will it pay." The people rightfully look to him for guidance in the economics as well as the physics of public works, and the vast majority of engineers engaged in federal development projects are believed to measure up to this standard of of responsibility.

There is no great line of demarcation discernible among the various groups of engineers in the several governmental departments as regards professional training, talent, or principle. Their interests are directed toward different ends, and they have sharp differences of opinion as to the relative importance of their various objectives. These differences are becoming more and more the subjects of wholesome discussion and compromise and are being worked out in regular inter-agency committee meetings. The participating engineers have somewhat the same professional backgrounds and conform to the same engineering standards; except for the more selective screening accorded army officers, they have been trained in the same schools and traditions. In fact, it has been found that the personnel of the various departments are somewhat interchangeable. Under the prevailing circumstances, it is hardly conceivable that one large group should be guilty of all the possible professional shortcomings and misdeeds to the exclusion of all the other similar groups, yet that is what many vociferous critics of the waterways development program would have the public believe.

---

[2] *River and Harbor Act*, approved June 13, 1902, 57th Cong., 2d Session, Section 541, Stat., Title 33, U. S. Code, 372.

This is not to say that no mistakes have been made or that no better methods or tests for soundness of the waterway projects can be devised. Constant practice and experimentation have been improving the techniques of investigating, planning, estimating, and constructing these projects for many years and will continue to do so. The problem of coordinating the various desirable purposes within the national water-resource development program has become increasingly complex, as has the problem of coordinating the various media of transportation into an integrated system while making the best use of the inherent advantages of each medium. These problems have increasingly challenged the best minds of the nation for the past twenty-five years.

ENGINEERS VERSUS ECONOMISTS

During the last quarter of a century there has grown into prominence a branch of the profession of "pure economics" that is attempting to solve all these problems by the application of a number of somewhat abstract and radical theories and a glossary of new words descriptive of the process. Their approach seems to differ from that of the engineers; they rely mainly on reference libraries for their basic information in the absence of first-hand experience or knowledge of the engineering problems involved—that is, practical contact with harnessing of water resources or carrying goods in commercial transportation. For some reason not entirely clear to the writer, this school of economists has singled out and set a vogue for concerted critical attack on all the analytical methods, findings, and accomplishments of the army engineers (Corps of Engineers, United States Department of the Army) in their administration of public works, largely to the exclusion of other groups of engineers similarly engaged. Because these economists are omnivorous readers and diligent transcribers, this critical bibliography has grown into a cumulative flood of censure. Their reports, articles, and books have followed closely upon one another, each author compiling and quoting the allegations of his predecessors, sometimes adding new ones of his own, apparently without any very diligent effort at verification. In some respects they seem to enjoy an astonishing immunity to the impact of cold, hard facts but, because the bulk of their criticisms have gone unanswered by those in a position to refute them, many of the allegations by frequent repetition have gained public currency as facts—more by default than by any proven validity. That this situation is resented by the profession-at-large is indicated by the following excerpts from an editorial:[3]

> "During the past few months no less than three congressional committee attacks and a critical book have been directed against the civil works activities of the Corps of Engineers. * * *
>
> "Silence in the face of these criticisms is not in the national interests, and is, moreover, damaging to the standing of the civil engineering profession. The fact that the criticisms are in many respects unfair and in others not factual makes the silent acceptance of them surprising as well as to be regretted."

---

[3] *Engineering News-Record*, November 29, 1951, p. 21.

The writer's position coincides with the editorial opinion which he accepts as an "ear-to-the-ground" report on the reaction of the civil engineers of the nation. If it is in conflict with the position of representatives of the Corps of Engineers, it can be offered in extenuation that these are the independent views and observations of the writer and do not necessarily imply acquiescence of the Corps of Engineers.

The railroads and their financial backers constitute the principal opposition to waterway development. In view of their competitive position their attitude is natural and logical. Their interests, however, do not necessarily coincide with the public interest, which is the concern of the engineers in charge of waterway development. It is felt that the engineers responsible for the administration of the program of river and harbor development have carried forbearance under invalid criticism too far. The task of refuting some of the most ill-founded allegations has been appropriately dealt with by others.[4,5,6,7,8] There are, however, certain less obvious fallacies familiar to this writer because of his close association with particular phases of the problem that have unjustifiably won popular acceptance merely through unchallenged repetition. The writer's choice of topics has been frankly selective in order that he may dispose of the most flagrant, and hence the most vulnerable, misstatements.

TRAFFIC ESTIMATES

Probably the least warranted, most easily disproved, yet most universal indictment brought against waterway engineers is that of overoptimism in estimating the volume of future water-borne tonnage for proposed navigation improvements. In his monumental work[9] in the report of the Federal Coordinator of Transportation—"Public Aids to Transportation"—the Director of Research, Charles S. Morgan, an eminent transportation economist of exceptionally broad viewpoint, indicated in highly critical statements his belief that most of the tonnage forecasts of the engineers were overestimated. For example, one finds this statement:[10]

> "The commercial canvasses and economic surveys are not nearly critical enough. The Board of Engineers and its staff have not been equipped with trained traffic men and economists to an extent that would assure a sound appraisal of the ever enthusiastic claims of waterway advocates or to make comprehensive independent analyses. The contributions of the Board of Engineers to the engineering phases of waterway improvements and flood control have, of course, been of the highest order, but economic questions having such broad ramifications as a major waterway project require more varied expert talents than have been available."

Again the report states:[11]

> "This skepticism arises from the fact that in many instances these waterways have not developed the volume of traffic which had been anticipated."

---

[4] "Waterway Growth in the United States," by C. H. Chorpening, *Transactions*, ASCE, Vol. CT, 1953, p. 976.

[5] "History and Future of Flood Control," by George R. Schneider, *ibid.*, p. 1042.

[6] "One Hundred Years of Improvement on Lower Mississippi River," by P. A. Feringa and Charles W. Schweizer, *ibid.*, p. 1100.

[7] "Development of the Tennessee River Waterway," by C. E. Blee, *ibid.*, p. 1132.

[8] "American Hydraulic Dredges," by Carl H. Giroux, *ibid.*, p. 1180.

[9] "Public Aids to Transportation by Water," by Charles S. Morgan, U. S. Govt. Printing Office, Washington, D. C., 1939, Vol. III, pp. 206–207.

[10] *Ibid.*, p. 207.

[11] "Public Aids to Transportation," by Charles S. Morgan, U. S. Govt. Printing Office, Washington, D. C., 1940, Vol. I, pp. 48, 52, 79, 115.

The skepticism of the Director of Research was based on a per-ton-mile evaluation of the waterways in 1936 when several of them were still in the construction stage. A comparison of the growth of traffic on six typical waterways from 1936 to 1950 is shown in the following tabulation:

Project	Water-borne ton-mileage, 1936	Water-borne ton-mileage, 1950
Upper Mississippi River	154,130,000	2,220,513,000
Lower Mississippi River	3,477,489,000	13,518,732,000
Ohio River	2,652,870,000	8,800,451,000
Kanawha River	88,381,000	325,747,000
Cumberland River	63,818,000	229,634,000
Illinois Waterway	174,875,000	2,734,327,000
Total	6,611,563,000	27,829,404,000

Although the Federal Coordinator's report[9] was compiled during a period when some of the major waterways were still in the development stage of modernized improvement and insufficient time had elapsed for the attraction of prospective commerce, the remarkable growth of traffic on the waterways during the ensuing years has shown—in contrast to the critics' charge that forecasts of future traffic have been greatly overestimated—that in many instances the forecasts were overconservative, as may be seen from the following tabulation which lists, in ton-miles, the inland traffic on the Mississippi River system:

Year	Ton-miles
1934	5,872,777,000
1939	9,896,943,000
1944	19,004,643,000
1950	30,281,638,000

Nearly all the criticisms of the waterway development program rest on the fallacy, disproved by factual record, that prospective water-borne traffic has not developed as anticipated by the engineers. Notwithstanding the facts revealed by commercial statistics, many of the more recent critics still persist in adhering to the discredited assumptions of the earlier critics, as shown in the following excerpt:[12]

> "The [Illinois] waterway is being enlarged at the expense of the Federal Government, although the traffic using the waterway has thus far been less than expected."

The enlargement operations referred to extended from 1933 to 1939, when the 9-ft channel of the Illinois Waterway was finally secured. In 1930 the Corps of Engineers estimated a prospective volume of freight of 7,500,000 tons annually when water-borne commerce matured. The traffic was only 257,000 tons in 1934 but had reached 7,677,000 tons, or more than the predicted volume, by 1944; in 1947, when the book[12] was released, the traffic had exceeded the volume of traffic forecast by one third. (It had doubled by 1950.) In view of this trend, publication of the quoted passage indicates an astonishing disregard of the facts.

---

[12] "Transport Facilities, Services and Policies," by Emory Johnson, Univ. of Pennsylvania, Philadelphia, Pa., 1947, p. 319.

In another book[13] it is stated:

> "On the whole the Engineers have been overoptimistic in their estimates of waterway traffic. According to a report of the Federal Coordinator (1939) in certain areas it would require more traffic than moves by all agencies of transport combined to bring waterway use up to effective working capacity."

The author also states:[14]

> "The staff of the Board of Investigation and Research, after careful review of waterway use statistics—(1938 and 1940)—concluded that results attained on individual waterways are occasionally better—but more often worse—than predictions contained in the project documents."

These conclusions of the period from 1938 to 1940 were passed along to the public in 1951 as authoritative, with no apparent effort at verification.

A report of the Secretary of Commerce in December, 1949,[15] stated, with regard to reports of the Board of Engineers on waterway improvements:

> "For purposes of this report, no survey has been made to determine whether the anticipated benefits from particular projects have actually materialized, although there is a general impression that, in many cases the traffic which subsequently developed on the waterway was far less than that assumed when the project was recommended."

It is to be regretted that lack of time prevented verification of the popular but threadbare allegations of earlier investigators, which were thus given further impetus.

The office of the Federal Coordinator of Transportation officially ceased to exist in June, 1936, but the report by the director of its Section of Research was finally published in 1939. It was the source of most of the later criticisms of the capacity of the Board of Engineers and its staff to make comprehensive, independent analyses of waterway projects. The "Prefatory Note" to the report acknowledges the outstanding services rendered by eight traffic and transportation specialists and economists on the director's staff. A typical circumstance bearing on criticisms of this kind is that, when the Federal Coordinator's report[16] was published in 1939, three of the eight specialists given this special acclaim by the Director had been members of the staff of the Corps of Engineers for two years. Later, after the Board of Investigation and Research was disbanded in 1944, the services of two of its top transportation economists were also secured for the staff of the Board of Engineers. Nevertheless, the original criticism,[9] penned in 1936 before the establishment of the economics division of the Board of Engineers, has been avidly quoted and repeated in the works of most of the subsequent critics up to the present time. The report of the Board of Investigation and Research[17] as well as the Federal Coordinator's report[9] was also cited in the book, "National Transportation Policy,"[18] by two economists of the new order. The book was intended as a guide for the Hoover Commission's reorganization plan but is understood to have been rejected by that body. This book furnishes additional examples of the acceptance of obsolete, unverified criticisms. The attitude of its authors can be summarized by the following:[19]

---

[13] "Muddy Waters—The Army Engineers and the Nation's Rivers," by Arthur Maass, Harvard University Press, Cambridge, Mass., 1951, p. 185.

[14] *Ibid.*, p. 186.

[15] "Issues Involved in a Unified and Coordinated Federal Program for Transportation," A Report to the President from the Secretary of Commerce, U. S. Govt. Printing Office, Washington, D. C., 1949, p. 7.

[16] "Public Aids to Transportation by Water," Prefatory Note, by Charles S. Morgan, U. S. Govt. Printing Office, Washington, D. C., Vol. III, 1939, p. III.

[17] "Public Aid to Domestic Transportation," Board of Investigation and Research, Transportation Act of 1940, *House Document 159*, 79th Cong., 1st Session, 1945, pp. 337, 338, and 352, and Appendix h, p. 706.

> "Because of the multiple operations of the Corps of Engineers in the field of water resource development however, it is not suggested that the Corps itself be transferred to the Department of Transportation * * * all navigation projects should be reviewed by the Transportation Department to determine the economic desirability * * *.
>
> "The highly questionable economic justification of a large part of the federal government's river and harbor development program has been pointed out repeatedly in studies of transportation. The fact that several hundred million dollars are committed each year to inland waterway improvements, many of which could not conceivably be justified from a transportation viewpoint, is one of the most serious indictments of federal transportation policy."

These allegations simply do not conform with the recorded facts. Contrary to the impression given by numerous critics it is only within the past twenty-five years that definite forecasts of the volume of commerce and the magnitude of transportation savings have been incorporated in the published reports of the engineers on proposed navigation projects. Among the major waterway projects that have been completed and in operation long enough for water-borne commerce to develop, only five were authorized on the basis of specific estimates of future traffic. Their actual performance records are shown in Table 1. Unfortunately, the mere fact that time has proved the Corps of Engineers right and the earlier critics wrong in this respect does not seem to have exerted any deterrent effect on later critics. When it is recognized that this barge-borne tonnage has materialized, despite every competitive device accessible to competing agencies to prevent its growth, the inherent utility of this means of transportation is evident.

TABLE 1.—RESULTS OF WATERWAY IMPROVEMENT

Project	TRAFFIC FORECAST		Traffic development in 1950, in tons
	Year authorized	Tons	
Upper Mississippi	1930	9,000,000	11,025,000
Gulf Intracoastal	1945	7,000,000	18,971,000
Illinois Waterway	1933	8,330,000	16,421,000
Kanawha River	1931	2,300,000	6,388,000
Ohio River	1910	13,000,000	48,598,000

METHOD OF EVALUATION

Surveys to reveal the potential traffic and probable savings in transportation costs that will be made available by a proposed navigation improvement are usually coordinated with surveys to determine the most suitable plan and estimated cost of the project. It is thus possible by mutual adjustment to arrive at the optimum compromise between standards of improvement and desirable objectives. Information as to prospective commerce is obtained through (1) statistical studies of production, manufacture, and marketing; (2) freight waybill sampling; and (3) direct contact with both potential users and competitors of the proposed water route by means of hearings and field canvasses. Current scales of transportation charges from primary origin to final destination are compared with estimated charges including necessary transfers that would be remunerative to water carriers and their connections under the conditions of the proposed water route. Potential commerce thus developed is screened for volume, demand, accessibility, and adaptability to water movement; the magnitude of prospective benefits is computed by applying the unit savings derived as described. The probable annual benefits are then compared with the estimated cost of construction, operation, and maintenance, which is reduced to an annual carrying charge to determine the ratio of benefits to costs. The purpose of the canvasses is not so much to disclose the temporary traffic and transportation conditions of the current period as to develop the firmest possible trends on which to base logical forecasts of conditions bearing on the usefulness of the projects under investigation throughout the period of their useful life.

---

[18] "National Transportation Policy," by Charles L. Dearing and Wilfred Owen, Brookings Institution, Washington, D. C., 1949, pp. 86–89.

[19] *Ibid.*, section on "Reorganization of Federal Agencies," p. 394.

If the method used to estimate benefits were as simple as alleged by some critics of waterway development, a good calculating machine would suffice to carry these analytical processes to the proper conclusion. On the contrary, there are many complex aspects of the problem that have to be resolved by trained and experienced traffic and transportation specialists before a valid decision can be reached. The need for a more economical transportation must be established. The effect of the project on existing transportation agencies and their probable reaction to the competition have to be considered from the public viewpoint. Commercial data secured from local interests have to be critically scrutinized for overly optimistic or pessimistic predictions in the light of conditions revealed by the field canvass. For the past twenty-five years in particular, the technique of traffic analysis has been constantly revised and perfected in accordance with progressive thought among the agencies concerned with the national transportation problem. The trends in agricultural, industrial, and commercial activities of the areas tributary to proposed improvements and the influence of these trends on the pattern of commodity movements have had to be determined.

PERSONNEL

During the last quarter of a century there has been progressively built up within the staff organization of the Board of Engineers a mobile group of technically trained transportation specialists who have broad experience in dealing with those practical traffic problems pertaining to waterways that are related to the collection and distribution of basic commodities and to other modes of carriage in the national transportation network. Included among these seasoned specialists are licensed practitioners before the ICC, certified cost accountants, transportation analysts of national reputation, tariff computers, economic geographers with practical experience in—or contact with—barge-rail, barge-truck, and terminal operation, and engineers practiced in the coordination of structural and economic surveys and analyses of navigation projects. This staff is maintained to furnish guidance and assistance to the district offices of the Board of Engineers in organizing and conducting field canvasses, analyses, and evaluations of data on the most important waterway projects secured from shippers, carriers, producers of raw materials and fuels, manufacturers, and consumers. They maintain investigative relationships of mutual confidence with operators of the leading common, contract, and private waterway carrier lines; they are recognized and consulted by most public agencies as disinterested and authoritative sources of information on vessel operating practices, costs, and related fields. Great pains have been taken to gather the ablest personnel obtainable in this particular field. After all the data have been collected, screened, and tabulated, it is the experienced judgment of these men that derives the most reliable answer from the available material.

One of the problems that tax the judgment and tact of the field investigators is how to evaluate the traffic estimates furnished by interested persons in the potential tributary area in the light of conditions disclosed by the field canvass. Shippers are naturally optimistic in their estimates. They want as many alternative means of transportation available to them as possible, especially if the cost of providing the facilities is borne by the Treasury Department and not by local interests. Communities without direct access to inland waterways observe that other communities so favored have the advantage of freight rates adjusted to meet low-cost water transportation. That fact is the source of much of the promotional activity for extension of the waterway system. It is not, however, a guarantee that the facilities thus provided will actually be used to the capacity indicated after competitive adjustments among the carriers have been made. Profitably established carriers by the various modes of transportation, including existing waterway routes, frequently prefer the status quo to conjectural benefits—and possible competition—that may result from enlargements or extensions of navigation facilities. This attitude is a phase of the familiar problem that engineers must meet; they are constantly required to arbitrate between the claims of two factions—both fundamentally honest, with just motives, but with viewpoints colored by opposing financial interests in the outcome. The investigators have to weigh the conflicting evidence tactfully in the light of the public interest, which does not always correspond with either of the opposing viewpoints. In addition to those unfavorably reported upon, many proposed improvement projects are abandoned before reaching the stage of formal reports because their economic merits are expertly screened in the preliminary examination stage.

VALIDITY OF NAVIGATION SAVINGS

Reviewing the comparatively short period since the federal government embarked on its program of modernized improvement of inland rivers, two aspects stand out in prominent relief—on the one hand, the remarkably rapid growth of inland waterway commerce and, on the other hand, the insistence of waterway opponents that the benefits are illusory. The oppenents claim that barge operators could not offer service at rates lower than those of alternative modes of transport if the navigation facilities were not furnished to the operators without cost. Otherwise, they say, very little traffic would be attracted to the waterways. This claim is not borne out by recorded facts. As will be shown in a current analysis of the performance of leading inland waterways, the annual savings in transportation costs substantially exceed the annual charges for improvement.

Actually, the genesis of specious arguments of the foregoing kind may be traced back to the appraisal, in the 1936 report of the Federal Coordinator, of inland waterway improvements either in their incomplete state or at a stage of development retarded by the business recession of that period. However, opponents of the potentially serious competition that waterway improvements offered avidly seized on this circumstantial analysis as effective ammunition in a campaign calculated to discredit the navigation program before it had a chance to prove its inherent value. The wide publicity given to these figures, by frequent repetition, helped them take on the appearance of authority and fact. Many of the more gullible transportation analysts of recent years have been led to base their conclusions in regard to the merits of inland waterways on these premature conclusions of the depression era, when barge-borne commerce was but a small fraction of its present volume.

Illustrative of the manner in which this basis of evaluation unfairly disparages the economy of waterway transportation is the method of appraisal appropriated from the Federal Coordinator by the Board of Investigation and Research in its 1944 report[20] and by busy transcribers among the authors of much later treatises on the subject. This method applies the annual cost of improvement, which of course is greater during the early years of development, to the volume of traffic that has developed by that time. The Federal Coordinator's report[21] even matched the expenses for the fiscal year ending June 30th to the traffic for the preceding calendar year, which by no sort of economic gymnastics could be expected to benefit by improvements made six months after that traffic had moved. For the purpose of revealing the distortion that results from such a method of appraisal it is sufficient to refer to the history of the Illinois Waterway (between Chicago, Ill., and Alton, Ill., as an example). This waterway was officially opened for 9-ft-navigation in 1933, although that controlling depth was not secured until 1938. The engineers estimated an eventual matured annual traffic of 7,500,000 tons. The Federal Coordinator's evaluation of this waterway was based on conditions obtaining in 1935 when the total traffic was 620,313 tons, which amount was used in comparison with annual cost to obtain the unit rating of this waterway in cost per ton-mile. However, during the ensuing years between 1933 and 1950 the traffic on the Illinois Waterway steadily increased in volume as anticipated in the Corps of

---

[20] "Public Aids to Domestic Navigation," Board of Investigation and Research, Transportation Act of 1940, *House Document 159*, 79th Cong., 1st Session, 1945, p. 375 and Appendix E, pp. 568 to 593.

[21] "Public Aids to Transportation by Water," by Charles S. Morgan, U. S. Govt. Printing Office, Washington, D. C., 1939, Vol. III, Waterway Unit Cost Tables, pp. 148–157.

Engineers' original report and, by 1944,[22] had surpassed the original estimate. In 1950 this traffic amounted to more than 16,000,000 tons whereas the unit cost of boat-line operation, responsive to technological advances in the design of equipment and this ample reservoir of tonnage, dropped to an all-time low in mills per ton-mile. Thus, the differential between barge rates and rates by alternative routes, which represents savings to the shippers, has continued to increase with the growth in volume of traffic. The federal cost per ton-mile in 1950 for handling this large volume of traffic was less than one fourteenth of the unit cost assigned by the Federal Coordinator's staff as an indication of the economic value of this waterway.

It is an interesting commentary on this whole investigation of the justification of public aids to water transportation that the Federal Coordinator risked the following conclusions[23] on the basis of his findings in 1936:

> "Generally, the forecasts of traffic that would move over rivers and canals have exceeded by wide margins the traffic which actually developed, even with due allowance for the period required to develop traffic after waterway improvements have been completed. * * * Past experience indicated that in the future estimates will continue to require substantial discounting for overestimating."

The truly remarkable fact is that the significant upset in the Federal Coordinator's forecasts has apparently escaped the notice of the critical transcribers who depend on others to compile the basic data for their economic treatises.

In 1949, the two economists with the Brookings Institution (Washington, D. C.) still rested their conclusions on the Federal Coordinator's report of 1939 and (from another report) on[24]

> "* * * some indications of waste of general tax funds resulting from the overenthusiastic development of waterways provided by the public aid studies of the Board of Investigation and Research."

The studies[25] of the Board of Investigation and Research were made in 1942 on water-borne traffic for both 1940 and 1938. The investigators regarded the 1940 data as too high to be representative. However, actual statistics of waterway-borne commerce, current when "National Transportation Policy" was written, more than doubled the ton-mileage for 1940 and almost tripled the 1938 figures, affecting a corresponding decrease in the unit cost of improvement. With clear proof available to the authors that the basis of their findings as to overestimated traffic forecasts was no longer valid, publication of these findings in 1949 seems inexcusable.

RISING CONSTRUCTION COSTS

The most controversial waterway projects have purposely been selected for examination in this paper because each one exemplifies one or more elements in the prevalent pattern of criticism and its weakness. However, the writer does not mean to imply that all such projects are necessarily considered justified under present conditions. The unprecedented rise in the costs of materials and manpower characterizing the post-war era, coupled with the remarkable drop in productivity of migrant labor working on heavy construction as compared with those steadily employed, have completely upset the previously established balance between costs and benefits. It would have required almost superhuman prescience to have anticipated these trends, and the Corps of Engineers is by no means alone in having underestimated them. Some ambitious projects, recommended in prewar years, have subsequently been unfavorably reported on; others are being held in abeyance under a procedure resembling the pocket veto, while a firmer stabilization of outlook than is possible under 1952 conditions is being awaited. These adverse trends have provided the critics with a fine opportunity for "second-guessing" of which they have not been loathe to avail themselves.

---

[22] "The Illinois Waterway," Report of the Corps of Engrs. on the Illinois Waterway Project; *Senate Document 130*, 69th Cong., 1st Session, *Senate Document 126*, 71st Cong., 2d Session, 1930, p. 57; *House Document 184*, 73d Cong., 2d Session, U. S. Govt. Printing Office, Washington, D. C.

[23] "Public Aids to Transportation by Water," by Charles S. Morgan, U. S. Govt. Printing Office, Washington, D. C., 1939, Vol. III, p. 61.

[24] "National Transportation Policy," by Charles L. Dearing and Wilfred Owen, Brookings Institution, Washington, D. C., 1949, pp. 87-89.

[25] "Public Aids to Domestic Transportation," Board of Investigation and Research, Transportation Act of 1940, *House Document 159*, 79th Cong., 1st Session, 1945, pp. 373-376 and Table 64, Unit Project Costs.

Competing Projects

Frequently, betterments of waterway projects, instead of involving the widening or deepening of existing channels or the increase of lock dimensions, take the form of completely new by-pass channels which create advantages, such as savings in vessel operating costs, to water-borne traffic that already enjoys some measure of navigation improvement on the old channels. A simplified example is the lateral canal, now nearing completion, which by-passes the dangerous reach of the Mississippi River known as "Chain of Rocks" upstream from St. Louis, Mo. As its name implies, the river in this reach flows for about ten miles over a series of rock reefs that have always constituted a troublesome obstruction and hazard to navigation. Improvement measures had been conducted in the main river channel at this locality for many years, since the days of the pre-Civil War operations of Maj. Robert E. Lee, finally yielding dependable controlling depths of about 7 ft, which constituted a bottleneck in a system otherwise affording a 9-ft draft. A substantial through barge traffic was gradually built up that has made increasing use of this channel between the Ohio Basin and Lower Mississippi River sections of the waterway system on the one hand and the Illinois, Missouri, and Upper Mississippi River sections on the other. Without doubt, the benefits to this traffic have been justly cited as warranting former expenditures for improvement and maintenance of the river channel at this point.

Chain-Of-Rocks By-Pass Canal

Repeated attempts to establish the standard controlling depth of 9 ft over these dangerous shoals, needed to facilitate through commerce between the sections above and below St. Louis, were unfavorable. A dependable 9-ft, by-pass canal (long advocated by the Corps of Engineers) around this bottleneck was finally authorized and adopted by Congress in 1945. The benefits provided by previous improvement works in the main channel, enjoyed by existing traffic, will be duplicated in the new by-pass canal. In addition, the new project will facilitate the loading of barge tows to standard depths, in contrast to the light-loading now required to negotiate the Chain-of-Rocks reach; the improvement will result in substantial incremental savings in transportation costs all the way from origins to destinations on distant parts of the system. The benefits now provided in the main channel (and preserved in the new canal) are properly being charged off against the corresponding cost of the old works; only the additional savings from the increased draft are to be used in justification of the by-pass canal improvement. These savings are more than ample to warrant the expenditures made on the improvement. Not even the most exacting critic of the Corps of Engineers has challenged the soundness of justifying the by-pass canal project on the basis of incremental benefits or has claimed that the costly blasting, dredging, and contraction works that would be required to maintain the river channel over Chain of Rocks ought to be continued because of its former usefulness.

Diversion of Upbound Mississippi River Traffic

In 1939, and again in 1945, the Corps of Engineers proposed a provision for a waterway connection between the Tennessee and Tombigbee rivers that would provide a canalized route between Mobile, Ala., on the Gulf Intracoastal Waterway and Paducah, Ky., on the improved Ohio River. This canal also would connect northern and southern parts of the waterway system. The Board of Engineers accepted as a minor part of the justification of the project the savings estimated to result from diversion of a part of the through upbound traffic from the open Mississippi River channel to the connecting canal route. Major benefits were expected from new traffic generated by the improvement. In 1939 it was found that a through upbound movement of 925,000 tons per annum between New Orleans (La.) and the mouth of the Ohio River could be diverted from the adverse current of the open river to the slack water of the Tennessee-Tombigbee route at annual savings of $1,000,000. Upbound tonnage on the Lower Mississippi River continued its steady increase from 2,955,479 tons in the calendar year 1938 to 11,027,584 tons in the calendar year 1944. The central statistical control office at St. Louis was asked to compute the upbound tonnage passing through without stop for each year; it was estimated as a total volume of 3,066,000 tons which could be considered as divertible to the canal in the 1945 report. Because of an observed trend manifested during the six-year interval toward increased speed and power of tow-boats engaged in certain specialized services, the savings in vessel operating time and cost resulting from use of the alternative northbound route was estimated to be $1,200,000 a year. The increase in the estimate of savings from the proposed diversion of only 20% over the 1939 figure instead of the 200% indicated by the statistics of actual commerce in 1945 represented the conservative judgment of the water-carrier specialists on the Board of Engineers' staff. They were inclined to discount the sharp increase of the war years and believed that the trend toward streamlining and integrating tows in specialized services tended to minimize the operating time and cost differential between the two routes so as to render the proposed canal unattractive as an upbound route to certain new types of traffic. The readers are invited to attend closely the foregoing estimating procedure and figures, both clearly set out[26,27] in the reports themselves, when reading the adverse comments of critics to be quoted subsequently. No rate comparison is involved; what is involved is merely the saving in time and consequently in operating costs of the same equipment on the alternative routes. Thus, only the incremental savings provided by the proposed route as compared with the existing route were used in justification of the Tennessee-Tombigbee connection. As stated in the report,[27]

> "The propriety of claiming savings on tonnage diverted to the proposed improvement is apparent when it is considered that the traffic already enjoys the benefits of water transportation and that it is only the incremental savings in distance and time that are credited to the connecting waterway project."

The author of "Muddy Waters" and the investigative staff of the Appropriations Committee of the United States House of Representatives, among others, were highly critical of the use of the incremental-savings principle in justifying this proposed waterway. The author of "Muddy Waters" cites the Tennessee-Tombigbee project as an example of unsound engineering for projects that compete with each other for the same traffic.[28] He records the concurrence of the Board of Engineers in the item of estimated annual benefits in the 1939 report[26] of $1,000,000 from traffic to be diverted and the doubts expressed by the Chief Engineer of the Corps of Engineers. The author of "Muddy Waters" continues:[29]

> "After the Congress rejected the project on the basis of the 1939 report, the Board of Engineers for Rivers and Harbors made a reexamination (in 1945) in order to bring up to date the data with respect to economic benefits. * * * The allocation of annual benefits from savings to upbound Mississippi River traffic to be diverted to the Tombigbee waterway was revised upward to $1.2 million. This time, the Chief of Engineers interposed no objection to the consideration of this annual benefit, without which the project could not have obtained a favorable cost-benefit ratio. He stated, 'in addition, traffic already moving advantageously upstream against Mississippi River currents will be able to use the new waterway at additional savings estimated at $1.2 million, annually'. * * * [footnote reference 30]
>
> "Congress [had] turned down the Tennessee-Tombigbee in the Rivers and Harbors bill of 1945 [on the basis of the 1939 report] and the debate reveals that in doing so it in effect rejected the benefits claimed for national defense. Thus in the reexamination of the waterway conducted by the Board of Engineers in 1945, all of the imponderable benefits of national defense, land enhancement, or recreation, which had been rejected in the previous report were eliminated. It was this action which compelled allocation of the greater benefits to upbound Mississippi River traffic, referred to above."

---

[26] "Report on Tennessee-Tombigbee Connecting Canal Project," by the Corps of Engineers, *House Document 269*, 76th Cong., 1st Session, December 23, 1938, U. S. Govt. Printing Office, Washington, D. C., p. 53.

[27] "Report on Tennessee-Tombigbee Connecting Canal Project," by the Board of Engineers for Rivers and Harbors, *House Document 486*, 79th Cong., 2d Session, September 29, 1945, U. S. Govt. Printing Office, Washington, D. C., p. 175.

[28] "Muddy Waters—The Army Engineers and the Nation's Rivers," by Arthur Maass, Chapter on "Responsibility to the Profession," Harvard University Press, Cambridge, Mass., 1951, p. 183.

[29] *Ibid.*, pp. 185-186.

[30] "Report on Tennessee-Tombigbee Connecting Canal Project," by the Board of Engineers for Rivers and Harbors, *House Document 486*, 79th Cong., 2d Session, September 29, 1945, U. S. Govt. Printing Office, Washington, D. C.

Readers are urged to ponder the implications in the foregoing concluding sentence in the light of the statistically supported facts previously reported.

Additional criticism is as follows:[31]

> "For reasons not known, the Bureau of the Budget did not hold the new proposal contrary to the President's program, and the Congress authorized the waterway in the Rivers and Harbors Act of 1946 * * *. The Corps had no doubt used the upbound Mississippi traffic to justify the improvement of that [Lower Mississippi] river."

The foregoing comment typifies the persistence of critics to ignore the growth of water-borne commerce. They cling to the thesis that there is only a fixed volume of traffic, and that growth on one route must be offset by an equal shrinkage on some other route in spite of the overwhelming statistical evidence to the contrary throughout the history of industrial and commercial development of the interior of the country. It was not the through divertible traffic that was used to justify the improvement of the Lower Mississippi River for navigation. As a matter of record, the annual increase in upbound traffic on the Mississippi River between New Orleans and the mouth of the Ohio River from the date of the 1939 report to the present has averaged more each year than the entire estimated diversion to the Tombigbee route. Ignoring altogether the benefits enjoyed by southbound traffic on the Lower Mississippi River, expenditures on the navigation features of that improvement would be justified by substantial savings on the scheduled local, northbound, wayport commerce of the common-carrier barge lines alone, which service would continue on the river altogether uninterrupted by through traffic diversions.

INCREMENTAL BENEFITS

Arguments along the preceding lines are beside the point, however, in establishing the validity of the principle attacked in "Muddy Waters." It would make no difference in principle if the proposed diversion took every ton of commerce from the Lower Mississippi River and consigned that improvement to abandonment. If the Tombigbee River route were better than the Lower Mississippi route—enough to pay for itself in additional benefits—the project would be justified. There is no fundamental difference in theory between diverting the Chain-of-Rocks traffic to the by-pass canal and using the Tennessee-Tombigbee canal route—except that the latter by-pass, instead of being 8 miles long, would be 800 miles long. The diverted traffic would be afforded the benefits it now enjoys on the open Mississippi River, which are not counted in justification of the connecting canal, but are, in effect, charged off against the improvement of the open river. The diverted traffic would enjoy additional benefits in the saving of distance and time reflected in vessel operating expenses via the new route. These additional, incremental benefits are properly creditable to the proposed improvement. The same theory applies to the replacement of an icebox with an electric refrigerator. The theory is emphasized herein because it is intended to invoke the incremental-savings principle in a broad application to other current criticisms of the waterway improvement program.

---

[31] "Muddy Waters—The Army Engineers and the Nation's Rivers," by Arthur Maass, Harvard University Press, Cambridge, Mass., 1951, p. 184.

ECONOMIC RESULTS OF IMPROVEMENT

Of the 28,000 miles of improved channels shown on the waterway map, only approximately 9,000 miles comprise the interconnected inland and intracoastal system with facilities fully improved to modern standards, upon which barge service has become firmly enough established to be an important factor in domestic transportation. It is this system upon which most of the money has been spent and by which most of the tonnage is carried. The fact that the Corps of Engineers' forecasts of traffic volume expected to develop on these waterways have been considerably exceeded in actuality is confirmed by the steadily increasing annual ton-mileage shown in the following tabulation and presented graphically in Fig. 1:

Year	Ton-miles	Year	Ton-miles
1927	5,553,912,000	1939	9,896,943,000
1928	5,662,743,000	1940	11,578,418,000
1929	4,982,631,000	1941	14,960,979,000
1930	5,172,389,000	1942	15,339,165,000
1931	5,507,976,000	1943	15,874,740,000
1932	5,083,119,000	1944	19,004,643,000
1933	6,990,028,000	1945	17,737,830,000
1934	5,872,777,000	1946	16,210,079,000
1935	6,291,232,000	1947	20,740,265,000
1936	7,416,822,000	1948	24,871,700,000
1937	8,151,861,000	1949	24,153,321,000
1938	8,463,127,000	1950	30,281,638,000

That this growth has taken place under adverse circumstances is attested by the Federal Coordinator of Transportation in his pioneer report[32] on federal aids in 1940:

> "They [advocates of waterways] point out that when such a waterway is opened and water carriers begin to use it, immediately competing modes of transportation, particularly the railroads, reduce their rates, thus depriving the waterway of traffic it would otherwise carry. It is true that the results of construction and improvement of waterways are as they describe."

The assistant general counsel of the Association of American Railroads (AAR) in his testimony[33] on Senate Resolution 50 explained:

> "In the effort to prevent traffic diversion, [rail] rates on commodities that are most vulnerable to competition will tend toward * * * 'out-of-pocket' costs."

Commenting on this universal practice of rate depression the chairman of the ICC in the Petroleum Products Case[34] said: "The railroads will have a new hole in their revenues which they must fill at the expense of some other traffic." It is worthy of note that the water-borne ton-mileage shown in Fig. 1 has been built up despite the previously described practices of competitors. Traffic has been attracted to water routes in preference to land routes by the differential between competitively depressed rail rates and compensatory water-carrier service charges that do not include improvement costs.

---

[32] "Public Aids to Transportation," by Joseph B. Eastman, U. S. Govt. Printing Office, Washington, D. C., 1940, Vol. 1, Foreword, p. IV.

[33] Hearings before the Senate Interstate and Foreign Commerce Subcommittee on a Study of Domestic Land and Water Transportation, *Senate Resolution 50*, 81st Cong., 2d Session, 1950, April 20, 1950, pp. 203-204.

[34] *I. C. C. Decisions*, Vol. 235, 1939, p. 115. (The *I. C. C. Decisions* of the Interstate Commerce Comm. are published by the U. S. Govt. Printing Office, Washington, D. C.)

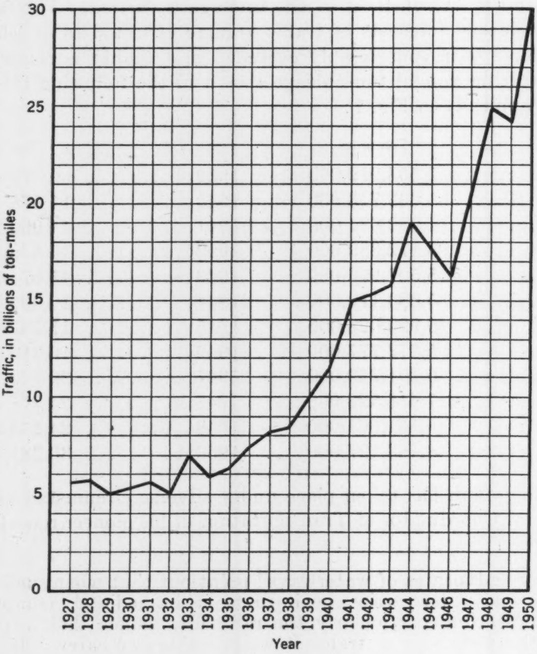

FIG. 1.—INLAND TRAFFIC ON THE MISSISSIPPI RIVER SYSTEM FROM 1927 TO 1950

The report[35] of the volunteer Engineers Joint Council (EJC) committee on national water policy dismisses the remarkable growth of water-borne commerce under these conditions with the following observation:

> "Since the general taxpayer provides and maintains, free of charge, the right-of-way on which the inland waterway operator conducts his business, and since the subsidy payments show a sharp upward trend, it is not surprising that traffic on these artificial channels show an impressive increase in recent years."

The EJC proposes this somewhat unrealistic remedy:

> "By imposition of a system of toll charges, the margin between waterway costs and rail rates would, in many cases, be eliminated or substantially

---

[35] "Principles of a Sound National Water Policy," prepared under the auspices of the Engineers Joint Council, Edwards Bros., Ann Arbor, Mich., July, 1951, pp. 70, 81, 86, and 87.

> reduced. In such cases a large part of the traffic would abandon the waterway. * * *
>
> "In consideration of the imposition of user charges equivalent to the complete cost of waterway transportation, the railroad rates should likewise be [made] compensatory."

The personnel of the EJC task force committee on inland waterway transportation included a group of eminent businessmen and professional men. It is difficult to find reasons for the apparent inconsistencies between their findings and their conclusions except unavoidable haste and insufficient time for consideration of all the facts brought out by their investigations, as stressed in the foreword to the report. Parts of the report devoted to waterways seem to have been "farmed out" to different individuals without complete coordination of the findings. However they may have been formulated, these parts indicate misconception of the competitive situation actually existing.

TABLE 2.—COMPARISON OF COSTS AND BENEFITS FOR 1948, IN DOLLARS

Section of waterway system	Charges for amortization, interest, and maintenance and operation (1)	Savings in cost of transportation (2)	Net savings after deduction of waterway costs (3)
Lower Mississippi River	13,455,000	67,979,000	54,524,000
Middle Mississippi River	2,560,000	8,620,000	6,060,000
Upper Mississippi River	8,295,000	11,521,000	3,226,000
Ohio River	10,235,000	41,827,000	31,592,000
Monongahela River	1,344,000	19,913,000	18,569,000
Allegheny River	871,000	946,000	75,000
Illinois Waterway	2,128,000	12,094,000	9,966,000
Missouri River[a]	11,456,000	303,000	(−11,153,000)
Cumberland River	899,000	1,582,000	683,000
Warrior-Tombigbee Waterway	1,271,000	2,471,000	1,200,000
Ouachita River[b]	315,000	22,000	(−293,000)
Gulf Intracoastal	4,068,000	55,270,000	51,202,000
Columbia River[a]	2,005,000	689,000	(−1,316,000)
Sacramento River	1,054,000	2,499,000	2,345,000
Kanawha River	1,026,000	1,981,000	955,000
Total	60,082,000	227,717,000	167,635,000

[a] Projects are currently under construction, and present traffic is that which uses the waterway in spite of the interruptions occasioned by improvement activities; it is not a valid indication of the economic value that the completed waterway will have in the integrated transportation system. [b] Improved to inferior standards which do not permit interchange of traffic with standard waterway system. Proposed enlargement pending.

As a matter of fact, the competitive rates available to waterway users via the alternative rail routes do not cover the costs of "right of way" either, because they are depressed rates admittedly based on the "out-of-pocket" cost of handling added traffic to meet water competition. The rate differentials now in effect actually average substantially less than would the differentials if competitive rail rates were held at the normal level (as recommended by the EJC) and the water carrier costs were raised to include public improvement costs. This fact has been established in studies of going waterways made from time to time by the Corps of Engineers and is exemplified in a brief analysis of the fifteen most important projects of the waterway system made for the EJC task force committee in 1950. These projects accounted for 80% of the total annual charges for all waterways of the Mississippi-Intracoastal system and handled over 80% of all barge-borne freight; thus, they may be considered reasonably representative. Table 2 is submitted as giving a sufficiently accurate picture of waterway economics to dispose of many of the assumptions on which opponents of the federal improvement program have based their criticisms.

In order to obtain as reliable a measure as possible of the transportation savings earned on the fifteen waterways in 1948, the principal commodities conveyed were analyzed; representative cargo movements on each section and from one section to another, both by all-water routes and combination rail-and-water routes, were analyzed for comparison with the most economical available alternative routes from primary origins to final destinations. The difference between the charges actually incurred by the shippers, including the extra transfer costs, and those that would have applied to shipping by the cheapest alternative route (in the absence of the waterway) were developed as unit savings. Full barge-line service costs plus a reasonable return on investment in equipment were used in the analysis in place of barge-line tariff rates because the great preponderance of water-borne freight was known to have been moved by contract or in industry-owned carrier services that did not establish rates. The unit savings thus derived for each of the selected waterway projects were applied to the ton-mileage of the sample commodity movements; the results were tabulated in Col. 2, Table 2, as indicating actual savings made in freight charges. This table represents, of course, the results of a sampling process; there was neither time nor funds for a complete analysis of each movement. It is believed, however, that Table 2 affords the closest approximation that can be made, short of an exhaustive waybill analysis of each separate shipment. The significant figures are verifiable. Approved sampling methods were used by competent statisticians who prepared data, to which was applied the experienced knowledge of a staff of traffic specialists. Every effort was made to obtain a representative cross section of waterway commerce. Improvement costs were reduced to annual charges from the detailed cost records dating from the inception of the projects.

As previously explained, Table 2 limits the savings for each section of the waterway system to the amount saved on operations on that section alone. If the feeder value of some of the branch waterways had been computed on the basis of traffic contributed to the main stream, the savings on the branches would have been increased and those on the main stems commensurately diminished, so that the benefits would have been more uniform throughout. The estimates of savings differ from the various published analyses not only in reflecting the increased tonnages of later years but also in another significant particular: The normal fully remunerative level of rates was used in the comparison, rather than rates that had been depressed to uneconomic levels to meet existing waterway competition. This clearly gives the true measure of savings enjoyed by the shippers, who would have had to pay the normal rates had not the water improvements been available. In all the proposals of economists for applying user charges to waterway transportation in order to reimburse the national Treasury, the tests for economic justification laid down by them have been given the aspect of fairness, but it is evident that few projects were expected to survive the tests. Table 2 indicates that the principal completed waterways not only would have passed the tests but also would provide net annual savings in transportation costs sufficient to pay the annual improvement charges, leaving an ample margin for profitable operation of the water carriers and for the attraction of an even greater volume of tonnage under the framework of a normal, fully compensatory rate structure, recommended by the EJC.

SYSTEM VALUE

In the foregoing analysis of typical sections of the existing waterway system are compared the computed annual charges covering interest, amortization, maintenance, and operation with the transportation savings earned separately on each component section. This is the only feasible means of measuring the economic results of improvement of completed individual projects without duplicating savings made in the transportation of through freight passing over two or more sections in its progress from primary origin to final destination.

In the method is ignored the very important element of system value whereby, because of standard interconnection, freight can travel without transshipment in continuous voyages between such distant ports as Pittsburgh (Pa.) on the Ohio River; Chicago, the terminus of the Illinois Waterway; Minneapolis (Minn.) on the Upper Mississippi River; Kansas City (Mo.) on the Missouri River; St. Louis, Memphis (Tenn.), and New Orleans, on the Lower Mississippi River; and Mobile (Ala.), Port St. Joe (Fla.), Beaumont, Houston, and Corpus Christi (Texas) on the Gulf of Mexico. It would obviously be impracticable, for instance, to credit the whole saving on a tow-load of industrial alcolol from its origin at a refinery in Texas City (Tex.) to an anti-freeze manufacturing plant in Charleston (W. Va.) to the originating Gulf Intracoastal Canal; the saving might, by the same reasoning, be attributed to the existence of the terminating Kanawha River improvement to Charleston. The only means of evaluating the element of continuity of the interconnected navigable channels is to treat the improved system as a whole. When the problem, however, is to determine the probable economic justification of a proposed extension, enlargement, or cross connection, the element of system value can be given due weight.

FEEDER VALUE

Official orders and regulations that have governed for many years the procedure of the Corps of Engineers in arriving at estimates of the benefits of a proposed navigation improvement contain the following stipulation:[36]

> "If the proposed improvement will develop new waterway movements that include increased traffic to existing waterways, the estimated saving for the complete water movement will be included as a benefit, and no part of such saving should be deducted on the theory that it should be assigned to the connecting waterway. On the other hand, when a proposed improvement will result in the extension of waterway movements already developed, only savings which result from the extension of the movements should be included as a benefit, and no part of the saving already being realized by movement on the existing waterway will be included as a benefit for the new improvement."

---

[36] "Orders and Regulations," Corps of Engineers, Chapter IV, Pt. II, Paragraph 4206.23, October 15, 1952 (revised August 3, 1953), pp. 37, 38, 38a, U. S. Govt. Printing Office, Washington, D. C.

It is fundamental to sound analysis that proposed additions to existing improvements are responsible for transportation savings on the traffic from origins to destinations if, without the improvement, the traffic would move from origin to destination by other means or would not move at all. In other words, when a proposed extension or enlargement of a waterway is under consideration, the engineers are not concerned with the degree of justification attained by the completed parts of the system. They need to determine only whether the proposed addition will provide added benefits equal to its cost, whether those benefits accrue from the project itself, or whether they are contributed by the project to the system as a whole. This kind of benefit is, in transportation parlance, a measure of the "feeder value" of the project, and its comparative magnitude determines the justification of the proposed improvement. The question of whether the completed waterway connections are or are not already earning savings sufficient for their justification is not pertinent. It is evident, however, that any proposed extension or enlargement that will swell the volume of profitable, long-haul, trunk-line traffic tends to increase the return on the public investment already made in the waterway system.

A typical reaction[37] of waterway opponents to the recognition of feeder value in estimating benefits to result from navigation improvements appeared in 1946, under the name of a prominent economist of the AAR. This article is essentially an abridgment of testimony[38] introduced before the Committee on Rivers and Harbors of the United States House of Representatives on May 7, 1946, on the proposed improvement of the Big Sandy River and the Tug and Levisa forks (Kentucky-West Virginia). The contents were briefly summarized[39] by the author in the following subtitle:

> "Curious reasoning employed by Army Engineers to 'justify' a branch-line river project. —— Since the venture will cost more than it will 'save,' Engineers seek to make the figures balance by imputing main waterway 'savings' to the feeder."

The author continues[39] in reference to the Corps of Engineers' report on the highly controversial Big Sandy River project:

> "This is a startling new device for securing economic justification. * * * For this project the Engineers propose to pump in water to make it navigable and also to pump in 'savings' to make it pay."

In 1945, the Board of Engineers approved the project for improving the Big Sandy River for navigation from its mouth in the Ohio River up its two principal forks running through the coal fields of West Virginia and eastern Kentucky. Railroads occupying the banks of the Ohio River and the Big Sandy River and one bank of each fork were moving a large tonnage of high-grade coal from these fields to distant industrial markets on the Ohio River, the Illinois River, the Upper Mississippi River, and the Great Lakes. Although this activity had been going on for almost forty years, no facilities had ever been provided at the mouth of the Big Sandy River for the trans-shipment of this coal to destination by barge. Waterfront property suitable for interchange tipples is almost invariably owned, occupied, or controlled by the rail lines. It has never been the practice of the railroads to surrender freight already loaded into their cars to competing modes of transportation even though a considerable saving in the cost of providing the carrier service may be shown. No substantial part of the traffic estimated as prospective to the Big Sandy River improvement would be in a position to benefit from the availability of the Ohio River, Mississippi River, or the Illinois Waterway, without construction of this project to provide a navigable access route.

---

[37] "Feeder Value of Tributary Waterways," by C. S. Duncan, *Railway Age*, March 30, 1946, pp. 668–669.

[38] Hearings on *House Resolution 3961* to authorize the Tennessee-Tombigbee Connecting Canal, May 7, 1946, *House Document 486*, 79th Cong., 2d Session, pp. 331–335.

[39] "Feeder Value of Tributary Waterways," by C. S. Duncan, *Railway Age*, March 30, 1946, p. 668, Subcaption.

It was planned, therefore, to canalize the Big Sandy River and its tributaries in order to barge coal directly from the extensive undeveloped seams on the sides of the forks not accessible to rail service and thence to transport the coal in the same barges to distant markets by way of the existing Ohio River improvement and its navigable connections. It was found that stand-by facilities to insure adequate water supply for lockages during the short periods of drought could be supplied either by providing regulating reservoirs on the headwaters or by pumping the occasional water deficiency into the locks from the pools below them. The choice of pumping was a routine decision based on simple engineering calculations and was a workable feature of minor importance in the general design. The magnitude of the coal reserves and the demand at specific markets along the existing waterway system had been established by survey. Transportation of the prospective tonnage by barge on the Big Sandy River and its tributaries alone could not be accomplished at sufficient savings to justify the expense of the project, but savings to be realized on the water movement from primary origin to final destination on the interconnected system were indicated as ample. Because it was evident that the prospective movement of this coal over the existing waterways with its consequent savings in transportation costs would not occur without adoption of the Big Sandy River project, the entire estimated saving was credited to the proposed improvement in accordance with the long-established provisions previously quoted.[36] The ratio of benefits to project costs were thus computed on the basis of the value of the proposed improvement to the existing waterway system as a feeder.

However, the article[40] continues to reject the principle of feeder value and, in so doing, overlooks the fundamental difference between evaluating an existing interlocked waterway system and measuring the probable effects of an additional feeder to that system. The author states[40] that in his opinion:

> "The Army Engineers cannot have stopped long enough to think this matter out, in their haste to find justification for the Big Sandy project. * * *
>
> "It is a fact also that the Ohio River has other tributaries. The principle should be made to apply to them in the same manner as to the Big Sandy. Let us see what happens in that case.
>
> "For the year 1940 the Chief of Engineers in his annual report on 'Commercial Statistics' for water-borne traffic gives the total vessel traffic on the Ohio River as 29,546,388 tons. In the same year there floated out into that river 'outbound traffic,' preponderantly coal, defined as being 'traffic moving from one waterway into another,' in tonnage as follows:

---

[40] "Feeder Value of Tributary Waterways," by C. S. Duncan, *Railway Age*, March 30, 1946, p. 669.

	Tons
From the Monongahela	10,908,024
From the Allegheny	1,388,297
From the Kanawha	2,473,340
From the Cumberland	87,484
Total	14,757,145

> "If to the above figure there be added the tonnage of sand and gravel dredged from the bottom of the river, a commodity for which no expensive improvements can be or ever have been justified, amounting to 5,257,945 tons, there is a total of 20,014,090 tons to be excluded from the Ohio River. This would leave a total tonnage for its economic justification of 9,532,298 tons.
>
> "On this river prior to the inauguration of the present canalization project in 1910 there was carried over 10,000,000 tons annually of freight traffic, a greater amount than is left to the river after all the expenditures for improvements."

The force of the foregoing comparison is lost when it is considered that, of the 10,000,000 tons using the Ohio River before the present canalization, coal from the same tributaries, together with sand and gravel, contributed almost the same proportion, leaving a balance of less than half the 10,000,000 tons as originating on the Ohio River proper. A fair comparison for the enlightenment of impartial readers would have stripped the 10,000,000 tons down to 4,000,000 tons in the same manner that the 29,000,000 tons were stripped down to 9,000,000 tons. As a matter of fact, the 10,000,000 tons moving in 1910 was short-haul traffic handled in old, light-draft equipment over facilities fast becoming obsolete. The Chesapeake and Ohio Railway Company was then extending its main line along the banks of the Ohio River; had the waterway not been modernized, it would soon have ceased to be a significant factor in the transportation of the region. As it is now, the Ohio River canalization project is a highly successful and profitable improvement with an annual barge-borne commerce of more than 52,000,000 tons, much of it long-haul through traffic representing substantial savings above its cost.

Oddly enough, the very railroads in whose behalf the article was written submitted testimony in the same case indicating an opposite view of feeder value as a legitimate element of justification. The chairman of their coal traffic committee testified[41] at a hearing before the Board of Engineers on November 14, 1945:

> "Every coal mine, whether served by the main line of any of the numerous branches and subbranches of those railroads, is accorded the opportunity to compete with every other mine in the group at any and all markets on equal railroad freight rates."

In other words, the railroads are glad to build feeder branches to productive mines for the sake of the long-haul business thus brought to the main line. However, because they charge only main-line rates, the railroads earn no extra revenue for service on the branch lines. They justify the expense of feeder-branch construction to stockholders and the regulatory commissions completely on the basis of the feeder value of the branches. A vice-president of the Chesapeake and Ohio Railway Company testified[41] at the same hearing:

---

[41] Hearing before the Board of Engrs. for Rivers and Harbors on the Big Sandy River Project, Louisa, Ky., November 14, 1945, Archives of the Board of Engrs. for Rivers and Harbors, Washington, D. C.

> "It is a long-time policy of the Railway to furnish service by the building lines or short spurs of those who want to develop coal mines, if they can show that they have the coal reserves in quantity and quality to justify * * * and if they can show reasonable market prospects."

Because the same blanket rates have applied for years to main line and branch line alike, it is evident that branch-line construction is financed on the feeder-value basis

A review of decisions by the ICC involving the feeder value of branch railroad lines throughout the past sixty years shows that this basis is not "a startling new device" nor does it involve "curious" or "fallacious" reasoning. The following are firmly fixed as precedents:

> "They [small subsidiary roads] are feeders to the main lines, and help to swell the revenues of those lines. Their profitableness is not to be measured solely by what they earn themselves, but by the increase of business they bring to the main-line."[42]
>
> "These branch lines, however, are operated as part of a great and prosperous system. They are feeders to the main-line and help swell the revenue of that line."[43]
>
> "It is not expected that the extension will be profitable in itself, but as a feeder of the Union Pacific system, it will probably earn a fair return on the investment."[44]
>
> "The applicant states that the proposed extension will probably not be profitable in itself, but only as a feeder for its system * * *."[45]
>
> "It is not expected that the extension will be profitable claimed that its utility as a feeder line justifies construction."[46]

The same principle, recognized by the Board of Engineers in their report[47] on the Big Sandy River project, would seem to have ample support by transportation authorities.

John Overton, chairman of the Senate Subcommittee on Interstate and Foreign Commerce, referring to the nationwide scope of the waterways program at a hearing on the Red River project (Louisiana) in 1946, called particular attention to the prospective feeder value of the Red River canal:[48]

> "By the very nature and magnitude of the work, individual projects going to make up the [nation-wide] comprehensive development program have to be proposed, analyzed, adopted and prosecuted piece-meal. Each waterway extension, enlargement, feeder branch, or inter-connection adds to the efficiency and usefulness of the whole system. Through the construction of the proposed Red River canal, for instance, its tributary area will be

---

[42] *I. C. C. Decisions*, Vol. 4, 1891, p. 588.

[43] *Ibid.*, Vol. 19, 1899, p. 71.

[44] *Ibid.*, Vol. 86, 1924, p. 264.

[45] *Ibid.*, Vol. 99, 1925, p. 432.

[46] *Ibid.*, Vol. 150, 1929, p. 126.

[47] "Report of Board of Engineers for Rivers and Harbors on Big Sandy River and Tug and Levisa Forks, W. Va. and Ky.," *House Document 264*, 80th Cong., 1st Session, April 24, 1946, U. S. Govt. Printing Office, Washington, D. C.

[48] Address before the Board of Engrs. for Rivers and Harbors on the Red River Lateral Canal Project, Louisiana, *House Document 320*, 80th Cong., 1st Session, 1946, January 14, 1946, Archives of Board of Engrs. for Rivers and Harbors, Washington, D. C.

> connected with practically the entire inland waterway network of the nation and will share in the benefits of public expenditures already made in all other parts of the country. Similarly, the regions already provided with water transportation will benefit by the added accessibility of the markets and sources of raw material of the Red River area. I am reliably informed that the increase in average length of haul by inland river barge from year to year has kept pace with the progressive extensions and betterments that have been made—the increase in the past 15 years amounting to about 75 percent. Furthermore, the extension of the waterway system brings in its wake the extension of joint barge-rail and barge-truck transportation that extends the benefits of low-cost truck carrier service to expanded belts of territory not directly accessible to barge service."

COMPETITION

The ton-mileage of freight transported on the inland waterways is only about 6% of that carried on the railroads of the country. The fluctuation in rail ton-mileage from one year to another averages several times more than the total annual ton-mileage of waterway commerce. If the waterways were shut down and all waterway freight that could be handled were diverted to the railroads, it would not make nearly as much difference in their revenues as the normal annual fluctuation. Nevertheless, the railroads' opposition to the federal waterway improvement program is readily understandable when it is recognized that they have to pay for their roadways whereas the waterway carriers do not. Because some of their competitive practices are termed uneconomical in this paper, this does not mean to imply that they are unlawful or reprehensible in any sense. Together with the Federal Coordinator of Transportation, however, the writer believes that railroad practices are often detrimental to the public and sometimes injurious to the railroads themselves. He finds that, as stated[32] by the Federal Coordinator:

> "When a waterway is open, immediately competing modes of transportation, particularly the railroads, reduce their rates thus depriving the waterway of traffic which it would otherwise carry.
>
> "The public gets the benefit of those reductions but the waterway does not get the benefit of that traffic; and if you included all the traffic on all the reduced rates for which waterways were responsible, there would be a very different showing * * *."

and believes, with the Federal Coordinator, in his capacity as chairman of the ICC in 1939,[49] that

> "* * * a system of rates based on the cost of rendering the service would be better than any system of competitive rates, for all concerned including the country and its industries."

In their sixty-fifth annual report[50] the ICC declared: "Reductions to meet competition have been made possible in part by the high level of charges on other rail traffic." However, in their decision in the 15 Percent Rate Case, the ICC stated:[51]

---

[49] Hearings before the House Committee on Interstate and Foreign Commerce on the "Omnibus Transportation Bill" of 1939, *House Resolution 4862*, 76th Cong., 1st Session, Vol. 2 of transcript, p. 1091 and p. 1727, March 29, 1939.

[50] "Sixty-Fifth Annual Report of I. C. C.," November 1, 1951, reference to the "Fifteen Percent Rate Case," p. 4, U. S. Govt. Printing Office, Washington, D. C.

[51] *I. C. C. Decisions*, Ex Parte No. 115, Vol. 223, 1937, p. 739.

> "In their need for increased revenue, the applicants [railroads] have been careful to avoid proposing any increases in rates which have been published to meet the competition of other forms of transportation, although these are the depressed rates which are so largely responsible for their financial troubles."

In addition to the practice of depressing rates between waterway ports on barge-adapted traffic, the railroads have adopted another means of discouraging water-borne freight movements. Usually, a large part of the barge freight either reaches the waterway through a preliminary rail haul or reaches its destination through a final rail haul from the river ports, or both. Although the usually long water component of these joint movements can be performed by the barge lines at considerable saving, this benefit is offset, if possible, by excessively high rates charged on the short accessory and delivery hauls by rail. The high access rates charged by the railroads on coal from the southern Illinois fields to Alton on the Mississippi River and the high delivery rates on these same rail-barge-rail movements to inland points through the Twin Cities and other river ports on the upper Illinois River and the Mississippi River are examples in which little savings are allowed under the depressed all-rail rates on these movements.

The assistant general counsel of the AAR testified[52] before the Senate Subcommittee on Interstate and Foreign Commerce in 1950, touching on the diversion of traffic from rail to waterway:

> "The loss or revenue from the tonnage actually diverted to the waterways because of Federal subsidy is serious, but it is only a part of the loss suffered from this cause. The railroads also suffer the loss of much revenue because of depressed rates they must maintain in order to prevent the diversion of a large additional tonnage to subsidized waterways."

Quotation from "National Transportation Policy:"[53]

> "In the effort to prevent traffic diversion, rates on the commodities that are most vulnerable to competition will tend toward the level of out-of-pocket costs. Revenue required to obtain the level of earnings needed to induce new capital into the industry can then be secured only by increasing rates on the less vulnerable traffic."

Actually, the economic loss from these competitive practices (which is, of course, eventually passed on to the public) is greater than described by the railroad representative. There is always a substantial part of any block of traffic that is not susceptible to attraction by water transportation but will seek rail service at normal rail-rate levels for various sound reasons unconnected with comparative freight charges. When rates are depressed, the railroads suffer a material and unnecessary loss on this kind of traffic, in addition to the tonnage described in the foregoing testimony. It should be clear that, when the rail lines offer these uneconomical rates to potential shippers by water and make up their revenue deficits on noncompetitive movements elsewhere, they are in effect subsidizing one group of shippers at the expense of the other, just as they accuse the water carriers of doing.

---

[52] Hearings on a Study of Domestic Land and Water Transportation, *Senate Resolution 50*, **81st Cong.** 2d Session, p. 203, April 20, 1950.

[53] "National Transportation Policy," by Charles L. Dearing and Wilfred Owen, Brookings Institution, Washington, D. C., 1949, p. 300.

Another basic weakness of this competitive policy is that merely meeting the rate of a low-cost competitor at a noncompensatory level secures no permanent benefit to the high-cost carrier. The only logical objective from the viewpoint of those interested in the financial solvency of the competing enterprise is to drive out competition with a subsequent return to the previous high level or even a higher level to recuperate the losses incurred in the venture. In all these cases the inevitable injury to the public, to whom the bill is finally passed, is manifest. It is the conviction of the writer that a restoration of competitive rates to a normal fully compensatory level would eliminate a large part of the losses of the high-cost carriers. The transportation of low-grade bulk freight and other freight adapted to barge movement could profitably be left to the water lines, and the resulting stimulation of industry would be reflected generally in a more remunerative class of freight business for the high-cost transportation agencies.

THE ADDED-TRAFFIC THEORY

In order that transportation agencies of all types remain in business, their revenues in the aggregate must exceed their expenses. It has been shown that, when confronted with water-carrier competition, railroads depress their rates on the relatively small contested part of their traffic to less than the full cost of handling it and shift the excess revenue burden to the large blocks of noncompetitive tonnage that usually make up the bulk of their business. They seek to justify this rate manipulation on the theory that the added freight, attracted or recaptured from their competitors by noncompensatory rates, can be transported without incurring commensurate increases in carrier costs. The railroads claim to be better off handling the additional tonnage at a loss than surrendering it to competitors. Evidently the soundness of the theory depends on whether the short-term or the long-term effect is under consideration. For the long-term effect it can be shown that the formula is altogether unsound and would not be tolerated in any well-run engineering office.

The representative Illinois Central Railroad serves as an example. Its freight tonnage has increased tenfold in the past sixty years. Without doubt it was found that occasionally during that period of expansion a few more tons could be added to a freight car or a few more cars added to a train, without a horizontal, proportionate rise in the out-of-pocket costs of operation. However, the continuing process of adding tonnage throughout the sixty-year period has required progressively adding trains to the service; increasing the number and power of locomotives, number and size of rolling stock, and capacity of terminals; enlarging yards and servicing facilities; replacing light rail by heavy rail, double-tracking, and a corresponding expansion of operating and administrative personnel; and supplying machinery for attracting and servicing the required capital. All these additions, improvements, renewals, and expansions have been required by the added traffic until at the end the added traffic is no longer identifiable. It has merged and become practically all the traffic, and the out-of-pocket costs per ton-mile have caught up with the full costs.

In his opinion in the 15 Percent Rate Case,[51] Interstate Commerce Commissioner Joseph B. Eastman warned that:

> "Carriage for a supposed margin over 'out-of-pocket cost' is becoming the rule instead of the exception, and it will work only as the exception."

Stuart Daggett[54] points out that: "Few carrier costs are constant (that is, do not fluctuate with volume of traffic) over long periods * * *." Kent Healy[55] has found that: "The unit cost of additional traffic in the long run may be almost the same as the average over-all cost." W. Z. Ripley refuses to recognize the difference between "added traffic" and normal traffic:[56]

> "The moment the old traffic has outgrown the existing plant, the new expenditure becomes chargeable to all the business alike. * * * Each ton, both of old and new traffic, beyond the capacity of the facilities then in service, is equally responsible for the expense of the new equipment."

The former director of the Bureau of Economics and Statistics of the ICC concluded that:[57] "In the long run, every item of expense is variable with traffic changes 'although all items' do not increase or decrease in direct proportion." The usual explanation for assuming the constancy of the unassignable items of carrier expense is the existence of unutilized capacity. As the former director further states:[57]

> "Such explanation may have been justified when carriers were in their infancy * * *. However, in an industry such as the railroads, where the original excess capacity with which the carriers started operation has long since been utilized, and the pressure of added traffic during the past 50 years or more has required an almost continuous expansion of their facilities, this explanation loses much of its force."

Nevertheless, the opponents of inland waterway transportation continue to invoke the added-traffic theory in their petitions for relief from the laws against discrimination. The dangerous extent to which the theory is recognized as valid by the regulatory commissions may be judged from a few instances of rate reductions approved on this principle.

The following example involved the shipment of 100,000 tons of blackstrap molasses annually from the New Orleans river port area to Peoria (Ill.) and Pekin (Ill.) waterfront refineries on the Illinois River for processing into industrial alcohol.[58] During the initial period (from 1928 to 1937), this traffic paid the regular rail rate of $6.00 per ton, which yielded about 7 mills per ton-mile. Seeking to lower its costs of production, the molasses industry acquired a towboat and fleet of tank barges in which it was found that this raw material could be transported for a cost of $2.60 per ton, or 43% of the rail charge it had been paying. With the intention of increasing the volume of this profitable business, this shipper had begun negotiations for the purchase of an additional fleet when the railroads abruptly reduced their rate to $3.50 per ton, and thence to $3.00 per ton on trainload lots of the commodity, or 3.5 mills per ton-mile.

---

[54] "Principles of Inland Transportation," by Stuart Daggett, Harper Bros., New York, N. Y., 1941, pp. 314–319.

[55] "The Economics of Transportation in America," by Kent T. Healy, The Ronald Press, New York, N. Y., 1940, p. 197.

[56] "Railroads, Rates, and Regulations," by W. Z. Ripley, Longsman-Greene, New York, N. Y., 1912, pp. 61–62.

[57] "Rail Freight Service Cost Tables," by Ford K. Edwards, *Senate Document 63*, 78th Cong., 1st Session, 1943, p. 1 and p. 19.

[58] *I. C. C. Decisions*, Vol. 233, 1937, p. 271; Vol. 235, 1939, p. 485; and Vol. 241, 1940, p. 177.

Out of this revenue the carriers had to pay approximately 1 mill per ton-mile rental for special tank-car equipment leased to them by the industry. Compared with the average of 9.9 mills per ton-mile then being collected for rail traffic in general, this traffic obviously was not paying its share of the rail-service cost, but it was sufficient to hold the movement on the rails and forestall the purchase of barge equipment. Meanwhile, the rail rates on blackstrap molasses between intermediate points not accessible to the waterway were held at the previous high level, which has since been raised and, together with other noncompetitive rail traffic, is carrying the revenue burden. The improved river thus lost a substantial block of traffic, which the water carriers could have transported profitably, to rail carriers which could not transport it profitably. However, this and many hundreds of similar rate adjustments were approved by the ICC after thorough investigation.

A more recent typical example of the granting of regulatory authority to the railroads to reduce rates to meet competition between waterway ports while maintaining intermediate rates at a higher level occurred in Alabama. The rail rate in effect on coal from mines in the Birmingham area to Mobile (in Alabama) at the beginning of the proceeding was $2.55 a ton. In 1950, the ICC permitted a reduction to $1.28 per ton.[59] The distances varied from 334 miles to 370 miles, yielding revenues of from 3.8 mills to 3.5 mills per ton-mile and involved interchange among three individual lines. To intermediate dry-land points averaging 106 miles, 294 miles, and 365 miles from the mines, maintenance of the previous rates of $1.55, $2.80, and $1.90 per ton was authorized, yielding 14.6 mills, 9.5 mills, and 5.2 mills, respectively. In 1943, the director of the Bureau of Economics of the ICC had found that the average full cost of moving bulk freight, such as coal in hopper cars, in the Southern Region was 8.2 mills per ton-mile. The result of this adjustment, however, was to attract an annual movement of more than 300,000 tons of coal from these mines to Mobile by rail, leaving 72,000 tons to travel by waterway.

In March, 1951, a decision of the ICC[60] authorized a reduction in the rail rate for sulfur from Port Sulphur (La.) to Nashville (Tenn.) of from $10.20 a ton to $7.00 a ton to "meet" barge competition. The rail distance is 667 miles. The railroads were granted authority to maintain higher rates to intermediate points not reached by water service, as for instance $7.80 per ton to Hurricane (Ala.), only 203 miles from Port Sulphur, and $10.20 per ton to Prospect (Tenn.), only 577 miles. An earlier case[61] decided in January, 1942, granted a reduction on iron and steel articles from Newport (Ky.) to Memphis of from $5.40 per ton to $3.60 per ton to meet waterway competition. A similar case[62] in August, 1941, authorized a reduction on cotton linters from Cairo (Ill.) to Chattanooga (Tenn.) of from $5.00 per ton to $3.60 per ton for the same reason. As in the many other "relief" cases, authority is granted to maintain higher rates for shorter hauls between those origins and destinations that are not subject to competition from the water carriers.

---

[59] *I. C. C. Decisions*, Fourth Section Application 19085, Vol. 253, 1950, p. 458.

[60] *I. & S. Dockets 5781 and 5794*, Vol. 280, 1951, p. 423.

[61] *I. C. C. Decisions*, Vol. 248, 1942, p. 453.

[62] *Ibid.*, Vol. 246, 1941, p. 516.

In its sixty-fifth annual report,[50] the ICC observed:

> "As we said in our last report, reductions to meet competition have been made possible in part by the high level of charges on other rail traffic."

Testifying before the Interstate and Foreign Commerce Subcommittee, the general freight agent of the American Barge Line Company remarked:[63]

> "Although the railroads are willing to cut their rates as much or more than 50 percent on traffic moving between the river banks, they are not willing to interchange interior traffic with the water lines even upon the same basis as they do with their railroad connections, unless forced to do so."

A considerable volume of the competitive tonnage will always travel by rail for various reasons other than the scale of charges, so that the revenue losses occasioned by competitive rate depression are not confined to the recaptured tonnage. When it is realized that freight held on the rails by such added-traffic rate reductions could travel, as provided for by waterway, at a profit to carrier and shipper alike—the magnitude of the economic loss to the public as well as to the transportation agencies becomes manifest. A further deplorable result of the form which this kind of competition has been allowed to take is the conviction held among local interests not served by waterways that the only way to bring excessive freight rates down to reasonable levels is to promote local waterway projects. The EJC included among its recommendations[64] the following: "The use of inland waterways as a regulatory agency to force reductions in rates on land carriers should be abandoned." Such use is not contemplated by the Corps of Engineers. Of course, there is no valid defense for spending public money on navigation projects merely to regulate freight rates in the public interest—that being, ostensibly at least, the function of the regulatory commissions. The Chief of Engineers, in a letter[65] to the chairman of the Interstate and Foreign Commerce Committee of the House of Representatives dated February 25, 1939, in reference to a navigation project report, said:

> "My report most emphatically does not recommend the construction of the canal at public expense for the purpose of reducing rail freight rates * * *."

These practices, however, do create an uneven and uneconomical distribution of tonnage among the several agencies of transport, diverting traffic from adapted carriers to nonadapted carriers, thus defeating the whole purpose for which low-cost water transportation is provided.

The following excerpts are taken from some particularly pertinent testimony which was presented in the Barge-Rail Rate Case[66] by the traffic manager of the Mississippi Valley Barge Line, a typical victim of competition based on this spurious theory—

---

[63] **Hearing before the Senate Interstate and Foreign Commerce Subcommittee, *Senate Resolution 50*, 81st Cong., 2d Session, 1950, p. 1483.**

[64] "Principles of a Sound National Water Policy," prepared under the auspices of Engineers Joint Council, July 21, 1951, "Summary and Conclusions," p. 95, Edwards Bros., Inc., Ann Arbor, Mich.

[65] Letter from Julian L. Schley, Chief of Engrs., U. S. Army, to the Chairman, House Committee on Interstate and Foreign Commerce, dated February 25, 1939, in transcript of hearings on *House Resolution 2531* and *House Resolution 4862*, 76 Cong., 1st Session, Vol. 2 of transcript, March 29, 1939, p. 1091, U. S. Govt. Printing Office, Washington, D. C.

[66] ***I. C. C. Docket 26712*. Hearings at New Orleans, La., March 25, 1935, U. S. Govt Printing Office, Washington, D. C.**

> "Counsel: You have referred several times to this question of 'added traffic' basis for justifying rate reductions.
>
> "Traffic Manager: That is another theoretical proposition. It is based on the premise that once a railroad is built, trains are in operation, supervisory staffs are employed, and a certain volume of traffic is moving on normal rates, the out-of-pocket cost of handling additional business is but a fractional part of the full cost.
>
> * * *
>
> "Counsel: In computing the so-called out-of-pocket expense, can you state what percentage of the actual expense is ordinarily used as a basis of computation?
>
> "Traffic Manager: * * * I have seen where 40 percent was used and I have seen where 60 percent was used. * * * I would say that 50 percent [of full cost] is a fair average of the various amounts used."

In the same proceeding, the counsel for the Mississippi Valley Association (MVA), an organization of industrial, commercial, agricultural, and consumer interests of the midcontinent area, testified in reply to questions by railroad counsel in part as follows:

> "MVA Counsel: If you make money, that would be a sound doctrine, but by making money I do not refer to your so-called added traffic theories and out-of-pocket costs. You cannot make money on such theories as that. * * * I think the theory is false and illusory all the way through.
>
> "Railroad Counsel: Well, do I understand that the members of the Mississippi Valley Association advocate putting the railroads in a place where they cannot meet competition?
>
> "MVA Counsel: We take this position, that a railroad cannot meet the rates of a lower-cost carrier successfully. The barge is inherently a lower-cost carrier. The railroads can never meet those rates without going below a profitable rate for a railroad carrier."

The same thought was expressed in a joint letter from the United States Secretary of War, the Secretary of Agriculture, and the chairman of the United States Maritime Commission to the chairman of the Senate Committee on Commerce on February 16, 1940, as follows:[67]

> "The shipping public is thus led to forego the real economic benefits provided by the waterways at public expense, and to accept in lieu thereof rail rate reductions which work injury to the railroads themselves. The very questionable advantages which the rail carriers derive from the practice are a depletion of water-adapted tonnage, a consequently misleading rise in waterway improvement costs per ton-mile, and the discrediting of the policy of river improvement by the Federal Government."

The chairman of the ICC, in characterizing the use of added-traffic rates as a weapon against less favored competitors, said:[51]

> "It may be used, for example, at the expense of such [exclusive blocks of noncompetitive] rail traffic, for the purpose of maintaining an unfair and destructive warfare with competitors who are not fortunate enough to possess such a reserve of exclusive business."

The trouble with this, as with many of these sound and forward-looking pronouncements, is that it was a minority opinion and did not deter the majority of the ICC from protecting the revenues of the carriers from erosion threatened by these discriminatory practices. However, looking into the future, it is not being too optimistic to hope that the fallacy of the added-traffic theory will become increasingly manifest to the regulatory agencies or that they will be required by legislation to desist from granting relief to carriers invoking this unsound doctrine.

---

[67] *Congressional Record*, March 4, 1940, pp. 3481 to 3485.

USER CHARGES

All serious students of transportation must concede that, whereas rail carriers pay all expenses (including roadway) out of earnings and water carriers pay nothing for the navigation facilities they use, an inequitable situation results. The railroads should not be criticized, when trying to offset this handicap, for taking all lawful measures they deem advantageous to their interest in profitable operation of their own properties. The writer believes that some of the measures they take are harmful to themselves as well as to their competitors. He is convinced that the corrective solution most universally advocated—that of imposing tolls on the users of waterways—would, under the prevailing regulatory leniency, constitute a remedy worse than the disease.

The ostensible objective advanced by those who advocate user charges is reimbursement of the national Treasury for outlays made in providing and maintaining the improvements. If this were indeed the governing purpose, the advocates could logically be expected to devise and propose some fair and practical system of collection whose cost of administration would not exceed the revenues and which would not progressively "dry up" the traffic of waterways representing public funds already irrevocably invested. Reading between the lines of even the most academic treatise on the subject leads to the conclusion, however, that it is not concern for the taxpayers' money but for removal of the element of unequal competition inherent in the present system of inland waterway transportation that motivates the advocates of tolls. Otherwise, no distinction would be drawn between inland river carriers and users of the Great Lakes and coastal harbor improvements. The difference is that the service of river-boat lines is within reach of competitive rate adjustments by the surface carriers, whereas the Great Lakes carriers' costs are inherently too low to be reached by competing carriers, and the coastal harbor channels are actually a necessary supplement to rail service.

The general counsel for the ARA in his testimony[68] on the Transportation Bill S.2009, in April, 1939—explaining the inclusion (in the railroads' draft of this bill) of exemptions of Great Lakes carriers and coastal-channel operators—said:

> "That particular language was put in with special reference to conditions on the Great Lakes, where the bulk of the tonnage there is carried by contract carriers who are, generally speaking, not in competition with anybody. Grain, ore, stone, coal, and some other commodities * * * move in large quantities at relatively low rates which the railroads could never hope to meet."

---

[68] Hearing before the House Committee on Interstate and Foreign Commerce, February 8, 1939, on the "Omnibus Transportation Bill," *House Resolution 2531*, pp. 382-383 of transcript, 76th Cong., 1st Session.

The Director of Research for the Federal Coordinator of Transportation[9] presents what is probably the fairest, most intelligent, and most objective analysis of the problem of tolls that has been published up to 1952. In lifting passages from the director's report out of context (always a potential source of injustice), the writer has attempted to project fairly the director's apparent attitude toward the practical effect of imposing user charges to recover various proportions of the expenditures already made on waterway projects and charges on recommended extensions and enlargements of the system.[69]

> "Questions of Policy for the Future"
>
> "The Tolls Question. * * * The following assumptions are laid down:
>
> (a) That all principles and methods will be laid down uniformly.
> (b) That the newer existing waterway improvements and those now approaching completion will be permitted to develop without tolls * * *
> (c) That traffic which does not * * * benefit * * * will be excluded.
> (d) That the question of assessing tolls will be considered from the point of view of covering (i) total costs or (ii) the costs of maintenance and operation, only.
>
> "The charging of tolls would (1) contribute to placing the several forms of transportation on more nearly equal competitive terms, lay the basis for a more effective cooperation of the different forms of transportation in the public interest, and lessen trade dislocations that result from competition between self-sustaining and subsidized services. (2) Promote adequate control and a rational planning of future waterway improvements. (3) To a minor extent, contribute to the public Treasury funds needed for the general purposes of government."

In studying the stated objectives, one is disturbed by the dislocations and discriminations that would inevitably result from acceptance of those recommendations. If user charges were to be imposed commensurate with the cost of improving and maintaining the various channels and locks, as proposed, there would be an almost infinite variation in toll rates, and the cost of allocation, assessment, and collection could well exceed the total revenue received. Inland waterway routes are now on a rational competitive basis with rail-lake-rail routes such as that from Pittsburgh to Minneapolis (Minn.), and with rail-coastwise routes such as that from Pittsburgh to Houston. These relationships would be unwarrantably destroyed by the imposition of tolls on one group of carriers and not on the others, when all are using federally provided facilities. Before 1952, no workable system for avoiding these discriminations had been proposed by the advocates of user charges.

The Director of Research also stated:[70]

> "In a memorandum to the Federal Coordinator of Transportation from railroad representatives the following suggestion was offered:
>
> > "The Association of Railway Executives recommends that charges be assessed against all commercial users of improved waterways to

---

[69] "Public Aids to Transportation," by Charles S. Morgan, U. S. Govt. Printing Office, Washington, D. C., 1939, Vol. III, "User Charges," pp. 120–127.

[70] *Ibid.*, p. 125.

> compensate taxpayers for their investment in such waterways and for amounts which have been expended for administration, maintenance, and operation. To this end we propose that Congress provide by law that navigable inland waterways be made self-supporting and self-liquidating; that tolls should be provided for the use of the improved navigable inland waterways of the United States when commercially used.
>
> * * *
>
> 'There is no thought in the minds of the Association to suggest tolls so heavy as to destroy the traffic * * *.'"

Gregory S. Prince, the representative of the AAR before the Subcommittee on Interstate and Foreign Commerce at the hearings on Senate Resolution 50 (1950) testified as follows:[71]

> "The railroads do have a rightful basis of complaining when as here, the inroads [on rail freight traffic] are due to artificial advantages resulting from subsidies to inland waterway transportation.
>
> "Since no user charge of any kind or description is imposed for the use of inland waterways, the entire [federal] expenditure for new work and for operation and maintenance on rivers and canals constitutes a subsidy * * *.
>
> "The Presiding Officer: Those expenditures also aid the railroads to a certain extent. Do you get a portion of that share?
>
> "Answer: From the seacoast harbors and channels?
>
> "The Presiding Officer: Yes.
>
> "AAR Representative: That is correct, sir."

At least five bills have been introduced since 1935 proposing tolls for the use of improved inland waterways, all of which have died in the legislative mill.

The Federal Coordinator has reported that:[72]

> "Only if the carriers were subject to tolls adequate to carry the cost-reasonably assigned to them could they demonstrate what water transportas tion is able to do and begin a reckoning of true savings. It is only too obvious from this report that if tolls in such amounts were assessed a large part and in some cases all of the traffic now carried on various of the rivers and canals would disappear.
>
> * * *
>
> "Competition between public capital and private capital * * * cannot be brought under sensible control until the railroads' competitors are forced to meet the same kinds of costs the railroads themselves do, or some balancing favor is given the railroads by the Government."

The foregoing pronouncements bring into prominence an attitude evinced in varying degree by all opponents of inland waterway development. On the one hand, they advocate the imposition of tolls on the users of inland waterways, to the end that the United States be reimbursed for its expenditures on inland waterway projects; on the other hand, however, they voice the opinion that such action will drive a large part of the traffic off the water. In that case, obviously the stated purpose would be defeated.

---

[71] Hearings before the Senate Resolution Subcommittee on Interstate and Foreign Commerce on a Study of Domestic Land and Water Transportation, *Senate Resolution 50*, 81st Cong., 2d Session, 1950, p. 200.

[72] "Public Aid to Transportation," by Charles S. Morgan, U. S. Govt. Printing Office, Washington, D.C., 1939, Vol. III, p. 206.

The author of "Muddy Waters" advocates user charges on waterways as a sound water-development policy, sound transportation policy, and sound general national policy. He lists among those advocating tolls the ICC, the President's "Committee of Six" (railroad executives), the National Resources Planning Board, Charles L. Dearing and Wilfred Owen in their book, "National Transportation Policy," and Secretary Charles Sawyer of the Department of Commerce. He claims that it is a sound, established fiscal policy generally to require recipients of special economic benefits from governmental activities to pay directly, "at least in part," for those benefits. He states that, by placing the burden of waterway costs directly on those who use the facilities, the collection of user payments would "tend to promote sounder planning of waterway projects" and "greater care in the prediction of benefits from proposed projects."

Alone among the many treatises advocating user charges, the author of "Muddy Waters" recognizes the present unsatisfactory competitive situation but dismisses the dangers in the situation that would be created by the imposition of tolls with scant consideration.

He concedes that:[73]

> "To compete with subsidized water transportation, the railroads, subject to whatever limitations are imposed by regulatory agencies, often depress to an uneconomic level their rates on freight that competes with waterways. They 'lose' money on these out-of-pocket-costs rates, but make up the loss by charging higher rates on freight for which there is no water competition."

The foregoing pronouncements bring into prominence an attitude evinced in varying degree by most opponents of inland waterways development. None of the many economists who propose the imposition of tolls appear willing to face squarely the situation which would result if their recommendations were to be followed. The imposition of tolls on waterway commerce without positive legislative protection of the water carriers against destructive rate-cutting by the more firmly entrenched rail carriers would probably end in complete elimination of barge service from the inland navigation system. The reason lies in the uneconomic competitive practices of the overland carriers and the lenient attitude of regulatory agencies toward these practices. There can be no fair and workable application of user charges to waterway transportation unless and until a rigid cost-of-service basis of competitive rates is imposed on competing agencies as far as the contested traffic is concerned. Railroads, because they go almost everywhere and transport all kinds of freight, can handle any commodity movement available to any of the other modes of transportation. Under the prevailing system, they can and do depress their rates, frequently below the actual cost of handling, on any particular block of competitive traffic they choose to select for attack and raise their rates proportionately on other traffic that is not available to their restricted competitor. Boat lines have no such blocks of exclusive, noncompetitive traffic within the limited scope of their transportation activities upon which they can shift their revenue burden through higher rates. All their freight movements must carry their full share of the total expense of transportation if the water-carrier enterprises are not to collapse.

---

[73] "Muddy Waters—The Army Engineers and the Nation's Rivers," by Arthur Maass, Harvard University Press, Cambridge, Mass., 1951, p. 163.

If tolls are imposed upon such operations, the taxes would have to be passed along to the shippers and through the shippers to the ultimate consumers of the goods in proportionate additions to each rate. It is clear that, under the competitive conditions just described, these water lines would be at the mercy of competitors possessing diversified traffic until they had been eliminated from the field, one by one, by selective rate cutting. The shipping public would thus be deprived of a genuinely economical means of transportation in its special field.

The author of "Muddy Waters" evinces little concern over this state of affairs, merely stating:[73]

> "If the collection of tolls were not to eliminate uneconomic rail rates automatically, then it would be the responsibility of the Interstate Commerce Commission to compel railroads to establish rates that truly represent their relative economies."

There is nothing in the long record of rate decisions by the ICC that would offer any assurance of protection from that source. The railroads themselves have maintained that they cannot fix individual rates at cost. The ICC has always permitted the railroads to establish low rates where the existence of waterway competition could be shown, permitting the maintenance of higher rates on shorter intermediate hauls not subject to competion. It is only when the courts intervene, as in the Ex-Barge Grain Case (1943), that the barge lines can obtain some measure of protection against discriminatory rate cutting.

This case was on appeal to the United States Supreme Court[74] growing out of an ICC decision.[75,76,77] In the dissenting opinion of Supreme Court Justice Hugo Black on this case is an illuminating quotation:[74]

> "The District Court, which held that the Interstate Commerce Commission's order 'discriminates against water competition by users of the barges' understood the issue. The railroads which proposed the increase in the cost to barge shippers, also understood the issue as is shown by the frank statement of their representative at the Commission hearing:
>
> > 'We made this proposal, as I have stated several times, and filed these tariffs with the hope that we could drive this business off the water and back onto the rails where it belongs * * *. We are not in love with water transportation * * * and we believe we are entitled to that grain business.'"

The decision of the Supreme Court required the ICC to reverse itself and protect the barge users from discrimination.[74]

The attitude of the competitors of waterway transportation was well understood by the chairman of the ICC. In his dissenting opinion he denied the railroads the right to establish obviously noncompensatory rates in the

---

[74] Interstate Commerce Comm. vs. Inland Waterways Corp., U. S. Code, 319 U. S., p. 671.

[75] *I. C. C. Decisions*, Vol. 248, 1949, p. 307.

[76] *Ibid.*, Vol. 256, 1950, p. 353.

[77] "Fifty-Seventh Annual Report of I. C. C.," U. S. Govt. Printing Office, Washington, D. C., 1943, p. 88.

Petroleum Products Case of 1933—in which the railroads sought to reduce their rates below cost to regain traffic that had been lost to barge lines:[78]

> "This promises to be a return to a policy of railroad rate-making which existed for many years * * *. The railroads in their early years encountered stiff competition from steamboat lines * * * and they proceeded to meet this competition ruthlessly. Eventually they swept the waters clean of competing craft except on the ocean and Gulf, and even there the competition was greatly weakened.
>
> "This was done by cutting rates where competition existed, to whatever extent was necessary to paralyze it, at the same time maintaining rates at a very high level elsewhere. The steamboats did not have this reservoir of non-competitive traffic (upon which to shift the revenue burden of a rate war) to help them out, and hence perished in the unequal struggle. * * * All of this made, of course, for a very uneven development of the country, and it was one of the main factors which precipitated the creation of this Commission."

In 1939, in testimony before the Committee on Interstate and Foreign Commerce of the House of Representatives on the Interstate Commerce Bill, R. V. Fletcher, the vice-president and general counsel of the AAR defined the attitude of the railroads toward any regulatory attempt to prescribe rates on a cost-of-service basis. He proposed that the wording of the act require that only in the aggregate must the rates of railroads meet their revenue requirements. It is at once apparent what they could do, with that leeway, in adjusting their rates to competitive conditions. He quoted a proposed provision in the draft of the bill that was later eliminated:[79]

> "It [the Interstate Commerce Commission] shall give due consideration to the undesirability, in the public interest, of permitting any carrier to establish and maintain any rate, fare, or charge which is the same as, or less than, the full cost of performing the service."

The AAR counsel continued:

> "Now we think that, with great deference of course, we think that an objectionable and dangerous thing to undertake to give so much emphasis upon the full cost of performing the service.
>
> * * *
>
> "You cannot make rates on that basis, although many thoughtful students have endeavored to do so. It is impracticable. It is impossible to find the proper figure and impossible to apply it if you found it in view of the competitive conditions we have."

In continued hearings on the same bill, the counsel proposed a rate-making rule containing the following language:[79]

> "We [the railroads] propose, therefore, a rate-making rule to read as follows:
>
> > "It shall be the duty of the Interstate Commerce Commission * * * to permit the establishment * * * of rates which, as a whole, will be adequate * * *.'"

---

[78] *I. C. C. Decisions*, Vol. 94, 1933, p. 31.

[79] Hearings before the House Committee on Interstate and Foreign Commerce on the "Omnibus Transportation Bill" of 1939, April 3 and 4, 1939, 76th Cong., 1st Session, p. 383 and p. 578.

It is difficult to believe that the railroads, with their fully detailed statistical records and their elaborate facilities for research, do not actually know within reasonable approximation what their costs are. It was made abundantly clear in the prolonged hearings on the Class Rate Case[80] that they do not relish having such costs established for official use (and possible misuse); such an attitude is readily understandable. The Bureau of Economics and Statistics of the ICC, however, has compiled[57] from railroad records, and keeps reasonably current, a voluminous analysis of the varying costs per ton-mile of handling and transporting more than 700 different commodities in the various freight territories. These cost figures are based on the relative use characteristically made by shippers of each kind of commodity of available rail equipment and facilities. Some elements of cost have to be prorated on a more or less arbitary basis, but the method has received the acclaim of traffic men in general and is being relied on increasingly by the ICC in important decisions involving the justness and reasonableness of rates.

This cost-finding system has been applied by the Corps of Engineers to the detailed statistical records of representative barge-line operators on various sections of the waterway system and in various kinds of service. A set of base costs has thus been compiled for modification to fit any specific set of conditions expected to be encountered on individual waterway projects, and for comparison with "Rail Freight Service Cost Tables."[57] The general acceptance of the cost basis by traffic and transportation specialists as a yardstick for measuring the reasonableness of rates and the tendency toward greater reliance upon it, even by the regulatory agencies, are encouraging. The Corps of Engineers look ahead with some confidence to an eventual legislative ban on the system that now permits rates to deflect tonnage from an economical to an uneconomical agency of transport.

In "Muddy Waters" is a fairly accurate statement of the engineers' position (paraphrased from "Rationale of Inland Waterway Transportation,"[81] prepared under the direction of the Chief of Engineers in 1940) as follows:[82]

> "Cost of service is not the governing factor in fixing the rates of competing railroads. Railroads establish uneconomic rates [out-of-pocket-costs rates] on freight that competes with waterways.
>
> "The effect of such differential rating is to keep freight that economically should travel on waterways, on the railroads instead, because of the better service which railroads can offer. Therefore, waterways are not used to the extent they should be, economically, and as a result, unit costs are relatively high.
>
> "The most disastrous effect of the current system of permitting high cost, high grade carriers to compete with low cost, low grade carriers for low grade traffic, is the diversion from waterways, without profit to anybody, of traffic which they could serve adequately, and economically. In thus curtailing water-borne tonnage it produces misleading unit cost statistics applied to the provision of channels and locks—statistics which are used with skill and effectiveness by opponents of the national waterway policy.

---

[80] *I. C. C. Docket No. 28300*, investigation, 1939. Hearings in Indianapolis, Ind., September 22 to October 1, 1942, U. S. Govt. Printing Office, Washington, D. C.

[81] "Transportation and National Policy," National Resources Planning Board, Washington, D. C., May, 1942, Pt. II, Section IV, "Inland Water Transport," by Julian L. Schley, pp. 443–446.

[82] "Muddy Waters—The Army Engineers and the Nation's Rivers," by Arthur Maass, Harvard University Press, Cambridge, Mass., 1951, p. 165.

> "For these reasons, at least until such time as water-borne tonnage is allowed to swell to the predicted volume when permitted freely to seek water routes, uninfluenced by competitive rail rate depression, improvement costs should not be included in comparative rate figures for economic justification, and tolls should not be charged."

It could be wished that the text had been quoted, verbatim. The rearrangement in the last sentence states in effect that improvement costs are disregarded in determining economic justification and that tolls should not be charged under any circumstances. This impression of the attitude of the Corps of Engineers, created by the writings of various opponents of waterways, has certainly lodged in the minds of the public.

The author of "Muddy Waters" aims this final blast at the engineers' procedure:[83]

> "If water rate figures used in survey reports were revised to include both carrier costs and public improvement costs, the economic justification for any project would be determined by a simple comparison of rail and water rates. That is, assuming the water rates to be lower, the differential between the two rates would be multiplied by the amount of traffic (in ton-miles) which, after a development period, could be expected to move if asked to bear full costs. This would not give the same result as the Engineers now obtain by establishing a ratio between the annual costs of a project (derived by amortizing the investment and adding annual maintenance costs) and the annual benefits (derived by comparing rail rates to subsidized water carrier rates), for the simple reason that estimated volume of traffic is likely to be much greater where the rates comparisons are based on the lower subsidized water rates, which include no allowance for waterway improvement costs.
>
> "In the second place, even if the present rail rates are already uneconomically depressed, or if it is feared that an uneconomic reduction in rail rates after a project is built will adversely affect its economic justification then the duty of the Chief of Engineers as a public servant is not to recommend the construction of additional costly water projects on a justification which fails to include in water rates the public costs of improvements, but to estimate the traffic distribution which will result from rail and water rates, both based upon full cost of service, and then, if the project appears justified, to recommend its construction and at the same time to recommend that the railroads be made to establish fully economic rates by regulation if they fail to do so on their own accord."

The engineers have ample reason to doubt the possibility of any effective protection of waterway traffic against rate-cutting raids, through regulation. They include annual charges covering interest, amortization, and maintenance and operation of navigation facilities among the costs to be offset by transportation savings in measuring their economic justification. They do not add hypothetical tolls to the water rates because Congress has flatly rejected tolls. It may be assumed from the record that Congress does not intend to impose tolls for the valid reasons set forth in this paper. If and when Congress adopts tolls by legislation, the engineers can naturally be expected to modify their formula accordingly.

---

[83] "Muddy Waters—The Army Engineers and the Nation's Rivers," by Arthur Maass, Harvard University Press, Cambridge, Mass., 1951, p. 166.

THE NATIONAL TRANSPORTATION SYSTEM

An additional criterion, popular with theorists in the field of traffic economics, is that all navigation improvements, in order to justify themselves, should be susceptible of being fitted into what they term the "National Transportation System" to advantage. Like most other theories, this one sounds reasonable; but it has no logical application because there is no national transportation system. That is, factually speaking, there is not any logically planned, coordinated organization of carriers of all types to take care of the national freight burden in the most efficient and economical way. The criteria observed by the Corps of Engineers in investigating the merits of any project require an appraisal of existing transportation facilities of all types in the area tributary to the proposed waterway and a determination of the net contribution it can be expected to make toward proper disposal of the local transport needs; but apparently that is not what the theorists mean. They mean that, if there is already a physical adequacy of transportation, no matter how improvidently conceived, badly managed, expensive, or obsolescent, an economical waterway should not be introduced into the "system" unless the weakest of the existing transport agencies are either supported in relative idleness or paid to stand aside. That is the theory under which the existing carriers have successfully opposed the Riverlake Belt Conveyor scheme for moving ore and coal between lake ports and the Pittsburgh-Youngstown steel-producing area. Until the beginning of World War II, they successfully opposed the crossing of their rights of way by an oil pipe line from a port on the Gulf of Mexico into the Southeast, until the exigencies of war disposed of their opposition. It is a position entirely comprehensible from the standpoint of the ownership of existing facilities, but if it is generally adopted, it will deprive the country of most efficient and economical transportation for certain commodities needed in great volume by basic industries.

The existing carriers have grown and spread and joined in response to the needs of commerce, and whereas they might have done better, they have not done badly on the whole. The existing transportation plant, such as it is, needs both cultivation and pruning. Parts of the country are still undersupplied with transportation whereas other parts seem to be oversupplied, but they seem to respond eventually to the law of supply and demand.

Some railroads are favorably located, suitably designed, well managed, and prosperous, rendering an indispensable service to the public at reasonable rates. Others successfully attract a large enough share of the commerce to remain solvent and useful without being able to recompense their owners with much of a return on their investment. Still other ventures, unsoundly launched in the first place, are poorly supplied and maintained, exploited by their creditors, constitute a drain on their financial backing and contend for traffic that one of the sounder companies could more profitably handle. According to the integration theory, however, all these existing agencies, efficient or inefficient, must be sustained in "healthy financial condition"[84] by holding freight rates high enough to allow them a profit. That was the theory of the ICC in its adverse report on the Lake Erie-Ohio River Canal, with respect to the probable effect of the proposed canal on the existing carriers between Lake Erie and the Youngstown-Pittsburgh area. The report states:[85]

---

[84] "Muddy Waters—The Army Engineers and the Nation's Rivers," by Arthur Maass, Harvard University Press, Cambridge, Mass., 1951, p. 167.

> "Included in these lists are carriers which will be recognized as basically strong and others whose present condition is very bad and whose long-term outlook is unfavorable."

However, it was held that all these carriers should be maintained in financially sound condition, even though the steel industry in the eastern United States and the coal-using industries in the western states had to continue without a more economical and efficient means of transportation. It is not apparent to the writer why those carriers whose condition and outlook were bad should be maintained in service at a loss any more than that the old Mississippi River channel through Chain of Rocks should be maintained after the more efficient by-pass canal is opened to navigation. If the entrance of an efficient and economical waterway into the transportation field creates a surplus of carrier facilities, it is clearly in the interest of a healthy transportation system that the most costly and inefficient units be displaced and traffic be distributed among those agencies that can profitably render the required service at reasonable rates. There would not seem to be any logical obligation on the general taxpayers or shippers to forego the benefits of economical water transportation in order to maintain a wasteful and inefficient competitor in business.

LEGISLATION

Three bills having important bearing on the future of waterway transportation were pending at the close of the 82d Congress. The significance of two of them, S-2742 and S-2743, imposing tolls on water carriers and abolishing restraints on the competitive depression of rates, has been explained. The third bill, S-2744, provided that final determination of the public necessity for providing and maintaining waterways shall be vested in the ICC. This paper is not concerned with the questions of policy involved in pending legislation but whether the proposals can be made to work in actual practice. Drafters of this bill have inserted some odd provisions that seem incompatible with the practical attainment of the stated objectives. One provision is that the economic investigations by the Corps of Engineers and the ICC are not to be coordinated as might be expected. The Corps of Engineers must complete its surveys and reports and make its recommendations before the project is referred to ICC. The assistant general counsel of the AAR in presenting the proposal before a Senate Committee said:[86]

> "Both because of the experience and qualifications of the Commission and because of its broad responsibilities in the field of transportation, the determination of whether additional waterway facilities for navigation proposed should be constructed is one which should be vested in the Interstate Commerce Commission."

A further shift of responsibility is contemplated by this witness:[87]

> "The policies with respect to the improvement of inland waterways are essentially a part of our national transportation policy. Accordingly we

---

[85] I. C. C. Report on the Lake Erie and Ohio River Canal Project, *House Document 178*, 76th Cong., 1st Session, 1938. Also *I. C. C. Decisions*, Vol. 235, 1939, p. 753.

[86] Hearings before the Senate Interstate and Foreign Commerce Committee on Bill S-2744, 82d Cong., 2d Session, 1952, p. 1520, April 9, 1952.

[87] *Ibid.*, pp. 1371 to 1380.

> believe the Congress might well give consideration to the transfer of jurisdiction over inland waterway navigation projects from the Committees on Public Works to the Committees on Interstate and Foreign Commerce, the latter being the ones charged with the responsibility for transportation problems generally."

The sponsors of these bills are evidently not interested in the fact that the improvement of inland waterways is likewise essentially a part of the national water-resource development policy under the jurisdiction of the Committees on Public Works of Congress. That the conflict might be awkward is substantiated by the following stipulation in the bill[88] which finally emerged from the Senate Subcommittee on Interstate and Foreign Commerce in February, 1952:

> "No Federal project for the improvement of any inland waterway designed, in whole or in part, to aid navigation shall hereafter be undertaken, nor shall any Federal funds by expended on or allocated to any project heretofore authorized by the Congress but construction of which is less than 25 per centum complete, * * * until the Interstate Commerce Commission after full hearing shall have submitted a report as hereinafter provided concerning justification and the public convenience and necessity for the transportation features of the project."

This provision obviously applies to multiple-purpose projects featuring flood control, hydroelectric power, irrigation, and drainage—with navigation facilities of possibly minor importance. It is apparent what the proposed procedure would do to a project like the Columbia River valley improvement. According to the bill[89] it would operate as follows:

> "Whenever a detailed survey of proposed inland waterway improvement project designed, in whole or in part, to aid navigation, has been made, and the report based on said survey shall contain a recommendation in favor of such project, said survey and report shall be submitted by the Chief of Engineers, United States Army, to the Interstate Commerce Commission for investigation and report as hereinafter provided. * * * Upon receipt of the report of the Interstate Commerce Commission, the Chief of Engineers shall submit it, together with the engineering survey and report, to the Board of Engineers for Rivers and Harbors for its review and recommendation."

Taking into consideration the procedural machinery of the ICC and the average time it requires to process transportation cases of similar scope, it is doubtful whether a full report on any important project could possibly reach Congress while the original survey data were current.

The bill contains other interesting provisions. The report that the ICC would receive from the Chief of Engineers would already embody a complete economic analysis of the project supported by the necessary canvass of potential users and competitors in the field, data secured through the usual public hearings, waybill and commodity studies, and rate analyses and computations. The ICC would then institute a similar investigation of the same sources to determine the present or future public convenience and necessity; it must publish notice of the investigation in the Federal Register and serve a copy of its order, with a description of the nature and location of the project, upon all carriers which might be affected. It must afford opportunity for fair hearing to all parties having an interest therein. All this will have been done by personnel of recognized competence in the prior survey by the engineers. The bill[88] contains the provision:

---

[88] Hearings before the Senate Interstate and Foreign Commerce Committee on Bill S-2744, 82nd Cong., 2d Session, 1952, p. 1520, April 9, 1952, p. 1511.

[89] *Ibid.*, p. 3, Section 5.

> "It shall have the power on its own motion, and it shall be its duty upon proper application and showing of any party at interest, to require by subpoena the attendance and testimony of witnesses at the hearing on said investigation, including the engineer or engineers who prepared the report upon which the investigation is based and the production of the records and documents relating to matters pertinent to the purpose of the investigation."

NATIONAL DEFENSE

The value of waterways to national defense has been ably demonstrated in the paper of Chester C. Thompson, president of the American Waterways Operators, and the instances he cites are convincing.[90] There are, however, certain other elements of national security value that merit consideration in the intervals between wars. Before World War II, opponents of the waterways naively claimed that, because railroads, motor trucks, and pipe lines were also capable of performing service valuable to the security of the country, no recognition should be accorded waterways for their unique role in national defense. That premise completely ignored the impending shortage of all means of transportation, as succinctly conceded by the National Resources Planning Board in its "afterword" to the report[91] on "Transportation and National Policy."

> "What once plagued us as a surplus of transportation facilities, we must now recognize as a grave shortage that imperils the attainment of war production goals. * * * The nation is fortunate to have at its disposal in the present emergency the great increase in facilities of all kinds which seemed so disturbing in 1932."

In view of that candid admission, it would be unfair to quote the following passage from the body of the same report were it not for the deterrent warning to be drawn from it for future guidance. The earlier passage reads:[92]

> "There no longer exists either a general undersupply of transport facilities or a deficiency of other controls. * * * Defense objectives cited on behalf of transport promotion, however, have in the past been more often a high-sounding phrase invoked to obtain funds, than a disinterested desire to preserve the Nation, and the same applies to many current pleas for defense funds."

No nation can long maintain transportation facilities on an "all-out" war basis if these facilities do not also fit into a peacetime economy. Conversely, it is even more dangerous for a nation to attempt to maintain its transportation facilities—especially its rivers and harbors—on a scale that is suitable only for a peacetime economy. The occurrences since 1940 have emphasized the kind of peacetime economy that can be expected in the future.

More than three years before the involvement of the United States in World War II, Gen. Julian L. Schley, the Chief of Engineers, in a public address had called attention to the military importance of inland waterways in the following words:

---

[90] "Inland Waterway Transportation and National Defense," by Chester C. Thompson, presented before Inland Waterways Division, ASCE, Chicago, Ill., September 11, 1952.

[91] "Transportation and National Policy," National Resources Planning Board, Washington, D. C., May, 1942, "Summary Statement of Findings," by Ralph W Watkins, p. 2.

[92] *Ibid.*, p. 9.

> "Let us examine for a moment this great inland waterway transportation system in the event of a national war emergency. The lesson of 1918 should be remembered. * * * The development of improved interconnected systems places us in a far better position today. I visualize tremendous use of this inland system during any future war."

The difficulty was that a recurring peacetime philosophy, which was a desire to avoid unpleasant thoughts of war, had the public in its grip in 1938. Peacetime economies prevailed. The situation is well described in an editorial[93] of 1943:

> "In May of last year Hon. Clyde Reed, transportation authority of the U. S. Senate, was warning that body that [footnote reference 94]:
>
> > 'We are in a critical hour so far as transportation is concerned * * *. The critical outlook for the movement of coal next fall and winter cannot be overestimated.'"

Three years prior to that ominous pronouncement, however, Senator Reed was not yet worried about the impending scarcity of transportation. He was assuring the National Industrial Traffic League that:[94]

> "The United States has a surplus of commercial transportation facilities of all classes. * * * As long as I am a member of the United States Senate, I shall oppose this inland waterway racket."

At the same time, a vice-presidnet of the ARA was making the following public statement:[95]

> "The action taken at the meeting of the railway executives in Washington on September 19, 1939, much in the same manner as that of 1923, and the results accomplished since that time, have proven conclusively that the railroads can meet any demand for transportation, present or prospective, that may be made."

The director of the Office of Defense Transportation in September, 1942, sent out the following plea to the traffic organizations of the nation:[96]

> "Those of you who deal with transportation can make a substantial contribution to the war effort if you will use the inland waterways to the greatest extent possible, thereby relieving other transportation systems."

This same official, however, as Chairman of the ICC, in 1939, had stated:[34]

> "It would be more economical for the Government not to construct and maintain the waterways but instead to use an equivalent amount of money as a subsidy to the railroads in exchange for lower rates."

The editorial of 1943 continues with the following observation:[93]

> "The point is that these civil officials are not and were not conscious obstructionists, but on the other hand exceptionally able patriotic men,

---

[93] "These Rivers Belong in the War," *Waterways*, March, 1943, p. 20.

[94] *Ibid.*, pp. 20–21.

[95] *Ibid.*, p. 21.

[96] Bulletin issued by Joseph B. Eastman to the transportation industry, September, 1942, Archives of the Office of Defense Transportation, Archives Building, Washington, D. C.

> performing, within the scope of their special knowledge, talents and training, a splendid and indispensable service to the nation at this critical time. They simply were not thinking of war. Nevertheless, it is equally obvious that if the policies advocated by them between wars had been followed we would be entirely unable to carry out their present recommendations."

There is, furthermore, another aspect of national security value that is largely economic in character and that should also be given consideration. In the 176 years of the independence of this country we have been at war eight times for a total duration of twenty-five years, or almost one year out of each seven. The present world outlook certainly does not offer any assurance of a more favorable future ratio for many years. Any set of conditions that occurs so frequently for such long periods must be recognized in the permanent national economy. The sinking of coast-wise vessels during World War II in a service that could have been replaced through protected waterways was not just an isolated catastrophe that threatened the success of the military effort. Twice in twenty-three years the United States has had to replace costly vessels and their cargos with what can be considered an expanding sequence of recurring expense.

The allocation of steel for the construction of coal barges and tank barges was sought by the director of the Office of Defense Transportation in the early months of World War II, but the War Production Board did not even acknowledge the request for more than eight months. Good dry-cargo barges were converted into poor tank barges and their normal useful life curtailed to the duration of the war. Wooden tank barges totally unfit for peacetime operation had to be built as a temporary wartime expedient. All these losses are susceptible of being placed on an annual cost basis and charged to the peacetime lag in providing waterway equipment and facilities. As the *Waterways* editorial[97] concluded: "Clearly we cannot expect to utilize waterways in war time if we neglect to build them in peacetime."

With reference to the future peacetime need of facilities found so useful in war, even the ICC, in its sixty-third annual report (1949), conceded that:[98]

> "In the 4 years since the close of armed hostilities, it has become increasingly clear that the peacetime economy of the country will require most of the transportation facilities which were believed, ten years ago, to have been provided too far ahead of the traffic."

Again the estimates of the Corps of Engineers, made in the face of the vociferous dissent of the economists, are found to be vindicated by time.

CONCLUSION

This paper has attempted to counter some of the protests of opponents of waterway transportation against the administration of the improvement program. It is realized that many important aspects of the subject have not been mentioned and that there is room for wide divergence of opinion about those that have been considered. It is hoped that at least some light has been thrown on obscure facets of the problem of determining justification of federal projects.

---

[97] "These Rivers Belong in the War," *Waterways*, March, 1943, p. 22.

[98] "Sixty-Third Annual Report of I. C. C.," 1949, "Transportation During the Year," p. 2 and p. 9, U. S. Govt. Printing Office, Washington, D. C.

The field-survey and office-analysis processes have been briefly explained, and the efforts to staff the Board of Engineers for Rivers and Harbors with qualified specialists has been described. The complications arising from conflicts among transportation interests have been detailed, and the basis adopted for evaluation of navigation benefits explained. The bearing of waterway development on national security has been studied briefly in its predominantly economic aspects, and the significance of pending legislation interpreted from the standpoint of the general public interest. The vital role that the waterways are playing in the national economy has been demonstrated.

The paper has also attempted to bring light to bear on the sources of some of the most widely held, popular misconceptions with regard to the manner in which waterway projects are tested for economic soundness. In contradiction to the allegation that the public costs are customarily ignored in comparing water-carrier service with other modes of transportation, the authorized routine procedures followed in evaluating proposed improvements have been set forth in detail. Published project reports on all major improvements of the last two decades furnish corroboration. The allegation that forecasts of tonnage for waterway projects are uniformly overly optimistic is refuted by the tabulated performance records of the principal component sections of the waterway system, previously recommended by the engineers. The validity of savings in transportation charges is supported by comparison of service costs, including estimated toll charges potentially assessable against users of the inland waterways. The discouraging effect of prevailing competitive practices on the growth of barge-borne traffic, now sanctioned by the regulatory agencies, has been diagnosed and a remedy has been prescribed. The essential unsoundness of the added-traffic theory of rate-making has been explained and the self-defeating element in a tolls system exposed.

It is difficult to coordinate the development of the water resources of the country for the various desirable objectives so as to obtain the maximum net benefit for all concerned. It is difficult to coordinate the various elements of national transportation so that the freight burden may be most efficiently and economically handled to the end that commerce and industry may be wholesomely promoted. It is doubly difficult to coordinate both of these general purposes into a single program. There is only one field of transportation in which both programs impinge one upon the other and that is in the field of inland waterways. None of the many articles, reports, or books of individual authorities or commissions that have lately flooded the publishing houses and printing plants has even attempted to offer a workable formula for the solution of these conflicting objectives. It is the writer's conviction that over-all planning for the future and adherence to an accepted plan will accomplish much toward simplifying these vital problems; but eventually the projects will have to be approached individually, with the most thorough possible analysis of their relation to the over-all task, by experienced engineers of proven knowledge and judgment in the fields of both transportation and the coordinated development of national water resources.

DISCUSSION

DUANE ORR.[99]—Mr. Faison emphasizes many of the controversial issues between advocates of waterway improvement projects and those opposed to federal expenditures on such projects. His report concerns mostly inland waterway projects because such projects are the ones universally condemned by the interests that oppose waterway improvements.

The question is raised whether economists are more qualified than engineers to evaluate and determine the feasibility of a project. Very few, if any, engineers will concede that a specialist in pure economics is more qualified than an engineer of broad experience. In most instances economists become so highly theoretical as to lose all sight of the practical aspects of the problem. Likewise, no one questions that proper evaluation of a waterways project requires a person with special training and with practical engineering experience in waterways and transportation. The fact that the Corps of Engineers has been assigned the responsibility of evaluating, constructing, and maintaining the nation's waterways is not a temporary phenomenon to be deplored but such a policy has been brought about by the thinking of the public spirited citizens of this country.

The over-all results of the waterway improvement program in the past few years have definitely shown that the expenditure of federal funds was fully justified, although in some isolated instances a particular project may not have fulfilled all expectations. The fact that one project may prove uneconomical does not warrant a condemnation of all waterway projects. In most cases with which the writer is familiar, changing conditions between the time the report was prepared and the time the project was completed have accounted for the decrease in actual tonnage below the original estimate. By the same token, in other cases, changing conditions after the project was authorized have caused the tonnage to exceed original estimates. In either case the estimates were wrong, yet the criticism leveled at the engineers preparing the reports was made only when the actual tonnage was less than that estimated—not when the tonnage exceeded the estimate. The writer acknowledges that in some instances borderline cases should have received futher study and verification before feasibility reports were submitted. However, in many cases, it is extremely difficult, if not impossible, to develop all the information about a project within the time allotted for preparation of the report.

The Gulf Intracoastal Waterway, extending from New Orleans to Brownsville, Tex., is a typical example of an internal waterway that has exceeded the Corps of Engineers' estimate of potential tonnage sixfold; the tonnage is still increasing, although few of the feeder canals projected for the waterway have been completed. Completion of the feeder canals will further increase the tonnage on the main artery, although dredging of the feeder canals may in some instances divert the origin of tonnage from one feeder to the other. However, the net result will be an increased use of the waterway because new tonnage not previously available to the waterway will originate from points on the new canals.

---

[99] Dist. Engr., Port of Corpus Christi, Nueces County Nav. Dist., Corpus Christi, Tex.

The criticism that the cost of construction of a project exceeds the engineers' estimate and that the tonnage using the waterway during the early periods after the project is completed fails to equal the estimates shown in the report authorizing the project is hardly justified in many cases. In some instances criticism may be warranted, but in most cases a study of the background of the project will reveal that it was authorized several years before the first appropriation was made and that several more years elapsed before construction was completed. Because of this delay, construction costs may have changed greatly from those estimated in the original report, and likewise the tonnage may vary from the original estimate because of changes which have occurred between the time of the original report and the time the waterway was opened for traffic. It appears that a plan should be developed whereby the lag between authorization and construction of a project would be limited to a reasonable period of time. If this is not feasible, a plan should be formed whereby every project is reviewed prior to the expenditure of the first construction funds, to determine whether conditions have changed to such an extent as to affect its feasibility.

It is the writer's opinion that the over-all development of a waterway or basin project should be authorized at one time rather than on a "piecemeal" basis, as was formerly the policy. A long-range, over-all plan for developing the potential waterways is certainly a more desirable and a more sensible approach to the problem even though many years may elapse before some sections of a project can be completed to project dimensions. A master plan, based on existing conditions, for the development of all potential waterways, with priority assigned to each waterway and to each section of a project, would certainly be a step forward in solving the dilemma that exists in developing the nation's waterways. An over-all plan for the complete development of a waterway would permit a more proper evaluation of the potential tonnage that would use the waterway, and under this plan the potential tonnage on feeder canals and the main waterway could be properly credited to the respective sections.

There are those who continually insist that user charges be placed on users of the nation's waterways. As explained by Mr. Faison, this idea involves a highly complex policy of many years standing in this country and is one that can be debated pro and con without an agreement ever being reached.

The national defense aspect of waterways is certainly one that cannot be overlooked or taken lightly, for the use made of the inland waterways during World War II conclusively proved their value, and the results justified all the money that the federal government spent on improving and maintaining the nation's inland waterways. In the event of another war the rail and highway transportation facilities of this country will no doubt be far more heavily burdened than they were during World War II. Also, based on past experience, the use of ships in coastwise service would not be feasible even if the ships were available. A well-developed national waterway system can in times of emergency carry large tonnages with little equipment and is subject to few of the hazards experienced by ocean shipping. Full utilization of the waterways will permit the railroads and highways to carry finished products and war materials that are so urgently needed in time of war.

In conclusion, the only test of a public-works project is the extent of public benefit. Waterways projects are within this category, and, if after careful engineering analysis benefits or savings exceed all legitimate costs chargeable to the project, the project must be considered possible and is justified from the standpoint of public benefit.

L. Perry Cookingham.[100]—The interest of Kansas City in the development of inland waterway projects is twofold—first, interest in the development of bulk cargo shipping on the Missouri River, and second, interest in effective control of the river flow in times of flood and drought. The vital position of greater Kansas City in the economy of the United States and its future growth rest heavily on the public's understanding of the importance of a forward-looking national policy in the development of water resources. Mr. Faison has performed a commendable public service by presenting a factual analysis of a widely misunderstood problem.

Greater Kansas City is located at the confluence of two rivers, the Missouri River and the Kansas River. The local flood protection works, now nearly complete, are designed to work in conjunction with upstream reservoirs that are capable of retaining large volumes of water in time of flood and of releasing the impounded water in periods of drought. Unfortunately, these reservoirs have not been completed, and Kansas City is still subject to wide fluctuations in the river flows.

The Kansas City area is widely recognized as a large and important industrial, marketing, and transportation center. The facilities of the city also serve a wide trade territory extending in all directions. Approximately twenty-six square miles of greater Kansas City lie in the area that depends on the local flood-protection structures. It is estimated that from 85% to 90% of the city's industrial facilities, representing a property value alone of approximately $936,000,000, are located in this area.

The great flood in Kansas City in 1951 resulted in an economic disaster without parallel in the nation's history. Estimates of damage range from one-half billion dollars upward. Local protection works prevented flood damage of approximately $264,000,000. Had the planned upstream reservoirs in the Kansas River Basin been in operation, almost the entire tragic loss could have been prevented.

In 1952, the Missouri River rose to record heights in Kansas City, but local protection works operating in conjunction with upstream reservoirs on the Missouri, then completed, prevented a recurrence of the flood disaster. Savings resulting from the operation, during 1951 and 1952, of local flood protection works constructed at an approximate cost of $49,000,000 amount to almost eight times the construction cost.

The construction of upstream reservoirs to permit a regulated flow of the two great rivers at Kansas City is not only essential to flood protection and navigation but is also necessary to assure an adequate supply of water in times of drought and to meet the needs of the city's growing population.

---

[100] City Manager, City of Kansas City, Mo.

Water supply and sewage disposal alike depend on the maintenance of adequate flow in the rivers. The partly completed system of reservoirs on the upper Missouri River provided the storage whence came approximately 75% of the river flow below Sioux City (Iowa) during the severe drought conditions of the summer and fall of 1953. A current employee magazine has this to say about the use of water in industry.[101]

> "When Du Pont engineers set out to scout new plant sites, a prime concern is a source of water. The reason is basic: water is Du Pont's most valuable raw material."

Reasonable assurance of both flood protection and water supply is necessary if Kansas City is to compete favorably for the location of new and expanding industry.

Kansas City had its beginning as a landing on the Missouri River and became a principal channel of trade in the 1880's. The growth of other methods of transportation decreased the importance of river shipping for a time, but today expanding industries urgently require the greatest, most complete, integrated system of all modes of transport. Evidence of renewed interest in transportation by water is reflected by the fact that two competing barge lines have recently inaugurated service. No less impressive is the fact that, although the only regularly scheduled service through Kansas City in the past was the government subsidized federal barge line, tonnage handled at the city's municipal wharf increased from 27,143 tons in 1949 to 44,957 tons in 1953, or 65.6%. Vessel traffic in tons, from Kansas City to Sioux City, increased from 275,354 tons in 1946 to 1,646,048 tons in 1952; from Kansas City to the mouth of the river, traffic increased from 748,556 tons to 1,198,656 tons in the same period, exclusive of rafted shipments.

The system of inland waterways may well be considered among the nation's greatest assets, both in time of peace and war. Certainly it is easily understood that Kansas City must again become an important river port, a well-integrated part of the inland waterway system. Gen. T. Q. Ashburn said before the Society,[102]

> "If our navigable highways are developed as they should be, it will be only a matter of a few years till such cities as the Twin Cities, Kansas City, Omaha, and many others will be actually if not geographically seaports."

The expansion and improvement of air transportation and rail transportation in Kansas City have resulted in an indisputable economic gain to the area. Transportation by water represents a relatively undeveloped potential which will contribute importantly to the increasing prosperity of the metropolitan area and trade territory alike. Indeed, use of the Missouri River as an inland waterway may result in a presently unforeseeable economic and industrial development for Kansas City. Col. L. J. Lincoln of the Corps of Engineers, in an address in Kansas City on June 2, 1953, remarked:

---

[101] "Dams, Drouth and Industry," Editorial, *The Topeka State Journal*, Topeka, Kans., September 10, 1953.

[102] "The Steamboat and the Great Plains Empire, Louisiana Purchase V Part II," *Waterways*, December, 1953, p. 46.

> "Greater Kansas City would be short-sighted if it did not include in its plans additional wharf sites and facilities to cope with the increased river traffic that is bound to come."

William G. Oliphant, president of the now privately-owned Federal Barge Lines, and Captain Dave Parker, president of the Sioux-New Orleans Line which recently inaugurated service on the Missouri River, speaking before the Kansas City Council of the MVA on January 29, 1954, informed the the group that, in view of commitments then existing, it was anticipated that the tonnage of freight handled in the Mississippi Valley in 1954 would be double the volume handled there in 1953. Officials of Kansas City were urged to provide adequate facilities to accommodate the increased river traffic. The City of Kansas City has included in the immediate work program the expansion and improvement of the municipal wharf. Long-range programming includes the expenditure of substantial sums for the construction of an additional municipal freight terminal and attendant facilities. Adequate facilities will be provided to keep pace with this important and expanding complement to the transportation system.

Estimates of the potential traffic load on the Missouri River range from four million tons to five million tons annually, according to recent surveys.[103] Previous estimates of the economic potential of the Kansas City area have proven far too conservative. It appears probable that these predictions of waterway traffic may likewise be underestimated. If so, the situation will be far from unique in view of the numerous similar examples cited by Mr. Faison.

The writer has recently returned from an extensive official tour of western Germany. Personal observation of the amazing economic recovery attained in a relatively short period of time has resulted in the firm conclusion that the extensive use of the extremely well-developed inland waterway transportation system is responsible, in large part, for this phenomenal progress.

MARVIN B. MARSH.[104]—In presenting his paper on the economic aspects of inland water way projects, Mr. Faison has made a great contribution to the systematic and economical development of the transportation resources of the United States. He has clarified the important place inland waterway facilities occupy in meeting the over-all transportation needs of the country.

Unfortunately, for many years there has appeared in widely circulated publications of various types a procession of nonfactual statements and allegations minimizing the function of inland waterway projects in the transportation system of the United States and misleading the public as to the true ratio of costs to benefits of such projects. In the absence of complete information, the validity of these statements has been accepted by the general public to the detriment of waterway development. Mr. Faison's paper is of great importance in establishing by professional discussion the true values of the many facets of water transportation.

---

[103] "The Missouri River Basin Development Program," Missouri Basin Inter-Agency Committee and The Missouri River States Committee, U. S. Govt. Printing Office, Washington, D. C., June, 1952, p. 23.

[104] Pres., Marsh Steel Corp., Kansas City, Mo.

Mr. Faison's examples did not include specific reference to Missouri River navigation, except as a part of the national inland waterway system, but navigation on this river could well have been selected as an excellent example of a sound, economic, and greatly needed waterway development. This conclusion is based on the writer's experience in recent years as a member of the River Navigation Committee of the Kansas City Chamber of Commerce and as chairman of the Kansas City Council of the MVA, whereby he had the responsibility of reviewing and studying all available data pertaining to navigation on inland waterways. Furthermore, the writer is engaged in a business of such a nature and location that the dependable and economic transportation of approximately 50,000 tons of steel per year is the most vital factor in its operation. At least one quarter of the total cost of steel delivered in the Kansas City trade area is composed of freight costs alone, unless water transportation is used; if, however, barge shipment is used, the freight charges become a relatively unimportant item in the final cost of the finished product. For example, all steel products coming into Kansas City in 500-ton minimum barge-loads from the two major producing points (Chicago and Pittsburgh), are subject to the following comparative freight charges, given in dollars per ton:

	From Chicago	From Pittsburgh
Rail charges to Kansas City	15.40	20.85
Barge cost to Kansas City	6.52	8.43
Savings using barge transportation	8.88	12.42

In the foregoing tabulation the barge cost to Kansas City includes an unloading charge of $1.00 per ton at the Kansas City wharf, plus a charge of 65¢ per ton for drayage to any plant in Greater Kansas City.

The time of the cargo in transit by barge is only a few days longer than by rail; the cargo in a barge is never damaged by rough handling through hump yards or by switching; it is never damaged by moisture due to condensation in transit, as is so often the case in rail transit in which a car moves through chilly nights and warm days, because the cargo in a barge is kept at constant temperature by being always below the water line. Furthermore, barge equipment that brings steel and other commodities into the Kansas City area for consumption is then available to take out grain and other commodities produced in this region to markets that could not otherwise be reached because of the transportation cost and to many markets already being reached by other means of transportation—at a tremendous saving to both producer and consumer.

Mr. Faison's findings that the actual development of traffic volume usually exceeds estimates made to substantiate planning recommendations are also supported by experience with transportation on the Missouri River. The important use of this river during World War II is so well known that elaboration is not necessary. In 1953 (*a*) only a small number of the potential users of barge transportation were unaware of its benefits; (*b*) loading of all barge equipment had to be limited to approximately 60% of capacity in order to navigate a 6-ft-deep channel because the standard 9-ft-deep channel was not yet completed; (*c*) the wharf facilities were very limited and somewhat awkward for large tonnages; and (*d*) obsolete, inefficient equipment was used for most of the tonnage hauled during the entire season (a few modern towboats and barges made a trip or two at the end of the season). In spite of the foregoing, commercial traffic on the Missouri River in 1953 exceeded 50,000,000 ton-miles. River conditions are constantly improving (a 9-ft-deep channel is now available for more than 90% of the distance between Kansas City and the mouth of the river); additional and improved wharf facilities are being planned; operators of new, privately owned barge lines are placing in service modern equipment especially designed for Missouri River conditions; and there is an ever-growing appreciation by the public of this great natural resource in the Missouri Valley. There is no question in the mind of the writer that the trend shown in Fig. 1 for the Mississippi River system (1927–1950) will soon be duplicated on the Missouri River.

The author, under the heading, "Competition," states that the chief opponents of the federal waterway improvements are the railroads. This is true on the Missouri River, where a few of the railroads serving Kansas City are constantly fighting navigation on the Missouri River with nonfactual and unprovable statements. These same railroads can gain tremendously in the future by the benefits of new and greater industrial enterprises and enlarged agricultural activity, all created by Missouri River navigation. Railroad economists lose sight of the fact that federal funds spent for stabilization of the Missouri River, which prevents their roadbeds and bridges from being washed away by a meandering, uncontrolled river, is the main expenditure required for the development and maintenance of a navigable channel. A desirable channel for navigation purposes is a natural by-product of river stabilization, especially on the Missouri River where locks are not necessary.

The quantity and quality of the services that can be provided by river barges have been established beyond any question for hundreds of important commodities. The only need that remains is public appreciation of the advantages of competitive waterway transportation.

Businessmen, as well as engineers, should study Mr. Faison's paper carefully so that the admittedly difficult problems concerning development of transportation can reflect a proper evaluation of all resources in this field. His conclusions are especially pertinent for the part of the United States known as the "heart of America" for in this area the development of industrial and agricultural potentials can be advanced tremendously by the rapid development of river transportation.

OWEN G. STANLEY,[105] M. ASCE.—Mr. Faison's excellent article constitutes a long-delayed answer to much unjust, untrue, and unwarranted criticism of navigation projects and the work of the Corps of Engineers in general. It is unfortunate that this adverse criticism has been left unanswered for so long. This discussion will merely be an attempt to amplify some of the points made by the author and possibly to promote a better understanding of some parts of his paper.

---

[105] Special Assistant to Div. Engr., Corps. of Engrs., U. S. Dept. of the Army, San Francisco, Calif.

The statement in Mr. Faison's paper (under the heading, "Engineers versus Economists") that there has been a multitude of critical articles,

> "* * * each author compiling and quoting the allegations of his predecessors, sometimes adding new ones of his own, apparently without any very diligent effort at verification"

expresses a typical situation. Apparently the truth of an allegation is of no particular importance to these authors if it appears to support the point they wish to make. Later, Mr. Faison points out several such instances appearing in the book entitled "Muddy Waters." There were flagrant instances of such tactics in that book.[106] The book contains a tabulation[107] which shows, for the Kings River project in California, the annual benefits assigned to flood control and irrigation in various reports by the Corps of Engineers. In the last column of this tabulation the author of the book purports to quote the figures for the benefits of the Kings River project given by the Corps of Engineers in the "Supplement to Comprehensive Report."[108] The annual flood-control benefit is quoted as $2,126,000 and the annual irrigation benefit as $3,382,000. The values quoted in "Muddy Waters" as being given by the Corps of Engineers differ materially from those given in previous reports of the Corps of Engineers; the author of that book subsequently presents his version of the reasons for the change noted. His narrative on this subject is, to say the least, very uncomplimentary to the Corps of Engineers. He implies that the Corps of Engineers was shifting flood-control benefits accruing at Tulare Lake from the Kings River project (then already under construction) to the Kaweah River, Tule River, and Kern River projects in order to justify those projects and obtain funds for their initiation by the Corps of Engineers. Astonishing as it may seem, a perusal of *House Document 367*[109] shows that the figures quoted by the author of "Muddy Waters" are not those which appear in the report. The annual benefit for irrigation given in *House Document 367* for the Kings River Project is $2,656,000. The total annual flood-control benefits accruing to the Kings River project are not separately given. They are listed in that document as $312,000 along Kings River itself and $4,311,000 for Tulare Lake, into which Kings River flows. The benefits at Tulare Lake, however, would be the combined effect of reservoirs on the Kings River, Kern River, Tule River, and Kaweah River. It therefore would seem quite evident that the figures quoted in "Muddy Waters" in this instance were given, regardless of the facts, merely to furnish foundation for the derogatory argument that followed.

Mr. Faison's treatment of the objections raised in "Muddy Waters" to counting benefits incremental to those already accruing on traffic diverted from the Mississippi River emphasizes the need for a more widespread understanding of the sound economic principle underlying the Tombigbee waterway analysis. In effect, the same principle which is the basis for the Tombigbee waterway analysis is invoked whenever an old building, still useful, is torn down and replaced by a larger and more modern structure. If construction of the new building is to be a sound economic proposition, the income from it must be sufficiently higher than the income from the old building to justify all the final charges; that is, the increment of income must be sufficient to meet all the costs involved in tearing down the old building and erecting the new structure and to provide a profit. The author's statement (under the heading, "Incremental Benefits") that

---

[106] "Muddy Waters—The Army Engineers and Nation's Rivers," by Arthur Maass, Harvard University Press, Cambridge, Mass., 1951, pp. 249–250.

[107] *Ibid.*, p. 249.

[108] "Supplement to Comprehensive Report," *House Document 367*, 81st Cong., 1st Session, January, 1951.

[109] *Ibid.*, p. 26 and p. 44.

> "It would make no difference in principle if the proposed diversion took every ton of commerce from the Lower Mississippi River and consigned that improvement to abandonment"

is definitely sound, as illustrated by the foregoing reference to the replacement of an old structure by a modern one. The new structure must merely provide benefits sufficiently greater than the benefits from the old structure to justify all the costs involved in making the change.

In computing the saving due to certain navigation projects, the author (under the heading, "Economic Results of Improvement") uses the "normal fully remunerative rate" to obtain the rate of saving; from the description of the method of analysis used, however, it seems that the rate of saving was probably applied only to that traffic which actually moved over the waterway projects. As far as the shippers in the affected areas are concerned, the rate of saving could also be properly applied to the quantity of traffic still being carried by the railroads at depressed rates—in order to obtain the total savings resulting from the navigation projects. This is so because, if it were not for the navigation projects, the shippers concerned would still be paying the "normal fully remunerative rate" on all traffic, whether or not it now moves by water or by railroad.

The author's analysis of the value of a proposed feeder to an existing system is perfectly sound but could be expressed more simply by stating that the value of a proposed feeder to an existing system of waterways is the total value of the whole system with that feeder included minus the total value of the whole system without that feeder. The correctness of the proposition as expressed could hardly be denied.

The author's contention that, in effect, the objective of depressed rail rates is to drive out competing water transportation and then, after the competition is gone, to return to the previous high, or even higher, rates is evidently true. Such tactics are undoubtedly disturbing to industry and, in certain instances, might even cause industrial establishments to fail. The procedure recommended by the author—that the railroads return their rates to the "normal fully compensatory" level and leave the low-grade freight to seek the low-cost water transportation—would be better for railroads, shippers, and navigation interests alike.

In addition to the author's objection to "user charges", the following might be added: (*a*) The cost of administration and collection would be very great in proportion to the funds collected. (*b*) Obviously, if charge is made for the use of one public improvement of this sort, it should be made for all—and even the railroads do not advocate any charge on certain waterway developments. (*c*) It would be very difficult to make and collect fair assessments. The first thought would be to base the charge on a ton-mileage scale. However, that would not be fair to a barge which would draw 10 ft but would use a waterway having a 30-ft depth. The cost of furnishing the requirements of the barge might be little because of the natural condition of the waterway, whereas the costs of the 30-ft-deep project might be great. Naturally, under these circumstances, the barge should not be required to pay the same per-ton rate as the deep-draft vessel that necessitated building the 30-ft depth.

This will be the situation in the Sacramento Deep Water Channel in California when that project is completed. Shallow-draft boats and barges plying from and to Sacramento are expected to use the deep-water channel at material reductions in operating time as compared with the natural river route because of shorter distance, straighter alinement, and avoidance of river current. Of course, the shallow-draft boats and barges will make no use of any depth below approximately 12 ft. Any user charge, in fairness, should not be the same for this light-draft traffic as for the deep-draft vessels, and any attempt to collect such a charge probably would tend to drive a large part of the light-draft traffic back to the natural river channel and thus deprive the project of benefits it should develop.

Under the heading, "User Charges," the sentence reading "They do not add hypothetical tolls to the water rates because [the United States] Congress has flatly rejected tolls * * *" might give the impression that the formula used by the Corps of Engineers leaves out some element of the cost because Congress has refused to authorize tolls. Such is not the case. All costs are included in the accounting by the Corps of Engineers. If tolls were charged and the estimates of traffic remained the same, the form of the accounting formula would have to be modified, but the end result—the benefit-cost ratio—would be the same.

The statement (under the heading, "The National Transportation System") that

> "There would not seem to be any logical obligation on the general taxpayers or shippers to forego the benefits of economical water transportation in order to maintain a wasteful and inefficient competitor in business"

presents perfectly sound logic. In this era of good highways and large trucking facilities, it seems probable that some of the less efficient railroads could be liquidated to advantage without material loss to the general public. That traffic of the eliminated railroads which could not be transported by waterways and the more efficiently operated railroads could be satisfactorily moved by truck.

HERMAN W. SCHULL, JR.,[110] M. ASCE.—The author's illustrations of the essential accuracy and conservative nature of the traffic forecasts of the Corps of Engineers, as exemplified in Table 1, are well substantiated by experience in Florida. The channel referred to in the following discussion is the Intracoastal Waterway from Jacksonville to Miami, which provides a 370-mile inland sheltered route along the east coast of Florida. The waterway is part of the Atlantic Intracoastal Waterway System extending northward to Trenton, N. J., and southward to Key West, Fla.

The original Intracoastal Waterway from Jacksonville to Miami was constructed by a private corporation and operated as a toll channel. When completed to Miami in 1912, the waterway was nominally 5 ft deep and 50 ft wide. Freight traffic on the waterway reached an all-time high in 1926 during the Florida "boom." At that time a railroad parallel to the waterway, unable to carry the increased traffic, imposed an embargo on building materials and many other commodities. In the years immediately following the lifting of the embargo, traffic on the waterway dropped to the more normal average of 150,000 tons per year.

In 1926 the Corps of Engineers estimated that normal traffic on the waterway would increase to at least 373,000 tons annually following enlargement to an 8-ft depth and a 100-ft width. Enlargement to those dimensions was completed as a federal toll-free project in 1935. Traffic increased rapidly thereafter, as is illustrated by the following statistics for the five-year periods before and after the improvement was effected.

Period	Average annual traffic, in tons
1931–1935, inclusive	241,000
1936–1940, inclusive	460,000

Thus, the improved waterway almost immediately exceeded the tonnage estimate used for its justification. The five-year average tonnage movements have consistently exceeded the original estimate since the improvement was completed. Although tonnage did not appreciably increase during the war years of 1942–1945, the more intensive use is reflected in greater haul distances, causing ton-mileage figures to show an increase of more than 250% in excess of normal levels. Much of that increase resulted from the wartime necessity of barging certain critical commodities via the protected waterway rather than in ocean-going vessels. The toll exacted by enemy submarines in the near-shore ocean routes was quite apparent in wrecked hulks and cargoes scattered along the Florida coast. At one time three separate ship casualties were visible from the same point on the beach.

In 1942 the Corps of Engineers recommended further enlargement to a 12-ft depth and a 125-ft width. The principal basis for that recommendation was a traffic forecast of 707,000 tons annually following the enlargement. Nearly all the northern half of the waterway has now been enlarged as recommended. When the enlargement is completed southward to Miami, it is confidently expected that developing traffic will quickly increase to proportions that will again prove the Corps of Engineers' forecast to be conservatively accurate.

---

[110] Col., Corps of Engrs., U. S. Dept. of the Army, Jacksonville, Fla.

Nels C. Magnuson,[111] M. ASCE.—The Constitution of the United States gives the federal government jurisdiction over navigation by the "Commerce Clause" which states that the Constitution shall have power: "To regulate commerce with foreign nations, and among the several States and with the Indian tribes."

The Report of the President's Water Resources Policy Commission reviews the development of water resource policy under the Commerce Clause and states the following:[112]

> "The exercise of federal commerce authority to protect navigation including the prevention of interference with and obstructions to navigation—even those created under prior state or federal sanction— was repeatedly sustained. Correspondingly, exercise of that power in the construction of navigable channels and the Panama Canal was upheld."

Opponents of the waterways improvement projects do not usually dispute the right of the federal government to engage in such improvement but attempt to discredit it by a deluge of criticism. Mr. Faison has described the growth of water-borne commerce to a volume far beyond that estimated when the projects were recommended. Table 2 indicates a benefit-cost ratio of 3.79 to 1. A complete discussion of the savings per ton is not practicable herein, but the Ohio River seems typical. Table 2 shows that in 1948 annual charges were $10,235,000 and savings, $41,827,000. The annual report of the Chief of Engineers for 1949 shows that 42,792,000 tons of commerce were handled in 1948; as shown in Table 1, it had increased to 48,598,000 tons by 1950. Total charges for amortization, interest, and maintenance and operation averaged $0.24 per ton in 1948; the savings averaged $0.98 per ton. The net savings after deduction of costs were thus $0.74 per ton.

It is stated, under the heading, "Economic Results of Improvement," that the analyses cover the most important projects in the waterway system. It is believed that the smaller projects will show equal savings. Excluding the Atlantic Intracoastal Waterway (Wilmington District), the Wilmington (N.C.) District had six projects that handled between 28,000 tons and 600,000 tons of commerce in 1952; the total commerce moving over those projects was approximately 1,200,000 tons. Transportation savings are estimated at $1.00 per ton, or more. The greatest cost per ton for interest, amortization, and operation and maintenance was approximately $0.25 per ton on the Cape Fear River upstream from Wilmington. Other projects in North Carolina are of primary interest to commercial fishermen but they also handle various items of commerce in substantial quantities.

Several times in Mr. Faison's paper the statement is made that opponents allege that waterways are subsidized. In this regard it is well to remember that the railroads were heavily subsidized during their period of development. The following[113] is quoted from the Texas Almanac for 1943–1944:

---

[111] Chief, Planning and Reports Branch, Wilmington Dist., Corps. of Engrs., U. S. Dept. of the Army, Wilmington, N. C.

[112] "Water Resources Law," Report of the Presidents' Water Resources Policy Comm., Vol. 3, Chapter 2, U. S. Govt. Printing Office, Washington, D. C., 1950, pp. 11–12.

[113] "The Texas Almanac for 1943–1944," *Dallas Morning News*, Dallas, Tex., 1944, p. 282.

> "Railroad building in Texas was encouraged during its early stages by large grants of land from the public domain, grants to railroads totaling 32,153,878 acres. Partly as a consequence of these grants and partly due to the intense competition to pre-empt territory in a region with obviously great potentialities, railroad building became a turbulent procedure characterized by ruthless methods and much abuse of privilege."

If charges for transportation are based on the costs of providing transportation services, certain types of commerce will increase on the nation's waterways. On the other hand, it is believed that when the cost of moving freight by water approaches the cost of moving freight by land it will be transported by land. The rapidly expanding economy of the United States provides opportunity for the optimum development of all types of transportation, with each type handling the commodities for which it is best adapted. Those charged with the development of natural resources would be remiss in their duty if they did not seek full economical development of navigable waters.

Braxton B. Carr.[114]—Mr. Faison presents an interesting and timely discussion of some important problems involved in waterways development that have too long been obscured. The fact that critical attacks on some phases of waterways development have been carefully designed to get attention rather than discuss the issues involved has tended to leave the public poorly informed on many of the problems explored by Mr. Faison.

Continuing critical attack on waterways development over the years has succeeded in creating adverse opinion which must be counteracted, not only in the interest of waterways transportation but in the interest of a sound national transportation system. Criticism that seeks constantly to pit the weight of opinion against one basic form of transportation not only obscures facts necessary to progress but operates in the long run to the detriment of the promulgators of the attack as well as the system attacked.

Mr. Faison has rendered a service not only to the waterways interests but to railroad interests also if the railroad interests will consider his findings objectively. The need is not for less transportation, but for more transportation with all phases integrated to complement each other. Water-borne commerce has demonstrated its value. Critical attacks aimed at the destruction of waterways transportation ill becomes any responsible interests having a stake in the continued growth of this country.

There are related benefits in waterways development that have a bearing on any ultimate assessment of the value of many projects which Mr. Faison has not discussed: In the Warrior-Tombigbee Waterway project, which is the primary interest of the writer's organization, a more useful and a more efficient navigation project is the objective. However, in achieving full development for navigation, water supply must be stabilized, and as a natural by-product better available water supplies will be created, health guards will be established by better pollution controls, and certain flood-control features will be incorporated as a matter of course and at little or no additional expense. Many other projects having navigation as their primary purpose incorporate such features. Any ultimate assessment of their true worth to the basic economy must be based on a consideration of these features as benefits. The writer's organization fully realizes that these features are by-products of navigation in its project, but such features are tremendously valuable and are accessible as benefits.

---

[114] Executive Vice-Pres., Warrior-Tombigbee Development Assn., Birmingham, Ala.

Cyril E. Childe.[115]—If civil engineers believe that they have a responsibility to guide the public in the wise and economical expenditure of public money, they should be critically and vocally aroused by Mr. Faison's paper, which combines a defense and explanation of the methods of the Corps of Engineers with a study of the growth of inland waterways and important questions of public policy raised through their development. Because engineers are particularly qualified to form and express intelligent opinions on the economy, efficiency, and practical worth of engineering works, their views as informed citizens and taxpayers concerned with the country's welfare should be of special value to members of Congress, public officials, and the general public. However, in the clamor of controversy about this country's national policies and expenditures for control and use of water resources, the writer finds little comment of a general nature from engineering sources and much misinformation and ignorance which the views of informed engineers could counteract.

Mr. Faison directs attention to charges of certain economists supporting contentions of the railroads that inland waterways are uneconomical; that subsidized inland water transportation is unfair competition; that reports of the Corps of Engineers approving such waterway improvements habitually underestimate costs and overestimate benefits; and that, if true economic costs and value were taken into consideration, there would be no justification for construction or continuance of many or most inland waterways.

Statistics cited by Mr. Faison effectively refute the contention that the Corps of Engineers overestimate the tonnage and consequent savings resulting from inland waterway improvements which they recommend in their reports. The contrary is shown to be true—the completed inland waterways are currently carrying much larger tonnages than the engineers estimated and savings in transportation charges are correspondingly greater than originally predicted. It is true that sharply rising prices since World War II have increased costs of waterway improvements and other public works in excess of original estimates, but it is also generally true that benefits have correspondingly risen. The soundness of the estimates of the Corps of Engineers has not been impaired by the changes in price levels. Generally speaking, projects that were justified under the earlier price levels are equally justified under the higher prices prevailing when the projects were actually constructed.

It seems rather strange that so many economists, and even some public officials, continue to brand inland waterway improvements as unjustifiable and quote old and inaccurate figures without taking the trouble to investigate the results actually achieved and the trends plainly indicated for the future. Is this because the cry of "pork-barrel" is sufficient to prejudice some minds, and because interests opposed to waterway development, desiring the preservation of the status quo, are more effectively promoting their cause than are those favoring the waterways? Engineers in government service are understandably reluctant to engage in public controversy. It is a good thing, therefore, that a man of Mr. Faison's ability and eminence has spoken.

---

[115] Transportation Consultant, Washington, D. C.; formerly Member, Board of Investigation and Research (Transportation Act of 1940); Chairman, Committee on Water Transportation Policy, President's Water Resources Policy Commission.

After disposing of the contentions that the Corps of Engineers' construction-cost estimates and tonnage estimates are overoptimistic, Mr. Faison proceeds to an examination of the arguments that inland water transport is not truly economical and competes unfairly against railroads.

Unquestionably, it is the present policy of the railroads, as it has been from the beginning, to maintain depressed rates below the full cost of the service on traffic for which water carriers can compete so as to keep the traffic moving by rail. This policy, which is approved by the ICC, is so deep-seated that it could only be corrected by legislation forbidding the charging by common carriers of below-cost rates to meet competition of other lower-cost carriers. Until such a change in rate policy is adopted, the establishment of tolls or user charges on the inland waterways would tend to be self-defeating, except as an aid to railroads in suppressing water transportation. Moreover, the assumption is unjustified that the competition of toll-free water transportation is really injurious to the railroads. Analyses of the traffic and earnings of railroads in the Mississippi Valley show that they have been enjoying greater prosperity than the railroads and areas that are not served by waterways. They have gained much more through increased rail movements of high-grade manufactured goods, supplied by industries which located on the inland waterways in order to obtain the benefits of low-cost water transportation of raw and semi-manufactured materials, than they have lost by reason of the water transportation of these low-grade commodities. Low-cost inland waterway transportation is thus proved to be essentially complementary, rather than competitive, to rail transportation. Mr. Faison is over-generous in conceding that toll-free waterways are inequitable to the railroads because actually the railroads fare better where such waterways exist than where they are absent. Another point that must be considered is that the railroads themselves are direct beneficiaries of the federal expenditures for flood protection on rivers in the Mississippi Valley and elsewhere, which in the aggregate exceed in amount the expenditures for navigation. As long as the railroads pay nothing for flood-control works preserving their rights of way, they cannot consistently demand that the barges moving on the same rivers paralleling the railroad rights-of-way pay tolls for the water rights of way they use. A policy of requiring direct beneficiaries of public facilities to pay user charges, making them self-sustaining and self-liquidating, might conceivably be as successfully applied to river and harbor works as to highways. In the final analysis, the public would pay the cost either way, whether by general taxation or by tolls; but Mr. Faison effectively warns against the application of discriminatory or burdensome tolls that would impair or destroy the public value of the facilities.

Proposals of the railroads and some economists that reports and recommendations of the Corps of Engineers should not be adopted until they are investigated and approved by some other agency, such as the ICC or the Department of Commerce, are obviously for purposes of delaying and preventing construction of the projects. The public interest would not be served by such tactics.

Analysis of the facts presented by Mr. Faison may fairly lead to the conclusion that the fault of the Corps of Engineers is not that they have been overoptimistic and extravagant in the estimates and recommendations for waterway improvements, but rather that they have been overconservative, thereby failing to justify and support a program of expenditures for waterway improvement large enough for the country's needs. Examples of important projects long-delayed or yet to be undertaken include the Missouri River, the Tennessee-Tombigbee Waterway, and the Lake Erie-Ohio River Canal.

A point of perhaps greater significance than underestimating tonnage is that the Corps of Engineers in measuring the economic merits of a project seldom, if ever, do more than compute savings in transportation charges which would result from construction of the new project. The benefits derived from cheaper transportation are more widespread than this. They are measured by the greater growth and prosperity of the community resulting from stimulation of industry and increased utilization of human and natural resources. Such benefits are difficult to measure fully in dollars but they are nonetheless real and important. The Corps of Engineers, instead of being labeled as overoptimistic and reckless spenders of public money, might well be warned that an excess of caution may be a more serious fault.

The Corps of Engineers' recommendations are sometimes criticized on the grounds that they deal in piecemeal fashion with water-resource development, without due consideration of over-all national needs. There are indeed some conflicts of both public and private aims with respect to transportation and other water-resource development, in which the Corps of Engineers' activities may clash with other agencies. The separate agencies cannot justly be held responsible for this situation. The fault lies in the lack of coordinating legislation. It could not be cured by switching engineering-economic functions from the Department of the Army to either the Departments of the Interior or Commerce, or to the ICC, as variously proposed. The President's Water Resources Policy Commission's report of 1950 has proposed that a coordinating Commission be created. Certainly the nation's transportation system of railways, highways, waterways, pipe lines, and airways must be considered as a whole if the United States is to achieve and maintain a transportation system of greatest fitness and adequacy for commerce and national defense. Coordination of all types of transportation service with competition limited to striving for greater economy and excellence of service must be the goal. To this end a federal transportation authority should be created to study continuously national transportation needs, capacity, and performance. It should make recommendations to the President and to Congress as to the desirability of public and private expenditures, as well as service needs and best methods of supplying them, and the legislative and organizational changes needed for a coordinated national transportation system of greatest economy and efficiency. Within the framework of such coordinating authority, the Corps of Engineers' able and impartial services could be utilized in conducting a program of waterway improvements to the nation's utmost advantage.

Francis J. Wilson,[116] M. ASCE, and Newton R. Graham.[117]—The author has performed a public service in explaining the procedures used for economic analyses of proposed inland waterways by the federal government and in refuting criticisms made by the opponents of waterway improvement in their attempts to discredit these projects. As is usually the case with regard to any proposed public development, the opponents and critics are the greatest in number and most vociferous. Unfortunately, they are not always respectful of cold, hard facts—with the result that the general public is left with a distorted picture of the issues involved.

No one denies that domestic freight transportation is one of the most important national activities. Its significance as a factor in unifying the states and in maintaining a high standard of living is incalculable. Approximate information is available on the extent and costs of this activity. The 1950 volume of inter-city traffic as reported by the ICC was more than one trillion ton-miles, or 24,000 ton-miles for each head of a household in the United States. Freight revenues during 1950 for transportation movements reported to the ICC amounted to $11,750,000,000, or approximately $275 per household head. This value should be considered only as a general indication of the costs of supporting the transportation system. Included in these data are taxes to support federal and local governments and excluded are costs of public aids and regulatory bodies and the costs of important transportation movements that are not reported to the ICC. It is evident that domestic freight transportation is exceedingly important and requires large expenditures for its upkeep. The importance of maintaining minimum total costs to the public cannot be overemphasized.

The trend of the volume of freight transportation has been upward, the previous peak year of 1929 having been exceeded every year since 1940 and the 1950 value being almost 165% of the 1929 value. However, the most interesting fact to be noted in a comparison of the annual transportation data for the past twenty years is the change in the relative parts of the total transportation load carried by the various transportation agencies. Current indications are that this redistribution is continuing. In 1929, the railroads carried almost 74% of the total ton-mile traffic. By 1950 this had shrunk to approximately 59% of the total, despite the fact that their 1950 ton-mile traffic was substantially larger than in 1929. The decrease in the railroads' percentage of the total national traffic was occasioned by traffic increases in the pipe lines, motor lines, and inland waterways, with the larger increases gained by the first two agencies. The waterways traffic, excluding the Great Lakes, while still relatively minor, increased from approximately 1.5% in 1929 to 5% in 1950.

An important factor in the increase of the inland waterways' share of the total traffic is the technological advances that have tended to reduce towing costs and increased the dependability of water-borne movements. Radar, channel depth indicators, more efficient propulsion units, and streamlined and integrated tows are some of the recent innovations. These advances undoubtedly are one of the reasons why the traffic has exceeded the originally predicted values.

---

[116] Cons. Engr. and Technical Adviser to Oklahoma Planning and Resources Board, Tulsa, Okla.

[117] Pres., Tulsa Clearing House Assn., Tulsa, Okla.

The inter-agency shifting of the transportation load has initiated a determined effort by the railroads toward a cessation and reversal of the current trend. Pipe-line traffic and Great Lakes traffic seem to be relatively immune to any such action on the part of the railroads. However, the railroads stoutly resisted the expansion of the Great Lakes system in their opposition to the St. Lawrence Seaway. Highway and inland-waterway transportation seem to be the two fields most susceptible to the competitive and political efforts of the railroads.

Most transportation specialists agree that vessel costs per ton-mile of lake-borne and sea-borne traffic make them the most economical forms of transportation. Costs per ton-mile for inland-waterway transportation are similar, the main difference in total costs being the difference in costs required to construct and maintain the inland channels as compared to harbor works. It follows that the total costs of inland water traffic decrease as the volume increases until the capacity of the waterway is reached. At some value, usually far below the capacity of the waterway, the point is reached where the total costs of inland-waterway traffic become more economical than overland transportation. The tabulation of savings earned by the fifteen most important inland waterways in 1948 indicates that the point of equal costs and benefits has been passed. The 1951 volume in ton-miles of all inland-waterway traffic excluding the Great Lakes, which was approximately 44% greater than the 1948 volume, indicates that the economy of the improvements is now even more favorable.

CHARLES L. HALL,[118] M. ASCE.—The writer is in complete sympathy with the reasons given by Mr. Faison in the "Introduction" for writing this highly informative professional paper. Its preparation was certainly not an easy task. European engineers think it impossible, with the statistical evidence available to them, to determine the economic value of most waterways already in existence. In commenting on the writer's paper on the economic value of the improvement of the Ohio River, the general reporter, Jean Aubert, stated:[119]

> "We consider that application of the method suggested by Colonel Hall would be difficult on most waterways, owing to the meagreness [insuffisance] of the statistical information usually available."

Statistical information in Europe is believed to be plentiful. The difficulty lies in applying the information to a given concrete case so as to produce statistical evidence. If that is true after a project is completed and in operation, these difficulties must be greatly multiplied in the case of a project existing only as a blueprint. If this question of economic justification were to be more vigorously contested, it might prove interesting to produce the advertisements for the original bond issues of all the railroad companies and compare them with the subsequent fate of the bonds.

---

[118] Washington, D. C.; formerly Col., Corps of Engrs., U. S. Dept. of the Army, Washington, D. C.

[119] "General Report on Third Communication, 17th International Navigation Congress," by Jean Aubert, Imprimerie Lesigne, Brussels, 1949, p. 4.

The writer, as a member of the Navigation and Inland Waterway Transportation Task Committee of the EJC which was criticized in Mr. Faison's paper under the heading, "Economic Results of Improvement," feels required to defend that committee. It is probably true that, as with all engineering committees with which this writer is familiar, the work of the task committee was farmed out, but a most intense effort was made to prepare coordinated findings satisfactory to all committee members. In reference to the quotation[35] from "Principles of a Sound National Water Policy," the task committee recommended in Appendix III[120] " * * * that study be given to the practicability of levying charges upon the users * * * ." This system of charging the users of federal services has now been suggested for a great variety of beneficiaries and is economically sound if it can be placed in practice. Under the heading, "Waterways and National Transportation Policy," of the cited report[121] some of the difficulties in the matter of waterway tolls and the complexities of the study required are indicated. When reread after four years, the report seems eminently fair.

One matter referred to by the author worried the writer when he was a member of the Board of Engineers for Rivers and Harbors. Under the heading, "Feeder Value," the author writes:

> "They need to determine only whether the proposed addition will provide added benefits equal to its cost, whether those benefits accrue from the project itself, or whether they are contributed by the project to the system as a whole."

There is no flaw in the logic here, but such reasoning may result in justifying costs by counting benefits twice. The upper Mississippi improvement was partly justified on the basis of commerce expected to originate in western Iowa and eastern Nebraska. The commerce from this area was later used to justify the upper Missouri River improvement. Criticism of such duplication may readily result from perfectly honest study at different times by different groups of engineers.

Mr. Faison apparently believes that the railroads will be permitted to depress competing rates forever, using the added traffic theory as justification. This difficulty can be avoided by requiring all carriers to fix their freight rates on a per-ton-mile basis. The writer was severely criticized for suggesting this remedy in a previous professional paper.[122] At that time Mr. Faison was one of the few persons who came to the writer's support. Under the heading, "User Charges," Mr. Faison states his belief that waterway transportation would disappear under a regime of tolls unless a rigid cost-of-service basis of competitive rail rates were to be imposed. Anyone who has struggled with any sort of rate fixing can imagine the endless litigation before the ICC that could arise concerning the cost-of-service basis for charges. Only an automatic device, such as the per-ton-mile charge, will settle this mass of potential disputes.

---

[120] "Principles of a Sound National Water Policy," prepared under the auspices of the Engineers Joint Council, Edwards Bros., Ann Arbor, Mich., July, 1951, Appendix III, p. 94.

[121] *Ibid.*, pp. 86 and 87.

[122] "The Logical System of Freight Rates," by Charles L. Hall, *Transactions*, ASCE, Vol. 115, 1950, p. 33.

James Warren Davis,[123] A. M. ASCE.—An analysis and public scrutiny of the typical criticisms directed at the civil works activities of the Corps of Engineers have long been necessary. Mr. Faison's paper contributes much toward this end.

Attacks against the Corps of Engineers' policy on waterway improvements are not unusual. This policy has survived congressional committee investigations and many derogatory articles by well-known authors in various publications. Because it has been able to survive the past allegations the Corps of Engineers has been staisfied to ignore any new attacks.

The writer agrees that engineers responsible for the administration of river and harbor development have been too tolerant of invalid criticism. However, because such criticism is quite popular material for nontechnical publications, the task of refuting the charges would be almost a full-time occupation.

Although Mr. Faison's article deals mainly with inland-waterway development, the principles involved are equally pertinent to tidal waterways. The same procedures used to determine the economic feasibility of an inland-waterway improvement by the federal government are used to determine whether a coastal waterway merits improvement. Those who emphasize the fact that that government subsidy of inland water carriers through federal maintenance of the waterways creates unfair competition to land carriers are conspicuously absent from the ranks of those who oppose improvement of coastal harbors and their approaches. Perhaps it is not generally known that federal improvement of any waterway—coastal or inland—requires three separate acts of congress. Is it not presumptuous therefore to maintain that the Corps of Engineers could conceivably provide a waterway improvement that was contrary to the desires of the general public?

Federal improvement of waterways has been termed by its opponents a subsidy of water carriers and a waste of taxpayers' money. However, these critics of the Corps of Engineers' policies do not seem to object to subsidies by nonfederal agencies. With the exception of the Port of Baltimore, every major seaport in the United States, Canada, and South America contains extensive terminal facilities constructed by the states or municipalities in which the ports are located. The facilities are leased to users at rates that can never be hoped to realize a return that will approach retirement of the cost of the facilities and debt service during the normal lives of the structures. The economic theory behind this latter form of subsidy is identical to that motivating the practice of federal improvement of waterways.

The author has shown by painstaking analysis and relevant statistics the soundness of public investment in waterway improvement and has masterfully pointed out that it is easier to be critical than correct.

---

[123] Director, Port of Baltimore Comm., Baltimore, Md.

Haywood R. Faison,[124] M. ASCE.—The generous comments of those who have discussed this paper have fulfilled the writer's hope that fallacies in some of the most common allegations about inland waterways might be brought to light. It was candidly admitted that the aspects selected for treatment were chosen for their obviously favorable bearing. The writer readily conceded that there were unfavorable angles not considered in the paper.

Mr. Orr illuminates the most important factor of uncertainty in estimating water-resources development when he deplores the unnecessary time lag between authorizations and actual construction of projects. The phenomenal growth of the benefit-cost ratios of the Texas oil ports and the Gulf Intracoastal canal might have been reversed if the trend, during the long waiting period, had been on the opposite slope of economic fluctuation. The writer is inclined to join in Mr. Orr's advocacy of the basin-wide, multiple-purpose approach to water-resources development and Mr. Cookingham's application of the principle, narrowed down to its effect on the Greater Kansas City region. That important area in the nation's economy experienced a disastrous flood in 1951, and the potential benefits of all-purpose river control were well exemplified by its obvious needs. The writer has, however, found it difficult to fit improvements like the Lake Erie-Ohio River Canal, the Tennessee-Tombigbee navigable connection, the Intracoastal waterways, and the Cross-Florida and Cape Cod canal projects into such a segregated river-basin program.

In view of the enthusiastic response to the exposure of nonfactual assertions which have tended to discount the benefits of waterway transportation, the writer's reluctance to give the issues such broad application as do some of the commentators may seem ungracious. Messrs. Cookingham, Marsh, and Childe all take the writer to task for not indicating the Upper Missouri River as promising the most generally beneficial results among proposed major navigation improvements. The omission had but little significance, resulting as it did from the writer's unfamiliarity with the traffic potentialities of the region and his ignorance of the adaptablility of the stream to modern navigation requirements. He does not challenge the validity of the claims of more fully informed critics but he is conscious of the fact that there are many more economically worthy projects on which to spend public money than there are funds available for the spending.

Mr. Marsh is joined by Messrs. Wilson and Graham in recognizing, among other trends, the remarkable technological advances that have been made in the design of nautical floating equipment and motive power and the consequently-accelerated growth of water-borne tonnage as a percentage of total domestic freight movements. The experience of these gentlemen in the comparatively arid regions of the western United States qualifies them to attest to the advantages of inland barge transportation as well as to the stultifying effect of retarding canalization of the natural water courses on industrial and commercial activity.

Mr. Stanley's remarks furnish a welcome amplification and clarification of some of the points the writer attempted to make in the paper, and the examples of the incremental principle of project justification are particularly apt. Mr. Stanley regards the writer's method of computing transportation savings as ultraconservative because the rate differential factors are applied "only to that traffic which actually moved over the waterway" and not to tonnage continuing to move via overland routes at competitively depressed rates. The writer does not consider the latter differentials to constitute true economic savings because the surface carriers granting them have to make up such revenue concessions to shippers by shifting the burden to noncompetitive freight. This principle seems to be recognized in a later paragraph conceding that such tactics are prejudicial to the public and the carriers alike.

---

[124] Chf. Navigation Analyst, Hoover Comm., Washington D. C.; formerly Chf. Engr.-Economist, Board of Engrs. for Rivers and Harbors, U. S. Dept. of the Army, Washington, D. C.

Mr. Stanley attributes to the writer a basic objection to the imposition of tolls for the use of public waterways. Actually, the writer is not opposed to user charges in principle. He believes that some practical method of exacting special contributions for special benefits will have to be developed before the competitive situation among the carriers can be fairly adjusted. He is frankly at a loss to devise an equitable formula for collecting tolls that will not do more harm than good.

Colonel Schull contributes welcome statistical support for the conservative estimating techniques of the Corps of Engineers. It might be held that vessel traffic on the Florida Intracoastal canal, comprising, as it does, such a large proportion of yachts, cabin cruisers, sports-fishing boats, and similar luxury craft, is not the most appropriate choice of projects to demonstrate the broad incidence of public benefits. However, it can be argued that the beneficiaries also pay a disproportionately large share of income taxes into the federal treasury, from which come the improvement funds. The provision of commercial navigation facilities at the expense of the general public—specifically including yachting and sports-fishing as legitimate commerce—is a policy laid down by congressional statute, and not merely an administrative interpretation originating with the Corps of Engineers.

Mr. Magnuson brings to the discussion a wealth of experience with the provision of relatively short "feeders" to the Intracoastal Waterway system. He finds that they, too, in the main, show a favorable ratio of transportation savings to construction costs when the continuous water movements they originate or terminate are considered.

Mr. Carr evidently concurs with the writer that the general public has been misled by constantly repeated but carelessly verified propaganda with regard to the economic justification of typical inland waterways. In concurrence with Mr. Childe, he, too, finds that waterway projects necessarily involve indirect beneficial results to the public in addition to the primary purposes of the improvements.

Mr. Childe's background in the service of the federal government as chairman of the navigation committee of the President's Water Resources Policy Commission and consultant on transportation problems to executive departments, congressional committees, and various national traffic associations eminently qualifies him to comment constructively on the economic aspects of waterway projects. The writer, in his official capacity, has profited extensively in the past from Mr. Childe's wise and disinterested counsel. Mr. Childe correctly interprets the paper not as an attempt to vindicate all projects for navigation improvement but to analyze the practices of the Corps of Engineers and defend them from the burgeoning of unwarranted criticism that seems to flourish for lack of effective refutation.

Mr. Childe believes that low-cost water transportation has become a vital necessity to the industrial prosperity of the country and he views engineers' excess of caution in evaluating its net effects on the carrier agencies as a more serious fault than those ascribed by hostile critics. He readily concedes, however, that competition among the various elements of the nation's transportation system must be fairly coordinated, and to further that end he recommends the establishment of a comprehensive federal transportation authority within the executive branch of the government.

In view of Colonel Hall's many profound contributions not only to international technical literature on water transportation but also to the practical construction and administration of some of the most important national river and harbor projects, the writer considers him to be the pre-eminent authority on improvements for navigation in the United States. It is therefore highly gratifying to have him discuss this paper at some length and highly appropriate that his comments should be the most keenly critical among those contributed.

As to the report of the task committee of the EJC of 1950 on inland waterway transportation, the only passage therein that was challenged by the writer attributed the growth of barge-borne freight tonnage to the absence of charges covering the use of the waterways. Before that report was published, there had been made available to the EJC by the Corps of Engineers a detailed statistical tabulation of the economic results of improving the nation's principal waterways which showed annual transportation savings so far in excess of improvement costs as to provide ample margin for the attraction of traffic that could readily have absorbed potential user charges. Of course, the writer should have recognized it as well within the province of the task committee to question the accuracy of the tabulation.

In the example cited by Colonel Hall of overlapping benefits used in justification of both the Upper Mississippi River canalization and the proposed Upper Missouri River open-channel work, the probable improvement of the latter stream should have been foreseen and the overlapping potential savings allocated between the two projects in accordance with the most likely probability. This problem frequently arises in connection with both river projects and harbor projects that tap identical sources of potential water-borne commerce. Perhaps the resolution of such problems should be referred to an independent board or authority such as that suggested by Mr. Childe. Despite this problem, the writer still maintains the fundamental validity of the incremental approach, as clarified in Mr. Stanley's discussion.

Colonel Hall was probably justified in ascribing to the writer a pessimistic attitude toward the probability of regulation of transportation rates to reflect carrier service costs. The record of decisions of the regulatory commissions in this field certainly offers scant encouragement. However, the writer does not actually entertain so negative an outlook for the future. It is believed that the obvious advantages to all the interests involved, including the general public, will eventually bring about the adoption of some such rational basis of rate-making as that advocated[122] by Colonel Hall.

Most engineers charged with the development of water resources for navigation will be willing to concede the justness of Mr. Davis's impeachment of their tolerance toward invalid and nonfactual criticism. Without doubt, this tolerance has permitted the general public to acquire an altogether distorted concept of some of the economic aspects treated herein. On the other hand, Mr. Davis presents a sound and refreshing view of the analogies between inland waterways and improved tidal harbors and estuaries. His discussion challenges many commonly accepted misconceptions which would deny that similarity. Users of publicly provided harbor facilities do indeed display a peculiar logic in cheerfully accepting federal subsidies for their improvement while clamoring for tolls on light-draft inland waterways to reimburse the federal treasury for inland-waterway construction and maintenance.

As previously stated, the writer did not undertake to deal with the more valid criticisms of the inland waterways program. It was felt that these aspects had received more than adequate publicity through the publications of the critics and their press agents. If opponents had been willing to rest the case on valid censures alone, there would have been no occasion to take up the cudgels in behalf of the Corps of Engineers and its procedures.

One point that the writer had hoped to emphasize was scarcely touched on by the commentators. That point is the propensity of many national associations in favor of developments for navigation to extol the economic virtues of practically all proposals for waterway improvements more or less indiscriminately. It is felt that the uncritical support of any and all projects militates against a sound program.

AMERICAN SOCIETY OF CIVIL ENGINEERS
Founded November 5, 1852
TRANSACTIONS

Paper No. 2782

BACKSIGHTS AND FORESIGHTS

(GLIMPSES AHEAD IN THE LIGHT OF HISTORY AS DIRECTED BY SCIENCE)

ADDRESS AT THE SUMMER CONVENTION
ST. LOUIS, MO., JUNE 15, 1955

BY WILLIAM ROY GLIDDEN,[1] PRESIDENT, ASCE

The final repository of all experience is history, and new experience in its turn becomes history. Science is systematized knowledge, and the accumulation of this knowledge becomes history—every branch of science and engineering, which is applied science, has its own distinct record of failure, discovery, and success. It is a truism that like causes produce like effects.

Given a set of conditions or sequence of events, it is possible to predict trends and consequences based on past experience. The accuracy of these predictions depends on the accuracy of the antecedents, and inquiry into variations from results anticipated develops new discovery and adds to the sum total of our knowledge. It is therefore necessary, before venturing a prediction, that we possess a thorough comprehension of existing data and that we consider the possible influence of modifying conditions; our knowledge of the historical evidence must be complete.

On our journey into the darkness of the future—into the mysteries of the unknown—the headlights of history and the reliable methods of science reveal the road ahead.

The idea of progress, the idea of unlimited advance, is a comparatively new concept. People of today have become so accustomed to the expectation that the future will surpass the present and the past that we overlook the fact that, prior to the industrial revolution and the beginnings of modern science, the world was static, that adherence to ancient methods, ideas, and thought processes was the accepted and generally unquestioned way of life. The few who did question it were made uncomfortable; they were martyrs to science and progress.

---

[1] Asst. Chf. Engr., Virginia Dept. of Highways, Richmond, Va.

Progress is measured by the creation of new wealth, tangible and intangible; the wealth of durable goods, the abundance of consumer goods, and the dissemination of culture to enrich the minds and well-being of mankind. It results from universal effort and is most effective when directed to avenues of ever-increasing number rather than being confined to the worn, hard-beaten paths of yesterday. A concentration of effort in familiar lines of endeavor will create an enormous amount of goods of restricted variety, but does this surfeit denote progress? When production becomes more varied and directed to the creation of new kinds of goods or to the development of more efficient production of staple goods, real progress will be made in the creation of new wealth.

There are those who advocate a social order similar to that of certain collectivist species of hymenopterous insects, in which the family groups, the reproductives, the workers, and the soldiers function under terms of absolute equality. Insects are well adapted by nature for life on this planet and may eventually, so some say, survive humanity—humanity which requires so much that is artificial and extraneous for its existence and well-being. For thousands of centuries mutations in insect forms have been almost imperceptible. There has been no progress or improvement in their condition except that imposed by nature through the process of natural selection in meeting changing environments.

The greatest joy in human existence lies in the anticipation of improved conditions and changes for the better, or what is commonly known to Americans as the pursuit of happiness. What chance then is there for happiness in a fixed social order such as that which communism or some other egalitarian political system would force upon us? We might as well be termites and live in eternal darkness. To create increased wealth and happiness, men must be different and have divergent abilities. The accent should be on quality, not equality.

It is reasonable to concede that the greatest progress is made by peoples whose individuals show greatest divergence in lines of ability. As we advance into the future, conditions are met which are entirely unrelated to recorded historical events and which cannot be anticipated by the most discerning minds. Decisions must be governed by chance, whose influence widens as the historical period lengthens. Because the probability of success in any play of chance increases with the number of trials, the more varied the trials become, the more rapidly will progress be made.

The inflexibility of all systems of centralized control inhibits the necessary variety of means available to cope with a mode of action whose consequences are unpredictable. Any single decision adopted because of the laws of chance is likely to be wrong.

Centralized control is not confined to authoritarian forms of government. To promote the common good—even under democratic government—we must surrender some of our freedoms, and the necessity for making decisions confronts any government. In a democracy the majority, or a highly organized minority under the guise of a majority, rules. However, authority resides with the dominant element, and where chance is to decide this element

—whether a majority or otherwise—is predestined to be wrong most of the time.

There is probably less government under majority rule than under more concentrated forms. Certainly, history tends to demonstrate maximum progress under an intelligent majority. Therefore, since progress is made in inverse proportion to the extent of governmental control, we may safely conclude that greatest progress would be made where rule is reduced to a minimum. We recognize certain necessary functions of government. But it has been aptly said that those people are best governed who are least governed. Unfortunately, effective self-government can be achieved only by those peoples whose individuals possess highest character and moral stamina.

Almost any form of government will succeed when its citizens are honest and intelligent. No government can long succeed, however exalted in conception, when its people individually or in organized pressure groups are selfish, dishonest, and ignorant. Until we have good people we will not have good government.

In primitive times, bridge building was done by cut-and-try methods, and there were many failures. There are numerous records in the history of bridge engineering of attempted construction overtaken by disaster several times before a permanent structure rewarded the efforts of the builders. Today, bridge failures are so rare that when they do occur they make news of spectacular importance. In modern times, failures often can be attributed to insufficient funds to do the job properly and a willingness of those responsible for policy to accept calculated risks. The most spectacular failures in recent years have been or could have been predicted from the accumulated knowledge of bridge design available at the time of construction.

The development of bridge engineering to its present high state of perfection illustrates what can be done under no rule at all. The discovery and utilization of the basic mathematical and physical laws and processes have been entirely independent of governmental regulations. In science and engineering, only the laws of nature govern. In contrast to the fiat of government, nature's laws compel absolute obedience. What is true in science and engineering is true in all lines of human endeavor—progress is greatest when least hampered by regulation; discovery and advance are accelerated where there is greatest diversity of activity.

Students of history agree that the most important civilizations were those whose people displayed superior ability, and the development of these civilizations has contributed to the greatest advances in knowledge and culture. In seven millenniums of Mediterranean history there have been eight wide periods in which there has been great fluctuation of human ability.

Beginning with a foreign invasion, each period is followed by a stage of assimilation through from six to eight centuries. Then follows rapid development culminating successively in the arts, techniques, and finally in wealth. Wealth induces a period of luxury and consequent decay which continues until the old race becomes "too weak to initiate anything, when a fresh race comes in, and utilizes the old stock to graft on both in blood and culture. As soon as the mixture is well started it grows on the old soil, and produces a new wave of civilization."

Some historians aver that western civilization, which includes the United States, is in the period which began with the fall of the Roman Empire. We have passed the peak in the fine arts, literature, and great music and are now making stupendous advances in science. This will rapidly bring us into the next and forward state which is that of great wealth. After this, according to the cycles of Mediterranean history, we may expect the great decline. This is a very gloomy prospect.

We have observed, however, that in evaluating effects from a given set of causes there may be some modifying influences not found in the original conditions.

If we had no additional historical or other evidence upon which to base a conclusion, we would be compelled to accept the idea of another great decline as inevitable. Happily, the laws of cause and effect may be applied to historical events and their influence on forecasting the future just as they are applied to discovery and advances in science and engineering. The study of influences not found in the usual pattern of former events may lead to conclusions quite different from those normally expected. Let us examine the record of civilization in other parts of the world and the changing conditions induced by man's ever-expanding conquest over time and space.

There is in existence today a civilization which, except for a few minor fluctuations, is substantially the same as it was four thousand years ago. In the arts, literature, and philosophy, no civilization has produced anything to surpass that of the Chinese. They were civilized at a time when our own ancestors wore skins for clothing and painted their bodies blue to express their cultural instincts. Do not forget that silk and fine fabrics, porcelain, paper, block printing, the navigation compass, and gunpowder came to us from China centuries ago. To be sure, China has been invaded many times, but its population is so vast that the spawn of the conqueror has been completely dissolved in the turbulence of the great life stream of its humanity. The depth and effect of recent ideological developments remain to be determined and observed. An ideological change may produce consequences much more profound than a military conquest.

The fellahin of Egypt still cultivate the lands of the Nile much as they did six thousand years ago in the days of the Pharaohs. Except for gunpowder, old-world vices and superstitions, and the scourge of military art, what did the Spanish conquistadores bring to the Aztecs of Mexico and the Incas of Peru? It is questionable whether the descendants of these peoples enjoy as high a state of civilization as they did in the thirteenth century.

We have been taught that the fall of Rome was a cataclysm of transcendent importance—that in the year 410 the civilized world came to an end. Removed from the possibility of verification, the idea of a serene and splendid Roman world-supremacy grew up in the imagination of mankind. The tradition of the world empire of Rome and the legend of the supremacy of the Caesars hold to this day.

What are the real facts? H. G. Wells points out about the kingdom taken by the vandals that "facts and figures" are available that show very clearly the true nature of these barbarian eruptions. They were not really the conquest and replacement of one people or race by another; what happened was something very different—it was a social revolution started and masked by a superficial foreign conquest.

Because of the advance of science and engineering, the drudgery of the slave is disappearing from the face of the earth. He is being supplanted by the machine. In many communities, the humblest citizen can command the services of a thousand slaves by the flick of an electric switch. The possibilities inherent in the impending use of atomic power stagger the imagination.

Although we are still living in the penumbra of the dark ages and slavery has not been entirely eliminated from the earth—as, for example, in certain totalitarian states—we can hope that the dawn will break eventually on a free world with slavery reduced to a thing of unpleasant memory. There will be no dangerous or effective fifth columns in lands where the people are reasonably contented, and opposition to the invader will be vigorous and determined.

We may safely conclude that the day is probably passing when wholesale invasion and permanent occupation by one people of the domain of another will be the mode of conquest and government. The system of colonial empires of the British and others will be succeeded by patterns of infiltration such as the ideological imperialism of the Russians or the economic imperialism of the United States. Swift means of travel and communication will make actual military occupation of "spheres of influence" unnecessary or even undesirable. Invasion is being replaced by immigration. In this country, for example, Boston has been "captured" by the Irish, New York by the old world, and the Northwest by the Scandinavians.

The diversity resulting from the amalgamation of conquered races with the invaders which can be construed to be essential to successive peaks of advanced civilization as in the past is becoming a continuous process. The population of the United States contains large groups from all the important nations. Few of these people have been here for ten generations and most of them for less than five. Mixing of those racial elements now here has only begun and will not become complete for four or five centuries. The civilization based upon this mixture is advancing rapidly, and still the old civilization transplanted from Europe has not ended.

Under the laws of natural selection, species unsuited to a particular environment disappear and only those better fitted to survive remain. The surviving forms become more or less alike and are less adaptable to a changed environment—and are lost when conditions change. In mankind, the influence of society reduces individuals to a common denominator. From infancy to old age those who conform to the conventions encounter less resistance and find life more comfortable. Divergent types leave fewer descendants, and ability is lowered to a dead level.

The elements which characterize a higher state of civilization spring from the efforts of a small group in a given population, including educators, scientists, and engineers—those individuals who are divergent from the general type and who are more subject to elimination in the leveling process. Without these people, civilization cannot be long maintained.

As Professor Arnold Toynbee seeks to demonstrate in his recent work, "A Study of History," there appears to be no direct connection between a civilization's technical achievements and its growth or decline. Techniques have often continued unimpaired or have even been improved long after a society is clearly on the downward path of disintegration. Witness the Greeks and Romans, who had accumulated an impressive array of technical achievements by the beginning of the Christian era and who were still steadily pressing forward on the technical front—but whose civilization had begun its breakdown four centuries before in the Atheno-Peloponnesian War.

Breakdown of a civilization occurs when the creative minority, the leaders, lose their creative power—that is, when normal or spiritual sterility sets in. And it may well be that the great challenge our society must meet in order to survive is its own materialism.

From the time of antiquity down to the present, humanity has been plagued with some fundamental questions which constantly recur and which have been explored by many of our best minds.

Is man destroying the resources of his world and at the same time continually increasing his numbers by spawning in geometrical progression and increasing his life expectancy through the advance in medical science so that he is doomed to die of starvation? We have been inclined to scoff at the warnings of Malthus since the introduction of farm machinery and improved methods of agronomy. Perhaps the evil day has merely been postponed. It has been said that humanity is but a scrofulous itch on the face of an insignificant planet. Will mankind, like the pathogenic microorganism of a major infection, perish after it has destroyed its host? Surely, we have no more worlds to conquer. We have made great strides in production, but how about an equitable and benign world distribution so that a minimum living may be had for all, especially in those areas we choose to call backward? We must recognize that there are many who do not look on our civilization with favor and that within our own midst we harbor slums, whose denizens, often wilful ones, resent the efforts of uplifters, professional and more nobly inspired. Is it enough to provide food, clothing, and shelter to satisfy the optimum in human needs? We must consider the satisfaction of the intellect, or what is known to many as matters of the spirit. Will specialized education result in more wisdom, health, safety, and happiness for our people? There is danger that in creating brilliant specialists the best use of their talents will be denied to society—that the most important decisions affecting mankind will be left to ordinary intellects.

With the growth of great institutions and the expansion of the activities of government, we are compelled to surrender some of our freedom. Will this destroy initiative and dim or extinguish the light of the true spirit of free inquiry, the light that has already brought us so far?

The answers to most of these questions must await the judgment of posterity as gained by the crystallization of experience. Yesterday's seven thousand years of recorded history is but as a watch in the night in the long eons of planetary existence, and one would be foolhardy in the extreme to attempt a projection of historical experience that far into the future. It is more probable than not that life as we know it will some day be extinct. The many portents of the doom to come are well known to science, but it seems not unreasonable to hope that the day is so far removed that we need have no immediate concern. Nevertheless, recent developments in atomic science—like the first rays of a new day's early dawn—however welcome, bring unpleasant apprehension of storms ahead.

Discounting the possibilities of man's destruction by his own folly, we can derive some comfort from the scene now appearing on the horizon. We can conclude that with the constant agitation of society by continuous accretions of new elements there is a chance that the diversity so necessary to progress will be maintained. Differences in geography and climate will prevent a dead level of uniformity among the peoples of the earth.

The dissemination of knowledge and the dispersal of advanced culture throughout the world constitute our main hope for the future of civilization—that it will never be utterly destroyed. Its seed has now been scattered over wide areas, it takes root apace, and growth becomes luxuriant as the years roll down the highway to eternity. We have the necessary differences in population, and varieties of climate, and other world conditions to prevent the deadening effect of uniformity, and unless there is complete moral bankruptcy the majority of mankind can look forward to many centuries of the enjoyment of the fruits of progress and the pursuit of happiness.

MEMOIRS OF DECEASED MEMBERS

ABSTRACTS

Past-President

Ernest Emmanuel Howard 1558

Other Members

Lorin Theodore Blodget 1558
Louis Philip Blum 1559
Frank Leonard Bolton 1560
Harold Edgar Butcher 1560
Leland Clapper 1561
Osborne Joel Dempster 1561
John Wilson Dougherty 1562
James Frankland 1563
Leslie Holmes Garlinghouse 1563
Frederick Ernest Giesecke 1564
George Williams Gosline 1564
Donald Gunn 1565
Harry Parker Hammond 1566
Roy Cordis Hardman 1566
Judson Clifford Heindel 1567
Frank Hutchinson 1568
Edward Hyatt 1568
Paul Eells Jeffers 1569
Frank Arthur Johnson 1569
Owen Meriwether Jones 1570
Vivian Gregor Kaufman 1571
Spencer William Lowden 1571
Conrad Olai Mannes 1572
Thomas Alwyn Middlebrooks 1572
Emery Oliver 1573
Ralph Mallory Palmer 1574
Oren Reed 1574
Leo Bond Roberts 1575
Robert Laurence Ryan 1575
Harry Augustus Shuptrine 1576
Rush Tabor Sill 1576
William Everett Swift 1577
Henry Whitney Tabor 1578
Earle Everett Teeter 1578
William Foster Trimble, Jr. 1579
Dana Melvin Wood 1579
William Herbert Watt Yeo 1580

ERNEST EMMANUEL HOWARD, PAST-PRESIDENT, ASCE[1]

DIED AUGUST 19, 1953

Ernest Emmanuel Howard, the son of Henry A. and Emma (Skipp) Howard, was born on February 29, 1880, in Toronto, Canada. He was graduated from the University of Texas at Austin in 1900 with the degrees of Bachelor of Science and Civil Engineer.

Throughout his professional career he was associated with the same firm (now Howard, Needles, Tammen & Bergendoff). Mr. Howard and his associates were recognized nationally and internationally as bridge designers. They were responsible for work in almost every state, for two bridges in Russia and several in Manchuria, Canada, and Mexico. Among Mr. Howard's many accomplishments was the origination of the double lift bridge over the Willamette River at Portland, Ore.—as of 1955 the only bridge in the world with separately movable upper and lower decks. His firm was engaged in several federal projects and in the design of several toll roads.

Mr. Howard was an active member of several technical societies. He was Vice-President and then President of the Kansas City Section of the Society. He was elected a Director of the Society in 1941, Vice-President in 1945, and President in 1950. He received the honorary degree of Doctor of Engineering from the University of Nebraska at Lincoln and that of Doctor of Science from the University of Missouri at Columbia. He was a member of the commission for the recent renovation of the White House (Washington, D. C.).

Mr. Howard was a founder of the University of Kansas City (Mo.) and the chairman of its board of trustees for twenty-three years. He was widely traveled and actively interested in ancient engineering, archeology, and civilizations.

On June 6, 1942, he was married to Josephine Tiernan. He is survived by his widow; a brother, Henry; and two half sisters.

Mr. Howard was elected a Junior of the American Society of Civil Engineers on December 3, 1901; an Associate Member on September 6, 1905; and a Member on March 4, 1913. He became a Life Member in January, 1940.

LORIN THEODORE BLODGET, A. M. ASCE[2]

DIED AUGUST 17, 1954

Lorin Theodore Blodget, the son of Lorin and Theodora Blodget, was born in Woodbury, N. J., on August 16, 1901. He received the degree of Bachelor of

---

NOTE.—Complete manuscripts have been deposited in the Engineering Societies' Library, 29 West 39 St., New York, N. Y., and are available for consultation. Many of these memoirs have been considerably abbreviated for printing in *Transactions*.

[1] Memoir prepared by Ashley B. Taylor, M. ASCE.

[2] Memoir prepared by Julian R. Fleming, A. M. ASCE.

Science in Civil Engineering from Princeton University in Princeton, N. J., in 1922.

Between 1925 and 1943 his professional experience included work with the New York, New Haven, and Hartford Railroad, the Pennsylvania Railroad, the Hadley Contracting and Construction Company, the Quartermaster Corps (United States Department of the Army), and the United States Engineers and Constructors. He was a civil engineer for the Navigation and Transportation Branch of the Tennessee Valley Authority from 1943 until the time of his death.

Mr. Blodget was a member of the Tennessee Valley Authority Engineers Association, a member of the supervisory committee of the Tennessee Valley Authority Credit Union, and a member of the Knoxville (Tenn.) Technical Society.

He was married to Georgiana Mallon on July 4, 1942, at Gadsden, Ala. Mr. Blodget is survived by his widow; his mother; a sister, Louise; and a brother, Robert.

Mr. Blodget was elected an Associate Member of the American Society of Civil Engineers on February 23, 1932.

LOUIS PHILIP BLUM, M. ASCE[1]

DIED NOVEMBER 4, 1952

Louis Philip Blum, the son of Jacob and Katherine (Hoffman) Blum, was born in Philadelphia, Pa., on April 28, 1873.

In 1916 he formed a partnership with William Archie Weldin, M. ASCE. His practice included service as borough engineer and consultant to the Controller of Allegheny County (Pennsylvania). He also served railroads entering Pittsburgh and many manufacturing companies. He was an expert on surveys and a frequent witness in court on such matters. His firm was responsible for the layout of many subdivisions and for the design and supervision of construction of paving and drainage structures in municipalities surrounding Pittsburgh. After his retirement in 1945, Mr. Blum was associated with the Chester Engineers of Pittsburgh in sanitary engineering practice.

Mr. Blum was a member of the Engineers Society of Western Pennsylvania and served as chairman of the civil engineers section. He was also President of the Pittsburgh Section of the Society in 1940–1941.

He was married to Clara A. Mendel on February 21, 1906. He is survived by his daughter, Katherine Caroline; his sons, Louis Mendel, George Walter, and Howard Edward; his sisters, Mrs. Emma Moore and Ella Blum; and his brothers, William, Charles, and Edward.

Mr. Blum was elected a Member of the American Society of Civil Engineers on May 31, 1910. He became a Life Member in January, 1944.

---

[1] Memoir prepared by John F. Laboon, M. ASCE.

FRANK LEONARD BOLTON, A. M. ASCE[1]

DIED SEPTEMBER 16, 1954

Frank Leonard Bolton, the son of Charles F. and Mary E. (Davis) Bolton, was born in Portland, Me., on June 22, 1885. He received the degree of Bachelor of Science in Civil Engineering from the University of Michigan at Ann Arbor in 1909.

He served as a captain in the Corps of Engineers, United States Army. Later he became general manager of the Cayuga Rock Salt Company, Inc., a salt mine industry on Cayuga Lake near Ithaca, N. Y. He was director of the Watkins Salt Company at Watkins Glen, N. Y., and of the Tompkins County Trust Company of Ithaca. Mr. Bolton also served as a director of the Atlantic Deeper Waterways Association and was elected vice-president and then president of the New York State Waterways Association. He was director of this association at the time of his death. In 1944 he was a delegate to the Republican National Convention. He was a member of the American Legion and St. John's Episcopal Church of Ithaca.

On December 26, 1924, he was married to Lucie G. Wilkinson. He is survived by his widow.

Mr. Bolton was elected a Junior of the American Society of Civil Engineers on June 30, 1910, and an Associate Member on May 15, 1917. He became a Life Member in January, 1952.

HAROLD EDGAR BUTCHER, J. M. ASCE[2]

DIED JUNE 10, 1954

Harold Edgar Butcher, the son of Herbert Edgar and Lillis Nola (Shelby) Butcher, was born on November 6, 1924, near Maynardville, Tenn. He received the degrees of Bachelor of Science in Civil Engineering and Master of Science in Civil Engineering from the University of Tennessee at Knoxville.

During his undergraduate vacations, Mr. Butcher was employed by the Corps of Engineers, United States Department of the Army, in flood control work on the Mississippi River. For the two years following his graduation he was employed by Skidmore, Owings, and Merrill, architects and engineers, at Oak Ridge, Tenn. In 1950, he became employed by the Carbide and Carbon Chemicals Company at Oak Ridge. He continued to work for that firm until his death, an accidental death by drowning.

Mr. Butcher was a member of the Junior Chamber of Commerce of Oak Ridge and served as Secretary-Treasurer of the Oak Ridge Subsection of the Tennessee Valley Section of the Society in 1951–1952.

---

[1] Memoir prepared by John E. Perry, M. ASCE.

[2] Memoir prepared by Joseph P. Laws and Robert H. Nagel, Associate Members, ASCE.

He is survived by his mother; two sisters, Marian (Mrs. J. L. Balch) and Mary Ellen (Mrs. R. D. Harvey); and a brother, Kendall.

Mr. Butcher was elected a Junior Member of the American Society of Civil Engineers on September 7, 1948.

LELAND CLAPPER, M. ASCE[1]

DIED NOVEMBER 1, 1953

Leland Clapper, the son of Marion O. and Emma J. (Porter) Clapper, was born on July 31, 1886, in Washington, Iowa. He was graduated from Iowa State College at Ames with the degree of Bachelor of Science in Civil Engineering. He did graduate work at the Massachusetts Institute of Technology at Boston.

He began his engineering career with the Great Northern Railway Company. In 1910 he became employed by the Duluth and Iron Range Railway Company as an assistant engineer and, later, as engineer of bridges and buildings. He served as City Engineer of Two Harbors, Minn., for several years. At the time of his retirement he was chief engineer of the Duluth and Iron Range Railway. Mr. Clapper's innovations contributed considerably to the efficient handling of ore at the upper Great Lakes ports.

After his retirement he became actively engaged in the community affairs of Van Nuys, Calif. He was also an ardent sportsman.

He was married to Linnie Perry and is survived by his widow and daughter, Roberta.

Mr. Clapper was elected an Associate Member of the American Society of Civil Engineers on August 31, 1915, and a Member on November 25, 1919. He became a Life Member in January, 1950.

OSBORNE JOEL DEMPSTER, M. ASCE[2]

DIED SEPTEMBER 25, 1954

Osborne Joel Dempster, the son of Delos C. and Jennie (Bradt) Dempster, was born in Herkimer, N. Y., on November 26, 1873. He was graduated from Union College (Schenectady, N. Y.) in 1897.

After graduation, Mr. Dempster entered New York State employment in the Division of the State Engineer and Surveyor. His work was concerned with the survey and design for the State Barge Canal, particularly along the Hudson and Mohawk rivers and in the Adirondack Mountains. In 1926 he was made District Engineer of District No. 6 at Hornell, N. Y. Mr. Dempster was in complete charge of all the public works in that district, which included Allegany, Steuben, Chemung, Tioga, Schuyler, and Yates counties. His responsibilities included the design, construction, and maintenance of state highways and bridges and the elimination of grade crossings. He continued in this position until his retirement in 1936.

---

[1] Memoir prepared by Wayne A. Clark, M. ASCE, and Robert B. Rhode, A.M. ASCE.

[2] Memoir prepared by William J. Dennis, A. M. ASCE.

He was married to Harriet A. Weller of Frankfort, N. Y. He is survived by one daughter, Harriet.

Mr. Dempster was elected an Associate Member of the American Society of Civil Engineers on January 3, 1906, and a Member on April 30, 1912. He became a Life Member in January, 1941.

JOHN WILSON DOUGHERTY, M. ASCE[1]

DIED MAY 1, 1954

John Wilson Dougherty, the son of John Edward and Ella May (Turner) Dougherty, was born at Edmore, N. Dak., on January 1, 1913. He received the degree of Bachelor of Science in Civil Engineering in 1934 from Oregon State College at Corvallis. In 1938 he received the degree of Master of Science from the Carnegie Institute of Technology (Pittsburgh, Pa.).

In May, 1942, he became Executive Officer for the 1303d Engineer General Service Regiment. Mr. Dougherty rose to the rank of Lieutenant Colonel and received the Bronze Star for service in Europe.

In 1946, Mr. Dougherty joined the Bechtel Corporation in Los Angeles, Calif.; his responsibilities included the design of a hydroelectric project in the high Sierras and work involving flumes, tunnels, and inverted syphons.

Mr. Dougherty was Chairman of the Reception Committee of the Los Angeles Section of the Society in 1952 and a member of the Regional Subsection Committee in 1953. He was a registered professional engineer in California and Oregon and a member of several technical associations.

On May 28, 1942, Mr. Dougherty was married to Ruth Alexeena Sanger. He is survived by his widow; a son, John Wilson, Jr.; a daughter, Patricia; his mother; and two sisters, Irene (Mrs. C. R. Hansen) and Mildred (Mrs. G. E. Lacey).

Mr. Dougherty was elected a Junior of the American Society of Civil Engineers on October 29, 1934; an Associate Member on January 13, 1947; and a Member on March 19, 1951.

---

[1] Memoir prepared by Leslie A. Irvin, M. ASCE.

JAMES FRANKLAND, M. ASCE[1]

DIED MARCH 12, 1954

James Frankland, the son of Henry Morton and Harriet (Kalberg) Frankland, was born in Seattle, Wash., on January 13, 1889. He attended the University of Washington in Seattle.

In 1913, after working for the Public Utilities Department of the City of Seattle, Mr. Frankland won a permanent appointment in the United States Forest Service. He served with the United States Army from 1917 to 1919 and rose to the rank of Colonel in the Army Reserve. In 1919 Mr. Frankland became assistant engineer for the Port of Tacoma (Wash.). He worked on bridge design and construction from 1922 until 1924. He then returned to the United States Forest Service and was assigned to the Division of Engineering, Portland (Ore.) Regional Office. In 1936 he was appointed assistant regional forester in charge of engineering.

Mr. Frankland served for many years as a member of the Board of Trustees of Lewis and Clark College at Portland and was board chairman from 1945 to 1948. He was a member of technical and fraternal organizations.

He was married in 1920 to Olga Everett. He is survived by his widow; a foster son, Allen; a foster daughter, Judith (Mrs. Alan Becker); and three sisters, Mrs. Bert Gagnon, Mrs. William Dirkee Smith, and Mrs. Jack Merriott.

Mr. Frankland was elected a Member of the American Society of Civil Engineers on March 11, 1929.

LESLIE HOLMES GARLINGHOUSE, A. M. ASCE[2]

DIED JUNE 26, 1954

Leslie Holmes Garlinghouse, the son of Holmes Spalding and Emma (Sherman) Garlinghouse, was born in Leadville, Colo., on October 19, 1887. He was graduated in 1910 from Rensselaer Polytechnic Institute in Troy, N. Y.

For fourteen years he was associated with the Blaw-Knox Company (Pittsburgh, Pa.) where he gained a reputation in the design and field service of steel forms for concrete. During World War I, he was chief engineer of the Great Western Electro Chemical Company and built plants in Cartago, Calif., and Pittsburg, Calif., for the production of special equipment for the armed services.

From 1923 until his death Mr. Garlinghouse participated in the establishment and operation of the firms of Garlinghouse Bros. and Gar-Bro Manufacturing Company, distributors and manufacturers of construction machinery in Los Angeles, Calif. Under his supervision, many machines were designed and produced which have materially speeded up concrete-construction techniques—bottom-dump concrete buckets, barrows, and buggies for transporting concrete and chutes and other implements for fast and accurate moving and placing of the important construction material.

---

[1] Memoir prepared by Robert M. Bonney, A. M. ASCE.

[2] Memoir prepared by Albert F. Garlinghouse, A. M. ASCE.

He was married in August, 1912, to Elsie Lee Armstrong, who died in 1944. He was married to Marjorie Mason Johnson on August 18, 1950. He is survived by his widow; a son, Leslie; a daughter, Lucy Lee (Mrs. W. F. Dexter); and two brothers, Ralph L. and Albert F.

Mr. Garlinghouse was elected an Associate Member of the American Society of Civil Engineers on August 9, 1920.

FREDERICK ERNEST GIESECKE, M. ASCE[1]

DIED JUNE 27, 1953

Frederick Ernest Giesecke, the son of Julius and Wilhelmina (Groos) Giesecke, was born in Latium, Washington County, Texas, on January 28, 1869. He received the degrees of Bachelor of Science in Mechanical Engineering and Mechanical Engineer from the Agricultural and Mechanical College of Texas at College Station. He also received the degree of Bachelor of Science in Architecture in 1904 from the Massachusetts Institute of Technology at Boston and the degrees of Doctor of Philosophy and Civil Engineer from the University of Illinois at Urbana.

In 1888 he became head of the Department of Mechanical Drawing at the Agricultural and Mechanical College of Texas. In 1912 he became professor of architecture and head of that department at the University of Texas at Austin. In 1914 he was appointed director of the Engineering Experiment Station. His experiments pioneered the way for the premixed concrete industry of today. Mr. Giesecke returned to the Agricultural and Mechanical College of Texas in 1927 as head of the Department of Architecture and college architect. He was the author of many works—among them the book,[2] "Mechanical Drawing."

Mr. Giesecke was president of the American Society of Heating and Ventilating Engineers in 1940 and was awarded a medal by that society for outstanding work in that field.

In 1891 Mr. Giesecke was married to Hulda Gruene of New Braunfels, Tex. He is survived by his widow and three daughters, Mrs. Alma Hodges, Linda (Mrs. P. M. Geren), and Minnie (Mrs. E. Wight).

Mr. Giesecke was elected a Member of the American Society of Civil Engineers on March 4, 1913. He became a Life Member in January, 1940.

GEORGE WILLIAMS GOSLINE, A. M. ASCE[3]

DIED MAY 9, 1954

George Williams Gosline, the son of George William and Irene (Kelley) Gosline, was born in Carnegie, Pa., on February 29, 1904. He attended the University of Nevada at Reno.

---

[1] Memoir prepared by Preston M. Geren, M. ASCE.

[2] "Mechanical Drawing," by Frederick E. Giesecke, Macmillan Co., New York, N. Y., Pt. I, 1900, Pt. II, 1904, Pt. III, 1909.

[3] Memoir prepared by Francis K. Muceus, A. M. ASCE.

Mr. Gosline became project engineer of the 40,000-acre soil and water conservation demonstration project of the Soil Conservation Service, United States Department of Agriculture (SCS), near Watsonville, Calif. Under his leadership soil and water conservation practices that today are standard were pioneered and evaluated. Mr. Gosline continued his work for the SCS as an engineering supervisor and consultant for the states of Oregon and Washington and later as a specialist in the Pacific Coast Regional Office at Portland, Ore., in charge of irrigation and drainage for northern California. In 1951 he joined the Bureau of Water Works of the City of Portland as a hydraulic engineer.

He was married to Marian Atmore on December 31, 1924, in Los Angeles, Calif. He is survived by two sons, William and Michael; two grandchildren; his parents; and a brother, James.

Mr. Gosline was elected an Associate Member of the American Society of Civil Engineers on September 14, 1936.

DONALD GUNN, A. M. ASCE[1]

DIED OCTOBER 22, 1952

Donald Gunn, the son of William Saunders and Lillian Arrington (Rice) Gunn, was born on December 3, 1902, in Rome, Ga. He received the degree of Bachelor of Science in Electrical Engineering from the Georgia School of Technology at Atlanta.

From 1930 until the time of his death he was employed by the Safe Harbor Water Power Corporation and the Pennsylvania Water & Power Company, affiliated companies which have large hydroelectric plants on the lower Susquehanna River. Mr. Gunn made a detailed study of depreciation of medium-head and low-head hydroelectric developments of early origin in the eastern parts of the United States and Canada. He was a depreciation witness in proceedings before the Federal Power Commission and the Pennsylvania Public Utility Commission, a member of a depreciation committee of the Pennsylvania Electric Association, and an alternate of the Society's Subcommittee on Depreciation. He was also a director of the Susquehanna Transmission Company of Maryland.

In 1929 Mr. Gunn was married to Mary E. Dillon. He is survived by his widow; three daughters, Mary Virginia, Marguerite S., and Nancy Ellen; and two sisters, Elsie (Mrs. T. S. Stokes) and Edith (Mrs. W. Rose).

Mr. Gunn was elected an Associate Member of the American Society of Civil Engineers on April 14, 1941.

---

[1] Memoir prepared by Rolland W. Chase, M. ASCE.

HARRY PARKER HAMMOND, M. ASCE[1]

DIED OCTOBER 21, 1953

Harry Parker Hammond, the son of George A. and Sarah J. (Snyder) Hammond, was born at Asbury Park, N. J., on December 21, 1884. He received the degree of Bachelor of Science in Civil Engineering from the University of Pennsylvania at Philadelphia in 1909.

He then began his career in education as an instructor in civil engineering at that university. In 1927 he became head of the department of civil engineering at Polytechnic Institute of Brooklyn (N. Y.) and in 1937 he became dean of the School of Engineering of the Pennsylvania State College (at State College); he retired as Dean Emeritus in 1951. During this period enrollment grew enormously, and many changes were made in instruction—research was especially emphasized.

In 1923 the Society for the Promotion of Engineering Education, now the American Society for Engineering Education (ASEE), began an investigation of engineering education, with W. E. Wickenden as director and Mr. Hammond as associate director, culminating with the publication[2] of the "Wickenden Report," a summary of conditions then existing. This investigation stimulated great interest in engineering education and resulted in the formation of the Engineers' Council for Professional Development. During World War II Mr. Hammond was chairman of an ASEE committee which produced the report,[3] "Engineering Education After the War," which has had far-reaching effects on engineering education in recent years.

Mr. Hammond had considerable experience in engineering practice and served on advisory committees for several governmental organizations. He was awarded many honors in recognition of his services, among them the Lamme Medal and the McGraw award of the ASEE.

On September 7, 1913, he was married to Margaret Leonard Raymond. He is survived by his widow.

Mr. Hammond was elected an Associate Member of the American Society of Civil Engineers on January 14, 1918, and a Member on May 8, 1922. He became a Life Member in January, 1953.

ROY CORDIS HARDMAN, M. ASCE[4]

DIED APRIL 20, 1954

Roy Cordis Hardman, the son of Owen Cordis and Sarah Hardman, was born in Washington, Iowa, on December 4, 1880. He was graduated from the State

---

[1] Memoir prepared by B. A. Whisler, M. ASCE, assisted by Lawrence Perez, A. M. ASCE, and E. B. Stavely.

[2] "Report of the Investigation of Engineering Education, 1923–1929," by W. E. Wickenden and Harry Parker Hammond, Office of the Secretary, S.P.E.E., Univ. of Pittsburgh, Pittsburgh, Pa., Vol. I, 1930; Vol. II, 1934.

[3] "Engineering Education After the War," *Journal of Engineering Education*, Vol. 34, No. 9, May, 1944, pp. 589–614.

[4] Memoir prepared by Mrs. Clare Hardman.

University of Iowa at Iowa City in 1904 with the degree of Bachelor of Science in Civil Engineering. In 1909 he was awarded the degree of Civil Engineer from the same university.

After graduation Mr. Hardman worked in the Philippine Islands. He later became a superintendent of construction for the War Department. He served at the Panama Canal, for the Republic of El Salvador, and the city of San Salvador, Salvador. He then became director general of highways and construction for the Republic of Costa Rica. In 1934 Mr. Hardman was made P.W.A. (Public Works Administration) inspector for Colorado, Utah, Idaho, Wyoming, and Montana. In 1935 he was the P.W.A. representative to and regional director for Puerto Rico and the Virgin Islands. Mr. Hardman retired early in 1943 and remained at Los Angeles until his death.

He was married in 1908 to Mary Martin who died a year later. In 1911 he was married to Clare Lyon. He is survived by his widow; a son, Robert Lyon; and a daughter, Mrs. J. C. Egan.

Mr. Hardman was elected an Associate Member of the American Society of Civil Engineers on October 7, 1908, and a Member on May 13, 1918. He became a Life Member in January, 1943.

JUDSON CLIFFORD HEINDEL, A. M. ASCE[1]

DIED NOVEMBER 27, 1953

Judson Clifford Heindel, the son of George Mathias and Martha Wise Heindel, was born on December 6, 1894, at Albany, N. Y. He received the degree of Bachelor of Science in Civil Engineering in 1923 from Union College at Schenectady, N. Y.

From 1917 until 1919 Mr. Heindel saw service with the 303d Engineers, United States Department of the Army, including the battles of St. Mihiel and Meuse Argonne in France. From 1923 until 1925 he was employed as a field engineer by the Koppers Company of Pittsburgh, Pa. In 1931 he joined the New York Power and Light Company at Albany. He became employed as principal engineering draftsman in the structural division of the power engineering and construction division of the Tennessee Valley Authority in 1937 and at the time of his death was a civil engineer in this division.

Mr. Heindel was a member of the Masonic Blue Lodge of Albany and the Signal Mountain Presbyterian Church (Signal Mountain, Tenn.). He was active in the civic affairs of Signal Mountain.

On June 20, 1936, Mr. Heindel was married to Mary Watson Craig. He is survived by his wife and son, Clifford Craig.

Mr. Heindel was elected an Associate Member of the American Society of Civil Engineers on October 9, 1941.

---

[1] Memoir prepared by L. A. Schmidt, Jr., M. ASCE.

FRANK HUTCHINSON, M. ASCE[1]

DIED JANUARY 5, 1953

Frank Hutchinson, the son of Timothy Wilbur and Anna (Canby) Hutchinson, was born on September 27, 1874, in Olney, Ill. After intensive training in drafting and engineering by the Ohio and Mississippi Railroad, he entered the University of Illinois at Urbana as a special student.

He then worked on relocation and construction for the Union Pacific Railroad in Wyoming and later became office engineer for the St. Louis Valley Railroad at St. Louis, Mo. In 1913 he became engineer and superintendent of an iron ore property in Minnesota for the Pittsburgh Steel Ore Company. In 1919 he opened a consulting office in Duluth, Minn., and was actively engaged in various studies, examinations, and reports. Among his major projects were the examination of the Krivoi Rog Iron Range in Russia and preparation of plans for the mines; examination of and reports on manganese ores in Cuba; patent litigation concerning iron ore concentrating machines; and investigation of the iron ore reserves of the Lake Superior area and their competitive position in relation to imported ores.

On October 15, 1901, he was married to Blanch Barnard of Olney. He is survived by a son, Lynne B.; a sister, Ethel; and two grandchildren.

Mr. Hutchinson was elected a Member of the American Society of Civil Engineers on March 13, 1917. He became a Life Member in January, 1945.

EDWARD HYATT, M. ASCE[2]

DIED JUNE 17, 1954

Edward Hyatt, the son of Edward and Margaret (Gill) Hyatt, was born near San Jacinto, Calif., on July 21, 1888. He received degrees in civil engineering from Stanford University at Stanford, Calif.

He began his thirty-five-year career in the service of his native state as an engineer for the California Highway Commission. In 1916 he transferred to the State Water Commission, an agency created to administer state laws pertaining to water rights. In 1921 the State Water Commission became part of the Division of Water Rights of the State Department of Public Works; Mr. Hyatt was appointed deputy chief and then chief of that division. In 1927 he was appointed State Engineer of California. Mr. Hyatt directed surveys which led to the development of the State Water Plan, the basis for the water conservation program in California, and of the Central Valley Project.

He was a member of several governmental planning committees, technical associations, and honorary societies. He was a Past-President of the Sacramento Section of the Society.

---

[1] Memoir prepared by Wayne A. Clark, M. ASCE.

[2] Memoir prepared by Gordon Zander, Arthur D. Edmonston, and Thomas B. Waddell, Members, ASCE.

On June 22, 1916, he was married to Delta A. Garst. He is survived by his widow; two daughters, Dolly Margaret and Janice (Mrs. H. D. McClure); and three granddaughters.

Mr. Hyatt was elected an Associate Member of the American Society of Civil Engineers on October 11, 1920, and a Member on April 8, 1924.

PAUL EELLS JEFFERS, M. ASCE[1]

DIED AUGUST 7, 1953

Paul Eells Jeffers, the son of Charles Addison and Lulu (Eells) Jeffers, was born at Los Angeles, Calif., on February 14, 1889. He received the degree of Bachelor of Science in Civil Engineering from Stanford University in Stanford, Calif., in 1913. He also spent two years as a special student at the Massachusetts Institute of Technology in Cambridge.

From 1919 until his death, Mr. Jeffers maintained his own office. He was responsible for the structural design of many outstanding buildings in Southern California. He became president of the State Board of Registration for Professional Engineers in 1947. He served several other local and state agencies in an advisory capacity and was a consultant for the National Research Council (Washington, D. C.). Interest in earthquake research led Mr. Jeffers to become an expert in seismic effects on structures; as a result, he had an active part in formulating various California earthquake ordinances.

Mr. Jeffers was a member of many technical organizations and held official positions in several of them. Among these organizations was the Structural Engineers Association of Southern California of which he was an organizer and also the first president.

On August 14, 1914, he was married to Florence Mackey. He is survived by his widow; a son, Sheldon; a daughter, Elizabeth (Mrs. James Cuthill); and a brother, John.

Mr. Jeffers was elected a Member of the American Society of Civil Engineers on June 9, 1930.

FRANK ARTHUR JOHNSON, M. ASCE[2]

DIED JUNE 21, 1954

Frank Arthur Johnson, the son of Andrew and Lena (Samuelson) Johnson, was born on August 22, 1888, in San Francisco, Calif. He attended the University of California at Berkeley.

From the time of the San Francisco earthquate and fire, Mr. Johnson was continuously engaged in structural engineering in California. In 1911 he entered the office of H. J. Brunnier, M. ASCE, consulting structural engineer, and was responsible for the design of some of the major buildings in San Francisco. His employment with the California State Division of Architecture began in 1933. He helped to formulate policy and supervised reconstruction of damaged public school buildings following the Long Beach earthquake; he also had a large part in the preparation of the state code for earthquake-resistant design and construction. He was transferred to the design section of the same division and was responsible for the structural design of all state buildings.

---

[1] Memoir prepared by Ernest C. Hillman, M. ASCE, and Robert Wilder.

[2] Memoir prepared by Allen H. Brownfield, A. M. ASCE.

Mr. Johnson was active in the Structural Engineers Association of California and was director of the Central California Association in 1952–1953.

On June 27, 1917, he was married to Abby Gibson. He is survived by his widow; two daughters, Mary Alice Lien and Frances Wilson; and six grandchildren.

Mr. Johnson was elected an Associate Member of the American Society of Civil Engineers on November 25, 1919, and a Member on June 19, 1953. He became a Life Member in January, 1954.

OWEN MERIWETHER JONES, M. ASCE[1]

Died April 7, 1951

Owen Meriwether Jones, the son of Richard Wood and Margaret Jane (Coleman) Jones, was born in Nashville, Tenn., on November 8, 1878. He was graduated from Vanderbilt University in Nashville in 1900.

In 1903 he became an instructor in civil engineering at Syracuse (N. Y.) University and later head of the department of civil engineering at Tulane University (New Orleans, La.). In 1910 he began studies on the regulation of water flow from Lake Superior for the Michigan-Lake Superior Power Company. In later years he served as vice-president of this company. Mr. Jones was in charge of the construction of eight sluice gates on the St. Mary's River and of the dike which completed the control of the waters of Lake Superior. In 1923 he was made chief engineer of the New-Kanawha Power Company. He then became chief engineer of the Electro Metallurgical Division, Union Carbide and Carbon Corporation, and consultant on the hydroelectric facilities of that company.

He served as president of the West Virginia State Registration Board for Professional Engineers and as a director and president of the West Virginia Society of Professional Engineers.

On May 5, 1905, he was married to Elizabeth McMillin. He is survived by his widow; two sons, Owen and John; and a daughter, Elizabeth Jones Godley.

Mr. Jones was elected a Member of the American Society of Civil Engineers on April 2, 1913. He became a Life Member in January, 1948.

---

[1] Memoir prepared by Junius T. Moore, M. ASCE.

VIVIAN GREGOR KAUFMAN, A. M. ASCE[1]

Died March 14, 1954

Vivian Gregor Kaufman, the son of Charles and Daisy (Murfield) Kaufman, was born at LeRoy, Ill., on October 20, 1898. He was awarded the degree of Bachelor of Science in Civil Engineering in 1934 by the University of Illinois at Urbana. He served for one year as President of the Student Chapter of the Society.

After a period of training in hydraulic model work at the Waterways Experiment Station of the Corps of Engineers (United States Department of the Army) in Vicksburg, Miss., he was placed in charge of the Mississippi River Flood Control Model, at the time the largest model of its type in the world. He assisted materially in the development of the present system of cutoffs and levees on the Mississippi River. His duties with the Mississippi River Commission included the planning for and publication of standard operating procedures for flood fighting, a detailed plan of the activities of the Commission in preparation for and during flood emergencies.

On August 18, 1928, he was married to Adelaide Rhodes of Champaign, Ill. He is survived by his widow; a son, Robert Charles; and a daughter, Virginia Ann.

Mr. Kaufman was elected an Associate Member of the American Society of Civil Engineers on November 13, 1939.

SPENCER WILLIAM LOWDEN, A. M. ASCE[2]

Died January 13, 1953

Spencer William Lowden, the son of William J. and Annie (Ryan) Lowden, was born at Lowden's Ranch, Trinity County, California, on April 27, 1888. He attended St. Mary's College (at St. Mary's College, Calif.) and Vander Naillens School of Engineering (in Oakland, Calif.).

He served the California Highway Commission for more than forty years; he located and constructed many miles of the first state highways in Trinity, Siskiyou, Shasta, Tehama, Lassen, and Modoc counties. He was also responsible for the improvement and maintenance of approximately 900 miles of state highways in Inyo and Mono counties and the eastern part of Kern County. In 1950 he was made district engineer of District VIII in San Bernardino. His work included the development of U. S. 395 to multilane divided standards, the planning and construction of the eastern part of Ramona Freeway, and the improvement of many other routes.

In 1914, Mr. Lowden was married to Mildred Gaige Smith. He is survived by his widow; his daughters, Margaret (Mrs. D. Young) and Patricia (Mrs. W. Cain); his son, William Earl; three grandchildren; three brothers; and two sisters.

---

[1] Memoir prepared by Frederick R. Brown, M. ASCE.

[2] Memoir prepared by Perry R. Lowden, Marysville, Calif.

Mr. Lowden was elected an Associate Member of the American Society of Civil Engineers on October 8, 1918.

CONRAD OLAI MANNES, M. ASCE[1]

Died August 14, 1953

Conrad Olai Mannes, the son of Peter K. and Helen (Hoye) Mannes, was born in Norway on November 17, 1885.

From 1905 to 1914, he was engaged in railroad construction in North Dakota, Washington, Minnesota, and Oregon. For the next two years he maintained a private engineering practice in Washington. He then served as Thurston County engineer in Olympia, Wash., until 1919. After doing highway construction work for the Washington State Highway Department, he became city engineer for Shelton, Wash.; he then spent fourteen years in Seattle, Wash., in private practice in design and construction work. Mr. Mannes later was superintendent for the Valley Construction Company in Seattle. He served as King County Engineer in Seattle and then became a civil engineer for the firm of Dewitt C. Griffin in Seattle. In 1951 he was made city engineer of Kelso, Wash.; he also worked as a construction engineer.

Mr. Mannes was a member of the National Society of Professional Engineers and was also a past national director of the American Public Works Association.

On June 18, 1911, Mr. Mannes was married to Verda V. Scott. He is survived by his widow and two children, Conrad Olai, Jr., and Arlene Helen (Mrs. Hollis M. Ramsay).

Mr. Mannes was elected an Associate Member of the American Society of Civil Engineers on April 7, 1924, and a Member on November 4, 1948.

THOMAS ALWYN MIDDLEBROOKS, A. M. ASCE[2]

Died February 3, 1954

Thomas Alwyn Middlebrooks, the son of Benjamin H. and Ethel (Crawford) Middlebrooks, was born in Yatesville, Ga., on December 13, 1903. He received the degree of Bachelor of Science in Civil Engineering from the Georgia Institute of Technology at Atlanta. He also studied at the Massachusetts Institute of Technology at Cambridge under the direction of Karl Terzaghi, Hon. M. ASCE, and thus was one of those who pioneered the application of modern soil mechanics in the United States.

---

[1] Memoir prepared by Robert M. Bonney, A.M. ASCE.

[2] Memoir prepared by Mason C. Prichard, M. ASCE.

He became the chief of the Soil Section, Vicksburg District, Corps of Engineers (United States Department of the Army). In 1933, Mr. Middlebrooks transferred to Fort Peck, Mont.; he was responsible for the design and construction of Fort Peck Dam—by some standards the largest earth dam in the world. Among his many published works is the paper,[1] "Fort Peck Slide," for which he was awarded the James Laurie Medal by the Society. During World War II, he served as a consultant on many military projects.

He was an active member of several technical organizations and was chairman of the United States delegation to the Second International Soil Mechanics Conference in Rotterdam in 1948.

On November 23, 1933, he was married to Jeannette Meacham. He is survived by his widow, three children, his mother, a sister, and two brothers.

Mr. Middlebrooks was elected a Junior of the American Society of Civil Engineers on November 23, 1931, and an Associate Member on May 13, 1935.

EMERY OLIVER, M. ASCE[2]

DIED JULY 26, 1954

Emery Oliver was born in Newton, Iowa, on April 29, 1863.

In 1887, he began his twenty-three-year career as a railroad locator and construction engineer. For a proposed railroad from Salt Lake City, Utah, to San Francisco, Calif., he located a line down the Middle Fork of Feather River—the first known passage of Bald Rock Canyon. He also began location for the first railroad between Portland, Ore., and Seattle, Wash., and discovered the route adopted by the Southern Pacific Company for its main line from San Francisco to Portland. Mr. Oliver's familiarity with the Feather River country led to the discovery of a route of 1% grade across the Sierra Nevadas for the Western Pacific Railway.

He became general manager and chief engineer of Natomas Consolidated of California in 1912. This company operated a fleet of thirteen gold dredges in Sacramento and Butte Counties (California) and owned 100,000 acres of land in Sacramento Valley that were inundated annually. Under Mr. Oliver's direction, 140 sq miles of overflowed land were reclaimed.

On November 1, 1893, Mr. Oliver was married to Annette E. Sylvester. She died in 1915, leaving two sons, Graydon and Boyd. In 1917 he was married to Mary Gabriele Driscol Lindsay. He is survived by his sons, six grandchildren, three great-grandchildren, and a brother.

Mr. Oliver was elected a Member of the American Society of Civil Engineers on March 7, 1906. He became a Life Member in January, 1934.

---

[1] "Fort Peck Slide," by Thomas A. Middlebrooks, *Transactions*, ASCE, Vol. 107, 1942, p. 723.

[2] Memoir prepared by Norwood Silsbee and Walter E. Stoddard, Associate Members, ASCE.

RALPH MALLORY PALMER, A.M. ASCE[1]

Died January 15, 1954

Ralph Mallory Palmer, the son of John and Kate (Mallory) Palmer, was born in Knapp, Wis., on November 13, 1885. He received the degree of Civil Engineer from Valparaiso University at Valparaiso, Ind., in 1914.

During World War I, he served overseas as a First Lieutenant in the Corps of Engineers, United States Army. In 1919 he was employed by the City of Duluth (Minn.) as assistant civil engineer. He was promoted to construction engineer in 1923, the position he held at the time of his death. His work included the planning, designing, and supervising of construction for projects of the City of Duluth. One of his most valuable contributions was the layout and supervision of construction of the sewage disposal system of Duluth. His thorough knowledge of the requirements resulted in many economies without the sacrifice of any necessary features.

Mr. Palmer was a licensed professional engineer in the State of Minnesota. He was a member of the American Society for Testing Materials and the Duluth Engineers' Club. He was also very active in fraternal organizations.

He was married to Lois Mae Sivalia, who died in 1937. He was married in 1939 to Mary Oksanen. He is survived by his widow, his mother, a sister, and three brothers.

Mr. Palmer was elected an Associate Member of the American Society of Civil Engineers on October 15, 1923.

OREN REED, M. ASCE[2]

Died October 29, 1953

Oren Reed, the son of William A. and Ella Copeland Reed, was born at St. Paul, Ind., on March 5, 1896. He received the degrees of Bachelor of Science in Civil Engineering and Civil Engineer from Purdue University at Lafayette, Ind. He also studied in Norway.

In 1923 he was employed as assistant design engineer on hydroelectric power development for the San Joaquin Light and Power Corporation at Fresno, Calif.; he was sent to Germany as an inspector of steel pipe. After responsibilities for the development of Indiana state parks and forests, he joined the Tennessee Valley Authority; he did work on Pickwick Dam, Hales Bar Dam, Watts Bar Dam, Fontana Dam, and Watauga Dam. In 1950 he was transferred to the Widows Creek Steam Plant at Stevenson, Ala., as construction engineer.

In 1946 Mr. Reed made reports on hydroelectric potentialities in Brazil. In 1951 he attended the World Power Conference in Sweden and studied modern hydroelectric developments in Europe. He was a frequent contributor to various technical publications and was a member of Tau Beta Pi, Sigma Xi, and Theta Chi.

---

[1] Memoir prepared by Walter A. Hurtley, A.M. ASCE.
[2] Memoir prepared by L. A. Schmidt, Jr., M. ASCE.

On March 1, 1930, he was married to Lucia Janssen at Vasteras, Sweden. He is survived by his widow.

Mr. Reed was elected a Junior of the American Society of Civil Engineers on January 14, 1924; an Associate Member on October 10, 1927; and a Member on July 13, 1936.

LEO BOND ROBERTS, M. ASCE[1]

Died January 16, 1954

Leo Bond Roberts, the son of David James and Effie (Bond) Roberts, was born on May 19, 1887, at Osage City, Kans. He attended the University of Kansas at Lawrence.

During World War I he served in France rising to the rank of Major and receiving military honors. He also served in the Corps of Engineers (United States Department of the Army) during World War II.

Mr. Roberts was best known for his work in topographic surveying. Among his accomplishments were: The mapping of a route for an expedition led by Roy Chapman Andrews across Inner and Outer Mongolia and the Gobi Desert to Kalzan, China; and the aerial mapping of southern Chile. Mr. Roberts also led two reconnaissance survey parties into the interior of Ethiopia. From 1937 until 1939, Mr. Roberts was assistant chief engineer for the New York World's Fair Corporation. In 1941 he became project manager on construction for advanced naval bases in Northern Ireland and Scotland. After the war he made studies and reports on proposed port construction projects. From 1949 until his death he was associated with the architectural firm, Skidmore, Owings and Merrill (New York, N. Y.), as a construction engineer. He was the author of a widely used textbook,[2] "Topographic Mapping."

In 1913, he was married to Gertrude Mullett of Kansas City, Mo. He is survived by his widow; two sons, David and Richard; and a sister, Mrs. Mona Johnston.

Mr. Roberts was elected an Associate Member of the American Society of Civil Engineers on November 27, 1917, and a Member on July 16, 1928.

ROBERT LAURENCE RYAN, A. M. ASCE[3]

Died July 31, 1954

Robert Laurence Ryan, the son of Laurence Robert and Margaret (McChesney) Ryan, was born on January 17, 1894, in Galesburg, Ill. He received the degree of Bachelor of Science in Civil Engineering in 1917 from the University of California at Berkeley.

In 1928 he entered private practice in Santa Paula, Calif. In 1935 he was elected County Surveyor of Ventura County (California). He was also responsible, in other official capacities, for most major planning.

---

[1] Memoir prepared by Eugene E. Halmos, M. ASCE.

[2] "Topographic Mapping," by Leo Bond Roberts, Society of American Military Engineers, 1924.

[3] Memoir prepared by Vernon M. Freeman, M. ASCE.

In World War II, Mr. Ryan was awarded the Legion of Merit for taking a reconnaissance group ashore on New Georgia (Solomon Islands) and a naval citation for outstanding service. He had many civic, fraternal, and military affiliations. He was President of the Santa Barbara-Ventura Counties Branch of the Los Angeles Section of the Society at the time of his death. He was also a past-president of the Ventura Engineers Club.

On October 14, 1926, Mr. Ryan was married to Ida Mae Shively of Santa Paula. He is survived by his widow; a daughter, Donna; a son, Robert; three sisters, Harriet (Mrs. Neil Bailard), Marian, and Helen.

Mr. Ryan was elected an Associate Member of the American Society of Civil Engineers on October 19, 1942.

HARRY AUGUSTUS SHUPTRINE, M. ASCE[1]

DIED DECEMBER 6, 1954

Harry Augustus Shuptrine, the son of Willard B. and Caroline (Smith) Shuptrine, was born on February 17, 1887, in Savannah, Ga. In 1909 he received the degree of Bachelor of Science in Civil Engineering from the University of Michigan at Ann Arbor.

In 1917 he joined the bridge division of the Michigan Central Railroad and later was employed as the first bridge engineer of the Wayne County (Michigan) Road Commission; he had charge of the design and construction of all bridges and grade separations—among them, the bascule bridges over the Rouge River and the county bridge to Grosse Ile. He was also in charge of design and construction of the Davison and John C. Lodge expressways in the cities of Highland Park and Detroit.

Mr. Shuptrine was a Past-President of the Michigan Section of the Society and also of the Michigan Engineering Society, and a member of the Engineering Society of Detroit. He was a registered Civil Engineer in the State of Michigan.

On November 11, 1918, he was married to Vera M. Ezard at Detroit. He is survived by his widow; two sons, Harry and Calvert; a daughter, Vera Elizabeth; and a brother, Willard.

Mr. Shuptrine was elected an Associate Member of the American Society of Civil Engineers on October 10, 1921, and a Member on April 22, 1935.

RUSH TABOR SILL, M. ASCE[2]

DIED AUGUST 19, 1954

Rush Tabor Sill, the son of J. A. and Martha (French) Sill, was born on November 27, 1882, near Fremont, Nebr. He received the degree of Engineer of Mines from the Colorado School of Mines at Golden in 1906.

---

[1] Memoir prepared by Julian C. Mead, M. ASCE.

[2] Memoir prepared by Donald McCord Baker, M. ASCE.

After work in the Mesabi Range and in Mexico, he began a practice examining and managing mines in this country, Alaska, British Columbia, and Mexico. He served as a consultant for several large earthfill dams and tunnels in the western United States. In 1942 he and his associates formed the firm of Ruscardon Engineers. Mr. Sill continued to serve as a consultant on dam and tunnel construction. He was appointed a consultant on the Tecolote Tunnel in Santa Barbara (Calif.) by the Bureau of Reclamation, United States Department of the Interior.

Mr. Sill was a past-president of the Los Angeles section of the American Institute of Mining and Metallurgical Engineers.

In November, 1918, he was married to Lizette F. Nicholas, who died in 1947. In 1948 he was married to Mildred N. Dickie. He is survived by his widow; a sister, Mrs. Tom F. Williams; and a brother, Harley.

Mr. Sill was elected a Member of the American Society of Civil Engineers on February 16, 1948.

WILLIAM EVERETT SWIFT, M. ASCE[1]

Died February 28, 1953

William Everett Swift, the son of Charles Rufus and Mary (Everett) Swift, was born in Cornwall, Conn., on January 1, 1871. He attended Amherst College (Amherst, Mass.) and was graduated from the Massachusetts Institute of Technology at Boston in 1895 with a degree in civil engineering.

Mr. Swift was responsible for planning the 42nd Street section of the New York City subway and was in charge of special studies for construction of the Panama Canal. He was in charge of the location and construction of the first project of the United States Reclamation Service, the Truckee-Carson Irrigation Project in Nevada. Other work in the western United States included the design and construction of Swift Dam at Valier, Mont. (at that time the highest rock-filled dam in the world), and the location, design, and construction of the Huntley irrigation system near Billings, Mont. He also located the Hudson River Division of the Catskill Viaduct for the New York Board of Water Supply. Mr. Swift's work also took him to Alaska, Greece, The Dominican Republic, and Costa Rica.

Mr. Swift was married on June 30, 1902, to Mabel Alice Runner. He is survived by his widow; two daughters, Margaret (Mrs. W. G. Humphrey) and Mary Everett (Mrs. F. E. Calhoun); a son, Dr. William E. Swift, Jr.; and six grandchildren.

Mr. Swift was elected an Associate Member of the American Society of Civil Engineers on September 2, 1903, and a Member on June 30, 1910. He became a Life Member in January, 1938.

---

[1] Memoir prepared by Mabel Alice Swift, Cornwall, Conn.

HENRY WHITNEY TABOR, A. M. ASCE[1]

DIED NOVEMBER 30, 1954

Henry Whitney Tabor, the son of Ernest and Gertrude (Smith) Tabor, was born in Escondido, Calif., on February 20, 1894. He received the degrees of Bachelor of Science in Civil Engineering and Civil Engineer from the University of Wisconsin at Madison.

He became an instructor in civil engineering at the University of Wisconsin and later was employed as an engineer by several firms in California. In 1930, when the engineering staff of the Bureau of Reclamation (United States Department of the Interior) was expanded to prepare designs and specifications for dams, Mr. Tabor was employed as a civil engineer in the chief engineer's office at Denver, Colo. He supervised the designs and specifications for Hoover Dam, Grand Coulee Dam, and Norris Dam, among others. Mr. Tabor became head of the Outlet Works Section and finally head of the Spillway and Outlet Works Section.

On August 30, 1929, Mr. Tabor was married to Ruth Johnson. He is survived by his widow; a daughter, Sybella Anne (Mrs. S. S. Winston); and a son, Rowland Whitney.

Mr. Tabor was elected an Associate Member of the American Society of Civil Engineers on November 14, 1927.

EARLE EVERETT TEETER, M. ASCE[2]

DIED OCTOBER 24, 1954

Earle Everett Teeter, the son of Dennis P. and Margaret (Reid) Teeter, was born at Monticello, Ind., on May 6, 1882. He received the degree of Bachelor of Science in Civil Engineering from Purdue University at Lafayette, Ind., in 1907. He also studied at the University of Washington in Seattle, Chattanooga (Tenn.) College of Law, American University in Washington, D. C., and Southeastern University in Washington, D. C.

He made investigations in the Gulf Coast area and on the Pecos River, including the planning of power, flood control, and navigation projects for both the United States and Mexico. Subsequently, he was made assistant director of irrigation in the Republic of Haiti; he then made investigations on the Tennessee River and its tributaries for power development and flood control. Mr. Teeter later planned high navigation dams on the Ohio and Kanawha rivers. In 1938 he began studies of national scope pertaining to stream control and development of hydroelectric resources for the Federal Power Commission.

Mr. Teeter was an active member of national and local technical societies.

---

[1] Memoir prepared by George C. Rouse, Denver, Colo.

[2] Memoir prepared by Mrs. Edward R. Leyendecker, Jr., Laredo, Tex.

On August 12, 1918, he was married to Katherine Staton. He is survived by his widow and two daughters, Dulcie (Mrs. R. H. Randall, Jr.) and Virginia (Mrs. E. R. Leyendecker, Jr.).

Mr. Teeter was elected an Associate Member of the American Society of Civil Engineers on December 31, 1913, and a Member on January 19, 1925. He became a Life Member in January, 1949.

WILLIAM FOSTER TRIMBLE, JR., A.M. ASCE[1]

DIED JUNE 18, 1954

William Foster Trimble, Jr., the son of Anthony H. and Margaret (Clark) Trimble, was born on June 27, 1893, in Pittsburgh, Pa. He received the degree of Bachelor of Science in Civil Engineering in 1916 from the University of Pittsburgh.

During World War I he worked for the American Shipping Board in Philadelphia, Pa., and as a civil engineer for the Pennsylvania Railroad Company. He succeeded his uncle as president of W. F. Trimble & Sons Company, general contractors of Pittsburgh, in 1937.

He was an officer of banking, insurance, and other business organizations. He also served on various committees for the University of Pittsburgh Engineering School and was a member of the board of trustees of that university for two terms. He was an active member of several fraternal and religious groups in Pittsburgh.

On June 14, 1917, he was married to Lois Turkle. He is survived by his widow; two sons, William Foster, III, and Anthony H.; a brother, T. Lee Trimble; a sister, Eleanor (Mrs. W. F. Peel); and three grandsons.

Mr. Trimble was elected an Associate Member of the American Society of Civil Engineers on April 25, 1921.

DANA MELVIN WOOD, M. ASCE[2]

DIED MAY 10, 1954

Dana Melvin Wood, the son of Henry B. and Emily W. (Eaton) Wood, was born in St. Louis, Mo., on April 22, 1884. He attended the Massachusetts Institute of Technology at Boston.

His professional career began with service for the Water Resources Branch of the Geological Survey (United States Department of the Interior) as an assistant engineer. In 1934 Mr. Wood began his work for the Tennessee Valley Authority. He held the positions of senior and head hydraulic engineer and chief of the power studies branch in the division of water control planning. He retired in 1954. One of his outstanding traits was his interest in young engineers—his desire to help them assume added responsibilities and to help them toward professional development. He received the Desmond Fitzgerald Medal of the Boston Society of Civil Engineers and was the author of numerous scientific and technical articles.

---

[1] Memoir prepared by William Foster Trimble, III.

[2] Memoir prepared by Julian R. Fleming, A. M. ASCE.

On April 22, 1909, he was married to Marion R. Elliott in Belmont, Mass. He is survived by his widow and three children, James E., Emily S. (Mrs. Bruno L. Bucit), and Charles D.

Mr. Wood was elected an Associate Member of the American Society of Civil Engineers on December 6, 1915, and a Member on January 18, 1921. He became a Life Member in January, 1950.

WILLIAM HERBERT WATT YEO, A.M. ASCE[1]

Died October 1, 1954

William Herbert Watt Yeo, the son of William and Mary (Watt) Yeo, was born in Carnegie, Pa., on January 6, 1877. He received the degree of Bachelor of Philosophy in engineering from Franklin College at New Athens, Ohio.

His field investigations led to the comprehensive (unpublished) report, "Hydrographic and Irrigation Conditions in the Rio Grande Valley—New Mexico"—currently the only reliable source of information on the subject. After military service, he entered private practice and also served as Dona Ana County (New Mexico) Surveyor. He was later appointed State Engineer of New Mexico. From 1934 until 1942 he participated in the investigation and construction of numerous projects for the Soil Conservation Service (United States Department of Agriculture) and made studies and reports of silt problems on the Rio Grande in New Mexico as well as other streams. He then joined the Corps of Engineers (United States Department of the Army) in Albuquerque, N. Mex. His studies provided information needed for the control of floods and sediment in the Middle Rio Grande Valley.

On April 24, 1907, he was married to Lodalee Patton. Mr. Yeo is survived by a nephew.

Mr. Yeo was elected an Associate Member of the American Society of Civil Engineers on February 1, 1910. He became a Life Member in January, 1945.

---

[1] Memoir prepared by Floy E. French, Las Cruces, N. Mex.

TRANSACTIONS

OF THE

AMERICAN SOCIETY OF CIVIL ENGINEERS

INDEX
VOLUME 120
1955

Subject Index, Page 1583
Author Index, Page 1628

Titles of papers are in quotation marks when given with the author's name.

VOLUME 120

SUBJECT INDEX

ACCOUNTS AND ACCOUNTING
See COSTS . . . ; *also* subheading Financing under relative subject

ADDRESSES
See AMERICAN SOCIETY OF CIVIL ENGINEERS—Addresses; *see also* under subject of address

AERATION
See also HYDRAULIC JUMP; TANKS, AERATION
Aeration in composting of refuse, 897, 904, 909, 916.
"Flocculation and Flocculation Basins," Thomas R. Camp, 1.

AERATION TANKS
See TANKS, AERATION

AERIAL . . .
See also AIR . . .

AERIAL MAPS AND MAPPING
See MAPS AND MAPPING, AERIAL

AERIAL SURVEYS AND SURVEYING
See SURVEYS AND SURVEYING, AERIAL

AERODYNAMIC MODELS
See MODELS, AERODYNAMIC

AERODYNAMICS
See also under relative subject
"Aerodynamic Stability of Suspension Bridges": 1952 Report of the Advisory Board on the Investigation of Suspension Bridges, E. F. Kelley, Raymond Archibald, A. A. Jakkula, Raymond Archibald, C. B. McCullough, G. S. Paxson, F. H. Frankland, C. F. Goodrich, Jonathan Jones, C. Earl Webb, Russell G. Cone, Shortridge Hardesty, Charles M. Spofford, O. L. Grover, E. F. Kelley, R. B. McMinn, Leon S. Moisseiff, C. H. Purcell, Norman C. Raab, George D. Whittle, Theodor von Karman, Frank M. Masters, P. L. Pratley, John G. Little, Leon H. Nishkian, R. W. Crum, Franklin N. Wray, Charles C. Sunderland, H. L. Dryden, G. B. Schubauer, O. H. Ammann, Elmer K. Timby, Emil H. Praeger, F. B. Farquharson, Charles E. Andrew, Glenn B. Woodruff, and Hardy Cross, 721.
"Wind Velocities during Hurricanes," Robert C. Gentry, 169.

AGGREGATES AND AGGREGATION
"Flocculation and Flocculation Basins," Thomas R. Camp, 1.
"Movements in Structural Concrete in a Powerhouse," Stanley Moyer and Viggo Hansen (with discussion), 1183.

AGREEMENTS
See CONTRACTS

AGRICULTURE
See DRAINAGE; FERTILIZERS (cross references thereunder); FLOODS (cross references thereunder); IRRIGATION; LAND . . . ; SOIL . . .

AIR . . .
See also AERIAL . . . (cross references thereunder); AERO- . . .

AIR CHAMBERS
See PIPE LINES

AIRCRAFT
See also AIRPLANE . . .
"Determination of Radii of Curvature of Taxiways," John H. Jones and Robert Horonjeff, 27.

AIRFIELDS
See AIRPORTS

AIR FLOW
"Aerodynamic Stability of Suspension Bridges": 1952 Report of the Advisory Board on the Investigation of Suspension Bridges, E. F. Kelley, Raymond Archibald, A. A. Jakkula, Raymond Archibald, C. B. McCullough, G. S. Paxson, F. H. Frankland, C. F. Goodrich, Jonathan Jones, C. Earl Webb, Russell G. Cone, Shortridge Hardesty, Charles M. Spofford, O. L. Grover, E. F. Kelley, R. B. McMinn, Leon S. Moisseiff, C. H. Purcell, Norman C. Raab,

AIR FLOW (*Continued*)
George D. Whittle, Theodor von Karman, Frank M. Masters, P. L. Pratley, John G. Little, Leon H. Nishkian, R. W. Crum, Franklin N. Wray, Charles C. Sunderland, H. L. Dryden, G. B. Schubauer, O. H. Ammann, Elmer K. Timby, Emil H. Praeger, F. B. Farquharson, Charles E. Andrew, Glenn B. Woodruff, and Hardy Cross, 721.

AIRPLANE PARKING
Passenger and cargo parking requirements at an international airport in relation to basic planning and design, 367.

AIR POLLUTION
See AIR SANITATION (cross reference thereunder)

AIRPORTS (structures and localities)
See also TRAFFIC, AIRPORT
"Determination of Radii of Curvature of Taxiways," John H. Jones and Robert Horonjeff, 27.
Planning an international airport terminal building, 370.
Summary of building requirements and personnel needs, actual and estimated, at an international airport, 1950–1970, 368.

AIR SANITATION
See ODORS

AIR TERMINALS
See AIRPORTS

AIR TESTING
See AERODYNAMICS

ALINEMENT CURVES
See CURVES (alinement curves)

ALKALIES
See CONCRETE—Alkalies

ALLOYS
See STRESS AND STRAIN—Alloys; *see also* under relative metal, e.g., ALUMINUM

ALLUVIATION
See BARS (alluvia); EROSION . . . ; SEDIMENT AND SEDIMENTATION; SILT AND SILTING . . . ; VALLEYS

ALUMINUM
See also ALLOYS (cross references thereunder)
Eccentrically loaded aluminum alloy columns, 1116.
Testing for plastic strength of rolled rectangular aluminum alloy bars, 1117, 1125.
Welded aluminum in ships and bridge stringers, 115, 140.

AMERICAN SOCIETY OF CIVIL ENGINEERS

Addresses
1955—Address at the Summer Convention, St. Louis, Mo., June 15, 1955, William R. Glidden, 1550.

Committee Reports—Plasticity
"Plastic Strength of Structural Members": A Symposium, Robert L. Ketter, Edmund L. Kaminsky, and Lynn S. Beedle; Paul P. Bijlaard, Gordon P. Fisher, and George Winter; John W. Clark; and W. Gordon Brady and Daniel C. Drucker (with discussion), 1019.

Committee Reports—Structures (General)
"Plastic Strength of Structural Members": A Symposium, Robert L. Ketter, Edmund L. Kaminsky, and Lynn S. Beedle; Paul P. Bijlaard, Gordon P. Fisher, and George Winter; John W. Clark; and W. Gordon Brady and Daniel C. Drucker (with discussion), 1019.

Memoirs of Members. *See* name of member in Author Index. (*See also* p. 1557)

ANALYSIS, DESIGN
See under relative subject, e.g., WATER HAMMER

ANALYSIS OF DATA
See EQUATIONS; GRAPHICAL CHARTS (cross references thereunder); MATHEMATICS; PROBABILITY, THEORY OF; STRUCTURES, THEORY OF; *also* under relative subject, e.g., SOILS

ANALYSIS, STRUCTURAL
See EQUATIONS; STRESS AND STRAIN; STRUCTURES, THEORY OF . . .

ANEMOMETERS
See WIND MEASURING INSTRUMENTS

APPARATUS
See under relative subject, e.g., WELLS; *also* INSTRUMENTS (cross references thereunder); *also* under general types of apparatus

APPARATUS, TRIAXIAL COMPRESSION
See SOILS—Tests and Testing

AQUIFERS
See WELLS

ARCHITECTS AND ARCHITECTURE

See type of structure or structural part, e.g., BRIDGES; BUILDINGS

ARCHITECTURE, NAVAL

See NAVAL ARCHITECTURE (cross reference thereunder)

ASSOCIATIONS

See SOCIETIES, TECHNICAL

ATMOSPHERIC POLLUTION

See AIR SANITATION (cross reference thereunder)

ATMOSPHERIC PRESSURE

"Wind Velocities during Hurricanes," Robert C. Gentry, 169.

AUTHORITIES

See MUNICIPAL AUTHORITIES

AUTOMOBILE . . .

See MOTOR . . . (cross references thereunder)

BACKWATER

"Backwater Effects of Open-Channel Constrictions," Hubert J. Tracy and Rolland W. Carter (with discussion), 993.

"Backwater Functions by Numerical Integration," Clint J. Keifer and Henry H. Chu, 429. *Discussion:* Francis F. Escoffier; Henry J. Miles; Richard Silvester; and Clint J. Keifer and Henry H. Chu, 443.

Computing of a sketch of a typical backwater flow, 985.

Short cut method of computing backwater depths, 1011.

Tables of functions to facilitate computing of water surface profiles in circular conduits, 429, 443.

BACTERIA

Bacterial decomposition as related to composting processes, 897, 910, 917.

BAFFLES

See WATER, FLOW OF . . .

BANKS AND BANK PROTECTION, RIVER

See RIVER BANKS AND BANK PROTECTION (cross references thereunder)

BARGES

Bridge erection by floating the spans into position, 249.

BARS (alluvia)

Investigations of increased shoaling conditions in inner harbor navigation channels, Charleston, South Carolina, 1948–1953, 687, 689, 695.

"Sediment Sampling in Tidal Waterways," Edward A. Schultz, 687.

BASINS (depression in earth's surface)

See DRAINAGE; VALLEYS; *see also* RIVER BASINS (cross references thereunder)

BASINS, FLOCCULATION

See FLOCCULATION BASINS (cross references thereunder)

BASINS, SETTLING (water supply)

See SETTLING BASINS

BEACHES

See SAND DUNES

BEAMS (General)

See also BRIDGES; BUCKLING; CONNECTORS AND CONNECTIONS (cross references thereunder); FLANGES (cross reference thereunder); GIRDERS . . . (cross references thereunder); STRESS AND STRAIN—Beams (General); STRUCTURES, THEORY OF—Beams and Girders (General); TORSION; WHEEL LOADS

"Deflections of a Circular Beam Out of Its Initial Plane," Enrico Volterra, 65. *Discussion:* I. Oesterblom, and Enrico Volterra, 87.

Effect of coped holes in web of beams and resultant cracking tendencies, 120, 121.

"Impulsive Motion of Elasto-Plastic Beams," Hans H. Bleich and Mario G. Salvadori (with discussion), 499.

"Inelastic Behavior of Reinforced Concrete Members," Lawrence H. N. Lee (with discussion), 181.

Stringer detail design in long span bridges, 221.

Bibliography

Circular beams on elastic foundations, 309.

Deflections of circular beams, 84, 87, 88, 91.

BEAMS, CONTINUOUS

See also STRESS AND STRAIN—Beams, Continuous

"Constrained Circular Beams on Elastic Foundations," Enrico Volterra and Randall Chung, 301.

"Lateral Buckling of I-Beams," Mario G. Salvadori (with discussion), 1165.

"Stress Measurements, San Leandro Creek Bridge," Ray W. Clough and Charles F. Scheffey, 939.

BEARING CAPACITY (foundations, rocks, soils)
For more general interpretation *see* cross references under LOAD
"Reduction in Soil Strength with Increase in Density," Charles R. Foster, 803. *Discussion:* Edward S. Barber, George R. Halton, and Charles R. Foster, 816.
"Strength Characteristics of Compacted Clays," Gerald A. Leonards (with discussion), 1420.
"The Undisturbed Consolidation Behavior of Clay," John H. Schmertmann (with discussion), 1201.

BED LOAD
See CHANNELS; SILT AND SILTING . . . ; TURBULENCE; WATER, FLOW OF, IN OPEN CHANNELS

BENDING
See BUCKLING; MOMENTS; STRESS AND STRAIN; *also* under relative structure, structural part or material, e.g., BEAMS; CONCRETE

BIBLIOGRAPHY
See subheading Bibliography under relative subject. (Comprehensive bibliographical footnotes existing in individual papers in which books and other material are cited)

BIOGRAPHIES OF DECEASED MEMBERS
See cross reference under MEMOIRS OF DECEASED MEMBERS. (*See also* p. 1557)

BOGS
See MARSHES; PEAT

BOLTED JOINTS
See JOINTS, BOLTED (cross reference thereunder)

BOLTS
See JOINTS

BORINGS
"Sand Compaction by Vibroflotation," Elio D'Appolonia, Callix E. Miller, Jr., and Thomas M. Ware, 154.

BOUNDARIES (land ownership)
See RIGHTS OF WAY (land strips)

BOUNDARY LAYER, THEORY OF (fluid flow)
See FLUIDS, FLOW OF (cross references thereunder); WATER, FLOW OF . . .

BOW GIRDERS
See GIRDERS

BRACING
See TRUSSES . . .

BREAKWATERS
See WATER PRESSURE; WAVES

BRIDGE CABLES
Construction of suspension spans, Chesapeake Bay Bridge, 251.

BRIDGE FAILURES
See FAILURES, BRIDGE

BRIDGE PIERS
See also CONCRETE
Computing backwater from channel obstructions caused by bridge piers, 1007, 1008, 1013.

BRIDGES (General)
See also BEAMS . . . ; COLUMNS; COSTS, BRIDGE; FAILURES, BRIDGE; GIRDERS; MASONRY (cross reference thereunder); STRESS AND STRAIN—Bridges; STRUCTURES, THEORY OF—Bridges; TRUSSES . . . ; VIBRATION; WATER, FLOW OF, IN OPEN CHANNELS; WHEEL LOADS
"Chesapeake Bay Bridge," Ethan F. Ball, 245.
Requirements for weldable bridge steel, 108, 116.

BRIDGES, GIRDER
"Erection of Main River Span, Passaic River Bridge," Jonathan Jones, 208.
Failures of welded bridges in Canada, 132, 135, 144.
"Stress Measurements, San Leandro Creek Bridge," Ray W. Clough and Charles F. Scheffey, 939.

BRIDGES, MOVABLE (LIFT)
Origination of the double lift bridge, 1558.

BRIDGES, SUSPENSION
See also STRESS AND STRAIN—Bridges, Suspension
"Aerodynamic Stability of Suspension Bridges": 1952 Report of the Advisory Board on the Investigation of Suspension Bridges, E. F. Kelley, Raymond Archibald, A. A. Jakkula, Raymond Archibald, C. B. McCullough, G. S. Paxson, F. H. Frankland, C. F. Goodrich, Jonathan Jones, C. Earl Webb, Russell G. Cone, Shortridge Hardesty, Charles M. Spofford, O. L. Grover, E. F. Kelley, R. B. McMinn, Leon S. Moisseiff, C. H. Purcell, Norman C. Raab, George D. Whittle, Theodor von

BRIDGES, SUSPENSION (*Cont.*)

Karman, Frank M. Masters, P. L. Pratley, John G. Little, Leon H. Nishkian, R. W. Crum, Franklin N. Wray, Charles C. Sunderland, H. L. Dryden, G. B. Schubauer, O. H. Ammann, Elmer K. Timby, Emil H. Praeger, F. B. Farquharson, Charles E. Andrew, Glenn B. Woodruff, and Hardy Cross, 721.

Flutter theory as related to bridge oscillation problems, 742, 744, 751, 758, 762.

Negative slope theory as related to bridge oscillation problems, 729, 739, 744, 748.

Weight in relation to vibration, 760, 767.

Bibliography

Bibliography on stability of suspension bridges, 768.

BRIDGES, TRUSS

See STRESS AND STRAIN—Bridges, Truss; TRUSSES . . .

BUCKLING

Interaction curves for I-beams under thrust and end moments, 1170, 1172, 1173, 1178.

"Lateral Buckling of I-Beams," Mario G. Salvadori, 1165. *Discussion:* Robert V. Whitman, Michael R. Horne, and Mario G. Salvadori, 1178.

"Plastic Strength of Structural Members": A Symposium, Robert L. Ketter and Edmund L. Kaminsky, and Lynn S. Beedle; Paul P. Bijlaard, Gordon P. Fisher, and George Winter; John W. Clark; and W. Gordon Brady and Daniel C. Drucker (with discussion), 1019.

BUILDING (process)

See CONSTRUCTION

BUILDING MATERIALS

See MATERIALS OF CONSTRUCTION

BUILDINGS

See also EARTHQUAKES; FAILURES, BUILDING; FOUNDATIONS . . . ; MATERIALS OF CONSTRUCTION; ROOFS AND ROOFING; STRESS AND STRAIN . . . ; STRUCTURES, THEORY OF . . . ; *also* under type of building, e.g., AIRPORTS

Buildings in the United States using bolt connectors in lieu of rivets, 1395, 1398.

Evolution of the taller building, 147.

BUILDING STONE

See STONE (cross references thereunder)

BULKHEADS

See also RETAINING WALLS; WAVES

Usage of bulkheads to combat landslides, 286.

BULKHEAD WALLS

See RETAINING WALLS

BUTTERFLY VALVES

See VALVES

CABLES, BRIDGE

See BRIDGE CABLES

CANALS (General)

See also CHANNELS; EROSION, STREAM; IRRIGATION CANALS; SEDIMENT AND SEDIMENTATION; SILT AND SILTING, CHANNEL; WATER, FLOW OF, IN OPEN CHANNELS; WATER TRANSPORTATION; WATERWAYS; WAVES

CANALS (Geographical)

Illinois Waterway. *See* WATERWAYS (Geographical)—Illinois Waterway

United States

"Some Economic Aspects of Waterway Projects," Haywood R. Faison (with discussion), 1480.

CANALS, IRRIGATION

See IRRIGATION CANALS

CARRIERS

See AIRCRAFT; MOTOR . . . (cross references thereunder); RAIL . . . ; RATE MAKING; TRANSPORTATION (cross references thereunder); WATER . . .

CARS

See MOTOR VEHICLES (cross references thereunder)

CARTOGRAPHY

See CHARTS (cross references thereunder); MAPS AND MAPPING; SURVEYS AND SURVEYING

CAR WHEELS

See WHEEL LOADS

CAVITATION

"Applications of the Relaxation Technique in Fluid Mechanics," John S. McNown, En-Yun Hsu and Chia-Shun Yih (with discussion), 650.

"Hydraulic Model Studies of Martin Dam Draft Tubes," Carl E. Kindsvater and Richard R. Randolph, Jr., (with discussion), 1399.

CHAMBERS, AIR
See PIPE LINES

CHANNELS (waterways)
See also EROSION, STREAM; HYDRAULIC JUMP; RIVERS; SILT AND SILTING, CHANNEL; WATER, FLOW OF, IN OPEN CHANNELS
"Design of Stable Channels," Emory W. Lane, 1234. *Discussion:* Serge Leliavsky; A. Nizery and G. Braudeau; N. K. Bose; Jose S. Gandolfo; and Emory W. Lane, 1261.
Effects of bends in stable channel design, 1256, 1259.

CHARTS
See GRAPHICAL CHARTS (cross references thereunder); *see also* MAPS AND MAPPING . . . ; *also* under relative subject, e.g., WATER HAMMER

CIRCULAR BEAMS
See BEAMS

CITIES
See also AIRPORTS; BUILDINGS; CITY PLANNING; COSTS . . . ; EMPLOYEES AND EMPLOYMENT; ENGINEERS AND ENGINEERING—Government Relationships; GAS AND GASWORKS . . . ; INDUSTRIAL . . . ; MUNICIPAL . . . ; ODORS; PARKING . . . (cross reference thereunder); PUBLIC HEALTH; REFUSE DISPOSAL; SEWAGE . . . ; SEWERS; TRAFFIC . . . ; *also* geographical subheadings under relative subject, e.g., HARBORS—Charleston, S. C.
"Community and Neighborhood Development," Russell H. Riley, 449.
Importance of waterway development in the Kansas City, Missouri area, 1528, 1531, 1546.

CITY PLANNING (General)
See also EDUCATION; HIGHWAYS AND ROADS
Noteworthy examples of neighborhood planning and development in the United States, 453.
Remedies suggested for the restoration and improvement of the older neighborhood, 452.
"The Training of City Planners," Howard K. Menhinick (with discussion), 608.

CITY PLANNING (Geographical)
Florida
"Community and Neighborhood Development," Russell H. Riley, 449.
West Palm Beach, Fla.
"Community and Neighborhood Development," Russell H. Riley, 449.

CIVIL ENGINEERS AND ENGINEERING
See AMERICAN SOCIETY OF CIVIL ENGINEERS; ENGINEERS AND ENGINEERING (and cross references thereunder)

CLASSIFICATION OF SOILS
See SOILS—Classification

CLAY
See also SHEAR; SOILS
"Reduction in Soil Strength with Increase in Density," Charles R. Foster (with discussion), 803.
"Strength Characteristics of Compacted Clays," Gerald A. Leonards, 1420. *Discussion:* Harold J. Gibbs and Jack W. Hilf; James K. Mitchell; Preston T. Bennett and Paul E. Wohlt; and Gerald A. Leonards, 1455.
"The Undisturbed Consolidation Behavior of Clay," John H. Schmertmann (with discussion), 1201.
Bibliography
List of references on the strength characteristics of compacted soils, including clays, 1452.

COAGULANTS AND COAGULATION
See WATER TREATMENT

COFFERDAMS
Forty-five foot rock excavation with rock slide problems as undertaken at Hales Bar Hydroelectric Plant, in Tennessee, 555, 559.

COLLEGES AND SCHOOLS, ENGINEERING
See EDUCATION

COLUMNS
See also STRESS AND STRAIN—Columns; STRUCTURES, THEORY OF—Columns
"Inelastic Behavior of Reinforced Concrete Members," Lawrence H. N. Lee (with discussion), 181.
"Lateral Buckling of I-Beams," Mario G. Salvadori (with discussion), 1165.

COMMERCE
See AIRPORTS; CANALS; CHANNELS; CITIES; FREIGHT; HARBORS; RIVERS; TRANSPORTATION (cross references thereunder); WATER TRANSPORTATION; WATERWAYS

COMMITTEE REPORTS
See AMERICAN SOCIETY OF CIVIL ENGINEERS—Committee Reports; *see also* under subject of report

COMPACTION
See BEARING CAPACITY; SOILS

COMPOST AND COMPOSTING
See under type of waste, e.g., REFUSE DISPOSAL; *see also* BACTERIA

COMPRESSION
See STRESS AND STRAIN

COMPRESSION MEMBERS
See COLUMNS

COMPRESSION TESTS, SOIL
See SOILS—Tests and Testing

CONCRETE (General)
See also AGGREGATES AND AGGREGATION; FAILURES, CONCRETE; GRAVEL; SAND; SEEPAGE; SLABS; STRESS AND STRAIN—Concrete; STRUCTURES, THEORY OF—Concrete, Reinforced; *also* under special structure or structural part
"Movements in Structural Concrete in a Powerhouse," Stanley Moyer and Viggo Hansen, 1183. *Discussion:* E. A. Woodhead; Herbert A. Kammer; and Stanley Moyer and Viggo Hansen, 1193.

Alkalies
"Movements in Structural Concrete in a Powerhouse," Stanley Moyer and Viggo Hansen (with discussion), 1183.

Construction
Installation of pyramids in Martin Dam draft tubes, Tallapoosa River, Alabama, 1416.

Effect of Natural Processes
"Stress Measurements, San Leandro Creek Bridge," Ray W. Clough and Charles F. Scheffey, 939.

Expansion and Contraction
Map indicating location of structures in United States where expansive concrete exists, 137.
"Movements in Structural Concrete in a Powerhouse," Stanley Moyer and Viggo Hansen (with discussion), 1183.
Special shrinkage problems relating to long-span cylindrical shell roofs, 637, 640, 644, 645.

Linings. *See* under structure, e.g., TUNNEL LININGS

Plastic Flow
"Inelastic Behavior of Reinforced Concrete Members," Lawrence H. N. Lee (with discussion), 181.

Shrinkage. *See* Expansion and Contraction (hereunder)

Slabs. *See* SLABS

Temperature
"Movements in Structural Concrete in a Powerhouse," Stanley Moyer and Viggo Hansen (with discussion), 1183.

Tests and Testing
"Inelastic Behavior of Reinforced Concrete Members," Lawrence H. N. Lee, 181. *Discussion:* Boris Bresler, Alfred J. Ashdown, and Lawrence H. N. Lee, 203.

CONCRETE-METAL
See cross reference under REINFORCED CONCRETE

CONCRETE, REINFORCED
See CONCRETE . . .

CONDUITS
See also FLUMES; PENSTOCKS; PIPE LINES; TUNNELS . . .
"Backwater Functions by Numerical Integration," Clint J. Keifer and Henry H. Chu (with discussion), 429.
"Flow in Rough Conduits," Henry M. Morris, Jr. (with discussion), 373.
"High-Velocity Tests in a Penstock," Maxwell F. Burke (with discussion), 863.

CONNECTORS AND CONNECTIONS
See JOINTS . . . ; WELDS AND WELDING

CONSOLIDATION TESTS, SOIL
See SOILS—Tests and Testing

CONSTRICTION
See WATER, FLOW OF, IN OPEN CHANNELS

CONSTRUCTION
See also BUILDINGS; CONCRETE—Construction; CONTRACTS;

CONSTRUCTION (*Continued*)
COSTS . . . ; CURVES (alinement curves); FAILURES . . . ; INSPECTORS AND INSPECTION (cross reference thereunder); MATERIALS OF CONSTRUCTION; SOILS—Construction; SPECIFICATIONS; STRESS AND STRAIN . . . ; STRUCTURES, THEORY OF . . . ; *also* under type of construction, e.g., BRIDGES; TUNNELS
"Chesapeake Bay Bridge," Ethan F. Ball, 245.
Installation of pyramids in Martin Dam draft tubes, Tallapoosa River, Alabama, 1416.
"Structural Observations of the Kern County Earthquake," Henry J. Degenkolb, 1280.
Value of construction roadway requirement in contracts, 223.
"Welded Structures": A Symposium, Simon A. Greenberg, La Motte Grover, and C. L. Kreidler (with discussion), 103.

CONSTRUCTION CURVES
See CURVES (alinement curves)

CONSTRUCTION MATERIALS
See MATERIALS OF CONSTRUCTION

CONSTRUCTION, UNDERWATER
See UNDERWATER CONSTRUCTION (cross reference thereunder)

CONTINUOUS BEAMS
See BEAMS, CONTINUOUS

CONTINUOUS FRAMES
See STRUCTURES, THEORY OF—Frames, Continuous

CONTINUOUS GIRDERS
See GIRDERS, CONTINUOUS (cross reference thereunder)

CONTINUOUS STRUCTURES
See STRUCTURES, THEORY OF

CONTRACTION
See under relative subject, e.g., CONCRETE—Expansion and Contraction; WATER, FLOW OF, IN OPEN CHANNELS

CONTRACTS
See also SPECIFICATIONS
Securing and preliminaries of fulfilling a structural steel contract, 148.

CONVENTIONS (American Society of Civil Engineers)
See AMERICAN SOCIETY OF CIVIL ENGINEERS—Addresses

COSTS (General)
See also subheading Financing under relative subject

COSTS (of work)
See COSTS . . .

COSTS, BRIDGE
Value of construction roadway requirement in contracts as related to overall erection cost, 223.

COSTS, DAM
Summary of total and itemized costs of changes, additions and improvements at Hales Bar Dam, in Tennessee, 555, 557.

COSTS, FILTRATION PLANT (SEWAGE)
Economical designing of single and two stage biofiltration plants, 823, 834.

COSTS, FLOOD
Flood damage costs as related to open channel constrictions, 1009.

COSTS, HIGHWAY AND ROAD
Turnpike design standards and other features influencing control of cost estimates, 56, 57, 64.

COSTS, INDUSTRIAL PLANT
Plant location selection as related to cost factors, 418.

COSTS, JOINT
Bolt and riveted connections compared, 1390, 1392, 1395, 1397, 1398.

COSTS, LANDSLIDE
Prevention and correction of slides in relation to cost, 289.

COSTS, PUMP AND PUMPING
Pump characteristics in relation to relative cost and performance efficiency by type, 18.

COSTS, RAILROAD TRACK
Reduction of costs by usage of simplified method of transit lining of high speed tracks, 521, 537, 538.

COSTS, REFUSE DISPOSAL
Factors influencing composting costs, 909, 912, 913, 918, 920.

COSTS, SAND COMPACTION
Sand compaction process cost comparisons, 155.

COSTS, SEWAGE DISPOSAL
Construction contract costs (total and partially itemized) for certain municipal authorities in Pennsylvania, 844, 859.

COSTS, STEEL
Welded steel in relation to cost, 104, 110, 111, 128.

COSTS, TANK (SEWAGE TANKS)
Building costs of circular and rectangular tanks compared, 361.

COSTS, TRANSPORTATION
See COSTS, WATER TRANSPORTATION

COSTS, TUNNEL
Most economical type of tunnel, 423.

COSTS, WATER HAMMER ANALYSIS
Inexpensive water hammer analysis method as installed at Tracy Pumping Plant, in California, 697, 715.

COSTS, WATER TRANSPORTATION
Methods of determining cost requirements in relation to ratio of future benefits, 1480.

COSTS, WELD AND WELDING
Radiographic inspection and radiographic plate costs, 243, 244.

COURT DECISIONS
See under relative subject (under the subject law heading, e.g., RATE MAKING LAW)

CRACKS AND CRACKING
See under relative subject, e.g., BEAMS (General)

CRANES, DERRICKS AND POWER SHOVELS
"Erection of Main River Span, Passaic River Bridge," Jonathan Jones, 208.

CREEP
See STRESS AND STRAIN; STRUCTURES, THEORY OF

CURRENT METERS
See METERS AND METERING, CURRENT

CURRENTS
See TIDES; WAVES

CURVED BEAMS
See BEAMS

CURVED STRUCTURES
See STRUCTURES, THEORY OF—Curved Structures

CURVES (alinement curves)
"Determination of Radii of Curvature of Taxiways," John H. Jones and Robert Horonjeff, 27.
Solution of compound curves by simultaneous equations, 532.
"Transit Lining of High-Speed Track," Neil R. Berndt, 521. *Discussion:* Harry Rubey, 538.

CURVES (backwater)
See BACKWATER

CURVES (construction curves)
See CURVES (alinement curves)

CURVES (design curves)
See under relative subject of design, e.g., BUCKLING; STRUCTURES (General)

CURVES (elastic curves)
See STRUCTURES, THEORY OF

CURVE TANGENTS
See RAILROAD TRACKS

CYLINDRICAL SHELLS
See STRUCTURES, THEORY OF—Shell Structures

DAMPING
See STRESS AND STRAIN; STRUCTURES, THEORY OF

DAMS (General)
See COFFERDAMS; COSTS, DAM; FOUNDATIONS, DAM; LOCKS; MODELS, HYDRAULIC; WATER PRESSURE

DEFENSE
See NATIONAL DEFENSE

DEFINITIONS
See TERMINOLOGY

DEFLECTIONS
See STRESS AND STRAIN; STRUCTURES, THEORY OF . . . ; *see also* under relative structure or structural part, e.g., BEAMS; GIRDERS

DEFORMATION
See FAILURES . . . ; STRESS AND STRAIN; STRUCTURES, THEORY OF; *also* under type of material, e.g., CONCRETE; *also* under specific type of stress, e.g., BUCKLING, TORSION; *also* under type of structure, e.g., BRIDGES

DEFORMATION, THERMAL
See TEMPERATURE

DERRICKS
See CRANES, DERRICKS AND POWER SHOVELS

DESIGN
See under relative subject, e.g., CHANNELS; PUMPS AND PUMPING; *see also* SPECIFICATIONS; STRUCTURES, THEORY OF

DESIGN ANALYSIS
See under relative subject, e.g., WATER HAMMER

DESIGN CURVES
See CURVES (design curves) (cross reference thereunder)

DIAGRAMS
See GRAPHICAL CHARTS (cross references thereunder); *see also* under relative subject

DIESEL ENGINES
See ENGINES

DIFFUSER FLOW
See DRAFT TUBES

DISCHARGE
See WATER, FLOW OF . . .

DISCHARGE COEFFICIENTS
See under relative subject, e.g., WATER, FLOW OF, IN OPEN CHANNELS

DISTORTION
See STRESS AND STRAIN; TORSION

DRAFT TUBES
"Hydraulic Model Studies of Martin Dam Draft Tubes," Carl E. Kindsvater and Richard R. Randolph, Jr., 1399. *Discussion:* Richard S. Woodruff; and Carl E. Kindsvater and Richard R. Randolph, Jr., 1416.

DRAINAGE
See also SEWERS; WELLS
Drainage of ground water in landslides, 283, 285, 288.
"Effect of Well Screens on Flow into Wells," Jack S. Petersen, Carl Rohwer and Maurice L. Albertson (with discussion), 563.
"Selection and Design of High-Volume, Low-Head Pumps," George F. Snodgrass, 17.
"Total Sediment Load Measured in Turbulence Flume," Paul C. Benedict, Maurice L. Albertson and Donald Q. Matejka (with discussion), 457.

DRAWDOWN
See WELLS

DRAWINGS
See under relative subject

DUNES
See SAND DUNES

DYNAMICS OF FLUIDS
See HYDRODYNAMICS

DYNAMICS OF GASES
See AERODYNAMICS

DYNAMICS OF STRUCTURES
See STRUCTURAL DYNAMICS

EARTH . . .
See also GROUND . . . ; LAND . . . ; SOIL . . .

EARTH FLOW
See LANDSLIDES

EARTH MOVEMENTS
See EARTHQUAKES; LANDSLIDES

EARTH PRESSURE
"Reduction in Soil Strength with Increase in Density," Charles R. Foster (with discussion), 803.

EARTHQUAKES
See also SEISMOLOGY; STRUCTURES, THEORY OF—Earthquake Problems; VIBRATION
Effect of earthquakes on masonry buildings, 1282.
"Structural Observations of the Kern County Earthquake," Henry J. Degenkolb, 1280.

EARTHS
See SOILS

EARTHWORK
See also DRAINAGE; EMBANKMENTS; FOUNDATIONS . . . ; LEVEES (cross reference thereunder)
"Design of Stable Channels," Emory W. Lane (with discussion), 1234.

ECONOMICS
See also CONTRACTS; COSTS . . . ; RATE MAKING; *also* under relative subject, subheading Financing
The added traffic theory in railroad economics, 1506.
"Industrial Development in the South," Carl O. Hoyer (with discussion), 411.
"Planning and Operating Turnpikes," Charles M. Noble, 54.

EDUCATION
Attitudes toward standardization of curricula, 344, 345.

EDUCATION (*Continued*)

Early engineering schools in France and United States, 342.

"Issues in Highway Engineering Education," Harmer E. Davis and Ralph A. Moyer, 340.

Specific curricula recommendations for undergraduate and graduate courses and research and extension programs in highway engineering, 347, 349.

"The Training of City Planners," Howard K. Menhinick, 608. *Discussion:* Jorma J. Salovaara, 613.

ELASTIC CURVES

See CURVES (elastic curves) (cross reference thereunder)

ELASTICITY

See also PHOTOELASTICITY; PLASTICITY; STRESS AND STRAIN

"Analysis and Tests of a Cylindrical Shell Roof Model," Bruno Thurlimann and Bruce G. Johnston (with discussion), 615.

"Aseismic Design of Firmly Founded Elastic Structures," Lawrence E. Goodman, Emilio Rosenblueth and Nathan M. Newmark, 782.

"Constrained Circular Beams on Elastic Foundations," Enrico Volterra and Randall Chung, 301.

"Impulsive Motion of Elasto-Plastic Beams" Hans H. Bleich and Mario G. Salvadori (with discussion), 499.

ELASTICITY, PHOTO-

See PHOTOELASTICITY

ELECTRIC POWER PLANTS

See POWER PLANTS

ELECTRONIC INSTRUMENTS

See SURVEYING INSTRUMENTS

EMBANKMENTS

See also LEVEES (cross reference thereunder); SOILS

Embankments on peat foundations, 98.

EMPLOYEES AND EMPLOYMENT

Actual and estimated personnel needs at an international airport, 1950–1970, 368.

Advantages of pneumatic impact wrench in reducing operator's physical effort in joint connector tightening, 1392.

Qualifications testing and duties of automatic and semi-automatic welders and welding inspectors, 238, 239.

Shortage of riveters in United States in relation to need for newer type of joint fasteners, 1391, 1392, 1396.

Turnpike personnel requirements, organization and training, 57, 61, 62, 63, 64.

ENERGY

See AERODYNAMICS; ENGINES; HYDRODYNAMICS; POWER (cross references thereunder); STRUCTURAL DYNAMICS; STRUCTURES, THEORY OF; WATER, FLOW OF, IN OPEN CHANNELS

ENERGY, KINETIC

See DYNAMICS . . . (cross references thereunder)

ENERGY, LOSS OF

See FRICTION; HYDRAULIC JUMP; VALVES; WATER, FLOW OF . . . ; WATER HAMMER

ENGINEERING

See ENGINEERS AND ENGINEERING

ENGINEERING AND WAR

See cross reference under WAR AND ENGINEERING

ENGINEERING BIBLIOGRAPHY

See BIBLIOGRAPHY (cross references thereunder)

ENGINEERING COLLEGES AND SCHOOLS

See EDUCATION

ENGINEERING EDUCATION

See EDUCATION

ENGINEERING GLOSSARIES

See TERMINOLOGY

ENGINEERING HISTORY

See under relative subject, e.g., JOINTS, BOLTED (cross reference thereunder); POWER PLANTS

ENGINEERING MECHANICS

See MECHANICS . . . (cross references thereunder)

ENGINEERING SOCIETIES

See SOCIETIES, TECHNICAL; *see also* AMERICAN SOCIETY OF CIVIL ENGINEERS

ENGINEERS AND ENGINEERING (General)

See also AMERICAN SOCIETY OF CIVIL ENGINEERS. (For memoirs of deceased members, *see* name of member in Author Index.) (*See*

ENGINEERS AND ENGINEERING (General) (*Continued*)
also p. 1557); ARCHITECTS AND ARCHITECTURE (cross reference thereunder); CONTRACTS; EDUCATION; EMPLOYEES AND EMPLOYMENT; RESEARCH; SOCIETIES, TECHNICAL; TERMINOLOGY
Government Relationships
Duties of the consulting engineer under trust indentures securing bonds issued by municipal authorities in Pennsylvania, for sewage works construction and operation, 860.
Refutation of allegations of malpractice of the United States Corps of Engineers in relation to waterway projects by former Chief Engineer-Economist of United States Board of Engineers for Rivers and Harbors, 1480.
Philosophy
"Backsights and Foresights—Glimpses Ahead in the Light of History as Directed by Science": Address at the Summer Convention, St. Louis, Missouri, June 15, 1955, William R. Glidden, 1550.
Professional Relationships
Characteristics essential to an engineer's success according to national technical society members, 343.
Responsibility of civil engineer and economist in waterway development, 1480.
ENGINES
See also TURBINES . . .
Powering pumps of varying size with diesel and oil engines, 20.
EQUATIONS
See also under relative subject, e.g., BACKWATER; WATER, FLOW OF . . .
Equations of elasticity for point-isotropic materials, 36.
Integration of partial differential equations (the Laplaçian, the Poisson, the biharmonic and other types), by application of relaxation procedure, 651, 661, 667.
Monte Carlo statistical method of solving of partial differential equations, 675.
Usage of Hazen-Williams equation to analyze pipe network velocities for high rates of flow, 894.
ERECTION
See CONSTRUCTION
EROSION (General)
See also CAVITATION
EROSION, FOUNDATION
Apron tests to prevent scour below a dam, 544.
EROSION, STREAM
"Design of Stable Channels," Emory W. Lane (with discussion), 1234.
Forces causing scour, 1237.
ESTIMATES
See COSTS
ESTUARIES
See RIVERS
ETHICS
See ENGINEERS AND ENGINEERING—Professional Relationships
EXCAVATION
See FOUNDATIONS; *also* under specific substructure, e.g., TUNNELS . . .
EXCAVATORS (machinery)
See CRANES, DERRICKS AND POWER SHOVELS
EXPANSION
See under relative subject, e.g., CONCRETE—Expansion and Contraction
EXPERIMENTS AND EXPERIMENTATION
See LABORATORIES . . . (cross references thereunder); MODELS; TESTS AND TESTING (cross references thereunder); *also* under material, structure or structural part tested; *also* under relative subject, e.g., WATER, FLOW OF . . .
EXPLORATION
See BORINGS; EXCAVATION (cross references thereunder); FOUNDATIONS . . .
EXTENSOMETERS
See GAGES, STRAIN
FABRICATION
See under relative subject, e.g., BRIDGES; STEEL; *see also* CONSTRUCTION
FACT FINDING
See RESEARCH
FACTOR OF SAFETY
See under relative subject
FACTOR, ROUGHNESS
See cross reference under ROUGHNESS FACTOR

FAILURES (General)

See also BEARING CAPACITY; STRESS AND STRAIN; STRUCTURES, THEORY OF; *also* under relative subject, e.g., BRIDGES . . .

FAILURES, BRIDGE

Determining contributory failure factors in welded girder spans in Canada, 132, 135, 144.

Fatigue failure causes and remedies in floor beam hangers in railway bridges, 1353, 1391.

Official reports of Tacoma Narrows Bridge, Puget Sound, Washington, 721.

FAILURES, BUILDING

Structural observation of earthquake resisting qualities of materials and design deficiencies, 1280.

FAILURES, CONCRETE

"Inelastic Behavior of Reinforced Concrete Members," Lawrence H. N. Lee (with discussion), 181.

FAILURES, JOINT

Fatigue failure causes and remedies in riveted and bolted structural joints, 1353.

Bibliography

Bibliographic sources for results of numerous fatigue tests, 1379.

FAILURES, PLATE

"High-Strength Bolts in Structural Joints": A Symposium, W. C. Stewart; William H. Munse, D. T. Wright, and Nathan M. Newmark; Frank Baron and Edward W. Larson, Jr.; R. A. Hechtman, D. R. Young, A. G. Chin, and E. R. Savikko; Jack W. Carter, Kenneth H. Lenzen, and Lawrence T. Wyly; and T. R. Higgins and E. J. Ruble (with discussion), 1295.

FAILURES, POWER

Power failure and its transient effects at Tracy Pumping Plant, Central Valley Project, in California, 697.

FAILURES, PUMP AND PUMPING

Effects of power failure at Tracy Pumping Plant, Central Valley Project, in California, 697.

FASTENERS

See BOLTS (cross reference thereunder); CONNECTORS AND CONNECTIONS (cross references thereunder); RIVETS AND RIVETING

FATIGUE

See under relative subject, e.g., STRESS AND STRAIN—Joints; ***see also*** FAILURES

FERTILIZERS

See COMPOST AND COMPOSTING (cross references thereunder); SEWAGE SLUDGE

FILTERS AND FILTRATION, SEWAGE

See also SEWAGE DISPOSAL; TANKS, SEDIMENTATION (sewage)

"Evaluation of the Performance of Biofiltration Plants," Renville S. Rankin, 823. *Discussion:* Peter Homack, and Renville S. Rankin, 836.

National Research Council formula for biological filtration in plants serving military installations during World War II, 827, 831, 836.

Reduction of biochemical oxygen demand (B.O.D.) in biofiltration plants, and lack of evidence of nitrification, 824, 831, 840.

FILTERS AND FILTRATION, WATER

"Effect of Well Screens on Flow into Wells," Jack S. Petersen, Carl Rohwer and Maurice L. Albertson (with discussion), 563.

FILTRATION PLANTS, SEWAGE

See also COSTS, FILTRATION PLANT (SEWAGE)

Operating data for biofiltration plants, 828.

Operation data for representative single and two stage municipal biofiltration plants, under various climatic conditions, in the United States, 830, 834, 837.

FINANCE

See COSTS . . . ; ECONOMICS; ***see also*** subheading Financing under relative subject, e.g., HIGHWAYS AND ROADS—Financing; SEWAGE DISPOSAL—Financing

FINITE DIFFERENCES, THEORY OF

See MATHEMATICS

FIRE STREAMS

See WATER, FLOW OF, THROUGH ORIFICES

FLANGES

See STRESS AND STRAIN—Flanges

FLEXURE

See STRESS AND STRAIN; STRUCTURES, THEORY OF

FLOCCULATION BASINS

See SETTLING BASINS (water supply); TANKS, SEDIMENTATION (sewage)

FLOCS AND FLOCCULATION

See AGGREGATES AND AGGREGATION

FLOOD CONTROL

See RESERVOIRS, FLOOD CONTROL

FLOODS (General)

See COSTS, FLOOD; RESERVOIRS, FLOOD CONTROL

FLOOR BEAMS

See BEAMS . . .

FLOW

See AIR FLOW; CONCRETE—Plastic Flow; DIFFUSER FLOW (cross reference thereunder); EARTH FLOW (cross reference thereunder); FLOODS (cross references thereunder); GROUND WATER; LIQUIDS, FLOW OF . . . ; NONUNIFORM FLOW (cross reference thereunder); RUNOFF; SEEPAGE; SEWAGE . . . ; TURBULENCE; WATER, FLOW OF . . .

FLOW, LAMINAR

See WATER, FLOW OF, IN PIPES

FLOW METERS

See METERS AND METERING; WEIRS (cross references thereunder)

FLOW OF FLUIDS

See GAS . . . ; LIQUIDS, FLOW OF; WATER, FLOW OF . . .

FLOW OF LIQUIDS

See LIQUIDS, FLOW OF . . .

FLOW OF OIL

See WELLS

FLOW OF SOLIDS

See SOLIDS, FLOW OF (cross refences thereunder)

FLOW OF WATER

See WATER, FLOW OF . . .

FLUID FRICTION COEFFICIENTS

See FRICTION COEFFICIENTS, FLUID

FLUID MECHANICS

See WATER, FLOW OF

FLUIDS, DYNAMICS OF

See HYDRODYNAMICS

FLUIDS, FLOW OF

See GAS . . . ; LIQUIDS, FLOW OF; WATER, FLOW OF . . .

FLUMES

See also WATER, FLOW OF, IN OPEN CHANNELS

"Total Sediment Load Measured in Turbulence Flume," Paul C. Benedict, Maurice L. Albertson and Donald Q. Matejka (with discussion), 457.

FLUTTER, THEORY OF

See BRIDGES, SUSPENSION

FLUVIAL MODELS

See MODELS, HYDRAULIC

FOOTINGS

See FOUNDATIONS, BUILDING

FORMULAS

See under relative subject, e.g., STRUCTURES, THEORY OF—Shell Structures

FOUNDATIONS (General)

See also BEARING CAPACITY; BORINGS; COFFERDAMS; EARTH PRESSURE; EARTHQUAKES; EROSION, FOUNDATION; SEEPAGE; SOILS; STRESS AND STRAIN—Foundations; WATER PRESSURE

Interbedded sand and rock foundations, 101.

"Unusual Foundation Conditions in the Everglades," Paul H. Shea, 92.

FOUNDATIONS, BUILDING

"Constrained Circular Beams on Elastic Foundations," Enrico Volterra and Randall Chung, 301.

"Sand Compaction by Vibroflotation," Elio D'Appolonia, Callix E. Miller, Jr., and Thomas M. Ware, 154.

Bibliography

Circular beams on elastic foundations, 309.

FOUNDATIONS, DAM

"Modernization of the Hales Bar Plant," Adolf A. Meyer (with discussion), 539.

FOUNDATIONS, LEVEE

"Unusual Foundation Conditions in the Everglades," Paul H. Shea, 92.

FRAMES (General)

See STRESS AND STRAIN—Frames . . . ; *see also* BEAMS; COLUMNS

FRAMES, CONTINUOUS

See STRUCTURES, THEORY OF—Frames, Continuous

FRAMES, RIGID

See STRESS AND STRAIN—Frames, Rigid

FRAMEWORKS

See STRUCTURES, THEORY OF

FREIGHT

Actual and estimated air cargo (imports and exports) at Puerto Rico International Airport, at San Juan, 1940–1970, 366.

"Some Economic Aspects of Waterway Projects," Haywood R. Faison (with discussion), 1480.

Ton mileage percentage of freight transported on United States inland waterways, 1504, 1506.

FRICTION

See also TURBULENCE

"Determination of Radii of Curvature of Taxiways," John H. Jones and Robert Horonjeff, 27.

"Flow in Rough Conduits," Henry M. Morris, Jr. (with discussion), 373.

"Motion of Particles on Bed of a Turbulent Stream," Arthur T. Ippen and Ramjee P. Verma, 921.

"Open Channels with Nonuniform Discharge," Wen-Hsiung Li (with discussion), 255.

"Pressure Surges in Pump Installations," John Parmakian (with discussion), 697.

FRICTION COEFFICIENTS, FLUID

"Backwater Effects of Open-Channel Constrictions," Hubert J. Tracy and Rolland W. Carter (with discussion), 993.

"High-Velocity Tests in a Penstock," Maxwell F. Burke (with discussion), 863.

"Motion of Particles on Bed of a Turbulent Stream," Arthur T. Ippen and Ramjee P. Verma, 921.

Pipe friction test data for San Gabriel Dam, in California, 870.

"Tranquil Flow through Open-Channel Constrictions," Carl E. Kindsvater and Rolland W. Carter (with discussion), 955.

FUEL

See GAS . . . ; OIL . . . (cross references thereunder)

GAGES (General)

See also METERS AND METERING . . . ; *also* cross references under INSTRUMENTS

GAGES, PRESSURE

"High-Velocity Tests in a Penstock," Maxwell F. Burke (with discussion), 863.

GAGES, STRAIN

"Stress Measurements, San Leandro Creek Bridge," Ray W. Clough and Charles F. Scheffey, 939.

Usage of Whittemore strain gage, 315, 317.

GAGES, STREAM

"High-Velocity Tests in a Penstock," Maxwell F. Burke (with discussion), 863.

GARBAGE DISPOSAL

See REFUSE DISPOSAL

GAS AND GASWORKS LAW

Early law and interstate control of oil and gas in the United States, 496, 498.

GATES

See under type of gate, e.g., WATER GATES, MOVABLE

GAUGES (measuring instruments)

See GAGES

GEODETIC SURVEYS AND SURVEYING

See SURVEYS AND SURVEYING, GEODETIC

GEOMETRY

See under relative subject, e.g., CURVES (alinement curves); WATER, FLOW OF . . .

GIRDER BRIDGES

See BRIDGES, GIRDER

GIRDERS (General)

See also BEAMS; BRIDGES; STRESS AND STRAIN . . .

"Deflections of a Circular Beam Out of Its Initial Plane," Enrico Volterra (with discussion), 65.

GIRDERS, CONTINUOUS

See BRIDGES, GIRDER

GLOSSARIES

See TERMINOLOGY

GOVERNMENT

See also AUTHORITIES (cross reference thereunder); ENGINEERS AND ENGINEERING—Government Relationships; PUBLIC HEALTH; *also* LAW subject heading under related topic, e.g., SEWAGE DISPOSAL LAW; WATERWAY LAW

"Some Economic Aspects of Waterway Projects," Haywood R. Faison (with discussion), 1480.

GRAPHICAL CHARTS

See NOMOGRAPHS; *also* under relative subject

GRAVEL

See also SAND; SOILS

Analyzing problems of water flow into well screens surrounded by different sized gravel, 563.

GROUND . . .

See also EARTH . . . ; LAND . . . ; SOIL . . .

GROUND MOVEMENTS

See EARTHQUAKES; LANDSLIDES

GROUND WATER

See also SEEPAGE; WATER SUPPLY

Action of ground water in relation to landslides, 283.

Confined and unconfined percolating water differentiated, 491.

"Effect of Well Screens on Flow into Wells," Jack S. Petersen, Carl Rohwer and Maurice L. Albertson (with discussion), 563.

GROUND WATER LAW

Formation of county water districts in California for protection of landowners in ground water suits, 494, 498.

"Statutory Control of Ground Water in the Western United States," S. T. Harding, 490.

GROUNDWORK

See EARTHWORK; FOUNDATIONS

GUSTS

See WIND . . .

HARBORS (General)

See also CHANNELS; FREIGHT; TRAFFIC, WATERWAY; WATER TRANSPORTATION; WAVES

HARBORS (Geographical)

Charleston, S. C.

Investigations of increased shoaling conditions in inner harbor navigation channels, 1948–1953, 687, 689, 695.

HEAD, LOSS OF

See AERATION; FRICTION; WATER, FLOW OF . . .

HEALTH, PERSONAL

See EMPLOYEES AND EMPLOYMENT

HEALTH, PUBLIC

See PUBLIC HEALTH

HIGHWAY AND ROAD LAW

Drafting the essential features of enabling turnpike legislation, 55.

HIGHWAY BRIDGES

See BRIDGES

HIGHWAY CURVES

See CURVES (alinement curves)

HIGHWAY ENGINEERS AND ENGINEERING

See ENGINEERS AND ENGINEERING; HIGHWAYS AND ROADS; *see also* under relative subject, e.g., EDUCATION; EMPLOYEES AND EMPLOYMENT

HIGHWAYS AND ROADS (General)

See also BRIDGE . . . ; COSTS, HIGHWAY AND ROAD; CURVES (alinement curves); MOTOR . . . (cross references thereunder); RIGHTS OF WAY (land strips); SOILS; TRAFFIC, HIGHWAY AND ROAD (cross reference thereunder); TUNNEL . . .

The highway problem following World War II and contributing factors enumerated, 340.

Suggested staff organization, with charts, for large turnpike projects during design, construction and operation phases, 60, 61, 64.

Financing

Turnpike financing methods, 54, 58.

Operation

"Planning and Operating Turnpikes," Charles M. Noble, 54.

Planning and Design

"Planning and Operating Turnpikes," Charles M. Noble, 54.

HIGHWAYS AND ROADS (Geographical)

California

"Correction of Landslides and Slipouts," Arthur W. Root, 281.

Maryland

Chesapeake Bay Bridge as important link in highway system of the United States, 245.

HISTORY, ENGINEERING

See under relative subject, e.g., JOINTS, BOLTED (cross reference thereunder); POWER PLANTS

HOISTING MACHINERY

See under specific types of machines, e.g., CRANES, DERRICKS AND POWER SHOVELS

HOSE

See under relative technical subject, e.g., WATER, FLOW OF . . . ; *see also* NOZZLES (cross reference thereunder)

HUMUS

See COMPOST AND COMPOSTING (cross references thereunder)

HURRICANES

See WIND . . .

HYDRAULIC JUMP

See also WATER, FLOW OF . . .

"Discharge Characteristics of Tainter Gates," Arthur Toch, 290.

"Open Channels with Nonuniform Discharge," Wen-Hsiung Li (with discussion), 255.

HYDRAULIC LABORATORIES

See also MODELS, HYDRAULIC

Test equipment and procedure for open channel constriction investigations, 999, 1000.

HYDRAULIC MACHINERY

See under type of machinery, e.g., PUMPS AND PUMPING

HYDRAULIC MODELS

See MODELS, HYDRAULIC

HYDRAULICS

See also AERATION; BREAKWATERS (cross references thereunder); BULKHEADS; CANALS; CAVITATION; CHANNELS (waterways); CONDUITS; COSTS . . . ; DAMS (cross references thereunder); DRAINAGE; EROSION . . . ; FILTERS AND FILTRATION . . . ; FLOODS (cross references thereunder); FLOW . . . (cross references thereunder); FLUID (cross references thereunder); FLUMES; FOUNDATIONS . . . ; FRICTION . . . ; GAGES . . . ; GROUND WATER; HARBORS; HYDRAULIC . . . ; HYDRO- . . . ; IRRIGATION . . . ; LEVEES (cross reference thereunder); LIQUIDS . . . ; LOCKS; METERS AND METERING; MODELS, HYDRAULIC; MULTI-PURPOSE PROJECTS; PENSTOCKS; PIPE . . . ; POWER . . . ; PUMPS AND PUMPING; RESERVOIRS . . . ; RIVER . . . ; RUNOFF; SEDIMENT AND SEDIMENTATION; SEEPAGE; SEWAGE . . . ; SEWERS; SILT AND SILTING . . . ; TANKS . . . ; TERMINOLOGY; TIDES; TURBINES, WATER; TURBULENCE; VALLEYS; VALVES; VISCOSITY; WATER . . . ; WAVES; WELLS

"Applications of the Relaxation Technique in Fluid Mechanics," John S. McNown, En-Yun Hsu and Chia-Shun Yih (with discussion), 650.

"Backwater Functions by Numerical Integration," Clint J. Keifer and Henry H. Chu (with discussion), 429.

"Flow in Rough Conduits," Henry M. Morris, Jr. (with discussion), 373.

"High-Velocity Tests in a Penstock," Maxwell F. Burke (with discussion), 863.

"Open Channels with Nonuniform Discharge," Wen-Hsiung Li (with discussion), 255.

HYDRAULIC TURBINES

See TURBINES, WATER

HYDRODYNAMICS

"Applications of the Relaxation Technique in Fluid Mechanics," John S. McNown, En-Yun Hsu and Chia-Shun Yih (with discussion), 650.

"Effect of Well Screens on Flow into Wells," Jack S. Petersen, Carl Rohwer and Maurice L. Albertson (with discussion), 563.

"Motion of Particles on Bed of a Turbulent Stream," Arthur T. Ippen and Ramjee P. Verma, 921.

HYDROELECTRIC PLANTS

See POWER PLANTS

HYDROELECTRIC POWER PLANTS

See POWER PLANTS

HYDROLOGY
See DRAINAGE; FLOOD . . . ; GROUND WATER; MARSHES; RAINFALL (cross references thereunder); RIVERS; RUNOFF; WATER . . .

HYDROMETRY
See WATER, FLOW OF . . .

HYDROSTATIC UPLIFT
See WATER PRESSURE

IMPACT
See also IMPULSE (cross reference thereunder); VIBRATION; WHEEL LOADS
"Welded Structures": A Symposium, Simon A. Greenberg, La Motte Grover, and C. L. Kreidler (with discussion), 103.

IMPULSE
See STRUCTURAL DYNAMICS; *see also* IMPACT

INDUSTRIAL PLANTS
See also COSTS, INDUSTRIAL PLANT; *see also* under specific type of plant, e.g., POWER PLANTS; *also* cross references under WORKS
Difficulties of choosing best plant site, 417.
"Industrial Development in the South," Carl O. Hoyer (with discussion), 411.

INDUSTRIAL WASTE
See ODORS; REFUSE DISPOSAL; SEWAGE DISPOSAL; SEWAGE SLUDGE

INDUSTRIAL WATER SUPPLY
See IRRIGATION; WATER SUPPLY

INDUSTRY
See under relative technical classification; *see also* EMPLOYEES AND EMPLOYMENT; *also* under type of industry or industrial plant, e.g., STEEL PLANTS

INFILTRATION
See FLOODS (cross references thereunder); GROUND WATER; LAND . . . ; SEEPAGE

INLAND WATERWAYS
See WATERWAYS

INSPECTORS AND INSPECTION
See under relative subject, e.g., WELDS AND WELDING—Inspection

INSTRUMENTS
See GAGES; METERS AND METERING . . . ; *also* under general types of instruments, e.g., SURVEYING INSTRUMENTS; WIND MEASURING INSTRUMENTS; *also* cross reference under specific type of instrument, e.g., ANEMOMETERS; *also* cross references under APPARATUS; *also* under usage

IRRIGATION (General)
See also WATER SUPPLY

IRRIGATION (Geographical)
California
"Statutory Control of Ground Water in the Western United States," S. T. Harding, 490.
Western States
"Statutory Control of Ground Water in the Western United States," S. T. Harding, 490.

IRRIGATION CANALS
"Design of Stable Channels," Emory W. Lane (with discussion), 1234.

JETS
See WATER, FLOW OF, THROUGH ORIFICES

JOINTS (General)
See also COSTS, JOINT; FAILURES, JOINT; RIVETS AND RIVETING; STRESS AND STRAIN—Joints; STRUCTURES, THEORY OF—Joints; WELDS AND WELDING
Advantage of pneumatic impact wrench in reducing physical effort required, and reducing noise, in bolt connector tightening, 1392.
Approved specifications for control of the assembly of high-tensile bolts, 1298.
"High-Strength Bolts in Structural Joints": A Symposium, W. C. Stewart; William H. Munse, D. T. Wright, and Nathan M. Newmark; Frank Baron and Edward W. Larson, Jr.; R. A. Hechtman, D. R. Young, A. G. Chin, and E. R. Savikko; Jack W. Carter, Kenneth H. Lenzen, and Lawrence T. Wyly; and T. R. Higgins and E. J. Ruble, 1295. *Discussion:* A. J. Francis; and William H. Munse, D. T. Wright, and Nathan M. Newmark; Glenn B. Woodruff; Karl de Vries; Harry C. Prince; and Jack W. Carter, Kenneth H. Lenzen, and Lawrence T. Wyly, 1299, 1353.

JOINTS (General) (*Continued*)

History of the use of high strength bolts, 1296, 1389, 1391.

Relative fatigue strength of bolted, riveted butt-type joints, and lap joints, 1313, 1315.

JOINTS, BOLTED

See JOINTS (General)

JOINTS, RIVETED

"High-Strength Bolts in Structural Joints": A Symposium, W. C. Stewart; William H. Munse, D. T. Wright, and Nathan M. Newmark; Frank Baron and Edward W. Larson, Jr.; R. A. Hechtman, D. R. Young, A. G. Chin, and E. R. Savikko; Jack W. Carter, Kenneth H. Lenzen, and Lawrence T. Wyly; and T. R. Higgins and E. J. Ruble (with discussion), 1295.

JOINTS, WELDED

"Welded Structures": A Symposium, Simon A. Greenberg, La Motte Grover, and C. L. Kreidler (with discussion), 103.

JUMP, HYDRAULIC

See HYDRAULIC JUMP

KINETIC ENERGY

See DYNAMICS . . . (cross references thereunder)

LABOR

See EMPLOYEES AND EMPLOYMENT

LABORATORIES

See under specific type of laboratory, e.g., HYDRAULIC LABORATORIES; *also* under relative subject; *also* under MODELS . . . ; TESTS AND TESTING (cross references thereunder); *also* under material, structure, or structural part tested, e.g., CLAY

LABORATORIES, HYDRAULIC

See HYDRAULIC LABORATORIES

LAKES

See WATER . . . ; WAVES

LAMINAR FLOW

See WATER, FLOW OF, IN PIPES

LAND . . .

See also EARTH . . . ; GROUND . . . ; MARSHES; SOIL . . . ; SURVEYS AND SURVEYING . . .

LAND SETTLEMENT

"Unusual Foundation Conditions in the Everglades," Paul H. Shea, 92.

LANDSLIDES

See also COSTS, LANDSLIDE

"Correction of Landslides and Slipouts," Arthur W. Root, 281.

LAND SURVEYS

See SURVEYS AND SURVEYING, PLANE

LATERAL FORCES

See EARTHQUAKES; WIND . . .

LAW

See LAW subject heading under related topic, e.g., GROUND WATER LAW; HIGHWAY AND ROAD LAW; *see also* CONTRACTS

LEAST SQUARES, THEORY OF

See PROBABILITY, THEORY OF

LEGISLATION

See under relative subject (under the subject law heading, e.g., HIGHWAY AND ROAD LAW)

LEVEES

See FOUNDATIONS, LEVEE

LIBRARIES

Searches

See SURVEYS (research data) (cross references thereunder)

LIFT BRIDGES

See BRIDGES, MOVABLE (LIFT)

LIFTING MACHINERY

See HOISTING MACHINERY (cross reference thereunder)

LIGHTING

See GAS . . .

LIMESTONE

Mississippian limestone formation at Hales Bar Dam and Hydroelectric Plant, in Tennessee, 541.

"Unusual Foundation Conditions in the Everglades," Paul H. Shea, 92.

LIMIT DESIGN, THEORY OF

Investigation and limit analysis of net area in tension as related to plastic strength, with testing apparatus, 1133, 1136, 1148, 1164.

LININGS

See under relative type, e.g., TUNNEL LININGS; *also* under relative subject

LIQUIDS, FLOW OF (General)

See also VALVES; VISCOSITY; WATER, FLOW OF . . .

LIQUIDS, FLOW OF (General) (*Continued*)

"Applications of the Relaxation Technique in Fluid Mechanics," John S. McNown, En-Yun Hsu and Chia-Shun Yih (with discussion), 650.

Usage of the theory of finite differences, 651, 669.

LIQUIDS, FLOW OF, OVER WEIRS

"Applications of the Relaxation Technique in Fluid Mechanics," John S. McNown, En-Yun Hsu and Chia-Shun Yih (with discussion), 650.

LITIGATION

See under relative subject (under the subject law heading, e.g., GROUND WATER LAW)

LOAD

See BEARING CAPACITY; BUCKLING; EARTH PRESSURE; FAILURES . . . ; IMPACT; STRESS AND STRAIN; STRUCTURES; STRUCTURES, THEORY OF; VIBRATION; WATER PRESSURE; WHEEL LOADS; WIND PRESSURE (cross references thereunder); *also* under structure, structural member or part, e.g., BEAMS . . . ; JOINTS; SLABS

LOAD, BED

See CHANNELS; SILT AND SILTING . . . ; TURBULENCE; WATER, FLOW OF, IN OPEN CHANNELS

LOAD, SUSPENDED

See SEDIMENT AND SEDIMENTATION; SILT AND SILTING . . .

LOCKS

Improving locks at Hales Bar Dam, in Tennessee, 545.

LOSS OF ENERGY

See FRICTION; HYDRAULIC JUMP; VALVES; WATER, FLOW OF . . . ; WATER HAMMER

LOSS OF HEAD

See AERATION; FRICTION; WATER, FLOW OF . . .

MACHINERY

See under specific type of machine, e.g., CRANES, DERRICKS AND POWER SHOVELS; TURBINES; *also* under usage

MAPPING INSTRUMENTS

See SURVEYING INSTRUMENTS

MAPS AND MAPPING (General)

See also SURVEYS AND SURVEYING; *also* under relative subject

MAPS AND MAPPING, AERIAL

"The Importance of Shoran Surveying," Carl I. Aslakson, 225.

MARINE ENGINEERS AND ENGINEERING

See under relative subject, e.g., SHIPBUILDING

MARSHES

"Unusual Foundation Conditions in the Everglades," Paul H. Shea, 92.

MASONRY

See EARTHQUAKES

MATERIALS OF CONSTRUCTION

See also AGGREGATES AND AGGREGATION; ALUMINUM; CLAY; CONCRETE; COSTS . . . ; EARTHQUAKES; EROSION . . . ; GRAVEL; LIMESTONE; METALS (cross references thereunder); PEAT; PERMEABILITY OF MATERIALS (cross references thereunder); SAND; SEEPAGE; SOILS; STEEL; STRENGTH OF MATERIALS (cross references thereunder); STRESS AND STRAIN . . . ; STRUCTURES, THEORY OF . . . ; *also* under usage

"Plastic Strength of Structural Members": A Symposium, Robert L. Ketter, Edmund L. Kaminsky, and Lynn S. Beedle; Paul P. Bijlaard, Gordon P. Fisher, and George Winter; John W. Clark; and W. Gordon Brady and Daniel C. Drucker (with discussion), 1019.

MATERIALS, PERMEABILITY OF

See PERMEABILITY OF MATERIALS (cross references thereunder)

MATERIALS, STRENGTH OF

See STRENGTH OF MATERIALS (cross references thereunder)

MATERIALS, TESTING OF

See TESTS AND TESTING (cross references thereunder)

MATERIALS, WASTE

See cross references under WASTE DISPOSAL

MATHEMATICS

See also EQUATIONS; GRAPHICAL CHARTS (cross references thereunder); PROBABILITY, THEORY OF; *also* under relative subject

MATHEMATICS (*Continued*)
"Applications of the Relaxation Technique in Fluid Mechanics," John S. McNown, En-Yun Hsu and Chia-Shun Yih (with discussion), 650.
Successful usage of theory of finite differences, 651.
Use of theory of finite differences to solve design problems of stable channels, 1242, 1260.

MEASURING INSTRUMENTS
See GAGES; METERS AND METERING; SURVEYING INSTRUMENTS; WIND MEASURING INSTRUMENTS

MECHANICAL ENGINEERS AND ENGINEERING
See under relative subject, e.g., MACHINERY (cross references thereunder); MOTOR . . . (cross references thereunder); TURBINES . . .

MECHANICS
See also DYNAMICS . . . (cross references thereunder); FLUID . . . (cross references thereunder); HYDRAULICS; MATHEMATICS; STRENGTH OF MATERIALS (cross references thereunder); STRUCTURAL . . . ; STRUCTURES, THEORY OF; TESTS AND TESTING (cross references thereunder)

MECHANICS, FLUID
See WATER, FLOW OF

MECHANICS, SOIL
See SOILS

MEMBERS (ASCE)
See AMERICAN SOCIETY OF CIVIL ENGINEERS. (For memoirs of deceased members, *see* name of member in Author Index. *See also* p. 1557)

MEMBERS, COMPRESSION
See COLUMNS

MEMBERS, STRUCTURAL
See BEAMS . . . ; COLUMNS; GIRDERS; STRUCTURES (General); STRUCTURES, THEORY OF; *also* under name of material, e.g., CONCRETE; *also* under structure, e.g., BRIDGES

MEMOIRS OF DECEASED MEMBERS
See name of member in Author Index. (*See also* p. 1557)

MERCHANT MARINE
See WATER TRANSPORTATION

METALS
See ALLOYS (cross references thereunder); MATERIALS OF CONSTRUCTION; REINFORCED CONCRETE (cross reference thereunder); STRENGTH OF MATERIALS (cross references thereunder); STRESS AND STRAIN . . . ; WELDS AND WELDING; *also* under specific metal or its alloy, e.g., ALUMINUM; STEEL

METEOROLOGY
See ATMOSPHERIC . . . ; WIND

METERS AND METERING (General)
See also GAGES . . . ; INSTRUMENTS (cross references thereunder); WEIRS (cross references thereunder)

METERS AND METERING, CURRENT
Gas-operated pitot tube installation, 877, 878, 889, 890, 891, 894.
"High-Velocity Tests in a Penstock," Maxwell F. Burke (with discussion), 863.
A pitot tube for small pipes, 892.

METERS AND METERING, VENTURI
"High-Velocity Tests in a Penstock," Maxwell F. Burke (with discussion), 863.

METERS AND METERING, WATER (stream velocity)
See METERS AND METERING, CURRENT

MILITARY ENGINEERS AND ENGINEERING
See NATIONAL DEFENSE; *also* under relative technical subject, e.g., AIRPORTS; BRIDGES; FILTERS AND FILTRATION, SEWAGE; WATER SUPPLY

MINERALS
See under relative technical subject, e.g., CONCRETE; MATERIALS OF CONSTRUCTION; ROCK (cross references thereunder)

MODELS (General)
"Photoelastic Analogy for Nonhomogeneous Foundations," Allen J. Curtis and F. E. Richart, Jr., 35.

MODELS, AERODYNAMIC
Value of aerodynamic model testing for suspension bridge problem investigations, 748.

MODELS, HYDRAULIC

"Discharge Characteristics of Tainter Gates," Arthur Toch, 290.

"Hydraulic Model Studies of Martin Dam Draft Tubes," Carl E. Kindsvater and Richard R. Randolph, Jr. (with discussion), 1399.

"Total Sediment Load Measured in Turbulence Flume," Paul C. Benedict, Maurice L. Albertson and Donald Q. Matejka (with discussion), 457.

MODELS, STRUCTURAL

"Aerodynamic Stability of Suspension Bridges": 1952 Report of the Advisory Board on the Investigation of Suspension Bridges, E. F. Kelley, Raymond Archibald, A. A. Jakkula, Raymond Archibald, C. B. McCullough, G. S. Paxson, F. H. Frankland, C. F. Goodrich, Jonathan Jones, C. Earl Webb, Russell G. Cone, Shortridge Hardesty, Charles M. Spofford, O. L. Grover, E. F. Kelley, R. B. McMinn, Leon S. Moisseiff, C. H. Purcell, Norman C. Raab, George D. Whittle, Theodor von Karman, Frank M. Masters, P. L. Pratley, John G. Little, Leon H. Nishkian, R. W. Crum, Franklin N. Wray, Charles C. Sunderland, H. L. Dryden, G. B. Schubauer, O. H. Ammann, Elmer K. Timby, Emil H. Praeger, F. B. Farquharson, Charles E. Andrew, Glenn B. Woodruff, and Hardy Cross, 721.

"Analysis and Tests of a Cylindrical Shell Roof Model," Bruno Thurlimann and Bruce G. Johnston (with discussion), 615.

MOISTURE

See CONCRETE—Effect of Natural Processes; REFUSE DISPOSAL; SOILS

MOMENTS

See also STRESS AND STRAIN; STRUCTURES, THEORY OF; *also* under specific type of stress, e.g., BUCKLING; TORSION

"Analysis and Tests of a Cylindrical Shell Roof Model," Bruno Thurlimann and Bruce G. Johnston (with discussion), 615.

"Inelastic Behavior of Reinforced Concrete Members," Lawrence H. N. Lee (with discussion), 181.

"Plastic Strength of Structural Members": A Symposium, Robert L. Ketter, Edmund L. Kaminsky, and Lynn S. Beedle; Paul P. Bijlaard, Gordon P. Fisher, and George Winter; John W. Clark; and W. Gordon Brady and Daniel C. Drucker (with discussion), 1019.

MOMENTUM

See WATER, FLOW OF . . .

MOTOR TRUCKS

See WHEEL LOADS

MOTOR VEHICLES

See TUNNELS, VEHICULAR; WHEEL LOADS

MOTORWAYS

See HIGHWAYS AND ROADS

MOVABLE BRIDGES

See BRIDGES, MOVABLE

MOVABLE WATER GATES

See WATER GATES, MOVABLE

MULTI-PURPOSE PROJECTS (RIVER PROJECTS)

"Modernization of the Hales Bar Plant," Adolf A. Meyer (with discussion), 539.

MUNICIPAL AUTHORITIES

"Financing of Sewage Works in Pennsylvania," Samuel I. Zack, 843.

MUNICIPAL ENGINEERS AND ENGINEERING

See ENGINEERS AND ENGINEERING; *see also* AIRPORTS; BRIDGES; CITIES; CITY PLANNING; COSTS . . . ; DRAINAGE; FILTERS AND FILTRATION . . . ; FIRE . . . (cross reference thereunder); GAS . . . ; HARBORS; POWER . . . ; PUBLIC HEALTH; REFUSE DISPOSAL; SANITATION; SEWAGE . . . ; SEWERS; TRAFFIC . . . ; WATER . . . ; and similar relative subjects

MUNICIPALITIES

See CITIES

NATIONAL DEFENSE

See also cross references under WAR AND ENGINEERING

Value of inland waterways in national defense, 1522, 1527.

NAVAL ARCHITECTURE

See SHIPBUILDING

NAVIGATION

See CANALS; CHANNELS; DAMS (cross references thereunder); FLOODS (cross references thereunder); HARBORS; LOCKS; MULTI-PURPOSE PROJECTS; RIVERS; TIDES; WATER TRANSPORTATION; WATERWAYS

NEIGHBORHOOD PLANNING
See CITY PLANNING
NETWORKS
See MATHEMATICS
NOMENCLATURE
See TERMINOLOGY
NOMOGRAPHS
Nomograph for backwater curves, 447, 448.
NONUNIFORM FLOW
See WATER, FLOW OF . . .
NOZZLES
See WATER, FLOW OF, THROUGH ORIFICES
NUISANCES, ABATEMENT OF
See INDUSTRIAL WASTE (cross references thereunder); ODORS; PUBLIC HEALTH
OBITUARIES OF MEMBERS
See name of member in Author Index. (*See also* p. 1557)
OCEAN . . .
See WAVES
OCEAN BARS
See BARS (alluvia)
OCEAN BEACHES
See SAND DUNES
OCEAN CURRENTS
See WAVES
OCEAN WAVES
See WAVES
ODORS
Odor as related to refuse composting, 897, 910, 911.
OIL ENGINES
See ENGINES
OIL, FLOW OF
See WELLS
OIL WELLS
See WELLS
OPEN CHANNELS
See CHANNELS; WATER, FLOW OF, IN OPEN CHANNELS
ORDNANCE
See METALS (cross references thereunder)
ORGANIZATIONS
See SOCIETIES, TECHNICAL; *see also* AMERICAN SOCIETY OF CIVIL ENGINEERS
ORIFICES
See WATER, FLOW OF, THROUGH ORIFICES
OSCILLATION
See VIBRATION; WAVES
PARKING, AIRPLANE
See AIRPLANE PARKING
PAVEMENT AND PAVING (General)
See SOILS; WHEEL LOADS
PEAT
Results of shear test and other physical characteristics of peat in the Everglades, 98, 99.
"Unusual Foundation Conditions in the Everglades," Paul H. Shea, 92.
PEDOLOGY
See SOILS—Classification
PENSTOCKS
"High-Velocity Tests in a Penstock," Maxwell F. Burke, 863. *Discussion:* Steponas Kolupaila, Frank B. Campbell, Arthur L. Collins, R. Clifford Youngquist, and Maxwell F. Burke, 884.
PERCOLATION
See GROUND WATER; SEEPAGE
PERMEABILITY OF MATERIALS
See SEEPAGE; STRENGTH OF MATERIALS; *also* under type of material, e.g., CONCRETE; SOILS
PERSONNEL
See EMPLOYEES AND EMPLOYMENT
PETROLEUM
See OIL (cross references thereunder)
PHILOSOPHY, ENGINEERING
See ENGINEERS AND ENGINEERING—Philosophy
PHOTOELASTICITY
"Photoelastic Analogy for Nonhomogeneous Foundations," Allen J. Curtis and F. E. Richart, Jr., 35.
Photoelastic investigations of stress concentrations, 1353.
PHOTOGRAMMETRY
See SURVEYS AND SURVEYING, AERIAL
PIERS, BRIDGE
See BRIDGE PIERS
PILES AND PILE DRIVING
See also BEARING CAPACITY
Usage of piles to combat landslides, 286.

PILLARS
See COLUMNS

PIPE LINES
See also PENSTOCKS; PUMPS AND PUMPING; WATER, FLOW OF, IN PIPES; WATER HAMMER
"Pressure Surges in Pump Installations," John Parmakian (with discussion), 697.

PIPES AND PIPING (fluid conveyance)
See CONDUITS; PENSTOCKS; PIPE LINES; SEWERS; SILT AND SILTING; WATER, FLOW OF, IN PIPES; WATER HAMMER

PITOT TUBES
See METERS AND METERING, CURRENT

PITTING
See CAVITATION

PLANE SURVEYS AND SURVEYING
See SURVEYS AND SURVEYING, PLANE

PLANNING
See AIRPORTS; CITY PLANNING; HIGHWAYS AND ROADS—Planning and Design; NEIGHBORHOOD PLANNING (cross reference thereunder); POSTWAR PLANNING (cross references thereunder)

PLANTS (industrial buildings and equipment)
See INDUSTRIAL PLANTS; *see also* under type of plant, e.g., POWER PLANTS; STEEL PLANTS; *also* WORKS (cross references thereunder)

PLASTIC FLOW
See CONCRETE—Plastic Flow

PLASTICITY
See also CONCRETE—Plastic Flow; ELASTICITY
"Impulsive Motion of Elasto-Plastic Beams," Hans H. Bleich and Mario G. Salvadori (with discussion), 499.
Plastic analysis in structural design, 122, 128, 131.
"Plastic Strength of Structural Members": A Symposium, Robert L. Ketter, Edmund L. Kaminsky and Lynn S. Beedle; Paul P. Bijlaard, Gordon P. Fisher and George Winter; John W. Clark; and W. Gordon Brady and Daniel C. Drucker, 1019. *Discussion:* George Winter; and Robert L. Ketter, Edmund L. Kaminsky, and Lynn S. Beedle; Robert L. Ketter and Lynn S. Beedle; J. F. Baker and Michael R. Horne; and Paul P. Bijlaard, Gordon P. Fisher, and George Winter; William H. Munse; Paul P. Bijlaard; and W. Gordon Brady and Daniel C. Drucker, 1028, 1070, 1133.

PLASTIC THEORY
See PLASTICITY

PLATES
See also FAILURES, PLATE; JOINTS . . . ; SLABS; STRESS AND STRAIN—Plates
"Dead-Load Stress Measurement in a Long Span Bridge," Lawrence T. Wyly, Maurice B. Lagaard, Ralph W. Kluge, Kenneth H. Lenzen, Edward W. Larson, Jr., and Lewis B. McCammon, Jr. (with discussion), 311.

POLLUTION, AIR
See AIR SANITATION (cross reference thereunder)

POPULATION
Ratio and rate of increase of population in the South, 1950, 413.

PORE WATER PRESSURE
See WATER PRESSURE

POROSITY
See SEEPAGE

PORTS
See AIRPORTS; HARBORS

POSTWAR PLANNING
See ENGINEERS AND ENGINEERING—Philosophy; *also* under relative subject

POWER (General)
See DAMS (cross references thereunder); DYNA- . . . (cross references thereunder); ENGINES; FAILURES, POWER; FUEL (cross references thereunder); PUMPS AND PUMPING; TURBINES, WATER; WATER HAMMER; WATER POWER (cross references thereunder)

POWERHOUSES
See POWER PLANTS

POWER PLANTS (General)
See also PENSTOCKS; TURBINES, WATER

POWER PLANTS (General) (*Cont.*)
- "Movements in Structural Concrete in a Powerhouse," Stanley Moyer and Viggo Hansen (with discussion), 1183.

POWER PLANTS (Geographical)

Alabama
- "Hydraulic Model Studies of Martin Dam Draft Tubes," Carl E. Kindsvater and Richard R. Randolph, Jr. (with discussion), 1399.

Maryland
- Conowingo Powerhouse cross section, 1199.

Tennessee River Valley
- History and plan of Hales Bar Dam and Hydroelectric Plant, a pioneer hydroelectric plant in the United States, 539, 540.
- "Modernization of the Hales Bar Plant," Adolf A. Meyer, 539. *Discussion:* George R. Rich, Clarence E. Blee, George A. Jessop, and Adolf A. Meyer, 557.
- Plans of Hales Bar Hydroelectric Plant powerhouse and transformer yard, in Tennessee, 547, 549, 551, 552.

PRESIDENTIAL ADDRESSES (American Society of Civil Engineers)
- *See* AMERICAN SOCIETY OF CIVIL ENGINEERS—Addresses; *see also* under subject of address

PRESSURE
- *See* ATMOSPHERIC PRESSURE; CAVITATION; EARTH PRESSURE; IMPACT; PUMPS AND PUMPING; STRESS AND STRAIN; WATER HAMMER; WATER PRESSURE; WAVES; WIND PRESSURE (cross references thereunder)

PRESSURE GAGES
- *See* GAGES, PRESSURE

PRIME MOVERS
- *See* ENERGY (cross references thereunder); POWER (cross references thereunder)

PROBABILITY, THEORY OF
- Probability theory of large numbers applied to aseismic design of structures, 782.
- Usage of least squares method for computing straight line curves in friction tests, 872.

Bibliography
- Bibliography on engineering seismology, 801.

PROFESSIONAL STANDARDS
- *See* ENGINEERS AND ENGINEERING—Professional Relationships

PROPERTY (landed property)
- *See* LAND . . . ; RIGHTS OF WAY (land strips)

PROTOTYPES AND MODELS
- *See* MODELS

PUBLIC HEALTH
- *See also* SANITATION; WATER SUPPLY
- Pneumatic impact wrench as related to noise reduction in bolted construction work, 1395.

PUBLIC HEALTH ENGINEERS AND ENGINEERING
- *See* ENGINEERS AND ENGINEERING; PUBLIC HEALTH

PUBLIC SERVICES
- *See* under type of service, e.g., SEWAGE DISPOSAL

PUBLIC UTILITIES
- *See* GAS . . . ; POWER (cross references thereunder); POWER PLANTS; RAILROAD . . . ; RATE MAKING . . .

PUBLIC WORKS

Financing
- *See* under type of structure or project, e.g., WATERWAYS—Financing

PUMPING ENGINES
- *See* ENGINES

PUMPING STATIONS
- *See* DRAINAGE

PUMPS AND PUMPING (General)
- *See also* COSTS, PUMP AND PUMPING; FAILURES, PUMP AND PUMPING
- Characteristics of an axial-flow pump, 25.
- General arrangement of Tracy Pumping Plant, in California, 699.
- "Selection and Design of High-Volume, Low-Head Pumps," George F. Snodgrass, 17.

PURIFICATION
- *See* AIR SANITATION (cross reference thereunder)

RADIAL GATES
- *See* WATER GATES, MOVABLE

RAILROAD BRIDGES
See BRIDGES
RAILROAD CURVES
See CURVES (alinement curves)
RAILROADS (General)
See also BRIDGES; CURVES (alinement curves); TRAFFIC, RAILROAD
Design and Construction. *See* under relative subject, e.g., BRIDGES; RAILROAD TRACKS
RAILROAD TRACKS
See also COSTS, RAILROAD TRACK; CURVES (alinement curves); EMBANKMENTS
Simplified standardized method of transit lining of high-speed tracks with specified advantages and disadvantages, 521, 537.
RAILROAD TRAFFIC
See TRAFFIC, RAILROAD
RAINFALL (General)
See DRAINAGE; FLOODS (cross references thereunder); SEEPAGE; *see also* RUNOFF
RATE MAKING
"Some Economic Aspects of Waterway Projects," Haywood R. Faison (with discussion), 1480.
RATE MAKING LAW
Inland water traffic rate fixing case appealed to United States Supreme Court, and 82nd Congress pending legislation, as a result of an Interstate Commerce Commission decision, 1515, 1520.
RECORDING APPARATUS
See under general type of apparatus; *see also* under relative subject
RECORDING INSTRUMENTS
See under relative subject
RECORD KEEPING
See NOMOGRAPHS; *also* under relative subject, e.g., VIBRATION; WIND
RECREATIONAL FACILITIES
See CITY PLANNING
REDUNDANCE, STRUCTURAL
See STRUCTURES, THEORY OF
REFUSE DISPOSAL
See also COSTS, REFUSE DISPOSAL; ODORS; SEWAGE DISPOSAL; SEWAGE SLUDGE
Moisture in relation to successful composting, 903, 909, 910.
"Stabilization of Municipal Refuse by Composting," Percy H. McGauhey and Harold B. Gotaas, 897. *Discussion:* Arthur W. Furbank; and Percy H. McGauhey and Harold B. Gotaas, 916.
Bibliography
Bibliography of composting, 914.
REGIONAL PLANNING
See HIGHWAYS AND ROADS—Planning and Design
REINFORCED CONCRETE
See CONCRETE . . .
RELAXATION (numerical analysis)
See under relative subject, e.g., LIQUIDS, FLOW OF
REPORTS OF COMMITTEES
See AMERICAN SOCIETY OF CIVIL ENGINEERS—Committee Reports; *see also* under subject of report
RESEARCH
See also AMERICAN SOCIETY OF CIVIL ENGINEERS; HYDRAULIC LABORATORIES; MODELS; PROBABILITY, THEORY OF; STRUCTURES, THEORY OF; TESTS AND TESTING (cross references thereunder); *also* under relative subject, e.g., ROOFS AND ROOFING; WELDS AND WELDING
Future studies of United States Bureau of Reclamation for improving canal design procedures, 1258, 1261.
Research needed in aerodynamic stability of suspension bridges, 766.
Research needed in relationship between compressive strength and void ratio, 1451, 1452, 1479.
RESERVOIRS (General)
See also DAMS (cross references thereunder)
RESERVOIRS, FLOOD CONTROL
"High-Velocity Tests in a Penstock," Maxwell F. Burke (with discussion), 863.
RESONANCE
See VIBRATION; WATER HAMMER; WAVES
RETAINING WALLS
See also BULKHEADS; EARTH PRESSURE; EMBANKMENTS
Usage of retaining walls to combat landslides, 286.

REVETMENT
See WAVES

RIGHTS OF WAY (land strips)
Acquiring turnpike rights of way, 60.

RIGID FRAMES
See STRESS AND STRAIN—Frames, Rigid

RIVER BANKS AND BANK PROTECTION
See FLOODS (cross references thereunder); SEDIMENT AND SEDIMENTATION; SILT AND SILTING, CHANNEL

RIVER BASINS
See DRAINAGE; VALLEYS

RIVER CHANNELS
See CHANNELS

RIVER RECTIFICATION
See RIVER REGULATION (cross references thereunder)

RIVER REGULATION
See BARS (alluvia); IRRIGATION CANALS; RIVERS; WATER, FLOW OF, IN OPEN CHANNELS

RIVERS (General)
See also BARS (alluvia); BRIDGE . . . ; CHANNELS; COSTS . . . ; DRAINAGE; EROSION, STREAM; GAGES, STREAM; HYDRAULIC LABORATORIES; LOCKS; MODELS, HYDRAULIC; MULTI-PURPOSE PROJECTS (RIVER PROJECTS); RUNOFF; SEDIMENT AND SEDIMENTATION; SILT AND SILTING, CHANNEL; TIDES; TRAFFIC, RIVER; TRAFFIC, WATERWAY; TUNNELS, VEHICULAR; VALLEYS; WATER, FLOW OF, IN OPEN CHANNELS; WATER TRANSPORTATION; WATERWAY . . . ; WAVES
Estuary characteristics complicating total sediment measuring problems, 688.
"Sediment Sampling in Tidal Waterways," Edward A. Schultz, 687.

Financing
"Some Economic Aspects of Waterway Projects," Haywood R. Faison (with discussion), 1480.

RIVERS (Geographical)

Mississippi River
"Some Economic Aspects of Waterway Projects," Haywood R. Faison (with discussion), 1480.

Passaic River
"Erection of Main River Span, Passaic River Bridge," Jonathan Jones, 208.

RIVER TIDES
See TIDES

RIVER TRAFFIC
See TRAFFIC, RIVER

RIVER TRANSPORTATION
See WATER TRANSPORTATION

RIVER VALLEYS
See VALLEYS

RIVETED JOINTS
See JOINTS, RIVETED

RIVETS AND RIVETING
See also CONNECTORS AND CONNECTIONS (cross references thereunder); STRESS AND STRAIN—Rivets and Riveting
"High-Strength Bolts in Structural Joints": A Symposium, W. C. Stewart; William H. Munse, D. T. Wright, and Nathan M. Newmark; Frank Baron and Edward W. Larson, Jr.; R. A. Hechtman, D. R. Young, A. G. Chin, and E. R. Savikko; Jack W. Carter, Kenneth H. Lenzen, and Lawrence T. Wyly; and T. R. Higgins and E. J. Ruble (with discussion), 1295.

ROADBEDS
See DRAINAGE; RAILROAD TRACKS; TUNNELS . . .

ROADS
See HIGHWAYS AND ROADS

ROCK
See FOUNDATIONS; LIMESTONE

ROOFS AND ROOFING
See also STRUCTURES, THEORY OF—Roofs and Roofing
"Analysis and Tests of a Cylindrical Shell Roof Model," Bruno Thurlimann and Bruce G. Johnston (with discussion), 615.
Ancient and first modern shell roof in the United States, 615, 616.

Bibliography
Problems relative to cylindrical shell roofs, 642.

ROUGHNESS
See FRICTION
ROUGHNESS FACTOR
See FRICTION COEFFICIENTS . . .
RUBBISH DISPOSAL
See REFUSE DISPOSAL
RUNOFF (General)
See also RAINFALL (cross references thereunder)
RUNOFF (Geographical)
California
"High-Velocity Tests in a Penstock," Maxwell F. Burke (with discussion), 863.
RUNWAYS
See AIRPORTS
SAFETY
See EARTHQUAKES
SAFETY FACTOR
See under relative subject
SAMPLING
See under relative subject, e.g., SEDIMENT AND SEDIMENTATION; *also* under relative material, e.g., SOILS
SAND
See also BARS (alluvia); COSTS, SAND . . . ; GRAVEL; SEDIMENT AND SEDIMENTATION; SEEPAGE; SILT AND SILTING . . . ; SOILS
"Design of Stable Channels," Emory W. Lane (with discussion), 1234.
Interbedded sand and rock foundations, 101.
"Motion of Particles on Bed of a Turbulent Stream," Arthur T. Ippen and Ramjee P. Verma, 921.
"Sand Compaction by Vibroflotation," Elio D'Appolonia, Callix E. Miller, Jr., and Thomas M. Ware, 154.
SAND BARS
See BARS (alluvia)
SAND DUNES
"Total Sediment Load Measured in Turbulence Flume," Paul C. Benedict, Maurice L. Albertson and Donald Q. Matejka (with discussion), 457.
SANITARY ENGINEERS AND ENGINEERING
See ENGINEERS AND ENGINEERING; SANITATION
SANITATION
See also COSTS . . . ; DRAINAGE; ENGINEERS AND ENGINEERING; FILTERS AND FILTRATION . . . ; ODORS; PIPES AND PIPING (cross references thereunder); REFUSE DISPOSAL; SEWAGE DISPOSAL; SEWAGE SLUDGE; SEWERS; TANKS . . . ; WATER . . .
"Flocculation and Flocculation Basins," Thomas R. Camp, 1.
SCHOOLS AND COLLEGES, ENGINEERING
See EDUCATION
SCIENTIFIC SOCIETIES
See AMERICAN SOCIETY OF CIVIL ENGINEERS; SOCIETIES, TECHNICAL; *see also* ENGINEERS AND ENGINEERING
SCOUR
See EROSION . . .
SCREENS, WELL
See WELLS
SEA . . .
See MARINE . . . (cross reference thereunder); OCEAN . . . (cross references thereunder)
SEACOAST
See HARBORS; TIDES; WAVES
SEAPORTS
See HARBORS
SEARCHES, LIBRARY
See LIBRARIES—Searches (cross reference thereunder)
SEASHORE
See SHORES AND SHORE PROTECTION (cross references thereunder)
SEA WALLS
See WATER PRESSURE; WAVES
SEAWAYS
See WATERWAYS
SEDIMENT AND SEDIMENTATION
See also SILT AND SILTING; TURBULENCE
"Design of Stable Channels," Emory W. Lane (with discussion), 1234.
"Evaluation of the Performance of Biofiltration Plants," Renville S. Rankin (with discussion), 823.
"Flocculation and Flocculation Basins," Thomas R. Camp, 1.

SEDIMENT AND SEDIMENTATION (*Continued*)
"Sediment Sampling in Tidal Waterways," Edward A. Schultz, 687.
"Total Sediment Load Measured in Turbulence Flume," Paul C. Benedict, Maurice L. Albertson and Donald Q. Matejka, 457. *Discussion:* W. H. Corbett, O. C. Hansen, and W. M. Borland; and Paul C. Benedict, Maurice L. Albertson and Donald Q. Matejka, 485.
Usage of baffles and battens to force sediment dunes into suspension, 457, 462, 463.

SEDIMENTATION TANKS (sewage)
See TANKS, SEDIMENTATION (sewage)

SEEPAGE
See also GROUND WATER
"Applications of the Relaxation Technique in Fluid Mechanics," John S. McNown, En-Yun Hsu and Chia-Shun Yih (with discussion), 650.
"Movements in Structural Concrete in a Powerhouse," Stanley Moyer and Viggo Hansen (with discussion), 1183.
"Unusual Foundation Conditions in the Everglades," Paul H. Shea, 92.

SEISMOLOGY
See also EARTHQUAKES
Bibliography
Aseismic design problems, 801.

SETTLEMENT, LAND
See LAND SETTLEMENT

SETTLEMENT OF STRUCTURES
See BEARING CAPACITY; EMBANKMENTS; FOUNDATIONS . . . ; SOILS . . .

SETTLING BASINS (water supply)
"Flocculation and Flocculation Basins," Thomas R. Camp, 1.

SETTLING TANKS (sewage)
See TANKS, SEDIMENTATION (sewage)

SEWAGE COLLECTION
See SEWERS

SEWAGE DISPOSAL (General)
See also COSTS, SEWAGE DISPOSAL; FILTERS AND FILTRATION, SEWAGE; SEWAGE SLUDGE; SEWERS; TANKS . . .
"Flocculation and Flocculation Basins," Thomas R. Camp, 1.
Financing
"Financing of Sewage Works in Pennsylvania," Samuel I. Zack, 843.

SEWAGE DISPOSAL (Geographical)
Chicago, Ill.
"Sewage Aeration Practice in Chicago," Norval E. Anderson, 351.
Pennsylvania
"Financing of Sewage Works in Pennsylvania," Samuel I. Zack, 843.
Industrial waste regulations under sewer rental system in certain Pennsylvania communities, 853, 859.

SEWAGE DISPOSAL LAW
"Financing of Sewage Works in Pennsylvania," Samuel I. Zack, 843.

SEWAGE FILTERS AND FILTRATION
See FILTERS AND FILTRATION, SEWAGE

SEWAGE SLUDGE
See also SEWAGE DISPOSAL; TANKS . . .
"Sewage Aeration Practice in Chicago," Norval E. Anderson, 351.
"Summary operation information and tabulated data for major activated sludge plants, Chicago, Illinois Sanitary District, processing pioneers, 352, 353, 357, 362.

SEWAGE TANKS
See cross references under TANKS, SEWAGE

SEWAGE TREATMENT
See SEWAGE DISPOSAL

SEWAGE WORKS
See FILTRATION PLANTS, SEWAGE; SEWAGE DISPOSAL

SEWERAGE
See SEWERS

SEWERS (General)
See also BACKWATER; RAINFALL (cross references thereunder); RUNOFF; WATER, FLOW OF, IN PIPES

SEWERS (Geographical)
Pennsylvania
Municipal sewer rental charge system as existing in certain Pennsylvania communities, 843, 846.

SHEAR
"Analysis and Tests of a Cylindrical Shell Roof Model," Bruno Thurli-

SHEAR (*Continued*)
mann and Bruce G. Johnston (with discussion), 615.
"Design of Stable Channels," Emory W. Lane (with discussion), 1234.
"Flocculation and Flocculation Basins," Thomas R. Camp, 1.
"High-Strength Bolts in Structural Joints": A Symposium, W. C. Stewart; William M. Munse, D. T. Wright, and Nathan M. Newmark; Frank Baron and Edward W. Larson, Jr.; R. A. Hechtman, D. R. Young, A. G. Chin, and E. R. Savikko; Jack W. Carter, Kenneth H. Lenzen, and Lawrence T. Wyly; and T. R. Higgins and E. J. Ruble (with discussion), 1295.
Investigation and limit analysis of net area in tension, 1133, 1153.
"Strength Characteristics of Compacted Clays," Gerald A. Leonards (with discussion), 1420.

SHEARING STRESS
See SHEAR

SHELL STRUCTURES
See FLUMES; PIPE LINES; PIPES AND PIPING (cross references thereunder); ROOFS AND ROOFING; STRESS AND STRAIN—Shell Structures; STRUCTURES, THEORY OF—Shell Structures

SHIPBUILDING
Ship fracture problems, 113.

SHIP CANALS
See CANALS

SHIPS AND SHIPPING
See WATER TRANSPORTATION (and cross references thereunder)

SHORAN
See under usage, e.g., TRIANGULATION

SHORES AND SHORE PROTECTION (lands adjacent to lake, ocean or sea water)
See SAND DUNES; WAVES; *also* cross references under RIVER BANKS AND BANK PROTECTION

SHRINKAGE, CONCRETE
See CONCRETE—Shrinkage (cross reference thereunder)

SIDEWALKS (General)
See CONCRETE

SIEVES
See SCREENS, WELL (cross reference thereunder)

SILT AND SILTING (General)
See also AGGREGATES AND AGGREGATION; SEDIMENT AND SEDIMENTATION
"Total Sediment Load Measured in Turbulence Flume," Paul C. Benedict, Maurice L. Albertson and Donald Q. Maejka (with discussion), 457.
"Motion of Particles on Bed of a Turbulent Stream," Arthur T. Ippen and Ramjee P. Verma, 921.

SKIN FRICTION
See FRICTION

SLABS
See also PLATES
"Stress Measurements, San Leandro Creek Bridge," Ray W. Clough and Charles F. Scheffey, 939.

SLIDES
See LANDSLIDES

SLIPS AND SLIPPAGE (movement of surfaces)
See JOINTS, BOLTED (cross reference thereunder); JOINTS, RIVETED; LANDSLIDES

SLOPING CHANNELS
See CHANNELS

SLUDGE, SEWAGE
See SEWAGE SLUDGE

SOCIETIES, TECHNICAL
See also AMERICAN SOCIETY OF CIVIL ENGINEERS; ENGINEERS AND ENGINEERING; *also* under relative subject, e.g., WATERWAYS
Organization and activities of American Society for Engineering Education, Engineers' Council for Professional Development and Society for the Promotion of Engineering Education, 342, 343.

SOIL . . .
See also EARTH . . . ; GROUND . . . ; LAND . . .

SOIL MECHANICS
See SOILS

SOIL PRESSURE
See EARTH PRESSURE

SOILS (General)
See also BEARING CAPACITY; CLAY; DRAINAGE; EARTH

SOILS (General) (*Continued*)
PRESSURE; EROSION . . . ; FOUNDATIONS . . . ; FRICTION; GRAVEL; GROUND . . . ; LAND . . . ; PEAT; SAND; SEDIMENT AND SEDIMENTATION; SEEPAGE; SILT AND SILTING; STRESS AND STRAIN—Soils; *also* under name of soil structure, e.g., LEVEES (cross reference thereunder)

Compost as a soil conditioner, 897.

Coulomb Law on soil resistance and its historical usage, 1422, 1450, 1467, 1475.

"Effect of Well Screens on Flow into Wells," Jack S. Petersen, Carl Rohwer and Maurice L. Albertson (with discussion), 563.

Bibliography

Bibliography on the strength characteristics of soils, 1452.

Classification

Fort Union formation, North Dakota clay, Mississippi River bank, and Fort Belvoir, Virginia soil characteristics, 1425, 1435, 1464, 1469.

Compaction. *See* BEARING CAPACITY

Construction

"Design of Stable Channels," Emory W. Lane (with discussion), 1234.

Tests and Testing

Mechanical analysis tests of Bartow, Florida soils, 154.

"Photoelastic Analogy for Nonhomogeneous Foundations," Allen J. Curtis and F. E. Richart, Jr., 35.

"Reduction in Soil Strength with Increase in Density," Charles R. Foster (with discussion), 803.

"Strength Characteristics of Compacted Clays," Gerald A. Leonards (with discussion), 1420.

Three bay triaxial compression testing apparatus with schematic piping diagram, with data, 1432, 1434, 1436, 1455, 1471.

"The Undisturbed Consolidation Behavior of Clay," John H. Schmertmann, 1201. *Discussion:* Robert L. Crisp, and John H. Schmertmann, 1228.

SOIL TRANSPORTATION

See SEDIMENT AND SEDIMENTATION; SILT AND SILTING

SOLIDS, FLOW OF

See EARTH FLOW (cross reference thereunder); PUMPS AND PUMPING; SEDIMENT AND SEDIMENTATION; SILT AND SILTING . . . ; WATER, FLOW OF, IN OPEN CHANNELS; WATER, FLOW OF, IN PIPES

SPACE STRUCTURES

See STRUCTURES, THEORY OF . . . ; *also* under specific type of structure

SPACE TRUSSES

See STRUCTURES, THEORY OF—Trusses and Trussed Structures; TRUSSES

SPECIFICATIONS

See also under relative subject, e.g., JOINTS (General); WELDS AND WELDING; *see also* CONTRACTS

"Plastic Strength of Structural Members": A Symposium, Robert L. Ketter and Edmund L. Kaminsky, and Lynn S. Beedle; Paul P. Bijlaard, Gordon P. Fisher, and George Winter; John W. Clark; and W. Gordon Brady and Daniel C. Drucker (with discussion), 1019.

SPEED

See RAILROADS . . .

SPIRALS

See CURVES (alinement curves)

SPLICE PLATES

See PLATES

STABILITY

See AERODYNAMICS; BUCKLING; HYDRODYNAMICS; SOIL . . .

STANDARDS, PROFESSIONAL

See ENGINEERS AND ENGINEERING—Professional Relationships

STATICALLY INDETERMINATE STRUCTURES

See STRUCTURES, THEORY OF

STATIONS

See under relative type of station, e.g., PUMPING STATIONS (cross reference thereunder); *see also* cross references under TERMINALS

STATISTICS

See relative subject

STEEL (General)

See also COSTS, STEEL; MATERIALS OF CONSTRUCTION; STRESS AND STRAIN—Steel; WELDS AND WELDING; *also* under special structure or structural part

"Welded Structures": A Symposium, Simon A. Greenberg, La Motte Grover, and C. L. Kreidler (with discussion), 103.

STEEL PLANTS

Organization and operation of a steel company, 148.

STIFFENING TRUSSES

See TRUSSES, STIFFENING

STIFFNESS

"Aerodynamic Stability of Suspension Bridges": 1952 Report of the Advisory Board on the Investigation of Suspension Bridges, E. F. Kelley, Raymond Archibald, A. A. Jakkula, Raymond Archibald, C. B. McCullough, G. S. Paxson, F. H. Frankland, C. F. Goodrich, Jonathan Jones, C. Earl Webb, Russell G. Cone, Shortridge Hardesty, Charles M. Spofford, O. L. Grover, E. F. Kelley, R. B. McMinn, Leon S. Moisseiff, C. H. Purcell, Norman C. Raab, George D. Whittle, Theodor von Karman, Frank M. Masters, P. L. Pratley, John G. Little, Leon H. Nishkian, R. W. Crum, Franklin N. Wray, Charles C. Sunderland, H. L. Dryden, G. B. Schubauer, O. H. Ammann, Elmer K. Timby, Emil H. Praeger, F. B. Farquharson, Charles E. Andrew, Glenn B. Woodruff, and Hardy Cross, 721.

"Plastic Strength of Structural Members": A Symposium, Robert L. Ketter, Edmund L. Kaminsky, and Lynn S. Beedle; Paul P. Bijlaard, Gordon P. Fisher, and George Winter; John W. Clark; and W. Gordon Brady and Daniel C. Drucker (with discussion), 1019.

STONE

See GRAVEL; LIMESTONE; ROCK (cross references thereunder)

STORMS

See RAINFALL (cross references thereunder); WIND . . .

STORM WATER

See DRAINAGE; SEWAGE DISPOSAL; SEWERS

STRAIN

See STRESS AND STRAIN

STRAIN GAGES

See GAGES, STRAIN

STRAINMETERS

See GAGES, STRAIN

STREAM EROSION

See EROSION, STREAM

STREAM FLOW

See WATER, FLOW OF, IN OPEN CHANNELS

STREAM GAGES

See GAGES, STREAM

STREAMS

See RIVERS and cross references thereunder

STREAMS, FIRE

See FIRE STREAMS (cross reference thereunder)

STREETS

See BRIDGES; CITIES; CITY PLANNING; CONDUITS; CURVES (alinement curves); *see also* HIGHWAYS AND ROADS

STRENGTH OF MATERIALS

See FAILURES . . . ; STRESS AND STRAIN; *also* under specific material (*see* list of materials under MATERIALS OF CONSTRUCTION); *also* under fabricated structure or structural part, e.g., STRUCTURES

STRESS AND STRAIN (General)

See also CONCRETE—Temperature; EARTH PRESSURE; EARTHQUAKES; ELASTICITY; FAILURES . . . ; GAGES, STRAIN; IMPACT; MOMENTS; PHOTOELASTICITY; STIFFNESS; STRENGTH OF MATERIALS (cross references thereunder); STRUCTURES, THEORY OF; TEMPERATURE; VIBRATION; WATER PRESSURE; WAVES; WHEEL LOADS; WIND . . . ; *also* under specific type of stress, e.g., BUCKLING; SHEAR; TORSION

Usage of whitewash as a valuable strain indicating device, 1097, 1106, 1107.

Alloys

Aluminum alloy testing to failure for plastic strength, 1135.

Beams (General). *See also* BUCKLING; SHEAR; STRESS AND STRAIN—Flanges; TORSION

"Deflections of a Circular Beam Out of Its Initial Plane," Enrico Volterra (with discussion), 65.

STRESS AND STRAIN (General) (*Continued*)

Beams (General) (*Continued*)

Test arrangement and impact test procedure for welded beams, 116, 117, 130.

Beams, Continuous

"Plastic Strength of Structural Members": A Symposium, Robert L. Ketter, Edmund L. Kaminsky, and Lynn S. Beedle; Paul P. Bijlaard, Gordon P. Fisher, and George Winter; John W. Clark; and W. Gordon Brady and Daniel C. Drucker (with discussion), 1019.

Breakwaters. *See* WATER PRESSURE

Bridges (General). *See also* SHEAR

Bridges, Girder

"Stress Measurements, San Leandro Creek Bridge," Ray W. Clough and Charles F. Scheffey, 939.

Bridges, Suspension

"Aerodynamic Stability of Suspension Bridges": 1952 Report of the Advisory Board on the Investigation of Suspension Bridges, E. F. Kelley, Raymond Archibald, A. A. Jakkula, Raymond Archibald, C. B. McCullough, G. S. Paxson, F. H. Frankland, C. F. Goodrich, Jonathan Jones, C. Earl Webb, Russell G. Cone, Shortridge Hardesty, Charles M. Spofford, O. L. Grover, E. F. Kelley, R. B. McMinn, Leon S. Moisseiff, C. H. Purcell, Norman C. Raab, George D. Whittle, Theodor von Karman, Frank M. Masters, P. L. Pratley, John G. Little, Leon H. Nishkian, R. W. Crum, Franklin N. Wray, Charles C. Sunderland, H. L. Dryden, G. B. Schubauer, O. H. Ammann, Elmer K. Timby, Emil H. Praeger, F. B. Farquharson, Charles E. Andrew, Glenn B. Woodruff, and Hardy Cross, 721.

Damping characteristics, 745, 759, 765, 766, 771.

Bridges, Truss

"Dead-Load Stress Measurement in a Long Span Bridge," Lawrence T. Wyly, Maurice B. Lagaard, Ralph W. Kluge, Kenneth H. Lenzen, Edward W. Larson, Jr., and Lewis B. McCammon, Jr., 311. *Discussion:* Almon H. Fuller; and Lawrence T. Wyly, Maurice B. Lagaard, Ralph W. Kluge, Kenneth H. Lenzen, Edward W. Larson, Jr., and Lewis B. McCammon, Jr., 336.

Clay. *See* SHEAR

Columns

"Plastic Strength of Structural Members": A Symposium, Robert L. Ketter, Edmund L. Kaminsky, and Lynn S. Beedle; Paul P. Bijlaard, Gordon P. Fisher, and George Winter; John W. Clark; W. Gordon Brady and Daniel C. Drucker (with discussion), 1019.

Concrete

"Inelastic Behavior of Reinforced Concrete Members," Lawrence H. N. Lee (with discussion), 181.

Curved Structures. *See* STRUCTURES, THEORY OF—Curved Structures

Flanges

"Plastic Strength of Structural Members": A Symposium, Robert L. Ketter, Edmund L. Kaminsky, and Lynn S. Beedle; Paul P. Bijlaard, Gordon P. Fisher, and George Winter; John W. Clark; and W. Gordon Brady and Daniel C. Drucker (with discussion), 1019.

Usage of drawn rectangular aluminum alloy tubes for testing plastic strength in flanges, 1117.

Foundations

"Constrained Circular Beams on Elastic Foundations," Enrico Volterra and Randall Chung, 301.

"Photoelastic Analogy for Nonhomogeneous Foundations," Allen J. Curtis and F. E. Richart, Jr., 35.

Frames, Rigid

"Plastic Strength of Structural Members": A Symposium, Robert L. Ketter, Edmund L. Kaminsky, and Lynn S. Beedle; Paul P. Bijlaard, Gordon P. Fisher, and George Winter; John W. Clark; and W. Gordon Brady and Daniel C. Drucker (with discussion), 1019.

"Welded Structures": A Symposium, Simon A. Greenberg, La Motte Grover, and C. L. Kreidler (with discussion), 103.

Joints

Action of joints as to variance in load and slip relationship, 1295.

Correlation between stresses determined photoelastically and by strain gages, 1362.

Fatigue testing apparatus, 1307.

"High-Strength Bolts in Structural Joints": A Symposium, W. C. Stewart; William H. Munse, D. T. Wright, and Nathan M. Newmark;

STRESS AND STRAIN (General) (*Continued*)

Joints (*Continued*)

Frank Baron and Edward W. Larson, Jr.; R. A. Hechtman, D. R. Young, A. G. Chin, and E. R. Savikko; Jack W. Carter, Kenneth H. Lenzen, and Lawrence T. Wyly; and T. R. Higgins and E. J. Ruble (with discussion), 1295.

"Plastic Strength of Structural Members": A Symposium, Robert L. Ketter, Edmund L. Kaminsky, and Lynn S. Beedle; Paul P. Bijlaard, Gordon P. Fisher, and George Winter; John W. Clark; and W. Gordon Brady and Daniel C. Drucker (with discussion), 1019.

Plates

"Plastic Strength of Structural Members": A Symposium, Robert L. Ketter, Edmund L. Kaminsky, and Lynn S. Beedle; Paul P. Bijlaard, Gordon P. Fisher, and George Winter; John W. Clark; and W. Gordon Brady and Daniel C. Drucker (with discussion), 1019.

Reinforced Concrete. *See* Concrete (hereunder)

Rivets and Riveting

"High-Strength Bolts in Structural Joints": A Symposium, W. C. Stewart; William H. Munse, D. T. Wright, and Nathan M. Newmark; Frank Baron and Edward W. Larson, Jr.; R. A. Hechtman, D. R. Young, A. G. Chin, and E. R. Savikko; Jack W. Carter, Kenneth H. Lenzen, and Lawrence T. Wyly; and T. R. Higgins and E. J. Ruble (with discussion), 1295.

Hot-driven and cold-driven rivet behavior and fatigue characteristics under stress, 1322.

Shell Structures

"Analysis and Tests of a Cylindrical Shell Roof Model," Bruno Thurlimann and Bruce G. Johnston, 615. *Discussion:* G. C. Ernst; Charles S. Whitney; Boyd G. Anderson; and Bruno Thurlimann and Bruce G. Johnston, 644.

Soils

"Reduction in Soil Strength with Increase in Density," Charles R. Foster (with discussion), 803.

"Strength Characteristics of Compacted Clays," Gerald A. Leonards (with discussion), 1420.

"The Undisturbed Consolidation Behavior of Clay," John H. Schmertmann (with discussion), 1201.

Steel. *See also* Plates (hereunder)

Laboratory tests of bolted joints, 1295.

"Plastic Strength of Structural Members": A Symposium, Robert L. Ketter, Edmund L. Kaminsky, and Lynn S. Beedle; Paul P. Bijlaard, Gordon P. Fisher, and George Winter; John W. Clark; and W. Gordon Brady and Daniel C. Drucker (with discussion), 1019.

"Welded Structures": A Syposium, Simon A. Greenberg, La Motte Grover, and C. L. Kreidler (with discussion), 103.

Structures (General)

"Plastic Strength of Structural Members": A Symposium, Robert L. Ketter, Edmund L. Kaminsky, and Lynn S. Beedle; Paul P. Bijlaard, Gordon P. Fisher, and George Winter; John W. Clark; and W. Gordon Brady and Daniel C. Drucker (with discussion), 1019.

STRESS, SHEARING

See SHEAR

STRINGERS

See BEAMS

STRUCTURAL ANALYSIS

See EQUATIONS; STRESS AND STRAIN; STRUCTURES, THEORY OF . . .

STRUCTURAL DYNAMICS

See also AERODYNAMICS; EARTHQUAKES; STRUCTURES, THEORY OF; VIBRATION

"Aerodynamic Stability of Suspension Bridges": 1952 Report of the Advisory Board on the Investigation of Suspension Bridges, E. F. Kelley, Raymond Archibald, A. A. Jakkula, Raymond Archibald, C. B. McCullough, G. S. Paxson, F. H. Frankland, C. F. Goodrich, Jonathan Jones, C. Earl Webb, Russell G. Cone, Shortridge Hardesty, Charles M. Spofford, O. L. Grover, E. F. Kelley, R. B. McMinn, Leon S. Moisseiff, C. H. Purcell, Norman C. Raab, George D. Whittle, Theodor von Karman, Frank M. Masters, P. L. Pratley, John G. Little, Leon H. Nishkian, R. W. Crum, Franklin N. Wray, Charles C. Sunderland, H. L. Dryden, G. B. Schubauer, O. H. Ammann, Elmer K. Timby, Emil H.

STRUCTURAL DYNAMICS (*Cont.*)
Praeger, F. B. Farquharson, Charles E. Andrew, Glenn B. Woodruff, and Hardy Cross, 721.
"Impulsive Motion of Elasto-Plastic Beams," Hans H. Bleich and Mario G. Salvadori (with discussion), 499.

STRUCTURAL ENGINEERS AND ENGINEERING
See STRUCTURES . . . ; *see also* under relative structure, e.g., BRIDGES . . . ; BUILDINGS

STRUCTURAL JOINTS
See JOINTS

STRUCTURAL MATERIALS
See MATERIALS OF CONSTRUCTION

STRUCTURAL MEMBERS
See MEMBERS, STRUCTURAL (cross references thereunder)

STRUCTURAL MODELS
See MODELS, STRUCTURAL

STRUCTURAL REDUNDANCE
See STRUCTURES, THEORY OF

STRUCTURAL STEEL
See STEEL

STRUCTURES (General)
See also BUILDINGS; CONSTRUCTION; FOUNDATIONS . . . ; MATERIALS OF CONSTRUCTION; MODELS, STRUCTURAL; STRESS AND STRAIN . . . ; STRUCTURES, THEORY OF . . . ; VIBRATION; *also* under specific type of structure or related subject; *also* under general types of structures, e.g., SHELL STRUCTURES (cross references thereunder)
"Plastic Strength of Structural Members": A Symposium, Robert L. Ketter and Edmund L. Kaminsky, and Lynn S. Beedle; Paul P. Bijlaard, and Gordon P. Fisher, and George Winter; John W. Clark; and W. Gordon Brady and Daniel C. Drucker (with discussion), 1019.

STRUCTURES, CONTINUOUS
See STRUCTURES, THEORY OF

STRUCTURES, CURVED
See CURVED STRUCTURES (cross reference thereunder)

STRUCTURES, SETTLEMENT OF
See BEARING CAPACITY; EMBANKMENTS; FOUNDATIONS . . . ; SOILS . . .

STRUCTURES, SHELL
See SHELL STRUCTURES (cross references thereunder)

STRUCTURES, SPACE
See SPACE STRUCTURES (cross references thereunder)

STRUCTURES, STATICALLY INDETERMINATE
See STATICALLY INDETERMINATE STRUCTURES (cross reference thereunder)

STRUCTURES, THEORY OF (General)
See also STRESS AND STRAIN; *also* under type of structure or structural part
"Plastic Strength of Structural Members": A Symposium, Robert L. Ketter, Edmund L. Kaminsky, and Lynn S. Beedle; Paul P. Bijlaard, Gordon P. Fisher and George Winter; John W. Clark; and W. Gordon Brady and Daniel C. Drucker (with discussion), 1019.

Bibliography
Bibliography on engineering seismology, 801.

Beams and Girders (General)
"Impulsive Motion of Elasto-Plastic Beams," Hans H. Bleich and Mario G. Salvadori, 499. *Discussion:* P. S. Symonds; and Hans H. Bleich and Mario G. Salvadori, 516.

Bridges
"Aerodynamic Stability of Suspension Bridges": 1952 Report of the Advisory Board on the Investigation of Suspension Bridges, E. F. Kelley, Raymond Archibald, A. A. Jakkula, Raymond Archibald, C. B. McCullough, G. S. Paxson, F. H. Frankland, C. F. Goodrich, Jonathan Jones, C. Earl Webb, Russell G. Cone, Shortridge Hardesty, Charles M. Spofford, O. L. Grover, E. F. Kelley, R. B. McMinn, Leon S. Moisseiff, C. H. Purcell, Norman C. Raab, George D. Whittle, Theodor von Karman, Frank M. Masters, P. L. Pratley, John G. Little, Leon H. Nishkian, R. W. Crum, Franklin N. Wray, Charles C. Sunderland, H. L. Dryden, G. B. Schubauer, O. H. Ammann, Elmer K. Timby, Emil H. Praeger, F. B. Farquharson, Charles E. Andrew, Glenn B. Woodruff, and Hardy Cross, 721.

STRUCTURES, THEORY OF (General (*Continued*)

Columns

"Plastic Strength of Structural Members": A Symposium, Robert L. Ketter, Edmund L. Kaminsky, and Lynn S. Beedle; Paul P. Bijlaard, Gordon P. Fisher, and George Winter; John W. Clark; and W. Gordon Brady and Daniel C. Drucker (with discussion), 1019.

Concrete, Reinforced

"Inelastic Behavior of Reinforced Concrete Members," Lawrence H. N. Lee (with discussion), 181.

Curved Structures

"Constrained Circular Beams on Elastic Foundations," Enrico Volterra and Randall Chung, 301.

Earthquake Problems

"Aseismic Design of Firmly Founded Elastic Structures," Lawrence E. Goodman, Emilio Rosenblueth and Nathan M. Newmark, 782.

Frames (General). *See also* Beams and Girders (hereunder); Columns (hereunder)

Frames, Continuous

"Lateral Buckling of I-Beams," Mario G. Salvadori (with discussion), 1165.

Girders (General). *See* Beams and Girders (General) (hereunder)

Joints

Working hypothesis explaining rationally cause and remedy for fatigue failures in structural joints, 1353, 1356, 1380.

Roofs and Roofing

"Analysis and Tests of a Cylindrical Shell Roof Model," Bruno Thurlimann and Bruce G. Johnston (with discussion), 615.

Shell Structures

"Analysis and Tests of a Cylindrical Shell Roof Model," Bruno Thurlimann and Bruce G. Johnston (with discussion), 615.

Trusses and Trussed Structures

"Plastic Strength of Structural Members": A Symposium, Robert L. Ketter, Edmund L. Kaminsky, and Lynn S. Beedle; Paul P. Bijlaard, Gordon P. Fisher, and George Winter; John W. Clark; and W. Gordon Brady and Daniel C. Drucker (with discussion), 1019.

STRUCTURES, TRUSSED

See STRUCTURES, THEORY OF —Trusses and Trussed Structures; TRUSSES . . .

STRUCTURES, UNDERGROUND

See UNDERGROUND STRUCTURES (cross references thereunder)

STRUTS

See COLUMNS

SUB- . . .

See also UNDER- . . .

SUBSTRUCTURES

See CONCRETE; FOUNDATIONS (and cross references thereunder); MASONRY (cross reference thereunder); *also* under type of substructure, e.g., TUNNELS

SURFACE PROFILES

See WATER SURFACE PROFILES (cross reference thereunder)

SURFACE RUNOFF

See RUNOFF

SURFACES, SLIPPAGE OF

See SLIPS AND SLIPPAGE (movement of surfaces) (cross references thereunder)

SURGES (water surface)

See WATER HAMMER; WAVES

SURVEYING

See SURVEYS AND SURVEYING

SURVEYING INSTRUMENTS

"The Importance of Shoran Surveying," Carl I. Aslakson, 225.

Bibliography

Shoran as a surveying instrument, 233.

SURVEYS (research data)

See under relative subject, e.g., CONCRETE; *see also* RESEARCH

SURVEYS AND SURVEYING (General)

See also MAPS AND MAPPING . . . ; PROPERTY (landed property) (cross references thereunder); TRIANGULATION

SURVEYS AND SURVEYING, AERIAL

See also MAPS AND MAPPING, AERIAL

"The Importance of Shoran Surveying," Carl I. Aslakson, 225.

Bibliography

Shoran in aerial surveying, 233.

SURVEYS AND SURVEYING, GEODETIC
"The Importance of Shoran Surveying," Carl I. Aslakson, 225.

SURVEYS AND SURVEYING, PLANE
"Transit Lining of High-Speed Track," Neil R. Berndt (with discussion), 521.

SUSPENDED LOAD
See SEDIMENT AND SEDIMENTATION; SILT AND SILTING . . .

SUSPENSION BRIDGES
See BRIDGES, SUSPENSION

SWAMPS
See MARSHES

SYMBOLS
See under relative subject, e.g., HYDRAULICS; MATHEMATICS

TAINTER GATES
See WATER GATES, MOVABLE

TANGENTS, CURVE
See RAILROAD TRACKS

TANKS (General)
See WATER, FLOW OF, IN OPEN CHANNELS

TANKS, AERATION
"Flocculation and Flocculation Basins," Thomas R. Camp, 1.
"Sewage Aeration Practice in Chicago," Norval E. Anderson, 351.

TANKS, SEDIMENTATION (sewage)
See also SETTLING BASINS (water supply)
"Flocculation and Flocculation Basins," Thomas R. Camp, 1.
"Sewage Aeration Practice in Chicago," Norval E. Anderson, 351.

TANKS, SETTLING (sewage)
See TANKS, SEDIMENTATION (sewage)

TANKS, SEWAGE
See COSTS, TANK (SEWAGE TANKS); TANKS, AERATION; TANKS, SEDIMENTATION (sewage)

TAXIWAYS
See AIRPORTS

TECHNICAL SCHOOLS
See EDUCATION

TECHNICAL SOCIETIES
See SOCIETIES, TECHNICAL; *see also* AMERICAN SOCIETY OF CIVIL ENGINEERS; ENGINEERS AND ENGINEERING

TEMPERATURE
See also CONCRETE—Temperature
"Analysis and Tests of a Cylindrical Shell Roof Model," Bruno Thurlimann and Bruce G. Johnston (with discussion), 615.
"Dead-Load Stress Measurement in a Long Span Bridge," Lawrence T. Wyly, Maurice B. Lagaard, Ralph W. Kluge, Kenneth H. Lenzen, Edward W. Larson, Jr., and Lewis B. McCammon, Jr. (with discussion), 311.
"Stress Measurements, San Leandro Creek Bridge," Ray W. Clough and Charles F. Scheffey, 939.
Temperature in relation to composting, 905, 910.

TENSILE STRESS
See STRESS AND STRAIN

TENSION
See STRESS AND STRAIN

TERMINALS (structures and localities)
See AIR TERMINALS (cross reference thereunder)

TERMINOLOGY (Arranged hereunder by specific or comprehensive subject word when possible)

Beams. (Balk as a military term for stringer beams of aluminum alloys), 141.
City planning. (Neighborhood and urban sprawl as city planning terms), 450, 451.
Clay compaction. (Relative soil resistance terms), 1450.
Columns. (Secant formula as a stress term), 1124.
Consolidation test terms defined, 1203, 1204, 1209.
Hurricane terms, 179.
Landslide and slipout differentiated, 281.
Plastic flow. (Usage of terms, contained plastic flow, limit load, and impending plastic flow), 1137, 1153.
Refuse disposal. (Aerobic and anaerobic composting processes compared, 899.
Sediment as a term, 1235.

TERMINOLOGY *(Continued)*
Sewage disposal. (Biofiltration as a term), 823.
Sewage disposal. (Sludge age, solids aeration period, and solids rate as sewage disposal terms used by designer and operator), 355.
Stable and unstable channel defined, 1235, 1276.
Steel. (Scratching, laying out, and fitting as used in steel plants), 151.
Submergence, as vertical distance in pumping operations, 23.
Theory of limit design. (Statically admissible stress field, and kinematically admissible velocity field, 1137, 1138.
Water flow. (Wake interference flow and skimming flow defined), 377.
Wind. (High velocity wind terms), 179.

TESTING MACHINES
See under use, material, structure or structural part tested

TESTS AND TESTING
See BUCKLING; ELASTICITY; FAILURES . . . ; LABORATORIES (cross references thereunder); MODELS . . . ; SHEAR; STRENGTH OF MATERIALS (cross references thereunder); STRESS AND STRAIN; STRUCTURES, THEORY OF; TORSION; WATER, FLOW OF . . . ; *also* under material, structure or structural part tested, e.g., ROOFS AND ROOFING; SOILS—Tests and Testing

THEORIES
See cross references hereunder and under ANALYSIS OF DATA; *see also* under relative subject or its relative science, e.g., HYDRAULICS; MATHEMATICS

THEORY OF BOUNDARY LAYER (fluid flow)
See BOUNDARY LAYER, THEORY OF (cross references thereunder)

THEORY OF ELASTICITY
See ELASTICITY

THEORY OF FINITE DIFFERENCES
See MATHEMATICS

THEORY OF FLUTTER
See BRIDGES, SUSPENSION

THEORY OF LEAST SQUARES
See PROBABILITY, THEORY OF

THEORY OF LIMIT DESIGN
See LIMIT DESIGN, THEORY OF

THEORY OF PLASTICITY
See PLASTICITY

THEORY OF PROBABILITY
See PROBABILITY, THEORY OF

THEORY OF STRUCTURES
See STRUCTURES, THEORY OF

THEORY, PLASTIC
See PLASTICITY

THERMAL DEFORMATION
See TEMPERATURE

THROW, WATER
See JETS (cross reference thereunder)

THRUST
See under relative structure, structural part or material, e.g., BEAMS . . . ; ROOFS AND ROOFING

TIDES
See also WAVES
"Sediment Sampling in Tidal Waterways," Edward A. Schultz, 687.

TOLLS (General)
Establishing the toll system on turnpikes, 62.

TOOLS
See under usage

TORSION
"Lateral Buckling of I-Beams," Mario G. Salvadori (with discussion), 1165.
"Plastic Strength of Structural Members": A Symposium, Robert L. Ketter, Edmund L. Kaminsky, and Lynn S. Beedle; Paul P. Bijlaard, Gordon P. Fisher, and George Winter; John W. Clark; and W. Gordon Brady and Daniel C. Drucker (with discussion), 1019.

TOWBOATS AND TOWING
See BARGES

TRACKS
See under type of track, e.g., RAILROAD TRACKS

TRADE WASTE
See INDUSTRIAL WASTE (cross references thereunder)

TRAFFIC (General)
See also FREIGHT; TRANSPORTATION (cross references thereunder); WHEEL LOADS

TRAFFIC, AIRPORT

Actual and estimated traffic (passenger and cargo) at Puerto Rico International Airport, at San Juan, 1940–1970, 366.

"Traffic at an International Airport," Walther Prokosch, 364.

TRAFFIC, HIGHWAY AND ROAD

See TOLLS

TRAFFIC, RAILROAD

Waterway competition, including rate making practices, in the United States, 1480, 1504, 1506, 1540.

TRAFFIC, RIVER

Inland traffic on the Mississippi River system, 1927–1950, 1496.

TRAFFIC, VEHICULAR

See TRAFFIC, HIGHWAY AND ROAD (cross reference thereunder)

TRAFFIC, WATERWAY

See also specific type of waterway (hereunder)

"Some Economic Aspects of Waterway Projects," Haywood R. Faison (with discussion), 1480.

Traffic growth statistics for six inland waterways in the United States, 1936–1950, 1484.

TRAIN . . .

See RAILROAD . . .

TRAJECTORY, WATER

See JETS (cross reference thereunder)

TRANSPORTATION

See CANALS; FREIGHT; RIVERS; SOIL TRANSPORTATION (cross references thereunder); TRAFFIC; WATER TRANSPORTATION; WATERWAYS

TRAVELING CRANES

See CRANES, DERRICKS AND POWER SHOVELS

TRIANGULATION

See also SURVEYS AND SURVEYING

"The Importance of Shoran Surveyng," Carl I. Aslakson, 225.

TRIAXIAL COMPRESSION APPARATUS

See SOILS—Tests and Testing

TRUCKS

See MOTOR TRUCKS (cross reference thereunder)

TRUSS BRIDGES

See BRIDGES, TRUSS (cross references thereunder)

TRUSSED STRUCTURES

See STRUCTURES, THEORY OF—Trusses and Trussed Structures; TRUSSES . . .

TRUSSES (General)

See also BRIDGES, TRUSS (cross references thereunder); STRUCTURES, THEORY OF—Trusses and Trussed Structures

TRUSSES, STIFFENING

"Aerodynamic Stability of Suspension Bridges": 1952 Report of the Advisory Board on the Investigation of Suspension Bridges, E. F. Kelley, Raymond Archibald, A. A. Jakkula, Raymond Archibald, C. B. McCullough, G. S. Paxson, F. H. Frankland, C. F. Goodrich, Jonathan Jones, C. Earl Webb, Russell G. Cone, Shortridge Hardesty, Charles M. Spofford, O. L. Grover, E. F. Kelley, R. B. McMinn, Leon S. Moisseiff, C. H. Purcell, Norman C. Raab, George D. Whittle, Theodor von Karman, Frank M. Masters, P. L. Pratley, John G. Little, Leon H. Nishkian, R. W. Crum, Franklin N. Wray, Charles C. Sunderland, H. L. Dryden, G. B. Schubauer, O. H. Ammann, Elmer K. Timby, Emil H. Praeger, F. B. Farquharson, Charles E. Andrew, Glenn B. Woodruff, and Hardy Cross, 721.

TUBES

See CONDUITS; DRAFT TUBES; NOZZLES (cross reference thereunder); PIPE LINES; PIPES AND PIPING (cross references thereunder); PITOT TUBES (cross reference thereunder); SHELL STRUCTURES (cross references thereunder); TUNNELS; WATER, FLOW OF, IN PIPES

TUNNEL LININGS

"Construction of the Elizabeth River Tunnel," Joseph Peraino, 423.

TUNNELS (General)

See also COSTS, TUNNEL

TUNNELS, VEHICULAR

"Construction of the Elizabeth River Tunnel," Joseph Peraino, 423.

TURBINES, WATER

See also PENSTOCKS

"Hydraulic Model Studies of Martin Dam Draft Tubes," Carl E. Kindsvater and Richard R. Randolph, Jr. (with discussion), 1399.

TURBINES, WATER (*Continued*)

Turbine design as developed for Hales Bar Hydroelectric Plant, in Tennessee, 559, 562.

TURBULENCE (water agitation)

See also FRICTION . . . ; HYDRAULIC JUMP; WATER, FLOW OF . . .

"Flow in Rough Conduits," Henry M. Morris, Jr. (with discussion), 373.

"Motion of Particles on Bed of a Turbulent Stream," Arthur T. Ippen and Ramjee P. Verma, 921.

Procedures for forcing bed load into suspension by increased turbulence, 461.

"Total Sediment Load Measured in Turbulence Flume," Paul C. Benedict, Maurice L. Albertson and Donald Q. Matejka (with discussion), 457.

TURBULENCE, WIND

See WIND . . .

TURNPIKES

See HIGHWAYS AND ROADS; TOLLS

TWISTING

See TORSION; *also* under relative material, structure or structural part, e.g., BEAMS

UNDER- . . .

See also SUB- . . .

UNDERFLOW

See SEEPAGE; WELLS

UNDERGROUND STRUCTURES

See under type of structure, e.g., CONDUITS; SEWERS; *see also* under related subject, e.g., SOILS

UNDERGROUND WATER

See GROUND WATER

UNDERWATER CONSTRUCTION

See under type of construction, e.g., TUNNELS

UNITED STATES WEATHER BUREAU

See under relative subject, e.g., FLOODS (cross references thereunder); WIND . . .

UNIT STRESSES

See STRESS AND STRAIN

UPLIFT, HYDROSTATIC

See WATER PRESSURE

URBAN . . .

See CITIES

UTILITIES

See PUBLIC UTILITIES (cross references thereunder)

VALLEYS (Geographical)

Loup River Basin, Nebr.

"Total Sediment Load Measured in Turbulence Flume," Paul C. Benedict, Maurice L. Albertson and Donald Q. Matejka (with discussion), 457.

VALVES

Binding of butterfly valves in conjunction with concrete movement, 1183, 1185.

Butterfly valves used at Tracy Pumping Plant, in California, 697, 706.

"High-Velocity Tests in a Penstock," Maxwell F. Burke (with discussion), 863.

VEHICLES

See under general types of vehicles, e.g., MOTOR VEHICLES (cross references thereunder)

VEHICULAR TRAFFIC

See TRAFFIC, HIGHWAY AND ROAD (cross reference thereunder)

VEHICULAR TUNNELS

See TUNNELS, VEHICULAR

VELOCITY

See AERODYNAMICS; CURVES (alinement curves); HYDRODYNAMICS; VIBRATION; WATER, FLOW OF . . . ; WIND

VELOCITY DISTRIBUTION

See WATER, FLOW OF . . .

VELOCITY METERS

See WATER VELOCITY METERS (cross reference thereunder)

VENTURI METERS

See METERS AND METERING, VENTURI

VESSELS

See SHIP . . . ; *see also* BARGES

VIBRATION

See also EARTHQUAKES; IMPACT

"Aerodynamic Stability of Suspension Bridges": 1952 Report of the Advisory Board on the Investigation of Suspension Bridges, E. F. Kelley, Raymond Archibald, A. A. Jakkula, Raymond Archibald, C. B. McCullough, G. S. Paxson, F. H. Frankland, C. F. Goodrich, Jonathan Jones, C. Earl Webb, Russell G. Cone, Shortridge Hardesty, Charles M. Spofford, O. L. Grover, E. F. Kelley,

VIBRATION (*Continued*)
R. B. McMinn, Leon S. Moisseiff, C. H. Purcell, Norman C. Raab, George D. Whittle, Theodor von Karman, Frank M. Masters, P. L. Pratley, John G. Little, Leon H. Nishkian, R. W. Crum, Franklin N. Wray, Charles C. Sunderland, H. L. Dryden, G. B. Schubauer, O. H. Ammann, Elmer K. Timby, Emil H. Praeger, F. B. Farquharson, Charles E. Andrew, Glenn B. Woodruff, and Hardy Cross, 721.
Elasto-plastic vibrations of free-free beams, 502.
Instability, noise, flashes and vibration in draft tubes at Martin Dam, Tallapoosa River, in Alabama, 1400, 1406.
Interpretation of dynamic records, 951.
Natural vibrations of a suspension bridge, 731, 735.
"Sand Compaction by Vibroflotation," Elio D'Appolonia, Callix E. Miller, Jr., and Thomas M. Ware, 154.
Suspension bridges subject to aerodynamic oscillation, in the United States, Canada and Norway, 753, 775.

VIBROFLOTS AND VIBROFLOTATION
See COMPACTION (cross references thereunder)

VISCOSITY
See also WATER, FLOW OF . . .
"Flocculation and Flocculation Basins," Thomas R. Camp, 1.
"Flow in Rough Conduits," Henry M. Morris, Jr. (with discussion), 373.
"High-Velocity Tests in a Penstock," Maxwell F. Burke (with discussion), 863.

VOID RATIO
See SOILS

WALLS
See under relative structure or type of wall, e.g., BULKHEADS; RETAINING WALLS

WAR AND ENGINEERING
See NATIONAL DEFENSE; *also* cross references under MILITARY ENGINEERS AND ENGINEERING; POSTWAR PLANNING

WASTE DISPOSAL
See INDUSTRIAL WASTE (cross references thereunder); ODORS; REFUSE DISPOSAL; SANITATION; SEWAGE DISPOSAL; SEWAGE SLUDGE; SEWERS

WASTE MATERIALS
See cross references under WASTE DISPOSAL

WASTE WATER
See SEWAGE DISPOSAL; SEWERS

WATER . . .
See also AERATION; BACKWATER; CAVITATION; CONDUITS; COSTS . . . ; DAMS (cross references thereunder); DRAINAGE; DRAWDOWN (cross reference thereunder); EROSION . . . ; FILTERS AND FILTRATION . . . ; FLOODS (cross references thereunder); FLUMES; GOVERNMENT; GROUND WATER; HYDRAULIC . . . ; HYDRO- . . . ; IRRIGATION; MARSHES; METERS AND METERING . . . ; MODELS, HYDRAULIC; OCEAN . . . (cross references thereunder); PIPES AND PIPING (cross references thereunder); RAINFALL (cross references thereunder); RESERVOIRS; RUNOFF; SANITATION; SEEPAGE; SEWAGE DISPOSAL; SEWERS; STORM WATER (cross references thereunder); TANKS . . . ; TERMINOLOGY; TURBULENCE; WAVES; WELLS

WATER COLLECTION
See INFILTRATION (cross references thereunder); WELLS

WATER DISTRIBUTION
See CANALS; CONDUITS; IRRIGATION

WATER FILTERS AND FILTRATION
See FILTERS AND FILTRATION, WATER

WATER, FLOW OF (General)
See also FLOODS (cross references thereunder); FLUMES; FRICTION . . . ; GROUND WATER; HYDRAULICS; LIQUIDS, FLOW OF; MODELS, HYDRAULIC; TURBULENCE; VALVES; VISCOSITY; WATER GATES, MOVABLE; WATER HAMMER; WELLS
"Applications of the Relaxation Technique in Fluid Mechanics," John S. McNown, En-Yun Hsu and Chia-Shun Yih, 650. *Discussion:* Fred W. Blaisdell; Henry M. Paynter and Ronald F. Scott; Mladen Boreli;

WATER, FLOW OF (General) (*Continued*)

Turgut Sarpkaya; and John S. McNown, En-Yun Hsu and Chia-Shun Yih, 670.

Basic types of flow, including wake interference flow, 373, 377, 403.

"Flow in Rough Conduits," Henry M. Morris, Jr., 373. *Discussion:* Victor L. Streeter, Walter Rand, Harry H. Ambrose, and Henry M. Morris, Jr., 399.

WATER, FLOW OF, IN FLUMES

See WATER, FLOW OF, IN OPEN CHANNELS

WATER, FLOW OF, IN OPEN CHANNELS

See also BACKWATER; SEDIMENT AND SEDIMENTATION; SILT AND SILTING, CHANNEL; WAVES

"Backwater Effects of Open-Channel Constrictions," Hubert J. Tracy and Rolland W. Carter, 993. *Discussion:* Paul V. Hodges; Carl F. Izzard; Harold R. Henry; and Hubert J. Tracy and Rolland W. Carter, 1007.

"Backwater Functions by Numerical Integration," Clint J. Keifer and Henry H. Chu (with discussion), 429.

Channels having nonuniform discharge, 255.

Computing backwater from channel obstructions caused by bridge piers, 1007, 1008, 1013.

Constriction geometry in open channel flow, 993.

Equation based on the conservation of momentum and its successful use in the study of hydraulic jump, 256.

"Flocculation and Flocculation Basins," Thomas R. Camp, 1.

"Flow in Rough Conduits," Henry M. Morris, Jr. (with discussion), 373.

Geometry of open channel constrictions, 955.

"Motion of Particles on Bed of a Turbulent Stream," Arthur T. Ippen and Ramjee P. Verma, 921.

"Open Channels with Nonuniform Discharge," Wen-Hsiung Li, 255. *Discussion:* Turgut Sarpkaya and Wen-Hsiung Li, 275.

Three reports on water flow through bridge openings, 991, 994.

"Total Sediment Load Measured in Turbulence Flume," Paul C. Benedict, Maurice L. Albertson and Donald Q. Matejka (with discussion), 457.

Tractive force distribution from velocity distribution, 1234.

"Tranquil Flow through Open-Channel Constrictions," Carl E. Kindsvater and Rolland W. Carter, 955. *Discussion:* Emmett M. Laursen and Arthur Toch; Fred W. Blaisdell; Pin-nam Lin; Carl F. Izzard; Chesley J. Posey; and Carl E. Kindsvater and Rolland W. Carter, 981.

Usage of baffles and battens to force sediment dunes into suspension, 457, 462, 463.

Bibliography

Review of literature on theory and methods of computing flow, 957.

WATER, FLOW OF, IN PIPES

See also PIPE LINES; PIPES AND PIPING (cross references thereunder); PUMPS AND PUMPING; SEWERS; WATER HAMMER; WATER PRESSURE

"Flow in Rough Conduits," Henry M. Morris, Jr. (with discussion), 373.

"High-Velocity Tests in a Penstock," Maxwell F. Burke (with discussion), 863.

"Hydraulic Model Studies of Martin Dam Draft Tubes," Carl E. Kindsvater and Richard R. Randolph, Jr. (with discussion), 1399.

WATER, FLOW OF, IN TANKS

See WATER, FLOW OF, IN OPEN CHANNELS

WATER, FLOW OF, THROUGH ORIFICES

"Applications of the Relaxation Technique in Fluid Mechanics," John S. McNown, En-Yun Hsu and Chia-Shun Yih (with discussion), 650.

"Effect of Well Screens on Flow into Wells," Jack S. Petersen, Carl Rohwer and Maurice L. Albertson (with discussion), 563.

"High-Velocity Tests in a Penstock," Maxwell F. Burke (with discussion), 863.

The orifice analogy for open channel constrictions, 961.

WATER GATES, MOVABLE

"Discharge Characteristics of Tainter Gates," Arthur Toch, 290.

WATER, GROUND

See GROUND WATER

WATER HAMMER

See also COSTS, WATER HAMMER ANALYSIS; WATER PRESSURE

Charts for solution of water hammer problems, 697, 713.

"Pressure Surges in Pump Installations," John Parmakian, 697. *Discussion:* Carroll E. Withers, Peter Linton, and John Parmakian, 717.

WATER INSTRUMENTS

See under types of instruments, e.g., GAGES . . . ; METERS AND METERING . . .

WATER LAW

See LAW subject heading under WATER . . . , e.g., WATERWAY LAW

WATER METERS AND METERING (stream velocity)

See METERS AND METERING, CURRENT

WATER PIPES AND PIPING

See PIPES AND PIPING (cross references thereunder)

WATER POWER (General)

See MULTI-PURPOSE PROJECTS (RIVER PROJECTS); POWER PLANTS; TURBINES, WATER

WATER PRESSURE

See also GAGES, PRESSURE; PIPE LINES; WATER HAMMER

"Applications of the Relaxation Technique in Fluid Mechanics," John S. McNown, En-Yun Hsu and Chia-Shun Yih (with discussion), 650.

"Hydraulic Model Studies of Martin Dam Draft Tubes," Carl E. Kindsvater and Richard R. Randolph, Jr. (with discussion), 1399.

"Reduction in Soil Strength with Increase in Density," Charles R. Foster (with discussion), 803.

"Strength Characteristics of Compacted Clays," Gerald A. Leonards (with discussion), 1420.

"The Undisturbed Consolidation Behavior of Clay," John H. Schmertmann (with discussion), 1201.

WATER, STORM

See DRAINAGE; SEWAGE DISPOSAL; SEWERS

WATER SUPPLY (General)

See also FILTERS AND FILTRATION, WATER; GROUND WATER; IRRIGATION; METERS AND METERING; PIPE LINES; PUMPS AND PUMPING; SETTLING BASINS; WATER . . . (related subject headings thereunder); WELLS

"Effect of Well Screens on Flow into Wells," Jack S. Petersen, Carl Rohwer and Maurice L. Albertson (with discussion), 563.

WATER SURFACE PROFILES

See BACKWATER

WATER SURFACE SURGES

See WATER HAMMER; WAVES

WATER THROW

See JETS (cross reference thereunder)

WATER TRAJECTORY

See JETS (cross reference thereunder)

WATER TRANSPORTATION (General)

See also CANALS; COSTS, WATER TRANSPORTATION; FREIGHT; HARBORS; RIVERS; TRAFFIC . . . ; TUNNELS, VEHICULAR; WATERWAYS

The "Commerce Clause" in the United States Constitution, 1537.

WATER TRANSPORTATION (Geographical)

United States

"Some Economic Aspects of Waterway Projects," Haywood R. Faison (with discussion), 1480.

WATER TREATMENT

See also FILTERS AND FILTRATION, WATER

"Flocculation and Flocculation Basins," Thomas R. Camp, 1.

WATER TURBINES

See TURBINES, WATER

WATER, UNDERGROUND

See GROUND WATER

WATER VELOCITY METERS

See METERS AND METERING, CURRENT

WATER, WASTE

See SEWAGE DISPOSAL; SEWERS

WATER WAVES

See WAVES

WATERWAY LAW

United States Supreme Court decision and 82nd Congress legislation pending relating to inland waterway rate making and other problems, 1515, 1520.

WATERWAYS (General)
See also CANALS; CHANNELS; COSTS . . . ; FREIGHT; HARBORS; OCEAN . . . (cross references thereunder); RIVERS; SEA . . . (cross references thereunder); TRAFFIC, WATERWAY; WATER TRANSPORTATION
Financing
"Some Economic Aspects of Waterway Projects," Haywood R. Faison (with discussion), 1480.
WATERWAYS (Geographical)
Illinois Waterway
Economic aspects and history of the Illinois Waterway, 1480, 1489.
United States
Report of Engineers Joint Council (EJC) committee on national water policy recommendations criticized and defended, 1496, 1544.
"Some Economic Aspects of Waterway Projects," Haywood R. Faison, 1480. *Discussion:* Duane Orr; L. Perry Cookingham; Marvin B. Marsh; Owen G. Stanley; Herman W. Schull, Jr.; Nels C. Magnuson; Braxton B. Carr; Cyril E. Childe; Francis J. Wilson and Newton R. Graham; Charles L. Hall; James W. Davis; and Haywood R. Faison, 1526.
WATERWAY TRAFFIC
See TRAFFIC, WATERWAY
WATER TRAJECTORY
See JETS (cross reference thereunder)
WATERWAY TRANSPORTATION
See WATER TRANSPORTATION
WATERWORKS (General)
See DAMS (cross references thereunder); ENGINES; METERS AND METERING, VENTURI; PIPE LINES; PIPES AND PIPING (cross references thereunder); PUMPS AND PUMPING; SEDIMENT AND SEDIMENTATION; WATER SUPPLY; WATER TREATMENT; WELLS
WAVES
See also SEISMOLOGY; TIDES; WATER PRESSURE
Relaxation method usage in determining certain types of wave motion, including seiche, 651, 681, 686.
WEATHER
See ATMOSPHERIC PRESSURE; FLOODS (cross references thereunder); HYDROLOGY (cross references thereunder); RAINFALL (cross references thereunder); TEMPERATURE; WIND . . .
WEATHER BUREAU, UNITED STATES
See under relative subject, e.g., FLOODS (cross references thereunder); WIND . . .
WEBS
See BEAMS
WEIGHTS
See under relative subject, e.g., BRIDGES, SUSPENSION
WEIRS
See LIQUIDS, FLOW OF, OVER WEIRS; WATER, FLOW OF, IN OPEN CHANNELS; WATER, FLOW OF, IN PIPES
WELDED JOINTS
See JOINTS, WELDED
WELDS AND WELDING
See also COSTS, WELD AND WELDING; METALS (cross references thereunder)
Specifications controlling welding of structural steel, 236, 244.
"Welded Structures": A Symposium, Simon A. Greenberg, La Motte Grover, and C. L. Kreidler, 103. *Discussion:* Jack R. Benjamin, George W. Lamb, F. J. Tamanini, Norman B. Jones, and La Motte Grover, 112.
Inspection
Radiographic inspection in bridge welding, 242.
"Structural Welding Inspection," John L. Beaton and Paul G. Jonas, 235.
Uses of penetrant dye method of inspection, 240.
WELLS
See also GROUND WATER
"Applications of the Relaxation Technique in Fluid Mechanics," John S. McNown, En-Yun Hsu and Chia-Shun Yih (with discussion), 650.
Early law and interstate control of oil and gas in the United States, 496, 498.
"Effect of Well Screens on Flow into Wells," Jack S. Petersen, Carl Rohwer and Maurice L. Albertson, 563. *Discussion:* Wen-Hsiung Li; Arthur L. Collins; Mohammad Nazir and Nazir Ahmad; Matthew I. Rorabaugh; Dean F. Peterson, Jr.; G. Cohen de Lara; Gerard Tison, Jr.;

WELLS (*Continued*)
and Jack S. Petersen, Carl Rohwer, and Maurice L. Albertson, 586.
Test apparatus for determining water flow into and through well screens, 571, 573, 593.

WHEEL LOADS
"Stress Measurements, San Leandro Creek Bridge," Ray W. Clough and Charles F. Scheffey, 939.

WIND (General)
See also WAVES
"Aerodynamic Stability of Suspension Bridges": 1952 Report of the Advisory Board on the Investigation of Suspension Bridges, E. F. Kelley, Raymond Archibald, A. A. Jakkula, Raymond Archibald, C. B. McCullough, G. S. Paxson, F. H. Frankland, C. F. Goodrich, Jonathan Jones, C. Earl Webb, Russell G. Cone, Shortridge Hardesty, Charles M. Spofford, O. L. Grover, E. F. Kelley, R. B. McMinn, Leon S. Moisseiff, C. H. Purcell, Norman C. Raab, George D. Whittle, Theodor von Karman, Frank M. Masters, P. L. Pratley, John G. Little, Leon H. Nishkian, R. W. Crum, Franklin N. Wray, Charles C. Sunderland, H. L. Dryden, G. B. Schubauer, O. H. Ammann, Elmer K. Timby, Emil H. Praeger, F. B. Farquharson, Charles E. Andrew, Glenn B. Woodruff, and Hardy Cross, 721.
High frequency hurricane localities, in United States, 1900–1951, 178.
Hurricane recording by the United States Weather Bureau, including gust factor, 173, 175.
Maximum velocities recorded for hurricane winds, including gusts, 174, 179.
"Wind Velocities during Hurricanes," Robert C. Gentry, 169.

WIND MEASURING INSTRUMENTS
Designing and using wind measuring instruments in extremely high winds, 173.
Methods of using anemometers, 174, 176.

WIND PRESSURE
See AERODYNAMICS; STRUCTURES, THEORY OF—Bridges

WIRE ROPES AND ROPING
See CABLES . . . (cross reference thereunder)

WORK, COST OF
See COSTS

WORKS (industrial buildings and equipment)
See under general types of works, e.g., PUBLIC WORKS (cross reference thereunder); *also* under specific type of works, e.g., GAS AND GASWORK . . . ; SEWAGE WORKS (cross references thereunder); WATERWORKS (cross references thereunder); *see also* cross references under PLANTS

AUTHOR INDEX

(including Memoirs of deceased members)

Ahmad, Nazir
Well screens, 593.

Albertson, Maurice L.
"Effect of Well Screens on Flow into Wells," 563.
"Total Sediment Load Measured in Turbulence Flume," 457.

Ambrose, Harry H.
Rough conduits, 402.

Ammann, O. H.
"Aerodynamic Stability of Suspension Bridges": 1952 Report of the Advisory Board on the Investigation of Suspension Bridges, 768.

Anderson, Boyd G.
Cylindrical shell roofs, 646.

Anderson, Norval
"Sewage Aeration Practice in Chicago," 351.

Andrew, Charles E.
"Aerodynamic Stability of Suspension Bridges": 1952 Report of the Advisory Board on the Investigation of Suspension Bridges, 768.

Archibald, Raymond
"Aerodynamic Stability of Suspension Bridges": 1952 Report of the Advisory Board on the Investigation of Suspension Bridges, 767.

Ashdown, Alfred J.
Inelastic behavior, 205.

Aslakson, Carl I.
"The Importance of Shoran Surveying," 225.

Baker, J. F.
Plastic strength, 1104.

Ball, Ethan F.
"Chesapeake Bay Bridge," 245.

Barber, Edward S.
Soil strength, 816.

Baron, Frank
"High-Strength Bolts in Structural Joints (symposium): Comparison of Bolted and Riveted Joints," 1322.
"Plastic Strength of Structural Members (symposium): Foreword," 1020.

Beaton, John L.
"Structural Welding Inspection," 235.

Beedle, Lynn S.
Plastic strength, 1097.
"Plastic Strength of Structural Members (symposium): Foreword," 1020.
"Plastic Strength of Structural Members (symposium): Plastic Deformation of Wide-Flange Beam-Columns," 1028.

Benedict, Paul C.
"Total Sediment Load Measured in Turbulence Flume," 457.

Benjamin, Jack R.
Welded structures, 134.

Bennett, Preston T.
Compacted clays, 1467.

Berndt, Neil R.
"Transit Lining of High-Speed Track," 521.

Bijlaard, Paul P.
Plastic strength, 1156.
"Plastic Strength of Structural Members (symposium): Eccentrically Loaded, End-Restrained Columns," 1070.

Blaisdell, Fred W.
Open channel constrictions, 981.
Relaxation techniques, 670.

Blee, Clarence E.
Hydroelectric plants, 558.

Bleich, Hans H.
"Impulsive Motion of Elasto-Plastic Beams," 499.

Blodget, Lorin Theodore
Memoir of, 1558.

Blum, Louis Philip
Memoir of, 1559.

Bolton, Frank Leonard
Memoir of, 1560.

Boreli, Mladen
Relaxation techniques, 677.

Borland, W. M.
Turbulence flumes, 485.

Bose, N. K.
Stable channels, 1269.

Brady, W. Gordon
"Plastic Strength of Structural Members (symposium): Investigation and Limit Analysis of Net Area in Tension," 1133.

Braudeau, G.
Stable channels, 1266.

Bresler, Boris
Inelastic behavior, 203.

Burke, Maxwell F.
"High-Velocity Tests in a Penstock," 863.

Butcher, Harold Edgar
Memoir of, 1560.

Camp, Thomas R.
"Flocculation and Flocculation Basins," 1.

Campbell, Frank B.
Penstock tests, 887.

Carr, Braxton B.
Waterway economics, 1538.

Carter, Jack W.
"High-Strength Bolts in Structural Joints (symposium): Fatigue in Riveted and Bolted Single-Lap Joints," 1353.

Carter, Rolland W.
"Backwater Effects of Open-Channel Constrictions," 993.
"Tranquil Flow through Open-Channel Constrictions." 955.

Childe, Cyril E.
Waterway economics, 1539.

Chin, A. G.
"High-Strength Bolts in Structural Joints (symposium): Slip of Joints under Static Loads," 1335.

Chu, Henry H.
"Backwater Functions by Numerical Integration," 429.

Chung, Randall
"Constrained Circular Beams on Elastic Foundations," 301.

Clapper, Leland
Memoir of, 1561.

Clark, John W.
"Plastic Strength of Structural Members (symposium): Eccentrically Loaded Aluminum Columns," 1116.

Clough, Ray W.
"Stress Measurements, San Leandro Creek Bridge," 939.

Collins, Arthur L.
Penstock tests, 888.
Well screens, 590.

Cone, Russell G.
"Aerodynamic Stability of Suspension Bridges": 1952 Report of the Advisory Board on the Investigation of Suspension Bridges, 767.

Cookingham, L. Perry
Waterway economics, 1528.

Corbett, W. H.
Turbulence flumes, 485.

Crisp, Robert L., Jr.
Undisturbed consolidation, 1228.

Cross, Hardy
"Aerodynamic Stability of Suspension Bridges": 1952 Report of the Advisory Board on the Investigation of Suspension Bridges, 768.

Crum, R. W.
"Aerodynamic Stability of Suspension Bridges": 1952 Report of the Advisory Board on the Investigation of Suspension Bridges, 768.

Curtis, Allen J.
"Photoelastic Analogy for Nonhomogeneous Foundations," 35.

D'Appolonia, Elio
"Sand Compaction by Vibroflotation," 154.

Davis, Harmer E.
"Issues in Highway Engineering Education," 340.

Davis, James W.
Waterway economics, 1545.

Degenkolb, Henry J.
"Structural Observations of the Kern County Earthquake," 1280.

de Lara, G. Cohen
Well screens, 598.

Dempster, Osborne Joel
Memoir of, 1561.

de Vries, Karl
High strength bolts, 1381.

Dougherty, John Wilson
Memoir of, 1562.

Drucker, Daniel C.
"Plastic Strength of Structural Members (symposium): Foreword." 1020.

Drucker, Daniel C. (*Continued*)
"Plastic Strength of Structural Members (symposium): Investigation and Limit Analysis of Net Area in Tension," 1133.

Dryden, H. L.
"Aerodynamic Stability of Suspension Bridges": 1952 Report of the Advisory Board on the Investigation of Suspension Bridges, 768.

Ernst, G. C.
Cylindrical shell roofs, 644.

Escoffier, Francis F.
Backwater functions, 443.

Faison, Haywood R.
"Some Economic Aspects of Waterway Projects," 1480.

Farquharson, F. B.
"Aerodynamic Stability of Suspension Bridges": 1952 Report of the Advisory Board on the Investigation of Suspension Bridges, 768.

Fisher, Gordon P.
"Plastic Strength of Structural Members (symposium): Eccentrically Loaded, End-Restrained Columns," 1070.

Foster, Charles R.
"Reduction in Soil Strength with Increase in Density," 803.

Francis, A. J.
High strength bolts, 1319.

Frankland, F. H.
"Aerodynamic Stability of Suspension Bridges": 1952 Report of the Advisory Board on the Investigation of Suspension Bridges, 767.

Frankland, James
Memoir of, 1563.

Fuller, Almon H.
Stress measurement, 336.

Furbank, Arthur W.
Municipal composting, 916.

Gandolfo, Jose S.
Stable channels, 1271.

Garlinghouse, Leslie Holmes
Memoir of, 1563.

Gentry, Robert C.
"Wind Velocities during Hurricanes," 169.

Gibbs, Harold J.
Compacted clays, 1455.

Giesecke, Frederick Ernest
Memoir of, 1564.

Glidden, William R.
"Backsights and Foresights—Glimpses Ahead in the Light of History as Directed by Science": Address at the Summer Convention, St. Louis, Mo., June 15, 1955, 1550.

Goodman, Lawrence E.
"Aseismic Design of Firmly Founded Elastic Structures," 782.

Goodrich, C. F.
"Aerodynamic Stability of Suspension Bridges": 1952 Report of the Advisory Board on the Investigation of Suspension Bridges, 767.

Gosline, George Williams
Memoir of, 1564.

Gotaas, Harold B.
"Stabilization of Municipal Refuse by Composting," 897.

Graham, Newton R.
Waterway economics, 1542.

Greenberg Simon A.
"Welded Structures (symposium): Steel Requirements," 104.

Griffiths, John D.
"Plastic Strength of Structural Members (symposium): Foreword," 1020.

Grover, La Motte
"Welded Structures (symposium): Design and Research," 112.

Grover, O. L.
"Aerodynamic Stability of Suspension Bridges": 1952 Report of the Advisory Board on the Investigation of Suspension Bridges, 767.

Gunn, Donald
Memoir of, 1565.

Hall, Charles L.
Waterway economics, 1543.

Halton, George R.
Soil strength, 817.

Hammond, Harry Parker
Memoir of, 1566.

Hansen, O. C.
Turbulence flumes, 485.

Hansen, Viggo
"Movements in Structural Concrete in a Powerhouse," 1183.

Hardesty, Shortridge
"Aerodynamic Stability of Suspension Bridges": 1952 Report of the Advisory Board on the Investigation of Suspension Bridges, 767.

Harding, S. T.
"Statutory Control of Ground Water in the Western United States," 490.

Hardman, Roy Cordis
Memoir of, 1566.

Hechtman, R. A.
"High-Strength Bolts in Structural Joints (symposium): Slip of Joints under Static Loads," 1335.

Heindel, Judson Clifford
Memoir of, 1567.

Henry, Harold R.
Open channel constrictions, 1013.

Higgins, T. R.
"High-Strength Bolts in Structural Joints (symposium): Structural Uses of High-Strength Bolts," 1389.

Hilf, Jack W.
Compacted clays, 1455.

Hodges, Paul V.
Open channel constrictions, 1007.

Hognestad, Eivind
"Plastic Strength of Structural Members (symposium): Foreword," 1020.

Homack, Peter
Biofiltration plants, 836.

Horne, Michael R.
Lateral buckling, 1179.
Plastic strength, 1104.

Horonjeff, Robert
"Determination of Radii of Curvature of Taxiways," 27.

Howard, Ernest Emmanuel
Memoir of, 1558.

Hoyer, Carl O.
"Industrial Development in the South," 411.

Hsu, En-Yun
"Applications of the Relaxation Technique in Fluid Mechanics," 650.

Hutchinson, Frank
Memoir of, 1568.

Hyatt, Edward
Memoir of, 1568.

Ippen, Arthur T.
"Motion of Particles on Bed of a Turbulent Stream," 921.

Izzard, Carl F.
Open channel constrictions, 985, 1008.

Jakkula, A. A.
"Aerodynamic Stability of Suspension Bridges": 1952 Report of the Advisory Board on the Investigation of Suspension Bridges, 767.

James, R. L.
"Plastic Strength of Structural Members (symposium): Foreword," 1020.

Jeffers, Paul Eells
Memoir of, 1569.

Jessop, George A.
Hydroelectric plants, 559.

Johnson, Frank Arthur
Memoir of, 1569.

Johnston, Bruce G.
"Analysis and Tests of a Cylindrical Shell Roof Model," 615.
"Plastic Strength of Structural Members (symposium): Foreword," 1020.

Jonas, Paul G.
"Structural Welding Inspection," 235.

Jones, John H.
"Determination of Radii of Curvature of Taxiways," 27.

Jones, Jonathan
"Aerodynamic Stability of Suspension Bridges": 1952 Report of the Advisory Board on the Investigation of Suspension Bridges, 767.
"Erection of Main River Span, Passaic River Bridge," 208.

Jones, Norman B.
Welded structures, 143.

Jones, Owen Meriwether
Memoir of, 1570.

Kaminsky, Edmund L.
"Plastic Strength of Structural Members (symposium): Plastic Deformation of Wide-Flange Beam-Columns," 1028.

Kammer, Herbert A.
Concrete movement, 1196.

Kampmeier, Roland A.
Southern industry, 422.

Kaufman, Vivian Gregor
Memoir of, 1571.

Keifer, Clint J.
"Backwater Functions by Numerical Integration," 429.

Kelley, E. F.
"Aerodynamic Stability of Suspension Bridges": 1952 Report of the Advisory Board on the Investigation of Suspension Bridges, 767.

Ketter, Robert L.
Plastic strength, 1097.
"Plastic Strength of Structural Members (symposium): Plastic Deformation of Wide-Flange Beam-Columns," 1028.

Kindsvater, Carl E.
"Hydraulic Model Studies of Martin Dam Draft Tubes," 1399.
"Tranquil Flow through Open-Channel Constrictions," 955.

Kluge, Ralph W.
"Dead-Load Stress Measurement in a Long Span Bridge," 311.

Kolupaila, Steponas
Penstock tests, 884.

Kreidler, C. L.
"Welded Structures (symposium): Fabrication and Construction," 147.

Lagaard, Maurice B.
"Dead-Load Stress Measurement in a Long Span Bridge," 311.

Lamb, George W.
Welded structures, 135.

Lane, Emory W.
"Design of Stable Channels," 1234.

Larson, Edward W., Jr.
"Dead-Load Stress Measurement in a Long Span Bridge," 311.
"High-Strength Bolts in Structural Joints (symposium): Comparison of Bolted and Riveted Joints," 1322.

Laursen, Emmett M.
Open channel constrictions, 981.

Lee *See also* Li

Lee, Lawrence H. N.
"Inelastic Behavior of Reinforced Concrete Members," 181.

Leliavsky, Serge
Stable channels, 1261.

Lenzen, Kenneth H.
"Dead-Load Stress Measurement in a Long Span Bridge," 311.
"High-Strength Bolts in Structural Joints (symposium): Fatigue in Riveted and Bolted Single-Lap Joints," 1353.

Leonards, Gerald A.
"Strength Characteristics of Compacted Clays," 1420.

Li. *See also* Lee

Li, Wen-Hsiung
"Open Channels with Nonuniform Discharge," 255.
Well screens, 586.

Lin, Pin-Nam
Open channel constrictions, 982.

Linton, Peter
Pressure surges, 717.

Little, John G.
"Aerodynamic Stability of Suspension Bridges": 1952 Report of the Advisory Board on the Investigation of Suspension Bridges, 768.

Lowden, Spencer William
Memoir of, 1571.

Lundquist, Eugene E.
"Plastic Strength of Structural Members (symposium): Foreword," 1020.

Magnuson, Nels C.
Waterway economics, 1537.

Mannes, Conrad Olai
Memoir of, 1572.

Marsh, Marvin B.
Waterway economics, 1530.

Masters, Frank M.
"Aerodynamic Stability of Suspension Bridges": 1952 Report of the Advisory Board on the Investigation of Suspension Bridges, 768.

Matejka, Donald Q.
"Total Sediment Load Measured in Turbulence Flume," 457.

McCammon, Lewis B., Jr.
"Dead-Load Stress Measurement in a Long Span Bridge," 311.

McCullough, C. B.
"Aerodynamic Stability of Suspension Bridges": 1952 Report of the Advisory Board on the Investigation of Suspension Bridges, 767.

McGauhey, Percy H.
"Stabilization of Municipal Refuse by Composting," 897.

McMinn, R. B.
"Aerodynamic Stability of Suspension Bridges": 1952 Report of the Advisory Board on the Investigation of Suspension Bridges, 767.

McNown, John S.
"Applications of the Relaxation Technique in Fluid Mechanics," 650.

Menhinick, Howard K.
"The Training of City Planners," 608.

Meyer, Adolf A.
"Modernization of the Hales Bar Plant," 539.

Middlebrooks, Thomas Alwyn
Memoir of, 1572.

Miles, Henry J.
Backwater functions, 444.

Miller, Callix E.
"Sand Compaction by Vibroflotation," 154.

Mitchell, James K.
Compacted clays, 1462.

Moisseiff, Leon S.
"Aerodynamic Stability of Suspension Bridges": 1952 Report of the Advisory Board on the Investigation of Suspension Bridges, 767.

Morris, Henry M., Jr.
"Flow in Rough Conduits," 373.

Moyer, Ralph A.
"Issues in Highway Engineering Education," 340.

Moyer, Stanley
"Movements in Structural Concrete in a Powerhouse," 1183.

Munse, William H.
"High-Strength Bolts in Structural Joints (symposium); Laboratory Tests of Bolted Joints," 1299.
Plastic strength, 1155.
"Plastic Strength of Structural Members (symposium): Foreword," 1020.

Nazir, Mohammad
Well screens, 593.

Newmark, Nathan M.
"Aseismic Design of Firmly Founded Elastic Structures," 782.
"High-Strength Bolts in Structural Joints (symposium): Laboratory Tests of Bolted Joints," 1299.

Nishkian, Leon H.
"Aerodynamic Stability of Suspension Bridges": 1952 Report of the Advisory Board on the Investigation of Suspension Bridges, 768.

Nizery, A.
Stable channels, 1266.

Noble, Charles M.
"Planning and Operating Turnpikes," 54.

Oesterblom, I.
Circular beams, 87.

Oliver, Emery
Memoir of, 1573.

Orr, Duane
Waterway economics, 1526.

Palmer, Ralph Mallory
Memoir of, 1574.

Parmakian, John
"Pressure Surges in Pump Installations," 697.

Paxson, G. S.
"Aerodynamic Stability of Suspension Bridges": 1952 Report of the Advisory Board on the Investigation of Suspension Bridges, 767.

Paynter, Henry M.
Relaxation techniques, 671.

Peraino, Joseph
"Construction of the Elizabeth River Tunnel," 423.

Petersen, Jack S.
"Effect of Well Screens on Flow into Wells," 563.

Peterson, Dean F., Jr.
Well screens, 597.

Posey, Chesley J.
Open channel constrictions, 990.

Praeger, Emil H.
"Aerodynamic Stability of Suspension Bridges": 1952 Report of the Advisory Board on the Investigation of Suspension Bridges, 768.

Pratley, P. L.
"Aerodynamic Stability of Suspension Bridges": 1952 Report of the Advisory Board on the Investigation of Suspension Bridges, 768.

Prince, Harry C.
High strength bolts, 1382.

Prokosch, Walther
"Traffic at an International Airport," 364.

Purcell, C. H.
"Aerodynamic Stability of Suspension Bridges": 1952 Report of the Advisory Board on the Investigation of Suspension Bridges, 767.

Raab, Norman C.
"Aerodynamic Stability of Suspension Bridges": 1952 Report of the Advisory Board on the Investigation of Suspension Bridges, 767.

Rand, Walter
Rough conduits, 400.

Randolph, Richard R., Jr.
"Hydraulic Model Studies of Martin Dam Draft Tubes," 1399.

Rankin, Renville S.
"Evaluation of the Performance of Biofiltration Plants," 823.

Reed, Oren
Memoir of, 1574.

Rich, George R.
Hydroelectric plants, 557.

Richart, F. E., Jr.
"Photoelastic Analogy for Nonhomogeneous Foundations," 35.

Riley, Russell H.
"Community and Neighborhood Development," 449.

Roberts, Leo Bond
Memoir of, 1575.

Rohwer, Carl
"Effect of Well Screens on Flow into Wells," 563.

Root, Arthur W.
"Correction of Landslides and Slipouts," 281.

Rorabaugh, Matthew I.
Well screens, 595.

Rosenblueth, Emilio
"Aseismic Design of Firmly Founded Elastic Structures," 782.

Rubey, Harry
Transit lining of railway curves, 538.

Ruble, E. J.
"High-Strength Bolts in Structural Joints (symposium): Structural Uses of High-Strength Bolts," 1389.

Ryan, Robert Laurence
Memoir of, 1575.

Salovaara, Jorma J.
City planners and education, 613.

Salvadori, Mario G.
"Impulsive Motion of Elasto-Plastic Beams," 499.
"Lateral Buckling of I-Beams," 1165.

Sarpkaya, Turgut
Open channels, 275.
Relaxation techniques, 681.

Savikko, E. R.
"High-Strength Bolts in Structural Joints (symposium): Slip of Joints under Static Loads," 1335.

Scheffey, Charles F.
"Stress Measurements, San Leandro Creek Bridge," 939.

Schmertmann, John H.
"The Undisturbed Consolidation Behavior of Clay," 1201.

Schubauer, G. B.
"Aerodynamic Stability of Suspension Bridges": 1952 Report of the Advisory Board on the Investigation of Suspension Bridges, 768.

Schull, Herman W., Jr.
Waterway economics, 1536.

Schultz, Edward A.
"Sediment Sampling in Tidal Waterways," 687.

Scott, Ronald F.
Relaxation techniques, 671.

Shea, Paul H.
"Unusual Foundation Conditions in the Everglades," 92.

Shuptrine, Harry Augustus
Memoir of, 1576.

Sill, Rush Tabor
Memoir of, 1576.

Silvester, Richard
Backwater functions, 445.

Snodgrass, George F.
"Selection and Design of High-Volume, Low-Head Pumps," 17.

Spofford, Charles M.
"Aerodynamic Stability of Suspension Bridges": 1952 Report of the Advisory Board on the Investigation of Suspension Bridges, 767.

Stanley, Owen G.
Waterway economics, 1532.

Stewart, W. C.
"High-Strength Bolts in Structural Joints (symposium): History of the Use of High-Strength Bolts," 1296.

Streeter, Victor L.
Rough conduits, 399.

Sunderland, Charles C.
"Aerodynamic Stability of Suspension Bridges": 1952 Report of the Advisory Board on the Investigation of Suspension Bridges, 768.

Swift, William Everett
Memoir of, 1577.

Symonds, P. S.
Elasto-plastic beams, 516.
"Plastic Strength of Structural Members (symposium): Foreword," 1020.

Tabor, Henry Whitney
Memoir of, 1578.

Tamanini, F. J.
Welded structures, 140.

Teeter, Earle Everett
Memoir of, 1578.

Thurlimann, Bruno
"Analysis and Tests of a Cylindrical Shell Roof Model," 615.

Timby, Elmer K.
"Aerodynamic Stability of Suspension Bridges": 1952 Report of the Advisory Board on the Investigation of Suspension Bridges, 768.

Tison, Gerard, Jr.
Well screens, 601.

Toch, Arthur
"Discharge Characteristics of Tainter Gates," 290.
Open channel constrictions, 981.

Tracy, Hubert J.
"Backwater Effects of Open-Channel Constrictions," 993.

Trimble, William Foster, Jr.
Memoir of, 1579.

Verma, Ramjee P.
"Motion of Particles on Bed of a Turbulent Stream," 921.

Volterra, Enrico
"Constrained Circular Beams on Elastic Foundations," 301.
"Deflections of a Circular Beam Out of Its Initial Plane," 65.

von Karman, Theodor
"Aerodynamic Stability of Suspension Bridges": 1952 Report of the Advisory Board on the Investigation of Suspension Bridges, 768.

Ware, Thomas M.
"Sand Compaction by Vibroflotation," 154.

Webb, C. Earl
"Aerodynamic Stability of Suspension Bridges": 1952 Report of the Advisory Board on the Investigation of Suspension Bridges, 767.

Whitman, Robert V.
Lateral buckling, 1178.

Whitney, Charles S.
Cylindrical shell roofs, 645.

Whittle, George D.
"Aerodynamic Stability of Suspension Bridges": 1952 Report of the Advisory Board on the Investigation of Suspension Bridges, 767.

Wilson, Francis J.
Waterway economics, 1542.

Winter, George
Plastic strength, 1062.
"Plastic Strength of Structural Members (symposium): Eccentrically Loaded, End-Restrained Columns," 1070.
"Plastic Strength of Structural Members (symposium), Foreword," 1020.

Withers, Carroll E.
Pressure surges, 717.

Wohlt, Paul E.
Compacted clays, 1467.

Wood, Dana Melvin
Memoir of, 1579.

Woodhead, E. A.
Concrete movement, 1193.

Woodruff, Glenn B.
"Aerodynamic Stability of Suspension Bridges": 1952 Report of the Advisory Board on the Investigation of Suspension Bridges, 768.
High strength bolts, 1381.

Woodruff, Richard S.
Draft tubes, 1416.

Wray, Franklin N.
"Aerodynamic Stability of Suspension Bridges": 1952 Report of the Advisory Board on the Investigation of Suspension Bridges, 768.

Wright, D. T.
"High-Strength Bolts in Structural Joints (symposium): Laboratory Tests of Bolted Joints," 1299.

Wyly, Lawrence T.
"Dead-Load Stress Measurement in a Long Span Bridge," 311.
"High-Strength Bolts in Structural Joints (symposium): Fatigue in Riveted and Bolted Single-Lap Joints," 1353.

Yeo, William Herbert Watt
Memoir of, 1580.

Yih, Chia-Shun
"Applications of the Relaxation Technique in Fluid Mechanics," 650.

Young, D. R.
"High-Strength Bolts in Structural Joints (symposium): Slip of Joints under Static Loads," 1335.

Youngquist, R. Clifford
Penstock tests, 893.

Zack, Samuel I.
"Financing of Sewage Works in Pennsylvania," 843.